Virchows Arch (2008) 452:1–10
DOI 10.1007/s00428-007-0532-2

REVIEW AND PERSPECTIVE

MicroRNA—implications for cancer

Stefanie Sassen · Eric A. Miska · Carlos Caldas

Received: 18 August 2007 / Revised: 9 October 2007 / Accepted: 18 October 2007 / Published online: 27 November 2007
© Springer-Verlag 2007

Abstract MicroRNAs (miRNAs) are small RNA molecules that regulate gene expression post-transcriptionally. After the discovery of the first miRNA in the roundworm *Caenorhabditis elegans*, these short regulatory RNAs have been found to be an abundant class of RNAs in plants, animals, and DNA viruses. About 3% of human genes encode for miRNAs, and up to 30% of human protein coding genes may be regulated by miRNAs. MicroRNAs play a key role in diverse biological processes, including development, cell proliferation, differentiation, and apoptosis. Accordingly, altered miRNA expression is likely to contribute to human disease, including cancer. This review will summarize the emerging knowledge of the connections between human miRNA biology and different aspects of carcinogenesis. Various techniques available to investigate miRNAs will also be discussed.

Keywords MicroRNA · miRNA · Cancer · Pathogenesis · Development

S. Sassen (✉) · C. Caldas
Breast Cancer Functional Genomics Laboratory, Cancer Research UK Cambridge Research Institute and Department of Oncology, University of Cambridge, Li Ka Shing Centre,
Robinson Way,
Cambridge CB2 0RE, UK
e-mail: stefanie.sassen@cancer.org.uk

E. A. Miska
Wellcome Trust/Cancer Research UK Gurdon Institute and Department of Biochemistry, University of Cambridge,
Cambridge, UK

The "small RNA revolution"

Small ribonucleic acid (RNA) can act as a specific regulator of gene expression. This discovery has been an exciting breakthrough in Biological Sciences of the past decade, culminating in last year's Nobel Prize in Physiology or Medicine awarded to Andrew Fire and Craig Mello. Building on previous work mainly in plants [50], Fire et al. [23] discovered that exogenous double-stranded RNA can be used to specifically interfere with gene function. This phenomenon was called RNA interference (RNAi). They also speculated that organisms might use double-stranded RNA naturally as a way of silencing genes. It was then shown that RNA interference was mediated by 22 nucleotide single-stranded RNAs termed small interfering RNAs (siRNAs) derived from the longer double-stranded RNA precursors [87]. The small interfering RNAs were found to repress genes by eliminating the corresponding messenger RNA transcripts, and thus, preventing protein synthesis.

Over the following years, many new small functional RNAs have been found. RNA is usually thought of as messenger RNA that serves as the template for translation of genes into proteins. In contrast, functional or non-coding RNA molecules are transcribed from a DNA sequence, but not translated into protein. The encoding DNA sequence is often referred to as an RNA gene. Functional RNA genes in the human genome include transfer RNA (tRNA), ribosomal RNA (rRNA), and various other small non-coding RNAs. Several hundred genes in our genome encode small functional RNA molecules collectively called microRNAs (miRNAs). Precursors of these miRNA molecules form structures of double-stranded RNA that can activate the RNA interference machinery. MicroRNAs downregulate

gene expression either by degradation of messenger RNA through the RNA interference pathway or by inhibiting protein translation.

The first miRNA was discovered in 1993 by Victor Ambros and colleagues Rosalind Lee and Rhonda Feinbaum [42]. A genetic screen in the roundworm *Caenorhabditis elegans*, a millimeter-long animal used as a model organism in biological research, identified genes involved in developmental timing [42]. Surprisingly, one of the genes, termed *lin-4*, did not encode a protein but instead a novel 22-nucleotide small RNA. Seven years later, Reinhart et al. [70] discovered a second 22-nucleotide small RNA of this type, *let-7*, a gene also involved in *C. elegans* developmental timing. The *lin-4* and *let-7* small regulatory RNAs soon became very exciting for two reasons. Firstly, homologs of the *let-7* gene were identified in other animals including humans [65]. The conservation of *let-7* across species suggested an important and fundamental biological role for this small RNA. Secondly, the mechanism of RNA interference (RNAi) was discovered at that time, and it became clear that miRNA and RNAi pathways were intricately linked and shared common components. Within the following year, more than 100 additional small regulatory RNAs similar to *lin-4* and *let-7* were identified in worms, the fruit fly *Drosophila*, and in humans [38, 40, 41]. These small non-coding RNAs were named microRNAs (miRNAs) [38, 40, 41].

Subsequently, many more short regulatory RNAs were identified in almost all multicellular organisms, including flowering plants, worms, flies, fish, frogs, mammals [38, 40, 41, 48, 71], and in single cellular algae and DNA viruses [66, 75]. To date, more than 500 human miRNAs have been experimentally identified. Computational predictions of miRNA targets suggest that up to 30% of human protein coding genes may be regulated by miRNAs [46, 68]. This makes miRNAs one of the most abundant classes of regulatory genes in humans. MicroRNAs are now perceived as a key layer of post-transcriptional control within the networks of gene regulation.

MicroRNAs are sequentially processed from longer precursor molecules that are encoded by the miRNA genes [1] (Fig. 1). MiRNA genes are referred to by the same name (termed *mir*) written in italics to distinguish them from the corresponding mature miRNA (termed miR) followed by a number, e.g., *mir-1* or miR-1. The encoding DNA sequence is much longer than the mature miRNA. Two ribonuclease enzymes, Drosha and Dicer, subsequently process the primary transcripts (or pri-miRNA) to generate mature miRNAs. The primary transcripts contain one or more stem-loop structures of about 70 bases. Stem-loops are double-stranded RNA structures consisting of a nucleotide sequence that can fold back on itself to form a double helix with a region of imperfect base pairing that forms an open loop at the end (Fig. 1a). The ribonuclease Drosha excises the stem-loop structure to form the precursor miRNA (or pre-miRNA) [43]. After export into the cytoplasm, the pre-miRNA is cleaved by the ribonuclease Dicer to generate a short RNA duplex [6, 28]. After untwisting, one RNA strand becomes the mature single-stranded miRNA, while the complementary strand, termed miRNA*, is usually rapidly degraded (Fig. 1b).

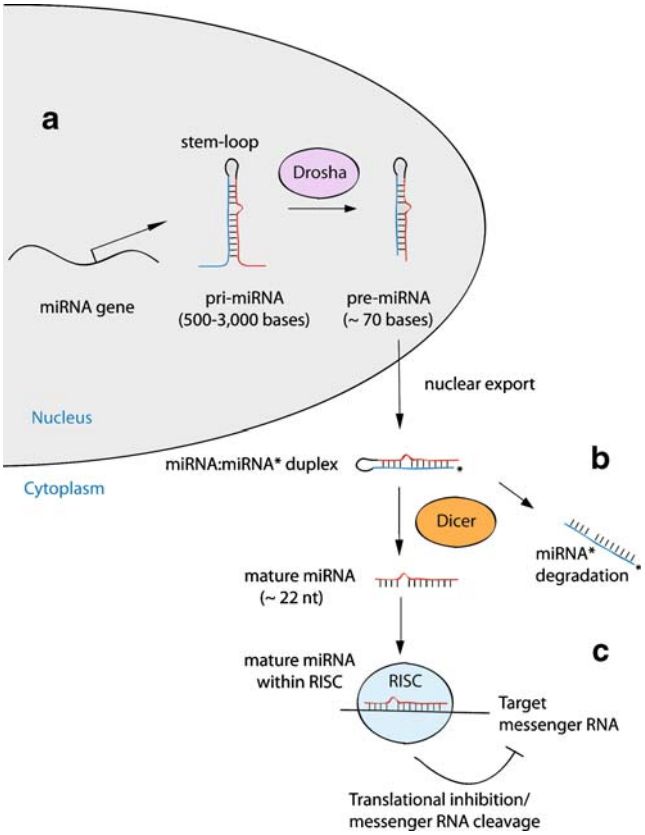


Fig. 1 The biogenesis and function of miRNAs. **a** Primary miRNAs (*pri-miRNA*) are transcribed from longer encoding DNA sequences (miRNA genes). The pri-miRNA contains one or more stem-loop structures of about 70 bases. In the nucleus, the ribonuclease enzyme Drosha excises the stem-loop structure to form the precursor miRNA (*pre-miRNA*). **b** After export into the cytoplasm, the pre-miRNA is cleaved by the ribonuclease Dicer to generate a short RNA duplex (miRNA:miRNA*). **c** The mature single-stranded miRNA is incorporated into the RNA-induced silencing complex (*RISC*), while the complementary strand (miRNA*) is usually rapidly degraded. The miRNA incorporated into the silencing complex can bind to the target messenger RNA by base pairing, causing inhibition of protein translation and/or degradation of the target messenger RNA

MicroRNAs recognize their targets based on sequence complementarity [10]. The mature miRNA is partially complementary to one or more messenger RNAs. In humans, the complementary sites are usually within the 3′-untranslated region of the target messenger RNA. To become effective, the mature miRNA forms a complex with proteins, termed the RNA-induced silencing complex. The miRNA incorporated into the silencing complex can bind to

the target messenger RNA by base pairing. This base pairing subsequently causes inhibition of protein translation and/or degradation of the messenger RNA (Fig. 1c). The potential mechanisms underlying this process were recently reviewed [30, 67]. Protein levels of the target gene are consequently reduced, whereas messenger RNA levels may or may not be decreased. In humans, miRNAs mainly inhibit protein translation of their target genes and only infrequently cause degradation or cleavage of the messenger RNA [1].

The biological role and in vivo functions of most mammalian miRNAs are still poorly understood. In invertebrates, miRNAs regulate developmental timing (e.g., *lin-4*), neuronal differentiation, cell proliferation, growth control, and programmed cell death [9, 33, 42]. In mammals, miRNAs have been found to play a role in embryogenesis and stem cell maintenance [7], hematopoietic cell differentiation [17], and brain development [59, 60]. To date, knowledge of human miRNAs has been primarily descriptive. MicroRNA expression has been found to be deregulated in a wide range of human diseases including cancer. However, it remains uncertain whether altered miRNA expression is a cause or consequence of pathological processes. The underlying mechanisms of why and how miRNAs become deregulated are largely unknown. Although bioinformatics approaches can predict thousands of genes that are potentially targeted and regulated by miRNAs based on sequence complementarity, only very few miRNA target genes have been functionally validated. Our group is currently investigating the role of miRNAs in mammary gland development and breast cancer pathogenesis. A comparison of miRNA and gene expression identified miRNAs that classify molecular breast cancer subtypes [8]. As cancer is ultimately a consequence of disordered gene expression, miRNAs have been suggested to contribute to the development of cancer [11]. This review will focus on the connection between human miRNA biology and different aspects of carcinogenesis. Various techniques available to investigate miRNAs will also be discussed.

MicroRNAs and cancer

Three important observations early in the history of miRNAs suggested a potential role in human cancer. Firstly, the earliest miRNAs discovered in the roundworm *C. elegans* and the fruit fly *Drosophila* were shown to control cell proliferation and apoptosis [9, 42]. Their deregulation may therefore contribute to proliferative diseases such as cancer. Secondly, when human miRNAs were discovered, it was noticed that many miRNA genes were located at fragile sites in the genome or regions that are commonly amplified or deleted in human cancer [14]. Thirdly, malignant tumors and tumor cell lines were found to have widespread deregulated miRNA expression compared to normal tissues [12, 24, 52]. The question remained whether the altered miRNA expression observed in cancer is a cause or consequence of malignant transformation.

MicroRNAs as causal cancer genes at genomic breakpoints

Five years ago, the first direct evidence for an involvement of miRNAs in cancer was reported [13]. Calin et al. studied a well-known deletion on chromosome 13, which is the most frequent chromosomal abnormality in chronic lymphocytic leukemia (CLL). This deletion had long been suspected to contribute to leukemogenesis. However, extensive studies had failed to identify a causal gene. Calin et al. [13] found that two miRNA genes, *mir-15* and *mir-16*, were located within this 30-kb deletion. They subsequently analyzed the expression of miR-15 and miR-16 in blood samples from patients with CLL. Both miRNAs were absent or downregulated in the majority (68%) of cases when compared to normal tissue or lymphocytes. This finding suggested that these two miRNAs were causally involved in the pathogenesis of chronic lymphocytic leukemia.

In 2005, three reports provided the first mechanistic insight into how miRNAs might contribute to carcinogenesis. Two independent studies described the relationship between a miRNA cluster, *mir-17-92*, and the Myc oncogenic pathway [27, 63]. A third report demonstrated an interaction between *let-7* miRNA and the RAS proto-oncogene [32].

The mir-17-92 cluster—small RNAs with oncogenic potential

A cluster of six miRNAs, the *mir-17-92* cluster, was found to be located within a region on chromosome 13 that is commonly amplified in human B-cell lymphomas [64]. He et al. [27] demonstrated that the miRNAs from the *mir-17-92* cluster were overexpressed in lymphoma cell lines carrying this amplification, and expression levels correlated with gene copy number of the *mir-17-92* locus [27]. Further, the miR-17-92 primary transcript was found to be overexpressed in tumor samples from lymphoma patients. To test their hypothesis that *mir-17-92* actively contributes to lymphomagenesis, the authors took advantage of a mouse model of human B-cell lymphoma. These mice develop lymphomas due to an overexpression of the Myc oncogene. The Myc oncogene encodes the transcription factor c-Myc that regulates cell proliferation, growth, and apoptosis, and overexpression of c-Myc is common in cancer. He et al. [27] demonstrated that additional expres-

sion of the *mir-17-92* cluster accelerated c-Myc-induced tumorigenesis in mice. The authors therefore suggested that *mir-17-92* was the first potential non-coding oncogene, referred to as oncomir-1.

The cellular function of miR-17-92 was not identified in these experiments. Nevertheless, the pathology of the tumors indicated lower rates of apoptosis as compared to tumors with Myc overexpression alone. Three recent studies contributed towards our understanding of the oncogenic potential of miR-17-92. Two reports demonstrated an anti-apoptotic effect of miR-17-92 through various pathways that promote cell proliferation and growth [55, 76]. A third study identified mir-17-92 as a mediator of angiogenesis in tumors induced by the oncogene c-Myc [19].

O'Donnell et al. [63] independently identified the same cluster of miRNAs, *mir-17-92*, to be regulated by the transcription factor c-Myc. The transcription factor Myc induces expression of E2F1 growth factor. The *mir-17-92* cluster which is also induced by c-Myc does, in contrast, inhibit E2F1 expression. The authors therefore suggested a novel regulatory mechanism by which c-Myc fine-tunes gene expression by activating the transcription of target genes and by simultaneously inducing inhibitory miRNAs that reduce their translation.

The example of the *mir-17-92* cluster highlights that a distinction between oncogenic and tumor suppressor miRNAs is likely to be an oversimplification. The same miRNAs may have oncogenic or tumor suppressor activity depending on the context and the cell type they are expressed in. A single miRNA may regulate various unrelated target genes and thereby control opposing activities such as cellular proliferation and apoptosis. The ultimate function of a miRNA may depend on the tissue type they are expressed in and what target genes are present.

MicroRNAs with tumor suppressor potential

The *let-7* family of miRNAs was the first group of miRNAs shown to regulate expression of a proto-oncogene, the RAS protein. RAS proteins are membrane-associated signaling proteins that regulate cell growth and differentiation. A miRNA that controls expression of these potentially oncogenic proteins would be predicted to possess tumor suppressor activity.

Mutations in the RAS oncogene are present in approximately 15–30% of all human cancers, and overexpression of the RAS oncogene is common in lung cancer. Johnson et al. [32] showed that overexpression of RAS protein in lung cancer tissue correlated with reduced expression of *let-7* miRNA. They experimentally confirmed that *let-7* can inhibit RAS expression in human cancer cell lines. Loss or reduction of *let-7* in lung cancer leads to RAS overexpression, thus, promoting cellular growth and contributing to tumorigenesis. The authors therefore suggested that *let-7* acts as tumor suppressor [32]. Another group independently reported reduced expression of *let-7* in lung cancers and found that this correlated with a poor prognosis [77].

Global loss of miRNA expression in cancer

A global decrease in miRNA levels has been observed in human cancers, indicating that small RNAs may have an intrinsic function in tumor suppression. Lu et al. [52] were the first to show that the expression levels of many miRNAs were significantly reduced in cancers compared to the corresponding normal tissues. They analyzed a total of 217 human and mouse miRNAs across 334 human cancers, cancer cell lines, and normal tissues. Cancers had significantly reduced global miRNA expression. Poorly differentiated tumors had lower miRNA levels compared with more-differentiated tumors. The authors hypothesized that miRNAs can function to drive terminal differentiation and prevent cell division. Global changes in miRNA expression may reflect the degree of cell differentiation [52]. A recent study examined the expression of 241 human miRNAs in a comprehensive panel of human cancer cell lines, the NCI-60 panel, and in normal tissues [24]. The authors confirmed the finding that most miRNAs were expressed at lower levels in human tumor-derived cell lines compared with the corresponding normal tissue [24].

Until recently, considerable uncertainty remained as to whether the altered miRNA expression observed in cancer was a cause or consequence of malignant transformation. Earlier this year, a study by Kumar et al. [37] proved for the first time that widespread reduction in miRNA expression does, indeed, promote tumorigenesis. The authors globally reduced the production of mature miRNAs through a knockdown of the miRNA-processing enzymes Drosha and Dicer in cell lines. The mouse and human cancer cells consequently showed decreased steady-state miRNA levels. These cells with global miRNA loss showed enhanced cellular growth in vitro [37]. When injected into nude mice, these cells generated faster growing and more invasive tumors compared to controls. To assess the effect of global miRNA loss in vivo, the authors deleted the miRNA-processing enzyme Dicer in a mouse model of lung cancer. The Dicer mutant mice who had impaired miRNA processing developed an increased tumor burden, with an expansion in tumor number and tumor size, as well as tumors which were less well differentiated compared to controls [37]. Overall, these data clearly suggest that global miRNA loss enhances tumorigenesis. Kumar et al. demonstrated that loss of miRNAs leads to upregulation of proto-oncogenes such as RAS and c-Myc. However, it remains to

be elucidated whether loss of all miRNAs is necessary or whether reduction of a subgroup of key tumor suppressor miRNAs, such as *let-7*, is the event that promotes malignant transformation.

MicroRNAs in the p53 tumor suppressor network

Transcriptional networks are often deregulated in cancer cells and may lead to altered transcription of miRNA genes. Two recent studies identified a miRNA, miR-34, to be regulated by the p53 transcription factor [16, 26]. The p53 protein, also called "the guardian of the genome", regulates the cellular response to stress and cancer-initiating events such as DNA damage. He et al. [26] found that a miRNA, miR-34, is directly activated by the transcription factor p53 after DNA damage. Expression of miR-34 induces cell cycle arrest and thereby acts together with other effectors of the p53 tumor suppressor network to inhibit inappropriate cell proliferation. Another group independently demonstrated that miR-34 is upregulated by p53 upon DNA damage and promotes apoptosis [16].

Together, these data indicate that altered expression of miRNAs is not simply a secondary event that reflects the less differentiated state of cancer cells. In contrast, at least in some cases, miRNA expression is specifically driven by tumor suppressors and oncogenes.

MicroRNAs with a role in tumor invasion and metastasis

Transcriptional networks may drive miRNA expression in cancers. Recent work from Ma et al. [54] suggested a model by which a pleiotropic transcription factor, Twist, induces expression of a specific miRNA, which suppresses its direct target and in turn activates a pro-metastatic gene, leading to tumor cell invasion and metastasis. The expression of miR-10b induced by the transcription factor Twist promoted cell migration and invasion in mouse and human breast cancer cells. Furthermore, the expression level of miR-10b in primary human breast carcinomas correlated with clinical progression [54]. These findings, if confirmed, suggest that specific miRNAs may have a role beyond the tumor-initiating event and directly participate in tumor progression and metastasis.

Regulation of miRNAs in cancer—who regulates the regulators?

In few cases, the underlying cause of miRNA deregulation in cancer is clear. As discussed above, the overexpression of miR-17-92 correlates with amplification of its gene locus [27]. Similarly, decreased expression of miR-15 and miR-16 is associated with a corresponding chromosomal deletion [13].

Transcriptional or epigenetic regulation of miRNAs has been recently reported [53, 73]. The transcription of a miRNA gene, *mir-124a*, was shown to be inactivated by hypermethylation of its promoter in various human tumors. This process of epigenetic silencing is a well-known mechanism to inactivate protein-coding genes in cancer cells and may similarly apply to miRNAs. The miRNA gene *mir-127* is usually expressed in normal cells but not in cancer cells. Saito et al. [73] demonstrated that miR-127 was highly induced in cultured human cancer cells after treatment with demethylating drugs, suggesting that it is subject to epigenetic silencing through promoter hypermethylation.

A novel mechanism of miRNA regulation was suggested by Mayr et al. [56] and Lee and Dutta [44]. They demonstrated that miRNA function could be regulated through loss of miRNA binding sites in the target gene. Both groups independently demonstrated that chromosomal translocations in a known oncogene, high mobility group A2 (Hmga2), led to loss of the *let-7* miRNA binding sites in its messenger RNA. Disrupted repression of Hmga2 by *let-7* promoted oncogenic transformation and growth in mammalian cells. These two studies provide the first evidence that disrupting the interaction of a single miRNA and its target can produce an abnormal phenotype in mammalian cells [44, 56].

In addition, there is evidence that miRNAs are regulated indirectly through control of their processing enzymes. Thomson et al. [81] showed that a downregulation of miRNAs in human cancer was not associated with reduced levels of the primary miRNA transcripts. The authors therefore suggested regulation of miRNAs during subsequent processing steps, e.g., through altered function of the enzyme Drosha [81].

MicroRNA profiling—implications for cancer diagnosis

Lu et al. [52] asked the question whether global miRNA expression profiles could classify human cancer. MicroRNA expression profiles clearly differentiated human cancers according to their developmental origin.

Cancers of epithelial and hematopoietic origin had distinct miRNA profiles. A subgroup of gastrointestinal tumors, which arise from endoderm, was distinguished by miRNA expression patterns. Furthermore, tumors within a single cell lineage such as acute lymphoblastic leukemia were further differentiated according to their underlying genetic abnormality into BCR/ABL-positive tumors, T-cell tumors, and those with MLL gene rearrangement [52]. Finally, the authors applied the miRNA expression profiles they had established to an independent series of 17 poorly differentiated tumors of unknown origin. Based on the differential expression of 217 miRNAs, a correct diagnosis could be established in 12 out of 17 of the tumors. In

contrast, gene expression profiling based on ~16,000 messenger RNAs did not accurately classify the tumors [52]. This has potential important clinical implications. If miRNAs prove useful for clinical diagnosis, their key advantage might be their high stability. In contrast to most messenger RNAs, they are long-lived in vivo [49] and very stable in vitro [78], which might allow analysis of paraffin-embedded samples for routine diagnostic applications.

MicroRNAs—novel therapeutic targets?

Regulatory RNAs may also have therapeutic applications by which disease-causing miRNAs could be antagonized or functional miRNAs restored. The most intuitive choice of molecules to correct altered miRNA–messenger RNA interactions are RNA oligonucleotides. These oligonucleotides need to be chemically modified to allow for stability in serum and cellular uptake. Modified antisense oligonucleotides are already being developed to utilize the intrinsic RNAi pathway for delivery of gene therapy. If the delivery problem can be overcome, then miRNA therapies may also be possible.

Two studies have successfully applied 2′-*O*-Methyl-modified antisense RNAs to inhibit miRNA function in cultured cells [29, 57]. Recent work by Krutzfeldt et al. [36] demonstrated that modified cholesterol-conjugated antisense RNAs designated "antagomirs" could effectively inhibit miRNA function in vivo in the adult mouse. The authors applied three daily intravenous injections of antagomirs and achieved effective inhibition of four miRNAs over a period of weeks in most tissues except brain [36]. A novel approach was recently reported by Ebert et al. [21]. They developed miRNA inhibitors that can be transiently expressed in cultured mammalian cells. These competitive inhibitors termed "miRNA sponges" derepressed miRNA targets at least as strongly as chemically modified antisense oligonucleotides [21]. A different approach was taken by Tsuda et al. [83]. The authors designed synthetic miRNAs to target overexpressed tumor proteins, such as HER-2 protein. A synthetic miRNA targeting HER-2 messenger RNA successfully inhibited HER-2 protein expression in ovarian cancer cells [83]. Together, these studies hold some promise of miRNAs as future therapeutic targets.

One limitation of antisense RNA therapies is the restricted number of cells that can be targeted. Any approach to knock down a particular miRNA with antisense oligonucleotides will only result in partial knockdown. This may represent a limitation for cancer therapies. It remains to be seen whether indirectly mediated bystander effects on cancer cells that have not been directly targeted may partly overcome this limitation. In contrast, a partial effect on function may be of therapeutic value in neurodegenerative diseases, such as Parkinson's or Alzheimer's disease. A partial restoration of dopamine production by antisense therapy might result in a significant clinical improvement in Parkinson patients. Similarly, a partial reduction of the disease-causing proteins in Alzheimer's disease may lead to a clinical improvement and might be achievable by RNA based or miRNA gene therapy.

Techniques and approaches to study miRNAs

All known miRNAs are registered in a public web-based registry, the "miRBase" database that provides up-to-date information on all published miRNAs [25]. Novel miRNA genes can be discovered by bioinformatics approaches searching for evolutionary conserved stem-loop structures in the genome (reviewed in [3, 5]). Experimentally, miRNAs are discovered by cloning all small RNAs from a certain tissue type or developmental stage and subsequent sequencing to identify the subgroup of small RNAs that fulfill the criteria for miRNAs [38, 51]. Both computational and experimental approaches indicate that many more miRNAs are likely to be identified [4, 5], which is reflected by the rapidly increasing number of annotated miRNAs which increased from less than 300 to more than 4,000 over the past 4 years [58].

MicroRNA expression studies

Northern blot analysis is a well-established technique for studying messenger RNA expression and was soon adapted to detect miRNAs in cells or tissues [42, 84]. Subsequently, conventional DNA microarray technology was modified to form miRNA microarrays, allowing for the detection of multiple miRNAs simultaneously across various samples [15, 60, 62, 82].

Lu et al. [52] developed a novel microarray strategy to improve probe specificity, which is critical due to the short nature of mature miRNAs. They performed hybridization in solution using polystyrene capture beads that are coupled to oligonucleotide probes complementary to the miRNAs of interest. The solution hybrids are then analyzed using a multicolor flow cytometer measuring bead color, denoting miRNA identity, and labeling intensity, denoting miRNA abundance [52].

In parallel to microarray platforms, commercial assays for quantitative reverse transcriptase polymerase chain reaction (RT-PCR) have become available. These allow for the analysis of miRNAs in small tissue samples or even single cells [79], as well as validation of microarray data. In addition to mature miRNAs, these quantitative RT-PCR assays can be applied to analyze miRNA precursors and primary transcripts [31]. In situ hybridization for the

detection of mature miRNAs has recently become possible by using special high-affinity locked nucleic acid (LNA)-modified DNA oligonucleotide probes and holds promise for the application on human formalin-fixed and paraffin embedded tissue [35, 61].

Functional characterization of miRNAs

Various strategies have been used to investigate the function of specific miRNAs. In worms and flies, loss-of-function mutants for specific miRNAs or miRNA families allow us to draw conclusions regarding possible physiological functions of miRNAs from the resulting abnormal phenotype [34, 39, 86]. The knockdown of miRNAs or pre-miRNAs using modified antisense oligonucleotides has proven particularly useful in cell lines [29, 45, 57]. LNA-modified antisense oligonucleotides have been successfully utilized to knock down specific miRNAs in cultured cells [22]. This approach allowed identification of a crucial role for a miRNA, miR-223, in granulocytic differentiation [22]. In addition, the modified antisense RNAs (antagomirs) described by Krutzfeldt et al. [36], which inhibit miRNA function in the adult mouse, may provide a potential research tool to study miRNA function in vivo.

In mammals, induced defects in miRNA biogenesis are a useful tool for investigating the biological roles of miRNAs, as loss-of-function mutants are not available for most miRNA genes. Dicer knockout mouse models have revealed essential roles for miRNAs in murine organogenesis [88]. A recent study utilized a combined knockdown of the miRNA-processing enzymes Drosha, Dicer1, and DGCR8 to study the consequences of a global decrease in mature miRNAs in cancer cell lines and in a mouse model for lung cancer [37].

Earlier this year, four independent groups have, for the first time, deleted genes for single miRNAs in mice [72, 80, 85, 88]. Two of the groups deleted the same DNA sequence for *mir-155* and described severe immune defects [72, 80]. Mice lacking miR-155 showed impaired function of B and T lymphocytes and dendritic cells [72]. In particular, T helper cell differentiation and the germinal center reaction to produce a T-cell-dependent antibody response were defective [80]. Together, these two studies demonstrated a key role for miR-155 in normal immune function. The two other groups deleted different miRNAs, miR-1-2 and miR-208, and reported cardiac defects. Mice lacking miR-208 showed inadequate cardiac growth in response to stress [85], while mice lacking miR-1-2 had defects in cardiac morphogenesis and electrical conduction [88].

MicroRNA target sites

A validated biochemical strategy for identifying miRNA targets would be highly desirable. Two groups have recently reported promising approaches to experimentally identify miRNA targets. Both approaches apply biochemical methods to purify the effector complexes of miRNAs associated with proteins and bound messenger RNA targets [2, 20].

An increasing number of sophisticated bioinformatics approaches are being developed to predict putative miRNA target genes [3, 10, 69, 74]. This is based on the fact that miRNA target recognition is at least partly based on simple sequence complementarity. Interestingly, exact base pairing between miRNAs and their targets commonly appears to be required only in the first six to eight bases from the 5′ end of the miRNA. The short nature of this designated "seed region" allows a single miRNA to act on up to a hundred different target sites, and all human miRNAs together may regulate up to one third of protein coding genes [10, 47]. A different approach to discovering miRNA target genes is to knock out or overexpress a particular miRNA and use conventional microarrays to identify genes that show changes in expression. This approach is based on the observation that some miRNAs can also downregulate messenger RNA levels in addition to downregulating protein levels of their target genes [49]. Experimental validation of miRNA target sites has been limited to date. A common approach has been to express a miRNA in vivo while simultaneously expressing and monitoring the target messenger RNA linked to a reporter gene, i.e., Luciferase [10, 18, 55, 56, 76]. The fact that a single miRNA can regulate multiple targets and a particular target may be regulated by various miRNAs suggests a highly complex network of miRNA-target interactions, which is only beginning to be unraveled.

Conclusions

Over recent years, miRNAs have emerged as major players in the complex networks of gene regulation and have been implicated in various aspects of human disease. Only 5 years after the first study reported a direct involvement of miRNAs in cancer, these small RNAs have already significantly improved our understanding of carcinogenesis. In addition to protein-coding oncogenes and tumor suppressor genes, we will have to take into account miRNAs and their regulatory networks if we aim to understand the complex processes underlying malignant transformation.

References

1. Bartel DP (2004) MicroRNAs: genomics, biogenesis, mechanism, and function. Cell 116:281–297

2. Beitzinger M, Peters L, Zhu JY, Kremmer E, Meister G (2007) Identification of Human microRNA targets from isolated Argonaute protein complexes. RNA Biol 4(2)
3. Bentwich I (2005) Prediction and validation of microRNAs and their targets. FEBS Lett 579:5904–5910
4. Bentwich I, Avniel A, Karov Y, Aharonov R, Gilad S, Barad O, Barzilai A, Einat P, Einav U, Meiri E, Sharon E, Spector Y, Bentwich Z (2005) Identification of hundreds of conserved and nonconserved human microRNAs. Nat Genet 37:766–770
5. Berezikov E, Cuppen E, Plasterk RH (2006) Approaches to microRNA discovery. Nat Genet 38 Suppl:S2–S7
6. Bernstein E, Caudy AA, Hammond SM, Hannon GJ (2001) Role for a bidentate ribonuclease in the initiation step of RNA interference. Nature 409:363–366
7. Bernstein E, Kim SY, Carmell MA, Murchison EP, Alcorn H, Li MZ, Mills AA, Elledge SJ, Anderson KV, Hannon GJ (2003) Dicer is essential for mouse development. Nat Genet 35:215–217
8. Blenkiron C, Goldstein LD, Thorne NP, Spiteri I, Chin SF, Dunning M, Barbosa-Morais NL, Teschendorff A, Green AR, Ellis IO, Tavaré S, Caldas C, Miska EA (2007) MicroRNA expression profiling of human breast cancer identifies new markers of tumour subtype. Genome Biol 8(10):R214
9. Brennecke J, Hipfner DR, Stark A, Russell RB, Cohen SM (2003) bantam encodes a developmentally regulated microRNA that controls cell proliferation and regulates the proapoptotic gene hid in Drosophila. Cell 113:25–36
10. Brennecke J, Stark A, Russell RB, Cohen SM (2005) Principles of microRNA-target recognition. PLoS Biol 3:e85
11. Caldas C, Brenton JD (2005) Sizing up miRNAs as cancer genes. Nat Med 11:712–714
12. Calin GA, Croce CM (2006) MicroRNA signatures in human cancers. Nat Rev Cancer 6:857–866
13. Calin GA, Dumitru CD, Shimizu M, Bichi R, Zupo S, Noch E, Aldler H, Rattan S, Keating M, Rai K, Rassenti L, Kipps T, Negrini M, Bullrich F, Croce CM (2002) Frequent deletions and down-regulation of micro- RNA genes miR15 and miR16 at 13q14 in chronic lymphocytic leukemia. Proc Natl Acad Sci USA 99:15524–15529
14. Calin GA, Sevignani C, Dumitru CD, Hyslop T, Noch E, Yendamuri S, Shimizu M, Rattan S, Bullrich F, Negrini M, Croce CM (2004) Human microRNA genes are frequently located at fragile sites and genomic regions involved in cancers. Proc Natl Acad Sci USA 101:2999–3004
15. Castoldi M, Schmidt S, Benes V, Noerholm M, Kulozik AE, Hentze MW, Muckenthaler MU (2006) A sensitive array for microRNA expression profiling (miChip) based on locked nucleic acids (LNA). RNA 12:913–920
16. Chang TC, Wentzel EA, Kent OA, Ramachandran K, Mullendore M, Lee KH, Feldmann G, Yamakuchi M, Ferlito M, Lowenstein CJ, Arking DE, Beer MA, Maitra A, Mendell JT (2007) Transactivation of miR-34a by p53 broadly influences gene expression and promotes apoptosis. Mol Cell 26:745–752
17. Chen CZ, Li L, Lodish HF, Bartel DP (2004) MicroRNAs modulate hematopoietic lineage differentiation. Science 303:83–86
18. Cimmino A, Calin GA, Fabbri M, Iorio MV, Ferracin M, Shimizu M, Wojcik SE, Aqeilan RI, Zupo S, Dono M, Rassenti L, Alder H, Volinia S, Liu CG, Kipps TJ, Negrini M, Croce CM (2005) miR-15 and miR-16 induce apoptosis by targeting BCL2. Proc Natl Acad Sci USA 102:13944–13949
19. Dews M, Homayouni A, Yu D, Murphy D, Sevignani C, Wentzel E, Furth EE, Lee WM, Enders GH, Mendell JT, Thomas-Tikhonenko A (2006) Augmentation of tumor angiogenesis by a Myc-activated microRNA cluster. Nat Genet 38:1060–1065
20. Easow G, Teleman AA, Cohen SM (2007) Isolation of microRNA targets by miRNP immunopurification. RNA 13:1198–1204
21. Ebert MS, Neilson JR, Sharp PA (2007) MicroRNA sponges: competitive inhibitors of small RNAs in mammalian cells. Nat Methods 4:721–726
22. Fazi F, Rosa A, Fatica A, Gelmetti V, De Marchis ML, Nervi C, Bozzoni I (2005) A minicircuitry comprised of microRNA-223 and transcription factors NFI-A and C/EBPalpha regulates human granulopoiesis. Cell 123:819–831
23. Fire A, Xu S, Montgomery MK, Kostas SA, Driver SE, Mello CC (1998) Potent and specific genetic interference by double-stranded RNA in *Caenorhabditis elegans*. Nature 391:806–811
24. Gaur A, Jewell DA, Liang Y, Ridzon D, Moore JH, Chen C, Ambros VR, Israel MA (2007) Characterization of microRNA expression levels and their biological correlates in human cancer cell lines. Cancer Res 67:2456–2468
25. Griffiths-Jones S, Grocock RJ, van Dongen S, Bateman A, Enright AJ (2006) miRBase: microRNA sequences, targets and gene nomenclature. Nucleic Acids Res 34:D140–D144
26. He L, He X, Lim LP, de Stanchina E, Xuan Z, Liang Y, Xue W, Zender L, Magnus J, Ridzon D, Jackson AL, Linsley PS, Chen C, Lowe SW, Cleary MA, Hannon GJ (2007) A microRNA component of the p53 tumour suppressor network. Nature 447:1130–1134
27. He L, Thomson JM, Hemann MT, Hernando-Monge E, Mu D, Goodson S, Powers S, Cordon-Cardo C, Lowe SW, Hannon GJ, Hammond SM (2005) A microRNA polycistron as a potential human oncogene. Nature 435:828–833
28. Hutvagner G, McLachlan J, Pasquinelli AE, Balint E, Tuschl T, Zamore PD (2001) A cellular function for the RNA-interference enzyme Dicer in the maturation of the let-7 small temporal RNA. Science 293:834–838
29. Hutvagner G, Simard MJ, Mello CC, Zamore PD (2004) Sequence-specific inhibition of small RNA function. PLoS Biol 2:E98
30. Jackson RJ, Standart N (2007) How do microRNAs regulate gene expression? Sci STKE 2007:re1
31. Jiang J, Lee EJ, Gusev Y, Schmittgen TD (2005) Real-time expression profiling of microRNA precursors in human cancer cell lines. Nucleic Acids Res 33:5394–5403
32. Johnson SM, Grosshans H, Shingara J, Byrom M, Jarvis R, Cheng A, Labourier E, Reinert KL, Brown D, Slack FJ (2005) RAS is regulated by the let-7 microRNA family. Cell 120:635–647
33. Johnston RJ, Hobert O (2003) A microRNA controlling left/right neuronal asymmetry in *Caenorhabditis elegans*. Nature 426:845–849
34. Jones-Rhoades MW, Bartel DP, Bartel B (2006) MicroRNAS and their regulatory roles in plants. Annu Rev Plant Biol 57:19–53
35. Kloosterman WP, Wienholds E, de Bruijn E, Kauppinen S, Plasterk RH (2006) In situ detection of miRNAs in animal embryos using LNA-modified oligonucleotide probes. Nat Methods 3:27–29
36. Krutzfeldt J, Rajewsky N, Braich R, Rajeev KG, Tuschl T, Manoharan M, Stoffel M (2005) Silencing of microRNAs in vivo with 'antagomirs'. Nature 438:685–689
37. Kumar MS, Lu J, Mercer KL, Golub TR, Jacks T (2007) Impaired microRNA processing enhances cellular transformation and tumorigenesis. Nat Genet 39:673–677
38. Lagos-Quintana M, Rauhut R, Lendeckel W, Tuschl T (2001) Identification of novel genes coding for small expressed RNAs. Science 294:853–858
39. Lai EC, Tam B, Rubin GM (2005) Pervasive regulation of Drosophila Notch target genes by GY-box-, Brd-box-, and K-box-class microRNAs. Genes Dev 19:1067–1080
40. Lau NC, Lim LP, Weinstein EG, Bartel DP (2001) An abundant class of tiny RNAs with probable regulatory roles in *Caenorhabditis elegans*. Science 294:858–862
41. Lee RC, Ambros V (2001) An extensive class of small RNAs in *Caenorhabditis elegans*. Science 294:862–864

42. Lee RC, Feinbaum RL, Ambros V (1993) The *C. elegans* heterochronic gene lin-4 encodes small RNAs with antisense complementarity to lin-14. Cell 75:843–854
43. Lee Y, Ahn C, Han J, Choi H, Kim J, Yim J, Lee J, Provost P, Radmark O, Kim S, Kim VN (2003) The nuclear RNase III Drosha initiates microRNA processing. Nature 425:415–419
44. Lee YS, Dutta A (2007) The tumor suppressor microRNA let-7 represses the HMGA2 oncogene. Genes Dev 21:1025–1030
45. Lee YS, Kim HK, Chung S, Kim KS, Dutta A (2005) Depletion of human micro-RNA miR-125b reveals that it is critical for the proliferation of differentiated cells but not for the down-regulation of putative targets during differentiation. J Biol Chem 280:16635–16641
46. Lewis BP, Burge CB, Bartel DP (2005) Conserved seed pairing, often flanked by adenosines, indicates that thousands of human genes are microRNA targets. Cell 120:15–20
47. Lewis BP, Shih IH, Jones-Rhoades MW, Bartel DP, Burge CB (2003) Prediction of mammalian microRNA targets. Cell 115:787–798
48. Lim LP, Glasner ME, Yekta S, Burge CB, Bartel DP (2003) Vertebrate microRNA genes. Science 299:1540
49. Lim LP, Lau NC, Garrett-Engele P, Grimson A, Schelter JM, Castle J, Bartel DP, Linsley PS, Johnson JM (2005) Microarray analysis shows that some microRNAs downregulate large numbers of target mRNAs. Nature 433:769–773
50. Lindbo JA, Silva-Rosales L, Proebsting WM, Dougherty WG (1993) Induction of a highly specific antiviral state in transgenic plants: implications for regulation of gene expression and virus resistance. Plant Cell 5:1749–1759
51. Lu C, Tej SS, Luo S, Haudenschild CD, Meyers BC, Green PJ (2005) Elucidation of the small RNA component of the transcriptome. Science 309:1567–1569
52. Lu J, Getz G, Miska EA, Alvarez-Saavedra E, Lamb J, Peck D, Sweet-Cordero A, Ebert BL, Mak RH, Ferrando AA, Downing JR, Jacks T, Horvitz HR, Golub TR (2005) MicroRNA expression profiles classify human cancers. Nature 435:834–838
53. Lujambio A, Ropero S, Ballestar E, Fraga MF, Cerrato C, Setien F, Casado S, Suarez-Gauthier A, Sanchez-Cespedes M, Gitt A, Spiteri I, Das PP, Caldas C, Miska E, Esteller M (2007) Genetic unmasking of an epigenetically silenced microRNA in human cancer cells. Cancer Res 67:1424–1429
54. Ma L, Teruya-Feldstein J, Weinberg RA (2007) Tumour invasion and metastasis initiated by microRNA-10b in breast cancer. Nature 449:682–688
55. Matsubara H, Takeuchi T, Nishikawa E, Yanagisawa K, Hayashita Y, Ebi H, Yamada H, Suzuki M, Nagino M, Nimura Y, Osada H, Takahashi T (2007) Apoptosis induction by antisense oligonucleotides against miR-17-5p and miR-20a in lung cancers overexpressing miR-17-92. Oncogene 26:6099–6105
56. Mayr C, Hemann MT, Bartel DP (2007) Disrupting the pairing between let-7 and Hmga2 enhances oncogenic transformation. Science 315:1576–1579
57. Meister G, Landthaler M, Dorsett Y, Tuschl T (2004) Sequence-specific inhibition of microRNA- and siRNA-induced RNA silencing. RNA 10:544–550
58. miRBase. [Online Database] (2007) Available from: http://microrna.sanger.ac.uk/
59. Miska EA (2005) How microRNAs control cell division, differentiation and death. Curr Opin Genet Dev 15:563–568
60. Miska EA, Alvarez-Saavedra E, Townsend M, Yoshii A, Sestan N, Rakic P, Constantine-Paton M, Horvitz HR (2004) Microarray analysis of microRNA expression in the developing mammalian brain. Genome Biol 5:R68
61. Nelson PT, Baldwin DA, Kloosterman WP, Kauppinen S, Plasterk RH, Mourelatos Z (2006) RAKE and LNA-ISH reveal microRNA expression and localization in archival human brain. RNA 12:187–191
62. Nelson PT, Baldwin DA, Scearce LM, Oberholtzer JC, Tobias JW, Mourelatos Z (2004) Microarray-based, high-throughput gene expression profiling of microRNAs. Nat Methods 1:155–161
63. O'Donnell KA, Wentzel EA, Zeller KI, Dang CV, Mendell JT (2005) c-Myc-regulated microRNAs modulate E2F1 expression. Nature 435:839–843
64. Ota A, Tagawa H, Karnan S, Tsuzuki S, Karpas A, Kira S, Yoshida Y, Seto M (2004) Identification and characterization of a novel gene, C13orf25, as a target for 13q31-q32 amplification in malignant lymphoma. Cancer Res 64:3087–3095
65. Pasquinelli AE, Reinhart BJ, Slack F, Martindale MQ, Kuroda MI, Maller B, Hayward DC, Ball EE, Degnan B, Muller P, Spring J, Srinivasan A, Fishman M, Finnerty J, Corbo J, Levine M, Leahy P, Davidson E, Ruvkun G (2000) Conservation of the sequence and temporal expression of let-7 heterochronic regulatory RNA. Nature 408:86–89
66. Pfeffer S, Zavolan M, Grasser FA, Chien M, Russo JJ, Ju J, John B, Enright AJ, Marks D, Sander C, Tuschl T (2004) Identification of virus-encoded microRNAs. Science 304:734–736
67. Pillai RS, Bhattacharyya SN, Filipowicz W (2007) Repression of protein synthesis by miRNAs: how many mechanisms? Trends Cell Biol 17:118–126
68. Rajewsky N (2006) microRNA target predictions in animals. Nat Genet 38 Suppl:S8–S13
69. Rajewsky N, Socci ND (2004) Computational identification of microRNA targets. Dev Biol 267:529–535
70. Reinhart BJ, Slack FJ, Basson M, Pasquinelli AE, Bettinger JC, Rougvie AE, Horvitz HR, Ruvkun G (2000) The 21-nucleotide let-7 RNA regulates developmental timing in *Caenorhabditis elegans*. Nature 403:901–906
71. Reinhart BJ, Weinstein EG, Rhoades MW, Bartel B, Bartel DP (2002) MicroRNAs in plants. Genes Dev 16:1616–1626
72. Rodriguez A, Vigorito E, Clare S, Warren MV, Couttet P, Soond DR, van Dongen S, Grocock RJ, Das PP, Miska EA, Vetrie D, Okkenhaug K, Enright AJ, Dougan G, Turner M, Bradley A (2007) Requirement of bic/microRNA-155 for normal immune function. Science 316:608–611
73. Saito Y, Liang G, Egger G, Friedman JM, Chuang JC, Coetzee GA, Jones PA (2006) Specific activation of microRNA-127 with downregulation of the proto-oncogene BCL6 by chromatin-modifying drugs in human cancer cells. Cancer Cell 9:435–443
74. Sethupathy P, Megraw M, Hatzigeorgiou AG (2006) A guide through present computational approaches for the identification of mammalian microRNA targets. Nat Methods 3:881–886
75. Sullivan CS, Ganem D (2005) MicroRNAs and viral infection. Mol Cell 20:3–7
76. Sylvestre Y, De Guire V, Querido E, Mukhopadhyay UK, Bourdeau V, Major F, Ferbeyre G, Chartrand P (2007) An E2F/miR-20a autoregulatory feedback loop. J Biol Chem 282:2135–2143
77. Takamizawa J, Konishi H, Yanagisawa K, Tomida S, Osada H, Endoh H, Harano T, Yatabe Y, Nagino M, Nimura Y, Mitsudomi T, Takahashi T (2004) Reduced expression of the let-7 microRNAs in human lung cancers in association with shortened postoperative survival. Cancer Res 64:3753–3756
78. Tang F, Hajkova P, Barton SC, Lao K, Surani MA (2006) MicroRNA expression profiling of single whole embryonic stem cells. Nucleic Acids Res 34:e9
79. Tang F, Hajkova P, Barton SC, O'Carroll D, Lee C, Lao K, Surani MA (2006) 220-plex microRNA expression profile of a single cell. Nat Protoc 1:1154–1159
80. Thai TH, Calado DP, Casola S, Ansel KM, Xiao C, Xue Y, Murphy A, Frendewey D, Valenzuela D, Kutok JL, Schmidt-Supprian M, Rajewsky N, Yancopoulos G, Rao A, Rajewsky K (2007) Regulation of the germinal center response by microRNA-155. Science 316:604–608

81. Thomson JM, Newman M, Parker JS, Morin-Kensicki EM, Wright T, Hammond SM (2006) Extensive post-transcriptional regulation of microRNAs and its implications for cancer. Genes Dev 20:2202–2207
82. Thomson JM, Parker J, Perou CM, Hammond SM (2004) A custom microarray platform for analysis of microRNA gene expression. Nat Methods 1:47–53
83. Tsuda N, Kawano K, Efferson CL, Ioannides CG (2005) Synthetic microRNA and double-stranded RNA targeting the 3′-untranslated region of HER-2/neu mRNA inhibit HER-2 protein expression in ovarian cancer cells. Int J Oncol 27:1299–1306
84. Valoczi A, Hornyik C, Varga N, Burgyan J, Kauppinen S, Havelda Z (2004) Sensitive and specific detection of microRNAs by Northern blot analysis using LNA-modified oligonucleotide probes. Nucleic Acids Res 32:e175
85. van Rooij E, Sutherland LB, Qi X, Richardson JA, Hill J, Olson EN (2007) Control of stress-dependent cardiac growth and gene expression by a microRNA. Science 316: 575–579
86. Wightman B, Ha I, Ruvkun G (1993) Posttranscriptional regulation of the heterochronic gene lin-14 by lin-4 mediates temporal pattern formation in *C. elegans*. Cell 75:855–862
87. Zamore PD, Tuschl T, Sharp PA, Bartel DP (2000) RNAi: double-stranded RNA directs the ATP-dependent cleavage of mRNA at 21 to 23 nucleotide intervals. Cell 101:25–33
88. Zhao Y, Ransom JF, Li A, Vedantham V, von Drehle M, Muth AN, Tsuchihashi T, McManus MT, Schwartz RJ, Srivastava D (2007) Dysregulation of cardiogenesis, cardiac conduction, and cell cycle in mice lacking miRNA-1-2. Cell 129:303–317

Virchows Arch (2008) 452:11–18
DOI 10.1007/s00428-007-0505-5

REVIEW AND PERSPECTIVE

Guidelines for autopsy investigation of sudden cardiac death

Cristina Basso · Margaret Burke · Paul Fornes · Patrick J Gallagher · Rosa Henriques de Gouveia · Mary Sheppard · Gaetano Thiene · Allard van der Wal · on behalf of the Association for European Cardiovascular Pathology*

Received: 30 May 2007 / Revised: 8 August 2007 / Accepted: 21 August 2007 / Published online: 20 October 2007
© Springer-Verlag 2007

Abstract Although sudden cardiac death is one of the most important mode of death in Western Countries, pathologists and public health physicians have not given this problem the attention it deserves. New methods of preventing potentially fatal arrhythmias have been developed, and the accurate diagnosis of the causes of sudden cardiac death is now of particular importance. Pathologists are responsible for determining the precise cause of sudden death but there is considerable variation in the way in which they approach this increasingly complex task. The Association for European Cardiovascular Pathology developed guidelines, which represent the minimum standard that is required in the routine autopsy practice for the adequate assessment of sudden cardiac death, including not only a protocol for heart examination and histological sampling, but also for toxicology and molecular investigation. Our recommendations apply to university medical centres, regional and district hospitals and all types of forensic medicine institutes. If a uniform method of investigation is adopted throughout the European Union, this will lead to improvements in standards of practice, allow meaningful comparisons between different communities and regions and, most importantly, permit future trends in the patterns of disease causing sudden death to be monitored.

Keywords Autopsy · Guidelines · Protocol · Sudden cardiac death

Introduction

Sudden cardiac death (SCD) is the leading mode of death in all communities of the United States and of the European Union, but its precise incidence is unknown. Internationally

*http://anpat.unipd.it/aecvp/

C. Basso · G. Thiene (✉)
Pathological Anatomy, Department of Medical Diagnostic Sciences and Special Therapies,
University of Padua Medical School,
Padua, Italy
e-mail: gaetano.thiene@unipd.it

C. Basso
e-mail: cristina.basso@unipd.it

M. Burke
Department of Histopathology, Royal Brompton & Harefield NHS Trust, Harefield Hospital,
Harefield, UK
e-mail: M.Burke@rbht.nhs.uk

P. Fornes
Department of Pathology, Hopital Européen G. Pompidou,
Paris, France
e-mail: Paul.Fornes@wanadoo.fr

P. J. Gallagher
Department of Pathology, Southampton University Hospital,
Southampton, UK
e-mail: P.J.Gallagher@soton.ac.uk

R. H. de Gouveia
Department of Pathology, Hospital de Santa Cruz,
Lisbon, Portugal
e-mail: rhgouveia@mail.telepac.pt

M. Sheppard
Department of Pathology, Royal Brompton Hospital,
London, UK
e-mail: M.Sheppard@rbht.nhs.uk

A. van der Wal
Pathology, Academic Medical Center, University of Amsterdam,
Amsterdam, The Netherlands
e-mail: a.c.vanderwal@amc.uva.nl

accepted methods of death certification do not include a specific category of SCD. Estimates for the United States range from 250,000 to 400,000 adult people dying suddenly each year due to cardiovascular causes with an overall incidence of 1 to 2/1,000 population per year [13, 18, 29]. A task force of the European Society of Cardiology has adopted the incidence ranges from 36 to 128 deaths per 100,000 population per year [3, 19]. More than 60% of these are the result of coronary heart disease. Among the general population of adolescents and adults younger than the age of 30 years, the overall risk of SCD is 1/100,000 and a wider spectrum of diseases can account for the final event [9].

The major difficulties in interpreting epidemiological data on sudden death are the lack of standardization in death certificate coding and the variability in the definition of sudden death. Sudden death has been defined as "a natural, unexpected fatal event occurring within one hour from the onset of symptoms in an apparently healthy subject or whose disease was not so severe as to predict an abrupt outcome" [14]. This well describes many witnessed deaths in the community or in emergency departments. It is less satisfactory in pathological practice where autopsies may be requested on patients whose deaths were not witnessed, occurred during sleep or at an unknown time before their bodies were discovered. Under the latter circumstances, it is probably more satisfactory to assume that the death was sudden if the deceased was known to be in good health 24 h before death occurred [28]. Moreover, for practical purposes, a death can be classified as sudden if a patient is resuscitated after cardiac arrest, survives on life support for a limited period of time and then dies due to irreversible brain damage.

Pathologists are responsible for determining the precise cause of sudden death but there is considerable variation in the way in which they approach this increasingly complex task. A variety of book chapters, professional guidelines and articles have described how pathologists should investigate sudden death [1, 5, 11, 20, 23, 27]. However, there is little consistency among centres, even in individual countries. In this report, we describe the minimum standard that is required in the routine autopsy practice for the adequate assessment of SCD in the general population, excluding sudden infant death syndrome. Our recommendations apply to university medical centres, regional and district hospitals and all types of forensic medicine institutes. If a uniform method of investigation is adopted throughout the European Union, this will lead to improvements in standards of practice, allow meaningful comparisons between different communities and regions and, most importantly, permit future trends in the patterns of disease causing sudden death to be monitored.

The role of the autopsy in sudden death

To establish or consider:

- whether the death is attributable to a cardiac disease or to other causes of sudden death;
- the nature of the cardiac disease, and whether the mechanism was arrhythmic or mechanical;
- whether the cardiac condition causing sudden death may be inherited, requiring screening and counselling of the next of kin;
- the possibility of toxic or illicit drug abuse and other unnatural deaths.

Clinical information relevant to the autopsy

In practice the amount of information that is available before autopsy is variable. Any potential source of information should be interrogated (e.g. family members, general practitioner, etc), preferentially before autopsy is carried out. Ideally, the following information is required:

- age, gender, occupation, lifestyle (especially alcohol or smoking), usual pattern of exercise or athletic activity;
- circumstances of death: date, time interval (instantaneous or <1 h), place of death (e.g. at home, at work, in hospital, at recreation), circumstances (at rest, during sleep, during exercise—athletic or non-athletic—, during emotional stress), witnessed or un-witnessed, any suspicious circumstances (carbon monoxide, violence, traffic accident, etc);
- medical history: general health status, previous significant illnesses (especially syncope, chest pain, and palpitations, particularly during exercise, myocardial infarction, hypertension, respiratory and recent infectious disease, epilepsy, asthma, etc), previous surgical operations or interventions, previous ECG tracings and chest X-rays, results of cardiovascular examination, laboratory investigations (especially lipid profiles);
- prescription and non-prescription medications;
- family cardiac history: ischaemic heart disease and premature sudden death, arrhythmias, inherited cardiac diseases;
- ECG tracing taken during resuscitation, serum enzyme and troponin measurements.

The autopsy procedure

All sudden death autopsies should be sequential structured examinations. They should specifically address the major causes of extra-cardiac and cardiac sudden death. Principles

Table 1 SCD at postmortem

Cardiovascular substrates	
Mechanical	Others
Intrapericardial haemorrhage and cardiac tamponade	Fibromuscular dysplasia
Ascending aorta rupture (hypertension, Marfan, bicuspid aortic valve, coarctation, others)	Intramural small vessel disease
Post myocardial infarction free wall rupture	Cardiac allograft rejection, acute or chronic
Pulmonary embolism	Previous surgical or interventional procedures
Acute mitral valve incompetence with pulmonary edema	Coronary artery by-pass (saphenous vein, mammary and radial arteries, etc)
Post myocardial infarction papillary muscle rupture	Percutaneous balloon coronary angioplasty, stents
Chordae tendineae rupture (floppy mitral valve)	Myocardium
Intracavitary obstruction (e.g. thrombus/neoplasms)	Cardiomyopathy, hypertrophic
Abrupt prosthetic valve dysfunction (e.g. laceration, dehiscence, thrombotic block, poppet escape)	Cardiomyopathy, arrhythmogenic right ventricular
Congenital partial absence of the pericardium with strangulation	Cardiomyopathy, dilated
Arrhythmic	Cardiomyopathy, inflammatory (myocarditis)
Coronary arteries (±post-myocardial infarction scar)	Secondary cardiomyopathies (storage, infiltrative, sarcoidosis, etc)
Congenital anomalies	Hypertensive heart disease
Origin from the aorta	Idiopathic left ventricular hypertrophy
Wrong sinus (RCA from the left sinus, LCA from the right sinus)	Unclassified cardiomyopathies (spongy myocardium, fibroelastosis)
LCx from the right sinus or from RCA	Valve
High take off from the tubular portion	Aortic valve stenosis
Ostia plication	Myxoid degeneration of the mitral valve with prolapse
Origin from the pulmonary trunk	Conduction system
Course: intra-myocardial course (“myocardial bridge”)	Sinoatrial disease
Acquired	AV block (Lev–Lenegre disease, AV node cystic tumor)
Atherosclerosis	Ventricular pre-excitation (Wolff–Parkinson–White syndrome, Lown Ganong Levine syndrome)
Complicated (thrombus, haemorrhage)	Congenital heart disease (operated and un-operated) with or without Eisenmenger syndrome
Uncomplicated	Normal heart (“sine materia” or unexplained SCD or sudden arrhythmic death syndrome)
Embolism	Long and short QT syndromes
Arteritis	Brugada syndrome
Dissection	Catecholaminergic polymorphic ventricular tachycardia
	Idiopathic ventricular fibrillation

AV atrioventricular; *LCA* left coronary artery; *LCx* left circumflex branch; *RCA* right coronary artery

and rules relating to autopsy procedures should adhere to the Recommendations on the Harmonisation of Medico-Legal Autopsy Rules produced by the Committee of Ministers of the Council of Europe [5].

External examination of the body

- Establish body weight and height (to correlate with heart weight and wall thickness [16, 21, 22]).
- Check for recent intravenous access, intubation, ECG pads, defibrillator and electrical burns, drain sites and traumatic lesions;
- Check for implantable cardioverter defibrillator (ICD)/pacemaker; if in situ, see MDA Safety Notice 2002 for safe removal and interrogation [17].

Full autopsy with sequential approach to the causes of sudden death

Exclusion of non-cardiac causes of sudden death

Any natural sudden death can be considered cardiac in origin after the exclusion of non-cardiac causes. Thus, a full autopsy with sequential approach should be always performed to exclude common and un-common extra-cardiac causes of sudden death, especially:

– Cerebral (e.g. sub-arachnoid or intra-cerebral haemorrhage, etc)
– Respiratory (e.g. asthma, anaphylaxis, etc)
– Acute haemorrhagic shock (e.g. ruptured aortic aneurysm, peptic ulcer, etc)
– Septic shock (Waterhouse–Friderichsen syndrome)

Search for cardiac causes of sudden death

Many cardiovascular diseases can cause SCD, either through an arrhythmic mechanism (electrical SCD) or by compromising the mechanical function of the heart (mechanical SCD). These disorders may affect the coronary arteries, the myocardium, the cardiac valves, the conducting system, the intra-pericardial aorta or the pulmonary artery, the integrity of which is essential for a regular heart function (Table 1).

The standard gross examination of the heart

1. Check the pericardium, open it and explore the pericardial cavity.
2. Check the anatomy of the great arteries before transecting them 3 cm above the aortic and pulmonary valves.
3. Check and transect the pulmonary veins. Transect the superior vena cava 2 cm above the point where the crest of the right atrial appendage meets the superior vena cava (to preserve sinus node). Transect the inferior vena cava close to the diaphragm.
4. Open the right atrium from the inferior vena cava to the apex of the appendage. Open the left atrium between the pulmonary veins and then to the atrial appendage. Inspect the atrial cavities, the inter-atrial septum and determine whether the foramen ovale is patent. Examine the mitral and tricuspid valves (or valve prostheses) from above and check the integrity of the papillary muscles and chordae tendineae.
5. Inspect the aorta, the pulmonary artery and the aortic and pulmonary valves (or valve prosthesis) from above.
6. Check coronary arteries:
   (a) examine the size, shape, position, number and patency of the coronary ostia;
   (b) assess the size, course and "dominance" of the major epicardial arteries;
   (c) make multiple transverse cuts at 3 mm intervals along the course of the main epicardial arteries and branches such as the diagonal and obtuse marginal, and check patency;
   (d) heavily calcified coronary arteries can sometimes be opened adequately with sharp scissors. If this is not possible, they should be removed intact, decalcified and opened transversely;
   (e) coronary artery segments containing a metallic stent should be referred intact to labs with facilities for resin embedding and subsequent processing and sectioning;
   (f) coronary artery bypass grafts (saphenous veins, internal mammary arteries, radial arteries, etc) should be carefully examined with transverse cuts. The proximal and distal anastomoses should be examined with particular care. Side branch clips or sutures may facilitate their identification, particularly when dealing with internal mammary grafts.
7. Make a complete transverse (short-axis) cut of the heart at the mid-ventricular level and then parallel slices of ventricles at 1 cm intervals towards the apex and assess these slices carefully for morphology of the walls and cavities.
8. Once emptied of blood, note the following measurements:
   (a) Total heart weight: assess weight of heart against tables of normal weights by age, gender and body weight [16, 21, 22];
   (b) Wall thickness: inspect endocardium, measure thickness of mid cavity free wall of the left ventricle, right ventricle and of the septum (excluding trabeculae) against tables of normal thickness by age, gender and body weight [16, 21, 22];
   (c) Heart dimensions: the transverse size is best calculated as the distance from the obtuse to the acute margin in the posterior atrioventricular sulcus. The longitudinal size is obtained from a measurement of the distance between the crux cordis and the apex of the heart on the posterior aspect.
9. Dissect the basal half of the heart in the flow of blood and complete examination of atrial and ventricular septa, atrioventricular valves, ventricular inflows and outflows, and semi-lunar valves. In case of ECG documented ventricular pre-excitation, the atrioventricular rings should be maintained intact.

The standard histologic examination of the heart Myocardium: take mapped labelled blocks from a representative transverse slice of the ventricles to include the free wall of the left ventricle (anterior, lateral and posterior), the ventricular septum (anterior and posterior), and the free wall of the right ventricle (anterior, lateral and posterior), and right ventricular outflow tract and one block from each atria. In addition, any area with significant macroscopic abnormalities should be sampled. H & E and a connective tissue stain (van Gieson, trichrome or Sirius red) are standard. Other special stains and immunohistochemistry should be performed as required.

Coronary arteries: in the setting of coronary artery disease, most severe focal lesions should be sampled for histology in labelled blocks and stained as before.

Other cardiac samples (such as valvular tissue, pericardium and aorta) as indicated.
If the clinical history or ECG tracing suggest a conduction abnormality, conduction system investigation by serial sections technique should be performed.

Electron microscopy investigation If there is the suspicion of rare cardiomyopathies (mitochondrial, storage, infiltrative, etc) a small sample of myocardium (1 mm) should be fixed in 2.5% glutaraldehyde for ultrastructural examination.

Referral of hearts to specialised centres Best practice is that the entire heart is retained and sent to specialized centres. The referring pathologist should complete steps 1–5 of the standard gross examination of the heart, make a transverse apical section of the heart and empty the heart of blood. Tissues, blood and other fluids for toxicology and molecular pathology should be taken before fixing the heart in formalin 10% (see "Molecular pathology" below). If the heart cannot be retained, it is essential that extensive photographic documentation is made, indicating where individual blocks are taken.

Other tissues for histological examination

Specimens from the main other organs should be taken routinely and stained with H & E and a connective tissue stain.

Further laboratory tests

Molecular or toxicologic studies may be required at some stage in the future. To this end, appropriate storage of autopsy tissues/fluids is essential in SCD autopsies. If these laboratory tests are needed and no on-site facilities are available, the stored material should be sent to specialised labs established at regional or national levels.

Toxicology In investigating out-of-hospital deaths, the question is almost always raised of whether toxic substances are involved. Depending on the circumstances surrounding the death and toxicological data, the manner of death can be natural, accidental or criminal. Even when the heart is found to be abnormal at gross and/or microscopic examination, and death occurred suddenly,

Table 2 Certainity of diagnosis in SCD autopsies

Certain	Highly Probable	Uncertain
Massive pulmonary embolism	Stable atherosclerotic plaque with luminal stenosis >75% with or without healed myocardial infarction	Minor anomalies of the coronary arteries from the aorta (RCA from the left sinus, LCA from the right without inter-arterial course, high take-off from the tubular portion, LCx originating from the right sinus or RCA, coronary ostia plication, fibromuscular dysplasia, intramural small vessel disease)
Haemopericardium due to aortic or cardiac rupture	Anomalous origin of the LCA from the right sinus and inter-arterial course	Intra-myocardial course of a coronary artery (myocardial bridge)
Mitral valve papillary muscle or chordae tendineae rupture with acute mitral valve incompetence and pulmonary edema	Cardiomyopathies (hypertrophic, arrhythmogenic right ventricular, dilated, others)	Focal myocarditis, hypertensive heart disease, idiopathic left ventricular hypertrophy
Acute coronary occlusion due to thrombosis, dissection or embolism	Myxoid degeneration of the mitral valve with prolapse, with atrial dilatation or left ventricular hypertrophy and intact chordae	Myxoid degeneration of the mitral valve with prolapse, without atrial dilatation or left ventricular hypertrophy and intact chordae
Anomalous origin of the coronary artery from the pulmonary trunk	Aortic stenosis with left ventricular hypertrophy	Dystrophic calcification of the membranous septum (±mitral annulus/aortic valve)
Neoplasm/thrombus obstructing the valve orifice	ECG documented ventricular pre-excitation (Wolff–Parkinson–White syndrome, Lown Ganong Levine syndrome)	Atrial septum lipoma
Thrombotic block of the valve prosthesis	ECG documented sinoatrial or AV block	AV node cystic tumor without ECG evidence of AV block, conducting system disease without ECG documentation
Laceration/dehiscence/poppet escape of the valve prosthesis with acute valve incompetence	Congenital heart diseases, operated	Congenital heart diseases, un-operated with or without Eisenmenger syndrome
Massive acute myocarditis		

AV atrioventricular; *ECG* electrocardiogram; *LCA* left coronary artery; *LCx* left circumflex branch; *RCA* right coronary artery

the question still remains of whether a substance may have triggered the death, acting as additional factor to the anatomic substrate. Particularly in the athlete and in the young, doping and recreational drugs may precipitate SCD. Moreover, SCD may be caused by medications with cardiac side effects, such as neuroleptic or even cardiac drugs. The proper selection, collection, and submission of specimens for toxicological analyses is mandatory if analytical results are to be accurate and scientifically useful. The types and minimum amounts of tissue specimens and fluids needed for toxicological evaluation are frequently dictated by the analytes that must be identified and quantitated. For the purpose of sudden death investigation, the following amounts are adapted from the Guidelines of the Society of Forensic Toxicologists and the American Academy of Forensic Sciences [24]: heart blood 25 ml, peripheral blood from femoral veins 10 ml, urine 30–50 ml, bile 20–30 ml (when urine is not available). All samples are stored at 4°C. A lock of hair (100–200 mg) should be cut from the back head (or from the pubic hair when head hair is not available). Toxicological analyses should be quantitative.

Molecular pathology Molecular studies of SCD include both detection of viral genomes in inflammatory cardiomyopathies, and gene mutational analysis in both structural and non-structural genetically determined heart diseases [1, 7, 8, 26]. For these purposes, 10 ml of EDTA blood and 5 g of heart and spleen tissues are either frozen and stored at −80°C, or alternatively stored in RNA *later* at 4°C for up to 2 weeks.

Formulation of a diagnosis and the clinicopathological summary

The report should conclude with a clear clinicopathological summary (epicrisis). As far as possible this should relate the pathological findings to the clinical history, the circumstances of the death and any investigation performed close to the time of the death. There will be inevitable variations in the format of the death certificate between the states of the European Union.

In the majority of SCDs, a clear pathological cause can be identified, albeit with varying degrees of confidence. Wherever possible, the most likely underlying cause should be stated and the need for familial clinical screening and genetic analysis clearly indicated [4, 27].

It is important to accept that *different degrees of certainty* exist in defining the cause–effect relationship between the cardiovascular substrate and the sudden death event. Table 2 lists the commonest substrates of SCD, classifying each as *certain*, *highly probable* or *uncertain*. In the probable, and especially the uncertain categories, each case should be considered on its individual merits. The clinical history and the circumstances of death may influence the decision making process.

Finally, there are myocardial diseases in which the border between physiological and pathological changes is poorly defined. Some of these *diagnostic gray zones* are described in Table 3 [2, 6, 15, 25]. In everyday practice, pathologists should make a detailed macroscopic and

Table 3 The gray zone between physiological and pathological changes in myocardial disease

Physiological change	Pathological Change	Comments
Fatty infiltration of the right ventricular wall	Arrhythmogenic right ventricular cardiomyopathy	Massive fatty infiltration of the right ventricle without any evidence of replacement-type fibrosis and myocyte degeneration should not be considered "per se" a substrate of SCD, especially in obese and elderly people [2, 25].
Exercise induced left ventricular hypertrophy (athlete's heart)	Hypertrophic cardiomyopathy	An enlarged left ventricular cavity with increased wall thickness up to 13–14 mm is present in more than one third of highly trained athletes. Detailed histology is essential [15].
Focal myocardial disarray without hypertrophy	Hypertrophic cardiomyopathy without hypertrophy	Macroscopic changes are not always present in hypertrophic cardiomyopathy. At microscopy, the amount of fibres disarray should exceed 5–10% of fibres to be diagnostic. Isolated myocardial disarray confined to the anteroseptal and posteroseptal junctions should be considered normal. For a confident diagnosis, additional findings, such as interstitial and/or replacement fibrosis and abnormal intra-myocardial small vessels should be searched for [15].
Scattered inflammatory foci with or without small foci of fibrosis	Borderline/focal myocarditis	In the absence of myocyte necrosis, small foci of inflammatory cells (even after immunohistochemistry), are not sufficient evidence of myocarditis. Scattered small foci of fibrosis are also insignificant. Both findings should prompt examination of additional blocks. Viral infection should be excluded by molecular techniques [6].

microscopic description of their findings without implying a cause and effect relationship. If there is real doubt as to whether the changes are physiological or pathological, an expert opinion should be sought (see "Referral of hearts to specialised centres" above).

Deaths that remain unexplained after careful macroscopic, microscopic and laboratory investigation should be classified as sudden arrhythmic death syndrome [4, 10, 12]. We strongly suspect that the numbers of these unexplained deaths have been under-estimated in the past. There is increasing evidence that SCD in these instances might be due to inherited ion channel disorders, such as long QT and short QT syndromes, Brugada syndrome and catecholaminergic polymorphic ventricular tachycardia, which present with well-defined abnormalities of basal or effort ECG. In this setting, the availability of ECG tracings may be crucial for the diagnosis and molecular studies are essential. First degree relatives should undergo clinical screening and subsequent genetic analysis when indicated.

Conclusions

Although SCD is one of the most important mode of death in the European Union, pathologists and public health physicians have not given this problem the attention it deserves. Ventricular fibrillation is the nightmare of Western countries' populations. New methods of preventing potentially fatal arrhythmias have been developed and the accurate diagnosis of SCD is now of particular importance. The guidelines we produced represent the minimum standards of practice that should be adopted throughout the European Union and elsewhere. Further detailed information on the investigation of SCD and the diagnosis of specific entities will be available on the web site of the Association for European Cardiovascular Pathology (http://anpat.unipd.it/aecvp/).

References

1. Basso C, Calabrese F, Corrado D, Thiene G (2001) Postmortem diagnosis in sudden cardiac death victims: macroscopic, microscopic and molecular findings. Cardiovasc Res 50:290–330
2. Basso C, Thiene G (2005) Adipositas cordis, fatty infiltration of the right ventricle, and arrhythmogenic right ventricular cardiomyopathy. Just a matter of fat? Cardiovasc Pathol 14:37–41
3. Becker LB, Smith DW, Rhodes KV (1993) Incidence of cardiac arrest: a neglected factor in evaluating survival rates. Ann Emerg Med 22:86–91
4. Behr E, Wood DA, Wright M, Syrris P, Sheppard MN, Casey A, Davies MJ, McKenna W (2003) Sudden arrhythmic death syndrome steering group. Cardiological assessment of first-degree relatives in sudden arrhythmic death syndrome. Lancet 362:1457–1459
5. Brinkmann B (1999) Harmonization of medico-legal autopsy rules. Committee of Ministers. Council of Europe. Int J Legal Med 113:1–14
6. Calabrese F, Thiene G (2003) Myocarditis and inflammatory cardiomyopathy: microbiological and molecular biological aspects. Cardiovasc Res 60:11–25
7. Carturan E, Tester DJ, Brost BB, Basso C, Thiene G, Ackerman MJ (2007) Postmortem genetic testing for conventional autopsy negative sudden unexplained death: an evaluation of different DNA extraction protocols and the feasibility of mutational analysis from archival paraffin embedded heart tissue. Am J Clin Pathol (in press)
8. Chugh SS, Senashova O, Watts A, Tran PT, Zhou Z, Gong Q, Titus JL, Hayflick SJ (2004) Postmortem molecular screening in unexplained sudden death. J Am Coll Cardiol 43:1625–1629
9. Corrado D, Basso C, Pavei A, Michieli P, Schiavon M, Thiene G (2006) Trends in sudden cardiovascular death in young competitive athletes after implementation of a preparticipation screening program. JAMA 296:1593–1601
10. Corrado D, Basso C, Thiene G (2001). Sudden cardiac death in young people with apparently normal heart. Cardiovasc Res 50:399–408
11. Davies MJ (1999) The investigation of sudden cardiac death. Histopathology 34:93–98
12. Fabre A, Sheppard MN (2006) Sudden adult death syndrome and other non-ischaemic causes of sudden cardiac death. Heart 92:316–320
13. Gillum RF (1989) Sudden coronary death in the United States: 1980–1985. Circulation 79:756–765
14. Goldstein S (1982) The necessity of a uniform definition of sudden coronary death: witnessed death within 1 hour of the onset of acute symptoms. Am Heart J 103:156–159
15. Hughes SE (2004) The pathology of hypertrophic cardiomyopathy. Histopathology 44:412–427
16. Kitzman DW, Scholz DG, Hagen PT, Ilstrup DM, Edwards WD (1988) Age-related changes in normal human hearts during the first 10 decades of life. Part II (maturity): a quantitative anatomic study of 765 specimens from subjects 20 to 99 years old. Mayo Clin Proc 63:137–146
17. Medical Devices Agency Safety Notice 2002(35) (2002) Removal of implantable cardioverter defibrillators (ICDs). http://www.mhra.gov.uk/home/idcplg?IdcService=SS_GET_PAGE&useSecondary=true&ssDocName=CON008731&ssTargetNodeId=420 (pp 1–3)
18. Myerburg RJ, Castellanos A (2001) Cardiac arrest and sudden cardiac death. In: Braunwald E (ed) Heart disease: a textbook of cardiovascular medicine. Saunders, Philadelphia, PA, pp 890–931
19. Priori SG, Aliot E, Blomstrom-Lundqvist C, Bossaert L, Breithardt G, Brugada P, Camm AJ, Cappato R, Cobbe SM, Di Mario C, Maron BJ, McKenna WJ, Pedersen AK, Ravens U, Schwartz PJ, Trusz-Gluza M, Vardas P, Wellens HJ, Zipes DP (2001) Task force on sudden cardiac death of the European Society of Cardiology. Eur Heart J 22:1374–1450
20. Royal College of Pathologists (2005) Guidelines on autopsy practice 2005, scenario 1: sudden death with likely cardiac pathology. http://www.rcpath.org/index.asp?PageID=687 (pp 1–7)
21. Scholz DG, Kitzman DW, Hagen PT, Ilstrup DM, Edwards WD (1988) Age-related changes in normal human hearts during the first 10 decades of life. Part I (growth): a quantitative anatomic study of 200 specimens from subjects from birth to 19 years old. Mayo Clin Proc 63:126–136
22. Schulz DM, Giordano DA (1962) Hearts of infants and children: weights and measurements. Arch Pathol 73:464–471

23. Sheppard M, Davies MJ (1998) Investigation of sudden cardiac death. In: Sheppard M, Davies MJ (eds) Practical cardiovascular pathology. Arnold, London, pp 191–204
24. SOFT and AAFS (2002) Forensic toxicology laboratory guidelines. www.soft-tox.org/docs/Guidelines.2002.final.pdf pp 1–23
25. Tansey DK, Aly Z, Sheppard MN (2005) Fat in the right ventricle of the normal heart. Histopathology 46:98–104
26. Tester DJ, Ackerman MJ (2006) The role of molecular autopsy in unexplained sudden cardiac death. Curr Opin Cardiol 21:166–172
27. Thiene G, Basso C, Corrado D (2001). Cardiovascular causes of sudden death. In: Silver MD, Gotlieb AI, Schoen FJ (eds) Cardiovascular pathology. Churchill Livingstone, Philadelphia, pp 326–374
28. Virmani R, Burke AP, Farb A (2001) Sudden cardiac death. Cardiovasc Pathol 10:211–218
29. Zheng ZJ, Croft JB, Giles WH, Mensah GA (2001) Sudden cardiac death in the United States, 1989 to 1998. Circulation 104:2158–2163

Virchows Arch (2008) 452:19–25
DOI 10.1007/s00428-007-0527-z

ORIGINAL ARTICLE

Guidelines for neuropathologic diagnostics of perinatal unexpected loss and sudden infant death syndrome (SIDS)—a technical protocol

Luigi Matturri · Giulia Ottaviani · Anna Maria Lavezzi

Received: 8 June 2007 / Revised: 17 September 2007 / Accepted: 15 October 2007 / Published online: 22 November 2007
© Springer-Verlag 2007

Abstract In light of the growing information on the pathophysiology and clinical aspects of unexpected perinatal loss and sudden infant death syndrome (SIDS), a novel approach to the inherent problems by pathologists has become necessary. Herein, we propose an up-to-date protocol for accurate examination of the central autonomic nervous system and of the cardiac conduction system, which can encompass morphological and/or functional abnormalities of reliable epicritical value in unexplained perinatal loss and SIDS, particularly in those cases (still quite numerous) lacking adequate clinical documentation. Anatomo-pathologic examination of the central autonomic nervous system includes an in-depth study on histological serial sections of the brainstem, cerebellum, and spinal cord, where the main structures participating in control of the vital functions are located. For the histological study of the cardiac conductions system, serial sections were obtained from two blocks, including the sino-atrial node and the atrio-ventricular system, respectively. This type of updated investigation is yielding important arguments for a broader discussion of the pathogenesis of unexpected stillbirth, early neonatal death, and SIDS, besides allowing a more complete forensic-medical documentation of individual cases.

"Lino Rossi" Research Center for the study and prevention of unexpected perinatal death and SIDS, Institute of Pathology, University of Milan, Italy.

L. Matturri (✉) · G. Ottaviani · A. M. Lavezzi
Institute of Pathology, University of Milan,
Via della Commenda, 19,
20122 Milan, Italy
e-mail: luigi.matturri@unimi.it
URL: http://users.unimi.it/~pathol/pathol.html

Keywords Anatomo-pathological protocol · Autonomic nervous system · Cardiac conduction system · Stillbirth · SIDS

Introduction

Unexpected perinatal loss, which includes stillbirth or fetal death after 22 completed weeks (154 days) and early neonatal death occurring during the first 7 days of life [30] and sudden infant death syndrome (SIDS), represent facets of a multifactorial problem that has not yet found a universally recognized approach on the clinical plane. The fundamental component is pathological anatomy.

These tragic events are still frequent despite the progress in the field of maternal–infant health care. SIDS strikes one infant every 700–1,000 live births, being the most frequent cause of death within the first year of life [5, 17]. Worldwide, there are over 6.3 million perinatal deaths a year, almost all of which occur in developing countries, where the risk of death around birth is six times greater than in developed countries. Stillbirths account for over half of all perinatal deaths, and two-thirds of stillbirths are unexplained [4, 30].

Recently, the International Stillbirth Alliance and the USA Academy of Pediatrics [4, 29] stressed the need to submit all victims of such deaths to neuropathologic studies. In fact, the possibility of preventing perinatal unexpected death and SIDS relies mainly on a better knowledge of the underlying alterations of the central autonomic nervous system (ANS) and of the cardiac conduction system (CCS), which functions under the control of the nervous system.

So far, neuropathological studies have been focused on the consequences of hypoxic cerebral damages (gliosis,

etc.) and infections [3]. Instead, studies addressing the identification of peculiar lesions of the structures and/or the nuclei modulating the vital functions, are fundamental for pathogenic evaluations of the reflexogenic sudden death.

Therefore, the pathogenesis of stillbirth and SIDS must be taken in most cases to include some autonomic nervous dysfunctions in the control of the vital functions. A histopathological substrate should be searched for in a wide neuropathology field, including the brainstem nuclei, the cerebellum (cortex and deep nuclei), and the cardiac conduction system, subjected to strict autonomic control [2, 10, 11, 23, 26, 28].

The aim of this work is to propose a more accurate and up-to-date version of the previous guidelines [22], particularly with regard to the protocol for the examination of the nuclei and/or structures presiding over the vital activities (cardiorespiratory, arousal, upper digestive tract, etc.), which in all cases of unexpected perinatal loss and SIDS studied by our group, have shown congenital alterations.

Autopsy, neuropathological, and cardiac sampling and the method of examination of the ANS and the CCS

This protocol was applied in a very wide population of unexpected and unexplained perinatal and infant death victims. This was a selected set of cases, addressed to our Institute on the basis of a specific decree of the Lombardy Region [16]. This project, in fact, imposes that all the cases of unexplained perinatal death and/or of suspected SIDS must be sent to us, as Reference Center, for the in-depth anatomo-pathological examination. Therefore, cases with a defined cause of death (genetic abnormalities, infections, malformations, etc.) were excluded from this study.

In all cases of unexpected perinatal and infant death, a complete autopsy is performed according to the International Standardized Autopsy Protocol of the Global Strategy Task Force of SIDS International [6].

These autopsy guidelines include examination of the placental disk, umbilical cord, and membranes in fetuses and, in all cases, an in-depth histological examination of the cardiorespiratory autonomic nervous system [20, 22].

Protocol for examination of the central ANS

Anatomo-pathologic study of the central autonomic nervous system includes an in-depth study of the brainstem, cerebellum, and spinal cord, where the main structures participating in control of the vital functions are located (cardiorespiratory, arousal, upper digestive tract, etc.).

Brainstem (medulla oblongata, pons, and midbrain)

Examination of the brainstem includes sampling of three specimens, as shown in Fig. 1. The first specimen, ponto-mesencephalic, includes the upper third of the pons and the adjacent portion of midbrain. The second extends from the upper third of the medulla oblongata to the portion adjacent to the pons. The third specimen takes as reference point the obex and extends 2–3 mm above it and below it.

Transverse serial sections are made at intervals of 30 μm. For each level, twelve 5-μm sections are obtained, two of which are routinely stained for histological

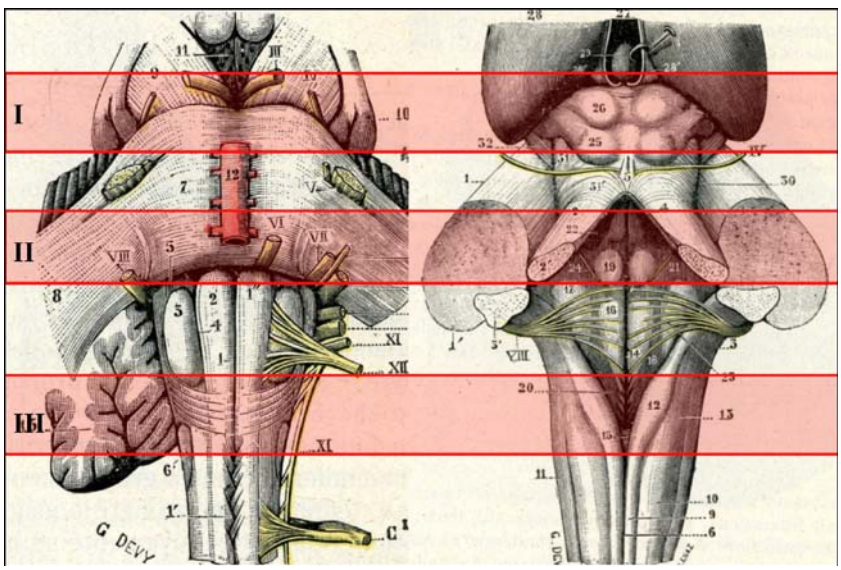


Fig. 1 Sampling of the brainstem: ventral (*left*) and dorsal (*right*) surface. Modified from L. Testut, "Anatomia Umana", Unione Tipografico-Editrice Torinese, Torino, 1923

examination alternately using hematoxylin–eosin and Klüver–Barrera stains, and three additional sections at each level are subjected to immunohistochemistry to study the functional activities. The remaining sections are saved and stained as deemed necessary for further investigations.

The routine histological evaluation of the brainstem is focused on the locus coeruleus, the parafacial nucleus, the parabrachial/Kölliker–Fuse complex in the pons/mesencephalon, and on the hypoglossus, the dorsal motor vagal, the tractus solitarius, the ambiguus, the pre-Bötzinger, the inferior olivary, and the arcuate nuclei in the medulla oblongata.

Figure 2 shows the histological sections corresponding to the three brainstem specimens of Fig. 1 indicating the main nuclei and structures to be examined.

Cerebellum

It is essential to make an accurate examination of the cerebellum, too, in view of its role in controlling the respiratory muscles and of the observation of developmental anomalies of the cortex and deep nuclei in cases of perinatal unexpected death and SIDS. To examine both the cerebellar cortex and the nuclei (dentate, etc.), a specimen of hemisphere extending all along the major diameter should be sampled.

Spinal cord (cervico-thoracic tract)

The removal of the first five thoracic levels of the spinal cord enables examination of the orthosympathetic intermediolateral nucleus.

Protocol for examination of the functional activities of the central ANS

To analyze the immunoexpression of neurotransmitters, particularly somatostatin, substance P and tyrosine-hydroxylase, sections are subjected to immunohistochemical methods with specific primary antibodies after application of the avidin–biotin–peroxidase technique, in conformity with conventional immunohistochemical procedures. Immunohistochemical visualization of apoptotic cells was obtained by the TUNEL method (TdT-mediated dUTP-biotin nick end labeling).

A detailed description of the immunohistochemical methods, including the immunopositivity evaluation, applied in this study is available in our previous works [9, 12–14].

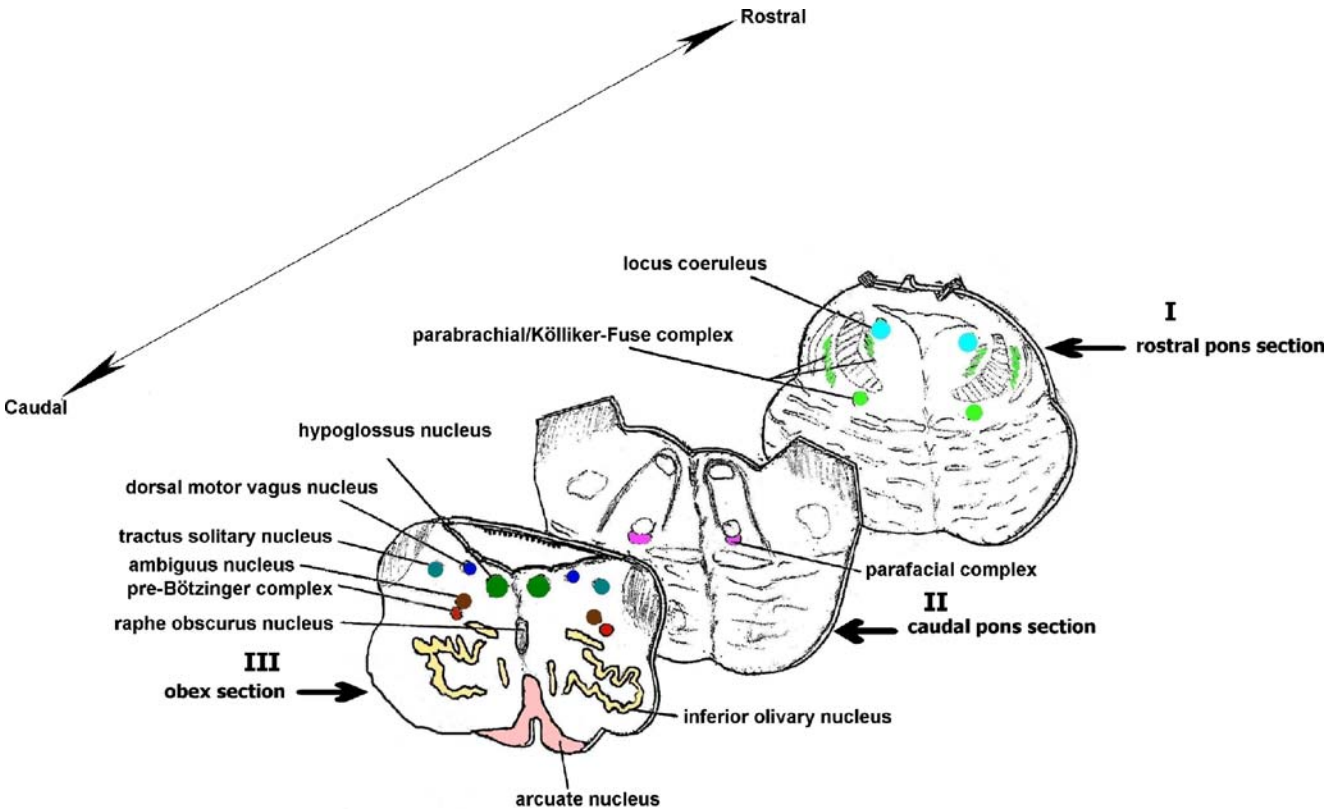


Fig. 2 Brainstem: the histological sections corresponding to the three specimens, indicating the main nuclei and structures to be examined

Protocol for morphometric analysis of the central ANS

The morphologic examination of the main nuclei and structures of the brainstem and cerebellum is usually supplemented by morphometric analysis, performed with an image analyzer. The following parameters are evaluated and indicated as mean values and standard deviation: area (expressed in mm^2), neuronal density (expressed as number of neurons per mm^2), and neuronal size (cell body area, expressed in μm^2). An in-depth description of the methodology can be found in our previous works [7, 8, 13, 15, 19, 21].

Protocol for examination of the CCS

The neonatal and infant hearts are regularly examined for pathologic changes in the atria, septa, ventricles, pericardium, endocardium, and coronary arteries. Samples of the myocardium are stained with hematoxylin–eosin and trichromic Heidenhain (azan).

Histological observations of the heart are focused on the cardiac conduction system. The conducting tissue, although fairly constant in layout and structure, is subject to noteworthy individual variations; hence, histological examination on serial sections is expected to provide the necessary data on both topography and pathology of the specialized tissue. The CCS is removed in two blocks for paraffin embedding.

Block 1 This contains the sinu-atrial (SA) node, its atrial approaches, and the *Crista Terminalis* and the SA node gangliar plexus. The main visual reference for removal is centered upon the *Sulcus–Crista Terminalis*. Two longitudinal cuts are driven, parallel to the *Sulcus–Crista* line, through the atrial wall, with a medial prolongation on the right side to encompass the anterior aspect of the inlet of the superior vena cava; on the left side, the cava-cava bridge has to be sectioned very medially, prolonging the cut on the superior vena cava wall. Of the two transverse cuts, the superior one is oriented to remove as much as possible of the cava funnel in between the longitudinal sections. The inferior cut removes, more or less distally (according to the atrial volume), the fan of pectinate muscles that radiate from the *Crista Terminalis* (Fig. 3).

Block 2 This contains the atrium–ventricular (AV) system with its atrial approaches: the reference points of the excision are, on the right side, the outlet of the coronary sinus and the *pars membranacea septi*. By holding the already opened heart so as to expose the interventricular septum against a fairly intense light source, the transparent area of the *pars membranacea* can be clearly spotted and pinned between thumb and index; thereupon, the procedure continues with excision of the interventricular septum together with the central fibrous body, the lowermost part of the atrial septum, and the adjacent segments of the AV fibrous annuli. The cuts will be driven as follows: (a) an inferior, longitudinal incision through the posterior part of the septum, across the AV annulus fibrous and up to the superior margin of the coronary sinus ostium; (b) an anterior longitudinal incision parallel to the former, through the superior part of the septum, extending to the aortic valvular ring; (c) and (d) two cuts perpendicular to (a) and (b), to remove the tissue block, with its upper margin about 1.5 cm above the AV ring and its lower margin encompassing the base of the medial tricuspid papillary muscle and possibly the moderator band.

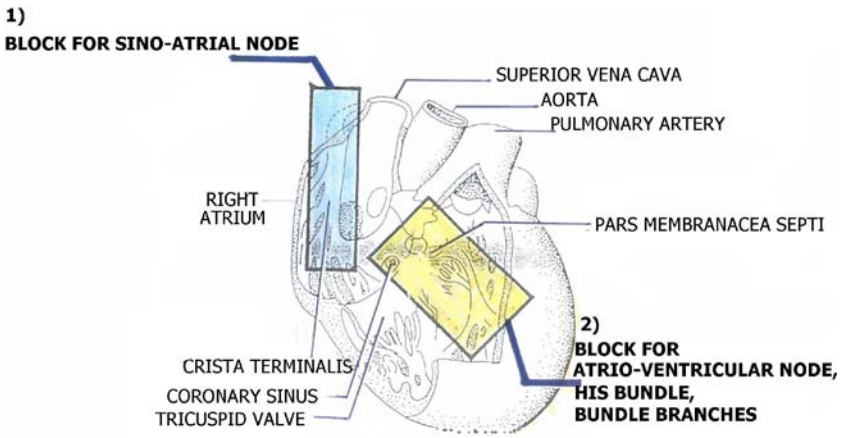


Fig. 3 The procedure for removing the two blocks for the study of the cardiac conduction system. Block 1 contains the sino-atrial node (*SAN*), its atrial approaches, the *Crista Terminalis*, and the sinu-atrial node gangliar plexus. The main visual reference for the removal is centered upon the *Sulcus-Crista Terminalis*. Block 2 contains the atrio-ventricular node (*AVN*), the His bundle (*HB*), and bundle branches. The reference points for the excision are, on the right side, the outlet of the coronary sinus and the pars membranacea septi

Both blocks 1 and 2 are routinely fixed in 10% buffered formalin that, besides simplicity, has the advantage of allowing further silver impregnations of the nervous system, whenever needed. On paraffin embedding, it is advisable to place the medial margin of block 1 and the posterior–inferior margin of block 2 at the bottom. The resulting section plane of block 1 is perpendicular to the atrial endocardial surface and parallel to the major axis of the *Crista Terminalis*. The block 2 section is also perpendicular to both endocardial surfaces, along the major septal axis. Besides the generic differences from these oversimplified models, individual variations must be expected, due to the remarkable variability of the conduction system and to the slight discrepancies occurring in the excision of the heart fragments from case to case.

Regarding fetal hearts, the small hearts from fetuses aged 22–35 gestational weeks are processed entire and serially cut. The section plane of this paraffin block is perpendicular to the interatrial and interventricular septa and parallel to the anterior heart surface. For near to term and term fetuses aged 36–42 gestational weeks, the hearts are sampled according to the above-described method for infant and neonatal hearts with the exception of fetuses that are small for gestational age (Fig. 4).

For the histological examination of the conduction tissue, the one or two paraffin blocks are cut serially at intervals of 20–40 μm (levels). For each level, three sections are retained and mounted, and one of the mounted sections is stained alternately with hematoxylin–eosin, azan, and terminal uridine deoxynucleotidyl transferase dUTP nick end labeling for apoptosis. All intervening sections are kept and stained as deemed necessary. For each heart, in our experience, the average number of histological sections stained and examined was about 100. A 3-D reconstruction of the conduction system can be obtained from the series of 2-D slides [18, 24, 25, 27].

The morphological investigations of both ANS and CCS should be completed by the application of molecular biology methods with the purpose of disclosing genetic abnormalities (particularly mutations and genetic polymorphisms) and the presence of any microorganisms, including viruses.

Results of the application of the guidelines in perinatal and infant unexpected death

Our morphological investigations in 71 cases of sudden perinatal death (57 late fetal and 14 neonatal deaths) and 138 cases of SIDS have disclosed a variety of congenital lesions, as reported in our previous studies, of the autonomic nervous system (particularly of the brainstem and cerebellum) [7–11, 12–15, 19, 21] and of the cardiac conduction system [18, 24, 25, 27].

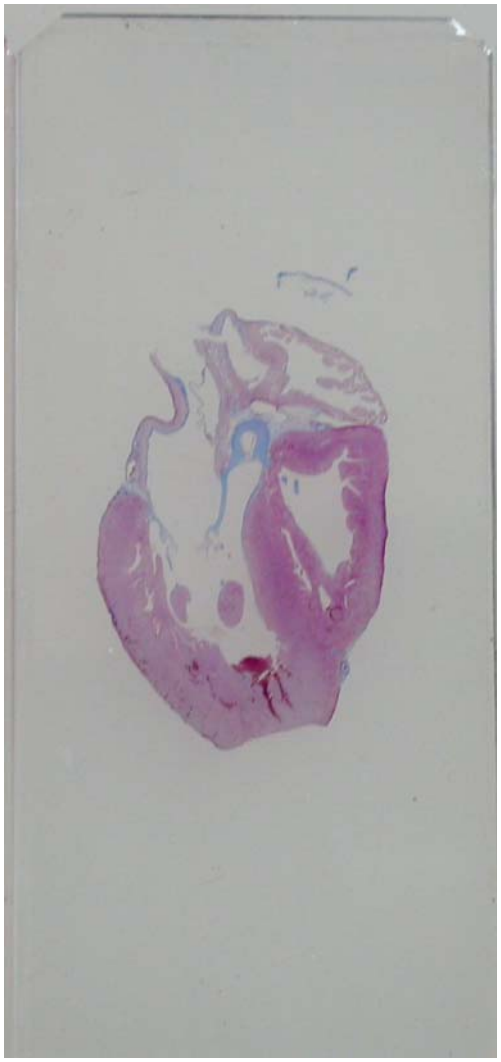


Fig. 4 Histological slide, trichromic Heidenhain (azan) stained, of a heart from a female fetus aged 23^{+4} gestational weeks. The heart was processed entire and serially cut. The section plane of the heart's paraffin block was perpendicular to the interatrial and interventricular septa and parallel to the anterior heart surface

From the overall analysis of the neuropathological results, the following prominent data emerged:

1. In all cases of sudden perinatal and infant death, one or more congenital morphological and/or functional abnormalities of the brainstem and cerebellum were observed.
2. In the SIDS victims, the main alteration was hypoplasia of the arcuate nucleus, sometimes associated to hypoplasia of the reticular formation and of the hypoglossus nucleus. This hypoplasia was present with the same incidence in fetal and infant unexpected deaths.
3. Hypoplasia of the facial/parafacial complex was a very frequent and specific anomaly of sudden fetal deaths never observed after birth.

4. Hypoplasia of the Kölliker–Fuse nucleus was frequently observed in perinatal deaths (stillbirths and early neonatal deaths).
5. The cerebellar cortex showed in many cases delayed maturation particularly in SIDS victims.
6. Among the functional alterations, altered expression of neurotransmitters in the brainstem was frequently diagnosed, particularly of catecholamine in the locus coeruleus and of somatostatin in the hypoglossus nucleus, besides defective apoptotic programs in cerebellum (precisely in the Purkinje and internal granular layers of the cerebellar cortex and in the dentate nucleus).

From the overall analysis of the cardiac conduction system results, the following prominent data emerged:

1. Accessory atrioventricular pathways, mostly Mahaim fibers, in 27% of stillbirth and in 23% of SIDS victims.
2. Cartilaginous hypermetaplasia in 20% of stillbirth and in 12% of SIDS.

All of these cardiac conduction findings may be isolated or associated with central nervous system alterations. These associations were observed in 30% of cases of our studies.

Discussion

In light of the growing information on the pathophysiology and clinical aspects of unexpected perinatal loss and SIDS, a novel approach to the inherent problems by pathologists (particularly by those entrusted with forensic medical authority) has become necessary.

This type of updated investigation, extending from the cardiac conduction system up to the brainstem and cerebellar vital centers, has heretofore been neglected even in the recent standardization of diagnostic criteria of SIDS proposed by a very wide group of researchers in this field [1].

Herein, we have reported a new and more updated version of the standard technical protocol for performing accurate examination of the central autonomic nervous system and of the cardiac conduction system in cases of unexplained perinatal loss and SIDS.

Our studies, performed according to this protocol, have revealed frequent structural and/or functional alterations of the autonomic nervous system and of the cardiac conduction system in the victims of perinatal unexpected death and SIDS [7–9, 12–15, 19, 21]. These alterations, which are frequently associated, are mainly of a congenital nature and therefore represent a common morphological substrate in both perinatal and infant unexplained death.

A particularly common finding in these pathologies was hypoplasia of the arcuate nucleus, a chemoreceptorial component of the ventral surface, which was present in over 50% of the victims, albeit with different degrees of extension and severity. In perinatal deaths, in addition to hypoplasia of the arcuate nucleus, we observed hypodevelopment of the reticular formation, consisting of the presence of very sparse branching of the dendrites into the neuropil, prevalently in the ambiguous and pre-Bötzinger nuclei areas, besides hypoplasia of the parabrachial/Kölliker–Fuse complex. Moreover, exclusively in unexplained fetal death victims, apart from hypoplasia of the arcuate nucleus, we frequently observed hypoplasia of the parafacial nucleus. In unexplained death victims, we also observed functional alterations of different nuclei and/or structures of the brainstem, mainly consisting of severe disturbances of the neuroreceptoral activities (particularly in the locus coeruleus and in the hypoglossus nucleus) [9, 13].

Among the abnormalities of the cardiac conduction system, sometimes associated with abnormalities of the autonomic nervous system, the most frequent were accessory atrioventricular pathways, mostly Mahaim fibers [18, 24, 25, 27].

Subtle isolated or associated lesions involving these structures are likely responsible for the disruption of the neuronal pathways. In particular, neuropathological involvement of the vagal-glossopharyngeal neuronal circuit may explain some lethal reflexogenic mechanisms of sudden perinatal death (in both the near term fetus and the newborn) and early infant death, including SIDS.

Already in 2002 at the International Congress on SIDS [20], we indicated the need to analyze all these structures in the context of an in-depth neuropathological examination of the autonomic nervous system and proposed the new definition of SIDS as the “sudden death of an infant under one year of age which remains unexplained after a thorough case investigation, including performance of a complete autopsy and in-depth histology of the cardiorespiratory autonomic nervous system, examination of the death scene, and a review of the clinical history.”

All in all, the above-illustrated autopsy examination procedures enable analysis of the morpho-functional substrates of perinatal loss and of SIDS, namely, the reflexogenic histopathology focused upon the vital (namely cardiorespiratory) neuronal circuitry. In conclusion, neuropathology is an integral component and a consistent substrate of both SIDS and unexpected perinatal loss; an updated appraisal of fundamental aspects of the histopathology of the autonomic nervous system and the cardiac conduction system could help to foster a better understanding of the problem at issue.

It is hoped that the neuropathological protocol we propose will prove useful to the pathologist faced with victims of unexpected perinatal loss and SIDS, in the autopsy room, to explain their deaths and hopefully, in the future, to save other lives.

Acknowledgments This study was supported by the Italian Lombardy Region target project n. 49210/2000 (Program of research and intervention for the reduction of the risk of SIDS and unexpected fetal death), by the agreement Lombardy Region-Pfizer Italia S.r.l. n. 814/2006, and by Ministry of Foreign Affairs (joined projects of particular relevance "Anatomopathologic and genetic study of the unexplained perinatal death and SIDS") n. 269/P/0085087/2004 and n. 0083227/20006.

References

1. Bajanowski T, Vege A, Byard RW, Krous HF, Arnestad M, Bachs L, Banner J, Blair PS, Borthne A, Dettmeyer R, Fleming P, Gaustad P, Gregersen M, Grøgaard J, Holter E, Isaksen CV, Jorgensen JV, de Lange C, Madea B, Moore I, Morland J, Opdal SH, Råsten-Almqvist P, Schlaud M, Sidebotham P, Skullerud K, Stoltenburg-Didinger G, Stray-Pedersen A, Sveum L, Rognum TO (2007) Sudden infant death syndrome (SIDS)—standardised investigations and classification: recommendations. Forensic Sci Int 165:129–143
2. Blanco CE, Dawes GS, Hanson MA, McCooke HB (1984) The response to hypoxia of arterial chemoreceptors in fetal sheep and new-born lambs. J Physiol 351:25–37
3. Grafe MR, Kinney H (2002) Neuropathology associated with stillbirth. Sem Neuropathol 26:83–88
4. International Stillbirth Alliance (2007) http://www.stillbirthalliance.org/. Cited June 9, 2007
5. Kochanek KD, Murphy SL, Anderson RN, Scott C (2004) Deaths: final data for 2002. Natl Vital Stat Rep 53:1–115
6. Krous HF (1996) Instruction and reference manual for the International Standardise Autopsy Protocol for sudden unexpected infant death. J SIDS Infant Mortal 1:203–246
7. Lavezzi AM, Ottaviani G, Mauri M, Matturri L (2003) Hypoplasia of the arcuate nucleus and maternal smoking during pregnancy, in perinatal and infant sudden unexpected death. Neuropathology 24:284–289
8. Lavezzi AM, Ottaviani G, Ballabio GM, Rossi L, Matturri L (2004) Preliminary study on the cytoarchitecture of the human parabrachial/Kölliker–Fuse complex with reference to sudden infant death syndrome and sudden intrauterine unexplained death. Pediatr Dev Pathol 7:171–179
9. Lavezzi AM, Ottaviani G, Matturri L (2004) Role of somatostatin and apoptosis in breathing control in sudden perinatal and infant unexplained death. Clin Neuropathol 23:304–310
10. Lavezzi AM, Ottaviani G, Rossi L, Matturri L (2004) Cytoarchitectural organization of the parabrachial/Kölliker–Fuse complex in man. Brain Dev 26:316–320
11. Lavezzi AM, Ottaviani G, Rossi L, Matturri L (2004) Hypoplasia of the Parabrachial/Kölliker–Fuse complex in perinatal death. Biol Neonate 86:92–97
12. Lavezzi AM, Ottaviani G, Matturri L (2005) Adverse effects of prenatal tabacco smoke exposure on biological parameters of the developing brainstem. Neurobiol Dis 20:601–607
13. Lavezzi AM, Ottaviani G, Mingrone R, Matturri L (2005) Analysis of the human locus coeruleus in perinatal and infant sudden unexplained death. Possible role of the cigarette smoking in the development of this nucleus. Dev Brain Res 154:71–80
14. Lavezzi AM, Ottaviani G, Mauri M, Matturri L (2006) Alterations of biological features of the cerebellum in sudden perinatal and infant death. Curr Mol Med 6:429–435
15. Lavezzi AM, Matturri L (2007) Functional neuroanatomy of the human pre-Bötzinger complex with particular reference to sudden unexplained perinatal and infant death. Neuropathology (in press)
16. Lombardy Regional Decree n. 11693 of 06-20-02 (2007) "Legislative measures on adoption of anatomo-pathological and forensic-pathological intervention targeted on the prevention, knowledge, and identification of the sudden infant death cases." http://users.unimi.it/~pathol/pdf/decreto.pdf. Cited August 21, 2007
17. Matthews T, McDonnell M, McGarvey C, Loftus G, O'Regan M (2004) A multivariate time based analysis of SIDS risk factors. Arch Dis Child 89:267–271
18. Matturri L, Ottaviani G, Ramos SG, Rossi L (2000) Sudden infant death syndrome (SIDS): a study of cardiac conduction system. Cardiovasc Pathol 9:137–145
19. Matturri L, Biondo B, Suarez-Mier MP, Rossi L (2002) Brain stem lesions in the sudden infant death syndrome: variability in the hypoplasia of the arcuate nucleus. Acta Neuropathol (Berl) 104:12–20
20. Matturri L, Lavezzi AM, Rossi L (2002) Proposal to modify the definition of SIDS, with regard to the post mortem exam In: Proceed. 7th SIDS International Conference. Florence, Italy; August 31-September 4, 2002, p. 103
21. Matturri L, Minoli I, Lavezzi AM, Cappellini A, Ramos S, Rossi L (2002) Hypoplasia of medullary arcuate nucleus in unexpected late fetal death (stillborn infants): a pathologic study. Pediatrics 109:1–5
22. Matturri L, Ottaviani G, Lavezzi AM (2005) Techniques and criteria in pathologic and forensic-medical diagnostics of sudden unexpected infant and perinatal death. Am J Clin Pathol 124:259–268
23. McKay LC, Janczewski WA, Feldman JL (2005) Sleep-disordered breathing after targeted ablation of preBötzinger complex neurons. Nat Neurosci 8:1142–1144
24. Ottaviani G, Matturri L, Rossi L, James TN (2003) Crib death: further support for the concept of fatal cardiac electrical instability as the final common pathway. Int J Cardiol 92:17–26
25. Ottaviani G, Matturri L (2007) Histopathology of the cardiac conduction system in sudden intrauterine unexplained death (SIUD). Cardiovasc Pathol (in press)
26. Rekling JC, Feldman JL (1998) PreBötzinger complex and pacemaker neurons: hypothesized site and kernel for respiratory rhythm generation. Annu Rev Physiol 60:385–405
27. Rossi L, Matturri L (1990) Clinicopathological approach to cardiac arrhythmias. Centro Scient Torinese, Turin. Distributed by Futura, Mount Kisco, NY
28. Teitel DF (1996) Fetal chemoreception: a developing story. Reprod Fertil Dev 8:471–482
29. USA Academy of Pediatrics (2005) http://www.msnbc.msn.com/id/9649335/. Cited June 9, 2007
30. World Health Organization (WHO) (2006) Neonatal and perinatal mortality: country, regional and global estimates. WHO, Geneva, pp 1–75

Virchows Arch (2008) 452:27–32
DOI 10.1007/s00428-007-0524-2

ORIGINAL ARTICLE

C-kit protein expression correlated with activating mutations in KIT gene in oral mucosal melanoma

Rosario S. Rivera · Hitoshi Nagatsuka · Mehmet Gunduz · Beyhan Cengiz · Esra Gunduz · Chong Huat Siar · Hidetsugu Tsujigiwa · Ryo Tamamura · Kok Ng Han · Noriyuki Nagai

Received: 27 June 2007 / Revised: 27 August 2007 / Accepted: 4 October 2007 / Published online: 8 December 2007
© Springer-Verlag 2007

Abstract C-kit is a trans-membrane receptor tyrosine kinase (RTK) encoded by the proto-oncogene KIT located at 4q11-12. Gain-of-function mutations arising to c-kit activation independent of its ligand were observed in various tumors related to germ cells, mast cells, and interstitial cells of Cajal. C-kit also participates in melanocyte development; hence, its involvement in oral mucosal melanoma (OMM) tumorigenesis was investigated. Immunohistochemistry and mutation analysis were performed using 18 cases of human primary OMM. Results revealed 16 cases positive to c-kit protein. Atypical melanocytes expressed c-kit. All in situ components expressed c-kit, but only four cases exhibited intense expression in the invasive component. Missense mutations were observed in four cases, and two of those correlated with increased protein expression. C-kit expression in atypical melanocytes suggests the role of c-kit in the early stage of OMM tumorigenesis. C-kit protein expression correlated with activating mutations indicating the pertinent role of the proto-oncogene KIT in the tumorigenesis of OMM.

Keywords Oral mucosal melanoma · C-kit mutation · Immunohistochemistry

R. S. Rivera · H. Nagatsuka (✉) · M. Gunduz · B. Cengiz · E. Gunduz · H. Tsujigiwa · R. Tamamura · N. Nagai
Department of Oral Pathology and Medicine,
Graduate School of Medicine,
Dentistry and Pharmaceutical Sciences, Okayama University,
2-5-1 Shikata-cho,
Okayama 700-8525, Japan
e-mail: jin@md.okayama-u.ac.jp

R. S. Rivera
College of Dentistry, University of the East,
Manila, Philippines

C. H. Siar
Department of Oral Pathology,
Oral Medicine and Periodontology, Faculty of Dentistry,
University of Malaya,
Kuala Lampur, Malaysia

K. N. Han
Unit of Stomatology, Cancer Research Centre,
Institute for Medical Research,
Kuala Lumpur, Malaysia

Introduction

Oral mucosal melanoma (OMM) is a rare malignant soft tissue neoplasm, which comprises 0.5% of oral malignancies [5, 13]. The mechanism involved in its progression and aggressiveness is not clearly understood. Because of the slow progress in the treatment of melanoma, significant advances may require new insights into melanoma biology. Molecular analysis may give better perception and selection of therapy, targeting signaling molecules responsible for OMM progression.

Melanocytes are specialized melanin-producing cells that originate from the neural crest and migrate to the skin, hair follicle, and retina. Melanocytes can also be found in the oral mucosa, but their existence and function are unknown [13]. C-kit is one of the receptor tyrosine kinases (RTK) that influences proliferation, migration, and survival of melanocytes. C-kit, a protein encoded by the proto-oncogene KIT, is activated by its ligand, stem cell factor, during melanogenesis [1]. However, in tumors, c-kit activation independent of its ligand through oncogenic mutations enables the receptor to phosphorylate various substrate proteins. This will then lead to activation of signal transduction cascades that regulate cell proliferation, apoptosis, chemotaxis, and adhesion [21, 23].

Gain-of-function mutations in c-kit were identified in various solid tumors particularly in gastrointestinal stromal tumor (GIST) [4, 7, 9, 10, 14, 15, 18, 19, 23, 26, 32, 37, 38]. The in-frame mutations vary from single base pair substitutions to complex deletions and insertions [7, 38]. The identification of c-kit mutation led to further studies on molecular therapy of GIST and other tumors with imatinib mesylate (STI-571, Gleevec), a specific competitive inhibitor of c-kit [39]. C-kit mutations most commonly involve the juxta-membrane domain (JMD) encoded by exon 11, although mutations in other domains were also found [8, 21, 26, 38].

C-kit is an important receptor for melanocyte growth and maturation and its expression might be inferred in melanoma [19]. Likewise, the detection of c-kit activating mutation in OMM may give an insight to the value of specific RTK inhibitor in a subset of melanoma. Although several studies involving c-kit and melanoma have been reported, there has been no research done on OMM. Thus, we investigated the protein expression and activating mutations in c-kit exons 11 and 13. C-kit protein expression correlated with activating mutations, which might be in part responsible for OMM tumorigenesis.

Materials and methods

Paraffin-embedded tissue samples

Hematoxylin and eosin (HE) sections from 18 cases of formalin-fixed, paraffin-embedded primary OMM were retrospectively analyzed. The cases were histologically classified according to the Western Society of Teachers in Oral Pathology classification [5, 28].

Immunohistochemistry

New sections of tissue samples were cut for immunohistochemistry (IHC). Deparaffinized tissue sections were blocked for endogenous peroxidase activity using 3% hydrogen peroxide in methanol for 30 min, washed with Tris-buffered saline solution, and treated for antigen retrieval in citrate buffer, pH 6.0 (heat pressure for 5 min at 121°C). The slides were covered with serum-free protein block (DakoCytomation, Carpinteria, USA) for 15 min, followed by C-kit antibody (DakoCytomation) with a dilution of 1:100 and incubated overnight at 4°C. Immunoreaction was carried out with Envision™ Detection Reagent Peroxidase (DakoCytomation) and detected with 3-amino-ethylcarbazole substrate chromogen (DakoCytomation). Immunoreaction was defined as negative (−) when no immunoreaction was observed and focal (±) when less than 20% melanoma cells were positive and if the degree of staining was weak. When the degree of staining was strong, it was regarded as moderate (+) when 20–50% melanoma cells were positive and intense (++) when more than 50% melanoma cells were positive. Immunoreactions for in situ and invasive components were recorded separately.

Mutation analysis

Genomic deoxyribonucleic acid (DNA) was extracted from formalin-fixed paraffin blocks with Dexpat Kit (Takara Bio, Shiga, Japan) following the manufacturer's procedure. Although hot spots for c-kit include exons 9, 11, 13, and 17, the study focused on exons 11 and 13 because most mutations in GIST were found in these exons. Exons 11 and 13 were amplified by polymerase chain reaction (PCR) using primers shown in Table 1. PCR was performed in 20-μl reactions containing 2 μl reaction buffer, 1.6 μl dexoyribonucleotide triphosphate, 0.5 μl of primer, and 0.1 μl r*Taq* (Takara Bio) and diluted to volume with sterile water. PCR-cycling conditions were as follows: initial denaturation at 94°C for 3 min, 45 cycles of denaturation at 94°C for 30 s, annealing at 58 (exon 11) and 62°C (exon 13) for 1 min, and extension at 72°C for 1 min. A final extension at 72°C for 7 min was also performed. PCR products were purified with Geneclean III Kit, and others were treated with ExoSAP-IT (USB, Ohio, USA) before sequence-specific PCR. For confirmation purposes, new sets of PCR products were subjected to single-strand confirmation polymorphism (SSCP); aberrant bands were cut and subjected to PCR followed by ExoSAP-IT treatment and sequence-specific PCR.

Direct sequencing was performed using Big Dye Terminator v1.1 Cycle Sequencing Kit (Applied Biosystems, CA, USA). Sequence reactions were purified with ethanol and ethylenediamine tetraacetic acid precipitation and analyzed on a 3130xl ABI Prism Genetic Analyzer (Applied Biosystems, Hitachi, Japan).

Results

Immunohistochemistry

Figure 1a (in situ) and c (invasive) are representative HE sections of OMM. The expressions observed were mem-

Table 1 Primer sequences for C-kit

Exon	Sequence	
Exon 11	Forward	5′-CTCTCCAGAGTGCTCAATGAC-3′
	Reverse	5′-AGCCCCTGTTTCATACTGACC-3′
Exon 13	Forward	5′-CGGCCATGACTGTCGCTGTAA-3′
	Reverse	5′-CTCCAATGGTGCAGGCTCCAA-3′

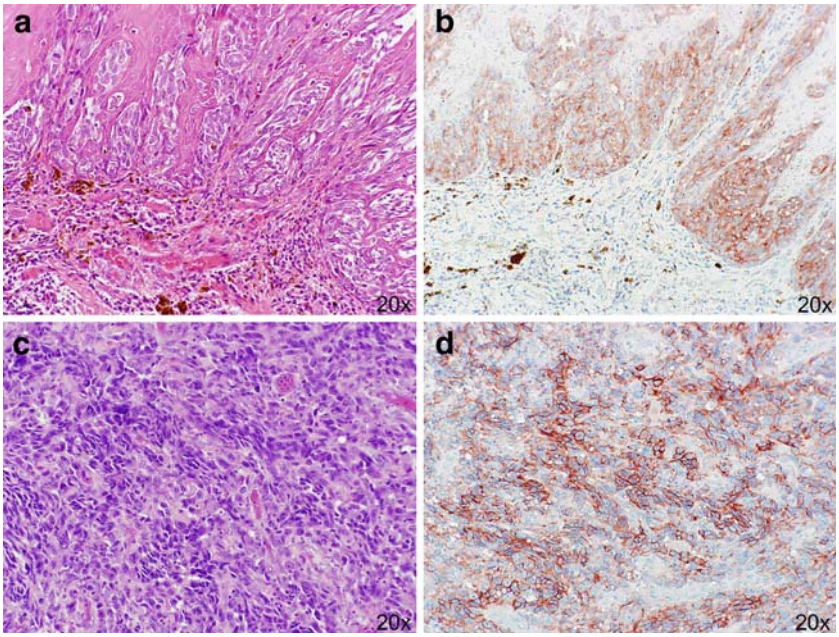


Fig. 1 C-kit expression in OMM. HE sections of the in situ component (**a**) and invasive components (**c**). This figure shows intense expression of c-kit protein in the in situ component (**b**) and invasive component (**d**)

branous and cytoplasmic. C-kit expression was detected in atypical melanocytes. Furthermore, c-kit expression was detected in all in situ components (Fig. 1b). Only one case exhibited focal staining, and the rest were moderate to intense. In invasive components, c-kit expression was observed in 16 out of 18 cases. C-kit expression varied from focal to intense, and only four cases were intensely positive (Fig. 1d).

Mutation analysis

All cases were subjected to mutation analysis including the two IHC-negative cases. Many aberrant bands were observed in SSCP gels for exons 11 and 13 (Fig. 2). When these bands were sequenced, few missense and silent mutations were obtained. Missense mutations were detected in 4 out of 15 cases with DNA amplification (27%), two mutations in exon 11 and two in exon 13. Mutations W557R and K642E have been reported in GIST [4, 9, 14, 15, 18, 19, 23, 26, 37, 38], but K642E was also reported specifically in mucosal melanoma [8]. Our literature search did not reveal any report on the mutation V569G (Fig. 3).

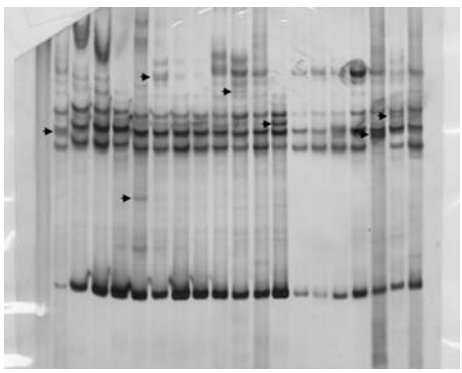


Fig. 2 Single strand confirmation polymorphism. Aberrant bands from PCR products with exon 13 were evident (*arrows*)

Results in Table 2 show that in the four cases with mutations, two showed intense c-kit protein expression (cases 6 and 15). Case 6 exhibited several recurrences, and case 15 was of the amelanotic type. Moreover, two cases with mutations exhibited an increase in protein expression from in situ phase to invasive phase (cases 6 and 9).

Discussion

OMM has a poor prognosis with a 5–20% survival rate [33]. The poor prognosis of OMM has caused some deliberations as to whether OMM has a more aggressive behavior than its cutaneous counterpart or was it due to the delay in diagnosis. Surgical excision, radiation therapy, and targeting specific molecules were employed in the management of melanoma [12, 22]. However, analysis of the molecular biology of the tumor is one important leap toward understanding the nature of the neoplasm and for the provision of ample management.

C-kit expression has been detected mostly in the in situ components of melanoma [27, 29, 30, 35]. The expression of c-kit in basally growing acral lentiginous melanoma cells suggested that the cells expressing the protein were essential in the initial stage of tumor progression [30]. Atypical melanocytic proliferation may indicate early

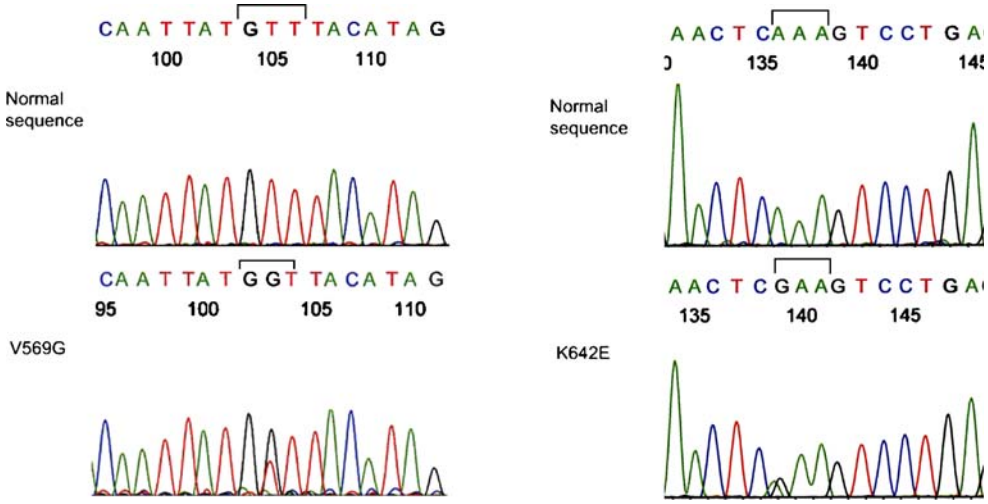


Fig. 3 Direct sequence. The figure shows normal sequence and missense mutations in exon 11 (*V569G*) and exon 13 (*K642E*)

progression of OMM [13, 28]. Therefore, c-kit expression in atypical melanocytes indicates the role of c-kit in the early stage of OMM tumorigenesis.

C-kit mutation in skin melanoma was rarely observed, but several mutations have been found in acral and mucosal melanoma with protein overexpression and increased DNA copy [8]. Although two from our cases failed to express c-kit protein, all cases were subjected to mutation analysis. It is interesting to note that one mutation (W557R) was found in a negative case. The significance of weak and focal c-kit staining is not clear [39]. The negative case might have probably expressed the receptor at a level below the detection limit of IHC assay. Thus, c-kit mutation may also be present, although the immunohistochemical assay gave a negative response.

Table 2 Summary of immunohistochemistry results and mutation analysis

Case	Histological type	IHC		Mutation analysis
		In situ	Invasive	
1	Invasive with in situ	++	+	Wild type
2	Invasive with in situ	+	±	Wild type
3[a]	Invasive	NA	±	Wild type
4	Invasive	NA	±	Wild type
5[a]	Invasive with in situ	++	++	Wild type
6[b]	Invasive with in situ	+	++	K642E[c], P585P
7	Invasive with in situ	+	±	Wild type
8	Invasive	NA	+	Wild type
9	Invasive with in situ	±	+	V569G
10	Invasive	NA	−	W557R[c]
11	Invasive	NA	−	Insufficient DNA amount
12	Invasive with in situ	++	+	Wild type
13	Invasive	NA	±	Insufficient DNA amount
14	Invasive	NA	++	Insufficient DNA amount
15[a]	Invasive	NA	++	K642E[c], S645S
16	Invasive	NA	±	Wild type
17	Invasive with in situ	+	±	Wild type
18	Invasive with in situ	+	+	Wild type

[a] Amelanotic type
[b] With several recurrences
[c] Reported in other tumors

Although a decrease in c-kit protein from in situ to invasive phase was observed, an increased expression was also detected in two cases (cases 6 and 9). Incidentally, these cases conformed to the mutation analysis suggesting the correlation between increased c-kit protein expression and the presence of activating mutation. Furthermore, case 6 exhibited several recurrences suggesting that c-kit protein overexpression and gene mutation may contribute to the high recurrence rate. Moreover, amelanotic melanoma has been associated with a more aggressive type and poor prognosis. Although only three samples from our cases were amelanotic, incidentally, one case (case 15) had intense protein expression and activating mutation. This result suggests that c-kit has a role in the aggressiveness of OMM.

Therapies targeting tyrosine kinase activities have been promising in cases of melanoma expressing the c-kit protein [11, 16, 20]. However, lack of response to imatinib has also been reported in melanoma [2, 6, 36, 40]. Phase II studies with imatinib until know failed to show efficacy in melanoma patients [6]. Overexpression of the c-kit protein has been previously observed without the occurrence of mutation, so it is possible that the driving force toward tumorigenesis is not solely related to mutation [3, 31]. Furthermore, it may also be speculated that a specific RTK inhibitor may only be of value in subtypes of melanoma [8]. Although it is unclear whether the presence of mutation or protein overexpression might be of significance for tumor behavior, the use of RTK inhibitors may have a significant outcome in melanoma subtypes with increased protein expression or activating mutation [34]. In addition,

(vascular endothelial growth factor) VEGF expression might be regulated by a c-kit signal transduction cascade. Several RTK inhibitors have antitumor effects by blocking c-kit activation as well as suppressing VEGF transcription and translation [17, 24, 25]. Because VEGF is highly expressed by OMM cells (unpublished data), the use of specific RTK inhibitor may block c-kit activation as well as suppress angiogenesis.

In summary, c-kit expression suggests a role in the early stage of OMM tumorigenesis. Increased c-kit protein expression correlated with activating mutations suggesting pertinent role of the proto-oncogene KIT in the tumorigenesis of OMM. Further studies may be carried out to elucidate the molecular mechanisms that underlie the correlation of activating mutation and protein expression with clinical outcome.

Acknowledgments This work was supported in part by grants-in-aid for scientific research from the Ministry of Education, Culture, Sports, Science and Technology (B17406027, C19592109). The authors would also like to thank Ms. Kazuko Funakoshi for her technical expertise. The experiments complied with the current laws of Japan.

References

1. Alexeev V, Yoon K (2006) Distinctive role of the cKit receptor tyrosine kinase signaling in mammalian melanocytes. J Invest Dermatol 126:1102–1110
2. Alexis JB, Martinez AE, Lutzky J (2005) An immunohistochemical evaluation of c-kit (CD-117) expression in malignant melanoma, and results of imatinib mesylate (Gleevec) therapy in three patients. Melanoma Res 15:283–285
3. All-Ericsson C, Girnita L, Muller-Brunotte A, Brodin B, Seregard S, Ostman A, Larsson O (2004) c-Kit-dependent growth of uveal melanoma cells: a potential therapeutic target? Invest Ophthalmol Vis Sci 45:2075–2082
4. Andersson J, Bumming P, Meis-Kindblom JM, Sihto H, Nupponen N, Joensuu H, Oden A, Gustavsson B, Kindblom LG, Nilsson B (2006) Gastrointestinal stromal tumors with KIT exon 11 deletions are associated with poor prognosis. Gastroenterology 130:1573–1581
5. Barker BF, Carpenter WM, Daniels TE, Kahn MA, Leider AS, Lozada-Nur F, Lynch DP, Melrose R, Merrell P, Morton T, Peters E, Regezi JA, Richards SD, Rick GM, Rohrer MD, Slater L, Stewart JC, Tomich CE, Vickers RA, Wood NK, Young SK (1997) Oral mucosal melanomas: the WESTOP Banff workshop proceedings. Western Society of Teachers of Oral Pathology. Oral Surg Oral Med Oral Pathol Oral Radiol Endod 83:672–679
6. Becker JC, Brocker EB, Schadendorf D, Ugurel S (2007) Imatinib in melanoma: a selective treatment option based on KIT mutation status? J Clin Oncol 25:e9
7. Corless CL, McGreevey L, Haley A, Town A, Heinrich MC (2002) KIT mutations are common in incidental gastrointestinal stromal tumors one centimeter or less in size. Am J Pathol 160:1567–1572
8. Curtin JA, Busam K, Pinkel D, Bastian BC (2006) Somatic activation of KIT in distinct subtypes of melanoma. J Clin Oncol 24:4340–4346
9. Daum O, Grossmann P, Vanecek T, Sima R, Mukensnabl P, Michal M (2007) Diagnostic morphological features of PDGFRA-mutated gastrointestinal stromal tumors: molecular genetic and histologic analysis of 60 cases of gastric gastrointestinal stromal tumors. Ann Diagn Pathol 11:27–33
10. Do I, Araujo ES, Kalil RK, Bacchini P, Bertoni F, Unni KK, Park YK (2007) Protein expression of KIT and gene mutation of c-kit and PDGFRs in Ewing sarcomas. Pathol Res Pract 203:127–134
11. Fiorentini G, Rossi S, Lanzanova G, Biancalani M, Palomba A, Bernardeschi P, Dentico P, De Giorgi U (2003) Tyrosine kinase inhibitor imatinib mesylate as anticancer agent for advanced ocular melanoma expressing immunohistochemical C-KIT (CD 117): preliminary results of a compassionate use clinical trial. J Exp Clin Cancer Res 22:17–20
12. Flaherty KT (2006) Chemotherapy and targeted therapy combinations in advanced melanoma. Clin Cancer Res 12:2366s–2370s
13. Hicks MJ, Flaitz CM (2000) Oral mucosal melanoma: epidemiology and pathobiology. Oral Oncol 36:152–169
14. Hirota S, Ohashi A, Nishida T, Isozaki K, Kinoshita K, Shinomura Y, Kitamura Y (2003) Gain-of-function mutations of platelet-derived growth factor receptor alpha gene in gastrointestinal stromal tumors. Gastroenterology 125:660–667
15. Isozaki K, Terris B, Belghiti J, Schiffmann S, Hirota S, Vanderwinden JM (2000) Germline-activating mutation in the kinase domain of KIT gene in familial gastrointestinal stromal tumors. Am J Pathol 157:1581–1585
16. Ivan D, Niveiro M, Diwan AH, Eton O, Kim KB, Lacey C, Gonzalez C, Prieto VG (2006) Analysis of protein tyrosine kinases expression in the melanoma metastases of patients treated with Imatinib Mesylate (STI571, Gleevec). J Cutan Pathol 33:280–285
17. Jin T, Nakatani H, Taguchi T, Nakano T, Okabayashi T, Sugimoto T, Kobayashi M, Araki K (2006) STI571 (Glivec) suppresses the expression of vascular endothelial growth factor in the gastrointestinal stromal tumor cell line, GIST-T1. World J Gastroenterol 12:703–708
18. Kang DY, Park CK, Choi JS, Jin SY, Kim HJ, Joo M, Kang MS, Moon WS, Yun KJ, Yu ES, Kang H, Kim KM (2007) Multiple gastrointestinal stromal tumors: clinicopathologic and genetic analysis of 12 patients. Am J Surg Pathol 31:224–232
19. Kinoshita K, Isozaki K, Hirota S, Nishida T, Chen H, Nakahara M, Nagasawa Y, Ohashi A, Shinomura Y, Kitamura Y, Matsuzawa Y (2003) C-kit gene mutation at exon 17 or 13 is very rare in sporadic gastrointestinal stromal tumors. J Gastroenterol Hepatol 18:147–151
20. Lefevre G, Glotin AL, Calipel A, Mouriaux F, Tran T, Kherrouche Z, Maurage CA, Auclair C, Mascarelli F (2004) Roles of stem cell factor/c-Kit and effects of Glivec/STI571 in human uveal melanoma cell tumorigenesis. J Biol Chem 279:31769–31779
21. Lennartsson J, Blume-Jensen P, Hermanson M, Ponten E, Carlberg M, Ronnstrand L (1999) Phosphorylation of Shc by Src family kinases is necessary for stem cell factor receptor/c-kit mediated activation of the Ras/MAP kinase pathway and c-fos induction. Oncogene 18:5546–5553
22. Leslie MC, Bar-Eli M (2005) Regulation of gene expression in melanoma: new approaches for treatment. J Cell Biochem 94:25–38
23. Lin SC, Liu CL, Wang TI, Chang WS, Tzen CY, Huang MJ (2006) Clinical implications of C-kit gene mutation in patients with large gastrointestinal stromal tumors. J Gastroenterol Hepatol 21:1604–1608
24. Litz J, Krystal GW (2006) Imatinib inhibits c-Kit-induced hypoxia-inducible factor-1alpha activity and vascular endothelial growth factor expression in small cell lung cancer cells. Mol Cancer Ther 5:1415–1422
25. Litz J, Sakuntala Warshamana-Greene G, Sulanke G, Lipson KE, Krystal GW (2004) The multi-targeted kinase inhibitor SU5416 inhibits small cell lung cancer growth and angiogenesis, in part by blocking Kit-mediated VEGF expression. Lung Cancer 46:283–91

26. Lux ML, Rubin BP, Biase TL, Chen CJ, Maclure T, Demetri G, Xiao S, Singer S, Fletcher CD, Fletcher JA (2000) KIT extracellular and kinase domain mutations in gastrointestinal stromal tumors. Am J Pathol 156:791–795
27. Montone KT, van Belle P, Elenitsas R, Elder DE (1997) Proto-oncogene c-kit expression in malignant melanoma: protein loss with tumor progression. Mod Pathol 10:939–944
28. Nagatsuka H, Rivera RS, Gunduz M, Lee YJ, Tamamura R, Gunduz E, Naito I, Sado Y, Nagai N (2005) Immunolocalization and distribution patterns of type IV collagen alpha chains in oral mucosal melanoma. Virchows Arch 447:710–716
29. Natali PG, Nicotra MR, Winkler AB, Cavaliere R, Bigotti A, Ullrich A (1992) Progression of human cutaneous melanoma is associated with loss of expression of c-kit proto-oncogene receptor. Int J Cancer 52:197–201
30. Ohashi A, Funasaka Y, Ueda M, Ichihashi M (1996) c-KIT receptor expression in cutaneous malignant melanoma and benign melanotic naevi. Melanoma Res 6:25–30
31. Pache M, Glatz K, Bosch D, Dirnhofer S, Mirlacher M, Simon R, Schraml P, Rufle A, Flammer J, Sauter G, Meyer P (2003) Sequence analysis and high-throughput immunohistochemical profiling of KIT (CD 117) expression in uveal melanoma using tissue microarrays. Virchows Arch 443:741–744
32. Puputti M, Tynninen O, Sihto H, Blom T, Maenpaa H, Isola J, Paetau A, Joensuu H, Nupponen NN (2006) Amplification of KIT, PDGFRA, VEGFR2, and EGFR in gliomas. Mol Cancer Res 4:927–934
33. Rapidis AD, Apostolidis C, Vilos G, Valsamis S (2003) Primary malignant melanoma of the oral mucosa. J Oral Maxillofac Surg 61:1132–1139
34. Shen SS, Zhang PS, Eton O, Prieto VG (2003) Analysis of protein tyrosine kinase expression in melanocytic lesions by tissue array. J Cutan Pathol 30:539–547
35. Stefanou D, Batistatou A, Zioga A, Arkoumani E, Papachristou DJ, Agnantis NJ (2004) Immunohistochemical expression of vascular endothelial growth factor (VEGF) and C-KIT in cutaneous melanocytic lesions. Int J Surg Pathol 12:133–138
36. Ugurel S, Hildenbrand R, Zimpfer A, La Rosee P, Paschka P, Sucker A, Keikavoussi P, Becker JC, Rittgen W, Hochhaus A, Schadendorf D (2005) Lack of clinical efficacy of imatinib in metastatic melanoma. Br J Cancer 92:1398–1405
37. Wardelmann E, Losen I, Hans V, Neidt I, Speidel N, Bierhoff E, Heinicke T, Pietsch T, Buttner R, Merkelbach-Bruse S (2003) Deletion of Trp-557 and Lys-558 in the juxtamembrane domain of the c-kit protooncogene is associated with metastatic behavior of gastrointestinal stromal tumors. Int J Cancer 106:887–895
38. Willmore C, Holden JA, Zhou L, Tripp S, Wittwer CT, Layfield LJ (2004) Detection of c-kit-activating mutations in gastrointestinal stromal tumors by high-resolution amplicon melting analysis. Am J Clin Pathol 122:206–216
39. Willmore-Payne C, Holden JA, Tripp S, Layfield LJ (2005) Human malignant melanoma: detection of BRAF- and c-kit-activating mutations by high-resolution amplicon melting analysis. Hum Pathol 36:486–493
40. Wyman K, Atkins MB, Prieto V, Eton O, McDermott DF, Hubbard F, Byrnes C, Sanders K, Sosman JA (2006) Multicenter phase II trial of high-dose imatinib mesylate in metastatic melanoma: significant toxicity with no clinical efficacy. Cancer 106:2005–2011

Virchows Arch (2008) 452:33–39
DOI 10.1007/s00428-007-0523-3

ORIGINAL ARTICLE

Expression of CCN3 protein in human Wilms' tumors: immunohistochemical detection of CCN3 variants using domain-specific antibodies

Manish Mani Subramaniam · Noureddine Lazar · Samuel Navarro · Bernard Perbal · Antonio Llombart-Bosch

Received: 11 August 2007 / Revised: 14 September 2007 / Accepted: 28 September 2007 / Published online: 8 December 2007
© Springer-Verlag 2007

Abstract We aimed to detect truncated CCN3 protein variants in formalin-fixed paraffin-embedded samples of eight Wilms' tumors using anti-K19M and novel domain-specific antibodies, anti-NH2, anti-NH3, anti-NH4, and anti-NH5 raised against C-terminal (CT) domain and modules 1, 2, 3, and 4 of the CCN3 protein, respectively. In Wilms' tumors, all the domain antibodies except anti-NH4 exhibited both nuclear and cytoplasmic staining in blastema as well as primitive tubules. NH4 was detected only in the cytoplasm of tumor cells. Normal fetal kidneys revealed mainly cytoplasmic immunoreactivity for all antibodies in tubules and glomeruli, except for K19 and NH5, which showed some nuclear staining. Our data suggest expression of a truncated nuclear CCN3 variant lacking the thrombospondin type-1-like domain and cytoplasmic full-length CCN3 protein in Wilms' tumor cells. In addition, normal fetal kidneys express mainly full-length protein mostly localized to cytoplasm. Truncated CCN3 protein in Wilms' tumor cells may provide evidence for its tumorigenic role in these tumors. Uniform NH5 staining compared to variable expression of K19M indicates that using NH5 is a better approach for detecting the CT domain of CCN3 protein in archival specimens. Thus, the domain-specific antibodies represent valuable tools for detecting CCN3 protein variants in normal and neoplastic kidneys.

Keywords CCN3 · Nov · Wilms' tumors · Truncated protein · Domain-specific antibodies

Abbreviations

NOV	Nephroblastoma overexpressed gene
MAV-1	Myeloblastosis-associated virus type 1
SIOP	International Society of Pediatric Oncology
CTGF	Connective tissue growth factor
IGFBP	Insulin-like growth factor binding protein
VWC	Von Willebrand complex
CT	C-terminal domain
TSP1	Thrombospondin type 1 repeat
WT1	Wilms' tumor gene 1

Introduction

Wilms' tumor is a pediatric renal neoplasm that affects 1 in 10,000 children with a peak occurrence between 3 and 6 years of age [3]. They can be sporadic (99%) and unilateral (93%) or heritable (1%) and bilateral (18%). The revised International Society of Pediatric Oncology working classification classifies Wilms' tumors into low-risk (cystic nephroblastomas), intermediate-risk (epithelial, stromal with muscle, cartilage or bone, mixed, focal anaplastic), and high-risk (blastemal and anaplastic types) categories [7].

Besides WT1 gene alterations, the induction of avian nephroblastomas by integration of myeloblastosis-associated virus type 1 in CCN3 (NOV, nephroblastoma overexpressed) gene has emerged as a recent model in the development of

Manish Mani Subramaniam and Noureddine Lazar made an equal contribution to this work.

M. M. Subramaniam · S. Navarro · A. Llombart-Bosch (✉)
Department of Pathology, Medical School, University of Valencia,
Avda. Blasco Ibañez, 17,
46010 Valencia, Spain
e-mail: antonio.llombart@uv.es

N. Lazar · B. Perbal
Laboratoire d' Oncologie Virale et Moléculaire,
UFR de Biochimie, Université Paris 7-D.Diderot,
Paris, France

Wilms' tumor. The CCN3 protein belongs to the CCN family of proteins involved in basic biological processes such as cell adhesion, migration, proliferation, and differentiation. The CCN proteins are numbered from CCN1 to CCN6 according to the order in which they were described in the literature: CCN1 (cysteine-rich CYR61), CCN2 (CTGF, connective tissue growth factor), CCN3 (NOV), CCN4 (WISP-1/ELM-1, wnt-1-induced secreted proteins), CCN5 (WISP-2/rCop-1/CTGF-L), and CCN6 (WISP-3) [4]. With the exception of CCN5, which lacks the C-terminal (CT) module, all CCN proteins show a common multimodular organization with four distinct structural modules sharing partial identity with: insulin-like growth factor proteins (IGFBP), Willebrand factor C (VWC), thrombospondin type 1 repeat (TSP1), and several extracellular proteins containing a cysteine knot motif (CT) [2].

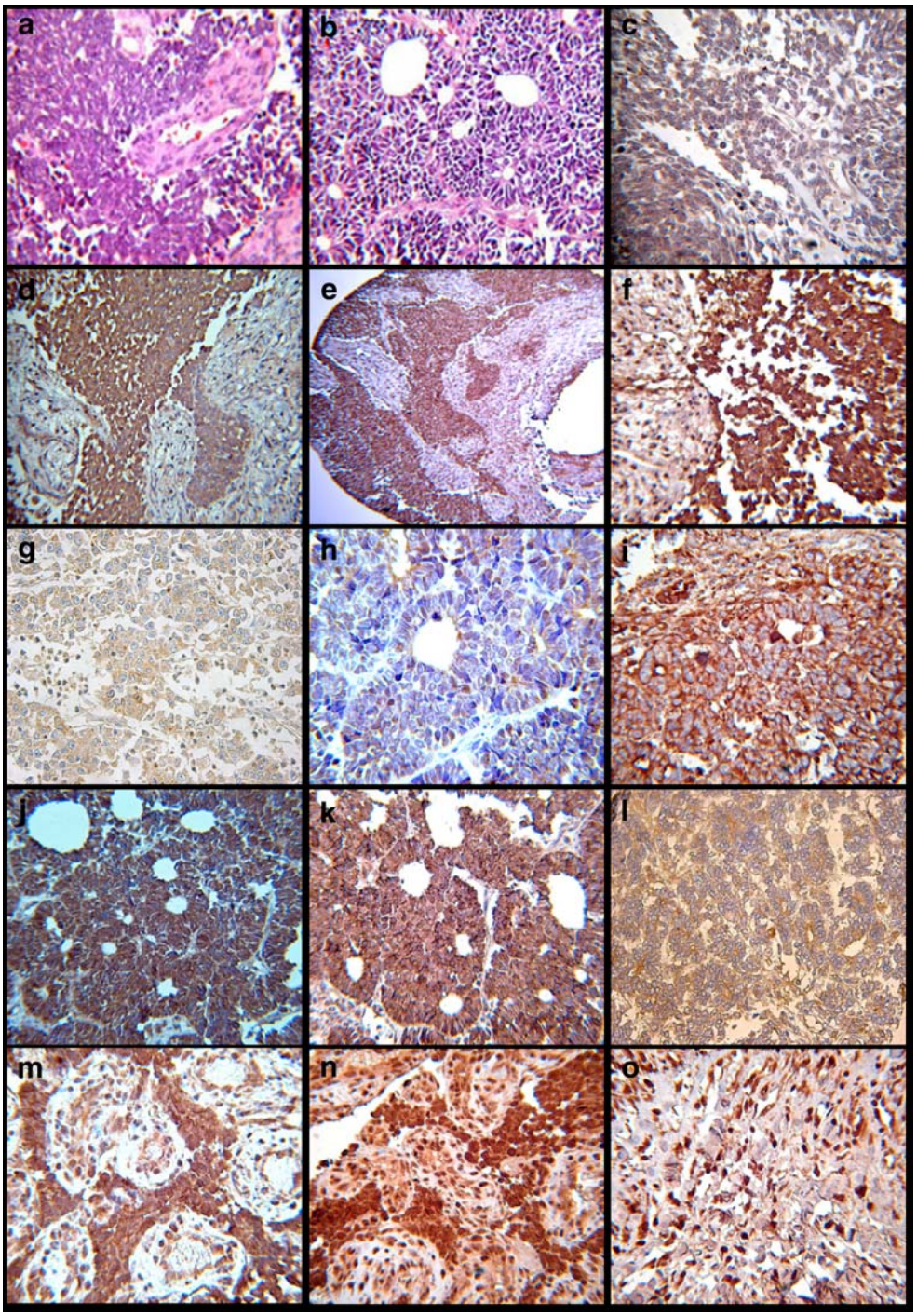


Fig. 1 Histopathological features (**a–d**): **a** blastemal type of Wilms' tumor showing sheets of undifferentiated round blastemal cells. **b** Predominant primitive tumor tubules in a tubular subtype of Wilms' tumor (**a** and **b**: H&E, original magnification ×400); immunohistochemical staining of CCN3 in Wilms' tumors (**c–o**): **c–f** intense nuclear and cytoplasmic staining of the blastemal cells by anti-K19M, anti-NH2, anti-NH3, and anti-NH5 antibodies, respectively (**c** anti-K19M, original magnification ×400, **d**, **e,** and **f** anti-NH2, NH3, and NH5, respectively; original magnification ×200). **g** Pure cytoplasmic staining of the blastema and absent nuclear expression observed with anti-NH4 suggest a truncated nuclear CCN3 variant lacking TSP-1 module (**g**: anti-NH4, original magnification ×400). **h–k** Intense nuclear and cytoplasmic signals seen in the primitive tubules for K19M, NH2, NH3, and NH5, respectively (**h** to **k**: K19M, NH2, NH3, and NH5 immunostains, respectively; original magnification ×400). **l** Anti-NH4 antibody stains intensely the cytoplasm of the tubules, while the nucleus is negative also indicating a truncated CCN3 protein (**l**: anti-NH4, original magnification ×400). **m–o** Stromal staining with anti-NH2, anti-NH3, and anti-NH5 antibodies, respectively (**m–o**: anti-NH2, anti-NH3, and anti-NH5 stains, respectively; original magnification ×400)

Full-length secreted CCN3 protein is associated with differentiation of rhabdomyosarcomas [11, 30], neuroblastomas [23], cartilaginous tumors [23], and inhibition of the growth and decrease in tumorigenicity of several tumor cell lines including glioblastoma [10], choriocarcinoma [9], and musculoskeletal Ewing's sarcomas [1, 24]. CCN3 expression is also implicated in the differentiation of glomerular podocytes during normal nephrogenesis and heterotypic mesenchymal differentiation in Wilms' tumors [6]. Down-regulation of CCN3 protein has also been related to poor prognosis in various tumors [6, 11, 17, 18, 22–24, 29].

However, it has been postulated that the expression of a 32-kDa amino-truncated CCN3 protein, lacking the signal peptide and the IGFBP module, is responsible for tumorigenesis due to its altered intracellular addressing [26]. Truncated variants of CCN3 protein have been proposed to induce morphological transformation of embryonic fibroblasts in experimental models [12] and have also been detected in nucleus of several cancers [5, 25] and cancer cell lines [20]. These data suggest that expression of truncated CCN3 protein has implications in tumorigenesis [21, 22]. Therefore, it is important to address their production under normal and pathological conditions.

The previously described K19M marker identified only the CT domain of the CCN3 protein [6, 17]. In this paper, we report the use of newly developed domain-specific antibodies such as anti-NH2, anti-NH3, anti-NH4, and anti-NH5 raised against modules 1, 2, 3, and 4 of the CCN3 protein to determine whether truncated CCN3 protein variants or full-length CCN3 protein is produced in archival specimens of human Wilms' tumors.

Materials and methods

Tumor samples and tissue microarray assembly

A total of eight Wilms' tumors including four purely blastemal, three mixed blastemal and tubular, and one predominantly tubular were included in the study. The diagnosis of Wilms' tumors was confirmed by established histological criteria [2] as well as standard panel of diagnostic markers [2]. Six of the eight tumors showed positive immunostaining for WT1; one was positive for cytokeratin, while desmin expression was noted in four cases. Although two cases lacked WT1 immunostaining, they displayed the typical blastemal areas (Fig. 1a) and primitive tubules (Fig. 1b) suggestive of nephroblastoma. All these samples were assembled in a tissue microarray (TMA). Each case in the TMA was represented by four 1-mm tissue cores. In addition, four normal fetal kidney samples (22 weeks gestation) were also included in the TMA.

CCN3 immunohistochemistry

TMA sections of 5 μm were deparaffinized, and antigen retrieval was performed by pressure cooking the tissue sections in citrate buffer (pH 6.0) at 1.5 ATM for 3 min. The endogenous peroxidase was blocked using 3% hydrogen peroxidase for 5 min at room temperature. Immunohistochemistry (IHC) was performed using the following polyclonal rabbit anti-CCN3 antibodies: (1) anti-K19M antibody directed against a peptide specific to the CT module, (2) anti-NH2 serum raised against module 1 (IGFBP), (3) anti-NH3 serum against module 2 (VWC), (4) anti-NH4 serum against module 3 (TSP-1), and (5) anti-NH5 serum against module 4 (CT). The dilutions of the antibodies were as follows: anti-K19M (1:800), anti-NH2, anti-NH3, anti-NH4 (1:400), and anti-NH5 at 1:600. The immunohistochemical procedure included incubation of primary antibodies for 1 h, immunodetection using Chem-Mate™ DAKO ENVISION™/HRP Rabbit/Mouse (ENV) system followed by revelation of the reaction product by exposure to 3,3′-diaminobenzidine chromogen. Normal fetal kidneys in the TMA served as positive controls, while specimens lacking primary antibody were used as negative control. The CCN3 immunostains were scored as follows: score 1 (mild), limited positivity (<50%) and weak immunostaining; score 2 (moderate), diffuse positivity (>50%) and moderate immunostaining; and score 3 (intense), diffuse (>75%) and strong immunostaining [17]. The immunostains were evaluated independently by three investigators (MMS, SN, and ALB), and in case of disagreement in the IHC scoring, the consensus was recorded as the final score.

Results

Immunoreactivity of K19M and domain-specific CCN3 antibodies in Wilms' tumors

Immunostaining score for all antibodies was compared between the four tissue cores of each case. No significant differences in the immunostain results were observed between the tissue cores. The mean of observations in the four cores was taken into consideration for the final score. Overall, the mean concordance level of IHC score obtained among all the three observers for all the CCN3 antibodies was 92%. Out of the total 40 sample cores (including tumor and normal samples) in each TMA section, concordance was reached by all the three investigators for K19M, NH2, NH3, NH4, and NH5 in 33/40 (83%), 38/40 (95%), 36/40 (90%), 35/40 (95%), and 38/40 (95%) sample cores, respectively.

All the CCN3 antibodies revealed both cytoplasmic as well as nuclear immunoreactivity except anti-NH4 which

showed predominant cytoplasmic staining. The undifferentiated blastemal cells showed both cytoplasmic and nuclear expression of K19M with intense staining noted in three cases (38%; Fig. 1c), moderate in four cases (50%), and mild in one case (13%). Anti-NH2 (Fig. 1d), anti-NH3 (Fig. 1e), and anti-NH5 (Fig. 1f) gave intensely positive nuclear and cytoplasmic signals in the blastemal cells of all Wilms' tumors. The primitive tubules of the majority of the nephroblastomas displayed mild to moderate cytoplasmic and nuclear immunoreactivity to K19M (Fig 1h) and intense reaction for anti-NH2 (Fig. 1i), anti-NH3 (Fig. 1j), and anti-NH5 (Fig. 1k). Variable immunostaining pattern was observed with anti-NH4 antibody. The blastema was mild to moderately positive for anti-NH4 in four (50%), intense in one (13%), and negative in two (25%) cases. Nuclear staining of NH4 was observed neither in the blastema nor in tubules. For an equal intensity of immunoreactivity, blastemal and tubules that were both nuclear and cytoplasmic positive for K19M, anti-NH2, anti-NH3, and anti-NH5 antibodies exhibited only cytoplasmic positivity for anti-NH4 (Fig. 1g,l). The latter findings suggest that full-length CCN3 protein is expressed in cytoplasm, while the nuclear CCN3 variant is a truncated protein lacking the TSP1 module. Stromal cells were mildly immunoreactive to K19M and anti-NH4 but intensely stained for NH2, NH3, and NH5 (Fig. 1m–o).

CCN3 expression in normal kidneys

The normal fetal kidneys revealed intense cytoplasmic staining for all domain antibodies in the proximal and distal convoluted tubules and mild reactivity in the glomeruli suggesting cytoplasmic accumulation of full-length CCN3 protein (Fig. 2a–e). In addition to cytoplasmic staining, some nuclear reaction was also observed for K19M (Fig. 2a) and NH5 (Fig. 2e) in normal fetal kidneys. Similar immunoreactivity of CCN3 as that of normal fetal kidneys was also observed in the nonneoplastic renal tissue present adjacent to neoplastic areas in the tumor samples.

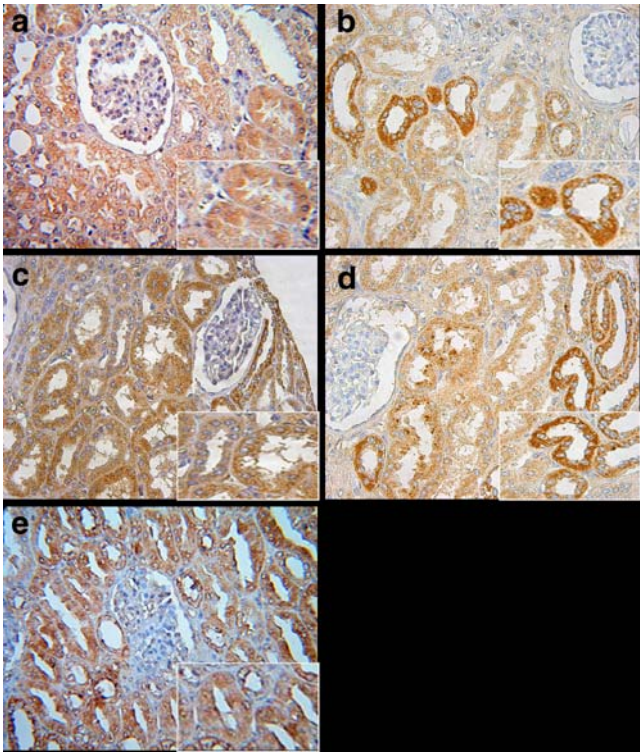


Fig. 2 Immunoexpression of CCN3 in normal fetal kidneys (**a**–**e**): Intense predominant cytoplasmic immunoreactivity is observed with anti-K19M, anti-NH2, anti-NH3, anti-NH4, and anti-NH5 antibodies, respectively, suggestive of full-length CCN3 protein in the cytoplasm. In addition, weak nuclear positivity was also observed with K19M (**a**) and NH5 (**e**; **a** to **e**: anti-K19M, anti-NH2, anti-NH3, anti-NH4, and anti-NH5 immunostains; original magnification ×400; *insets*, original magnification ×600)

Discussion

Accumulating evidence supports the fact that CCN3 protein has a dual effect on cell proliferation, which is dependent on the relative amount of secreted full-length and intracellular truncated isoforms [26, 27]. When this balance between full-length and truncated CCN3 isoforms is disrupted, either at the level of posttranslational processing or through aberrant production of truncated variant (by viral insertion or any other genetic event), cells would respond to the constant positive effects of nuclear CCN3, a situation that would provide ground for occurrence of further tumorigenic events [27]. Amino-truncated CCN3 variants lacking signal peptide cause modifications in their intracellular addressing thereby resulting in altered fate of these truncated proteins [27]. Considering the fact that expression of such a truncated CCN3 variant induced morphological transformation of chicken embryo fibroblasts, taken together, these findings suggested that transcriptional repression of genes possessing antiproliferative activity resulted in oncogenic transformation [12] and cancer development [26].

In this paper, we used rabbit polyclonal antibodies directed against the various structural domains of CCN3 protein to detect truncated CCN3 variants in human nephroblastomas to provide insights into its tumorigenic role in these tumors. To date, only the K19M antibody which recognizes the CT domain of the CCN3 protein has been published. The use of K19M alone is inadequate to identify missing domains of the CCN3 protein, as it is raised against only one module of the CCN3 protein. As a solution to this issue, we used newly developed domain-specific antibodies NH2, NH3, NH4, and NH5 targeting modules 1, 2, 3, and 4 of the CCN3 protein in formalin-

fixed and paraffin-embedded clinical specimens of Wilms' tumors and normal kidneys.

Domain-specific antibodies NH2, NH3, and NH5 showed similar intense nuclear and cytoplasmic staining in the blastema and tubules of all the Wilms' tumors. However, variable immunoreactivity was observed with K19M and NH4. K19M revealed moderate to intense nuclear and cytoplasmic staining in blastemal cells, while mild to moderate reaction in the tubules. Stronger uniform staining was observed with NH5 compared to K19M, although both detect the same module (CT domain) of CCN3. This discrepancy may be due to the fact that K19M recognizes only a CT peptide, whereas NH5 is directed against the entire module 4 of CCN3 protein. Alternatively, this finding can be explained based on the observation by Kyurkchiev et al. [13] that the CT domain of CCN3 is not easily accessible and exists in different configurations depending on its interaction with other proteins or self-dimerization and cellular location. Thus, our data demonstrate that anti-NH5 antibody easily detects the CT domain of CCN3 protein as compared to K19M and is a better approach for detecting the CT module. NH4 showed lower immunoexpression in Wilms' tumors compared to other antibodies. The staining was limited mainly to the cytoplasm of blastemal and tubular cells in all cases. Furthermore, in cases with similar staining intensity for NH4 as well as rest of the domain-specific CCN3 antibodies, NH4 displayed pure cytoplasmic reaction, while the other antibodies stained both cytoplasm and nucleus suggesting the presence of a truncated nuclear protein lacking the TSP1 domain.

In the normal fetal kidneys, all the domain-specific antibodies showed predominantly cytoplasmic immunoreactivity in the tubules and glomeruli. No nuclear staining, except for NH5 and K19, was observed.

Taking together the patterns of CCN3 expression in normal and neoplastic kidneys, we suggest that full-length CCN3 protein is confined mainly to the cytoplasmic component in normal kidneys as well as Wilms' tumors, while the nuclear CCN3 variant detected only in Wilms' tumors is a truncated CCN3 protein lacking the TSP-1 module.

Based on our results, we discuss below some possible implications of truncated CCN3 proteins that might be relevant to our study.

Truncated CCN3 proteins interact with other transcription regulatory proteins and act as transcriptional corepressors of certain genes controlling cell proliferation. Quantitative transcription assays performed with deletions of CT module of the CCN3 protein failed to inhibit transcription implying that the transcription inhibitory domain lies in the CT module [27]. Furthermore in our study, truncated CCN3 variants were detected only in the nucleus of Wilms' tumors and were lacking in normal fetal kidneys. In addition, the CT module as detected by K19M and NH5 antibodies was consistently observed in the nuclear truncated protein of all our cases. Summing up these observations, our results seem to support the previously established hypothesis.

One possible mechanism for the production of truncated protein variants might be the chromosomal rearrangements and translocations that occur in cancer cells. An alternative speculation is that certain proteolytic mechanisms, probably between modules 2 and 3, might be responsible for the cleavage of secreted full-length CCN3 protein [20, 21].

The second important factor is the underlying mechanisms responsible for the nuclear translocation of truncated CCN3 variant. Planque et al. [27] observed that CCN3 variants lacking both CT module and signal peptide was localized to the cytoplasm, but those with intact CT module and deficient signal peptide were retained in the nucleus. Additionally, they showed that a putative nuclear localization signal at position 280–303 of the CT module directed the recombinant green fluorescent protein (GFP)-tagged CCN3 variants to the nucleus. In our cases, the CT module was detected in both full-length CCN3 variant located in the cytoplasm as well as in truncated nuclear variant as demonstrated by the intense nuclear and cytoplasmic staining of K19M and NH5 antibodies. Although our findings partially support the nuclear addressing role of CT module, as we did not assess the status of signal peptide and did not perform GFP-tagged immunofluorescence assays, this hypothesis cannot be concretely established in our series.

Interestingly, nuclear import of regulatory proteins was also reported to be a feature of CCN2, another member of CCN family [28]. Besides CCN proteins, nuclear localization has also been documented in variety of protein families including growth factors, hormones, cytokines, and transmembrane receptors [19].

Another issue which is worth discussing is the regulation of angiogenesis by truncated CCN3 variants. The T1 sequence of TSP1 domain of CCN proteins is reported to be a ligand for binding of integrin alpha 6 beta 1 ($\alpha_6\beta_1$) [15]. In addition to $\alpha_6\beta_1$, interaction of CCN3 with integrins alpha v beta 3 ($\alpha_v\beta_3$) and alpha 5 beta 1($\alpha_5\beta_1$) is also responsible for its pro-angiogenic activities [8, 14, 16]. However, TSP1 of CCN3 does not directly bind to $\alpha_6\beta_1$ [8]. Therefore, altered angiogenesis due to lack of TSP1 domain in the CCN3 protein might be less likely in our setting.

In this report, we show that novel domain-specific antibodies directed against the different modules of CCN3 protein are demonstrated to be effective tools in the immunodetection of CCN3 protein in formalin-fixed and paraffin-embedded clinical specimens of human Wilms'

tumors as well as normal kidneys. In Wilms' tumors, the blastemal and tubular cells displayed cytoplasmic immunoreactivity to all domain-specific CCN3 antibodies suggestive of full-length CCN3 protein, while the nucleus expressed all the domain-specific antibodies except anti-NH4 indicating a truncated CCN3 variant lacking TSP1 domain. In the normal kidneys, only full-length CCN3 protein was detected in the cytoplasm as demonstrated by intense cytoplasmic staining to all CCN3 antibodies, with the exception of some nuclear decoration for NH5 and K19 in fetal and embryonal kidneys. Uniform intense staining with NH5 antibodies compared to variable expression of K19M suggests that the NH5 epitopes are easily accessible to these polyclonal antibodies and therefore constitute a better approach for detecting the CT domain of CCN3 protein, whose accessibility was reported to depend upon conformational state [13]. Nuclear localization of truncated CCN3 proteins deficient in TSP1 demonstrated in our study may provide insights into the development of human Wilms' tumors. In addition, it can open new fields of investigation into the regulatory functions of CCN family of proteins.

Our study may serve as a useful model in addressing the question of protein variant production in normal and pathological conditions. Further investigations on mechanisms underlying the nuclear addressing of CCN proteins will help to provide a better understanding of this novel family of cell growth regulators.

Acknowledgment This work was supported by a grant (PI-04/0822) from the FIS (Instituto Carlos-III, Madrid, Spain) and PROTHETS (Prognosis and therapeutic targets of Ewing's family of tumors) FP6 contract number 503036. Manish Mani Subramaniam is a holder of a grant from the Hospital Clinic of University and the Spanish Association Against Cancer (AECC) of Valencia, Spain.

References

1. Benini S, Perbal B, Zambelli D, Colombo MP, Manara MC, Serra M, Parenza M, Martinez V, Picci P, Scotlandi K (2005) In Ewing's sarcoma CCN3(NOV) inhibits proliferation while promoting migration and invasion of the same cell type. Oncogene 24:4349–4361
2. Bork P (1993) The modular architecture of a new family of growth regulators related to connective tissue growth factor. FEBS Lett 327:125–130
3. Breslow N, Beckwith JB, Ciol M, Sharples K (1988) Age distribution of Wilms' tumor: report from the National Wilms' Tumor Study. Cancer Res 48:1653–1657
4. Brigstock DR, Goldschmeding R, Katsube KI, Lam SC, Lau LF, Lyons K, Naus C, Perbal B, Riser B, Takigawa M, Yeger H (2003) Proposal for a unified CCN nomenclature. Mol Pathol 56:127–128
5. Cervello M, Giannitrapani L, Labbozzetta M, Notarbartolo M, D'Alessandro N, Lampiasi N, Azzolina A, Montalto G (2004) Expression of WISPs and of their novel alternative variants in human hepatocellular carcinoma cells. Ann N Y Acad Sci 1028:432–439
6. Chevalier G, Yeger H, Martinerie C, Laurent M, Alami J, Schofield PN, Perbal B (1998) novH: differential expression in developing kidney and Wilms' tumors. Am J Pathol 152:1563–1575
7. Eble JN, Sauter G, Epstein JI, Sesterhenn IA (2002) Pathology and genetics of tumors of the urinary system and male genital organs. In: Eble JN, Sauter G, Epstein JI, Sesterhenn IA (eds) World Health Organization classification of tumors. IARC Press, Lyon
8. Ellis PD, Metcalfe JC, Hyvonen M, Kemp PR (2003) Adhesion of endothelial cells to NOV is mediated by the integrins alphavbeta3 and alpha5beta1. J Vasc Res 40:234–243
9. Gellhaus A, Dong X, Propson S, Maass K, Klein-Hitpass L, Kibschull M, Traub O, Willecke K, Perbal B, Lye SJ, Winterhager E (2004) Connexin43 interacts with NOV: a possible mechanism for negative regulation of cell growth in choriocarcinoma cells. J Biol Chem 279:36931–36942
10. Gupta N, Wang H, McLeod TL, Naus CC, Kyurkchiev S, Advani S, Yu J, Perbal B, Weichselbaum RR (2001) Inhibition of glioma cell growth and tumorigenic potential by CCN3 (NOV). Mol Pathol 54:293–299
11. Jiang WG, Watkins G, Fodstad O, Douglas-Jones A, Mokbel K, Mansel RE (2004) Differential expression of the CCN family members Cyr61, CTGF and Nov in human breast cancer. Endocr Relat Cancer 11:781–791
12. Joliot V, Martinerie C, Dambrine G, Plassiart G, Brisac M, Crochet J, Perbal B (1992) Proviral rearrangements and overexpression of a new cellular gene (nov) in myeloblastosis-associated virus type 1-induced nephroblastomas. Mol Cell Biol 12:10–21
13. Kyurkchiev S, Yeger H, Bleau AM, Perbal B (2004) Potential cellular conformations of the CCN3 (NOV) protein. Cell Commun Signal 2:9–17
14. Leu SJ, Liu Y, Chen N, Chen CC, Lam SC, Lau LF (2003) Identification of a novel integrin alpha 6 beta 1 binding site in the angiogenic inducer CCN1 (CYR61). J Biol Chem 278:33801–33808
15. Lin CG, Leu SJ, Chen N, Tebeau CM, Lin SX, Yeung CY, Lau LF (2003) CCN3 (NOV) is a novel angiogenic regulator of the CCN protein family. J Biol Chem 278:24200–24208
16. Lin CG, Chen CC, Leu SJ, Grzeszkiewicz TM, Lau LF (2005) Integrin-dependent functions of the angiogenic inducer NOV (CCN3): implication in wound healing. J Biol Chem 280:8229–8237
17. Manara MC, Perbal B, Benini S, Strammiello R, Cerisano V, Perdichizzi S, Serra M, Astolfi A, Bertoni F, Alami J, Yeger H, Picci P, Scotlandi K (2002) The expression of ccn3 (nov) gene in musculoskeletal tumors. Am J Pathol 160:849–859
18. McCallum L, Price S, Planque N, Perbal B, Pierce A, Whetton AD, Irvine AE (2006) A novel mechanism for BCR-ABL action: stimulated secretion of CCN3 is involved in growth and differentiation regulation. Blood 108:1716–1723
19. Olsnes S, Klingenberg O, Wiedlocha A (2003) Transport of exogenous growth factors and cytokines to the cytosol and to the nucleus. Physiol Rev 83:163–182
20. Perbal B (1999) Nuclear localisation of NOVH protein: a potential role for NOV in the regulation of gene expression. Mol Pathol 52:84–91
21. Perbal B (2001) NOV (nephroblastoma overexpressed) and the CCN family of genes: structural and functional issues. Mol Pathol 54:57–79
22. Perbal B (2004) CCN proteins: multifunctional signalling regulators. Lancet 363:62–64
23. Perbal B (2006) The CCN3 protein and cancer. Adv Exp Med Biol 587:23–40
24. Planque N, Bleau AM, Perbal B (2005) The CCN3 protein: a multifunctional cell growth regulator. In: Perbal B, Takigawa M (eds) The CCN proteins: a new family of cell growth and differentiation regulators. Imperial College Press, London, pp 239–257

25. Planque N, Perbal B (2003) A structural approach to the role of CCN (CYR61/CTGF/NOV) proteins in tumourigenesis. Cancer Cell Int 3:1–15
26. Planque N, Perbal B (2003) The CCN Proteins, a new family of cell growth regulators. In: Pandalai SG (ed) Recent research developments in human pathology, vol 1. 2003 Part II. Transworld Research Network, Trivandrum, pp 333–369
27. Planque N, Long Li C, Saule S, Bleau AM, Perbal B (2006) Nuclear addressing provides a clue for the transforming activity of amino-truncated CCN3 proteins. J Cell Biochem 99:105–116
28. Wahab NA, Brinkman H, Mason RM (2001) Role of connective tissue growth factor in the pathogenesis of diabetic nephropathy. Biochem J 359:77–87
29. Xie D, Yin D, Wang HJ, Liu GT, Elashoff R, Black K, Koeffler HP (2004) Levels of expression of CYR61 and CTGF are prognostic for tumor progression and survival of individuals with gliomas. Clin Cancer Res 10:2072–2081
30. Yeger H, Chevalier G, Alami J, Perbal B (1998) Expression of novH in rhabdomyosarcoma. Proc Am Assoc Cancer Res 39 (Abstract 265)

Virchows Arch (2008) 452:41–47
DOI 10.1007/s00428-007-0528-y

ORIGINAL ARTICLE

3-D reconstruction and virtual ductoscopy of high-grade ductal carcinoma in situ of the breast with casting type calcifications using refraction-based X-ray CT

Shu Ichihara · Masami Ando · Anton Maksimenko · Tetsuya Yuasa · Hiroshi Sugiyama · Eiko Hashimoto · Katsuhito Yamasaki · Kensaku Mori · Yoshinori Arai · Tokiko Endo

Received: 15 July 2007 / Revised: 4 October 2007 / Accepted: 11 October 2007 / Published online: 14 November 2007
© Springer-Verlag 2007

Abstract Stereomicroscopic observations of thick sections, or three-dimensional (3-D) reconstructions from serial sections, have provided insights into histopathology. However, they generally require time-consuming and laborious procedures. Recently, we have developed a new algorithm for refraction-based X-ray computed tomography (CT). The aim of this study is to apply this emerging technology to visualize the 3-D structure of a high-grade ductal carcinomas in situ (DCIS) of the breast. The high-resolution two-dimensional images of the refraction-based CT were validated by comparing them with the sequential histological sections. Without adding any contrast medium, the new CT showed strong contrast and was able to depict the non-calcified fine structures such as duct walls and intraductal carcinoma itself, both of which were barely visible in a conventional absorption-based CT. 3-D reconstruction and virtual endoscopy revealed that the high-grade DCIS was located within the dichotomatous branches of the ducts. Multiple calcifications occurred in the necrotic core of the continuous DCIS, resulting in linear and branching (casting

S. Ichihara (✉)
Department of Pathology, Nagoya Medical Center,
Sannomaru 4-1-1, Naka-ku,
Nagoya 460-0001, Japan
e-mail: shu-kkr@umin.ac.jp

M. Ando
DDS Center, Research Institute for Science and Technology,
Tokyo University of Science,
2451 Yamasaki,
Noda, Chiba 278-8510, Japan

M. Ando · A. Maksimenko · H. Sugiyama
Photon Factory, IMSS, KEK,
Oho 1-1,
Tsukuba, Ibaraki 305-0801, Japan

M. Ando · H. Sugiyama · E. Hashimoto
Department of Photo-Science, GUAS,
Oho 1-1,
Tsukuba, Ibaraki 305-0801, Japan

T. Yuasa
Department of Bio-system Engineering, Faculty of Engineering,
Yamagata University,
4-3-16 Jonan,
Yonezawa, Yamagata 992-8510, Japan

K. Yamasaki
Genome Informatics Center, Kobe University,
Kusunoki-Cho 7-5-2,
Kobe, Hyogo 650-0017, Japan

K. Mori
Graduate School of Engineering, Nagoya University,
Furo-cho, Chikusa-ku,
Nagoya 464-8603, Japan

Y. Arai
Institutes for Oral Science, Matsumoto Dental University,
1780 Gobara Hirooka,
Shiojiri 399-0781, Japan

T. Endo
Department of Radiology, Nagoya Medical Center,
Sannomaru 4-1-1, Naka-ku,
Nagoya 460-0001, Japan

type) calcifications, a hallmark of high-grade DCIS on mammograms. In conclusion, refraction-based X-ray CT approaches the low-power light microscopic view of the histological sections. It provides high quality slice data for 3-D reconstruction and virtual ductosocpy.

Keywords Microcalcification · Radiologic–pathologic correlation · Virtual endoscopy

Introduction

Three-dimensional (3-D) approaches have provided insights into the histopathology of the breast [10, 16, 21–25]. They are particularly fruitful in understanding the pathology of ductal carcinomas in situ (DCIS) of the breast. For example, through stereomicroscopic observation of thick sections, Welling and his associates [24, 25] have revealed that the epithelial cells of the breast lobules are the major sources of mammary DCIS. With a complete 3-D solid model of the full extent of all mammary duct lobular systems throughout the breast, Ohtake et al. [16] have indicated that DCIS basically involves a single mammary duct lobular system. Based on two-dimensional (2-D) and 3-D large section histology images, Tot [22] has proposed a new theory that DCIS, especially if high grade, develops within a single sick lobe of the breast. The casting type calcifications in these cases may be located within duct-like structures that have been formed by DCIS itself [21, 23]. An unsolved problem with 3-D studies is that they generally require time-consuming and laborious work.

Recently, our group has developed a new algorithm for refraction-based X-ray computed tomography (CT) and has attained a spatial resolution of approximately 10 μm with a much higher contrast than conventional absorption-based CT [1, 8, 12, 13, 26, 27]. The aim of this study is to apply this emerging technology to visualize the 3-D structure of a high-grade DCIS of the breast with linear and branching microcalcifications. Although the radiologic and histologic correlation in high-grade DCIS of the breast has been extensively studied [5–7, 10, 18–20], we selected this material because there have been few 3-D studies addressing the pathological site of mammographic microcalcifications.

Materials and methods

A system for synchrotron radiation imaging with refraction-based X-rays has been designed and built at Photon Factory, KEK, a synchrotron radiation facility in Tsukuba, Japan. The system has been operational since 2002. Figure 1 shows an overview of the data acquisition system for 3-D reconstruction. The X-ray optics used was diffraction-enhanced imaging (DEI) [4]. DEI is accomplished by inserting a Bragg type analyzer crystal in the beam path between the sample and the detector. A new algorithm for 3-D CT has been developed [13, 26, 27]. The outgoing beam from an asymmetrically cut collimator crystal is directed onto the sample. This beam is almost plane wave due to the asymmetry of the collimator crystal. The plane wave incident onto the sample may receive both absorption and refraction effect. The X-ray that may receive absorption will penetrate the sample without changing its direction while the refraction component may change its direction at the boundaries of the internal structure of the sample. An angle analyzer crystal can detect to separate these two types of X-ray components from the sample. To extract the refraction component of this beam, the CT data were acquired on both sides of the diffraction peak of the analyzer crystal. The data were stored in an X-ray CCD camera (X-FDI, Photonics Science, East Sussex UK) that has a view size of 8.7 mm (h)×6.9 mm (w) with 16-bit and 1,392×1040 pixels. The size of each pixel is 6.3×6.6 μm. The upper limit of the specimen size was determined by the detector (CCD camera) size rather than the beam size. The beam size at Photon Factory (Tsukuba) and that at SPring-8 (Kobe) is 30×30 and 90×90 mm, respectively. When this work was done, the upper limit of the specimen was 8.7×6.9 mm because of the limited detector size. In 2006, we upgraded the detector at Photon Factory, and the upper limit of the specimen is now 20×20 mm.

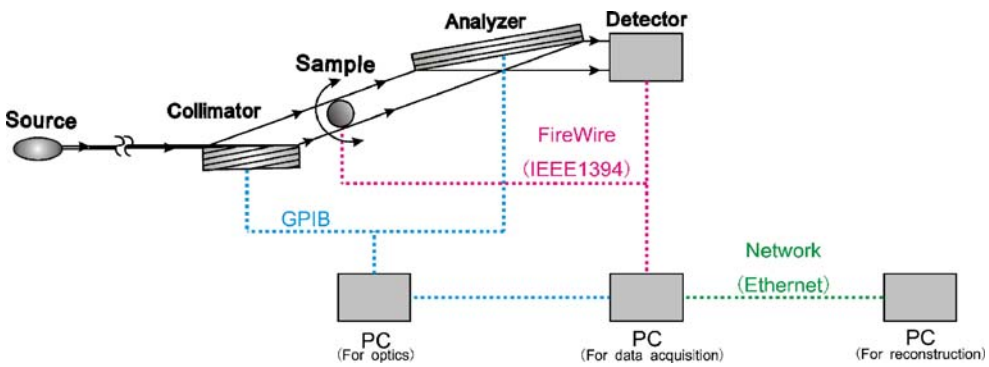


Fig. 1 Overview of the new data acquisition system for 3-D reconstruction of soft tissue. The X-ray optics used is DEI

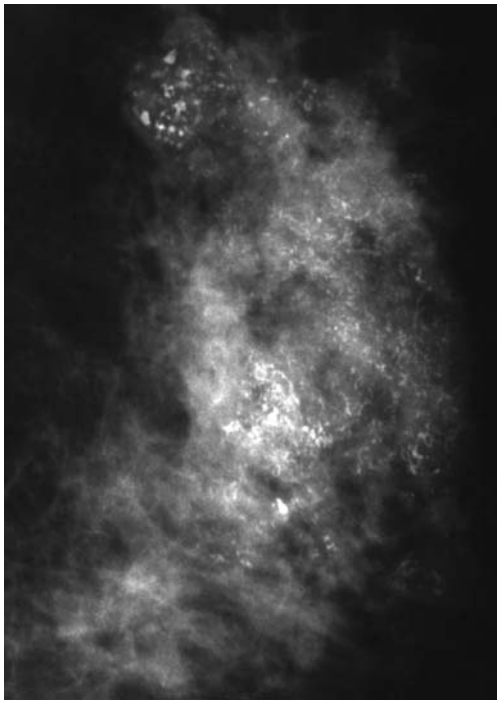


Fig. 2 Magnified view of the left breast (medio-lateral oblique view). There were fine linear and branching calcifications in the left breast. These fine linear and branching calcifications are believed to be a hallmark of high-grade DCIS

A case of extensive high-grade DCIS with typical linear and branching microcalcifications on mammograms was selected (Fig. 2). The patient was a 55-year-old Japanese woman. Aspiration cytology was reported as malignant, and the core needle biopsy was reported as noninvasive ductal carcinoma. Magnetic resonance imaging also suggested widespread DCIS. The patient underwent a mastectomy. The sentinel lymph nodes were negative for metastasis. After 48-h fixation in buffered formalin, the mastectomy specimen was serially sectioned and examined by pathologists. The mapping of the cancer distribution in the slices indicated that the whole upper outer quadrant of the left breast was affected by DCIS. Microscopically, comedo-type necrosis was observed within intraductal carcinoma and chronic inflammatory infiltrate in the surrounding tissue. Dystrophic calcifications were seen in the comedo-type necrosis within intraductal carcinoma. Extensive sampling revealed one small invasive focus measuring 4 mm in diameter in one slice. The maximum dimension of the DCIS was about 80 mm. A cylindrical tissue containing only DCIS (3.6 mm in diameter and 4.7 mm in height) was taken out of the slice, as a sample to be visualized by the new system. The diameter of the sample was a little more than that obtained from ten-gauge core needle biopsy. Data from 900 projections with an interval of 0.2° were used.

After all CT data were obtained, the entire cylindrical tissue was serially sectioned and stained with hematoxylin and eosion (HE) for histology and CT correlation studies (Fig. 3). The plane of the histological sections was the same as that of the CT scan in direction (i.e., cross-sections), to simplify the comparison of the slice images on CT with the histological sections. The total number of the sequential histological sections was 283. The images of the refraction-based CT was compared with those of an absorption-based micro-CT that had been newly developed for in vivo small animal imaging [2, 3] (Fig. 4).

Before the 3-D reconstruction, fine structures other than the DCIS, were eliminated from the original CT images to make it easy to understand histologic-mammographic correlation. This step was accomplished by comparing the

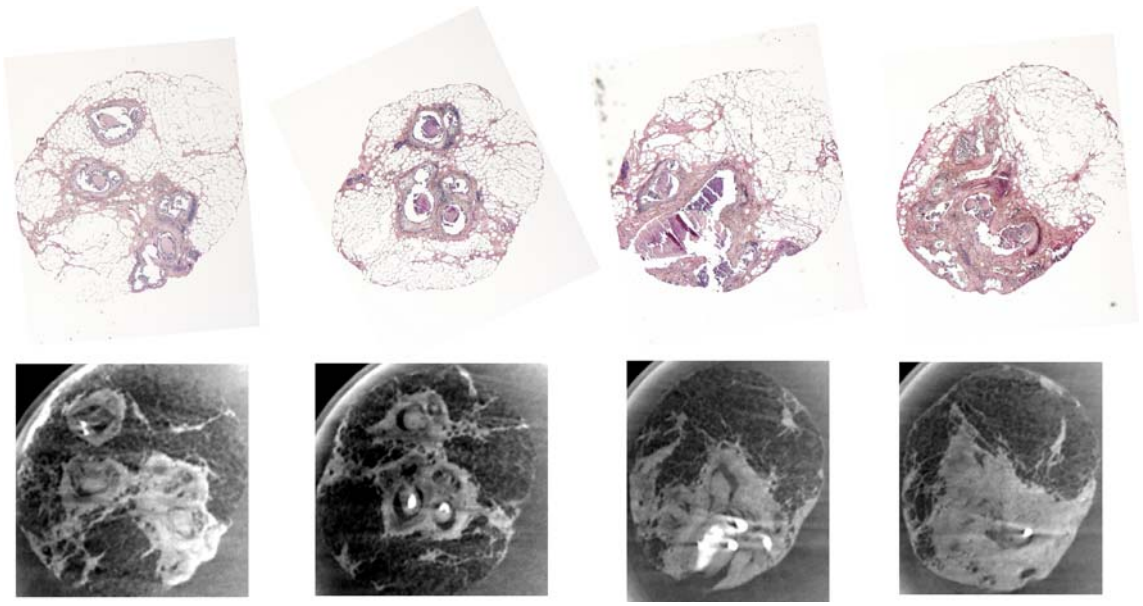


Fig. 3 Four representative images obtained with the new system (lower row) and the corresponding histological sections stained with HE (upper row)

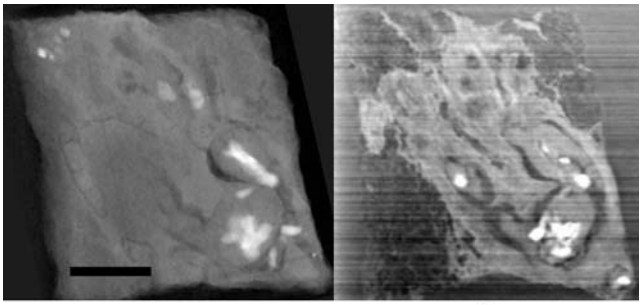


Fig. 4 Comparison of the images obtained with an absorption-based micro-CT (**a**, *left*) and refraction-based CT (**b**, *right*). In the refraction-based CT, we can easily distinguish the walls of ducts, intraductal carcinoma (*a gray mass in the ducts*), and calcifications (*white areas*). These fine structures are hardly visible in the absorption-based micro-CT (Scale bar: 1 mm)

CT images with the corresponding histological images and marking the outline of the ducts containing carcinoma cells. Based on these CT images, computer graphic 3-D images were created using VS studio Max Volume Graphics, Heidelberg, Germany (Fig. 5). The software program used was a voxel data visualization and analysis system.

As a virtual endoscopy system, we used a high-speed software-based volume rendering method on a PC platform developed by one of the coauthors, Mori and his associates [14, 15]. This volume-rendering method can generate virtual endoscopic images of a 3-D volume of 512×512×4,898 voxel size of volume rendering. This is characterized by perspective projection, specular reflection, and on-the-fly normal vector computation on a conventional PC without any special hardware at 13 frames per second (Fig. 6).

Results

To verify refraction-based CT images, the serial 2-D images from the new system were compared by both radiologists and pathologists with the serial histological sections. Figure 3 shows four representative histological images (upper row) and the corresponding refraction-based CT images (lower row). The high contrast white materials observed in the lumen of the ducts were microcalcifications in the conventional histological sections. The maximum size of the microcalcifications was 1.1 mm. The grayish material surrounding the microcalcifications corresponded to the intraductal carcinoma with necrosis, although necrotic and non-necrotic areas were distinguished only in histological sections. The black zone between the carcinoma and the duct wall was a vacant space, which may be in part due to tissue shrinkage or fixation artifact during the specimen preparation. Virtual endoscopic observation was performed utilizing these vacant spaces between the carcinoma and the duct wall. The grayish white area around the ducts in the refraction-based CT was found to be normal fibroglandular tissue. The dark gray areas filling the space between the ducts and the fibroglandular tissue were adipose tissue. There were at least four ducts in the upper cross-sections, but they gradually decreased in the lower cross-sections and finally fused to become one large duct measuring around 2.0 mm at the bottom. This suggests that the multiple ducts in the specimen belonged to the same duct system.

The 2-D longitudinal images obtained with the new system were compared with those obtained with the absorption-based micro-CT [3] (Fig. 4). In both CT, microcalcifications were recognized as discrete high contrast masses. However, the dilated and branching ducts containing the intraductal mass, fibroglandular tissue, and adipose tissue were depicted only in the refraction-based CT findings. The fine structures, except for mirocalcificatcions, were barely visible in the absorption-based micro-CT findings, suggesting a limitation of conventional CTs for soft tissue imaging.

The serial 2-D images obtained with the new system (n=900) were reconstructed into the 3-D structure using a commercially available voxel data visualization software (Fig. 5a and b). The fine structures other than the DCIS had been erased in advance. The reconstructed 3-D structures can be rotated freely on the computer display. The branching ducts at the upper level gradually approach each other and finally merge into a large duct at the lower level of the specimen. This confirms that the branching ducts in the

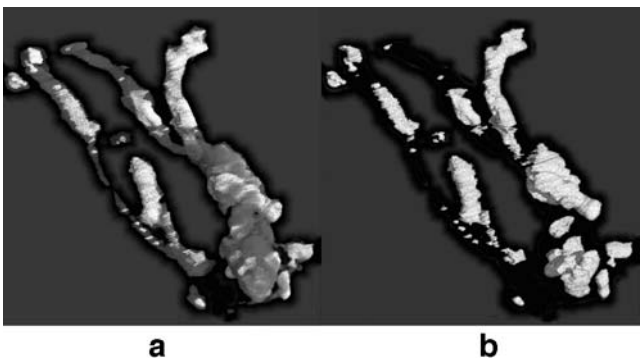


Fig. 5 The reconstructed 3-D images of the DCIS from the serial 2-D images (n=900) obtained with the new system. The reconstructed 3-D structure can be rotated freely on the computer display. Prior to the 3-D reconstruction, the fine structures of the breast parenchyma, other than the DCIS, were eliminated from the original CT images to make it easy to understand histologic–mammographic correlation. The ducts have a dichotomous branching and the branching ducts formed acute angles. **a** The reconstructed DCIS exhibiting both calcifications (*white*) and non-calcified tumor (*gray*). **b** The reconstructed DCIS only exhibiting calcifications (*white*). Comparison of these two figures indicates that the pathognomonic linear and branching type microcalcifications on the mammograms result from multifocal calcifications (*white*) that developed within the necrotic zone of the continuous DCIS (*gray*)

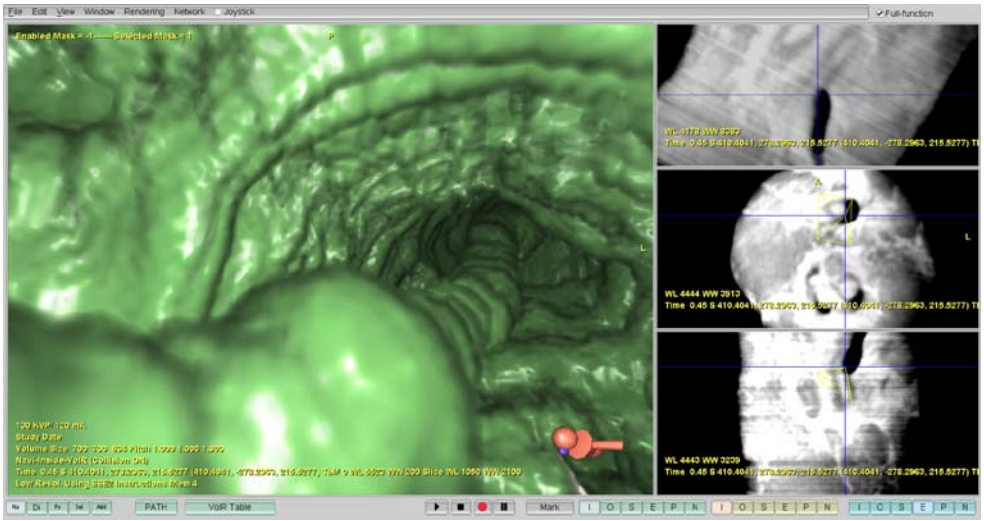


Fig. 6 Virtual endoscopy of the mammary DCIS. The comedo-type necrosis appeared as a continuous rope-like structure within the duct. The size of the duct is around 0.6 mm

specimen belong to the same duct system. The ducts showed dichotomous branching twice, and the branching ducts formed acute angles. Figure 5a and b are the magnified views of the reconstructed DCIS, while only the calcifications of the DCIS are shown in Fig. 5b. These figures indicate that the DCIS (grayish material that fills ductal lumen) was located within the ducts because repeated dichotomatous branching is not the feature of the terminal ductal lobular unit. Comparing these two figures indicates that multiple calcifications (white areas within the grayish material) occurred in the necrotic zone of the continuous DCIS, resulting in the linear and branching microcalcifications. Dicotomatous branching of the ducts was also confirmed with virtual endoscopic observation [14, 15] (Fig. 6). In virtual endoscopy, comedo-type necrosis appeared as a rope-like material occupying the center of the ducts.

Discussion

The appearance of microcalcifications on mammograms is an important diagnostic clue that can lead to the detection of DCIS of the breast [5, 6, 19]. This article focused on the subtype of DCIS characterized by coarse, branching, longish, histologically amorphous calcifications. This type of microcalcifications, called as casting type, believed to be a hallmark of high-grade DCIS. However, the exact pathological site of mammographic microcalcifications remains unclear from conventional histological sections because they are only a few microns in thickness. In 2-D histological sections, DCIS appears as multiple duct-like structures containing malignant epithelial cells. These spaces are separated by the connective tissue stroma; the relationship between these spaces is obscured in histological sections. Whereas 3-D reconstructions are suitable for correlating 2-D histologic findings and panoramic mammographic findings, few 3-D studies have addressed the pathological site of mammographic microcalcifications. To the authors' knowledge, this is the first 3-D reconstruction and virtual endoscopic observation of mammary DCIS to elucidate the pathological site of mammographic calcifications.

The refraction-based CT depicted not only the microcalcifications but also the fine structures such as the cancerous tissue in the branching ducts, the outline of the duct lumen, fibroglandular tissue, and adipose tissue. Most of these fine structures were hardly visible in absorption-based micro-CT. The images obtained with refraction-based CT were validated by comparing them with the corresponding histological sections. There was a close relationship between the refraction-based CT and the HE-stained histological sections. The refraction-based X-ray CT images approached a low-power light microscopic view of the histological sections. It is important to note that the new CT does not require any contrast medium. Based on the high quality slice data, DCIS in a large core biopsy specimen was successfully visualized as a 3-D reconstruction model as well as a virtual endoscopy. Although a small portion of the widespread DCIS was reconstructed in this study, the DCIS was continuous in a branching duct system. This is consistent with the current view that the vast majority of high-grade DCIS is a continuous and unifocal process, as opposed to the perceived multifocality implied by 2-D histological sections [9, 11, 17].

This 3-D reconstruction model indicated that the linear and branching microcalcifications occurred in the central necrotic zone of the DCIS, involving ducts with a tree-like structure. The microcalcifications in the necrotic tumor at the branching points of the duct created branching calcifications. Our findings agree with the previous studies that focused on the correlation between mammographic and pathological findings of linear and branching microcalcifications. Stomper et al. [19] found that the comedo subtype of

DCIS is more likely to be accompanied by linear calcifications than are the noncomedo subtypes, and noncomedo DCIS is more likely to be associated with granular calcifications than is the comedo subtype. Evans and Pinder [7] suggested that granular calcifications are formed in necrotic DCIS as a result of the necrotic debris within the ducts undergoing dystrophic calcification. These granular calcifications can coalesce to form rod-shaped calcifications. If these rod-shaped calcifications occur where the breast duct is branching, then branching calcifications may result. Similar assertions have also been advocated by Rubin [18]. Tabar [20] considered that the pathological site of the casting type (linear and branching) calcifications is the distended ducts and their branches, whereas that of crushed stone-like calcifications is distended terminal duct lobular units.

Virtual endoscopy is a noninvasive technique that can examine the inside of a virtualized human body. This system has many advantages, such as (1) observation that is impossible by real endoscopes, (2) quantitative measurements, and (3) application to individual patient with no pain [15]. So far, virtual endoscopy has been applied to the colon, bronchi, blood vessels, urinary tract. But there have been no reports as to virtual endoscopy (ductoscopy) of the breast. In this study we demonstrated that refraction-based X-ray CT provides high-quality slice data for virtual endoscopy in the breast.

In conclusion, refraction-based X-ray CT is almost equivalent to the low-power light microscopic view of the histological sections. Using its high quality slice data, this 3-D study successfully located the high grade DCIS with casting type calcifications in the dicotomatous branches of the duct. Because the epithelial proliferations in the breast primarily occur within the 3-D mammary duct lobular systems, 3-D approach with refraction-based CT could shed light on radiologic and pathologic correlations.

Acknowledgments This research project was financially supported by a Grant-in-Aid for Exploratory research (No.15654042) and a Grant-in-Aid for Scientific Research (A) (No.18206011) from the Japanese Ministry of Education, Culture, Sports, Science and Technology (MEXT), a Grant-in-Aid for the policy-based medical services network for breast cancer screening pathology from the National Hospital Organization in Japan and the Suzuken Research Fund. The experiment was performed under the approval of the KEK Program Advisory Board under No. 2005G085 for the use of the Photon Factory. The specimen used in this study was with the consent of the patient. We would like to thank Mr. Katsuhito Tamaoki and Mr. Kazuki Matsui for their excellent technical assistance and Dr. Chiho Ohbayashi, Dr. Keisuke Hanioka, and Dr. Yoshiko Sakuma for providing clinical data. We are also grateful to Dr. Mitsuhiro Tozaki, Dr. Suzuko Moritani, Dr. Masaki Hasegawa, and Dr. Shinji Mii for their useful comments regarding this study. None of the authors has any conflict of interest to declare. This work was presented in part at XXXVI International Congress of the International Academy of Pathology in Montreal, Canada, September 16–21, 2006.

References

1. Ando M, Akatsuka T, Bando H, Chikaura Y, Endo T, Hashimoto E, Hirano K, Hyodo K, Ichihara S, Maksimenko A, Sugiyama H, Ueno E, Yamasaki K, Yuasa T (2006) First attempt at 3D X-ray visualization of DCIS due to refaction contrast—in good relation to pathological view. In: Astley SM, Brady M, Rose C, Zwiggelaar R (eds) Proceedings IWDM. Springer, Berlin Heidelberg New York, pp 525–532
2. Arai Y, Ninomiya T, Tanimoto H (2007) Development of in vivo micro computed tomography using flat panel detector. Dent Jpn 143:109–111
3. Arai Y, Yamada A, Ninomiya T, Kato T, Masuda Y (2005) Micro-computed tomography newly developed for in vivo small animal imaging. Oral Radiol 21:14–18
4. Chapman D, Thomlinson W, Johnston R, Washburn D, Pisano E, Gmur N (1997) Diffraction enhanced X-ray imaging. Phys Med Biol 42:2015–2025
5. Dershaw DD, Abramson A, Kinne DW (1989) Ductal carcinoma in situ: mammographic findings and clinical implications. Radiology 170:411–415
6. Evans A, Ellis I, Pinder S, Wilson R (2002) Breast calcification: a diagnostic manual. Greenwich Medical Media, London
7. Evans A, Pinder S, Wilson R, Sibbering M, Poller D, Elston C, Ellis I (1994) Ductal carcinoma in situ of the breast: correlation between mammographic and pathologic findings. AJR Am J Roentgenol 162:1307–1311
8. Hashimoto E, Maksimenko A, Sugiyama H, Hyodo K, Shimao D, Nishio Y, Ishikawa T, Ando M (2006) First application of X-Ray refraction-based computed tomography to a biomedical object. Zoological Science 23:809–813
9. Holland R, Hendriks JH, Vebeek AL, Mravunac M, Schuurmans Stekhoven JH (1990) Extent, distribution, and mammographic/histological correlations of breast ductal carcinoma in situ. Lancet 335:519–522
10. Ichihara S, Moritani S, Ohtake T, Ohuchi N (2005) Ductal carcinoma in situ of the breast: the pathological reason for the diversity of its clinical imaging. In: Ueno E, Shiina T, Kuboto M (eds) Research and development in breast ultrasound. Springer, Tokyo, pp 104–113
11. Lagios MD, Westdahl PR, Margolin FR, Rose MR (1982) Duct carcinoma in situ. Relationship of extent of noninvasive disease to the frequency of occult invasion, multicentricity, lymph node metastases, and short-term treatment failures. Cancer 50:1309–1314
12. Maksimenko A, Ando M, Sugiyama H, Yuasa T (2005) Computed tomographic reconstruction based on X-ray refraction contrast. Appl Phys Lett 86:124105–124101~124505–124103
13. Maksimenko A, Ando M, Sugiyama H, Yuasa T (2005) Possibility of computed tomographic reconstruction of cracks from X-ray refraction contrast. Jpn J Appl Physics 44:L633–L635
14. Mori KS, Suenaga Y, Toriwaki J (2003) Fast software-based volume rendering using multimeda instructions on PC platforms and its application to virtual endoscopy. In: Proc. of SPIE, Medical Imaging 2003, Physiology and Function: Methods, Systems, and Applications. The International Society for Optical Engineering, San Diego, Calfornia, USA, pp 111–122
15. Mori K, Urano A, Hasegawa J, Toriwaki J, Anno H, Katada K (1996) Virtualized endoscope system—an application of virtual reality technology to diagnostic aid. IEICE Trans Inf Syst 79-D:809–819
16. Ohtake T, Kimijima I, Fukushima T, Yasuda M, Sekikawa K, Takenoshita S, Abe R (2001) Computer-assisted complete three-dimensional reconstruction of the mammary ductal/lobular sys-

tems: implications of ductal anastomoses for breast-conserving surgery. Cancer 91:2263–2272
17. Page DL, Rogers LW, Schuyler PA, Dupont WD, Jensen RA (2002) Ductal carcinoma in situ of the breast. Williams & Wilkins, Philadelphia
18. Rubin E (2002) Ductal carcinoma in situ: a radilogical perspective. Williams & Wilkins, Philadelphia
19. Stomper PC, Connolly JL (1992) Ductal carcinoma in situ of the breast: correlation between mammographic calcification and tumor subtype. AJR Am J Roentgenol 159:483–485
20. Tabar L, Gad A, Parsons WC, Neeland DB (2002) Mammographic appearances of in situ carcinomas. Williams & Wilkins, Philadelphia
21. Tabar L, Tot T, Dean PB (2007) Casting type calcifications: sign of a subtype with deceptive features. Thieme, Stuttgart
22. Tot T (2005) DCIS, cytokeratins, and the theory of the sick lobe. Virchows Arch 447:1–8
23. Tot T, Tabar L (2005) Mammographic–pathologic correlation of ductal carcinoma in situ of the breast using two- and three-dimensional large histologic sections. Semin Breast Dis 8:144–151
24. Wellings SR, Jensen HM (1973) On the origin and progression of ductal carcinoma in the human breast. J Natl Cancer Inst 50:1111–1118
25. Wellings SR, Jensen HM, Marcum RG (1975) An atlas of subgross pathology of the human breast with special reference to possible precancerous lesions. J Natl Cancer Inst 55:231–273
26. Yuasa T, Maksimenko A, Hashimoto E, Sugiyama H, Hyodo K, Akatsuka T, Ando M (2006) Hard-X-ray region tomographic reconstruction of the refractive-index gradient vector field: imaging principles and comparisons with diffraction-enhanced-imaging-based computed tomography. Opt Lett 31:1818–1820
27. Yuasa T, Sugiyama H, Zhong Z, Maksimenko A, Dilmanian FA, Akatsuka M, Ando M (2005) High-pass-filtered diffraction microtomography by coherent hard x rays for cell imaging: theoretical and numerical studies of the imaging and reconstruction principles. JOSA 22:2622–2634

Virchows Arch (2008) 452:49–55
DOI 10.1007/s00428-007-0530-4

ORIGINAL ARTICLE

Prognostic role of CD44 cell adhesion molecule expression in primary and metastatic renal cell carcinoma: a clinicopathologic study of 125 cases

So Dug Lim · Andrew N. Young · Gladell P. Paner · Mahul B. Amin

Received: 30 August 2007 / Revised: 5 October 2007 / Accepted: 17 October 2007 / Published online: 20 November 2007
© Springer-Verlag 2007

Abstract Possible prognostic utility of CD44 in renal cell carcinoma (RCC) prompted a comparison of its expression in primary and metastatic RCC. A total of 164 paraffin-embedded tissues of primary RCC and metastatic RCCs from 125 patients were immunostained with CD44 (standard form) antibody. It consisted of 86 primary RCCs (50 with subsequent metastasis [MET+] and 36 with no known metastasis [MET−]) during follow up and 78 metastatic RCCs (39 metastatic RCCs only and 39 with matched RCC primary from RCC MET + category). Immunoreactivity for CD44 was scored semiquantitatively as 0, 1, or 2 (0, <5%; 1, 5–50%; 2, ≥50%). Expression of CD44 was significantly higher in metastatic RCCs compared to primary RCCs (p= 0.036). CD44 immunoreactivity in the primary RCC (MET− and MET+) correlated with progression-free survival (p= 0.027). In metastatic RCCs, CD44 immunoreactivity also correlated with survival after detection of first metastasis (p=0.011). In multivariate analysis, stage (p=0.0001) and CD44 immunoreactivity (p=0.03) in primary RCC were independent predictors of progression-free survival. Our study suggests that CD44 status in RCC provides useful prognostic information both in primary and metastatic RCCs and may have applicability in stratifying patients for therapeutic decisions.

Keywords Renal cell carcinoma · Prognosis · CD44 · Immunohistochemistry · Metastasis

S. D. Lim
Department of Pathology, Konkuk University School of Medicine,
4-12 Hwayang-dong, Gwangjin-gu,
143-729 Seoul, Republic of Korea

S. D. Lim
Center for Geriatric Neuroscience Research,
Institute of Biomedical Science and Technology,
Konkuk University,
4-12 Hwayang-dong, Gwangjin-gu,
143-729 Seoul, Republic of Korea

A. N. Young
Department of Pathology and Laboratory Medicine,
Emory University School of Medicine,
1364 Clifton road, NE,
Atlanta, GA 30322, USA

G. P. Paner
Department of Pathology, Loyola University Medical Center,
IL 2160 S First Avenue,
Maywood, IL 60153, USA

M. B. Amin (✉)
Department of Pathology and Laboratory Medicine,
Cedars-Sinai Medical Center,
8700 Beverly Blvd., Suite 8728,
Los Angeles, CA 90048, USA
e-mail: aminm@cshs.org

Introduction

Tumor stage, nuclear grade, and histologic type including sarcomatoid change are considered to be the main pathologic prognostic factors in renal cell carcinoma (RCC) [1, 3, 6]. However, these parameters are not always sufficient to predict the clinical behavior such that there is a need to identify additional prognostic markers of clinical outcome in patients with RCC. Several studies have suggested the prognostic value of cell proliferation markers [5, 17], *p53* mutation [21], growth factor expression [15], and intratumoral microvessel density [17]; although the results are not always concordant. Hence, the search for additional prognostic markers remains active.

The CD44 group of transmembrane glycoproteins encompasses a predominant form (CD44 standard form) and several variant isoforms, which differ mainly in primary structure. The standard form CD44 is the main receptor for hyaluronate and has been implicated in various human malignancies, playing a vital role in determining the fate of hematogenous dissemination of tumor cells [14]. Although CD44 is closely associated with proliferation, metastasis, cancer recurrence, and prognosis, contradictory results have been reported concerning the overexpression of CD44 by immunohistochemistry in relation to tumor development and progression in different tumors at different sites [7, 18, 19]. Meanwhile, CD44 expression has been suggested as a useful prognostic marker in RCC [2, 7, 17], and the presence of CD44 has been shown to confer increased metastatic potential [8, 10].

We therefore examined the expression of CD44 (standard form) in both primary RCCs and RCCs at metastatic sites and correlated its expression in these tumors with the usual prognostic factors and progression-free survival after nephrectomy. We specifically studied the expression of CD44 in primary RCCs and their corresponding metastasis to ascertain if acquisition of CD44 immunoreactivity correlated with metastatic potential. Finally, we assessed whether there was heterogeneity of CD44 expression in patients with multiple metastases and if CD44 immunoreactivity correlated with survival after detection of a metastasis.

Materials and methods

Clinicopathologic data

A total of 164 formalin-fixed, paraffin-embedded tissues of primary RCC and metastatic lesions from 125 patients were randomly selected from the archives of the Emory University Hospital, Atlanta, GA, on the basis of available paraffin blocks for the analysis of CD44 expression. It consisted of 86 primary RCCs (50 with subsequent metastasis [MET+] and 36 with no known metastasis [MET−] during follow-up period) and 78 metastatic RCCs (39 metastatic RCCs only and 39 with matched RCC primary from RCC MET+ category).

The following histopathological criteria were evaluated: histologic subtype [1], Fuhrman nuclear grade [6], and pathologic stage according to the 2006 American Joint Committee on Cancer (AJCC) TNM staging system (6th edition) [9]. Follow-up data, including date of initial diagnosis, date of detection of first metastasis, date of death, and/or date of last follow-up, status (development of recurrence, metastasis, and death), and adjuvant therapy were obtained from medical records.

Overall survival and progression-free survival were both calculated from the date of surgery. Progression-free period was defined as the period of time during which there was no evidence of disease progression (recurrence, metastasis, or death from disease). For analysis of overall survival in relation to CD44 expression in metastatic RCCs, the duration of overall survival was calculated from the date of first detection of metastasis until death or last follow-up.

The Emory University Institutional Review Board approved this research under protocol 255–2002.

Immunohistochemistry

Representative formalin-fixed paraffin-embedded tissues for each case were deparaffinated and subjected to antigen retrieval in citrate buffer (pH 6) using an electric pressure cooker set at 120°C for 5 min. Sections were incubated for 5 min in 3% hydrogen peroxide to quench endogenous tissue peroxidase. Immunohistochemistry was performed using primary antibody (anti-human mouse IgG CD44 monoclonal antibody, standard form, Pharmingen, San Diego, CA) at a dilution of 1:640, an avidin–biotin complex kit (LSAB2; Dako, Carpinteria, CA) and the Dako autostainer (Dako). After 25 min incubation with primary antibody, sections were washed and treated with biotinylated secondary anti-immunoglobulin, followed by avidin coupled to biotinylated horseradish peroxidase, according to manufacturer's instructions. The immunohistochemical reactions were visualized using diaminobenzidine as the chromogenic peroxidase substrate. Sections were counterstained with hematoxylin for 1 min. Specificity of the procedure was verified by negative control reactions with primary antibody replaced with buffer and by positive control using palatine tonsilar tissue. CD44 immunoreactivity was analyzed by a semiquantitative method using three scores based on percent of cells staining as follows: 0, negative to <5%; 1, 5–50% positive tumor cells; and 2, ≥50% tumor cells immunopositive. Cases were blinded for outcome during the immunohistochemistry evaluation.

Statistics

Statistical analysis was done with Statistical Package for the Social Sciences (SPSS) software (SPSS, Chicago, IL, USA). The relationships between the clinicopathologic data were analyzed using the χ^2 test. The Kaplan–Meier survival curves and log-rank tests were used to determine statistical significance of survival data. Cox proportional hazard model was performed to evaluate the independent predictive value of significant pathologic variables by univariate analysis. A value of $p<0.05$ was considered statistically significant.

Results

The pertinent clinicopathologic data of the 86 cases of primary RCCs are summarized in Table 1. Of 86 primary tumors, 36 cases had no known metastasis of the tumor (RCC MET−), and 50 cases showed subsequent metastasis (RCC MET+) during follow-up period (mean, 60 months; median, 46 months). Of 78 metastatic RCCs, 39 cases were matched with the primary RCCs from RCC MET+ category. The mean follow-up time for metastatic RCC patients was 51 months (median, 55 months). About 30 of 78 patients with the metastatic RCC had the multifocal sites of metastasis including lung, bone, lymph nodes, and soft tissue. The 36 cases of RCC MET− included 34 clear cells, 1 papillary, and 1 chromophobe RCCs. The 50 cases with RCC MET+ included 45 clear cells, 3 papillary, and 2 unclassified RCCs. Besides 39 metastatic RCC matched with the primary RCCs from RCC MET+ category, the remaining 39 metastatic RCC consisted of 38 clear cell RCCs and 1 unclassified RCC.

All RCC subtypes were included in the statistical analysis because there was no significant difference between the analysis including all RCC subtypes and the analysis confined only to clear cell RCC (data not shown).

Table 1 Summary of primary RCCs and metastatic RCCs examined for analysis of CD44 expression

	Type of lesion	Number examined
Primary RCCs		86
	RCC MET−	36
	RCC MET+	50
Follow-up period (months)	Mean(median)	60 (46)
Metastatic RCCs		78
	With matched primary RCC	39
	Only metastatic lesions	39
Follow-up period (months)	Mean(median)	51(55)
No. of metastatic sites	Single	48
	Multifocal(>1)	30
Metastatic sites examined		78
	Lung	17
	Bone	15
	Lymph nodes	14
	Soft tissue	13
	Brain	5
	Liver	5
	Intestine	4
	Pancreas	2
	Ovary	1
	Testis	2

RCC MET− No known metastasis during follow-up; *RCC MET+* subsequent metastasis during follow-up

Table 2 Clinicopathologic findings in 36 RCC MET− and 50 RCC MET+

	Primary RCC	Primary RCC		*p* value
		RCC MET−	RCC MET+	
No. of cases	86	36	50	
Age (years, mean+SD)	59+12	60+11	59+13	0.8
Sex (M/F)	1.6: 1	1.1: 1	2.2: 1	0.152
Tumor size (cm, mean+SD)	6.7+4	5.4+3	7.7+4	**0.003**
Fuhrman grade				
1 and 2	33.7%	55.6%	18.0%	**<0.001**
3 and 4	66.3%	44.4%	82.0%	
TNM stage				
I and II	47.6%	82.9%	22.4%	**<0.001**
III and IV	52.4%	17.1%	77.6%	
Adjuvant treatment	15.1%	8.3%	20.0%	0.222

RCC MET− No known metastasis during follow-up; *RCC MET+* Subsequent metastasis during follow-up

The mean tumor diameter of 86 cases of primary RCCs was 6.7 cm. The tumor size difference between RCC MET− and RCC MET+ tumors was statistically significant (p=0.003; Table 2). The Fuhrman nuclear grade and TNM stage also showed statistically significant differences between two groups (p<0.001, p<0.001, respectively; Table 2). About 15.1% of 86 patients received adjuvant treatment after nephrectomy.

An intense membranous staining pattern of tumor cells with CD44 was considered positive. CD44 immunoreactivity correlated with Fuhrman nuclear grade (p=0.003; Table 3; Fig. 1). CD44 immunoreactivity was not signifi-

Table 3 Comparison of clinicopathological findings between primary RCCs and CD44 immunoreactivity

	CD44 immunoreactivity[a]				
	Total	0	1	2	*p* value
No. of cases	86	48	26	12	
Tumor size (cm)					
<6 cm	41.7%	54.3%	25.7%	20.0%	0.39
≥6 cm	58.3%	55.1%	34.7%	10.2%	
Fuhrman grade					
1 and 2	33.7%	79.3%	29.7%	0.0%	**0.003**
3 and 4	66.3%	43.9%	35.1%	21.0%	
TNM stage					
I and II	47.6%	60.0%	30.0%	10.0%	0.32
III and IV	52.4%	52.3%	29.5%	18.2%	

[a] CD44 immunoreactivity: 0, <5%; 1, ≥5 to <50%; 2, ≥50%

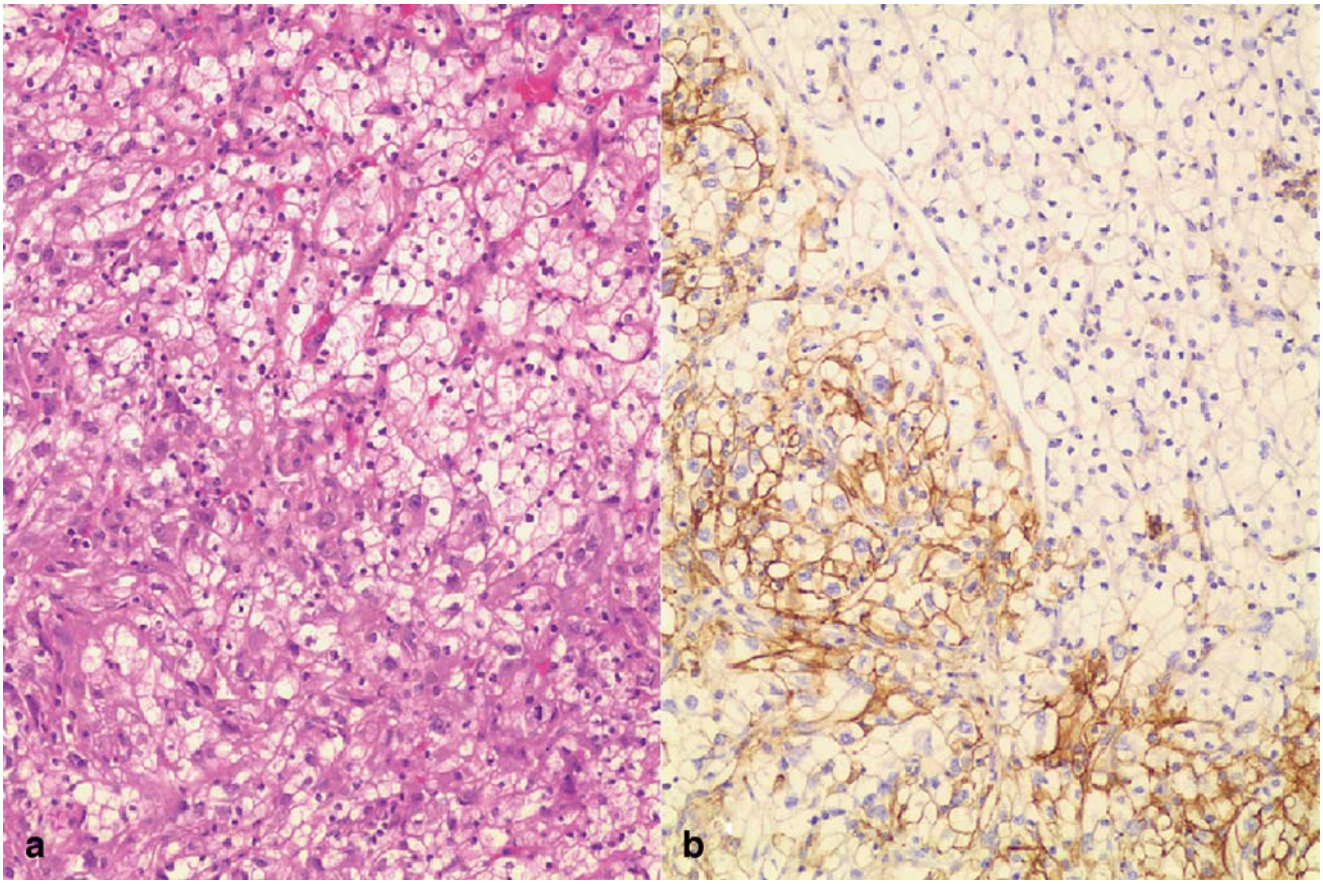


Fig. 1 CD44 immunoreactivity in a case of primary RCC MET+ to illustrate the trend in immunoreactivity between different Fuhrman nuclear grades in same tumor. **a** Hematoxylin and eosin showing grade 2 areas in a tumor (*right side*) and grade 3 areas in the *left*; **b** overexpression of CD44 in grade 3 areas as opposed to negative staining in the grade 2 area of the tumor

cantly different between organ confined (pT1 and pT2) and non-organ confined (pT3 and pT4) tumors (p=0.32).

More than 50% immunoreactivity of CD44 was seen in 5.6% of primary RCCs in the RCC MET−, in 20% of RCC MET+ , and in 43.6% of all metastatic RCCs (Fig. 2). CD44 immunoreactivity tended to be higher in primary RCC MET+ than in primary RCC MET−, although this difference was not statistically significant (p=0.146; Fig. 2). There was significant difference of CD44 immunoreactivity between primary RCCs and its matched metastatic RCCs (p=*0.036*). Overall, CD44 immunoreactivity was higher in metastatic RCCs compared to primary RCCs (p=0.018; Fig. 2). CD44 immunoreactivity in RCC MET+ tends to show more diffuse and strong positivity in RCC within vascular-lymphatic spaces and its corresponding metastasis (Fig. 3).

By univariate analysis, tumor grade and stage correlated with progression-free survival (p=0.013, p<0.001, respectively; Fig. 4a,b). A significant decrease in progression-free survival was observed for patients having high CD44 expression (p=0.027; Fig. 4c). This significance was maintained when adjusted for adjuvant treatment and TNM stage (p=0.025, p=0.035, respectively, data not shown).

Of 78 patients with the metastatic RCCs, CD44 immunoreactivity in metastatic RCCs correlated with overall survival (p=0.011; Fig. 5). In patients with metastases to multiple sites, there was no difference in CD44 immunoreactivity between the different metastatic RCCs (as studied in 38 samples from 17 cases).

Cox regression analysis, including variables significantly associated with survival in univariate analysis, showed that TNM stage (p=0.0001) and CD44 immunoreactivity (p=0.03) were independent prognostic factors for progression-free survival (Table 4).

Discussion

RCC is well recognized as a malignancy with an unpredictable clinical course [1, 3, 8]. Although several pathologic parameters, including histologic stage, grade, and sarcomatoid change provide independent prognostic information, the outcome after surgery in an individual patient

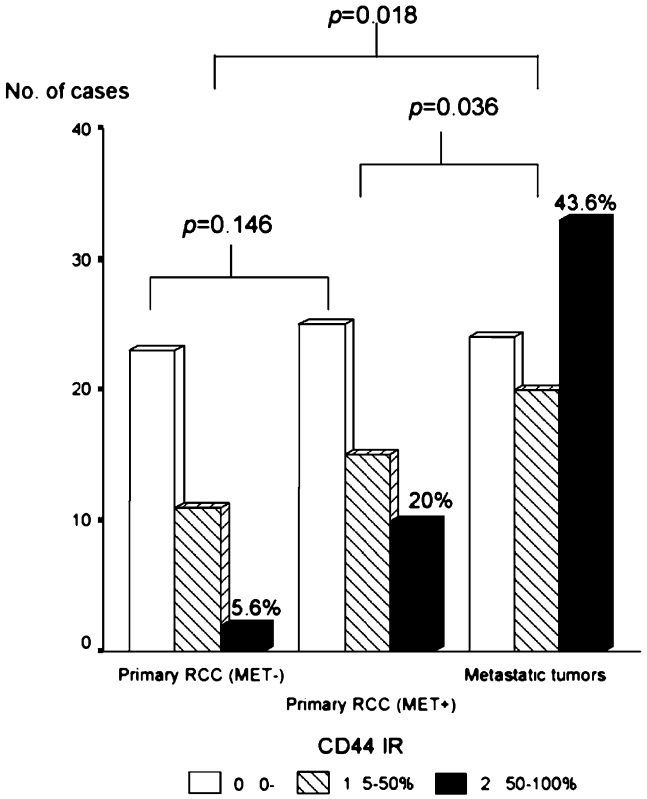


Fig. 2 Comparison of CD44 immunoreactivity between primary RCC (MET−), primary RCC (MET+) and metastatic RCC tumors

remains uncertain, and studies to discover additional prognostic markers are still under investigation [14, 17, 20].

In this study, majority of the RCCs exhibited some degree of CD44 positivity, the frequency of which is consistent with the results observed in other studies [7, 16]. Although a contradictory result has been reported concerning the prognostic significance of CD44 immunoexpression in RCC [23], most other studies have shown that high CD44 expression in RCC is associated with poor survival [7, 13, 17], a significant risk of progression [5, 16], and poor tumor differentiation [23]. CD44 expression was shown to be correlated with tumor grade, with higher immunoreactivity observed in higher grade tumors [2, 7, 23]. CD44 expression was also shown to be correlated with RCC tumor size and stage [2, 7]. Paradis et al [16] demonstrated that CD44 expression in organ-confined clear cell RCCs was an independent prognostic factor for both overall and disease-free survival by univariate and multivariate analysis. While their study was limited only to patients with early stage tumors, we showed that CD44 expression in primary RCC including tumors that subsequently developed metastasis has prognostic value for lower progression-free survival by multivariate analysis, which was independent of stage and grade. Moreover, this correlation maintained significance when adjusted for adjuvant treatment.

Our study reaffirmed the importance of TNM staging of RCC in predicting disease progression, and its documentation is quintessential in the surgical pathology report. However, with the rise of non-surgical ablation (laser and cryotherapy) for kidney mass lesions, the biopsy is the only available histologic material for documentation of the pathology [11, 23]. Because such treatment, thus, not permit pathologic staging, CD44 immunohistochemistry may be helpful in limited tissue material as a surrogate predictor marker for prognostic outcome and consequent stratification for active patient surveillance of metastatic disease.

Gilcrease et al [8] showed increased expression of CD44 in some tumors showing evidence of extrarenal invasion or with known metastasis at the time of nephrectomy. In this study, although CD44 expression between RCC MET− and RCC MET+ was not statistically different, CD44 expression was higher in RCC MET+ than in RCC MET−, which tends to suggest that tumors with increased CD44 expression have potential metastatic ability and that perhaps acquisition of CD44 positively is one of the molecular events that confers metastatic potential. This is well in

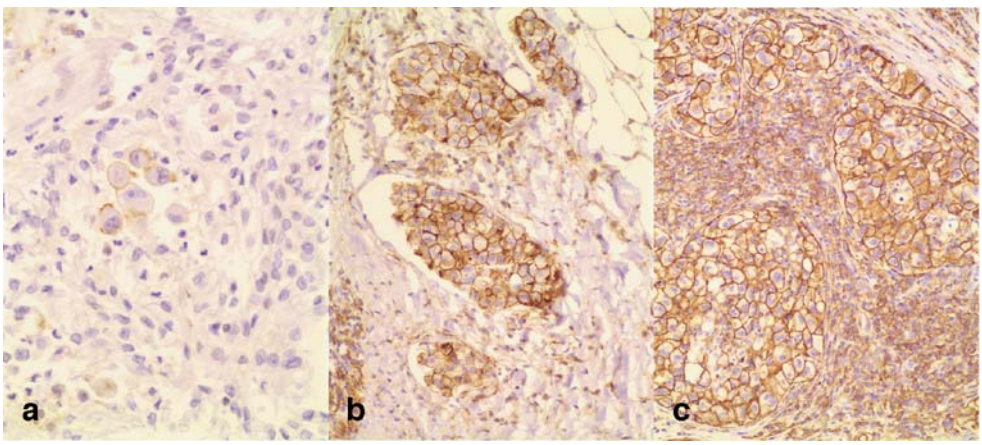


Fig. 3 CD44 immunoreactivity in a case of RCC MET+ and its corresponding metastasis. **a** Focal CD44 immunoreactivity in primary tumor; **b** strong positivity in RCC within vascular-lymphatic spaces; **c** in the metastasis site of the hilar lymph node with score 2 + immunoreactivity. Note that the native lymphoid population is also CD44 positive (positive internal control)

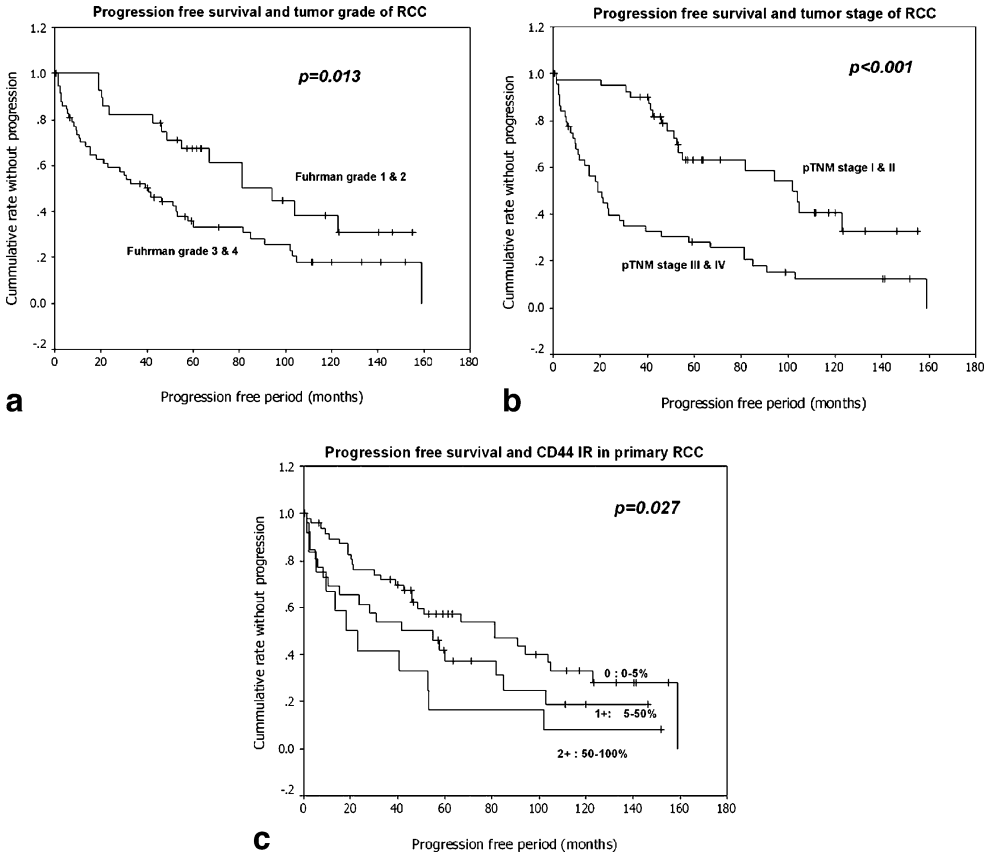


Fig. 4 Kaplan–Meier curves demonstrating the relationship between progression-free survival and **a** tumor grade, **b** tumor stage, and **c** CD44 immunoreactivity in primary RCCs

keeping with the understanding of the pathobiology of metastasis and the understanding of the role of CD44 in tumor biology [4, 12].

To the best of our knowledge, this is the first report to show clearly that a high expression of CD44 in metastatic lesions of RCC is also associated with poor survival. RCC has potential to metastasize early, present with metastasis or present several years after the nephrectomy. Even in patients with metastasis, RCC pursues an enigmatic clinical course. This biologic vagary permits metastasectomy in patients after nephrectomy or even before nephrectomy. Thus, while stage, grade, histologic subtype, and sarcomatoid change are useful for the primary tumor and overall survival, CD44 would be a useful marker to analyze in patients with metastasis. Our findings suggest the potential applicability of determination of CD44 expression in RCC and its metastatic lesions for further accurate prognostication of patients.

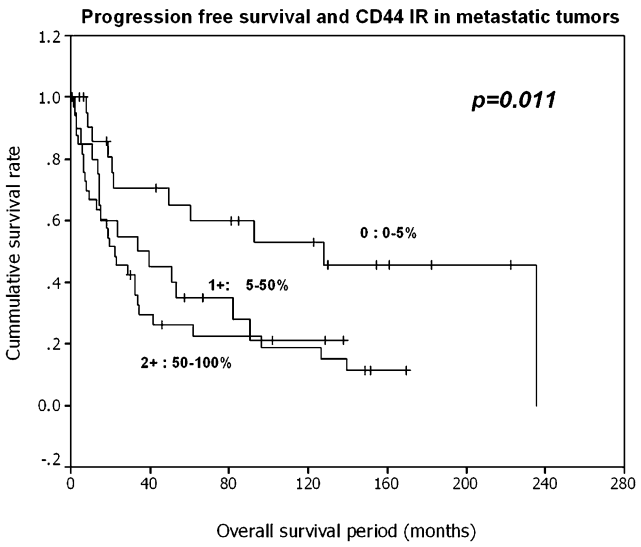


Fig. 5 Kaplan–Meier curves demonstrating the relationship between overall survival and CD44 immunoreactivity in the metastatic RCCs

Table 4 Multivariate analysis for progression-free survival

	Univariate analysis	Multivariate analysis		
	p value	RR	95% CI	*p* value
TNM stage	<0.001	3.29	1.79–6.05	**0.0001**
Nuclear grade	0.0088	1.94	0.74–3.09	0.271
CD44 immunoreactivity	0.0181	2.46	1.16–5.23	**0.03**

Acknowledgement This work was supported by the Second-Phase of BK (Brain Korea) 21 Project in 2006.

References

1. Amin MB, Amin MB, Tamboli P, Javidan J, Stricker H, de-Peralta Venturina M, Deshpande A, Menon M (2002) Prognostic impact of histologic subtyping of adult renal epithelial neoplasms: an experience of 405 cases. Am J Surg Pathol 26:281–291
2. Daniel L, Lechevallier E, Giorgi R, Lindner V, De Fromont M, Vieillefond A, Coulange C, Figarella-Branger D (2001) CD44s and CD44v6 expression in localized T1–T2 conventional renal cell carcinomas. J Pathol 193:345–349
3. de Peralta-Venturina M, Moch H, Amin M, Tamboli P, Hailemariam S, Mihatsch M, Javidan J, Stricker H, Ro JY, Amin MB (2001) Sarcomatoid differentiation in renal cell carcinoma: a study of 101 cases. Am J Surg Pathol 25:275–284
4. Draffin JE, McFarlane S, Hill A, Johnston PG, Waugh DJ (2004) CD44 potentiates the adherence of metastatic prostate and breast cancer cells to bone marrow endothelial cells. Cancer Res 64:5702–5711
5. Fischer C, Georg C, Kraus S, Terpe HJ, Luedecke G, Weidner W (1999) CD44s, E-cadherin and PCNA as markers for progression in renal cell carcinoma. Anticancer Res 19:1513–1517
6. Fuhrman SA, Lasky LC, Limas C (1982) Prognostic significance of morphologic parameters in renal cell carcinoma. Am J Surg Pathol 6:655–663
7. Gilcrease MZ, Guzman-Paz M, Niehans G, Cherwitz D, McCarthy JB, Albores-Saavedra J (1999) Correlation of CD44S expression in renal clear cell carcinomas with subsequent tumor progression or recurrence. Cancer 86:2320–2326
8. Gilcrease MZ, Truong L, Brown RW (1996) Correlation of very late activation integrin and CD44 expression with extrarenal invasion and metastasis of renal cell carcinomas. Hum Pathol 27:1355–1360
9. Greene FL, Compton CC, Fritz AG et al (eds) (2006) American Joint Committee on Cancer. *AJCC Cancer Staging Manual*, 6th edn. Springer, New York, NY, pp 315–322
10. Günthert U, Hofmann M, Rudy W, Reber S, Zöller M, Haussmann I, Matzku S, Wenzel A, Ponta H, Herrlich P (1991) A new variant of glycoprotein CD44 confers metastatic potential to rat carcinoma cells. Cell 65:13–24
11. Harik LR, Pashaei S, Humphrey PA, Tamboli P, Amin MB (2005) Needle core biopsy of the kidney for mass lesions: A clinicopathologic perspective based on 196 cases. Mod Pathol 18:144A (Abstract)
12. Hill A, McFarlane S, Johnston PG, Waugh DJ (2006) The emerging role of CD44 in regulating skeletal micrometastasis. Cancer Lett 237:1–9
13. Li N, Tsuji M, Kanda K, Murakami Y, Kanayama H, Kagawa S (2000) Analysis of CD44 isoform v10 expression and its prognostic value in renal cell carcinoma. Br J Urol Int 85:514–518
14. Liao HX, Lee DM, Levesque MC, Haynes BF (1995) N-terminal and central regions of the human CD44 extracellular domain participate in cell surface hyaluronan binding. J Immunol 155:3938–3945
15. Moch H, Sauter G, Buchholz N, Gasser TC, Bubendorf L, Waldman FM, Mihatsch MJ (1997) Epidermal growth factor receptor expression is associated with rapid tumor cell proliferation in renal cell carcinoma. Hum Pathol 28:1255–1259
16. Paradis V, Ferlicot S, Ghannam E, Zeimoura L, Blanchet P, Eschwége P, Jardin A, Benoît G, Bedossa P (1999) CD44 is an independent prognostic factor in conventional renal cell carcinomas. J Urol 161:1984–1987
17. Rioux-Leclercq N, Epstein JI, Bansard JY, Turlin B, Patard JJ, Manunta A, Chan T, Ramee MP, Lobel B, Moulinoux JP (2001) Clinical significance of cell proliferation, microvessel density, and CD44 adhesion molecule expression in renal cell carcinoma. Hum Pathol 32:1209–1215
18. Ross JS, Sheehan CE, Williams SS, Malfetano JH, Szyfelbein WM, Kallakury BV (2001) Decreased CD44 standard form expression correlates with prognostic variables in ovarian carcinomas. Am J Clin Pathol 116:122–128
19. Ross JS, del Rosario AD, Bui HX, Kallakury BV, Okby NT, Figge J (1996) Expression of the CD44 cell adhesion molecule in urinary bladder transitional cell carcinoma. Mod Pathol 9:854–860
20. Russo P (2004) Surgical intervention in patients with metastatic renal cancer: current status of metastasectomy and cytoreductive nephrectomy. Nat Clin Pract Urol 1:26–30
21. Tannapfel A, Hahn HA, Katalinic A, Fietkau RJ, Kuhn R, Wittekind CW (1997) Incidence of apoptosis, cell proliferation and P53 expression in renal cell carcinomas. Anticancer Res 17:1155–1162
22. Tawfik OW, Kramer B, Shideler B, Danley M, Kimler BF, Holzbeierlein J (2007) Prognostic significance of CD44, platelet-derived growth factor receptor alpha, and cyclooxygenase 2 expression in renal cell carcinoma. Arch Pathol Lab Med 131 (2):261–267
23. Terpe HJ, Störkel S, Zimmer U, Anquez V, Fischer C, Pantel K, Günthert U (1996) Expression of CD44 isoforms in renal cell tumors. Positive correlation to tumor differentiation. Am J Pathol 148:453–463

Virchows Arch (2008) 452:57–63
DOI 10.1007/s00428-007-0540-2

ORIGINAL ARTICLE

Lymphangiogenesis in Crohn's disease: an immunohistochemical study using monoclonal antibody D2-40

F. Pedica · C. Ligorio · P. Tonelli · S. Bartolini · P. Baccarini

Received: 17 September 2007 / Revised: 24 October 2007 / Accepted: 26 October 2007 / Published online: 27 November 2007
© Springer-Verlag 2007

Abstract Crohn's disease (CD) is a chronic inflammatory bowel disorder of unknown etiology. An involvement of the intestinal lymphatic system has been suggested. Recently, monoclonal antibodies have become available to distinguish lymphatic vessels from blood vessels. The aim of the study was to examine the distribution of lymphatic vessels in ileal and colic walls of patients affected by CD and compare it with healthy controls and other inflammatory bowel diseases. Twenty-eight cases of CD, 13 cases of other inflammatory bowel diseases, and 10 normal ileal and colic walls were studied. Immunohistochemical staining was performed using the monoclonal antibody D2-40. Quantification of lymphatic vessels was performed by identifying four fields with high density of lymphatics and then counting the number of lymphatic vessels at high resolution. Lymphatic diameter was also evaluated by using an ocular micrometer. Lymphatic vessels showed the highest density in CD specimens. The median number of lymphatics was significantly higher both in ileal and colic samples of CD than the other inflammatory diseases as well as normal controls. Moreover, in patients with CD, diffuse lymphangiectasia was also observed. The present data suggest that lymphangiogenesis and lymphangiectasia probably play a role in the pathogenesis of CD.

Keywords Inflammatory bowel disease · Crohn's disease · D2-40 · Lymphatic vessels · Immunohistochemistry

F. Pedica (✉) · C. Ligorio · P. Baccarini
Section of Pathology, Bellaria Hospital, University of Bologna,
Via Altura 3,
40139 Bologna, Italy
e-mail: f.pedica@alice.it

P. Tonelli
General Surgery 1, Department of Medicine and General Surgery,
Azienda Ospedaliero-Universitaria Careggi,
Firenze, Italy

S. Bartolini
Unity of Oncology, Bellaria Hospital,
Bologna, Italy

Introduction

Crohn's disease (CD) is a chronic relapsing disorder of the gastrointestinal tract characterized by segmental transmural inflammation. Although several theories have been proposed regarding genetic, immunological, bacterial, and vascular factors, a definite etiology is still unknown [1, 2]. At present, most of the published data point toward a disregulated immune response that occurs in genetically predisposed individuals [14]. In 1976, Kalima et al. [12] created an experimental model of CD in pigs. They produced long-lasting obstruction of the mesenteric lymphatics of the terminal ileum by injecting formalin into regional lymph nodes. They obtained clinical and morphological changes nearly identical to CD, suggesting a possible role of the intestinal lymphatic system in the etiopathogenesis of this disease. Because of the lack of specific lymphatic endothelial markers, studies about lymphatics have been scanty and nonconclusive. Recently, antibodies became available to distinguish lymphatic vessels from blood vessels. D2-40 is a monoclonal antibody that reacts with a 40-kDa O-linked sialoglycoprotein found on lymphatic endothelium, fetal testis, and on the surface of testicular germ cell tumors [16]. Several studies have shown that D2-40 is a highly selective marker of lymphatic endothelium in formalin-fixed, paraffin-embedded tissue specimens [7, 11]. In the only study regarding intestinal lymphatic vessels in patients with chronic idiopathic

inflammatory bowel disease (IBD) to date, Geleff et al. [8] observed an increased number of lymphatics in both CD and ulcerative colitis (UC).

The current study was performed to determine the number and distribution of lymphatic vessels in the ileal and colic walls of patients affected by CD and compare the results with healthy controls as well as other IBDs, such as UC, diverticulitis, ischemic disease, and pseudomembranous colitis.

Materials and methods

A total of 67 samples from 51 patients were selected from the files of the Department of Pathology of Bellaria Hospital in Bologna.

Thirty-four samples of CD were taken from surgical resections of small and large bowel (25 blocks from the small bowel and 9 from the large bowel) of 28 patients (17 men and 11 women) with a mean age of 34.6 years (range 18–61). Elective surgery was performed for severe intestinal stricturing in 19 of 28 patients (67.9%) and for fistulizing disease in nine patients (32.1%). The average duration of disease was 5.1 years with a range between 0 (diagnosis performed at the time of surgery) and 19 years.

For comparison, four cases of surgical resection for UC were studied. The patients were two men and two women with a mean age of 50.5 years (range 32–65). The average duration of the disease was 8 years (range 1–12). Three patients underwent surgery for medically resistant disease. Emergency surgery for toxic megacolon was performed in one case.

Moreover, four cases of ischemic ileitis, three cases of complicated diverticulitis, one case of ischemic colitis, and one case of pseudomembranous colitis were studied.

Ten samples of normal ileum and ten samples of normal colon, obtained from intestinal resections for adenocarcinoma of the large bowel, were chosen as normal controls.

All tissues were fixed in neutral-buffered 10% formalin and were paraffin embedded: 4-μm-thick sections were stained with hematoxylin and eosin, and immunohistochemistry was performed on subsequent sections, using monoclonal antibody D2-40 (1:25, Signet Laboratories, Dedham, MA). Sections were immersed in buffer citrate pH 6.0 for 25 min at 95°C. Endogenous peroxidase activity was blocked by 3% hydrogen peroxide in methanol for 10 min. After a 5-min wash in phosphate-buffered saline, the sections were incubated with anti-human D2-40 monoclonal antibody for 60 min at room temperature. The processing was carried on an automated stainer (Ventana Benchmark, Ventana Medical System, Tucson, AZ).

The quantification of lymphatic vessels was performed, as previously described [8], by identifying four fields with a high density of lymphatics ("hot spots") at low resolution (40×) and then counting the number of lymphatic vessels (D2-40 positive) at middle power (250×). For each section, the range and the median value of lymphatics were calculated, and evaluation for statistical significance was achieved using paired groups in the Mann–Whitney test.

Measurement of lymphatic diameter was obtained employing an ocular micrometer. The lymphatic diameter was calculated by identifying the largest lymphatic vessel in each hot spot field and recording its smallest diameter, as previously described [15]. Values from the four fields were then averaged to give the mean lymphatic diameter. Moreover, the largest value for each group of diseases was reported.

Using the ocular micrometer, we also evaluated the thickness of the bowel wall in the same samples analyzed for density and diameter of microvessels.

Results

Morphological evaluation

D2-40 immunoreactivity was evaluated taking in account only vessels with visible lumens. In doubtful cases, immunohistochemistry was repeated on step sections. Lymphatic count was focused on the submucosal layer, and the results are summarized in Table 1.

Crohn's disease In ileal specimens (25 cases), a prominent transmural inflammatory infiltrate with lymphoid aggregates was present, together with severe edema and dilation of capillary vessels, especially in the lamina propria and submucosa. Scattered non-necrotizing granulomas were found in 20 of 28 cases (71.4%). Aftoid ulcers and a diffuse neural hyperplasia were also seen. The lymphatic capillary vessels were strongly stained with monoclonal antibody D2-40, and their lumens were obviously patent

Table 1 Lymphatic microvessel density in intestinal submucosa expressed as number of D2-40 positive vessels per middle power field (0,5 mm^2, ×250)

Cases	Median value (range)
CD (terminal ileum)	14 (8–32)
CD (colon)	21 (15–29)
UC (colon)	8.25 (6–11)
Ischemic ileitis	4.25 (1–9)
Diverticulitis (colon)	6.5 (4–9)
Ischemic colitis	5.75 (4–7)
Pseudomembranous colitis	2.75 (2–3)
Normal ileum	3.87 (2–7)
Normal colon	5.37 (2–10)

CD: Crohn's disease, *UC*: ulcerative colitis

(Fig. 1a,b). The median number of lymphatics in the submucosa of terminal ileum was 14 per middle power field (range 8–32).

The affected colon (five cases) of CD patients was very thick (7.52 mm with a range of 5.33–11.52) as a consequence of severe inflammation, with some mucosal ulceration and glandular distortion present. There were a large number of D2-40-positive lymphatic capillaries at each level of the bowel wall, except in the lamina propria (Fig. 1c,d). In the colic submucosa, the lymph vessels appeared dilated and tortuous, sometimes containing lymphocytes. The median number of lymphatics was 21 per middle power field (range 15–29). Moreover, a diffuse lymphangiectasia was clearly evident. Cecal samples (four cases) of patients that had undergone ileo-colic resection for CD were also investigated. Despite a grossly normal appearance of the colic segment and a normal appearance of the mucosa histologically, immunohistochemical evaluation with D2-40 revealed a significant increase in the number of lymph vessels. The median number of lymph vessels was 12.87 (range 10–17) compared to the median value of 5.37 for the normal colon, as reported below. In these cases, the bowel thickness was quite normal (average value of 4.58 mm with a range of 4.25–5.04).

Normal controls In normal ileum (ten cases), lymphatics appeared as tiny vessels scattered throughout each layer (Fig. 2a). They were more concentrated between the submucosa and lamina propria, and their median number was 3.87 per middle power field (range 2–7).

In normal large bowel (ten cases), a low number of lymph vessels was noted in every layer. Lymphatics were completely absent in the lamina propria, as has been well described (Fig. 2b). The median number of lymphatics was 5.37 per middle power field (range 2–10).

Ulcerative colitis In UC (four cases), inflammatory changes were mainly confined to the lamina propria and submucosa.

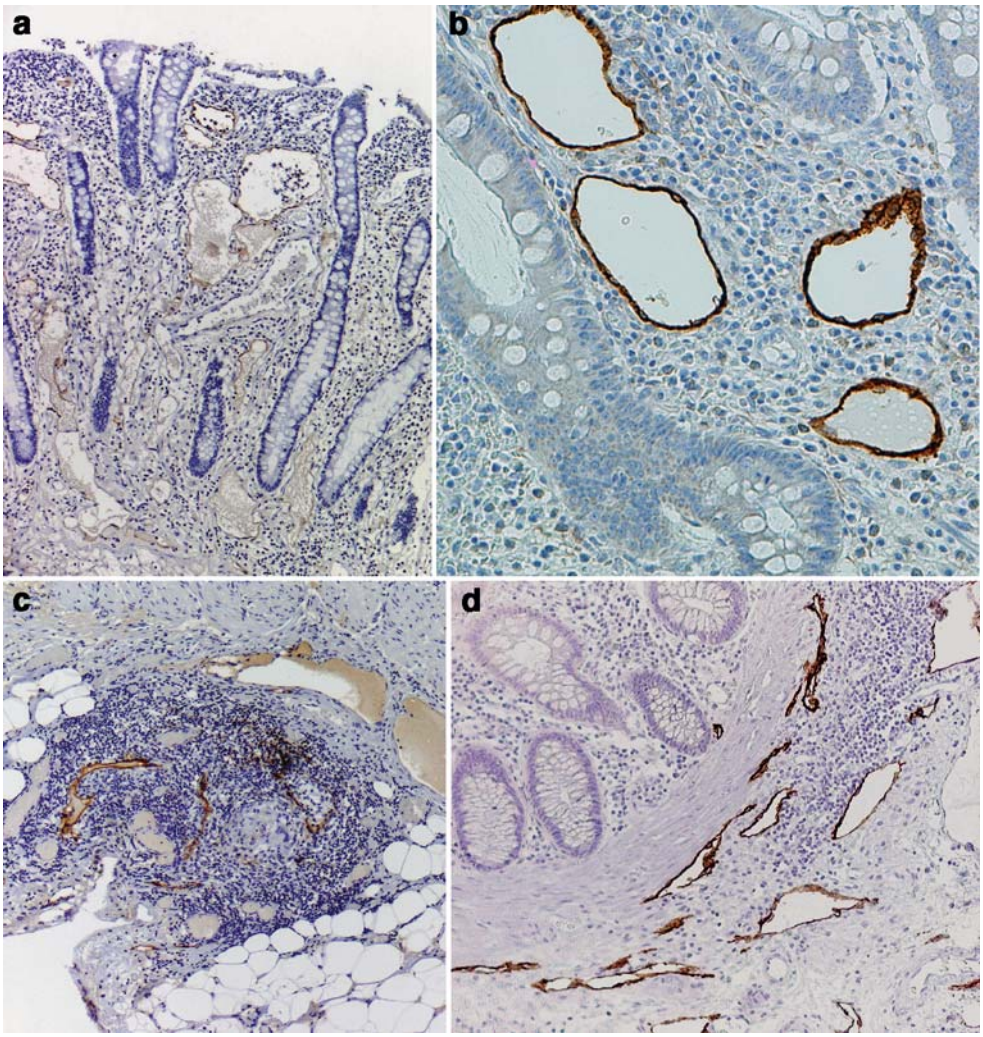


Fig. 1 D2-40 expression in Crohn's disease. Immunohistochemical staining evidenced lymphatic vessels, which appear numerous and dilated, in the lamina propria of the ileum (**a**, ×100)(**b**, ×250), in subserosal layer of the colon, within a granuloma (**c**, ×100), and in the submucosa of the colon (**d**, ×100)

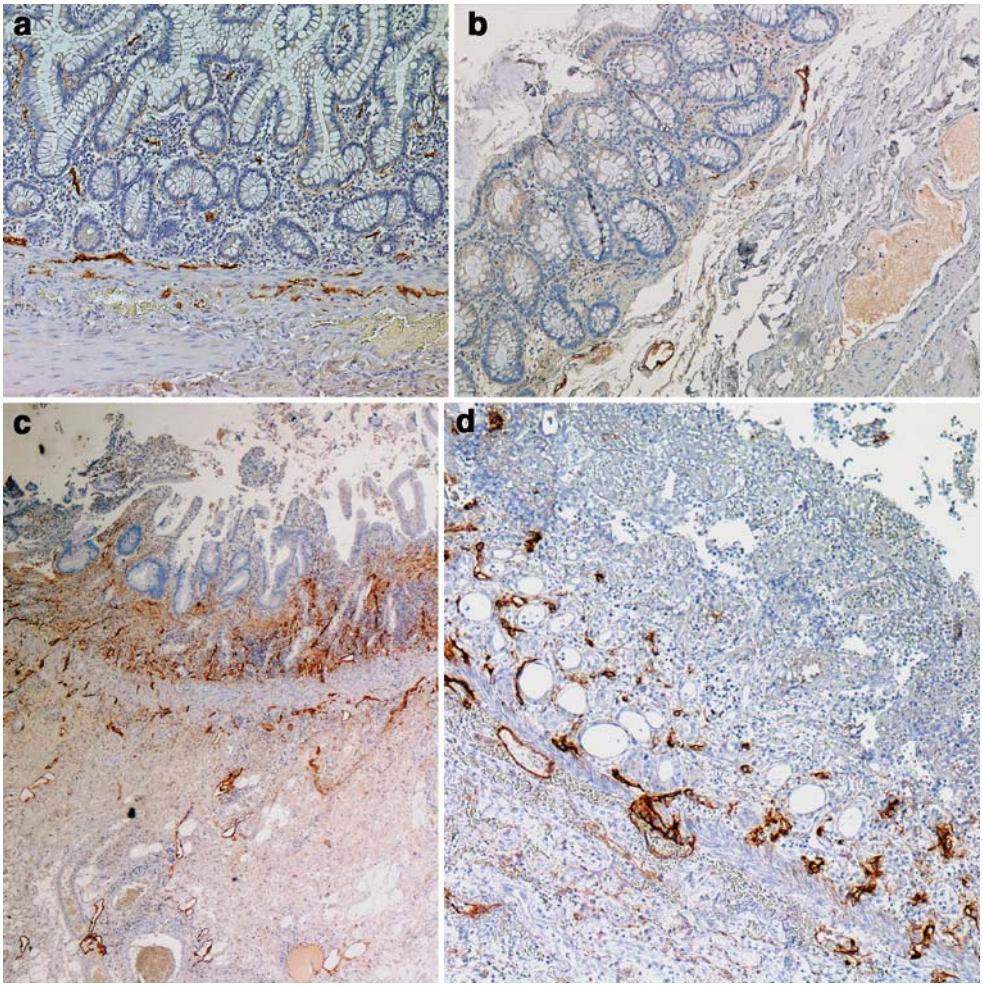


Fig. 2 Immunostaining for D2-40 in normal ileum (**a**, ×100) and normal colon (**b**, ×100): Lymph vessels are scanty and not dilated. Lymphatics density is slightly increased in UC, both in lamina propria and in submucosa (**c**, ×40). Ischemic ileitis shows several lymphatic microvessels (**d**, ×100)

Both acute and chronic changes with prominent crypt abscess formation were seen, and architectural distortion was characteristically present. The case of toxic megacolon showed severe chronic active inflammation of the mucosa and ulceration extending into the deep portions of the mucosa and superficial muscolaris propria. The lamina propria was characterized by small but numerous blood vessels and rare D2-40-positive tiny lymphatics (Fig. 2c). The lymph vessels were moderately increased in number but rarely dilated, with a median number of 8.25 per middle power field (range 6–11).

Ischemic ileitis In ischemic small bowel specimens (four cases), the intestinal wall thickness was reduced, and the mucosa was often lost. Inflammation and hemorrhage were diffusely present, and lymph vessels appeared compressed (Fig. 2d). The median number of lymphatic vessels was 4.25 per middle power field (range 1–9).

Diverticulitis In the four cases of complicated diverticulitis, the colic wall was disorganized, and the mucosa was thrown into prominent accordion-like folds. The mucosal folds were surrounded by acute and chronic inflammatory infiltrates. There were only a few lymphatics that were not dilated. The median number of lymphatics was 6.5 per middle power field (range 4–9).

Ischemic colitis In the case of ischemic colitis, the bowel had lost the mucosal layer in most of the specimen. The number of lymphatics was slightly increased, and they were noticeably dilated. The number of lymphatics was 5.75 per middle power field (range 4–7).

Pseudomembranous colitis In the case of pseudomembranous colitis, the mucosal layer was almost completely destroyed by inflammation and necrosis. There were only a few lymphatics located in the submucosa, and they were not dilated. The number of lymph vessels per middle power field was 2.75 (range 2–3).

Diameter of lymphatics In CD, the diameter of lymphatic vessels in the ileal submucosa was increased almost ten times compared to normal controls (172.8 vs 18 μm). In colon samples of CD, the diameter of lymph vessels was

increased six times that of normal controls (116.6 vs 19.8 μm). In ischemic ileum, the lymphatic vessels were also increased in diameter (50.4 μm), although not to the extent of ileum samples of CD. Likewise, lymph vessels in ischemic colitis were noticeably increased (90 μm), although not to the extent of the colon samples of CD. The lymphatic vessels of other IBDs showed a moderate increase in diameter and did not exceed 54 μm. The values for average and maximum diameters of lymphatic vessels are summarized in Table 2.

Thickness of the bowel wall The mean thickness in CD was 5.85 (range 4–9.72) for ileum and 7.52 (5.33–11.52) for colon. In UC, the average value of bowel wall thickness was 4.95 (range 4.07–6.98) while in normal controls was 3.58 in ileal samples (range 2.3–4.32) and 3.37 in colon samples (range 3.28–3.53).

Statistical evaluation

In the small bowel, paired groups of normal ileum vs CD and CD vs ischemic disease both showed a high statistically significant difference applying the Mann–Whitney test ($p<0.0001$).

In addition, in the large bowel, the test gave a high statistically significant difference in normal vs CD colonic specimens ($p=0.001$), in UC vs CD ($p=0.016$), and in CD vs all the other diseases combined (UC, diverticulitis, ischemic colitis, and pseudomembranous colitis) with $p=0.001$. Finally, the Mann–Whitney test gave a high statistically significant difference comparing the "histologically normal" colon of patients with CD vs normal controls ($p=0.001$; Table 3).

Table 2 Diameters of lymphatics (μm) in intestinal submucosa in descending order

Cases	Mean maximal diameter	Maximum diameter
Ileal CD	172.8	187.2
Colic CD	116.6	154
Ischemic colitis	90	126
Pseudomembranous colitis	54	75.6
UC	51.3	90
Ischemic ileitis	50.4	54
Diverticulitis	39.6	46.8
Normal colon	19.8	21.6
Normal ileum	18	25.2

CD: Crohn's disease, *UC*: ulcerative colitis

Table 3 Statistical evaluation of lymphatic microvessel density in intestinal submucosa, applying the Mann–Whitney test

Comparisons	*p* value
Ileal CD vs normal ileum	$p<0.0001$
Ileal CD vs ischemic ileum	$p<0.0001$
Colic CD vs normal colon	$p=0.001$
"histologically normal" colon of CD vs normal colon	$p=0.001$
Colic CD vs other colic inflammatory disorders[a]	$p=0.001$
Colic CD vs UC	$p=0.016$

CD: Crohn's disease, *UC*: ulcerative colitis
[a] UC, diverticulitis, ischemic colitis, pseudomembranous colitis

Discussion

The lymphatic system plays an essential role in the maintenance of tissue homeostasis, draining interstitial fluid and macromolecules from the extracellular space to the blood circulation and thus preventing edema. The lymphatic system is also a basic component of the immune response, allowing the antigen-presenting cells to activate immune cells in the lymph nodes and contributing in the transport of immune-competent cells in the blood stream [10]. Submucosal edema is a characteristic feature of CD, and it was accurately described since the first report by Crohn et al. in 1932 [5].

Despite several later descriptions regarding the edema and the dilation of lymphatic vessels in the intestinal wall of CD, only a few studies have focused about the role of lymphatics in this disorder [13, 17, 19, 20].

Recently, several markers specific for human lymphatic endothelium have been identified [3, 4, 16]. Zeng et al. [22], using a D2-40 monoclonal antibody, performed immunohistochemistry on endoscopical biopsies of children affected by several diseases of the intestinal tract, including CD. They found "lymphatic abnormality" in four of four cases of CD of the ileum and in 8 of 12 cases of CD of the colon, but they did not provide any quantitative data. Geleff et al. [8], using anti-human podoplanin antibody, observed an increased number of lymphatic vessels in the submucosal layer in both CD and UC.

In the present study, we applied the D2-40 monoclonal antibody to a series of patients affected by CD, UC, and non-IBD intestinal disorders (diverticulitis, ischemic disease, and pseudomembranous colitis). We confirmed a significant increase in the number of lymphatics in CD, both in the small and large bowel, with an increase of almost four times when compared with normal controls.

In addition, we found statistically significant differences in lymphatic microvessel density between CD and the other inflammatory disorders considered. Geleff et al. found a slightly higher density of lymphatics in CD relative to UC

(15.82 vs 11.46) and suggested that the increased number of lymphatics might be caused by the same mechanism in both. In our study, the median number of lymphatics in CD was considerably higher than in UC (21 vs 8.25) and in the other inflammatory disorders (see Table 1). Although the size of the field was slightly larger in the study by Geleff (0.739 mm^2, ×200 vs 0.5 mm^2, ×250), we adjusted for this difference in our calculations to make a proper comparison. The discrepancy between the two studies might be due to methodological differences or variable inflammatory activity in the intestinal samples. The present data are superimposable to those of Fogt et al. [6] who found the number of lymphatic vessels in the submucosa of UC (ten cases) to be between 7.2 and 9 (in a field of 0.5 mm^2, ×250). Furthermore, in our study, for the first time, lymphatic vessels of cecal samples from patients with ileal CD were analyzed. A statistically significant difference between these "histologically normal" samples and normal controls was found, with a median number of lymphatics of 12.87 vs 5.37 (see Table 3). Moreover, measurement of lymph vessel diameter in all cases demonstrated that lymphangiectasia is a constant feature of CD. In fact, the caliber of lymphatic vessels was noticeably higher in CD when compared to normal controls and other inflammatory bowel disorders. We did not find any other report that considers lymphatic diameters in IBD.

Both in ileal and colic samples of CD, the bowel wall was thicker than in UC and normal controls. Nevertheless, we did not observe any significant correlation between thickness of the bowel wall, duration of disease, and number of lymphatic vessels.

It is well known that a lymphangiogenetic process is present in every pathological condition characterized by inflammation. Nevertheless, it is difficult to explain the marked increased density of lymphatic vessels in CD compared to the other inflammatory bowel disorders. It could be hypothesized that these differences may be a consequence of different grades of inflammatory activity, but we did not find any statistically significant correlation between density of lymphatics and severity of inflammation.

In four cases of ileal CD in which the number of lymphatics was higher than 23 per middle power field, the intensity of acute and chronic inflammation was very mild.

In all UC cases, despite the severe inflammation, the density of lymphatic vessels did not show such an increase, and the microvessels were not dilated.

Furthermore, because lymphangiogenesis and lymphangiectasia were present in both affected and histologically normal intestinal samples of CD, it is reasonable to suggest that the alteration of the lymphatic system represents a primary etiopathogenetic factor.

Several hypotheses can be made regarding possible mechanisms for lymphedema in CD, including congenital agenesia, obstruction, or alterations in the course of lymphatic drainage in the mesentery [9, 19, 20]. It is well known that different genes control the development of lymphatics. One of most important is the homebox gene Prox-1, which regulates the expression of podoplanin [10]. Podoplanin-null mice (−/−) die soon after birth for lung failure and present with an increased number of severely dilated ileal submucosal lymphatic vessels and cutaneous lymphedema [18]. In podoplanin-deficient mice (+/−), slightly enlarged submucosal lymphatic vessels in the small intestine are found, without any other macroscopical phenotypic abnormality. The authors concluded that podoplanin is required to control different aspects of normal lymphatic vasculature formation and its deficiency results in impaired patterning of lymphatic capillary networks [18]. Other mechanisms such as defective contractile activity or an altered permeability of lymphatic vessels could be implicated in CD lymphatic stasis.

Recently, Wu et al. [21] created a model of guinea pig ileitis by inducing ileal inflammation with intraluminal injection of 2,4,6-trinitrobenzenesulfonic acid. They observed that lymphatic diameters were increased and spontaneous constriction of lymphatics was dramatically reduced, resulting in engorgement of the lymphatics and marked submucosa edema.

We believe that our results together with those of previous reports indicate that lymphatic vessels may play an important etiopathogenetic role in CD and deserve to be further studied.

Acknowledgments The authors wish to thank Prof. M.P. Foschini and Prof. V. Eusebi for critical reading of the manuscript and valuable discussion. A special thanks to Dr. Jeff Brown for editing the manuscript.

References

1. Abraham C, Cho JH (2006) Functional consequences of NOD2 (CARD15) mutations. Inflamm Bowel Dis 12:641–650
2. American Gastroenterological Association (1997) Crohn's disease: yesterday, today and tomorrow. Gastroenterology 112:1028–1030
3. Banerji S, Ni J, Wang SX, Clasper S, Su J, Tammi R, Jones M, Jackson DG (1999) LYVE-1, a new homologue of the CD44 glycoprotein, is a lymph-specific receptor for hyaluronan. J Cell Biol 144:789–801
4. Breiteneder-Geleff S, Soleiman A, Horvat R, Amann G, Kowalski H, Kerjaschki D (1999) Podoplanin—a specific marker for lymphatic endothelium expressed in angiosarcoma. Verh Ges Pathol 83:270–275
5. Crohn BB, Ginzburg L, Oppenheimer GD (1932) Regional ileitis: a pathologic and clinical entity. J Am Med Assoc 99:1323–1329
6. Fogt F, Pascha TL, Zhang PJ, Gausas RE, Rahemtulla A, Zimmerman RL (2004) Proliferation of D2-40-expressing intestinal lymphatic vessels in lamina propria in inflammatory bowel disease. Int J Mol Med 13:211–214

7. Fukunaga M (2005) Expression of D2-40 in lymphatic endothelium of normal tissues and vascular tumours. Histopathology 46:396–402
8. Geleff S, Schoppmann SF, Oberhuber G (2003) Increase in podoplanin-expressing intestinal lymphatic vessels in inflammatory bowel disease. Virchows Arch 442:231–237
9. Heatley RV, Bolton PM, Hughes LE, Owen EW (1980) Mesenteric lymphatic obstruction in Crohn's disease. Digestion 20:307–313
10. Hong YK, Shin JW, Detmar M (2004) Development of the lymphatic vascular system: a mystery unravels. Dev Dyn 231:462–473
11. Kahn HJ, Bailey D, Marks A (2002) Monoclonal antibody, D2-40, a new marker of lymphatic endothelium, reacts with Kaposi's sarcoma and a subset of angiosarcomas. Mod Pathol 15:434–440
12. Kalima TV, Saloniemi H, Rahko T (1976) Experimental regional enteritis in pigs. Scand J Gastroenterol 11:353–362
13. Kovi J, Duong HD, Hoang CT (1981) Ultrastructure of intestinal lymphatics in Crohn's disease. Am J Clin Pathol 76:385–394
14. Kucharzik T, Maaser C, Lugering A, Kagnoff M, Mayer L, Targan S, Domschke W (2006) Recent understanding of IBD pathogenesis: implications for future therapies. Inflamm Bowel Dis 12:1068–1083
15. Liang P, Hong JW, Ubukata H, Liu HR, Watanabe Y, Katano M, Motohashi G, Kasuga T, Nakada I, Tabuchi T (2006) Increased density and diameter of lymphatic microvessels correlate with lymph node metastasis in early stage invasive colorectal carcinoma. Virchows Arch 448:570–575
16. Marks A, Sutherland DR, Bailey D, Iglesias I, Law J, Lei M, Yeger H, Banerjee D, Baumal R (1999) Characterization and distribution of an oncofetal antigen (M2A antigen) expressed on testicular germ cell tumours. Br J Cancer 80:569–578
17. Mooney EE, Walker J, Hourihane DO'B (1995) Relation of granulomas to lymphatic vessels in Crohn's disease. J Clin Pathol 48:335–338
18. Schacht V, Ramirez MI, Hong YK, Hirakawa S, Feng D, Harvey N, Williams M, Dvorak AM, Dvorak HF, Oliver G, Detmar M (2003) T1α-podoplanin deficiency disrupts normal lymphatic vasculature formation and causes lymphedema. EMBO J 22:3546–3556
19. Tonelli P (2000) New developments in Crohn's disease: solution of doctrinal mysteries and reinstatement as a surgically treatable disease. The process is not a form of enteritis but lymphedema contaminated by intestinal contents. Chir Ital 52:109–121
20. Wu TF, MacNaughton WK, von der Weid P-Y (2005) Lymphatic vessel contractile activity and intestinal inflammation. Mem Inst Oswaldo Cruz 100(Suppl 1):107–110
21. Wu TF, Carati CJ, MacNaughton WK, von der Weid P-Y (2006) Contractile activity of lymphatic vessels is altered in the TNBS model of guinea pig ileitis. Am J Physiol Gastrointest Liver Physiol 291:G566–G574
22. Zeng Y, Wanf F, Williams ED, Chow CW (2005) Lymphatics in the alimentary tract of children in health and disease: study on mucosal biopsies using the monoclonal antibody D2-40. Pediat Dev Pathol 8:541–549

Virchows Arch (2008) 452:65–74
DOI 10.1007/s00428-007-0535-z

ORIGINAL ARTICLE

Prognostic significance of the Fas-receptor/Fas-ligand system in cervical squamous cell carcinoma

Enrique Lerma · Marisa Romero · Alberto Gallardo · Cristina Pons · Josefina Muñoz · Josefina Fuentes · Belen Lloveras · Lluis Catasus · Jaime Prat

Received: 14 August 2007 / Revised: 17 October 2007 / Accepted: 22 October 2007 / Published online: 14 November 2007
© Springer-Verlag 2007

Abstract We studied whether Fas-receptor (Fas-R; CD95) expression, single-nucleotide polymorphisms (SNPs) in the Fas promoter region, and/or Fas-ligand (Fas-L) production could determine individual susceptibility to cervical cancer progression. The clinicopathologic features of 38 patients with cervical squamous carcinomas (22 stage I, 8 stage II, and 8 stage III+) were reviewed and related with: (a) Fas-R expression by immunohistochemistry; (b) Fas-R SNPs at -670 and -1377 locations by restriction fragment length polymorphism and DNA sequencing; and (c) Fas-L expression by immunohistochemistry. Overall and disease-free survival curves showed significant differences in relation to stage ($p<0.001$). Fas-R was identified in 20 of 38 (52.6%) tumors without statistical differences in survival, stage, or Fas-L overproduction. Fas-R GG genotype was more common than expected in advanced tumors ($p=0.065$). The Fas-R-1377A allele and AA genotype were unrelated with survival, stage, or Fas-R expression. Fas-L overproduction was detected in 20 of 38 (52.6%) tumors; it was more frequent in advanced-stage tumors and was inversely related to survival ($p=0.03$) and decrease in host inflammatory response ($p=0.01$). Fas-R expression by tumor cells seems unrelated to stage or lymphoid infiltrate. Tumor production of Fas-L may represent an attempt to destroy the host's lymphocytic reaction.

E. Lerma (✉) · M. Romero · A. Gallardo · C. Pons · J. Muñoz · J. Fuentes · B. Lloveras · L. Catasus · J. Prat
Department of Pathology, Hospital de la Santa Creu i Sant Pau, Autonomous University of Barcelona,
Avda. Sant Antoni Ma Claret 167,
08025 Barcelona, Spain
e-mail: elerma@santpau.es

B. Lloveras
Department of Pathology, Bellvitge Hospital,
Barcelona, Spain

Keywords Cervix · Squamous cell carcinoma · Fas (CD95-APO-1) · Fas ligand · Single-nucleotide polymorphisms · Immunohistochemistry

Introduction

Cervical carcinoma is the second most prevalent cancer affecting women worldwide, and 500,000 new cases are reported per year. The incidence is higher in Asia, South America, and Africa [30, 45]. Human papilloma virus (HPV) infection is the most prevalent etiologic agent [16, 25, 27].

Most viral infections of the cervical mucosa are controlled by the host's immune response, either mediated by antibodies against viral proteins [mainly class immunoglobulin (Ig)G and mucosal IgA] or by the cellular inflammatory response [natural-killer (NK) cells and CD4 and CD8 T lymphocytes]. By these mechanisms, the defense effect of Ig together with the cellular inflammatory response induces apoptosis of infected keratinocytes in the majority of cases [28]. When the immune system is unable to destroy infected cells, the HPV genome may be integrated into the host's cellular DNA, and a preneoplastic lesion appears. This process is mediated by disruption of the viral open reading frame (ORF), resulting in loss of E2 function, a regulatory protein for E6 and E7 oncogenes [14, 23]. Then, E6 protein binds to p53 protein and targets it for accelerated ubiquitin-mediated degradation, allowing cell proliferation without p53 control [23]; and E7 contributes to cellular transformation by interfering with the $p16^{INK4a}$/CDK4/cyclinD1/pRb cell cycle regulatory pathway [14].

The Fas (APO-1/CD95) system regulates diverse physiologic and pathologic mechanisms for apoptosis, and interaction between Fas ligand and a transmembrane cell-surface Fas receptor induces cell death [13, 18, 40]. Fas is a

death receptor from the tumor necrosis factor (TNF) superfamily. The Fas ligand induces Fas trimerization, recruitment of Fas-associated death domain and procaspase 8, and activation of apoptosis [31]. This mechanism could help to destroy HPV-infected keratinocytes. Reduced Fas-mediated apoptosis has been described in cervical carcinogenesis, and this may facilitate cellular proliferation [6]. Decreased Fas-R (CD95) expression has recently been described in cervical carcinomas by immunohistochemistry (IHC) [34] and polymerase chain reaction (PCR) [6].

Fas gene mutations and single-nucleotide polymorphisms (SNP) in its promoter region have also been described. Mutations occur in immune diseases [10, 33] and only occasionally in tumors [4, 5, 21, 37]; however, to our knowledge, they have never been reported in cervical carcinomas. Promoter-region SNPs are known to occur in various carcinomas such as esophageal and cervical carcinoma [7, 9, 20, 41, 43]. Lai et al. [20] recently reported that the frequency of the Fas 670-A allele increased from high-grade squamous intraepithelial lesions to invasive carcinomas, being approximately twice as frequent in patients with invasive carcinoma than the general population; however, this finding has not been confirmed by other investigators [7, 9, 43].

Overproduction of Fas-L has also been described in several gynecological cancers including squamous cell carcinomas (SCC) of the cervix [6] and vulva [43]. The paracrine overproduction of Fas-L could facilitate tumor progression by inducing apoptosis of the immune cells which usually express Fas in their membrane, such as CD8 and natural-killer cells.

In this study, we tried to determine whether the IHC expression of Fas receptor and the tumor production of Fas-L correlate with invasiveness, immune response, and prognosis in squamous cell carcinomas of the cervix, particularly in early-stage tumors. We also investigated the relationship between the IHC expression of the Fas receptor and gene promoter SNP at Fas-670 and -1377.

Materials and methods

Thirty-eight patients with invasive squamous cell carcinomas were identified from the surgical pathology files of the of Department Pathology of the Hospital de la Santa Creu i Sant Pau (HSCSP), Autonomous University of Barcelona, Spain. Standard treatment consisted in radiotherapy followed by radical hysterectomy and bilateral salpingo-ooforectomy, and pelvic and/or para-aortic lymphadenectomy in most cases. Occasional modifications of this procedure are specified in "Results." The study design was approved by the HSCSP Ethic Committee. The age of the patients varied from 29 to 79 years. Clinical charts, pathology reports, and the hematoxylin- and eosin-stained microscopic slides were reviewed to re-assess the conventional clinicopathological features (clinical symptoms, parity, pathology stage, histologic type, grade, tumor size, depth of invasion, status of margins, inflammatory infiltrate, vascular space invasion, survival, and HIV status). The inflammatory infiltrate was subclassified based on types of cells (lymphoplasmocytic vs mixed, when a moderate number of leucocytes were also present) and density (nonflorid vs florid, when a marked inflammatory infiltrate was located in the peritumoral stroma and focally in the neoplasia).

One paraffin block was selected for each case, and several tissue sections were made for special studies. Molecular studies consisted in HPV identification by PCR and assessment of Fas promoter polymorphism in -670 and -1377 positions. Immunohistochemical staining for Fas-R (CD95), Fas-L, and various lymphocyte populations were also done.

HPV-DNA analysis

HPV-DNA analysis was done in all cases. The method consisted in amplification of 450-bp long fragment of the L1 region from the ORF. This region conserves its sequence and presents a highly characteristic restriction pattern for each type of HPV. Briefly, DNA was obtained from a tissue section by xylene/ethanol deparaffinization and subsequent digestion with proteinase K in a PCR buffer solution. After proteinase inactivation by heating, the sample was subjected to DNA amplification and restriction with Rsa I. Positive controls were cervical biopsies with known HPV infection. Negative controls were also used.

Immunohistochemistry

Immunohistochemical staining was performed with the Dako Autostainer and CSA II amplification kit in 5-μm tissue sections in pretreated slides. Origin and dilution of primary antibodies are shown in Table 1. Specificity was controlled for each antibody-staining tumor sections incubated without primary antibodies (internal negative control).

Fas-R staining was considered positive when more than 10% of cells showed a well-defined membrane pattern.

Table 1 Primary antibodies and working dilution

Primary antibodies	Working dilution
Fas-L (Clone 5D1, Novocastra)	1:50
Fas-CD95 (Clone DX2–1, DAKO)	1:50
CD4 (Clone 1F6, Novocastra)	1:50
CD8 (Clone C-8/144B, DAKO)	1:50
CD20 (Clone L-26, DAKO)	1:50
CD56 (Clone 1B6, Novocastra)	1:50

Fas-L was considered positive when a cytoplasmic staining appeared in more than 10% of tumor cells. With this 10% threshold, randomly selected, we only would exclude cases with very few positive cells.

Inflammatory cell subpopulations were evaluated in the most cellular areas with CD20 to identify B lymphocytes, CD4 for helper T lymphocytes, CD8 for cytotoxic T lymphocytes, and CD56-NK for natural-killer cells, even though it is known that a subpopulation of activated T lymphocytes could also stain for CD56. A modification of a previously described method was used to count lymphocyte subpopulations [44]. Briefly, a square grid of 1×1 cm was placed in the eyepiece of the microscope. This grid has a network of 10×10 lines, making 100 intersections and covering a tumor area of 0.0625 mm^2 with a ×40 objective. Ten fields in the representative areas of tumor/stroma intersection were measured for each immunohistochemical stain, and the mean value was then calculated and transformed into number of cells per square millimeter multiplying by 16 ($0.0625 \times 16 = 1$ mm^2).

A section of tonsil was used as positive external control. Endocervical, basal cells from the exocervix (Fig. 1), and neoplasm-related lymphocytic infiltrate served as internal controls.

Assessment of Fas-R promoter polymorphisms

Genomic DNA was extracted by proteinase K digestion and QUIAamp DNA Mini Kit (Quiagen GmbH, Hilden, Germany), following the manufacturer's instructions, from ten consecutive 5 μm thick tissue sections. PCR-restriction fragment length polymorphism (RFLP) protocols were carried on to determine SNP at -670 and -1377 locations in the Fas-R promoter.

SNP at -670 was amplified by polymerase chain reaction using oligonucleotide primers (Fas F: 5′-CTACCTAAGAGC TATCTACCGTTC-3′; Fas R: 5′-GGCTGTCCA TGTTGTGGCTGC-3′). PCR was carried out in a GeneAmp PCR System 9700 thermocycler (Applied Biosystems, Foster City, CA, USA) for 35 cycles of amplification (95°C for 30 s, 56°C for 45 s, 72°C for 1 min; first cycle, 95°C for 12 min; last cycle, 72°C for 15 min). The PCR product was checked in 1.8% agarose gels containing ethidium bromide. The PCR product of 331 bp band-size contains two MvaI (CCAGG) restriction sites: the first, located at -857, is a nonpolymorphic target, and the second, at -670, is the polymorphic target. PCR products were digested at 37° for 4 h 30 min with *MvaI* restriction enzyme (New England Biolabs, Beverly, MA, USA). Restriction products were also checked in agarose gels. When the polymorphic site was conserved (G genotype), three bands of 100, 188, and 44 bp were generated; if it was destroyed (A genotype), two bands of 100 and 232 bp (188+44 bp) were generated.

For comparison and as a reference in various general populations for different races, the estimated frequencies for genotypes GG, GA, and AA were 26, 51, and 23%, respectively [7, 9, 12].

Primers used for Fas-R-1377 polymorphism determination were FasF: 5′-TGTGTGCACAAGGCTGGCGC-3′ and FasR: 5′-TGCATCTGTCACTGCACTTACCACCA-3′ and gave a 122 bp-sized band. To be able to use the BstUI restriction enzyme (New England Biolabs), we created an artificial BstUI restriction site by changing CAC to CGC in Fas F-3′end. Thus, it was possible to distinguish G-genotype (conserved restriction site) to A-genotype (destroyed restriction site). The size of the fragments was determined in a 9% acrilamide gel.

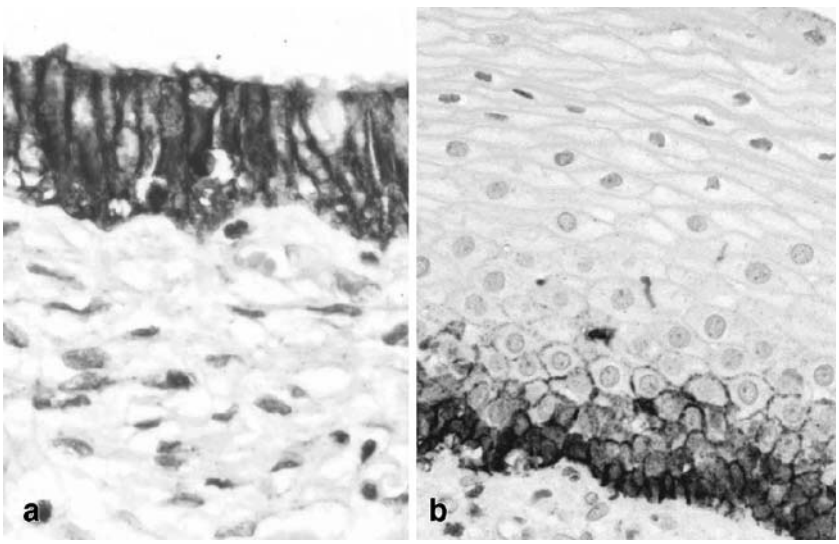


Fig. 1 Immunohistochemical Fas (CD95) expression in normal endocervical (**a**), and squamous exocervical cells (**b**)

For comparison and as a reference in a general population, the estimated frequencies of the genotypes GG, GA, and AA were 76, 22, and 2%, respectively [12].

Statistical analysis

The categorical variables were analyzed by means of contingency tables and Fisher's exact test to assess significant differences between pairs of features (percentages). Chi-square test was used for tables with more than two levels and Yates corrections were applied if necessary. The quantitative variables were analyzed by means of mean and standard deviation, and the analysis of variance was used for comparisons. Survival was evaluated according to the Kaplan–Meier method and log-rank test for comparison. Additionally, these data were submitted to the Cox regression analysis as a multivariate approach.

The level of significance was set at 0.05, and all the analyses were performed with the Statistical Package for the Social Sciences (v 11.5). The p value will be cited only when the correlations were statistically significant or showed a trend, at least.

Results

Clinicopathologic features

The mean age of the patients at diagnosis was 45 years (range: 29–79). Surgical treatment consisted of conization in two cases (small low-stage tumors), hysterectomy and bilateral salpingo-ooforectomy (HBSO) in five, and HBSO and pelvic/iliac lymph node dissection in 31 cases. Exceptions for the standard treatment were the addition of chemotherapy in four advanced-stage patients, another advanced case was treated only with palliative chemotherapy, and two Stage IA1 women, initially diagnosed of cervical intra-epithelial neoplasia (CIN) III, who wanted to preserve the fertility and had a wide conization with negative margins.

Clinicopathologic features are summarized in Table 2.

Metrorrhagia was the initial symptom in 27 patients; 5 were HIV (+). Mean tumor diameter was 2.9 (range 0.5–8) cm, and depth of invasion 1.5 (range 0.3–5) cm. All tumors were squamous cell carcinomas with a histologic grade of I in 11 patients, II in 18, and III in 9. Reactive mononuclear infiltrate was mainly composed of lymphocytes and plasma cells in 21 cases (13 stage I, 4 stage II, and 4 in stage III), whereas the remaining 15 cases showed a mixed infiltrate with a significant number of leukocytes (estimated from 10 to 30%), unrelated with necrosis or ulceration. The lymphocytic reaction was florid in 14 tumors (12 stage I and 1 each of stages II and III; Table 2). Vascular space invasion was found in 13 tumors, and lymph node metastases in 6. Surgical-pathologic stage was IA in 2 patients, IB in 20, IIA in 5, IIB in 3, and IIIB or higher in the remaining 8 patients. Twenty-four patients are alive without evidence of disease, four alive with residual disease (follow-up of 6, 12, 24, and 30 months), seven died of tumor, and three died of other causes. The mean follow-up was 56 months (range 11–222). As expected, overall and disease-free survival curves showed significant differences according to stage ($p<0.001$).

Table 2 Cervical squamous cell carcinomas

	TOTAL
Number of cases	38
Mean age	45 (range, 29–79)
Metrorragia	27 (71%)
HIV(+)	5 (13.2%)
Parity	13 (34.2%)
Tumor diameter (cm)	2.9 (range, 0.5–8)
Depth invasion (cm)	1.5 (range 0.3–5)
Histological grade 1	11 (28.9%)
Histological grade 2	18 (47.4%)
Histological grade 3	9 (23.7%)
Lympho-plasmacytic infiltrate	21 (55.3%)
Florid lymphoid infiltrate	14 (36.8%)
Vascular invasion	13 (34.2%)
Lymph Node + (over 31 cases)	6 (19.4%)
IA	2 (5.3%)
IB	20 (53.6%)
II	8 (21%)
III-IV	8 (21%)
No evidence of disease	24 (mean 73 months)
Alive with disease	4 (mean 18 months)
Death of tumor	7 (mean 12 months)
Death of other causes	3 (mean 40 months)

Clinicopathologic data

HPV-DNA Analysis

HPV-16 DNA was detected in all cases.

Immunohistochemical results

Fas-R (CD95) expression

Cell membrane immunohistochemical expression of Fas-R was identified in 20 of 38 (52.6%) tumors without statistical differences between stages. Fifty percent stage I tumors, 37.5% stage II, and 75% stage III showed the immunohistochemical expression (Fig. 2). Percentages for all three groups are shown in Table 3.

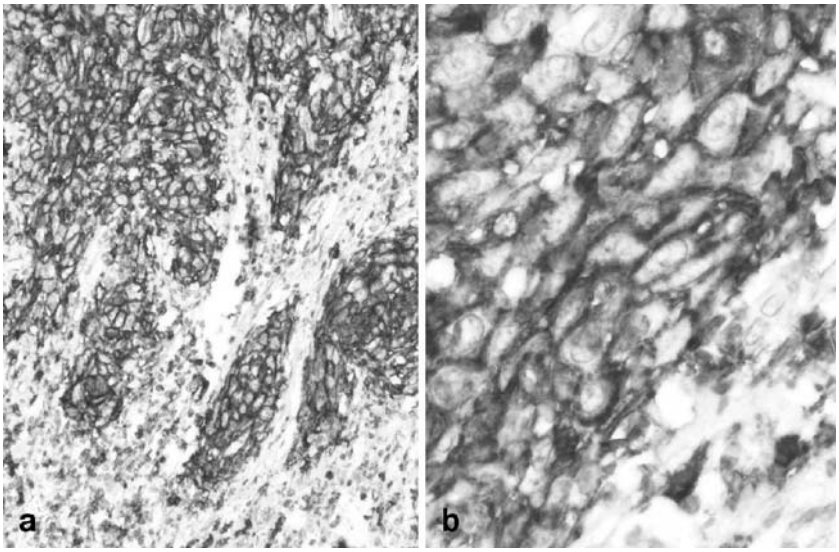


Fig. 2 Immunohistochemical Fas expression in a squamous cell carcinoma; note the membrane and cytoplasmic staining (magnification, **a** ×20; **b** ×40)

Fas-L expression

Overall, cytoplasmic Fas-L immunohistochemical expression was detected in 20 of 38 (52.6%) tumors (Table 3). It was inversely related with survival (p=0.03; Fig. 3) and showed only a trend in relation with stage (p=0.07). Cytoplasmic Fas-L expression (Fig. 4) was detected in eight stage I tumors (36.4%), only one of which was associated with a dense inflammatory infiltrate; four had a nondense mononuclear infiltrate, and three had a mixed inflammatory reaction. In higher stage tumors, Fas-L expression was detected in 4 of 8 (50%) stage II carcinomas and 6 of 8 (75%) stage III; a dense lymphocytic infiltrate was found only in one of these patients who had a stage III carcinoma. Thus, host's inflammatory response decreased as Fas-L expression increased (p=0.01)

Lymphocyte subpopulations

We analyzed the frequency of cells stained with CD20, CD4, CD8, and CD56 to determine lymphocyte subpopulations within the host's inflammatory reaction. The mean number of positive cells both in the neoplastic epithelium and the stroma were evaluated separately (Table 4).

Although some isolated cells were located in the epithelium, most B lymphocytes (CD 20) were located in stroma, and they often exhibited a nodular pattern. B stromal lymphocytes were more frequent in stage I tumors (mean number of 98 lymphocytes per square millimeter) than in stage II (72) and III (49). Helper T lymphocytes (CD4) were only rarely found in the epithelium, and most were seen in the stroma, irrespective of HIV status. The mean number of CD4 cells per square millimeter in the epithelium/stroma was 17 of 508 in stage I tumors, 13 of 426 in stage II, and 27 of 272 in stage III. Cytotoxic lymphocytes (CD8) constituted the highest component of the inflammatory infiltrate, and although more abundant in the stroma, they were also found within the tumor in the following proportions: 80 of 896 in stage I, 288 of 688 in stage II, and 432 of 752 in stage III. Thus, the number of CD8 lymphocytes in the epithelium increased in relation with the stage. NK cells (CD56) were few in epithelium and scanty in stroma; a mean of 32 of 80 cells were detected in stage I tumors, 32 of 192 in stage II, and 48 of 144 in stage III. Although we found differences between stages and type of lymphocytes, they were not statistically significant.

Fas-R immunostaining in tumor cells correlated neither with the Fas-L expression, density of lymphocytic reaction,

Table 3 Cervical squamous cell carcinomas

Stage	I (22 cases)	II (8 cases)	III (8 cases)	Total (38 cases)
Fas-R (CD95)	11 (50%)	3 (37.5%)	6 (75%)	20 (52.6%)
Fas-Ligand	8 (36.4%)	4 (50%)	6 (75%)	20 (52.6%)
Lympho-plasmacytic I	13 (59.1%)	4 (50%)	4 (50%)	21 (55.2%)
Florid inflammatory infiltrate	12 (54.5%)	1 (12.5%)	1 (12.5%)	14 (36.8%)

Correlation by stages of type and density of lymphoid infiltrates and inmunohistochemical expression of Fas-R and Fas-L

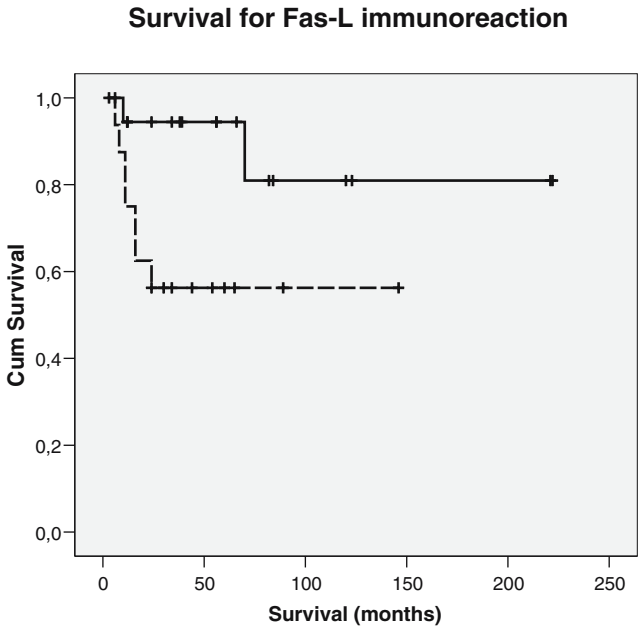


Fig. 3 Kaplan–Meier's survival distribution for Fas-L negative (*upper line*) and Fas-L positive tumors (*lower line*). The differences between the two groups are statistically significant ($p=0.02$)

nor the percentage of lymphocyte subpopulations. Some correlation was encountered between Fas-L production and the density and subtypes of lymphocytes but without statistical significance.

Fas SNP studies

SNPs were assessed for Fas-R-670 in 34 cases and cases for Fas-R-1377 in 37. The results and their relationship with Fas-R immunohistochemical expression are summarized below.

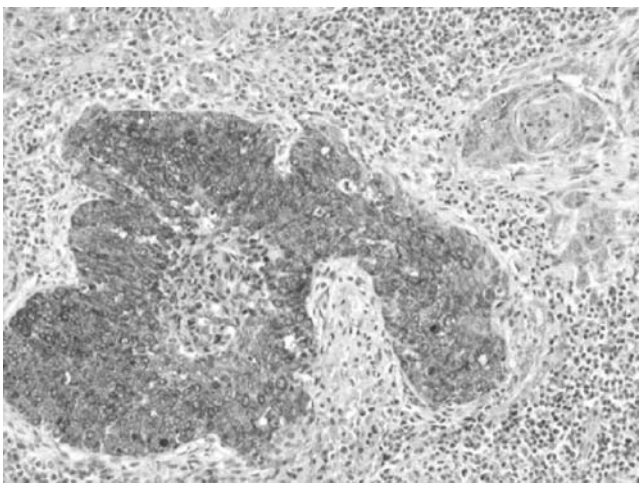


Fig. 4 Immunohistochemical Fas-L cytoplasmic expression in a cervical squamous cell carcinoma (magnification, ×40)

Table 4 Cervical squamous cell carcinomas

	I (22 cases)	II (8 cases)	III (8 cases)
CD 20	16/98	12/72	17/49
CD 4	17/508	13/426	27/272
CD 8	80/896	288/688	432/752
CD 56	32/80	32/192	48/144

Correlation between type of lymphocytes and stage
Expressed by the mean number of cells by square millimeter in tumoral epithelium/stroma

Fas-R-670

Frequencies of A and G alleles were 0.47 and 0.53, respectively (Fig. 5). A mild increase of G allele was detected in stage I carcinomas versus more advanced tumors. Nevertheless, there were no significant differences between stages for the overall frequencies of the Fas-R-670 genotypes GG, GA, and AA, which in various ethnic populations [23, 24, 28] have been estimated in 26, 51, and 23%, respectively (Table 5).

The frequency of the Fas-R-670 GG genotype was higher in stage III tumors (50%) than in stages I (22.2%) and II (37.5%; $p=0.16$), whereas the GA genotype was less common in patients with advanced tumors. Although these differences had no statistical significance, a trend between GG genotype and adverse prognosis was observed ($p=0.065$). Three of four HIV (+) patients had the GA genotype.

Comparison between SNP-670 genotypes and membrane expression of Fas-R was analyzed in 34 cases, including the 20 positive cases (58.8%). Percentages of all groups of patients are shown in Table 6. Fas-R expression was positive in 45.5% of the patients with the GG genotype, 55.5% of those with the AA genotype, and 71.4% with the GA genotype. Fas-R genotypes did not correlate with stage or Fas-R expression.

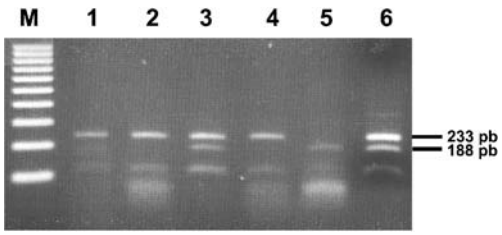


Fig. 5 SNP at -670 in Fas promoter. Two polymorphic bands, of 188 or 233 bp, were produced depending on the presence of G or A allele at -670 position. *Lane M* Marker (100 bp ladder). *Lanes 1–6* correspond to tumor samples with genotypes GA (*lanes 3*, *6*), AA (*lanes 1*, *2*, *4*) and GG (*lane 5*), respectively

Table 5 Cervical squamous cell carcinomas

	Stage I	Stage II	Stage III	Mean
A allele	0.54	0.41	0.44	0.47
G allele	0.46	0.59	0.56	0.53
GG genotype	4/18 (22.2%)	3/8 (37.5%)	4/8 (50%)	11/34 (32.4%)
GA genotype	9/18 (50%)	4/8 (50%)	1/8 (12%)	14/34 (41.2%)
AA genotype	5/18 (27.7%)	1/8 (12.5%)	3/8 (38%)	9/34(26.5%)

Frequency of alleles and genotypes of Fas SNPs -670

Fas-R-1377

The mean allele frequencies were 0.08 for Fas-R-1377A and 0.92 for Fas-R-1377G. The A allele appeared exclusively in DNA of low-stage patients (0.16; p=0.033), whereas its frequency in general population is 0.13 [21]. Frequencies of Fas-R-1377 GG, GA, and AA genotypes were 86.5% (32 cases), 10.8% (4 cases), and 2.7% (1 case), respectively. For comparison, and as a reference in a general population, the estimated frequencies of the genotypes GG, GA, and AA were 76, 22, and 2%, respectively [28].

Correlation between SNP-1377 and membrane expression of Fas-R was done in 37 tumors, 20 (54.1%) of which were Fas-R positive. Fas-R was detected in 56.3% of tumors from patients with the GG genotype and in 40% of those with the GA or AA genotype. No relation was found between -1377 alleles or genotypes and Fas-R expression or stage.

Discussion

Cervical cancer is the second most prevalent cancer worldwide and is the fifth cause of cancer death in women. The mean age for its development is the fifth decade of life [31, 45]. Well-established etiologic factors for cervical carcinoma are earlier sexual intercourse, lifetime number of sexual partners, multiparity, smoking habits, genetic factors, suppressed immunity, and particularly, HPV infection [16]. HPV-16 DNA was identified by PCR in all patients in the present study. The genetic risk for cervical cancer has recently been estimated to be about twice as high in women whose mother or sister has had cervical carcinoma [1, 2, 22]. Immunity and genetics are closely related and play an important role in the resistance to HPV infections. This could be associated with human leukocyte antigens (HLA): loss of the B44 locus in HLA-I has been linked with progression of precancerous cervical lesions in HPV16 positive cases [8], and diverse HLA-II haplotypes such as DQ6, DR1501, and DRB1 connect HPV infections and neoplasia [2, 3].

Besides interactions between HPV and HLA haplotypes, Fas/CD 95 expression could help to explain why persistent viral infections may be associated with the development of preneoplastic lesions and invasive cervical tumors.

The Fas (APO-1/CD95) system regulates apoptosis through the interaction between the Fas-L and the transmembrane cell surface Fas-R. Fas-R is a member of the tumor necrosis factor receptor family [18] and is encoded by a gene located in the long arm of chromosome 10 [13]. Since keratinocytes are reported to be susceptible to apoptosis by interferon via Fas-R, [42] two Fas-related mechanisms may be taken into consideration during HPV-induced cervical carcinogenesis: (a) suppression of apoptosis in infected keratinocytes by downregulated Fas-R expression [5, 21, 37]; and (b) active immunosuppression by Fas-L overproduction by tumor cells [6, 11, 40].

Fas-R gene mutations have been reported in immune diseases and in several cancers [4, 5, 10, 21, 33, 37] but, to our knowledge, not in cervical carcinomas where, nevertheless, a decreased production of Fas-R mRNA [6] has been

Table 6 Cervical squamous cell carcinomas

	Stage I/Fas-R(+)	Stage II/Fas-R(+)	Stage III/Fas-R(+)	Mean
GG genotype	2/5 (40%)	1/2 (50%)	2/4 (50%)	5/11 (45.5%)
GA genotype	6/8 (75%)	3/4 (75%)	1/1 (100%)	10/14 (71.4%)
AA genotype	1/5 (20%)	1/2 (50%)	3/3 (100%)	5/9 (55.5%)
Total	9/18 (50%)	5/8 (62.5%)	6/8 (75%)	20/34 (58.8%)

Relation between Fas-R (CD95) expression and SNPs -670

described. Fas-R expression could be regulated by various cytokines, especially interferon and TNF [24, 35] which are produced by HPV-infected keratinocytes or the inflammatory reaction associated with cervical carcinomas. Granular cytoplasmic and membranous Fas-R stains are identified by IHC in the normal cervix, and their loss has been reported in approximately 50% of squamous intraepithelial lesion (SIL) and SCC [14]. In our series, Fas-R expression was preserved in only 52.6% of the tumors, without any relationship with stage, histologic grade, inflammatory reaction, or prognosis. These findings prompted us to investigate a relationship between Fas-R expression and SNP in the promoter region of this gene, which has been previously described in cervical carcinomas [7, 9, 19, 20, 43].

SNP A/G in position -670 of the Fas-R gene has been related with longevity and Fas-R expression. Fas-R expression in the 670 G allele homozygotes is said to be lower than in the A allele homozygote [32]. However, it has also been recently reported that women with the -670 A allele and AA genotype have a higher susceptibility to HPV infection, increased risk for intraepithelial lesions, and more frequent invasive cervical carcinomas than the general population [19, 20]. These findings have been confirmed neither by us nor by other investigators [7, 9, 43]. In fact, although in our cases the G allele had the same frequency as in the general population, the GG genotype was more common in advanced carcinomas (50 vs 26%). Furthermore, Fas-R expression was more frequently lost in higher-stage tumors with the 670-GG genotype: only 45.5% of cases with this genotype showed positive staining, whereas Fas-R was identified in 71.4% of tumors from patients with the 670-GA genotype. In agreement with our findings, a Fas-R-670 GG genotype has been related with an increased risk of esophageal squamous cell carcinoma [41]. Such results suggest an association between the -670-G allele and low Fas-R expression, resistance to apoptosis, and probably more aggressive tumors.

Although it has been stated that the Fas-R 1377 A allele and the AA genotype confer a more efficient Fas-R expression in response to interferon (IFN) stimuli [12], no relation was detected in our study between the -1377 genotype and Fas-R expression. Moreover, no relation has been found between Fas-R-1377 SNP and cervical carcinomas either in our series or in others [19]. Other polymorphisms such as p53 [15], TGF-β1 [39], MMP-1 [29], and IL-10 promoter [38] have also been associated with cervical carcinomas, but results were inconclusive.

Fas-L production by keratinocytes may significantly increase upon IFN effect in a time- and dose-dependent manner inducing apoptosis of cocultured T lymphocytes [40]. Furthermore, overexpression of Fas-L at the periphery of vulvar SCC may contribute to tumor-associated immunosuppression by increased apoptosis of the lymphoid cells surrounding the tumor [26]. Although Fas-L mRNA production has been rarely demonstrated in cervical SCC [6], Fas-L expression was detected in 56% of invasive neoplasms [34]. In our series, Fas-L immunostaining in tumor cells correlated with tumor stage: 36.4% in stage I, 50% in stage II, and 75% in stage III. Fas-L expression inversely correlated, although without statistical significance, with the presence of a florid lymphoid infiltrate; it was present in 54.5% of stage I tumors but only in 12.5% of stage II/III tumors. These findings strongly suggests that Fas-L production by tumor cells results in decreased lymphoid cell reaction and is likely a defense mechanism of the tumor against host's immunity.

The immune response to cervical neoplasia varies with the extension of disease. In SIL, typically associated with persistent HPV infection and high viral load, the lymphocytic reaction varies, but according to Kobayashi et al. [17], the estimated percentages of lymphocyte subpopulations by image analysis were 41% for CD4, 45% for CD8, 7% for CD20, and 7% for CD56. In invasive carcinomas, lymphocyte populations also vary with the stage, and reduction of CD4 lymphocytes, mild increase of CD8, and marked increase of CD56 have been found by flow cytometry in metastatic SCC [36]. In our series, although there was an overall decrease of lymphocytes in relation with stage, the proportion of the various lymphocyte populations remained almost unchanged, except for a mild decrease in CD4 cells, an increase in CD8 lymphocytes particularly in the epithelium, and a mild increase in CD56 positive cells in advanced SCC.

In summary, Fas-R expression by tumor cells seems to be unrelated to stage or quantity of the lymphoid infiltrate. It is a constitutive event independent of tumor progression. Tumor production of Fas-L may represent an attempt to destroy the host's lymphocytic reaction. Further studies are needed to confirm these findings.

References

1. Ahlbom A, Lichtenstein P, Malmstrom H, Feychting M, Hemminki K, Pedersen NL (1997) Cancer in twins: genetic and nongenetic familial risk factors. J Natl Cancer Inst 89:287–293
2. Allen M, Lalantari M, Ylitalo N, Pettersson B, Hagmar B, Scheibenpflug L, Johansson B, Petterson U, Gyllensten U (1996) HLA DQ-DR haplotype and susceptibility to cervical carcinomaL indications of increased risk for development of cervical carcinoma in individuals infected with HPV 18. Tissue Antigens 48:32–37
3. Apple RJ, Erlich HA, Klitz W, Manos MM, Becker TM, Wheeler CM (1994) HLA DR-DQ associations with cervical carcinoma show papillomavirus-type specificity. Nat Genet 6:157–162
4. Boldrini L, Faviana P, Pistolesi F, Gisfredi S, Di Quirico D, Lucchi M, Mussi A, Angeletti CA, Baldinotti F, Fogli A, Simi P, Basolo F, Fontanini G (2001) Alterations of Fas (APO-1/CD 95) gene and its relationship with p53 in non small cell lung cancer. Oncogene 20:6632–6637

5. Butler LM, Hewett PJ, Butler WJ, Couled PA (1998) Down-regulation of fas gene expression in colon cancer is not a result of allelic loss or gene rearrangement. Br J Cancer 77:1454–1459
6. Das H, Koizumi T, Sugimoto T, Chakraborty S, Ichimura T, Hasegawa K, Nishimura R (2000) Quantitation of Fas and Fas ligand gene expression in human ovarian, cervical and endometrial carcinomas using real-time quantitative RT-PCR. Br J Cancer 82:1682–1688
7. Dybikowska A, Sliwinski W, Emerich J, Podhajska AJ (2004) Evaluation of Fas gene promoter polymorphism in cervical cancer patients. Int J Mol Med 14:475–478
8. Ellis JR, Keating PJ, Baird J, Hounsell EF, Renouf DV, Rowe M, Hopkins D, Duggan-Keen MF, Bartholomew JS, Young LS (1995) The association of an HPV16 oncogene variant with HLA-B7 has implications for vaccine design in cervical cancer. Nature Med 1:464–470
9. Engelmark MT, Renkema KY, Gyllensten UB (2004) No evidence of the involvement of the Fas-670 promoter polymorphism in cervical cancer in situ. Int J Cancer 112:1084–1085
10. Fisher GH, Rosenberg FJ, Straus SE, Dale JK, Middleton LA, Lin AY, Strober W, Lenardo MJ, Puck JM (1995) Dominant interfering Fas gene mutations impair apoptosis in human autoimmune lymphoproliferative syndrome. Cell 81:935–946
11. Griffith TS, Brunner T, Fletcher SM, Green DR, Ferguson TA (1995) Fas ligand-induced apoptosis as a mechanism of immune privilege. Science 270:1189–1192
12. Huang QR, Morris D, Manolios N (1997) Identification and characterization of polymorphism's in the promoter region of the human Apo-1/Fas (CD95) gene. Mol Immunol 34:577–582
13. Inazawa J, Itoh N, Abe T, Nagata S (1992) Assignment of the human Fas antigen gene (Fas) to 10q24.1. Genomics 14:821–822
14. Jones DL, Munger K (1996) Interactions of the human papillomavirus E7 protein with cell cycle regulators. Semin Cancer Biol 7:327–337
15. Kim JW, Lee CG, Park YG, Kim KS, Kim IK, Sohn YW, Min HK, Lee JM, Namkoong SE (2000) Combined analysis of germline polymorphism's of p53, GSTM1, GSTT1, CYP1A1 and CYP2E1. Relation to the incidence rate of cervical carcinomas. Cancer 88:2082–2091
16. Kjellberg L, Hallmans G, Ahren AM, Johansson R, Bergman F, Wadell G, Angstrom T, Dillner J (2000) Smoking, diet, pregnancy and oral contraceptive use as risk factors for cervical intraepithelial neoplasia in relation to human papillomavirus infection. Br J Cancer 82:1332–1338
17. Kobayashi A, Greenblatt RM, Anastos K, Minkoff H, Massad LS, Young M, Levine AM, Darragh TM, Weinberg V, Smith-McCune KK (2004) Functional attributes of mucosal immunity in cervical intraepithelial neoplasia. Cancer Res 64:6766–6774
18. Krammer DH (2000) CD95's deadly mission in the immune system. Nature 407:789–795
19. Lai HC, Lin WY, Lin YW, Chang CC, Yu MH, Chen CC, Chu TY (2005) Genetic polymorphism's of FAS and FASL (CD95/CD95L) genes in cervical carcinogenesis: An analysis of haplotype and gene–gene interaction. Gynecol Oncol 99:113–118
20. Lai HC, Sytwu HK, Sun CA, Yu MH, Yu CP, Liu HS, Chang CC, Chu TY (2003) Single nucleotide polymorphism at Fas promoter is associated with cervical carcinogenesis. Int J Cancer 103:221–225
21. Lee SH, Shin MS, Park WS, Kim SY, Dong SM, Pi JH, Lee HK, Kim HS, Jang JJ, Kim CS, Kim SH, Lee JY (1999) Alterations of Fas gene in transitional cell carcinomas of urinary bladder. Cancer Res 59:3068–3072
22. Magnusson PK, Sparen P, Gyllensten UB (1999) Genetic link to cervical tumors. Nature 400:29–30
23. Mantovani F, Banks L (2001) The human papilloma virus E6 protein and its contribution to malignant progression. Oncogene 20:7874–7887
24. Matsue H, Kobayashi H, Hosokawa T, Akitaya T, Ohkawara A (1995) Keratinocytes constitutively express the Fas antigen that mediates apoptosis in IFN gamma-treated cultured keratinocytes. Arch Dermatol Res 287:315–320
25. Milde-Langosch K, Schreiber C, Becker G, Löning T, Stegner HE (1993) Human papillomavirus a detection in cervical adenocarcinomas by polymerase chain reaction. Hum Pathol 24:590–594
26. Moers C, Warskulat U, Müschen M, Even J, Niederacher D, Josien R, Koldovsky U, Beckmann MW, Häussinger D (1999) Regulation of CD95 (Apo-1/Fas) ligand and receptor expression in squamous-cell carcinoma by interferon-gamma and cisplatin. Int J Cancer 80:564–572
27. Muñoz N, Bosch FX, de Sanjosé S, Herrero R, Castellsagué X, Shah KV, Snijders PJ, Meijer CJ, International Agency for Research on Cancer Multicenter Cervical Cancer Study Group (2003) Epidemiologic classification of human papillomavirus types associated with cervical cancer. N Engl J Med 348:518–527
28. Nguyen HH, Broker TR, Chow LT, Alvarez RD, Vu HL, Andrasi J, Brewer LR, Jin G, Mestecky J (2005) Immune response to human HPV in genital tract of women with cervical cancer. Ginecol Oncol 96:452–461
29. Nishioka Y, Sagae S, Nishikawa A, Kudo R (2003) A relationship between Matrix metalloproteinase-1 (MMP-1) promoter polymorphism and cervical cancer progression. Cancer Lett 200:49–55
30. Parkin DM, Bray F, Ferlay J, Pisani P (2001) Estimating the world cancer burden: Globocan 2000. Int J Cancer 94:153–156
31. Peter ME, Krammer PH (2003) TheCD95(Apo-/Fas) DISC and beyond. Cell Death Differ 10:26–35
32. Pinti M, Troiano L, Nasi M, Moretti L, Monterastelli E, Mazzacani A, Mussi C, Ventura P, Olivieri F, Franceschi C, Salvioli G, Cossarizza A (2002) Genetic polymorphisms of Fas (CD95) and FasL (CD178) in human longevity: studies on centenarians. Cell Death Differ 9:431–438
33. Ramenghi U, Bonissoni S, Migliaretti G, DeFranco S, Bottarel F, Gambaruto C, DiFranco D, Priori R, Conti F, Dianzani I, Valesini G, Merletti F, Dianzani U (2000) Deficiency of the Fas apoptosis pathway without Fas gene mutations is a familial trait predisposing to development of autoimmune disease and cancer. Blood 95:3176–3182
34. Reesink-Peters N, Hougardy BM, van den Heuvel FA, Ten Hoor KA, Hollema H, Boezen HM, de Vries EG, de Jong S, van der Zee AG (2005) Death receptors and ligands in cervical carcinogenesis: an immunohistochemical study. Gynecol Oncol 96:705–713
35. Sayama K, Yonehara S, Watanabe Y, Miki Y (1994) Expression of Fas antigen on keratinocytes in vivo and induction of apoptosis in cultured keratinocytes. J Invest Dermatol 103:330–334
36. Sheu BC, Hsu SM, Ho HN, Lin RH, Torng PL, Huang SC (1999) Reversed CD4/CD8 ratios of tumor-infiltrating lymphocytes are correlated with progression of human cervical carcinoma. Cancer 86:1537–1543
37. Shimonishi T, Isse K, Shibata F, Aburatani I, Tsuneyama K, Sabit H, Harada K, Miyazaki K, Nakanuma Y (2000) Up-regulation of Fas ligand at early stages and down regulation of Fas at progressed stages of intrahepatic cholangiocarcinoma reflect evasion from immune surveillance. Hepatology 32:761–769
38. Stanczuk GA, Sibanda EN, Perrey C, Chivara M, Pravica V, Hutchinson IV, Tswana SA (2001) Cancer of the uterine cervix may be significantly associated with gene polymorphism's coding for increased IL10 production. Int J Cancer 94:792–794
39. Stanczuk GA, Tswana SA, Bergstrom S, Sibanda EN (2002) Polymorphism's in codons 10 and 25 of TGF gene in patients with invasive squamous cell carcinoma of the uterine cervix. Eur J Immunogenet 29:417–421
40. Strand S, Hofmann WJ, Hug H, Muller M, Otto G, Strand D, Mariani SM, Stremmel W, Krammer PH, Galle PR (1996) Lymphocyte apoptosis induced by CD95 (APO-1/Fas) ligand-expressing tumor cells—a mechanism of immune evasion? Nat Med 2:1361–1366

41. Sun T, Miao X, Zhang X, Tan W, Xiong P, Lin D (2004) Polymorphism's of death pathway genes FAS in esophageal squamous-cell carcinoma. J Natl Cancer Inst 96:1030–1036
42. Trautmann A, Akdis M, Kleemann D, Altznauer F, Simon HU, Graeve T, Noll M, Brocker EB, Blaser K, Akdis CA (2000) T cell-mediated Fas-induced keratinocyte apoptosis plays a key pathogenetic role in eczematous dermatitis. J Clin Invest 106:25–35
43. Ueda M, Hung YC, Terai Y, Yamaguchi H, Saito J, Nunobiki O, Noda S, Ueki M (2005) Fas gene promoter -670 polymorphism (A/G) is associated with cervical carcinogenesis. Gynecol Oncol 98:129–133
44. Vidal D, Matias X, Alomar A (2004) Open study of the efficacy and mechanism of action of topical imiquimod in basal cell carcinoma. Clin Exp Dermatol 29:518–525
45. Waggoner SE (2003) Cervical cancer. Lancet 361:2217–2225

Virchows Arch (2008) 452:75–81
DOI 10.1007/s00428-007-0531-3

ORIGINAL ARTICLE

Analysis of follicular lymphoma by dual-color fluorescence in situ hybridization

Dakeun Lee · Jinwon Seo · YoungLyun Oh · Jinman Kim · YoungHyeh Ko

Received: 14 August 2007 / Revised: 21 September 2007 / Accepted: 18 October 2007 / Published online: 27 November 2007
© Springer-Verlag 2007

Abstract Follicular lymphoma (FL) is divided into two groups: one with the t(14;18)(q32;q21) and the other without this translocation but with other chromosomal abnormalities including t(3q27) break. The majority of FLs in Western countries have the former chromosomal changes with characteristic clinical features and low histological grades. The goal of this study was to investigate the characteristics of Korean FLs with regard to the underlying molecular defects. Sixty-one cases of FL were evaluated from two centers in Korea by immunostaining for CD10, bcl-2, and bcl-6 proteins. Fluorescence in situ hybridization was performed to detect the t(14;18) and t(3q27) break. Cases with FL grade 3 accounted for 57% of all 61 cases. The t (14;18) was detected in 43.9% of the cases studied, and the frequency was 80, 50, 34.8, and 9.1% from grade 1 through grade 3b. The t(3q27) was detected in 16.1% of cases. Cases without a t(14;18) were mainly histological grade 3 ($P<$ 0.001) and had a tendency to have the t(3q27) and bcl-2 amplification. The incidence of t(14;18)-positive low-grade FL was found to be lower in Korea than in Western countries. The increased frequency of t(14;18)-negative grade 3 FL attributes to the lower incidence of t(14;18) in Korean FL.

Keywords Bcl-2 · Bcl-6 · FISH · Follicular lymphoma · Translocation

D. Lee · J. Seo · Y. Oh · Y. Ko (✉)
Department of Pathology, Samsung Medical Center,
Sungkyunkwan University School of Medicine,
Kangnam-gu, Ilwon-dong 50,
135-710 Seoul, South Korea
e-mail: yhko@smc.samsung.co.kr

J. Kim (✉)
Department of Pathology,
Chungnam National University School of Medicine,
Joong-gu, Moonwha 1-dong,
301-131 Daejeon, South Korea
e-mail: jinmank@cnu.ac.kr

Introduction

Follicular lymphoma (FL) is a relatively common type of malignant non-Hodgkin lymphoma (NHL); it accounts for about 30% of NHL, in the Western world [1]. In contrast to Western countries, the frequency of FLs is relatively low in Asian countries [1, 4]. Among Asian groups, the frequency of FL in Korea is similar to or slightly lower than other countries: Korea (6.2%, 1998) [14], Japan (6.7%, 2000) [33], Hong Kong (8%, 1998) [1], Thailand (11.1%, 1998 [32]; 3.8%, 1996 [11]), and Taiwan (6.3%, 1991) [30]. This geographic heterogeneity is widely accepted but unexplained.

The t(14;18)(q32;q21) chromosome abnormality is the genetic hallmark of FL. This abnormality juxtaposes the VDJ region of the immunoglobulin heavy chain (IgH) gene on chromosome 14q32 with the B cell leukemia/lymphoma-2 (BCL-2) gene on chromosome 18q21, placing BCL-2 under the regulatory control of the IgH promotor and causing an overexpression of the bcl-2 protein [34]. Because the bcl-2 protein is an inhibitor of apoptosis, its overexpression prevents neoplastic cells from undergoing apoptosis, and this causes their accumulation. However, this is not sufficient to produce lymphomagenesis as demonstrated by the finding of the t(14;18) in healthy persons [16].

The Bcl-2 translocation is detected by routine cytogenetic analysis, polymerase chain reaction (PCR) techniques,

and fluorescence in situ hybridization (FISH). Unlike conventional cytogenetics, FISH does not need a fresh sample and can be applied to formalin-fixed, paraffin-embedded tissue, thus enabling retrospective analysis of archival material, which can provide a convenient additional diagnostic tool for FLs [5]. In addition, FISH can improve the detection rate of the t(14;18) [26], especially in cases that involve variant breakpoints, which are not detectable by PCR targeting at the major breakpoint and minor cluster regions.

In a small subset of FLs, there are translocations involving the bcl-6 gene at chromosome 3q27. The partner chromosome is usually 14q32 at the IgH locus. In FL without the bcl-2 translocation, the bcl-6 genetic rearrangement is considered to play an important role [12]. The t(3;14)(q27;q32) leads to rearrangements of the bcl-6 proto-oncogene, encoding a POZ/zinc-finger transcriptional repressor [19]. In the reactive germinal center, bcl-6 interacts with Blimp-1 (transcriptional repressor of cMYC), which causes growth arrest, terminal plasmacytic differentiation, or apoptotic cell death. Therefore, repression of Blimp-1, by deregulated expression of bcl-6, might be important to lymphomagenesis permitting continued cell growth [29]. However, the relationship between the bcl-6 rearrangement and its expression is uncertain [31].

On the other hand, it has been reported that FLs without the t(14;18), including cases with the bcl-6 rearrangements and other cytogenetic abnormalities such as trisomy 18 are usually histological grade 3b [10, 22, 28]. This may suggest that FLs without the t(14;18) are pathophysiologically distinct from those cases with the bcl-2 translocation.

Recently, several studies have demonstrated that FL exhibits various morphologies, phenotypes, genetic aberrations, and clinical behaviors. These features vary greatly across geographic regions, suggesting geographic heterogeneity as a characteristic of this type of lymphoma. Therefore, this study was undertaken to determine the features of FLs in Koreans, with regard to genetic changes including the bcl-2 and bcl-6 translocation. We also investigated the relationship between these genetic aberrations and the histological grade, as well as the antigen expression profile of bcl-2, CD10, and bcl-6.

Materials and methods

Patient samples

The study population included 61 Korean patients who were diagnosed histopathologically with FL, of which 45 cases were from the Samsung Medical Center and 16 cases were from Chungnam University Hospital, from August 1995 to September 2005. There were 34 male and 27 female patients who ranged in age from 16 to 79 years (mean, 55 years; median 57 years). Two pathologists reviewed each case for confirmation of the diagnosis of FL. The histopathologic subclassification was determined according to the World Health Organization Classification [35]. This study was approved by the institutional review board, in accordance with the Declaration of Helsinki.

Immunohistochemistry

Immunohistochemical studies were performed on formalin-fixed, paraffin-embedded tissues using a labeled streptavidin–biotin method and a microwave-induced antigen retrieval method with citrate buffer (pH 6.0). The antibodies used were for Bcl-2 (124, 1:40, DakoCytomation, Glostrup, Denmark), Bcl-6 (Polyclonal, 1:60, Santa Cruz, CA), and CD10 (56C6, 1:100, Novocastra, Newcastle upon Tyne, UK). The cutoff level for bcl-2 and CD10 was staining of at least 30% of the tumor cell's cytoplasm. We used high bcl-6 reactivity (more than 60% cells with nuclear staining) as a cutoff, approximately equivalent to the percentage of bcl-6-positive cells encountered in non-neoplastic follicle centers.

Fluorescence in situ hybridization

FISH was performed using LSI IgH Spectrum Green/LSI Bcl2 Spectrum Orange Dual-color dual-fusion probe (Vysis, Downers Grove, IL) and the LSI Bcl6 Dual Color breakapart probe (Vysis) to detect the t(14;18) and t(3q27) break; 3–4-μm sections from formalin-fixed, paraffin-embedded tissues were placed on silane-coated glass slides. The slides were heated at 56°C for 2 h for adherence of the samples. Then, they were immediately deparaffinized with xylene three times at room temperature (RT), for 15 min each. Each slide was dehydrated in ethanol three times, for 2 min each. After that, they were treated with Tris/ethylenediamine tetraacetic acid buffer in the microwave at 98°C for 25 min, rinsed in phosphate-buffered saline (PBS), and digested in Digest-All 3 (pepsin; Zymed, California, USA) at 37°C for 6–8 min, followed by washing in PBS. The slides were fixed in 10% formalin for 1 min and washed with PBS. Dehydration was performed with four consecutive changes of 70, 85, 95, and 100% ethanol. After the slides were air dried, we placed 10 μl of a probe on the slides, covered them with a 22×22-mm coverslip, and sealed them with Ruber cement. Denaturation was achieved by incubating the slides at 94°C for 3 min in a humidifier chamber; they were then hybridized at 37°C overnight.

For the signal detection, the slides were washed with 0.5× sodium chloride–sodium citrate (SSC) at RT and placed in 0.5× SSC for 5 min at 76°C. In a Triton bath, the antifade nuclei were counterstained with diamidinopheny-

lindole and then mounted with an antifade solution. The slides were analyzed under a fluorescence microscope with ×1,000 magnification. The hybridization signals were evaluated by analyzing 100 to 150 nuclei on each slide. The cutoff value was determined from the normal-value study conducted on five reactive lymph nodes and was set at the mean percentage of cells plus three standard deviations (Fig. 1).

Statistical analysis

Statistical analysis of the data collected from the current study was performed using Fisher's exact test and the χ^2 test with SPSS software. A P value less than 0.05 was regarded as statistically significant.

Results

Grade distribution

In the present study, the grade distribution of FL from the 61 cases was as follows: 18 grade 1 (30%); 8 grade 2 (13%); 24 grade 3a (39%), and 11 grade 3b (18%).

Immunohistochemical study

Among the 61 cases with FL, 55 cases (90.2%) were bcl-2 positive. The bcl-2-positive cases accounted for 88.9% of grade 1, 75% of grade 2, 91.7% of grade 3a, and 100% of grade 3b cases. CD10 positivity was observed in 54.1% of all cases, accounting for 88.9% of grade 1, 62.5% of grade 2, 45.8% of grade 3a, and 9.1% of grade 3b cases. Bcl-6 positivity was detected in 57.4% of the 61 cases, accounting for 72.2% of grade 1, 62.5% of grade 2, 62.5% of grade 3a, and 18.2% of grade 3b cases (Table 1).

The expression rate of the bcl-2 protein was high and similar regardless of the histological grade (P=0.423). By contrast, the frequency of CD10 expression was inversely associated with the tumor grade (P<0.001). CD10 expression was much higher in low-grade (grade 1 and 2) cases than in high-grade (grade 3a and 3b) cases (P<0.001). The rate of bcl-6 protein expression was similar from grade 1 to grade 3a but significantly lower in grade 3b (P=0.005). There was no statistical difference between low- and high-grade cases in bcl-6 expression (P=0.088).

Analysis by fluorescence in situ hybridization

Among the 61 cases, FISH was successful in 57 cases for the bcl-2 translocation and in 56 cases for the bcl-6 translocation. The cutoff point was determined as 4.17% (mean, 1.51%; SD, 0.89) based on the normal value study conducted on five non-neoplastic-reactive lymphoid tissue sections. The bcl-2 translocation was identified in 43.9% of all cases. The frequency of the t(14;18) was highest in

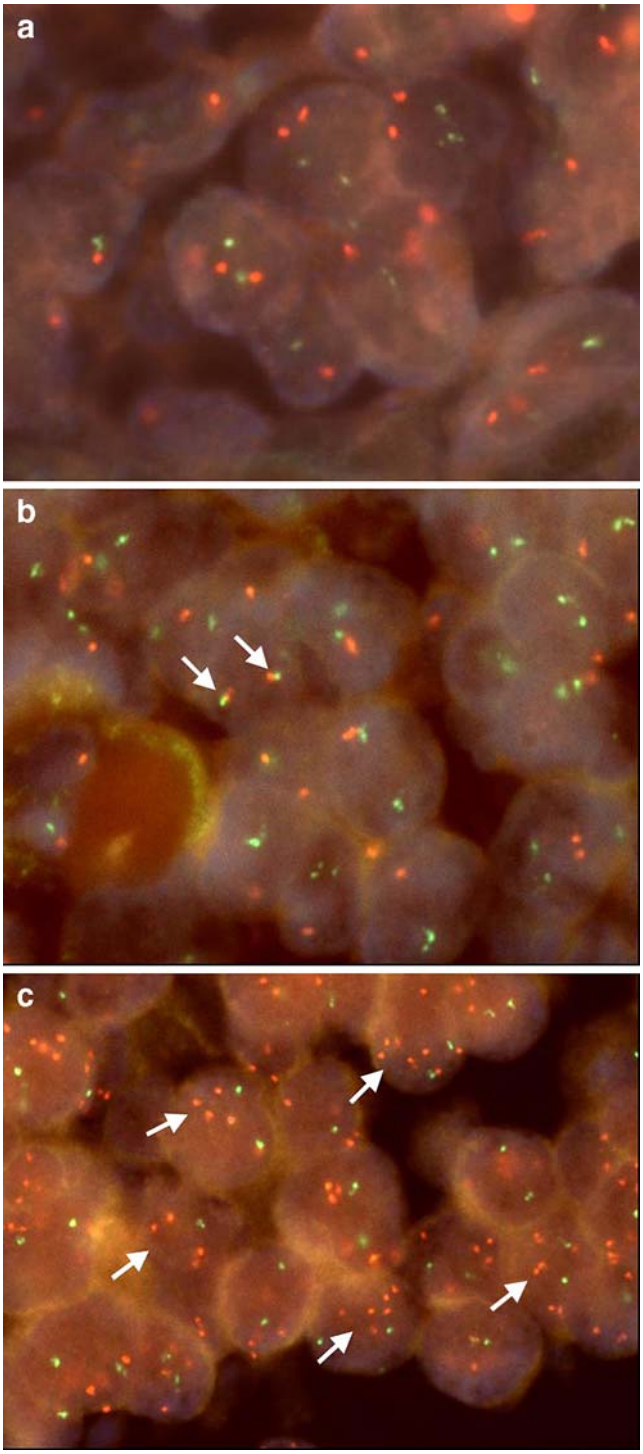


Fig. 1 Representative fluorescence in situ hybridization for bcl-2 gene translocation using dual-color dual-fusion probe (Vysis, Downers Grove, IL). **a** In a normal nucleus, there are two separate green (14q32) and orange (18q21) signals. **b** In a nucleus harboring t(14;18), one fused signal and two separate green and orange signals are present (*arrows*). **c** In a case with bcl-2 amplification, there are many red signals representing bcl-2 genes in a nucleus (*arrows*)

Table 1 Immunohistochemical results according to histological grades

Grade	CD10			Bcl-2			Bcl-6		
	+	−	Positivity (%)	+	−	Positivity (%)	+	−	Positivity (%)
1	16	2	88.9	16	2	88.9	13	5	72.2
2	5	3	62.5	6	2	75	5	3	62.5
3a	11	13	45.8	22	2	91.7	15	9	62.5
3b	1	10	9.1	11	0	100	2	9	18.2
Total	33	28	54.1	55	6	90.2	35	26	57.4

grade 1 (80%), followed by grade 2 (50%), grade 3a (34.8%), and grade 3b (9.1%) cases. The frequency of the bcl-6 translocation was much lower, 16.1%, for all FL specimens, including grade 1 (11.8%), grade 2 (0%), grade 3a (19%), and grade 3b (27.3%; Table 2). The bcl-2 duplication was detected in seven cases, including one grade 1, two grade 2, one grade 3a, and three grade 3b. Among them, two cases (grade 1, one; grade 2, one) had a bcl-2 translocation and an amplification simultaneously.

The frequency of the bcl-2 translocation was statistically different when the disease grades were compared ($P<0.001$). This translocation was more frequently detected in the low-grade compared to the high-grade FL cases ($P<0.001$). By contrast, there were no significant differences in the disease grades with the t(3q27) break ($P=0.298$). However, higher-grade FLs tended to have the t(3q27) break more frequently than did low-grade FLs, but this difference was not statistically significant ($P=0.160$).

Of all cases studied, 16 (25.8%) were negative for the t (14;18), t(3q27) break and bcl-2 amplification. They included one grade 1 (5.6%), two grade 2 (25%), seven grade 3a (29.2%), and six grade 3b (54.5%) cases. The cases without genetic alterations of bcl-2 and bcl-6 were more common among samples with grade 3 histology ($P=0.022$).

Comparison between the cases with and without bcl-2 gene rearrangement

The frequency of grade 3 FL was much lower in cases with t(14;18) than cases without t(14;18). While 9 of 26 cases (34.6%) with t(14;18) were histological grade 3, 25 of 31 cases (81%) without t(14;18) were grade 3. There was no significant difference in the expression of bcl-2 and bcl-6 between t(14;18)-positive and t(14;18)-negative cases. However, the CD10 expression was significantly associated with the presence of the t(14;18) ($P<0.001$); it was expressed in 20 of 26 (76.9%) of the cases carrying the t (14;18) but in only 10 of 31 (32.3%) of the cases without the t(14;18).

The Bcl-6 translocation was found in 7 of 27 (25.9%) of the cases without a t(14;18), while it was identified in only 2 of 26 (7.7%) of the cases with the t(14;18). However, the association between the bcl-6 translocation and the absence of the t(14;18) was not statistically significant ($P=0.832$) A bcl-2 amplification was detected in 16.1% of the cases that did not have the t(14;18), while it was found in 7.7% of the cases with the t(14;18) (Table 3).

Discussion

In the current study, the distribution of grade 1, 2, and 3 FL was 30, 13, and 57%; high-grade tumors (grade 3) accounted for more than half of the total FL archives. The incidence of grade 3 FL varies according to the geographic area and has been thought to be higher in Asian countries (Table 4). However, some recent Japanese studies showed that grade 3 FLs were relatively uncommon and that the grade distributions were more consistent with those reported from Western countries [9, 20]. The frequency of

Table 2 Chromosomal alterations according to histological grades

Grade	t(14;18)			t(3q27) break		
	+	−	Positivity (%)	+	−	Positivity (%)
1	12	3	80	2	15	11.8
2	4	4	50	0	7	0
3a	8	15	34.8	4	17	19
3b	1	10	9.1	3	8	27.3
Total	25	32	43.9	9	47	16.1

Table 3 Comparison between the groups with or without bcl-2 gene arrangement

	t(14;18)				*P* value
	+	Positivity (%)	−	Positivity (%)	
Bcl-2	24/26	92.3	28/31	90.3	0.585
CD10	20/26	76.9	10/31	32.3	<0.001
Bcl-6	15/26	57.7	17/31	54.8	0.521
t(3q27) break	2/26	7.7	7/27	25.9	0.079
Bcl-2 amplification	2/26	7.7	5/31	16.1	0.291

grade 3 FLs in our data and in one previous study [7] was considerably higher than that from other Asian countries. The ratio of grades 3a to 3b was 2.2:1. The proportion of FL grade 3b was similar to that of prior reports from Japan but was much higher than rates reported from England and Malaysia [6, 24].

The t(14;18) has been considered the hallmark of FL. However, this translocation has been identified in other NHLs [15]. Furthermore, it is not a constant finding even in diagnosed cases of FL; its presence is quite variable among the histological grades. A number of studies have associated the absence of the bcl-2 rearrangement with higher histological grades of disease [8–10, 18, 28]. This observation is also consistent with our findings; the frequency of the t(14;18) was 80, 50, 34.8, and 9.1% in cases with grade 1 through grade 3b. The frequency of the bcl-2 rearrangement also has been reported to be variable and differs by geographic region, showing a significant gradient from the relatively low rate of 48 to 55% among Asian and European studies to approximately 80% in a series reported from the USA [4]. However, recent FISH studies from Southeast Asia demonstrated a relatively high frequency of the bcl-2 gene rearrangement, 56–81% [9, 18, 24, 28]; the investigators attributed the differences observed between the results of studies from the East and the West in part to technical factors. The work of Peh et al. [24] supported this notion; they performed FISH on cases without a detectable t(14;18) translocation by PCR and demonstrated a bcl-2 rearrangement in an additional 4 out of 11 cases.

In the current study, 57 out of 61 cases were tested by FISH for the bcl-2 translocation, and only 25 cases (43.9%) were found to have the t(14;18), which is a much lower detection rate than the results reported from other recent Asian studies [9, 18, 24, 28]. In regard to histological grade, grades 1 and 2 tumors showed a high frequency of the bcl-2 translocation, which is compatible with the findings reported from other countries. However, high-grade tumors were strongly associated with the absence of the t(14;18) ($P<0.001$), and most of the t(14;18)-negative cases (81%) were grade 3 in the current study. Therefore, the lower frequency of t(14;18) in our study is likely due to the existence of a higher proportion of t(14;18)-negative grade 3 FLs.

The frequency of the t(14;18) in our study was especially low in grade 3 cases compared to previous studies (Table 5). It was even lower in grade 3b (9.1%) than grade 3a (34.8%). The higher proportion of grade 3b cases in previous studies attributes to the low frequency of the t(14;18) in Korea. FL grade 3 is a heterogeneous disease group; FL grade 3a is frequently accompanied by bcl-2 rearrangement, while bcl-2 rearrangement is not common in FL grade 3b [22].

The Bcl-6 translocation is another important genetic aberration in FLs. It is identified in up to 30% of diffuse large B cell lymphoma, but it may be found in a small number of other types of lymphomas such as marginal zone B cell lymphoma, nodular lymphocyte predominant Hodgkin lymphoma, as well as FL. In FLs, the frequency of the t(3q27) break has been reported to be low with an overall detection rate of 10–20% [3, 9, 17, 21, 25]. We detected the bcl-6 translocation in 16.1% of cases (9 out of 56 cases). The bcl-6 translocation has been associated with the absence of the t(14;18) or grade 3 histology, especially grade 3b with a diffuse large B cell component [12, 13]. Our findings were consistent with prior studies; the t(3q27) break was detected in cases with grade 3 histology more frequently; however, this difference was not statistically significant ($P=0.160$).

Bcl-6 expression did not correlate with the t(3q27) break ($P=0.614$); 67% of cases with t(3q27) break were bcl-6 protein positive, and 59% of cases without t(3q27) break were bcl-6 protein positive. Cases with chromosome alterations at the bcl-6 gene locus do not always express the bcl-6 protein [25]. Skinnider et al. [31] suggested possible mechanisms to explain this phenomenon; the breakpoint at the 3q27 region may not affect the bcl-6

Table 4 Overview of FISH analyzed studies of follicular lymphoma distribution according to histological grades

	Grade 1 (%)	Grade 2 (%)	Grade 3 (%)	Grade 3a/3b
Current study	30	13	57	2.2:1
Chau et al. [6] (England, 2003)	43	32	25	4:1
Miyazato et al. [20] (Japan, 2002)	38	29	33	–
Guo et al. [9] (Japan, 2005)	26	48	26	2:1
Peh et al. [24] (Malaysia, 2004)	22	39	39	3.8:1

Table 5 Overview of distribution of bcl-2 gene rearrangement according to histological grades

	Grade 1 (%)	Grade 2 (%)	Grade 3 (%)
Peh et al. [24] (Malaysia, 2004)	100	83	82
Guo et al. [9] (Japan, 2005)	100	92	44
Matsumoto et al. [18] (Japan, 2004)	67	50	50
Current study	80	50	27

gene, the rearrangement may disrupt the gene during translocation, or bcl-6 gene deregulation may be an early step in lymphomagenesis, and its expression may not be necessary once a malignant clone has been established. However, the exact mechanisms remain unknown and are still under investigation.

Bcl-2 expression was seen in 24 out of 26 (92.3%) cases with the t(14;18), while 28 out of 31 cases (90.3%) without the t(14;18) stained for bcl-2 protein. This observation supports the hypothesis that the bcl-2 protein can be upregulated by other mechanisms than translocation, such as other types of chromosomal alterations involving the bcl-2 gene on chromosome 18, viral infection, cytokine effects, or interaction with cell cycle regulators [2, 10, 23, 27].

In conclusion, the incidence of t(14;18)-positive low-grade FL in Korea is relatively low compared to Western countries. The high incidence of t(14;18)-negative grade 3 FL attributes to the relatively low incidence of t(14;18) in Korean FL and suggests genetic and geographic heterogeneity for this type of lymphoma.

References

1. Anderson JR, Armitage JO, Weisenburger DD (1998) Epidemiology of the non-Hodgkin's lymphomas: distributions of the major subtypes differ by geographic locations. Non-Hodgkin's Lymphoma Classification Project. Ann Oncol 9:717–720
2. Aster JC, Longtine JA (2002) Detection of BCL2 rearrangements in follicular lymphoma. Am J Pathol 160:759–763
3. Bastard C, Deweindt C, Kerckaert JP, Lenormand B, Rossi A, Pezzella F, Fruchart C, Duval C, Monconduit M, Tilly H (1994) LAZ3 rearrangements in non-Hodgkin's lymphoma: correlation with histology, immunophenotype, karyotype, and clinical outcome in 217 patients. Blood 83:2423–2427
4. Biagi JJ, Seymour JF (2002) Insights into the molecular pathogenesis of follicular lymphoma arising from analysis of geographic variation. Blood 99:4265–4275
5. Blough RI, Smolarek TA, Ulbright TM, Heerema NA (1997) Bicolor fluorescence in situ hybridization on nuclei from formalin-fixed, paraffin-embedded testicular germ cell tumors: comparison with standard metaphase analysis. Cancer Genet Cytogenet 94:79–84
6. Chau I, Jones R, Cunningham D, Wotherspoon A, Maisey N, Norman AR, Jain P, Bishop L, Horwich A, Catovsky D (2003) Outcome of follicular lymphoma grade 3: is anthracycline necessary as front-line therapy? Br J Cancer 89:36–42
7. Chi JG, Shin SS, Ahn GH, Lee SK (1985) Malignant lymphomas in Korea. Jpn J Clin Oncol 15:653–659
8. Gaulard P, d'Agay MF, Peuchmaur M, Brousse N, Gisselbrecht C, Solal-Celigny P, Diebold J, Mason DY (1992) Expression of the bcl-2 gene product in follicular lymphoma. Am J Pathol 140:1089–1095
9. Guo Y, Karube K, Kawano R, Yamaguchi T, Suzumiya J, Huang GS, Ohshima K (2005) Low-grade follicular lymphoma with t (14;18) presents a homogeneous disease entity otherwise the rest comprises minor groups of heterogeneous disease entities with Bcl2 amplification, Bcl6 translocation or other gene aberrances. Leukemia 19:1058–1063
10. Horsman DE, Okamoto I, Ludkovski O, Le N, Harder L, Gesk S, Siebert R, Chhanabhai M, Sehn L, Connors JM, Gascoyne RD (2003) Follicular lymphoma lacking the t(14;18)(q32;q21): identification of two disease subtypes. Br J Haematol 120:424–433
11. Intragumtornchai T, Wannakrairoj P, Chaimongkol B, Bhoopat L, Lekhakula A, Thamprasit T, Suwanwela N, Suthipinthawong C, Prayoonwiwat W, Meekungwal P, Sirijerachai C, Pairojkul C (1996) Non-Hodgkin's lymphomas in Thailand. A retrospective pathologic and clinical analysis of 1391 cases. Cancer 78:1813–1819
12. Jardin F, Gaulard P, Buchonnet G, Contentin N, Lepretre S, Lenain P, Stamatoullas A, Picquenot JM, Duval C, Parmentier F, Tilly H, Bastard C (2002) Follicular lymphoma without t(14;18) and with BCL-6 rearrangement: a lymphoma subtype with distinct pathological, molecular and clinical characteristics. Leukemia 16:2309–2317
13. Katzenberger T, Ott G, Klein T, Kalla J, Muller-Hermelink HK, Ott MM (2004) Cytogenetic alterations affecting BCL6 are predominantly found in follicular lymphomas grade 3B with a diffuse large B-cell component. Am J Pathol 165:481–490
14. Ko YH, Kim CW, Park CS, Jang HK, Lee SS, Kim SH, Ree HJ, Lee JD, Kim SW, Huh JR (1998) REAL classification of malignant lymphomas in the Republic of Korea: incidence of recently recognized entities and changes in clinicopathologic features. Hematolymphoreticular Study Group of the Korean Society of Pathologists. Revised European-American lymphoma. Cancer 83:806–812
15. Lai R, Arber DA, Chang KL, Wilson CS, Weiss LM (1998) Frequency of bcl-2 expression in non-Hodgkin's lymphoma: a study of 778 cases with comparison of marginal zone lymphoma and monocytoid B-cell hyperplasia. Mod Pathol 11:864–869
16. Limpens J, Stad R, Vos C, de Vlaam C, de Jong D, van Ommen GJ, Schuuring E, Kluin PM (1995) Lymphoma-associated translocation t(14;18) in blood B cells of normal individuals. Blood 85:2528–2536
17. Lo Coco F, Ye BH, Lista F, Corradini P, Offit K, Knowles DM, Chaganti RS, Dalla-Favera R (1994) Rearrangements of the BCL6 gene in diffuse large cell non-Hodgkin's lymphoma. Blood 83:1757–1759
18. Matsumoto Y, Nomura K, Matsumoto S, Ueda K, Nakao M, Nishida K, Sakabe H, Yokota S, Horiike S, Nakamine H, Nakamura S, Taniwaki M (2004) Detection of t(14;18) in follicular lymphoma by dual-color fluorescence in situ hybridization on paraffin-embedded tissue sections. Cancer Genet Cytogenet 150:22–26
19. Miki T, Kawamata N, Hirosawa S, Aoki N (1994) Gene involved in the 3q27 translocation associated with B-cell lymphoma, BCL5, encodes a Kruppel-like zinc-finger protein. Blood 83:26–32
20. Miyazato H, Nakatsuka S, Miyanaga I, Hanamoto H, Tatsumi Y, Matsuda M, Maeda Y, Kanamaru A, Aozasa K (2002) Follicular lymphoma in Osaka, Japan: histological features and chronological change. Int J Hematol 76:333–337
21. Otsuki T, Yano T, Clark HM, Bastard C, Kerckaert JP, Jaffe ES, Raffeld M (1995) Analysis of LAZ3 (BCL-6) status in B-cell non-Hodgkin's lymphomas: results of rearrangement and gene expression studies and a mutational analysis of coding region sequences. Blood 85:2877–2884
22. Ott G, Katzenberger T, Lohr A, Kindelberger S, Rudiger T, Wilhelm M, Kalla J, Rosenwald A, Muller JG, Ott MM, Muller-Hermelink HK (2002) Cytomorphologic, immunohistochemical, and cytogenetic profiles of follicular lymphoma: 2 types of follicular lymphoma grade 3. Blood 99:3806–3812
23. Papakonstantinou G, Verbeke C, Hastka J, Bohrer M, Hehlmann R (2001) bcl-2 expression in non-Hodgkin's lymphomas is not

associated with bcl-2 gene rearrangements. Br J Haematol 113:383–390
24. Peh SC, Shaminie J, Tai YC, Tan J, Gan SS (2004) The pattern and frequency of t(14;18) translocation and immunophenotype in Asian follicular lymphoma. Histopathology 45:501–510
25. Pittaluga S, Ayoubi TA, Wlodarska I, Stul M, Cassiman JJ, Mecucci C, Van Den Berghe H, Van De Ven WJ, De Wolf-Peeters C (1996) BCL-6 expression in reactive lymphoid tissue and in B-cell non-Hodgkin's lymphomas. J Pathol 179:145–150
26. Rack KA, Salomon-Nguyen F, Radford-Weiss I, Gil MO, Schmitt C, Belanger C, Nusbaum S, Vekemans M, Valensi F, Macintyre EA (1998) FISH detection of chromosome 14q32/IgH translocations: evaluation in follicular lymphoma. Br J Haematol 103:495–504
27. Seite P, Hillion J, d'Agay MF, Gaulard P, Cazals D, Badoux F, Berger R, Larsen CJ (1993) BCL2 gene activation and protein expression in follicular lymphoma: a report on 64 cases. Leukemia 7:410–417
28. Sekiguchi N, Kobayashi Y, Yokota Y, Kusumoto S, Tanimoto K, Watanabe T, Matsuno Y, Tobinai K (2005) Follicular lymphoma subgrouping by fluorescence in situ hybridization analysis. Cancer Sci 96:77–82
29. Shaffer AL, Lin KI, Kuo TC, Yu X, Hurt EM, Rosenwald A, Giltnane JM, Yang L, Zhao H, Calame K, Staudt LM (2002) Blimp-1 orchestrates plasma cell differentiation by extinguishing the mature B cell gene expression program. Immunity 17:51–62
30. Shih LY, Liang DC (1991) Non-Hodgkin's lymphomas in Asia. Hematol Oncol Clin North Am 5:983–1001
31. Skinnider BF, Horsman DE, Dupuis B, Gascoyne RD (1999) Bcl-6 and Bcl-2 protein expression in diffuse large B-cell lymphoma and follicular lymphoma: correlation with 3q27 and 18q21 chromosomal abnormalities. Human Pathol 30:803–808
32. Sukpanichnant S, Sonakul D, Piankijagum A, Wanachiwanawin W, Veerakul G, Mahasandana C, Tanphaichitr VS, Suvatte V (1998) Malignant lymphoma in Thailand: changes in the frequency of malignant lymphoma determined from a histopathologic and immunophenotypic analysis of 425 cases at Siriraj Hospital. Cancer 83:1197–1204
33. Lymphoma Study Group of Japanese Pathologists (2000) The World Health Organization classification of malignant lymphomas in Japan: incidence of recently recognized entities. Pathol Int 50:696–702
34. Tsujimoto Y, Finger LR, Yunis J, Nowell PC, Croce CM (1984) Cloning of the chromosome breakpoint of neoplastic B cells with the t(14;18) chromosome translocation. Science 226:1097–1099
35. World Health Organization Classification of Tumours (2001) Pathology and genetics of tumours of haematopoietic and lymphoid tissues. IARC, Lyon

Virchows Arch (2008) 452:83–90
DOI 10.1007/s00428-007-0526-0

ORIGINAL ARTICLE

Differential expression of stromal MMP-1, MMP-9 and TIMP-1 in basal cell carcinomas of immunosuppressed patients and controls

Sonja Boyd · Kalle Tolvanen · Susanna Virolainen · Tiina Kuivanen · Lauri Kyllönen · Ulpu Saarialho-Kere

Received: 20 June 2007 / Revised: 20 September 2007 / Accepted: 14 October 2007 / Published online: 22 November 2007
© Springer-Verlag 2007

Abstract Matrix metalloproteinases (MMPs) have an important role in the initiation, growth, and invasion of malignant tumors. Basal cell cancer (BCC) is the most common human malignancy. The risk of BCC is 10–16 times higher among organ transplant recipients compared with the nontransplanted population. The aim of this study was to compare the expression of several MMPs and their tissue inhibitors (TIMPs) in BCCs from kidney transplant recipients and controls. Expression of MMPs-1, -7, -8, -9, -10, -13, -26, and TIMPs-1 and -3 was evaluated by immunohistochemistry in 25 samples of BCC of kidney transplant recipients and 25 matched controls representing superficial and nodular subtypes. No significant differences were detected in MMP expression of BCC tumor cells between immunocompetent and immunodeficient patients. However, MMPs-1 and -9 and TIMP-1 were expressed more frequently in stromal macrophages in the BCCs of immunocompetent patients. When tumor subtypes were compared irrespective of the patient group, more MMP-1-positive fibroblasts and MMP-9-positive neutrophils were detected in the superficial subtype, while stromal MMP-10 expression was more abundant in nodular tumors. Our results suggest that abundant peritumoral expression of TIMP-1 in non-immunocompromised patients limits ECM degradation permissive for cancer cell migration.

Keywords MMP-7 · MMP-10 · MMP-13 · MMP-26 · TIMP-3

S. Boyd · S. Virolainen
Department of Pathology, Helsinki University Central Hospital and Biomedicum Helsinki, University of Helsinki, Helsinki, Finland

K. Tolvanen · S. Virolainen · T. Kuivanen · U. Saarialho-Kere
Department of Dermatology, Helsinki University Central Hospital and Biomedicum Helsinki, University of Helsinki, Helsinki, Finland

L. Kyllönen
Department of Transplantation Surgery, Helsinki University Central Hospital and University of Helsinki, Helsinki, Finland

U. Saarialho-Kere
Department of Dermatology, Clinical Science and Education, Karolinska Institutet, Södersjukhuset, Stockholm, Sweden

U. Saarialho-Kere (✉)
Department of Dermatology, Helsinki University Central Hospital, Meilahdentie 2, Helsinki, Finland
e-mail: ulpu.saarialho-kere@helsinki.fi

Abbreviations

BCC	basal cell carcinoma
ECM	extracellular matrix
NMSC	non-melanoma skin cancer

Introduction

Basal cell carcinoma (BCC) is the most common malignancy among white individuals worldwide. It rarely metastasizes but is locally invasive and may thus cause morbidity and mortality. Age-standardized rate of BCC in whites is 32–407 per 100,000 population in Europe and the U.S., and its incidence is increasing [15]. The risk factors of BCC include sun exposure, smoking [8], arsenic exposure [20], ionizing radiation, and immunosuppression. BCCs

generally occur on sun-exposed areas such as the head and neck [44]. Patients with BCC located in the trunk have an increased risk of developing multiple BCCs, and these tumors develop at a faster rate [32].

Organ transplant recipients are at increased risk for skin cancer. Risk for BCC in kidney transplant recipients is 10–16 times higher than in non-immunocompromised individuals [21, 45]. Immunosuppressive treatment, age at the time of transplantation, male sex, skin type II, and environmental exposure to UV radiation are major risk factors in the development of non-melanoma skin cancer (NMSC) in organ transplant recipients [6, 16–18]. BCCs in transplant recipients develop at younger age, occur more frequently on extracranial locations, are more often of superficial type, have poorer inflammatory response and show slightly more frequent squamous differentiation compared with the non-transplanted population [21, 25].

Matrix metalloproteinases (MMPs) are a family of 23 zinc-binding proteolytic enzymes that are capable of degrading practically all components of the extracellular matrix (ECM). MMPs enhance tumor-induced angiogenesis, tumor invasion, tumor survival and metastatic spread, modulate immunologic responses, and activate cytokines, such as TNF-α, TGF-β1, and IGF [10, 43]. Tumor cells not only secrete MMPs but induce stromal cells, such as fibroblasts, inflammatory cells, and endothelial cells, to produce them [10]. MMPs are divided into six main classes: collagenases (MMPs-1, -8 and -13), gelatinases (MMPs-2 and -9), stromelysins (MMPs-3, -10, -12, and -11), matrilysins (MMPs -7 and -26), membrane-type MMPs (MMPs-14, -15, -16, -24, -17, and -25), and other MMPs (MMPs-19, -20, -21, and -28) [29]. Several studies have shown that MMPs-1, -7, -9, -10, -13 and -26 are not present in normal skin but need wounding or tumorigenesis for induction [1, 26, 28, 36, 40].

Tissue inhibitors of matrix metalloproteinases (TIMPs 1-4) are natural inhibitors of MMPs. They are multifunctional proteins that not only inhibit MMPs but promote cell growth, induce apoptosis, and inhibit angiogenesis [9]. With some exceptions, all TIMPs are able to inhibit all MMPs. TIMPs are expressed by several cell types [19], and all, except the ECM-bound TIMP-3, are soluble.

The aim of this study was to compare the expression of several MMPs and their inhibitors, TIMPs, at the protein level, between BCCs of renal transplant and immunocompetent patients, to determine whether they could play a role in the more frequent occurrence and possibly more aggressive behavior of BCCs in transplant patients.

Materials and methods

Patients and tissues Formalin-fixed, paraffin-embedded samples from immunosuppressed renal transplant patients and their matched nonimmunosuppressed controls were obtained from the Departments of Dermatopathology and Pathology, Helsinki University Central Hospital, Finland (Table 1). The immunosuppressed group included 25 BCC specimens from 13 patients. The BCCs had appeared between 2 and 29 years after transplantation (mean 13.8 years). The nonimmunosuppressed group included 25 BCC specimens from 25 patients. Diagnoses were made by an experienced dermatopathologist (SV). The WHO classification was used in grading of the tumors [33]. The use of archival specimens was approved by the corresponding ethical committee of the Helsinki University Central Hospital, Finland.

Immunohistochemistry Immunohistochemistry was performed on 4-μm-thick paraffin sections by the avidin–biotin–peroxidase complex technique (Dako StreptABComplex/HRP Duet, Mouse/Rabbit, Glostrup, Denmark) or by the antibody-polymer detection technique (PowerVision Poly-HRP IHC Kit, ImmunoVision Technologies Co, Brisbane, CA, USA). Sections were incubated in 3% H_2O_2 for 10 min at room temperature to block endogenous peroxidase. Sections were pretreated with 10 mg/ml trypsin or incubation in citrate buffer in a +95°C water bath. We used mostly mouse monoclonal antibodies to study the localization of MMP-1 (1:500, IM35L, Oncogene Research Products, San Diego, CA, USA), MMP-7 (1:100, IM40L, Calbiochem, La Jolla, CA, USA), MMP-8 (1:20, IM38L, Calbiochem), MMP-9 (1:100, GE-213, Labvision Neomarkers, Fremont, CA, USA), MMP-10 (1:300, 5E4, Novocastra Laboratories, Newcastle upon Tyne, UK), MMP-13 (1:10, Labvision Neomarkers), MMP-26 (1:150) [24], TIMP-1 (1:100, IM63L, Calbiochem), and TIMP-3 (1:400, IM43L, Calbiochem) as previously described [23, 30]. Diaminobenzidine (DAB) or aminoethylcarbazole (AEC) were used as chromogenic substrates and Mayer hematoxylin as counterstain. Positive controls were samples of chronic wounds and placenta that were known to express the respective MMPs or TIMPs.

Evaluation of immunohistochemistry Immunohistochemical staining was analyzed independently by three (SB, US-K, SV) investigators through light microscopic observation. The expression of MMPs and TIMPs was determined in the tumor epithelium (invasive front, central part, superficial part), in the intact epidermis adjacent to the tumor as well as in macrophages, neutrophils, lymphocytes, and fibroblasts surrounding the tumor. Three hot spots were selected at ×40 magnification, whereas counting was performed at ×400 magnification. The total number of positive cells was counted from three distinct high-power fields. Grading was performed semiquantitatively as follows: 0=0–9 positive cells, 1=10–50 positive cells, 2=51–100 positive cells, 3=over 100 positive cells.

Statistical analysis Mann–Whitney *U* and chi-square tests were performed to investigate the significance of results with SPSS 15.0 for Windows. A *p* value under 0.05 was considered as significant.

Results

Collagenases Almost all tumors expressed MMP-1 centrally inside the tumor. The invading front of the tumor epithelium

Table 1 Clinical features of the patients and tumors

Number	Sex/age	Site	Histology	Immunosuppression
1A	M/53	Back	Superficial	AzaSter
1B	F/44	Shoulder	Superficial	No
2A	M/57	Shoulder	Superficial	AzaSter
2B	M/84	Back	Superficial	No
3A	M/64	Scalp	superficial	AzaSter
3B	F/78	Scalp	Superficial + micronodular	No
4A	M/66	Chest	Nodular	CyaAzaSter
4B	F/56	Chest	Superficial + Nodular	No
5A	M/67	Temple	Nodular	CyaAzaSter
5B	M/81	Temple	Nodular	No
6A	M/67	Chin	Nodular	CyaAzaSter
6B	M/74	Chin	Nodular	No
7A	M/68	Temple	Nodular	CyaAzaSter
7B	F/78	Temple	Nodular	No
8A	M/68	Nose	Nodular	CyaAzaSter
8B	F/74	Nose	Superficial + nodular	No
9A	M/45	Neck	Superficial	AzaSter
9B	M/73	Neck	Superficial	No
10A	M/48	Earlobe	Nodular+sclerosing	AzaSter
10B	M/71	Earlobe	Nodular	No
11A	M/49	Back	Nodular + infiltrating	AzaSter
11B	M/84	Chest	Nodular + infiltrating	No
12A	M/50	Back	Nodular	AzaSter
12B	F/70	Back	Nodular	No
13A	M/52	Forehead	Nodular	AzaSter
13B	F/72	Forehead	Nodular	No
14A	M/52	Scalp	Nodular	AzaSter
14B	M/75	Scalp	Nodular	No
15A	M/60	Back	Nodular + superficial	CyaAzaSter
15B	M/75	Back	Superficial + nodular	No
16A	M/60	Chest	Nodular	CyaAzaSter
16B	F/83	Chest	Superficial + nodular	No
17A	M/67	Chest	Nodular	CyaAzaSter
17B	F/83	Chest	Nodular	No
18A	M/70	Back	Nodular	MMFCyaSter
18B	M/77	Back	Nodular	No
19A	M/63	Back	Superficial	CyaSter
19B	M/81	Back	Superficial	No
20A	M/56	Neck	Superficial	MMFCyASter
20B	M/86	Neck	Superficial	No
21A	F/66	Nose	Nodular	TacMMF
21B	M/78	Nose	Nodular	No
22A	M/70	Neck	Nodular	MMFCyaSter
22B	M/71	Neck	Nodular	No
23A	M/68	Forehead	Nodular	CyaAzaSter
23B	M/86	Forehead	Nodular	No
24A	M/74	Temple	Superficial	CyaAzaSter
24B	M/76	Forehead	Superficial	No
25A	M/75	Arm	Nodular	CyaAzaSter
25B	F/76	Forearm	Nodular	No

Cya Cyclosporin, *Tac* tacrolimus, *Aza* azathioprine, *MMF* mycophenolate mofetil; *Ster* methylprednisolone

expressed MMP-1 in 6 of 25 tumors of the immunosuppressed group compared with 11 of 25 cases in the nonimmunosuppressed group (Fig. 1a,b; Table 2), the difference not being statistically significant. Stromal macrophages were MMP-1 immunopositive in 19 of 25 samples in the immunosuppressed group compared with 23 of 25 samples in the control group (Fig. 1a,b; Tables 2 and 3). However, the degree of semiquantitatively assessed MMP-1 immunopositivity in macrophages was higher in the non-immunosuppressed group (p=0.026) (Tables 2 and 3). Stromal fibroblasts were frequently MMP-1 positive in both groups, but a tendency for stromal fibroblasts to express MMP-1 (p=0.073) more abundantly in controls was noted (Table 3). There were 13 superficial and 28 nodular tumors (Table 1). When the histological subtypes were compared irrespective of immune status, there were more often MMP-1-positive stromal fibroblasts and cancer cells at the migration front of superficial than nodular tumors. The expression of MMP-1 in stromal fibroblasts of superficial tumors was 0.846 (mean) compared with 0.607 in nodular tumors, and the expression of MMP-1 in tumor cells of the superficial tumors was 0.465 (mean) compared with 0.250 in nodular tumors (Fig. 1c).

MMP-8 was not expressed by epithelial cells in any of the BCCs, and no difference between the number of stromal neutrophils near the pushing border in the two patient groups was detected either (Table 2). There were no statistically significant differences in MMP-13 staining in tumor cells at the invasive front or in stromal macrophages and fibroblasts of immunocompetent and transplanted patients (Table 2).

Gelatinase B MMP-9 was not expressed by epithelial cells in any of the tumors (Tables 2 and 3). MMP-9-positive macrophages were seen in 11 of 25 samples of the immunosuppressed group compared with 18 of 25 in the control group (Table 2), the semiquantitatively assessed difference being statistically significant (p=0.037) (Fig. 1d,e; Table 3). Neutrophils were MMP-9 immunopositive in 7 of 25 samples of the immunosuppressed group and in 3 of 25 of the nonimmunosuppressed group (Table 3). There were more often MMP-9 positive neutrophils (data not shown) in superficial than nodular BCCs (means, 0.462 vs 0.179).

Matrilysins Expression of MMP-7 by tumor cells at the invasive front, by mitotic tumor cells inside the tumor (Fig. 1f) or by stromal cells did not differ significantly between the groups (Table 2). The expression of MMP-26 in cancer cells or stroma did not differ significantly between immunodeficient and control subjects (Table 2).

Stromelysin-2 No statistically significant differences were noted between the groups when staining for MMP-10 in cancer cells, stromal cells (Fig. 2a; Table 2), or endothelium (Fig. 2b). When superficial and nodular subtypes were compared irrespective of immune status, there were more often stromal MMP-10 positive macrophages and fibroblasts in the nodular subtype (means 0.462 vs 0.929, respectively).

TIMPs BCC epithelium was rarely TIMP-1 immunopositive (Tables 2 and 3). Peritumoral macrophages were

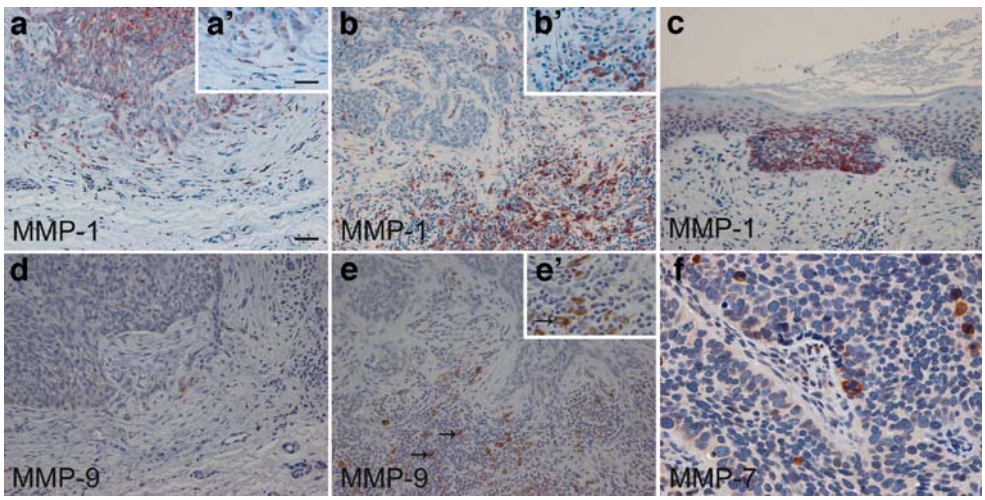


Fig. 1 MMP-1, MMP-9, and MMP-7 in basal cell cancer. **a** MMP-1 is expressed in basal cell cancer and stromal cells in a BCC of an immunosuppressed patient. *Inset a′*: Higher magnification of MMP-1-positive fibroblasts. **b** Stromal macrophages in particular are positive for MMP-1 in a BCC of an immunocompetent patient. *Inset b′*: Higher magnification of MMP-1 positive macrophages. **c** In superficial BCCs, MMP-1 was more frequently expressed at the migration front than in the nodular tumors. **d** Stromal expression of MMP-9 in a BCC of a kidney-transplant patient. **e** MMP-9 positive macrophages (*arrows*) in a BCC of an immunocompetent patient. *Inset b′*: Higher magnification of MMP-9 positive macrophages (*arrow*). **f** MMP-7 was frequently expressed by mitotic tumor cells inside BCC. *Scale bars*: (**a**–**e**), 25 μm; (*a′*, *b′*, *e′*, **f**), 12.5 μm

Table 2 Expression of MMPs-1, -7, -8, -9, -10, -13, and -26 and TIMPs -1 and -3 in BCCs of immunosuppressed and nonimmunosuppressed patients

Parameter	MMP-1			MMP-7		MMP-8		MMP-9		MMP-10		MMP-13		MMP-26		TIMP-1			TIMP-3	
	T	MF	FL	T	S	T	NF	T	MF	T	S	T	S	T	S	T	MF	FL	T	S
IS	6	19	14	1	1	0	3	0	11	3	12	4	18	2	1	1	2	4	9	13
C	11	23	20	2	2	0	1	0	18	1	15	7	19	3	1	2	9	10	12	14

n=25 in both groups
T Invading front, *S* stromal macrophages and fibroblasts, *MF* macrophages, *FL* fibroblasts, *NF* neutrophils, *IS* immunosuppressed, *C* controls

TIMP-1 immunopositive in 2 of 25 tumors of immunosuppressed patients compared with 9 of 25 in the controls. The amount of semiquantitatively assessed TIMP-1 immunopositivity was significantly more frequent in the control group (p=0.017) (Table 3). Fibroblasts in the immunocompetent group tended to express TIMP-1 more abundantly than corresponding cells in the immunosuppressed group (p=0.056) (Fig. 2c,d; Table 3). There were no significant differences in TIMP-3 immunopositivity of cancer cells at the invasive front or of macrophages, fibroblasts, and endothelial cells (data not shown) between immunosuppressed and control patients (Table 2).

Discussion

Skin cancer is the most common post-transplant malignancy with a rate 50 times higher than in the general population [37]. BCCs of transplant recipients are more often superfi-

Table 3 Expression of MMP-1, MMP-9, and TIMP-1 in BCCs

Number	MMP-1			MMP-9			TIMP-1			Number	MMP-1			MMP-9			TIMP-1		
IS	T	MF	FL	T	MF	NF	T	MF	FL	C	T	MF	FL	T	MF	NF	T	MF	FL
1A	2	1	1	0	0	1	0	0	0	1B	0	2	1	0	0	0	0	0	0
2A	0	1	0	0	1	0	0	0	0	2B	0	2	1	0	1	0	0	0	0
3A	0	2	2	0	1	2	0	0	1	3B	1	2	1	0	0	0	0	1	1
4A	0	2	1	0	1	0	0	0	0	4B	0	2	1	0	1	0	0	0	0
5A	0	2	1	0	1	1	0	1	0	5B	1	2	1	0	1	0	0	0	1
6A	0	1	1	0	1	0	0	0	0	6B	0	2	1	0	1	0	0	1	2
7A	0	2	1	0	1	0	0	0	0	7B	1	2	2	0	1	0	0	1	0
8A	0	2	1	0	1	1	0	0	0	8B	0	2	1	0	1	0	0	1	1
9A	1	1	1	0	0	0	0	0	0	9B	1	2	2	0	1	0	0	1	0
10A	1	2	1	0	1	0	1	1	1	10B	0	3	1	0	2	0	0	2	1
11A	0	1	1	0	0	0	0	0	0	11B	1	1	1	0	1	0	0	0	0
12A	0	1	1	0	0	0	0	0	0	12B	1	0	0	0	0	0	0	0	0
13A	0	0	0	0	0	0	0	0	0	13B	0	1	1	0	1	0	0	0	0
14A	0	0	0	0	0	0	0	0	0	14B	0	1	1	0	0	0	0	0	0
15A	0	1	1	0	0	0	0	0	0	15B	1	1	1	0	1	0	0	0	0
16A	0	2	1	0	1	1	0	0	0	16B	1	2	1	0	1	0	0	0	0
17A	0	1	0	0	0	0	0	0	0	17B	1	2	1	0	1	0	1	1	1
18A	0	1	0	0	0	0	0	0	0	18B	0	1	1	0	1	0	1	0	0
19A	0	0	0	0	0	1	0	0	0	19B	0	1	1	0	0	1	0	1	1
20A	1	0	0	0	0	0	0	0	0	20B	1	2	1	0	1	1	0	0	1
21A	0	0	0	0	0	0	0	0	1	21B	1	1	0	0	1	0	0	0	0
22A	1	1	0	0	1	0	0	0	0	22B	0	1	0	0	0	0	0	0	1
23A	1	1	0	0	0	0	0	0	0	23B	0	2	1	0	1	0	0	1	1
24A	0	0	1	0	0	0	0	0	1	24B	0	1	0	0	1	0	0	0	0
25A	0	1	0	0	1	1	0	0	0	25B	0	0	0	0	0	1	0	0	0
Sum	7	26	15	0	11	8	1	2	4		11	38	22	0	19	3	2	10	11
P value	NS	0.026	0.073	NS	0.037	NS	NS	0.017	0.056										

Semiquantitative grading is described in the Materials and methods section.
IS Immunosuppressed, *C* immunocompetent, *T* invading front, *MF* macrophages, *NF* neutrophils, *FL* fibroblasts

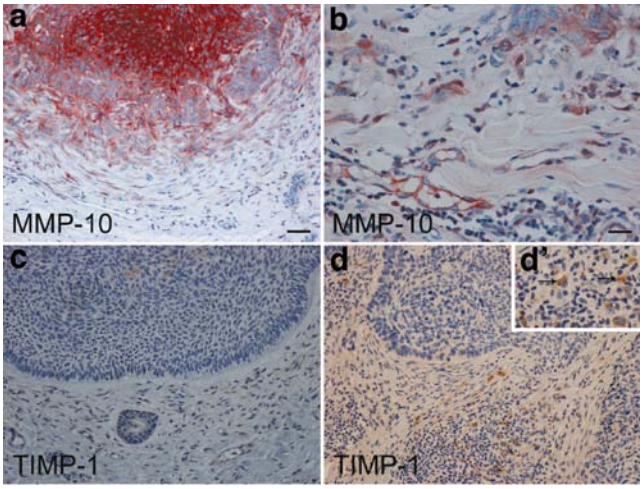


Fig. 2 MMP-10 and TIMP-1 in basal cell cancer. **a** MMP-10 was expressed by tumor and stromal cells in BCC. **b** MMP-10 expression in macrophages and endothelial cells of the pushing border. **c** TIMP-1 immunostaining in a BCC of a kidney-transplanted patient. **d** Expression of TIMP-1 in macrophages in a BCC of a control patient. *d′*: Higher magnification of TIMP-1 positive macrophages (*arrows*). *Scale bars*: (**a**, **c**, **d**), 25 μm; (**b**, *d′*), 12.5 μm

cial, occur predominantly on males and at a younger age, and are often located extracranially. In our material, 44% of BCCs were extracranial, and 28% were superficial in both groups, as tumors were site- and histology-matched. The majority of patients in the transplanted group were male, 24 of 25 compared with 15 of 25 in the control group. Mean age in the immunosuppression group was 61.4 years compared with 75.4 years in the control group. Our material was thus representative compared to previous reports [16, 21].

This is the first study examining MMP and TIMP profiles in BCC of transplant vs nonimmunocompromised patients. Investigation of the expression patterns of MMPs in pathological conditions can contribute to the rational design of anti-MMP therapy [42]. Each MMP degrades a particular subset of matrix proteins, activates growth factors, or sheds various cell surface molecules. Collagenases cleave preferably various collagens but a number of other proteins as well [29]. MMP-1 is the major collagenolytic enzyme detected in BCC [47], and in this study, MMP-1 was detected in BCC epithelium and stromal cells in agreement with previous reports [38, 46]. MMP-1 immunopositivity was significantly weaker in macrophages of the immunosuppressed, while fibroblasts tended to be more often immunopositive in the control group. Immunosuppressive therapy to inhibit allograft rejection could influence this finding, as at least, the use of corticosteroids or cyclosporin may downregulate levels of MMP-1 [2, 31]. Tumor-associated fibroblasts are unique in BCC secreting growth factors acting on tumor cells and angiogenic molecules [35]. Tumor-associated macrophages have a dual role: although they may kill neoplastic cells, they may secrete angiogenic growth factors, cytokines, and proteases, all of which can potentiate neoplastic progression [13]. Interestingly, increased expression of MMP-1 was also detected in macrophages surrounding regressing Kaposi's sarcomas [41], suggesting that MMP-1 positive macrophages may participate in host response reactions raised by the growth of BCC. Lymphocytes are the main inflammatory cell type in the vicinity of BCCs [27], but no MMPs were present in them.

The pathway of diminishing host response and gain of permissive tissue environment characterizes development of a BCC from the superficial to the nodular subtype [27]. Besides, there is a clear association of nodular BCC with sun-damaged skin and the superficial type with non-sunexposed skin [27]. When the expression of MMPs was compared in superficial vs nodular BCCs irrespective of the immune status, MMP-1 was more often detected in fibroblasts and epithelial cells at the invasive front in superficial than nodular BCCs, implicating that MMP-1 may be important in the early stages of tumor growth in degrading the ECM and cleaving active forms of growth factors that then stimulate epithelial cancer cells.

Of the other collagenases, MMP-8 was occasionally found only in neutrophils, and no differences were seen between the groups. Among MMPs, MMP-8 possesses an exceptional protective role in cancer in murine models [5] and, based on our current results, does not seem to be important in the biological behavior of BCC. MMP-13 expression is associated with malignant transformation in keratinocytes [4]. Surprisingly, it was not overrepresented at the invasive front of BCCs in immunosuppressed patients, and no significant differences in the dermal infiltrate were noted either.

MMP-9 is able to degrade collagens and gelatin among others and enhances angiogenesis by releasing VEGF [7]. MMP-9 and MMP-10 protect tumor cells from protein kinase C/p53-induced apoptosis [34]. In this study, MMP-9 was not detected in the BCC epithelium, but in neutrophils and macrophages surrounding it. MMP-9 immunopositivity was significantly more frequent in the macrophages of the nonimmunosuppressed. This may promote slower growth of these tumors by higher production of anti-angiogenic molecules [12]. MMP-9 is selectively involved in squamous carcinogenesis [13] and overexpressed in the epidermis surrounding SCCs of kidney transplant recipients compared to nonimmunocompromised patients [11]. However, our results do not support its role in mediating the growth of BCCs, which also have a different cell of origin. MMP-9 was more abundantly expressed in neutrophils of superficial than nodular BCCs, supporting data that infiltrating neutrophils play a crucial role in activating angiogenesis during the early stages of carcinogenesis [39].

To our knowledge, this is the first comprehensive study on MMP-10 protein expression in BCC. MMP-10 degrades collagens, fibronectin, elastin, and gelatin among others [29]. MMP-10 mRNA has been detected in BCC epithelium [28] but not in stromal cells. In this study, MMP-10 protein was seen in both groups in the BCC epithelium, adjacent epidermis, stromal cells, and endothelium at the invasive front. Furthermore, MMP-10 was more common in the stromal infiltrate of nodular tumors, suggesting that it may have a role in the aggressiveness of BCCs. This agrees with our previous findings on the mRNA level, showing that particularly, the aggressive sclerosing subtype of BCC expresses MMP-10 most abundantly [28].

MMP-7 has been found in recurrent and infiltrative BCC, but not in other BCC subtypes [26]. In this study, MMP-7 was detected in BCC epithelium in three nodular BCCs. The finding of MMP-7 expression associated with mitoses agrees with findings in cell culture [3]. Previous studies have shown the transformation specific nature of MMP-7 [23, 30], but our current data do not support the idea that this MMP would be upregulated by immunosuppression. The other matrilysin now studied for the first time in a large set of BCCs, MMP-26, was only rarely seen in the BCC epithelium or stromal cells, suggesting that it is not essential for the growth or angiogenesis in BCCs.

TIMPs are multifunctional molecules that can have antitumor or antimetastatic effects, but also a positive correlation between TIMP level, and poor outcome in individual types of tumors has been reported [14]. TIMP-1 was rarely detected in invasive BCC epithelium, while stromal expression was abundant in accordance with gene array data [22]. Macrophages showed significantly more TIMP-1 immunopositivity in the nonimmunosuppressed group, whereas the total amount of macrophages did not differ significantly between the groups as assessed by CD163 immunostaining (data not shown). Our results suggest that in non-immunocompromised subjects TIMP-1 prevents MMP degradation of the collagenous ECM and, thus, inhibits easy migration of tumor cells. This is the first study on TIMP-3 protein expression in a substantial number of BCCs. In contrast to TIMP-1, TIMP-3 produced by cancer cells at the margins of tumor nodules may be a host-response to inhibit MMP-mediated migration of tumor cells through the stroma.

In conclusion, we found no difference in the expression of most MMPs in the BCC tumor cells of immunocompetent and immunodeficient kidney transplant recipients. However, our results on MMP-1 and MMP-9 emphasize the role of tumor-associated macrophages and fibroblasts in the behavior of BCCs in conjunction with immunosuppression. Furthermore, strong peritumoral expression of TIMP-1 may limit matrix degradation permissive for cancer cell migration in tumors of immunocompetent patients. Future studies are needed to evaluate whether these differences could have an implication in the prevention and/or treatment of BCCs.

Acknowledgements We thank Ms. Alli Tallqvist for skillfull technical assistance and Prof. K. Isaka, Tokyo Medical University, for MMP-26 antibodies.

This study was supported by the Academy of Finland, Sigrid Juselius Foundation, Finnish Cancer Research Foundation, Ida Montin Foundation (TK), Maud Kuistila Foundation (TK), Emil Aaltonen Foundation (TK), and Helsinki University Central Hospital Research Fund (TYH 6241), Finland and Cancerfonden and Swedish Research Council, Sweden.

References

1. Ahokas K, Skoog T, Suomela S, Jeskanen L, Impola U, Isaka K, Saarialho-Kere U (2005) Matrilysin-2 (Matrix metalloproteinase-26) is upregulated in keratinocytes during wound repair and early skin carcinogenesis. J Invest Dermatol 124:849–856
2. Bolzani G, Della Coletta R, Martelli Junior H, Graner E (2000) Cyclosporin A inhibits production and activity of matrix metalloproteinases by gingival fibroblasts. J Periodontal Res 35:51–58
3. De Angelis T, Noè A, Chatterjee M, Mulholland J (2002) Stromelysin-1 activation correlates with invasiveness in squamous cell carcinoma. J Invest Dermatol 118:759–766
4. Airola K, Johansson N, Kariniemi AL, Kähäri VM, Saarialho-Kere UK (1997) Human collagenase-3 is expressed in malignant squamous epithelium of the skin. J Invest Dermatol 109:225–231
5. Balbin M, Fueyo A, Tester AM, Pendás AM, Pitiot AS, Astudillo A, Overall CM, Shapiro SD, López-Otín C (2003) Loss of collagenase-2 confers increased skin tumor susceptibility to male mice. Nat Genet 35:252–257
6. Berg D, Otley CC (2002) Skin cancer in organ transplant recipients: epidemiology, pathogenesis, and management. J Am Acad Dermatol 47:1–17
7. Bergers G, Brekken R, McMahon G, Vu TH, Itoh T, Tamaki K, Tanzawa K, Thorpe P, Itohara S, Werb Z, Hanahan D (2000) Matrix metalloproteinase-9 triggers the angiogenic switch during carcinogenesis. Nat Cell Biol 2:737–744
8. Boyd AS, Shyr Y, King LE (2002) Basal cell carcinoma in young women: an evaluation of the association of tanning bed use and smoking. J Am Acad Dermatol 46:706–709
9. Brew K, Dinakarpandian D, Nagase H (2000) Tissue inhibitors of metalloproteinases: evolution, structure and function. Biochim Biophys Acta 7:267–283
10. Chang C, Werb Z (2001) The many faces of metalloproteases: cell growth, invasion, angiogenesis and metastasis. Trends Cell Biol 11:S37–S43 (Review)
11. Chebassier N, Leroy S, Tenaud I, Knol AC, Dreno B (2002) Overexpression of MMP-2 and MMP-9 in squamous cell carcinomas of immunosuppressed patients. Arch Dermatol Res 294:124–126
12. Cornelius L, Nehring LC, Harding E, Bolanowski M, Welgus HG, Kobayashi DK, Pierce RA, Shapiro SD (1998) Matrix metalloproteinases generate angiostatin: effects on neovascularization. J Immunol 161:6845–6852
13. Coussens L, Werb Z (2002) Inflammation and cancer. Nature 420:860–867
14. Curran S, Murray G (1999) Matrix metalloproteinases in tumour invasion and metastasis. J Pathol 189:300–308

15. Diepken TL, Mahler V (2002) The epidemiology of skin cancer. Br J Dermatol 146(Suppl 61):1–6
16. Euvrard S, Kanitakis J, Pouteil-Noble C, Dureau G, Touraine JL, Faure M, Claudy A, Thivolet J (1995) Comparative epidemiologic study of premalignant and malignant epithelial cutaneous lesions developing after kidney and heart transplantation. J Am Acad Dermatol 33:222–229
17. Ferrándiz C, Fuente MJ, Ribera M, Bielsa I, Fernández MT, Lauzurica R, Roca J (1995) Epidermal dysplasia and neoplasia in kidney transplant recipients. J Am Acad Dermatol 33:590–596
18. Fortina AB, Piaserico S, Caforio AL, Abeni D, Alaibac M, Angelini A, Iliceto S, Peserico A (2004) Immunosuppressive level and other risk factors for basal cell carcinoma and squamous cell carcinoma in heart transplant recipients. Arch Dermatol 140:1079–1085
19. Gomez DE, Alonso DF, Yoshiji H, Thorgeirsson UP (1997) Tissue inhibitors of metalloproteinases: structure, regulation and biological functions. Eur J Cell Biol 74:111–122
20. Guo HR, Yu HS, Hu H, Monson RR (2001) Arsenic in drinking water and skin cancers: cell-type specificity (Taiwan, ROC). Cancer Causes Control 12:909–916
21. Harwood CA, Proby CM, McGregor JM, Sheaff MT, Leigh IM, Cerio R (2006) Clinicopathologic features of skin cancer in organ transplant recipients: a retrospective case-control series. J Am Acad Dermatol 54:290–300
22. Howell B, Solish N, Lu C, Watanabe H, Mamelak AJ, Freed I, Wang B, Sauder DN (2005) Microarray profiles of human basal cell carcinoma: insights into tumor growth and behavior. J Dermatol Sci 39:39–51
23. Impola U, Jeskanen L, Ravanti L, Syrjänen S, Baldursson B, Kähäri V-M, Saarialho-Kere U (2005) Expression of matrix metalloproteinase (MMP)-7 and MMP-13 and loss of MMP-19 and p16 are associated with malignant progression in chronic wounds. Br J Dermatol 152:720–726
24. Isaka K, Nishi H, Nakai H, Nakada T, Feng Li Y, Ebihara Y, Takayama M (2003) Matrix metalloproteinase-26 is expressed in human endometrium but not in endometrial carcinoma. Cancer 97:79–89
25. Kanitakis J, Alhaj-Ibrahim L, Euvrard S, Claudy A (2003) Basal cell carcinomas developing in solid organ transplant recipients: clinico-pathologic study of 176 cases. Arch Dermatol 139:1133–1137
26. Karelina T, Goldberg GI, Eisen AZ (1994) Matrilysin (PUMP) correlates with dermal invasion during appendageal development and cutaneous neoplasia. J Invest Dermatol 103:482–487
27. Kaur P, Mulvaney M, Carlson J (2006) Basal cell carcinoma progression correlates with host immune response and stromal alterations: a histologic analysis. Am J Dermatopathol 28:293–307
28. Kerkelä E, Ala-aho R, Jeskanen L, Lohi J, Kähäri V-M, Saarialho-Kere U (2001) Differential patterns of stromelysin-2 (MMP-10) and MT1-MMP (MMP-14) expression in epithelial skin cancers. Br J Cancer 84:659–669
29. Kerkelä E, Saarialho-Kere U (2003) Matrix metalloproteinases in tumor progression: focus on basal and squamous cell skin cancer. Exp Dermatol 12:109–125
30. Kuivanen T, Jeskanen L, Kyllönen L, Impola U, Saarialho-Kere U (2006) Transformation-specific matrix metalloproteinases, MMP-7 and MMP-13 are present in epithelial cells of keratoacanthomas. Modern Pathol 19:1203–1212
31. Kylmäniemi M, Oikarinen A, Oikarinen K, Salo T (1996) Effects of dexamethasone and cell proliferation on the expression of matrix metalloproteinases in human mucosal normal and malignant cells. J Dent Res 75:919–926
32. Lear JT, Smith AG, Strange RD, Fryer AA (1998) Patients with truncal basal cell carcinoma represent a high-risk group. Arch Dermatol 134:373
33. LeBoit PE, Burg G, Weedon D, Sarasain A (eds) (2006) World Health Organization classification of tumours. Pathology and genetics of skin tumours. IARC, Lyon
34. Meyer E, Vollmer J, Bovey R, Stamenkovic I (2005) Matrix metalloproteinases 9 and 10 inhibit protein kinase C potentiated, p53-mediated apoptosis. Cancer Res 65:4261–4272
35. Micke P, Kappert K, Oshima M, Sundquist C, Scheidl S, Lindahl P, Heldin C-H, Botling J, Ponten F, Östman A (2007) In situ identification of genes regulated specifically in fibroblasts of human basal cell carcinoma. J Invest Dermatol 127:1516–1523
36. Mirastschijski U, Impola U, Jahkola T, Karlsmark T, Ågren M, Saarialho-Kere U (2002) Ectopic localization of matrix metalloproteinase-9 in chronic cutaneous wounds. Hum Pathol 33:355–364
37. Moloney FJ, Comber H, O, Lorcain P, O, Kelly P, Conlon PJ, Murphy GM (2006) A population-based study of skin cancer incidence and prevalence in renal transplant recipients. Brit J Dermatol 154:498–504
38. Monhian N, Jewett B, Baker S, Varani J (2006) Matrix metalloproteinase expression in normal skin associated with basal cell carcinoma and in distal skin from the same patients. Arch Facial Plast Surg 7:238–243
39. Nozawa H, Chiu C, Hanahan D (2006) Infiltrating neutrophils mediate the initial angiogenic switch in a mouse model of multistage carcinogenesis. Proc Natl Acad Sci USA 103:12493–12498
40. Ohnishi Y, Tajima S, Akiyama M, Ishibashi A, Kobayashi R, Horii I (2000) Expression of elastin-related proteins and matrix metalloproteinases in actinic elastosis of sun-damaged skin. Arch Dermatol Res 292:27–31
41. Pantanowitz L, Dezube BJ, Hernandez-Barrantes S, Tahan SR, Dabbous MK (2006) Matrix metalloproteinases in the progression and regression of Kaposi's sarcoma. J Cutan Pathol 33:793–796
42. Rosenthal E, Matrisian L (2006) Matrix metalloproteinases in head and neck cancer. Head Neck 28:639–648
43. Tanaka M, Itai T, Adachi M, Nagata S (1998) Downregulation of Fas ligand by shedding. Nat Med 4:31–36
44. Tilli CM, van Steensel MA, Krekels GA, Neumann HA, Ramaekers FC (2005) Molecular aetiology and pathogenesis of basal cell carcinoma. Br J Dermatol 152:1108–1124 (review)
45. Tran H, Chen K, Shumack S (2003) Epidemiology and aetiology of basal cell carcinoma. Br J Dermatol 149(Suppl 66):50–52
46. Varani J, Hattori Y, Chi Y, Schmidt T, Perone P, Zeigler ME, Fader DJ, Johnson TM (2000) Collagenolytic and gelatinolytic matrix metalloproteinases and their inhibitors in basal cell carcinoma of skin: comparison with normal skin. Br J Cancer 82:657–665
47. Yucel T, Mutnal A, Fay K, Fligiel SE, Wang T, Johnson T, Baker SR, Varani J (2005) Matrix metalloproteinase expression in basal cell carcinoma: relationship between enzyme profile and collagen fragmentation pattern. Exp Mol Pathol 79:151–160

Virchows Arch (2008) 452:91–95
DOI 10.1007/s00428-007-0486-4

CASE REPORT

Thyroid follicular carcinoma-like renal tumor: a case report with morphologic, immunophenotypic, cytogenetic, and scintigraphic studies

Sterlacci William · Verdorfer Irmgard · Gabriel Michael · Mikuz Gregor

Received: 24 July 2007 / Accepted: 24 July 2007 / Published online: 18 August 2007
© Springer-Verlag 2007

Abstract In this report, a rare renal tumor that morphologically resembles a thyroid follicular carcinoma is described. To date, this subtype has not been integrated into a known form of renal carcinoma. A 29-year-old female patient without relevant family or social history underwent nephrectomy because of a renal tumor measuring 5 cm by the largest diameter. The macroscopically white-yellow tumor showed follicular structures with abundant eosinophilic colloidal material and focal papillary differentiation by light microscopy. Immunohistochemically, the tumor cells stained positively for cytokeratin (CK-7, CK-20, CAM 5.2) and vimentin. CD-10, CD-117, thyroid transcription factor-1, and thyreoglobulin remained completely negative. Chromosomal losses of 1, 3, 7, 9p21, 12, 17, and X were detected by fluorescence in situ hybridization. Scintigraphs showed an inconspicuous thyroid gland and no extrathyroidal pathological accumulations, making metastatic spread to the kidney highly unlikely. To our knowledge, this is the second fully documented case of a thyroid follicular carcinoma-like renal tumor. This uncommon variant is important to keep in mind to prevent unnecessary or inappropriate treatment.

Keywords Thyroid follicular carcinoma-like · Renal tumor · Immunophenotypic

S. William (✉) · V. Irmgard · M. Gregor
Department of Pathology, Medical University of Innsbruck,
Muellerstr. 44, 6020 Innsbruck, Austria
e-mail: william.sterlacci@i-med.ac.at

G. Michael
Department of Nuclear Medicine,
Medical University of Innsbruck,
Anichstr. 35, Innsbruck, Austria

Introduction

Cancer of the kidney and renal pelvis represent 3–4% of all adult malignancies [12] with renal cell carcinoma accounting for 80–85% [16]. Renal cell carcinoma occurs twice as often in men than in women [16], and patients are generally older than 40 years at diagnosis, being predominantly in the seventh decade of life [3]. Other less common histologic types include transitional cell carcinoma of the renal pelvis and Wilms' tumor (nephroblastoma) in children [16]. Renal cell carcinoma can be classified as clear cell or conventional (approximately 60%), papillary (7–14%), chromophobe (6–11%), oncocytoma (7–10%), collecting duct, and medullary cell type (<1%) [26]. One unusual form of renal cell carcinoma, which morphologically resembles that of thyroid follicular carcinoma, has yet been fully documented in a single case report [13]. Herein, we describe another such entity.

Clinical history

A 29-year-old woman without relevant family or social history was found to have a mass in the middle of her left kidney measuring 3.4×4.3×4.4 cm by ultrasonography. The structure was echo-inhomogeneous with a 5-mm broad edematous border and showed displacement of the blood vessels, without evidence of capsule penetration or infiltrative growth.

The histologic aspects of the nephrectomy specimen strongly suggested a thyroid follicular carcinoma becoming manifest by metastasis to the kidney. The tumor was therefore ultimately signed off as a renal metastasis by a thyroid follicular carcinoma.

Table 1 Antibodies used for immunohistochemical staining

Antibody	Source	Dilution
CAM5.2	Becton, Dickinson and Company	1:5
CD10	Novocastra	1:50
CD117	DAKO	1:100
CK7	DAKO	1:50
CK20	DAKO	1:1000
Thyreoglobulin	DAKO	1:6000
Thyroid transcription factor-1	DAKO	1:100
Vimentin	DAKO	1:250

Despite scintigraphic results without discernable pathology, total thyroidectomy with subsequent bilateral excision of the jugulary lymph nodes was performed.

Approximately 2 months after nephrectomy, a focus in the lower left lung lobe was biopsied, presenting identical histomorphology as the described renal tumor.

Five years after primary diagnosis, the patient is still in good health without recurring disease or related complaints. She also gave birth to a healthy child after an uneventful pregnancy.

Materials and methods

Tissue was fixed in 10% neutral-buffered formalin, embedded in paraffin, and stained with hematoxylin and eosin. Immunohistochemistry was performed using the automated staining system NexES with a diaminobenzidine detection kit, both by Ventana Medical Systems. The primary antibodies used and their dilutions are listed in Table 1.

Fluorescence in situ hybridization (FISH) was performed with a panel of centromere and locus specific probes (Vysis, Downers Grove, IL) according to the protocol of the manufacturer.

Results

The nephrectomy specimen revealed a well-circumscribed tumor measuring 5 cm by the largest diameter, white-yellow on cross-section, and without presentable connection to the renal pelvis. By histological examination, the tumor was made up of flat cells forming one layered micro-, normo-, and macrofollicular structures containing abundant eosinophilic colloidal material (Fig. 1a). Some parts also showed papillary differentiation. The lesion was delimitable from the surrounding normal kidney tissue by a poorly developed fibrous pseudocapsule.

Immunhistochemically, the tumor cells showed staining for cytokeratin (CK-7, CK-20, CAM 5.2) as well as vimentin (Fig. 1b, c). CD-10, CD-117, thyroid transcription factor-1 (TTF-1) and thyroglobulin (Tg) remained completely negative (Fig. 1d). FISH analysis was performed for detection of abnormal chromosomal copy number changes, demon-

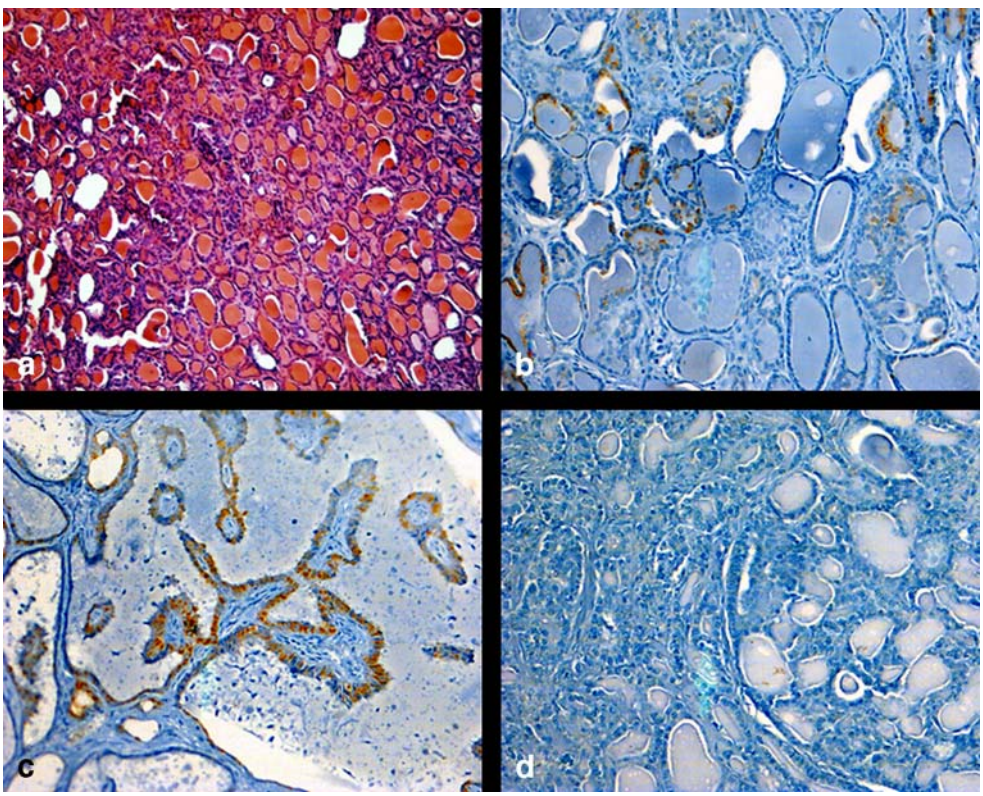


Fig. 1 Histologic and immunophenotypic features of thyroid follicular like renal carcinoma. **a** Hematoxylin and eosin (original magnification 20×). **b** Cytokeratin cocktail CAM 5.2 stain (original magnification 20×). **c** Cytokeratin 7 stain in an area with papillary differentiation (original magnification 20×). **d** Thyreoglobulin stain remaining negative (original magnification 20×)

strating a loss of chromosomes 1 (23.7%), 3 (29.4%), 7 (22%), 9p21 (31.2%), 12 (17.8%), 17 (31.2%), and X (46.7%).

99-Tc-Scintigraphy and ultrasound of the neck demonstrated no suspicious findings, and laboratory parameters were also in a normal range, making thyroid pathology very unlikely. Abnormal extrathyroidal findings or pathological accumulations of specific markers were also not observed. Furthermore, 18-fluorodeoxyglucose positron emission tomography (18-FDG-PET) did not reveal areas with an increased uptake. 131-I whole-body scans performed before, as well as after thyroidectomy, did not show areas suspicious for thyroid cancer (Fig. 2).

The thyroidectomy specimen and all excised lymph nodes were without pathological findings.

The biopsy of the focus in the lower left lung lobe presented identical histomorphology as the described renal tumor, although it differed immunhistochemically by positive staining for TTF-1, without expressing CK-20.

Discussion

The kidney tumor described in this case primarily pointed toward a renal metastasis of a thyroid follicular carcinoma. The immunhistochemical findings did not completely support this diagnose, as staining for TTF-1 and Tg repeatedly remained entirely negative. Tg is generally a reliable marker for thyroid follicular carcinoma, although it has been shown that not all such tumors stain positively, particularly poorly differentiated forms [6, 10, 24]. TTF-1 is also usually only absent in anaplastic thyroid carcinomas [20]. In contrast, this particular tumor was histomorphologically highly differentiated. Additionally, no increased uptake during 18-FDG-PET could be demonstrated, referring to a poorly differentiated thyroid carcinoma [4]. Furthermore, considering the rather low Tg levels (preoperative=4.4 ng/μL, postoperative=2.9 ng/μL), metastatic disease deriving from the thyroid gland was unlikely [22]. It is interesting to note that the secondary lung focus with identical hematoxylin and eosin morphology did indeed express TTF-1, the meaning of which remains unclear.

Attempts have been made to characterize common renal epithelial neoplasms by a panel of different antibodies, mainly CK-7, CD-10, and vimentin, which were also part of our diagnostic workup. Bazille et al. [1] found positive staining for CK 7 and vimentin to be rather specific for papillary renal carcinomas. This is interesting because some parts of our tumor showed papillary differentiation as well. On the other hand, 65% of papillary renal tumors examined by Bazille et al. [1] also expressed CD-10, which remained negative in our case. Kim and Kim [15] even stated in their study that papillary renal carcinomas predominantly express CD-10, while also being positive for CK-7 and vimentin. The only other renal epithelial neoplasm found with similar immunohistochemistry was the chromophobe subtype, expressing CK-7 without staining positive for CD-10 [5, 15]. Although, Bazille et al. demonstrated 39% of their chromophobe carcinomas with positive CD-10 staining. Furthermore, the chromophobe variants did not express vimentin [1, 5]. The one existing fully documented case of thyroid follicular carcinoma-like tumor of the kidney by Jung et al. [13] showed intense staining for cytokeratin cocktail AE1/AE3 and CD-10, without expressing CK-7 or CK-20. In addition, the tumor cells revealed a focal cytoplasmic vimentin reaction, while TTF-1 and Tg remained negative. Keeping in mind the existing immunohistochemical discrepancies of common renal epithelial neoplasms, our described tumor, also considered renal, prompts considerable diagnostic difficulties.

Renal cell carcinomas are characterized by different histological patterns and clinical courses, caused by different cytogenetic profiles. Deletions of three regions on chromosome 3p are a consistent early aberration in tumorgenesis of clear cell carcinoma. In addition, structural and numerical abnormalities of 5p, 7, 6q, 8p, 9p, 14q, 17p, and XY are fre-

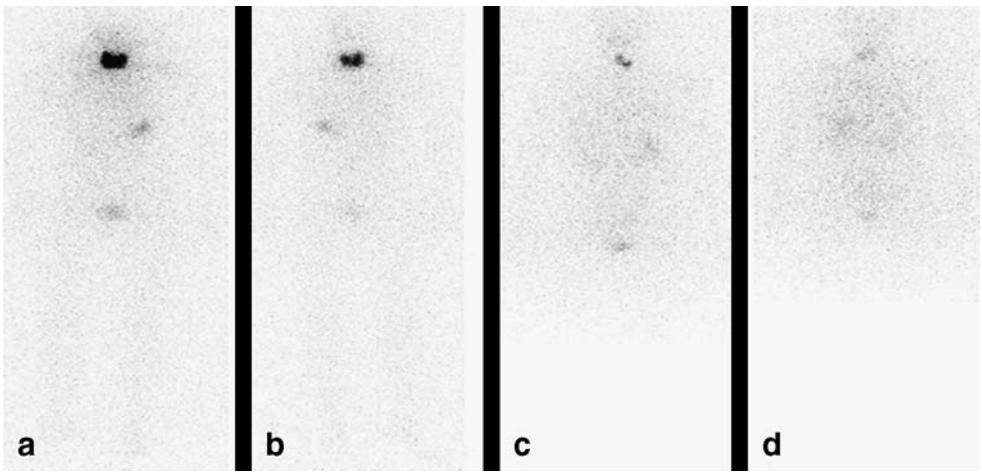


Fig. 2 131-I whole-body scintigrams. **a** Prethyroidectomy anterior. **b** Prethyroidectomy posterior. **c** Post-thyroidectomy anterior. **d** Post-thyroidectomy posterior

quent findings in this tumor type. The described cytogenetic characteristics of the papillary (chromophilic) carcinoma are gains of 3q, 7, 12, 16, 17, and 20 and loss of Y. The chromophobe renal cell carcinoma has been associated predominantly with losses of chromosomes 1, 2, 6, 10, 13, 17, 21, and X [14, 17, 18, 25, 27, 28]. Our cytogenetic profile is not typical for clear cell or papillary renal cell carcinoma but is more similar to the findings in the chromophobe variant. Our data are discrepant with the cytogenetic data by Jung et al. [13]. These authors found chromosomal gains of 7q36, 8q14, 12, 16, 17, 19q, 20q, 21q, and Xp and losses of 1p36, 3, and 9q21–33 in a thyroid follicular-like renal carcinoma.

When assuming a thyroid carcinoma, not only the thyroid gland itself but also ectopic thyroid tissue must be considered, which is reported in 7% of adults [31] especially in a thyroglossal duct or the close vicinity of the thyroid gland [8]. Ninety percent of reported cases of ectopic thyroid are found in the anterior midline at the base of the tongue [19]. Other possible sites are the anterior tongue, larynx, trachea, esophagus, mediastinum, pericardium, diaphragm, and neck branchial cysts [8]. Malignant transformation of ectopic thyroid tissue is extremely uncommon, and most cases are characterized as papillary carcinomas [19]. Scintigraphs performed before and after surgery could not detect suspicious accumulations in the thyroid gland, an ectopic area, or in the suspected pulmonary lesion.

Struma ovarii metastasizing to the kidney would be a possible, although extremely seldom occurrence, which must also be excluded for the sake of completeness. Struma ovarii, a rare ovarian teratoma consisting mainly of thyroid tissue, represent 2% of all ovarian tumors [21, 29]. Malignancy occurs in 5–10% [7, 9, 11, 23, 30], and only in approximately 5% do they metastasize, primarily to the liver and peritoneum [2]. In our case, no ovarian abnormalities were encountered sonographically or scintigraphically, although it must be noted that malignant strumae ovarii demonstrate a relatively poor iodine uptake and do not usually secrete thyroid hormones [2, 30]. Additionally, the fact that the patient experienced an uneventful pregnancy and child birth makes a struma ovarii very unlikely.

References

1. Bazille C, Allory Y, Molinie V, Vieillefond A, Cochand-Priollet B, Cussenot O, Callard P, Sibony M (2004) Immunohistochemical characterisation of the main histologic subtypes of epithelial renal tumours on tissue-microarrays. Study of 310 cases. Ann Pathol 24: 395–406
2. Berghella V, Ngadiman S, Rosenberg H, Hoda S, Zuna RE (1997) Malignant struma ovarii. A case report and review of the literature. Gynecol Obstet Invest 43:68–72
3. Cao Y, Paner GP, Perry KT, Flanigan RC, Campbell SC, Picken MM (2005) Renal neoplasms in younger adults: analysis of 112 tumors from a single institution according to the new 2004 World Health Organization classification and 2002 American Joint Committee on Cancer Staging System. Arch Pathol Lab Med 129:487–491
4. Chung JK, So Y, Lee JS, Choi CW, Lim SM, Lee DS, Hong SW, Youn YK, Lee MC, Cho BY (1999) Value of FDG PET in papillary thyroid carcinoma with negative 131I whole-body scan. J Nucl Med 40:986–992
5. Dai L, Lu XH, Li ZH, Li R, Liu H, Liu YL, Hui YZ (2004) Value of special stains and immunohistochemistry in the diagnosis of renal epithelial neoplasms. Zhonghua Bing Li Xue Za Zhi 33:140–142
6. de Micco C, Ruf J, Carayon P, Chrestian MA, Henry JF, Toga M (1987) Immunohistochemical study of thyroglobulin in thyroid carcinomas with monoclonal antibodies. Cancer 59:471–476
7. Devaney K, Snyder R, Norris HJ, Tavassoli FA (1993) Proliferative and histologically malignant struma ovarii: a clinicopathologic study of 54 cases. Int J Gynecol Pathol 12:333–343
8. Fumarola A, Trimboli P, Cavaliere R, Coletta I, Veltri A, Di Fiore A, Ciardi A, Piccirilli F (2006) Thyroid papillary carcinoma arising in ectopic thyroid tissue within a neck branchial cyst. World J Surg Oncol 4:24
9. Gonzalez-Angulo A, Kaufman RH, Braungard CD, Chapman FC, Hinshaw AJ (1963) Adenocarcinoma of thyroid arising in struma ovarii (malignant struma ovarii). Report of two cases and review of the literature. Obstet Gynecol 21:567–576
10. Harach HR, Franssila KO (1988) Thyroglobulin immunostaining in follicular thyroid carcinoma: relationship to the degree of differentiation and cell type. Histopathology 13:43–54
11. Hasleton PS, Kelehan P, Whittaker JS, Burslem RW, Turner L (1987) Benign and malignant struma ovarii. Arch Pathol Lab Med 102:180–184
12. Jemal A, Siegel R, Ward E, Murray T, Xu J, Thun MJ (2007) Cancer statistics, 2007. CA Cancer J Clin 57:43–66
13. Jung SJ, Chung JI, Park SH, Ayala AG, Ro JY (2006) Thyroid follicular carcinoma-like tumor of kidney: a case report with morphologic, immunohistochemical, and genetic analysis. Am J Surg Pathol 30:411–415
14. Junker K, Schlichter A, Junker U, Knofel B, Kosmehl H, Schubert J, Claussen U (1997) Cytogenetic, histopathologic, and immunologic studies of multifocal renal cell carcinoma. Cancer 79:975–981
15. Kim MK, Kim S (2002) Immunohistochemical profile of common epithelial neoplasms arising in the kidney. Appl Immunohistochem Mol Morphol 10:332–338
16. Kosary CL, McLaughlin JK (1993) Kidney and renal pelvis. In: Miller BA, Ries LAG, Hankey BF et al (eds) SEER cancer statistics review. 1973–1990. NIH publication no. 93-2789, XI.1-XI.22. National Cancer Institute, Bethesda, MD
17. Kovacs G (1993) Molecular cytogenetics of renal cell tumors. Adv Cancer Res 62:89–124
18. Lau LC, Tan PH, Chong TW, Foo KT, Yip S (2007) Cytogenetic alterations in renal tumors: a study of 38 Southeast Asian patients. Cancer Genet Cytogenet 175:1–7
19. Ling L, Zhou SH, Wang SQ, Wang LJ (2004) Misdiagnosed ectopic thyroid carcinoma: report of two cases. Chin Med J (Engl) 117:1588–1589
20. Miettinen M, Franssila KO (2000) Variable expression of keratins and nearly uniform lack of thyroid transcription factor 1 in thyroid anaplastic carcinoma. Human Pathol 31:1139–1145
21. Nieminen U, Vonnumers C, Widholm O (1964) Struma ovarii acta. Obstet Gynecol Scand 42:399–424
22. Pacini F, Molinaro E, Lippi F, Castagna MG, Agate L, Ceccarelli C, Taddei D, Elisei R, Capezzone M, Pinchera A (2001) Prediction of disease status by recombinant human TSH-stimulated serum Tg in the postsurgical follow-up of differentiated thyroid carcinoma. J Clin Endocrinol Metab 86:5686–5690
23. Pardo-Mindan FJ, Vazquez JJ (1983) Malignant struma ovarii. Light and electron microscopic study. Cancer 51:337–343

24. Ratnatnga N, Ramadasa S (1993) Immunohistochemical staining for thyroglobulin in poorly differentiated carcinoma of the thyroid. Ceylon Med J 38:113–116
25. Receveur AO, Couturier J, Molinie V, Vieillefond A, Desangles F, Guillaud-Bataille M, Danglot G, Coullin P, Bernheim A (2005) Characterization of quantitative chromosomal abnormalities in renal cellcarcinomas by interphase four-color fluorescence in situ hybridization. Cancer Genet Cytogenet 158:110–118
26. Reuter VE, Presti JC Jr (2000) Contemporary approach to the classification of renal epithelial tumors. Semin Oncol 27:124–137
27. Speicher MR, Schoell B, du Manoir S, Schrock E, Ried T, Cremer T, Storkel S, Kovacs A, Kovacs G (1994) Specific loss of chromosomes 1, 2, 6, 10, 13, 17, and 21 in chromophobe renal cell carcinomas revealed by comparative genomic hybridization. Am J Pathol 145:356–364
28. Verdorfer I, Hobisch A, Hittmair A, Duba HC, Bartsch G, Utermann G, Erdel M (1999) Cytogenetic characterization of 22 human renal cell tumors in relation to a histopathological classification. Cancer Genet Cytogenet 111:61–70
29. Woodruff JD, Rauh JT, Markley RL (1966) Ovarian struma. Obstet Gynecol 27:94–201
30. Yannopoulos D, Yannopoulos K, Ossowski R (1976) Malignant struma ovarii. Pathol Annu 11:403–413
31. Yildiz K, Koksal H, Ozoran Y, Muhtar H, Telatar M (1993) Papillary carcinoma in a thyroglossal duct remnant with normal thyroid gland. J Laryngol Otol 107:1174–1176

Virchows Arch (2008) 452:97–101
DOI 10.1007/s00428-007-0518-0

CASE REPORT

Brucellosis of the lung: case report and review of the literature

Dirk Theegarten · Sven Albrecht · Martin Tötsch · Helmut Teschler · Heinrich Neubauer · Sascha Al Dahouk

Received: 7 June 2007 / Revised: 6 September 2007 / Accepted: 26 September 2007 / Published online: 20 October 2007
© Springer-Verlag 2007

Abstract Human brucellosis is a worldwide re-emerging zoonosis. However, its histological appearance has only been occasionally described. We report the case of a young girl who had been suffering from a spontaneous fracture of the eighth thoracic vertebra at the age of 7. At the age of 15, X-ray showed a translucence of the seventh and ninth thoracic vertebra, and additionally, a bi-lateral episcleritis was detected. Three months later, she was admitted to the hospital because of perspiration at night and moderate fever. Computer tomography revealed coarsely spotted infiltrates in the lower fields of both lungs. Serology for rheumatic diseases was negative. Thoracoscopical wedge resection was done for histological clarification of pulmonary changes. Microscopically, a granulomatous inflammation with central necrosis was seen. A Ziehl–Neelsen stain did not demonstrate acid-fast bacteria. In spite of negative serology, real-time polymerase chain reaction detected *Brucella melitensis* deoxyribonucleic acid in the formalin-fixed tissue samples of the lung. Interrogation of the patient revealed visits in different Arabian countries during childhood as a presumable source of infection. In conclusion, granulomatous inflammation negative for Ziehl–Neelsen and Grocott stains presenting together with other localized lesions should lead to specific investigations on brucellosis.

Keywords Brucellosis · Lung · Granulomatosis · Zoonosis

D. Theegarten (✉) · M. Tötsch
Institute of Pathology and Neuropathology,
University Hospital Essen, University of Duisburg-Essen,
Hufelandstrasse 55,
45122 Essen, Germany
e-mail: dirk.theegarten@uk-essen.de

S. Albrecht · H. Teschler
Department of Pneumology, Ruhrlandklinik,
University Hospital Essen,
Tueschener Weg 40,
45239 Essen, Germany

H. Neubauer · S. Al Dahouk
Department of Bacteriology,
Bundeswehr Institute of Microbiology,
Neuherbergstrasse 11,
80937 Muenchen, Germany

Present address:
H. Neubauer
Institute of Bacterial Infections and Zoonoses,
Friedrich-Loeffler-Institut,
Naumburger Strasse 96a,
07743 Jena, Germany

Present address:
S. Al Dahouk
Department of Internal Medicine III, RWTH Aachen University,
Pauwelsstrasse 30,
52074 Aachen, Germany

Introduction

Brucellosis is a worldwide re-emerging zoonosis caused by organisms belonging to the genus *Brucella*, which are Gram-negative, non-spore-forming, facultative intracellular bacteria [5, 25]. *Brucella* infections cause reproductive failure in domestic animals and acute and chronic disease in affected humans. The most pathogenic species are *B. melitensis*, responsible for small ruminant brucellosis (sheep, goats), *B. abortus*, the main etiologic agent of bovine brucellosis, and *B. suis* responsible for swine brucellosis [7, 10]. Wildlife animals (bisons, elks, wild boars, marine mammals) may be affected as well [9, 18]. Animal brucellosis is still endemic in Mediterranean countries [7], in Africa, the Middle East,



Fig. 1 High-resolution computertomography reveals a localized pericardial infiltrate

South Asia and Central and South America. In non-endemic countries with a successful eradication of animal brucellosis like Germany, disease is imported by travelling [3]. Brucellosis is mainly transmitted through the consumption of non-pasteurized milk or cheese from infected goats, sheep or cattle, consumption of contaminated meat or by direct contact with infected animals and their abortion material. Brucellosis is the most frequently laboratory-acquired bacterial infection, and *Brucella* might even be used in bioterrorism [5, 23].

Uncharacteristic symptoms like undulant fever and malaise are seen in most patients. Focal manifestations are found in joints and bones (spondylitis, sacroiliitis, arthritis), the respiratory tract (pneumonia, pleuritis), in the cardiovascular (endocarditis, pericarditis, vasculitis), and nervous system (radiculitis, meningoencephalomyelitis), in the urogenital system (nephritis, epididymitis, orchitis) as well as in the liver, spleen and the skin [3, 5, 14, 25]. Histology of brucellosis shows a granulomatous reaction; additionally, uncharacteristic features are described [1, 2, 8, 11, 16, 18–22], which can be seen in a large number of other lung diseases as well [6, 12].

Clinical history

A 15-year-old German girl had suffered from back pain at the age of 7 for the first time. Magnetic resonance imaging (MRI) revealed cyphosis and a spontaneous fracture of the eighth thoracic vertebra. A very small biopsy was taken, which allowed no clear-cut diagnosis. An eosinophilic granuloma was considered. However, after anti-biotic therapy, recurrent regression of symptoms and of MRI changes were observed. Seven years later, severe back pain re-occurred. This time, MRI showed translucence of the seventh and ninth thoracic vertebra. A subsequently performed positron emission tomography combined with computer tomography for the detection of additional foci revealed two pulmonary lesions in the right apical lung. Clinically, the patient was complaining about perspiration at night, moderate undulant fever and weakness. Clinical examinations showed a bi-lateral episcleritis and slightly decreased haemoglobin (11.1 g/dl), whereas liver enzymes were within normal range. Serology for rheumatic or immunological diseases, complement fixation test (CFT) for brucellosis and tuberculin skin test were negative. High-resolution computer tomography showed coarsely spotted infiltrates in both lower fields of the lungs (Fig. 1). Bodyplethysmography revealed slight obstruction. Clinical differential diagnostic considerations included bronchiolitis obliterans with organizing pneumonia, Langerhan's cell histiocytosis, tuberculosis and sarcoidosis. Thoracoscopic wedge resection was carried out for histological clarification of pulmonary changes. After diagnosis of brucellosis, anti-biotic treatment using rifampicin and doxycycline combined with prednison was administered for 3 months, which resulted in the disappearance of all symptoms. Sacroiliitis developed after ending medication. Serology remained negative at this time (IgG in enzyme-linked immunosorbent assay [ELISA]<5 U/ml, questionable 20–30; IgM ELISA<5 U/ml, questionable 15–20). Anti-microbial treatment was continued. During therapy, temporary rifampicin-induced renal failure developed. At the moment (33 months after initial start of treatment) the patient shows no signs of a relapse of the disease.

Materials and methods

The lung specimen was fixed in 3.5% buffered formaldehyde and conventionally stained (haematoxylin–eosin, Elastica van Gieson, periodic acid Schiff, Ziehl–Neelsen, Grocott, Whartin–Starry, Brown–Hopps). Tissue samples selected for investigation by polymerase chain reaction (PCR) were dried using liquid nitrogen and homogenized mechanically. Subsequently, deoxyribonucleic acid (DNA) samples were prepared using a lysis buffer (5× buffer D [PCR Optimation Kit; Invitrogen, DeShelp, The Netherlands, 1:5 diluted in Aqua dest.]; 0.5% Tween 20™ [ICI, American Limited, Merck, Germany]; 2 mg/ml proteinase K [Roche Diagnostics, Germany]). After incubation at 56°C for 1 h and inactivation for 10 min at 95°C, 2 µl of the cleared lysate were used as a template in an in-house genus-specific *bcsp31* real-time PCR [3] as well as in the species-specific automated multiplex oligonucleotide synthesizer (AMOS) PCR according to Redkar et al. [17].

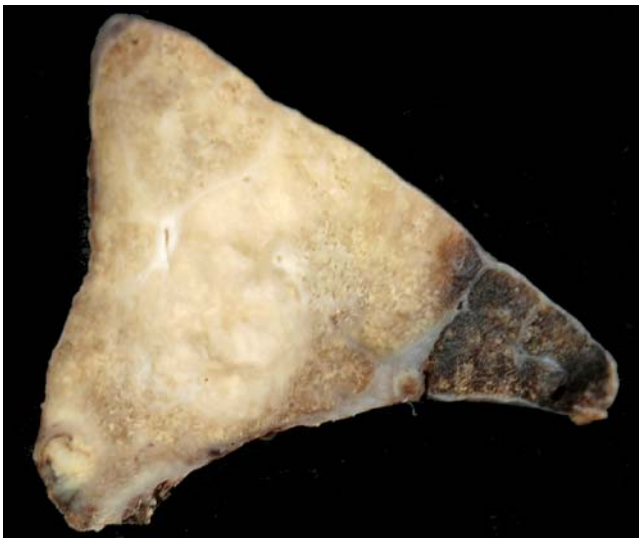


Fig. 2 Macroscopy of the wedge resection shows a central necrosis with a surrounding rim of mesenchymal tissue

Results

Wedge resection specimen showed a yellow-white map-like consolidation of the lung with a crumbly cut (Fig. 2). Microscopically, in the haematoxylin–eosin stain, irregular foci of extensive caseous necrosis containing neutrophils with a granulomatous inflammation in the surrounding tissue were seen (Fig. 3a, b). Multi-nuclear giant cells were often large and did not show the typical arrangement in the periphery as found in tuberculosis (Fig. 3c). In some areas, epitheloid cells were densely aggregated showing pallisading. Foreign bodies, vasculitis or prominent eosinophiles were not seen. Adjacent lung parenchyma revealed dystelectasis, focal intra-alveolar granulation tissue and minor infiltrations of lymphocytes and plasma cells. Scarring in the surrounding tissue was demonstrated particularly in the Elastica van Gieson stain. Using periodic acid Schiff reaction, Grocott and Whartin–Starry stains, no fungi or bacteria could be detected. Ziehl–Neelsen stain showed no acid-fast bacteria. Brown Hopps stain (modified Gram stain) revealed coccoid agents within the necrotic areas (Fig. 3d).

By the genus-specific *bcsp31* real-time PCR, *Brucella* DNA was detected, and the modified AMOS-PCR revealed *B. melitensis*.

Discussion

Brucellosis is a disease rarely seen by pathologists. Generally, histological findings vary widely and include abscesses, ulcerations and vasculitis, granulation tissue, histiocytic reactions and non-caseating or caseating granulomatous patterns [1]. Summarizing the results of three larger studies with a total of 78 cases, non-specific chronic inflammation is dominating (56.4%), and granulomatous patterns without necrosis are found in 29.5% and with necrosis in 14.1% [1,

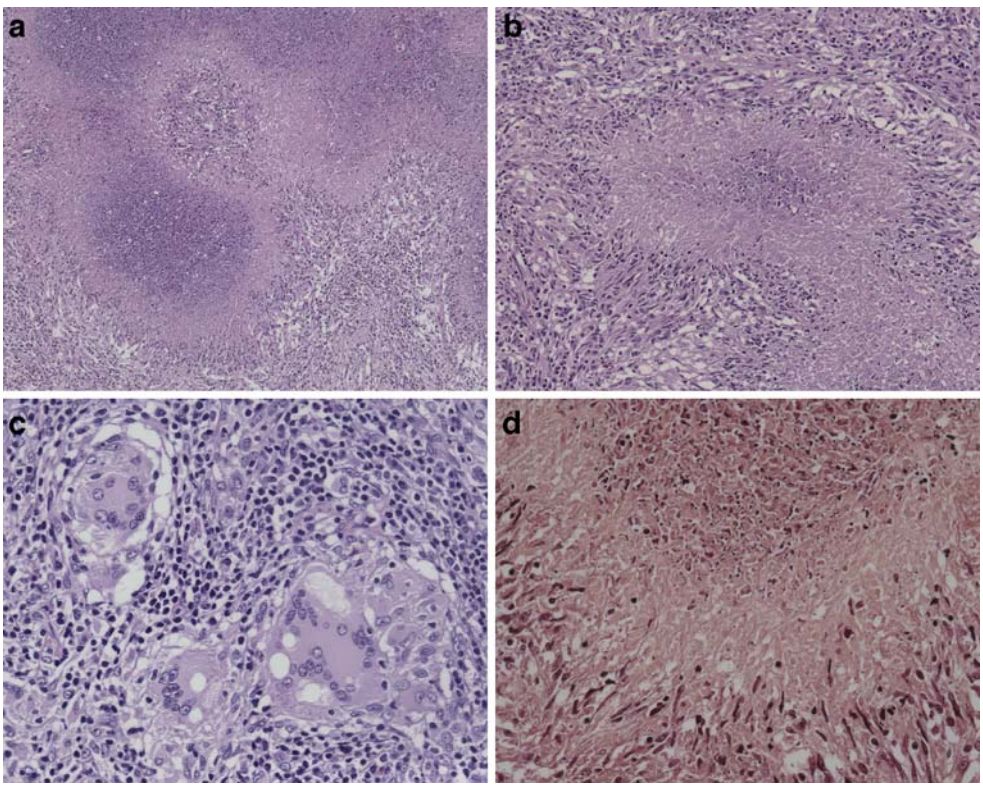


Fig. 3 Histology reveals caseating granulomatous inflammation (**a**, haematoxylin–eosin, original magnification ×100) with densely aggregated epitheloid cells (**b**, haematoxylin–eosin, original magnification ×200) and often irregular-shaped and large multi-nuclear giant cells (**c**, haematoxylin–eosin, original magnification ×400). Within the central necrosis dark coccoid structures can be seen (**d**, Brown–Hopps, original magnification ×400)

Table 1 Summary of organ manifestations and histology in three major reports [1, 11, 21]

	Chronic non-specific	Granulomatous without necrosis	Granulomatous with necrosis	Total
Skin	3	0	0	3 (3.8%)
Lymph nodes	4	1	1	6 (7.7%)
Spleen	0	2	1	3 (3.8%)
Liver	11	9	0	20 (25.6%)
Gallbladder	0	1	0	1 (1.3%)
Endocard	10	0	0	10 (12.8%)
Myocard	0	1	0	1 (1.3%)
Lung	0	0	1	1 (1.3%)
Kidney	1	0	1	2 (2.6%)
Testis	0	1	0	1 (1.3%)
Bone	7	4	1	12 (15.4%)
Synovia	2	1	1	4 (5.1%)
Spinal cord	1	0	3	4 (5.1%)
Soft tissue	5	3	2	10 (12.8%)
total (n=78)	44 (56.4%)	23 (29.5%)	11 (14.1%)	78 (100%)

11, 21]. The most frequently affected organs are the liver, bones, endocard and soft tissues (Table 1). Pleuropulmonary manifestations and their histology are described in different case reports [2, 4, 8, 16, 19–22]. Tuberculosis-like changes are dominant, and men are more often affected (Table 2). Intra-pulmonal nodules with hyalinization and focal calcification are seen as well [4, 16, 20].

Clinically, osteoarticular complications occur in 20 to 40% of patients with brucellosis [25]. In a large study with a clinical cohort from the Balkan Peninsula (n=450), respiratory manifestations were reported in 6.9%. Most of these patients (75.6%) exhibited spondylitis, endocarditis and meningoencephalitis as well [14]. Fever was noticed in 94.5%, cough in 67.6% and dyspnoea in 21.6%. Respiratory involvement showed typical lobar pneumonia in 32.4% (mostly in the basal lobes), interstitial pneumonia in 40.5% and a honeycomb pattern and pleural effusions in 10.8% each. In a series from Germany, 37% of the patients with brucellosis suffered from osteoarticular and 30% from respiratory complications, mostly bronchopneumonia [3]. The routine use of chest radiographs in patients with fever of unknown origin could be a possible reason for the increased percentage of pulmonary manifestations of brucellosis in Germany.

Infectious diseases with various organ manifestations (e.g. osteoarticular) should be regarded as suspicious for brucellosis, especially when there is a potential exposure. In these cases, clinical investigations are necessary to prove or exclude brucellosis. Successful diagnosis depends on the verification by microbiological means, usually by culture or serology [15, 19–21]. A negative CFT does not necessarily exclude brucellosis [15, 24]. Rarely, brucellosis is diagnosed by histology. However, negative Ziehl–Neelsen and Grocott stains, the occurrence of various other lesions and in our case atypical arranged and large giant multinucleated cells as well as densely aggregated epitheloid cells should raise substantial doubt on the diagnosis of tuberculosis and provoke suspicion of brucellosis. Primarily, PCR or in situ hybridization should be applied for exclusion of infection by mycobacteria [13]. Subsequent immunohistochemical investigations may be helpful in the diagnosis of brucellosis [18]. The most sensitive method is a real-time PCR, e.g. our genus-specific *bcsp31* PCR, which can be performed on routinely processed formalin-fixed and paraffin-embedded tissue [3, 16].

The final question to be answered is the route of infection for our young patient. In the past, pulmonary brucellosis was mainly reported in agricultural workers or abattoirs [8, 21, 25], but in this case, it seems to be most likely that the disease had been acquired in childhood during visits in different Arabic countries in connection with her father's employment in this region. This is well fitting to the results of an epidemiological study, which proved that more than 90% of infections in Germany are acquired in endemic countries, mostly around the Mediterranean Sea [3]. In the European Community, a total of

Table 2 Histology in nine cases with pleuropulmonary manifestations [2, 4, 8, 16, 19, 20, 22]

	Age (range)	Male/female	Chronic non-specific	Granulomatous without necrosis	Granulomatous with necrosis	Total
Pleura	27–37	1:1	1	1	0	2
Lung	33–68	6:	1	0	6	7

1,080 confirmed cases were reported in 2005; in Germany, 31 cases were detected [7]. Highest incidences are reported in Portugal, Italy, Spain and Greece. In 2005, raw milk from cows in Greece was found positive for *Brucella* in 6.1%, which provides a persisting source for infections [7].

References

1. Akhtar M (2001) Histopathological features. In: Madkour MM (ed) Makour's brucellosis. Springer, Berlin, pp 65–73
2. Al-Anazi AR, Aziz S, Fouda MA (2005) Brucellosis: haemorrhagic pleural effusion. Med Princ Pract 14:118–120
3. Al Dahouk S, Nöckler K, Hensel A, Tomaso H, Scholz HC, Hagen RM, Neubauer H (2005) Human brucellosis in a non-endemic country: a report from Germany, 2002 and 2003. Eur J Clin Microbiol Infect Dis 24:450–456
4. Chavez CA, Veach GE (1976) Brucellosis. Localized pulmonary nodule due to *Brucella suis*. J Kansas Med Soc 76:434–437
5. Corbel MJ (1997) Brucellosis: an overview. Emerg Infect Dis 3:213–221
6. El-Zammar OA, Katzenstein ALA (2007) Pathological diagnosis of granulomatous lung disease: a review. Histopathology 50:289–310
7. European Food Safety Authority (2006) The community summary report on trends and sources of zoonoses, zoonotic agents, antimicrobial resistance and foodborne outbreaks in the European Union in 2005: *Brucella*. The EFSA Journal 94:146–159
8. Garcia-Rodriguez JA, Garcia-Sanchez JE, Munoz Bellido JL, Ortiz de la Tabla V, Bellido Barbero J (1988) Review of pulmonary brucellosis: a case report on brucellar pulmonary empyema. Diagn Microbiol Infect Dis 11:53–60
9. Godfroid J (2002) Brucellosis in wildlife. Rev Sci Tech 21:277–286
10. Godfroid J, Cloeckaert A, Liautard J-P, Kohler S, Fretin D, Walravens K, Garin-Bastuji B, Letesson J-J (2005) From the discovery of the Malta fever's agent to the discovery of a marine mammal reservoir, brucellosis has continuously been a re-emerging zoonosis. Vet Res 36:313–326
11. Hunt AC, Bothwell PW (1967) Histological findings in human brucellosis. J Clin Path 20:267–272
12. Lack EE, Connor DH (1997) Tuberculosis. In: Connor DH, Chandler FW, Schwartz DA, Manz HJ, Lack EE (eds) Pathology of infectious diseases. Appleton & Lange, Stamford, pp 857–868
13. Lefmann M, Schweickert B, Buchholz P, Gobel UB, Ulrichs T, Seiler P, Theegarten D, Moter A (2006) Evaluation of peptide nucleic acid-fluorescence in situ hybridization for identification of clinically relevant mycobacteria in clinical specimens and tissue sections. J Clin Microbiol 44:3760–3767
14. Pappas G, Bosilkovski M, Akritidis N, Mastora M, Krteva L, Tsianos E (2003) Brucellosis and the respiratory system. Clin Infect Dis e37:95–99
15. Potasman I, Even L, Banai M, Cohen E, Angel D, Jaffe M (1991) Brucellosis: an unusual diagnosis for a seronegative patient with abscesses, osteomyelitis, and ulcerative colitis. Rev Infect Dis 13:1039–1042
16. Ramah SJ, Chomet B, McLean J, Lemke C (1959) Pulmonary granuloma due to brucellosis. JAMA 170:1665–1667
17. Redkar R, Rose S, Bricker B, DelVecchio V (2001) Real-time detection of *Brucella abortus*, *Brucella melitensis* and *Brucella suis*. Mol Cell Probes 15:43–52
18. Rhyan JC, Gidlewski T, Roffe TJ, Aune K, Philo LM, Ewalt DR (2001) Pathology of brucellosis in bison from Yellowstone National Park. J Wildl Dis 37:101–109
19. Takahashi H, Tanaka S, Yoshida K, Hoshino H, Sasaki H, Takahashi K, Kimura K, Fuji N, Kimura H, Mori M, Abe S (1996) An unusual case of brucellosis in Japan: Difficulties in the differential diagnosis from pulmonary tuberculosis. Intern Med 35:310–314
20. Webb WA, Thoroughman JC (1966) Solitary pulmonary nodule due to *Brucella suis*. Report of a case. Dis Chest 49:222–224
21. Weed LA, Dahlin DC, Pugh DG, Ivins JC (1952) *Brucella* in tissues removed at surgery. Am J Clin Pathol 22:10–21
22. Weed LA, Sloss PT, Clagett OT (1956) Chronic localized pulmonary brucellosis. JAMA 161:1044–1047
23. Yagupsky P, Baron EJ (2005) Laboratory exposures to Brucellae and implications for bioterrorism. Emerg Infect Dis 11:1180–1185
24. Yavuz T, Ozaydin M, Ulusan V, Ocal A, Ibrisim E, Kutsal A (2004) A case of mitral stenosis complicated with seronegative *Brucella endocarditis*. Jpn Heart J 45:353–358
25. Young EJ (1997) Brucellosis. In: Connor DH, Chandler FW, Schwartz DA, Manz HJ, Lack EE (eds) Pathology of infectious diseases. Appleton & Lange, Stamford, pp 447–452

Virchows Arch (2008) 452:103–107
DOI 10.1007/s00428-007-0533-1

CASE REPORT

Small cell carcinoma with concomitant adenocarcinoma arising in a Barrett's oesophagus: report of a case with a favourable behaviour

Frédéric Bibeau · Marie-Christine Chateau · Michel Guiu · Eric Assenat · David Azria · Rosy Lavaill · Marc Ychou · Florence Boissière-Michot

Received: 3 August 2007 / Revised: 27 September 2007 / Accepted: 21 October 2007 / Published online: 16 November 2007
© Springer-Verlag 2007

Abstract Most Barrett's oesophagus-associated cancers are adenocarcinomas which occur in a pure form. They are rarely combined with another type of malignancy, such as endocrine tumours. Within the endocrine spectrum, small cell carcinomas (SmCC) usually have a highly aggressive behaviour with a poor prognosis. We report a case of composite SmCC and adenocarcinoma in the setting of a Barrett's oesophagus, in a 54-year-old man. This tumour was identified on a surgical specimen after neoadjuvant treatment with radiotherapy and 5-FU-Cis-platin based chemotherapy. The SmCC component was positive for chromogranin A, synaptophysin, neural cell adhesion molecule and neuron-specific enolase and negative for high molecular weight cytokeratin. The adenocarcinoma component showed a converse phenotype. In our case, the origin of the SmCC component could be explained by the numerous chromogranin A-positive cells observed in the Barrett's oesophagus or by the potential progenitor cells that may be located in the submucosal oesophageal gland ducts and the Barrett's metaplasia. Our report is thus indicative of the high and totipotential risk of Barrett's oesophagus. Moreover, it is particular because of its favourable behaviour, with a 6-year disease-free survival, after neoadjuvant chemoradiation, surgery and postoperative chemotherapy.

Keywords Barrett's oesophagus · Small cell carcinoma · Composite tumour

F. Bibeau (✉) · M.-C. Chateau · R. Lavaill · F. Boissière-Michot
Department of Pathology, Centre Régional de Lutte Contre le Cancer Val d'Aurelle,
208 Rue des Apothicaires,
34298 Montpellier Cedex 5, France
e-mail: fbibeau@valdorel.fnclcc.fr

M. Guiu
Centre de Pathologie,
2 Avenue des Palmiers,
66000 Perpignan, France

E. Assenat · D. Azria · M. Ychou
Department of Oncology, Centre Régional de Lutte Contre le Cancer Val d'Aurelle,
Montpellier, France

Introduction

Most malignant tumours of the oesophagus are squamous cell carcinomas or adenocarcinomas. These latter types usually occur in a pure form, associated with Barrett's oesophagus, which is a well-known premalignant condition [1]. Other carcinomas are rare, but the occurrence of neoplasms such as composite tumours and endocrine tumours have been reported [1, 8, 24]. Within the endocrine spectrum, small cell carcinomas (SmCC) represent a highly aggressive neoplasm with a very poor prognosis [22]. We report herein a case of a composite SmCC well differentiated adenocarcinoma, arising in a Barrett's oesophagus, and characterized by a favourable behaviour 6 years after neoadjuvant chemoradiotherapy, surgery and postoperative chemotherapy. We describe the histopathological and immunohistochemical features of this composite tumour and discuss the different mechanisms predisposing to the development of an endocrine component, notably the role

of Barrett's metaplasia. We also point out the significance of a SmCC component in terms of therapeutic management.

Clinical history

A 54-year-old man with a known history of gastro-oesophageal reflux disease and Barrett's oesophagus, complained of epigastric discomfort. Endoscopic studies showed a tumour mass in the distal third of the oesophagus, and biopsy specimens established a diagnosis of well-differentiated adenocarcinoma, in the setting of a Barrett's oesophagus with high grade dysplasia. Preoperative endo-oesophageal ultrasonography classified this lesion as locally advanced with invasion of the muscularis propria and the lymph nodes. Clinical workup via computed tomographic scans revealed a cardial extension but no other distant lesions. The patient underwent concomitant radiotherapy and 5-FU-cisplatin-based chemotherapy that led to a significant tumour regression. It was followed 6 weeks later by a subtotal oesophagectomy with a lymphadenectomy. A mass, measuring 2×1.5×0.6 cm, was found in the lower oesophagus which morphologically corresponded to a composite SmCC adenocarcinoma. The 12 lymph nodes recovered were free of metastases. Post-therapeutical TNM staging was evaluated as ypT2N0M0. The patient received four courses of postoperative chemotherapy, similar to those previously administered. He remained free of disease 6 years after treatment.

Materials and methods

The surgical specimen was fixed in 10% formalin and embedded in paraffin. Four-micron sections were stained for conventional histopathological examination with hematoxylin and eosin and processed for immunohistochemistry using a standard avidin–biotin peroxidase complex technique. The following primary antibodies were used: pan-cytokeratin (mouse monoclonal, clone KL1, diluted 1:50, Immunotech, France), high molecular weight cytokeratin (CK) (mouse monoclonal, clone 34ßE12, diluted 1:50, Dako, Denmark), CK 5/6 (clone D5/16 B4, diluted 1:100, Dako, Denmark), CK 14 (clone LL002, diluted 1:75, DBS, USA), CK 19 (clone RCK108, diluted,1:50, Dako, Denmark), chromogranin A (rabbit polyclonal, ref A0430, diluted 1:500, Dako, Denmark), synaptophysin (rabbit polyclonal, ref A0010, diluted 1:150, Dako, Denmark), neural cell adhesion molecule (NCAM, mouse monoclonal, clone 123C3, diluted 1:50, Zymed, USA), neuron-specific enolase (NSE, mouse monoclonal, clone BBS/NC/VI-H14, diluted 1:100, Dako, Denmark), thyroid transcription factor-1 (TTF-1, mouse monoclonal, clone 8G7G3/1, diluted 1:100, Dako, Denmark) and Ki67 (mouse monoclonal, clone MIB-1, diluted 1:100, Dako, Denmark). Appropriate positive and negative controls were introduced for each immunoperoxidase stain. Acidic mucin in the goblet cells of the Barrett's oesophagus was detected using Alcian blue at pH 2.5.

Results

The tumour from the surgical specimen consisted of a SmCC admixed with a well differentiated adenocarcinoma (Fig. 1a). It deeply invaded the muscularis propria of the oesophagus, but the adventitia was not infiltrated. Each malignant component represented approximately half of the whole tumour and was clearly distinct from the other (Fig. 1a). The SmCC was arranged in solid and trabecular patterns without rosette formation (Fig. 1c). It was composed of small to intermediate cells with scant cytoplasm, irregular hyperchromatic nuclei with moulding and focal single-cell necrosis (Fig. 1c). Salt-and-pepper chromatin was also noted, as well as a high mitotic rate averaging 36 per ten high-power fields. The SmCC component was located beneath a squamous island

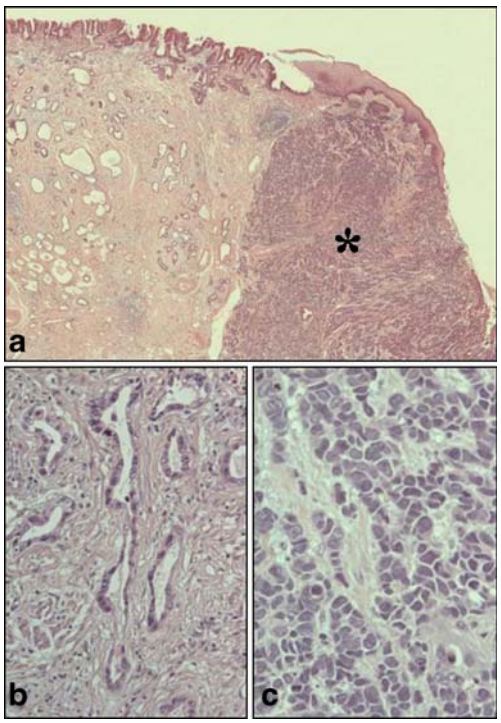


Fig. 1 **a** Composite tumour with adenocarcinoma and small cell carcinoma (*star*) components arising in a setting of a Barrett's oesophagus (H&E, ×20); **b** Adenocarcinoma component: well differentiated proliferation composed of tubular structures with cytologic atypia (H&E, ×200); **c** Small cell carcinoma (SmCC): poorly differentiated proliferation with a trabecular pattern and nuclear moulding (H&E, ×400)

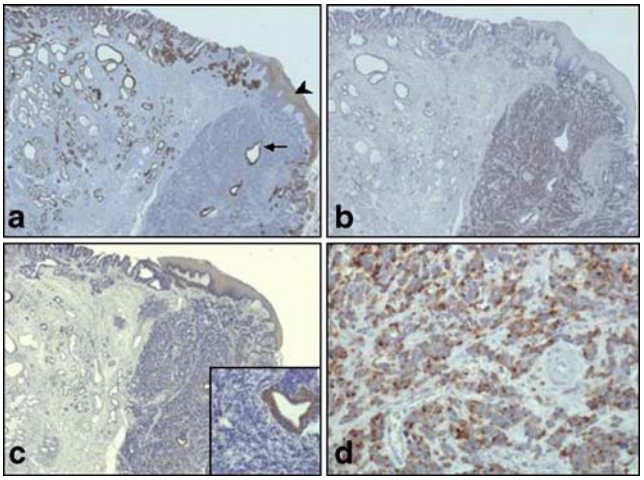


Fig. 2 **a** Strong pan-cytokeratin staining of the adenocarcinoma (KL1, immunoperoxydase ×20); note the positive squamous island (*arrowhead*) and gland ducts (*arrow*), above and within the SmCC, respectively; **b** NCAM expression restricted to the SmCC (immunoperoxydase ×20); **c** CK 5/6 negativity of both components. *Inset*: positive staining of submucosal oesophageal gland ducts (immunoperoxydase ×20 and 200); **d** Strong chromogranin staining of the SmCC component (immunoperoxydase ×100)

(Fig. 2a). Moreover, a remaining oesophageal gland duct was observed in the center of the SmCC area (Fig. 2a). The adenocarcinoma was exclusively composed of tubular structures with cytologic atypia (Fig. 1b). Barrett's oesophagus was characterized by a metaplastic specialized-type epithelium with columnar and goblet cells, showing features of low- and high-grade dysplasia. The goblet cells displayed an intense alcian blue staining. The SmCC component was strongly positive for chromogranin (Fig. 2d) and showed a lower intensity for other endocrine markers such as synaptophysin, NSE and NCAM (Fig. 2b). It also displayed a dot-like staining for pan-cytokeratin and a negativity for high molecular weight cytokeratin, an immunohistochemical pattern characteristic of endocrine cells [10, 14]. In addition, negativity for CK 5/6 (Fig. 2c), CK 14 and CK 19 was also observed, ruling out a basaloid squamous cell carcinoma [21]. Seventy percent of the SmCC component showed a nuclear staining with Ki67. TTF-1 was negative. On the other hand, the adenocarcinomatous component diffusely expressed the pan-cytokeratin and the high molecular weight cytokeratin, while it was negative for CK5/6 and all the previously mentioned endocrine markers (Fig. 2a–c). Submucosal gland ducts within the SmCC component were highlighted with pan-cytokeratin, high molecular weight cytokeratin and CK5/6 (Fig. 2c). Chromogranin A-positive cells were only found scattered throughout the adenocarcinomatous areas, but interestingly appeared as variable number of single cells or clusters in the metaplastic epithelium of Barrett's oesophagus (Fig. 3). Histology and immunohistochemistry reviewing of

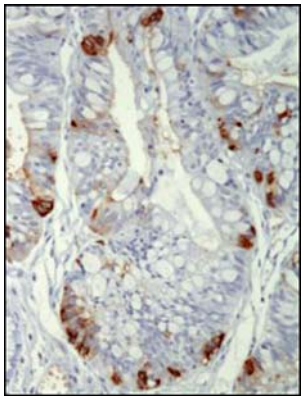


Fig. 3 Barrett's oesophagus. Metaplastic epithelium with goblet cells and numerous chromogranin positive cells (immunoperoxydase ×200)

the preoperative biopsies did not reveal any endocrine component associated with the invasive adenocarcinoma.

Discussion

Most of Barrett's oesophagus-associated cancers are adenocarcinomas which occur in a pure form [1, 15]. They are rarely combined with another type of malignancy, such as squamous cell carcinomas or endocrine tumours [8, 13]. Within the endocrine spectrum, SmCC account for 1% of oesophageal neoplasms, but oesophagus represents the most common SmCC location after the lung [1]. Oesophageal SmCC usually share the same aggressive behaviour and poor prognosis as their pulmonary counterparts, requiring a specific chemotherapy. To our knowledge, very few examples of long-term survivors, treated for a pure or combined primary oesophageal SmCC, have been documented [6, 16, 23]. We report, herein, a case of a primary SmCC with concomitant adenocarcinoma arising in a Barrett's oesophagus, with a 6-year favourable follow-up. The origin of endocrine tumours in the oesophagus is poorly understood, but some authors have reported that the number of endocrine cells increases in the metaplastic epithelium of Barrett's oesophagus, in comparison with the usual sparse number found in the normal gastro-oesophageal junction [3, 20]. Similarly, numerous endocrine cells have been identified in intestinal metaplasia of the gallbladder, notably associated with large cell endocrine carcinoma [14]. It is thus plausible, in our case, that Barrett's metaplasia with numerous endocrine cells could favour the development of a SmCC component. Moreover, it has been postulated that composite tumours might derive from totipotent stem cells, leading to a proliferation with multidirectional differentiation. Some authors have proposed that these totipotent cells could originate from the oesophageal epithelium or in the submucosal gland ducts of the distal third of the oesophagus [5, 9]. This could thus explain the reported observations with combined squamous cell carcinomas, adenocarcinomas, endocrine carcinomas and sarcomas of the oesophagus

[8, 24] and the presence of small foci of squamous, glandular or mucoepidermoid differentiation sometimes found in predominant SmCC [19]. Furthermore, the totipotent cells may be the source of regenerative squamous islands lying within Barrrett's metaplasia [5, 9]. In our case, the SmCC component was located beneath a squamous island and encompassed, in its center, a remaining oesophageal gland duct. Taken together, these observations suggest the possibility that the potential progenitor cell of the SmCC component could also be located in the depth of an oesophageal gland duct. The alternative of distinct progenitor cells, respectively, located in gland ducts for the SmCC component and in Barrett's metaplasia for the adenocarcinomatous component, might also explain the origin of this composite SmCC-adenocarcinoma. At least, neoadjuvant chemoradiotherapy has been proposed as a possible mechanism to induce endocrine differentiation in tumour cells, notably in rectal adenocarcinomas [18]. However, the cell morphology after treatment is different from those observed in SmCC, characterized by an ample amount of eosinophilic cytoplasm and a very low Ki67 labelling index. This pattern of morphologic alteration lacked any significant association with outcome and has been regarded as a state of tumour cell degeneration [17]. Thus, in our case, the identification of a SmCC component in the surgical specimen but not in the preoperative biopsy, could rather be explained by an insufficient endoscopic sampling than by a chemoradiation induction. The recognition of the SmCC counterpart could have relevant clinical implications, as it is considered as a highly aggressive neoplasm that worsens the prognosis. It usually involves the use of chemotherapeutic agents different from those used in the treatment of oesophageal adenocarcinomas or squamous cell carcinomas, including VP16 [12]. In our observation, surgical resection combined with neoadjuvant radiochemotherapy, using 5-FU-cisplatin, led to a six-year disease-free survival. Such a long-term survival has rarely been reported [6, 16, 23] and contrasts with most of the oesophageal SmCC characterized by a survival period of less than 6 months, even when the primary growth is limited [2, 22]. The 5-FU-cisplatin combination has produced good response in squamous and glandular carcinomas and has showed synergistic effects with radiotherapy [7]. In high grade endocrine tumours, cisplatin-VP16 is the conventional treatment. However, some reports have described the effectiveness of chemotherapy using either a single agent (i.e., 5-FU) or other combinations (i.e., cyclophosphamide/5-FU, cyclophosphamide/doxorubicin, hydrochloride/vincristine or cyclophosphamide/doxorubicine, hypochloride/vincristine/cisplatin) with or without radiotherapy [4, 11]. The favourable evolution of the patient could be linked, in our case, to the given radiochemotherapy protocol, effective on both tumour components, even without VP16. In conclusion, we described a primary composite SmCC-adenocarcinoma of the oesophagus, in which chromogranin-A positive cells of Barrett's metaplasia or totipotent stem cells could be involved in the endocrine neoplastic initiation. Moreover, our case was characterized by a favourable behaviour with a long-lived response to the treatment. This could be linked to the effectiveness of the neoadjuvant radiochemotherapy, surgery and postoperative chemotherapy.

References

1. Aaltonen LA, Hamilton SR (2007) (ed) World Health Organization classification of tumours. Pathology and genetics of tumours of the digestive system. Lyon 2000 ed. IARC
2. Brenner B, Tang LH, Klimstra DS, Kelsen DP (2004) Small-cell carcinomas of the gastrointestinal tract: a review. J Clin Oncol 22:2730–2739
3. Buchan AM, Grant S, Freeman HJ (1985) Regulatory peptides in Barrett's oesophagus. J Pathol 146:227–234
4. Caldwell CB, Bains MS, Burt M (1991) Unusual malignant neoplasms of the esophagus. Oat cell carcinoma, melanoma, and sarcoma. J Thorac Cardiovasc Surg 101:100–107
5. Coad RA, Woodman AC, Warner PJ, Barr H, Wright NA, Shepherd NA (2005) On the histogenesis of Barrett's oesophagus and its associated squamous islands: a three-dimensional study of their morphological relationship with native oesophageal gland ducts. J Pathol 206:388–394
6. Hama Y, Uematsu M, Ichikura T, Tamura E, Aida S, Kohno M, Kusano S (1999) A case of primary small cell carcinoma of the cervical esophagus with long-term survival following concurrent chemoradiotherapy: case report and review of the literature. Tumori 85:284–287
7. Jani AB, Connell PP, Vesich VJ, O'Brien KM, Chen LM (2000) Analysis of the role of adjuvant chemotherapy for invasive carcinoma of the esophagus. Am J Clin Oncol 23:554–558
8. Kanamoto A, Nakanishi Y, Ochiai A, Shimoda T, Yamaguchi H, Tachimori Y, Kato H, Watanabe H (2000) A case of small polypoid esophageal carcinoma with multidirectional differentiation, including neuroendocrine, squamous, ciliated glandular, and sarcomatous components. Arch Pathol Lab Med 124: 1685–1687
9. Li H, Walsh TN, O'Dowd G, Gillen P, Byrne PJ, Hennessy TP (1994) Mechanisms of columnar metaplasia and squamous regeneration in experimental Barrett's esophagus. Surgery 115:176–181
10. Lyda MH, Weiss LM (2000) Immunoreactivity for epithelial and neuroendocrine antibodies are useful in the differential diagnosis of lung carcinomas. Hum Pathol 31:980–987
11. McFadden DW, Rudnicki M, Talamini MA (1989) Primary small cell carcinoma of the esophagus. Ann Thorac Surg 47:477–480
12. Mitry E, Baudin E, Ducreux M, Sabourin JC, Rufie P, Aparicio T, Aparicio T, Lasser P, Elias D, Duvillard P, Schlumberger M, Rougier P (1999) Treatment of poorly differentiated neuroendocrine tumours with etoposide and cisplatin. Br J Cancer 81: 1351–1355
13. Noguchi T, Uchida Y, Fumoto S, Wada S, Sato T, Takeno S (2002) Adenosquamous carcinoma arising in Barrett's esophagus. Jpn J Thorac Cardiovasc Surg 50:537–540

14. Papotti M, Cassoni P, Sapino A, Passarino G, Krueger JE, bores-Saavedra J (2000) Large cell neuroendocrine carcinoma of the gallbladder: report of two cases. Am J Surg Pathol 24:1424–1428
15. Sarbia M, Becker KF, Hofler H (2004) Pathology of upper gastrointestinal malignancies. Semin Oncol 31:465–475
16. Saw EC, Yu GS, Wagner G, Heng Y (1997) Synchronous primary neuroendocrine carcinoma and adenocarcinoma in Barrett's esophagus. J Clin Gastroenterol 24:116–119
17. Shia J, Guillem JG, Moore HG, Tickoo SK, Qin J, Ruo L, Suriawinata A, Paty PB, Minsky BD, Weiser MR, Temple LK, Wong WD, Klimstra DS (2004) Patterns of morphologic alteration in residual rectal carcinoma following preoperative chemoradiation and their association with long-term outcome. Am J Surg Pathol 28:215–223
18. Shia J, Tickoo SK, Guillem JG, Qin J, Nissan A, Hoos A, Stojadinovic A, Ruo L, Wong WD, Paty PB, Weiser MR, Minsky BD, Klimstra DS (2002) Increased endocrine cells in treated rectal adenocarcinomas: a possible reflection of endocrine differentiation in tumor cells induced by chemotherapy and radiotherapy. Am J Surg Pathol 26:863–872
19. Takubo K, Nakamura K, Sawabe M, Arai T, Esaki Y, Miyashita M, Mafune K, Tanaka Y, Sasajima K (1999) Primary undifferentiated small cell carcinoma of the esophagus. Hum Pathol 30:216–221
20. Tateishi R, Taniguchi H, Wada A, Horai T, Taniguchi K (1974) Argyrophil cells and melanocytes in esophageal mucosa. Arch Pathol 98:87–89
21. Tsubochi H, Suzuki T, Suzuki S, Ohashi Y, Ishibashi S, Moriya T, Fujimura S, Sasano H (2000) Immunohistochemical study of basaloid squamous cell carcinoma, adenoid cystic and mucoepidermoid carcinoma in the upper aerodigestive tract. Anticancer Res 20:1205–1211
22. Wu Z, Ma JY, Yang JJ, Zhao YF, Zhang SF (2004) Primary small cell carcinoma of esophagus: report of 9 cases and review of literature. World J Gastroenterol 10:3680–3682
23. Yachida S, Matsushita K, Usuki H, Wanibuchi H, Maeba T, Maeta H (2001) Long-term survival after resection for small cell carcinoma of the esophagus. Ann Thorac Surg 72:596–597
24. Yamamoto J, Ohshima K, Ikeda S, Iwashita A, Kikuchi M (2003) Primary esophageal small cell carcinoma with concomitant invasive squamous cell carcinoma or carcinoma in situ. Hum Pathol 34:1108–1115

Virchows Arch (2008) 452:109–111
DOI 10.1007/s00428-007-0546-9

CASE REPORT

Mature cystic teratoma of the ovary with male accessory sexual glands including seminal vesicles, prostatic tissue, and bulbo-urethral glands: a case report

Ksenya V. Shelekhova · Vaclav Hejda · Dmitry V. Kazakov · Michal Michal

Received: 21 May 2007 / Revised: 31 October 2007 / Accepted: 1 November 2007 / Published online: 8 December 2007
© Springer-Verlag 2007

Abstract We present an extremely rare case of a benign cystic ovarian teratoma with structures of male accessory sexual glands. The patient was a 30-year-old woman. A unilocular cystic tumor, measuring 5cm in the largest diameter, was found in her right ovary and was removed. The teratoma contained epidermis, skin appendages, respiratory and intestinal epithelia, cartilage, muscle, and nervous and connective tissue. In addition to these histologically mature tissues, there were nodules with prostatic acini, prostate duct-like structures strongly positive for prostate-specific antigen and acid prostatic phosphatase, structures resembling Cowper's glands, and seminal vesicles surrounded by fibromuscular stroma. To our knowledge, this is the first case in the English literature describing seminal vesicles associated with prostatic tissue and bulbo-urethral glands in a mature ovarian teratoma.

Keywords Ovary · Cystic teratoma · Prostatic tissue · Seminal vesicles

K. V. Shelekhova
Department of Pathology, Petrov's Institute of Oncology, Saint Petersburg, Russia

V. Hejda
Department of Pathology, Institute for the Care of Mother and Child, Prague, Czech Republic

D. V. Kazakov · M. Michal (✉)
Sikl's Department of Pathology, Charles University, Medical Faculty Hospital, Alej Svobody 80, 304 60 Pilsen, Czech Republic
e-mail: michal@medima.cz

Introduction

Mature cystic teratomas of the ovary containing structures from all three germ layers are common neoplasms in this localization. Epidermis, cutaneous appendages, respiratory and intestinal epithelia, cartilage, muscle, and nervous and connective tissue are almost always detected in the tumors. Other tissues including pancreas, kidney, brain, and thymus are rarely found. Foci of urothelial epithelium in association with prostatic tissue have been described in teratomas of the ovary in a small number of reports [1, 2, 3, 6, 8, 9, 12].

The present case revealed male accessory sexual glands, such as prostatic and Cowper's glands, and seminal vesicles occurring in a benign ovarian teratoma. To our knowledge, such a combination of male accessory sexual glands in an ovarian teratoma has not been previously reported.

Clinical history

A 30-year-old woman, nulligravida, nullipara, who had been treated for Hashimoto thyreoiditis, presented with a 1-week history of pain in the lower abdomen. Ultrasound investigation disclosed a cyst of the right ovary approximately 4cm in diameter. An ovarectomy was performed by a laparoscopy, and the cystic lesion was removed. The postoperative course was uneventful.

Material and methods

The tumorous tissue was fixed in 4% formalin, routinely processed and stained with hematoxylin and eosin. Immunohistochemical studies were performed on formalin-fixed, paraffin-embedded sections using prostate-specific antigen

(PSA; polyclonal; Glostrup) and prostatic alkaline phosphatase (polyclonal; Dakocytomation, Glostrup).

Results

On gross examination, the lesion measured 5 × 3.5 × 1.5cm, was multilocular, and contained oily material found in some cysts.

Histologically, the neoplasm contained the usual tissues of a mature cystic adult teratoma, including epidermis, skin appendages, respiratory and intestinal epithelia, cartilage, muscle, and nervous and connective tissue. In addition, one area in the fibromuscular wall of the teratoma revealed structures identical to prostatic glands, Cowper glands, and seminal vesicles (Fig. 1a,b). The prostatic glands were composed of simple ducts and acini lined by luminal cuboidal cells supported by a layer of basal cells and surrounded by a fibromuscular stroma (Fig. 1c). The Cowper glands were lined by cuboidal epithelial cells with very pale cytoplasm and basally located nuclei; these glands had the appearance of mucinous minor salivary glands embedded within a skeletal muscle (Fig. 1d). The seminal vesicles with highly complex mucosal folds were lined by the epithelium made up of columnar and basal cells, with occasional brown pigment in the cytoplasm of the columnar cells.

Immunohistochemically, the prostatic glands showed positivity for PSA and acid prostatic phosphatase (Fig. 1e). In contrast, the cells of the Cowper's glands and seminal vesicles were negative for these markers.

Discussion

Prostatic gland, Cowper's (bulbo-urethral) glands, and seminal vesicles are the main male accessory sexual glands. They form a functionally common group because they excrete liquid substances for slurring spermatozoons. Seminal vesicles in the male have no homologue in the

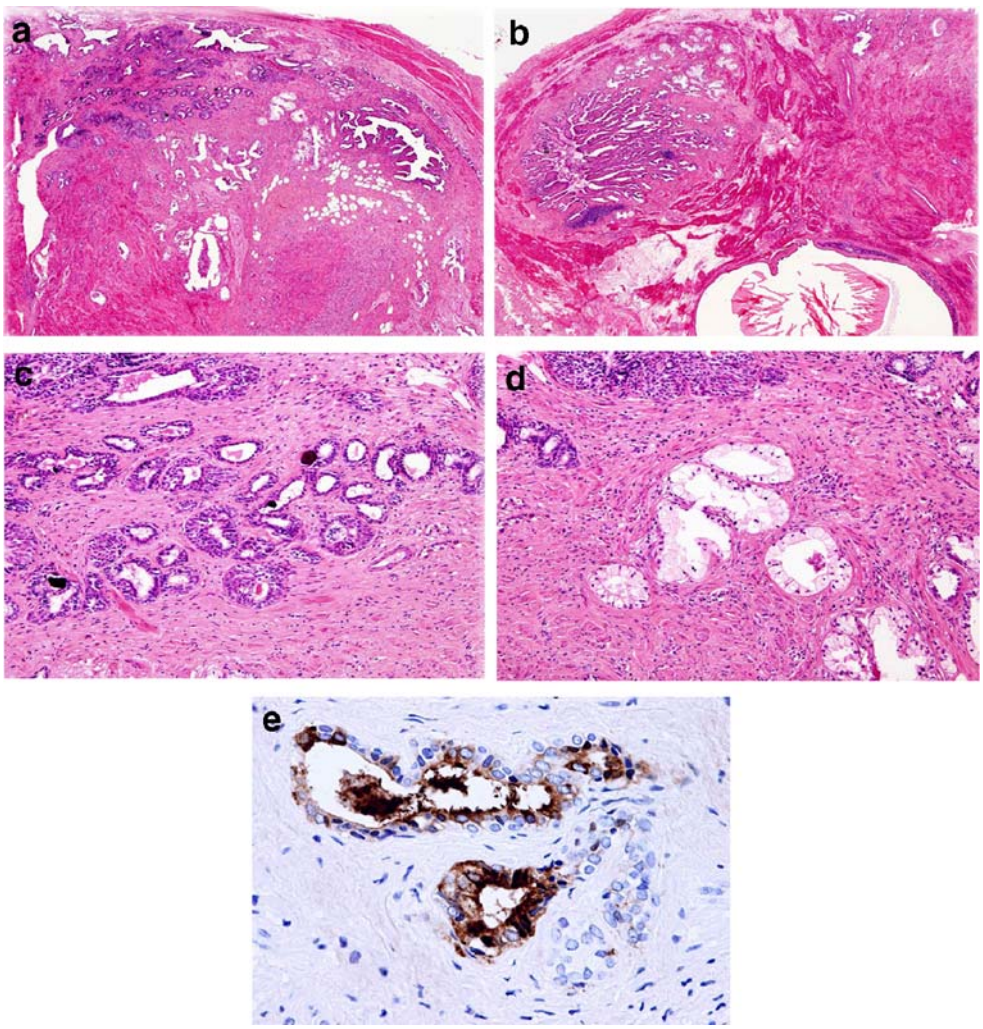


Fig. 1 **a** Part of the teratoma with a structures identical to prostatic glands, Cowper glands, and seminal vesicles embedded in a fibromuscular tissue. **b** Complex folded seminal vesicles can be seen. The cyst in the lower portion was lined by intestinal epithelium. **c** Close-up view of the prostatic glands: Note simple ducts and acini lined by luminal cuboidal cells supported by a layer of basal cells and surrounded by a fibromuscular stroma. **d** Close-up view of the Cowper glands: glands lined by cuboidal epithelial cells with very pale cytoplasm and basally located nuclei. Note the resemblance to mucinous minor salivary glands embedded within a skeletal muscle. **e** The prostatic glands showed positivity for PSA

female. Paraurethral (Skene's) glands in the female are mesonephric derivates and represent the underdeveloped homologue of the prostatic glands. The Bartholin glands are the homologue of male bulbo-urethral glands (Cowper's glands).

Prostatic tissue has rarely been described in the female genital tract [1–12]. Most reports documented the occurrence of prostatic tissue as a component of teratoma; however, ectopic prostatic tissue has also been found in the uterine cervix and vagina [5], including a patient with adrenogenital syndrome [4]. A unique case of benign prostatic tissue unassociated with a teratoma located at the ovarian hilum and merging with hyperplastic mesonephric remnants, which demonstrated various forms of epithelial metaplasia, is also on record [10].

Our review of the literature revealed about 19 cases of prostatic tissue being a component of an ovarian teratoma [9]. In addition, some of these reports described the presence of urothelium, Cowper's excretory ducts and glands, and a vascularized area with sinusoids surrounded by a fibromuscular wall of the cavernous type [3, 6, 7, 8, 9]. A case of prostatic adenocarcinoma in a mature cystic teratoma of the ovary has also been reported [3]. Our case seems to be the first report describing seminal vesicles in association with the foresaid male urogenital sinus structures in an ovarian mature teratoma. Interestingly, we have not found a single case report that would describe the occurrence of prostatic glands in the testicular teratoma in the literature.

Male accessory sexual glands derive from mesonephric ducts and urogenital sinus; the common embryogenital origin of these structures in men and in women seems to be a logical explanation for the development of the prostate tissue, Cowper's glands, and seminal vesicles in ovarian teratomas.

Conflict of interest statement We declare that we have no conflict of interest.

References

1. Bertrand GM (1986) Unique finding of prostatic tissue in a benign cystic ovarian teratoma. Arch Pathol Lab Med 110:683–684
2. Brumback RA, Brown BS, di Sant'Agnese PA (1985) Unique finding of prostatic tissue in a benign cystic ovarian teratoma. Arch Pathol Lab Med 109:675–677
3. Halabi M, Oliva E, Mazal PR, Breitenecker G, Young RH (2002) Prostatic tissue in mature cystic teratomas of the ovary: a report of four cases, including one with features of prostatic adenocarcinoma, and cytogenetic studies. Int J Gynecol Pathol 21:261–267
4. Kim KR, Park KH, Kim JW, Cho KJ, Ro JY (2004) Transitional cell metaplasia and ectopic prostatic tissue in the uterine cervix and vagina in a patient with adrenogenital syndrome: report of a case suggesting a possible role of androgen in the histogenesis. Int J Gynecol Pathol 23:182–187
5. McCluggage WG, Ganesan R, Hirschowitz L, Miller K, Rollason TP (2006) Ectopic prostatic tissue in the uterine cervix and vagina: report of a series with a detailed immunohistochemical analysis. Am J Surg Pathol 30:209–215
6. McLachlin CM, Srigley JR (1992) Prostatic tissue in mature cystic teratomas of the ovary. Am J Surg Pathol 16:780–784
7. Melniker LA, Slavutin LJ (1980) Prostatic tissue in a benign cystic teratoma of the ovary. Diagn Gynecol Obstet 2:139–145
8. Nogales FF, Vergara E, Medina MT (1995) Prostate in ovarian mature cystic teratoma. Histopathology 26:373–375
9. Resta L, Marzullo A, Pellegrino M, Rizzi E, Piscitelli D (2004) Male urogenital sinus structures in mature cystic teratomas of the ovary. Report of two cases. Histopathology 45:303–305
10. Smith CE, Toplis PJ, Nogales FF (1999) Ovarian prostatic tissue originating from hilar mesonephric rests. Am J Surg Pathol 23:232–236
11. Uzoaru I, Nadimpalli V (1993) Prostate in ovarian teratoma. Am J Surg Pathol 17:531
12. Vadmal M, Steven I (1996) Prostatic tissue in cystic ovarian teratomas. Hum Pathol 27:428–429

Virchows Arch (2008) 452:113–114
DOI 10.1007/s00428-007-0537-x

LETTER TO THE EDITOR

Pagetoid melanocytes in nevi simulant of melanoma

Aikaterini Zioga · Anna Batistatou

Received: 15 October 2007 / Accepted: 23 October 2007 / Published online: 20 November 2007
© Springer-Verlag 2007

Dear Editor,

We read with great interest the review article by Massi [1] on the melanocytic nevi simulant of melanoma and found it particularly useful in everyday pathology practice. We would like to draw some further attention to the pagetoid spread, observed occasionally in benign melanocytic lesions. Since the early residency years, pathologists consider pagetoid melanocytic spread as the histological hallmark of melanoma. Later on, the appreciation of the histological picture is refined, based on widely accepted and personalized criteria, formulated by continuous reading and experience. However, although we know that benign nevi can exhibit some pagetoid spread of melanocytes, when we see this feature under the microscope, we still have the fear that we are possibly under diagnosing a melanoma.

As mentioned in the article, when dealing with ascending melanocytes, it is important to pay attention to the architectural details, such as the pagetoid spread being only at the center of the lesion and not significant for nevi, and at the boarders of the lesion and significant in melanoma [1]. In this study, we would like to draw attention to the cytological details as well because, as it is pointed by G. Massi, they are providing the main clue in the differential diagnosis. In particular, the presence of fine delicate dendrites in ascending melanocytes is indicative of benign lesions. We studied a series of six melanocytic nevi with pagetoid melanocytosis [2] (five women, one man; age range, 32–47; mean age, 39 years) and five melanomas (three women, two men; age range, 36–70; mean age, 55 years), none of which was acral. To be able to visualize the dendrites immunohistochemical staining for Melan-A (MART-1, clone A103, Biogenex, CA, USA) was performed. We used the alkaline phosphatase anti-alkaline phosphatase (APAAP) technique and fast red as chromogen (fast red substrate pack, Biogenex). Sections were counterstained with Mayer hematoxylin and mounted in glycerol gelatin.

With the immunohistochemical stain for Melan-A, the normal melanocytes located in the basal layer of the epidermis were stained as well. These melanocytes possess an elaborate network of delicate dendrites (Fig. 1a), which enables them to communicate with associated keratinocytes (1 melanocyte with approximately 36 keratinocytes) [3]. We have noted that ascending melanocytes in benign melanocytic lesions had delicate dendrites as well (Fig. 1b,c), whereas in melanomas, they were round and devoid of dendrites (Fig. 1d–f). We believe that the presence of delicate dendrites is another cytological feature that aids in the differential diagnosis between benign nevus and melanoma, if pagetoid spread is present.

Because, to ascend, the melanocyte must decouple from the basement membrane and the keratinocytes and retract its dendrites, it is conceivable that the presence of delicate dendrites in melanocytes located into suprabasal layers of the epidermis is an indirect indicator of chronicity. That is, the benign melanocyte, besides being differentiated, it has

A. Zioga · A. Batistatou (✉)
Department of Pathology, University Hospital of Ioannina, Ioannina, Greece
e-mail: abatista@cc.uoi.gr

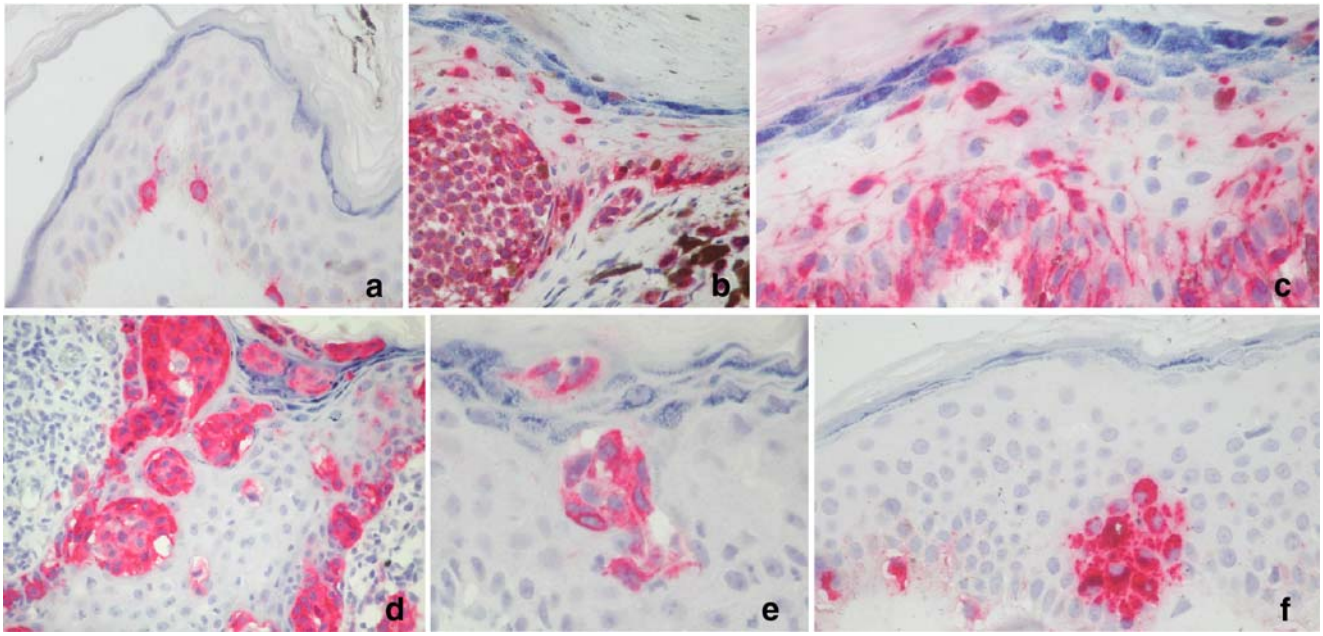


Fig. 1 Immunohistochemical staining with Melan-A (fast red; original magnification, ×400). **a** Normal melanocytes with thin elaborate dendrites. **b**, **c** Benign pagetoid melanocytosis in two cases of nevi. Note the presence of dendrites in ascending melanocytes. **d**–**f** Pagetoid spread in melanoma. Note the round contour of ascending malignant melanocytes arranged singly or in nests and the absence of discernible dendrites

had the time needed to elaborate dendrites in its new ascended position. On the other hand, the malignant melanocyte does not have this ability, either because it is not differentiated enough or because of its fast ascend up the epidermis. The only exception are the melanocytes in acral lesions. As pointed in the article, their malignant melanocytes have long and thick dendrites that are usually heavily pigmented [1].

References

1. Massi G (2007) Melanocytic nevi simulant of melanoma with medicolegal relevance. Virchows Arch 451:623–647
2. Petronic-Rosic V, Shea CR, Krausz T (2004) Pagetoid melanocytosis: when is it significant. Pathology 36:435–444
3. Haass NK, Smalley KS, Li L, Herlyn M (2005) Adhesion, migration and communication in melanocytes and melanoma. Pigment Cell Res 18:150–159

Virchows Arch (2008) 452:115–117
DOI 10.1007/s00428-007-0539-8

LETTER TO THE EDITOR

Pigmented lipofibromatosis in unusual location: case report and review of the literature

Lobna Ayadi · Slim Charfi · Youssef Ben Hamed · Ibtissem Bahri · Naourez Gouiaa · Abdelmajid Khabir · Saloua Makni · Tahya Sellami-Boudawara

Received: 31 July 2007 / Revised: 28 September 2007 / Accepted: 23 October 2007 / Published online: 8 December 2007
© Springer-Verlag 2007

Dear Editor,

Lipofibromatosis is a rare, recently reported, fibrofatty pediatric tumor, which affects mainly extremities [1, 6]. Histopathological features of this tumor must be distinguished from fibrous hamartoma of child, fibromatosis, calcifying aponevrotic fibroma, and lipoblastoma [1]. Pigmented lipofibromatosis is a rare histological variant of lipofibromatosis, which is not yet clearly distinguished. We describe a case of pigmented lipofibromatosis in an unusual location (back).

We report the case of a 14-year-old female who presented with several years history of a slowly enlarging, painless mass of the back. Physical examination demonstrated a subcutaneous, firm, nodule measuring 3.5×2.5 cm. The nodule seems to be fixed at deep tissues without abnormality of the overlying skin. She was otherwise healthy, and no family history of cutaneous abnormalities was noted. Any radiological exam was done. An excisional biopsy was performed. A 4×3×3 cm ill-defined mass was excised. Grossly, the tumor presented an adipose appearance without encapsulation. The cut surface presented some black pigmented areas. Hematoxylin and eosin (HE) stained sections showed small lobules of mature adipose tissue, dissected by moderately cellular bundles, of spindle elements without atypia (Fig. 1). Some scattered cells were pigmented (Fig. 2) and Fontana–Masson stain was positive on these pigmented cells. On immunohistochemistry study, spindle cells were diffusely positive for vimentine and α smooth muscle actin (Fig. 3). Pigmented cells were positive for S100 protein and Melan A and negative for HMB45 (Fig. 4). At 15 months of follow-up, there was no evidence of recurrence.

Lipofibromatosis is a distinctive entity, rare, benign lesion recently described by Fetsch et al. in 2000 [1] and is recognized as a distinctive fibrofatty tumour of childhood in the World Health Organization classification of tumors in 2002 [4]. Since this report, which includes 45 cases, only four other cases of lipofibromatosis were published [1–3, 5, 6]. Lipofibromatosis is different and must be equally distinguished from the entity designated as "lipofibromatosis" observed in cases of congenital macrodactyly and local gigantism [1]. The tumor commonly occurs in extremities, rarely in the hands, arms, legs, and feet [1, 6]. Rarely, chest, abdomen, or head and neck are affected [1–5]. The present observation is the first report of lipofibromatosis in the back. There is an over 2:1 male predominance. The median age for initial surgery is 1 year (range from 11 days to 12 year) [1]. The lesion is typically ill defined, painless, and slowly growing [1]. Macroscopically, it is yellowish or tan-whitish appearance with a prominent fatty component. Very rare tumor have exceeded 5 cm [1, 3–6]. Histologically, the tumor is poorly marginated, often composed of more than 70% of adipose tissue. Fascicles of fibroblastic cells traversed, with a striking association, the adipose tissue. The fibroblastic component is weakly to moderately collagenized. In a few cases, more heavy foci of myxoid change are noted [1]. Small univacuolated cells at the interface between the fibroblastic element and mature fat are rarely observed [1, 5]. There was no nuclear atypia, and mitotic figures are

L. Ayadi · S. Charfi (✉) · I. Bahri · N. Gouiaa · A. Khabir · S. Makni · T. Sellami-Boudawara
Laboratoire d'anatomie et de cytologie pathologiques,
CHU Habib Bourguiba,
3029 Sfax, Tunisie
e-mail: charfislim@gmail.com

Y. Ben Hamed
Laboratoire privé d'anatomie et de cytologie pathologiques,
Sfax, Tunisie

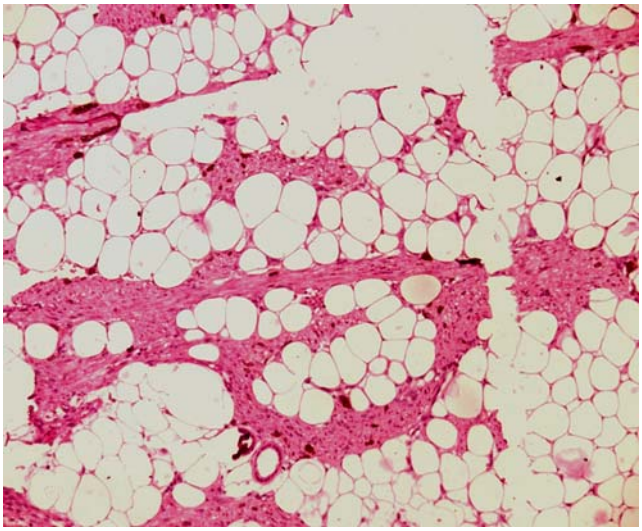


Fig. 1 Abundant adipose tissue with septa of spindle cells (HE ×100)

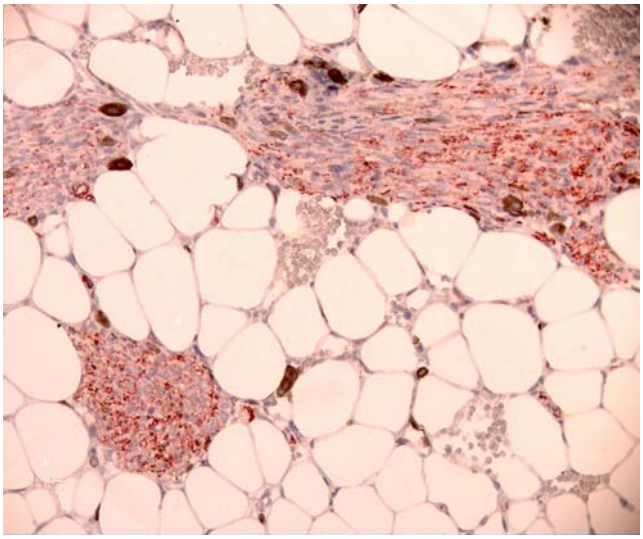


Fig. 3 Positive immunostaining for α smooth muscle actin (×200)

absent or low [1]. Only one instance of the report of Fetsch et al. had a mitotic rate higher than 5 per 50 high-power fields. The presence of a small number of scattered pigmented cells in the fibroblastic component is a rare finding. In the report of Fetsch et al., only two tumor cases with this finding were noted [1]. These two cases had a congenital development and were located in the foot and the forearm. Our case is the first report of noncongenital pigmented lipofibromatosis. According to Fetsch et al., pigmented cells are "bystander cells" that have become passively incorporated within the mass because their normal migration pathway has been disturbed by the lipofibromatous process [1]. We think that the number of reported pigmented lipofibromatosis is too small to allow a correct clinicopathological analysis of this variant. Differential diagnosis of lipofibromatosis includes fibrous hamartoma of child, fibromatosis, calcifying aponevrotic fibroma, and lipoblastoma. All distinctive criteria are cited in the work of Fetsch et al. [1]. Immunohistochemically, it is not primordial for diagnosis of lipofibromatosis. Tumor spindle cells are often focally positive for CD99, CD34, Bcl-2, S100, muscle actin, and EMA. There is no reactivity for desmin and keratins. Pigmented cells are positive for tyrosinase, Melan A, HMB-45, and S-100 protein [1, 3–5]. Complete excision of the lesion is recommended to prevent local recurrence [1, 2]. Congenital tumors, male sex, involvement of hands and feet, incomplete surgery, and a high mitotic activity are associated with a risk of recurrence [1, 2]. Today, no metastasis was reported [1].

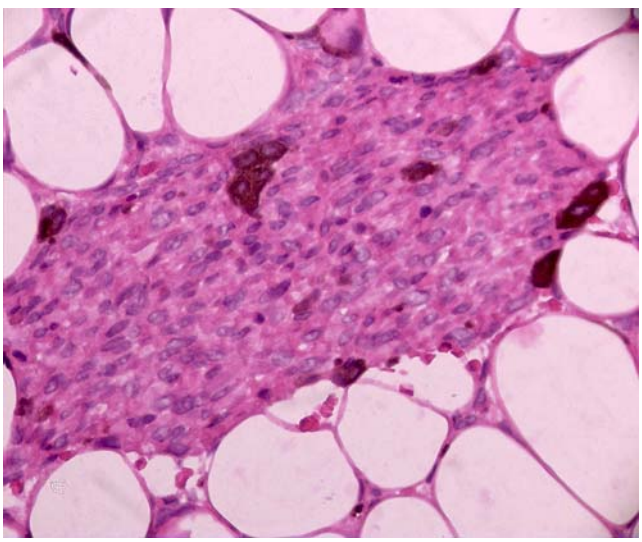


Fig. 2 Fascicles of spindle cells traversing mature adipose tissue. Note the pigmented cells (HE × 400)

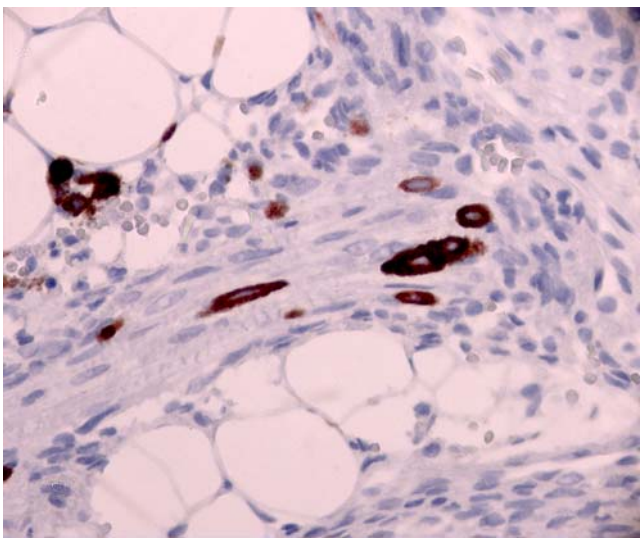


Fig. 4 Immunostaining of pigmented cells with Melan A (×200)

References

1. Fetsch JF, Miettinen M, Laskin WB, Michal M, Enzinger FM (2000) A clinicopathologic study of 45 pediatric soft tissue tumors with an admixture of adipose tissue and fibroblastic elements, and a proposal for classification as lipofibromatosis. Am J Surg Pathol 24:1491–1500
2. Herrmann BW, Dehner LP, Forsen JW (2004) Lipofibromatosis presenting as a pediatric neck mass. Int J Pediatr Otorhinolaryngol 68:1545–1549
3. Kabasawa Y, Katsube KI, Harada H, Nagumo K, Terasaki H, Perbal B (2007) A male infant case of lipofibromatosis in the submental region exhibited the expression of the connective tissue growth factor. Oral Surg Oral Med Oral Pathol Oral Radiol Endod 103:677–682
4. Miettinen M, Fetsch JF (2002) Lipofibromatosis. Pathology and genetics of tumours of soft tissue and bone. In: Fletcher CDM, Unni KK, Mertens F (eds) World Health Organisation classification of tumours. IARC, Lyon, p 85
5. Sasaki D, Hatori M, Hosaka M, Watanabe M, Kokubun S (2005) Lipofibromatosis arising in a pediatric forearm—a case report. Upsala J Med Sci 110:259–266
6. Teo HE, Peh WC, Chan MY, Walford N (2005) Infantile lipofibromatosis of the upper limb. Skeletal Radiol 34:799–802

Virchows Arch (2008) 452:119–132
DOI 10.1007/s00428-007-0509-1

REVIEW AND PERSPECTIVE

PEComas: the past, the present and the future

Guido Martignoni · Maurizio Pea · Daniela Reghellin · Giuseppe Zamboni · Franco Bonetti

Received: 7 August 2007 / Accepted: 6 September 2007 / Published online: 14 December 2007
© Springer-Verlag 2007

Abstract The perivascular epithelioid cell (PEC) is a cell type constantly present in a group of tumors called PEComas. PEC expresses myogenic and melanocytic markers, such as HMB45 and actin. Recently, recurrent chromosomal alterations have been demonstrated in PEC. At present, PEComa is a widely accepted entity. In the past 10 years, the use of this term has allowed to report and describe numerous cases permitting to start highlighting the biology of this group of lesions. PEComas are related to the genetic alterations of tuberous sclerosis complex (TSC), an autosomal dominant genetic disease due to losses of TSC1 (9q34) or TSC2 (16p13.3) genes which seem to have a role in the regulation of the Rheb/mTOR/p70S6K pathway. There are some open questions about PEComas regarding its histogenesis, the definition of epithelioid angiomyolipoma and the identification of the histological criteria of malignancy. An innovative therapeutic trial using rapamycin is under way for tumors occurring in TSC such as renal angiomyolipoma and lymphangioleiomyomatosis. Its success could provide the rationale for the use of the same drug in other lesions composed of PECs, especially in the malignant ones.

Keywords PEComa · PEC · Angiomyolipoma · Lymphangioleiomyomatosis · Sugar tumor · TSC · mTOR · Rapamycin

G. Martignoni · M. Pea · D. Reghellin · G. Zamboni · F. Bonetti
Department of Pathology, Università di Verona,
Verona, Italy

F. Bonetti (✉)
Anatomia Patologica, Università di Verona,
Strada Le Grazie n. 8,
Verona, Italy
e-mail: franco.bonetti@univr.it

What is the perivascular epithelioid cell?

The perivascular epithelioid cell (PEC) (Fig. 1) is a cell type constantly present in a group of tumors including angiomyolipoma (AML), clear-cell "sugar" tumor (CCST) of the lung and extrapulmonary sites, lymphangioleiomyomatosis, clear-cell myomelanocytic tumor of the falciform ligament/ligamentum teres and rare clear-cell tumors of other anatomical sites.

It has morphologic, immunohistochemical, ultrastructural and genetic distinctive features such as an epithelioid appearance with a clear to granular cytoplasm, a round to oval, centrally located nucleus and an inconspicuous nucleolus. PEC has mild to any atypia and a typical perivascular location [13]. At present, PEC has not a known normal counterpart.

Immunohistochemically, PEC expresses myogenic and melanocytic markers, such as HMB45, HMSA-1, MelanA/Mart1, microophtalmia transcription factor (Mitf), actin and, less commonly, desmin [13, 55, 126]. Its immunoreactivity for vimentin is usually incospicuous.

At ultrastructural analysis, PEC contains microfilament bundles with electron-dense condensation, numerous mithocondria and membrane-bound dense granules [11, 118].

It is thought that PEC can modulate its morphology and immunophenotype: given all the characteristics described above (Fig. 2), PEC can show muscular features with a spindle shape and a stronger positivity for actin than for HMB45 or it can have an epithelioid feature with a strong positivity for HMB45 and a mild, if any, reaction for actin (Fig. 3). PEC can also become vacuolized acquiring the feature of an adipocyte. Progesterone receptor positivity has been described in PEC with spindle morphology; this suggests a possible role of progesterone in this morphologic modulation [13, 107].

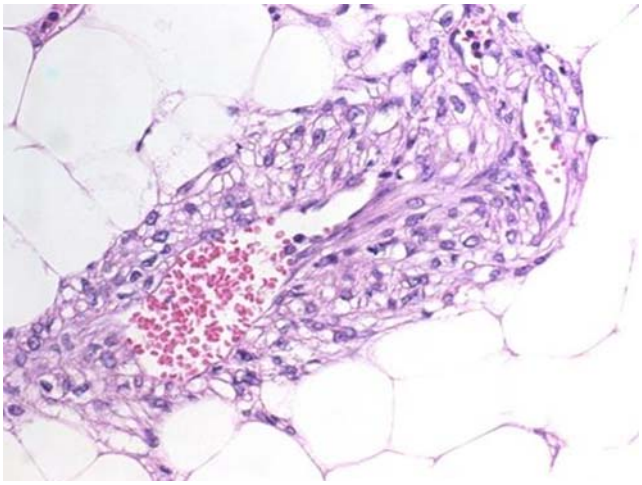


Fig. 1 Renal angiomyolipoma: perivascular epithelioid cells arranged around a blood vessel; H&E ×20

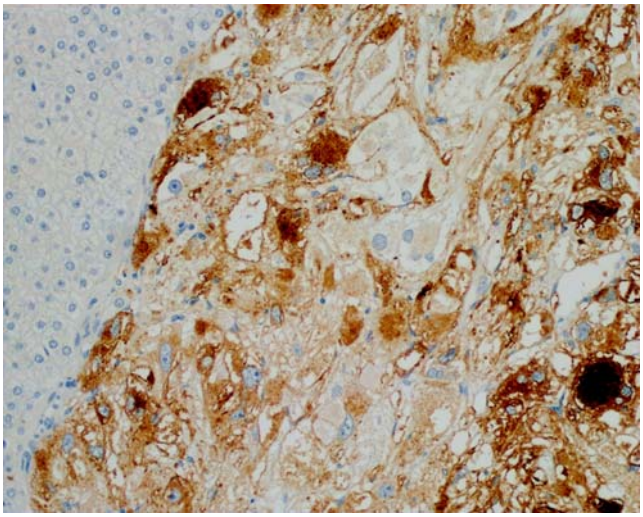


Fig. 3 Hepatic angiomyolipoma: strong granular HMB45 immunoreactivity in perivascular epithelioid cells; HMB45 ×20

Recently, recurrent chromosomal alterations have been demonstrated in PEC [87].

What is a PEComa?

The World Health Organization defines PEComa as "a mesenchymal tumor composed of histologically and immunohistochemically distinctive perivascular epithelioid cells" [37].

At present, this neoplasm is a widely accepted entity. However, some authors cast doubts on the existence of PEComa as a distinctive tumor, particularly as regards the uterine ones that they view as leiomyosarcoma with aberrant expression of HMB45 [102–104]. Although we understand their perplexity, we would like to underline some points. First, it has been demonstrated that there are different gene expression profiles among uterine smooth muscle tumors, demonstrating their heterogeneity [105, 106, 119]. Second, we think that it is difficult to explain, in uterine smooth muscle neoplasms, both HMB45 and Mitf positivity as an aberrant expression or antibody cross-reactivity involving both antigens [81]. Third, we think that the absence of a recognized normal counterpart for PEC is not a sufficient reason to reject the concept of PEComa; in fact, there are other well-accepted soft-tissue neoplasms, such as alveolar soft-part sarcoma and epithelioid sarcoma, that still have not a known normal counterpart.

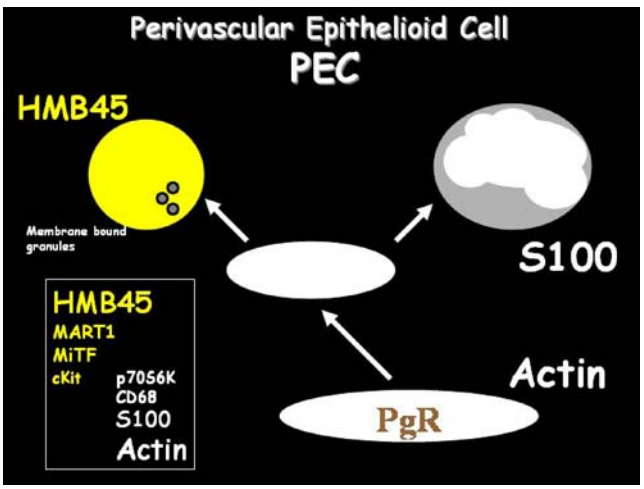


Fig. 2 Diagram demonstrating the modulation of morphology and immunophenotye of PECs

Some authors have questioned about the use of the term "PEComa". They consider it ambiguous because it is not clear whether this term should be restricted to purely epithelioid tumors as CCST or whether the term should be more broadly applied to include AML and lymphangioleiomyomatosis [80, 111].

We believe that AML, CCST and pulmonary lymphangioleiomyomatosis are composed of PECs in different stages of modulation, and these lesions, together with clear-cell myomelanocytic tumor of the falciform ligament/ligamentum teres, belong to the same family of tumors, the PEComas.

Nevertheless, we think that it is better to continue to name some of them (i.e. AML and pulmonary lymphangioleiomyomatosis) also with their established names which identify their clinical and morphological aspects and are well known by clinicians and pathologists [15].

Moreover, in the past 10 years, the use of the term PEComa has permitted to report and describe numerous cases with the morphological and immunohistochemical features of this tumor permitting to start to understand the biology of this group of lesions.

PEC and tuberous sclerosis

PEComas are related to the tuberous sclerosis complex (TSC) or, better, to the genetic alterations of TSC, an autosomal dominant genetic disease due to losses of TSC1 (9q34) or TSC2 (16p13.3) genes [112, 116] and characterized by mental retardation, seizures and cellular proliferations (AMLs, subependymal giant cell tumors, cutaneous angiofibromas, cardiac rabdomyomas, lymphangioleiomyomatosis, pulmonary multifocal micronodular hyperplasia). Similar alterations of the TSC genes have been demonstrated in a significant number of PEComas, both occurring within the TSC and in sporadic cases.

In recent years, great advances have been made in our knowledge of TSC and related lesions. In particular, TSC genes seem to have an important role in the regulation of the Rheb/mTOR/p70S6K pathway [62].

Kenerson et al. [59] have recently demonstrated increased levels of phospho-p70S6K, a marker of mTOR activity, in sporadic AMLs. The associated reduced phospho-AKT expression is consistent with the disruption of TSC1/2 function.

Similar findings were obtained analysing extrarenal PEComas.

PEComa: the past

PEC was first described in 1943 by Apitz [5] as an "abnormal myoblast" in renal AML, as reported by Masson [77] in his famous book.

The idea of a possible link between AML and other two lesions, CCST and lymphangioleiomyomatosis, came from the fact that the same epithelioid cell was observed in them. Moreover, this cell was HMB45-positive in all three lesions [9, 93, 94].

Later, ultrastructural examination revealed the presence of premelanosomes both in CCSTs of the lung and in epithelioid clear-cell component of renal and hepatic AMLs [9, 42, 43, 93, 94, 118].

In addition, the possibility of a relationship between AML and lymphangioleiomyomatosis was suggested by the fact that both occur in TSC [10].

We proposed that CCST should be also included in this syndrome [10], and the first description of this tumor in a patient with TSC confirmed this idea [35].

In 1996, we described the first case of pancreatic CCST and suggested the name PEComa for neoplasms composed of a pure proliferation of PECs [125].

Moreover, the fact that the same clear epithelioid cell composing pulmonary "sugar" tumor was present in AML and was the only component of some small renal microhamartoma (Fig. 4) suggested to us the idea of the existence of a monotypic epithelioid AML of the kidney. We looked for them, and we found them [96].

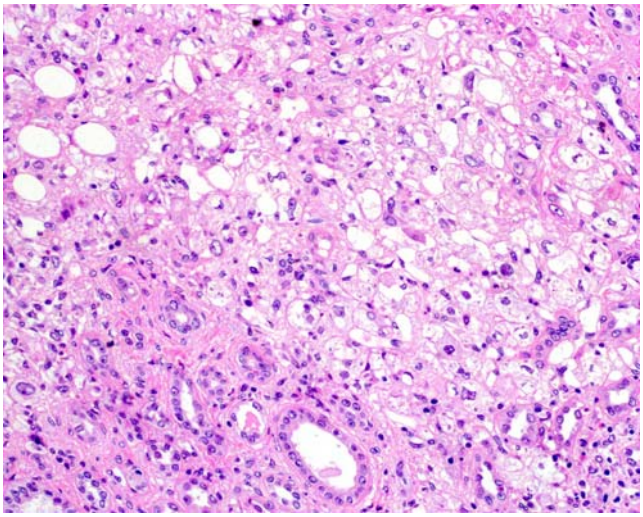


Fig. 4 Renal microhamartoma completely composed of perivascular epithelioid cells; H&E ×20

PEComa: the present

PEComas have been described in different organs and are considered ubiquitous tumors.

Kidney

PEComas of the kidney include classic AML, microscopic AML (so-called microhamartoma), intraglomerular lesions, cystic AML, epithelioid AML, oncocytoma-like AML and lymphangiomyomatosis of the renal sinus.

Classic angiomyolipoma is the most common mesenchymal tumor of the kidney. Being composed of a variable mixture of adipose tissue and spindle and epithelioid smooth muscle cells mixed together with abnormal thick-walled blood vessels, AML is the prototype of the capacity of PEC to modulate its morphology [29, 76].

For a long time, AML has been considered a hamartoma rather than a true neoplasm, but, at present, its clonal nature has been demonstrated [19, 57, 101]. In patients with TSC, renal AMLs are found in both sexes, in the third and fourth decades of life, with a female predominance; they are usually asymptomatic, bilateral, small and multifocal. Sporadic AMLs occur in older patients, in the fourth to sixth decades of life, with a female predominance; they are single, unilateral and larger than those associated with TSC [76]. Classic AML contains more than one cell type; if a particular cell type predominates, AML is consequently named (lipoma-like AML or leiomyoma-like AML) [6].

Classic AML has a benign outcome. Multifocality and regional lymph node involvement can occur, and this is considered to represent a multifocal growth pattern rather than a metastasis [1, 110]. Three cases of sarcoma developing in sporadic AML have been reported. Similar cases have not been described in TSC patients [22, 32, 73].

Both inherited and sporadic AML frequently demonstrates loss of heterozigosity of chromosome 16p (containing the TSC2 locus). The TSC1 gene occasionally shows loss of heterozigosity [17, 50].

Microscopic angiomyolipomas (so-called microhamartomas) They are small nodules often present in a kidney with an AML. They are not homogeneous in appearance and display all the heterogeneous morphologic aspects of AML; microscopic AMLs do not contain thick-walled blood vessels [13, 20].

Intraglomerular lesions with similar features of AML have been reported in patients with and without tuberous sclerosis and in the TSC2/PKD1 contiguous gene syndrome, a disease with a deletion disrupting both TSC2 and PKD1 (autosomal dominant polycystic disease gene) [74].

Cystic angiomyolipoma is a recently described variant of AML [25, 33]. It is a solid-cystic lesion that, microscopically, is composed of epithelial cysts lined by cuboidal to hobnail cells, positive for cytokeratin; a compact subepithelial "cambium-like" layer of stromal cells positive for HMB45, Melan-A, CD10, estrogen and progesterone receptors and a solid extracystic component with the morphology of a muscle-predominant (Fig. 5) AML, which is positive for HMB45, estrogen and progesterone receptors, smooth muscle actin and desmin and which is associated with irregular blood vessels. Some authors think that the subepithelial "cambium-like" layer is a manifestation of a mullerian differentiation of PEC. If the epithelial cysts represent entrapped renal tubular epithelium [33] or are also related to PEC is unknown.

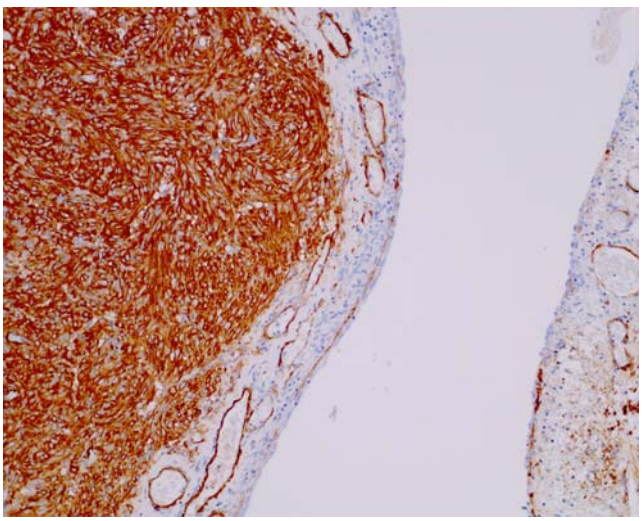


Fig. 5 Cystic angiomyolipoma: strong positivity for actin in the solid extracystic component; SM ACT ×10

Only 1 of the 16 cases described to date had a history of TSC [33].

Epithelioid angiomyolipoma is another recently described variant of AML. It is composed of purely epithelioid cells with melanogenesis markers immunoreactivity arranged in sheets. Both adipocytes and abnormal blood vessels are not present. The cytoplasm of the neoplastic cells varies from faintly eosinophilic to clear. Tumor cells can display considerable nuclear atypia, and necrosis can be present. This tumor can recur locally and metastasise causing death. On the basis of histology alone, it is not possible to predict malignant behaviour in these neoplasms, and further data are needed to better define it. However, at the present time, all epithelioid AMLs should be closely followed clinically. Epithelioid AMLs has been described in patient with or without evidence of TSC and in the TSC2/PKD1 contiguous gene syndrome.

Loss of heterozigosity of TSC2 have been reported in some cases of sporadic epithelioid AML [28, 72, 74, 84, 96].

Oncocytoma-like angiomyolipomas are tumors composed of a homogeneous population of HMB45-positive polygonal cells with strongly eosinophilic cytoplasm. They have been described in patients with and without TSC. Recognition of this variant is important because oncocytomas in the same kidney with AMLs have been reported repeatedly and in patients with TSC oncocytomas seem to occur more frequently than in general population [75].

Lymphangiomyomatosis of the renal sinus is a plaque-like mass in the wall of the renal pelvis. All three cases reported to date also had renal AMLs, but in only one of them careful postmortem examination of the lungs revealed pulmonary lymphangiomyomatosis [74, 78].

Bladder and prostate

In 2003, Pan et al. [85, 86] have reported two PEComas of the genitourinary tract in patients without TSC. Both tumors were composed of a variable percentage of epithelioid and spindle cells with clear to granular cytoplasm arranged in nests separated by a vascular stroma. Neoplastic cells were positive for HMB45 but not for epithelial markers, vimentin and S100 protein. The prostatic tumor (Fig. 6) showed a low mitotic activity, coagulative necrosis and a malignant behaviour, whereas the neoplasm

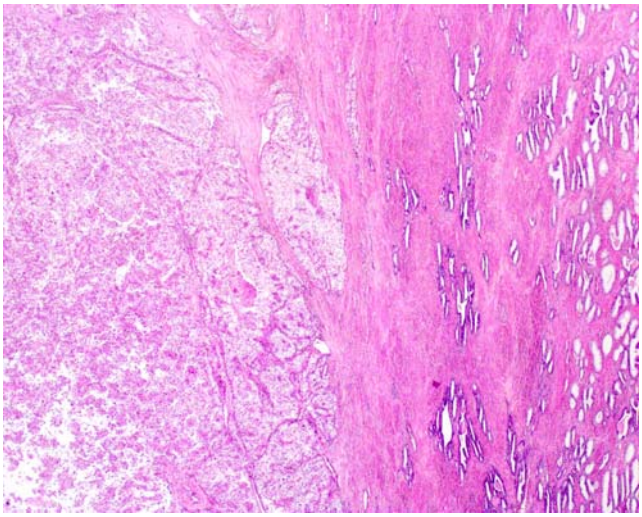


Fig. 6 Prostatic PEComa composed of epithelioid cells with clear cytoplasm arranged in nests; H&E ×4

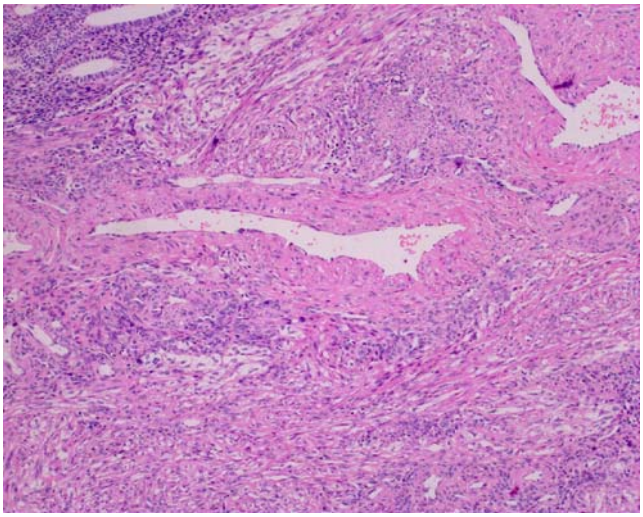


Fig. 8 Uterine PEComa composed of epithelioid cells with a clear cytoplasm and well-defined cell borders; H&E ×10

of the bladder (Fig. 7), lacking these histologic findings, behaved in a benign fashion. Another case of primary PEComa of the bladder has recently been described; also in this case, the patient is well and alive at 48 months after surgery [90].

Finally, Weinreb et al. [120] have recently described a case of PEComa of the urachal cyst composed of pleomorphic cells and containing necrosis and a high mitotic activity. In this case, they also found a peculiar aspect that they named "pecosis": remote from the tumor, there were isolated capillaries surrounded by a single layer of clear cells.

Uterus

The first case of PEC tumor of the uterus was reported by Pea et al. [95]: it was a polypoid neoplasm involving the endometrium, which showed morphological features overlapping those of the CCST of the lung (Fig. 8).

Vang and Kempson [115] described eight cases of uterine PEC tumor ("PEComa"). They distinguished a morphologic spectrum of neoplasms varying from tumors with a tongue-like growth pattern composed of sheets of HMB45-positive clear epithelioid cells, which they called group A, to circumscribed tumors composed of hyalinized stroma and neoplastic cells focally positive for HMB45 and extensively immunoreactive for actin and desmin, which they refer to as group B. In two of these eight cases, pelvic lymph nodes contained lymphangiomyomatosis.

Lesions considered to be uterine involvement of *lymphangioleiomyomatosis* are usually asymptomatic, and some of them correspond to an incidental finding in patients with TSC.

PEComas of the uterus have usually shown benign behaviour, but 13 tumors, 2 of them associated with TSC, were aggressive [16]. In two of six uterine PEComas described by Folpe et al. [39], patients have metastases and one of six patients died of PEComa.

Fadare et al. [31] described a case of uterine PEComa in a patient with TSC in which there was intra-abdominal "PEComatosis": surgeon found small foci of epithelioid cells in the lamina propria of the small intestine, myometrium and ovarian hilum.

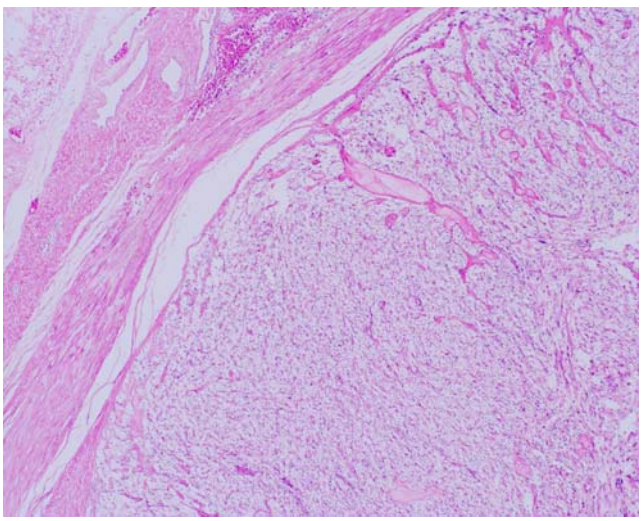


Fig. 7 Bladder PEComa composed of epithelioid cells with clear cytoplasm arranged in nests, H&E ×4

Ovary, vulva and vagina

A tumor with a strong and diffuse HMB45 expression morphologically corresponding to an *epithelioid angiomyolipoma* has been reported in the ovary [4].

Tazelaar et al. [111] reported a case described as primary extrapulmonary *clear-cell "sugar" tumor* of the vulva.

Finally, cases of vaginal PEComa have also been described [39, 83].

Lung

PEComas of the lung include lymphangioleiomyomatosis and *clear-cell "sugar" tumor.*

Lymphangioleiomyomatosis (LAM) (Fig. 9) is a rare and progressive disease that affects the lungs of women, usually in premenopausal age; occasionally, it can be extrapulmonary (as described above). It consists of a nodular, often widespread and bilateral interstitial proliferation of HMB45, actin and desmin-positive smooth muscle cells which can vary from small spindle-shaped cells to large epithelioid cells, usually arranged around thin-walled, branching vascular channels; this proliferation is associated with dilated lymphatics and cystic changes [9, 11, 18, 113].

LAM is usually sporadic; patients with TSC are frequently afflicted.

In many cases of LAM, there is a slow progression to pulmonary failure, and the only therapy is lung transplantation. In no-transplanted patient, there is a median survival of 8–10 years [113].

CCST (Fig. 10) was originally described in the lung [68]. It is a rare and benign neoplasm composed of a uniform population of round-to-polygonal epithelioid cells, with a clear or eosinophilic cytoplasm and well-defined cell borders. Tumor cells are surrounded by prominent and thin-walled vascular channels. CCST has a nested or alveolar appearance. We have also observed adipocytic cells in a few cases of CCST [12]. Tumor cells are positive for HMB45 (Fig. 11) [12, 41, 93].

Pulmonary CCST is rarely associated with TSC [35]; in the vast majority of cases, it is a sporadic lesion.

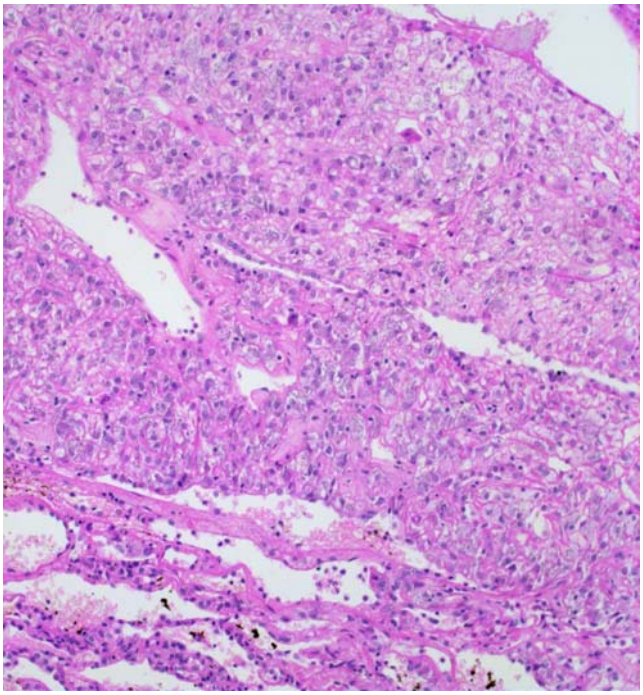


Fig. 10 Pulmonary clear-cell "sugar" tumor composed of epithelioid cells with a clear cytoplasm and well-defined cell borders. A prominent vascular channel is present; H&E ×10

Pancreas

PEComa of the pancreas was reported for the first time in 1996 by Zamboni et al. [125]. It was actually the first time that the very term PEC was introduced (Fig. 12).

The paper reported a tumor with overlapping features of the "benign clear-cell sugar tumor of the lung". This finding was in our opinion consistent with the hypothesis that similar tumors could possibly arise in many if not all locations.

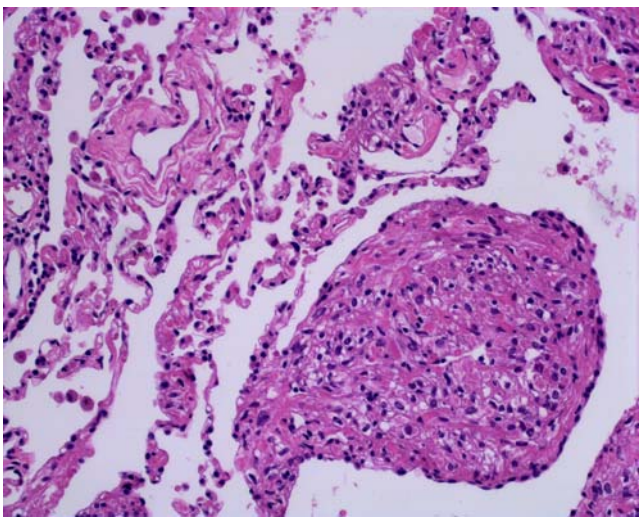


Fig. 9 Pulmonary lymphangioleiomyomatosis composed of epithelioid cells arranged around a vascular channel; H&E ×20

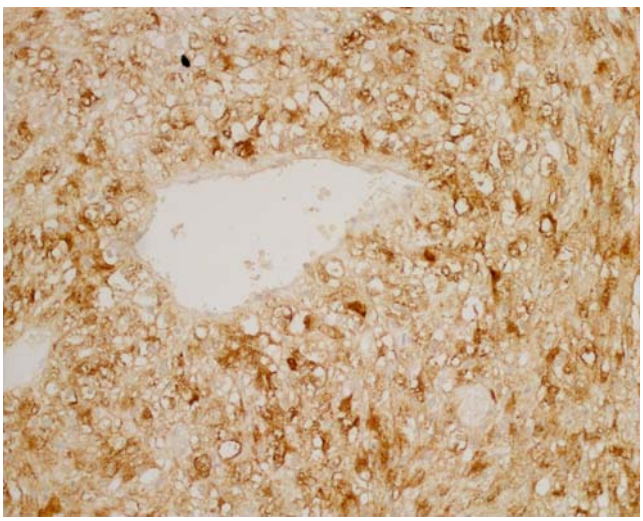


Fig. 11 Pulmonary clear-cell "sugar" tumor: HMB45 immunoreactivity in tumor cells; HMB45 ×20

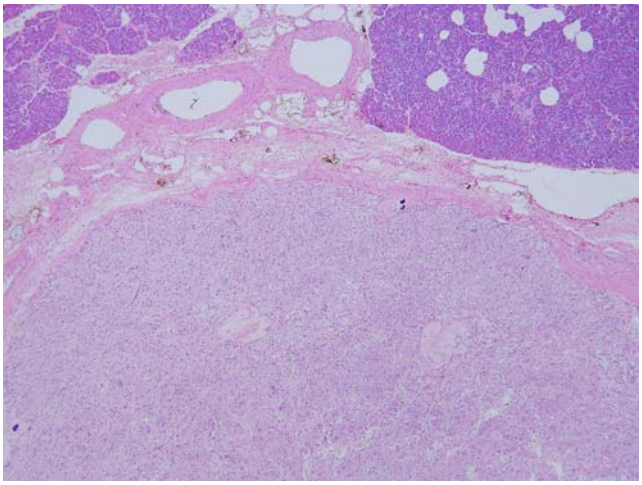


Fig. 12 Pancreatic clear-cell "sugar" tumor: this tumor has overlapping features of the clear-cell "sugar" tumor of the lung: epithelioid cells, with a clear cytoplasm and with a nested appearance; H&E ×4

Thus the term PEComa was introduced to include all similar lesions arising outside the lung. At the time, we believed this to be a unique case. However, in the following years we have observed other two cases of PEComa of the pancreas with overlapping morphological, phenotypical and clinical features.

Thus, while still a very rare disease of the pancreas, PEComa is not an extraordinary finding in this location.

The clinical aspects of PEComa of the pancreas are interesting because they are discovered incidentally during echography of the abdomen and then investigated usually with cyto-aspiration. The observation of clear epithelioid cells can understandably lead to the wrong diagnosis of clear-cell carcinoma of the pancreas and thus lead to duodenocephalopancreasectomy.

A primary *angiomyolipoma* of the pancreas has also been described. It was a cephalopancreatic nodule in a non-TSC woman [51].

Liver

Apart from kidney, liver is the most likely organ involved by *angiomyolipoma* (Fig. 13), either classic or epithelioid [44, 114, 118]. Frequently, hepatic AML shows a prominent component of large epithelioid cells [114]. There has also been described a case of CCST of the common bile duct [98].

Other sites

Lymphangioleiomyomatosis has also been reported in extrapulmonary sites including mediastinal and retroperitoneal lymph nodes, soft tissue of the mesentery and the renal sinus, as previously described. Usually, extrapulmonary LAM presents as a localized well-circumscribed mass called "lymphangiomyoma" [78].

Apart from kidney and liver, classic or even epithelioid *angiomyolipoma* can occur in different visceral and somatic sites as gastrointestinal tract, pelvis [14, 34, 47], nasal cavity [7], soft tissues [49] retroperitoneum [63], bone [53] and orbit [54].

Clear-cell "sugar" tumor has been described in a variety of extrapulmonary sites, apart from uterus and pancreas: skin [26], soft tissues [40], breast [45], skull base [66], gastrointestinal tract [8, 111], inter-atrial cardiac septum [111] and oral mucosa [61].

Clear-cell myomelanocytic tumour of the falciform ligament/ligamentum teres (*CCMMT*) is a PEComa showing predominantly spindled cell morphology.

It has been first described in 2000 by Folpe et al. [36] who presented seven cases of PEComa arising in the abdomen. All patients but one were women ranging from 3 to 21years of age. These neoplasms were composed of spindle cells arranged in fascicles and nests, positive for HMB45 and, in three cases, also for Melan-A, microophtalmia transcription factor (Mitf) and actin. Also in these cases, premelanosomes were ultrastructurally detected. At follow-up, in one patient presumed lung metastasis developed.

CCMMT has also been described in thigh [38] and in the skin [79].

PEComa: the future

PEComas are a group of ubiquitous neoplasms sharing morphological, immunohistochemical, ultrastructural and genetic distinctive features.

There are some open questions about PEComas: the histogenesis and the normal/physiological counterpart of

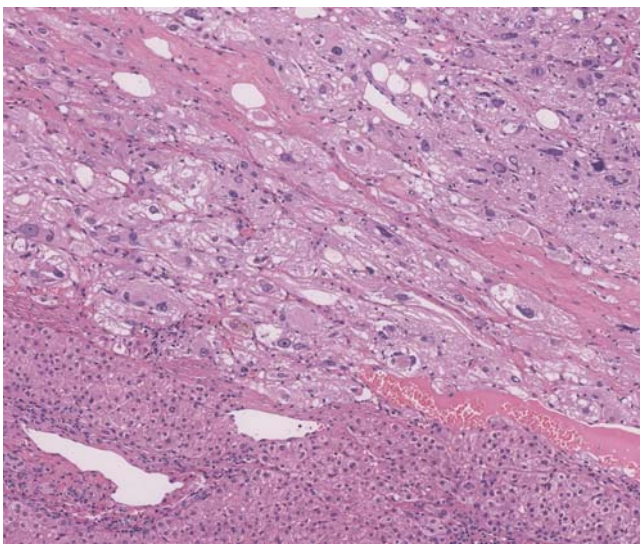


Fig. 13 Hepatic angiomyolipoma: solid component made of large epithelioid cells; H&E ×10

Table 1 Reported cases of malignant PEComas in literature

Reference	Diagnosis	Site	Sex/age	Outcome	Comments
Sale and Kulander [100]	CCST	Lung	n.a./n.a.	AWD at 10 years	Hepatic metastases at 10 years
Ferry et al. [32]	Epithelioid AML	Kidney	F/49	DOD at 5.5 months	
Al-Saleem et al. [3]	Epithelioid AML	Kidney	F/21	DOD at 3 months	
Pea et al. [96]	Epithelioid AML	Kidney	F/24	DOD at 1 year	Pelvic and hepatic metastases
Pea et al. [96]	Epithelioid AML	Kidney	M/29	DOD at 18 months	Pulmonary and hepatic metastases
Christiano et al. [21]	Epithelioid AML	Kidney	M/42	AWD at 15 months	
L'Hostis et al. [67]	Epithelioid AML	Kidney	F/71	DOD at 2 years	
Folpe et al. [36]	PEComa	Ligamentum teres falciform ligament	M/29	DOC at 1 year	Radiographically suspected lung metastasis at 3 months
Martignoni et al. [73]	Epithelioid AML	Kidney	F/50	AWD at 10 years	Local recurrence at 7 years; pulmonary, pelvic and abdominal metastases at 10 years
Bonetti et al. [14]	PEComa	Uterus	F/41	ANED at 6 months	Ovarian mass at presentation
Bonetti et al. [14]	PEComa	Uterus	F/19	AWD at 18 months	Aggressive local recurrence at 1 month; lung and bone metastases at 11 months
Bonetti et al. [14]	PEComa	Terminal ileum and cecum	F/28	DOD at 28 months	Hepatic metastasis
Cibas et al. [22]	Epithelioid AML	Kidney	F/49	AWD at 6 months	
Saito et al. [99]	CCST	Kidney	F/23	DOD at 1 year	Retroperitoneal recurrence at 3 months
Yamamoto et al. [122]	Epithelioid AML	Kidney	M/47	DOD	DOD with spinal, lung and lymph node metastases (autopsy case)
Dimmler et al. [27]	PEComa	Uterus	F/61	AWD at 7 years	Lung metastases
Greene et al. [46]	PEComa	Uterus and pelvic side wall	F/79	DOD at several months	Pelvic and mesenteric recurrence at 2 years
Lau et al. [63]	Epithelioid AML	Retroperitoneum	M/29	ANED at 18 years	Liver metastases at 9 years; thymus and lung metastases at 17 years
Leclerc et al. [64]	Epithelioid AML	Kidney	F/36	ANED	Lymph node metastases
Lin et al. [69]	Epithelioid AML	Kidney	n.a./58	AWD	Liver and lymph node metastases
Ong et al. [82]	Epithelioid AML	Kidney	F/74	AWD	Adrenal metastases
Pan et al. [85]	PEComa	Prostate	M/46	DOD at 4 years	Submitted to adjuvant chemotherapy; lung metastases at 3 years

Takahashi et al. [109]	Epithelioid AML	Kidney	F/40	DOD at 18 months	Submitted to adjuvant chemotherapy; pulmonary metastases
Takahashi et al. [109]	Epithelioid AML	Kidney	M/44	DOD at 60 months	Splenic and retroperitoneal metastases at 3 years; hepatic metastases at 60 months
Yanai et al. [123]	PEComa	Jejunum	F/32	AWD at 25 months	Pelvic wall recurrence/local metastases at 13 months; ovarian metastases at 25 months
Darai et al. [24]	Epithelioid AML	Urach	F/n.a.	AWD	Lymph node metastases
Harris et al. [49]	PEComa	Soft tissue near knee	M/87	AWD at 40 months	Inguinal lymph node and lung metastases at 13 months
Lehman [66]	PEComa	Skull base	F/49	DOD at 3 months	Paraspinal and lung metastasis at 6 weeks
Bosincu et al. [16]	PEComa	Uterus	F/59	DOD at 1 year	Pelvic recurrence at 6 months
Evert et al. [30]	PEComa	Rectovaginal space	F/56	AWD	Pulmonary metastases at presentation
Folpe et al. [39]	PEComa	Neck	F/77	ANED at 6 months	Re-excision and submitted to adjuvant radiotherapy
Folpe et al. [39]	PEComa	Forearm	M/71	ANED at 10 months	Re-excision and submitted to adjuvant radiotherapy
Folpe et al. [39]	PEComa	Broad ligament	F/16	ANED at 18 months	Re-excised
Folpe et al. [39]	PEComa	Falciform ligament	F/15	ANED at 35 months	Re-excised
Folpe et al. [39]	PEComa	Uterus	F/56	AWD at 11 years	Submitted to adjuvant radio and chemotherapy; lung and bone metastases
Folpe et al. [39]	PEComa	Pelvic soft tissue	F/72	AWD at 15 months	Local recurrence
Folpe et al. [39]	PEComa	Omentum	M/40	AWD at 24 months	Extensive intra-abdominal recurrence/local metastases
Folpe et al. [39]	PEComa	Uterus	F/59	AWD at 30 months	Submitted to adjuvant chemotherapy; liver and lung metastases at 30 months
Folpe et al. [39]	PEComa	Mesentery	F/46	DOD at 27 months	Submitted to adjuvant chemotherapy; extensive intra-abdominal recurrence and liver metastases at 22 months
Folpe et al. [39]	PEComa	Uterus	F/36	DOD at 39 months	Submitted to adjuvant chemotherapy; lung metastases at 12 months and liver metastases at 36 months
Svec and Velenska [108]	Epithelioid AML	Kidney	F/47	ANED at 5 months	Recurrence at 3 months
Yu et al. [124]	Epithelioid AML	Kidney	F/12	DOD at 9 months	Lymph node metastases; submitted to adjuvant chemotherapy
Agaimy and Wünsch 2006 [2]	PEComa	Ileum	F/63	AWD at 14 months	Abdomino-pelvic recurrence
Kim et al. [60]	CCMT	Broad ligament	F/12	AWD at 1 year	Iliac fossa recurrence
Mai and Belanger [70]	PEComa	Thigh	M/56	DOD at 1 year	Pulmonary and brain metastases
Mai and Belanger [70]	PEComa	Thigh	F/60	DOD at 1 year	Pulmonary metastases

Table 1 (continued)

Reference	Diagnosis	Site	Sex/age	Outcome	Comments
Mai and Belanger [70]	PEComa	Groin	M/46	DOD at 2 years	Lymph node metastases
Parfitt et al. [89]	PEComa	Liver	F/60	AWD at 10 years	Hepatic recurrence and pulmonary, pancreatic and muscular metastases at 9 years; bladder metastases at 10 years
Parfitt et al. [91]	PEComa	Lung/Adrenal gland	F/53	AWD	Brain metastases at several moths
Yamamoto et al. [121]	PEComa	Colon	F/43	DOD at 38 months	Peritoneal dissemination at 20 months
Gupta et al. [48]	Epithelioid AML	Retroperitoneum	F/80	AWD at 1 year	Hepatic and rib metastases
Huang et al. [52]	Epithelioid AML	Kidney	F/78	DOD at 5 months	
Park et al. [92]	Epithelioid AML	Kidney	M/69	AWD at 8 months	Hepatic and peritoneal metastases
Park et al. [92]	Epithelioid AML	Kidney	F/46	AWD at 12 months	Hepatic and lymph node metastases
Weinreb et al. [120]	PEComa	Retroperitoneum	F/49	AWD	Brain and lung metastases

ANED Alive, not evidence of disease; *AWD* alive with disease; *DOC* dead of other causes; *DOD* dead of disease; *n.a.* not available

PEC, the definition of epithelioid AML and the identification of the histological criteria of malignancy.

The histogenesis and the normal/physiological counterpart of PEC are unknown, but some hypotheses have been proposed. One hypothesis is that PEC derives from undifferentiated cells of the neural crest that can express dual smooth muscle and melanocytic phenotype; a second hypothesis is that PEC has a myoblastic, smooth muscle origin with a molecular alteration that brings to expression of melanogenesis and melanocytic markers [107]; a third hypothesis is that PEC has a pericytic origin. As regards PEComa's histogenesis, the involvement of TSC pathway in these neoplasms can suggest some possibilities: it has been previously proposed that B-raf activity in cells lacking TSC2 may play a role in cell differentiation [56]. Moreover, TSC pathway regulates negatively Wnt/beta-catenin pathway [71] and beta-catenin regulates transcription of genes involved in cell proliferation and differentiation. Nevertheless, more cases should be analysed to better understand PEC origin and PEComa's histogenesis.

The second issue regarding PEComas is which cases should be classified as epithelioid AML particularly in the kidney and liver, where AML occurs with higher frequency. We defined epithelioid AML as a neoplasm composed of purely epithelioid cells with melanogenesis markers immunoreactivity arranged in sheets, without adipocytes and abnormal blood vessels.

However, in otherwise classic AML, areas of epithelioid cells can be observed, raising the question how much they should be represented to call a tumor "epithelioid angiomyolipoma". The collection of such cases and a consensus meeting could be useful tools to answer to this problem.

Malignant PEComa can be a very aggressive disease leading to multiple metastases and death as expected with a high-grade sarcoma [3, 14, 16, 32, 39, 52, 66, 67, 70, 85, 96,

Fig. 14 Hepatic angiomyolipoma: cytoplasmic signal in immunohistochemical reaction for p70S6K; p70S6K ×10

99, 109, 121, 124]. A few malignant PEComas metastasised after several years (7–9 years) [27, 73, 89, 100] (Table 1).

Recently, Folpe et al. [39] reported 26 cases of PEComas of soft tissue and gynaecologic origin proposing criteria for the classification of these tumors as "benign", "of uncertain malignant potential" and "malignant". In this study, they observed a significant association between tumor size >5cm, infiltrative growth pattern, high nuclear grade, necrosis and mitotic activity >1/50 HPF and subsequent aggressive clinical behaviour of PEComas.

We think that this approach is the best available at the moment. While more cases with long follow-up are needed to verify the effectiveness of this prognostic classification, we believe that all cases of PEComa should be classified according to the criteria proposed by Folpe et al.

Another future challenge regarding PEComas is their management.

Surgery seems to be the only approach for aggressive cases, as chemio- and radiotherapy has not shown significant results. However, this derives from anecdotical cases as no therapeutic trial has so far been implemented. There are obvious difficulties to perform a therapeutic trial mainly due to the rarity of the disease. An international cooperative study is needed to address this problem.

A very different problem is posed by lymphangioleyomyomatosis. In fact, lymphangioleyomyomatosis is composed of a population of cells with no atypia. Mitotic activity is virtually absent or extremely low. In spite of this, the disease usually progresses inexorably towards lung-function impairment.

Recently, Kenerson et al. [59] demonstrated TSC1/2 inactivation and m-TOR hyperactivation in non-TSC AMLs and in extrarenal PEComas using immunohistochemistry and Western blot analysis. In particular, m-TOR hyperactivation can be studied in such lesions using immunohistochemical detection of p70S6K. As we have previously mentioned, p70S6K is a protein kinase activated by m-TOR. Immunohistochemical reaction for p70S6K can stain both p70S6K, which gives a cytoplasmic signal (Fig. 14), and a second isoform of kinase, p85S6K, which is also activated by m-TOR and which gives a nuclear signal.

Rapamycin is a specific inhibitor of m-TOR [23] which is approved by the US Food and Drug Administration for immunosuppression therapy after renal transplant [117], and it has recently been approved also for therapy of renal cell carcinomas and acute myeloid leukemia [88, 97]. Preclinical studies in animal models of TSC have shown significant in vivo response to rapamycin [58, 65].

As regards LAM, an innovative therapeutic trial is under way. Rapamycin seems to block signaling through the Akt cell growth and survival pathway (for up-to-date information, see http://www.thelamfoundation.org).

A similar trial has already shown a positive effect on renal AML, and we can hope to see the same effect on LAM.

If this will be the case, this could provide the rationale for the use of the same drug in other lesions composed of PECs.

Acknowledgements The authors thank Fondazione Cassa di Risparmio di Verona (Unicredit, Cariverona) for financial support.

References

1. Abdulla M, Bui HX, del Rosario AD, Ross JS (1994) Renal angiomyolipoma. DNA content and immunohistochemical study of classic and multicentric variants. Arch Pathol Lab Med 118:735–739
2. Agaimy A, Wünsch PH (2006) Perivascular epithelioid cell sarcoma (malignant PEComa) of the ileum. Pathol Res Pract 202:37–41
3. Al-Saleem T, Wessner LL, Scheithauer BW, Patterson K, Roach ES, Dreyer SJ, Fujikawa K, Bjornsson J, Bernstein J, Henske EP (1998) Malignant tumors of the kidney, brain, and soft tissues in children and young adults with the tuberous sclerosis complex. Cancer 83:2208–2216
4. Anderson AE, Yang X, Young RH (2002) Epithelioid angiomyolipoma of the ovary: a case report and literature review. Int J Gynecol Pathol 21:69–73
5. Apitz K (1943) Die Geschwülste und Gewebsmissbildungen der Nierenrinde. II Midteilung. Die mesenchymalen Neubildungen. Virchows Arch 311:306–327
6. Bacchi CE, Bonetti F, Pea M, Martignoni G, Gown AM (1996) HMB-45, a review. Appl Immunohistochem 4:73–85
7. Banerjee SS, Eyden B, Trenholm PW, Sheikh MY, Wakamatsu K, Ancans J, Rosai J (2001) Monotypic angiomyolipoma of the nasal cavity: a heretofore undescribed occurrence. Int J Surg Pathol 9:309–315
8. Birkhaeuser F, Ackermann C, Flueckiger T, Guenin MO, Kern B, Tondelli P, Peterli R (2004) First description of a PEComa (perivascular epithelioid cell tumor) of the colon: report of a case and review of the literature. Dis Colon Rectum 47:1734–1737
9. Bonetti F, Pea M, Martignoni G, Zamboni G, Iuzzolino P (1991) Cellular heterogeneity in lymphangiomyomatosis of the lung. Hum Pathol 22:727–728
10. Bonetti F, Pea M, Martignoni G, Zamboni G (1992) PEC and sugar. Am J Surg Pathol 16:307–308
11. Bonetti F, Chiodera PL, Pea M, Martignoni G, Bosi F, Zamboni G, Mariuzzi GM (1993) Transbronchial biopsy in lymphangiomyomatosis of the lung. HMB45 for diagnosis. Am J Surg Pathol 17:1092–1102
12. Bonetti F, Pea M, Martignoni G, Doglioni C, Zamboni G, Capelli P, Rimondi P, Andrion A (1994) Clear cell ("sugar") tumor of the lung is a lesion strictly related to angiomyolipoma–the concept of a family of lesions characterized by the presence of the perivascular epithelioid cells (PEC). Pathology 26:230–236
13. Bonetti F, Pea M, Martignoni G, Zamboni G, Manfrin E, Colombari R, Mariuzzi GM (1997) The Perivascular Epithelioid Cell and related lesions. Adv Anat Pathol 4:343–358
14. Bonetti F, Martignoni G, Colato C, Manfrin E, Gambacorta M, Faleri M, Bacchi C, Sin VC, Wong NL, Coady M, Chan JK (2001) Abdominopelvic sarcoma of perivascular epithelioid cells. Report of four cases in young women, one with tuberous sclerosis. Mod Pathol 14:563–568
15. Bonetti F, Martignoni G, Pea M (2002) Correspondence re: Bonetti F, Martignoni G, Colato C, Manfrin E, Gambacorta M, Faleri M et al. Abdominopelvic sarcoma of perivascular epithelioid cells. Report of four cases in young women, one with tuberous sclerosis. Mod Pathol 2001;14:563–8. And Tazelaar HD, Batts KP, Srigley JR. Primary extrapulmonary sugar tumor (PEST): a report of four cases. Mod Pathol 2001;14:615–22. Mod Pathol 15:87–90

16. Bosincu L, Rocca PC, Martignoni G, Nogales FF, Longa L, Maccioni A, Massarelli G (2005) Perivascular epithelioid cell (PEC) tumors of the uterus: a clinicopathologic study of two cases with aggressive features. Mod Pathol 18:1336–1342
17. Carbonara C, Longa L, Grosso E, Mazzucco G, Borrone C, Garrè ML, Brisigotti M, Filippi G, Scabar A, Giannotti A, Falzoni P, Monga G, Garini G, Gabrielli M, Riegler P, Danesino C, Ruggieri M, Magro G, Migone N (1996) Apparent preferential loss of heterozigosity at TSC2 over TSC1 chromosomal region in tuberous sclerosis hamartomas. Genes Chromosomes Cancer 15:18–25
18. Chan JK, Tsang WY, Pau MY, Tang MC, Pang SW, Fletcher CD (1993) Lymphangiomyomatosis and angiomyolipoma: closely related entities characterized by hamartomatous proliferation of HMB-45-positive smooth muscle. Histopathology 22: 445–455
19. Cheng L, Gu J, Eble JN, Bostwick DG, Younger C, MacLennan GT, Abdul-Karim FW, Geary WA, Koch MO, Zhang S, Ulbright TM (2001) Molecular genetic evidence for different clonal origin of components of human renal angiomyolipomas. Am J Surg Pathol 25:1231–1236
20. Chowdhury PR, Tsuda N, Anami M, Hayashi T, Iseki M, Kishikawa F, Kanetake H, Saito Y (1996) A histopathologic and immunohistochemical study of small nodules of renal angiomyolipoma: a comparison of small nodules with angiomyolipoma. Mod Pathol 9:1081–1088
21. Christiano AP, Yang X, Gerber GS (1999) Malignant transformation of renal angiomyolipoma. J Urol 161:1900–1901
22. Cibas ES, Goss GA, Kulke MH, Demetri GD, Fletcher CD (2001) Malignant epithelioid angiomyolipoma ('sarcoma ex angiomyolipoma') of the kidney: a case report and review of the literature. Am J Surg Pathol 25:121–126
23. Cohen E (2006) m-TOR inhibitors. Clin Adv Hematol Oncol 4:38–39
24. Darai E, Bazot M, Barranger E, Detchev R, Cortez A (2004) Epithelioid angiomyolipoma of the uterus: a case report. J Reprod Med 49:578–581
25. Davis CJ, Barton JH, Sesterhenn IA (2006) Cystic angiomyolipoma of the kidney: a clinicopathologic description of 11 cases. Mod Pathol 19:669–674
26. de Saint Aubain Somerhausen N, Gomez Galdon M, Bouffioux B, Courtin C, Theunis A, Vogeleer MN, Myant N (2005) Clear cell 'sugar' tumor (PEComa) of the skin: a case report. J Cutan Pathol 32:441–444
27. Dimmler A, Seitz G, Hohenberger W, Kirchner T, Faller G (2003) Late pulmonary metastasis in uterine PEComa. J Clin Pathol 56:627–628
28. Eble JN, Amin MB, Young RH (1997) Epithelioid angiomyolipoma of the kidney: a report of five cases with a prominent and diagnostically confusing epithelioid smooth muscle component. Am J Surg Pathol 21:1123–1130
29. Eble JN (1998) Angiomyolipoma of kidney. Semin Diagn Pathol 15:21–40
30. Evert M, Wardelmann E, Nestler G, Schultz HU, Roessner A, Röcken C (2005) Abdominopelvic perivascular epithelioid cell sarcoma (malignant PEComa) mimicking gastrointestinal stromal tumour of the rectum. Histopathology 46:115–117
31. Fadare O, Parkash V, Yilmaz Y, Mariappan MR, Ma L, Hileeto D, Qumsiyeh MB, Hui P (2004) Perivascular epithelioid cell tumor (PEComa) of the uterine cervix associated with intra-abdominal 'PEComatosis': a clinicopathological study with comparative genomic hybridization analysis. World J Surg Oncol 2:35
32. Ferry JA, Malt RA, Young RH (1991) Renal angiomyolipoma with sarcomatous transformation and pulmonary metastases. Am J Surg Pathol 15:1083–1088
33. Fine SW, Reuter VE, Epstein JI, Argani P (2006) Angiomyolipoma with epithelial cysts (AMLEC). A distinctive cystic variant of angiomyolipoma. Am J Surg Pathol 30:593–599
34. Fink D, Marsden DE, Edwards L, Camaris C, Hacker NF (2004) Malignant perivascular epithelioid cell tumor (PEComa) arising in the broad ligament. Int J Gynecol Cancer 14:1036–1039
35. Flieder DB, Travis WD (1997) Clear cell 'sugar' tumor of the lung: association with lymphangioleiomyomatosis and multifocal micronodular pneumocyte hyperplasia in a patient with tuberous sclerosis. Am J Surg Pathol 21:1242–1247
36. Folpe AL, Goodman ZD, Ishak KG, Paulino AF, Taboada EM, Meehan SA, Weiss SW (2000) Clear cell myomelanocytic tumor of the falciform ligament/ligamentum teres: a novel member of the perivascular epithelioid clear cell family of tumors with a predilection for children and young adults. Am J Surg Pathol 24:1239–1246
37. Folpe AL (2002) Neoplasms with perivascular epithelioid cell differentiation (PEComas). In: Fletcher CDM, Unni KK, Epstein J, Mertens F (eds) Pathology and genetics of tumours of soft tissue and bone. Series: WHO Classification of tumours. IARC Press, Lyon, pp 221–222
38. Folpe AL, McKenney JK, Li Z, Smith SJ, Weiss SW (2002) Clear cell myelomelanocytic tumor of the thigh: report of a unique case. Am J Surg Pathol 26:809–812
39. Folpe AL, Mentzel T, Lehr HA, Fisher C, Balzer BL, Weiss SW (2005) Perivascular epitheliod cell neoplasms of soft tissue and gynecologic origin: a clinicopathologic study of 26 cases and review of the literature. Am J Surg Pathol 29:1558–1575
40. Fukunaga M (2004) Perivascular epithelioid cell tumor (PEComa) of soft tissue. Case report with ultrastructural study. APMIS 112:98–104
41. Gaffey MJ, Mills SE, Askin FB, Ross GW, Sale GE, Kulander BG, Visscher DW, Yousem SA, Colby TV (1990) Clear cell tumor of th e lung. A clinicopathologic, immunohistochemical, and ultrastructural study of eight cases. Am J Surg Pathol 14:248–259
42. Gaffey MJ, Mills SE, Zarbo RJ, Weiss LM, Gown AM (1991) Clear cell tumor of the lung. Immunohistochemical and ultrastructural evidence of melanogenesis. Am J Surg Pathol 15:644–653
43. Gal AA, Koss MN, Hochholzer L, Chejfec G (1991) An immunohistochemical study of benign clear cell ('sugar') tumor of the lung. Arch Pathol Lab Med 115:1034–1038
44. Goodman ZD, Ishak KG (1984) Angiomyolipomas of the liver. Am J Surg Pathol 8:745–750
45. Govender D, Sabaratnam RM, Essa AS (2002) Clear cell 'sugar' tumor of the breast: another extrapulmonary site and review of the literature. Am J Surg Pathol 26:670–675
46. Greene LA, Mount SL, Schned AR, Cooper K (2003) Recurrent perivascular epithelioid cell tumor of the uterus (PEComa): an immunohistochemical study and review of the literature. Gynecol Oncol 90:677–681
47. Gronchi A, Diment J, Colecchia M, Fiore M, Santinami M (2004) Atypical pleomorphic angiomyolipoma localized to the pelvis: a case report and review of the literature. Histopathology 44:292–295
48. Gupta C, Malani AK, Gupta V, Singh J, Ammar H (2007) Metastatic retroperitoneal epithelioid angiomyolipoma. J Clin Pathol 60:428–431
49. Harris GC, McCulloch TA, Perks G, Fisher C (2004) Malignant perivascular epithelioid cell tumor ('PEComa') of soft tissue: a unique case. Am J Surg Pathol 28:1655–1658
50. Henske EP, Neumann HP, Scheithauer BW, Herbst EW, Short MP, Kwiatkowski DJ (1995) Loss of heterozigosity in the tuberous sclerosis (TSC2) region of chromosome band 16 p13

occurs in sporadic as well as TSC-associated renal angiomyolipomas. Genes Chromosomes Cancer 13:295–298
51. Heywood G, Smyrk TC, Donohue JH (2004) Primary angiomyolipoma of the pancreas. Pancreas 28:443–445
52. Huang KH, Huang CY, Chung SD, Pu YS, Shun CT, Chen J (2007) Malignant epithelioid angiomyolipoma of the kidney. J Formos Med Assoc 106(2 Suppl):S51–54
53. Insabato L, De Rosa G, Terracciano LM, Fazioli F, Di Santo F, Rosai J (2002) Primary monotypic epithelioid angiomyolipoma of bone. Histopathology 40:286–290
54. Iyengar P, Deangelis DD, Greenberg M, Taylor G (2005) Perivascular epithelioid cell tumor of the orbit: a case report and review of the literature. Pediatr Dev Pathol 8:98–104
55. Jungbluth AA, Busam KJ, Gerald WL et al (1998) A103: an anti-melan-a monoclonal antibody for the detection of malignant melanoma in paraffin-embedded tissues. Am J Surg Pathol 22:595–602
56. Karbowniczek M, Henske EP (2005) The role of tuberin in cellular differentiation: are B-Raf and MAPK involved? Ann N Y Acad Sci 1059:168–173
57. Kattar MM, Grignon DJ, Eble JN, Hurley PM, Lewis PE, Sakr WE, Cher ML (1999) Chromosomal analysis of renal angiomyolipoma by comparative genomic hybridization: evidence for clonal origin. Hum Pathol 30:295–299
58. Kenerson H, Dundon TA, Yeung RS (2005) Effects of rapamycin in the Eker rat model of tuberous sclerosis complex. Pediatr Res 57:67–75
59. Kenerson H, Folpe AL, Takayama TK, Yeung RS (2007) Activation of the mTOR pathway in sporadic angiomyolipomas and other epithelioid cell neoplasms. Hum Pathol 38:1361–1371
60. Kim HJ, Lim SJ, Choi H, Park K (2006) Malignant clear-cell myomelanocytic tumor of broad ligament-a case report. Virchows Arch 448:867–870
61. Koutlas IG, Pambuccian SE, Jessurun J, Manivel JC, Gopalakrishnan R (2005) Perivascular epithelioid cell tumor of the oral mucosa. Arch Pathol Lab Med 129:690–693
62. Kwiatkowski DJ (2003) Tuberous sclerosis: from tubers to mTOR. Ann Hum Genet 67:87–96
63. Lau SK, Marchevsky AM, McKenna RJ, Luthringer DJ (2003) Malignant monotypic epithelioid angiomyolipoma of the retroperitoneum. Int J Surg Pathol 11:223–228
64. Leclerc JC, Marchal F, Stines J, Régent D (2003) L'angiomyolipome rénal épithélioide: tumeur bénigne ou maligne? J Radiol 84:851–854
65. Lee L, Sudentas P, Donohue B, Asrican K, Worku A, Walker V, Sun Y, Schmidt K, Albert MS, El-Hashemite N, Lader AS, Onda H, Zhang H, Kwiatkowski DJ, Debora SL (2005) Efficacy of rapamycin analog (CCI-779) and IFN-gamma in tuberous sclerosis mouse models. Genes Chromosomes Cancer 42:213–227
66. Lehman NL (2004) Malignant PEComa of the skull base. Am J Surg Pathol 28:1230–1232
67. L'Hostis BA, Diminiere C, Ferriere JM, Coindre JM (1999) Renal angiomyolipoma: a clinicopathologic, immunohistochemical, and follow-up study of 46 cases. Am J Surg Pathol 23:1011–1020
68. Liebow AA, Castleman B (1971) Benign clear cell ('sugar') tumors of the lung. Yale J Biol Med 43:213–222
69. Lin WC, Wang JH, Wei CJ, Pan CC, Chang CY (2003) Malignant renal epithelioid angiomyolipoma with aggressive behaviour and distant metastases. J Chin Med Assoc 66:303–306
70. Mai KT, Belanger EC (2006) Perivascular epithelioid cell tumour (PEComa) of the soft tissue. Pathology 38:415–420
71. Mak BC, Takemaru K, Kenerson HL, Moon RT, Yeung RS (2003) The tuberin-hamartin complex negatively regulates beta-catenin signalling activity. J Biol Chem 278:5947–5951
72. Martignoni G, Pea M, Bonetti F, Zamboni G, Carbonara C, Longa L, Zancanaro C, Maran M, Brisigotti M, Mariuzzi GM (1998) Carcinomalike monotypic epithelioid angiomyolipoma in patients without evidence of tuberous sclerosis: a clinicopathologic and genetic study. Am J Surg Pathol 22:663–672
73. Martignoni G, Pea M, Rigaud G, Manfrin E, Colato C, Zamboni G, Scarpa A, Tardanico R, Roncalli M, Bonetti F (2000) Renal angiomyolipoma with epithelioid sarcomatous transformation and metastases: demonstration of the same genetic defects in the primary and metastatic lesions. Am J Surg Pathol 24:889–894
74. Martignoni G, Bonetti F, Pea M, Tardanico R, Brunelli M, Eble JN (2002) Renal disease in adults with TSC2/PKD1 contiguous gene syndrome. Am J Surg Pathol 26:198–205
75. Martignoni G, Pea M, Bonetti F, Brunelli M, Eble JN (2002) Oncocytoma-like angiomyolipoma. A clinicopathologic and immunohistochemical study of 2 cases. Arch Pathol Lab Med 126:610–612
76. Martignoni G, Amin M (2004) Angiomyolipoma. In: Eble JN, Sauter G, Epstein J, Sesterhenn I (eds) Pathology and genetics of tumours of the urinary system and male genital organs series: WHO classification of tumours. IARC Press, Lyon, pp 65–67
77. Masson P (1970) Origin of fibromyolipomas. In: Human tumors. Histology, diagnosis, and technique. Detroit: Wayne State University Press 735–736
78. Matsui K, Tatsuguchi A, Valencia J, Yu Z, Bechtle J, Beasley MB, Avila N, Travis WD, Moss J, Ferrans VJ (2000) Extrapulmonary lymphangioleiomyomatosis (LAM): clinicopathologic features in 22 cases. Hum Pathol 31:1242–1248
79. Mentzel T, Reisshauer S, Rütten A, Hantschke M, Soares de Almeida LM, Kutzner H (2005) Cutaneous clear cell myomelanocytic tumour: a new member of the growing family of perivascular epithelioid cell tumours (PEComas). Clinicopathological and immunohistochemical analysis of seven cases. Histopathology 46:498–504
80. Nuciforo PG, O'Hara CD (2002) Correspondence re: Bonetti F, Martignoni G, Colato C, Manfrin E, Gambacorta M, Faleri M et al. Abdominopelvic sarcoma of perivascular epithelioid cells. Report of four cases in young women, one with tuberous sclerosis. Mod Pathol 2001;14:563–8. And Tazelaar HD, Batts KP, Srigley JR. Primary extrapulmonary sugar tumor (PEST): a report of four cases. Mod Pathol 2001;14:615–22. Mod Pathol 15:87–90
81. Oliva E, Wang WL, Branton P, Logani S, Zannoni GF, Linkov I, Asher M, Soslow RA (2006) Expression of melanocytic ("PEComa") markers in smooth muscle tumors of the uterus: an immunohistochemical analysis of 86 cases. (Abstract) 95th USCAP Annual Meeting, Atlanta, Georgia
82. Ong A, Pinto P, Kim F, Kavoussi L (2003) Recurrent renal epithelioid angiomyolipoma. Urology 61:1035iii–1035v
83. Ong LY, Hwang WS, Wong A, Chan MY, Chui CH (2007) Perivascular epithelioid cell tumour of the vagina in an 8 year old girl. J Pediatr Surg 42:564–566
84. Pan CC, Chung MY (2006) Loss of heterozygosity of TSC2 and TSC1 gene in perivascular epithelioid cell tumor (PEComa). (Abstract) 95th USCAP Annual Meeting, Atlanta, Georgia
85. Pan CC, Yang AH, Chiang H (2003) Malignant perivascular epithelioid cell tumor involving the prostate. Arch Patol Lab Med 127:E96–E98
86. Pan CC, Yu IT, Yang AH, Chiang H (2003) Clear cell myomelanocytic tumor of the urinary bladder. Am J Surg Pathol 27:689–692
87. Pan CC, Jong YJ, Chai CY, Huang SH, Chen YJ (2006) Comparative genomic hybridization study of perivascular epithelioid cell tumor. Molecular genetic evidence of perivascular epithelioid cell tumor as a distinctive neoplasm. Hum Pathol 37:606–612
88. Pantuck AJ, Thomas G, Belldegrun AS, Figlin RA (2006) Mammalian target of rapamycin inhibitors in renal cell carcinoma: current status and future applications. Semin Oncol 33:607–613

89. Parfitt JR, Bella AJ, Izawa JI, Wehrli BM (2006) Malignant neoplasm of perivascular epithelioid cells of the liver. Arch Pathol Lab Med 130:1219–1222
90. Parfitt JR, Bella AJ, Wehrli BM, Izawa JI (2006) Primary PEComa of the bladder treated with primary excision and adjuvant interferon-alpha immunotherapy: a case report. BMC Urol 6:20
91. Parfitt JR, Keith JL, Megyesi JF, Ang LC (2006) Metastatic PEComa to the brain. Acta Neuropathol (Berl) 112:349–351
92. Park HK, Zhang S, Wong MK, Kim HL (2007) Clinical presentation of epithelioid angiomyolipoma. Int J Urol 14:21–25
93. Pea M, Bonetti F, Zamboni G, Martignoni G, Fiore-Donati L, Doglioni C (1991) Clear cell tumor and angiomyolipoma. Am J Surg Pathol 15:199–202
94. Pea M, Bonetti F, Zamboni G, Martignoni G, Riva M, Colombari R, Mombello A, Bonzanini M, Scarpa A, Ghimenton C et al (1991) Melanocyte-marker HMB-45 is regularly expressed in angiomyolipoma of the kidney. Pathology 23:185–188
95. Pea M, Martignoni G, Zamboni G, Bonetti F (1996) Perivascular epithelioid cell. Am J Surg Pathol 20:1149–1153
96. Pea M, Bonetti F, Martignoni G, Henske EP, Manfrin E, Colato C, Bernstein J (1998) Apparent renal cell carcinomas in tuberous sclerosis are heterogeneous: the identification of malignant epithelioid angiomyolipoma. Am J Surg Pathol 22: 180–187
97. Récher C, Dos Santos C, Demur C, Payrastre B (2005) mTOR, a new therapeutic target in acute myeloid leukemia. Cell Cycle 4:1540–1549
98. Sadeghi S, Krigman H, Maluf H (2004) Perivascular epithelioid clear cell tumor of the common bile duct. Am J Surg Pathol 28:1107–1110
99. Saito K, Fujii Y, Kasahara I, Kobayashi N, Kasuga T, Kihara K (2002) Malignant clear cell "sugar" tumor of the kidney: clear cell variant of epithelioid angiomyolipoma. J Urol 168:2533–2534
100. Sale GE, Kulander BG (1988) "Benign" clear-cell tumor (sugar tumor) of the lung with hepatic metastases ten years after resection of pulmonary primary tumor. Arch Pathol Lab Med 112:1177–1178
101. Sepp T, Yates JR, Green AJ (1996) Loss of heterozigosity in tuberous sclerosis hamartomas. J Med Genet 33:962–964
102. Silva EG, Deavers MT, Bodurka DC, Malpica A (2004) Uterine epithelioid leiomyosarcomas with clear cells. Reactivity with HMB-45 and the concept of PEComa. Am J Surg Pathol 28:244–249
103. Silva EG, Bodurka DC, Scouros MA, Ayala A (2005) A uterine leiomyosarcoma that became positive for HMB45 in the metastasis. Ann Diagn Pathol 9:43–45
104. Simpson KW, Albores-Saavedra J (2007) HMB-45 reactivity in conventional uterine leiomyosarcomas. Am J Surg Pathol 31:95–98
105. Skubitz KM, Skubitz APN (2003) Differential gene expression in uterine leiomyoma. J Lab Clin Med 141:297–308
106. Skubitz KM, Skubitz APN (2003) Differential gene expression in leiomyosarcoma. Cancer 98–1029–1038
107. Stone CH, Lee MW, Amin MB, Yaziji H, Gown AM, Ro JY, Tètu B, Paraf F, Zarbo RJ (2001) Renal angiomyolipoma: further immunophenotypic characterization of an expanding morphologic spectrum. Arch Pathol Lab Med 125:751–758
108. Svec A, Velenska Z (2005) Renal epithelioid angiomyolipoma–a close mimic of renal cell carcinoma. Report of a case and review of the literature. Pathol Res Pract 200:851–856
109. Takahashi N, Kitahara R, Hishimoto Y, Ohguro A, Hashimoto Y, Suzuki T (2003) Malignant transformation of renal angiomyolipoma. Int J Urol 10:271–273
110. Tallarigo C, Baldassarre R, Bianchi G, Comunale L, Olivo G, Pea M, Bonetti F, Martignoni G, Zamboni G, Mobilio G (1992) Diagnostic and therapeutic problems in multicentric renal angiomyolipoma. J Urol 148:1880–1884
111. Tazelaar HD, Batts KP, Srigley JR (2001) Primary extrapulmonary sugar tumor (PEST): a report of four cases. Mod Pathol 14:615–622
112. The European Chromosome 16 Tuberous Sclerosis Consortium (1993) Identification and characterization of the tuberous sclerosis gene on chromosome 16. Cell 75:1305–1315
113. Travis WD, Colby TV, Koss MN, Rosado-de-Christenson ML, Muller NL, King Jr TE (2002) Atlas of nontumor pathology: non-neoplastic disorders of the lower respiratory tract, First Series, Fascicle 2. American Registry of Pathology, Washington D.C
114. Tsui WM, Colombari R, Portmann BC, Bonetti F, Thung SN, Ferrell LD, Nakanuma Y, Snover DC, Bioulac-Sage P, Dhillon AP (1999) Hepatic angiomyolipoma: a clinicopathologic study of 30 cases and delineation of unusual morphologic variants. Am J Surg Pathol 23:34–48
115. Vang R, Kempson RL (2002) Perivascular epithelioid cell tumor ('PEComa') of the uterus: a subset of HMB-45-positive epithelioid mesenchymal neoplasms with an uncertain relationship to pure smooth muscle tumors. Am J Surg Pathol 26:1–13
116. van Slegtenhorst M, de Hoogt R, Hermans C, Nellist M, Janssen B, Verhoef S, Lindhout D, van den Ouweland A, Halley D, Young J, Burley M, Jeremiah S, Woodward K, Nahmias J, Fox M, Ekong R, Osborne J, Wolfe J, Povey S, Snell RG, Cheadle JP, Jones AC, Tachataki M, Ravine D, Sampson JR, Reeve MP, Richardson P, Wilmer F, Munro C, Hawkins TL, Sepp T, Ali JB, Ward S, Green AJ, Yates JR, Kwiatkowska J, Henske EP, Short MP, Haines JH, Jozwiak S, Kwiatkowski DJ (1997) Identification of the tuberous sclerosis gene TSC1 on chromosome 9q34. Science 277:805–808
117. Webster AC, Lee VW, Chapman JR, Craig JC (2006) Target of rapamycin inhibitors (sirolimus and everolimus) for primary immunosuppression of kidney transplant recipients: a systematic review and meta-analysis of randomized trials. Transplantation 81:1234–1248
118. Weeks DA, Malott RL, Arnesen M, Zuppan C, Aitken D, Mierau G (1991) Hepatic angiomyolipoma with striated granules and positivity with melanoma—specific antibody (HMB-45): a report of two cases. Ultrastruct Pathol 15:563–571
119. Wei J, Chiriboga L, Mizuguchi M, Yee H, Mittal K (2005) Expression profile of tuberin and some potential tumorigenic factors in 60 patients with uterine leiomyomata. Mod Pathol 18:179–188
120. Weinreb I, Howarth D, Latta E, Ghazarian D, Chetty R (2007) Perivascular epithelioid cell neoplasms (PEComas): four malignant cases expanding the histopathological spectrum and description of a unique finding. Virchows Archiv 450:463–470
121. Yamamoto H, Oda Y, Takashi Y, Oiwa T, Kobayashi C, Tamia S, Kawaguchi K, Hino O, Tsuneyoshi M (2006) Malignant perivascular epithelioid cell tumor of the colon: report of a case with molecular analysis. Pathol Int 56:46–50
122. Yamamoto T, Ito K, Suzuki K, Yamanaka H, Ebihara K, Sasaki A (2002) Rapidly progressive malignant epithelioid angiomyolipoma of the kidney. J Urol 168:190–191
123. Yanai H, Matsuura H, Sonobe H, Shiozaki S, Kawabata K (2003) Perivascular epithelioid cell tumor of the jejunum. Pathol Res Pract 199:47–50
124. Yu W, Fraser RB, Gaskin DA, Fernandez CV, Wright, JR, Jr (2005) C-Kit-positive metastatic malignant pigmented clear-cell epithelioid tumor arising from the kidney in a child without tuberous sclerosis. Ann Diagn Pathol 9:330–334
125. Zamboni G, Pea M, Martignoni G, Zancanaro C, Faccioli G, Gilioli E, Pederzoli P, Bonetti F (1996) Clear cell "sugar" tumor of the pancreas. A novel member of the family of lesions characterized by the presence of perivascular epithelioid cells. Am J Surg Pathol 20:722–730
126. Zavala-Pompa A, Folpe AL, Jimenez RE, Lim SD, Cohen C, Eble JN, Amin MB (2001) Immunohistochemical study of microophtalmia transcription factor and tyrosinase in angiomyolipoma of the kidney, renal cell carcinoma, and renal and retroperitoneal sarcomas: comparative evaluation with traditional diagnostic markers. Am J Surg Pathol 25:65–70

Virchows Arch (2008) 452:133–138
DOI 10.1007/s00428-007-0550-0

ORIGINAL ARTICLE

Peritumoural, but not intratumoural, lymphatic vessel density and invasion correlate with colorectal carcinoma poor-outcome markers

Adhemar Longatto-Filho · Céline Pinheiro · Luísa Ferreira · Cristovam Scapulatempo · Venancio A. F. Alves · Fátima Baltazar · Fernando Schmitt

Received: 3 September 2007 / Revised: 2 November 2007 / Accepted: 10 November 2007 / Published online: 18 December 2007
© Springer-Verlag 2007

Abstract To evaluate whether lymphatic vessel density (LVD) and lymphatic vessel invasion (LVI) are useful markers of worse outcome in colorectal carcinoma and if LVD and LVI correlate to the classical clinical-pathological parameters, we analysed 120 cases of colorectal carcinomas selected from the files of Division of Pathology, Hospital das Clinicas, São Paulo University, Brazil. Assessment of LVD and LVI was performed by immunohistochemical detection of lymphatic vessels, using the monoclonal antibody D2-40. Higher LVD was found in the intratumoural area, when comparing with normal and peritumoural areas ($p<0.001$). However, peritumoural LVD, but not intratumoural, correlated with both colonic-wall-invasion depth ($p=0.037$) and liver metastasis ($p=0.012$). Remarkably, LVI was found associated with local invasion ($p=0.016$), nodal metastasis ($p=0.022$) and hepatic metastasis ($p<0.001$). Peritumoural LVD and LVI are directly related to histopathological variables indicative of poor outcome such as lymph-node status and liver metastasis.

Keywords D2-40 · Colorectal carcinoma · Metastasis · Lymphatic vessel density · Lymphatic invasion · Lymph-node invasion

A. Longatto-Filho (✉) · C. Pinheiro · L. Ferreira · F. Baltazar
Life and Health Sciences Research Institute (ICVS),
School of Health Sciences, University of Minho,
4710-057 Braga, Portugal
e-mail: longatto@ecsaude.uminho.pt

A. Longatto-Filho
Instituto Adolfo Lutz,
São Paulo, Brazil

C. Scapulatempo · V. A. F. Alves
LIM14-Department of Pathology,
São Paulo University School of Medicine,
São Paulo, Brazil

F. Schmitt
IPATIMUP,
Porto, Portugal

F. Schmitt
Medical Faculty of the University of Porto,
Porto, Portugal

Introduction

Colorectal carcinoma is one of the most prevalent malignancies, being a common cause of cancer-related death, and its incidence is continuously increasing worldwide. The estimated 2006 cancer rates in Europe were 3,191,600 cancer cases diagnosed (excluding non-melanoma skin cancer) and 1,703,000 related deaths. Colorectal cancer was the second most common form of cancer (412,900, 12.9% of all cancer cases) and also the second most common cause of death from cancer (207,400 deaths or 12.2%) [6]. Since lymphatic-vessel network is recognized as the first conduit for colon-carcinoma metastasis, lymph-node invasion has been considered a marker of worse prognosis [11], as well as the number of lymph nodes examined and compromised by the carcinoma, distinguishing mesenteric tumour deposits from replaced lymph nodes. These variables should be searched together with the assessment of tumour grade, depth of wall penetration, blood-vessel invasion and tumour stage [21]. It must be acknowledged, however, that accurate identification of each criterion of this traditional checklist may not be straightforward [8]. Moreover, present assessment of these histo-

pathological features not always predicts individual outcome; therefore, additional approaches have been studied [4]. It is becoming increasingly clear that additional factors, both morphological and molecular, will be needed for future clinical management. Recent studies have also shown potential approaches for blocking the growth of lymphatic vessels to prevent tumour metastasis [1]. Blockade of vascular endothelial growth factor receptor (VEGFR)-3 pathway by specific antibodies has been reported to efficiently inhibit experimental tumour lymphangiogenesis and metastasis [24]. Moreover, recent experimental data recognized that mice lymphatic vessels have substantial plasticity during the early postnatal period, but not after that, thus suggesting that anti-lymphangiogenic therapy could possibly be safely applied to adults [9].

The search for more reproducible morphological markers and a better understanding of molecular signalling of lymphatic sprout in cancer scenario is a very motivating challenge due to the possible repercussion both in prognostic assessment and in most accurately understanding metastasis mechanisms. Recently, positive correlation between lymphatic vessel density (LVD), lymphatic vessel invasion (LVI), depth of invasion and metastases to regional lymph nodes and the liver has been reported [8]. Also, lymphatic vessel invasion was found to be related with lymph-node metastasis, and both lymphatic microvessel density and lymphatic vessel invasion were also correlated to poor outcome [13]. The preliminary findings have consistently found a positive correlation between LVD and LVI and adverse outcome [13]. However, these results are not unanimously accepted and should be cautiously considered because the degree of lymphangiogenesis alone was not recognised as an independent prognostic factor for colorectal cancer [16]. Furthermore, in spite of the potential usefulness of lymphatic microvessel density evaluations as prognostic factor, no clear-cut positive correlation has been reported between the degree of lymphangiogenesis and clinical outcome, and more data from different series are still necessary to validate these findings [20].

For this reason, herein we investigated if increased LVD as well as LVI in the primary tumour, in a large series of colon carcinomas, correlated to histopathological markers indicative of poor outcome, such as depth of tumour invasion, lymph node and liver metastasis.

Materials and methods

A series of formalin-fixed, paraffin-embedded samples from 120 colorectal carcinoma cases was retrieved from the files of the Division of Pathology, Hospital das Clinicas, São Paulo University School of Medicine (São Paulo, Brazil).

The tumours were primarily categorised according to WHO classification [7] and staged according to Tumor, Node, Metastases (TNM) classification. Clinic-pathological variables included: age, gender, macroscopic presentation, tumour size, depth of invasion, lymph-node status, TNM staging and hepatic metastasis.

D2-40 immunohistochemistry

Immunohistochemistry was carried out using the avidin–biotin–peroxidase complex assay, with the monoclonal antibody D2-40 (DAKO, Carpinteria, CA, USA) raised against an *O*-linked sialoglycoprotein. Briefly, deparaffinized and re-hydrated sections were immersed in 0.01 M citrate buffer (pH 6.0) and heated at 98°C for 20 min; slides were, then, incubated with 0.3% hydrogen peroxide in methanol for 30 min, followed by incubation with Normal Horse Serum (Vector Laboratories, CA, USA) for 20 min, at room temperature, before incubating with the primary antibody diluted 1:100, overnight at 4°C. Sections were then sequentially washed in phosphate-buffered saline 1× and incubated with Biotinylated Universal Secondary antibody (Vector Laboratories) for 30 min, Vectastain® Elite ABC reagent (Vector Laboratories) for 45 min at 37°C, developed with 3,3′-diamino-benzidine (DAKO) for 10 min and counterstained with hematoxylin–eosin. Negative controls were performed by omitting the primary antibody and, as positive control, tonsil tissue was used.

Immunohistochemical evaluation

Immunohistochemical reaction of D2-40 was evaluated considering its expression in the membrane/cytoplasm of endothelial cells. Evaluation was performed blindly, and LVD was assessed as described by Weidner et al [23] with slight modification. For LVD assessment, microvessel was defined as a single endothelial cell or a cluster of endothelial cells positive for D2-40, sitting around a visible lumen clearly separate from adjacent microvessels and from other connective-tissue components. Additionally, as lymphatic vessels could generally appear as distorted and overlapped structures in cancer setting, the packed vessels were assumed as one lymphatic unit. The number of vessels was quantified at ×200 magnification. The median of microvessels counted in ten hot-spot fields was defined as LVD. Each hot spot corresponds to a number of vessels confined to an area of 0.15 mm^2. Additionally, a cut-point of 4 micro-vessel invasion (median LVI value, evaluated in the same areas where LVD was analysed) was used for comparison with pathological variables. Both LVD and LVI were evaluated using D2-40 immunostained lymphatic vessels.

Statistical analysis

Data were stored and analyzed using the SPSS statistical software (for Windows, version 14.0, Chicago, IL, USA). The Shapiro–Wilk test was applied to assess normality of the results. Data was examined for statistical significance using the Student's *t*, the one-way analysis of variance (ANOVA), the Mann–Whitney *U*, the Kruskal–Wallis and the Pearson's chi-square (χ^2) tests, as appropriate, being threshold for significance *p* values <0.05.

Results

We have studied 120 colon carcinoma samples from patients with a median age of 64, ranging from 24 to 95 years, which included 53 women and 67 men.

The median value of LVD, assessed by D2-40 immunoexpression, in intratumoural areas was significantly higher than those in normal stroma ($p<0.001$, Fig. 1). In addition, intratumoural LVD counting exhibited about twofold more lymphatics than at the periphery of the tumour ($p<0.001$, Table 1).

Table 2 depicts the correlation between the clinical-pathological variables and LVD (peri- and intratumoural). No association was found between age or gender of patients and tumoural LVD (data not shown). Peritumoural LVD was associated with depth of wall invasion ($p=0.037$), hepatic metastasis ($p=0.012$) and TNM staging ($p=0.044$). We found significant differences ($p<0.001$) between the evaluation of lymphatic invasion with the specific lymphatic marker D2-40 and haematoxylin–eosin stain: 74.2% (89 of 120) against 48.3% (58 of 120), respectively.

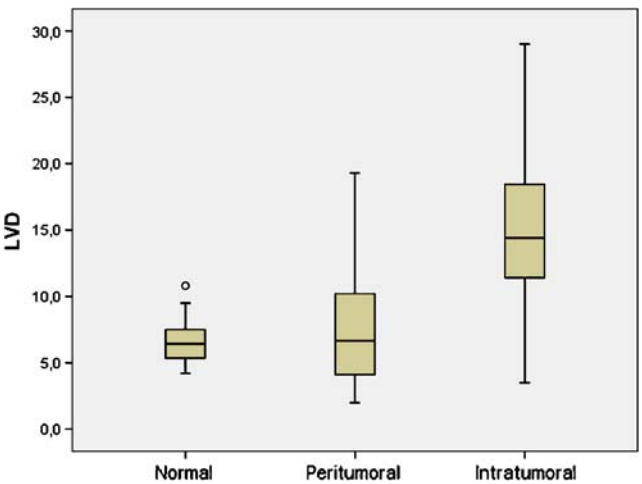


Fig. 1 Representation of lymphatic vessel density among the different colorectal areas

Table 1 Comparison of lymphatic vessel density (LVD) among the different tissue regions using the Student's *t* test

Tissue regions	LVD (median)	*p*
Normal vs peritumoural	6.4 vs 6.8	0.682
Normal vs intratumoural	6.4 vs 14.6	<0.001
Peritumoural vs intratumoural	6.8 vs 14.6	<0.001

The median values represent the number of lymphatic vessels counted in hot-spot areas.

Table 3 shows the correlation between invasion, presented both as positive and as number of invaded vessels (above the median value), and the histopathological variables. As for vessel density, no correlations were found between lymphatic invasion and age of diagnosis or gender (data not shown). Lymphatic invasion (Fig. 2) was significantly associated with presence of nodal metastasis ($p=0.022$), and a trend for cases with hepatic metastasis to present lymphatic invasion ($p=0.064$) was also observed. When considering the number of invaded lymphatic vessels (>4), we found a significant correlation with depth of invasion ($p=0.018$), the presence of both nodal and hepatic

Table 2 Associations of LVD with the histopathological data

Histopathological variables	*n*	Peritumoural LVD[a]		Intratumoural LVD[b]	
		Median	*P*	Mean	*p*
Tumour size			0.116		0.817
≤5	65	6.1		15.0	
>5	54	7.1		15.2	
Macroscopic type			0.574		0.792
Exofitic	24	6.4		15.6	
Ulcerative	45	6.0		14.5	
Infiltrative	12	8.9		14.5	
Sessile-ulcerated	39	6.8		15.6	
Depth of invasion			0.037		0.551
T1 + T2	22	5.4		14.4	
T3 + T4	98	7.2		15.2	
Nodal metastasis			0.414		0.660
Absent	60	6.8		14.8	
Present	60	6.4		15.3	
TNM			0.044		0.937
I	16	4.8		14.6	
II	33	7.1		14.9	
III	36	5.6		15.0	
IV	35	9.1		15.6	
Hepatic metastasis			0.012		0.559
Absent	85	5.8		14.9	
Present	35	9.1		15.6	

[a] Mann–Whitney *U* test and Kruskal–Wallis test were used when sample-grouping >2 (data do not follow a normal distribution)
[b] Student's *t* test and one-way ANOVA were used when sample-grouping >2 (data follow a normal distribution)

Table 3 Relationship between lymphatic invasion and clinical-pathological parameters using the Pearson's chi-square (χ^2) test

	n	Positive invasion		Invasion >4	
		%	*p*	%	*p*
Tumour size			0.696		0.790
≤5	65	75.4		29.2	
>5	54	72.2		31.5	
Macroscopic type			0.128		0.943
Exofitic	24	66.7		25.0	
Ulcerative	45	68.9		31.1	
Infiltrative	12	100.0		33.3	
Sessile-ulcerated	39	76.9		30.8	
Depth of invasion			0.212		0.018
T1 + T2	22	63.6		9.1	
T3 + T4	98	76.5		34.7	
Nodal metastasis			0.022		0.046
Absent	60	65.0		21.7	
Present	60	83.3		38.3	
TNM			0.107		0.009
I	16	68.8		12.5	
II	33	60.6		21.2	
III	36	77.8		25.0	
IV	35	85.7		51.4	
Hepatic metastasis			0.064		0.001
Absent	85	69.4		21.2	
Present	35	85.7		51.4	

metastasis (p=0.046 and p=0.001, respectively) and TNM staging (p=0.009).

Discussion

In the present study, we found a significant difference between LVD in the normal mucosa and intratumoural stroma (p<0.001). The results herein reported strongly correlated both peritumoural LVD and peritumoural LVI with the presence of hepatic metastasis. This association was already described within tumoural areas and reinforces the importance of our results. Recently, Parr and Jiang [18] elegantly described lymph-vessel expression by using real-time quantitative polymerase chain reaction assay for several lymphangiogenic markers and found that VEGFR-3, Prox-1, podoplanin and 5′-nucleotidase were higher expressed in colorectal carcinoma in comparison to the normal mucosa. Indeed, we found similar LVD in normal and peritumoural area but higher LVD in the intratumoural area (p<0.001). This is interesting because one can hypothesise that intratumoural area is more liable to receive lymphangiogenic stimulation during the carcinogenic development [15]. In spite of that, higher LVD does not necessarily mean that these conduits are more prone to facilitate metastatic spread; on the contrary, our results strengthened that intratumoural lymphatics in fact are not adequate route for malignant-cell escape and that functional lymphatics in the tumour margin are sufficient for lymphatic metastasis [17]. Recently, Kuroyama et al. [10] found higher intratumoural lymphatic density in cases with lymph-node metastasis than in those without metastasis but, as we found in our study, they did not observe correlation with tumour size, depth of tumour invasion, distant metastasis or TNM stage. Interestingly, we did not find significant correlations between both peritumoural and intratumoural LVD and lymph-node metastasis, even considering that we found a higher intratumoural LVD.

The number of lymph nodes evaluated after surgical resection is positively associated with survival of patients with stage II and stage III colon cancer [3]. Saad and collaborators [19] found that high LVD correlates with both depth of invasion and lymph-node metastasis. We found a significant association between peritumoural LVD and depth of invasion (p<0.037) and between the number of lymphatic vessels invaded by the tumour and depth of invasion (p<0.018). Liang et al. [11] emphasised that lymphatic microvessel density is important in colorectal carcinoma to predict lymph-node metastases mainly associated to lymphatic vessels' diameter (not assessed in the present study).

Importantly, we observed a strong correlation between peritumoural LVD and lymphatic invasion (≥4 lymphatic vessels invaded; p=0.0001) and hepatic metastasis (p=0.012). It is well known that, at the time of diagnosis of colorectal cancer, 20% of the patients already have liver metastasis, and 30% of the patients will develop metastasis afterwards [14, 19]. These findings could be decisive for future investigations regarding the surgical resection options of the colorectal hepatic metastasis [3]. Furthermore, tumour cells metastasized to the liver have certainly

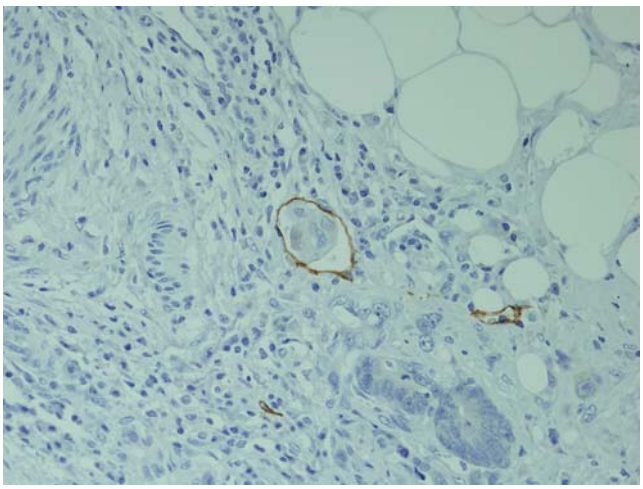


Fig. 2 Peritumoural lymphatic vessel invasion (D2-40 staining, ×40 magnification)

crossed the hepatic sinusoidal endothelial barrier and completed steps of metastatic cascade [2]. Accordingly, further studies exploring the earlier stages of colorectal metastasis, proliferation and new vessel formation as well as mechanisms to disturb cell survival are needed [5]. The more exciting results were observed with lymphatic invasion highlighted by D2-40, which positively correlated with the lymph-node status and liver metastasis. Cases with more than four lymphatic vessels invaded showed significantly more hepatic metastasis. Indeed, the correlation we observed between lymphatic invasion and TNM staging ($p=0.009$) also corroborates the above-mentioned findings. In contrast to these findings, some recent data indicate that extensive lymphangiogenesis indeed occurs in colorectal carcinoma, but there are controversial data concerning the value of the degree of lymphangiogenesis as an independent prognostic factor [13, 16]. The significant differences found between lymphatic invasion evaluated with haematoxylin–eosin stain and with the lymphatic marker D2-40 ($p<0.001$) emphasises the importance of the use of a specific marker to identify lymphatics. As compared with blood capillaries, lymphatic vessels, principally those within the tumour mass, have poorly developed junctions with frequently large inter-endothelial gaps, with discontinuous or completely absent basement membranes. The recent discovery of specific lymphatic vessel markers and their corresponding antibodies have aided the identification of lymphatic vessels. Indeed, D2-40 importantly enhances the lymphatic endothelial cells borders, highlighting the presence of lymphatic invasion in the tumours [19].

Colorectal carcinoma is one of the most prevalent cancers worldwide, and lymphatic metastatic route was long considered as an important parameter of worse outcome [8]. Due to the recent development of finer immunohistochemical markers, lymphangiogenesis was rediscovered in oncologic pathology enabling more accurate counting of LVD in all types of neoplasms, with special emphasis on carcinomas [12]. The results herein presented, using the specific lymphatic marker D2-40, indicate that peritumoural LVD and LVI are reliable parameters to predict poor prognosis and contribute to identify patients more prone to develop hepatic metastasis.

Conflict of interest statement We declare that we have no conflict of interest.

References

1. Achen MG, Mann GB, Stacker SA (2006) Targeting lymphangiogenesis to prevent tumour metastasis. Br J Cancer 94:1355–1360
2. Braet F, Nagatsuma K, Saito M, Soon L, Wisse E, Matsuura T (2007) The hepatic sinusoidal endothelial lining and colorectal liver metastases. World J Gastroenterol 13:821–825
3. Chang GJ, Rodriguez-Bigas MA, Skibber JM, Moyer VA (2007) Lymph node evaluation and survival after curative resection of colon cancer: systematic review. J Natl Cancer Inst 99:433–441
4. Compton CC (2003) Colorectal carcinoma: diagnostic, prognostic, and molecular features. Mod Pathol 16:376–388
5. Des Guetz G, Uzzan B, Nicolas P, Cucherat M, Morere JF, Benamouzig R, Breau JL, Perret GY (2006) Microvessel density and VEGF expressionz are prognostic factors in colorectal cancer. Meta-analysis of the literature. Br J Cancer 94:1823–1832
6. Ferlay J, Autier P, Boniol M, Heanue M, Colombet M, Boyle P (2007) Estimates of the cancer incidence and mortality in Europe in 2006. Ann Oncol 18:581–592
7. Hamilton SR, Aaltonen LA (eds) (2000). World Health Organization classification of tumours. Tumours of the disgestive system. IARC Press, Lyon, France
8. Jass JR, O'brien MJ, Riddell RH, Snover DC, on behalf of the Association of Directors of Anatomic and Surgical Pathology (2007) Recommendations for the reporting of surgically resected specimens of colorectal carcinoma. Hum Pathol 38:537–545
9. Karpanen T, Wirzenius M, Mäkkinen T, Veikkola T, Haisma HJ, Achen MG, Stacker SA, Pytowski B, YlA-Herttuala S, Alitalo K (2006) Lymphangiogenic growth factor responsiveness is modulated by postnatal lymphatic vessel maturation. Am J Pathol 169:708–718
10. Kuroyama S, Kobayashi N, Ohbu M, Ohtani Y, Okayasu I, Kakita A (2005) Enzyme histochemical analysis of lymphatic vessels in colon carcinoma: occurrence of lymphangiogenesis within the tumour. Hepatogastroenterology 52:1057–1061
11. Liang P, Hong JW, Ubukata H, Liu HR, Watanabe Y, Katano M, Motohashi G, Kasuga T, Nakada I, Tabuchi T (2006) Increased density and diameter of lymphatic microvessels correlate with lymph node metastasis in early stage invasive colorectal carcinoma. Virchows Arch 448:570–575
12. Longatto-Filho A, Pinheiro C, Pereira SM, Etlinger D, Moreira MA, Jubé LF, Queiroz GS, Baltazar F, Schmitt FC (2007) Lymphatic vessel density and epithelial D2-40 immunoreactivity in pre-invasive and invasive lesions of the uterine cervix. Gynecol Oncol 107:45–51
13. Matsumoto K, Nakayama Y, Inoue Y, Minagawa N, Katsuki T, Shibao K, Tsurudome Y, Hirata K, Nagata N, Itoh H (2007) Lymphatic microvessel density is an independent prognostic factor in colorectal cancer. Dis Colon Rectum 50:308–314
14. Nishio H, Hamady ZZ, Malik HZ, Fenwick S, Rajendra Prasad K, Toogood GJ, Lodge JP (2007) Outcome following repeat liver resection for colorectal liver metastases. Eur J Surg Oncol 33:729–734
15. Oliver G, Alitalo K (2005) The lymphatic vasculature: recent progress and paradigms. Annu Rev Cell Dev Biol 21:457–483
16. Omachi T, Kawai Y, Mizuno R, Nomiyama T, Miyagawa S, Ohhashi T, Nakayama J (2007) Immunohistochemical demonstration of proliferating lymphatic vessels in colorectal carcinoma and its clinicopathological significance. Cancer Lett 246:167–172
17. Padera TP, Kadambi A, di Tomaso E, Carreira CM, Brown EB, Boucher Y, Choi NC, Mathisen D, Wain J, Mark EJ, Munn LL, Jain RK (2002) Lymphatic metastasis in the absence of functional intratumor lymphatics. Science 296:1883–1886
18. Parr C, Jiang WG (2003) Quantitative analysis of lymphangiogenic markers in human colorectal cancer. Int J Oncol 23:533–539
19. Saad RS, Kordunsky L, Liu YL, Denning KL, Kandil HA, Silverman JF (2006) Lymphatic microvessel density as prognostic marker in colorectal cancer. Mod Pathol 19:1317–1323

20. Sugarbaker PH (2007) Peritoneum as the first-line of defense in carcinomatosis. J Surg Oncol 95:93–96
21. Sundlisaeter E, Dicko A, Sakariassen PO, Sondenaa K, Enger PO, Bjerkvig R (2007) Lymphangiogenesis in colorectal cancer-Prognostic and therapeutic aspects. Int J Cancer 121:1401–1409
22. Walgenbach-Bruenagel G, Tolba RH, Varnai AD, Bollmann M, Hirner A, Walgenbach KJ (2006) Detection of lymphatic invasion in early stage primary colorectal cancer with the monoclonal antibody D2-40. Eur Surg Res 38:438–444
23. Weidner N, Semple JP, Welch WR, Folkman J (1991) Tumour angiogenesis and metastasis—correlation in invasive breast carcinoma. N Engl J Med 324:1–8
24. Wissmann C, Detmar M (2006) Pathways targeting tumour lymphangiogenesis. Clin. Cancer Res 12:6865–6868

Virchows Arch (2008) 452:139–146
DOI 10.1007/s00428-007-0558-5

ORIGINAL ARTICLE

Increased expression of monocarboxylate transporters 1, 2, and 4 in colorectal carcinomas

Céline Pinheiro · Adhemar Longatto-Filho · Cristovam Scapulatempo · Luísa Ferreira · Sandra Martins · Luc Pellerin · Mesquita Rodrigues · Venancio A. F. Alves · Fernando Schmitt · Fátima Baltazar

Received: 10 September 2007 / Revised: 5 November 2007 / Accepted: 6 December 2007 / Published online: 10 January 2008
© Springer-Verlag 2007

Abstract Tumour cells are known to be highly glycolytic, thus producing high amounts of lactic acid. Monocarboxylate transporters (MCTs), by promoting the efflux of the accumulating acids, constitute one of the most important mechanisms in the maintenance of tumour intracellular pH. Since data concerning MCT expression in colorectal carcinomas (CRC) are scarce and controversial, the present study aimed to assess the expressions of MCT1, 2, and 4 in a well characterized series of CRC and assess their role in CRC carcinogenesis. CRC samples (126 cases) were analyzed for MCT1, MCT2, and MCT4 immunoexpression and findings correlated with clinico-pathological parameters. Expression of all MCT isoforms in tumour cells was significantly increased when compared to adjacent normal epithelium. Remarkably, there was a significant gain of membrane expression for MCT1 and MCT4 and loss of plasma membrane expression for MCT2 in tumour cells. Plasma membrane expression of MCT1 was directly related to the presence of vascular invasion. This is the larger study on MCT expression in CRC and evaluates for the first time its clinico-pathological significance. The increased expression of these transporters suggests an important role in CRC, which might justify their use, especially MCT1 and MCT4, as targets in CRC drug therapy.

Keywords Monocarboxylate transporter · Colorectal carcinoma

C. Pinheiro · A. Longatto-Filho · L. Ferreira · S. Martins · F. Baltazar (✉)
Life and Health Sciences Research Institute (ICVS), School of Health Sciences, University of Minho, Campus de Gualtar, 4710-057 Braga, Portugal
e-mail: fbaltazar@ecsaude.uminho.pt

A. Longatto-Filho
Instituto Adolfo Lutz, São Paulo, Brazil

C. Scapulatempo · V. A. F. Alves
Department of Pathology, University of São Paulo School of Medicine, São Paulo, Brazil

S. Martins · M. Rodrigues
S. Marcos Hospital, Braga, Portugal

L. Pellerin
Faculty of Biology and Medicine, University of Lausanne, Lausanne, Switzerland

F. Schmitt
Institute of Pathology and Immunology of University of Porto (IPATIMUP), Porto, Portugal

F. Schmitt
Medical Faculty of the University of Porto, Porto, Portugal

Introduction

Highly proliferative cancer cells maintain a high rate of glycolysis, producing large amounts of acids, mainly lactic acid. Despite this fact, only the interstitial pH of tumours is low, while the intracellular pH of tumours is either normal or higher than that of normal tissues [3, 10]. In order to prevent apoptosis by cellular acidosis, tumour cells increase proton efflux through pH regulators, such as proton pumps, sodium-proton exchangers, bicarbonate transporters, and

monocarboxylate transporters (MCTs), which are described to be up-regulated in tumour cells [11].

MCTs play a central role in cellular metabolism and are essential for transport of monocarboxylates, such as lactate, across the plasma membrane. Based on sequence homologies, 14 MCT family members were identified, although only a few have been functionally characterized. MCT1–MCT4 isoforms are proton symporters, which have lactate as a common substrate, each isoform exhibiting different biochemical properties [9]. Substrate specificity has been associated with the tissue distribution of each transporter, depending on their metabolic activity: MCT1 has an ubiquitous distribution [6], while MCT2, having a high affinity for the substrate, is found in tissues that use lactate as a substrate (e.g., liver) [2]. MCT4, which is a low-affinity transporter, is present in highly glycolytic tissues (e.g., slow-twitch muscle) [4] and MCT3 is exclusively found in the retinal pigment epithelium and in the choroid plexus epithelium [16].

Using in vitro and ex vivo models, Wahl et al. [19] demonstrated that MCTs are major players in the regulation of pH in melanoma cells and proposed that MCT inhibitors may be particularly effective against malignant melanoma. There are also evidence for the upregulation of MCTs in other tumours such as alveolar sarcoma of soft tissues [13], high grade glial neoplasms [7, 15], and colorectal carcinomas (CRC) [12].

Lactate release from tumour cells is a common endpoint of several metabolic alterations, raising the hypothesis of an association with tumour progression [21]. Some evidence support this hypothesis: low interstitial pH is associated with the upregulation of various angiogenic molecules, which support tumour growth, invasion, and metastasis such as vascular endothelial growth factor [8]. Lactate accumulation has also been associated with metastization and lower disease-free and overall survival in squamous cell carcinomas of the uterine cervix and head and neck carcinomas [1, 20]. Targeting MCT activity would not only induce apoptosis due to cellular acidosis, but would also lead to reduction in tumour angiogenesis, invasion, and metastasis. Thus, MCTs can constitute an attractive target for cancer therapy.

Data concerning expression of MCTs in CRC are scarce and controversial. While Lambert et al. [14] described a decrease in MCT1 expression during transition to malignancy, Koukourakis et al. [12] reported an increase in MCT1 expression in tumour cells, which is supported by the metabolic alterations induced by anaerobic glycolysis. The latter study also assessed the expression of MCT2 and MCT4, finding a strong cytoplasmic expression of MCT2 in cancer cells, but a weak expression of MCT4 in the tumour environment, suggesting a minimal role of this MCT isoform in CRC metabolic homeostasis.

Our study aimed to contribute to the elucidation of the role of MCTs in CRC, by assessing the immunohistochemical expression of the MCT isoforms 1, 2, and 4 in a large and well characterized series of CRC and evaluating its clinico-pathological significance.

Materials and methods

A series of formalin-fixed, paraffin-embedded tissues from 126 CRC was retrieved from the files of the Medical School of the University of São Paulo (Brazil). Tissue samples were analyzed for MCT1, MCT2, and MCT4 immunohistochemical expression using specific antibodies. Comparison of MCT expression in tumour vs normal cells was also possible since, for most cases, the same paraffin section contained both tumour and normal colonic epithelium. MCT immunohistochemical expression was correlated with the available clinico-pathological data, which included: age, gender, tumour size, macroscopic presentation, histological type, tumour localization, depth of invasion, vascular invasion, nodal metastasis, and TNM classification. Normal colorectal mucosa, liver, and skeletal muscle samples were obtained prospectively from patients undergoing surgery: colorectal mucosa and abdominal wall skeletal muscle were obtained from a patient with diagnosis of diverticulosis; liver was from a patient with a diagnosis of metastatic colon carcinoma. Informed written consent was obtained from the individuals prior to removal of the tissue.

Western blotting

The specificity of the antibodies used in immunohistochemistry was evaluated by Western blotting. Tissue samples from human colon, liver, and muscle were used as positive controls for the expression of MCT1, 2, and 4, respectively. Briefly, fresh samples were collected, homogenized in a lysis buffer and then centrifuged at 6,000 rpm, 20 min at 4°C. The supernatants were collected and protein concentrations were determined by the method of Lowry. Protein was separated on a 10% (*w*/*v*) polyacrylamide gel and transferred onto a nitrocellulose membrane (Amersham Pharmacia Biotech, Piscataway, NJ, USA). Membranes were blocked with 1% Tween, 10% milk, and 1% bovine serum albumin in TBS for 1 h. Membranes were then incubated overnight at 4°C with primary polyclonal antibodies for MCT1 (AB3538P, Chemicon International, Temecula, CA, USA), MCT2 (sc-14926, Santa Cruz Biotechnology, Santa Cruz, CA, USA), and MCT4 (AB3316P, Chemicon International), diluted 1:200 for MCT1 and MCT4, and 1:100 for MCT2. Membranes were then incubated with the secondary

antibody coupled to horseradish peroxidase (SantaCruz Biotechnology) and bound antibodies were visualized by chemiluminescence (Supersignal West Femto kit, Pierce, Rockford, IL, USA).

Immunohistochemistry

Immunohistochemistry was performed according to avidin–biotin–peroxidase complex principle (R.T.U. VECTASTAIN Elite ABC Kit (Universal), Vector Laboratories, Burlingame, CA, USA), with the primary antibodies for MCT1, MCT2, and MCT4, used in Western blotting, diluted 1:200. Briefly, deparaffinized and rehydrated sections were incubated in 0.3% hydrogen peroxide for 30 min, to inactivate endogenous peroxidases, and washed in PBS. Antigen retrieval was performed by immersing slide-mounted sections in 0.01 M citrate buffered solution (pH 6.0) and microwaving (600 W) for 15 min then washed in PBS. Tissue sections were then incubated with a protein blocking solution for 20 min and incubated with the primary antibody overnight at room temperature. Sections were then sequentially washed in PBS and incubated with biotinylated secondary antibody for 30 min, R.T.U. Vectastain® Elite ABC reagent for 45 min at 37°C and developed with 3,3′-diamino-benzidine (DAB+ Substrate System, DakoCytomation, Carpinteria, CA, USA) for 10 min. Negative controls were performed by using the adequate serum controls for the primary antibodies used (N1699 and X0907, DakoCytomation, Carpinteria, CA, USA). Normal colon, kidney, and skeletal muscle tissues were used as positive controls for MCT1, MCT2, and MCT4, respectively. Tissue sections were counterstained with haematoxylin and permanently mounted.

Immunohistochemical evaluation

Sections were scored semi-quantitatively for immunoreaction extension as follows: 0: 0% of immunoreactive cells; 1: <5% of immunoreactive cells; 2: 5–50% of immunoreactive cells; and 3: >50% of immunoreactive cells. Also, intensity of staining was scored semi-qualitatively as 0: negative; 1: weak; 2: intermediate; and 3: strong. Immunoreaction final score was defined as the sum of both parameters (extension and intensity), and grouped as negative (0), weak (2), moderate (3), and strong (4–6). For statistical purposes, only moderate and strong immunoreaction final scores were considered as positive. Finally, positive plasma membrane staining was also assessed. Evaluation of MCT immunohistochemical expression was performed blindly by two independent observers and discordant cases were discussed in a double-head microscope in order to determine a final score.



Fig. 1 Western blotting of human tissue lysates for *MCT1*, *2*, and *4*. Normal colon, liver, and skeletal muscle were used for *MCT1*, *2*, and *4* detection, respectively

Statistical analysis

Data were stored and analyzed using the SPSS statistical software (version 14.0, SPSS Inc., Chicago, IL, USA). The comparison of MCT expression between tumour and normal cells as well as the relationship between MCT expressions and the clinico-pathological parameters were examined for statistical significance using Pearson's chi-square (χ^2) test, with the threshold for significant p values being <0.05.

Results

One hundred and twenty six cases of CRC, corresponding to 56 women and 70 men with a median age of 64 (range 24–95), were analyzed for MCT1, MCT2, and MCT4 immunohistochemical expression. Western blot analyses of normal human tissues, using the antibodies for the three MCT isoforms, revealed protein bands around 50 kDa (Fig. 1), consistent with the molecular weight described for these membrane proteins [7].

Table 1 summarizes the frequency of MCT isoforms 1, 2, and 4 expressions in tumour cells and normal adjacent epithelium. In positive cases, cytoplasmic staining was always present while the frequency of plasma membrane staining differed for each isoform, being more frequent for

Table 1 Pattern of MCT staining in tumour vs normal adjacent epithelium

Isoform	*n*	Immunoreaction		Plasma membrane	
		Positive (%)	*p*	Positive (%)	*p*
MCT1			<0.001		<0.001
Normal	86	34.9		9.3	
Tumour	126	85.7		51.6	
MCT2			0.017		0.031
Normal	84	83.3		14.3	
Tumour	126	93.7		5.6	
MCT4			<0.001		<0.001
Normal	89	55.1		9.0	
Tumour	126	96.0		38.1	

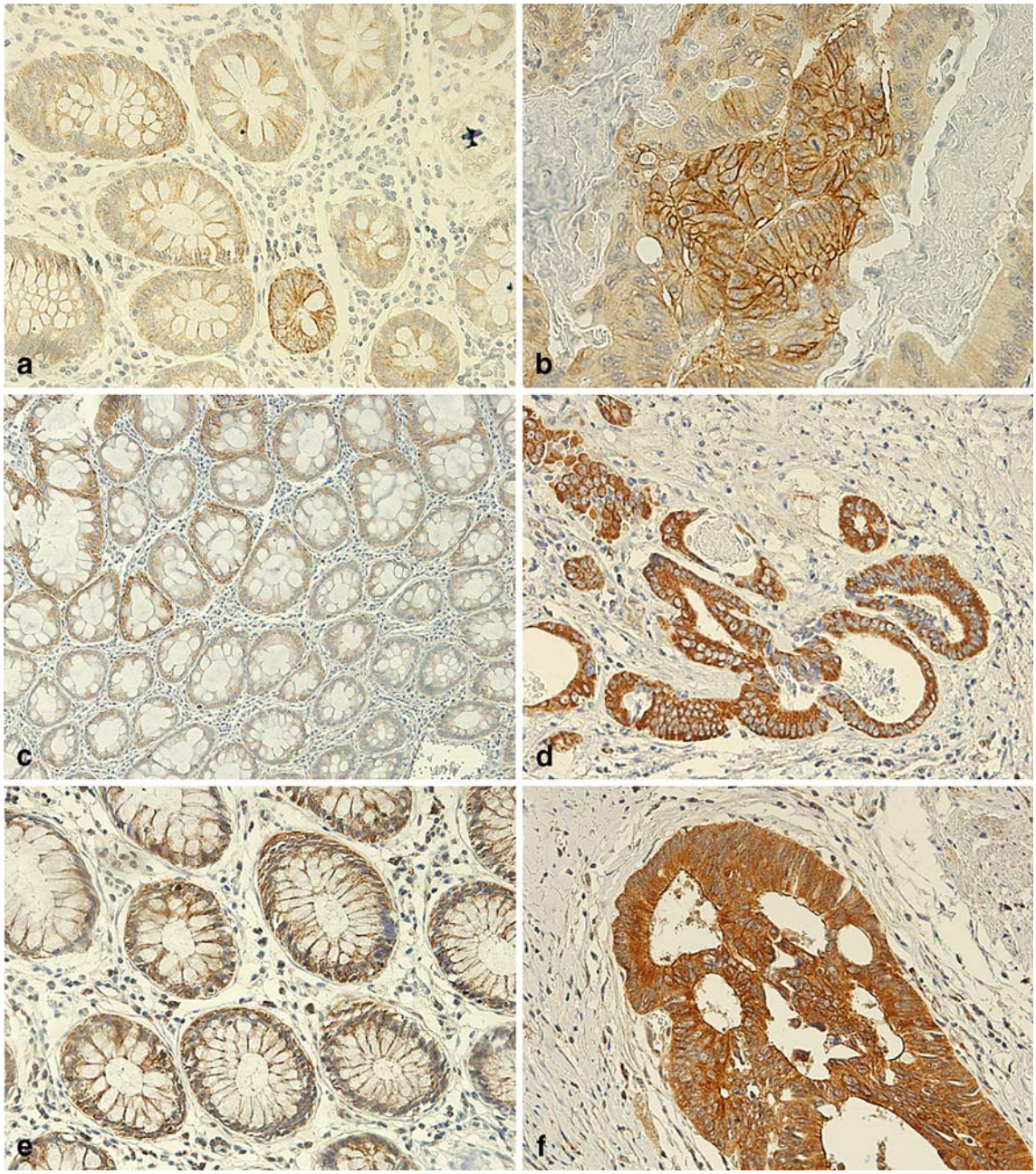


Fig. 2 Immunohistochemical expression of MCT1, 2, and 4 in colon carcinoma samples. Staining in tumour cells (**b**, **d**, and **f**: MCT1, 2, and 4, respectively) was stronger than in the adjacent normal epithelium (**a**, **c**, and **e**: MCT1, 2, and 4, respectively). MCT1 plasma membrane staining (**b**) was frequently observed in tumour cells

MCT1 than for the other isoforms (51.6% vs 38.1% for MCT4 vs 5.6% for MCT2).

MCT1 immunoexpression in tumour cells was significantly increased, when compared to adjacent normal epithelium (85.7% vs 34.9%, $p<0.001$, Table 1). Importantly, plasma membrane staining was also significantly more frequent in tumour than in normal cells (51.6% vs 9.3%, $p<0.001$, Table 1). Plasma membrane expression of MCT1 (Fig. 2) was directly related to the presence of vascular invasion ($p=0.003$, Table 2).

Staining for MCT2 in tumour cells was also more frequent than in the adjacent normal epithelium (93.7% vs 83.3%; $p=0.017$, Table 1). Remarkably, there was a significant loss of plasma membrane staining in tumour cells (14.3% vs 5.6%; $p<0.001$, Table 1). Although it was possible to observe "granule" like cytoplasmic staining for all MCT isoforms, this pattern was much more common for MCT2 in tumour cells (Fig. 2).

MCT4 was the most frequently expressed isoform in tumour cells, with 96% of the cases showing positive

Table 2 Assessment of correlation between MCTs membrane expression and the clinico-pathological data

Clinical data	Plasma membrane						
	MCT1			MCT2		MCT4	
	n	Positive (%)	*p*	Positive (%)	*p*	Positive (%)	*p*
Tumour size (cm)			0.897		0.117		0.572
<5	53	50.9		1.9		35.8	
≥5	71	52.1		8.5		40.8	
Macroscopic type			0.826		0.360		0.548
Exophytic	26	46.2		0.0		30.8	
Ulcerative	49	55.1		8.2		40.8	
Infiltrative	12	58.3		0.0		25.0	
Sessile-ulcerated	39	48.7		7.7		43.6	
Histological type			0.563		0.551		0.586
Adenocarcinoma	111	50.5		5.4		38.7	
Mucinous	10	60.0		10.0		30.0	
Localization[a]			0.261		0.474		0.923
Right colon	21	42.9		4.8		38.1	
Left colon	40	45.0		2.5		40.0	
Rectum	61	59.0		8.2		36.1	
Invasion			0.251		0.208		0.829
T1+T2	22	40.9		0.0		36.4	
T3+T4	103	54.4		6.8		38.8	
Vascular invasion[b]			0.003		0.090		0.400
Absent	57	36.8		1.8		42.1	
Present	69	63.8		8.7		34.8	
Nodal metastasis			0.212		0.697		1.000
Absent	63	46.0		4.8		38.1	
Present	63	57.1		6.3		38.1	
TNM			0.408		0.722		0.276
Stage I	16	43.8		0.0		31.3	
Stage II	35	42.9		5.7		40.0	
Stage III	38	60.5		7.9		28.9	
Stage IV	36	55.6		5.6		50.0	

[a] Tumour localization was grouped as follows: right colon—cecum and ascendant colon; left colon—splenic flexure, descendant colon, sigmoid and rectosigmoid.
[b] Vascular invasion includes both lymph and blood vessel invasion.

staining, and expression was significantly more frequent than adjacent normal epithelium ($p<0.001$, Table 1). Figure 2 shows representative cases of MCT4 positive staining in tumour cells and in adjacent normal epithelium. As observed for MCT1, MCT4 plasma membrane staining in tumour cells was significantly more frequent than in the adjacent normal epithelium ($p<0.001$, Table 1). Assessment of correlation between MCT4 expression and the clinico-pathological data revealed a positive association between MCT4 positivity and small size tumours ($p=0.049$, Table 3).

Discussion

Experimental evidence point at MCTs as potential targets for cancer therapy [5, 15, 19]. However, the role of these membrane proteins in solid tumour development and survival is not fully understood. In the present study, we showed an evident increase in MCT immunoexpression in CRC cells when compared to adjacent normal epithelium. Most importantly, we evaluated the correlation between MCT expression in CRC and clinico-pathological data for the first time.

Although MCT1 is described as having a ubiquitous distribution, it appears that this MCT isoform plays an important role in the bidirectional transport of lactate and other short-chain fatty acids across the colonic luminal membrane [17]. Unexpectedly, when analysing MCT expression in the available adjacent normal epithelium, we found that MCT1 was the least expressed isoform. However, since these normal tissue areas are in the surroundings of tumour cells, we cannot rule out the possibility that these areas are under the influence of

Table 3 Assessment of correlation between MCTs immunoreaction and the clinico-pathological data

Clinical data	Immunoreaction					
	N	MCT1		MCT2		MCT4	
		Positive (%)	*p*	Positive (%)	*P*	Positive (%)	*p*
Tumour size (cm)			0.383		0.117		0.049
<5	53	88.7		98.1		100.0	
≥5	71	83.1		91.5		93.0	
Macroscopic type			0.267		0.967		0.480
Exophytic	26	76.9		92.3		100.0	
Ulcerative	49	89.8		93.9		93.9	
Infiltrative	12	75.0		91.7		91.7	
Sessile-ulcerated	39	89.7		94.9		97.4	
Histological type			0.509		0.413		0.542
Adenocarcinoma	111	87.4		93.7		96.4	
Mucinous	10	80.0		100.0		100.0	
Localization[a]			0.586		0.714		0.900
Right colon	21	81.0		90.5		95.2	
Left colon	40	82.5		95.0		95.0	
Rectum	61	88.5		95.1		96.7	
Invasion			0.220		0.570		0.292
T1+T2	22	77.3		90.9		100.0	
T3+T4	103	87.4		94.2		95.1	
Vascular invasion[b]			0.942		0.081		0.810
Absent	57	86.0		89.5		96.5	
Present	69	85.5		97.1		95.7	
Nodal metastasis			0.611		1.000		0.648
Absent	63	84.1		93.7		95.2	
Present	63	87.3		93.7		96.8	
TNM			0.610		0.591		0.238
Stage I	16	75.0		87.5		100.0	
Stage II	35	85.7		97.1		91.4	
Stage III	38	86.8		92.1		94.7	
Stage IV	36	88.9		94.4		100.0	

[a] Tumour localization was grouped as follows: right colon—cecum and ascendant colon; left colon—splenic flexure, descendant colon, sigmoid and rectosigmoid.
[b] Vascular invasion includes both lymph and blood vessel invasion.

tumour microenvironment and could show altered MCT expression. It would then be important to further analyze MCT expression in a series of normal colorectal samples. Data concerning MCT1 expression in solid tumours is scarce and there are conflicting data related to CRC [12, 14, 17]. Our immunohistochemical findings are in agreement with the results of Koukourakis et al. [12]. Although using different antibodies from this previous study, we were also able to detect a high percentage of positive cases for MCT1 expression as well as MCT1 plasma membrane expression in a high number of cases. However, these findings diverge from previous reports, where the authors described a decrease in MCT1 expression in CRC during transition from normality to malignancy [14, 17]. Concerning the clinico-pathological data, we found a significant correlation between MCT1 plasma membrane staining and vascular invasion. MCT1 plasma membrane localization is essential for transporter activity and, assuming a role in the efflux of accumulating acids, MCT1 activity would lead to extracellular acidification. Then, the positive correlation between MCT1 plasma membrane staining and vascular invasion would be in harmony with previous reports which stated that extracellular acidification induces invasion [10].

Data concerning MCT2 expression in solid tumour is also limited. Contrasting with the results presented by Lambert et al. [14], we found expression of MCT2 in both adjacent normal epithelium and tumour cells in CRC. The staining pattern was cytoplasmic and, in a low number of cases, associated with the plasma membrane. Notably, we found a significant decrease in plasma membrane staining in tumour cells, when comparing to adjacent normal epithelium. This finding is in agreement with the results of Koukourakis et al. [12], who described lack of plasma membrane expression in tumour cells but a strong cyto-

plasmic expression. The authors hypothesized that this cytoplasmic expression was probably associated with the presence of MCT2 in mitochondrial membranes. Taking into consideration the physiological role of MCT2 in the transport of pyruvate into the mitochondria, one could hypothesize that the highly glycolytic tumour cell would up-regulate MCT2 in an attempt to oxidize the excess pyruvate produced. This process would also contribute to the "removal" of the acid accumulated in the cytoplasm.

Concerning MCT4, we found it to be the most frequently expressed isoform in tumour cells, an expression which was significantly increased when compared to the adjacent normal epithelium. These findings contrast with the results of Lambert et al. [14], who did not find MCT4 expression in colon carcinoma and with the results of Koukourakis et al. [12], who described weak MCT4 expression in the tumour environment. This discrepancy could be related to the specificity of the antibodies used. In our study, the frequency of MCT4 staining in tumour cells was significantly different from the adjacent normal epithelium, which, together with the Western blot results, led us to believe in the specificity of the antibody used. We also found an increase in MCT4 plasma membrane staining in tumour cells when comparing with the adjacent normal epithelium. This fact supports the hypothesis that MCTs are important in the efflux of accumulated acids in tumour cells, specially MCT4 which, due to its low affinity for lactate, would be important in highly glycolytic cells [4]. We can thus postulate that MCT4 presence in the plasma membrane will allow continuous glycolytic rate (by "removing" the end product), prevention of apoptosis due to intracellular acidification and contribution to cancer cell survival. Evaluation of the correlation between MCT4 expression and clinico-pathological data revealed positive associations with tumour size, however the correlation is weak ($p=0.049$). Nevertheless, assuming that the glycolysis rate in smaller tumours is higher than in bigger tumours [18], and considering the role of MCT4 in lactate efflux, it is understandable that MCT4 activity would not be so crucial in bigger-sized tumours.

One of the most notable findings in this study was the significant gain of MCT1 and MCT4 plasma membrane expression and loss of MCT2 plasma membrane expression in cancer cells. Since MCTs need to be in the plasma membrane in order to export the accumulating acids in highly glycolytic cells, and taking into consideration the substrate affinities of the different isoforms, MCT1 and MCT4 expression in the membrane is in agreement with the metabolic alterations observed in cancer cells. On the other hand, MCT2, which is involved in the uptake of monocarboxylates into the cells in normal cell metabolism [2], does not appear to have an important role in highly glycolytic cancer cells.

This is the most comprehensive study on MCT expression in CRC and the above findings point to MCTs, specially MCT1 and MCT4, as playing an important role in CRC. MCT aberrant expression might justify future studies using these proteins as targets in CRC drug therapy. So far, however, the level of human toxicity and efficacy of the known MCT inhibitors are not currently known [7] and the search for effective and safe inhibitors would be of great value.

Acknowledgments CP received a PhD fellowship from Fundação para a Ciência e Tecnologia (SFRH/BD/27465/2006).

Conflict of interest statement We declare that we have no conflict of interest.

References

1. Brizel DM, Schroeder T, Scher RL, Walenta S, Clough RW, Dewhirst MW, Mueller-Klieser W (2001) Elevated tumour lactate concentrations predict for an increased risk of metastases in head-and-neck cancer. Int J Radiat Oncol Biol Phys 51:349–353
2. Broer S, Broer A, Schneider HP, Stegen C, Halestrap AP, Deitmer JW (1999) Characterization of the high-affinity monocarboxylate transporter MCT2 in *Xenopus laevis* oocytes. Biochem J 341:529–535
3. Dang CV, Semenza GL (1999) Oncogenic alterations of metabolism. Trends Biochem Sci 24:68–72
4. Dimmer KS, Friedrich B, Lang F, Deitmer JW, Broer S (2000) The low-affinity monocarboxylate transporter MCT4 is adapted to the export of lactate in highly glycolytic cells. Biochem J 1:219–227
5. Fang J, Quinones QJ, Holman TL, Morowitz MJ, Wang Q, Zhao H, Sivo F, Maris JM, Wahl ML (2006) The H+-linked monocarboxylate transporter (MCT1/SLC16A1): a potential therapeutic target for high-risk neuroblastoma. Mol Pharmacol 70:2108–2115
6. Fishbein WN, Merezhinskaya N, Foellmer JW (2002) Relative distribution of three major lactate transporters in frozen human tissues and their localization in unfixed skeletal muscle. Muscle Nerve 26:101–112
7. Froberg MK, Gerhart DZ, Enerson BE, Manivel C, Guzman-Paz M, Seacotte N, Drewes LR (2001) Expression of monocarboxylate transporter MCT1 in normal and neoplastic human CNS tissues. Neuroreport 12:761–765
8. Fukumura D, Xu L, Chen Y, Gohongi T, Seed B, Jain RK (2001) Hypoxia and acidosis independently up-regulate vascular endothelial growth factor transcription in brain tumors in vivo. Cancer Res 61:6020–6024
9. Halestrap AP, Meredith D (2004) The SLC16 gene family—from monocarboxylate transporters (MCTs) to aromatic amino acid transporters and beyond. Pflugers Arch 447:619–628
10. Helmlinger G, Sckell A, Dellian M, Forbes NS, Jain RK (2002) Acid production in glycolysis-impaired tumors provides new insights into tumor metabolism. Clin Cancer Res 8:1284–1291
11. Izumi H, Torigoe T, Ishiguchi H, Uramoto H, Yoshida Y, Tanabe M, Ise T, Murakami T, Yoshida T, Nomoto M, Kohno K (2003) Cellular pH regulators: potentially promising molecular targets for cancer chemotherapy. Cancer Treat Rev 29:541–549
12. Koukourakis MI, Giatromanolaki A, Harris AL, Sivridis E (2006) Comparison of metabolic pathways between cancer cells and stromal cells in colorectal carcinomas: a metabolic survival role for tumor-associated stroma. Cancer Res 66:632–637
13. Ladanyi M, Antonescu CR, Drobnjak M, Baren A, Lui MY, Golde DW, Cordon-Cardo C (2002) The precrystalline cytoplasmic

granules of alveolar soft part sarcoma contain monocarboxylate transporter 1 and CD147. AJP 160:1215–1221
14. Lambert DW, Wood IS, Ellis A, Shirazi-Beechey SP (2002) Molecular changes in the expression of human colonic nutrient transporters during the transition from normality to malignancy. Br J Cancer 86:1262–1269
15. Mathupala SP, Parajuli P, Sloan AE (2004) Silencing of monocarboxylate transporters via small interfering ribonucleic acid inhibits glycolysis and induces cell death in malignant glioma: an in vitro study. Neurosurgery 55:1410–1419
16. Philp NJ, Yoon H, Lombardi L (2001) Mouse MCT3 gene is expressed preferentially in retinal pigment and choroid plexus epithelia. Am J Physiol Cell Physiol 280:1319–1326
17. Ritzhaupt A, Wood IS, Ellis A, Hosie KB, Shirazi-Beechey SP (1998) Identification and characterization of a monocarboxylate transporter (MCT1) in pig and human colon: its potential to transport L-lactate as well as butyrate. J Physiol 513:719–732
18. Vaupel P (2004) The role of hypoxia-induced factors in tumor progression. Oncologist 9:10–17
19. Wahl ML, Owen JA, Burd R, Herlands RA, Nogami SS, Rodeck U, Berd D, Leeper DB, Owen CS (2002) Regulation of intracellular pH in human melanoma: potential therapeutic implications. Mol Cancer Ther 1:617–628
20. Walenta S, Wetterling M, Lehrke M, Schwickert G, Sundfor K, Rofstad EK, Mueller-Klieser W (2000) High lactate levels predict likelihood of metastases, tumor recurrence, and restricted patient survival in human cervical cancers. Cancer Res 60:916–921
21. Walenta S, Schroeder T, Mueller-Klieser W (2004) Lactate in solid malignant tumors: potential basis of a metabolic classification in clinical oncology. Curr Med Chem 11:2195–2204

Virchows Arch (2008) 452:147–155
DOI 10.1007/s00428-007-0551-z

ORIGINAL ARTICLE

Downregulated parafibromin expression is a promising marker for pathogenesis, invasion, metastasis and prognosis of gastric carcinomas

Hua-chuan Zheng · Hiroyuki Takahashi · Xiao-han Li · Takuo Hara · Shinji Masuda · Yi-fu Guan · Yasuo Takano

Received: 5 October 2007 / Revised: 9 November 2007 / Accepted: 10 November 2007 / Published online: 14 December 2007
© Springer-Verlag 2007

Abstract Parafibromin is a protein encoded by the hyperparathyroidism 2 oncosuppressor gene and its downregulated expression is involved in pathogenesis of parathyroid carcinomas. To clarify the roles of parafibromin expression in tumourigenesis and progression of gastric carcinomas, it was examined by immunohistochemistry (IHC) on tissue microarray containing gastric carcinomas (n=508), adenomas (n=45) and gastritis (n=49) with a comparison of its expression with clinicopathological parametres of carcinomas. Gastric carcinoma cell lines (MKN28, AGS, MKN45, KATO-III and HGC-27) were studied for parafibromin expression by IHC and western blot. Parafibromin expression was localised in the nucleus of gastric epithelial cells, adenoma, carcinoma cells and cell lines. Its expression was gradually decreased from gastritis to gastric carcinoma, through gastric adenomas ($p<0.05$) and inversely correlated with tumour size, depth of invasion, lymphatic invasion, lymph node metastasis and Union Internationale Contre le Cancer (UICC) staging ($p<0.05$) but not with sex or venous invasion ($p>0.05$). Parafibromin was strongly expressed in older carcinoma patients compared with younger ones ($p<0.05$). There was stronger positivity of parafibromin in intestinal-type than diffuse-type carcinomas ($p<0.05$). Univariate analysis indicated cumulative survival rate of patients with positive parafibromin expression to be higher than without its expression ($p<0.05$). Multivariate analysis showed that age, tumour size, depth of invasion, lymphatic invasion, lymph node metastasis, UICC staging and Lauren's classification but not sex, venous invasion or parafibromin expression were independent prognostic factors for carcinomas($p<0.05$). Downregulated parafibromin expression possibly contributed to pathogenesis, growth, invasion and metastasis of gastric carcinomas. It was considered as a promising marker to indicate the aggressive behaviours and prognosis of gastric carcinomas.

Keywords Gastric carcinoma · Parafibromin · Pathogenesis · Progression · Prognosis

H.-c. Zheng (✉) · Y.-f. Guan
Department of Biochemistry and Molecular Biology,
College of Basic Medicine, China Medical University,
Shenyang, China
e-mail: zheng_huachuan@hotmail.com

H. Takahashi · Y. Takano
Department of Diagnostic Pathology,
Graduate School of Medicine and Pharmaceutical Sciences,
University of Toyama,
2630 Sugitani,
Toyama 930-0194, Japan

X.-h. Li
Division of Pathology,
Shenjing Hospital of China Medical University,
Shenyang, China

T. Hara · S. Masuda
Kouseiren Takaoka Hospital,
Takaoka, Japan

Introduction

Parafibromin is a protein encoded by the hyperparathyroidism 2 (HRPT2) oncosuppressor gene, whose mutation causes the hyperparathyroidism–jaw tumour syndrome. The disease is an autosomal dominant disorder characterised by the occurrence of parathyroid adenoma or carcinoma, fibro-osseous jaw tumours of the mandible or maxilla and renal neoplastic and non-neoplastic abnormalities, such as Wilms' tumour, hamar-

toma or cystic renal disease [1, 16, 20]. HRPT2 gene is located in human chromosome 1q31.2, consists of 17 exons and spans 18.5 kb in the genome. It encodes a 2.7-kb transcript which is translated into a 531-amino-acid parafibromin protein with a molecular weight of 60 kd [3, 4, 23]. The 200-amino-acid C-terminal segment of parafibromin shares 32% identity and 54% homology with cell division cycle 73, a *Saccharomyces cerevisiae* protein forming the polymerase-associated factor 1 (Paf1) complex, which is associated with ribonucleic acid (RNA) polymerase II and involved in transcript site selection, transcriptional elongation, histone H2B ubiquitination, histone H3 methylation, poly (A) length control and coupling of transcriptional and posttranscriptional events [10, 17, 18, 24, 27]. Parafibromin overexpression was documented to inhibit colony formation and cellular proliferation and induce cell cycle arrest in the G1 phase, indicating that parafibromin has a critical role in cell growth [28]. Northern blot analysis showed HRPT2 expression in heart, brain, placenta, lung, liver, skeletal muscle, kidney and pancreas [4]. Western blot study revealed parafibromin expression as a 60-kd band in the adrenal gland, heart, pancreas and kidney but 40-kd immunoreactive bands in the heart and skeletal muscle of human [25]. Immunohistochemically, higher expression of parafibromin was found widespread in glomerular mesangial cell, hepatocytes, cells of the base of gastric glands, renal cortex tubules and the pars intermedia of the hypophysis [17]. Subsequent investigations have revealed that mutations in HRPT2 are present in 66–100% of sporadic parathyroid carcinomas [7, 20]. Hyperparathyroidism–jaw-tumours-syndrome-related and sporadic parathyroid carcinomas are characterised by loss of parafibromin nuclear immunoreactivity [5, 22]. Selvarajan et al. [19] found that parafibromin expression was inversely linked to tumour size, pathologic stage and lymphovascular invasion of breast carcinomas using immunohistochemistry in a tissue microarray (TMA) study. These findings suggested the potential roles of parafibromin in pathogenesis and progression of malignancies.

Gastric carcinoma ranks as the world's second leading cause of cancer mortality behind lung cancer despite a sharp worldwide decline in both its incidence and mortality since the second half of the 20th century [9]. Tumourigenesis and progression of gastric carcinoma is a multistage process with the involvement of a multifactorial aetiology, which mainly results from gene–environment interactions [32, 33]. Gastric carcinomas are classified into early and advanced ones on the basis of whether the carcinomas invade into the muscularis propria of the stomach [12]. In 1965, Lauren [13] classified gastric carcinomas into intestinal- and diffuse-type ones based on the morphological appearances. Intestinal-type carcinomas are characterised by cohesive carcinoma cells forming gland-like tubular structures with expanding or infiltrative growth pattern. However, the cell cohesion is less apparent or absent in diffuse-type carcinoma and cancer cells diffusely spread in the gastric wall [31]. Generally, there is a favorable prognosis for the patients with early or intestinal carcinoma compared with the other type. In our study, parafibromin expression was examined in gastric carcinoma, adenoma, gastritis and gastric carcinoma cell lines and compared with the clinicopathological parametres of carcinomas, as well as prognosis to explore the clinicopathological significance and molecular roles of parafibromin expression in stepwise development of gastric carcinoma.

Materials and methods

Subjects

Gastric carcinomas (n=508) were collected from the surgical resection, adenoma (n=45) from endoscopic biopsy or polypectomy and gastritis (n=49) from the endoscopic biopsy in our affiliated hospital, Himi Citizen Hospital and Kouseiren Takanoka Hospital between 1993 and 2006. All carcinomas were adenocarcinomas and the adenoma group was free from non-neoplastic polyp types, leiomyomas and benign gastrointestinal stromal tumours. The patients with gastric carcinoma were 354 men and 154 women (29~91 years, mean=65.4 years). Among them, 191 cases have carcinomas accompanied with lymph node metastasis. None of the patients underwent chemotherapy or radiotherapy before surgery. They all provided consent for use of tumour tissue for clinical research and our University Ethical Committee approved the research protocol. We followed up all patients by consulting their case documents or through telephone.

Pathology

All tissues were fixed in 4% neutralised formaldehyde, embedded in paraffin and incised into 4-μm sections. These sections were stained by haematoxylin and eosin (HE) to confirm their histological diagnosis and other microscopic characteristics. The staging for each gastric carcinoma was evaluated according to the Union Internationale Contre le Cancer (UICC) system for the extent of tumour spread [21]. Histological architecture of gastric carcinoma was expressed in terms of Lauren's [13, 31] classification. Furthermore, tumour size, depth of invasion, lymphatic and venous invasion were determined.

Tissue microarray

Representative areas of solid tumours were identified in HE-stained sections of the selected tumour cases and a 2-mm-in-

diametre tissue core per donor block was punched out and transferred to a recipient block with a maximum of 48 cores using a Tissue Microarrayer (AZUMAYA KIN-1, Japan). Four-micrometre-thick sections were consecutively incised from the recipient block and transferred to polylysine-coated glass slides. HE staining was performed on TMA for confirmation of tumour tissue.

Cell lines and culture

Gastric carcinoma cell lines come from the Japanese Physical and Chemical Institute, including MKN28 (well-differentiated adenocarcinoma), AGS (moderately differentiated adenocarcinoma), MNK45 (poorly differentiated adenocarcinoma), KATO-III (poorly differentiated adenocarcinoma) and HGC-27 (undifferentiated adenocarcinoma). They were maintained in Roswell Park Memorial Institute 1640 (MKN28, MKN45 and KATO-III), minimum essential (HGC-27) or Ham's F12 (AGS) medium supplemented with 10% foetal bovine serum, 100-units/ml penicillin, and 100-μg/ml streptomycin in a humidified atmosphere of 5% CO_2 at 37°C. Total protein was prepared from all cells by cell disruption buffer according to Protein And RNA Isolation System manual (Arctiris Bioscience, USA). All cells were collected by centrifugation, rinsed with phosphate-buffered saline, fixed by 10% formalin and then embedded in paraffin as routinely processed.

Immunohistochemistry

Consecutive sections were deparaffinised with xylene, dehydrated with alcohol and subjected to antigen retrieval by irradiating in target retrieval solution citrate pH 6.0 (TRS, DAKO, Carpinteria, CA 93013, USA) for 15 min with microwave oven (Oriental Rotor Lmt. Co., Tokyo, Japan). Five percent bovine serum albumin was then applied for 1 min to prevent non-specific binding. The sections were incubated with mouse anti-parafibromin antibody (Clone 2H1, SC-33638, Santa Cruz, CA, USA; 1:40) for 15 min, then treated with the anti-mouse Envison-PO (DAKO, CA, USA) antibody for 15 min. Binding sites were visualised with 3, 3′-diaminobenzidine with the 5-min reaction. All the incubations were performed in a microwave oven to allow intermittent irradiation as described previously [11]. After each treatment, the slides were washed with Tris-buffered saline with Tween 20 (TBST; 10 mM Tris-HCl, 150 mM NaCl, 0.1% Tween 20) three times for 1 min. After being counterstained with Mayer's haematoxylin, the sections were dehydrated, cleared and mounted. Omission of the primary antibody was used as a negative control.

One hundred cells were randomly selected and counted from five representative fields of each section blindly by three independent observers (Takano Y, Li XH and Zheng HC). The positive percentage of counted cells was graded semi-quantitatively according to a four-tier scoring system: negative (−), 0~5%; weakly positive (+), 6~25%; moderately positive (++), 26~50%; and strongly positive (+++), 51~100%.

Western blot

Fifty-microgramme denatured protein was separated on an SDS-polyacrylamide gel (10% acrylamide) and transferred to Hybond membrane (Amersham, Germany), which was then blocked overnight in 5% milk in TBST. For immunoblotting, the membrane was incubated for 1 h with mouse anti-parafibromin antibody as described above. Then, it was rinsed by TBST and incubated with anti-mouse immunoglobulin G conjugated to horseradish peroxidase (DAKO, CA, USA, 1:1,000) for 1 h. Bands were visualised with X-ray film (Fujifilm, Japan) by ECL-Plus detection reagents (Amersham, Germany). After that, membrane was washed with WB Stripping Solution (pH 2–3, Nacalai, Tokyo, Japan) for 30 min and treated as described above except mouse anti-β-actin antibody (Sigma, MO, USA, 1:5,000) as an internal control.

Statistical analysis

Statistical evaluation was performed using *Spearman* correlation test to analyse the rank data. *Kaplan–Meier* survival plots were generated and comparisons between survival curves were made with the log–rank statistic. The Cox's proportional hazards model was employed for multivariate analysis. $P<0.05$ was considered as statistically significant. SPSS 10.0 software was employed to analyse all data.

Results

Parafibromin expression in gastric tumours and carcinoma cell lines

As shown in Fig. 1, parafibromin was positively immunostained in the nucleus of MKN28, AGS, MKN45, KATO-III and HGC-27, and its expression level was consistent with the data of Western blot. Parafibromin was strongly expressed in the nucleus of gastric epithelial cells, adenomas and early carcinomas but not in given advanced carcinomas. Occasionally, it also appeared in stromal fibroblasts and lymphocytes but much weaker than epithelial cells or adenomas (Fig. 2).Generally, the stromal lymphocytes and fibroblasts were negative in cases where the tumour was negative. Overall, parafibromin expression was detected respectively in all gastritis (100.0%), 36 out of

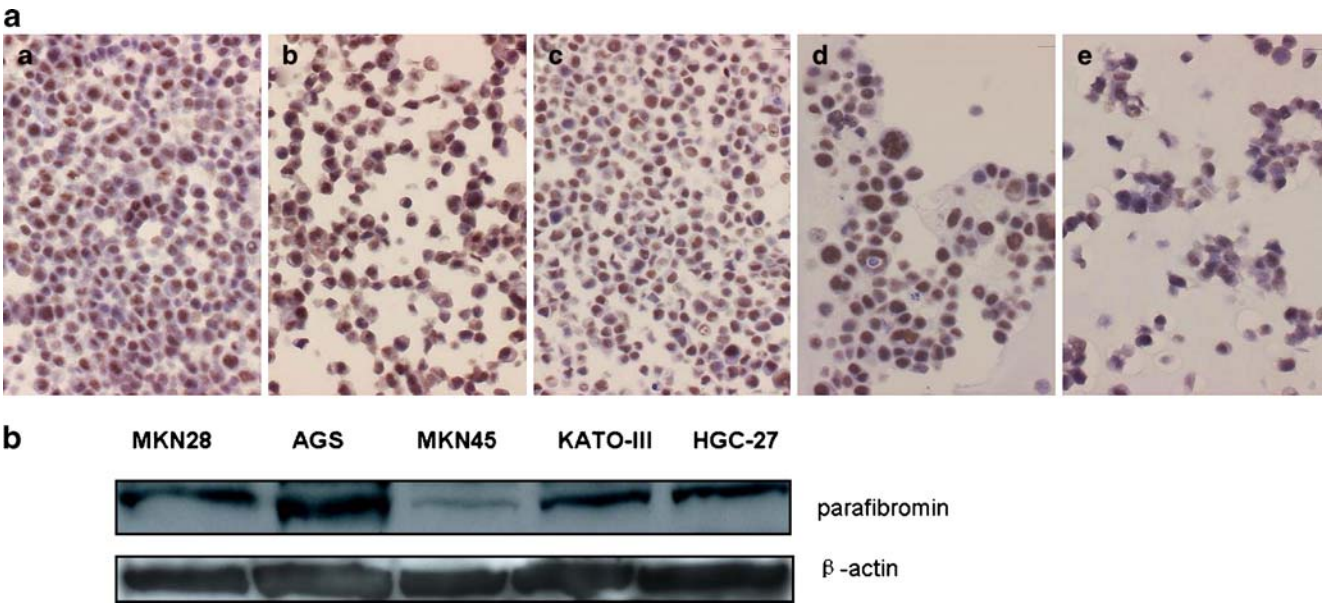


Fig. 1 Parafibromin expression in gastric carcinoma cell lines. **a** Parafibromin was positively immunostained in the nucleus of MKN28 (*a*), AGS (*b*), MKN45 (*c*), KATO-III (*d*) and HGC-27(*e*). **b** Cell lysate (50 μg) was loaded and probed with anti-human parafibromin antibody (60 kd) with β-actin (42 kd) as an internal control. *Lane #1*: MKN28; *#2* AGS; *#3* MKN45; *#4* KATO-III; *#5* HGC-27

45 adenoma patients (80.0%) and 233 out of total 508 gastric carcinoma patients (45.9%). Statistically, gradually reduced expression of parafibromin was seen from gastritis to gastric carcinoma through gastric adenoma ($p<0.05$, Table 1). As summarised in Table 2, parafibromin expression was inversely correlated with tumour size, depth of invasion, lymphatic invasion, lymph node metastasis and UICC staging ($p<0.05$) but not with sex or venous invasion ($p>0.05$). Parafibromin was strongly expressed in older carcinoma patients compared with younger ones ($p<0.05$). Intestinal-type carcinomas exhibited more frequent expression of parafibromin than diffuse-type ones ($p<0.05$).

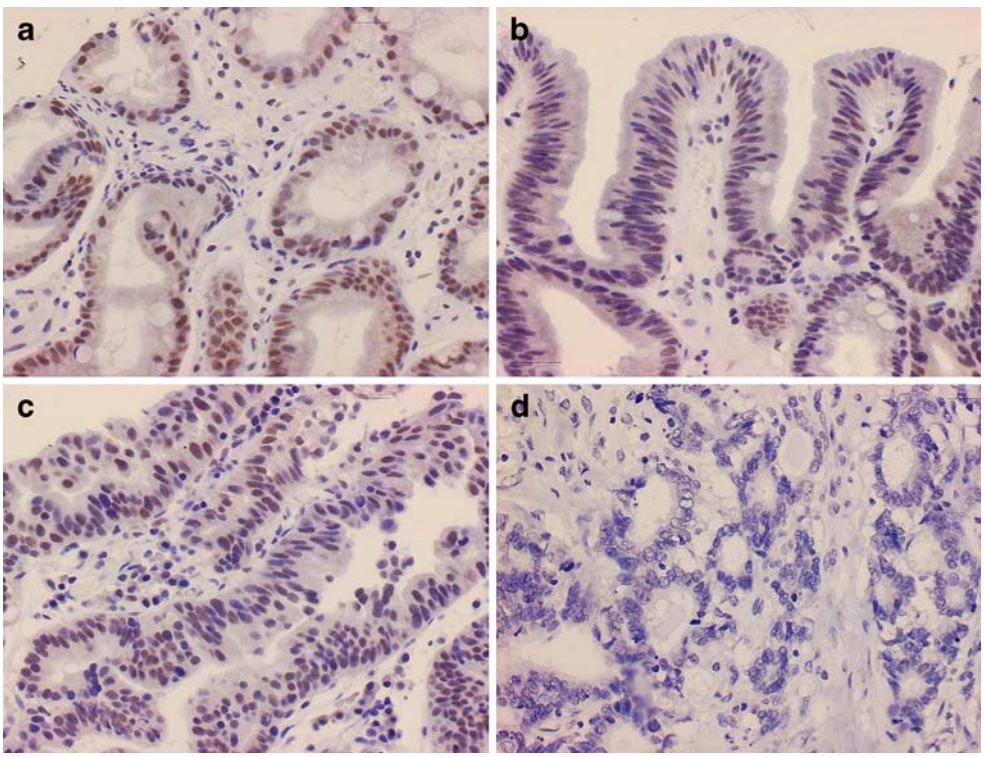


Fig. 2 Immunohistochemical staining of parafibromin in gastritis, adenoma and carcinoma. Note parafibromin positivity was strongly observed in the nucleus of gastric superficial epithelium (**a**), and adenoma (**c**) and early gastric carcinoma (**b**), occasionally weaker in the stromal fibroblasts and lymphocytes (**a**, **c**), but not in given advanced gastric carcinomas (**d**), indicating that the internal positive control (stromal cells) was negative adjacent to the negative staining carcinoma cells but positive adjacent to the positive epithelial cells

Table 1 Parafibromin expression in gastric tissue samples

Groups	Number	Parafibromin expression				
		–	+	++	+++	PR (%)
Gastritis	49	0	1	7	41	100.0[a]
Gastric adenoma	45	9	5	8	23	80.0[b]
Gastric carcinoma	508	275	55	60	118	45.9

PR Positive rate
[a] Compared with gastric adenoma or carcinoma, $p<0.001$
[b] Compared with gastric carcinoma, $p<0.001$

Univariate and multivariate survival analysis

Follow-up information was available on 508 gastric carcinoma patients for periods ranging from 0.2 months to 12.2 years (median=67.2 months). Figure 3 showed survival curves stratified according to parafibromin expression for gastric carcinomas. Univariate analysis using the *Kaplan–Meier* method indicated cumulative survival rate of patients with weak, moderate or strong parafibromin expression to be obviously higher than without its expression ($p<0.05$; Fig. 3a). The significant difference disappeared if stratified according to the depth of invasion (Fig. 3b, c). Multivariate analysis using Cox' s proportional hazard model indicated that age, tumour size, depth of invasion, lymphatic invasion, lymph node metastasis, UICC staging and Lauren's classification ($p<0.05$) but not sex,

Table 2 Relationship between parafibromin expression and clinicopathological features of gastric carcinomas

Clinicopathological features	Number	Parafibromin expression						
		–	+	++	+++	PR (%)	Rs	*p* value
Age (years)								
<65	209	125	24	24	36	40.2	0.095	<0.05
≥65	299	150	31	36	82	49.8		
Sex								
Male	354	188	37	38	91	46.9	0.054	>0.05
Female	154	87	18	22	27	43.5		
Tumour size (cm)								
<4	263	116	26	34	85	55.9	−0.237	<0.001
≥4	245	159	27	26	33	35.1		
Depth of invasion								
T_{is-1}	263	102	30	40	91	61.2	−0.344	<0.001
T_{2-4}	245	173	25	20	27	29.4		
Lymphatic invasion								
–	331	157	42	45	87	52.6	−0.168	<0.001
+	177	118	13	15	31	33.3		
Venous invasion								
–	443	236	49	51	107	46.7	−0.051	>0.05
+	65	39	6	9	11	40.0		
Lymph node metastasis								
–	317	138	38	44	97	56.5	−0.285	<0.001
+	191	137	17	16	21	28.3		
UICC staging								
0–I	292	123	36	41	92	57.9	−0.292	<0.001
II-IV	216	152	19	19	26	29.6		
Lauren's classification								
Intestinal-type	273	108	34	38	93	60.4	−0.322	<0.001
Diffuse-type	225	157	21	22	25	30.2		

PR Positive rate, T_{is} carcinoma in situ, T_1 lamina propria and submucosa, T_2 muscularis propria and subserosa, T_3 exposure to serosa, T_4 invasion into serosa, *UICC* Union Internationale Contre le Cancer

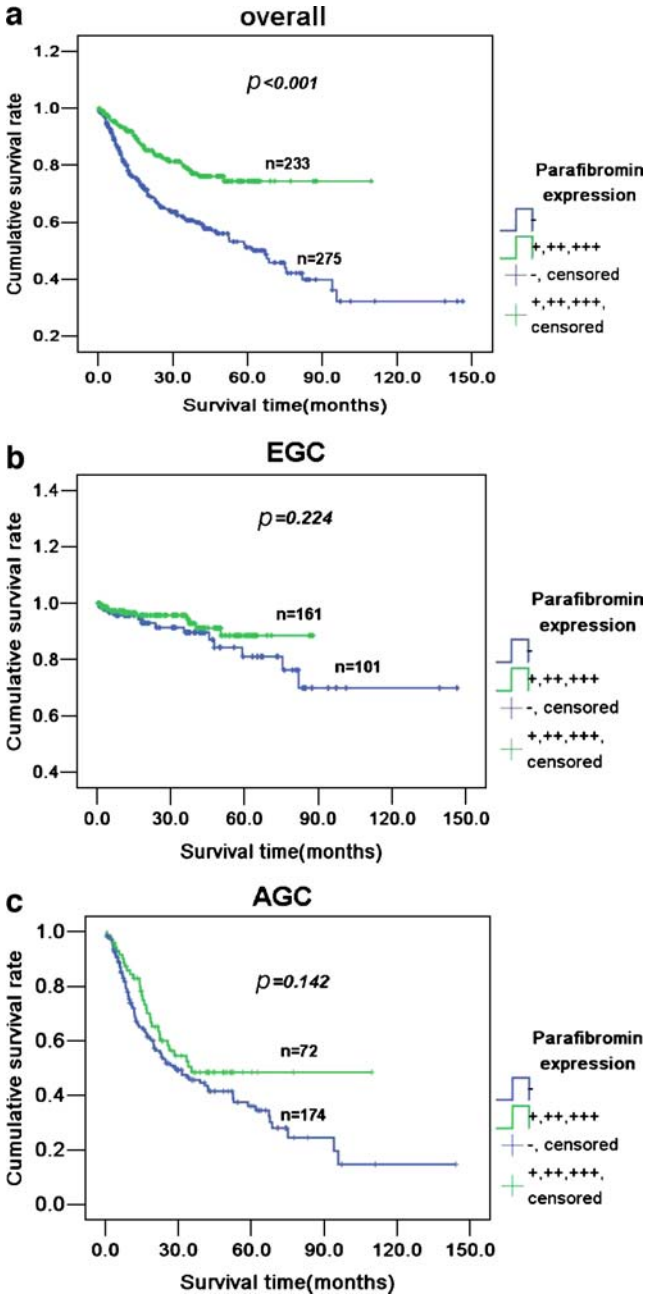


Fig. 3 Correlation between parafibromin status and prognosis of the gastric carcinoma patients. *Kaplan–Meier* curves for cumulative survival rate of patients with gastric carcinomas according to the parafibromin expression in overall (**a**), early (**b**, *EGC*) and advanced (**c**, *AGC*) gastric carcinomas

venous invasion or parafibromin expression were independent prognostic factors for overall gastric carcinomas ($p>0.05$; Table 3).

Discussion

HRPT2 has been isolated from complementary DNA libraries of parathyroid, kidney and bone tissue and encodes tumour suppressor protein parafibromin [4]. In the present study, the nuclear expression pattern was observed in the gastric epithelial cells, adenomas, adenocarcinomas and carcinoma cell lines consistent with previous reports in the gastric superficial mucosa, hepatocytes, kidney cortex tubules, adrenal gland, spleen lymphocytes, parathyroid tissue, adenoma and carcinomas, breast carcinoma [5, 8, 17, 19]. Although the result was in contrast with the paper of Porzionato et al. [17] possibly due to different incubation times of primary antibody, the great majority of immunohistochemical and cell transfection studies supported our observation of the nuclear staining [2, 5, 6, 8, 14, 19]. This study again demonstrates that parafibromin is nuclear and not cytoplasmic or nucleocytoplasmic in location as initially thought. The weaker expression of parafibromin in stromal cells than epithelial cells and adenoma might be due to the specificity of its cellular distribution as described previously [17]. It was found that the translocation of parafibromin to the nuclear compartment involved a function monopartite nuclear localisation signal at residues 136–139 [2, 6]. Parafibromin is a component of Paf1 complex in the nucleus, where it plays a role in cell cycle regulation, histone methylation, lipid and nucleic acid metabolism [10, 17]. The distribution pattern of parafibromin protein in gastric epithelial cells or tumour cells demonstrated its biological function in the nucleus.

Statistically, parafibromin expression was gradually reduced from gastritis to carcinoma through adenoma in line with parathyroid carcinogenesis, suggesting that downregulated parafibromin expression might contribute to the malignant transformation of gastric epithelial cells as an early event. The positive rate of parafibromin expression was reduced to 80% in gastric adenoma and reached about 46% of gastric adenocarcinoma, supporting the involvement of parafibromin in the gastric adenoma–adenocarcinoma sequence. Actually, the adenoma can progress into and be incorporated with gastric well-differentiated carcinoma when it grows bigger and de novo carcinogenesis is well understood, especially in diffuse-type gastric carcinomas [34]. Higher parafibromin expression in adenoma and intestinal-type carcinoma indicated that decreased parafibromin expression might play an important role in de novo diffuse-type carcinogenesis but less in intestinal carcinogenic pathway.

A body of evidences indicated that downregulation of tumour suppressor protein expression was due to genetic or epigenetic changes, like allelic loss, mutation, loss of heterozygosity (LOH), hypermethylation and microsatellite instability in malignancies [29, 30]. In the sporadic parathyroid carcinomas and hyperparathyroidism–jaw tumours, LOH or mutation of HRPT2 might cause the loss and inactivation of parafibromin protein [20, 25, 26]. Furthermore, the reduced expression of parafibromin was

Table 3 Multivariate analysis of clinicopathological variables for survival with gastric carcinomas

Number	Clinicopathological parametres	Relative risk (95%CI)	*p* value
A	Age (≥65 years)	1.929 (1.357–2.743)	<0.001
B	Sex (female)	1.463 (0.983–2.179)	>0.05
C	Tumour size (≥4 cm)	1.606 (1.013–2.547)	<0.05
D	Depth of invasion ($T_{2–4}$)	6.530 (3.110–13.710)	<0.001
E	Lymphatic invasion (+)	2.626 (1.516–3.374)	<0.001
F	Venous invasion (+)	0.959 (0.633–1.452)	>0.05
G	Lymph node metastasis (+)	2.773 (1.525–5.043)	<0.01
H	UICC staging (II-IV)	0.294 (0.139–0.622)	<0.01
I	Lauren's classification (diffuse-type)	1.796 (1.212–2.661)	<0.01
J	Parafibromin expression (+~+++)	0.792 (0.529–1.187)	>0.05

CI Confidence interval, *UICC*= Union Internationale Contre le Cancer

found to closely link to the tumour size, depth of invasion, lymphatic or venous invasion and UICC staging in line with the observation in breast carcinomas [19], indicating the inhibitory effects of parafibromin on tumour growth, invasion, metastasis and progression of gastric carcinomas. Drosophila Hyrax and its human orthologue, parafibromin, are required for nuclear transduction of the Wnt/Wg signal and bind directly to the C-terminal region of beta-catenin–Armadillo, thereby controlling transcriptional initiation and elongation by RNA polymerase II [15]. Parafibromin overexpression can inhibit colony formation, anchorage-dependent cell growth and cellular proliferation and induce cell cycle arrest in the G1 phase [28]. These findings demonstrated that loss of parafibromin expression had impact on the pathogenesis and progression of malignancies by promoting cellular proliferation. Additionally, parafibromin was expressed with a higher incidence in intestinal-type gastric cancer, which is presumed to arise from preceding dysplastic lesions, than diffuse-type one, which evolves without any precedent dysplastic changes. It is also demonstrated that distinct parafibromin expression underlies the molecular mechanisms for the differentiation of intestinal- and diffuse-type carcinomas.

Until now, there is yet no paper describing the prognostic significance of parafibromin expression in malignancies. Here, for the first time, we analysed the relation of parafibromin expression with the survival rate of 508 patients with gastric carcinoma. The results revealed a close link between its loss and worse survival. If stratified according to the depth of invasion, the significant link disappeared, indicating that the relationship between parafibromin expression and prognosis depends on the depth of invasion. The multivariate analysis demonstrated that age, depth of invasion, lymphatic invasion, lymph node metastasis, UICC staging and Lauren's classification but not parafibromin expression, venous invasion or sex were independent prognostic factors for carcinomas. These findings suggested that parafibromin expression is a promising indicator for the favorable prognosis of gastric carcinoma patients, albeit not independent.

In the present study, a large number of gastric carcinoma cases were screened by TMA, which takes the advantages of high throughput, identical immunohistochemical conditions, and economy of samples, antibodies and time [33]. Although we used 2-mm-in-diametre needles, which are large enough to evaluate the morphological appearance and carefully selected representative regions with the reference of HE slides, it was difficult to avoid selection bias. Gill et al. [5] found that stronger parafibromin staining and more positive cells sometimes appeared at the edges of the parathyroid tumour than in the centre. This could be due to fixation methods, other processing issues or a biological phenomenon, for example tissue hypoxia in the centre of large tumours. Additionally, the collection of our samples (e.g. gastritis, adenoma and adenocarcinoma) respectively from the endoscopic biopsy, polypectomy, or surgical resection put forward their another possibility of selection bias because of different fixation and processing methods. Selvarajan et al. [19] found that parafibromin underexpression was correlated particularly with large tumour size which is in line with our finding. It was possible that weaker staining could be attributable to poor fixation properties in the centre of large tumours. Because tumour size is a key prognostic indicator, this artifact could explain the prognostic significance of parafibromin in gastric carcinomas. Therefore, it is a limitation of the present study not to separate the edge and centre of gastric carcinomas when establishing TMA. In the current study, the negatively staining carcinomas are associated with a negative internal control (stromal cells and lymphocytes) whereas the positive staining epithelium is adjacent to positive staining internal controls. Therefore, the negative staining of the carcinoma might be artificial, which should be considered as another limitation of the study. Our study might be mentioned as a preliminary experiment and the staining with original-size sections is an extensive work in

the future using the gastric carcinoma samples, fixed and processed by the same approach.

In summary, downregulated parafibromin expression might play an important role in malignant transformation of gastric epithelial cells. Its reduced expression was closely related to growth, invasion, metastasis and worse prognosis of gastric carcinomas. Its expression could be employed to differentiate the intestinal- and diffuse-type carcinomas and underlay the molecular mechanism about the differentiation of both carcinomas. It was considered as a promising marker to indicate the pathobiological behaviours and prognosis of gastric carcinomas.

Acknowledgements We particularly thanked Kanako Yasuyoshi, Tokimasa Kumada and Hideki Hatta for their technical help and Yukari Inoue for her secretarial assistance. This work was partially supported by the Japanese Ministry of Education, Science, Sports and Culture, Grant-in-Aid for Scientific Research 14770072, Japanese Smoking Foundation and Shenyang Outstanding Scholar Foundation.

Conflict of interest statement No conflict of interest

References

1. Aldred MJ, Talacko AA, Savarirayan R, Murdolo V, Mills AE, Radden BG, Alimov A, Villablanca A, Larsson C (2006) Dental findings in a family with hyperparathyroidism–jaw tumour syndrome and a novel HRPT2 gene mutation. Oral Surg Oral Med Oral Pathol Oral Radiol Endod 101:212–218
2. Bradley KJ, Bowl MR, Williams SE, Ahmad BN, Partridge CJ, Patmanidi AL, Kennedy AM, Loh NY, Thakker RV (2007) Parafibromin is a nuclear protein with a functional monopartite nuclear localization signal. Oncogene 26:1213–1221
3. Bradley KJ, Cavaco BM, Bowl MR, Harding B, Young A, Thakker RV (2005) Utilisation of a cryptic non-canonical donor splice site of the gene encoding PARAFIBROMIN is associated with familial isolated primary hyperparathyroidism. J Med Genet 42:e51
4. Carpten JD, Robbins CM, Villablanca A, Forsberg L, Presciuttini S, Bailey-Wilson J, Simonds WF, Gillanders EM, Kennedy AM, Chen JD, Agarwal SK, Sood R, Jones MP, Moses TY, Haven C, Petillo D, Leotlela PD, Harding B, Cameron D, Pannett AA, Hoog A, Heath H, James-Newton LA, Robinson B, Zarbo RJ, Cavaco BM, Wassif W, Perrier ND, Rosen IB, Kristoffersson U, Turnpenny PD, Farnebo LO, Besser GM, Jackson CE, Morreau H, Trent JM, Thakker RV, Marx SJ, Teh BT, Larsson C, Hobbs MR (2002) HRPT2, encoding parafibromin, is mutated in hyperparathyroidism–jaw tumour syndrome. Nat Genet 32:676–680
5. Gill AJ, Clarkson A, Gimm O, Keil J, Dralle H, Howell VM, Marsh DJ (2006) Loss of nuclear expression of parafibromin distinguishes parathyroid carcinomas and hyperparathyroidism –jaw tumour (HPT-JT) syndrome-related adenomas from sporadic parathyroid adenomas and hyperplasias. Am J Surg Pathol 30:1140–1149
6. Hahn MA, Marsh DJ (2005) Identification of a functional bipartite nuclear localization signal in the tumour suppressor parafibromin. Oncogene 24:6241–6248
7. Howell VM, Haven CJ, Kahnoski K, Khoo SK, Petillo D, Chen J, Fleuren GJ, Robinson BG, Delbridge LW, Philips J, Nelson AE, Krause U, Hammje K, Dralle H, Hoang-Vu C, Gimm O, Marsh DJ, Morreau H, Teh BT (2003) HRPT2 mutations are associated with malignancy in sporadic parathyroid tumours. J Med Genet 40:657–663
8. Juhlin C, Larsson C, Yakoleva T, Leibiger I, Leibiger B, Alimov A, Weber G, Hoog A, Villablanca A (2006) Loss of parafibromin expression in a subset of parathyroid adenomas. Endocr Relat Cancer 13:509–523
9. Kelley JR, Duggan JM (2003) Gastric cancer epidemiology and risk factors. J Clin Epidemiol 56:1–9
10. Krogan NJ, Dover J, Wood A, Schneider J, Heidt J, Boateng MA, Dean K, Ryan OW, Golshani A, Johnston M, Greenblatt JF, Shilatifard A (2003) The Paf1 complex is required for histone H3 methylation by COMPASS and Dot1p: linking transcriptional elongation to histone methylation. Mol Cell 11:721–729
11. Kumada T, Tsuneyama K, Hatta H, Ishizawa S, Takano Y (2004) Improved 1-h rapid immunostaining method using intermittent microwave irradiation: practicability based on 5 years application in Toyama Medical and Pharmaceutical University Hospital. Mod Pathol 17:1141–1149
12. Kurokawa T, Fuchigami A (1967) Gastric carcinoma in its early stages. Naika 20:824–829
13. Lauren P (1965) The two histological main types of gastric carcinoma: diffuse and so-called intestinal-type carcinoma. An attempt at a histo-clinical classification. Acta Pathol Microbiol Scand 64:31–49
14. Lin L, Czapiga M, Nini L, Zhang JH, Simonds WF (2007) Nuclear localization of the parafibromin tumor suppressor protein implicated in the hyperparathyroidism–jaw tumor syndrome enhances its proapoptotic function. Mol Cancer Res 5:183–193
15. Mosimann C, Hausmann G, Basler K (2006) Parafibromin/hyrax activates Wnt/Wg target gene transcription by direct association with beta-catenin/Armadillo. Cell 125:327–341
16. Pimenta FJ, Gontijo Silveira LF, Tavares GC, Silva AC, Perdigao PF, Castro WH, Gomez MV, Teh BT, De Marco L, Gomez RS (2006) HRPT2 gene alterations in ossifying fibroma of the jaws. Oral Oncol 42:735–739
17. Porzionato A, Macchi V, Barzon L, Masi G, Iacobone M, Parenti A, Palu G, De Caro R (2006) Immunohistochemical assessment of parafibromin in mouse and human tissues. J Anat 209:817–827
18. Rozenblatt-Rosen O, Hughes CM, Nannepaga SJ, Shanmugam KS, Copeland TD, Guszczynski T, Resau JH, Meyerson M (2005) The parafibromin tumour suppressor protein is part of a human Paf1 complex. Mol Cell Biol 25:612–620
19. Selvarajan S, Sii LH, Lee A, Yip G, Bay BH, Tan MH, Teh BT, Tan PH (2007) Parafibromin expression in breast cancer: a novel marker for prognostication? J Clin Pathol (in press)
20. Shattuck TM, Valimaki S, Obara T, Gaz RD, Clark OH, Shoback D, Wierman ME, Tojo K, Robbins CM, Carpten JD, Farnebo LO, Larsson C, Arnold A (2003) Somatic and germ-line mutations of the HRPT2 gene in sporadic parathyroid carcinoma. N Engl J Med 349:1722–1729
21. Sobin LH, Wittekind CH (2002) TNM classification of malignant tumours, 6th edn. Wiley, Hoboken
22. Tan MH, Morrison C, Wang P, Yang X, Haven CJ, Zhang C, Zhao P, Tretiakova MS, Korpi-Hyovalti E, Burgess JR, Soo KC, Cheah WK, Cao B, Resau J, Morreau H, Teh BT (2004) Loss of parafibromin immunoreactivity is a distinguishing feature of parathyroid carcinoma. Clin Cancer Res 10:6629–6637
23. Wang PF, Tan MH, Zhang C, Morreau H, Teh BT (2005) HRPT2, a tumour suppressor gene for hyperparathyroidism-jaw tumour syndrome. Horm Metab Res 37:380–383
24. Wood A, Krogan NJ, Dover J, Schneider J, Heidt J, Boateng MA, Dean K, Golshani A, Zhang Y, Greenblatt JF, Johnston M, Shilatifard A (2003) Bre1, an E3 ubiquitin ligase required for recruitment and substrate selection of Rad6 at a promoter. Mol Cell 11:267–274

25. Woodard GE, Lin L, Zhang JH, Agarwal SK, Marx SJ, Simonds WF (2005) Parafibromin, product of the hyperparathyroidism–jaw tumour syndrome gene HRPT2, regulates cyclin D1/PRAD1 expression. Oncogene 24:1272–1276
26. Yang GY, Zhang YC, Liu XD, Wu YQ, Li MS, Gong CY, Guan BW, Mi DH, Liu S (1992) Geographic pathology on the precursors of stomach cancer. J Environ Pathol Toxicol Oncol 11: 339–344
27. Yart A, Gstaiger M, Wirbelauer C, Pecnik M, Anastasiou D, Hess D, Krek W (2005) The HRPT2 tumour suppressor gene product parafibromin associates with human PAF1 and RNA polymerase II. Mol Cell Biol 25:5052–5060
28. Zhang C, Kong D, Tan MH, Pappas DL, Wang PF, Chen J, Farber L, Zhang N, Koo HM, Weinreich M, Williams BO, Teh BT (2006) Parafibromin inhibits cancer cell growth and causes G1 phase arrest. Biochem Biophys Res Commun 350:17–24
29. Zheng HC, Sun JM, Li XH, Yang XF, Zhang YC, Xin Y (2003) Role of PTEN and MMP-7 expression in growth, invasion, metastasis and angiogenesis of gastric carcinoma. Pathol Int 53: 659–666
30. Zheng H, Takahashi H, Murai Y, Cui Z, Nomoto K, Niwa H, Tsuneyama K, Takano Y Low expression of FHIT and PTEN correlates with malignancy of gastric carcinomas. Appl Immunohistochem Mol Morphol (in press)
31. Zheng H, Takahashi H, Murai Y, Cui Z, Nomoto K, Miwa S, Tsuneyama K, Takano Y (2007) Pathobiological characteristics of intestinal and diffuse-type gastric carcinoma in Japan: an immunostaining study on the tissue microarray. J Clin Pathol 60:273–277
32. Zheng HC, Takahashi H, Murai Y, Cui ZG, Nomoto K, Miwa S, Tsuneyama K, Takano Y (2006) Upregulated EMMPRIN/CD147 might contribute to growth and angiogenesis of gastric carcinoma: a good marker for local invasion and prognosis. Br J Cancer 95:1371–1378
33. Zheng H, Takahashi H, Nakajima T, Murai Y, Cui Z, Nomoto K, Tsuneyama K, Takano Y (2006) MUC6 down-regulation correlates with gastric carcinoma progression and a poor prognosis: an immunohistochemical study with tissue microarrays. J Cancer Res Clin Oncol 132:817–823
34. Zheng HC, Tsuneyama K, Takahashi H, Miwa S, Sugiyama T, Popivanova BK, Fujii C, Nomoto K, Mukaida N, Takano Y (2007) Aberrant Pim-3 expression is involved in gastric adenoma-adenocarcinoma sequence and cancer progression. J Cancer Res Clin Oncol (in press)

Virchows Arch (2008) 452:157–167
DOI 10.1007/s00428-007-0549-6

ORIGINAL ARTICLE

Proteomic identification of heat shock protein 27 as a differentiation and prognostic marker in neuroblastoma but not in Ewing's sarcoma

Cristina Zanini · Francesco Pulerà · Franco Carta · Giuliana Giribaldi · Giorgia Mandili · Milena Maria Maule · Marco Forni · Franco Turrini

Received: 24 September 2007 / Revised: 31 October 2007 / Accepted: 11 November 2007 / Published online: 8 December 2007
© Springer-Verlag 2007

Abstract Neuroblastoma (NB) and Ewing's sarcoma (ES) cell lines were analysed by two-dimensional gel electrophoresis (2-DE) searching for new diagnostic/prognostic markers. Protein expression profiles displayed a high degree of similarity with the exception of marked heat shock protein (HSP) 27 and less marked HSP60 and HSP70 family up-modulations in NB cells. HSP27, which showed peculiar variability in different NB cell preparations, responded to all trans-retinoic acid treatment in NB cells but not in ES cells at gene and protein expression levels. Immunohistochemistry studies showed different behaviours of HSP27 and HSP70 expression in NB and ES biopsies. HSP27 was less expressed, whereas HSP70 was more expressed in the immature areas of NB. HSP27 expression showed positive and statistically significant correlation with favourable prognosis, and HSP27 expression also negatively correlated with increasing aggressiveness of histological type. In ES, both chaperones were expressed without characteristic patterns. Our results suggest that HSP27, after further clinical validations, could be used as a marker of neuronal differentiation in vivo for the assessment of the biological behaviour of NB and for the risk stratification of patients.

Keywords Ewing's sarcoma · Gene expression · Immunohistochemistry · HSP · Neuroblastoma · Proteomic

C. Zanini (✉) · F. Carta · G. Giribaldi · F. Turrini
Department of Genetics, Biology and Biochemistry,
University of Turin,
Via Santena 5 bis,
10126 Turin, Italy
e-mail: cristina.zanini@unito.it

F. Pulerà · M. Forni
Division of Pediatric Pathology,
Ospedale Infantile Regina Margherita of Turin,
Piazza Polonia 96,
10126 Turin, Italy

G. Mandili
Center for Experimental Research and Medical Studies (CERMS),
University of Turin,
Via Santena 5,
10126 Turin, Italy

M. M. Maule
Epidemiology Unit, CPO Piemonte, CERMS, University of Turin,
Via Santena 5,
10126 Turin, Italy

Introduction

Neuroblastoma (NB) and Ewing's sarcoma (ES) are very aggressive tumours with a long-term survival rate that, in unfavourable clinical settings, may be as low as 15% for NB [34]. They are both members of the so-called small round blue-cell tumours of infancy and childhood, a broad category of neoplasia with undifferentiated histology that also includes lymphoma and rhabdomyosarcoma [32]. Their differential diagnosis has been facilitated with the introduction of improved diagnostic tools. Even so, the discovery of new prognostic markers would be very valuable in both cases. NB and ES are currently thought to derive from the neural crest and may originate from a progenitor neuroectodermal cell during its differentiation. They nevertheless display different cytogenetic and chromosome aberrations and also differ in their clinical presentation and prognosis [5, 10]. NB is an enigmatic tumour. It ranges from a very immature neoplasm, morphologically similar to ES, to a fully differentiated form known as ganglioneuroma, a benign tumour that is the endpoint of the maturation of neuroblasts to ganglion cells.

Its prognostic factors are widely applied in paediatric oncology. Histology (the International Neuroblastoma Pathology Classification [INPC] and the mitosis karyorrhexis index), proto-oncogene MYCN amplification, deletion of the short arm of chromosome 1 and ploidy (cellular deoxyribonucleic acid [DNA] content) are currently used for risk stratification [27]. New markers that identify areas of cellular differentiation/maturation on histological sections and with more sensitivity or precocity than morphology alone may provide additional factors and help to stratify patients according to risk groups. ES is microscopically more uniform. Its prognostic factors are mainly confined to the type of chromosomal translocation and the extension of the neoplasia, as well as its origin in the dermis [13]. We undertook a comparative proteomic analysis of NB and ES cell lines to gain a clearer understanding of the differences in their behaviour and look for new diagnostic or prognostic markers. Protein expression profiles displayed a very high degree of similarity with the exception of marked HSP27 up-modulation in NB cells. Quantitative gene expression and Western blot findings were compared with the proteomic data. Little is known about the role of heat shock proteins (HSPs) in the central nervous system. Their role in neuroprotection following thermal stress and ischemia/reperfusion injury has been described in neurons [2, 37]. A correlation has been demonstrated between NB stage and HSP27 expression [33]. Induction of alpha B-crystallin (small HSP family) after chemotherapy in NB has also been described [14]. A growing body of evidence suggests a relationship between HSP expression and prognosis in different types of malignancies [16, 18, 25, 29, 31]. HSP27 exerts both a caspase-dependent [6] and an caspase-independent [8, 22] anti-apoptotic activity. Moreover, in the present study, biopsy specimens were studied immunohistochemically to determine HSP27 and HSP70 expression patterns in primary and metastatic NB and ES.

Materials and methods

Cell culture and retinoic acid treatment

Established human neuroectodermal tumour cell lines (NB lines AF8, IMR-5 and SJ-N-KP and ES lines TC106, 6647 and PDE02) [3, 24, 26, 30] were cultured (2×10^4/mL) at 37°C, 5% CO_2 in RPMI 1640 (Sigma) supplemented with 10% heat-inactivated foetal bovine serum (EuroClone), 100 μg/mL streptomycin and 100 U/mL penicillin (Sigma). To reduce cell preparation variability, we cultured the cell for 5 days after thawing of new aliquots.

For induction of differentiation, cells were cultured for 24 h in the presence of 10 μM all trans-retinoic acid (ATRA; Sigma) suspended in dimethyl sulphoxide as previously described [12]. Control cultures contained the same concentration of dimethyl sulphoxide. The maximum concentration of dimethyl sulphoxide was maintained below 0.001%.

Tissue samples

Paraffin-embedded tissue blocks were retrieved from the files of the Pathology Department of Regina Margherita Children's Hospital (Turin, Italy). NB was diagnosed according to the INPC classification (including mitosis karyorrhexis index for stroma poor histology) and assigned to favourable and unfavourable prognostic groups. All the tumours were also reviewed by the Italian Neuroblastoma Pathology Panel, to validate the diagnosis. MYCN status, 1p deletion and ploidy were determined by the Centre of Reference—Gaslini Institute (Genoa, Italy) [28]. For ES, six blocks were selected from five patients including the five primary tumours and one methachronous lung metastasis from the third ES patient. For NB, 33 blocks from 26 patients were selected (Table 1). These cases were originally diagnosed as ganglioneuroblastoma intermixed (GNB-I), GNB nodular (GNB-N), NB Stroma Poor (SP) undifferentiated (NB-U), SP poorly differentiated (NB-PD) and SP differentiating (NB-D). All blocks were selected after a review of the corresponding haematoxylin and eosin slides to sample areas of differentiating tumour and Schwannian stroma (if represented) as well as the more immature clusters and nodules (if present). The blocks included first diagnostic biopsies of primary tumours (16 cases), bone marrow metastasis (three cases), liver metastasis (one case) and a central nervous system tumour resection for cerebral metastatic spread (one case) or lymph node metastasis (five cases). To investigate HSP expression during tumour progression, one or more bone marrow biopsies with metastatic disease were examined in parallel to the primary tumours (Table 1, cases number 15, 18, 22 and 23). The expression of HSP27 and HSP70 was also assessed in several normal tissues present in the blocks selected for the study. Areas of reactive gliosis were selected in the NB metastatic to central nervous system.

Two-dimensional gel electrophoresis

Cells (10^7) from each cell line were washed three times in phosphate-buffered saline, harvested with a scraper, suspended in 0.5 mL of a solution containing 8 M urea, 2% w/v CHAPS, 40 mM Tris and protease inhibitors (5 mM ethylenediamine tetraacetic acid and 2 mM phenylmethanesulphonylfluoride) and analysed by 2-DE, as previously described [7]. Briefly, 2-DE was performed using ready-made immobilized pH gradient strips (17 cm, pH 4–7, Nurex). Each sample, 150 μg of protein for analytical gels

Table 1 Molecular prognostic factors and immunohistochemistry analysis of HSP70 and HSP27 in neuroblastic tumours

Patient	Age (years)	Diagnosis[a]	INPC AGE/ PROG[b]	Survival[c]	MYCN amp[d]	1p36 deletion[e]	MKI index[f]	DNA index[g]	HSP70[h]	HSP27[i]	Tumour sampled[j]
NB 1	2	GNB-I	FH	ned	*n.r.*[k]	*n.r.*	*n.r.*	1.27	−	+++	PT
NB 2	2	NB-D	FH	ned	NA	I	Low	1.61	++++	+/++	PT
NB 3	3	NB-D	FH	ned	*n.d.*[l]	*n.d.*	Intermediate	1.47	+++	++	PT
NB 4	1	NB-PD	FH	ned	NA	ND	Low	1.46	+++	++	PT
NB 5	1	NB-PD	FH	ned	NA	ND	Low	1.22	+++	++	PT
NB 6	1	NB-PD	FH	ned	NA	ND	Low	1.47	+++	+	PT
NB 7	0.4	NB-PD	FH	ned	NA	ND	Low	*n.d.*	+++	+/++	PT
NB 8	0.01	NB-PD	FH	ned	NA	ND	Intermediate	1.52	+++	−/+	PT
NB 9	1	NB-PD	FH	ned	NA	ND	Intermediate	1.27	++/+	+	PT
NB 10	1.7	NB-PD	UH	dead 36	NA	ND	Intermediate	1.00	+++/++++	+	PT
NB 11	2	NB-PD	UH	ned	NA	ND	Low	1.49	+++	−	PT
NB 12	8.5	NB-PD	UH	pd	G	I	High	1.47	+++	−/+	PT
NB 13	5	NB-PD	UH	dead 51	G	D	Low	*n.d.*	++++	+++	PT
NB 14	4	GNB-N	UH	dead 30	G	ND	High	2.00	+/++	−/+	PT
NB 15	4	GNB-N	UH	dead 196	G	ND	Low	1.47	+++/++	−/+	PT
NB 15 a	4	GNB-N	UH	dead 196	G	ND	Low	1.47	+++/++	−	MTS BM
NB 15 b	4	GNB-N	UH	dead 196	G	ND	Low	1.47	+++/++	−	MTS BM
NB 15 c	4	GNB-N	UH	dead 196	G	ND	Low	1.47	+++/++	−	MTS BM
NB 16	4	NB-U	UH	dead 19	G	I	High	2.36	+++	−	PT
NB 17	0.8	NB-PD	FH	ned	NA	ND	Intermediate	1.40	++++	+/++	MTS LN
NB 18	18	NB-PD	UH	ned	NA	ND	Low	*n.d.*	+++	−/+	MTS BM
NB 18 a	18	NB-PD	UH	ned	NA	ND	Low	*n.d.*	+++	−/+	MTS BM
NB 18 b	18	NB-PD	UH	ned	NA	ND	Low	*n.d.*	+++	−/+	MTS BM
NB 19	7	NB-PD	UH	ned	NA	ND	Intermediate	1.00	+++	−/+	MTS LN
NB 20	4	NB-PD	UH	pd	NA	ND	Intermediate	1.00	+++	−	MTS LN
NB 21	5	NB-PD	UH	pd	*n.d.*	*n.d.*	Low	*n.d.*	++	++	MTS BM
NB 22	3	NB-PD	UH	pd	G	*n.d.*	Intermediate	*n.d.*	++++	+++	MTS BM
NB 22 a	3	NB-PD	UH	pd	G	*n.d.*	Intermediate	*n.d.*	++++	−	MTS BM
NB 23	3	NB-PD	UH	dead 4	NA	ND	Intermediate	1.00	++++	−/+	MTS LN
NB 23 a	3	NB-PD	UH	dead 4	NA	ND	Intermediate	1.00	++++	−	MTS BM
NB 24	2	NB-PD	UH	dead 37	A	D	High	*n.d.*	+++	−	MTS LN
NB 25	0.3	NB-U	UH	dead 5	NA	*n.d.*	*n.d.*	*n.d.*	++/+++	−	MTS L
NB 26	1	NB-U	UH	ned	NA	D	High	1.00	+++	−	MTS CNS

[a] Histological diagnosis: *GNB-I* ganglioneuroblastoma intermixed, *GNB-N* ganglioneuroblastoma nodular, *NB-D* neuroblastoma differentiating, *NB-PD* neuroblastoma poorly differentiated, *NB-U* neuroblastoma undifferentiated

[b] INCP age/prognosis: *FH* favourable histology and *UH* unfavourable histology according to age-related INCP [36]

[c] Survival: *ned* no evidence of disease, *pd* progressive disease (survival was expressed in months)

[d] MYCN amplification test: *NA* not amplified, *A* amplified, *G* gain, an up to fourfold excess of gene copies or chromosomal regions in relation to the reference probe on the same chromosome

[e] 1p36 deletion: *ND* non-deleted, *D* deleted, *I* allelic imbalanced

[f] Mitosis karyorrhexis index

[g] Cellular DNA content

[h, i] HSP27 and HSP70 immunostaining: scores (− negative, + positive) were referred to the immature areas

[j] *PT* Primary tumour, *MTS* metastatic disease, *BM* bone marrow, *CNS* central nervous system, *L* liver, *LN* lymph node

[k] Prognostic factor determination is routinely not requested for stroma-rich component

[l] Not detected for tissue sample limitations

and 1 mg for preparative gels, was loaded onto each isoelectric focussing gel and separated. The second-dimensional separation was performed on 10% polyacrylamide gel; gels were stained with silver stain [19] and Coomassie Blue R-250 stain. All experiments were performed three or more times. Stained gels were scanned with ImageMaster VDS-CL (Pharmacia), and gel image files were subsequently analysed with ImageMaster 2D Elite (Amersham Biosciences). The protein level of each spot was expressed as the percentage of total spot volume in the whole gel (relative abundance). Gels were run for each NB (three cell lines) and ES (three cell lines) cell lines. The average relative abundances and standard deviations were calculated for each spot. Significance of differences between NB and ES spot abundance was calculated with Student's *t* test from the abundance values in each gel.

Mass spectrometric analysis and peptide mass fingerprinting

Coomassie blue-stained spots were excised from 2-DE gels of SJ-N-KP and PDE02 cell lines and destained by washing twice with 50% acetonitrile (ACN) in 5 mM ammonium bicarbonate. Gel pieces were then dried for 30 min in ACN. Dried pieces of gel were subjected to protein digestion by trypsin using previous published protocols [38]. Mass spectrometry (MS) analysis of peptides from 2-DE gel spots were performed with a matrix-assisted laser desorption/ionization time of flight micro-MX (Micromass) equipped with a delayed extraction unit, according to the tuning procedures suggested by the manufacturer. Samples were loaded onto MALDI target using 1 μL of the tryptic digest mixed 1:1 with a solution of alpha-cyano hydroxycinnamic acid (10 mg/mL in 40% ACN, 0.1% v/v trifluoroacetic acid). Peak lists were generated with ProteinLynx Data Preparation using the following parameters: external calibration with lock mass using mass 2,465.1989 Da of ACTH, background subtract type adaptive combining all scans, performing deisotoping with a threshold of 5%. Peak lists created as above described were sent to ProteinLynx Global Server 2.2.5 (PLGS) search using Swiss-Prot database (release 51.0 of Oct 2006). Search settings allowed one missed cleavage with the trypsin enzyme selected, carboxymethylated cysteine as fixed modification and oxidation of methionine as potential variable modification, peptide tolerance of 100 ppm, taxa human, molecular weight range 10–100 kDa and p*I* range 3–10. Only identification with PLGS score major than 9 were taken in consideration.

Protein score=1*n*(probability of Protein GIVEN Data and Initial Assumptions)/(probability of Protein GIVEN Initial Assumptions). If there are *N* proteins in the databank, each protein in a databank has a probability of 1/*N*. Therefore, the maximum possible score is ln(*N*), and the minimum possible score is zero when the data provide no information, relative to the databank.

Western blot analysis

Cells (1×10^6) were solubilized, and proteins were separated in a 8% polyacrylamide gel and transferred to nitrocellulose membrane as described [11]. Five micrograms of proteins were loaded for each lane. Membranes were incubated with anti-GAPDH (rabbit polyclonal, FL-335; Santa Cruz Biotechnology), anti-HSP27 (rabbit polyclonal, SPP-715, Stressgen), anti-HSP60 (mouse monoclonal, SPA-806, Stressgen) and anti-HSP70 (mouse monoclonal, H-5147; Stressgen) antibodies. After incubation with the appropriate secondary antibody, immunoreactive bands were detected with an enhanced chemiluminescence kit (Bio-Rad).

Gene expression

SJ-N-KP and PDE02 cells (1×10^6) were resuspended in 500 μL sol A (ribonucleic acid [RNA] extraction Kit Nurex), and total RNA was purified according to the manufacturer's instructions. Complementary DNA (cDNA) was prepared with the iScript cDNA Synthesis Kit (Bio-Rad) according to the manufacturer's instructions. Different primer pairs were used for HSP and reference gene polymerase chain reaction (PCR) amplification. Oligonucleotide sequences and annealing temperatures were obtained with the Beacon Designer Software (PREMIER Biosoft International; Table 2). The efficiency values for each set of primers ranged from 90.2 to 100%. Primers were obtained from Invitrogen. Real-time quantitative reverse transcriptase (RT)-PCR was performed with the iCycler (Bio-Rad) instrument. PCR amplification was carried out in 25 μL of reaction mixture. Two microlitres of cDNA and primers using concentrations indicated in Table 2 were added to the amplification mixture (iQ SYBR Green Supermix, Bio-Rad). DNA polymerase was pre-activated for 2 min at 94°C, and the amplification was performed by a 45-cycle PCR (94°C, 30 s, annealing temperature, as indicated in Table 2, 30 s and 72°C, 30 s). Quantification of PCR results was assessed with the $2^{\Delta\Delta Ct}$ method [17]. Ribosomal protein (S14) was used as reference gene to normalize cDNA across samples. Similar result were obtained using GAPDH and Beta2-microglobulin(β2M) (data not shown). To validate the use of the $2^{\Delta\Delta Ct}$ method, serial dilutions of LNCaP (prostatic cancer cell line) standard cDNA (Nurex) were tested. The efficiency values for each set of primers are indicated in Table 2. The range obtained confirmed that the expressions of each gene could be directly compared. All the transcripts displayed high linearity amplification plots ($r>0.98$). The specificity of the PCR results was confirmed by melt curve analysis. The significance of the differences between NB and ES in the triplicate experiments was determined with a two-tailed Student's *t* test.

Immunohistochemistry

Four 4-μm sections from the NB and ES blocks were immunostained with the iVIEW 3,3′-diaminobenzidine tetrahydrochloride (DAB) Detection Kit (Ventana Medical System) on a Benchmark automatic stainer. Standard antigen retrieval treatment and biotinylated secondary antibodies were used. Incubation was for 30 min at 37°C. Anti-HSP27 antibody was diluted at 1:800 and anti-HSP70 antibody at 1:1,600. Standard streptavidin–horseradish peroxidase conjugate treatment was applied. Immunostaining was visualized with hydrogen peroxide substrate and DAB chromogen, which is readily detected by light microscopy.

Table 2 Real-time PCR primers and conditions

Gene	Primers (nM)	$T_{(a)}$[a]	Efficiency[b]	Primers 5′–3′	PCR product[c]	$T_{(m)}$[d]
HSPA8 Ac. NM_153201	400	60	95.8	AACCGAACCACTCCAAGCTATTATCAGACTGGACAACAGCATCA	157	88.6
HSP70 Ac. NM_005346	300	60	100.5	CTTGGCCGAGAAGGACGAGTTAGTCCGCTGATGATGGGGTTAC	75	86.2
GRP75 Ac. NM_004134	200	60	108.3	CGGCGATATGATGATCCTGAAGTTGACTCGGAGAATACAATTTCCCA	119	84.8
HSP60 Ac. BC002676	200	60	99.9	TCGCTGAAGATGTTGATGGAGATTGTCACCAAACCCTGGAGC	103	85.5
HSP27 Ac. NM_001540	300	52	99.1	GCTGACGGTCAAGACCAAGGATGTAGCCATGCTCGTCCTG	78	89.5
HSPA5 Ac. NM_005347	300	58	95.4	GCTGAGGCTTATTTGGGAAAGAACTTGGCGTTGGGCATCATTAA	79	82.2
Disulphide isomerase Ac. NM_005313	200	62	99.9	TTCCTGTTGTTGCTATCAGAACTGACCTCTCCAGAGCCTTCCCA	87	84.9
β2M Ac. NM_004048	600	56	94.9	AGCAAGGACTGGTCTTTCTATCTCATGTCTCGATCCCACTTAACTATCTT	128	84.6
GAPDH Ac. BC020308	300	58	92.2	GAAGGTGAAGGTCGGAGTCATGGGTGGAATCATATTGGAA	155	86.5
S14 Ac. BC001126	200	60	95.4	AGGTGCAAGGAGCTGGGTATTCCAGGGGTCTTGGTCCTATTT	78	87.8

[a] Annealing temperature (°C)
[b] PCR efficiency expressed as percentage (%)
[c] PCR products lengths (bp)
[d] Amplicons melting temperature (°C)

Statistical analysis of immunohistochemistry results

Protein expression in patients with favourable prognosis was compared with protein expression in patients with unfavourable prognosis by testing the equality of proportions and the two-sided Fisher's exact test. Similarly, the association between MYCN amplification and prognosis was assessed through the two-sided Fisher's exact test [36]. The sensibility and specificity (with 95% confidence intervals) of HSP27 expression and MYCN non-amplification in predicting a favourable prognosis were calculated [1]. Protein expression in undifferentiated (NB-U) vs more differentiated (GNB-I, NB-D and NB-PD) tumours was compared through the two-sided Fisher's exact test [36]. Spearman's rank correlation coefficient between protein expression and both prognosis benignancy and aggressiveness of histological types (from GNB-I to NB-U) was calculated [36].

Results

2-DE gel analysis of differentially expressed proteins in NB and ES

In a first round of experiments, we performed 2-DE in NB and ES cell lines in the 4–7 pH range. We subsequently performed 2-DE separations also in the 3–10 pH range (see below). Our 2-DE protocol allowed efficient separation of proteins of molecular weights ranging between 90 and 15 kDa. We detected 810+45 resolved spots in NB cells and 784+17 resolved spots in ES cells. Figure 1 shows representative 2-DE gel images of NB (SJ-N-KP; Fig. 1a) and ES (PDE02; Fig. 1b) cell lines. Although several differences seem to be present comparing the two 2-DE images presented in Fig 1, after statistical analysis of the normalized quantities of matched spots of 2-DE maps originated from different cell preparations of three NB and three ES cell lines (see "Materials and methods"), only five proteins displayed significant differences (Table 3). Figure 1c displays an enlargement of the significantly diverging spots. It is interesting to note that we observed larger quantitative variations of protein spots in NB cells preparation than in ES cells (Table 3). We therefore speculated that variability may be related to the known tendency of NB cells to undergo spontaneous differentiation under standard culture conditions [23]; in particular, spot no. 6 (HSP27) showed the largest variability. Of note, all differentially expressed proteins were chaperones (HSP70 family, HSP60 and HSP27) or stress-related proteins. No additional significant differences between the NB and ES lines were found when 2-DE was performed at pH 3–10 (data not shown).

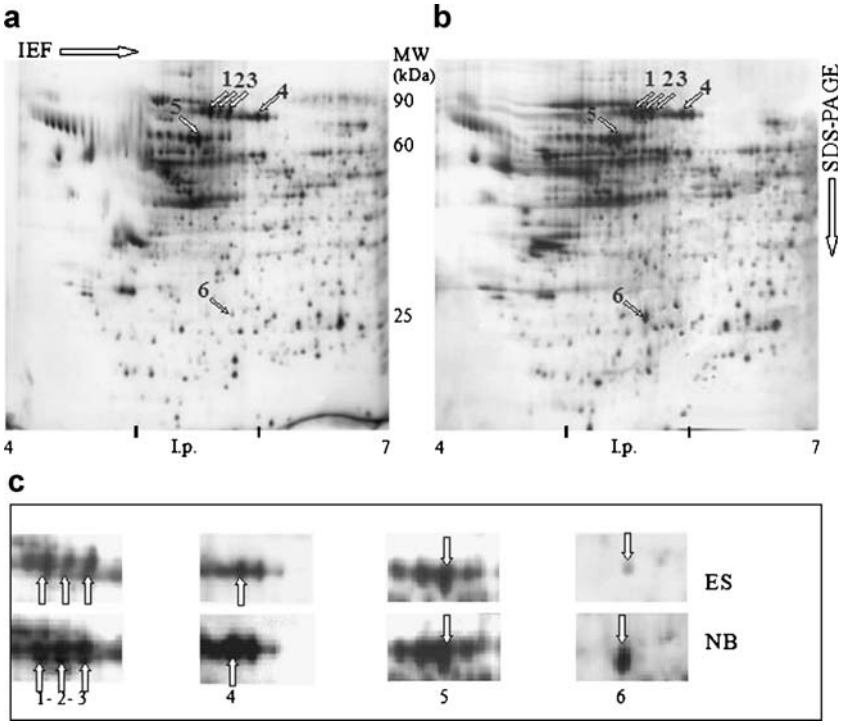


Fig. 1 2-DE analysis of NB and ES cell lines. **a**, **b** Representative silver-stained 2-DE patterns of ES cell line (PDE02) and NB cell line (SJ-N-KP). Proteins were separated using 17-cm, pH-4–7 strips followed by SDS-PAGE on 10%, 18×20-cm gels. Proteins showing apparent differential expression were identified by progressive numbers. Corresponding identifications are reported in Table 3. Among them, protein spots showing significant differential expression after the analysis of three NB and three ES cell lines are evidenced by *underline characters*. **c** Spots corresponding to significantly diverging proteins are magnified

Western blotting and quantitative gene expression analysis

In accordance to 2-DE results, NB cell lines showed higher blot intensities for HSP27 than ES cells; less marked differences were observed for HSP70, and no apparent differences were observed for HSP60 (Fig. 2a). To verify if observed HSP27 variability in 2-DE gels was due to spontaneous differentiation of NB cells under culture conditions, we treated three NB cell lines and three ES cell lines with ATRA, known to induce NB cells differentiation [4, 21, 35]. ATRA treatment caused increase of HSP27 blot intensity in all NB cell lines but not in ES cell lines (Fig. 2b), and HSP70 and HSP60 blots displayed no apparent changes both in NB and ES cells (data not shown). Anti-GAPDH Western blots were included to verify that comparable protein amounts were loaded on each lane.

Gene expression of proteins differentially expressed in NB and ES cell lines was performed by real-time RT-PCR. Figure 3a illustrates the ratio between messenger RNA levels in NB (SJ-N-KP) cells and ES (PDE02) cells. In

Table 3 Differentially expressed proteins identified by 2-DE

Spot number[a]	Protein name	Accession number[b]	ΔMr(Da)/ ΔpI[c]	Matching / no matching peptides[d] ES	Cover (%)[e]	Score[f]	Matching / no matching peptides[d] NB	Cover (%)[e]	Score[f]	Relative Abundance[g] + SD[h] NB	Relative Abundance[g] + SD[h] ES	Ratio[i]	p[l]
1	HSPA8	P11142	1,200/0.34	20/5	36.8	9.3517	29/11	46.6	9.3517	3.03±1.93	1.06±0.34	2.85	S
2–3	HSP70	P08107	1,450/0.38	10/24	18.1	9.3509	18/17	30.4	9.3509	2.59±1.78	0.58±0.19	4.46	S
4	GRP75	P38646	2,200/0.22	12/16	17.2	9.3517	7/4	14.3	9.3517	0.58±0.34	0.25±0.09	2.32	S
5	HSP60	P10809	1,750/0.11	10/6	26	9.3517	10/14	29.5	9.3517	4.33±2.15	1.63±0.78	2.66	S
6	HSP27	P04792	1,260/0.33	6/9	32.7	9.0164	7/11	40.0	9.3502	1.05±0.91	0.03±0.01	31.8	HS

[a] Spot number as reported in Fig. 1
[b] SWISS-PROT accession number
[c] Difference (Δ) of experimental Mr and p*I* compared to theoretical values
[d] Number of peptides matching with the protein sequence identified
[e] The sequence coverage expressed as percentage
[f, g] Protein level of each spot expressed as the percentage of total spot volume in the whole gel and standard deviation (SD)
[h] Protein level in NB vs ES
[i] The significance (HS=$p<0.01$; S=$p<0.05$) of the differences between NB and ES was determined with a two-tailed Student's *t* test. Values were calculated in duplicate experiments using three different NB and three different ES cell lines

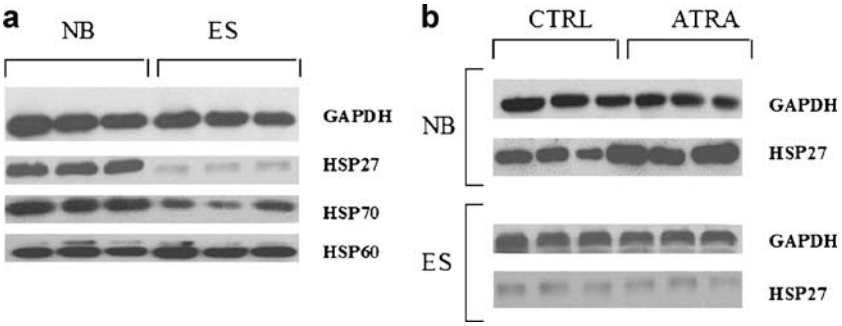


Fig. 2 Western blot analysis of HSP27 and HSP70 protein (**a**), Western blot of NB (AF8, IMR-5 and SJ-N-KP) and ES (TC106, 6647 and PDE02) cell lines stained by anti-GAPDH, anti-HSP27, anti-HSP70 and anti-HSP60 antibodies. **b** Western blot of the NB (AF8, IMR-5 and SJ-N-KP) and ES (TC106, 6647 and PDE02) cell lines after treatment by ATRA: Proteins were stained by anti-HSP27 and anti-GAPDH antibodies

agreement to protein expression data, HSP27 gene expression was markedly over expressed in NB. Furthermore, chaperones belonging to the HSP70 family (HSPA8, HSP70, GRP75) but not HSP60 showed higher gene expression levels in NB than in ES cells. Figure 3b shows that 24-h ATRA treatment caused a substantial HSP27 gene expression induction (7.62+0.9-fold increase) in NB cells; ATRA did not cause HSP27 induction in ES cells. All additionally tested HSP were not consistently over or down-regulated in NB and ES cells after ATRA treatment.

Immunohistochemistry analysis of HSP27 and HSP70 in NB and ES tissue

We focussed immunohistochemistry analysis on HSP27 and HSP70. HSP60 was not further investigated because proteomic results were not confirmed by Western blotting and gene expression analysis. All cases of ES displayed diffuse and intense HSP27 and HSP70 reactivity without characteristic staining patterns (Fig. 4a and b). On the contrary, in NB biopsies, HSP27 and HSP70 showed very

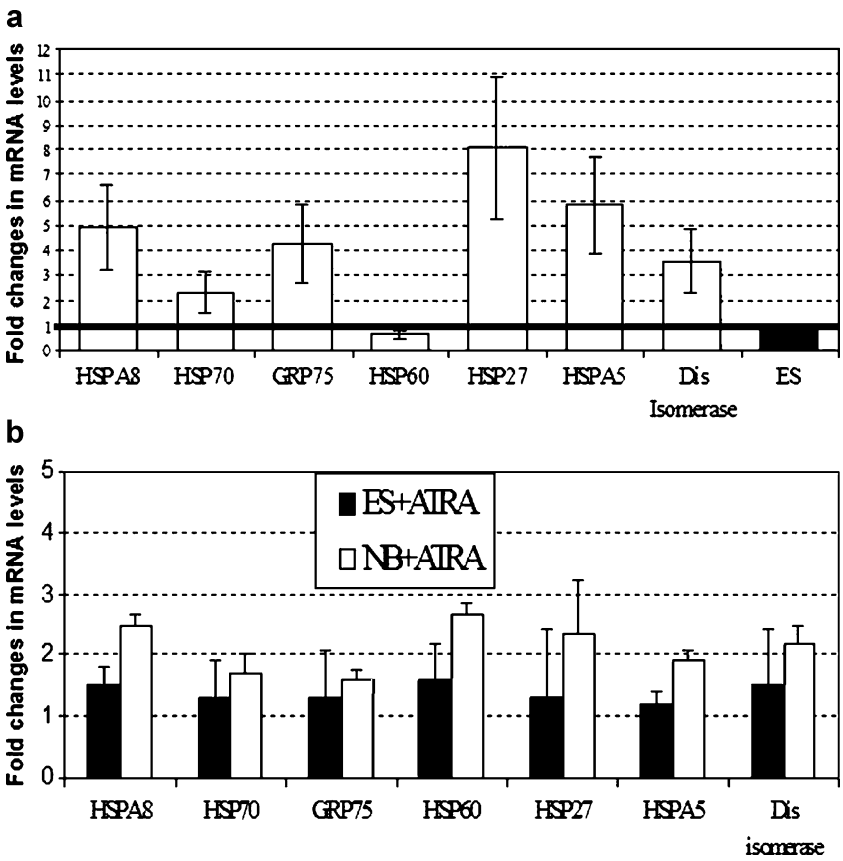


Fig. 3 Quantitative gene expression analysis of differentially expressed proteins in ES and NB cells. **a** mRNA expression levels in NB vs ES cells. The changes in NB mRNA expression were measured using real-time RT-PCR. Values are expressed as fold increase in NB vs ES cells. **b** mRNA expression levels in NB and ES cells after 10 μM ATRA treatment. Results are presented as fold increase in treated cells vs untreated controls. Data presented were normalized to S14 mRNA expression and are mean±SD of three experiments

characteristic staining patterns according to different stages of disease. Table 1 shows the results obtained on 26 NB patients. First diagnostic biopsies were from primary tumours (patients 1 to 16) or metastases (patients 17 to 26). Biopsies both from primary tumour and metastases were available in some patients (number 15, 18, 22 and 23). According to INPC classification, patients were assigned to favourable and unfavourable prognostic groups. We observed very low HSP27 expression only in 10% (1 of 10) of patients with favourable prognosis; on the opposite, 75% (12 of 16) of patients with unfavourable prognosis showed very low or absent HSP27 expression. In more differentiated tumours (GNB-I, NB-D and NB-PD), HSP27 was expressed (with the exception of patient number 11), while in undifferentiated tumours (NB-U), HSP27 was absent (P value for the two-sided Fisher's exact test=0.008). A positive and statistically significant correlation was found between HSP27 expression and favourable prognosis (Spearman ρ=0.52, P value=0.006), whereas no correlation was found between HSP70 and prognosis (Spearman ρ= 0.06, P value=0.763). HSP27 expression negatively correlated with increasing aggressiveness of histological type (Spearman ρ=−0.44, P value=0.026), whereas no correlation was found for HSP70 and histological type (Spearman ρ=0.19, P value=0.35). In GNB-N, the mature areas were positive, while the neuroblastic cells present in the undifferentiated nodule were negative (Fig. 4c; a reversal staining pattern is observed with HSP70 Fig. 4d). In 17 out of 18 NB-PD cases, the immature neuroblasts were prevalently positive, although in 11 cases, small foci of negative neuroblasts were present. In the three cases of NB-U and in their corresponding metastatic nodules, HSP27 was diffusely negative (Fig. 4e to h). It is interesting to note that in the liver biopsy of a case of NB-U, neuroblasts were

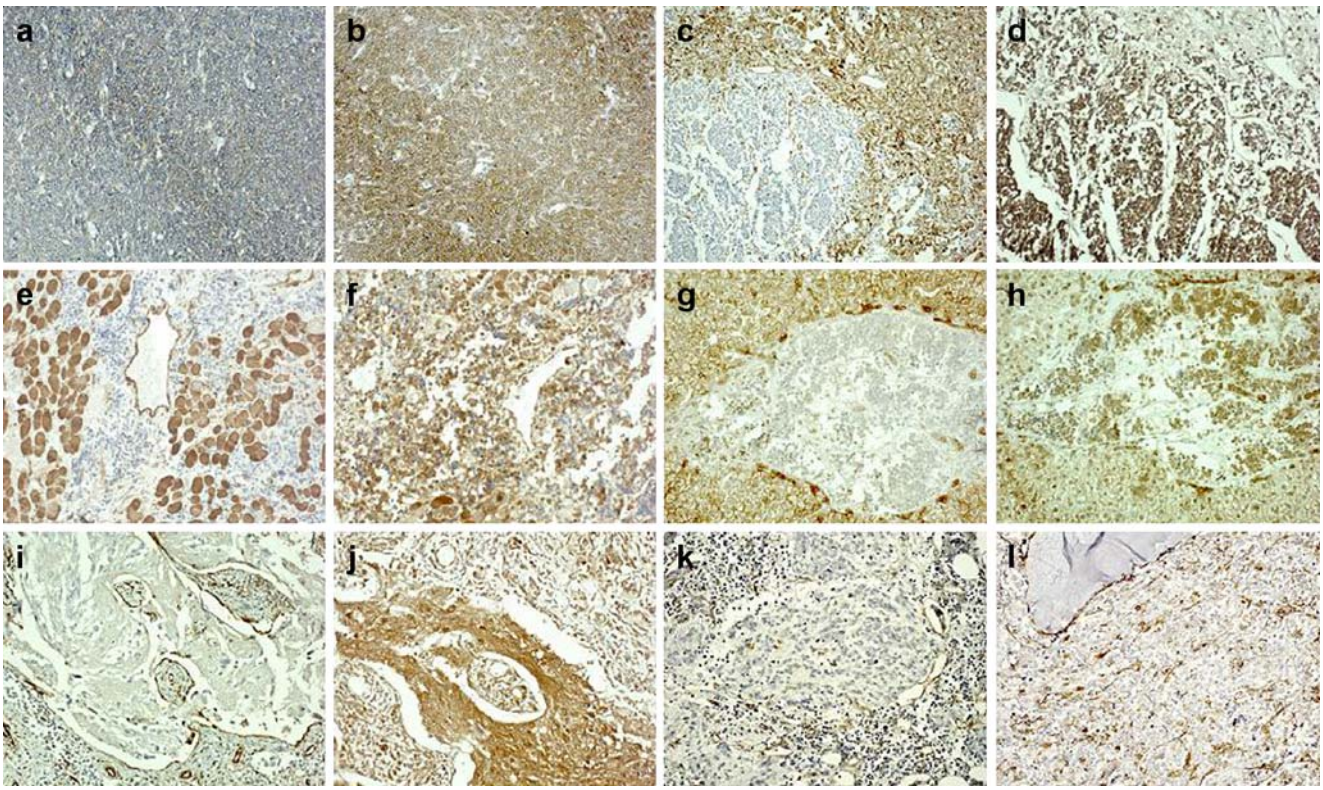


Fig. 4 HSP27 and HSP70 protein detection by peroxidase immunohistochemistry on paraffin-embedded materials in ES (**a**–**b**) and in NB (**c**–**j**). ES is diffusely positive for HSP27 with moderate positivity (**a**); a more intense decoration is seen with HSP70 (**b**). HSP expression in nodular ganglioneuroblastoma (GNB-N) (**c**, **d**). The nodule of neuroblasts in GNB-N: in **c**, the nodular undifferentiated component is negative for HSP27 while the more differentiated component at the periphery is strongly positive; in **d**, stained for HSP70, a reversal image is seen with the immature nodule intensely positive and the surrounding tumour is only weakly stained. **e**, **f** Undifferentiated NB (NB10, see Table 1) invading skeletal muscle: in **e**, the neuroblasts are negative for HSP27 and sharply contrast the positive skeletal fibers, while in **f**, neuroblasts are positive for HSP70 as are the skeletal fibers. [**g**, **h**], neuroblastoma metastatic (NB7, see Table 1) to a portal space of the liver: in **g** the neuroblasts are negative for HSP27 while in **h** are strongly positive for HSP70. Hepatocytes are differently decorated by the two HSP: in **g**, HSP27 is more expressed in the hepatocytes, whereas in **h**, HSP70 is more expressed in biliary ducts. **i**, **j** Small metastatic deposit in lymphonode (NB8, see Table 1): in **i**, the abundant neuropile is only weakly positive for HSP27; in **j**, staining for HSP70 shows intense positivity of neuroblastic cells and neuropile. **k**, **l** Progression of NB-U metastatic in bone marrow. In **k**, the neuroblasts metastatic are discrete nodules rimmed by haemopoietic cells. The occasional cells positive for HSP 27 are stromal elements. In a later marrow biopsy **l**, there is diffuse marrow infiltration by neuroblasts which are diffusely negative for HSP27. Only intermingled stromal cells are positive. Original magnifications, ×20 (**a**, **b**, **c**, **d**, **g**, **h**, **i** and **j**) ×40 (**e** and **f**)

negative, but HSP27 was positive in hepatocytes membranes and in bile ducts (Fig. 4g; in h, the staining pattern with HSP70). In the four cases (NB patients number 15, 18, 22, 23) in which tumour progression was evidenced in bone marrow biopsies, the expression of HSP27 was greatly diminished or completely negative in comparison to the primitive tumour. Case 15 is paradigmatic: The child abdominal mass was diagnosed as GNB-N (with undifferentiated histology of the nodule) at the age of 4 years. The tumour was successfully treated for almost 2 years, and the child was off therapy at the age of 7 years. At the age of 14 years, a bone marrow relapse was detected. The histology was that of NB-U. Despite aggressive therapy, the patient died of progressive disease at 20 months from relapse. Successive bone marrow biopsies of the late relapse, showing massive marrow invasion by undifferentiated NB, were analysed for HSP. In the three successive bone marrow biopsies available, no HSP27 immunoreactivity was detected (Fig. 4k and l).

By contrast with HSP27, HSP70 showed a reverse pattern of staining with the immature component more strongly decorated than the more mature areas (Fig. 4f,h and j). HSP70 was strongly positive in very immature cells without signs of differentiation and less positive in ganglion cells at the end of the maturation pathway. The metastatic spread to lymph nodes showed strongly positive HSP70 staining (Fig. 4j).

Discussion

The present work was aimed to find prognostic/diagnostic markers of NB and ES by differential proteomic analysis of NB and ES cell lines. Despite the clear chromosomal and clinical presentation distinction between both types of tumors, only five proteins came out as differentially expressed by proteomic analysis. This unexpected finding could be originated by two major factors. (1) 2-DE profiling is limited to the more expressed components of the cellular proteome, and less expressed proteins could easily escape from the analysis. Sodium dodecyl sulphate–polyacrylamide gel electrophoresis profiles followed by MS/MS analysis previously revealed that all the major protein components are shared by the two cell types [38]. (2) The number of statistically significant differences was greatly reduced by the observed variability between different cell preparations. As a matter of fact, because of their complexity and costs, proteomic studies are usually performed on a limited number of replicates. In our study, the statistical analysis was performed comparing nine different samples for each condition (three different cellular preparation for each NB or ES cell lines). To establish the analytical error, we also performed several comparisons of 2-DE results running identical samples. It is interesting to note that variability was not depending on the analytical error but on the actual variability between different cell culture preparations hampering the chances to identify significant differences.

Variability between different cell preparations was particularly marked in NB cells and HSP27 appeared to be the most variable protein. We then raised the hypothesis that HSP27 over-expression may be related to NB cells tendency to undergo spontaneous differentiation in vitro [23]. This hypothesis was supported by HSP27 response to short-term ATRA treatment of NB cells. This finding is supported by previous findings [33]. A number of additional proteins was recently found by Cimmino et al. [9] to undergo expression variations after ATRA treatment of NB cells; also in this study, large variations were observed between different cell lines, and the proteomic analysis was therefore limited to one cell line. In this last report, data do not support HSP27 variations induced by ATRA as shown by our results and data form Ungar et al. [33]; this may depend on different analytical methods or on different cell lines utilized.

To verify HSP27 relationship to NB differentiation in vivo, we collected an extensive sample of clinical cases to allow all aspects of the differentiation/maturation process from immature neuroblasts to ganglion cells to be represented on microscopic sections.

Surgical specimens were studied by immunohistochemistry to investigate the expression of HSP27 and HSP70 in vivo; this approach is of particular interest in the case of non-uniform protein expression in different areas of cancer. As a matter of fact, while variability may be theoretically present within all kinds of tumours, it is particularly relevant in NB that, in the same specimen, generally contains areas of varying degrees of maturation. The recent definition of prognosis-related criteria in the evaluation of tumour histology in the nodular ganglioneuroblastoma and the recognition of several variants in the nodular sub-type are in keeping with the importance of relating biological data to tumour morphology [20]. Immunostaining showed that HSP27 behaves as an early marker of tumour differentiation/maturation: It is completely negative in aggressive tumours in which maturation is blocked and discretely positive in the immature component of NB, which displays some tendency to mature. The positive cells in immature component in NB-PD may, in fact, reflect an early commitment to maturation. In the same clusters, no signs of cell differentiation were detectable by morphology alone. On the other hand, HSP27 expression is evident in the maturing neuroblasts, which produce abundant neuropile and show signs of maturation not strictly related to such production but to maturation itself, which is one of the important phenomena related to a favourable biological behaviour. HSP70 showed a reverse pattern of staining with the immature component more strongly decorated than the

more mature areas. In ES, immunostaining revealed diffuse expression of HSP27 and HSP70. In cutaneous ES, no difference of staining was noted even if primary cutaneous ES has a more favourable course than soft tissue or bone localizations. The distinct behaviour of HSP27 and HSP70 observed by immunostaining in NB tissue and after retinoic acid treatment of NB cells suggests that they can be independently regulated. In accordance with our results, parallel regulation of all chaperones genes was previously rendered questionable by the observation that in prostate adenocarcinoma cell lines, elevated levels of HSP transcription factor, HSF1, are associated with elevated levels of HSP27 but not HSP90 or HSP70 [14].

In conclusion, proteomic and gene expression experiments have provided fresh information about HSP expression and regulation in NB and ES cell lines; in particular, HSP27 variability and response to ATRA in NB cells suggested its relationship with cellular differentiation. HSP27 immunostaining in NB tissue revealed positive and statistically significant correlation between HSP27 expression and favourable prognosis; HSP27 expression also negatively correlated with increasing aggressiveness of histological type. In our study (26 patients), HSP27 showed similar prognostic value to MYCN expression, therefore, suggesting its use as new histological prognostic marker in NB. Larger clinical validation, although, is required to assess its practical application.

Acknowledgement We thank Paola Angelini MD—Centre of Reference—Gaslini Istitute, Genoa, Italy, and Daniele Bertin, Ospedale Infantile Regina Margherita, Turin, Italy. This study was partially supported by the "ONCOLOGY SPECIAL PROJECT" Compagnia di San Paolo/FIRMS and Regione Piemonte, Turin, Italy.

Conflict of interest statement We declare that we have no conflict of interest.

References

1. Armstrong BK, White E, Saracci R (1992) Principles exposure measurement in epidemiology. Oxford University Press, New York, pp 66–67
2. Bando Y, Katayama T, Kasai K, Taniguchi M, Tamatani M, Tohyama M (2003) GRP94 (94 kDa glucose-regulated protein) suppresses ischemic neuronal cell death against ischemia/reperfusion injury. Eur J Neurosi 18:829–40
3. Biedler JL, Roffler-Tarlov S, Shachner M, Freedman LS (1978) Multiple neurotransmitter synthesis by human neuroblastoma cell lines and clones. Cancer Res 38:3751–3757
4. Biedler JL, Spengler BA, Chang TD, Ross RA (1988) Transdifferentiation of human neuroblastoma cells results in coordinate loss of neuronal and malignant properties. Prog Clin Biol Res 271:265–276
5. Brodeur GM, Maris JM (2002) Neuroblastoma. In: Pizzo PA, Poplack DG (eds) Principles and practice of pediatric oncology. Lippincott Williams & Wilkins, Philadhelphia, pp 895–937
6. Bruey JM, Ducasse C, Bonniaud P, Ravagnan L, Susin SA, Diaz-Latoud C, Gurbuxani S, Arrigo AP, Kroemer G, Solary E, Garrido C (2000) Hsp27 negatively regulates cell death by interacting with cytochrome c. Nat Cell Biol 2:645–652
7. Carta F, Demuro PP, Zanini C, Santona A, Castiglia D, D'Atri S, Ascierto PA, Napoletano M, Cossu A, Tavolini B, Turrini F, Manca A, Sini MC Palmieri G, Rozzo AC (2005) Analysis of candidate genes through a proteomics-based approach in primary cell lines from malignant melanomas and their metastases. Melanoma Res 15:235–244
8. Charette SJ, Lavoie JN, Lambert H, Landry J (2000) Inhibition of Daxx-mediated apoptosis by heat shock protein 27. Mol Cell Biol 20:7602–7612
9. Cimmino F, Spano D, Capasso M, Zambrano N, Russo R, Zollo M, Iascolan A (2007) Comparative proteomic expression profile in all-trans retinoic acid differentiated neuroblastoma cell line. J Proteome Res 6:2550–2564
10. Ginsberg JP, Woo SY, Johnson ME, Hicks MJ, Horowitz ME (2002) Ewing's sarcoma family of tumors: Ewing's sarcoma of bone and soft tissue and the peripheral primitive neuroectodermal tumors. In: Pizzo PA, Poplack DG (eds) Principles and practice of pediatric oncology. Lippincott Williams & Wilkins, Philadhelphia, pp 937–1016
11. Giribaldi G, Ulliers D, Mannu F, Arese P, Turrini F (2001) Growth of *Plasmodium falciparum* induces stage-dependent haemichrome formation, oxidative aggregation of band 3, membrane deposition of complement and antibodies, and phagocytosis of parasitized erythrocytes. Br J Haematol 13:492–499
12. Harris MN, Ozpolat B, Abdi F, Gu S, Legler A, Mawuenyega KG, Tirado-Gomez M, Lopez-Berestein G, Chen X (2004) Comparative proteomic analysis of all-trans-retinoic acid treatment reveals systematic posttranscriptional control mechanisms in acute promyelocytic leukemia. Blood 104:1314–1323
13. Hasegawa SL, Davison JM, Rutten A, Fletcher JA, Fletcher CD (1998) Primary cutaneous Ewing's sarcoma: immunophenotypic and molecular cytogenetic evaluation of five cases. Am J Surg Pathol 22:310–8
14. Hoang AT, Huang J, Rudra-Ganguly N, Zheng J, Powell WC, Rabindran SK, Wu C, Roy-Burman P (2000) A novel association between the human heat shock transcription factor 1 (HSF1) and prostate adenocarcinoma. Am J Pathol 156:857–864
15. Ishiguro Y, Kato K, Akatsuka H, Iwata H, Nagaya M (1997) Chemotherapy-induced expression of alpha B-crystallin in neuroblastoma. Med Pediatr Oncol 29:11–5
16. Jolly C, Morimoto RI (2000) Role of the heat shock response and molecular chaperones in oncogenesis and cell death. J Natl Cancer Inst 92:1564–1572
17. Livak KJ, Schmittgen TD (2001) Analysis of relative gene expression data using real-time quantitative PCR and the 2(-Delta Delta C(T)) Method. Methods 25:402–408
18. Miyazaki T, Kato H, Faried A, Sohda M, Nakajima M, Fukai Y, Masuda R, Fukuchi M, Ojima H, Tsukada K, Kuwano H (2005) Predictors of response to chemo-radiotherapy and radiotherapy for esophageal squamous cell carcinoma. Anticancer Res 25:2749–2755
19. Oakley BR, Kirsch DR, Morris NR (1980) A simplified ultrasensitive silver stain for detecting proteins in polyacrylamide gels. Anal Biochem 105:361–363
20. Peuchmaur M, d'Amore SG, Joshi VV, Hata J, Roald B, Dehner LP, Gerbing RB, Stram DO, Lukens JN, Matthay KK, Shimada H (2003) Revision of the International Neuroblastoma Pathology Classification: confirmation of favorable and unfavorable prognostic subsets in ganglioneuroblastoma, nodular. Cancer 98: 2274–2281
21. Ponthan F, Borgstrom P, Hassan M, Wassberg E, Redfem CP, Kogner P (2001) The vitamin A analogues: 13-cis retinoic acid, 9-cis retinoic

acid, and Ro 13-6307 inhibit neuroblastoma tumour growth in vivo. Med Pediatr Oncol 36:127–131
22. Rane MJ, Pan Y, Singh S, Powell DW, Wu R, Cummins T, Chen Q, McLeish KR, Klein JB (2003) Heat shock protein 27 controls apoptosis by regulating Akt activation. J Biol Chem 278:27828–27835
23. Rettig WJ, Splenger BA, Chesa PG, Old LJ, Biedler JL (1987) Coordinate changes in neuronal phenotype and surface antigen expression in human neuroblastoma cell variants. Cancer Res 47: 1383–1389
24. Rocchi P, Ferreri AM, Simone G, Prodi G (1987) Epirubicin-induced differentiation of human neuroblastoma cells in vitro. Anticancer Res 7:247–250
25. Sarto C, Valsecchi C, Magni F, Tremolada L, Arizzi C, Cordani N, Cesellato S, Doro G, Favoni P, Perego RA, Raimondo F, Ferrero S, Mocarelli P, Galli-Kienle M (2004) Expression of heat shock protein 27 in human renal cell carcinoma. Proteomics 4:2252–2260
26. Schlesinger HR, Gerson JM, Moorhead PS, Maguire H, Hummeler K (1976) Establishment and characterization of human neuroblastoma cell lines. Cancer Res 36:3094–3100
27. Schwab M, Shimada H, Joshi V, Brodeur GM (2000) Neuroblastic tumours of adrenal gland and sympathetic nervous system. In: Kleihues P, Canavee WK (eds) Pathology and genetics of tumours of the nervous system. IARC, Lyon, pp 153–161
28. SIOP (2004) Europe Neuroblastoma AIEOP LNESG2 Study: guidelines for the treatment of patients with localized resectable neuroblastoma and analysis of prognostic factors. Ist. G. Gaslini
29. Thanner F, Sutterlin MW, Kapp M, Rieger L, Morr AK, Kristen P, Dietl J, Gassel AM, Muller T (2005) Heat shock protein 27 is associated with decreased survival in node-negative breast cancer patients. Anticancer Res 25:1649–1653
30. Thiele CJ, McKeon C, Triche TJ, Ross RA Reynolds CP, Israel MA (1987) Differential protooncogene expression characterizes histopathologically indistinguishable tumors of the peripheral nervous system. J Clin Invest 80:804–811
31. Thomas X, Campos L, Mounier C, Cornillon J, Flandrin P, Le QH, Piselli S, Guyotat D (2005) Expression of heat-shock proteins is associated with major adverse prognostic factors in acute myeloid leukemia. Leuk Res 29:1049–1058
32. Triche T, Askin FB, Kissane JM (1986) Neuroblastoma, Ewing Sarcoma and the differential diagnosis of small- round- blue-cell tumor. In: Finegold M (ed) Pathology of neoplasia in children and adolescents. Sauders, Philadelphia, pp 145–195
33. Ungar DR, Hailat N Strahler JR, Kuick RD, Brodeur GM, Seeger RC, Reynolds CP, Hanash SM (1994) Hsp27 expression in neuroblastoma: correlation with disease stage. J Nat Can Inst 86:780–4
34. Ushigome S, Machinami R, Soresens PH (2002) Ewing sarcoma/primitive neuroectodermal tumour (PNET). In: Fletcher CDM, Unni KK, Mertens F (eds) Pathology and genetics of tumours of soft tissue and bone. IARC, Lyon, pp 298–300
35. Voight A, Zintl F (2003) Effects of retinoic acid on proliferation, apoptosis, cytotoxicity, migration, and invasion of neuroblastoma cells. Med Pediatr Oncol 40:205–213
36. Woolson RF, Clarke WR (2002) Statistical methods for the analysis of biomedical data, 2nd edn. Wiley, New York, pp 226–232, 286–288
37. Yenari MA (2002) Heat shock proteins and neuroprotection. Adv Exp Med Biol 513:281–289
38. Zanini C, Giribaldi G, Mandili G, Carta F, Crescenzio N, Bisaro B, Doria A, Foglia L, di Montezemolo LC, Timeus F, Turrini F (2007) Inhibition of heat shock proteins (HSP) expression by quercetin and differential doxorubicin sensitization in neuroblastoma and Ewing's sarcoma cell lines. J Neurochem 103:1344–1354

Virchows Arch (2008) 452:169–174
DOI 10.1007/s00428-007-0525-1

ORIGINAL ARTICLE

Mucosal colonization of gastric endocrine tumors mimicking mixed neoplasms

Tu Vinh Luong · Emanuela Pilozzi · Italo Bearzi · Cesare Bordi

Received: 29 August 2007 / Revised: 27 September 2007 / Accepted: 4 October 2007 / Published online: 14 December 2007
© Springer-Verlag 2007

Abstract Two cases of gastric tumors showing mixed composition of endocrine cell clusters and exocrine glands and originally diagnosed as mixed neoplasms are described. In both cases, the exocrine glandular component was restricted to the upper third of the neoplasms being consistently absent in areas of muscular wall invasion and, in case 2, in nodal metastases. These glands were in close anatomical contiguity with the glands of the overlying gastric mucosa or, in case 1, apparently derived from deep pouch-like invaginations of the mucosa. They showed either lack of dysplasia (case 1) or mild dysplasia (case 2) with a Ki67 proliferation index consistently lower than that of the intramucosal glands. The intratumoral glands presented intestinal metaplastic features confirmed by intense Cdx2 immunostaining that, conversely, was absent in the endocrine component of the tumors. The latter showed intense vesicular monoamine transporter 2 immunoreactivity consistent with its origin from the enterochromaffin-like cells of the gastric oxyntic mucosa. On the basis of these findings, it is proposed that the exocrine glands do not represent a true neoplastic component of the tumors. Although mucosal entrapment by the tumor cannot be ruled out, they more likely reflect a hitherto unrecognized mechanism of mucosal colonization of gastric endocrine tumors.

Keywords Endocrine gastric tumors · Intestinal metaplasia · Mixed tumors

T. V. Luong · C. Bordi (✉)
Department of Pathology and Laboratory Medicine,
Section of Anatomic Pathology, University of Parma,
14 via Gramsci.,
43100 Parma, Italy
e-mail: cesare.bordi@unipr.it

E. Pilozzi
Department of Experimental Medicine and Human Pathology,
Section of Immunopathology,
La Sapienza University 2nd School of Medicine,
Rome, Italy

I. Bearzi
Department of Pathology, School of Medicine,
The Polytechnic University of the Marche Region,
Ancona, Italy

Introduction

The occurrence of tumors with mixed endocrine and exocrine components in the gastrointestinal tract is well recognized. The association of the two components can vary in a spectrum ranging from nonendocrine neoplasms—either adenomas or carcinomas—with interspersed neuroendocrine cells to truly composite tumors showing an intimate mixture of endocrine and exocrine tumor aggregates and to collision tumors in which the carcinoid and the adenoma/adenocarcinoma are closely juxtaposed but not admixed [10]. Tumors can be classified as truly mixed only if both components are present in significant proportions, comprising at least one third of the whole tumor mass [9].

It is generally assumed that in mixed tumors, both components are of neoplastic origin. We describe herein two cases of gastric tumors received in consultation with the diagnosis of mixed tumors in which evidence was presented for a non-neoplastic nature of the exocrine component likely reflecting colonization of the endocrine tumor by extensions of the overlying gastric mucosa.

Case reports

Clinical findings

Case 1 A 76-year-old man, with proven hepatitis C virus infection, underwent surgery for hepatocarcinoma. Preoperative investigations included gastric endoscopy, which showed the convergence of the folds but no tumor evidence even after collection of gastric biopsies. At surgery, an unexpected gastric mass measuring 1.8 cm in major axis was found at the junction between the corpus and the fundus and was removed together with wide margins of unaffected gastric wall. Six month later, during surgery for removal of a recurrent hepatocarcinoma mass, the stomach was found to be unremarkable. Pre- and postoperative serum gastrin levels proved to be within the normal values.

Case 2 A 55-year-old man complaining of hematemesis was diagnosed as having a gastric polyp by endoscopic examination. Preoperative laboratory data showed hypergastrinemia (1,110 pg/ml, normal<40), high titer of circulating *Helicobacter pylori* antibodies (36 U/ml, normal<9), and lack of parietal cell antibodies. Subtotal gastrectomy was performed, and on the basis of the tumor findings, a total gastrectomy was eventually performed.

Materials and methods

In both cases, representative samples of gastric tumors and of extratumoral gastric mucosa were obtained from surgical specimens. After formalin fixation and paraffin embedding, 4-μm-thick sections were stained with hematoxylin and eosin, and an immunohistochemical procedure for chromogranin A (CgA; Neomarker, California, USA; dilution 1:2,000), vesicular monoamine transporters 2 (Chemicon, California, USA; dilution 1:1000), Cdx2 (Novocastra, Newcaslte, UK; dilution 1:300), somatostatin receptor subtype 2 (Biotrend, Koln, Germany; dilution 1:2,000), and Ki67 (MIB1, Dako, Copenhagen, Denmark; dilution 1:100) was performed using the polymer system (Advanced HRP, Dako) in accordance with the manufacturer's specifications.

Results

Case 1 On histological examination, the mucosal surface of the tumor showed deep, irregular pouches covered by either foveolar or intestinal metaplastic epithelium, a pattern reminiscent of ulcer re-epithelization (Fig. 1a). Such epithelial extensions deeply penetrated a thickened muscularis mucosae and the upper third of the underlying tumor where they ramified into smaller glands intimately admixed with the cell clusters of the endocrine tumor (Fig. 1b). These glands were mostly lined by intestinalized epithelium and consistently devoid of any cytological or architectural atypia (Fig. 1c). The remaining tumor showed a well-defined organoid pattern mostly with a solid trabecular arrangement and appeared to extensively infiltrate through the muscularis propria up to the subserosa. Nonendocrine glands were consistently absent in the lower two thirds of the tumor including the tumor front invading the muscular wall (Fig. 1b). The tumor cells were characterized by relatively abundant cytoplasm and fairly large vesicular nuclei with occasional prominent eosinophilic nucleoli or by smaller, hyperchromatic nuclei with irregular chromatin clumps and small nucleoli. Necrosis was absent, and mitoses were virtually absent. It is interesting to note that in spite of their diffuse distribution in the tumor-associated exocrine epithelium, intestinal metaplastic changes were consistently absent in the remaining oxyntic mucosa, which did not present significant pathological lesions. On immunohistochemical analysis, the endocrine tumor cells strongly expressed CgA (Fig. 1d) and VMAT-2 and presented membranous staining for somatostatin receptor subtype 2. The Ki67 proliferation index was below 1%. Nuclear immunostaining for Cdx2 was selectively restricted to the intermixed intestinalized glands (Fig. 1e). In several instances, linear collections of cells sharing the same immunophenotype of tumor endocrine cells were seen at the base of the epithelium of these glands, being in intimate anatomical relation with the surrounding endocrine cell clusters (Fig. 1d). No enterochromaffin-like (ECL) cell-proliferating changes was detected by appropriate immunostaining in the extratumoral mucosa.

Case 2 In the surgical specimen of partial proximal gastrectomy, a raised and circumscribed lesion measuring 1.8 cm in diameter was observed. Histologically, the tumor extended from the basal part of the mucosa to the submucosa and extensively infiltrated the muscularis propria. Its surface was covered by gastric mucosa with extensive intestinal metaplasia. Hypertrophy of the underlying muscularis mucosae resulted in ramifying bundles of smooth muscle cells extending to both the mucosal lamina propria and the submucosa. Gland-like structures indistinguishable from the metaplastic mucosal glands were diffusely interspersed among the tumor clusters in the region of submucosal invasion (Fig. 2a) but were consistently absent in the areas of muscular wall infiltration (Fig. 2b). These exocrine glands shared with the intestinalized glands of the gastric mucosa a mild degree of cytological atypia. They were intimately admixed with well-differentiated endocrine tumor aggregates that showed an organoid, solid trabecular

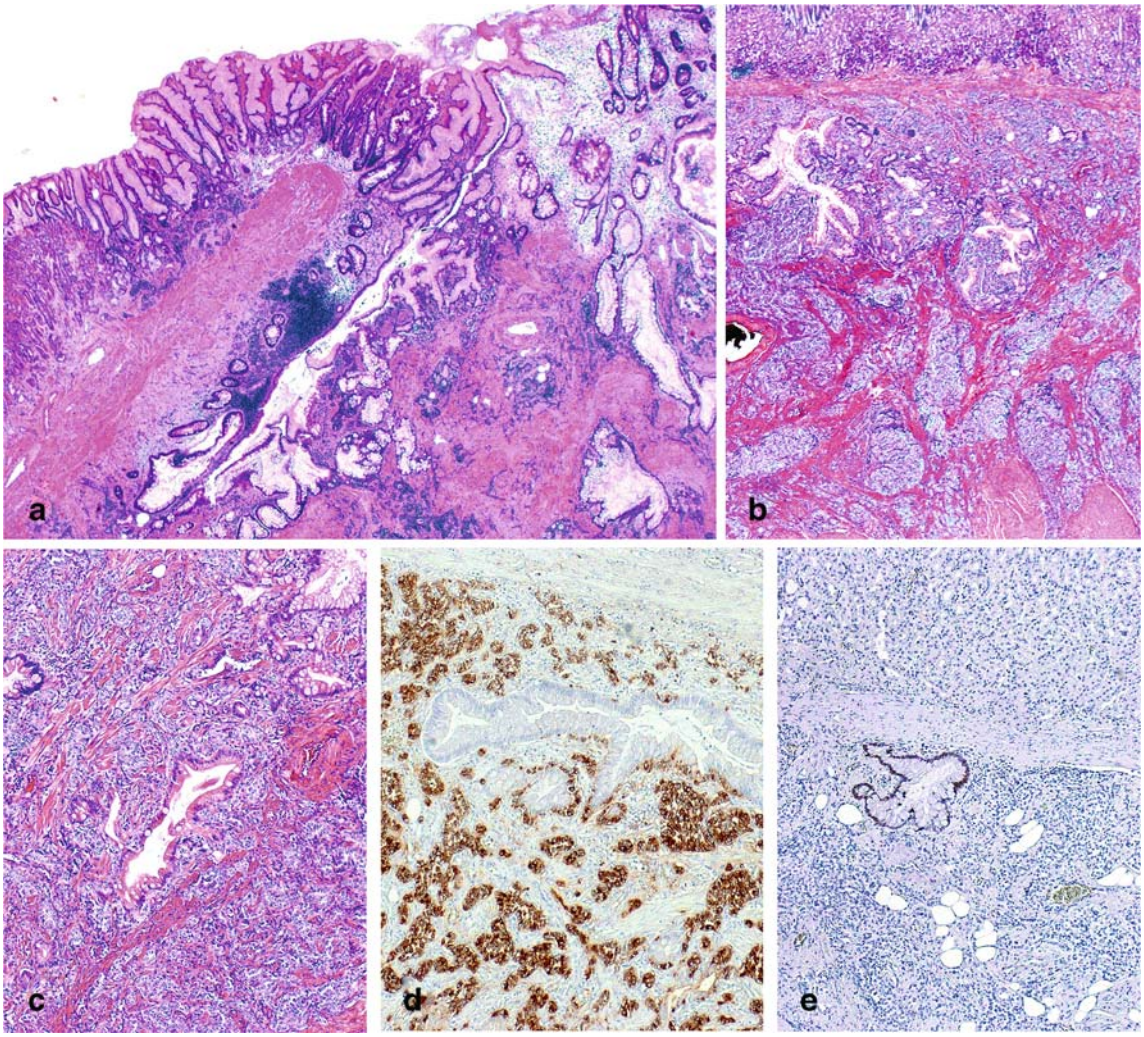


Fig. 1 Case 1. **a** Low-power view showing deep pouch-like extensions of the mucosa extending downward into the underlying tumor. Note the hypertrophy of the muscularis mucosae and the nonatrophic oxyntic mucosa. **b** Branching gland-like structures mixed with clusters of endocrine tumor in the submucosal area but not in the deep tumor regions infiltrating the muscular wall. **c** Glands lined by metaplastic intestinal epithelium intermixed with solid tumor cell clusters and smooth muscle cell bundles derived from the muscularis mucosae. **d** Heavy, selective expression of chromogranin A by endocrine tumor cells with rows of immunoreactive cells along the basal side of the unreactive intestinal type epithelium. **e** Nuclear labeling of the nonendocrine glands for the intestinal marker Cdx2 with no staining in endocrine tumors cells and in the overlying nonatrophic oxyntic mucosa

pattern and represented the only tumor component infiltrating the muscularis propria. Endocrine tumor cells showed relatively abundant cytoplasm and fairly regular vesicular nuclei with well-represented nucleoli. Neither mitoses nor tumor necrosis was seen. Lymphatic and perineural invasion were present. The extratumoral oxyntic mucosa was characterized by multifocal atrophic gastritis with frequent, extensive foci of intestinal metaplasia interspersed among areas featuring well-preserved oxyntic glands. Moreover, an additional carcinoid tumor with entirely intramucosal extension was found. By immunohistochemistry, endocrine tumor cells heavily expressed CgA and VMAT-2 (Fig. 2c), with a low Ki67 proliferation index (<1%) and a consistently absent immunoreactivity for Cdx2 (Fig. 2d). In contrast, the exocrine glands admixed with the carcinoid cell clusters showed strong Cdx2 labeling (Fig. 2d) while exhibiting a negligible Ki67 proliferation rate clearly lower than that of the above non-neoplastic mucosal glands. Accumulations of endocrine cells were present in the basal side of the gland epithelium often extending into the neighboring endocrine cell tumor aggregates (Fig. 2c). In the extratumoral oxyntic mucosa, extensive proliferative changes of ECL endocrine cells with linear and micronodular changes were disclosed by CgA immunostaining.

Three local lymph nodes removed at the time of total gastrectomy proved to be involved by metastatic tumor tissue exclusively showing endocrine features.

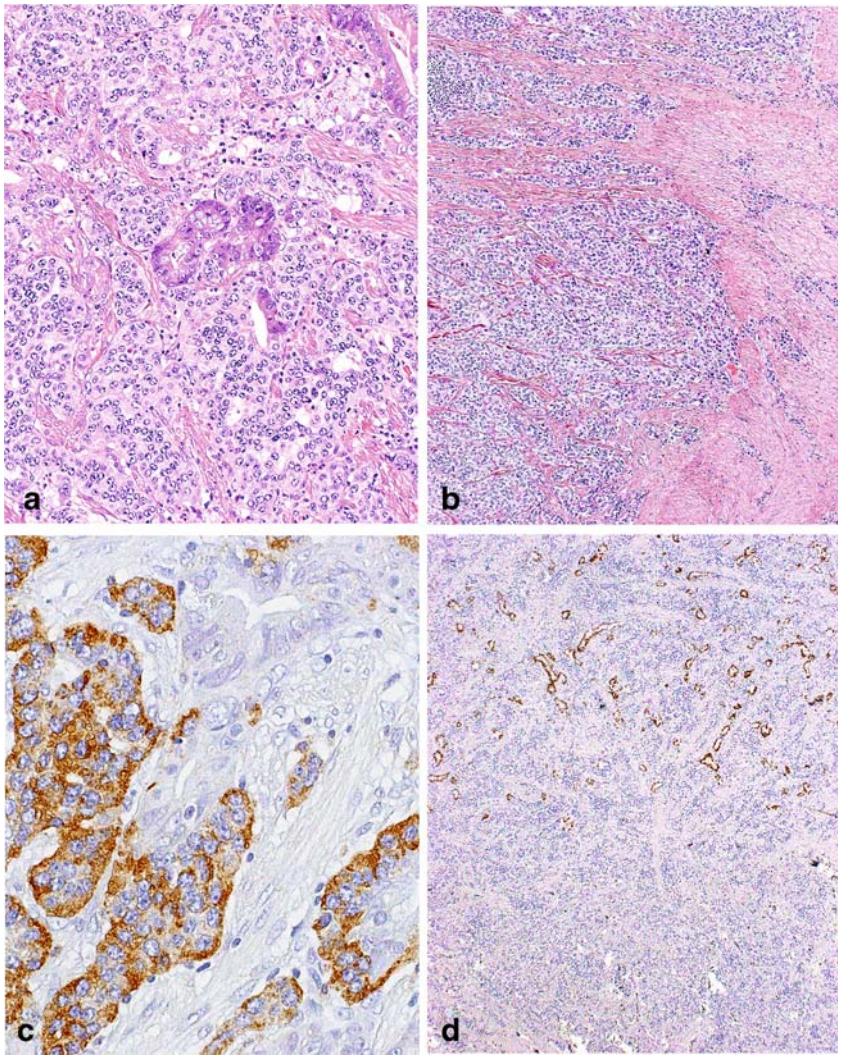


Fig. 2 Case 2. **a** Hyperchromic nonendocrine glands mixed with solid clusters of well-differentiated endocrine tumors. **b** Absence of exocrine glands in the tumor regions infiltrating the muscularis propria. **c** VMAT-2 immunostaining of endocrine neoplastic clusters that are in close contact with the unreactive intestinal-type epithelium and sometimes extend into the basal epithelial layer. **d** Cdx2 immunoreactivity restricted to the nonendocrine component of the tumor and highlighting the clear cut upper zonation of intestinalized glands

Discussion

We describe here two cases of gastric tumors with apparent mixed endocrine–exocrine composition in which topographical, cytological, and immunohistochemical features supported a nontumoral origin of the exocrine component and suggested a previously unrecognized mechanism of downward displacement of gastric mucosa within gastric endocrine tumors. The origin of the exocrine component of the tumor from the covering non-neoplastic mucosa was readily appreciated in case 1 showing close anatomical relation of the intratumoral exocrine glands with deep pouch-like extensions of the mucosa, coupled with the lack of dysplasia in these metaplastic, intestinalized, and Cdx2-expressing glands. In case 2, in spite of the lack of deep mucosal invaginations and occurrence of mild cell atypia, the absence of frank dysplasia and the negligible Ki67-labeling index clearly lower than that of overlying metaplastic mucosa glands also were against a neoplastic nature of the Cdx2-expressing glands intermingled with the endocrine tumor aggregates. In keeping with this suggestion was in both cases the clear-cut topographical restriction of the exocrine glands to the upper third of the tumors together with their absence in tumor areas of the muscular wall invasion as well as in nodal metastases of case 2.

On the basis of our findings, we propose that the occurrence of exocrine glands lacking frank atypia and segregated in the upper, nonmuscular invading regions of gastric endocrine tumors does not reflect mixed neoplasms. Although a process of mucosal entrapment by the tumor as proposed for exocrine ductules associated with pancreatic endocrine tumors [18] cannot be ruled out, we favor a still unrecognized ability of gastric endocrine tumors to be colonized by the non-neoplastic overlying mucosa for several reasons: First, anatomical contiguity of intratumoral glands with deep pouch-like invaginations of the mucosa was clearly observed in case 1, and second, the intratumoral glands were also found at the submucosal level where they

are not present under normal conditions. The frequency of this phenomenon requires to be evaluated in additional cases. In this regard, a previous case from our laboratory, originally interpreted as a composite tumor [4], has been found on re-examination to largely fit the criteria indicated above, suggesting that the present findings may be more common than previously realized.

In both cases, the endocrine component of the tumors appeared to be well differentiated deserving the designation of well-differentiated endocrine carcinoma according to the World Health Organization classification [16] on the basis of tumor infiltration beyond the submucosa and, in case 2, of lymph node metastases. The practical diagnostic importance of distinguishing a pure well-differentiated endocrine carcinoma from a malignant mixed endocrine–exocrine tumor resides in the fact that the prognosis of the latter does not differ from that pure gastric adenocarcinomas [3].

The immunohistochemical characteristics of tumor cells and in particular the strong expression of VMAT-2 coupled with the absent labeling for the intestinal marker Cdx2 were consistent with those of ECL cells of the oxyntic mucosa of the stomach [14]. On the basis of the Rindi's classification of gastric carcinoids [13], the endocrine tumor of case 2 was fully consistent with the type I ECL cell carcinoid, in view of its multiplicity and its association with chronic atrophic gastritis of the oxyntic mucosa, hypergastrinemia, and with the background of diffuse ECL cell precursor lesions in the extratumoral mucosa, a hallmark of hypergastrinemia [2]. The malignant behavior of the tumor, documented by the deep infiltration of the muscular wall and nodal metastases, however, is unusual for this tumor type [13, 16]. In contrast, the characteristics of the tumor in case 1, with the absence of pathological changes in the extratumoral mucosa including ECL cell proliferation but with the peculiar exception of the intestinal metaplastic changes in intratumoral glands (discussed below), were consistent with those of the sporadic, type III ECL cell carcinoid.

Hypertrophy of the muscularis mucosae associated with the tumors was present in both cases. This is a well-recognized feature of gastric ECL cell endocrine tumors that has been regarded to reflect a field effect of growth factor(s), possibly basic fibroblast growth factor, produced by tumor cells [1]. Such association with a hypertrophied muscularis mucosae and the distribution circumscribed to the submucosal area make the present phenomenon of downward mucosal gland displacement very similar to that occurring in gastritis cystica profunda [6].

The intratumoral exocrine glands showed in both cases morphological features of metaplastic intestinalization confirmed by the strong immunoreactivity with the intestinal marker Cdx2. In case 2, this finding could be explained in view of the extensive metaplastic changes related to multifocal atrophic gastritis of the mucosa from which the tumor originated. Such event could not be documented in case 1 where the extratumoral mucosa was histologically normal and intestinal metaplasia was selectively restricted to the exocrine glands associated with the tumor. In this case, it is tempting to speculate that the intestinal differentiation of the exocrine glands was driven by factors released by endocrine tumor cells. Alternatively, it may depend on changes in the microenvironment as supported by recent studies on the role of environmental influences on Cdx2 expression within the upper gastrointestinal tract [11, 12, 15]. Normal acidic conditions were found to suppress gastric Cdx2 expression, whereas hypoacidity may induce upregulation of Cdx2 leading to intestinal metaplasia [5]. Indeed, the pouches seen in case 1 and created by the gastric epithelium invaginating within the submucosal tumor may have modified the microenvironment in the sense of increased luminal pH leading to subsequent aberrant expression of Cdx2 and local intestinal differentiation in the absence of extratumoral intestinal metaplasia.

Finally, the intimate relationship observed in both cases between the endocrine tumor cells and the interspersed exocrine glands is intriguing. Indeed, in the basal side of their epithelium, the latter often presented accumulations of endocrine cells sharing identical cytological and immunophenotypic characteristics of and displaying direct extension to the neighboring neoplastic endocrine cell clusters. Whether such intraglandular endocrine cells reflect precursor lesions for the extraglandular tumor development, a well-recognized feature of gastrin-depending types I and II gastric carcinoids but not of sporadic type III tumors [2], is contradicted by the immunohistochemical results. Cdx2 immunoreactivity, an intestinal phenotypic marker not only for exocrine cells but also for carcinoids of intestinal origin [7, 8], was diffusely expressed by exocrine glands but absent in endocrine cells in both our cases. Furthermore, tumoral and intraglandular endocrine cells were heavily immunoreactive for VMAT-2, a marker typical for ECL cell tumors of gastric origin but absent in intestinal enterochromaffin cell neoplasms [17]. Infiltration of the intestinal-type exocrine glands by the adjacent endocrine tumor cells of gastric type may, therefore, represent a more plausible explanation for the finding observed.

In conclusion, this report present two cases of low-grade malignant endocrine tumor of the stomach in which colonization of the overlying mucosa led to an inadequate diagnosis of a mixed tumor. Immunohistochemistry reveals the gastric type of the cells of the endocrine tumors and the intestinal type of the colonizing glands suggesting infiltration of the latter by endocrine tumor cells.

Acknowledgment This study was supported by grant no. 20050-69205_001 from the Italian Ministry of Education, University and Research.

References

1. Bordi C, Caruana P, D'Adda T, Azzoni C (1995) Smooth muscle cell abnormalities associated with gastric ECL cell carcinoids. Endocr Pathol 6:103–113
2. Bordi C, D'Adda T, Azzoni C, Pilato P, Caruana P (1995) Hypergastrinemia and gastric enterochromaffin-like cells. Am J Surg Pathol 19(Suppl 1):S8–S19
3. Capella C, La Rosa S, Uccella S, Billo P, Cornaggia M (2000) Mixed endocrine–exocrine tumors of the gastrointestinal tract. Semin Diagn Pathol 17:91–103
4. Caruso ML, Pilato FP, D'Adda T, Baggi MT, Pucci L, Valentini AM, Lacatena M, Bordi C (1989) Composite carcinoid–adenocarcinoma of the stomach associated with multiple gastric carcinoids and non-antral gastric atrophy. Cancer 64:1534–1539
5. Faller G, Kirchner T (2005) Immunological and morphogenic basis of gastric mucosa atrophy and metaplasia. Virchows Arch 446:1–9
6. Franzin G, Novelli P (1981) Gastritis cystica profunda. Histopathology 5:535–547
7. Jaffee IM, Rahmani M, Singhal MG, Younes M (2006) Expression of the intestinal transcription factor CDX2 in carcinoid tumors is a marker of midgut origin. Arch Pathol Lab Med 130: 1522–1526
8. La Rosa S, Rigoli E, Uccella S, Chiaravalli AM, Capella C (2004) CDX2 as a marker of intestinal EC-cells and related well-differentiated endocrine tumors. Virchows Arch 445:248–254
9. Lewin K (1987) Carcinoid tumors and the mixed (composite) glandular–endocrine cell carcinomas. Am J Surg Pathol 11(Suppl 1): 71–86
10. Lewin KJ, Appelman HD (1996) Tumors of the esophagus and stomach. In: Rosai J, Sobin LH (eds) Atlas of tumor pathology, 3rd series, Fasc. 18. Armed Forces Institute of Pathology, Washington, DC, pp 351–352
11. Marchetti M, Caliot E, Pringault E (2003) Chronic acid exposure leads to activation of the cdx2 intestinal homeobox gene in a long-term culture of mouse esophageal keratinocytes. J Cell Sci 116: 1429–1436
12. Phillips RW, Frierson HF Jr, Moskaluk CA (2003) Cdx2 as a marker of epithelial intestinal differentiation in the esophagus. Am J Surg Pathol 27:1442–1447
13. Rindi G, Luinetti O, Cornaggia M, Capella C, Solcia E (1993) Three subtypes of gastric argyrophil carcinoid and the gastric neuroendocrine carcinoma: a clinicopathologic study. Gastroenterology 104:994–1006
14. Rindi G, Paolotti D, Fiocca R, Wiedenmann B, Henry JP, Solcia E (2000) Vesicular monoamine transporter 2 as a marker of gastric enterochromaffin-like cell tumors. Virchows Arch 436:217–223
15. Silberg DG, Sullivan J, Kang E, Swain GP, Moffett J, Sund NJ, Sackett SD, Kaestner KH (2002) Cdx2 ectopic expression induces gastric intestinal metaplasia in transgenic mice. Gastroenterology 122:689–696
16. Solcia E, Capella C, Klöppel G, Heitz PU, Sobin LH, Rosai J (2000) Endocrine tumours of the gastrointestinal tract. In: Solcia E, Klöppel G, Sobin LH (eds) Histological typing of endocrine tumours, 2nd edn. Springer, Berlin, pp 61–68
17. Uccella S, Cerutti R, Vigetti D, Furlan D, Oldrini R, Carnevali I, Pelosi G, La Rosa S, Passi A, Capella C (2006) Histidine decarboxylase, DOPA decarboxylase, and vesicular monoamine transporter 2 expression in neuroendocrine tumors: immunohistochemical study and gene expression analysis. J Histochem Cytochem 54:863–875
18. Van Eeden S, de Leng WWJ, Offerhaus GJA, Morsink FH, Weterman MAJ, de Krijger RR, Kloppel G, Klimstra DS (2004) Ductuloinsular tumors of the pancreas—endocrine tumors with entrapped nonneoplastic ductules. Am J Surg Pathol 28:813–820

Virchows Arch (2008) 452:175–180
DOI 10.1007/s00428-007-0543-z

ORIGINAL ARTICLE

Hypomethylation of *hepatocyte nuclear factor-1beta (HNF-1beta)* CpG island in clear cell carcinoma of the ovary

Noriko Kato · Gen Tamura · Teiichi Motoyama

Received: 10 August 2007 / Revised: 22 October 2007 / Accepted: 30 October 2007 / Published online: 8 December 2007
© Springer-Verlag 2007

Abstract Expression of *hepatocyte nuclear factor-1beta (HNF-1beta)* is significantly up-regulated in ovarian clear cell carcinoma (CCC). The mechanism of up-regulation, however, remains unclear. It has been recognized that hypomethylation of specific gene promoters is involved in aberrant gene expression in carcinogenesis. In the present study, ovarian CCCs were examined whether there was a correlation between the methylation and expression status of *HNF-1beta*, using combined bisulfite restriction analysis (COBRA), bisulfite-sequencing and immunocyto/histochemistry. In 2 CCC cell lines, hypomethylation of *HNF-1beta* CpG island strongly correlated with *HNF-1beta* expression, at both the mRNA and protein levels. In archival surgical specimens, 20 of 20 CCCs were immunohistochemically positive for HNF-1beta, whereas none of 20 serous adenocarcinomas (SAs) or 12 normal ovaries were positive for it. By COBRA, methylation of *HNF-1beta* CpG island was less frequently detected in CCCs (8 of 20, 40%) than SAs (18 of 20, 90%) or normal ovaries (12 of 12, 100%) ($p<0.01$), which was confirmed by bisulfite-sequencing. In addition, *HNF-1beta* hypomethylation correlated with a high HNF-1beta immunostaining score in CCCs. These results strongly suggest that hypomethylation of the *HNF-1beta* CpG island participates in the *HNF-1beta* up-regulation in ovarian CCC.

N. Kato (✉) · T. Motoyama
Department of Pathology, Yamagata University School of Medicine, 2-2-2 Iida-nishi, Yamagata, Japan
e-mail: nkato@med.id.yamagata-u.ac.jp

G. Tamura
Department of Pathology, Yamagata Prefectural Central Hospital, Yamagata, Japan

Keywords Clear cell carcinoma · Ovary · *HNF-1beta* · Hypomethylation

Abbreviations

CCC	clear cell carcinoma
SA	serous adenocarcinoma
HNF-1beta	*hepatocyte nuclear factor-1beta*
COBRA	combined bisulfite restriction analysis

Introduction

A transcription factor, hepatocyte nuclear factor-1beta (HNF-1beta), also called transcription factor 2 (TCF2), is now recognized as an excellent marker for clear cell carcinoma (CCC) of the ovary because the expression is significantly up-regulated in ovarian CCC compared with non-CCC ovarian cancers [6, 11–14, 18]. The mechanism of *HNF-1beta* up-regulation in CCC, however, remains unclear. In normal human tissues, *HNF-1beta* expression is tissue-specific: In human embryos, *HNF-1beta* transcripts were detected in various organs, including kidney, genital tract, pancreas, biliary tract, duodenum, and stomach, whereas in human adults, *HNF-1beta* transcripts were predominantly detected in kidney and pancreas [5]. It is most likely that the tissue-specific *HNF-1beta* expression in normal tissues is controlled at the epigenetic level. In humans, one of the epigenetic mechanisms that regulate expression of genes is methylation of the clusters of CpG dinucleotides, called CpG islands [9]. The CpG islands are most often found in the promoter and first exon of genes, and they are generally protected from methylation. Genes can be transcribed from methylation-free promoters [9]. It is well known that

hypermethylation of promoter CpG island of tumor suppressor genes is responsible for the gene inactivation and development of cancers [4, 10]. On the other hand, some oncogenes or cancer-related antigen genes, which are usually silent by promoter hypermethylation, are activated by demethylation of the CpG islands in several cancers [2, 3, 8, 15]. Recently, Terasawa et al. showed that methylation of the *HNF-1beta* CpG island was rare in ovarian CCC, but common in non-CCC ovarian cancers or various cancer cell lines [17], suggesting that hypomethylation of *HNF-1beta* CpG island might contribute to overexpression of HNF-1beta in CCC. However, it has not been analyzed at all whether there is a correlation between the methylation and expression status of *HNF-1beta*.

In the present study, we first examined ovarian CCC cell lines for status of *HNF-1beta* CpG island methylation, as well as expression of *HNF-1beta* mRNA and protein. Subsequently, primary CCCs were examined to determine whether there was a correlation between the protein expression and methylation status of *HNF-1beta* by using paraffin-embedded tissue specimens.

Materials and methods

Cell lines and surgical specimens

We examined four ovarian cancer cell lines, including 2 CCC cell lines (JHOC-5 and HAC-2) and two serous adenocarcinoma (SA) cell lines (JHOS-2 and JHOS-3). JHOC-5, JHOS-2, and JHOS-3 were kindly provided by Dr. H. Ishikawa (Tokyo Jikei Medical School, Tokyo, Japan), and HAC-2 was a generous gift from Dr. M. Nishida (Kasumigaura Medical Center, Tsuchiura, Japan). All cell lines were cultured in RPMI1640 supplemented with 10% fetal bovine serum in a humidified 5% CO_2 atmosphere at 37°C. Log-phase cultured cells were fixed in 10% formalin and embedded in paraffin for preparation of cell blocks. For analysis of primary tumors, 20 ovarian CCCs were examined. Of the 20 CCCs, 14 were stage I, 2 were stage II, and 4 were stage III, according to the criteria of the International Federation of Gynecology and Obstetrics (FIGO) [1]. The histologic grade (FIGO) was 2 (15 cases) or 3 (5 cases). Two patients died of the tumor, whereas 18 are alive with recurrence (2 patients) or without recurrence (16 patients) for 1–6 years after surgery. For comparison, 20 ovarian SAs and 12 normal ovaries were examined. SA was chosen for a comparative study, since SA was a histological type showing the least frequent *HNF-1beta* expression among non-CCC ovarian carcinomas [6, 11, 18]. The normal ovaries were obtained from females ranging in age from 21 to 46 years, and they did not bear any pathological changes, including endometriosis. All of the primary tumors and normal ovaries were obtained by surgery, fixed in 10% formalin and embedded in paraffin.

Bisulfite treatment of genomic DNA and combined bisulfite restriction analysis

Genomic DNA was extracted from cell lines using a SepaGene Kit (Sankyo Junyaku, Tokyo, Japan), or extracted from paraffin-embedded surgical specimens by manual microdissection followed by phenol-chloroform extraction, and then treated with sodium bisulfite as described previously. Briefly, 1 μg of genomic DNA denatured with NaOH was treated with sodium bisulfite for 16 h at 55°C, and then purified. The methylation status of *HNF-1beta* was examined using combined bisulfite restriction analysis (COBRA), a method for semiquantitative bisulfite-PCR analysis [19]. A 195-bp fragment encompassing the CpG island of *HNF-1beta* exon 1 was amplified using primers 5′-GGG GTY GAG TTY GAT ATT AAG T-3′ (forward) and 5′-TAC CTA AAC ATC CRA TCC ACC T-3′ (reverse), which would equally amplify both methylated and unmethylated DNAs [17]. The PCR products were digested with the restriction enzyme *Tai* I (Fermentas Life Sciences, Ontario, Canada), which cleaves CpG sites retained because of methylation. The DNA was analyzed by electrophoresis on a 6% polyacrylamide gel.

Direct-sequencing of bisulfite-PCR products

The bisulfite-PCR products of four cell lines (two CCCs and two SAs), four primary CCCs, six primary SAs, and eight normal ovaries were used for direct sequencing. Briefly, 20 μl of bisulfite-PCR products were purified using a QIA quick PCR purification kit (Qiagen, Tokyo, Japan), and were sequenced using a BigDye terminator cycle sequencing kit (PE Applied Biosystems, Foster City, CA, USA) with an ATGC DNA sequencer (Genetyx, Tokyo, Japan).

Reverse transcription-PCR

Total RNA was extracted by use of Trizol reagent (Invitrogen, Carlsbad, CA), from 2 CCC and 2 SA cell lines. One microgram of total RNA was used as the template for RT-PCR, to amplify a 133-bp fragment of *HNF-1beta*. The primer sequences used were: 5′-GCC CAC ACA CCA CTT ACT TCG-3′ (sense) and 5′-GTC CGT CAG GTA AGC AGG GAC-3′ (antisense). As an internal control, a 587-bp fragment of beta-actin was amplified. Reverse transcription was performed at 50°C for 30 min, and was followed by a PCR protocol including

35 cycles at an annealing temperature of 56°C. The PCR products were analyzed by electrophoresis on a 6% polyacrylamide gel.

Immunocytochemistry and immunohistochemistry

Immunocytochemistry or immunohistochemistry for HNF-1beta was performed on paraffin-embedded sections of cell blocks or surgical specimens. For antigen retrieval, the slides were pretreated with microwave heating at 95°C for 21 min in sodium citrate buffer (10 mM sodium-citrate monohydrate, pH 6.0). The slides were treated with 0.3% hydrogen peroxide in methanol for 20 min, preincubated in 2% normal rabbit serum (DAKO, Glostrup, Denmark) for 30 min, then incubated with goat polyclonal antibody for HNF-1beta (sc-7411; dilution 1/400; Santa Cruz Biotechnology, CA, USA) at 4°C overnight. The immunocytochemical and immunohistochemical reactions were visualized using a LSAB2 kit (DakoCytomation, Carpinteria, CA) with diaminobenzidine as a chromogen. As positive and negative controls, tissue sections of normal kidney were included in each run: renal tubules as positive control and glomeruli as negative control. Staining was judged as positive if the intensity of staining was as strong as that of positive control. Immunoreactivity was scored on the basis of the percentage of tumor cells positive for HNF-1beta (0, no positive cells; 1, <5%; 2, 5–25%; 3, 26–50%; 4, >50% positive cells).

Statistical analysis

Fisher's exact probability test was used to analyze the statistical significance of the relationship between the *HNF-1beta* methylation status and the clinicopathological variables. Differences were considered significant if P values were less than 0.05.

Results

Expression and methylation status of *HNF-1beta* in ovarian cancer cell lines

Two of two CCC cell lines showed *HNF-1beta* expression at both the mRNA and protein levels, whereas two of two SA cell lines did not show *HNF-1beta* expression at either level (Fig. 1a and b). Using COBRA, methylation of *HNF-1beta* was not detected in the two CCC cell lines, whereas it was detected in the two SA cell lines (Fig. 1c). Direct sequencing of the bisulfite-PCR products revealed that the two CCC cell lines showed diffuse unmethylation of their CpGs, whereas the two SA cell lines showed diffuse methylation (Fig. 1d).

Expression and methylation status of *HNF-1beta* in primary ovarian cancers and normal ovaries

All 20 primary CCCs examined showed distinct immunoreactivity for HNF-1beta. The immunostaining score was four in two (10%) cases, three in eight (40%) cases, two in nine (45%) cases, and one in one (5%) case. In contrast, neither 20 SAs nor 12 normal ovaries showed immunoreactivity for it (Fig. 2a). Using COBRA, *HNF-1beta* methylation was detected in 8 of 20 (40%) CCCs, 18 of 20 (90%) SAs, and 12 of 12 (100%) normal ovaries (Fig. 2b). Methylation was significantly less frequently detected in CCCs than SAs or normal ovaries ($p<0.01$). In normal ovaries, not only methylated alleles but also unmethylated alleles were detected. Among ten primary tumors (four CCCs and six SAs) that were subjected to direct sequencing of the bisulfite-PCR products, three CCCs showed unmethylation of most of the CpGs, whereas three SAs showed methylation of them. The others showed both unmethylation and methylation of the CpGs. All eight normal ovaries sequenced showed a mixed pattern of unmethylation and methylation of the CpGs (Fig. 2c).

Correlation between *HNF-1beta* methylation status and HNF-1beta immunostaining score in CCC

Ten of twelve CCCs shown by COBRA not to be methylated had a high (4 or 3) HNF-1beta immunostaining score. In contrast, eight of eight CCCs shown to be methylated had a low (2 or 1) HNF-1beta immunostaining score (Table 1).

Correlation between *HNF-1beta* methylation status and clinicopathological variables in CCC

HNF-1beta methylation status was not significantly correlated with FIGO stage, histological grade or patients' prognoses.

Discussion

In the present study, we first examined ovarian cancer cell lines in vitro for the expression and methylation status of *HNF-1beta*. *HNF-1beta* expression, at both the mRNA and protein levels, strongly correlated with hypomethylation of *HNF-1beta* CpG island. To assess methylation status, we carried out not only COBRA but also bisulfite-sequencing to examine whether the methylation detected by COBRA reflects the overall level of methylation of the *HNF-1beta* CpG island. Most of the CpGs were unmethylated in CCC cell lines, whereas they were methylated in SA cell lines, except for a few CpGs showing a mixed pattern of

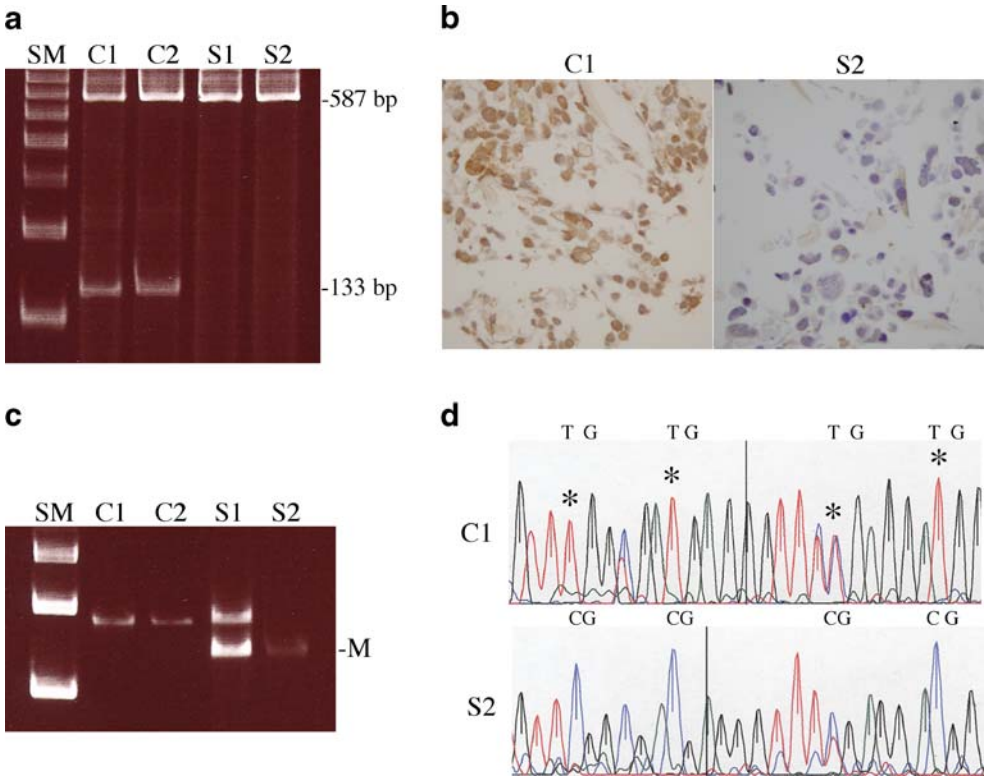


Fig. 1 **a** RT-PCR for *hepatocyte nuclear factor-1beta (HNF-1beta)* in ovarian cancer cell lines. Clear cell adenocarcinoma (CCC) cell lines (*C1* and *C2*) expressed *HNF-1beta* mRNA (133 bp), whereas serous adenocarcinoma (SA) cell lines (*S1* and *S2*) did not express it. *Beta-actin* served as an internal control. *C1*, JHOC-5; *C2*, HAC-2; *S1*, JHOS-2; *S2*, JHOS-3; *SM*, size marker. **b** Immunocytochemistry for HNF-1beta. A CCC cell line (*C1*) showed distinct nuclear immunoreactivity for HNF-1beta, whereas a SA cell line (*S2*) did not show significant immunoreactivity for it (SAB with hematoxylin counterstain, ×400). **c** Combined bisulfite restriction analysis (COBRA) for *HNF-1beta* exon 1 CpG island in ovarian cancer cell lines. The PCR products contained a restriction site for *Tai* I, which recognizes ACGT. The PCR products were digested only when the CpG sites were retained after bisulfite treatment because of methylation. *M*, methylated alleles; *SM*, size marker. **d** Direct sequencing of bisulfite PCR products of cell lines. Bisulfite treatment of the C1 DNA converted cytosines to thymines, although some cytosines also remained as cytosines. In contrast, all cytosines remained as cytosines in S2; *asterisk*, converted thymines

unmethylation and methylation. The present study clearly demonstrated that the *HNF-1beta* CpG island was hypomethylated in CCC cell lines, and the hypomethylation correlated with HNF-1beta overexpression.

It has been reported that normal ovaries scarcely expressed *HNF-1beta* transcripts [5], and this was also supported by our immunohistochemical analysis. Using COBRA, both unmethylated and methylated alleles were detected in normal ovaries, and bisulfite-sequencing confirmed that most of the CpGs showed a mixed pattern of methylation and unmethylation. It seems that COBRA can be reliably applied for DNA obtained from paraffin-embedded tissue samples, as previously mentioned by Xiong et al. [19]. Our results indicated that partial unmethylation, which might occur either randomly or in mono-allelic manner, is common in normal ovaries, and that partial unmethylation alone does not result in *HNF-1beta* expression in normal ovaries. In primary ovarian cancers, all 20 CCCs but none of 20 SAs showed immunoreactivity for HNF-1beta, which was consistent with previous data [6, 11–14, 18]. COBRA using DNAs extracted from the paraffin sections corresponding to those analyzed by immunohistochemistry revealed that *HNF-1beta* methylation was significantly less frequently detected in CCC (8 of 20, 40%) than in SA (18 of 20, 90%) ($p<0.01$). Again, this result was confirmed by bisulfite-sequencing: the CpGs of the island were mostly unmethylated in CCCs whereas they were mostly methylated in SAs. In some cases of CCC and SA, the CpGs showed a mixed pattern of methylation and unmethylation, at least a part of which might have represented the pattern of non-neoplastic tissues contaminating the tumor. Collectively, these data indicate that the *HNF-1beta* CpG island is hypomethylated in primary CCCs, and the hypomethylation correlates with HNF-1beta overexpression in primary CCCs. It is most likely that the hypomethylation of *HNF-1beta* CpG island is at least one of the contributors to HNF-1beta overexpression. Alternatively, other potential contributors to the HNF-1beta overexpression are histone acetylation and gene amplification. A previous study showed that methylation was associated with histone deacetylation, and when treating cells with histone

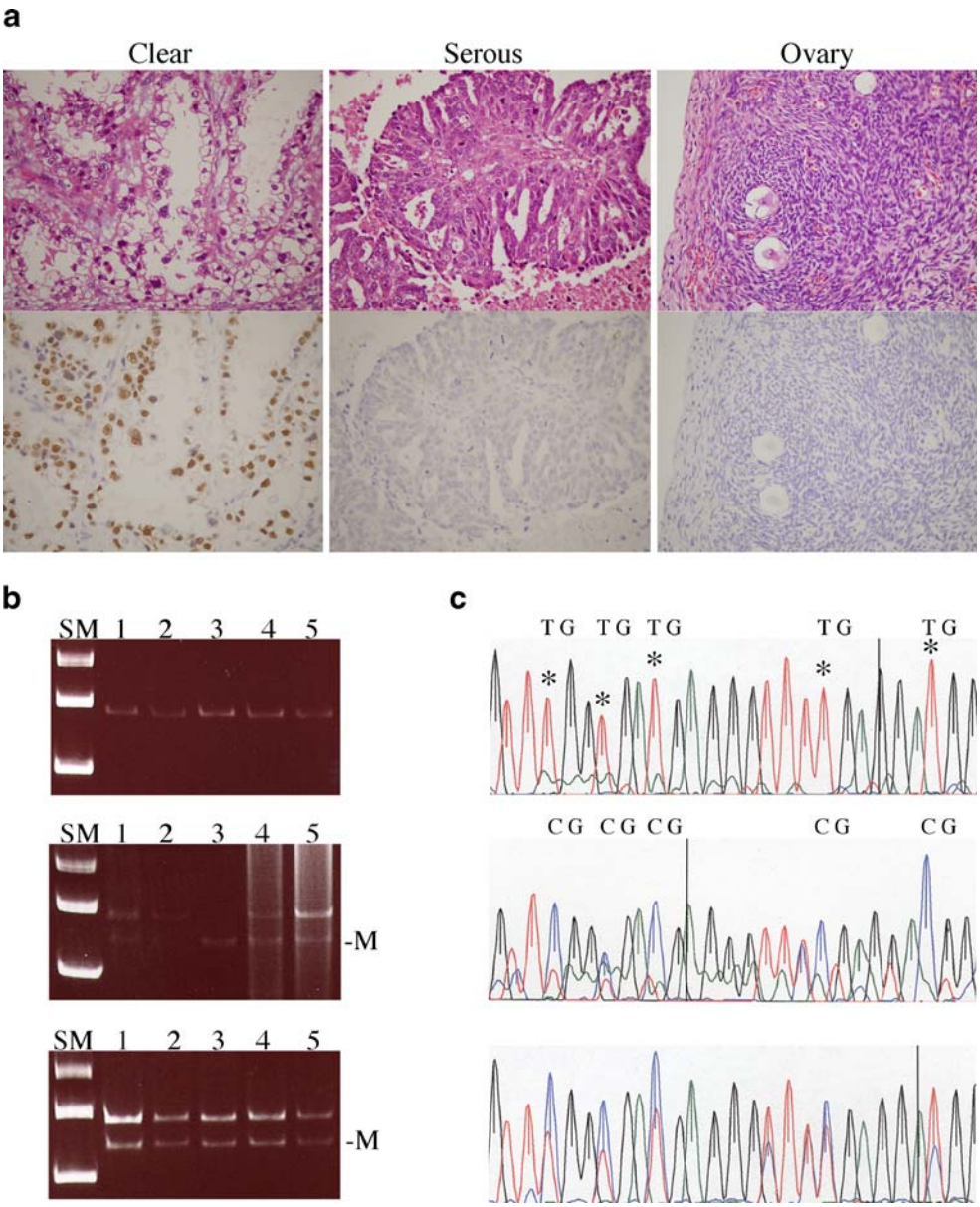


Fig. 2 **a** Immunohistochemistry for HNF-1beta in CCC, SA and normal ovary. CCC showed distinct nuclear immunoreactivity for HNF-1beta, whereas SA or normal ovary did not show any immunoreactivity for it (SAB with hematoxylin counterstain, ×400). **b** Analysis of *HNF-1beta* methylation in CCC (*upper*), SA (*middle*) and normal ovary (*lower*). Methylation was rarely detected in CCC, whereas it was common in SA and the normal ovary; *M* methylated alleles, *SM* size marker. **c** Direct sequencing of bisulfite PCR products of CCC (*upper*), SA (*middle*) and normal ovary (*lower*). Bisulfite treatment of the CCC DNA converted all cytosines to thymines, whereas cytosines remained as cytosines in SA. In the normal ovary, the CpGs contained a mixture of cytosines and thymines; *asterisk*, converted thymines

deacetylase inhibitor combined with methyltransferase inhibitor, *HNF-1beta* expression was synergistically induced [17]. Although all SAs examined here were negative for HNF-1beta, we failed to detect methylation in a few SAs, implying not only methylation but also other mechanisms, such as histone modification, regulate *HNF-1beta* expression. As for gene amplification, the gain of 17q21-q24 was found in 40% of CCC cases using comparative genomic hybridization [7]. Since *HNF-1beta* is located at 17q12, this gain might possibly involve the amplification of *HNF-1beta* and result in overexpression of HNF-1beta. Further study of the correlation between the chromosomal gain and *HNF-1beta* expression status will be necessary to verify this speculation.

Table 1 Correlation between *HNF-1beta* methylation status and HNF-1beta immunostaining score in clear cell carcinoma of the ovary

	HNF-1beta immunostaining score*	
	Low	High
HNF-1beta CpGs methylation		
Detected	8	0
Not detected	2	10

**low*, <25%; *high*, >25% tumor cells were positive for HNF-1beta

The present study further demonstrated that *HNF-1beta* hypomethylation was linked to high HNF-1beta immunostaining score in primary CCCs. The primary CCCs shown by COBRA not to be methylated had a high HNF-1beta immunostaining score, whereas those shown to be methylated had a low HNF-1beta immunostaining score. Although

the methylation detected in primary CCCs might be derived from contaminating non-neoplastic tissues to a greater or lesser degree, our findings suggest that primary CCCs contain a wide range of demethylation ratios, so that some CCCs have a large number of tumor cells whose CpG island is demethylated enough to express HNF-1beta, whereas others do not. In the present study, there was no correlation between the clinicopathological features and the methylation status of *HNF-1beta*, which was concordant with previous data on the correlation between clinicopathological variables and expression status of HNF-1beta [11, 18]. This, together with the fact that partial unmethylation of the *HNF-1beta* CpG island was common in normal ovaries, indicates that *HNF-1beta* hypomethylation is not likely to be related to cancer progression in CCC. Our previous study showed that HNF-1beta was also expressed in benign or borderline clear cell tumors and endometriosis [11], which are probable origins of CCC. It is possible that the demethylation of *HNF-1beta* CpG island is related to early transformation into the clear cell lineage, rather than to malignant transformation. Further study of the *HNF-1beta* methylation status in benign/borderline clear cell tumors or endometriosis would clarify the significance of the demethylation of *HNF-1beta* CpG island in the histogenesis of ovarian CCC. From the clinical point of view, HNF-1beta is expected to be one of the potential molecular targets for therapy because CCC is resistant to cisplatinum-based chemotherapy [16]. More understanding of the mechanism of *HNF-1beta* expression might shed light on developing therapeutic strategies targeting HNF-1beta.

In summary, the *HNF-1beta* CpG island is hypomethylated in ovarian CCC, and the hypomethylation correlates with HNF-1beta overexpression in this tumor. Hypomethylation of the *HNF-1beta* CpG island probably participates in the up-regulation of *HNF-1beta* in ovarian CCC.

Acknowledgement

Conflict of interest statement We declare that we have no conflict of interest.

References

1. Benedet JL, Bender H, Jones HW III, Ngan HY, Pecorelli S (2000) FIGO staging classifications and clinical practice guidelines in the management of gynecologic cancers. FIGO committee on Gynecologic Oncology. Int J Gynecol Obstet 70:209–262
2. Cheah MS, Wallace CD, Hoffman RM (1984) Hypomethylation of DNA in human cancer cells: a site-specific change in the c-myc oncogene. J Natl Cancer Inst 73:1057–1065
3. De Smet C, De Backer O, Faraoni I, Lurquni C, Brasseur F, Boon T (1996) The activation of human gene *MAGE-1* in tumor cells is correlated with genome-wide demethylation. Proc Natl Acad Sci USA 93:7149–7153
4. Goodman JI, Watson RE (2002) Altered DNA methylation: a secondary mechanism involved in carcinogenesis. Ann Rev Pharacol Toxicol 42:501–525
5. Haumaitre C, Fabre M, Cormier S, Baumann C, Delezoide AL, Cereghini S (2006) Severe pancreas hypoplasia and multicystic renal dysplasia in two human fetuses carrying novel *HNF1beta/MODY5* mutations. Hum Mol Genet 15:2363–2375
6. Higashiguchi A, Yamada T, Susumu N, Mori T, Suzuki A, Aoki D, Sakamoto M (2007) Specific expression of hepatocyte nuclear factor-1beta in the ovarian clear cell adenocarcinoma and its application to cytological diagnosis. Cancer Sci 98:387–391
7. Hirasawa A, Saito-Ohara F, Inoue J, Aoki D, Susumu N, Yokoyama T, Nozawa S, Inazawa J, Imoto I (2003) Association of 17q21-q24 gain in ovarian clear cell adenocarcinomas with poor prognosis and identification of PPM1D and APPBP2 as likely amplification targets. Clin Cancer Res 9:1995–2004
8. Honda T, Tamura G, Waki T, Kawata S, Terashima M, Nishizuka S, Motoyama T (2004) Demethylation of *MAGE* promoters during gastric cancer progression. Br J Cancer 90:838–843
9. Jones PA, Takai D (2001) The role of DNA methylation in mammalian epigenetics. Science 293:1068–1070
10. Jones PA, Baylin SB (2002) The fundamental role of epigenetic events in cancer. Nat Rev Genet 3:415–428
11. Kato N, Sasou S, Motoyama T (2006) Expression of hepatocyte nuclear factor-1beta (HNF-1beta) in clear cell tumors and endometriosis of the ovary. Mod Pathol 19:83–89
12. Kato N, Toukairin M, Asanuma I, Motoyama T (2007) Immunocytochemistry for hepatocyte nuclear factor-1beta (HNF-1beta): A marker for ovarian clear cell carcinoma. Diagn Cytopathol 35:193–197
13. Lu KH, Patterson AP, Wang L, Marquez RT, Atkinson EN, Baggerly KA, Ramoth LR, Rosen DG, Liu J, Hellstrom I, Smith D, Hartmann L, Fishman D, Berchuck A, Schmandt R, Whitaker R, Gershenson DM, Mills GB, Bast RC Jr (2004) Selection of potential markers for epithelial ovarian cancer with gene expression arrays and recursive descent partition analysis. Clin Cancer Res 10:3291–3300
14. Schwartz DR, Kardia SL, Shedden KA, Kuick R, Michailidis G, Taylor JM, Misek DE, Wu R, Zhai Y, Darrah DM, Reed H, Ellenson LH, Giordano TJ, Fearon ER, Hanash SM, Cho KR (2002) Gene expression in ovarian cancer reflects both morphology and biological behavior, distinguishing clear cell from other poor-prognosis ovarian carcinomas. Cancer Res 62:4722–4729
15. Sharrard RM, Royds JA, Rogers S, Shorthouse AJ (1992) Patterns of methylation of the c-myc gene in human colorectal cancer progression. Br J Cancer 65:667–672
16. Sugiyama T, Kamura T, Kigawa J, Terakawa N, Kikuchi Y, Kita T, Suzuki M, Sato I, Taguchi K (2000) Clinical characteristics of clear cell carcinoma of the ovary: a distinct histologic type with poor prognosis and resistance to platinum-based chemotherapy. Cancer 88:2584–2589
17. Terasawa K, Toyota M, Sagae S, Ogi K, Suzuki H, Sonoda T, Akino K, Maruyama R, Nishikawa N, Imai K, Shinomura Y, Saito T, Tokino T (2006) Epigenetic inactivation of *TCF2* in ovarian cancer and various cancer cell lines. Br J Cancer 94:914–921
18. Tsuchiya A, Sakamoto M, Yasuda J, Chuma M, Ohta T, Ohki M, Yasugi T, Taketani Y, Hirohashi S (2003) Expression profiling in ovarian clear cell carcinoma. Identification of hepatocyte nuclear factor-1beta as a molecular marker and a possible molecular target for therapy of ovarian clear cell carcinoma. Am J Pathol 163:2503–2512
19. Xiong Z, Laird PW (1997) COBRA: a sensitive and quantitative DNA methylation assay. Nucleic Acids Res 25:2532–2534

Virchows Arch (2008) 452:181–191
DOI 10.1007/s00428-007-0542-0

ORIGINAL ARTICLE

Expression of aromatase and estrogen receptors in human adrenocortical tumors

Luisa Barzon · Giulia Masi · Monia Pacenti · Marta Trevisan · Francesco Fallo · Andrea Remo · Guido Martignoni · Daniela Montanaro · Vincenzo Pezzi · Giorgio Palù

Received: 30 July 2007 / Revised: 8 October 2007 / Accepted: 30 October 2007 / Published online: 21 December 2007
© Springer-Verlag 2007

Abstract We recently demonstrated that adrenocortical carcinoma cells express aromatase and estrogen receptors (ERs) and that 17β-estradiol enhances adrenocortical cell proliferation. To provide a clue to the role of estrogens in adrenal tumorigenesis, we investigated the expression profile of genes involved in sex steroid hormone production and activity in a large series of normal and neoplastic human adrenocortical tissues. Quantitative reverse transcriptase–polymerase chain reaction, Western blotting, and immunohistochemistry showed that ERα and ERβ, androgen receptor (AR), and aromatase were expressed in the adrenal cortex and in adrenocortical tumors. ERβ was the predominant ER subtype and was mainly expressed in the zona glomerulosa and fasciculata. Western blot analysis revealed the presence of a truncated form of AR in adrenocortical tissues. With respect to the normal adrenal cortex and adrenocortical adenomas, carcinomas were characterized by significantly lower ERβ levels, ERα upregulation, and aromatase overexpression. ER expression correlated with expression of nuclear hormone receptors, suggesting they could be involved in ER modulation. In agreement with our in vitro findings, the results of this study suggest that estrogens, locally produced by aromatase, could enhance adrenocortical cell proliferation though autocrine/paracrine mechanisms. This study opens new perspectives on the potential use of antiestrogens and aromatase inhibitors as therapeutic agents against ACC.

Keywords Estrogen receptors · Androgen receptor · Adrenocortical tumors · Aromatase

L. Barzon (✉) · G. Masi · M. Pacenti · M. Trevisan · G. Palù
Department of Histology,
Microbiology and Medical Biotechnologies,
University of Padova,
Via A. Gabelli 63,
35121 Padova, Italy
e-mail: luisa.barzon@unipd.it

F. Fallo
Department of Medical and Surgical Sciences,
University of Padova,
Padova, Italy

A. Remo · G. Martignoni
Department of Pathology, University of Verona,
Verona, Italy

D. Montanaro · V. Pezzi
Department of Pharmaco-biology, University of Calabria,
Arcavacata di Rende,
Cosenza, Italy

Introduction

Estrogens and androgens have been demonstrated to play a critical role in the etiology and progression of several endocrine-related malignancies, such as breast, ovarian, and prostate cancers. Some epidemiological and experimental studies suggest that sex steroid hormones could also be involved in adrenocortical tumorigenesis. In fact, adrenocortical tumors are more frequent in women than in men, especially in those exposed to estro-progestins [5, 12]. Moreover, we recently demonstrated that 17β-estradiol enhances proliferation of the human adrenocortical carcinoma (ACC) cell line NCI-H295R, whereas antiestrogens inhibit ACC cell growth [19]. At variance, androgens have been shown to inhibit NCI-H295R cell proliferation, an effect that is reverted by antiandrogens [27, 36].

To date, only a few studies have investigated expression of estrogen receptors (ERs), androgen receptor

(AR), and aromatase—the enzyme responsible for estrogen biosynthesis—in the human adrenal cortex and in adrenocortical tumors.

The effects of estrogens are mediated by two ER subtypes, ERα and ERβ. While estrogens induce cancer cell proliferation through ERα, ERβ seems to exert a protective effect [4]. ER expression has been studied in the human fetal adrenal cortex, where ERβ is expressed at markedly higher levels than ERα [6, 34], and in pubertal human adrenal tissues, where ERβ is detectable in the zona reticularis, whereas ERα is undetectable [3]. Only anecdotal reports of ER expression in adrenal tumors are available in the literature [9, 22, 28]. Likewise, data on AR expression in the adrenal gland are limited to a few reports, which demonstrated the presence of AR messenger ribonucleic acid (mRNA) in normal and neoplastic human adrenocortical tissues [27]. The presence of aromatase has been recently demonstrated in the fetal adrenal gland [24], in the zona glomerulosa and medulla of the normal adrenal gland [3], in feminizing human adrenocortical tumors [25], and in NCI-H295R cells [19].

Expression and activity of ERs and AR are inhibited by the orphan nuclear hormone receptors DAX-1 (dosage-sensitive sex reversal, adrenal hypoplasia critical region, on chromosome X, gene 1) and SHP (small heterodimer partner) [11, 13, 37], which are also negative regulators of steroidogenic factor 1 (SF-1) and liver receptor homolog 1 (LRH-1) [33]. At variance, SF-1 and LRH-1 stimulate the expression of several steroidogeneic enzymes and nuclear hormone receptors. In breast adipose stromal cells, LRH-1 enhances aromatase expression, thus contributing to the growth of estrogen-positive breast tumors [7, 38].

Following our experimental studies on the effects of estrogens and antiestrogens on ACC cells and on the basis of the above evidence from the literature, in the present study, we investigated expression of genes involved in sex steroid hormone production and activity in normal and neoplastic human adrenocortical tissues to provide a clue to the role of estrogens in adrenal tumorigenesis.

Materials and methods

Adrenocortical samples

We investigated archived fresh-frozen or paraffin-embedded samples of adrenocortical tumors removed at surgery, normal adrenal cortex macroscopically dissected from adrenal glands of kidney donors, and fetal adrenal glands obtained at autopsy (Table 1). Tissue samples were obtained with the approval of local ethics committees and consent from patients, in accordance with the Declaration of Helsinki guidelines.

Table 1 Characteristics of the study population (n=68)

Characteristics	Value
Normal adrenal cortex	N=14
Female/male	9/5
Median age (range)	45 (24–62)
Fetal adrenal gland	N=5
Gestation weeks	13, 16, 19, 20, 25
Adrenocortical adenomas	N=33
Female/male	24/9
Median age (range)	42 (19–70)
Cortisol-producing	4
Aldosterone-producing	13
Androgen-producing	1
Nonfunctioning	15
Adrenocortical carcinomas	N=16
Female/male	11/5
Median age (range)	46 (27–69)
Cortisol-producing	4
Aldosterone-producing	1
Cortisol and androgen-producing	5
Nonfunctioning	6

Diagnosis of malignancy was performed according to the histopathologic criteria proposed by Weiss et al. [35], with modification proposed by Aubert et al. [2]. Briefly, an adrenocortical neoplasm was defined as malignant in the presence of three or more of the following criteria: (1) high nuclear grade, according to the Fuhrman criteria [10], (2) greater than five mitoses per 50 high-power fields, (3) atypical mitotic figures, (4) less than 25% of tumor cells are clear cells, (5) diffuse architecture (>33% of tumor), (6) necrosis, (7) venous invasion, (8) sinusoidal invasion, and (9) capsular invasion.

Immunohistochemistry

Immunohistochemical evaluation of ERα, ERβ, and AR protein expression was performed in a group of archive adrenocortical samples, including 16 ACCs, 5 normal adult adrenal glands, and 5 fetal normal adrenal glands. Specimens were fixed in 10% neutral buffered formalin. Immunohistochemical analysis was performed on deparaffinized sections pretreated for 30 min in 10 mM citrate buffer in steam. Mouse anti-human monoclonal antibodies to ERα (clone SP1, dilution 1:400, Lab-Vision, Neomarkers, Fremont, CA), ERβ1 (clone PPG5/10, dilution 1:50, Serotec, Oxford, UK), and AR (clone AR441, dilution 1:20, Dako Italia S.p.A, Milan, Italy) were tested with a polymeric-labeling two-step method (Super sensitiveTM IHC detection system, Biogenex, San Ramon) in an automated staining system (GenoMx i6000, Biogenex). For ERβ, an overnight incubation was done. Three carcinomas of the breast and three

adenocarcinomas of the prostate were used as external controls. Neoplastic cells were considered positive when they showed nuclear immunoreactivity, which was scored as follows: 0, undectable or equivocal individual single cells positivity; 1+, weak intensity; 2+, strong intensity. For each case, the percentage (%) of positive neoplastic cells was reported. Cytoplasmatic imunoreactivity, which was present in all cases of human adrenal glands, adrenal carcinomas, and in four of five fetal adrenal glands, was ignored.

Quantitative RT-PCR

Fifty-six adrenal tumor tissues, including 15 nonfunctioning adrenocortical adenomas (NFAs), 4 cortisol-producing adenomas (CPAs), 13 aldosterone-producing adenomas (APAs), 1 androgen-producing adenoma, and 9 ACCs (six functioning, three nonfunctioning), and 14 normal adrenal cortex samples were studied. Reference RNA from human adrenal cortex (Human Adrenal Total RNA, Ambion, Austin, TX) was also employed as control. Total RNA was isolated using the RNeasy kit (Qiagen S.p.A. Milan, Italy), reverse transcribed, and subjected to quantitative real-time reverse transcriptase–polymerase chain reaction (RT-PCR) analysis of *ERα*, *ERβ*, *AR*, *PGR* (i.e., the progesterone receptor gene), *CYP19* (i.e., the aromatase gene), *SF-1*, *DAX-1*, *LRH-1,* and *SHP* mRNA levels by using the oligonucleotide primer sequences reported in Table 2 and SYBR green reagents (Applied Biosystems, Foster City, CA). Absolute quantification was performed against a standard curve obtained by amplification of correspondent complementary deoxyribonucleic acids (DNAs) subcloned into the pCR2.1 vector (Invitrogen Life Technologies S.p.A, San Giuliano Milanese, Italy), as reported [8]. mRNA values are reported as copies per microgram total RNA, after statandardization against the housekeeping gene *RPLP0*, which was also quantified by real-time RT-PCR.

Western blot analysis

Western blot analysis was performed as previously described [9, 19] in a subset of the above adrenocortical tissue samples, including two normal adrenal tissues, two CPAs, one APA, three NFAs, and four ACCs. Briefly, total protein extracts were separated on sodium dodecyl sulfate–polyacrylamide 11% gel and then electroblotted onto a nitrocellulose membrane. Blots were incubated overnight at 4°C with anti-ERβ antibody against the C-terminal region of ERβ (1:500; Serotec), anti-ERα (F-10) against the C-terminal region of ERα (1:1,000; Santa Cruz Biotech, Santa Cruz, CA), mouse anti-human aromatase (1:1,000; Serotec); anti-SF-1 (1:2,000; Prof. Ken-ichirou Morohashi, National Institute for Basic Biology, Okazaki, Japan), anti-DAX-1 (2F4; 1:1,000) raised against amino acids 135–166 of human DAX-1 (Prof. Paolo Sassone-Corsi, School of Medicine University of California, Irvine, CA), and anti-AR (441; 1:1,000; Santa Cruz Biotech). Membranes were incubated with horseradish peroxidase-coniugated antibodies (Santa Cruz Biotech), and immunoreactive bands were visualized with ECL Plus Western blotting detection system (Amersham Pharmacia Biotech, UK) and quantified with Scion Immage software (Frederich, MD). As control loading, membranes were stripped and reprobed with actin antiserum.

Statistical analysis

Data are presented as mean±SD or median and range. Comparisons were performed by Mann–Whitney *U* test and Spearman Rank *R* correlation, setting the significance level to $p<0.05$ (Statistica 7.1, StatSoft Italia srl, Italy).

Table 2 Sequences of the oligonucleotide primers employed for real-time RT-PCR analysis

Gene	Forward primer	Reverse primer	Amplicon length (bp)	Annealing temperature (°C)
ER-α	CCACCAAACCAGTGCACCATT	GGTCTTTTCGTATCCCACCTTC	108	64
ER-β	AGAGTCCCTGGTGTGAAGCAAG	GACAGCGCAGAAGTGAGCATC	143	68
AR	CCTGGCTTCCGCAACTTACAC	GGACTTGTGCATGCGGTACTCA	168	64
PGR	CGCGCTCTACCCTGCACTC	TGAATCCGGCCTCAGGTAGTT	121	66
CYP19	TCACTGGCCTTTTTCTCTTGGT	GGGTCCAATTCCCATGCA	83	60
SF-1	GGAGTTTGTCTGCCTCAAGTTCA	CGTCTTTCACCAGGATGTGGTT	80	60
DAX-1	CCAAGGAGTACGCCTACCTCAA	ACTGGAGTCCCTGAATGTACTTCC	90	60
LRH-1	TACCGACAAGTGGTACATGGAA	CGGCTTGTGATGCTATTATGGA	89	60
SHP	CCTCAATGCTGTCTGGAGTCCTT	CTGCAGGTGCCCAATGTG	132	60
RPLP0	GGCGACCTGGAAGTCCAACT	CCATCAGCACCACAGCCTTC	149	68

Results

Expression of sex steroid hormone receptors

Normal fetal and adult adrenal gland Immunohistochemical analysis of adult adrenal glands demonstrated heterogeneous expression of ERβ (Fig. 1a–c) with nuclear positivity in the zona glomerulosa and fasciculata (score 1) but no expression in the zona reticularis and medulla. Fetal adrenal glands were negative for ERβ expression, with the exception of a case with nuclear immunoreactivity (score 2) in all adrenal zones (Fig. 1d–f). Both adult and fetal normal adrenal glands were negative for AR and ERα immunostaining. The adenocarcinomas of the prostate used as controls were positive for AR and the carcinomas of the breast immunoreacted for both ERα and ERβ1 (data not shown).

In agreement with immunohistochemical results, Western blot analysis of two normal adrenal cortex samples demonstrated strong ERβ expression and relatively low ERα levels (Fig. 2). As observed in MCF-7 control cells, ERα appeared as an immunopositive band corresponding to the full-length 66-kDa protein and a faint smaller band of 46 kDa, which could possibly represent the N-terminally deleted isoform of ERα with antagonist activity on ERα 66-kDa function [23]. In addition, ERβ appeared as two bands, i.e., a faint band corresponding to a 55 kDa-protein variant and a more intense band corresponding to the expected full-length 59-kDa isoform of ERβ1 [21]. At variance with immunohistochemistry, Western blot analysis of normal adrenocortical tissues allowed to detect the AR protein, which appeared as a double band with the highest of 75 kDa, whereas the full-length AR form of 110 kDa was absent. The apparent discrepancy between immunohistochemical and Western blot results could be explained by the relatively low levels of ERα and AR expression in the adrenal gland, which could be detected by Western blot but not by immunohistochemistry.

Quantitative RT-PCR analysis of sex steroid hormone receptors was performed in 14 normal adrenal cortex samples. It demonstrated variable levels of *ERs*, *PGR*, and *AR* mRNA (Fig. 3). In particular, mean *ERα* mRNA was 25,000±17,650 copies per μg total RNA; *ERβ* mRNA levels were about twofold higher than *ERα* mRNA levels, in agreement with protein expression data, and there was a positive association between the amount of *ERβ* mRNA and *ERα* mRNA levels (Spearman Rank *R* correlation, $p<0.05$). *AR* mRNA was 17,700±8,300 copies per μg total RNA; *PGR* mRNA was 300,000±290,000 copies per μg total RNA.

Adrenocortical tumors Immunohistochemical analysis of sex steroid hormone receptors expression in ACCs demonstrated that all ACCs were negative for ERα, with the exception of one case of ACC, which showed rare positive cells (Table 3). Western blot and RT-PCR analyses demonstrated higher levels of ERα protein and transcripts in ACCs than in the normal adrenal cortex (Figs. 2 and 3). At variance, quantitative real-time RT-PCR did not demonstrated any significant difference in ERα mRNA levels between normal adrenal cortex and adrenocortical adenomas, either functioning or nonfunctioning. No significant variation in the proportion of ERα protein isoforms was observed in the different tumor types at Western blot analysis.

Immunohistochemical staining demonstrated that 12 out of 16 (65%) ACCs were immunoreactive for ERβ, including six ACCs composed by large, eosinophilic and pleomorphic score 2 cells and six ACCs composed of smaller cells that were frequently scored 1 (Table 3, Fig. 4a–d). A single tumor showing both types of cells showed both scores of intensity. The results of immunohistochemistry were concordant with Western blot and RT-PCR analyses, which showed variable ERβ expression among adrenocortical tumors. In fact, ERβ levels were relatively low in several cases of ACCs and NFAs as compared to control normal adrenal tissues but increased in other cases. Statistical analysis demonstrated that, overall, *ERβ* mRNA levels were significantly lower in ACCs than in the normal adrenal cortex (mean, 11,200±2,550 vs 44,580±8,050 copies per μg total RNA, $p<0.01$). Moreover, in ACCs, the ERα/ERβ ratio was significantly higher in ACCs than in the normal adrenal cortex (ERα/ERβ ratio, 21.5±35.4 vs 0.51±0.29, $p<0.05$; Fig. 3), and ERβ mRNA expression tended to be inversely related to ERα expression, although the correlation was not statistically significant. *PGR* mRNA levels in ACCs were about fourfold higher (1,250,00±1,600,000 copies per μg total RNA) than in control normal adrenocortical tissues and correlated with that of *ERα*.

Six out of the 16 ACCs (38%) were positive for AR at immunohistochemical analysis and also displayed higher AR protein and mRNA levels than AR-negative ACCs at Western blot and quantitative RT-PCR analyses (Table 3). Among AR-positive ACCs, two displayed rare positive cells, whereas the other four cases were scored 2 with a percentage of positive cells ranging from 5 to 100%. (Table 3; Fig. 4e and f). AR expression was unrelated to any morphological features (e.g., mitotic rate, necrosis, vascular invasion, capsular invasion) present in ACCs. In benign adrenocortical tumor samples, Western blot and real-time RT-PCR analyses showed a wide variability of AR expression, with undetectable AR levels in four cases of NFAs and in the androgen-producing adenoma and high levels in four APAs (Figs. 2 and 3). Statistical analysis

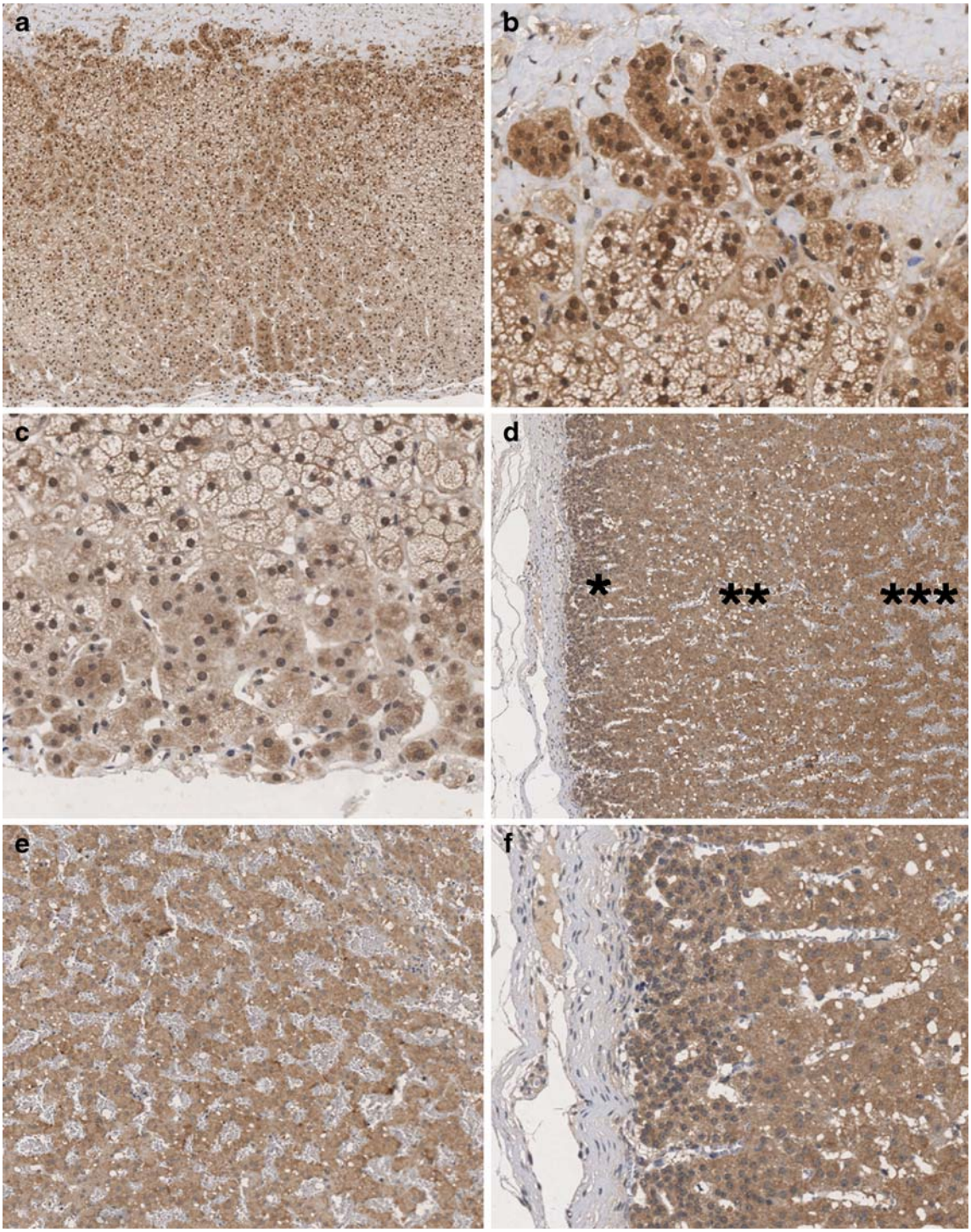


Fig. 1 Immunohistochemical evaluation of ERα, ERβ, and AR in normal adult and fetal adrenal cortex. **a** Adrenal cortex with a heterogeneous ERβ expression into three different areas. **b** The normal cells of the zona glomerulosa and zona fasciculata show nuclear and cytoplasmatic expression of ERβ. **c** The normal cells of the zona reticularis display a strong cytoplasmatic ERβ expression, but their nuclei are prevalently negative. **d** Fetal adrenal with cytoplasmatic ERβ expression without nuclear staining (*asterisk*, subcapsular definitive zone; *double asterisk*, transitional zone; *triple asterisk*, fetal zone). **e** Fetal zone: the cells show cytoplasmatic immunostaining. **f** Definitive and transitional zone: like the fetal zone, cells show cytoplasmatic immunostaining, but their nuclei are negative

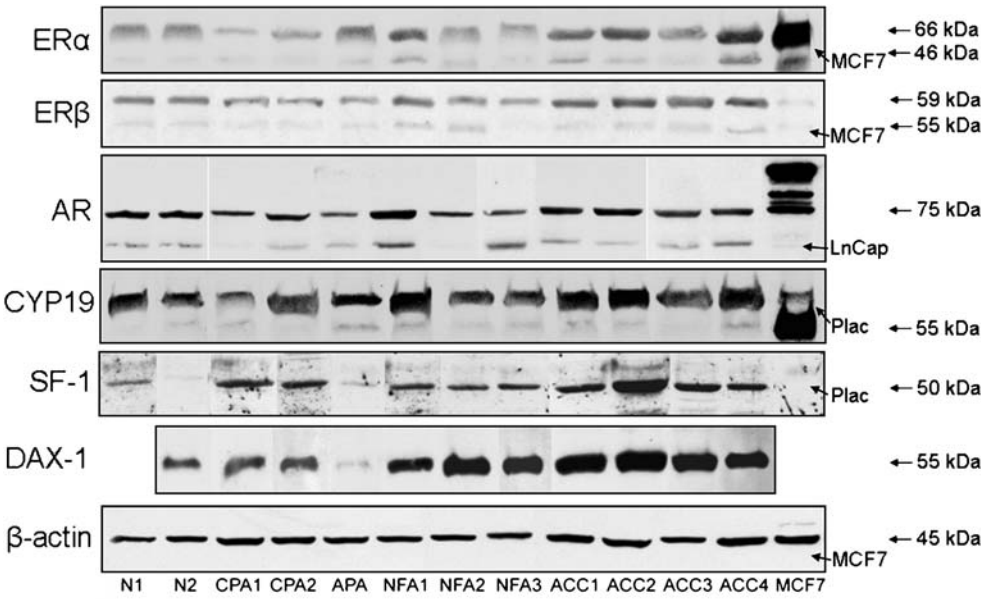


Fig. 2 Western blots of ERα, ERβ, AR, CYP19, SF-1, and DAX-1 on normal and pathological (CPA, APA, NFA, ACC) adrenocortical tissue extracts (50 μg). β-Actin was used as loading control. Results are representative of three independent experiments

demonstrated that, overall, *AR* mRNA levels were significantly lower in NFAs (6,700±9,010 copies per μg total RNA) than in the normal adrenal cortex ($p<0.01$).

Expression of aromatase

Aromatase protein was expressed in normal adrenocortical tissues, although at lower levels than in human placenta, and was visualized at Western blot as a double band of 55 and 60 kDa. The small variation in molecular mass could be due to the level of glycosylation; however, glycosylation does not seem to have an impact on the enzymatic activity [20, 30]. Increased expression of aromatase protein and *CYP19* mRNA was observed in ACCs, especially in cortisol- and androgen-secreting ACCs, than in the normal adrenal gland (16,090±9,140 vs 2,500±1,280 copies per μg total RNA; Figs. 2 and 3). *CYP19* mRNA levels showed a positive association with ERα mRNA expression (Spearman Rank *R* correlation, $p<0.05$) but not with ERβ expression.

Expression of orphan nuclear hormone receptors

In the normal adrenal cortex, SF-1 and DAX-1 were highly expressed, whereas *LRH-1* and *SHP* mRNA levels were about tenfold lower (Fig. 3). Expression of *SF-1*, *DAX-1*, and *LRH-1* was variable, with no significant differences between normal and neoplastic adrenal tissues, whereas *SHP* mRNA expression in APAs and NFAs was lower than in the normal adrenal cortex (Figs. 2 and 3). In the normal and neoplastic adrenal cortex, *SF-1* and *DAX-1* mRNA levels showed a positive correlation with *LRH-1* mRNA but a negative correlation with *SHP* mRNA ($p<0.05$). As for sex steroid hormone receptors, *ERβ* and *ERα* mRNAs showed a positive association with *LRH-1* expression but a negative correlation with *SHP*.

Discussion

This study represents the first investigation on expression of ERs and aromatase in the normal adrenal cortex and tumors derived thereof. It demonstrates that (1) ERs, AR, and aromatase are expressed in the human adrenal cortex and in adrenocortical tumors, (2) *ERβ* is the predominant ER subtype in the adrenal cortex, (3) ACCs are characterized by low ERβ levels and/or increased amount of ERα and abnormal AR expression, (4) aromatase is expressed in the adrenal cortex and adrenocortical tumors and it is overexpressed in ACCs, and (5) expression of ERs correlates with nuclear hormone receptor expression.

By immunohistochemistry, Western blot, and real-time RT-PCR analyses, we demonstrated that both ERs are expressed in the normal adrenal cortex but that the amount of ERβ is about twofold that of ERα. In adult normal adrenal cortex, we could localize ERβ expression in the zona glomerulosa and fasciculata, at variance with findings in the prepubertal adrenal gland, where ERβ was detectable in the zona reticularis [3]. ERβ expression seems to be variable also during fetal adrenal development, as ERβ has been detected in the definitive zone but not in the fetal zone of 20- and 38-gestational week fetuses [6], whereas, in neonates, ERβ is expressed in the fetal zone but not in other zones [3]. In our experience, ERβ was generally undetectable in fetal adrenal glands. Thus, the expression pattern of ERs in the adrenal cortex seems to change during adrenal development, suggesting a role for estrogens in this process.

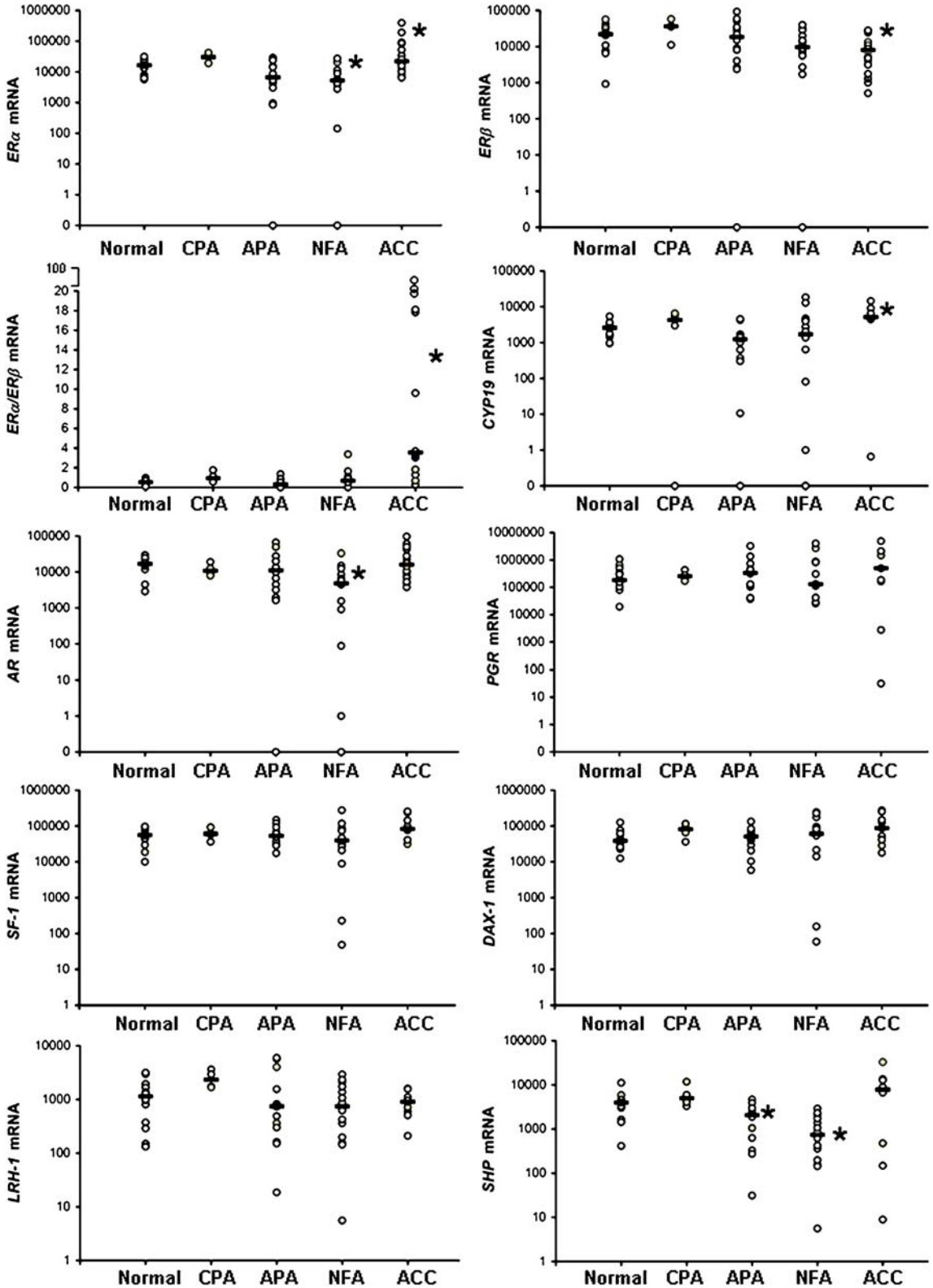


Fig. 3 Expression of transcripts of sex steroid hormone receptors, aromatase (CYP19), and orphan nuclear receptors as determined by quantitative real-time RT-PCR in normal and neoplastic adrenal glands. Individual values and medians (*horizontal bars*) are shown. *Normal* Normal adrenal cortex, *CPA* cortisol-producing adenoma, *APA* aldosterone-producing adenoma, *NFA* nonfuntioning adenoma, *ACC* adrenocortical carcinoma; *asterisk*, values significantly different from those of the normal adrenal cortex (Mann–Whitney *U* test, $p<0.05$)

Table 3 Analysis of ERα, ERβ, and AR expression in ACCs

	Immunohistochemical analysis[a]			Real-time RT-PCR analysis[b]		
ACC no.	ERα score	ERβ1 score	AR score	ERα mRNA	ERβ mRNA	AR mRNA
1	0	2 (70%)	0	7,640	27,900	22,280
2	0	1 (90%)	2 (80%)	16,940	13,280	9,370
3	0	1 (40%)	0	34,240	9,920	4,900
4	0	0	0	25,770	7,190	17,430
5	0	2 (100%)	0	12,300	12,800	7,410
6	0	1 (70%)	2 (5%)	39,320	4,020	42,830
7	0	2 (100%)	0	16,570	24,150	10,690
8	0	2 (100%)	2 (10%)	18,420	10,760	61,080
9	0	2 (100%)	0 (rare cells)	86,560	4,780	14,460
10	0 (rare positive cells)	0	0 (rare cells)	91,800	1,200	28,000
11	0	0	2 (5%)	51,860	508	50,440
12	0	1 (90%)	2 (100%)	84,500	27,890	98,000
13	0	1 (70%)	0	10,100	3,120	3,760
14	0	2 (10%)	0	15,750	8,620	6,890
15	0	0	2 (10%)	6,460	1,750	5,340
16	0	1 (70%)	0	91,150	997	15,070

[a] Neoplastic cells were considered positive when they showed nuclear immunoreactivity, which was scored as follows: 0 undectable or equivocal individual single cells positivity, 1+ weak intensity, and 2+ strong intensity. The percentage (%) of reactive neoplastic cells is reported within parenthesis. Cytoplasmatic imunoreactivity was ignored.
[b] mRNA values are expressed as copies per μg total RNA.

Adrenocortical tumors were characterized by variable levels of ERs. Remarkably, several cases of ACCs showed lower ERβ expression and/or higher ERα levels, resulting in increased ERα/ERβ ratio, than the normal adrenal cortex. These results are in agreement with findings in other estrogen-dependent cancers, such as breast, ovary, colon, and prostate cancer, which show ERα overexpression and/or reduced ERβ levels [4]. It is interesting to note that aromatase was also expressed at relatively high levels in the normal adrenal cortex and its expression markedly increased in ACCs. Based of these observations, we hypothesize that estrogens could contribute to adrenal tumorigenesis through an autocrine/paracrine loop. Estrogens could be produced locally in ACC cells by aromatase and exert their proliferative effect through ERα, while the counteracting antiproliferative activity of ERβ would be lost in cancer cells.

In this regard, we have recently demonstrated that H295R ACC cells express high levels of aromatase and are able to convert androgens to estrogens, which, through a short autocrine loop mediated by ERα, enhance H295R cell proliferation [19]. Treatment with the antiestrogens ICI 182,780 and 4-hydroxytamoxifen upregulated ERβ expression and inhibited basal and 17β-estradiol-induced H295R cell proliferation. In particular, ICI 182,780 determined cell growth arrest, whereas treatment with 4-hydroxytamoxifen activated the Fas/FasL pathway, which in turn induced apoptosis. This effect could be due to 4-hydroxytamoxifen interaction with ERβ and binding to the AP-1 site on the FasL promoter in H295R cells. A dose-dependent inhibition of H295R cell proliferation was also observed after treatment with the aromatase inhibitor Letrozole, thus further confirming the role of estrogens in H295R cell proliferation [19].

Androgens have been shown to inhibit H295R cell proliferation through their receptor [27]. This study demonstrates that AR was overexpressed in a subset of ACCs, whereas it was undetectable in some cases of NFA. It is interesting to note that at Western blot analysis, the full-length AR form of 110 kDa was absent, and AR appeared as a 75-kDa protein. The 75-kDa form has been also identified in prostate carcinoma and represents a truncated form of AR, generated by proteolytic cleavage [18]. This truncated AR has constitutive transcriptional activity, as it lacks a ligand binding domain, but it can bind androgen-responsive elements through its DNA-binding domain. We hypothesize that in adrenocortical cells, this truncated AR with androgen-independent activity could compete with the androgen-dependent negative regulation of adrenocortical cell growth. An imbalance toward the androgen-independent pathway could contribute to unrestrained cell proliferation in ACCs. This hypothesis is being investigated with experiments that are ongoing.

Finally, we investigated expression of orphan nuclear receptors to find clues on the regulation of sex steroid hormone receptors and aromatase expression in adrenocortical cells. We demonstrated variable expression of SF-1, DAX-1, LRH-1, and SHP in the adrenal cortex and its tumors, with increased DAX-1 and SF-1 levels in ACCs

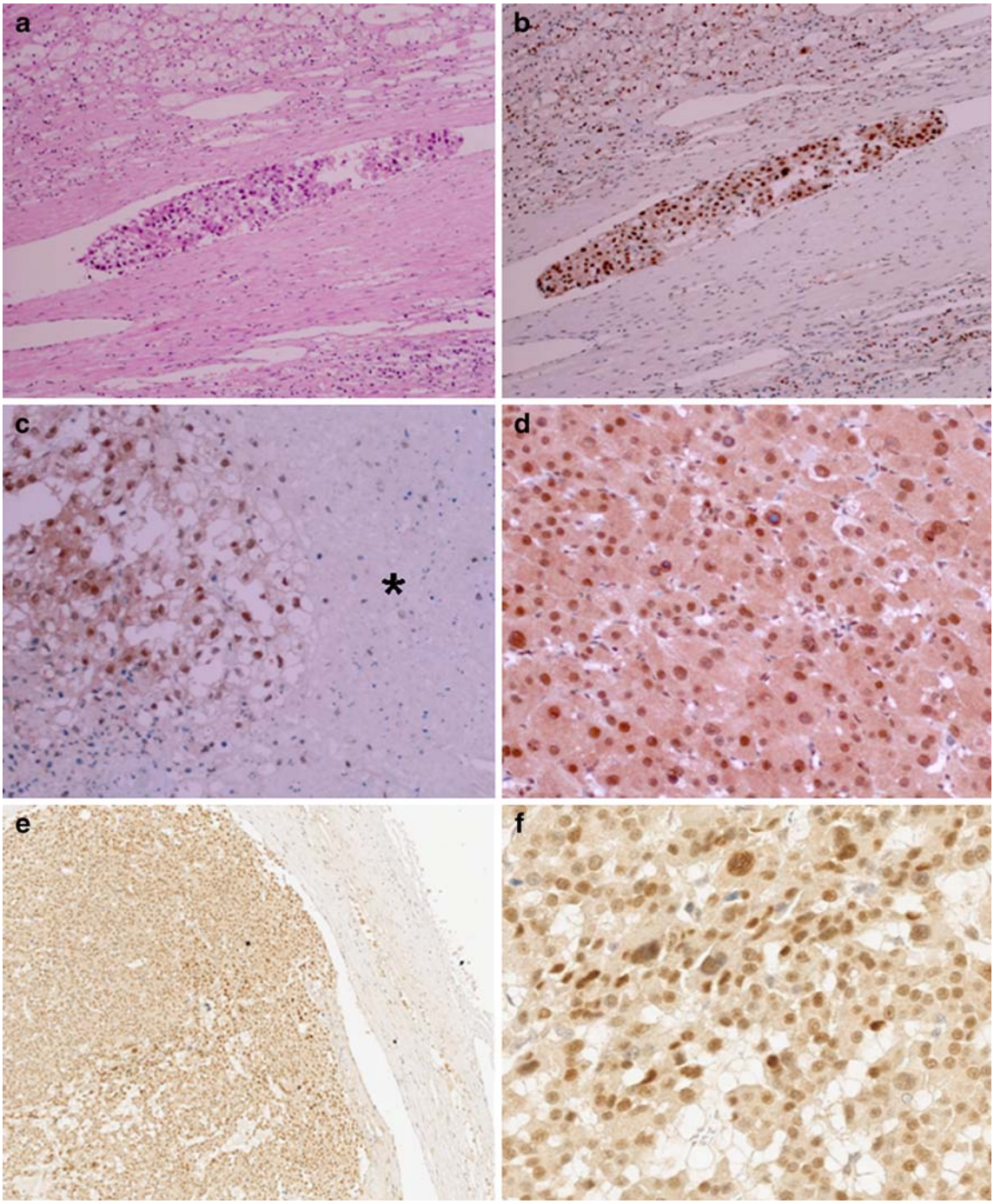


Fig. 4 Immunohistochemical evaluation of ERβ and AR expression in ACCs. **a–b** Vascular invasion by neoplastic emboli in an ACC. In **b**, the nuclei of neoplastic cells exhibit ERβ expression. **c** ACC cells around a focus of necrosis (*asterisk*) showing nuclear ERβ staining. **d** Large eosinophilic ACC cells displaying a ERβ positivity. **e–f** Diffuse immunostaning of AR in pleomorphic neoplastic cells of on ACC

and decreased SHP levels in APAs and NFAs. Variable SF-1 and DAX-1 expression in adrenocortical tumors has been reported also in the literature [17, 26, 29, 31, 32], whereas no data are available on LRH-1 and SHP expression. The positive correlation between *LRH-1* expression and *ER*s mRNA levels, as well as the negative association between *SHP* and *ER*s, suggest that *LRH-1* and *SHP* might be transcriptional targets of ERs, as shown in other cell types [1, 16]. On the other hand, increased *LRH-1* expression and decreased *SHP* expression in ER-positive adrenal tumors could enhance estrogen-mediated effects on cell proliferation, as LRH-1 has been shown to induce aromatase expression [7, 38], whereas SHP has been demonstrated to repress ERα and ERβ transcriptional activity [14, 15].

In conclusion, our results demonstrate that ACCs are characterized by an imbalance between ERα and ERβ

levels and increased aromatase expression. Abnormal expression of AR and orphan nuclear hormone receptors could also contribute to the effects of estrogens in adrenocortical tumorigenesis. Because estrogens have a proliferative effect on ACC cells, the results of this study suggest that estrogens could contribute to adrenocortical tumorigenesis though autocrine/paracrine effects. This study opens new perspectives on the potential use of antiestrogens and aromatase inhibitors as therapeutic agents against ACC.

Acknowledgments Giulia Masi is a recipient of a fellowship from IRCCS-IOV (Instituto Oncologico Veneto). This work was supported by AIRC funds to Giorgio Palù.

References

1. Annicotte JS, Chavey C, Servant N, Teyssier J, Bardin A, Licznar A, Badia E, Pujol P, Vignon F, Maudelonde T, Lazennec G, Cavailles V, Fajas L (2005) The nuclear receptor liver receptor homolog-1 is an estrogen receptor target gene. Oncogene 24:8167–8175
2. Aubert S, Wacrenier A, Leroy X, Devos P, Carnaille B, Proye C, Wemeau JL, Lecomte-Houcke M, Leteurtre E (2002) Weiss system revisited: a clinicopathologic and immunohistochemical study of 49 adrenocortical tumors. Am J Surg Pathol 26:1612–1619
3. Baquedano MS, Saraco N, Berensztein E, Pepe C, Bianchini M, Levy E, Goni J, Rivarola MA, Belgorosky A (2007) Identification and developmental changes of aromatase and estrogen receptor expression in prepubertal and pubertal human adrenal tissues. J Clin Endocrinol Metab 92:2215–2222
4. Bardin A, Boulle N, Lazennec G, Vignon F, Pujol P (2004) Loss of ERβ expression as a common step in estrogen-dependent tumor progression. Endocr-Relat Cancer 11:537–551
5. Barzon L, Sonino N, Fallo F, Palù G, Boscaro M (2003) Prevalence and natural history of adrenal incidentalomas. Eur J Endocrinol 149:273–285
6. Brandenberger AW, Tee MK, Lee JY, Chao V, Jaffe RB (1997) Tissue distribution of estrogen receptors α (ER-α) and β (ER-β) mRNA in the midgestational human fetus. J Clin Endocrinol Metab 82:3509–3512
7. Clyne CD, Speed CJ, Zhou J, Simpson ER (2002) Liver receptor homologue-1 (LRH-1) regulates expression of aromatase in preadipocytes. J Biol Chem 277:20591–20597
8. Fallo F, Pezzi V, Barzon L, Mulatero P, Veglio F, Sonino N, Mathis JM (2002) Quantitative assessment of *CYP11B1* and *CYP11B2* expression in aldosterone-producing adenomas. Eur J Endocrinol 147:795–802
9. Fallo F, Pezzi V, Sonino N, Altavilla G, Barzon L (2005) Adrenal incidentaloma in pregnancy. A case report. J Endocrinol Investig 28:459–463
10. Greene LF, Page DL, Fritz A, Batch M, Haller DG, Morrow M (2002) American Joint Committee on Cancer (AJCC) Cancer staging manual, 6th edn. Springer, New York
11. Holter E, Kotaja N, Makela S, Strauss L, Kietz S, Janne OA, Gustafsson JA, Palvimo JJ, Treuter E (2002) Inhibition of androgen receptor (AR) function by the reproductive orphan nuclear receptor DAX-1. Mol Endocrinol 16:515–528
12. Hsing AW, Nam JM, Co Chien HT, McLaughlin JK, Fraumeni JF Jr (1996) Risk factors for adrenal cancer: an exploratory study. Int J Cancer 65:432–436
13. Iyer AK, Zhang YH, McCabe ER (2006) Dosage-sensitive sex reversal adrenal hypoplasia congenita critical region on the X chromosome, gene 1 (DAX1) (NR0B1) and small heterodimer partner (SHP) (NR0B2) form homodimers individually, as well as DAX1-SHP heterodimers. Mol Endocrinol 20:2326–2342
14. Johansson L, Thomsen JS, Damdimopoulos AE, Spyrou G, Gustafsson JA, Treuter E (1999) The orphan nuclear receptor SHP inhibits agonist-dependent transcriptional activity of estrogen receptors ERα and ERβ. J Biol Chem 274:345–353
15. Klinge CM, Jernigan SC, Risinger KE (2002) The agonist activity of tamoxifen is inhibited by the short heterodimer partner orphan nuclear receptor in human endometrial cancer cells. Endocrinology 143:853–867
16. Lai K, Harnish DC, Evans MJ (2003) Estrogen receptor alpha regulates expression of the orphan receptor small heterodimer partner. J Biol Chem 278:36418–36429
17. Lefrancois-Martinez AM, Bertherat J, Val P, Tournaire C, Gallo-Payet N, Hyndman D, Veyssiere G, Bertagna X, Jean C, Martinez A (2004) Decreased expression of cyclic adenosine monophosphate-regulated aldose reductase (AKR1B1) is associated with malignancy in human sporadic adrenocortical tumors. J Clin Endocrinol Metab 89:3010–3019
18. Libertini SJ, Tepper CG, Rodriguez V, Asmuth DM, Kung HJ, Mudryj M (2007) Evidence for calpain-mediated androgen receptor cleavage as a mechanism for androgen independence. Cancer Res 67:9001–9005
19. Montanaro D, Maggiolini M, Recchia AG, Barzon L, Fallo F, Andò S, Pezzi V (2005) Antiestrogens upregulate ERβ expression and inhibit human adrenocortical cell proliferation. J Mol Endocrinol 35:245–256
20. Moslemi S, Vibet A, Papadopoulos V, Camoin L, Silberzahn P, Gaillard JL (1997) Purification and characterization of equine testicular cytochrome P-450 aromatase: comparison with the human enzyme. Comp Biochem Physiol B Biochem Mol Biol 118:217–227
21. Murphy LC, Watson PH (2006) Is oestrogen receptor-β a predictor of endocrine therapy responsiveness in human breast cancer. Endocr Relat Cancer 13:327–334
22. Nakao M, Sato B, Koga M, Noma K, Kishimoto S, Matsuda M, Sonoda T, Matsumoto K (1986) Biochemical and immunological characterization of estrogen binding components in human neoplastic adrenocortical tissues. J Steroid Biochem 25:1–9
23. Penot G, Le Peron C, Merot Y, Grimaud-Fanouillere E, Ferriere F, Boujrad N, Kah O, Saligaut C, Ducouret B, Metivier R, Flouriot G (2005) The human estrogen receptor-α isoform hERα46 antagonizes the proliferative influence of hERα66 in MCF7 breast cancer cells. Endocrinology 146:5474–5484
24. Pezzi V, Mathis JM, Rainey WE, Carr BR (2003) Profiling transcript levels for steroidogenic enzymes in fetal tissues. J Steroid Biochem Mol Biol 87:181–189
25. Phornphutkul C, Okubo T, Wu K, Harel Z, Tracy TF, Pinar H, Chen S, Gruppuso PA, Goodwin G (2001) Aromatase P450 expression in feminizing adrenal adenoma presenting as isosexual precocious puberty. J Clin Endocrinol Metab 86:649–652
26. Reincke M, Beuschlein F, Lalli E, Arlt W, Vay S, Sassone-Corsi P, Allolio B (1998) DAX-1 expression in human adrenocortical neoplasms: implications for steroidogenesis. J Clin Endocrinol Metab 83:2597–2600
27. Rossi R, Zatelli MC, Valentini A, Cavazzini P, Fallo F, del Senno L, degli Uberti EC (1998) Evidence for androgen receptor gene expression and growth inhibitory effect of dihydrotestosterone on human adrenocortical cells. J Endocrinol 159:373–380

28. Sanfilippo JS, Wittliff JL (1984) Steroid hormone receptors in adrenal cortical carcinoma. Am J Obstet Gynecol 150:326–327
29. Sasano H, Shizawa S, Suzuki T, Takayama K, Fukaya T, Morohashi K, Nagura H (1995) Ad4BP in the human adrenal cortex and its disorders. J Clin Endocrinol Metab 80:2378–2380
30. Sethumadhavan K, Bellino FL, Thotakura NR (1991) Estrogen synthetase (aromatase). The cytochrome P-450 component of the human placental enzyme is a glycoprotein. Mol Cell Endocrinol 78:25–32
31. Shibata H, Ando T, Suzuki T, Kurihara I, Hayashi K, Hayashi M, Saito I, Murai M, Saruta T (1998) COUP-TFI expression in human adrenocortical adenomas: possible role in steroidogenesis. J Clin Endocrinol Metab 83:4520–4523
32. Shibata H, Ikeda Y, Mukai T, Morohashi K, Kurihara I, Ando T, Suzuki T, Kobayashi S, Murai M, Saito I, Saruta T (2001) Expression profiles of COUP-TF, DAX-1, and SF-1 in the human adrenal gland and adrenocortical tumors: possible implications in steroidogenesis. Mol Genet Metab 74:206–216
33. Sirianni R, Seely JB, Attia G, Stocco DM, Carr BR, Pezzi V, Rainey WE (2002) Liver receptor homologue-1 is expressed in human steroidogenic tissues and activates transcription of genes encoding steroidogenic enzymes. J Endocrinol 174:R13–R17
34. Takeyama J, Suzuki T, Inoue S, Kaneko C, Nagura H, Harada N, Sasano H (2001) Expression and cellular localization of estrogen receptors α and β in the human fetus. J Clin Endocrinol Metab 86:2258–2262
35. Weiss LM, Medeiros LJ, Vickery AL Jr (1989) Pathologic features of prognostic significance in adrenocortical carcinoma. Am J Surg Pathol 13:202–206
36. Zatelli MC, Rossi R, degli Uberti EC (2000) Androgen influences transforming growth factor-β1 gene expression in human adrenocortical cells. J Clin Endocrinol Metab 85:847–852
37. Zhang H, Thomsen JS, Johansson L, Gustafsson JA, Treuter E (2000) DAX-1 functions as an LXXLL-containing corepressor for activated estrogen receptors. J Biol Chem 275:39855–39859
38. Zhou J, Suzuki T, Kovacic A, Saito R, Miki Y, Ishida T, Moriya T, Simpson ER, Sasano H, Clyne CD (2005) Interactions between prostaglandin E2, liver receptor homologue-1, and aromatase in breast cancer. Cancer Res 65:657–663

Virchows Arch (2008) 452:193–200
DOI 10.1007/s00428-007-0541-1

ORIGINAL ARTICLE

Renal oncocytoma with and without intravascular extension into the branches of renal vein have the same morphological, immunohistochemical, and genetic features

Ondrej Hes · Michal Michal · Radek Šíma · Tomáš Vaněček · Matteo Brunelli · Guido Martignoni · Naoto Kuroda · Isabel Alvarado Cabrero · Delia Perez-Montiel · Milan Hora · Tomáš Ürge · Miroslav Dvořák · Marie Jarošová · Ximing Yang

Received: 21 August 2007 / Revised: 16 October 2007 / Accepted: 23 October 2007 / Published online: 8 December 2007
© Springer-Verlag 2007

Abstract We attempted to investigate the clinicopathological correlation of renal oncocytoma (RO) with renal vein extension. We identified seven ROs with extension into the branches of renal vein. The age of seven patients ranged from 61 to 82 years. Five cases were identified incidentally; two patients had gross hematuria. After surgery, all patients were alive and free of tumors with follow-up of 1 to 5 years (mean=3.6). Oncocytomas measured from 2.2 to 7.5 cm. Renal vein extension was grossly suspected in five of seven cases and histologically confirmed in all seven cases. Tumor cells were positive for cytokeratins, mitochondrial-antigen (MIA), epithelial membrane antigen (EMA), and parvalbumin; five of seven tumors were focally positive for CD117. Ultrastructurally, the cytoplasm was packed by mitochondria. Molecular genetic analysis did not detect abnormal numbers of chromosomes 1, 2, 6, 7, 10, 17, and XY by fluorescence in situ hybridization, loss of heterozygosity on 3p and mutation of von Hippel–Lindau gene in all cases. Array comparative genomic hybridization analysis of two cases did not show any major genetic changes. Our conclusions are as follows: (1) renal oncocytomas may have intravascular extension to the branches of the renal

O. Hes · M. Michal · R. Šíma · T. Vaněček
Department of Pathology, Charles University Hospital Plzeň, Pilsen, Czech Republic

M. Brunelli · G. Martignoni
Department of Pathology, Verona University, Verona, Italy

N. Kuroda
Department of Pathology, Red Cross Hospital Kochi, Kochi, Japan

I. Alvarado Cabrero
Department of Pathology, Centro Medico Mexico City, Mexico, USA

D. Perez-Montiel
Department of Pathology, Institute Nacional de Cancerología, Mexico City, Mexico, USA

M. Hora · T. Ürge
Department of Urology, Charles University Hospital Plzeň, Pilsen, Czech Republic

M. Dvořák
Department of Forensic Medicine, Charles University Plzeň, Pilsen, Czech Republic

M. Jarošová
Department of Hematooncology, University Hospital Olomouc, Olomouc, Czech Republic

X. Yang
Department of Pathology, Northwestern University Feinberg School of Medicine, Chicago, IL, USA

O. Hes (✉)
Department of Pathology, Laboratore Spec. Diagnostiky Medical Faculty and University Hospital, Alej Svobody 80, 323 18 Pilsen, Czech Republic
e-mail: hes@medima.cz

vein; (2) renal oncocytomas with intravascular extension to the branches of the renal vein have the same morphological, immunohistochemical, and cytogenetic findings as have their counterparts without evidence of intravascular invasion; (3) the absence of metastases suggests an overall benign behavior of this tumor, but this has to be substantiated by further studies with a long-term follow-up; and (4) in a renal tumor with granular cytoplasm showing renal vein extension, it is necessary to carefully exclude renal cell carcinomas such as chromophobe RCC, oncocytic variant of papillary RCC, and granular variant of clear cell RCC.

Keywords Kidney · Renal oncocytoma · Intravascular · Intravenous extension · Molecular biology

Introduction

Renal oncocytoma (RO) is currently considered within the spectrum of benign tumors of the kidney [1, 10, 14, 18, 22]. Almost all cases originally described as "malignant" were subsequently reclassified as renal cell carcinomas [13]. There is a single case of authentic RO with aggressive behavior in the English literature [18]. For many years, we have been aware of an interesting feature that can be seen in an otherwise perfectly benign RO and that simulates a malignant behavior, namely, the extension of the tumor to branches of the renal vein. In this paper, we present morphological, ultrastructural, and molecular cytogenetical study of seven such cases.

Materials and methods

The seven cases of RO with protrusion into the renal vein were found among 324 cases of RO in the archives of the authors. The diagnosis of intravital vascular extension was accepted only in cases with CD34, CD31, or factor VIII positivity of the surface of the intravenous tumor. Histological sections of formalin-fixed, paraffin-embedded tissue were stained with hematoxylin and eosin and Hale colloidal iron stain. Immunohistochemical studies were performed on paraffin-embedded tissues. Primary antibodies to the following antigens were employed: cytokeratins (CAM5.2, at 1:50, Becton-Dickinson, San Jose, CA, USA; AE1-AE3, at 1:500, Boehringer, Mannheim, Germany; CK7, at 1:200, Dako, Glostrup, Denmark), EMA (E29, at 1:1,000, Dako), Ki-67 (MIB1, at 1:200, Dako), mitochondrial antigen (MIA; 113–1, at 1:500, Dako), parvalbumin (parv-19, 1:1,000, Sigma, Steinheim), CD117 (polyclonal, at 1:150, Dako), Melan A (A 103, at 1:100, Dako), HMB45 (HMB45, at 1:300, Dako), S100 protein (S1/61/69, at 1:50, Novocastra, Newcastle), TFE3 (polyclonal, at 1:500, Santa Cruz, Santa Cruz, CA, USA), CD34 (at 1:800, NeoMarkers, Fremont, CA, USA), CD31 (JC70A, at 1:50, Dako), and factor VIII (F8/86, at 1:4000, Dako). The primary antibodies were visualized using the supersensitive streptavidin-biotin-peroxidase complex (BioGenex, San Ramon, CA, USA). Small pieces of the formaldehyde-fixed wet tissue of three cases (cases 1, 2, and 4) were postfixed in glutaraldehyde and routinely processed for electron microscopy.

Analysis of the von Hippel–Lindau gene mutation and 3p loss of heterozygosity

Five 10-μm-thick sections of tumor and normal tissue were cut from the formalin-fixed paraffin-embedded blocks and DNA was extracted by the NucleoSpin Tissue Kit (Macherey Nagel, Duren, Germany) according to manufacturer's protocol. Polymerase chain reaction (PCR) for von Hippel–Lindau (VHL) gene analysis was carried out using primers listed in Table 1. PCR for loss of heterozygosity (LOH) analysis of chromosome 3p was performed using short tandem repeat (STR) markers and primers shown in Table 2. The reaction conditions were as follows: 12.5 μl of HotStart Taq PCR Master Mix (QIAgen, Hilden, Germany), 10 pmol of each primer, 100 ng of template DNA, and distilled water up to 25 μl. Amplification program for all fragments, except the marker D3S666, consisted of denaturation at 95°C for 15 min, then 40 cycles of denaturation at 95°C for 1 min, annealing at 55°C for 1 min, and extension at 72°C for 1 min. The program was finished by 72°C incubation for 7 min. Annealing temperature for fragment D3S666 was 58°C.

Successfully amplified PCR products of the VHL gene were purified with a Montage PCR Centrifugal Filter

Table 1 Primers used in PCR analysis of VHL gene

Exon	Name	Sequence 5′ → 3′
Exon 1	VHL e1–1	CGCGAAGACTACGGAGGT
	VHL e1–2	GTCTTCTTCAGGGCCGTA
	VHL e1–3	GAGGCAGGCGTCGAAGAG
	VHL e1–4	GCGATTGCAGAAGATGACCT
	VHL e1–5	GCCGAGGAGGAGATGGAG
	VHL e1–6	CCCGTACCTCGGTAGCTGT
	VHL e1–7	CCGTATGGCTCAACTTCGAC
	VHL e1–8	GCTTCAGACCGTGCTATCGT
Exon 2	VHL e2–1	ACCGGTGTGGCTCTTTAACA
	VHL e2–2	TCCTGTACTTACCACAACAACCTT
Exon 3	VHL e3–1	GCAAAGCCTCTTGTTCGTTC
	VHL e3–2	ACATTTGGGTGGTCTTCCAG
	VHL e3–3	CAGGAGACTGGACATCGTCA
	VHL e3–4C	CCATCAAAAGCTGAGATGAAAC

Table 2 STR markers and primers used in PCR LOH analysis of chromosome 3p

Marker	Name	Sequence 5` → 3`
D3S1768	D3S1768SF	GGTTGCTGCCAAAGATTAGA
	D3S1768A	CACTGTGATTTGCTGTTGGA
D3S1300	D3S1300SF	AGCTCACATTCTAGTCAGCCT
	D3S1300A	GCCAATTCCCCAGATG
D3S1317	D3S1317–1.1	TACAAGTTCAGTGGAGAACC
	D3S1317–1.2	CCTCCAGGCCATACACAGTCA
D3S666	D3S666-SK 15	CAAGGCATTAAAGTGGCCACGC
	D3S666- SK 16	GTTTGAACCAGTTTCCTACTGAG

Devices (Millipore, Billerica, MA, USA) and sequenced using a Big Dye Terminator Sequencing kit (PE/Applied Biosystems, Foster City, CA, USA). Samples were then run on an automated sequencer ABI Prism 310 (PE/Applied Biosystems) at a constant voltage of 11.3 kV for 20 min.

Successfully amplified PCR products of STR markers were mixed with size marker and run on an automated sequencer ABI Prism 310 (PE/Applied Biosystems) at a constant voltage of 15 kV for 28 min.

Fluorescence in situ hybridization

Fluorescence in situ hybridization analysis was performed independently at two institutions. Analysis of chromosomes 7, 17, and XY was performed at the Charles University Hospital (Czech Republic). Analysis of chromosomes 1, 2, 6, 10, and 17 was performed at the Verona University (Italy).

Fluorescence in situ hybridization on chromosomes 7, 17, and XY

From each tumor, 5-μm sections were cut from paraffin-embedded blocks and placed on the slides. Tissues were deparaffinized in xylen three times for 5 min and then washed twice in 100% ethanol, once in 95% ethanol and once in deionized water for 5 min. Then, the slides were heated in the Target Retrieval Solution (DAKO) for 40 min at 95°C and subsequently cooled at room temperature (RT) for 20 min in the Target Retrieval Solution. The slides were washed in deionized water for 5 min at RT, and tissue were covered with 150 μl (or enough to cover the specimen) of the Proteinase K (DAKO) solution for 4–7 min. Then, the slides were rinsed several times over 5 min with deionized water, dehydrated in 95 and 100% ethanol for 1 min each and air dryed. Afterwards, the probe mixtures consisted of 7 μl LSI hybridization buffer, 1 μl CEP probe and 2 μl purified H_2O in case of chromosome 7 and 17, or prepared XY probe mix (Vysis, Downers Grove, IL, USA) were applied on the samples and covered with coverslips. The slides were denatured at 85°C for 10 min and incubated in humidified box at 37°C overnight. Then, the coverslips were carefully removed, and the slides were washed for 2 min in 0.4× saline-sodium citrate (SSC)/0.3% NP-40 at 73°C and for 1 min in 2× SSC/0.1% NP-40 at RT. After that, the slides were placed in a dark room until completely dry, counterstained with DAPI II (Vysis) and viewed under a fluorescence microscope Olympus BX 60.

The criteria for evaluating the FISH signals were the same as in the paper of Hes et al. [9].

Fluorescence in situ hybridization on chromosomes 1, 2, 6, 10, and 17

Interphase cytogenetic FISH analysis was performed using centromeric probes [SpectrumGreen for chromosomes 6, 10, and 17 and SpectrumOrange for chromosomes 1 and 2 (Vysis)]. Paraffin was removed from the sections with two 10-min washes in xylene. After hydrating in 100, 85, and 70% ethanol solutions (10 min each), rinsing in distilled water (10 min), and twice in phosphate buffer solution (pH 7, 10 min each), the slides were fixed in methanol-acetic acid 3:1 for 10 min and air dried. Next, the sections were treated with a 2× SSC solution for 15 min at 37°C, and then dehydrated in consecutive 70, 85, and 100% ethanol solutions for 1 min each and then dried. Next, the sections were incubated in 0.1 mM citric acid (pH 6) solution at 85°C for 1 h. Then, they were again dehydrated in a series of ethanol solutions and dried. The tissue was digested by applying 0.75 ml of pepsin (Sigma, St. Louis, MO, USA) solution (4 mg/ml in 0.9% NaCl, pH 1.5) to each slide and incubating them in a humidified box for 30 min at 37°C. Afterwards, the slides were rinsed with distilled water for few seconds, dehydrated again in graded ethanol solutions and dried. Each probe was diluted 1:100 in tDenHyb1 buffer (Insitus, Albuquerque, NM). Ten microliters of the diluted probe were applied to each slide, and coverslips were placed over the slides. Denaturation was achieved by incubating the slides at 80°C for 10 min in a humidified box; then, hybridization was performed at 37°C for 3 h. The coverslips were then removed, and the slides were immersed at the room temperature in 0.5× SSC for 2 min, in 50% formamide/1× SSC for 5 min, and in 2× SSC for 2 min. The slides were air dried and counterstained with 10 μl DAPI/Antifade (DAPI in Fluorguard, 0.5 μg/ml, Insitus, Albuquerque, NM).

The slides were examined using an Axioplan microscope (Zeiss, Germany) with appropriate filters for SpectrumOrange, SpectrumGreen, and DAPI nuclear counterstain. The signals were recorded with a CCD camera (Axiocam HRm).

FISH signals were evaluated as previously described; 100–200 neoplastic nuclei were counted. The criteria for loss of chromosome were described previously [3].

Array comparative genomic hybridization

Array comparative genomic hybridization (CGH) analysis was performed using the GenoSensor Array 300 system, following the manufacturer's instructions (Vysis). Each array contains 287 target clone DNA (P1, PAC, or BAC clones) representing loci previously shown to be commonly altered in human cancers or to be involved in congenital syndromes and telomeres. The clones are printed in triplicate, and the average resolution of the array is 10 Mb. Briefly, 100 ng of genomic DNA were labeled by a random primer reaction. Tumor DNA was labeled with Cy3 and the normal reference DNA with Cy5. The hybridization mixture consisted of 2.5 μl of each of the differentially labeled DNAs and 25 μl of hybridization buffer containing human Cot-1 DNA. This mixture was denatured at 80°C for 10 min, and this probe was applied onto the spotted area of the array under a coverslip and hybridized in a humid chamber containing 50% formamide/2× SSC at 37°C for 72 h. After hybridization, the arrays were washed three times in 50% formamide/2× SSC at 45°C for 10 min, followed by four 5 min washes in 1× SSC at room temperature, and a brief rinse in distilled water. Finally, the slides were counterstained with DAPI IV solution (Vysis). Each hybridized slide was captured using Genosensor 300 microarray scanner (Vysis Abbott Molecular). As each spot in the array is present in triplicates, the median of the three spots of each probe in the array was calculated. Using the default settings of the GenoSensor, the clones were accepted only if the coefficient of variation between the triplicate spots was less than 10 and if the average correlation coefficient was greater than or equal to 0.9. The normalized ratio for each target was calculated relative to the modal DNA copy number, and the statistical significance of each change was reported as p value [19]. A p value of <0.01 indicated the significant difference between the copy numbers of a targets and the modal clones. A fluorescence ratio >1.25 (log2=0.32) was considered as DNA gains, while DNA losses were scored when the ratio was <0.75 (log2=-0.41).

Results

From 324 RO in our registry, we identified 7 RO with extension into the branches of renal vein. The essential clinicopathological data are summarized in Table 3. The patients were two women and five men, with ages ranging from 61 to 82 years (mean 72.9 years). Whereas in five patients the renal tumors were found incidentally (as for example in Case 2 in whom the kidney neoplasm was identified during a staging procedure for glioblastoma of the right temporal lobe), two patients presented with hematuria. All but one patient were treated by nephrectomy only; one patient (case 6) underwent artificial embolization of blood supply of the tumor and subsequent nephrectomy. Neither adjuvant chemotherapy nor actinotherapy was administered. The clinical follow-up ranged from 1 to 5 years (mean, 3.6 years): All patients are currently well, without signs of recurrences and metastases. Patient 1 underwent irradiation of the prostate because of a prostatic adenocarcinoma (PSA serum level 14 ng/ml, Gleason grade 6 from needle biopsy) 4 years after the nephrectomy for RO, and at the last check-up, there were no signs of generalization of prostatic or renal neoplasia.

Grossly, the tumors were confined to the kidney. Extension into the vascular structures was grossly suspected in five cases (Fig. 1). In all cases, the tumor was bulging into the renal sinus. On cut section, the tumors were dark tan to brown in color. Central fibrous scar was noted in three cases. The tumors ranged in the largest diameter from 2.2 to 7.5 cm (mean, 4.97 cm). A small papillary adenoma (diameter, 0.3 cm) was incidentally found in the same kidney of patient 7.

Microscopically, the tumors were composed of large eosinophilic cells with granular cytoplasm. Nuclei were usually oval, with only focal slightly polymorphism. Mitotic activity was absent. The tumor cells were mainly arranged in a solid-alveolar pattern, and only rarely were small tubular structures present (Fig. 2a, b). Areas of hyaline scars were documented in three cases. No morphological differences were noted in the intravascular compo-

Table 3 Main clinicopathological features

	Sex/age	Side	Diameter	Localization	Grossly suspect extension	Follow-up
Case 1	M/69	Right	7.5 cm	Pole and hilus	Yes	5 years AW
Case 2	F/61	Left	4.6 cm	Hilus	Yes	1 year AW
Case 3	M/77	Right	7.5 cm	Hilus	Yes	2 years AW
Case 4	M/75	Left	5.5 cm	Pole and hilus	No	4 years AW
Case 5	F/82	Right	5 cm	Central part	Yes	4 years AW
Case 6	M/78	Left	5.5 cm	Hilus	No	4 years AW
Case 7	M/68	Left	2.2 cm	Pole and hilus	Yes	4 years AW

F Female, *M* male, *AW* alive and well

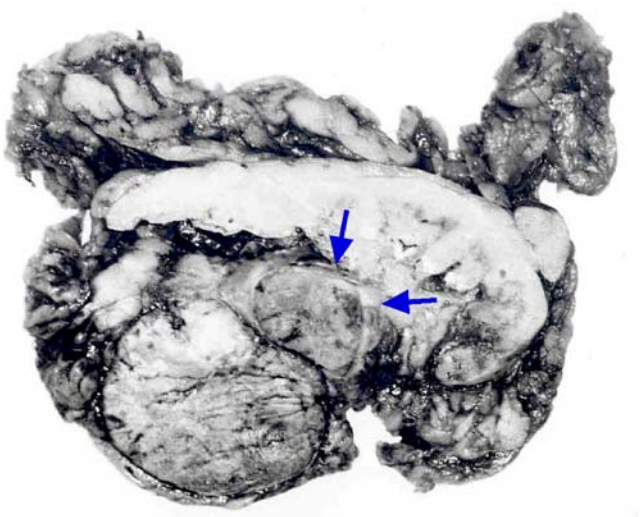


Fig. 1 Renal oncocytoma extending into the dilated vein (*blue arrows*)

nent of the tumors localized within the renal vein and the main tumorous mass. In no case did we find cytologic features typical of chromophobe renal cell carcinomas. All intravenous structures were covered by a single layer of endothelial cells. All cases were Hale colloidal iron stain negative.

Results of immunohistochemical findings are summarized in Table 4. All cases were CAM5.2, EMA and MIA positive in the epithelial component. Furthermore, all but one case were AE1-AE3 positive. Six of the seven cases manifested positive reaction for CK 7, including two cases were a focal staining for this marker and four cases in which only single cells were labeled with CK7. CD117 was focally positive in five out of the seven cases. The surface endothelial layer of intravascular tumors was positive with antibodies to factor VIII, CD31, and CD34 in all seven cases (Fig. 3a, b). The proliferating index (Ki-67) was very low in all cases, with less than 1% of the nuclei labeled. All cases were negative for TFE3, HMB45, Melan A, and S100 protein.

Ultrastructural examination was performed in three cases. Nuclei were oval in shape with small nucleoli. The cytoplasm of tumorous cells was packed with predominantly lamellar mitochondria. Occasionally, small intracytoplasmic lumina covered by short microvilli were present. The luminal aspect of the oncocytic cells was covered by microvilli as well.

The results of molecular biology findings are shown in Table 5. No mutation of the VHL gene was found in all cases. Likewise, no LOH was observed in all successfully analyzed samples. Analysis of chromosome 1, 2, 6, 7, 10, 17, X, and Y copy number did not show any abnormalities.

The results of array CGH performed on patients 2 (Fig. 4a, b) and 3 are shown (Fig. 4c, d).

The CGH analysis of these two cases did not reveal any major chromosomal changes. Overall, four clones display losses, while one clone revealed gain with a 0.001–0.0001 probability.

Discussion

Almost all "malignant" RO published in the older literature are currently thought to represent one of the following "carcinomas of the kidney with granular cytoplasm": chromophobe renal cell carcinomas, granular variant of clear renal cell carcinomas, collecting duct carcinoma of the kidney, or papillary renal cell carcinoma [1, 2].

Vascular invasion is an important factor in the disease prognosis. In cases of renal cell carcinoma, gross evidence of vascular invasion allowed the authors to designate the tumors as stage III [8, 17]. The situation is probably

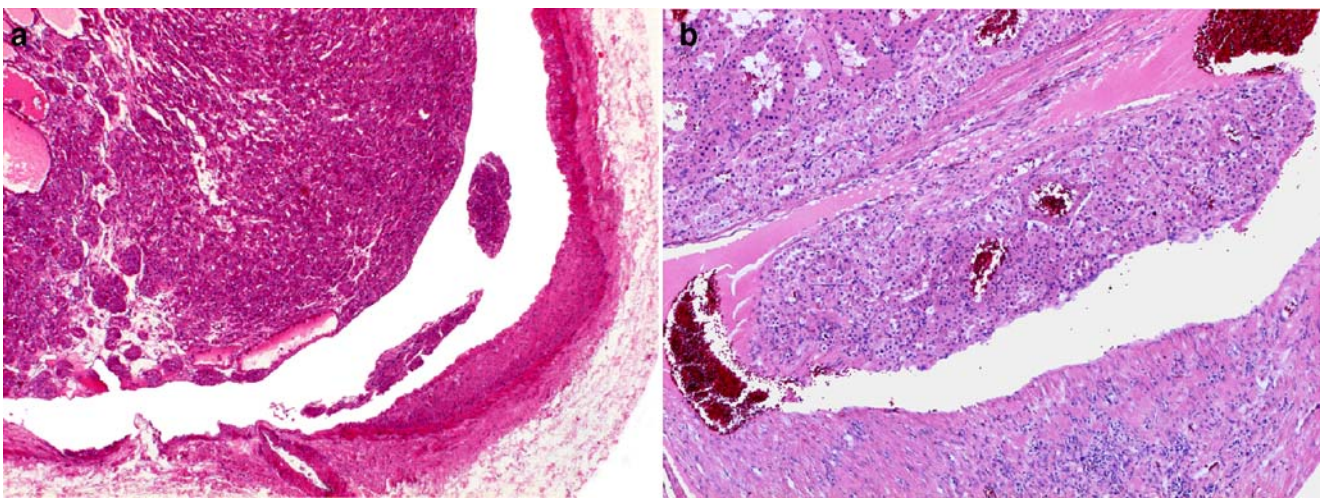


Fig. 2 **a**, **b** Renal oncocytoma within an obvious sinus vein

Table 4 Immunohistochemical results

	AE1-AE3	CAM5.2	CK 7	EMA	TFE3	MIA	CD 117	HMB45	Melan A	Parvalbumin	S100	Ki-67
Case 1	++	++	–	+++	–	+++	foc++	–	–	+	–	0–2/hpf
Case 2	+	++	foc++	++	–	+++	foc++	–	–	–	–	0/hpf
Case 3	+	+++	single cells	+	–	+++	–	–	–	+	–	0–1/hpf
Case 4	+	+++	single cells	+++	–	+++	–	–	–	++	–	0–2/hpf
Case 5	+++	++	foc++	+	–	+++	foc++	–	–	–	–	0–1/hpf
Case 6	+	+	single cells	+++	–	+++	foc++	–	–	–	–	0–1/hpf
Case 7	+	+	single cells	++	–	+++	foc+	–	–	+	–	0–1/hpf

AE1–AE3 Cytokeratin, *CAM5.2* cytokeratin, *CK 7* cytokeratin, *EMA* epithelial membrane antigen, *MIA* antimitochondrial antigen, *foc* focally positive

different with RO. Davis et al. [6] reported vascular invasion in 9 cases (5.4%) from 166 RO patients, and this feature had apparently no influence on their clinical behavior. Lieber et al. [13] identified three cases of RO with angioinvasion but without further progression of the disease in their disputable paper.

Another case was described by Psihramis et al. The patient had bilateral RO with unilateral invasion of the renal vein and perinephric fat. The diagnosis of RO was supported by genetic analysis in which a loss of chromosomes 1 and Y (−1, −Y) was detected. Unfortunately, no follow-up of the patient was provided [20].

Perez-Ordonez et al. suggested that the presence of vascular invasion portend a more aggressive clinical behavior. One of their patients had a biopsy-proven liver metastasis, and the second individual developed liver and bone metastases. The authors had only a core biopsy of the metastasis of the former patient, while there were no biopsies or autopsy findings in the second patient in their series who eventually died with a disseminated disease [18]. It seems that the above-mentioned case with the stable liver metastasis could be accepted as metastasing renal RO from all the papers published in the English language literature.

No signs of aggressive biological behavior were noted in our patients, but, admittedly, the follow-up period of our patients is not long (mean, 3.8 years). We agree with the conclusions of Davis et al. [6] who assumed that angioinvasion have no connotation with a worse prognosis.

One possible explanation of vascular involvement seems to be mechanical abruption of the wall of the renal vein. Four tumors in our series were localized in the central region of the kidney, and the remaining three neoplasms were situated in the renal pole with the extension into the region of the hilus. All tumors grossly compressed vascular structures, and in five patients the vascular extension was grossly visible.

The intrarenal veins are unique in that they have extremely thin walls. They have a wall structure that is very similar to or fundamentally the same is as that of renal capillaries. Moreover, they appear to have no intrinsic shape attributable to their own wall structure but instead fill irregular spaces between tubules [12]. It could be one of the reasons why tumorous mass can relatively easily bulge into

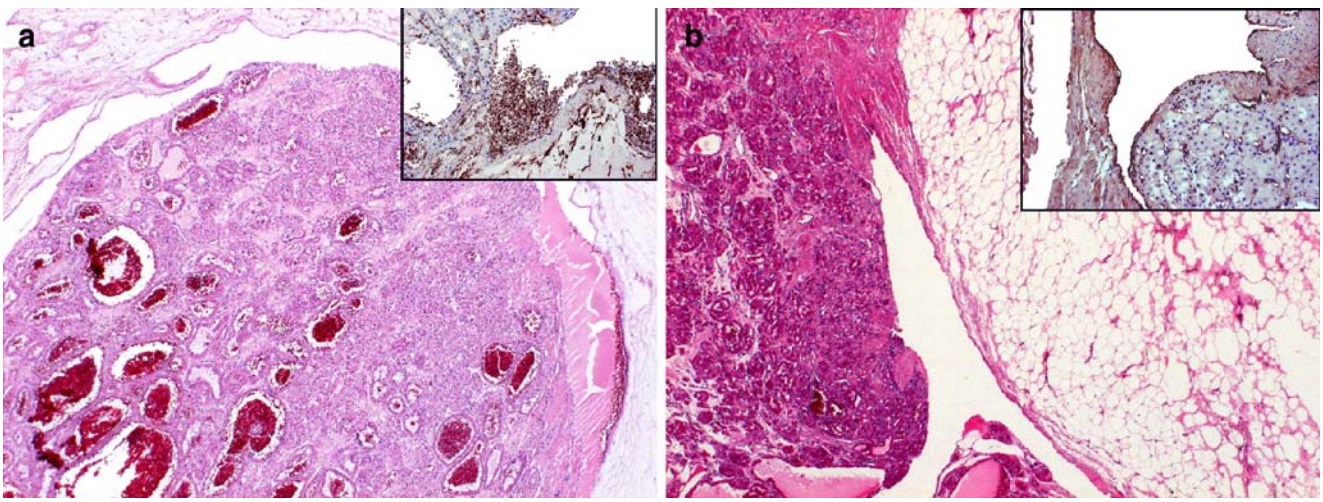


Fig. 3 **a**, **b** Renal oncocytoma within the sinus vein. The surface endothelial layer of intravascular tumors reacts positively with antibodies to factor VIII, CD31 and CD 34 in all seven cases (*insets*)

Table 5 Molecular biology

	LOH				FISH						MA	
	d3 s666	d3 s1300	d3 s1768	d3 s1317	1	2	6	7	10	17	XY	VHL
Case 1	NI	na	na	na	D	D	D	na	D	na	na	WT
Case 2	–	–	–	NI	D	D	D	D	D	D	XX	WT
Case 3	NI	NI	–	–	D	D	D	D	D	na	XY	WT
Case 4	NI	na	na	–	D	D	D	D	D	D	XY	WT
Case 5	NI	–	NI	–	D	D	D	D	D	D	XX	WT
Case 6	–	–	–	NI	D	D	D	D	D	D	XY	WT
Case 7	–	–	NI	–	D	D	D	D	D	D	XY	WT

LOH Loss of heterozygosity, *FISH* fluorescence in situ hybridization, *MA* mutation analysis, *na* not analyzable, *NI* non-informative, *D* disomy, *WT* wild type

the intravascular space. To do so, it is not necessary for a tumor to be located exactly within the hilar region; expansion into the renal vein can occur from a more remote location in the kidney parenchyma.

A similar situation exists in renal angiomyolipoma. Renal angiomyolipoma also rarely invades the venous structures in the hilus, or extends into the vena cava inferior [5, 7]. An extension into the right atrium has also been reported [21], with a possible misdiagnosis of malignant angiomyolipoma in such cases [4]. The analysis of the seven presented cases of RO shows that angioinvasion or renal vein extension seems to have no prognostic significance whatsoever. Nonetheless, the differential diagnostic considerations of RO with intravenous extension are very important and include three relatively common entities. The first one is chromophobe renal cell carcinoma (CRCC) namely the eosinophilic type, which can be easily misdiagnosed as RO. In chromophobe renal cell carcinoma, the presence of raisinoid nuclei, which are absent in RO, is a very important differential diagnostic feature. Moreover, it is possible to find perinuclear clearing in chromophobe renal cell carcinoma, a feature not encountered in RO. Hale colloidal iron stain positivity could assist in the differential diagnosis between RO and CRCC, but the intensity and the quality of staining are dependent on the type of fixation. Unfortunately, both RO and CRCC have no specific genetic changes that would allow one to make diagnosis by molecular biology only [23]. However, the hallmark of chromophobe renal cell carcinoma is multiple chromosomal losses involving chromosomes 1, 2, 6, 10, and 17 [3]. The results of CGH analysis of our two cases did not reveal any major chromosomal changes, which could rise a suspicion for a chromophobe renal cell carcinoma.

Moreover, FISH did not detected abnormal numbers of chromosomes 1, 2, 6, 10, and 17.

Another very similar entity to RO is the recently described papillary renal cell carcinoma, oncocytic variant. This type of carcinoma is composed of typical oncocytic cells arranged in a solid/papillary pattern. All published tumors contained papillary areas, which can be very

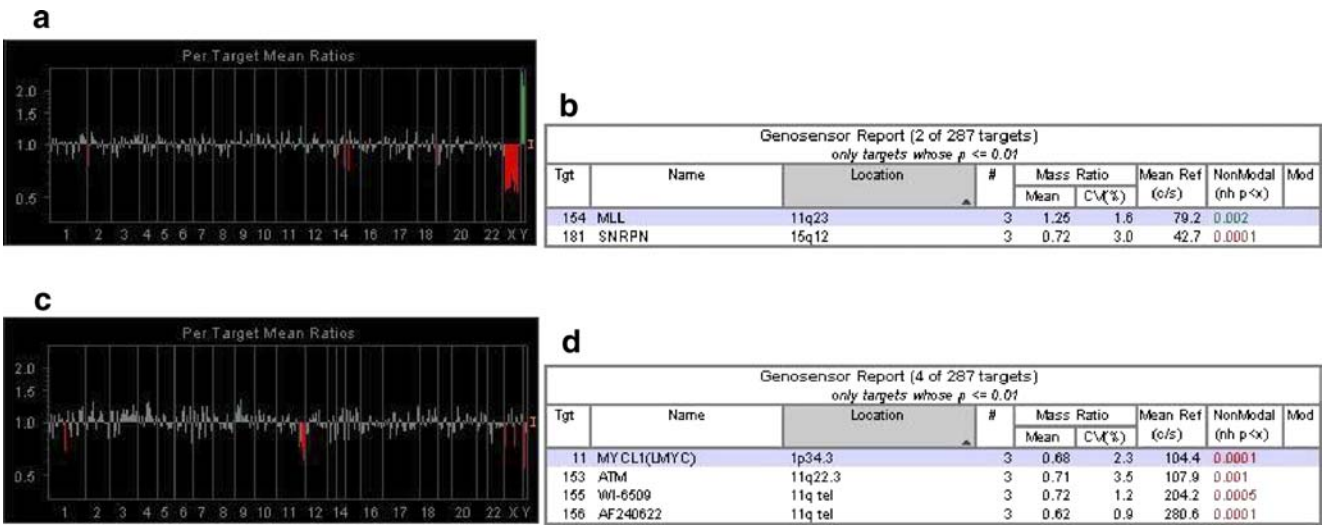


Fig. 4 **a**–**d** Results of array CGH in cases 2 and 3 showing Target report tables and Target Main Ration Plot. The plot displays the target ration in a genomically ordered bar chart with significant gain colored in *green* and significant loss colored in *red*. Modified Target Report Table tabulates statistics for each of spots considering to be changed

limited. In well-sampled cases, it is possible to detect such a pattern. Molecular genetic findings can assist in the differential diagnosis because of the presence of trisomy of chromosomes 7, 17 altogether with the loss of Y chromosome in male patients. These changes never occur in RO [9, 11].

The last common tumor that should be taken into the consideration in the differential diagnosis is the granular variant of clear cell RCC. This tumor can be distinguished from RO by nuclear polymorphism and by the absence of diffuse MIA cytoplasmic positivity. Moreover, nearly 50% of clear RCC carry the VHL gene mutation. Another common finding is deletion of chromosome 3p [8]. We were not able to detect such changes in our cases.

Two very rare tumorous entities should be taken into the consideration. The first one is the so-called oncocytoma-like angiomyolipoma. This tumor could be easily excluded by HMB45 immunoreaction, which is always negative in RO, like in our cases [15]. The second entity is a rare, so-called oncocytoid renal cell carcinoma occurring after neuroblastoma [16]. No patient in our series had a history of neuroblastoma. The tumors in our series were arranged in a solid-alveolar pattern, occasionally with small tubular formations. No papillary component was detected.

In summary: (1) renal oncocytomas may have intravascular extension into the branches of the renal vein; (2) renal oncocytomas with intravascular extension to the branches of the renal vein have morphological, immunohistochemical, and cytogenetic findings identical to those seen in renal oncocytomas without evidence of intravascular invasion; (3) the absence of metastases suggest an overall benign behavior of these tumors, however, as the follow-up period in our series is relatively short, further studies are needed to prove this statement; and (4) in a renal tumor with granular cytoplasm showing renal vein extension, it is necessary to carefully exclude renal cell carcinomas such as chromophobe RCC, oncocytic variant of papillary RCC and granular variant of clear cell RCC.

References

1. Amin MB, Crotty TB, Tickoo SK, Farrow GM (1997) Renal oncocytoma: a reappraisal of morphologic features with clinicopathologic findings in 80 cases. Am J Surg Pathol 21:1–12
2. Amin MB, Amin MB, Tamboli P, Javidan J, Stricker H, de Peralta-Venturina M, Deshpande A, Menon M (2002) Prognostic impact of histologic subtyping of adult renal epithelial neoplasms. Am J Surg Pathol 26:281–291
3. Brunelli M, Eble JN, Zhang S, Martignoni G, Delahunt B, Cheng L (2005) Eosinophilic and classic chromophobe renal cell carcinomas have similar frequent losses of multiple chromosomes from among chromosomes 1, 2, 6, 10, and 17, and this pattern of genetic abnormality is not present in renal oncocytoma. Mod Pathol 18:161–169
4. Byrne DJ, Hamilton Steward PA, Lowe JW (1988) Malignant angiomyolipoma of the kidney associated with hypercalcemia. Br J Urol 62:89–90
5. Chen SS, Lin AT, Chen KK, Chang LS, Chang KK, Chiang H (1996) Renal angiomyolipoma with extension into renal vein. Br J Urol 77:927–928
6. Davis CJ, Sesterhenn IA, Mostofi FK, Ho CK (1991) Renal oncocytoma: clinicopathological study of 166 patients. J Urogenital Pathol 1:41–52
7. Eble JN (1998) Angiomyolipoma of kidney. Sem Diagn Pathol 15:21–40
8. Eble JN, Sauter G, Epstein JI, Sesterhenn IA (eds) (2004) In: Tumours of the urinary system and male genital organs. Pathology and genetics. IARC Press, Lyon
9. Hes O, Brunelli M, Michal M, Cossu Rocca P, Hora M, Chilosi M, Mina M, Boudová L, Menestrina F, Martignoni G (2006) Oncocytic papillary renal cell carcinoma: a clinicopathologic, immunohistochemical, ultrastructural, and interphase cytogenetic study of 12 cases. Ann Diagn Pathol 10:133–139
10. Kovacs G, Akhtar M, Beckwith BJ, Bugert P, Cooper CS, Delahunt B, Eble JN, Fleming S, Ljungberg B, Medeiros LJ, Moch H, Reuter VE, Ritz E, Roos G, Schmidt D, Srigley JR, Storkel S, van Den Berg E, Zbar B (1997) The Heidelberg classification of renal cell tumours. J Pathol 183:131–133
11. Lefevre M, Couturier J, Sibony M, Bazille C, Boyer K, Callard P, Vieillefond A, Allory Y (2005) Adult papillary renal tumor with oncocytic cells: clinicopathologic, immunohistochemical, and cytogenetic features of 10 cases. Am J Surg Pathol 29:1576–1581
12. Lemley KV, Kriz W (1994) Structure and function of the renal vasculature. In: Tisher CC, Brenner BM (eds) Renal pathology with clinical and functional correlations. 2nd edn. Lippincott, Philadelphia, pp 981–1026
13. Lieber MM, Tomera KM, Farrow GM (1993) Renal oncocytoma: clinical and biological correlates. J Urol 150:1380–1383
14. Ligato S, Ro JY, Tamboli P, Amin MB, Ayala AG (1999) Benign tumours and tumour-like lesions of the adult kidney part I: Benign renal epithelial neoplasms. Adv Anat Pathol 6:1–11
15. Martignoni G, Pea M, Brunelli M, Eble JN (2002) Oncocytoma-like angiomyolipoma. A clinicopathologic and immunohistochemical study of 2 cases. Arch Pathol Lab Med 126:610–612
16. Medeiros LJ, Palmedo G, Krigman HR, Kovacs G, Beckwith JB (1999) Oncocytoid renal cell carcinoma after neuroblastoma: a report of four cases of a distinct clinicopathologic entity. Am J Surg Pathol 23:772–780
17. Mostofi FK, Davies CJ (1998) Histological typing of kidney tumors, 2nd edn. Springer, Berlin Heidelberg New York
18. Perez-Ordonez B, Hamed G, Campbell S, Erlandson RA, Russo P, Gaudin PB, Reuter VE (1997) Renal oncocytoma: a clinicopathologic study of 70 cases. Am J Surg Pathol 21:871–883
19. Piper J, Stegenga S, Pestova E, Marble H, Lucas M, Wilber K, King W (2002) An objective method for detecting copy-number changes in CGH microarray experiments. Proceedings of the Third Euroconference on Quantitative Molecular Cytogenetics, Rosenon, Sweden, July 4–6, pp 109–114
20. Psihramis KE, Dal Cin P, Dretler SP, Prout GR, Sanberg AA (1988) Further evidence that renal oncocytoma has malignant potential. J Urol 139:585–587
21. Rothenberg DM, Brandt TD, D'Cruz I (1986) Computed tomography of renal angiomyolipoma presenting as right atrial mass. J Comput Assist Tomogr 10:1054–1056
22. Storkel S, Eble JN, Adlakha K, Amin M, Blute ML, Bostwick DG, Darson M, Delahunt B, Iczkowski K (1997) Classification of renal carcinoma. Workgroup No. 1. Cancer 80:987–989
23. Yang XJ, Sugimura J, Schafernak KT, Tretiakova MS, Han M, Vogelzang NJ, Furge K, Teh BT (2006) Classification of renal neoplasms based on molecular signatures. J Urol 175:2302–2306

Virchows Arch (2008) 452:201–207
DOI 10.1007/s00428-007-0548-7

ORIGINAL ARTICLE

Feasibility of percutaneous organ biopsy as part of a minimally invasive perinatal autopsy

A. C. G. Breeze · F. A. Jessop · A. L. Whitehead · P. A. K. Set · L. Berman · G. A. Hackett · C. C. Lees · for the Cambridge post mortem MRI Study Group

Received: 10 July 2007 / Revised: 5 November 2007 / Accepted: 9 November 2007 / Published online: 18 December 2007
© Springer-Verlag 2007

Abstract To determine the feasibility of percutaneous fetal organ biopsies in the context of a 'minimally invasive' perinatal autopsy after stillbirth and termination for abnormality is the aim of this study. We assessed successful biopsy rate and the proportion adequate for histological examination in 30 fetuses undergoing organ sampling before autopsy. The relationship between gestational age, body weight, death–biopsy interval, operator experience and successful biopsy rate was investigated. Significant findings from conventional block histology were compared with corresponding percutaneous biopsies. Of 210 organ biopsies attempted from seven target organs, 107 were obtained, of which 94 were adequate for pathological comment. The median delivery–autopsy interval was 4 (range 2–11) days. Adequate samples were obtained from the lung in 86% cases (95% CI 68, 96%), liver 76% (95% CI 56, 90%) and less frequently for the myocardium, kidney, adrenal, thymus and spleen. There was no relationship between biopsy success and time to biopsy, gestational age, body weight and user experience. No histological abnormalities found at autopsy were diagnosed from needle biopsies. Although targeted percutaneous biopsies appear feasible for some organs, fewer than 50% of all biopsies are adequate for histological examination. This technique cannot be considered to provide useful clinical information as part of a 'minimally invasive' perinatal autopsy.

Keywords Fetus · Congenital anomaly · Autopsy · Pregnancy loss · Fetal death · Organ biopsy · Feasibility studies

A. C. G. Breeze · G. A. Hackett · C. C. Lees (✉)
Division of Maternal–Fetal Medicine, Addenbrooke's Hospital,
Cambridge University Hospitals NHS Foundation Trust,
Box 228, Hills Road,
Cambridge CB2 0QQ, UK
e-mail: Christoph.Lees@addenbrookes.nhs.uk

P. A. K. Set · L. Berman
Department of Radiology, Addenbrooke's Hospital,
Cambridge University Hospitals NHS Foundation Trust,
Box 219, Hills Road,
Cambridge CB2 0QQ, UK

F. A. Jessop · A. L. Whitehead
Department of Histopathology, Addenbrooke's Hospital,
Cambridge University Hospitals NHS Foundation Trust,
Box 235, Hills Road,
Cambridge CB2 0QQ, UK

L. Berman
Addenbrooke's Hospital,
Box 111, Hills Road,
Cambridge CB2 0QQ, UK

Introduction

Perinatal deaths due to fetal abnormality, late miscarriage and stillbirth complicate around 1% of pregnancies [16]. Even when there is an identifiable clinical cause for fetal death or pregnancy loss, the results of specialist investigations, including autopsy by an experienced paediatric/fetal pathologist, may modify or correct this [5], or modify the estimation of recurrence risk in cases of fetal abnormality [2]. Despite this information, increasing numbers of parents decline consent for an autopsy [11], and there are significant problems of recruitment and retention into the specialty of pediatric and perinatal pathology [5]. Furthermore, perinatal pathology services have become centralised in regional centres, requiring transport of the body of the fetus or neonate to another centre for autopsy [14].

In view of the declining post mortem consent rates and recent publicity regarding post mortem organ retention, studies have compared magnetic resonance imaging with conventional perinatal autopsy [1, 3, 4, 9, 10, 18]. Worldwide experience with perinatal post mortem magnetic resonance imaging (MRI) remains limited, and the technique remains largely unproven, with a number of questions remaining about its feasibility and implementation as a clinical service [8, 15].

A major concern relates to the inability of MRI alone to provide tissue for microscopic examination, despite providing excellent macroscopic information in many cases. The possibility of combining post mortem imaging with percutaneous organ biopsies has been raised [8, 15], thereby, providing a 'less invasive autopsy'—but its feasibility has not been determined. This study (performed as part of an MRI-based minimally invasive autopsy), reports on the feasibility of obtaining tissue that is adequate for histological assessment from percutaneous organ biopsy and compares significant histopathological findings from organ block histology with the corresponding percutaneous biopsies.

Material and methods

This was part of a prospective comparative study from 2003 to 2005 of post mortem MRI combined with percutaneous needle biopsy vs conventional autopsy. Local research ethics committee approval was obtained (Cambridge REC reference 02/004). This institution has 5,000 maternities per year and a subregional fetal medicine unit, receiving referrals from a delivery population of approximately 24,000/year. The study group consisted of 30 fetuses, comprising those that were either miscarried or stillborn (15 fetuses) or pregnancies terminated because of fetal abnormalities (15). Gestational age ranged from 16–39 weeks and birth weight from 61–3,270 g.

Table 1 Frequency of successful organ sampling (n=29)

Organ	Observed organ sampling	Observed organ sampling rate for histopathological comment
	Proportion (95% CIs)	Proportion (95% CIs)
Lung	0.90 (0.73, 0.98)	0.86 (0.68, 0.96)
Liver	0.83 (0.64, 0.94)	0.76 (0.56, 0.90)
Myocardium	0.52 (0.33, 0.71)	0.52 (0.33, 0.71
Kidney	0.52 (0.33, 0.71)	0.34 (0.18, 0.54)
Adrenal	0.41 (0.24, 0.61)	0.41 (0.21, 0.61)
Thymus	0.34 (0.18, 0.54)	0.17 (0.06, 0.36)
Spleen	0.17 (0.06, 0.36)	0.17 (0.06, 0.36)

Fig. 1 **a** Relationship between fetal weight and number of successful biopsies obtained per fetus. Axis legends: *y-axis* Number of adequate biopsies obtained, *x-axis* fetal weight (g). **b** Relationship between gestational age and number of successful biopsies obtained per fetus. Axis legends: *y-axis* Number of adequate biopsies obtained, *x-axis* gestational age of fetus (completed weeks). **c** Relationship between number of adequate biopsies and interval between death and biopsy. Axis legends: *y-axis* Number of adequate biopsies obtained, *x-axis* interval between diagnosis of fetal death and biopsy. **d** Relationship between case number and number of adequate biopsies. Axis legends: *y-axis* Number of adequate biopsies obtained, *x-axis* case number

Percutaneous organ biopsies were performed by an obstetric research fellow (ACGB) and specialist radiologist using ultrasound guidance ± surface landmarks in the first three cases; in the following 27 cases, they were performed using surface landmarks only. The target organs were the fetal lungs, heart, spleen, liver, kidneys, adrenals and thymus. Sampling was attempted in all cases irrespective of whether or not abnormality was suspected on ultrasound or MRI, using a 16- to 18-G 'Temno' cutting biopsy needle (Cardinal Health, IL, USA), a device commonly used for needle biopsy in radiology practice. These were performed just before autopsy. The biopsies were batch reported by one of two specialist perinatal pathologists, whichever did not subsequently perform the conventional post mortem.

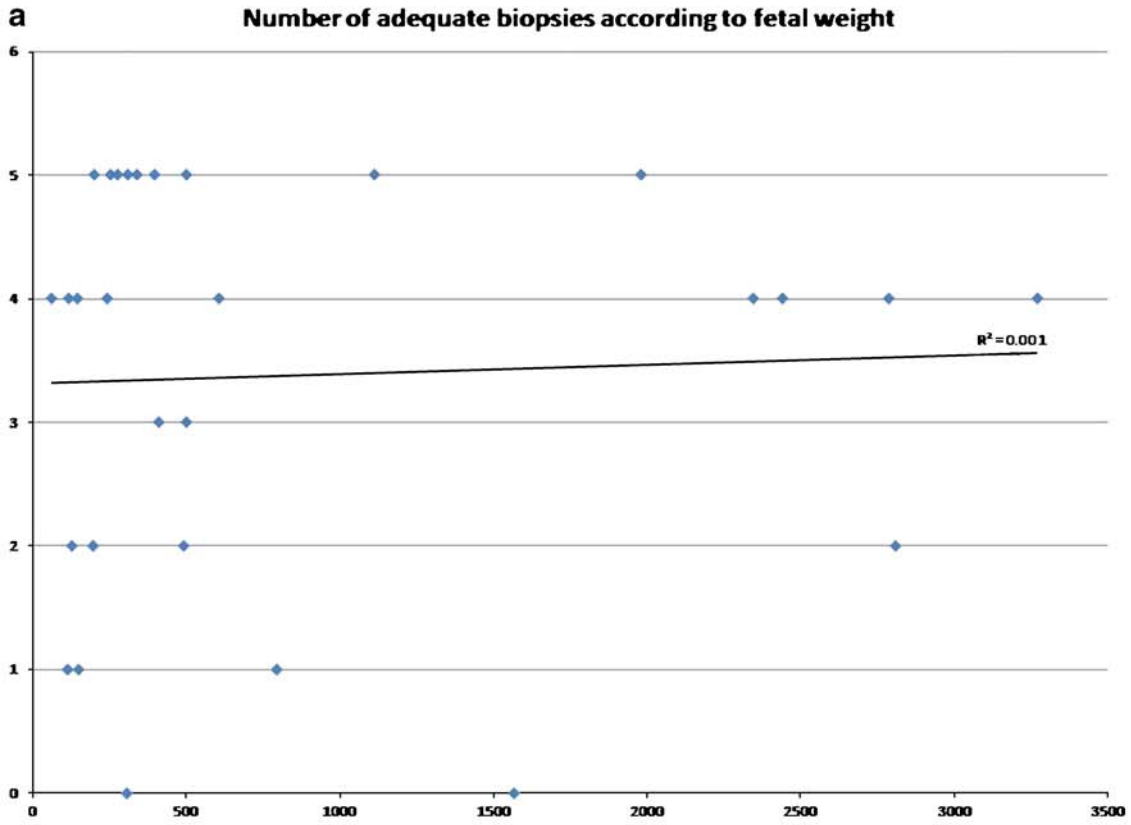
Conventional post mortem examinations were performed by one of two consultant perinatal pathologists working in our hospital, according to Royal College of Pathologists guidelines [13]. The pathologists were informed of the clinical and ultrasound findings but were 'blinded' to post mortem MRI findings. The written report for the organ biopsies and conventional block histology were compared.

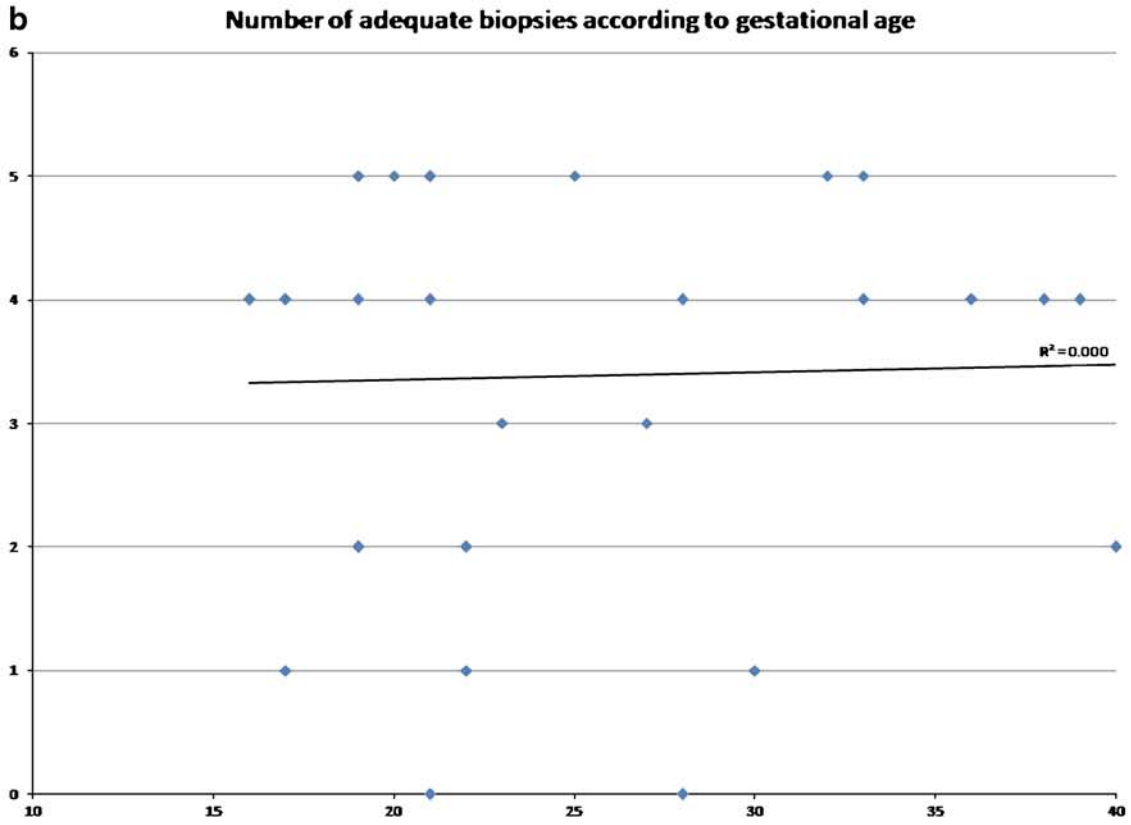
Results

The median interval from delivery to autopsy was 4 days, and 95% of autopsies were performed within 7 days from delivery (range 2 – 11 days).

In one case, the parents requested biopsy blocks and slides to be returned to them before reporting. Therefore, of 210 biopsies attempted from 30 fetuses, 203 biopsies from 29 fetuses were analysed. One hundred and seven (53%) were confirmed histologically to be of the seven target organs. However, in only 94 of the 107 (46%) were these biopsies considered adequate for histopathological comment. The median number of confirmed target organ biopsies was 4 (range 0–6) per fetus. Other biopsies demonstrated connective tissue, further samples of other target organs (each organ only counting once per case) or unrecognisable tissue.

In two cases, six organs were sampled, in ten cases, five organs were successfully biopsied, in seven cases four, in three cases three, in two cases two, and in four cases only


a
Number of adequate biopsies according to fetal weight
R² = 0.001
0
1
2
3
4
5
6
0
500
1000
1500
2000
2500
3000
3500


b
Number of adequate biopsies according to gestational age
R² = 0.000
0
1
2
3
4
5
6
10
15
20
25
30
35
40

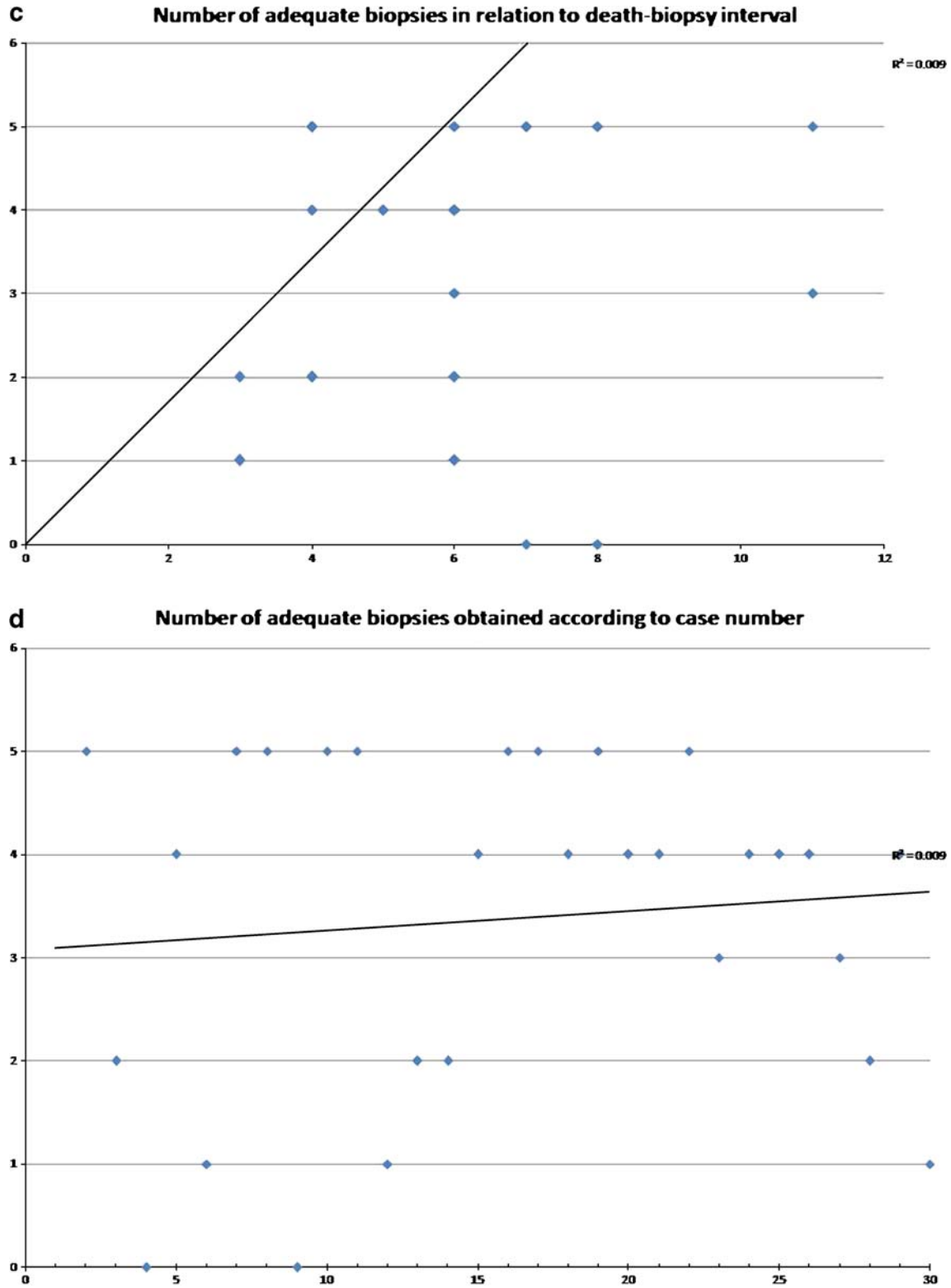


Fig. 1 (continued)

Table 2 Correlation between significant block histology findings and corresponding percutaneous biopsy

Organ	Significant block findings	Corresponding biopsy findings
Lung	Case 1—chronic inflammatory infiltrate around bronchioles extending into lung parenchyma	Case 1—no biopsy available
	Case 2—focal necrosis	Case 2—apparently normal lung
	Case 4—focal necrosis	Case 4—lung biopsy inadequate
	Case 8—interstitial inflammatory cell infiltrate	Case 8—apparently normal lung
	Case 21—poorly formed potential airspaces	Case 21—lung biopsy inadequate
Liver	Case 28—Congested liver	Case 28—normal liver
Myocardium	Case 4—focal necrosis	Case 4—no biopsy available
Kidney	Case 16—multicystic dysplastic kidneys	Case 16—no biopsy available
Adrenal	Case 1—congested, haemorrhagic adrenals	Case 1—no biopsy available
	Case 11—haemorrhagic adrenals	Case 11—normal adrenals
Thymus	Case 11—cortical depletion	Case 11—normal
	Case 23—cortical depletion	Case 23—inadequate biopsy
	Case 29—large cystic Hassall's corpuscles	Case 29—no biopsy available
Spleen	Case 11—haemorrhagic spleen	Case 11—no biopsy available

one. In one case, none of the attempted biopsies could be confirmed by microscopy. Of these 107 biopsies, 13 were considered inadequate for pathological comment.

The highest biopsy success (in terms of samples adequate for comment) was for the lungs and liver (86.0 and 76%, respectively) and lowest for the spleen (17%; see Table 1). No relationships between gestational age and success rate, nor birth weight and success rate were observed, nor for interval between death and biopsy. There was no obvious 'learning curve' for the technique. The regression lines in Fig. 1a,b,c and d illustrate this. In those cases in which ultrasound guidance was used, five biopsies were obtained adequate for histopathological comment in each case.

Table 2 shows the potentially significant findings at block histology and the corresponding findings (if available) of the percutaneous core biopsies from the same fetus. In most cases, organ histology was normal, or organs were too autolysed for comment at full post mortem. However, there was one case with significant liver block findings, five cases with significant lung block findings, one case with significant myocardial block findings, one case with significant renal block findings, two cases with adrenal block findings, one case with significant spleen findings, and three cases with significant thymus block findings. In no cases were the significant block histology findings replicated in the organ biopsies; these were all reported as either normal, inadequate or no biopsy available.

Discussion

The aim of this study was to determine whether samples adequate for pathological comment could be obtained by percutaneous needle sampling from fetuses after stillbirth or termination for abnormality. The two questions addressed by this study are represented by Tables 1 and 2, namely, how frequently are adequate samples obtained from fetal organs and how do percutaneous biopsy results compare with those of conventional block histology?

While for some fetal organs, such as lungs and liver, adequate samples could be obtained in the majority of cases, for others, most samples were inadequate. These difficulties reflect the relatively small size of many fetal organs, particularly in the mid-trimester and possibly also the lack of imaging guidance in this study. It is also noteworthy that where histological abnormalities were found at conventional autopsy, in no cases were these identified in the needle biopsies taken of the same organs—either because the biopsies failed, were inadequate or were reported as normal. This must be regarded as a significant weakness of organ biopsy in this study; in comparison with histology from conventional autopsy, the false negative rate of percutaneous biopsy was 100%.

In many perinatal autopsies, organ histology does not reveal histological abnormalities in most organs; a frequent finding is that many internal organs are too autolysed for pathological comment. In cases of termination for fetal abnormality, histological abnormalities may only be expected in a small number of organs, usually suspected in advance on prenatal imaging. In antepartum fetal death, histological abnormalities may be most commonly found in the liver or lungs, for example, showing evidence of fetal bacterial or viral infection [16]. In this context, adequate samples were most easily obtained from the fetal lungs and liver potentially allowing assessment of fetal organ development and maturation—and the histological investigation of perinatal infection. However, none of the biopsies in this study revealed such findings, even when, for example, block histology from the same fetus showed evidence of

infection. Abnormalities in the fetal thymus ("cortical depletion") may be seen in cases of chronic hypoxia. The thymus was successfully sampled in only 17% of biopsy attempts, and fetal spleen and adrenal were sampled with most difficulty. We must therefore be guarded about recommending percutaneous biopsy of any fetal organs after stillbirth as the likelihood of successful biopsy for some organs, and then disclosing abnormalities may be low.

The results presented are comparable with those described previously for adults, with adequate samples obtained from the liver in 92% of cases, the heart in 55%, the lung in 46% and the kidney in 34% [17]. A more recent—but smaller—study reported successful biopsy of the adult lung in 100% of 21 cases to only 9.5% for the kidney [7]. To our knowledge, the only previous reported data on needle biopsy in the context of perinatal loss was that described in one neonate after death after neonatal encephalopathy [12]; it is unclear whether imaging guidance was used in this case. The only experience of percutaneous organ biopsy in children used ultrasound guidance to obtain biopsies of organs in 19 children [6], although the data reported do not allow direct comparisons with this study, as they concentrated on agreement on cause of death.

The success rates for organ sampling that we describe provide pragmatic data on what could be expected to be achieved without highly trained individuals or imaging guidance and suggest that tissue can be obtained by percutaneous biopsy of certain major fetal organs using surface landmarks. There was no apparent learning curve relating to increasing experience. Our data suggest that we must be cautious about the interpretation of apparently adequate percutaneous biopsies, as in all cases in which there were histological abnormalities on block histology, these were not detected by biopsy. Furthermore, in many of the cases in which significant histological abnormalities were identified on conventional organ blocks, inadequate or no tissue from the organ of interest was obtained by percutaneous biopsy (Table 2). While it is possible, therefore, that imaging-directed biopsy (whether by ultrasound or MRI) might provide a higher proportion of samples that are both adequate for comment, and able to replicate the findings of block histology, this remains to be proven.

This paper details the feasibility of percutaneous organ biopsies as part of a "minimally invasive" perinatal autopsy—not its comparability to conventional autopsy. Although approximately one half of the organs were successfully sampled, even where this was the case, it did not allow an accurate histological diagnosis to be made. We detected none of the histological abnormalities that were found by conventional tissue-block histology, although the sample of abnormal cases is admittedly small. We therefore demonstrate no utility for percutaneous needle biopsy. Whether percutaneous biopsy would make any practical difference to achieving a diagnosis and counselling parents where specific pathologies were suspected remains to be demonstrated. Furthermore, the role of percutaneous biopsies as a stand alone investigation or in combination with imaging in perinatal death would appear on the basis of these findings to be limited.

Acknowledgements Members of the Cambridge post mortem MRI study group also include: Dr Justin Cross, Professor David J Lomas, and Ms Ilse Joubert (of the Department of Radiology, University of Cambridge and Addenbrooke's Hospital). We are indebted to the parents who agreed to take part in this study at a very difficult time. We also acknowledge the assistance of Andrew F Dean (Department of Histopathology, Addenbrooke's Hospital), and Dr Nicholas Coleman (Hutchison-MRC Centre, Cambridge), and the paediatric pathology service staff of Addenbrooke's Hospital: Nicola Wood, Gillian Kenyon, Simon Brown, and Michelle Macer. We also wish to thank the midwives and medical staff of the Rosie Hospital, Cambridge for their support.

This study was supported by a grant from the Trustees of the Addenbrooke's Charities, and ACGB's salary was supported by Cambridge Fetal Care.

Conflict of interest statement The authors have no conflicts of interest to declare.

References

1. Alderliesten ME, Peringa J, van der Hulst VP, Blaauwgeers HL, van Lith JM (2003) Perinatal mortality: clinical value of postmortem magnetic resonance imaging compared with autopsy in routine obstetric practice. BJOG 110:378–382
2. Boyd PA, Tondi F, Hicks NR, Chamberlain PF (2004) Autopsy after termination of pregnancy for fetal anomaly: retrospective cohort study. BMJ 328:137
3. Breeze AC, Cross JJ, Hackett GA, Jessop FA, Joubert I, Lomas DJ, Set PA, Whitehead AL, Lees CC (2006) Use of a confidence scale in reporting postmortem fetal magnetic resonance imaging. Ultrasound Obstet Gynecol 28:918–924
4. Brookes JA, Hall-Craggs MA, Sams VR, Lees WR (1996) Non-invasive perinatal necropsy by magnetic resonance imaging. Lancet 348:1139–1141
5. Cox P, Scott R (2001) Perinatal pathology in 2001. Arch Dis Child 84:457–458
6. Farina J, Millana C, Fdez-Acenero MJ, Furio V, Aragoncillo P, Martin VG, Buencuerpo J (2002) Ultrasonographic autopsy (echopsy): a new autopsy technique. Virchows Arch 440:635–639
7. Foroudi F, Cheung K, Duflou J (1995) A comparison of the needle biopsy post mortem with the conventional autopsy. Pathology 27:79–82
8. Griffiths PD, Paley MN, Whitby EH (2005) Post-mortem MRI as an adjunct to fetal or neonatal autopsy. Lancet 365:1271–1273
9. Griffiths PD, Variend D, Evans M, Jones A, Wilkinson ID, Paley MN, Whitby E (2003) Postmortem MR imaging of the fetal and stillborn central nervous system. AJNR Am J Neuroradiol 24:22–27
10. Huisman TA, Wisser J, Stallmach T, Krestin GP, Huch R, Kubik-Huch RA (2002) MR autopsy in fetuses. Fetal Diagn Ther 17:58–64
11. Khong TY, Tanner AR (2006) Foetal and neonatal autopsy rates and use of tissue for research: The influence of 'organ retention' controversy and new consent process. J Paediatr Child Health 42:366–369

12. Nicholl RM, Balasubramaniam VP, Urquhart DS, Sellathurai N, Rutherford MA (2007) Postmortem brain MRI with selective tissue biopsy as an adjunct to autopsy following neonatal encephalopathy. Eur J Paediatr Neurol 11:167–174
13. Royal College of Obstetricians and Gynaecologists, Royal College of Pathologists. *Fetal and perinatal pathology: report of a joint working party.* London: RCOG Press, 2001
14. Rushton DI (1998) Perinatal pathology: centralise or perish. Br J Obstet Gynaecol 105:5–7
15. Sebire NJ (2006) Towards the minimally invasive autopsy. Ultrasound Obstet Gynecol 28:865–867
16. Silver RM (2007) Fetal death. Obstet Gynecol 109:153–167
17. Wellman KF (1969) The needle autopsy. A retrospective evaluation of 294 consecutive cases. Am J Clin Pathol 52:441–444
18. Woodward PJ, Sohaey R, Harris DP, Jackson GM, Klatt EC, Alexander AL, Kennedy A (1997) Postmortem fetal MR imaging: comparison with findings at autopsy. AJR Am J Roentgenol 168:41–46

Virchows Arch (2008) 452:209–213
DOI 10.1007/s00428-007-0519-z

CASE REPORT

Primary clear cell meningioma of the orbit mimicking a metastatic carcinoma: usefulness of immunohistochemistry and cytogenetic analysis

Maxime Benchetritt · Véronique Hofman · Elodie Long · Guillaume Odin · Elodie Basc · Basile Pasquier · Florence Pedeutour · Paul Hofman

Received: 3 July 2007 / Revised: 19 September 2007 / Accepted: 27 September 2007 / Published online: 10 January 2008
© Springer-Verlag 2007

Abstract Clear cell meningiomas (CCM) are rare tumors of the nervous system that usually occur in young patients and display high recurrence rates and potentially aggressive behavior. In this report, we describe a primary CCM of the orbit in an 84-year-old man with a previous history of a clear cell carcinoma of the kidney. Histologically, the tumor demonstrated a sheet-like proliferation of clear polygonal cells. Differential diagnosis includes metastasis of clear cell carcinomas. Immunohistochemistry, by showing that tumor cells expressed vimentin, epithelial membrane antigen, and progesterone antigens, and cytogenetic analysis, by identifying a monosomy 22, confirmed the diagnosis of CCM.

M. Benchetritt · V. Hofman · E. Long · P. Hofman (✉)
Laboratory of Clinical and Experimental Pathology,
Louis Pasteur Hospital,
30 avenue de la voie romaine,
06002 Nice, France
e-mail: hofman.p@chu-nice.fr

G. Odin
Department of Otorhinolaryngology,
Louis Pasteur Hospital,
30 avenue de la voie romaine,
06002 Nice, France

E. Basc · F. Pedeutour
Laboratory of Solid Tumors Genetics, Faculty of Medicine,
Centre Hospitalier Universitaire de Nice and CNRS UMR,
6543 Nice, France

B. Pasquier
Department of Pathology, Albert Michallon Hospital,
38043 Grenoble, France

P. Hofman
Human Biobank CHU-CAL-UNSA/CRB INSERM,
Louis Pasteur Hospital,
Nice, France

Keywords Orbit · Meningioma · Clear cell meningioma · Metastasis · Immunohistochemistry · Cytogenetics

Introduction

Orbital meningiomas represent between 0.4 and 2% of all intracranial meningiomas and account for 3 to 9% of all orbital tumors [7, 22]. Primary orbital meningiomas arise from the optic nerve sheath and may infiltrate the sphenoid wing producing hyperostosis [1, 21]. Clear cell meningioma (CCM) is a peculiar variant of meningioma affecting young patients which typically arises in spinal or cerebellopontine locations and shows high incidence of recurrence [14, 16–18, 27]. CCM is one of the rarest histologic forms of meningiomas, representing 0.2% of these tumors. Because of its aggressive behavior, it must be distinguished from other meningioma varieties. Differential diagnosis of CCM can be very difficult to make histologically, particularly in some unusual locations and in the absence of cytogenetic analyses [8].

We report a case of a primary CCM of the orbit, for which the diagnosis, suspected histologically, was confirmed by immunohistochemistry and cytogenetic studies. To our knowledge, this has not been reported previously.

Clinical history

The patient was an 84-year-old man, with a previous history of both prostatic adenocarcinoma and clear cell renal adenocarcinoma treated by radical prostactectomy and nephrectomy, who presented with left exophtalmia for 2 months, without other symptoms. Physical examination

showed a severely impaired vision. Computed tomographic scan of the orbit showed a well-circumscribed mass of the left orbit measuring 30×12 mm that was inseparable from the sphenoid bone, with an extracranial extension in the temporal fosse (Fig. 1a) and a hyperosteosis (Fig. 1b). Surgical biopsies were followed by endovascular embolization in conjunction with open resection of the tumor. However, aggressive resection and complete tumor removal were not possible. Despite secondary radiation therapy, the tumor invaded the cavernous sinus and the sella turcica, and the patient died 1 year after the diagnosis.

Materials and methods

Histological and immunohistological studies

For histological analysis, different specimens were taken from the tumor, fixed in 10% formaldehyde, and embedded in paraffin blocks. Four-micrometer sections of the paraffin blocks were stained with hematoxylin–eosin–safran (HES) and periodic acid-Schiff (PAS) with and without diastase digestion. Immunohistochemical staining for epithelial membrane antigen (EMA; Dako, Carpinteria, CA, USA; 1:60), AE1/3 (Dako; 1:50), cytokeratin 20 (Ck20, Ventana, Illrich, France; 1:200), cytokeratin 19 (Ck19, Ventana; 1:200), cytokeratin 8 (Ck8, Ventana; 1:200), cytokeratin 7 (Ck7, Ventana; 1:200), prostatic specific antigen (PSA; Dako; 1:100), renal cell carcinoma marker (RCC Ma; Vector Laboratories, Burlingame, CA, USA; 1:50), HMB45 (Immunotech, Luminy, France; 1:50), Ki67 (Dako: 100), S-100 (Immunotech; 1:50), vimentin (Ventana; 1:100), glial

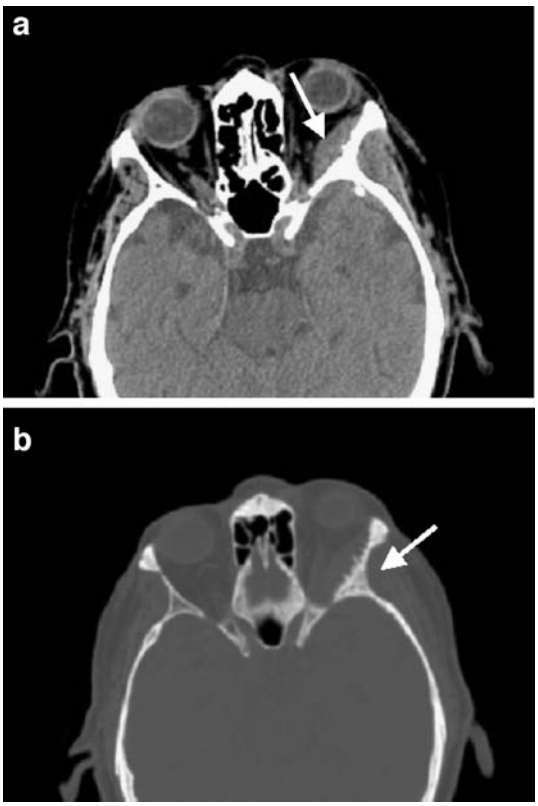


Fig. 1 Axial computed tomography demonstrating an intraorbital tumor (*arrow*) in contact with sphenoid wing (**a**) and associated with osseous involvement characterized by a hyperostosis (*arrow*; **b**)

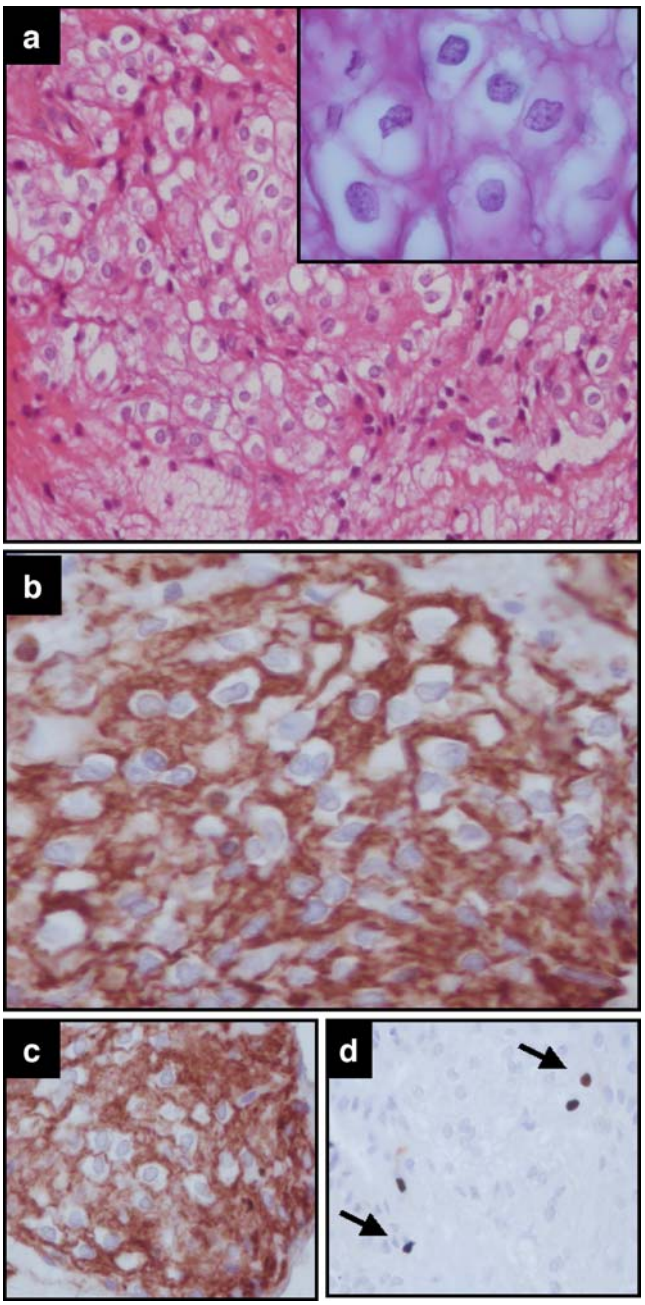


Fig. 2 Sheets of polygonal cells with abundant clear cytoplasm and small round nuclei and lack of intranuclear cytoplasmic invaginations or psammomatous bodies (**a**; HES ×200; *inset* HES ×800). Membranous reactivity for EMA (**b**; ×320). Diffuse and strong staining of the tumor cells for vimentin (**c**; ×320). A few nuclei are stained for progesterone (*arrows*; **d**; ×320)

fibrillary acidic protein (Dako, prediluted), neurofilament (Dako; 1:50), chromogranin A (Ventana; 1: 100), synaptophysin (Ventana), CD56 (Dako; 1:50), muscle actin (HHF-35, Dako; 1:50), desmin (Dako; 1:50), CD45 (Immunotech; 1:200), CD20 (Immunotech; 1:200), CD10 (Dako; 1:100), CD68 (Ventana; 1:100), CD34 (Immunotech; 1:100), CD57 (Becton-Dickinson, San José, CA, USA; 1:100), progesterone (Ventana; 1:100), inhibin (Dako; 1:50), and CD117 (Dako; 1:100) were performed using the streptavidin–biotin complex method.

Cytogenetic analysis

Two fresh fragments of the tumor were reserved for cytogenetic analysis. After mechanical and enzymatic dissociation of the fragment and short-term culture of cells (8 days), metaphase cell analyses were performed according to established procedures [13].

Results

Histologic findings

The resected specimens consisted of seven fragments from 0.3 to 0.7 cm in diameter. Histologically, the tumor showed proliferation of uniform noncohesive polygonal clear cells and contained bands of collagen without necrosis (Fig. 2a). Occasional nucleoli were seen (Fig. 2a, inset). Mitoses, nuclear cytoplasmic inclusions, and psammoma bodies were not observed (Fig. 2a, inset). Glycogen was identified within the tumor cells by diastase-digestible PAS-positive cytoplasm staining.

Immunohistochemical findings

Immunohistochemically, tumor cells showed widespread positivity for EMA (Fig. 2b) and vimentin (Fig. 2c). A few cells were positive for progesterone (Fig. 2d). Anti-Ki67 immunostaining showed some positive nuclei, and the MIB-1 labeling index was evaluated as 15%. Other immunostainings performed in this study were uniformly negative in the tumor cells.

Cytogenetic findings

RHG-banded karyotypes showed an abnormal chromosome 2 in seven cell metaphases: Additional material from unknown origin was present at the extremity of the long arm of a chromosome 2, at band 2q37 (Fig. 3). This additional fragment was intensely stained by the 4,6-diamino-2-phenyl-indole, suggesting that it was mainly made up of heterochromatin. In addition, a monosomy 22 was observed in four cells (Fig. 3). According to the International System for Human Cytogenetic Nomenclature [9], the karyotype was: 46,XY,add(2)(q37)[7]/45,idem,22[4].

Discussion

Orbital lesions are a heterogeneous array of diseases which can be classified based on origin, (1) primary lesions, which

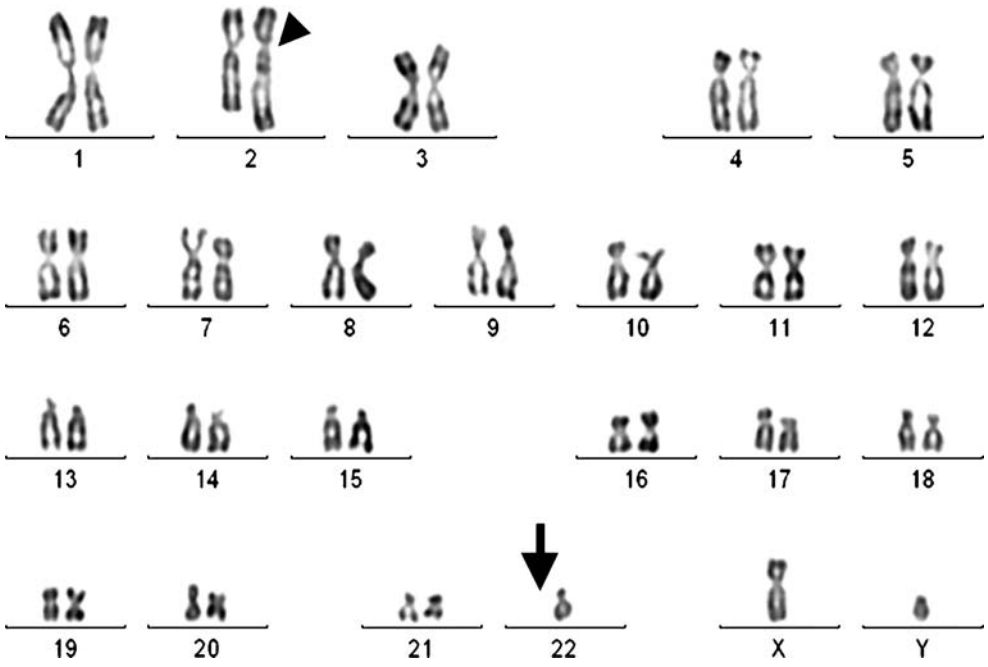


Fig. 3 RHG-banded karyotype of a metaphase cell. The *arrowhead* indicates the abnormal chromosome 2 with additional material of unknown origin at 2q37 and loss of a chromosome 22 (*arrow*), respectively

originate from the orbit itself, (2) secondary lesions, which extend to the orbit from neighboring structures and include such lesions as intracranial tumors and tumors of the paranasal sinuses that by contiguity extend to involve the orbit, and (3) metastatic tumors [5, 7, 22]. Among orbital tumors, meningiomas can be either primary or secondary in origin [1, 7]. Primary orbital meningiomas arise from the orbit nerve sheath and may extend through the optic canal intracranially, or as in the present reported case, they may infiltrate the sphenoid wing producing hyperostosis [1]. Orbital meningiomas, as with those located in other regions, have a predilection for afflicting females [1, 7]. Unilateral visual loss and progressive painless exophthalmos are the most common presentations [7]. Finally, orbital meningiomas share pathological characteristics with other intracranial meningiomas [7].

CCM is a very rare meningioma variant of which fewer than 50 cases have been described in the literature [10]. CCM seems to occur mostly in young patients, although both pediatric and elderly patients have been reported [10]. CCM shows a strong predilection for occurring in the cerebellopontine angle and the spinal column [3, 4, 10, 25]. However, other exceptional locations have been reported, including brainstem parenchyma, fourth ventricle, and sacro-coccygeal regions [2, 4, 24]. CCM has been classified in the categories of grade II by the WHO classification because of its high rates of local recurrence and aggressive clinical course [12]. Histologically, CCM manifests sheets of glycogenated polygonal cells with small round nuclei and a relative lack of intranuclear cytoplasmic invaginations, whorling growth, or psammomatous bodies. The cells have an abundant clear cytoplasm with round, uniform, bland-appearing nuclei lacking significant mitotic activity. The appearance of the distinctive hyalinized stroma along with intermixed, bland tumor cells forms a characteristic histological picture. Immunostains for CCMs reveal diffuse and strong staining of the tumor cells for vimentin and membranous reactivity for EMA. Positivity for progesterone has been reported [16]. Previous reports have shown that the MIB-1 labeling index is a significant prognostic marker for meningiomas [11, 15]. MIB-1 labeling index for CCM is usually intermediate, ranging between that of grades II and III meningiomas [12, 19, 20, 23]. Finally, ultrastructural features of CCM clearly show meningothelial differentiation in the form of cytoplasmic intermediate filaments, interdigiting cell membranes, and intercellular junctions. Although loss or structural rearrangement of chromosome 22 has been largely described in typical meningiomas, the cytogenetic finding of CCM has not been reported to date [12, 19, 20, 23]. Recently, Hartmann et al. [6] reported 22% NF2 mutations in CCMs by single-strand conformational polymorphism.

To the best of our knowledge, the present reported case is the first observation of a CCM of the orbit and the first described loss of chromosome 22 by cytogenetic analysis.

Differential diagnosis of CCM mainly includes lesions with clear cell appearance [10, 27]. Other nervous system tumors such as microcystic meningiomas, clear cell ependymomas, oligodendrogliomas, and lipid-rich glioblastomas can be considered [10, 27]. More exceptionally, a clear cell carcinoma metastasis can be also discussed [8].

In the present case, because orbital metastatic lesions are not infrequent, and considering the previous history of the patient, metastasis of a prostatic or a renal carcinoma of the orbit was first discussed [5, 8]. Tumor cells were not stained with anti-CD10, anti-Ck 8, and anti-RCC Ma antibodies which was not in favor of a metastasis of a renal clear cell adenocarcinoma. Moreover, negative immunostaining with anti-PSA antibody made unlikely the diagnosis of a metastasis of a prostatic adenocarcinoma. Other nervous system tumors, pleomorphic xanthoastrocytoma, hemangioblastoma, and solitary fibrous tumor of the orbit with epithelioid features were also considered [8, 26]. However, these diagnoses were eliminated because the tumors cells expressed EMA, vimentin, and progesterone antigens. Finally, immunohistochemical results and the presence of loss of chromosome 22 allowed us to differentiate CCM from other primary and metastatic clear cell tumors of the orbit.

This case highlights the usefulness of combined morphological and cytogenetic approaches to perform an accurate diagnosis of rare variants of meningioma from small resected specimens and particularly when these tumors are developed in unusual locations.

Acknowledgment The authors thank Rita Attias for her skilfull technical assistance and Dr. Ellen Van Obberghen-Schilling for editing this manuscript. This work was supported by a grant from the Comité des Alpes-Maritimes de la Ligue Nationale contre le Cancer.

References

1. Boulos PT, Dumont AS, Mandell JW, Jane JA Sr. (2001) Meningiomas of the orbit: contemporary considerations. Neurosurg Focus 10:1–10
2. Carlotti CG Jr., Neder L, Colli BO, dos Santos MB, Garcia AS, Elias J Jr, Chimelli LC (2003) Clear cell meningioma of the fourth ventricle. Am J Surg Pathol 27:131–135
3. Dhall SS, Tumialan LM, Brat DJ, Barrow DL (2005) Spinal intradural clear cell meningioma following resection of a suprasellar clear cell meningioma. Case report and recommendations for management. J Neurosurg 103:559–563
4. Epstein NE, Drexler S, Schneider J (2005) Clear cell meningioma of the cauda equina in an adult: case report and literature review. J Spinal Disord Tech 18:539–543
5. Goldberg RA, Rottman J, Cline RA (1990) Tumors metastatic to the orbit: a changing picture. Surv Ophthalmol 35:1–24

6. Hartmann C, Sieberns J, Gehlhar C, Simon M, Paulus W, von Deimling A (2006) NF2 mutations in secretory and other rare variants of meningiomas. Brain Pathol 16:15–19
7. Henderson JW (1994) Orbital tumors, 3rd edn. Raven, New York
8. Inoue T, Miyamoto K, Kodama H, Hosoe H, Shimokawa K, Shimizu K (2005) Cervical clear cell meningioma mimicking a vertebral metastasis. J Clin Neurosci 12:685–687
9. ISCN (2005) An international system for human cytogenetic nomenclature. In: Shaffer LG, Tommerup N (eds) S. Karger, Basel 2005
10. Jain D, Sharma MC, Sarkar C, Suri V, Garg A, Singh M, Sharma BS, Mahapatra AK (2007) Clear cell meningioma, an uncommon variant of meningioma: a clinicopathologic study of nine cases. J Neurooncol 81:315–321
11. Kim Y-J, Ketter R, Henn W, Zang KD, Steudel W-I, Feiden W (2006) Histopathologic indicators of recurrence in meningiomas: correlation with clinical and genetic parameters. Virchows Arch 449:529–538
12. Kleihues P, Cavenee WK (eds) (2000) Pathology and genetics of tumours of the nervous system. IARC Press, Lyon, pp 176–184
13. Limon J, Dal Cin P, Sandberg AA (1986) Application of long-term collagenase disaggregation for the cytogenetic analysis of human solid tumors. Cancer Genet Cytogenet 23:305–313
14. Liu PI, Liu GC, Tsai KB, Lin CL, Hsu JS (2005) Intraspinal clear-cell meningioma: case report and review of literature. Surg Neurol 63:285–288
15. Ming-Tak Ho D, Hsu C-Y, Ting L-T, Chiang H (2002) Histopathology and MIB-1 labeling index predicted recurrence of meningiomas. Cancer 94:1538–1547
16. Oviedo A, Pang D, Zovickian J, Smith M (2005) Clear cell meningioma: case report and review of the literature. Pediatr Dev Pathol 8:386–390
17. Payano M, Kondo Y, Kashima K, Daa T, Yatsuka T, Kida H, Nakayama I, Yokoyama S (2004) Two cases of nondura-based clear cell meningioma of the cauda equina. APMIS 112: 141–147
18. Prinz M, Patt S, Mitrovics T, Cervos-Navarro J (1996) Clear cell meningioma: report of a spinal case. Gen Diagn Pathol 141:261–267
19. Ragel BT, Jensen RL (2005) Molecular genetics of meningiomas. Neurosurg Focus 19:1–8
20. Riemenschneider MJ, Perry A, Reifenberger G (2006) Histological classification and molecular genetics of meningiomas. Lancet Neurol 5:1045–1054
21. Roser F, Nakamura M, Jacobs C, Vorkapic P, Samii M (2005) Sphenoid wing meningiomas with osseous involvement. Surgical Neurol 64:37–43
22. Shields JA, Shields CL, Scartozzi R (2004) Survey of 1264 patients with orbital tumors and simulating lesions. Ophtalmology 111:997–1008
23. Schneider BF, Shashi V, von Kap-Herr C, Golden WL (1995) Loss of chromosomes 22 and 14 in the malignant progession of meningiomas. A comparative study of fluorescence in situ hybridization (FISH) and standard cytogenetic analysis
24. Teo JG, Goh KY, Rosenblum MK, Muszynski CA, Epstein FJ (1998) Intraparenchymal clear cell meningioma of the brainstem in a 2-year-old child. Case report and literature review. Pediatr Neurosurg 28:27–30
25. Vural M, Arslantas A, Ciftci E, Artan S, Atasoy MA (2007) An unusual case of cervical clear-cell meningioma in pediatric age. Childs Nerv Syst 23:225–229
26. Warraich I, Dunn DM, Oliver JW (2006) Solitary fibrous tumor of the orbit with epithelioid features. Arch Pathol Lab Med 130:1039–1041
27. Zorludemir S, Scheithauer BW, Hirose T, Van Houten C, Miller G, Meyer FB (1995) Clear cell meningioma. A clinicopathologic study of a potentially aggressive variant of meningioma. Am J Surg Pathol 19:493–505

Virchows Arch (2008) 452:215–219
DOI 10.1007/s00428-007-0536-y

CASE REPORT

Primary adrenocortical sarcomatoid carcinoma: case report and review of literature

Nathalie Sturm · Nabila Moulai · Marie-Hélène Laverrière · Olivier Chabre · Jean-Luc Descotes · Elisabeth Brambilla

Received: 25 June 2007 / Revised: 18 October 2007 / Accepted: 23 October 2007 / Published online: 14 December 2007
© Springer-Verlag 2007

Abstract Adrenocortical carcinoma (AC) mixed with a sarcoma or sarcoma-like component is exceptional, and only six cases have been detailed in the literature, three including osteo-, chondro-, or rhabdomyosarcoma components, and three others only showing a malignant spindle cell component. These histological subtypes, respectively called adrenal carcinosarcomas and sarcomatoid AC, represent poorly differentiated and extremely aggressive forms of carcinoma, with locoregional recurrence and metastases rapidly arising from the sarcomatous or sarcomatoid component, and death occurring in a few months. We report a case of AC in a 31-year-old man presenting as a nonfunctional tumor, with a histological biphasic pattern combining few areas of differentiated AC and extensive areas of sarcomatoid spindle cell proliferation. The patient died 3 months of locoregional and distant recurrences after surgery despite apparently total tumor resection and VP16-cisplatinum chemotherapy. This case underlines the necessity to identify and isolate these carcinoma's subtypes with worse prognosis and the difficulties to distinguish them from metastatic carcinomas and retroperitoneal sarcomas, in relation to the particular adrenal cortex immunoprofile. According to the World Health Organization principles of terminology, we suggest these tumors be collectively classified as "adrenal sarcomatoid carcinomas," a designation that tends to unify all carcinomas with "pleomorphic, sarcomatoid, or sarcomatous elements."

Keywords Adrenal gland · Carcinosarcoma · Sarcomatoid and sarcomatous components · Adrenocortical carcinoma

N. Sturm · N. Moulai · M.-H. Laverrière · E. Brambilla
Department of Pathology, CHU Albert Michallon,
38043, Grenoble, France

J.-L. Descotes
Department of Surgery, CHU Albert Michallon,
38043, Grenoble, France

O. Chabre
Department of Endocrinology, CHU Albert Michallon,
38043, Grenoble, France

N. Sturm (✉)
Département d'Anatomie et de Cytologie Pathologiques,
CHU Albert Michallon,
BP 217, 38043, Grenoble Cedex 9, France
e-mail: NSturm@chu-grenoble.fr

Introduction

Adrenocortical carcinoma (AC) is a rare tumor with a reported yearly incidence between 1.5 and 2 cases per million individuals and a poor prognosis. A significant proportion of patients have distant metastasis at the time of presentation. It presents as functional or nonfunctional tumor, depending on the presence or absence of clinical syndromes caused by excessive hormonal secretion. Curative surgery is the most effective treatment, and chemotherapy is better in patients treated early after the first surgery [8]. In most studies, the disease was diagnosed at an advanced stage, with recurrence and metastases often occurring within the first 12 months and a mortality rate for adults ranging from 50% within 2 years, 84% at 5 years, and 90% at 10 years [11]. More recently, the common use of modern imaging techniques favoring early detection and the use of large curative resection had positive influence on the natural history of the disease, and better survival rate have been reported with a 5-year overall survival ranging between 38 and 60% [8]. Discerning malignancy in adrenocortical tumors may be difficult when invasion into

surrounding tissues or metastases are missing, and algorithms of histological features have been established to help pathologists to diagnose malignancy. High mitotic rate with atypical mitoses, necrosis, high cellular pleomorphism, and capsular and vascular invasion are main histological features associated with much more aggressive tumor behavior [10, 12, 13]. Biphasic tumors such as sarcomatoid carcinoma and carcinosarcoma contain a sarcoma-like or sarcoma component and regroup all these aggressive histological criteria. They correspond to subtypes of poorly differentiated carcinomas with worse prognosis than conventional AC. We describe a new case of sarcomatoid carcinoma with rapid fatal behavior and review the literature on this extremely rare entity presenting high differential diagnosis difficulties. We, thus, suggest to classify these tumors as "sarcomatoid carcinomas," in agreement with the World Histological Organization (WHO) terminology applied to such identical carcinomas "with pleomorphic, sarcomatoid, or sarcomatous elements" arising in others epithelial organs [9].

Clinical history

A 31-year-old man was admitted to the hospital with a 2-month history of asthenia and left upper abdominal pain, without weight loss or fever. These clinical symptoms lead to the discovery of a 13-cm heterogeneous hypoechogenic left adrenal mass on abdominal ultrasound. On admission, physical examination was normal, without palpable abdominal mass or symptoms of steroid hormone or catecholamine excess (absence of arterial hypertension, flush, diarrhea, palpitation, Cushing's syndrome, virilization). Laboratory studies did not show steroid secretion abnormality; serum catecholamines were within normal levels. Abdominal computed tomography scan showed a large (11.7 × 9 cm) well-demarcated hypodense left adrenal mass impinging on the pancreas and the spleen, without connection with the kidney. After intravenous contrast injection, the lesion became inhomogeneous, with a central hypointense necrotic area and peripheral small calcifications. Locoregional invasion, distant lymph node, and liver or pulmonary metastasis were not seen. Left adrenalectomy was performed, complicated by rupture of the tumor capsule during surgery. Locoregional recurrence occurred 2 months later, with infiltration of the spleen hilus leading to abdominal and retroperitoneal compression, pleural effusion, and ascitis. One cure of VP16-cisplatinum chemotherapy was administrated, but the patient died 3 months after the surgery.

Material and methods

Tissues were fixed in 10% formalin, embedded in paraffin, sectioned, and stained with routine hematoxylin–eosin–safron (HES). Representative sections from each component of the tumor were immunostained using the avidin–biotin–

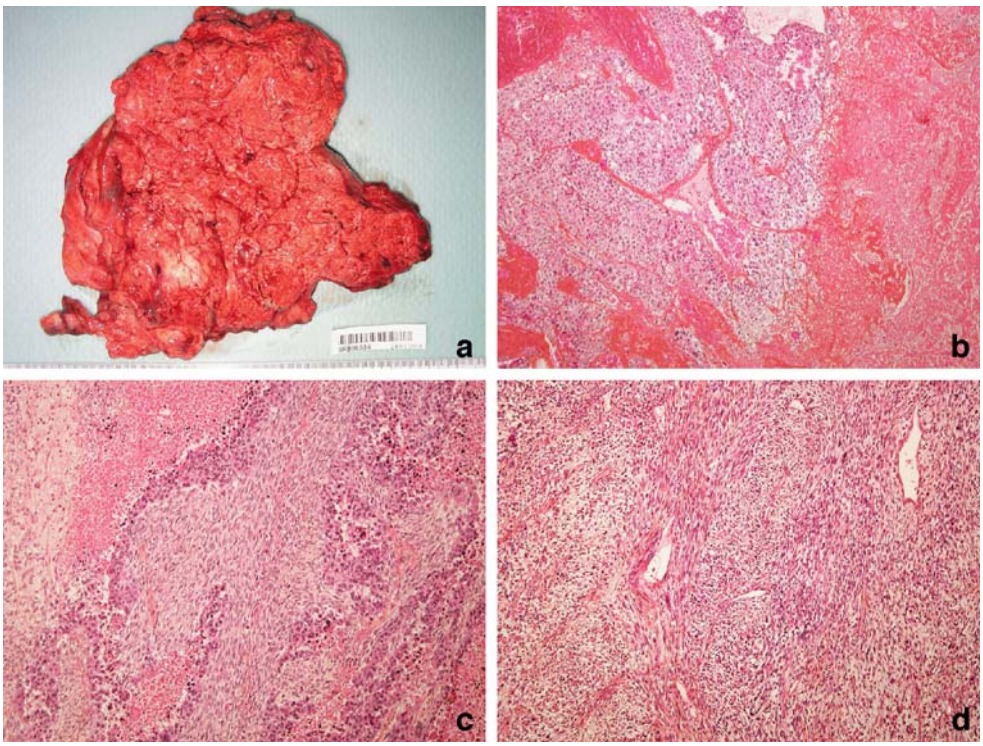


Fig. 1 **a** Gross appearance of the adrenalectomy with variegated polypoid and lobulated cut surface and extensive necrosis of the tumor. **b** Carcinomatous component showing "well-differentiated" clear adrenocortical tumorous cells, arranged in massive or trabecular pattern, mixed with areas of necrosis. **c** Biphasic appearance with closely intermingled sarcomatoid and "poorly differentiated" carcinomatous areas. **d** Sarcomatoid component composed of uniform spindle cells arranged in a fascicular pattern (original magnification ×100, HES stain)

peroxidase complex method, with the following antibodies: cytokeratin AE1-AE3 (AE1-AE3, 1/75, Dako), cytokeratin 8–18 (5D3, 1/150, Novocastra), cytokeratin 19 (RCK108, 1/500, Biogenex), cytokeratin 1–5–10–14 (34betaE12, 1/50, Dako), epithelial membranous antigen (MC-5, 1/200, Biogenex), chromogranin A (LK2H10, 1/1500, Chemicon), CD56 (123-C3, 1/20, Monosan), synaptophysin (1/100, Dako), actin (HHF35, 1/25, Dako), desmin (1/100, Dako), smooth muscle alpha-actin (1A4, 1/50, Zymed), myogenin (LO26, 1/100, Novocastra), S-100 protein (1/1500, Dako), vimentin (1/100, Boehringer), alpha-inhibin (R1, 1/30, Dako), Ki67 (KiS5, 1/25, Dako), and melan A (A103, 1/100, Dako).

Results

The surgical specimen weighted 620 g. It was fragmented and presented as a tumoral well-demarcated encapsulated mass of about 12 × 7 × 5.5 cm, with a widely cystic degenerative cut surface, necrosis and hemorrhage, and a rim of white to gray and pink soft tissue (Fig. 1a). There was little recognizable residual adrenal gland, laminated at the periphery of the tumor. Vascular invasion was noted outside the main tumor mass in vessels located in the periadrenal fat. Histologically, the tumor was composed of both carcinomatous and sarcomatoid components focally intermingled (Fig. 1b–d). The main component showed uniform spindle-shaped tumor cells arranged in a fascicular haphazard pattern. There were also areas of well-differentiated clear and eosinophilic adrenocortical cells resembling those of normal adrenal cortex and forming nests and lobules, and few foci of poor differentiated carcinomatous cells (grades III to IV using Fürhman's nuclear criteria) arranged in a diffuse and solid growth pattern. Few high pleomorphic giant cells with one or more bizarre, hyperchromatic, and anisokaryotic nuclei were present. Mitotic rate in both components was high, with three mitoses per

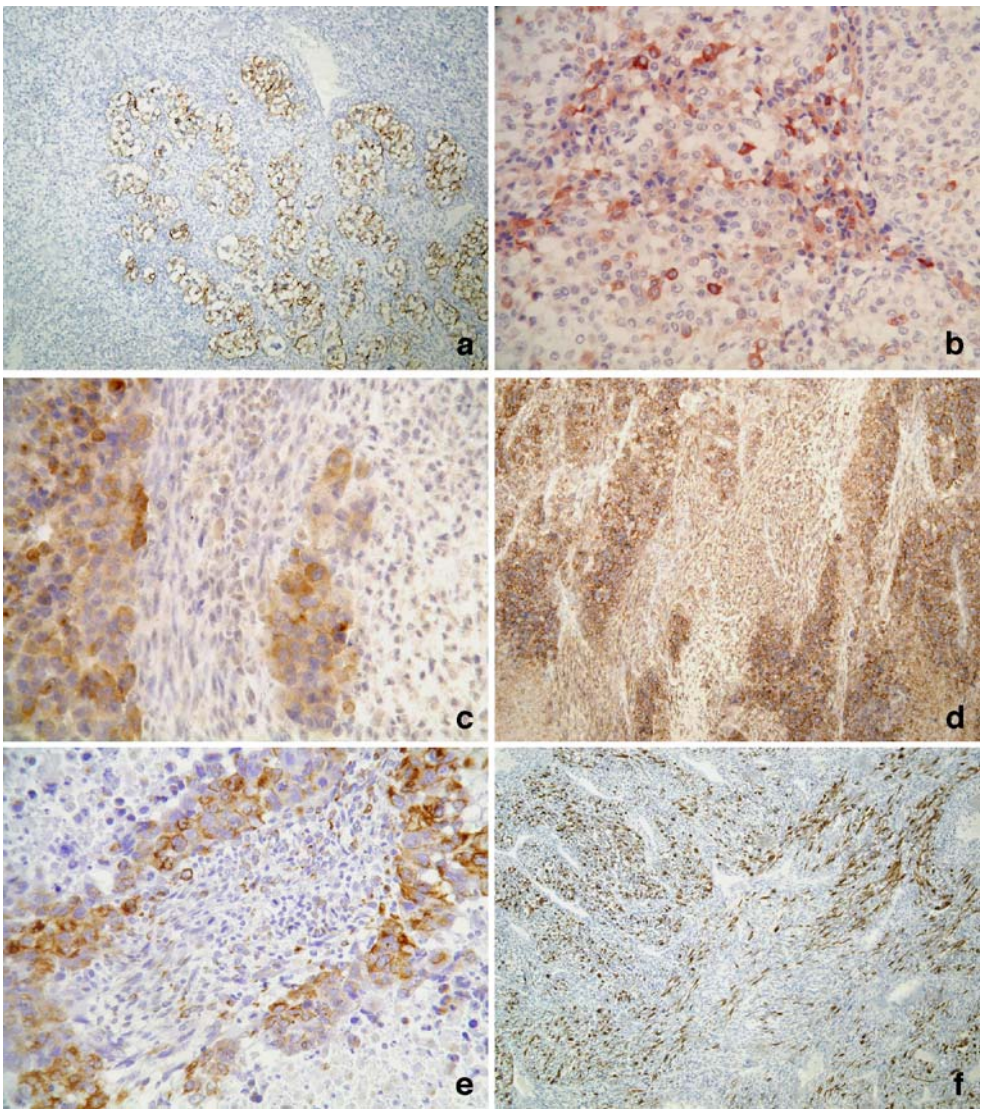


Fig. 2 **a**. Foci of clear carcinomatous cells, reacted with AE1–AE3 cytokeratin, mixed with negative spindle cells. **b** Clear carcinomatous cells showing cytoplasmic reactivity with alpha-inhibin. **c** Carcinomatous areas reacted with synaptophysin. **d** Biphasic reactivity of carcinomatous and sarcomatoid components with CD56. **e** Carcinomatous areas and scattered spindle cells reacted with desmin. **f** Sarcomatoid areas showing strong reactivity with HHF35 actin (original magnification ×100, **a**, **d**, and **f;** ×200, **b**, **c**, and **e**)

high-power field (HPF) in average and atypical mitoses, associated with large areas of necrosis. Vascular invasion observed at gross examination was composed of spindle malignant cells forming tumor thrombi in large veins into periadrenal fat. Foci of capsular invasion were also observed. Areas of rhabdomyosarcoma, chondrosarcoma, or osteosarcoma were not seen despite extensive sampling of the tumor. Eight of the nine Weiss's histological criteria were present. Indeed, areas of diffuse pattern represented less than one third of the tumor, and the spindle sarcoma-like component, histological hallmark in sarcomatoid carcinoma, was not included in the Weiss's scoring system applied to conventional AC. Tumor cells in the carcinomatous component were focally positive for cytokeratin AE1–AE3, alpha-inhibin, and synaptophysin (Fig. 2a–c). Both the carcinomatous and sarcomatoid components in the tumor diffusely and intensively expressed 123-C3 and vimentin, and showed a focal immunoreactivity with smooth muscular markers (Fig. 2d–f). Immunostains for epithelial-membrane antigen (EMA), PS100, MYF-4, chromogranin A, melan A, cytokeratins 19, 8–18, and 1–5–10–14 were negative. Ki67 staining index was over 50%.

Discussion

Adrenal sarcomatoid carcinoma represent an extremely rare variant and a poorly differentiated form of AC, with only six detailed reported cases in the literature (Table 1) [1–4, 6, 7]. As in our case, all presented with a dramatically aggressive behavior. Despite aggressive multi-modality therapy, they rapidly developed recurrences or metastases and died in 3 to 8 months (mean, 6 months). Age of initial presentation ranged from 29 to 79 years (mean, 53) with a female/male ratio of 1.33, and these tumors most often lacked any endocrine dysfunction. Age, disease stage, and completeness of resection are essential criteria in the assessment of prognosis of AC, along with a careful sampling and morphologic evaluation. Histopathological features have a significant impact on the outcome of the disease, such as size and weight of the tumor, high mitotic rate and atypical mitoses, necrosis, high nuclear pleomorphism, diffuse growth pattern and decreased number of cells with clear cytoplasm, and vascular and capsular invasion [10, 12, 13]. In the widely applied multifactorial scoring system proposed by Weiss et al., tumor mitotic activity has been indicated to be the most significant determinant of survival [12, 13]. In a more recent study, patients with high mitotic rate (>20 mitoses per 50 HPF) had significantly worse survival than those with a low rate of mitosis (5–20 mitoses per 50 HPF), and patients with high cellular pleomorphism (defined as giant cells with bizarre and hyperchromatic nuclei and multinucleated cells) or sarcoma-like component within AC had a worse outcome [8]. Carcinosarcoma combines features of conventional AC and areas of sarcoma including heterologous tissues such as rhabdomyosarcomas or areas with chondroid and/or osteogenic differentiation. Sarcomatoid carcinoma, also referred as carcinoma with sarcoma-like component, is mostly composed of spindle malignant cells without heterologous tissue component and often associated (but not necessarily) with more conventional carcinomatous areas. Giant cells (alone or in association with spindle cells and defined as very large and pleomorphic discohesive cells with one or multiple hyperchromatic, anisokaryotic, and multilobated nuclei) are also a feature of sarcomatoid carcinoma in lung cancer classification when this component represents at least 10% of the surface. As regard to AC, high cellular pleomorphism is often present as a Weiss's criteria. Therefore, whether giant cells alone per se

Table 1 Clinicopathological features of adrenocortical sarcomatoid carcinomas reported to date

Authors year of publication	Sex/age	Size (cm), weight (g)	Clinical features and symptoms	Non carcinomatous component	Time of death postoperatively
Okazumi et al. [7]	M, 46	14 cm, 880 g	NF, thrombus into right atrium genex and ventricle	Spindle	206 days
Collina et al. [2]	F, 68	NA	NF	Spindle	7 months
Decorato et al. [3]	F, 42	19 cm	NF	Rhabdomyosarcoma	7 months
Fischler et al. [4]	F, 29	12,5 cm, 610 g	Virilization	Rhabdomyosarcoma spindle	8 months
Barksdale et al. [1]	F, 79	5 cm	NF	Osteosarcoma chondrosarcoma	4 months
Lee et al. [6]	M, 61	12 cm	NF, liver metastasis	Spindle	Postoperative days
our case	M, 31	12 cm	NF, abdominal pain	Spindle	3 months

NA Non-available, *NF* non-functioning

would qualify an adrenal carcinoma as sarcomatoid is an open question, and the answer could also depend on the surface component. In agreement with recommendations provided by WHO in other epithelial malignant neoplasms, we propose that the sarcoma-like component should be well circonscribed and represent at least 10% of the tumor bulk to consider the diagnosis of sarcomatoid AC.

In epithelial organs other than the adrenal gland, when the conventional carcinomatous component is absent, expression of epithelial markers in the spindle and/or giant cell component is required for the diagnosis of sarcomatoid carcinoma, using a panel of cytokeratins, EMA, and carcinoembryonic antigen antibodies [9]. Reasoning is somewhat different in the adrenal gland because normal adrenal cortex and AC express vimentin but usually not cytokeratins. Therefore, foci of the sarcomatoid component are not likely to express cytokeratins. Consequently, diagnosis of adrenal sarcomatoid carcinoma relies on the presence of unequivocal areas of differentiated AC, with its suggestive immunohistochemical profile including synaptophysin, vimentin, 123-C3, Melan A, alpha-inhibin, NSE positivity, and chromogranin A negativity. A generous sampling (at least one section per centimeter of tumor diameter) is necessary to confirm the biphasic pattern and disclose a clear-cut carcinomatous component, allowing (1) to prove the adrenal origin and (2) to rule out two important differential diagnoses in this site such as retroperitoneal sarcoma, leiomyosarcoma, and poorly differentiated metastatic carcinoma. An important feature to keep in mind in this diagnostic challenge is the common occurrence of focal smooth muscle differentiation in sarcomatoid carcinoma, well described in numerous localizations and also observed in the present case [5].

At present, there is no general consensus on the distinction between carcinosarcoma and sarcomatoid carcinoma. Over the past, some authors have synonymously used these entities, whereas others have considered them separately. Trying to distinguish between these two tumor categories may be just an academic exercise because both tumors are highly aggressive malignancies with similarly poor outcomes, regardless of histological findings and treatment. Current concept tends to consider that both represent malignant epithelial neoplasms that have undergone an epithelial to mesenchymal transition. This hypothesis supports the contention that both epithelial and mesenchymal components originate from a single clone and justifies to unify these unusual complex carcinomas with a pleomorphic, sarcomatoid, or sarcomatous biphasic appearance under the collective designation of "sarcomatoid carcinoma."

In conclusion, thorough sampling and careful morphologic examination of the tumor remains, to date, essential in determining prognosis for patients, especially based on cellular pleomorphism and dedifferentiation, mitotic count, and tumor stage. Identification of the sarcomatoid carcinoma histological subtype is also very important because of its worse prognosis, requiring the most aggressive treatment.

References

1. Barksdale SK, Marincola FM, Jaffe G (1993) Carcinosarcoma of the adrenal cortex presenting with mineralocorticoid excess. Am J Surg Pathol 17:941–945
2. Collina G, Maldarizzi F, Betts CM, Eusebi V (1989) Primary sarcomatoid carcinoma of the adrenal gland. First case report. Virchows Arch A Pathol Anat Histopathol 415:161–167
3. Decorato JW, Gruber H, Petti M, Levowitz BS (1990) Adrenal carcinosarcoma. J Surg Oncol 45:134–136
4. Fischler DF, Nunez C, Levin HS, McMahon JT, Sheeler LR, Adelstein DJ (1992) Adrenal carcinosarcoma presenting in a woman with clinical signs of virilization. A case report with immunohistochemical and ultrastructural findings. Am J Surg Pathol 16:626–631
5. Guarino M, Tricomi P, Giordano F, Cristofori E (1996) Sarcomatoid carcinomas: pathological and histopathogenic considerations. Pathology 28:298–305
6. Lee MS, Park IA, Chi JG, Ham EK, Lee KC, Lee CW (1997) Adrenal carcinosarcoma. A case report. J Korean Med Sci 12: 374–377
7. Okazumi S, Asano T, Ryu M, Nagashima T, Odaka M, Isono K, Nishizowa T (1987) Surgical resection of adrenal carcinoma extending into the vena cava, right atrium and ventricle: case report and review of the literature. Nippon Geka Gakkai Zasshi 88: 231–238
8. Tauchmanova L, Colao A, Marzano L, Sparano L, Camera L, Rossi A, Palmieri G, Marzano E, Salvatore M, Pettinato G, Lombardi G, Rossi R (2004) Adrenocortical carcinomas: twelve-year prospective experience. World J Surg 28:896–903
9. Travis WD, Brambilla E, Muller-Hermelink HK, Harris CC (2004) World Health Organization classification of tumours. pathology and genetics of tumours of the lung, pleura, thymus and heart. IARC Press, Lyon
10. Van't Sant HP, Bouvy ND, Kazemier G, Bonjer HJ, Hop WCJ, Feelders RA, de Herder WW, de Krijger RR (2007) The prognostic value of two different histopathological scoring systems for adrenocortical carcinomas. Histopathology 51: 239–245
11. Wajchenberg BL, Albergaria Pereira MA, Medonca BB, Latronico AC, Carneiro PC, Ferreira-Alves VA, Zerbini MC, Liberman B, Gomes GC, Kirschner MA (2000) Adrenocortical carcinoma. Clinical and laboratory observations. Cancer 88:711–736
12. Weiss LM (1984) Comparative histologic study of 43 metastasizing and non-metastasizing adrenocortical tumors. Am J Surg Pathol 8:163–169
13. Weiss LM, Medeiros LJ, Vickety AL (1989) Pathologic features of prognostic significance in adrenocortical carcinoma. Am J Surg Pathol 13:202–206

Virchows Arch (2008) 452:221–227
DOI 10.1007/s00428-007-0538-9

CASE REPORT

Systemic Erdheim–Chester disease

Brendan Craig Dickson · Vaijayanti Pethe · Catherine Tse-Shing Chung · David John Charles Howarth · Juan Manuel Bilbao · Victor Lodovico Fornasier · Catherine Joanne Streutker · Linda Marilyn Sugar · Bharati Bapat

Received: 27 June 2007 / Revised: 16 October 2007 / Accepted: 23 October 2007 / Published online: 10 January 2008
© Springer-Verlag 2007

Abstract Erdheim–Chester disease is a rare xanthomatosis that may present with characteristic radiologic and histologic features. There have been conflicting reports regarding the nature of this process, including whether it represents a reactive or neoplastic lesion. We present the clinical histories, pathologic findings, and an analysis of clonality using the HUMARA assay in two patients diagnosed with Erdheim–Chester disease. One case has previously been documented in the literature. Histologically, both cases demonstrated sheets of foamy xanthomatous histiocytes with widespread infiltration of the viscera. These regions were punctuated by variable amounts of inflammation, including lymphocytes, plasma cells, and occasional Touton-type giant cells. The histiocytes were immunoreactive for CD68 and CD163; they did not stain with S100 or CD1a. One case was found to be monoclonal; however, the second case had extensive DNA degradation; thus, clonality could not be assessed. In addition to contributing an additional report of this rare disease to the literature, we demonstrate the histiocytes to express CD163, thereby further supporting a monocyte/macrophage basis. Moreover, in confirming clonality, our observations lend additional evidence to the view that Erdheim–Chester disease represents a neoplastic process.

Keywords Erdheim–Chester disease · Clonality · HUMARA assay · Neoplasm · Xanthomatosis · Case report · CD163

Introduction

Erdheim–Chester disease (ECD) is a rare xanthomatosis, of unknown etiology, that is frequently denoted by a characteristic radiologic and histologic pattern. It generally occurs in adults and demonstrates a slight male predominance [28]. The clinical course is variable, depending on the location and extent of disease; however, death as a result of extensive systemic involvement is well documented. Lesions may be skeletal and/or extra-skeletal in location;

B. C. Dickson · V. Pethe · C. T.-S. Chung · D. J. C. Howarth · B. Bapat
Department of Pathology and Laboratory Medicine,
Mount Sinai Hospital,
Toronto, ON, Canada

B. C. Dickson · V. Pethe · C. T.-S. Chung · D. J. C. Howarth · J. M. Bilbao · V. L. Fornasier · C. J. Streutker · L. M. Sugar · B. Bapat
Department of Laboratory Medicine and Pathobiology,
University of Toronto,
Toronto, ON, Canada

V. Pethe · B. Bapat
Samuel Lunenfeld Research Institute, Mount Sinai Hospital,
Toronto, ON, Canada

V. L. Fornasier · C. J. Streutker
Division of Pathology, St. Michael's Hospital,
Toronto, ON, Canada

J. M. Bilbao · L. M. Sugar
Department of Anatomic Pathology,
Sunnybrook Health Science Center,
Toronto, ON, Canada

B. Bapat (✉)
Department of Pathology and Laboratory Medicine,
Samuel Lunenfeld Research Institute, Mount Sinai Hospital,
60 Murray Street, Room L6-304B,
Toronto, ON M5T 3L9, Canada
e-mail: bapat@mshri.on.ca

the former yielding characteristic bilateral cortical sclerosis of the long bones [11]. While virtually any tissue site may be involved, all tend to share a similar histologic pattern of widespread infiltration by foamy histiocytes, with variable numbers of concomitant lymphocytes, plasma cells, and Touton-type giant cells; fibrosis is frequently also a feature [29]. The histiocytes are immunoreactive with lysozyme, alpha-1-antichymotrypsin, alpha-1-antitrypsin, and CD68 [29]; consequently, the lesion is presumed to be of macrophage/monocyte lineage, although none of these markers are lineage specific. There are conflicting reports regarding whether ECD represents a reactive polyclonal [2], or a neoplastic monoclonal lesion [7, 27]. Here, we add an additional case of this rare entity to the literature, demonstrate the novel expression of CD163 in these lesions, and confirm clonality using the X-linked human androgen-receptor gene (HUMARA) assay.

Clinical histories

Patient 1

This case has previously been documented in the literature [19]. In May 2000, a 32-year-old woman with hereditary hemorrhagic telangectasia underwent a screening magnetic resonance imaging (MRI) of the head, which revealed a left posterior fossa mass. Initially interpreted as a meningioma, the decision was made to monitor the patient conservatively. In December 2000, she presented with hypoalbuminemia, anasarca and ascites, anemia, diabetes mellitus, hypothyroidism, right exophthalmos, as well as ataxia, dysarthria, and peripheral limb weakness. A repeat MRI of the head showed bilateral retro-orbital masses. The posterior fossa tumour was resected in March 2001, and the diagnosis of ECD was rendered on histopathologic evaluation of the specimen. Radiologic survey of the long bones subsequently confirmed the presence of bilateral cortical sclerosis. She had a normal lipid profile and no history of a metabolic storage disease or hypercholesterolemia. The following month, the patient presented to the hospital with an abdominal mass. Imaging confirmed hepatomegaly and bilateral perirenal soft tissue masses. She declined radiation and was treated variably with steroids and cyclophosphamide. By August 2002, she had developed diabetes insipidus, and had progressive dyspnea. In June 2003, her weakness precipitously worsened, and she was unable to void. An MRI confirmed severe cord compression due to an intraspinal thoracic mass, and she was found to have free air in the abdomen, although exploratory laparotomy failed to identify the source. She ultimately developed sepsis, endocarditis, renal failure, and refractory hypoxemia. Upon institution of supportive management and comfort methods, the patient died in July 2003, and permission was granted for a complete autopsy.

Patient 2

A 77-year-old woman presented with a history of progressive dyspnea and peripheral edema in November 1995. Her relevant past medical history included hypothyroidism, hypertension, and anemia. There was no history of a metabolic storage disease, hypercholesterolemia, or lipid abnormalities. Computed tomography (CT) imaging of the thorax and abdomen revealed mediastinal and lung changes consistent with metastatic carcinoma and multiple suspicious, albeit small, liver lesions. A CT-guided biopsy of the latter proved non-diagnostic. A sanguinous 1.4-l pericardial effusion was drained, but the patient continued to have severe right heart failure that was attributed to constrictive pericarditis. A pericardial window offered little benefit, and a pericardial stripping was performed. Histologic evaluation of the pericardial tissue revealed fibrous pericarditis and abundant foamy macrophages, but the possibility of ECD was not raised. There was no documented history of leg or knee/ankle pain, and imaging of the lower limbs was not obtained. The patient's symptoms progressed, and she developed sepsis, renal failure, hypoalbuminemia, hypotension, and atrial fibrillation. She ultimately died in April 1996, and permission for autopsy, excluding the CNS, was granted.

Materials and methods

Tissue samples

Pursuant to departmental approval, the two cases of ECD were identified from the records of the Division of Pathology, St. Michael's Hospital, Toronto, ON. Tissue was obtained from autopsy specimens that were fixed in 4% formalin and paraffin-embedded. The cases were externally reviewed by a pathologist specializing in bone and soft tissue (DJCH) to confirm the diagnosis.

Immunohistochemistry

Immunohistochemistry was performed using standard techniques. Briefly, 4-μm paraffin-embedded tissue sections were dewaxed in xylene and rehydrated in graded alcohol solutions. Endogenous peroxidase was blocked with 3% hydrogen peroxide. After performing antigen retrieval using 10 mM citrate buffer (pH 6.0) in TT Mega Milestone (ESBE Scientific, Markham, Ontario, Canada), endogenous avidin and biotin were blocked using goat serum, avidin blocking reagent, and biotin-blocking reagents (R&D,

Minneapolis, MN, USA), respectively. The slides were then incubated with primary antibody overnight with either CD68 (KP-1, 1:200; PGM-1, 1:100), CD163 (1006, 1:300), S100 (polyclonal, 1:3,000), or CD1a (010, 1:150). Next, slides were rinsed with Tris-buffered saline (TBS) and incubated with biotinylated secondary antibody (R&D). This was followed by a rinse in TBS, incubation with high-sensitivity streptavidin conjugated to horse-radish peroxidase, followed by 3,3′-diaminobenzidine (HSS-HRP, DAB) chromogen and counterstaining with Mayers Haematoxylin blue in Scott's water.

Microdissection and DNA extraction

Hematoxylin and eosin (H&E) slides from each case were reviewed; blocks containing Erdheim–Chester disease, with the least amount of potential contamination from visceral tissues and inflammatory cells, were selected for analysis. Using a sterile microtome, 7 μm sections were cut onto sterile glass slides (three slides per case). Slides were deparaffinized, rehydrated in graduated alcohol solutions, and stained with Toluidine blue to help visualize the cells. A dissecting microscope (×10) was used to identify the xanthomatous regions, which were then were manually scraped into sterile 1.5-ml tubes using sterile 18-gauge needles. The samples were processed for genomic DNA extraction according the manufacturers protocol using the QIAamp DNA Mini Kit [22].

PCR and analysis of clonality using HUMARA

The human androgen receptor (HUMARA) gene on chromosome X contains a restriction site for methylation-sensitive *HpaII* enzyme and highly polymorphic CAG repeats adjacent to exon 1 of this gene. Clonality analysis was performed as described previously [31], based on digestion of genomic DNA with the methylation-sensitive restriction enzyme *HpaII*, followed by polymerase chain reaction (PCR) amplification of the CAG repeat of human androgen receptor on X-chromosome. Briefly, 250–400 ng of the extracted DNA was digested with 10 U *HpaII* (NEB, Beverly, MA) in a reaction volume of 20 μl at 37°C, overnight. The reaction mixture was brought to 65°C for 20 mins to inactivate *HpaII*. PCR was performed in a total volume of 30 μl reaction mixture consisting of 100–400 ng of undigested or digested DNA, 3 μl of 10× reaction buffer, 250 μM of dNTPs, 2 mM $MgCl_2$, 100 ng of each primer, and 0.3 μl Taq polymerase (5 U/μl, Invitrogen). The PCR reaction conditions were as follows: initial denaturation at 95°C for 5 min, followed by 45 cycles each consisting of denaturation at 95°C for 45 s, annealing at 63°C for 45 s, and extension at 72°C for 30 s, with final extension at 72°C for 10 mins. PCR products (200–400 bp) of undigested DNA templates were electrophoresed on 2.5% agarose gel. Heterozygous cases were identified by the presence of two bands of different sizes on the agarose gel, each representing a parental allele. PCR products generated from *Hpa II* digested DNA for such heterozygous, thus informative, cases were then electrophoresed on to 2.5% agarose gel to assess clonality. Cases were considered monoclonal if only a single band is observed after PCR of *HpaII*-digested DNA. Positive and negative controls included a diffuse large B-cell lymphoma and reactive granulomatous infiltrate obtained from unrelated females, respectively. The primer sequences for the amplification of the HUMARA locus were used as previously published: F: 5′-GCT GTG AAG GTT GCT GTT CCT CAT-3′; R: 5′-TCC AGA ATC TGT TCC AGA GCG TGC–3′ [31].

Results

Autopsy findings

Patient 1

Gross External examination failed to reveal xanthelasma or stigmata of hypercholesterolemia. Internal examination confirmed extensive involvement of the abdomen by diffuse fibrosis encasing the kidneys and adrenals and extending through the intervertebral spaces into the spinal cord. There was involvement of the pericardium, heart, and great vessels. There was encasement of the optic chiasm and pituitary, and compression of the heart and main vessels within the mediastinum.

Microscopic The involved tissues had a similar appearance, with sheets of foamy macrophages admixed with a smaller number of lymphocytes, plasma cells, and occasional Touton-type giant cells; interspersed was mild-to-moderate fibrosis. The macrophages showed slight variability in appearance, but were bland with minimal nuclear pleomorphism, and mitotic activity was not readily identified (Fig. 1a). Immunohistochemistry showed the cells to be positive for CD68 (Fig. 1b), CD163 (Fig. 1c), HAM-56, lysozyme alpha-1-antichymotrypsin, and vimentin, and negative for S-100, CD1a and keratin (not shown). Electron microscopy confirmed the presence of lipid vacuoles, but failed to demonstrate Birbeck granules (not shown).

Patient 2

Gross External examination of the patient did not reveal xanthelasma or stigmata of hypercholesterolemia. Bilateral kidneys and adrenals were encased by a white-yellow

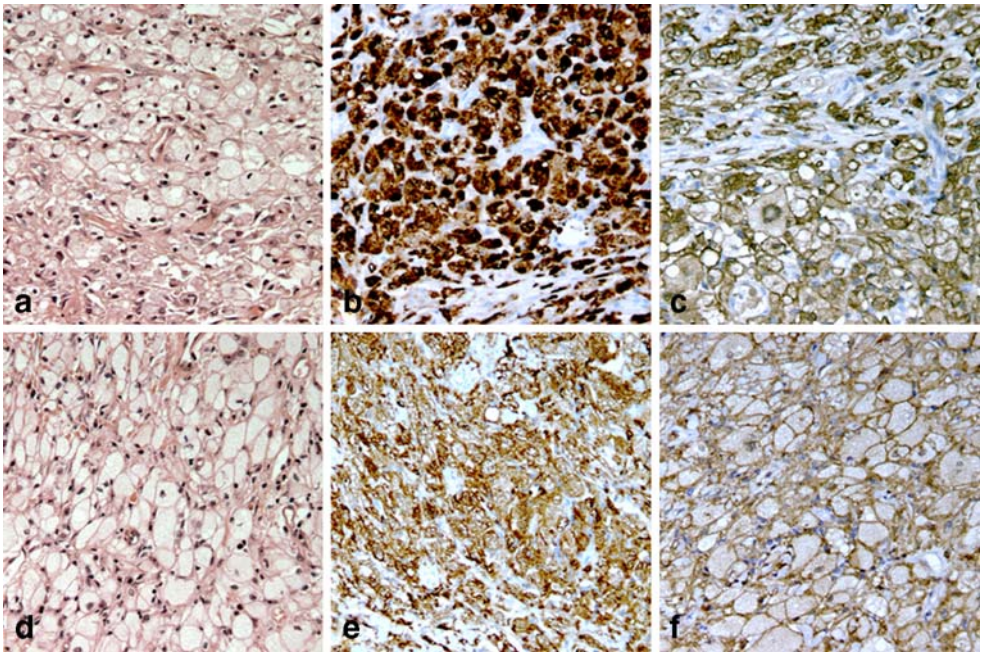


Fig. 1 Erdheim–Chester disease showing diffuse infiltration by foamy histiocytes, admixed with smaller numbers of lymphocytes and plasma cells. patient 1: H&E (**a** ×200), and immunohistochemistry showing expression of CD68 (**b** ×200), and CD163 (**c** ×200). patient 2: H&E (**d** ×200), and immunohistochemistry showing expression of CD68 (**e**, ×200) and CD163 (**f** ×200)

fibrosis. This fibrotic process extended throughout the retroperitoneum, abdominal and pelvic soft tissues, encasing the thoracic and abdominal aorta, and tracked along the major vessels and portal tracts, to penetrate the liver. It involved the bowel and spleen and essentially replaced the pancreas. The process involved the mediastinal great vessels, remaining pericardial tissue and heart, which showed biventricular hypertrophy that was more pronounced on the right. There was extension along the septae of the lungs; however, the regional lymph nodes were grossly unremarkable. The bone marrow was involved.

Microscopic All of the involved sections examined essentially demonstrated a similar process with sheets of foamy macrophages and scattered lymphocytes, plasma cells, and occasional Touton-type giant cells. Rare fibroblasts and variable amounts of collagen were also identified. The macrophages were uniform, with minimal nuclear pleomorphism and no mitotic activity (Fig. 1d). Special stains confirmed that the macrophages contained neutral lipid. Immunohistochemistry showed the cells to be positive for CD68 (Fig. 1e), CD163 (Fig. 1f), lysozyme alpha-1-antichymotrypsin, and vimentin; and negative for S-100, CD1a, and high molecular weight keratin (not shown). Electron microscopy confirmed the presence of lipid vacuoles, but did not show Birbeck granules (not shown).

Many tissues that were grossly unremarkable were, on histology, shown to be diffusely infiltrated by the xanthogranulomatous infiltrate. There was involvement of the lung alveoli, liver sinusoids, spleen, Bowman's space in the kidney, vessels of the uterus and ovary, submucosa of the small and large bowel, and bone marrow. Aggregates of histiocytes were focally identified within vascular spaces. Incidental note was also made of the presence of lymphocytic thyroiditis, chronic pancreatitis, and focal membranous colitis.

Analysis of clonality

DNA amplified from both patients showed heterozygous band pattern; hence, both patients were informative and were deemed suitable for clonality analysis. X-chromosome inactivation due to DNA methylation with lyonization is random, and polyclonal tissue from informative cases contain both methylated (inactive) and unmethylated (active) alleles in roughly equal proportions; in some instances, "skewed" lyonization can occur, whereby, there is deviation from this ratio [33]. By contrast, monoclonal tissue originating from a single progenitor cell contains only one methylated allele, and therefore, yields only a single band after amplification of *HpaII*-digested DNA, as was the case with patient 2 (Fig. 2). Of note, in patient 1, there appeared to be extensive DNA degradation, thereby, precluding assessment of clonality in the specimen examined (not shown).

Discussion

William Chester in 1930, working under Jakob Erdheim, is reported to have been the first to describe the exuberant xanthogranulomatous infiltrate that now bears

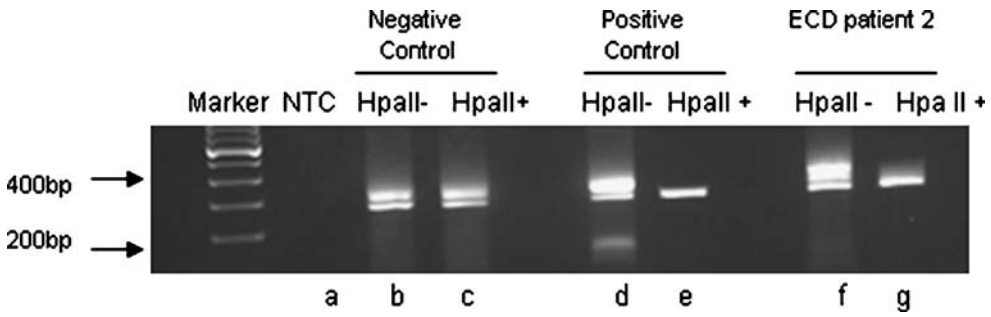


Fig. 2 Analysis of clonality in a patient with Erdheim–Chester disease (ECD), based on the pattern of X-chromosome inactivation using the human androgen receptor gene (HUMARA) assay. DNA undigested with methylation-sensitive enzyme HpaII (HpaII−) produced a heterozygous, thus informative, band pattern of HUMARA alleles in the DNA extracted from a reactive granulomatous infiltrate (negative control, *lane B*), diffuse large B-cell lymphoma (positive control; *lane D*) and lesional autopsy tissue from ECD patient 2 (*lane F*). After HpaII digestion (HpaII+), only a single band was observed in the positive control and ECD patient 2 (*lanes E and G*, respectively), indicating a monoclonal cell origin. In contrast, reactive granulomatous infiltrate demonstrates a heterozygous pattern post-HPaII digestion, confirming the reactive infiltrate is polyclonal (*NTC* No template control)

their names [6]. Similar descriptions subsequently appeared in the literature including those by Oberling in 1935 [21] and Sorenson in 1964 [26]. It was Jaffe, who, in 1972, proposed the eponymous Erdheim–Chester disease to describe a patient population with widespread systemic involvement and classic radiologic features [16]. Difficulties can arise in applying this term to lesions with non-prototypic presentations. This is further compounded by the multitude of xanthogranulomatous lesions bearing a related histologic and immunophenotypic pattern, such as juvenile xanthogranuloma [17], adult xanthogranuloma of the orbit [25], histiocytic sarcoma [30], and xanthoma disseminatum [23]. In most of the aforementioned cases, distinction is readily achieved on the basis of their differing clinical features; however, by virtue of its similar morphologic features and propensity for widespread involvement, the latter may potentially be confused with ECD. Xanthoma disseminatum is generally characterized as a benign disseminated mucocutaneous xanthomatosis [5]; nevertheless, there are reports of cases bearing overlapping features with ECD, including diabetes insipidus [1, 15], and long bone involvement [18], and fatal outcome.

Erdheim–Chester disease is characterized by a widespread xanthogranulomatous infiltrate that can involve the bones and/or soft tissues. Many consider the radiologic features of bilateral symmetrical osteosclerosis of the metaphyseal and diaphyseal regions of long bones pathognomonic for ECD; lytic lesions are also known to occur in about one-third of cases [11]. The nature of the disease early in its course remains poorly understood, perhaps in part because of delays in reaching a correct diagnosis [3]. As a disease of macrophages/monocytes, it is unclear whether ECD initially presents as a disease of marrow cavities, or whether—similar to many lymphoid neoplasms—extramedullary analogs exist; such cases would presumably not be amenable to early radiographic detection. Histologically, sheets and cords of foamy histiocytes diffusely infiltrate the tissues and viscera. This is frequently associated with variable amounts of fibrosis and the presence of inflammatory cells such as lymphocytes, plasma cells, and Touton-type giant cells. Immunohistochemistry demonstrates the histiocytes to be positive for markers of macrophage lineage, including CD68, lysozyme, alpha-1-anti-trypsin, and alpha-1-anti-chymotrypsin; they fail to express CD1a, a marker of dendritic lineage; and there are conflicting reports on the expression of S100, another marker of dendritic cells. Whether this represents a reactive process or a neoplasm of histiocytes has been recently debated.

Neoplasia is somewhat surprisingly difficult to define, although most would agree it represents a growth "...that tends to be atypical, autonomous, and aggressive" [20]. The observation of clonality, in and of itself, is not a *conditio sine qua non* for neoplasia; nevertheless, in the above context, it is extremely useful in confirming such a suspicion and contributing towards elucidating the pathophysiology of a disease. In assessing clonality from paraffin-embedded tissue, HUMARA has become a widely accepted technique of choice for such investigations. Using the HUMARA locus to assess clonality, Chetritt et al. studied five patients with ECD and demonstrated clonality in two cases of ECD and in one case of ECD associated with Langerhan's cell histiocytosis; one case was uninformative for HUMARA, and another was found to be polyclonal likely due to contamination from a heavy inflammatory cell infiltrate [7]. Conflicting results were reported by Al-Quran and colleagues who analyzed a single case of ECD using the same assay, but determined that the process was polyclonal in origin [2]. Of note, in their study, they estimated that the histiocytes in their study represented >50% of the cells taken for DNA examination,

while some estimates would suggest that this is sufficient for detection of clonality; it is conceivable that sampling contributed to their discordant findings. More recently, cytogenetic evidence of clonality was recently postulated, with a complex pattern of balanced translocations reported [27]. This finding is important because the presence of clonal cytogenetic abnormalities may point to a neoplastic etiology, rather than that of a clonal expansion in response to an inciting stimulus.

We describe two cases of ECD with rapidly progressive systemic involvement and fatal outcomes; one of these cases represents a new addition of this rare disease to the literature. In both of our cases, there were overlapping symptoms that likely reflected the progressive involvement of multiple organ systems. Both patients had diabetes insipidus, which is commonly observed in ECD and a reflection of pituitary involvement; progressive dyspnea, with infiltration of the lungs and widespread mediastinal involvement; anemia, possibly due to the observed bone marrow involvement; and hepatomegaly, edema, ascites, and hypoalbuminemia, in part, stemming from the liver infiltration. Both patients also showed diffuse retroperitoneal xanthogranulomas, which has previously been observed in ECD [10, 14, 24]. Our first patient had proptosis and paralysis due to spinal cord involvement; the latter is a feature that very rarely complicates ECD [9]. She also had diabetes mellitus, presumably because of widespread pancreatic replacement and/or chronic pancreatitis. The second patient had lymphocytic thyroiditis; a link between hyopothyroidism and ECD has previously been proposed [8]. Prognosis in ECD appears to be based on the extent of extraosseous involvement [28], and in both of our cases, the clinical course progressed rapidly to death.

The first patient had a history of hereditary hemorrhagic telangectasia and, as part of a screening MRI of the brain, had an incidentally discovered posteria fossa mass. Radiologically the lesion was thought to represent a meningioma, and the decision was made to observe the lesion. Less than a year later, she became symptomatic, and a craniotomy was performed to resect the tumour. On the basis of histopathology, ECD was diagnosed; imaging of the long bones subsequently confirmed the diagnosis, with the observation of sclerotic long bone lesions. Little is known about the early behavior of ECD, and it is unclear whether the lesion arose de novo in the CNS or was the result of spread from elsewhere. Certainly, it is unlikely that in early lesions with skeletal involvement would there be sufficient gross changes to allow detection using traditional plain film imaging, thus, placing greater diagnostic importance on the histopathologic observation of atypical histiocytic infiltrates. A related point is illustrated from the second patient where the diagnosis of ECD was not suspected clinically. Had there been an attempt to obtain diagnostic material for histologic evaluation, the diagnosis could have been raised ante mortem.

In examining these cases of ECD, we are the first to report expression of CD163—a marker of almost exclusive expression in cells of monocyte/macrophage lineage [30]; positivity for this marker lends strong support to a macrophage/monocyte origin. Staining with this antibody was found to be both membranous and/or cytoplasmic. Similar to other cases of ECD, we confirmed expression of CD68; of note, staining with the PGM-1 clone was somewhat more widespread compared to the KP-1 clone (not shown). The lesional tissue in both patients failed to stain with CD1a and S100. Electron microscopy failed to identify the presence of Birbeck granules.

Utilizing the HUMARA assay, we were able to confirm clonality in one of our two patients. Our results, therefore, lend additional support to the view that ECD is a clonal neoplastic process. Nevertheless, classification of this entity as an aggressive benign neoplasm, outright malignancy, or an expansion of clonally derived cells in response to a stimulus (e.g., cytokines [12], or landscaping effect [32]) merits further investigation and consensus. It has been suggested that skewed lyonization can, in some instances, lead to the false impression of clonality in a polyclonal population [4]. While this remains a possibility in our case, the possibility of an erroneous conclusion is lessened by the fact these findings have been independently reached in previous HUMARA-based studies of clonality in multiple female patients [7], and through unrelated studies using cytogenetic analysis [27].

In conclusion, we contribute an additional case of Erdheim–Chester disease to the existing literature. Our immunohistochemical results, with the novel observation of CD163 expression in this disease, supports the hypothesis that these lesions are derived from a monocyte/macrophage mediator, and our analysis using the HUMARA assay confirms a clonal basis for this disease. There remain uncertainties in our understanding of early histiocyte differentiation, particularly as this pertains to dendritic cells, macrophages/monocytes, and their precursors [13]; the same can be said for the relationship, if any, among the various xanthoses. Further studies are needed to better characterize the pathogenesis of Erdheim–Chester disease and related lesions.

References

1. Alexander AS, Turner R, Uniate L, Pearcy RG (2005) Xanthoma disseminatum: a case report and literature review. Br J Radiol 78:153–157
2. Al-Quran S, Reith J, Bradley J, Rimsza L (2002) Erdheim–Chester disease: case report, PCR-based analysis of clonality, and review of literature. Mod Pathol 15:666–672

3. Barnes PJ, Foyle A, Hache KA, Langley RG, Burrell S, Juskevicius R (2005) Erdheim–Chester disease of the breast: a case report and review of the literature. Breast J 11:462–467
4. Boudewijns M, van Dongen JJ, Langerak AW (2007) The human androgen receptor X-chromosome inactivation assay for clonality diagnostics of natural killer cell proliferations. J Mol Diagn 9:337–344
5. Caputo R, Veraldi S, Grimalt R, Gianotti R, Tosti A, Varotti C, de Kaminsky AR (1995) The various clinical patterns of xanthoma disseminatum. Considerations on seven cases and review of the literature. Dermatology 190:19–24
6. Chester W (1930) Über lipoidgranulomatose. Virchows Arch Pathol Anat 279:561–602
7. Chetritt J, Paradis V, Dargere D, Adle-Biassette H, Maurage CA, Mussini JM, Vital A, Wechsler J, Bedossa P (1999) Chester–Erdheim disease: a neoplastic disorder. Hum Pathol 30:1093–1096
8. Cruz AA, de Alencar VM, Falcao MF, Elias J Jr., Chahud F (2006) Association between Erdheim–Chester disease, Hashimoto thyroiditis, and familial thrombocytopenia. Ophthal Plast Reconstr Surg 22:60–62
9. Curgunlu A, Karter Y, Ozturk A (2003) Erdheim–Chester disease: a rare cause of paraplegia. Eur J Intern Med 14:53–55
10. Eble JN, Rosenberg AE, Young RH (1994) Retroperitoneal xanthogranuloma in a patient with Erdheim–Chester disease. Am J Surg Pathol 18:843–848
11. Egan AJ, Boardman LA, Tazelaar HD, Swensen SJ, Jett JR, Yousem SA, Myers JL (1999) Erdheim–Chester disease: clinical, radiologic, and histopathologic findings in five patients with interstitial lung disease. Am J Surg Pathol 23:17–26
12. Egeler RM, Pritchard J, Gadner H, D'Angio GJ (1995) An international histiocytic language. Blood 85:2281–2282
13. Favara BE, Feller AC, Pauli M, Jaffe ES, Weiss LM, Arico M, Bucsky P, Egeler RM, Elinder G, Gadner H (1997) Contemporary classification of histiocytic disorders. The WHO committee on histiocytic/reticulum cell proliferations. Reclassification working group of the histiocyte society. Med Pediatr Oncol 29:157–166
14. Gauthier V, Cauchon R (1958) Retroperitoneal xanthogranuloma: 2 cases. Laval Med 26:316–337
15. Hisanaga Y, Akaike Y, Kuroda K (2004) Xanthoma disseminatum with large plaques confined to the back, pulmonary involvement and multiple intestinal xanthomas. Dermatology 208:164–166
16. Jaffe HL (1972) Lipid (cholesterol) granulomatosis. Metabolic, degenerative and inflammatory diseases of bones and joints. Lea & Fibiger, Philadelphia, pp 535 –541
17. Jaffe R (2004) Dendritic histiocytoses: an update. Companion meeting: society for hematopathology (USCAP 2004). Vancouver, British Columbia
18. Khandpur S, Manchanda Y, Sharma VK, Singh MK, Tandon N (2003) Rare association of xanthoma disseminatum with skeletal involvement. Australas J Dermatol 44:190–193
19. Kovacs K, Bilbao JM, Fornasier VL, Horvath E (2004) Pituitary pathology in Erdheim–Chester disease. Endocr Pathol 15:159–166
20. Majno G, Joris I (2004) Cells, tissues, and disease: principles of general pathology, 2nd edn. Oxford University Press, New York, p 1040
21. Oberling C (1935) Retroperitoneal xanthogranuloma. Am J Cancer 23:477–489
22. QIAGEN (2003) QIAamp DNA Mini Kit and QIAamp DNA Blood Mini Kit Handbook
23. Rush WL, Andriko JA, Galateau-Salle F, Brambilla E, Brambilla C, Ziany-bey I, Rosado-de-Christenson ML, Travis WD (2000) Pulmonary pathology of Erdheim–Chester disease. Mod Pathol 13:747–754
24. Simpson FG, Robinson PJ, Hardy GJ, Losowsky MS (1979) Erdheim–Chester disease associated with retroperitoneal xanthogranuloma. Br J Radiol 52:232–235
25. Sivak-Callcott JA, Lim WK, Seah LL, Oestreicher J, Rossman D, Nijhawan N, Rootman J, White V, Williams HJ, Chang WW, DiBartolomeo A, Howarth D (2005) Xanthogranulomatous disease in the lacrimal gland. Br J Ophthalmol 89:1375–1377
26. Sorensen EW (1964) Hyperlipidemia. A report of an unusual case complicated by bone-lesions, macrocytic anaemia and leukemoid bone marrow. Acta Med Scand 175:207–214
27. Vencio EF, Jenkins RB, Schiller JL, Huynh TV, Wenger DD, Inwards CY, Oliveira AM (2007) Clonal cytogenetic abnormalities in Erdheim–Chester disease. Am J Surg Pathol 31:319–321
28. Veyssier-Belot C, Cacoub P, Caparros-Lefebvre D, Wechsler J, Brun B, Remy M, Wallaert B, Petit H, Grimaldi A, Wechsler B, Godeau P (1996) Erdheim–Chester disease. Clinical and radiologic characteristics of 59 cases. Medicine (Baltimore) 75:157–169
29. Vinh TN, Sweet DE (2002) Erdheim–Chester disease. In: Fletcher CDM, Unni KK, Mertens F (eds) Pathology and genetics of tumours of soft tissue and bone. IARC, Lyon, p 347
30. Vos JA, Abbondanzo SL, Barekman CL, Andriko JW, Miettinen M, Aguilera NS (2005) Histiocytic sarcoma: a study of five cases including the histiocyte marker CD163. Mod Pathol 18:693–704
31. Wang L, Zhu H (2006) Clonal analysis of palmar fibromatosis: a study whether palmar fibromatosis is a real tumor. J Transl Med 4:21
32. West RB, Rubin BP, Miller MA, Subramanian S, Kaygusuz G, Montgomery K, Zhu S, Marinelli RJ, De Luca A, Downs-Kelly E, Goldblum JR, Corless CL, Brown PO, Gilks CB, Nielsen TO, Huntsman D, van de Rijn M (2006) A landscape effect in tenosynovial giant-cell tumor from activation of CSF1 expression by a translocation in a minority of tumor cells. Proc Natl Acad Sci U S A 103:690–695
33. Willman CL, Busque L, Griffith BB, Favara BE, McClain KL, Duncan MH, Gilliland DG (1994) Langerhans'-cell histiocytosis (histiocytosis X)—a clonal proliferative disease. N Engl J Med 331:154–160

Virchows Arch (2008) 452:229–231
DOI 10.1007/s00428-007-0529-x

LETTER TO THE EDITOR

Tissue transfer to pathology labs: under vacuum is the safe alternative to formalin

Gianni Bussolati · Luigi Chiusa · Antonio Cimino · Giuseppe D'Armento

Received: 16 October 2007 / Accepted: 16 October 2007 / Published online: 21 December 2007
© Springer-Verlag 2007

The time-honoured use of formalin, both as a preserver and fixative for histological processing is encountering increasing criticisms because of toxicity and environmental concerns. Moreover, the declaration recently issued by the International Agency for Research on Cancer [1] which classified formaldehyde as a class 1 carcinogen has definitely increased the request by health authorities, technicians and practicing pathologists to reduce exposure. Such requests contrast with the considerable advantages offered by this safe, chip, reliable fixative. Although it should be acknowledged that in modern pathology laboratories, visitors are not any more met by the permeating flavour of a stingy scent because formalin processing is mostly carried out under aspiration hoods, a critical passage is still represented by the transfer of tissues from the surgical theatre to the pathology lab. Apart from the small biopsies, which are directly collected into pre-filled containers and cause no concern, problems are encountered with the immersion of large specimens and organs into large boxes to be filled with formalin. A list of such problems follows:

1. Plastic containers are large and relatively heavy, while on occasion spilling may occur.
2. Immersion into formalin prevents the collection of fresh material for tissue banking. Fixation starts, but only at the periphery. Discoloration occurs, while a delay in the transfer to pathology labs is somehow justified by the fact that 'the tissue is already in formalin'.
3. Nurses at the surgical theatre are becoming increasingly concerned for toxicity and cancerogenicity issues because the fluid has to be managed freely and not under hood.
4. When the container arrives at the pathology lab, its opening, extraction of the specimen and reduction of the latter constitutes a major cause of diffusion of formaldehyde fumes.

To circumvent such problems, we adopted a transfer under vacuum. We selected a semi-professional machine, of a relatively limited cost and size (Mod. VAC 10, by Milestone, Bergamo, Italy; see http://www.milestonemedsrl.com) (Fig. 1) and capable of handling large bags. After testing the use of such machine on different tissue specimens and organs (colon, gallbladder, spleen and kidney) and checking the safety of the processing from the point of view of histological preservation, we trans-



Fig. 1 The under vacuum machine used in our hospital

G. Bussolati (✉) · L. Chiusa · A. Cimino · G. D'Armento
Department of Biomedical Sciences and Human Oncology,
University of Turin,
Via Santena n. 7,
10126 Torino, Italy
e-mail: gianni.bussolati@unito.it

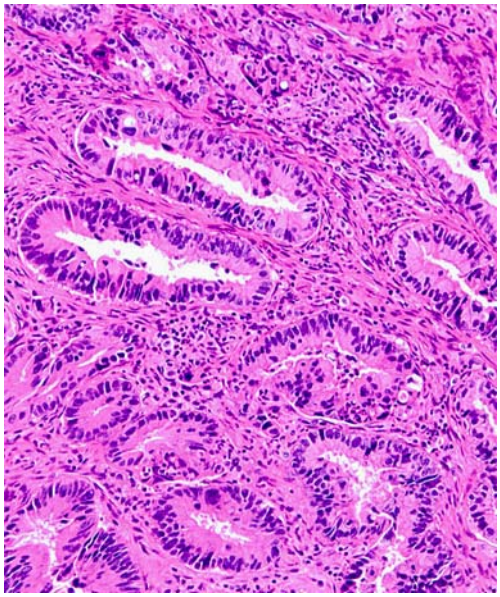


Fig. 2 Adenocarcinoma of the colon. The specimen was kept under vacuum at 4°C for 48 h, then routinely processed with formalin fixation and paraffin embedding. The structure is preserved and diagnosis is feasible. H&E. 150×

ferred the machine to a surgical theatre of our Hospital, where it is now in use by nurses for one year. Large surgical specimens (from thyroid, breast, colon and other organs) immediately after removal are put in plastic bags with or without an identification label (which can alternatively be attached on the surface of the bag). Vacuum and sealing processes takes approximately 15 s. The specimen is then kept in a refrigerator for up to a few hours, although preferentially soon transferred to the pathology lab inside a container (we routinely use a pick-nick box with chilling devices inside). On rare occasions, because of urgency operations during the weekend, the under-vacuum tissues are kept in the refrigerator for 1–2 days and arrived in the laboratory after a long delay.

Upon arrival of the specimen to the pathology lab, reduction takes place so that selected block are inserted into cassettes for routinary fixation in formalin and paraffin embedding, or frozen for tissue banking. The rest of the specimen is kept under formalin in sealed boxes as a reserve.

As a review of the results of the above processing, the experiences gained after 1 year can be summarized as follows:

1. No drawbacks or problems were encountered in approximately 2,000 cases so far processed, as far as the morphological preservation or the immunohistochemical reactivity are concerned. Preservation was less optimal in cases when the under-vacuum specimen had been stored at the surgical theatre for long time, but even this did not prevent histopathological processing and reading (Fig. 2).
2. Under-vacuum processing is very well accepted by the personnel of the surgical theatre, who find it safe and easy. Previously, the consumption of formalin in that place was 15 l per week, and it is now reduced to null.
3. Under-vacuum processing routinely provides material for tissue banking. The quality of RNA preservation is of course related to the time of processing, but even tissues kept in the fridge under vacuum for long time provided nucleic acids of acceptable quality (Fig. 3a,b). This finding is in agreement with reports on the stability of RNA in non-fixed surgical specimens kept on ice [2].

In conclusion, tissue transfer in under-vacuum conditions meets the request of health authorities and involved personnel to reduce exposure to formaldehyde. Absence of air decreases autolytic processes, favours the cooling of specimens (because of the absence of insulating air) and

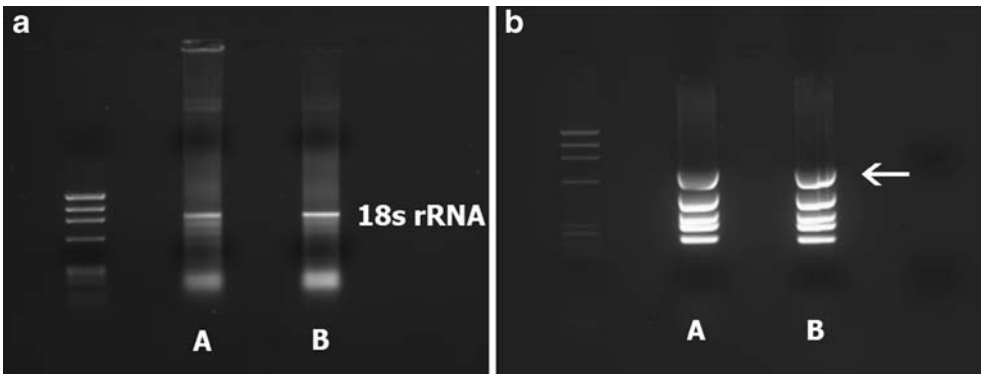


Fig. 3 Colon mucosa either (*A*) frozen immediately after removal or (*B*) preserved under vacuum at 4°C for 48 h. The extracted RNA is of acceptable and similar quality. **a** Shows 1% denaturing agarose gel of total RNA running: the 18s band is visible and no degradation is appreciable. **b** Represents RT-PCR products of cytokeratine 20 mRNA of different bp number. The upper band (*arrow*) is related to a 716-bp product

gives rise to a relatively small and light bag, easy to carry as compared to formalin-filled containers.

The goal of a formalin-free Hospital is still far away, but the present proposal represents a step forward.

Acknowledgement Work supported by a grant from Regione Piemonte Ricera Sanitaria Finalizzata.

References

1. International Agency for Research on Cancer (2006) Monographs on the evaluation of Carcinogenic Risk to humans, vol 88. IARC, Lyon, France
2. Micke P, Ohshima M, Tahmasebpoor S, Ren ZP, Ostman A, Ponten F, Botling J (2006) Biobanking of fresh frozen tissue: RNA is stable in non-fixed surgical specimens. Lab Invest 86:202–211

Virchows Arch (2008) 452:233–240
DOI 10.1007/s00428-008-0577-x

ORIGINAL ARTICLE

A score based on microscopic criteria proposed for analysis of papillary carcinoma of the thyroid

Priscilla Verhulst · Patrick Devos · Sébastien Aubert · David Buob · Isaac Cranshaw · Christine Do Cao · François Pattou · Bruno Carnaille · Jean-Louis Wemeau · Emmanuelle Leteurtre

Received: 12 September 2007 / Revised: 29 December 2007 / Accepted: 5 January 2008 / Published online: 1 February 2008
© Springer-Verlag 2008

Abstract Morphologic examination is the gold standard for diagnosing papillary thyroid carcinoma (PTC). This diagnosis, especially for the follicular variant, may be variable even among experts. Our objective was to analyze the frequency of PTC microscopic criteria in a series of thyroid tumors including follicular adenoma (FA) and PTC to build a score which could constitute a novel way for microscopic analysis of such thyroid tumors. Sixty-six PTC and 66 FA were matched for age, sex, and thyroiditis. Two independent observers delineated the classical PTC microscopic criteria. PTC microscopic criteria were variably expressed in individual tumors. Under univariate analysis, all criteria were significantly more frequent in PTC than in FA ($p<0.05$). Under multivariate analysis, the most important criteria were: dark staining colloid >25%, nuclear grooves, enlarged nuclei, ovoid nuclei >5% of tumor cells, and lack of polarization. Using linear discriminant analysis, these five criteria allowed us to build a scaled score. The score proposed did not allow the making of a definite distinction between FA and PTC in routine practice. It represents the variety of microscopic presentations of FA and PTC on the basis of a statistical analysis and could help in further evaluation of immunohistochemical or molecular markers.

Keywords Score · Microscopic criteria · Papillary carcinoma · Thyroid · Diagnosis

P. Verhulst · S. Aubert · D. Buob · E. Leteurtre (✉)
Pôle Pathologie, Centre de Biologie Pathologie, CHR-U de Lille,
2 Avenue Oscar Lambret,
59037 Lille, France
e-mail: e-leteurtre@chru-lille.fr

I. Cranshaw · F. Pattou · B. Carnaille
Service de Chirurgie Générale et Endocrinienne, CHR-U de Lille,
59037 Lille, France

C. Do Cao · J.-L. Wemeau
Service de Médecine Interne et d'Endocrinologie,
CHR-U de Lille,
59037 Lille, France

P. Devos · S. Aubert · D. Buob · F. Pattou · B. Carnaille · J.-L. Wemeau · E. Leteurtre
Faculté de Médecine de Lille,
59045 Lille, France

Introduction

Papillary thyroid carcinoma (PTC) is a "malignant epithelial tumor showing evidence of follicular cell differentiation and characterized by distinctive nuclear features" [26]. These nuclear features classically include: nuclear pseudoinclusions, nuclear grooves, ground glass nuclei, overlapping and crowded nuclei, ovoid nuclei, and enlarged and irregularly shaped nuclei [26, 33]. Their presence is both necessary and sufficient for the diagnosis of PTC. In everyday practice, the diagnosis of PTC with invasive growth and/or with papillary structures is easily made on standard examination. In contrast, the diagnosis of encapsulated follicular variant of PTC (FVPTC) is often difficult. Indeed, the diagnosis mainly relies on nuclear features which are sometimes incomplete and/or only present focally. The number of criteria and the percentage of tumor cells with the nuclear features required for a diagnosis of encapsulated FVPTC are not clearly defined in the literature. So, Chan [7] proposed a subset of criteria for the diagnosis of encapsulated FVPTC, including nuclear features, psammoma bodies, and subsidiary features such as abortive papillae, elongated or irregularly shaped follicles,

dark staining colloid, and multinucleated histiocytes in lumens of follicles.

Currently, the difficulties encountered in this field of pathology lead to a low reproducibility for this diagnosis even between experienced pathologists [19, 21, 27]. Moreover, when microscopic criteria for a diagnosis of PTC are incomplete or focal, some authors have suggested that the case should not be placed into a definite benign or malignant category and should rather be termed "well-differentiated tumor of uncertain malignant potential" [37].

Actually, the distinction between follicular adenoma (FA) and FVPTC remains one of the most difficult and controversial area in thyroid surgical pathology [2, 7, 8, 20, 23, 25, 32]. Moreover, advances are limited by the excellent prognosis of the majority of PTC when patients are correctly treated and surveyed. More precisely, mortality from thyroid cancer in the US was stable between 1973 and 2002 (approximately 0.5 deaths per 100,000) and in a recent study, the long-term outcome of FVPTC was similar to that of classical PTC [12, 24]. Overdiagnosing PTC may lead to excessive treatment including unnecessary total thyroidectomy and radioactive iodine therapy, and in contrast underdiagnosing PTC may increase the risk of recurrence or distant metastasis. Currently, no immunohistochemical or molecular marker allows us to make a definite distinction between FA and PTC and the "gold standard" is still based on morphologic criteria, with less than perfect results [18, 25, 36].

The objectives of this study were:

1. To analyze the presence, the percentage of tumor cells with each microscopic criterion of PTC in individual tumor, and the frequency of PTC microscopic criteria in a series of 66 PTC.
2. To propose a score illustrating the variety of morphologic presentations in the histopathological categories of FA and PTC.

Materials and methods

Patients and tumors

This study has been conducted on two distinct populations:

1. A training set of 132 thyroid tumors (66 PTC and 66 FA) allowing us to analyze the presence and frequency of PTC microscopic criteria and to elaborate the score.
2. A validation set including 58 thyroid tumors (29 PTC and 29 FA).

The training set included 66 PTC (tumor size≥1 cm) collected retrospectively and consecutively from August 2000 to September 2001 at the University Hospital of Lille. Selected PTC were matched for age, sex, and presence or not of thyroiditis with 66 FA.

The validation set included 29 PTC (tumor size≥1 cm) collected retrospectively from January 2004 to September 2004 at the same institution. These 29 PTC were also matched for age, sex, and presence or not of thyroiditis with 29 FA.

Pathology

Specimens were fixed in 10% buffered formalin for 24–48 h and embedded in paraffin wax, colored by hematoxylin and eosin. All available histological slides of each tumor were reviewed by one pathologist (PV) who analyzed on the training set the presence and the percentage of tumor cells with each PTC microscopic criterion classically described in the literature. For each tumor, one representative slide was selected. Then, a consensual microscopic analysis was established on a double-headed light microscope by two observers (PV and EL).

Some microscopic criteria were studied on all tumor slides: papillary architecture, psammoma bodies, abortive papillae, elongated or irregularly shaped follicles, dark staining colloid, and multinucleated histiocytes in lumens of follicles. While other criteria were studied on a representative tumor slide: nuclear pseudoinclusions, nuclear grooves, enlarged nuclei (1.5×normal size), ground glass nuclei, overlapping and crowded nuclei, lack of polarization in the cells that line a follicle (nuclei observed at variable levels in the cytoplasm), ovoid nuclei, and irregularly shaped nuclei.

A semiquantitative microscopic analysis in four categories (absence; presence ≤25%; >25% and ≤75%; >75% of tumor) was realized for the following criteria: papillary architecture, abortive papillae, elongated or irregularly shaped follicles, dark staining colloid, nuclear grooves, enlarged nuclei, overlapping nuclei, and lack of polarization.

For ground glass nuclei, ovoid nuclei, and irregularly shaped nuclei, quantitative analysis included six categories (absence; presence ≤1%; >1% and ≤5%; >5% and ≤25%; >25 and ≤75%; > 75% of tumor).

A qualitative analysis (absence or presence) was realized for the following criteria: psammoma bodies, multinucleated histiocytes in lumens of follicles, and nuclear pseudoinclusions.

Only the criteria selected by statistical methods and which allowed us to define a scaled score were further analyzed on the validation set.

Statistical methods

Firstly, a descriptive analysis was performed in order to check and resume the data. Semiquantitative parameters

were recoded into two classes. Secondly, comparisons of frequencies among the two groups (FA–PTC) were performed using the Chi-square test or Fisher exact test if necessary. A linear discriminant analysis was performed on all significant parameters at level 0.15. Finally, a stepwise analysis was performed in order to determine the best subset of parameters useful to establish the score. Receiving operating characteristic curve was used to determine the optimal threshold for differentiating FA and PTC. The score was evaluated on a training set and a validation set.

Results

Training set

The training set included 100 women (76%) and 32 men (24%). The mean age of patients with PTC was 41 years (range 9–73 years). The mean age of patients with FA was 44 years (range 21–75 years). Amongst the 132 patients, 22 (16%) presented with a thyroiditis. Table 1 summarizes the histopathological characteristics of PTC in the training set. The presence, the frequency of each PTC microscopic criterion, was evaluated in PTC of the training set, according to the percentage of tumor with the microscopic criteria (Table 2). Enlarged nuclei were the only feature present in more than 75% of tumor cells in the majority of the cases (94%). Some other criteria such as papillary architecture, abortive papillae, elongated follicles, dark staining colloid, lack of polarization in the cells and ovoid nuclei, were present in a wide range from 0% to more than 75% of the tumor. Other criteria such as nuclear grooves, overlapping nuclei, ground glass nuclei, or irregularly shaped nuclei, were present in less than 25% of the tumor in the majority of the cases. Psammoma bodies, multinucleated histiocytes and pseudoinclusions were respectively observed in 28 (42%), 28 (42%), and 36 (55%) cases of the PTC (Table 3).

Table 1 Histopathological characteristics of papillary thyroid carcinomas included in the training set (n=66) and in the validation set (n=29)

Histopathological characteristics of PTC	Training set, n (%)	Validation set, n (%)	p value
Presence of thyroiditis	11 (16)	6 (21)	0.63
Histological subtype			
Classical type	43 (65)	10 (35)	0.005
Follicular variant	12 (18)	17 (59)	<0.0001
Diffuse sclerosing variant	3 (5)	0 (0)	0.24
Tall cell contingent	6 (9)	1 (3)	0.33
Columnar cell contingent	2 (3)	0 (0)	0.34
Warthin-like variant	0 (0)	1 (3)	0.12
Encapsulated–circumscribed or invasive carcinoma			
Encapsulated–circumscribed carcinoma	17 (26)	17 (59)	0.002
Invasive carcinoma	49 (74)	12 (41)	0.002
Presence of lymph node metastasis	25 (38)	5 (8)	0.046

Table 2 Frequency of papillary thyroid carcinomas microscopic criteria in PTC of the training set (n=66) according to the percentage of tumor with the microscopic criteria

	Percentage of tumor with the PTC microscopic criteria[a]			
	0% (%)	≤25% (%)	25–75% (%)	>75% (%)
PTC microscopic criteria: frequency in PTC of the training set				
Papillary architecture	18	33	26	23
Abortive papillae	1	29	50	20
Elongated follicles	0	17	47	36
Dark staining colloid	3	24	35	38
Nuclear grooves	1	99	0	0
Enlarged nuclei	0	1	5	94
Overlapping nuclei	1	65	34	0
Lack of polarization in the cells	5	38	56	1
Ground glass nuclei	1	82	17	0
Ovoid nuclei	0	34	65	1
Irregularly shaped nuclei	0	97	3	0

[a] Results are presented in four semiquantitative categories (0 when the morphologic feature was absent; ≤25% when present in less or equal 25% of the tumor; >25 et ≤75% when present in strictly more than 25% and less or equal 75% of the tumor; >75% when present in strictly more than 75% of the tumor)

Secondly, threshold values (i.e., percentage of tumor presenting the microscopic criteria of PTC) were determined for these different criteria allowing a more efficient distinction between PTC and FA. The threshold value was determined at 5% for the ground glass nuclei, ovoid nuclei, and irregularly shaped nuclei and at 25% for dark staining colloid, elongated or irregularly shaped follicles, and abortive papillae. For other criteria, the presence of this feature, whatever the percentage, was effective to differentiate PTC from FA. Under univariate analysis, all the criteria defined were significantly more frequently observed in PTC than in FA (p<0.05; Table 3). Nevertheless, none of these criteria were totally specific and sensitive for the diagnosis of malignancy. Under multivariate analysis, by a stepwise analysis, the best subset of criteria useful to establish the score included the presence of dark staining colloid in more than 25% of the tumor, presence of nuclear grooves, presence of enlarged nuclei, presence of ovoid nuclei in more than 5% of tumor cells, and lack of polarization in the cells. The microscopic criteria are illustrated in Figs. 1, 2 and 3.

Stepwise regression analysis included these five criteria and allowed us to build a score: ovoid nuclei (0 when absent

Table 3 Comparison of the frequency of papillary thyroid carcinoma microscopic criteria between PTC and follicular adenomas in the training set

PTC microscopic criteria[a]	PTC; $n=66$ Number (%)	FA; $n=66$ Number (%)	p value
Papillary architecture	54 (82)	0 (0)	<0.0001
Abortive papillae >25%	46 (70)	9 (14)	<0.0001
Elongated or irregularly shaped follicles >25%	55 (83)	12 (18)	<0.0001
Dark staining colloid >25%	48 (73)	6 (9)	<0.0001
Nuclear grooves	65 (98)	14 (21)	<0.0001
Enlarged nuclei	66 (100)	14 (21)	<0.0001
Overlapping and crowded nuclei			
>0 and <25%	43 (65)	22 (33)	<0.0001
≥25 and <75%	22 (33)	0 (0)	<0.0001
Lack of polarization in the cells	63 (95)	5 (8)	<0.0001
Ground glass nuclei >5%	32 (48)	5 (8)	<0.0001
Ovoid nuclei >5%	61 (92)	1 (2)	<0.0001
Irregularly shaped nuclei >5%	23 (35)	7 (11)	<0.0001
Psammoma bodies	28 (42)	0 (0)	<0.0001
Multinucleated histiocytes in lumens of follicles	28 (42)	2 (3)	<0.0001
Nuclear pseudoinclusions	36 (55)	0 (0)	<0.0001

[a] Threshold values were determined in terms of percentage of tumor presenting the morphologic feature of PTC

or 30 when present) + lack of polarization (0 when absent or 22 when present) + nuclear grooves (0 when absent or 14 when present) + enlarged nuclei (0 when absent or 7 when present) + dark staining colloid (0 when absent or 6 when present). The manner to calculate the score in a given tumor is presented in Table 4. Thus, each tumor was graded from 0 to 79, determining a total score according to the total number of criteria present. On the training set, 65/66 PTC scored >30 and only one PTC scored <30. In contrast, none of the FA scored >30 (Fig. 4). Therefore, when the threshold score was set at >30, it had a sensitivity of 98.5% and a specificity of 100% for the original diagnosis of PTC. Further analysis showed that the total score was not statistically different between PTC with lymph node metastasis and PTC without lymph node metastasis.

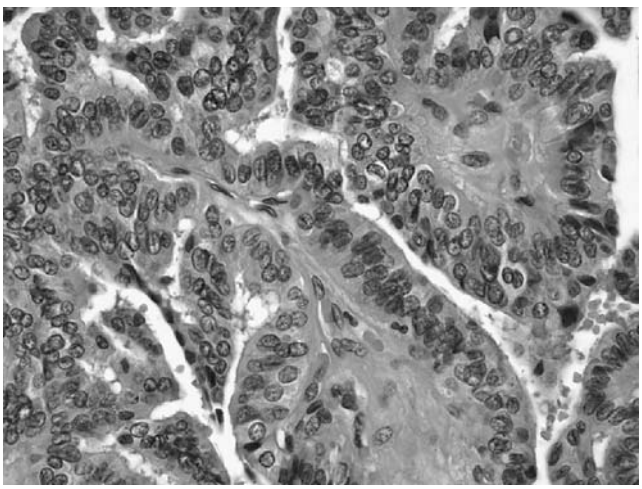


Fig. 1 Papillary thyroid carcinoma. Ovoid nuclei and lack of polarization in the cell that line papillae or follicle. The nuclei are not regularly observed at the base of the cell but are located at variable level in the cytoplasm of the cell. Standard examination ×400

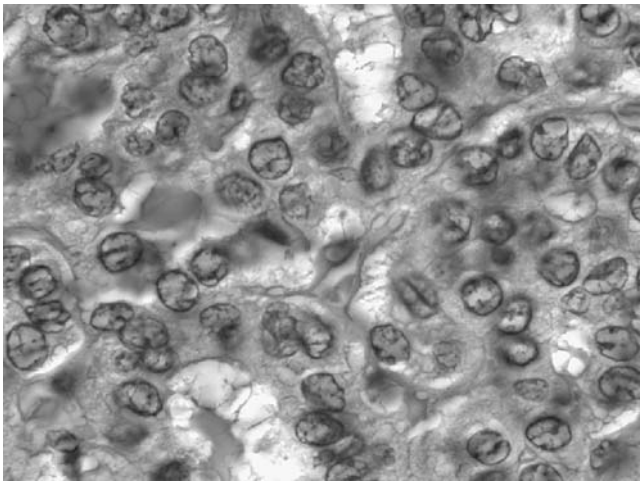


Fig. 2 Papillary thyroid carcinoma. Ovoid nuclei with some nuclear grooves. Standard examination ×1000

Validation set

The histopathological characteristics of PTC in the validation set are summarized in Table 1. The score was tested on this validation set which contained 29 FA and 29 PTC (Fig. 5): 21/29 PTC scored >30 and 8/29 PTC scored ≤30 but >7; 21/29 FA scored ≤7 and 8/29 FA scored >7 but ≤30. None of the FA scored >30. On this validation set of 58

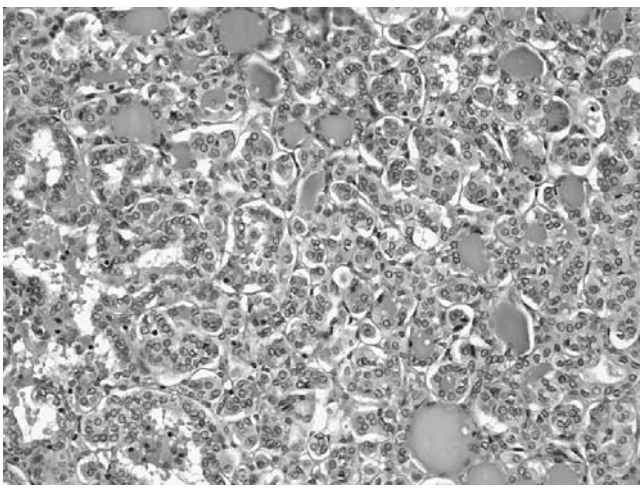


Fig. 3 Papillary thyroid carcinoma. Elongated and irregularly shaped follicles with dark staining colloid. Standard examination ×200

Table 4 Calculation of the total score for a thyroid tumor

Microscopic criteria	Result	Points
Ovoid nuclei >5%	Absent 0 or present 30	…..
Lack of polarization	Absent 0 or present 22	…..
Nuclear grooves	Absent 0 or present 14	…..
Enlarged nuclei	Absent 0 or present 7	…..
Dark staining colloid >25%	Absent 0 or present 6	…..
Total score (0 to 79)		…..

thyroid tumors, a total score of >30 had a sensitivity of 72.4% and a specificity of 100% for the original diagnosis of PTC. Therefore, in the analysis of the validation set, we observed a "gray zone" between 7 and 30 which contained both FA and PTC.

More precisely, eight PTC and eight FA scored between 7 and 30. These 16 cases were reviewed. Of the eight PTC that scored between 7 and 30, five tumors had focal or incomplete microscopic criteria of PTC. In one of these cases, technical problems prevented accurate analysis of nuclear features which led to a wrongfully low score. In three other cases, PTC features, which are not included in the score (ground glass nuclei and crowded nuclei), were present leading to a morphologic diagnosis of PTC but with a low score. Of the eight FA that scored between 7 and 30, five cases had very focal morphologic features of PTC while the last three cases were indisputably benign lesions including two oxyphilic adenomas and one adenoma with hyperplastic papillae.

Discussion

The current study reviewed the presence, the percentage of tumor presenting with a microscopic criteria of PTC, the

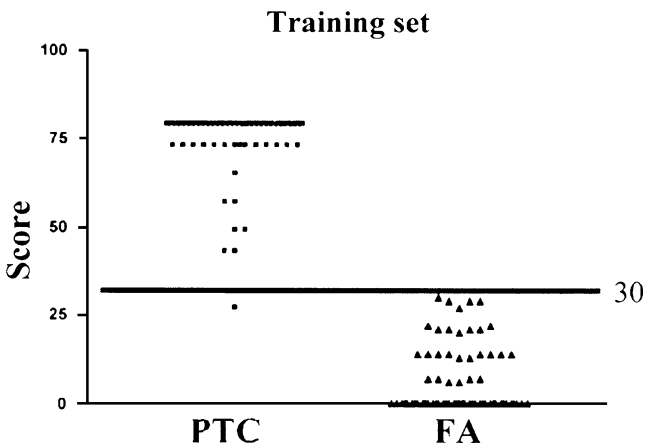


Fig. 4 Repartition of patients according to the result of the scaled score in the training set. Papillary thyroid carcinoma (*PTC*); follicular adenoma (*FA*)

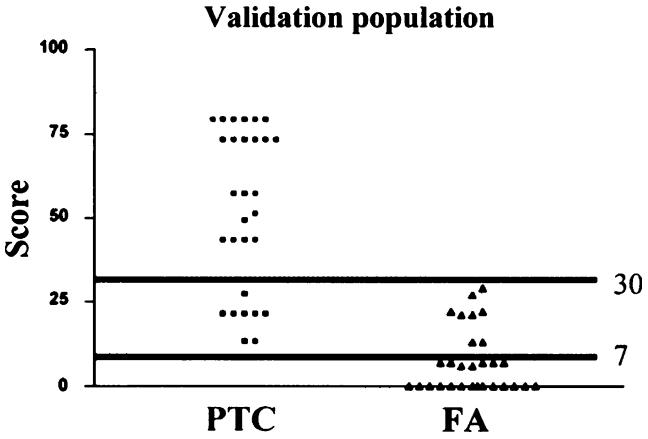


Fig. 5 Repartition of patients according to the result of the scaled score in the validation set. Papillary thyroid carcinoma (*PTC*); follicular adenoma (*FA*)

frequency of PTC microscopic criteria in a series of PTC and devised a score based on statistical analysis of microscopic criteria to propose a novel approach for the microscopic analysis of FA and PTC. This score included five criteria with specific weight: ovoid nuclei>5% (0 when absent or 30 when present) + lack of polarization (0 when absent or 22 when present) + nuclear grooves (0 when absent or 14 when present) + enlarged nuclei (0 when absent or 7 when present) + dark staining colloid>25% (0 when absent or 6 when present). The "gold standard" for the diagnosis of PTC still relies on microscopic features. Most PTC are easily diagnosed on standard examination when invasion and/or papillary structures are present. In contrast, for encapsulated FVPTC, the diagnosis is made on the basis of nuclear features whose identification remains quite subjective and causes high interobserver variability even among experts [19, 21, 27]. An international panel of ten experienced thyroid pathologists was requested to rank the criteria that were the most helpful in the diagnosis of FVPTC. For these authors, the most important criteria included cytoplasmic invagination into the nucleus (nuclear pseudoinclusion), abundant nuclear grooves, and ground glass nuclei [27]. Interestingly, other authors analyzed the PTC nuclear features using confocal microscopy and obtained a tridimensional model of the nuclei with crateriform areas, clefts, and tunnel-like structures [30]. Chan et al. proposed an association of microscopic features to diagnose FVPTC. This system includes not only nuclear features (ovoid nuclei, crowded nuclei, clear nuclei, grooves, nuclear pseudoinclusions) but also psammoma bodies, abortive papillae, irregularly shaped follicles, dark staining colloid, and multinucleated histiocytes in the lumens of follicles [7]. More precisely, Chan et al. determined four major features: (1) ovoid nuclei; (2) crowded nuclei, lack of polarization in the cells; (3) nuclear clearing or prominent grooving; (4) psammoma bodies. If one of these four major features was lacking, four or more of the following subsidiary

features were necessary for a diagnosis of FVPTC: (1) abortive papillae; (2) irregularly shaped follicles; (3) dark staining colloid; (4) presence of rare nuclear pseudoinclusions; (5) multinucleated histiocytes [7]. In another approach, the Chernobyl pathologists group proposed a subset of "well-differentiated thyroid tumor of uncertain malignant potential" for encapsulated follicular neoplasm that only shows some of the nuclear features or whose features are unconvincing [37].

In our study, we first analyzed the presence, the percentage of tumor presenting with the microscopic criteria of PTC, and the frequency of PTC microscopic criteria in a series of 66 PTC. The combination and frequency of microscopic criteria present in PTC have not been clearly reported in the literature. In our series, the first observation was that the percentage of tumor with a microscopic criteria for PTC is highly variable from case to case. Indeed, features such as papillary architecture, abortive papillae, elongated follicles, dark staining colloid, lack of polarization in the cells or ovoid nuclei were present in a wide range from 0% to more than 75% of the tumor. Other nuclear criteria such as nuclear grooves, overlapping nuclei, ground glass nuclei, or irregularly shaped nuclei were present in less than 25% of the tumor in the majority of our cases. Finally, enlarged nuclei was the only feature present in more than 75% of tumor cells in the majority of cases (94%). Some of the nuclear criteria for PTC underlined in the literature, in particular nuclear grooves or ground glass nuclei, were only observed in a minority of tumor cells in our series. Psammoma bodies, multinucleated histiocytes, and pseudoinclusions were noted in 28 (42%), 28 (42%), and 36 (55%) cases of PTC. Our results are comparable with those of Adeniran et al. [1] who also found that nuclear enlargement was present in a high proportion of tumors cells, optically clear nuclei in a slightly smaller proportion, and nuclear grooves to a variable degree from case to case. For these authors, presence of nuclear pseudoinclusions was the less frequent finding among all tumors (54%) [1].

After determination of threshold values, the univariate analysis demonstrated that all criteria were significantly more frequently observed in PTC than in FA but none of them was totally sensitive and specific for the diagnosis of malignancy. By a stepwise regression analysis, we proposed a scaled score based on the best subset of criteria. This is the first study to determine morphologic criteria helpful for the diagnosis of PTC on the basis of statistical methods. In the training set, when the threshold for malignancy was determined above 30, this score presented a sensitivity of 98.5% and a specificity of 100% for malignancy. On the validation set, there was a "gray zone" for cases which total score was between 7 and 30. This "gray zone" includes eight PTC and eight FA. Review of these 16 cases revealed that the majority were encapsulated neoplasms with a follicular pattern ($n=10$) that showed very focal morphologic features of PTC. In the other three cases, PTC morphologic features were convincing but were not included in the score (ground glass nuclei and crowded nuclei). The "gray zone" also included two cases of oxyphilic adenoma and one case of adenoma with hyperplastic papillae identified on standard examination. In fact, although the selection of the training and validation sets was realized during different periods in the same institution, the two populations of the study were distinct in the proportion of classical PTC (65% in the training set versus 35% in the validation set, $p=0.005$), follicular variant of PTC (18% versus 59%, $p<0.0001$), invasive tumors (74% versus 41%, $p=0.002$), and lymph node metastasis (38% versus 8%, $p=0.046$). This discrepancy could explain the decreased sensitivity of the score in the validation set. Indeed, the gray zone observed with the score system on the validation population underlines the difficulties encountered in this field of pathology, in particular for encapsulated and follicular variant of PTC. It is in accordance with the subset of "well-differentiated thyroid tumor of uncertain malignant potential" defined by the Chernobyl pathologists group for encapsulated follicular neoplasm that only shows some of the nuclear features or whose features are unconvincing [37].

Numerous studies have investigated immunohistochemical and molecular markers for separating FVPTC from other benign conditions [5, 9, 13, 15–17, 28, 29, 34, 35]. Unfortunately, such markers have been deemed to be insufficiently discriminatory to make a reliable diagnosis in difficult encapsulated follicular thyroid tumors.[4, 18, 25, 31, 35, 36]. Recently, many advances have been made in the pathogenesis of PTC. The genetic events include rearranged during transfection (RET)/PTC rearrangements, RAS and BRAF gene mutations [3]. Some correlations have been described between the subtype of PTC (FVPTC versus classic PTC) and the type of gene mutations [6, 14]. Interestingly, Adeniran et al. [1] found that tumors with RAS mutations had significantly lower prevalence of microscopic features of PTC whereas in tumors with RET/PTC rearrangement these features were significantly more frequent. Moreover, BRAF mutation is a significant risk factor for locoregional lymph node metastasis and has been found to correlate with older age of patients, more frequent extrathyroidal extension, advanced tumor stage at presentation, and tumor recurrence [10, 11, 22].

The score proposed did not allow us to make a definite distinction between FA and PTC in routine practice but it does successfully reflect the gradient of morphologic

presentation between FA and PTC, in particular for cases of FVPTC. Such a scaled score may be a useful tool in this field of thyroid pathology. This score could be further tested by different teams of pathologists and in different pathological populations, such as metastatic or aggressive forms of PTC. It could also have a role in the evaluation of immunohistochemical or molecular markers which are proposed in this area of pathology.

Acknowledgement Mrs D'Herbomez M. contributed to the elaboration of the figures.

Conflict of interest statement We declare that we have no conflict of interest.

References

1. Adeniran AJ, Zhu Z, Gandhi M, Steward DL, Fidler JP, Giordano TJ, Biddinger PW, Nikiforov Y (2006) Correlation between genetic alterations and microscopic features, clinical manifestations and prognostic characteristics of thyroid papillary carcinomas. Am J Surg Pathol 30:216–222
2. Baloch ZW, Livolsi VA (2002) Follicular-patterned lesions of the thyroid: the bane of the pathologist. Am J Clin Pathol 117:143–150
3. Baloch ZW, LiVolsi VA (2005) Pathologic diagnosis of papillary thyroid carcinoma: today and tomorrow. Expert Rev Mol Diagn 5:573–584
4. Baloch ZW, LiVolsi VA (2007) Our approach to follicular-patterned lesions of the thyroid. J Clin Pathol 60:244–250
5. Barroeta JE, Baloch ZW, Lal P, Pasha TL, Zhang PJ, LiVolsi VA (2006) Diagnostic value of differential expression of CK19, Galectin-3, HBME-1, ERK, RET, and p16 in benign and malignant follicular-derived lesions of the thyroid: an immunohistochemical tissue microarray analysis. Endocr Pathol 17:225–234
6. Castro P, Rebocho AP, Soares RJ, Magalhaes J, Roque L, Trovisco V, Vieira de Castro I, Cardoso-de-Oliveira M, Fonseca E, Soares P, Sobrinho-Simoes M (2006) PAX8-PPARgamma rearrangement is frequently detected in the follicular variant of papillary thyroid carcinoma. J Clin Endocrinol Metab 91:213–220
7. Chan JK (2002) Strict criteria should be applied in the diagnosis of encapsulated follicular variant of papillary thyroid carcinoma. Am J Clin Pathol 117:16–18
8. Chan JKC (2002) The author's reply. Am J Clin Pathol 118:605
9. Chevillard S, Ugolin N, Vielh P, Ory K, Levalois C, Elliott D, Clayman GL, El-Naggar AK (2004) Gene expression profiling of differentiated thyroid neoplasms: diagnostic and clinical implications. Clin Cancer Res 10:6586–6597
10. Ciampi R, Nikiforov YE (2007) Minireview: RET/PTC rearrangements and BRAF mutations in thyroid tumorigenesis. Endocrinology 148:936–941
11. Cohen Y, Xing M, Mambo E, Guo Z, Wu G, Trink B, Beller U, Westra WH, Ladenson PW, Sidransky D (2003) BRAF mutation in papillary thyroid carcinoma. J Natl Cancer Inst 95:625–627
12. Davies L, Welch HG (2006) Increasing incidence of thyroid cancer in the United States, 1973–2002. JAMA 295:2164–2167
13. De Matos PS, Ferreira AP, De Oliveira Facuri F, Assumpçao LVM, Metze K, Ward LS (2005) Usefulness of HBME-1, cytokeratin 19 and galectin-3 immunostaining in the diagnosis of thyroid malignancy. Histopathology 47:391–401
14. Di Cristofaro J, Marcy M, Vasko V, Sebag F, Fakhry N, Wynford-Thomas D, De Micco C (2006) Molecular genetic study comparing follicular variant versus classic papillary thyroid carcinomas: association of N-ras mutation in codon 61 with follicular variant. Hum Pathol 37:824–830
15. Finley DJ, Arora N, Zhu B, Gallagher L, Fahey III TJ (2004) Molecular profiling distinguishes papillary carcinoma from benign thyroid nodules. J Clin Endocrinol Metab 89:3214–3223
16. Finley DJ, Zhu B, Barden CB, Fahey TJ (2004) Discrimination of benign and malignant thyroid nodules by molecular profiling. Ann Surg 240:425–437
17. Finn SP, Smyth P, Cahill S, Streck C, O'Regan EM, Flavin R, Sherlock J, Howells D, Henfrey R, Cullen M, Toner M, Timon C, O'Leary JJ, Sheils OM (2007) Expression microarray analysis of papillary thyroid carcinoma and benign thyroid tissue: emphasis on the follicular variant and potential markers of malignancy. Virchows Arch 450:249–260
18. Franc B (2003) Cherche marqueur désespérément pour tumeurs thyroïdiennes de diagnostic incertain. Ann Pathol 23:7–10
19. Hirokawa M, Carney JA, Goellner JR, DeLellis RA, Heffess CS, Katoh R, Tsujimoto M, Kakudo K (2002) Observer variation of encapsulated follicular lesions of the thyroid gland. Am J Surg Pathol 26:1508–1514
20. Hunt JL, Dacic S, Barnes EL, Bures JC (2002) Encapsulated follicular variant of papillary thyroid carcinoma. Am J Clin Pathol 118:602–606
21. Kakudo K, Katoh R, Sakamoto A, Asa S, DeLellis RA, Carney JA, Naganuma H, Kameyama K, Takami H (2002) Thyroid gland: international case conference. Endocr Pathol 13:131–134
22. Kim J, Giuliano AE, Turner RR, Gaffney RE, Umetani N, Kitago M, Elashoff D, Hoon DSB (2006) Lymphatic mapping establishes the role of BRAF gene mutation in papillary thyroid carcinoma. Ann Surg 244:799–804
23. Kondo T, Ezzat S, Asa S (2006) Pathogenetic mechanisms in thyroid follicular-cell neoplasia. Nat Rev Cancer 6:292–306
24. Lang BHH, Lo CY, Chan WF, Lam AKY, Wan KY (2006) Classical and follicular variant of papillary thyroid carcinoma: a comparative study on clinicopathologic features and long-term outcome. World J Surg 30:752–758
25. LiVolsi VA (2003) Can we agree to disagree? Hum Pathol 34:1081–1082
26. LiVolsi VA, Albores-Saavedra J, Asa SL, Baloch ZW, Sobrinho-Simoes M, Wenig B, DeLellis RA, Cady B, Mazzaferri EL, Hay I, Fagin JA, Weber AL, Caruso P, Voutilainen PE, Franssila KO, Williams ED, Schneider AB, Nikiforov Y, Rabes HM, Akslen L, Ezzat S, Santoro M, Eng C, Harach HR (2004) Papillary carcinoma. In: WHO classification of tumours. Pathology and genetics. Tumours of endocrine organs. IARC, Lyon, pp 57–66
27. Lloyd RV, Erickson LA, Casey MB, Lam KY, Lohse CM, Asa SL, Chan JK, DeLellis RA, Harach HR, Kakudo K, LiVolsi VA, Rosai J, Sebo TJ, Sobrinho-Simoes M, Wenig BM, Lae ME (2004) Observer variation in the diagnosis of follicular variant of papillary thyroid carcinoma. Am J Surg Pathol 28:1336–1340
28. Mehrotra P, Okpokam A, Bouhaidar R, Johnson SJ, Wilson JA, Davies BR, Lennard TWJ (2004) Galectin-3 does not reliably distinguish benign from malignant thyroid neoplasms. Histopathology 45:493–500
29. Nakamura N, Erickson LA, Jin L, Kajita S, Zhang H, Qian X, Rumilla K, Lloyd RV (2006) Immunohistochemical separation of follicular variant of papillary thyroid carcinoma from follicular adenoma. Endocr Pathol 17:213–223

30. Papotti M, Manazza AD, Chiarle R, Bussolati G (2004) Confocal microscope analysis and tridimensional reconstruction of papillary thyroid carcinoma nuclei. Virchows Arch 444:350–355
31. Papotti M, Rodriguez J, De Pompa R, Bartolazzi A, Rosai J (2005) Galectin-3 and HBME-1 expression in well-differentiated thyroid tumors with follicular architecture of uncertain malignant potential. Mod Pathol 18:541–546
32. Renshaw AA, Gould EW (2002) Why there is the tendency to "overdiagnose" the follicular variant of papillary thyroid carcinoma. Am J Clin Pathol 117:19–21
33. Rosai J, Carcangiu ML, DeLellis RA (1992) Atlas of tumor pathology. Tumors of the thyroid gland. Armed Forces Institute of Pathology, Washington, DC
34. Rosen J, He M, Umbricht C, Alexander HR, Dackiw APB, Zeiger MA, Libutti SK (2005) A six-gene model for differentiating benign from malignant thyroid tumors on the basis of gene expression. Surgery 138:1050–1057
35. Scognamiglio T, Hyjek E, Kao J, Chen YT (2006) Diagnostic usefulness of HBME1, galectin-3, CK19 and CITED1 and evaluation of their expression in encapsulated lesions with questionable features of papillary thyroid carcinoma. Am J Clin Pathol 126:700–708
36. Suster S (2006) Thyroid tumors with a follicular growth pattern. Arch Pathol Lab Med 130:984–988
37. Williams ED (2000) Guest editorial: two proposals regarding the terminology of thyroid tumors. Int J Surg Pathol 8:181–183

Virchows Arch (2008) 452:241–250
DOI 10.1007/s00428-007-0570-9

ORIGINAL ARTICLE

Molecular characterisation of breast cancer patients at high and low recurrence risk

Serena Bonin · Davide Brunetti · Elena Benedetti · Isabella Dotti · Nader Gorji · Giorgio Stanta

Received: 23 August 2007 / Accepted: 20 December 2007 / Published online: 31 January 2008
© Springer-Verlag 2008

Abstract The ability to predict the recurrence risk in breast cancer patients is not available for the individual. It is commonly accepted that the different clinical course of tumours with identical histology and stage are the result of differences at the molecular level. This case study of 80 patients affected by breast cancer looked at the messenger ribonucleic acid expression level of 22 genes, by using quantitative reverse transcriptase–polymerase chain reaction. Our results showed that a panel of seven genes is associated to patients' survival. Moreover, the combination of two couples of genes is able to define short- and long-living cohorts of patients. In particular, our findings strongly demonstrate that retinoblastoma (RB) and cyclin-dependent kinase 2 (CDK2) on one side and cytokeratin 8 (CK8) and epidermal growth factor receptor 2 (HER2) on the other may affect the clinical course of the disease in 56% of patients. Groups characterised by low RB and high CDK2 as with low CK8 and high HER2 have a higher risk of recurrences and death in 5 years. The identification of these sub-groups of patients with higher risk of early relapse could have further involvement in the selection of the cases to submit to therapy against HER2 or CDK2 as a possible therapy target.

Keywords Breast cancer · Formalin-fixed paraffin-embedded tissues · Quantitative RT-PCR · RB · CDK2 · HER2 · CK8

S. Bonin · I. Dotti · G. Stanta
Department of Clinical,
Morphological and Technological Sciences,
International Centre for Genetic Engineering and Biotechnology,
University of Trieste,
Trieste, Italy

D. Brunetti
Friuli-Venezia Giulia Cancer Registry,
Udine, Italy

E. Benedetti
International Centre for Genetic Engineering and Biotechnology,
Trieste, Italy

N. Gorji
Surgical Pathology Unit, S. Andrea Hospital,
La Spezia, Italy

G. Stanta (✉)
Surgical Pathology Unit, Cattinara Hospital,
Strada di Fiume 447,
34149 Trieste, Italy
e-mail: stanta@icgeb.org

Introduction

Breast cancer is the leading cause of death among women in developed countries [30]. Despite important advances in therapy, more than half of the affected patients undergoes relapses [17].

Many studies on gene expression carried out by microarrays have identified expression profiles and gene sets that are prognostic and/or predictive of outcome of breast cancer patients. Unfortunately, genes identified by these studies show only a slight overlap, even if they seem to be able to predict the outcome of the same group of patients [7]. The major concern related to the use of microarray platforms is the requirement of high-quality ribonucleic acid (RNA), generally derived from frozen samples. Such tumour sets are often small, and an extensive clinical history is not yet available, whereas formalin-fixed paraffin-embedded (FFPE) materials are abundant and allow the possibility of selecting samples related to patients that have been

followed-up for long periods. Although reverse transcriptase–polymerase chain reaction (RT-PCR)-based methods from FFPE samples can have clinical application, genome-wide microarray analysis has proven to be difficult. A recent paper by Penland et al. [19], has demonstrated that only a minority of FFPE blocks could be analysed by microarray.

To investigate the progression of breast carcinoma, we analysed the level of expression of a well-defined panel of genes involved in the maintenance/abrogation of the cell senescence machinery in primary breast cancers. This study represents an extension of a previous paper where we analysed a part of this cohort of patients for cell cycle-related molecules, such as cyclins, cyclin-dependent kinases (CDKs) and the phosphatase cell division cycle 25a (CDC25a) [2].

Recent studies have demonstrated that the first step in creating an in vitro model of human cancer involves the abrogation of the cellular senescence mechanism. In fact, a tumour will develop only if it has bypassed all senescence controls [5]. Two tumour suppressor genes, retinoblastoma and p53, are central factors in replicative and premature senescence. Suppression or down-regulation of the retinoblastoma pathway together with the activation of immortalisation factors, such as telomerase activation and RAS pathway activation, is essential to define breast cancer tumourigenesis and progression [12], also at a clinical level. By using quantitative RT-PCR, we looked at the messenger RNA (mRNA) expression level of 22 genes belonging to the RAS pathway (epidermal growth factor receptor 1 [EGFr1] and 2 [HER2], k-RAS, v-raf-1 murine leukaemia viral oncogene homolog 1 [RAF-1], mitogen-activated protein kinase 1 [ERK1], phosphatidylinositol 3 kinase [PI3K], protein kinase B isoform 3 [AKT3]), cell cycle regulation/senescence (Cyclin A, D1 and E1, CDK2, CDK4, CDK6, CDK inhibitor 2A [p16], retinoblastoma 2 [p130-RB2], retinoblastoma [RB], CDC25a), telomerase complex (mRNA coding for catalytic component and RNA component, hTRT and hTR, respectively) and differentiation/metastasis suppression genes such as non-metastatic cells 1 protein (NM23), sel-1 suppressor of lin-12-like (SEL-1L) and cytokeratin 8 (CK8). Genes were selected according to their known links to malignant cell behaviour in breast cancer and their importance in major cancer hallmarks, such as cell senescence/proliferation and survival. Our main goal was to investigate whether the gene expression profiles of the reported molecular markers in primary tumours are predictive of metastatic potential.

Materials and methods

Eighty women were selected who were residents in the Northeastern Italian province of Trieste and whose first primary cancer was unilateral infiltrating duct breast carcinoma. Cancers were diagnosed at the age of 34 or older,

Table 1 Oligonucleotide sequences

Genes	Primer sequences
AKT3	up: 5′-TCT GCC TTG GAC TAT CTA CA-3′ sense
	dw: 5′-AAT TTT TAT GTG GCC ATC T-3′ antisense
	Probe: 5′-CCG TGA TCT CAA GTT GGA GAA TCT AAT G-3′ sense
Cytokeratin 8	up: 5′-AGG AGA AGC TGA AGC TGG A-3′ sense
	dw: 5′-CTC TGT ACG CTT ATT GAT C-3′ antisense
	probe: 5′-GAG GAC TTC AAG AAC AAG TAT GAG G-3′ sense
ERK1	up: 5′-GTT CCC AAA TGC TGA CTC-3′ sense
	dw: 5′-CAG AGC CTG TTC TAC TTC AA-3′ antisense
	probe: 5′-TGG ACA AAA TGT TGA CAT TCA A-3′ sense
NM-23	up: 5′-CAG AAA GGA TTC CGC CTT-3′ sense
	dw: 5′-GGT CCT TCAGGT CAA CGT A-3′ antisense
	probe: 5′-CAT GCA AGC TTC CGA AGA TCT TCT C-3′ sense
PI3K	up: 5′-CCA AAA TTA CTG CTG TCA AT -3′ sense
	dw: 5′- TAG GCC AAA TCT GAA GCA -3′ antisense
	probe: 5′-GAT GTT GCT CAG CTT CAG GCG C-3′ sense
p130 (RB2)	up: 5′-GGC AGC AGT GAT AGC AGA-3′ sense
	dw: 5′-AAG GTG CTG CTT GAC CTC-3′ antisense
	Probe: 5′-CTG GAG TCT CTA CTG GTT CTA TCT TTG-3′ sensed
RAF-1	up: 5′-GGA TTG GGT CAG GCT CTT-3′ sense
	dw: 5′-GGG TCG ACA ACC TTT AGG A-3′ antisense
	probe: 5′-TAA ATG GCA CGG AGA TGT TGC AG-3′ sense
SEL-1L	up: 5′-TTC TAG AGT CTC CAA ATC CAG-3′ sense
	dw: 5′-ATG TGC TGT GCC TTC AAT-3′ antisense
	probe: 5′-GTA CGG AAA CCA GCT TTG ACC G-3′ sense

Primers up and down (dw) were used in the PCR reaction. The probe was used in the hybridisation of the dot blots.

Table 2 RT-PCR and hybridisation conditions

Marker	PCR conditions			Hybridisation conditions	
	RNA[a] (ng)	T_a[b] (°C)	PCR cycles[c]	T[d] (°C)	Formamide %[e]
AKT3	125	50	45	52	3.0
Cytokeratin 8	500	50	50	46	0.0
ERK1	30	50	35	52	3.0
NM23	100	50	40	50	0.0
PI3K	60	50	30	52	8.0
p130 (RB2)	250	55	55	45	0.0
RAF-1	120	55	40	52	4.2
SEL-1L	15	51	45	45	0.0

[a] Quantity of total RNA used in the cDNA synthesis
[b] Annealing temperature for PCR reaction
[c] Number of PCR cycles
[d] Hybridisation Temperature
[e] Percentage of Formamide included in the hybridisation solution

between 1971 and 1989 and treated only with Halsted radical mastectomy and complete axillary dissection, without any additional chemotherapy or radiotherapy. Seventy-three patients belonging to this cohort were also part of a previous study [2]. All the slides from the primary tumour were reviewed by one of the authors (Stanta). Carcinomas were histologically graded according to Elston and Ellis [6] and grouped in stages according to the *TNM Classification of Malignant Tumours*, 6th edition [10].

The cohort of women was followed through the general population-based Friuli–Venezia Giulia Cancer Registry [1] from diagnosis of breast cancer to death or until 31 December 2006, whichever came first [18]. One patient was lost in 1993, after 4 years of follow-up. During the observation period, 69 women died, and all of them underwent complete autopsy at the Surgical Pathology Department of the University of Trieste.

FFPE specimens from primary breast cancers were microdissected and used to extract and quantify the RNA as described in detail elsewhere [3, 24, 27]. RT-PCR was performed as previously reported [24]. Cyclins A, D1 and E, CDK2, 4 and 6 and CDC25a were previously analysed in 73 patients [2] and seven additional patients. Oligonucleotides and RT-PCR conditions were already described for: cyclins A, D1 and E, CDK2, 4 and 6 and CDC25a [2], p16, RB, k-RAS, EGFr1, HER2 [25] and telomerase component genes [26]. For AKT3, CK8, ERK1, NM23, RAF-1, PI3K and SEL-1L and p130 (RB2) oligonucleotides, PCR and hybridisation conditions are reported in Tables 1 and 2. We used paraffin blocks without tissues as negative controls. The basal level of expression of the genes was quantified by analysing ten normal mammary glands, from biopsies negative for cancer performed in the same range of time as the cases. The baseline expression level was therefore detected for epithelial, myoepithelial and fibrous tissue but not adipose tissue elements of the normal gland. RNA extracted from the breast cancer cell line (BT-549) was used as a positive control. To test the reproducibility of the method, for every gene analysed, we randomly selected ten samples from the case study for re-submission for RT-PCR analyses. Amplification products were quantified by dot hybridisation as previously reported [24]. Standardisation using housekeeping genes was reported in detail elsewhere [2, 3].

T test analysis was applied to compare the mean value of expression of each gene in patients with recurrences and in those without metastasis. To estimate the joint effects of the analysed covariates on patients' survival, the data were analysed by fitting the Cox proportional hazard regression model as previously reported [2]. Cox proportional hazard analysis included age at diagnosis, stage and grade of the tumours and the complete set of the molecular markers. In this analysis, tumours with expression of molecular markers lower or higher than the mean value were classified as low or high status of expression, respectively.

To investigate possible associations among the genes detected by Cox regression analysis, we chose pairs of molecular markers involved in opposite or conflicting functions. We considered groups defined by: high expression status of one marker and low expression status of the other marker as well as the opposite situation. The chosen pairs of genes were: HER2 and CK8 as de-differentiation/differentiation markers, CDK2 and RB as markers of cell cycle progression/senescence, PI3K-RAF1 and AKT3-RAF1 as markers of the main branches of the RAS pathways and PI3K and AKT3 as markers of activation of cell transcription factors. The log-rank test was used to compare the survival between the above mentioned groups.

Statistical analyses were performed with the package Stata/SE 9.0 (Stata, College Station, TX).

Table 3 Characteristics of the 80 breast carcinomas by stage, grading and patients' age at diagnosis

Stage	Grading[a]			Number of cases	Age at diagnosis (years)	
	G1	G2	G3		Mean	Range
I	14	15	4	33	65	38–79
IIA	7	14	5	26	63	35–87
IIB	1	4	1	6	56	48–63
IIIA	3	6	2	11	57	34–76
IIIC	0	3	1	4	70	47–90
All stages	25	42	13	80	61	34–90

[a] *G1* Well differentiated, *G2* moderately differentiated, *G3* poorly differentiated

Table 4 Results of Cox multivariate analysis

Variables	Hazard ratio (p)[a]	95%CI[b]
CDK2	5.3 (0.04)	1.1–25.4
HER2	3.8 (0.02)	1.2–12.2
PI3K	3.2 (0.06)	0.9–10.8
CYCLIN E	2.4	0.8–6.5
RAF1	2.3 (0.05)	1.0–5.6
ERK1	2.0	0.8–4.9
CDK4	1.8	0.4–9.1
STAGE	1.5	0.9–2.5
HTR	1.5	0.6–3.5
CYCLIN A	1.5	0.7–3.0
CDC25a	1.4	0.3–7.5
CDK6	1.3	0.5–3.3
EGFR1	1.1	0.5–2.4
SEL1L	1.1	0.5–2.8
CYCLIN D1	1.0	0.3–3.5
P16	1.0	0.5–2.1
AGE	1.0	0.9–1.0
RB2	0.8	0.3–2.4
GRADE	0.7	0.3–1.4
NM23	0.6	0.2–2.1
K-RAS	0.6	0.3–1.2
HTRT	0.6	0.2–1.4
RB	0.3 (0.03)	0.1–0.9
CK8	0.3 (0.04)	0.1–1.0
AKT3	0.2 (0.01)	0.09–0.7

[a] Probability value is reported only for markers that affected significantly patients' survival.
[b] Confidence interval

Results

The cohort of 80 women affected by breast cancer showed a median age at diagnosis of 61 years (25th–75th percentile=51–70). All of them were affected by infiltrating duct carcinoma of the breast, the diameter of which was not larger than 3.0 cm at pathological examination. Staging and grading of tumours are shown in Table 3. The axillary lymph nodes were tumour negative in 43 patients, while they were positive in 37 patients at the time of diagnosis of the primary tumour. The median number of positive nodes was 3 (range=1–15). During the period of observation, 42 patients developed distant metastases.

The median duration of follow-up was 6 years (25th–75th percentile=3–12 years). Of the 69 deceased patients, 42 died of breast cancer metastases, one patient died of ovary carcinoma and 26 of non-neoplastic diseases.

This study confirms our previous findings on CDC25a (p=0.01), CDK2 (p=0.01) and CDK4 (p=0.03) expression in the groups of patients who developed recurrences and the patients that did not [2]. Moreover, the present study also confirms that CDK2 and CDC25a affected patients' survival in univariate analysis (p=0.0001 and p=0.02, respectively) as previously reported [2].

The results of the Cox proportional hazard regression analysis are reported in detail in Table 4. An independent influence on cancer-specific death was detected for AKT3 (p=0.01), RAF-1 (p=0.05), CDK2 (p=0.04), CK8 (p=0.04), RB (p=0.03) and HER2 (p=0.02). A borderline influence on patients' survival was detected for PI3K (p=0.06). Conversely, tumour stage and grade, patients' age at diagnosis and the remaining molecular markers analysed did not show an effect on survival. After dividing the stage into lymph node status (positive or negative for metastasis) and tumour dimension (diameter expressed in centimetres), the results of Cox proportional hazard regression analysis were restated. In this analysis, lymph node status and tumour diameter did not affect patients' survival (p=0.1 and p=0.5, respectively).

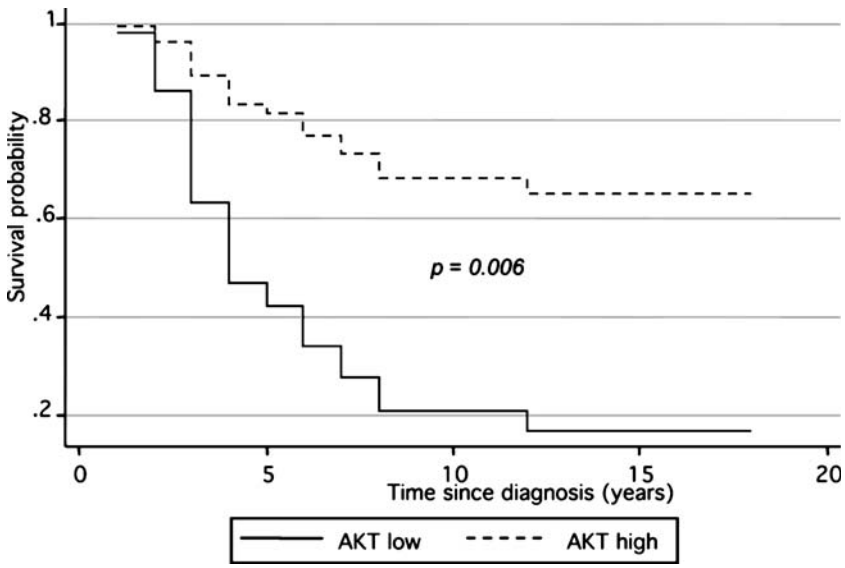


Fig. 1 Survival curves related to Cox proportional hazard regression with respect to AKT3 expression level in the sub-groups of low AKT3 (AKT3 expression lower than the mean value) or high AKT3 (AKT3 expression higher than the mean value)

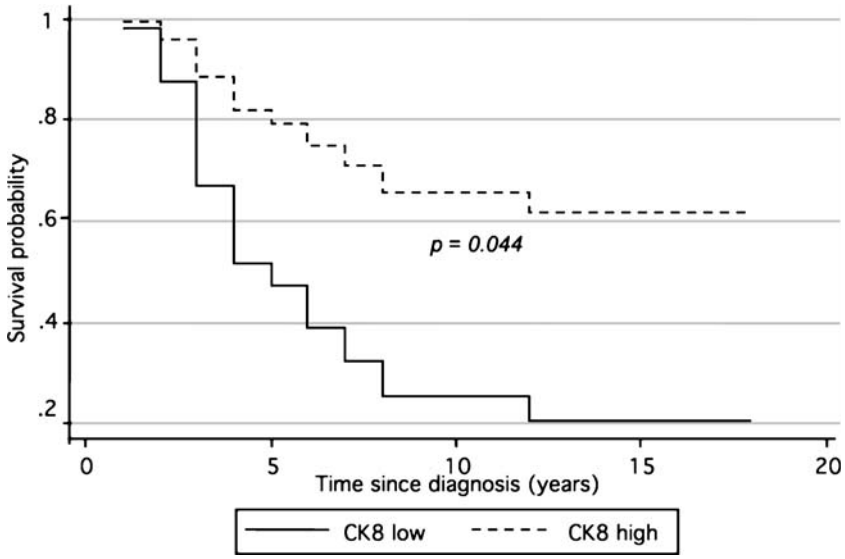


Fig. 2 Survival curves related to Cox proportional hazard regression with respect to cytokeratin 8 expression level in the sub-groups of low cytokeratin 8 (cytokeratin 8 expression lower than the mean value) or high cytokeratin 8 (cytokeratin 8 expression higher than the mean value)

Among the genes related to survival, AKT3, CK8 and RB seem to have a protective effect. Higher expression levels were indeed associated with better prognosis (Figs. 1, 2 and 3, respectively). Conversely, CDK2, HER2, PI3K and RAF-1 showed a worse effect on patient survival (Figs. 4, 5, 6 and 7, respectively). In particular, CDK2 and HER2 high-expression statuses seem to be associated with early relapses, and patients' survival decreased to 27 and 36% at 5 years, respectively (Figs. 4 and 5).

Moreover, groups of patients with a high-expression status of RB but a low-expression status of CDK2 showed a longer disease-free survival in comparison to the group characterised by low RB status and high CDK2 status (p= 0.001) as described in Fig. 8. A borderline significance (p= 0.07) was detected when pairing CK8 and HER2 statuses (Fig. 9). The associations RAF1–PI3K and PI3K–AKT3 as well as the pairing between RAF1 and AKT3 did not affect patients' survival (p=0.9 and p=0.7, respectively).

Seventy-three percent of patients belonging to the group with low RB and high CDK2 statuses died during the first 5 years of follow-up. A similar pattern was found for the group described by low CK8 and high HER2, in which 47% of patients died within the fifth year of follow-up. Moreover, the groups described by these two couples did not share any patient. Conversely, breast cancer patients described by high RB and low CDK2 showed a 5- and a 10-year survival probability of 77 and 68%, respectively. Similarly, the survival probability of patients with high CK8 and low HER2 was 81 and 69% at 5 and 10 years, respectively. These two groups overlapped for three patients. The four groups identified by these couples of markers included 45 of the 80 patients (56%).

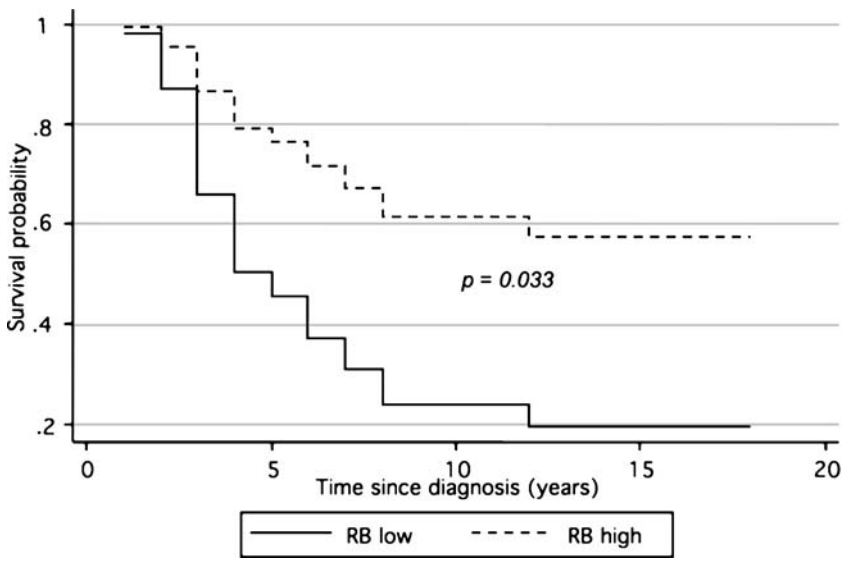


Fig. 3 Survival curves related to Cox proportional hazard regression with respect to retinoblastoma expression level in the sub-groups of low retinoblastoma (RB expression lower than the mean value) or high retinoblastoma (RB expression higher than the mean value)

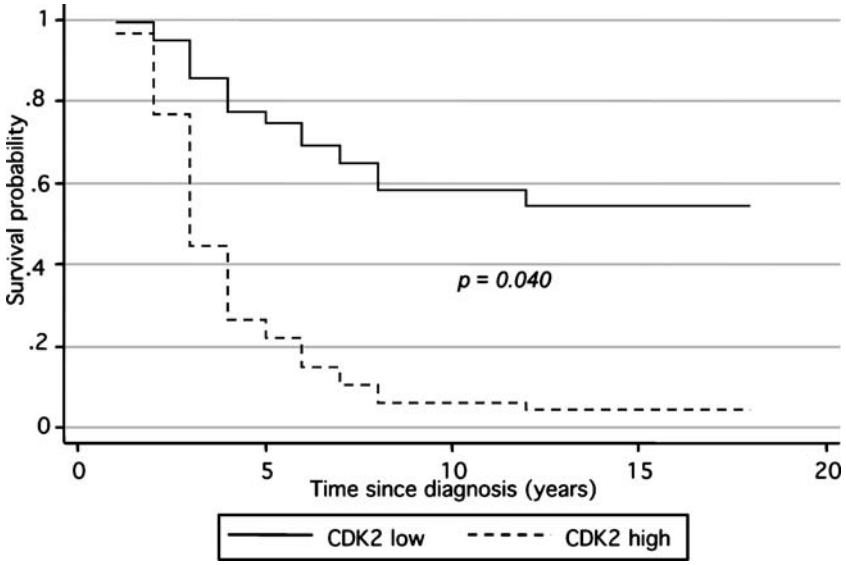


Fig. 4 Survival curves related to Cox proportional hazard regression with respect to CDK2 expression level in the sub-groups of low CDK2 (CDK2 expression lower than the mean value) or high CDK2 (CDK2 expression higher than the mean value)

Discussion

The ability to define the risk of recurrence is useful in medical decision making. Several clinical and pathological factors have been proposed to predict the recurrence of breast cancer. However, at the present time, it is not possible to predict recurrence vs no recurrence at an individual level. It is commonly accepted that the different clinical courses of patients characterised by the same histology and stage are the result of molecular differences among cancers [21]. Different single molecular markers have been assessed in the past 20 years but failed to be considered for clinical use for various reasons [21]. Micro-array studies have identified expression profiles and gene sets that are prognostic or predictive or both for patients with breast cancer. Comparison of the lists of genes derived from these studies shows only a slight overlap probably because of differences in the cohorts of patients, micro-array platforms and mathematical methods of analysis [7]. Understanding the molecular alterations connected with progression to eventual recurrence is of particular importance, especially for therapeutic decisions.

In the present study, carried out on 80 women with infiltrating duct carcinoma of the breast, quantitative RT-PCR was performed for a set of 22 genes involved in cell senescence, malignant transformation and tumour suppression. This study confirms our previous findings on the expression level of CDK2, CDK4 and CDC25a in breast cancer progression [2] and their correlation with recurrences. As previously reported [2], CDK2 over-expression seems to have an influence on the patient's survival both by uni- and multi-variate analysis, while data on CDC25a and

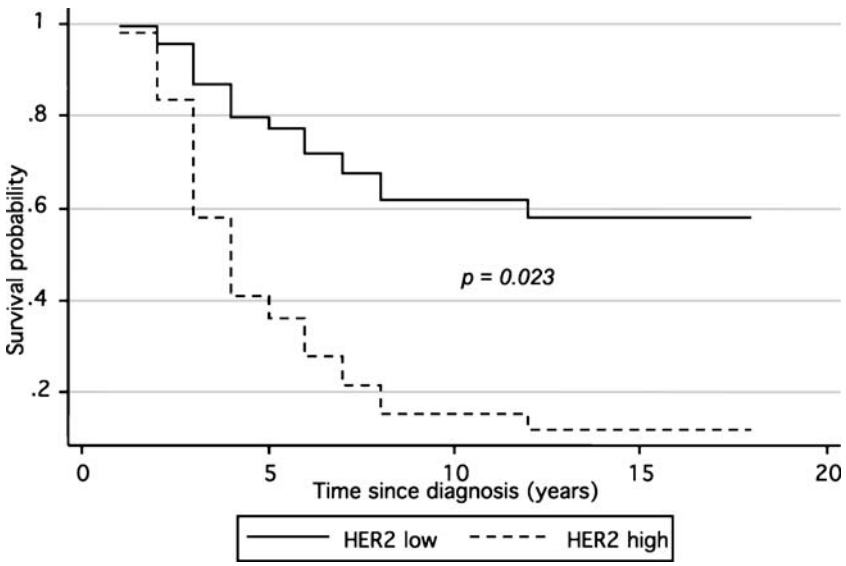


Fig. 5 Survival curves related to Cox proportional hazard regression with respect to HER2 expression level in the sub-groups of low HER2 (HER2 expression lower than the mean value) or high HER2 (HER2 expression higher than the mean value)

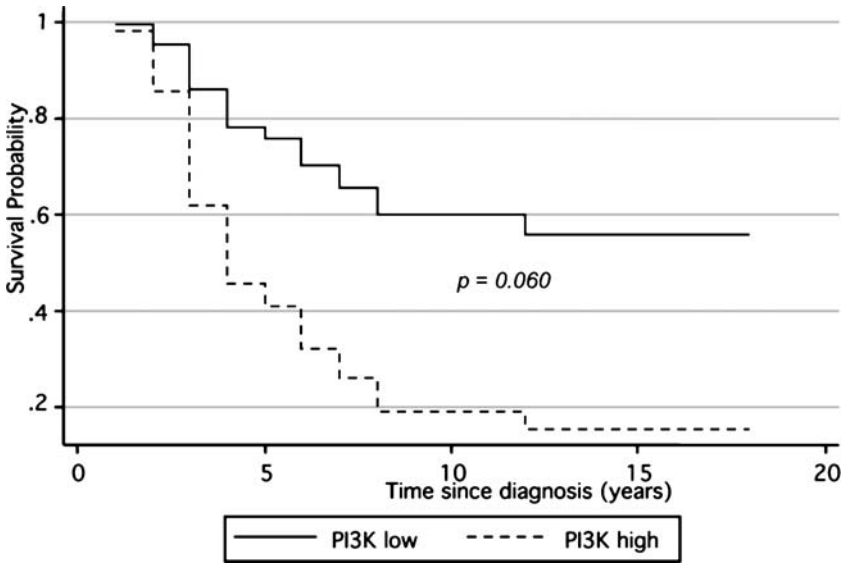


Fig. 6 Survival curves related to Cox proportional hazard regression with respect to PI3K expression level in the sub-groups of low PI3K (PI3K expression lower than the mean value) or high PI3K (PI3K expression higher than the mean value)

survival were confirmed only by uni-variate analysis. In our study, Cox proportional hazard analysis did not identify tumour stage as significantly affecting survival in these patients (p=0.1). The main differences between the previous and the present study is the enrolment of seven women in the cohort of patients and 15 new molecular markers that have been compared with the previous ones.

Patients' survival was analysed by the Cox proportional hazard regression method. We divided the cases with a high level of expression (over the average value) from those with lower expression (below the average value). In this analysis, only those genes that showed a significant level of survival between the two groups are discussed.

Cox proportional hazard analysis identified different molecules involved in patients' survival. In particular, our results showed that patients with a higher expression level of HER2 and/or PI3K and a lower expression level of AKT seem to have the worst outcome. Our data agree with previous reports. It is well known that alteration in the PI3K/AKT signalling cascade is common in human cancers and results in hyper-activation of the pathway that leads to tumour progression [8]. In particular, our data associate a worse outcome to patients over-expressing HER2 and/or PI3K but not AKT. The association of higher AKT3 mRNA expression level with better prognosis shown in our study is discordant with a previous paper [29]. A possible explanation of this discrepancy is related to methodological issues, as Totunaka et al. detected AKT in its activated status, i.e. the expression of phosphorylated AKT by immunohistochemistry (IHC). Our primer set was able to identify only isoform 3 of the transcript (AKT3). In fact recently, Maroulakou et al. reported that AKT2 ablation accelerates

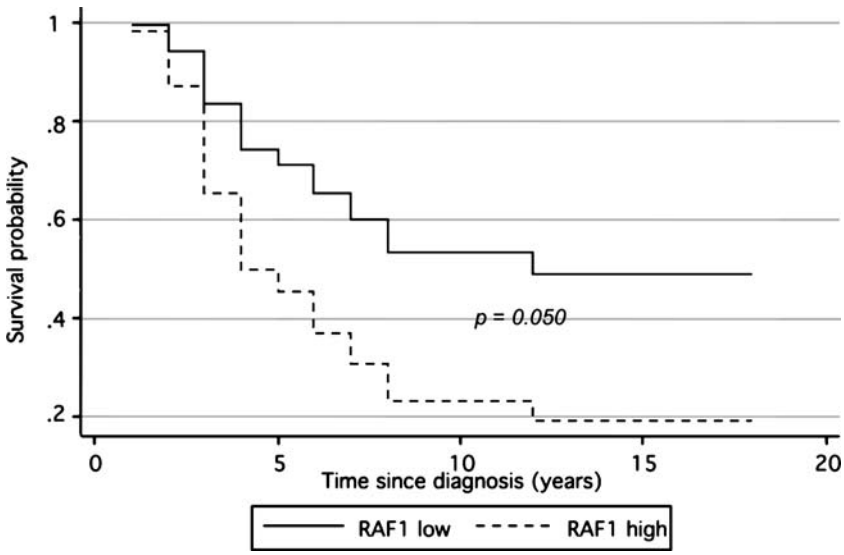


Fig. 7 Survival curves related to Cox proportional hazard regression with respect to RAF-1 expression level in the sub-groups of low RAF-1 (RAF-1 expression lower than the mean value) or high RAF-1 (RAF-1 expression higher than the mean value)

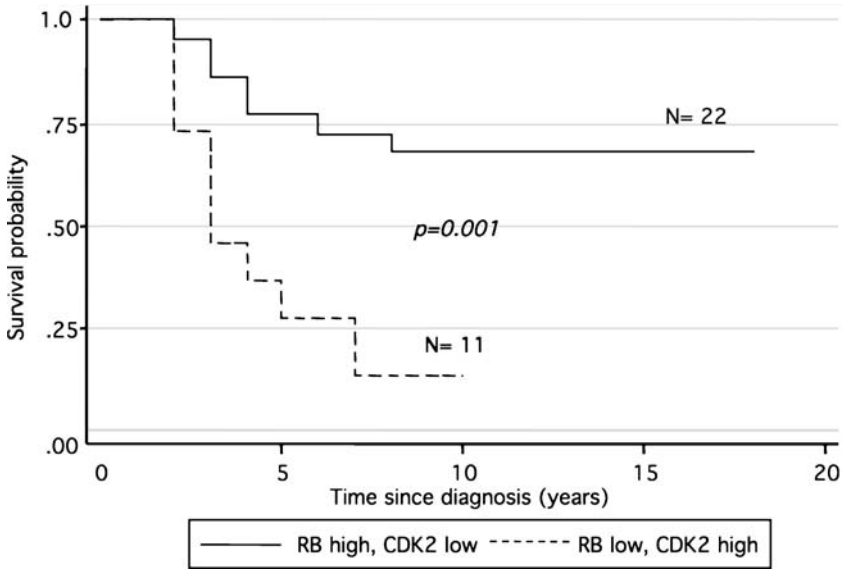


Fig. 8 Kaplan–Meier survival curves for patients with respect to RB and CDK2 expression level in the sub-groups of high RB and low CDK2 or low RB and high CDK2 status

whilst AKT1 and AKT3 ablation seem to inhibit the development of mammary adenocarcinoma in mice [13] suggesting a complex functional pattern for this group of proteins.

RAF-1 is a protein serine–threonine kinase that plays an important role in cell growth, proliferation and survival. Our results show that patients with high RAF-1 status had a decreased disease survival as detected by Cox multivariate analysis (Fig. 7). These data agree with previous findings by Mewani et al. [15], these authors reported that an over-expression of RAF-1 in mammary epithelial cells induced the expression of genes promoting cell proliferation, invasiveness, angiogenesis, cell survival and also with mitogen-activated protein kinase kinase/extracellular regulated kinase-independent functions [14].

It is well-documented that the RB pathway plays a critical role in cell cycle progression, acting as a crucial negative regulator of cellular proliferation [23]. Our latest results on RB expression level and survival indicate a protective role of this molecule in breast cancer progression; patients with high RB seem to have a longer survival time (Fig. 3). Our findings agree with Derenzini et al. [4], who found that patients with low RB mRNA and a high level of phosphorylated RB labelling index had shorter disease-free intervals and overall survival time. Moreover, our data show that the CDK2 and RB expression levels, when combined together, are well able to predict patients' survival. The fact that patients characterised by a high status of CDK2 and a low status of RB presented a worse prognosis agrees with the role of these molecules in

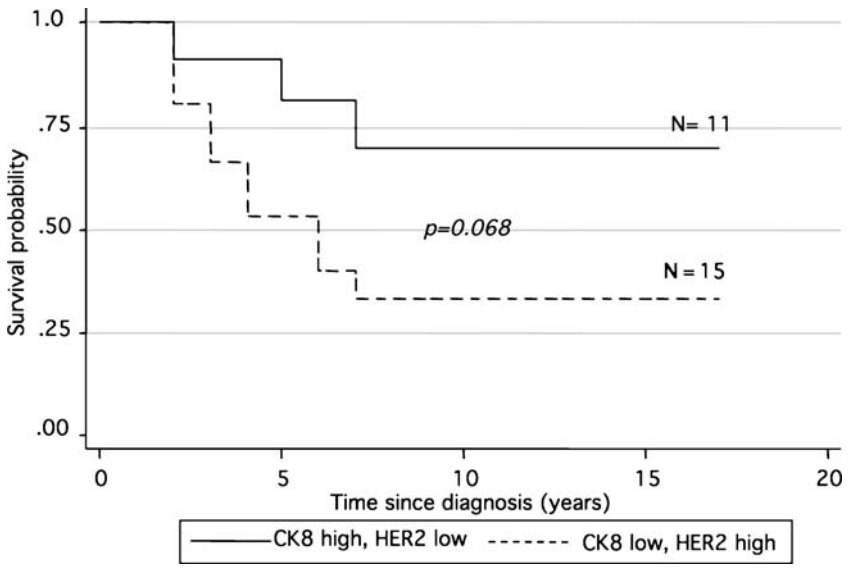


Fig. 9 Kaplan–Meier survival curves for patients with respect to Cytokeratin 8 and HER2 expression level in the sub-groups of high CK8 and low HER2 or low CK8 and high HER2 status

progression of the cell cycle through the G1/S phase and even indicated overcoming of this control checkpoint.

CK8 is characteristically present in luminal cells of a normal mammary gland. A wide range of cytokeratin expression is often seen in invasive breast cancer, which may be caused by loss of differentiation of the tumour cells [28]. In our study, higher expression levels of CK8 were associated in Cox multivariate analysis with better prognosis, and CK8 has a protective influence on patients' survival. Our data are concordant with the investigation by Fuchs et al. [9] based on IHC in breast carcinomas and breast cancer cell lines. That study revealed that suppression of CK8 was significantly correlated with short survival. Moreover, in cell lines with increasing invasion potential, epithelial keratins were also lost [9]. In our case study, CK8 (at high-expression status) in association with HER2 (low-expression status) identifies a group of patients with better prognosis. In this group of patients, the oestrogen receptor (ER) status was analysed by RT-PCR as previously reported [16] (data not shown). The patients of the group characterised by a high expression level of CK8 and low expression levels of HER2 were all positive for ER at the mRNA level. On the contrary, the other group, defined by the opposite pattern of the two markers (high HER2 and low CK8 levels), presented very low or no expression levels of the ER. These data agree with the recently reported molecular classification of breast cancer [20]. Patients with negative or weakly positive ER status and higher expression levels of HER2 presented a worse outcome, in accordance with Perreard et al. [20] who found ER-negative tumours more aggressive.

Of the 22 markers analysed in our study, 15 genes did not show influence on patients' survival. Among them, telomerase components need a comment. This enzyme catalyses the de novo synthesis of telomere repeats, which is necessary for unlimited cellular proliferation. The telomerase reverse transcriptase hTRT was detected at mRNA levels both in normal breast and breast cancer tissues [11]. Recently, Salhab et al. [22] investigated the expression level of the key telomere-related genes in human breast cancer and found that hTRT levels predicted the patients' overall survival. In our study, we did not find any association among telomerase components (hTR, the RNA template, and hTRT, the catalytic component), pathological parameters and patients' survival. One possible explanation is the normalisation methodology used by Salhab. Indeed, the authors normalised the expression levels of the telomerase genes against cytokeratin 19 (CK19) and not against one or more reliable housekeeping genes. This could modify the expression level of the telomerase machinery according to the level of CK19 expressed in cancer epithelial cells. From our study, it seems that telomerase expression could be a prerequisite for the early phase of tumorigenesis rather than a mechanism connected with progression. The presence and relative abundance of epithelial cells expressing telomerase within normal breast tissues could suggest that breast tumours arise from these highly expressing telomerase epithelial cells [11].

The molecular tumour progression analysed in the present study shows the natural history of the disease because the enrolled patients were only treated with the same type of surgical therapy. Our findings strongly demonstrate that the combination of two pairs of functionally conflicting markers (RB and CDK2 on one side, CK8 and HER2 on the other) may be divided into sub-groups that cover more than 50% of the patients, and these pairs of markers are able to identify sub-groups of patients with shorter relapse-free and survival times from those with long survival without recurrences. Groups characterised by low RB and high CDK2 (27% of survivors at 5 years and 14% at 10 years) as with low CK8 and high HER2 (53% of survivors at 5 years and 33% at 10 years) have a higher risk of early recurrence and death, suggesting that breast cancer progression in these patients could be related to these markers. Moreover, the recognition of these sub-groups of patients with higher risk of early relapse could have further relevance for the selection of patients to submit to therapy against HER2 or also against CDK2 as possible therapy targets. On the contrary, those with low CDK2 expression and high RB (68% of survival after 15 years) and those with high CK8 and low HER2 (69% of survival after 15 years) present a very good prognosis.

These results are preliminary because the real predictive value of these double-biomarker groups could result only from larger retrospective and prospectively randomised studies to evaluate that the use of these molecular assays yield better clinical outcome than current clinical decision-making systems. Moreover, a possible use of IHC markers as surrogates for the reported genes could represent a further simplification with the prospective of introducing them into routine tumour management.

References

1. Agenzia Regionale della Sanità (2002) Registro tumori regionale—dati di incidenza 1995–1998. Agenzia Regionale della Sanità, Italy
2. Bonin S, Brunetti D, Benedetti E, Gorji N, Stanta G (2006) Expression of cyclin-dependent kinases and CDC25a phosphatase is related with recurrences and survival in women with peri- and post-menopausal breast cancer. Virchows Arch 448(5):539–544
3. Bonin S, Pascolo L, Croce LS, Stanta G, Tiribelli C (2002) Gene expression of ABC proteins in hepatocellular carcinoma, perineoplastic tissue, and liver diseases. Mol Med 8(6):318–325
4. Derenzini M, Montanaro L, Vici M, Barbieri S, Ceccarelli C, Santini D, Taffurelli M, Martinelli GN, Trere D (2007) Relationship between the RB1 mRNA level and the expression of phosphorylated RB protein in human breast cancers: their relevance in cell proliferation

activity and patient clinical outcome. Histol Histopathol 22(5):505–513
5. Dimri GP (2005) What has senescence got to do with cancer? Cancer Cell 7(6):505–512
6. Elston CW, Ellis IO (1991) Pathological prognostic factors in breast cancer. I. The value of histological grade in breast cancer: experience from a large study with long-term follow-up. Histopathology 19 (5):403–410
7. Fan C, Oh DS, Wessels L, Weigelt B, Nuyten DS, Nobel AB, van, t Veer LJ, Perou CM (2006) Concordance among gene-expression-based predictors for breast cancer. N Engl J Med 355(6):560–569
8. Fresno Vara JA, Casado E, de Castro J, Cejas P, Belda-Iniesta C, Gonzalez-Baron M (2004) PI3K/Akt signalling pathway and cancer. Cancer Treat Rev 30(2):193–204
9. Fuchs IB, Lichtenegger W, Buehler H, Henrich W, Stein H, Kleine-Tebbe A, Schaller G (2002) The prognostic significance of epithelial–mesenchymal transition in breast cancer. Anticancer Res 22(6A):3415–3419
10. Greene FL, Page DL, Fleming ID, Fritz A, Balch MC, Haller DG, Morrow M (2002) AJCC cancer staging manual. Springer, New York
11. Hines WC, Fajardo AM, Joste NE, Bisoffi M, Griffith JK (2005) Quantitative and spatial measurements of telomerase reverse transcriptase expression within normal and malignant human breast tissues. Mol Cancer Res 3(9):503–509
12. Kendall SD, Linardic CM, Adam SJ, Counter CM (2005) A network of genetic events sufficient to convert normal human cells to a tumorigenic state. Cancer Res 65(21):9824–9828
13. Maroulakou IG, Oemler W, Naber SP, Tsichlis PN (2007) Akt1 ablation inhibits, whereas Akt2 ablation accelerates, the development of mammary adenocarcinomas in mouse mammary tumor virus (MMTV)-ErbB2/neu and MMTV-polyoma middle T transgenic mice. Cancer Res 67(1):167–177
14. McCubrey JA, Steelman LS, Abrams SL, Lee JT, Chang F, Bertrand FE, Navolanic PM, Terrian DM, Franklin RA, D'Assoro AB, Salisbury JL, Mazzarino MC, Stivala F, Libra M (2006) Roles of the RAF/MEK/ERK and PI3K/PTEN/AKT pathways in malignant transformation and drug resistance. Adv Enzyme Regul 46:249–279
15. Mewani RR, Tian S, Li B, Danner MT, Carr TD, Lee S, Rahman A, Kasid UN, Jung M, Dritschilo A, Gokhale PC (2006) Gene expression profile by inhibiting Raf-1 protein kinase in breast cancer cells. Int J Mol Med 17(3):457–463
16. Nardon E, Buda I, Stanta G, Buratti E, Fonda M, Cattin L (2003) Insulin-like growth factor system gene expression in women with type 2 diabetes and breast cancer. J Clin Pathol 56(8):599–604
17. Paredes J, Lopes N, Milanezi F, Schmitt FC (2007) P-cadherin and cytokeratin 5: useful adjunct markers to distinguish basal-like ductal carcinomas in situ. Virchows Archiv 450:73–80
18. Parkin DM, Whelan SL, Ferlay J, Raymond L, Young J (1997) Cancer incidence in five continents, vol. VII. International Agency for Research on Cancer, Lyon, pp 562–565
19. Penland SK, Keku TO, Torrice C, He X, Krishnamurthy J, Hoadley KA, Woosley JT, Thomas NE, Perou CM, Sandler RS, Sharpless NE (2007) RNA expression analysis of formalin-fixed paraffin-embedded tumors. Lab Invest 87(4):383–391
20. Perreard L, Fan C, Quackenbush JF, Mullins M, Gauthier NP, Nelson E, Mone M, Hansen H, Buys SS, Rasmussen K, Orrico AR, Dreher D, Walters R, Parker J, Hu Z, He X, Palazzo JP, Olopade OI, Szabo A, Perou CM, Bernard PS (2006) Classification and risk stratification of invasive breast carcinomas using a real-time quantitative RT-PCR assay. Breast Cancer Res 8(2):R23
21. Pusztai L, Mazouni C, Anderson K, Wu Y, Symmans WF (2006) Molecular classification of breast cancer: limitations and potential. Oncologist 11(8):868–877
22. Salhab M, Jiang WG, Newbold RF, Mokbel K (2007) The expression of gene transcripts of telomere-associated genes in human breast cancer: correlation with clinico-pathological parameters and clinical outcome. Breast Cancer Res Treat (in press)
23. Sherr CJ, McCormick F (2002) The RB and p53 pathways in cancer. Cancer Cell 2(2):103–112
24. Stanta G, Bonin S (1998) RNA quantitative analysis from fixed and paraffin-embedded tissues: membrane hybridization and capillary electrophoresis. Biotechniques 24(2):271–276
25. Stanta G, Bonin S, Losi L, Eusebi V (1998) Molecular characterization of intraductal breast carcinomas. Virchows Arch 432(2):107–111
26. Stanta G, Bonin S, Niccolini B, Raccanelli A, Baralle F (1999) Catalytic subunit of telomerase expression is related to RNA component expression. FEBS Lett 460(2):285–288
27. Stanta G, Schneider C (1991) RNA extracted from paraffin-embedded human tissues is amenable to analysis by PCR amplification. Biotechniques 11(3):304, 306, 308
28. Su L, Morgan PR, Lane EB (1996) Expression of cytokeratin messenger RNA versus protein in the normal mammary gland and in breast cancer. Human Pathol 27(8):800–806
29. Tokunaga E, Kimura Y, Mashino K, Oki E, Kataoka A, Ohno S, Morita M, Kakeji Y, Baba H, Maehara Y (2006) Activation of PI3K/Akt signaling and hormone resistance in breast cancer. Breast Cancer 13(2):137–144
30. Yankaskas BC (2005) Epidemiology of breast cancer in young women. Breast Dis 23:3–8

Virchows Arch (2008) 452:251–258
DOI 10.1007/s00428-007-0554-9

ORIGINAL ARTICLE

Advantage of FISH analysis using FKHR probes for an adjunct to diagnosis of rhabdomyosarcomas

Tadaki Matsumura · Takehiko Yamaguchi · Kunihiko Seki · Tadakazu Shimoda · Takuro Wada · Toshihiko Yamashita · Tadashi Hasegawa

Received: 23 May 2007 / Revised: 5 November 2007 / Accepted: 29 November 2007 / Published online: 20 December 2007
© Springer-Verlag 2007

Abstract Translocations can be detected using fluorescence in situ hybridization (FISH) in formalin-fixed paraffin-embedded tissues. Recently, a commercially available FKHR (13q14) dual-color, break-apart rearrangement probe has been developed. However, the advantages of using this probe have not been reported. This study demonstrated the usefulness of this probe for the clinical diagnosis of rhabdomyosarcomas (RMS). We studied 33 RMS (19 embryonal rhabdomyosarcomas [ERMS], including three sclerosing-type RMS, and 14 alveloar rhabdomyosarcomas [ARMS]). Fluorescence signals were detected for 18 of the 19 (94.7%) ERMS and 13 of the 14 (92.8%) ARMS. A split-signal pattern was detected in 12 of 13 (92.3%) ARMS but was not detected in any of the ERMS, including the three sclerosing-type RMS. Amplification and polyploidy were present in both the ERMS and the ARMS. Our FISH study highlighted the excellent performance of the presently reported commercial break-apart probe for the detection of FKHR gene rearrangements in RMS. Because amplification and polyploidy were detected in both the ERMS and the ARMS, sufficient care should be taken when counting the nuclear signals. No rearrangements of the FKHR gene were found in any of the three sclerosing-type RMS when examined using a FISH assay, supporting the hypothesis that sclerosing RMS can be included as an ERMS.

Keywords Rhabdomyosarcoma · FISH · FKHR · Formalin-fixed paraffin-embedded tissue · Sclerosing rhabdomyosarcoma

T. Matsumura · T. Yamaguchi · T. Hasegawa (✉)
Department of Surgical Pathology, Sapporo Medical University School of Medicine,
South 1, West 16, Chuo-ku,
Sapporo 060-8543, Japan
e-mail: hasetada@sapmed.ac.jp

T. Matsumura · T. Wada · T. Yamashita
Department of Orthopedic Surgery, Sapporo Medical University School of Medicine,
South 1, West 16, Chuo-ku,
Sapporo 060-8543, Japan

K. Seki
Department of Diagnostic Pathology, Kanto Medical Center NTT EC,
5-9-22 Higashi-gotanda, Shinagawa-ku,
Tokyo 141-8625, Japan

T. Shimoda
Division of Clinical Laboratory, National Cancer Center Hospital,
5-1-1 Tsukiji, Chuo-ku,
Tokyo 104-0045, Japan

Abbreviations

RMS	rhabdomyosarcomas
ERMS	embryonal rhabdomyosarcomas
ARMS	alveolar rhabdomyosarcomas
PRMS	pleomorphic rhabdomyosarcomas
RT-PCR	reverse transcriptase–polymerase chain reaction
FFPE	formalin-fixed paraffin-embedded
FISH	fluorescence in situ hybridization
H&E	hematoxylin and eosin,
DAPI II	4',6-diamidino-2-phenylindole
CCD	charge-coupled-device

Introduction

Rhabdomyosarcomas (RMS) are the most common malignant soft-tissue tumor in children. RMS are currently classified into three categories: embryonal (ERMS), alveo-

lar (ARMS) and pleomorphic RMS (PRMS) [15, 22]. ERMS, including botryoid [25], spindle cell [7, 17], and sclerosing variants [8, 10, 18], typically occur in young children, whereas ARMS, including its solid pattern [23, 27, 31], usually occur in older children and young adults, and PRMS occur in older adults [35]. These histologic subtypes are one of the most useful prognostic parameters in RMS, as ERMS are generally associated with a more favorable prognosis [16].

Most ARMS are cytogenetically associated with one of two translocations: t(2;13)(q35;q14) or t(1;13)(p36;q14) [1, 9, 12, 29]. Physical mapping and cloning studies have revealed that these translocations fuse the FKHR locus on chromosome 13 to either PAX3 on chromosome 2 or PAX7 on chromosome 1, leading to the generation of the chimeric genes PAX3–FKHR or PAX7–FKHR, respectively. The remaining ARMS are translocation negative or fusion negative and form a basically unexplored group. In contrast, cytogenetic studies of ERMS have failed to show any consistent structural chromosomal translocations.

Although PAX3–FKHR or PAX7–FKHR fusion genes can be readily detected using reverse transcriptase–polymerase chain reaction (RT-PCR), fresh frozen tissues may not always be available. These translocations can also be detected using RT-PCR and formalin-fixed paraffin-embedded (FFPE) tissues. However, RT-PCR is less sensitive in FFPE than in frozen tissues. Thus, the application of fluorescence in situ hybridization (FISH) methodology has significantly improved our diagnostic ability through the establishment of specific deoxyribonucleic acid (DNA) probes capable of detecting chromosomal aberrations in FFPE tissues and some soft-tissue sarcomas [6, 19, 20, 24, 30, 36].

A commercially available FKHR (13q14) dual-color, break-apart rearrangement probe was recently developed and has been tested extensively by Vysis (http://www.vysis.com). This probe identifies not only the two most common ARMS-associated fusion genes but also potential atypical variants. However, the advantages of using this probe have not been reported in a systematic study.

In this paper, we report our findings using this newly developed probe for the detection of FKHR rearrangements in interphase nuclei extracted from FFPE tissues and demonstrate the usefulness of this technique for the clinical diagnosis of RMS.

Materials and methods

Sample selection

The archival pathological files of the Surgical Pathology, Sapporo Medical University Hospital, Sapporo, Japan, and the Laboratory of Pathology, National Cancer Center Hospital, Tokyo, Japan, were screened for patients with a diagnosis of RMS. A series of patients whose lesions morphologically and immunophenotypically resembled RMS and who were diagnosed and treated at these hospitals were selected for further study. Nineteen ERMS samples, including one spindle cell-type and three sclerosing-type RMS, and 14 ARMS samples, including two solid-type ARMS, were analyzed (Table 1). In addition, 12 non-RMS tumors (three Ewing's sarcomas/primitive neuroectodermal tumors, three desmoplastic small round tumors, three clear-cell sarcomas, and three synovial sarcomas) were chosen as negative controls.

The histopathologic types of the samples that were studied are listed in Table 1. For the light microscopy examinations, all the specimens were routinely fixed in 10% formalin and embedded in paraffin wax, and 4-μm-thick sections were then cut and stained with hematoxylin and eosin (H&E). Tumor slides of all RMS specimens, stained with H&E, were reviewed, and representative sections from paraffin wax blocks were examined by the labeled polymer method, with the appropriate use of positive and negative controls. The sections were dewaxed, rehydrated, and moistened with phosphate-buffered saline (pH 7.4). They were pretreated in an autoclave at 121°C for 10 min in 10 mmol/l citrate buffer (pH 6.0), before being incubated with antibodies to the following molecules on an automated immunostatining system (Dako Autostainer, Dako, Carpinteria, CA) for 30 min: vimentin (clone V9; prediluted; BioGenex, San Ramon, CA), desmin (clone D33; prediluted; BioGenex), muscle specific actin (clone HHF35; prediluted; BioGenex), and myogenin (clone F5D; 1/50 dilution; Dako, Glostrup, Denmark). All tumors were positive for these skeletal muscle markers and were classified according to their morphological subtype.

Conventional ERMS exhibited a loose and dense pattern created by variable condensation of the tumor cells, separated by a loose, myxoid stroma that was often rich in connective tissue mucins (Fig. 1a). Spindle cell RMS were composed mainly of elongated spindle cells mimicking fetal myotubes at a late stage of differentiation, and a storiform or fascicular pattern, reminiscent of smooth-muscle tumors, was present (Fig. 1b). Sclerosing RMS were characterized by prominent hyaline sclerosis and a pseudovascular growth pattern (Fig. 1c). This variant of RMS was sometimes difficult to differentiate from ARMS. Conventional ARMS produce a collagenous fibrovascular septum that divides mixtures of undifferentiated tumor cells and rhabdomyoblasts into discrete nests (Fig. 2a). Solid RMS were characterized by unorganized sheets of undifferentiated small cells and the absence of a discrete fibrous septum (Fig. 2b). These lesions were sometimes misdiag-

Table 1 Clinical, histological, and FISH data for 33 rhabdomyosarcomas

Case	Age (year)	Sex	Site	Histologic type	FISH[a]	Signal pattern
1	45	M	Foot	ARMS	SS (60)	
2	20	M	Hand	ARMS	SS (82)	Amplification, polyploidy
3	28	F	Face	ARMS	SS (76)	
4	22	F	Thigh	ARMS	SS (72)	
5	16	F	Foot	ARMS	SS (56)	
6	19	F	Jaw	ARMS	SS (54)	Amplification
7	0.17	M	Face	ARMS	SS (70)	Amplification
8	7	M	Buttock	ARMS	SS (76)	Amplification, polyploidy
9	6	F	Face	ARMS	ND	
10	19	F	Inguina	ARMS (solid type)	SS (52)	Amplification, polyploidy
11	27	M	Inguina	ARMS	SS (78)	Amplification, polyploidy
12	38	M	Inguina	ARMS (solid type)	SS (72)	Amplification
13	20	M	Hand	ARMS	FS	Amplification, polyploidy
14	11	M	Nasal cavity	ARMS	SS (60)	Amplification, polyploidy
15	20	M	Orbit	ERMS	FS	Amplification
16	19	M	Prostate	ERMS	FS	
17	30	M	Thigh	ERMS	FS	Amplification
18	18	F	Orbit	ERMS	FS	
19	12	F	Jaw	ERMS	FS	
20	17	M	Testis	ERMS	FS	Amplification
21	39	M	Foot	ERMS (sclerosing type)	FS	
22	47	M	Prostate	ERMS (spindle cell type)	FS	Amplification
23	21	M	Foot	ERMS	FS	Amplification
24	11	M	Orbit	ERMS	FS	
25	5	F	Thigh	ERMS	FS	Amplification
26	14	F	Parotid gland	ERMS	FS	
27	22	M	Thigh	ERMS	FS	
28	14	F	Orbit	ERMS	FS	Polyploidy
29	61	M	Retroperitoneum	ERMS (sclerosing type)	FS	
30	12	M	Orbit	ERMS	FS	
31	15	M	Orbit	ERMS	FS	Polyploidy
32	46	M	Foot	ERMS (sclerosing type)	ND	
33	2	M	Elbow	ERMS	FS	Polyploidy

ARMS Alveolar rhabdomyosarcoma, *ERMS* embryonal rhabdomyosarcoma, *SS* split signal, *ND* not detected, *FS* fusion signal
[a] Positive cells with split signals (%)

nosed as ERMS because of the lack of a distinctive alveolar architecture.

Fluorescence in situ hybridization

Dual-color FISH studies were performed using FFPE specimens sectioned into 4-μm-thick tissue sections. Briefly, after dewaxing and hydration, the sections were immersed in 0.2 N HCl for 20 min followed by a pretreatment solution (Vysis, Downer's Grove, IL) at 80°C for 30 min. After digestion in protease for 60 min at 37°C, the sections were washed in phosphate-buffered saline for 5 min at room temperature, fixed in 10% formaldehyde for 10 min at room temperature, washed in phosphate-buffered saline for 5 min at room temperature, and placed into prewarmed denaturation solution (Vysis) for 5 min at 72°C. They were then dehydrated in an ethanol series (70, 85, and 100%) at room temperature for 1 min each and air dried. Ten microliters of solution containing an LSI FKHR (13q14) dual-color, break-apart rearrangement probe (Vysis) was added to the sample area of the slides at 45°C. According to the manufacturer's instructions, the probe consisted of a mixture of two FISH DNA probes. The first probe was a 720-kb probe labeled with spectrum green at a site proximal to the FKHR gene. The second probe was an approximately 650-kb probe labeled with spectrum orange at a site extending distally from the FKHR gene. The slides were covered with a coverslip, sealed with rubber cement, and incubated at 37°C for 48 h in a humidified chamber. Posthybridization washing was performed in a wash buffer at

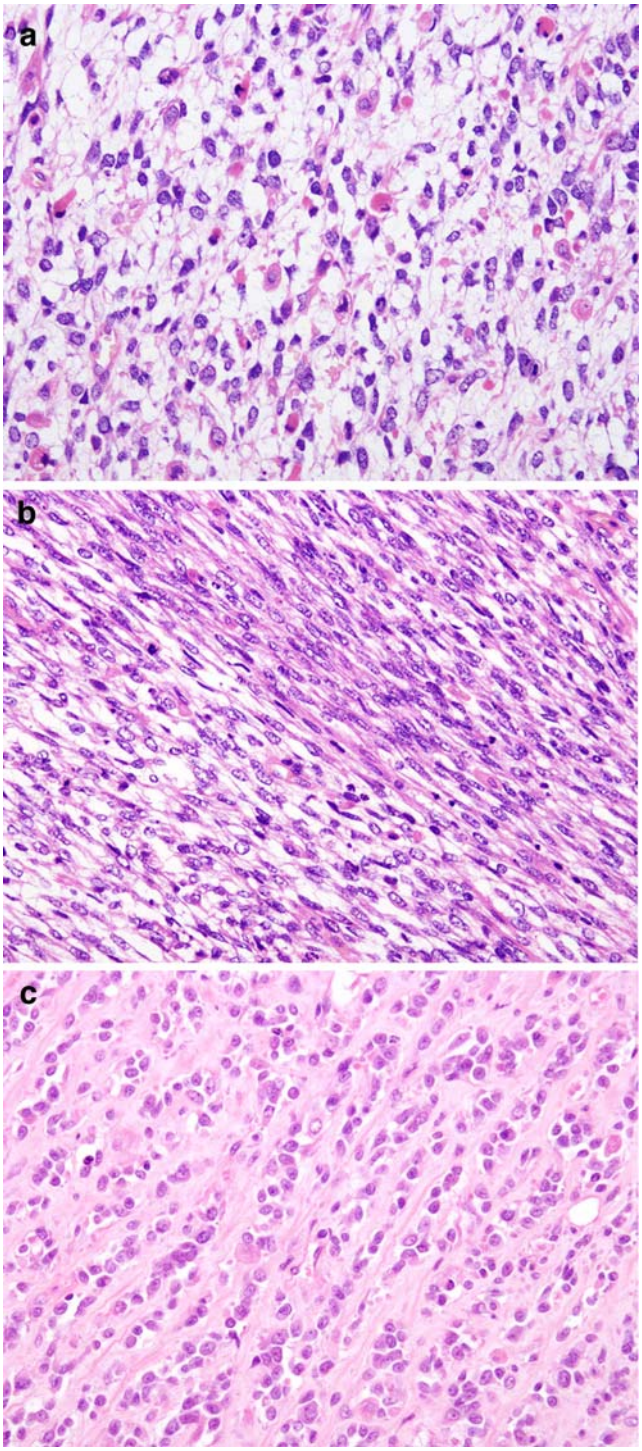


Fig. 1 **a** Conventional embryonal rhabdomyosarcoma composed of many rhabdomyoblasts and stellate cells with deeply eosinophilic cytoplasm (original magnification, ×200). **b** Spindle cell rhabdomyosarcoma characterized by spindle-shaped rhabdomyoblasts with a fascicular pattern (original magnification, ×200). **c** Sclerosing rhabdomyosarcoma composed of abundant intercellular hyalinized collagen and rhabdomyoblasts with a pseudoalveolar growth pattern (original magnification, ×200)

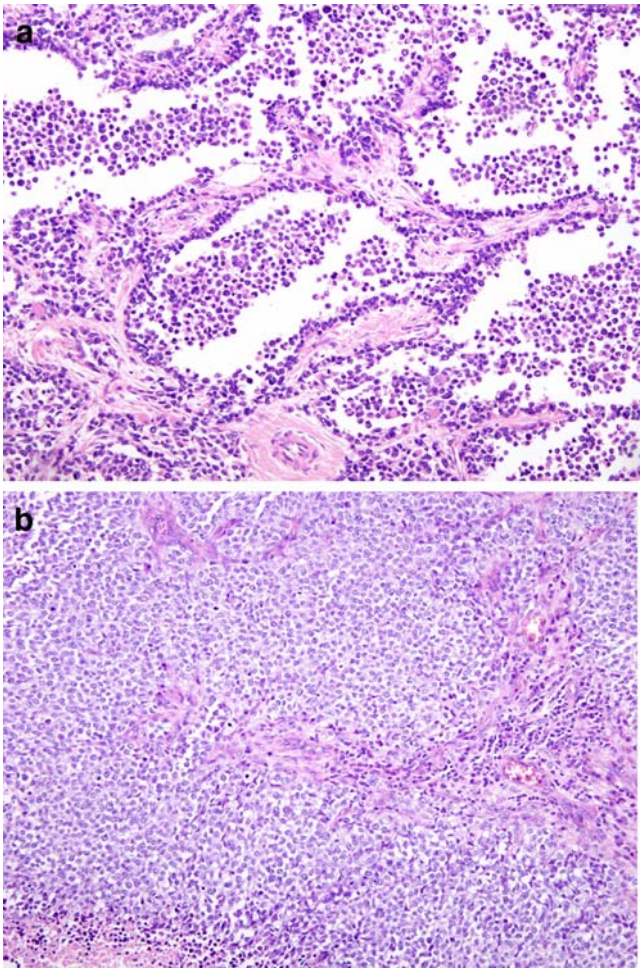


Fig. 2 **a** Conventional alveolar rhabdomyosarcoma with fibrovascular septa containing small round-shaped rhabdomyoblasts (original magnification, ×100). **b** Solid rhabdomyosarcoma with monotonous sheets of small round cells and without fibrous septa (original magnification, ×200)

72°C for 2 min. Subsequently, 10 μL of 4′,6-diamidino-2-phenylindole counterstain (Vysis) was placed on the slide, which was then covered with a coverslip.

We performed the FISH assay after confirming the most histologically typical areas using H&E-stained sections. The slides were observed using a fluorescence microscope with appropriate filters, and the resulting images were captured using a charge-coupled-device camera. Fifty to 60 nuclei exhibiting both green and orange signals were counted by two different individuals, and the percentages of green, orange, and fused signals were calculated. A positive result was defined as the presence of split signals in more than 10% of the cells when the distance between the flanking signals was twice or three times the estimated signal diameter. We regarded extra signals of either orange or green as amplification and more than three pairs of orange and green signals as polyploidy. A positive result was defined as the presence of amplified signals in more

than 11% of the cells. The cutoff value of amplification was based on counts in non-RMS tumors. A positive result was defined as the presence of polyploid signals in any cell.

Results

FISH analysis

The FISH findings are summarized in Table 1. The FISH assay failed to produce results in 2 of the 33 RMS samples because of poor tissue preservation. Thus, FISH findings were available for 18 of 19 (94.7%) ERMS and 13 of 14 (92.8%) ARMS specimens. Fusion of the orange and green signal patterns was detected in 18 of the 18 (100%) ERMS samples (Fig. 3a). No rearrangements of the FKHR gene were found in the one spindle cell-type and all three sclerosing-type cases. In contrast to the ERMS specimens, a split-signal pattern of one green and one orange, demonstrating a rearrangement of the FKHR gene, was detected in a mean of 66.9% (range: 55–82%) cells in 12 of the 13 (92.3%) ARMS samples (Fig. 3b). The two solid-type cases both exhibited rearrangements of the FKHR gene. All non-RMS tumors were negative for the FKHR gene rearrangements detected using FISH, and split signals were seen in a mean of 0.7% (range=0–4%).

A FISH analysis using the FKHR probe revealed the amplification of the green signal located proximal to the FKHR gene and polyploidy. Amplification was observed in 33.3% (6 of 18) of the ERMS (Fig. 4a) and 53.8% (7 of 13) of the ARMS specimens. In these cases, there was on average 44.8% (range=38–96%) cells with amplified signals. Polyploidy was observed in 38.9% (7 of 18) of the ERMS (Fig. 4b) and 69.2% (9 of 13) of the ARMS

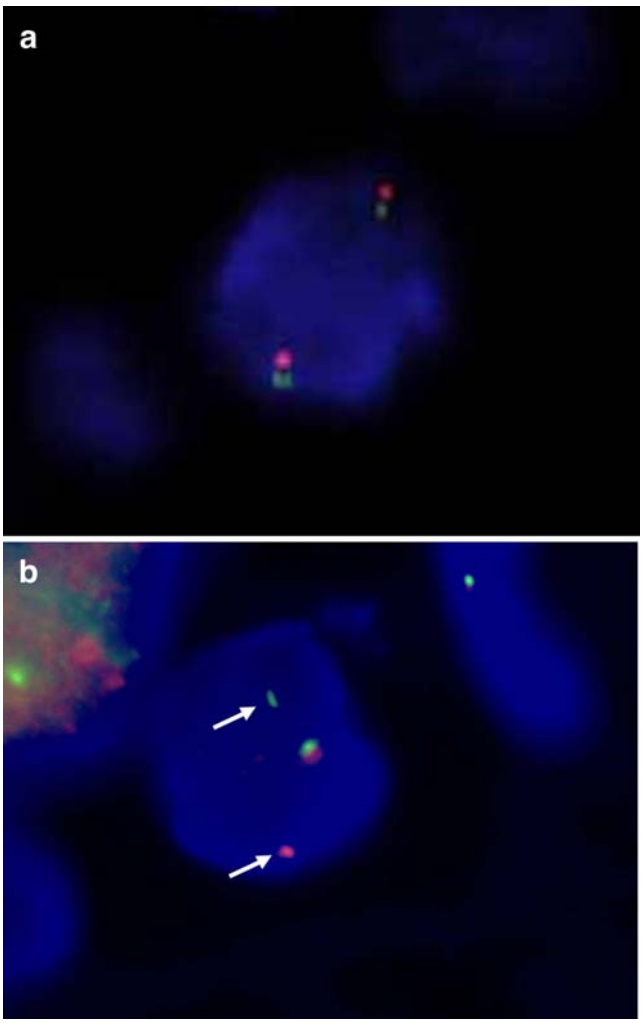


Fig. 3 Rhabdomyosarcomas analyzed by FISH using FKHR probes (centromeric, *green*; telomeric, *orange*). **a** Fusion signals in an embryonal rhabdomyosarcoma (original magnification, ×100). **b** Split signals (*arrows*) in an alveolar rhabdomyosarcoma (original magnification, ×100)

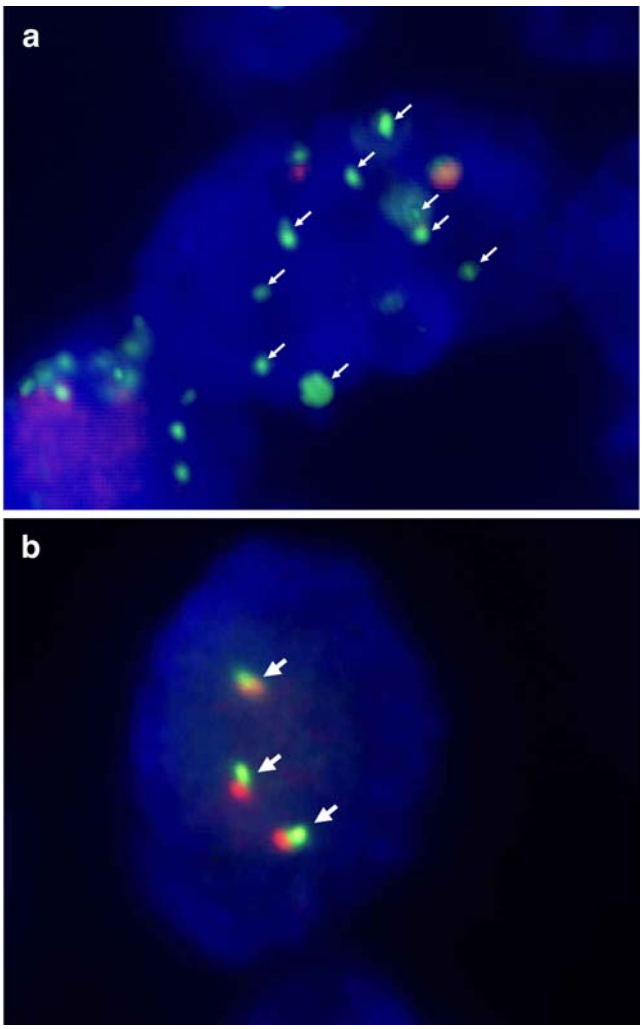


Fig. 4 Rhabdomyosarcomas analyzed by FISH using FKHR probes (centromeric, *green*; telomeric, *orange*). **a** Amplification of centromeric green (*arrows*) in an embryonal rhabdomyosarcoma (original magnification, ×100). **b** Polyploidy pattern of an embryonal rhabdomyosarcoma with three fusion signal (*arrows*; original magnification, ×100)

specimens. In these cases, there was on average 12% (range=0–30%) cells with polyploid signals. In non-RMS specimens, amplified and polyploid signals were seen in a mean of 3.3 (range=0–10) and 4.5% (range=0–38%), respectively. Polyploidy was observed in 41.7% (5 of 12) of the non-RMS specimens. In amplified and non-amplified specimens of split-signal-positive ARMS, there was on average 68 and 64.8% cells with split signals, respectively. In polyploid and nonpolyploid specimens of these, there was on average 69.6 and 65% cells with split signals, respectively.

Discussion

Although the different PAX-FKHR fusion genes can be identified using RT-PCR, RT-PCR analysis for routine diagnosis requires fresh or frozen tissues and various primers to avoid false-negative or false-positive results. However, such tissues are not always available for analysis, and such analyses are expensive and time consuming. In contrast, FISH is a very appealing technique for several reasons; it can be performed using FFPE specimens, and it is easy to use in clinical settings. Therefore, we explored the use of FISH assays for the diagnosis of RMS.

Nishio et al. [20] reported that FISH was more sensitive than RT-PCR for the diagnosis of ARMS. Previous RT-PCR studies have reported that approximately 80% of ARMS are associated with PAX3–FKHR or PAX7–FKHR fusion transcripts [1, 29]. Our FISH study indicated that the percentage of positive results using a commercial probe for detecting rearrangements of the FKHR gene in ARMS samples was 92.3%. As in a previous study [20], our FISH results indicated an excellent performance.

Approximately 20% of ARMS are translocation negative, forming a more heterogenous, unexplored group in which unambiguous classification and discrimination from ERMS is based on classical methods. Recent studies have indicated that PAX3–AFX or PAX3–NCPA1 have been detected in some cases [3, 33]. In the current FISH assay, a split-signal pattern was not detected in one ARMS sample. This result suggests a variant translocation, but the FKHR gene could be associated with PAX3–AFX, PAX3–NCPA1, or an otherwise unknown fusion transcript. Two cases (one ERMS and one ARMS) were FISH negative. The reason for these negative results may have been that the specimens were decalcified.

Nishio et al. [20] used single-fusion probes and detected a rearrangement of the FKHR gene in 34.5% (15 of 39) of their ARMS specimens. In our FISH analysis using break-apart probes, a rearrangement of the FKHR gene was detected in 92.3% of our ARMS specimens. The results using the break-apart probes were more detectable and easier to interpret because the abnormality that was sought (the separation of two signals) was readily recognizable [6, 32]. However, the normal pattern must be carefully defined because normal signals may occasionally appear to be slightly separated when using break-apart probes.

Amplification and polyploidy were detected in both the ERMS and ARMS specimens, so care must be taken when counting the nuclear signals. In particular, both amplification and polyploidy were more frequent in ARMS than in ERMS. In split-signal-positive ARMS, the amplified or polyploid ARMS specimens showed almost an equal amount of split-signal cells compared to the nonamplified and nonpolyploid ARMS specimens. In this study, we defined a positive result of polyploidy as the presence of polyploid signals in any cell. In fact, amplification was observed characteristically in RMS, but polyploidy was not. However, it is difficult to define these extra signals as amplification and polyploidy precisely because this type of probe does not contain a centromere control probe. Previous studies have shown that genomic amplification was detected predominantly in ARMS [5, 13, 21, 34]. In contrast, Bridge et al. [4] reported that genomic amplification was detected equally in 26 and 23% of ERMS and ARMS specimens, respectively. Their study revealed amplifications involving 2q31-32, 11q14-25, 12q13-15, 13q14, 15q25-26, 17p11-12, 17q23-25, and 18q21. The 12q13-15 region contains growth-related genes like SAS, GLI, CDK4, GADD153, and MDM2 [11, 14, 26], whereas the 15q25-26 region contains transformation-related and antiapoptosis-related genes like the insulin-like growth factor type I receptor [28]. Barr et al. [2] demonstrated that amplification was detected in 21% of PAX3– or PAX7–FKHR-positive cases. The amplification was detected in the majority of ARMS specimens, while the amplification was only detected in one of 22 PAX3–FKHR-positive ARMS specimens. Additional studies are required to determine the relationship between genetic characteristics and histologic categories.

Recently, an unusual RMS with prominent hyaline sclerosis has been described as “sclerosing rhabdomyosarcoma” [8, 10, 18]. This variant of RMS is sometimes difficult to differentiate from ARMS because the lesion occurs in the extremities of adults and histologically exhibits a microalveolar pattern. Previous studies on this variant indicated that PAX3–FKHR or PAX7–FKHR fusion transcripts were not found during an RT-PCR analysis, ruling out a relationship with ARMS [8, 10, 18]. This cytogenic profile supports the classification of adult sclerosing RMS as a clinical and morphological variant of ERMS. We described three cases of sclerosing-type RMS in adult patients (average age, 49 years) in whom the RMS

were characterized by prominent hyaline sclerosis and psudoalveolar patterns. Two of the three cases occurred in the extremities. No rearrangements of the FKHR gene were found in all three sclerosing-type cases when examined using the FISH assay. These findings support the inclusion of sclerosing RMS in the ERMS category.

In conclusion, we analyzed 33 RMS specimens using FISH and a commercial FKHR break-apart rearrangement probe. Our FISH study highlighted the excellent performance of the commercial break-apart probe for detecting rearrangements of the FKHR gene in RMS specimens. Amplification and polyploidy were detected in both ERMS and ARMS specimens, so care should be taken when counting the nuclear signals. No rearrangements of the FKHR gene were found in all three of the sclerosing-type RMS specimens when examined using the FISH assay, supporting the inclusion of sclerosing RMS in the ERMS category.

Conflict of interest statement We declare that we have no conflict of interest.

References

1. Barr FG (1997) Molecular genetics and pathogenesis of rhabdomyosarcoma. J Pediatr Hematol Oncol 19:483–491
2. Barr FG, Nauta LE, Davis RJ, Schäfer BW, Nycum LM, Biegel JA (1996) In vivo amplification of the PAX3–FKHR and PAX7–FKHR fusion genes in alveolar rhabdomyosarcoma. Hum Mol Genet 5:15–21
3. Barr FG, Qualman SJ, Macris MH, Melnyk N, Lawlor ER, Strzelecki DM, Triche TJ, Bridge JA, Sorensen PH (2002) Genetic heterogeneity in the alveolar rhabdomyosarcoma subset without typical gene fusions. Cancer Res 62:4704–4710
4. Bridge JA, Liu J, Qualman SJ, Suijkerbuijk R, Wenger G, Zhang J, Wan X, Baker KS, Sorensen P, Barr FG (2002) Genomic gains and losses are similar in genetic and histologic subsets of rhabdomyosarcoma, whereas amplification predominates in embryonal with anaplasia and alveolar subtypes. Genes Chromosomes Cancer 33:310–321
5. Bridge JA, Liu J, Weibolt V, Baker KS, Perry D, Kruger R, Qualman S, Barr F, Sorensen P, Triche T, Suijkerbuijk R (2000) Novel genomic imbalances in embryonal rhabdomyosarcoma revealed by comparative genomic hybridization and fluorescence in situ hybridization: an intergroup rhabdomyosarcoma study. Genes Chromosomes Cancer 27:337–344
6. Bridge RS, Rajaram V, Dehner LP, Pfeifer JD, Perry A (2006) Molecular diagnosis of Ewing sarcoma/primitive neuroectodermal tumor in routinely processed tissue: a comparison of two FISH strategies and RT-PCR in malignant round cell tumors. Mod Pathol 19:1–8
7. Cavazzana AO, Schmidt D, Ninfo V, Harms D, Tollot M, Carli M, Treuner J, Betto R, Salviati G (1992) Spindle cell rhabdomyosarcoma. A prognostically favorable variant of rhabdomyosarcoma. Am J Surg Pathol 16:229–235
8. Croes R, Debiec-Rychter M, Cokelaere K, De Vos R, Hagemeijer A, Sciot R (2005) Adult sclerosing rhabdomyosarcoma: cytogenetic link with embryonal rhabdomyosarcoma. Virchows Arch 446:64–67
9. Davis RJ, D'Cruz CM, Lovell MA, Biegel JA, Barr FG (1994) Fusion of PAX7 to FKHR by the variant t(1;13)(p36;q14) translocation in alveolar rhabdomyosarcoma. Cancer Res 54:2869–2872
10. Folpe AL, McKenney JK, Bridge JA, Weiss SW (2002) Sclerosing rhabdomyosarcoma in adults: report of four cases of a hyalinizing, matrix-rich variant of rhabdomyosarcoma that may be confused with osteosarcoma, chondrosarcoma, or angiosarcoma. Am J Surg Pathol 26:1175–1183
11. Forus A, Florenes VA, Maelandsmo GM, Meltzer PS, Fodstad O, Myklebost O (1993) Mapping of amplification units in the q13-14 region of chromosome 12 in human sarcomas: some amplica do not include MDM2. Cell Growth Differ 4:1065–1070
12. Galili N, Davis RJ, Fredericks WJ, Mukhopadhyay S, Rauscher FJ 3rd, Emanuel BS, Rovera G, Barr FG (1993) Fusion of a fork head domain gene to PAX3 in the solid tumour alveolar rhabdomyosarcoma. Nat Genet 5:230–235
13. Gordon AT, Brinkschmidt C, Anderson J, Coleman N, Dockhorn-Dworniczak B, Pritchard-Jones K, Shipley J (2000) A novel and consistent amplicon at 13q31 associated with alveolar rhabdomyosarcoma. Genes Chromosomes Cancer 28:220–226
14. Khatib ZA, Matsushime H, Valentine M, Shapiro DN, Sherr CJ, Look AT (1993) Coamplification of the CDK4 gene with MDM2 and GLI in human sarcomas. Cancer Res 53:5535–5541
15. Kodet R, Newton WA Jr, Hamoudi AB, Asmar L, Jacobs DL, Maurer HM (1993) Childhood rhabdomyosarcoma with anaplastic (pleomorphic) features. A report of the Intergroup Rhabdomyosarcoma Study. Am J Surg Pathol 17:443–453
16. Koscielniak E, Harms D, Henze G, Jurgens H, Gadner H, Herbst M, Klingebiel T, Schmidt BF, Morgan M, Knietig R, Treuner J (1999) Results of treatment for soft tissue sarcoma in childhood and adolescence: a final report of the German Cooperative Soft Tissue Sarcoma Study CWS-86. J Clin Oncol 17:3706–3719
17. Leuschner I, Newton WA Jr, Schmidt D, Sachs N, Asmar L, Hamoudi A, Harms D, Maurer HM (1993) Spindle cell variants of embryonal rhabdomyosarcoma in the paratesticular region. A report of the Intergroup Rhabdomyosarcoma Study. Am J Surg Pathol 17:221–230
18. Mentzel T, Katenkamp D (2000) Sclerosing, pseudovascular rhabdomyosarcoma in adults. Clinicopathological and immunohistochemical analysis of three cases. Virchows Arch 436:305–311
19. Mhawech-Fauceglia P, Herrmann F, Penetrante R, Beck A, Sait S, Block AM, Odunsi K, Fisher J, Balos L, Cheney RT (2006) Diagnostic utility of FLI-1 monoclonal antibody and dual-colour, break-apart probe fluorescence in situ (FISH) analysis in Ewing's sarcoma/primitive neuroectodermal tumour (EWS/PNET). A comparative study with CD99 and FLI-1 polyclonal antibodies. Histopathology 49:569–575
20. Nishio J, Althof PA, Bailey JM, Zhou M, Neff JR, Barr FG, Parham DM, Teot L, Qualman SJ, Bridge JA (2006) Use of a novel FISH assay on paraffin-embedded tissues as an adjunct to diagnosis of alveolar rhabdomyosarcoma. Lab Invest 86:547–556
21. Pandita A, Zielenska M, Thorner P, Bayani J, Godbout R, Greenberg M, Squire JA (1999) Application of comparative genomic hybridization, spectral karyotyping, and microarray analysis in the identification of subtype-specific patterns of genomic changes in rhabdomyosarcoma. Neoplasia 1:262–275
22. Parham DM, Barr FG (2002) Embryonal rhabdomyosarcoma. In: Fletcher CDM, Unni KK, Mertens F (eds) WHO classification of

tumours, pathology and genetics of tumours of soft tissue and bone. IARC, Lyon, France, pp 146–154
23. Parham DM, Shapiro DN, Downing JR, Webber BL, Douglass EC (1994) Solid alveolar rhabdomyosarcomas with the t(2;13). Report of two cases with diagnostic implications. Am J Surg Pathol 18:474–478
24. Patel RM, Downs-Kelly E, Weiss SW, Folpe AL, Tubbs RR, Tuthill RJ, Goldblum JR, Skacel M (2005) Dual-color, break-apart fluorescence in situ hybridization for EWS gene rearrangement distinguishes clear cell sarcoma of soft tissue from malignant melanoma. Mod Pathol 18:1585–1590
25. Qualman SJ, Coffin CM, Newton WA, Hojo H, Triche TJ, Parham DM, Crist WM (1998) Intergroup Rhabdomyosarcoma Study: update for pathologists. Pediatr Dev Pathol 1:550–561
26. Roberts WM, Douglass EC, Peiper SC, Houghton PJ, Look AT (1989) Amplification of the gli gene in childhood sarcomas. Cancer Res 49:5407–5413
27. Sartelet H, Lantuejoul S, Armari-Alla C, Pin I, Delattre O, Brambilla E (1998) Solid alveolar rhabdomyosarcoma of the thorax in a child. Histopathology 32:165–171
28. Shapiro DN, Jones BG, Shapiro LH, Dias P, Houghton PJ (1994) Antisense-mediated reduction in insulin-like growth factor-I receptor expression suppresses the malignant phenotype of a human alveolar rhabdomyosarcoma. J Clin Invest 94:1235–1242
29. Sorensen PH, Lynch JC, Qualman SJ, Tirabosco R, Lim JF, Maurer HM, Bridge JA, Crist WM, Triche TJ, Barr FG (2002) PAX3-FKHR and PAX7-FKHR gene fusions are prognostic indicators in alveolar rhabdomyosarcoma: a report from the children's oncology group. J Clin Oncol 20:2672–2679
30. Surace C, Panagopoulos I, Palsson E, Rocchi M, Mandahl N, Mertens F (2004) A novel FISH assay for SS18-SSX fusion type in synovial sarcoma. Lab Invest 84:1185–1192
31. Tsokos M, Webber BL, Parham DM, Wesley RA, Miser A, Miser JS, Etcubanas E, Kinsella T, Grayson J, Glatstein E (1992) Rhabdomyosarcoma. A new classification scheme related to prognosis. Arch Pathol Lab Med 116:847–855
32. Ventura RA, Martin-Subero JI, Jones M, McParland J, Gesk S, Mason DY, Siebert R (2006) FISH analysis for the detection of lymphoma-associated chromosomal abnormalities in routine paraffin-embedded tissue. J Mol Diagn 8:141–151
33. Wachtel M, Dettling M, Koscielniak E, Stegmaier S, Treuner J, Simon-Klingenstein K, Buhlmann P, Niggli FK, Schafer BW (2004) Gene expression signatures identify rhabdomyosarcoma subtypes and detect a novel t(2;2)(q35;p23) translocation fusing PAX3 to NCOA1. Cancer Res 64:5539–5545
34. Weber-Hall S, Anderson J, McManus A, Abe S, Nojima T, Pinkerton R, Pritchard-Jones K, Shipley J (1996) Gains, losses, and amplification of genomic material in rhabdomyosarcoma analyzed by comparative genomic hybridization. Cancer Res 56:3220–3224
35. Weiss SW, Goldblum JR (2001) Enzinger and Weiss's soft tissue tumors, 4th edn. Mosby, St. Louis
36. Yamaguchi U, Hasegawa T, Morimoto Y, Tateishi U, Endo M, Nakatani F, Kawai A, Chuman H, Beppu Y, Endo M, Kurotaki H, Furuta K (2005) A practical approach to the clinical diagnosis of Ewing's sarcoma/primitive neuroectodermal tumour and other small round cell tumours sharing EWS rearrangement using new fluorescence in situ hybridisation probes for EWSR1 on formalin fixed, paraffin wax embedded tissue. J Clin Pathol 58:1051–1056

Virchows Arch (2008) 452:259–268
DOI 10.1007/s00428-007-0557-6

ORIGINAL ARTICLE

Molecular genetic aberrations of ovarian and uterine carcinosarcomas—a CGH and FISH study

Alexander Schipf · Doris Mayr · Thomas Kirchner · Joachim Diebold

Received: 8 June 2007 / Revised: 23 November 2007 / Accepted: 30 November 2007 / Published online: 10 January 2008
© Springer-Verlag 2007

Abstract The origin of carcinosarcomas of the ovary and uterus has long been discussed. In this study, we used a molecular–genetic approach to elucidate the tumorigenesis of carcinosarcomas of these organs correlating our findings with the specific biphasic pattern of these tumors. We analyzed a series of 30 paraffin-embedded carcinosarcomas of the ovary and the uterus using comparative genomic hybridization (CGH) and fluorescence in-situ hybridization (FISH). In general, gains (85%) were observed more frequently, than losses (30%). Characteristic and frequent chromosomal amplification was observed on chromosome 8q and 20q (42 and 70%). FISH revealed c-myc (8q24.12) and ZNF217 (20q13.2) amplification in 78 and 87%. Amplification of ZNF217 was mostly seen in both tumor components, whereas amplification of c-myc was observed less often in the sarcomatous than in the carcinomatous tumor component. Analysis of the proliferation index using Ki67 immunohistochemistry revealed a strong or moderate expression in all cases, wherein the carcinomatous tumor component showed significantly a higher proliferation index compared to the sarcomatous tumor areas. Although our results are in agreement with a monoclonal origin of ovarian and uterine carcinosarcomas, the carcinomatous component seems to be the more aggressive part of the tumor. Furthermore, the observed patterns of genetic aberrations are highly similar to those of serous carcinomas. This is compatible with the current opinion that these neoplasms should be considered as metaplastic carcinomas.

Keywords Carcinosarcoma · CGH · FISH · Immunohistology · Ovary

A. Schipf (✉) · J. Diebold
Institute of Pathology, KSL Luzern,
6000 Luzern 16, Switzerland
e-mail: alexander.schipf@ksl.ch

D. Mayr · T. Kirchner
Institute of Pathology, LMU,
Munich, Germany

Introduction

Carcinosarcomas of the female genital tract, also called malignant mixed Mullerian tumors, are highly aggressive biphasic neoplasms composed of carcinomatous and sarcomatous components. They usually occur in the uterus, ovaries, Fallopian tubes, and vagina, in descending order of frequency. Histologically, the carcinomatous component is usually of the endometrioid, serous, or clear-cell type. The sarcomatous component may be either homologous (endometrial stromal sarcoma, fibrosarcoma, leiomyosarcoma) or heterologous. These uncommon tumors are usually found in postmenopausal women, frequently at an advanced stage, and have a very poor prognosis.

The histogenesis of carcinosarcomas of the female genital tract has been an issue of great controversy. To explain the characteristic biphasic pattern, several theories have been proposed with two major theories being favored. One theory suggests that these tumors develop through two independent neoplastic processes, forming a biclonal tumor ("collision" theory). According to the other theory, the tumor consists of a monoclonal tumor cell population undergoing partially metaplastic transformation ("conversion" theory). Other histogenetic theories, such as the

"combination" theory where both tumor components derive from a single stem cell, which differentiates very early in tumorigenesis in diverging directions, or the "composition" theory, interpreting the sarcomatous component as pseudosarcomatous stromal reaction, were largely dismissed [27].

In the last few years, evidence in favor of a monoclonal origin particularly supporting the conversion hypothesis has accumulated, based on a number of studies using sensitive morphological, cytogenetic, ultrastructural, and immunohistochemical techniques [2, 4, 6, 8, 13, 16, 29, 30].

Cytogenetic studies of carcinosarcomas have revealed extremely complex karyotypes with multiple chromosomal gains and losses. Multiple chromosomal alterations were described, such as polysomy 8, loss of heterozygosity (LOH), or p53 mutations. Deoxyribonucleic acid (DNA) cytometry showed nondiploidy in most carcinosarcomas [1, 3, 7, 21, 25–28, 35].

All these studies were based on small number of cases or in vitro cell cultures. The genetic mechanism determining the intratumoral heterogeneity of the biphasic carcinosarcomatous phenotype is still unknown.

A comprehensive analysis of carcinosarcomas by comparative genomic hybridization (CGH) and fluorescence in situ hybridization (FISH) has not been performed so far. Therefore, in the present study, we investigated the molecular aberrations in 30 carcinosarcomas by these techniques. We correlated our findings with the biphasic phenotype to elucidate the clonal relationship between the epithelial and mesenchymal tumor component and the possible mode of development of the biphasic pattern. Our observations provide evidence that the two tumor components are very closely related and support the "conversion" theory.

Materials and methods

Specimen

Formalin-fixed and paraffin-embedded tissue of 30 patients diagnosed with carcinosarcoma of the ovary and uterus were retrieved from archives of the Institute of Pathology of the University of Munich.

Twenty-four cases were located in the ovary, six cases in the endometrium. Ten tumors showed heterologous differentiation of the sarcomatous component. All the other carcinosarcomas were of homologous differentiation.

All patients had been treated surgically between 1988 and 2004 at the same institution (Department of Gynecology of the Klinikum Grosshadern, University of Munich). No patient received any other treatment before the operation.

According to the criteria of the International Federation of Gynecologists and Obstetricians and the International Union against Cancer, they were stage IC to IVB.

Per case, between 1 and 20 representative histological slides were available.

Comparative genomic hybridization

Chromosome preparation and karyotype analysis were performed as previously described [34]. Total tumor DNA was extracted from tissue sections—without differentiation of carcinomatous or sarcomatous components. One microgram of tumor DNA was labeled by a standard nick-translation reaction with biotin-16-deoxyuridine triphosphate (dUTP) and 1 μg reference DNA from a healthy male donor with digoxigenic-11-dUTP (each from Boehringer Mannheim). The purification of the labeled DNA fragments of less than 100 bp was achieved by applying column chromatography (Sephadex-G50, Amersham Biosciences Pharmacia GE Healthcare, Munich). Repetitive sequences were blocked with 70 μg of Cot 1 DNA.

Gray-band images of 4′,6-diamidino-2-phenylindole, fluorescein isothiocyanate, and rhodamine fluorescence were taken using a charge-coupled-device camera coupled to a Zeiss microscope. For digital image analysis and subsequent karyotyping, the ISIS QUIPS-XL (MetaSystems, Altlussheim) software package was used. Only metaphase spreads showing a high green-to-red intensity were taken in account. Between 8 and 20 metaphases (mean=12.2) for each chromosome were analyzed. Corresponding ratio profiles were evaluated only within the 99% confidence limit. The 50% threshold (upper threshold, 1.2; lower threshold, 0.8) were applied to define the chromosomal regions of DNA sequence losses and gains.

Fluorescence in situ hybridization

After removal of excess normal tissue, FISH was performed on tumor tissue sections. To recognize and distinguish carcinomatous or sarcomatous tumor components, FISH sections were carefully compared with serial hematoxylin–eosin-stained sections.

The in situ hybridization was performed as described previously [10]. The hybridization mix was prepared according to the manufacturer's protocol with DNA-specific probes for 8q24.12 and 20q13.2 (c-myc and ZNF217, Abbott/Vysis, Wiesbaden) [5].

The slides were evaluated under a ZEISS (Göttingen, Germany) axioscope fluorescence microscope equipped with an HBO 100-W mercury lamp and dual- and triple-band pass filters (Applied Imaging, Vysis, AF Analysentechnik, Tuebingen). Hybridization signals were counted in 60 to 120 nuclei per case. Only discrete signals in nonoverlapping nuclei with distinct nuclear borders were evaluated. Split signals were counted as one signal. Amplification was defined as a ratio of gene to centro-

mere signals of greater than 2, whereas polysomy was defined as an increase of gene copy numbers with a constant gene-to-centromere ratio less than 2 in all examined tumor cells. In 13 cases, the enumeration of FISH signals was performed twice. The difference between the first and the second count was 0.25±0.21 hybridization signal per nucleus for centromere signals and 0.33±0.35 for gene signals. Thus, the results proved to be highly reproducible.

Immunhistochemistry

All paraffin-embedded specimens were cut at 2–3 μm and mounted on SuperFrost/Plus microscope slides (Menzel, Germany). After deparaffinization and rehydration, sections were immunhistochemically stained with a streptavidin–biotin complex system (Dako, Hamburg). Anticytokeratin monoclonal antibodies (Dako) were used for detection of the epithelial component. To detect the mesenchymal tumor components, antivimentin monoclonal antibody (Dako) and antidesmin monoclonal antibody (Dako) were used.

For Ki67, the monoclonal antibody MIB1 (Dako, Glostrup, Denmark) was used at a dilution of 1:50. The immunohistochemical results of Ki67 were scored quantitatively. Carcinomatous and sarcomatous tumor cells were counted, and the percentage of the immunoreactive cells was determined.

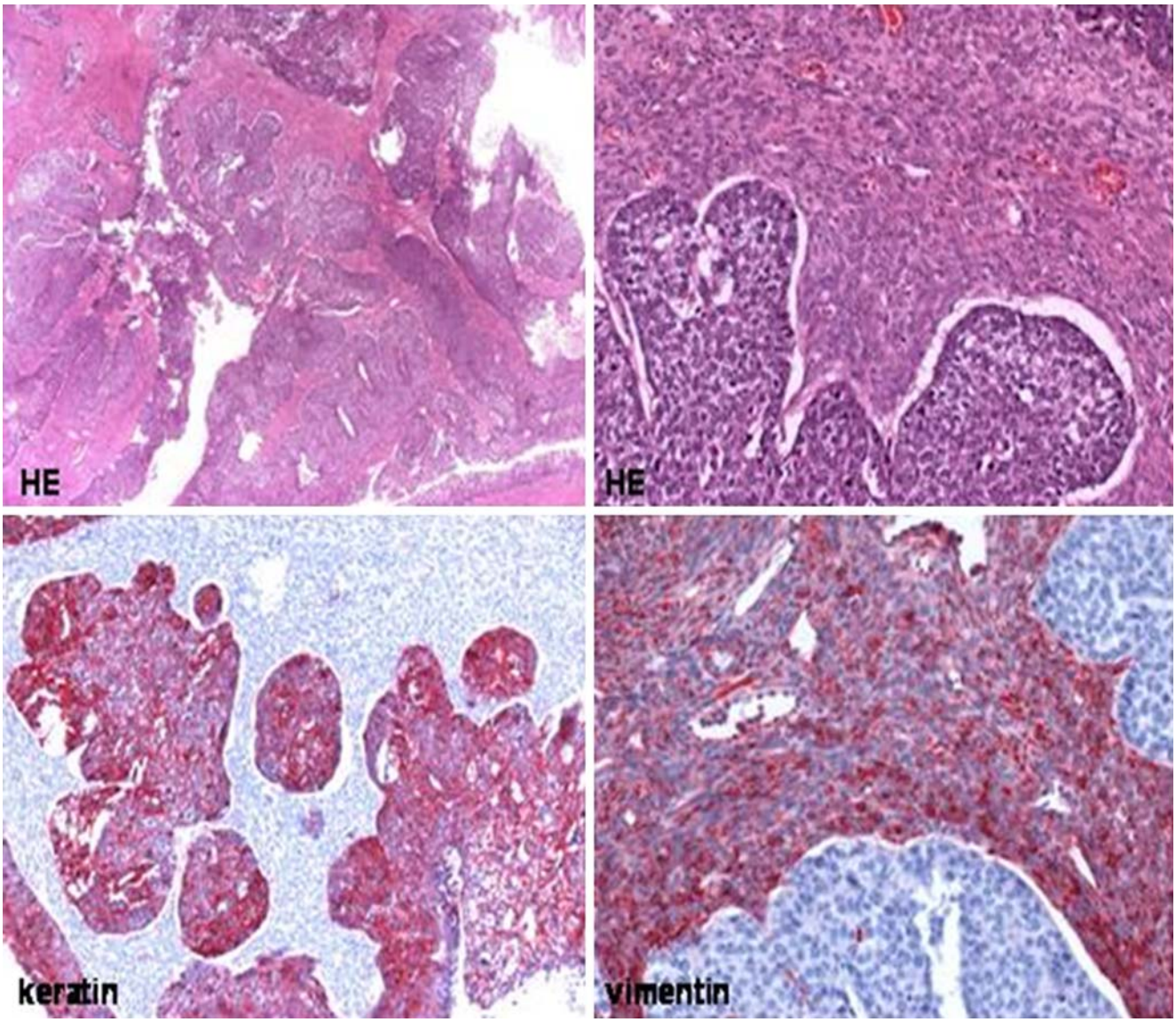


Fig. 1 Representative hematoxylin–eosin-stained and immunhistochemistry sections of a carcinosarcoma. Epithelial components were marked by keratin staining, mesenchymal by vimentin

Results

Histology

Histologically, all tumors were composed of an admixture of malignant epithelial and mesenchymal stromal cells. To differentiate into distinct tumor components, immunohistochemistry was performed in all cases (Fig. 1). Epithelial and mesenchymal neoplastic cells were clearly distinguished.

Histological features of investigated carcinosarcomas are summarized in Table 1. Sixteen of 24 ovarian and four of six uterine tumors showed homologous differentiation of the sarcomatous component such as endometrial stromal sarcoma, fibrosarcoma, and leiomyosarcoma. The carcinomatous component was of endometrioid or serous type.

In seven cases, the carcinomatous tumor component predominated, whereas in 18 cases, sarcomatous areas prevailed.

Comparative genomic hybridization

To get a general idea of chromosomal aberrations in the carcinomatous and sarcomatous tumor components, we analyzed 25 cases using CGH technology. In general, the tumors showed a large number of chromosomal imbalances, and almost all chromosomes were affected (Fig. 2).

Gains (85%) were observed more frequently than losses (30%). The most frequently occurring CGH changes were gains on chromosomes 1q, 2p, 8q, 12p, 19q, and 20q. Wherein, amplifications on chromosome 8q and 20q were particularly frequent (42 and 70%) and were correlated with each other in more than 50%. Losses were observed most frequently on chromosome 4q, 9q, and 13q. CGH profiles of cases with predominance of carcinomatous areas were highly similar to CGH ideograms of cases with preponderance of sarcomatous tissue (Fig. 3).

Fluorescence in situ hybridization

FISH analysis for chromosome 8 and 20 was successful in 23 of 30 cases. Many carcinosarcomas contained aberrations on chromosomes 8 and 20 detectable by FISH.

Increase of c-myc gene copy number and a gene-to-centromere ratio less than 2 in all examined tumor cells (polysomy) was observed in five tumors. Amplification of

Table 1 Stage, age at time of diagnosis, tumor localization, and histological differentiation of the carcinomatous and sarcomatous components (n=30)

Case number	Stage	Age	Localization	Epithelial differentiation	Sarcomatous differentiation
1	IIIB	70	Ovarian	Serous	Homologous
2	IIIC	75	Ovarian	Endometrioid	Heterologous
3	IIB	59	Ovarian	Serous	Homologous
4	IC	64	Ovarian	Serous	Homologous
5	IIIC	80	Uterine	Serous	Homologous
6	IIB	77	Ovarian	Serous	Homologous
7	IIA	73	Ovarian	Serous	Heterologous
8	IIIC	68	Uterine	Serous	Homologous
9	IIA	68	Uterine	Serous	Homologous
10	IIIB	42	Ovarian	Endometrioid	Heterologous
11	IIIB	73	Ovarian	Serous	Homologous
12	IVB	48	Ovarian	Serous	Homologous
13	IIIC	67	Ovarian	Endometrioid	Homologous
14	IIIC	68	Uterine	Serous	Homologous
15	IIIC	63	Ovarian	Endometrioid	Homologous
16	IIIC	79	Ovarian	Serous	Homologous
17	IVB	81	Ovarian	Serous	Heterologous
18	IIIB	74	Ovarian	Endometrioid	Heterologous
19	IIIC	87	Uterine	Serous	Heterologous
20	IVB	72	Ovarian	Endometrioid	Homologous
21	IIICB	79	Uterine	Serous	Heterologous
22	IVB	X	Ovarian	Serous	Heterologous
23	IVB	48	Ovarian	Serous	Homologous
24	IIIB	67	Ovarian	Serous	Homologous
25	IIIB	70	Ovarian	Serous	Homologous
26	IIIB	65	Ovarian	Endometrioid	Homologous
27	IIIB	53	Ovarian	Serous	heterologous
28	IIIC	75	Ovarian	Serous	heterologous
29	IVB	79	Ovarian	Endometrioid	Homologous
30	IVA	68	Ovarian	Serous	Homologous

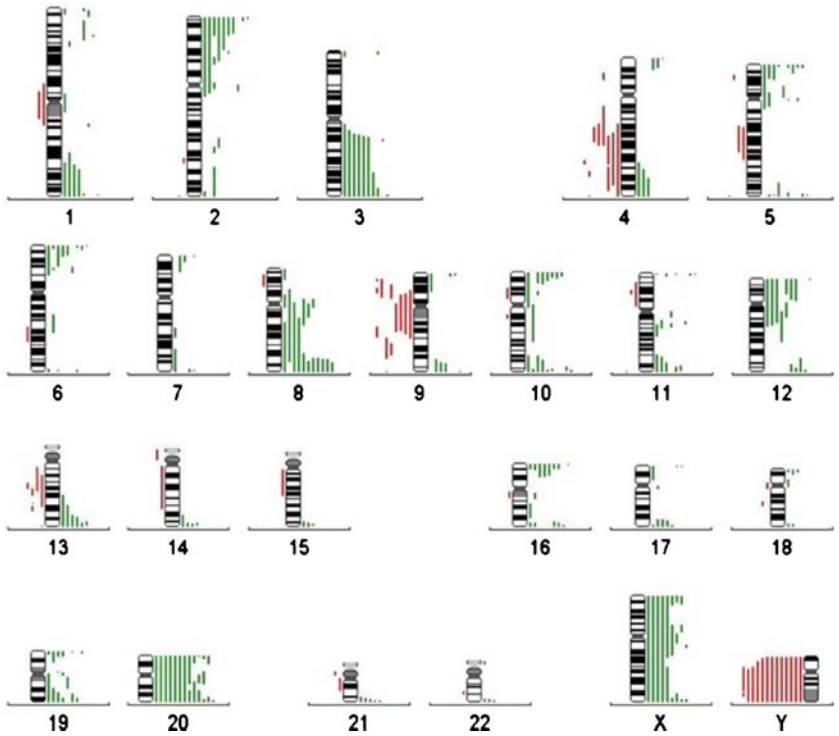


Fig. 2 Ideogram showing comparative genomic hybridization findings in 25 carcinosarcomas of the ovary and uterus (*red bars on the left* of chromosomes are losses, and *green bars on the right* are gains)

c-myc (gene/centromere signals greater than 2) was observed in 18 cases (Table 2A).

Comparing gene and centromere 8 copy numbers, 16 of the 18 cases showed amplification for c-myc in the carcinomatous tumor component. The median number of c-myc hybridization signals per nucleus was three in five cases and greater than three in nine cases. In contrast, c-myc amplifications in the sarcomatous component were observed in only four (of 18) cases wherein two cases showed amplification in both tumor components simultaneously (Table 2B, Figs. 4 and 5).

For znf217 analysis, the median number of hybridization signals per nucleus was three and higher in 19 cases. Four tumors showed polysomy, and in 19 cases, we observed

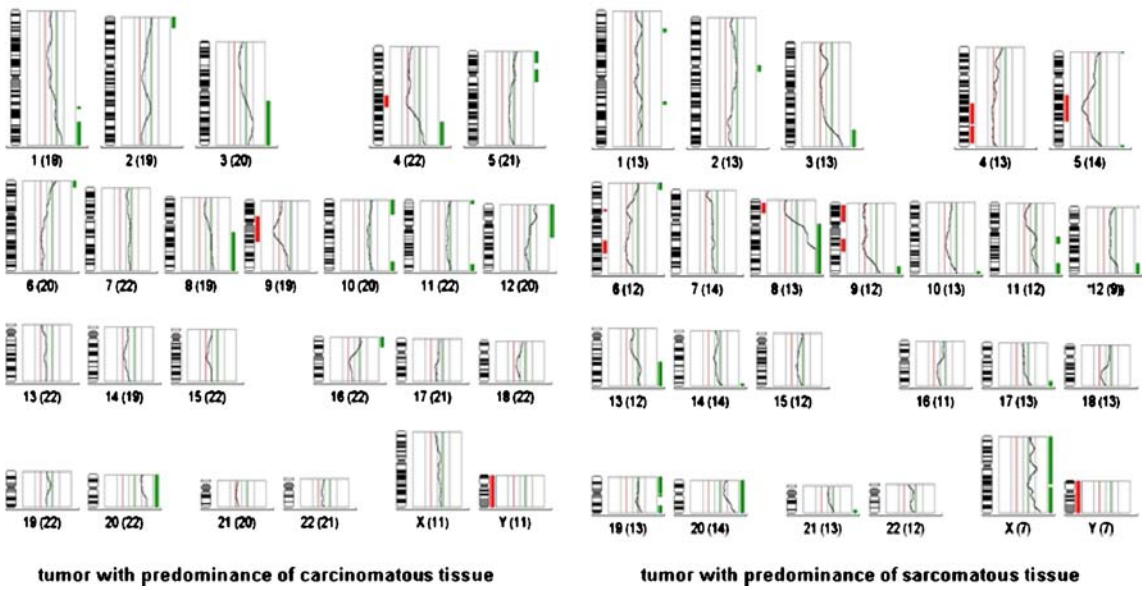


Fig. 3 Two examples of CGH ideograms of a tumor with predominance of carcinomatous and sarcomatous areas, respectively, revealing a high grade of similarity

Table 2 Overview of c-myc and znf217 FISH analysis (n=23, polysomy: increase of gene copy number and constant gene to centromere ratio less than 2; amplification: gene to centromere index greater than 2, A), comparison of genetic aberrations in carcinomatous and sarcomatous components of tumors with gene amplification (**B**)

	c-myc	znf217
A		
tumors with polysomy	5	4
tumors with amplification	18	19
Total	23	23
B		
Cases with gene amplification in		
Carcinomatous area only	14	14
Sarcomatous area only	4	15
Carcinomatous and sarcomatous area	2	10
Total	18	19

amplification of znf217 chromosome regions. In contrast to c-myc amplifications, a high level of homology was seen between the two components in each tumor. Fourteen of 19 cases showed amplification of znf217 in the carcinomatous and 15 cases in the sarcomatous tumor area, whereas simultaneous amplification in both tumor components was seen in ten (of 19) cases (Table 2B, Fig. 5).

Comparison of CGH and FISH

Comparison of CGH and FISH results showed that most of the chromosomal gains in CGH on chromosomes 8 and 20 could be detected by FISH (52 and 70%). Negative findings in CGH analysis also correlated with negative FISH results. Gains on chromosome 8q24 (c-myc) were observed on

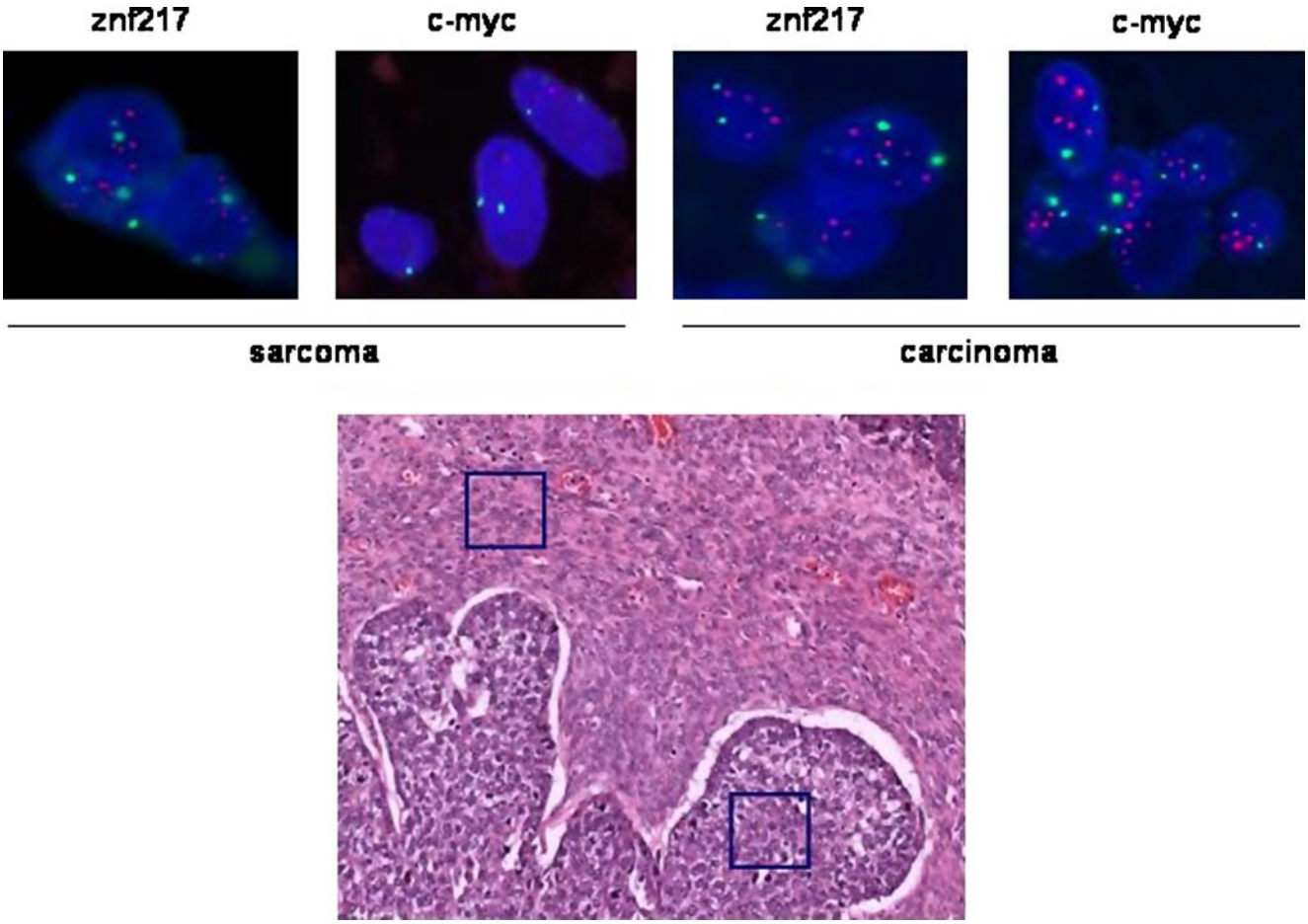


Fig. 4 Fluorescence in situ hybridization analyses. Examples for 20q13 and 8q24 in sarcomatous and carcinomatous tumor components. Three to six nuclei display multiple, red hybridization signals in both components for 20q13 and 8q24 hybridization signals amplified in the carcinomatous tumor component

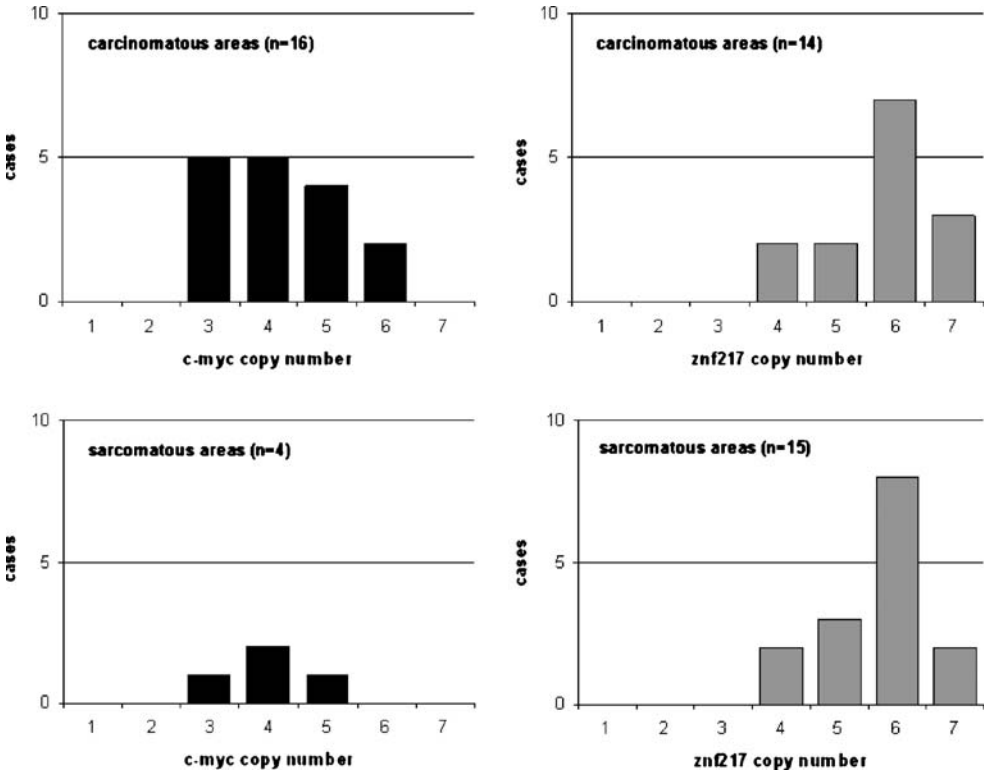


Fig. 5 Comparison of c-myc and znf217 gene copy numbers in carcinomatous and sarcomatous areas of tumors with gene amplification

CGH analysis in 14 cases, and nine tumors showed no amplification in CGH. Using FISH analysis, we detected among these negative tumors six cases with amplification on chromosome 8q24. For znf217 (20q13), the majority of gene amplifications could be demonstrated in both techniques (Table 3). The Chi-squared test revealed a statistically significant correlation ($p<0.05$).

Immunohistochemistry

Twenty-five cases were analyzed in epithelial and mesenchymal areas for the proliferation-associated antigen Ki67 to assess the growth fraction in both tumor areas. Ki67 was strongly or moderately expressed in all cases, wherein the carcinomatous tumor component showed a significantly ($p<0.001$) higher proliferation index (mean 70%) compared to the sarcomatous tumor areas (mean 28%; Table 4, Fig. 6).

Discussion

Despite many histological, immunohistochemical, cytogenetic, and ultrastructural analyses, the histogenesis of carcinosarcomas still remained a matter of controversy [2, 4, 16–20, 22, 23, 29, 33, 36].

In this study, we used a molecular–genetic approach to elucidate the tumorigenesis of carcinosarcomas of the ovary and the uterus correlating our findings with the biphasic pattern of these tumors. For the first time, a combination of CGH and FISH techniques was used for this purpose.

Histologically, the tumors included in this study showed a great variety of epithelial and mesenchymal differentiation. Most tumors were of advanced stage, and the majority showed homologous differentiation of the sarcomatous tumor component.

Investigating the cytogenetic pattern of the carcinosarcomas, we used molecular–genetic techniques to character-

Table 3 Comparison of CGH and FISH results

CGH amplifications for 8q24.12 and 20q13.2 (rows) and FISH gene/centromere index (columns), $n=23$
Chi-squared test, $p<0.05$

		Positive	Negative
		FISH 8q24 ($n=23$)	
CGH 8q24	Positive	12	2
	Negative	6	3
		Fish 20q13 ($n=23$)	
CGH 20q13	Positive	16	1
	Negative	4	2

Table 4 Proliferation index in carcinomatous and sarcomatous tumor components (immunhistochemical Ki67 staining)

Case number	Carcinomatous tumor area (Ki67 staining, %)	Sarcomatous tumor area (Ki67 staining, %)
1	80	5
3	75	20
4	75	40
5	60	33
6	80	10
7	80	20
8	50	20
9	45	10
11	60	25
12	60	10
13	40	40
14	90	50
15	90	20
16	80	40
17	60	40
20	75	10
21	75	70
22	60	50
23	80	20
24	60	33
25	80	10
27	60	50
28	75	25
29	80	20
30	80	40

ize chromosomal changes with special consideration of the intratumoral heterogeneity of carcinosarcomas. It is well known that chromosomal aberrations occur commonly in carcinosarcomas of the female genital tract. Cytogenetic studies have shown that p53 and K-ras mutations, LOH, and microsatellite instability arise in both tumor components [1, 14, 15, 25, 38]. Wada et al. [38] found identical mutations of p53 and K-ras in the two different tumor components. Identical p53 point mutations were also observed in both tumor areas, by other groups supporting a common monoclonal origin of both carcinoma and sarcoma [25, 37].

p53 mutations seem to be an early event in tumorigenesis occurring before the separate development of epithelial and mesenchymal differentiation. p53, C-erbB-2, and c-myc protein expression has been shown in the carcinomatous as well in the sarcomatous tumor areas [8, 9, 24–26].

Regarding LOH, molecular analysis frequently showed aberrations, which were almost identically in the two tumor components [1].

Emoto et al. [12] reported the results of cell culture studies and analysis of the c-myc gene revealing concordant karyotype abnormalities and c-myc amplifications in the carcinomatous and sarcomatous subclones.

On cytogenetic level, our results demonstrate a uniform pattern of chromosomal gains and losses on the majority of the chromosomes in CGH analysis. Most aberrations were clustered on distinct chromosomal segments, and gains (chromosome 1q, 2p, 8q, 12p, 19q, and 20q) were observed more frequently than losses (4q, 9q, and 13q). The amplicons mentioned contain a number of well known oncogenes, e.g., BTAK (20q), KRAS (12p), or PIK3CA (3q).

Because total tumor DNA was used, carcinoma areas and sarcoma components were not separately analyzed by CGH. However, the comparison of cases with predominance of sarcomatous areas with those that mainly showed carcinomatous differentiation revealed a high similarity. In addition, no difference was seen in CGH patterns of carcinosarcomas with different epithelial differentiation (endometrioid vs serous), exemplarily amplification of

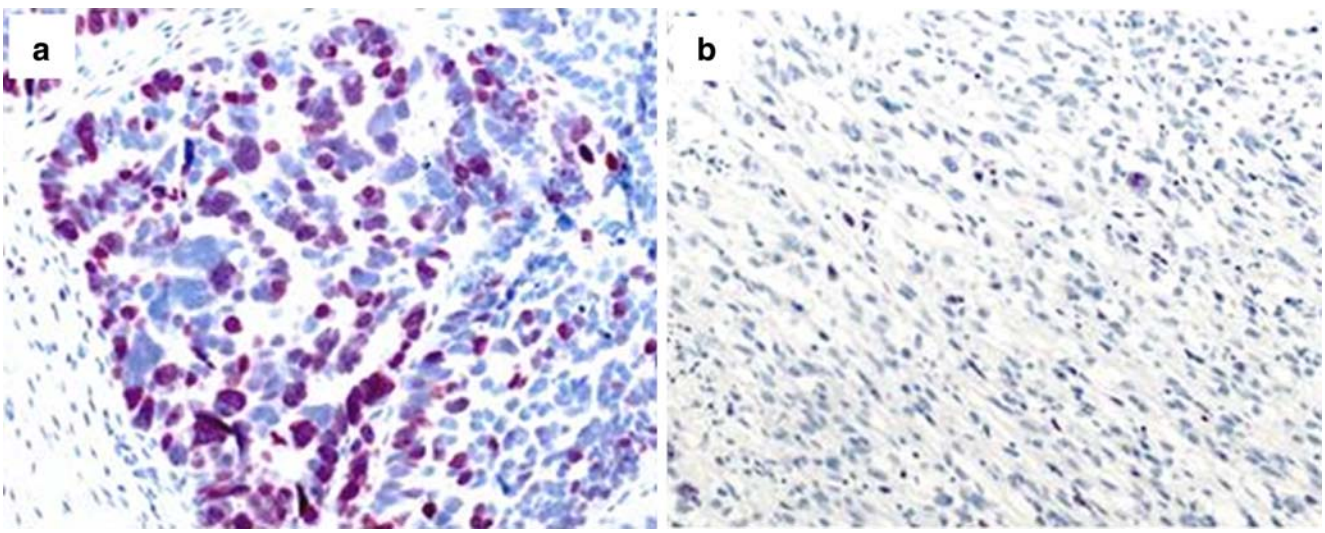


Fig. 6 Representative immunohistochemical detection of nuclear Ki67 accumulation in carcinomatous (**a**) and sarcomatous (**b**) tumor component. The original magnification of each, ×40 objective

chromosome 8 was observed in 54% of serous and 62% of endometrioid carcinosarcomas, equally to amplifications on chromosome 20 (72 and 75%). These results show that the two tumor components are genetically closely related and support the "conversion" hypothesis. Furthermore, the CGH patterns observed in our study are almost identical to those of high-grade serous ovarian carcinomas and very similar to CGH patterns of endometrial carcinomas [32]. These findings suggest that carcinosarcomas are particularly aggressive variants of conventional ovarian carcinomas.

To gain more detailed information about the two tumor components, we investigated the carcinomatous and sarcomatous tumor component separately using FISH technique. Because amplifications on chromosome 8q and 20q were particularly frequent (about 70%), comparative FISH analysis of the carcinomatous and sarcomatous tumor components focused on these regions. Amplification of znf217 was seen equally in both tumor components, whereas high-level amplifications of c-myc were more prominent in carcinomatous than in sarcomatous tumor areas. Overall, results of CGH and FISH analysis correlated well. C-myc amplifications were less evident in CGH than in FISH analysis. In six cases, amplification of c-myc was seen only by FISH. These results underline the lower sensitivity of CGH for detection of small chromosomal aberrations.

In agreement with molecular–genetic analyses of other investigators [1, 21, 25, 30], we were able to demonstrate that the majority of the tumors harbored a substantial number of gene amplifications in the carcinomatous tumor area indicating a high level of chromosomal instability in these areas.

Separate assessment of the proliferation activity of both tumor components by Ki67 immunohistochemistry are in agreement with this hypothesis. A higher proliferation index was revealed in the carcinomatous areas, whereas the sarcomatous component showed inhomogeneous and focal expression of Ki67 in tumor cells. Other investigators have also demonstrated a higher proliferation index and apoptotic activity in the carcinomatous than in the sarcomatous component [31, 39]. In agreement with this view, it is noteworthy that metastases of carcinosarcomas often only contain carcinomatous tissue. Furthermore, it has been shown by immunohistochemistry of the vascular endothelial growth factor that angiogenic activity is also more pronounced in the carcinomatous areas [11]. These results also suggest that the carcinomatous element is the biologically dominant one in these mixed tumors.

In summary, molecular cytogenetic analysis of 30 cases of ovarian and uterine carcinosarcomas revealed a high level of homology of chromosomal aberrations between the different tumor components suggesting a monoclonal origin of these tumors. However, the carcinomatous element seems to be the driving force of tumorigenesis. The sarcomatous tumor component is either derived from the carcinoma by transdifferentiation or from a common stem cell undergoing divergent differentiation. For confirmation of these results, additional molecular–genetic analyses will be needed.

Furthermore, the striking similarity of molecular genetic aberrations of carcinosarcomas and high-grade ovarian carcinomas supports the notion that similar treatment protocols for adjuvant therapy should be used for these groups of patients.

Acknowledgments The authors thank Beate Luthardt for excellent technical assistance.

References

1. Abeln EC, Smit VT, Wessels JW, de Leeuw WJ, Cornelisse CJ, Fleuren GJ (1997) Molecular genetic evidence for the conversion hypothesis of the origin of malignant mixed Mullerian tumours. J Pathol 183:424–431
2. Auerbach HE, LiVolsi VA, Merino MJ (1988) Malignant mixed Mullerian tumors of the uterus. An immunohistochemical study. Int J Gynecol Pathol 7:123–130
3. Blom R, Guerrieri C, Stal O, Malmstrom H, Sullivan S, Simonsen E (1988) Malignant mixed Müllerian tumors of the uterus: A clinicopathologic, DNA flow cytometry, p53, and mdm-2 analysis of 44 cases. Gynecol Oncol 68:18–24
4. de Brito PA, Silverberg SG, Orenstein JM (1993) Carcinosarcoma (malignant mixed mullerian (mesodermal) tumor) of the female genital tract: immunohistochemical and ultrastructural analysis of 28 cases. Hum Pathol 24:132–142
5. Collins C, Rommens JM, Kowbell D (1998) Positional cloning of ZNF217 andNABC1: genes amplified at 20q13.2 and overexpression in breast carcinoma. Proc Natl Acad Sci USA 95: 8703–8708
6. Chung MT, Mukai K, Teshima S, Kishi K, Shimosato Y (1988) Expression of various antigens by different components of uterine mixed Mullerian tumors. An immunohistochemical study. Acta Pathol Jpn 38:35–45
7. Costa MJ, Vogelsan J, Young LJ (1994) p53 gene mutation in female genital tract carcinosarcomas (malignant mixed Mullerian tumors): a clinicopathologic study of 74 cases. Mod Pathol 7: 619–627
8. Costa MJ, Khan R, Judd R (1991) Carcinoma (malignant mixed mullerian [mesodermal] tumor) of the uterus and ovary. Correlation of clinical, pathologic, and immunohistochemical features in 29 cases. Arch Pathol Lab Med 115:583–590
9. Costa MJ, Walls J (1996) Epidermal growth factor receptor and c-erbB-2 oncoprotein expression in female genital tract carcinosarcomas (malignant mixed Mullerian tumors). Clinicopathologic study of 82 cases. Cancer 77:533–542
10. Diebold J, Mosinger K, Peiro G, Pannekamp U, Kaltz C, Lohrs U et al (2000) 20q13 and cyclin D1 in ovarian carcinomas. Analysis by fluorescence in situ hybridization. J Pathol 190:564–571
11. Emoto M, Iwasaki H, Ishiguro M, Kikuchi M, Horiuchi S, Kawarabayashi T et al (1999) Angiogenesis in carcinosarcomas of the uterus: differences in the microvessel density and expression of vascular endothelial growth factor between the epithelial and mesenchymal elements. Hum Pathol 30:1232–1241
12. Emoto M, Iwasaki H, Oshima K, Kikuchi M, Kaneko Y, Kawarabayashi T (1997) Characteristics of rhabdomyosarcoma

cell lines derived from uterine carcinosarcomas. Virchows Arch 431:249–256
13. Emoto M, Iwasaki H, Kikuchi M, Ishiguro M, Kubota T, Kaneko J et al (1992) Two cell lines established from mixed mullerian tumors of the uterus. Morphologic, immunocytochemical, and cytogenetic analyses. Cancer 69:1759–1768
14. Fujii H, Yoshida M, Gong ZX, Matsumoto T, Hamano Y, Shirai T et al (2000) Frequent genetic heterogeneity in the clonal evolution of gynecological carcinosarcoma and its influence on phenotypic diversity. Cancer Res 60:114–120
15. Gallardo A, Matias-Guiu X, Lagarda H, Catasus L, Bussaglia E, Prat J et al (2002) Malignant mullerian mixed tumor arising from ovarian serous carcinoma: a clinicopathologic and molecular study of two cases. Int J Gynecol Pathol 21:268–272
16. Geisinger KR, Dabbs DJ, Marshall RB (1987) Malignant mixed Mullerian tumors. An ultrastructural and immunohistochemical analysis with histogenetic considerations. Cancer 59:1781–1790
17. George E, Manivel JC, Dehner LP, Wick MR (1991) Malignant mixed Mullerian tumors: an immunohistochemical study of 47 cases, with histogenetic considerations and clinical correlation. Hum Pathol 22:215–223
18. Gorai I, Doi C, Minaguchi H (1993) Establishment and characterization of carcinosarcoma cell line of the human uterus. Cancer 71:775–786
19. Gorai I, Yanagibashi T, Taki A, Udagawa K, Miyagi E, Minaguchi H et al (1997) Uterine carcinosarcoma is derived from a single stem cell: an in vitro study. Int J Cancer 72:821–827
20. Gorstein F, Anderson TL (1991) Malignant mixed mesodermal tumors: carcinoma, sarcoma, or both? Hum Pathol 22:207–209
21. Gunawan B, Baumhoer D, Schulten HJ, Emons G, Fuzesi L (2003) Polysomy 8 in three cases of homologous malignant mixed Mullerian tumors of the uterus. Anticancer Res 23:1379–1383
22. Haba R, Kobayashi S, Miki H, Hirakawa E, Mori S, Ishii Y et al (1993) Mixed mesodermal tumor of the ovary: immunohistochemical study with histogenetic consideration. Acta Pathol Jpn 43:696–701
23. Ishikawa S, Kaneko H, Sumida T, Sekiya M (1979) Ultrastructure of mesodermal mixed tumor of the uterus. Acta Pathol Jpn 29:801–809
24. Jeffers MD, Richmond JA, Macaulay EM (1995) Overexpression of the c-myc proto-oncogene occurs frequently in uterine sarcomas. Mod Pathol 8:701–704
25. Kounelis S, Jones MW, Papadaki H, Bakker A, Swalsky P, Finkelstein SD (1998) Carcinosarcomas (malignant mixed mullerian tumors) of the female genital tract: comparative molecular analysis of epithelial and mesenchymal components. Hum Pathol 29:82–87
26. Mayall F, Rutty K, Campbell F, Goddard H (1994) p53 immunostaining suggests that uterine carcinosarcomas are monoclonal. Histopathology 24:211–214
27. McCluggage WG (2002) Malignant biphasic uterine tumors: carcinosarcomas or metaplastic carcinomas? J Clin Pathol 55:321–325
28. McCluggage WG (2002) Uterine carcinosarcomas (malignant mixed Mullerian tumors) are metaplastic carcinomas. Int J Gynecol Cancer 12:687–690
29. Meis JM, Lawrence MD (1990) The immunohistochemical profile of malignant mixed mullerian tumor. Overlap with endometrial adenocarcinoma. Am J Clin Pathol 94:1–7
30. Micci F, Teixeira MR, Haugom L, Kristensen G, Abeler VM, Heim S (2004) Genomic aberrations in carcinomas of the uterine corpus. Genes Chromosomes Cancer 40:229–246
31. Nicotina PA, Ferlazzo G, Vicelli AM (1997) Proliferation indices and p53 immunocytochemistry in uterine mixed mullerian tumors. Histol Histopathol 12:967–972
32. Schulten HJ, Gunawan B, Enders C, Donhuijsen K, Emons G, Füzesi L (2004) Overrepresentation of 8q in carcinosarcomas and endometrial adenocarcinomas. Am J Clin Pathol 122:546–551
33. Silverberg SG, Major FJ, Blessing JA, Fetter B, Askin FB, Miller A et al (1990) Carcinosarcoma (malignant mixed mesodermal tumor) of the uterus. A Gynecologic Oncology Group pathologic study of 203 cases. Int J Gynecol Pathol 9:1–19
34. Simon R, Burger H, Brinkschmidt C, Bocker W, Hertle L, Terpe HJ (1998) Chromosomal aberrations associated with invasion in papillary superficial bladder cancer. J Pathol 185:345–351
35. Soong R, Knowles S, Hammond IG, Michael C, Iacopetta BJ (1999) p53 protein overexpression and gene mutation in mixed Mullerian tumors of the uterus. Cancer Detect Prev 23:8–12
36. Sreenan JJ, Hart WR (1995) Carcinosarcomas of the female genital tract. A pathologic study of 29 metastatic tumors: further evidence for the dominant role of the epithelial component and the conversion theory of histogenesis. Am J Surg Pathol 19:666–674
37. Thompson L, Chang B, Barsky SH (1996) Monoclonal origins of malignant mixed tumors (carcinosarcomas). Evidence for a divergent histogenesis. Am J Surg Pathol 20:277–285
38. Wada H, Enomoto T, Fujita M, Yoshino K, Nakashima R, Tsujimoto M et al (1997) Molecular evidence that most but not all carcinosarcomas of the uterus are combination tumors. Cancer Res 57:5379–5385
39. Yoshida Y, Kurokawa T, Fukuno N, Nishikawa Y, Kamitani N, Kotsuji F (2000) Markers of apoptosis and angiogenesis indicate that carcinomatous components play an important role in the malignant behavior of uterine carcinosarcoma. Hum Pathol 31:1448–1454

Virchows Arch (2008) 452:269–276
DOI 10.1007/s00428-007-0561-x

ORIGINAL ARTICLE

Consistent numerical chromosome aberrations in thecofibromas of the ovary

Francesca Micci · Lisbeth Haugom · Vera M. Abeler · Claes G. Tropé · Håvard E. Danielsen · Sverre Heim

Received: 24 September 2007 / Revised: 6 December 2007 / Accepted: 11 December 2007 / Published online: 10 January 2008
© Springer-Verlag 2007

Abstract Sex cord-stromal tumors of the ovary comprise 8% of all ovarian neoplasms. Because they consist of cells that resemble embryonic sex cord and/or specialized ovarian stroma cells, their cytologic and histologic features can be viewed as reflecting a continuum from fibromas to thecomas with thecofibromas in between. Existing cytogenetic knowledge about ovarian thecomas–thecofibromas–fibromas is restricted to 44 cases with chromosomal abnormalities. The most common aberration has been trisomy 12, identified either by karyotyping or using fluorescence in situ hybridization (FISH). We wanted to obtain more information about the genomic composition of these tumors, and, therefore, examined 29 new thecoma–thecofibroma–fibroma tumors of the ovary using karyotyping, comparative genomic hybridization, interphase FISH, and DNA ploidy analysis. We detected aneuploidy in 21 tumors. Trisomy and/or tetrasomy 12 was the most common chromosomal aberration, found in 15 tumors (71.5% of the aneuploid tumors or 51.5% of all analyzed tumors), followed by trisomy for chromosomes 10, 18, 4, and 9. Some monosomies (for chromosomes 4, 9, 10, and 18) were also identified, either as the sole change or in combination with trisomies. The nonrandom occurrence of these aneuploidies in these benign tumors strongly indicates that they play a major pathogenetic role, but how trisomies and other aneuploidies contribute to tumorigenesis remains unknown.

Keywords Thecofibroma · Trisomy 12 · IP-FISH · Karyotyping · Ploidy analysis · Aneuploidy

Addendum After submission of this manuscript, an article by Streblow et al. describing a similar study of thecoma–thecofibroma–fibroma tumors was published in Cancer Genetics and Cytogenetics (178:135–140). That study too found that imbalances of other chromosomes than chromosome 12 may represent nonrandom genomic changes in this group of tumors.

F. Micci (✉) · L. Haugom · S. Heim
Department of Medical Genetics,
Rikshospitalet-Radiumhospitalet Medical Centre,
0310 Oslo, Norway
e-mail: francesca.micci@labmed.uio.no

V. M. Abeler
Department of Pathology,
Rikshospitalet-Radiumhospitalet Medical Centre,
Oslo, Norway

C. G. Tropé
Department of Gynecologic Oncology,
Rikshospitalet-Radiumhospitalet Medical Centre,
Oslo, Norway

H. E. Danielsen
Department of Medical Informatics,
Rikshospitalet-Radiumhospitalet Medical Centre,
Oslo, Norway

H. E. Danielsen
Centre for Cancer Biomedicine, University of Oslo,
Oslo, Norway

H. E. Danielsen
Department of Informatics, University of Oslo,
Oslo, Norway

S. Heim
Faculty of Medicine, University of Oslo,
Oslo, Norway

Introduction

Sex cord-stromal tumors are ovarian neoplasms made up of a mixture of fibroblasts of gonadal stroma origin and granulosa cells, theca cells, and/or their luteinized derivatives Sertoli and Leydig cells [12]. Altogether, they account for 8% of all ovarian tumors. At the two ends of the histological continuum are thecomas and fibromas, whereas

thecofibromas per definition occupy the middle ground with variable amounts of theca cells and fibroblasts [29]. Thecofibromas, thecomas, and fibromas of the ovary are almost invariably unilateral, only 3% are bilateral, and they are almost never malignant [12].

Trisomy and tetrasomy for chromosome 12 have been demonstrated in tumors belonging to the thecoma–thecofibroma–fibroma group by karyotypic analysis and fluorescence in situ hybridization (FISH) [13, 14, 19, 23, 25–28]. Gain of chromosome 12 is not, however, specific for tumors of this group even in the ovarian context, since it has also been seen in some benign and borderline epithelial tumors and in occasional granulosa cell tumors [23, 25].

We report here 29 thecoma–thecofibroma–fibroma tumors, including two pairs of bilateral tumors, that were investigated for numerical chromosomal changes by means of karyotyping, comparative genomic hybridization (CGH), interphase FISH (IP-FISH), and DNA ploidy analysis.

Material and methods

Tumors

All tumors were examined at the Rikshospitalet-Radiumhospitalet Medical Centre as part of a research off-shoot from our diagnostic cytogenetic work on female genital tract tumors. The pathological examination yielded the following diagnoses: thecofibroma (24 tumors), thecofibroma and cystadenoma (one tumor), thecofibroma and adenofibroma (one tumor), thecofibroma and fibroma (one tumor), thecoma (one tumor), and fibroma (one tumor). The tumors were unilateral in most of the patients, but tumors 26a and 26b were from the right and left ovary of the same woman, as were also tumors 27a and 27b. Thus, a total of 29 tumors of the thecoma–thecofibroma–fibroma group (henceforth sometimes referred to collectively as thecofibromas) from altogether 27 patients (from 46 to 90 years of age; mean age 55 years) were analyzed.

In seven instances, fresh tumor material was sent to the cytogenetics laboratory, allowing cell culturing with subsequent karyotyping and DNA extraction; the findings made by karyotyping these seven tumors (see "Results") formed the starting point for the entire study and provided the rationale for choosing the chromosome-specific probes for the later examinations of archival material. This latter part of the study consisted of DNA content measurement and IP-FISH and was undertaken on formalin-fixed, paraffin-embedded tissue from 28 tumors.

Cell culturing and karyotyping

Only on seven tumors (see Table 1), from which fresh material was available, was it possible to perform cell culturing with subsequent karyotypic analysis. The tumor samples were manually minced and treated with Collagen II (Worthington, Freehold, NJ, USA) until a suitable suspension of cells and cell clumps was obtained. After 6–7 days of culturing in a selective medium, colchicine was added and the cultures harvested according to Mandahl [16]. The chromosomes of the dividing cells were then G-banded and a karyotype established following the recommendations of the ISCN (Fig. 1) [6].

Comparative genomic hybridization (CGH)

DNA was isolated by the phenol–chloroform method as previously described [2]. Comparative genomic hybridization [9] was performed according to our modifications of standard procedures [17] on the same seven tumors (Table 1) that had already been cell cultured and karyotyped. Chromosomes were karyotyped based on their inverted DAPI appearance, and the relative hybridization signal intensity was determined along each chromosome. An average of 10–15 cells was analyzed to generate ratio profiles with 95% confidence interval for each chromosome. The threshold values 1.25 and 0.75 were used to score gain and loss of DNA sequences, respectively. A negative (normal versus normal) and a positive (a cell line with known copy number changes) control were included in the experiments. The description of the CGH copy number changes was based on the recommendation of the ISCN [6].

DNA ploidy analysis

DNA image cytometry was performed on the 28 tumors from which formalin-fixed, paraffin-embedded tissue was available (Table 1). The procedures for measurement of DNA content and the criteria for ploidy classification were as previously described [11], with but minor modifications. A region of a paraffin block rich in tumor cells was selected for preparation of monolayers. Two 50-μm sections were cut and enzymatically digested (SIGMA protease, type XXIV, Sigma Chemical Co., St Louis, MO, USA) for the preparation of cell monolayers. The DNA content of at least 1,000 Feulgen–Schiff-stained nuclei was measured and analyzed using the Fairfield DNA Ploidy System (Fairfield Imaging Ltd, Kent, UK) and assessed according to an established protocol (Fig. 2) [11].

Interphase fluorescence in situ hybridization (IP-FISH)

Interphase-FISH analysis was performed on the 28 tumors from which archival material was available (Table 1). Interphase-FISH with α-satellite probes specific for the centromeres of chromosomes 4, 9, 10, 12, and 18 (Vysis,

Table 1 Overview of the findings obtained with ploidy analysis, IP-FISH experiments, karyotyping and CGH imbalances of the 29 cases of tumors of the ovaries

Case no.	Patient no.	Age of patient (years)	Diagnosis	Ploidy	IP-FISH	Karyotype	CGH imbalances
1	00/01935	54	Thecofibroma + fibroma	Aneuploid	+4; +10; +12; +18	46, XX[161]	Rev ish enh (4q12q22, 4q31)
2	00/21952	60	Thecofibroma + adenofibroma	No material available	No material available	46, XX[13]	Rev ish enh (4, 6, 10, 12, 14, 15, 18, 20)
3	00/28277	68	Thecofibroma	Diploid	+9; +12	50, XX, +9, +12, +18, +21[27]	Rev ish enh (9, 12, 18, 21)
4	00/28803	76	Thecofibroma	Diploid	+4; +10; +12; +12	50, XX, +4, +10, +12, +12[5]/46, XX[6]	Rev ish enh (4, 10, 12)
5	01/12660	86	Thecofibroma + cystadenoma	Diploid	+9; −10; +12	48, XX, +9, +12[6]	Not informative
6	02/01497	74	Thecofibroma	Diploid	−4; +10	45, XX, −6[7]/46, XX[82]	Not informative
7	03/20559	50	Thecofibroma	Diploid	−9	46, XX[2]	No imbalances
8	02/17538	52	Thecofibroma	Aneuploid	−4; +9; +12; +12	–	–
9	03/01383	51	Thecofibroma	Diploid	Normal	–	–
10	03/05656	55	Thecofibroma	Aneuploid	+4; +9; +9; +10; +12; +12; +18; +18	–	–
11	03/07193	72	Thecofibroma	Diploid	Normal	–	–
12	03/07996	90	Thecofibroma	Diploid	Normal	–	–
13	03/09346	50	Thecoma	Diploid	+4; −9; +12	–	–
14	03/12052	52	Thecofibroma	Diploid	+12	–	–
15	03/13113	47	Thecofibroma	Diploid	+12; −18	–	–
16	03/13358	74	Thecofibroma	Diploid	+12	–	–
17	03/19463	49	Fibroma	Diploid	Normal	–	–
18	04/00723	48	Thecofibroma	Diploid	+12	–	–
19	04/02959	54	Thecofibroma	Aneuploid	+10; +12; +18	–	–
20	04/04772	51	Thecofibroma	Diploid	+12	–	–
21	04/08312	67	Thecofibroma	Aneuploid DNA index 1, 10	Normal	–	–
22	04/10494	53	Thecofibroma	Diploid	Normal	–	–
23	04/15325	71	Thecofibroma	Diploid	Normal	–	–
24	04/15697	58	Thecofibroma	Diploid	+12	–	–
25	04/16640	46	Thecofibroma	Aneuploid	+9; +10; +18	–	–
26a	04/02297 right ovary	65	Thecofibroma	Diploid	Normal	–	–
26b	04/02297 left ovary	65	Thecofibroma	Diploid	−18	–	–
27a	04/08151 right ovary	72	Thecofibroma	Diploid	Normal	–	–
27b	04/08151 left ovary	72	Thecofibroma	Diploid	−9; −18	–	–

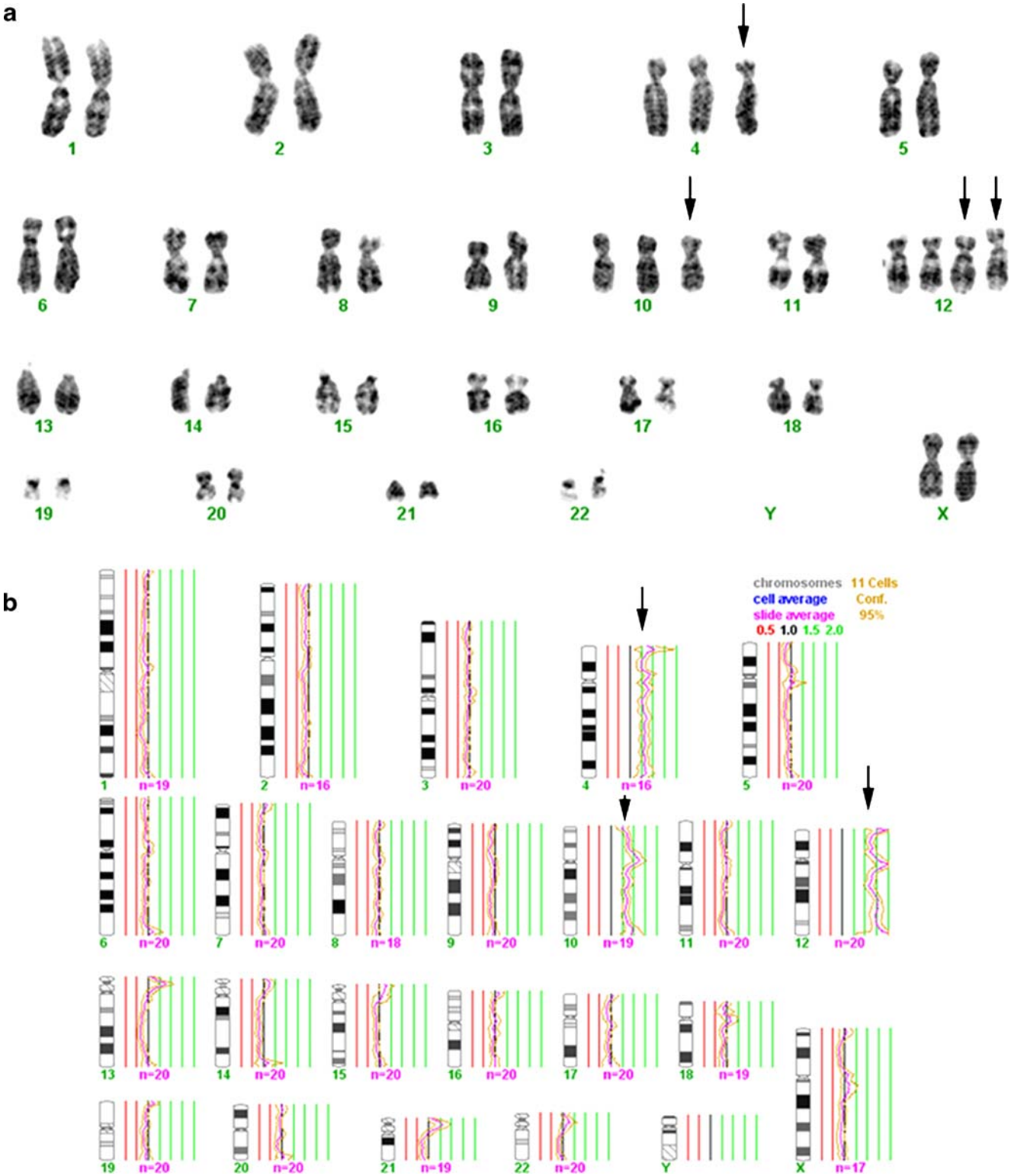


Fig. 1 Composite G-banding karyogram (**a**) and CGH profile (**b**) of the thecofibroma of case 4. All aberrations detected by karyotyping matched the imbalances scored by CGH. *Vertical arrows* indicate gained chromosomes

Abbott, Norway) was performed on nuclei extracted from formalin-fixed, paraffin-embedded tumor tissue. These probes were selected because their corresponding chromosomes had been found gained in at least two different cases by karyotyping and/or CGH analysis of the seven tumors that could be examined using these techniques (see below). The nuclei were extracted as described by Liehr et al. [15]. The nuclear suspension was pretreated as described earlier,

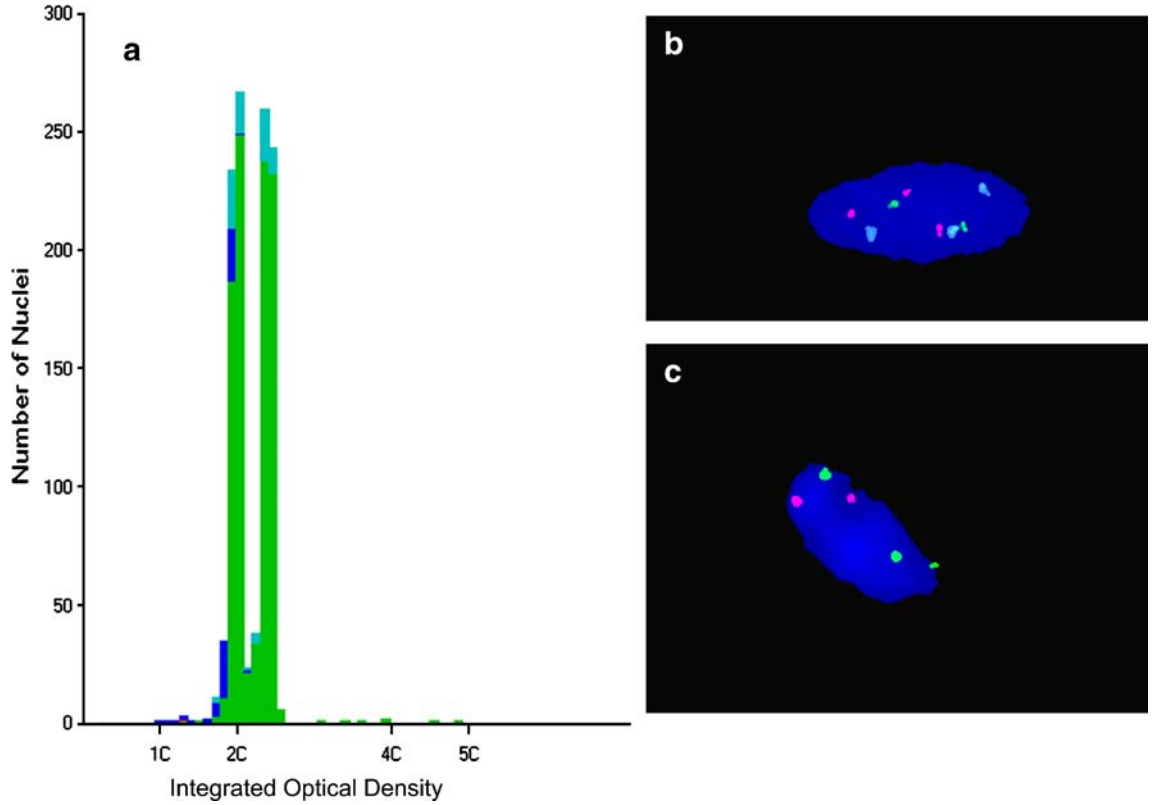


Fig. 2 **a** Ploidy distribution of the thecofibroma of case 25. The *green* area shows the distribution of the tumor cells, whereas the *blue* marks the distribution of the internal control cells. **b** IP-FISH picture of a cell from case 25 showing trisomy 9 and trisomy 18. The probes used were CEP 9 (*blue color*), CEP 12 (*green color*), and CEP 18 (*red color*). **c** IP-FISH picture from case 25 showing trisomy 10. The probes used were CEP 4 (*red color*) and CEP 10 (*green color*)

with but minor modifications [10], and the denaturation and washing steps were as published by Persons [24]. Two hundred consecutive, whole, and single nuclei were evaluated. The specificity of the probes was validated by FISH experiments on slides with metaphases and interphase nuclei from a karyotypically normal person. A cut-off of 10% was chosen for all probes based on the findings on these control slides.

Results

The main clinicopathologic data, karyotypic features, CGH imbalances, IP-FISH, and DNA ploidy classification results are summarized in Table 1. The karyotypic analysis of the seven thecofibromas from which fresh material was available showed simple numerical chromosome aberrations in four tumors and a normal chromosome complement in the remaining three. Trisomy 12 was found in two tumors (cases 3 and 5), in both of them together with also other numerical changes. Tetrasomy 12 was detected in case 4, again together with other numerical changes. Trisomy 9 was seen in tumors 3 and 5, whereas trisomies for chromosomes 4, 10, 18, and 21 were detected in one tumor each. Case 6 presented a small clone with monosomy of chromosome 6.

The CGH analysis gave informative results in five of the seven tumors showing imbalances in four (Table 1). With the exception of case 1, which showed gain of only some bands from chromosome arm 4q, the other imbalances were gains of entire chromosomes. Chromosome 12 was gained in three tumors (cases 2, 3, and 4), and chromosomes 4 and 10 were gained in two tumors (cases 2 and 4), as was also chromosome 18 in cases 2 and 3. An extra copy of chromosomes 6, 14, 15, and 20 was seen in only one tumor (case 2), whereas gain of chromosomes 9 and 21 was seen only in case 3.

Based on these karyotyping and CGH results, we decided to investigate the genomic composition of the thecofibroma group of tumors more closely, making use of also whatever archival material in the form of paraffin-embedded blocks that could be retrieved from our Department of Pathology. We chose to investigate for the presence of those whole-chromosome gains that had been detected in at least two different tumors by means of karyotyping and/or CGH analysis. A total of 28 thecofibroma tumors were found, including six of the seven we had received for karyotyping at the beginning of our study, i.e., 22 additional

tumors were available for study. All these 28 tumors were then investigated for ploidy classification by measurement of DNA content and for numerical chromosome aberration by IP-FISH analysis. In 22 of the tumors, the DNA content was classified as diploid, whereas in six tumors, it was clearly aneuploid (cases 1, 8, 10, 19, 21, and 25; Table 1).

The IP-FISH analysis performed with α-satellite probes for chromosomes 4, 9, 10, 12, and 18 showed a normal, diploid content of the investigated chromosomes in nine tumors, whereas the remaining 19 showed copy number alterations (Table 1). Trisomy or tetrasomy for chromosome 12 was the most common abnormality (14 tumors). Gain(s) of chromosome 12 was found together with other numerical changes in nine tumors (cases 1, 3, 4, 5, 8, 10, 13, 15, and 19) and as the sole change in five tumors (cases 14, 16, 18, 20, and 24). The other abnormalities detected in this series were trisomy 10 in six tumors and trisomy for chromosomes 4 and 9 in four tumors each. Trisomy 18 was detected in three tumors, whereas, in case 10, tetrasomy 18 was seen. Some monosomies were also detected either as the sole chromosomal change or in combination with gains and/or losses of other chromosomes. Monosomy for chromosomes 4 and 10 was seen only together with chromosomal gains. Monosomy 9 was present in case 7 as the sole abnormality and in tumor 27b together with monosomy 18. Monosomy for chromosome 18 was also seen in case 15, together with a +12, and in tumor 26b as the sole aberration.

Discussion

The cytogenetic literature on the thecoma–thecofibroma–fibroma group of ovarian tumors is quite limited, inasmuch as only seven thecomas [3, 14, 19, 23, 28], 15 thecofibromas [3, 7, 14, 26], and 22 fibromas [13, 14, 23, 25, 27, 28] have been reported with cytogenetic abnormalities detected by karyotyping or FISH analysis. The most common aberration found in these tumors has been an extra chromosome 12, seen equally frequently in thecomas, thecofibromas, and ovarian fibromas. We wanted to find out how often trisomy 12 could be seen in a larger series of such tumors and also to search for other numerical changes that might characterize them, alone or in combination with +12.

Trisomy and/or tetrasomy for chromosome 12 was the most common change also in our series, detected in 15 out of 29 tumors. The common finding of trisomy 12 in thecomas, thecofibromas, and fibromas of the ovary supports the notion that these are but three variants of the same group of tumors. In addition to thecofibromas, trisomy 12 is known to occur also in benign, borderline, and even (mostly well differentiated) malignant epithelial ovarian tumors [22]. The aberration is by no means organ specific, however, since +12 also occurs nonrandomly, and often as the only cytogenetic change, in chronic lymphocytic leukemia [4, 5], various non-ovarian adenocarcinomas [8, 30], Wilms tumors [1], and leiomyomas [21, 20]. The molecular mechanism whereby +12 might contribute to tumorigenesis is unknown, but some kind of dosage effect may be stipulated. In addition, the origin of the third copy of chromosome 12 is unknown; whether it comes from duplication of one homologue or from triplication with concomitant loss of the other homologue needs investigation.

Tetrasomy 12 was identified in three tumors (cases 4, 8, and 10), always together with other abnormalities. Liang et al. [14] suggested a relationship between tetrasomy 12 in ovarian tumors and the patients' age; however, in our study, this was not borne out since the three patients were 52, 55, and 76 years old, i.e., below, equal to and well beyond the median age for the entire patient group.

Other numerical chromosome aberrations were also seen to different degrees and, with the exception of monosomy for chromosomes 9 and 18 in cases 7 and 26b, respectively, always in combination with other changes. Trisomy for chromosomes 10 and 18 was seen in seven and six cases, respectively. Although none of these trisomies has been reported before in this tumor type, their finding here in 35% (seven tumors out of 20 with abnormalities) and 30% (six tumors out of 20) clearly identify them as nonrandom chromosomal changes in the thecoma–thecofibroma–fibroma group of ovarian tumors. Trisomy for chromosomes 4 and 9 was detected in five cases each. Trisomy 4 has previously been reported in two thecomas, together with +12 in the case described by Mrozek et al. [19], and in combination with +9 and +12 in the case reported by Pejovic et al. [23]. As for trisomy 12, and indeed for all whole-chromosome gains, the pathogenetic role of these trisomies is presently unknown, in ovarian tumors as elsewhere. Be that as it may, all these numerical chromosomal abnormalities, +4, +9, +10, +12, and +18, have also been found in other tumor types at different frequencies both as sole aberrations and together with other changes [18].

Also, monosomies for chromosomes 4, 9, 10, and 18 were detected in the present study. They were present in a total of eight cases, in five of them together with trisomies, whereas in cases 7 and 26b, only a −9 and a −18 were seen, respectively. In tumor 27b, both −9 and −18 were detected. Monosomy 4 was identified in cases 6 and 8, whereas monosomies for chromosomes 9, 10, and 18 were identified in cases 13, 5, and 15, respectively, together with trisomies. The monosomies were seen at frequencies from 10% to 17.5% by IP-FISH, meaning that they were generally detected in fewer cells than were the trisomies, making them difficult to be detected by other techniques. This is the first time that chromosome losses have been detected in thecoma–thecofibroma–fibroma tumors of the ovary. Their

pathogenetic role needs further investigation, although the standard assumption is that loss of tumor suppressor genes on the lost chromosome(s) may be the important outcome.

Bilateral thecofibromas are rare, found only in 3% of the patients. It was, therefore, of some interest that we could analyze two bilateral tumors in the present study. Case 26a showed no numerical chromosome aberrations, whereas in its counterpart, case 26b, monosomy 18 was detected. Case 27a again showed no numerical chromosome aberration, whereas the contralateral tumor (case 27b) showed monosomy for chromosomes 9 and 18. The only bilateral thecofibroma previously analyzed showed a cytogenetically normal karyotype in both ovaries [3]. It is impossible to assess, based on the examination of these three tumor pairs, whether bilateral thecofibromas involve a spreading from one side to the other or whether the two tumors are double de novo primaries.

The somewhat variable information obtained with the different techniques used in the present study needs some commenting. Measurement of DNA content detected only six aneuploidies in 28 tumors, whereas IP-FISH, performed on nuclei extracted from the same paraffin blocks as the nuclei for ploidy analysis, identified 19 cases with numerical aberrations. This discrepancy may be because of false positive or false negative results with each of the methods used. One well-known cause of false negative results is that cytometry-based measurement of DNA ploidy analysis is not able to identify the presence of aneuploidies involving only one and/or two chromosomes, especially if they are small. This is because the gain or loss has to be more than 2–5% (which typically is the coefficient of variation of the single peaks in the DNA histograms from paraffin-embedded tumors) of the total DNA content of the nucleus in order to give rise to a clearly separate peak in this type of measurement. By way of example, the tumor of case 4 was found to be diploid by DNA content measurement, whereas trisomy for chromosomes 4 and 10 and tetrasomy 12 were identified by IP-FISH, karyotyping, and CGH. The opposite situation was seen in case 21, which showed an aneuploid DNA content but had a normal, diploid content for the chromosomes investigated by IP-FISH. This tumor may have had in its genome other unbalanced chromosome rearrangements, including trisomies, than those selected for testing in this study. Adding credibility to this explanation is the fact that chromosomes 6, 14, 15, 20, and 21 were found gained in single tumors of the present series, making them candidates for aneuploidies less frequent than gain of the chromosomes here investigated. Although the findings in most tumors were the same with the different techniques used, the combination of alternative methods for scoring numerical chromosome aberrations, each with its inherent advantages and disadvantages, in ovarian thecomas–thecofibromas–fibromas as indeed for all tumor types, obviously reduces the likelihood of obtaining false positive and/or false negative results.

Conflict of interest statement We declare that we have no conflict of interest.

References

1. Bown N, Cotterill SJ, Roberts P, Griffiths M, Larkins S, Hibbert S, Middleton H, Kelsey A, Tritton D, Mitchell C (2002) Cytogenetic abnormalities and clinical outcome in Wilms tumor: a study by the U.K. cancer cytogenetics group and the U.K. Children's Cancer Study Group. Med Pediatr Oncol 38:11–21
2. Brandal P, Bjerkehagen B, Heim S (2004) Molecular cytogenetic characterization of tenosynovial giant cell tumors. Neoplasia 6:578–583
3. Fletcher JA, Gibas Z, Donovan K, Perez-Atayde A, Genest D, Morton CC, Lage JM (1991) Ovarian granulosa-stromal cell tumors are characterized by trisomy 12. Am J Pathol 138:515–520
4. Garcia-Marco JA, Price CM, Ellis J, Morey M, Matutes E, Lens D, Colman S, Catovsky D (1996) Correlation of trisomy 12 with proliferating cells by combined immunocytochemistry and fluorescence in situ hybridization in chronic lymphocytic leukemia. Leukemia 10:1705–1711
5. Geisler CH, Philip P, Christensen BE, Hou-Jensen K, Pedersen NT, Jensen OM, Thorling K, Andersen E, Birgens HS, Drivsholm A, Ellegaard J, Larsen JK, Plesner T, Brown P, Andersen PK, Hansen MM (1997) In B-cell chronic lymphocytic leukaemia chromosome 17 abnormalities and not trisomy 12 are the single most important cytogenetic abnormalities for the prognosis: a cytogenetic and immunophenotypic study of 480 unselected newly diagnosed patients. Leuk Res 21:1011–1023
6. Shaffer LG, Tommerup N (eds) (2005) An international system for human cytogenetic nomenclature. Karger S, Basel
7. Izutsu T, Kudo T, Miura F, Nishiya I (1995) Numerical and structural chromosome abnormalities in an ovarian fibrothecoma. Cancer Genet Cytogenet 83:84–86
8. Jenkins RB, Bartelt D Jr., Stalboerger P, Persons D, Dahl RJ, Podratz K, Keeney G, Hartmann L (1993) Cytogenetic studies of epithelial ovarian carcinoma. Cancer Genet Cytogenet 71:76–86
9. Kallioniemi A, Kallioniemi OP, Sudar D, Rutovitz D, Gray JW, Waldman F, Pinkel D (1992) Comparative genomic hybridization for molecular cytogenetic analysis of solid tumors. Science 258:818–821
10. Knuutila S, Nylund SJ, Wessman M, Larramendy ML (1994) Analysis of genotype and phenotype on the same interphase or mitotic cell. A manual of MAC (morphology antibody chromosomes) methodology. Cancer Genet Cytogenet 72:1–15
11. Kristensen GB, Kildal W, Abeler VM, Kaern J, Vergote I, Trope CG, Danielsen HE (2003) Large-scale genomic instability predicts long-term outcome for women with invasive stage I ovarian cancer. Ann Oncol 14:1494–1500
12. Kurman RJ (ed) (2002) Blaustein's pathology of the female genital tract. Springer-Verlag, New York
13. Leung WY, Schwartz PE, Ng HT, Yang-Feng TL (1990) Trisomy 12 in benign fibroma and granulosa cell tumor of the ovary. Gynecol Oncol 38:28–31
14. Liang SB, Sonobe H, Taguchi T, Takeuchi T, Furihata M, Yuri K, Ohtsuki Y (2001) Tetrasomy 12 in ovarian tumors of thecoma–fibroma group: a fluorescence in situ hybridization analysis using paraffin sections. Pathol Int 51:37–42

15. Liehr T, Grehl H, Rautenstrauss B (1995) FISH analysis of interphase nuclei extracted from paraffin-embedded tissue. Trends Genet 11:377–378
16. Mandahl N (2001) Methods in solid tumors cytogenetics. In: Rooney DE (ed) Human cytogenetics—malignancy and acquired abnormalities. Oxford University Press, Oxford, pp 165–203
17. Micci F, Teixeira MR, Haugom L, Kristensen G, Abeler VM, Heim S (2004) Genomic aberrations in carcinomas of the uterine corpus. Genes Chromosomes Cancer 40:229–246
18. Mitelman, F., Johansson, B., Mertens, F. (2006) Mitelman database of chromosome aberrations in cancer. http://cgap.nci.nih.gov/Chromosomes/Mitelman
19. Mrozek K, Limon J, Debniak J, Emerich J (1992) Trisomy 12 and 4 in a thecoma of the ovary. Gynecol Oncol 45:66–68
20. Nilbert M, Heim S, Mandahl N, Floderus UM, Willen H, Mitelman F (1990) Characteristic chromosome abnormalities, including rearrangements of 6p, del(7q), +12, and t(12;14), in 44 uterine leiomyomas. Hum Genet 85:605–611
21. Nilbert M, Heim S, Mandahl N, Floderus UM, Willen H, Mitelman F (1990) Trisomy 12 in uterine leiomyomas. A new cytogenetic subgroup. Cancer Genet Cytogenet 45:63–66
22. Pejovic T (1995) Genetic changes in ovarian cancer. Ann Med 27:73–78
23. Pejovic T, Heim S, Mandahl N, Elmfors B, Floderus UM, Furgyik S, Helm G, Willen H, Mitelman F (1990) Trisomy 12 is a consistent chromosomal aberration in benign ovarian tumors. Genes Chromosomes Cancer 2:48–52
24. Persons DL, Hartmann LC, Herath JF, Borell TJ, Cliby WA, Keeney GL, Jenkins RB (1993) Interphase molecular cytogenetic analysis of epithelial ovarian carcinomas. Am J Pathol 142:733–741
25. Persons DL, Hartmann LC, Herath JF, Keeney GL, Jenkins RB (1994) Fluorescence in situ hybridization analysis of trisomy 12 in ovarian tumors. Am J Clin Pathol 102:775–779
26. Shashi V, Golden WL, Kap-Herr C, Andersen WA, Gaffey MJ (1994) Interphase fluorescence in situ hybridization for trisomy 12 on archival ovarian sex cord-stromal tumors. Gynecol Oncol 55:349–354
27. Smith LM, Hu P, Meyer LJ, Coffin CM (2002) Complex karyotypic abnormality in ovarian fibroma associated with Gorlin syndrome. Am J Med Genet 112:61–64
28. Taruscio D, Carcangiu ML, Ward DC (1993) Detection of trisomy 12 on ovarian sex cord stromal tumors by fluorescence in situ hybridization. Diagn Mol Pathol 2:94–98
29. Tavassoli FA, Devilee P (eds) (2003) World health organization classification of tumors: pathology and genetics of tumors of the breast and female genital organs. IARC, Lyon
30. Thompson FH, Liu Y, Emerson J, Weinstein R, Makar R, Trent JM, Taetle R, Alberts DS (1994) Simple numeric abnormalities as primary karyotype changes in ovarian carcinoma. Genes Chromosomes Cancer 10:262–266

Virchows Arch (2008) 452:277–283
DOI 10.1007/s00428-007-0563-8

ORIGINAL ARTICLE

Influence of preoperative core biopsies on uPA/PAI-1 expression in breast cancer tissue

Susanne Haas · Tjoung-Won Park · Jens Claus Hahne · Hans-Peter Fischer

Received: 27 September 2007 / Revised: 21 November 2007 / Accepted: 14 December 2007 / Published online: 15 January 2008
© Springer-Verlag 2007

Abstract The urokinase-type plasminogen activator (uPA) and the plasminogen activator inhibitor-1 (PAI-1) are involved in tumor invasion and metastasis as well as wound healing and inflammation. We investigated the impact of tissue injury by preoperative sampling on the level of uPA/PAI-1 in paraffin tissue of 55 breast cancer cases by immunohistochemistry. The tumor area surrounding the biopsy channel was compared with distant intact tumor tissue. uPA and PAI-1 were constantly expressed by the tumor cells. Fibroblastic expression was higher in the tumor area surrounding the biopsy channel than in intact tissue with 47 vs 29 positive cases for uPA ($p<0.001$) and 35 vs 25 positive cases for PAI-1 ($p=0.055$). A decrease in fibroblastic enzyme expression from the biopsy area to the intact tumor tissue was seen in 21 cases for uPA and 16 cases for PAI-1. This difference was most evident in cases with an interval of 6 days and longer between biopsy and surgery. In conclusion, fibroblastic inflammatory reaction around the biopsy channel affects stromal uPA and PAI-1 expression, which possibly leads to falsely increased enzyme levels in ELISA. Tissue specimen for ELISA analysis should not be taken from the tumor area around the biopsy channel in the resection specimen.

S. Haas (✉) · J. C. Hahne · H.-P. Fischer
Institute of Pathology,
Sigmund Freud Str. 25,
D-53127, Bonn, Germany
e-mail: Susanne.Haas@ukb.uni-bonn.de

T.-W. Park
Department of Obstetrics and Gynecology,
Medical Faculty of the University of Bonn,
Bonn, Germany

Keywords Breast cancer · uPA · PAI-1 · Inflammation · Preoperative sampling

Introduction

Invasion and metastasis of cancer cells is a result of their capacity to interact with extracellular tissue. Degradation of extracellular matrix and basement membranes by proteolytic enzymes is an important step for tumor invasion [1, 2].

Serine proteinases, including the plasminogen activator system as well as matrix metalloproteinases (MMPs), play an essential role in this process. These proteases are produced as pro-enzymes. The urokinase plasminogen activator (uPA) is activated after proteolysis by serine proteases (e.g. plasmin, trypsin or plasma kallikrein) or by cysteine proteases (e.g. cathepsin B or L). After activation, uPA is tightly regulated by the specific plasminogen activator inhibitor-1 (PAI-1). uPA is involved in proteolytic activation of some MMPs [17]. Furthermore uPA converts plasminogen to plasmin, which plays a major part in tissue remodelling. uPA and PAI-1 also take part in physiological processes such as embryogenesis, wound healing and clot lysis [18].

In cancer growth, uPA supports cell migration and invasion by plasmin-independent mechanisms, including multiple interactions between uPA, uPAR, PAI-1, extracellular matrix proteins, integrins, endocytosis receptors and growth factors [1]. It has been suggested that expression of PAI-1 by the stromal cells of the tumor, especially in areas surrounding the tumor vessels, serves to protect the tumor stroma from the ongoing uPA-mediated proteolysis [14].

Numerous experimental and clinical studies have demonstrated that uPA/PAI-1 play a pivotal role in some solid tumors [5, 7–9]. A pooled analysis performed by the

EORTC including a total of 8,377 breast cancer patients with a median follow-up of 6.5 years validated the prognostic power of uPA/PAI-1. High tumor levels of uPA/PAI-1 were associated with poor disease-free and overall survival. Further studies provided evidence for the predictive impact of uPA/PAI-1 on the response to adjuvant chemotherapy particularly in the clinically important subgroup of node-negative patients [11]. For patients with node-negative breast cancer, the clinical benefit of adjuvant chemotherapy is relatively low considering that almost 70% of patients are cured by locoregional treatment alone. Recent studies indicate that uPA/PAI-1 could help to select those patients who benefit from adjuvant chemotherapy. Taken together these findings underline the clinical potential of uPA/PAI-1.

Over the past decade the diagnostic algorithm for breast abnormalities has changed significantly and an increasing number of well-organized multidisciplinary breast units have been established across Europe. In this setting and with the improvement of image-guided tissue sampling techniques, the majority of patients with breast cancer will undergo preoperative tissue sampling (i.e. core biopsy, vacuum assisted biopsy).

In view of this change of diagnostic work-up we investigated the influence of preoperative tissue sampling on the expression of uPA and PAI-1 in breast cancer as taking of a preoperative punch needle biopsy leads to acute inflammation and fibroblastic reaction in the tumor tissue that might enhance expression of uPA and PAI-1.

The local expression in the biopsy area was compared with the expression of intact tumor tissue by immunohistochemistry. The data were correlated with the uPA/PAI-protein levels determined by a commercially available enzyme-linked immunosorbent assay (ELISA), which has been used in numerous clinical studies and has been assessed by the Receptor and Biomarker Group of the EORTC.

Material and methods

Patients

Tissue sampling and use for this study were performed in accordance with standard guidelines of the ethic committee of the Medical Faculty of the University of Bonn. Immunohistochemistry was performed on paraffin tissue of 55 invasive breast cancer resection specimens in which a biopsy channel could be clearly identified retrospectively (localized bleeding, granulation tissue with fibroblasts). In each case, one specimen from the area surrounding the biopsy channel (BC) and one from intact tumor tissue (IT, distance from the biopsy channel at least 0.5 cm) was chosen for immunohistochemistry.

In all cases, uPA and PAI-1-levels had been determined on unprocessed tissue by ELISA.

Immunohistochemistry

Tissue specimens were fixed in 4% buffered formaldehyde and embedded in paraffin. Immunohistochemical stainings were performed on 4-μm sections with an immunostainer (Techmate 500; DAKO). The antigen–antibody binding was visualized by means of the avidin–biotin complex (ABC-method) using AEC (3-amino-9-ethylcarbazol) as chromogen.

The following primary antibodies were used: anti-PAI-1 monoclonal mouse antibody IgG1κ and anti-uPA monoclonal mouse antibody IgG1 (both from DCS diagnostic, Hamburg, Germany). Both antibodies were incubated over night at 4°C. Dilutions were 1:50 for anti-uPA and 1:20 for anti-PAI-1.

Evaluation of immunohistochemistry and statistical analysis

Immunohistochemical staining in the tumor tissue less than 1 cm around the core biopsy injury was compared to intact tumor tissue more than 1 cm distant from the biopsy channel. Cytoplasmic immunohistochemical staining of tumor cells and stromal cells was evaluated separately. Scoring levels were: 0 = absent staining, 1 = week staining intensity (equal to non neoplastic breast tissue), 2 = moderate and 3 = strong staining intensity. For statistical analysis, chi square analysis and Fisher's exact test were used, if appropriate.

ELISA

uPA and PAI-1 levels were determined on unprocessed tumor tissue of the resection specimen by a standardized ELISA (Femtelle, American Diagnostica Inc, Stanford, USA). Tissue weighing 100–300 mg was pulverized by means of a microdismembrator. For tissue extraction, 2 ml cold extraction buffer (0.2 ml 10% Triton X-100 and 1.8 ml Tris-buffer, pH 8.5) was added for 14–16 h at 4°C. The suspension was centrifuged at 100,000×*g* for 1 h at 4°C. After determination of the total protein level (BC Protein assay, Pierce), the supernatants were stored at−80°C for further analysis.

Standards, controls and tissue extracts were diluted (1:20) in phosphate buffered saline (PBS) containing 1% bovine serum albumin (BSA). One hundred microliters were added to the microtiter plate and incubated at 4°C over night. After washing with PBS-Triton, the detection antibody incubated for 1 h at room temperature, followed by another washing step. The reaction was visualized by streptavidin peroxidase (incubated at 1 h by room temper-

ature) and tetramethylbenzidine perborate (TMB) as a substrate (20 min at room temperature). Reaction was stopped by adding 0.5 N H_2SO_4. Adsorbances were read at 450 nm wavelength.

Cut-off values were 3 ng/mg total protein for uPA and 14 ng/mg total protein for PAI-1.

Results

Patients and tumor specimen

Patients' age ranged from 28–82 years, median was 61 years. Histology of the invasive carcinomas was ductal in 40 and lobular in 15 cases. The tumors showed poor (27 cases) or moderate (28 cases) differentiation. Lymph node metastasis was present in 16 cases at time of diagnosis.

The mean interval between core biopsy and surgery was 6 days (1–16 days).

Immunohistochemical (IHC) expression of uPA and PAI-1 in non neoplastic epithelium and breast cancer cells

In most cases, uPA and PAI-1 were expressed simultaneously with anti-uPA generally showing a stronger staining intensity. Moderate or strong uPA and PAI-1 expression was a constant finding within the cytoplasma of the tumor cells. Staining of the cancer cells showed only slight heterogeneity throughout the tumor which was independent of the distance from the biopsy channel.

In non neoplastic epithelium, expression of both enzymes was variable, but never stronger than in the tumor glands. In some cases a gradual increase of staining intensity from non neoplastic glands to in situ carcinoma and invasive cancer cells could be seen (Fig. 1a–c).

Expression of uPA and PAI-1 (IHC) in fibroblasts of the tumor stroma

The tumor associated stromal cells showed a greater variation of the staining intensity comparing different tumors and tumor areas of the same tumor. These differences in staining intensity were not generally related to the number of stromal cells. (Fig. 1f–h). Stromal expression of uPA/PAI-1 was independent of a diffuse pre-existing lymphocytic infiltrate (Fig. 1e).

Fibroblastic uPA and PAI-expression in the area of the biopsy channel (BC) and in intact tumor tissue (IT)

Stromal enzyme expression in the area from which the core biopsy or vacuum assisted biopsy was taken (referred to as biopsy channel, BC) was compared to distant intact tumor tissue by immunohistochemistry.

Generally, enzyme expression was higher in the BC area. This difference was significant for uPA (Table 1, Fig. 1d,e). Looking at the single tumors, a decrease in enzyme expression from the biopsy area to the distant intact tumor tissue could be seen in 21 cases for uPA and 16 cases for PAI-1. Homogeneous positive or negative expression was seen in 31 (uPA) and 22 (PAI-1) cases. Only a minority of cases revealed stronger enzyme expression in the intact tumor tissue (three cases uPA, six cases PAI-1).

Correlation of ELISA results with uPA/PAI-1 expression (IHC) in the tumor stroma

Immunohistochemical stromal enzyme expression was correlated with ELISA results (Table 1). The number of cases with high ELISA analyte levels was higher for PAI-1 than for uPA (35 vs 20 cases).

In cases with positive uPA/PAI-1 immunostaining around the biopsy channel (BC) and in peripheral intact tumor (IT), ten out of 26 cases also demonstrated high ELISA levels for uPA and 13 out of 19 cases for PAI-1.

In the tumors that showed no expression around the BC but positive staining in intact tumor stroma, two out of three cases demonstrated high levels of uPA and two out of six cases high levels of PAI-1.

In the group of tumors with a positive immunoreaction around the BC, but not in intact tumor stroma, pathologically elevated ELISA levels were found in eight out of 21 cases for uPA and in 11 out of 16 cases for PAI-1.

All five tumors with negative stromal enzyme expression of uPA in both areas (BC and IT) also had a low ELISA result (Table 1).

There were five cases with extraordinary high ELISA levels for PAI-1 (>70–181 ng/mg protein). These tumors revealed positive stromal enzyme expression in the punch biopsy area, but only two of them were also positive in the periphery. Therefore, this group of tumors did not show a remarkably strong expression in immunohistochemistry corresponding to the high ELISA levels.

Temporal relationship between preoperative punch biopsy and expression of uPA and PAI-1 in the resection specimen

In the BC area, immunohistochemical expression levels in fibroblastic cells were independent of the period of time between punch biopsy and surgery. In contrast, expression in the intact distant tumor areas was weaker or absent if surgery was done 6 or more days after punch needle biopsy (Tables 2 and 3). In consequence, the number of tumors with positive expression in both areas was lower

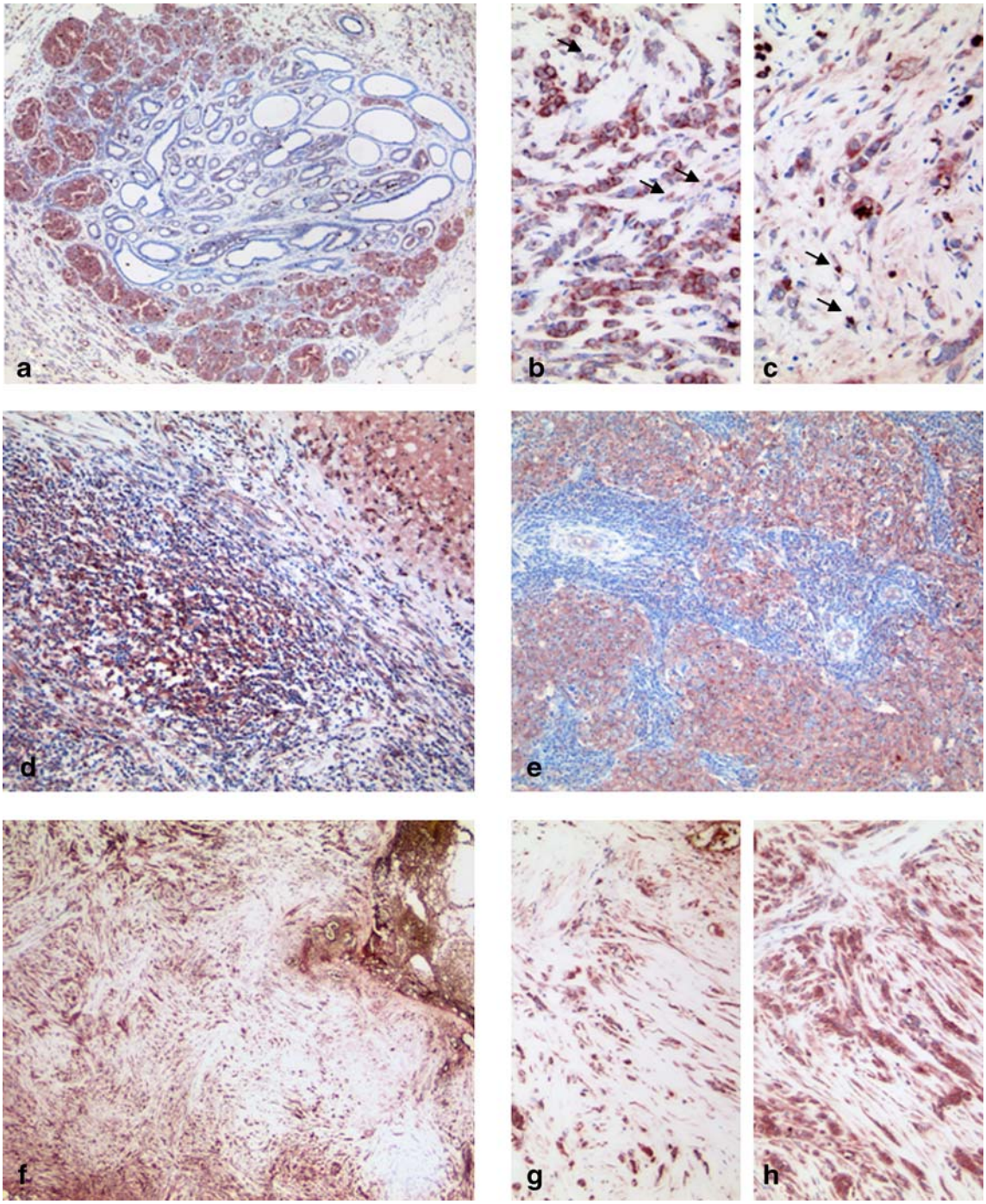


Fig. 1 **a**–**c** uPA/PAI-1 expression in a lobular invasive carcinoma. Faint staining of uPA in pre-existing non neoplastic ducts compared to strongly increased expression in the surrounding lobular in situ carcinoma (**a**). Strong staining of the invasive tumors cells as well as stromal cells (*arrows*, **b**). Weaker expression of PAI-1 by the stromal cells. PAI-1 positive macrophages (**c**, *arrows*). **d**, **e** High grade ductal invasive carcinoma with a dense lymphocytic infiltrate and numerous fibroblastic cells with strong expression of uPA closely related to the BC area (*right corner*, **d**). Decreased expression in fibroblasts of the intact distant tumor stroma compared to uPA positive tumor cells (**e**) Strong pre-existing stromal lymphocytic infiltrate. **f**–**h** Lobular invasive carcinoma with strong expression of uPA in the stromal cells in the BC area (**f**, **g**), but also in intact tumor areas (**h**)

after 9 days. This observation was most obvious for uPA and, to a lesser degree, for PAI-1. ELISA levels for uPA also decreased after 9 days, while they remained high for PAI-1.

In the five tumors with very high ELISA levels for PAI-1, the time between biopsy and surgery ranged from 1 to 9 days (two patients after 1 day, three patients after 6 days and later).

Table 1 Immunohistochemical expression of uPA and PAI-1 in the area surrounding the biopsy channel (BC) and intact tumor tissue (IT)

	uPA IHC		uPA ELISA high	PAI-1 IHC		PAI-1 ELISA high
Number of cases	55		20	55		35
BC						
Positive (+)	47		18	35		24
Negative (−)	8		2	20		11
IT		$p<0.001$			p 0.055	
Positive (+)	29		12	25		15
Negative (−)	26		8	30		20
BC+/IT+	26		10	19		13
BC−/IT−	5		0	14		9
BC+/IT−	21		8	16		11
BC−/IT+	3		2	6		2

Comparison with ELISA results.

Correlation of uPA and PAI-1 expression (IHC, ELISA) with tumor growth and prognostic factors

We could not establish a relationship between (immuno-) histological tumor features (histologic tumor typing, stromal reaction, stromal uPA/PAI-1 expression and inflammation) with tumor size, grading, nodal status and hormonal receptor status. This was also observed for uPA and PAI-1 ELISA results (data not shown).

Discussion

Diagnosis and therapy of breast cancer are under continual development. ELISA analyte levels of uPA and PAI-1 are supposed to be novel prognostic factors and selection criterions of adjuvant chemotherapy in axillary node-negative breast cancer patients [8, 9, 11]. Because uPA and PAI-1 ELISA results may have direct impact on the treatment modality, it should be carefully considered whether analyte levels may be influenced by other factors. One of these factors is taking of preoperative core biopsies for confirmation of the tumor diagnosis. Especially for PAI-1 a possible strong increase in ELISA enzyme levels is assumed after this iatrogenically induced tissue injury (see declaration of the manufacturer for ELISA kit, Femtelle®).

uPA and PAI-1 are involved in manifold extracellular processes. Both enzymes are not only expressed by the cancer cells themselves pointing to their function in cancer cell migration and invasion [1, 4]. They are also expressed by fibroblast-like stromal cells, macrophages, mastcells and endothelial cells [2, 4, 6, 12]. Secretion of matrix-degrading proteases, as well as their downstream activators such as

Table 2 Levels of uPA in relation to time interval between core biopsy and surgery

	N	1–5 days	6–8 days	>9 days
N		17	23	15
BC+	47	13	20	14
BC−	8	4	3	1
IT+	29	12	12	5
IT−	26	5	11	10
BC+/IT+	26	10	11	5
BC−/IT−	5	2	2	1
BC+/IT−	21	3	9	9
BC−/IT+	3	2	1	0
ELISA high	20	7	9	4

BC Tumor area surrounding the biopsy channel, *IT* intact tumor tissue

Table 3 Levels of PAI-1 in relation to time interval between core biopsy and surgery

	N	1–5 days	6–8 days	>9 days
N		17	23	15
BC+	35	10	14	11
BC−	20	7	9	4
IT+	25	8	13	4
IT−	30	9	10	11
BC+/IT+	19	7	8	4
BC−/IT−	14	6	4	4
BC+/IT−	16	3	6	7
BC−/IT+	6	1	5	0
ELISA high	35	10	13	12

BC Tumor area surrounding the biopsy channel, *IT* intact tumor tissue

uPA by fibroblasts of the tumor stroma underlines their critical role for tumor growth [3, 10, 13, 15].

In order to differentiate between these different tissue components, we used immunohistochemistry. According to the biological function of uPA/PAI-1 as outlined above, we found both enzymes constantly expressed in the carcinoma cells. In contrast to this, expression in the fibroblasts of the tumor stroma was more heterogeneous.

This tissue heterogeneity may be one reason for the discrepancy between immunohistochemistry and ELISA results in the present as well as in former studies [6]. In our cases, a correspondence was only seen in tumors lacking stromal uPA expression which also showed negative ELISA results. Another reason for the differences between IHC and ELISA may be the fact that both enzymes are present in the cytoplasm of the cells as well as in the extracellular space [1, 6]. In contrast to the semiquantitative data achieved by immunohistochemistry, ELISA gives objective quantitative data of protein levels in the tissue [19]. Therefore, both methods have their specific advantages but they are not directly comparable.

Referring to the immunohistochemical expression of uPA and PAI-1, a considerable number of tumors with increased fibroblastic enzyme expression in the tumor tissue surrounding the biopsy channel compared to distant tumor areas was seen. This difference was most remarkable in tumors with a pre-existing hypocellular stroma and absence of necrosis. This indicates that fibroblastic stromal reaction induced by tissue injury leads to increased levels of enzyme expression.

The time interval between biopsy and operation had an influence on stromal enzyme expression in tumor areas without a punch biopsy lesion. In these intact tumor areas, fibroblastic uPA and PAI-1 expression decreased 9 and more days after preoperative biopsy, while expression remained high in the area surrounding the biopsy channel. In most tumors with strong enzyme expression in both areas, surgery was done within 5 days after biopsy. This may be explained by uPA-dependent plasminogen activation which was found to be most intense in days 6–10 of wound healing [16]. Obviously, the peripheral tumor stroma is less affected by the inflammatory process as the level of fibroblastic uPA und PAI-1 expression is generally lower and decreases earlier.

These results were most evident for uPA immunohistochemistry. ELISA levels of uPA were also decreased 9 days after biopsy, similar to the immunohistochemical expression levels in the intact tumor stroma. PAI-1 ELISA was independent of the interval of time. These results indicate that the course of wound healing after preoperative biopsy may also influence enzyme levels in ELISA.

Therefore both the time and the point of specimen collection for ELISA in relation to the preoperative biopsy may influence levels of uPA and PAI-1 in the tumor tissue. Obviously, the distant, intact tumor tissue is less affected by the wound healing processes. For practical use, tissue samples for ELISA should not be taken from tumor areas with macroscopically discernible punch biopsy injury in order to avoid false positive results.

Conflict of interest statement We declare that we have no conflict of interest.

References

1. Andreasen PA, Egelund R, Petersen HH (2000) The plasminogen activation system in tumor growth, invasion, and metastasis. Cell Mol Life Sci 57(1):25–40
2. Andreasen PA, Kjoller L, Christensen L, Duffy MJ (1997) The urokinase-type plasminogen activator in cancer metastasis: a review. Int J Cancer 72:1–22
3. Camps JL, Chang SM, Hsu TC, Freeman MR, Hong SJ, Zhau HE, von Eschenbach AC, Chung LW (1990) Fibroblast mediated acceleration of human epithelial tumor growth in vivo. Proc Natl Acad Sci USA 87:75–79
4. Dublin E, Hanby A, Patel NK, Liebman R, Barnes D (2000) Immunohistochemical expression of uPA, uPAR, and PAI-1 in breast carcinoma. Am J Pathol 157:1219–1227
5. Duffy MJ, Reilly D, O'Sullivan C, O'Higgins N, Fennelly JJ, Andreasen P (1990) Urokinase-plasminogen activator, a new and independent prognostic marker in breast cancer. Cancer Res 50:6827–6829
6. Ferrier CM, de Witte HH, Straatman H, van Tienoven DH, van Geloof WL, Rietveld FJR, Sweep CGJ, Ruiteer DJ, van Muijen GNP (1999) Comparison of immunohistochemistry with immunoassay (ELISA) for the detection of components of the plasminogen activation system in human tumour tissue. Br J Cancer 79:1534–1541
7. Ganesh S, Sier CF, Griffioen G, Vloedgraven HJ, de Boer A, Welvaart K, de Velde CJ, van Krieken JH, Verheijen JH, Lamers CB (1994) Prognostic relevance of plasminogen activators and their inhibitors in colorectal cancer. Cancer Res 54:4065–4071
8. Harbeck N, Kates RE, Look MP, Meijer-van Gelder ME, Klijn JGM, Jänicke F, Krüger A, Kiechle M, Schmitt M, Foekens JA (2002) Enhanced benefit from adjuvant systemic chemotherapy in breast cancer patients classified high risk according to uPA and PAI-1 (n=3424). Cancer Res 62:4617–4622
9. Jänicke F, Prechtl A, Thomssen C, Harbeck N, Meisner C, Untch M, Sweep CG, Selbmann HK, Graeff H, Schmitt M, for the German Chemo N0 Study group (2001) Randomized adjuvant chemotherapy trial in high-risk lymph node-negative breast cancer patients identified by urokinase-type plasminogen activator and plasminogen activator inhibitor type I. J Natl Cancer Inst 93:913–920
10. Lee AHS, Gillett CE, Ryder K, Fentiman IS, Miles DW, Millis RR (2006) Different patterns of inflammation and prognosis in invasive carcinoma of the breast. Histopathology 48:692–701
11. Liotta LA, Kohn EC (2001) The microenvironment of the tumour–host interface. Nature 411:375–379
12. Look MP, van Putten WLJ, Duffy MJ, Harbeck N, Christensen IJ, Thomssen C, Kates R, Spyratos F, Fernö M, Eppenberger- Castori S, Sweep CGJ, Ulm K, Peyrat JP, Martin PM, Magdelenat H, Brünner N, Duggan C, Lisboa BW, Bendahl PO, Quillien V, Daver A, Ricolleau G, Meijer-van Gelder ME, Mander P, fiets E, Blankenstein MA, Broet P, Romain S, Daxenbichler G,

Windbichler G, Cufer T, Borstnar S, Kueng W, Beex LVAM, Klijn JGM, O'Higgins NO, Eppenberger U, Jänicke F, Schmitt M, Foekens JA (2002) Pooled analysis of prognostic impact of urokinase-type plasminogen activator and its inhibitor PAI-1 in 8377 breast cancer patients. J Natl Cancer Institute 94:116–128

13. Nielsen BS, Sehested M, Suun S, Rank F, Timshel S, Rygaard J, Johnsen M, Dano K (2001) Urokinase plasminogen activator is localized in stromal cells in ductal breast cancer. Lab Invest 81:1485–1501
14. Olumi AF, Dazin P, Tlsty TD (1998) A novel coculture technique demonstrates that normal human prostatic fibroblasts contribute to tumor formation of LNCaP cells by retarding cell death. Cancer Res 58:4525–4530
15. Pappot H, Gardsvoll H, Romer J, Pedersen AN, Grondahl-Hansen J, Pyke C, Brunner N (1995) Plasminogen activator inhibitor type 1 in cancer: therapeutic and prognostic implications. Biol Chem Hoppe Seyler 376(5):259–267
16. Pyke C, Ralfkiaer E, Tryggvason K, Dano K (1993) Messenger RNA for two type IV collagenases is located in stromal cells in human colon cancer. Am J Pathol 142:359–365
17. Schäfer BM, Maier K, Eickhoff U, Todd RF, Kramer MD (1994) Plasminogen activation in healing human wounds. Am J Pathology 144:1269–1280
18. Schmitt M, Janicke F, Moniwa N, Chucholowski N, Pache L, Graeff H (1992) Tumor-associated urokinase-type plasminogen activator: biological and clinical significance. Biol Chem Hoppe Seyler 373(7):611–22
19. Sweep CGJ, Geurts-Moespot J, Grebenschikov N, de Witte JH, Heuvel JJTM, Schmitt M, Duffy MJ, Jänicke F, Kramer MD, Foekens JA, Brünner N, Brugal G, Pedersen AN, Benraad TJ (1998) External quality assessment of trans-European multicentre antigen determinations (ELISA) of urokinase-type plasminogen activator (uPA) and its type-1 inhibitor (PI-1) in human breast cancer tissue extracts. Br J Cancer 78:1434–1441

Virchows Arch (2008) 452:285–293
DOI 10.1007/s00428-007-0564-7

ORIGINAL ARTICLE

Renal oncocytoma with and without intravascular extension into the branches of renal vein have the same morphological, immunohistochemical and genetic features

Ondrej Hes · Michal Michal · Radek Šíma · Tomáš Vaněček · Matteo Brunelli · Guido Martignoni · Naoto Kuroda · Isabel Alvarado Cabrero · Delia Perez-Montiel · Milan Hora · Tomáš Ürge · Miroslav Dvořák · Marie Jarošová · Ximing Yang

Received: 21 August 2007 / Revised: 16 October 2007 / Accepted: 23 October 2007 / Published online: 15 January 2008
© Springer-Verlag 2007

Abstract We attempted to investigate the clinicopathological correlation of renal oncocytoma (RO) with renal vein extension. We identified seven ROs with extension into the branches of renal vein. The age of seven patients ranged from 61 to 82 years. Five cases were identified; incidentally, two patients had gross hematuria. After surgery, all patients were alive and free of tumors with follow-up of 1 to 5 years (mean=3.6). Oncocytomas measured from 2.2 to 7.5 cm. Renal vein extension was grossly suspected in 5/7 cases and histologically confirmed in all seven cases. Tumor cells were positive for cytokeratins, mitochondrial antigen, epithelial membrane antigen, and parvalbumin; 5/7 tumors were focally positive for cluster of differentiation 117. Ultrastructurally, the cytoplasm was packed by mitochondria. Molecular genetic analysis did not detect abnormal numbers of chromosomes 1, 2, 6, 7, 10, 17, and XY by fluorescence in situ hybridization, loss of heterozygosity on 3p, and mutation of Von Hippel–Lindau gene in all cases. Array comparative genomic hybridization analysis of two cases did not show any major genetic changes. Conclusions are: (1) renal oncocytomas may have intravascular extension to the branches of the renal vein; (2) renal oncocytomas with intravascular extension to the branches of the renal vein have the same morphological, immunohistochemical, and cytoge-

O. Hes · M. Michal · R. Šíma · T. Vaněček
Department of Pathology, Charles University Hospital,
Pilsen, Czech Republic

M. Brunelli · G. Martignoni
Department of Pathology, Verona University,
Verona, Italy

N. Kuroda
Department of Pathology, Red Cross Hospital Kochi,
Kochi, Japan

I. A. Cabrero
Department of Pathology, Centro Medico,
Mexico City, Mexico

D. Perez-Montiel
Department of Pathology, Institute Nacional de Cancerología,
Mexico City, Mexico

M. Hora · T. Ürge
Department of Urology, Charles University Hospital,
Pilsen, Czech Republic

M. Dvořák
Department of Forensic Medicine, Charles University,
Pilsen, Czech Republic

M. Jarošová
Department of Hematooncology, University Hospital,
Olomouc, Czech Republic

X. Yang
Department of Pathology, Northwestern University
Feinberg School of Medicine,
Chicago, IL, USA

O. Hes (✉)
Sikl's Department of Pathology, Laboratore Spec. Diagnostiky
Medical Faculty and University Hospital,
Alej Svobody 80,
323 18 Pilsen, Czech Republic
e-mail: hes@medima.cz

netic findings as have their counterparts without evidence of intravascular invasion; (3) the absence of metastases suggests an overall benign behavior of this tumor, but this has to be substantiated by further studies with a long-term follow-up; (4) in a renal tumor with granular cytoplasm showing renal vein extension, it is necessary to carefully exclude renal cell carcinomas (RCC) such as chromophobe RCC, oncocytic variant of papillary RCC, and granular variant of clear cell RCC.

Keywords Kidney · Renal oncocytoma · Intravascular · Intravenous extension · Molecular biology

Introduction

Renal oncocytoma (RO) is currently considered within the spectrum of benign tumors of the kidney [1, 10, 14, 18, 22]. Almost all cases originally described as "malignant" were subsequently reclassified as renal cell carcinomas [13]. There is a single case of authentic RO with aggressive behavior in the English literature [18]. For many years, we have been aware of an interesting feature that can be seen in an otherwise perfectly benign RO and that simulates a malignant behavior, namely the extension of the tumor to branches of the renal vein. Here we present morphological, ultrastructural, and molecular cytogenetical study of seven such cases.

Materials and methods

The seven cases of RO with protrusion into the renal vein were found among 324 cases of RO in the archives of the authors. The diagnosis of intravital vascular extension was accepted only in cases with cluster of differentiation (CD) 34, CD31, or factor VIII positivity of the surface of the intravenous tumor. Histological sections of formalin-fixed, paraffin-embedded tissue were stained with hematoxylin and eosin and Hale colloidal iron stain. Immunohistochemical studies were performed on paraffin-embedded tissues. Primary antibodies to the following antigens were employed: cytokeratins (CK; CAM5.2, at 1:50, Becton-Dickinson, San Jose, CA, USA; AE1-AE3, at 1:500, Boehringer, Mannheim, Germany; CK7, at 1:200, DAKO), epithelial membrane antigen (EMA) (E29, at 1:1000, DAKO, Glostrup, Denmark), Ki-67 (MIB1, at 1:200, DAKO), mitochondrial antigen (MIA; 113–1, at 1:500, DAKO), parvalbumin (parv-19, 1:1000, Sigma, Steinheim, Germany), CD117 (polyclonal, at 1:150, DAKO), Melan A (A 103, at 1:100, DAKO), human melanoma black (HMB) 45 (HMB45, at 1:300, DAKO), S100 protein (S1/61/69, at 1:50, Novocastra, Newcastle, UK), TFE3 (polyclonal, at 1:500, Santa Cruz, Santa Cruz, CA, USA), CD34 (at 1:800, NeoMarkers, Fremont, CA, USA), CD31 (JC70A, at 1:50, DAKO) and factor VIII (F8/86, at 1:4000, DAKO). The primary antibodies were visualized using the supersensitive streptavidin–biotin–peroxidase complex (BioGenex, San Ramon, CA, USA). Small pieces of the formaldehyde-fixed wet tissue of three cases (cases 1, 2, 4) were postfixed in glutaraldehyde and routinely processed for electron microscopy.

Analysis of the VHL gene mutation and 3p LOH

Five 10-μm-thick sections of tumor and normal tissue were cut from the formalin-fixed paraffin-embedded blocks and DNA was extracted by the NucleoSpin Tissue Kit (Macherey Nagel, Duren, Germany) according to manufacturer's protocol. Polymerase chain reaction (PCR) for Von Hippel–Lindau (VHL) gene analysis was carried out using primers listed in Table 1. PCR for loss of heterozygosity (LOH) analysis of chromosome 3p was performed using short tandem repeat (STR) markers and primers shown in Table 2. The reaction conditions were as follows: 12.5 μl of HotStart Taq PCR Master Mix (QIAgen, Hilden, Germany), 10 pmol of each primer, 100 ng of template DNA and distilled water up to 25 μl. Amplification program for all fragments, except the marker D3S666, consisted of denaturation at 95°C for 15 min, then 40 cycles of denaturation at 95°C for 1 min, annealing at 55°C for 1 min, and extension at 72°C for 1 min. The program was finished by 72°C incubation for 7 min. Annealing temperature for fragment D3S666 was 58°C.

Successfully amplified PCR products of the VHL gene were purified with a Montage PCR Centrifugal Filter Devices (Millipore, Billerica, MA, USA) and sequenced using a Big Dye Terminator Sequencing kit (PE/Applied Biosystems, Foster City, CA, USA). Samples were then run

Table 1 Primers used in PCR analysis of VHL gene

Exon	Name	Sequence 5′ → 3′
Exon 1	VHL e1-1	CGCGAAGACTACGGAGGT
	VHL e1-2	GTCTTCTTCAGGGCCGTA
	VHL e1-3	GAGGCAGGCGTCGAAGAG
	VHL e1-4	GCGATTGCAGAAGATGACCT
	VHL e1-5	GCCGAGGAGGAGATGGAG
	VHL e1-6	CCCGTACCTCGGTAGCTGT
	VHL e1-7	CCGTATGGCTCAACTTCGAC
	VHL e1-8	GCTTCAGACCGTGCTATCGT
Exon 2	VHL e2-1	ACCGGTGTGGCTCTTTAACA
	VHL e2-2	TCCTGTACTTACCACAACAACCTT
Exon 3	VHL e3-1	GCAAAGCCTCTTGTTCGTTC
	VHL e3-2	ACATTTGGGTGGTCTTCCAG
	VHL e3-3	CAGGAGACTGGACATCGTCA
	VHL e3-4C	CCATCAAAAGCTGAGATGAAAC

Table 2 Analysis of chromosome 7, 17, X and Y copy number by FISH

Marker	Name	Sequence 5′ → 3′
D3S1768	D3S1768SF	GGTTGCTGCCAAAGATTAGA
	D3S1768A	CACTGTGATTTGCTGTTGGA
D3S1300	D3S1300SF	AGCTCACATTCTAGTCAGCCT
	D3S1300A	GCCAATTCCCCAGATG
D3S1317	D3S1317-1.1	TACAAGTTCAGTGGAGAACC
	D3S1317-1.2	CCTCCAGGCCATACACAGTCA
D3S666	D3S666-SK#15	CAAGGCATTAAAGTGGCCACGC
	D3S666-SK#16	GTTTGAACCAGTTTCCTACTGAG

on an automated sequencer Applied Biosystems Inc. (ABI) Prism 310 (PE/Applied Biosystems) at a constant voltage of 11.3 kV for 20 min.

Successfully amplified PCR products of STR markers were mixed with size marker and run on an automated sequencer ABI Prism 310 (PE/Applied Biosystems) at a constant voltage of 15 kV for 28 min.

Fluorescence in situ hybridization

Fluorescence in situ hybridization (FISH) analysis was performed independently at two institutions. Analysis of chromosomes 7, 17, and XY was performed at the Charles University Hospital (Czech Republic). Analysis of chromosomes 1, 2, 6, 10, and 17 was performed at the Verona University (Italy).

FISH on chromosomes 7, 17, and XY

From each tumor, 5-μm sections were cut from paraffin-embedded blocks and placed on the slides. Tissues were deparaffinized in xylene three times for 5 min and then washed twice in 100% ethanol, once in 95% ethanol, and once in deionized water for 5 min. Then, the slides were heated in the Target Retrieval Solution (DAKO) for 40 min at 95°C and subsequently cooled at room temperature (RT) for 20 min in the Target Retrieval Solution. The slides were washed in deionized water for 5 min at RT and tissue were covered with 150 μl (or enough to cover the specimen) of the Proteinase K (DAKO) solution for 4–7 min. Then, the slides were rinsed several times over 5 min with deionized water, dehydrated in 95% and 100% ethanol for 1 min each, and air dried. Afterwards, the probe mixtures consisted of 7 μL large-scale integration hybridization buffer, 1-μL chromosome enumeration probe and 2-μL purified H_2O in case of chromosome 7 and 17, or prepared XY probe mix (Vysis, Downers Grove, IL, USA) were applied on the samples and covered with coverslips. The slides were denatured at 85°C for 10 min and incubated in humidified box at 37°C overnight. Then, the coverslips were carefully removed and the slides were washed for 2 min in 0.4× standard saline citrate (SSC)/0.3% NP-40 at 73°C and for 1 min in 2× SSC/0.1% NP-40 at RT. After that, the slides were placed in a dark room until completely dry, counterstained with 4′,6-diamidino-2-phenylindole (DAPI) II (Vysis), and viewed under a fluorescence microscope Olympus BX 60.

The criteria for evaluating the FISH signals were the same as in the paper of Hes et al. [9].

FISH on chromosomes 1, 2, 6, 10, and 17

Interphase cytogenetic FISH analysis was performed using centromeric probes (SpectrumGreen for chromosomes 6, 10, and 17 and SpectrumOrange for chromosomes 1 and 2 (Vysis)). Paraffin was removed from the sections with two 10-min washes in xylene. After hydrating in 100%, 85%, and 70% ethanol solutions (10 min each), rinsing in distilled water (10 min) and twice in phosphate buffer solution (pH 7, 10 min each), the slides were fixed in methanol–acetic acid 3:1 for 10 min and air dried. Next, the sections were treated with a 2× SSC solution for 15 min at 37°C, then dehydrated in consecutive 70%, 85%, and 100% ethanol solutions for 1 min each, and then dried. Next, the sections were incubated in 0.1-mM citric acid (pH 6) solution at 85°C for 1 h. Then they were again dehydrated in a series of ethanol solutions and dried. The tissue was digested by applying 0.75 ml of pepsin (Sigma, St. Louis, MO, USA) solution (4 mg/ml in 0.9% NaCl, pH 1.5) to each slide and incubating them in a humidified box for 30 min at 37°C. Afterwards, the slides were rinsed with distilled water for few seconds, dehydrated again in graded ethanol solutions, and dried. Each probe was diluted 1:100 in tDenHyb1 buffer (Insitus, Albuquerque, NM, USA). Ten microliters of the diluted probe were applied to each slide and coverslips were placed over the slides. Denaturation was achieved by incubating the slides at 80°C for 10 min in a humidified box; then hybridization was performed at 37°C for 3 h. The coverslips were then removed and the slides were immersed at the room temperature in 0.5× SSC for 2 min, in 50% formamide/1× SSC for 5 min, and in 2× SSC for 2 min. The slides were air dried and counterstained with 10 μl DAPI/Antifade (DAPI in Fluorguard, 0.5 μg/ml, Insitus, Albuquerque, NM).

The slides were examined using an Axioplan microscope (Zeiss, Germany) with appropriate filters for SpectrumOrange, SpectrumGreen, and DAPI nuclear counterstain. The signals were recorded with a charge-coupled device camera (Axiocam HRm).

FISH signals were evaluated as previously described; 100–200 neoplastic nuclei were counted. The criteria for loss of chromosome were described previously [3].

Array CGH

Array comparative genomic hybridization (CGH) analysis was performed using the GenoSensor Array 300 system, following the manufacturer's instructions (Vysis). Each array contains 287 target clone DNA (P1, PAC, or BAC clones) representing loci previously shown to be commonly altered in human cancers or to be involved in congenital syndromes and telomeres. The clones are printed in triplicate and the average resolution of the array is 10 Mb. Briefly, 100 ng of genomic DNA were labeled by a random primer reaction. Tumor DNA was labeled with Cy3 and the normal reference DNA with Cy5. The hybridization mixture consisted of 2.5 μl of each of the differentially labeled DNAs and 25 μl of hybridization buffer containing human Cot-1 DNA. This mixture was denatured at 80°C for 10 min and this probe was applied onto the spotted area of the array under a coverslip and hybridized in a humid chamber containing 50% formamide/2× SSC at 37°C for 72 h. After hybridization, the arrays were washed 3× in 50% formamide/2× SSC at 45°C for 10 min, followed by four 5-min washes in 1× SSC at room temperature and a brief rinse in distilled water. Finally, the slides were counterstained with DAPI IV solution (Vysis). Each hybridized slide was captured using Genosensor 300 microarray scanner (Vysis Abbott Molecular). Since each spot in the array is present in triplicates, the median of the three spots of each probe in the array was calculated. Through the use of the default settings of the GenoSensor, the clones were accepted only if the coefficient of variation between the triplicate spots was less than 10 and if the average correlation coefficient was ≥0.9. The normalized ratio for each target was calculated relative to the modal DNA copy number, and the statistical significance of each change was reported as *p*-value [19]. A *p*-value of <0.01 indicated the significant difference between the copy numbers of targets and the modal clones. A fluorescence ratio of >1.25 (log2=0.32) was considered as DNA gains, while DNA losses were scored when the ratio was <0.75 (log2=−0.41).

Results

From 324 RO in our registry, we identified seven RO with extension into the branches of renal vein. The essential clinicopathological data are summarized in Table 3. The patients were two women and five men, with ages ranging from 61 to 82 years (mean 72.9 years). Whereas in five patients the renal tumors were found incidentally (as for example in Case 2 in whom the kidney neoplasm was identified during a staging procedure for glioblastoma of the right temporal lobe), two patients presented with hematuria. All but one patient were treated by nephrectomy; only one patient (case 6) underwent artificial embolization of blood supply of the tumor and subsequent nephrectomy. Neither adjuvant chemotherapy nor actinotherapy was administered. The clinical follow-up ranged from 1 to 5 years (mean 3.6 years); all patients are currently well, without signs of recurrences and metastases. Patient no. 1 underwent irradiation of the prostate because of a prostatic adenocarcinoma (prostate-specific antigen serum level 14 ng/ml, Gleason grade 6 from needle biopsy) 4 years after the nephrectomy for RO and at the last checkup there were no signs of generalization of prostatic or renal neoplasia.

Grossly, the tumors were confined to the kidney. Extension into the vascular structures was grossly suspected in five cases (Fig. 1). In all cases, the tumor was bulging into the renal sinus. On cut section, the tumors were dark tan to brown in color. Central fibrous scar was noted in three cases. The tumors ranged in the largest diameter from 2.2 to 7.5 cm (mean 4.97 cm). A small papillary adenoma (diameter 0.3 cm) was incidentally found in the same kidney of patient no. 7.

Microscopically, the tumors were composed of large eosinophilic cells with granular cytoplasm. Nuclei were usually oval, with only focal slight polymorphism. Mitotic activity was absent. The tumor cells were mainly arranged in a solid-alveolar pattern, and only rarely were small tubular structures present (Fig. 2a,b). Areas of hyaline scars were documented in three cases. No morphological differ-

Table 3 Main clinicopathological features

	Sex/age	Side	Diameter	Localization	Grossly suspect extension	Follow up
Case 1	M/69	Right	7.5 cm	Pole and hilus	Yes	5 years AW
Case 2	F/61	Left	4.6 cm	Hilus	Yes	1 year AW
Case 3	M/77	Right	7.5 cm	Hilus	Yes	2 years AW
Case 4	M/75	Left	5.5 cm	Pole and hilus	No	4 years AW
Case 5	F/82	Right	5 cm	Central part	Yes	4 years AW
Case 6	M/78	Left	5.5 cm	Hilus	No	4 years AW
Case 7	M/68	Left	2.2 cm	Pole and hilus	Yes	4 years AW

F Female, *M* male, *AW* alive and well

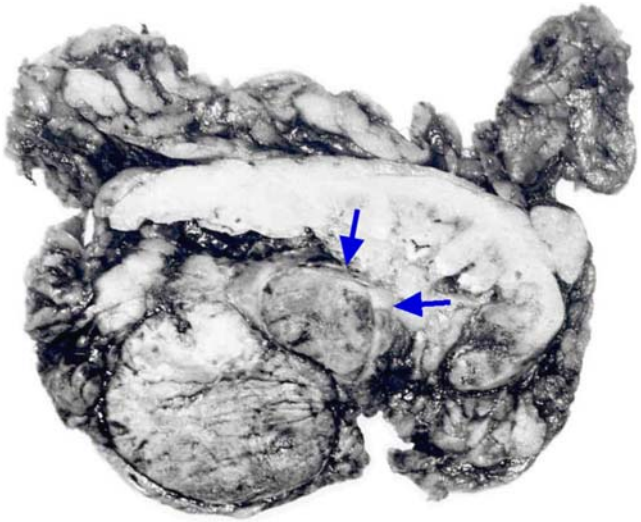


Fig. 1 Renal oncocytoma extending into the dilated vein (*blue arrows*)

ences were noted in the intravascular component of the tumors localized within the renal vein and the main tumorous mass. In no case did we find cytologic features typical of chromophobe renal cell carcinomas (CRCC). All intravenous structures were covered by a single layer of endothelial cells. All cases were Hale colloidal iron stain negative.

Results of immunohistochemical findings are summarized in Table 4. All cases were CAM5.2, EMA, and MIA positive in the epithelial component. Also, all but one case were AE1–AE3 positive. Six of the seven cases manifested positive reaction for CK7, including two cases which were a focal staining for this marker and four cases in which only single cells were labeled with CK7. CD117 was focally positive in five out of the seven cases. The surface endothelial layer of intravascular tumors was positive with antibodies to factor VIII, CD31, and CD34 in all seven cases (Fig. 3a,b). The proliferating index (Ki-67) was very low in all cases, with less than 1% of the nuclei labeled. All cases were negative for transcription factor binding to immunoglobulin heavy constant mu enhancer 3, HMB45, Melan A, and S100 protein.

Ultrastructural examination was performed in three cases. Nuclei were oval in shape with small nucleoli. The cytoplasm of tumorous cells was packed with predominantly lamellar mitochondria. Occasionally, small intracytoplasmic lumina covered by short microvilli were present. The luminal aspect of the oncocytic cells was covered by microvilli as well.

The results of molecular biology findings are shown in Table 5. No mutation of the VHL gene was found in all cases. Likewise, no LOH was observed in all successfully analyzed samples. Analysis of chromosome 1, 2, 6, 7, 10, 17, X, and Y copy number did not show any abnormalities.

The results of array CGH performed on patients no. 2 (Fig. 4a,b) and 3 are shown (Fig. 4c,d).

The CGH analysis of these two cases did not reveal any major chromosomal changes. Overall, four clones display losses, while one clone revealed gain with a 0.001–0.0001 probability.

Discussion

Almost all "malignant" RO published in the older literature are currently thought to represent one of the following "carcinomas of the kidney with granular cytoplasm": chromophobe renal cell carcinomas, granular variant of clear renal cell carcinomas, collecting duct carcinoma of the kidney, or papillary renal cell carcinoma [1, 2].

Vascular invasion is an important factor in the disease prognosis. In cases of renal cell carcinoma, gross evidence of vascular invasion allowed the authors to designate the tumors as stage III [8, 17]. The situation is probably different with RO. Davis et al. [6] reported vascular invasion in nine cases (5.4%) from 166 RO patients, and

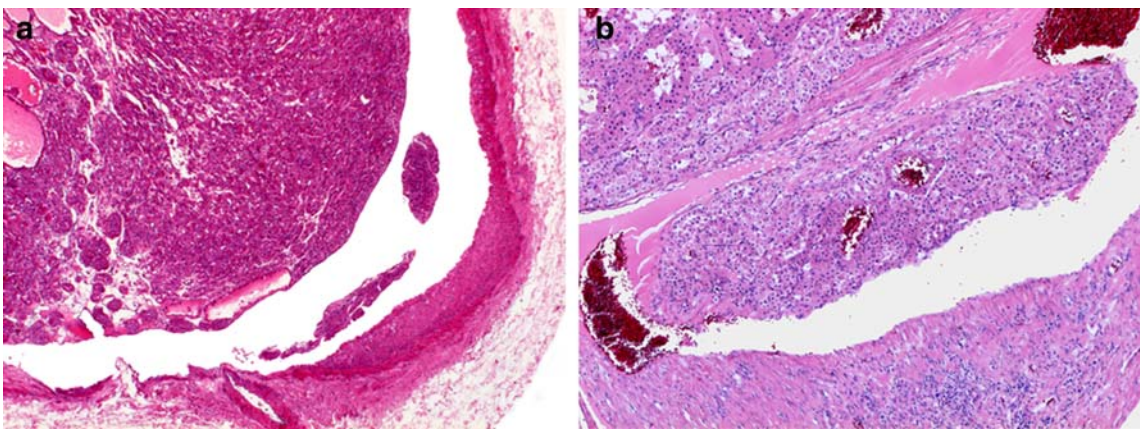


Fig. 2 **a** and **b** Renal oncocytoma within an obvious sinus vein

Table 4 Immunohistochemical results

	AE1–AE3	CAM5.2	CK 7	EMA	TFE3	MIA	CD 117	HMB45	Melan A	Parvalbumin	S100	Ki-67
Case 1	++	++	–	+++	–	+++	foc++	–	–	+	–	0–2/hpf
Case 2	+	++	foc++	++	–	+++	foc++	–	–	–	–	0/hpf
Case 3	+	+++	single cells	+	–	+++	–	–	–	+	–	0–1/hpf
Case 4	+	+++	single cells	+++	–	+++	–	–	–	++	–	0–2/hpf
Case 5	+++	++	foc++	+	–	+++	foc++	–	–	–	–	0–1/hpf
Case 6	+	+	single cells	+++	–	+++	foc++	–	–	–	–	0–1/hpf
Case 7	+	+	single cells	++	–	+++	foc+	–	–	+	–	0–1/hpf

AE1–AE3 Cytokeratin, *CAM5.2* cytokeratin, *CK 7* cytokeratin, *EMA* epithelial membrane antigen, *MIA* antimitochondrial antigen, *foc* focally positive

this feature had apparently no influence on their clinical behavior. Lieber et al. [13] identified three cases of RO with angioinvasion but without further progression of the disease in their disputable paper.

Another case was described by Psihramis et al. [20]. The patient had bilateral RO with unilateral invasion of the renal vein and perinephric fat. The diagnosis of RO was supported by genetic analysis in which a loss of chromosomes 1 and Y (−1,−Y) was detected. Unfortunately, no follow-up of the patient was provided.

Perez-Ordonez et al. [18] suggested that the presence of vascular invasion portend a more aggressive clinical behavior. One of their patients had a biopsy-proven liver metastasis and the second individual developed liver and bone metastases. The authors had only a core biopsy of the metastasis of the former patient, while there were no biopsies or autopsy findings in the second patient in their series who eventually died with a disseminated disease. It seems that the above-mentioned case with the stable liver metastasis could be accepted as metastasing renal RO from all the papers published in the English language literature.

No signs of aggressive biological behavior were noted in our patients, but, admittedly, the follow-up period of our patients is not long (mean 3.8 years). We agree with the conclusions of Davis et al. [6] who assumed that angioinvasion has no connotation with a worse prognosis.

One possible explanation of vascular involvement seems to be mechanical abruption of the wall of the renal vein. Four tumors in our series were localized in the central region of the kidney, and the remaining three neoplasms were situated in the renal pole with the extension into the region of the hilus. All tumors grossly compressed vascular structures, and in five patients the vascular extension was grossly visible.

The intrarenal veins are unique in that they have extremely thin walls. They have a wall structure that is very similar to or fundamentally the same as that of renal capillaries. Moreover, they appear to have no intrinsic shape attributable to their own wall structure but instead fill irregular spaces between tubules [12]. It could be one of the reasons why tumorous mass can relatively easily bulge into the intravascular space. To do so, it is not necessary for a tumor to be located exactly within the hilar region; expansion into the renal vein can occur from a more remote location in the kidney parenchyma.

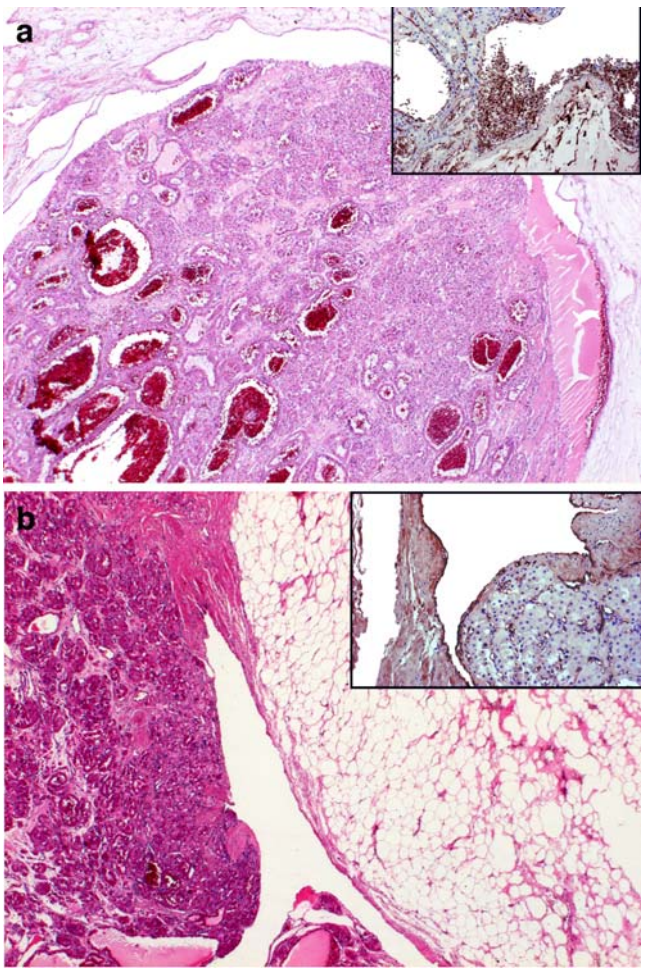


Fig. 3 **a** and **b** Renal oncocytoma within the sinus vein. The surface endothelial layer of intravascular tumors reacts positively with antibodies to factor VIII, CD31 and CD34 in all seven cases (*insets*)

Table 5 Molecular biology

	LOH				FISH							MA
	d3 s666	d3 s1300	d3 s1768	d3 s1317	1	2	6	7	10	17	XY	VHL
Case 1	NI	na	na	na	D	D	D	na	D	na	na	WT
Case 2	–	–	–	NI	D	D	D	D	D	D	XX	WT
Case 3	NI	NI	–	–	D	D	D	D	D	na	XY	WT
Case 4	NI	na	na	–	D	D	D	D	D	D	XY	WT
Case 5	NI	–	NI	–	D	D	D	D	D	D	XX	WT
Case 6	–	–	–	NI	D	D	D	D	D	D	XY	WT
Case 7	–	–	NI	–	D	D	D	D	D	D	XY	WT

LOH Loss of heterozygosity, *FISH* fluorescence in situ hybridization, *MA* mutation analysis, *na* not analyzable, *NI* non-informative, *D* disomy, *WT* wild type

A similar situation exists in renal angiomyolipoma. Renal angiomyolipoma also rarely invades the venous structures in the hilus, or extends into the vena cava inferior [5, 7]. An extension into the right atrium has also been reported [21], with a possible misdiagnosis of malignant angiomyolipoma in such cases [4]. The analysis of the seven presented cases of RO shows that angioinvasion or renal vein extension seems to have no prognostic

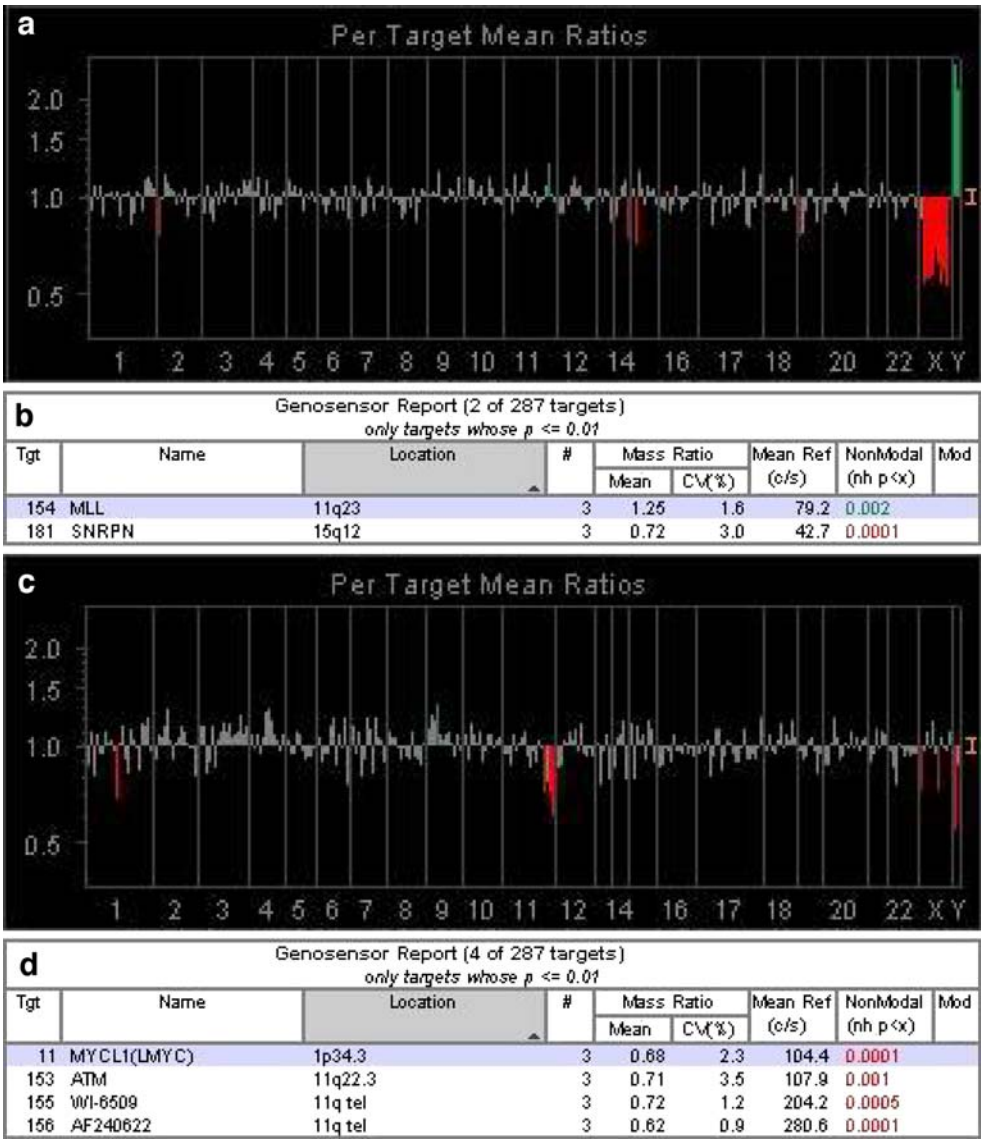


Fig. 4 a–d: Results of array CGH in cases No. 2 and No. 3 showing target report tables and target main ration plot. The plot displays the target ration in a genomically ordered bar chart with significant gain colored *green* and significant loss colored in *red*. Modified target report table tabulates statistics for each of spots considering to be changed

significance whatsoever. Nonetheless, the differential diagnostic considerations of RO with intravenous extension are very important and include three relatively common entities. The first one is chromophobe renal cell carcinoma (CRCC), namely the eosinophilic type, which can be easily misdiagnosed as RO. In chromophobe renal cell carcinoma, the presence of raisinoid nuclei, which are absent in RO, is a very important differential diagnostic feature. Moreover, it is possible to find perinuclear clearing in chromophobe renal cell carcinoma, a feature not encountered in RO. Hale colloidal iron stain positivity could assist in the differential diagnosis between RO and CRCC, but the intensity and the quality of staining are dependent on the type of fixation. Unfortunately, both RO and CRCC have no specific genetic changes that would allow one to make diagnosis by molecular biology only [23]. However, the hallmark of chromophobe renal cell carcinoma is multiple chromosomal losses involving chromosomes 1, 2, 6, 10, and 17 [3]. The results of CGH analysis of our two cases did not reveal any major chromosomal changes which could raise a suspicion for a chromophobe renal cell carcinoma.

Moreover, FISH did not detect abnormal numbers of chromosomes 1, 2, 6, 10, and 17.

Another very similar entity to RO is recently described papillary renal cell carcinoma, oncocytic variant. This type of carcinoma is composed of typical oncocytic cells arranged in a solid–papillary pattern. All published tumors contained papillary areas, which can be very limited. In well-sampled cases, it is possible to detect such a pattern. Molecular genetic findings can assist in the differential diagnosis because of the presence of trisomy of chromosomes 7 and 17 altogether with the loss of Y chromosome in male patients. These changes never occur in RO [9, 11].

The last common tumor which should be taken into the consideration in the differential diagnosis is the granular variant of clear cell RCC. This tumor can be distinguished from RO by nuclear polymorphism and by the absence of diffuse MIA cytoplasmic positivity. Moreover, nearly 50% of clear RCC carry the VHL gene mutation. Another common finding is deletion of chromosome 3p [8]. We were not able to detect such changes in our cases.

Two very rare tumorous entities should be taken into the consideration. The first one is so-called oncocytoma-like angiomyolipoma. This tumor could be easily excluded by HMB45 immunoreaction, which is always negative in RO, like in our cases [15]. The second entity is a rare, so-called oncocytoid renal cell carcinoma occurring after neuroblastoma [16]. No patient in our series had a history of neuroblastoma. The tumors in our series were arranged in a solid-alveolar pattern, occasionally with small tubular formations. No papillary component was detected.

In summary: (1) renal oncocytomas may have intravascular extension into the branches of the renal vein; (2) renal oncocytomas with intravascular extension to the branches of the renal vein have morphological, immunohistochemical, and cytogenetic findings identical to those seen in renal oncocytomas without evidence of intravascular invasion; (3) the absence of metastases suggest an overall benign behavior of these tumors; however, as the follow-up period in our series is relatively short, further studies are needed to prove this statement; (4) in a renal tumor with granular cytoplasm showing renal vein extension, it is necessary to carefully exclude renal cell carcinomas such as CRCC, oncocytic variant of papillary RCC, and granular variant of clear cell RCC.

References

1. Amin MB, Crotty TB, Tickoo SK, Farrow GM (1997) Renal oncocytoma: a reappraisal of morphologic features with clinicopathologic findings in 80 cases. Am J Surg Pathol 21:1–12
2. Amin MB, Amin MB, Tamboli P, Javidan J, Stricker H, de Peralta-Venturina M, Deshpande A, Menon M (2002) Prognostic impact of histologic subtyping of adult renal epithelial neoplasms. Am J Surg Pathol 26:281–291
3. Brunelli M, Eble JN, Zhang S, Martignoni G, Delahunt B, Cheng L (2005) Eosinophilic and classic chromophobe renal cell carcinomas have similar frequent losses of multiple chromosomes from among chromosomes 1, 2, 6, 10, and 17, and this pattern of genetic abnormality is not present in renal oncocytoma. Mod Pathol 18:161–169
4. Byrne DJ, Hamilton Steward PA, Lowe JW (1988) Malignant angiomyolipoma of the kidney associated with hypercalcemia. Br J Urol 62:89–90
5. Chen SS, Lin AT, Chen KK, Chang LS, Chang KK, Chiang H (1996) Renal angiomyolipoma with extension into renal vein. Br J Urol 77:927–928
6. Davis CJ, Sesterhenn IA, Mostofi FK, Ho CK (1991) Renal oncocytoma: clinicopathological study of 166 patients. J Urogenital Pathol 1:41–52
7. Eble JN (1998) Angiomyolipoma of kidney. Sem Diagn Pathol 15:21–40
8. Eble JN, Sauter G, Epstein JI, Sesterhenn IA (2004) Tumours of the urinary system and male genital organs. Pathology and genetics. IARC, Lyon
9. Hes O, Brunelli M, Michal M, Cossu Rocca P, Hora M, Chilosi M, Mina M, Boudová L, Menestrina F, Martignoni G (2006) Oncocytic papillary renal cell carcinoma: a clinicopathologic, immunohistochemical, ultrastructural, and interphase cytogenetic study of 12 cases. Ann Diagn Pathol 10:133–139
10. Kovacs G, Akhtar M, Beckwith BJ, Bugert P, Cooper CS, Delahunt B, Eble JN, Fleming S, Ljungberg B, Medeiros LJ, Moch H, Reuter VE, Ritz E, Roos G, Schmidt D, Srigley JR, Storkel S, van Den Berg E, Zbar B (1997) The Heidelberg classification of renal cell tumours. J Pathol 183:131–133
11. Lefevre M, Couturier J, Sibony M, Bazille C, Boyer K, Callard P, Vieillefond A, Allory Y (2005) Adult papillary renal tumor with oncocytic cells: clinicopathologic, immunohistochemical, and cytogenetic features of 10 cases. Am J Surg Pathol 29:1576–1581
12. Lemley KV, Kriz W (1994) Structure and function of the renal vasculature. In: Tisher CC, Brenner BM (eds) Renal pathology with clinical and functional correlations. 2nd edn. Lippincott, Philadelphia, pp 981–1026

13. Lieber MM, Tomera KM, Farrow GM (1993) Renal oncocytoma: clinical and biological correlates. J Urol 1993 150:1380–1383
14. Ligato S, Ro JY, Tamboli P, Amin MB, Ayala AG (1999) Benign tumours and tumour-like lesions of the adult kidney part I: benign renal epithelial neoplasms. Adv Anat Pathol 6:1–11
15. Martignoni G, Pea M, Brunelli M, Eble JN (2002) Oncocytoma-like angiomyolipoma. A clinicopathologic and immunohistochemical study of 2 cases. Arch Pathol Lab Med 126:610–612
16. Medeiros LJ, Palmedo G, Krigman HR, Kovacs G, Beckwith JB (1999) Oncocytoid renal cell carcinoma after neuroblastoma: a report of four cases of a distinct clinicopathologic entity. Am J Surg Pathol 23:772–780
17. Mostofi FK, Davies CJ (1998) Histological typing of kidney tumors, 2nd edn. Springer, Berlin
18. Perez-Ordonez B, Hamed G, Campbell S, Erlandson RA, Russo P, Gaudin PB, Reuter VE (1997) Renal oncocytoma: a clinicopathologic study of 70 cases. Am J Surg Pathol 21:871–883
19. Piper J, Stegenga S, Pestova E, Marble H, Lucas M, Wilber K, King W (2002) An objective method for detecting copy-number changes in CGH microarray experiments. In: Proceedings of the Third Euroconference on Quantitative Molecular Cytogenetics, Rosenon, Sweden, 4–6 July 2002, pp. 109–114
20. Psihramis KE, Dal Cin P, Dretler SP, Prout GR, Sanberg AA (1988) Further evidence that renal oncocytoma has malignant potential. J Urol 1988 139:585–587
21. Rothenberg DM, Brandt TD, D'Cruz I (1986) Computed tomography of renal angiomyolipoma presenting as right atrial mass. J Comput Assist Tomogr 10:1054–1056
22. Storkel S, Eble JN, Adlakha K, Amin M, Blute ML, Bostwick DG, Darson M, Delahunt B, Iczkowski K (1997) Classification of renal carcinoma. Workgroup No 1.. Cancer 80:987–989
23. Yang XJ, Sugimura J, Schafernak KT, Tretiakova MS, Han M, Vogelzang NJ, Furge K, Teh BT (2006) Classification of renal neoplasms based on molecular signatures. J Urol 175:2302–2306

Virchows Arch (2008) 452:295–304
DOI 10.1007/s00428-007-0560-y

ORIGINAL ARTICLE

Clinical significance of nuclear factor (NF)-κB levels in urothelial carcinoma of the urinary bladder

Georgia Levidou · Angelica A. Saetta · Penelope Korkolopoulou · Polyanthi Papanastasiou · Katerina Gioti · Petros Pavlopoulos · Kalliopi Diamantopoulou · Eupthemia Thomas-Tsagli · Konstantinos Xiromeritis · Efstratios Patsouris

Received: 6 September 2007 / Revised: 13 November 2007 / Accepted: 6 December 2007 / Published online: 10 January 2008
© Springer-Verlag 2007

Abstract Nuclear factor (NF)-κB has been reported to be constitutively activated in various human neoplasms. However, its clinical significance in bladder urothelial carcinoma (UC) remains an unresolved issue. We conducted this study trying to elucidate the role of NFκB in bladder UC and its potential prognostic significance, by quantifying immunohistochemically the levels of p65/RelA expression in paraffin-embedded tissue from 116 patients. Some of the cases had previously been stained for cellular FLICE-like inhibitory protein (c-FLIP) and bcl-2. Seventy-four cases displayed concurrent cytoplasmic and nuclear immunoreactivity, whereas 18 only nuclear immunoexpression and 21 only cytoplasmic immunoexpression, and the remaining three cases were negative for p65/RelA. Nuclear p65/RelA expression was positively associated with tumour grade and T-category (p=0.0001 in both cases). In addition, cytoplasmic p65/RelA expression was lower in advanced T-category (p=0.0030). Moreover, p65/RelA nuclear expression was positively correlated with c-FLIP (p=0.0109) and bcl-2 (p=0.0452). p65/RelA nuclear expression adversely affected survival in both univariate and multivariate analysis in superficial (Ta–T1; p=0.0010 and p=0.0008) as well as in muscle-invasive carcinomas (T2–T4; p=0.0004 and p=0.0003). Our results demonstrate that NF-κB nuclear expression is correlated with histologic grade and T category in bladder UC. Moreover, NF-κB nuclear expression emerges as an independent prognosticator of adverse significance, conveying information beyond that obtained by standard clinicopathological prognosticators.

Keywords NFκB · Immunoexpression · Bladder urothelial carcinoma

Introduction

Urothelial carcinoma (UC) of the urinary bladder is considered to be the fifth most common cancer in industrialized countries [44] and the second most common cancer of the genitourinary tract [16]. Even after complete transurethral resection, 75% of patients will recur [44], a fact highlighting the necessity for the identification of molecular markers that could possibly predict disease aggressiveness and clinical course. Moreover, gaining insight into the molecular determinants of the biologic behaviour of detrusor muscle-invasive bladder cancer is imperative to the development of more rational biologically oriented treatment strategies. Current belief holds that bladder cancer development is a multi-step process, in which, apart from genetic and environmental factors several oncogenes, tumour suppressor genes, cell cycle regulators as well as perturbations in apoptotic cell death regulation are implicated [9, 44].

By virtue of its pivotal role in many biological decisions affecting cell fate, nuclear factor (NF)-κB is the point of convergence of most metabolic and oncogenic pathways [4, 5, 53]. It is a family of transcription factors, whose

Georgia Levidou, Angelica A. Saetta, Penelope Korkolopoulou have equally contributed to the manuscript.

G. Levidou (✉) · A. A. Saetta · P. Korkolopoulou · P. Papanastasiou · K. Gioti · P. Pavlopoulos · K. Diamantopoulou · E. Thomas-Tsagli · K. Xiromeritis · E. Patsouris
Department of Pathology,
National and Kapodistrian University of Athens,
75 Mikras Asias Street,
Athens 11527, Greece
e-mail: glevidou@yahoo.gr

members share a Rel homology domain (RHD), subjecting them to a particular type of regulation centered on nuclear–cytoplasmic shuttling [13]. The RHD is an approximately 300-amino acid terminal domain, which is composed of two immunoglobulin-like repeats and serves several functions: It is the dimerization and DNA-binding domain for this class of proteins, it contains the nuclear localization signal (NLS) and most importantly, it is the binding site of NF-κB inhibitors [23, 40]. The NF-κB family consists of five RHD proteins namely, p50/NFκB1, p52/NF-κB2, c-Rel, RelB and p65/RelA [6]. Under resting conditions, NF-κB is localized in the cytoplasm and consists of three subunits: p50 and p65 (both DNA-binding capacity) and the inhibiting subunit IκBa, which is bound to p65. NF-κB activation may be caused by several cytokines and mitogens, as well as during oxidative stress, cell damage and viral infections [21, 38]. This activation entails the phoshorylation of IκBa by tyrosine kinases IκB kinase (IKK) [49], which in turn are phosphorylated by multiple signalling pathways, including members of the mitogen-activated protein kinase kinase family [23]. IκBa, β and ε contain two conserved serine residues in their N-terminal domain, the phosphorylation of which targets them to polyubiquitination and subsequent degradation by the 26S proteasome [40, 48]. This permits the liberation of the nuclear localization signal of NF-κB and consequently its translocation in the nucleus [6]. Activated NF-κB regulates the transcription of a wide variety of reporter genes, by binding to enhancers of target genes inducing their transcription [6]. The genes regulated by NF-κB include anti-apoptotic genes (such as survivin, cellular FLICE-like inhibitory protein [c-FLIP] and bcl-2), cell cycle regulators (such as cyclin D1), angiogenic factors (such as Cox-2), as well as genes encoding adhesion molecules and inflammatory cytokines (such as interleukin [IL]-8) [22, 31, 45].

Accumulating evidence highlights NF-κB as a major determinant of human tumourigenesis of several human neoplasms. Several investigators have reported constitutive activation of NF-κB in various tumour cells and cell lines, such as those of lymphoid origin [3, 11, 15], as well as those of ovarian [4], breast [35], pancreatic [52] and thyroid [51] origin. Moreover, its immunoexpression has been correlated with worse patients overall survival in human lung [57], prostatic [31, 45], gastric [32], esophageal [19] and tonsillar squamous carcinoma [56], as well as adenoid cystic carcinoma of salivary glands [55]. However, little information is available about the expression of NF-κB protein in urothelial bladder cancer (UC) [54], and, to the best of our knowledge, there is no published investigation addressing the potential prognostic significance of this molecule in bladder UC.

This study analyzes the immunohistochemical expression of NF-B protein in bladder UC specimens, assessing the expression of RelA/p65 subunit, in an effort to elucidate whether this molecule is correlated with tumour aggressiveness. We were also interested in the relationship of p65/RelA expression with other conventional inhibitors of apoptosis, such as the c-FLIP and bcl-2 protein. Finally, we aimed to clarify the role of NF-κB role in patients' prognosis in the presence of standard clinicopathological prognosticators.

Materials and methods

Patients

This is a study of 116 consecutive patients with primary bladder UC diagnosed, treated and followed up at Asklepeion Voula and IKA hospitals in Athens between 1985 and 1995, for which sufficient paraffin-embedded tissue and follow-up information were available. Informed consent was obtained from all patients before enrolment in the study. The study follows the principles of the Declaration of Helsinki and was approved by the ethical committee of the University of Athens Medical School. The mean age of patients was 65.48±11.90 ranging from 29 to 89 years, whereas the male-to-female ratio was 103:13. All cases were reviewed by two experienced pathologists (Levidou, Korkolopoulou) and assigned a histological grade and T-category according to the latest World Health Organization (WHO) classification [10] and the fifth edition of the TNM classification [46] taking into account the report of Mikulowski and Hellsten [34]. There were 17 tumours of low malignant potential (papillary neoplasms of low malignant potential, PNLMP), 42 low-grade carcinomas (LG) and 57 high-grade carcinomas (HG). Staging was based on combination of clinical (cystoscopy, computed tomography and ultrasound) and histological data to determine the absence (Ta, n=17) or presence (T1, n=34) of invasion of the lamina propria or invasion into or beyond the detrusor muscle (T2–T4, n=65).

Follow-up information was available in all but three patients. Follow-up period for the remaining 113 patients ranged from 3 to 86.7 months (median=36 months). During this period, 26 patients had died of their disease after a median survival of 20 months (range 7–48 months). The median follow-up for the remaining 87 patients was 41.5 months (range 3–86.7).

Immunohistochemical staining

Four-micrometre serial sections were cut from each specimen on Superfrost plus glass slides and left to dry overnight at 37°C. After deparaffinization, immunostaining was performed by using a rabbit polyclonal anti-RelA/p65 antibody (18–7308, California, USA, Zymed Laboratories)

diluted 1:300. The antibody was incubated overnight at 37°C. For p65 detection, antigen retrieval with microwaving for 30 min, at 750 W, in citrate buffer, pH 6.0, was required. Immunostaining was performed using the standard ABC (Ultravision Detection system, Labvision) and visualized with 3,3′-diaminobenzidine tetrachloride solution. The slides were counterstained with hematoxylin. Known positive controls (i.e. breast carcinoma) as well as negative controls (sections in which p65/RelA antibody was substituted by non-specific rabbit serum) were also stained in each run. In addition, 51 and 49 cases were stained for c-FLIP and bcl-2 proteins, respectively, some of which were available from our previous investigations [27, 28].

Light microscopic evaluation of immunostained slides was performed independently by two pathologists without knowledge of the clinical information. If a discrepancy occurred between the two assessments, the slides were reassessed jointly without information of the previous scores. In each case, 1,000–1,500 neoplastic cells throughout the section were counted at high-power magnification. Nuclear and cytoplasmic p65/RelA expression was evaluated separately. Nuclear p65/RelA labelling index was defined as the percentage of neoplastic cells with nuclear immunoreactivity out of the total number of neoplastic cells counted. Cytoplasmic p65/RelA expression was categorized in three levels according to the percentage of neoplastic cells with cytoplasmic staining, as follows: absent/low (level 1): 0–20% of neoplastic cells with cytoplasmic staining, moderate (level 2): 21–60% of neoplastic cells with cytoplasmic staining and extensive (level 3): >60% of neoplastic cells with cytoplasmic staining.

Statistical methods

In the basic statistical analysis, p65/RelA nuclear expression was treated as a continuous variable, whereas cytoplasmic p65/RelA expression as ordinal. Correlation between nuclear and cytoplasmic p65/RelA expression was tested with Kruskal–Wallis analysis of variance (ANOVA) along with Spearman's rank correlation coefficient. Associations of p65/RelA nuclear expression with other clinicopathological parameters, such as grade, T-category, tumour size and patients' sex and gender, were tested with Kruskal–Wallis ANOVA, whereas the corresponding associations of cytoplasmic p65/RelA expression were tested with Chi-square or Fisher's exact test, as appropriate. Associations of p65/RelA nuclear and cytoplasmic expression with c-FLIP and bcl-2 were calculated with Spearman's rank correlation coefficient and Kruskal–Wallis ANOVA, respectively.

The survival analysis was performed using death of disease as the endpoint. The effect of various parameters (age, sex, tumour size, T-category, grade and p65/RelA nuclear and cytoplasmic expression) on clinical outcome was assessed by plotting survival curves according to the Kaplan–Meier method and comparing groups using the log-rank test. In univariate survival analysis, p65/RelA nuclear expression was categorized on the basis of the median value (3%). Multivariate analysis was performed using Cox's model with stepwise forward selection to evaluate the predictive power of each power independently of others. As in basic statistical calculations, p65/RelA nuclear expression was treated as a continuous variable, whereas cytoplasmic as ordinal. Given that c-FLIP and bcl-2 were not available in many cases and their prognostic utility has been the subject of previous investigations [27, 28], these two variables were not included in survival analysis. Statistical calculations were performed using the Statistical package STATA 9.0/SE for Windows. All results with a two-sided p level less than or equal to 0.05 were considered statistically significant.

Results

Expression of p65/RelA in bladder UCs

Immunoreactivity of p65/RelA was nuclear and cytoplasmic. Seventy-four cases displayed concurrent cytoplasmic and nuclear immnoreactivity, 18 cases displayed only nuclear immunoexpression, 21 cases displayed only cytoplasmic immunoexpression and the remaining three cases were devoid of p65/RelA immunoreactivity. The overall rate of p65/RelA nuclear immunoexpression rose to 79.3% (92 of 116 cases). Positive neoplastic cells (with nuclear or cytoplasmic staining) were diffusely distributed throughout neoplastic tissue with little variation among individual cases. Normal urothelium displayed mainly a cytoplasmic p65/RelA staining with only a few scattered positive nuclei (Fig. 1a). Tumour-infiltrating lymphocytes invariably expressed p65/RelA, serving therefore as an internal positive control for each case.

Nuclear p65/RelA immunoexpression decreased with increasing levels of cytoplasmic p65/RelA (Kruskal–Wallis ANOVA, $p=0.0049$, Fig. 2), a relationship that remained significant when the analysis was restricted to muscle-invasive carcinomas (T2–T4; Kruskal–Wallis ANOVA, $p=0.0272$), but failed to retain its statistical significance in superficial (Ta–T1) bladder UCs ($p>0.10$). This negative correlation was confirmed with the Spearman's rank correlation coefficient ($R=-0.3012$, $p<0.0001$) in the entire cohort, as well as in muscle-invasive carcinomas ($R=-0.3223$, $p=0.0100$).

Correlations of p65/RelA with clinicopathological parameters

Nuclear p65/RelA expression increased with increasing histological grade in the entire cohort (Kruskal–Wallis, ANOVA, $p=0.0001$, Table 1, Fig. 1b,c,d, 3a), as well as in

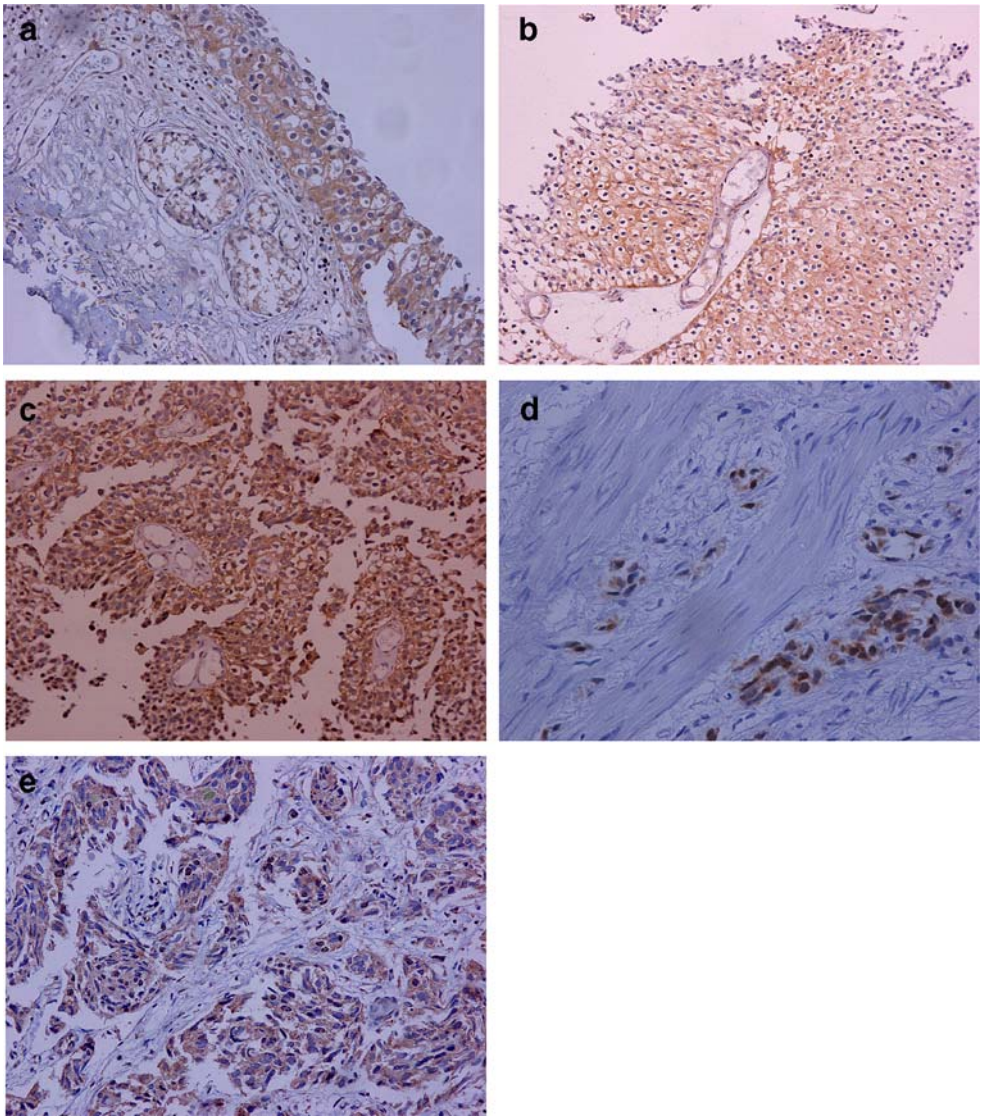


Fig. 1 **a** Normal urothelium displaying mainly cytoplasmic p65/RelA immunoreactivity. **b**, **c**, **d** Immunohistochemical expression of p65/RelA in a papillary neoplasm of low malignant potential, Ta (MX200, **b**), low grade, T1 (MX200, **c**), high grade, T2 (**d**, MX400) and high grade, T1 (MX200, **e**) bladder urothelial carcinomas (original magnification, ×40)

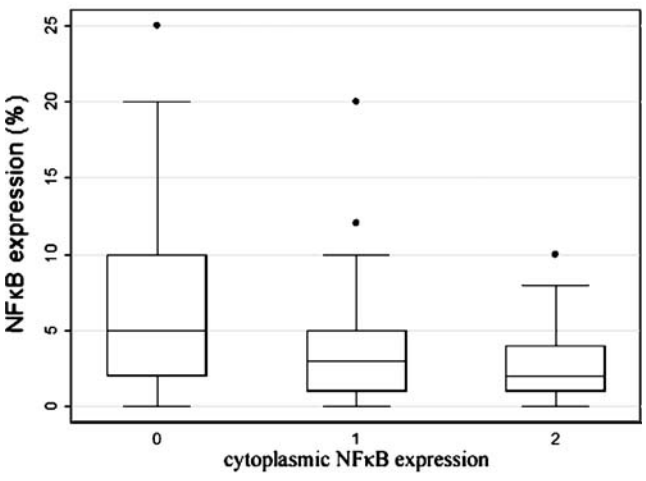


Fig. 2 Schematic representation of the association of p65/RelA nuclear with cytoplasmic p65/RelA expression

superficial (Ta–T1, Kruskal–Wallis, ANOVA, $p=0.0011$) and muscle-invasive carcinomas (T2–T4 Kruskal–Wallis, ANOVA, $p=0.0001$). Moreover, nuclear p65/RelA immunostaining was positively correlated with tumour T-category in the entire cohort (Kruskal–Wallis, ANOVA, p=0.0001, Table 1, Fig. 1b,c,d, 3b) and in muscle-invasive carcinomas (Kruskal–Wallis, ANOVA, $p=0.0047$), but this relationship failed to attain statistical significance when analysis was restricted to superficial (Ta–T1) bladder UCs ($p>0.10$). In addition, nuclear p65/RelA was marginally correlated with tumour size ($p=0.0611$, Table 1) but was unrelated to patients' age and gender ($p>0.10$).

Accordingly, cytoplasmic p65/RelA reactivity was marginally correlated with histological grade in the entire cohort ($p=0.0810$, Table 2). Furthermore, cytoplasmic p65/RelA immunoreactivity decreased with increasing tumour T-category in the entire cohort and in muscle-invasive carcinomas ($p=0.0030$ and $p=0.0073$, respectively, Table 2).

Table 1 Relationship between nuclear p65/RelA expression and clinicopathological parameters in 116 patients with urothelial bladder carcinoma

	p65/RelA nuclear expression (%)			
	Number	median	Range	*p* value
Age (years)	116	70	39–89	>0.10[a]
Grade				0.0001[b]
Papillary neoplasms of low malignant potential, PNLMPs	17	1	0–5	
Low-grade carcinomas, LG	42	2	0–8	
High-grade carcinomas, HG	57	5	0–25	
Stage				0.001[b]
Ta	17	1	0–5	
T1	34	2	0–12	
T2	40	3	0–20	
T3	16	5	0–20	
T4	7	5	0–25	
Tumour size (cm)	116	2	0.1–25	0.0611[a]
Sex				>0.10[c]
Female	13	5	0–15	
Male	103	2	0–25	

[a] Results of Spearman's correlation coefficient
[b] Results of Kruskal–Wallis ANOVA
[c] Results of Mann Whitney *U* test

The respective relationships between p65/RelA cytoplasmic expression and tumour grade or T-category in superficial bladder UCs (Ta–T1) failed to attain statistical significance ($p>0.10$). However, patients' age, sex and tumour size were unrelated to cytoplasmic p65/RelA ($p>0.10$).

Relationship of p65/RelA with c-FLIP and bcl-2

The associations of c-FLIP and bcl2 with clinicopathological parameters in bladder UCs have been examined in detail previously [28, 27] and therefore will not be mentioned.

Nuclear p65/RelA expression was positively correlated with c-FLIP and bcl-2 expression (Spearman's rank correlation coefficient, $R=0.3178$, $p=0.0109$). Moreover, nuclear expression was increased in bcl-2-positive neoplasms compared to bcl-2-negative ones (Kruskal–Wallis, ANOVA, $p=0.0452$). Cytoplasmic p65/RelA expression was not associated with c-FLIP or bcl2 expression levels (Kruskal–Wallis, ANOVA, $p>0.10$).

Survival analysis

Survival analysis was performed separately for Ta–T1 and T2–T4 UCs because of the substantially worse behaviour of the latter group (T4–T2 vs Ta–T1, $p>0.0001$, log-rank test). In univariate analysis of Ta–T1 urothelial bladder carcino-

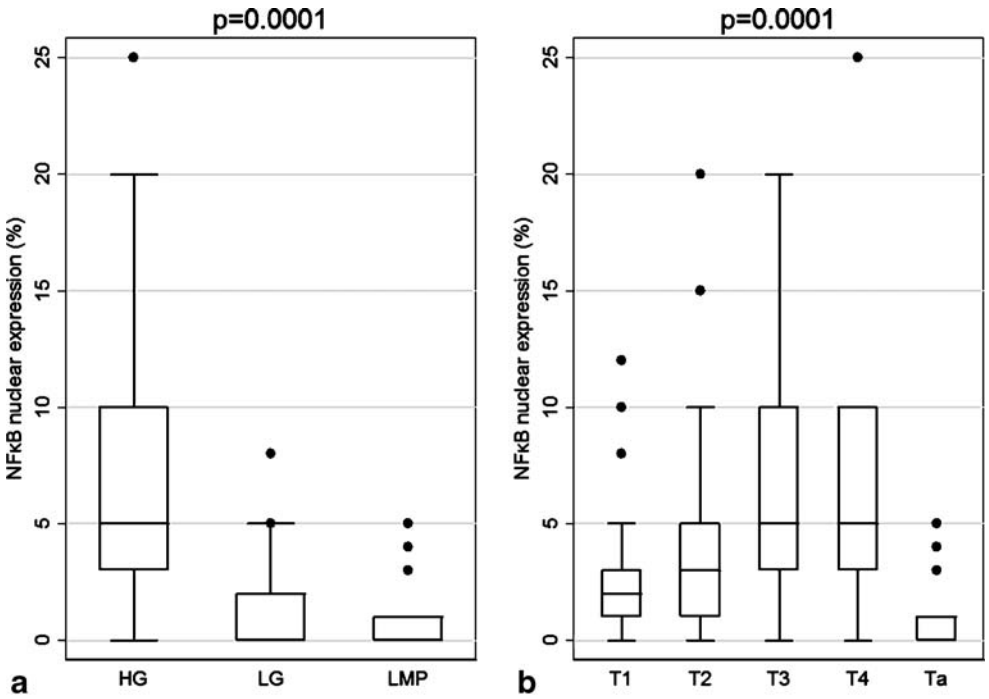


Fig. 3 Schematic representation of the association of p65/RelA nuclear expression with **a** histologic grade and **b** T-category in the entire cohort. p65/RelA increases with increasing grade and T-category

Table 2 Associations of cytoplasmic p65/RelA expression with clinicopathological parameters in 116 patients with urothelial bladder carcinoma (results of Fisher's exact test)

	Cytoplasmic p65/RelA			*p* value
	Absent/ low	Medium	Excessive	
Grade				0.0810
Papillary neoplasms of low malignant potential, PNLMPs	15	25	17	
Low-grade carcinomas, LG	5	16	21	
High-grade carcinomas, HG	1	6	10	
Stage				0.0030
Ta	1	6	10	
T1	2	19	13	
T2	9	12	19	
T3	6	5	5	
T4	3	3	1	
Sex				>0.10
Female	3	5	5	
Male	18	41	44	

mas, higher p65/RelA nuclear expression levels (>3 vs ≤3%, Fig. 4a), higher T-category (T1 vs Ta) and histological grade (HG vs LG vs PNLMP, $p<0.0001$) implied a lesser probability of survival (Table 3). The parameters affecting survival in muscle-invasive carcinomas (T2–T4) were p65/RelA overexpression (>3 vs ≤3%, Fig. 4b), low p65/RelA cytoplasmic expression (0 vs 1 vs 2,), histological grade (HG vs LG vs PNLMP, $p=0.0031$) and T-category (T2 vs T3 vs T4; Table 3). The median survival time for patients whose tumours overexpressed nuclear p65/RelA was 66.6 and 30 months in superficial and muscle-invasive bladder UCs, respectively. It is to be noted that none of the patients within the low-expressor group in both Ta–T1 and T2–T4 bladder UCs had a disease-specific event, and therefore median and mean survival time for this group cannot be calculated.

In multivariate analysis of superficial carcinomas (Ta/T1), p65/RelA expression was the only parameter that remained significant. High p65/RelA nuclear expression and T-category turned out to be the independent prognostic factors for muscle-invasive carcinomas. The final models are presented in Table 4.

Discussion

Although bladder UC is often detected at an early stage, the identification of those tumours prone to progress or recur remains a difficult and challenging issue [44]. Several molecular markers have been suggested for the stratification of patients in terms of clinical course and outcome, among which cell cycle regulators, such as p53, p27, pRb and cyclin D1 [8, 9, 26, 25, 36, 42, 44], as well as apoptotic coordinators, such as c-FLIP and bcl-2 family proteins [27, 28, 44], figure prominently. Published studies, however, have yielded contradictory results, mainly because of the presence of influential methodological issues (i.e. small sample size, the ratio of superficial to muscle-invasive cases and the administration of different therapeutic protocols), which confound their outcomes and consequently hamper

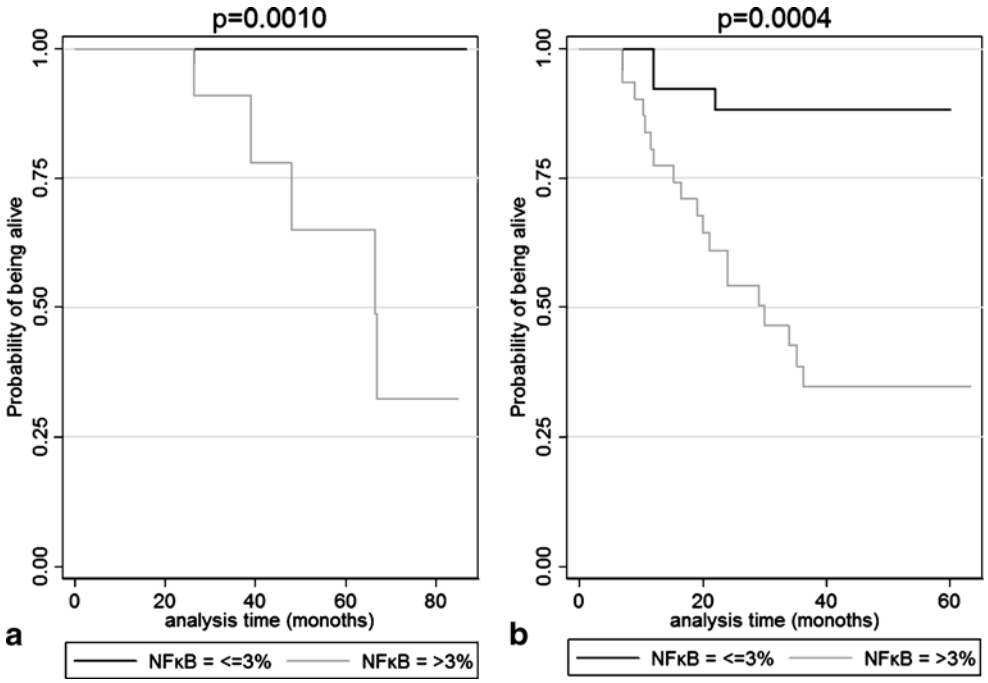


Fig. 4 Kaplan–Meier survival curves according to p65/RelA expression in **a** 51 patients with superficial and **b** 62 patients with muscle-invasive bladder urothelial carcinoma

Table 3 Univariate analysis in Ta–T1 and in T2–T4 bladder UCs

Parameter	Ta/T1 bladder UCs, n=51	T2–T4 bladder UCs, n=62
Grade (PNLMP vs LG vs HG)	<0.0001	0.0031
T-category	Ta vs T1 0.0341	T2 vs T3 vs T4, p<0.0001
Age (>35 vs ≤35)	0.1193	0.4734
Gender (1: male, 2: female)	0.7095	0.9969
Tumour size (<1.5 vs ≥1.5 cm)	0.0870	0.7681
P65/RelA nuclear LI (≤3 vs >3%)	0.0010	0.0004
P65/RelA cytoplasmic expression (0 vs 1 vs 2)	0.6546	0.0244

Analysis using the log-rank test (p values)

the identification of a universally approved prognostic marker.

Accumulating evidence suggests that NF-κB is constitutively activated and exhibits a strong transactivation potential in several human cancer tissues [4, 14, 24, 35, 41, 50, 51]. Accordingly, nuclear translocation of the p65 subunit has been reported to be markedly higher in gastric, colon and prostatic adenocarcinoma cells when compared to their normal counterparts [33, 43, 45]. However, published information regarding the role of NF-κB activation in tumours of the genitourinary tract is limited to a few reports describing aberrant activation in renal cell and prostatic carcinomas [31, 38, 45]. Importantly, in a recent Chinese study, NF-κB expression is higher in bladder UC cells in comparison to that of non-neoplastic mucosa [54]. In our cohort, we observed that normal urothelium displayed a mainly cytoplasmic p65/RelA immunoexpression, whereas in the majority of the studied tumours (79.3%), p65/RelA was seen in the nucleus. Cytoplasmic NF-κB immunolocalization is considered to correspond to the inactive form of NF-κB protein, whereas nuclear immunoreactivity is regarded as a surrogate marker for the activated NF-κB protein. This staining pattern is broadly in line with investigations concerning other neoplasms, such as gastric and prostatic adenocarcinomas [32, 45].

The detailed mechanisms underlying NF-κB activation in bladder UC remain unclear, and the analysis of NFκB regulating pathways and molecules for the detection of mutations that possibly promote NF-κB activation in many other human cancers is still in progress. NFκB activation has been reportedly attributed to the phosphorylation of IκB protein by IKK kinase. However, it is conceivable that NF-κB activation is a multi-step process in which several molecules interact to initiate a highly coordinated response [41]. Differential activation and expression of these molecules under different conditions could possibly account for the apparently contradictory data obtained in different tissues. For example, although NF-κB-inducing kinase plays the major role in constitutive activation of NF-κB in melanoma cells [7], in prostate cancer cells, this appears to result from the increased activity of the IKK kinase complex [12, 39, 47]. Clearly, the question of the alterations in the upstream signalling pathways that result in the constitutive activation of the NF-κB protein remains to be addressed in bladder UC cell lines.

Another interesting issue emerging from the present investigation relates to the differential nuclear expression of NF-κB during the progression of bladder UC. Thus, p65/RelA nuclear expression levels increased in higher tumour grade and advanced T-category cases, whereas cytoplasmic p65/RelA immunoreactivity decreased with increasing tumour histologic grade and invasive potential, in muscle-invasive (T2–T4) carcinomas. Taking into account that the normal urothelium displayed minimal nuclear p65/RelA immunoreactivity, our results speak in favour of the potential role of this molecule in urothelial bladder tumourigenesis as well in the acquisition of a more aggressive phenotype. It is worthy of note, however, that the significant overlap in the nuclear expression levels of p65/RelA across the various grade and stage categories hampers its use as a diagnostic tool supplementing the existing WHO criteria. Our observations are in alignment with previous studies concerning prostate and renal cell carcinomas [37, 45], in which p65/RelA nuclear immunoreactivity was related to tumour invasiveness and aggressive behaviour. Along this line, it has been postulated that NF-κB can stimulate the transcription of genes that may be essential for malignant transformation with consequent genomic instability, accelerating neoplastic progression [17]. Moreover, our results are in accordance with experimental data in a panel of human bladder UC cell lines with varying metastatic potential indicating that highly

Table 4 Cox's proportional hazard estimation, in superficial (Ta–T1; model A) and in muscle invasive (T2–T4; model B)

Models	Parameter	Hazard ratio (HR)	p value	95% confidence interval of HR	
A	p65/RelA nuclear LI	1,972	0,0080	1,194	3,257
B	p65/RelA nuclear LI	1,107	0,0003	1,034	1,184
	T category T2 vs T3 vs T4	4,152	<0,0001	2,252	7,651

metastatic bladder UC cells constitutively expressed high levels of NF-κB, in comparison to that of cells with low metastatic potential [22]. In addition, the role of the NF-κB protein in bladder UC tumourigenesis has previously been speculated because of its relationship with interstitial cystitis [2], given that the development of bladder cancer is related to urinary tract infection [30, 52]. Thus, NF-κB is more often activated in urothelial cells from interstitial cystitis as compared to controls [2].

Perhaps, the most intriguing finding of our study was the fact that p65/RelA nuclear overexpression connotes a poor survival probability and remains a prognostic factor after multivariate analysis in both superficial and muscle-invasive UCs. It is worthy of note that this is the first attempt to link NF-κB expression with survival in bladder UC. Cytoplasmic p65/RelA expression does not seem to be informative in this regard. A plausible explanation for this finding is that the relationship between cytoplasmic p65/RelA immunoreactivity and survival that was elicited in univariate survival analysis in muscle-invasive carcinomas largely resides in its relationship with nuclear p65/RelA, the latter thus acting as a confounding factor. Our results are in line with previous studies in gastric and prostatic adenocarcinomas, in which nuclear immunolocalization of the NF-κB protein was proposed as a useful prognostic marker [31, 32]. Although the median period of surviving patients in our study was approximately 3.5 years, it should be acknowledged that the vast majority of bladder UCs progress clinically during the first 3 years after presentation [41], which allows meaningful conclusions to be drawn at the end of this period. Furthermore, our results in survival analysis recapitulate most of the parameters that have been established as determinants of clinical outcome in patients with bladder UC (i.e. histologic grade, T- category), advocating that our cohort is representative and leads to valid results. Moreover, the percentage of high-grade cases in the group of muscle-invasive carcinomas (57 in 65 cases) is broadly in line with the figure quoted in previously published studies [29]. The fact that nuclear p65/RelA expression maintained its statistical significance in multivariate survival analysis along with tumour stage in muscle-invasive carcinomas indicates that the prognostic significance of p65/RelA nuclear overexpression cannot be attributed to its relationship with this parameter and that there should be other reasons accounting for this finding, e.g. the inhibition of apoptosis that results from NF-κB activation [1, 23]. Our preliminary results of a positive relationship between p65/RelA nuclear immunoexpression with both c-FLIP and bcl-2 expression that emerged in our cohort, despite the small number of cases studied, raise the hypothesis that NF-κB may exert anti-apoptotic effects in bladder UCs. Of course, validation of these results in a larger number of cases is mandatory to verify this assumption. In this context, the NF-κB protein has been shown to induce anti-apoptotic effects in cells treated with apoptotic agents, such as tumour necrosis factor-α, ionizing radiation or chemotherapeutic agents [18, 20], therefore enhancing chemoresistance and radioresistance. Horiguchi et al. investigated the use of a dehydroxymethyl derivative of epoxuquinomycin C—a NF-κB function inhibitor in bladder cancer—and suggested that it represents a possible new treatment strategy by virtue of its role in the promotion of apoptosis against advanced bladder cancer [18]. An additional mechanism could relate to the involvement of NF-κB in the activation of a number of cell cycle regulators (i.e. cyclin D1) that have been implicated in patients' overall survival in bladder cancer [8, 36, 42], as well as genes participating in the process of tumour metastasis (i.e. metalloproteinases 3) or angiogenesis (i.e. Cox-2 and IL-8) [21, 22].

In conclusion, our study demonstrates that p65/RelA nuclear expression and therefore NF-κB activation parallels histologic grade and T-category especially in muscle-invasive bladder UC, directly implicating NF-κB in the acquisition of the malignant and more aggressive phenotype in urothelial bladder carcinomas. More importantly, p65/RelA nuclear overexpression emerges as a valuable adverse prognostic marker in both superficial and muscle-invasive tumours, retaining its significance in multivariate analysis, in the presence of tumour T-category and histologic grade, thus conveying supplementing information obtained by standard clinicopathological prognosticators. These results encourage further investigations into the use of NF-κB inhibitors as an adjunct to the currently available treatment options in bladder UC [18]. Analysis of the potential role of such molecules in human urothelial bladder carcinoma cell lines is warranted to validate our observations and to provide more insight into their function in bladder UC.

Conflict of interest statement We declare that we have no conflict of interest.

References

1. Abdel-Latif MMM, O'Riodan J, Windle HJ, Carton E, Ravi N, Kelleher D, Reynolds JV (2004) NF-κB activation in esophageal adenocarcinoma. relationship to Barrett's metaplasia, survival, and response to neoadjuvant chemoradiotherapy. Ann Surg 239:491–499
2. Abdel-Mageed AB, Ghoniem GM (1998) Potential role of Rel/Nuclear factor-jB in the pathogenesis of interstitial cystitis. J Urol 160:2000
3. Baldwin AS (1996) The NF-κB and IκB proteins: new discoveries and insights. Annu Rev Immunol 14:649–683
4. Bours V, Dejardin E, Goujon-Letawe F, Merville MP, Castronovo V (1994) The NF-κB transcription factor and cancer: high expression of NF-κB and IκB-related proteins in tumour cell lines. Biochem Pharmacol 47:145–149
5. Chen FE, Ghosh G (1999) Regulation of DNA binding by Rel/NFκB transcription factors: structural reviews. Oncogene 18:6845–6852

6. Dejardin E, Deregowski V, Chapelier M, Jacobs N, Gielen J, Merville MP, Bours V (1999) Regulation of NF kappa B activity by I kappaB-related proteins in adenocarcinoma cells. Oncogene 18:2567–2577
7. Dhawan P, Singh AB, Ellis DL, Richmond A (2002) Constitutive activation of Akt/protein kinase B in melanoma leads to up-regulation of nuclear factor-kappaB and tumor progression. Cancer Res 62:7335–7342
8. Dolcet X, Llobet D, Pallares J, Matias-Guiu X (2005) NF-κB in development and progression of human cancer. Virchows Arch 5:475–482
9. Eble JN, Young RH (1997) Carcinoma of the urinary bladder: a review of its diverse morphology. Semin Diagn Pathol 14:98–108
10. Eble JN, Epstein JI, Seternhenn IA (2004) World Health Organization classification of tumours. Pathology and genetics, tumours of the urinary system and male genital track. IARC, Lyon, pp 89–115
11. Feinman R, Koury J, Thames M, Barlogie B, Epstein J, Siegel DS (1999) Role of NF- B in the rescue of multiple myeloma cells from glucocorticoid-induced apoptosis by bcl-2. Blood 93:3044–3052
12. Gasparian AV, Yao YJ, Kowalczyk D, Lyakh LA, Karseladze A, Slaga TJ, Budunova IV (2002) The role of IKK in constitutive activation of NF-kappaB transcription factor in prostate carcinoma cells. J Cell Sci 115:141–151
13. Ghosh S, May M, Kopp EB (1998) NFκB and Rel proteins: evolutionary conserved mediators of immune responses. Annu Rev Immunol 16:225–260
14. Gilmore TD (2006) Introduction to NF-kappaB: players, pathways, perspectives. Oncogene 25(51):6680–6684
15. Giri DK, Aggarwal BB (1998) Constitutive activation of NF- B causes resistance to apoptosis in human cutaneous T cell lymphoma HuT-78 cells. Autocrine role of tumour necrosis factor and reactive oxygen intermediates. J Biol Chem 273:14008–14014
16. Greenlee RT, Murray T, Bolden S, Wingo PA (2000) Cancer statistics 2000. CA Cancer J Clin 50:7–33
17. Hayashi S, Yamamoto M, Ueno Y, Ikeda K, Ohshima K, Soma G et al (2001) Expression of nuclear factor-kappa B, tumor necrosis factor receptor type 1, and c-Myc in human astrocytomas. Neurol Med Chir (Tokyo) 41(4):187–195
18. Horiguchi Y, Kuroda K, Nakashima J, Murai M, Umezawa K (2003) Antitumor effect of a novel nuclear factor-kappa B activation inhibitor in bladder cancer cells. Expert Rev Anticancer Ther 6:793–798
19. Izzo JG, Malhotra U, Wu TT, Ensor J, Luthra R, Lee JH, Swisher SG, Liao Z, Chao KS, Hittelman WN, Aggarwal BB, Ajani JA (2006) Association of activated transcription factor nuclear factor kappab with chemoradiation resistance and poor outcome in esophageal carcinoma. J Clin Oncol 5:748–754
20. Jacobson SH, Hylander B, Wretlind B, Brauner A (1994) Interleukin-6 and interleukin-8 in serum and urine in patients with acute pyelonephritis in relation to bacterial-virulence-associated traits and renal function. Nephron 67(2):172–179
21. Kang S, Kim YB, Kim MH, Yoon KS, Kim JW, Park NH, Song YS, Kang D, Yoo KY, Kang SB, Lee HP (2005) Polymorphism in the nuclear factor kappa-B binding promoter region of cyclooxygenase-2 is associated with an increased risk of bladder cancer. J Can Let 217(1):11–16
22. Karashima T, Sweeney P, Kamat A, Huang S, Kim SJ, Bar-Eli M, McConkey DJ, Dinney CPN (2003) Nuclear factor-κB mediates angiogenesis and metastasis of human bladder cancer through the regulation of interleukin-8. Clin Cancer Res 9:2786–2797
23. Karin M (1999) How NF-kappaB is activated: the role of the IkappaB kinase (IKK) complex. Oncogene 18(49):6867–6874
24. Karin M, Cao Y, Greten FR, Li AW (2002) NFκB in cancer: from innocent bystander to major culprit. Nat Rev Cancer 2:301–310
25. Korkolopoulou P, Konstantinidou AE, Christodoulou P, Patsouris E, Thomas-Tsangli E, Kapralos P, Davaris P (2000) Apoptosis in bladder carcinomas detected with monoclonal antibody to single-stranded DNA: relation to cell cycle regulators and survival. Urology 56(3):516–520
26. Korkolopoulou P, Christodoulou P, Lazaris A, Thomas-Tsagli E, Kapralos P, Papanikolaou A, Kalliteraki I, Davaris P (2001) Prognostic implications of aberrations in p16/pRb pathway in urothelial bladder carcinomas: a multivariate analysis including p53 expression and proliferation markers. Eur Urol 39(2):167–177
27. Korkolopoulou P, Lazaris AC, Konstantinidou AE, Kavantzas N, Patsouris E, Christodoulou P, Thomas-Tsagli E, Davaris P (2002) Differential expression of bcl-2 family proteins in bladder carcinomas. Relationship with apoptotic rate and survival. Eur Urol 41(3):274–283
28. Korkolopoulou P, Goudopoulou A, Voutsinas G, Thomas-Tsagli E, Kapralos P, Patsouris E, Saetta AA (2004) C-Flip expression in bladder urothelial carcinomas: its role in resistance to Fas-mediated apoptosis and clinicopathologic correltations. J Urol 63(6):1198–1204
29. Kruger S, Thorns C, Bohle A, Feller AC (2003) Prognostic significance of a grading system considering tumour heterogenetity in muscle invasive urothelial carcinoma of the urinary bladder. Int Urol Nephrol 35(2):169–173
30. La Vecchia C, Negri E, D'Avanzo B, Savoldelli R, Franceschi S (1991) Genital and urinary tract diseases and bladder cancer. Cancer Res 51:629–631
31. Lessard L, Mes-Masson AM, Lamarre L, Wall L, Lattouf JB, Saad F (2003) NF-κB nuclear localization and its prognostic significance in prostate cancer. BJU Int 91:417–420
32. Levidou G, Korkolopoulou P, Nikiteas N, Tzanakis N, Thymara I, Saetta AA et al (2007) Expression of nuclear factor kappaB in human gastric carcinoma: relationship with IkappaBa and prognostic significance. Virchows Arch 450(5):519–527
33. Lind DS, Hochwald SN, Malaty J, Rekkas S, Hebig P, Mishra G, Moldawer LL, Copeland EM 3rd, Mackay S (2001) Nuclear factor-kappa B is upregulated in colorectal cancer. Surgery 2:363–369
34. Mikulowski P, Hellsten S (2005) T1G1 urinary bladder carcinoma: Fact or fiction? Scand J Urol Nephrol 39:135–137
35. Nakshatri H, Bhat-Nakshatri P, Martin DA, Goulet RJ, Sledge GW (1997) Constitutive activation of NF- B during progression of breast cancer to hormone-independent growth. Mol Cell Biol 17:3629–3639
36. Osman I, Scher H, Zhang ZF, Soos TJ, Hamza R, Eissa S, Khaled H, Koff A, Cordon-Cardo C (1997) Expression of cyclin D1 but not cyclins E and A, is related to progression in bilharzial bladder cancer. Clin Cancer Res 3:2247–2251
37. Oya M, Takayanagi A, Horiguchi A, Mizuno R, Ohtsubo M, Marumo K, Shimizu N, Murai M (2003) Increased nuclear factor-kappa B activation is related to the tumor development of renal cell carcinoma. Carcinogenesis 24(3):377–384
38. Pahl HL (1999) Activators and target genes of Rel/NF-kappaB transcription factors. Oncogene 18(49):6853–6866
39. Palayoor ST, Youmell MY, Calderwood SK, Coleman CN, Price BD (1999) Constitutive activation of IκB kinase α and NF-κB in prostate cancer cells is inhibited by ibuprofen. Oncogene 18:7389–7394
40. Perkins ND (2000) The Rel/NF-kappa B family: friend and foe. Trends Biochem Sci 9:434–440
41. Pryor JP (1973) Factors influencing the survival of patients with transitional cell tumours of the urinary bladder. Br J Urol 45:586–591
42. Rayet B, Gelinas C (1999) Aberrant rel/nfkb genes and activity in human cancer. Oncogene 18(49):6938–6947
43. Sasaki N, Morisaki T, Hashizume K, Yao T, Tsuneyoshi M, Noshiro H, Nakamura K, Yamanaka T, Uchiyama A, Tanaka M, Katano M

(2001) Nuclear factor-kappaB p65 (RelA) transcription factor is constitutively activated in human gastric carcinoma tissue. Clin Cancer Res 12:4136–4142
44. Schulz WA (2006) Understanding urothelial carcinoma through cancer pathways. Int J Cancer 119(7):1513–1518
45. Shukla S, MacLennan GT, Fu P, Patel J, Marengo SR, Resnick MI, Gupta S (2004) Nuclear factor-kappaB/p65 (Rel A) is constitutively activated in human prostate adenocarcinoma and correlates with disease progression. Neoplasia 6(4):390–400
46. Sobin LH, Wittekind C (1997) TNM classification of malignant tumors. Wiley, New York
47. Suh J, Payvandi F, Edelstein LC, Amenta PS, Zong WX, Gelinas C, Rabson AB (2002) Mechanisms of constitutive NF-kappaB activation in human prostate cancer cells. Prostate 52 (3):183–200
48. Thanos D, Maniatis T (1995) NF-κB: a lesson in family values. Cell 80:529–532
49. Tojima Y, Fujimoto A, Delhase M, Chen Y, Hatakeyama S, Nakayama K, Kaneko Y, Nimura Y, Motoyama N, Ikeda K, Karin M, Nakanishi M (2000) NAK is an IkappaB kinase-activating kinase. Nature 404(6779):778–782
50. Visconti R, Cerutti J, Battista S, Fedele M, Trapasso F, Zeki K, Miano MP, Nigris F, Casalino L, Curcio F, Santoro M, Fusco A (1997) Expression of the neoplastic phenotype by human thyroid carcinoma cell lines requires NF-κB p65 protein expression. Oncogene 15:1987–1994
51. Wang W, Abbruzzese JL, Evans DB, Larry L, Cleary KR, Chiao PJ (1999) The nuclear factor-κB/RelA transcription factor is constitutively activated in human pancreatic adenocarcinoma cells. Clin Cancer Res 5:119–127
52. Wang XC, Saban R, Kaysen JS, Saban MR, Allen PL, Benes EN, Hammond TG (2000) Nuclear factor kappa B mediates lipopolysaccharide-induced inflammation in the urinary bladder. J Urol 163(3):993–998
53. Williams GT (1991) Programmed cell death: apoptosis and oncogenesis. Cell 65(7):1097–1098
54. Xie DH, Tang XD, Xia SJ, Tan JM, Wang XH, Cai Y (2002) Expression of NF-kappa B in human bladder cancer and its clinical significance. Ai Zheng 21(6):663–667
55. Zhang J, Peng B, Chen X (2005) Expressions of nuclear factor kappaB, inducible nitric oxide synthase, and vascular endothelial growth factor in adenoid cystic carcinoma of salivary glands: correlations with the angiogenesis and clinical outcome. Clin Cancer Res 20:7334–7343
56. Zhang PL, Pellitteri PK, Law A, Gilroy PA, Wood GC, Kennedy TL, Blasick TM, Lun M, Schuerch C 3rd, Brown RE (2005) Overexpression of phosphorylated nuclear factor- kappa B in tonsillar squamous cell carcinoma and high-grade dysplasia is associated with poor prognosis. Mod Pathol 7:924–932
57. Zhang Z, Ma J, Li N, Sun N, Wang C (2006) Expression of nuclear factor-kappaB and its clinical significance in non small-cell lung cancer. Ann Thorac Surg 1:243–248

Virchows Arch (2008) 452:305–312
DOI 10.1007/s00428-008-0584-y

ORIGINAL ARTICLE

A procedure for tissue freezing and processing applicable to both intra-operative frozen section diagnosis and tissue banking in surgical pathology

Susanne Steu · Maya Baucamp · Gabriela von Dach · Marion Bawohl · Susanne Dettwiler · Martina Storz · Holger Moch · Peter Schraml

Received: 21 September 2007 / Revised: 10 January 2008 / Accepted: 15 January 2008 / Published online: 6 February 2008
© Springer-Verlag 2008

Abstract Different methods for snap freezing surgical human tissue specimens exist. At pathology institutes with higher work loads, solid carbon dioxide, freezing sprays, and cryostat freezing are commonly used as coolants for diagnosing frozen tissue sections, whereas for tissue banking, liquid nitrogen or isopentane cooled with liquid nitrogen is preferred. Freezing tissues for diagnostic and research purposes are therefore often time consuming, laborious, even hazardous, and not user friendly. In tissue banks, frozen tissue samples are stored in cryovials, capsules, cryomolds, or cryocassettes. Tissues are additionally embedded using freezing media or wrapped in plastic bags or aluminum foils to prevent desiccation. The latter method aggravates enormously further tissue handling and processing. Here, we describe an isopentane-based workflow which concurrently facilitates tissue freezing and processing for both routine intra-operative frozen section and tissue banking and satisfies the qualitative demands of pathologists, cancer researchers, laboratory technicians, and tissue bankers.

Keywords Rapid frozen section · Tissue banking · Tissue freezing procedures · OCT

S. Steu · M. Baucamp · G. von Dach · M. Bawohl · S. Dettwiler · M. Storz · H. Moch · P. Schraml (✉)
Department of Pathology, Institute of Surgical Pathology,
Zurich University Hospital,
Schmelzbergstrasse 12,
Zurich, Switzerland
e-mail: Peter.Schraml@usz.ch

Introduction

The use of modern technologies in genomics and proteomics permits the identification of disease-associated mechanisms at molecular levels. Research data are mostly derived from cell lines or animal models. To translate this knowledge into clinical applications, it is necessary to examine numerous, well-documented human tissues of high quality. Tissue collections appropriate for such investigations exist, particularly in pathology institutes at universities.

For diagnostic purposes, tissue samples are generally treated in two ways. Almost all specimens are formalin fixed and paraffin embedded (FFPE). This procedure is routinely used for hematoxylin staining and immunohistochemical analysis of tissue sections cut from paraffin blocks. For rapid intra-operative sections, tissue samples are generally directly placed onto a metal chuck provided with optimal cutting temperature (OCT) compound and frozen either using solid carbon dioxide or the cooling chamber of a cryostat [8]. Slow freezing of tissues produces artifacts due to aggregation of water molecules into ice crystals, which is significantly reduced with liquid nitrogen [8, 11]. Because of the very low temperature of liquid nitrogen, extremely soft tissues, such as brain, spleen, or lymph node, become brittle and rigid and therefore are difficult to cut. In addition, liquid nitrogen evaporates rapidly particularly in small containers, which consequently have to be refilled several times a day.

As FFPE tissue is of limited quality for molecular analyses [12], additional tissue pieces are also kept frozen for future diagnostic and research purposes in many pathology institutes at universities. However, as with rapid sectioning, the protocols designed for freezing tissues for

tissue banks commonly differ and are not always standardized. For tissue banking, "superfluous" tissue pieces not needed for diagnostic purposes are commonly frozen in liquid nitrogen or in cooled isopentane. Different strategies are applied to preserve tissue specimens for tissue banks. Cold-resistant cryovials or cryomolds are commonly used because they can be labeled easily and do not require much space [1, 2, 6]. Freezing medium is also added to protect tissue pieces from desiccation. Alternatively, tissue samples can also be wrapped in plastic bags or aluminum foils [1, 3]. Sometimes tissues were brought into shape depending on the size of the containers/tissue cassettes. All these methods are disadvantageous as tissues are difficult to handle for further processing. Snap-frozen, non-embedded tissues pieces are also transferred directly into plastic bags, which are placed in a box containing numerous other plastic bags with different tissue samples. The storage of a growing number of plastic bags in a cryocontainer may hamper determining the location of the tissues of interest and thus becomes, as the tissue collection may grow rapidly, more and more unmanageable. An additional important and critical issue of tissue banking is that in most of the cases the quality of the morphology of stored frozen tissue is unknown. Consequently, there is no guarantee for which purposes/methods the collected tissues may ideally be used for research projects.

Here, we describe a protocol that is applicable to both rapid intra-operative section and tumor tissue banking. The effects of solid carbon dioxide, isopentane, and liquid nitrogen on tissue morphology and molecular structures (RNA, DNA, and protein) of tumor tissues embedded in OCT are also discussed.

Materials and methods

Tissue samples Eleven tumors derived from patients who underwent surgery (between May and June 2006) at Zurich University Hospital were randomly selected for this study. There were one renal cell carcinoma, two breast carcinomas, three lung carcinomas, one endometrial carcinoma, one stomach carcinoma, one seminoma, and two ovarian carcinomas. Three different protocols were applied to test and compare the effects of different freezing media on the morphological structure of each of the tumor samples. (a) For rapid sectioning, macro-dissected tumor material was frozen using the carbon dioxide quick-freeze method (carbon dioxide gas), where the coolant flows directly over the tissue [8]. This procedure has routinely been applied at our institute for the last two decades. (b) In parallel, one tissue piece of each of the 11 tumors not further needed for diagnostic purposes was wrapped in a plastic bag, put into a cryocassette, and snap frozen in liquid nitrogen for 10 s. This method has been used for collecting frozen tissues for our tissue bank since 1992. (c) An additional piece of tissue from each of the tumors was transferred to a cryocassette provided with a plastic mold. The tissue in the plastic mold was covered with OCT compound and snap frozen by immersing the closed cryocassette in pre-cooled isopentane at −80°C for 30 s using the mechanic freezer SnapFrost® (Alphelys, France). HE sections from all frozen tissue specimens were reviewed by a pathologist (H.M.).

Immunohistochemistry Frozen sections (4 μm) were treated with acetone (10 min) and then fixed in buffered formalin for 30 min. Following antigen retrieval for 10 min at 96°C in 0.1 M citrate buffer, tissue sections were incubated using MIB-1 (1:20 dilution; DAKO, Glostrup, Denmark). Standard immunohistochemical detection of bound antibody was performed using goat anti-rabbit IgG secondary antibodies followed by the ABC (Vectastain) and peroxidase substrate kits (1:200 dilution; Vector Laboratories, Burlingame, CA, USA).

DNA and RNA extraction Ten 20-μm sections were cut from each of the tumor samples either frozen in liquid nitrogen at −196°C or in isopentane at −80°C. DNA (five sections from each tumor) and RNA (five sections from each tumor) were extracted using the Biorobot EZ1 workstation (Qiagen) in combination with the recommended kit (EZ1 DNA tissue and EZ1 RNA Universal Tissue, respectively) according to the instructions of the manufacturer. DNA and RNA yield and purity was analyzed using a NanoDrop 1000 spectrophotometer. RNA integrity was assessed using the 2100 bioanalyzer (Agilent).

PCR mRNA expression of β-actin was determined in all isopentane and liquid nitrogen frozen tumors using conventional reverse transcriptase polymerase chain reaction (RT-PCR). Briefly, 1 μg total RNA was reverse transcribed using 50 ng of random hexamers, 100 U of M-MLV reverse transcriptase, and 20 U of RNAse Out (all reagents and enzymes from Invitrogen) for 10 min at 25°C and 60 min at 37°C. cDNA (2 μl each) was serially diluted (1:50, 1:250, and 1:500). A 485-bp fragment of β-actin was amplified using 2 μl GeneAmp® 10× PCR buffer (Applied Biosystems), 2 mM $MgCl_2$, 0.5 μM primers (forward primer: agc ctc gcc ttt gcc ga; reverse primer: gag gcg tac agg gat agc ac), and 1 U of AmpliTaq Gold® Taq polymerase (Applied Biosystems). PCR was performed in a total volume of 20 μl for 10 min at 94°C and 35 cycles with 30 s at 94°C, 30 s at 55°C, and 1 min at 72°C. Fifty nanograms of genomic DNA of each of the 11 tumors was used to amplify sequences of exon 1 of the von Hippel Lindau gene (267 and 503 bp) [7] and the PAX-2 gene (927 bp; forward primer: ggg tac aag acg ccc agt agt agt; reverse primer: ctt cct tcc tct ctt tct ggt cct).

Immunoblot Protein was extracted from 20-μm tissue sections using RIPA buffer (Sigma). Total protein concentration was measured using the bicinchoninic acid protein assay (Pierce) and NanoDrop 1000 spectrophotometer. Twenty micrograms of protein of each sample was separated on NuPage™ 4–12% Bis–Tris gels (Invitrogen) and transferred to nitrocellulose membrane following standard protocols. The membrane was incubated for 1 h at room temperature with mouse-monoclonal antibody against β-actin (1:5,000, MAB1501, Chemikon) in 1% fat-free dry milk in 1× TBST. HRP-conjugated rabbit anti-mouse secondary antibody (1:5,000, ab6728, Abcam) was used to detect β-actin. For signal detection, the ECL™ Western Blotting analysis system in combination with Hyperfilm™ (Amersham Pharmacia) was used.

Statistics Paired Student's *t* tests were applied to assess significant variances between the DNA, RNA, and protein values obtained from differentially treated tumors.

Results

Tissue pieces from 11 different tumor tissue specimens were snap frozen either with carbon dioxide snow, liquid nitrogen, or isopentane, which was pre-cooled at −80°C using the mechanical freezer SnapFrost®. The procedure for the latter method is outlined in Fig. 1a–c. HE sections were reviewed to study the effects of the three freezing media on tumor tissue morphology. As demonstrated in Fig. 2, the carbon dioxide quick-freeze method damaged the tissue structure due to ice crystal formation. In contrast, no artifacts were seen in tissues that were frozen in isopentane or liquid nitrogen. The morphological evaluation and the amounts of RNA, DNA, and protein obtained from each of the differently treated tumors are listed in Table 1. Statistical comparison of RNA, DNA, and protein concentrations showed no significant differences between tumors frozen in isopentane or liquid nitrogen (Table 2).

Positive results of immunohistochemical, Western blot, RNA and DNA analyses were obtained from all tumors that were frozen in liquid nitrogen or isopentane. Examples of protein, DNA, and RNA data of one seminoma and one endometrial carcinoma embedded in OCT and frozen in isopentane are illustrated in Fig. 3.

Discussion

In view of the different procedures used for rapid intraoperative section and tissue banking in many pathology institutes, our study aimed at establishing a reliable method which is applicable to both fields of activity. The use of a mechanical freezer and isopentane not only improves significantly the quality of the diagnosis of rapid sections, but also preserves the cellular and molecular structures of tumor tissues, which is a requisite for high-quality tissue banking.

Compared to tissues treated with carbon dioxide gas, the morphology of the tissues frozen with isopentane and liquid nitrogen was significantly more homogeneous and representative. It also seems obvious that the morphology of tumor types displaying more complex and irregular patterns, such as carcinomas of the lung, endometrium, and kidney, was best preserved with isopentane (Table 1, Fig. 2b). In contrast to isopentane, which directly transmits the temperature to the specimen, liquid nitrogen creates a layer of nitrogen gas around the tissue, which delays the freezing rate. This may explain our observation that certain tissues frozen in isopentane retain a slightly better morphology. Accordingly, this method is superior to quick-freeze procedures commonly used for routine frozen section examination and clearly facilitates evaluating routine rapid sections.

Embedding tissues in a frozen tissue matrix, such as OCT compound (Tissue Tek®), is required for reviewing properly HE sections from tumors. We used plastic molds in which tissue pieces of a maximal volume of 20×15×5 mm can be placed and embedded in OCT and which fit exactly in cryocassettes. Freezing tissues in plastic molds results in regular-shaped tissue blocks (Fig. 1c). To generate frozen sections, the OCT tissue block can easily be fixed on a chuck in a cryostat by gently pressing against the base of the plastic mold. This procedure has been used for both rapid section and tissue banking. For the latter method, it is important to prevent the cut tissue from desiccation. As OCT protects tissues from the freeze-burn effect of liquid nitrogen, we re-sealed transparently the tissue surface with OCT diluted 1:1 with aqua bidest using a brush (Fig. 1d). The tissue block was then transferred to a mechanically labeled cryocassette and stored in a cryobox at −80°C for arranging concisely archived frozen tissue until reuse (Fig. 1e).

Knowing the histological composition and the quality of stored tissue is a basic prerequisite for tumor tissue banking (Fig. 1f). Morphological features, such as tumor area, non-neoplastic area, and percentage of tumor cells within the tumor area, are directly documented on the glass slide with the HE section. This allows tracking precisely those tumor tissue specimens suited for the molecular method required for future cancer research projects. For analyzing reliably gene mutations, gene or protein expression patterns in tumors, tissue samples used for extractions should preferably not or only be low contaminated with non-neoplastic

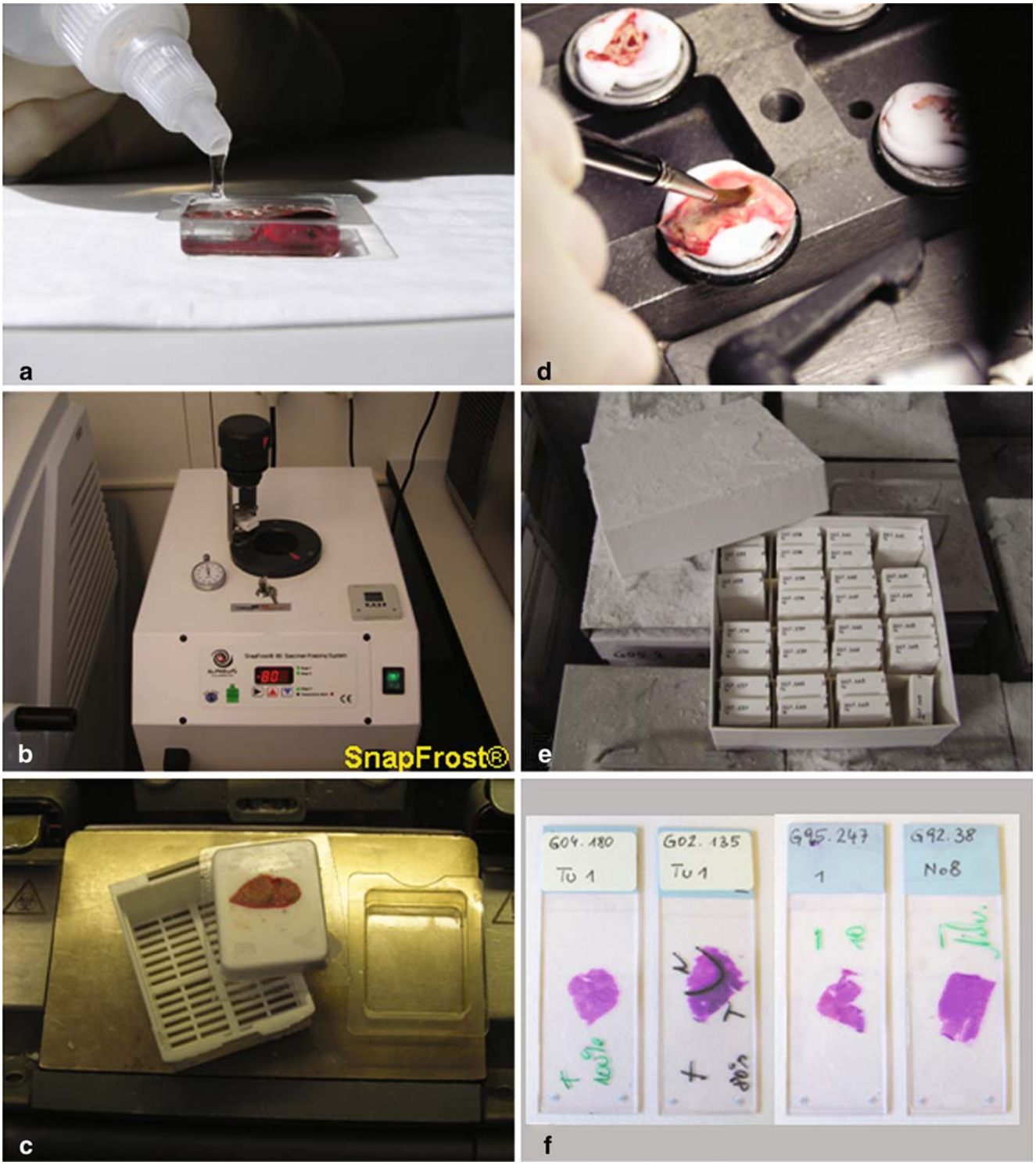


Fig. 1 Tissue processing for rapid section (**a**–**c**) and tumor tissue banking (**a**–**f**). Tumor tissue in plastic mold embedded with OCT (**a**). Tissue holder with cryocassette containing tissue prepared for freezing at −80°C in isopentane using the SnapFrost® (**b**). Resulting OCT tissue block (**c**). Resealing of the cut tissue surface with diluted OCT (**d**). Tissue storage (**e**). Quality control of tumor tissue for biobanking (**f**). +/− Good/bad morphology, *T* tumor, *N* normal, *Necr* necrosis, *%* tumor cells

cells. It is of note, however, that RNA extracted from tumors with more than 50% tumor cells is apparently still sufficient for yielding a gene expression signature as predictor of survival in breast cancer [10]. Very heterogeneous tumors, in which the cell population of interest constitutes only a small fraction, can still be used for in situ analyses, immunostainings, laser micro-dissection, or PCR-based microbial DNA/RNA detection.

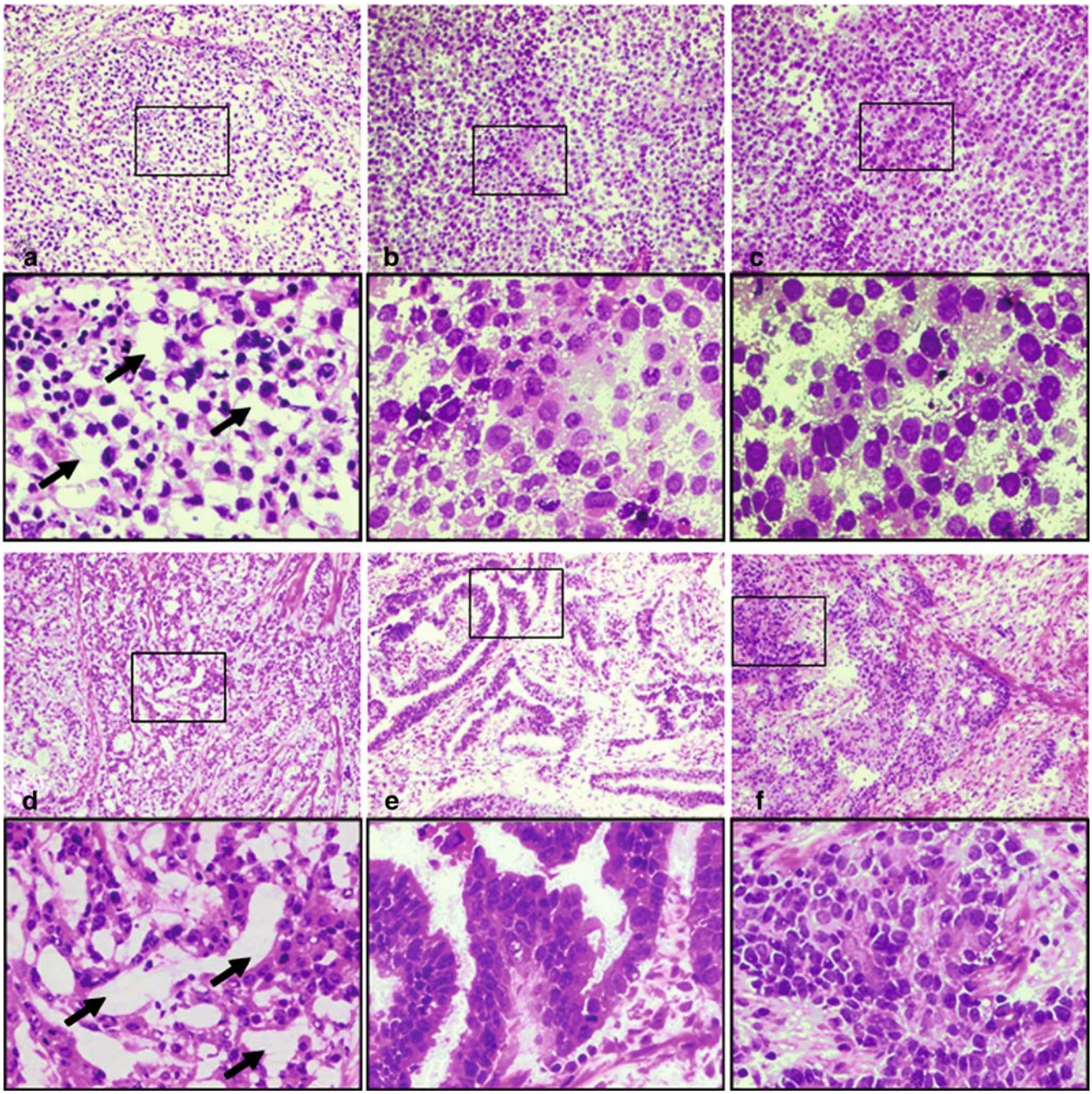


Fig. 2 Examples of HE stained sections of a seminoma (**a–c**) and an endometrial carcinoma (**d–f**) (magnifications ×10 and ×40). Tissue frozen with carbon dioxide snow (**a**, **d**), isopentane (**b**, **e**), and liquid nitrogen (**c**, **f**). Arrows indicate artifacts due to ice crystal formation

According to the recommendations of the European Human Frozen Tumour Tissue Bank (TuBaFrost) [5] and the guidelines for the collection, handling, and storage of specimens from the Breast International Group (BIG) and National Cancer Institute (NCI) Cooperative Group breast cancer clinical trials (http://ctep.cancer.gov/forms/guidelines_fresh_tissue.pdf), isopentane is the medium of choice for snap freezing tissues as it is a very efficient cryoconductor and in comparison to liquid nitrogen, causes fewer cryo-artifacts. In addition, OCT is an option for tumor biobanking as it gives high-quality results for histology study, preserves morphology by protecting tissue from the lyophilization effect of liquid nitrogen, and minimizes biological cross contamination. However, there is hardly any literature data that described the possible chemical reactions of isopentane and OCT with cellular structures and its impact on molecular assays. Using a modified protocol for immunostaining frozen tissue sections and Western blot, we observed Ki-67 and β-actin expression patterns that were detectable in all tumor types and virtually identical between the differently treated tissue pairs. By

Table 1 The impact of freezing medium on tumor morphology, RNA, DNA, and protein quality

Tumor type	Medium	Morphology[a]	RNA (μg/μl)[b]	260/280 nm	rRNA ratio	RIN	DNA (μg/μl)[b]	Protein (μg/μl)[b]
Renal cell carcinoma	Isopentane	+++	1.43	2.1	1.5	8.4	0.71	4.32
	Liquid nitrogen	++	1.01	2.08	1.7	8.5	0.56	4.0
	CO_2	+	nd	nd	nd	nd	nd	nd
Breast carcinoma	Isopentane	++	0.97	2.07	1.2	8.1	0.34	5.4
	Liquid nitrogen	++	8.2	2.06	1.3	8.3	0.42	4.2
	CO_2	+	nd	nd	nd	nd	nd	nd
Lung adenocarcinoma	Isopentane	++	1.09	2.05	1.2	7.9	0.67	3.8
	Liquid nitrogen	++	1.31	2.08	1.1	7.3	0.59	4.5
	CO_2	+	nd	nd	nd	nd	nd	nd
Endometrial carcinoma	Isopentane	+++	2.46	2.11	1.6	7.4	1.56	5.6
	Liquid nitrogen	++	2.18	2.12	1.7	7.6	1.72	6.8
	CO_2	+	nd	nd	nd	nd	nd	nd
Stomach carcinoma	Isopentane	++	1.55	2.09	1.4	7.9	0.89	3.9
	Liquid nitrogen	++	2.48	2.1	1.7	7.5	1.47	5.8
	CO_2	+	nd	nd	nd	nd	nd	nd
Lung adenocarcinoma	Isopentane	++	1.28	2.1	1.4	7.5	0.36	4.1
	Liquid nitrogen	++	0.84	2.07	1.1	7.9	0.29	3.5
	CO_2	+	nd	nd	nd	nd	nd	nd
Seminoma	Isopentane	++	0.78	2.01	1.3	6.4	0.14	6.0
	Liquid nitrogen	++	0.91	2.04	1.3	6.3	0.16	6.4
	CO_2	+	nd	nd	nd	nd	nd	nd
Ovarian carcinoma	Isopentane	++	0.81	2.04	1.8	8.3	0.32	3.8
	Liquid nitrogen	++	0.77	2.08	1.6	8.2	0.4	3.6
	CO_2	+	nd	nd	nd	nd	nd	nd
Ovarian carcinoma	Isopentane	++	1.37	2.09	1.0	7.2	0.96	4.9
	Liquid nitrogen	++	1.35	2.11	1.0	7.3	0.78	4.5
	CO_2	+	nd	nd	nd	nd	nd	nd
Breast carcinoma	Isopentane	++	0.88	2.11	1.4	8.8	0.56	2.2
	Liquid nitrogen	++	1.23	2.08	1.3	8.5	0.72	3.0
	CO_2	+	nd	nd	nd	nd	nd	nd
Lung adenocarcinoma	Isopentane	+++	0.92	2.07	1.3	7.9	0.7	4.8
	Liquid nitrogen	++	0.57	2.02	1.4	7.9	0.46	4.2
	CO_2	+	nd	nd	nd	nd	nd	nd

nd Not done

[a] Evaluation of morphology: + problematic; ++, +++ well evaluable; +++ morphology better than ++

[b] Total volume: 50 μl

comparing the results obtained with liquid nitrogen, we conclude that IHC and Western results were not influenced negatively, neither by isopentane nor by OCT.

Previous studies suggested that the presence of OCT in DNA extracts can inhibit amplification by polymerase chain reactions [9]. Using a column-based system, which highly purifies DNA from any residual components, we were able to amplify DNA fragments ranging from 267 to 927 bp in all tumors. This strongly suggests that a successful amplification of larger PCR products mainly depends on the protocol used for extracting DNA from OCT embedded tumors. It is also of note that there were no

Table 2 Mean values ± standard deviations of RNA, DNA, and protein extracted from tissues frozen in isopentane and liquid nitrogen

Medium	RNA (μg/μl)	260/280 nm	rRNA ratio	RIN	DNA (μg/μl)	Protein (μg/μl)
Isopentane	1.18+0.54	2.08+0.03	1.41+0.22	7.89+0.47	0.66+0.37	4.44+1.01
Liquid nitrogen	1.15+0.65	2.08+0.03	1.38+0.25	7.85+0.45	0.69+0.46	4.59+1.17
p value	ns	ns	ns	ns	ns	ns

ns Not significant

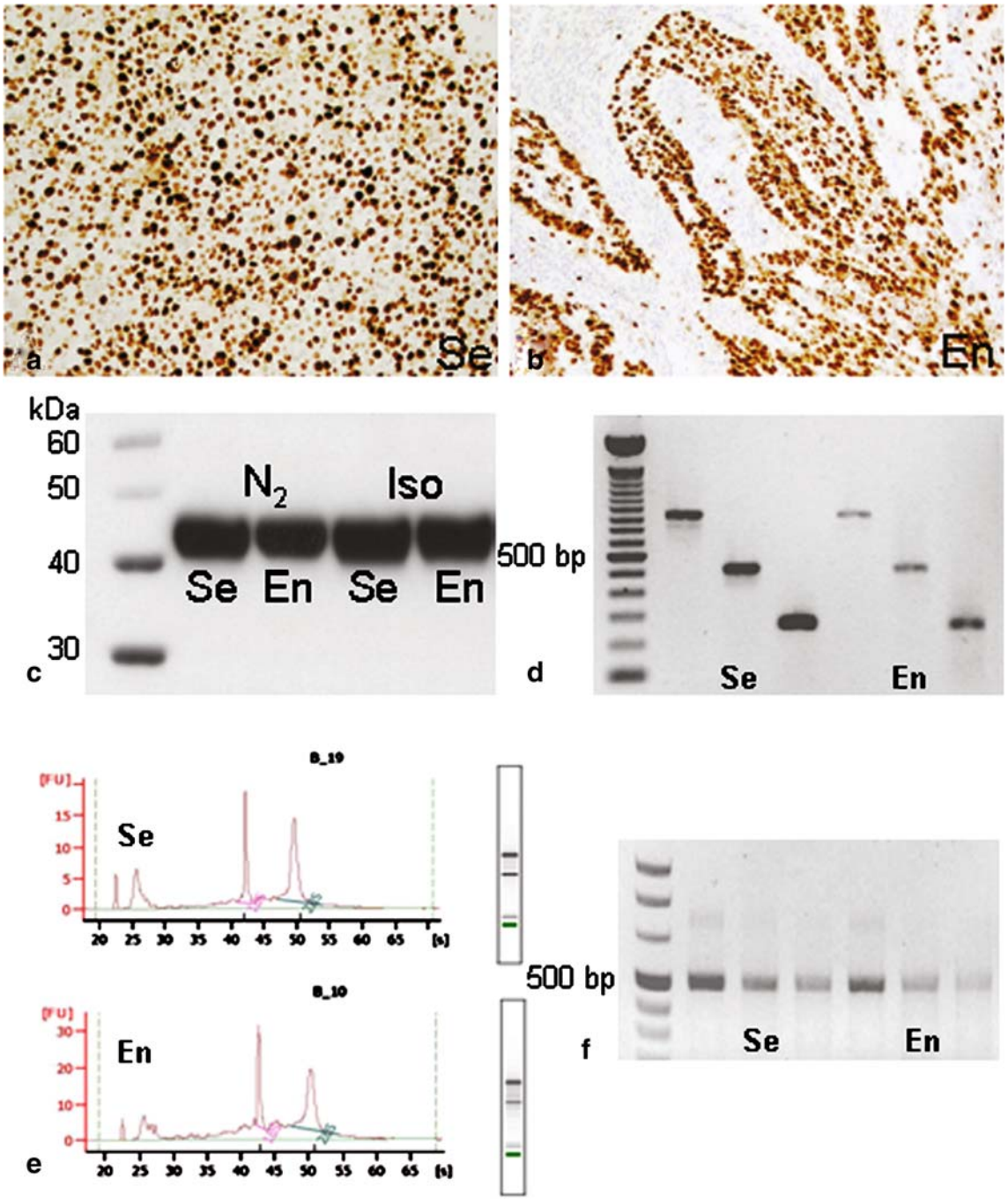


Fig. 3 Examples of protein, DNA, and RNA quality analyses of OCT embedded tumors frozen in isopentane. Ki-67 stained tissue sections (**a**, **b**). Western blot showing β-actin expression in matched tumors frozen in liquid nitrogen or isopentane (**c**). DNA amplification of VHL (267 and 503 bp) and PAX-2 (927 bp) gene fragments (**d**). Bioanalyzer scans of extracted total RNA (**e**). RT-PCR of β-actin mRNA (485 bp) with diluted cDNA (1:50, 1:250, and 1:500; **f**). *Se* Seminoma, *En* endometrial carcinoma, N_2 liquid nitrogen, *Iso* isopentane

significant differences between the freezing media, tumor types, and DNA yields (Table 1).

Although RNA seems to be stable in non-fixed surgical specimens for up to 16 h [4], it is widely accepted that comprehensive gene expression profiling studies rely on RNA of high quality. To test the integrity of the RNA of our tissue samples, snap freezing was done as recommended [5] within 30 min after surgery. As shown in Table 1, RNA integrity numbers (RIN) were comparable between the differently treated tumor pairs being highest for one breast carcinoma (8.8) and lowest for one seminoma (6.3). RIN, ribosomal RNA ratios, optical density, RNA yields, and RT-PCR results showed that intact RNA was obtained from all tumor types (Table 1, Fig. 3e,f) embedded in OCT.

Long-term storage of tissue samples is one of the most challenging issues for tissue banking. As our protocol was first established in January 2006 at our institute, we currently do not know whether the integrity of cellular and molecular structures of our tissues becomes compromised after storage for a longer period of time. By following strictly the guidelines of TuBaFrost [5], BIG, and NCI (http://ctep.cancer.gov/forms/guidelines_fresh_tissue.pdf) for tissue banking, the procedure described here should ensure the quality of tissue samples. In fact, re-analysis of the tumor tissues after 1 year of storage at −80° C demonstrated clearly that the high quality of morphology, DNA, and RNA remained unchanged (data not shown).

Safety reasons also strongly argue for using a system like the SnapFrost®. Carbon dioxide originating from liquid carbonic acid stored in a cylinder is often used for rapid section. Depending on the type of disease, treating tissues using this method may cause formation of harmful aerosol, which may be infectious when inhaled. For tissue banking, liquid nitrogen is commonly filled in containers that have to be opened many times for freezing tissues, which causes strong evaporation. In contrast, isopentane is a non-degassing fluid which is kept in a closable freezing chamber. This considerably lowers the risks for cold burns and infections.

We developed an isopentane-based protocol that may help to standardize snap-freezing tissues for both routine rapid section and tumor biobanking in pathology institutes. This procedure is time saving, simplifies significantly tissue handling and processing, and preserves excellently the integrity of cellular and molecular structures in different tumor types, thus satisfying the demands of pathologists, scientists, technicians, and tissue bankers.

Acknowledgments We thank Dr. Kirsten Struckmann and Silvia Behnke for their excellent technical support. This study was supported by UBS AG (made possible by an anonymous donor), Zurich Cancer League, and the Foundation Biobank-Suisse. We declare that the experiments comply with the current laws of the Kanton Zürich.

Conflict of interest statement We declare that we have no conflict of interest.

References

1. Grizzle WE, Aamodt R, Clausen K, LiVolsi V, Pretlow TG, Qualman S (1998) Providing human tissues for research: how to establish a program. Arch Pathol Lab Med 122:1065–1076
2. Loken SD, Demetrick DJ (2005) A novel method for freezing and storing research tissue bank specimens. Hum Pathol 36:977–980
3. McElroy HH, Shih MS, Parfitt AM (1993) Producing frozen sections of calcified bone. Biotech Histochem 68:50–55
4. Micke P, Ohshima M, Tahmasebpoor S, Ren ZP, Ostman A, Ponten F, Botling J (2006) Biobanking of fresh frozen tissue: RNA is stable in nonfixed surgical specimens. Lab Invest 86:202–211
5. Morente MM, Mager R, Alonso S, Pezzella F, Spatz A, Knox K, Kerr D, Dinjens WN, Oosterhuis JW, Lam KH, Oomen MH, van Damme B, van de Vijver M, van Boven H, Kerjaschki D, Pammer J, Lopez-Guerrero JA, Llombart Bosch A, Carbone A, Gloghini A, Teodorovic I, Isabelle M, Passioukov A, Lejeune S, Therasse P, van Veen EB, Ratcliffe C, Riegman PH (2006) TuBaFrost 2: standardising tissue collection and quality control procedures for a European virtual frozen tissue bank network. Eur J Cancer 42:2684–2691
6. Naber SP (1996) Continuing role of a frozen-tissue bank in molecular pathology. Diagn Mol Pathol 5:253–259
7. Schraml P, Struckmann K, Hatz F, Sonnet S, Kully C, Gasser T, Sauter G, Mihatsch MJ, Moch H (2002) VHL mutations and their correlation with tumour cell proliferation, microvessel density, and patient prognosis in clear cell renal cell carcinoma. J Pathol 196:186–193
8. Silva EG, Kraemer BB (1987) Intraoperative pathologic diagnosis. Frozen section and other techniques. Williams & Wilkins, Baltimore
9. Turbett GR, Sellner LN (1997) The use of optimal cutting temperature compound can inhibit amplification by polymerase chain reaction. Diagn Mol Pathol 6:298–303
10. van de Vijver MJ, He YD, van't Veer LJ, Dai H, Hart AA, Voskuil DW, Schreiber GJ, Peterse JL, Roberts C, Marton MJ, Parrish M, Atsma D, Witteveen A, Glas A, Delahaye L, van der Velde T, Bartelink H, Rodenhuis S, Rutgers ET, Friend SH, Bernards R (2002) A gene-expression signature as a predictor of survival in breast cancer. N Engl J Med 347:1999–2009
11. Vonsattel JP, Aizawa H, Ge P, DiFiglia M, McKee AC, MacDonald M, Gusella JF, Landwehrmeyer GB, Bird ED, Richardson EP Jr. et al (1995) An improved approach to prepare human brains for research. J Neuropathol Exp Neurol 54:42–56
12. Went PT, Dirnhofer S, Bundi M, Mirlacher M, Schraml P, Mangialaio S, Dimitrijevic S, Kononen J, Lugli A, Simon R, Sauter G (2004) Prevalence of KIT expression in human tumors. J Clin Oncol 22:4514–4522

Virchows Arch (2008) 452:313–318
DOI 10.1007/s00428-008-0576-y

ORIGINAL ARTICLE

Cut-resistant protective gloves in pathology—effective and cost-effective

Florian R. Fritzsche · Manfred Dietel · Wilko Weichert · Ann-Christin Buckendahl

Received: 22 October 2007 / Revised: 19 December 2007 / Accepted: 28 December 2007 / Published online: 31 January 2008
© Springer-Verlag 2008

Abstract Cutting injuries and needle-stitch injuries constitute a potentially fatal danger to both pathologists and autopsy personnel. We evaluated such injuries in a large German institute of pathology from 2002 to 2007 and analysed the effect of the introduction of cut-resistant gloves on the incidence of these injuries. In the observation period, 64 injuries (48 cutting injuries and 16 needle-stitch injuries) were noted in the injury report books. Most injuries were located at the non-dominant hand, preferentially at the index finger and the thumb. Around one fifths of the injuries were at the side of handedness. The average number of injuries per month was 1.22 for the 50months prior to the introduction of cut-resistant gloves, more than seven times higher than after their introduction (0.158; 19months; $p < 0.001$). Considering the medical and administrational costs of such injuries, cut-resistant protective gloves are an effective and cost-effective completion of personal occupational safety measures in surgical pathology and autopsy. We strongly recommend the use of such gloves, especially for autopsy personnel.

Keywords Cutting injury · Protective gloves · Cut-resistant · Pathology · Occupational safety

F. R. Fritzsche (✉) · M. Dietel · W. Weichert · A.-C. Buckendahl
Institute of Pathology, Charité Universitätsmedizin Berlin,
Campus Mitte. Charitéplatz 1,
10117 Berlin, Germany
e-mail: florian.fritzsche@charite.de

F. R. Fritzsche
Institute of Surgical Pathology, UniversitätsSpital Zürich,
Schmelzbergstr. 12,
8091 Zürich, Schweiz
e-mail: florian.fritzsche@usz.ch

Introduction

Besides histological diagnostics, conducting autopsies and preparing and dissecting surgical pathology specimen are the main tasks of surgical pathologists. Because precision is paramount for pathological workup of tissue, both former activities include the use of various extremely sharp blades and scalpels (Fig. 1a). Suturing bodies at autopsies further implicates the use of solid-core needles (Fig. 1a). Not surprisingly, the constant use of such instruments quite frequently leads to injuries. Cutting injuries and needle-stitch injuries could vary from harmless superficial wounds to deep lacerations.

An additional danger associated with the handling of fresh or partially fixed human tissue is the danger of transmission of blood-borne diseases. The possibility of disease transmission by autopsies was first recognised by the Austrian–Hungarian physician Ignaz Philipp Semmelweiss in the nineteenth century [4, 7]. Although many infectious diseases from Semmelweiss' times would probably be less fatal today, serious blood-borne disease like viral hepatitis B and C (HCV) or human immunodeficiency virus (HIV) remain a potentially fatal thread [3, 11]. The theoretical career risk for pathologists and autopsy assistants is definitely not negligible [17]. Moreover, several other infectious diseases were found transmittable at autopsies or by cutting/needle-stitch injuries [2, 5, 6, 8, 19, 25, 27].

In 1987, Steger analysed the life expectancy and causes of death of pathologists in Germany and found that their life expectancy was reduced in comparison to the normal population due to a rather high rate of occupational infections, accidents and suicides [22]. If unnatural causes of deaths and occupational infections were excluded, the life expectancy converged to that of the normal population [22]. Personal safety measures have strongly evolved over

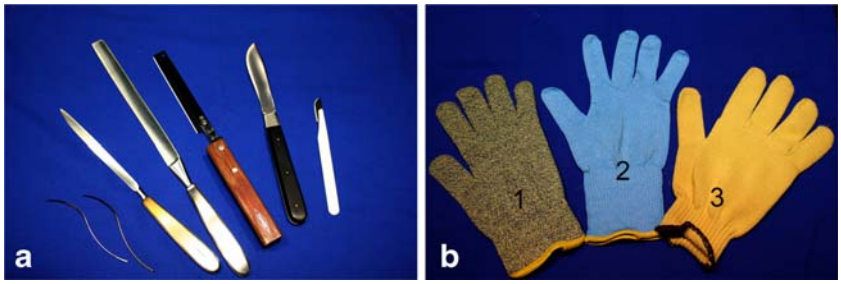


Fig. 1 **a** Selection of blades and needles used in the dissection and autopsy divisions. **b** Three different cut-resistant gloves (1: Vantage™ 2: proFood® Safe-Knit®; 3: GoldKnit™). The gloves differ in thickness, dexterity, elasticity and price

time (Fig. 2). The improvements made could mainly be contributed to a better understanding of the causes and origins of diseases.

In this study, we analysed cutting and needle-stitch injuries before and after the introduction of cut-resistant gloves as an additional routine safety measure for pathologists and autopsy assistants. Some laboratories have already used such *protective gloves* before. We hope that the results of this study will persuade more pathologists to introduce this easy, effective and cheap safety measure.

Materials and methods

Data collection

Our analysis was performed at the Institute of Pathology (Charité Campus Mitte (CCM) and Campus Virchow Klinikum (CVK)) of the Charité Universitätsmedizin Berlin. This large institution is the service provider of pathologic diagnostics for two university campuses of the Charité and several peripheral hospitals and physicians. For our analysis, we reviewed the injury report books (IRB) from the central preparation and dissection laboratory (CPDL) for surgical specimen and from two autopsy divisions (CCM–CVK). We included all cutting and needle-stitch injuries from January 2002 until September 2007. Cutting injuries of medical laboratory assistants with microtome blades (different division) and cutting injuries aside the hands were excluded.

Year, type and side of injury were noted. Handedness and protective measures used at the time of injury were assessed from the IRB and personnel interviews if possible.

In addition, we assessed the number of autopsies for each year and the annual number of surgical specimen processed. Information about costs for the treatment of needle-stitch and cutting injuries were obtained from the compulsory accident insurance companies in Berlin, Munich (Bavaria) and Düsseldorf (North Rhine–Westphalia (NRW)).

Change of occupational safety measures

Standard safety measures for autopsies and dissection of surgical specimen included cotton protective clothing, protective shoes, plastic skirts and single or double layers of latex or vinyl gloves. Furthermore, surgical masks and protective eyewear were used in the autopsy divisions.

Starting February 2006 cut-resistant gloves (different types (Fig. 1b), Ansell Healthcare Europe NV, Brussels, Belgium) were introduced at both autopsy divisions for all physicians, autopsy assistants and students working with blades and needles. From April till the beginning of July, extra-thin cut-resistant gloves (Fig. 1b, proFood® Safe-Knit® and Vantage™, Ansell) and protective eyewear (Uvex Arbeitsschutz GmbH, Fürth, Germany) were introduced at the central preparation and dissection laboratory. Additionally, in all three divisions, highly fluid resistant respirators (Health Care Respirator 1873V FFP3 with valve, 3M St. Paul, MN, USA) of the highest protection level (filter face piece protection level 3 = FFP3) against airborne particles (e.g. fungal spores) aerosols (e.g. tuberculosis [9, 10, 18, 24])

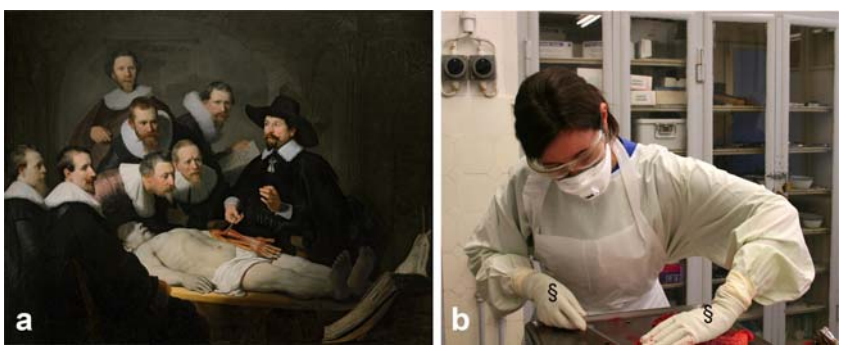


Fig. 2 Personal safety measures at different times: **a** The anatomy lesson of Dr. Tulp (Rembrandt, Royal Picture Gallery Mauritshuis, The Hague, the Netherlands). **b** Pathology resident at the Charité Universitätsmedizin Berlin with the new standard personal safety measures (protective clothing, protective eyewear, FFP3 respirator, doubled-latex gloves and cut-resistant gloves (§))

and viruses (e.g. HIV, HCV, H5N1 flu) replaced the conventional surgical mask as standard protection.

Statistics

For statistical analysis, we used SPSS 14.0 (SPSS Inc. Chicago, IL, USA). To asses differences in incidence rates, number of autopsies and number of surgical specimen, the Mann–Whitney *U* test and the Kruskal–Wallis test were applied. Correlation analyses were performed applying Spearman's rank order correlation. *P*-values < 0.05 were considered significant.

Results

In the observation period, 48 cutting injuries and 16 needle-stitch injuries were reported. Most injuries occurred in the autopsy divisions, where pathologists reported three cutting injuries and autopsy personnel reported the remaining 33 cutting injuries as well as all needle-stitch injuries. The remaining 12 cutting injuries occurred to pathologists in the dissection division. Typical activities associated with the occurrence of injuries were organ exenteration, suturing the body at the end of the autopsy, cutting and slicing surgical specimen or changing blades.

Detailed characterisation of the injuries is provided in Table 1. Thirty-six of the injuries (56%) affected the non-dominant hand, while the dominant hand was injured in 20% (13 cases). For the remaining cases, either the handedness or the hand injured was unknown. Concerning the exact location, the index finger was most often affected (20×) closely followed by the thumb (15×) and further behind the middle finger (7×), little finger (3×) and the ring finger (2×).

Sixty-one of the injuries happened between January 2002 and February 2006 (before the introduction of cut-resistant gloves in the specific divisions), which results in an average of 1.22 injuries per month. The remaining three injuries (two needle stitches and one cutting injury) took place 19months after introduction of the new safety concept, resulting in an average of 0.158 injuries per month. This difference in the incidence rate was statistically highly significant (Mann–Whitney *U* test: $p < 0.001$, Fig. 3). If July 2006 but not February (completed introduction in CPDL) was used as the cutoff, the values changed to 1.15 injuries per month before and 0.13 injuries per months after the introduction of the gloves ($p = 0.001$). Interestingly, the cutting injury and one of the needle-stitch injuries reported after February 2006 occurred to persons who did not wear cut-resistant gloves at this time. One needle-stitch injury happened although cut-resistant gloves were worn.

The average number of surgical specimen investigated and autopsies performed varied around 41,500 (range 39,000–44,000) for the former procedure and around 470 (range 440–510) per year for the latter procedure. The differences in the number of surgical specimen diagnosed and autopsies performed were not statistically significant between years ($p = 0.416$ for both autopsies and surgical specimen), indicating that changes in the incidence of injuries were not due to differences in yearly work load. Furthermore, there was no correlation between the number of injuries and that of autopsies or surgical specimen ($p = 0.468$ and $p = 0.623$). Although a normal fluctuation of employees took place in all three included divisions, the number of employees in the respective division at a given time remained constant (data not shown). To test for a general trend of not reporting injuries in certain times, we compared the frequencies of all other injuries in the IRB for the respective years (2002, 2; 2003, 11, 2004, 5; 2005, 13; 2006, 12; 2007, 7). To improve intra- and inter-institutional comparability, we related cutting and needle-stitch injuries to the number of autopsies and surgical specimens. Per 100 autopsies, 2.5 injuries occurred before and 0.4 after the introduction of cut-resistant gloves. The equivalent numbers for 10,000 surgical specimens were 0.7 and 0.0.

Only ten of the cutting and needle-stitch injuries noted were reported to the accident insurance company and

Table 1 Characteristics of cutting injuries (CI) and needle-stitch injuries (NS) for the respective years (2007: January–September)

Characteristic	2002		2003		2004		2005		2006		2007	
Type of injury	CI	NS	CI	NS	CI	NS	CI	NS	CI	NS	CI	NS
Number of injuries	12	6	19	3	8	3	7	2	2	1	0	1
Right hand	3		8	3	1			1				
Left hand	6	6	11		6	3	6	1	2	1		1
Unknown hand	3				1		1					
At side of handedness	2		6	3	1	1						
At contralateral hand	5	5	12		4	1	4	1	2	1		1
Unknown handedness	5	1	1		3	1	3	1				
Cut-resistant gloves used										1		
Latex–vinyl gloves only	12	6	19	3	8	3	6	2	2			1
Total injuries	18		22		11		9		3		1	

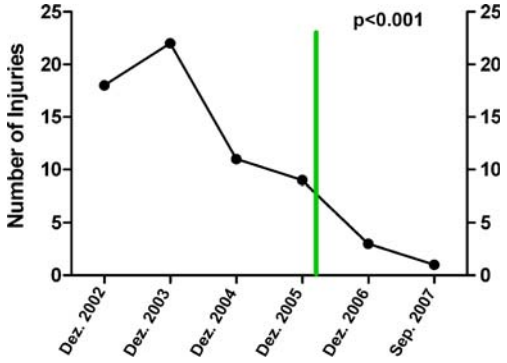


Fig. 3 Graph displaying the reduction of cutting and needle-stitch injuries after the introduction of cut-resistant gloves (*vertical bar*)

resulted in a medical examination. The mean costs for a medical examination and laboratory analyses in Berlin for a cutting–needle-stitch injury were 187.66 Euro in 2001. This is in line with the average costs reported from Bavaria and NRW. Costs due to administrational effort and lost working time were estimated above 200 Euro per case. Infections and further medical treatment were not included in these estimates. If included, the costs per case were above 4,000 Euro per year according to the accident insurance company of NRW. In the observation period, one of the cutting injuries included in our study resulted in a month-long prophylactic anti-retroviral therapy. Prices of the cut-resistant gloves were 7.45, 11.40 and 17.50 Euro (recommended retail price) per pair, respectively. For an institute with about 20 persons working in the analysed divisions, the overall costs for individual cut-resistant gloves would be between 149 and 350 Euro (about 210–495 US dollar).

Additionally, to the cutting injuries, four splashes in the eye were reported in the CPDL before the introduction of protective eyewear. Three of those splashes were officially registered and resulted in medical examinations. After the introduction of protective eyewear, no further incidences were reported.

Discussion

Blood-borne diseases like HCV and HIV are a global phenomenon with disease focusing mainly outside Western Europe. Still, also in this region, they do remain epidemiologically important diseases and constitute a potential danger for medical staff including pathologists [1, 3, 11–13, 17]. Standard occupational safety measures should take into account that an infection of a patient might be unknown to both clinician and pathologist at the time of tissue examination. Therefore, the mere enhancement of otherwise insufficient standard safety measures in the case of known infectious disease should be considered substandard and careless.

Concordant with our results, two orthopaedic studies found the thumb and the index finger, respectively, thumb, index finger, middle finger and palm most often affected by glove-perforating injuries [16, 23]. Dominant and non-dominant hand were affected almost alike [16, 23]. Although the number of cases was small (n = 8), Pritt and Waters [21] reported similar results in their study of cutting injuries in a pathology department. A possible explanation for the predominance of injuries at the non-dominant hand in our larger study could be the use of different, mainly larger, blades and needles with larger handles in comparison with surgical disciplines, which might make injuries of the cutting hand less likely. Differences in the results might also be attributed to the 15 cases with unknown handedness or side of injury in our study, although it seems very unlikely that all these cases could be attributed to the dominant hand.

From the eight cases in Pritt's study, two were especially interesting because cut-resistant gloves were worn by the affected physicians. In one case, the cutting injury occurred at the non-gloved cutting hand while the non-cutting hand was protected. In the other case, a microtome blade obviously cut through the cut-resistant glove and into the thumb of a resident [21]. Notwithstanding the institute in Pritt's study, microtome blades are not used for the dissection of surgical specimen in our department. Anyhow, we had only few microtome-caused injuries (n = 4) in the respective laboratory section and because we have not introduced cut-resistant gloves in this section we excluded them from our analysis. In a probatory experiment, when we tried to cut through the thin cut-resistant gloves from the CPDL (both types) with a microtome blade, we were unable to permeate the glove.

Kelly et al. compared doubled-latex gloves with the same combination of latex and cut-resistant gloves we used in a series of 12 consecutive intermaxillary fixation procedures and a test set of six cadaver heads. They demonstrated a significant reduction of glove perforation when using cut-resistant gloves [14]. Likewise, Pieper et al. have compared double-latex gloving, triple-latex gloving and gloving with Kevlar or stainless steel glove liners in 30 oral surgical procedures [20]. Although perforations in the Kevlar and stainless steel group occurred, protection was superior to that of double-latex gloving. Importantly, cut resistance was not tested in this study because all perforations could be attributed to wire puncture [20]. In a study on 50 orthopaedic procedures, no advantage for cut-resistant gloves was found [16]. Again, the punctures in this study were rather not attributable to blade injuries. However, in contrast, another randomised orthopaedic study on 118 operations did show a significantly higher perforation rate without cut-resistant gloves [23].

The relevance of percutaneous injuries in surgical disciplines has already been described and cut-resistant gloves are seen as potentially useful [15]. The majority of

injuries was due to needle stitches [15]. Considering the inferior protection of Kevlar-based cut-resistant gloves against puncture injuries in comparison with cutting injuries, the benefit of cut-resistant gloves is probably limited in these circumstances. Although puncture-resistant polyethylene gloves are commercially available, the cutaneous sensibility with these gloves was markedly reduced, questioning their usability [26].

As two injuries took place at unprotected hands after the introduction of cut-resistant gloves, it is obvious that wearing habits differed among the staff. An exact analysis of how often cut-resistant gloves were worn was not possible retrospectively. Generally, the younger residents (first to fourth year) accepted the use of cut-resistant gloves better than older physicians. The wearing habits of the autopsy staff varied from seldom to constantly. In the majority of cases, the cut-resistant gloves were worn on the non-dominant hand only. Arguments for this practice as well as for not wearing the gloves were better dexterity and sensitivity, for example when searching lymph nodes. Routine wearers of the gloves reported good adjustment to the gloves and only minimal restrictions, especially when wearing them only on the non-dominant side. Adjustment was even better in the autopsy divisions, probably attributable to the fact that less often microscopically small probes had to be handled.

Because needles were able to penetrate the used cut-resistant gloves, a reduction of these injuries could not be expected. That we still experienced a reduction in the year 2006 and 2007 might be due to a better care in the usage of needles possibly caused by an increased attention to occupational safety with the introduction of cut-resistant gloves. Because, for autopsy personnel, skin sensitivity is not of that high importance for exenteration, it is possible that the new puncture-resistant polyethylene gloves could prevent or at least further reduce needle-stitch injuries in this field of work. Until now, there exist no data on this issue, but we plan to test such gloves for this purpose in the future.

Another point to address is that possible important external parameters influencing the incidence rates of cutting injuries like number of employees in a division, number and type of cutting instruments, number of autopsies and number of surgical specimen did not relevantly change from 2002 to 2007. The number of injuries other than the included forms was rather low. These injuries were also infrequent in years with the highest cutting and needle-stitch injuries (2002 and 2004), increased in 2005 and 2006 and decreased little again in 2007. This argues against the possibility of a changed injury-reporting behaviour and supports the attribution of the observed changes to the use of cut-resistant gloves. However, the just significant drop ($p = 0.046$) in the number of injuries between 2002–2003 and 2004–2005 is difficult to explain. Meanwhile, even the drop from 2004–2005 to 2006–2007 is highly significant ($p = 0.009$). The observational study design does not allow for an absolutely doubtless attribution of the demonstrated improvements (decrease) in the numbers of injuries to the cut-resistant gloves, but considering all data given this seems at least to be a very likely and well-founded assumption.

Based on the authors' experiences, the study results and the review of literature, recommendations for the safe use of blades and needles in dissection and autopsy divisions are summarised in Table 2. Further experiments should be performed concerning the usefulness of polyethylene gloves instead of conventional cut-resistant gloves (see Table 2 point 4), especially for autopsy personnel.

Financially, even considering only the officially reported cases (15%, which is in line with estimations from the accident insurance company of NRW with around 80% unreported cases), the expenditures for medical treatments by the accident insurance companies exceed the costs for cut-resistant gloves by far. The use of cut-resistant gloves

Table 2 Recommendations for the safe use of blades and needles in pathologic dissection and autopsy divisions

Number	Recommendation
1	If blades are not necessary, they should be omitted and should be out of the normal elbowroom. Ideally, they could be placed in troughs or drawers but in clear view of the user. Blunt blades and needles should not be used but carefully replaced. Waste blades should be dropped into special one-way-open containers only—not just stored besides. The containers should be regularly emptied.
2	Direct pressure should not be executed on a blade with the hands (especially not without wearing cut-resistant gloves). Using hands–fingers to exercise counter-pressure for suturing should be avoided. If unavoidable, as much space as possible for the penetrating needle should be given.
3	External disturbance for the cutting or suturing person should be minimised.
4	Cut-resistant gloves should be worn in addition to doubled-latex–vinyl gloves ideally on both hands whenever possible. At least for the non-dominant hand, such gloves should be used whenever working with blades.
5	If an injury occurred, work should be stopped and the wound should be treated according to wound-adapted treatment plans. Injuries with blades or needles should be reported. Although time pressure and shortage of staff seem often to seriously hinder this, it is the responsibility for one's own health next to insurance-related reasons that should promote compliance in this essential matter.

seems therefore reasonable not only from the medical but also from a macro-economical point of view.

In conclusion, we demonstrated that cut-resistant protective gloves are a reasonable, effective and cost-effective safety measure in pathologic autopsy and dissection divisions. Although certainly underestimated, cutting injuries are not very frequent; however, they still constitute a relevant and specific danger to pathologists and autopsy staff. The procedures described in this study could significantly reduce their incidence rate.

Acknowledgements The support in financial data collection by the Unfallkasse Berlin, Unfallkasse München and Unfallkasse Nordrhein-Westfalen is greatly acknowledged. We thank our chief autopsy assistants Mr. Rudi Schweiger and Mr. Anistan Sebastiampillai for their continuous support and Dr. Marius Fritzsche for discussion.

Conflict of interest statement We declare that we have no conflict of interest.

References

1. Alter MJ (2007) Epidemiology of hepatitis C virus infection. World J Gastroenterol 13:2436–2441
2. Aoki M (2004) Transmission of tuberculosis (II). Kekkaku 79:693–703
3. Bellentani S, Miglioli L, Bedogni G, Croce LS, Tiribelli C (2005) Epidemiology of hepatitis C virus infection. Minerva Gastroenterol Dietol 51:15–29
4. Best M, Neuhauser D (2004) Ignaz Semmelweis and the birth of infection control. Qual Saf Health Care 13:233–234
5. Burton JL (2003) Health and safety at necropsy. J Clin Pathol 56:254–260
6. Cone LA, Curry N, Wuestoff MA, O, ' SJ, Feller JF (1998) Septic synovitis and arthritis due to *Corynebacterium striatum* following an accidental scalpel injury. Clin Infect Dis 27:1532–1533
7. De Costa CM (2002) "The contagiousness of childbed fever": a short history of puerperal sepsis and its treatment. Med J Aust 177:668–671
8. Ganczak M, Boron-Kaczmarska A, Dziuba I (2003) Pathologist and HIV—are safe autopsies possible? Pol J Pathol 54:143–146
9. Gerston KF, Blumberg L, Gafoor H (1998) Viability of mycobacteria in formalin-fixed tissues. Int J Tuberc Lung Dis 2:521
10. Gerston KF, Blumberg L, Tshabalala VA, Murray J (2004) Viability of mycobacteria in formalin-fixed lungs. Human Pathol 35:571–575
11. Hamouda O, Marcus U, Voss L, Kollan C (2007) Epidemiology of HIV infections in Germany. Bundesgesundheitsblatt Gesundheitsforschung Gesundheitsschutz 50:399–411
12. Ippolito G, The Studio Italiano Rischio O (1996) Scalpel injury and HIV infection in a surgeon. The Studio Italiano Rischio Occupazionale da HIV (SIROH). Lancet 347:1042
13. Johnson MD, Schaffner W, Atkinson J, Pierce MA (1997) Autopsy risk and acquisition of human immunodeficiency virus infection: a case report and reappraisal. Arch Pathol Lab Med 121:64–66
14. Kelly KE, Lee KC, Tami TA (1993) Surgical glove perforations in otolaryngology: prevention with cut-resistant gloves. Otolaryngol Head Neck Surg 108:91–95
15. Lewis FR Jr., Short LJ, Howard RJ, Jacobs AJ, Roche NE (1995) Epidemiology of injuries by needles and other sharp instruments. Minimizing sharp injuries in gynecologic and obstetric operations. Surg Clin North Am 75:1105–1121
16. Louis SS, Steinberg EL, Gruen OA, Bartlett CS, Helfet DL (1998) Outer gloves in orthopaedic procedures: a polyester/stainless steel wire weave glove liner compared with latex. J Orthop Trauma 12:101–105
17. Nolte KB, Yoon SS (2003) Theoretical risk for occupational blood-borne infections in forensic pathologists. Infect Control Hosp Epidemiol 24:772–773
18. Okochi Y (2005) Hospital outbreak of *Mycobacterium tuberculosis* resulting from autopsy exposure. Kansenshogaku Zasshi 79:534–542
19. Paul N, Jacob ME (2006) An outbreak of cadaver-acquired chickenpox in a health care setting. Clin Infect Dis 43:599–601
20. Pieper SP, Schimmele SR, Johnson JA, Harper JL (1995) A prospective study of the efficacy of various gloving techniques in the application of Erich arch bars. J Oral Maxillofac Surg 53:1174–1176 discussion 1177
21. Pritt BS, Waters BL (2005) Cutting injuries in an academic pathology department. Arch Pathol Lab Med 129:1022–1026
22. Steger G (1987) Life expectancy and causes of death of pathologists. Pathologe 8:108–111
23. Sutton PM, Greene T, Howell FR (1998) The protective effect of a cut-resistant glove liner. A prospective, randomised trial. J Bone Joint Surg 80:411–413
24. Walls T, Shingadia D (2007) The epidemiology of tuberculosis in Europe. Arch Dis Child 92:726–729
25. Wang JF, Cao Z, Chen XS (2004) The advance of protection for hazard factor during autopsy. Fa Yi Xue Za Zhi 20:110–112
26. Woods JA, Leslie LF, Drake DB, Edlich RF (1996) Effect of puncture resistant surgical gloves, finger guards, and glove liners on cutaneous sensibility and surgical psychomotor skills. J Biomed Mater Res 33:47–51
27. Yazdanpanah Y, De Carli G, Migueres B, Lot F, Campins M, Colombo C, Thomas T, Deuffic-Burban S, Prevot MH, Domart M, Tarantola A, Abiteboul D, Deny P, Pol S, Desenclos JC, Puro V, Bouvet E (2005) Risk factors for hepatitis C virus transmission to health care workers after occupational exposure: a European case-control study. Clin Infect Dis 41:1423–1430

Virchows Arch (2008) 452:319–324
DOI 10.1007/s00428-007-0544-y

CASE REPORT

Thymoma with ganglioneuroblastomatous component: case report

Kenji Kashiwabara · Hayato Ikota · Shigebumi Tanaka · Chie Ohta · Toshiki Yajima · Hideki Endoh · Ei Yamaki · Hiroyuki Kuwano · Takashi Nakajima

Received: 7 September 2007 / Revised: 30 October 2007 / Accepted: 31 October 2007 / Published online: 20 December 2007
© Springer-Verlag 2007

Abstract A mediastinal tumor in a 49-year-old woman with myasthenia gravis is reported. The tumor was well-demarcated and located in the supero-anterior mediastinum. Microscopically, the tumor consisted of thymic and neuroblastic tumor components, the latter of which consisted of immature and maturing neuronal cells, abundant neuropils, and Schwannian stroma. The two components intermingled with each other inside the tumor capsule. The tumor was diagnosed as thymoma with a ganglioneuroblastomatous component. The coexistence of epithelial and neuronal tissues in the thymic neoplasm is extremely rare.

Keywords Thymus · Thymoma · Neuroblastic tumor · Bimorphic tumor

K. Kashiwabara (✉)
Department of Clinical Pathology, Saiseikai Maebashi Hospital,
564-1 Kamishinden-machi,
Maebashi, Gunma, 371-0821, Japan
e-mail: ke-kashiwabara@maebashi.saiseikai.or.jp

H. Ikota
Department of Clinical Pathology, Fukaya Red Cross Hospital,
Fukaya, Japan

S. Tanaka · C. Ohta · T. Yajima · H. Endoh · E. Yamaki · H. Kuwano
Department of General Surgical Science,
Gunma University Graduate School of Medicine,
Maebashi, Japan

T. Nakajima
Department of Pathology, Gunma University Hospital,
Maebashi, Japan

Introduction

Various types of neoplasms develop in the thymic area [25], of which thymic epithelial tumors are the most common. In rare cases, tumors with bimorphic or heterogeneous morphology appear within a single tumor and are designated as carcinosarcoma, metaplastic thymoma, and so on [4, 11, 13, 20–23, 26, 27]. However, thymic epithelial tumors with neuroectodermal differentiation are exceptionally rare. In this report, an unusual presentation of a seemingly benign thymic epithelial tumor with a neuroblastic tumor component is documented.

Clinical history

A 49-year-old woman complaining of fatigue, dyspnea, and dysphasia for 1 month was admitted to our hospital. A blood examination revealed an elevated level of anti-acetylcholine receptor antibody. The patient was diagnosed with myasthenia gravis. She had no other endocrine or immunological symptoms or abnormalities. Chest computed tomography scan detected a mass in the superior to anterior mediastinum. The patient underwent an extended thymectomy to remove the mass. During the surgery, an encapsulated mass was noted in the supero-anterior mediastinal fat, cephalic to the left brachiochephalic vein. The clinical stage was Masaoka's stage I. The postoperative course was uneventful 1 year after tumor removal.

Materials and methods

Tissues were fixed in 10% formalin, serially sectioned and routinely processed in paraffin and stained with hematoxylin

and eosin. Immunohistochemical studies were performed using an automated slide preparation system (Benchmark LT, Ventana, Tucson, AZ, USA). Primary antisera used were as below: CD99 (12E7, Dakocytomation, Glostrup, Denmark, 1:50), CD3 (polyclonal, Ventana, prediluted), CD5 (SP19, Ventana, prediluted), CD20 (L26, Ventana, prediluted), pankeratin (AE1/AE3 and PCK26, Ventana, prediluted), CK7 (OV-TL12/30, Ventana, prediluted), CK20 (Ks 20.8, Ventana, prediluted), CK19 (Novocastra, B170, Newcastle upon Tyne, UK, 1:100), leu7 (Becton Dickinson, HNK-1, San Jose, CA, USA, 1:25), S-100 (4C4.9, Ventana, prediluted), GFAP (6F2, Dakocytomation, 1:100), and chromogranin A (LK-2H10, Ventana, prediluted).

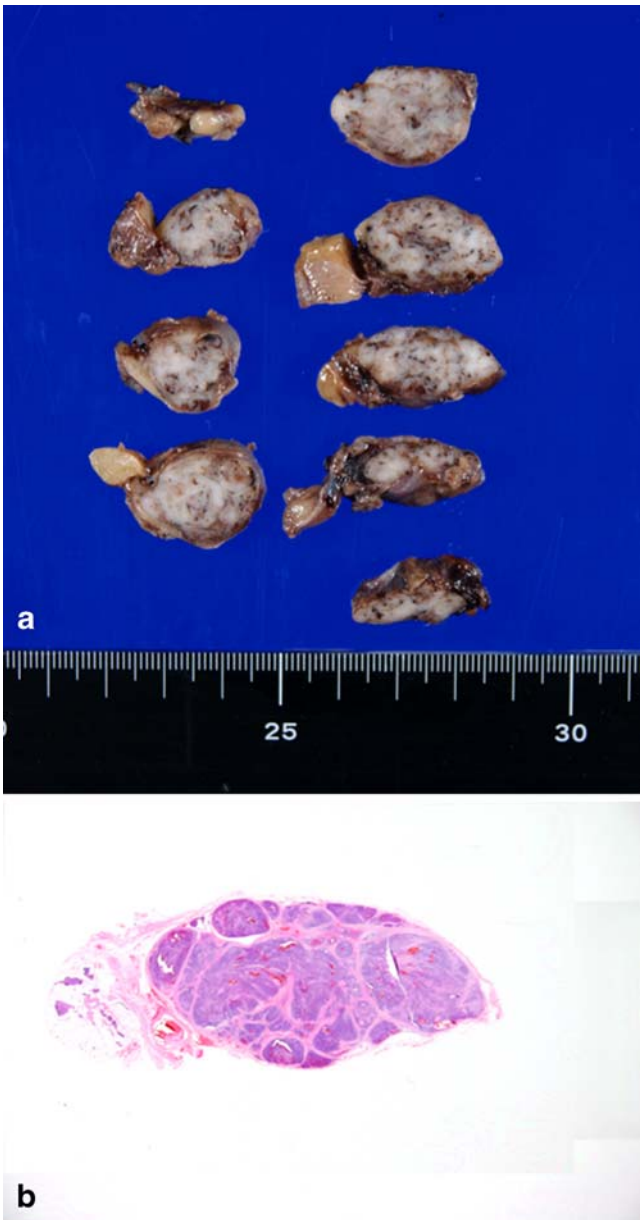


Fig. 1 **a** Cut surfaces of the tumor. Note the well-demarcated tumor with variegated appearance with white and gray-brown areas throughout the tumor. **b** Loupe view of a section. The tumor has lobular architecture divided by fibrous septa (hematoxylin and eosin)

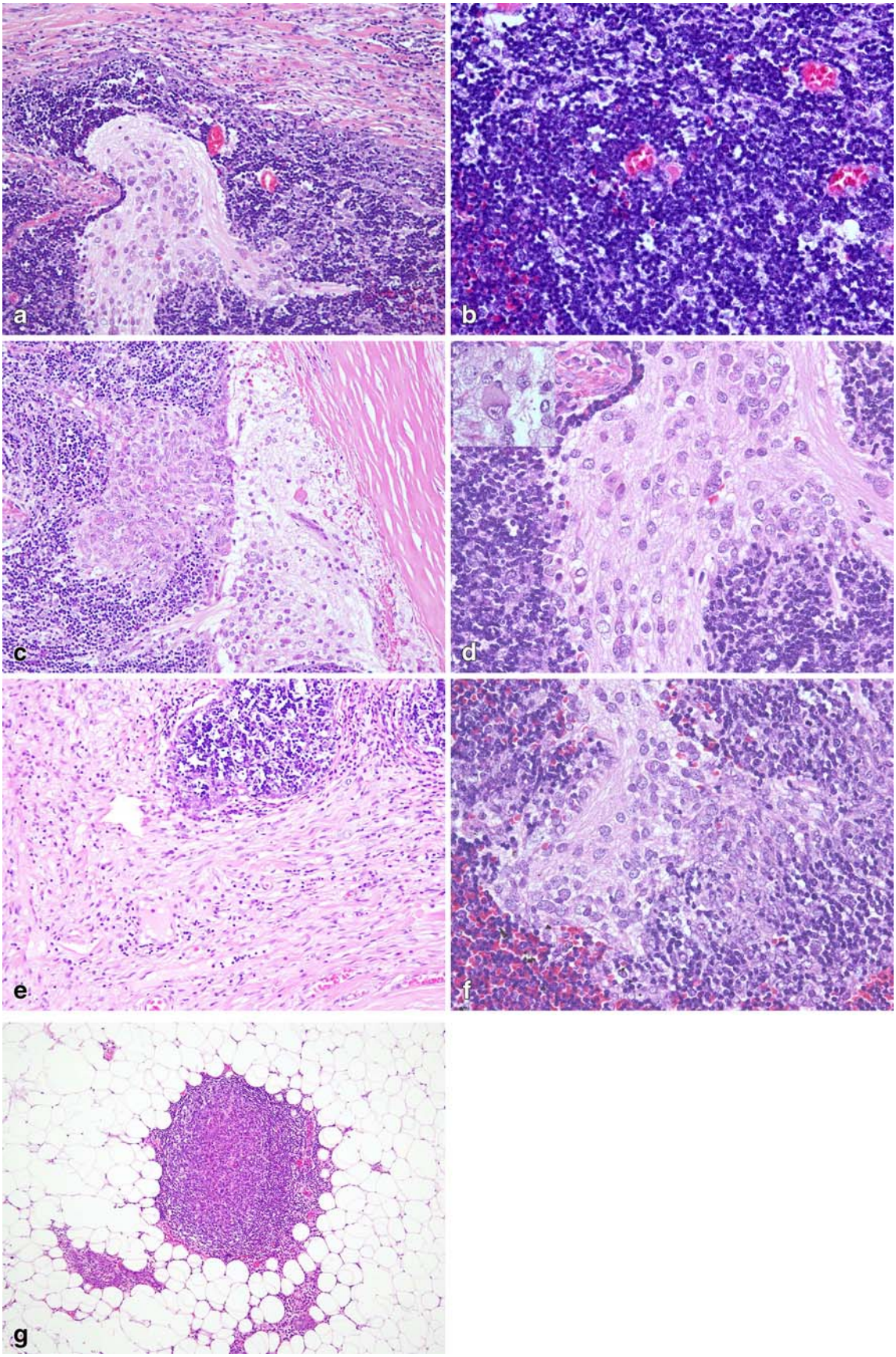
Results

The specimen was a well-circumscribed mass embedded in mediastinal fat tissue. The mass was approximately 2.0 cm in maximum diameter. The cut surface revealed a lobulated growth pattern with a white and gray-brown mottled appearance (Fig. 1a).

Microscopically, the mass was completely encapsulated by fibrous tissue and compartmentalized by fibrous tissue extending from the capsule. Invasion outside the capsule was not observed (Fig. 1b). The parenchyma consisted of two distinct components (Fig. 2a). One component resembled the normal thymus and was composed of epithelial cell elements with round nuclei (Fig. 2b) that were arranged as a mesh with a prominent small lymphocytic infiltrate. In some portions, spindle-shaped epithelial cells were growing as fascicles or nests (Fig. 2c). Mitotic figures, nuclear atypia, and nucleoli were inconspicuous in the epithelial cells. Tingeble body macrophages, perivascular spaces, and Hassall's corpuscles were not seen. This component was compatible with the histology of type AB thymoma based on the WHO classification [25].

The other component was located in the periphery of each compartment of the thymic area or within it, and seen as multifocal pale islands or eosinophilic septa. It was distributed throughout the tumor. In this component, neuronal cells of several stages of differentiation were proliferating in random distribution (Fig. 2d). Immature cells were small and round with dispersed fine chromatin and indiscernible cytoplasm. More mature cells had prominent eosinophilic cytoplasm and deviated nuclei. The cells were immersed in abundant neuropil-like fine fibrillary tissue. Mature cells were more predominant than immature cells. Occasionally, completely matured ganglion cells were present. Foci of undifferentiated neuroblasts

Fig. 2 Histopathologic appearance of the tumor (hematoxylin and eosin). **a** The pale island in the left half of the field represents the neuroblastic element in the thymoma element. The upper eosinophilic area represents the Schwannian stroma (×200). **b** A higher magnification of the thymic area. Thymic epithelial cells with round nuclei proliferate with abundant small lymphocytes (×400). **c** Spindle-shaped epithelial cells are growing as a solid nest in some portions (×200). **d** Proliferation of small round cells with immature and maturing neuronal cells in the neuropil stroma. Occasional ganglion cells are shown in the *inset* (×400). **e** Schwannian stroma. Slender cells with wavy nuclei are forming fascicles around the thymic area (×100). **f** Transition between neuronal component and thymic epithelial cells (×200). **g** Involuted thymus with lymphoid follicle outside the tumor capsule (×100)


a
b
c
d
e
f
g

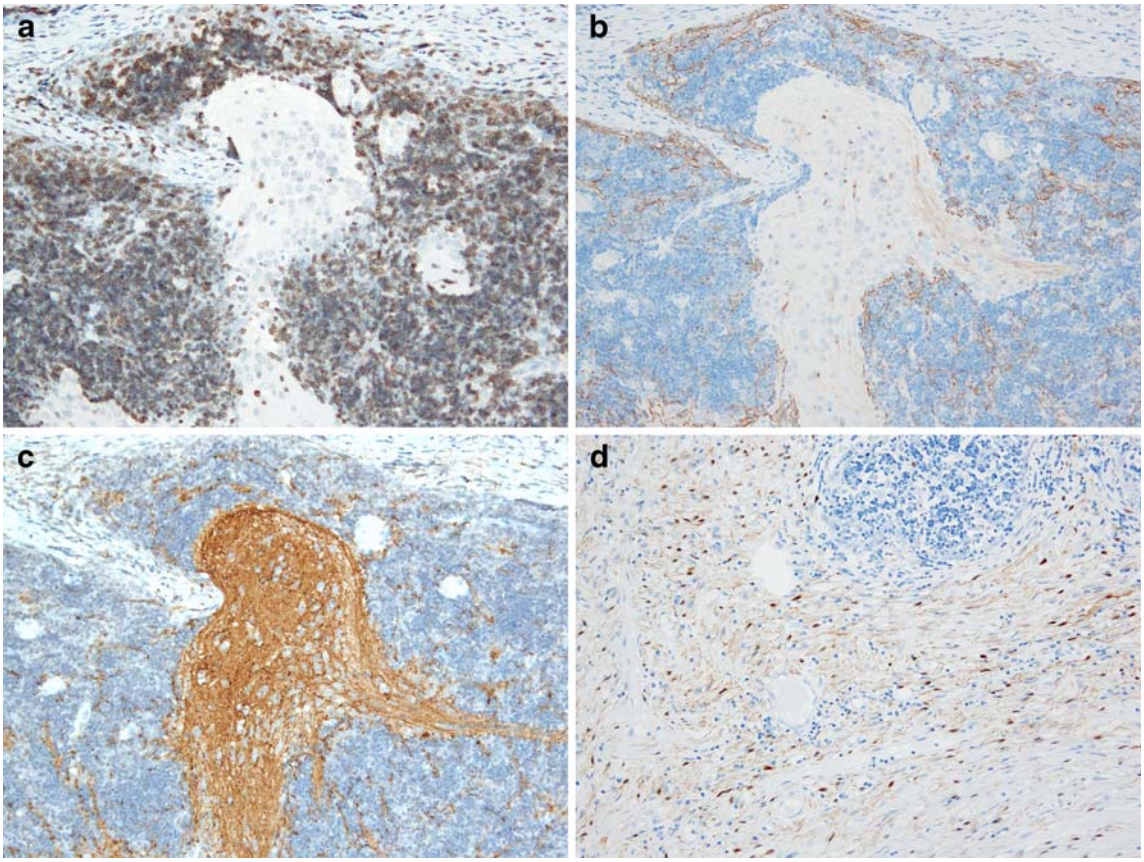


Fig. 3 Immunohistochemical findings of the tumor. **a** Infiltrating small lymphoid cells were CD 3 positive (×200). **b** Cytokeratin staining demonstrated a network of epithelial cells (CK19, ×200). **c** Synaptophysin highlighted the neural area (×200). **d** Schwannian stroma was positive for S-100 protein (×200)

were inconspicuous. In the periphery of the two components, slender cells with wavy nuclei were growing as fascicles that resembled the peripheral nerve (Fig. 2e). This was comparable with the Schwannian stroma of neuroblastic tumors. The Schwannian stroma occupied about half of the neuronal component. This morphological constellation was consistent with ganglioneuroblastoma, an intermixed subtype according to the International Neuroblastoma Pathology Classification [16, 17]. The thymic and ganglioneuroblastomatous components transited or intermingled with each other (Fig. 2f). Surrounding adipose tissue contained the involuted thymus with lymphoid follicular hyperplasia (Fig. 2g).

To characterize tumor cell differentiation, immunohistochemical studies were performed. Infiltrating lymphocytes were positive for CD99, CD3, and CD5 (Fig. 3a) but negative for CD20. Several cytokeratins (AE1/AE3 and PCK26, CK7, CK 19) clearly showed an epithelial framework in the thymoma component (Fig. 3b). The ganglioneuroblastoma component was positive for synaptophysin and leu7 (Fig. 3c). Antisynaptophysin antibody stained the cell membrane of neuronal cells and the neuropil-like tissue, and anti-leu7 antibody stained the cytoplasm of some neuronal cells and neuropil-like tissue. Antisynaptophysin and leu 7 antibodies demonstrated the fine processes emanating into thymic areas. S-100 was positive in the Schwannian area (Fig. 3d). Pancytokeratin

Table 1 Summary of immunohistochemistry

	Thymic	Neuronal	Lymphocytes
AE1/AE3	+	+/–[a]	–
CK7	+	–	–
CK19	+	–	–
CK20	–	–	–
CD3	–	–	+
CD5	–	–	+
CD99	–	–	+
CD20	–	–	+[b]
Synaptophysin	–	+	–
S-100	–	+	–
Leu7	–	+	–
GFAP	–	–	–
Chromogranin A	–	–	–

[a] Occasionally stained cells and less intensely stained fibrillary matrix
[b] Only lymphoid follicles

(AE1/AE3 and PCK26) was positive in occasional neural cells and neuropil-like tissue. Other cytokeratins (CK7, CK19, CK20) were negative. GFAP and chromogranin A were negative in both areas. These observations are summarized in Table 1.

Discussion

The supero-anterior mediastinal mass reported herein was a unique thymic tumor containing a ganglioneuroblatomatous component. As proliferating thymic epithelial cells showed no atypical, necrosis, mitosis or invasive growth, this tumor was comparable with ordinal thymoma. Moreover, neuronal cells of various stages of differentiation within the neuropil and Schwannian stroma were seen within the same tumor. The latter component was comparable with ganglioneuroblastoma of intermixed subtype based on the recent classification of neuroblastic tumors [16, 17]. As the thymic and ganglioneuroblastic areas were intermixed, we tentatively diagnosed this unusual tumor as thymoma with a ganglioneuroblastomatous component, considering it a single neoplasm. Pathological differential diagnosis of this tumor includes teratoma, other unknown thymic epithelial tumors, and collision tumors.

The thymus is the most prevalent organ for extragonadal germ cell tumors. Teratomas often include neuroectodermal tissue. However, the present tumor did not include such tissue elements as the epidermis, skin appendages, or respiratory and alimentary tract that can be frequently observed in teratomas. In addition, mediastinal teratomas rarely contain thymus tissue [18].

Some thymic epithelial tumors are characterized by biphasic or combined morphology [25]. However, thymic epithelial tumors containing definite neuronal elements are quite rare. Carcinosarcomas or sarcomatoid carcinomas are infrequent carcinomas of thymic origin partly showing a sarcomatous appearance. Many reports described myogenic or osteogenic differentiation but did not mention neuroectodermal differentiation in these carcinomas [4, 11, 13, 20–22, 26].

Metaplastic thymoma is another bimorphic thymoma with epithelial islands and fascicles of spindle cells [23, 27]. For metaplastic thymomas, the spindle cells are distinctly positive for cytokeratin and epithelial membrane antigen. Some cells are positive for glioneuronal markers in a few tumor cells, but they do not show distinct neuroectodermal morphology [27]. Additionally, the location of the present case deviated to the superior mediastinum, which is comparable with ectopic hamartomatous thymoma. Similar to metaplastic thymoma, ectopic hamartomatous thymoma is characterized by a mixture of epithelial and spindle cells that are positive for epithelial markers [5, 15]. Thus, the current case did not satisfy the definition of any known thymic tumor.

Most neuroectodermal tumors arise in the posterior mediastinum and rarely develop in the thymus [2, 3, 12]. We did not regard this tumor as a collision of a thymoma and a ganglioneuroblastoma tumor because the two elements were confined within a single encapsulated mass and intermingled with each other rather than distinctly separated. Nevertheless, the thymic neuroblastic tumor might be a unique entity different from the conventional neuroblastic tumor. It develops in adults and is often accompanied by the syndrome of inappropriate secretion of antidiuretic hormone (SIADH) [2, 3]. Argani et al. postulated that thymic epithelial cell progenitors have the potential to differentiate along neural lineage based on their analysis of three cases of thymic neuroblastoma [2]. In our patient, plasma hyponatremia and hypoosmolarity suggestive of SIADH were not preoperatively present.

There has been only one previously reported case of a bimorphic thymic epithelial and neuroblastic tumor similar to our case [1]. Alguacil-Garcia et al. reported a thymic epithelial tumor with neuroblastomatous differentiation that was a thymic carcinoma with scattered islands and clusters of small round immature cells with a fine fibrillary background structure. Immunohistochemistry and ultrastructural studies confirmed their neuroblastic or neuroendocrine characteristics. The previous case differed from ours in that more mature components such as ganglion cells or Schwannian stroma were not present, and the thymic epithelial cells were malignant. However, both cases suggest that thymic epithelial neoplasms have the potential to differentiate to neuroectodermal cells.

The histogenesis of the present case is difficult to explain. Immunohistochemical investigation of neuropeptides has revealed the presence of neuroendocrine cells in the normal thymus [7]. Thymic carcinomas are already known to exhibit neuroendocrine differentiation [8, 9]. It is hypothesized that there are progenitor cells in the thymus that may have the potential to differentiate toward thymic epithelium and neuroendocrine cells. Therefore, we speculate that, during tumor genesis, progenitor cells also differentiated to neuroectodermal cells and additionally achieved further maturation of ganglion cells to constitute a combination of thymoma and ganglioneuroblastoma.

In other organs, combinations of epithelial and neuronal tumors are very rarely observed. In the sinonasal area, olfactory neuroblastomas may contain carcinomatous elements, and teratocarcinosarcomas often show neuroectodermal differentiation admixed with other malignant teratoma and carcinosarcomatous areas [10, 14]. Tanimoto et al. reported a rare teratocarcinosarcoma of the ovary with prominent neuroectodermal differentiation [24]. Freeman et al. described a combined carcinoid tumor and ganglioneuro-

blastoma of the lung [6]. Thus, the tumors of most reported cases are malignant. Also, in the thymus, neuroendocrine differentiation in benign thymoma is infrequent [8, 19]. Accordingly, although thymic epithelial cells are otherwise benign and the neuroblastic component indicates favorable histology [17], it was necessary to regard this extraordinary thymic epithelial tumor as a thymoma of uncertain malignant potential for the purpose of clinical management.

In summary, we have reported an unusual thymoma with ganglioneuroblastoma component that developed in the mediastinum and discussed its differential diagnosis.

Acknowledgements The authors thank Miss Kaori Satoh (Department of Pathology, Gunma University Hospital) for her technical and clerical assistance.

Conflict of interest statement We declare that we have no conflicts of interest.

References

1. Alguacil-Garcia A, Halliday WC (1987) Thymic carcinoma with focal neuroblastoma differentiation. Am J Surg Pathol 11:474–479
2. Argani P, Erlandson RA, Rosai J (1997) Thymic neuroblastoma in adults: report of three cases with special emphasis on its association with the syndrome of inappropriate secretion of antidiuretic hormone. Am J Clin Pathol 108:537–543
3. Asada Y, Marutuka K, Mitsukawa T, Mitsukawa T, Kuribayashi T, Taniguchi S, Sumiyoshi A (1996) Ganglioneuroblastoma of the thymus: an adult case with syndrome of inappropriate secretion of antidiutetic hormone. Hum Pathol 27:506–509
4. Eimoto T, Kitaoka M, Ogawa H, Niwa H, Murase T, Tateyama H, Inagaki H, Soji T, Wang HJ (2002) Thymic sarcomatoid carcinoma with skeletal muscle differentiation: report of two cases, one with cytogenetic analysis. Histopathology 40:46–57
5. Fletch JF, Weiss SW (1990) Ectopic hamartomatous thymoma: clinicopathologic, immunohistochemical, and histogenetic considerations in four new cases. Hum Pathol 21:662–668
6. Freeman JK, Otis CN (2001) Combined carcinoid tumor and ganglioneuroblastoma of the lung. Int J Surg Pathol 9:169–173
7. Geenen V, Defresne MP, Robert F, Legros JJ, Franchimont P, Boniver J (1988) The neurohormonal thymic microenvironment; immunohistochemical evidence that thymic nurse cells are neuroendocrine cells. Neuroendocrinology 47:365–368
8. Hishima T, Fukayama M, Hayashi Y, Fujii T, Arai K, Shiozawa Y, Funata N, Koike M (1998) Neuroendocrine differentiation in thymic epithelial tumors with special reference to thymic carcinoma and atypical thymoma. Hum Pathol 29:330–338
9. Lauriola L, Erlandson RA, Rosai J (1998) Neuroendocrine differentiation is a common feature of thymic carcinoma. Am J Surg Pathol 22:1059–1066
10. Miller DC, Goodman ML, Pilch BZ, Shi SR, Dickersin GR, Halpern H, Norris CM Jr (1984) Mixed olfacroty neuroblastoma and carcinoma. A report of two cases. Cancer 54:2019–2028
11. Murakami S, Shamoto M, Miura K, Takeuchi J (1984) A thymic tumor with massive proliferation of myoid cells. Acta Pathol Jpn 34:1375–1383
12. Nagashima Y, Miyagi Y, Tanaka Y, Miyashita A, Shigematsu S, Aoki I, Nakatani Y, Misugi K (1997) Adult ganglioneuroblastoma of the anterior mediastinum. Pathol Res Pract 193:727–732
13. Nishimura M, Kodama T, Nishiyama H, Nishiwaki Y, Yokose T, Shimosato Y (1997) A case of sarcomatoid carcinoma of the thymus. Pathol Int 47:633–636
14. Pai SA, Naresh KN, Masih K, Ramarao C, Borges AM (1998) Teratocarcinosarcoma of the paranasal sinuses: a clinicopathologic and immunohistochemical study. Hum Pathol 29:718–722
15. Rosal J, Limas C, Husband EM (1984) Ectopic hamatromatous thymoma. A distinctive benign lesion of lower neck. Am J Surg Pathol 8:501–513
16. Shimada H, Ambros IM, Dehner LP, Hata J, Joshi VV, Roald B (1999) Terminology and morphologic criteria of neuroblastic tumors: recommendations by the International Neuroblastoma Pathology Committee. Cancer 86:349–363
17. Shimada H, Ambros IM, Dehner LP, Hata J, Joshi VV, Roald B, Stram DO, Gerbing RB, Lukens JN, Matthay KK, Castleberry RP (1999) The International Neuroblastoma Pathology Classification (the Shimada system). Cancer 86:364–372
18. Shimosato Y, Mukai K (1997) Tumors of mediastinum. Atlas of tumor pathology, 3rd series, fascicle 21. Armed Force Institute of Pathology, Washington, DC
19. Shiraishi J, Nomori H, Orisaka H, Mori T, Yamazaki K (2006) Atypical thymoma (WHO B3) with neuroendocrine differentiation: report of a case. Virchows Arch 449:234–237
20. Snover DC, Levine GD, Rosai J (1982) Thymic carcinoma. Five distinctive histological variants. Am J Surg Pathol 6:451–470
21. Suarez Viela D, Salas Valien JS, Gonzalez Moran MA, Izquierdo Garcia F, Riera Velasco JR (1992) Thymic carcinosarcoma associated with a spindle cell thymoma. An immunohistochemical study. Histopathology 21:263–268
22. Suster S, Rosai J (1991) Thymic carcinoma. A clinicopathological study of 60 cases. Cancer 67:1025–1032
23. Suster S, Moran CA, Chan JKC (1997) Thymoma with pseudosarcomatous stroma: report of an unusual histologic variant of thymic epithelial neoplasm that may simulate carcinosarcoma. Am J Surg Pathol 21:1316–1323
24. Tanimoto A, Arima N, Hayashi R, Hamada T, Matsuki Y, Sasaguri Y (2001) Teratoid carcinosarcoma of the ovary with prominent neuroectodermal differentiation. Pathol Int 51: 829–832
25. Travis WD, Brambilla E, Muiller-Hermelink KK, Harris CC (2004) Tumours of the lung, pleura, thymus and heart. World Health Organization Classification of tumors. IARC Press, Lyon
26. Wick MR, Weiland LH, Sceithause BW, Bernatz PE (1982) Primary thymic carcinomas. Am J Surg Pathol 6:613–630
27. Yoneda S, Marx A, Heimann S, Shirakusa T, Kikuchi M, Müller-Hermelink HK (1999) Low grade metaplastic carcinoma of the thymus. Histopathology 35:19–30

Virchows Arch (2008) 452:325–330
DOI 10.1007/s00428-007-0547-8

CASE REPORT

Huge renal cyst with parietal renal cell carcinoma, osseous metaplasia and a papillary adenoma: a case report with unique clinicopathological features and literature review

Giacomo Puppa · Andrea Gervasio · Kutsal Yorukoglu · Romano Colombari · Francesco De Marchi · Vincenzo Canzonieri

Received: 10 August 2007 / Revised: 6 November 2007 / Accepted: 8 November 2007 / Published online: 14 December 2007
© Springer-Verlag 2007

Abstract The unique clinicopathological features of a giant solitary renal cyst with a parietal clear cell carcinoma in contiguity with a focus of osseous metaplasia and a papillary adenoma are reported. Ultrasonography and computed tomography showed a single cyst with a focal wall irregularity. During surgery, a frozen section revealed the presence of a renal cell carcinoma of clear cell type, so a nephrectomy was performed. After extensive pathological sampling of the cyst's wall, a focus of osseous metaplasia in contiguity with the main tumour and a microscopic papillary adenoma were found. Diagnostic implications for the present case are discussed within a pertinent literature review.

G. Puppa (✉) · V. Canzonieri
Division of Pathology, CRO-Istituto Nazionale Tumori, Aviano, Italy
e-mail: gpuppa@yahoo.com

A. Gervasio
Division of Radiology, Istituto Clinico Città di Brescia, Brescia, Italy

K. Yorukoglu
Department of Pathology, Dokuz Eylul University, Izmir, Turkey

R. Colombari
Division of Pathology, 'G. Fracastoro' City Hospital, Verona, Italy

F. De Marchi
Surgical Oncology, CRO-Istituto Nazionale Tumori, Aviano, Italy

Present address:
G. Puppa
Division of Pathology, 'G. Fracastoro' City Hospital, Verona, Italy

Keywords Renal cell carcinoma · Cyst · Papillary adenoma · Osseous metaplasia

Introduction

The occurrence of malignant epithelial tumours arising in a renal cyst is rare. At present, only about 20 cases are reported in the English literature [1, 2, 7, 8, 13, 14, 16–18]. From the radiologic–pathologic point of view, the differential diagnosis includes the few presentations of cystic renal cell carcinomas (RCC) [3].

The recognition of cyst-associated malignancies is usually made by pathological examination of the nephrectomy specimen, performed for tumoural and for non-tumoural causes, or by frozen section examination during surgery and then confirmed after extensive pathologic examination of the cyst to exclude the presence of other neoplastic foci (multifocal tumour), other cystic lesions and regressive changes such as necrosis.

We report a case of RCC with osseous metaplasia and a papillary adenoma, both present within the wall of a solitary renal cyst. A review of the literature revealed the uniqueness of this case.

Clinical history

An asymptomatic 46-year-old man was in treatment for a history of hypertension due to primary hyperaldosteronism, which was diagnosed at the age of 35 years. The prescribed treatment for this condition was an anti-hypertensive therapy including diuretics. His medical history was significant only for Gilbert's syndrome.

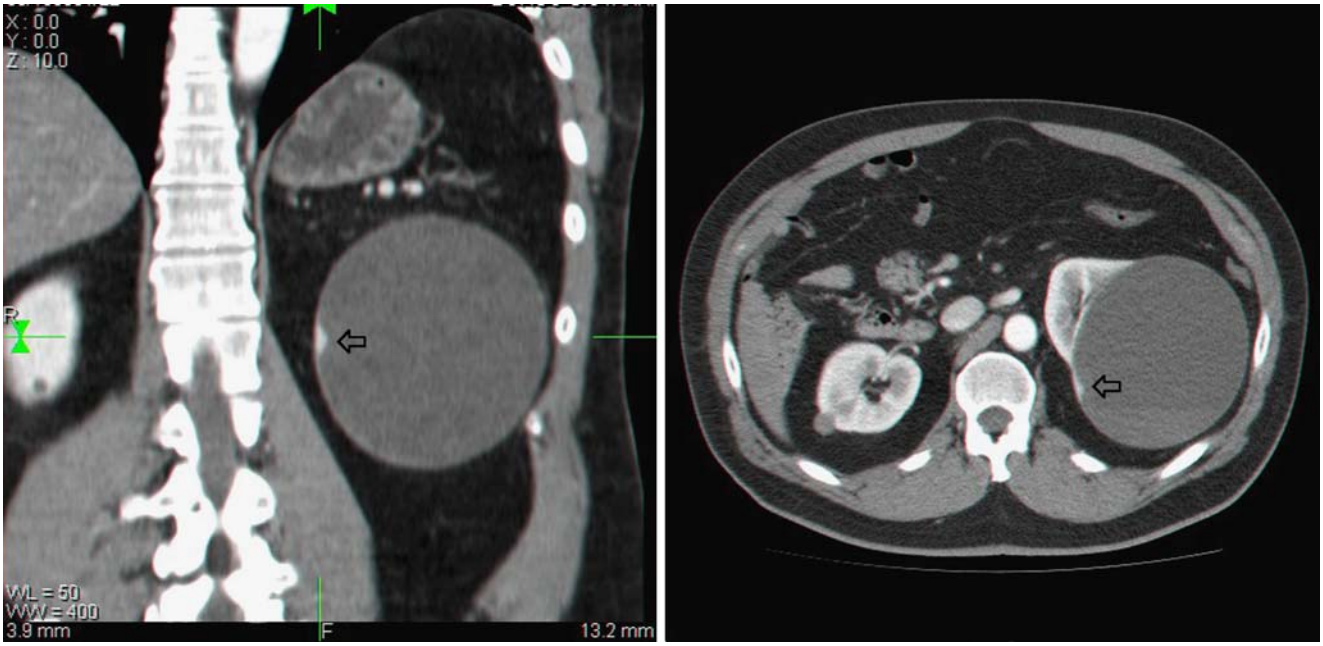


Fig. 1 The CT scanning after intravenous contrast injection. The *arrow* indicates the cyst mural nodule

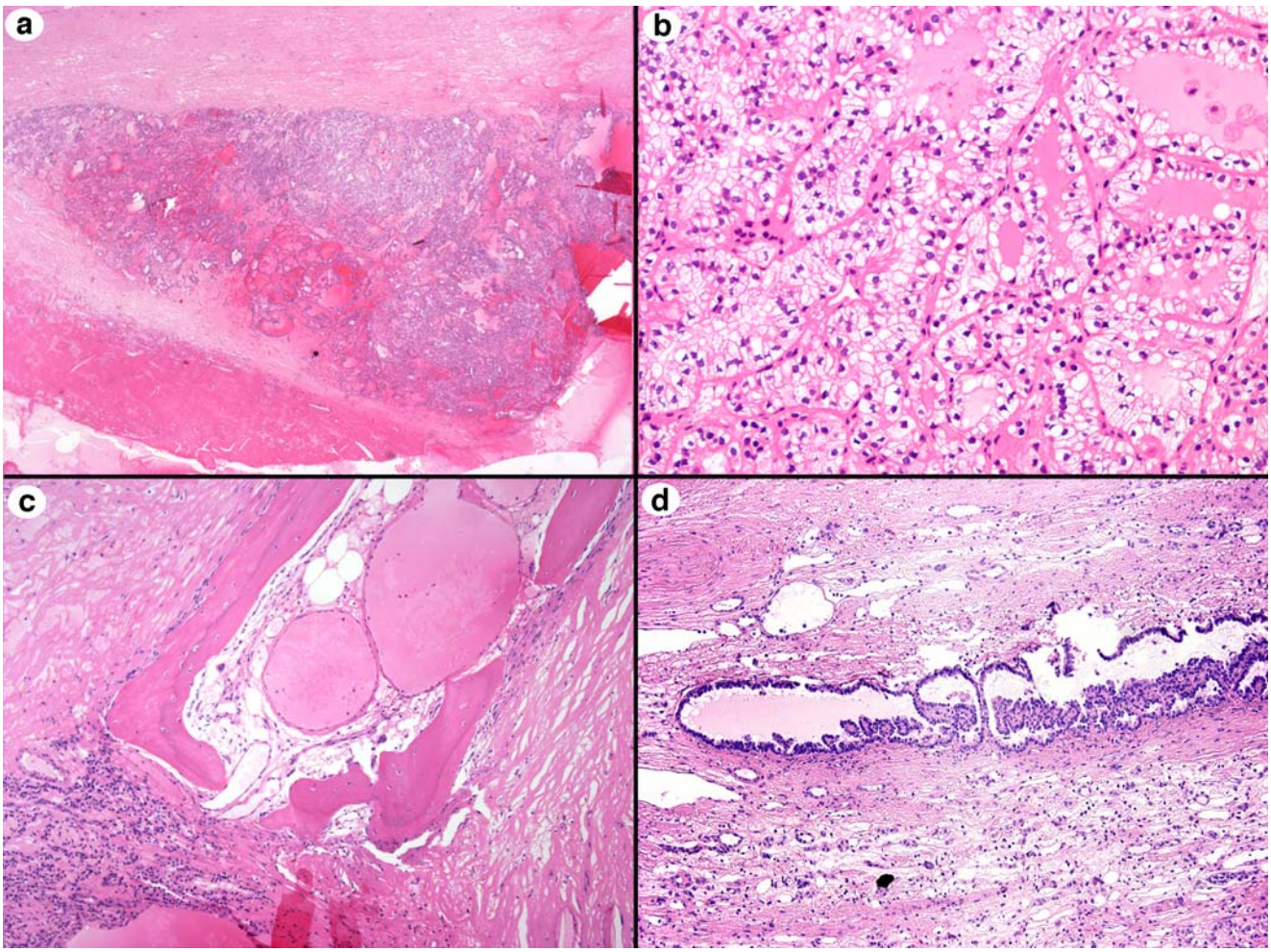


Fig. 2 Histology of the mural nodule at low (**a**) and higher (**b**) magnification. **c** Osseous metaplasia in contiguity with the tumour. **d** The distant cyst wall harbouring a papillary adenoma

Due to the recent appearance of a renal cystic lesion with a parietal irregularity, incidentally discovered by ultrasound scan, further radiological studies were performed. The CT scan confirmed the presence of a 12-cm left renal cyst with a single small mural nodule along its wall. After the injection of the contrast medium, the nodule was clearly enhanced (Fig. 1), meeting the criteria for a Bosniak category IV cystic lesion. No other lesions were seen in the same kidney or in the contra-lateral one. During surgery, a frozen section confirmed the malignant nature of the neoplasm, revealing a RCC in the cystic wall, so a radical nephrectomy was performed.

Materials and methods

The tissues were fixed in 10% formalin and embedded in paraffin for light microscopic examination. Sections of 3-μm thickness were stained with haematoxylin and eosin.

Immunohistochemical stainings were performed on the Ventana BenchMark XT Automated Platform (Ventana Medical Systems, Tucson, AZ, USA), using Ventana UltraView™ DAB detection KIT (Ventana Medical Systems, Tucson, AZ, USA) with the following antibodies: CD10 (Clone 56C6, Ventana), CK7 (Clone OV-TL 12/30, Ventana), racemase (Clone 13H4, Cell Marque).

Results

On macroscopic examination, the kidney weighed 700 g and measured 10×5×5 cm; no other lesions were observed except for the remnants of the cyst. The wall of the cyst, both in the area of the tumour and at distance, was extensively sampled. Microscopic examination revealed a 1-cm clear cell type RCC, Fuhrman grade 1, in contiguity with a focus of osseous metaplasia within the cyst wall (Fig. 2a–c). The cyst wall appeared multi-layered and fibrous; and no clear cells were present among the inner lining. The remnant of the cystic fluid appeared as a blood clot with numerous cholesterol crystals attached to the inner cyst surface (Fig. 2a). In one of the numerous samples taken from the cyst, far from the RCC

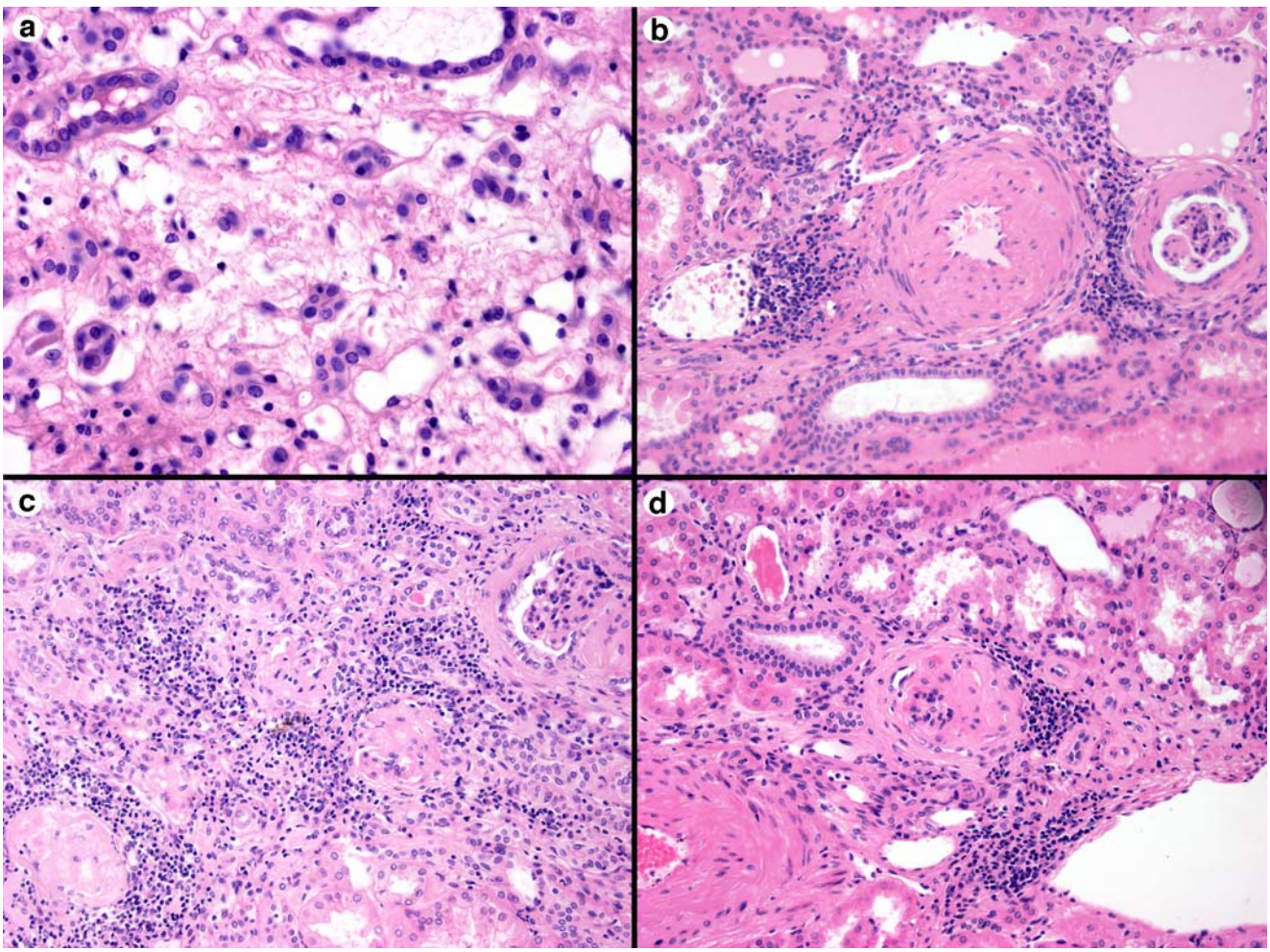


Fig. 3 Histology of the renal parenchyma adjacent to the cyst (**a**) and at distance (**b**–**d**) showing typical hypertension-associated damages

Table 1 Major criteria distinguishing the four types of RCC with cystic features

	Percentage	Appearance	Histotype (usual)
RCC with intrinsic multi-loculated cystic growth	40	Multi-locular; solid component <10%	c.c.
RCC with intrinsic unilocular cystic growth (cystoadenocarcinoma)	30	Unilocular; the tumour is lined by a continuous layer of epithelial (tumour) cells	pap.
RCC arising in a pre-existing renal simple cyst	20	Unilocular; discrete nodule in an otherwise simple cyst; the cyst epithelium is often absent (compressive atrophy)	c.c.
RCC with cystic necrosis	10	2 sub-sets based on amount of necrosis: extensively necrotic cystic RCC and necrotic cystic RCC with readily identifiable nests of tumour cells	c.c.

Extracted from Bisceglia et al. [3] and Hartman et al. [13].
c.c.: clear cell, *pap.*: papillary

in the distal parietal wall, a papillary adenoma (Fig. 2d) was a further incidental finding. The pericystic renal parenchyma showed atrophic tubules and atypical reactive changes associated with fibrosis (nephrosclerosis; Fig. 3a), whereas the remaining parenchyma displayed areas of vascular–interstitial damage, including perivascular lymphocyte infiltrates, arteriolar myointimal hyperplasia and thrombotic microangiopathy combined with focal glomerulosclerosis (Fig. 3b–d). Immunohistochemically, the RCC was positive for CK7 and CD10, negative for racemase. The small papillary adenoma was consumed for diagnostic purposes.

Discussion

Renal cysts are commonly encountered as an incidental finding both on radiological imaging and on macroscopic pathological examination. The Bosniak classification distinguishes cystic renal lesions in four categories according to the CT findings. Essentially, the classification is based on the evaluation of the number and appearance of the septa, the wall thickness, interface with the kidney parenchyma, the presence of calcification and the contrast enhancement characteristics of the lesion, allowing the determination of the nature of the cystic lesions and their separation into surgical and non-surgical lesions [5].

An enhancing solid renal lesion, even small and localised within a cyst's wall, as the one described in this paper, should always be considered malignant until proven otherwise [6].

Four sub-types of RCC with cystic changes have been identified based on radiologic and pathologic examination: (1) RCC with intrinsic multi-loculated cystic growth; (2) RCC with intrinsic unilocular cystic growth; (3) RCC

Table 2 RCC arised as parietal nodules within renal cyst previously described

Author, year	No. of cases	Age, sex	Kidney	Location	Diameter of cyst	Diameter of tumour	Histology RCC	Follow-up
Srimannarayana, 1975	1	49, M	L	l.p.	6 cm	n.s.	c.c.	n.s.
Ambrose, 1976	3	56, M	L	m.p.	n.s.	n.s.	c.c.	Well, 3 years
		50, M	L	u.p.	3 cm	n.s.	c.c.	Well, 3.5 years
		67, M	L	u.p.	6.5 cm	2.5 cm	c.c.	Well, 4.5 years
Anderson, 1977	1	71, M	L	l.p.	n.s.	n.s.	c.c.	n.s.
Bruun, 1986	2	60, M	L	u.p.	n.s.	n.s.	c.c.	p.d., 1.5 years
		48, M	R	m.p.	5 cm	n.s.	c.c.	Well, 2 years
Ljungberg, 1990	1	71, M	R	l.p.	n.s.	0.7 cm	c.c.	Well, 1.5 years
Waguespack, 1996	1	69, M	L	l.p.	5 cm	1 cm	pap.	n.s.
Ulker, 1995	1	73, F	L	Posterior	18 cm	2 cm	c.c.	n.s.
Bowers, 1997	1	25, F	R	m.p.	5 cm	n.s.	c.c.	n.s.

For case reports precedent to 1975, see the review in Hartman et al. [13].
l.p.: lower pole, *u.p.*: upper pole, *m.p.*: middle part, *n.s.*: not specified, *c.c.*: clear cell, *pap.*: papillary, *p.d.*: progression disease

arising in a pre-existing simple renal cyst and (4) RCC with cystic necrosis [3, 13]. This classification encompasses both clear cell and papillary RCC [3, 13]. The major criteria for the differential diagnosis between the four types of RCC with cystic features are summarised in Table 1.

In the case that we present in this paper, the cyst mural nodule corresponds to a RCC arising in a pre-existing simple renal cyst because the extensive sampling of the cyst demonstrated only a small papillary adenoma at distance and excluded the presence of other carcinomatous foci, i.e. the RCC with intrinsic unilocular cystic growth. In addition, no necrosis was observed, allowing the exclusion of a RCC with cystic necrosis. Among the sub-types of RCC with cystic changes, the case we present in this paper, that is, a carcinoma arising in a unilocular cyst, is the rarest of the group [3].

A review of the literature showed that about 20 such cases of clear type RCC have been reported, most likely originating within a pre-existing cyst [1, 2, 7, 8, 13, 14, 16, 17]. The clinical and morphological data of the cases of cysts with parietal RCC nodules previously described are summarised in Table 2. In addition, the present case has unique features, as it is the first reported association of a clear cell type RCC with osseous metaplasia and a papillary adenoma within a renal cyst's wall.

Osseous metaplasia has already been described in cystic RCC, in particular in association with multi-loculated cystic type [4, 12]. Papillary adenomas can be encountered in association with various renal diseases: among neoplastic conditions, they tend to occur more often in patients with papillary renal cell carcinoma with the two lesions being considered as a continuum of the same biological process, as recently suggested [19].

When a renal cyst-associated neoplasm is encountered in the kidney, some clinicopathological settings must be considered, both hereditary and acquired, because these conditions are associated with both RCC and papillary adenoma. These include: (1) autosomal-dominant polycystic kidney disease; (2) Birt–Hogg–Dubè syndrome; (3) acquired renal cystic disease in patients with end-stage kidney diseases leading to chronic renal failure and long-term dialysis [3]. Acquired cystic renal disease is a well-known phenomenon in dialysis patients, and renal tumours develop in one fifth of these patients [11].

Our patient did not meet any of the abovementioned conditions, and no other kidney diseases were present in the family clinical records.

As the presence of a single cyst per se is not considered to be a risk factor for RCC development, we considered other factors that may possibly have had a tumour-promoting role. From this viewpoint, the diuretic therapy that the patient was taking has been shown to increase the risk of RCC, although controversies still exist on this point because it is not yet clear if it is the hypertension itself or its therapy that may be specifically correlated with the risk of developing RCC [15].

The neoplastic conditions that we have described were associated not only with atrophic parenchymal changes, probably due to compression caused by the cyst, but also with histological alterations typically caused by the hypertension and the anti-hypertensive treatment. Such changes (arteriolonephrosclerosis) have been described as more often associated in kidneys with renal cell neoplasms [9], whilst on the other hand, the development of acquired cysts and renal cell carcinoma have been reported in patients with nephrosclerosis who had not undergone haemodialysis [10].

Acknowledgments The authors gratefully thank Mrs. Anna Maria Colussi for her assistance with editing.

Conflict of interest statement We declare that we have no conflict of interest.

References

1. Ambrose SS, Lewis EL, O'Brien DP III, Walton KN, Ross JR (1977) Unsuspected renal tumors associated with renal cysts. J Urol 117:704–707
2. Anderson JD, Lieber M, Smith RB (1977) Latent adenocarcinoma in renal cysts. J Urol 118:861–862
3. Bisceglia M, Galliani CA, Senger C, Stallone C, Sessa A (2006) Renal cystic diseases: a review. Adv Anat Pathol 13:26–56
4. Bloom TL, Gray Sears CL, Williams TR, Linfesty RL, Amling CL (2003) Multilocular cystic renal cell carcinoma with osseous metaplasia in a 25-year-old woman. Urology 61:462
5. Bosniak MA (1986) The current radiological approach to renal cysts. Radiology 158:1–10
6. Bosniak MA (1991) The small (less than or equal to 3.0 cm) renal parenchymal tumor: detection, diagnosis, and controversies. Radiology 179:307–317
7. Bowers DL, Ikeguchi EF, Sawczuk IS (1997) Transition from renal cyst to a renal carcinoma detected by ultrasonography. Br J Urol 80:495–496
8. Bruun E, Nielsen K (1986) Solitary cyst and clear cell adenocarcinoma of the kidney: report of 2 cases and review of the literature. J Urol 136:449–451
9. Budin RE, McDonnell PJ (1984) Renal cell neoplasms. Their relationship to arteriolonephrosclerosis. Arch Pathol Lab Med 108:138–140
10. Chung-Park M, Ricanati E, Lankerani M, Kedia K (1983) Acquired renal cysts and multiple renal cell and urothelial tumors. Am J Clin Pathol 79:238–242
11. Dunnill MS, Millard PR, Oliver D (1977) Acquired cystic disease of the kidneys: A hazard of long-term intermittent maintenance haemodialysis. J Clin Pathol 30:868–877
12. Halat SK, MacLennan GT (2007) Multilocular cystic renal cell carcinoma. J Urol 177:343
13. Hartman DS, Davis CJ Jr, Johns T, Goldman SM (1986) Cystic renal cell carcinoma. Urology 28:145–153
14. Ljungberg B, Holmberg G, Sjodin JG, Hietala SO, Stenling R (1990) Renal cell carcinoma in a renal cyst: a case report and review of the literature. J Urol 143:797–799
15. Messerli FH (2005) Risk factors for renal cell carcinoma: hypertension or diuretics? Kidney Int 67:774–775

16. Srimannarayana A, Kelly DG, Duff FA (1975) Renal cell carcinoma in the free wall of a simple renal cyst. Br J Urol 47:152
17. Ulker V, Ozyurt C, Gursan A (1996) Renal cell carcinoma in a giant renal cyst. A case report and review of the literature. Int Urol Nephrol 28:141–144
18. Waguespack RL, Kearse WS Jr (1996) Renal cell carcinoma arising from the free wall of a renal cyst. Abdom Imaging 21: 71–72
19. Wang KL, Weinrach DM, Luan C, Han M, Lin F, Teh BT, Yang XJ (2007) Renal papillary adenoma—a putative precursor of papillary renal cell carcinoma. Hum Pathol 38:239–246

Virchows Arch (2008) 452:331–336
DOI 10.1007/s00428-007-0555-8

OpenAccess

CASE REPORT

Occurrence of ocular melanoma thirteen years after skin melanoma: two separate primaries or metastatic disease? A case solved with *NRAS* and *CDKN2A (INK4A-ARF)* mutational analysis

Heidi V. N. Küsters-Vandevelde · Jan E. E. Keunen · Pieter Wesseling · Marian A. J. Verdijk · Marjolijn J. L. Ligtenberg · Willeke A. M. Blokx

Received: 28 November 2007 / Accepted: 29 November 2007 / Published online: 17 January 2008
© The Author(s) 2007

Abstract The differential diagnosis between primary uveal melanoma and cutaneous melanoma metastasis in the eye may be difficult, both clinically and histologically. We report successful application of combined mutational analysis of the *NRAS* and the *CDKN2A* gene to discriminate between these two entities. The patient had a history of a superficial spreading cutaneous melanoma of the left shoulder. Nine years later, she developed a lymph node metastasis in the left axilla, and 13 years later she presented with an atypical, pigmented tumor in the uvea. Histologically, the origin of the uveal melanoma could not be determined with certainty. We performed molecular analysis on the skin melanoma, the lymph node metastasis and the uveal melanoma. We detected an *NRAS* codon 61 mutation (c.182A>G, p.Gln61Arg) in all three tumor specimens. This mutation was absent in the normal control tissue of the patient, thereby excluding a germline mutation. To confirm a clonal relationship between the tumors, we also performed *CDKN2A* mutational analysis. We detected a *CDKN2A* mutation ((p16) c.238C>T, p.Arg80X, (p14) c.404C>T, p.Pro135Leu)) in the tumor samples, but not in the normal control tissue of the patient. We concluded that the uveal melanoma is a metastasis from the cutaneous melanoma removed 13 years before.

Keywords Melanoma · Metastasis · Uveal · *NRAS* · *CDKN2A*

H. V. N. Küsters-Vandevelde (✉) · P. Wesseling · M. A. J. Verdijk · M. J. L. Ligtenberg · W. A. M. Blokx
Department of Pathology C66,
Canisius Wilhelmina Hospital,
P.O. Box 9015, 6500 GS Nijmegen,
The Netherlands
e-mail: H.vandevelde@pathol.umcn.nl

J. E. E. Keunen
Department of Ophthalmology,
Radboud University Nijmegen Medical Centre,
Nijmegen, The Netherlands

M. J. L. Ligtenberg
Department of Human Genetics,
Radboud University Nijmegen Medical Centre,
Nijmegen, The Netherlands

Introduction

Especially in case of two cutaneous melanomas or a combination of an ocular and cutaneous melanoma, the clinical and histological differential diagnosis between a second primary melanoma and a melanoma metastasis can be very difficult, as both organs show a relative high frequency of primary melanomas. The commonest primary intraocular malignancy of adults is uveal melanoma [10]. Metastatic melanoma to the eye is rare and generally occurs in patients with widespread metastatic disease [17]. The most common site of metastatic cutaneous melanoma involvement of the eye is the choroid (46%). Metastatic melanoma to the vitreous and anterior chamber is rare (11–18% of all intraocular cutaneous melanoma metastases) [6]. Differentiation between a primary uveal melanoma and an intraocular metastasis is of prognostic and clinical importance, as intraocular metastases imply systemic spread and have a poor prognosis with a patient survival rarely exceeding more than 1 year [17].

Mutations in *BRAF* and less frequently in *NRAS* are involved in cutaneous melanoma development [4, 11]. In

Table 1 Primers used in the analysis of *CDKN2A, BRAF, NRAS* and *HRAS*, and the size of their PCR products

Exon *CDKN2A (INK4a-ARF)**	Forward	Reverse	Size PCR product (bp)
1B	TCAGGGAAGGCGGGTGCGCG	GCCGCGGGATGTGAACCAC	244
1B	CGCCGCGAGTGAGGGTTTT	CACCGCGGTTATCTCCTCC	263
1A	GAGAGGGGGAGAGCAGGCAG	GCACCTCCTCTACCCGACC	122
1A	GGAGCAGCATGGAGCCTTC	AGTCGCCCGCCATCCC CTG	177
2	AGCTTCCTTTCCGTCATGC	GCAGCACCACCAGCGTGTC	202
2	AGCCCAACTGCGCCGACCC	CCAGGTCCACGGGCAGACG	146
2	TGGACGTGCGCGATGCCTG	GGAAGCTCTCAGGGTACAAATTC	188
3	CGGTAGGGACGGCAAGAGAG	GAGGGACCTTCGGTGACTGATG	162
*BRAF** exon 15	CCTTTACTTACTACACCTCAG	AAAAATAGCCTCAATTCTTAC	197
*NRAS** exon 2	GGTTTCCAACAGGTTCTTGC	TGGGTAAAGATGATCCGACA	240
*NRAS** exon 3	GATTCTTACAGAAAACAAGTGG	TAATGCTCCTAGTACCTGTAGAG	230
*HRAS** exon 3	CTGCAGGATTCCTACCGGA	ACTTGGTGTTGTTGATGGCA	196

*All forward primers contained the M13 consensus sequence TGT AAA ACG ACG GCC AGT at the 5′ end. All reverse primers contained the M13 consensus sequence CAG GAA ACA GCT ATG ACC.

contrast, in primary uveal melanomas, *BRAF* and *NRAS* do not appear to be involved in tumorigenesis [3, 8, 15].

CDKN2A mutations have been detected in cutaneous melanoma, both in sporadic melanoma and especially in familial melanoma, with frequencies ranging up to 30% for the latter [16]. Both in primary sporadic ocular melanoma and in familial cases of primary uveal melanoma, *CDKN2A* mutations are very rarely detected (5%) [9, 14].

We present a case of a rare and relatively late occurrence of an intraocular melanoma metastasis 13 years after development of a primary cutaneous melanoma, and illustrate the diagnostic use of *RAS* and *CDKN2A* mutational analysis.

Clinical history

In November 2005, a 47-year-old caucasian female presented to her local ophthalmologist because of mouches volantes in her left eye. She had a history of a superficial spreading cutaneous melanoma of the left shoulder (Clark level IV) removed in 1994, and a lymph node metastasis in the left axilla excised in 2003. Since then no systemic metastasis was detected at annual control. Visual acuity was 20/20 in both eyes and the vitreous of the left eye showed some opacities. These opacities increased gradually over a 2-month period, but resolved spontaneously thereafter. In July 2006, she again developed complaints of recurrent mouches volantes. The diagnosis revealed uveitis, and the patient was treated with local steroids. However, local treatment was not effective and the patient was referred to our center. Examination of the right eye revealed no abnormalities. The visual acuity in the left eye was 20/40, and non-pigmented cells were noticed in the anterior chamber, along with a vitreous haze. As an extensive uveitis screening revealed no abnormalities, intraocular metastasis of the cutaneous melanoma removed 13 years earlier was suspected. A focal, white, and preretinal condensation of vitreous cells developed within a few weeks and some pigmented cells became visible in the vitreous. Subsequently, the intraocular pressure increased to 25 mmHg due to non-pigmented cells in the anterior chamber. A diagnostic vitrectomy was performed. Vitreous samples were positive for malignant melanoma cells. A total body examination excluded systemic metastasis outside the eye. Progressive worsening of the condition of the left eye turned into a visual acuity of 20/80 and a secondary glaucoma up to 50 mmHg occurred, refractive to topical medication. On patient's request, no eye salvaging treatment such as external beam radiation was performed, and the affected eye was enucleated. Histological examination of the eye ball revealed an atypical melanocytic lesion in the iris and ciliary body, with extension under the retina and invasion of the sclera. Although histologically the growth pattern was consistent with primary uveal melanoma, an intraocular metastasis could not be excluded with certainty. As discrimination between second primary and metastatic melanoma was of prognostic importance, we decided to perform mutational analysis for the *BRAF, NRAS, HRAS,* and *CDKN2A* genes on all tumor samples, as well as on the normal control skin of this patient.

Materials and methods

BRAF, *NRAS,* and *HRAS* mutational analysis

DNA isolation was performed as previously described [1, 2]. Briefly, of all tissue samples about three 10-μm unstained sections of formalin-fixed paraffin-embedded

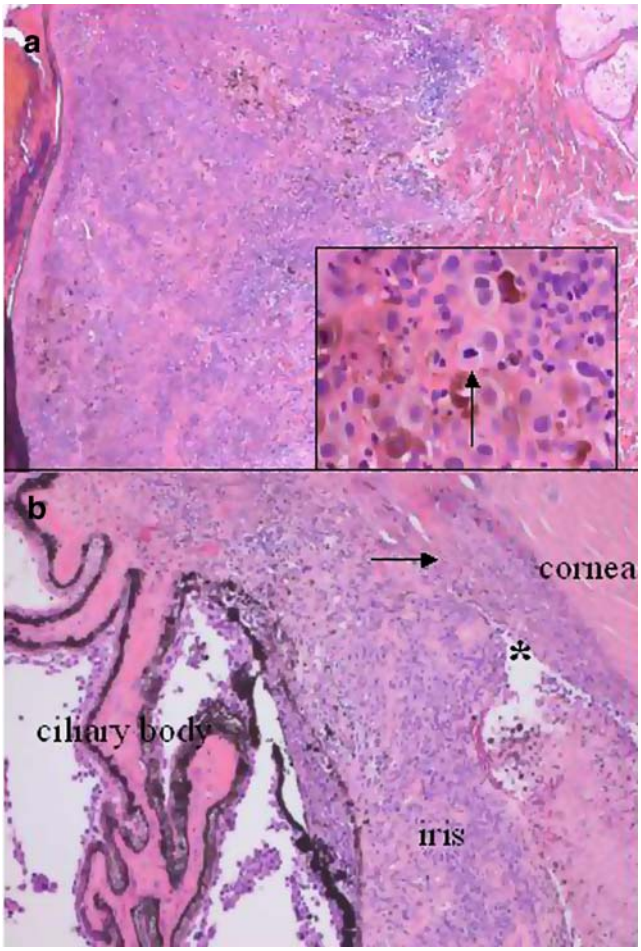


Fig. 1 **a**. The cutaneous melanoma in 1994 was a superficial spreading melanoma, Breslow thickness 1.5 mm, growing into the reticular dermis (hematoxylin and eosin staining, original magnification ×50). The *inset* shows a detail of the deep portion of the tumor with epithelioid melanocytes, melanin pigment, and mitotic figure (*arrow*, original magnification ×400). **b**. The intraocular melanoma, located in the ciliary body and iris with invasion of the sclera, anterior angle (*asterisk*) and canal of Schlemm (*arrow*) (hematoxylin and eosin staining, original magnification ×50)

tissue were manually microdissected, using H&E stained sections as a reference. The tumor cell percentage in the microdissected specimens was estimated as 70% for the cutaneous and uveal melanoma and as 90% for the lymph node metastasis. DNA was purified using the DNeasy Blood and Tissue kit (Qiagen). Primer sequences are shown in Table 1. Polymerase chain reaction (PCR) amplification of *BRAF* exon 15, *NRAS* exons 2 and 3, and *HRAS* exon 3 was performed in a total volume of 50-µl PCR mix containing 50 ng template DNA, 5 µl PCR buffer IV (Integro), 10 µl dNTP 0.2 mM, 6.0 µl $MgCl_2$ 3.0 mM, 0.125 µl Taq DNA polymerase (Integro, 5 U/µl), and 22.9 µl mQ. An initial denaturation at 92°C for 5 min was followed by 35 cycles of denaturation at 94°C for 45 s, annealing at 60°C for 45 s, and extension at 72°C for 45 s with a final extension of 5 min at 72°C. DNA amplification was performed in a MJ PTC 200 PCR cycler (Biozym). After purification of the PCR products using a Qiaquick PCR purification kit (Qiagen), sequence analysis was performed using BigDye terminator version 2 of Applied Biosystems on an ABI 3730 automatic sequencer (Applied Biosystems).

CDKN2A mutational analysis

The *CDKN2A* mutation analysis was performed as previously described [1, 2]. Briefly, PCR was performed with AmpliTaq Gold DNA Polymerase (Applied Biosystems) using an optimized $MgCl_2$ concentration (varying from 1 to 2 mM) in a MJ PTC 200 PCR cycler (Biozym). All primers used in the analysis contained either an M13 forward or M13 reverse consensus sequence. All primers and sizes of the PCR products are listed in Table 1. The entire open reading frames of *CDKN2A* were analyzed in DNA isolated from the tumor samples and normal skin.

Results

Revision of the primary cutaneous melanoma removed in 1994 revealed an asymmetric compound melanocytic lesion with focal ulceration and lack of maturation toward the base of the lesion. The melanocytes showed an epithelioid phenotype with anisokaryosis and prominent nucleoli. Deep mitotic figures were present (Fig. 1). A satellite lesion was present at the junction of the dermis toward the subcutis. Tumor thickness measured 1.5 mm, not including the satellite. Focally, a preexistent nevus was present. Resection margins were at least 2 mm free of tumor. Revision of the lymph node metastasis in the left axilla that was excised in 2003 revealed a large tumor surrounded by limited preexistent lymphoid tissue. The tumor cells showed morphological resemblance to the cutaneous melanoma cells with an epithelioid phenotype and frequent mitotic figures. In addition, in the lymph node metastasis large areas of necrosis were present.

Histological examination of the eye ball revealed an atypical melanocytic lesion in the iris and ciliary body, with extension under the retina and invasion of the sclera. Tumor cells were also present at the surface of the ciliary body in the anterior angle, and showed invasion in the area containing the canal of Schlemm (Fig. 1). The melanocytic cells showed an epithelioid morphology, with focally spindle cell pattern, marked pleiomorphism of tumor cell nuclei, and occasional mitotic figures. Tumor thickness measured 3 mm.

Molecular analysis of the *NRAS* gene revealed a codon 61 mutation (c.182A>G, p.Gln61Arg) in all three tumor

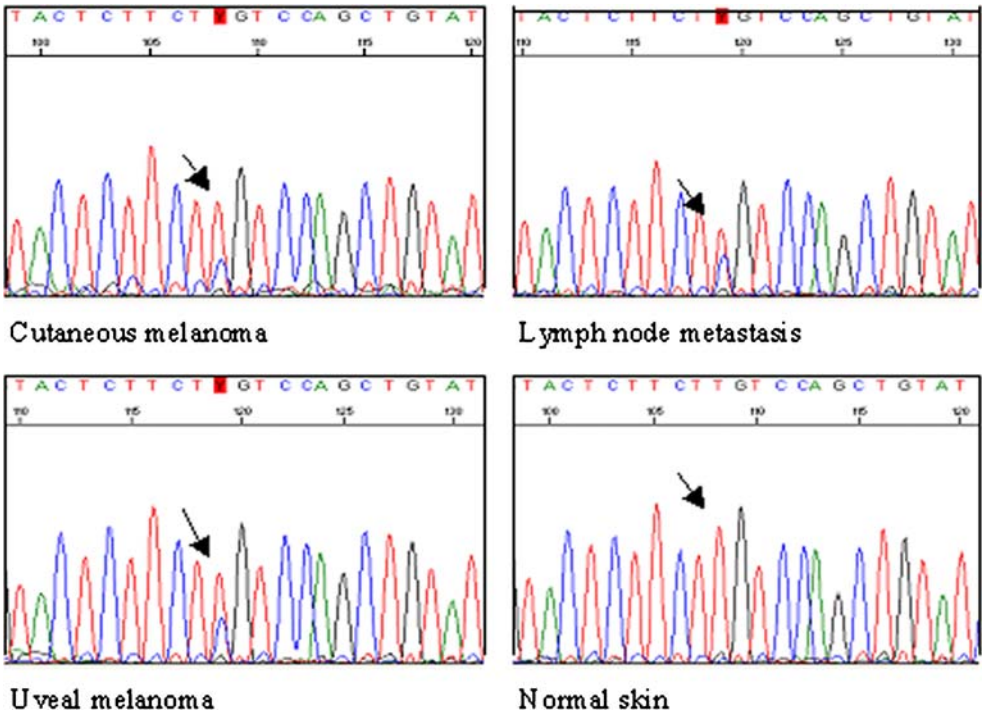


Fig. 2 *NRAS* exon 3 mutation, c.182A>G, p.Gln61Arg, detected in the primary cutaneous melanoma, the lymph node metastasis and the uveal melanoma. Reverse sequence

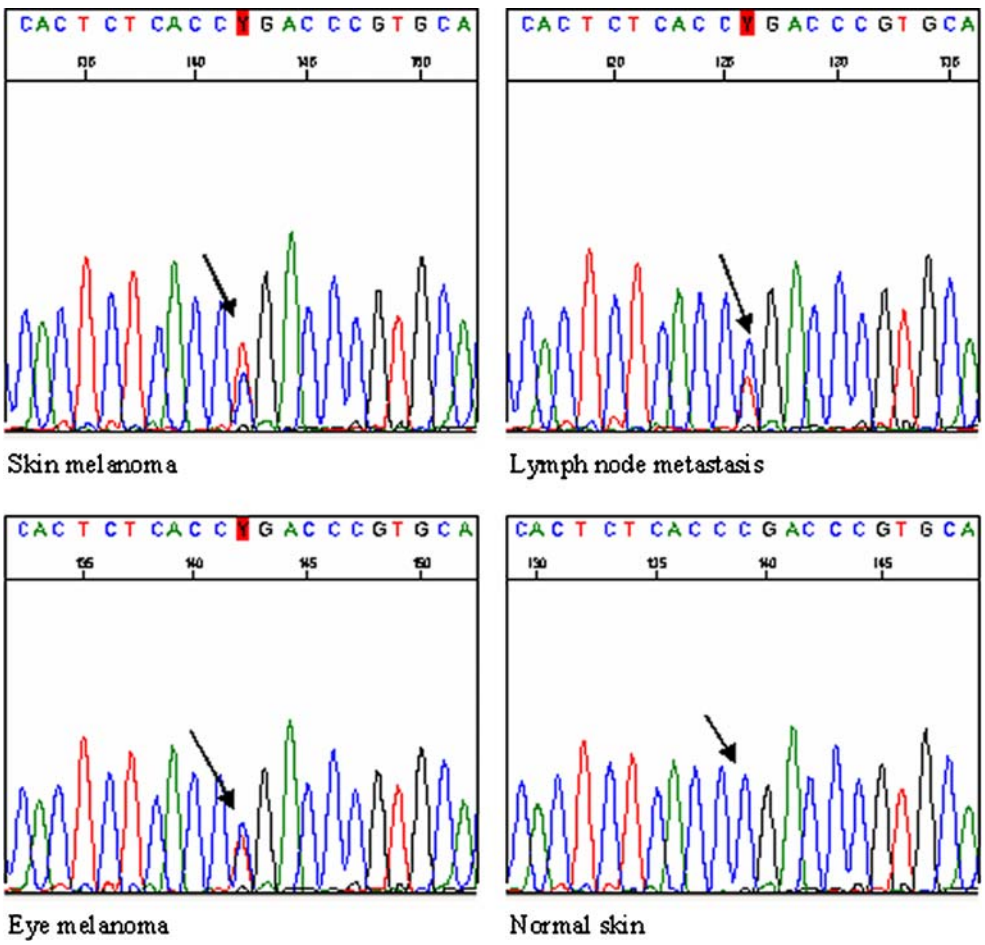


Fig. 3 *CDKN2A* exon 2 mutation, (p16) c.238C>T, p. Arg80X; (p14) c.404C>T, p.Pro135Leu, detected in the primary cutaneous melanoma, the lymph node metastasis and the uveal melanoma. Forward sequence

samples. This mutation was not present in the normal control skin of the patient (Fig. 2). No mutations were detected in *NRAS* exon 2, *BRAF* exon 15, and *HRAS* exon 3. We also performed *CDKN2A* mutational analysis on all samples. A *CDKN2A* mutation ((p16)c.238C>T, p.Arg80X, (p14)c.404C>T, p.Pro135Leu)) was present in all three tumor samples, but absent in the normal control tissue of the patient, indicating that this is a somatic mutation (Fig. 3). It was concluded that the ocular melanoma should be considered as a metastasis of the cutaneous melanoma diagnosed 13 years before.

Discussion

This case report illustrates that molecular analysis can be very helpful in the differential diagnosis between a second primary melanoma and a melanoma metastasis. We chose for mutational analysis of the *BRAF* gene and the *RAS* proto-oncogenes *NRAS* and *HRAS*, because these genes are frequently involved in cutaneous melanocytic lesions, with a reported total mutation frequency for *NRAS* or *BRAF* of 82% in cutaneous melanoma [4]. Furthermore, these mutations are described to occur early in tumorigenesis, before the development of metastasis [4, 11]. We detected in all three tumor samples an *NRAS* codon 61 mutation (c.182A>G, p.Gln61Arg). *NRAS* mutations are known to occur in up to 30% of all cutaneous melanoma cases, the most common being mutations in NRAS codon 61 [4, 7, 11]. In contrast, *NRAS* mutations have been reported to be absent in primary uveal melanoma [3, 15]. The *NRAS* mutation thus strongly supports the metastatic nature of the intraocular melanoma in our patient. The finding of the same somatic mutation in *CDKN2A* in both cutaneous and intraocular melanoma confirms the metastatic nature of the disease in this patient. In contrast to *NRAS* mutations that are limited to codon 61 and codon 12 in cutaneous melanoma, somatic *CDKN2A* mutations are much more tumor specific and thus are not expected to be identical in two different primary melanomas [7]. Furthermore, activating *CDKN2A* mutations are described to be very rare in primary ocular melanomas [9, 13].

Eskandarpour et al. reported specific activating mutations in *NRAS* codon 61 in 95% of primary hereditary cutaneous melanomas (20/21), but in only 10% of sporadic cutaneous melanomas (1/10) [5]. Therefore, the presence of a somatic *NRAS* codon 61 mutation might indicate a familial predisposition to melanoma instead of a clonal relationship.

Discriminating between a second primary intraocular melanoma and metastatic disease is of prognostic importance. Intraocular metastases of melanoma are associated with a poor prognosis with a mean interval between diagnosis of the intraocular metastasis and death of 8.8 months [17]. In contrast, survival in patients diagnosed with a primary intraocular melanoma is more variable, with a reported 5-year cumulative survival rate of up to 60% [12].

In conclusion, this case report illustrates that mutational analysis for the *RAS* proto-oncogenes and *CDKN2A* can be useful in the clinically relevant, but sometimes difficult, differential diagnosis between a second primary intraocular melanoma and an intraocular metastasis of a cutaneous melanoma.

Conflict of interest statement We declare that we have no conflict of interest.

We declare that the molecular analyses comply with the current laws in The Netherlands.

Open Access This article is distributed under the terms of the Creative Commons Attribution Noncommercial License which permits any noncommercial use, distribution, and reproduction in any medium, provided the original author(s) and source are credited.

References

1. Blokx WA, Lesterhuis JJ, Andriessen MP, Verdijk MA, Punt KJ, Ligtenberg MJ (2007) CDKN2A (INK4A-ARF) mutation analysis to distinguish cutaneous melanoma metastasis from a second primary melanoma. Am J Surg Pathol 31:637–641
2. Blokx WA, Ruiter DJ, Verdijk MA, de Wilde PC, Willems RW, de Jong EM, Ligtenberg MJ (2005) INK4-ARF and p53 mutations in metastatic cutaneous squamous cell carcinoma: case report and archival study on the use of Ink4a-ARF and p53 mutation analysis in identification of the corresponding primary tumor. Am J Surg Pathol 29:125–130
3. Cruz F III, Rubin BP, Wilson D, Town A, Schroeder A, Haley A, Bainbridge T, Heinrich MC, Corless CL (2003) Absence of BRAF and NRAS mutations in uveal melanoma. Cancer Res 63:5761–5766
4. Edlundh-Rose E, Egyhazi S, Omholt K, Mansson-Brahme E, Platz A, Hansson J, Lundeberg J (2006) NRAS and BRAF mutations in melanoma tumours in relation to clinical characteristics: a study based on mutation screening by pyrosequencing. Melanoma Res 16:471–478
5. Eskandarpour M, Hashemi J, Kanter L, Ringborg U, Platz A, Hansson J (2003) Frequency of UV-inducible NRAS mutations in melanomas of patients with germline CDKN2A mutations. J Natl Cancer Inst 95:790–798
6. Gunduz K, Shields JA, Shields CL, Eagle RC Jr (1998) Cutaneous melanoma metastatic to the vitreous cavity. Ophthalmology 105:600–605
7. Hocker T, Tsao H (2007) Ultraviolet radiation and melanoma: a systematic review and analysis of reported sequence variants. Hum Mutat 28:578–588
8. Kilic E, Bruggenwirth HT, Verbiest MM, Zwarthoff EC, Mooy NM, Luyten GP, de KA (2004) The RAS-BRAF kinase pathway is not involved in uveal melanoma. Melanoma Res 14:203–205
9. Lamperska K, Mackiewicz K, Kaczmarek A, Kwiatkowska E, Starzycka M, Romanowska B, Heizman J, Stachura J, Mackiewicz A (2002) Expression of p16 in sporadic primary uveal melanoma. Acta Biochim Pol 49:377–385

10. Lyons CJ, Hungerford J (1990) Detection of ocular malignancies. J R Soc Med 83:165–167
11. Omholt K, Karsberg S, Platz A, Kanter L, Ringborg U, Hansson J (2002) Screening of N-ras codon 61 mutations in paired primary and metastatic cutaneous melanomas: mutations occur early and persist throughout tumor progression. Clin Cancer Res 8:3468–3474
12. Park WL, Jenison-Williams T, Pasqua-Darnell T (2003) Uveal melanoma and poor treatment compliance: an atypical outcome with literature review. Optom Vis Sci 80:344–355
13. Smith JH, Padnick-Silver L, Newlin A, Rhodes K, Rubinstein WS (2007) Genetic study of familial uveal melanoma: association of uveal and cutaneous melanoma with cutaneous and ocular nevi. Ophthalmology 114:774–779
14. Smith JH, Padnick-Silver L, Newlin A, Rhodes K, Rubinstein WS (2007) Genetic study of familial uveal melanoma: association of uveal and cutaneous melanoma with cutaneous and ocular nevi. Ophthalmology 114:774–779
15. Soparker CN, O'Brien JM, Albert DM (1993) Investigation of the role of the ras protooncogene point mutation in human uveal melanomas. Invest Ophthalmol Vis Sci 34:2203–2209
16. Soufir N, Basset-Seguin N (2001) The INK4a-ARF locus: role in the genetic predisposition to familial melanoma and in skin carcinogenesis. Bull Cancer 88:1061–1067
17. Zografos L, Ducrey N, Beati D, Schalenbourg A, Spahn B, Balmer A, Othenin-Girard CB, Chamot L, Egger E (2003) Metastatic melanoma in the eye and orbit. Ophthalmology 110:2245–2256

Virchows Arch (2008) 452:337–341
DOI 10.1007/s00428-007-0556-7

CASE REPORT

Primary acinar cell carcinoma of the liver

Valérie Hervieu · Catherine Lombard-Bohas · Jérôme Dumortier · Olivier Boillot · Jean-Yves Scoazec

Received: 13 August 2007 / Revised: 9 November 2007 / Accepted: 1 December 2007 / Published online: 10 January 2008
© Springer-Verlag 2007

Abstract We report a case of acinar cell carcinoma primary to the liver. The tumor was diagnosed in a 35-year-old woman complaining of abdominal pain and asthenia; serum alpha-fetoprotein (AFP) levels were increased at 6,000 IU/mL; imaging studies showed a hypervascular mass located in the left lobe of the liver. A left lobectomy was performed. The tumor had a heterogeneous appearance. In well-differentiated areas, tumor cells formed acinar structures, had a pyramidal shape and a highly eosinophilic, granular cytoplasm, PAS diastase resistant. In less-differentiated areas, tumor cells were endocrinelike. The immunohistochemical study showed that tumor cells expressed trypsin. Alpha-fetoprotein and alpha1-antritrypsin were detected in about 30% of cells; HepPar1 was present in 15% of cells. Chromogranin A and synaptophysin were detected in rare cells. After surgery, serum AFP levels quickly returned to normal; no evidence of recurrence or metastasis was observed during follow-up. The final diagnosis, based on histological, immunohistochemical, and ultrastructural arguments, was extra-pancreatic acinar cell carcinoma, primary to the liver. This unusual lesion is likely to be the result of an abnormal differentiation pathway involving a transformed multipotential progenitor cell.

Keywords Liver tumor · Pancreatic carcinoma · Acinar cell carcinoma · Immunohistochemistry · Alpha-fetoprotein

V. Hervieu · J.-Y. Scoazec (✉)
Service Central d'Anatomie et Cytologie Pathologiques,
Hospices Civils de Lyon, Hôpital Edouard Herriot,
69437 Lyon Cedex 03, France
e-mail: jean-yves.scoazec@chu-lyon.fr

V. Hervieu · O. Boillot · J.-Y. Scoazec
Université Claude Bernard Lyon 1, Université de Lyon,
Villeurbanne, France

C. Lombard-Bohas
Unité d'Oncologie Médicale, Hospices Civils de Lyon,
Hôpital Edouard Herriot,
Lyon, France

J. Dumortier · O. Boillot
Fédération des Spécialités Digestives, Hospices Civils de Lyon,
Hôpital Edouard Herriot,
Lyon, France

Introduction

Acinar cell carcinoma is a rare form of tumor of the pancreas [9–11, 17]. Its diagnosis relies on the demonstration of acinar cell differentiation, including: (a) the existence of an acinar architecture; (b) the presence of characteristic morphological features in tumor cells, such as a pyramidal shape and a highly eosinophilic, granular, cytoplasm; (c) the ultrastructural demonstration of zymogen granules; and (d) the immunohistochemical detection of characteristic acinar markers, such as trypsin, present in more than 95% of cases, chymotrypsin, lipase, amylase, phospholipase A2, or elastase 1 [10].

The pathological spectrum of acinar cell carcinomas of the pancreas is large [10]. The degree of cell differentiation is variable from one case to another and may even be heterogeneous within the same tumor: The histological picture may range from that of a well-differentiated tumor with typical architectural and cytological features to that of a less-differentiated tumor formed by solid nests of endocrine-like tumor cells. The immunohistochemical profile is often complex: various lineage markers, including endocrine or neuro-endocrine markers [10, 19] and alpha-fetoprotein (AFP) [3, 8, 10], may be expressed by a proportion of tumor cells. Finally, tumor cells with acinar differentiation may be associated with other neoplastic

populations, in cases of mixed tumors, usually endocrine-acinar, or of multilineage tumors, such as pancreatoblastoma [10].

Very few cases of extra-pancreatic acinar cell carcinomas have been described in the literature. Three tumors were located in the stomach [5, 15, 20], one in the ampullary region [16] and one in the jejunum [13]; at least three arose in an ectopic pancreas [13, 15, 16]; two were classified as mixed acinar-endocrine tumors [5, 16]. In addition, an acinar cell component has been observed in three cases of tumors otherwise classified as mixed glandular-endocrine carcinomas of the stomach [7]. Finally, a case of acinar cell carcinoma has been described as part of a mediastinal teratoma [3].

We report here the first case of acinar cell carcinoma primary to the liver, in order to draw attention to this so far undescribed type of liver tumor, to underline the diagnostic difficulties encountered in this highly unusual location, and to discuss the possible histogenesis of the lesion.

Clinical history

A 35-year-old female was referred in 2001 to our institution for abdominal pain associated with asthenia, anorexia, and weight loss (>5 kg in 6 months). The patient was known to be HBsAg positive since 1991; there was no alteration of liver blood tests and no evidence of chronic hepatitis at a liver biopsy performed in 1993. Serum AFP levels were markedly increased at 6,000 IU/mL; the serum levels of CA19-9, CEA, and CA125 were within the normal range. Imaging studies revealed the presence of a large tumor mass, measuring 5 cm in diameter, located in the left lobe of the liver; the tumor was well limited and hypervascular. The clinical diagnosis was hepatocellular carcinoma. A left lobectomy was performed. Recovery was uneventful. Serum AFP levels returned to the normal range immediately after surgery. At the date of submission of the manuscript, the patient was well, without evidence of recurrence or metastasis.

Materials and methods

The surgical specimen was received fresh. Tissue samples were taken from the tumor and the adjacent liver tissue, fixed in buffered formalin, and embedded in paraffin. They were processed according to standard techniques for histological, histochemical, and immunohistochemical investigations. For immunohistochemical study, the following markers were tested: cytokeratins (KL1 and AE1/AE3, Dako, Trappes, France), cytokeratins 7 (OV-TL12/30, Dako) and 20 (K_s20.8, Dako), vimentin (V9, Dako), AFP (polyclonal antibody, Dako), alpha1-antitrypsin (polyclonal antibody, Dako), hepatocyte antigen or HepPar1 (OCH1E5, Dako), chromogranin A (polyclonal antibody, Dako), synaptophysin (SY38, Sigma), trypsin (polyclonal antibody, Bioadvance, Emerainville, France), E-cadherin (NCH38, Dako), beta-catenin (5H10, Zymed), Ki67 (MIB-1, Dako). An unsuccessful attempt to perform an ultrastructural study was made by using tissue samples retrieved from a formalin-fixed material.

Results

At macroscopical examination, the surgical specimen was found to contain a large polycyclic tumor mass, well circumscribed, unencapsulated, and measuring 4 cm in its largest diameter. The cut surface was whitish, with small hemorrhagic areas; there was no necrosis. The adjacent liver appeared normal, without cirrhosis or fibrosis. No satellite nodule was detected. At histological examination, the tumor was formed by large lobules separated by thin fibrous bands. The morphological appearance of the lesion was heterogeneous (Fig. 1). In most areas, tumor cells were arranged in solid nests and presented an endocrine-like morphology (Fig. 1c and d); they were medium-sized, with a high nucleo-cytoplasmic ratio, a scant cytoplasm, and a regular nucleus with finely dispersed chromatin; mitoses were frequent. In some areas, the architecture was ribbon-like or acinar: Large tumor cells, with a pyramidal shape, were arranged in cords or in acinar structures with a central lumen usually containing eosinophilic deposits (Fig. 1a); tumor cell cytoplasm was abundant, usually strongly eosinophilic (Fig. 1b), PAS diastase resistant. There was no area containing cells with hepatoid features. The tumor stroma was formed by thin fibrous bands containing numerous small vessels. There was no evidence of angioinvasion or perineural invasion. The adjacent liver presented a normal overall architecture without significant inflammation or fibrosis.

At immunohistochemical investigation (Fig. 2), tumor cells were uniformly cytokeratin positive and vimentin negative. Trypsin was detected as extracellular deposits located either in the lumen of acinar structures (Fig. 2a) or more rarely in the cytoplasm of tumor cells (Fig. 2b). Some scattered cells expressed cytokeratin 7; there was no detectable expression of cytokeratin 20. Alpha-fetoprotein was detected in about 30% cells, with variable levels of intensity (Fig. 2c); alpha1-antitrypsin was detected in a proportion of tumor cells, but, as usual, the staining was difficult to interpret because of the important reactivity of the plasma and of the extracellular matrix. HepPar1 reacted with 15% of tumor cells; the staining was cytoplasmic, granular, and faint (Fig. 2d); positive tumor cells did not

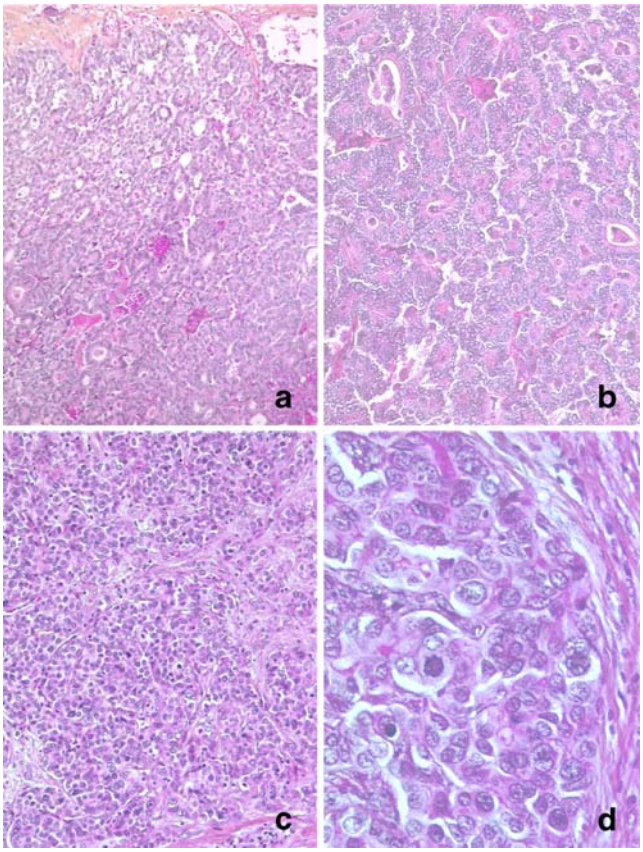


Fig. 1 Histological features. This well-differentiated area (**a**) shows a typical acinar architecture; at higher magnification (**b**), tumor cells are arranged in acinar structures around a central lumen containing an eosinophilic material; their cytoplasms are strongly eosinophilic. In contrast, a less-differentiated region (**c**) shows a compact architecture formed by tumor cells with an endocrine-like appearance showing numerous mitoses (**d**). H & E, **a** ×120, **b** ×280, **c** ×100, **d** ×340

present any hepatoid morphological feature but were endocrinelike in appearance. Chromogranin A and synaptophysin were expressed by about 10% of tumor cells, isolated or grouped in small clusters. E-cadherin and beta-catenin were expressed by all tumor cells, with a normal membrane distribution. The proliferation index, evaluated with MIB-1 antibody, ranged from <5% in the most differentiated areas to 15% in the less-differentiated regions.

Discussion

This case raised several related issues: (a) how to properly classify this unusual liver tumor; (b) how to affirm its primary nature; and (c) how to manage the patient.

Clinically, the detection of an apparently primary liver tumor, hypervascular at imaging studies and associated with elevated AFP levels, in a patient with a previous history of HBV infection, was highly suggestive of hepatocellular carcinoma. The much unexpected histological diagnosis of acinar cell carcinoma was raised on several arguments. A first element was the presence of morphological evidence of acinar differentiation, including the presence of a characteristic architectural pattern and the occurrence of typical cytological features (pyramidal shape, strongly eosinophilic cytoplasm, diastase resistant PAS positivity). These well-differentiated regions coexisted, as frequently observed in acinar cell carcinomas of the pancreas [10], with less-differentiated regions in which tumor cells assumed a poorly suggestive, endocrine-like appearance, which, alone, may have been much confusing and may have led to a diagnosis of poorly differentiated hepatocellular carcinoma.

The immunohistochemical profile of the tumor was, therefore, essential to assess the diagnosis. A most suggestive feature was the positivity of the acinar cell marker trypsin: The sensitivity and specificity of this marker for the diagnosis of acinar cell carcinoma have been well demonstrated [10]. The demonstration of zymogen granules by ultrastructural examination, which may

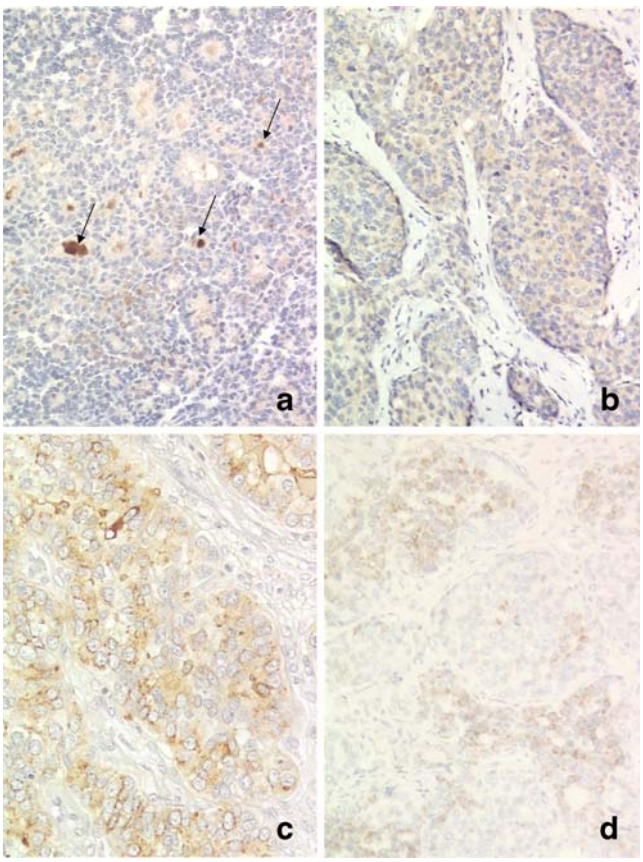


Fig. 2 Immunohistochemical features. Trypsin (**a**, **b**) is detected either in extracellular deposits in the lumen of acinar structures (**a**, *arrows*) or as a faint cytoplasmic labeling (**b**). Some tumor cells express AFP (**c**) and HepPar1 (**d**); the labeling for HepPar1 is cytoplasmic, granular, and very faint. Indirect immunoperoxidase technique according to the streptavidin–biotin technique, followed by nuclear counterstaining with Mayer's hematoxylin; **a** and **b** ×80, **c** ×140, **d** ×220

have strengthened this immunohistochemical result, was unfortunately hampered by the poor technical conditions in which it was attempted. The positivity of several "hepatocellular" markers, including AFP, alpha1-antitrypsin, and hepatocyte antigen, did not rule out the diagnosis of acinar cell carcinoma: (a) the expression of AFP, as well as of alpha1-antitrypsin, has been described in a significant proportion of acinar cell carcinomas of the pancreas [6, 11, 19]; (b) the expression of another hepatocellular marker, HepPar1, has not been described so far in acinar cell carcinoma of the pancreas but is not unexpected because of the frequent expression of hepatocellular markers in this type of tumor. The immunoreactivity observed in our case was faint and recalled that observed in nonhepatoid adenocarcinomas (such as those of the small intestine or of the thyroid) [12]. In the same way, the expression of endocrine and neuro-endocrine markers, as observed in our case, is frequent in acinar cell carcinoma of the pancreas, in which it is observed in up to 42% of cases [10]; as in our case, this expression is usually restricted to a small proportion of tumor cells. Only tumors with >25% of cells showing evidence of endocrine or acinar differentiation have to be classified as mixed endocrine-acinar cells [10].

The histological diagnosis of acinar cell carcinoma made in our case immediately raised the question of the primary or secondary nature of this liver tumor, since acinar cell carcinomas frequently metastasize to the liver. Several arguments strongly support the primary nature of the lesion: (a) No evidence of pancreatic lesion was found at imaging studies and during surgical exploration; (b) the surgical resection of the liver lesion induced a rapid decrease in serum AFP levels, which returned to the normal; (c) there was no evidence of recurrence or metastasis even after a long follow-up. In view of the primary nature of the lesion, no treatment other than surgery was attempted in our patient, and a regular follow-up was set up. It must be noted that, owing to the rarity of acinar cell carcinoma, no consensus has emerged about the most adequate therapeutic management of this tumor [9].

The histogenesis of such an unusual tumor is difficult to assess. A first hypothesis is that the tumor arose from an ectopic pancreas, as previously suggested for other cases of extra-pancreatic acinar cell carcinoma. This possibility is, however, unlikely in our case because of the location of the lesion at the distal extremity of the left lobe. The occurrence of intra-hepatic ectopic pancreatic tissue is extremely rare. In the very few cases reported so far [18], the ectopic pancreas tissue has been more often found close to the common bile duct and was usually associated with developmental abnormalities of the biliary tree [1]. Another hypothesis is that this unusual lesion resulted from an abnormal differentiation process. It must be noted that, ontogenetically, both liver and pancreatic cells are derived from a common progenitor cell [4] and that, experimentally, liver cells retain the capacity to transdifferentiate into acinar pancreatic cells under certain conditions [2, 14]. It may, therefore, be hypothesized that, in our case, an abnormal differentiation pathway resulted in the acquisition of acinar pancreatic features by a transformed clone deriving from a multipotential progenitor cell.

In conclusion, we report the first case of primary acinar cell carcinoma of the liver and point out the potential diagnostic pitfalls raised by this unusual tumor, such as the possible association with elevated AFP serum levels. We suggest that this diagnosis may be considered for morphologically atypical primary tumors of the liver lacking the conventional features of hepatocellular carcinoma despite the expression of hepatocellular markers.

Conflict of interest statement We declare that we have no conflict of interest.

References

1. Bahadir B, Ozdamar SO, Gun BD, Bektas S, Numanoglu KV, Kuzey GM (2006) Ectopic pancreas associated with choledochal cyst and multiseptate gallbladder. Pediatr Dev Pathol 9:312–315
2. Ber I, Shternhall K, Perl S, Ohanuna Z, Goldberg I, Barshack I, Benvenisti-Zarum L, Meivar-Levy I, Ferber S (2003) Functional, persistent, and extended liver to pancreas transdifferentiation. J Biol Chem 278:31950–31957
3. Cingolani N, Shaco-Levy R, Farruggio A, Klimstra DS, Rosai J (2000) Alpha-fetoprotein production by pancreatic tumors exhibiting acinar cell differentiation: study of five cases, one arising in a mediastinal teratoma. Hum Pathol 31:938–944
4. Deutsch G, Jung J, Zheng M, Lora J, Zaret KS (2001) A bipotential precursor population for pancreas and liver within the embryonic endoderm. Development 128:871–881
5. Fukunaga M (2002) Gastric carcinoma resembling pancreatic mixed acinar-endocrine carcinoma. Hum Pathol 33:569–573
6. Hoorens A, Lemoine NR, McLellan E, Morohoshi T, Kamisawa T, Heitz PU, Stamm B, Ruschoff J, Wiedenmann B, Kloppel G (1993) Pancreatic acinar cell carcinoma. An analysis of cell lineage markers, p53 expression, and Ki-ras mutation. Am J Pathol 143:685–698
7. Jain D, Eslami-Varzaneh F, Takano AM, Ayer U, Umashankar R, Muller R, Klimstra DS (2005) Composite glandular and endocrine tumors of the stomach with pancreatic acinar differentiation. Am J Surg Pathol 29:1524–1529
8. Kawamoto S, Hiraoka T, Kanemitsu K, Kimura M, Miyauchi Y, Takeya M (1992) Alpha-fetoprotein-producing pancreatic cancer—a case report and review of 28 cases. Hepatogastroenterology 39:282–286
9. Kitagami H, Kondo S, Hirano S, Kawakami H, Egawa S, Tanaka M (2007) Acinar cell carcinoma of the pancreas. Clinical analysis of 115 patients from Pancreatic Cancer Registry of Japan Pancreas Society. Pancreas 35:42–46
10. Klimstra DS (2007) Nonductal neoplasms of the pancreas. Mod Pathol 20(Suppl 1):S94–S12
11. Klimstra DS, Heffess CS, Oertel JE, Rosai J (1992) Acinar cell carcinoma of the pancreas. A clinicopathologic study of 28 cases. Am J Surg Pathol 16:815–837

12. Lugli A, Tornillo L, Mirlacher M, Bundi M, Sauter G, Terracciano LM (2004) Hepatocyte paraffin 1 expression in human normal and neoplastic tissues: tissue microarray analysis on 3,940 tissue samples. Am J Clin Pathol 122:721–727
13. Makhlouf HR, Almeida JL, Sobin LH (1999) Carcinoma in jejunal pancreatic heterotopia. Arch Pathol Lab Med 123:707–711
14. Meivar-Levy I, Ferber S (2003) New organs from our own tissues: liver-to-pancreas transdifferentiation. Trends Endocrinol Metab 14:460–466
15. Mizuno Y, Sumi Y, Nachi S, Ito Y, Marui T, Saji S, Matsutomo H (2007) Acinar cell carcinoma arising from an ectopic pancreas. Surg Today 37:704–707
16. Moncur JT, Lacy BE, Longnecker DS (2002) Mixed acinar-endocrine carcinoma arising in the ampulla of Vater. Hum Pathol 33:449–451
17. Mulkeen AL, Yoo PS, Cha C (2006) Less common neoplasms of the pancreas. World J Gastroenterol 12:3180–3185
18. Pujari BD, Deodhare SG (1979) Intrahepatic ectopic pancreas: report of a case. Indian J Med Sci 33:157–159
19. Skacel M, Ormsby AH, Petras RE, McMahon JT, Henricks WH (2000) Immunohistochemistry in the differential diagnosis of acinar and endocrine pancreatic neoplasms. Appl Immunohistochem Mol Morphol 8:203–209
20. Sun Y, Wasserman PG (2004) Acinar cell carcinoma arising in the stomach: a case report with literature review. Hum Pathol 35:263–265

Virchows Arch (2008) 452:343–345
DOI 10.1007/s00428-007-0559-4

CASE REPORT

Hibernoma-like brown fat in the bone marrow: report of a unique case

C. Thorns · C. Schardt · D. Katenkamp · C. Kähler · H. Merz · A. C. Feller

Received: 12 November 2007 / Revised: 3 December 2007 / Accepted: 6 December 2007 / Published online: 10 January 2008
© Springer-Verlag 2007

Abstract We report on a bone-marrow biopsy of a 61-year-old female patient that was performed because of the clinical suspicion of a myeloproliferative disease. The trephine biopsy showed morphological features that were consistent with an essential thrombocythaemia (ET). The diagnosis of a myeloproliferative disease could be corroborated by demonstration of the V617F mutation of JAK2. Besides the histological features of ET, the marrow showed a peculiar infiltrate that consisted of multivacuolated cells that were immunohistochemically identified as brown adipose tissue with a hibernoma-like picture. To the best of our knowledge, this is the first report on brown adipose tissue in the bone marrow.

Keywords Trephine bone marrow biopsy · Immunohistochemical stainings · Brown adipose tissue

C. Thorns (✉) · C. Kähler · H. Merz · A. C. Feller
Institut für Pathologie und Konsultations-und Referenzzentrum für Lymphknotendiagnostik und Hämatopathologie, Universitätsklinikum Schleswig-Holstein, Campus Lübeck, Ratzeburger Allee 160, 23538 Lübeck, Germany
e-mail: thorns@patho.uni-luebeck.de

C. Schardt
Onkologische Schwerpunktpraxis, Gelsenkirchen, Germany

D. Katenkamp
Institut für Pathologie und Konsultations-und Referenzzentrum für Weichgewebstumoren, Universitätsklinikum Jena, Jena, Germany

Introduction

Trephine bone marrow biopsies are routinely taken during the diagnostic workup of haematological diseases and for staging of malignant tumours. The normal bone marrow, besides the haematopoietic lineages, does possess fat cells in a very variable number. However, the fat of the normal bone marrow is generally considered to consist of white univacuolated fat cells. Multivacuolated brown adipose tissue in the adult is essentially confined to the perirenal, posterior cervical and intercostal regions. In this paper, we report on brown adipose tissue as a peculiar coincidental finding in a bone marrow that was biopsied during the diagnostic workup of a myeloproliferative disease.

Case history

We report on a bone-marrow biopsy of a 61-year-old female patient who presented with marked thrombocythaemia and mild leucocytosis (haemoglobin 15.6 g/dl, white blood cells 10.200/μl, platelets 742.000/μl). A trephine bone-marrow biopsy was performed because of the suspicion of a myeloproliferative disease.

Materials and methods

The morphologic features of the trephine bone marrow biopsy were assessed on haematoxylin and eosin-, periodic acid–Schiff (PAS)-, Giemsa-, Alcian blue- and Gomori-stained sections of formalin-fixed, paraffin-embedded tissue. Bone-marrow aspirate and peripheral-blood smears were stained for Pappenheim.

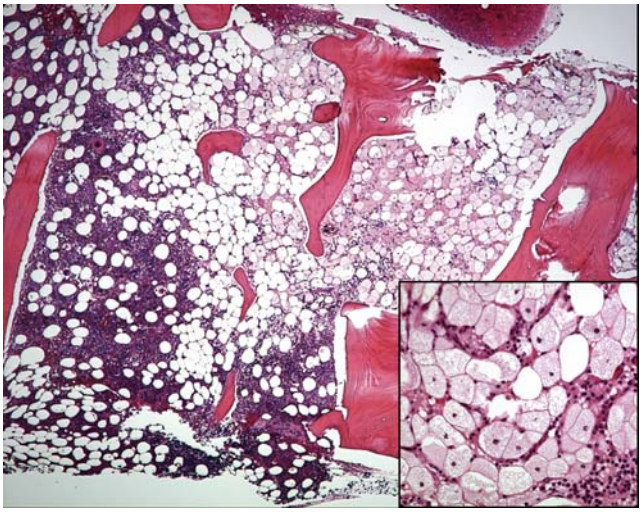


Fig. 1 Low-power magnification of the bone marrow biopsy with haematopoietic marrow on the *left* and brown adipose tissue on the *right*. *Inset* High-power magnification of multivacuolated fat cells

Immunohistochemical stainings were performed according to a standard three-step immunoperoxidase technique with diaminobenzidine as chromogen. The following antibodies were used: CD117, HMB45, Lysozyme, S100, Melan A, Mac387, Vimentin (Dako, Denmark), CD42, PGM1 (Lab Vision, Fremont, USA), KL1 (ImmunoTech, Marseilles, Francs) and CD 34 (Novocastra, Newcastle, UK).

Molecular analysis for the V617F mutation of JAK2 was performed on peripheral blood using an allele-specific polymerase chain reaction approach [1].

Results

The trephine biopsy was more or less divided in two distinct areas, both of which will be described separately: one representing the haematopoietic marrow, the other showing a peculiar infiltrate.

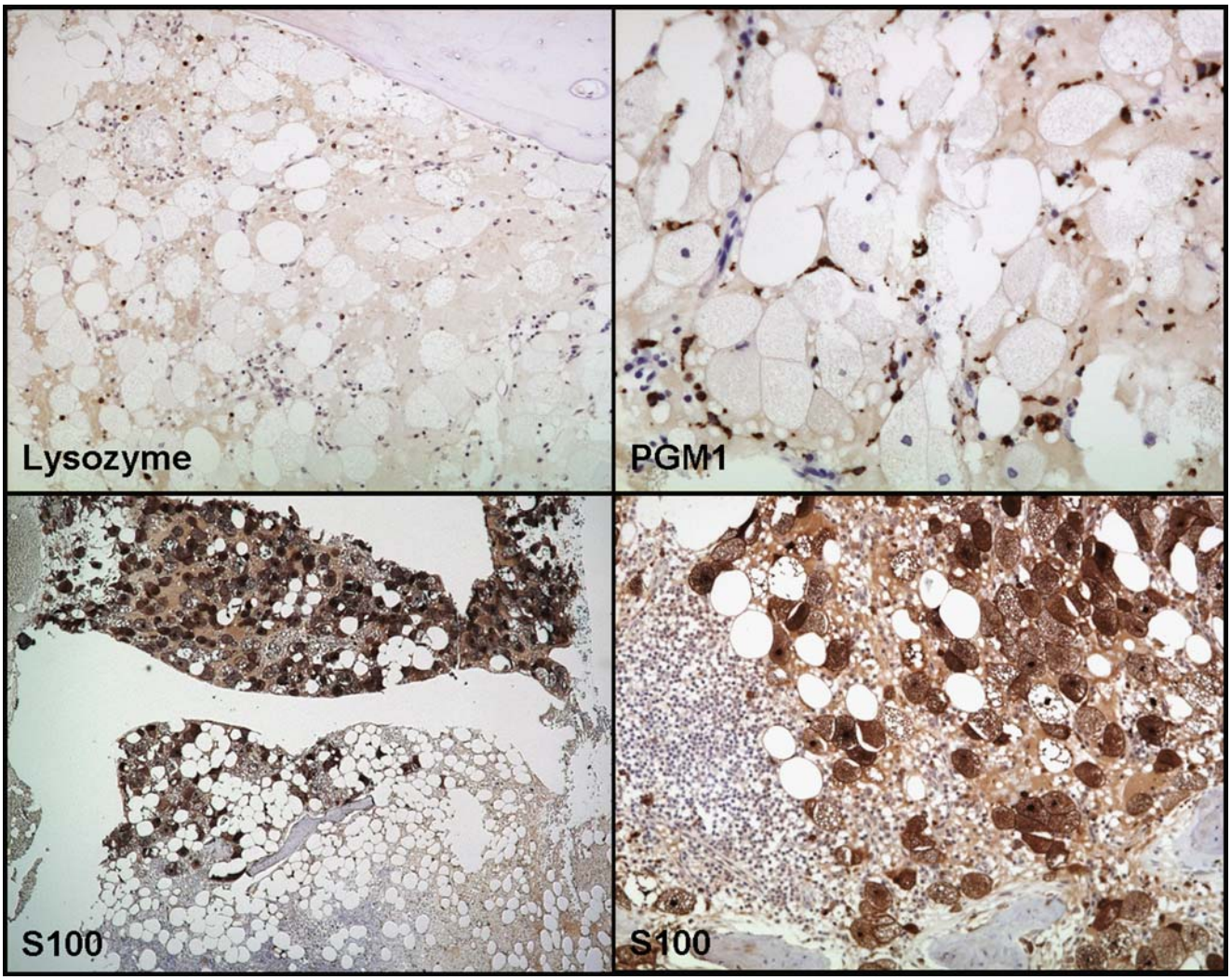


Fig. 2 Negative staining for lysozyme and PGM1 and positive staining for S100 on brown fat cells

The haematopoietic bone marrow was mildly hypercellular with a particular prominent megakaryopoiesis. The size of megakaryocytes was normal to slightly increased; only very few megakaryocytes showed hyperchromatic nuclei. Large clusters of megakaryocytes were not present. Reticulin fibrosis was present only focally and very mild. The bone-marrow aspirate showed an increase in megakaryocytes and a mild increase in overall cellularity. There were no dysplastic features. Peripheral blood smears revealed an increased number of platelets with only occasional giant forms. Mild leucocytosis was present. There was no pathological left shift of the granulocytic lineage and no absolute basophilia. Immunohistochemical stains revealed no excess of blasts (CD34, CD117) and confirmed the increase of megakaryocytes (CD42). Molecular analysis of peripheral blood revealed a V617F mutation of JAK2. The findings were consistent with the diagnosis of essential thrombocythaemia [6].

The other part of the bone-marrow biopsy showed a peculiar infiltrate that was clearly separated from the haematopoietic marrow (Fig. 1). The infiltrate consisted of diffusely arranged large cells with abundant foamy cytoplasm. The nuclei were small and uniform and did not show any features of malignancy. The cytology was consistent with foamy macrophages or multivacuolated brown fat cells. The PAS and Alcian-blue reactions revealed no intracellular storage of mucins. Immunohistochemical staining for macrophage-associated markers (PGM1, lysozyme, and MAC387) gave negative results, whereas staining for S100 was clearly positive (Fig. 2). For the sake of completeness, staining for HMB45, Melan A and KL1 were performed and resulted in negative reactions on the suspicious cell population. In consideration of the cytological features and the immunohistochemical results, these cells were interpreted as brown adipose tissue.

Discussion

In humans, brown adipose tissue is well established early in the fifth month of fetal life and has a wide distribution in the early years. In adult life, it progressively disappears and is confined to the more central parts of the body, which leads to a vest-like arrangement with the greatest yields of brown fat in perirenal, posterior cervical and intercostal localization [3, 5]. In contrast, brown adipose tissue is very common in animals, especially hibernators. Brown fat cells have the capacity to directly transform chemical energy in heat and, therefore, are the site of non-shivering heat production. Several types of brown fat cells, which are distinguished mostly on the basis of a different size and number of intracellular vacuoles, can be identified morphologically. The different types probably represent different stages of activity (reviewed in [4]).

White fat is an integral part of the normal bone marrow, and hence, lipomas of the bone marrow have been well described [2]. However, to the best of our knowledge, brown adipose tissue in the bone marrow has not yet been described in the literature. And we are not aware of any other case in our own files (with a couple of thousand trephine bone-marrow biopsies per year). Whether the brown fat cells in the present case are non-neoplastic resting cells or represent an early stage of a hibernoma is arguable. The fact that the cells were confined to the marrow spaces without developing a tumour or mass is clearly in favour of the former.

One must bear in mind that the brown fat cell, when inactive, becomes univacuolated and is nearly indistinguishable from the white fat cell on light microscopy [3]. Therefore, it may very well be that inactive brown fat cells are not as rare in the bone marrow as it seems to be but are missed on routine light microscopy. It seems to be unlikely that brown adipose tissue is physiologically part of the bone marrow for local heat production. However, it may be that this is the case under certain pathological or extreme circumstances.

In the presented case, the differential diagnosis to brown adipose tissue was foamy macrophages, clear-cell carcinoma and less likely, more because of the reactivity for S100 than for cytology, melanoma.

The presented case may bring to mind again that one should be prepared to encounter curiosities in bone marrows with otherwise diagnostically straight forward features.

References

1. Baxter EJ, Scott LM, Campbell PJ, East C, Fourouclas N, Swanton S, Vassiliou GS, Bench AJ, Boyd EM, Curtin N, Scott MA, Erber WN, Cancer Genome Project, Green AR (2005) Acquired mutation of the tyrosine kinase JAK2 in human myeloproliferative disorders. Lancet 365:1054–1061
2. Döhler R, Harms D (1981) Intraosseous lipomas. Z Orthop Ihre Grenzgeb 119(1):138–141
3. Heaton JM (1972) The distribution of brown adipose tissue in the human. J Anat 112(1):35–39
4. Ito T, Tanuma Y, Yamada M, Yamamoto M (1991) Morphological studies on brown adipose tissue in the bat and humans of various ages. Arch Histol Cytol 54(1):1–39
5. Merklin RJ (1974) Growths and distribution of human fetal brown fat. Anat Rec 178(3):637–646
6. Tefferi A, Thiele J, Orazi A, Kvasnicka HM, Barbui T, Hanson CA, Barosi G, Verstovsek S, Birgegard G, Mesa R, Reilly JT, Gisslinger H, Vannucchi AM, Cervantes F, Finazzi G, Hoffman R, Gilliland DG, Bloomfield CD, Vardiman JW (2007) Proposals and rationale for revision of the World Health Organization diagnostic criteria for polycythemia vera, essential thrombocythemia, and primary myelofibrosis: recommendations from an ad hoc international expert panel. Blood 110(4): 1092–1097

Virchows Arch (2008) 452:347–348
DOI 10.1007/s00428-008-0579-8

LETTER TO THE EDITOR

CXCR7 transcription in human non-small cell lung cancer and tumor-free lung tissues; possible regulation upon chemotherapy

Torsten Goldmann · Daniel Drömann · Janine Radtke · Sebastian Marwitz · Dagmar S. Lang · Holger Schultz · Ekkehard Vollmer

Received: 19 November 2007 / Revised: 7 January 2008 / Accepted: 8 January 2008 / Published online: 24 January 2008
© Springer-Verlag 2008

Keywords HOPE · CXCR7 · Lung · Cancer

Various chemokine receptors are expressed by malignant tumors and have been associated with tumor progression and metastasis [4]. A recent study demonstrated the promotion of tumor growth in breast and lung cancer by CXCR7, formerly known as orphan receptor CMKOR1/RDC1 utilizing cell lines and animal models. CXCR7 expression in human breast and lung cancer specimens, as well as in the tumor vasculature was shown on the protein level by immunohistochemistry. Here, we employed human lung tissues treated with the novel hepes–glutamic acid buffer-mediated organic solvent protection effect (HOPE) technique [5] to analyze the overall expression of CRCX7 on the mRNA level in non-small cell lung cancer (NSCLC) and tumor-free lung tissues. Additionally, the effect of chemotherapy upon the transcription of CRXR7 was addressed, employing a currently established human model system [1, 3].

Applying RT-PCR with a specific primer set spanning an amplicon of 156 bp (5′–TGCTGGACATCTTCTCCATC-3′ forward, 5′-CTTCATCAGCTCCTACCT-3′ reverse), we found transcription of CXCR7 in all of the 30 NSCLC samples analyzed. A set of ten examples is shown in Fig. 1a. Specificity of the reverse-transcription polymerase chain reaction (RT-PCR) was verified by sequencing of the PCR products. The results of RT-PCR were then validated by in situ hybridization (N=21) using a double stranded DNA probe labeled with digoxigenin, which revealed transcripts of CXCR7 within the tumor cells of 17 samples (Fig. 1b) with only some occasional signals in the tumor-associated vasculature [2]. Moreover, 20 specimens of tumor-free human lungs were also subjected to in situ hybridization and all revealed transcripts localized mainly in alveolar macrophages (Fig. 1c) and in cells, which reflect the morphology of alveolar epithelial cells type II (Fig. 1d).

Stimulation of tumor tissues with physiological concentrations of carboplat and gemcitabine (N=30) was performed within the human model system designated short-term stimulation of tissues in comparison to corresponding tissues, which received cultivation without stimulation [3]. Here, we found an upregulation of CXCR7 transcription upon chemotherapy in 13.4% of the cases, downregulation in 33.3%, and no regulation in 53.3%, as determined by semiquantitative RT-PCR in relation to glyceraldehyde-3-phosphate dehydrogenase (exemplified in the lower panel of Fig. 1a; note upregulation of CXCR7 in sample 4 upon chemotherapy).

Taken together, our study verifies the recently reported results on the mRNA level in a comparably large amount of specimens [4]. However, although some signals were occasionally observable, we did not detect strong expression within the tumor-associated vasculature on the RNA level. The effects of chemotherapy onto CXCR7 are heterogeneous. Nevertheless, the same holds true for the overall characteristics of the tumors themselves and their

T. Goldmann (✉) · J. Radtke · S. Marwitz · D. S. Lang · H. Schultz · E. Vollmer
Clinical and Experimental Pathology,
Research Center Borstel, Parkallee 1-40,
23845 Borstel, Germany
e-mail: tgoldmann@fz-borstel.de

D. Drömann
Medical Clinic,
Research Center Borstel, Parkallee 1-40,
23845 Borstel, Germany

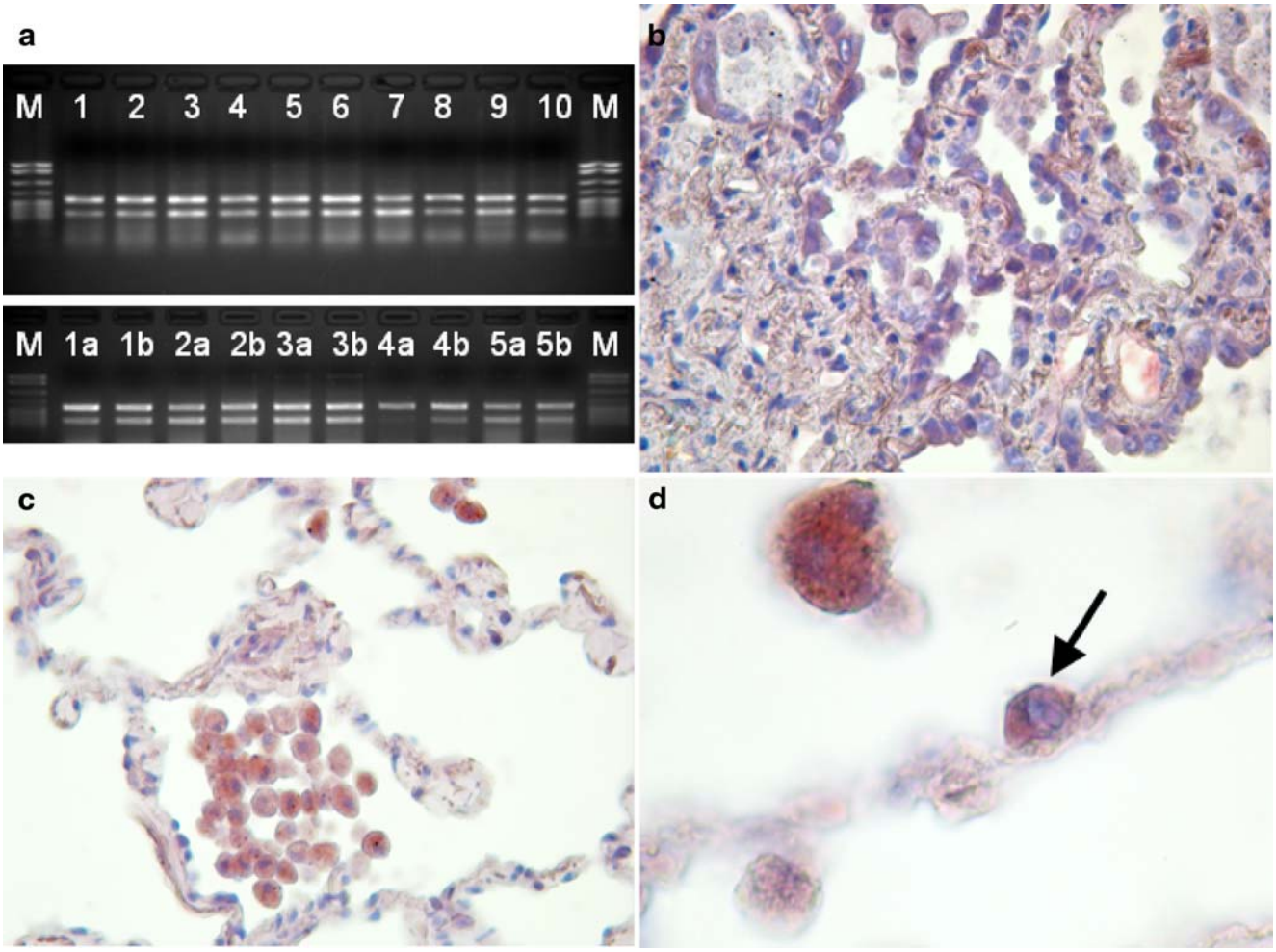


Fig. 1 **a***Upper panel*: RT-PCR targeting CXCR7 and GAPDH mRNA in human NSCLC: *M*=pBr322 Msp1; *upper signals*: A 257-bp fragment of GAPDH; *lower signals*: CXCR7. *Lower panel*: RT-PCR targeting CXCR7 and GAPDH mRNA in human NSCLC after STST: *a*: medium controls; *b*: stimulation with carboplat and gemcitabine. *M*=pBr322 Msp1; *upper signals*: A 257-bp fragment of GAPDH; *lower signals*: CXCR7. **b**, **c**, **d** In situ hybridization targeting mRNA of CXCR7 in human lung tissues using a digoxigenin-labeled DNA probe and new fuchsine as a chromogen: **b** Adenocarcinoma of the lung (×400). **c** Alveolar macrophages (×400). **d** Alveolar epithelial cell type II, see *arrow* (×1,000)

behavior upon chemotherapeutic interventions within the patients. Therefore, the effects of chemotherapy onto CXCR7 might be valuable hints towards an understanding of the broad chemotherapy resistance found in NSCLC. We have additionally shown a consistent transcription of CXCR7 within tumor-free lung tissues, suggesting a possible new function of this receptor in nonmalignant processes within the human lung.

Conflict of interest statement We declare that we have no conflict of interest.

References

1. Droemann D, Rupp J, Goldmann T, Uhlig U, Branscheid D, Vollmer E, Kujath P, Zabel P, Dalhoff K (2007) Disparate innate immune responses to persistent and acute *Chlamydia pneumoniae* infection in COPD. Am J Respir Crit Care Med 175:791–797
2. Goldmann T, Wiedorn KH, Kühl H, Olert J, Branscheid D, Pechkovsky D, Zissel G, Galle J, Müller-Quernheim J, Vollmer E (2002) Assessment of transcriptional gene activity in situ by application of HOPE-fixed, paraffin-embedded tissues. Pathol Res Pract 198:91–95
3. Lang DS, Droemann D, Schultz H, Branscheid D, Martin C, Ressmeyer A, Zabel P, Vollmer E, Goldmann T (2007) A novel human *ex vivo* model for the analysis of molecular events during lung cancer chemotherapy. Resp Res 14:43
4. Miao Z, Luker KE, Summers BC, Berahovich R, Bhojani MS, Rehemtulla A, Kleer CG, Essner JJ, Nasevicius A, Luker GD, Howard MC, Schall TJ (2007) CXCR7 (RDC1) promotes breast and lung tumor growth in vivo and is expressed on tumor-associated vasculature. PNAS 104:15735–15740
5. Olert J, Wiedorn KH, Goldmann T, Kühl H, Mehraein Y, Scherthan H, Niketeghad F, Vollmer E, Müller AM, Müller-Navia J (2001) HOPE-fixation: a novel fixing method and paraffin embedding technique for human soft tissues. Pathol Res Pract 197:823–826

Virchows Arch (2008) 452:349–350
DOI 10.1007/s00428-008-0581-1

LETTER TO THE EDITOR

A case of pararenal PEComa with extensive bone metaplasia

Carmen L. Menéndez · Rodrigo Gil Ugarteburu · Jesús M. Capilla Ampudia · Gabriela Corte Torres · Eduardo Fuente · Mario Argüelles

Received: 6 December 2007 / Revised: 5 January 2008 / Accepted: 11 January 2008 / Published online: 5 February 2008
© Springer-Verlag 2008

Dear Editor,

The group of perivascular epithelioid cell tumours (PEComas; a family of rare mesenchymal neoplasms arising at different visceral and soft tissue sites) has a wide spectrum of morphology. We present a case with a very unusual feature: wide bone metaplasia.

The patient was a 63-year-old hypertensive woman complaining from left flank pain and cystitis. Laboratory data were normal, except *E. coli* in urine. Results of an abdominal simple X-ray showed a 4-cm calcified round tumour at the upper left renal pole, very evident with the computed tomography (CT) scan (Fig. 1). It was excised through laparoscope. The mass was covered by fatty tissue and had good cleavage from adjacent kidney.

The gross specimen was a 28-g, 4-cm-sized, smooth-surfaced tumour with very loose attachments to the fat nearby. It showed haemorrhagic and cystic areas alternating with a few white solid ones. The consistency was so hard that it required decalcification. Microscopically, it was composed by aggregates of clear or light eosinophilic epithelioid cells with relatively bland nuclei and some giant cells, among fine arborizing capillaries or around thick-walled, often hyalinized blood vessels, alternating with hypocellular collagenous–hyalinized areas, sometimes calcified. Endochondral ossification and lamellar bone was frequent (Fig. 2). Occasionally, mature adipose tissue was found. Cellular areas were 21% of the total. There was no mitosis or necrosis. The tumour was entirely circumscribed by a fine connective capsule. Fatty tissue and adrenal gland had no abnormalities. Immunohistochemically, neoplastic cells expressed vimentin, frequent human melanoma black (HMB)45 (more intense in larger epithelioid–clear cells, with paranuclear accentuation; Fig. 3) and melan-A (same staining pattern), also S100, smooth muscle antigen, clusters of differentiation (CD)10, CD68 and occasionally pan-cytokeratin. They were desmin, myogenin, α-inhibin, epithelial membrane antigen, CD117, cyclin D1, CD34 and CD31 negative. Ki 67 was inapparent.

This immunohistochemical profile is specific of PEComa. Other clear cell tumours of that area can be excluded [4]. HMB45-positive large neoplastic cells (proliferating PEC cells) were sometimes located very close to endothelial lined spaces. In sum, this unusual case belongs to the PEComa family, a recently defined group of tumours originated from perivascular epithelioid (PEC) cells [1, 2] at multiple sites, encompassing angiomyolipoma, lymphangiomyomatosis, clear cell "sugar" tumour and rare tumours in other locations. They have a wide range of clinical, pathological and immunohistochemical features: clearly malignant [3, 5], some of uncertain malignant potential and a few benign. This case would fulfil the criteria of the

C. L. Menéndez (✉) · G. Corte Torres · E. Fuente · M. Argüelles
Pathology Department, Hospital de Cabueñes,
C/ Los Prados 395, Cabueñes,
33203 Gijón, Asturias, Spain
e-mail: carluznr@telecable.es

R. Gil Ugarteburu
Department of Urology, Hospital de Cabueñes,
Gijón, Spain

J. M. Capilla Ampudia
Department of Radiology, Hospital de Cabueñes,
Gijón, Spain



Fig. 1 CT scan showed a calcified round tumour at the upper left renal pole

benign group: small (<5 cm), bland cellularity, no mitosis–necrosis–vascular invasion [1]; it had wide hyalinised areas and frequent calcification and osseous metaplasia, an unusual feature (which made it more evident in the CT scan). Six months after it was excised there was no evidence of recurrence or metastases.

Acknowledgement We thank Dr A. López-Beltrán, Department of Pathology, Córdoba University, Spain, for his appreciated remarks about this case.

Conflict of interest statement We declare that we have no conflict of interest.

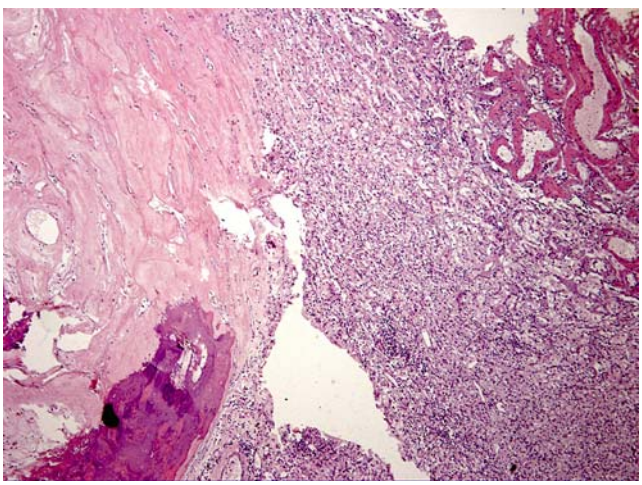


Fig. 2 Aggregates of neoplastic cells around prominent vessels, alternating with hyalinised areas and mature bone formation

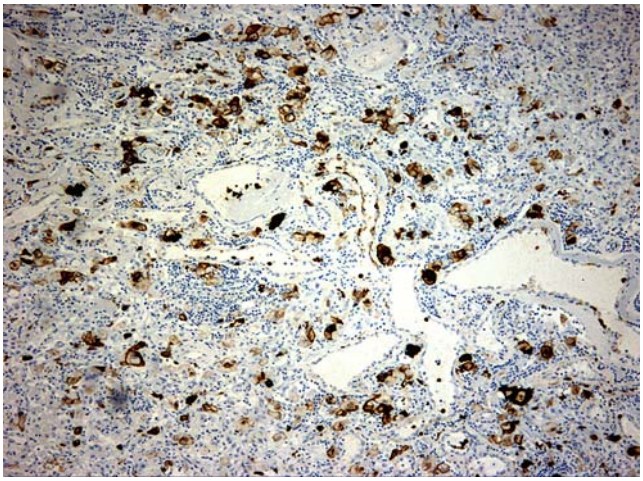


Fig. 3 Clear–epithelioid cells, positive for HMB45, have a close relationship with nearby vessels

References

1. Folpe AL, Mentzel T, Lehr HA, Fisher C, Balzer B, Weiss C (2005) Perivascular epithelioid cell neoplasms of soft tissue and gynecologic origin. A clinicopathologic study of 26 cases and review of the literature. Am J Surg Pathol 29:1558–1574
2. Hornick JL, Fletcher CD (2006) PEComa: what do we know so far?. Histopathology 48:75–82
3. Kim HJ, Lim SJ, Choi H, Park K (2006) Malignant clear cell myomelanocytic tumor of broad ligament—a case report. Virchows Arch 448:867–870
4. Merran S, Vieillefond A, Peyromaure M, Dupuy C (2004) Renal angiomyolipoma with calcification: CT-pathology correlation. Br J Radiol 77:782–783
5. Weinreb I, Howarth D, Latta E, Ghazarian D, Chetty R (2007) Perivascular epithelioid cell neoplasms (PEComas): four malignant cases expanding the histopathological spectrum and a description of a unique finding. Virchows Arch 450:463–470

Virchows Arch (2008) 452:351–352
DOI 10.1007/s00428-007-0553-x

LETTER TO THE EDITOR

Adenohibernoma of the breast

Nilgun Kapucuoglu · Sibel Percınel · Antonio Angelone

Received: 29 October 2007 / Revised: 15 November 2007 / Accepted: 16 November 2007 / Published online: 14 December 2007
© Springer-Verlag 2007

Dear Sir,

Brown fat is mainly found in infants and children and gradually disappears from most sites of the body with increasing age. During adulthood, deposits of brown fat persist around kidneys, adrenal glands, and aorta and within the mediastinum and neck. Tumors composed of brown fat (hibernomas) are rare in breast [1, 2, 4, 5]. A rare case of hamartoma containing brown fat has been reported by Garijo et al. [5]. Adenohibernoma, hibernoma-containing glands, is also a very rare lesion as one case only has been described until now [2]. Here, we are reporting a second case.

The patient, a 57-year-old lady, underwent excisional biopsy 2 cm across due to right breast lesion detected mammographically. The family history was unremarkable. Histologically, in addition to tubular carcinoma, an incidental lesion was detected nearby *which had not been detected on mammograms*. This latter lesion was well circumscribed *and measuring 3 mm*. It was formed partly by a fibroepithelial proliferation reminiscent of fibroadenoma with myxoid stroma (Fig. 1). Nuclear atypia and epithelial proliferation were not present. The remaining part of the nodular lesion showed dilated glands immersed within fat tissue, which showed uniform, normochromatic, and centrally located nuclei with vacuolated granular eosinophilic cytoplasms consistent with brown fat (Fig. 2). Accordingly, the vacuolated granular *brown fat* cells were positive with avidin–biotin complex peroxidase for S-100 protein (Dako, polyclonal, 1:1500; Fig. 3) and negative for wide spectrum keratin (Dako, MNF116, 1:200) and cluster of differentiation (CD)68 (Neomarkers, monoclonal, MAC387, 1:200). There was no residual lesion within the re-excision specimen which consisted of fibrofatty tissue measuring 4 cm. Seven lymph nodes from lower axillary level were reactive. There is no evidence of disease after a 6-year follow-up.

Adenolipomas are lesions composed of glands immersed in adult classical adipous tissue and are closely associated with hamartomas. Both lesions are fibroglandular and are well circumscribed [3] and the amount of fat is by definition conspicuous in adenolipomas compared with hamartomas. Hamartomas are lesions that result from faulty development in an organ, composed of an abnormal mixture of normally occurring tissue elements or an abnormal proportion of a single element normally present at that site. Brown fat is not a normal constituent of adult breast tissue and in this respect adenohibernomas cannot be regarded as hamartomas. Damiani and Panarelli [2] suggested a hamartomatous origin from remnants of fetal brown adipose tissue or, alternatively, the possibility of de novo mixed proliferation showing brown fat differentiation in its mesenchymal component for adenohibernomas. In addition, the focus that the granular cells are associated to a fibroadenoma is a further proof that the adenohibernoma is not a hamartoma. This situation was favored by Fisher et al. [3] who believed that fibroadenomas and hamartomas were

N. Kapucuoglu (✉)
Department of Pathology, Faculty of Medicine,
Suleyman Demirel University,
32260 Isparta, Turkey
e-mail: nilgunkap@hotmail.com

S. Percınel
Department of Pathology, Faculty of Medicine,
Ankara University,
Sihhiye,
Ankara, Turkey

A. Angelone
Servizio di Anatomia Patologica,
Ospedale Civile dello Spirito Santo,
Via Fonte Romana 9,
Pescara, Italy

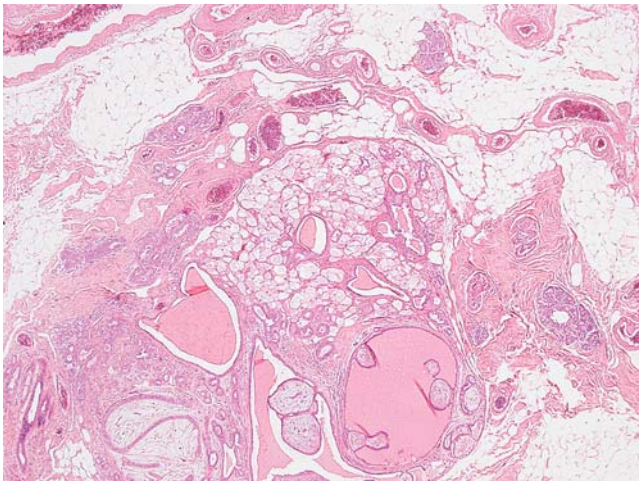


Fig. 1 Well-circumscribed lesion consisting of *areas reminiscent of fibroadenoma* and of glands intermingling with brown fat. H & E

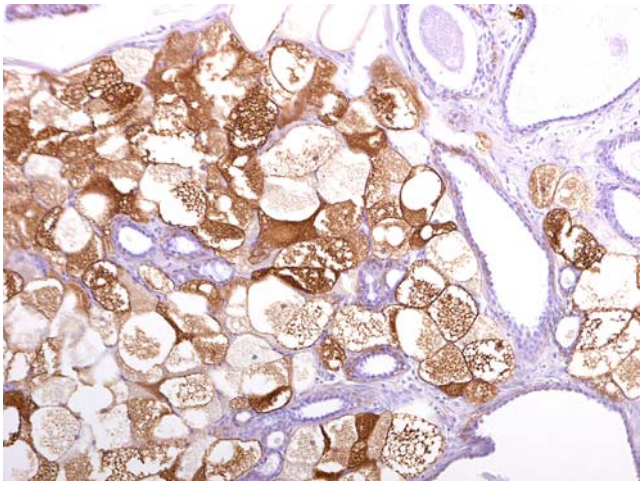


Fig. 3 The brown fat cells are strongly positive for S-100 protein (ABC peroxidase)

completely different lesions. Fibroadenomas with adult fat are rare but well described. Fibroadenoma showing brown fat has been reported only in one case previously [4].

Whether the adenohibernomas are part of the group of fibroadenomas containing brown fat is open to question. However, the case of adenohibernoma reported so far was not associated to a fibroadenoma. This indicates that, although rare adenohibernoma can be regarded as a genuine entity, it is different from fibroadenoma.

In differential diagnosis, due to eosinophilic granular cells in adenohibernomas, granular cell tumor which contains finely granular cells are positive for CD68 and invasive breast carcinomas with apocrine features which are positive for keratin should be kept in mind. However, indolent features of the brown fat cells together with CD68 and keratin negativity make this possibility unlikely.

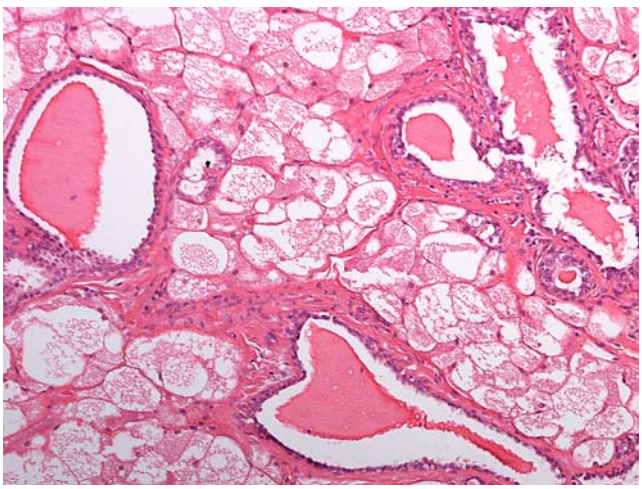


Fig. 2 Brown fat showing vacuolated granular eosinophilic cytoplasm and small normochromatic nuclei. H & E

Acknowledgement The authors are grateful to Professor V. Eusebi for critical reading of this paper.

Conflict of interest statement We declare that we have no conflict of interest.

References

1. Collville J, Feigin K, Tang L, Keating D, Cohen MA (2006) Mammary hibernoma. Breast J 12:563–565
2. Damiani S, Panarelli M (1996) Mammary adenohibernoma. Histopathology 28:554–555
3. Fisher CJ, Hanby AM, Robinson L, Millis RR (1992) Mammary hamartoma—a review of 35 cases. Histopathology 20:99–106
4. Furlong MA, Fanburg-Smith JC, Miettinen M (2001) The morphologic spectrum of hibernoma. A clinicopathologic study of 170 cases. Am J Surg Pathol 25:809–814
5. Garijo MF, Torio B, Val-Bernal JF (1997) Mammary hamartoma with brown adipose tissue. Gen Diagn Pathol 143:243–246

Virchows Arch (2008) 452:353–362
DOI 10.1007/s00428-008-0585-x

ORIGINAL ARTICLE

Diagnostic algorithm for papillary urothelial tumors in the urinary bladder

Jung-Weon Shim · Kang Su Cho · Young-Deuk Choi · Yong-Wook Park · Dong-Wha Lee · Woon-Sup Han · Sang-In Shim · Hyun-Jung Kim · Nam Hoon Cho

Received: 28 September 2007 / Revised: 19 December 2007 / Accepted: 19 January 2008 / Published online: 1 March 2008
© Springer-Verlag 2008

Abstract Papillary urothelial neoplasms with deceptively bland cytology cannot be easily classified. We aimed to design a new algorithm that could differentiate between these neoplasms based on a scoring system. We proposed a new scoring system that enables to reproducibly diagnose non-invasive papillary urothelial tumors. In this system, each lesion was given individual scores from 0 to 3 for mitosis and cellular thickness, from 0 to 2 for cellular atypia, and an additional score for papillary fusion. These scores were combined to form a summed score allowing the tumors to be ranked as follows: 0–1 = UP, 2–4 = low malignant potential (LMP), 5–7 = low-grade transitional cell carcinoma (TCC), and 8–9 = high-grade TCC. In addition to the scoring system, ancillary studies of MIB and p53 indexes with CK20 expression pattern analyses were compared together with clinical parameters. The MIB index was strongly correlated with disease progression. Four of the 22 LMP patients (18.2%) had late recurrences, two of these four (9.1%) had progression to low-grade carcinoma. The MIB index for LMP patients was strongly associated with recurrence (recurrence vs. non-recurrence, 16.5 vs. 8.1, $p<0.001$). The proposed scoring system could enhance the reproducibility to distinguish papillary urothelial neoplasms.

Keywords Papillary urothelial neoplasm of low malignant potential · Recurrence · MIB

Introduction

According to the 1998 World Health Organization/International Society of Urological Pathology (WHO/ISUP) [7, 23], the 1999 WHO blue book [15], and 2004 WHO blue book

J.-W. Shim
Department of Pathology, Hangang Sacred Heart Hospital,
Seoul, South Korea

K. S. Cho · Y.-D. Choi
Department of Urologic Oncology,
Yonsei University College of Medicine,
Seoul, South Korea

Y.-W. Park
Department of Pathology, Hanyang University Guri Hospital,
Seoul, South Korea

D.-W. Lee
Department of Pathology, Soonchunhyang University Hospital,
Seoul, South Korea

W.-S. Han
Department of Pathology,
Ewha Womans University Mokdong Hospital,
Seoul, South Korea

S.-I. Shim
Department of Pathology,
Catholic University of Korea St. Mary's Hospital,
Seoul, South Korea

H.-J. Kim
Department of Pathology, Inje University Sanggye Paik Hospital,
Seoul, South Korea

N. H. Cho
Korean Urologic Pathology Society,
Seoul, South Korea

N. H. Cho (✉)
Department of Pathology, Yonsei University College of Medicine,
Seodaemoon-ku Sinchon-dong 134,
Seoul 120-752, South Korea
e-mail: cho1988@yumc.yonsei.ac.kr

[12], papillary urothelial neoplasms (PUNs) have been categorized as urothelial papilloma (UP), inverted papilloma (IP), papillary urothelial neoplasm of low malignant potential (PUNLMP), low-grade papillary urothelial carcinoma (LGPUC), and high-grade papillary urothelial carcinoma (HGPUC). The main aim of the 1998 WHO/ISUP classification guidelines was to develop a universally accepted and reproducible classification system. However, the reproducible classification and diagnostic criteria between non-invasive superficial PUN, a constellation of well-known papillary tumors of low progression incidence, remains in dispute. In particular, PUNLMP terminology has been the main point of discussion in the field since the introduction of the 1998 WHO/ISUP classification system.

UP or IP, whether exophytic or inverted, is well defined because it usually presents as a small single mass. PUNLMP is defined as papillary urothelial tumors which resemble exophytic UP, except for an increased cellular proliferation that exceeds a normal thickness [7, 12, 15, 23]. LGPUC is defined as complex papillary fronds with easily recognizable architectural and cytological variations. Tumors with moderate-to-marked atypia are defined as HGPUC [7, 12, 15, 23]. However, from the pathologic viewpoint, the diagnostic boundary between stage 0 (Ta) LGPUC and the non-carcinoma group is vague. By definition, the critical point for deciphering between PUNLMP and UP is the identification of layers exceeding an accepted urothelial thickness. This step can be very subjective and confusing, which regard to the section axes [6]. Moreover, architectural and cytologic atypia favor a LGPUC classification over PUNLMP or UP classification and are even less reproducible. Through survey of a consensus trial of papillary urothelial tumors, a severe discrepancy was observed in PUNLMP by even the most experienced urologic pathologists [16, 23]. Thus, the clinical significances and biological differences in PUNLMP are still inconclusive due to ambiguous diagnostic criteria [5, 17–19].

We designed an algorithm based on the scoring system defined by several histopathological findings. For confirmation, we surveyed the clinical manifestation and recent 5-year follow-up data on 175 papillary urothelial tumors. In addition, we also assessed ancillary studies of MIB and p53 indexes with CK20 expression pattern analysis. While both ends of the MIB and p53 index spectrums were easily categorized as UP and LGPUC, cases within the shaded zone were reviewed clinically and re-assessed by our scoring system.

Materials and methods

Materials

One hundred seventy-five cases were selected from the medical records and archival slides. These cases were selected from a large collection of papillary urothelial tumors in Urologic Oncology Files of Yonsei University College of Medicine since 1990.

Demographic data with regard to age, sex, the site involved, tumor number, size, time to recurrence, frequency of recurrence, progression, associated malignancy, and survival time were obtained from each patient's medical records. The time of recurrence was calculated from the time from a complete response (no evidence of disease) to the time of the first evidence of tumor recurrence at the latest follow-up. All patients underwent transurethral resection (TUR) of the bladder tumor. After the initial TUR was performed at 6-month interval for 2 years and yearly thereafter, patients did not receive any additional intravesical treatment until the first recurrence.

All cases were independently reanalyzed by seven pathologists specialized in urological pathology, in the first round of the consensus review. Each participant rendered a diagnosis after a prior training session based on the 2004 WHO classification. After completing the first round, all cases were reviewed with our new scoring system by all participants of the present study.

Scoring system

Well-known parameters used in different point systems were adopted for the new scoring scheme. The most critical, highly reproducible findings including thickness of layers and mitosis with cytologic atypia were depicted in Fig. 1. According to consensus rate between peer reviewers, relevant impact was given differently. Three points were given in the best reproducible criteria, thickness of layers and mitosis, and cytologic atypia. One point was given in the parameter with wide range of variation, papillae fusion.

Because increased cellular proliferation exceeding to seven layers is the minimal criteria for a score, indicating a more progressive disease than PUNLMP, this particular criteria should be emphasized. Our general rule was to judge areas of the section where the papillae are sectioned perpendicular to the surface and basement membrane and thus include the central fibrovascular stalk while avoiding areas of oblique or longitudinally cut. However, despite unequivocal LGPUC, the loss of umbrella cells leads to a section that is thinner than seven layers. The scoring criteria for cellular thickness in the sample was as follows: 0 point if all fronds had less than seven layers and intact umbrella cells were present, 1 point if any fronds had less than seven layers but no obvious umbrella cells were present, 2 points if samples had more than one frond with more than seven layers and intact umbrella cells, and 3 points if any fronds had more than seven layers and no umbrella cells were present (Fig. 1a).

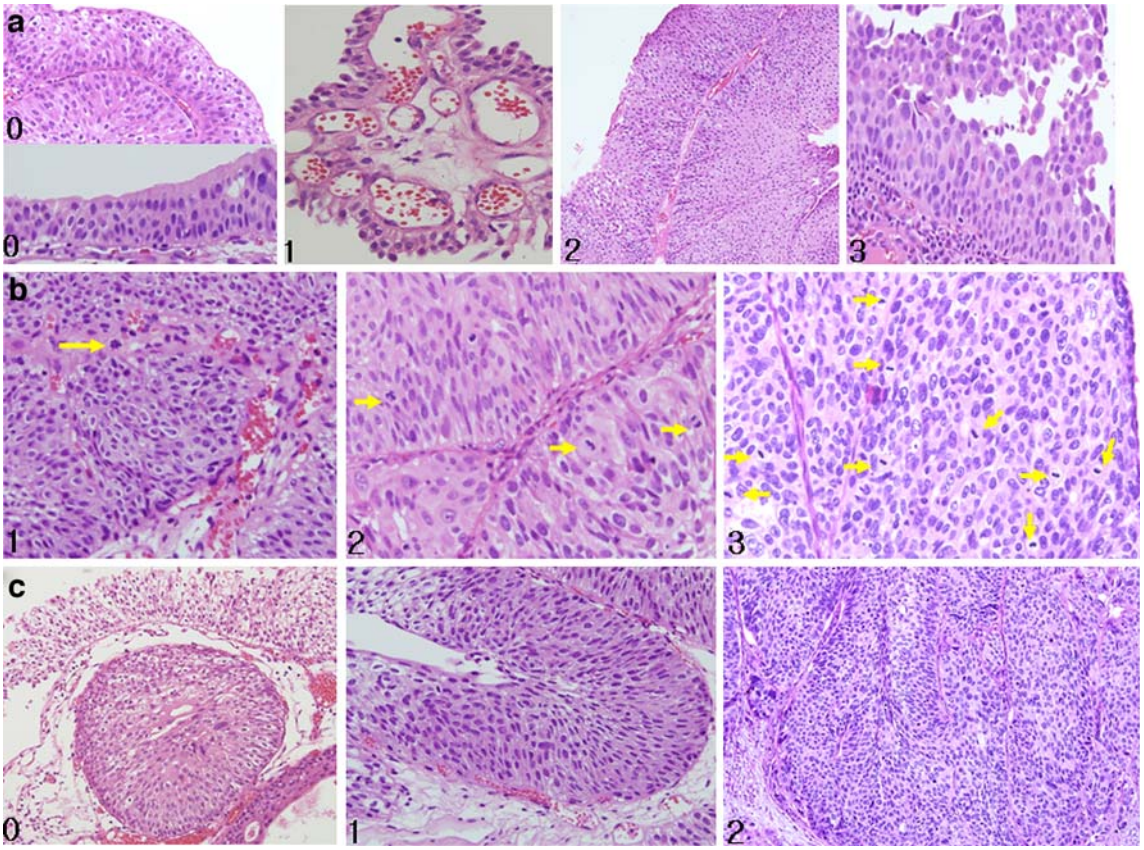


Fig. 1 Histopathological findings of papillary urothelial tumors. **a** Thickness of layers. Each number represents the corresponding score: 0 means a thickness less than seven layers with intact umbrella cells, 1 means a thickness less than seven layers with the loss of umbrella cells, *2* means a thickness more than seven layers with intact umbrella cells, and *3* means a thickness more than seven layers with the loss of umbrella cells. **b** Mitosis. *1* means a few mitoses less than five per high power field, *2* means mitotic index between five and ten mitoses per ten HPF, and *3* means more than ten mitoses per ten HPF. **c** Cytologic atypia. *0* Atypia restricted to the surface is not considered true atypia. *1* Diffuse cellular atypia in a random fashion, but with a mild degree is score 1. *2* Diffuse cellular atypia in a random fashion and a moderate to severe degree of atypia is defined score 2

Mitotic figures were assessed by recording the total numbers from ten high power (×400) fields (HPF) selected at random in each case (Fig. 1b). If more than ten mitoses/ten HPF were identified, 3 points were given. In case between five and ten mitosis/ten HPF, 2 points were given. In case with mitotic index less than 5/10 HPF, 1 point was given. Samples that did not show any mitosis were given a 0 score.

Although cellular atypia can be another parameter that can distinguish benign or malignant tumors, caution should be taken when interpreting this criterion because the cellular distribution for this characteristic is variable. If the cellular atypia is restricted to superficial cells, this is less significant with regard to determining whether a sample is benign or malignant (Fig. 2). In our scoring system, samples with randomly and frequently distributed cellular atypia with moderate to severe degree were given 2 points. One point was assigned to samples with randomly distributed mild atypia. Samples with no pleomorphism were given 0 scores (Fig. 1c). The moderate to severe atypia are defined to be easily recognized in low power field, whereas mild atypia is observed as slightly variable nuclear size and clumping of chromatin in high power field. Cell morphology could be another additive feature that can distinguish benign and malignant tumors, but not included in this category. Spindle cells frequently appear in the benign cases with a gradual transition to epithelioid cells occasionally as the tumor progresses.

Another mechanism for distinguishing papillary urothelial tumors is by assessing architectural atypia. Because papillary fusion and branching is an easily recognized and fairly reproducible finding, a maximum of 1 point was given when this characteristic was observed. Unequivocal papillary fusion was given 1 point, and no branching or fused papillae was given 0 point. Although the palisading basal layer is another clue to polarity preservation, it is not definitely diagnostic. However, we experienced this feature as a strong supportive finding with approaching to the specific diagnosis of PUNLMP.

The entire scoring system is summarized in Table 1. Seemingly clear, a diagnostic conundrum occasionally occurs when a sample falls in the boundary zone. In such

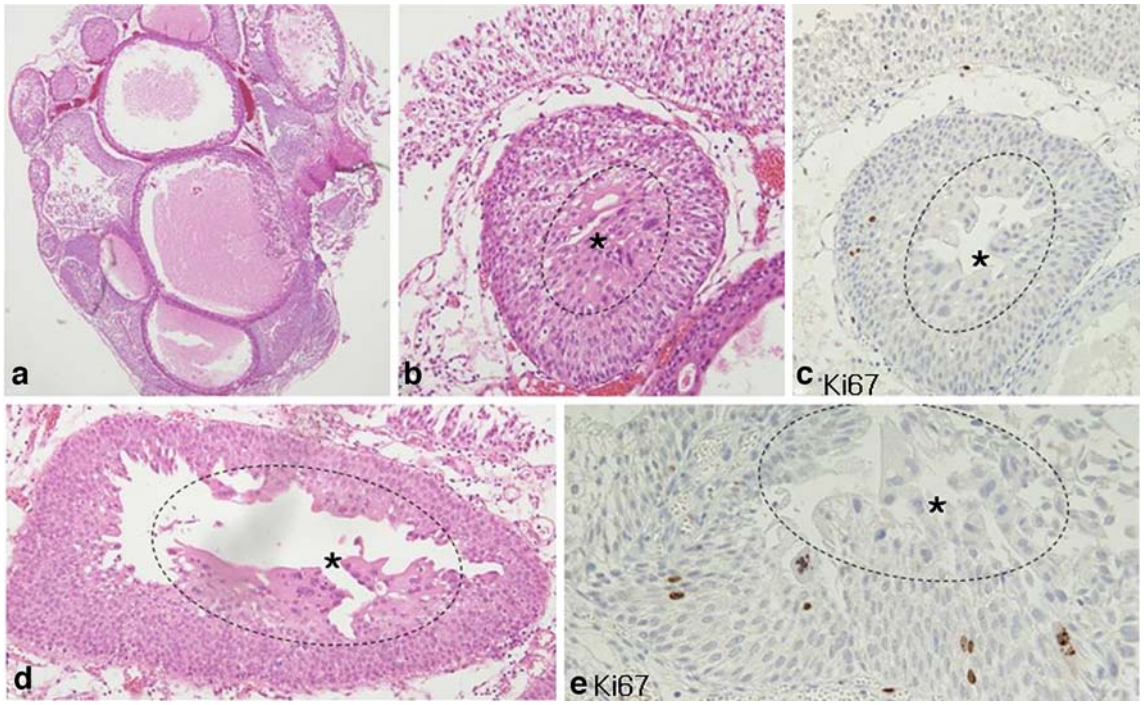


Fig. 2 Atypia in surface cells of urothelial papilloma or inverted papilloma. **a** Polypoid mass with an inverted pattern of urothelial nests. **b** Atypia (*asterisk*) is noted in the surface (*circle*) of the inverted nest. **c** Atypical cells are not immunoreactive to MIB. **d** Syncytial changes of atypical cells (*asterisk*) are restricted to the surface (*circle*). **e** MIB is scattered, but not expressed in the atypical cells (*asterisk*) of the surface (*circle*)

cases, diagnostic ancillary studies can be adopted for further clarification.

Immunohistochemical analysis

Three consecutive serial sections from each case were immunostained for MIB, p53, and CK20. In brief, the 4-μm-thick sections of paraffin-embedded tissue were deparaffinized and rehydrated. After a treatment with a 3% hydrogen peroxide solution for 10 min to block endogenous peroxidases, the sections were boiled in 10 mmol/L citrate buffer (pH 6.0) in a microwave oven for 20 min. The sections were subsequently incubated at 4°C overnight with the aforementioned primary antibodies. After a thorough rinsing in phosphate-buffered saline, the sections were treated with the DAKO LSAB (labeled streptavidin–biotin) kit, stained with amino-ethyl carbazole and then counter-stained with Mayer's hematoxylin.

Table 1 Diagnostic scoring system for papillary urothelial tumors

Variables	Features	Score
Mitosis	No mitosis	0
	<5/10 HPF	1
	5–10/10 HPF	2
	>10/10 HPF	3
Thickness of layers	<7, with intact umbrella cells	0
	<7, with the loss of umbrella cell	1
	>7, with intact umbrella cells	2
	>7, with the loss of umbrella cell	3
Cytologic atypia	None	0
	Diffuse mild atypia	1
	Diffuse moderate–severe atypia	2
Papillae fusion	No	0
	Yes	1

Quantitative method

The immunohistochemical staining results were assessed by a quantitative immunoreactivity score [(ratio of stained urothelial cells per the total number of tumor cells)×100]. The MIB index was interpreted by counting the number of MIB-positive cells out of a total of 1,000 epithelial cells in the most staining area under the high power magnification (×400). The p53 index was scored by the ratio derived from the number of p53-positive cells out of a total of 1,000 epithelial cells. This ratio was then semi-quantitatively reassorted as 0, 1 (<15%), and 2 (>15%). CK20 focally stained the surface cells in normal urothelium. Whereas this focal and patch staining pattern restrictive to the surface (periphery) was considered negative in our study, we defined CK20 staining as positive only when CK20 antibodies diffusely stained through the entire epithelium. Cells with nuclear MIB

and p53 staining as well as cytoplasmic and membranous CK20 staining were regarded as positive cells. The immunohistochemical staining results were analyzed by two independent investigators.

Recurrence and progression in long-term follow-up

Individual follow-up times were calculated as the number of months from the date of the diagnostic surgical procedure, which was usually a transurethral resection of the bladder, to the date of the most recent cystoscopy. The length of the follow-up for the whole series ranged from 15 to 195 months (median, 127 months). A recurrence was defined as a tumor which was fulgurated (no histopathological material) or resected (confirmed to be malignant by histological examination). Stage progression was defined as a recurrence with a lamina propria invasion (pT1) or the development of metastatic disease.

Statistical analysis

Statistical analysis was carried out using SPSS (Windows version 10.0). A Student's *t* test was used to evaluate the associations among the continuous variables. The correlation between immunoreactive variables was analyzed using the Pearson correlation study, and frequency distributions were generated using descriptive statistics (analysis of variance). $p < 0.05$ was considered to be statistically significant. Associations between histological categories and immunoreactivities as well as with tumor recurrence or progression were assessed by a Chi test. The inter-observer agreement (kappa) was measured for each diagnostic category as well as for each score component. The kappa value was interpreted as follows: 0–0.2, slight; 0.21–0.4, fair; 0.41–0.6, moderate; 0.61–0.8, substantial; and 0.81–1.0, almost perfect.

Results

In the first round, seven pathologists unanimously agreed on the overall diagnosis in 97 of the 175 subjects (55.4%). The lowest consensus rate between the pathologists was in classifying the PUNLMP (27.3%), and the highest consensus rate was in classifying the HGPUC (92.85%). The overall inter-observer agreement in the first round was moderate (kappa = 0.587). After the completion of the first round, all cases were reviewed by all study participants, and a consensus diagnosis was reached. This consensus diagnosis was used as the introduction for a newly designed scoring system combined with ancillary tools mainly based on the MIB index and clinical factors.

The scoring system, as shown in Tables 1 and 2, consists of six separately graded components, the scores for which were then added to determine the total score equivalent to a diagnostic category. This scoring system was significantly improved with the adoption of the new scoring scheme in the second round (kappa = 0.832). The inter-observer agreement on separate components of this scoring system showed a substantially increased the classification to a perfect level of agreement: a kappa of 0.754 for mitosis (substantial agreement), a kappa of 0.635 for cellular thickness (substantial), and a kappa of 0.556 for cellular atypia (moderate agreement). With specific regards to PUNLMP, the result of which had the least consensus, the inter-observer agreement was substantially improved (kappa = 0.670). The most consistent findings in low magnification of PUNLMP were long and slender papillae with partly fused and branched papillae, and no obvious cytologic atypia (Fig. 3). Basal palisading features in each papilla can be accounted for the PUNLMP (Fig. 3c,d). It should be pointed that thickness more than seven layers with loss of surface cells in any papillae should never be seen in PUNLMP. The best diagnostic reproducibility for PUNLMP was mitosis. Randomly scattered mitosis was the most important finding against the diagnosis of PUNLMP.

Clinicopathological classification of PUN

The mean patient age at the first diagnosis of UP, PUNLMP, PULC, and PUHC was 62.6, 68.4, 67.1, and 69.3 years, respectively. The following clinical parameters were included: single vs. multiple, small (less than 1–2 cm)

Table 2 Total score ranges in papillary urothelial tumors

Dx	Mitosis	Thickness of layers	Atypia	Fused papilla	Total score
UP	0–1	0	0	0	0–1
IP	0–1	0–1	0–1	1	1–3
PUNLMP	0–1	1–2	0	1	2–4
LGPUC	2	1–3	1	1	5–7
HGPUC	3	2–3	2	1	8–9

Atypia means hyperchromacia, irregular nuclear contours and prominent nucleoli.
UP Urothelial papilloma, *IP* inverted papilloma, *PUNLMP* papillary urothelial neoplasm low malignant potential, *LGPUC* low-grade papillary urothelial carcinoma, *HGPUC* high-grade papillary urothelial carcinoma

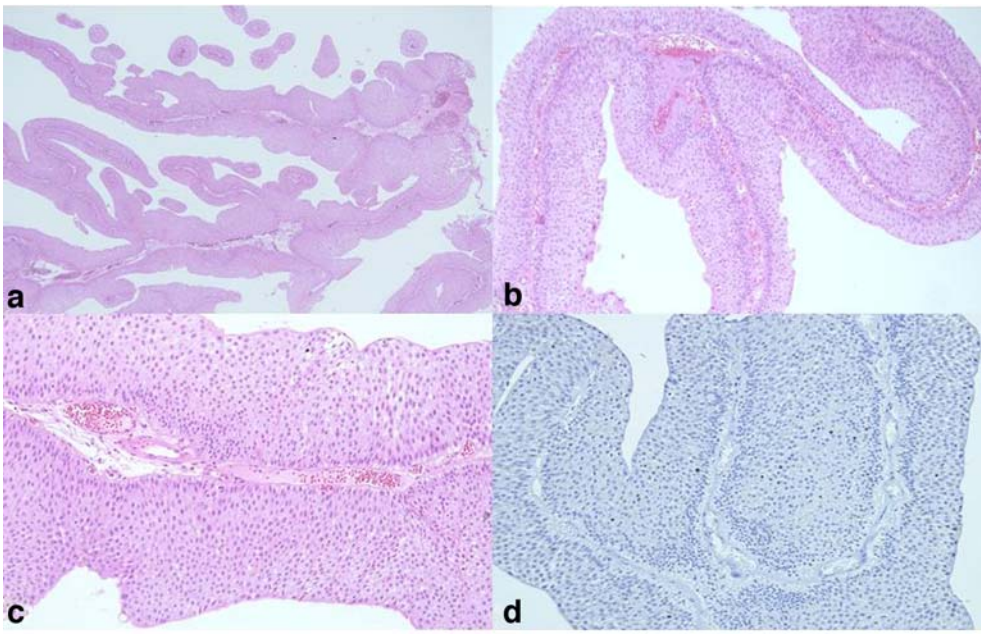


Fig. 3 Visualization of PUNLMP with light microscopy. **a** Long- and slender-branched papillae is a characteristic histological clue for a diagnosis of PUNLMP. **b** Branched papillae are fused. **c** Basal palisading feature is another indicator of PUNLMP. **d** Branched fused papillae with basal palisading feature are a characteristic feature of PUNLMP

vs. large (more than 2 cm), no recurrence vs. recurrence, and no progression vs. progression. UP was all single and small, but recurred in one patient (14.3%). No progression or association with LGPUC was found in any of the UP cases. IP was predominantly single, but 27.3% (6/22) of the cases were multiple, and 13.6% (3/22) of the cases were associated with LGPUC. Three cases of IP associated with LGPUC were typically benign, which were easily differentiated from inverted urothelial carcinoma. None of the IP cases progressed to LGPUC. PUNLMP frequently presents with a single and small lesion. Of the PUNLMP cases, 13.6% (3/22) had two or more lesions, but all of them were small, which were less than 1 cm. Of the PUNLMP patients, 18.2% (4/22) had a late recurrence (average 21.5 months) and 9.1% (2/22) progressed to LGPUC (after 5 and 56 months, respectively), but never underwent stage progression to invade muscle proper. Of the LGPUC patients, 70.4% (38/54) demonstrated a significantly higher recurrence frequency and 9.3% (5/54) progressed to higher stages.

MIB, p53 indices, and cytokeratin 20 expression according to papillary urothelial tumors

Immunohistochemical results of papillary urothelial tumors based on new scoring system were summarized in Table 3. The MIB index was variably expressed and increased proportionately with disease progression (Fig. 4). The mean MIB index was 5.85, 8.29, 38.74, and 58.32 in UP, LMP, LGPUC, and HGPUC (p value<0.001), respectively. The MIB index was relatively and significantly higher in recurred PUNLMP than in non-recurrent cases (16.5 vs. 8.1, $p<0.001$). Atypia in surface cells occasionally seen in papillomas were not immunoreactive to MIB (Fig. 2c,d, and e). p53 had variable expression ranges in urothelial tumors and no significant association with recurrence in spite of an apparent tendency towards disease progression. CK20 was diffusely immunoreactive in all layers of some PUNs, whereas these cells are negative or focally reactive in the superficial cells of UP and IP cases (Fig. 5). However, CK20 staining had no significant association with clinicopathological variables.

Discussion

PUNs are a common characteristic of the indolent nature of papillary tumors with cytologically banal features. They are often difficult to define with solid classifying criteria for the low-grade, non-invasive PUNs, benign papillomas, papillary urothelial neoplasms of low malignant potential (PUNLMP), and low-grade papillary urothelial carcinomas (LGPUC). The classification of PUNLMP was initially introduced to replace the previously designated WHO grade 1 urothelial carcinoma that was defined by the 1998 WHO/ISUP classification system [7, 23]. Murphy [17] interpreted some of the 1973 WHO grade 1 tumors as PUNLMP and some as LGPUC, Bostwick and Mikuz [3] translated the 1973 WHO grade 1, 2, and 3 tumors as PUNLMP, LGPUC, and HGPUC, respectively. Reuter and Melamed [20] interpreted the 1973 WHO grade 1 tumors as PUNLMP, grade 2 as LGPUC or HGPUC, and grade 3 as HGPUC.

Based on the histopathological findings, both architectural atypia and cellular atypia are prime parameters that

Table 3 Immunohistochemical results in papillary urothelial tumors

	Summing score	MIB (avg. Nc. index) cut-off >15%	p53 (no. of strong index, cut-off >15%)	CK20 (intense /diffuse)
UP (*n*=7)	0.42±0.01	5.85±0.12	0	2 (28.6%)
IP (*n*=22)	1.63±2.54	7.63±3.57	5 (22.7%)	7 (*n*=31.8%)
PUNLMP (*n*=22)	3.08±1.91	8.29±2.14	7 (31.8%)	10 (*n*=45.5%)
LGPUC (*n*=54)	6.28±1.04	38.74±12.25	25 (46.3%)	18 (*n*=33.3%)
HGPUC (*n*=70)	8.5±0.5	58.32±3.69	48 (68.6%)	25 (*n*=35.7%)

Avg. Nc. index Average nuclear index

include thickness of papillae, fused papillae, cellular pleomorphism, and mitosis. However, some cases can often have overlapping findings. In a multi-institutional survey in the Korean Urologic Pathology Society, PUNs diagnoses were given little consensus by urologic pathologists, despite the fixed criteria introduced by the WHO guide. Our substantial discrepancies in diagnoses are quite similar to data collected from other institutes [16, 23]. Architectural atypia, such as a thickness more than seven layers and fused papillae, are very useful in differentiating benign from worse lesions, but are sometimes confusing due to tangential sections. In general, cytological atypia is much more reproducible than architectural atypia. Cellular atypia can be recognized only along superficial layers or in a random distribution, whether mild or severe. We found that the former lacks ki67 expression, which may represent degenerative changes, not proliferation. Cytologic atypia that is restricted to the superficial layer can be found in urothelial benign tumors [4, 6]. Mitosis can be the most representative and the highly reproducible variable, when using the total number of mitoses from ten HPF (×400) selected at random. The benign category of PUN demonstrated rare, but regular mitoses near the basal layer of the urothelium. The loss of umbrella cells, degree of the nuclear groove preservation, cytologic spindling or epithelioid feature, and palisading basal layers can be another

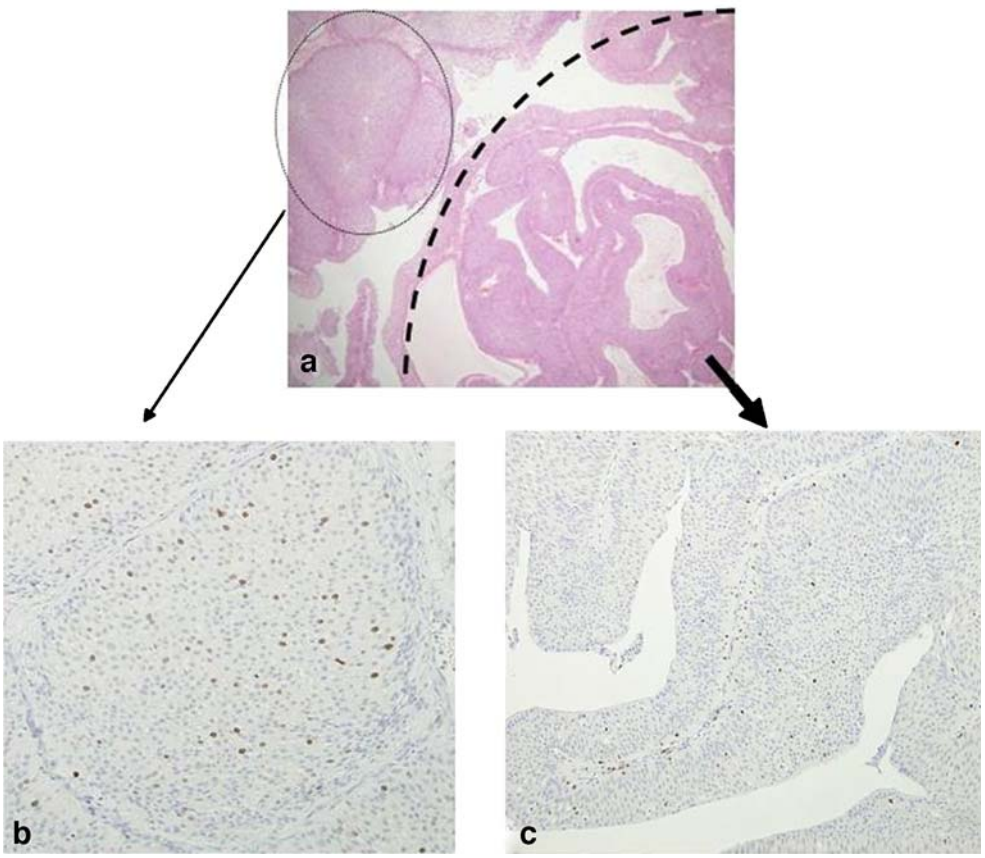


Fig. 4 MIB index of LGPUC. **a** Areas of thick trabeculated papillae (*closed circle*) are opposed to areas of PUNLMP (*semicircle*). **b** Notice many scattered MIB indexes in the portion of thick trabeculae, which represents LGPUC. **c** Little MIB indexes were recognized in areas of PUNLMP

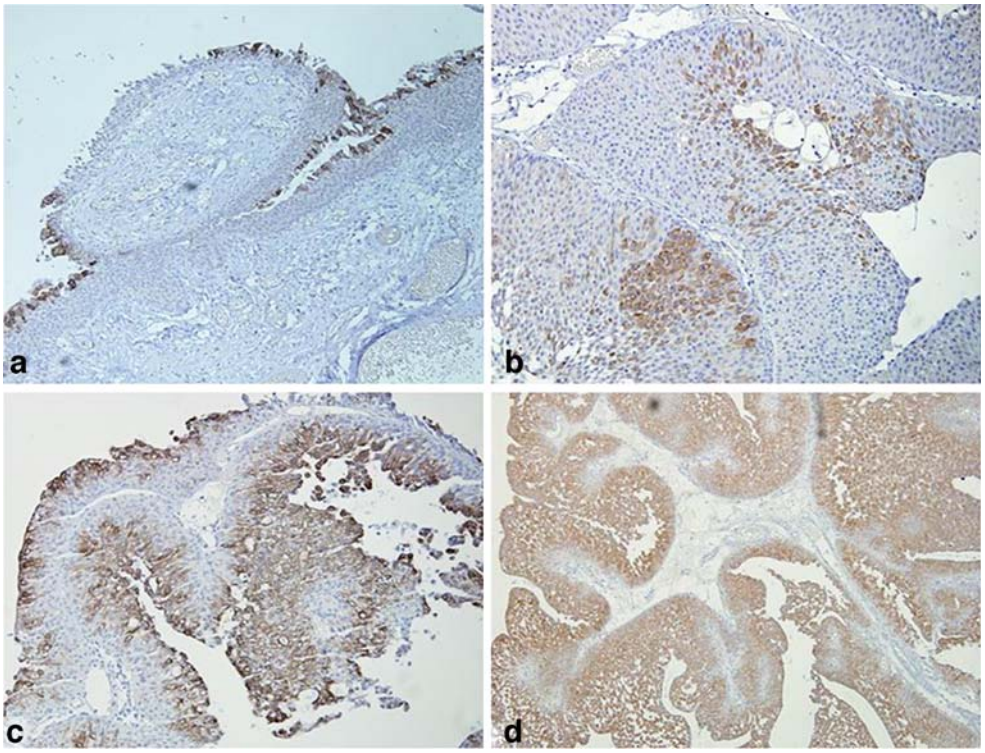


Fig. 5 Cytokeratin 20 expression pattern analysis in PUNs. **a** CK20 expression was restricted to the surface. **b** Patchy areas of CK20 immunoreactivity had spread. **c** Solid compactum of positive expression was noted. **d** Diffuse CK20 expression was observed

supportive findings, but excluded in this algorithm, because these findings appear too subjective and less reproducible. For instance, the loss of umbrella cells may be caused by a manipulation or a biopsy procedure. Conversely, well-preserved umbrella cells can be observed in overt carcinoma. Basal palisading features in each papilla can be, however, useful in PUNLMP or IP, whereas overt epithelioid features instead of spindling can be a supportive finding to favor carcinoma over PUNLMP or papilloma.

For the purpose of achieving a reproducible diagnosis for PUN, a scoring method based on pathological parameters was recently proposed by the Korean Urologic Pathology Society. The main principle behind this scoring system is for each parameter to be scored differently with different weights of implication. For instance, more concordant parameters such as mitosis and with thickness of layers were scored by a three-tiered system. The scoring of atypia was two tiered, and fused papillae was one tiered. Each diagnosis can be clearly divided when using this system. Furthermore, PUNs were well categorized with a high consensus rate upon the application of this algorithm. A useful tool under the routine microscopy would be an algorithm derived from our peer-review data in the form of flow diagram starting features seen at low power (modest thickness with focal fused papillae) progressing to medium power (no obvious atypia) and high power (scanty mitosis) ending up at a diagnosis of PUNLMP.

The helpful ancillary findings for this new scoring system were the MIB index and clinical findings of multiplicity, size, and recurrences. Since the MIB index has been widely known as an independent prognostic predictor of recurrence [2, 10, 14], it was introduced to distinguish between PUNs. Most authors reported that the MIB index of recurrent predictors and poor prognostic factors is around 10% of the cut-off level. Using the same method, the MIB index varies according to the time of fixation [22]. The MIB index in specimens fixed for 50 h (over the weekend) was significantly lower than the overnight-fixed specimens. High p53 and MIB expression could be significant prognostic factors in the univariate analysis of bladder cancer [8], while p53 is an independent factor [21].

CK20 showed diffuse immunoreactivity in all layers of certain PUNs, while negative or focally reactive in the superficial cells of UP and IP cases. The diffuse and strong expression of CK20 was correlated to the tumor severity. Although highly controversial with regard to their implication of CK20 expression loss, Harnden et al. [9] found a decreased CK20 expression to be an independent ($p<0.0001$) predictor of tumor recurrence in papillary tumors. Unlike the findings reported by Alsheikh et al. [1], our data did not reveal a significant correlation with tumor recurrence.

Upon our survey of clinicopathological correlations, UP recurred in 14.3% of the patients, but demonstrated no progression or association with PULC. IP was associated with LGPUC in 13.6% of the cases, but never progressed to LGPUC. PUNLMP showed two or more lesions in 13.6%

of the cases, but all of the lesions were less than 1 cm. Of patients with PUNLMP, 18.2% demonstrated late recurrence (average 21.5 months) and 9.1% of the PUNLMP cases progressed to LGPUC in either 5 or 56 months. Of the patients with PULC, 70.4% (38/54) demonstrated a significantly higher frequency of recurrence and 9.3% (5/54) of these patients progressed to higher stage. With regard to the labile nomenclature and diagnostic criteria of PUNLMP, the biological behavior of PUNLMP remains controversial.

Jordan et al. [13] concluded in a study of 91 cases with grade 1 urothelial tumors that low-grade lesions, usually designated transitional cell carcinoma, grade 1, are benign and should be called papilloma rather than carcinomas. In contrast, a study by Cheng et al. [6] of 112 PUNLMP cases found that those with PUNLMP are at risk of cancer progression and death from bladder cancer. Thus, it is prudent not to consider a constellation of low-grade papillary urothelial neoplasms to be benign. Pich et al. [18] studied 19 LMP cases and found that PUNLMP had a relatively high recurrence rate (47.4%) with no progression. These results were also in accordance with the study of 95 LMP cases by Holmang et al. [11]. We apparently observed that PUNLMP cases demonstrated late recurrences and progression with relatively lower frequencies, a finding that represents LMP. Statistical variations of recurrence and progression depend on many factors, including follow-up intervals, a definition of recurrence or progression, and sample size. However, reaching an accurate diagnosis may be most important. Therefore, we invented an algorithm by which a greater number of uniform diagnoses with less discrepancy can be achieved.

In conclusion, the mitotic index and thickness of layers with cytologic atypia could be useful and reproducible parameters for the scoring algorithm to discriminate between papillary urothelial tumors. Based on the new scoring algorithm, PUNLMP can be clinicopathologically listed as an intermediary stage between UP and LGPUC.

Acknowledgments This study was supported by The Genitourinary Pathology Study Group of the Korean Society of Pathologists (2006). We appreciate all participants who screened and surveyed each case.

Conflict of interest statement We declare that we have no conflict of interest.

References

1. Alsheikh A, Mohamedali Z, Jones E, Masterson J, Gilks CB (2001) Comparison of the WHO/ISUP classification and cytokeratin 20 expression in predicting the behavior of low grade papillary urothelial tumors. World Health Organization/International Society of Urologic Pathology. Mod Pathol 14:267–272
2. Bol MG, Baak JP, van Dierman B, Buhr-Wildhagen S, Janssen EA, Kjellevold KH, Kruse AJ, Mestad O, Ogreid P (2003) Proliferation markers and DNA content analysis in urinary bladder TaT1 urothelial cell carcinomas: identification of subgroups with low and high stage progression risks. J Clin Pathol 56:447–452
3. Bostwick DG, Mikuz G (2002) Urothelial papillary (exophytic) neoplasm. Virchows Arch 441:109–116
4. Broussard JN, Tan PH, Epstein JI (2004) Atypia in inverted urothelial papillomas: pathology and prognostic significance. Hum Pathol 35:1499–1504
5. Busch C, Algaba F (2002) The WHO/ISUP 1998 and WHO 1999 systems for malignancy grading of bladder cancer. Scientific foundation and translation to one another and previous systems. Virchows Arch 44:105–108
6. Cheng L, Neumann RM, Bostwick DG (1999) Papillary urothelial neoplasms of low malignant potential. Clinical and biologic implications. Cancer 86:2102–2108
7. Epstein JI, Amin MB, Reuter VR, Mostofi FK (1999) The Bladder Consensus Conference Committee (1999) The World Health Organization/International Society of Urologic Pathology consensus classification of urothelial (transitional cell) neoplasms of the urinary bladder. Am J Surg Pathol 22:14435–14448
8. Gontero P, Casetta G, Zitella A, Ballario R, Pacchioni D, Magnani C, Muir GH, Tizzani A (2000) Evaluation of p53 protein overexpression, ki67 proliferative activity and mitotic index as markers of tumor recurrence in superficial transitional cell carcinomas of the bladder. Eur Urol 38:287–296
9. Harnden P, Mahmood N, Southgate J (1999) Expression of cytokeratin 20 redefines urothelial papillomas of the bladder. Lancet 353:974–977
10. Helpap B, Schmitz-Drager BJ, Hamilton PW, Muzzonigro G, Galosi AB, Kurth KH, Lubaroff D, Waters DJ, Droller MJ (2003) Molecular pathology of non-invasive urothelial carcinomas. Virchows Arch 442:309–316
11. Holmang S, Andius P, Hedelin H, Wester K, Busch C, Johansson SL (2001) Stage progression in Ta papillary urothelial tumors: relationship to grade, immunohistochemical expression of tumor markers, mitotic frequency and DNA ploidy. J Urol 165:1124–1130
12. Johansson SL, Busch C (2004) Papillary urothelial neoplasm of low malignant potential. In: Eble JN, Sauter G, Epstein JI, Sesterhenn IA (eds) Pathology and genetics of tumors of the urinary system and male genital organs. IARC, Lyon, pp 115–117
13. Jordan AM, Weingarten MA, Murphy WM (1987) Transitional cell neoplasms of the urinary bladder: can biologic potential be predicted from histologic grading? Cancer 60:2766–2774
14. Mai KT, Elmontaser G, Perkins G, Yazdi HM, Stinson WA (2004) Histopathological and immunohistochemical study of papillary urothelial neoplasm of low malignant potential and grade associated with extensive invasive low-grade urothelial carcinoma. BJU Int 94:544–547
15. Mostofi FK, Davis CJ, Seterhenn IA (eds) (1999) Histological typing of urinary bladder tumors. World Health Organization international histological classification of tumors. Springer, New York
16. Murphy WM, Takezawa K, Maruniak NA (2002) Interobserver discrepancy using the 1998 World Health Organization/International Society of Urologic Pathology Classification of urothelial neoplasm: practical choices for patient care. J Urol 168:968–972
17. Murphy WM (1999) Bladder cancer redefined. Cancer 86:1890–1892
18. Pich A, Chiusa L, Formiconi A, Galliano D, Bortolin P, Navone R (2001) Biologic difference between noninvasive papillary urothelial neoplasm of low malignant potential and low grade (grade 1) papillary carcinomas of the bladder. Am J Surg Pathol 25:1528–1533
19. Pich A, Chiusa L, Formiconi A, Galliano D, Bortolin P, Comino A, Navone R (2002) Proliferative activity is the most significant

predictor of recurrence in noninvasive papillary urothelial neoplasm of low malignant potential and grade 1 papillary carcinomas of the bladder. Cancer 95:784–790
20. Reuter VE, Melamed MR (1997) The urothelial tract. In: Stenberg SS (ed) Diagnostic surgical pathology. Lippincott Williams & Wilkins, Philadelphia
21. Rodriguez-Alonso A, Pita-Fernandez S, Gonzalez-Carrero J, Nogueria-March JL (2002) P53 and ki67 expression as prognostic factors for cancer-related survival in stage T1 transitional cell bladder carcinoma. Eur Urol 41:182–189
22. Wester K, Adnersson A, Ranefall P, Bengtsson E, Malmstrom P, Busch C (2000) Cultured human fibroblasts in agarose gel as a multi-functional control for immunohistochemistry. Standardization of Ki67 (MIB1) assessment in routinely processed urinary bladder carcinoma tissue. J Pathol 190:503–511
23. Yorukoglu K, Tuna B, Dikicioglu E, Duzcan E, Isisag A, Sen S, Mungan U, Kirkali Z (2003) Reproducibility of the 1998 World Health Organization/International Society of Urologic Pathology Classification of papillary urothelial neoplasms of the urinary bladder. Virchow Arch 443:734–740

Virchows Arch (2008) 452:363–368
DOI 10.1007/s00428-007-0568-3

ORIGINAL ARTICLE

Where we publish

An analysis of the publications of German institutes of pathology

Florian Rudolf Fritzsche · Manfred Dietel · Glen Kristiansen

Received: 14 September 2007 / Revised: 12 December 2007 / Accepted: 14 December 2007 / Published online: 10 January 2008
© Springer-Verlag 2007

Abstract Pathologists provide the link between the clinical and the natural science aspect of medicine and are often integrated in translational research projects. We wanted to analyse the spread and position of research led by pathologists in the scientific literature. Publications from institutes of pathology of 21 randomly chosen German university cities between 2004 and 2006 were analysed. To validate our findings we subsequently extended our analysis to 45 university cities from Italy, France and the Nordic countries (Denmark, Finland, Iceland, Norway and Sweden). We detected publications directed by pathologists in numerous biomedical journals, most of which not categorised as "pathology" journals. In the analyses from Germany and Italy, Virchows Archiv led the ranking in terms of absolute number of publications. Meanwhile, Anticancer Research and the International Journal of Cancer took the lead concerning publications from pathologists from the Nordic countries. Our results mirror the wide diversification in scientific pathology and the overlap with other medical subspecialties, especially oncology, cell biology and biochemistry. This explains the problem of defining "pathology" journals and deducting pathological research activity from these publications. However, the general notion that pathology journals are the most important communication medium of pathology research was affirmed.

F. R. Fritzsche (✉) · M. Dietel
Institute of Pathology, Charité—Universitätsmedizin Berlin,
Charité Campus Mitte, Charitéplatz 1,
10117 Berlin, Germany
e-mail: florian.fritzsche@charite.de

G. Kristiansen
Institute of Pathology, Universitätsspital Zürich,
Zurich, Switzerland

Keywords Pathology · Research · Publications · Journals · Impact factors · Bibliometric

Introduction

In contrast to other physicians, pathologists do typically neither see nor treat patients directly [9]. Defining and detecting diseases on morphologic grounds are the main tasks of pathologists, making them close consultants of unique therapeutic relevance to their clinical colleagues especially those from the surgical, interventional and oncological medical specialties [1, 3, 4, 12, 16]. These extensive and close interactions with various medical disciplines not only display the importance of this subject in the clinico-therapeutic and diagnostic relation but also explain for the frequent integration and contributions of pathologists in and to research projects led by clinical colleagues [2]. The resulting publications from such interdisciplinary cooperation may either be published in journals of a certain clinical specialty, general medical journals or journals with a focus on pathology. Analysing the cumulative publications of research with dominant responsibility of pathologists on the one hand and the wide range of contributions of pathologists to primarily non-pathological but clinically-led research on the other hand, would certainly result in publications in various biomedical journals with diverse foci. This omnipresent pathological research is the logical consequence of the interlinked position of this discipline. Anyhow, it dilutes the analysis of originally pathological research topics. In this study, we wanted to analyse where pathologists from institutes in 21 German university cities published in the years 2004 to 2006. To validate our findings, we subsequently included 45 additional university cities from Italy, the Nordic

countries and France in our analysis. Apart from giving a comprehensive enumeration of journals, we evaluated the journals according to their subject categories listed in the ISI Web of Sciences (www.portal.isiknowledge.com) and provided a rank order of the leading journals of pathological research. Furthermore, we analysed the impact factors (IF) of the average pathological article and of the journals with primarily pathological publications.

Materials and methods

Publications were analysed from university institutes of pathology from 21 randomly chosen German university cities: Aachen, Berlin, Bochum, Bonn, Dresden, Erlangen, Essen, Freiburg, Greifswald, Halle, Hamburg, Hannover, Heidelberg–Mannheim, Jena, Kiel, Magdeburg, Munich, Münster, Regensburg, Rostock and Würzburg. Medline-based (www.pubmed.gov) analyses were conducted with the following specifications: We used the term "Pathology AND *City*" (name of the respective university city) in the "search"-field. Limits were specified as a specific date range was provided in the "published in the last"-field (e.g. 2004.01.01–2004.12.31). Publications with differing publication date entries were assorted to the earliest date provided. "Journal article" as chosen from the "type of article" menu and "affiliation" was specified as the default tag. All articles in the search results had to be screened to confirm that a member of an institute of pathology of the included university cities was first or last/corresponding author of the specific article. Publications with contributions from pathologists not resulting in first- or last authorships were not considered. Publications that did not fit into the "original article" category like reviews, communications and case reports were also excluded. To avoid missing publications from cities with umlaut or aberrant English city names, searches were performed for all possible spellings (e.g. München, Munich, Muenchen, Munchen). For cities with more than one university institute (e.g. Berlin and Munich), the publications of the institutes were summarised. Publications explicitly conducted by neuropathological departments or clinical research subunits were

Table 1 Journals with primarily pathological publications from German institutes in the years 2004 to 2006

Journals with primarily pathological publications
1. Journals (5–39 publications) Virchows Arch; J Pathol; Int J Cancer; Histopathology; Int J Oncol; Oncogene; Mod Pathol; Clin Cancer Res; Am J Surg Pathol; Cancer Res; J Clin Pathol; Human Pathol; Lab Invest; Pathol Res Pract; Cancer Lett; Oncol Rep; Am J Pathol; Br J Cancer; Histol Histopathol; Biochem Biophys Res Commun; Int J Gynecol Pathol; Int J Mol Med; Leuk Res; Am J Clin Pathol; Blood; Breast Cancer Res Treat; Cancer Genet Cytogenet; J Mol Diagn; Methods Mol Med
2. Journals (2–4 publications) Anticancer Res; Cancer; Genes Chromosomes Cancer; Gut; J Cancer Res Clin Oncol; Neoplasia; World J Gastroenterol; Ann Rheum Dis; Appl Immunohistochem Mol Morphol; BMC Cancer; Br J Haematol; Carcinogenesis; Cell Oncol; Clin Exp Rheumatol; Diagn Mol Pathol; Diagn Pathol; Exp Cell Res; Gastroenterology; Gynecol Oncol; Histochem Cell Biol; Int J Gynecol Cancer; Invest Ophthalmol Vis Sci; Liver Int; Lung Cancer; Melanoma Res; Pathobiology; Acta Histochem; Am J Respir Crit Care Med; Anal Quant Cytol Histol; Ann Neurol; Arthritis Res Ther; Arthritis Rheum; Breast Cancer Res; Cancer Gene Ther; Cells Tissues Organs; Cytocine; Cytogenet Genome Res; Dig Dis; Endoscopy; Eur J Cancer; Eur J Haematol; FASEB J; Gene Expr Patterns; Genesis; J Am Soc Nephrol; J Biol Chem; J Chemother; J Infect Dis; J Mol Biol; Kidney Int; Mol Biol Evol; Nephrol Dial Transplant; Nucleic Acids Res; Oncology; Pathology; Prostate; Rom J Morphol Embryol; Scand J Gastroenterol; Stem Cells Dev; Transpl Int
3. Journals (1 publication) Acta Cytol; Acta Neuropathol; Adv Enzyme Regul; Am J Physiol Cell Physiol; Am J Transplant; Ann Hum Genet; Ann Vasc Surg; APMIS; Arch Dermatol; Arch Pathol Lab Med; Atherosclerosis; Biochem J; Biochim Biophys Acta; Biotechniques; BJU Int; BMC Infect Dis; BMC Musculoskelet Disord; Br J Nutr; Br J Ophthalmol; Brain Pathol; Breast; Cancer Immun; Cell Immunol; Cell Mol Life Sci; Cell Prolif; Cell Tissue Res; Chest; Clin Chem; Clin Exp Dermatol; Clin Exp Metastasis; Clin Gastroenterol Hepatol; Clin Immunol; Clin Orthop Relat Res; Cornea; Diabetologia; Dis Colon Rectum; Eur Arch Otorhinolaryngol; Eur J Surg Oncol; Eur Respir J; Exp Mol Pathol; Exp Toxicol Pathol; Foot Ankle Int; Front Biosci; Genome Res; Graefes Arch Clin Exp Ophthalmol; Haematologica; Hepatol Res; Hepatology; Hum Antibodies; Hum Genet; Hum Mutat; Hum Reprod; Inflamm Res; Int J Legal Med; J Autoimmun; J Biochem Biophys Methods; J Biotechnol; J Clin Endocrinol Metab; J Clin Oncol; J Histochem Cytochem; J Immunol; J Invest Dermatol; J Med Genet; J Med Virol; J Microsc; J Mol Evol; J Mol Med; J Natl Cancer Inst; J Neural Transm; J Neurosurg; J Pharmacol Exp Ther; J Proteome Res; J Rheumatol; J Urol; J Vasc Res; Klin Padiatr; J Lab Clin Med; Lancet Oncol; Laryngoscope; Lasers Surg Med; Med Hypotheses; Methods Mol Biol; Micron; Mol Biol Cell; Mol Cancer Ther; Mol Hum Reprod; Mol Ther; Mutat Res; Mycoses; N Engl J Med; Neuroimmunomodulation; Oligonucleotides; Oral Oncol; Pankreas; Pediatr Dev Pathol; Pigment Cell Res; PLoS Biol; Proc Natl Acad Sci U S A; Proteomics; Rapid Commun Mass Spectrom; Respiration; Rheumatol Int; Scand J Rheumatol; Spine; Stud Health Technol Inform; Syst Biol; Technol Health Care; Transplantation; Xenotransplantation; Zhonghua Bing Li Xue Za Zhi

The journal names are ordered according to the numbers of total publications and alphabetically respectively. Journal names are abbreviated according to Medline.

excluded. For applicable publications, the journal name and the related publications in the specific years were noted.

The impact factor of the journal and the accordant year, as well as the subject category of the journal, were included from the ISI web of Science (www.portal.isiknowledge.com) and the ISI Journal Citation Report (JCR®). To validate our results, we extended the analysis described above to 45 university cities from France, Italy, Norway, Sweden, Finland, Denmark and Iceland (Rome, Milan, Pisa, Catania, Naples, Turin, Verona, Perugia, Bari, Novara, Ferrara, Parma, Palermo, Padua, Bologna, Paris, Angers, Rennes, Bordeaux, Clermont-Ferrand, Strasbourg, Toulouse, Limoges, Montpellier, Lille, Lyon, Grenoble, Nantes, Saint-Etienne, Rouen, Bergen, Oslo, Tromso, Helsinki, Tampere, Oulu, Turku, Kuopio, Aarhus, Copenhagen, Lund, Stockholm, Linkoping, Goteborg and Reykiavik).

Results

Publications with leading contributions from institutes of pathology in Germany from the 21 university cities were

Table 2 Leading journals for publications from pathologists in the different cohorts

Journals	IF 2004 (N)	IF 2005 (N)	IF 2006 (N)
A Germany			
Virchows Archiv	2.227(12)	2.224 (14)	2.251 (13)
The Journal of Pathology	5.333 (11)	6.213 (17)	5.759 (5)
International Journal of Cancer	4.416 (5)	4.700 (6)	4.693 (8)
Histopathology	2.955 (1)	2.608 (9)	3.216 (6)
International Journal of Oncology	3.056 (7)	2.601 (8)	2.556 (1)
Oncogene	6.310 (5)	6.872 (3)	6.582 (8)
Modern Pathology	3.643 (5)	3.426 (5)	3.753 (5)
Clinical Cancer Research	5.623 (2)	5.715 (7)	6.177 (5)
American Journal of Surgical Pathology	4.690 (3)	4.377 (6)	4.144 (4)
Cancer Research	7.690 (4)	7.616 (4)	7.656 (4)
Journal of Clinical Pathology	2.619 (2)	2.170 (2)	2.245 (8)
Human Pathology	3.369(2)	2.550 (4)	2.810 (5)
Median journal IF: 3.902–4.030	Mean IF: 4.198		
B Italy			
Virchows Archiv	2.227(4)	2.224 (7)	2.251 (6)
Journal of Immunology	6.486 (4)	6.387 (7)	6.293 (3)
Modern Pathology	3.643 (5)	3.426 (3)	3.753 (4)
Clinical Cancer Research	5.623 (3)	5.715 (3)	6.177 (5)
Journal of Biological Chemistry	6.355 (7)	5.854 (1)	5.808 (1)
Journal of Virology	5.398 (3)	5.178 (2)	5.341 (4)
Proceedings of the National Academy of Sciences of the USA	10.452 (4)	10.231 (3)	9.643 (2)
Blood	9.782 (3)	10.131 (3)	10.370 (2)
Cancer Research	7.690 (4)	7.616 (2)	7.656 (2)
Carcinogenesis	5.375 (5)	5.108 (0)	5.366 (3)
Transplantation Proceedings	0.511 (0)	0.799 (6)	0.962 (2)
Histopathology	2.955 (2)	2.608 (1)	3.216 (4)
Median journal IF: 5.477–5.587	Mean IF: 5.372		
C Nordic countries			
Anticancer Research	1.395 (10)	1.604 (8)	1.479 (5)
International Journal of Cancer	4.416 (6)	4.700 (10)	4.693 (7)
Gynecologic Oncology	2.083 (5)	2.251 (6)	2.319 (5)
APMIS	1.500 (5)	2.127 (3)	1.875 (7)
Journal of Biological Chemistry	6.355 (6)	5.854 (5)	5.808 (3)
Experimental Cell Research	4.007 (5)	4.140 (4)	3.777 (3)
Cancer Research	7.690 (4)	7.616 (4)	7.656 (4)
Oncogene	6.310 (2)	6.872 (4)	6.582 (6)
Clinical Cancer Research	5.623 (2)	5.715 (4)	6.177 (5)
Diagnostic Cytopathology	0.962 (1)	0.987 (6)	0.786 (4)
European Journal of Cancer	3.302 (4)	3.706 (0)	4.167 (6)
Genes Chromosomes and Cancer	4.276 (4)	3.937 (3)	3.900 (3)
Median journal IF: 4.034–4.142	Mean IF: 3.912		

The journals Blood, Cancer Genet Cytogent, Genes Chromomsomes Cancer, J Clin Pathol and Virchows Arch had nine publications each from the Nordic countries. For Table 2 one of these was randomly chosen.
The impact factors (*IF*) for the different years are given with the respective numbers of publications (*N*) in the specific year in brackets.

detected in more than 200 different biomedical journals in the observation period (Table 1). The analyses of the Italian and Nordic university cities also revealed publications in more than 200 different journals for each cohort. The total number of publications was 566 from the Italian, 598 from the German and 610 from the Nordic cohort without relevant differences between the single years. The analysis of the French cities resulted in only 87 publications in 48 different journals.

The journals with the most publications from pathologists in Germany were Virchows Archiv, the Journal of Pathology and the International Journal of Cancer. These and the other top ranking journals are listed in Table 2a. The composition of the 12 top ranking journals for the Italian and Nordic cohort (Table 2b,c) differed from each other and that of the German cohort. However, journals like Cancer Research, Clinical Cancer Research and Virchows Archiv were present in all three rankings. If categorised according to the JCR subject categories, the 12 leading journals from the German cohort were categorised as "Pathology" (seven: *Virchows Archiv*, *J Pathol*, *Histopathology*, *Modern Pathology*, *Am J Surg Pathol*, *J Clin Pathol* and *Human Pathol*), "Oncology" (five: *Int J Cancer*, *Int. J Oncol*, *Oncogene*, *Clin Cancer Res* and *Cancer Res*) and "Cell Biology" (two: *Histopathology* and *Oncogene*). "Surgery" (*Am J Surg Pathol*), "Genetics and Heredity" (*Oncogene*) and "Biochemistry and Molecular Biology" (*Oncogene*) occurred only once.

The most frequent categories for the leading journals form the Italian cohort were "Pathology" (three), "Oncology" (three) and "Immunology" (two). Those of the Nordic cohort were "Oncology" (nine), "Biochemistry and Molecular Biology" (two) "Cell Biology" (two) "Genetics and Heredity" (two) and "Pathology" (two).

Publications in the 12 top ranking journals (Table 2) accounted for 28.4%, 22.5% and 37.2% of the total categorised publications from the Nordic, Italian and German cohort respectively.

The leading journals for the French cohort were Human Pathology, Histopathology, the American Journal of Surgical Pathology, Modern Pathology and Virchows Archiv (all categorised as "Pathology" plus once "Cell Biology" and "Surgery").

The impact factors gained in all four cohorts ranged between 0.507 (*Folia Neuropathologica*, 2004) to 51.296 (*New England Journal of Medicine*, 2006). The mean IF for a publication was 3.437, 3.655, 3.748 and 3.865 in the French, Nordic, German and Italian cohort respectively. The median impact factor of the journals remained below these values (France: 2.955–3.277; Nordic countries: 2.729–2.887; Germany: 2.623–2.775; Italy: 2.704–2.855). Consequently, it is not surprising that the mean IF of the publications in the 12 leading journals and the median IF of these journals was even higher (Table 2).

If all journals and publications in the German, Italian and Nordic cohort were considered and analysed according to the respective subject category available from the ISI web of Science, the following results were obtained.

In all cohorts the most frequent journal category was "Oncology" followed by "Biochemistry and Molecular Biology", "Pathology" and "Cell Biology" Figs. 1a, 2b and 3a). If the number of publications in the specific journal category was evaluated (Figs. 1b, 2b and 3b), the "Pathology" became the leading category in the German and Italian cohort and distanced itself from "Biochemistry and Molecular Biology" and "Cell Biology" in all cohorts. The overall proportion of publications in journals categorised

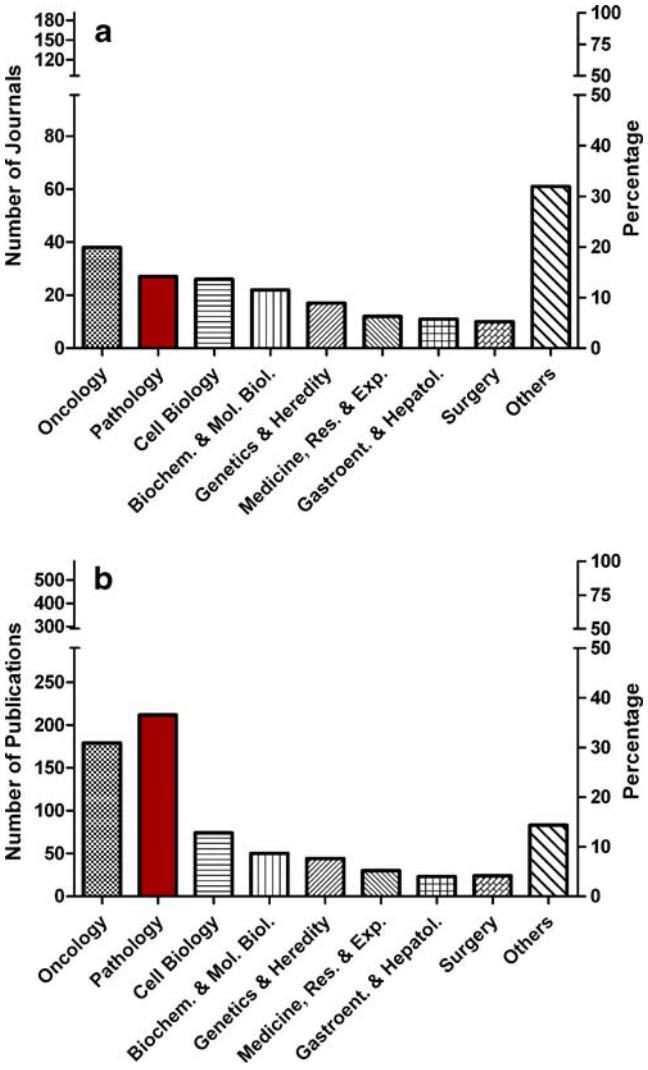


Fig. 1 Germany—journal categories and publications. **a** Ranking of the most frequent journal categories (Oncology, Pathology; Cell Biology; Biochemistry and Molecular Biology; Genetics and Heredity; Medicine, Research and Experimental; Gastroenterology and Hepatology; Surgery; Others) and their share in all journals (n=191). **b** Absolute numbers and proportions of publications in journals of the respective category related to all publications in journals with a given category (n=580)

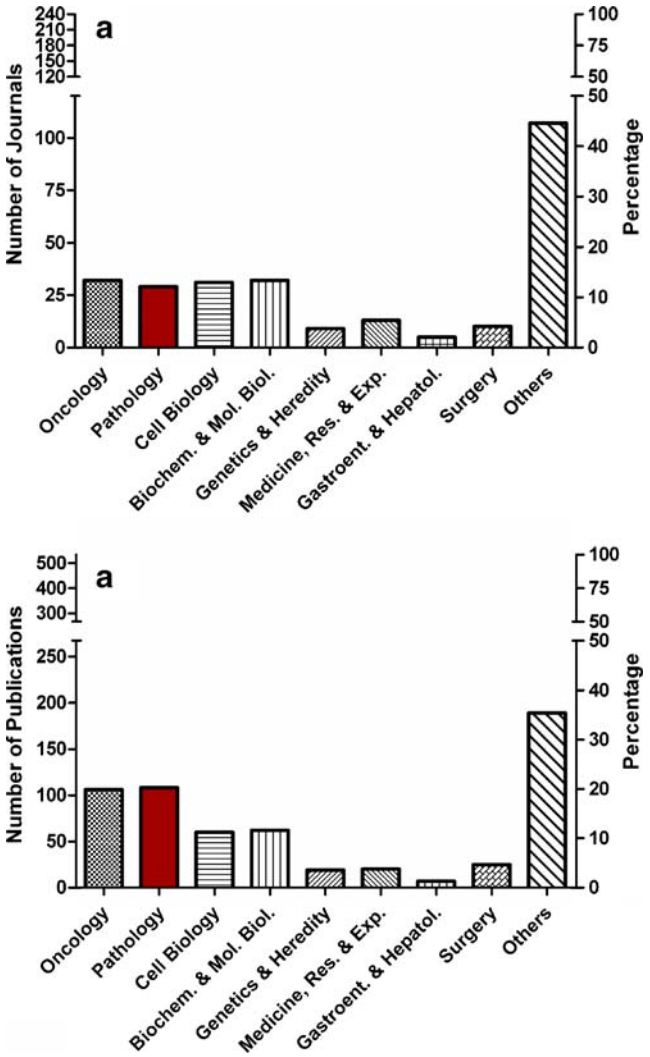


Fig. 2 Italy—journal categories and publications. **a** Ranking of the most frequent journal categories (see Fig. 1) and their share in all journals (n=240). **b** Absolute numbers and proportions of publications in journals of the respective category related to all publications in journals with a given category (n=534)

as "Pathology" was 19.1%, 20.2% and 36.6% for the Nordic, Italian and German cohort, respectively.

Discussion

Although pathologists provide the diagnostic gold standard in oncological medicine and research, very few studies have analysed the publication habits of pathologists in a representative fashion [5, 7, 10, 11, 19]. Several studies have analysed the scientific output on a national or international basis related for various medical discipline based on an analysis of accordingly categorised journals [6–8, 13, 15, 17–19]. The main presumption in these publications is that from the analysis of research outputs in biomedical journals of a specific medical category, the research output of the related medical discipline could be inferred. To our knowledge, this is the first study to analyse the scientific output on the basis of national institutes and cities in a certain medical specialty including all Medline-listed biomedical journals and focusing on pathologists. Our results mirror the interconnection and diversification of modern pathological research with a broad range of clinical and paraclinical specialties resulting in a huge range of journals and biomedical categories applicable for publications. Particularly, the overlap with journals having an oncological, cell biological or biochemical focus is not surprising. Since histological tumour diagnostic is probably the most important subsection in anatomic pathology, the high rate of publications in oncology-focused journals found in all cohorts is certainly comprehensible.

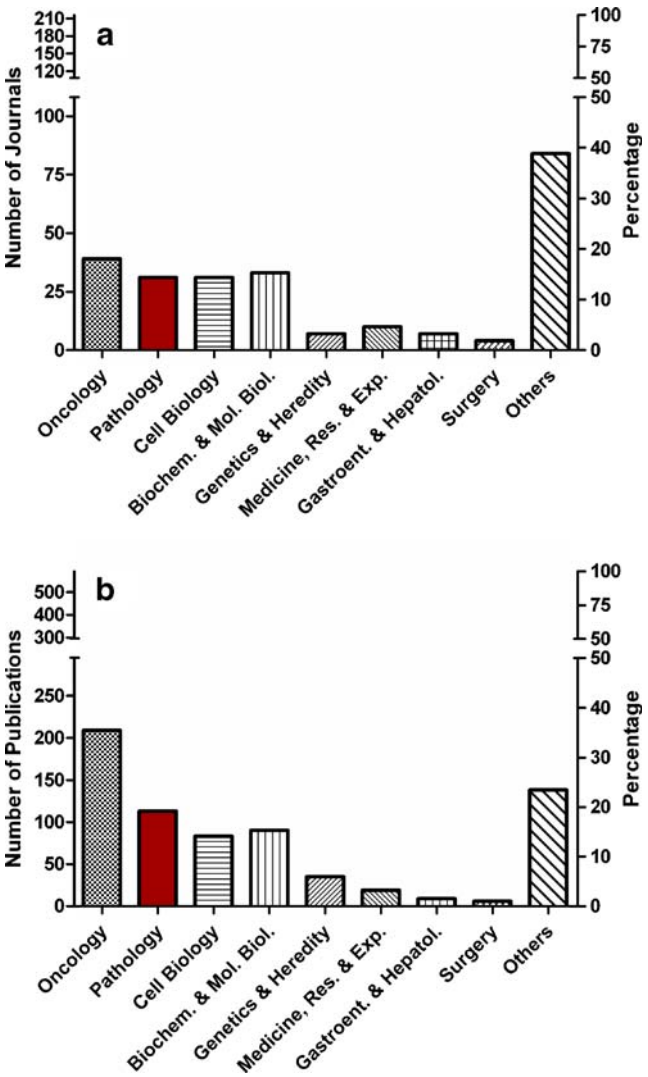


Fig. 3 Nordic countries—journal categories and publications. **a** Ranking of the most frequent journal categories (see Fig. 1) and their share in all journals (n=216). **b** Absolute numbers and proportions of publications in journals of the respective category related to all publications in journals with a given category (n=591)

The analysis of the French cohort was limited and is only seen as supplemental since the high rate of dropouts in the internet-based search for publications severely questions the representativeness of this cohort. The reason for these dropouts was that most authors from France, in contrast to the vast majority of authors from the other analysed countries, used the national language instead of the English language for the affiliation declaration.

A limit of this study is our inability to differentiate between the authors as being biologists, other natural scientists or physicians, since in many institutes of pathology research is not only done by physicians but also to a significant extent by associated natural scientists. This differentiation is difficult because specifying information is not always available from the homepages of the institutes and the affiliation given in Medline is also often not helpful in this direction. On the other hand, the integration of biologists in the pathological molecular diagnostics, as well as the full-time dedication of physicians to pathobiological research, questions the reasonability of such differentiations. A further point to be addressed is the use of the word "pathology" not only in departments of pathology but also for various research subunits of clinical departments. We excluded publications from such subunits if no actual connection to the specialty of pathology was detected.

Having analysed three large international cohorts, our results demonstrate that most articles from pathologists are published in a wide spectrum of non-pathological journals with main focuses in oncology and cell biology and biochemistry. Still, journals with a focus on histopathology, accounting for 1/5 up to 1/3 of all these publications, remain the most or second most important category and representation of pathological research. In this regard, our results differ from those of Mela et al. who have analysed radiological research (including editorials, short reports and technical notes) in selected European countries from 1995 to 2000 and concluded that only one third of publications from radiologists were published in non-radiological journals [14]. The mean impact factor for publications from German radiologists in this study was 1.177 [14]. A possible explanation for the differences to our results could be the broader spectrum of research outputs included and differences in the assessment of primary contributions.

The availability of published articles via the internet might be responsible for a greater independence of scientists from their traditional subject-related journals and print versions. The decision for a certain journal is supposedly more influenced by its impact factor with its related monetary implications than by the question whether the own peer group will be optimally reached.

Acknowledging that only 690 of the 6,166 biomedical journals listed in the JCR® in 2006 achieved an impact factor of more than 3.5 and only 530 of more than 4.0, the mean impact factor of pathological publications can be considered rather high (upper 8 to 12% of biomedical journals) consistently in the different cohorts.

Acknowledgements The contributions of Dr. Marius Fritzsche and Ilka Kristiansen are greatly appreciated.

Conflict of interest statement We declare that we have no conflict of interest.

References

1. Crawford JM, Tykocinski ML (2005) Pathology as the enabler of human research. Lab Invest 85:1058–1064
2. Denk H (2001) Pathology and clinical medicine in the 21st Century. Verh Dtsch Ges Pathol 85:80–86
3. Dietel M (2007) Predictive pathology of cytostatic drug resistance and new anti-cancer targets. Targeted therapies in cancer. Springer, Berlin, pp 25–32
4. Dietel M, Sers C (2006) Personalized medicine and development of targeted therapies: the upcoming challenge for diagnostic molecular pathology. A review. Virchows Arch 448:744–755
5. Donato HM, De Oliveira CF (2006) Breast pathology: evaluation of the Portuguese scientific activity based on bibliometric indicators. Acta Med Port 19:225–234
6. Falagas ME, Papastamataki PA, Bliziotis IA (2006) A bibliometric analysis of research productivity in Parasitology by different world regions during a 9-year period (1995–2003). BMC Infect Dis 6:56
7. Fritzsche FR, Oelrich B, Dietel M, Jung K, Kristiansen G (2007) European and US publications in the 50 highest ranking pathology journals from 2000 to 2006 J Clin Pathol in press
8. Fuentes-Arderiu X, Lacambra MJ (2005) Publications in clinical chemistry journals in the European Union. Clin Chim Acta 362:189–191
9. Holland L, Bosch B (2006) Medical students' perceptions of pathology and the effect of the second-year pathology course. Human Pathol 37:1–8
10. Jones AW (2005) Creme de la creme in forensic science and legal medicine. The most highly cited articles, authors and journals 1981–2003. Int J Leg Med 119:59–65
11. Jones AW (2007) The distribution of forensic journals, reflections on authorship practices, peer-review and role of the impact factor. Forensic Sci Int 165:115–128
12. Masood S (2003) The expanding role of pathologists in the diagnosis and management of breast cancer: worldwide excellence in breast pathology program. Breast J 9(Suppl 2):S94–S97
13. Mela GS, Cimmino MA (1998) An overview of rheumatological research in the European Union. Ann Rheum Dis 57:643–647
14. Mela GS, Martinoli C, Poggi E, Derchi LE (2003) Radiological research in Europe: a bibliometric study. Eur Radiol 13:657–662
15. Michalopoulos A, Falagas ME (2005) A bibliometric analysis of global research production in respiratory medicine. Chest 128:3993–3998
16. Nizze H (2001) Pathology for the 21st century. Invitation to the 85th Congress of the German Society for Pathology in Munster, 6–9 June 2001. Der Pathologe 22:1–3
17. Oelrich B, Peters R, Jung K (2007) A bibliometric evaluation of publications in urological journals among European Union countries between 2000–2005. Eur Urol 52(4):1238–48
18. Rahman M, Sakamoto J, Fukui T (2003) Japan's share of research output in urology and nephrology. Int J Urol 10:353–355
19. Ugolini D, Casilli C, Mela GS (2002) Assessing oncological productivity. is one method sufficient? Eur J Cancer 38:1121–1125

Virchows Arch (2008) 452:369–375
DOI 10.1007/s00428-008-0590-0

ORIGINAL ARTICLE

Down-regulation of the metastasis suppressor protein KAI1/CD82 correlates with occurrence of metastasis, prognosis and presence of HPV DNA in human penile squamous cell carcinoma

C. Protzel · C. Kakies · B. Kleist · M. Poetsch · J. Giebel

Received: 12 November 2007 / Revised: 13 January 2008 / Accepted: 23 January 2008 / Published online: 28 February 2008
© Springer-Verlag 2008

Abstract In penile squamous cell carcinoma (PSCC), the outcome largely depends on early detection and resection of inguinal lymph node metastases. We investigated the role of metastasis suppressor protein kang ai 1 (KAI1)/cluster of differentiation 82 (CD82), which is known to be of prognostic significance for a wide variety of cancers. Moreover, we analysed the tumours for human papillomavirus (HPV) DNA and loss of heterozygosity at the 11p11.2 locus. Tissue samples of 30 primary PSCCs were investigated immunohistochemically using an anti-KAI1/CD82 polyclonal antibody. The expression was assessed according to the degree of KAI1/CD82-positive tumour cells as positive, decreased or negative. The presence of HPV6/11, HPV16 and HPV18 DNA was analysed by polymerase chain reaction. All patients with decreased or negative expression of KAI1/CD82 in primary lesions had lymph node metastases (p=0.0002). Patients with positive KAI1/CD82 expression showed a significant better prognosis for survival compared to the other groups (p=0.0042). Presence of HPV DNA was associated with decreased or negative KAI1/CD82 expression. Lacking or decreased expression of metastasis suppressor gene *KAI1/CD82* appears to be a prognostic parameter for the occurrence of lymph node metastases in PSCC. Our study suggests an association of decreased KAI1/CD82 expression with tumour progression, development of metastases and disease-specific death.

Keywords Penile carcinoma · Metastasis · KAI1/CD82 · HPV · LOH

C. Protzel (✉) · C. Kakies
Department of Urology, Ernst Moritz Arndt University,
Fleischmannstr. 42–44,
17475, Greifswald, Germany
e-mail: protzel@uni-greifswald.de

B. Kleist
Department of Pathology,
Ernst Moritz Arndt University of Greifswald,
Greifswald, Germany

M. Poetsch
Institute of Forensic Medicine, University Hospital Essen,
Essen, Germany

C. Kakies · J. Giebel
Department of Anatomy and Cell Biology,
Ernst Moritz Arndt University of Greifswald,
Greifswald, Germany

Introduction

Penile squamous cell carcinoma (PSCC) is an uncommon tumour entity in North America and Europe. Although PSCC is known for slow local tumour growth, metastases are frequently found in inguinal lymph nodes even in early tumour stages [4]. PSCC may be cured by resection of the primary lesion and the involved regional lymph nodes. The presence of lymph node metastases is the main variable able to affect the survival in patients with PSCC.

Because inguinal lymphadenectomy is known to be associated with a high morbidity and a high percentage of non-palpable inguinal lymph nodes is not affected by metastasis (up to 75–90% of patients), reliable predictors for metastasis are necessary [13].

Despite current studies concerning p53, matrix metallopeptidase 9 and Ki67 [3, 20, 23, 29], there is only rare information about the predictive value of tumour markers,

expression of tumour suppressor and metastasis suppressor genes in penile carcinomas.

The cell membrane protein KAI1 ("kang ai" = Chinese for "anti-cancer"), also known as cluster of differentiation 82 (CD82), was originally described as a metastasis suppressor gene in prostate cancer [5]. This gene located on chromosome 11p11.2 is a member of the glycoprotein transmembrane-4 superfamily [21]. KAI1/CD82 is a 40–75-kDa tetraspanin cell surface protein and plays a role in signal transduction, cell activation, development, proliferation and motility [2, 37]. Down-regulation of KAI1/CD82 is associated with metastatic progression and poor prognosis in several carcinomas [35, 44, 46]. Because KAI1/CD82 is reported to be down-regulated in other squamous cell carcinomas, e.g. cervical carcinomas or oral carcinomas, it is an interesting candidate for additional prognostic information on PSCC [8, 11, 17].

The mechanism of down-regulation of KAI1/CD82 is not fully elucidated (e.g. an association with p53 is discussed) [24]. Loss of heterozygosity (LOH) is a common indicator for the involvement of tumour suppressor genes in the pathogenesis of carcinomas and LOH of 11p11.2 has been reported infrequently [15].

Therefore, we investigated immunohistochemically the value of KAI1/CD82 as prognostic marker for metastasis and survival in patients with PSCC and compared KAI1/CD82 expression with the presence of human papillomavirus (HPV) DNA known for disturbance of the 14^{ARF}/MDM2/p53 pathway [39]. Additionally, we also analysed the 11p11.2 locus by amplification of adequate microsatellite markers.

Materials and methods

Patients

Thirty patients (median patient age 66.5 years, range 35 to 89 years) with invasive PSCC treated at the University Hospital of Greifswald and Helios Hospital Schwerin were available for investigation. Patient data and tissues were obtained and used after advice from the Medical Ethics Committee of the University of Greifswald in accordance with the declaration of Helsinki and the International Conference of Harmonisation–Good Clinical Practice. The anonymity of the patients investigated was preserved corresponding to rules of data protection of the Human Medical Faculty Greifswald and the county Mecklenburg–Vorpommern.

Nine patients underwent tumour resection, 15 partial penectomy while total penectomy was necessary in six patients. The median follow-up for patients with invasive carcinomas was 46.1 months (range 2 to 125 months). Fourteen patients were alive and showed no evidence of disease; two patients were alive with disease. Eleven patients died of tumour and two patients of non-tumour-related causes (one patient lost to follow-up).

Representative tumour tissue samples with adjacent non-neoplastic tissue allowing sufficient classification and grading were obtained during surgery and subjected to 4% buffered formalin. Pathological classification was done on haematoxylin-and-eosin-stained specimen. The age of the specimens was mainly between 1 and 10 years. Two specimens were older than 10 years. All specimens underwent additional independent histopathological review (BK). Tumours were staged according to the 2002 tumour–node–metastasis system; histological grading was classified as grade 1—well differentiated, grade 2—moderately differentiated and grade 3—poorly differentiated [34]. The tumours were additionally histologically subtyped according to the World Health Organisation (WHO) classification [7].

Immunohistochemistry

Immunohistochemistry was carried out on paraffin sections (4 μm). In detail, endogenous peroxidase activity was blocked prior to immunohistochemistry by incubation in 0.3% H_2O_2 in methanol for 40 min (22°C). Sections were subjected to heat antigen retrieval (microwave oven, 700 W, 20 min) using 10 mM citrate buffer (pH 6.0). After cooling in citrate buffer and subsequent washings in phosphate-buffered saline (PBS), immunohistochemistry was done using a staining kit (Vectastain, Santa Cruz Biotechnology, Santa Cruz, CA, USA). Blocking with goat serum (Vectastain kit, 20 min) was followed by incubation with anti-KAI1 polyclonal antibody (Santa Cruz Biotechnology, Santa Cruz, CA, USA) for 45 min at 22°C and two washes in PBS (2×5 min). The antibody was previously used by several authors for immunohistochemistry and Western blot [10]. Incubation with secondary antibody (30 min, 22°C) was followed by washing in PBS (2×5 min). Slides were subjected to avidin–biotin–peroxidase complex reagent (45 min). Visualisation was performed after washing in PBS (2×5 min) with 0.1% diamine–benzidine in PBS per 0.01% H_2O_2 followed by haematoxylin counterstaining and mounting in glycerol-gelatine (Merck, Darmstadt, Germany). Control reactions were (1) incubating slides with PBS alone, (2) using PBS instead of primary antibody and (3) replacing the KAI1 antibody with a monoclonal antibody (β1-integrin, Biomol, Hamburg, Germany) not reactive in paraffin sections. Photographs were taken on an Olympus B ×50 microscope equipped with an Olympus DP 10 digital camera.

The percentage of KAI1 positive tumour cells was evaluated by three independent observers (CP, CK, BK) and intensity was measured by percentage of stained tumour cells. According to previous studies, expression of KAI1 was classified as negative (less than 10% of the

tumour cells positive), decreased (10–50% of tumour cells positive) or positive (more than 50% of the tumour cells positive) [6, 25, 43].

Because poor prognosis has been described for tumours with reduced KAI1 expression, we compared survival data of patients with decreased or negative expression (KAI1/CD82<50%) with the data of patients with positive expression (cutoff level of 50% for plotting and comparing of survival curves) [12].

DNA extraction, LOH analysis and HPV DNA detection

Due to limited material, only 21 carcinomas were available for DNA extraction. First, haematoxylin–eosin-stained slides were carefully inspected by light microscopy to identify areas which carry a sufficient amount (at least 3 mm^2) of tumour tissue measured by a scaled optical adjustment. This same area was then identified on the unstained 10-μm dewaxed, rehydrated and airdried tissue section, which was fixed in an optical installation allowing the separate isolation of predominant tumour tissue without adherent non-tumourous structures under microscopical control with a cannula (used for intravenous injections). DNA isolation from paraffin-embedded tissue was performed as previously described [27, 28] with the High Pure polymerase chain reaction (PCR) Template Preparation Kit (Roche Molecular Biochemicals, Mannheim, Germany).

The following six microsatellite loci were studied: D11S986 and D11 S4133 at 11p11.2 (in the vicinity of KAI1), and D11S1353, D11S4144, D11S4167 and D11S528 at 11q23 (as controls). Primer sequences were obtained from Genome Data Base (http://www.gdb.org); cytogenetic locations are according to Ensembl (http://www.ensembl.org). PCR amplification was performed in multiplex assays with fluorochrome-labelled primers (6-FAM, JOE, or TAMRA) in 12.5 μl sample volumes with 2–5 ng of genomic tumour or normal DNA as template in 15 mM Tris–HCl, 50 mM KCl, with 200 μM dNTPs, 1.5 mM $MgCl_2$, 0.1 nM primers, and one unit HotStart Taq Polymerase (Qiagen, Hilden, Germany). An initial denaturation and activation step of 12 min at 95°C was followed by 30–35 cycles of 1 min at 95°C, 1 min at 55–58°C and 2 min at 72°C and a 30 min final elongation step at 72°C. PCR products were analysed on an ABI310 genetic analyser (Applied Biosystems, Darmstadt, Germany) with ROX-labelled internal lane standard. All PCR assays were repeated at least once. LOH was scored if one allele was >90% decreased in tumour DNA when compared with the same allele in normal control DNA in both PCR assays.

Because HPV6/11, HPV16 and HPV18 DNA is most frequently found in PSCC and especially HPV16 DNA is correlated with disturbance of several cellular pathways, we selected them for PCR diagnostics [32, 39].

The amplification of HPV6/11 DNA with specific primer sequences F-TACACTGCTGGACAACATGC and R-GTGCGCAGATGGGACACAC and HPV16 DNA with specific primer sequences F-CCCAGCTGTAATCATGCATGGAGA and R-GTGTGCCCATTAACAGGTCTTCCA was detected in a duplex PCR as described by Husnjak et al. [14]. For the amplification of HPV18 DNA, we used specific primer sequences F-GAATTCACTCTATGTGCAG and R-TAGTTGTTGCCTGTAGGTG as published by Riethdorf et al. [30]. The products were analysed by electrophoresis on polyacrylamide gels and detected by silver staining. To prove the presence of amplifiable DNA in the extractions, all of them were amplified with primers for the human beta-globin gene.

Statistical analysis

Descriptive statistical data have been reported in terms of mean values and standard deviation. Chi Square Test and Kendall Tau Test were used to examine the correlation between KAI1 expression and clinical parameters.

Furthermore, we used the Kaplan Meier method to plot survival function and the log rank test to compare survival curves. A p value <0.05 was considered statistically significant.

Results

Pathological findings

The samples from 30 patients comprised 13 pT1, eight pT2, eight pT3 and one pT4 tumours. Lymph node metastases were diagnosed in 17 patients. In detail, metastases were evident in six pT1, five pT2 and six pT3–4 tumours.

Fifteen tumours were keratinising conventional squamous cell carcinoma (SCC), seven tumours were non-keratinising conventional SCCs. Moreover, three patients with basaloid variants of SCC, two patients with papillary variants, two patients with verrucous variants and one patient with a condylomatous variant of SCC were included in this study.

Occurrence of lymph node metastases correlated significantly to clinical outcome, i.e. disease associated death (p=0.004) whereas stage and grade of tumours did not correlate with the occurrence of metastases or clinical outcome.

Immunohistochemical localisation of KAI1/CD82

Immunohistochemical staining for KAI1/CD82 was found in the cytoplasm and plasma membranes of tumour cells. In every tumour demonstrating KAI1/CD82 expression, positive membranous and cytoplasmatic staining was detected. According to the KAI1/CD82 score, 17 samples were KAI1/

CD82 positive; ten were decreased and three tumours were negative. Examples for different kind of KAI1/CD82 expression are shown in Fig. 1.

KAI1/CD82 expression was also found in adjacent non-neoplastic tissue especially in vascular and nerve structures.

Association of KAI1/CD82 expression with clinicopathological data

There was no significant association of KAI1/CD82 expression and local tumour stage (T-stage). Otherwise, KAI1/CD82 staining was significantly associated with the histological grading of the primary tumour (p=0.027).

A decrease in KAI1/CD82 expression in primary tumours was significantly associated with the occurrence of lymph node metastases (p=0.0002). All patients with decreased or negative KAI1/CD82 expression in primary lesions showed lymph node metastases. However, metastases were also found in four patients with positive KAI1/CD82 expression. WHO tumour stage (including local tumour stage and presence of metastases) showed a significant association with KAI1/CD82 expression. Statistical comparison between KAI1/CD82 expression and histopathological data are shown in Table 1. Due to the low number of cases with rare histological subtypes, statistical analysis concerning subtypes did not show significant differences in our study.

KAI1/CD82 expression and prognosis

We selected 50% as a cutoff level for KAI1 expression (negative and decreased expression vs. positive expression) with the purpose of plotting and comparing survival curves. KAI1 expression at the cutoff level exhibited a prognostic value for disease-specific death with a log rank test of 0.0042 (Fig. 2).

Analysis for HPV DNA and for loss of heterozygosity on chromosome 11

Twenty-one tumours were analysed for HPV DNA by PCR. Twelve tumours were negative for HPV DNA, whereas nine tumours showed HPV DNA presence. Seven tumours presented HPV16 DNA, while two tumours were positive for HPV6/11 DNA. HPV18 DNA was not found in primary tumours of patients of our study.

We further analysed a possible role of loss of the *KAI1/CD82* gene in down-regulation of KAI1/CD82 protein by LOH. None of the 21 tumours that were available for LOH analysis showed LOH in the examined two microsatellite loci from 11p11 or in one of the control microsatellite repeats from chromosome 11.

Association of HPV DNA presence with KAI1/CD82 expression and clinical data

Nine tumours showed HPV DNA presence. Most tumours with HPV DNA presence showed a reduced KAI1/CD82 expression (seven tumours with decreased or negative expression KAI1/CD82 vs. two tumours with HPV DNA and positive expression of KAI1/CD82). In all tumours negative for KAI1/CD82, an expression of HPV DNA was detected. Seven out of 12 tumours without HPV DNA presence were positive for KAI1/CD82 expression (p=

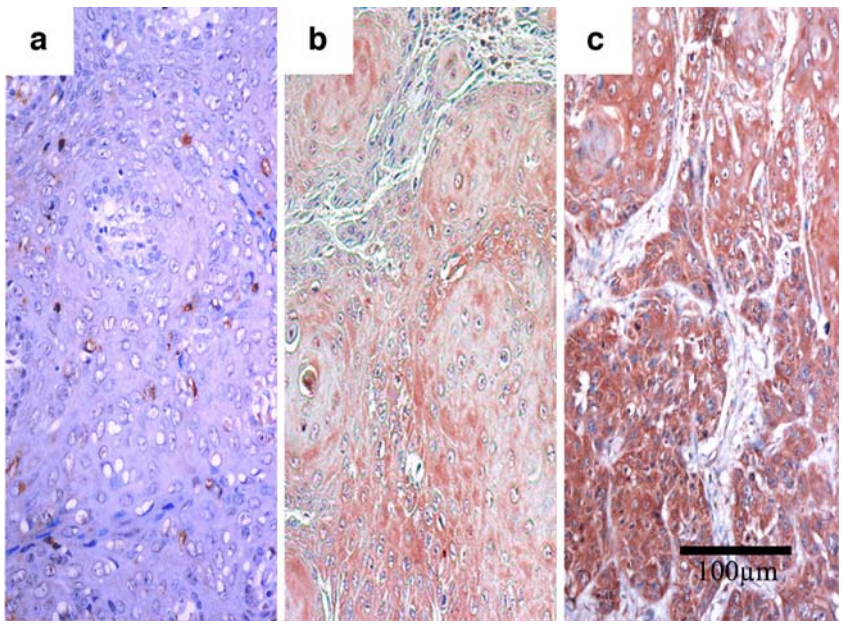


Fig. 1 Different expression of KAI1/CD82 in penile carcinomas. Negative (**a**), decreased expression (**b**) and positive staining (**c**)

Table 1 Association of KAI1/CD82 with tumour stage, grading, metastasis and WHO stage

		No. of patients	KAI1/CD82 status			Chi square *p*
			Negative	Decreased	Positive	
T	1	13	1	3	9	0.790
	2	8	1	3	4	
	3	8	1	3	4	
	4	1	0	1	0	
G	1	5	0	1	4	0.027
	2	21	1	7	13	
	3	4	2	2	0	
N	0	13	0	0	13	<0.001
	+	17	3	10	4	
M	0	24	1	6	17	<0.001
	+	6	2	4	0	
WHO stage	I	7	0	0	7	0.005
	II	7	1	1	5	
	III	8	1	2	5	
	IV	8	1	7	0	

0.013). Both carcinomas with HPV 6/11 DNA were KAI1/CD82 negative.

Statistical analysis did not show a correlation between HPV DNA presence and occurrence of lymph node metastasis or prognosis.

Discussion

Carcinogenesis and development of metastasis are complex processes comprising multiple mechanisms whose details are still unknown. Metastasis suppressor gene *KAI1/CD82* originally described in prostate cancer [5] seems to play a crucial role in invasion and migration of tumour cells. Several previous studies described the prognostic role of KAI1/CD82 expression for the development of metastasis in various tumour entities [6, 9, 19, 25]. For instance, down-regulation of KAI1/CD82 has been shown to be significantly associated with occurrence of lymph node metastasis in oral squamous cell carcinomas [42] and with poor differentiation in cervical squamous cell carcinomas [7]. Because PSCC is known to share several prognostic markers with cervical carcinomas, KAI1/CD82 expression status in PSCC may provide further information about risk of progression and metastases.

In this study, we found a significant association of KAI1/CD82 expression with WHO tumour stage and grading in penile carcinomas which is in line with the observations in breast cancer, cervical carcinomas and gastric carcinomas [7, 41, 44]. Also, in accordance to previous findings in other tumour entities [9], our study showed a significant association between reduced KAI1/CD82 expression and the occurrence of metastasis in PSCC. Consistently, this suggests an important role of KAI1/CD82 down-regulation in the process of tumour cell dissemination in penile carcinomas.

Several studies elucidated the function of KAI1/CD82 in the development of metastasis. In vitro expression of KAI1/CD82 decreased invasive growth and mobility of cancer cells [45]. In addition, KAI1/CD82 transfected colorectal cancer cell line LOVO showed increased normotopic cell adhesion [18].

Recently, it was demonstrated that an interaction of KAI1/CD82 and Duffy blood group protein Duffy antigen receptor for chemokines (gp-Fy) led to an attachment of cancer cells to vascular endothelial cells followed by an inhibition of tumour cell proliferation [31]. These results hint at KAI1/CD82 not only as an indicator for lymph node metastases but also as a potential target for new therapeutics [40] which could probably improve the prognosis of patients with penile carcinomas. The first results after adenoviral transduction of KAI1/CD82 into lung cancer tumour cells are promising [38].

The mechanisms resulting in the loss of KAI1/CD82 expression are still unknown. According to previous findings down-regulation of KAI1/CD82 is a complex process involving multiple regulatory mechanisms like p53-dependent regulation, while promotor hypermethylation, gene mutation and loss of heterozygosity seem not to be essentially involved in KAI1/CD82 loss [16, 25, 36]. Loss of heterozygosity in the *KAI/CD82* gene locus could not be shown in the penile carcinomas of our study, thus confirming previous results.

HPV infection frequently found in PSCC is known for disturbance of several pathways of cell cycle regulation such as 14^{ARF}/MDM2/p53 [39]. The tumour suppressor gene *p53* activates expression of KAI1/CD82 by interaction

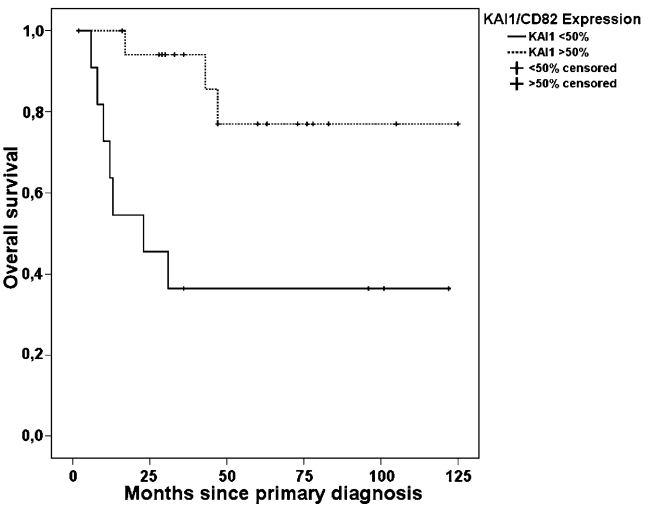


Fig. 2 Kaplan Meier survival curves for KAI1/CD82 expression. Log rank $p=0.0042$

with the KAI1/CD82 promotor region [24]. Therefore, we additionally compared the HPV DNA status of the carcinomas with the KAI1/CD82 expression. In contrast to the results of Schindl et al. [33] for cervical cancer, we were able to demonstrate a possible association of HPV DNA detection and down-regulation of KAI1/CD82 expression, although this may be caused by the small number of carcinomas investigated. While HPV infection is frequently linked to carcinomas of the cervix uteri, only 30% of conventional PSCC show HPV DNA presence [26, 32]. Thus, our data may underline the different roles of HPV DNA in cervical and penile carcinomas. Because a synergistic effect of several factors in regulation of KAI1/CD82 expression was demonstrated, different effects of associated proteins (e.g. junB or AP2) in cervical and penile carcinomas have to be taken into account [22].

Because different histological subtypes like the basaloid subtype are more strongly associated with HPV DNA presence, further elucidation of the role of HPV in down-regulation of KAI1/CD82 in rare subtypes of PSCC is needed [32]. Analysis concerning HPV DNA types and KAI1/CD82 expression on a higher number of cases of rare histological subtypes might be useful in the explanation of different pathways of tumour growth and development of metastasis.

Our data hint at a possible prognostic significance of KAI1/CD82 for the survival of patients with penile carcinoma, despite the low number of cases investigated. These findings are in accordance with previous studies for gastric cancer, colorectal cancer, lung cancer and oral squamous carcinomas [1, 8, 19, 41]. Because occurrence of metastasis is the main variable affecting prognosis in patients with PSCC, a strong association between KAI1/CD82 expression, development of metastases and prognosis as demonstrated in this study seems possible. Further studies with higher number of cases are needed to confirm our data.

In conclusion, the loss of expression of metastasis suppressor gene *KAI1/CD82* demonstrated in this study seems to play an essential role in the development of metastases in PSCC and is therefore a promising marker to indicate the necessity of inguinal lymphadenectomy.

Furthermore, our results of decreased KAI1/CD82 expression in context with the known KAI1/CD82 functions and novel findings suggest KAI1/CD82 as a possible target for future therapeutics in gene therapy which could improve the prognosis of patients with penile carcinomas.

Acknowledgements We thank Mrs. M. Bansemir (Department of Anatomy and Cell Biology, Greifswald, Germany) for the skilful technical assistance.

Patient data and tissues were obtained and used after advice from the Medical Ethics Committee of the University of Greifswald in accordance with the declaration of Helsinki and the International Conference of Harmonisation–Good Clinical Practice. The anonymity of the patients investigated was preserved corresponding to rules of data protection of the Human Medical Faculty Greifswald and the county Mecklenburg–Vorpommern.

Conflict of interest statement We declare that we have no conflict of interest.

References

1. Adachi M, Taki T, Ieki Y, Huang CL, Higashiyama M, Miyake M (1996) Correlation of KAI1/CD82 gene expression with good prognosis in patients with non-small cell lung cancer. Cancer Res 56:1751–1755
2. Bienstock RJ, Barrett JC (2001) KAI1, a prostate metastasis suppressor: prediction of solvated structure and interactions with binding partners; integrins, cadherins, and cell-surface receptor proteins. Mol Carcinog 32:139–153
3. Campos RS, Lopes A, Guimaraes GC, Carvalho AL, Soares FA (2006) E-cadherin, MMP-2, and MMP-9 as prognostic markers in penile cancer: analysis of 125 patients. Urology 67:797–802
4. Doehn C, Baumgartel M, Jocham D (2001) Surgical therapy of penis carcinoma. Urologe A 40:303–307
5. Dong JT, Lamb PW, Rinker-Schaeffer CW, Vukanovic J, Ichikawa T, Isaacs JT, Barrett JC (1995) KAI1, a metastasis suppressor gene for prostate cancer on human chromosome 11p11.2. Science 268:884–886
6. Dong JT, Suzuki H, Pin SS, Bova GS, Schalken JA, Isaacs WB, Barrett JC, Isaacs JT (1996) Down-regulation of the KAI1 metastasis suppressor gene during the progression of human prostatic cancer infrequently involves gene mutation or allelic loss. Cancer Res 56:4387–4390
7. Eble JN, Sauter G, Epstein JI, Sesterhenn IA (2004) World Health Organization classification of tumours. Pathology and genetics of tumours of the urinary system and male genital organs. IARC, Lyon, pp 280–290
8. Farhadieh RD, Smee R, Ow K, Yang JL, Russell PJ, Crouch R, Jackson P, Jacobson IV (2004) Down-regulation of KAI1/CD82 protein expression in oral cancer correlates with reduced disease free survival and overall patient survival. Cancer Lett 213:91–98
9. Friess H, Guo XZ, Berberat P, Graber HU, Zimmermann A, Korc M, Buchler MW (1998) Reduced KAI1 expression in pancreatic cancer is associated with lymph node and distant metastases. Int J Cancer 79:349–355
10. Gellersen B, Briese J, Oberndörfer M, Redlin K, Samalecos A, Richter DU, Löning T, Schulte HM, Bamberger AM (2007) Expression of the metastasis suppressor KAI1 in decidual cells at the human maternal–fetal interface: regulation and functional implications. Am J Pathol 170:126–139
11. Geradts J, Maynard R, Birrer MJ, Hendricks D, Abbondanzo SL, Fong KM, Barrett JC, Lombardi DP (1999) Frequent loss of KAI1 expression in squamous and lymphoid neoplasms. An immunohistochemical study of archival tissues. Am J Pathol 154:1665–1671
12. Higashiyama M, Kodama K, Yokouchi H, Takami K, Adachi M, Taki T, Ishiguro S, Nakamori S, Yoshie O, Miyake M (1998) KAI1/CD82 expression in non-small cell lung carcinoma is a novel, favorable prognostic factor. Cancer 83:466–474
13. Horenblas S (2001) Lymphadenectomy for squamous cell carcinoma of the penis. Part 2: the role and technique of lymph node dissection. BJU Int 88:473–483
14. Husnjak K, Grce M, Magdic L, Pavelic K (2000) Comparison of five different polymerase chain reaction methods for detection of

human papillomavirus in cervical cell specimens. J Virol Methods 88:125–134
15. Kawana Y, Komiya A, Ueda T, Nihei N, Kuramochi H, Suzuki H, Yatani R, Imai T, Dong JT, Imai T, Yoshie O, Barrett JC, Isaacs JT, Shimazaki J, Ito H, Ichikawa T (1997) Location of KAI1 on the short arm of human chromosome 11 and frequency of allelic loss in advanced human prostate cancer. Prostate 32:205–213
16. Liu FS, Dong JT, Chen JT, Hsieh YT, Ho ES, Hung MJ (2000) Frequent down-regulation and lack of mutation of the KAI1 metastasis suppressor gene in epithelial ovarian carcinoma. Gynecol Oncol 78:10–15
17. Liu FS, Chen JT, Dong JT, Hsieh YT, Lin AJ, Ho ES, Hung MJ, Lu CH (2001) KAI1 metastasis suppressor gene is frequently down-regulated in cervical carcinoma. Am J Pathol 159:1629–1634
18. Liu L, Wu DH, Li ZG, Yang GZ, Ding YQ (2003) Effects of KAI1/CD82 on biological behavior of human colorectal carcinoma cell line. World J Gastroenterol 9:1231–1236
19. Lombardi DP, Geradts J, Foley JF, Chiao C, Lamb PW, Barrett JC (1999) Loss of KAI1 expression in the progression of colorectal cancer. Cancer Res 59:5724–5731
20. Lopes A, Bezerra AL, Pinto CA, Serrano SV, de Mell OC, Villa LL (2002) p53 as a new prognostic factor for lymph node metastasis in penile carcinoma: analysis of 82 patients treated with amputation and bilateral lymphadenectomy. J Urol 168:81–86
21. Maecker HT, Todd SC, Levy S (1997) The tetraspanin superfamily: molecular facilitators. Faseb J 11:428–442
22. Marreiros A, Dudgeon K, Dao V, Grimm MO, Czolij R, Crossley M, Jackson P (2005) KAI1 promoter activity is dependent on p53, junB and AP2: evidence for a possible mechanism underlying loss of KAI1 expression in cancer cells. Oncogene 24:637–649
23. Martins AC, Faria SM, Cologna AJ, Suaid HJ, Tucci S Jr. (2002) Immunoexpression of p53 protein and proliferating cell nuclear antigen in penile carcinoma. J Urol 167:89–92 discussion 92–83
24. Mashimo T, Watabe M, Hirota S, Hosobe S, Miura K, Tegtmeyer PJ, Rinker-Shaeffer CW, Watabe K (1998) The expression of the KAI1 gene, a tumor metastasis suppressor, is directly activated by p53. Proc Natl Acad Sci U S A 95:11307–11311
25. Miyazaki T, Kato H, Shitara Y, Yoshikawa M, Tajima K, Masuda N, Shouji H, Tsukada K, Nakajima T, Kuwano H (2000) Mutation and expression of the metastasis suppressor gene KAI1 in esophageal squamous cell carcinoma. Cancer 89:955–962
26. Munoz N, Bosch FX, de Sanjose S, Herrero R, Castellsague X, Shah KV, Snijders PJ, Meijer CJ (2003) Epidemiologic classification of human papillomavirus types associated with cervical cancer. N Engl J Med 348:518–527
27. Poetsch M, Dittberner T, Woenckhaus C (2001) PTEN/MMAC1 in malignant melanoma and its importance for tumor progression. Cancer Genet Cytogenet 125:21–26
28. Poetsch M, Zimmermann A, Wolf E, Kleist B (2005) Loss of heterozygosity occurs predominantly, but not exclusively, in the epithelial compartment of pleomorphic adenoma. Neoplasia 7:688–695
29. Protzel C, Knoedel J, Zimmermann U, Woenckhaus C, Poetsch M, Giebel J (2007) Expression of proliferation marker Ki67 correlates to occurrence of metastasis and prognosis, histological subtypes and HPV DNA detection in penile carcinomas. Histol Histopathol 22:1197–1204
30. Riethdorf S, Riethdorf L, Milde-Langosch K, Park TW, Loning T (2000) Differences in HPV 16- and HPV 18 E6/E7 oncogene expression between in situ and invasive adenocarcinomas of the cervix uteri. Virchows Arch 437:491–500
31. Rinker-Schaeffer CW, Hickson JA (2006) Stopping cancer before it colonizes. Nat Med 12:887–888
32. Rubin MA, Kleter B, Zhou M, Ayala G, Cubilla AL, Quint WGV, Pirog EC (2001) Detection and typing of human papillomavirus DNA in penile carcinoma. Am J Pathol 159:1211–1218
33. Schindl M, Bachtiary B, Dreier B, Birner P, Latinovic L, Karner B, Breitenecker G, Oberhuber G (2001) Impact of human papillomavirus infection on the expression of the KAI1 metastasis suppressor protein in invasive cervical cancer. Cancer Lett 162:261–266
34. Sobin LH, Wittekind C, International Union Against Cancer (2002) TNM classification of malignant tumours. Wiley-Liss, New York
35. Son BH, Choi JS, Lee JH (2005) Prognostic values of KAI1 and surviving expression in an infiltrating ductal carcinoma of the breast. Pathology 37(2):131–136 Apr
36. Tagawa K, Arihiro K, Takeshima Y, Hiyama E, Yamasaki M, Inai K (1999) Down-regulation of KAI1 messenger RNA expression is not associated with loss of heterozygosity of the KAI1 gene region in lung adenocarcinoma. Jpn J Cancer Res 90:970–976
37. Takaoka A, Hinoda Y, Satoh S, Adachi Y, Itoh F, Adachi M, Imai K (1998) Suppression of invasive properties of colon cancer cells by a metastasis suppressor KAI1 gene. Oncogene 16:1443–1453
38. Takeda T, Hattori N, Tokuhara T, Nishimura Y, Yokoyama M, Miyake M (2007) Adenoviral transduction of MRP-1/CD9 and KAI1/CD82 inhibits lymph node metastasis in orthotopic lung cancer model. Cancer Res 67:1744–1749
39. Thomas M, Pim D, Banks L (1999) The role of the E6-p53 interaction in the molecular pathogenesis of HPV. Oncogene 18:7690–7700
40. Tonoli H, Barrett JC (2005) CD82 metastasis suppressor gene: a potential target for new therapeutics? Trends Mol Med 11:563–570
41. Tsutsumi S, Shimura T, Morinaga N, Mochiki E, Asao T, Kuwano H (2005) Loss of KAI1 expression in gastric cancer. Hepatogastroenterology 52:281–284
42. Uzawa K, Ono K, Suzuki H, Tanaka C, Yakushiji T, Yamamoto N, Yokoe H, Tanzawa H (2002) High prevalence of decreased expression of KAI1 metastasis suppressor in human oral carcinogenesis. Clin Cancer Res 8:828–835
43. Wu DH, Liu L, Chen LH, Ding YQ (2004) KAI1 gene expression in colonic carcinoma and its clinical significances. World J Gastroenterol 10:2245–2249
44. Yang X, Wei L, Tang C, Slack R, Montgomery E, Lippman M (2000) KAI1 protein is down-regulated during the progression of human breast cancer. Clin Cancer Res 6:3424–3429
45. Yang X, Wei LL, Tang C, Slack R, Mueller S, Lippman ME (2001) Overexpression of KAI1 suppresses in vitro invasiveness and in vivo metastasis in breast cancer cells. Cancer Res 61:5284–5288
46. Zheng H, Tsuneyama K, Cheng C, Takahashi H, Cui Z, Nomoto K, Murai Y, Takano Y (2007) Expression of KAI1 and tenascin, and microvessel density are closely correlated with liver metastasis of gastrointestinal adenocarcinoma. J Clin Pathol 60:50–56

Virchows Arch (2008) 452:377–382
DOI 10.1007/s00428-008-0597-6

ORIGINAL ARTICLE

Frequent epigenetic silencing of the *FHIT* gene in penile squamous cell carcinomas

Naoki Yanagawa · Mitsumasa Osakabe · Masahiro Hayashi · Gen Tamura · Teiichi Motoyama

Received: 1 October 2007 / Revised: 28 January 2008 / Accepted: 10 February 2008 / Published online: 26 February 2008
© Springer-Verlag 2008

Abstract Methylation of normally unmethylated CpG-rich islands in or near the promoter region has been associated with transcriptional inactivation of tumor-suppressor and tumor-related genes in human cancers. However, so far, only a few studies have searched for DNA methylation in penile carcinoma (PC). On the other hand, human papillomavirus (HPV) has been reported to be associated with the pathogenesis of PC. To elucidate the methylation status of PC and HPV infection, the methylation status of eight genes (*DAPK, FHIT, MGMT, p14, p16, RAR-β, RASSF1A, and RUNX3*), the incidences of the HPV status, and the expression of Fhit protein were examined in 25 PCs. The frequencies of methylation were: 28% for *DAPK*, 92% for *FHIT*, 20% for *MGMT*, 4% for *p14*, 24% for *p16*, 24% for *RAR-β*, 12% for *RASSF1A*, and 44% for *RUNX3*. Negative expression of Fhit protein was observed in 22 of the 25 cancers (88%). Among those 22, 20 showed methylation of the *FHIT* gene. HPV-DNA was detected in three of the 25 cancers (12%). Methylation of *FHIT* gene was frequently found than HPV infection, therefore methylation of the *FHIT* gene is suggested to play an important role in the pathogenesis of penile squamous cell carcinoma.

N. Yanagawa (✉) · M. Osakabe · T. Motoyama
Department of Pathology,
Yamagata University School of Medicine,
2-2-2 Iida-Nishi,
Yamagata 990-9585, Japan
e-mail: nyanagaw@med.id.yamagata-u.ac.jp

M. Hayashi
Department of Dermatology,
Yamagata University School of Medicine,
Yamagata 990-9585, Japan

G. Tamura
Division of Pathology, Yamagata Prefectural Central Hospital,
Yamagata 990-2292, Japan

Keywords Penile carcinoma · *FHIT* · methylation-HPV

Penile carcinoma (PC) is a rare disease in Japan. However, the incidence rates of PC vary markedly among different populations. The highest cumulative rate, 1% by age 75, is seen in parts of Uganda and the lowest, 300-fold less, is found among Israeli Jews [5]. For rare disease, only limited data are available regarding such molecular change.

Methylation of normally unmethylated CpG-rich islands in or near the promoter region has been reported to be associated with the transcriptional inactivation of tumor-suppressor and tumor-related genes in human cancers [17], however there is little information available regarding the epigenetic factors related to the pathogenesis of PC [7, 25]. On the other hand, there have been several reports suggesting an association between human papillomavirus (HPV) and PC, however the reported prevalence of HPV in PC is also highly variable, namely from 15 to 71% [4, 6, 10, 13, 16, 19, 22], and therefore the epidemiology of PC thus remains uncertain.

In the present study, we elucidated the methylation status of tumor-suppressor and tumor-related genes (*DAPK*, *FHIT*, *MGMT*, *p14*, *p16*, *RAR-β*, *RASSF1A*, and *RUNX3*), which have been shown to be silenced by promoter hypermethylation in human cancers [17, 28, 31, 32], in addition to the incidences of HPV infection and the expression of Fhit protein for PCs in Japanese males.

Materials and methods

Tissue specimens

Twenty-five Japanese patients with invasive PC were selected from the pathology files of Yamagata University

Hospital and affiliated hospitals. Twenty specimens were obtained by penile amputation and five by multiple biopsies.

Histological classification

The tumors were classified according to the classification of Armed Forces Institute of Pathology (AFIP) [30].

DNA extraction

Tumor DNA was extracted according to Goelz et al. [8] from 10–15 μm-thick formalin-fixed, paraffin-embedded serial sections. A microdissection was performed using a surgical blade under microscopy.

Methylation-specific PCR (MSP)

The methylation status of the examined genes was determined by MSP [11]. Before MSP, DNA samples were treated with bisulfite to convert all unmethylated cytosines to uracils, while leaving methylated cytosines unaffected. Briefly, 2 μg of genomic DNA was denatured by treatment with NaOH and modified by sodium bisulfite. DNA samples were then purified using a Wizard DNA purification resin (Promega, Madison, WI), treated with NaOH, recovered in ethanol, and then resuspended in 30 μl of distilled water. Modified DNA was amplified in a total volume of 20 μl using GeneAmp PCR Gold Buffer (PE Applied Biosystems) containing 1.0 mM $MgCl_2$, 20 μM of each primer, 0.2 mM dNTPs, and 1 unit of Taq polymerase (AmpliTaq Gold DNA Polymerase, PE Applied Biosystems). After the activation of the Taq Polymerase at 95°C for 8 min, PCR was performed in a thermal cycler (GeneAmp 2400, PE Applied Biosystems) for 35 cycles, each cycle consisting of denaturation at 95°C for 15 s, annealing at 55–63°C for 15 s, and extension at 72°C for 30 s, followed by a final 7 min extension at 72°C. A positive control and negative control (diluted water without DNA) were included for each amplification. The PCR products were then separated on a non-denaturing 6% polyacrylamide gel, stained with ethidium bromide, and visualized under UV illumination. MSP primer sequences have been listed elsewhere [28, 31, 32]. All DNA samples were checked for bisulfite modification using an unmethylated *DAPK* primer set.

Immunohistochemical analysis of Fhit protein expression

Immunohistochemical staining for Fhit protein was performed on formalin-fixed paraffin-embedded specimens. Deparaffinized 3-m thick sections were immunohistochemically stained with a streptavidin–biotin complex system (Nichirei, Tokyo, Japan). A rabbit polyclonal antibody to Fhit protein was obtained from IBL (Takasaki, Japan). In accordance with Sozzi et al. [26], the staining was determined to show a negative expression, when the tumor cells were definitely stained less than 10%, and when over 10%, it was determined to show a positive expression. Non-neoplastic squamous cell epithelium or non-neoplastic urothelial epithelium or sebaceous gland epithelium, which were present in the vicinity of the tumor on the same slide, were used as positive internal controls. The slide examination was performed by two independent observers (NY and TM).

HPV-DNA detection and typing

Tumor DNA was analyzed for HPV-DNA using polymerase chain reaction–restriction fragment length polymorphism (PCR-RFLP) analysis. At least nine types of HPV-DNA (HPV 6, 11, 16, 18, 31, 33, 42, 52, 58) can be identified by the combination of L1C1/L1C2 consensus primers and restriction enzyme digestion [29].

Results

Histological type

Histological examinations revealed that all PC cases examined were usual types of squamous cell carcinoma (well-differentiated type, 16 cases; moderately differentiated type, 9 cases; Table 1). There were no special types such as basaloid, warty, or verrucous carcinoma. The patients ranged in age from 46 to 87 years (average, 67.4 years).

Methylation status

The results concerning gene methylation are shown (Fig. 1 and Table 1). The frequencies of methylation were as follows: 28% (seven of 25) for *DAPK*, 92% (23 of 25) for *FHIT*, 20% (five of 25) for *MGMT*, 4% (one of 25) for *p14*, 24% (six of 25) for *p16*, 24% (six of 25) for *RAR-β*, 12% (three of 25) for *RASSF1A*, and 44% (11 of 25) for *RUNX3*.

Immunohistochemistry

Negative expression of Fhit protein was observed in 22 of 25 cases (88%; Fig. 2).

Correlation between immunohistochemistry and methylation of *FHIT* gene

Among the 22 cases with a negative Fhit protein expression, 20 demonstrated methylation of the *FHIT* gene (Table 1).

Table 1 Methylation status, Fhit protein expression, and HPV-DNA analysis in penile carcinomas

Case	Age	Histology	Methylation status								IHC	HPV
			DAPK	*FHIT*	*MGMT*	*p14*	*p16*	*RAR-β*	*RASS*	*RUNX3*	Fhit exp.	
1	67	Usual, wel	M	M	M	U	M	U	U	U	N	−
2	68	Usual, wel	U	M	U	U	U	U	U	M	N	−
3	72	Usual, mod	U	M	U	U	M	U	U	M	N	−
4	72	Usual, wel	U	U	U	U	M	U	U	U	N	−
5	64	Usual, mod	M	M	M	U	U	U	U	M	N	−
6	46	Usual, wel	M	M	M	U	U	U	M	M	N	−
7	69	Usual, mod	M	M	U	U	M	M	M	M	P	−
8	77	Usual, wel	U	M	U	U	U	U	U	U	N	−
9	77	Usual, wel	U	M	U	U	U	M	U	M	N	−
10	62	Usual, mod	U	M	U	U	U	U	U	U	N	+
11	60	Usual, wel	U	M	U	U	U	U	U	U	N	−
12	64	Usual, wel	U	M	U	U	U	M	U	U	N	−
13	51	Usual, mod	U	U	U	U	U	M	U	U	N	−
14	60	Usual, mod	U	M	U	U	U	U	U	U	N	−
15	52	Usual, wel	U	M	M	U	U	U	U	M	N	−
16	73	Usual, mod	M	M	U	U	M	M	M	M	P	−
17	72	Usual, mod	U	M	M	U	U	U	U	M	N	−
18	81	Usual, wel	U	M	U	U	U	U	U	U	N	+
19	57	Usual, wel	U	M	U	U	U	U	U	U	N	−
20	74	Usual, wel	M	M	U	U	U	U	U	U	P	−
21	68	Usual, wel	U	M	U	U	M	U	U	U	N	−
22	87	Usual, wel	U	M	U	U	U	U	U	U	N	−
23	66	Usual, wel	M	M	U	U	U	U	U	U	N	−
24	79	Usual, wel	U	M	U	U	U	M	U	M	N	−
25	67	Usual, mod	U	M	U	M	U	U	U	M	N	+

IHC Immuhistochemistry, *Fhit exp.* Fhit protein expression, *RASS RASSF1A*, *Usual* usual types of squamous cell carcinoma, *wel* well differentiated, *mod* moderately differentiated, *M* methylated, *U* unmethylated, *N* negative, *P* positive, + present, − absent

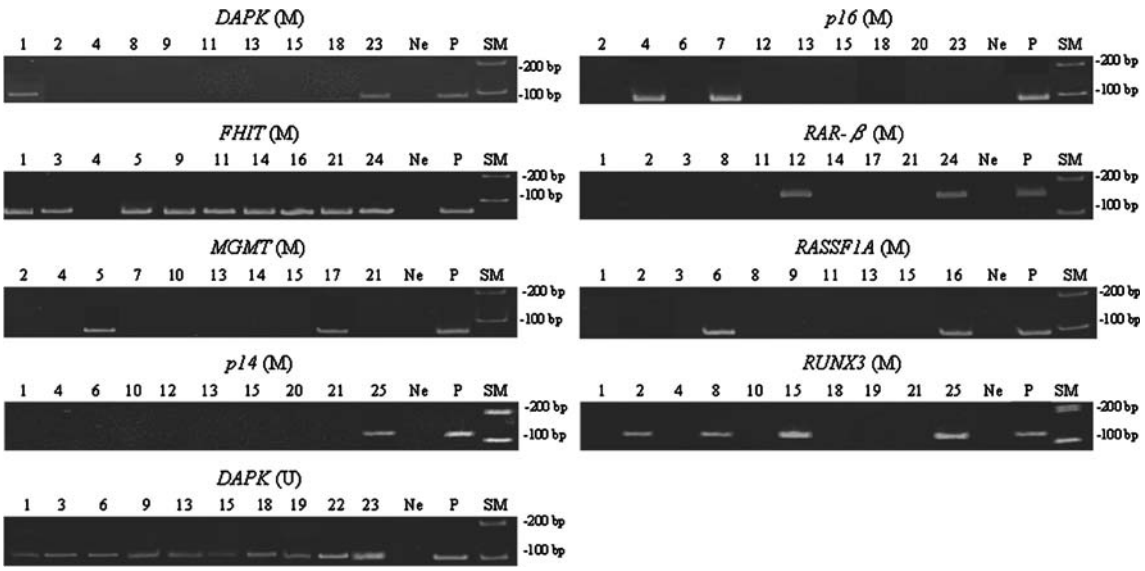


Fig. 1 A methylation analysis of eight genes in PCs by MSP. The unmethylated form of *DAPK* was run as a control for DNA integrity. *M*, methylated-specific sequence; *U*, unmethylated-specific sequence; *Ne*, negative control (water blanks); *P*, positive control; *SM*, size marker

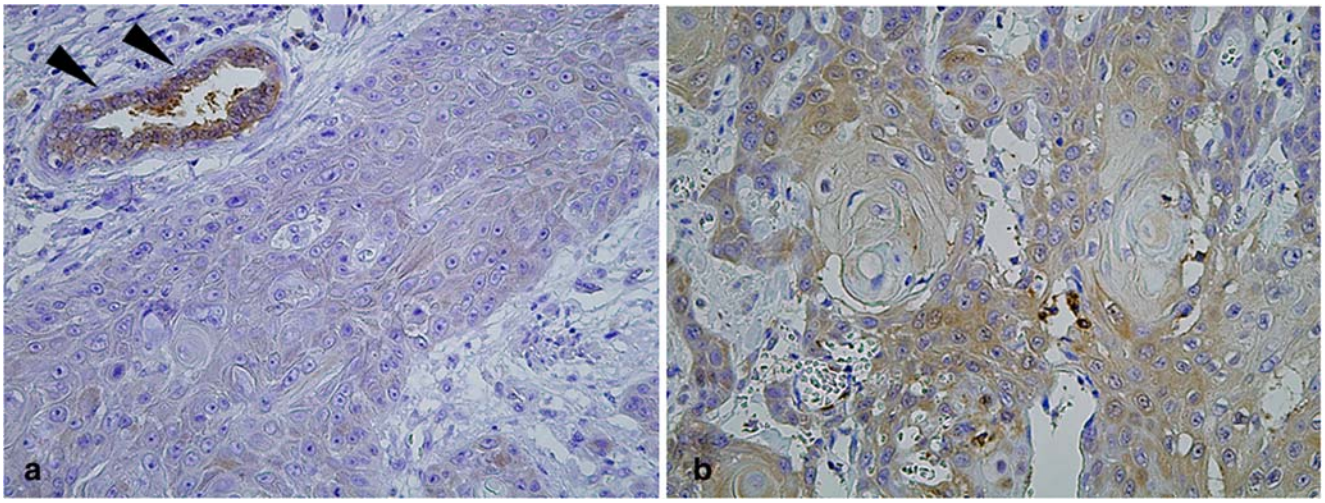


Fig. 2 Immunohistochemistry of the Fhit protein expression. **a** A negative expression of Fhit protein is observed in case 9 (*arrowheads* indicate non-neoplastic urothelial epithelium as internal positive control; ×400). **b** A positive expression of Fhit protein is observed in case 7 (×400)

HPV-DNA

HPV-DNA was detected in three of 25 cases (12%), all cases were type 16 (Fig. 3).

Discussions

Penile carcinoma is a rare disease, only a few studies have so far investigated the molecular change in such cases, and the results also vary greatly. Soufir et al. [25] suggested a mutation of *p53* gene to have been observed in three of three cases (100%), Levi et al. [15] in seven of 21 cases (33%), but both Castern et al. [3] and Suzuki et al. [27] suggested no mutation of *p53* gene was observed. Alves et al. [1] presented deletions in 13q21-22 and 4q21-32 on chromosome region and Poetsch et al. [20] presented deletions in 2q,6p,8q, 9p, 21q, and 17p13 on chromosome region. For methylation, besides a few, only two literatures discussed PC. Ferruex et al. [7] suggested *p16* methylation was observed in nine of 53 cases (17%), Soufir et al. [25] observed no methylation of *p14* and *p16* gene. To our knowledge, no further information about the methylation of multiple genes in PC has been reported until now.

In the present study, methylation was found in all of the examined genes especially high in *FHIT* (92%). The *FHIT* gene is located in the chromosome region 3p14.2 and inactivated by mainly intragenic deletion and methylation [18, 31]. Although the function of this gene is uncertain, the loss of Fhit protein expression is frequent in various carcinomas [2, 9, 31]; accordingly, this gene is thought to be a tumor-suppressor gene [14, 21, 23, 24, 31]. Recent data strongly indicated an association between *FHIT* gene inactivation and an increased survival after DNA damage, which is based on over-active checkpoints regulated by the ATR/CHK1 pathway [12]. Furthermore, the authors argued that because Fhit protein is known to be directly or indirectly proapoptotic, the differential behavior of Fhit-positive and -negative cells at the G2/M boundary might not rely on checkpoint or cycling defects but in sending or responding to an apoptotic signal [9]. Immunohistochemically, negative expression of Fhit protein was observed in 22 of 25 cases (88%). Among 22, 20 cases demonstrated methylation of *FHIT* gene. This result suggests the inactivation of the *FHIT* gene mainly occurs by the methylation of its promoter in PC. Sozzi et al. [25] reported that smoking exposure affects the inactivation of *FHIT* gene in lung carcinoma; Butler et al. [2] reported an association between HPV infection and the inactivation of *FHIT* gene in cervical cancer, but due to uncertainly in PC, further examinations are called for. For the other five cases, three methylated cases also showed a mild decrease in Fhit protein although our criteria were not completely fulfilled.

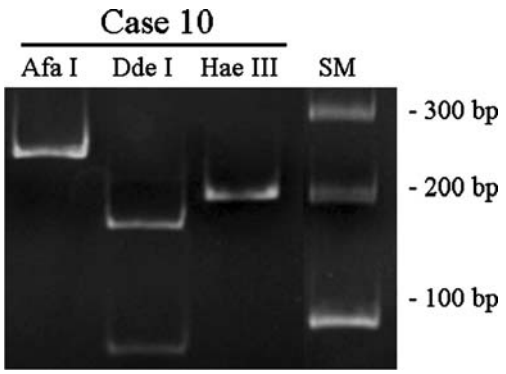


Fig. 3 Detection and typing of HPV-DNA. Following PCR amplification, equal aliquots of the PCR products were digested with the restriction enzymes *AfaI*, *DdeI* or *HaeIII*, and HPV-DNA typing performed based on the restriction patterns. Example of HPV type 16 DNA detected in PCs is shown. *SM*, size marker

Two cases showed that a negative expression of Fhit protein might occur due to some other mechanism (such as deletion or mutation), although these mechanisms have not yet been investigated in our present study.

At least one gene was methylated in all examined cases. Except for *FHIT*, five genes (*DAPK, MGMT*, *p16*, *RAR-β*, and *RUNX3*) also were methylated by more than 20%. The present examined genes have been reported as tumor-suppressor or tumor-related genes, and the methylation of these genes is thus considered to affect the pathogenesis of PC as well as other carcinomas.

HPV-DNA was detected in three cases (12%), less frequently than previous reports [4, 6, 10, 13, 16, 19, 22]. We consider the reason for this to be as follows: (1) differences in the sensitivity of the detection method. (2) Differences in the ethnic origin of population analyzed. Previously, Iwasawa et al. [13] suggested HPV-DNA was detected in 63% of Japanese PC, Suzuki et al. [27] suggested in 54%. However, our present study demonstrates a low rate, and this rate might be different even between Japanese. (3) Tumor subtype. Rubin et al. [22] divided carcinomas into four subtypes, for example, keratinizing squamous cell carcinoma (SCC), verrucous carcinoma, basaloid carcinoma, and warty carcinoma, and suggest SCC and verrucous carcinoma were positive for HPV-DNA in only 34.9% and 33.3% of examined cases, respectively, HPV-DNA was detected in 80% of basaloid and 100% of warty tumor subtypes. Our cases were all usual types of squamous cell carcinoma, and no special types were observed. For this reason, the frequency of the HPV status may thus have demonstrated a low rate in our study.

In conclusion, the methylation of the *FHIT* gene was frequently found in PC, these findings suggest that the *FHIT* gene therefore plays an important role in the pathogenesis of penile squamous cell carcinoma.

Acknowledgements We are grateful to Dr. S. Sasou (Yamagata Prefectural Central Hospital), Dr. S. Arai (Yamagata Prefectural Nihonkai Hospital), Dr. K. Nemoto (Niigata Cancer Center Hospital), and Drs. M. Fukase and S. Uchigasaki (Tsuruoka municipal hospital) for kindly providing the samples.

Conflict of interest statement We declare that we have no conflict of interest.

References

1. Alves G, Heller A, Fiedler W, Campos MM, Claussen U, Omellas AA, Liehr T (2001) Genetic imbalances in 26 cases of penile squamous cell carcinoma. Genes Chromosomes Cancer 31:48–53
2. Butler D, Collins C, Mabruk M, Leader MB, Kay EW (2002) Loss of Fhit expression as a potential marker of malignant progression in preinvasive squamous cervical cancer. Gynecol Oncol 86:144–149
3. Castrén K, Vähäkangas K, Heikkinen E, Ranki A (1998) Absence of p53 mutations in benign and pre-malignant male genital lesions with over-expressed p53 protein. Int J Cancer 77:674–678
4. Chan KW, Lam KY, Chan AC, Lau P, Srivastava G (1994) Prevalence of human papillomavirus types 16 and 18 in penile carcinoma: a study of 41 cases using PCR. J Clin Pathol 47:823–826
5. Cubilla AL, Dillner J, Schelhammer PF, Horenblas S, Ayala AG, Reuter VE, Von Krogh G (2004) Tumors of the penis. Malignant epithelial tumors. In: Eble JN et al (ed) World Health Organization Classification of Tumors. Pathology & Genetics. Tumors of the Urinary System and Male Genital Organs. IARC, Lyon, pp 281–290
6. Cupp MR, Mlek RS, Goellner JR, Smith TF, Espy MJ (1995) The detection of human papillomavirus deoxyribonucleic acid in intraepithelial, in situ, verrucous and invasive carcinoma of the penis. J Urol 154:1024–1029
7. Ferreux E, Lont AP, Horenblas S, Gallee MP, Raaphorst FM, von Knebel Doeberitz M, Meijer CJ, Snijders PJ (2003) Evidence for at least three alternative mechanisms targeting the p16INK4A/cyclin D/Rb pathway in penile carcinoma, one of which is mediated by high-risk human papillomavirus. J Pathol 201:109–118
8. Goldberg M, Rummelt C, Laerm A, Helmbold P, Holbach LM, Ballhausen WG (2006) Epigenetic silencing contributes to frequent loss of the fragile histidine triad tumour suppressor in basal cell carcinomas. Br J Dermatol 155:1154–1158
9. Goelz SE, Hamilton SR, Vogelstein B (1985) Purification of DNA from formaldehyde fixed and paraffin embedded human tissue. Biochem Biophys Res Commun 130:118–126
10. Gregoire L, Cubilla AL, Reuter VE, Haas GP, Lancaster WD (1995) Preferential association of human papillomavirus with high-grade histologic variants of penile-invasive squamous cell carcinoma. J Natl Cancer Inst 87:1705–1709
11. Herman JG, Graff JR, Myohane S, Nelkin BD, Baylin SB (1996) Methylation-specific PCR:a novel PCR assay for methylation status of CpG islands. Proc Natl Acad Sci USA 93:9821–9826
12. Hu B, Han SY, Wang X, Ottey M, Potocrek MB, Dicker A, Huebner K, Wang Y (2005) Involvement of the Fhit gene in the ionizing radiation-activated ATR/CHK1 pathway. J Cell Physiol 202:518–523
13. Iwasawa A, Kumamoto Y, Fijinaga K (1993) Detection of human papillomavirus deoxyribonucleic acid in penile carcinoma by polymerase chain reaction and in situ hybridization. J Urol 149:59–63
14. Ji L, Fang B, Yen N, Fong K, Minna JD, Roth JA (1999) Induction of apoptosis and inhibition of tumorigenicity and tumor growth by adenovirus vector-mediated fragile histidine triad (FHIT) gene overexpression. Cancer Res 59:3333–3339
15. Levi JE, Rahal P, Sarkis AS, Villa L (1998) Human papillomavirus DNA and p53 status in penile carcinomas. Int J Cancer 76:779–783
16. Maden C, Sherman KJ, Beckmann AM, Hislop TG, The CZ, Ashley RL, Daling JR (1993) History of circumcision, medical conditions, and sexual activity and risk of penile cancer. J Natl Cancer Inst 85:19–24
17. Merlo A, Herman JG, Mao L, Lee DJ, Gabrielson E, Burger PC, Baylin SB, Sidransky D (1995) 5'¢ CpG island methylation is associated with transcriptional silencing of the tumour suppressor p16/CDKN2/MTS1 in human cancers. Nat Med 1:686–692
18. Pekarsky Y, Zanesi N, Palamarchuk A, Huebner K, Croce CM (2002) FHIT: from gene discovery to cancer treatment and prevention. Lancet Oncol 3:748–754
19. Picconi MA, Eijan AM, Distefano AL, Pueyo S, Alonio LV, Gorostidi S, Teyssie AR, Casebe A (2000) Human papillomavirus (HPV) DNA in penile carcinomas in Argentina: analysis of primary tumors and lymph nodes. J Med Virol 61:65–69
20. Poetsch M, Schuart BJ, Schwesinger G, Kleist B, Protzel C (2007) Screening of microsatellite markers in penile cancer reveals

differences between metastatic and nonmetastatic carcinomas. Mod Pathol 20:1069–1077
21. Roz L, Gramegna M, Ishii H, Croce CM, Sozzi G (2002) Restoration of fragile histidine triad (FHIT) expression induces apoptosis and suppresses tumorigenicity in lung and cervical cancer cell lines. Proc Natl Acad Sci U S A 99:3615–3620
22. Rubin MA, Kleter B, Zhou M, Ayala G, Cubilla AL, Quint WG, Pirog EC (2001) Detection and typing of human papillomavirus DNA in penile carcinoma: evidence for multiple independent pathways of penile carcinogenesis. Am J Pathol 159:1211–1218
23. Sard L, Accornero P, Tornielli S, Delia D, Bunone G, Campiglio M, Colombo MP, Gramegna M, Croce CM, Pierotti MA, Sozzi G (1999) The tumor-suppressor gene FHIT is involved in the regulation of apoptosis and in cell cycle control. Proc Natl Acad Sci U S A 96:8489–8492
24. Sevignani C, Calin GA, Cesari R, Sarti M, Ishii H, Yendamuri S, Vecchione A, Trapasso F, Croce CM (2003) Restoration of fragile histidine triad (FHIT) expression induces apoptosis and suppresses tumorigenicity in breast cancer cell lines. Cancer Res 63: 1183–1187
25. Soufir N, Queille S, Liboutet M, Thibaudeau O, Bachelier F, Delestaing G, Balloy BC, Breuer J, Janin A, Dubertret L, Vilmer C, Basset-Seguin N (2007) Inactivation of the CDKN2A and the p53 tumour suppressor genes in external genital carcinomas and their precursors. Br J Dermatol 156:448–453
26. Sozzi G, Pastorino U, Moiraghi L, Tagliabue E, Pezzella F, Ghirelli C, Tornielli S, Sard L, Huebner K, Pierotti MA, Croce CM, Pilotti S (1998) Loss of FHIT function in lung cancer and preinvasive bronchial lesions. Cancer Res 58:5032–5037
27. Suzuki H, Sato N, Kodama T, Okano T, Isaka S, Shirasawa H, Simizu B, Shimazaki J (1994) Detection of human papillomavirus DNA and state of p53 gene in Japanese penile cancer. Jpn J Clin Oncol 24:1–6
28. Yanagawa N, Tamura G, Oizumi H, Takahashi N, Shimazaki Y, Motoyama T (2003) Promoter hypermethylation of tumor suppressor and tumor-related genes in non-small cell lung cancers. Cancer Sci 94:589–592
29. Yoshikawa H, Kawana T, Kitagawa K, Mizuno M, Yoshikura H, Iwamoto A (1991) Detection and typing of multiple genital human papillomaviruses by DNA amplification with consensus primers. Jpn J Cancer Res 82:524–531
30. Young RH, Srigley JR, Amin MB, Ulbright TM, Cubilla AL (2000) Tumors of the prostate gland, seminal vesicle, male urethra, and penis. Atlas of Tumor Pathology, 3rd series, Fasc. 28. Armed Forces Institute of Pathology, Washington DC, pp 417–435
31. Zochbauer-Muller S, Fong KM, Maitra A, Lam S, Geradts J, Ashfag R, Virmani AK, Milchgrub S, Gazdar AF, Minna JD (2001) 5′ CpG island methylation of the *FHIT* gene is correlated with loss of gene expression in lung and breast cancer. Cancer Res 61:3581–3585
32. Zochbauer-Muller S, Fong KM, Virmani AK, Geradts J, Gazdar AF, Minna JD (2001) Aberrant promoter methylation of multiple genes in non-small cell lung cancers. Cancer Res 61:249–255

Virchows Arch (2008) 452:383–392
DOI 10.1007/s00428-007-0508-2

ORIGINAL ARTICLE

Augmented β cell loss and mitochondrial abnormalities in sucrose-fed GK rats

Hiroki Mizukami · Ryuichi Wada · Motoi Koyama · Teruko Takeo · Sechiko Suga · Makoto Wakui · Soroku Yagihashi

Received: 8 June 2007 / Revised: 22 August 2007 / Accepted: 2 September 2007 / Published online: 31 January 2008
© Springer-Verlag 2007

Abstract Progressive decline of islet β cell mass is a hallmark of type 2 diabetes, where nutritional insults are invoked in the pathologic process. Its detailed mechanisms are, however, incompletely understood. We explored the effect of sucrose diet on mitochondria in Goto Kakizaki (GK) rats, a spontaneously diabetic model. Six-week-old male GK rats were given 30% sucrose orally for 2 weeks. Normal Wistar rats fed with sucrose served as controls. Compared to untreated GK rats, sucrose-fed GK rats showed severe degeneration and death of β cells with disrupted and swollen mitochondria and a greater β cell loss. Submicroscopic analysis disclosed a smaller mean volume and a greater number of mitochondria in β cells in GK rats compared to those in Wistar rats. Mitochondria in sucrose-fed GK rats were 2.4-fold greater in mean volume than those in untreated state. Without sucrose feeding, there was no significant difference in mitochondrial membrane potentials (MmPs) of isolated islets between Wistar and GK rats. MmPs were reduced by 44% in sucrose-fed GK rats but not influenced in sucrose-fed Wistar rats. Current results suggest that nutritional insults like sucrose feeding may exert deleterious effects on mitochondria, resulting in augmented β cell loss in type 2 diabetes.

H. Mizukami · R. Wada · M. Koyama · S. Yagihashi (✉)
Department of Pathology and Molecular Medicine,
Hirosaki University Graduate School of Medicine,
5 Zaifu-cho,
Hirosaki 036-8562, Japan
e-mail: yagihasi@cc.hirosaki-u.ac.jp

T. Takeo · S. Suga · M. Wakui
Department of Physiology,
Hirosaki University Graduate School of Medicine,
Hirosaki, Japan

Keywords Type 2 diabetes · Mitochondria · Oxidative stress · β cell death

Introduction

Recent studies indicated that long-standing hyperglycemic milieu with insulin resistance attributes to progressive decline of β cell mass, implicating a role of glucotoxicity and/or lipotoxicity in the pathogenesis of islet lesions in type 2 diabetes [5, 19, 29]. Increased flux of glucose to β cells exerts enhanced production of oxidative stress, glycation of structural proteins, or activation of cellular signaling that leads to cell death [30, 31]. In recent studies, mitochondria-derived oxidative stress through superoxide production or nitric oxide release is proposed to underlie the glucotoxicity that accounts not only for impaired insulin secretion but also for induction of premature β cell death [17, 36]. Vulnerability of islet β cells to nutritional insults is a salient feature in type 2 diabetic animal models in which impaired mitochondrial function related to excessive oxidative stress is proposed to contribute to islet pathology [8, 11, 16]. Importance of mitochondria in islet pathology has also been supported by the fact that cases with mutated mitochondrial DNA develop impaired β cell function and β cell loss, resulting in insulin-deficient diabetes [14, 25].

The Goto Kakizaki (GK) rat, a spontaneous nonobese type 2 diabetic animal model, is widely used for studies on the pathogenesis of type 2 diabetes and its complications [9, 10, 12, 22, 23, 27]. In our previous studies, we found severe loss of islet β cells in sucrose-fed GK rats compared to untreated GK rats, whereas islets in normal Wistar rats were not affected by the same diet [16]. It is still unknown, however, how mitochondria are involved in such augment-

ed β cell injury in sucrose-fed GK rats and whether the changes of mitochondria if any are specific to this model. Due to the fact that mitochondria play a central role in the process of cellular death related to oxidative stress [3, 13, 20], information on mitochondrial changes in type 2 diabetic animal models may be extremely valuable. In the present study, we therefore investigated functional and structural changes of mitochondria in GK rats maintained on a sucrose diet.

Materials and methods

Animals

GK and normal control Wistar rats were obtained from the colony bred in Takeda Research Institute (Takeda Chemical Industries, Osaka, Japan). The animals had a free access to tap water and were given standard laboratory diet (Oriental Yeast, Tokyo, Japan). At 6 weeks of age, both GK and Wistar rats were divided into two balanced groups, one fed with 30% sucrose in drinking water (*v*/*v*) and the other without sucrose for 2 weeks.

During the experimental period, body weight was measured at weekly intervals, and all animals received oral glucose tolerance tests (2 g/kg body weight). Blood samples were obtained from tail vessels, and blood glucose values were determined by glucose oxidase method (Toecho Super 2, Kagawa, Japan). Plasma concentrations of immunoreactive insulin were estimated in animals after overnight fasting using an insulin kit (Morinaga, Yokohama, Japan). Under intravenous anesthesia with 50 mg/kg pentobarbital (Abbott Laboratories, Chicago, IL, USA), the animals were killed by exsanguination. Then pancreas tissues were excised for structural investigations. All experiments followed the guideline for animal experimentation, Hirosaki University (approval number M00075).

Sampling for structural investigations and mitochondrial membrane potentials

Pancreatic tissues were fixed in 10% buffered formalin and embedded in paraffin. Serial 4-μm-thick paraffin sections were stained with hematoxylin–eosin (HE) for islet pathology and double immunostained for insulin and glucagon to identify β and α cells, as described previously [16]. Quantitative evaluation of islet β cells and α cells was conducted adopting a computer-assisted point-counting methods on an Olympus AX80 microscope (Olympus, Tokyo, Japan) connected to a personal computer using NIH image (version 1.56, Wayne Rasband, National Institutes of Health) [16]. In each animal, 25 to 80 fields (average, 45) were subjected to quantitation of endocrine cells. The ratio of areas of α cells and β cells to the parenchymal pancreatic area was presented as the volume density of α cells and β cells, respectively.

For electron microscopy, a small portion of the pancreatic tail tissue in each rat from all groups was fixed in ice-cold 2.5% glutaraldehyde in 0.05 mol/l cacodylate buffer (pH 7.4) overnight at 4°C and postfixed with 1% osmium tetroxide for 1 h at room temperature. After dehydration through an ascending series of ethanol, the samples were embedded in epon.

For the analysis of mitochondrial membrane potentials (MmPs), pancreatic islets were isolated from groups of animals with the modified method of Lacy and Kostianovsky [18]. Rhodamine fluorescence was measured for MmPs [6, 7].

Ultrastructure of β cells and morphometry of mitochondria

Ultrathin sections from epon-embedded blocks were stained with uranyl acetate and lead citrate. They were examined by a JEOL TEM-2000EX electron microscope (Nihon Densi, Tokyo, Japan). Ultrastructure of two to three islets was examined in each animal, and features of nuclei and cytoplasmic organelles were observed. Identification of β cells and α cells was possible by their specific cytoplasmic secretory granules. Because β cells in GK rats and sucrose-fed GK rats showed degenerative changes characterized by nuclear pyknosis, cytoplasmic vacuoles, as well as dark smudgy appearance of whole cells, frequencies of these cells were counted among 80 to 120 islet β cells in each animal at a magnification of ×5,000. Cells with nuclear pyknotic changes and cytoplasmic vacuolar changes were designated as degenerated cells, whereas cells with smudgy nuclei and dark vacuolar cytoplasm showing distorted contour and electron-dense appearance were designated as dead cells (see Fig. 4). Mean value of the frequencies of dead cells was then calculated in each group and compared among groups.

For morphometric analysis on mitochondria in β cells, 30 to 40 electron micrographs at a magnification of ×15,000 of β cells randomly chosen from two to three islets were prepared in each rat. β cells were identified by the characteristic features of secretory granules. About 240 micrographs in total were used for analysis in each group. Morphometry of mitochondria was based on the method previously described by Serradas et al. [33]. The volume of mitochondria per unit tissue volume (*V*v), the surface area of mitochondria per unit tissue volume (*S*v), and the number of mitochondria per unit tissue volume (*N*v) were determined by a computer-assisted image analyzing system using the NIH image. The average mitochondrial volume (*V*v/*N*v) and the average mitochondrial surface area (*S*v/*N*v) were then calculated.

Evaluation of mitochondrial membrane potentials

Isolated islets obtained from each experimental group were dispersed and incubated overnight in 60-mm dishes in RPMI 1640 with 10% fetal bovine serum and 0.1 mg/ml penicillin and streptomycin (Gibco, Grand Island, NY, USA). The fluorescent probe rhodamine 123 (Rh123; Sigma, St. Louis, MO, USA) was used to assess MmPs ($\Delta\Psi$) of islets by stimulating with glucose perifusion [6, 7]. Before starting recordings, islets were perifused with 5.6-mM glucose solution and set for 30 min in the dark. To detect MmPs ($\Delta\Psi$), an isolated islet was preincubated with 10 μg/ml Rh123 for 10 min at 37° C (final concentration of 2 mM=400 μl in one dish). The rhodamine fluorescein was excited at 490 nm and measured at 530 nm. In each islet, fluorographic alterations were recorded for 24 min under the continuous perifusion with 5.6-mM glucose for 4 min, 22.2-mM glucose for 14 min, 5.6-mM glucose for 4 min, and completed with 1 mM NaCN (respiratory chain blocker) for 2 min.

Fluorescence intensity in each islet was calculated automatically with a digital imaging processor by a computer-assisted image analyzing system (NT 5783, Hamamatsu photonics, Hamamatsu, Japan). With this method, intensity of rhodamine fluorescence at 5.6-mM glucose stimulation was set to 100%, and percent changes of fluorescence in response to hyperpolarization by stimulation with 22.2-mM glucose were calculated as MmPs ($\Delta\Psi$).

Statistical analysis

All morphometric analyses were performed in a double-masked manner. Comparisons were made using a one-way analysis of variance, followed by post hoc Bonferroni's corrections. Values of p less than 0.05 were considered statistically significant.

Results

Body weight, blood glucose, and insulin concentrations

Mean body weight in GK rats was significantly smaller at 6 and 8 weeks of age compared to those in age-related control Wistar rats (Table 1). Sucrose diet reduced body weight by 8% in Wistar rats but did not affect GK rats. Fasting glucose levels in GK rats were elevated 1.5- to 2.2-fold in GK rats during the experiment but were not affected by sucrose feeding. Blood glucose concentrations on oral glucose tolerance test in sucrose-fed GK rats were, however, elevated, representing 128% of 60-min values of untreated GK rats (Fig. 1). In contrast, control Wistar rats well tolerated the glucose challenge showing normal values at both 60 and 120 min.

Plasma insulin concentrations at fast were elevated 1.8- to 2.5-fold in GK rats compared to those in Wistar rats. These levels were further elevated by sucrose diet in both Wistar rats and GK rats, suggesting the augmentation of insulin resistance.

Immunohistochemistry on β cells and α cells

At 8 weeks of age, the islet of GK rats already showed fibrosis, and the islet contour was disorganized (Fig. 2). After sucrose feeding, islets in normal Wistar rats were slightly hypertrophic, but there was no apparent degenerative change. In contrast, islets in sucrose-fed GK rats were severely fibrotic, and endocrine cells appeared atrophic and disorganized. Morphometric analysis demonstrated a significant reduction in β cells in untreated GK rats compared to normal Wistar rats (Fig. 3). Sucrose-fed GK rats showed further reduction in β cells, and the difference between sucrose-fed GK and untreated GK rats was significant ($p<0.01$). There was no significant alteration in the population of α cells in untreated GK and sucrose-fed GK rats,

Table 1 Body weight, blood glucose, and insulin concentrations of experimental animals

Group	Body weight (g)		Fasting blood glucose (mmol/l)		Fasting plasma insulin (ng/ml)	
	6 week	8 week	6 week	8 week	6 week	8 week
W	180±8 (10)	288±7 (9)	3.12±0.28 (10)	3.86±0.51 (9)	0.33±0.13 (7)	0.45±0.36 (7)
W+S		259±6 (8)		3.50±0.48 (8)		1.02±0.26 (7)**
GK	152±4 (10)*	242±9 (9)*	4.75±0.62 (10)*	5.87±0.86 (9)*	0.94±0.25 (7)*	0.85±0.35 (7)**
GK+S		237±8 (8)*, ***		6.06±0.59 (8)*		1.71±0.41 (6)*, ***, ****

Values are expressed as mean±SEM. The number of animals is shown in parentheses.
W Untreated Wistar rats, *W+S* sucrose-fed Wistar rats, *GK* untreated GK rats, *GK+S* sucrose-fed GK rats
*$p<0.01$ vs W
**$p<0.05$ vs W
***$p<0.01$ vs W+S
****$p<0.01$ vs GK

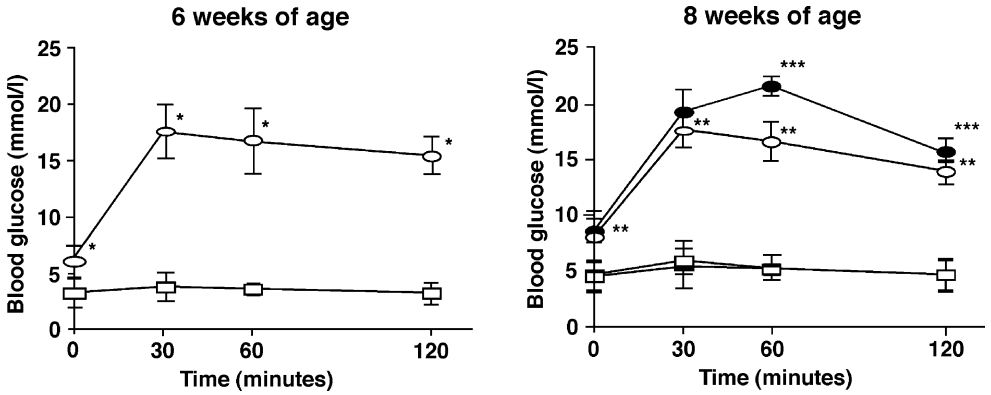


Fig. 1 Serial changes of blood glucose values on 2 g/kg oral glucose tolerance test. At the beginning of the experiment (*left panel*), blood glucose concentrations were all elevated in GK rats before and after glucose challenge. The increase in blood glucose values was further augmented at 60 and 120 min after glucose challenge in sucrose-fed GK rats at 8 weeks of age, indicating worsening of glucose intolerance (*right panel*). *Open circle* represents for GK, *open square* for Wistar, *filled circle* for sucrose-fed GK, and *filled square* for sucrose-fed Wistar rats. *$p<0.01$ vs untreated Wistar rats; **$p<0.01$ vs untreated and sucrose-fed Wistar rats, ***$p<0.05$ vs untreated GK rats and sucrose-fed Wistar and untreated Wistar rats. *Bar* stands for mean± SEM

indicating that the effects of sucrose were specific to β cells.

Ultrastructure of β cells and mitochondria morphometry

Normal Wistar rats showed normal architecture of islet endocrine cells (Fig. 4a). There were no apparent changes in sucrose-fed Wistar rats. Islets in GK rats contained some β cells (about 10%) with dilated endoplasmic reticula and vacuoles but were replete with specific secretory granules (Fig. 4b). Their nuclei showed clumping of chromatin and pyknosis. These cells were considered to be degenerated (Fig. 4b and c). They occasionally showed a dark, smudgy appearance with dense organellar degeneration and myelin figures (Fig. 4d). Such affected cells were distorted and exhibited features consistent with dead necrotic cells, often phagocytized by infiltrated macrophage (Fig. 4e and f). In contrast to degenerated or dead β cells, adjacent non-β cells like α cells as well as δ cells were intact (Fig. 4g and h).

Frequencies of dead β cells with smudgy appearance in Wistar, sucrose-fed Wistar, GK, and sucrose-fed GK rats were 0 ($n=4$), 0.17±0.16% ($n=4$), 0.83±0.31% ($n=4$), and 2.75±0.48% ($n=4$), respectively. The average value in sucrose-fed GK rats was greater than that in untreated GK

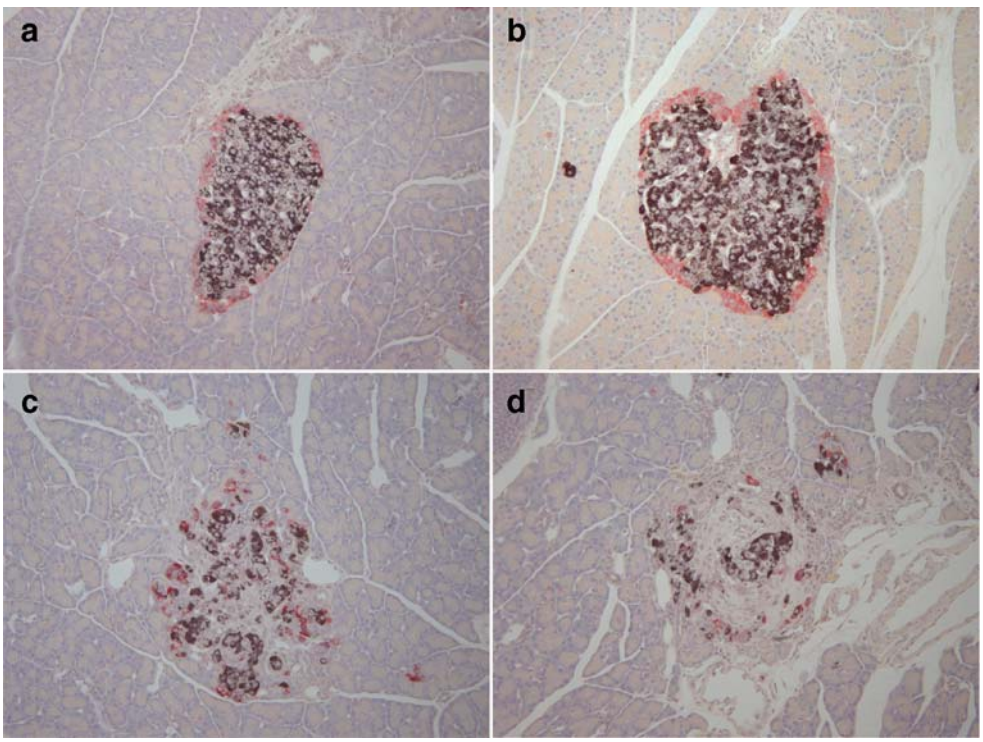


Fig. 2 Immunohistochemistry of pancreatic islets double-stained for insulin (*black*) and glucagon (*red*) in normal Wistar (**a**), sucrose-fed Wistar (**b**), GK (**c**), and sucrose-fed GK rat (**d**). There appeared to be slight hyperplasia of the islet in sucrose-fed Wistar rat compared to untreated Wistar rat. The islet in GK rat is markedly disorganized with depletion of insulin-positive cells. The islet contour is further deteriorated with severe fibrosis in sucrose-fed GK rat. There appeared to be further depletion of insulin-positive cells

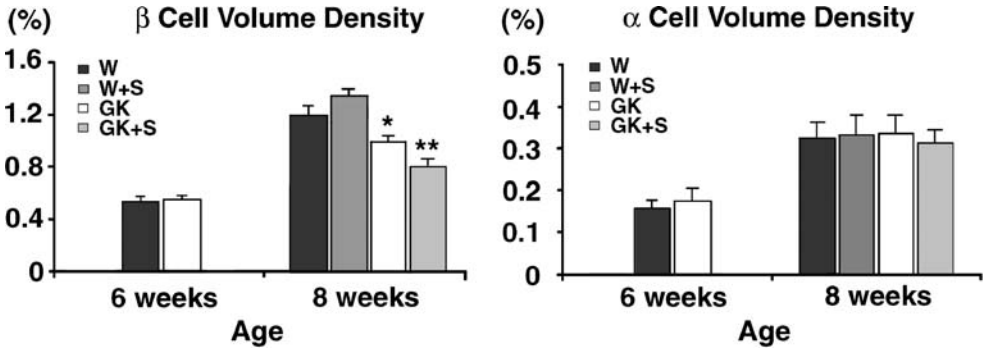


Fig. 3 Morphometric data of islet α and β cells in experimental animals. At 6 weeks of age, there was no significant difference in the volume density of β and α cells between normal Wistar (*W*) and GK rats (*GK*). At 8 weeks of age, there was a significant reduction in β cell volume density in GK rats compared to normal Wistar rats (*left panel*). Sucrose-fed GK rats (*GK+S*) showed further reduction in average β cell volume density compared to that in untreated GK rats. No significant difference was found in α cell volume density among groups (*right panel*). *Bar* stands for mean±SEM. *$p<0.05$ vs W, **$p<0.01$ vs W, sucrose-fed Wistar rats (*W+S*), and untreated GK rats

or in sucrose-fed Wistar rats ($p<0.001$ for all other groups). Similarly, degenerated β cells with cytoplasmic vacuolation were frequent in sucrose-fed GK rats (23.7±2.5%) but less in untreated GK rat (9.7±1.7%). They were rare in sucrose-fed Wistar (0.3±0.2%) and untreated Wistar rats (nil).

β cells in control Wistar rats contained well-developed cytoplasmic organelles and mitochondria (Fig. 5a). In sucrose-fed Wistar rats, only a few β cells appeared to show slightly swollen mitochondria (<10% of mitochondria), but they appeared almost normal (Fig. 5b). Mitochondria in GK rats appeared smaller compared with those in normal Wistar rats (Fig. 5c), but their cristae were well preserved. Sucrose-fed GK rats showed markedly swollen mitochondria with disruption of cristae (>90% of mitochondria; Fig. 5d).

The mean volume (*V*v) of mitochondria per unit tissue volume in β cells was 47.8% smaller in 8-week-old GK rats than that in age-matched control Wistar rats ($p<0.01$; Fig. 5e). By contrast, GK rats contained a significantly greater number (*N*v) of mitochondria per unit tissue volume than control Wistar rats ($p<0.01$). In sucrose-fed GK rats, mean *V*v was 25% greater than that in untreated GK rats ($p<0.01$). In addition, mean *N*v in sucrose-treated GK rats was significantly reduced compared with untreated GK rats. Average mitochondrial volume (*V*v/*N*v) in untreated GK rats was significantly smaller than that in control Wistar rats ($p<0.01$), whereas *V*v/*N*v was significantly increased (2.4-fold increase) in sucrose-fed GK rats compared with that in untreated GK rats ($p<0.01$). Conversely, *V*v/*N*v was significantly smaller in sucrose-fed Wistar rats compared with that in untreated control Wistar rats ($p<0.05$).

Mitochondrial membrane potentials

When the islets in normal Wistar rats were stimulated with 22.2-mM glucose after 5.6-mM glucose perifusion, there was significant hyperpolarization of the mitochondrial membrane as reflected by an 18–20% change in MmPs ($\Delta\Psi$; Fig. 6a). The islets from sucrose-fed Wistar rats showed similar reactions. The levels of MmPs in untreated GK rats were slightly greater than those in Wistar rats, indicating hypersecretion of insulin at basal levels. By contrast, sucrose-fed GK rats expressed a significant attenuation of MmPs to 56% the level of untreated GK rats ($p<0.02$). The addition of NaCN confirmed the membrane integrity in all the experiments. All of the mean values of MmPs are shown in Fig. 6b.

Discussion

The present study demonstrated both structural and functional mitochondrial abnormalities in islet β cells of GK rats. On a sucrose diet, disruption of mitochondria was only found in GK rats. Islet MmP levels in response to glucose stimuli were markedly reduced in sucrose-fed GK rats, while MmPs in normal Wistar rats were not influenced by sucrose feeding. Ultrastructure showed features of β cell death in sucrose-fed GK rats but not in sucrose-fed Wistar rats. The effects of sucrose feeding on β cells were therefore specific to GK rats. It was thus indicated that genetic background may underlie the vulnerability of β cells to sucrose. Our current results also suggest that the augmented β cell loss in sucrose-fed GK rats may possibly be related to functional and structural impairments of mitochondria in this model. Decrease in β cell mass in GK rats was apparent at 8 weeks of age in our study. Other groups also found a similar time course of β cell reduction in this model [12, 23], while much earlier reduction in β cell volume has also been reported in French group [27, 33]. Environmental factors to augment an early expression of diabetes-related genes may be involved in the early depletion of β cells in this model [33].

While the vulnerability of β cells to sucrose is known to be dependent on animal species [28], the mechanism is still

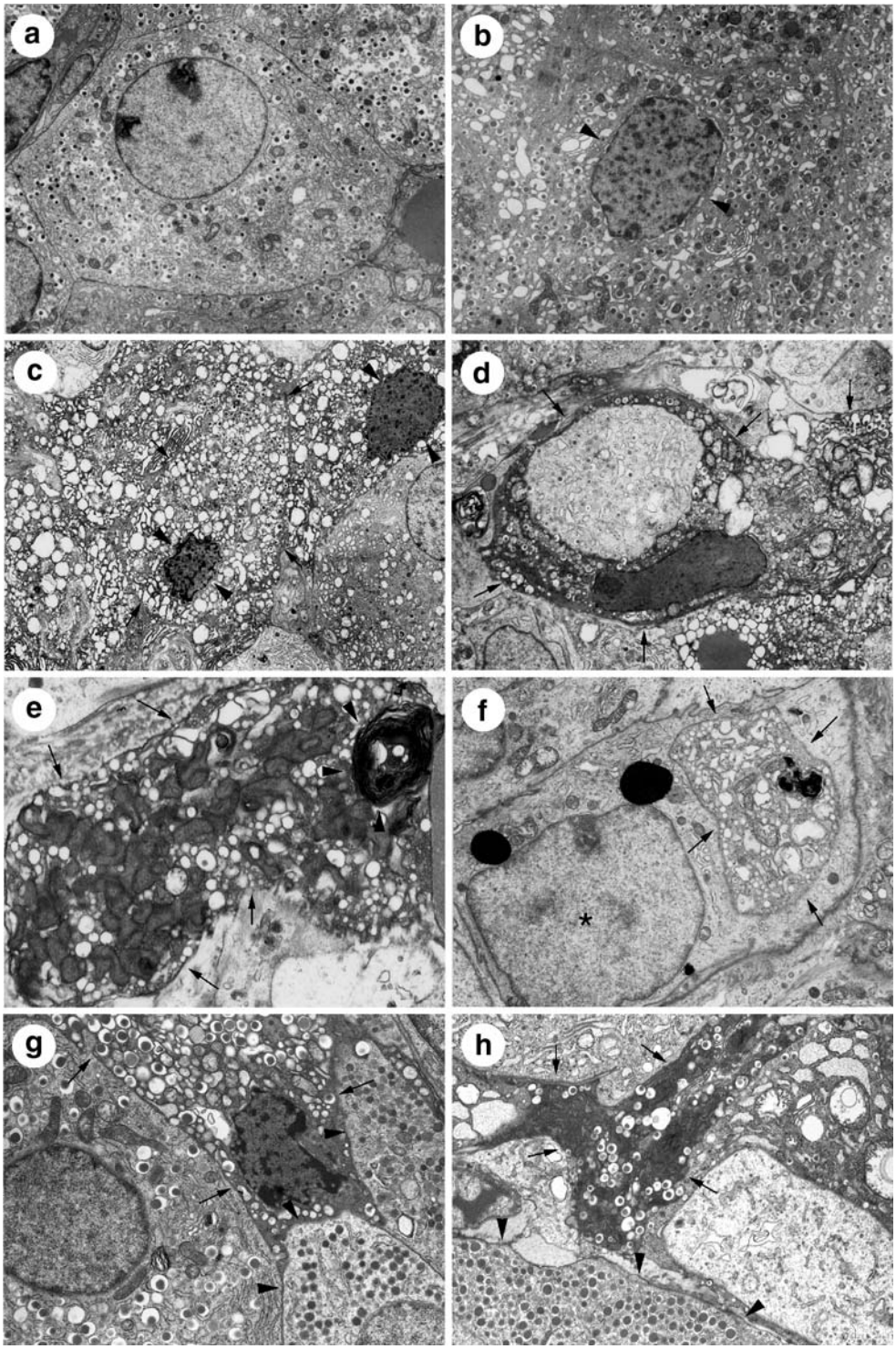


Fig. 4 Ultrastructure of islets in Wistar rats and GK rats at 8 weeks of age. **a** Islets of Wistar rat showed normal structure (×5,200). **b** Mild degenerative changes of β cells in GK rat showing irregular contour of nucleus with clumping of chromatin (*arrowhead*; ×5,200). **c** Severely degenerated β cells (*arrows*) in sucrose-fed GK rats showing nuclear pyknosis (*arrowhead*) and vacuolar changes of organelles (×4,200). **d** Dead β cell (*arrows*) in sucrose-fed GK rat showing encircled dark cytoplasmic elongation with smudgy appearance of nucleus and degenerated organelles (×4,500). **e** Dead β cell (*arrows*) in sucrose-fed GK rat showing dark cytoplasm with myelin figures (*arrowhead*; ×10,200). **f** Entrapment of dead β cell (*arrows*) by macrophage (*asterisk*) in sucrose-fed GK rat (×11,000). **g** Intact non-β cells (*arrowhead*) adjacent to severely degenerated β cell (*arrows*) in sucrose-fed GK rat (×3,900). **h** Intact non-β cell (*arrowhead*) neighboring dead β cell (*arrows*) in sucrose-fed GK rat (×3,900)

controversial [26, 35]. Enhanced postprandial hyperglycemia, severe insulin resistance, and hyperlipidemia, all of which were depicted in sucrose-fed GK rats, could contribute to β cell toxicity [23, 24]. In our previous studies, we could demonstrate a greater percentage of β cells undergoing apoptosis (TUNEL positive cells) in sucrose-fed GK rats indicating that the loss may be accounted for by a greater rate of apoptosis rather than reduced rate of replication compared to untreated GK rats [16]. The current study is the first to demonstrate that mitochondrial alterations are intimately related to β cell death in sucrose-fed rats. The dead cells with dense irregular cytoplasmic contour were often phagocytosed. Adjacent α and δ cells appeared to be intact, and thus, the

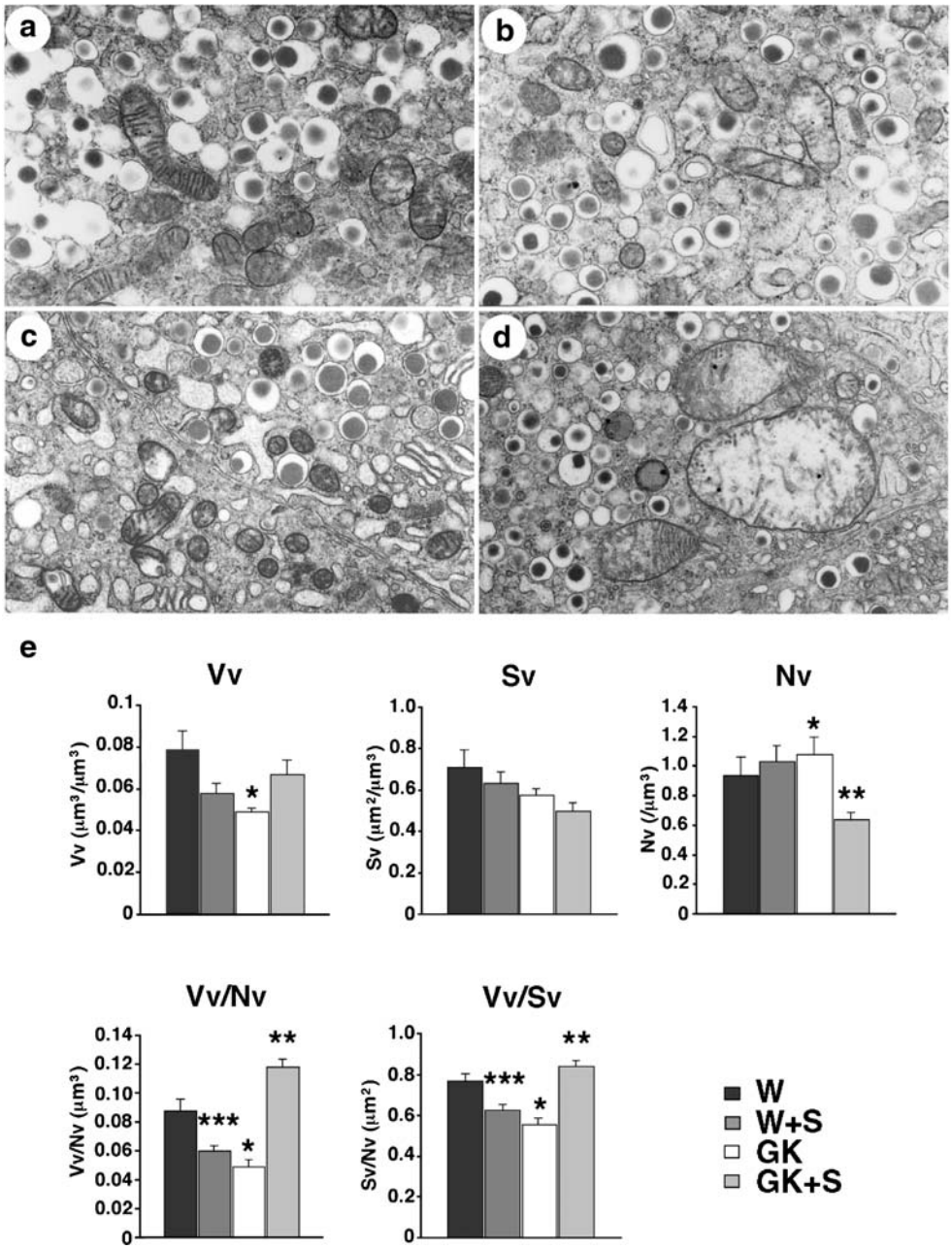


Fig. 5 Mitochondrial morphology in experimental animals at 8 weeks of age. Wistar rats showed normal morphology of mitochondria mixed with abundant insulin granules (**a**), and sucrose feeding slightly decreased the volume with wider granular areas (**b**). In contrast, mitochondria in GK rats appeared to be small and round (**c**), and they became markedly swollen after sucrose-diet (**d**) (figures are all ×12,000). Morphometric data confirmed the alterations of mitochondrial structure (**e**). *Bars* are expressed as means±SEM. *Vv* Average volume per unit tissue volume, *Sv* average surface area per unit tissue volume, *Nv* average number per unit tissue volume, *Vv/Nv* average volume per mitochondrium, *Vv/Sv* average volume per surface area, *W* Wistar rats, *W+S* sucrose-fed Wistar rats, *G* GK rats, *G+S* sucrose-fed GK rats. *$p<0.01$ vs Wistar rats, **$p<0.01$ vs untreated GK rats, ***$p<0.01$ vs Wistar rats

effect was specific to β cells. Our findings suggest that excessive flux of glucose by sucrose diet possibly induced mitochondrial disruption, releasing free radicals to promote premature β cell death, which in turn led to a reduced β cell volume density. The results are in keeping with our previous results that the correction of postprandial hyperglycemia by α-glucosidase inhibitor to suppress the hyperglycemic stress to mitochondria successfully prevented β cell loss in GK rats [15]. There also remains a possibility, however, that hyperosmotic damage due to excessive intake of sucrose in conjunction with diabetic polydipsia might have caused membrane disruption of mitochondria in sucrose-fed GK rats. This issue should be explored by further investigations.

Mitochondria in β cells alter their structure when exposed to oxidative stress or under exposure to high-fat diet [8]. We found a decrease in mean mitochondrial volume (*V*v/*N*v) and an increase in number (*N*v) of mitochondria per single β cell in 8-week-old GK rats compared to control Wistar rats. Serradas et al. [33] also found smaller mitochondria and increased number of mitochondria per unit cell area but decreased mitochondrial DNA in adult GK rats but not in fetal GK rats, compared to age-matched control rats. They interpreted that those changes were consequences of long-

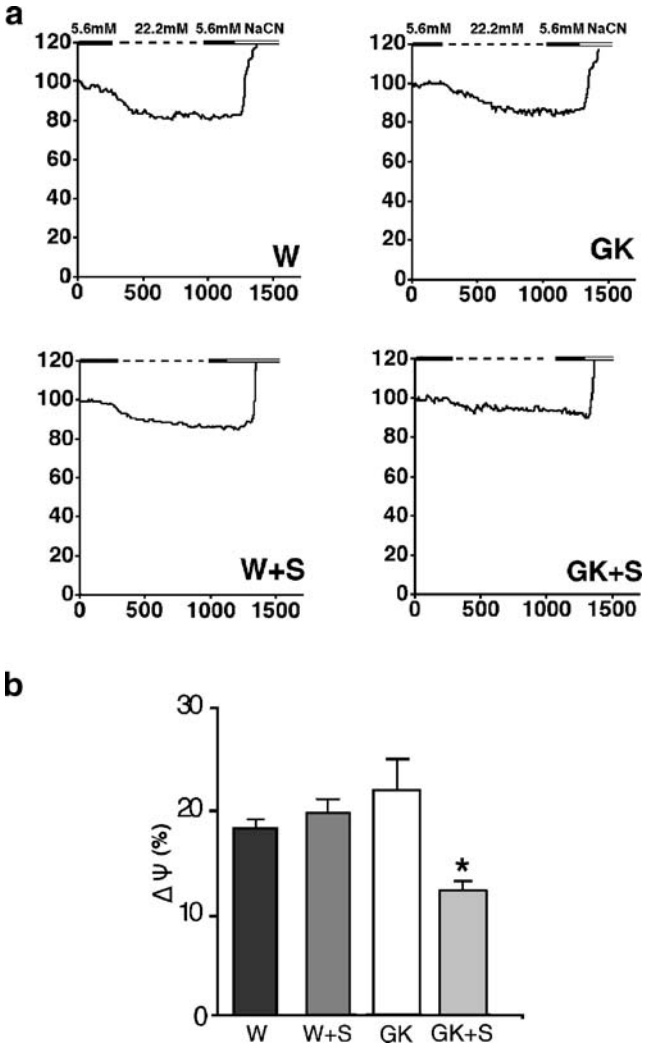


Fig. 6 Changes in MmPs ($\Delta\Psi$) of isolated islets from 8-week-old rats in response to glucose stimulation, recorded by rhodamine fluorescence (**a**). Representative traces from at least eight experiments in each group are shown. The average peak values of MmPs ($\Delta\Psi$) in each group is summarized (**b**). See the text for explanation of the figure. *Bar* stands for mean±SEM. *W* Wistar rats, *W+S* sucrose-fed Wistar rats, *GK* GK rats, *GK+S* sucrose-fed GK rats. *$p<0.01$ vs W, W+S, and GK

term metabolic impairment. The increased number of mitochondria may reflect compensatory adaptation to raise much energy in response to glucose stimuli to maintain glucose homeostasis, although it was still insufficient to maintain normal glucose values in GK rats [7, 21]. In the present study, while sucrose-fed Wistar rats showed a decreased volume of mitochondria, sucrose-fed GK rats showed reciprocal results: an increase in mitochondrial volume and decrease in number in sucrose-fed GK rats compared with those in untreated animals. Mitochondrial changes in sucrose-fed Wistar rats may be interpreted as their potency adapting to sucrose-induced metabolic changes by replicating mitochondria to supply the energy for the synthesis and secretion of insulin. In contrast, abnormally swollen mitochondria (2.4-fold increase in *V*v/*N*v) with disruption of cristae in sucrose-fed GK rats may reflect a limited capacity of mitochondria to overcome a sucrose load in β cells in this model.

In accord with structural changes, we detected mitochondrial dysfunction in islets of sucrose-fed GK rats. Attenuation of MmPs was much more conspicuous in sucrose-fed GK rats. Such an immediate deterioration of MmPs in the islets of GK rats after an exposure to high glucose suggests that mitochondria in GK rats are indeed susceptible to ambient hyperglycemia and may well account for a poor potency of mitochondria to respond to stimuli in sucrose-fed GK rats. Low MmPs are associated with opening of a permeability transition pore (PTP) in the mitochondrial membrane which enables a release of apoptosis-initiating factor and cytochrome C, leading to the activation of apoptotic processes [3, 13]. Concurrently, PTP opening impairs oxidative phosphorylation, increases free radical generation and causes swelling of mitochondria, which in turn activates uncoupling protein (UCP)-2, finally reducing ATP levels [3, 17, 20], and ultimately resulting in cell death [37]. Although mitochondria isolated from GK rats were reported to show a different susceptibility to oxidative stress depending on the organs [32], islets are vulnerable to oxidative stress due to paucity of antioxidant enzymes [34, 36]. As such, sucrose feeding in GK rats may have enhanced the oxidative-stress-induced cell injury in islets of GK rats. This contention may be in keeping with the recent report that 6 weeks of high-fat feeding caused upregulation of UCP-2 in islets of GK rats [2].

Mitochondrial ATP production is most crucial for glucose-induced insulin secretion. Oxidative phosphorylation of glucose exerts NADH transport to mitochondria in which NADH and pyruvate complicatedly shuttle with potentiatin of MmPs [7]. This process is followed by opening of ATP-sensitive K-channel leading to Ca-dependent insulin secretion. Impairment of this shuttle may attribute to the impaired insulin secretion in response to glucose in GK rat [23, 24, 27]. In contrast, despite the marked impairment of mitochondrial function, insulin concentrations in the fasting state were greater in GK rats compared to normal Wistar rats, suggesting the presence of insulin resistance in this model. This paradoxical phenomenon may be accounted for by the fact that ATP-independent insulin release, distinct from mitochondria-mediated secretion, is enhanced via cAMP- or adenyl-cyclase-related exocytosis in this model [1, 4].

In summary, the present study underscored the implication of mitochondria in augmented β cell loss in sucrose-fed GK rats. The finding suggests that dietary factors such as sucrose in addition to genetic factors contribute to rapid β cell depletion and that poor potency of mitochondria to accommodate to environmental insults may possibly lead to an earlier onset of diabetes in humans.

Acknowledgment This study was not possible without the kind supply of GK rats from Drs. Hitoshi Ikeda and Hiroyuki Odaka, Research Institute, Takeda Pharmaceuticals. The authors are indebted to Ms. Yuko Sasaki for her expert technical assistance. This study was supported by grants to Soroku Yagihashi from the Ministry of Education, Science, Sports and Culture, Japan.

References

1. Abdel-Halim SM, Guenifi A, He B, Yang B, Mustafa M, Hojeberg B, Hillert J, Bakhiet M, Efendic S (1998) Mutations in the promoter of adenylyl cyclase (AC)-III gene, overexpression of AC-III mRNA, and enhanced cAMP generation in islets from the spontaneously diabetic GK rat model of type 2 diabetes. Diabetes 47:498–504
2. Briaud I, Kelpe CL, Johnson LM, Tran PO, Poitout V (2002) Differential effects of hyperlipidemia on insulin secretion in islets of Langerhans from hyperglycemic versus normoglycemic rats. Diabetes 51:662–668
3. Daugas E, Susin SA, Zamzami N, Ferri KF, Irinopoulou T, Larochette N, Prevost MC, Leber B, Andrews D, Penninger J, Kroemer G (2000) Mitochondrial-nuclear translocation of AIF in apoptosis and necrosis. FASEB J 14:729–739
4. Dolz M, Bailbe D, Giroix MH, Calderari S, Gangnerau MN, Serradas P, Rickenbach K, Irminger JC, Portha B (2005) Restitution of defective glucose-stimulated insulin secretion in diabetic GK rat by acetylcholine uncovers paradoxical stimulatory effect of beta-cell muscarinic receptor activation on cAMP production. Diabetes 54:3229–3237
5. Donath MY, Ehses JA, Maedler K, Schumann DM, Ellingsgaard H, Eppler E, Reinecke M (2005) Mechanisms of β-cell death in type 2 diabetes. Diabetes 54(Suppl 2):S108–S113
6. Emaus RK, Grunwald R, Lemasters JJ (1986) Rhodamine 123 as a probe of transmembrane potential in isolated rat-liver mitochondria: spectral and metabolic properties. Biochim Biophys Acta 850:436–448
7. Eto K, Tsubamoto Y, Terauchi Y, Sugiyama T, Kishimoto T, Takahashi N, Yamauchi N, Kubota N, Murayama S, Aizawa T, Akanuma Y, Aizawa S, Kasai H, Yazaki Y, Kadowaki T (1999) Role of NADH shuttle system in glucose-induced activation of mitochondrial metabolism and insulin secretion. Science 283: 981–985
8. Fex M, Nitert MD, Wierup N, Sundler F, Ling C, Mulder H (2007) Enhanced mitochondrial metabolism may account for the adaptation to insulin resistance in islets from C57BL/6J mice fed a high fat diet. Diabetologia 50:74–83
9. Goto Y, Kakizaki M, Masaki N (1975) Spontaneous diabetes produced by selective breeding of normal Wistar rats. Proc Jpn Acad 51:80–85
10. Goto Y, Suzuki K, Ono T, Sasaki M, Toyota T (1988) Development of diabetes in the non-obese NIDDM rat (GK rat). Adv Exp Med Biol 246:29–31
11. Gross DJ, Leibowitz G, Cerasi E, Kaiser N (1996) Increased susceptibility of islets from diabetes-prone *Psammomys obesus* to the deleterious effects of chronic glucose exposure. Endocrinology 137:5610–5615
12. Guenifi A, Abdel-Halim SM, Hoog A, Falkmer S, Östenson CG (1995) Preserved β-cell density in the endocrine pancreas of young, spontaneously diabetic Goto-Kakizaki (GK) rats. Pancreas 10:148–153
13. Kim JS, He L, Lemasters JJ (2003) Mitochondria permeability transition: a common pathway to necrosis and apoptosis. Biochem Biophys Res Comm 304:463–470
14. Kobayashi T, Nakanishi K, Nakase H, Kajio H, Okubo M, Murase T, Kosaka K (1997) In situ characterization of islets in diabetes with a mitochondrial DNA mutation at nucleotide position 3243. Diabetes 46:1567–1571
15. Koyama M, Wada R, Mizukami H, Sakuraba H, Odaka H, Ikeda H, Yagihashi S (2000) Inhibition of progressive reduction of islet β-cell mass in spontaneously diabetic Goto-Kakizaki rats by α-glucosidase inhibitor. Metabolism 49:1–7
16. Koyama M, Wada R, Sakuraba H, Mizukami H, Yagihashi S (1998) Accelerated loss of islet β cells in sucrose-fed Goto-Kakizaki rats, a genetic model of non-insulin-dependent diabetes mellitus. Am J Pathol 153:537–545
17. Krauss S, Zhang CY, Scorrano L, Dalgaard LT, St-Pierre J, Grey ST, Lowell BB (2003) Superoxide-mediated activation of uncoupling protein 2 causes pancreatic beta cell dysfunction. J Clin Invest 112:1831–1842
18. Lacy PE, Kostianovsky M (1967) Method for the isolation of intact islets of Langerhans from the rat pancreas. Diabetes 16: 35–39
19. Lee Y, Hirose H, Ohneda M, Johnson JH, McGarry JD, Unger RH (1994) β-cell lipotoxicity in the pathogenesis of non-insulin-dependent diabetes mellitus of obese rats: impairment in adipocyte-β-cell relationships. Proc Natl Acad Sci U S A 91: 10878–10882
20. Leonard JV, Schapira AHV (2000) Mitochondrial respiratory chain disorders II: neurodegenerative disorders and nuclear gene defects. Lancet 355:389–394
21. Lowell BB, Schulman GI (2005) Mitochondrial dysfunction in type 2 diabetes. Science 307:384–387
22. Odaka H, Sugiyama Y, Ikeda H (1991) Effect of pioglitazone on sucrose-deteriorated diabetic states in spontaneously diabetic GK rats. J Jpn Diab Soc 34:523–530
23. Östenson C-G, Abdel-Halim SM, Andersson A, Guenifi A, Khan A, Larsson O, Berggren PO, Efendic S (1996) Studies on the pathogenesis of NIDDM in the GK (Goto-Kakizaki) rat. In: Shafrir E (ed) Lessons from animal diabetes, VI. Birkhäuser, Boston, pp 299–315
24. Östenson CG, Khan A, Abdel-Halim SM, Guenifi A, Suzuki K, Goto Y, Efendic S (1993) Abnormal insulin secretion and glucose metabolism in pancreatic islets from the spontaneously diabetic GK rat. Diabetologia 36:3–8
25. Otabe S, Yasuda K, Mori Y, Shimokawa K, Kadowaki H, Jimi A, Nonaka K, Akanuma Y, Yazaki Y, Kadowaki T (1999) Molecular and histological evaluation of pancreata from patients with a mitochondrial gene mutation associated with impaired insulin secretion. Biochem Biophys Res Commun 259:149–156
26. Portha B, Giroix MH, Picon L (1982) Effect of diet on glucose tolerance and insulin response in chemically diabetic rats. Metabolism 31:1194–1199
27. Portha B, Serradas P, Bailbe D, Suzuki K, Goto Y, Giroix MH (1991) β-cell insensitivity to glucose in the GK rat, a spontaneous non-obese model for type II diabetes. Diabetes 40:486–491
28. Reiser S, Michaelis O IV, Putney J, Hallfrisch J (1975) Effects of sucrose feeding on the intestinal transport of sugars in two strains of rats. J Nutr 105:894–905
29. Rhodes CJ (2005) Type 2 diabetes: a matter of beta-cell life and death? Science 307:380–384
30. Robertson RP, Harmon J, Tran PO, Poitout V (2003) Glucose toxicity in beta-cells: type 2 diabetes, good radicals gone bad, and the glutathione connection. Diabetes 52:581–587
31. Sakuraba H, Mizukami H, Yagihashi N, Wada R, Hanyu C, Yagihashi S (2002) Reduced beta-cell mass and expression of oxidative stress-related DNA damage in the islet of Japanese Type II diabetic patients. Diabetologia 45:85–96
32. Santos MS, Santos DL, Palmeira CM, Seica R, Moreno AJ, Oliveira CR (2001) Brain and liver mitochondria isolated from

diabetic Goto-Kakizaki rats show different susceptibility to induced oxidative stress. Diabetes Metab Res Rev 17:223–230
33. Serradas P, Giroix MH, Saulnier C, Gangnerau MN, Borg LA, Welsh M, Portha B, Welsh N (1995) Mitochondrial deoxyribonucleic acid content is specifically decreased in adult, but not fetal, pancreatic islets of the Goto-Kakizaki rat, a genetic model of non-insulin-dependent diabetes. Endocrinology 136:5623–5631
34. Tiedge M, Lortz S, Drinkgern J, Lenzen S (1997) Relation between antioxidant enzyme gene expression and antioxidative defense status of insulin-producing cells. Diabetes 46:1733–1742
35. Vallerand AL, Lupien J, Bukowiecki LJ (1986) Synergistic improvement of glucose intolerance by sucrose feeding and exercise training. Am J Physiol 250:E607–E614
36. Wu L, Nicholson W, Knobel SM, Steffner RJ, May JM, Piston DW, Powers AC (2004) Oxidative stress is a mediator of glucose toxicity in insulin-secreting pancreatic islet cell lines. J Biol Chem 279:12126–12134
37. Yang S, Zhu H, Li Y, Lin H, Gabrielson K, Trush MA, Diehl AM (2000) Mitochondrial adaptations to obesity-related oxidant stress. Arch Biochem Biophys 378:259–268

Virchows Arch (2008) 452:393–403
DOI 10.1007/s00428-007-0520-6

ORIGINAL ARTICLE

Kidney biopsies can be used for estimations of glomerular number and volume: a pig study

Anders Bergh Lødrup · Kristian Karstoft · Thomas Heide Dissing · Michael Pedersen · Jens Randel Nyengaard

Received: 14 July 2007 / Accepted: 27 September 2007 / Published online: 24 January 2008
© Springer-Verlag 2007

Abstract In this study, we wanted to evaluate the use of kidney biopsies for estimation of N(glom) and V(glom) in both healthy and chronically diseased kidneys. Danish Landrace pigs with mean weight of 29 kg (range: 25–35 kg) were either subjected to unilateral ureteral obstruction (UUO) or non-obstruction (healthy). N(glom) and V(glom) was estimated by design-based methods using biopsies, $N(\text{glom})^{\text{biopsy}}$ and $V(\text{glom})^{\text{biopsy}}$. From each kidney, six biopsies were withdrawn at six topographically different sites. All estimates were done following stereological principles and reference methods estimated number with the physical fractionator, $N(\text{glom})^{\text{PF}}$, and volume with test point system, $V(\text{glom})^{\text{TPS}}$. $N(\text{glom})^{\text{PF}}$ was $1.30 \pm 0.28 \times 10^6$ for UUO kidneys and $1.59 \pm 0.28 \times 10^6$ for healthy kidneys. $N(\text{glom})^{\text{biopsy}}$ was $1.18 \pm 0.28 \times 10^6$ ($p > 0.05$) for UUO and $1.33 \pm 0.24 \times 10^6$ ($p = 0.04$) for healthy kidneys. When UUO and healthy kidneys were grouped, $N(\text{glom})^{\text{PF}}$ was $1.46 \pm 0.31 \times 10^6$, and $N(\text{glom})^{\text{biopsy}}$ was $1.28 \pm 0.25 \times 10^6$ ($p > 0.05$). $V(\text{glom})^{\text{TPS}}$ was 1,079±126 mm^3 for UUO and 1,707±263 mm^3 for healthy kidneys. $V(\text{glom})^{\text{biopsy}}$ was 1,048±291 mm^3 for UUO ($p > 0.05$) and 1,373±393 mm^3 for healthy kidneys ($p > 0.05$). When UUO and healthy kidneys were grouped, $V(\text{glom})^{\text{TPS}}$ was 1,180±229 mm^3 and $V(\text{glom})^{\text{biopsy}}$ 1,129±334 mm^3 ($p > 0.05$). Biopsy sites were tested for any systematic differences between site- and mean values, and no significant difference was found ($p > 0.05$). This study showed that biopsies can be used for estimating N(glom) and V(glom) by design-based methods, but more precise determination of biopsy volume is needed.

Keywords Biopsy · Kidney glomerulus · Pathology · Microscopy · Animal model

A. B. Lødrup · K. Karstoft · J. R. Nyengaard
Stereology and Electron Microscopy Research Laboratory and MIND Center, Aarhus University,
Aarhus, Denmark

A. B. Lødrup · K. Karstoft · T. H. Dissing · M. Pedersen
MR Research Centre, Aarhus University Hospital,
Aarhus, Denmark

A. B. Lødrup · K. Karstoft · T. H. Dissing · M. Pedersen · J. R. Nyengaard (✉)
Institute of Clinical Medicine, Aarhus University Hospital,
Aarhus, Denmark
e-mail: nyengaard@ki.au.dk

Introduction

In daily clinical routines, kidney biopsies are occasionally withdrawn for predicting renal allograft outcome and diagnosing and monitoring kidney diseases. Microscopic investigation of extracted biopsies allows information about the glomerular number and volume, parameters that have proven to be clinically important since Brenner et al. showed that development of chronic kidney disease is associated with a low number of glomeruli [4, 5]. Later studies have demonstrated a relationship between an abnormal number or size of glomeruli and kidney-related diseases, often suggesting that the histological findings were determined by the degree of kidney disease: Nyengaard and Bendtsen demonstrated a loss of total number of glomeruli in cortex, N(glom), in cases of severe diabetic glomerulonephropathy [3], and Keller et al. have shown that a reduction in nephrons could be associated with development of essential hypertension [13]. In different studies, total glomerular volume, V(glom), has shown to be significantly increased in patients with insulin-dependent diabetes mellitus (IDDM) with albuminuria, but not in

IDDM patients without albuminuria [22], and mean glomerular volume, V_N(glom), have varied from normal [16] to increased [1] in diseased kidneys. However, most studies have been performed using ex vivo investigations of total kidney, and only a few studies have estimated glomerular number and volume using biopsies. In 1994, Basgen et al. estimated *N*(glom) by combining magnetic resonance imaging (MRI) volumetric measures of the kidney and biopsies of the renal cortex in a dog model [2]. In 2003, a similar approach was applied by Fulladoza et al. to patients subjected to renal allograft transplantation [8]. Both studies used one biopsy per kidney and a model-based method (referred to as the Weibel and Gomez method) [21], assuming a spherical shape of the glomerulus.

The aim of our study was to evaluate the use of biopsies. This was done by comparing estimations of *N*(glom) and *V*(glom) in biopsy with those in total kidney. To avoid the above-mentioned assumption of the spherical glomerular shape, we used design-based methods for estimating *N*(glom) and *V*(glom). Furthermore, we took six biopsies from six topographically different sites from each kidney and made comparative analysis of glomerular number density. The study was conducted in both healthy and chronically ill kidneys. Experimentally created unilateral ureteral obstruction (UUO) was used in this study, allowing for renal impairment with adverse effects on both the renophysiology and ureteral system [12].

Method and materials

Animal handling

This study included Danish Landrace pigs with mean weight of 29 kg (range, 25–35 kg). For estimation of *N*(glom) and *V*(glom), nine pigs underwent UUO. Pigs with healthy non-obstructed kidneys were also included, ten for estimations of *N*(glom) and three for estimations of *V*(glom). Preanesthesia was given using ketamin (10 mg/kg) and midazolam (0.5 mg/kg) i.m. Pigs were intubated and connected to a respirator (Servo Ventilator 900 A; Siemens, Solna, Sweden) set to a flow rate of 0.1 l/min/kg and a O_2:N_2O ratio of 1:2. Anesthesia and analgesia were maintained using 1.5% isofluran mixed with O_2:N_2O. Pulse, HgB-saturation and end-expiratory pCO_2 were monitored (Oxicap 4700, Ohmeda, Louisville, CO) and the blood pressure was monitored through a catheter placed in the profound femoral artery (CardioMed 4008, InVivo, Tulsa, OK). Hydration was maintained during the entire study using saline i.v. (10 ml/kg/h), and urine was collected through an indwelling bladder catheter. The study was carried out according to the Danish legislation considering animal experiments. The pigs were housed in dedicated animal facilities. Initial exclusion of kidneys with morphological and physiological pathology was based on anatomical MRI and serum creatinine values.

Unilateral ureteral obstruction

UUO was performed by approaching the ureter retroperitoneally under sterile conditions. The ureter was reached through a flank incision and was exposed and presented with a Baltimore. A silicone tube (duodenal tube, CH 14, with a luminal diameter of 3.0 mm) was placed around the ureter 15 mm distally to the ureteropelvine junction, and the tube was ligated with two or three ligatures (silk 0-0). The muscle was sewed with polysorb™ 3-0 and skin with nylon 3-0. Ampicillin i.m. (1.0 g) was given pre- and postoperatively. Ultrasonography of the kidneys was performed 7 days later to evaluate the level of hydronephrosis (Diagnostic Ultrasound System 3535; Brüel, Copenhagen, Denmark), and urine was collected with an indwelling bladder catheter for measurements of protein and leukocytes by stix. The UUO was released by removal of the silicone tube (incision and closing of incision as described above).

Biopsies and nephrectomy

The abdominal cavity was reached through a longitudinal incision through linea alba. Kidneys and their vessels were presented, and retroperitoneum and connective tissue were removed. Kidney capsules were kept intact. Biopsies were withdrawn using a biopsy pistol (Pro Mag I TM 2.5; MD TECH; Gainesville, FL) and an 18-gauge needle (Pro Mag MD Tech). Six biopsies per kidney were withdrawn at six topographically different sites: one in the upper pole, four in the margo lateralis, and one in the lower pole (Fig. 1). Biopsies were immediately immersed in phosphate-buffered formaldehyde (4%). Subsequently, nephrectomy was per-

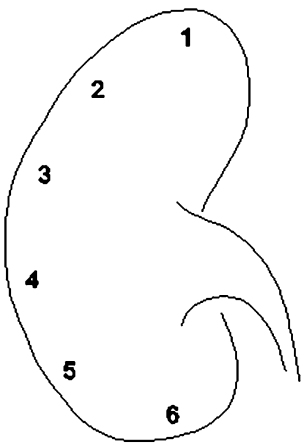


Fig. 1 Schematic drawing of kidney showing the six sites wherefrom biopsies were withdrawn

formed, and the renal arteries and veins were ligated and cut through. The kidney was removed and brought to a fume cupboard, where a catheter was placed in the remaining part of the renal artery. The kidney was flushed with 200 ml phosphate buffer to wash out coagulated blood and was perfused using a peristaltic pump (Watson Marlow, Medford, MA) with phosphate-buffered formaldehyde 4% for 5 min at a rate of 250 ml/min. After perfusion fixation, the kidney was immersed in the same fixative.

Stereology

Total kidney estimates of *N*(glom) and *V*(glom) were done using the physical fractionator and test point system, respectively.

Biopsy volume, number of glomeruli, and glomerular profile area were estimated for all biopsies. Knowledge of renal cortical volume, *V*(cor), allowed for estimations of *N* (glom) and *V*(glom). For single-kidney details, see Table 1.

V(cor) by point counting

The kidneys were embedded in agar and cut into 3 mm thick slabs of which one out of five were sampled, the slab sampling fraction (SSF), using systematic uniformly random sampling (SURS). Renal cortical volume was estimated from these slabs (3 mm) ad modum Cavalieri by point counting of cortex using a stereomicroscope.

N(glom) by physical fractionator, $N(\text{glom})^{\text{PF}}$

The physical fractionator (PF) introduced in 1986 by Gundersen et al [9, 10], is today a profoundly validated method for making precise and unbiased estimates of *N* (glom).

Each slab was cut into a variable number of blocks (1–16), wherefrom two 30 μm thick slices were taken and used for sampling of glomeruli by light microscope and computer software designed for stereological investigations. The two slices was denoted as a disector-pair. *N*(glom) was estimated using the equation:

$$N(\text{glom}) = Q^{-} \times (\text{SSF} \times \text{BSF} \times \text{HSF} \times \text{ASF})^{-1} \quad (1)$$

where SSF was the above-mentioned slab sampling fraction (1/5); BSF was the block sampling fraction, 1/1–1/16, depending on how many blocks was cut from one slab; HSF was the height sampling fraction, constituted by the disector-pair taken from one block. Due to shrinkage during plastic embedding, HSF was 1/41; ASF was the area sampling fraction, constituted by the area of the slices used for sampling glomeruli, in our study 1/7; Q^{-} was the number of glomeruli sampled from a disector pair. Glomeruli were sampled using the disector and a counting frame, both explained in detail elsewhere [9, 20]. For details concerning estimations of *N*(glom) by PF see Appendix I.

N(glom) by biopsies, $N(\text{glom})^{\text{biopsy}}$

Each biopsy was divided into a medullary part and a cortical part using a stereomicroscope. The mass of the cortical part was measured (Struers Kebo Lab, Struer, Denmark), and a volume for each cortical biopsy was calculated assuming that the mass density of renal cortex was 1.04 g/cm^3. The biopsies were embedded in plastic and cut exhaustively into 20 μm thick slices. Using the analysis

Table 1 Parameters for estimating *N*(glom) by PF and biopsy and estimating *V*(glom) by test point system and biopsy

Method	Parameters	UUO	Healthy
$N(\text{glom})^{\text{PF}}$	Number of kidneys	9	10
	Number of biopsies per kidney	6	6
	Number of disector pair sampled per kidney	7 (6–7)	7 (6–8)
	Number of glomeruli sampled per disector pair	21 (15–34)	22 (17–28)
	Number of glomeruli sampled per kidney	138 (90–235)	157 (125–199)
$N(\text{glom})^{\text{biopsy}}$	Mass of biopsy (mg)	2.2 (2.1–2.8)	2.8 (1.7–3.7)
	Number of glomeruli in biopsy	54 (38–67)	49 (29–68)
	Number of kidneys	9	3
	Number of biopsies per kidney	6	6
$V(\text{glom})^{\text{TPS}}$	FOV sampled per kidney	7 (6–7)	7 (6–8)
	P(glom)/*P*(cor) sampled per FOV	37/102 (18–58/57–171)	42/129 (52–28/75–162)
	P(glom)/*P*(cor) sampled per kidney	249/681 (131–404/401–1,196)	304/933 (372–227/600–1,295)
$V(\text{glom})^{\text{biopsy}}$	Number of glomeruli sampled from biopsy	6.4 (3–9)	6.3 (2–9)
	Number of glomeruli sampled from kidney	29 (28–45)	29 (26–30)

Data presented as mean (range). $N(\text{glom})^{PF}$:*N*(glom) by PF; $N(\text{glom})^{biopsy}$:*N*(glom) by biopsy; $V(\text{glom})^{TPS}$:*V*(glom) by test point system; $V(\text{glom})^{biopsy}$:*V*(glom) by biopsy; disector pair: two consecutive slices, each 30 μm thick, which constitute a 1/50 of a kidney block

FOV Field of view during microscopy, *P*(glom)/*P*(cor) test points hitting glomeruli/cortex

software VIS (Visiopharm, Copenhagen, Denmark) digital images were acquired of all slices, and glomeruli were counted using the dissector. The volume and number of glomeruli for each biopsy was used to calculate the glomerular density, N_v(glom/cor), for each biopsy and for each kidney, the latter being a mean of all six biopsies. N(glom) was then given by:

$$N(\text{glom}) = N_V(\text{glom/cor}) \times V(\text{cor}) \quad (2)$$

V(glom) by test point system, $V(\text{glom})^{\text{TPS}}$

We estimated the volume density of glomeruli, V_v(glom/cor), by point counting on 3-μm-thick slices of renal cortex. Using the software CAST, a test point system was displayed on a computer monitor together with live images of the slices, sampled by SURS. Test points hitting glomerular tuft, P(glom), and cortex (glomeruli included), P(cor), were sampled, and V_v(glom/cor) could be calculated as:

$$V_v(\text{glom/cor}) = \frac{\sum P(\text{glom}) \times p(\text{cor})}{\sum P(\text{cor}) \times p(\text{glom})} \quad (3)$$

where p(glom) and p(cor) were the number of test points per field-of-view used to count cortex and glomeruli, which were 48 and 30, respectively. dx and dy was 5,000 μm.

Knowing the total volume of renal cortex, we could calculate the total volume of glomeruli in renal cortex:

$$V(\text{glom}) = V_V(\text{glom/cor}) \times V(\text{cor}) \quad (4)$$

V(glom) by biopsy, $V(\text{glom})^{\text{biopsy}}$

A random set of 10–12 consecutive slices from the middle of the biopsies were sampled. Using the disector principle, a set of glomeruli was sampled from these slices (Fig. 2). We then estimated the profile area of these glomeruli using the 2D nucleator (Fig. 2), which is a stereological tool capable of making unbiased area-estimates of 2D structures. The volume of each sampled glomeruli could be estimated using the Cavalieri principle. Glomerular mean volume, V_N(glom), was calculated as the volume of sampled glomeruli divided by the number of sampled glomeruli. V(glom) for each kidney was given by:

$$V(\text{glom}) = V_N(\text{glom}) \times N(\text{glom}) \quad (5)$$

where N(glom) was estimated by PF.

Shrinkage

Shrinkage of the renal tissue was followed closely. The average total shrinkage from in situ tissue to slices used for microscopy was 32% for perfusion-fixed tissue and 63% for non-perfused tissue (biopsies). For details see Appendix II.

Statistics

Results were reported as mean±SD, and $p<0.05$ was considered statistically significant. The difference between methods for estimating N(glom) and V(glom) were analyzed using single-factor analysis of variance (ANOVA) and presented with Bland–Altman plots. Biopsies were analyzed with single-factor repeated measurements ANOVA. Outlier analysis was performed using Dixon's Test for outliers [6].

Results

Hydronephrosis in UUO kidneys was confirmed by ultrasonography. No urine stix showed any sign of leukocytes or blood in the urine. One biopsy had to be

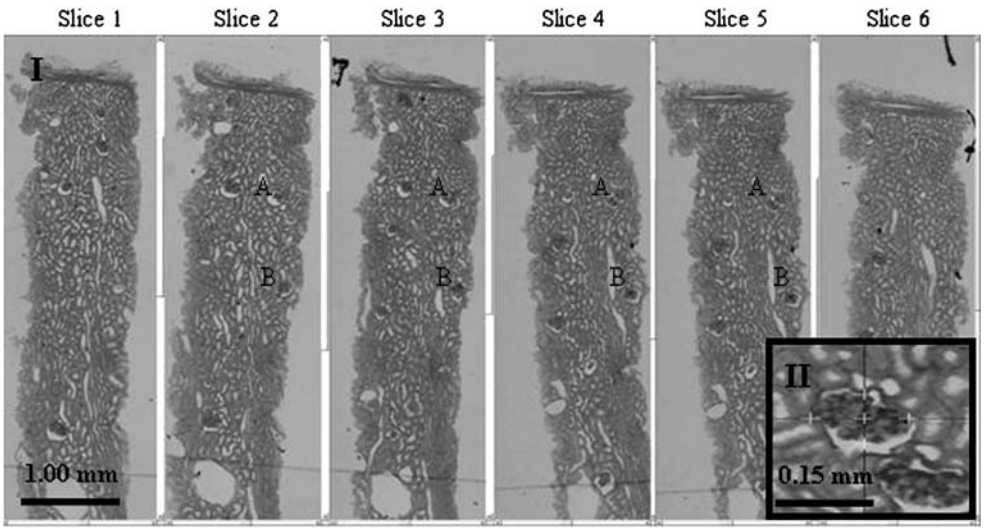


Fig. 2 *I* Digital images of biopsy, slices 1–6. Two glomeruli (*A* and *B*) can be sampled using the disector principle. *Bar* indicates 1.0 mm. *II* The 2D nucleator. The area of the sampled glomerulus profile can be estimated using the known lengths of the test lines. *Bar* indicates 0.15 mm

excluded because it contained no cortical tissue (kidney, nine; biopsy, two), and one biopsy was excluded for estimations of V(glom) on the basis of outlier analysis (kidney, four; biopsy, two). Results for each kidney are shown in Tables 2 and 3.

V(cor) by point counting

Volume of renal cortex was 48.5±8.6 cm^3 for UUO kidneys and 74.4±10.8 cm^3 for healthy kidneys.

N(glom) by PF and biopsy

$N(glom)^{PF}$ was $1.30 \pm 0.28 \times 10^6$ for UUO kidneys and $1.59 \pm 0.28 \times 10^6$ for healthy kidneys. $N(glom)^{biopsy}$ was $1.18 \pm 0.28 \times 10^6$ ($p>0.05$) for UUO and $1.33 \pm 0.24 \times 10^6$ ($p=0.04$) for healthy kidneys. When UUO and healthy kidneys were grouped, $N(glom)^{PF}$ was $1.46 \pm 0.31 \times 10^6$ and $N(glom)^{biopsy}$ was $1.28 \pm 0.25 \times 10^6$ ($p>0.05$) (Fig. 3).

V(glom) by test point system and biopsy

$V(glom)^{TPS}$ was 1,079±126 mm^3 for UUO and 1,707±263 mm^3 for healthy kidneys. $V(glom)^{biopsy}$ was significantly lowered for both groups ($p<0.001$). However, when the results were corrected for shrinkage, $V(glom)^{biopsy}$ was 1,048±291 mm^3 for UUO ($p>0.05$) and 1,373±393 mm^3 for healthy kidneys ($p>0.05$). When UUO and healthy kidneys were grouped, $V(glom)^{TPS}$ was 1,180±229 mm^3 and $V(glom)^{biopsy}$ 1,129±334 mm^3 ($p>0.05$) (Fig. 3).

Table 2 Results of estimating N(glom)

Pig (L/R)	$N(glom)^{PF}$ ($\times 10^6$)	$N(glom)^{biopsy}$ ($\times 10^6$)	N_v(glom/cor) (mm^{-3})
UUO			
1(L)	1.05	0.80	22
2(L)	1.10	1.01	25
3(l)	1.59	0.97	22
4(R)	1.11	0.88	20
5(R)	1.75	1.62	27
6(L)	1.32	1.23	21
7(L)	1.02	1.44	29
8(R)	1.17	1.31	28
9(R)	1.62	1.36	23
Healthy			
10(L)	1.43	1.29	19
11(R)	1.43	0.90	15
12(R)	1.92	1.30	18
13(L)	1.47	1.65	18
14(L)	1.34	1.33	21
15(R)	1.69	1.29	15
16(L)	1.47	1.46	21
17(R)	2.07	1.72	19
18(L)	1.22	1.10	14
19(R)	1.90	1.28	17

L/R Left kidney/right kidney, $N(glom)^{PF}$ N(glom) by physical fractionator, $N(glom)^{biopsy}$ N(glom) by biopsies, $N_v(glom/cor)$ glomerular density, mean obtained from all six biopsies

Table 3 Results of estimating V(glom) in mm^3

Pig (L/R)	$V(glom)^{TPS}$ (mm^3)	$V(glom)^{biopsy}$ β (mm^3)	V_v(glom/cor) (%)
UUO			
1(L)	882	680	2.4
2(L)	996	1,013	2.4
3(l)	957	1,162	2.2
4(R)	1,161	1,476	2.7
5(R)	1,199	1,178	2.0
6(L)	1,202	902	2.0
7(L)	1,000	728	2.0
8(R)	1,084	841	2.3
9(R)	1,231	1,452	2.1
Healthy			
10(R)	1,261	1,350	2.2
11(L)	1,528	1,777	1.8
12(L)	1,658	992	2.4

L/R Left kidney/right kidney, $V(glom)$ total glomerular volume in mm^3, $V_V(glom/cor)$ glomerular volume density, β corrected for shrinkage

Estimation of volume and number of glomeruli by biopsies

For each kidney, two means of N_V(glom/cor) were produced: one from all six biopsies, denoted as biopsy-mean, and one from total kidney using $N(glom)^{PF}$ and $V(cor)^{TSP}$, denoted as reference-mean. Biopsy sites were tested for any systematic differences between site- and mean values ($p>0.05$ for biopsy site one to six compared to both biopsy- and reference-mean for both UUO and healthy kidneys). N_V(glom/cor) and difference between biopsy-site and reference-mean were plotted for all six biopsy sites for both UUO and healthy kidneys (Fig. 4). Similar analysis was carried out for V_N(glom) for UUO and healthy kidneys, demonstrating no significant differences between biopsy sites and mean values ($p>0.05$, Fig. 5). Reference-mean was calculated by dividing $V(glom)^{TPS}$ with $N(glom)^{PF}$.

Discussion

This study evaluated the use of biopsies for estimating N(glom) and V(glom) with two design-based methods. These methods were compared to the reference methods, the physical fractionator and test point system. Estimations were made for both healthy and diseased kidneys.

Choice of model

Ureteral obstruction is known to result in kidneys with hyperactive RAS-system [7], hypoxia and a decreased GFR. Single-nephron hypertension and hyperfiltration can be seen and may be worsened by the loss of nephrons [11]. The total UUO performed in this study mimicked a chronic state of this pathogenesis. Due to relief of obstruction, we were able to avoid states like acute renal failure and excessive renal fibrosis, which would have caused a heterogeneous group of diseased kidneys less adequate for statistical analysis. Pigs were chosen because of their renal macroscopically similarities with humans, e.g., poly-calyces. Biopsies were handled in accordance with modern guidelines [20].

Validation of reference methods, $N(\text{glom})^{\text{PF}}$ and $V(\text{glom})^{\text{TPS}}$

The total variation, expressed as the coefficient of variance, CV_{total}, of $N(\text{glom})^{\text{PF}}$ for all groups was 18.7%. CV_{total} resulted from both biological variation, CV_{bio}, between kidneys and imprecision due to the physical fractionator (coefficient of error, CE). The CE of the physical fractionator was 9.0%. Taking into account that $CV^2_{total} = CV^2_{bio} + CE^2$, biological variance was 16.3%. So sampling more glomeruli would not improve the precision of our estimates, as the majority of total variance was due to biological variance. Previous studies suggested a preferable ratio in the range of $0.25 < \frac{CE^2}{CV^2} < 0.5$, and in our study, we obtained the ratio: $\frac{CE^2}{CV^2} = 0.23$, suggesting the contribution from CE was acceptable.

$V(\text{glom})^{\text{TPS}}$ was based on estimations of $V_v(\text{glom/cor})$. CV_{total} and the CE of $V_v(\text{glom/cor})$ was 13.1 and 9.3%, resulting in a CV_{bio} at 9.2%. We obtained a ratio of $\frac{CE^2}{CV^2} = 0.51$, suggesting that the imprecision had an increased, but still acceptable, influence on the CV.

Validation of $N(\text{glom})^{\text{biopsy}}$

Although biopsy method tended to underestimate $N(\text{glom})$ compared to PF, no significant difference was found between the methods for UUO kidneys. For healthy kidneys, a statistical significant difference was observed between the two methods, and the highest estimates of $N(\text{glom})$ was also obtained by PF for this group. The twofold SD for the differences between methods was approximately 0.5×10^6. The maximum intra-individual difference between the two methods was 65% for UUO and 60% for healthy kidneys.

Inaccurate estimations of $N_v(\text{glom/cor})$ may explain the significant intra-individual difference between $N(\text{glom})^{\text{PF}}$ and $N(\text{glom})^{\text{biopsy}}$. Our ex vivo analyses of biopsies included measurements of volume of biopsies and estima-

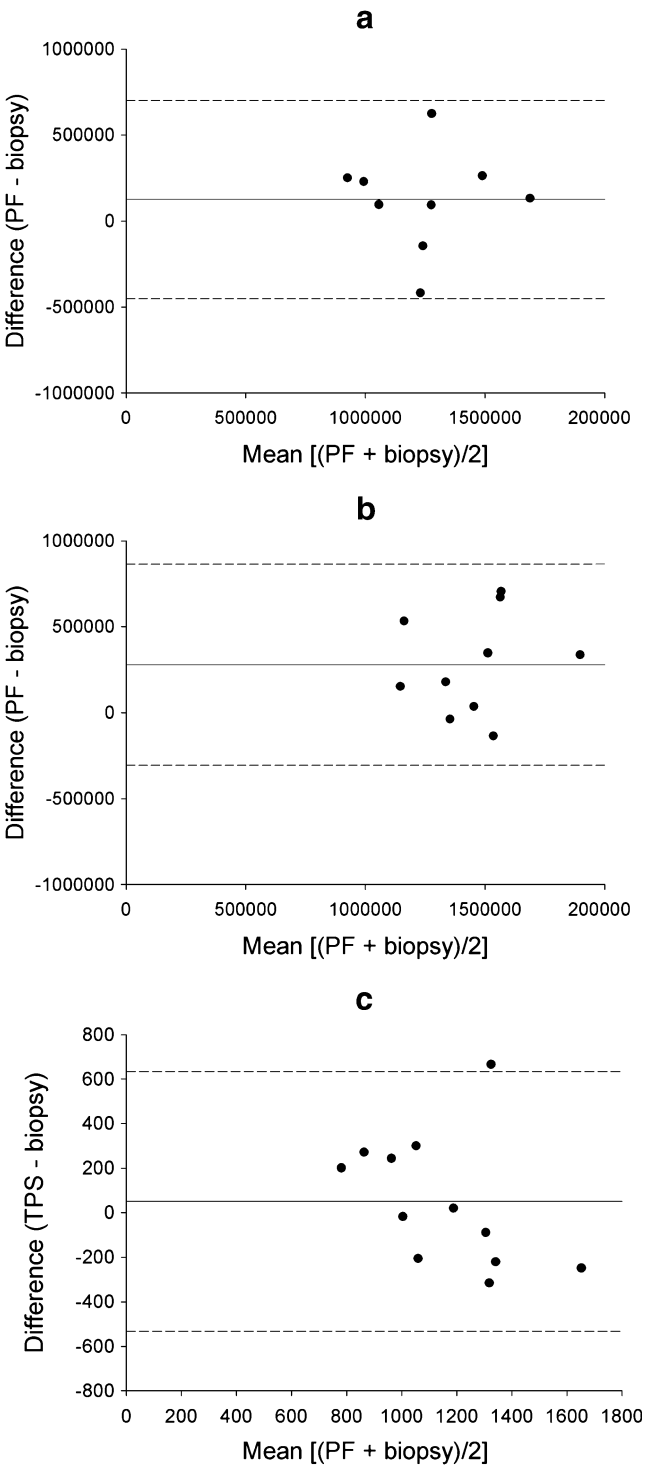


Fig. 3 **a**, **b** Bland–Altman plots with $N(\text{glom})$ by physical fractionator (PF) and biopsy for UUO kidneys. *X*-axis: mean of $N(\text{glom})$ by PF and biopsy. *Y*-axis: difference in $N(\text{glom})$ between PF and biopsy. **c** Bland–Altman plots with $V(\text{glom})$ by test point system (TPS) and biopsy for UUO and healthy kidneys. *X*-axis: mean of $V(\text{glom})$ by TPS and biopsy. *Y*-axis: difference in $V(\text{glom})$ (mm^3) between TPS and biopsy method. *Dotted line*: $\pm 2 \times \text{SD}$. *Full line*: mean difference

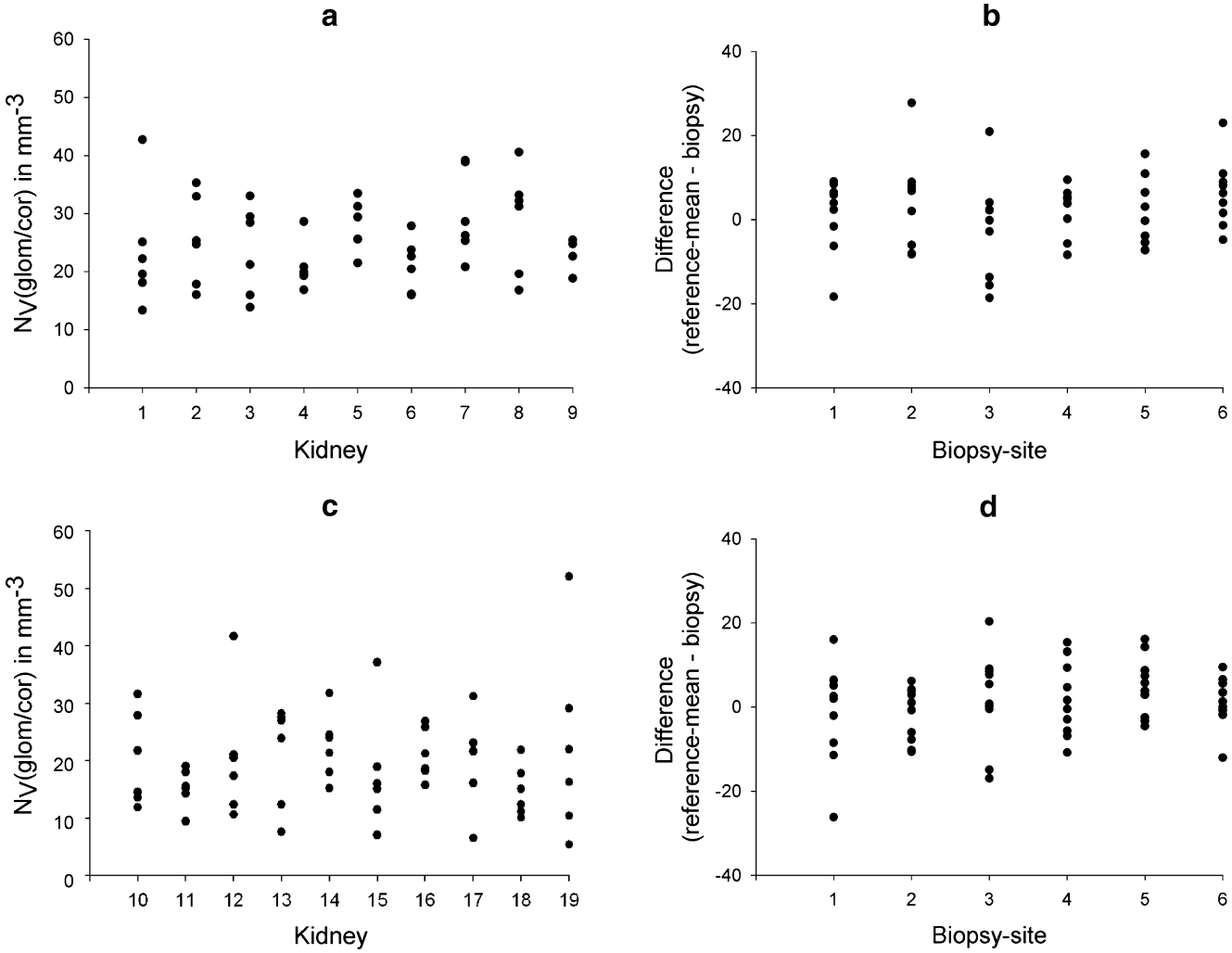


Fig. 4 **a** UUO kidneys. N_V(glom/cor) (mm^{-3}) at all six biopsy sites for each kidney. **b** UUO kidneys. Difference in N_V(glom/cor) (mm^{-3}) between biopsies and reference-mean. **c** Healthy kidneys. N_V(glom/cor) (mm^{-3}) at all six biopsy sites for each kidney. **d** Healthy kidneys. Difference in N_V(glom/cor) (mm^{-3}) between biopsies and reference-mean

tion of number of glomeruli in the biopsies. As for the latter, using 20 μm thick sections and keeping track of every glomeruli within the biopsies, only counting those which met the criteria of the disector counting rule, we were able to minimize the errors that may occur during this procedure. However, getting solid reproducible estimates of biopsy volume was more difficult. The major problem in this procedure was evaporation during the measurements of biopsy mass, because a relatively large amount of formaldehyde, the size of the biopsy taken into consideration, was likely to evaporate during the procedure. However, over- and underestimation of in vivo biopsy weight were not systematically demonstrated according to the Bland–Altman plots, and imprecision rather than bias may have been introduced.

When Basgen et al. used the model-based method (Weibel and Gomez), they compared it with the PF and found no significant difference between methods. Qua model-based, the result would be biased if the model did not fit the examined tissue, that is, if the glomeruli did not have the assumed spherical shape. The porcine glomeruli in our study presented themselves with varying shapes—some spherical, some ellipsoid and many with a more heterogeneous shape—and a model-based approach would certainly have biased our results. The designed-based unbiased method was preferable and could benefit by a more precise determination of the biopsy volume.

Validation of $V(\text{glom})^{\text{biopsy}}$

Corrected for shrinkage, the biopsy method tended to overestimate V(glom), especially for kidneys with large glomerular volume, as revealed from the Bland–Altman plot. The twofold standard deviation for differences between methods was approximately 600 mm^3. The

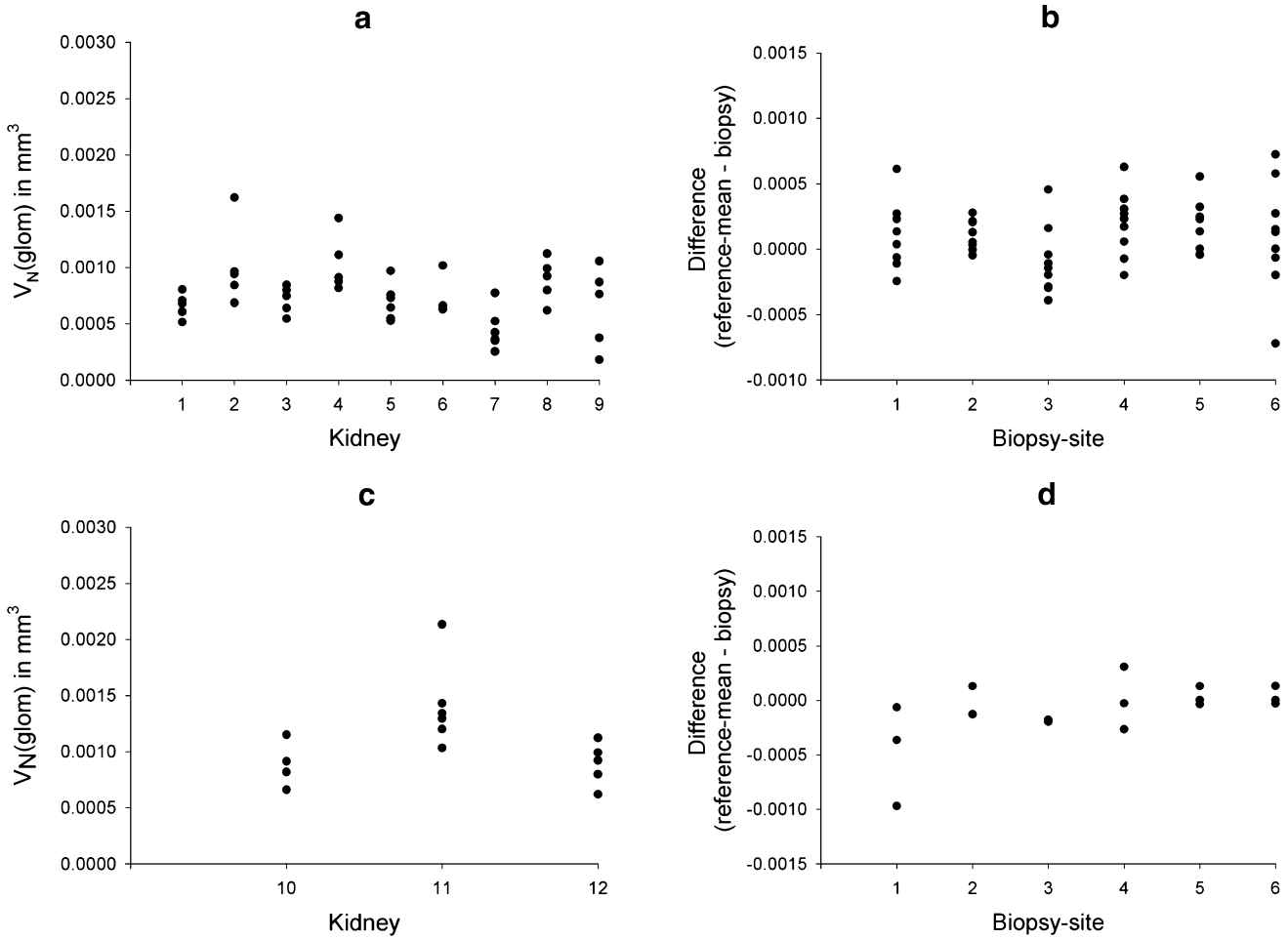


Fig. 5 **a** UUO kidneys. V_N(glom) (mm^3) at all six biopsy sites for each kidney. **b** UUO kidneys. Difference in V_N(glom) (mm^3) between biopsies and reference-mean. **c** Healthy kidneys. V_N(glom) (mm^3) at all six biopsy sites for each kidney. **d** Healthy kidneys. Difference in V_N(glom) (mm^3) between biopsies and reference-mean

maximum intra-individual difference was 27% for UUO and 40% for healthy kidneys. $V(\text{glom})^{\text{biopsy}}$ was not affected by determination of biopsy volume, as it was calculated using N(glom) by PF. We speculate that the decreased intra-individual difference for $V(\text{glom})^{\text{biopsy}}$ compared to $N(\text{glom})^{\text{biopsy}}$ may be due to the absence of imprecision otherwise introduced with the biopsy volume. Furthermore, we did not sample all glomeruli in the

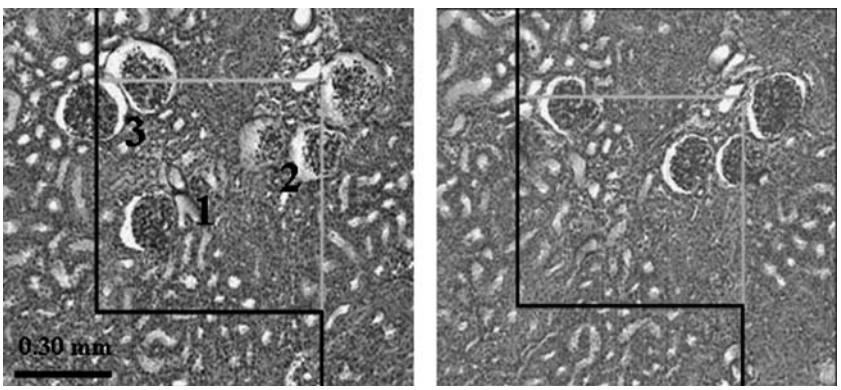


Fig. 6 The disector and the counting frame explained by use of three glomeruli and two consecutive sections, 30 μm thick. *Left image* is the sampling section and *right image* the look-up section. Exclusion line is *black*, inclusion line is *grey*. Glomerular profiles inside counting frame or touching the inclusion line are sampled by counting frame (no. 1 and 2). Glomerular profiles outside counting frame or touching the exclusion line cannot be sampled by counting frame (no. 3). Of those sampled by the counting frame, only glomeruli that are visible in sampling- and not look-up section can be sampled by the disector, here no. 1

biopsies when estimating V_N(glom). Increasing the number of sampled glomeruli may have reduced the differences between TPS and biopsy method further.

The results regarding glomerular volume were corrected for shrinkage, and we found that the obstructed and non-obstructed kidney tissue shrunk equally. However, it is possible that severely sclerotic and inflamed kidneys may behave differently during plastic embedding, stressing the importance of control and monitoring of shrinkage.

Validation of biopsies

V(cor)^{TPS} was used for estimating N(glom)^{biopsy} and N(glom)^{PF} for estimating V(glom)^{biopsy}, which reduced the imprecision/bias caused by the method and allowed for an analysis of the difference between biopsies. The kidney is a complex organ with certain biological dispositions, and it is fair to ask whether or not an 18-gauge needle biopsy can be regarded as a representative fraction for this organ. In monkey kidneys, it has been shown that glomerular density and mean glomerular volume changes from the periphery of the cortex to the juxtamedullary cortex; thus, the glomerular density is high and mean glomerular volume low at the periphery and vice versa [18], and similar findings were done in dogs by Basgen et al. [2] in their study. However, this should not affect our results with bias or imprecision, as all our biopsies were taken perpendicular to the surface of the cortex. In our experimental study, we found substantial variation in N_v(glom/cor) between the six biopsy sites within the same kidney (sometimes more than fourfold), but we found no significant systematically demonstrated difference between the sites (Fig. 4). As for V_N(glom), which was used to estimate V(glom)^{biopsy}, we found a similar pattern: the variation within one kidney was substantial (in most cases within two- or threefold), although not as markedly as for N(glom), but without significant difference between the biopsy sites (Fig. 5).

To evaluate the possibilities for clinical application, we estimated glomerular number and volume for UUO kidneys, using just one biopsy (site four) and using V(cor) by MRI and N(glom)^{biopsy}. No significant difference was found for either method compared to the reference method (data not shown), and a promising perspective on this, is the combination of quantitative analysis and immunohistochemistry of kidney biopsy. It is suspected that obesity may be associated with a reduction in kidney function and N(glom) [14, 15], and alcohol and tobacco [17] are known to be associated with chronic kidney disease. One or all three factors are very often seen in patients admitted to departments for internal medicine. Biopsies may reveal more information about the renal state of patients not yet diagnosed with—but who are at risk for developing chronic kidney disease. However, the disadvantages and risks during such an invasive procedure must be compared to the benefits, and although the latter looks promising, further research is needed.

Conclusion

Using biopsies for estimating N(glom) and V(glom) is a promising alternative for monitoring the healthy and chronically ill kidney. Further development of the design-based method for estimating N(glom) is however needed, and we have shown that a major contributor to error of the method is determining biopsy volume. The distribution of glomeruli in the cortex still needs further research, but our data suggest no significant systematic difference between biopsy-site regarding number density or mean volume.

Acknowledgements The skillful technical assistance of Maj-Britt Lundorf is gratefully acknowledged. This study was financially supported by The Research Foundation, Aarhus University and the Becket Foundation. The study complied with the current Danish laws for scientific research.

Appendix

Appendix I—N(glom)

Each slab was cut into a variable number of blocks (1–16) of which one was sampled, the block sampling fraction (BSF), and embedded in plastic: tissue was dehydrated in alcohol (70, 96, 99%), infiltrated with plastic, and the solution was mixed with Hardner I followed by Hardner II (Technovit, Kuzler, Germany). The block was cut into slices on microtome (HM 355, Brock & Michelsen Instruments, Copenhagen, Denmark). Slices were put on glass slides and stained with Mayers hematoxylin. From the middle of each block, two consecutive slices were sampled, each 30 μm thick, a so-called disector pair, which constituted a 1/50 of a block, denoted the height sampling fraction (HSF). However, due to shrinkage caused by the plastic embedding, the actual fraction was 1/41. The one slice was denoted as the sampling section, and the other as the look-up section. Using an Olympus BX50 microscope, objective 2 and ×90 magnification, connected with a SIS-1 digital camera (Olympus Soft Imaging Solutions GmbH, Münster, Germany) and the software CAST (Visiopharm, Copenhagen, Denmark), real-time magnified images of the two sections could be displayed on a computer monitor, enabling the investigator to identify glomeruli within the cortex. A counting frame, developed by Gundersen and explained in detail elsewhere [9], was displayed on the monitor. Glomeruli hitting the exclusion line were not sampled, whereas glomeruli hitting the inclusion line and

glomeruli inside the counting frame were sampled (Fig. 6). Glomeruli were sampled according to the disector principle, which is an unbiased sampling technique explained in detail elsewhere [19]. The microscope stage could be moved by a motor in predetermined, equidistant steps in two orthogonal directions, allowing the counting frame to cover a known fraction of the sampling section (and the look-up section). Knowing the area of the counting frame, a(frame), and the length of the equidistant steps, dx and dy, the area sampling fraction (ASF) could be estimated as:

$$\mathrm{ASF} = \frac{a(\mathrm{frame})}{\mathrm{dx} \times \mathrm{dy}} \tag{6}$$

where a(frame)=291×10^4 μm^2, dx and dy=4,500 μm, resulting in ASF=1/7. N(glom) can be estimated by multiplying number of sampled glomeruli, Q^-, with the inverse fractions mentioned above:

$$N(\mathrm{glom}) = Q^- \times (\mathrm{SSF} \times \mathrm{BSF} \times \mathrm{HSF} \times \mathrm{ASF})^{-1} \tag{7}$$

The total number of glomeruli in one kidney was calculated as the sum of blocks multiplied with the inverse fractions:

$$N(\mathrm{glom})_{\mathrm{kidney}} = \frac{\sum \mathrm{Q^-block}}{1/2} \times \left(\frac{1}{5} \times \left[\frac{1}{1}; \frac{1}{16}\right] \times \frac{1}{41} \times \frac{1}{7}\right)^{-1} \tag{8}$$

Where $\sum Q^-$ is the number of glomeruli sampled from all blocks. As the glomeruli were sampled from both sample- and look-up section, Q^- was divided with 1/2.

Appendix II—Shrinkage

Uncontrolled shrinkage of the renal tissue would affect our estimations of both N(glom) and V(glom).In this study, the shrinkage was reduced by both perfusion with formaldehyde and embedding in plastic. Only the tissue used in the reference method, PF and TPS, was perfusion fixed. Biopsies were immersion fixed.

Estimation of shrinkage/collapse caused by nephrectomy.

Nineteen kidneys, nine UUO and ten healthy, underwent MRI both before and immediately after nephrectomy and perfusion fixation. Both UUO and healthy kidneys were MRI scanned 1, 2, 3, and 6 weeks after nephrectomy. Furthermore, ten healthy kidneys underwent MRI before nephrectomy and immersion fixation. The volume of immersion-fixed kidneys was estimated by fluid displacement 1 or 2 weeks after nephrectomy.

Estimation of shrinkage caused by plastic-embedding

Kidneys, UUO and healthy, were cut into 3 mm thick blocks, and the area of three blocks per kidney was estimated by point counting both before and after plastic embedding. Slices from blocks, 30 μm, were cut using microtome, and the area of slices was estimated by point counting. One block per kidney was cut exhaustively into a number of 20 μm slices. By counting the number of slices which constituted a block, the thickness of the block after plastic-embedding was estimated.

Total shrinkage

The post-nephrectomy MRI showed no significant changes in renal cortical volume for perfusion-fixed kidneys, and this did not change over time. In average, immersion-fixed kidneys shrunk/collapsed with 37% after nephrectomy. Shrinkage caused by plastic-embedding cutting on microtome was 32% for both UUO and healthy kidneys. The total shrinkage for immersion fixed tissue was 58%.

References

1. Aratacho-Perula E, Roldan-Villalobos R, Salcedo-Leal I, Vaamonde-Leos R (1993) Stereological estimates of volume-weighted mean glomerular volume in streptozotocin-diabetic rats. Lab Invest 68: 56–61
2. Basgen JM, Steffes MW, Stillman AE, Mauer SM (1994) Estimating glomerular number in situ using magnetic resonance imaging and biopsy. Kidney Int 45:1668–1672
3. Bendtsen TF, Nyengaard JR (1992) The number of glomeruli in type 1 (insulin-dependent) and type 2 (non-insulin-dependent) diabetic patients. Diabetologia 35:844–850
4. Brenner BM (1983) Hemodynamically mediated glomerular injury and the progressive nature of kidney disease. Kidney Int 23:647–655
5. Brenner BM, Lawler EV, MacKenzie HS (1996) The hyperfiltration theory: a paradigm shift in nephrology. Kidney Int 49:1774–1777
6. Dixon WJ (1953) Processing data for outliers. Biometrics 9 (1):74–89
7. Frøkiær J, Nielsen AS, Knudsen L et al (1992) Enhanced intrarenal angiotensin II generation in the renal hemodynamic response to acute unilateral complete obstruction of the pig ureter. Am J Physiol 263:527–533
8. Fulladosa X, Moreso F, Narvaez JA, Hueso M, Caldes A, Gil-Vernet S, Castelao AM, Alsina J, Grinyo JM, Seron D (2002) Total glomerular number in stable renal allografts. Transplant Proc 34:343–344

9. Gundersen HJ, Bagger P, Bendtsen TF, Evans SM, Korbo L, Marcussen N, Møller A, Nielsen K, Nyengaard JR, Pakkenberg B, Sørensen FB, Vesterby A, West MJ (1988) The new stereological tools: Disector, fractionator, nucleator and point sampled intercepts and their use in pathological research and diagnosis. Acta Pathol Microbiol Immunol Scand 96:857–881
10. Gundersen HJ (2002) The smooth fractionator. J Microsc 3 (9):191–210
11. Hostetter TH, Olson JL, Rennke HG, Venkatachalam MA (1981) Hyperfiltration in remnant nephrons: a potentially adverse response to renal ablation. Am J Physiol 241:85–93
12. Hvistendahl JJ, Pedersen TS, Jørgensen HH, Rehling M, Frøkiær J (1996) Renal hemodynamic response to graded ureter obstruction in the pig. Nephron 74:168–174
13. Keller G (2003) Nephron number in patients with primary hypertension. N Engl J Med 348:101–108
14. Praga M (2005) Synergy of low nephron number and obesity: a new focus on hyperfiltration nephropathy. Nephrol Dial transplant 20:2549–2597
15. Rea DJ, Heimbach JK, Grande JP, Textor SC, Taler SJ, Prieto M, Larson TS, Cosio FG, Stegall MD (2006) Glomerular volume and renal histology in obese and non-obese living kidney donors. Kidney Int 70:1636–1641
16. Schmitz A, Nyengaard JR, Bendtsen TF (1994) Glomerular volume in type 2 (noninsulin dependent) diabetes estimated by a direct and unbiased stereological method. J Hypertens 62:108–113
17. Shankar A, Klein R, Klein BEK (2006) The association among smoking, heavy drinking and chronic kidney disease. Am J Epidemiol 164:263–271
18. Skov K, Nyengaard JR, Patwardan A, Mulvany MJ (1999) Large juxtamedullary glomeruli and afferent arterioles in healthy primates. Kidney Int 55:1462–1469
19. Sterio DC (1984) The unbiased estimation of number and sizes using the disector. J Microsc 134:127–136
20. Walker PD, Cavallo T, Bonsib SM (2004) Practice guidelines for the renal biopsy. Modern Pathology 17:1553–1563
21. Weibel ER, Gomez DM (1962) A principle for counting tissue structures on random sections. J Appl Physiol 17:343–348
22. Østerby R, Asplund J, Bangstad HJ, Nyberg G, Rudberg S, Viberti GC, Walker JD (1997) Glomerular volume and the glomerular vascular pole area in patients with insulin-dependent diabetes mellitus. Virchows Arch 431:351–357

Virchows Arch (2008) 452:405–410
DOI 10.1007/s00428-007-0534-0

OpenAccess

ORIGINAL ARTICLE

High JC virus load in tongue carcinomas may be a risk factor for tongue tumorigenesis

Tomohiko Kutsuna · Huachuan Zheng · Hekmat Osman Abdel-Aziz · Yoshihiro Murai · Koichi Tsuneyama · Isao Furuta · Yasuo Takano

Received: 21 August 2007 / Revised: 17 October 2007 / Accepted: 21 October 2007 / Published online: 19 February 2008
© The Author(s) 2008

Abstract The John Cunningham virus (JCV) asymptomatically infects a large proportion (~90%) of the population worldwide but may be activated in immunodeficient patients, resulting in progressive multifocal leukoencephalopathy. Recent reports demonstrated its oncogenic role in malignancies. In this paper, the presence of JCV-targeting T antigen was investigated in tongue carcinoma (TC, $n=39$), dysplastic tongue epithelium (DTE, $n=15$) and glossitis ($n=15$) using real-time polymerase chain reaction (PCR) and in situ PCR and immunohistochemistry, and JCV copies were analyzed with the clinicopathological parameters of TCs. The results demonstrated that glossitis and DTEs had significantly lower copies of JCV (410.5±44.3 and 658.3±53.3 copies/μg DNA respectively) than TCs (981.5±14.0, $p<0.05$). When they were divided into three groups with 0–200 copies/μg DNA (low), 201–1,000 (moderate) and more than 1001 (high), TCs showed 3 (7.6%) in the low group, 21 (53.8%) in the moderate group and 15 (38.4%) in the high group and glossitis showed 11 (73.3%) in the low group, 0 (0%) in the moderate group and 4 (26.6%) in the high group. The DTEs occupied an intermediate position between them ($p<0.001$). In situ PCR demonstrated that the nuclei of TC and DTE cells are sporadically *T-antigen* positive but not in nasal turbinate epithelial cells. Immunohistochemistry for T-antigen protein revealed four positive cases only in TCs. The existence of JCV T-antigen DNA was not associated with the clinicopathological variables of TCs. In conclusion, the presence of JCV may be a risk factor of tongue carcinogenesis.

Keywords Tongue cancer · JC virus · Carcinogenesis

T. Kutsuna · H. Zheng · H. O. Abdel-Aziz · Y. Murai · K. Tsuneyama · Y. Takano (✉)
Department of Diagnostic Pathology,
Graduate School of Medicine and Pharmaceutical Sciences,
University of Toyama,
2630 Sugitani,
Toyama 930-0194, Japan
e-mail: ytakano@med.u-toyama.ac.jp

T. Kutsuna · I. Furuta
Department of Oral and Maxillofacial Surgery,
Graduate School of Medicine and Pharmaceutical Sciences,
University of Toyama,
Toyama, Japan

H. Zheng
Department of Biochemistry, College of Basic Medicine,
China Medical University,
Shenyang, China

Introduction

John Cunningham virus (JCV), firstly isolated from the brain of patients with progressive multifocal leukoencephalopathy [12], is a member of the polyomavirus group together with simian virus 40 (SV40) and BK virus. These share major characteristics, such as non-enveloped virions, double-stranded circular DNA genomes, and oncogenic potential under the appropriate conditions [7]. It has been generally thought that JCV has neurotropic oncogenicity both in rodents and humans [14]. The JCV infects a large proportion of the population worldwide, and 80–90% of all adults are seropositive for the virus. Primary infection occurs during childhood and remains asymptomatic with the virus persisting quiescent in the kidneys and lymphoid tissues. However, JCV may be activated when the immune system is impaired [18]. JCV can be detected in tonsillar tissue [10], and the respiratory and digestive tracts are thought to be the primary sites for JCV to enter human body. A recent report described that lung tissue expresses

abundant levels of JCV receptor-type sialic acids which mediate JCV infection [5].

JCV has been detected in human brain tumors [2, 3] and also in several epithelial malignancies, such as colon, prostate, and esophageal carcinomas [4, 6, 19]. A transgenic mouse strain expressing the JCV T antigen is reported to exhibit pituitary tumors in approximately 50% of the animals by 1 year of age, some progressing to malignant peripheral nerve-sheath tumors [14]. T antigen is considered to play an important role in JCV oncogenesis as it interferes with two tumor suppressor proteins that regulate cell-cycle progression, including pRb and p53. T antigen binds to pRb and displaces E2F, thereby promoting cell-cycle progression and the inappropriate cell proliferation of ontogenetically transformed cells [9]. The release of E2F from Rb normally activates p14ARF expression that leads to stabilization of p53. However, T antigen binds to and inactivates p53 to prevent inhibition of the cell cycle, providing an optimal cell environment for viral replication and packaging during the JCV lytic infection and then facilitating the transformation in non-permissive cells [17]. T antigen can increase the stability of β-catenin and cause its accumulation by directly binding so that the protein then translocates to the nucleus where it enhances the expression of such genes as c-myc and cyclin D1, which are typical of the deregulation in the Wnt signaling pathway [8]. In this paper, we examined JCV-targeting T antigen in combination with real-time polymerase chain reaction (PCR), in situ PCR, and immunohistochemistry to clarify the oncogenic role of JCV in tongue carcinogenesis.

Materials and methods

Cases

Formalin-fixed and paraffin-embedded samples were selected from the pathological archive of the University of Toyama Hospital from 1982 to 1999 with informed consent of the patients [39 cases of tongue squamous cell carcinoma (TC), 58.5±15.2 years (mean±SD), male/female=23:16; 15 cases of dysplastic tongue epithelium (DTE), 60.2± 10.4 years, 11:4; 15 cases of glossitis; 67.7±9.8 years, 9:6]. Among the 39 TCs, 14 cases had lymph node metastasis, and the average longitudinal tumor size was 3.1±0.95 cm (mean±SD). The staging for each tongue carcinoma was evaluated according to the Union Internationale Contre le Cancer system showing stage I in 7 cases, stage II in 15, stage III in 11, and stage IV in 6. Twenty-seven patients were followed-up for more than 5 years and are still alive, but 12 patients died due to tumor progression within 5 years. The Ethics Committee of the Hospital gave approval for genetic experiments restricted to JCV.

DNA extraction

Paraffin-embedded specimens were cut into consecutive 10 μm sections for microdissection with reference to hematoxylin-and-eosin staining. Then tissues were deparaffinized in xylene followed by incubation with proteinase K and sodium dodecyl sulfate at 55°C overnight. DNA was extracted using phenol–chloroform–isoamyl method (25:24:1 ratio) and dissolved in Tris-EDTA buffer (TE, 10mM Tris-HCI+1mM EDTA, pH 7.4) after ethanol precipitation. Before DNA extraction, their DNAs were amplified using glyceraldehyde-3-phosphate dehydrogenase (GAPDH) primers (sense, 5′-ACATCAAGAAGGT GGTGAGC-3′ and anti-sense, 5′-CTGTTGCTGTAGCC AAATTCGT-3′; 199 bp) by 35 cycles of denaturation at 95°C for 60 s, annealing 53°C for 60 s, and extension at 72°C for 60 s followed by an additional 7 min at 72°C to confirm the integrity of the DNA. All reactions were modulated using the Gene Amp 9700 PCR System™ (Applied Biosystem, Forster City, USA). Ten-microliter aliquots of each PCR product were examined by electrophoresis on 8% polyacrylamide gels. Finally, the gels were stained with ethidium bromide and photographed under ultraviolet light. The cases examined in the present study were limited to the ones that showed a clear single band of GAPDH.

Quantitation of JCV DNA by real-time PCR

A real-time, fluorescence probe-based PCR method was employed for quantitative assessment of JCV in samples using the Mx3000P™ Real-Time PCR system (Stratagene, La Jolla, CA, USA). For establishment of the quantitative technique, a JCV-containing plasmid (pBS-JCVMad1, kindly provided by Associate Professor H Sawa, Department of Neuropathology, Hokkaido University, Graduate School of Medicine) was serially diluted and served as a standard reference. This standard and DNA samples of TCs, DTEs, and nasal turbinate epithelial cells (NTEs) were subjected to PCR amplification of the 128-bp sequence of the *T-antigen* using RT-JCV1, nucleotides 3492–3511, 5′-GCCACCCCAGCCATATATTG-3′ and RT-JCV-2, nucleotides 3619–3595, 5′-GTTGACAGTATCCATATGACCAG AGAA-3′ as the forward and reverse primers, respectively. The monitoring of the amplicon development was performed using a double-dye probe, RT-JCV-3, nucleotides 3515–3539, 5′-[FAM]-TAAAACAGCATTGCCATG TGCCCC A-[TAMRA]-3′. The reactions were performed using the 2x TaqMan® Universal PCR Master Mix (Applied Biosystems). Reaction mixtures (25 μl) contained 12.5 μl TaqMan® Universal PCR master mix with 2.25 μl (10 μM) of each primer, 2.5 μl (2.5 μM) of double-dye probe, and 100 ng of template DNA. The protocol included the following parameters: an initial 10 min of incubation at

95°C for TaqMan® DNA polymerase activation followed by 60 cycles of denaturation at 95°C for 30 s, annealing at 55°C for 1 min, and extension at 72°C for 30 s.

In situ PCR

Sections (10 μm thick) were digested with proteinase K (10 μg/ml) for 15 min at 37°C, then topoisomerase I was applied for 30 min at room temperature. After rinsing with phosphate-buffered saline (PBS), the tissue was fixed in 4% neutralized paraformaldehyde and subjected to washing with 2× saline sodium citrate (SSC). Then a 125-μl aliquot of the PCR solution (1 μM primers of JCT-1A, nucleotides 3052–3069, 5′-CCTGTAAAGTTCTAGGCA-3′ and JCT-1AS, nucleotides 3225–3207, 5′-AGTCAAGGGATT TACCTTC-3′, 200 μM DIG-11-dUTP, 4.5 mM $MgCl_2$, PCR buffer, 2 U *Taq* polymerase) was placed on the tissue under membrane sealing, and then PCR was performed on the slide griddle of a programmable thermal controller: 94°C for 3 min, followed by 15 cycles of 92°C for 15 s, 55°C for 15 s, 72°C for 30 s, and finally 72°C for 5 min. These primers result in the amplification of a 174-bp fragment of JCV. In the next step, the tissue was washed with 2× SSC and incubated with blocking solution, 100 μg/ml Salmon Testis DNA (Sigma, Germany), 10 μg/ml yeast tRNA (Sigma), and 5% bovine serum albumin in PBS, for 1 h. Finally, the sections were incubated with an anti-digoxigenin antibody coupled to alkaline phosphatase overnight, followed by DAKO® Fuchsin + Substrate-Chromogen System (DakoCytomation) and then were counterstained with methyl green. JCV infected neuroblastoma (JCI) cells (kindly provided by Dr. Kazuo Nagashima, Hokkaido University, Sapporro, Japan) were used as positive controls in this experiment.

DNA direct sequencing for PCR products

PCR amplicons were further confirmed by direct sequencing because there is some homology between polyomaviruses SV40, BK virus, and JCV [20]. After 35 cycles of PCR under the same conditions as real-time or in situ PCR, DNA was purified on MicroSpin Columns (Amersham Biosciences) before sequencing according to the manufacturer's instructions using a BigDye® Terminator v3.1 cycle sequencing kit and an ABI PRISM® 3100 genetic analyzer (Applied Biosystems). All sequences were analyzed for homology using the nucleotide–nucleotide "BLAST" search feature located on the National Center for Biotechnology Information Web site.

Immunohistochemistry

For immunohistochemistry, 4 μm thick sections of formalin-fixed and paraffin-embedded TCs, DTEs, NTEs, and JCI cells were deparaffinized with xylene, dehydrated through an alcohol gradient, immersed in heated target-retrieval buffered solution (DAKO) with intermittent microwave irradiation for 15 min. A methanol solution with H_2O_2 was applied for 5 min to block endogenous peroxidase. The primary antibody used was a mouse monoclonal anti-simian virus T antigen that cross-reacts with JCV T antigen (1:100 dilution; clone Pab 101; Santa Cruz Biotechnology, Santa Cruz, CA, USA). The tissue was incubated with the primary antibody overnight, followed by exposure to DAKO EnVision™ Labeled Polymer (DAKO) for 30 min. Staining was developed by a reaction with diaminobenzidine chromogen, and counterstaining for 1 min with hematoxylin was then performed.

Statistical analysis

A statistical evaluation was performed using the chi-square test to compare the positive rate and Mann-Whitney *U* test to differentiate the non-parametric means. SPSS 10.0 software was employed to analyze all data, and $p<0.05$ was considered to be statistically significant.

Results

Real-time PCR for T antigen was successful with all cases examined with a quantitative standard using plasmid pBS-JCVMad1. The PCR products for the T-antigen sequence amplified by real-time PCR were verified to be JCV (not the BK or SV40 species of polyomavirus) by DNA sequencing. The viral DNA loads were 981.6±14.0 copies/μg DNA (mean±SE; standard error range 37.8–2,338.4) in TCs, 658.3±53.3 copies/μg DNA (3.5–2,883) in DTEs and 410.5±44.3 copies/μg DNA (0–2,070.0) in glossitis. There were significant differences between TCs and DTEs and glossitis ($p<0.05$, Fig. 1a). When the JCV copy numbers in the TCs, DTEs and glossitis were divided into three groups, low (0–200 copies/μg DNA), moderate (201–1000), and high (≥1001), there were significant differences among them ($p<0.01$, Table 1). Figure 1b,c, and d show the average copy numbers in each group. The value for the control of JCI cells was 4.39×10^6 copies/μg DNA. In the TCs, the correlation between JCV copy number (low, 0–1000; high, ≥1001) and such clinicopathological variables as tumor size, stage, differentiation, and lymph node metastasis was examined, but no correlation was observed (Table 2).

In situ PCR amplification and immunohistochemical staining was accompanied by a positive control for JCV using the genomic DNA from JCI cells, which persistently is infected with JCV. In situ PCR demonstrated clear positive staining in 20–30% of the JCI cells (Fig. 2a). Some

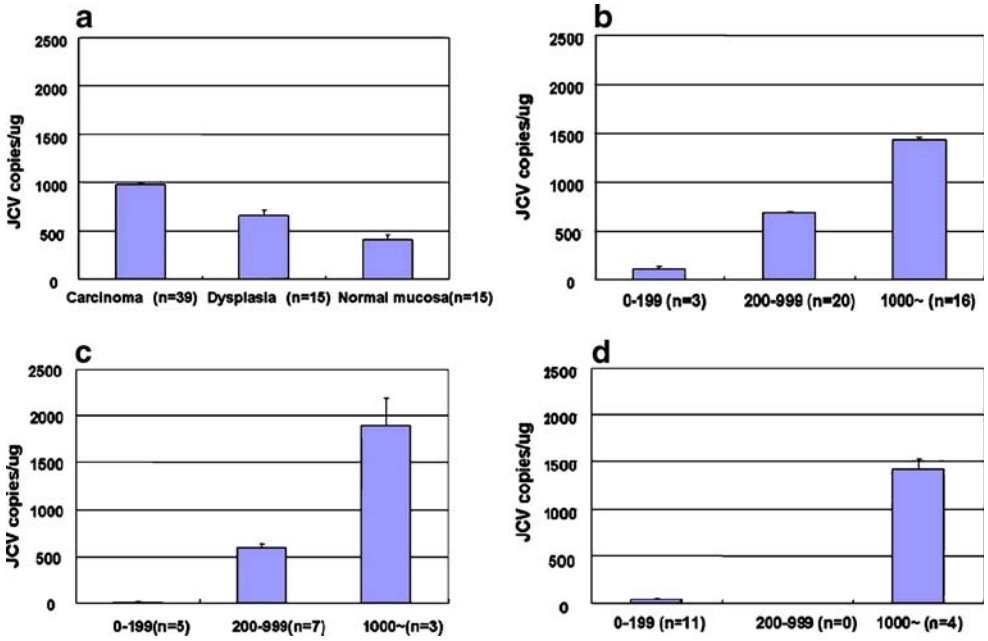


Fig. 1 JCV viral DNA loads (data are mean±SE). Distribution of JCV copies in tongue carcinoma, dysplastic tongue epithelium, and glossitis (**a**). If JCV viral DNA loads are divided into low, moderate, and high groups, numbers of different groups were indicated for TC (**b**), DTE (**c**), and glossitis (**d**). Compared with TCs, glossitis and DTC had significantly lower copies of JCV ($p<0.05$). After grouping, there were significant differences among them ($p<0.01$)

positive cells were also noted in DTEs (Fig. 2b). In some cases, positive cells were sporadically found in areas of the TCs (Fig. 2c). In the glossitis, no signals were observed in any of the cases. However, each of these PCR amplicons was confirmed further through DNA sequencing; and in each instance, the presence of JCV was validated. In this study, we observed JCV T-Ag expression occasionally in TC samples (4 of 39, 10.3%). Figure 3 shows the immunohistochemical data obtained from JCI cell line and TC. Positive nuclear staining was observed in the positive control JCI cells (Fig. 3a). The nuclear expression pattern of T antigen also appeared in TC (Fig. 3b), and no detection of T antigen was noted in glossitis. Direct cycle sequencing indicated no variation in the DNA sequences of PCR amplicons (data not shown).

Discussion

In the present study, the results of real-time PCR for determining JCV T-antigen load revealed significantly higher levels in TCs compared with DTEs and glossitis. An earlier report described that colon cancers and adenomas similarly demonstrated a higher JCV T-antigen load calculated by real-time PCR than background tissue or normal colonic mucosa [15]. From the available data, the viral DNA loads in formalin-fixed and paraffin-embedded samples in colon [15], gastric [11], and lung [20] cancers appear to be similar to our finding. According to the results of the real-time PCR, the JCV copy number was calculated to be around one copy per ten cells in TCs on the basis of the DNA extraction procedure from oral squamous cell carcinoma cells (about 100,000 cells/μg DNA, data not shown). If the presence of JCV is associated with the development of cancer, then one might expect to find one virus genome per human genome in cancer tissue but not in normal tissue. In a previous study of gastric cancers using fresh frozen samples, the JCV DNA loads were found to be about 4,800 copies/μg DNA in gastric cancers, about 5,400

Table 1 JCV viral DNA loads divided into low, moderate and high groups in TCs, DTEs, and glossitis

Groups	0–200 copies/μg DNA	201–1,000 copies/μg DNA	≥1001 copies/μg DNA
TC	3	21	15
DTE	5	7	3
NTE	11	0	4

Footnotes: $p<0.01$

Table 2 Correlation between the clinicopathological variables and JCV viral DNA loads

Groups	0 – 1000 copies/μg DNA	1001 – copies/μg DNA	*p* value
Size	29.7±7.7 cm	32.8±11.4 cm	>0.05
Stage			
0–II	14	8	
III, IV	10	7	
Differentiation			>0.05
Well	16	8	
Mod, poor	8	7	
Metastasis			>0.05
–	17	8	
+	7	7	

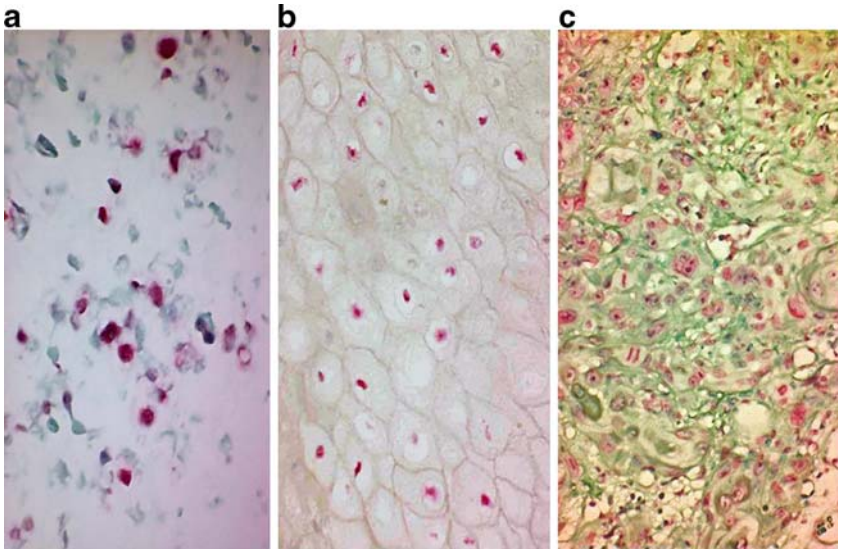


Fig. 2 In situ PCR for T-antigen. **a** JCI cells infected by JCV as positive control, of which 20–30% cells are positive for T-antigen. **b** DTE, low grade dysplasia in line with so-called leukoplakia. Clear positive signals can be seen in the nuclei. **c** TC, moderately differentiated squamous cell carcinoma. Moderately intense but clear signals are noted in the nuclei

in paired adjacent noncancerous tissues, and 540 in normal gastric tissues. When the corresponding samples were processed by formalin fixation and paraffin embedding, the JCV DNA load was reduced to one sixth in gastric cancers, 1/20 in adjacent non-cancerous tissues, and one fifth in normal gastric mucosa [11]. The value of 981.5 copies/μg DNA in TCs in the present study may thus correspond to 4,900 (×5) to 19,630 (×20) in fresh frozen samples. Those numerical values of JCV copies may indicate its oncogenic role in the malignancies, including TCs.

When the viral DNA loads were divided into three groups, low, moderate and high, the TCs included 15 high cases (38.4%), 21 moderate (53.8%), and 3 low (7.7%), on the contrary, glossitis had only 4 high cases (26.6%) and almost none of JCV DNA in the other 11 cases. DTEs occupied an intermediate position between them. It is possible that a JCV infection of the glossitis is a major risk factor for tongue carcinomas, and some of them develop into dysplasia and finally carcinoma. In fact, Epstein–Barr virus was not detected by in situ RNA hybridization in our cases. It was the same for human papilloma virus type 16 and 18 by PCR (data not shown). The presence of high viral DNA loads was not correlated with any clinicopathological variables that may support the hypothesis that JCV infection is not directly linked to cancer progression. However, it is still possible that JCV may play some role in the oncogenesis of tongue carcinoma.

While Zambrano et al. [19] used in situ hybridization (ISH) to reveal the sporadic presence of JCV in normal prostatic glandular epithelium, data on the actual infection levels were not available. No signals were detected by ISH in the current study except in the positive controls (data not shown), possibly due to the small copy number. In contrast, in situ PCR can detect even a few viral copies per cell [16], and sporadic nests of positive cells were detected in TCs and DTEs but not in glossitis, which is consistent with the viral DNA loads observed. T-antigen protein expression was observed by immunohistochemistry in only four cases of TCs and DTE as opposed to the observations of Shin et al. [13]. Although we employed the antibody against SV40 T antigen, our data should be reliable enough to confirm the JCV localization because we evaluated the immunolabeling positivity of JCV T antigen taken together with the data of real-time PCR. In these experiments, it was difficult to prove the clear positivity of T-antigen protein, but the antibody used in the present study had limited success. It is thought that the half-life of T-antigen protein might be very short, and it is not easy to detect the T-antigen positivity

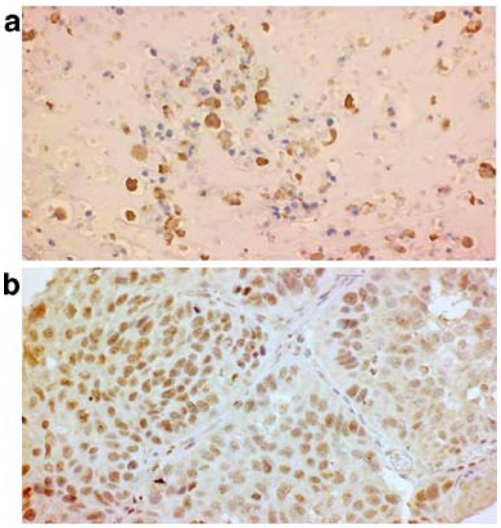


Fig. 3 Immunohistochemistry for T-antigen protein. **a** JCI cells as a positive control, of which 20–30% cells are positive. **b** TC, well differentiated squamous cell carcinoma. Moderately intense but clearly positive localization is visible in the nuclei

when formalin-fixed and paraffin-embedded tissues are used.

An earlier study demonstrated the presence of replicating JCV DNA in B lymphocytes from peripheral blood, tonsil, and spleen, and it has been hypothesized that lymphocytes may thus be one site of JCV persistence [10]. The detection of viral gene products in renal tubules and the excretion of JC virions in the urine indicate JCV persistence in the kidney [1]. In the present study, JCV DNA contamination from JCV persistent B lymphocytes in the oral mucosa, which contain B lymphocytes, could not be ruled out. However, the majority of JCV-infected cells observed by in situ PCR were tonsil stromal cells rather than B lymphocytes with using tonsil tissues (data not shown), which is consistent with the findings of Monaco et al. [10].

In conclusion, the presence of JCV in normal tongue tissue may be a risk factor for tumorigenesis of tongue carcinoma, and the possibility that JCV may play some oncogenetic role can thus not be ruled out. Further investigations to explore this possibility therefore appear to be warranted.

Acknowledgment We particularly thank Ms. Kanako Yasuyoshi and Mr. Tokimasa Kumada and Hideki Hatta for their expert technical support for the tissue preparation and immunohistochemistry. This work was supported by Japanese Smoking Science Foundation.

Open Access This article is distributed under the terms of the Creative Commons Attribution Noncommercial License which permits any noncommercial use, distribution, and reproduction in any medium, provided the original author(s) and source are credited.

References

1. Boldorini R, Veggiani C, Barco D, Monga G (2005) Kidney and urinary tract polyomavirus infection and distribution: molecular biology investigation of 10 consecutive autopsies. Arch Pathol Lab Med 129:69–73
2. Del Valle L, Gordon J, Assimakopoulou M, Enam S, Geddes JF, Varakis JN, Katsetos CD, Croul S, Khalili K (2001) Detection of JC virus DNA sequences and expression of the viral regulatory protein T-antigen in tumors of the central nervous system. Cancer Res 61:4287–4293
3. Del Valle L, Gordon J, Enam S, Delbue S, Croul S, Abraham S, Radhakrishnan S, Assimakopoulou M, Katsetos CD, Khalili K (2002) Expression of human neurotropic polyomavirus JCV late gene product agnoprotein in human medulloblastoma. J Natl Cancer Inst 94:267–273
4. Del Valle L, White MK, Enam S, Oviedo SP, Bromer MQ, Thomas RM, Parkman HP, Khalili K (2005) Detection of JC virus DNA sequences and expression of viral T antigen and agnoprotein in esophageal carcinoma. Cancer 103:516–527
5. Eash S, Tavares R, Stopa EG, Robbins SH, Brossay L, Atwood WJ (2004) Differential distribution of the JC virus receptor-type sialic acid in normal human tissues. Am J Pathol 164:419–428
6. Enam S, Del Valle L, Lara C, Gan DD, Ortiz-Hidalgo C, Palazzo JP, Khalili K (2002) Association of human polyomavirus JCV with colon cancer: evidence for interaction of viral T-antigen and β-catenin. Cancer Res 62:7093–7101
7. Frisque RJ, Bream GL, Cannella MT (1984) Human polyomavirus JC virus genome. J Virol 51:458–469
8. Gan DD, Reiss K, Carrill T, Del Valle L, Croul S, Giordano A, Fishman P, Khalili K (2001) Involvement of Wnt signaling pathway in murine medulloblastoma induced by human neurotropic JC virus. Oncogene 20:4864–4870
9. Krynska B, Gordon J, Otte J, Franks R, Franks R, Knobler R, DeLuca A, Giordano A, Khalili K (1997) Role of cell cycle regulators in tumor formation in transgenic mice expressing the human neurotropic virus, JCV, early protein. J Cell Biochem 67:223–230
10. Monaco MC, Jensen PN, Hou J, Durham LC, Major EO (1998) Detection of JC virus DNA in human tonsil tissue: evidence for site of initial viral infection. J Virol 72:9918–9923
11. Murai Y, Zheng HC, Aziz HO, Mei H, Kutsuna T, Nakanishi Y, Tsuneyama K, Takano Y (2007) High JC virus load in gastric cancer and adjacent non-cancerous mucosa. Cancer Sci 98:25–31
12. Padgett BL, Walker DL (1973) Prevalence of antibodies in human sera against JC virus, an isolate from a case of progressive multifocal leukoencephalopathy. J Infect Dis 127:467–470
13. Shin SK, Li MS, Fuerst F, Hotchkiss E, Meyer R, Kim IT, Goel A, Boland CR (2006) Oncogenic T-antigen of JC virus is present frequently in human gastric cancers. Cancer 107:481–488
14. Shollar D, Del Valle L, Khalili K, Otte J, Gordon J (2004) JCV T-antigen interacts with the neurofibromatosis type 2 gene product in a transgenic mouse model of malignant peripheral nerve sheath tumors. Oncogene 23:5459–5467
15. Theodoropoulos G, Panoussopoulos D, Papaconstantinou I, Gazouli M, Perdiki M, Bramis J, Lazaris ACh (2005) Assessment of JC polyoma virus in colon neoplasms. Dis Colon Rectum 48:86–91
16. Ueki K, Richardson EP Jr., Henson JW, Louis DN (1994) In situ polymerase chain reaction demonstration of JC virus in progressive multifocal leukoencephalopathy, including an index case. Ann Neurol 36:670–673
17. Vogelstein B, Lane D, Levine AJ (2000) Surfing the p53 network. Nature 408:307–310
18. Weber T, Major EO (1997) Progressive multifocal leukoencephalopathy: molecular biology, pathogenesis and clinical impact. Intervirology 40:98–111
19. Zambrano A, Kalantari M, Simoneau A, Jensen JL, Villarreal LP (2002) Detection of human polyomaviruses and papillomaviruses in prostatic tissue reveals the prostate as a habitat for multiple viral infections. Prostate 53:263–276
20. Zheng H, Abdel Aziz HO, Nakanishi Y, Masuda S, Saito H, Tsuneyama K, Takano Y (2007) Oncogenic role of JC virus in lung cancer. J Pathol 212:306–315

Virchows Arch (2008) 452:411–414
DOI 10.1007/s00428-008-0589-6

ORIGINAL ARTICLE

Expression of Epstein–Barr-virus-encoded small nuclear RNA in nasopharyngeal carcinomas of Aegean Turkish patients

Yeşim Ertan · Mine Hekimgil · Serap Karaarslan · Saliha Soydan

Received: 9 October 2007 / Revised: 11 January 2008 / Accepted: 23 January 2008 / Published online: 26 February 2008
© Springer-Verlag 2008

Abstract Nasopharyngeal carcinomas (NPC) are epithelial neoplasms which show a distinct geographical distribution and have a characteristic histology. These tumors have multifactorial etiology, including virological, environmental, and genetic components. The aim of the present study is to assess the relation between Epstein–Barr-virus (EBV) and subtypes of NPC in Aegean Turkish patients. In the present study, nasopharyngeal biopsies of 84 cases diagnosed as nasopharyngeal carcinoma, between 1998 and 2004, were reevaluated. In situ hybridization with the fluorescein-conjugated EBV-encoded small nuclear RNA (EBER) oligonucleotide probe was performed on paraffin-embedded tissue sections using an automated slide stainer system. Of 84 patients, 55 were men and 29 were women with ages ranging between 7 and 77 years (median 50, mean 46.73). Seventy-three of 84 cases were EBER positive. All of 62 cases (100.0%) with undifferentiated carcinoma, 8 of 16 (50.0%) with differentiated nonkeratinizing carcinoma, and three of six (50.0%) with keratinizing squamous cell carcinoma were EBV positive. EBER positivity was statistically significantly higher in undifferentiated carcinomas, compared to the other morphological subtypes ($p=0.000$). Our results showed that all morphological subtypes of NPC are highly associated with EBV latent infection in our region, and a higher prevalence was found for the undifferentiated subtype.

Keywords Nasopharyngeal carcinoma · EBER · *in situ* hybridization

Y. Ertan (✉) · M. Hekimgil · S. Karaarslan · S. Soydan
Department of Pathology, Ege University Faculty of Medicine, Izmir, Turkey
e-mail: yesim.ertan@ege.edu.tr

Introduction

Nasopharyngeal carcinoma (NPC) is a rare epithelial tumor that has been classified into three types by the World Health Organization (WHO): squamous cell carcinoma (WHO type 1), nonkeratinizing carcinoma, differentiated (WHO type 2) or undifferentiated (WHO type 3), and basaloid squamous cell carcinoma [3]. The incidence varies greatly with geographical location, age, and race, occurring mainly in Southeast Asia but rare in Europe and North America [22]. NPC has a multifactorial etiology, including genetic predisposition and viral and environmental factors, but Epstein–Barr virus (EBV) appears to be the strongest related factor worldwide. As well known, EBV is associated with certain lymphoid malignancies such as Burkitt's lymphoma [5], Hodgkin's lymphoma [26], and T cell lymphoma [13]. EBV is also frequently present in the carcinomas of nasopharynx, stomach, lung, thymus, and salivary gland [9, 15, 16, 19, 23, 27].

Serology [14], Southern blotting [21], polymerase chain reaction (PCR) [1], immunohistochemistry [17], and DNA in situ hybridization (ISH) [16] are used to demonstrate an association between EBV and NPC. But the rate of positive cases of EBV in NPCs varies with each method used [12]. ISH techniques that target viral DNA or mRNA are of limited use in NPC because of the low genomic copy numbers and low mRNA transcription in latent infections, but the abundant expression of nuclear EBV-encoded small nonpolyadenylated RNAs (EBERs) in latently infected cells makes them ideal targets for ISH [22]. EBER was shown to be a target nucleic acid for ISH detection of EBV in formalin-fixed, paraffin-embedded tissue sections because of its high copy number in latent EBV-infected cells [11].

In the literature, to our knowledge, there has been no previous study using EBER ISH for the detection of latent EBV in NPCs of the Turkish population. Thus, this study was performed to assess EBV status in Turkish patients with NPC using EBER ISH.

Materials and methods

Patients

In this study, 84 cases with nasopharyngeal carcinoma which were diagnosed during the period 1998–2004 in our pathology department were included. The nasopharyngeal biopsies were examined histologically and subclassified according to the WHO classification. Tissue sections were available for EBER ISH in all cases.

Methods

ISH for EBER was performed on 5-μm-thick paraffin-embedded tissue sections using an automated slide stainer system (Benchmark XT**,** Ventana Medical Systems, Tucson, AZ, USA). Briefly, after deparaffinization and rehydration, tissues were treated with proteinase K and hybridized with the fluorescein-conjugated EBER oligonucleotide probe (INFORM EBER Probe, Ventana Medical Systems, Tucson, AZ, USA). The hybridized probe was detected by using an in situ hybridization detection system (ISH iVIEW Blue Detection Kit, Ventana Medical Systems, Tucson, AZ, USA) utilizing an anti-fluorescein primary antibody which binds to the EBER probe and a biotinylated secondary antibody formulation that binds to the primary mouse antibody. This step is followed by an indirect biotin streptavidin system coupled to an enzyme substrate (5-bromo-4-chloro-3-indolyl phosphate–nitro blue tetrazolium). First, a streptavidin enzyme conjugate binds to the biotin present on the secondary antibody. The specific antibody, secondary antibody, and the streptavidin enzyme complex are then visualized by light microscopy utilizing a precipitating enzyme-generated product. Each step is incubated for a precise time and temperature. At the end of each incubation step, the automated slide stainer washes the sections to stop the reaction and remove the unbound material that would hinder the desired reaction in subsequent steps. Liquid Coverslip is applied which minimizes the evaporation of aqueous reagents on the surface of the specimen-containing slide. Serial sections of lymph nodes of a case of infectious mononucleosis and five cases diagnosed as Hodgkin's disease which previously demonstrated to harbor EBV-latent membrane protein 1 (LMP1) were used as positive controls.

Statistical analysis

Statistical analyses were carried out by computer-based program SPSS (version 14.0). Student's *t* test was used to compare means of continuous variables and Pearson's chi-square and Fisher's exact tests to compare the association between the histological subtypes and EBER positivity. *p* value less than 0.05 was accepted to display the significance of differences.

Results

Of 84 patients, 55 were men and 29 were women with ages ranging between 7 and 77 years (median 50, mean 46.73). According to the WHO classification, 62 cases (73.9%) of undifferentiated carcinoma, 16 cases (19.0%) of differentiated nonkeratinizing carcinoma and six (7.1%) of keratinizing squamous cell carcinoma were included in the study.

In the present study, EBER ISH was positive in 73 (86.9%) of the 84 samples. According to histological subtypes, all of 62 cases (100.0%) with undifferentiated carcinoma (Fig. 1a), eight of 16 (50.0%) with differentiated nonkeratinizing carcinoma (Fig. 1b), and three of six (50.0%) with keratinizing squamous cell carcinoma were EBV positive.

Of the 73 EBER-positive cases, 62 (84.9%) were undifferentiated carcinoma; eight (11.0%) were differentiated nonkeratinizing carcinoma, and three (4.1%) were keratinizing squamous cell carcinoma. In our study, EBER positivity was statistically significantly higher in undifferentiated carcinomas, compared to the other morphological subtypes ($p=0.000$).

Among those patients who were EBER positive, almost all tumor nuclei had EBER signals. There was no statistically significant difference between age, sex, and EBER positivity.

Discussion

ISH for EBER is the most sensitive and specific method for identification of EBV in specific cells [4, 8, 22, 25]. This method relies on the natural biological amplification of the target sequence, which results in numerous EBER transcripts [22]. These EBERs are highly transcribed in all latently infected cells with up to 10^6 copies in EBV-infected cells [2, 10]. This study confirms the relationship between EBV and various histological subtypes of NPC in Aegean Turkish patients and demonstrates that ISH for EBER detects the presence of latent EBV infection in the tumor tissue of most cases.

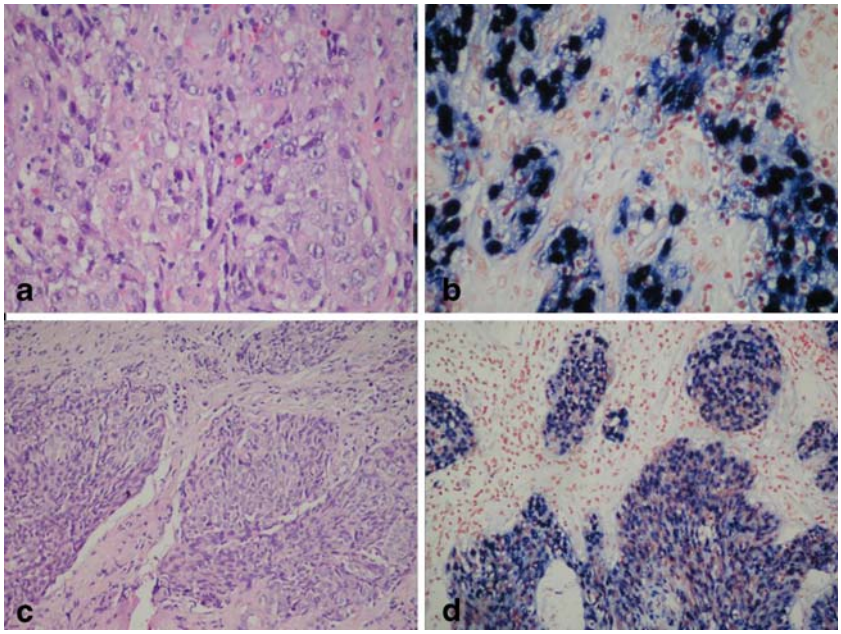


Fig. 1 **a** Undifferentiated carcinoma stained with hematoxylin and eosin (original magnification ×400) **b** Nuclear staining for EBER by in situ hybridization in undifferentiated carcinoma (original magnification ×400) **c** Non-keratinizing squamous cell carcinoma stained with hematoxylin and eosin (original magnification x 200) **d** Nuclear staining for EBER by *in situ* hybridization in nonkeratinizing squamous cell carcinoma (original magnification ×200)

In the literature, there are several studies from different regions of the world which have demonstrated EBER in NPC (Table 1). Because NPC is one of the predominant tumors in the population in Southern China, reaching 80 cases per 100,000 population per year, the largest series are reported from this region [22]. In a study of 120 cases of NPC in which the patients were predominantly Chinese, EBER were expressed in most neoplastic cells of NPC, including all three WHO types of NPC [18]. In that same study, it was also found that EBER in nonkeratinizing carcinoma and undifferentiated carcinoma were higher than in differentiated squamous cell carcinoma. In the study of 107 cases of NPC from Taiwan [24], EBV was detected by PCR in 97 cases and by EBER in situ hybridization in 105 cases. They reported that sensitivity of EBER ISH was somewhat higher compared to that of PCR. Because of the high sensitivity and specificity of EBER ISH, they suggested that this method can be useful for the routine histology in the evaluation of materials from patients who have a high risk of NPC. In a study on Japanese patients, it was found that EBER1 transcripts were localized to the nucleus of tumor cells in all 39 cases of NPC, including the keratinizing subtype and was suggested that all morphological subtypes of NPC were highly associated with EBV latency which has been detected by EBER ISH; thus, EBV would appear to be essential for the oncogenesis of all NPCs [12].

But the incidence of NPC in Western countries is lower than that in the far east and an intermediate incidence of NPC has been noted in countries of the Mediterranean basin. A study from Spain reported EBV positivity in 29 of 30 NPC by EBER ISH [20]. And another study from Italy demonstrated that 16 of 24 cases of nonkeratinizing NPC were positive by EBER ISH [6]. The study from Israel found a relatively high association of NPC and latent EBV infection, in which 40 of 45 patients were positive by EBER ISH [22].

In the present study, 100% of nonkeratinizing carcinoma, undifferentiated type were positive with EBER ISH and most of the previous studies report a high correlation of EBER expression [7, 16, 22], similar to our results. An association between EBER1 expression and undifferentiated histology was also found in a study from the US and Canada that included 32 of 45 cases of NPC, but lymphoepithelioma-like carcinomas of the bladder were uniformly EBV negative [7]. In both of these two studies, LMP1 immunohistochemistry was less sensitive in detecting EBV latency in NPC, compared to EBER ISH [7, 22].

Table 1 Increasing frequency of EBER positivity of nasopharyngeal carcinomas according to different geographic locations

Gabusi E et al. Italy, 2001 [6]	*Gulley ML et al.* United States and Canada, 1995 [7]	*Ertan Y et al.* Turkey, 2007 (current study)	*Sela GB et al.* Israel, 2004 [22]	*Plaza G et al.* Spain, 2002 [20]	*Tsai ST et al.* Taiwan, 1998 [24]	*Pathmanathan R et al.* Malaysia, 1995 [18]	*Inoue H et al.* Ja pan, 2002 [12]
16/24 (66.6%)	32/45 (71.1%)	73/84 (86.9%)	40/45 (88.8%)	29/30 (96.6%)	105/107 (98.1%)	120/120 (100%)	39/39 (100%)

This study was performed to assess EBV status in our patients with NPC because there has been no previous study in the literature using EBER ISH in the Turkish population. In the present study, our results were intermediate compared to previous studies reported from the eastern and western parts of the world; EBER ISH were found positive in 86.9% of all histologic types of NPCs and in 100% of those with undifferentiated histology. In conclusion, as detected by EBER ISH, latent EBV infection was statistically significantly more prevalent in patients with undifferentiated carcinoma, compared to other types of NPC, in Aegean Turkish patients, similar to earlier studies.

Acknowledgement Authors thank Mrs. H. Uluer for her help in assessing the statistical analysis.

Conflict of interest statement We declare that we have no conflict of interest.

References

1. Akao I, Sato Y, Mukai K, Uhara H, Furuya S, Hoshikawa T, Shimosato Y, Takeyama I (1991) Detection of Epstein–Barr virus DNA in formalin-fixed paraffin-embedded tissue of nasopharyngeal carcinoma using polymerase chain reaction and *in situ* hybridization. Laryngoscope 101:279–283
2. Arrand JR, Rymo L (1982) Characterization of the major Epstein–Barr virus-specific RNA in Burkitt Lymphoma-derived cells. J Virol 41:376–389
3. Barnes L, Eveson J, Reichart P, Sidransky D (2005) Tumours of the nasopharynx. World Health Organization classification of tumours. Pathology and genetics of tumours of the head and neck tumours. IARC, Lyon, pp 83–97
4. Chang KL, Chen Y-Y, Shibata D, Weiss LM (1992) Description of an *in situ* hybridization methodology for detection of Epstein–Barr virus RNA in paraffin-embedded tissues, with a survey of normal and neoplastic tissues. Diag Mol Pathol 1:246–255
5. Epstein MA, Achong BG, Barr YM (1964) Virus particles in cultured lymphoblasts from Burkitt's lymphoma. Lancet 1:702–703
6. Gabusi E, Lattes C, Fiorentino M, D'Errico A, Grigioni WF (2001) Expression of Epstein–Barr virus-encoded RNA and biological markers in Italian nasopharyngeal carcinomas. J Exp Clin Cancer Res 20:371–376
7. Gulley ML, Amin MB, Nicholls JM, Banks PM, Ayala AG, Srigley JR, Eagan PA, Ro JY (1995) Epstein–Barr virus is detected in undifferentiated nasopharyngeal carcinoma but not in lymphoepithelioma-like carcinoma of the urinary bladder. Hum Pathol 26:1207–1214
8. Hamilton-Dutoit SJ, Pallesen G (1994) Detection of Epstein–Barr virus small RNAs in routine paraffin sections using non-isotopic RNA/RNA *in situ* hybridization. Histopathology 25:101–111
9. Hamilton-Dutoit SJ, Therkildsen MH, Neilsen NH, Jensen H, Hansen JP, Pallesen G (1991) Undifferentiated carcinoma of the salivary gland in Greenlandic Eskimos: demonstration of Epstein–Barr virus DNA by *in situ* nucleic acid hybridization. Hum Pathol 22:811–815
10. Howe JG, Steitz J (1986) Localization of Epstein–Barr virus-encoded small RNAs by *in situ* hybridization. Proc Natl Acad Sci U S A 83:9006–9010
11. Howe JG, Shu MD (1988) Isolation and characterization of the genes for two small RNAs of herpesvirus papio and their comparison with Epstein–Barr virus-encoded EBER RNAs. J Virol 62:2790–2798
12. Inoue H, Sato Y, Tsuchiya B, Nagai H, Takahashi H, Kameya T (2002) Expression of Epstein–Barr virus-encoded small nuclear RNA1 in Japanese nasopharyngeal carcinomas. Acta Otolaryngol Suppl 547:113–117
13. Jones JF, Shurin S, Abramowsky C, Tubbs RR, Sciotto CG, Wahl R, Sands J, Gottman D, Katz BZ, Sklar J (1988) T-cell lymphomas containing Epstein–Barr viral DNA in patients with chronic Epstein–Barr virus infections. N Engl J Med 318:733–741
14. Lanier AP, Bornkamm GW, Henle W, Henle G, Bender TR, Talbot ML, Dohan PH (1981) Association of Epstein–Barr virus with nasopharyngeal carcinoma in Alaskan native patients: serum antibodies and tissue EBNA and DNA. Int J Cancer 28:301–305
15. Leyvraz S, Henle W, Chahinian AP, Perlmann C, Klein G, Gordon RE, Rosenblum M, Holland JF (1985) Association of Epstein–Barr virus with thymic carcinoma. N Engl J Med 312:1296–1299
16. Niedobitek G, Hansmann ML, Herbst H, Young LS, Dienemann D, Hartmann CA, Finn T, Pitteroff S, Welt A, Anagnostopoulos I et al (1991) Epstein–Barr virus and carcinomas: undifferentiated carcinomas but not squamous cell carcinomas of the nasopharynx are regularly associated with the virus. J Pathol 165:17–24
17. Niedobitek G, Fahraeus R, Herbst H, Latza U, Ferszt A, Klein G, Stein H (1992) The Epstein–Barr virus encoded membrane protein (LMP) induces phenotypic changes in epithelial cells. Virchows Arch B Cell Pathol Incl Mol Pathol 62:55–59
18. Pathmanathan R, Prasad U, Chandrika G, Sadler R, Flynn K, Traub RN (1995) Undifferentiated, nonkeratinizing, and squamous cell carcinoma of the nasopharynx: variants of Epstein Barr virus-infected neoplasia. Am J Pathol 146:1355–1367
19. Pittaluga S, Wong MP, Chung LP, Loke SL (1993) Clonal Epstein–Barr virus in lymphoepithelioma-like carcinoma of the lung. Am J Surg Pathol 17:678–682
20. Plaza G, Manzanal AI, Fogué L, Santón A, Martínez-Montero JC, Bellas C (2002) Association of Epstein–Barr virus and nasopharyngeal carcinoma in Caucasian patients. Ann Otol Rhinol Laryngol 111:210–216
21. Raab-Traub N, Flynn K, Pearson G, Huang A, Levine P, Lanier A, Pagano J (1987) The differentiated form of nasopharyngeal carcinoma contains Epstein–Barr virus DNA. Int J Cancer 39:25–29
22. Sela GB, Kuten A, Minkov I, Ari GE (2004) Prevalence and relevance of EBV latency in nasopharyngeal carcinoma in Israel. J Clin Pathol 57:290–293
23. Shibata D, Weiss LM (1992) Epstein–Barr virus-associated gastric carcinoma. Am J Pathol 140:769–774
24. Tsai ST, Jin YT, Mann RB, Ambinder RF (1998) Epstein–Barr virus detection in nasopharyngeal tissues of patients with suspected nasopharyngeal carcinoma. Cancer 82:1449–1453
25. Weiss LM, Chang KL (1996) Association of Epstein-Barr virus with hematolymphoid neoplasia. Adv Anat Pathol 3:1–15
26. Weiss LM, Movahed LA, Warnke RA, Sklar J (1989) Detection of Epstein–Barr viral genomes in Reed–Sternberg cells of Hodgkin's disease. N Engl J Med 320:502–506
27. Weiss LM, Movahed LA, Butler AE, Swanson SA, Frierson HF Jr, Cooper PH, Colby TV, Mills SE (1989) Analysis of lymphoepithelioma and lymphoepithelioma-like carcinomas for EBV genomes by *in situ* hybridization. Am J Surg Pathol 13:625–631

Virchows Arch (2008) 452:415–426
DOI 10.1007/s00428-007-0545-x

ORIGINAL ARTICLE

Mitochondrial expression of the two-pore domain TASK-3 channels in malignantly transformed and non-malignant human cells

Zoltán Rusznák · Gábor Bakondi · Lívia Kosztka · Krisztina Pocsai · Beatrix Dienes · János Fodor · Andrea Telek · Mónika Gönczi · Géza Szűcs · László Csernoch

Received: 17 July 2007 / Revised: 20 October 2007 / Accepted: 31 October 2007 / Published online: 20 December 2007
© Springer-Verlag 2007

Abstract The presence of TASK-3 channels has been described in a number of healthy and malignantly transformed cells, showing mainly intracellular distribution with relatively insignificant labelling of the cell surface membrane. In this work, immunochemical and molecular biology methods were utilised to establish the intracellular organelle whose TASK-3 expression accounts for this strong intracellular labelling using cultured melanoma and HaCaT cells. Before the immunocytochemical experiments, the presence of TASK-3 mRNA was also confirmed in melanoma cells. Comparison of the results of the TASK-3- and mitochondrion-specific labelling indicated that the TASK-3 channel subunits were strongly expressed by mitochondria in both investigated cell types. Moreover, prominent TASK-3 expression of keratinocytes could also be demonstrated in histological sections excised from the human skin. These results indicate that TASK-3 channels are present in the mitochondria in both malignantly transformed and healthy cells, suggesting that they might have roles in ensuring mitochondrial functions.

Keywords TASK-3 channel · Melanoma · HaCaT cells · Keratinocytes · Mitochondrion

Z. Rusznák · G. Bakondi · L. Kosztka · K. Pocsai · B. Dienes · J. Fodor · A. Telek · M. Gönczi · G. Szűcs · L. Csernoch (✉)
Department of Physiology,
Research Centre for Molecular Medicine,
Medical and Health Science Centre, University of Debrecen,
Debrecen, P.O. Box 22, 4012, Hungary
e-mail: csl@phys.dote.hu

Introduction

TASK-3 channels [5, 18] are representatives of the two-pore domain K^+ channel family [17]. As their name indicates [TWIK (Tandem pore-domain in weak inward rectifier K^+ channels)-related acid-sensitive K^+ channels], they are sensitive to alterations of the extracellular pH, closing on acidification with a p*K* of 6.4–6.8 [5, 18, 22, 28]. Many functional studies have indicated that TASK-3 channels are involved in a number of physiological functions, including regulation of aldosterone secretion [7], adjustment of neuronal excitability [1, 3, 11, 12, 14, 16, 21, 23,], providing hypoxia and acid sensitivity of the peripheral chemoreceptors [13, 32, 33] and shaping the duration of postsynaptic events [6]. Interestingly, TASK-3 channels also participate in some other phenomena where their exact functions are less obvious. TASK-3 channel subunits, for example, seem to have essential roles in the induction of apoptotic cell death of cerebellar granule cells [20]. Although the TASK-channel-induced apoptosis may be the consequence of the cell volume decrease occurring as the result of the K^+, Cl^- and water movements, and/or the reduction of the intracellular K^+ concentration leading to the activation of caspases and nucleases, the exact connection between the activity of TASK channels and the apoptotic cell death is still unclear.

Despite the pro-apoptotic functions, TASK-3 channels may also serve tumourigenic functions. Amplification of the kcnk9 gene (encoding the TASK-3 protein) has been noted in a number of malignant tumours, accompanied by a 5- to 100-fold overexpression of the channel protein in a significant portion (44%) of the investigated breast and

lung cancers [24]. TASK-3 expression was also reported in malignant stomach and large intestinal tumours [19], and in a recent study, very strong TASK-3 expression has been noted in malignant melanoma cells both in vitro and in vivo [26]. Immunocytochemical and immunohistochemical studies pointed out that the TASK-3 expression was present mostly intracellularly, with relatively insignificant cell surface labelling, suggesting that there might be cell organelles with significant TASK-3 expression. However, the suitable explanation of this unexpected distribution pattern of the TASK-3 channel protein is still missing. In fact, information about the possible intracellular targets of the TASK-3 channel subunits would be particularly important, as their presence in some well-specified organelles might significantly aid further studies trying to establish the precise link between the TASK-3 expression and the tumourigenic potential of these channels. Furthermore, as TASK-3 channels are considered as potential future targets of tumour therapy, it would be essential to establish where they are situated and what they exactly do in either malignantly transformed or healthy cells.

The primary aim of the present work was to find the intracellular structure whose TASK-3 expression is mainly responsible for the significant intracellular localisation of the TASK-3-specific immunopositivity. Before commencing the immunocyto- and immunohistochemical work, the TASK-3 expression of melanoma cells was confirmed at the mRNA level. Moreover, it was also shown that the sequence of mRNA isolated from the melanoma cells did not show mutation. For the first time, intense TASK-3 expression was demonstrated in HaCaT cells maintained in cell culture as well as in keratinocytes of the human epidermis and hair follicles. Most importantly, the results indicated that the previously noted but hitherto unexplained intracellular localisation of the TASK-3 immunopositivity was the consequence of the mitochondrial expression of these channels.

Materials and methods

Cell culture: WM35 malignant melanoma, HaCaT human keratinocyte and C2C12 murine skeletal myoblast cell lines

The WM35 is an established melanoma cell line isolated from a primary, radial growth phase tumour site. Melanoma cells were cultured in RPMI 1640 medium containing 10% fetal bovine serum (FBS), 2 mM L-Glutamine, 50 U/ml penicillin, 50 μg/ml streptomycin and 1.25 μg/ml fungizone (Biogal, Debrecen, Hungary). HaCaT keratinocytes were continuously cultured in endotoxin-free Dulbecco's modified Eagle's medium (DMEM) solution on sterilized coverslips as described before [10]. For the transfection experiments, C2C12 cells (a murine skeletal myoblast cell line) were cultured in DMEM medium supplemented with 10% FBS, 50 U/ml penicillin, 50 μg/ml streptomycin and 1.25 μg/ml fungizone. In all cases, cell passage was performed when the confluence was about 80%. All chemicals were purchased from Sigma-Aldrich (St. Louis, MO, USA) unless indicated otherwise.

Amplification and sequencing of the TASK-3-specific mRNA isolated from melanoma cells

Total RNA was extracted from melanoma cells and was reverse transcribed to cDNA. The following polymerase chain reaction (PCR) primer pairs for the human TASK-3 gene were designed to enable the individual amplification of three specific parts of the entire coding sequence from the purified samples: FW 5′ ATGAAGAGGCAGAACGTGCG and Rev 5′ TCGCTGCTGATGTTGTACTTC (beginning from the start codon and 199 bases from the start codon of human TASK-3, respectively); FW 5′ GCTGAAGCGCATT AAGAAGTG and Rev 5′ AACTGACTTCCGGCGTTTCA (466 and 1152 bases from the start codon, respectively); FW 5′ GCGAGGAGGAGAAACTCAAAGC and Rev 5′ GAGAAGAAGCCCACAGTCACCAT (156 and 524 bases from the start codon, respectively). The amplified PCR products (the first 169 base pairs, encoding the N terminus of the protein; the last 708 base pairs, encoding the C terminus of the protein; and the middle 391 base pairs, encoding the first pore-forming region) were gel-extracted, purified and sequenced.

Transient transfection of C2C12 cells

C2C12 cells were transfected with a human TASK-3-encoding plasmid (pcDNA3 hTASK3/7; a kind gift from Prof. Peter R. Stanfield and Dr. Ian Ashmole). The TASK-3 cDNA was blunt end cloned into the *Eco*RV site of the vector pcDNA3 (Invitrogen, Carlsbad, CA, USA). Transient transfection was performed on cells seeded onto coverslips (with 2 μg plasmid DNA on each coverslip) using Superfect transfection reagent (Qiagen, Hilden, Germany). Cells were allowed to express the introduced gene for 48 h after the transfection under tissue culture conditions (5% CO_2, 37°C).

Mitochondrial labelling

Mitochondrial labelling was achieved by employing a mitochondrion-selective fluorescent dye [MitoTracker® Red CMXRos (M-7512) probe, Molecular Probes, Leiden, The Netherlands] in a final working concentration of 100 nM. Adherent cells were grown on coverslips, the culture medium was removed, and the medium containing

MitoTracker® was applied. Cells were incubated with the loading medium for 30 min under cell culture conditions, followed by TASK-3-specific immunolabelling. The same technique was applied before the separation of the mitochondria.

Immunocytochemistry

The immunocytochemistry was performed 12–18 h and 30–72 h after the latest subculturing of the melanoma and HaCaT cells, respectively. For immunocytochemistry, the cells were gently fixed in 4% paraformaldehyde (15 min, room temperature) and rinsed in phosphate-buffered saline (PBS, 0.02 M NaH_2PO_4, 0.1 M NaCl) supplemented with 100 mM glycine (3×5 min). Permeabilisation was achieved by applying PBS containing 0.1% Triton X-100 (10 min) followed by three rinses in PBS. Blocking was performed with PBS containing 1% bovine serum albumin for 30 min at room temperature followed by the application of the primary antibody (4°C, overnight). When immunolabelling was performed on whole cells, a monoclonal antibody (1:200–1:2,000) was employed (KO514, Clone KCNK75, Sigma) whose specificity was confirmed elsewhere [26]. The cells were rinsed in PBS (three times) on the following day, incubated with the secondary antibody [fluorescein isothiocyanate (FITC)-conjugated horse anti-mouse antibody; 1:200; Vector Laboratories, Burlingame, CA, USA] for 1 h at room temperature followed by three rinses with PBS. At the end of the procedure, the labelled cells were mounted using Vectashield mounting medium containing DAPI (Vector Laboratories). Control experiments were regularly performed by omitting the primary antibody from the reactions.

Immunohistochemistry

The immunohistochemical methods were similar to those reported earlier [26]. All experiments on human tissues were conducted with the authorization of the Ethical Committee of the University of Debrecen as well as with the written consent of the patients. The tissue samples were surgically removed for postoperative histopathological diagnosis. After removal, the specimens were immediately fixed in 4% buffered formaldehyde (24 h), embedded in paraffin wax, and 4-μm-thick sections were cut.

In some cases, antigen retrieval was applied. In these instances, the sections were incubated in 8 mM Tris–buffer (pH=8.4) for 15 min in a microwave oven (750 W) or they were treated with 0.1 M citrate buffer [pH=6.0] for 2 min in a pressure cooker. Both methods increased the intensity of the immunoreactions and provided identical results. In the next step, the endogenous peroxidase activity was blocked with 3% H_2O_2 in water (10 min, room temperature). Non-specific binding was prevented by incubating the sections with Protein Block serum-free reagent (DAKO, Glostrup, Denmark; 5 min, room temperature). The tissue sections were then incubated overnight at 4°C with an anti-TASK-3-specific primary antibody [either with the same monoclonal antibody (Sigma) that was employed for the immunocytochemical investigations or with a polyclonal one that was raised in goat (Santa-Cruz Biotechnology, Santa Cruz, CA, USA; 1:200)]. Although the two antibodies recognised different epitopes of the TASK-3 channel protein, they labelled identical structures.

When the monoclonal antibody was applied, the tissue sections were incubated with the EnVision system (DAKO). In the case of the polyclonal antibody, the sections were incubated in biotinylated anti-goat secondary antibodies (raised in rabbit) for 30 min (1:100, DAKO), then rinsed with PBS (3×5 min) and incubated with horseradish-peroxidase-conjugated streptavidin (30 min; 1:500; room temperature). In both cases, visualisation was achieved by employing VIP SK4600 kit (Vector). At the end of the procedure, slight counterstaining was performed (methyl green).

Control experiments were regularly performed. In these cases, the polyclonal antibody was co-incubated with the antibody-specific blocking peptide (supplied by the manufacturer of the primary antibody), according to the instructions provided by the supplier. When the monoclonal antibody was employed, control experiments were completed by leaving the primary antibody out of the reaction.

Preparation of mitochondria separated from melanoma cells

Isolated mitochondria were obtained using an established protocol [2]. Cultured melanoma cells were trypsinised and centrifuged at 1,000×*g* for 10 min. The pellet was first washed with Buffer 1 solution (250 mM mannitol, 75 mM sucrose, 100 μM K^+–EDTA, 10 mM K^+–HEPES and protease inhibitor cocktail) to remove the residuals of the culture medium. Then it was resuspended in Buffer 1 containing 500 μM K^+–EGTA. The cell suspension was incubated on ice for 20 min, and then the cells were lysed with a glass homogeniser. When approximately 50–70% of the cells were lysed (the ratio of lysed cells was estimated with trypan blue staining), the cell suspension was centrifuged at 1,000×*g* for 10 min. The pellet was discarded, and the supernatant was centrifuged again at 10,000×*g* for 15 min. The pellet, now containing the mitochondrial fraction of the melanoma cells, was resuspended in Buffer 1 containing 0.5% bovine serum albumin, centrifuged again (10,000×*g*, 15 min), and resuspended in Buffer 1 solution. Before the immunolabelling, the pellet was resuspended in

4% paraformaldehyde and transferred onto poly-D-lysine-coated coverslips.

Immunolabelling of isolated mitochondria

The basic steps of the immunolabelling were the same as in the cases of the immunoreactions performed on whole cells. Mitochondrion-specific labelling was either achieved by incubating the melanoma cells with MitoTracker® followed by the isolation of the mitochondria or using a monoclonal, cytochrome-c-specific primary antibody (BD PharMingen San Diego, CA, USA; 1:100) after completing the isolation procedure. The TASK-3-specific immunoreaction was always conducted after the isolation, either with the monoclonal antibody or (when the cytochrome-c-specific reaction was employed for labelling the mitochondria) with a polyclonal anti-TASK-3-specific antibody raised in rabbit (Alomone Labs., Jerusalem, Israel; 1:800–1:2,000; the specificity of this antibody was established elsewhere [19]). In these instances, the cytochrome-c-specific and TASK-3-specific immunoreactions performed on isolated mitochondria were completed by applying Texas red-conjugated horse anti-mouse (1:200; Vector Laboratories) and FITC-conjugated goat anti-rabbit secondary antibodies (1:200; Vector Laboratories), respectively, followed by mounting (Vectashield mounting medium with DAPI; Vector Laboratories).

Microscopy

The non-fluorescent immunoreactions were investigated using a Nikon Eclipse 600-W microscope (Nikon, Tokyo, Japan) equipped with an RT Color CCD camera. The images were acquired using 4× and 20× air as well as 60× oil immersion objectives (numerical apertures, 0.13, 0.5 and 1.4, respectively) and the Spot RT v3.5 software.

The presence and distribution of fluorescent labelling were assessed at room temperature using a laser scanning confocal microscope (Zeiss LSM 510 microscope, Oberkochen, Germany) equipped with 40× oil or 63× water immersion objectives (numerical apertures 1.3 and 1.2, respectively). For the excitation of the FITC- and Texas red-conjugated secondary antibodies, a 488-nm and a 543-nm laser were employed, respectively; the latter wavelength was used for the excitation of MitoTracker® too. In some instances, "Z-stack" images were obtained from the areas or cells of interest; in these cases, the thickness of the individual optical sections varied between 0.5 and 1.0 μm. The images were analysed and reconstructed using the Zeiss LSM Image Browser; the final forms of the illustrations were created using Adobe Photoshop 7.0. In some cases, digital images were corrected for brightness and contrast; in these instances, the entire image was processed in the same way.

Results

Co-localisation of the TASK-3- and mitochondrion-specific labellings in melanoma cells

Our earlier studies describing the presence and distribution of the TASK-3 channel protein in various tumour cells demonstrated that the immunopositivity was present mainly intracellularly [19, 26]; thus, it appeared to be essential to establish which cell organelle the strong intracellular TASK-3 expression could be associated with. To answer this question, TASK-3-specific immunolabelling was performed in combination with the application of melanosoma, endoplasmic reticulum and mitochondrion-specific markers. These experiments indicated that neither the melanosomes nor the endoplasmic reticulum was responsible for the intense intracellular TASK-3 positivity observed before (not shown). However, as Fig. 1 demonstrates, the TASK-3-specific immunocytochemistry (Fig. 1a,d,g) and the mitochondrial labelling (Fig. 1b,e,h) produced essentially the same distribution patterns, apart from the strong nuclear TASK-3 positivity, as described in our earlier reports [19, 26]. Co-localisation of the TASK-3- and mitochondrion-specific stainings was particularly evident in the overlay images (Fig. 1c,f,i). The strong co-localisation of the mitochondria and the TASK-3 channels was verified using 0.5-μm-thick optical sections as well, covering the entire depth of the melanoma cells. A representative example is shown in Fig. 2, proving that the co-localisation presented in Fig. 1 was not the result of a mere vertical overlap of the two labelling patterns, but it was explained by the mitochondrial expression of the TASK-3 channel protein.

The images presented in Figs. 1 and 2 suggested a very strong co-localisation of the mitochondria and the TASK-3 channel subunits. However, to ensure that the mitochondrial expression of the TASK-3 channels was not an experimental artifice, several experiments were carried out to rule out non-specific binding between the anti-TASK-3 monoclonal antibody and the mitochondria. Although the specificity of the antibody has been demonstrated earlier [26], given the potential significance of the TASK-3 expression in the mitochondria, the presence of the TASK-3 channel was sought and confirmed at the mRNA level too. In these experiments, TASK-3-specific mRNA was isolated from the melanoma cells, and it was established that the full length of this mRNA showed exactly the same sequence as expected from the sequence of the human TASK-3 gene (GeneBank accession number BC075080; [31]). This result not only supported the hypothesis about the TASK-3 expression of the melanoma cells but also suggested that the TASK-3 channel protein found in the melanoma cells did not show mutation.

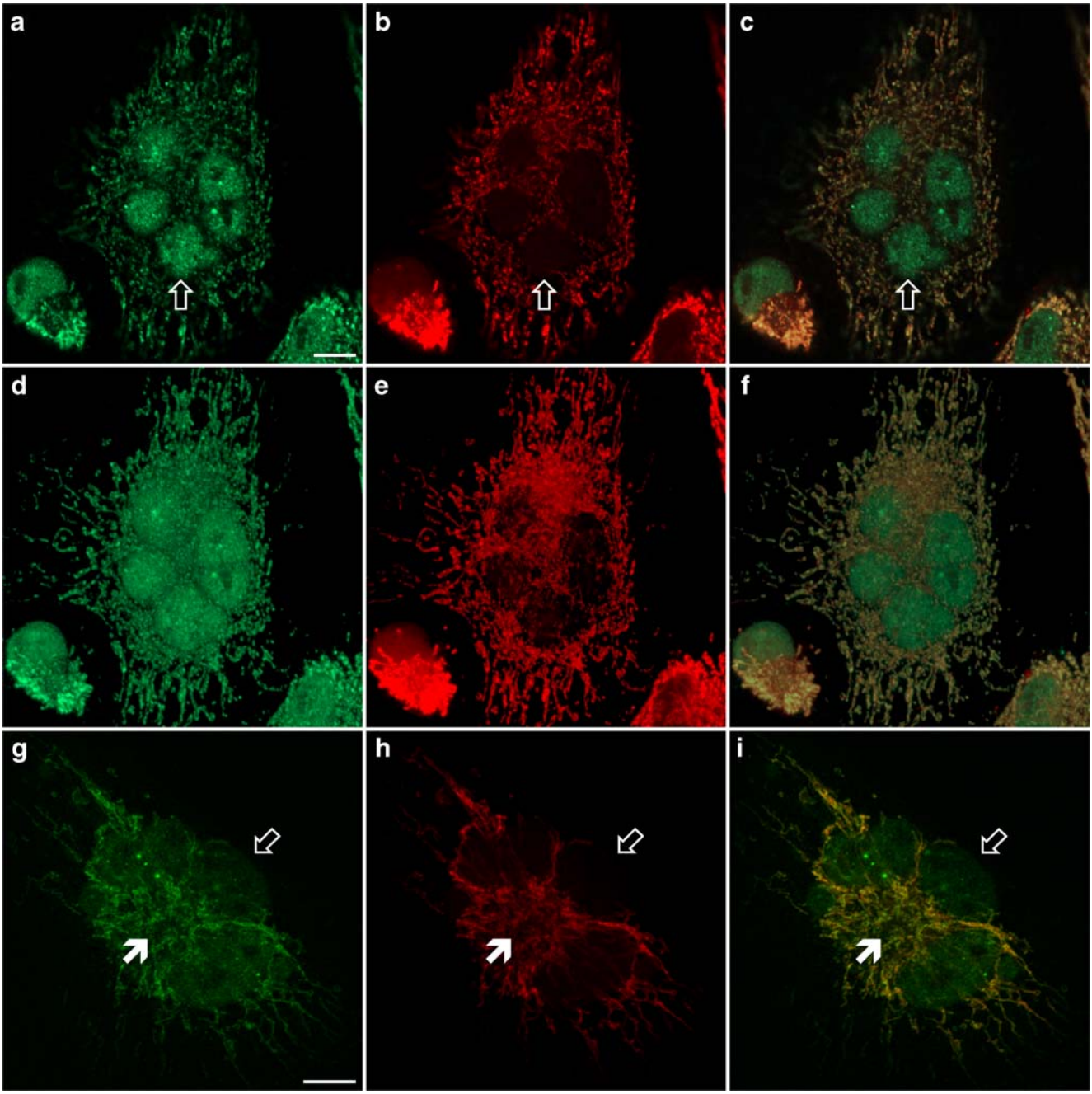


Fig. 1 Co-localisation of the TASK-3-specific immunopositivity and mitochondrion-specific labelling in melanoma cells maintained in cell culture. **a** TASK-3-specific immunopositivity taken 3 μm above the bottom of a melanoma cell 18 h after the latest subculturing employing the monoclonal antibody. **b** The result of the mitochondrion-specific labelling (MitoTracker®) of the same area and plane. **c** Overlay of **a** and **b**. The nuclei are strongly positive for TASK-3, but not labelled with the mitochondrion-specific marker (such a nucleus is indicated by the *arrow*). **d**–**f** Composite images [TASK-3-specific labelling (**d**), mitochondrion-specific labelling (**e**) and overlay (**f**)] of the cell presented in **a**–**c**. The image was obtained by producing the vertical overlap of 29 individual sections taken at 0.5-μm intervals. **g**–**i** Same as **a**–**c**, but the immunoreaction and mitochondrial labelling were performed 12 h after the latest subculturing. Empty *arrow* indicates a nucleus, *filled arrow* shows strongly TASK-3-positive mitochondria situated in the proximity of the nuclei of the presented melanoma cell. Calibration, 10 μm

The demonstration of the TASK-3 channels at mRNA level was an important step of the control experiments, but it was not enough to exclude a potential cross-reaction arising from non-specific binding of the antibody to some of the mitochondrial proteins. To address this possibility, human TASK-3-negative C2C12 cells were transiently transfected with hTASK-3-encoding vectors, followed by mitochondrial labelling and the application of TASK-3-specific immunocytochemistry (Fig. 3). In these experiments, only the successfully transfected C2C12 cells

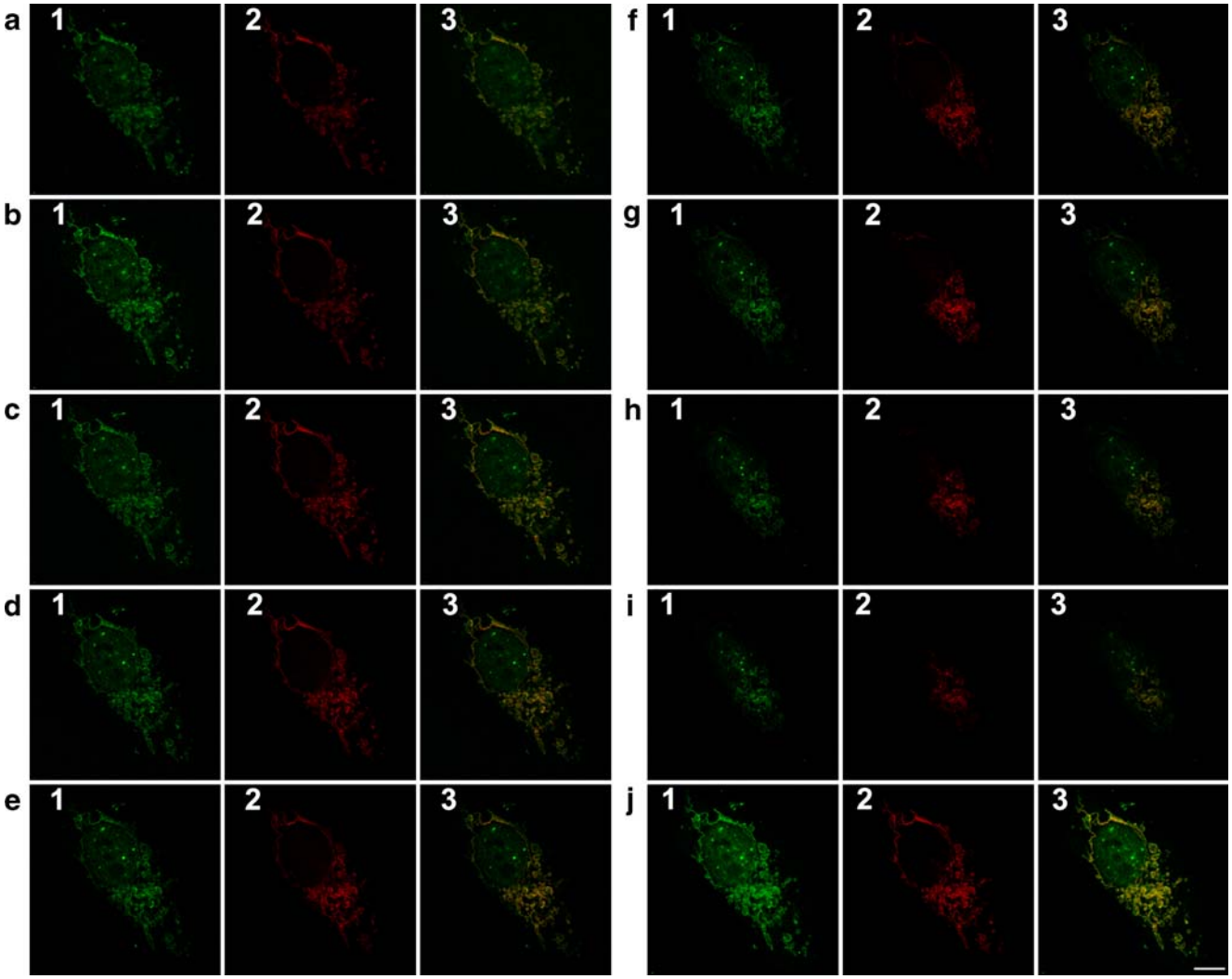


Fig. 2 Individual sections demonstrating the co-localisation of the TASK-3-specific immunopositivity and the mitochondrial labelling in a cultured melanoma cell. TASK-3-specific immunoreaction was performed using a monoclonal, anti-TASK-3-specific antibody on melanoma cells maintained in cell culture and labelled with a mitochondrion-specific marker (MitoTracker®) beforehand. The cell culture used for this experiment was subcultured 12 h before fixation and commencing the immunolabelling. The first optical section (**a**, *1–3*) was taken just above the coverslip at the bottom of the melanoma cell. Green signal (**a**, *1*) represents the result of the TASK-3-specific immunolabelling, red signal (**a**, *2*) reflects the distribution of the mitochondrial marker, whereas the third picture is the overlay image (**a**, *3*). The organisation of the subsequent images (**b**–**i**) is the same, and they were taken at 0.5-μm intervals until the top of the cell was reached. **j**, *1–3* demonstrate the composite images produced by the vertical overlap of the individual sections. Calibration, 10 μm

showed TASK-3-specific immunoreaction (Fig. 3a), whereas all of them demonstrated strong mitochondrion-specific labelling (Fig. 3b), indicating that the previously demonstrated strong co-localisation of the mitochondria and the TASK-3 subunits was the result of a specific reaction. In fact, the mitochondrial expression of the TASK-3 channels in malignant melanoma cells could very well explain our earlier findings, describing that the TASK-3-specific immunolabelling within the cells often concentrated around or between the individual nuclei of the melanoma cells, and it was also strongly present in the developing processes. This distribution pattern of the TASK-3 immunopositivity corresponded to locations where the density of mitochondria was especially high.

The strong TASK-3-specific immunopositivity of the mitochondria suggested that they might have significant TASK-3 expression, but further studies, including functional experiments, are necessary to establish whether the integrity of these channels is preserved. As most of these experiments would require isolated mitochondria, it was important to establish that mitochondria isolated from the melanoma cells also possessed TASK-3-specific immunopositivity. The result of the mitochondrial isolation protocol is demonstrated in Fig. 4. The separation procedure resulted in a suspension containing small (0.5–2 μm) granules, some of them standing alone, others forming groups of varying size. As these granules showed strong positivity for the mitochondrial tracer (Fig. 4b and e), they were

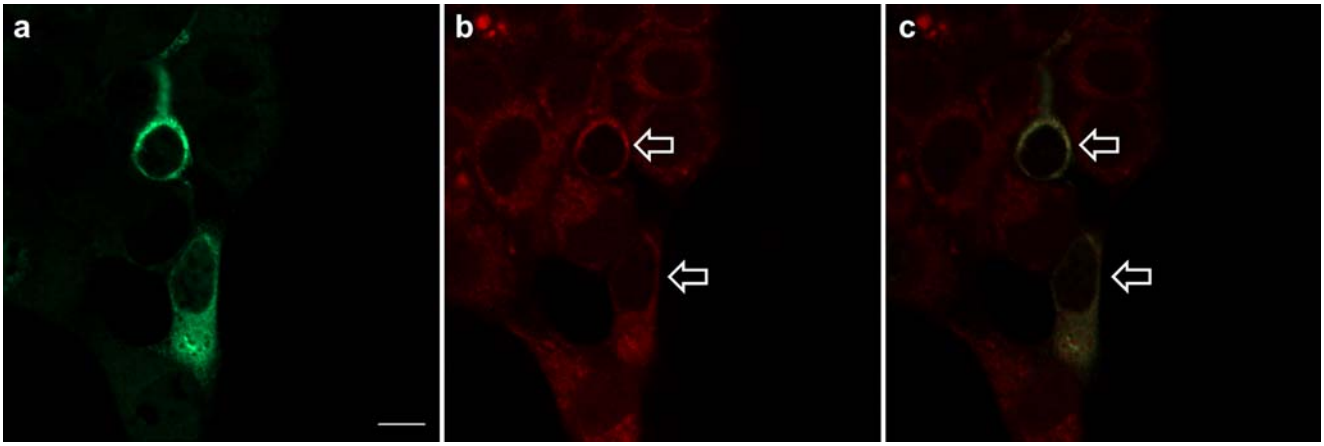


Fig. 3 Transfection experiment showing the lack of non-specific reaction between the TASK-3-specific monoclonal antibody and mitochondrial proteins. **a** Otherwise TASK-3-negative, cultured C2C12 cells were transfected with a human TASK-3 protein-encoding plasmid, then subjected to TASK-3-specific immunolabelling using the monoclonal antibody. The cells, where the transfection was successful, show strong and clear TASK-3 positivity. **b** Before the fixation and initiation of the immunolabelling, a mitochondrial labelling (MitoTracker®) was also employed. All cells are strongly positive for the mitochondrial dye; the two TASK-3-positive cells are indicated by *arrows*. **c** Overlay image of **a** and **b**. While the mitochondrial positivity is obvious in every cell present, only two cells are positive when the TASK-3-specific immunoreaction is visualised (*arrows*). Calibration, 10 μm

identified as separated mitochondria. The obtained mitochondrial suspension was also TASK-3-positive (Fig. 4a and d), and co-localisation could be established of the mitochondrion- and TASK-3-specific labellings (Fig. 4c and f). These results not only proved the applicability of the isolation protocol but also demonstrated that the TASK-3 channel protein was present in the isolated mitochondria too. To seek further confirmation of the TASK-3 positivity of the isolated mitochondria, experiments were also conducted using an entirely different labelling strategy (Fig. 4g–i). In these instances, the mitochondria were labelled by a cytochrome-c-specific monoclonal antibody (Fig. 4h) in combination with a polyclonal anti-TASK-3 antibody, recognising a different epitope of the channel protein (Fig. 4g). The co-localisation of the TASK-3- and cytochrome-c-specific labellings was evident (Fig. 4i), confirming the presence of TASK-3 channels in the isolated mitochondria.

TASK-3 positivity of keratinocytes in vitro and in vivo

The results presented so far indicated that TASK-3 channels were present in the mitochondria of the melanoma cells, and the mitochondrial TASK-3 expression could be demonstrated in separated mitochondria too. However, it was also a very important question whether the mitochondrial TASK-3 expression was a specific feature of tumour cells, or this channel had similar distribution in other (healthy) cells as well. As our preliminary experiments on various cell lines indicated that HaCaT cells were strongly positive for TASK-3, as a model for non-malignant cells, HaCaT keratinocytes were employed for the investigation of their TASK-3 expression pattern (Fig. 5). As seen in the low magnification images (Fig. 5a–d), cultured HaCaT keratinocytes demonstrated strong TASK-3-specific immunopositivity, and the distribution of the TASK-3-specific immunolabelling pattern was similar to that seen in the cases of the melanoma cells. After investigating the distribution of the mitochondrion-specific labelling in the HaCaT cells, it could also be demonstrated that (similarly to the melanoma cells) the characteristic TASK-3-labelling pattern was the consequence of their mitochondrial expression. The strong co-localisation of the TASK-3- and mitochondrion-specific labelling of the HaCaT cells could be further emphasised by demonstrating high-magnification confocal images (Fig. 5e–h). The mitochondrial expression of the TASK-3 channel protein was also evident in HaCaT cells committed to cell division (see the cell marked with arrow in Fig. 5a–d as well as the high magnification images obtained from a different cell shown in Fig. 5i–l).

As the presence of a protein in an immortalised cell line maintained in cell culture does not necessarily reflect the true behaviour of the original cells (keratinocytes in the present case) in vivo, immunohistochemical experiments were conducted on wax-embedded human tissue sections investigating whether keratinocytes or other structures of the healthy skin possessed noticeable TASK-3 expression too. As seen in Fig. 6, several cell types showed distinct and very strong TASK-3 immunopositivity. Figure 6a and b demonstrates that the keratinocytes were strongly positive for TASK-3, whereas the surrounding connective tissue showed no noteworthy immunoreaction. Besides keratinocytes of the squamous epithelium, secretory cells (Fig. 6c) and keratinocytes of the hair follicles also produced strong TASK-3-specific immunopositivity (Fig. 6d and e). The distribution of the TASK-3 labelling was similar to that observed in

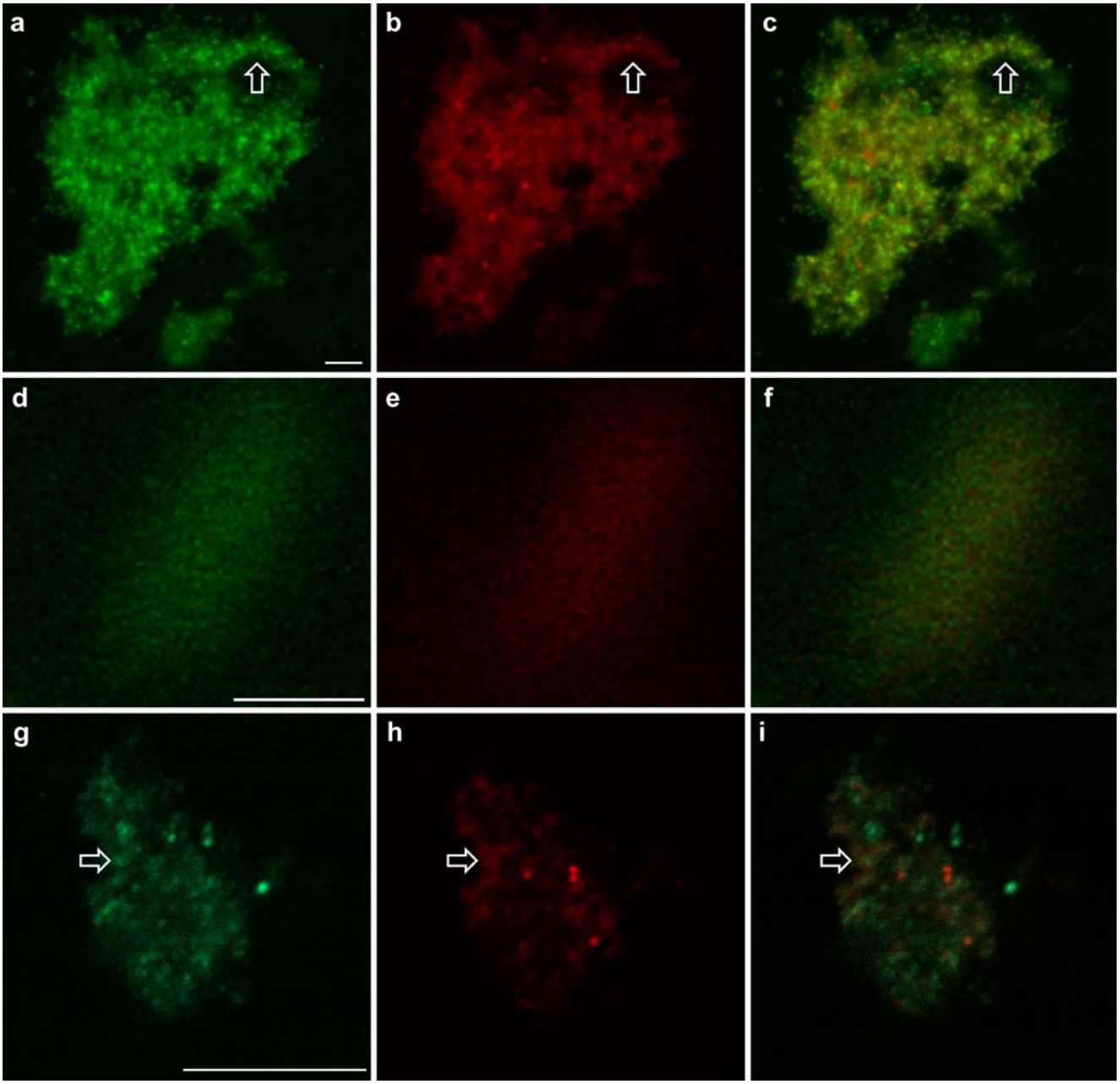


Fig. 4 TASK-3 immunopositivity of isolated mitochondria prepared from cultured melanoma cells. Mitochondria were isolated according to the protocol described in "Materials and methods". Before the isolation, the mitochondrion-specific fluorescent dye, MitoTracker® was employed, selectively marking the mitochondria (*red signal*, **b** and **e**). **a** and **d** Show the result of the TASK-3-specific immunoreaction (with the monoclonal antibody). The overlay images are also presented (**c** and **f**). *Arrow* marks a region where the granular appearance of the TASK-3- and mitochondrion-specific labelling is particularly obvious in **a**–**c**. **d**–**f** Show the TASK-3-positivity of a single mitochondrion. **g**–**i** Both the mitochondria and TASK-3 channel protein were labelled differently than in **a**–**f**. In these instances, mitochondria and TASK-3 channels were labelled using cytochrome-c-specific monoclonal and TASK-3-specific polyclonal antibodies. *Green signal* reflects the distribution of the TASK-3-specific (**g**), whereas *red signal* demonstrates the presence of the cytochrome-c-specific reactions (**h**). The overlay image is also presented (**i**); *arrow* indicates a location within the mitochondrial suspension where the granular nature of the immunopositivities is evident. Calibration, 10 μm (*top* and *bottom* panels) and 1 μm (*middle* panels)

melanoma and HaCaT cells: The TASK-3-specific immunopositivity was present mainly intracellularly, often demonstrating a clearly granular pattern, which was usually present in the proximity of the cell nuclei. The often present, distinctly granular distribution of the TASK-3-specific immunopositivity observed in the cytoplasm of keratinocytes might have corresponded to the mitochondrial localisation of the TASK-3 channel protein in vivo. This expression pattern could be reliably and consistently reproduced with primary antibodies recognising different epitopes of the channel

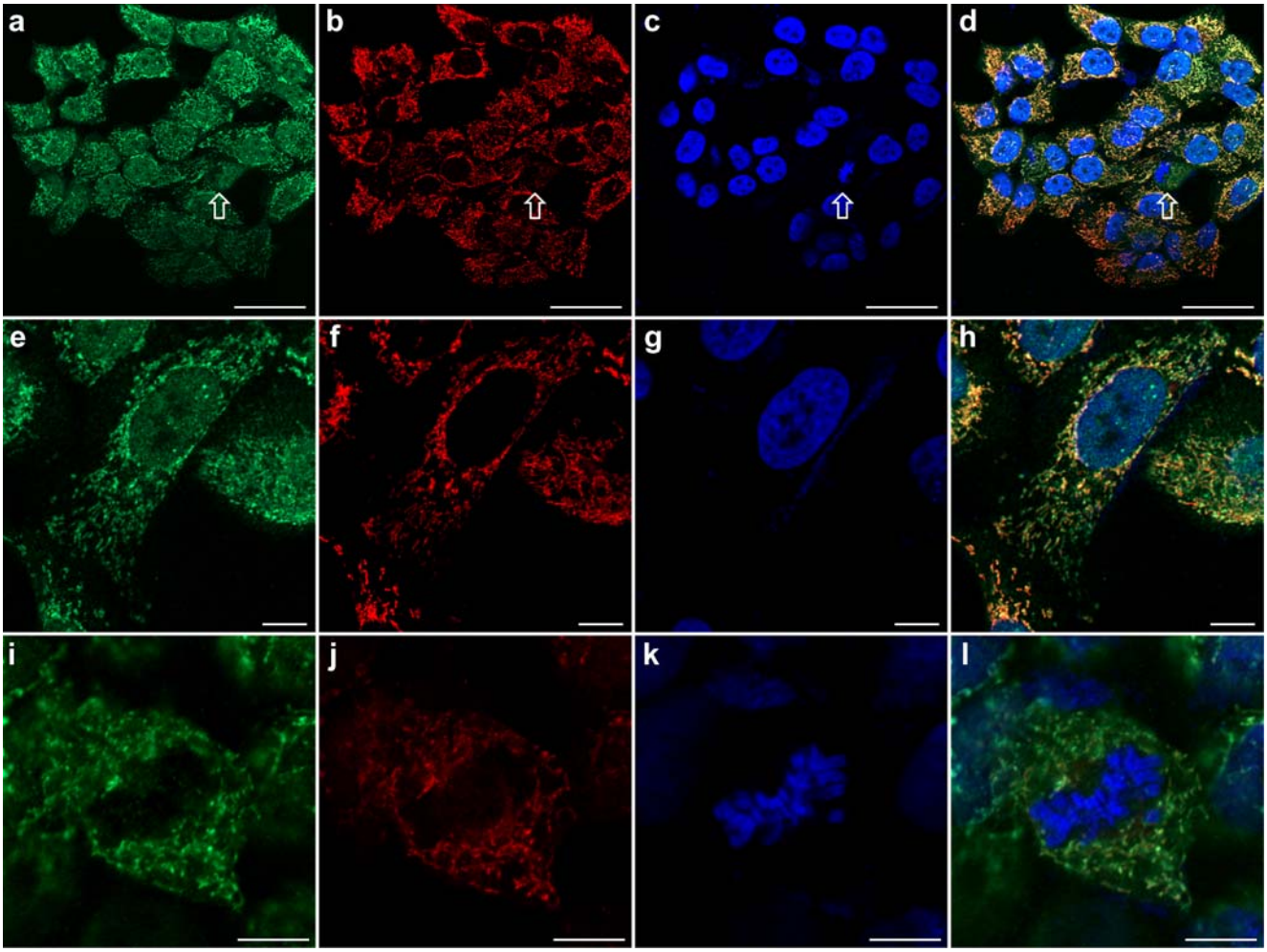


Fig. 5 TASK-3 positivity of HaCaT cells maintained in cell culture. **a** TASK-3-specific immunopositivity of cultured HaCaT cells. The presented photomicrographs demonstrate the results of the TASK-3- (**a**) and mitochondrion-specific (**b**) reactions as well as the result of the DAPI labelling (**c**). The overlay image is also presented (**d**). *Arrow* indicates a dividing HaCaT cell. **e**–**h** A single HaCaT cell presented at higher magnification; the organisation of the panels is the same as in **a**–**d**. **i**–**l** High magnification view of a single, dividing HaCaT cell. Calibration, 50 μm (**a**–**d**) and 10 μm (all other panels)

protein as well (not shown). Regardless of the antibodies applied, the control experiments (either pre-adsorption experiments or when the monoclonal primary antibody was omitted from the reaction) never produced notable immunopositivity in any of the previously reported strongly positive structures (Fig. 6f).

Discussion

The experimental findings presented in this study elucidate the previously noted but yet unexplained findings that TASK-3-specific immunopositivity was present mainly intracellularly in a number of malignantly transformed cells [19, 24, 26]. The present results established the mitochondrial expression of TASK-3 channels in both malignantly transformed (melanoma) and non-malignant (HaCaT) cells.

In addition to the various heterologous expression systems stably or transiently transfected with TASK-3 channel encoding vectors [4, 8, 26], the presence of TASK-3 immunopositivity has been described in several malignantly transformed and healthy human tissues in vitro and in vivo as well [19, 26, 29]. In these experiments, not only the presence of the TASK-3 channel protein could be successfully demonstrated, but it was also reported that the TASK-3 immunoreactivity was not restricted to the surface membrane but was present intracellularly as well. It must be noted that the intracellular presence of a channel protein is not unexpected, especially in the expression systems where the intense biosynthesis of the channel protein is responsible for the intense intracellular immunopositivity. As the antibodies recognising channel proteins may bind to molecules being currently synthesised, stored and transported to their final destination, intracellular appearance of the TASK-3 immunopositivity is not surprising either.

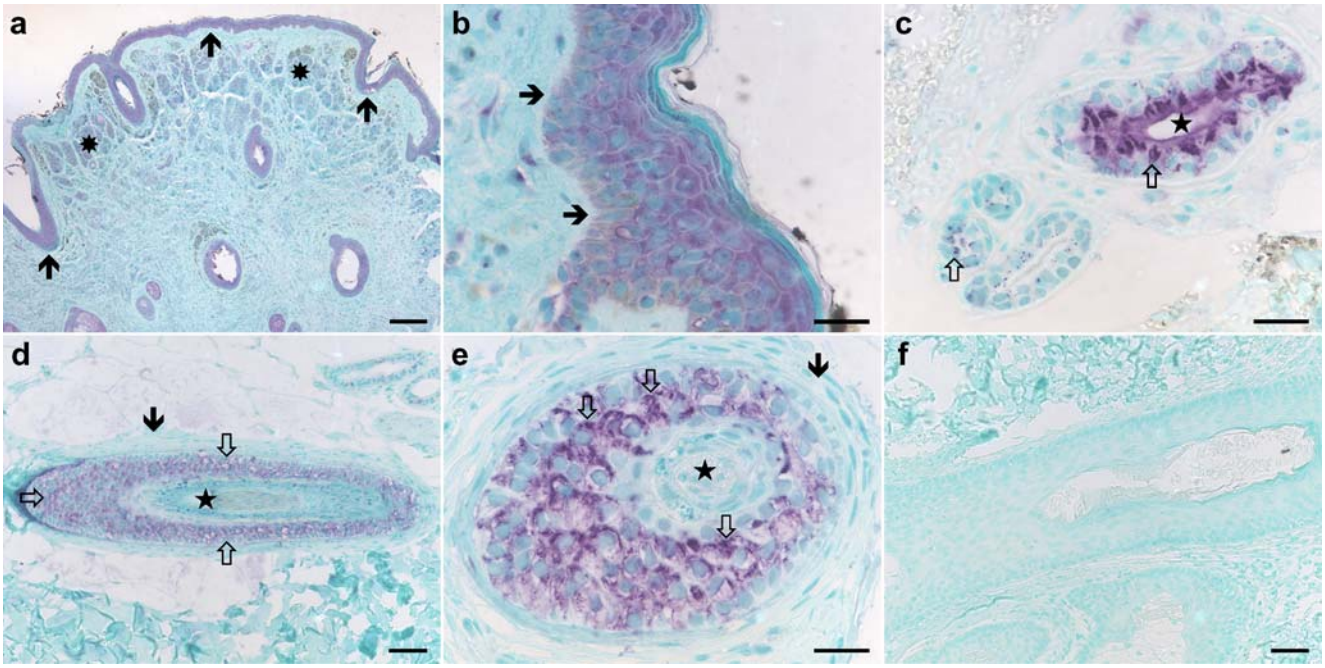


Fig. 6 TASK-3-specific immunolabelling of the human skin. **a** Low magnification image of a benign mole. The strongly positive (*purple* immunoreaction) epidermis is indicated by *arrows*; *stars* mark cellular nests composed of TASK-3-positive melanocytes. **b** High magnification image of the epidermis; *filled arrows* demonstrate TASK-3-positive stratum basale cells. **c** Strong TASK-3-specific immunopositivity presented by secretory cells of the sweat gland. *Star* indicates the lumen of the gland; *empty arrows* demonstrate the strong and often punctate appearance of the TASK-3 immunopositivity. **d** Longitudinal section of a hair follicle; *star* indicates the hair radix. The strong immunopositivity of the keratinocytes is obvious (*empty arrows*), and it is in sharp contrast with the TASK-3-negative connective tissue (*filled arrow*). **e** High magnification view of the cross-section of a hair follicle. The TASK-3-negative hair radix and connective tissue are labelled with a *star* and *filled arrow*, respectively. *Empty arrows* demonstrate a few examples of strongly TASK-3-positive keratinocytes showing clearly punctate TASK-3-specific reaction. The immunopositive granules often concentrated around or in the proximity of the cell nuclei. **f** Control reaction performed by leaving the primary antibody out of the reaction. Calibration, 250 μm (**a**); 50 μm (**d**, **f**); 25 μm (**b**, **c**, **e**)

Besides the channel protein naturally present in the endoplasmic reticulum, other possibilities may also be considered as an explanation of the intracellular accumulation and the lack of the TASK-3 channel protein in the surface membrane. It has been described that trafficking of the TASK-3 channels to the cell surface membrane requires the binding of the adapter protein 14-3-3 [27]. This adapter protein binds to the C terminus of the channel protein, and it seems to be essential for the expression of the TASK-3 channels in the cell surface. The exact mechanism by which it affects the trafficking of the TASK-3 channel protein is still not known, but it has been suggested that it may permit the binding of an accessory protein facilitating the traffic of the ready dimers from the endoplasmic reticulum to the cell surface, or it may mask a retention domain which is necessary for the binding of yet another protein required for the withdrawal of the channel protein from the cell membrane. Overexpression of the 14-3-3 protein resulted in increased TASK-3 current amplitude, whereas modification of the C terminus of the channel protein (making the binding between the channel protein and the 14-3-3 protein impossible) significantly reduced the current amplitude in *Xenopus* oocytes and resulted in the retention of the channel protein in the cytoplasm. Interestingly, deletion of even a single amino acid from the C terminus of the TASK-1 and TASK-3 channels abolished the binding of the 14-3-3 protein, impeding, therefore, the expression of the channel in the cell membrane. Considering the above, one of the possibilities to explain the lack of TASK-3-specific immunopositivity in the surface membrane of the melanoma cells would be that a mutation affecting the C-terminal region of the melanoma TASK-3 channels hinders the interaction between the channel protein and the adapter protein. However, as no alteration was found in the TASK-3-specific mRNA sequence of the melanoma cells in the present study, this possibility appears to be unlikely. An alternative explanation of the insignificant cell surface labelling may be the lack or modification of the adapter protein itself.

Interestingly, intracellular localisation of the TASK-3 immunopositivity has been reported in the rat central nervous system as well [4, 29]. In this case, the most significant intracellular structures to which TASK-3 immunopositivity could be associated were the Golgi apparatus, endoplasmic reticulum and certain intracellular vesicles. The observation that no TASK-3-specific immunopositivity was seen in the mitochondria and in the nucleus of the rat neurones raised the possibility that the intracellular TASK-3

immunopositivity observed in melanoma cells was also related to the endoplasmic reticulum. However, when TASK-3/SERCA-pump double labelling was performed on melanoma cells, very limited co-localisation could be observed only (unpublished observations), indicating that the TASK-3 channels had to be mostly present elsewhere in the cell, in the mitochondria, as evidenced by the strong co-localisation of the TASK-3 channels and the mitochondria.

Although the data presented in the present study do not allow the determination of the exact localisation of the TASK-3 channels within the mitochondria, it can be hypothesised that they are most likely associated to either the inner or the outer mitochondrial membrane. In fact, a mitochondrial ATP-sensitive K^+ channel (mtK_{ATP}) has already been described in the inner membrane [15, 25] whose function is to control mitochondrial volume by ensuring mitochondrial K^+ movement [9]. These channels also contribute to the establishment of the H^+ gradient and the transmembrane electric potential of the mitochondria known to be essential for their oxidative functions. It is reasonable to assume that if TASK-3 channels are situated in the inner mitochondrial membrane, they may possess similar functions. However, if the mitochondrial TASK-3 channels are situated in the outer mitochondrial membrane, their function may be similar to those of the Bcl channels: When functional, Bcl channels are cationic channels, and their activation causes mitochondrial membrane hyperpolarisation, reduced cytochrome-c release and maintained mitochondrial osmotic homeostasis [30].

On the basis of the experimental findings presented in this work, it is a tempting possibility that TASK-3 channels may be somehow involved in the mitochondrial function, and their activity might be important for the energy production of both healthy and malignantly transformed cells. An increased TASK-3 biosynthesis may be beneficial for the development, proliferation and growth of tumour cells, especially in the poorly oxygenated regions of solid tumours. Although functional studies are necessary to test this hypothesis, the data presented here seem to support the previous notion that selective inhibition of TASK-3 channels might offer a new possibility to inhibit proliferation and growth of tumour cells. Nevertheless, the results also point out that this therapeutical approach, however promising it might appear, should be considered with caution. Previous data have already indicated that TASK-3 expression is most likely present in various healthy cells, including but not restricted to cerebellar Purkinje and granule cells, gastrointestinal epithelial cells, endocrine cells situated in the Langerhans islets of the pancreas as well as benign melanocytes [19, 26, 29]. The present work not only extended the list of healthy cells by showing strong TASK-3 expression of the keratinocytes and sweat glands in the healthy skin but also demonstrated strong co-localisation of their TASK-3 channels and mitochondria. All in all, a TASK-3-specific therapeutical approach can only be seriously considered if tumour cell-targeted delivery of the appropriate compounds can be ensured.

Acknowledgement This work was supported by grants from the Hungarian Science Foundation (OTKA T46067, T49151, K61442, NK61412) and the Ministry of Health (ETT-151/2006). MG received an OTKA Postdoctoral Fellowship.

References

1. Aller MI, Veale EL, Linden AM, Sandu C, Schwaninger M, Evans LJ, Korpi ER, Mathie A, Wisden W, Brickley SG (2005) Modifying the subunit composition of TASK channels alters the modulation of a leak conductance in cerebellar granule neurons. J Neurosci 25:11455–11467
2. Bednarczyk P, Kicinska A, Kominkova V, Ondrias K, Dolowy K, Szewczyk A (2004) Quinine inhibits mitochondrial ATP-regulated potassium channel from bovine heart. J Membr Biol 199:63–72
3. Berg AP, Talley EM, Manger JP, Bayliss DA (2004) Motoneurons express heteromeric TWIK-related acid-sensitive K^+ (TASK) channels containing TASK-1 (KCNK3) and TASK-3 (KCNK9) subunits. J Neurosci 24:6693–6702
4. Callahan R, Labunskiy DA, Logvinova A, Abdallah M, Liu C, Cotton JF Yost CS (2004) Immunolocalization of TASK-3 (KCNK9) to a subset of cortical neurons in the rat CNS. Biochem Biophys Res Commun 319:525–530
5. Chapman CG, Meadows HJ, Godden RJ, Campbell DA, Duckworth M, Kelsell RE, Murdock PR, Randall AD, Rennie GI, Gloger IS (2000) Cloning, localisation and functional expression of a novel human, cerebellum specific, two pore domain potassium channel. Mol Brain Res 82:74–83
6. Chemin J, Girard C, Duprat F, Lesage F, Romey G, Lazdunski M (2003) Mechanisms underlying excitatory effects of group I metabotropic glutamate receptors via inhibition of 2P domain K^+ channels. EMBO J 22:5403–5411
7. Czirják G, Enyedi P (2002a) TASK-3 dominates the background potassium conductance in rat adrenal glomerulosa cells. Mol Endocrinol 16:621–629
8. Czirják G, Enyedi P (2002b) Formation of functional heterodimers between the TASK-1 and TASK-3 two-pore domain potassium channel subunits. J Biol Chem 277:5426–5432
9. Garlid KD (1996) Cation transport in mitochondria—the potassium cycle. Biochim Biophys Acta 1275:123–126
10. Gönczi M, Papp H, Bíró T, Kovács L, Csernoch L (2002) Effect of protein kinase C on transmembrane calcium fluxes in HaCaT keratinocytes. Exp Dermatol 11:25–33
11. Han J, Gnatenco C, Sladek CD, Kim D (2003) Background and tandem-pore potassium channels in magnocellular neurosecretory cells of the rat supraoptic nucleus. J Physiol 546:625–639
12. Han J, Truell J, Gnatenco C, Kim D (2002) Characterization of four types of background potassium channels in rat cerebellar granule neurons. J Physiol 542:431–444
13. Hartness ME, Lewis A, Searle GJ, O'Kelly I, Peers C, Kemp PJ (2001) Combined antisense and pharmacological approaches implicate hTASK as an airway O_2 sensing K^+ channel. J Biol Chem 276:26499–26508
14. Hopwood SE, Trapp S (2005) TASK-like K^+ channels mediate effects of 5-HT and extracellular pH in rat dorsal vagal neurones in vitro. J Physiol 568:145–154
15. Inoue I, Hagase H, Kishi K, Higuti T (1991) ATP-sensitive K^+ channel in the mitochondrial inner membrane. Nature 352:244–247

16. Kang D, Han J, Talley EM, Bayliss DA, Kim D (2003) Functional expression of TASK-1/TASK-3 heteromers in cerebellar granule cells. J Physiol 554:64–77
17. Ketchum KA, Joiner WJ, Sellers AJ, Kaczmarek LK, Goldstein SA (1995) A new family of outwardly rectifying potassium channel protein with two pore domains in tandem. Nature 376: 690–695
18. Kim Y, Bang H, Kim D (2000) TASK-3, a new member of the tandem pore K^+ channel family. J Biol Chem 275:9340–9347
19. Kovács I, Pocsai K, Czifra G, Sarkadi L, Szűcs G, Nemes Z, Rusznák Z (2005) TASK-3 immunoreactivity is present but shows differential distribution in the human gastrointestinal tract. Virchows Arch 446:402–410
20. Lauritzen I, Zanzouri M, Honoré E, Duprat F, Ehrengruber MU, Lazdunski M, Patel A (2003) K^+-dependent cerebellar granule neuron apoptosis. J Biol Chem 278:32068–32076
21. Lesage F, Lazdunski M (2000) Molecular and functional properties of two-pore-domain potassium channels. Am J Physiol 279:F793–F801
22. Meadows HJ, Randall AD (2001) Functional characterisation of human TASK-3, an acid-sensitive two-pore domain potassium channel. Neuropharmacology 40:551–559
23. Meuth SG, Budde T, Kanyshkova T, Broicher T, Munsch T, Pape H-C (2003) Contribution of TWIK-related acid-sensitive K^+ channel 1 (TASK1) and TASK3 channels to the control of activity modes in thalamocortical neurons. J Neurosci 23: 6460–6469
24. Mu D, Chen L, Zhang X, See L, Koch CM, Yen C, Tong JJ, Spiegel L, Nguyen CQ, Servoss A, Peng Y, Pei L, Marks JR, Lowe S, Hoey T, Jan LY, McCombie WR, Wigler MH, Powers S (2003) Genomic amplification and oncogenic properties of the *KCNK9* potassium channel gene. Cancer Cell 3:297–302
25. Paucek P, Mironove G, Mahdi F, Beavis AD, Woldegiorgis G, Garlid KD (1992) Reconstitution and partial purification of the glibenclamide-sensitive, ATP-dependent K^+ channel from rat liver and beef heart mitochondria. J Biol Chem 267:26062–26069
26. Pocsai K, Kosztka L, Bakondi G, Gönczi M, Fodor J, Dienes B, Szentesi P, Kovács I, Feniger-Barish R, Kopf E, Zharhary D, Szűcs G, Csernoch L Rusznák Z (2006) Melanoma cells exhibit strong intracellular TASK-3-specific immunopositivity in both tissue sections and cell culture. Cell Mol Life Sci 63: 2364–2376
27. Rajan S, Preisig-Müller R, Wischmeyer E, Nehring R, Hanley PJ, Renigunta V, Musset B, Schlichthörl G, Derst C, Karschin A, Daut J (2002) Interaction with 14-3-3 proteins promotes functional expression of the potassium channels TASK-1 and TASK-3. J Physiol 545:13–26
28. Rajan S, Wischmeyer E, Xin Liu G, Preising-Müller R, Daut J, Karschin A, Derst C (2000) TASK-3, a novel tandem pore domain acid-sensitive K^+ channel. An extracellular histidin as pH sensor. J Biol Chem 275:1650–1657
29. Rusznák Z, Pocsai K, Kovács I, Pór Á, Pál B, Bíró T, Szűcs G (2004) Differential distribution of TASK-1, TASK-2 and TASK-3 immunoreactivities in the rat and human cerebellum. Cell Mol Life Sci 61:1532–1542
30. Schendel SL, Xie Z, Oblatt Montal M, Matsuyama S, Montal M, Reed JC (1997) Channel formation by antiapoptotic protein Bcl-2. Proc Natl Acad Sci U S A 94:5113–5118
31. Strausberg RL, Feingold EA, Grouse LH, Derge JG, Klausner RD, Collins FS, Wagner L, Shenmen CM, Schuler GD, Altschul SF, Zeeberg B, Buetow KH, Schaefer CF, Bhat NK, Hopkins RF, Jordan H, Moore T, Max SI, Wang J, Hsieh F, Diatchenko L, Marusina K, Farmer AA, Rubin GM, Hong L, Stapleton M, Soares MB, Bonaldo MF, Casavant TL, Scheetz TE, Brownstein MJ, Usdin TB, Toshiyuki S, Carninci P, Prange C, Raha SS, Loquellano NA, Peters GJ, Abramson RD, Mullahy SJ, Bosak SA, McEwan PJ, McKernan KJ, Malek JA, Gunaratne PH, Richards S, Worley KC, Hale S, Garcia AM, Gay LJ, Hulyk SW, Villalon DK, Muzny DM, Sodergren EJ, Lu X, Gibbs RA, Fahey J, Helton E, Ketteman M, Madan A, Rodrigues S, Sanchez A, Whiting M, Madan A, Young AC, Shevchenko Y, Bouffard GG, Blakesley RW, Touchman JW, Green ED, Dickson MC, Rodriguez AC, Grimwood J, Schmutz J, Myers RM, Butterfield YS, Krzywinski MI, Skalska U, Smailus DE, Schnerch A, Schein JE, Jones SJ, Marra MA, (Mammalian Gene Collection Program Team) (2002) Generation and initial analysis of more than 15,000 full-length human and mouse cDNA sequences. Proc Natl Acad Sci U S A 99:16899–16903
32. Washburn CP, Bayliss DA, Guyenet PG (2003) Cardiorespiratory neurons of the rat ventrolateral medulla contain TASK-1 and TASK-3 channel mRNA. Resp Physiol Neurobiol 138:19–35
33. Washburn CP, Sirois JE, Talley EM, Guyenet PG, Bayliss DA (2002) Serotonergic raphe neurons express TASK channel transcripts and a TASK-like pH- and halothane-sensitive K^+ conductance. J Neurosci 22:1256–1265

Virchows Arch (2008) 452:427–434
DOI 10.1007/s00428-007-0552-y

ORIGINAL ARTICLE

Developing human minor salivary glands: morphological parallel relation between the expression of TGF-beta isoforms and cytoskeletal markers of glandular maturation

Silvia Vanessa Lourenço · Sabrina Hitomi Uyekita · Dirce Mary Correia Lima · Fernando Augusto Soares

Received: 26 June 2007 / Revised: 15 October 2007 / Accepted: 14 November 2007 / Published online: 14 December 2007
© Springer-Verlag 2007

Abstract Morphogenesis of salivary glands involves complex coordinated events. Synchronisation between cell proliferation, polarisation and differentiation, which are dependent on epithelial–mesenchymal interactions and on the microenvironment, is a requirement. Growth factors mediate many of these orchestrated biological processes and transforming growth factor-beta (TGF-beta) appear to be relevant. Using immunohistochemistry and immunofluorescence, we have mapped the distribution of TGF-beta 1, 2 and 3 and compared it with the expression of maturation markers in human salivary glands obtained from foetuses ranging from weeks 4 to 24 of gestation. TGF-beta 1 first appeared during canalisation stage in the surrounding mesenchyme and, in the more differentiated stages, was expressed in the cytoplasm of acinar cells throughout the adult gland. TGF-beta 2 was detected since the bud stage of the salivary gland. Its expression was observed in ductal cells and increased along gland differentiation, TGF-beta 3 was detected from the canalisation stage of the salivary gland, being weakly expressed on ductal cells, and it was the only factor detected on myoepithelial cells. The data suggest that TGF-beta have a role to play in salivary gland development and differentiation.

Keywords Transforming growth factor-beta · Salivary glands · Development

S. V. Lourenço · F. A. Soares
Department of General Pathology, Dental School,
University of São Paulo,
São Paulo, Brazil

S. V. Lourenço · D. M. C. Lima
Laboratory of Immunopathology, Institute of Tropical Medicine,
São Paulo, Brazil

S. V. Lourenço · S. H. Uyekita
Department of Dermatology, Medical School,
University of São Paulo,
São Paulo, Brazil

F. A. Soares
Hospital do A.C. Camargo,
São Paulo, Brazil

S. V. Lourenço (✉)
Disciplina de Patologia Geral, Faculdade de Odontologia,
Universidade de São Paulo,
Av Prof Lineu Prestes, 2227,
CEP: 05508-000 São Paulo, Brazil
e-mail: sloducca@usp.br

Introduction

All salivary glands develop in a similar manner. Formation starts with the proliferation of a solid cord of cells from the epithelium of the stomatodeum into the underlying ectomesenchyme. This cord of cells extends deeply into the ectomesenchyme and branches extensively. These cells then canalise by degradation of the central cells to form the ductal system and the terminal secretory end pieces. The epithelial ingrowths constitute the parenchyme of a salivary gland. The ectomesenchyme differentiates to form the connective tissue component of the gland, which supports the parenchyma.

Minor salivary glands begin to develop at 4–6 weeks of embryonic life. Branches from parasympathetic and sympathetic nerves migrate to the gland and the collecting veins are formed. Salivary gland development consists of a series of ducts ending in terminal secretory end pieces, grape-like in structure.

Table 1 Primary serum, clones, source and details of working protocol

Primary serum	Clone	Source	Antigen retrieval	Working dilution
CK14	LL002	Neomarker	Citrate buffer pH 6.0	1:50
CK low-MW	35βH11	DAKO	Citrate buffer pH 6.0	1:50
SMA	1A4	DAKO	Citrate buffer pH 6.0	1:50

To date, little is known of the key regulators of human salivary gland development and function. In most systems, there is a requirement of co-ordination between cell proliferation, polarisation and differentiation. These processes are dependent on epithelial–mesenchymal interactions and on the microenvironment. Temporal and spatial regulation of these events is likely to be important to salivary gland development and for proper tissue function, and our group has been investigating several of these aspects [20].

Hormones and growth factors mediate many of these highly orchestrated biological processes that occur during development, and the transforming growth factor-beta (TGF-beta) family is probably relevant for these processes. TGF-beta is a multifunctional growth factor that has several biological effects in vivo, including control of cell growth and differentiation, cell migration, lineage determination, motility, adhesion, apoptosis, synthesis and degradation of extracellular matrix, and it plays an important role in regulating tissue repair and regeneration [10, 22, 26, 28]. Multiple TGF-beta subunits are expressed during early embryonic morphogenesis in different order and levels which appear to have specific transcriptional regulation, fundamental in the induction and maintenance of differentiated cell types during craniofacial development [2].

The aim of this study was to study the expression and distribution of TGF-beta 1, 2 and 3 in the developing human salivary gland and its parallel relationship with morphology and maturation markers of these glands.

Materials and methods

Tissue preparation

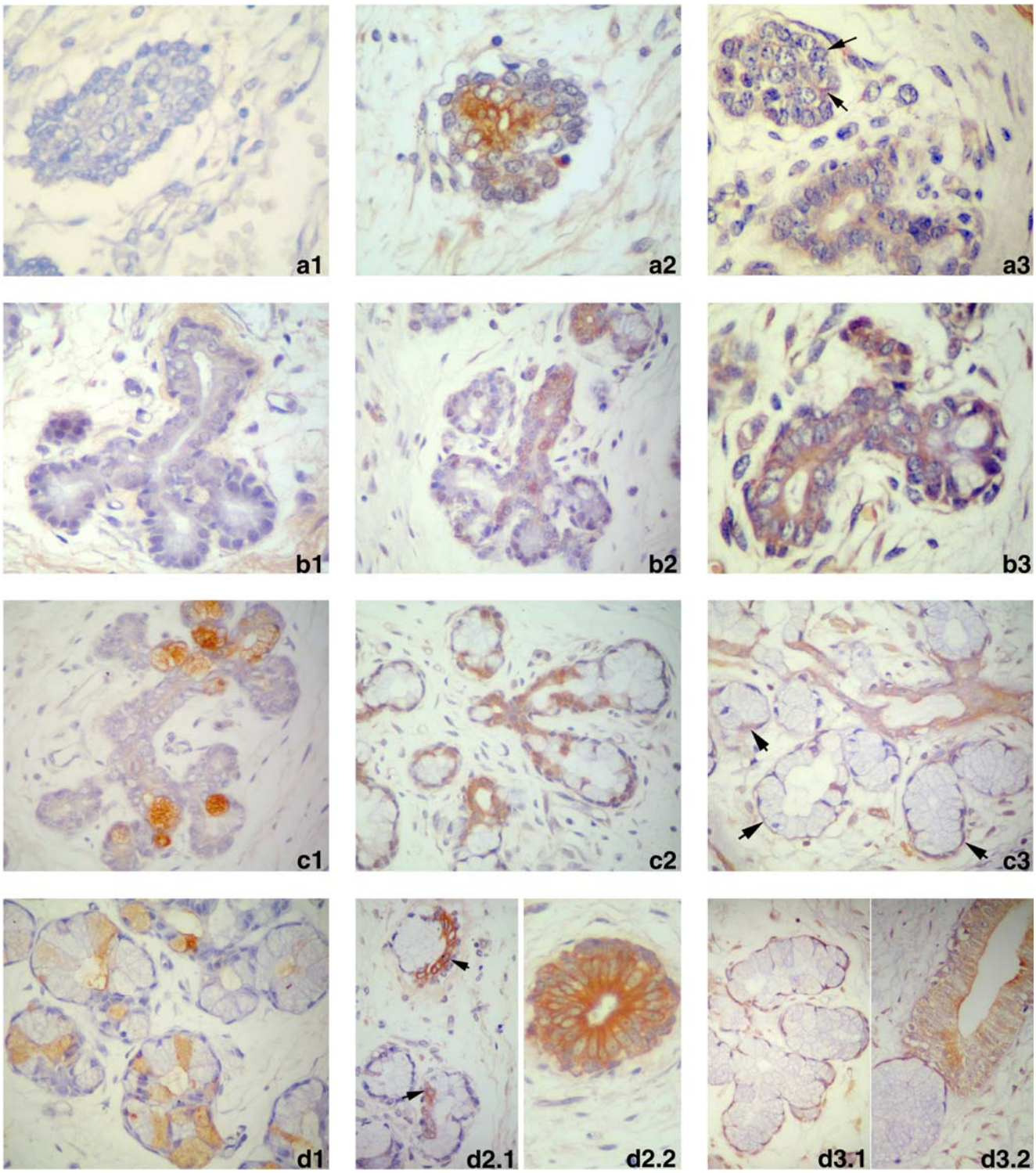
Thirty post-mortem human foetuses at 4th to 24th weeks of gestation were obtained from the Medical School of the University of São Paulo (in accordance with authorisation of the Ethical Committee of this institution). Specimens of oral cavity were collected from different sites, including buccal mucosa, tongue, mandible and hard palate. Fully developed salivary gland specimens were retrieved from the archives of the Laboratory of Dermatopathology of the same institution and were used as controls. All specimens were fixed in 10% buffered formalin for 24 h and embedded in paraffin. Haematoxylin and eosin slides were used to check for the presence of salivary glands and to study their morphology. Those presenting developing minor salivary glands were selected for the present analysis.

Immunohistochemistry

Three-micrometer serial sections of the specimens were incubated in 3% aqueous hydrogen peroxide for 30 min to quench endogenous peroxidase activity and with 1% bovine serum albumin (BSA) and 5% foetal calf serum (FCS) in Tris–HCl pH 7.4 for 60 min at room temperature to suppress non-specific binding of subsequent reagents.

Fig. 1 TGF-beta isoforms expression in developing salivary glands. ▶ **a1**, **a2**, **a3** Bud stage. **a1** There is no evidence of TGF-beta 1 expression in epithelial cells of the very initial phase of salivary gland development (streptavidin–biotin peroxidase, original magnification ×400). **a2** Expression of TGF-beta 2 in the cytoplasm of a few cells of the solid nest of developing salivary gland (streptavidin–biotin peroxidase, original magnification ×400). **a3** Weak expression of TGF-beta 3 around epithelial cells of the budding human minor salivary gland (*arrow*) (streptavidin–biotin peroxidase, original magnification ×400). **b1**, **b2**, **b3** Canalisation stage. **b1** Expression of TGF-beta 1 in the stroma surrounding the canalising ductal system (streptavidin–biotin peroxidase, original magnification ×400). **b2** Strong TGF-beta 2 expression in the cytoplasm of scattered epithelial cells of the canalising ductal system (streptavidin–biotin peroxidase, original magnification ×400). **b3** Weak expression of TGF-beta 3 on the luminal pole of the ductal cells of the canalising ductal system (streptavidin–biotin peroxidase, original magnification ×400). **c1**, **c2**, **c3** Branching stage. **c1** Strong expression of TGF-beta 1 in the cytoplasm of the initial developing mucous cells at the end tips of the branching salivary gland (streptavidin–biotin peroxidase, original magnification ×400). **c2** Strong expression of TGF-beta 2 in the cytoplasm of epithelial cells that compose the entire ductal system of the branching salivary gland including the intercalated duct located at the junction of the future acinar lobules (streptavidin–biotin peroxidase, original magnification ×400). **c3** Expression of TGF-beta 3 in the cytoplasm of the epithelial cells of the ductal system and in the myoepithelial cells that surround the developing mucous cells at the end tips of the branching salivary gland (*arrows*) (streptavidin–biotin peroxidase, original magnification ×400). **d1**, **d2**, **d3** Cytodifferentiation stage. **d1** Strong expression of TGF-beta 1 in scattered well-developed acinar cells forming the acinic lobules at the end tips of the developing salivary gland (streptavidin–biotin peroxidase, original magnification ×400). **d2.1**, **d2.2** Strong expression of TGF-beta 2 in the cytoplasm of the well-developed ducts including the intercalated duct at the ductal/acinar junction (**d2.1** *arrow*). **d3.1**, **d3.2** Strong expression of TGF-beta 3 in myoepithelial cells surrounding the well-differentiated acinar lobules (**d3.1**) and mild expression of TGF-beta 3 in the cytoplasm of epithelial cells forming an excretory duct (**d3.2**) (streptavidin–biotin peroxidase, original magnification ×400)

They were then incubated with 0.5% pepsin in phosphate-buffered saline (PBS) at 37°C pH 1.8 for 30 min for antigen retrieval, followed by incubation overnight with the primary antibodies—rabbit polyclonal against TGF-beta 1 (clone sc-146), TGF-beta 2 (clone sc-90) and TGF-beta 3 (clone sc-82), all obtained from Santa Cruz Biotechnology (Santa Cruz, CA, USA), used in a title of 1:150. The reaction followed with incubation with the indirect dextran polymer detection system (En Vision—Dako, Carpinteria, CA, USA). Staining was completed by incubation with 3′3 diaminobenzidine tetrachloride (DAB) for 3 min. Counter-staining with Mayer's haematoxylin, dehydrating and



mounting the slides with glass coverslip and xylene-based mountant completed the procedure.

Negative controls were achieved by substituting primary specific antibodies with non-immune serum and internal positive controls were considered according to primary serum manufacturer's datasheet recommendation.

All immunohistochemical reactions were carried out in triplicate.

Immunofluorescence

The 3-μm serial sections of developing minor salivary glands specimens were submitted to double labelling immunofluorescence reactions, performed in two steps: sections were incubated with the first primary antibody, followed by incubation with goat anti-mouse IgG labelled with green fluorescent Alexa 488 (Molecular Probes, Carlsbad, CA, USA) at a concentration of 1:100 in BSA–PBS. Incubation with the second primary antibody was performed, followed by incubation with goat anti-mouse IgG labelled with red fluorescent Alexa 594 (Molecular Probes) at a concentration of 1:100. Primary antibodies used, source, clone and working dilutions are described in Table 1. The sections were then air dried and mounted with Vecta Shield.

The results were analysed under Zeiss microscope equipped with epi-illumination and filters for fluorescein and rodamin and registered with a digital camera.

Specimens incubated with normal serum were used as negative controls. Internal positive controls such as basal layer of epithelium and blood vessels were present.

Results

Immunohistochemistry and immunofluorescence

The specimens studied were of the minor human salivary glands in various stages of development, which were bud, proliferation, canalisation, branching and cytodifferentiation. Salivary glands at bud/proliferation stages of development were negative for TGF-beta 1 (Fig. 1**a1**). In these stages, a few TGF-beta 2 positive cells could be detected (Fig. 1**a2**), and weak expression of TGF-beta 3 was observed around cells of the solid bud (Fig. 1**a3,** arrow). At bud/proliferation stage of salivary gland development, only a few cells were weakly positive for CK14 (Fig. 2**a**).

During canalisation stage, developing salivary gland ducts could be observed. TGF-beta 1 was detected in the stroma surrounding the canalising glandular structures (Fig. 1**b1**). Cells of the rudimentary canalised glandular structures were strongly positive for TGF-beta 2 (Fig. 1**b2**), and TGF-beta 3 was seen with a weak intensity in the apical pole of cells in contact with the lumen (Fig. 1**b3**). During this development stage, CK14 and low-molecular-weight cytokeratin (CK LMW) were present in the ductal epithelial cells. Smooth-muscle actin (SMA) (red) was only found in rare cells (Fig. 2**b**, **c**, **g**, **h**).

In the stage of branching and initial cytodifferentiation, TGF-beta 1 was strongly expressed in the cytoplasm of rudimentary mucous cells at the end of the branching glandular structure (Fig. 1**c1**). Ductal cells were intensely positive for TGF-beta 2 (Fig. 1**c2**), and TGF-beta 3 was weakly expressed in the apical pole of the luminal cells of the developing salivary glands. TGF-beta 3 was also positive around the rudimentary acinic lobules in the myoepithelial cells (Fig. 1**c3**, arrows). In the stage of branching and initial cytodifferentiation, ductal cells were positive for CK 14 (Fig. 2**d**). Luminal cells of the developing ductal system were positive for CK LMW. SMA (red) was detected in cells of the terminal portion of the ductal system and in cells that surrounded the rudimentary acinic lobules (Fig. 2**i**, **j**).

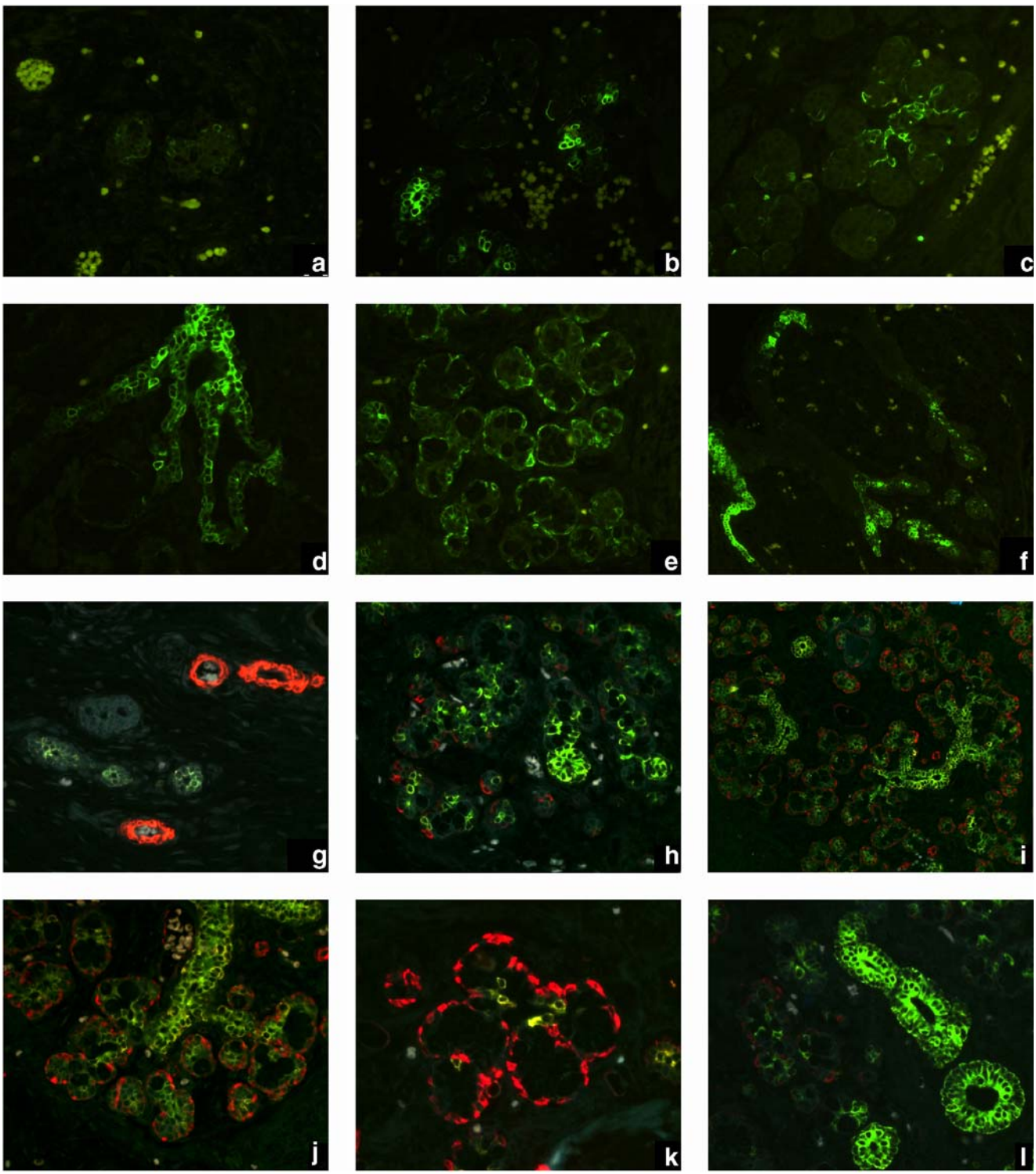
In a further differentiation stage (advanced cytodifferentiation), TGF-beta 1 was positive in the cytoplasm of a few acinar cells of the well-established acinic lobules (Fig. 1**d1**). TGF-beta 2 showed a strong expression in the cytoplasm of ductal cells of the entire glandular system (Fig. 1**d2.1**, arrow, and **d2.2**) and TGF-beta 3 was present in the myoepithelial cells surrounding the acinar lobules (Fig. 1**d3.1**). Yet, a weak expression of this factor was observed in ductal cells of well-developed excretory ducts (Fig. 1**d3.2**). In late acinar cytodifferentiation, CK14 was detected in the cytoplasm of basal cells of the ductal system. Myoepithelial cells were positive for CK14 (green)

Fig. 2 Markers of cytoskeletal differentiation in human developing minor salivary gland. **a** Bud stage of salivary gland development: weak expression of CK14 in a few cells of the epithelial islet of the developing gland. **b**, **c** Proliferation/canalisation phase: expression of CK14 in the cytoplasm of ductal cells. **d** Branching phase: presence of CK 14 in a greater number of cells of the ductal system of the developing gland. **e** Acinar differentiation: immunoexpression of CK14 in myoepithelial cells surrounding the acinar lobules. **f** Strong expression of CK14 in the basal layer of the epithelium and in the well-formed ductal system of the salivary gland. Note that the ductal portion of the duct next to the covering epithelium is still negative for this marker. **g** Initial phase of proliferation/canalisation: a few structures presenting positivity for CK LMW (*green*). SMA (*red*) is only detected in blood vessels walls in this phase. **h**, **i** Canalisation/branching phase: strong expression of CK LMW (*green*) in the cells of the ductal system. Initial expression of SMA (*red*) in myoepithelial cells surrounding mainly the terminal portion of the ductal system. **j** Initial phase of acinar differentiation: expression of CK LMW (*green*) in the ductal system and SMA (*red*) surrounding the acinic structures. **k** Well-formed acinar lobules: strong expression of SMA (*red*) around the acinar structures. A few cells are positive for CK LMW (*green*), probably representing the intercalated duct structure. **l** Well-developed ductal system strongly positive for CK LMW (*green*)

and SMA (red). CK LMW was seen in luminal cells of the ductal system (Fig. 2**e**, **f**, **k**, **l**).

The specimens of normal fully developed salivary glands studied comprised minor glands composed of mucous secretory units, myoepithelial cells and intercalated, striated and excretory ducts. TGF-beta 1 was intensely expressed on the cytoplasm of mucous acinar cells, and TGF-beta 2 and 3 were detected on epithelial cells of the ductal system (Fig. 3**a**, **b**, **c**).

Semi-quantitative analysis of TGF-beta isoforms expression in developing and adult salivary glands was performed and classified according to the intensity of the immunohistochemical stain as negative (0), weak (+), mild (++) and strong (+++). These results are illustrated in Table 2.



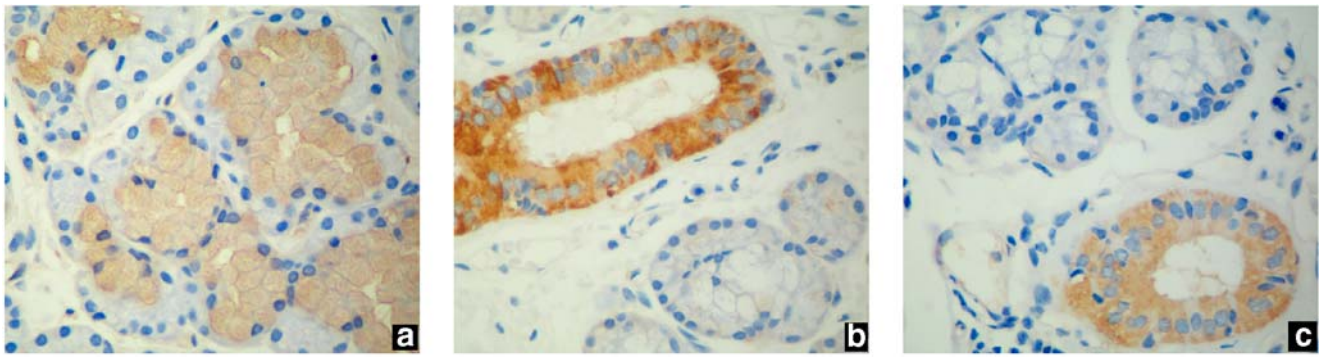


Fig. 3 TGF-beta expression in human normal adult minor salivary gland. **a** Expression of TGF-beta 1 in the cytoplasm of numerous acinar mucous cells (streptavidin–biotin peroxidase, original magnification ×400). **b** Strong expression of TGF-beta 2 in the cytoplasm of excretory ducts (streptavidin–biotin peroxidase, original magnification ×400). **c** Expression of TGF-beta 3 in the cytoplasm of excretory ducts (streptavidin–biotin peroxidase, original magnification ×400)

Discussion

The molecular mechanisms involved in salivary gland development have been described in some detail in the mouse and hamster [8, 16, 24]. To date, there is little known of the expression of growth factors during pre-natal and post-natal development of human salivary gland. Just as other glands and tissues, it is very likely that development is coordinated via several integrated events affecting proliferation, morphogenesis and cell-substratum interactions. These events are tightly regulated both temporally and spatially [4].

Our results revealed that TGF-beta 1, 2 and 3 are present in complementary patterns in the various phases of salivary gland development, branching, morphogenesis and cytodifferentiation. This pattern is dynamic and changes with the stage of development, and this tendency is also reported in the development of mammary glands and other glandular organs [1, 7, 15, 19, 25, 27, 29]. Moreover, the overlapping patterns of TGF-beta expression in morphogenetically active epithelial structures are reported in structures of murine head and neck, such as whisker follicle, salivary gland and tooth bud [25]. The TGF-beta superfamily is involved in many aspects of development and includes TGF-betas, BMPs, activins, inhibins and others [3]. Specifically, TGF-betas, activin and BMPs are reported to control salivary gland branching morphogenesis in studies that investigated these factors in mouse submandibular glands [13, 27].

During the initial stages of salivary gland morphogenesis, the bud stage, TGF-beta 1 was not present and TGF-beta 2 and 3 were detected in rare cells. This stage represents a highly proliferative phase, with little or no evidence of differentiation markers. Taking this into

Table 2 Semi-quantitative analysis of immunohistochemical expression of TGF-beta isoforms in developing and adult human minor salivary glands

		TGF-beta 1	TGF-beta 2	TGF-beta 3
Developing human minor salivary gland				
Bud stage	Epithelial cells	0	++	+
	Stroma	0	0	0
Canalisation stage	Ductal cells (epithelial)	0	+++	+
	Stroma	++	0	0
Branching stage	Ductal cells (epithelial)	0	+++	+
	Rudimentary acinar cells	+++	0	0
	Myoepithelial cells	0	0	++
	Stroma	0	0	0
Cyto-differentiation stage	Ductal cells (epithelial)	0	+++	++
	Acinar cells	+++	0	0
	Myoepithelial cells	0	0	++
	Stroma	0	0	0
Adult human minor salivary gland	Acinar cells	+++	0	0
	Ductal cells (epithelial)	0	+++	++
	Myoepithelial cells	0	0	0

Intensity of immunohistochemical stain: negative (0), weak (+), mild (++) and strong (+++)

consideration, it is predictable that TGF-beta expression is not a feature, as it has been previously reported that the factor inhibits proliferation and is more related to salivary gland differentiation and morphogenesis [6, 11, 14, 23]. Expression of cytokeratins is also not detected in this stage, in which cell proliferation is the main event. At this stage, none of the differentiation markers were present in the developing salivary glands, indicating that the glandular tissue is very immature and is establishing new connections with the extracellular matrix to prepare for a later stage of differentiation when phenotypic markers will be then detected. This result is in accordance with a previous report by Martins et al., in 2002 [21], who did not find any markers of differentiation in the very early stage of salivary gland development.

As salivary glands develop with increased tissue differentiation (canalisation/branching stage), TGF-beta 1 is detected in the mesenchyme surrounding the canalising and branching epithelial cords. This pattern of TGF-beta 1 expression imitates the one reported by Robinson et al., in 1991 [29], in branching morphogenesis of murine breast, and it is also reported in lung development [12]. This distribution of TGF-beta 1 during canalisation/branching phase may reflect an autocrine function of the growth factor, which would stimulate growth of the end-bud parenchymal cells. TGF-beta 2 and 3 are expressed in the epithelial cells of the initial ductal system. These results are only partially coincident with those published by Jaskoll and Melnick in 1999 [15], who reported the presence of TGF-1 and 2 in the branching epithelia and TGF-beta 3 in an epithelial and mesenchymal distribution. In this phase, the glandular system continues to display substantial epithelial cell proliferation, mainly at the tips of the canalising ductal system, where TGF-beta subunits are not yet detected. However, it is also characterised by the formation of ductal lumena and a significant change in the expression of cytoskeletal differentiation markers. At this stage (canalisation), positivity for CK14 and 35βH11 are observed, being indicative that cytodifferentiation progressed.

In advanced canalisation/branching stage and early cytodifferentiation of the salivary gland, the phenotype of the cells that compose the main structure of the developing gland is being well defined by the expression of CK14, CK LMW and SMA. TGF-beta 1 showed strong expression in the cytoplasm of immature mucous cells at the terminal end of the branched ductal system. TGF-beta 2 and 3 were distributed along all the luminal cells of the ductal system, including the intercalated ducts. TGF-beta 3 was also observed in the myoepithelial cells surrounding the immature mucous cells at the tip of the ductal system. This result agrees with the data reported by Robinson et al., 1991 [29], which described the expression of TGF-beta 3 in myoepithelial cells of the developing breast. This expression can also be compared with the expression of TGF-beta 3 in other organs composed of cells that present contractile components, such as skeletal and cardiac muscle and cells associated with blood vessels [25, 29]. Myoepithelial cells of salivary glands form the outermost layer of acinic lobules and ducts and act as both contractile cells to aid saliva secretion and cells with high capacity of synthesising basal lamina that ensheaths these structures [5]. Robinson et al., in 1991 [29], described the expression of TGF-beta 3 in myoepithelial stem cells, speculating on a possible function of inhibition of terminal differentiation, which would allow the formation of lateral buds in the developing breast. They also suggested that TGF-beta 3 could be involved in the elaboration of basal lamina components. These aspects could not be assessed in our study and remain to be elucidated in the formation of human salivary glands.

In late stages of salivary gland histogenesis, branching and cytodifferentiation of acinar cells, CK14, 35βH11 and SMA are present in this phase of gland development in a specific pattern. SMA is expressed when acinar lobules start to differentiate, stressing the presence of myoepithelial cells around these structures. CK14 is expressed by the basal cells of the excretory ducts and 35βH11 is found in the luminal cells of the ductal system. CK 14, according to other authors, will provide a strong base for the connection of basal cells with the basement membrane, functioning as integrators of the cytoplasm and allowing resistance to mechanical stress and maintenance of the ductal system architecture [9]. In this phase, TGF-beta 1 is seen in sparse, well-developed mucous acinar cells, and in adult salivary glands, the acinar cells conserved the expression of this growth factor. This pattern may be indicative that TGF-beta 1 is synthesised by acinar cells and is important for salivary gland maintenance. However, expression of TGF-beta 1 in adult normal salivary glands is disputable, and while Kizu et al. [17] reported its expression on acini and ducts, Kusafuka et al., in 2001 [18], found no evidences of its presence. TGF-beta 2 is exclusively detected along the epithelial cells of the ductal system, and TGF-beta 3 conserved its expression along the ductal system and in the myoepithelial cells that surround the mucous acinar lobules and these patterns and maintained in the adult structures.

The shifting prototype of TGF-beta subunits during maturation of salivary glands suggests changing stimuli requirements during the complex developmental stages of these glands. The present study adds strength to this evidence, showing that TGF-beta subunits are important factors during salivary gland differentiation, being developmentally regulated.

Acknowledgements Supported by *Fundacao de Amparo a Pesquisa do Estado de Sao Paulo* grants 02/02676-7 and 03/00450-4 and British Council Academic Link SPA/881/155.

References

1. Bartram U, Speer CP (2004) The role of transforming growth factor-beta in lung development and disease. Chest 125:754–765
2. Chai Y, Mah A, Crohin C, Groff S, Bringas P Jr, Le T, Santos V, Slavkin HC (1994) Specific transforming growth factor beta subtypes regulate embryonic mouse Meckel's cartilage and tooth development. Dev Biol 162:85–103
3. Chang H, Lau AL, Matzuk MM (2001) Studying TGF-beta superfamily signalling by knockouts and kcnokins. Mol Cell Endocrinol 180:39–46
4. Cutler LS (1989) Functional differentiation of salivary glands. In: Forte J (ed) Handbook of physiology, salivary, pancreatic, gastric and hepatobiliary secretion, vol 3. American Physiological Society Press, New York, pp 93–105
5. Cutler LS (1990) The role of extracellular matrix in the morphogenesis and differentiation of salivary glands. Adv Dent Res 4:27–33
6. Derynck R (1994) TGF-beta-receptor mediated signalling. Trends Biochem Sci 19:548–553
7. Faure E, Heisterkamp N, Groffen J, Kaartinen V (2000) Differential expression of TGF-beta isoforms during postlactational mammary gland involution. Cell Tissue Res 300:89–95
8. Fernandes RP, Cotanche DA, Lennon-Hopkins K, Erkan F, Menko AS, Kukuruzinska MA (1999) Differential expression of proliferative, cytoskeletal, and adhesive proteins during postnatal development of the hamster submandibular gland. Histochem Cell Biol 111(2):153–162
9. Fuchs E, Cleveland DW (1998) A structural scaffolding of intermediate filaments in health and disease. Science 279 (5350):514–519
10. Grande JP (1997) Role of transforming growth factor-beta in tissue injury and repair. Proc Soc Exp Biol Med 214:27–40
11. Hardman P, Landels E, Woolf AS, Spooner BS (1994) TGF-beta 1 inhibits growth and branching morphogenesis in embryonic mouse submandibular and sublingual glands in vivo. Dev Growth Differ 36:567–577
12. Heine UI, Muñoz EF, Flanders KC, Roberts A, Sporn MB (1990) Colocalization of TGF-beta 1 and collagen I and III, fibronectin and glycosaminoglycans during lung branching morphogenesis. Development 109:29–36
13. Heine U, Muñoz EF, Flanders KC, Ellingsworth LR, Lam HY, Thompson NL, Roberts AB, Sporn MB (1987) Role of transforming growth factor-beta in the development of the mouse embryo. J Cell Biol 105:2861–1876
14. Hu PP, Datto MB, Wang XF (1998) Molecular mechanisms of transforming growth factor-beta signalling. Endocr Rev 19:349–363
15. Jaskoll T, Melnick M (1999) Submandibular gland morphogenesis: stage-specific expression of TGF-alpha/EGF, IGF, TGF-beta, TNF, and IL-6 signal transduction in normal embryonic mice and the phenotypic effects of TGF-beta 2, TGF-beta 3, an EGF-R null mutations. Anat Rec 256:252–268
16. Kashimata M, Gresik EW (1996) Contemporary approaches to the study of salivary gland morphogenesis. Eur J Morphol 34:143–147
17. Kizu Y, Sakurai S, Katagiri S, Shinozaki N, Ono M, Tsubota K, Saito I (1996) Immunohistochemical analysis of tumour growth factor-beta 1 in normal and inflamed salivary glands. J Clin Pathol 49:728–732
18. Kusafuka K, Yamaguchi A, Kayano T, Takemura T (2001) Immunohistochemical localization of members of the transforming growth factor –beta superfamily in normal human salivary glands and pleomorphic adenomas. J Oral Pathol Med 30:413–420
19. Liu J, Tseu I, Wang J, Tanswell K, Post M (1996) Transforming growth factor-beta 2, but not beta 1 and beta 3, is critical for early rat lung branching. Dev Dyn 217:343–360
20. Lourenço SV, Kapas S (2005) Integrin expression in developing salivary glands. Histochem Cell Biol 124:391–399
21. Martins MD, Araújo VC, Raitz R, Araújo NS (2002) Expression of cytoskeletal proteins in developing human minor salivary glands. Eur J Oral Sci 110:316–32120
22. Massagué J (1998) TGF beta signal transduction. Annu Rev Biochem 67:753–791
23. Melnick M, Cehn H, Buckley S, Warburton D, Jaskoll T (1998) Insulin-like growth factor II receptor, transforming growth factor-beta, and Cdk4 expression and the developmental epigenetics of mouse palate morphogenesis and dysmorphogenesis. Dev Dyn 211:11–25
24. Menko AS, Kreidberg JA, Ryan TT, Van Bockstaele E, Kukuruzinska MA (2001) Loss of a3ß1 integrin function results in an altered differentiation program in the mouse submandibular gland. Dev Dyn 220(4):337–349
25. Millan FA, Denhez F, Kondaiah P, Akhurst RJ (1991) Embryonic gene expression patterns of TGF-beta 1, beta 2 and beta 3 suggest different developmental functions in vivo. Development 11:131–144
26. Moustakas A, Pardali K, Gaal A, Heldin CH (2002) Mechanisms of TGFβ signaling in regulation of cell growth and differentiation. Immunol Lett 82:85–91
27. Patel VN, Rebustini IT, Hoffman MP (2006) Salivary gland branching morphogenesis. Differentiation 74:349–364
28. Roberts AB, Sporn MB (1993) Physiological actions and clinical applications of transforming growth factor beta. Growth Fact 8:1–9
29. Robinson SD, Silberstein GB, Roberts AB, Flanders KC, Daniel CW (1991) Regulated expression and growth inhibitory effects of transforming growth factor-beta isoforms in mouse mammary gland development. Development 113:867–878

Virchows Arch (2008) 452:435–442
DOI 10.1007/s00428-007-0569-2

ORIGINAL ARTICLE

Ontogeny of human intrahepatic innervation

Dina G. Tiniakos · Joseph Mathew · Christos Kittas · Alastair D. Burt

Received: 10 October 2007 / Revised: 14 December 2007 / Accepted: 18 December 2007 / Published online: 15 January 2008
© Springer-Verlag 2007

Abstract Intrahepatic nerves serve important metabolic, sensory and motor functions. Their ontogeny in human liver has not been elucidated. We aimed to characterise the ontogeny of human intrahepatic innervation, to assess its relationship with biliary structures and to examine the distribution and nature of peptidergic nerves during development. We used immunohistochemistry on archival normal human liver tissue from 63 fetuses [8–40 gestational weeks (gw)] and 10 adults with antibodies to pan-neural markers and neuropeptides. Few nerve fibers appeared in portal tracts at 8 gw. Their density increased gradually from 12 gw and reached adult levels at 32–33 gw. Rare intra-acinar nerves, restricted to periportal areas, appeared at 40 gw. Galanin-, somatostatin- and calcitonin-gene-related peptide-positive nerve fibers were noted only in portal tracts from 22, 26 and 32 gw, respectively. In human adult liver, dense portal and intra-acinar neural supply was observed. Human fetal liver contains a neural network distributed mainly in portal tracts with a density that increases progressively towards term. Intra-acinar innervation appears at term, suggesting that is not required for normal liver function during development, while peptidergic nerves are important for intrauterine liver functions. Developmentally regulated expression of galanin and somatostatin may play a role in liver morphogenesis.

Keywords Liver innervation · Development · Peptidergic · Immunohistochemistry · Bile ducts

D. G. Tiniakos (✉) · C. Kittas
Laboratory of Histology and Embryology, Medical School,
National and Kapodistrian University of Athens,
75, M. Asias str, Goudi,
Athens 11527, Greece
e-mail: dtiniak@med.uoa.gr

J. Mathew
Department of Histopathology, Royal Cornwall Hospital,
Truro TR1 3 LJ, UK

A. D. Burt
Institute of Cellular Medicine, Newcastle University,
Newcastle upon Tyne NE2 4HH, UK

Introduction

The liver of most mammalian species, including man, is richly innervated by afferent and efferent sympathetic and parasympathetic fibers. Efferent nerve fibers are implicated in the regulation of hepatic hemodynamics [16, 20], microvasculature [35] and carbohydrate and lipid metabolism [16, 26], while afferent nerve fibers may serve sensory functions, such as ionoreception, baroreception, osmoregulation and control of metabolic receptors [2, 8]. Recent studies have shown that sympathetic nerves may regulate liver repair by modulating hepatic stellate cells and hepatic epithelial progenitors [23–25]. The latter may also be activated by stimulation of the vagal nerve [6] and may receive nerve endings [7]. The putative anatomical "niche" of hepatic progenitor cells in human liver lies in the canal of Hering, which conducts bile from canaliculi to terminal bile ducts in portal tracts [28]. It is not as yet clear whether intrahepatic nerves exert their influence on hepatic progenitor cells through direct nerve–progenitor cell contact, nerve contact with intermediate cell effectors or through diffusion of neurotransmitters.

Portal tract innervation is remarkably consistent across mammalian species [4, 13–15, 20] with adrenergic nerves forming an intrinsic plexus around the walls of portal tract blood vessels and less frequently in relation to bile duct radicles [4]. The latter, including bile ductules and canals of

Hering, are the site of close nerve–cholangiocyte contact [36].

The extent and acinar distribution of intra-acinar nerve fibers is very variable and shows significant differences between species. While rat and mouse livers have only limited intrasinusoidal innervation, the livers of man and guinea pig show rich intra-acinar innervation [3, 4, 13, 14, 19, 20]. In human adult liver, afferent and efferent nerve aminergic and peptidergic fibers are distributed unevenly in the acini running along the sinusoidal walls, predominating in the periportal region [29] but also extending to the terminal hepatic venules [4]. Nerve fibers are identified within the space of Disse, between hepatocytes and in close contact with perisinusoidal, endothelial and Kupffer cells [3, 4, 20].

Neuropeptide Y (NPY)-, substance P- and somatostatin-containing nerve fibers are demonstrated in portal tracts and along sinusoidal walls in close contact with hepatocytes and hepatic stellate cells [1, 4, 12, 34]. Vasoactive intestinal peptide (VIP)- and calcitonin-gene related peptide (CGRP) nerve fibers are mainly detected around portal blood vessels and may co-exist in cholinergic and sensory nerves [20, 33]. Nerves containing glucagon, glucagon-like peptide, neurotensin and galanin are found mainly in portal tracts [20, 11]. Cholinergic nerves are restricted in portal tracts with only a few fibers reaching periportal hepatocytes and sinusoids [3, 20].

Few studies have been conducted on the ontogeny of liver innervation [8]. In developing mice and rats, intrahepatic NPY-ergic nerve fibers first appear at the late fetal period, increase in density with age and reach adult levels at 2 weeks postnatal [9, 10]. In infant guinea pig liver (3 and 7 days postnatal), the distribution and density of NPY-ergic fibers is similar to that observed in the adult [9]. The ontogeny of human intrahepatic innervation has not been studied extensively, and the anatomical relationship of nerve fibers with bile ducts and possibly with proximal biliary structures (bile ductules and canals of Hering), a putative hepatic progenitor cell "niche", has not been assessed during liver development. Our group has already published a preliminary study in a small number of second- and third-trimester fetuses, showing the presence of nerve fibers in portal tracts from 20 gestational weeks (gw), reaching adult levels at 32 gw. Intrasinusoidal innervation was detected in human fetal liver only at term [31].

The present immunohistochemical study defines the ontogeny of human intrahepatic innervation using more detail in a large number of cases, including first-trimester fetuses, to assess the distribution and the nature of peptidergic nerves in human fetal liver and to examine the relationship of intrahepatic nerve fibers with biliary structures during development.

Materials and methods

Our material consisted of archival normal liver tissue from 63 human fetuses (gestational ages, 8–40 weeks) and 10 adults (normal areas from surgical liver specimens). The fetal material was obtained from therapeutic and spontaneous abortions; no fetal malformations or other pathology was detected at autopsy. According to the autopsy protocols at that time, one tissue block from the right lobe of the liver was collected per case. Tissue blocks from first-trimester cases, however, may have included part of other lobes and the hilum. Normal adult liver tissue was obtained from surgical specimens of liver resection for benign tumour distant from the neoplasm. The study was performed in accordance with National Bioethical Standards and ethical standards of the Helsinki Declaration of World Medical Association (2000) and with appropriate consent for use of anonymised archival tissue for research.

Tissue blocks were fixed in either Bouin's fixative or 10% buffered formalin (with mercuric chloride post-fixation) and then were routinely paraffin-embedded. Approximately 5 μm serial sections were cut from each block and were mounted onto poly-L-lysine- (Sigma, St. Louis, MO, USA) coated slides. The peroxidase–antiperoxidase immunohistochemical technique with antibodies specific for "pan-neural" markers and neuropeptides (Table 1) was performed. All steps were carried out in a 0.25 M phosphate buffer saline (PBS, pH= 7.4) at 25°C. After deparaffinization and rehydration in a series of graded ethanols, sections were incubated in 0.9% hydrogen peroxide (H_2O_2, Sigma) in methanol for 30 min in the dark, to inactivate endogenous peroxidase, and then were rinsed in tap and subsequently in distilled water. After 4× 4 min treatment with citric acid 0.001 M in a microwave oven (800 W), sections were rinsed in distilled water, PBS and then incubated for 20 min in 20% normal rabbit serum (NRS, Dako A/S Denmark) or 20% normal swine serum (NSS, Dako, Denmark) in PBS. Sections were then incubated for 1 h at room temperature with the primary antibodies diluted in 0.25 M PBS containing 0.5% NRS or NSS (dilutions shown in Table 1). After thorough rinse with PBS, the sections were incubated with the secondary antibody (rabbit anti-mouse or swine anti-rabbit), diluted in PBS (1:200 for monoclonal antibodies and 1:300 for polyclonal antisera) for 30 min at room temperature. The sections were then washed in PBS and incubated with the peroxidase–antiperoxidase complex (Dako), diluted 1:100 in PBS, for 25 min. Following rinses with PBS, sections were incubated with a solution of 3,3′diaminobenzidine tetrahydrochloride (DAB) 25 g/100 ml in PBS (Sigma) containing 80 μl H_2O_2 (Sigma). Nickel enhancement was applied in some experiments. Sections were then washed in tap water, counterstained with haematoxylin for 15 s, dehydrated in graded ethanols, cleared

Table 1 Specificity, origin, working dilution and source of antibodies used in the immunohistochemical study

Antibody specificity	Origin	Dilution	Source
PGP9.5	Rabbit	1:20	Ultraclone, UK
Neurofilaments	Mouse	1:20	Novocastra Laboratories, UK
Neurone-specific enolase	Rabbit	1:200	Dako, Denmark
S100 protein	Rabbit	1:500	Dako, Denmark
N-CAM	Mouse	1:500	Sigma, USA
Synaptophysin	Rabbit	1:10	Dako, Denmark
Neuropeptide Y	Rabbit	1:1,500	J.M. Polak (Imperial College, London, UK)
Somatostatin	Rabbit	1:2,500	J.M. Polak (Imperial College, London, UK)
Galanin	Rabbit	1:2,500	J.M. Polak (Imperial College, London, UK)
CGRP	Rabbit	1:750	J.M. Polak (Imperial College, London, UK)

in xylene, mounted with dibutyl polystyrene xylene (DPX) (BDH, England) and coverslipped. Negative control sections were used for each case in every immunostaining run, consisting of a duplicate section from each case treated as above with the exception that the incubation with the primary antibody was omitted. Nerve fibers in normal colonic wall tissue sections were used as positive control. Where applicable, distinction between immunopositive fibers and cells was based on known differences in their shape and size aided by the identification of nucleus in the latter.

The density of immunostained nerve fibers was scored semi-quantitatively with a scale of «−» to «+++» as previously described in studies on the ontogeny of solid-organ intraparenchymal innervation [32]. Briefly, «+++» corresponds to the highest density of portal or intra-acinar nerves, «++» refers to an intermediate nerve fiber density, «+» is used when only few immunopositive nerve fibers are recognized, and «−» shows that there are no immunostained nerve fibers. The slides were scored separately by two pathologists (D.G.T., J.M.). There were no significant differences between observers' scoring results.

Results

The topography and density of the intrinsic innervation of human fetal and adult liver is summarised in Table 2, while the distribution and density of peptidergic nerves is shown

Table 2 Immunolocalisation of nerve fibers in human fetal and adult liver using antibodies to pan-neural markers

Age	Liver																	
	NSE			NF			S-100			PGP9.5			N-CAM			Synaptophysin		
	PT	HAc	CV	PT	HAc	CV	PT	HAc	CV	PT	HAc	CV	PT	HAc	CV	PT	HAc	CV
Fetal (gw), n=63																		
8–10, n=4	−	−	−	+	−	−	−	−	−	−	−	−	−	−	−	−	−	−
12–18, n=14	+	−	−	+	−	−	+	−	−	+	−	−	+	−	−	+	−	−
20–24, n=9	+	−	−	+	−	−	+	−	−	++	−	−	+	−	−	+	−	−
26–27, n=5	+	−	−	+	−	−	+	−	−	++	−	−	+	−	−	+	−	−
28, n=2	++	−	−	+	−	−	++	−	−	+++	−	−	+	−	−	+	−	−
29, n=3	++	−	−	+	−	−	++	−	+[a]	+++	−	+[a]	+	−	−	+	−	−
30, n=3	++	−	−	++	−	−	++	−	−	+++	−	−	+	−	−	+	−	−
32, n=2	++	−	−	++	−	−	++	−	+[a]	+++	−	+[a]	+	−	−	+	−	−
33–38, n=14	++	−	−	++	−	−	++	−	−	+++	−	−	+	−	−	+	−	−
39, n=3	+++	−	−	++	−	−	++	−	−	+++	−	−	++	−	−	++	−	−
40, n=4	+++	−	−	++	−	−	++	+[b]	−	+++	+[b]	−	++	−	−	++	−	−
Adult, n=10	+++	+	−	++	+	−	++	+	−	+++	++	+	++	+	−	++	++	−

gw Gestational week; *PT* portal tracts; *HAc* hepatic acini; *CV* central veins; + low density;++ moderate density; +++ high density
[a] Large hepatic veins only
[b] Periportal zone (acinar zone 1) only

in Table 3. There were no significant differences in the density of immunostained nerve fibers between cases within in each of the time periods shown.

The distribution of neurone-specific enolase (NSE)-, neurofilament-, S-100 protein-, protein gene product 9.5 (PGP9.5)-, neural cell adhesion molecule (N-CAM)- and synaptophysin-positive nerve bundles in the portal tracts of fetal liver appeared similar to that observed in the human adult liver, i.e. many fibers were identified in close apposition to hepatic artery branches, fewer were related to portal vein branches, and only occasional fibers were detected close to bile duct radicles (Fig. 1). However, the latter were observed more frequently in fetal liver than in adult liver, at least until the 32nd gestational week. Occasional PGP9.5-positive fibers were detected close to the ductal plate, and in some first- and early second-trimester fetuses, scattered neurofilament- and N-CAM-positive cells were identified in close proximity to the ductal plate. Rare S100- and PGP9.5-immunoreactive fibers were identified in the walls of large hepatic veins at 29–32 gw, while there was no immunoreactivity for any marker within the walls of terminal hepatic veins. The density of the portal nerve bundles increased with the gestational age and reached adult levels at 32nd–33rd gestational week.

Few neurofilament-positive nerve fibers were observed in the portal tracts of 8–10 gw fetal liver, while all other "pan-neural" markers failed to identify intrahepatic nerve fibers at this stage. In a single case at 8 gw, sections included the hilum where the neurofilament-positive nerve fibers were most abundant. The density of nerves in portal tracts increased from 12th gestational week onwards and were identified with all the pan-neural markers used. Greater numbers of nerve fibers were detected using PGP9.5 than any of the other markers. There were no differences in immunostaining intensity with these markers between portal tracts of different sizes.

Intra-acinar nerve fibers, positive only for S-100 protein and PGP9.5, first appeared in human fetal liver only at the 40th gestational week, and they were restricted in periportal areas (acinar zone 1). In adult liver, dense intra-acinar innervation was identified using all "pan-neural" markers. Most intrasinusoidal nerve fibers were positive to PGP9.5, while lesser numbers were detected using the other markers. N-CAM detected the fewest intra-acinar nerve fibers. Occasional PGP9.5-positive nerve fibers were identified within the walls of terminal hepatic vein radicles.

Peptidergic nerves in human fetal liver were identified in portal tracts from 22 gw (Fig. 2). Intrasinusoidal peptidergic nerves fibers were not identified in fetal liver at any gestation. In detail, galaninergic intrahepatic nerve fibers were distributed mainly around hepatic arteries in portal tracts from 22nd gestational week, and they were present until term. However, they were absent from all adult liver cases. Galanin-positive nerve fibers were also noted close to portal vein branches and occasionally in close apposition to interlobular bile ducts in contact with their basement membrane (Fig. 2a,b). CGRP-ergic nerves were detected in low density in the portal tracts of human fetal liver from 32nd gestational week until term (Fig. 2c). Somatostatinergic nerves were detected in portal tracts only between the 26th and 33rd gestational weeks with a distribution similar to that of galaninergic nerves (Fig. 2d–f). A few somatostatinergic nerve fibers were identified around portal bile duct radicles until the 29th week of gestation (Fig. 2d,e). NPY-containing nerves were not demonstrated in any of the human fetal liver cases examined. In contrast, in human adult liver, NPY-ergic nerves were the only peptidergic nerves identified in portal tracts and acini, forming an extensive intrahepatic network.

Table 3 Immunolocalisation of nerve fibers in human fetal and adult liver using antibodies to neuropeptides

Age	Liver											
	NPY			Galanin			Somatostatin			CGRP		
	PT	HAc	CV	PT	HAc	CV	PT	HAc	CV	PT	HAc	CV
Fetal (gw), *n*=63												
8–21, *n*=21	−	−	−	−	−	−	−	−	−	−	−	−
22–24, *n*=6	−	−	−	+	−	−	−	−	−	−	−	−
26–28, *n*=7	−	−	−	+	−	−	+	−	−	−	−	−
29–30, *n*=6	−	−	−	+	−	−	++	−	−	−	−	−
32, *n*=2	−	−	−	++	−	−	++	−	−	+	−	−
33, *n*=3	−	−	−	++	−	−	++	−	−	+	−	−
34–40, *n*=18	−	−	−	++	−	−	−	−	−	+	−	−
Adult, *n*=10	++	+	+	−	−	−	−	−	−	−	−	−

gw Gestational week; *PT* portal tracts; *HAc* hepatic acini; *CV* central veins; + low density; ++ moderate density; +++ high density

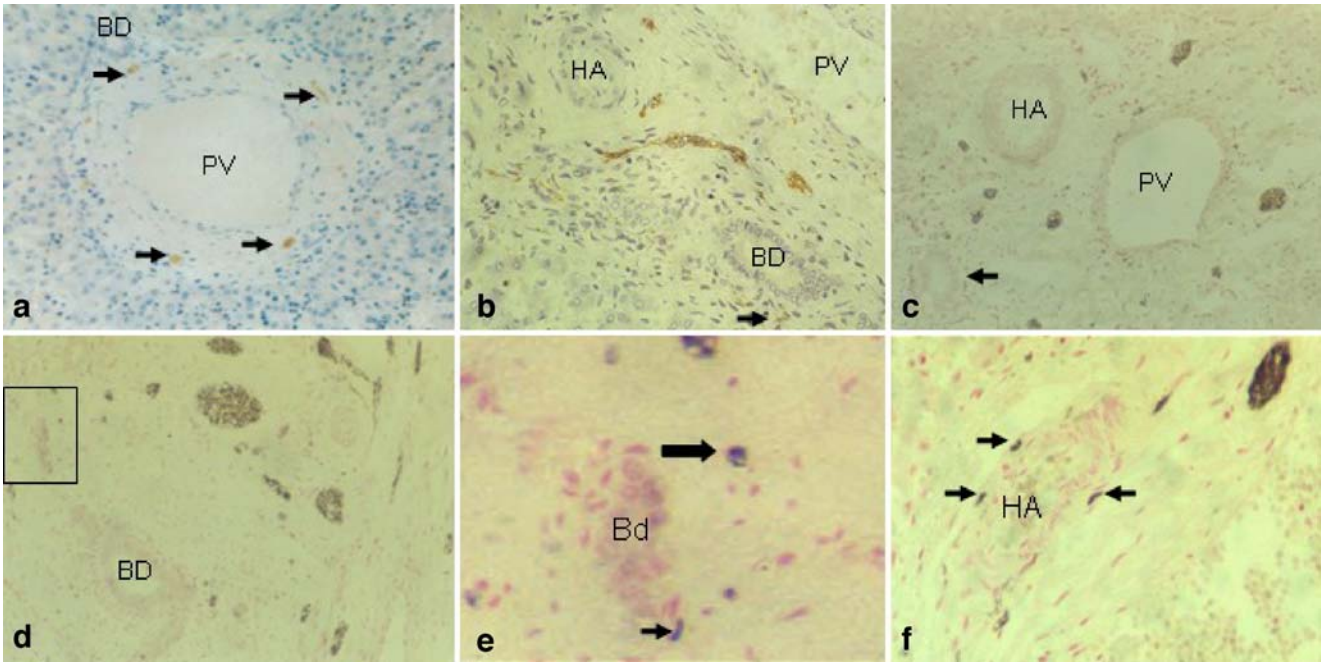


Fig. 1 Fetal liver, portal tract. **a** 20 gw, NSE-positive nerve fibers (*arrows*), DAB chromogen, ×100. **b** 29 gw, NSE-positive nerve fibers. Few nerve fibers are noted in the vicinity of a bile duct (*arrow*), DAB, ×200. **c** 29 gw, PGP9.5-positive nerve bundles. Some nerve fibers are shown close to the interlobular bile duct (*arrow*), nickel-DAB chromogen, ×200. **d** 29 gw, S-100-positive nerve bundles and fibers in a large portal tract. In the *rectangle*, a bile ductule is shown, nickel-DAB, ×200. **e** Magnification of the area in rectangle of **d**. An S-100-positive nerve fiber (*thin arrow*) is present in close apposition to the wall of the bile ductule (*Bd*), while a small nerve bundle is noted in the vicinity (*thick arrow*), nickel-DAB. **f** 33 gw, S-100-positive nerve fibers (*arrows*), probably originating from the nerve bundle showing at the upper right, in the wall of a terminal hepatic artery, nickel-DAB, ×400. *PV* Terminal portal vein branch, *HA* terminal hepatic artery branch, *BD* interlobular bile duct

Discussion

We studied the development of intrahepatic innervation in human fetuses using immunohistochemistry with antibodies to pan-neural markers and neuropeptides. We have previously shown that among the pan-neural markers, antibodies to PGP9.5 and S-100 are the most effective in identifying intra-acinar nerve fibers [18]. In the present study, the density of PGP9.5-positive nerve fibers was greater than that of S-100-positive fibers. This is not unexpected as S-100 is reportedly present in the cytoplasm of Schwann cells and not in neural cell axoplasm. Electron microscopic studies have shown that intrasinusoidal nerve fibers are only partially covered by Schwann cell processes [17].

The distribution of intrahepatic innervation in normal human adult tissues in our study was similar to that previously reported [1, 3, 4, 11, 15, 19–21, 29, 33], showing a rich neural supply of portal tracts, mainly around hepatic artery and portal vein branches with less in relation to intralobular bile ducts. PGP9.5-, NSE-, synaptophysin, S-100 and N-CAM-immunoreactive nerve fibers were identified in hepatic acini, along sinusoidal walls, in the space of Disse and in the walls of a few terminal hepatic veins. The intra-acinar distribution of nerve fibers was denser in zone 1 in accordance with previous studies [22, 29]. The close relationship of intra-acinar nerve fibers with hepatocytes may reflect their influence in the regulation of carbohydrate and lipid metabolism [26], while nerve fiber distribution in portal tracts is likely related to their hemodynamic actions [20]. Their presence in the space of Disse appears to be related to their contact with hepatic stellate cells [34] which are thought to be involved in the regulation of hepatic sinusoidal microcirculation by contraction and relaxation [35]. It is known that human and rat hepatic stellate cells, which play significant role in tissue remodelling, production of extracellular matrix components and response to acute liver necrotic injury, express neurotrophins and neurotrophin receptors [5]. Close contact of N-CAM-positive nerve endings with N-CAM-immunoreactive hepatic stellate cells has been observed in human liver [22]. In human liver disease, alterations in the distribution of intrahepatic nerves have been reported. These may play a role in the metabolic disturbances observed in the final stages of chronic liver disorders and in the alterations of intrahepatic blood flow in cirrhosis which may be related to the development of portal hypertension [18].

Zanchi et al. [36] reported close contact between immunoreactive nerve fibers and cholangiocytes of interlobular bile ducts and proximal biliary structures (bile ductules and canals of Hering) in human normal adult liver

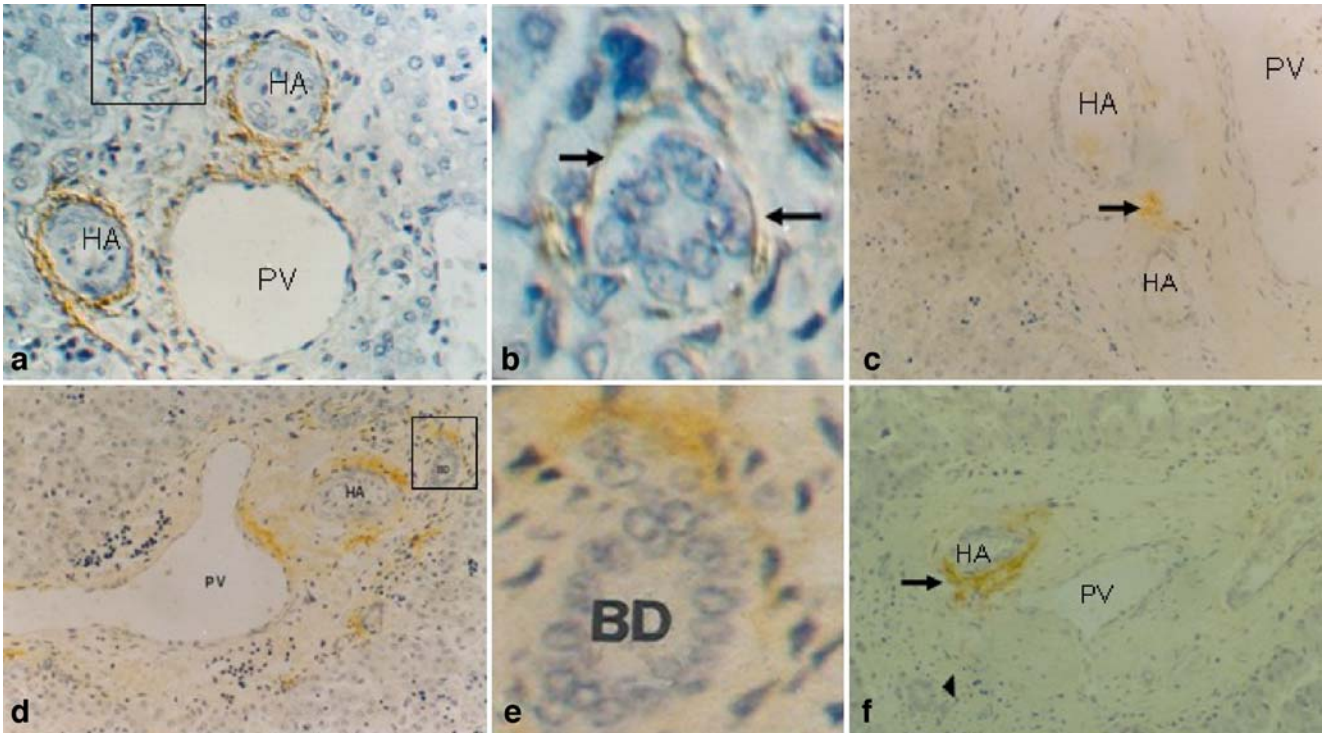


Fig. 2 Fetal liver, portal tract. **a** 32 gw, Galaninergic nerve fibers with characteristic portal distribution: dense innervation of terminal hepatic arteries, fewer nerve fibers in relation to terminal branch of portal vein and interlobular bile duct, DAB chromogen, ×400. **b** Magnification of the area in rectangle of **a**. Galanin-positive nerve fibers (*arrows*) attached to bile duct wall but not crossing the basement membrane or in between cholangiocytes. **c** 32 gw, CGRP-immunopositivity (*arrow*) between two terminal hepatic artery branches in portal tract, DAB, ×200. **d** 29 gw, somatostatin-positive nerve fibers, DAB, ×200. **e** Magnification of the area in rectangle of **d**. Somatostatin-positive nerve fiber in close apposition to the interlobular bile duct not extending between cholangiocytes. **f** 32 gw, somatostatinergic nerve: dense innervation of the terminal hepatic artery branch (*arrow*). Notice absence of immunopositive nerve fibers close to the bile duct radicle (*arrowhead*), DAB, ×200. *PV* Terminal portal vein branch, *HA* terminal hepatic artery branch, *BD* interlobular bile duct

using S-100 immunohistochemistry. We observed occasional nerve fibers in close contact with interlobular bile duct basement membranes in human fetal liver and less often in adult liver, but we did not observe nerve fibers crossing through the basement membrane and located between cholangiocytes. Terada and Nakanuma [30] detected nerve fibers in the walls of large-, medium-sized and septal bile ducts and surrounding peribiliary glands in normal human adult liver. In these branches of the biliary tree, some nerve fibers were seen in contact with epithelial cells. However, only sparse nerve fibers were detected around interlobular bile ducts and bile ductules [30]. This difference may be attributed to the fact that Zanchi et al. [36] examined many serially sectioned levels of the same portal tracts using computer-generated three-dimensional reconstructions and thus have examined in more detail the particular area of interest detecting the terminal location of some nerve fibers between cholangiocytes at the interface with the bile duct lumen. Recent studies have suggested a role for hepatic innervation in liver regeneration and hepatic epithelial progenitor cell modulation supporting the search for a possible anatomical link between intrahepatic nerves and the putative hepatic progenitor cell "niche" in the canals of Hering [6, 7, 22, 23]. It is still unclear, however, whether the cholangiocytes of the canal of Hering or other cells in the same location represent the progenitor cell compartment of the human liver [28].

The N-CAM- and neurofilament-positive cells close to the ductal plates of some first- and second-trimester fetuses could represent progenitor cells which are known to show neuroendocrine features including N-CAM immunoreactivity [27]. N-CAM is a cell-adhesion molecule with a significant regulatory role during development mainly through cell–cell and cell–matrix interactions. N-CAM may modulate the extension of hepatic progenitor cells through the extracellular matrix during fetal life by interacting with hepatic stellate cells, which also express N-CAM [22], and by binding to matrix components like heparan sulphate [27].

We have shown that human fetal liver is relatively poorly innervated during the first two trimesters of gestation with a neural network established in portal tracts, mainly around hepatic artery and portal vein branches and less often in relation to bile ducts. The relative paucity of nerve fibers in relation to ductal plates suggests that they are unlikely to play a major role in their remodelling during development. The density of nerve fibers in portal tracts reaches adult levels between 32nd and 33rd gestational

weeks. Intra-acinar nerve fibers are scarce in the human liver before birth suggesting that during human fetal life, direct innervation of hepatocytes and intrasinusoidal innervation is not required for normal liver function in utero. Peptidergic nerves were detected in human fetal liver as early as the 22nd gestational week and were localised in portal tracts mainly around hepatic arteries, in lesser extent close to portal vein branches and less often in relation to bile duct radicles. Some neuropeptides, such as galanin and somatostatin, were expressed only transiently during development. The latter suggests that fetal intrahepatic peptidergic nerves may play important roles in hepatic functions peculiar to life in utero and related to morphogenesis.

In human fetal liver, as in the mammalian adult liver, somatostatinergic nerves and CGRP-ergic nerves are thought to represent afferent sensory fibers [2]. NPY is present in sympathetic efferent nerves to the adult liver and may co-operate with noradrenaline in regulating hepatic blood flow [9, 15]. We have not observed NPY-ergic nerve fibers in human fetal liver. Ding et al. [9] have shown that NPY-immunoreactive fibers appear in the developing mouse liver only in late gestation and that they are present in the liver of neonatal guinea pigs both in portal tracts and in intra-acinar locations. We have shown that in human adult liver, NPY-ergic nerves are the most abundant peptidergic nerve fibers and are distributed in portal tracts in relation to blood vessels and in the acinus along sinusoids, in accordance with previous results of our group and others [1, 4, 9, 12, 21].

In human normal adult liver, many other types of immunoreactive peptidergic nerves may be detected including glucagon-, glucagon-like peptide-, somatostatin-, VIP, neurotensin-, gastrin/cholecystokinin C-terminus-, substance P- and serotoninergic nerve fibers [1, 11, 20, 33]. However, differences exist between studies on the intra-acinar distribution of VIP- and CGRP-ergic nerve fibers and the presence of galaninergic nerves. We have not observed somatostatinergic, galaninergic and CGRP-ergic nerve fibers in human adult liver. The disparities in the immunohistochemical results between studies may be attributed to the diversity in the specificity of the antibodies used, to differences in the methods applied and in the fixation of the specimens.

In conclusion, we showed that the human fetal liver is relatively poorly innervated during the first two trimesters of gestation with a neural network distributed mainly in portal tracts. There is a progressive increase in the density of intrahepatic nerve fibers towards term. The human adult liver receives dense portal and intra-acinar innervation in contrast to fetal liver where intra-acinar innervation appears only at term, suggesting that during development, intrasinusoidal nerves are not required for normal hepatic function. During the third trimester, a rich peptidergic neural network is identified within portal tracts with a transient expression of galanin, somatostatin and CGRP. In human adult liver, NPY-ergic nerve fibers dominate peptidergic innervation in both portal tracts and acini. The differences observed in peptidergic innervation between fetal and adult liver suggest that the fetal intrahepatic peptidergic network may play important role in liver morphogenesis and in hepatic functions peculiar to life *in utero*.

Acknowledgements This study was funded in part by "Kapodistrias" Research Program, Special Accounts Research Fund no 70/4/6549, University of Athens, Greece. The antibodies to somatostatin, NPY, galanin and CGRP were kindly supplied by Professor J.M. Polak, Imperial College, University of London, UK.

Conflict of interest statement We declare that we have no conflict of interest.

References

1. Akiyoshi H, Gonda T, Terada TA (1998) Comparative histochemical and immunohistochemical study of aminergic, cholinergic and peptidergic innervation in rat, hamster, guinea pig and human livers. Liver 18:352–359
2. Berthoud HR (2004) Anatomy and function of sensory hepatic nerves. Anat Rec 280A:827–835
3. Bioulac-Sage P, Lafon ME, Saric J, Balabaud C (1990) Nerves and perisinusoidal cells in human liver. J Hepatol 10:105–112
4. Burt AD, Tiniakos D, MacSween RNM, Griffiths MR, Wisse E, Polak JM (1989) Localization of adrenergic and neuropeptide tyrosine-containing nerves in the mammalian liver. Hepatology 9:839–845
5. Cassiman D, Denef C, Desmet VJ, Roskams T (2001) Human and rat hepatic stellate cells express neurotrophins and neurotrophin receptors. Hepatology 33:148–158
6. Cassiman D, Libbrecht L, Sinelli N, Desmet V, Denef C, Roskams T (2002) The vagal nerve stimulates activation of the hepatic progenitor cell compartment via muscarinic acetylcholine receptor 3. Am J Pathol 161:521–530
7. Cassiman D, Sinelli N, Bockx I, Vander Borght S, Petersen B, De Vos R, van Pelt J, Nevens F, Libbrecht L, Roskams T (2007) Human hepatic progenitor cells express vasoactive intestinal peptide receptor type 2 and receive nerve endings. Liver Int 27:323–328
8. Delalande JM, Milla PJ, Burns AJ (2004) Hepatic nervous system development. Anat Rec 280A:848–853
9. Ding WG, Kitasato H, Kimura H (1997) Development of neuropeptide Y innervation in the liver. Microsc Res Tech 15:365–371
10. El-Salhy M, Grimelius L, Emson PC, Falkmer S (1987) Polypeptide YY- and neuropeptide Y-immunoreactve cells and nerves in the endocrine and exocrine pancreas of some vertebrates: and onto- and phylogenetic study. Histochem J 19:111–117
11. El-Salhy M, Stenling R, Grimelius L (1983) Peptidergic innervation and endocrine cells in human liver. Scand J Gastroenterol 28:809–815
12. Feher E, Fodor M, Gorcs T, Feher J, Vallent K (1991) Immunohistochemical distribution of neuropeptide Y and catecholamine synthesizing enzymes in nerve fibers of the human liver. Digestion 50:194–201

13. Feher E, Fodor M, Feher J (1992) Ultrastructural localisation of somatostatin- and substance P immunoreactive nerve fibers in the feline liver. Gastroenterology 102:287–294
14. Goehler LE, Sternini C, Brecha NC (1988) Calcitonin gene-related peptide immunoreactivity in the biliary pathway and liver of the guinea pig: distribution and co-localization with substance P. Cell Tissue Res 253:145–150
15. Goehler LE, Sternini C (1991) Neuropeptide Y immunoreactivity in the mammalian liver: pattern of innervation and coexistence with tyrosine hydroxylase immunoreactivity. Cell Tissue Res 265:287–295
16. Jungermann K, Stumpel F (1999) Role of hepatic, intrahepatic and hepatoenteral nerves in the regulation of carbohydrate metabolism and hemodynamics of the liver and intestine. Hepatogastroenterol 46(suppl 2):1414–1417
17. Lafon ME, Bioulac-Sage P, LeBail B (1991) Nerves and perisinusoidal cells in human liver. In: Wisse E, Knook DL, McCuskey RS (eds) Cells of the hepatic sinusoid. Kupffer Cell Foundation, Rijswick, pp 230–234
18. Lee JA, Ahmed Q, Hines JE, Burt AD (1992) Disappearance of hepatic parenchymal nerves in human liver cirrhosis. Gut 33:87–91
19. Lin YS, Nosaka S, Amakata Y, Maeda T (1995) Comparative study of the mammalian liver innervation: an immunohistochemical study of PGP 9.5, dopamine-beta-hydroxylase and tyrosine hydroxylase. Comp Biochem Physiol A Physiol 110:289–298
20. McCuskey RS (2004) Anatomy of efferent hepatic nerves. Anat Rec 280A:821–826
21. Miyazawa Y, Fukuda Y, Imoto M, Koyama Y, Nagura H (1988) Immunohistochemical studies on the distribution of nerve fibers in chronic liver diseases. Am J Gastroenterol 83:1108–1114
22. Nakatani K, Seki S, Kawada N, Kobayashi K, Kaneda K (1996) Expression of neural cell adhesion molecule (N-CAM) in perisinusoidal stellate cells of human liver. Cell Tissue Res 283:159–165
23. Oben JA, Roskams T, Yang S, Lin H, Sinelli N, Li Z, Torbenson M, Huang J, Guarino P, Kafrouni M, Diehl AM (2003) Sympathetic nervous system inhibition increases hepatic progenitors and reduces liver injury. Hepatology 38:664–673
24. Oben JA, Diehl AM (2004) Sympathetic nervous system regulation of liver repair. Anat Rec 280A:874–883
25. Oben JA, Roskams T, Sinelli N, Li Z, Torbenson M, Yang S, Lin H, Smedh U, Moran TH, Thomas SH, Diehl AM (2004) Hepatic fibrogenesis requires sympathetic neurotransmitters. Gut 53:438–445
26. Püschel GP (2004) Control of hepatocyte metabolism by sympathetic and parasympathetic hepatic nerves. Anat Rec 280A:854–867
27. Roskams T, Cassiman D, De Vos R, Libbrecht L (2004) Neuroregulation of the neuroendocrine compartment of the liver. Anat Rec 280A:910–923
28. Saxena R, Theise N (2004) Canals of Hering: recent insights and current knowledge. Semin Liver Dis 24:43–48
29. Scoazec JY, Racine L, Couvelard A, Moreau A, Flejou JF, Bernuau D, Feldmann G (1993) Parenchymal innervation of normal and cirrhotic human liver: a light and electron microscopic study using monoclonal antibodies against neural cell-adhesion molecule. J Histochem Cytochem 41:899–908
30. Terada T, Nakanuma Y (1989) Innervation of intrahepatic bile ducts and peribiliary glands in normal human livers, extrahepatic biliary obstruction and hepatolithiasis: an immunohistochemical study. Hepatology 9:141–148
31. Tiniakos D, Tiniakos G, Burt AD (1994) Peptidergic innervation of human fetal liver (abstract). J Hepatol 21(suppl 1):S73
32. Tiniakos D, Anagnostou V, Stavrakis S, Karandrea D, Agapitos A, Kittas C (2004) Ontogeny of intrinsic innervation in the human kidney. Anat Embryol 209:41–47
33. Ueno T, Inuzuka S, Torimura T, Sakata R, Sakamoto R, Gondo K, Aoki T, Tanikawa K, Tsutsumi V (1991) Distribution of substance P and VIP in the human liver. Am J Gastroenterol 86:1633–1637
34. Ueno T, Tanikawa K (1996) Intralobular innervation and lipocyte contractility in the liver. Nutrition 13:141–148
35. Ueno T, Bioulac-Sage P, Balabaud C, Rosenbaum J (2004) Innervation of the sinusoidal wall: regulation of the sinusoidal diameter. Anat Rec 280A:868–873
36. Zanchi A, Feldman H, Reidy J, Qualter J, Theise N (2005) Innervation of a intraorgan hepatic progenitor cell “niche” in normal human liver (abstract). Hepatology 42(suppl 1):279A

Virchows Arch (2008) 452:443–448
DOI 10.1007/s00428-007-0571-8

ORIGINAL ARTICLE

Delta-like protein (DLK) is a novel immunohistochemical marker for human hepatoblastomas

Katalin Dezső · Judit Halász · Hanne Cathrine Bisgaard · Sándor Paku · Eszter Turányi · Zsuzsa Schaff · Peter Nagy

Received: 16 October 2007 / Revised: 18 December 2007 / Accepted: 27 December 2007 / Published online: 31 January 2008
© Springer-Verlag 2008

Abstract Delta-like protein (DLK) is a membrane protein with mostly unknown function. It is expressed by several embryonic tissues among others by the hepatoblasts of rodent and human fetal livers. We have investigated in the present study if this protein is expressed in human hepatoblastomas. The presence of DLK has been studied by standard immunohistochemistry in 31 hepatoblastomas and in several differential diagnostically related tumours: hepatocellular carcinomas and in undifferentiated childhood neoplasms. All the hepatoblastomas were positive for DLK; the surrounding liver tissue remained negative. The reaction was present in the epithelial component of the tumours. The staining pattern was mostly membranous, occasionally cytoplasmic. The other studied tumours were negative for DLK, except one hepatocellular carcinoma and the differentiating cells of two ganglioneuroblastomas. Therefore, DLK seems to be a highly sensitive and specific marker for hepatoblastomas.

Keywords Immunohistochemistry · Hepatoblastoma · DLK

K. D and J. H. contributed equally to this work.

K. Dezső · S. Paku · E. Turányi · P. Nagy (✉)
First Department of Pathology and Experimental Cancer Research,
Semmelweis University,
Üllői út 26,
Budapest 1085, Hungary
e-mail: nagy@korb1.sote.hu

J. Halász · Z. Schaff
Second Department of Pathology, Semmelweis University,
Budapest, Hungary

H. C. Bisgaard
The Danish Stem Cell Research Centre,
Department of Cellular and Molecular Medicine,
The Panum Institute, University of Copenhagen,
Copenhagen, Denmark

Abbreviations

DLK	delta-like protein
AFP	alpha-fetoprotein
TLCT	transitional liver cell tumour
MPNST	malignant peripheral nerve sheath tumour

Introduction

The DLK1 gene codes for an EGF-like homeotic protein called delta-like protein (DLK) [12]. Since DLK is expressed in a wide variety of embryonic tissues in the human, it has several alternative names: Preadipocyte factor 1 (Pref-1), pG2, SCP-1, ZOG or FA1 [23, 6, 7]. DLK is a transmembrane protein containing six EGF-like repeats, a signal sequence in the extracellular domain, a unique transmembrane domain and a short intracellular region [20]. The cysteine spacing and the amino acid sequence within the individual EGF-like repeats are similar to those of delta. Delta is a ligand of the Notch receptor in *Drosophila* [1]. The function of the DLK molecule is largely unknown.

Recently, DLK has been shown to be an important marker for the oval cells in rat liver [9, 22]. The oval cells are hepatic progenitor cells sharing phenotypic markers with the embryonic hepatoblasts [19]. DLK is also highly expressed in the hepatoblasts of the human embryonic and fetal liver [6]. In the present study, we wanted to investigate if DLK could be used as a marker for the primitive human childhood liver tumour, hepatoblastoma. DLK expression could be demonstrated in all the examined hepatoblastomas by standard immunohistochemistry, while it was not present in the majority of differential diagnostically related tumours. Therefore, we suggest that DLK can be used as a highly specific immunohistochemical marker for hepatoblastoma.

Materials and methods

Formalin-fixed, paraffin-embedded tissue was used for immunohistochemical staining. The most important parameters of the investigated tumours are listed in Tables 1, 2 and 3. In brief, after blocking the endogenous peroxidase activity in methanol and hydrogen peroxide, the antigens were retrieved by heating in 10 mmol citrate buffer (pH 7.0) in a microwave oven for 10 min. The sections were then blocked in pre-immune serum diluted in phosphate-buffered saline before overnight incubation with the primary antibodies [DLK, R&D Systems, catalog number AF1144, dilution 1:100, Minneapolis, MN, USA; alpha-fetoprotein (AFP), DAKO, catalog number A0008, dilution 1:100, Glostrup, Denmark; and CK19, Biogenex, catalog number MU246-UC, dilution 1:50, San Remon, CA, USA] at 4°C. The Vectastain ABC Elite Kit (Vector Laboratories, Burlingname, CA, USA) was used for developing the reactions with diaminobenzidine as chromogen. The pre-immune serum was not replaced with primary antibody in the negative control sections. Rat liver tissue with oval cells was used as positive control for DLK and AFP.

Statistical analysis was performed by Fisher's exact test using 3×3 and 3×4 contingency tables.

Results

Thirty-one formalin-fixed, paraffin-embedded hepatoblastomas were collected from our archives (Table 1). All of the hepatoblastomas were positive for DLK protein; that is, the

Table 1 Important characteristics of hepatoblastomas

Number	Age (year)	Gender	Classification		Positive reaction			Remarks
			Type	Dominant epithelial component	%	Intensity	Pattern	
1	3	Male	W	F	11–40	+	Ca	
2	5	Female	M	F	1–10	+	Cy	
3	5	Male	W	E	1–10	+	M	
4	1	Female	W	E	1–10	+	Cy	
5	0.5	Male	M	F	>40	+	M	
6	1	Male	M	F	>40	+	M	
7	1	Male	M	E	11–40	++	Cy	
8	2	Female	W	F	1–10	++	M	
9	0.5	Female	M	E	11–40	+	Ca	
10	1	Female	W	F	1–10	+	Cy	
11	7	Male	W	F	1–10	+	M	
12	1	Female	W	F	11–40	+	M	
13	4	Male	W	E	11–40	++	Ca	Splenic metastasis
14	1	Female	M	E	11–40	+	Ca	
15	1	Male	M	E	1–10	++	Cy	
16	10	Male	W f	F	1–10	+++	D	
17	3	Male	W	E	11–40	++	Cy	
18	3	Male	W	E	1–10	+	Ca	
19	3	Male	W	F	>40	++	M	Lung metastasis
20	2	Male	W	F	1–10	+	M	
21	5	Female	W	E	11–40	+	M	
22	1	Female	W	F	1–10	+	M	
23	2	Male	W	F	11–40	++	M	
24	14	Male	W f	F	1–10	+	Cy	
25	1	Female	M	F	1–10	+	M	
26	4.5	Female	W	E	1–10	+	Cy	
27	1	Female	W	E	1–10	+	M	
28	4	Male	M	F	1–10	+	Cy	
29	5	Female	W f	F	11–40	++	M	
30	5	Female	W f	F	>40	++	Cy/M	
31	0.5	Male	W	F	11–40	++	Ca	

Classification according to SIOPEL: *W* wholly epithelial, *M* mixed, *Wf* purely fetal, *E* embryonal, *F* fetal
Staining pattern: *Cy* cytoplasmic, *M* membranous, *Ca* canalicular, *D* dot like

Table 2 Important characteristics of hepatocellular carcinomas

Number	Age (year)	Gender	Histological type	Grade	AFP	CK19	DLK
1	56	Male	PG	II	+	–	–
2	73	Male	So	III	+	–	–
3	64	Male	Tr	III	+	+	–
4	57	Male	PG	II	–	–	–
5	77	Male	So	II	+	–	–
6	57	Male	So	III	+	–	–
7	70	Male	PG	III	+	+	–
8	53	Female	Tr	III	+	–	–
9	54	Male	PG	III	–	+	–
10	50	Male	PG	II	–	–	–
11	62	Male	Tr	II	+	+	+
12	54	Male	PG	III	+	–	–
13	78	Male	PG	II	–	–	–
14	53	Female	PG	II	+	–	–
15	59	Male	Tr	II	–	–	–
16	49	Male	So	III	+	–	–
17	51	Male	Tr	III	–	–	–
18	49	Male	Tr	II	–	–	–
19	68	Male	So	II	+	–	–
20	64	Male	PG	II	+	–	–
21	68	Male	So	III	+	–	–
22	68	Female	So	III	+	+	–
23	60	Male	Tr	II	–	+	–
24	79	Female	PG	II	–	+	–

Grading according to Edmondson and Steiner [4]
PG Pseudoglandular, *So* solid, *Tr* trabecular

sensitivity of this antibody on these tumours was 100%. The staining was usually focal, covering 5–50% of the tumour, while the surrounding liver always was negative. The DLK protein was exclusively located on the epithelial components of the tumours, while the mesenchymal part of the mixed hepatoblastomas stained negative. Within the epithelial part, there was no strictly consequent preferential staining. Although the reaction was usually stronger over the more differentiated fetal components compared to the embryonal areas (Fig. 1a–c). Two of our samples represented metastatic tumours, where the DLK staining was preserved in the metastases (Fig. 1d). The staining pattern at the cellular level was mostly membranous (Fig. 2a). Occasionally, the membrane staining was confined to some poles of the cells showing a canalicular-like pattern (Fig. 2b). Sometimes, the cytoplasm was decorated (Fig. 2c), or dot-like positive areas were present in the cells (Fig. 2d), but the nucleus always remained negative. The cellular distribution and the extent and intensity of the DLK staining did not show significant correlation with the histological subtype or any other parameters. All of the studied tumours were also positive for AFP, the established immunohistochemical

Table 3 Other tumours tested for DLK

Tumour type	Age range (years)	Mean age	Gender M/F	Number	Remarks
Germ cell tumour[a]	20–51	22.8	6/0	6	AFP+
Wilms tumour	1–11	5.7	4/1	5	
Ganglio/Neuroblastoma	0.5–17	3.2	3/6	9	
Medulloblastoma	1–19	7.6	3/2	5	
Rhabdoid tumour	1	–	1/0	1	
Infantile haemangioendothelioma	1–3[b]	2	2/0	2	
Mesenchymal hamartoma	0.5	–	0/1	1	
Liver MPNST	23	–	0/1	1	

[a] Two yolk sac tumours, one teratocarcinoma, one seminoma, two immature teratomas
[b] Months

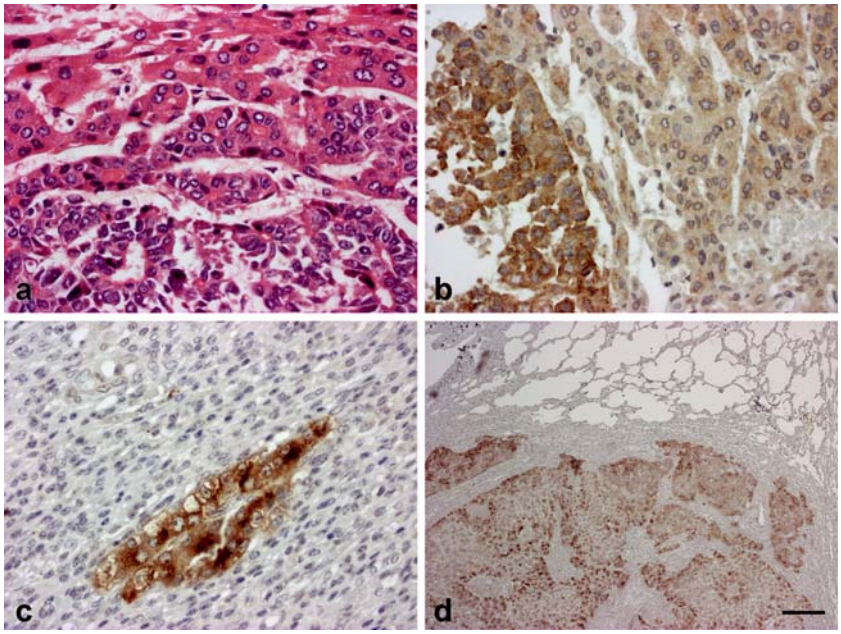


Fig. 1 **a** A hepatoblastoma with fetal (*lower part*) and embryonal components (H&E stain); **b** DLK stains preferentially the fetal component of the tumour shown in **a**. **c** Exclusive DLK staining in the epithelial part of a mixed hepatoblastoma; the mesenchymal component is negative. **d** Metastatic tumour in the lung, DLK is present only in the tumour tissue. *Scale bar* for **a**–**c**, 25 μm; **d**, 200 μm

marker of hepatoblastoma [5] (data not shown). The distribution of AFP and DLK occasionally overlapped, but this was not consistent.

We also examined several other tumour types for DLK expression. Twenty-four hepatocellular carcinomas were studied (Table 2). There was weak focal staining in one of these tumours; it is interesting to note that this hepatocellular carcinoma (HCC) was positive also for AFP and cytokeratin 19. In addition, the liver tumour of a 16-year-old girl showing transitional features between hepatoblastoma and hepatocellular carcinoma stained strongly for DLK (this tumour is not listed in the tables). Several other tumour samples have been stained with DLK antibody (Table 3), including six AFP-positive germ-cell tumours, a few undifferentiated childhood (Table 3) tumours covering neuroblastomas, Wilms tumours and medulloblastomas. The "small round cell" component of the tumours was consistently negative, but the enlarged, differentiating cells of two ganglioneuroblastomas reacted with the antibody. A few rare pediatric liver tumours (infantile haemangioendothelioma, mesenchymal hamartoma, malignant peripheral nerve sheath and rhabdoid tumour) were also examined, without any positive reactions. The specificity of DLK in the relation of all the tumours described above was 94%.

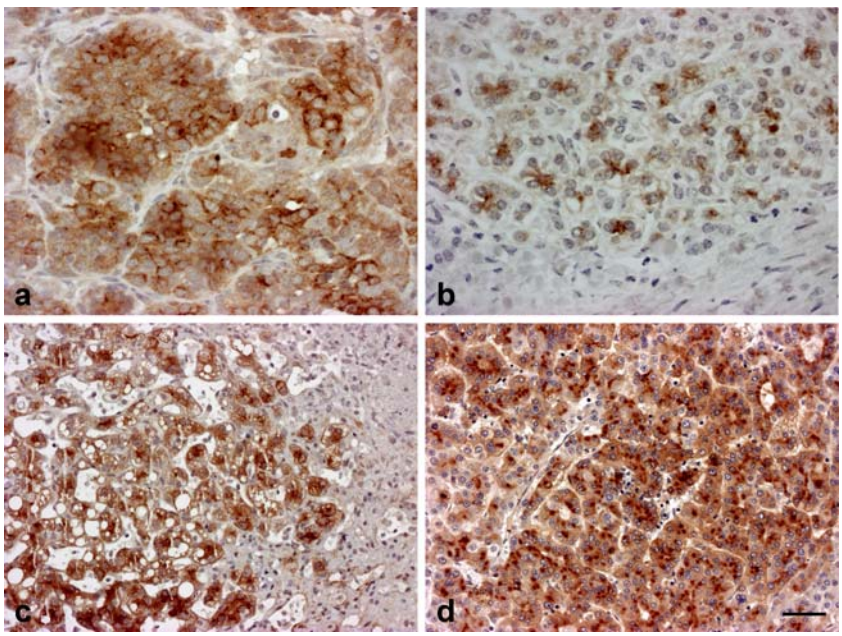


Fig. 2 Different staining pattern of DLK in hepatoblastomas: **a** membranous, **b** canalicular, **c** dot-like, **d** cytoplasmic. *Scale bar* for **a** and **b**, 25 μm; **c** and **d**, 50 μm

Discussion

Hepatoblastoma is the most common malignant liver tumour in children [17]. Its histological appearance is rather variable, but AFP is a stable hallmark for this tumour. In this paper, we report the finding of a novel reliable marker protein, namely DLK, which was detected in all the 31 studied hepatoblastomas. DLK was always expressed in the epithelial component, but its distribution did not show statistical correlation with the histological subtype. The staining pattern of DLK on the cells of hepatoblastomas is not uniform, but it is mostly associated with the cell surface. This is in agreement with the fact that DLK is a transmembrane protein with a large extracellular domain, but cytoplasmic staining of DLK also has been reported [8].

Both DLK and AFP mostly show focal staining pattern, but there was only partial overlap between the marked areas. Therefore, we believe that the application of both antibodies may increase the diagnostic sensitivity in case of limited availability of tumour sample, e.g. core biopsy or fine-needle aspiration biopsy. The divergent distribution of the two markers predicts that the regulation of the two genes is not identical. This is supported by the lack of DLK staining in all of the studied AFP-expressing germ-cell tumours. In addition, AFP can be present in HCCs, but we have detected focal staining for DLK only in one of the 24 examined HCCs. This particular tumour was positive for AFP and cytokeratin 19 as well. Lee et al. [14] defined recently a novel HCC subtype, which shares gene expression pattern with fetal hepatoblasts. This tumour type can be identified by microarray-based gene-expression profiling, but cytokeratin 19 and AFP co-immunostaining is characteristic for most of them. It is interesting to note that the only DLK-positive HCC sample is one of the three CK19+/AFP+ tumours, further supporting the relationship between these tumours and hepatoblasts. However, the great majority of the HCCs were negative for DLK. Consequently, DLK can be applied for the histological distinction between HCC and hepatoblastoma. DLK seemed to be useful, although with less stringent criteria for this distinction by a microarray-based global transciptome analysis [15]. In this study, elevated DLK expression was found only in a subset of hepatoblastomas. The partial disagreement between these and our results might be explained by the different methodology. Focally increased DLK expression was found in most of the hepatoblastomas by immunohistochemistry. The dilution effect of a sampling error might be responsible for the negative cases if the gene expression is analyzed on isolated RNA.

Recently, a malignant hepatocellular tumour developing in older children and adolescents have been termed transitional liver-cell tumour (TLCT) [16]. As its name implies, this highly aggressive neoplasm has a morphotype between hepatoblasts and hepatocytes. We have examined one liver tumour of a 16-year-old girl, which morphologically would fit into this category. This tumour was positive for hepatocyte-specific antigen and showed strong nuclear β-catenin reaction. However, differently from all the published TLCT cases, AFP could not be detected in the tumour by immunohistochemistry, and the serum value was also not elevated. This tumour showed strong, diffuse staining with DLK antibody. We are still uncertain on how to call this neoplasm, and thus it was not included in the listed cases in the tables. Nevertheless, we found DLK very useful to distinguish it from typical hepatocellular carcinoma.

DLK expression was conserved in the two hepatoblastoma metastases we examined, indicating that this immunophenotypic marker can be useful for the recognition of metastatic tumours. A few other undifferentiated childhood tumours were also tested for this marker, but they were negative except for the large ganglion cells of ganglioneuroblastomas (data not shown) in accordance with a previous report [8]. This is in line with the observation that DLK expression correlates with maturation along the chromaffin lineages [24].

In the adult rat liver, transcription and translation of the AFP and DLK1 genes are the only known reliable markers (which are not present in the biliary cells) for the bipotential oval/progenitor cells [19]. The human counterpart of the oval cells is still debated, but most results point to the ductular reaction which occurs in a wide variety of human liver diseases [18]. However, unlike murine oval cells [10], the cells of the human ductular reactions are consistently negative for AFP [11] and DLK (CH Jensen and HC Bisgaard, unpublished results) as well as the canals of Hering (P Nagy, unpublished results), which are the most likely candidates for the hepatic progenitor cell niche. These observations could indicate that oval cells expressing DLK and AFP in rat may recapitulate certain features of embryonic and fetal-liver development; this may not be the case in humans. Although the histogenesis of the hepatoblastomas is not clear, the presence of two embryonic liver-cell markers AFP and DLK supports the present notion about their hepatic embryonic or fetal progenitor-cell origin [25]. The function of DLK is not known. It is thought to play a role in cell-to-cell interactions controlling cell-fate determination during embryonic and fetal development and in adult organism [13]. DLK has been reported to interact with Notch1 in a specific manner using the yeast two-hybrid system [2, 3], and it may participate in the regulation of differentiation processes modulated by Notch1 activation and signalling [21]. If this is so, DLK may play a role in the growth and differentiation regulation of hepatoblastomas and may be a potential aim of molecularly targeted therapy.

In conclusion, DLK, a membrane protein of hepatoblasts and hepatocytes during embryonic and fetal development,

can be demonstrated by immunohistochemistry in hepatoblastomas but not in the majority of hepatocellular carcinomas or other related tumours. Therefore, DLK is a highly sensitive and specific immunophenotypic marker of this childhood liver tumour.

Acknowledgement This study was supported by OTKA K 67697, TS 049887 and ETT 32/2006.

Conflict of interest statement We declare that we have no conflict of interest.

References

1. Artavanis-Tsakonas S, Rand MD, Lake RJ (1999) Notch signalling: cell fate control and signal integration in developmentt. Science 284:770–776
2. Baladron V, Ruiz-Hidalgo MJ, Bonvini E, Gubina E, Notario V, Laborda J (2002) The EGF-like homeotic protein dlk affects cell growth and interacts with growth-modulating molecules in the yeast two hybrid system. Biochem Biophys Res Commun 291:193–204
3. Baladron V, Ruiz-Hidalgo MJ, Nueda ML, Diaz-Guerra MJ, Garcia-Ramirez JJ, Bonvini E, Gubina E, Laborda J (2005) Dlk acts as a negative regulator of NOTCH1 activation through interactions with specific EGF-like repeats. Exp Cell Res 303:343–359
4. Edmondson HA, Steiner PE (1954) Primary carcinoma of the liver. Cancer 7:462–503
5. Finegold MJ, Lopez-Terrada DH, Bowen J, Washington MK, Qualman SJ (2007) Protocol for the examination of specimens from pediatric patients with hepatoblastoma. Arch Pathol Lab Med 131:520–529
6. Floridon V, Jensen CH, Thorsen P, Nielsen O, Sunde L, Westergaard JG, Thomsen SG, Teisner B (2000) Does fetal antigen 1 (FA1) identify cells with regenerative, endocrine and neuroendocrine potentials? A study of FA1 in embryonic, fetal, and placental tissue and maternal circulation. Differentiation 66:49–59
7. Hedlund GP, Carlsson HE, Shieck E, Nilsson I, Lundblad C, Arons S, Iversen AK, Looman C Jensen HE, Hau J (2003) Fetal antigen 1 (FA1) in the adult rat adrenal gland, ovary and pituitary gland. In Vivo 17:1–4
8. Hsiao CC, Huang CC, Sheen JM, Tai MH, Chen CM, Huang LL, Chuang JH (2005) Differential expression of delta-like gene and protein in neuroblastoma, ganglioneuroblastoma and ganglioneuroma. Mod Pathol 18:656–662
9. Jensen CH, Jauho EI, Santoni-Rugiu E, Holmskov U, Teisner B, Tygstrup N, Bisgaard HC (2004) Transit-amplifying ductular (oval) cells and their hepatocytic progeny are characterized by a novel and distinctive expression of delta like protein/preadipocyte factor 1/fetal antigen 1. Am J Pathol 164:1347–1359
10. Jelnes P, Santoni-Rugiu E, Rasmussen M, Friis SL, Nielsen JH, Tygstrup N, Bisgaard HC (2007) Remarkable phenotypic heterogeneity displayed by oval cells in rat and mouse models of stem cell-mediated liver regeneration. Hepatology 45:1462–147
11. Kiss A, Schnur J, Szabó Z, Nagy P (2001) Immunohistochemical analysis of atypical ductular reaction in the human liver, with special emphasis on the presence of growth factors and their receptors. Liver 21:237–246
12. Laborda J, Susville EA, Hoffman T, Notario V (1993) Dlk: a putative mammalian homeotic gene differentially expressed in small cell lung carcinoma and neuroendocrine tumor cell line. J Biol Chem 268:3817–3820
13. Laborda J (2000) The role of the epidermal growth factor-like protein dlk in cell differentiation. Histol Histopathol 15:119–129
14. Lee JS, Heo J, Libbrecht L, Chi I, Kaposi-Novák P, Calvisi DF, Mikaelyan A, Roberts LR, Demetris AJ, Sun Z, Nevens F, Roskams T, Thorgeirsson SS (2006) A novel prognostic subtype of human hepatocellular carcinoma derived from hepatic progenitor cells. Nat Med 12:410–416
15. Luo J, Ren B, Keryanov S, Tseng GC, Rao UNM, Monga SP, Strom S, Demetris AJ, Nalesnik M, Yu YP, Ranganathan S, Michalopoulos GK (2006) Transcriptomic and genomic analysis of human hepatocellular carcinomas and hepatoblastomas. Hepatology 44:1012–1024
16. Prokurat A, Kluge P, Kosciesza A (2002) Transitional liver cell tumours (TLCT) in older children and adolescents: a novel group of agressive hepatic tumours expressing beta-catenin. Med Pediatr Oncol 39:510–518
17. Roebuck DJ, Perilongo G (2006) Hepatoblastoma: an oncological review. Pediatr Radiol 36:183–186
18. Roskams TA, Theise ND, Balabaud C, Bhagat G, Bhathal PS, Bioulac-Sage P (2004) Nomenclature of the finer branches of the biliary tree: canals, ductules, and ductular reactions in human livers. Hepatology 39:1739–1745
19. Santoni-Rugiu E, Jelnes P, Thorgeirsson SS, Bisgaard HC (2005) Progenitor cells in liver regeneration: molecular responses controlling their activation and expansion. APMIS 113:876–902
20. Smas CM, Sul HS (1993) Pref-1, a protein containing EGF-like repeats, inhibits adipocyte differentiation. Cell 73:725–734
21. Tanimizu N, Miyajima A (2004a) Notch signaling controls hepatoblast differentiation by altering the expression of liver-enriched transcription factors. J Cell Sci 117:3165–3174
22. Tanimizu N, Tsujimura T, Takahide K, Kodama T, Nakamura K, Miyajima A (2004) Expression of Dlk/Pref-1 defines a subpopulation in the oval cell compartment of rat liver. Gene Expression Patterns 5:209–218
23. Tornehave D, Jensen CH, Teisner B, Larson LI (1996) FA1 immunreactivity in endocrine tumours and during development of the human fetal pancreas, negative correlation with glucagon expression. Histochem Cell Biol 106:535–542
24. Van Limpt VA, Chan AJ, Van Sluis PG (2003) High delta-like 1 expression in a subset of neuroblastoma cell lines corresponds to a differentiated chromaffin cell type. Int J Cancer 105:61–69
25. Zimmermann A (2005) The emerging family of hepatoblastoma tumours: from ontogenesis to oncogenesis. Eur J Cancer 41:1503–1514

Virchows Arch (2008) 452:449–456
DOI 10.1007/s00428-008-0575-z

OpenAccess

ORIGINAL ARTICLE

Differential expression of mycobacterial antigen MPT64, apoptosis and inflammatory markers in multinucleated giant cells and epithelioid cells in granulomas caused by *Mycobacterium tuberculosis*

Tehmina Mustafa · Harald G. Wiker · Odd Mørkve · Lisbet Sviland

Received: 4 October 2007 / Revised: 20 November 2007 / Accepted: 28 December 2007 / Published online: 12 February 2008
© The Author(s) 2008

Abstract The development of granulomas is a major histopathological feature of tuberculosis. Very little information is available concerning the physiology and functions of different cell types in the tuberculous granulomas. The aim of this study was to compare the epithelioid cells (ECs) and multinucleated giant cells (MGCs) in the granulomas caused by *Mycobacterium tuberculosis* complex organisms. Lymph node biopsies from 30 cases of lymphadenitis were studied for expression of the secreted mycobacterial protein MPT64, caspase 3 as a marker of apoptosis, apoptosis-related proteins (Fas Ligand, Fas and Bax) and inflammatory cytokines (interleukin-10, transforming growth factor-β (TGF-β), tumour necrosis factor-α and interferon-γ) by immunohistochemistry. MGCs more often contained *M. tuberculosis* secretory antigen MPT64 ($p<0.001$) and expressed more TGF-β ($p=0.004$) than ECs. The total number of apoptotic MGCs was higher than the number of apoptotic ECs ($p=0.04$). Interestingly, there was a significant negative correlation between apoptosis and MPT64 expression in MGCs ($r=-0.569$, $p=0.003$), but not in ECs, implying that the heavy antigen load would lead to inhibition of apoptosis in these cells. When compared with ECs, higher percentage of MGCs expressed Fas Ligand and Fas ($p<0.004$). The role of MGCs may thus be different from surrounding ECs and these cells by virtue of higher mycobacterial antigen load, more TGF-β and reduced apoptosis may contribute towards persistence of infection.

Keywords Epithelioid cells · Multinucleated giant cells · Granulomas · MPT64 · Apoptosis · Cytokines · Tuberculosis

T. Mustafa · H. G. Wiker
Section for Microbiology and Immunology, The Gade Institute, University of Bergen,
Bergen, Norway

H. G. Wiker
Department of Microbiology and Immunology,
Haukeland University Hospital,
Bergen, Norway

O. Mørkve · L. Sviland
Centre for International Health, University of Bergen,
Bergen, Norway

L. Sviland
Department of Pathology, Haukeland University Hospital,
Bergen, Norway

T. Mustafa (✉)
Section for Microbiology and Immunology, The Gade Institute,
Armauer Hansens Building, Haukeland University Hospital,
Bergen, Norway
e-mail: tehmina.mustafa@gades.uib.no

Introduction

The development of granulomas in tuberculosis (TB) is an expression of acquired specific immune response in the host and is the main histopathological feature of tuberculosis. These granulomas are thought to contain the infection in a localised area, preventing bacterial spread to surrounding healthy tissues and to other organs [30, 31]. In humans, granuloma formation is essential for control of mycobacterial infections, as shown in children where a lack of granulomatous response is associated with unfavourable clinical outcome [7]. Immuno-deficient individuals without interferon (IFN)-γ-induced responses fail to develop granulomatous structures and subsequently die of mycobacterial

infection [3]. Paradoxically, granulomas are also responsible for the typical immunopathology caused by these infections.

Interleukin (IL)-10, transforming growth factor (TGF)-β, tumour necrosis factor (TNF)-α and IFN-γ are produced locally within tuberculous granulomas. In various experimental systems, it has been shown that TNF-α is associated with activation of macrophages [8] and enhances the bactericidal activity of monocytes and macrophages together with IFN-γ [9]. Both these cytokines are responsible for granuloma formation [5, 16]. On the other hand, IL-10 and TGF-β suppress the anti-mycobacterial immune responses and inhibit macrophage functions resulting in enhanced intracellular growth of bacteria [4, 13, 21, 34]. These cytokines by virtue of their anti-inflammatory properties play a role in limiting the excessive immune response, thus limiting tissue destruction. An optimal balance between various cytokines would lead to an effective protective immune response. *Mycobacterium tuberculosis* has evolved strategies to evade killing by the host response and this can affect the pattern of cytokine secretion in the granulomas. Pathogenic mycobacteria are shown to inhibit the apoptosis of the infected cells [15] by influencing the secretion of apoptosis-related proteins Fas, Fas Ligand (FasL) [22–24], Bcl2 and Bax [20], which leads to the bacterial persistence.

In vitro studies have shown the dynamics of granuloma formation. *M. tuberculosis* multiplies within macrophages and monocytes and the production of cytokines and chemokines by these infected macrophages induces the recruitment of macrophages, lymphocytes and dendritic cells at the infectious site. This cellular accumulation results in granuloma formation. Within granulomas, macrophages differentiate into epithelioid cells (ECs) and/or fuse to form multinucleated giant cells (MGCs), also called Langhans giant cells [11, 32]. Very little information is available concerning the physiology of granuloma-specific cell types such as ECs and MGCs. Are these two cell types different in their expression of various inflammatory markers and what role do they play in the host immunity? We have recently shown that there is a negative correlation between apoptotic markers and MPT64 expression in tuberculous granulomas [28]. It has been postulated that granulomas are responsible for the persistence of bacilli, but which cell types in the granulomas contribute towards this is not known.

The specific aim of this study was to compare the ECs and MGCs in the lesions caused by *M. tuberculosis* with respect to the expression of secreted mycobacterial protein MPT64 as a marker for mycobacterial infection, expression of caspase 3 as a marker of apoptosis, apoptosis-related proteins (FasL, Fas and Bax) and inflammatory cytokines (IL-10, TGF-β, TNF-α and IFN-γ).

Material and methods

Lymph node biopsies from 30 cases of tuberculous lymphadenitis were studied. Seventeen cases were obtained from the archives of Department of Pathology, Haukeland University Hospital, Norway. Thirteen cases were from patients diagnosed with mycobacterial lymphadenitis in an epidemiological study from rural Tanzania [19]. All these cases were confirmed to be caused by *M. tuberculosis* complex organisms based on the polymerase chain reaction done for amplification of IS6110 as described earlier [27]. All the cases were studied for the expression of mycobacterial antigen, apoptosis and all the proteins except Bax which was studied in 13 Tanzanian cases only. Ethical clearance was obtained from the Medical Research Coordinating Committee in Tanzania and the regional ethical committee in Norway. All participants from Tanzania gave verbal consent to the study.

Histology and immunohistochemistry

Parallel 5-μm-thick sections from each specimen were stained with haematoxylin and eosin, and immunostaining was done as described previously [25]. A kit (EnVision+ System-HRP) was used for immunostaining (DakoCytomation Denmark A/S, Glostrup, Denmark). Briefly, after deparaffinisation and rehydration, the sections were exposed to microwave antigen retrieval using citrate buffer pH 6.0 at 750 W for 10 min and at 350 W for 15 min. The sections were cooled for 20 min at room temperature and then incubated with H_2O_2 solution for 5 min. Primary antibodies were then applied to the sections for 45 min followed by incubation for 40 min with anti-rabbit or anti-mouse immunoglobulin conjugated with dextran polymer and horseradish peroxidase. The visualisation was with 3-amino-9-ethylcarbazol containing H_2O_2 (for cytokines and caspase 3) or diaminobenzidine for 10 min (for apoptosis-related proteins).

The following primary antibodies were used: MPT64 was detected using in-house-raised polyclonal rabbit antibodies [27]. Apoptotic cells were detected by caspase 3 staining (R&D Systems, Abingdon, Oxon, UK). IL-10, TNF-α and IFN-γ were detected with antibodies from ImmunoTools, Friesoythe, Germany, TGF-β with antibodies from Santa Cruz Biotechnology, Santa Cruz, CA, USA. Apoptosis-related protein FasL with antibodies from Alexis Biochemicals, San Diego, CA, USA, Fas, Bax and Bcl-2 with antibodies from Santa Cruz Biotechnology, Santa Cruz, California, USA. All of the antibodies were mouse monoclonal antibodies except anti-TGF-β, and anti-caspase-3 which were rabbit polyclonal antibodies as described previously [25].

Evaluation of histology, immunostaining and statistical analysis

The percentage of stained ECs was calculated by counting stained cells and the total number of nucleated cells in two to three areas from each biopsy, using a ×40 ocular fitted with a 10×10-mm grid. All the stained cells, irrespective of staining intensity, were counted. On average, 334 nucleated cells were present in one field–grid. For MGCs, the whole section was studied and all the MGCs were counted. Data were presented as a percentage of the stained MGCs. The number of MGCs varied in the biopsies ranging from 2 to 42 (median=15) MGCs. Non-parametric Wilcoxon signed-rank sum test for related samples was used for comparison of ECs and MGCs. Linear regression was performed to determine the relationship between the number of apoptotic cells and cells containing mycobacterial antigen. Bivariate correlations between number of cells stained for various proteins was determined by Spearman's rank correlations. p values less than 0.05 were considered as significant.

Results

Morphology

All the biopsies had necrotic granulomas. In 11 cases, there were additional non-necrotic granulomas. The morphology of MGCs varied. Some cells were relatively small with four to five nuclei in the centre of the cell, while others were large cells with many nuclei forming a ring in the cytoplasm. Both types of cells could be present in the same biopsy.

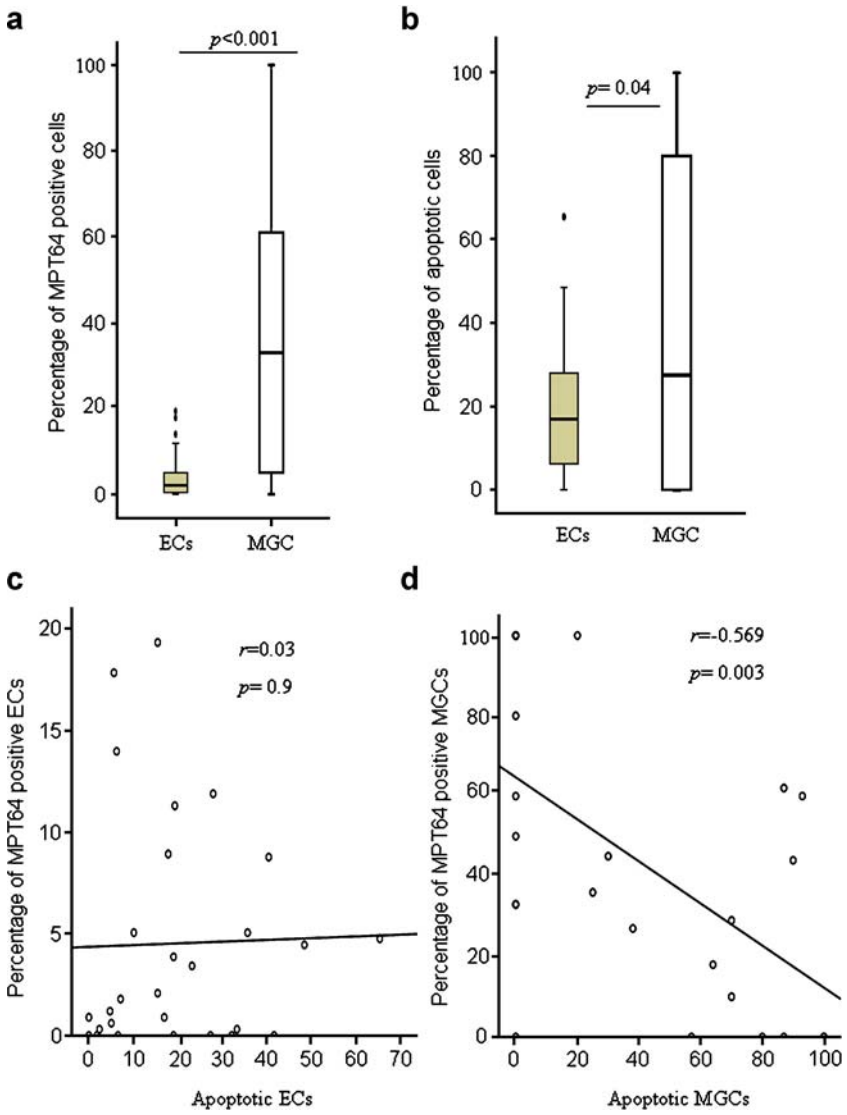


Fig. 1 **a–b** Percentage of epithelioid cells (*ECs*) and multinucleated giant cells (*MGCs*) expressing MPT64 antigen (**a**), and caspase 3 for apoptotic cells (**b**) detected by immunohistochemical staining in the lymphadenitis granulomas caused by *M. tuberculosis* (n=30). The median, 25th and 75th percentiles and minimum and maximum values are shown. The marks *filled circle* indicate the outliers. The statistically significant results are marked with p values. **c–d** Linear regression was performed to determine the relationship between apoptotic ECs and the MPT64-antigen-containing ECs (**c**), and apoptotic MGCs and MPT64-antigen-containing MGCs (**d**) among the tuberculous granulomas. There was a significant negative correlation between apoptotic MGCs and MPT64-antigen-containing MGCs

MPT64 expressing MGCs correlate negatively with apoptotic MGCs

MPT64 was expressed in the ECs and MGCs in the granulomas. Figure 1a shows the number of ECs and MGCs expressing MPT64 antigen. A higher proportion of MGCs (median=33%) expressed MPT64 antigen as compared to the ECs (median=2.1%, $p<0.001$). The intensity of staining in ECs and MGCs varied from weak to strong, indicating variation in the amount of antigen present in individual cells. Figure 2 shows granuloma cells with strong expression of MPT64 antigen.

Expression of caspase 3 was used to detect the apoptotic cells. Both ECs and MGCs in the granulomas expressed caspase 3 as shown in Fig. 2. Figure 1b shows the number of ECs and MGCs expressing this protein. The numbers of apoptotic ECs (median=17%) were lower than the apoptotic MGCs (median=27.5%, $p=0.04$). Interestingly, there was a significant negative correlation between the apoptotic MGCs and the MPT64 expressing MGCs ($r=-0.569$, $p=0.003$), while no significant correlation was found between apoptotic ECs and MPT64 expressing ECs (Fig. 1c–d), implying that the heavy antigen load would lead to inhibition of apoptosis in these cells.

MGCs express more FasL and Fas than ECs

Both the ECs and MGCs expressed FasL, Fas and Bax (Fig. 2). Figure 3a shows the number of these cells expressing the proteins. When compared with ECs, higher percentage of MGCs expressed FasL (median; EC=23.3%, MGC=45.7%, $p=0.008$) and Fas (median; EC=15.3%, MGC=44%, $p=0.005$). Table 1 shows the correlation between the numbers of ECs and MGCs expressing different proteins. The relationship of these proteins was different between the ECs and MGCs. FasL-expressing ECs correlated positively with Fas- ($p<0.001$) and Bax-expressing ($p<0.05$) ECs, and Fas-expressing ECs correlated

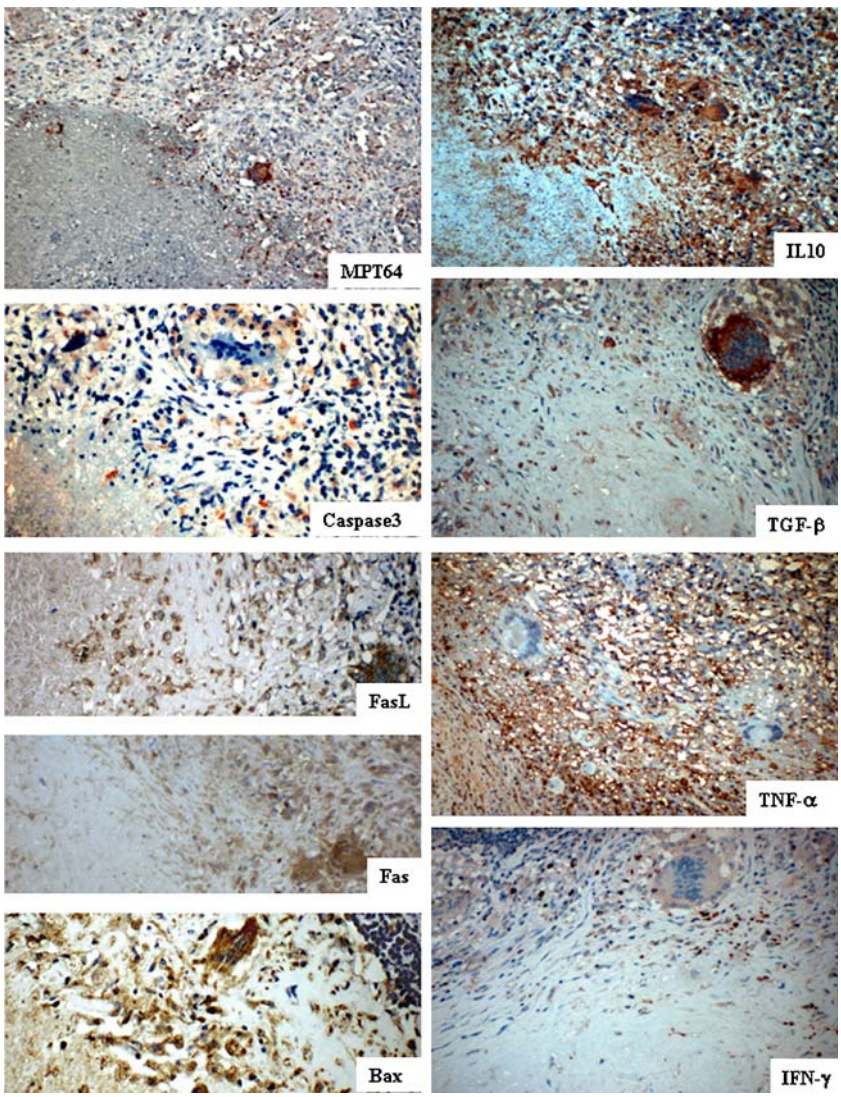


Fig. 2 Lymph node tissues showing the staining pattern of epithelioid cells and multinucleated giant cells in the tuberculous granulomas for mycobacterial secretory antigen MPT64, caspase 3 for detection of apoptotic cells, apoptosis-related proteins and cytokines, as detected by immunohistochemical staining

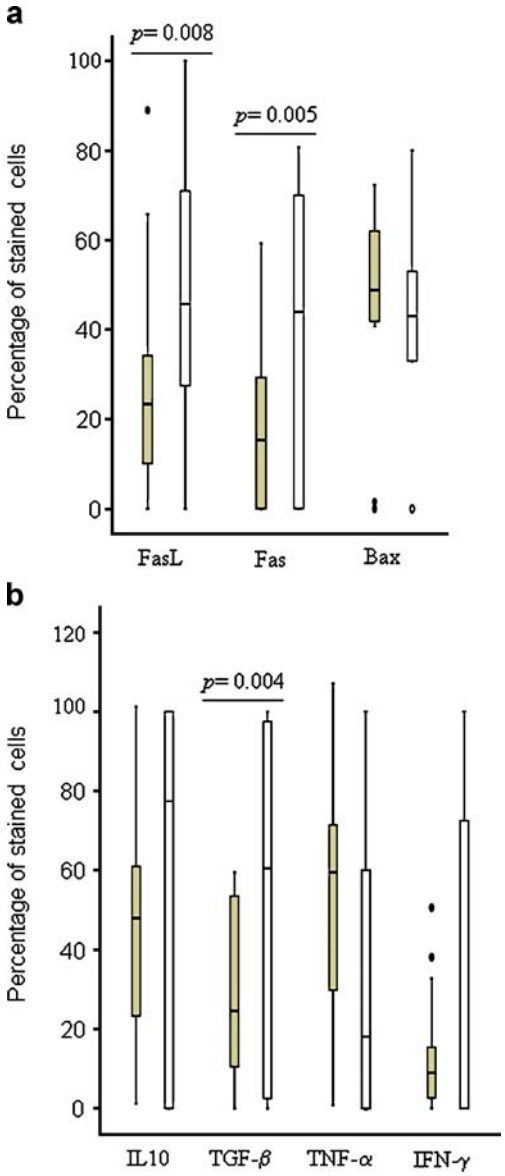


Fig. 3 Percentage of epithelioid cells ■ and multinucleated giant cells □ expressing apoptosis-related proteins (**a**) and cytokines (**b**) in the lymphadenitis granulomas caused by *M. tuberculosis*, detected by immunohistochemical staining. The median, 25th and 75th percentiles and minimum and maximum values are shown. The marks *filled circles* indicate the outliers. The statistically significant results are marked with *p* values

positively with Bax-expressing ECs ($p<0.05$). While among MGCs, FasL-expressing MGCs correlated positively with TGF-β- and IFN-γ-expressing MGCs, and Fas-expressing MGCs correlated positively with IL-10-expressing MGCs ($p<0.05$). Fas- and Bax-expressing ECs and MGCs correlated positively ($p<0.001$).

MGCs express more TGF-β than the ECs

Among the pro- and anti-inflammatory cytokines, ECs and MGCs expressed IL-10, TGF-β, TNF-α and IFN-γ (Fig. 2). Figure 3b shows the numbers of cells expressing these cytokines. Higher number of MGCs expressed TGF-β as compared with ECs (median; MGC=60.5%, EC=24.5%, $p=0.004$), while there was no statistically significant difference between the number of two cell types expressing IL-10, TNF-α or IFN-γ. The intensity of staining of IFN-γ was, however, stronger in the ECs than in the MGCs (Fig. 2), but the cell counts represent all stained cells irrespective of staining intensity. The number of TGF-β-expressing MGCs were higher than the numbers of IFN-γ- (median=0%, $p=0.004$) and TNF-α-expressing (median=18%, $p=0.01$) MGCs ($p<0.01$), while numbers of TGF-β-expressing ECs were lower than TNF-α- (median=59.5%, $p<0.001$) and IL-10-expressing (median=47.9%, $p=0.01$) ECs. The correlation between the numbers of ECs and MGCs expressing different proteins is shown in Table 1. The numbers of TGF-β-expressing ECs correlated positively with the numbers of IL-10- ($p<0.05$) and TNF-α-expressing ($p<0.001$) ECs, while the numbers of TGF-β-expressing MGCs correlated positively with IFN-γ-expressing MGCs ($p<0.05$). IL-10- and TNF-α-expressing MGCs also correlated positively ($p<0.001$).

Discussion

The differential expression of mycobacterial antigens, inflammatory and apoptosis markers by the ECs and MGCs suggests different functions of the two cell types. The ECs seem to have better mycobactericidal functions and consequently have lesser antigen load as determined by MPT64 expression. When these cells mature into MGCs, the expression of TGF-β increases which can lead to reduced mycobactericidal capability. Consequently, these cells carry a higher antigen load than the ECs. This transition in the pattern of cytokine expression can be attributed to the interaction of *M. tuberculosis* with the host cells to avoid killing by the host cells.

Both ECs and MGCs expressed caspase 3, which suggest that these cells are removed by apoptosis. This is in agreement with the observations that activated immune cells are eliminated by apoptosis which limits their destructive potential. However, the number of apoptotic MGCs and the MGCs with MPT64 antigen were higher than the respective ECs. Based on these findings, it can be hypothesised that the ECs which contain mycobacterial antigens may avoid apoptosis and preferentially fuse to form MGCs, while those without mycobacteria or its components are removed by apoptosis. The negative correlation of MPT64-antigen-expressing MGCs with the apoptotic MGCs implies that those with the most antigens may resist apoptosis. This is in agreement with studies showing that virulent mycobacteria cause inhibition of

Table 1 Relationship between the numbers of epithelioid cells and multinucleated giant cells expressing caspase 3, apoptosis-related proteins and various cytokines in granulomas caused by *M. tuberculosis* based on Spearman's rank correlation

	EC						MGC						
	Fas	Bax	IL-10	TNF-α	TGF-β	IFN-γ	FasL	Fas	Bax	IL-10	TNF-α	TGF-β	IFN-γ
EC													
FasL	0.7*	0.59**	−0.25	−0.17	−0.06	−0.30	0.24						
Fas		0.58**	−0.30	−0.37	−0.35	−0.31		0.64*					
Bax			−0.13	0.08	0.17	−0.07			0.85*				
IL-10				0.30	0.39**	0.05				0.16			
TNF-α					0.67*	0.22					−0.15		
TGF-β					0.12							0.26	
IFN-γ													0.26
MGC													
FasL								0.38	0.22	−0.02	0.15	0.55**	0.57**
Fas									0.45	0.51**	0.29	0.11	−0.07
Bax										0.24	0.29	0.07	0.20
IL-10											0.68*	0.08	−0.09
TNF-α												0.26	0.28
TGF-β													0.49**

The values shown are the correlation coefficients.
*$p<0.001$; **$p<0.05$

apoptosis and use these cells as a sanctuary to avoid immune response and persist in the host [15, 20, 22]. These MGCs may then prevent the granulomas to regress and heal, by antigen presentation to the surrounding lymphocytes and continuous recruitment of new cells. These suggestions are supported by findings from a previous work where an in vitro model of granulomas showed that only virulent species of the *M. tuberculosis* complex triggered the formation of MGCs, resembling natural Langhans giant cells found in human tuberculous granulomas [17]. These large MGCs are as active as macrophages, but they have reduced capacity of phagocytosis, despite a conserved ability to mediate antigen presentation.

Antigen-presenting cells with increased expression of FasL are shown to induce apoptosis in T-cells during antigen presentation, thus inducing antigen-specific T-cell tolerance [35]. In this study, more MGCs expressed FasL than ECs, and FasL-expressing MGCs correlated positively with TGF-β-expressing MGCs. As the infected MGCs are shown to possess antigen presentation capability by expression of major histocompatibility complex class II receptors [17], it can be assumed that FasL-expressing MGCs may lead to death of a subset of *M. tuberculosis*-specific T-cells, causing specific immune suppression in the host. This hypothesis is indirectly supported by studies in tuberculosis patients where constant apoptosis of T-cells has been shown to result in a reduction in T-cell numbers and depressed proliferative responses [14, 18]. Furthermore, the observation that FasL-expressing ECs correlate positively with Fas-expressing ECs while no significant correlation was found between these proteins among MGCs suggests that MGCs with increased expression of FasL do not simultaneously express Fas, which would help these cells to evade being killed via Fas–FasL pathway.

MPT64 is a 26-KD secreted mycobacterial protein shown to be specific for *M. tuberculosis* complex organisms [6, 12]. Secreted mycobacterial proteins are considered immunodominant and are involved in inducing protective immunity [1], but little is known about the role of MPT64 in host immunity. This antigen has been detected in the macrophages of human and mouse TB lesions [26, 27] and elicits T-cell responses in patients infected with TB [29]. The region encoding the corresponding *mpb64* gene is deleted from several bacillus Calmette–Guerin strains, and this has been correlated with a drop in virulence in animal infection models and reduced vaccine lesions in humans [2], suggesting a role of MPT64 in mycobacterial virulence. In this study, increased expression of MPT64 and TGF-β, FasL and Fas in MGCs as compared to ECs and a negative correlation between MPT64 expression and apoptosis in MGCs suggests that MPT64 may induce an increased expression of these proteins and inhibition of apoptosis of infected MGCs, making them more suitable for mycobacterial survival. There was, however, no significant correlation between MGCs expressing MPT64 and these proteins, and further studies are required to investigate the role of MPT64 in disease pathogenesis.

The difference in the pattern of relationship of cytokines between ECs and MGCs suggests different roles of these two cell types for control of the infection. Paradoxically, the number of MGCs expressing anti-inflammatory cytokines TGF-β and IL-10 correlated positively with MGCs

expressing pro-inflammatory cytokines IFN-γ and TNF-α, respectively. However, the intensity of staining for IFN-γ was less than TGF-β in MGCs as shown in Fig. 2, which may imply a reduced amount of IFN-γ as compared to TGF-β in these cells, while this difference in intensity was not reflected in the cell counts. Furthermore, TGF-β can block the mycobactericidal mechanisms induced by IFN-γ [33], and IL-10 has been shown to block the activity of TNF-α by inducing the release of soluble TNF-α receptor type 2 (TNFR2) from macrophages and the formation of inactive TNF-α-TNFR2 complexes [10]. These observations suggest that MGCs by virtue of increased levels of anti-inflammatory cytokines favour mycobacterial persistence.

In conclusion, we have found that a higher number of MGCs contain *M. tuberculosis* secretory antigen MPT64 and express more TGF-β as compared to ECs, implying that the maturation of ECs into MGCs is associated with reduction in mycobactericidal function which can lead to accumulation of mycobacterial antigen. The negative correlation between MPT64 in MGCs and caspase-3-expressing MGCs suggests that the infected MGCs avoid apoptosis. The MGCs and ECs may thus play different roles, EC being more fit to eliminate the bacilli, while MGCs harbour them. The relationship between these cells needs further analysis.

Acknowledgements We thank Dr. Sayoki G. Mfinanagi at the National Institute for Medical Research, Muhimbili Research Station, Tanzania for the provision of biopsies from Tanzania. This study was supported by funds from the University of Bergen, from Norwegian health-related research funding agency; Helse-Vest and Norwegian trusts for research funding; Gades Legat, Connie Gulberg Jansens Legat, and Skipsreder Tom Wilhelmsens Stiftelse.

Conflict of interest statement We declare that we have no conflict of interest.

Open Access This article is distributed under the terms of the Creative Commons Attribution Noncommercial License which permits any noncommercial use, distribution, and reproduction in any medium, provided the original author(s) and source are credited.

References

1. Andersen P (1997) Host responses and antigens involved in protective immunity to *Mycobacterium tuberculosis*. Scand J Immunol 45:115–131
2. Behr MA, Wilson MA, Gill WP, Salamon H, Schoolnik GK, Rane S, Small PM (1999) Comparative genomics of BCG vaccines by whole-genome DNA microarray. Science 284:1520–1523
3. Casanova JL (2000) Mendelian susceptibility to mycobacterial infection in man. Bull Acad Natl Med 184:1409–1416
4. Chantry D, Turner M, Abney E, Feldmann M (1989) Modulation of cytokine production by transforming growth factor-beta. J Immunol 142:4295–300
5. Cooper AM, Dalton DK, Stewart TA, Griffin JP, Russell DG, Orme IM (1993) Disseminated tuberculosis in interferon-gamma gene-disrupted mice. J Exp Med 178:2243–2247
6. Elhay MJ, Oettinger T, Andersen P (1998) Delayed-type hypersensitivity responses to ESAT-6 and MPT64 from *Mycobacterium tuberculosis* in the guinea pig. Infect Immun 66:3454–3456
7. Emile JF, Patey N, Altare F, Lamhamedi S, Jouanguy E, Boman F, Quillard J, LecomteHoucke M, Verola O, Mousnier JF, Dijoud F, Blanche S, Fischer A, Brousse N, Casanova JL (1997) Correlation of granuloma structure with clinical outcome defines two types of idiopathic disseminated BCG infection. J Pathol 181:25–30
8. Flesch IE, Kaufmann SH (1990) Activation of tuberculostatic macrophage functions by gamma interferon, interleukin-4, and tumor necrosis factor. Infect Immun 58:2675–2677
9. Flynn JL, Goldstein MM, Chan J, Triebold KJ, Pfeffer K, Lowenstein CJ, Schreiber R, Mak TW, Bloom BR (1995) Tumor necrosis factor-alpha is required in the protective immune response against *Mycobacterium tuberculosis* in mice. Immunity 2:561–572
10. Fratazzi C, Arbeit RD, Carini C, Balcewicz-Sablinska MK, Keane J, Kornfeld H, Remold HG (1999) Macrophage apoptosis in mycobacterial infections. J Leukoc Biol 66:763–4
11. Gasser A, Most J (1999) Generation of multinucleated giant cells in vitro by culture of human monocytes with *Mycobacterium bovis* BCG in combination with cytokine-containing supernatants. Infect Immun 67:395–402
12. Harboe M, Nagai S, Patarroyo ME, Torres ML, Ramirez C, Cruz N (1986) Properties of proteins MPB64, MPB70, and MPB80 of *Mycobacterium bovis* BCG. Infect Immun 52:293–302
13. Hernandez-Pando R, Orozco H, Arriaga K, Sampieri A, Larriva-Sahd J, Madrid-Marina V (1997) Analysis of the local kinetics and localization of interleukin-1 alpha, tumour necrosis factor-alpha and transforming growth factor-beta, during the course of experimental pulmonary tuberculosis. Immunology 90:607–617
14. Hirsch CS, Toossi Z, Vanham G, Johnson JL, Peters P, Okwera A, Mugerwa R, Mugyenyi P, Ellner JJ (1999) Apoptosis and T cell hyporesponsiveness in pulmonary tuberculosis. J Infect Dis 179:945–953
15. Keane J, Remold HG, Kornfeld H (2000) Virulent *Mycobacterium tuberculosis* strains evade apoptosis of infected alveolar macrophages. J Immunol 164:2016–2020
16. Kindler V, Sappino AP, Grau GE, Piguet PF, Vassalli P (1989) The inducing role of tumor necrosis factor in the development of bactericidal granulomas during BCG infection. Cell 56:731–740
17. Lay G, Poquet Y, Salek-Peyron P, Puissegur MP, Botanch C, Bon H, Levillain F, Duteyrat JL, Emile JF, Altare F (2007) Langhans giant cells from M-tuberculosis-induced human granulomas cannot mediate mycobacterial uptake. J Pathol 211:76–85
18. Manfredi AA, Heltai S, Rovere P, Sciorati C, Paolucci C, Galati G, Rugarli C, Vaiani R, Clementi E, Ferrarini M (1998) *Mycobacterium tuberculosis* exploits the CD95/CD95 ligand system of gammadelta T cells to cause apoptosis. Eur J Immunol 28:1798–1806
19. Mfinanga SG, Morkve O, Kazwala R, Cleaveland S, Sharp M, Kunda J, Nilsen R (2004) Mycobacterial adenitis: role of *Mycobacterium bovis*, non-tuberculous mycobacteria, HIV infection, and risk factors in Arusha, Tanzania. East Afr Med J 81:171–178
20. Mogga SJ, Mustafa T, Sviland L, Nilsen R (2002) Increased Bcl-2 and reduced Bax expression in infected macrophages in slowly progressive primary murine *Mycobacterium tuberculosis* infection. Scand J Immunol 56:383–391
21. Murray PJ, Wang L, Onufryk C, Tepper RI, Young RA (1997) T cell-derived IL-10 antagonizes macrophage function in mycobacterial infection. J Immunol 158:315–21
22. Mustafa T, Phyu S, Nilsen R, Bjune GRJ (1999) Increased expression of Fas ligand on *Mycobacterium tuberculosis* infected macrophages: a potential novel mechanism of immune evasion by *Mycobacterium tuberculosis*? Inflammation 23:507–521

23. Mustafa T, Bjune TG, Jonsson R, Pando RH, Nilsen R (2001) Increased expression of fas ligand in human tuberculosis and leprosy lesions: a potential novel mechanism of immune evasion in mycobacterial infection. Scand J Immunol 54:630–9
24. Mustafa T, Mogga SJ, Mfinanga SGM, Mørkve O, Sviland L (2005) Significance of Fas and Fas Ligand in tuberculous lymphadenitis. Immunology 114:255–262
25. Mustafa T, Mogga SJ, Mfinanga SGM, Morkve O, Sviland L (2006) Immunohistochemical analysis of cytokines and apoptosis in tuberculous lymphadenitis. Immunology 117:454–462
26. Mustafa T, Phyu S, Nilsen R, Jonsson R, Bjune G (1999) A mouse model for slowly progressive primary tuberculosis. Scand J Immunol 50:127–136
27. Mustafa T, Wiker HG, Mfinanga SGM, Morkve O, Sviland L (2006) Immunohistochemistry using a *Mycobacterium tuberculosis* complex specific antibody for improved diagnosis of tuberculous lymphadenitis. Mod Pathol 19:1606–1614
28. Mustafa T, Wiker HG, Morkve O, Sviland L (2007) Reduced apoptosis and increased inflammatory cytokines in granulomas caused by tuberculous compared to non-tuberculous mycobacteria: role of MPT64 antigen in apoptosis and immune response. Clin Exp Immunol 150:105–113
29. Roche PW, Triccas JA, Avery DT, Fifis T, Billmanjacobe H, Britton WJ (1994) Differential T-cell responses to mycobacteria-secreted proteins distinguish vaccination with Bacille Calmette-Guerin from infection with *Mycobacterium tuberculosis*. J Infect Dis 170:1326–1330
30. Sandor M, Weinstock JV, Wynn TA (2003) Granulomas in schistosome and mycobacterial infections: a model of local immune responses. Trends Immunol 24:44–52
31. Saunders BM, Frank AA, Orme IM (1999) Granuloma formation is required to contain bacillus growth and delay mortality in mice chronically infected with *Mycobacterium tuberculosis*. Immunology 98:324–328
32. Takashima T, Ohnishi K, Tsuyuguchi I, Kishimoto S (1993) Differential regulation of formation of multinucleated giant-cells from concanavalin-A-stimulated human blood monocytes by Ifn-Gamma and Il-4. J Immunol 150:3002–3010
33. Toossi Z, Ellner JJ (1998) The role of TGF beta in the pathogenesis of human tuberculosis. Clin Immunol Immunopathol 87:107–114
34. Toossi Z, Gogate P, Shiratsuchi H, Young T, Ellner JJ (1995) Enhanced production of TGF-beta by blood monocytes from patients with active tuberculosis and presence of TGF-beta in tuberculous granulomatous lung lesions. J Immunol 154:465–473
35. Zhang HG, Su X, Liu D, Liu W, Yang P, Wang Z, Edwards CK, Bluethmann H, Mountz JD, Zhou T (1999) Induction of specific T cell tolerance by Fas ligand-expressing antigen-presenting cells. J Immunol 162:1423–1430

Virchows Arch (2008) 452:457–463
DOI 10.1007/s00428-008-0583-z

CASE REPORT

Molecular genetic findings in two cases of sarcomatoid carcinoma of the ureter: evidence for evolution from a common pluripotent progenitor cell?

Hans-Ullrich Völker · Andreas Zettl · Georg Schön · Vitus Heller · Elmar Heinrich · Andreas Rosenwald · Mathias Handwerker · Hans-Konrad Müller-Hermelink · Alexander Marx · Philipp Ströbel

Received: 17 October 2007 / Revised: 14 January 2008 / Accepted: 16 January 2008 / Published online: 12 February 2008
© Springer-Verlag 2008

Abstract The current World Health Organization classification recommends the usage of the term sarcomatoid carcinoma (SC) for all biphasic malignant neoplasms of the urinary tract exhibiting morphologic and/or immunohistochemical evidence of epithelial and mesenchymal differentiation. While most SC have been described in the urinary bladder, ureteral SC are extremely rare tumors. Here, we report on the clinical, morphological, and molecular biological findings of two cases in this unusual location. The genetic alterations investigated by comparative genomic hybridization in the epithelial and the mesenchymal component of both cases showed considerable but not complete overlap. Moreover, in spite of many morphological differences between the two cases, both cases shared some genetic gains and losses. Our findings are compatible with the concept that SC originates from a common pluripotent progenitor cell with a potential for epithelial and mesenchymal differentiation.

Keywords Sarcomatoid carcinoma · Ureter · Immunohistochemistry · Comparative genomic hybridization · Histogenesis

H.-U. Völker (✉) · A. Zettl · A. Rosenwald · H.-K. Müller-Hermelink
Institute of Pathology, University of Würzburg,
Josef-Schneider-Straße 2,
97080 Würzburg, Germany
e-mail: hans-ullrich.voelker@t-online.de

G. Schön · E. Heinrich
Department of Urology, Missionsärztliche Klinik,
Würzburg, Germany

V. Heller
Department of Urology, Juliusspital,
Würzburg, Germany

M. Handwerker
Institute of Radiology and Neuroradiology,
Karlstadt, Germany

A. Marx · P. Ströbel
Institute of Pathology, University Medical Center Mannheim,
University of Heidelberg,
Mannheim, Germany

Introduction

Sarcomatoid carcinomas (SC) of the ureter are very rare neoplasms. Less than 20 cases have been described [1–3, 9, 10, 13, 17, 18, 23, 24, 27]. A confusing terminology with many different denominations (such as carcinosarcoma, heterologous sarcomatoid carcinoma, true malignant mixed tumor, biphasic sarcomatoid carcinoma, metaplastic carcinoma, or sarcomatoid carcinoma with heterologous differentiation) reflects the conceptual uncertainty as to whether this lesion represents dedifferentiated carcinoma or a genuine biphasic malignant neoplasm. The 2004 World Health Organization (WHO) classification of urothelial neoplasms recommends the term sarcomatoid carcinoma for all biphasic malignant neoplasms exhibiting evidence of epithelial and mesenchymal differentiation to overcome the previously tangled nomenclature [4].

SC can originate in the whole urinary tract, but the majority occurs in the urinary bladder. About 80 cases have

been reported at this site [19]. Most of these uncommon tumors are combinations of a transitional cell carcinoma and one or more different types of sarcoma, such as osteosarcoma, chondrosarcoma, or rhabdomyosarcoma. Apart from transitional cell carcinoma, other kinds of carcinoma have been described, including basaloid, squamous, and undifferentiated carcinoma [10, 18, 24].

The histogenesis of SC is unclear to date. Assumptions of a monoclonal origin exist, but only a few authors have performed genetic analysis [7, 8, 21].

Here, we describe the clinical, histomorphological, and genetic findings in two ureteral sarcomatoid carcinomas.

Clinical history

Patient 1 A 67-year-old female patient presented with a history of hydronephrosis for over 2 years. A 2-cm neoplasm was suspected in the distal right ureter on computed tomography (CT) scan and was confirmed by ureteroscopy. Nephroureterectomy, urocystectomy, and removal of the uterus and adnexa was performed. Neither recurrence nor distant metastases occurred until 18 months after surgery.

Patient 2 An 83-year-old male patient presented with painless macrohematuria and hydronephrosis. An obstructive segmental lesion located in the distal left ureter was diagnosed on CT scan and removed by nephroureterectomy. Thirty-six months after surgery the patient is free of relapsing tumor and distant metastases.

Materials and methods

Histological and immunohistochemical techniques

Tumor sections for light microscopy, immunohistochemistry, and genetic analysis were fixed in 10% buffered neutral formalin, embedded in paraffin, and stained with hematoxylin and eosin and periodic acid Schiff reagent (PAS). The primary antibodies used for immunohistochemistry are given in Table 1.

DNA extraction and comparative genomic hybridization

For extraction of DNA from the epithelial and mesenchymal tumor compartment, suitable paraffin blocks were

Table 1 Antibodies used for immunohistochemistry

Antigens–antibodies	Clone	Dilution	Source
α-fetoprotein (AFP)	Polyclonal	1:800	Dako
ß-HCG	Polyclonal	1:600	Dako
34ßE12	34ßE12	1:20	Dako
Actin	1A4	1:20	Immunotech
AE1/3	AE 1/AE3	1:100	Dako
CD10	56C6	1:40	Novocastra
CD117	104D2	1:100	Dako
CD30	BER-H2	1:10	Dako
CD31	JC70A	1:10	Dako
CD34	QBEnd10	1:100	Immunotech
CD99	HO36-1.1	1:50	Novocastra
CK7	OV-TL12/30	1:20	Dako
CK8/18 (CAM5.2)	–	1:2	Becton Dickinson
CK10/13	DE-K13	1:20	Dako
CK20	KS20.8	1:20	Dako
Desmin	D33	1:400	Dako
Estrogen receptor	SP1	1:10	Dako
HMB45	MO634	1:50	Dako
Inhibin	R1	1:10	Serotec
Ki67	MIB-1	1:200	Dako
Myogenin	F5D	1:50	Dako
PLAP	8A9	1:100	Dako
Progesterone receptor	SP2	1:10	Dako
Rb	XZ55	1:50	Neomarkers
S100 protein	Polyclonal	1:200	Dako
Vimentin	V9	1:800	Dako
WT1	6F-H2	1:20	Novocastra

selected and trimmed to exclude contamination with the respective other tumor component. Fifty serial 5-µm paraffin sections were cut from a tumor block. DNA extraction was performed using proteinase K and phenol–chloroform according to routine molecular biology protocols. Comparative genomic hybridization (CGH) was performed according to a standard protocol [12]. Briefly, equal amounts of tumor DNA nick labeled with biotin-16-deoxyuridine triphosphate (dUTP; Roche DiagnostiSC, Mannheim, Germany) and normal DNA labeled with digoxigenin-11-dUTP (Roche DiagnostiSC, Mannheim, Germany) were cohybridized on a commercially available metaphase slide (Vysis, Downers Grove, IL, USA). After overnight hybridization at 37°C, the different DNA labelings were visualized using fluorescein-isothiocyanate avidin (Vector Laboratories, Burlingame CA, USA) and Cy3-conjugated antidigoxigenin antibodies (Dianova, Hamburg, Germany), respectively. After counterstaining with 4,6-diamidino-2 phenylindole, 15 metaphases were recorded using a Zeiss Axiophot fluorescence microscope and analyzed with the ISIS digital image analysis system (MetaSystems, Altlussheim, Germany). Ratio values of 1.25 and 0.8 were used as upper and lower thresholds for identification of chromosomal gains or losses.

Results

Gross inspection and histopathological and immunohistochemical findings

Case 1

The distal ureter was thickened to a diameter of 1.8 cm over a length of 3.5 cm. The ureteral lumen was occluded by a soft papillary mass causing conspicuous hydronephrosis.

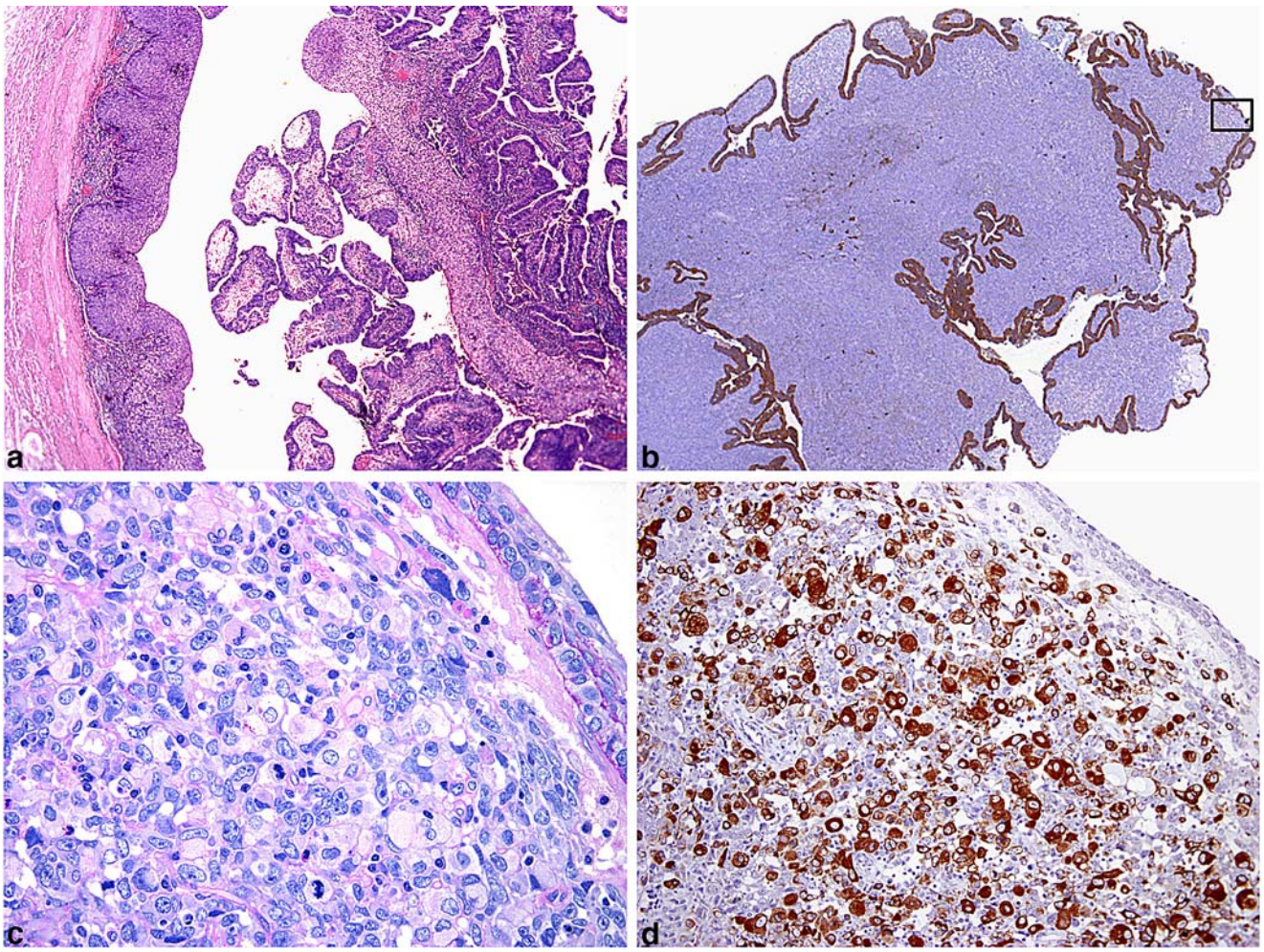


Fig. 1 Sarcomatoid carcinoma of the ureter, case 1. **a** Papillary tumor occluding the ureteral lumen, transitional carcinoma in situ of the ureteral mucosa (invasive carcinoma not shown, H & E, ×40). **b** Papillary tumor component, immunohistochemical staining of the surface epithelium with pan-cytokeratin, no staining of the underlying stroma (AE1/3 immunoperoxidase, ×20). **c** (framed in **b**): Focus of sarcoma with rhabdomyoid differentiation covered by an epithelial surface (PAS reaction ×400). **d** Corresponding immunohistochemistry to Fig. 2c with staining for desmin (immunoperoxidase, ×200)

Kidney, urinary bladder, uterus, and adnexa were inconspicuous on gross inspection.

Histological examination of the ureter revealed a biphasic tumor composed of a malignant epithelial and malignant mesenchymal component. The epithelial component consisted mainly of a conventional high grade transitional cell carcinoma with focal clear cell pattern, which invaded the ureteral wall (not shown). The invasive carcinoma was surrounded by an extensive carcinoma in situ (CIS). Another tumor component exhibited high-grade papillary features (Fig. 1a). On immunohistochemistry, both the invasive carcinoma and CIS showed a strong reaction with antibodies against pan-cytokeratin (CK) AE1/3, CAM5.2, and 34ßE12, with a rather weak reaction for CK7 and CK20. The epithelial surface of the papillary tumor was strongly positive for AE1/3 (Fig. 1b) and CK7, weakly positive for CK20, and negative for 34ßE12.

Below the papillary tumor component, there was a malignant mesenchymal spindle cell proliferation with conspicuous nuclear pleomorphism and focal rhabdomyosarcomatous features with a broad eosinophilic cytoplasm (Fig. 1c). On immunohistochemistry, the tumor was completely negative for pan-cytokeratin AE1/3, but positive for vimentin and focally for clusters of differentiation 117 (CD117) and CD10. The areas with rhabdomyoid morphology were strongly positive for actin, desmin (Fig. 1d), and myogenin. All other markers (including α-fetoprotein, ß-human chorionic gonadotropin (ß-HCG), CD31 and 34, CD99, human melanoma black 45, nuclear Wilm tumor 1 (WT1), inhibin, placental alkaline phosphatase (PLAP), and hormone receptors) were not expressed. p53 was overexpressed in both the epithelial and mesenchymal component, suggestive of an inactivating mutation. Rb was overexpressed in the mesenchymal part of the neoplasm.

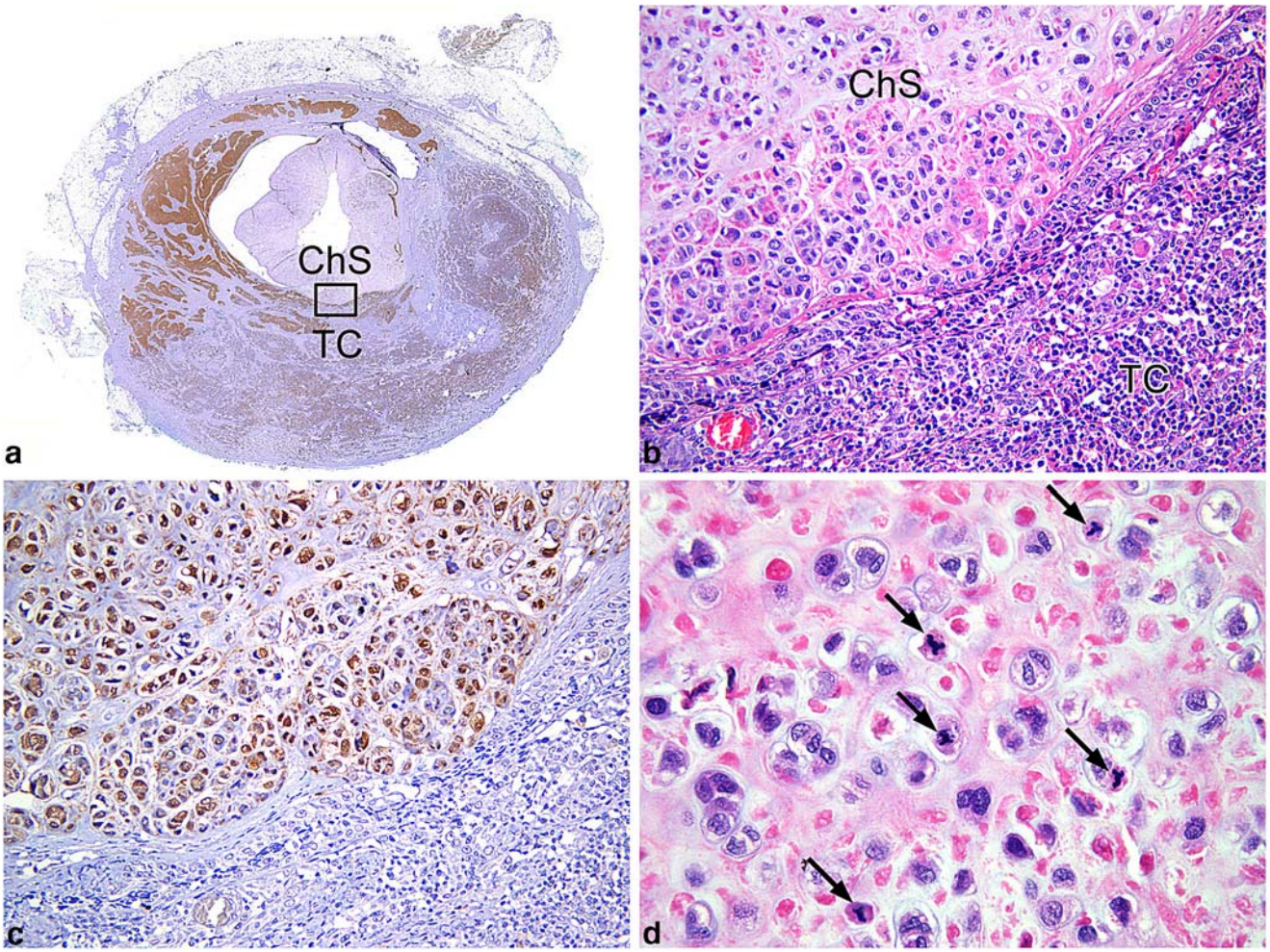


Fig. 2 Sarcomatoid carcinoma of the ureter, case 2. **a** Cross section of the ureter shows the invasive transitional cell carcinoma (*TC*) in the ureteral wall with expression of pan-cytokeratin. The weakly stained areas in the *lower right* correspond to undifferentiated carcinomatous areas. Ureteral lumen is occluded by a chondrosarcoma (*ChS*; AE1/3 immunoperoxidase, original magnification ×5). **b** (*framed* in **a**): Chondrosarcoma and carcinoma (H & E, ×200). **c** Strong expression of S100 protein exclusively in the chondrosarcoma but not in the epithelial tumor component (S100 immunoperoxidase, ×200). **d** Higher magnification reveals marked pleomorphism, the mitotic activity including atypical mitoses, and intermingled necrotic cells in the chondrosarcoma (H & E, ×400)

The proliferation index (Ki67) was approximately 80% in both components.

We diagnosed a sarcomatoid carcinoma with focal rhabdomyosarcomatous differentiation.

Three lymph node metastases showing exclusively the transitional cell carcinoma were detected in the surrounding soft tissue. The urinary bladder and the proximal ureter were free from dysplasia or tumor. The resected kidney, the uterus, and the adnexa were inconspicuous.

Case 2

On gross inspection, the distal ureter was occluded by a circumferential solid white mass with a diameter of 2.3 cm over a length of 4.5 cm. The kidney was unremarkable. Lymph nodes were not detectable.

Histologically, we found a biphasic malignant tumor with obvious epithelial and mesenchymal components. The epithelial component focally showed features of a conventional transitional cell carcinoma but consisted otherwise mainly of an undifferentiated carcinoma with marked nuclear pleomorphism and high mitotic activity and extensive infiltration of the ureter wall. Focally, the carcinoma displayed a sarcomatoid growth pattern with spindle cell appearance and minor areas of a PAS-negative myxoid stroma. In the undifferentiated carcinomatous and sarcomatoid areas, immunohistochemistry revealed strong reactivity for pan-cytokeratin AE1/3 (Fig. 2a), CAM5.2, and CK10/13, whereas CK7, CK20, ß-HCG, CD30, PLAP, WT1, and S100 were negative. The lumen of the ureter was occluded by a morphologically clearly distinct chondroid neoplasm showing hypercellularity, marked nuclear pleomorphism, and a mitotic activity up to five per high-power field and focal necrosis, corresponding to G2 chondrosarcoma. The areas corresponding to chondrosarcoma were strongly positive for S100 (Fig. 2b–d). p53 was overexpressed in both the epithelial and mesenchymal component; Rb was negative. The proliferation index (Ki67) was 50% in the epithelial and 30% in the mesenchymal component.

The diagnosis was sarcomatoid carcinoma with poor differentiated transitional cell carcinoma and G2 chondrosarcoma.

The kidney showed a moderate chronic pyelonephritis. Proximal ureter and kidney pelvis were free from tumor or dysplasia.

Results of comparative genomic hybridization analyses

CGH showed numerous gains and losses in both sarcomatoid carcinomas. In both cases, the genetic alterations were broadly overlapping between the two components, but there were also changes unique to either component. In both cases, at least one of the components showed gains on chromosomes 3q, 5p, and 6p and losses on chromosomes 5q, 11q, 13q, 14q, and 18q. Gains on chromosome 5p were the only alteration observed in the epithelial and mesenchymal component of both cases. The results are summarized in Table 2.

Discussion

A wide range of differentiations has been described for urinary tract SC. The epithelial component is most often a transitional cell carcinoma, but squamous cell carcinomas, adenocarcinomas, and in rare cases small cell neuroendocrine carcinomas may occur [10, 14, 23]. The mesenchymal component can consist of chondrosarcoma, osteosarcoma, rhabdomyosarcoma, or, rarely, liposarcoma [10, 19].

While the term s*arcomatoid carcinoma* sensu stricto implies a dedifferentiated carcinoma with mesenchymal features [11, 16, 20], the definition given by the WHO classification of urothelial neoplasms leaves open the possibility that not all biphasic malignant tumors might represent dedifferentiated carcinomas but also true mixed epithelial and mesenchymal neoplasms [22]. This concept

Table 2 Results of comparative genomic hybridization of tumor DNA isolated from the respective dissected malignant epithelial and mesenchymal components. Bold letters indicate genetic alterations found in both components (C+S)

	Case 1			Case 2		
	Carcinoma	C+S	Sarcoma	Carcinoma	C+S	Sarcoma
Gains	+3q	+2p +5p +11q13	+6p +7q32-qter ampl 8q24 +13q32-qter		+5p15-pter +6p21-p22 +16p +17	+1q +3q +9q31-qter
Losses	−3cen-p14 −13q	−4q −5q −9p −11p12-p14 −11q14-q22 −14q13-q21 −18q −Xp21	−6q −7p21 −8cen-q21	−5q15-q22 −14-q21	−13q	−10q −11q21-qter −18q

was supported by our molecular genetic findings showing a high but not absolute overlap of the genetic alterations identified. In both cases, there were alterations present exclusively in either the carcinoma or the sarcoma, which are an argument against origin of the sarcomatous component from a dedifferentiated carcinoma. Moreover, case 1 did not show an undifferentiated carcinoma component. In good agreement with the cases presented here, Fujii et al. [5] described an extensive overlap of genetic alterations in diverse gynecological biphasic tumors. Interestingly, in spite of the many morphological differences between the two cases, the overlap of the genetic alterations identified in both cases was remarkable. In detail, both cases shared gains of genetic material on chromosomes 3q (a region containing genes like, e.g., *cbl-b*, *rcc*), 5p, and 6p and losses of genetic material on chromosomes 5q, 11q, 13q, 14q, and 18q. It is thus tempting to speculate that one or several of these loci might harbor genes responsible for the malignant phenotype. In addition, case 1 showed loss of genetic material on chromosome 9p, the locus harboring the tumor suppressor gene cyclin-dependent kinase inhibitor 2A/p16. This alteration has repeatedly been reported also in sarcomatoid carcinomas of the urinary bladder [7, 8, 15].

To date, little is known about the histogenesis of SC in general. The most common theory assumes a monoclonal origin at different anatomic sites [5–8, 21, 22, 25, 26]. This concept is supported by findings of Sung et al. They have found an X-chromosome inactivation in both carcinomatous and sarcomatous components and a significant overlap of loss of heterozygosity in a series of urothelial SCs [21]. While the cell of origin in SC is unknown, most authors favor a primitive pluripotential stem cell, a concept that is also supported by our genetic findings. In experimental settings, cells separated from one part of a SC again induced a biphasic tumor when transferred into nude mice [19].

Ureteral SC seems to arise preferentially in the distal ureter. A few cases were located in the renal pelvis or proximal ureter [14, 17, 24]. Tobacco smoking and irradiation of the genital tract in gynecological patients have been considered risk factors for the development of SC [19]. Men appear to be affected more often [10, 18, 19]. Most of the patients are over 60 years of age. The symptoms are similar to conventional carcinomas in this location, i.e., gross hematuria and signs of ureteral obstruction [2, 18]. At the time of diagnosis, the tumors are often in advanced stages. Radical surgery is the only effective treatment; adjuvant radiotherapy or chemotherapy have not been shown to be beneficial [18]. The first patient presented here had had a history of hydronephrosis for over 2 years. A similar case with a protracted course was published by others [13]. In the majority of cases, however, the prognosis is poor and patients seldom survive longer than 3 years [10, 19, 24].

Conclusion

Sarcomatoid carcinomas comprise a group of tumors with heterogeneous morphology. Apart from the epithelial transitional cell component, a broad spectrum of mesenchymal differentiation is possible. An origin of both components from a pluripotent progenitor cell has been previously suggested. Our molecular genetic results in two cases which are compatible with this hypothesis and argue against sarcomatous dedifferentiation of preexisting carcinoma.

Acknowledgment Marx A and Ströbel P are supported by grants LSHB-CT-2003-503410 (Euro-Thymaide) and 10-1740 of the Deutsche Krebshilfe.

Conflict of interest statement We declare that we have no conflict of interest.

References

1. Burt JD, Murphy D, Heffernan EB (1995) Carcinosarcoma of the ureter presenting as biliary colic. Aust N Z J Surg 65:63–64
2. Byard RW, Bell ME, Alkan MK (1987) Primary carcinosarcoma: a rare cause of unilateral ureteral obstruction. J Urol 137:732–733
3. Darko A, Das K, Bhalla RS, Heller D (2006) Carcinosarcoma of the ureter: report of a case with unusual histology and review of the literature. Int J Urol 13:1528–1531
4. Eble JN, Sauter G, Epstein JI et al (2004) Pathology and genetics. Tumors of the urinary system and male genital organs. World Health Organization classification of tumours. IARC, Lyon, pp 102–103
5. Fujii H, Yoshida M, Gong ZX, Matsumoto T, Hamano Y, Fukunaga M, Hruban RH, Gabrielson E, Shirai T (2000) Frequent genetic heterogeneity in the clonal evolution of gynecological carcinosarcoma and its influence on phenotypic diversity. Cancer Res 60:114–120
6. Gotte K, Riedel F, Coy JF, Spahn V, Hormann K (2000) Salivary gland carcinosarcoma: immunohistochemical, molecular genetic and electron microscopic findings. Oral Oncol 36:360–364
7. Gronau S, Menz CK, Melzner I, Hautmann R, Moller P, Barth TF (2002) Immunohistomorphologic and molecular cytogenetic analysis of a carcinosarcoma of the urinary bladder. Virchows Arch 440:436–440
8. Halachmi S, DeMarzo AM, Chow NH, Halachmi N, Smith AE, Linn JF, Nativ O, Epstein JI, Schoenberg MP, Sidransky D (2000) Genetic alterations in urinary bladder carcinosarcoma: evidence of a common clonal origin. Eur Urol 37:350–357
9. Ishikura H, Kumagai F, Yoshiki T (1994) Carcinosarcoma of the ureter with unusual histologic features. Jpn J Clin Oncol 24:175–180
10. Johnin K, Kadowaki T, Kushima M, Ushida H, Koizumi S, Okada Y (2003) Primary heterologous carcinosarcoma of the ureter with necrotic malignant polyps. Report of a case and review of the literature. Urol Int 70:232–235
11. Lee G, Rankin A, Williamson M, Pope A (2004) Case report: sarcomatoid carcinoma arising from the ureter: a rare case and a treatment dilemma. Int Urol Nephrol 36:153–154
12. Lichter P, Bentz M, Joos S (1995) Detection of chromosomal aberrations by means of molecular cytogenetics: painting of chromosomes and chromosomal subregions and comparative genomic hybridization. Methods Enzymol 254:334–359

13. McDade HB, Armstrong EM, Graham AG (1974) Proceedings: a case of carcinosarcoma of ureter. J Clin Pathol 27:514
14. Mikuz G (1993) Non-urothelial tumors of the urinary tract. Verh Dtsch Ges Pathol 77:180–198
15. Mukhopadhyay S, Shrimpton AE, Jones LA, Nsouli IS, Abraham NZ Jr. (2004) Carcinosarcoma of the urinary bladder following cyclophosphamide therapy: evidence for monoclonal origin and chromosome 9p allelic loss. Arch Pathol Lab Med 128:e8–e11
16. Nagayoshi J, Kawakami T, Maruyama Y (1997) Sarcomatoid carcinoma of the ureter: a case report. Int J Urol 4:618–620
17. Orsatti G, Corgan FJ, Goldberg SA (1993) Carcinosarcoma of urothelial organs: sequential involvement of urinary bladder, ureter, and renal pelvis. Urology 41:289–291
18. Perimenis P, Athanasopoulos A, Geragthy J, Speakman M (2003) Carcinosarcoma of the ureter: a rare, pleomorphic, aggressive malignancy. Int Urol Nephrol 35:491–493
19. Perret L, Chaubert P, Hessler D, Guillou L (1998) Primary heterologous carcinosarcoma (metaplastic carcinoma) of the urinary bladder: a clinicopathologic, immunohistochemical, and ultrastructural analysis of eight cases and a review of the literature. Cancer 82:1535–1549
20. Petsch MJ, Planz B, Tschahargane C, Caspers HP (2004) Primary sarcomatoid carcinoma of the ureter. Aktuelle Urol 35:137–139
21. Sung MT, Wang M, MacLennan GT, Eble JN, Tan PH, Lopez-Beltran A, Montironi R, Harris JJ, Kuhar M, Cheng L (2007) Histogenesis of sarcomatoid urothelial carcinoma of the urinary bladder: evidence for a common clonal origin with divergent differentiation. J Pathol 211:420–430
22. Torenbeek R, Hermsen MA, Meijer GA, Baak JP, Meijer CJ (1999) Analysis by comparative genomic hybridization of epithelial and spindle cell components in sarcomatoid carcinoma and carcinosarcoma: histogenetic aspects. J Pathol 189: 338–343
23. Tsutsumi M, Kamiya M, Sakamoto M, Tobisu K, Kakizoe T (1993) A ureteral small cell carcinoma mixed with malignant mesodermal and ectodermal elements: a clinicopathological, morphological and immunohistochemical study. Jpn J Clin Oncol 23:325–329
24. Vermeulen P, Hoekx L, Colpaert C, Wyndaele JJ, Van Marck E (2000) Biphasic sarcomatoid carcinoma (carcinosarcoma) of the renal pelvis with heterologous chondrogenic differentiation. Virchows Arch 437:194–197
25. Volker HU, Muhlmeier G, Maier H, Kraft K, Muller-Hermelink HK, Zettl A (2007) True malignant mixed tumour (carcinosarcoma) of submandibular gland—a rare neoplasm of monoclonal origin? Histopathology 50:795–798
26. Watanabe M, Shimizu K, Kato H, Imai H, Nakano H, Sugawa M, Shiraishi T (2001) Carcinosarcoma of the uterus: immunohistochemical and genetic analysis of clonality of one case. Gynecol Oncol 82:563–567
27. Yano S, Arita M, Ueno F, Yoshida M, Ikegami K, Fukuda S (1984) Carcinosarcoma of the ureter. Eur Urol 10:71

Virchows Arch (2008) 452:465–467
DOI 10.1007/s00428-007-0565-6

LETTER TO THE EDITOR

Pigmented lipofibromatosis in unusual location: case report and review of the literature

Lobna Ayadi · Slim Charfi · Youssef Ben Hamed · Ibtissem Bahri · Naourez Gouiaa · Abdelmajid Khabir · Saloua Makni · Tahya Sellami-Boudawara

Received: 31 July 2007 / Revised: 28 September 2007 / Accepted: 23 October 2007 / Published online: 31 January 2008
© Springer-Verlag 2007

Dear Editor,

Lipofibromatosis is a rare, recently reported, *fibrofatty* pediatric tumour which affects mainly extremities [1, 6]. Histopathological features of this tumour must be distinguished from fibrous hamartoma of child, fibromatosis, calcifying aponevrotic fibroma and lipoblastoma [1]. Pigmented lipofibromatosis is a rare histological variant of lipofibromatosis which is not yet clearly distinguished. We describe a case of pigmented lipofibromatosis in an unusual location (back).

We report the case of a 14-year-old female who presented with several years history of a slowly enlarging, painless mass of the back. Physical examination demonstrated a subcutaneous, firm, nodule measuring 3.5 × 2.5cm. The nodule seems to be fixed at deep tissues without abnormality of the overlying skin. She was otherwise healthy and no family history of cutaneous abnormalities was noted. Any radiological exam was done. An excisional biopsy was performed. A 4 × 3 × 3cm ill-defined mass was excised. Grossly, the tumour presented an adipose appearance without encapsulation. The cut surface presented some black pigmented areas. Hematoxylin and eosin stained sections showed small lobules of mature adipose tissue, dissected by moderately cellular bundles, of spindle elements without atypia (Fig. 1). Some scattered cells were pigmented (Fig. 2) and Fontana–Masson stain was positive on these pigmented cells. On immunohistochemistry study, spindle cells were diffusely positive for vimentin and α smooth muscle actin (Fig. 3). Pigmented cells were positive for S100 protein and Melan A and negative for human melanoma black (HMB)-45 (Fig. 4). At 15 months of follow-up, there was no evidence of recurrence.

Lipofibromatosis is a distinctive entity of rare benign lesion recently described by Fetsch et al. [1, 4] in 2000 and recognised as a distinctive fibrofatty tumour of childhood in the World Health Organisation classification of tumours in 2002. Since this report, which includes 45 cases, only four other cases of lipofibromatosis were published [1–6]. Lipofibromatosis is different and must be equally distinguished from the entity designated as "lipofibromatosis," observed in cases of congenital macrodactyly and local gigantism [1]. The tumour commonly occurs in the extremities, rarely in the hands, arms, legs and feet [1, 6]. Chest, abdomen or head and neck are rarely affected [1–5]. The present observation is the first report of lipofibromatosis in the back. There is an over 2:1 male predominance. The median age for initial surgery is 1 year (range from 11 days to 12 year) [1]. The lesion is typically ill defined, painless and slow growing [1]. Macroscopically, it is yellowish or tan–whitish in appearance with a prominent fatty component. Very rare tumour have exceeded 5 cm [1, 3–6]. Histologically, the tumour is poorly marginated, often composed of more than 70% of adipose tissue. Fascicles of

L. Ayadi · S. Charfi (✉) · I. Bahri · N. Gouiaa · A. Khabir · S. Makni · T. Sellami-Boudawara
Laboratoire d'anatomie et de cytologie pathologiques,
CHU Habib Bourguiba,
3029 Sfax, Tunisia
e-mail: charfislim@gmail.com

Y. Ben Hamed
Laboratoire privé d'anatomie et de cytologie pathologiques,
Sfax, Tunisia

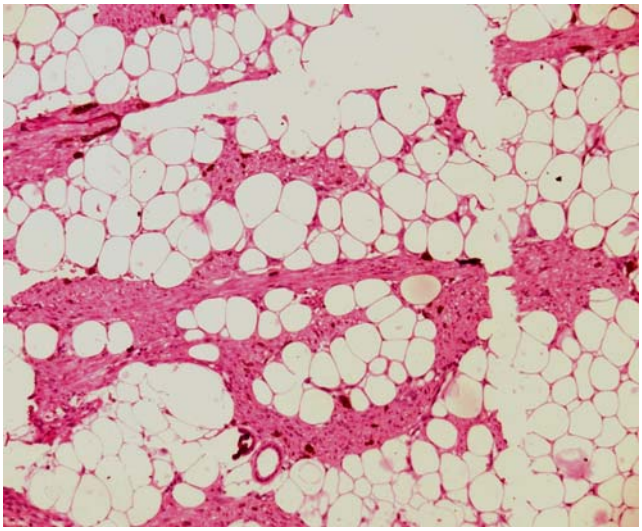


Fig. 1 Abundant adipose tissue with septa of spindle cells. H & E, ×100

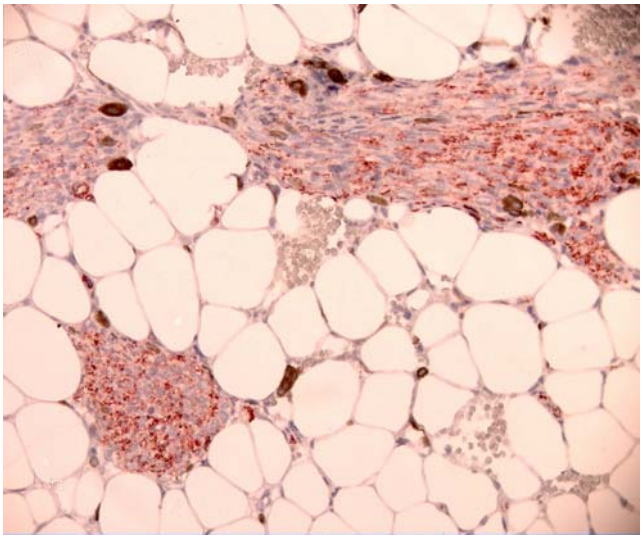


Fig. 3 Positive immunostaining for α smooth muscle actin. ×200

fibroblastic cells traversed, with a striking association, the adipose tissue. The fibroblastic component is weakly to moderately collagenised. In few cases, more heavily foci of myxoid change are noted [1]. Small univacuolated cells at the interface between the fibroblastic element and mature fat are rarely observed [1, 5]. There was no nuclear atypia and mitotic figures are absent or low [1]. Only one instance of the report of Fetsch et al. had a mitotic rate higher than 5 per 50 high-power fields. The presence of a small number of scattered pigmented cells in the fibroblastic component is a rare finding. In the report of Fetsch et al. [1], only two tumour cases with this finding were notably pigmented. These two cases had a congenital development and were located in foot and forearm. Our case is the first report of noncongenital pigmented lipofibromatosis. According to Fetsch et al., pigmented cells are "bystander cells" that have become passively incorporated within the mass because their normal migration pathway has been disturbed by the lipofibromatous process [1]. We think that the number of reported pigmented lipofibromatosis is too small to allow a correct clinicopathological analysis of this variant. Differential diagnosis of lipofibromatosis includes fibrous hamartoma of child, fibromatosis, calcifying aponevrotic fibroma and lipoblastoma. All distinctive criteria are cited in the work of Fetch et al. [1]. Immunohistochemically, it is not primordial for diagnosis of lipofiromatosis tumour. Tumor

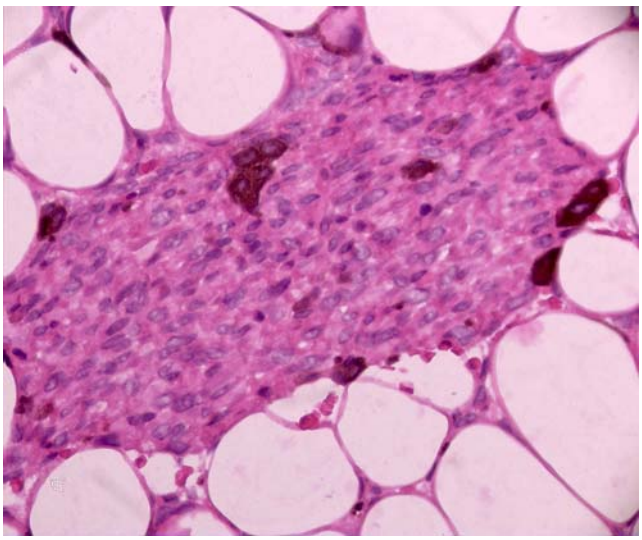


Fig. 2 Fascicles of spindle cells traversing mature adipose tissue. Note the pigmented cells H & E, ×400

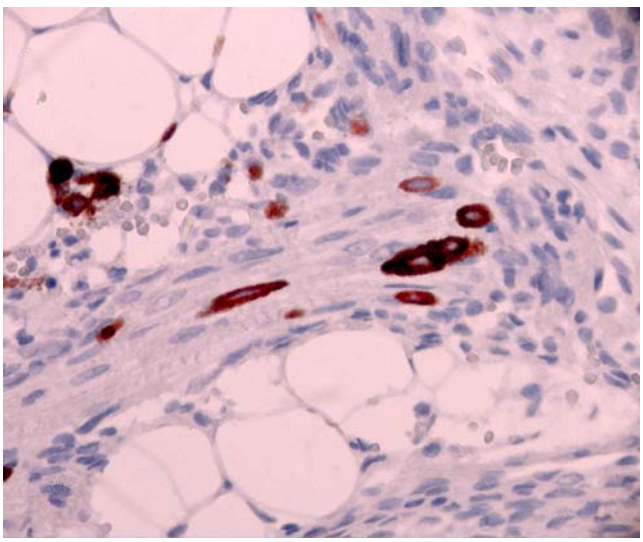


Fig. 4 Immunostaining of pigmented cells with Melan A. (×200)

spindle cells are often focally positive for CD99, CD34, Bcl-2, S100, muscle actin and epithelial membrane antigen. There is no reactivity for desmin and keratins. Pigmented cells are positive for tyrosinase, Melan A, HMB-45 and S-100 protein [1, 3–5]. Complete excision of the lesion is recommended to prevent local recurrence [1, 2]. Congenital tumours, male sex, involvement of hands and feet, incomplete surgery and a high mitotic activity are associated with a risk of recurrence [1, 2]. To date, no metastasis was reported [1].

References

1. Fetsch JF, Miettinen M, Laskin WB, Michal M, Enzinger FM (2000) A clinicopathologic study of 45 pediatric soft tissue tumors with an admixture of adipose tissue and fibroblastic elements, and a proposal for classification as lipofibromatosis. Am J Surg Pathol 24:1491–1500
2. Herrmann BW, Dehner LP, Forsen JW (2004) Lipofibromatosis presenting as a pediatric neck mass. Int J Pediatr Otorhinolaryngol 68:1545–1549
3. Kabasawa Y, Katsube KI, Harada H, Nagumo K, Terasaki H, Perbal B (2007) A male infant case of lipofibromatosis in the submental region exhibited the expression of the connective tissue growth factor. Oral Surg Oral Med Oral Pathol Oral Radiol Endod 103:677–682
4. Miettinen M, Fetsch JF (2002) In: Fletcher CDM, Unni KK, Mertens F (eds) Lipofibromatosis pathology and genetics of tumours of soft tissue and bone. World Health Organisation classification of tumours. IARC, Lyon, p 85
5. Sasaki D, Hatori M, Hosaka M, Watanabe M, Kokubun S (2005) Lipofibromatosis arising in a pediatric forearm—a case report. Upsala J Med Sci 110:259–266
6. Teo HE, Peh WC, Chan MY, Walford N (2005) Infantile lipofibromatosis of the upper limb. Skeletal Radiol 34:799–802

Virchows Arch (2008) 452:469–470
DOI 10.1007/s00428-007-0567-4

LETTER TO THE EDITOR

Mcl-1, an anti-apoptotic Bcl-2 family member, essentially overlaps with insulin-producing cells in neonatal nesidioblastosis

Makoto Sano · Emiko Hayashi · Hitohiko Murakami · Hiroshi Kishimoto · Ryuji Fukuzawa · Norimichi Nemoto

Received: 13 November 2007 / Revised: 1 December 2007 / Accepted: 14 December 2007 / Published online: 31 January 2008
© Springer-Verlag 2007

Dear Sirs,

We report here that anti-apoptotic protein Mcl-1 is closely related to the abnormal development of insulin-producing cells in neonatal nesidioblastosis. Nesidioblastosis, first reported by Dr. Laidlaw in 1938, was identified as the proliferation of endocrine cells differentiating from the pancreatic ductal epithelium to form islets, but the term "nesidioblastosis" has recently been used for histopathological abnormalities with hyperinsulinemic and hypoglycemic events [4]. Mcl-1, one of the anti-apoptotic Bcl-2 family members, is dispersed in fetal and adult pancreatic islets [1, 2, 6], and Mcl-1-positive cells have a distribution closely correspondent to that of glucagon-producing cells [2]. We have recently shown that Mcl-1 transgenic mice develop islet cell hyperplasia or insulinoma [3], indicating that constitutional persistent expression of Mcl-1 causes abnormal proliferation or new development of insulin-inducing cells in various islet cell disorders. This suggests that Mcl-1 is involved in pathogenesis of nesidioblastosis.

M. Sano (✉) · E. Hayashi · N. Nemoto
Department of Pathology,
Nihon University School of Medicine,
30-1 Oyaguchi-Kamimachi,
Itabashi-ku, Tokyo 173-8610, Japan
e-mail: msano@med.nihon-u.ac.jp

H. Murakami · H. Kishimoto
Pathology Laboratory,
Saitama Children's Medical Center, 2100 Magome,
339-8551 Iwatsuki, Saitama, Japan

R. Fukuzawa
Cancer Genetics Laboratory,
Department of Biochemistry,
University of Otago, P.O. Box 56,
Dunedin 9054, New Zealand

We have observed a neonate patient with intractable hyperinsulinemic and hypoglycemia whose histopathological findings showed typical features of diffuse nesidioblastosis. To clarify the anti-apoptotic role of Mcl-1 in nesidioblastosis, we carried out an immunohistochemical investigation using antibodies against Mcl-1 [5, 6] (1:50, rabbit polyclonal), insulin (1:400; rabbit polyclonal; DAKO Cytomation, Kyoto, Japan), glucagon (1:50; guinea pig polyclonal; DAKO Cytomation), and Ki-67 (1:50; mouse monoclonal, MIB-1; DAKO Cytomation). Staining was developed with a 3, 3′-diaminobenzidine (DAB) or True Blue (KPL, Gaithersburg, MD). Slides were counterstained with hematoxylin or nuclear fast red.

As opposed to reported in the normal fetal and adult pancreas, the distribution of Mcl-1-positive cells almost matched that of insulin-positive cells (Fig. 1a, Mcl-1; b, insulin) and rarely overlapped with that of glucagon-positive cells in nesidioblastosis (Fig. 1c). Mcl-1 was also expressed at low levels in the pancreatic ducts and intercalated ducts, which highlighted ductulo-insular proliferative lesions (Fig. 1d). We next addressed the question of whether or not these Mcl-1-positive cells possess proliferative properties. We performed double immunostaining for Mcl-1 and Ki-67. Most of the proliferating Mcl-1-positive cells in the pancreatic islets were devoid of Ki-67 labeling (Fig. 1e). Lack of Ki-67 staining was also observed in the Mcl-1-positive cells in the ductulo-insular proliferation (Fig. 1f). Thus, our results suggested that Mcl-1 expression contributes to development of new insulin-producing cells rather than cell proliferation.

We have shown overexpression of Mcl-1 in the ectopic and proliferative insulin-producing cells of human nesidioblastosis, which is consistent with the Mcl-1 transgenic mice model [3]. As endocrine cells derived from progenitor

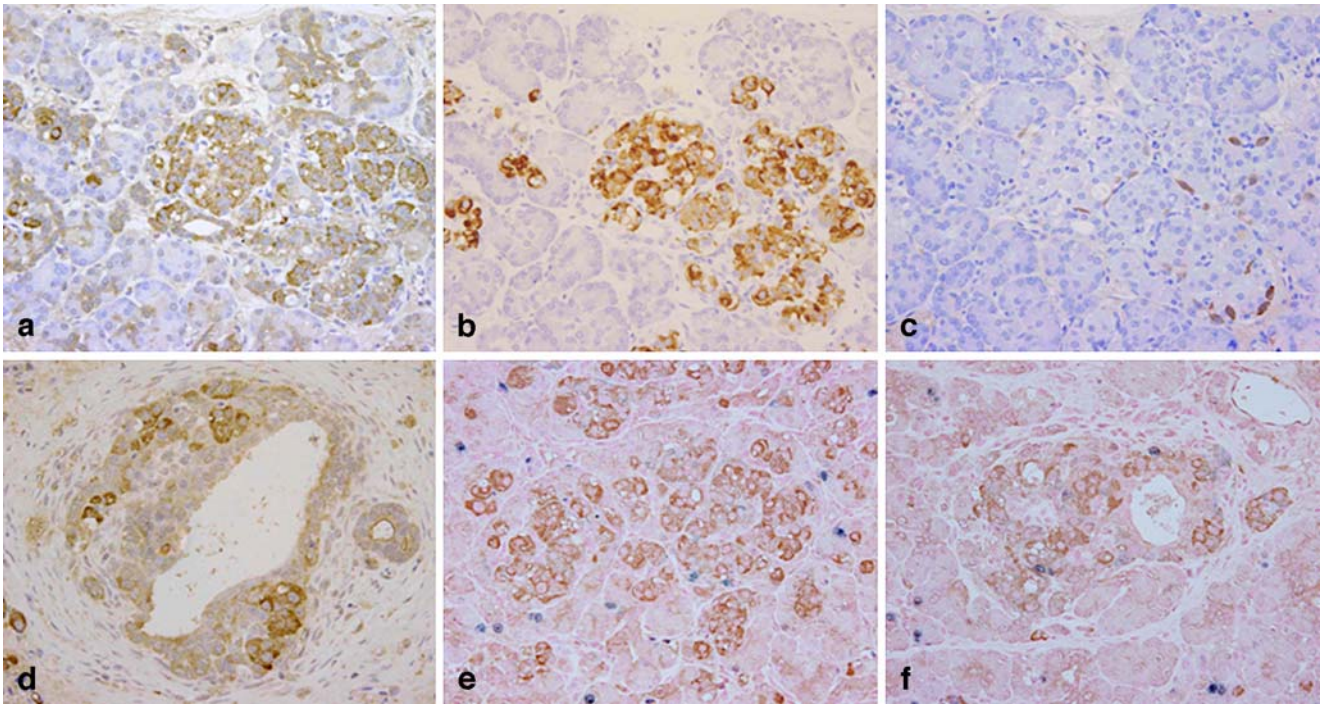


Fig. 1 Distribution of Mcl-1 expression in a neonatal nesidioblastosis. Mcl-1-positive cells essentially overlaps with insulin-positive cells, while weak expression of Mcl-1 is observed in the pancreatic and intercalated ducts (**a** Mcl-1, **b** insulin, **c** glucagon). In addition, prominent expression of Mcl-1 is also found in the ductulo-insular proliferative lesions (**d**). Ki-67-labeled cells (True Blue) are scattered among the proliferating Mcl-1-positive cells both in an islet (**e**, DAB) and a ductulo-insular complex (**f**)

cells in the ductal epithelium bud off newly formed islet, persistent overexpression of Mcl-1 in the putative progenitor cells committed to the insulin-producing cell lineage may enhance cell survival, thereby leading to abnormal development of insulin-producing cells in nesidioblastosis.

Acknowledgment This work was supported by Grant-in-Aid for Scientific Research of Japan Society for the Promotion of Science to M.S.

Conflict of interest statement The authors declare that we have no conflict of interest.

References

1. Kobayash H, Doi R, Hosotani R, Miyamoto Y, Koshiba T, Fujimoto K, Ida J, Tsuji S, Nakajima S, Kawaguchi M, Shiota K, Imamura M (2000) Immunohistochemical analysis of apoptosis-related proteins in human embryonic and fetal pancreatic tissues. Int J Pancreatol 27:113–122
2. Krajewski S, Bodrug S, Krajewska M, Shabaik A, Gascoyne R, Berean K, Reed JC (1995) Immunohistochemical analysis of Mcl-1 protein in human tissues. Differential regulation of Mcl-1 and Bcl-2 protein production suggests a unique role for Mcl-1 in control of programmed cell death in vivo. Am J Pathol 146:1309–1319
3. Matsushita K, Okita H, Suzuki A, Shimoda K, Fukuma M, Yamada T, Urano F, Honda T, Sano M, Iwanaga S, Ogawa S, Hata J, Umezawa A (2003) Islet cell hyperplasia in transgenic mice overexpressing EAT/mcl-1, a bcl-2 related gene. Mol Cell Endocrinol 203:105–116
4. Reinecke-Luthge A, Koschoreck F, Kloppel G (2000) The molecular basis of persistent hyperinsulinemic hypoglycemia of infancy and its pathologic substrates. Virchows Arch 436:1–5
5. Sano M, Nakanishi Y, Yagasaki H, Honma T, Oinuma T, Obana Y, Suzuki A, Nemoto N (2005) Overexpression of anti-apoptotic Mcl-1 in testicular germ cell tumours. Histopathology 46:532–539
6. Sano M, Umezawa A, Suzuki A, Shimoda K, Fukuma M, Hata J (2000) Involvement of EAT/mcl-1, an anti-apoptotic bcl-2-related gene, in murine embryogenesis and human development. Exp Cell Res 259:127–139

Virchows Arch (2008) 452:471
DOI 10.1007/s00428-008-0600-2

ERRATUM

Thyroid follicular carcinoma-like renal tumor: a case report with morphologic, immunophenotypic, cytogenetic and scintigraphic studies

William Sterlacci · Irmgard Verdorfer · Michael Gabriel · Gregor Mikuz

Published online: 12 March 2008
© Springer-Verlag 2008

Erratum to: Virchows Arch
DOI 10.1007/s00428-007-0486-4

Unfortunately, the author names were published incorrectly.

The online version of the original article can be found at http://dx.doi.org/10.1007/s00428-007-0486-4.

W. Sterlacci (✉) · I. Verdorfer · G. Mikuz
Department of Pathology, Medical University of Innsbruck,
Muellerstr. 44,
6020 Innsbruck, Austria
e-mail: william.sterlacci@i-med.ac.at

M. Gabriel
Department of Nuclear Medicine,
Medical University of Innsbruck,
Anichstr. 35,
Innsbruck, Austria

Virchows Arch (2008) 452:473–479
DOI 10.1007/s00428-008-0607-8

ORIGINAL ARTICLE

The significance of lobular neoplasia on needle core biopsy of the breast

S. Menon · G. J. R. Porter · A. J. Evans · I. O. Ellis · C. W. Elston · Z. Hodi · A. H. S. Lee

Received: 25 January 2008 / Revised: 28 February 2008 / Accepted: 9 March 2008 / Published online: 4 April 2008
© Springer-Verlag 2008

Abstract The management of a core biopsy diagnosis of lobular neoplasia is controversial. Detailed radiological–pathological review of 47 patients with cores showing classical lobular neoplasia was performed (patients with pleomorphic lobular carcinoma in situ (LCIS) or associated risk lesions were considered separately). Immediate surgical excision in 25 patients showed invasive carcinoma in 7, ductal carcinoma in situ (DCIS) in 1 and pleomorphic LCIS in 1; radiological–pathological review showed that the core biopsy missed a mass in 5, missed calcification in 2 and that calcification appeared adequately sampled in 2. Nineteen patients had follow-up of at least 2 years. Four patients developed malignancy at the site of the core biopsy (invasive carcinoma in three, DCIS in one); one carcinoma was mammographically occult, one patient had dense original mammograms and two had calcifications apparently adequately sampled by the core. In conclusion, most carcinomas identified at the site of core biopsy showing lobular neoplasia were the result of the core missing the radiological lesion, emphasising the importance of multidisciplinary review and investigation of any discordance. Some carcinomas were found after apparently adequate core biopsy, raising the question of whether excision biopsy should be considered after all core biopsy diagnoses of lobular neoplasia.

G. J. R. Porter · A. J. Evans
Department of Radiology, Nottingham University Hospital,
City Hospital Campus,
Nottingham, UK

S. Menon · I. O. Ellis · C. W. Elston · Z. Hodi · A. H. S. Lee (✉)
Department of Histopathology, Nottingham University Hospital,
City Hospital Campus, Hucknall Road,
Nottingham NG5 1PB, UK
e-mail: andrew.lee@nuh.nhs.uk

Keywords Lobular neoplasia · Atypical lobular neoplasia · Lobular carcinoma in situ · Pleomorphic lobular carcinoma in situ · Needle biopsy · Breast

Introduction

Lobular carcinoma in situ (LCIS) was described by Foot and Stewart [25]. The term atypical lobular hyperplasia (ALH) was later introduced to describe a similar lesion, but with less marked changes. We prefer the term lobular neoplasia [30], which includes both LCIS and ALH, particularly for core biopsies in which there is limited tissue, making distinction between ALH and LCIS difficult.

The relationship between lobular neoplasia and invasive carcinoma of the breast is controversial [28]. Lobular neoplasia is often multifocal and bilateral [4]. There is evidence that it is a risk factor for invasive carcinoma in both breasts: after a diagnosis of lobular neoplasia, there is an increased risk of subsequent invasive carcinoma in both breasts [30], and the majority are ductal in type. Recent evidence suggests that lobular neoplasia may, like ductal carcinoma in situ (DCIS), be a non-obligate precursor for invasive carcinoma at the same site. There is a higher risk of invasive carcinoma in the ipsilateral than in the contralateral breast. The proportion of subsequent carcinomas that are of lobular type is higher than in unselected series of carcinomas [45]. The morphology of the cells in lobular neoplasia and invasive lobular carcinoma is similar. The same truncating mutation in the E-cadherin gene has been found in invasive lobular carcinoma and adjacent LCIS [57].

The significance of lobular neoplasia in breast needle core biopsies is uncertain. Invasive carcinomas are sometimes identified after a core biopsy diagnosis of lobular

neoplasia. Some studies suggest this occurs because the core biopsy missed the lesion and so does not explain the clinical or radiological abnormality [41]. Other studies suggest that carcinomas may be identified after the diagnosis of lobular neoplasia on core biopsy even if the core biopsy explains the clinical or radiological abnormality [20]. An important consideration in radiological–pathological correlation is whether classical lobular neoplasia is associated with calcification. The traditional view is that lobular neoplasia does not have a radiological correlate [4], but recent reports have described an association between classical lobular neoplasia and calcification. We also wished to investigate our impression that, in core biopsies containing classical lobular neoplasia, calcification is often associated with columnar cell change.

Pleomorphic LCIS is a recently described variant of lobular neoplasia. The growth pattern and absence of E-cadherin expression resemble classical LCIS. However, the marked nuclear pleomorphism, frequent presence of central necrosis and calcification and expression of c-erbB-2 are similar to high-grade DCIS [50]. In the past, pleomorphic LCIS would usually have been diagnosed as high-grade DCIS.

The main aim of this study was to assess the risk of invasive carcinoma and DCIS at the site of classical lobular neoplasia diagnosed on breast needle core biopsies. In view of the clear morphological differences, pleomorphic LCIS was considered separately. A second aim was to investigate the localisation of calcification in core biopsies containing lobular neoplasia.

Materials and methods

This project was discussed with the chair of the Nottingham University Hospitals Research Ethics Committee who considered that it was a service evaluation and, therefore, did not require formal ethical approval. A multidisciplinary review of the pathology and radiology of patients with a core biopsy diagnosis of lobular neoplasia from July 1998 to June 2006 was performed. The biopsies from July 1998 to June 2000 were included in a previous study [35]. The diagnosis of lobular neoplasia was made on haematoxylin and eosin sections. Immunohistochemistry for E-cadherin was performed for lesions with a differential diagnosis including DCIS or pleomorphic LCIS. Lobular neoplasia was subdivided into ALH and LCIS using the criteria described by Page et al. [44]. Pleomorphic LCIS was defined as a high-grade dyscohesive intra-acinar proliferation that was E-cadherin negative.

Patients were excluded if they had synchronous or previous invasive carcinoma or DCIS in the same breast. Two patients with contralateral invasive carcinoma were included. Core biopsies containing invasive carcinoma, DCIS or an area suspicious of either diagnosis were excluded. Cores containing pleomorphic LCIS, an atypical intraductal epithelial proliferation (including atypical ductal hyperplasia), radial scar or a papillary lesion were considered separately. Thus, the main group of core biopsies studied contained classical lobular neoplasia with no other risk lesions: we termed this group "simple" classical lobular neoplasia.

The core biopsies were reviewed for the following features: location of any calcification and presence of columnar cell change. Six cores were not available, so could not be reviewed. The frequency of columnar cell change was compared with 87 consecutive core biopsies reported by one observer (AHSL) as normal or benign.

Results

Simple classical lobular neoplasia on core biopsy

Forty-nine core biopsies with lobular neoplasia from 47 women satisfied the entry criteria (0.3% of the 14,597 diagnostic core biopsies performed during this period). Two patients had two core biopsies from the same area of the breast containing lobular neoplasia: both are only counted once in the following results. The median age was 52 years (range 33 to 81).

Twenty-six patients presented with mammographic screening abnormalities: 20 with calcification, 3 with a mass, 2 with calcification and distortion and 1 with a mass and calcification. Nineteen patients presented symptomatically: ten with a mass, seven with a thickening and two with a thickening and calcification. Two women had calcification identified by mammography performed in one patient as part of the investigation of a contralateral carcinoma and, in the other, as follow-up of a contralateral carcinoma. Eight core biopsies were freehand, 14 were ultrasound guided and 25 were performed under stereotactic guidance.

There was an association between lobular neoplasia and columnar cell change (see Table 1). Calcification was seen in 25 of 41 cores with slides available for review. It was seen in lobular neoplasia in six biopsies (15%); in one the

Table 1 Extent of columnar cell change in cores with lobular neoplasia and controls

Columnar cell change	Core biopsy with lobular neoplasia	Controls (normal or benign core biopsy)
None	12 (29%)	58 (67%)
One lobule or duct	9 (22%)	14 (16%)
At least two lobules or ducts	20 (49%)	15 (17%)

$\chi^2 = 18$, $P = 0.0001$

calcification was only seen in the lobular neoplasia, but in the other five, it was also present in other changes (columnar cell change in three, sclerosing adenosis in one, fibroadenoma in one). Of the other 19 biopsies with calcification, columnar cell change was the most commonly associated pathology (10 biopsies).

Surgical excision within 2 months of core biopsy was performed in 25 patients. Excision showed malignancy in nine patients (see Table 2). In seven patients, pathology–radiology correlation showed that the core biopsy did not explain the radiological abnormality (a mass in five and calcification in two). Five of these seven patients were seen in the first 2 years of this study. Excision showed benign changes in 16, although one woman had invasive carcinoma of mixed ductal and lobular type diagnosed 33 months after the core biopsy in a separate quadrant of the same breast.

Nineteen patients who had not had a diagnostic surgical excision had follow-up of at least 2 years (range 25 to 105 months). None of these patients received radiotherapy to the breast. Malignancy was identified in seven women. In four, the malignancy was at the same site as the core biopsy (see Table 2), in one DCIS was found in a different quadrant of the same breast and two developed contralateral invasive carcinoma. Three women had no surgical excision and follow-up of less than 2 years. Neither of the two women with a previous history of contralateral invasive carcinoma developed carcinoma at the site of the core biopsy showing lobular neoplasia.

No significant relationships were found between the diagnosis of malignancy (DCIS, pleomorphic LCIS or invasive carcinoma) at the site of the core biopsy and the following features: age of the woman, diagnosis of ALH or LCIS on the core biopsy, whether core biopsy or vacuum-assisted biopsy was performed and the method of guidance (freehand, ultrasound or stereotactic).

Pleomorphic LCIS on core biopsy

Both patients with pleomorphic LCIS on core biopsy presented with calcification detected by mammographic screening. In both, calcification was seen histologically in association with the pleomorphic LCIS. Both had a diagnostic surgical excision, which showed cribriform DCIS in one and further LCIS in the other.

Atypical intraductal epithelial proliferation/radial scar/papillary lesion

Eight patients had atypical intraductal epithelial proliferation, radial scar or a papillary lesion in addition to lobular neoplasia

Table 2 Details of patients with invasive carcinoma, DCIS or pleomorphic LCIS at the site of the core biopsy showing simple lobular neoplasia

Age	Presentation	Core pathology	Time to excision/ months	Final diagnosis (surgical procedure)	Pathology–radiology correlation
60	Screen-detected mass	ALH, CCCh, calcs	1	13 mm IDC, G3, LN 0/4 (Mx)	Core missed mass
75	Symptomatic mass	LCIS, UEH, CCCh	2	6 mm IDC, G2, LN not examined (Mx)	Core missed mass
63	Screen-detected distortion and calcification. Mass on US	ALH	1	14 mm ILC, G2, LN 0/5 (WLE)	Core missed mass
54	Screen-detected calcification	ALH	1	4 mm tubulolobular carcinoma G1 + 50 mm DCIS, LN 0/6 (Mx)	Core missed calcs
43	Symptomatic mass	LCIS	1	9 mm IDLC, G2, LN 0/7 (Mx)	Core missed mass
68	Screen-detected mass	ALH	1	12 mm ILC, G2, LN 0/6 (Mx)	Core missed mass
64	Symptomatic mass, no mass on US. Mammographic calcification	ALH, cyst, calcs	1	7 mm DCIS (WLE)	Calcs sampled by core
54	Screen-detected calcification	ALH	1	12 mm tubular carcinoma + 35 mm DCIS, LN 0/4 (WLE)	Core missed calcs
45	Symptomatic cysts. Mammographic calcification	LCIS, calcs	1	5 mm pleomorphic LCIS (WLE)	Calcs sampled by core
52	Screen-detected calcification	ALH, UEH, CCCh, calcs	31	9 mm ILC, G2, LN 1/6 (Mx)	Mammographically occult mass
70	Screen-detected calcification	ALH, calcs	29	36 mm IDC, G3, LN 6/16 (Mx)	Dense original mammogram
51	Screen-detected calcification	ALH, CCCh, calcs	26	30 mm DCIS + extensive LCIS (Mx)	Calcs sampled by core
55	Screen-detected calcification	ALH, CCCh, calcs	29	IDC 8 mm, G3, 45 mm DCIS, LN 1/4 (Mx)	Calcs sampled by core

US ultrasound, *ALH* atypical lobular hyperplasia, *LCIS* lobular carcinoma in situ, *UEH* epithelial hyperplasia of usual type, *CCCh* columnar cell change, *calcs* calcification, *IDC* invasive ductal carcinoma, *ILC* invasive lobular carcinoma, *IDLC* invasive ductal and lobular carcinoma, *DCIS* ductal carcinoma in situ, *G* histological grade, *LN* axillary lymph nodes, *Mx* mastectomy, *WLE* wide local excision

on the core biopsy. All eight presented with abnormalities detected by mammographic screening: calcification in five, calcification and distortion in one, mass in one and distortion in one. Seven patients had a diagnostic surgical excision, and one patient had her lesion removed with vacuum-assisted mammotomy. DCIS was found in one of three women with core diagnosis of atypical intraductal epithelial atypia and in one of two with core diagnosis of radial scar. Papillary DCIS with a 3-mm focus of invasion was found after a core diagnosis of papillary lesion with atypical intraductal epithelial proliferation. One patient with a core diagnosis of radial scar with atypical intraductal epithelial proliferation and one with a papillary lesion had benign findings at excision.

Discussion

Relation between lobular neoplasia and calcification

An important question in the management of lobular neoplasia on core biopsy is the relationship between lobular neoplasia and calcification. Lobular neoplasia is not typically associated with any specific clinical abnormality, and there are no characteristic macroscopic features. Early papers suggested that classical lobular neoplasia does not have any diagnostic mammographic features [4]. In the past, surgical biopsies containing lobular neoplasia were frequently performed for mammographic calcification, but pathologically, the calcification was mostly associated with fibrocystic change and identified within the lobular neoplasia in about 20% [4, 11, 24, 55]. Calcification is associated with the lobular neoplasia in between 8% and 53% of core biopsies containing classical lobular neoplasia in different studies [1, 3, 14, 20, 41]. Benign calcification is frequently seen close to invasive carcinomas in surgical specimens [52]. It is well recognised that malignancy may be an incidental discovery on a biopsy for calcification that is associated only with benign disease [49].

The present study confirms the association between lobular neoplasia and columnar cell change [8, 41]. In older studies, the majority of surgical biopsies containing lobular neoplasia were performed for fibrocystic change [30]. In the present study, calcification was associated with lobular neoplasia in 15% of core biopsies, but commonly was also seen in fibrocystic change as well. Calcification was associated with columnar cell change in 32% of cores with lobular neoplasia. The association of calcification with columnar cell change is well recognised [27]. Our results support the view that, in biopsies containing lobular neoplasia, most of the calcification is associated with fibrocystic change, particularly columnar cell change. Importantly, the lobular neoplasia is incidental to the calcification in the majority of biopsies.

A recent study of collagenous spherulosis found that 15 of 59 patients had associated LCIS [48]. In contrast, only one of the patients in the present study with lobular neoplasia had associated collagenous spherulosis.

Relationship between simple classical lobular neoplasia and carcinoma

In this study, 44 women with simple classical lobular neoplasia on core biopsy had surgical excision or follow-up of at least 2 years. Twenty-five women had immediate surgical excision, which showed invasive carcinoma, DCIS or pleomorphic LCIS in nine (36%). In the majority, the core biopsy was judged to have missed the clinical/radiological lesion. This emphasises the importance of clinico-pathological review and further investigation of any discordance. Most of the missed lesions occurred in the early part of the study, suggesting that the accuracy of radiological localisation of core biopsies may have improved later in the series. A smaller number of carcinomas occurred after lobular neoplasia on core biopsy apparently incidental to the clinical or radiological lesion. This raises the question of whether excision biopsy should be considered after all core biopsy diagnoses of lobular neoplasia. The frequency of malignancy if the patients with radiological–pathological discordance are excluded is 11% (2/18).

Four of 19 patients with at least 2 years follow-up developed carcinoma at the site of the core biopsy. In one, the carcinoma was mammographically occult, although it was clinically palpable, in one the original mammogram was dense and two women had calcification apparently adequately sampled by the core biopsy. Definite comment cannot be made, but the clinical histories suggest that it is possible that the carcinoma may have been identified earlier in some of these patients if they had had an immediate surgical biopsy. If these women are added to those without radiological–pathological discordance in the above paragraph, the frequency of malignancy is 16% (6/37).

Previous published studies of simple lobular neoplasia on core biopsy were reviewed [1–3, 6, 9, 10, 12, 14, 16–18, 20, 21, 23, 25, 26, 31, 33, 36, 37, 39, 41–43, 46, 47, 51, 54, 58, 59]. The data in most studies are not representative. Probably the major bias is that only about half of the lesions had a surgical biopsy and it is not clear how patients were selected for excision biopsy. Furthermore, most studies only report image-guided or stereotactic biopsies. A surgical biopsy was performed in 561 patients with a core biopsy diagnosis of lobular neoplasia with invasive carcinoma found in 50 or 49 and DCIS in 32 or 33 (82 [15%] in total). It is ‘impossible to know if some of the reported cases are those in which the targeted lesion has been missed and re-excision was done for failure to

successfully sample the target' [15]. In reviewing the previous studies, we have assumed that sampling was adequate for core biopsy performed for calcification if calcification was present in the core biopsy. Of those 52 malignancies with details available, 25 (48%) had a radiological–pathological discordance (missed mass in 22 and missed calcification in 3), and 27 had apparently adequately sampled calcification.

One hundred four patients who did not have immediate surgical excision had reported follow-up. The only four patients (4%) with invasive carcinoma or DCIS on follow-up at the site of core biopsy are the four patients described in the present study. The absence of subsequent malignancy in other studies is very surprising given that lobular neoplasia is a well-established risk factor for later carcinoma. Nevertheless, the low rate suggests that the chance of invasive carcinoma or DCIS is lower in those not having immediate surgical excision.

It is difficult to estimate the chance of finding invasive carcinoma or DCIS if all patients had an excision biopsy. The 15% rate found in the subset of patients who had immediate excision biopsy is probably an overestimate. If the cases with radiological–pathological discordance are excluded, the risk is probably about half of this, approximately 8%. If one assumes that half of the patients who did not have an immediate excision did not have invasive carcinoma or DCIS at the core site, this gives an estimate of about 4%. This represents an estimate of the lower limit of risk.

Some studies suggest that the risk of finding invasive carcinoma or DCIS is a little higher if the core biopsy shows LCIS rather than ALH [13]. In view of the subjectivity of this distinction on core biopsy, it is probably of limited use in routine practice.

It is clearly appropriate to investigate patients with simple classical lobular neoplasia on core biopsy that does not explain the clinical or radiological abnormality. If a definitive diagnosis cannot be made with further core biopsy, then an excision biopsy is indicated.

The management of simple classical lobular neoplasia on core biopsy with no radiological–pathological discordance is less straightforward. As discussed above, the literature suggests that the risk of malignancy is in the range of 4% to 8%. This risk is comparable to that associated with radial scar or papillary lesion with no epithelial atypia [7, 34, 35, 40, 53]. Both radial scars and papillary lesions are excised in many centres according to current guidance [19]. The major difference with lobular neoplasia, however, is that both are usually clearly defined lesions on radiological examination and therefore easy to excise.

There is a need for prospective studies with surgical excision of all lesions so that an unbiased assessment of the risk of simple classical lobular neoplasia on core biopsy can be made. Careful radiology–pathology correlation is essential. It may be possible to stratify the risk within this group using clinical, radiological or pathological features.

Lobular neoplasia associated with radial scars, papillary lesions and atypical intraductal epithelial proliferations

Most centres excise radial scars, papillary lesions and atypical intraductal epithelial proliferations diagnosed on core biopsy. In the present study, carcinoma was found on excision of three of the eight lesions with these lesions in combination with lobular neoplasia. This supports the practice of excising such lesions.

Pleomorphic LCIS

In the present study, both cores with pleomorphic LCIS had associated calcification. In contrast to the controversial nature of the association between calcification and classical LCIS, the literature suggests that there is a clear relationship between calcification and pleomorphic LCIS [29, 50]. There are limited data on the significance of pleomorphic LCIS on core biopsy. One of the two patients in the present study had DCIS in the excision specimen. Three of the six patients described in the literature [5, 20, 37] had invasive carcinoma on excision, but radiology showed a density in one and an architectural distortion in another. Although the follow-up data are limited, we believe that, until there is further evidence, it is prudent to recommend that pleomorphic LCIS is managed as DCIS because of the morphological similarity of pleomorphic LCIS to high-grade DCIS. The present study may underestimate the frequency of pleomorphic LCIS, as E-cadherin immunohistochemistry was infrequently performed early in the study period and some cases may have been diagnosed as high-grade DCIS.

Some lobular neoplasia shows features overlapping with DCIS and is difficult to classify even with E-cadherin immunohistochemistry [32, 38]. Lobular neoplasia with comedo necrosis, but without marked nuclear pleomorphism, has recently been described [22]. The clinical significance of these rare clinico-pathological scenarios is uncertain. Until there is more evidence, it would be prudent to recommend surgical biopsy of such lesions because of the overlap of features with DCIS. Mass forming lobular neoplasia can occur rarely [56], but is an example of clinico-pathological discordance, so surgical biopsy is prudent.

In conclusion, we recommend excision after a core biopsy diagnosis of lobular neoplasia in the following circumstances:

1. Discordance of clinical or radiological findings with the pathological changes (this includes mass-forming lobular neoplasia)

2. Lobular neoplasia with atypical histological features including pleomorphic LCIS, lobular neoplasia with necrosis, and when it is not possible to exclude DCIS despite E-cadherin immunohistochemistry
3. If there is an associated risk lesion, such as atypical intraductal epithelial proliferation, radial scar or papillary lesion.

We suggest that further studies are needed to guide the management of simple classical lobular neoplasia, as the data on the risk of associated carcinoma remain unclear in this group of patients.

Conflict of interest statement We declare that we have no conflict of interest.

References

1. Arpino G, Allred DC, Mohsin SK, Weiss HL, Conrow D, Elledge RM (2004) Lobular neoplasia on core-needle biopsy—clinical significance. Cancer 101:242–250
2. Bauer VP, Ditkoff BA, Schnabel F, Brenin D, El-Tamer M, Smith S (2003) The management of lobular neoplasia identified on percutaneous core breast biopsy. Breast J 9:4–9
3. Berg WA, Mrose HE, Ioffe OB (2001) Atypical lobular hyperplasia or lobular carcinoma in situ at core-needle breast biopsy. Radiology 218:503–509
4. Beute BJ, Kalisher L, Hutter RVP (1991) Lobular carcinoma in situ of the breast: clinical, pathologic, and mammographic features. AJR Am J Roentgenol 157:257–265
5. Bibeau F, Chateau MC, Masson B (2003) Prise en charge des lésions mammaires infra-cliniques par macrobiopsies assistées par le vide (procédure Mammotome). Expérience du Centre Val d'Aurelle à propos d'une série de 560 procédures. [Management of non-palpable breast lesions with vacuum-assisted large core needle biopsies (Mammotome). Experience with 560 procedures at the Val d'Aurelle Center]. Ann Pathol 23:582–592
6. Bonnett M, Wallis T, Rossmann M, Pernick NL, Bouwman D, Carolin KA, Visscher D (2003) Histopathologic analysis of atypical lesions in image-guided core breast biopsies. Mod Pathol 16:154–160
7. Brenner RJ, Jackman RJ, Parker SH, Evans WP, Philpotts L, Deutch BM, Lechner MC, Lehrer D, Sylvan P, Hunt R, Adler SJ, Forcier N (2002) Percutaneous core needle biopsy of radial scars of the breast: when is excision necessary. AJR Am J Roentgenol 179:1179–1784
8. Brogi E, Oyama T, Koerner FC (2001) Atypical cystic lobules in patients with lobular neoplasia. Int J Surg Pathol 9:201–206
9. Burak WE, Owens KE, Tighe MB, Kemp L, Dinges SA, Hitchcock CL, Olsen J (2000) Vacuum-assisted stereotactic breast biopsy: histologic underestimation of malignant lesions. Arch Surg 135:700–703
10. Cangiarella J, Waisman J, Symmans WF, Gross J, Cohen JM, Wu H, Axelrod D (2001) Mammotome core biopsy for mammary microcalcification: analysis of 160 biopsies from 142 women with surgical and radiologic followup. Cancer 91:173–177
11. Carson W, Sanchez-Forgach E, Stomper P, Penetrante R, Tsangaris TN, Edge SB (1994) Lobular carcinoma in situ: observation without surgery as an appropriate therapy. Ann Surg Oncol 1:141–146
12. Cassano E, Urban LABD, Pizzamiglio M, Abbate F, Maisonneuve P, Renne G, Viale G, Bellomi M (2007) Ultrasound-guided vacuum-assisted core breast biopsy: experience with 406 cases. Breast Cancer Res Treat 102:103–110
13. Cohen MA (2004) Cancer upgrades at excisional biopsy after diagnosis of atypical lobular hyperplasia or lobular carcinoma in situ at core-needle biopsy: some reasons why. Radiology 231:617–621
14. Crisi GM, Mandavilli S, Cronin E, Ricci A (2003) Invasive mammary carcinoma after immediate and short-term follow-up for lobular neoplasia on core biopsy. Am J Surg Pathol 27:325–333
15. Dershaw DD (2003) Does LCIS or ALH without other high-risk lesions diagnosed on core biopsy require surgical excision. Breast J 9:1–3
16. Diebold T, Hahn T, Solbach C, Rody A, Balzer JO, Hansmann ML, Marx A, Viana F, Peters J, Jacobi V, Kaufmann M, Vogl TJ (2005) Evaluation of the stereotactic 8G vacuum-assisted breast biopsy in the histologic evaluation of suspicious mammography findings (BI-RADS IV). Invest Radiol 40:465–471
17. Dillon MF, McDermott EW, Hill AD, O'Doherty A, O'Higgins N, Quinn CM (2007) Predictive value of breast lesions of "uncertain malignant potential" and "suspicious of malignancy" determined by needle core biopsy. Ann Surg Oncol 14:704–711
18. Dmytrasz K, Tartter PI, Mizrachy H, Chinitz L, Rosenbaum Smith S, Estabrook A (2003) The significance of atypical lobular hyperplasia at percutaneous breast biopsy. Breast J 9:10–12
19. Ellis IO, Humphreys S, Michell M, Pinder SE, Wells CA, Zakhour HD (2004) Best Practice No 179. Guidelines for breast needle core biopsy handling and reporting in breast screening assessment. J Clin Pathol 57:897–902
20. Elsheikh TM, Silverman JF (2005) Follow-up surgical excision is indicated when breast core needle biopsies show atypical lobular hyperplasia or lobular carcinoma in situ: a correlative study of 33 patients with review of the literature. Am J Surg Pathol 29:534–543
21. Esserman LE, Lamea L, Tanev S, Poppiti R (2007) Should the extent of lobular neoplasia on core biopsy influence the decision for excision. Breast J 13:55–61
22. Fadare O, Dadmanesh F, Alvarado-Cabrero I, Snyder R, Mitchell JS, Tot T, Wang SA, Ghofrani M, Eusebi V, Martel M, Tavassoli FA (2006) Lobular intraepithelial neoplasia [lobular carcinoma in situ] with comedo-type necrosis: A clinicopathologic study of 18 cases. Am J Surg Pathol 30:1445–1453
23. Fajardo LL, Pisano ED, Caudry DJ, Gatsonis CA, Berg WA, Connolly J, Schnitt S, Page DL, McNeil BJ (2004) Stereotactic and sonographic large-core biopsy of nonpalpable breast lesions: results of the Radiologic Diagnostic Oncology Group V study. Acad Radiol 11:293–308
24. Fisher ER, Costantino J, Fisher B, Palekar AS, Paik SM, Suarez CM, Wolmark N (1996) Pathologic findings from the National Surgical Adjuvant Breast Project (NSABP) Protocol B-17. Five-year observations concerning lobular carcinoma in situ. Cancer 78:1403–1416
25. Foote FW, Stewart FW (1941) Lobular carcinoma in situ: a rare form of mammary cancer. Am J Pathol 17:491–496
26. Foster MC, Helvie MA, Gregory NE, Rebner M, Nees AV, Paramagul C (2004) Lobular carcinoma in situ or atypical lobular hyperplasia at core-needle biopsy: is excisional biopsy necessary. Radiology 231:813–819
27. Fraser JL, Raza S, Chorny K, Connolly JL, Schnitt SJ (1998) Columnar alteration with prominent apical snouts and secretions: a spectrum of changes frequently present in breast biopsies performed for microcalcifications. Am J Surg Pathol 22:1521–1527
28. Fulford LG, Reis-Filho JS, Lakhani SR (2004) Lobular in situ neoplasia. Curr Diagn Pathol 10:183–192

29. Georgian-Smith D, Lawton TJ (2001) Calcifications of lobular carcinoma in situ of the breast: radiologic–pathologic correlation. AJR Am J Roentgenol 176:1255–1259
30. Haagenson CD, Lane N, Lattes R, Bodian C (1978) Lobular neoplasia (so-called lobular carcinoma in situ) of the breast. Cancer 42:737–769
31. Irfan K, Brem RF (2002) Surgical and mammographic follow-up of papillary lesions and atypical lobular hyperplasia diagnosed with stereotactic vacuum-assisted biopsy. Breast J 8:230–233
32. Jacobs TW, Pliss N, Kouria G, Schnitt SJ (2001) Carcinoma in situ of the breast with indeterminate features: role of E-cadherin staining in categorisation. Am J Surg Pathol 25:229–236
33. Karabakhtsian RG, Johnson R, Sumkin J, Dabbs DJ (2007) The clinical significance of lobular neoplasia on breast core biopsy. Am J Surg Pathol 31:717–723
34. Kirwan SE, Denton ERE, Nash RM, Humphreys S, Michell MJ (2000) Multiple 14G stereotactic core biopsies in the diagnosis of mammographically detected stellate lesions of the breast. Clin Radiol 55:763–766
35. Lee AHS, Denley HE, Pinder SE, Ellis IO, Elston CW, Vujovic P, Macmillan RD, Evans AJ (2003) Excision biopsy findings of patients with breast needle core biopsies reported as suspicious of malignancy (B4) or lesion of uncertain malignant potential (B3). Histopathology 42:331–336
36. Liberman L, Sama M, Susnik B, Rosen PP, La Trenta LR, Morris EA, Abramson AF, Dershaw DD (1999) Lobular carcinoma in situ at percutaneous breast biopsy: surgical biopsy findings. Am J Roentgenol 173:291–299
37. Mahoney MC, Robinson-Smith TM, Shaughnessy EA (2006) Lobular neoplasia at 11-gauge vacuum-assisted stereotactic biopsy: correlation with surgical excisional biopsy and mammographic follow-up. AJR Am J Roentgenol 187:949–954
38. Maluf HM, Swanson PE, Koerner FC (2001) Solid low-grade in situ carcinoma of the breast: role of associated lesions and E-cadherin in differential diagnosis. Am J Surg Pathol 25:237–244
39. Margenthaler JA, Duke D, Monsees BS, Barton PT, Clark C, Dietz JR (2006) Correlation between core biopsy and excisional biopsy in breast high-risk lesions. Am J Surg 192:534–537
40. Mercado CL, Hamele-Bena D, Oken SM, Singer CI, Cangiarella J (2006) Papillary lesions of the breast at percutaneous core-needle biopsy. Radiology 238:801–808
41. Middleton LP, Grant S, Stephens T, Stelling CB, Sneige N, Sahin AA (2003) Lobular carcinoma in situ diagnosed by core needle biopsy: when should it be excised. Mod Pathol 16:120–129
42. O'Driscoll D, Britton P, Bobrow L, Wishart GC, Sinnatamby R, Warren R (2001) Lobular carcinoma in situ on core biopsy—what is the clinical significance. Clin Radiol 56:216–220
43. Orel SG, Rosen M, Mies C, Schnall MD (2006) MR imaging-guided 9-gauge vacuum-assisted core-needle breast biopsy: initial experience. Radiology 238:54–61
44. Page DL, Kidd TE, Dupont WD, Simpson JF, Rogers LW (1991) Lobular neoplasia of the breast: higher risk for subsequent invasive cancer predicted by more extensive disease. Hum Pathol 22:1232–1239
45. Page DL, Schuyler PA, Dupont WD, Jensen RA, Plummer WD, Simpson JF (2003) Atypical lobular hyperplasia as a unilateral predictor of breast cancer risk: a retrospective cohort study. [erratum in Lancet. 2003;361:1994]. Lancet 361:125–129
46. Philpotts LE, Shaheen NA, Jain KS, Carter D, Lee CH (2000) Uncommon high-risk lesions of the breast diagnosed at stereotactic core-needle biopsy: clinical importance. Radiology 216:831–837
47. Renshaw AA, Cartagena N, Derhagopian RP, Gould EW (2002) Lobular neoplasia in breast core needle biopsy specimens is not associated with an increased risk of ductal carcinoma in situ or invasive carcinoma. Am J Clin Pathol 117:797–799
48. Resetkova E, Albarracin C, Sneige N (2006) Collagenous spherulosis of breast: morphologic study of 59 cases and review of the literature. Am J Surg Pathol 30:20–27
49. Rosenfeld I, Tartter PI, Gajdos C, Hermann G, Bleiweiss I (2001) The significance of malignancies incidental to microcalcifications in breast spot localization biopsy specimens. Am J Surg 182:1–5
50. Sapino A, Frigerio A, Peterse JL, Arisio R, Coluccia C, Bussolati G (2000) Mammographically detected in situ lobular carcinomas of the breast. Virchows Arch 436:421–430
51. Sauer G, Deissler H, Strunz K, Helms G, Remmel E, Koretz K, Terinde R, Kreienberg R (2005) Ultrasound-guided large-core needle biopsies of breast lesions: analysis of 962 cases to determine the number of samples for reliable tumour classification. Br J Cancer 92:231–235
52. Selim A, Tahan SR (1998) Microscopic localization of calcifications in and around breast carcinoma: a cautionary note for needle core biopsies. Ann Surg 228:95–98
53. Shah VI, Flowers CI, Douglas-Jones AG, Dallimore NS, Rashid M (2006) Immunohistochemistry increases the accuracy of diagnosis of benign papillary lesions in breast needle core biopsy specimens. Histopathology 48:683–691
54. Shin SJ, Rosen PP (2002) Excisional biopsy should be performed if lobular carcinoma in situ is seen on needle core biopsy. Arch Pathol Lab Med 126:697–701
55. Sonnenfeld MR, Frenna TH, Weidner N, Meyer JE (1991) Lobular carcinoma in situ: mammographic–pathologic correlation of results of needle-directed biopsy. Radiology 181:363–367
56. Stein LF, Zisman G, Rapelyea JA, Schwartz AM, Abell B, Brem RF (2005) Lobular carcinoma in situ of the breast presenting as a mass. AJR Am J Roentgenol 184:1799–1801
57. Vos CBJ, Cleton-Jansen AM, Berx G, de Leeuw WJF, ter Haar NT, van Roy F, Cornelisse CJ, Peterse JL, van de Vijver MJ (1997) E-cadherin inactivation in lobular carcinoma in situ of the breast: an early event in tumorigenesis. Br J Cancer 76:1131–1133
58. Yeh IT, Dimitrov D, Otto P, Miller AR, Kahlenberg MS, Cruz A (2003) Pathologic review of atypical hyperplasia identified by image-guided breast needle core biopsy. Correlation with excision specimen. Arch Pathol Lab Med 127:49–54
59. Zuiani C, Londero V, Bestagno A, Puglisi F, Di Loreto C, Bazzocchi M (2005) Proliferative high-risk lesions of the breast: contribution and limits of US-guided core biopsy. Radiol Med 110:589–602

Virchows Arch (2008) 452:481–490
DOI 10.1007/s00428-007-0562-9

ORIGINAL ARTICLE

Glioblastomas: correlation between oligodendroglial components, genetic abnormalities, and prognosis

Luciana Wernersbach Pinto · Maria Betania Mahler Araújo · Andre L. Vettore · Liana Wernersbach · André Campana C. Leite · Leila Maria C. Chimelli · Fernando Augusto Soares

Received: 5 October 2007 / Revised: 7 December 2007 / Accepted: 13 December 2007 / Published online: 20 March 2008
© Springer-Verlag 2007

Abstract It has been demonstrated that a small percentage (approximately 15%) of glioblastomas (GBM) presents an oligodendroglial component with a variable frequency of chromosome 1p and 19q deletions, the genetic alteration related to chemotherapy response and longer survival in oligodendrogliomas. There is a growing interest in investigating 1p and 19q losses in hybrid gliomas and their impact on prognosis. A series of 88 GBMs was investigated regarding 1p and/or 19q losses, 24 with oligodendroglioma-like areas, using quantitative microsatellite analysis and/or fluorescent in situ hybridization. When present, the oligodendroglial and astrocytic components were independently investigated. Clinical data, histology, and 1p/19q status were correlated. Tumors with oligodendroglial components showed three cases each of 1p or 19q loss and one with combined 1p/19q loss. No difference in 1p or 19q status was observed between the oligodendroglial and astrocytic components. Conventional GBM demonstrated isolated 1p loss in four cases and 19q loss in five. No association was seen between 1p/19q status and histology. Deletions at 1p and/or 19q were infrequent in GBMs with oligodendroglial components. Despite the hybrid phenotype, the pattern of genetic changes at 1p and 19q was not different from that usually observed in conventional GBMs, nor did it show any correlation with survival.

Keywords Glioblastoma · Oligodendroglial component · 1p loss · 19q loss · Prognostic factors

L. W. Pinto · M. B. Mahler Araújo · F. A. Soares
Department of Anatomic Pathology, Hospital A C Camargo, São Paulo, SP, Brazil

A. L. Vettore
Ludwig Institute for Cancer Research, São Paulo, SP, Brazil

L. Wernersbach
Instituto Fernandes Figueira, Fundação Oswaldo Cruz, Rio de Janeiro, RJ, Brazil

A. C. C. Leite
Department of Radiotherapy, Hospital A C Camargo, São Paulo, SP, Brazil

L. M. C. Chimelli
Department of Pathology, School of Medicine, Universidade Federal do Rio de Janeiro, Rio de Janeiro, RJ, Brazil

L. W. Pinto (✉)
Laboratorio de Patologia, Instituto de Pesquisa Clínica Evandro Chagas, Fundação Oswaldo Cruz, Av. Brasil 4365, Manguinhos, 21040-900 Rio de Janeiro, RJ, Brasil
e-mail: luciana.wernersbach@ipec.fiocruz.br

Introduction

Glioblastoma (GBM) is the most aggressive yet most common primary brain tumor in adults, accounting for approximately 12–15% of all intracranial neoplasms. Despite widely available multimodal treatment that includes surgery, radiotherapy, and chemotherapy, the prognosis of GBM patients remains very poor, the mean survival rate being less than 1 year. Nevertheless, a few patients can survive longer, especially the under 50-year-olds [18].

GBMs are cellular, highly anaplastic, and morphologically highly heterogeneous tumors. They may be composed of many types of cells, including small anaplastic cells, spindle cells, fibrilar and gemistocytic astrocyte-like cells, and giant pleomorphic cells. Areas of metaplasia are sometimes seen. The presence of microvascular proliferation and/or necrosis is an essential criterion for diagnosis.

Two distinct morphological variants are recognized by the World Health Organization (WHO) classification: the giant cell GBM and the gliosarcoma, but additional patterns have also been identified. GBM with oligodendroglial components is one of these patterns [12, 15, 20]. It has been suggested that this term be used to designate tumors composed of a minor population of cells with oligodendroglial features and a major astrocytic component. The capacity to recognize an oligodendroglial component in a predominantly astrocytic tumor and to make a differential diagnosis with conventional GBMs and oligoastrocytomas is often difficult even for experienced neuropathologists [6, 20]. The prognostic significance of the presence of this component has been debated, and some studies have observed a better prognosis for tumors with an oligodendroglial component [7, 15].

Molecular genetic studies of GBMs with an oligodendroglial component have shown heterogeneous genetic alterations, with a variable frequency of losses on chromosomes 1p and 19q, the genetic hallmark of oligodendrogliomas [21]. The presence of 1p/19q loss has been associated with response to chemotherapy and prolonged survival in oligodendrogliomas [3, 4]. It has recently been suggested that oligodendrogliomas with 1p/19q loss are also more radiation sensitive [1]. This observation has led to an interest in investigating the presence of 1p/19q loss and its prognostic significance in astrocytic and mixed oligoastrocytic gliomas as well.

Conventional GBMs have shown chromosome 1p allelic loss in about 10% of all cases, while chromosome 19q loss occurs in 13–32% [10]. It has been speculated that GBMs with an oligodendroglial component may present 1p/19q loss more frequently than in conventional GBMs [6]. However, this issue remains controversial, and other studies have not been able to confirm this hypothesis [8]. Some studies have revealed that although 1p/19q loss is not common in GBMs, longer survival was associated with this genetic alteration. On the other hand, the presence or not of an oligodendroglial component was not associated with the chromosome loss [8, 22].

Another issue that remains poorly explored is whether the astrocytic and oligodendroglial areas of GBMs with an oligodendroglial component present identical genetic abnormalities, an important subject to consider when analyzing these tumors via molecular techniques in limited samples. A previous study by Walker et al. [24] on gliomas with histological intratumoral heterogeneity using tissue microdissection to verify if genetic losses on 1p36, 19q13, and 17p13 were present throughout the tumor or only in regions with an astrocytic or oligodendroglial phenotype found that, when present, losses were observed in all regions of the tumor. Moreover, the tumor suppressor genes mapped on chromosomes 1p and 19q certain to be involved in glioma development have not yet been identified. Many candidates have been proposed, and some submitted to mutational analysis, but no consistent results have been obtained to date. A recent approach, attempting to answer this question by evaluating the gene expression profiles of gliomas with and without 1p/19 losses using complementary deoxyribonucleic acid (DNA) microarrays, identified eight candidate genes with a significant lower expression in gliomas with 1p/19 loss [23].

The aim of the present study was to verify the status of chromosomes 1p and 19q in conventional GBMs and in GBMs with oligodendroglial features, analyzing both the astrocytic and oligodendroglial components in the second group. Genetic data were correlated with histological and clinical features, and survival analysis was also performed.

Materials and methods

Patients and histopathology review

Patients with a diagnosis of GBM who were seen at the Hospital do Câncer A. C. Camargo between 1982 and 2003 and had available tumor paraffin-embedded samples were included in the study. Tumor samples from another seven patients seen at the Universidade Federal do Rio de Janeiro and identified in a previous study were also included. All patients were submitted to tumor resection. Overall survival was calculated from the date of diagnostic surgery until death or the last known follow-up. This study was conducted with the approval of the Hospital's Ethics Committee (Protocol no. 626/04).

Pathological review was conducted by two pathologists (LWP and MBMA). The tumors that histologically demonstrated a major astrocytic component with obvious features of malignancy, along with a minor subpopulation of tumor cells with conspicuous oligodendroglial features, were considered GBM with an oligodendroglial component. The oligodendroglial features were represented by tumor cells with clear perinuclear halo and round, central nuclei, sometimes giving rise to a honeycomb aspect; a delicate vascular pattern ("chicken wire" pattern), and occasional microcalcifications. The criterion used to separate these tumors from anaplastic oligoastrocytomas was the presence of nuclear atypia, mitotic activity, microvascular proliferation, and necrosis in the predominant astrocytic component [6]. The sections were also accessed to determine if a viable tumor was available and to separate the oligodendroglial and astrocytic components for molecular genetic analysis. Eight samples containing nontumoral brain tissue were used as negative controls for the quantitative microsatellite analysis experiments and fluorescent in situ hybridization (FISH).

Quantitative microsatellite analysis for 1p and 19q loss

For quantitative microsatellite analysis, 10 to 20 sections from paraffin-embedded tumor samples were cut on glass slides, and the tumor tissue was hand dissected from the normal tissue. For GBMs with an oligodendroglial component, the astrocytic and oligodendroglial components were also separated, hand dissected, and independently evaluated. Tumor DNA was obtained using a proteinase K digestion followed by the phenol/chloroform extraction protocol. Quantitative microsatellite analysis was performed using real-time polymerase chain reaction (PCR) as described by Nigro et al. [17]. Microsatellite primer sets for loci on chromosomes 1p and 19q were used (Table 1), most of them located within the commonly deleted 1p36 and 19q13 regions observed in oligodendrogliomas. PCR reactions (25 μl) were performed in triplicate on a 96-well optical plate with an ABI prism 7500 (Applied Biosystems, Foster City, CA) using 12.5 μl of TaqMan Universal PCR Master Mix (Applied Biosystems), 2.0 μl (5 μM) of each primer, 0.15 μl (10 μM) probe (21-bp oligomer complementary to the microsatellite CA repeat: 5′-FAM-TGTGTGTGTGTGTGTGTGTGT-TAMRA-3′ [Applied Biosystems]), and genomic DNA (20–40 ng). Cycling parameters were 95°C for 12 min×one cycle and 40 cycles: 95°C for 20 s, 55°C for 20 s, and 72°C for 45 s. Primers were purchased from Applied Biosystems and Integrated DNA Technologies (Coralville, IA). The amplification of a reference pool of six microsatellite primer pairs (in a single well) was performed to normalize the differences in the amount of total input DNA. DNA was also isolated from eight normal brain tissues to calculate the average ΔCt. Calculations were performed for the PCR cycle number (Ct) average value, ΔCt [Ct (microsatellite)−Ct (reference pool)], ΔΔCt [ΔCt (tumor)−ΔCt (normal brain)], the relative copy number (2−ΔΔCt), and the tolerance interval (TI) with a confidence of 95%, determined from the pooled standard deviation of normal DNA for all microsatellite loci. According to this TI, copy numbers less than 1.1 were considered to represent losses.

Fluorescence in situ hybridization

A tissue microarray (TMA) was constructed using a Beecher tissue arrayer with cores (two 1.0-mm-diameter tissue cores from each donor block) representing areas from the astrocytic component of all tumors. Cases with an oligodendroglial component were additionally sampled on conventional slides. Both the TMA and the conventional slides were subjected to FISH. The 5-μm paraffin sections were deparaffinized, dehydrated in an ethanol series, and heat pretreated in pretreatment solution (Dako, Glostrup, Denmark) at 96°C for 10 min. Then, slides were washed and submitted to digestion with pepsin solution for 25 min at 37°C, rinsed in 2× salt–sodium citrate at room temperature, and air dried. Dual-color FISH hybridizations were performed using LSI probe sets 1p36/1q25 and 19q13/19p13 (spectrum orange-labeled 1p36 and 19q13 probes; spectrum green-labeled 1q25 and 19p13 probes; Vysis, Downers Grove, IL). Probes and target DNA were denatured simultaneously at 80°C for 5 min using a hybridizer (Dako), followed by overnight incubation at

Table 1 Sequence for the primers used in the quantitative microsatellite analysis

	Forward	Reverse
Primer		
D1S468	TAAAATATTAGGTCAAACCATG	ATGGCTGCATATAATGTTG
D1S2736	TACCTCCAGGATATTCTTGG	TTTTTGAGGTGTGAGAGCAG
D1S514	TGAATGCGTGGTCCCAACAT	GACTCAGACTTCCATCTGGACT
D1S199	GGTGACAGAGTGAGACCCTG	CAAAGACCATGTGCTCCGTA
D1S2620	AAGAGTTGTCCAACCAAATTG	GAATCTGGGATGGGATGTG
D1S2892	GCCTGGGCAACATGGCAAG	CTGGGACCACAGAGCCACC
D1S224	CATAATCCTTTGGCCCAATC	CATCACACATTTTAGAATACAGTGC
D19S424	AGCTGGTTATCTTGAGGGAG	TAGGCCACATGGAGGAGT
D19S867	CAATGAAAATGCTTTGTAAAAC	CCTTCAGAGGTGACCAG
D19S418	ACCAGGCATCCAGTGTTT	CAACTATCCCGCCTTTGT
D19S408	AGCTCTATGGGGTGGTGCC	GCCTCTTAGAGTTTTGGGAG
Reference pool		
D2S385	AGCTGTCAGTAGAAATAAGCAGAGA	TCAATAACACGCCAAAAGAC
D3S1554	ATTCATCTTGTTACTGTTCATTTGT	GGGCAAACCCAAAGACT
D5S643	TGGGCGACAGAGCCATC	TGTGGTGTGCCATTTATTGACT
D8S1800	CCATCAAATGTCGAACACTG	GTCCACCAATGCGTTAAAG
D12S1699	ACCTCATGCCTGTTAGG	TTCGTTCACATCCTGG
D21S1904	ATGAGTTCAGTGTTTCATGGACATC	AGCAAGATTACTGTCTGGTTTCCC

37°C and subsequent washes in a stringent wash buffer and Tris/HCl buffer (Dako). Nuclei were counterstained with 4′,6-diamidino-2-phenylindole (DAPI; 20 μl of fluorescence mounting medium with 100 μg/l DAPI, Dako). Sections were viewed under an Olympus® BX41-FL-III fluorescent microscope with appropriate filters, and 100 nonoverlapping nuclei were scored for the number of fluorescent signals. A ratio between p and q arms was calculated for chromosomes 1 and 19 in 500 non-neoplastic brain nuclei. A ratio of 0.86 or less was scored as a loss.

Statistical analysis

Survival analysis was performed using Kaplan–Meier product limit estimators, and the variables patient age, gender, histological diagnosis, location of the tumor, adjuvant treatment, extent of resection, 1p status, and 19q status were included in the analysis. The log-rank test was used for comparing the curves. Cox multivariate analysis was carried out to identify independent predictors with an effect on survival. Correlations between independent variables were determined using Fisher exact test, χ^2 test, and the contingency coefficient. A logistic regression model analysis was also performed to verify the associations between independent variables, and a *t* test for independent data was carried out to verify if the median ages in the two diagnostic groups were different. *P* values under 0.05 were considered significant. All analyses were carried out using the SPSS program (version 13.0).

Results

Patient characteristics

Only one patient with a previous diagnosis of low-grade astrocytoma was identified in this series of GBM patients. All the others were characterized as primary GBMs.

The age of the 88 patients (52 men and 36 women) ranged from to 6 to 81, and 23 patients were under 45. Adjuvant treatment with radiation therapy was administered to 58 patients and radiation plus chemotherapy to 12 patients. A number of chemotherapeutic approaches were employed. No adjuvant treatment was given to 16 patients, and there was not enough available information about adjuvant treatments on two. Tumors were most frequently found to have a combined location affecting more than one lobe, followed by the frontal lobe alone (19 cases) and the temporal lobe alone (16 cases). For 35 cases, the temporoparietal location was the most frequent. Three patients had multifocal tumors.

Forty-one patients were submitted to total tumor resection and 40 to subtotal resection. For seven patients, information about the extent of the resection was not available. Table 2 summarizes patient characteristics and treatments.

Identification of the oligodendroglial component

Twenty-four cases with an oligodendroglial component were identified, 17 of whom had been treated at the Hospital do Câncer A. C. Camargo, and seven were identified in a previous study at the Universidade Federal do Rio de Janeiro (Fig. 1). While the oligodendroglial component had a variable extent, it was always a minor component in tumors with a predominantly astrocytic morphology. The presence of this component was at least focal and characterized by areas with cells having oligodendroglioma-like features. The remaining 64 patients presented tumors demonstrating conventional morphology.

Among the 24 patients whose tumors had an oligodendroglial component, the median age was 52.3 (±2.8), and nine were under 45. These tumors frequently affected more than one lobe (combined location; $n=11$). Eight of these cases were treated with total resection and ten with subtotal resection. For six patients, information about the extent of resection was not available. Radiation therapy was given to 13 patients and radiation plus chemotherapy to five. Patients with tumors with an oligodendroglial component were not significantly younger than those with tumors without this component (52.3 vs 54.8 years of age; $P=0.49$; *t* test).

Table 2 Patient characteristics and treatment

Characteristics	Number of patients
Age (years)	
<45	23
≥45	65
Gender	
Female	36
Male	52
Tumor site	
Frontal	19
Parietal	10
Temporal	16
Occipital	5
Combined	35
Multifocal	3
Resection	
Total	41
Subtotal	40
NI	7
Adjuvant treatment	
RT	58
Chemo	12
None	16
NI	2

$n=88$
RT Radiation therapy, *Chemo* chemotherapy, *NI* not informed

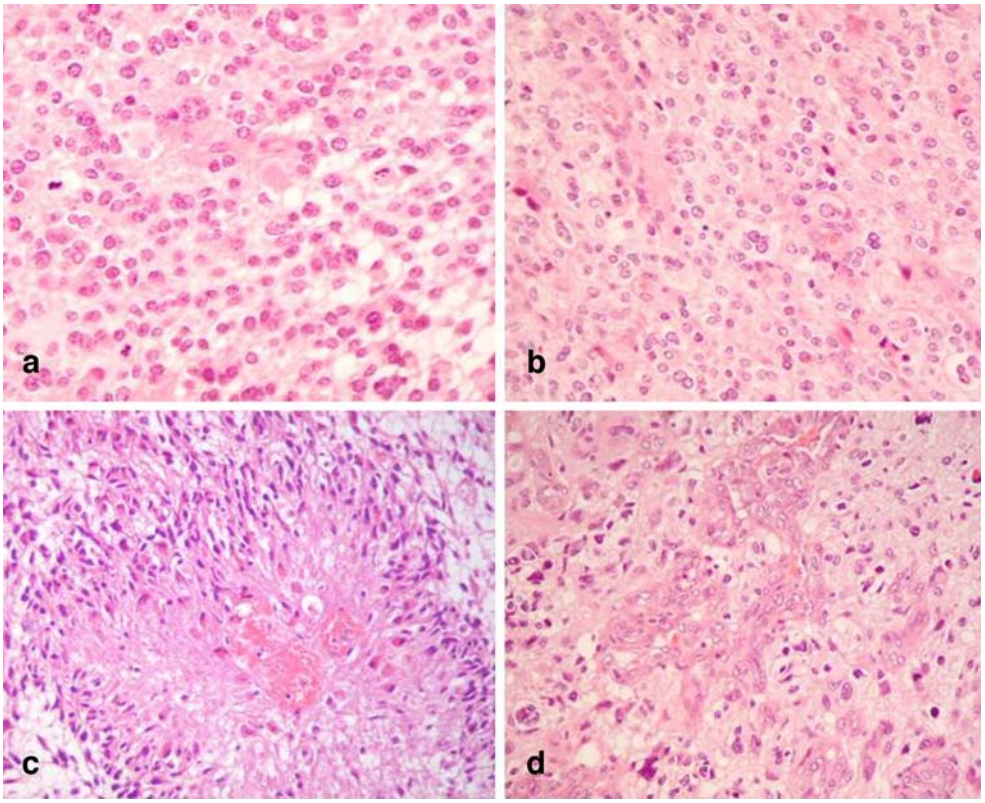


Fig. 1 **a**, **b** Glioblastoma with oligodendroglial features. Oligodendroglioma-like areas with relatively uniform, rounded nuclei and perinuclear halos. **c**, **d** Conventional GBM areas showing tumor cells with enlarged, irregularly or cigar-shaped hyperchromatic nuclei. Pseudopalisading necrosis and endothelial proliferation is noted (hematoxylin–eosin, original magnifications, ×400)

1p and 19q analysis

For the 88 patients (24 with GBMs with an oligodendroglial component and 64 conventional GBMs), 1p status was determined for 75 by one of the approaches (FISH and/or quantitative microsatellite analysis). Chromosome 19q status could be assessed for 73 patients. Combining FISH and quantitative microsatellite analysis data, three tumors with an oligodendroglial component showed a 1p loss, three had a 19q loss, and one was a combined 1p/19q deletion. Conventional GBMs demonstrated an isolated 1p loss in four cases and a 19q loss in another five cases. None of these tumors revealed a combined loss of 1p/19q. No difference was observed between the independently evaluated astrocytic and oligodendroglial components regarding the pattern of genetic alterations on chromosomes 1p and 19q. Table 3 summarizes the deletion frequencies in each tumoral group. Conventional GBMs studied by quantitative microsatellite analysis (ten cases) revealed loss of all 19q markers in one case and loss of the two D19S867 and D19S418 distal markers in another case. Via this approach, deletions of 1p involving the D1S2892 (1p34.2) and D1S2620 (1p36.12) markers were detected in one case. When cases with oligodendroglial components were evaluated by quantitative microsatellite analysis, one case lost the three markers analyzed at 19q and two had partial losses on the same chromosome arm. FISH hybridizations are illustrated in Fig. 2.

Table 3 Genetic patterns vs histological features

Histology	1p loss	19 q loss	1p/19q loss
GBM with an oligodendroglial component (n=24)	3	3	1
Conventional GBM (n=64)	4	5	0
Total (n=88)	7/75[a]	8/73[b]	1

[a] 1p status was determined for 75 patients.
[b] 19q status was determined for 73 patients.

Prognostic significance of clinical variables, histological features, and genetic abnormalities in GBM patients

The total 88 patients had an overall median survival of 13.8 months (±1.2). By Kaplan–Meier univariate analysis, survival was longer for patients under 45 (P=0.013). Kaplan–Meier curves also showed longer survival for patients receiving radiation and chemotherapy (P<0.001; Fig. 3). Although the median survival of patients who presented tumors containing an oligodendroglial component (14.9 months [±1.9]) was slightly longer than that of patients with conventional tumors (13.5 months [±1.4]), the difference was not statistically significant (P=0.566; Fig. 3).

Cox multivariate analysis was performed in 67 patients (Table 4). Age under 45 was related to a reduced risk of

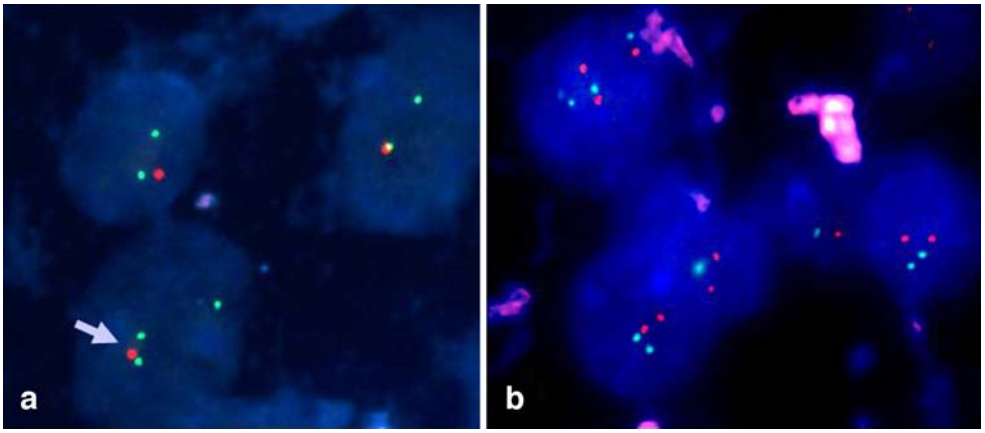


Fig. 2 FISH hybridizations from two cases: **a** GBM with an oligodendroglial component: deletion of 19q (one red signal, *arrow*). **b** GBM with an oligodendroglial component: Two red signals represent 19q retention

death (P=0.008). Adjuvant treatment also had a predictive value in that the patients who did not receive adjuvant radiation or chemotherapy showed an increased risk of death (P<0.001). Tumor histology, location, and extent of resection were not significantly associated with survival. Survival of patients with 1p or 19q deletions was also not different from those without these alterations. The significance of the 1p/19q codeletion could not be assessed because only one patient presented a codeletion.

Associations of 1p and 19q status with clinical data and histological features

Although the frequency of 1p and 19q deletions seems to be higher in the group of GBMs containing an oligodendroglial component than in the group with conventional morphology (19 vs 7.4% for 1p deletions and 20 vs 9.4% for 19q deletions), statistical significance was not observed (P=0.13 for 1p deletions and P=0.225 for 19q deletions; z test for proportion differences). No association was observed between 1p or 19q status and histological diagnosis (P=0.209 for 1p vs histology; and P=0.246 for 19q vs histology, Fisher's exact test). Associations between 1p and 19q status and clinical variables were also not identified in this series of patients.

Previous studies have reported that oligodendrogliomas and oligoastrocytomas located either in the temporal lobe or the diencephalon are less likely to be associated with 1p/19q loss [14, 16]. When the present series of GBMs was separated into temporal and extratemporal locations, no significant association was observed between the status of chromosomes 1p/19q and location or between histological diagnosis and location.

Discussion

The aim of this study was to investigate 1p and 19q chromosome losses in previously classified GBM tumors and compare the group of patients presenting tumors with an oligodendroglial component to the group presenting conventional morphology tumors.

Previous studies have demonstrated that the presence of an oligodendroglial component in GBM is associated with longer survival [7, 11]. Although the median survival was slightly longer for patients whose tumors had an oligodendroglial component, our study did not show a statistically significant difference in survival between these tumors and GBMs presenting conventional morphology. The frequency of genetic abnormalities on chromosomes 1p and 19q was also not significantly different in the two groups (P=0.065). GBMs with oligodendroglial components revealed the same alteration pattern on 1p and 19q as conventional GBMs. These data do not support the results of initial studies on molecular genetic findings in GBMs having an oligodendroglial component, demonstrating that these tumors presented a higher frequency of loss of heterozigosity on chromosomes 1p and 19q when compared with conventional GBMs. These studies likewise showed that the alterations usually observed in standard GBMs such as *EGFR* amplification, *PTEN* deletion, chromosome 10 deletion, *CDKN2A* deletion, and *TP53* mutations were also observed in GBMs with oligodendroglial components [6, 11].

Homma et al. [8] recently detected the presence of oligodendroglial components in 20% of the 403 GBMs studied. The conclusions reached in the above report were similar to those in the current study in regard to the frequency of deletions on 1p and 19q in GBMs having oligodendroglial components, showing no difference between these tumors and conventional ones. It is possible that the first studies to describe a higher frequency of 1p and 19q deletions included cases that would have been classified as anaplastic oligoastrocytomas or oligodendrogliomas in a more precise review. Nevertheless, the criteria used to identify GBMs with oligodendroglial components are not well established so that separating these tumors from anaplastic oligoastrocytomas is often a difficult and subjective task [20]. Although the oligodendroglioma-like

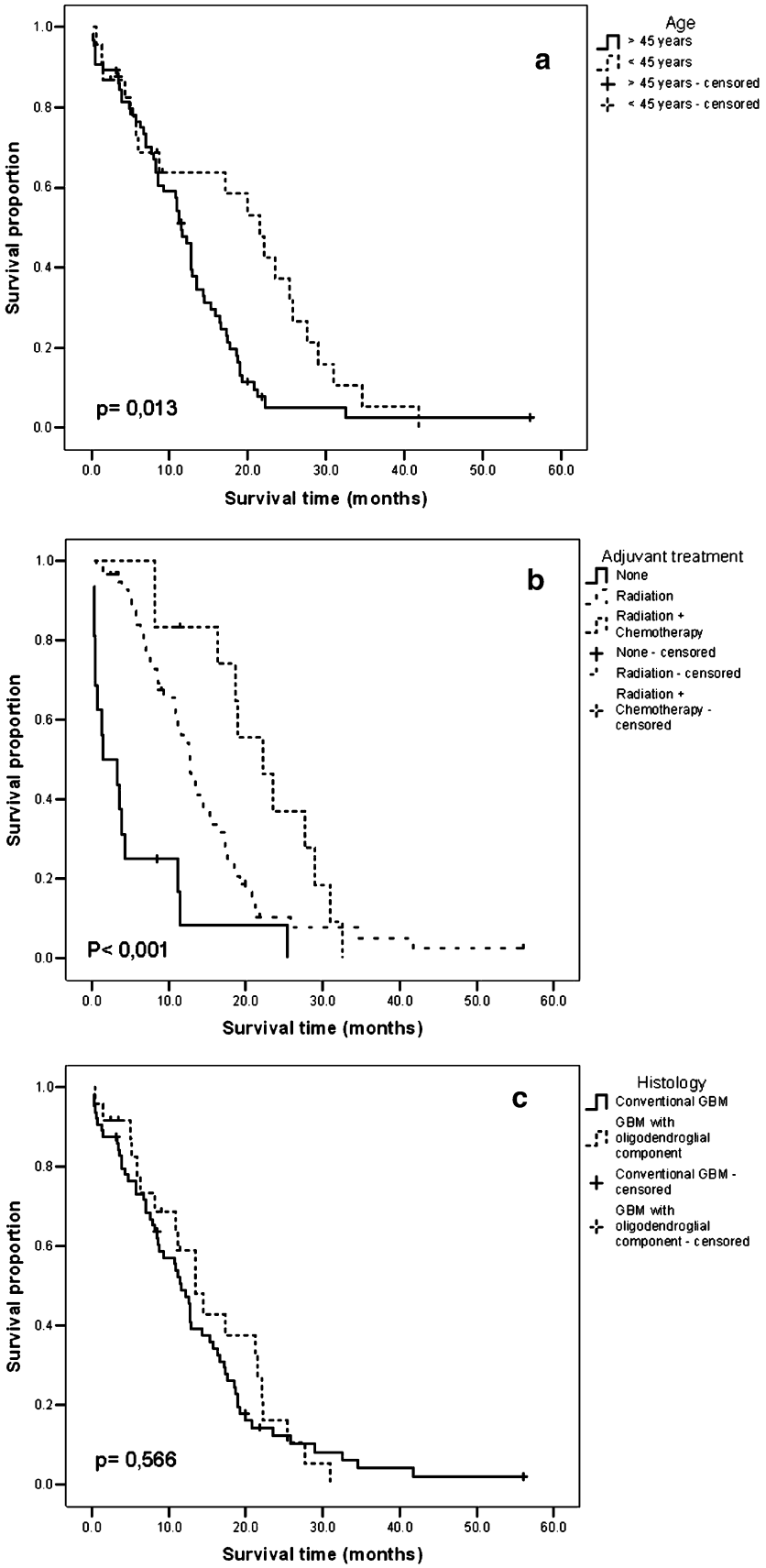


Fig. 3 Kaplan–Meier curves show that patient age under 45 and adjuvant treatment with radiation plus chemotherapy are associated with longer survival (**a**, **b**). The presence of an oligodendroglial component was not associated with longer survival in these series (**c**)

Table 4 Multivariate analysis results

Variable	Hazard ratio (95% CI)	*P* value
Age (years)		
≤45	1.00	0.008
>45	2.49 (1.26–4.91)	
Gender		
Female	1.00	0.896
Male	0.96 (0.54–1.72)	
Histology		
GBM-O	1.00	0.489
GBM	1.29 (0.62–2.69)	
Adjuvant treatment		
RT+chemotherapy	1.00	
RT	1.25 (0.57–2.71)	0.577
None	6.39 (2.34–17.45)	*0.001*
Resection		
Total	1.00	0.675
Subtotal	1.13 (0.64–1.99)	
1p status		
Deleted	1.00	0.439
Intact	0.71 (0.29–1.71)	
19q status		
Deleted	1.00	0.868
Intact	0.93 (0.38–2.24)	
Tumor location		
Combined	1.00	0.149
One lobe	0.66 (0.37–1.16)	

RT Radiation therapy, *GBM-O* GBM with oligodendroglial component, *GBM* conventional glioblastoma

areas were recognized as one of the possible cellular compositions of GBMs in the recently published WHO Classification of Tumors of the Central Nervous System (2007), definitive diagnostic criteria do not exist [12, 13].

Several studies have addressed the significance of 1p and 19q deletions in GBMs. Schmidt et al. [22] identified 1p/19q codeletion in 5 out of 73 GBMs and reported that this codeletion and not the isolated 1p or 19q deletion was associated with longer survival. These data could not be confirmed by subsequent studies that included the evaluation of 1p and 19q status in gliomas of various grades and histological aspects. These same studies failed to demonstrate the association of 1p/19q codeletions with tumors that are not classic oligodendrogliomas [2, 5, 24]. A study by Fuller et al. [5], involving morphologically ambiguous gliomas with hybrid oligoastrocytic features, did not show 1p/19q codeletions in grade IV gliomas, while isolated 19q deletions were predominately present in grade III and IV tumors. Walker et al. [24] found that the seven GBMs with oligodendroglial components investigated in their study had only chromosome 10 losses with no evidence of 1p or 19q losses in either of the independently evaluated astrocytic or oligodendroglial components. McDonald et al. [14] recently demonstrated that the presence of 1p/19q codeletions had an impact on prognosis only in tumors with a classic oligodendroglial histology after being reviewed by five neuropathologists. In tumors with an ambiguous morphology, 1p/19q deletions had no impact on survival. On the other hand, tumors with classic oligodendroglial morphology had a better prognosis even with intact 1p/19q [14].

These observations could also be applied to the present cases. In our study, 1p or 19q deletions had no impact on survival of patients with tumors with hybrid histology, i.e., GBMs with oligodendroglial areas. The significance of codeletion in our series could not be evaluated as only one patient showed both 1p and 19q losses. Nevertheless, this patient survived for 11 months after diagnosis and, thus, cannot be considered a long-term survivor. Although patients with isolated 19q deletion in our series had a median survival of 17.7 months, which was slightly longer than those without the deletion (14 months), this difference was also not statistically significant (P=0.372). This alteration has more frequently been observed in secondary GBMs. In our series, only one case was considered a secondary GBM, which was one of the GBMs containing oligodendroglial areas. This case showed 19q deletion, detected by both FISH and quantitative microsatellite analysis. Moreover, Miller and Perry [15] recently observed that solitary 19q deletions were more frequently detected in GBMs having oligodendroglial components (21% of the 58 cases analyzed). However, according to the authors, this alteration should not be used for diagnostic purposes because of its infrequent occurrence [15].

It should be pointed out that two types of deletions on chromosome 1 have been reported in the literature: complete 1p loss, commonly associated with 19q loss and oligodendroglial phenotype, and partial deletions of 1p, predominantly found in astrocytic gliomas and not associated with 19q deletions [9]. Our approach was not suitable for distinguishing between these two types of deletions. Nevertheless, when detected by quantitative microsatellite analysis, 1p loss involved only a few loci, most of which were located in the 1p36 region.

Another evaluation that was performed in our study consisted in verifying if the different components of the tumors having oligodendroglial areas would present different genetic profiles on chromosomes 1p and 19q. Both FISH and quantitative microsatellite analysis were used in this setting, but no difference was observed between the two components. It has previously been suggested that a separate evaluation of the two components would help in understanding the pathogenesis of tumors with an ambiguous morphology [6]. Studies investigating the genetic alterations of the different components in gliomas displaying intratumoral heterogeneity have found identical genetic changes in the different components, which tends to confirm a predominantly monoclonal origin of these tumors

[19, 24]. In their series of 11 oligoastrocytomas, Qu et al. [19] have shown that, in most cases, the oligodendroglial and astrocytic components displayed a similar genotype. Nevertheless, the components in two biphasic tumors revealed different genetic profiles, suggesting that, in some cases, these components may be derived from different cell clones [19].

Our study also confirmed the already-known relationship between survival and age as well as the impact of adjuvant treatment on prognosis. Patient age remains one of the most important prognostic factors for GBM patients, although other clinical characteristics also have an influence [18]. None of the genetic or molecular data have shown the same influence of age on survival of GBM patients.

In conclusion, our series of GBMs with oligodendroglial areas demonstrated slightly longer survival in comparison to conventional GBMs (not statistically significant) despite the infrequency of combined 1p/19q in these tumors. Notwithstanding the observed hybrid phenotype, the pattern of genetic changes on chromosomes 1p and 19q seems to be more closely related to astrocytic than oligodendroglial tumors. Moreover, in view of the fact that the classification of gliomas remains controversial, especially for those with a hybrid phenotype, new molecular markers could perhaps be utilized to resolve certain diagnostic issues. Our study contributes to the understanding of the GBM genetic profile, including tumors with an oligodendroglial component.

Acknowledgments The authors thank Carlos Ferreira Nascimento, Jose Ivanildo Neves, and Fabricio de Carvalho for their technical assistance and Judy Grevan for editing the text. This project was supported by the Fundação de Amparo à Pesquisa do Estado de São Paulo (FAPESP), grant ID 04/12360-2.

Conflict of interest statement We declare that we have no conflict of interest.

References

1. Aldape K, Burger PC, Perry A (2007) Clinicopathologic aspects of 1p/19q loss and the diagnosis of oligodendroglioma. Arch Pathol Lab Med 131:242–251
2. Barbashina V, Salazar P, Holland EC, Rosenblum MK, Ladanyi M (2005) Allelic losses at 1p36 and 19q13 in gliomas: correlation with histologic classification, definition of a 150-kb minimal deleted region on 1p36, and evaluation of CAMTA1 as a candidate tumor suppressor gene. Clin Cancer Res 11:1119–1128
3. Cairncross JG, Ueki K, Zlatescu MC, Lisle DK, Finkelstein DM, Hammond RR, Silver JS, Stark PC, Macdonald DR, Ino Y, Ramsay DA, Louis DN (1998) Specific genetic predictors of chemotherapeutic response and survival in patients with anaplastic oligodendrogliomas. J Natl Cancer Inst 90:1473–1479
4. Caskey LS, Fuller GN, Bruner JM, Yung WK, Sawaya RE, Holland EC, Zhang W (2000) Toward a molecular classification of the gliomas: histopathology, molecular genetics, and gene expression profiling. Histol Histopathol 15:971–981 (Review)
5. Fuller CE, Schmidt RE, Roth KA, Burger PC, Scheithauer BW, Banerjee R, Trinkaus K, Lytle R, Perry A (2003) Clinical utility of fluorescence in situ hybridization (FISH) in morphologically ambiguous gliomas with hybrid oligodendroglial/astrocytic features. J Neuropathol Exp Neurol 62:1118–1128
6. He J, Mokhtari K, Sanson M, Marie Y, Kujas M, Huguet S, Leuraud P, Capelle L, Delattre JY, Poirier J, Hoang-Xuan K (2001) Glioblastomas with an oligodendroglial component: a pathological and molecular study. J Neuropathol Exp Neurol 60:863–871
7. Hilton DA, Penney M, Pobereskin L, Sanders H, Love S (2004) Histological indicators of prognosis in Glioblastomas: retinoblastoma protein expression and oligodendroglial differentiation indicate improved survival. Histopathology 44:555–560
8. Homma T, Fukushima T, Vaccarella S, Yonekawa Y, Di Patre PL, Franceschi S, Ohgaki H (2006) Correlation among pathology, genotype, and patient outcomes in glioblastoma. J Neuropathol Exp Neurol 65:846–854
9. Idbaih A, Marie Y, Pierron G, Brennetot C, Hoang-Xuan K, Kujas M, Mokhtari K, Sanson M, Lejeune J, Aurias A, Delattre O, Delattre JY (2005) Two types of chromosome 1p losses with opposite significance in gliomas. Ann Neurol 58:483–487
10. Ino Y, Zlatescu MC, Sasaki H, Macdonald DR, Stemmer-Rachamimov AO, Jhung S, Ramsay DA, von Deimling A, Louis DN, Cairncross JG (2000) Long survival and therapeutic responses in patients with histologically disparate high-grade gliomas demonstrating chromosome 1p loss. J Neurosurg 92:983–990
11. Kraus JA, Lamszus K, Glesmann N, Beck M, Wolter M, Sabel M, Krex D, Klockgether T, Reifenberger G, Schlegel U (2001) Molecular genetic alterations in glioblastomas with oligodendroglial component. Acta Neuropathol 101:311–320
12. Kleihues P, Burger PC, Aldape KD, Brat DJ, Biernat W, Bigner DD, Nakazato Y, Plate KH, Giangaspero F, von Deimling A, Ohgaki H, Cavenee WK (2007) Glioblastoma. In: Louis DN, Ohgaki H, Wiestler OD, Cavenee WK (eds) WHO classification of tumours of the nervous system. IARC, Lyon, pp 33–49
13. Louis DN, Ohgaki H, Wiestler OD, Cavenee WK, Burger PC, Jouvet A, Scheithauer BW, Kleihues P (2007) The 2007 WHO classification of tumours of the central nervous system. Acta Neuropathol 114:97–109
14. McDonald JM, See SJ, Tremont IW, Colman H, Gilbert MR, Groves M, Burger PC, Louis DN, Giannini C, Fuller G, Passe S, Blair H, Jenkins RB, Yang H, Ledoux A, Aaron J, Tipnis U, Zhang W, Hess K, Aldape K (2005) The prognostic impact of histology and 1p/19q status in anaplastic oligodendroglial tumors. Cancer 104:1468–1477
15. Miller CR, Perry A (2007) Glioblastoma: morphologic and molecular genetic diversity. Arch Pathol Lab Med 131:397–406
16. Mueller W, Hartmann C, Hoffmann A, Lanksch W, Kiwit J, Tonn J, Veelken J, Schramm J, Weller M, Wiestler OD, Louis DN, von Deimling A (2002) Genetic signature of oligoastrocytomas correlates with tumor location and denotes distinct molecular subsets. Am J Pathol 161:313–319
17. Nigro JM, Takahashi MA, Ginzinger DG, Law M, Passe S, Jenkins RB, Aldape K (2001) Detection of 1p and 19q loss in oligodendroglioma by quantitative microsatellite analysis, a real-time quantitative polymerase chain reaction assay. Am J Pathol 158:1253–1262
18. Ohgaki H, Dessen P, Jourde B, Horstmann S, Nishikawa T, Di Patre PL, Burkhard C, Schuler D, Probst-Hensch NM, Maiorka PC, Baeza N, Pisani P, Yonekawa Y, Yasargil MG, Lutolf UM, Kleihues P (2004) Genetic pathways to glioblastoma: a population-based study. Cancer Res 64:6892–6899
19. Qu M, Olofsson T, Sigurdardottir S, You C, Kalimo H, Nistér M, Smits A, Ren ZP (2007) Genetically distinct astrocytic and oligodendroglial components in oligoastrocytomas. Acta Neuropathol 113:129–136

20. Reifenberger G, Collins VP (2004) Pathology and molecular genetics of astrocytic gliomas. J Mol Med 82:656–670
21. Reifenberger J, Reifenberger G, Liu L, James CD, Wechsler W, Collins VP (1994) Molecular genetic analysis of oligodendroglial tumors shows preferential allelic deletions on 19q and 1p. Am J Pathol 145:1175–1190
22. Schmidt MC, Antweiler S, Urban N, Mueller W, Kuklik A, Meyer-Puttlitz B, Wiestler OD, Louis DN, Fimmers R, von Deimling A (2002) Impact of genotype and morphology on the prognosis of Glioblastoma. J Neuropathol Exp Neurol 61:321–328
23. Tews B, Felsberg J, Hartmann C, Kunitz A, Hahn M, Toedt G, Neben K, Hummerich L, von Deimling A, Reifenberger G, Lichter P (2006) Identification of novel oligodendroglioma-associated candidate tumor suppressor genes in 1p36 and 19q13 using microarray-based expression profiling. Int J Cancer 119:792–800
24. Walker C, du Plessis DG, Joyce KA, Machell Y, Thomson-Hehir J, Al Haddad SA, Broome JC, Warnke PC (2003) Phenotype versus genotype in gliomas displaying inter- or intratumoral histological heterogeneity. Clin Cancer Res 9:4841–4851

Virchows Arch (2008) 452:491–497
DOI 10.1007/s00428-008-0592-y

ORIGINAL ARTICLE

Episomal amplification of *MYCN* in a case of medulloblastoma

Cecilia Surace · Florence Pedeutour · Domenico Trombetta · Fanny Burel-Vandenbos · Mariano Rocchi · Clelia Tiziana Storlazzi

Received: 6 September 2007 / Revised: 8 January 2008 / Accepted: 25 January 2008 / Published online: 20 February 2008
© Springer-Verlag 2008

Abstract Gene amplification, in the form of double minutes (dmin) and/or homogeneously staining regions (hsr), is frequently associated with tumor development. A well-known example is neuroblastoma for which *MYCN* gene (v-myc myelocytomatosis viral-related oncogene) amplification has a relevant prognostic significance. A third cryptic form of amplification, cytogenetically invisible and composed of episomes, has been also described, but it is very rarely seen in primary tumors. In this paper, we report on *MYCN* amplification, in the form of episomes, in a case of medulloblastoma. Detailed fluorescence in situ hybridization and real-time quantitative polymerase chain reaction analyses revealed an amplified genomic segment of approximately 590 kb containing only the genes *MYCN* and *N-cym* (v-myc myelocytomatosis viral-related oncogene, neuroblastoma-derived opposite strand). To the best of our knowledge, this is the first report of a solid primary tumor showing *MYCN* amplification in the form of episomes.

Keywords Episomes · *MYCN* · Medulloblastoma · FISH · RQ-PCR

C. Surace · D. Trombetta · M. Rocchi · C. T. Storlazzi
Department of Genetics and Microbiology,
University of Bari,
Bari, Italy

F. Pedeutour
Laboratory of Solid Tumors Genetics, Faculty of Medicine,
Nice University Hospital and CNRS UMR,
6543 Nice, France

F. Burel-Vandenbos
Department of Pathology, Nice University Hospital,
Nice, France

C. Surace (✉)
Laboratory of Cytogenetics and Molecular Genetics,
Ospedale Pediatrico "Bambino Gesù", IRCCS,
Piazza S.Onofrio 4,
00165 Rome, Italy
e-mail: cecilia.surace@opbg.net

Introduction

Gene amplification is a mechanism that can confer resistance to a wide range of drugs or that can activate cellular oncogenes to express abnormal levels of protein [5]. As a rule, the basic amplified elements are usually tandemly duplicated to form readily visible double minutes (dmin) and/or homogeneously staining regions (hsr).

The most consistent association between gene amplification and tumor development is shown in human neuroblastoma, where the *MYCN* (v-myc myelocytomatosis viral-related oncogene) gene, located at 2p24, is amplified in both primary tumors and established cell lines [5]. *MYCN* amplification is a significant predictor for clinical outcome because it correlates with aggressive tumor growth [12].

MYCN amplification has also been reported in a small group of primitive neuroectodermal tumors (PNET) that, as neuroblastoma, are malignant and invasive embryonal tumors of the central nervous system. These tumors predominantly show a neuronal differentiation and represent 20% of pediatric brain tumors [2]. Medullobastoma is an embryonal tumor arising in cerebellum [9].

Recently, an additional form of gene amplification has been reported by Graux et al. [8]. They found, in some T-ALL patients, a large number of episomal copies of *ABL1* and *NUP214* oncogenes, about 500 kb in size, which did not undergo tandem duplication, therefore remaining undetectable by conventional cytogenetics.

In the present study, we report a detailed analysis of a case of medulloblastoma carrying *MYCN* amplification in the form of episomes which can be revealed by appropriate fluorescence in situ hybridization (FISH).

Clinical history

In November 2004, a 15-year-old boy presented at the emergency room with headache, vomiting, static and kinetic cerebellar syndrome, and drowsiness. His medical history was unremarkable except for a posterior cervical pain that begun approximately 2 months before. The headaches and vomiting had started 1 week before. The cerebral magnetic resonance imaging (MRI) showed a heterogeneous tumor of the right cerebellar hemisphere, the consequence of which was a compression of the fourth ventricle and the cerebral trunk, hydrocephaly, and intracranial hypertension. A complete surgical removal of the tumor, diagnosed as cerebellar medulloblastoma according to World Health Organization classification [9], was done. In the next days after the excision, the cerebellar syndrome worsened and was associated with a right hemiparesy, a paralysis of the right VI nerve, a right facial palsy, a hypoesthesia of the right hemiface, and a right hypoacusis. After complete resection of the tumor in the posterior fossa, the excised tissue was subjected to histological examination. Histological analysis showed a round cell tumor displaying a high-cellular density. These cells were generally arranged in layers. More rarely, they formed pseudo-fibrillary rosettes of Homer–Wright type and perivascular pseudo-rosettes (Fig. 1a). Cells presented a rounded nucleus with thin chromatin, without nucleolus. The cytoplasm was not abundant, and it was eosinophilic or pale. The mitoses were numerous. Moreover, few foci composed of large cells were present. Within these foci, the large cells had an abundant eosinophilic cytoplasm and a large nucleus, sometimes with a large nucleolus (Fig. 1b). Because of the presence of these foci of large cells, the medulloblastoma was classified as a "large cell medulloblastoma."

Tumor showed a rich vascularization with thin capillaries presenting an endothelial hyperplasia. The lesion exhibited some microcalcifications.

The immunohistochemical study showed an intense positivity for neurofilaments in many tumoral cells. Glial fibrillary acidic protein was positive only in some regions of them. Synaptophysin showed positivity with variable intensity. Neuronal nuclei marked small cores like cerebellar grains. Melanin pigmentation was absent, and immunohistochemistry for melanocytic markers remained negative. Epithelial membrane antigen was negative. Cells were marked by the CD99. The index of proliferation (MIB1) was about 50%.

Medullar MRI and lumbar puncture were negative. Radiotherapy and chemotherapy (CCNU–chloroethylnitrosourea–cisplatinum and vincristine, two lines; CCNU and cisplatinum, three lines) were initiated in January and March 2005, respectively. The patient condition improved and was stable until October 2005. In October 2005, a clinical aggravation was observed with several neurological symptoms of a tumor recurrence. In December 2005, the MRI showed multiple cerebral lesions that confirmed the recurrence. The patient died 3 months after the recurrence.

Materials and methods

Cytogenetic analysis

The sample fragment of the tumor was obtained form a surgical excision. The cells were mechanically dissociated, incubated for 24 h, and treated by conventional cytogenetic methods for karyotype analysis. Sixteen RHG-banded metaphase cells were analyzed. The karyotype was described in accordance to the International System for Human Cytogenetic Nomenclature [14].

Fluorescence in situ hybridization probes

BAC clones for FISH analysis were selected according to their position in the human genome (UCSC database,

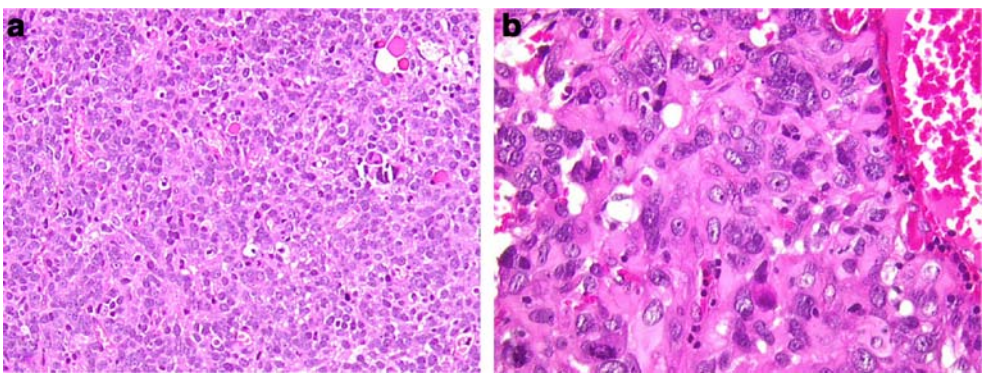


Fig. 1 **a** Histological section (stained with hematoxylin–eosin) of medulloblastoma showing a high cellular density and formation of Homer–Wright rosettes. **b** Large cells displaying abundant cytoplasm and pleomorphic, large nuclei with proeminent nucleoli (Hematoxylin–eosin–saffron ×400)

http://genome.ucsc.edu, March 2006 release). They are listed in Table 1.

The whole chromosome painting (WCP) probe specific for chromosome 2 was derived from flow-sorted chromosomes (kindly provided by Dr. Nigel Carter, Sanger Centre, Cambridge, UK) and polymerase chain reaction (PCR)-amplified using a degenerated oligonucleotide probe.

Fluorescence in situ hybridization

FISH experiments were carried out as previously described [10]. Chromosome preparations were hybridized in situ with probes directly and indirectly labeled by nick translation. Briefly, 600 ng of labeled probe was used for FISH experiments; hybridization was performed at 37°C in 2× saline-sodium citrate (SSC), 50% (vol/vol) formamide, 10% (wt/vol) dextran sulfate, 5 μg Cot-1 DNA (Bethesda Research Laboratories, Gaithersburg, MD, USA), and 3 μg sonicated salmon sperm DNA in a volume of 10 μl. Post-hybridization washing was performed at 42°C in 2× SSC/50% formamide (three times), followed by three washes in 0.1× SSC at 60°C. Biotin (Invitrogen Italia SRL, Milan, Italy)-labeled DNA was detected with streptavidin-diethylaminocoumarin (Molecular Probes, Milan, Italy). In co-hybridization experiments, other probes were directly labeled with fluorescein, Cy3, or Cy5. Chromosomes were identified by 4′,6-diamidino-2-phenylindole (DAPI) staining. Digital images were obtained using a Leica DMRXA epifluorescence microscope equipped with a cooled CCD camera (Princeton Instruments, Boston, MA, USA). Cy3 (red; New England Nuclear, Boston, MA, USA), fluorescein (green; Fermentas Life Sciences, Milan, Italy), Cy5 (IR; New England Nuclear), and DAPI (blue) fluorescence signals, which were detected using specific filters, were recorded separately as gray-scale images. Pseudocoloring and merging of images were performed with Adobe Photoshop software (Adobe Systems, Seattle, WA, USA).

Each FISH experiment was carried out co-hybridizing WCP 2, RP11-480N14 (*MYCN*), one clone proximal, and one clone distal to the *MYCN* gene. Reiterative FISH experiments were performed to ascertain bacterial artificial chromosome (BAC) clones encompassing the breakpoints of the amplified genomic segment in the episomes. These clones were identified because they showed fainter fluorescence signals on episomes when compared with the signals on the normal chromosomes 2 and because the partially overlapping more distal and more proximal clones produced no hybridization signals on episomes.

Table 1 BAC clones used in FISH experiments to characterize the episome extension

Probe	Accession no.	Map position on chr. 2	Signal on the episome
RP11–179D4	Ends	15,603,279–15,765,037	−
RP11–826H14	Ends	15,763,477–15,955,850	+
RP11–68A23	Ends	15,857,944–16,012,158	+
RP11–480N14	Ends	15,958,001–16,125,748	+
RP11–761F22	AC131095	15,996,264–16,163,147	+
RP11–153H16	Ends	16,225,552–16,381,172	+
RP11–652M18	Ends	16,268,891–16,452,618	+
RP11–945D18	Ends	16,384,833–16,564,423	+
RP11–637L15	Ends	16,454,615–16,611,450	+
RP11–542H15	AC104623	16,549,070–16,651,868	−
RP11–990G8	Ends	16,646,831–16,825,919	−

Their map positions is reported in the third column, along with their FISH results on the episomes (last column)

Real-time quantitative polymerase chain reaction

Real-time quantitative PCR (RQ-PCR) experiments were performed for a detailed characterization of the breakpoints at the sequence level. Multiple primer pairs were designed, with the Primer Express® software v2.0 (Applied Biosystems), on the sequence of the BACs RP11-826H14 and RP11-637L15 encompassing, respectively, the distal and the proximal breakpoint of the amplified genomic segment in episomes to identify regions of switch between amplified and not-amplified sequences. The segment encompassing each breakpoint was further narrowed down using the same approach, i.e., by selecting additional primer pairs within that region (Table 2). Tumor DNA was extracted from fresh tissue according to standard methods, and DNA from a healthy individual was used as a control. The DNA was amplified by means of Applied Biosystems Real-Time PCR System 7300 using the SYBR Green PCR kit (Applied Biosystems, Monza, Italy). The PCR conditions were as follows: 2 min at 50°C, 10 min at 95°C, 40 cycles of 15 s at 95°C, and 1 min at 60°C for all the primer pairs used. All measurements were performed at least in triplicate.

Long-range polymerase chain reaction

Long-range PCR experiments, using appropriate oligo primers, were performed to sequence the episome junction regions. The long-range PCR analyses were performed using TaKaRa LA Taq™ (Cambrex Bio Science, Milan, Italy).

Results

RGH-banding analysis of metaphase spreads derived from short-term cultured cells obtained before treatment revealed

Table 2 Primer pairs used in RQ-PCR studies, along with amplification results

Name	Sequence	Map on chr. 2	Amplified
826A F	GGCCAGACTTCCAGGAACATC	15,783,105–15,783,125	−
826A R	CAACTTCAGTAAATCAAGGACTTTTCA	15,783,146–15,783,172	
826B F	CAGTGTCTGAGGCCCCTTTC	15,823,171–15,823,190	−
826B R	TCCCTTCATTCACAGAGGCATA	15,823,210–15,823,231	
826C F	AGTGTCTTTGATTCCCTGTCAACA	15,882,999–15,883,021	−
826C R	CGTTCCCCTCTTCAGATGGA	15,883,039–15,883,058	
826CD1 F	TGGCCCCTTGACCTCTCTT	15,891,678–15,891,696	−
826CD1 R	AGGGTGCAGCCTCTGACATG	15,891,718–15,891,736	
826CD2 F	GGTCTTGAAGGAGGTGTGGATT	15,895,186–15,895,207	−
826CD2 R	CCTGGGATGCCCTTCTTTC	15,895,225–15,895,243	
826CD3 F	CCAAACCCAGCCTCTGACTCT	15,898,897–15,898,917	−
826CD3 R	GGACAGCATCATGAGCTAGGAA	15,898,938–15,898,958	
826CD7 F	TGCTTCTCACTGGGACTAGGATT	15,899,118–15,899,140	−
826CD7 R	AATCCGACCCCTGTTTCACA	15,899,160–15,899,179	
826CD8 F	CCTAGAGCATATCTAGGTTTAAAGTTGTTG	15,899,332–15,899,361	−
826CD8 R	GGGCAGAAGGCTGGATGAT	15,899,381–15,899,399	
826CD4 F	GGCCCAAGCCCCTTCTAGT	15,899,658–15,899,676	+
826CD4 R	TCTTGCTGGGTGCTCAGAGA	15,899,695–15,899,714	
826CD5 F	CTACCGTCCCCTAGCAAAACAG	15,900,682–15,900,703	+
826CD5 R	CCACACGTCCGCCCAAT	15,900,732–15,900,748	
826CD6 F	CCAACTCTCACGGCTTTGC	15,901,502–15,901,520	+
826CD6 R	ATCATTCCTGCCCCTTGCA	15,901,550–15,901,568	
826D F	GGGTCACCTCCCCCTTGAT	15,902,431–15,902,449	+
826D R	AGGGAGGGTCAAGGAGACTCA	15,902,469–15,902,489	
826E F	TGATTTTCCTGAAGCATTTTCCTTA	15,919,308–15,919,332	+
826E R	CTCACCTGGGCAGAAGCAA	15,919,352–15,919,370	
826F F	CGAGGGTTTGGGAAAGCATT	15,938,341–15,938,360	+
826F R	CAGCCGCCATTTGCAAGT	15,938,379–15,938,396	
637A F	GAAAGACAAGCAAAGGCAAGTGA	16,474,365–16,474,387	+
637A R	GAGCCCATGCAGGGATCTC	16,474,411–16,474,429	
637AB1 F	CCCTTTCTTAGAGGCCTTCCA	16,478,013–16,478,033	+
637AB1 R	CACCAGAGAGCTGCCCATTT	16,478,054–16,478,073	
637AB2 F	GGAGCGGTGGTGTGCTAGAT	16,483,116–16,483,135	+
637AB2 R	CCTGAGCTGGTTTTGAACTCTGA	16,483,155–16,483,177	
637AB3 F	GGCTCAACTGTAAGTCTTTCAGCAA	16,487,508–16,487,532	+
637AB3 R	TGGAGCACTGGCCGATCT	16,487,551–16,487,568	
637AB4 F	TGGTTCAGTTGGATAGGTTGCTT	16,488,030–16,488,052	+
637AB4 R	GAAGAGAAGATCACCGCCATTT	16,488,075–16,488,096	
637AB7 F	TGCAATAAAAAGACATCATATTCCACTAAC	16,488,290–16,488,319	+
637AB7 R	TGTTTAACCACCCAGTCTGTGGTA	16,488,339–16,488,362	
637AB9 F	AATGTAAAGCCATCCCCTAAATG	16,488,803–16,488,829	−
637AB9 R	TTGATGTTATACAAGGTCATGGACATC	16,488,757–16,488,777	
637AB8 F	TCTAGGCTGCTACACTTTACAATAACTTTT	16,490,032–16,490,061	−
637AB8 R	CCTTGAGATATGACTGCCTTTTTATTT	16,490,143–16,490,170	
637AB5 F	GCTTCAAGGCCCAGAGTATACAG	16,490,408–16,490,433	−
637AB5 R	CACCAGTCTGGCTATGTAGGCTTT	16,490,367–16,490,389	
637AB6 F	CAATAGAGGGTGATGAGGAGAGAAG	16,492,823–16,492,847	−
637AB6 R	TTTACAGTCCCCCCAAAATAGC	16,492,864–16,492,885	
637B F	CGGGTGAGGCTGGAATGT	16,494,613–16,494,630	−
637B R	CAGAGCAGCAGGAGCAAGTG	16,494,665–16,494,684	
637C F	AGGGCCTACTGTTTGCGCTAT	16,514,049–16,514,068	−
637C R	GGATTAGGCCAAATAAGCCAACT	16,514,087–16,514,109	

the presence of a mixture of hypodiploid and hypotetraploid cells with structural abnormalities of chromosomes 4, 6, and 11, loss of chromosomes 8 and 13, and the presence of three marker chromosomes. No double-minute chromosomes were observed, but with Giemsa staining, a slightly dark, large extra-band was noticed at 4q28. The karyotype can be described as follows: 43–44,X,-Y,add(4)(q28),add(6)(p11),-8, add(11)(q14),-13, +3mar[cp8]/86–88,idemx2[cp8].

Since the *MYCN* gene is frequently involved in this type of amplifications, we co-hybridized a FISH probe specific for the *MYCN*, with a chromosome-2-specific alpha-satellite 2 probe (Q-BIOgene, Illkirch, France). Both chromosomes 2 showed the normal *MYCN* signal at 2p24, and no signal was observed on the abnormal chromosome 4. Strikingly, multiple signals were observed as extra-chromosomal fluorescent dots, indicating a high-level of *MYCN* amplification (Fig. 2). The absence of a positive DAPI staining corresponding to fluorescent signals suggested that the amplification units were very small in size.

Reiterative FISH experiments using appropriate BAC clones (Table 1) located proximally and distally to the boundaries of the amplified segment. These boundaries were delineated by within the clones RP11-637L15 (chr2:16,454,615–16,611,450) and RP11-826H14 (chr2:15,763,477–15,955,850), respectively, (Fig. 3) which span a region of maximum ~850 kb. Co-hybridization experiments did neither detect deletions internal to the episomes nor deletions at the normal chromosomes 2.

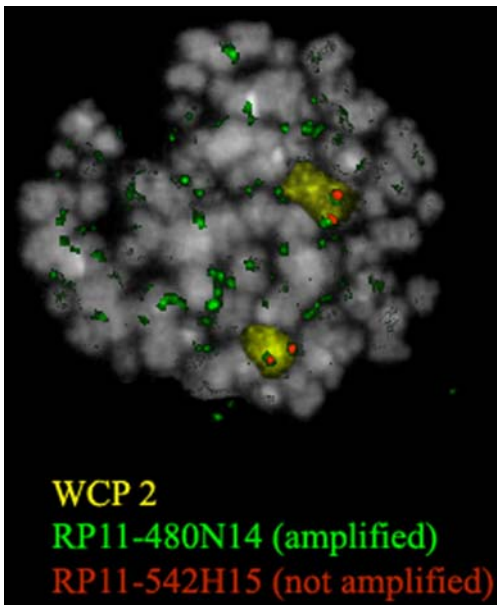


Fig. 2 Example of a co-hybridization FISH experiment, using the WCP specific for chromosome 2 (*yellow*), BACs RP11–480N14 (containing the *MYCN* probe, *green*), and RP11-542H15 (*red*, present only on normal chromosomes 2)

RQ-PCR analysis was exploited to refine the breakpoints at higher resolution. RQ-PCR experiments using primers located within the *MYCN* gene gave an approximate 30-fold copy number increase, yielding a very clear-cut distinction between amplified/non-amplified sequences. All the primer pairs used for the experiments are reported in Table 2. These experiments defined the telomeric and centromeric boundaries as falling within the genomic segments chr2:15,899,400–15,899,658 (258 bp), and chr2:16,488,363–16,488,757 (394 bp), respectively. Therefore, the size of the amplicon was determined to range from 588.705 to 589.357 bp.

To clone and sequence the internal junction of the episome, several PCR experiments were performed using forward and reverse primers designed on the proximal and distal amplicon borders and oriented towards the junction. All the experiments failed, and it was not possible, consequently, to define the junction at the sequence level.

Apart from *MYCN*, the genomic-amplified segment contains two putative genes: *N-cym* (v-myc myelocytomatosis viral related oncogene, neuroblastoma derived opposite strand) and AB073360 (Fig. 3).

Discussion

In the present study, we have described a case of medulloblastoma carrying *MYCN* amplification in the form of episomes. It represents, to the best of our knowledge, the first example of episomal amplification in a primary solid tumor.

FISH and RQ-PCR analyses precisely defined the size of the amplified genomic segment and the location of both proximal and distal breakpoints. PCR experiments designed to amplify the episomal junction were unsuccessful. The failure may indicate that the genomic architecture at the boundaries of the amplicon is more complex than a simple junction.

The model proposed for episome/dmin/hsr genesis, reported as the ‘episome model’, consists in the excision, circularization and subsequent amplification of the excised sequence [3, 15–17]. It implies that the excised segment is deleted on the donor chromosome. The finding that our case did not show a concomitant deletion of the *MYCN* region in one of the two chromosomes 2, however, is not in contrast with the model. It may only indicate that the excision event was post-replicative [16, 17]. The excised circular element, in fact, may segregate randomly with either the normal or the deleted chromatid. It is also possible that the deletion could be subsequently corrected as a result of somatic recombination between the two chromosomes 2 homologues.

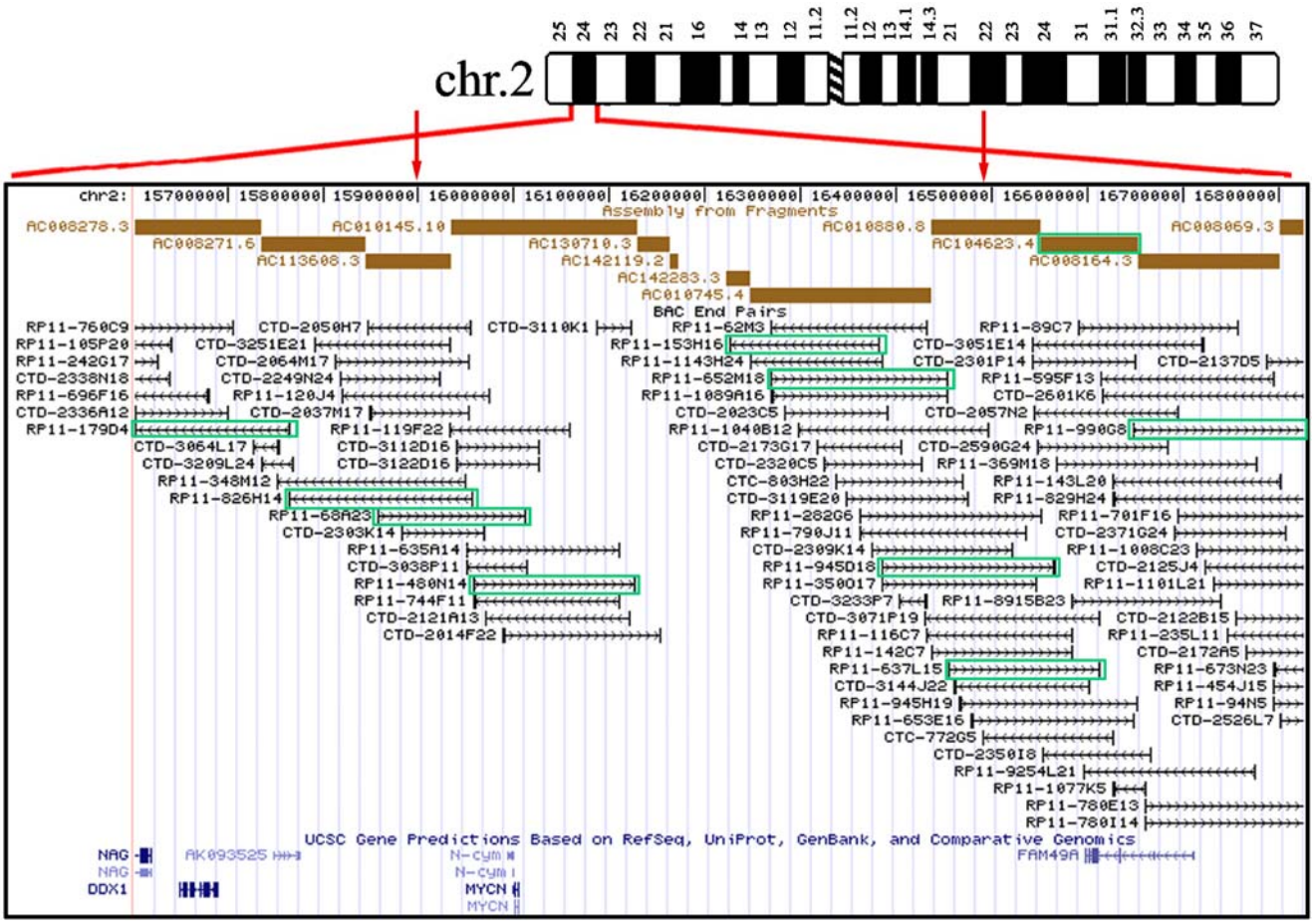


Fig. 3 The picture, from the UCSC database, graphically shows the map of the investigated region. The breakpoints of the amplified segment are indicated by *red arrows*. The clones used in FISH experiments are enclosed in *green rectangles*. The genes are reported at the bottom (in *blue*)

Episomes may result from a double-strand DNA break followed by the end-fusion by the non-homologous end joining mechanism. Although we could not corroborate this hypothesis at the sequence level because of the failure in sequencing the junction, the mapping of the amplicon breakpoints within non-homologous regions allow us exclude the involvement of homologous recombination.

Episomes may represent the initial step of gene amplification that, in the majority of cases, is immediately followed by concatenation, leading to double minutes formation and/or subsequent integration into chromosomal sites in the form of homogenously staining regions [11, 12]. It remains to be elucidated why, in rare cases, the episomes do not undergo the concatenation process.

The amplicon size is usually larger than the transcriptional unit of a single oncogene and includes several co-amplified genes. This situation complicates the identification of the actual target gene. It has been suggested that genes within the associated amplicon, apart from *MYCN,* may contribute to the oncogenic potential of this amplification and may correlate with poor prognosis [7]. Our case displayed an amplified region exceeding the *MYCN* gene, but only one known gene, named *N-cym*, was co-amplified (Fig. 3). This gene was reported to have a functional role during normal fetal development [1, 13], and it is expressed in the fetal brain, lung, liver, and kidney at low levels and in tumor cell lines containing amplified *MYCN*, where it is expressed at very high levels [1, 4]. Unfortunately, the lack of RNA material from the patient precluded any expression comparison of the two genes with respect to medulloblastoma cases lacking *MYCN*-containing episomes.

Some authors examined in detail the prognostic importance of *MYCN* expression in medulloblastomas, identifying a trend towards poorer outcomes in patients whose tumors had detectable levels of *MYCN* mRNA. Similar conclusions were also reached for *MYC* in the development of anaplasia [6].

The present case also indicates that the FISH analysis can disclose *MYCN* amplification in medulloblastoma in the absence of detectable episomes in Giemsa analysis, suggesting that amplification may be more frequent than expected by conventional cytogenetics.

Acknowledgments This work has been supported by AIRC (Associazione Italiana per la Ricerca sul Cancro), MIUR (Ministero dell'Istruzione, dell'Università e della Ricerca), Comité des Alpes-Maritimes de la Ligue Nationale contre le Cancer, and Institut National du Cancer. C. Surace was the recipient of FIRC (Fondazione Italiana per la Ricerca sul Cancro) 3 years fellowship (2003–2005). We are grateful to Rita Attias and Elodie Basc for their technical assistance. The experiments comply with the current Italian laws.

Conflict of interest statement We declare that we have no conflict of interest.

References

1. Armstrong BC, Krystal GW (1992) Isolation and characterization of complementary DNA for N-cym, a gene encoded by the DNA strand opposite to N-myc. Cell Growth Differ 3:385–390
2. Bayani J, Zielenska M, Marrano P, Ng YK, Taylor MD, Jay V, Rutka JT, Squire JA (2000) Molecular cytogenetic analysis of medulloblastomas and supratentorial primitive neuroectodermal tumors by using conventional banding, comparative genomic hybridization, and spectral karyotyping. J Neurosurg 93:437–448
3. Carroll SM, De Rose ML, Gaudray P, Moore CM, Needham-Vandevanter DR, Von Hoff DD, Wahl GM (1988) Double minute chromosomes can be produced from precursors derived from a chromosomal deletion. Mol Cell Biol 8:1525–1533
4. Chen QR, Bilke S, Wei JS, Whiteford CC, Cenacchi N, Krasnoselsky AL, Greer BT, Son CG, Westermann F, Berthold F, Schwab M, Catchpoole D, Khan J (2004) cDNA array-CGH profiling identifies genomic alterations specific to stage and MYCN-amplification in neuroblastoma. BMC Genomics 20:70
5. Corvi R, Amler LC, Savelyeva L, Gehring M, Schwab M (1994) MYCN is retained in single copy at chromsome 2 band p23–24 during amplification in human neuroblastoma cells. Proc Natl Acad Sci U S A 91:5523–5527
6. Eberhart CG, Kratz J, Wang Y, Summers K, Stearns D, Cohen K, Dang CV, Burger PC (2004) Histopathological and molecular prognostic markers in medulloblastoma: c-myc, N-myc, TrkC, and anaplasia. J Neuropathol Exp Neurol 63:441–449
7. Frühwald MC, O'Dorisio MS, Rush LJ, Reiter JL, Smiraglia DJ, Wenger G, Costello JF, White PS, Krahe R, Brodeur GM, Plass C (2000) Gene amplification in PNETs/medulloblastomas: Mapping of a novel amplified gene within the MYCN amplicon. J Med Genet 37:501–509
8. Graux C, Cools J, Melotte C, Quentmeier H, Ferrando A, Levine R, Vermeesch JR, Stul M, Dutta B, Boeckx N, Bosly A, Heimann P, Uyttebroeck A, Mentens N, Somers R, MavLeod RAF, Drexler HG, Look AT, Gilliland DG, Michaux L, Vandenberghe P, Wlodarska I, Marynen P, Hagemejijer A (2004) Fusion of *NUP214* to *ABL* on amplified episomes in T-cell acute lymphoblastic leukemia. Nat Genet 36:1084–1089
9. Kleihues P, Cavenee WK (eds) (2000) World Health Organization classification of tumors (Pathology and genetics of tumors of the nervous system). IARC Press, Lyon, France
10. Lichter P, Tang Chang CJ, Call K, Hermanson G, Evans GA, Housman D, Ward DC (1990) High resolution mapping of human chromosomes 11 by in situ hybridization with cosmid clones. Science 247:64–69
11. Savelyeva L, Schwab M (2001) Amplification of oncogenes revisited: from expression profiling to clinical application. Cancer Lett 167:115–123
12. Schwab M, Amler L (1990) Amplification of cellular oncogenes: a predictor of clinical outcome in human cancer. Genes Chromosomes Cancer 1:181
13. Scott D, Elsden J, Pearson A, Lunec J (2003) Genes co-amplified with MYCN in neuroblastoma: silent passengers or co-determinants of phenotype. Cancer Lett 197:81–86
14. Shaffer LG, Tommerup N (eds) (2005) ISCN: An international system for human cytogenetic nomenclature. Karger, Basel
15. Storlazzi CT, Fioretos T, Paulsson K, Strömbeck, Lassen C, Ahlgren T, Juliusson G, Mitelman F, Rocchi M, Johansson B (2004) Identification of a commonly amplified 4.3 Mb region with overexpression of C8FW, but not MYC in MYC-containing double minutes in myeloid malignancies. Hum Mol Genet 13:1479–1485
16. Storlazzi CT, Fioretos T, Surace C, Lonoce A, Mastrorilli A, Strömbeck B, D'Addabbo P, Iacovelli F, Minervini C, Aventin A, Dastugue N, Fonatsch C, Hagemeijer A, Jotterand M, Mühlematter D, Lafage-Pochitaloff M, Nguyen-Khac F, Schoch C, Slovak ML, Smith A, Solè F, Van Roy N, Johansson B, Rocchi M (2006) MYC-containing double minutes in hematologic malignancies: evidence in favor of the episome model and exclusion of MYC as the target gene. Hum Mol Genet 15:933–942
17. Vogt N, Lefèvre SH, Apiou F, Dutrillaux AM, Cör A, Leuraud P, Poupon MF, Dutrillaux B, Debatisse M, Malfoy B (2004) Molecular structure of double-minute chromosomes bearing amplified copies of the epidermal growth factor receptor gene in gliomas. Proc Natl Acad Sci U S A 101:11368–11373

Virchows Arch (2008) 452:499–505
DOI 10.1007/s00428-008-0606-9

ORIGINAL ARTICLE

The role of COX-2 in rectal cancer treated with preoperative radiotherapy

Hanifa Bouzourene · Pu Yan · Dominique Sandmeier · Abderrahim Zouhair · Maurice Matter · Henri Vuilleumier · Philippe Coucke

Received: 4 February 2008 / Accepted: 9 March 2008 / Published online: 5 April 2008
© Springer-Verlag 2008

Abstract Radiotherapy is one of the principal modalities of rectal cancer treatment, and the ability to predict radio resistance could potentially improve survival through a targeted treatment approach. Cyclooxygenase-2 (COX-2) may protect against damage by irradiation that would justify the use of COX-2 inhibitors. The purpose of this study was to investigate the potential role of COX-2 in tumor response and outcome of patients with rectal cancer treated preoperatively with radiotherapy. Using immunohistochemistry, we examined COX-2 expression in 88 surgical specimens of rectal cancer treated preoperatively and in 26 pretherapeutic biopsies. We tested whether COX-2 expression was correlated with clinico-pathologic parameters and with survival and local recurrence. COX-2 was expressed in 50% of the pretherapeutic tumor biopsies and in 88.6% of post-irradiated surgical samples. COX-2 expression was correlated only with enhanced tumor inflammation (p=0.03) and with tumor volume exceeding 30 cc (p=0.05). COX-2 was not significantly correlated with patient survival, but none of the patients with COX-2 negative tumors did recur locally, whereas 80% of patients with local recurrences have COX-2 positive tumors. We conclude that COX-2 expression is overexpressed in the majority of rectal cancers treated with radiotherapy and likely plays a role in local relapse.

Keywords Radiotherapy · Rectal cancer · Cyclooxygenase-2 · Survival · Recurrence

H. Bouzourene (✉) · P. Yan · D. Sandmeier
Institute of Pathology, Centre Hospitalier Universitaire Vaudois,
Bugnon 25, CH 1011 Lausanne, Switzerland
e-mail: Hanifa.Bouzourene@chuv.ch

A. Zouhair
Department of Radiooncology,
Centre Hospitalier Universitaire Vaudois,
CH 1011 Lausanne, Switzerland

M. Matter · H. Vuilleumier
Department of Surgery, Centre Hospitalier Universitaire Vaudois,
CH 1011 Lausanne, Switzerland

P. Coucke
Department of Radiation-Oncology,
Hôpital Maisonneuve-Rosemont,
5415, Boulevard de l'Assomption,
Montréal, QC, Canada H1T 2M4

Introduction

Nowadays, many therapeutic procedures are available for locally advanced rectal cancer (LARC). However, except the fact that surgery with total mesorectal excision is the mainstay of treatment [11–13, 16, 30], there is no consensus amongst the published literature about what should be the "standard" treatment and the primary endpoint in rectal cancer. Studies with systemic treatment do not show an impact of chemotherapy on overall survival or progression-free survival [1, 10]. In Europe, in contrast to the United States and Canada, a preoperative radiotherapy has been considered as the preferred treatment option for LARC to reduce the incidence of local recurrence [17, 38].

In addition to the problem of the best choice of a standard treatment, the therapeutic efficacy is often hindered by tumor resistance and especially tumor radio resistance. Recent studies indicate that COX-2, an enzyme involved in the metabolic conversion of arachidonic acid to prostaglandins, plays an important role in tumor growth and spread of established tumors by affecting mitogenesis, cellular adhesion, immune surveillance, apoptosis, and

angiogenesis [6, 21, 24, 34, 44, 41, 46]. Several studies have shown that COX-2 expression is elevated in human colorectal neoplasia as compared to normal mucosa, thus making COX-2 a potential target for chemoprevention [7, 15, 42]. A possible relationship between COX-2 expression in colorectal cancer tumors and patient survival has been investigated but nowadays data are inconclusive [8, 20, 22, 28, 33, 40, 48]. Because COX-2 may also be involved in tumor radio resistance, targeting of COX-2 or downstream products (prostaglandins) may eventually improve tumor response to radiotherapy [25, 26]. In vitro and in vivo studies have shown that treatment with selective COX-2 inhibitors significantly enhances tumor response to radiation without appreciably affecting normal tissue radio response [19, 23, 26, 29]. However, evidence of enhanced tumor response to radiation is less obvious in human models.

The purpose of this study was to investigate the relationship between the radiation resistance and the level of COX-2 on a retrospective series of patients with locally advanced rectal cancer (LARC) treated exclusively with radiotherapy. We therefore investigated COX-2 expression in pretherapeutic biopsies and surgical specimens and we tried to correlate it with histological response and clinical outcome.

Materials and methods

Patients

Between 1993 and 2002, 279 patients with locally advanced rectal cancer were included in a multicenter phase II trial on preoperative hyperfractionated and accelerated radiotherapy approved by the Human Investigations Committee of the radiation oncology centers [5]. Only 104 patients treated in our institution and already selected for a previously reported study were considered for this analysis [2].

Patients were eligible if they presented at preoperative work-up with cT3–cT4, whatever the N-stage, or cT1–cT2 with radiological evidence of positive lymph nodes. All patients were treated on protocol after obtaining informed consent for treatment. The age of the patients ranged from 28 to 85 (median, 63 years) and the sex ratio was 1.2 (female/male). Before initiation of the treatment, all patients underwent complete clinical examination, endoscopic biopsy, blood count, assessment of renal and hepatic function, and CEA determination. Distant metastatic disease was excluded by chest X-ray and abdominal ultrasound or computed tomography (CT scan). Assessment of the local extension of the tumor was done by digital rectal examination, rectal ultrasound, and/or CT scan. All patients were irradiated according to the same protocol [5]. The decision concerning the surgical technique, mainly abdominoperineal resection (APR) or low anterior resection, is left to the individual surgeons. The protocol stipulates that a total mesorectal excision with a sharp dissection is "the surgical standard" for those rectal tumors.

Biopsy specimens

Only 26 patients had pretherapeutic biopsies that were available for immunohistochemistry. Biopsies had been fixed in 10% neutral formalin for 12–24 h at room temperature. In the remainder cases, the tumor samples had been exhausted during previous studies and were no more present in the paraffin blocks or immunostaining failed because the material had been fixed in sublimated formol.

Macroscopical assessment of surgical specimens

The surgical specimens were fixed in 10% buffered neutral formalin for 24 h. The whole tumor and attached mesorectum were serially sliced at 3- to 4-mm intervals perpendicular to the longitudinal axis of the rectum, which allowed macroscopical identification of the areas of deepest invasion.

Histological assessment of surgical specimens

All irradiated rectal tumors were retrospectively reanalyzed (H.B). The tumors were classified according to the WHO classification of tumors of the digestive system [47] and staged according to the TNM classification [35]. Tumor downstaging was obtained by comparison of the clinical preoperative and postoperative pathological tumor staging. Tumor volume was calculated on the length and width evaluated on the macroscopical examination and on the tumor thickness assessed on slides. Tumor inflammation, tumor necrosis, and tumor regression were graded as previously described [2]. Tumor inflammatory reaction (mononuclear and granular cells) was graded as 1 when absent or mild, 2 when moderate, and 3 when extensive. Tumor necrosis was graded as 1 when absent or less than 25% of the tumor mass, 2 when it represented 25–50% of the tumor mass, 3 when it represented 50–75% of the tumor mass, and 4 when it represented 75% of the tumor mass. Tumor regression was graded in five grades, based on the presence of residual tumor cells and the extent of fibrosis. Grade 1 was defined as sterilization of the tumor, grade 2 by the presence of rare residual cancer cells scattered through the fibrosis, grade 3 by more residual tumor cells but fibrosis still predominates, grade 4 by more residual cancer cells than fibrosis, and grade 5 when the tumor shows no signs of regression. Vascular invasion was also recorded.

COX-2 immunohistochemistry

Four-micrometer-thick tissue sections were deparaffinized in xylene, rehydrated, treated with 0.3% H_2O_2 in methanol

for 30 min to block endogenous peroxidase activity. The antigen retrieval was done using a pressure cooker. After preheating 1 l of 0.01 M sodium citrate buffer, pH6.0 until boiling in a stainless steel pressure cooker, the sections were heated for 2 min, during which the pressure cooker reached operating temperature. Subsequently, the pressure cooker was removed from the heat source and placed under running cold water with the lid on to cool it down. The slides were placed in a container with running cold water and cooling continued for another 10 min. The sections were subsequently rinsed in phosphate-buffered saline (PBS) and conditioned with 10% normal goat serum for 30 min at room temperature (RT) and incubated with anti-COX-2 monoclonal antibody (Cayman Chemical, Ann Arbor, MI, USA) diluted at 1:200 in PBS with 0.1 M NaCl at RT for 2 h. After rinsing in PBS, the slides were incubated with DAKO EnVision™ (mouse) for 30 min at RT. After the slides were rinsed in PBS, peroxidase was revealed by immersion in diaminobenzidine (DAB; DAKO, Carpentiria, CA, USA) according to the manufacture's instructions and the sections were counterstained with hematoxylin and mounted for microscopic examination. The negative control was performed by using COX-2 blocking peptide diluted at 1:50 according to the manufacture's instructions (Cayman Chemical). Immunohistochemical expression of COX-2 was evaluated semiquantitatively by two observers using a double-headed microscope (H.B, P.Y) on blinded sections. There was no staining on the negative control slide. Staining for COX-2 in the normal rectal mucosa was used as a positive control. Absorptive epithelial cells bordering the luminal surface and especially basal part of the crypts showed COX-2 positivity, generally localized in the paranuclear region and cell membranes, less frequently in the nuclei. If no crypt staining was obtained after two attempts, the case was eliminated from the study on technical grounds. In tumor cells, COX-2 immunoreactivity was observed in the cytoplasm and/or in the nuclei (Fig. 1). The spindle-shaped stromal cells, intermingled with neoplastic glands, sometimes showed staining for COX-2. All cases were scored as following: score 0: <5% of positive cells; score 1: 5–30% of positive cells; score 2: 30–60% of positive cells; score 3: >60% of positive cells. Tumor cases with COX-2 score 0 were considered as negative.

Statistical analysis and follow-up

All patients were followed for local recurrence and distant metastasis every 6 months for the first 2 years and every year thereafter. A physical examination, serum carcinoembryonic antigen (CEA) assay, chest X-ray, abdominal ultrasound or CT scan, and a CT scan of the pelvis were included in the follow-up procedure. The events were death (all causes of death included) for overall survival (OS), distant metastases or locoregional relapse or death for disease-free survival (DFS), and local or locoregional relapse for local control (patients who died without local or locoregional relapse were censored at time of death), respectively.

All statistical analyses were conducted using the JUMP software (SAS, Cary, NC). A p value<0.05 was considered statistically significant. In univariate and multivariate analysis, OS, DFS, and local control were used as the end points. In univariate analysis survival curves were estimated according to the Kaplan–Meier method for the following variables: age, sex, pT, pN, tumor differentiation, tumor inflammation, tumor necrosis, tumor regression, tumor volume, and vascular invasion. The significance of their difference was estimated by the log-rank test. To increase the number of patients per group, the categories of the different pathological variables were also combined for these analyses, i.e., pT1–2 vs pT3–4; well and moderately differentiated adenocarcinomas vs poorly differentiated and mucinous carcinomas; absence or mild necrosis (score 1) vs moderate to extensive necrosis (scores 2–4); absence or mild inflammation (score 1) vs moderate to marked inflammation (scores 2 and 3); responder group (tumor regression grades 2–4) vs non-responder group (tumor regression grade 5).

Multivariate survival analysis according to the Cox's proportional hazards models was constructed by backward elimination of the following variables: age, sex, pT, pN, tumor differentiation, tumor inflammation, tumor necrosis, tumor regression, and vascular invasion.

Results

Pathological findings

Eighty-eight out of 104 patients with rectal cancer were selected for the COX-2 study. The remainder cases were excluded because the tumour was sterilized (tumor regression grade 1) or for technical reasons. There were 20 pT2 tumors (23%), 57 pT3 (65%), and 11 pT4 (12%). Tumor downstaging obtained after comparison of the clinical and pathological stages was observed in 44% of the cases. Regional lymph node metastases were found in 59% of patients. Of the tumors, 25% were well-differentiated adenocarcinomas, 42% were moderately differentiated adenocarcinomas, 10% were poorly differentiated adenocarcinomas, and 25% were mucinous carcinomas. Partial tumor regression (G2–4) was noted in 80% (G2=16%; G3=39%; G4=25%) and absence of regression (G5) was noted in 20% of the tumors. Tumor necrosis was absent or mild (score 1) in 66% of the tumors, moderate to extensive

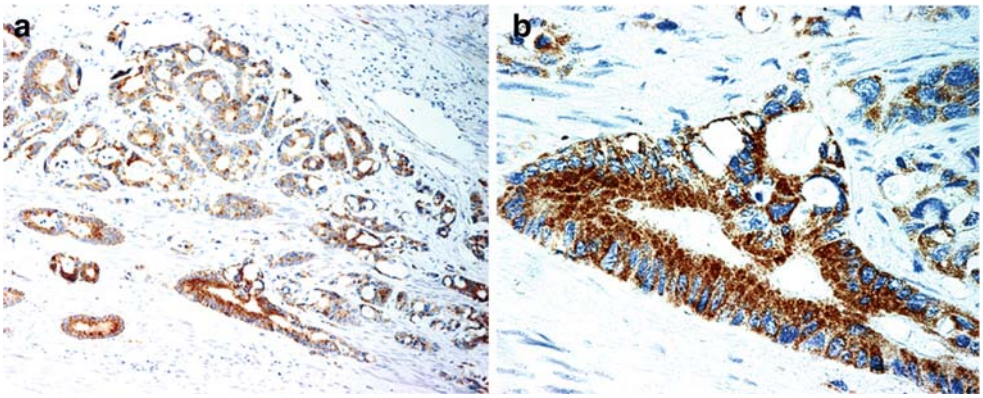


Fig. 1 Low (**a**) and high magnification (**b**) of COX-2 expression in a rectal adenocarcinoma treated preoperatively with radiotherapy

in 34% (scores 2–4) of the tumors. Tumors showed a mild or no inflammation (score 1) in 30% of cases, a moderate to marked inflammation in 70% (score 2 and 3) of cases. Vascular invasion was present in 29 patients.

Survival and local control

During follow-up (median=42 months), 24 patients developed distant metastasis and eight patients a local recurrence. Thirty-nine patients died, 29 of whom from rectal cancer.

The median OS was 53 months. The median actuarial OS was significantly lower in patients with lymph node metastases (p=0.005, log rank test) and for those patients presenting tumors with vascular invasion (p=0.003). There was no difference in OS between responders (G2–4) compared to non-responders (G5).

The median DFS was 46 months. The median actuarial DFS was significantly lower in patients with advanced pT stages (pT3–4) (p=0.03, log rank test) and with lymph node metastases (p=0.0008, log rank test). The DFS was longer in responders than in non responders (p=0.03, log rank test). Moreover, a significant correlation was found between the different grades of tumor regression and DFS (p=0.04, log rank test).

The actuarial locoregional recurrence rates at 2 and 5 years were 7.5% and 11.4%, respectively. There was a trend for a better local control in responders as compared to non-responders (p=0.10, log rank test).

Cyclooxygenase-2 immunostaining and pathologic analysis

By immunohistochemistry COX-2 was found to be absent in 13 (50%) out of 26 tumor biopsies taken before treatment (score 0). In tumor biopsies expressing COX-2, four cases were scored 1, four cases were scored 2, and five cases were scored 3.

In 88 surgical specimens, ten tumors (11%) did not express COX-2 (score 0). Of 78 COX-2 positive tumors (89%), 38 (44%) had a mild (score 1), 25 (28%) a moderate (score 2), and 15 (17%) a marked (score 3) COX-2 expression. The distribution of COX-2 expression and pathologic parameters is summarized in the Table 1. When comparing COX-2 expression in biopsies and surgical specimens we found that among 13 patients with negative tumor biopsies, ten (78%) became COX-2 positive in the surgical specimens with a scoring of expression varying from 1 to 3, whereas only three cases remained negative after irradiation. Among the cases with positive COX-2 in tumor biopsies, two had a higher score of expression, seven had the same score of expression, whereas four cases had a lower score of expression in the irradiated tumors.

COX-2 expression was not correlated with any of the following parameters: sex, age, tumor downstaging, pT, pN, tumor regression, tumor necrosis, vascular invasion. We found a trend of correlation between COX-2 and tumor differentiation (p=0.087). COX-2 was correlated with moderate and marked tumor inflammation (p=0.03) and with tumor volume exceeding 30 cc (p=0.05). Grouping according to level of expression of COX-2 with any of the tested pathological variables did not modify the conclusions of the present analysis.

We were not able to demonstrate any significant correlation between the expression level of COX-2 and OS and DFS. However, it is noteworthy that none of the patients having tumor without COX-2 expression did recur locally (0/10), in contrast to eight out of ten recurrences (80%) in 78 patients with tumor characterized by a COX-2 expression. It might well be that the number of local events is too small in the present series to allow us to highlight a significant difference.

Discussion

Colorectal cancer is a significant cause of morbidity and mortality in Western populations. Rectal cancer if treated by surgery alone is characterized by a high incidence of local recurrence (20 to 70%), regional lymph node and distant metastases [17, 38]. Until now, there is no consensus

Table 1 Correlations between COX-2 expression and histological parameters in 88 surgical specimens of rectal cancer treated with preoperative radiotherapy

Scores of COX-2 expression	COX- 2 expression								*p* value
	0		1		2		3		
	N	%	*N*	%	*N*	%	*N*	%	
Pathological staging									NS
pT2	4	4	7	8	4	5	5	6	
pT3	5	6	20	23	19	21	13	15	
pT4	1	1	5	6	3	3	2	2	
pN0	6	7	10	11	14	16	10	11	
pN1	4	5	21	24	10	11	10	11	
Tumor differentiation									0.087
Well differentiated	2	2	8	9	3	3	7	8	
Moderately differentiated	6	7	9	10	13	15	9	10	
Poorly differentiated	0	0	5	6	2	2	2	2	
Mucinous	2	2	9	10	9	10	2	2	
Tumor regression									NS
Partial (grades 2–4)	9	10	23	26	20	23	18	20	
Absent (grade 5)	1	1	9	10	3	3	5	6	
Tumor inflammation									
Mild (score 1)	4	5	10	11	6	7	6	7	
Moderate to marked (score 2,3)	6	7	23	26	20	23	13	15	0.03
Tumor necrosis									NS
Absent or mild (score 1)	10	11	30	34	22	25	16	18	
Moderate to marked (scores 2–4)	0	0	3	3	4	4	3	3	
Vascular invasion									NS
Present	5	6	9	10	10	11	5	6	
Absent	5	6	22	25	17	19	15	17	

NS non significant

among the published literature about what should be the "standard" treatment and the primary endpoint in rectal cancer (survival, disease-free survival, local control, sphincter sparing surgery or quality of life). However, neoadjuvant preoperative radiotherapy has been shown to induce tumor regression significantly, improving local control and overall survival [2, 5, 32]. Nevertheless, the tumor response, which is different from one patient to another, is probably limited by many genetic factors. Among those factors, the COX-2 appears to play an important role. Cyclooxygenase is a key enzyme that catalyses the conversion of prostaglandins and other eicosanoids from arachidonic acid. COX-2 is induced during pathologic conditions and is often overexpressed in premalignant lesions and malignant tumors [3, 6, 24, 43, 44]. This enzyme is linked to carcinogenesis, maintenance of progressive tumor growth, and facilitation of metastatic spread [4, 41]. Several studies have shown that COX-2 expression is elevated in human adenomas and colon cancers [7, 31, 33].

Data about the relationship between COX-2 expression and patient survival in colorectal cancer are inconclusive [8, 15, 20, 22, 28, 33, 36, 40, 48]. However, COX-2 protein expression has become the focus of active investigation because of its possible implication in tumor radio resistance. Indeed, it was reported that COX2 is upregulated by radiation, inducing radio resistance [25, 26, 29]. Preclinical studies have shown that treatment with selective COX-2 inhibitors significantly enhances tumor response to radiation without appreciably affecting normal tissue radio response [19, 26]. However, if in vitro and in vivo results support this hypothesis, the data available from human studies are scarce. In oral squamous cell carcinoma [39] and in laryngeal cancer [27] elevated COX-2 expression has been associated with radio resistance and diminished survival. Expression of COX-2 was also correlated with poor prognosis in squamous cell carcinoma of the uterine cervix treated with radiation therapy [9, 18].

In the present study, we investigated by immunohistochemistry the expression of COX-2 in 88 surgical specimens from a cohort of patients with rectal cancer treated preoperatively with radiotherapy and attempted to correlate this with pathologic parameters and clinical outcome. We also investigated the expression of COX-2 before neoadjuvant radiotherapy in a subset of rectal cancers with available tumor biopsies. COX-2 expression was present in

50% of pretherapeutic tumor biopsies and 89% of irradiated tumors. We found also that the large majority of negative tumor biopsies expressed COX-2 protein after radiotherapy and that a subset of positive tumor biopsies has an increased expression. This finding support the fact that, at least in a subgroup of rectal cancer, COX-2 is upregulated by radiation as already reported in some cancer cell lines [37]. However, this is in partial contradiction with a recent study that compared COX-2 expression in pretherapeutical rectal carcinoma biopsies and posttherapeutical surgical specimen and which found that COX-2 expression is present in nearly all pretherapeutical biopsies although there is an increase of the intensity of COX-2 expression in one third of posttherapeutical rectal cancer [45].

In the present analysis, COX-2 expression in post irradiated tumors was not correlated with any of the tested pathologic parameters in particular with tumor regression and tumor downstaging. We found that COX-2 was correlated with tumor inflammation which is in accordance with the fact that COX-2 is known to be induced by proinflammatory cytokines and that COX-2 is upregulated at sites of inflammation [14]. We also found that COX2 was more frequently expressed when tumor volume exceeds 30 cc. We were not able to provide an explanation for this finding especially as we did not find any correlation with tumor regression or tumor downstaging.

More importantly, we found that COX-2 expression is not a significant prognostic factor neither for overall patient survival nor for DFS in irradiated rectal carcinomas. These data are in line with one published study on human rectal cancer pretreated with chemoradiotherapy [45] but are not in accordance with the results reported in studies on squamous cell carcinoma of head and neck and cervix treated with radiotherapy alone or radiochemotherapy [39, 27, 9, 18].

Nevertheless, we found that there was a trend toward increased local failure in patients with treated tumors expressing COX-2. In contrast, all the patients with COX-2 negative tumors were free of local recurrence. The difference was not statistically significant, probably due to the small number of recurrences overall. However, testing of this hypothesis within the frame of a randomized trial could be interesting.

Conclusion

This study shows that radiotherapy induces an expression of COX-2 in the majority of rectal cancer patients and is correlated with tumor inflammation. COX-2 expression is not associated with rectal cancer survival and tumor response, but a possible association with local recurrence remains to be evaluated in a larger cohort of patients with rectal cancer treated by preoperative radiotherapy.

Acknowledgment This work was supported by grant from Fonds national Suisse de la recherche scientifique (FNRS 3100-63835).

Conflict of interest statement We declare that we have no conflict of interest.

References

1. Bosset JF, Calais G, Mineur L, Maingon P, Radosevic-Jelic L, Daban A, Bardet E, Beny A, Briffaux A, Collette L (2005) Enhanced tumorocidal effect of chemotherapy with preoperative radiotherapy for rectal cancer: preliminary results-EORTC 22921. J Clin Oncol 23:5620–5627
2. Bouzourene H, Bosman FT, Seelentag W, Matter M, Coucke P (2002) Importance of tumor regression assessment in predicting the outcome in patients with locally advanced rectal carcinoma treated with preoperative radiotherapy. Cancer 94:1121–1130
3. Chan G, Boyle JO, Yang EK, Zhang F, Sacks PG, Shah JP, Edelstein D, Soslow RA, Koki AT, Woerner BM, Masferrer JL, Dannenberg AJ (1999) Cyclooxigenase-2 expression is up-regulated in squamous cell carcinoma of the head and neck. Cancer Res 5:991–994
4. Coffey RJ, Hawkey CJ, Damstrup L, Graves-Deal R, Daniel VC, Dempsey PJ, Chinery R, Kirkland SC, DuBois RN, Jetton TL, Morrow JD (1997) Epidermal growth factor receptor activation induces nuclear targeting of cyclooxygenase-2, basolateral release of prostaglandins, and mitogenesis in polarizing colon cancer cells. Proc Natl Acad Sci U S A 94:657–662
5. Coucke P, Notter M, Stamm B, Matter M, Fasolini F, Schlumpf R, Matzinger O, Bouzourene H (2006) Preoperative hyperfractionated acccelerated radiotherapy (HART) in locally advanced rectal cancer (LARC) immediately followed by surgery. A prospective phase II trial. Radiother Oncol 79:52–58
6. Dubois RN, Abramson SB, Crofford L, Gupta RA, Simon LS, Van De Putte LB, Lipsky PE (1998) Cyclooxygenase in biology and disease. FASEB J 12:1063–1073
7. Eberhart CE, Coffey RJ, Radhika A, Giardiello FM, Ferrenbach S, Dubois RN (1994) Up-regulation of cyclooxigenase-2 gene expression in human colorectal adenomas and adenocarcinomas. Gastroenterology 107:1183–1188
8. Fux R, Schwab M, Thon KP, Gleiter CH, Fritz P (2005) Cyclooooxygenase-2 expression in human colorectal cancer is unrelated to overall patient survival. Clin Cancer Res 11:4754–4760
9. Gaffney DK, Holden J, Davis M, Zempolich K, Murphy KJ, Dodson M (2001) Elevated cyclooxygenase-2 expression correlates with diminished survival in carcinoma of the cervix treated with radiotherapy. Int J Radiat Oncol Biol Phys 49:1213–1217
10. Gérard JP, Conroy T, Bonnetain F, Bouché O, Chapet O, Closon-Dejardin MT, Untereiner M, Leduc B, Francois E, Maurel J, Seitz JF, Buecher B, Mackiewicz R, Ducreux M, Bedenne L (2006) Preoperative radiotherapy with or without concurrent fluorouracil and leucovorin in T3–4 rectal cancers: results of FFCD 9203. J Clin Oncol 24:4620–4625
11. Glimelius B (2003) Role of adjuvant chemoradiotherapy for abdominal malignancies. Dig Surg 20:169–179
12. Heald RJ, Ryall RD (1986) Recurrence and survival after total mesorectal excision for rectal cancer. Lancet 1:1479–1482
13. Hermanek P, Hermanek PJ (2000) Role of the surgeon as a variable in the treatment of rectal cancer. Sem Surg Oncol 19:325–329
14. Herschman HR, Xie W, Reddy S (1995) Inflammation, reproduction, cancer and all that.... The regulation and role of the inducible prostaglandin synthase. Bioessays 17:1031–1037

15. Joo YE, Kim HS, Min SW, Lee WS, Park CH, Park CS, Choi SK, Rew JS, Kim SJ (2002) Expression of cyclooxygenase-2 protein in colorectal carcinomas. Int J Gastrointest Cancer 31:147–154
16. Kapiteijn E, Putter H, van de Velde CJH and cooperative investigators of the Dutch Colorectal Cancer Group (2002) Impact of the introduction and training of total mesorectal excision on recurrence and survival in rectal cancer in the Netherlands. cooperative investigators of the Dutch Colorectal Cancer Group Br J Surgery 89:1142–1149
17. Kapiteijn E, Marijnen CA, Nagtegall ID Putter H, Steup WH, Wiggers T, Rutten HJ, Pahlman L, Glimelius B, van Krieken JH, Leer JW, van de Velde CJ, Dutch Colorectal Cancer Group (2001) Preoperative radiotherapy combined with total mesorectal excision for resectable rectal cancer. N Engl J Med 345:638–646
18. Kim YB, Kim GE, Cho NH, Cho HC, Pyo HR, Lee JD, Park TK, Koom WS, Chun M, Suh CO (2002) Overexpression of cyclooxigenase-2 is associated with a poor prognosis in patients with squamous cell carcinoma of the uterine cervix treated with radiation and concurrent chemotherapy. Cancer 95:531–539
19. Kishi K, Petersen S, Petersen C, Hunter N, Mason K, Masferrer JL, Tofilon PJ, Milas L (2000) Preferential enhancement of tumor radioresponse by an inhibitor of cyclooxygenase-2 inhibitor. Cancer Res 60:1326–1331
20. Konno H, Baba M, Shoji T, Ohta M, Suzuki S, Nakamura S (2002) Cyclooxygenase-2 expression correlates with uPAR levels and is responsible for poor prognosis of colorectal cancer. Clin Exp Metastasis 19:527–534
21. Masferrer JL, Leahy KM, Koki AT, Zweifel BS, Settle SL, Woerner BM, Edwards DA, Flickinger AG, Moore RJ, Seibert K (2000) Antiangiogenic and antitumor activities of cyclooxygenase-2 inhibitors. Cancer Res 60:1306–1311
22. Masunaga R, Kohno H, Dhar DK, Ohno S, Shibakita M, Kinugasa S, Yoshimura H, Tachibana M, Kubota H, Nagasue N (2000) Cyclooxygenase-2 expression correlates with tumor neovascularization and prognosis in human colorectal carcinoma patients. Clin Cancer Res 6:4064–4068
23. Milas L, Kishi K, Hunter N, Mason K (1999) Enhancement of tumor response to gamma-radiation by an inhibitor of cyclooxygenase-2 enzyme. J Natl Cancer Inst 91:1501–1504
24. Milas L (2003) Cyclooxygenase-2 (COX-2) enzyme inhibitors and radiotherapy: preclinical basis. Am J Clin Oncol 26:S66–69
25. Milas L, Mason KA, Crane CH, Liao Z, Masferrer J (2003) Improvement of radiotherapy or chemoradiotherapy by targeting COX-2 enzyme. Oncology 17:15–24
26. Nakata E, Mason KA, Hunter N, Husain A, Raju U, Liao Z, Ang KK, Milas L (2004) Potentiation of tumor response to radiation or chemoradiation by selective cyclooxygenase-2 enzyme inhibitors. Int J Radiat Oncol Biol Phys 58:369–375
27. Nix P, Lind M, Greenman J, Stafford N, Cawkwell L (2004) Expression of Cox-2 protein in radioresistant laryngeal cancer. Ann Oncol 15:797–801
28. Petersen S, Haroske G, Hellmich G, Ludwig K, Petersen C, Eicheler W (2002) COX-2 expression in rectal carcinoma: immunohistochemical pattern and clinical outcome. Anticancer Res 22:1225–1230
29. Pyo H, Choy H, Amorino GP, Kim JS, Cao Q, Hercules SK, DuBois RN (2001) A selective cyclooxigenase-2 inhibitor, NS-398, enhances the effect of radiation in vitro and in vivo preferentially on the cells that express cyclooxygenase-2. Clin Cancer Res 7:2998–3005
30. Quirke P, Durdey P, Dixon MF, Williams NS (1986) Local recurrence of rectal adeocarcinoma due to inadequate surgical resection: histopathological study of lateral tumor spread and surgical excision. Lancet 2:996–999
31. Sano H, Kawahito Y, Wilder RL, Hashiramoto A, Mukai S, Asai K, Kimura S, Kato H, Kondo M, Hla T (1995) Expression of cyclooxygenase-1 and-2 in human colorectal cancer. Cancer Res 55:3785–3789
32. Sauer R, Becker H, Hohenberger W, Rödel C, Wittekind C, Fietkau R, Martus P, Tschmelitsch J, Hager E, Hess CF, Karstens JH, Liersch T, Schmidberger H, Raab R (2004) Preoperative versus postoperative chemoradiotherapy for rectal cancer. German Rectal Cancer Study Group N Engl J Med 17:1731–1740
33. Sheehan KM, Sheahan K, O'Donoghue DP, MacSweeney F, Conroy RM, Fitzgerald DJ, Murray FE (1999) The relationship between cyclooxygenase-2 expression and colorectal cancer. JAMA 282:1254–1257
34. Smith WL, Garavito RM, Dewitt DL (1996) Prostaglandin endoperoxide H synthases (cyclooxygenases)-1 and -2. J Biol Chem 271:33157–33160
35. Sobin LH, Wittekind C (eds) (1997) TNM Classification of malignant tumours. 5th ed. John Wiley & Sons, New York
36. Soumaoro LT, Uetake H, Higuchi T, Takagi Y, Enomoto M, Sugihara K (2004) Cyclooxygenase-2 expression: a significant prognostic indicator for patients with colorectal cancer. Clin Cancer Res 10:8465–8471
37. Steinauer KK, Gibbs I, Ning S, French JN, Armstrong J, Knox SJ (2000) Radiation induces upregulation of cyclooxygenase-2 (COX-2) protein in PC-3 cells. Int J Radiat Oncol Biol Phys 48:325–328
38. Swedish Rectal Cancer Trial (1997) Improved survival with preoperative radiotherapy in resectable rectal cancer. N Engl J Med 336:980–987
39. Terakado N, Shintani S, Yano J, Chunnan L, Mihara M, Nakashiro K, Hamakawa H (2004) Overexpression of cyclooxygenase-2 is associated with radioresistance in oral squamous cell carcinoma. Oral Oncol 40:383–389
40. Tomozawa S, Tsuno NH, Sunami E, Hatano K, Kitayama J, Osada T, Saito S, Tsuruo T, Shibata Y, Nagawa H (2000) Cyclooxygenase-2 overexpression correlates with tumour recurrence, especially haematogenous metastasis, of colorectal cancer. Br J Cancer 83:324–328
41. Tsujii M, Dubois R (1995) Alterations in cellular adhesion and apoptosis in epithelial cells overexpressing prostaglandin endoperoxide synthase-2. Cell 83:493–501
42. Tsujii M, Kawano S, Dubois R (1997) Cyclooxigenase-2 expression in human colon cancer cells increases metastatic potential. Proc Natl Acad Sci U S A 94:3336–3340
43. Tucker ON, Dannenberg AJ, Yang EK, Zhang F, Teng L, Daly JM, Soslow RA, Masferrer JL, Woerner BM, Koki AT, Fahey TJ 3rd (1999) Cyclooxigenase-2 expression is upregulated in human pancreatic cancer. Cancer Res 59:987–990
44. Wambura C, Aoyama N, Shirasaka D, Kuroda K, Maekawa S, Ebara S, Watanabe Y, Tamura T, Kasuga M (2002) Effect of Helicobacter pylori-induced cyclooxygenase-2 on gastric epithelial cell kinetics: implication for gastric carcinogenesis. Helicobacter 7:129–138
45. Watwe V, Javle M, Lawrence D, Groth J, Iyer R, El-Hajjar D, Geradts J (2005) Cyclooxygenase-2 (COX-2) levels before and after chemotherapy: a study in rectal cancer. Am J Clin Oncol 28:560–564
46. Williams CS, Mann M, Dubois RN (1999) The role of cyclooxygenases in inflammation, cancer, and development. Oncogene 18:7908–7916
47. World Health Organization (1988) International histological classification of tumours. 2nd ed. Geneva: World Health Organization, 1969–1981. Springer-Verlag, Berlin
48. Zhang H, Sun XF (2002) Overexpression of cyclooxygenase-2 correlates with advanced stages of colorectal cancer. Am J Gastroenterol 97:1037–1041

Virchows Arch (2008) 452:507–514
DOI 10.1007/s00428-008-0602-0

OpenAccess

ORIGINAL ARTICLE

Validation of tissue microarray technology in squamous cell carcinoma of the esophagus

Judith Boone · Richard van Hillegersberg · Paul J. van Diest · G. Johan A. Offerhaus · Inne H. M. Borel Rinkes · Fiebo J. W. Ten Kate

Received: 6 December 2007 / Revised: 30 January 2008 / Accepted: 25 February 2008 / Published online: 8 April 2008
© The Author(s) 2008

Abstract Tissue microarray (TMA) technology has been developed to facilitate high-throughput immunohistochemical and in situ hybridization analysis of tissues by inserting small tissue biopsy cores into a single paraffin block. Several studies have revealed novel prognostic biomarkers in esophageal squamous cell carcinoma (ESCC) by means of TMA technology, although this technique has not yet been validated for these tumors. Because representativeness of the donor tissue cores may be a disadvantage compared to full sections, the aim of this study was to assess if TMA technology provides representative immunohistochemical results in ESCC. A TMA was constructed containing triplicate cores of 108 formalin-fixed, paraffin-embedded squamous cell carcinomas of the esophagus. The agreement in the differentiation grade and immunohistochemical staining scores of CK5/6, CK14, E-cadherin, Ki-67, and p53 between TMA cores and a subset of 64 randomly selected donor paraffin blocks was determined using kappa statistics. The concurrence between TMA cores and donor blocks was moderate for Ki-67 (κ=0.42) and E-cadherin (κ=0.47), substantial for differentiation grade (κ=0.65) and CK14 (κ=0.71), and almost perfect for p53 (κ=0.86) and CK5/6 (κ=0.93). TMA technology appears to be a valid method for immunohistochemical analysis of molecular markers in ESCC provided that the staining pattern in the tumor is homogeneous.

Keywords Biological markers · Esophageal neoplasms · Protein microarray analysis · Squamous cell carcinoma · Validation studies

J. Boone (✉) · R. van Hillegersberg · I. H. M. Borel Rinkes
Department of Surgery, University Medical Center Utrecht,
G04.228, Heidelberglaan 100,
3584 CX Utrecht, The Netherlands
e-mail: jboone2@umcutrecht.nl

P. J. van Diest · G. J. A. Offerhaus · F. J. W. Ten Kate
Department of Pathology, University Medical Center Utrecht,
Heidelberglaan 100,
3584 CX Utrecht, The Netherlands

Introduction

Esophageal carcinoma is the eighth most common type of cancer in the world [13]. Although the recent rise in incidence of esophageal cancer has predominantly been caused by an increase in adenocarcinomas, the majority of esophageal cancer cases globally are squamous cell carcinomas [13]. For both histological types, radical en bloc esophagectomy with an extensive lymph node dissection offers the best chance for cure, leading to an overall 5-year survival rate of around 30% [1, 20].

Well-known histopathological factors for prognostication of esophageal cancer include the TNM stage, the number of positive lymph nodes, and the presence of extracapsular lymph node involvement [16, 24, 26, 32]. Recently, there has been a growing interest in the prognostic value of molecular markers in (esophageal) cancer [21]. The expression of such markers is often studied by immunohistochemistry on formalin-fixed, paraffin-embedded tumor slides. Tissue microarray (TMA) technology has been developed to enable high-throughput immunohistochemical analyses [14]. By inserting small (diameter e.g. 0.6 mm) donor tissue core biopsies into a single recipient paraffin block, this technique allows for rapid analysis of large numbers of tissues under standardized laboratory and evaluation conditions without significantly damaging the patient's tissue. In addition, TMA technology leads to a significant

reduction of the amount of consumables used and time needed for interpretation, increasing cost-effectiveness.

A potential disadvantage compared to full tissue sections is that the donor cores may not be representative for the whole tumor, particularly in case of heterogeneous tumors and heterogeneously expressed molecular markers. Hence, some validation studies have been performed in various cancers using different kinds of antibodies [2, 4, 6, 7, 9, 12, 23, 35]. Although several studies have revealed novel prognostic biomarkers in esophageal squamous cell cancer (ESCC) by means of TMA technology [38, 39, 41], this technique has not yet been validated for these tumors.

The aim of the present study was, therefore, to validate TMA technology in ESCC by assessing the concurrence of immunohistochemical staining scores of established molecular markers with various expression patterns between triplicate 0.6 mm core biopsies of the TMA and their whole tissue section counterparts.

Materials and methods

TMA construction

Formalin-fixed, paraffin-embedded tissues from thoracic ESCCs of consecutive patients having undergone esophagolymphadenectomy at the authors' institute between 1989 and 2006 were retrieved from the archives of the Department of Pathology. Patients who received neoadjuvant therapy were excluded from this study. The study was carried out in accordance with the ethical guidelines of our institution concerning informed consent about the use of patient's materials after surgical procedures.

By an experienced pathologist (FtK), three representative tumor regions were marked on one selected hematoxylin and eosin (H&E)-stained section of each tumor, avoiding areas of necrosis. From these three tumor regions, a tissue cylinder with a diameter of 0.6 mm was punched out of the corresponding paraffin block ('donor block') and placed into the TMA paraffin block using a manual tissue arrayer (MTA-I, Beecher Instruments, Sun Prairie, USA), which was guided by the MTABooster® (Alphelys, Plaisir, France). The distribution and position of the cores was determined in advance with the TMA-designer Software (Alphelys-TMA Designer®, Version 1.6.8, Plaisir, France). Cores of normal esophageal mucosa, lymph node, kidney, liver, spleen, and prostate were incorporated in the tissue array block as internal controls.

Immunohistochemistry

For each marker, a 4-μm slide of the TMA and one of every selected donor paraffin block were immunohistochemically stained. Table 1 shows the details of all antibodies, dilutions, incubation times and antigen retrieval methods applied in this study.

For all stainings, sections were deparaffinized in xylene for 10 min followed by dehydration through graded alcohols. Endogenous peroxidase activity was blocked for 15 min in a buffer solution of pH 5.8 (containing 8.32 g citric acid, 21.52 g disodium hydrogen phosphate, 2 g sodium azide in 1 l of water) with hydrogen peroxide (0.3%). After antigen retrieval for 20 min, a cooling down period of 30 min was followed by incubation with the primary antibody. Depending on the antibody used, slides were incubated with the secondary antibody followed by

Table 1 Specification of antibodies used and details of tissue processing

Primary antibody	Staining pattern	Source[a]	Clone and code	Antigen retrieval	Dilution	Incubation time (min/room temperature)	Detection[b]	Positive control	Procedure
CK5/6	Cytoplasmic	Chemicon	D5/16 B4	EDTA pH 9.0	1:3,000	60	Strept ABC	Breast	Autostainer
CK14	Cytoplasmic	Neomarkers	LL002	EDTA pH 9.0	1:400	60	Powervision	Breast	Autostainer
E-cadherin	Membranous	Zymed	4A2C7	Citrate autoclave pH 6.0	1:200	60	Powervision	Breast	Autostainer
MIB-1 (Ki-67)	Nuclear	Dako	M7240	Citrate pH 6.0	1:100	60	Strept ABC	Tonsil	Autostainer
p53	Nuclear	Biogenex	BP53-12	Citrate pH 6.0	1:200	60	Strept ABC	Serous adenocarcinoma of the endometrium	Autostainer

[a] Biogenex, San Ramon, CA, USA; Chemicon, Chemicon International, Temecula, CA, USA; Dako, DakoCytomation, Glostrup, Denmark; Neomarkers, Fremont, USA; Zymed, Zymed Laboratories, San Francisco, CA, USA.
[b] Strept ABC is biotinylated horse–antimouse Vector BA-2000, diluted 1:500 in PBS, followed by streptavidin–biotin complex, diluted 1:1,000. Powervision ready to use (Poly-HRP-antiMs/Rb/RtIgG biotin-free; ImmunoVision Technologies, Norwell, CA, USA).

the streptavidin–biotin complex or slides were directly incubated with Powervision (details of both products shown in the legend of Table 1). Then, the peroxidase reactivity was developed by 3,3′-diaminobenzidine for 10 min and slides were counterstained with Mayer's hematoxylin. In between steps, slides were washed with phosphate-buffered saline (pH 7.4).

Immunohistochemical scoring

By two observers (FtK and JB) conjointly, the degree of differentiation and the percentage of immunohistochemically stained tumor cells were determined in all TMA cores and in the full sections of the selected donor blocks. Histologic grade was scored as well-differentiated (G1), moderately differentiated (G2), or poorly differentiated (G3) [37]. Staining of p53 and Ki-67 were marked as negative (<10% of tumor nuclei stained), weakly positive (10–50%), or strongly positive (≥50%) [10, 40]. Cytokeratin (CK)5/6 and CK14 staining were scored as negative (<10% of tumor cell cytoplasms stained), weakly positive (10–80%), or strongly positive (≥80%). E-cadherin expression was regarded negative when <50% of tumor cell membranes stained and positive when ≥50% stained [29, 30].

Cores were considered lost if <10% of cells contained tumor ('sampling error') or when <10% of tissue was present ('absent core'). Cases were excluded if two out of three cores were lost. When the scores between the cores of a particular case differed, the most frequent score determined the overall score. In case of three different scores in one case, the middle score was chosen. When only two cores were available with both a different score, the case was excluded from further analysis [11].

Statistical analysis

Statistical analyses were performed using the SPSS software for Windows (Version 12.0, SPSS, Chicago, IL, USA). Sixty-four donor blocks (60% of the tumors incorporated in the TMA) were randomly chosen by means of a random selection function of SPSS.

To determine the chance-corrected agreement between the immunohistochemical staining scores of TMA cores and large sections, the Cohen's weighted kappa statistic was calculated. Chance-corrected agreement was considered poor if $\kappa<0.00$, slight if $0<\kappa<0.20$, fair if $0.21<\kappa<0.40$, moderate if $0.41<\kappa<0.60$, substantial if $0.61<\kappa<0.80$, and almost perfect if $0.81<\kappa<1.00$ [17]. The overall agreement was defined as the percentage of correct agreement between the TMA and the donor blocks from the total number of cases [15].

Results

Of the 324 (3×108) tumor tissue cores that were transferred into the TMA paraffin block, a median of 295 (91%) was available for immunohistochemical scoring on the 6 TMA slides used in this study (Table 2). Of the 64 randomly selected cases, a median of 176 (92%) of 192 cores (3×64) was evaluable on the TMA slides.

On the H&E-stained TMA slide, 49 (76%) of the 64 randomly chosen cases were represented by 3 cores; 14 (22%) by 2 cores. One (1.6%) case was excluded from further analysis because only a single core was available. The agreement in the scores for the grade of differentiation between the TMA cores and the full sections is shown in Table 3. The weighted kappa score was 0.65.

Table 2 Overview of the amount of cores that were evaluable, absent or contained too little tumor in all 108 cases and in the 64 randomly selected cases on the TMA slides

	H&E	CK5/6	CK14	E-cadherin	Ki-67	p53	Median
Total TMA cases (n=108)							
No. of evaluable cores	293	309	294	306	293	295	295
Percentage	90	95	91	94	90	91	91
No. of absent cores	20	7	22	9	22	22	21
Percentage	6	2	7	3	7	7	6
No. of cores without tumor	11	8	8	9	9	7	9
Percentage	4	3	3	3	3	2	3
Randomly selected TMA cases (n=64)							
No. of evaluable cores	176	187	176	185	176	176	176
Percentage	92	97	92	96	92	92	92
No. of absent cores	13	3	13	4	13	13	13
Percentage	7	2	7	2	7	7	7
No. of cores without tumor	3	2	3	3	3	3	3
Percentage	2	1	2	2	2	2	2

H&E: hematoxylin and eosin

Table 3 Agreement in the degree of differentiation between TMA cores and full sections

		Full section				
		G1	G2	G3	Total	κ
TMA	G1	2	3	0	5	
	G2	2	21	2	25	
	G3	0	7	26	33	
	Total	4	31	28	63	0.65

G1: well-differentiated, *G2*: moderately differentiated, *G3*: poorly differentiated

Fifty-nine (92%) of the 64 randomly selected cases stained for CK5/6 were represented by 3 cores (Fig. 1); the 5 remaining cases by 2 cores. The immunohistochemical scores of the TMA and the donor blocks are shown in Table 4. Overall agreement in CK5/6 scores between the TMA and the donor blocks was 98% with a kappa of 0.93.

For CK14, two cases were excluded because only one tumor core was left and three cases were also excluded because the two available cores had discrepant immunohistochemical scores. Fifty (85%) of 59 cases had complete agreement (Table 4). Four cases were scored one class higher on TMA when compared with the full sections. Conversely, five other cases were classified lower on TMA with one case two classes lower. Kappa score was 0.71.

Regarding E-cadherin staining, three assessable cores were present in 89% of the cases; two cores in 11%. Overall agreement in E-cadherin staining scores was accomplished in 72% of cases (Table 5). In one case, a higher score was found on the TMA compared to the full section. In 17 cases, the expression of E-cadherin was scored lower on TMA than on the full sections. The observed kappa was 0.47.

Three-core analysis of Ki-67 staining could be performed in 78% of selected cases and two-core analysis in 19%. Two cases were represented by a single tumor core and were, therefore, excluded from further analysis. Ki-67 staining was scored as “moderate” on both TMA and full sections in 42 (69%) of 61 selected cases. In 79% of cases, the Ki-67 scores of the TMA were similar to that of the full sections. Thirteen cases were discordant (Table 6); kappa was 0.42.

With regard to p53 staining, two cores were present in 12 (19%) cases and 3 cores were available in 51 (80%) cases. One case was excluded as it was represented by only one TMA core. Complete agreement was achieved in 87% of the selected tumors (Table 6). In the eight nonconcordant cases, the difference was one class, resulting in a kappa of 0.86.

Discussion

After its introduction in 1998, TMA technology has been applied in the immunohistochemical analysis of various malignancies, including squamous cell carcinomas and adenocarcinomas of the esophagus [3, 5, 18, 19, 25, 41]. Although it seems a very attractive method for high-throughput analysis of hundreds of tissues simultaneously, it may have limitations as the evaluation of the marker

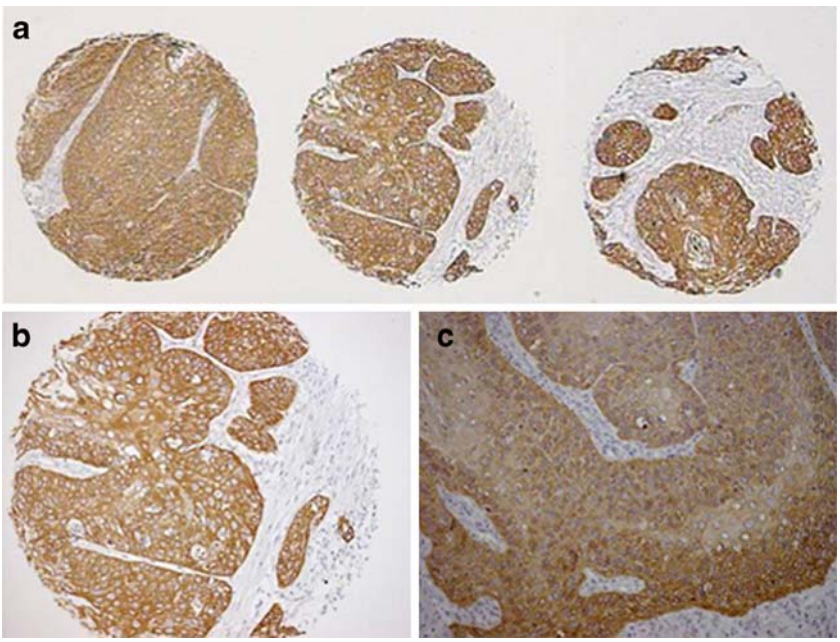


Fig. 1 Example of strong CK5/6 staining in TMA cores and the corresponding full section. **a** Three TMA cores representing one tumor; magnification ×20. **b** Enlargement of the middle TMA core depicted in **a**; magnification ×100. **c** Part of the slide of the donor block of the same tumor; magnification ×100

Table 4 Agreement in immunohistochemical scores between TMA cores and full slides stained for CK5/6 and CK14

		Full sections				
		<10%	10–80%	≥80%	Total	κ
TMAs	CK5/6					
	<10%	1	1	0	2	
	10–80%	0	4	0	4	
	≥80%	0	0	58	58	
	Total	1	5	58	64	0.93
	CK14					
	<10%	5	2	1	8	
	10–80%	0	11	2	13	
	≥80%	0	4	34	38	
	Total	5	17	37	59	0.71

Table 6 Agreement in immunohistochemical scores between TMA cores and full slides stained for Ki-67 and p53

		Full sections				
		<10%	10–50%	≥50%	Total	κ
TMAs	Ki-67					
	<10%	2	1	0	3	
	10–50%	3	42	3	48	
	≥50%	0	6	4	10	
	Total	5	49	7	61	0.42
	p53					
	<10%	19	3	0	22	
	10–50%	0	1	2	3	
	≥50%	0	3	35	38	
	Total	19	7	37	63	0.86

expression is reduced from full-section analysis to a few tissue cores of only 0.6 mm in diameter, especially for proteins that are heterogeneously expressed or that are cell cycle-dependent [36]. It is, therefore, essential to assess in each type of cancer individually and for every molecular marker whether TMA technology is feasible and valid [8, 33]. To our knowledge, this has not been done in esophageal cancer.

In our TMA containing triplicate cores of 108 ESCCs, a median of 9% of cores was uninformative (6% lost during tissue processing and 3% containing too little tumor), which is comparable to the results reported in other studies [7, 8, 27]. Improper selection of representative tumor areas on the donor block's H&E slide by the pathologist or incorrect punching of these representative areas out of the donor block can cause tissue cores that contain too little tumor. Possible causes of absent cores are the size and fragility of the tumor tissue used and the aggressiveness of tissue processing applied [31, 35, 42].

Moreover, the number of available cores on the TMA slide depends on the level at which the TMA paraffin block has been sectioned. The slides stained for H&E, CK14, Ki-67, and p53 were one of the first slides that were cut from our TMA block, whereas sections stained for CK5/6 and E-cadherin were taken slightly deeper. On these latter sections, a lower number of absent cores was observed (Table 2), showing that not all cores were placed at the exact same level in the TMA block during TMA construction, mainly due to dissimilar thicknesses of the donor paraffin blocks that were used to construct the TMA [34].

Table 5 Agreement in immunohistochemical scores between TMA cores and full slides stained for E-cadherin

		Full sections			
	E-cadherin	<50%	≥50%	Total	κ
TMA	<50%	22	17	39	
	≥50%	1	24	25	
	Total	23	41	64	0.47

The agreement in immunohistochemical results of the markers between our TMA and the full sections varied from moderate to almost perfect (κ=0.42 to 0.93), which is consistent with the results reported in other TMA validation studies [4, 7, 8, 31, 35]. The observed variation in agreement could be due to tumor heterogeneity, topographical variation in the expression pattern of the molecular marker, or to the scoring criteria used [31].

Regarding tumor heterogeneity, the optimal amount of tissue cores incorporated in the TMA has been a matter of debate. Several validation studies have shown that three cores are highly representative for the full section [6, 11, 12, 28]. The addition of a fourth core did not add to the percentage of agreement in a colorectal cancer TMA [12]. Moreover, the more cores punched per case, the fewer cases can be placed into the TMA reducing throughput. Adding a fourth core may nevertheless be worthwhile in tissues prone to uninformative cores due to small lesions such as dysplasias or carcinomas in situ [42]. In our TMA, the amount of uninformative cores was low (5–10%), probably because ESCCs have a large diameter, thereby increasing the chance of obtaining a core containing tumor tissue. Taken together, we consider it justified to utilize three biopsy cores in ESCCs. Nonetheless, using such a low amount of cores requires careful selection of the tumor regions by an experienced pathologist to deal with the heterogeneity of the tumor in the TMA [33].

The agreement between TMA and full sections was substantial to almost perfect for CK5/6 and CK14. Because 91% of cases have shown a very strong expression of CK5/

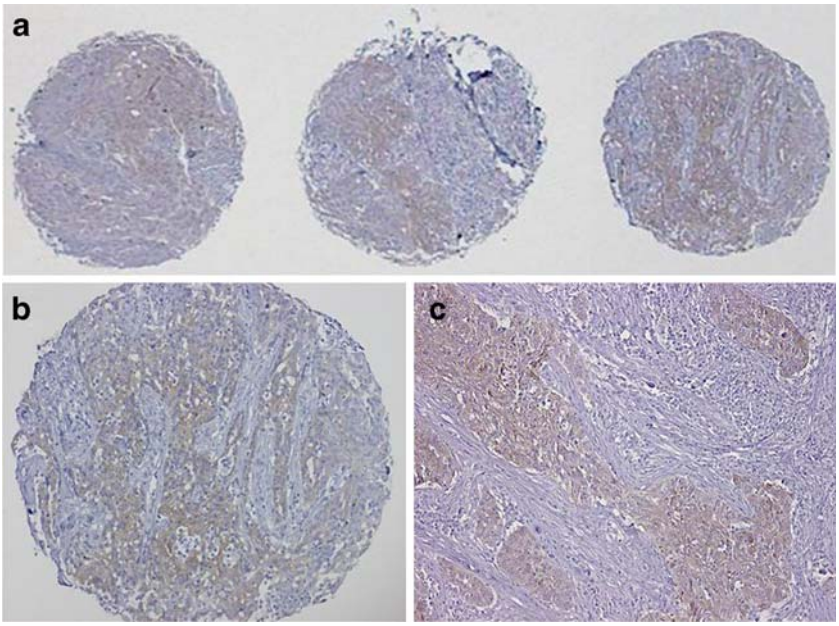


Fig. 2 Representative example of E-cadherin staining in TMA cores and the corresponding full section. **a** Three TMA cores representing one tumor; magnification ×20. **b** Enlargement of the right TMA core depicted in **a**; magnification ×100. **c** Part of the slide of the donor block of the same tumor; magnification ×100

6 and only 1 of 64 cases showed negative staining, this molecular marker does not subdivide ESCCs and consequently will not be a prognostic marker for this malignancy. CK14 was more evenly distributed over the three scoring groups, but because one case was scored two classes lower on TMA when compared to the full section, kappa was lower when compared to CK5/6.

The relatively moderate concordance in case of Ki-67 may be explained by the fact that almost 80% of cases were situated in one category (staining of 10–50% of tumor cells) with 13 discordant cases deviating from this category. E-cadherin also had a moderate concordance, mainly because the relatively faint staining intensity of this molecular maker made its assessment in our TMA very difficult (Fig. 2).

TMA technology was also found to be valid for determining the histologic grade of differentiation in ESCC. Complete agreement between TMA and full sections occurred in 78% (49 out of 63; κ=0.65) of selected cases, which is high when compared to the 40% agreement achieved in a TMA of bladder cancer [22]. Due to its homogeneous staining pattern, p53 showed excellent concordance (κ=0.86) in our microarray (Fig. 3).

The concurrence between the TMA and the full sections is affected by the cut-off values of the immunohistochemical scoring system of the stainings as well [7, 31]. The

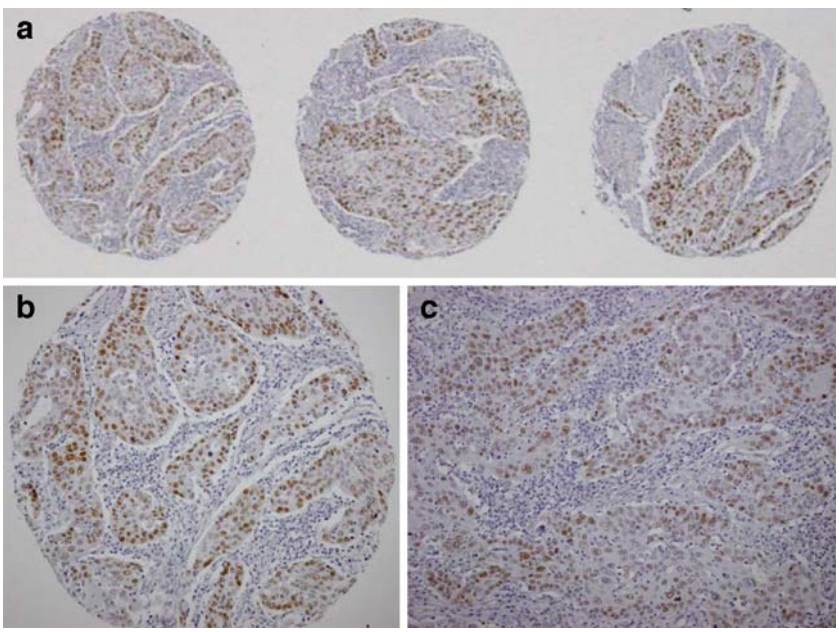


Fig. 3 Representative example of p53 staining in TMA cores and the corresponding full section. **a** Three TMA cores representing one tumor; magnification ×20. **b** Enlargement of the left TMA core depicted in **a**; magnification ×100. **c** Part of the slide of the donor block of the same tumor; magnification ×100

application of a two-class scoring system in an endometrial cancer TMA improved κ to 1.0 compared to 0.81 with a three-class system [7]. In our study, the two-class scoring system did not substantially affect the kappa (data not shown). Because the E-cadherin expression had a very low intensity in our ESCCs, we have chosen to apply a two-class system. In addition, the cut-off values indicating a strong immunohistochemical expression were set higher in the cytokeratins (80%) than in the other molecular markers (cut-off value 50%) because otherwise practically all tumors would be designated having a strong expression of cytokeratins.

Now that our esophageal cancer TMA has been validated, it will be used to correlate the expression of various molecular pathways with clinicopathologic data, aiming at detecting markers of prognostic significance and molecular targets for new therapies. Because the agreement between TMA slides and full sections depended on the molecular marker stained for, it should be considered to assess the expression pattern of a marker on a full section first, before staining a TMA slide. When a focal or heterogeneous expression pattern is noticed, it might be more valuable to assess marker expression by means of full sections instead of TMA. On the other hand, when a marker shows a homogeneously diffuse expression pattern, staining a TMA slide does allow for high-throughput screening of tumors. When a prognostic molecular marker has been identified by means of TMA technology, it is recommended to verify the results by full-section analysis.

In conclusion, this study has demonstrated TMA technology to be a valid method for immunohistochemical analysis in ESCC with agreement levels for well-known molecular markers with different staining potential between TMA and full sections ranging from moderate to almost perfect.

Conflict of interest statement We declare that we have no conflict of interest.

Open Access This article is distributed under the terms of the Creative Commons Attribution Noncommercial License which permits any noncommercial use, distribution, and reproduction in any medium, provided the original author(s) and source are credited.

References

1. Alexiou C, Khan OA, Black E, Field ML, Onyeaka P, Beggs L, Duffy JP, Beggs DF (2006) Survival after esophageal resection for carcinoma: the importance of the histologic cell type. Ann Thorac Surg 82:1073–1077
2. Camp RL, Charette LA, Rimm DL (2000) Validation of tissue microarray technology in breast carcinoma. Lab Invest 80:1943–1949
3. Chen AG, Yu ZC, Yu XF, Cao WF, Ding F, Liu ZH (2006) Overexpression of Ets-like protein 1 in human esophageal squamous cell carcinoma. World J Gastroenterol 12:7859–7863
4. Chen B, van den Brekel MW, Buschers W, Balm AJ, van Velthuysen ML (2003) Validation of tissue array technology in head and neck squamous cell carcinoma. Head Neck 25:922–930
5. Cheng MF, Tzao C, Tsai WC, Lee WH, Chen A, Chiang H, Sheu LF, Jin JS (2006) Expression of EMMPRIN and matriptase in esophageal squamous cell carcinoma: correlation with clinicopathological parameters. Dis Esophagus 19:482–486
6. Fernebro E, Dictor M, Bendahl PO, Ferno M, Nilbert M (2002) Evaluation of the tissue microarray technique for immunohistochemical analysis in rectal cancer. Arch Pathol Lab Med 126:702–705
7. Fons G, Hasibuan SM, Velden JV, Kate FJ (2007) Validation of tissue micro array technology in endometrioid cancer of the endometrium. J Clin Pathol 60:500–503
8. Gomaa W, Ke Y, Fujii H, Helliwell T (2005) Tissue microarray of head and neck squamous carcinoma: validation of the methodology for the study of cutaneous fatty acid-binding protein, vascular endothelial growth factor, involucrin and Ki-67. Virchows Arch 447:701–709
9. Griffin MC, Robinson RA, Trask DK (2003) Validation of tissue microarrays using p53 immunohistochemical studies of squamous cell carcinoma of the larynx. Mod Pathol 16:1181–1188
10. Han U, Can OI, Han S, Kayhan B, Onal BU (2007) Expressions of p53, VEGF C, p21: could they be used in preoperative evaluation of lymph node metastasis of esophageal squamous cell carcinoma? Dis Esophagus 20:379–385
11. Hoos A, Urist MJ, Stojadinovic A, Mastorides S, Dudas ME, Leung DH, Kuo D, Brennan MF, Lewis JJ, Cordon-Cardo C (2001) Validation of tissue microarrays for immunohistochemical profiling of cancer specimens using the example of human fibroblastic tumors. Am J Pathol 158:1245–1251
12. Jourdan F, Sebbagh N, Comperat E, Mourra N, Flahault A, Olschwang S, Duval A, Hamelin R, Flejou JF (2003) Tissue microarray technology: validation in colorectal carcinoma and analysis of p53, hMLH1, and hMSH2 immunohistochemical expression. Virchows Arch 443:115–121
13. Kamangar F, Dores GM, Anderson WF (2006) Patterns of cancer incidence, mortality, and prevalence across five continents: defining priorities to reduce cancer disparities in different geographic regions of the world. J Clin Oncol 24:2137–2150
14. Kononen J, Bubendorf L, Kallioniemi A, Barlund M, Schraml P, Leighton S, Torhorst J, Mihatsch MJ, Sauter G, Kallioniemi OP (1998) Tissue microarrays for high-throughput molecular profiling of tumor specimens. Nat Med 4:844–847
15. Kundel HL, Polansky M (2003) Measurement of observer agreement. Radiology 228:303–308
16. Lagarde SM, Ten Kate FJ, de Boer DJ, Busch OR, Obertop H, van Lanschot JJ (2006) Extracapsular lymph node involvement in node-positive patients with adenocarcinoma of the distal esophagus or gastroesophageal junction. Am J Surg Pathol 30:171–176
17. Landis JR, Koch GG (1977) The measurement of observer agreement for categorical data. Biometrics 33:159–174
18. Langer R, Von Rahden BH, Nahrig J, Von Weyhern C, Reiter R, Feith M, Stein HJ, Siewert JR, Hofler H, Sarbia M (2006) Prognostic significance of expression patterns of c-erbB-2, p53, p16INK4A, p27KIP1, cyclin D1 and epidermal growth factor receptor in oesophageal adenocarcinoma: a tissue microarray study. J Clin Pathol 59:631–634
19. Liu W, Yu ZC, Cao WF, Ding F, Liu ZH (2006) Functional studies of a novel oncogene TGM3 in human esophageal squamous cell carcinoma. World J Gastroenterol 12:3929–3932

20. Mariette C, Piessen G, Triboulet JP (2007) Therapeutic strategies in oesophageal carcinoma: role of surgery and other modalities. Lancet Oncol 8:545–553
21. Nair KS, Naidoo R, Chetty R (2005) Expression of cell adhesion molecules in oesophageal carcinoma and its prognostic value. J Clin Pathol 58:343–351
22. Nocito A, Bubendorf L, Tinner EM, Suess K, Wagner U, Forster T, Kononen J, Fijan A, Bruderer J, Schmid U, Ackermann D, Maurer R, Alund G, Knonagel H, Rist M, Anabitarte M, Hering F, Hardmeier T, Schoenenberger AJ, Flury R, Jager P, Fehr JL, Schraml P, Moch H, Mihatsch MJ, Gasser T, Sauter G (2001) Microarrays of bladder cancer tissue are highly representative of proliferation index and histological grade. J Pathol 194:349–357
23. Pacifico MD, Grover R, Richman P, Daley F, Wilson GD (2004) Validation of tissue microarray for the immunohistochemical profiling of melanoma. Melanoma Res 14:39–42
24. Pedrazzani C, deManzoni G, Marrelli D, Giacopuzzi S, Corso G, Bernini M, Roviello F (2007) Nodal staging in adenocarcinoma of the gastro-esophageal junction. Proposal of a specific staging system. Ann Surg Oncol 14:299–305
25. Reichelt U, Duesedau P, Tsourlakis MC, Quaas A, Link BC, Schurr PG, Kaifi JT, Gros SJ, Yekebas EF, Marx A, Simon R, Izbicki JR, Sauter G (2007) Frequent homogeneous HER-2 amplification in primary and metastatic adenocarcinoma of the esophagus. Mod Pathol 20:120–129
26. Rizk N, Venkatraman E, Park B, Flores R, Bains MS, Rusch V (2006) The prognostic importance of the number of involved lymph nodes in esophageal cancer: implications for revisions of the American Joint Committee on Cancer staging system. J Thorac Cardiovasc Surg 132:1374–1381
27. Rosen DG, Huang X, Deavers MT, Malpica A, Silva EG, Liu J (2004) Validation of tissue microarray technology in ovarian carcinoma. Mod Pathol 17:790–797
28. Rubin MA, Dunn R, Strawderman M, Pienta KJ (2002) Tissue microarray sampling strategy for prostate cancer biomarker analysis. Am J Surg Pathol 26:312–319
29. Sato F, Shimada Y, Watanabe G, Uchida S, Makino T, Imamura M (1999) Expression of vascular endothelial growth factor, matrix metalloproteinase-9 and E-cadherin in the process of lymph node metastasis in oesophageal cancer. Br J Cancer 80:1366–1372
30. Shiozaki H, Doki Y, Yamana H, Isono K (2002) A multi-institutional study of immunohistochemical investigation for the roles of cyclin D1 and E-cadherin in superficial squamous cell carcinoma of the esophagus. J Surg Oncol 79:166–173
31. Su Y, Shrubsole MJ, Ness RM, Cai Q, Kataoka N, Washington K, Zheng W (2006) Immunohistochemical expressions of Ki-67, cyclin D1, beta-catenin, cyclooxygenase-2, and epidermal growth factor receptor in human colorectal adenoma: a validation study of tissue microarrays. Cancer Epidemiol Biomarkers Prev 15:1719–1726
32. Takeno S, Noguchi T, Takahashi Y, Fumoto S, Shibata T, Kawahara K (2007) Assessment of clinical outcome in patients with esophageal squamous cell carcinoma using TNM classification score and molecular biological classification. Ann Surg Oncol 14:1431–1438
33. Tawfik El-Mansi M, Williams AR (2006) Validation of tissue microarray technology using cervical adenocarcinoma and its precursors as a model system. Int J Gynecol Cancer 16:1225–1233
34. Tzankov A, Went P, Zimpfer A, Dirnhofer S (2005) Tissue microarray technology: principles, pitfalls and perspectives—lessons learned from hematological malignancies. Exp Gerontol 40:737–744
35. Van den Eynden GG, Van dA I, Van Laere S, Colpaert CG, van Dam P, Merajver S, Kleer CG, Harris AL, Van Marck EA, Dirix LY, Vermeulen PB (2004) Validation of a tissue microarray to study differential protein expression in inflammatory and non-inflammatory breast cancer. Breast Cancer Res Treat 85:13–22
36. van Diest PJ, Vleugel M, van der Groep P, van der Wall E (2005) VEGF-D and HIF-1alpha in breast cancer. J Clin Pathol 58:335
37. Wittekind C, Greene FL, Hutter RVP, Klimpfinger M, Sobin LH (ed) (2004) TNM Atlas. Illustrated guide to the TNM/pTNM classification of malignant tumors. Springer, Berlin
38. Xu F, Zhong W, Li J, Shanshen Z, Cui J, Nesland JM, Suo Z (2005) Predictive value of EphA2 and EphrinA-1 expression in oesophageal squamous cell carcinoma. Anticancer Res 25:2943–2950
39. Xu FP, Xie D, Wen JM, Wu HX, Liu YD, Bi J, Lv ZL, Zeng YX, Guan XY (2007) SRC-3/AIB1 protein and gene amplification levels in human esophageal squamous cell carcinomas. Cancer Lett 245:69–74
40. Xu M, Jin YL, Fu J, Huang H, Chen SZ, Qu P, Tian HM, Liu ZY, Zhang W (2002) The abnormal expression of retinoic acid receptor-beta, p53 and Ki67 protein in normal, premalignant and malignant esophageal tissues. World J Gastroenterol 8:200–202
41. Xue LY, Hu N, Song YM, Zou SM, Shou JZ, Qian LX, Ren LQ, Lin DM, Tong T, He ZG, Zhan QM, Taylor PR, Lu N (2006) Tissue microarray analysis reveals a tight correlation between protein expression pattern and progression of esophageal squamous cell carcinoma. BMC Cancer 6:296
42. Yang XR, Charette LA, Garcia-Closas M, Lissowska J, Paal E, Sidawy M, Hewitt SM, Rimm DL, Sherman ME (2006) Construction and validation of tissue microarrays of ductal carcinoma in situ and terminal duct lobular units associated with invasive breast carcinoma. Diagn Mol Pathol 15:157–161

Virchows Arch (2008) 452:515–524
DOI 10.1007/s00428-008-0596-7

ORIGINAL ARTICLE

Helicobacter pylori-infection-associated CpG island hypermethylation in the stomach and its possible association with Polycomb repressive marks

Eun Joo Yoo · Seog-Yun Park · Nam-Yun Cho · Nayoung Kim · Hye Seung Lee · Gyeong Hoon Kang

Received: 6 November 2007 / Revised: 2 February 2008 / Accepted: 10 February 2008 / Published online: 12 March 2008
© Springer-Verlag 2008

Abstract *Helicobacter pylori* infection can induce CpG island (CGI) hypermethylation in gastric mucosa. Recently, genes occupied by Polycomb proteins in embryonic stem cells were shown to be vulnerable to aberrant DNA hypermethylation in cancers. To explore the relationship between *H. pylori* infection and DNA methylation changes in neoplastic and non-neoplastic stomach, we analyzed 25 CGIs and repetitive DNA elements from 82 chronic gastritis and 69 gastric carcinomas. Twenty-three CGIs showed significantly higher methylation levels in *H. pylori*-negative gastric carcinoma (n=28) than in *H. pylori*-negative chronic gastritis (n=39; P<0.05), indicating cancer-associated methylation. Eight CGIs exhibited significantly higher methylation levels in *H. pylori*-positive chronic gastritis (n=43) than in *H. pylori*-negative chronic gastritis (n=39; P<0.05). Six CGIs showed both cancer-associated and *H. pylori*-associated hypermethylation. Six (75%) of the eight *H. pylori*-associated hypermethylated genes contained at least one of three repressive marks (Suz12 occupancy, Eed occupancy, histone H3 K27 trimethylation), whereas 31% of the remaining cancer-associated hypermethylated genes had at least one mark. The findings suggest that *H. pylori* infection strongly induces CGI hypermethylation in gastric epithelial cells and that susceptibility to *H. pylori*-induced DNA hypermethylation may be determined by Polycomb repressive marks in stem or progenitor cells.

Keywords Chronic gastritis · CpG islands · DNA methylation · Gastric cancer · *Helicobacter pylori*

Electronic supplementary material The online version of this article (doi:10.1007/s00428-008-0596-7) contains supplementary material, which is available to authorized users.

Supported by the Korea Research Foundation Grant (MOEHRD; KRF-2005-041-E00081; G.H.K.) and by the second stage Brain Korea 21 Project.

E. J. Yoo · N.-Y. Cho · G. H. Kang
Laboratory of Epigenetics, Cancer Research Institute,
Seoul National University College of Medicine,
Seoul, South Korea

S.-Y. Park · H. S. Lee · G. H. Kang (✉)
Department of Pathology,
Seoul National University College of Medicine,
28 Yongon-dong, Chongno-gu,
Seoul 110-744, South Korea
e-mail: ghkang@snu.ac.kr

N. Kim
Department of Internal Medicine,
Seoul National University College of Medicine,
Seoul, South Korea

Introduction

Helicobacter pylori (*H. pylori*) has been designated as a human class I carcinogen of gastric malignancy by the International Agency for Research on Cancer [16]. Chronic infection with *H. pylori* generally increases the risk for gastric carcinoma by five- to six-fold [28]. The risk has been reported to be even greater when exposure to *H. pylori* infection is estimated based on the presence of serum antibodies to cytotoxin-associated gene product A [11]. Animal models have been developed to demonstrate a close association between *H. pylori* infection and gastric carcinoma [31, 35]. Although the exact mechanism of *H. pylori*-associated gastric carcinogenesis is unknown, long-standing bacterial infection, perpetuated chronic inflammation, and sustained mucosal epithelial cell proliferation are thought to produce a carcinogenic environment. Recently, *H. pylori*

infection was reported to be associated with enhanced hypermethylation of multiple CpG islands (CGIs) in chronic gastritis, and its eradication brings about reversal of the methylation status of multiple CGI loci [5, 6, 24, 25, 37]. This fact raises the possibility that aberrant methylation changes induced by *H. pylori* infection may contribute to *H. pylori* infection-associated gastric carcinogenesis. To date, however, only a limited number of CGI loci have been studied for their hypermethylation in association with *H. pylori* infection.

Aberrant DNA methylation in cancer cells is characterized by focal CGI hypermethylation and generalized genomic hypomethylation. Global hypomethylation contributes to chromosomal instability, as evidenced by recent cell line studies that induced genomic hypomethylation by knocking down DNA methyltransferases and demonstrated aberrant chromosomal structure or number in the cells [20]. It is known that the methylated DNA content of stomach-lining cells in chronic gastritis decreases with progression of the lesion along a multi-step progression to gastric carcinoma [8]. However, little is known about whether *H. pylori* infection leads to genomic hypomethylation.

Polycomb repressive complexes (PRCs) are involved in the initiation of gene repression through epigenetic modification of chromatin structure and three components, namely, enhancer of zeste homolog 2 (Ezh2), suppressor of zeste 12 homolog (Suz12) and embryonic ectodermal development (Eed), forms the core of PRC2 [34]. Ezh2 of PRC2 catalyzes histone H3 lysine 27 (H3K27) trimethylation, which is thought to provide a binding surface for PRC1 [3], which in turn facilitates a closed chromatin structure to repress gene expression. Recent studies have demonstrated that de novo hypermethylation of some promoter CGIs in human cancers may occur in a so-called "instructive manner", led by the chromatin "marks" of H3K27 trimethylation or binding of Polycomb group proteins Suz12 and Eed [29, 32, 43]. CGI loci carrying these chromatin marks in embryonic stem (ES) cells or normal tissue cells where these same loci are unmethylated may be preferentially targeted by aberrant DNA hypermethylation that occurs in association with cancer development [29, 32, 43]. In light of these facts, it can be speculated that in gastric epithelial stem or progenitor cells, CGI loci with these repressive chromatin marks may be vulnerable to hypermethylation induced by *H. pylori* infection. To date, nothing is known about whether CGI loci of *H. pylori*-related hypermethylation have some characteristic chromatin marks for preferred hypermethylation.

In this study, we analyzed the relationship of *H. pylori* infection to aberrant methylation in chronic gastritis and gastric carcinoma with respect to focal CGI hypermethylation and generalized genomic hypomethylation using quantitative methylation analysis. To determine the change of methylation content caused by *H. pylori* infection, we measured the methylation levels of LINE-1 and Alu repetitive elements as surrogates for global genomic methylation because these repetitive elements comprise about 30% of genomic DNA [22] and a strong correlation between 5-methylcytosine content in the human genome and measures of Alu and LINE-1 methylation using polymerase chain reaction has been demonstrated in a previous study [41]. Twenty-five CGI loci were analyzed for their methylation levels by quantitative methylation-specific real-time PCR (MethyLight technology). Using previously published information from stem cells [23], we were able to determine the occupancy by Suz12 and Eed and the trimethylation status of H3K27 for the 25 genes we examined.

Materials and methods

Patients

Four hundred sixty-seven patients who visited Seoul National University Bundang Hospital for gastroscopy from September 2003 to March 2005 were enrolled in the study. Patients underwent endoscopic mucosal biopsy and blood sampling for *H. pylori* detection. Patients with a history of gastric surgery and systemic disease requiring chronic medication were excluded from the enrollment. Neither chemical gastritis nor autoimmune gastritis was included. Written informed consent was obtained from all participating patients, and the study was approved by the Seoul National University Hospital's Institutional Review Board.

Gastroscopic biopsy and serologic evaluation

Three biopsy samples were taken from the greater curvature of the antrum and the body of the stomach. Two samples from the antrum and two samples from the stomach body were fixed in neutral buffered formalin solution and processed for hematoxylin–eosin (H&E) staining and modified Giemsa staining for histologic evaluation and assessment of the presence of *H. pylori*, respectively. The remaining two specimens were subjected to a rapid urease test (CLO test, Delta West, Bentley, Australia), which was monitored for up to 24 h. Blood samples were obtained from the patients and evaluated for the level of anti-*H. pylori* immunoglobulin (Ig) G using an enzyme-linked immunosorbent assay (Genedia *H. pylori* ELISA; Green Cross Sang A Co., Seoul, South Korea), and duplicate determinations were performed according to the manufacturer's protocol. Cases negative for three tests (CLO test, *H. pylori* IgG test, and histological *H. pylori* evaluation) were regarded as *H. pylori*-negative.

DNA extraction and bisulfite modification

Because previous studies [18, 26] revealed that intestinal metaplasia is accompanied by enhanced promoter CGI hypermethylation compared with chronic gastritis without intestinal metaplasia and our preliminary study revealed enhanced CGI hypermethylation in intestinal metaplasia regardless of *H. pylori* infection, cases that showed intestinal metaplasia or epithelial neoplasia in any of the four tissue samples were excluded from the study in order to focus on the effect of *H. pylori* infection on DNA methylation changes in chronic gastritis. Gastric carcinoma cases or chronic gastritis cases without intestinal metaplasia were included in the study. Twenty archival tissue sections of 4-μm thickness were used for DNA extraction. In gastric carcinoma cases, manual microdissection was performed in order not to include non-neoplastic mucosal epithelial cells. The dissected tissues were pooled together in a microtube containing lysis buffer and proteinase K. Sodium bisulfite conversion of genomic DNA was performed as described [41].

MethyLight assay

Twenty-five CGI loci were analyzed by the MethyLight technology using primers and probes targeting promoter sequences or the first exon [9, 41]. The oligonucleotide sequences of the primers and probes used have been described [42]. Briefly, two sets of primers and probes designed specifically to bind to bisulfite-converted DNA were used in each reaction; one set of primers and probe were used for every methylated target to be analyzed (methylated reaction), and another pair of primers and probe were for the reference locus, ALU (normalization control reaction). Normalization control reactions were methylation-independent measurements to control for DNA amplification and normalize for input DNA. *M.Sss*I-treated genomic DNA was used as a reference sample for complete methylation to determine the percentage of methylated reference (PMR) at a particular locus. PMR was defined as $100\times(\text{methylated reaction/normalization control reaction})_{\text{sample}}/(\text{methylated reaction/normalization control reaction})_{\text{M.SssI-Reference}}$.

Combined bisulfite restriction analysis (COBRA) assay

Bisulfite-modified genomic DNA was analyzed by COBRA to determine the methylation level of LINE-1 and Alu, as described [7]. In brief, LINE-1 and Alu were amplified with their respective primers that anneal to short sequences without CpG sites to amplify both methylated and unmethylated alleles equally. For the Alu reaction, *Taq*I was used to digest the methylated alleles, and the digested products were electrophoresed on a 12% polyacrylamide gel. The intensities of the digested and undigested bands were determined using Image J software (http://rsb.info.nih.gov/ij), and the percentage of methylated alleles was calculated by dividing the intensity of the digested band by the sum of the intensities of the digested band and the undigested band and multiplying by 100. For the LINE-1 reaction, *Taq*I and *Tas*I were used to digest the methylated alleles and unmethylated alleles, respectively. The percentage of methylated alleles was determined by dividing the intensity of *Taq*I-digested bands by the sum of *Taq*I-digested bands and *Tas*I-digested bands and multiplying by 100.

Statistical analysis

All statistical analyses were performed using SPSS software (SPSS, Ver.11.0, Chicago, IL). The relationship of CGI hypermethylation to *H. pylori* infection or cancer development was assessed by comparing the PMR values of examined CGIs using the Student's *t* test. The methylation levels of Alu or LINE-1 were compared between groups using the Student's *t* test. Comparison of the number of methylated CGI loci between groups was also performed using the Student's *t* test. A P value<0.05 was considered to be statistically significant.

Results

A total of 151 mucosal samples were analyzed for their methylation status in 25 CGI loci by MethyLight and in two repetitive elements (LINE-1 and Alu) by COBRA. The selected CGI loci except for *CDH1* were found to show higher methylation frequency or level in gastric carcinoma than in non-neoplastic gastric mucosa in our previous studies [17, 18] in which 170 CGI loci were analyzed for their methylation status in 16 gastric carcinoma and paired non-neoplastic gastric mucosa samples. *CDH1* was selected because of its known association of promoter CGI hypermethylation with *H. pylori* infection in the stomach [5, 6, 24]. The information regarding PRC2 occupancy was available for 153 of the 170 genes, and 60 genes contain occupancy of at least one component of PRC2. All of the PRC2-occupied 60 CGI loci showed promoter DNA hypermethylation in gastric carcinoma or non-neoplastic gastric mucosa samples, whereas 55 (59%) of 93 PRC2-nonoccupied genes exhibited CGI hypermethylation in gastric carcinoma or non-neoplastic gastric mucosa. Of the selected 24 CGI loci (except for *p14* for which PRC2 occupancy information is not available), 50% harbor occupancy of at least one component of PRC2, whereas 37.2% of the remaining 129 CGI loci contain occupancy of at least one component of PRC2. Forty three *H. pylori*-positive chronic gastritis samples (mean age, 55.1 years; range, 25–78 years), 39 *H. pylori*-negative chronic gastritis (mean age, 55.6 years; range, 24–85 years),

41 *H. pylori*-positive gastric carcinoma (mean age, 63.6 years; range, 40–82 years), and 28 *H. pylori*-negative gastric carcinoma (mean age, 64.7 years; range, 41–83 years) were included in the study. *H. pylori*-positive chronic gastritis cases were selected to match an age distribution and gender distribution comparable to those of the *H. pylori*-negative chronic gastritis cases. The *H. pylori*-positive chronic gastritis was composed of two subgroups, a current *H. pylori* infection group (n=33) and a prior *H. pylori* infection group (n=10). The current infection group was defined by the identification of *H. pylori* on H&E-stained biopsy slides or by a positive CLO test, and the prior infection group was defined by a positive *H. pylori* IgG test but negative CLO test and absence of *H. pylori* infection on histological examination.

CGI hypermethylation of chronic gastritis versus gastric carcinoma

To determine CGI loci showing cancer-related hypermethylation, the methylation levels of 25 CGI loci were compared between *H. pylori*-negative chronic gastritis (n=39) and *H. pylori*-negative gastric carcinoma (n=28). Twenty-three CGI loci (all except for *CDH1* and *DAPK1*) showed significantly higher methylation levels in *H. pylori*-negative gastric carcinoma than in *H. pylori*-negative chronic gastritis (P<0.05), indicating a cancer-related methylation (Fig. 1a). The remaining two loci showed apparent higher methylation levels in gastric carcinoma than in chronic gastritis, but the difference was statistically insignificant. When the methylation levels of examined CGI loci were compared between *H. pylori*-positive chronic gastritis (the current infection group, n=33) and *H. pylori*-positive gastric carcinoma, the cancer-related methylation loci except for seven loci (*p14*, *HOXA1*, *NEUROG1*, *SOCS1*, *CRABP1*, *MLH1*, and *SMAD9*) also displayed significantly higher methylation levels in gastric carcinoma than in chronic gastritis (P<0.05) (Fig. 1b). The level of global genomic methylation, represented by methylation levels of LINE-1 and Alu, was significantly lower in gastric carcinoma than in chronic gastritis (P<0.05), regardless of the status of *H. pylori* infection (Fig. 2a).

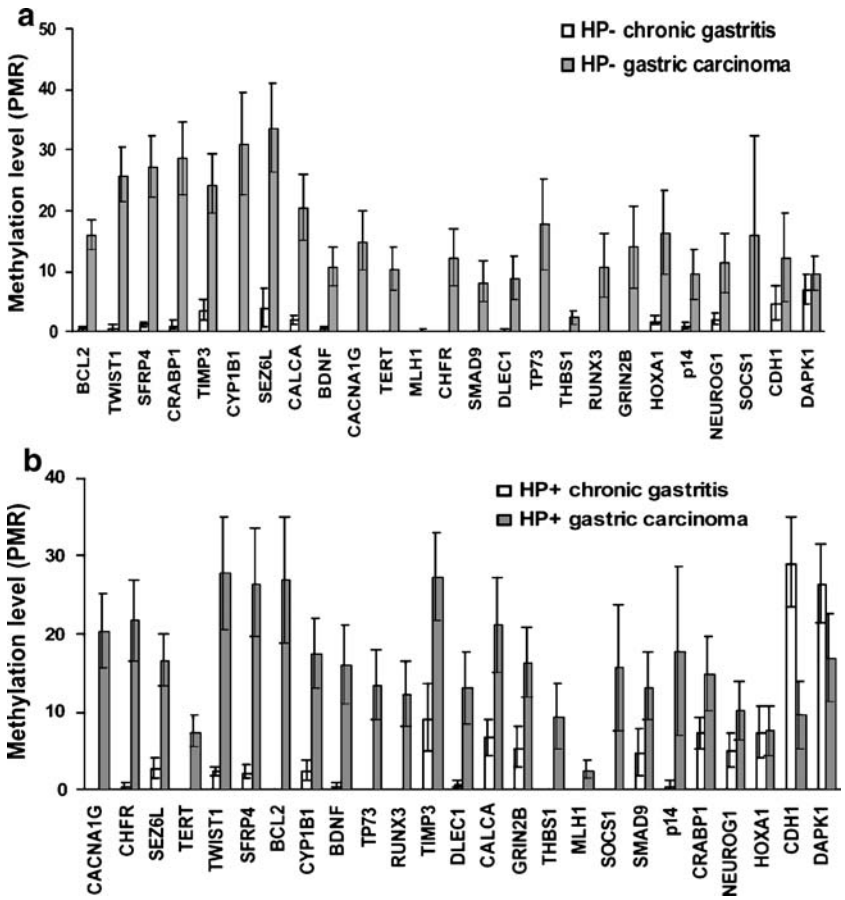


Fig. 1 **a** Comparison of the methylation levels of 25 CGI loci between *H. pylori*-negative (HP−) chronic gastritis specimens from non-cancer patients and HP− gastric carcinoma specimens. **b** Comparison between chronic gastritis cases with current *H. pylori* infection (from non-cancer patients) and *H. pylori*-positive gastric carcinoma cases. The examined CGI loci were sorted ordered from highest to lowest *P* values from left to right along the *x* axis. *Error bars* indicate S.E.M.

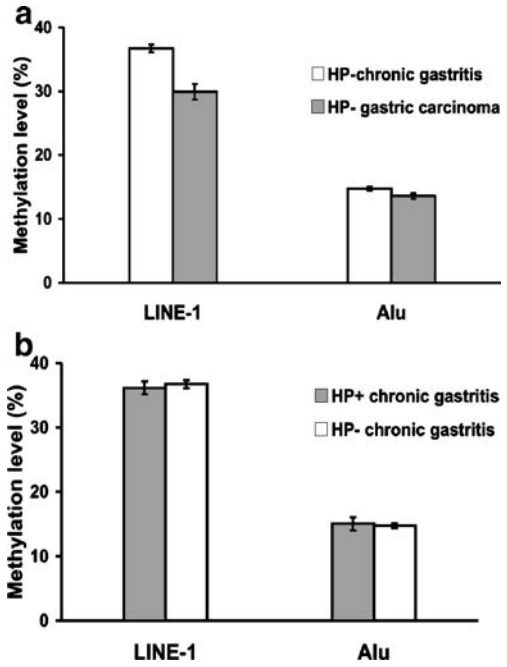


Fig. 2 **a** COBRA assay of LINE-1 and Alu repetitive elements reveal significantly lower methylation levels in *H. pylori*-negative gastric carcinoma than in *H. pylori*-negative chronic gastritis. *Error bars* indicate S.E.M. **b** COBRA assay of LINE-1 or Alu methylation levels demonstrated no difference between *H. pylori*-positive and *H. pylori*-negative chronic gastritis samples

CGI hypermethylation of *H. pylori*-positive chronic gastritis versus *H. pylori*-negative chronic gastritis

Of 25 CGI loci hypermethylated in gastric carcinoma, four loci (*RUNX3*, *SOCS1*, *TERT*, and *TP73*) were never methylated in chronic gastritis samples, regardless of *H. pylori* infection. Figure 3 depicts the summary of the PMR values generated by the MethyLight analysis. When the methylation levels of 21 CGI loci were compared between *H. pylori*-positive chronic gastritis (the current *H. pylori* infection group, n=33) and *H. pylori*-negative chronic gastritis, close association of hypermethylation with *H. pylori* infection was noted in eight CGI loci (*CACNA1G*, *CALCA*, *CDH1*, *CRABP1*, *CYP1B1*, *DAPK1*, *GRIN2B*, and *TWIST1*; Fig. 4). Of these, six loci (*CALCA*, *CACNA1G*, *CRABP1*, *CYP1B1*, *GRIN2B*, and *TWIST1*) showed both cancer-related and *H. pylori*-related hypermethylation. Of the 23 cancer-related methylation loci, 13 loci showed more than a two-fold increase in methylation levels in *H. pylori*-positive chronic gastritis samples than in *H. pylori*-negative chronic gastritis samples. No difference was noted in LINE-1 and Alu methylation levels between *H. pylori*-positive and *H. pylori*-negative chronic gastritis specimens (Fig. 2b).

When a CGI locus was arbitrarily regarded methylated when its PMR value was ≥4, the number of CGI loci methylated varied from 0 to 11 in the *H. pylori*-positive chronic gastritis samples (the current *H. pylori* infection group, n=33) and from 0 to 5 in the *H. pylori*-negative chronic gastritis samples (mean, 4.3 vs. 1.4; P<0.001) (Fig. 5a).

CGI hypermethylation in current *H. pylori* infection versus past *H. pylori* infection

The *H. pylori*-positive chronic gastritis cases were divided into two groups, namely current infection (n=33) and prior infection (n=10). Comparison of methylation levels of the examined CGI loci revealed that the methylation levels of the eight CGI loci showing *H. pylori*-related hypermethylation were apparently lower in the prior infection group than in the current infection group, but the differences were not significant (data not shown). When the number of methylated CGI loci (PMR≥4) was compared between the two groups, the current infection group showed a significantly higher number of methylated loci than the prior infection group (mean number, 4.3 vs. 2.6; P=0.014; Fig. 5b). Moreover, the number of CGI loci methylated was significantly higher in the prior infection group than in the *H. pylori*-negative chronic gastritis group (mean, 2.6 vs. 1.4; P=0.022).

CGI hypermethylation of *H. pylori*-positive gastric carcinoma versus *H. pylori*-negative gastric carcinoma

Although no significant difference was noted in the comparison of the methylation levels of the 24 CGI loci between *H. pylori*-positive and *H. pylori*-negative gastric carcinomas, *THBS1* showed a statistically insignificant 2-fold increase in methylation levels in *H. pylori*-infected gastric carcinoma samples. Alu and LINE-1 methylation levels did not differ between the *H. pylori*-positive and *H. pylori*-negative gastric carcinoma samples.

Discussion

In this study, *H. pylori*-positive and -negative chronic gastritis cases were analyzed for their methylation status of 25 promoter CGI loci using the MethyLight assay. The methylation levels of 15 CGI loci in *H. pylori*-positive chronic gastritis cases were elevated more than two-fold compared with those in *H. pylori*-negative chronic gastritis, and of these CGI loci the differences in the methylation levels in eight loci reached statistical significance. Furthermore, the number of CGI loci hypermethylated (PMR≥4) was significantly higher in the current infection group than in the prior *H. pylori* infection group. These results indicate that *H. pylori* infection is closely associated with aberrant CGI hypermethylation in chronic gastritis, consistent with

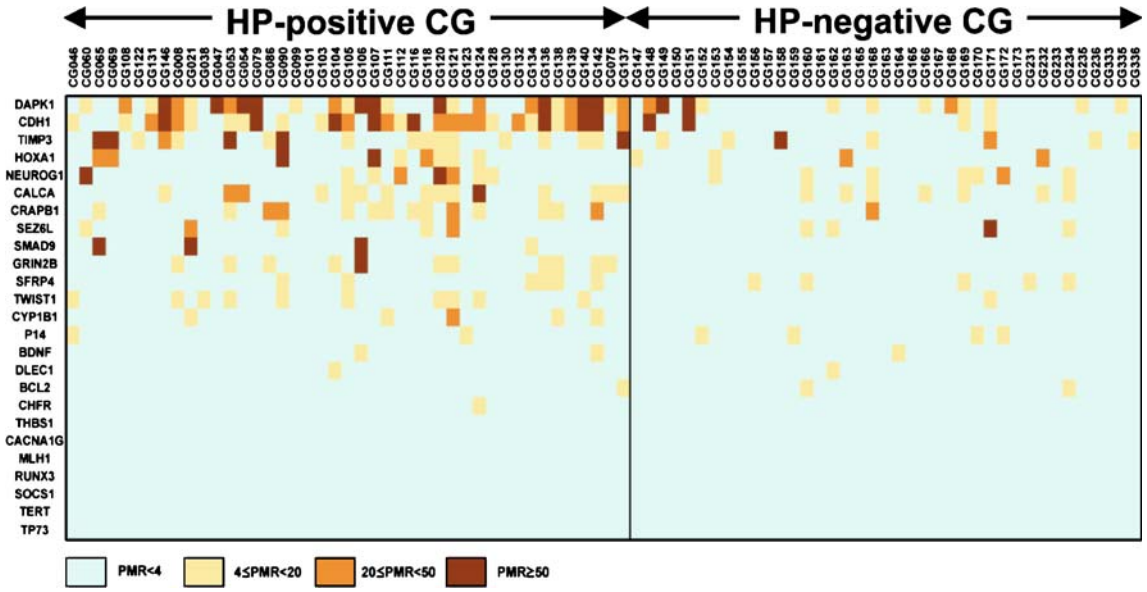


Fig. 3 Methylation map of the percent of methylated reference (*PMR*) values obtained for each CpG island (CGI) locus in *H. pylori*-positive (*HP-positive*) or *H. pylori*-negative chronic gastritis (*HP-negative CG*) cases. In total, 82 CG samples (horizontal axis) were examined for their methylation status at 25 CGI loci (*vertical axis*). The data shows that HP-positive CG samples tend to be more hypermethylated than HP-negative CG samples with regard to methylation levels or methylation frequencies. *Colored boxes* represent four classes of methylation levels [0<PMR<4 (*light blue*), 4≤PMR<20 (*light yellow*), 20≤PMR<50 (*light orange*), PMR≥50 (*brown*)], as indicated in the figure

the findings of other researchers [5, 24, 25]. However, it should be noted that variability existed in the susceptibility to hypermethylation induced by *H. pylori* infection depending on the type of CGI loci: 15 CGI loci showed more than two-fold increases in methylation levels in *H. pylori*-positive chronic gastritis compared to *H. pylori*-negative chronic gastritis cases, whereas the remaining ten CGI loci did not. Even within the current *H. pylori*-infection chronic gastritis subjects, the number of CGI loci hypermethylated per case displayed a wide distribution, indicating the existence of other factors, including host factors, in the vulnerability of CGIs to hypermethylation provoked by *H. pylori* infection. Host factors may include the duration of *H. pylori* infection and inflammatory response, and genetic variables. For example, genetic polymorphisms of the inflammatory cytokines involved in *H. pylori*

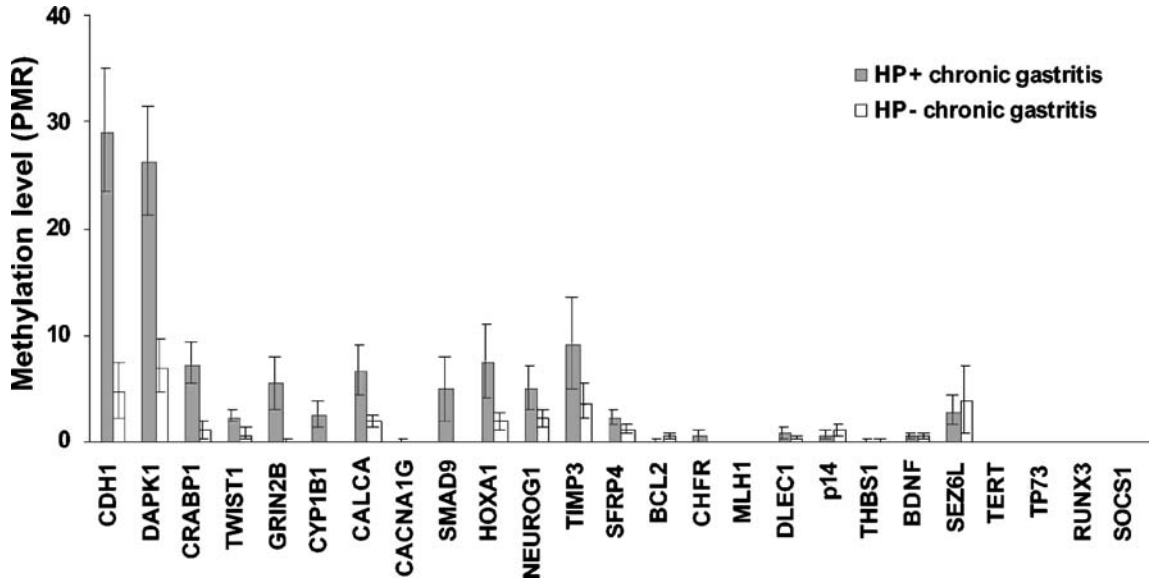


Fig. 4 Comparison between chronic gastritis cases with current *H. pylori* infection (from non-cancer patients) and chronic gastritis cases with no current *H. pylori* infection and no past history of *H. pylori* infection (from non-cancer patients). The examined CGI loci were sorted ordered from highest to lowest *P* values from *left to right* along the *x* axis. The *left eight CGI loci* showed a statistically significant difference in methylation levels ($P<0.05$)

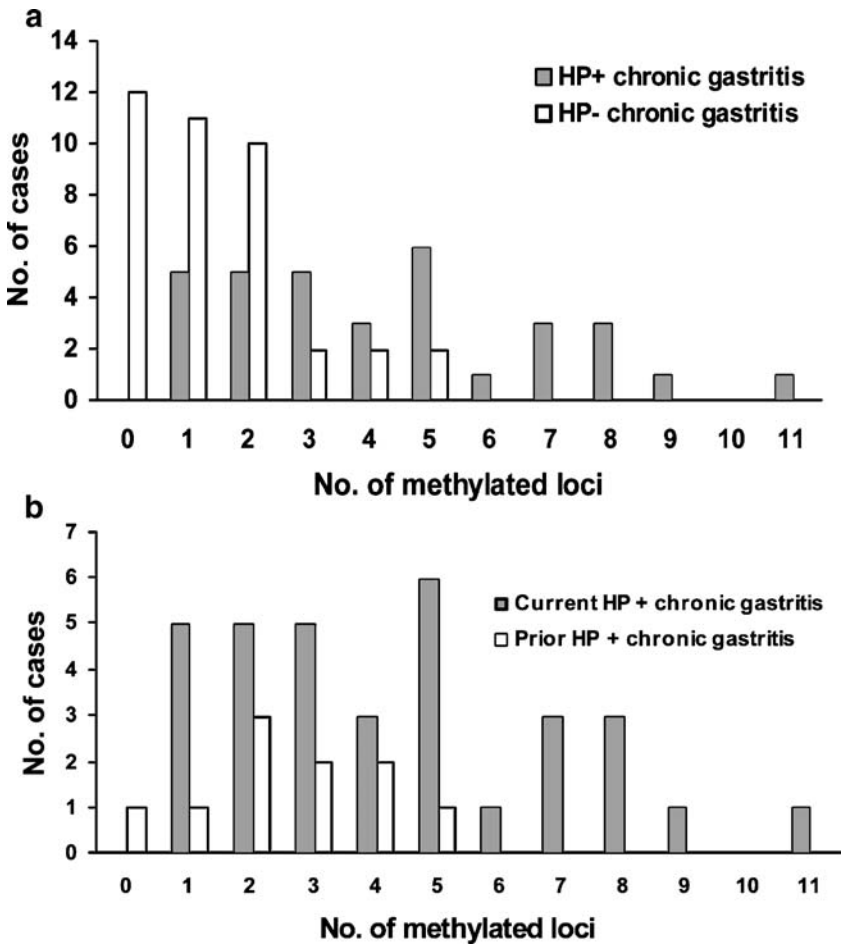


Fig. 5 **a** Distribution of the number of methylated CGI loci in *H. pylori*-positive chronic gastritis (current *H. pylori* infection) and *H. pylori*-negative chronic gastritis (no current *H. pylori* infection and no history of *H. pylori* infection). A CGI locus was considered methylated if the PMR was more than 4. **b** Comparison of the number of methylated CGI loci between chronic gastritis with current *H. pylori* infection and chronic gastritis with past *H. pylori* infection. Note the marked difference in the number of methylated CGI loci between the two groups

infection may affect susceptibility to *H. pylori*-induced hypermethylation [4].

Histologically, *H. pylori*-positive chronic gastritis tends to show more mononuclear and polymorphonuclear cell infiltration in the lamina propria than *H. pylori*-negative chronic gastritis, which was also the case in our study. Because we did not perform laser capture microdissection, inflammatory cells may give rise to a bias in the comparison of the methylation levels between *H. pylori*-positive and *H. pylori*-negative chronic gastritis. To identify whether the increased methylation levels of CGI loci in *H. pylori*-positive chronic gastritis were related to increased infiltration of inflammatory cells in the gastric mucosa, we examined peripheral blood leukocytes (from 50 healthy volunteers) for the methylation status of 25 CGI loci using the MethyLight technology. None of the CGI loci gave a PMR≥4 in peripheral blood leukocyte DNA (Supplementary data).

The present study provides supportive evidence that *H. pylori* infection is closely associated with aberrant CGI hypermethylation in the stomach. However, the mechanism of methylation induction in *H. pylori*-infected gastric mucosa remains unclear. A plausible explanation for the mechanism is as follows: an intense inflammatory response and an increased production of pro-inflammatory cytokines in the gastric mucosa provoked by *H. pylori* infection might participate in the induction of aberrant hypermethylation. (1) Interleukin-6, one of the cytokines produced in the *H. pylori*-infected gastric mucosa [1], has been shown to regulate the *DNMT1* promoter and the resulting enzyme activity [14, 15] and to increase methylcytosine content and modulate CGI hypermethylation [40]. (2) DNA methyltransferase expression has been reported to increase in the presence of *H. pylori* infection [36]. Overexpression of DNA methyltransferase is itself capable of bringing about de novo methylation of selective CGI loci [12]. (3)

5-Halogenated cytosine damage products, including 5-chlorocytosine and 5-bromocytosine, are formed in vivo by inflammation-mediated reactive molecules [2, 13] and it has been suggested that these modified pyrimidines mimic 5-methylcytosine and induce de novo methylation of previously unmethylated CpG sites [38].

CGI loci that are methylated in human cancers may be marked for preferred methylation. In recent studies, genes hypermethylated in human cancers were found to be often those genes which are marked by H3K27 trimethylation or Polycomb component occupancy in ES cells, where they are unmethylated [29, 32, 43]. In other words, PRC2 target genes of ES cells are predisposed to DNA hypermethylation occurring in association with cancer development. Because PRCs are not only essential regulators of embryonic development but also key players in the maintenance of adult stem cells [27, 39], gastric epithelial stem cells are expected to carry many genes under the control of PRCs and these Polycomb target genes may preferentially succumb to DNA hypermethylation induced by *H. pylori* infection. Although we could not explore the PRC occupancy of the examined 25 genes in gastric epithelial stem cells, published information about the occupancy by Polycomb group components (Suz12 and Eed) or H3K27 trimethylation at the genes in ES cells enabled us to analyze the association [23]. Based on the results of our methylation analysis, the examined 25 genes could be classified into three groups: (1) *H. pylori*-associated methylation only (*CDH1*, and *DAPK*), (2) cancer-associated methylation only (*BCL2*, *BDNF*, *CHFR*, *DLEC1*, *HOXA1*, *MLH1*, *NEUROG1*, *p14*, *RUNX3*, *SEZ6L*, *SFRP4*, *SMAD9*, *SOCS1*, *TERT*, *THBS1*, *TIMP3*, and *TP73*), and (3) both *H. pylori*- and cancer-associated methylation (*CACNA1G*, *CALCA*, *CRABP1*, *CYP1B1*, *GRIN2B*, and *TWIST1*). Seventy five percent of the genes showing *H. pylori*-associated methylation (the first and third groups) contain at least one of the three repressive marks, namely Suz12 occupancy, Eed occupancy, or H3K27 methylation, whereas 69% of the genes with cancer-associated methylation (the second group) do not carry any of the three repressive marks (Fig. 6). Furthermore, all of the genes with methylation associated with both *H. pylori* and cancer (the third group) contain one or more of the repressive marks. This fact suggests that repressive chromatin marks may leave genes vulnerable to later aberrant DNA hypermethylation induced by *H. pylori* infection, on the assumption that repressive chromatin marks established on genes early in development are maintained in gastric epithelial stem cells and progenitor cells. However, it should be noted that *CDH1* and *DAPK*, showing association of their hypermethylation with *H. pylori* infection, are not occupied by PRC2 in ES cells, and also that a large portion of the genes showing cancer-related methylation do not contain the repressive marks. Thus, other potential factors capable of directing targeted methylation should exist and may include the local DNA sequence motifs. Genome-wide DNA methylation studies have demonstrated the presence of such motifs which are significantly enriched in methylated promoter CGIs relative to the bulk of unmethylated CGIs [21, 33].

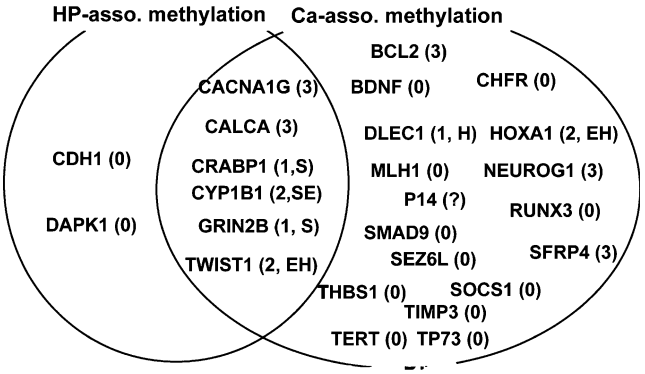


Fig. 6 Venn diagram showing CGI loci of *H. pylori*-associated methylation and those of gastric cancer-associated methylation. CGI loci having significantly higher methylation levels in *H. pylori*-negative gastric cancer specimens compared to *H. pylori*-negative chronic gastritis specimens are referred to as cancer-associated loci. The loci for which DNA hypermethylation was significantly associated with *H. pylori* infection are referred to as *H. pylori*-associated loci. The occupancy of the three components of PRC2 (Suz12 (*S*), Eed (*E*), and Ezh2 (*H*)) at the examined 25 genes in ES cells could be established from the published information and is given in parentheses and the numbers in parenthesis indicates the total number of occupying components. The status of PRC2 occupancy or H3K27 methylation for *p14* in ES cells is not known

Generalized genomic hypomethylation as well as focal CGI hypermethylation constitute aberrant methylation changes characteristic of human cancer cells and aged cells [10, 30]. Both methylation changes are frequently found in gastric carcinoma cells and even in multi-step lesions prior to gastric carcinoma [8, 19]. Given these facts, *H. pylori* infection was expected to affect the global genomic methylation status of the gastric epithelial cells. However, Alu and LINE-1 methylation levels, surrogates for genomic methylation levels, did not decrease in *H. pylori*-positive chronic gastritis samples compared with those of *H. pylori*-negative chronic gastritis samples, but they were significantly lower in gastric carcinoma compared with chronic gastritis cases, regardless of *H. pylori* infection. Although the number of analyzed cases was low, the findings suggest that *H. pylori* infection affects methylation changes of CGI loci but does not change the methylation content of the repetitive elements.

We have analyzed the relationship of aberrant DNA methylation changes in the stomach relative to *H. pylori* infection using the MethyLight assay on 25 genes and the COBRA assay on Alu and LINE-1 repetitive elements. The results suggest that *H. pylori* infection is strongly associated

with focal CGI hypermethylation but does not affect the genomic methylation contents. Identification of Polycomb group protein occupancy in stem cells of the 25 genes examined revealed that genes occupied by Polycomb group proteins during embryonic development seem to be vulnerable to *H. pylori*-related DNA hypermethylation.

Conflict of interest statement We declare that we have no conflict of interest.

References

1. Ando T, Kusugami K, Ohsuga M, Ina K, Shinoda M, Konagaya T, Sakai T, Imada A, Kasuga N, Nada T, Ichiyama S, Blaser MJ (1998) Differential normalization of mucosal interleukin-8 and interleukin-6 activity after *Helicobacter pylori* eradication. Infect Immun 66:4742–47
2. Badouard C, Masuda M, Nishino H, Cadet J, Favier A, Ravanat JL (2005) Detection of chlorinated DNA and RNA nucleosides by *H. pylori*LC coupled to tandem mass spectrometry as potential biomarkers of inflammation. J Chromatogr B Analyt Technol Biomed Life Sci 827:26–31
3. Cao R, Zhang Y (2004) The functions of E(Z)/EZH2-mediated methylation of lysine 27 in histone H3. Curr Opin Genet Dev 14:155–164
4. Chan AO, Chu KM, Huang C, Lam KF, Leung SY, Sun YW, Ko S, Xia HH, Cho CH, Hui WM, Lam SK, Rashid A (2007) Association between *Helicobacter pylori* infection and interleukin 1 beta polymorphism predispose to CpG island methylation in gastric cancer. Gut 56:595–597
5. Chan AO, Lam SK, Wong BC, Wong WM, Yuen MF, Yeung YH, Hui WM, Rashid A, Kwong YL (2003) Promoter methylation of E-cadherin gene in gastric mucosa associated with *Helicobacter pylori* infection and in gastric cancer. Gut 52:502–506
6. Chan AO, Peng JZ, Lam SK, Lai KC, Yuen MF, Cheung HK, Kwong YL, Rashid A, Chan CK, Wong BC (2006) Eradication of *Helicobacter pylori* infection reverses E-cadherin promoter hypermethylation. Gut 55:463–468
7. Cho NY, Kim BH, Choi M, Yoo EJ, Moon KC, Cho YM, Kim D, Kang GH (2007) Hypermethylation of CpG island loci and hypomethylation of LINE-1 and Alu repeats in prostate adenocarcinoma and their relationship to clinicopathological features. J Pathol 211:269–277
8. Cravo M, Pinto R, Fidalgo P, Chaves P, Gloria L, Nobre-Leitao C, Costa Mira F (1996) Global DNA hypomethylation occurs in the early stages of intestinal type gastric carcinoma. Gut 39:434–438
9. Eads CA, Lord RV, Wickramasinghe K, Long TI, Kurumboor SK, Bernstein L, Peters JH, DeMeester SR, DeMeester TR, Skinner KA, Laird PW (2001) Epigenetic patterns in the progression of esophageal adenocarcinoma. Cancer Res 61:3410–3418
10. Ehrlich M (2002) DNA methylation in cancer: too much, but also too little. Oncogene 21:5400–5413
11. Ekstrom AM, Held M, Hansson LE, Engstrand L, Nyren O (2001) *Helicobacter pylori* in gastric cancer established by CagA immunoblot as a marker of past infection. Gastroenterology 121:784–791
12. Feltus FA, Lee EK, Costello JF, Plass C, Vertino PM (2003) Predicting aberrant CpG island methylation. Proc Natl Acad Sci USA 100:12253–12258
13. Henderson JP, Byun J, Williams MV, Mueller DM, McCormick ML, Heinecke JW (2001) Production of brominating intermediates by myeloperoxidase. A transhalogenation pathway for generating mutagenic nucleobases during inflammation. J Biol Chem 276:7867–7875
14. Hodge DR, Peng B, Cherry JC, Hurt EM, Fox SD, Kelley JA, Munroe DJ, Farrar WL (2005) Interleukin 6 supports the maintenance of p53 tumor suppressor gene promoter methylation. Cancer Res 65:4673–4682
15. Hodge DR, Xiao W, Clausen PA, Heidecker G, Szyf M, Farrar WL (2001) Interleukin-6 regulation of the human DNA methyltransferase (HDNMT) gene in human erythroleukemia cells. J Biol Chem 276:39508–39511
16. IARC working group on the evaluation of carcinogenic risks to humans, schistosomes, liver flukes, Helicobacter pylori (1994) IARC monographs on the evaluation of carcinogenic risks to humans, vol 61. International Agency for Research on Cancer, Lyon, pp 1–241
17. Kang GH, Lee S, Cho NY, Gandamihardja T, Long TI, Weisenberger DJ, Campan M, Laird PW (2008) DNA methylation profiles of gastric carcinoma characterized by quantitative DNA methylation analysis. Lab Invest 88:161–170
18. Kang GH, Lee S, Kim JS, Jung HY (2003) Profile of aberrant CpG island methylation along multistep gastric carcinogenesis. Lab Invest 83:519–526
19. Kang GH, Shim YH, Jung HY, Kim WH, Ro JY, Rhyu MG (2001) CpG island methylation in premalignant stages of gastric carcinoma. Cancer Res 61:2847–2851
20. Karpf AR, Matsui S (2005) Genetic disruption of cytosine DNA methyltransferase enzymes induces chromosomal instability in human cancer cells. Cancer Res 65:8635–8639
21. Keshet I, Schlesinger Y, Farkash S, Rand E, Hecht M, Segal E, Pikarski E, Young RA, Niveleau A, Cedar H, Simon I (2006) Evidence for an instructive mechanism of de novo methylation in cancer cells. Nat Genet 38:149–153
22. Kochanek S, Renz D, Doerfler W (1993) DNA methylation in the Alu sequences of diploid and haploid primary human cells. EMBO J 12:1141–1151
23. Lee TI, Jenner RG, Boyer LA, Guenther MG, Levine SS, Kumar RM, Chevalier B, Johnstone SE, Cole MF, Isono K, Koseki H, Fuchikami T, Abe K, Murray HL, Zucker JP, Yuan B, Bell GW, Herbolsheimer E, Hannett NM, Sun K, Odom DT, Otte AP, Volkert TL, Bartel DP, Melton DA, Gifford DK, Jaenisch R, Young RA (2006) Control of developmental regulators by Polycomb in human embryonic stem cells. Cell 125:301–313
24. Leung WK, Man EP, Yu J, Go MY, To KF, Yamaoka Y, Cheng VY, Ng EK, Sung JJ (2006) Effects of *Helicobacter pylori* eradication on methylation status of E-cadherin gene in noncancerous stomach. Clin Cancer Res 12:3216–3221
25. Maekita T, Nakazawa K, Mihara M, Nakajima T, Yanaoka K, Iguchi M, Arii K, Kaneda A, Tsukamoto T, Tatematsu M, Tamura G, Saito D, Sugimura T, Ichinose M, Ushijima T (2006) High levels of aberrant DNA methylation in *Helicobacter pylori*-infected gastric mucosae and its possible association with gastric cancer risk. Clin Cancer Res 12:989–995
26. Mihara M, Yoshida Y, Tsukamoto T, Inada K, Nakanishi Y, Yagi Y, Imai K, Sugimura T, Tatematsu M, Ushijima T (2006) Methylation of multiple genes in gastric glands with intestinal metaplasia: a disorder with polyclonal origins. Am J Pathol 169:1643–1651
27. Molofsky AV, Pardal R, Morrison SJ (2004) Diverse mechanisms regulate stem cell self-renewal. Curr Opin Cell Biol 16:700–707
28. Normark S, Nilsson C, Normark BH, Hornef MW (2003) Persistent infection with *Helicobacter pylori* and the development of gastric cancer. Adv Cancer Res 90:63–89
29. Ohm JE, McGarvey KM, Yu X, Cheng L, Schuebel KE, Cope L, Mohammad HP, Chen W, Daniel VC, Yu W, Berman DM, Jenuwein T, Pruitt K, Sharkis SJ, Watkins DN, Herman JG, Baylin SB (2007) A

stem cell-like chromatin pattern may predispose tumor suppressor genes to DNA hypermethylation and heritable silencing. Nat Genet 39:237–242
30. Richardson B (2003) Impact of aging on DNA methylation. Aging Res Rev 2:245–261
31. Rieder G, Merchant JL, Haas R (2005) *Helicobacter pylori* cag-type IV secretion system facilitates corpus colonization to induce precancerous conditions in Mongolian gerbils. Gastroenterology 128:1229–1242
32. Schlesinger Y, Straussman R, Keshet I, Farkash S, Hecht M, Zimmerman J, Eden E, Yakhini Z, Ben-Shushan E, Reubinoff BE, Bergman Y, Simon I, Cedar H (2007) Polycomb-mediated methylation on Lys27 of histone H3 pre-marks genes for de novo methylation in cancer. Nat Genet 39:232–236
33. Shen L, Kondo Y, Guo Y, Zhang J, Zhang L, Ahmed S, Shu J, Chen X, Waterland RA, Issa JP (2007) Genome-wide profiling of DNA methylation reveals a class of normally methylated CpG island promoters. PLoS Genet 3:2023–2036
34. Sparmann A, van Lohuizen M (2006) Polycomb silencers control cell fate, development and cancer. Nat Rev Cancer 6:846–856
35. Sugiyama A, Maruta F, Ikeno T, Ishida K, Kawasaki S, Katsuyama T, Shimizu N, Tatematsu M (1998) *Helicobacter pylori* infection enhances *N*-methyl-*N*-nitrosourea-induced stomach carcinogenesis in the Mongolian gerbil. Cancer Res 58:2067–2069
36. Tamura G (2004) Promoter methylation status of tumor suppressor and tumor-related genes in neoplastic and non-neoplastic gastric epithelia. Histol Histopathol 19:221–228
37. Ushijima T, Nakajima T, Maekita T (2006) DNA methylation as a marker for the past and future. J Gastroenterol 41:401–407
38. Valinluck V, Sowers LC (2007) Endogenous cytosine damage products alter the site selectivity of human DNA maintenance methyltransferase DNMT1. Cancer Res 67:946–950
39. Valk-Lingbeek ME, Bruggeman SW, van Lohuizen M (2004) Stem cells and cancer; the polycomb connection. Cell 118: 409–418
40. Wehbe H, Henson R, Meng F, Mize-Berge J, Patel T (2006) Interleukin-6 contributes to growth in cholangiocarcinoma cells by aberrant promoter methylation and gene expression. Cancer Res 66:10517–10524
41. Weisenberger DJ, Campan M, Long TI, Kim M, Woods C, Fiala E, Ehrlich M, Laird PW (2005) Analysis of repetitive element DNA methylation by MethyLight. Nucleic Acids Res 33:6823–6836
42. Weisenberger DJ, Siegmund KD, Campan M, Young J, Long TI, Faasse MA, Kang GH, Widschwendter M, Weener D, Buchanan D, Koh H, Simms L, Barker M, Leggett B, Levine J, Kim M, French AJ, Thibodeau SN, Jass J, Haile R, Laird PW (2006) CpG island methylator phenotype underlies sporadic microsatellite instability and is tightly associated with BRAF mutation in colorectal cancer. Nat Genet 38:787–793
43. Widschwendter M, Fiegl H, Egle D, Mueller-Holzner E, Spizzo G, Marth C, Weisenberger DJ, Campan M, Young J, Jacobs I, Laird PW (2007) Epigenetic stem cell signature in cancer. Nat Genet 39:157–158

Virchows Arch (2008) 452:525–534
DOI 10.1007/s00428-007-0572-7

OpenAccess

ORIGINAL ARTICLE

Mixed-type gastric carcinomas exhibit more aggressive features and indicate the histogenesis of carcinomas

Hua-chuan Zheng · Xiao-han Li · Takuo Hara · Shinji Masuda · Xiang-hong Yang · Yi-fu Guan · Yasuo Takano

Received: 8 November 2007 / Revised: 27 December 2007 / Accepted: 27 December 2007 / Published online: 12 February 2008
© The Author(s) 2008

Abstract To investigate the pathobiological behaviors of gastric mixed-type (MT) carcinomas and gastric carcinogenesis, the clinicopathological characteristics of MT carcinomas were analyzed and compared with intestinal-type (IT) and diffuse-type (DT) carcinomas. The expression of Ki-67, caspase-3, p53, fragile histine triad (FHIT), maspin, extracellular matrix metalloproteinase inducer (EMMPRIN), vascular growth factor (VEGF), MUC-2, 4, 5AC and 6, CD44, E-cadherin, β-catenin, and phosphorylated glycogen synthase kinase 3β-ser^{9} (P-GSK3β-ser^{9}) was examined on tissue microarrays using immunohistochemistry. It was found that MT carcinomas exhibited large size, deep invasion, frequent local invasion, and lymph node metastasis in comparison with IT and DT carcinomas ($p<0.05$). All the markers except MUC-5AC showed higher expression in IT than DT carcinomas ($p<0.05$). The expression of maspin, EMMPRIN, VEGF, MUC-4, and membrane E-cadherin was stronger in MT intestinal than diffuse component ($p<0.05$). Immunoreactivities to Ki-67, EMMPRIN, and VEGF were weaker in IT carcinoma than in the MT intestinal portion ($p<0.05$), while the opposite was true for CD44, MUC-2, and MUC-6 ($p<0.05$). The MT diffuse component displayed a higher expression of FHIT, VEGF, and P-GSK3β-ser^{9} than DT carcinoma ($p<0.05$). The accumulative survival rate of the IT carcinoma patients was higher than the other types ($p<0.05$). The invasive depth, venous invasion, lymph node, peritoneal or liver metastasis, and Lauren's classification were independent prognostic factors for gastric carcinomas ($p<0.05$). These findings suggested that MT carcinomas were also indicated to be more aggressive than IT and DT carcinomas. Significant differences were observed in the proliferation, apoptosis, angiogenesis, mucin secretion, and cell adhesion between IT and DT carcinomas, whereas only a few of these characteristics showed differences between the MT intestinal and diffuse parts, thus suggesting that both the MT components might originate from the stem cells with similar genetic traits, but follow different histogenic pathways.

Keywords Gastric carcinoma · Mixed type · Lauren's classification · Pathobiological behaviors · Carcinogenesis

H.-c. Zheng (✉) · Y.-f. Guan
Department of Biochemistry and Molecular Biology,
College of Basic Medicine, China Medical University,
Shenyang, China
e-mail: zheng_huachuan@hotmail.com

H.-c. Zheng · X.-h. Li · Y. Takano
Department of Diagnostic Pathology,
Graduate School of Medicine and Pharmaceutical Science,
University of Toyama,
Toyama, Japan

T. Hara · S. Masuda
Kouseiren Takaoka Hospital,
Takaoka, Japan

X.-h. Li · X.-h. Yang
Division of Pathology,
Shengjing Hospital of China Medical University,
Shenyang, China

Introduction

Gastric carcinoma is the second leading cause of cancer-related death behind lung carcinoma despite a worldwide decline in both its incidence and mortality since the late half of the twentieth century [11]. It continues to be a major health problem because of the slow decrease in incidence in Asia and high mortality of diagnosed gastric carcinoma in

the West [23]. Generally, the prognosis of patients with gastric carcinoma is somewhat dependent on its histological type, such as intestinal type (IT) or diffuse type (DT) as defined by Lauren [16].

Although gastric carcinoma is a malignant tumor originating from the same gastric epithelium, its morphological features vary substantially among individual patients. Histologically, IT carcinoma principally includes papillary, well-differentiated, and moderately-differentiated or mucinous adenocarcinoma without signet ring carcinoma (SRC) cells, whereas DT mainly consists of the SRC, poorly differentiated and undifferentiated adenocarcinoma of WHO classification [7, 23]. Although Kushima and Hattori [12] firstly proposed an entity of gastric-type carcinoma and terminologically seemed homologous to the IT one, the carcinoma cells of this type closely resemble normal foveolar cells on the basis of tissue morphology and mucin properties and are considered to have been derived from foveolar hyperplasia or pyloric gland adenoma [12, 13]. Recently, our group also focused on Lauren's classification and found that IT carcinoma frequently occurred in old men, while DT was more frequent in comparatively young women. The latter group was more inclined to invasion into the muscularis propria, lymphatic invasion, and lymph node metastasis, and belonged to a higher TNM staging, in comparison to its IT counterparts. Further analysis demonstrated that IT gastric carcinomas with a more favorable prognosis were prone to high levels of proliferation and apoptosis and also always accompanied by a strong expression of the fragile histine triad (FHIT), phosphatase and tensin homology deleted from human chromosome 10 (PTEN), p53, and extracellular matrix metalloproteinase inducer (EMMPRIN) [30]. Additionally, many genetic and epigenetic changes, such as mutation, deletion, loss of heterozygosity, methylation, and microsatellite instability were differentially observed in both histological types of gastric carcinoma [27, 36]. These data indicate that different carcinogenic pathways exist for gastric IT and DT carcinomas. Although carcinogenesis is a multistage process which consists of a multi-factorial etiology resulting from gene–environment interaction, the intestinal type is frequently related to environmental factors like diet and predominates in areas with a high incidence of this disease. In contrast, the diffuse type is thought to be of genetic origin and evenly distributed worldwide [30, 24]. It is commonly believed that Lauren's classification is valuable for both the epidemiological studies and gastric carcinogenesis.

However, a small number of gastric carcinomas remain characterized as unclassified or mixed-type (MT) ones, which are comprised histologically of non-homogenous mixtures of IT and DT carcinomas. Stelzner and Emmrich [26] found that 28 MT carcinomas showed a deep infiltration of the gastric wall, frequent regional lymph node metastasis, and high staging in comparison to the other two types. Machado et al. [21] reported that inactivating E-cadherin mutations were exclusively observed in the diffuse component of the tumors, thus suggesting that MT carcinomas displayed phenotypic divergence. A recent study showed that bone-marrow-derived cells (BMDCs) could progress through metaplasia and dysplasia to intraepithelial cancer under the induction of the carcinogen, *Helicobacter pylori* [9]. Therefore, the analysis of distinct MT carcinoma components can be of remarkable pathogenic significance if it would be true that carcinoma cells originate from BMDCs. In the present study, 814 cases of gastric carcinomas were collected to further clarify the pathological characteristics of MT carcinoma and the gastric carcinogenesis pathways using a combination of tissue microarray (TMA) and immunohistochemical techniques.

Materials and methods

Subjects

A total of 814 gastric carcinomas were collected from surgical resection in Kouseiren Takaoka Hospital between 1998 and 2006. The patients with carcinomas included 573 men and 241 women (29–91 years, mean=65.7 years). Among them, 312 cases were demonstrated with lymph node metastasis and 24 with liver metastasis. None of these cases underwent either chemotherapy or radiotherapy before surgery. All patients gave their informed consent for the use of tumor tissue specimens for clinical research and the University Ethical Committee approved the research protocol. All patients were followed up by consulting their case documents and through telephone interviews.

Pathology

All tissue specimens were fixed in 4% neutralized formaldehyde, embedded in paraffin, and cut into 4-μm sections. These sections were stained by hematoxylin and eosin (HE) to confirm their histological diagnosis and other microscopic characteristics. The staging for each gastric carcinoma was evaluated according to the TNM system of the Internationale Contre le Cancer (UICC) indicating the extent of tumor spread [25]. The histomorphological architecture of the tumors was expressed according to Lauren's classification [7, 16, 30]. The growth patterns were divided into five groups based on a modification of Emmrich's method [26]. Briefly, group I showed a combination of two components with diffuse distribution.

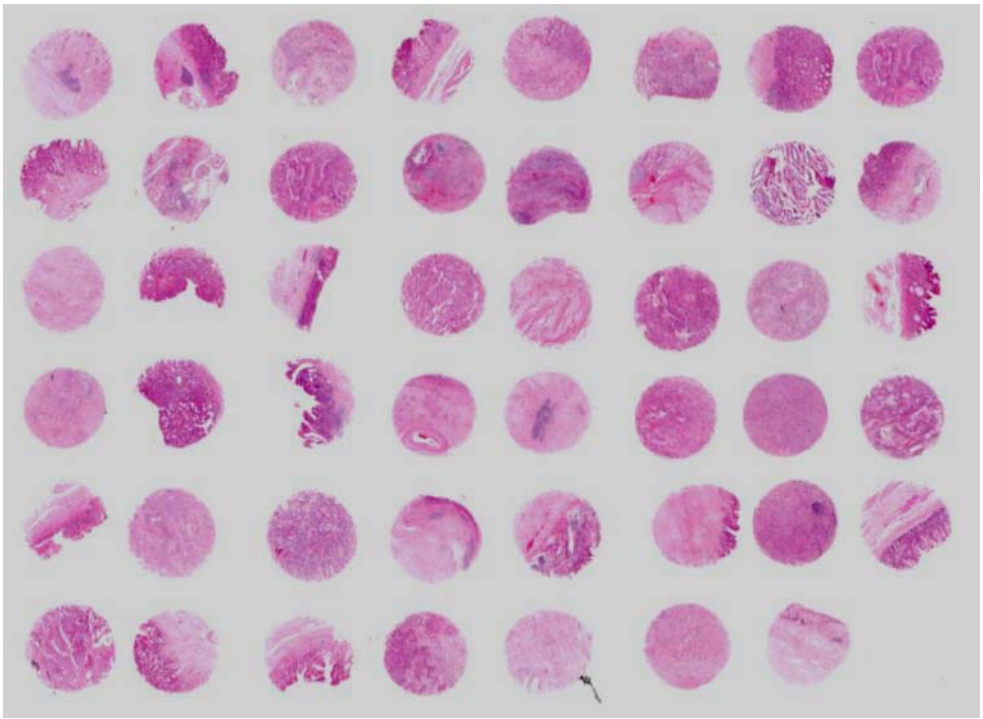


Fig. 1 HE staining of TMA of gastric carcinomas

Group II displayed both components with the border clearly visible. Group III represented some signet cells in the intestinal and diffuse components. Group IV were mucinous carcinomas with signet cells. Group V exhibited separately intestinal and diffuse components in the gastric wall. In addition, the depth of invasion, lymphatic and venous invasion, and peritoneal dissemination were all determined.

Tissue microarray

IT and DT carcinomas, as well as both components of the mixed type, were identified in HE stained sections of the selected tumor cases and a 2-mm-diameter tissue core of each donor block was punched out and transferred to a recipient block with a maximum of 48 cores using a Tissue Microarrayer (AZUMAYA KIN-1, Tokyo, Japan). Four-micrometer-thick sections were cut from the recipient block and transferred to poly-lysine-coated glass slides. HE staining was performed on TMA for confirmation of the tumor tissue (Fig. 1).

Immunohistochemistry

Consecutive sections were deparaffinized with xylene, dehydrated with alcohol, and subjected to antigen retrieval by irradiating in target retrieval solution (TRS, DAKO, Carpinteria, UAS) for 15 min in a microwave oven (Oriental rotor Lmt. Co. Tokyo, Japan). Five percent bovine serum albumin (BSA) was then applied for 15 min to prevent non-specific binding. The sections were incubated with primary antibodies for 15 min, then treated with the anti-mouse or anti-rabbit Envison-PO (DAKO, USA) antibodies for 15 min. All incubations were performed in the microwave oven for intermittent irradiation as described previously [15]. After each treatment, the slides were washed with TBST (10 mM Tris–HCl, 150 mM NaCl, 0.1% Tween 20) three times for 1 min. The primary antibodies are summarized in Table 1. All immunostaining was visualized with 3, 3′-diaminobenzidine (DAB) with 5-min reaction and counterstained with Mayer's hematoxylin.

Table 1 Primary antibodies used in this study

Names	Source	Company	Dilution
Ki-67	Rabbit	DAKO, Carpinteria, USA	1:25
Caspase-3	Rabbit	DAKO, USA	1:150
p53	Mouse	DAKO, USA	1:100
FHIT	Rabbit	Neomarkers, Fremont, USA	1:200
Maspin	Mouse	Novocastra, Newcastle upon Tyne, UK	Read-to-use
EMMPRIN	Mouse	Novocastra, UK	1:100
VEGF	Rabbit	Labvision, Fremont, USA	1:50
P-GSK3β-ser^{9}	Rabbit	SAT, USA	1:300
MUC-2	Mouse	Novocastra, UK	1:100
MUC-4	Mouse	Novocastra, UK	1:100
MUC-5AC	Mouse	Novocastra, UK	1:100
MUC-6	Mouse	Novocastra, UK	1:100
CD44	Mouse	DAKO, USA	1:50
E-cadherin	Mouse	Takara, Otsu, Japan	1:100
β-Catenin	Mouse	Calbiochem, CA, USA	1:200

Omission of the primary antibody was used as a negative control.

The immunoreactivity to Ki-67 and p53 was localized in the nucleus; FHIT, caspase-3, vascular growth factor (VEGF), maspin, phosphorylated glycogen synthase kinase 3β-ser^9 (P-GSK3β-ser^9), MUC-2, MUC-5AC, and MUC-6 in the cytoplasm; EMMPRIN and MUC-4 in the cytoplasm and membrane; CD44 and E-cadherin in the membrane; and β-catenin in the nucleus, cytoplasm, and membrane (Fig. 2). All evaluations were performed blindly by two independent observers (Takano Y and Zheng HC).

Statistical analysis

The statistical evaluation was performed using Fisher's exact possibility to differentiate the rates and the Mann–Whitney *U* test to differentiate the means of the different groups. Kaplan–Meier survival plots were generated and comparisons between the survival curves were made with the log-rank statistic. The Cox proportional hazards model was employed for multivariate analysis. $p<0.05$ was considered to represent a statistically significant difference. The SPSS 10.0 software program was employed to analyze all data.

Results

Clinicopathological characteristics of gastric IT, DT, and MT carcinomas

As summarized in Table 2, 415 IT cases were identified (51.0%), 221 DT (27.1%), and 178 MT (21.9%) among the 814 gastric carcinomas in this study. Patients with IT carcinoma were found to be significantly older than those with DT ($p<0.05$). The male and female ratios in the carcinoma cases gradually decreased from IT to DT through the MT groups ($p<0.05$). It was the same for lower TNM staging in the three groups ($p<0.05$). The positive rate of peritoneal spread was higher in the DT and MT cases than IT ($p<0.05$). MT carcinomas showed aggressive characteristics, such as large size, deep invasion, frequent local invasion, and lymph node metastasis, compared to the IT and DT ($p<0.05$). There was no significance between the three types of gastric carcinomas in the incidence of the liver metastasis ($p>0.05$).

Pathological behaviors of gastric MT carcinomas with different growth patterns or histological distribution of components

According to the growth pattern, the intestinal and diffuse components diffusely distributed without absolute border in group I of the MT carcinomas, which occurred more frequently (60.0%, 106/178) than the other four groups. As indicated in Table 3, most groups III and V gastric carcinomas were generally of early stage with less local invasion, infrequent lymph node metastasis and low TNM staging. In this study, only four advanced gastric carcinomas belonged to group IV, among which three cases were women and all were accompanied with lymphangiogenic invasion, lymph node metastasis, and high TNM staging. Although the main histological component was different from that in lymph node metastasis, the statistical data revealed that there was histological consistency between primary and lymph node metastasis foci ($p<0.05$). There were no remarkable differences in the pathological behaviors of MT carcinomas with different ratios of intestinal and diffuse portions ($p>0.05$).

Immunohistochemical analysis of intestinal or diffuse components from three types of gastric carcinomas

Table 4 demonstrates that all the markers except MUC-5AC were expressed at higher levels in IT carcinomas than in MT ones ($p<0.05$). The expression of maspin, EMMPRIN, VEGF, MUC-4, and E-cadherin was stronger in the intestinal component of MT carcinomas than in their diffuse counterpart ($p<0.05$). Immunoreactivities to Ki-67, EMMPRIN, and VEGF were weaker in the intestinal-type carcinomas than in the intestinal component of the MT ($p<0.05$), while it was the opposite for CD44, MUC-2, and MUC-6 ($p<0.05$). In contrast, the diffuse components of the MT carcinomas showed greater expression of Ki-67, FHIT, VEGF, and P-GSK3β-ser^9 than DT carcinomas ($p<0.05$).

Patients' outcome with different gastric carcinomas

Follow-up information for 500 carcinoma patients was used before 2002 for a period ranging from 5 days to 9.15 years (mean=49.4 months). Figure 3 shows the survival curves stratified according to Lauren's classification. Kaplan–Meier analysis indicated that the patients with IT carcinoma had a higher cumulative survival rate than those with the DT and MT lesions ($p<0.05$). Although the MT carcinoma patients' survival rate was comparatively lower than the DT ones,

Fig. 2 Immunostaining of TMA of gastric carcinomas. The immunoreactivity to Ki-67 (**a**) and p53 (**c**) was localized in the nucleus; FHIT (**d**), caspase-3 (**b**), VEGF (**g**), maspin (**e**), P-GSK3β-ser^9 (**h**), MUC-2 (**i**), MUC-5AC (**k**), MUC-6 (**l**) were seen in the cytoplasm, EMMPRIN (**f**) and MUC-4 (**j**) were seen in the cytoplasm and the plasma membrane, CD44 (**m**), and E-cadherin (**n**) in the plasma membrane; and β-catenin (**o**) in the nucleus, cytoplasm, and plasma membrane. These molecules were strongly expressed in the intestinal-type gastric carcinomas

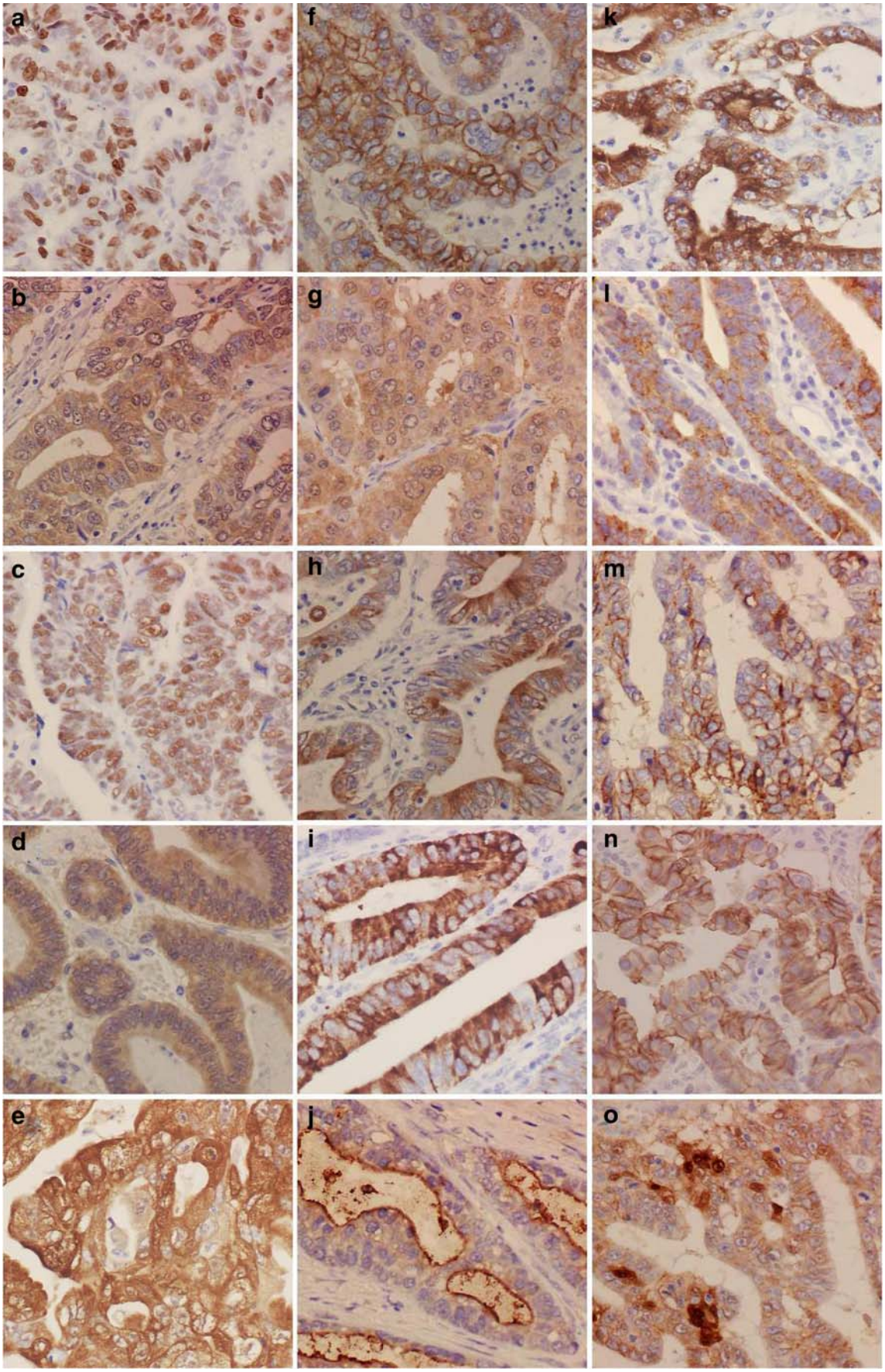

a
f
k
b
g
l
c
h
m
d
i
n
e
j
o

Table 2 Comparison of the clinicopathological features in gastric IT, DT, and MT carcinomas

Clinicopathological features	Intestinal-type carcinoma	Diffuse-type carcinoma	Mixed-type carcinoma
Case number	415 (51.0%)	221 (27.1%)	178 (21.9%)
Age (mean ± SD, years)	67.09±10.73	62.03±11.3*	65.80±13.28
Sex (male:female)	324:91	125:96	124:54**
Tumor size (mean ± SD, cm)	3.82±3.21	5.50±6.95	5.56±3.08**
Invasion into muscularis propria	153 (36.9%)	121 (54.8%)	123 (69.1%)**
Lymphatic invasion (+)	117 (28.2%)	83 (37.6%)	99 (55.6%)**
Venous invasion (+)	49 (11.8%)	32 (14.5%)	39 (21.9%)**
Lymph node metastasis (+)	113 (27.2%)	94 (42.5%)	105 (59.0%)**
Liver metastasis (+)	10 (2.4%)	8 (3.6%)	6 (3.4%)
Peritoneal spread (+)	14 (3.4%)***	22 (10.0%)	21 (11.8%)
TNM staging (O, I)	302 (72.8%)	69 (31.2%)	112 (63.0%)**

*$p<0.05$ compared with intestinal- and mixed-type carcinomas
**$p<0.05$ compared with intestinal- and diffuse-type carcinomas with both analyzed
***$p<0.05$ compared with diffuse- and mixed-type carcinomas

there was no statistical significance ($p>0.05$). Multivariate analysis demonstrated that invasive depth, venous invasion, lymph node, peritoneal or liver metastasis, and Lauren's classification were independent factors for the poor prognosis of gastric carcinoma patients ($p<0.05$; Table 5).

Discussion

Histologically, Lauren's classification of gastric carcinomas is based on the morphological appearances. IT carcinomas are characterized by cohesive carcinoma cells forming gland-like tubular structures with an expanding or infiltrative growth pattern, like a papillary and well-differentiated adenocarcinoma. However, the cell cohesion is less apparent or absent in DT carcinomas, and cancer cells diffusely spread in the gastric wall as poorly differentiated adenocarcinomas, SRC, or undifferentiated carcinomas [23, 30]. However, there are two types of histological distribution in the MT carcinoma, as described by Lauren [16]. In this study, carcinoma diagnosed as MT made up 21.9% of the whole series in this population, more than that reported by Borch et al. (13%), Lauren (14%), and Stelzner and Emmrich (14.1%), and less than that reported by Carneiro et al. (38.5%) [2, 5, 16, 26]. This discrepancy might be due to the differences in diagnosis criteria, geographical regions, human races, living habits, and so forth. The age and sex distribution of the patients with MT carcinoma was intermediate although IT carcinomas frequently occurred in old men, compared with DT carcinomas.

Morphologically, there are both intestinal and diffuse components in MT carcinomas, and they were found to be significantly larger, more advanced, and more frequently spread into local lymphatic and venous vessels or regional lymph nodes, compared with IT and DT carcinomas in the present study, consistent with other reports [6, 16, 30]. Kozuki et al. [14] found that prominent lymphatic permeation and lymph node metastasis were more frequently

Table 3 Pathological behaviors of gastric MT carcinomas

Clinicopathological features	*n*	Sex (male)	Invasion into MP	Lymphatic invasion	Venous invasion	Lymph node metastasis				Staging
						n	I>D	I=D	I<D	(O, I)
Growth pattern										
I	106	73 (68.9%)	82 (77.4%)	64 (60.4%)	26 (24.5%)	69 (65.1%)	32	14	23	35 (33.0%)
II	25	18 (78.3%)	21 (84.0%)	16 (64.0%)	7 (28.0%)	16 (64.0%)	5	5	6	7 (28.0%)
III	29	22 (75.9%)	11 (37.9%)	9 (31.0%)	3 (10.3%)	10 (34.5%)	4	3	3	18 (62.1%)
IV	4	1 (25.0%)	4 (100.0%)	4 (100.0%)	1 (25.0%)	4 (100.0%)	0	2	2	0 (0.0%)
V	14	10 (71.4%)	5 (35.7%)	6 (42.9%)	2 (14.3%)	6 (42.9%)	2	0	4	9 (64.3%)
Histological appearance										
Intestinal>diffuse	80	59 (73.8%)	54 (67.5%)	43 (53.8%)	20 (25.0%)	48 (60.0%)	30	8	10	33 (41.3%)
Intestinal=diffuse	20	15 (75.0%)	12 (60.0%)	9 (45.0%)	5 (25.0%)	10 (50.0%)	3	5	2	8 (40.0%)
Intestinal<diffuse	78	50 (64.1%)	57 (73.1%)	47 (60.3%)	14 (18.0%)	47 (60.3%)	10	11	26	28 (35.9%)

MP Muscularis propria; in lymph node metastatic foci: *I>D* intestinal>diffuse, *I<D* intestinal<diffuse, *I=D* intestinal=diffuse

Table 4 Immunohistochemical analysis in gastric IT, DT, and MT carcinomas

Biological markers	Intestinal-type carcinoma	Mixed-type carcinoma		Diffuse-type carcinoma
		Intestinal part	Diffuse part	
Ki-67	88/146 (60.3%)*,***	81/110 (73.6%)	78/110 (70.9%)*	57/119 (47.9%)
Caspase-3	84/152 (55.3%)*	52/119 (43.7%)	37/119 (31.1%)	24/115 (20.9%)
p53	76/151 (50.3%)*	37/118 (31.4%)	30/118 (25.4%)	25/120 (20.8%)
FHIT	90/150 (60.0%)*	63/113 (55.8%)	48/113 (42.5%)*	27/116 (23.3%)
Maspin	71/150 (47.3%)*	55/112 (49.1%)***	34/112 (30.4%)	38/120 (31.7%)
EMMPRIN	87/147 (59.2%)*,***	77/112 (68.8%)***	43/112 (38.4%)	32/117 (26.5%)
VEGF	95/151 (62.9%)*,***	90/114 (78.9%)***	61/114 (53.5%)*	31/121 (25.6%)
P-GSK3β-ser^{9}	88/144 (61.1%)*	74/113 (65.5%)	67/113 (59.3%)*	48/116 (41.4%)
MUC-2	55/145 (37.9%)*,***	31/118 (26.3%)	27/118 (22.9%)	23/117 (19.7%)
MUC-4	58/153 (37.9%)*	39/118 (33.1%)***	21/118 (17.8%)	18/118 (15.3%)
MUC-5AC	84/148 (56.8%)	57/106 (53.8%)	50/106 (47.2%)	54/113 (47.8%)
MUC-6	60/146 (41.1%)*,***	26/117 (22.2%)	18/117 (15.4%)	9/123 (7.3%)
CD44	64/152 (42.1%)*,***	32/114 (28.1%)	31/114 (27.2%)	32/120 (26.7%)
E-cadherin	91/142 (64.1%)*	58/112 (51.8%)***	38/112 (33.9%)	43/119 (36.1%)
Membrane β-catenin	57/144 (39.6%)*	36/117 (30.8%)	26/117 (22.2%)	26/118 (22.0%)

*$p<0.05$ compared with the diffuse-type carcinomas
**$p<0.05$ compared with intestinal-part carcinomas
***$p<0.05$ compared with diffuse-part carcinomas

observed in MT than in the pure type of gastric carcinomas. It was previously documented that the MT carcinomas showed a deeper infiltration of the gastric wall, a higher metastatic rate to the regional lymph nodes, and the need for higher staging with the TNM system of UICC classification, in contrast to IT and MT carcinomas [26]. These findings suggest that the pathobiological characteristics of the MT carcinomas were more aggressive than the other two types, which accounted for their comparatively poor prognosis observed in the present study although there was no statistical significance. Among the MT carcinomas, five groups were classified according to their growth pattern. Half of the present cases belonged to group I, which means there was diffuse distribution of the intestinal and diffuse component without clear borders in most of the MT cases. In general, groups III and IV of MT carcinomas did not exhibit deep invasion, comparatively high staging or frequent spreading, compared with other types. However, group IV of carcinomas with mucin and signet cells was more advanced with wide spreading, including local vessels and lymph node metastasis. Therefore, surgeons should carefully treat the patients with MT carcinomas in clinical practice because of their aggressive characteristics and poor prognosis, especially those classified as group IV. Furthermore, it was found that the major component in the MT primary foci morphologically paralleled to that in the

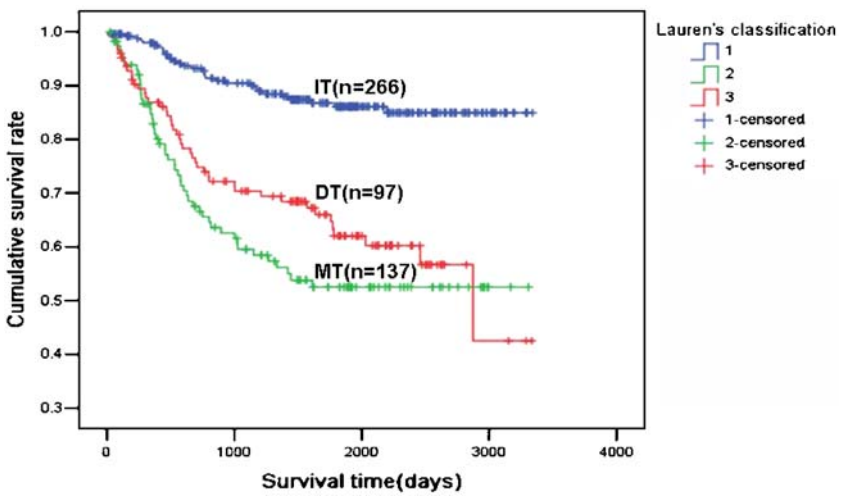


Fig. 3 Relationship between prognosis of carcinoma patients' and Lauren's classification Kaplan–Meier curves of cumulative survival rate for the patients with gastric carcinoma according to Lauren's classification. *IT* Intestinal type, *DT* diffuse type, *MT* mixed type

Table 5 Multivariate analysis of the clinicopathological variables of gastric carcinomas

Clinicopathological parameters	Relative risk (95% CI)	*p* Value
Age (≥65 years)	1.224 (0.849–1.764)	>0.05
Sex (male:female)	1.255 (0.827–1.904)	>0.05
Tumor size (≥4 cm)	1.466 (0.862–2.493)	>0.05
Invasive depth ($Ti_{s,1}/T_{2,3}$)	2.945 (1.533–5.657)	<0.05
Lymphatic invasion (−/+)	1.394 (0.865–2.247)	>0.05
Venous invasion (−/+)	1.692 (1.097–2.608)	<0.05
Lymph node metastasis (−/+)	1.983 (1.111–3.537)	<0.05
Peritoneal spread (−/+)	3.197 (2.031–5.031)	<0.05
Liver metastasis (−/+)	5.248 (2.575–10.697)	<0.05
Lauren's classification (intestinal/diffuse/mixed)	1.351 (1.084–1.683)	<0.05

CI Confidence interval

corresponding lymph node metastasis although the converse situation also appeared. This inconsistent phenomenon could be explained by sampling bias or the metastatic potential of individual carcinoma cells.

Compared with IT carcinomas, the MT counterpart always exhibited more severe characteristics, including invasion into muscularis propria, lymphatic invasion and lymph node metastasis, and high TNM staging in the present study, as observed by Lauren and other studies [16, 26, 30]. To clarify the pheno/genotypes of gastric carcinoma, the expression of Ki-67, caspase-3, p53, FHIT, maspin, VEGF, EMMPRIN, P-GSK3β-ser^9, MUC-2, MUC-4, MUC-5AC, MUC-6, E-cadherin, and β-catenin was examined by immunostaining. p53, FHIT, and maspin as tumor suppressor genes play important roles in regulating the balance between the proliferation and apoptosis of cancer cells [25, 30, 31, 34, 35]. Ki-67 antigen is present in the nuclei of cells undergoing proliferation and should be regarded as a good marker for cell proliferation [34]. Caspase-3 is responsible for the cleavage of poly (ADP-ribose) polymerase, actin, and sterol regulatory element binding protein and reflects the apoptotic level as a key protease in the cascade reaction of the apoptotic pathway [28]. In vivo and vitro evidences indicated that EMMPRIN and VEGF are involved in angiogenic processes in malignancies [29, 32]. Glycogen synthase kinase-3β (GSK3β) belongs to the serine/threonine protein kinase family and is also involved in regulating the balance between proliferation and apoptosis and can be inactivated via ser-9 phosphorylation by p70 S6 kinase, p90Rsk, Akt, certain isoforms of proteins kinase, and cyclic AMP-dependent protein kinase [1]. MUC-2, MUC-5AC, and MUC-6 are markers for intestinal goblet cells, superficial epithelium, and gastric pyloric gland cells, respectively, which can reflect the mucin secretion and variations in gastrointestinal malignancies. MUC-4 is a heterodimeric glycoprotein complex and expressed in several human epithelial carcinomas [3, 33]. CD44 is a cell surface glycoprotein involved in cell/cell and cell/matrix interactions. CD44 overexpression has been linked to the growth and spread of a range of different types of malignancies [8]. The E-cadherin can interact with β-catenin to form a complex, which is closely linked to cell adhesion and differentiation [19, 27, 36]. In the present study, all of the markers except MUC-5AC showed greater expression in the IT than in the DT carcinomas. Although some evidences indicate that MUC-5AC was strongly expressed in gastric DT carcinoma, in comparison with IT ones, there was no statistical difference in line with our finding [20, 22]. These data suggested that there were significant differences in the proliferation, apoptosis, angiogenesis, mucin production, and cell adhesion between the IT and DT carcinomas and these molecules mechanistically contributed to the molecular distinction in the morphological, behavioral, and histogenic aspects between both types of gastric carcinomas.

In general, DT carcinoma is believed to derive de novo from the peripheral stem cells of gastric gland neck proliferative zone without a recognizable precursor lesion except hereditary diffuse gastric cancer because in situ carcinoma or globoid dysplasia is its precancerous lesion, respectively, according to the Chinese and Western pathologists' opinions [4, 5, 9, 18,30]. When long-standing gastric inflammation causes tissue injury and stem cell failure with time, BMDCs are recruited and engrafted into the tissue stem cell niche, where BMDCs can behave in a way indistinguishable from endogenous tissue stem cells. With continued inflammation and injury, they can undergo sustained proliferation and malignant transformation into IT carcinomas, passing through precancerous stages of metaplasia and dysplasia when genetic defects, such as mutation, deletion, or rearrangement, are accumulated resulting in corruption of the balance between proliferation and apoptosis [17]. Likewise, dedifferentiation of intestinal to diffuse carcinoma had been identified as another histogenic pathway according to the histological heterogeneity of tumor cells, especially in the carcinomas containing moderately and poorly differentiated components with similar morphological appearance and diffuse distribution. If so, it is possible that the distinct components in MT carcinomas arise from the stem cells with common genetic traits and follow different carcinogenic pathways. Conversely, diffuse carcinoma could be derived from heterogeneity of the intestinal counterpart. According to our present data, no differences in the expression of Ki-67, caspase-3, FHIT, CD44, P-GSK3β-ser^9, MUC-2, MUC-5AC, MUC-6, and membrane β-catenin were observed between the intestinal and diffuse components of MT carcinomas, which supports the possibility of similar origin or dedifferentia-

tion. However, increased expression of EMMPRIN, VEGF, MUC-4, and E-cadherin in the intestinal component compared to the diffuse counterpart also provided evidence that the original carcinoma cells might undergo distinct carcinogenic routes resulting in the morphological distinction of both components. Both the intestinal and diffuse components in MT carcinomas had increased expression of Ki-67, EMMPRIN, and VEGF and reduced E-cadherin. Serum VEGF levels were found to be significantly higher in patients with MT gastric carcinomas than those with pure lesions [10]. It was proposed that MT carcinomas biologically displayed more aggressive behaviors than other types, including decreased cell adhesion, increased proliferation, and angiogenesis.

Most of the evidences in the present data indicated that the pathological behaviors of MT carcinomas were more aggressive than the other types, which was closely linked to the prognosis. It was previously documented that the MT patients' survival is significantly worse than those with IT or DT carcinomas regardless of their location [5]. However, this study demonstrated that there was no significance between the MT and DT carcinoma patients' survival rates although the former was lower than the latter. Additionally, both survival rates were lower than that with IT carcinomas. To avoid sampling bias from a shorter follow-up time, the older cases were chosen for the survival analysis, but they yielded consistent results. Furthermore, Cox's hazard proportional analysis indicated that the invasive depth, venous invasion, lymph node, peritoneal or liver metastasis, and Lauren's classification were independent prognostic factors for gastric carcinomas.

In summary, IT carcinoma, which is positively correlated with favorable prognosis, frequently displayed high levels of proliferation, apoptosis, angiogenesis, mucin production, and cell adhesion. Gastric MT carcinoma showed more aggressive behaviors than IT and DT ones. There was a significant difference in the proliferation, apoptosis, angiogenesis, mucin secretion, and cell adhesion between the IT and DT carcinomas, whereas only a few characteristics were differentially detected in the intestinal and diffuse component of the mixed-type carcinoma, suggesting that different components of MT carcinoma might originate from common stem cells, but follow distinct histogenic pathways. Furthermore, these results confirm that Lauren's classification is significant regarding the histopathogenesis and differentiation and considered as a guide to the clinical treatment of gastric carcinoma.

Acknowledgments We particularly thank Tokimasa Kumada and Hideki Hatta for their technical help and Yukari Inoue for her valuable secretarial assistance. This work was partially supported by the Japanese Ministry of Education, Science, Sports and Culture, Grant-in-Aid for Scientific Research 14770072, Japanese Smoking Foundation, Shenyang Outstanding Talent Foundation, and Natural Scientific Foundation of China (30600286).

Conflict of interest statement No conflict of interest.

Open Access This article is distributed under the terms of the Creative Commons Attribution Noncommercial License which permits any noncommercial use, distribution, and reproduction in any medium, provided the original author(s) and source are credited.

References

1. Ali A, Hoeflich KP, Woodgett JR (2001) Glycogen synthase kinase-3: properties, functions, and regulation. Chem Rev 101:2527–2540
2. Borch K, Jonsson B, Tarpila E, Franzen T, Berglund J, Kullman E, Franzen L (2000) Changing pattern of histological type, location, stage and outcome of surgical treatment of gastric carcinoma. Br J Surg 87:618–626
3. Byrd JC, Bresalier RS (2004) Mucins and mucin binding proteins in colorectal cancer. Cancer Metastasis Rev 23:77–99
4. Carneiro F, Huntsman DG, Smyrk TC, Owen DA, Seruca R, Pharoah P, Caldas C, Sobrinho-Simões M (2004) Model of the early development of diffuse gastric cancer in E-cadherin mutation carriers and its implications for patient screening. J Pathol 203:681–687
5. Carneiro F, Seixas M, Sobrinho-Simoes M (1995) New elements for an updated classification of the carcinomas of the stomach. Pathol Res Pract 191:571–584
6. Esaki Y, Hirayama R, Hirokawa K (1990) A comparison of patterns of metastasis in gastric cancer by histologic type and age. Cancer 65:2086–2090
7. Hamilton SR, Aaltonen LA (eds) (2000) In: WHO classification of tumors: pathology and genetics of tumors of the digestive system. IARC, Lyon, pp 39–50
8. Hong RL, Lee WJ, Shun CT, Chu JS, Chen YC (1995) Expression of CD44 and its clinical implication in diffuse-type and intestinal-type gastric adenocarcinomas. Oncology 52:334–339
9. Houghton J, Stoicov C, Nomura S, Rogers AB, Carlson J, Li H, Cai X, Fox JG, Goldenring JR, Wang TC (2004) Gastric cancer originating from bone marrow-derived cells. Science 306:1568–1571
10. Huang SP, Wu MS, Wang HP, Yang CS, Kuo ML, Lin JT (2002) Correlation between serum levels of interleukin-6 and vascular endothelial growth factor in gastric carcinoma. J Gastroenterol Hepatol 17:1165–1169
11. Kelley JR, Duggan JM (2003) Gastric cancer epidemiology and risk factors. J Clin Epidemiol 56:1–9
12. Kushima R, Hattori T (1993) Histogenesis and characteristics of gastric-type adenocarcinomas in the stomach. J Cancer Res Clin Oncol 120:103–111
13. Kushima R, Vieth M, Borchard F, Stolte M, Mukaisho K, Hattori T (2006) Gastric-type well-differentiated adenocarcinoma and pyloric gland adenoma of the stomach. Gastric Cancer 9:177–184
14. Kozuki T, Yao T, Nakamura S, Matsumoto T, Tsuneyoshi M (2002) Differences in p53 and cadherin–catenin complex expression between histological subtypes in diffusely infiltrating gastric carcinoma. Histopathology 41:56–64
15. Kumada T, Tsuneyama K, Hatta H, Ishizawa S, Takano Y (2004) Improved 1-h rapid immunostaining method using intermittent microwave irradiation: practicability based on 5 years application in Toyama Medical and Pharmaceutical University Hospital. Mod Pathol 17:1141–1149
16. Lauren P (1965) The two histological main types of gastric carcinoma: diffuse and so-called intestinal-type carcinoma. An attempt at a histo-clinical classification. Acta Pathol Microbiol Scand 64:31–49

17. Li HC, Stoicov C, Rogers AB, Houghton J (2006) Stem cells and cancer: evidence for bone marrow stem cells in epithelial cancers. World J Gastroenterol 12:363–371
18. Liu SC (1989) A newly recognized precancerous lesion of the stomach—histopathologic features of globoid dysplasia of human gastric epithelium. Zhonghua Zhong Liu Za Zhi 11:37–40
19. Lynch HT, Grady W, Suriano G, Huntsman D (2005) Gastric cancer: new genetic developments. J Surg Oncol 90:114–133
20. Machado JC, Nogueira AM, Carneiro F, Reis CA, Sobrinho-Simões M (2000) Gastric carcinoma exhibits distinct types of cell differentiation: an immunohistochemical study of trefoil peptides (TFF1 and TFF2) and mucins (MUC1, MUC2, MUC5AC, and MUC6). J Pathol 190:437–43
21. Machado JC, Soares P, Carneiro F, Rocha A, Beck S, Blin N, Berx G, Sobrinho-Simoes M (1999) E-cadherin gene mutations provide a genetic basis for the phenotypic divergence of mixed gastric carcinomas. Lab Invest 79:459–465
22. Reis CA, David L, Nielsen PA, Clausen H, Mirgorodskaya K, Roepstorff P, Sobrinho-Simões M (1997) Immunohistochemical study of MUC5AC expression in human gastric carcinomas using a novel monoclonal antibody. Int J Cancer 74:112–121
23. Roukos DH, Agnantis NJ, Fatouros M, Kappas AM (2002) Gastric cancer: introduction, pathology, epidemiology. Gastric & Breast Cancer 1:1–3
24. Shibata A, Longacre TA, Puligandla B, Parsonnet J, Habel LA (2001) Histological classification of gastric adenocarcinoma for epidemiological research: concordance between pathologists. Cancer Epidemiol Biomarkers Prev 10:75–78
25. Sobin LH, Wittekind CH (2002) TNM classification of malignant tumors, 6th edn. John Wiley, New York, pp 55–65
26. Stelzner S, Emmrich P (1997) The mixed type in Lauren's classification of gastric carcinoma. Histologic description and biologic behavior. Gen Diagn Pathol 143:39–48
27. Tahara E (2004) Genetic pathways of two types of gastric cancer. IARC Sci Publ 157:327–349
28. Zheng HC, Sun JM, Wei ZL, Yang XF, Zhang YC, Xin Y (2003) Expression of Fas ligand and caspase-3 contributes to formation of immune escape in gastric cancer. World J Gastroenterol 9:1415–1420
29. Zheng H, Takahashi H, Murai Y, Cui Z, Nomoto K, Niwa H, Tsuneyama K, Takano Y (2006a) Expressions of MMP-2, MMP-9 and VEGF are closely linked to growth, invasion, metastasis and angiogenesis of gastric carcinoma. Anticancer Res 26:3579–3583
30. Zheng H, Takahashi H, Murai Y, Cui Z, Nomoto K, Miwa S, Tsuneyama K, Takano Y (2007a) Pathobiological characteristics of intestinal- and diffuse-type gastric carcinoma in Japan: an immunostaining study on the tissue microarray. J Clin Pathol 60:273–277
31. Zheng H, Takahashi H, Murai Y, Cui Z, Nomoto K, Tsuneyama K, Masuda S, Takano Y (2007b) Low expression of FHIT and PTEN correlates with malignancy of gastric carcinoma: tissue-array findings. Appl Immunohistochem Mol Morphol 15(4):432–440
32. Zheng HC, Takahashi H, Murai Y, Cui ZG, Nomoto K, Miwa S, Tsuneyama K, Takano Y (2006d) Upregulated EMMPRIN/CD147 might contribute to growth and angiogenesis of gastric carcinoma: a good marker for local invasion and prognosis. Br J Cancer 95:1371–1378
33. Zheng H, Takahashi H, Nakajima T, Murai Y, Cui Z, Nomoto K, Tsuneyama K, Takano Y (2006b) MUC6 down-regulation correlates with gastric carcinoma progression and a poor prognosis: an immunohistochemical study with tissue microarrays. J Cancer Res Clin Oncol 132:817–823
34. Zheng H, Tsuneyama K, Cheng C, Takahashi H, Cui Z, Murai Y, Nomoto K, Takano Y (2006c) An immunohistochemical study of p53 and Ki-67 in gastrointestinal adenoma and adenocarcinoma using tissue microarray. Anticancer Res 26:2353–2360
35. Zheng H, Tsuneyama K, Cheng C, Takahashi H, Cui Z, Murai Y, Nomoto K, Takano Y (2007c) Maspin expression was involved in colorectal adenoma–adenocarcinoma sequence and liver metastasis of tumors. Anticancer Res 27:259–265
36. Zheng L, Wang L, Ajani J, Xie K (2004) Molecular basis of gastric cancer development and progression. Gastric Cancer 7:61–77

Virchows Arch (2008) 452:535–544
DOI 10.1007/s00428-008-0578-9

OpenAccess

ORIGINAL ARTICLE

Presence of HIF-1 and related genes in normal mucosa, adenomas and carcinomas of the colorectum

Astrid E. Greijer · Pien M. Delis-van Diemen · Remond J. A. Fijneman · Rachel H. Giles · Emile E. Voest · Victor W. M. van Hinsbergh · Gerrit A. Meijer

Received: 5 November 2007 / Revised: 7 January 2008 / Accepted: 7 January 2008 / Published online: 20 March 2008
© The Author(s) 2008

Abstract Expression of the transcription factor hypoxia-inducible factor 1 (HIF-1), which plays a key role in cellular adaptation to hypoxia, was investigated in normal colorectal mucosa (ten), adenomas (61), and carcinomas (23). Tissue samples were analyzed for HIF-1α, its upstream regulators, von Hippel–Lindau factor, AKT, and mammalian target of rapamycin (mTOR) and its downstream targets glucose transporter 1 (GLUT1), carbonic anhydrase IX, stromal-cell-derived factor 1 (SDF-1) by immunohistochemistry. In normal colorectal mucosa, HIF-1α was observed in almost all nuclei of surface epithelial cells, probably secondary to a gradient of oxygenation, as indicated by pimonidazole staining. The same staining pattern was present in 87% of adenomas. In carcinomas, HIF-1α was present predominantly around areas of necrosis (78%). Active AKT and mTOR, were present in all adenomas, carcinomas, and in normal colorectal mucosa. GLUT1 and SDF-1 were present in the normal surface epithelium of all adenoma cases, whereas in the carcinoma GLUT1 was located around necrotic regions and SDF-1 was present in all epithelial cells. In conclusion, HIF-1α appears to be physiologically expressed in the upper part of the colorectal mucosa. The present observations support that upregulation of HIF-1α and its downstream targets GLUT1 and SDF-1 in colorectal adenomas and carcinomas may be due to hypoxia, in close interaction with an active phosphatidylinositol 3-kinases–AKT–mTOR pathway.

Keywords HIF-1 · mTOR · SDF-1 · CA IX · Colon

Introduction

Colorectal carcinomas arise from normal epithelial cells of the colorectal mucosa through an adenoma stage. The transition from benign adenomas to malignant carcinomas, occurring in about 5% of all adenomas, is only beginning to be explored in appreciable detail. Biological changes involved in this process include important signaling pathways like the mammalian target of rapamycin (mTOR)–AKT pathway while recently also a role for hypoxia-driven signaling was shown [6, 14]. Both pathways are mediated by the transcription factor hypoxia-inducible factor 1 (HIF-1) as depicted in Fig. 1. HIF-1 is involved in cellular adaptation to hypoxia in solid tumors, including stimulation of angiogenesis and glycolysis [33]. HIF-1 consists of two subunits of which the β-subunit is constitutively expressed, whereas HIF-1α is regulated in particular by the oxygen level. Under normoxia, the HIF-1α protein is hydroxylated by prolyl hydroxylases [15, 16], which enables the von

Part of this work was financially supported by the 1st AEGON International Scholarship in Oncology (AEG, PMDvD, RJAF).

A. E. Greijer · P. M. Delis-van Diemen · R. J. A. Fijneman · G. A. Meijer (✉)
Department of Pathology, VU University Medical Centre, PO Box 7057, 1007 MB Amsterdam, The Netherlands
e-mail: ga.meijer@vumc.nl

A. E. Greijer · P. M. Delis-van Diemen · R. J. A. Fijneman
Department of Medical Oncology, VU University Medical Center, Amsterdam, The Netherlands

V. W. M. van Hinsbergh
Department of Physiology, VU University Medical Center, Amsterdam, The Netherlands

R. H. Giles · E. E. Voest
Department of Medical Oncology, University Medical Center Utrecht, Utrecht, The Netherlands

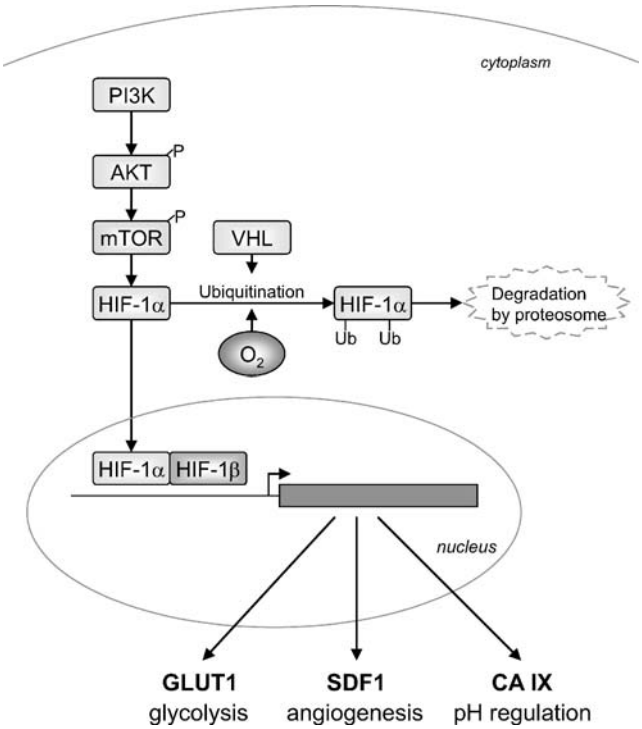


Fig. 1 Schematic representation of the interaction of the analyzed proteins. The PI3K–AKT–mTOR pathway is inducing HIF-1α. In addition, the absence of hypoxia prevents HIF-1α from degradation mediated by VHL. When HIF-1α is present, it binds to HIF-1 β in the nucleus. The formed complex activates target genes, like GLUT1, SDF1, and CA IX

Hippel–Lindau factor (VHL) to bind, resulting in ubiquination and rapid degradation by the proteosome [27]. HIF-1α is overexpressed in many solid tumors [38] and its presence has been correlated with, i.e., poor prognosis in breast and colorectal cancer patients [4, 36]. Stromal expression of hypoxia-regulated proteins is an adverse prognostic factor in colorectal carcinomas.

High protein levels of HIF-1α are not only caused by hypoxia but can also be induced by the absence of wild-type protein 53, mutated VHL and other tumor suppressor genes, as well as by activation of oncogenes like Her2neu (c-erbB-2) [24]. In addition, growth factors play a role. However, both hypoxia and signaling-mediated HIF-1 stimulation are mediated by the phosphatidylinositol 3-kinase (PI3K)–AKT, and the mTOR pathway [8]. Interestingly, both the serine–threonine protein kinase AKT as well as mTOR have been suggested to play a role in an early stage of colorectal carcinogenesis [2, 30]. Furthermore, the presence of a non-hypoxic HIF-1 induction has also been suggested, in colorectal adenomas [9].

Upon HIF-1 activation, multiple target genes become transcriptionally active, including genes involved in anaerobic glycolysis, metabolism, and angiogenesis. This includes glucose transporter 1 (GLUT1), which facilitates cellular glucose uptake [11, 26] and the angiogenesis-associated genes vascular endothelial growth factor and stromal-cell-derived factor 1 (SDF-1) also known as CXCL12 [5]. Furthermore, carbonic anhydrase IX (CA IX) which is prominently induced by hypoxia and is therefore considered to be an intrinsic hypoxia marker, which correlates with a chemical marker of hypoxia, pimonidazole [1, 17, 23, 28]. An additional function of CA IX is in the regulation of the maintenance of the physiological equilibrium in normal gastrointestinal tissue [31].

The present study aims to analyze the role HIF-1 in normal colorectal mucosa, adenomas, and carcinomas. To this end, the presence of HIF-1α as well as of its downstream targets GLUT1, SDF-1, and CA IX were analyzed in normal colon tissue, colorectal adenomas, and carcinomas. To explore the possible cause of HIF-1 overexpression, i.e., hypoxia or oncogenic stimulation, both the presence of the chemical hypoxia marker pimonidazole and of the HIF-1α upstream regulators, VHL, AKT, and mTOR, were investigated.

Materials and methods

Tumor material

A total of 84 tissue samples were studied, consisting of 61 colorectal adenomas, 20 of which contained already a focus of carcinoma and are therefore referred to as progressed adenomas, in contrast to the 41 adenomas with dysplasia only, which are referred to as nonprogressed adenomas. In addition, 23 colorectal carcinomas were analyzed. These samples were obtained from 75 patients, 37 of which were female and 38 male. Mean age was 67.8 years (range 40–89). Normal mucosa samples were obtained from the resection margins of colectomy specimens from ten patients with colorectal cancer. The study was approved by the Institutional Review Board and was in accordance with Dutch medical ethical guidelines.

Determination of hypoxic regions

Hypoxic regions in mouse tissues were visualized using the Hydroxyprobe-1 kit (Chemicon International, Temecula, CA, USA). These experiments were approved by the animal experimentation ethics committee, according to local and governmental regulations.

Briefly, mice were injected *intravenously* with pimonidazole (60-mg/kg body weight), which forms adducts from reductively activated pimonidazole in hypoxic cells. Mice were killed 90 min later by asphyxiation in CO_2. The Hydroxyprobe-1 monoclonal antibody was biotinylated using D-biotinyl-ε-aminocaproic acid *N*-hydroxysuccinimide ester (Boehringer Mannheim) and was used to stain

pimonidazole adducts in formalin-fixed paraffin-embedded tissues according to recommendations by the manufacturer.

Immunohistochemistry

Immunohistochemistry was performed on 4-μm-thick full-block consecutive sections. Slides were deparaffinized, followed by rehydration, and subsequently staining in batches with the antibodies described in Tables 1 and 2. HIF-1α staining was performed as described previously [3]. In brief, antigen retrieval was performed in antigen retrieval solution (DAKO, Glostrup, Denmark) for 45 min at 96°C. The primary antibody against HIF-1α was incubated at a dilution of 1:500 for 30 min at room temperature and the catalyzed signal amplification system (DAKO) was used for detecting HIF-1α staining.

For CA IX staining, no antigen retrieval step was used. Slides were incubated with a mouse primary antibody to CA IX in a 1:50 dilution for 30 min at room temperature. Detection was performed with the Envision+ system–horseradish peroxidase system for mouse primary antibodies (DAKO).

GLUT-1 staining was performed with a rabbit polyclonal anti-GLUT1 (antibody clone A 3536, DAKO, dilution 1:400) without antigen retrieval and subsequently developed with a standard avidin–biotinylated peroxidase complex (DAKO).

Staining procedures for AKT and mTOR were identical. After antigen retrieval, endogenous peroxidase activity was blocked for 10 min in methanol containing 0.3% hydrogen peroxide. The AKT antibody (Phospho-Akt (Ser473)) and mTOR antibody (Phospho-mTOR (Ser2448)) both obtained from Cell Signaling (Danvers, MA, USA) were incubated overnight at 4°C in a 1:50 dilution and subsequently detected with a standard avidin–biotinylated peroxidase complex.

SDF-1 staining was performed similar to the AKT and mTOR staining, except for the secondary antibody, which was a goat anti-rabbit antibody in this case.

For VHL staining, antigen retrieval was performed and endogenous peroxidase was blocked as the AKT and mTOR staining. Primary antibody against VHL was incubated for 60 min by room temperature, followed by Powervision (Immunologic, Duiven, the Netherlands) incubation for 30 min and subsequently the staining was detected with diaminobenzidine (SIGMA FAST™ 3,3′-diaminobenzidine tablets, Sigma Aldrich, St. Louis, MO, USA).

Before the slides were mounted with cover slips, all sections were counterstained for 30 s with Mayer's hematoxylin and dehydrated in 70%, 96%, and subsequently 100% ethanol and finally in xylene.

Evaluation and statistics

The intensity of the staining was compared between the normal mucosa, nonprogressed, progressed adenomas, and carcinomas and scored by two investigators. Staining intensity was scored in four classes (0 to 3) taking the negative control as a reference for score 0 and the positive control (clear cell renal adenocarcinomas (Grawitz tumor) as a reference for score 3). For HIF-1α, only nuclear staining was scored, for CA IX, membrane staining, and AKT and SDF-1 cytoplasmic staining, for mTOR predominantly cytoplasmic but also membrane staining was scored. Significance of differences between categories was analyzed by means of the Kruskal Wallis test. P-values<0.05 were considered to be significant.

Results

HIF-1α expression and its regulators hypoxia and VHL

In normal colorectal mucosa nine out of ten samples showed HIF-1α present in nuclei of the surface epithelium (Fig. 2). To evaluate whether hypoxia played a physiologic

Table 1 Details of the immunohistochemical stainings

Antibody	Species	Company and institutes	Dilution	Incubation	Antigen retrieval	Detection
HIF-1α	Mouse	BD Pharmingen	1/500	30′ RT	WB TRS 97°C 45′	CSA
Akt	Rabbit	Cell Signaling	1/50	o/n 4°C	WB Citr 97°C 10′	ABC
mTOR	Rabbit	Cell Signaling	1/50	o/n 4°C	WB Citr 97°C 10′	ABC
VHL	Mouse	BD Pharmingen	1/100	60′ RT	WB Citr 97°C 20′	Powervision
CA IX	Mouse	Lab Harris	1/50	30′ RT	none	Envision+
Glut-1	Rabbit	DAKO	1/400	60′ RT	WB Citr 97°C 20′	ABC
SDF-1	Mouse	R&D systems	1/400	o/n 4°C	WB Citr 97°C 10′	ABC
Hydroxyprobe-1	Mouse	Chemicon International	1/200	40′RT	0.01% pronase in PBS 40°C for 40′	ABC

BD Transduction laboratories, *Mab* monoclonal antibody, *PAb* polyclonal antibody, *RT* room temperature, *WB* water bath, *TRS* target retrieval solution (DAKO), *Citr* citrate buffer 10 mM pH 6.0, *CSA* catalyzed signal amplification system (DAKO), *ABC* avidin–biotinylated peroxidase complex, *Powervision* from immunologic R&D systems

Table 2 Number (and percentages) of HIF-1α, P-AKT, P-mTOR, VHL, CA IX, GLUT1, and SDF-1 expression in nonprogressed and progressed colorectal adenomas and adenocarcinomas in the respective categories of staining intensity

		Nonprogressed Adenoma, n=41	Progressed adenoma, n=20	Adenocarcinoma, n=23	Kruskal–Wallis test, P-value
HIF-1	Neg	6 (15)	2 (10)	5 (22)	0.8
	+	0 (0)	2 (10)	1 (4)	
	++	7 (17)	3 (15)	3 (13)	
	+++	28 (68)	13 (65)	14 (61)	
AKT	Neg	0 (0)	0 (0)	0 (0)	0.1
	+	12 (29)	7 (35)	0 (0)	
	++	11 (27)	5 (25)	10 (43)	
	+++	18 (78)	8 (40)	13 (57)	
mTOR	Neg	2 (5)	0 (0)[a]	0 (0)	0.4
	+	2 (5)	3 (16)	0 (0)	
	++	12 (29)	6 (32)	7 (30)	
	+++	25 (61)	10 (53)	16 (70)	
VHL	Neg	0 (0)[a]	1 (5)	0 (0)	0.9
	+	7 (18)	0 (0)	1 (4)	
	++	12 (30)	11 (55)	11 (48)	
	+++	21 (53)	8 (40)	11 (48)	
CA IX	Neg	10 (24)	4 (20)	1 (4)	0.3
	+	0 (0)	0 (0)	0 (0)	
	++	1 (2)	2 (10)	2 (9)	
	+++	30 (73)	14 (70)	20 (87)	
GLUT1	Neg	0 (0)	1 (5)	0 (0)	0.02
	+	8 (20)	6 (30)	0 (0)	
	++	15 (37)	4 (20)	6 (26)	
	+++	18 (44)	9 (45)	17 (74)	
SDF1	Neg	8 (20)[a]	7 (37)[a]	0 (0)	<0.005
	+	4 (10)	4 (21)	0 (0)	
	++	13 (33)	2 (11)	5 (22)	
	+++	15 (38)	6 (32)	18 (78)	

[a] One case not tested

role in the induction of HIF-1α in normal colorectal mucosa, we used mice that were injected with pimonidazole, a chemical marker of hypoxia that can be visualized by immunohistochemistry. The presence of tissue hypoxia was demonstrated in the surface epithelium of normal colon mucosa of the treated mice (Fig. 3). The pattern of hypoxic cells in the normal colorectal mucosa in mice matched with the distribution of HIF-1α immunohistochemical staining in human colorectal mucosa.

The presence of HIF-1α in normal colorectal mucosa was compared with that in adenomas and carcinomas. Adenomas displayed HIF-1α expression in 53 of the 61 cases, predominantly at the surface, gradually decreasing towards the center of the adenomas. No differences were seen between nonprogressed and progressed adenomas (85% and 90%, respectively), as shown in Table 2. Of the carcinomas, 78% (n=18) were positive, showing nuclear staining of HIF-1α in epithelial tumor cells. In carcinomas, a decreasing gradient of HIF-1α staining was observed from necrotic areas towards the well-vascularized stroma. Besides the epithelial tumor cells, in carcinomas, inflammatory cells in the tumor-associated stroma, and in five cases B-cells in lymph follicles, were positive for HIF-1α. Statistical analysis showed no significant differences in intensity of HIF-1α staining between normal mucosa, adenomas, and carcinomas.

VHL, the regulator of HIF-1α degradation, was also analyzed by means of immunohistochemistry (Fig. 2). VHL expression was observed in all epithelial cells in normal colorectal mucosa as well as in colorectal adenomas and carcinomas.

AKT and mTOR, oncogenic pathways regulating HIF-1α

To investigate whether, in addition to hypoxia, oncogenes and/or growth factors can contribute to the elevated HIF-1α, we studied the presence of phosphorylated forms of AKT and mTOR, which reflect an active state of the oncogene-driven pathway of HIF-1α activation. Low-intensity cytoplasmic staining for the active form of AKT (P-AKT) was seen in epithelial cells of normal mucosa in all tissues (Fig. 4). Positive staining was also seen in the smooth muscle cells of the muscularis propria and muscularis mucosae and in the walls of blood vessels. In

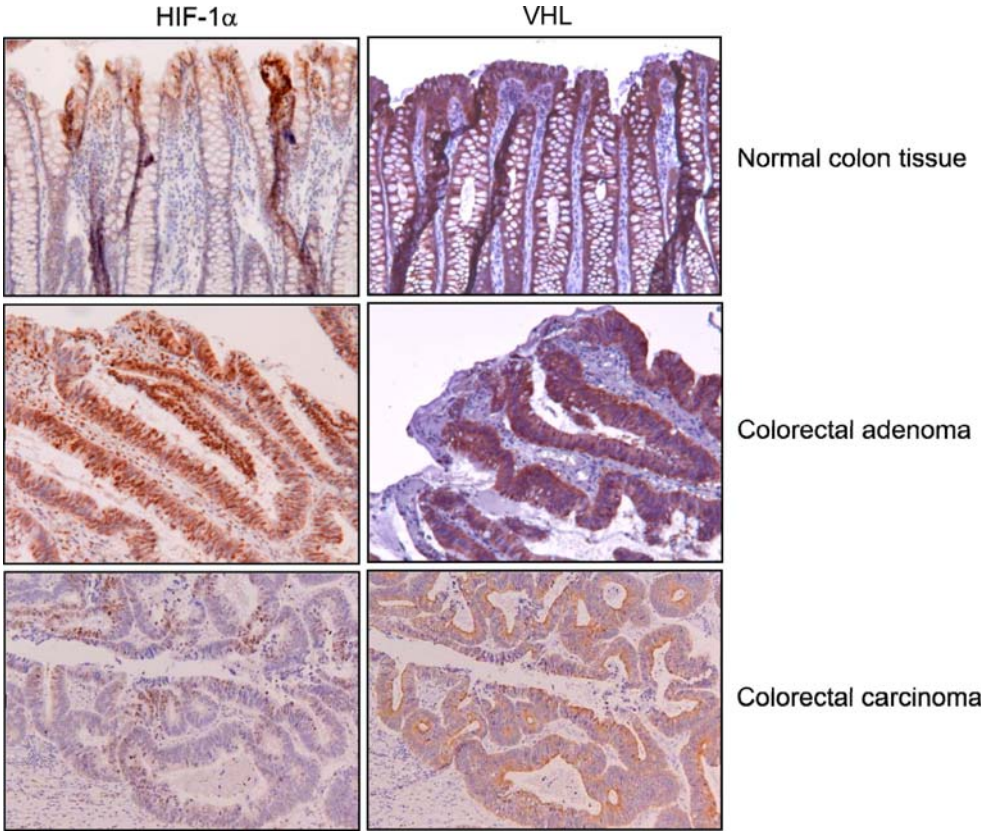


Fig. 2 Serial sections of normal colon mucosa, colorectal adenoma, and adenocarcinoma analyzed for HIF-1α and VHL expression. HIF-1α staining was observed in the nuclei of surface epithelium of normal mucosa and colorectal adenoma, whereas in adenocarcinomas HIF-1α was present near hypoxic regions with necrosis. VHL expression was observed in the cytoplasma of all epithelial cells of normal mucosa, adenomas, and adenocarcinomas

adenomas, staining in epithelial cells was more intense, present throughout the neoplastic tissue, and observed in all cases. Staining patterns in adenocarcinomas were similar and also observed in all samples analyzed.

Active mTOR was only present as a cytoplasmatic staining; nuclear staining was not observed in any of the cases (Fig. 4). In normal mucosa, mTOR was detected in the surface epithelium in all tissues. Likewise, in adenoma samples, mTOR was expressed in the surface epithelium but also more diffusely throughout the adenomas. In adenocarcinomas, staining patterns were diffused across the whole tumor, but more intense expression was detected in areas surrounding necrosis. Higher levels of active mTOR were observed at the invasive front of the tumor. In the adenocarcinomas, besides the cytoplasmic staining in some cells, a clear cellular membrane staining was observed. In all normal mucosa samples, adenomas, and carcinomas, mTOR was present, except for 5% of the nonprogressed adenomas, which were negative for mTOR (Table 2).

Expression of the HIF1 downstream targets Glut1 and SDF-1

To investigate to what extent downstream pathways were affected by HIF-1 upregulation, several HIF-1 target genes,

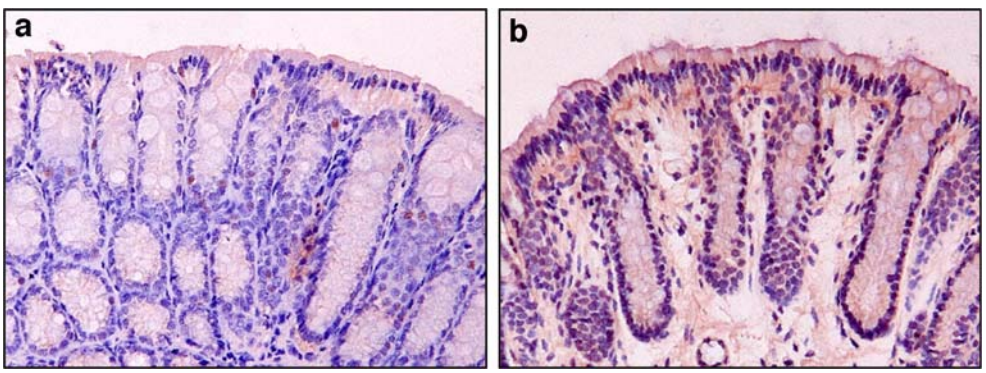


Fig. 3 Detection of hypoxia in murine colorectal mucosa by pimonidazole. **a** Colorectal mucosa of a non-injected mouse, **b** colorectal mucosa of a mouse that was injected intravenously with pimonidazole. After 90 min, the mouse was killed and colon tissue harvested and formalin fixed. Immunohistochemical staining against pimonidazole revealed hypoxia in the surface epithelium of the normal colon mucosa

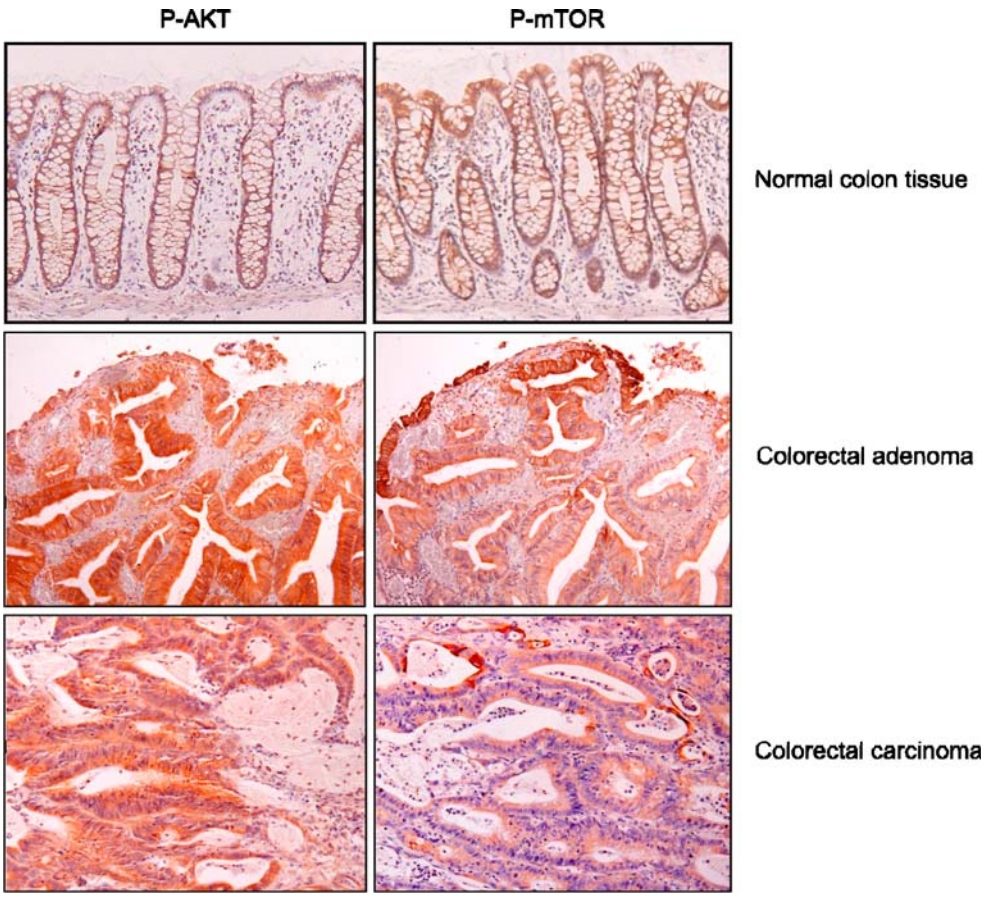


Fig. 4 Typical immunohistochemical staining patterns of the active forms of AKT (*P-AKT*) and mTOR (*P-mTOR*) in normal colon mucosa, colorectal adenoma, and adenocarcinomas. Presence of active AKT is seen in the cytoplasm of all epithelial cells with increasing intensities from the normal mucosa towards adenocarcinoma. Presence of active mTOR is restricted to the surface epithelium in normal mucosa and adenomas. In adenocarcinomas, cells surrounding necrotic areas show active mTOR as well. In addition, in adenocarcinomas, intracellular localization of mTOR changes from cytoplasm towards cellular membrane staining

including GLUT1 and SDF-1, were analyzed in normal mucosa, adenomas, and adenocarcinomas. Expression of GLUT1, which is involved in glucose metabolism, was closely correlated with HIF-1α in all colon tissues analyzed. In normal colon mucosa, GLUT1 expression showed a gradient from the surface epithelium towards the basis of the crypts (Fig. 5). All normal tissues showed a positive GLUT1 staining. In nonprogressed adenomas, all cases showed GLUT1 expression compared to 95% of progressed adenomas. All adenocarcinomas (n=23) were positive for GLUT1 as well. Staining was localized at the cell membrane of epithelial cells in normal mucosa, adenomas, and adenocarcinomas (Fig. 5). Most intense staining was seen at the surface epithelium of adenomas and in the vicinity of necrosis in carcinomas. As to staining intensity, a significant difference was detected between the adenomas and the carcinomas (Table 2).

In normal colon tissue, SDF-1 expression was comparable to that of HIF-1α, i.e., it was detected in a gradient from the surface epithelium towards the basis of the crypts. However, in all colorectal adenomas and adenocarcinomas, intense SDF-1 expression was observed in the epithelial cells, which was located in the cell membrane and cytoplasm (Fig. 5). Because this epithelial SDF-1 expression was seen in all epithelial cells, it co-localized only partly with HIF-1α presence. In contrast to the comparable intensity of the HIF-1α staining in adenomas and adenocarcinomas, the SDF-1 staining intensity was much higher in adenocarcinomas than in the adenomas (Table 2). In addition to the epithelial expression of SDF-1, endothelial cells of blood vessels stained positive for SDF-1 (Fig. 6).

Expression of CA IX

CA IX was originally identified in gastrointestinal tissues and later recognized as a HIF-1 target gene in many tissues. In normal mucosa, the presence of CA IX actually did not co-localize with that of HIF-1α. CA IX was observed in the bottom parts of the crypts, i.e., in the proliferative compartment, in contrast to HIF-1α, which was present in the surface epithelium. Seventy percent of the normal tissues showed CA IX expression. In adenomas and particular adenocarcinomas, CA IX and HIF-1 expressions had more resemblance. In adenomas, CA IX was present in a more diffuse pattern throughout the whole adenoma, including the surface epithelium (Fig. 5). In the adenocarcinomas, CA IX showed a perinecrotic staining, mainly co-localizing with the HIF-1α expression.

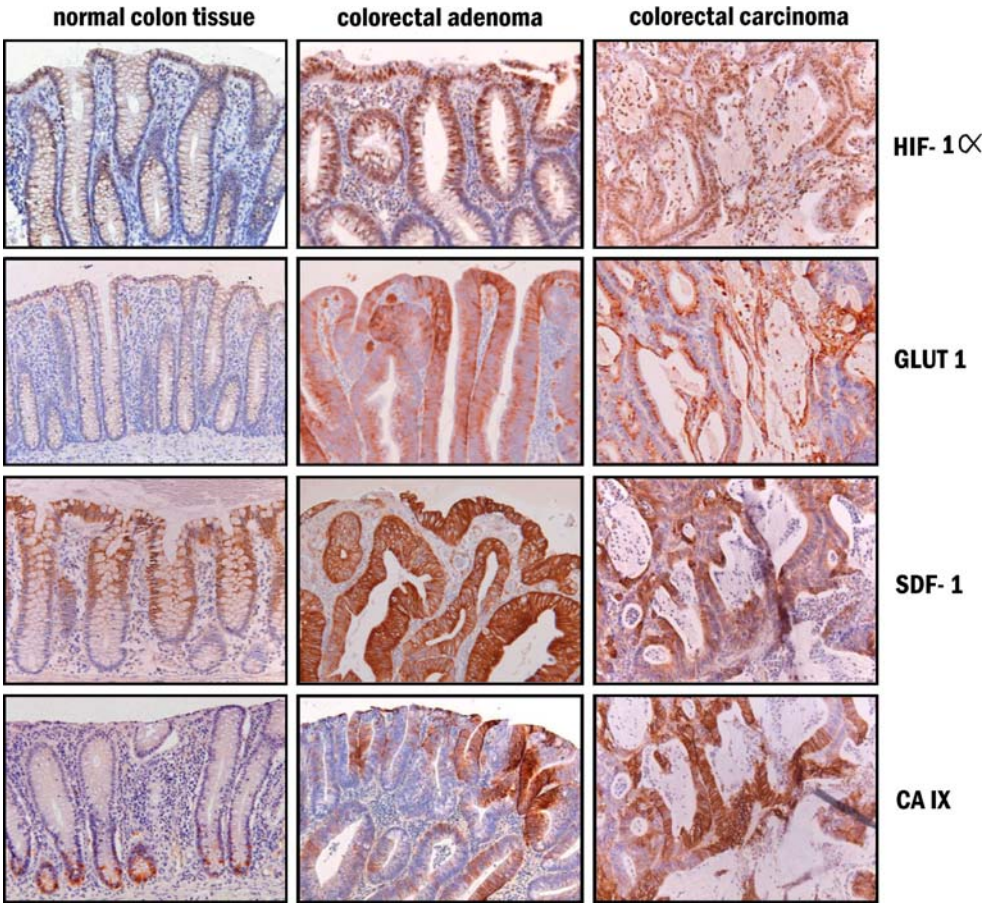


Fig. 5 Typical immunohistochemical staining patterns of HIF-1α, GLUT1, SDF-1, and CA IX in normal colon mucosa, colorectal adenomas, and adenocarcinomas. The downstream targets of HIF-1, i.e., SDF-1, GLUT1, and CA IX, have predominantly overlapping staining with the presence of HIF-1. However, in normal mucosa, CA IX is not expressed in the HIF-1α positive surface epithelium but is expressed in the basal of the crypts. In adenocarcinomas, SDF-1 is not only present in HIF-1α-positive cells but in all epithelial cells

Discussion

The present study demonstrates the presence of nuclear HIF-1α in the surface epithelium of normal colon and adenomas and in areas associated with peri-necrotic areas of colon adenocarcinoma. The data support a hypoxia-induced HIF-1 cascade, both in normal and neoplastic colorectal mucosa, as suggested by pimonidazole and HIF-1α patterns in association with GLUT1 and SDF-1 in normal colorectal mucosa and adenomas, as well as peri-necrotic HIF-1α and CA IX patterns in colorectal carcinomas. The occurrence of hypoxia around the surface epithelium was confirmed by pimonidazole staining of unaffected murine colon. Furthermore, hypoxia and the oncogenic activation of the AKT–mTOR pathway both contributed to HIF-1 expression in adenomas and adenocarcinomas. Moreover, the expression patterns of CA IX in normal mucosa and SDF-1 in neoplastic mucosa pointed to additional regulations independent from HIF-1.

The hypoxia–HIF-1 cascade

The presence of HIF-1α under physiological circumstances in the surface epithelium of normal colorectal mucosa observed in the present study may be due to the anaerobic environment in the lumen of the colon, which contributes to a relatively hypoxic state of especially this surface epithelium. Indeed, we observed accumulation of the chemical hypoxia marker pimonidazole particularly in the

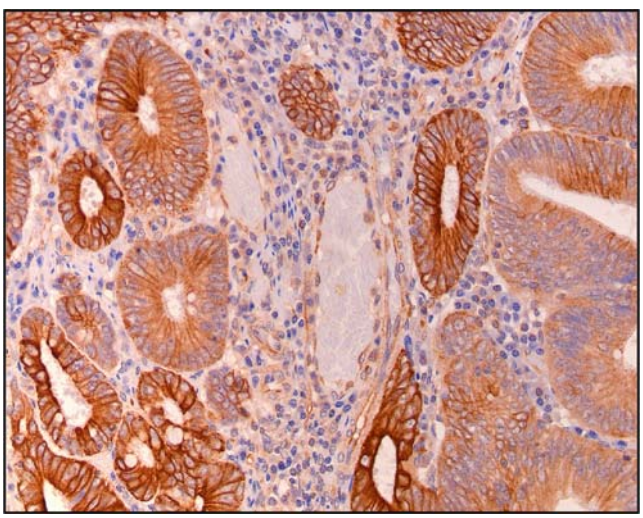


Fig. 6 SDF-1 expression in epithelial and endothelial cells of normal detected by immunohistochemistry

surface epithelium, indicating low oxygen levels [19]. The presence of pimonidazole showed a gradient towards the basis of the crypts, suggesting that the cause of hypoxia was indeed related to the anaerobic lumen. Apparently, the capillaries in the surface regions of the colon epithelium were unable to cope with the high oxygen demand of the tissue. This strongly suggests that these hypoxic areas may induce HIF-1α, which contributes to a sustained pressure on the stimulation of angiogenesis and glycolysis to adjust the energy levels of these cells.

Although immunohistochemical analysis of patient samples does not allow a formal analysis of functional relationships, it is highly likely that the HIF-1 detected in normal colorectal mucosa was transcriptionally active because HIF-1α was detected in the nuclei and the HIF-1 downstream targets GLUT1 and SDF-1 were present in the same regions where HIF-1α was found.

In 87% of colorectal adenomas, HIF-1α was present, showing staining predominantly in the nuclei of the surface epithelium. In colorectal adenocarcinomas, the presence of HIF-1α changes from the surface epithelium to epithelium cells surrounding regions of necrosis, indicating severe hypoxia. Presence of HIF-1α in the nuclei of epithelial cells went along with expression of the downstream targets GLUT1 and SDF1 in all different stages of the colon carcinogenesis.

In contrast to SDF-1 and GLUT1, the downstream target CA IX, known as a stringent hypoxia marker [35], did not co-localize with HIF-1α staining in normal colorectal mucosa. It should be noted that CA IX was originally described to have a role in maintaining the physiological equilibrium in the gastrointestinal tract. In fact, CA IX was more abundant in the basal half of the crypts, containing the proliferating compartment, rather than in the upper half of the mucosa where HIF-1α expression was observed. Indeed, co-localization of CA IX with Ki-67, a proliferation marker, has been found in colorectal cancer [31]. The lack of HIF-1α in the CA IX-positive regions indicates an HIF-1α-independent regulation of CA IX in normal colon epithelium. CA IX expression was reported to be also regulated by the transcription factor SP1 [18, 31].

Oncogenic upregulation of HIF-1

Oncogene-dependent regulation of HIF-1 can be mediated by the AKT–mTOR pathway [24, 39]. In the present study, in epithelium of all normal colorectal mucosa, a weak staining of P-AKT was observed, confirming data of Itoh et al. [14]. In all adenomas and adenocarcinomas analyzed, the active (phosphorylated) forms of AKT and mTOR were detected as well. Especially active mTOR showed co-localization with HIF-1α in normal tissue as well as in adenomas and adenocarcinomas. Co-localization of P-AKT with HIF-1α was less evident. Recently, in breast cancer, it has been shown that in the absence of P-AKT, only low levels of HIF-1α could be detected while in the presence of P-AKT high HIF-1α protein levels were observed [10]. In colorectal tumorigenesis, this regulation mechanism may be less relevant because staining was already observed in normal tissue. In addition, the presence of active AKT was not HIF-1 related because in adenocarcinomas P-AKT was present in a higher percentage of cells present than HIF-1α. The downstream target of AKT, mTOR, displayed comparable cellular expression patterns to HIF-1α in normal, adenomas, and carcinomas. This suggests that the AKT–mTOR–HIF-1α axis may be important in tumor growth and development as was seen in prostate epithelial cells [25].

Expression of VHL

An alternative mechanism that can lead to HIF-1α overexpression is loss of VHL expression. In normal colon mucosa, VHL is expressed, while in colorectal tumors VHL has been found to be lost or mutated in 11% of cases [7, 21]. Mutations in the VHL gene have been reported to result in cytoplasmic staining of HIF-1α in colorectal cancer in one study [22], while this could not be confirmed in another study of 80 patients [40]. Also in the present study, no cytoplasmic staining of HIF-1 α was seen at all, and VHL expression was seen in all epithelial cells of normal mucosa, colorectal adenomas, and carcinoma.

Expression of SDF1

SDF-1 was investigated in the present study as a downstream target of HIF-1 [13, 32]. Surprisingly, epithelial cells showed much stronger SDF-1 expression than endothelial cells lining blood vessels. In addition, expression was not merely restricted to areas showing HIF-1α staining but was observed in all epithelial adenomas and adenocarcinomas. SDF-1 staining in tumors cells has also been reported in breast cancer patients [29] and in clear cell–renal cell carcinomas, in which HIF-1α is constitutively expressed [37]. The intense staining of the colon tumor cells suggests that SDF-1 not only has a function in attracting circulating progenitor cells towards the angiogenic areas [12]. Indeed, SDF-1 stimulates intestinal epithelial cell migration and enhances the integrity of the mucosal barrier [34].

The level of expression of SDF-1 might also play a role in tumorigenesis because it is related with prognosis in colorectal cancer. The presence of its coding mRNA and the mRNA of its receptor, CXCR4, have been shown to be a poor prognostic factor [20]. In tumor formation, SDF-1 may bear impact on the recruitment of various types of progenitor cells needed for enhanced growth of the tumor tissue [29]. Our study supports a role of SDF-1 in

carcinogenesis because SDF-1 staining becomes more intense with the progression of normal colon tissue toward carcinomas. However, future studies are needed to substantiate such role.

Conclusion

The common expression of HIF-1α in the surface epithelium of the colorectal mucosa suggests that HIF-1 may play a role in the physiology of normal colon tissue. HIF-1α presence does not appear to be related to progression of colorectal carcinogenesis in contrast to GLUT1 and SDF-1, which are expressed more intensely at later stages of this process.

Acknowledgements The authors thank Cristel Snijckers and Helma van den Berg for technical assistance and Prof. A.L. Harris for providing the CA IX antibody. This work was supported in part by the 1st AEGON International Scholarship in Oncology.

Conflict of interest statement We declare that we have no conflict of interest.

Open Access This article is distributed under the terms of the Creative Commons Attribution Noncommercial License which permits any noncommercial use, distribution, and reproduction in any medium, provided the original author(s) and source are credited.

References

1. Airley RE, Loncaster J, Raleigh JA, Harris AL, Davidson SE, Hunter RD, West CM, Stratford IJ (2003) GLUT-1 and CAIX as intrinsic markers of hypoxia in carcinoma of the cervix: relationship to pimonidazole binding. Int J Cancer 104:85–91
2. Aoki K, Tamai Y, Horiike S, Oshima M, Taketo MM (2003) Colonic polyposis caused by mTOR-mediated chromosomal instability in Apc+/Delta716 Cdx2+/− compound mutant mice. Nat Genet 35:13–330
3. Bos R, Zhong H, Hanrahan CF, Mommers EC, Semenza GL, Pinedo HM, Abeloff MD, Simons JW, van Diest PJ, van Der Wall E (2001) Levels of hypoxia-inducible factor-1 alpha during breast carcinogenesis. J Natl Cancer Inst 93:309–314
4. Bos R, Van Der Groep P, Greijer AE, Shvarts A, Meijer S, Pinedo HM, Semenza GL, van Diest PJ, van Der Wall E (2003) Levels of hypoxia-inducible factor-1 alpha independently predict prognosis in patients with lymph node negative breast carcinoma. Cancer 97:1573–1581
5. Ceradini DJ, Kulkarni AR, Callaghan MJ, Tepper OM, Bastidas N, Kleinman ME, Capla JM, Galiano RD, Levine JP, Gurtner GC (2004) Progenitor cell trafficking is regulated by hypoxic gradients through HIF-1 induction of SDF-1. Nat Med 10:858–864
6. Cleven AH, Van Engeland M, Wouters BG, de Bruine AP (2007) Stromal expression of hypoxia regulated proteins is an adverse prognostic factor in colorectal carcinomas. Cell Oncol 29:229–240
7. Giles RH, Lolkema MP, Snijckers CM, Belderbos M, Van Der Groep P, Mans DA, van Beest M, van Noort M, Goldschmeding R, van Diest PJ, Clevers H, Voest EE (2006) Interplay between VHL/HIF1alpha and Wnt/beta-catenin pathways during colorectal tumorigenesis. Oncogene 25(21):3065–3070
8. Gingras AC, Raught B, Sonenberg N (2001) Regulation of translation initiation by FRAP/mTOR. Genes Dev 15:807–826
9. Goethals L, Debucquoy A, Perneel C, Geboes K, Ectors N, De Schutter H, Penninckx F, McBride WH, Begg AC, Haustermans KM (2006) Hypoxia in human colorectal adenocarcinoma: comparison between extrinsic and potential intrinsic hypoxia markers. Int J Radiat Oncol Biol Phys 65:246–254
10. Gort EH, Groot AJ, Derks van de Ven TL, Van Der Groep P, Verlaan I, van Laar T, van Diest PJ, van Der Wall E, Shvarts A (2006) Hypoxia-inducible factor-1alpha expression requires PI 3-kinase activity and correlates with Akt1 phosphorylation in invasive breast carcinomas. Oncogene 25(45):6123–6127
11. Greijer A, Van Der Groep P, Kemming D, Shvarts A, Semenza G, Meijer G, Van De Wiel M, Belien J, van Diest P, van Der Wall E (2005) Up-regulation of gene expression by hypoxia is mediated predominantly by hypoxia-inducible factor 1 (HIF-1). J Pathol 206(3):391–304
12. Grunewald M, Avraham I, Dor Y, Bachar-Lustig E, Itin A, Yung S, Chimenti S, Landsman L, Abramovitch R, Keshet E (2006) VEGF-induced adult neovascularization: recruitment, retention, and role of accessory cells. Cell 124:175–189
13. Heidemann J, Ogawa H, Rafiee P, Lugering N, Maaser C, Domschke W, Binion DG, Dwinell MB (2004) Mucosal angiogenesis regulation by CXCR4 and its ligand CXCL12 expressed by human intestinal microvascular endothelial cells. Am J Physiol Gastrointest Liver Physiol 286:G1059–G1068
14. Itoh N, Semba S, Ito M, Takeda H, Kawata S, Yamakawa M (2002) Phosphorylation of Akt/PKB is required for suppression of cancer cell apoptosis and tumor progression in human colorectal carcinoma. Cancer 94:3127–3134
15. Ivan M, Kondo K, Yang H, Kim W, Valiando J, Ohh M, Salic A, Asara JM, Lane WS, Kaelin WG Jr (2001) HIFalpha targeted for VHL-mediated destruction by proline hydroxylation: implications for O2 sensing. Science 292:464–468
16. Jaakkola P, Mole DR, Tian YM, Wilson MI, Gielbert J, Gaskell SJ, Kriegsheim A, Hebestreit HF, Mukherji M, Schofield CJ, Maxwell PH, Pugh CW, Ratcliffe PJ (2001) Targeting of HIF-alpha to the von Hippel–Lindau ubiquitylation complex by O2-regulated prolyl hydroxylation. Science 292:468–472
17. Kaanders JH, Wijffels KI, Marres HA, Ljungkvist AS, Pop LA, van den Hoogen FJ, de Wilde PC, Bussink J, Raleigh JA, van der Kogel AJ (2002) Pimonidazole binding and tumor vascularity predict for treatment outcome in head and neck cancer. Cancer Res 62:7066–7074
18. Kaluz S, Kaluzova M, Stanbridge EJ (2003) Expression of the hypoxia marker carbonic anhydrase IX is critically dependent on SP1 activity. Identification of a novel type of hypoxia- responsive enhancer. Cancer Res 63:917–922
19. Karhausen J, Furuta GT, Tomaszewski JE, Johnson RS, Colgan SP, Haase VH (2004) Epithelial hypoxia-inducible factor-1 is protective in murine experimental colitis. J Clin Invest 114:1098–1106
20. Kim J, Takeuchi H, Lam ST, Turner RR, Wang HJ, Kuo C, Foshag L, Bilchik AJ, Hoon DS (2005) Chemokine receptor CXCR4 expression in colorectal cancer patients increases the risk for recurrence and for poor survival. J Clin Oncol 23:2744–2753
21. Kuwai T, Kitadai Y, Tanaka S, Onogawa S, Matsutani N, Kaio E, Ito M, Chayama K (2003) Expression of hypoxia-inducible factor-1alpha is associated with tumor vascularization in human colorectal carcinoma. Int J Cancer 105:176–181
22. Kuwai T, Kitadai Y, Tanaka S, Hiyama T, Tanimoto K, Chayama K (2004) Mutation of the von Hippel–Lindau (VHL) gene in human

colorectal carcinoma: association with cytoplasmic accumulation of hypoxia-inducible factor (HIF)-1alpha. Cancer Sci 95:149–153
23. Lal A, Peters H, St Croix B, Haroon ZA, Dewhirst MW, Strausberg RL, Kaanders JH, Der Kogel AJ, Riggins GJ (2001) Transcriptional response to hypoxia in human tumors. J Natl Cancer Inst 93:1337–1343
24. Laughner E, Taghavi P, Chiles K, Mahon PC, Semenza GL (2001) Her2 (neu) signaling increases the rate of hypoxia-inducible factor 1alpha (hif-1alpha) synthesis: novel mechanism for hif-1-mediated vascular endothelial growth factor expression. Mol Cell Biol 21:3995–4004
25. Majumder PK, Sellers WR (2005) Akt-regulated pathways in prostate cancer. Oncogene 24:7465–7474
26. Manalo DJ, Rowan A, Lavoie T, Natarajan L, Kelly BD, Ye SQ, Garcia JG, Semenza GL (2005) Transcriptional regulation of vascular endothelial cell responses to hypoxia by HIF-1. Blood 105:659–669
27. Maxwell PH, Wiesener MS, Chang GW, Clifford SC, Vaux EC, Cockman ME, Wykoff CC, Pugh CW, Maher ER, Ratcliffe PJ (1999) The tumour suppressor protein VHL targets hypoxia-inducible factors for oxygen-dependent proteolysis. Nature 399:271–275
28. Olive PL, Aquino-Parsons C, MacPhail SH, Liao SY, Raleigh JA, Lerman MI, Stanbridge EJ (2001) Carbonic anhydrase 9 as an endogenous marker for hypoxic cells in cervical cancer. Cancer Res 61:8924–8929
29. Orimo A, Gupta PB, Sgroi DC, Arenzana-Seisdedos F, Delaunay T, Naeem R, Carey VJ, Richardson AL, Weinberg RA (2005) Stromal fibroblasts present in invasive human breast carcinomas promote tumor growth and angiogenesis through elevated SDF-1/CXCL12 secretion. Cell 121:335–348
30. Roy HK, Olusola BF, Clemens DL, Karolski WJ, Ratashak A, Lynch HT, Smyrk TC (2002) AKT proto-oncogene overexpression is an early event during sporadic colon carcinogenesis. Carcinogenesis 23:201–205
31. Saarnio J, Parkkila S, Parkkila AK, Haukipuro K, Pastorekova S, Pastorek J, Kairaluoma MI, Karttunen TJ (1998) Immunohistochemical study of colorectal tumors for expression of a novel transmembrane carbonic anhydrase, MN/CA IX, with potential value as a marker of cell proliferation. Am J Pathol 153:279–285
32. Schrader AJ, Lechner O, Templin M, Dittmar KE, Machtens S, Mengel M, Probst-Kepper M, Franzke A, Wollensak T, Gatzlaff P, Atzpodien J, Buer J, Lauber J (2002) CXCR4/CXCL12 expression and signalling in kidney cancer. Br J Cancer 86:1250–1256
33. Semenza GL (2003) Targeting HIF-1 for cancer therapy. Nat Rev Cancer 3:721–732
34. Smith JM, Johanesen PA, Wendt MK, Binion DG, Dwinell MB (2005) CXCL12 activation of CXCR4 regulates mucosal host defense through stimulation of epithelial cell migration and promotion of intestinal barrier integrity. Am J Physiol Gastrointest Liver Physiol 288:G316–G326
35. Wykoff CC, Beasley NJ, Watson PH, Turner KJ, Pastorek J, Sibtain A, Wilson GD, Turley H, Talks KL, Maxwell PH, Pugh CW, Ratcliffe PJ, Harris AL (2000) Hypoxia-inducible expression of tumor-associated carbonic anhydrases. Cancer Res 60:7075–7083
36. Yoshimura H, Dhar DK, Kohno H, Kubota H, Fujii T, Ueda S, Kinugasa S, Tachibana M, Nagasue N (2004) Prognostic impact of hypoxia-inducible factors 1alpha and 2alpha in colorectal cancer patients: correlation with tumor angiogenesis and cyclooxygenase-2 expression. Clin Cancer Res 10:8554–8560
37. Zagzag D, Krishnamachary B, Yee H, Okuyama H, Chiriboga L, Ali MA, Melamed J, Semenza GL (2005) Stromal cell-derived factor-1 alpha and CXCR4 expression in hemangioblastoma and clear cell-renal cell carcinoma: von Hippel–Lindau loss-of-function induces expression of a ligand and its receptor. Cancer Res 65:6178–6188
38. Zhong H, De Marzo AM, Laughner E, Lim M, Hilton DA, Zagzag D, Buechler P, Isaacs WB, Semenza GL, Simons JW (1999) Overexpression of hypoxia-inducible factor 1alpha in common human cancers and their metastases. Cancer Res 59:5830–5835
39. Zhong H, Chiles K, Feldser D, Laughner E, Hanrahan C, Georgescu MM, Simons JW, Semenza GL (2000) Modulation of hypoxia-inducible factor 1alpha expression by the epidermal growth factor/phosphatidylinositol 3-kinase/PTEN/AKT/FRAP pathway in human prostate cancer cells: implications for tumor angiogenesis and therapeutics. Cancer Res 60:1541–1545
40. Zhuang Z, Emmert-Buck MR, Roth MJ, Gnarra J, Linehan WM, Liotta LA, Lubensky IA (1996) von Hippel–Lindau disease gene deletion detected in microdissected sporadic human colon carcinoma specimens. Hum Pathol 27:152–156

Virchows Arch (2008) 452:545–557
DOI 10.1007/s00428-008-0604-y

ORIGINAL ARTICLE

Impact of rapamycin on liver regeneration

Daniel Palmes · Andree Zibert · Tymotheus Budny · Ralf Bahde · Evgeny Minin · Linus Kebschull · Jens Hölzen · Hartmut Schmidt · Hans-Ullrich Spiegel

Received: 5 November 2007 / Revised: 12 February 2008 / Accepted: 29 February 2008 / Published online: 9 April 2008
© Springer-Verlag 2008

Abstract The remarkable capacity of the liver to regenerate after injury and the prospects of organ self-renewal have attracted much interest in the understanding and modulation of the underlying molecular events. We investigated the effect of mammalian target of rapamycin (mTOR) inhibitor rapamycin (RAPA) on liver by correlating intravital microscopy, immunohistochemistry, and reverse transcriptase polymerase chain reaction in a rat model of 2/3 hepatectomy. RAPA significantly retarded proliferation of hepatocytes, endothelial cells, and hepatic stellate cells (HSCs) mostly between days 2 and 4 after hepatectomy and down-regulated major cytokines and growth factors (tumor necrosis factor alpha, hepatocyte growth factor, platelet-derived growth factor, platelet-derived growth factor receptor, insulin-like growth factor-1, transforming growth factor beta 1) important for liver regeneration. These effects were almost absent at later time points. RAPA also had a transient, but broad effect on angiogenesis, and impaired sinusoidal density as well as mRNA levels of vascular endothelial growth factor, vascular endothelial growth factor receptor 1, vascular endothelial growth factor receptor 2, and angiopoietin-1. Activation of HSC was also transiently suppressed as observed by smooth muscle protein 1 alpha protein expression and intercellular adhesion molecule-1 mRNA levels. The rate of apoptosis in liver was significantly increased by RAPA between day 3 and day 7. The effect of RAPA on liver repair, angiogenesis, and HSC activation is confined to the phase of active cell proliferation. This transient effect might allow further exploration of mTOR inhibitors in clinical situations that involve liver regeneration, and seems to have implications beyond immunosuppression.

Keywords Immunosuppression · Fibrosis · Antineoplastic · Transplantation · Small for size

Abbreviations

RAPA	rapamycin
HSC	hepatic stellate cell
NPC	non-parenchymal cell
mTOR	mammalian target of rapamycin
IVM	intravital microscopy
ECM	extracellular matrix

Introduction

In response to acute liver injury, hepatic cells can compensate parenchymal liver cell loss by cell proliferation [11, 42]. Compensatory liver cell proliferation is an important adaptive response in patients and gives unique insights into

Daniel Palmes and Andree Zibert contributed equally to this study.

D. Palmes · T. Budny · R. Bahde · L. Kebschull · J. Hölzen · H.-U. Spiegel
Surgical Research, Department of General Surgery,
Muenster University Hospital,
Waldeyerstr. 1,
48149 Muenster, Germany

A. Zibert · H. Schmidt (✉)
Experimental Transplant Hepatology,
Muenster University Hospital,
Domagkstr. 3A,
48149 Muenster, Germany
e-mail: hepar@ukmuenster.de

E. Minin
Institute of Pathology, Muenster University Hospital,
Domagkstr. 17,
48149 Muenster, Germany

the proliferation of hepatocytes and their interplay with non-parenchymal cells (NPCs), e.g., endothelial sinusoidal and hepatic stellate cells (HSC). Understanding the cellular and molecular events involved in liver regeneration is crucial for a further improvement of current therapy modalities of liver disease. The bacterial macrolide rapamycin (sirolimus, RAPA) was originally identified on the basis of its antifungal properties, and since then developed to a clinically well-known immunosuppressant that does not show nephrotoxicity unlike tacrolimus or cyclosporine [40]. Beyond immunosuppression, recent findings on the inhibition of tumor growth, fibrosis, and angiogenesis significantly added to the biologic properties of RAPA [14, 27, 38, 45]. The antineoplastic effect of RAPA has also offered new therapeutic options for inhibition of hepatocellular carcinoma (HCC) after liver transplantation [21, 44]. However, the diverse effects exerted by RAPA may also interfere with liver regeneration which becomes clinically important, e.g., in the course of reduced size liver grafts that have emerged to a standard method for the treatment of end-stage liver diseases and liver cancer in adults [41].

The molecular events following administration of RAPA are complex, and much knowledge has been perceived on its interaction with the mitogenic signaling pathway integrated by mammalian target of rapamycin (mTOR) kinases [1]. The selectivity of RAPA results from complex formation with intracellular immunophilin FK506 binding protein FKBP12 that specifically attacks mTORC1. Inhibition of mTORC1 leads to multiple changes in the signal cascade perturbing the function of downstream messengers p70S6 kinase and 4E-BP1. In many cells, mTORC1 inhibition is followed by abrogation of translation initiation and protein synthesis and in the arrest of the cell cycle at the G1 to S phase. Down-regulation of protein expression, proliferation, and cell cycle have been described for hepatocytes [18, 35] and stellate cells [12, 19, 22, 32]. Cyclin D1 and p21 seem to be important downstream messengers of the RAPA-mediated cell cycle arrest [13, 18, 29].

The antineoplastic and antifibrotic effects of RAPA in liver were associated with an interception of the macrolide with angiogenesis. In a mouse model of HCC, RAPA drastically reduced outgrowth of tumor cells, an effect that was paralleled by inhibition of tumor neovascularization [14]. Also, attenuation of liver injury by RAPA in a rat transplantation model was attributed to down-regulation of vascular endothelial growth factor (VEGF) [25]. During liver regeneration, reconstruction of sinusoids by proliferation of sinusoidal endothelial cells plays an important role in the blood supply for replicating hepatocytes [34]. In addition to interference of RAPA with genes involved in angiogenesis, important growth factors, transforming growth factor beta 1 (TGFβ), CTGF, and platelet-derived growth factor (PDGF), were also affected [3] suggesting that RAPA might have a long-lasting effect on factors that orchestrate liver regeneration. However, despite recent knowledge on individual time points with regard to signal transduction, fibrosis, and angiogenesis, the impact of RAPA on parenchymal cells and NPCs and the expression levels of various genes important for regenerating liver during and after hepatic cell proliferation have not been established.

Intravital microscopy (IVM) represents an innovative and powerful tool for simultaneous and serial analysis of morphological features in the regenerating liver particularly for the investigation of HSCs that can be specifically visualized because of their unique capability to store vitamin A [5, 23]. We used the well-characterized rat model of regenerating liver following 2/3 hepatectomy to gain insight into the temporal effects of RAPA on the proliferation of individual hepatic cells and expression of important cytokines and growth factors during and after liver cell proliferation. Using the IVM technique, histochemistry, and reverse transcriptase polymerase chain reaction (RT-PCR) analysis, we observed an early, broad impact of RAPA on hepatocytes, sinusoidal cells as well as HSCs, and on the expression of various factors crucial for liver regeneration. Importantly, the observed effects of RAPA were confined to the early phase of liver regeneration associated with a high cell proliferation. These effects were almost absent after proliferation has ceased implying an important time frame for an effective intervention by RAPA in the treatment of liver disease.

Materials and methods

Animals and materials

Rats were obtained from Charles River (Sulzfeld, Germany). RAPA was obtained from Wyeth Pharma (Münster, Germany). Sodium fluorescein, Hoechst 33342 (Ho342), and 4′,6-diamidino-2-phenylindole dihydrochloride (DAPI) were obtained by Sigma-Aldrich (Germany). Ki-67 (MIB-5) and smooth muscle protein 1 alpha (α-SMA) monoclonal antibodies (clone 1A4) were obtained from DakoCytomation (Hamburg, Germany). Streptavidin was obtained by Molecular Probes, Eugene (OR, USA). Single-stranded DNA (ssDNA) antibody was obtained by IBL (Fujioka, Japan). VEGF (ab2992) and vascular endothelial growth factor receptor 1 (VEGFR1; ab2350) antibodies were obtained by Abcam (Germany).

Experimental design

A pilot study was carried out in 49 male Lewis rats (250–300 g) in order to find out the clinically relevant serum

concentration of RAPA (5–15 ng/ml) [9]. RAPA (a kind gift of Wyeth Pharma GmbH, Münster, Germany) was orally administered via a gastric tube, and serum concentration of RAPA and liver and kidney parameters were daily measured. When RAPA was orally administered in 3-day intervals in different concentrations (1, 2, 3, 6, and 10 mg/kg body weight (b.w.) respectively), animals in these groups failed to maintain the clinically relevant serum concentration of RAPA. Therefore, we modified the protocol starting with a bolus of 6 mg/kg b.w. RAPA and continuing with 2 mg/kg b.w. per day. The main study consisted of 196 rats which were divided into four groups. In two groups (n=98), liver regeneration was induced as described below. Half of these animals (n=49) received daily RAPA at the previously described dose and half received vehicle (equivalent amount of saline). In the remaining groups (n=98), rats without liver resection received either RAPA (n=49) or saline (n=49) and served as controls. Seven animals per group were sacrificed at seven time points postoperatively (d0, d1, d2, d3, d4, d7, and d14) after intravital microscopy and withdrawal of blood and liver samples. Prior to the induction of liver regeneration, the rats were fasted for 24 h but had free access to water. Postoperatively, animals were fed ad libitum.

Rat model of liver regeneration

Liver regeneration was induced by a 2/3 hepatectomy as described previously [31]. In brief, two-thirds of the liver was resected so that only the left lobe, which makes up about 30% of total liver volume, remained in situ. All operations and handling procedures were in accordance with local animal welfare regulations and approved by the veterinary district administration of Muenster. All procedures were carried out under nitrous oxide/isoflurane anesthesia (N_2O/O_2=2:1+1.5% isoflurane).

Intravital microscopic analysis

Intravital microscopy was performed with a fluorescence microscope, Zeiss Axioscope, integrated in the Multi-Purpose Microscope system (100 W/2 HBO mercury lamp; eyepieces: ×10/20; objective Zeiss Achroplan ×20/0.5 w Ph 2 for water immersion; zoom lens 0.5–2.0; filter combinations of 450–490/515–565 nm (excitation/emission) for sodium fluorescein and 330–390/>430 nm for bisbenzamide and vitamin A autofluorescence) in epi-illumination technique [44]. Sodium fluorescein (2 μmol/kg body weight i.v., Sigma) was used to enhance contrast for assessing the sinusoid density. Hepatocyte nuclei were identified by admission of Hoechst 33342 (Ho342, 20 μmol/kg b.w., Sigma). HSCs were identified using their inherent vitamin A autofluorescence.

All experiments were performed under constant anesthesia and temperature conditions. Continuous arterial blood pressure was measured using a polyethylene catheter inserted into the carotid artery. For investigation of the liver regeneration, the lower surface of the left liver lobe was used. At first, sodium flourescein was injected via a central venous catheter. Using the filter for sodium flourescein, half of the acinus was visualized to identify the sinusoids and to measure the width of the hepatic cord in the later off-line analysis. Secondly, the filters were switched on to the filter for vitamin A autofluorescence and also for bisbenzimide to study the HSCs. By this, it is important to exactly focus on the acinus during the previous investigation of the sinusoids for having immediately a sharp picture of HSCs owing to their rapidly photobleaching characteristics. Six to 10 acini were randomly selected and recorded for the analysis of sinusoid density, hepatic cord width, and number of HSC [5, 23]. Next, the hepatocytes were studied because the same filter had to be used for the hepatocytes as for the HSCs and the fluorescence of the hepatic nuclei illuminated the vitamin A autofluorescence of the HSCs. Also, six to ten acini were randomly selected and recorded for the analysis of the hepatocytes.

All parameters were quantified off-line by a frame-to-frame analysis of video-recorded microscopic images via the computer-assisted image analysis system AnalySIS (SIS, Muenster, Germany). A final magnification of ×750 was employed for the assessment of the liver regeneration by the following parameters: The number of hepatocyte nuclei was counted per area (number per squared millimeter). The hepatocytes were identified by their regular, circular shape and enduring nature of their Ho342-related fluorescence. The hepatic cord width (in micrometer) was measured ten times per acinus. The sinusoid density was defined as the number of sinusoids per half acinus (number per squared millimeter). HSC frequency per area was calculated by counting the number of photobleaching sites per half acinus (number per squared millimeter). HSCs were identified as intense areas of fluorescence, which faded within 10–20 s of epi-illumination. HSCs were counted in the first second of UV epi-illumination because of its rapidly photobleaching characteristics [5, 23].

Serum parameter analysis

Ammonia (NH_3) was determined at 4°C, and bilirubin, aspartate aminotransferase (AST), and protein were determined at 37°C by standard enzymatic techniques (200L, micromethod, Ektachem-Kodak, Stuttgart, Germany).

Histological analysis

Morphologic parameters were recorded by hematoxylin and eosin staining and evaluated for proliferation, atrophy, and necrosis of the hepatic parenchyma. Liver regeneration was assessed using the monoclonal antibody MIB-5, specific for

the rat homologue of the Ki-67 proliferation-associated nuclear antigen, which detects cells outside the G0 stage of the cell cycle. The hepatocellular growth fraction, i.e., the proportion of MIB-5-decorated nuclei per 100 hepatocellular nuclei, was assessed by counting approximately 1,000 hepatocytes and NPCs. Apoptosis was assessed using the labeled streptavidin–biotin immunoperoxidase technique with an antibody against ssDNA. Nuclei were stained with DAPI. The proportion of ssDNA-decorated nuclei per 100 hepatocellular nuclei was semiquantitated by counting approximately 1,000 hepatocytes and NPCs each. Neoangiogenesis was assessed using antibodies specific for VEGF and VEGFR1 and evaluated according to a four-grade score: 0 = negative, 1 = partially (0–25%) weak positive stained cells, 2 = partially (25–50%) moderate or diffuse weak positive cells, 3 = diffuse moderate or strong positive cells (50–75%), and 4 = diffuse strong positive cells (>75%). Activated HSCs were detected by anti-α-SMA antibodies and assessed per 100 hepatocellular nuclei by counting approximately 1,000 hepatocytes and NPCs.

Real-time quantitative RT-PCR analysis

Randomly chosen samples from different regions of liver were snap-frozen immediately after resection and stored at −80°C. Total RNA was extracted after disruption of the tissue using a homogenizer and applied to RNeasy columns (Qiagen, Hilden, Germany) using DNAse I (30 U). The absence of overt RNA degradation was documented by ethidium bromide-stained agarose gels containing formaldehyde. Two micrograms of RNA was reverse-transcribed to complementary DNA (cDNA) using random hexamer and SuperScriptII (Invitrogen, Karlsruhe, Germany) according to the instructions of the manufacturer. Primers for PCR (presented in Table 1) were synthesized (MWG Biotech, Berlin, Germany) according to Primer 3 Express Software (Whitehead Institute for Biomedical Research, Cambridge, MD, USA). Primers were located such that exon–intron boundaries of the respective genes result in PCR amplicons of 90–120 bp. Optimization of the PCR was performed for each gene-specific primer pair to confirm specificity of the product by ethidium bromide-stained agarose gel. For quantitative real-time PCR, 0.05 μl of RT product was incubated with SYBER Green PCR Core Plus (Eurogenetec, Seraing, Belgium) using specific primers (150 nM). PCR was analyzed on the ABI Prism 7900 HT Sequence Detection System (PE Applied Biosystems, Foster City, CA, USA) by using a three-stage program parameter: 2 min at 50°C, 10 min at 95°C, and then 40 cycles of 14 s at 95°C, and 1 min at 60°C. Each sample

Table 1 Sequences and GenBank accession numbers of primers

Gene	Name	Accession number	Primer (forward/reverse)
Ang1	Angiopoietin-1	NM053546	GCACAAAGGACGCTGATAACG
			TAGATTGGAAGGGCCACAGG
HGF	Hepatocyte growth factor	NM017017	GTCAGCACCATCAAGGCAAG
			TGAGTGGGCCACCATAATCTC
ICAM	Intercellular adhesion molecule-1	BC081837	TTAGCTCCCGTGGGAGTATCAC
			CCGCAATGATCAGTACCAACAC
IGF1	Insulin-like growth factor-1	NM178866	CGCTGCAAGCCTACAAAGTC
			GGTCTTGTTTCCTGCACTTCC
PDGF	Platelet-derived growth factor	Z14117	CTGCTGCAATAACCGCAATG
			TGGCTTCTTTCTCACAATTTCG
PDGFR	Platelet-derived growth factor receptor	NM031525	CAAGCCTGATGCTGCTGATG
			GTCGCAGGAGATGGTGGAAG
αSMA	Smooth muscle alpha-actin	X06801	CCGTGACATCAAGGAGAAGC
			GCCCATCAGGCAGTTCGTAG
TGFβ	Transforming growth factor beta 1	NM021578	GCTCAACACCTGCACAGCTC
			GCTGCCGTACACAGCAGTTC
TNFα	Tumor necrosis factor alpha	X66539	CAAATGGGCTCCCTCTCATC
			TTTGCTACGACGTGGGCTAC
VEGF	Vascular endothelial growth factor	NM031836	CAGTTCGAGGAAAGGGAAAGG
			CAAATGCTTTCTCCGCTCTG
VEGFR1	FMS-like tyrosine kinase 1	NM019306	CAAAGCTCTGATGACCGAACTC
			TCCACGATCACCATCAGAGG
VEGFR2	Kinase insert domain protein receptor	NM013062	GAGCCCTCATGTCCGAACTC
			AGTCTTTCCCAGAGCGGAAG
HPRT	Hypoxanthine guanine phosphoribosyl transferase	NM012583	AAAGGACCTCTCGAAGTGTTGG
			AAGGGCATATCCAACAACAAAC

was tested in three independent experiments. Negative controls (cDNA-free solution) as well as a standard cDNA were included in each set of experiments. ct values were obtained as the number of cycles at which the fluorescence signal exceeded a standard threshold. The ct value produced by single primer sets was normalized to the expression of the house-keeping gene HPRT (Δct method).

Statistical analysis

Data are presented as mean ± SE. Statistical analysis was performed by the Mann–Whitney *U* test or by Student's *t* test using the SPSS 13.0 software. A level of significance of $p<0.05$ was considered as sufficient.

Results

RAPA does not affect survival after liver resection

A serum concentration between 5 and 15 ng/ml (median 11.8 ng/ml; range 7.3–14.6 ng/ml) could be achieved throughout the observation time of 14 days that was chosen in our study according to clinically therapeutic levels [25]. Blood levels of RAPA in rats were not perturbed by hepatectomy itself as was observed in a control group of rats that were subjected to the same protocol of RAPA treatment but without liver resection (median 10.8 ng/ml; range 6.8–14.5 ng/ml).

Survival of animals after hepatectomy was not affected by RAPA. All animals treated with RAPA ($n=49$) as well as animals of the untreated control ($n=49$) survived in a good general condition until their sacrifice.

RAPA transiently increases liver injury during early time points after hepatectomy

Hepatectomy led to significant changes in liver morphology not observed in sham-operated rats that displayed a regularly liver histology with homogeneous eosinophilic cytoplasm (Fig. 1). One day after liver resection, rats of both groups showed hepatocyte swelling and microvesicular steatosis predominantly in zone 1. Starting at day 3, numerous mitosis figures in hepatocytes and NPCs as well as clumps of small hepatocytes were visible which were surrounded by endothelial cells in the untreated control group. At day 7, liver histology was normally arranged but with larger lobules than preoperatively. In the RAPA treatment group, distinct dystrophic changes in hepatocytes with microvesicular steatosis, decreased mitosis figures, and delayed rearrangement of small hepatocyte clumps into sinusoids were observed. These changes of liver histology induced by RAPA treatment started usually around days 2–3 and were still present at day 7. At day 14, the liver histology was normal in specimens of both groups except scattered hepatocytes with dystrophic changes.

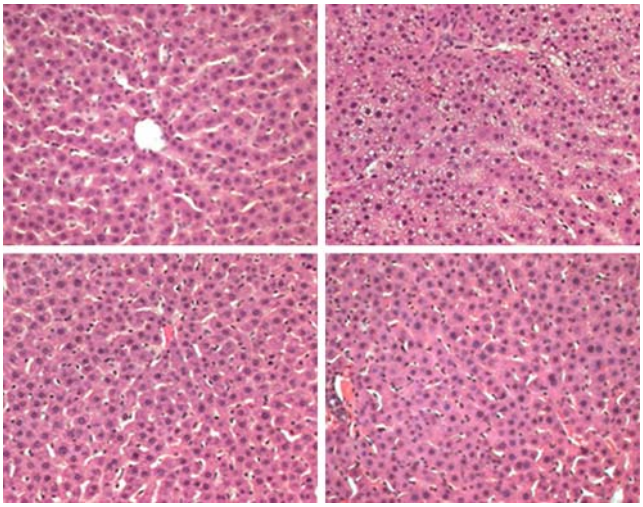


Fig. 1 RAPA induces morphologic changes in liver at early time points after hepatectomy. HE staining of liver in the non-treated control group (*left*) and in the RAPA-treated group (*right*). Representative liver sections after HE staining are shown at day 3 (*top*) and day 14 (*bottom*). For each time point and group, seven animals were subjected to analysis

Serum levels of AST, bilirubin, albumin, and ammonia were preoperatively within the normal range without significant differences among the groups (Table 2). Liver resection in combination with RAPA treatment led to a significant increase of AST at day 1 (1,728±17.8 vs. 2,497±333, respectively; $p=0.035$). However, following day 1 up to day 14, all serum levels were not found to be significantly altered between groups at any time point. The results suggest that at the end of the observation period (day 14) histological as well as serum parameters were almost restored to preoperative values indicating that liver regeneration has been completed in both groups.

Table 2 AST, bilirubin, albumin, and ammonia levels in RAPA-treated rats///

Parameter	Group	D0	D1	D14
AST (U/l)	RES	102±18	1728±18*	78±10
	RAPA	99±5	2497±333	83±10
Bilirubin (mg/dl)	RES	0.1±0.0	0.1±0.0	0.1±0.0
	RAPA	0.1±0.1	0.1±0.1	0.1±0.0
Albumin (g/dl)	RES	3.1±0.2	2.5±0.3	2.9±0.2
	RAPA	3.2±0.2	2.4±0.1	3.1±0.1
Ammonia (μg/dl)	RES	147±32	300±16	97±14
	RAPA	148±33	314±28	84±2

*$p<0.05$ (RES vs. RAPA)

RAPA inhibits proliferation of liver cells

In order to assess the effect of RAPA treatment on cell proliferation during liver regeneration, the presence of proliferation-associated nuclear antigen (rat homologue of Ki-67) was investigated in liver sections that allow detection of individual cells outside of the G0 stage of the proliferation cycle (Fig. 2). As expected from previous results observed in similar models of liver regeneration, the onset of hepatic cell proliferation was observed early after liver resection with significant increased proliferation rates of hepatocytes and NPCs starting at day 2 and day 3, respectively. The maximum of replication (up to 9-fold for hepatocytes and 2.5-fold for NPCs as compared to preoperative values, respectively) was observed at day 3 and day 4. Thereafter, proliferation rates of hepatic cells were slightly increased. RAPA treatment significantly reduced the proliferation of both hepatocytes (days 2, 3, and 4) and NPCs (day 3), while no significant difference of proliferation was observed at later time points suggesting that RAPA treatment led to a transient delay in hepatic cell proliferation.

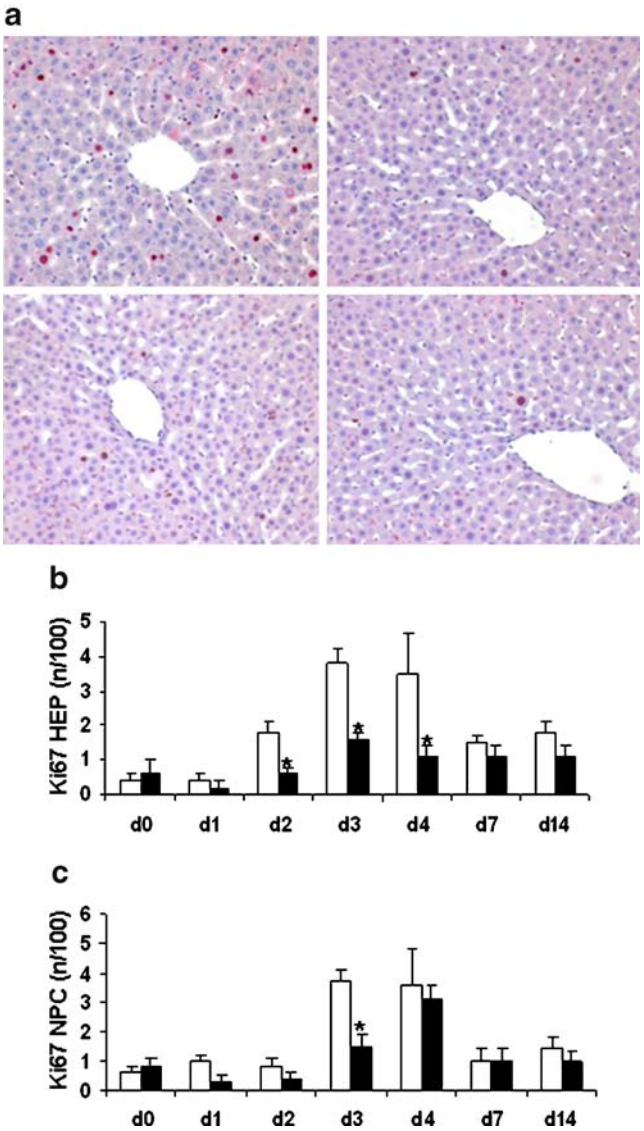


Fig. 2 Proliferation of hepatocytes and NPCs is down-regulated by RAPA. **a** Liver sections were stained with Ki-67-specific antibody obtained from non-treated control (*left*) and RAPA-treated animals (*right*). Representative liver sections obtained at day 3 (*top*) and day 14 (*bottom*) are shown. Quantitative analysis of Ki-67-positive hepatocytes (**b**) and NPCs (**c**) in the non-treated control group (*white columns*) and the RAPA-treated group (*black columns*) was obtained by counting 100 nuclei per field. For each time point, seven animals were subjected to analysis. *Asterisk* indicates significance ($p<0.05$) between groups

RAPA increases the rate of apoptotic liver cells

In addition to cell proliferation, we also investigated whether the rate of apoptosis was affected by RAPA treatment during liver regeneration. Apoptosis was assessed using antibodies against single-stranded DNA (Fig. 3).

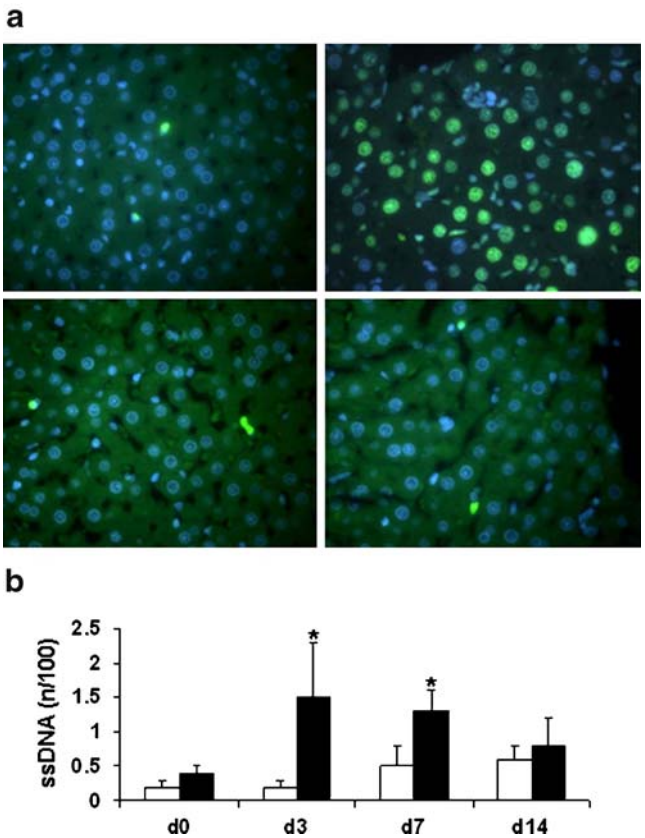


Fig. 3 Rate of apoptosis in hepatic cells is transiently increased after RAPA treatment. **a** Liver sections derived from non-treated control (*left*) and RAPA-treated animals (*right*) were subjected to staining with antibody directed against single-stranded DNA (ssDNA). Representative liver sections obtained at day 3 (*top*) and day 14 (*bottom*) are shown. **b** Quantitative analysis of positive hepatic cells in the non-treated control group (*white columns*) and the RAPA-treated group *(black columns*) was obtained by counting 100 nuclei per field. For each time point, seven animals were subjected to analysis. *Asterisk* indicates significance ($p<0.05$) between groups

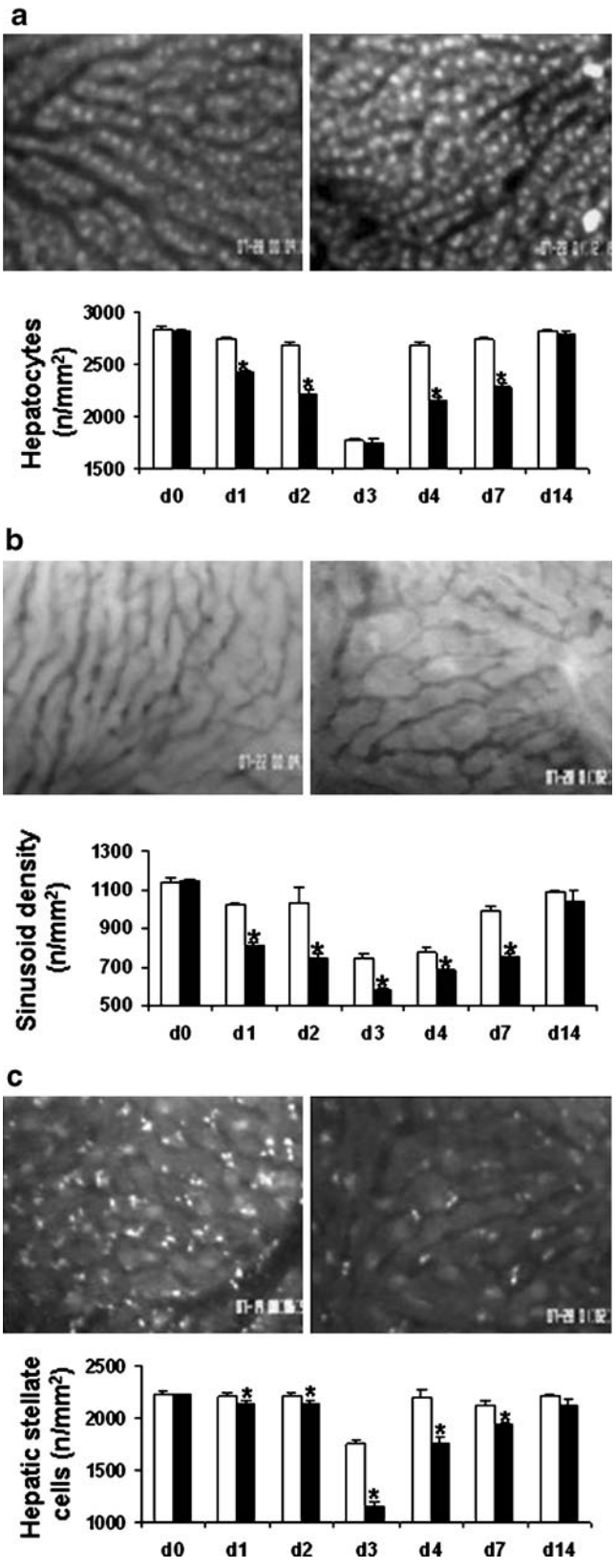


Fig. 4 Intravital microscopy reveals significant effects of RAPA on morphology in the regenerating liver. Representative intravital microscopic results of the regenerating liver in the non-treated control (*left*) and RAPA-treated animals (*right*). Representative pictures of **a** hepatocytes (day 3), **b** sinusoid density (day 7), and **c** autofluorescent HSCs (day 3) are shown. The diagrams show the semiquantitative analysis of hepatocyte number, sinusoid density, and HSC number after induction of liver regeneration in non-treated animals (*white column*) and RAPA-treated animals (*black column*). For each time point, seven animals were subjected to analysis. *Asterisk* indicates significance ($p<0.05$) between groups

Liver sections of the untreated control showed a minimal number of apoptosis of hepatocytes and NPCs at day 3 and a higher rate of apoptosis at day 7. In contrast, RAPA treatment significantly increased the rate of apoptosis of hepatic cells at day 3 and at day 7 suggesting that induction of apoptosis by RAPA may add to the transient delay in liver cell proliferation observed by Ki-67 staining.

Sinusoids, hepatocytes, and hepatic stellate cells are diminished by RAPA treatment

Intravital microscopy of liver was applied next for a simultaneous and serial in vivo analysis of the dynamic changes in individual numbers of sinusoids, hepatocytes, and hepatic stellate cells (Fig. 4). Liver resection led to a drop in the number of all three cell types at most early time points as compared to preoperative values. This drop was accompanied by a compensatory hypertrophy of the remaining hepatocytes as shown by an increase in hepatic cord width (Fig. 7). A minimum of cell number was observed for hepatocytes, sinusoids, and HSCs at day 3 for both animal groups. Following day 3, cell numbers increased continuously. In the non-treated control group, cell numbers of hepatocytes and HSCs reached almost identical levels starting already at day 4 as compared to the preoperative values, while sinusoidal cell density was still impaired at day 7.

In the RAPA-treated animals, significant lower cell numbers were observed for most time points between day 1 and day 7 as compared to the non-treated control indicating that RAPA suppresses the proliferation of sinusoids, hepatocytes, and HSCs. The remaining hepatocytes showed also signs of hypertrophy, e.g., an increased cord in comparison to normal-sized hepatocytes at day 0, but in a significantly lesser extent in comparison to the non-treated animals (Fig. 7). However, at the end of the observation period (day 14), the numbers of all three cell types were restored as compared to the postoperative controls indicating that despite continuous high serum levels of RAPA, inhibition of hepatocytes, HSCs, and sinusoidal density is confined to the early phase of liver regeneration.

α-SMA expressing cells are reduced by RAPA

To further investigate the role of activated HSCs during RAPA treatment in our model of liver regeneration, we performed measurement of smooth muscle protein 1 alpha expression in liver. α-SMA expression increased in liver of both groups starting from day 1 indicating that the degree of activated HSCs increased (Fig. 5). However, RAPA treatment significantly reduced α-SMA expression during day 3 to day 7 suggesting that RAPA has a dual effect on HSC proliferation and also on the accumulation of extracellular matrix (ECM) protein expression by these cells. At the end of the observation period (day 14), α-SMA expression was above preoperative levels, but RAPA treatment did not result in a significant inhibition of protein expression.

RAPA affects VEGF and VEGFR1 expressing cells

RAPA also affected hepatic neoangiogenesis. After liver resection, animals not treated with RAPA showed an increasing expression of VEGF and VEGFR1 between days 3 and 4 (Fig. 6) that dropped at day 7 reaching almost preoperative levels at day 14. However, RAPA treatment showed a bipartite effect with a significantly reduced (day 3 and day 4) or enhanced (day 7) expression of both molecules. At day 14, expression of VEGF and VEGFR1 was not affected between both groups.

To further analyze the effect of RAPA on angiogenesis, hepatic cord width was inspected by intravital microscopy (Fig. 7). Starting from day 1, RAPA treatment significantly enhanced hepatic cord width up to day 7 suggesting a

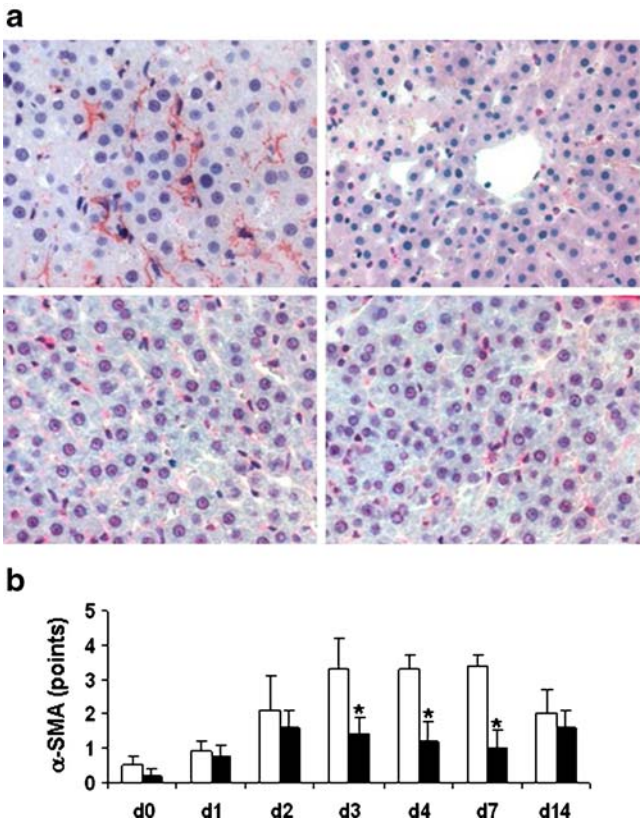


Fig. 5 Activation of HSCs was transiently suppressed by RAPA treatment. **a** Liver sections were stained with α-SMA-specific antibody obtained from non-treated control (*left*) and RAPA-treated animals (*right*). Representative liver sections obtained at day 7 (*top*) and day 14 (*bottom*) are shown. Semiquantitative analysis of α-SMA (**b**) in the non-treated control group (*white columns*) and the RAPA-treated group (*black columns*) was obtained using a four-grade score. For each time point 7 animals were subjected to analysis. *Asterisk* indicates significance ($p<0.05$) between groups

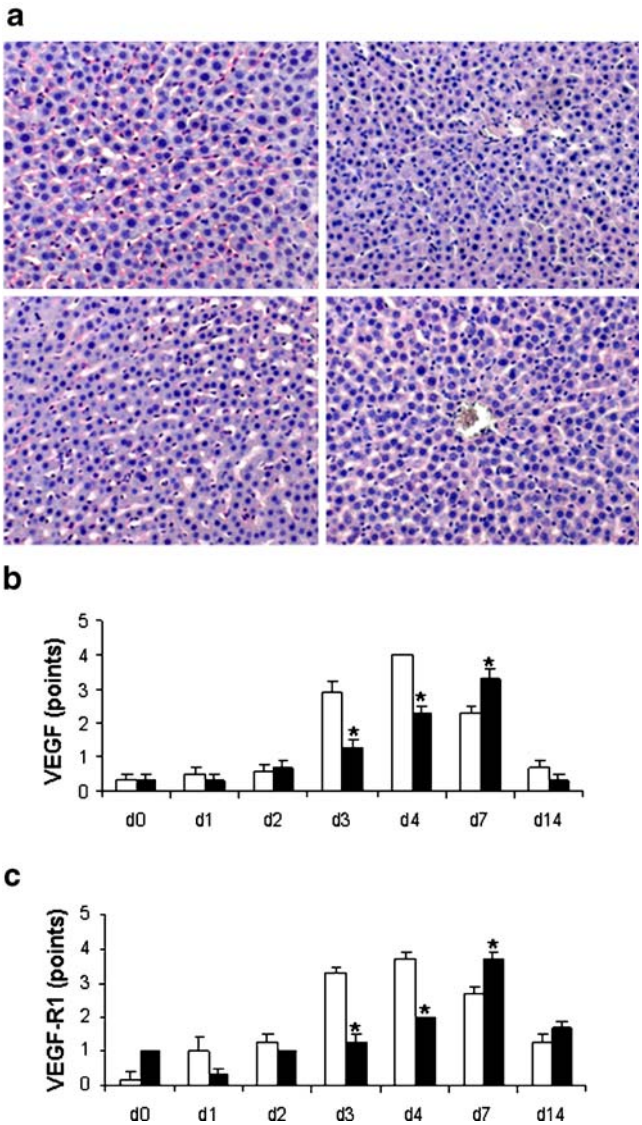


Fig. 6 VEGF and VEGFR1 expression is delayed after RAPA treatment. **a**. Liver sections were stained with VEGF-specific antibody obtained from non-treated control (*left*) and RAPA-treated animals (*right*). Representative liver sections obtained at day 3 (*top*) and day 14 (*bottom*) are shown. Semiquantitative analysis of VEGF (**b**) and VEGFR1 expression (**c**) in the non-treated control group (*white columns*) and the RAPA-treated group (*black columns*) was obtained using a four-grade score. For each time point, seven animals were subjected to analysis. *Asterisk* indicates significance ($p<0.05$) between groups

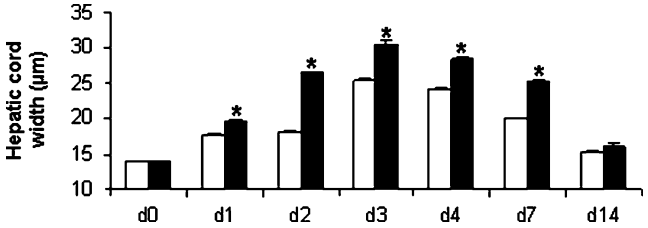


Fig. 7 RAPA treatment enhanced hepatic cord width. Semiquantitative analysis of hepatic cord width in the non-treated control group (*white columns*) and the RAPA-treated group (*black columns*) was obtained by intravital microscopy. For each time point, seven animals were subjected to analysis. *Asterisk* indicates significance ($p<0.05$) between groups

temporary compensatory growth (hypertrophy) of the regenerating liver that was initiated most likely due to the reduced sinusoidal density observed at these time points (Fig. 3). Hepatic cord width normalized at day 14 (14.3±0.4 µm).

RAPA suppresses expression of genes important for liver regeneration

In order to explore the expression of various genes important for liver regeneration, inflammation, ECM deposition, and angiogenesis, a real-time RT-PCR analysis of liver was performed. The relative mRNA levels were compared at early time points (24 and 48 h) as well as late time point (day 14) after hepatectomy between both groups (Fig. 8). Expression of important growth factors for liver regeneration, platelet-derived growth factor B (PDGFB) and its receptor (PDGFBR), hepatocyte growth factor, insulin-like growth factor-1 (IGF-1), and transforming growth factor beta 1 was significantly ($p<0.01$) down-regulated in rats treated with RAPA at early time points (24 and 48 h) underscoring our results of a delayed hepatocyte and NPC proliferation (Figs. 2 and 4). Likewise, pro-angiogenic genes, vascular endothelial growth factor A (VEGFA), and its receptors VEGFR1 and vascular endothelial growth factor receptor 2 (VEGFR2), as well as angiopoietin-1 (Ang-1), were down-regulated by RAPA treatment at early time points after hepatectomy as compared to the untreated control emphasizing the effect of a decelerated angiogenesis observed by IVM at early time points (Fig. 6). No differences were seen in α-SMA gene expression suggesting that the observed reduction of α-SMA protein (Fig. 5) might be due to posttranscriptional regulation. Intercellular adhesion molecule-1 (ICAM-1) expression that is up-regulated in activated HSC [26] was inhibited by RAPA at 24 h and also at day 14 after hepatectomy. A significant decreased tumor necrosis factor alpha (TNFα) expression level at early time points (24 and 48 h) was observed after RAPA treatment. Importantly, 14 days after hepatectomy when liver regeneration is completed in rats, a significant change in relative mRNA levels of most genes could not be detected suggesting that although RAPA has a broad and significant impact on various genes important for liver regeneration, this effect was not present after hepatic cell proliferation terminated.

Discussion

For analysis of the effects following RAPA treatment, we chose a model for which the kinetics of cell proliferation has been well documented. After 2/3 hepatectomy, the remnant rat liver cells almost double synchronously within 2 days [10, 41]. Liver regeneration was assessed using the Ki-67 proliferation-associated nuclear antigen, which detects cells outside the G0 stage of the cell cycle. In contrast to other methods, e.g., the assessment of liver weight or volume, this method is more precise and allows furthermore the discrimination between hepatocyte and NPC proliferation [5, 31]. Proliferation of hepatocytes starts almost at 12 h after liver resection, followed by a gradual decline. Replication of NPCs lags 24 h behind hepatocytes. The effects of RAPA upon proliferation of hepatocytes were analyzed by measurements of downstream p70S6 kinase and 4E-BP activities [4, 13, 20, 29, 35]. However, a direct measurement of RAPA upon proliferation of individual hepatic cells in vivo for different time points has not been established. Also, most previous studies involve analyses by biochemical approaches or histological stainings. Intravital microscopy represents an innovative tool for analysis of morphological features in the regenerating liver, particularly for the investigation of HSCs characteristics which can be specifically visualized because of their unique capability to store vitamin A, which possesses the characteristic of autofluorescence [5, 23]. Precisely, only non-activated HSCs are able to store vitamin A corresponding to the number of existing HSCs, whereas activated HSCs could furthermore be immunohistologically identified by detection of α-SMA. Using intravital microscopy, we observed a continuous increase in cell numbers following days 3–7, in line with previous results of hepatic cell proliferation that is initiated at 12–16 h after hepatectomy in rat, with a maximum at 24–48 h, ceasing at days 7–10. By this technique, we could follow a transient suppression of hepatocytes as well as NPCs that was induced by RAPA treatment. Impairment of cell numbers was pronounced during the phase of maximal hepatic cell proliferation and absent at later time points.

Cytokines and growth factors govern proliferation of liver cells during regeneration. One early event in liver regeneration is the transition of quiescent hepatocytes to respond to mitogens. This ‘priming’ event could be achieved in vivo by a single injection of TNFα [43]. Our results suggest that RAPA delays the onset of this ‘priming’ event probably by interference with the metabolism of

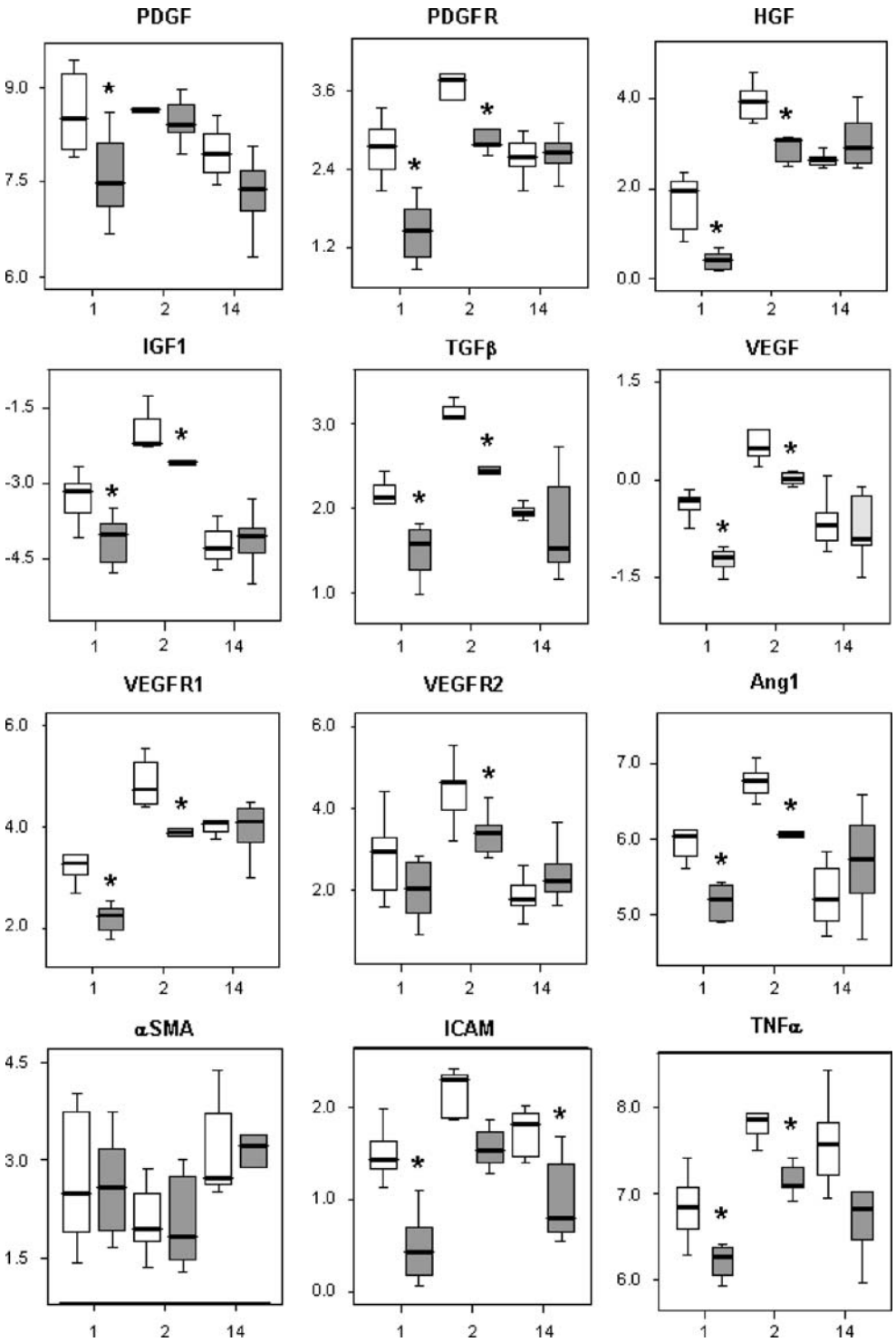


Fig. 8 RAPA suppresses expression of genes important for cell proliferation, angiogenesis, and HSC activation. Expression of individual genes was normalized to the HPRT house-keeping gene, and is given as Δct value (without unit) in a box-plot representation for the non-treated control group (*open box*) and the RAPA-treated group (*dark box*). RNA was obtained after 24 and 48 h and 14 days after hepatectomy and analyzed from five rats within each group. Results of three experiments are shown. *Asterisk* indicates significance ($p<0.01$) between groups

Kupffer cells located close to sinusoids, which are the main source for TNFα production. Likewise, other important growth factors, like PDGF and its receptor PDGFR as well as IGF-1, that are strong mitogens in liver, were observed to be transiently down-regulated suggesting that RAPA interferes at several levels with growth-factor-regulated induction of the cell cycle progression.

Another important finding was the inhibition of sinusoidal density in our liver regeneration model. The regulation of vasculogenesis, angiogenesis, and vascular permeability during liver regeneration is highly dependent on the presence of VEGFA and its two receptors VEGFR1 and VEGFR2 that are commonly expressed on hepatocytes and vascular endothelial cells, respectively [34, 39]. While impairment of

VEGFA expression by RAPA has been previously reported in animal models [14, 25], we detected here a concurrent down-regulation of its two receptors and also of pro-angiogenic factor angiopoietin-1 that regulates portal pressure [36] suggesting that RAPA has a broad antineogenic effect. For human endothelial cells, there is direct in vitro evidence that RAPA interferes with proliferation and differentiation [6]. Up-regulation of VEGF molecules was also linked to metastasis in several tumors [17] reinforcing emerging results that RAPA might possess a rather extended antineoplastic effect [7, 14, 27, 30]. A recent finding of mTOR inhibition via the tumor suppressor gene has linked mTOR pathways to the development of several human cancers [2] suggesting that the antineoplastic role of RAPA may apply to many tumor entities.

HSCs have a distinct role in liver growth after hepatectomy and also in the development of fibrosis, and are highly connected to proliferation and differentiation of other hepatic cells, e.g., hepatocytes, by the production of important paracrine effectors and ECM. In our model of liver regeneration, we observed a minimum of HSC numbers at day 3 and a rapid increase thereafter, which, however, lagged behind recovery of hepatocytes as was noticed before [11, 42]. RAPA was postulated to interfere directly with proliferation of HSC. In vitro findings demonstrated that phosphorylation of p70S6 kinase is blocked after RAPA treatment in cultivated HSCs [12, 22]. These findings were recently revised in animal models of fibrosis [3, 28, 45]. Our in vivo results on the determination of HSC numbers during RAPA treatment by intravital microscopy extend these findings that were mostly obtained by morphometry or RT-PCR analysis. PDGF that is known as the most potent mitogen for HSC [33] was down-regulated by RAPA. α-SMA, collagen α1, and ICAM-1 production are prominent markers for transformation of quiescent HSC to proliferative, fibrogenic, and contractile myofibroblasts. We and others [12, 28, 32] observed that RAPA decreased the production of α-SMA at the protein but not mRNA level. It seems likely that posttranscriptional factors might be involved in down-regulation of α-SMA or collagen after RAPA treatment. Down-regulation of ICAM-1 mRNA expression in liver after RAPA treatment was observed here first suggesting that transmigration of leucocytes in sinusoids during inflammation might be also affected [10, 16].

Induction of apoptosis by RAPA as observed here seems to be a rare event [37]. Whether apoptosis in liver that we concomitantly observed at early time points after RAPA treatment accounts in part for the lag in hepatocyte and NPC proliferation has to be determined in more detailed studies. However, it is known that TGFβ, produced mainly by HSC, is one of the most prominent antiproliferative factor within the liver, induces apoptosis, and is highly up-regulated during liver regeneration [8]. In regenerating liver, apoptosis is not induced in a pronounced rate, and it was therefore postulated that hepatocytes might not be sensitive to TGFβ-mediated apoptosis during regeneration [24]. Our observation of a significant rate of apoptosis after RAPA treatment suggests that the mechanism responsible for TGFβ resistance might be also affected by RAPA.

Early and late time points of liver disease were analyzed in different models, e.g., fibrosis or cirrhosis, to determine the effect of RAPA exerted on gene expression [3, 4, 13, 18, 20, 28, 29, 45]. In these studies, the portion and the individual cell type that proliferate at a given time point differ to some extent between animal models used, e.g., proliferation of biliary epithelium is involved after bile duct ligation, whereas mostly hepatocytes proliferate after chemical induced fibrosis. We believe that our study using the IVM technique and histochemistry as well as gene expression analysis at different time points after 2/3 hepatectomy, during and after a synchronous replication phase of hepatocytes, is the most direct evidence to date that the effect of RAPA on liver might be limited to the proliferation phase of hepatic cells. Nevertheless, beyond immunosuppression, RAPA has a significant impact on neoangeogenesis and can attenuate fibrosis and cirrhosis [3, 14, 25, 28] most likely as shown here due to perturbation of cells being in cycle. Our report is therefore relevant for recently emerging therapeutic strategies that take advantage of the unique capability of the liver to regenerate. Emerging new treatment options using RAPA and respective derivatives call for a timely application regime of these mTOR inhibitors for safe and efficient use in a clinical setting, e.g., after small-for-size liver transplantation.

Acknowledgements The authors thank K. Cebulla, G. Krull, and T. Möllers for technical assistance, and S. Stöppeler, S. Grothe, C. Meyer, and H. Grawe for animal care.

Conflict of interest statement We declare that we have no conflict of interest.

References

1. Abraham RT, Gibbons JJ (2007) The mammalian target of rapamycin signaling pathway: twists and turns in the road to cancer therapy. Clin Cancer Res 13:3109–3114
2. Bernardi R, Guernah I, Jin D, Grisendi S, Alimonti A, Teruya-Feldstein J, Cordon-Cardo C, Simon MC, Rafii S, Pandolfi PP (2006) PML inhibits HIF-1alpha translation and neoangiogenesis through repression of mTOR. Nature 442:779–785
3. Biecker E, De Gottardi A, Neef M, Unternährer M, Schneider V, Ledermann M, Sägesser H, Shaw S, Reichen J (2005) Long-term treatment of bile duct-ligated rats with rapamycin (sirolimus) significantly attenuates liver fibrosis: analysis of the underlying mechanisms. J Pharmacol Exp Ther 313:952–961

4. Boylan JM, Anand P, Gruppuso PA (2001) Ribosomal protein S6 phosphorylation and function during late gestation liver development in the rat. J Biol Chem 276:44457–44463
5. Budny T, Palmes D, Stratmann U, Minin E, Herbst H, Spiegel HU (2007) Morphologic features in the regenerating liver—a comparative intravital, lightmicroscopical and ultrastructural analysis with focus on hepatic stellate cells. Virchows Arch 451:781–791
6. Butzal M, Loges S, Schweizer M, Fischer U, Gehling UM, Hossfeld DK, Fiedler W (2004) Rapamycin inhibits proliferation and differentiation of human endothelial progenitor cells in vitro. Exp Cell Res 300:65–71
7. Del Bufalo D, Ciuffreda L, Trisciuoglio D, Desideri M, Cognetti F, Zupi G, Milella M (2006) Antiangiogenic potential of the mammalian target of rapamycin inhibitor temsirolimus. Cancer Res 66:5549–5554
8. Derynck R, Zhang YE (2003) Smad-dependent and Smad-independent pathways in TGF-beta family signalling. Nature 425:577–584
9. Dharancy S, Catteau B, Mortier L, Boleslawski E, Declerck N, Canva V, Piette F, Mathurin P, Pruvot FR (2006) Conversion to sirolimus: a useful strategy for recalcitrant cutaneous viral warts in liver transplant recipient. Liver Transpl 12:1883–1887
10. Elsharkawy AM, Wright MC, Hay RT, Arthur MJ, Hughes T, Bahr MJ, Degitz K, Mann DA (1999) Persistent activation of nuclear factor-kappaB in cultured rat hepatic stellate cells involves the induction of potentially novel Rel-like factors and prolonged changes in the expression of IkappaB family proteins. Hepatology 30:761–769
11. Fausto N (2004) Liver regeneration and repair: hepatocytes, progenitor cells, and stem cells. Hepatology 39:1477–1487
12. Gabele E, Reif S, Tsukada S, Bataller R, Yata Y, Morris T, Schrum LW, Brenner DA, Rippe RA (2005) The role of p70S6K in hepatic stellate cell collagen gene expression and cell proliferation. J Biol Chem 280:13374–13382
13. Goggin MM, Nelsen CJ, Kimball SR, Jefferson LS, Morley SJ, Albrecht JH (2004) Rapamycin-sensitive induction of eukaryotic initiation factor 4F in regenerating mouse liver. Hepatology 40:537–544
14. Guba M, von Breitenbuch P, Steinbauer M, Koehl G, Flegel S, Hornung M, Bruns CJ, Zuelke C, Farkas S, Anthuber M, Jauch KW, Geissler EK (2002) Rapamycin inhibits primary and metastatic tumor growth by antiangiogenesis: involvement of vascular endothelial growth factor. Nat Med 8:128–135
15. Guba M, Yezhelyev M, Eichhorn ME, Schmid G, Ischenko I, Papyan A, Graeb C, Seeliger H, Geissler EK, Jauch KW, Bruns CJ (2005) Rapamycin induces tumor-specific thrombosis via tissue factor in the presence of VEGF. Blood 105:4463–4469
16. Hellerbrand C, Wang SC, Tsukamoto H, Brenner DA, Rippe RA (1996) Expression of intracellular adhesion molecule 1 by activated hepatic stellate cells. Hepatology 24:670–676
17. Hiratsuka S, Nakamura K, Iwai S, Murakami M, Itoh T, Kijima H, Shipley JM, Senior RM, Shibuya M (2002) MMP9 induction by vascular endothelial growth factor receptor-1 is involved in lung-specific metastasis. Cancer Cell 2:289–300
18. Ilyin GP, Glaise D, Gilot D, Baffet G, Guguen-Guillouzo C (2003) Regulation and role of p21 and p27 cyclin-dependent kinase inhibitors during hepatocyte differentiation and growth. Am J Physiol Gastrointest Liver Physiol 285:G115–G127
19. Jiang F, Parsons CJ, Stefanovic B (2006) Gene expression profile of quiescent and activated rat hepatic stellate cells implicates Wnt signaling pathway in activation. J Hepatol 45:401–409
20. Jiang YP, Ballou LM, Lin RZ (2001) Rapamycin-insensitive regulation of 4e-BP1 in regenerating rat liver. J Biol Chem 276:10943–10951
21. Kneteman NM, Oberholzer J, Al Saghier M, Meeberg GA, Blitz M, Ma MM, Wong WW, Gutfreund K, Mason AL, Jewell LD, Shapiro AM, Bain VG, Bigam DL (2004) Sirolimus-based immunosuppression for liver transplantation in the presence of extended criteria for hepatocellular carcinoma. Liver Transpl 10:1301–1311
22. Le Pabic H, L'Helgoualc'h A, Coutant A, Wewer UM, Baffet G, Clément B, Théret N (2005) Involvement of the serine/threonine p70S6 kinase in TGF-beta1-induced ADAM12 expression in cultured human hepatic stellate cells. J Hepatol 43:1038–1044
23. Mabuchi A, Mullaney I, Sheard PW, Hessian PA, Mallard BL, Tawadrous MN, Zimmermann A, Senoo H, Wheatley AM (2004) Role of hepatic stellate cell/hepatocyte interaction and activation of hepatic stellate cells in the early phase of liver regeneration in the rat. J Hepatol 40:910–916
24. Macias-Silva M, Li W, Leu JI, Crissey MA, Taub R (2002) Up-regulated transcriptional repressors SnoN and Ski bind Smad proteins to antagonize transforming growth factor-beta signals during liver regeneration. J Biol Chem 277:28483–28490
25. Man K, Su M, Ng KT, Lo CM, Zhao Y, Ho JW, Sun CK, Lee TK, Fan ST (2006) Rapamycin attenuates liver graft injury in cirrhotic recipient—the significance of down-regulation of Rho–ROCK–VEGF pathway. Am J Transplant 6:697–704
26. Mayerhofer M, Aichberger KJ, Florian S, Valent P (2005) Identification of mTOR as a novel bifunctional target in chronic myeloid leukemia: dissection of growth-inhibitory and VEGF-suppressive effects of rapamycin in leukemic cells. FASEB J 19:960–962
27. Mayerhofer M, Valent P, Sperr WR, Griffin JD, Sillaber C (2002) BCR/ABL induces expression of vascular endothelial growth factor and its transcriptional activator, hypoxia inducible factor-1alpha, through a pathway involving phosphoinositide 3-kinase and the mammalian target of rapamycin. Blood 100:3767–3775
28. Neef M, Ledermann M, Saegesser H, Schneider V, Reichen J (2006) Oral imatinib treatment reduces early fibrogenesis but does not prevent progression in the long term. J Hepatol 44:167–175
29. Nelsen CJ, Rickheim DG, Tucker MM, Hansen LK, Albrecht JH (2003) Evidence that cyclin D1 mediates both growth and proliferation downstream of TOR in hepatocytes. J Biol Chem 278:3656–3663
30. Noh WC, Mondesire WH, Peng J, Jian W, Zhang H, Dong J, Mills GB, Hung MC, Meric-Bernstam F (2004) Determinants of rapamycin sensitivity in breast cancer cells. Clin Cancer Res 10:1013–1023
31. Palmes D, Spiegel HU (2004) Animal models of liver regeneration. Biomaterials 25:1601–1611
32. Park J, Ha H, Ahn HJ, Kang SW, Kim YS, Seo JY, Kim MS (2005) Sirolimus inhibits platelet-derived growth factor-induced collagen synthesis in rat vascular smooth muscle cells. Transplant Proc 37:3459–3462
33. Pinzani M, Knauss TC, Pierce GF, Hsieh P, Kenney W, Dubyak GR, Abboud HE (1991) Mitogenic signals for platelet-derived growth factor isoforms in liver fat-storing cells. Am J Physiol 260: C485–C491
34. Reynaert H, Chavez M, Geerts A (2001) Vascular endothelial growth factor and liver regeneration. J Hepatol 34:759–761
35. Rickheim DG, Nelsen CJ, Fassett JT, Timchenko NA, Hansen LK, Albrecht JH (2002) Differential regulation of cyclins D1 and D3 in hepatocyte proliferation. Hepatology 36:30–38
36. Sato T, El-Assal ON, Ono T, Yamanoi A, Dhar DK, Nagasue N (2001) Sinusoidal endothelial cell proliferation and expression of angiopoietin/Tie family in regenerating rat liver. J Hepatol 34:690–698
37. Schumacher G, Oidtmann M, Rosewicz S, Langrehr J, Jonas S, Mueller AR, Rueggeberg A, Neuhaus R, Bahra M, Jacob D, Gerlach H, Neuhaus P (2002) Sirolimus inhibits growth of human hepatoma cells in contrast to tacrolimus which promotes cell growth. Transplant Proc 34:1392–1393

38. Shegogue D, Trojanowska M (2004) Mammalian target of rapamycin positively regulates collagen type I production via a phosphatidylinositol 3-kinase-independent pathway. J Biol Chem 279:23166–23175
39. Shibuya M, Claesson-Welsh L (2006) Signal transduction by VEGF receptors in regulation of angiogenesis and lymphangiogenesis. Exp Cell Res 312:549–560
40. Smolewski P (2006) Recent developments in targeting the mammalian target of rapamycin (mTOR) kinase pathway. Anticancer Drugs 17:487–494
41. Soejima Y, Shimada M, Suehiro T, Hiroshige S, Ninomiya M, Shiotani S, Harada N, Hideki I, Yonemura Y, Maehara Y (2003) Outcome analysis in adult-to-adult living donor liver transplantation using the left lobe. Liver Transpl 9:581–586
42. Taub R (2004) Liver regeneration: from myth to mechanism. Nat Rev Mol Cell Biol 5:836–847
43. Webber EM, Bruix J, Pierce RH, Fausto N (1998) Tumor necrosis factor primes hepatocytes for DNA replication in the rat. Hepatology 28:1226–1234
44. Zhou J, Fan J, Wang Z, Wu ZQ, Qiu SJ, Huang XW, Yu Y, Sun J, Xiao YS, He YF, Wang YQ, Tang ZY (2006) Conversion to sirolimus immunosuppression in liver transplantation recipients with hepatocellular carcinoma: report of an initial experience. World J Gastroenterol 12:3114–3118
45. Zhu J, Wu J, Frizell E, Liu SL, Bashey R, Rubin R, Norton P, Zern MA (1999) Rapamycin inhibits hepatic stellate cell proliferation in vitro and limits fibrogenesis in an in vivo model of liver fibrosis. Gastroenterology 117:1198–1204

Virchows Arch (2008) 452:559–563
DOI 10.1007/s00428-008-0599-4

ORIGINAL ARTICLE

Trisomy of chromosome 6 in Merkel cell carcinoma within lymph nodes

Francesco Vasuri · Elisabetta Magrini · Maria Pia Foschini · Vincenzo Eusebi

Received: 6 December 2007 / Revised: 15 February 2008 / Accepted: 18 February 2008 / Published online: 2 April 2008
© Springer-Verlag 2008

Abstract Merkel cell carcinoma (MCC) of the skin is a neuroendocrine tumor with characteristic histological and immunohistochemical features. Among various cytogenetic changes, trisomy of chromosome 6 has been reported in 47% of cases using in situ hybridization. Primary tumors, morphologically and immunohistochemically identical to MCCs of the skin, have been described in other organs, including lymph nodes. Here, a cytogenetic study of four cases of MCC of lymph nodes is presented. Four cases of primary MCCs of lymph nodes and ten cases of cutaneous MCCs were studied for chromosome 6 using fluorescent in situ hybridization (FISH). All cases showed typical features of MCC both at hematoxylin and eosin (H&E) and immunohistochemistry. FISH showed trisomy 6 in two out of the four cases of MCCs of lymph node as well as in 6 out 10 cases of MCCs of skin. Lymph nodal and cutaneous MCCs share same histological and immunohistochemical features, as well as same cytogenetic alteration for chromosome 6. It seems that there are more similarities than differences between cutaneous and lymph nodal MCCs. Whether lymph nodal MCCs are primary tumors or metastases from regressed skin lesions is still questionable, although several findings indicate a primary origin.

F. Vasuri · E. Magrini · M. P. Foschini · V. Eusebi
Section of Anatomic and Cytopathology, University of Bologna, "M. Malpighi", Ospedale Bellaria, Bologna, Italy

V. Eusebi (✉)
Anatomia Patologica, University of Bologna, Ospedale Bellaria, Via Altura 3, 40139 Bologna, Italy
e-mail: vincenzo.eusebi@unibo.it

Keywords Merkel cell carcinoma · Lymph node · FISH · Trisomy 6

Introduction

Merkel cell carcinoma (MCC) of the skin is a neuroendocrine tumor affecting mostly elderly patients and occurring more commonly in the skin of face and lower extremities [9, 17]. It is generally characterized by poor prognosis. On morphological grounds MCC is formed by neoplastic cells with scanty acidophilic cytoplasm, round nuclei with granular chromatin, and one to two nucleoli. At electron microscopy, neuroendocrine granules and paranuclear dots of intermediate filaments are evident [9]. Immunohistochemically, MCC shows cytoplasmatic positivity for chromogranin, synaptophysin, and "dot-like" paranuclear positivity for cytokeratin 20 [3]. Several cytogenetic alterations have been described in these neoplasms, especially involving chromosomes 1, 11, and 13 as well as losses of 4p15-pter and gains of 8q21-q22 in common with squamous cell carcinoma of the skin [13–15]. Trisomy of chromosome 6 is the most frequent cytogenetic change having been seen in 47% of cases using in situ hybridization [10, 12].

Tumors morphologically and immunohistochemically identical to MCCs of the skin have been described in salivary glands, breast, and female genital tract [4, 7, 11, 18], including those believed to be primary of lymph nodes [5]. It was suggested for the latter to result from a malignant transformation of intranodal neuroectodermic rests or from an aberrant differentiation of stem cells of the lymphoreticular system [5].

Here, we report on a study based on fluorescent in situ hybridization (FISH) of four cases of MCC primary of

lymph nodes to see whether trisomy of chromosome 6 is also present in these neoplasms, a finding which would amplify the similarities between Merkel cell carcinomas of the skin and lymph nodes.

Materials and methods

Four cases of MCC with primary localization in lymph nodes were obtained from the consult cases of one of us (three cases) and from the files of the Section of Anatomic Pathology of the University of Bologna at Bellaria Hospital (one case). In addition ten consecutive cases of MCC of the skin, taken from the files of this same Institution, were selected. All cases were studied histologically with immunohistochemistry and FISH.

Histology and immunohistochemistry

All cases were formalin fixed and routinely processed to paraffin, sections were stained with hematoxylin–eosin (H&E) and immunostained for chromogranin, synaptophysin, and cytokeratin 20 (see Table 1). Immunohistochemistry was performed in an automatic immunostainer (Ventana).

Fluorescent in situ hybridization

Tissue sections (4-μm thick) of the most representative areas of the tumors were selected. Chromosome 6 copy number per cell was investigated by FISH using a centromere 6 probe alpha-satellite (Spectrum Orange Probe, Vysis, Abbott Laboratories, IL, USA). Sections were incubated at 60°C for 120 min, deparaffinized by washing in Bio Clear (Bio-Optica Spa, Milano) and dehydrated in 100% ethanol. After incubation in 2× saline sodium citrate buffer (2× SSC; pH 7.0) at 75°C for 10–15 min, sections were digested with proteinase K (0.25 mg/ml in 2× SSC; pH 7.0) at 45°C for 10–15 min, rinsed in 2× SSC (pH 7.0) at room temperature for 5 min, and dehydrated using ethanol in a series of increasing concentrations (70%, 85%, and 100%). The CEP6 probe was applied according to the manufacturer's instructions onto the selected area based on the presence of tumor foci on each slide, and the hybridization area was covered with a glass coverslip and sealed with rubber cement. The slides were incubated at 75°C for 8–10 min for codenaturation of chromosomal and probe DNA and incubated at 37°C for 20–24 h in order to allow the hybridization to occur. Posthybridization washes were performed in 0.3% NP-40 and 2× SSC (pH 7.0–7.5) at 75°C for 2 min. Samples were then dehydrated in ethanol as above and 4′,6′-diamidino-2-phenylindole (DAPI; 0.15 mg/ml in Vecta shield mounting medium, Vector Laboratories, Burlingame, CA, USA) was applied for chromatin counterstaining. Reactive non-neoplastic lymph node tissue was used as negative control.

Table 1 Antibodies used

Antibody	Source	Dilution	Clone	Antigen retrieval
Cytokeratin 20	Dako	1:40	KS 20.8	Wax Capture (WCAP)
Chromogranin	Biogenex	1:400	LK2H10	Wax Capture (WCAP)
Synaptophysin	Cell Marque	Prediluted	Polyclonal	Ventana

Evaluation of positivity

For the evaluation of positivity, we followed the same approach by Gancberg et al. [10], who regarded as trisomic the cases with more than 15% of nuclei showing three spots and monosomic those showing loss of one chromosome (one spot only) in more than 40% of cells. Internal control consisted of the use of chromosome 17 probes. To assess trisomy 6, in order to be even more stringent, we adopted a cut-off value of 20% of nuclei showing three spots.

Results

Clinical features

Patients with MCCs of lymph nodes were two men and two women with mean age of 71.7 years (range 58–85). The lymph nodes involved were inguinal in two cases and crural in the other two. All patients noticed nodal enlargement as the only clinical sign. After the diagnosis of nodal MCC, no primary tumor was found anywhere is spite of extensive investigation. Lower limbs in each patient were carefully studied, but no signs of primary or regressed lesion were found.

Two patients (cases 2 and 4) are alive and well after 15 and 18 months, respectively. One patient (case 1) showed after a month a nodal inguinal enlargement, in the same site of the first tumor, which proved to be an additional intranodal MCC; however, this patient was alive and well 36 months after excision, then was lost to follow-up. One patient (case 3) is alive and well after 96 months of follow-up.

Patients with MCCs of the skin were five men and five women with a mean age of 82.3 years (range 75–90). Tumors were located in the face in four cases, legs in three, buttocks in two, and dorsal region in one case.

Histology and immunohistochemistry

All cases showed typical features of MCC both at H&E and immunohistochemical levels, regardless of their localiza-

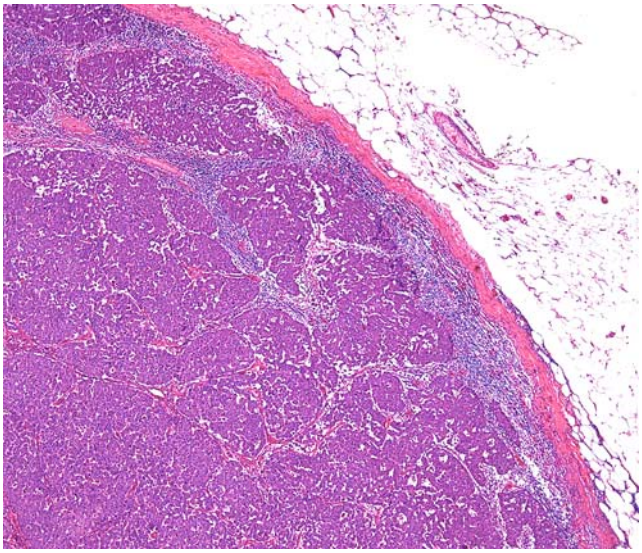


Fig. 1 Case 2: small cell carcinoma has effaced the structure of this lymph node

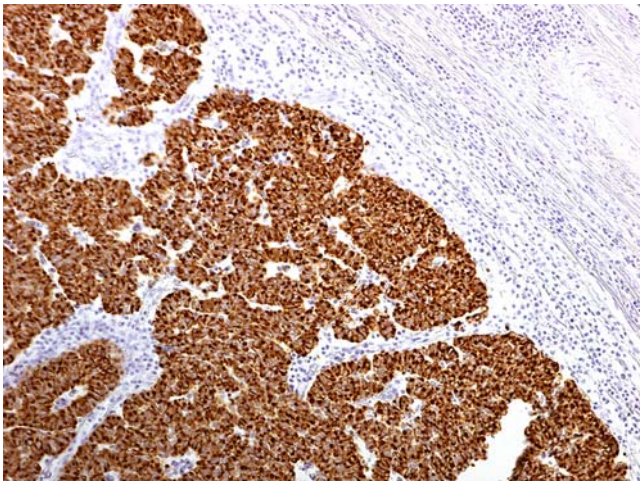


Fig. 3 Case 2: cytokeratin 20 highlights paranuclear dots of most of the neoplastic cells

tion. Accordingly, all tumors showed sheets or large clumps of neoplastic cells with round to ovoid nuclei and scanty eosinophilic cytoplasm. Chromatin was dispersed, nuclear membrane was well evident, and small nucleoli ranged from one to two. Mitoses were numerous and areas of necrosis were present. Tumors in lymph nodes effaced all the structure of the organ and only a small rim of peripheral lymphoid tissue, together with marginal sinus, was evident (Figs. 1 and 2). Lesions of the skin were all intradermal.

Cytokeratin 20 was positive in all cases with a mean percentage of positive cells of 86% (range 70–99%) in the lymph node group (Fig. 3) and of 87% (range 80–99%) in the skin group. All cases of both groups showed the typical paranuclear "dot-like" positivity. The mean percentage of chromogranin positive cells was 68% (range 30–95%) in the lymph node group (Fig. 4) and 77% (range 5–90%) in the skin group. The mean percentage of synaptophysin positive cells was 59% (range 0–80%) in the lymph node group (Fig. 5) and 72% (range 0–99%) in the skin group, with one case negative in each group (see Table 2). No differences in staining pattern or in intensity were evident between the two groups.

Cytogenetics

For FISH evaluation, a mean of 286 nuclei for case was evaluated (range 103–372). Two MCCs of lymph nodes and six MCCs of skin evidenced trisomy of chromosome 6 (50% and

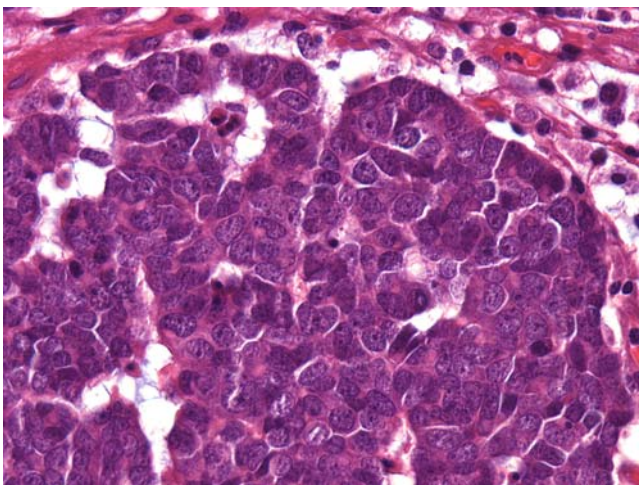


Fig. 2 Case 2: neoplastic cells show round nuclei, small nucleoli, and scanty cytoplasm

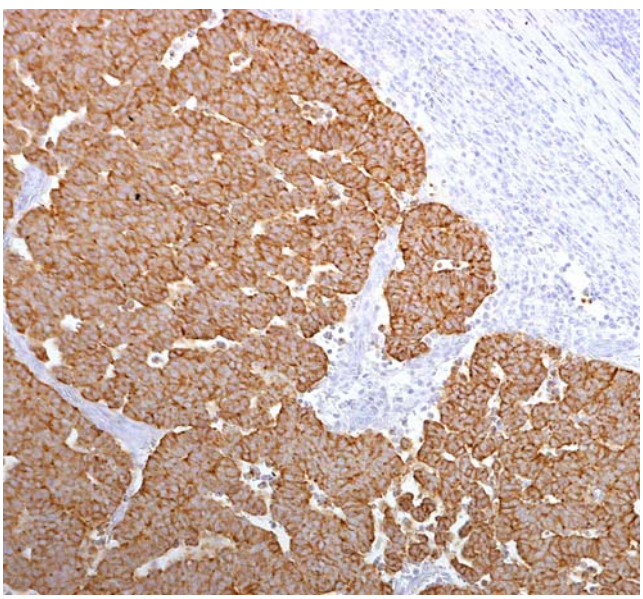


Fig. 4 Case 2: intense cytoplasmic positivity for chromogranin

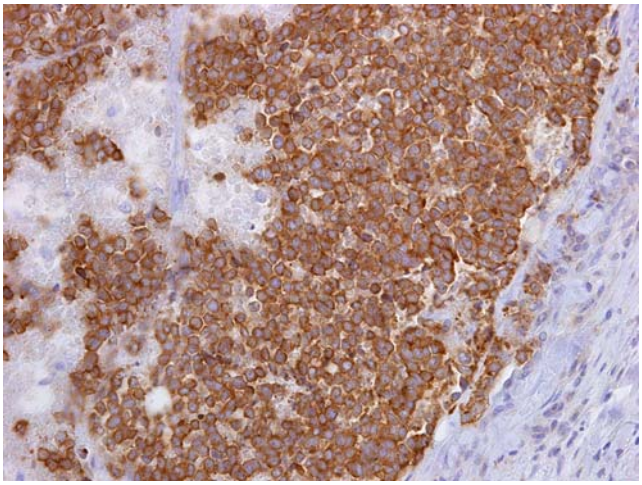


Fig. 5 Case 4: most of the cells are positive for synaptophysin

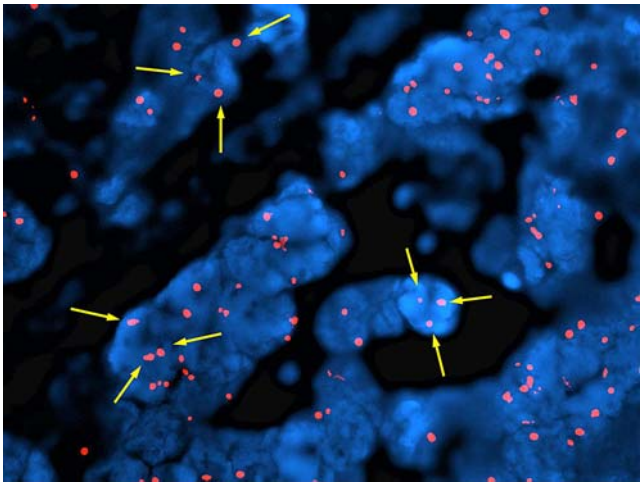


Fig. 6 Case 3: numerous nuclei show trisomy 6

60% of cases, respectively), with more than 20% of nuclei showing three spots (Fig. 6). The two MCCs of lymph node with trisomy 6 showed three spots in 27% and 30% of total cells, respectively, while the six MCCs of the skin with trisomy 6 showed three spots in a range of 23% to 43% (mean 30.5%) of the total neoplastic cell population (see also Table 2). No cases were observed in the lymph node or in the skin groups that had more than 40% of nuclei with one spot (range of nuclei with monosomy 4–24% in lymph node and 0–11% in skin).

Among the internal control cases, a mean of 104 nuclei for case was evaluated and three spots for chromosome 17 were found in 10% of nuclei (range 5–14%).

Discussion

Merkel cell carcinoma is a well-characterized neoplasm of the skin, but occasionally, it is also primarily observed in other sites including lymph nodes. All MCCs here studied, whether localized in skin or lymph nodes, shared same histological and immunohistochemical features. Several chromosomal irregularities have been documented in MCCs, the commonest aberrations involving chromosomes 1, 11, and 13 [14], as well as trisomy of chromosome 6 as a sole anomaly [10, 12]. Accordingly, when the FISH method was employed in this study, 50% of both cutaneous and nodal carcinomas showed a similar trisomy of chromosome 6. Therefore, it seems that it is not possible to separate lymph node and skin MCC on the account of this specific cytogenetic change.

All lymph nodal cases of our study were located in inguinal or crural regions. This seems to be an interesting finding, also consistent with the cases originally described [5], where five out of eight lymph nodal MCCs had an inguinal localization, and with some other case reports described in literature [2, 6, 8, 16].

Table 2 Clinical features and results of immunohistochemistry and FISH in each patient (percentages of positive cells)

Case	Sex	Age	Lymph node	CK20 (%)	Chromogranin (%)	Synaptophysin (%)	Three spots Chr 6 (%)
1	M	85	Inguinal	90	60	80	5
2	M	79	Crural	99	95	0	27
3	F	65	Inguinal	85	85	75	30
4	F	58	Crural	70	30	80	17
5	F	82	Face	85	85	70	11
6	F	90	Knee	80	85	70	26
7	M	86	Buttock	90	85	85	32
8	F	77	Lumbar region	85	85	85	43
9	M	75	Thigh	90	90	70	31
10	M	81	Thigh	85	85	85	13
11	F	81	Face	90	85	75	5
12	M	89	Nose	90	85	85	17
13	F	85	Face	80	5	0	23
14	M	77	Buttock	99	80	99	28

Whether MCCs of lymph nodes are real primary tumors or metastases from regressed skin lesions is still open to question, although several clinical features seem to indicate a primary origin in lymph nodes.

First of all, after the diagnosis of lymph nodal localization of MCC, all patients were extensively studied for skin lesions, but no primary neoplasms or signs of regression were found anywhere.

Admittedly, three cases had a relatively short follow-up (15, 18, and 36 months), with the exception of case 3, that is alive and well after 8 years. This same patient was one of the two showing trisomy of chromosome 6. Two of the cases originally described in lymph nodes [5] were also studied at postmortem (after 8 and 25 months, respectively) and in none of them a primary tumor was found. The case of MCC reported by Fornelli et al. [7] was found within an adenolymphoma of parotid, a benign tumor that often recognizes a primary origin in lymph nodes [1]. If MCCs of the skin are believed to be related to Merkel cells [9, 19] that harbor along the basal layer of epidermis, the origin of MCC of salivary glands, breast, genital tract, and lymph nodes from Merkel cells is highly questionable, as no native Merkel cells are present in these organs. It seems that this mystery is not solved by cytogenetic of MCC of lymph nodes.

Conflict of interest statement We declare we have no conflict of interest.

References

1. Azzopardi JG, Hou LT (1964) The genesis of adenolymphoma. J Pathol Bacteriol 88:213–218
2. Biering H, Bauditz J, Brenner N, Stein H, Lochs H, Strasburger CJ (2005) Primary neuroendocrine carcinoma of inguinal lymph node. Horm Res 64:16–19
3. Chan JKC, Suster S, Wenig BM, Tsang WYW, Chan JBK, Lau ALW (1997) Cytokeratin 20 immunoreactivity distinguishes Merkel cell (primary cutaneous neuroendocrine) carcinomas and salivary gland small cell carcinomas from small cell carcinomas of various sites. Am J Surg Pathol 21(2):226–234
4. Coleman NM, Smith-Zagone MJ, Tanyi J et al (2006) Primary neuroendocrine carcinoma of the vagina with Merkel cell carcinoma phenotype. Am J Surg Pathol 30:405–410
5. Eusebi V, Capella C, Cossu A, Rosai J (1992) Neuroendocrine carcinoma within lymph nodes in the absence of a primary tumor, with special reference to Merkel cell carcinoma. Am J Surg Pathol 16:658–666
6. Ferrara G, Ianniello GP, Di Vizio D, Nappi O (1997) Lymph node Merkel cell carcinoma with no evidence of cutaneous tumor-report of two cases. Tumori 83:868–872
7. Fornelli A, Eusebi V, Pasquinelli G, Quattrone P, Rosai J (2001) Merkel cell carcinoma of the parotid gland associated with Warthin tumor: report of two cases. Histopathology 39:342–346
8. Fotia G, Barni R, Bellan C, Neri A (2002) Lymph nodal Merkel cell carcinoma: primary or metastatic disease? A clinical case. Tumori 88:424–426
9. Frigerio B, Capella C, Eusebi V, Tenti P, Azzopardi JG (1983) Merkel cell carcinoma of the skin: the structure and origin of normal Merkel cells. Histopathology 7:229–249
10. Gancberg D, Feoli F, Hamels J et al (2000) Trisomy 6 in Merkel cell carcinoma: a recurrent chromosomal aberration. Histopathology 37:445–451
11. Kraemer BB, Mackay B, Batsakis JG (1983) Small cell carcinomas of the parotid gland. Cancer 52:2115–2121
12. Larsimont D, Verhest A (1996) Chromosome 6 trisomy as sole anomaly in a primary Merkel cell carcinoma. Virchows Arch 428:305–309
13. Leonard JH, Cook AL, Nancarrow D et al (2000) Deletion mapping on the short arm of chromosome 1 in Merkel cell carcinoma. Cancer Detect Prev 24:620–627
14. Leonard JH, Leonard P, Kearsley JH (1993) Chromosomes 1, 11, and 13 are frequently involved in karyotypic abnormalities in metastatic Merkel cell carcinoma. Cancer Genet Cytogenet 67:65–70
15. Popp S, Waltering S, Herbst C, Moll I, Boukamp P (2002) UV-B-type mutations and chromosomal imbalances indicate common pathways for the development of Merkel and skin squamous cell carcinomas. Int J Cancer 99:352–360
16. Samarendra P, Berkowitz L, Kumari S, Alexis R (2000) Primary nodal neuroendocrine (Merkel cell) tumor in a patient with HIV infection. South Med J 93:920–922
17. Sibley RK, Dahl D (1985) Primary neuroendocrine (Merkel cell?) carcinoma of the skin. Am J Surg Pathol 9:109–116
18. Tanda F, Scott C, Pittaluga S, Massarelli G (1983) Undifferentiated neuroendocrine (Merkel cell) carcinoma of the salivary glands; a light and electron microscopic study of two cases. Pathol Res Pract 178:167
19. Toker C (1982) Trabecular carcinoma of the skin. Am J Dermatopathol 4(6):497–500

Virchows Arch (2008) 452:565–570
DOI 10.1007/s00428-008-0603-z

ORIGINAL ARTICLE

Sarcoma of follicular dendritic cells with features of sinus lining cells—a new subtype of reticulum cell sarcoma?

Manuela Krokowski · Hartmut Merz · Christoph Thorns · Heinz-Wolfram Bernd · Ulrika Schade · Agnes Le Tourneau · Jacques Diebold · Alfred Christian Feller

Received: 18 September 2007 / Revised: 13 February 2008 / Accepted: 28 February 2008 / Published online: 2 April 2008
© Springer-Verlag 2008

Abstract Dendritic cell neoplasms of the World Health Organization classification comprise Langerhans cell histiocytosis, Langerhans cell sarcoma, interdigitating dendritic cell sarcoma, follicular dendritic cell sarcoma, and dendritic cell sarcoma, not otherwise specified. Several studies based on immunohistochemical and ultrastructural analysis tried to further clarify the origin of these neoplasms which are thought to derive from mesenchymal or bone marrow precursors. Lymphatic vessel endothelium hyaluronan receptor-1 (LYVE-1) was recently described as a marker for lymphatic endothelium which is expressed on normal liver blood sinusoid lining cells, spleen endothelium, activated tissue macrophages, blood vessels in the lung, endothelial cells of lymphatic sinuses, and in fibroblastic reticular cells in lymph nodes. We present a case of LYVE-1-positive reticulum cell neoplasm in an axillary lymph node. To the best of our knowledge, there has been no report about LYVE-1 expression in histiocytic or dendritic cell neoplasms so far. Due to the assumed specificity of this antibody, we propose designation of this reticulum cell sarcoma as lymphatic sinus lining cell sarcoma which might finally represent another subtype of reticulum cell sarcomas.

Keywords Sinus lining cell sarcoma · LYVE-1 · Follicular dendritic cell sarcoma

M. Krokowski (✉) · H. Merz · C. Thorns · H.-W. Bernd · U. Schade · A. C. Feller
Department of Pathology, Reference Center for Lymph Node Pathology and Hematopathology,
University Hospital of Schleswig-Holstein,
Campus Luebeck, Ratzeburger Allee 160,
23538 Luebeck, Germany
e-mail: krokowski@patho.mu-luebeck.de

A. Le Tourneau · J. Diebold
Assistance Hôpitaux Publique De Paris, Service Central D′ Anatomie Et Cytologie Pathologiques,
Hôtel-Dieu de Paris, 1, Place du Parvis Notre-Dame,
75181 Paris, France

Introduction

After the first description of a primary sarcoma in the lymph node with dendritic reticulum cell differentiation by Monda et al. in 1986 [11] a large number of histiocytic, dendritic, Langerhans, and respectively interdigitating dendritic cell sarcomas have been published. In 2002, the International Lymphoma Study Group developed the current classification of histiocytic and reticulum cell neoplasms. In this classification, distinction of the listed entities is based primarily on immunohistochemical data. Reticulum cell neoplasms comprise the following entities: Langerhans cell histiocytosis, Langerhans cell sarcoma, interdigitating dendritic cell sarcoma–tumor, follicular dendritic cell (FDC) sarcoma–tumor, and dendritic cell sarcoma, not otherwise specified [18].

As confirmed by earlier studies, an exact differentiation of the various above-described entities by means of morphology alone is not possible, and only thorough immunohistochemical analysis may prevent confusions with other mesenchymal tumors [7, 18]. Among reticulum cell neoplasms, fibroblastic reticular cell sarcoma has been described as a new subtype, based on the expression of vimentin, smooth muscle actin, and desmin [1].

Here, we report on a case of reticulum cell neoplasm expressing follicular dendritic cell antigens (cluster of differentiation 35 (CD35), CD23, CNA42, Kim4p, clusterin) and histiocytic associated antigens (CD14) as well as

mesenchymal antigens (vimentin) qualifying it as a dendritic reticulum cell sarcoma. The expression of LYVE-1 and CD31, which are additionally expressed to endothelial cells, on sinus lining cells clearly indicate the histogenetic relationship to this cell compartment of the lymph node. To the best of our knowledge, LYVE-1 expression in reticulum cell neoplasms has not been reported yet. Due to its assumed specificity, we propose such neoplasms to be designated as reticulum cell sarcoma of sinus lining cells possibly representing another subtype or differentiation step of reticulum cell sarcomas.

Materials and methods

Eight cases of reticulum cell neoplasms have been seen in the Service Central D'Anatomie Et Cytologie Pathologiques (Hôtel-Dieu de Paris) and the Reference Center for Lymph Node Pathology and Hematopathology (University Hospital of Schleswig-Holstein, Campus Luebeck) between the years 1999 and 2006: (1) lymph node of unknown localization of a 43-year-old woman, (2) breast biopsy of a 57-year-old woman, (3) splenectomy specimen of a 51-year-old woman, (4) osteolytic tumor in the os ileum of a 63-year-old woman, (5) cervical tumor of a 73-year-old man, (6) peritoneal nodule of a 26-year-old man with known FDC sarcoma of the appendix vermiformis, (7) axillary lymph node of a 52-year-old man, and (8) axillary lymph node of a 64-year-old man. Further clinical data were not available.

Five cases of chronic lymphadenitis and ten cases of angioimmunoblastic T-cell lymphoma were used as controls.

Additionally, ten cases of Langerhans cell histiocytosis including one malignant Langerhans cell histiocytosis and 5 cases of malignant histiocytosis were analyzed for LYVE-1-expression.

All specimens were formalin fixed and paraffin embedded. Sections were conventionally stained for hematoxylin–eosin, GIEMSA, and periodic acid–Schiff. In addition, all cases were stained with antibodies listed in Table 1 using a standard three-step immunoperoxidase technique with diaminobenzidine as chromogen.

Immunohistochemical slides were evaluated by three of the authors (H. M., A. C. F., and M. K.) on a multiheaded microscope to achieve consensus opinion for all stainings.

Table 1 Panel of antibodies

Antigen	Antibody clone	Dilution
CD35	Ber-MAC-DRC (DAKO)	1:50
CD21	1F8 (DAKO)	1:10
CNA42	CNA 42 (DAKO)	1:25
CD23	SP 23 (Lab vision)	1:100
Kim4p	Anti-IgG3	1:2
LYVE-1	Anti-LYVE-1 (Acris)	1:30
Vimentin	V9 (DAKO)	1:50
Clusterin	Clone 41D (Upstate)	1:50
Desmin	DE-R-11 (DAKO)	1:50
CD31	JC70A (DAKO)	1:40
CD8	BC/15A (Biocarta)	1:25
CD1a	010 (DAKO)	1:50
CD163	10 D6 (Novocastra)	1:50
CD14	Anti-CD14 (Novocastra)	1:50
SMA	1 A4 (DAKO)	1:50
EMA	MC-5 (Lab vision)	1:50
EBER	EBV probes and PNA in situ kit (DAKO)	

Results

Reticulum cell neoplasms

All cases were characterized by an infiltration of spindle cells with a predominantly solid, partly storiform, or fascicular growth pattern. Cases 1 and 8 exhibited additional large pseudovascular spaces (Fig. 1a). The spindle cells showed ovoid to elongated and partly polymorphic and vesicular nuclei with absent or small eosinophilic nucleoli and mainly indistinct cytoplasmic borders (Fig. 1b). A higher number of multinucleated cells could be found only in case 2. In addition, cases 3 and 4 showed a prominent inflammatory infiltrate with formation of abscesses and areas of necrosis. Circumscribed areas of myxoid changes were found in case 4.

Immunohistochemical analysis

All cases showed a positive reaction with vimentin. 6/8 cases were positive for CD23, CD14, and clusterin. Five out of eight cases showed a positivity for CD21 and 4/8 cases for CD35 (Fig. 1c) and CNA42. Four out of five cases were Kim4p positive; 3/6 cases showed a positivity for CD31. Smooth muscle actin was positive in one of eight cases. Case 8 was positive for LYVE-1 (Fig. 1d). All tumors were negative for desmin, CD68, CD163, CD1a, CD8 (0/7) as well as T- and B-cell antigens. All cases were negative for Epstein–Barr virus (Epstein–Barr-virus-encoded RNA in situ hybridization).

Clinical data and the immunohistochemical profiles are summarized in Table 2.

Reactive lymph nodes and angioimmunoblastic T-cell lymphomas

We selected five reactive lymph nodes with prominent follicular hyperplasia and prominent so called sinus histiocytosis. Herein, the follicular dendritic cells consis-

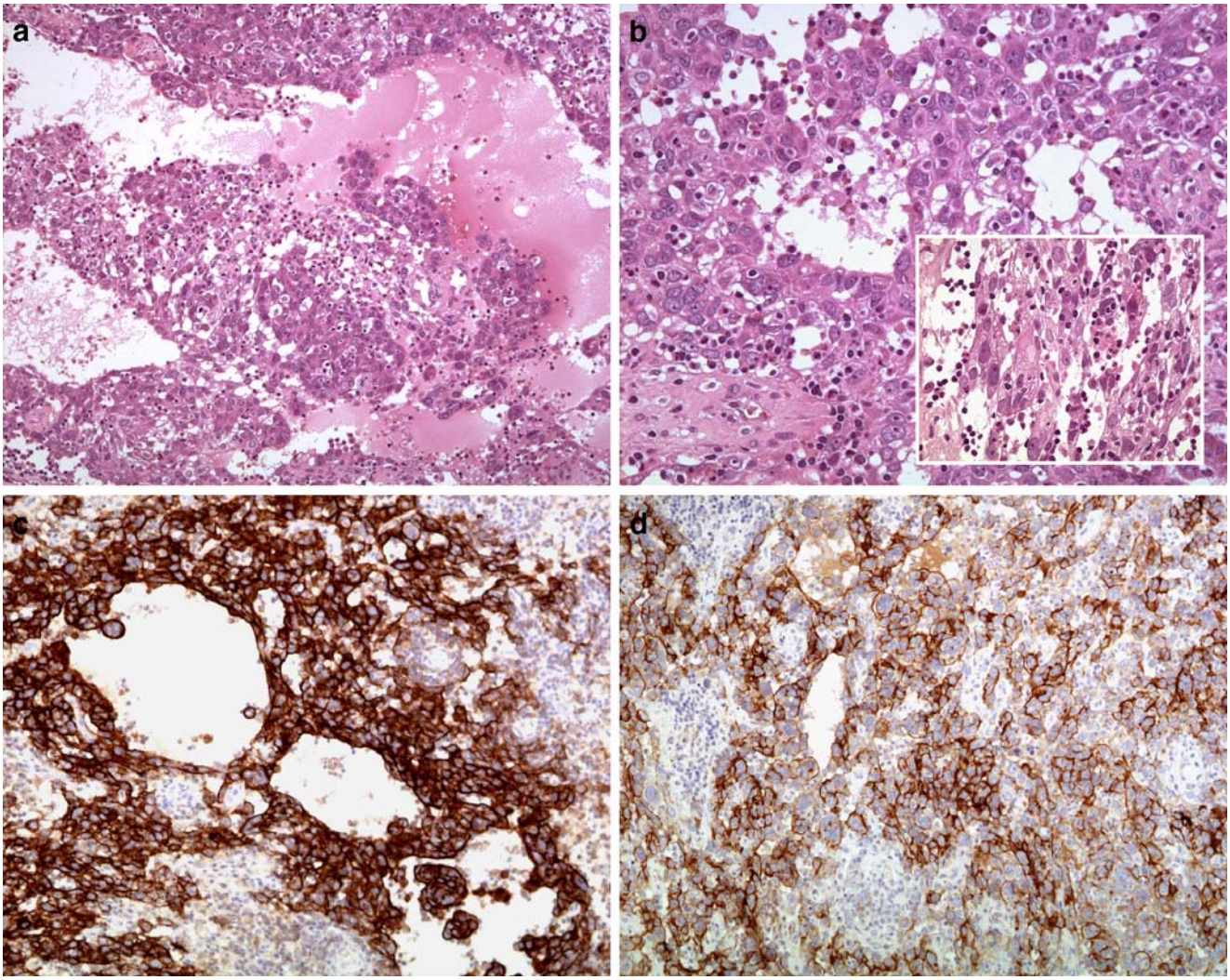


Fig. 1 Sinus lining cell sarcoma (case 8). **a** Large pseudovascular spaces (H & E, ×10). **b** Spindle cells with ovoid and polymorphic nuclei, small eosinophilic nucleoli, and abundant ill-defined eosinophilic cytoplasm (H & E, ×20, insert ×40). **c** CD35 shows strong membrane staining in the tumor cells (CD35, ×10). **d** Tumor cells demonstrate strong membrane staining with LYVE-1 (LYVE- 1, ×10)

tently showed positivity for CD35, CD23, clusterin, and partly CD14, but in all cases FDCs were negative for LYVE-1 and CD31. The sinus lining cells–fibroblastic reticulum cells and partly the histiocytes–macrophages in the sinuses showed a positive reaction for LYVE-1 (Fig. 2), CD14, and CD35.

We also analyzed ten cases of angioimmunoblastic lymphoma with prominent proliferation of FDCs. All FDC networks stained positive for CD35, CD23, and CNA42 but were consistently negative for LYVE-1.

LYVE-1 expression in other subtypes of reticulum cell neoplasms

Ten out of ten cases of Langerhans cell histiocytosis and 5/5 cases of malignant histiocytosis were negative for LYVE-1.

Discussion

Reticulum cells and their respective neoplasms, although rare, have been described since some decades. However, their cellular origin in terms of derivation from either immature precursor cells, monocytes, or fibroblastic cells has been elusive. Besides histiocytes and their malignant counterpart—histiocytic sarcomas—follicular and interdigitating cells are well characterized. Due to a quite well-defined immunophenotype, neoplasms of these cells can be readily identified. Thus, World Health Organization (WHO) included in their classification of histiocytic and dendritic cell neoplasms the following entities: histiocytic sarcoma, Langerhans cell histiocytosis, Langerhans cell sarcoma, interdigitating dendritic cell sarcoma–tumor, follicular dendritic cell sarcoma–tumor, and dendritic cell sarcoma, not otherwise specified [18].

Table 2 Summary of clinical data and immunohistochemical profiles

Case	1	2	3	4	5	6	7	8	
Age	43	54	51	63	73	26	52	64	–
Sex	m	f	f	f	m	m	m	m	–
Localization	Lymph node	Breast	Spleen	Os ileum	Cervical tumor	Lymph node (peritoneal)	Lymph node (axilla)	Lymph node (axilla)	Reactive lymph nodes (5) and angioimmunoblastic T-cell lymphoma (10)
Diagnosis	FDC sarcoma	FDC sarcoma	FDC sarcoma	FDC sarcoma	FDC sarcoma	FDC sarcoma	FDC sarcoma	Sarcoma of sinus lining cells	FDC–sinus lining cells
antibodies									
CD35	+	−	−	+	−	−	+	+	+/+
CD21	+	−	−	+	+	+	+	−	+/−
CNA42	+	−	+	+	−	−	−	+	
CD23	+	+	+	+	−	+	−	+	+/−
Kim4p	+	−	+	Not done	Not done	Not done	+	+	
Lyve-1	−	−	−	−	−	−	−	+	−/+
Vimentin	+	+	+	+	+	+	+	+	
Clusterin	+	+	+	+	−	+	−	+	
Desmin	−	−	−	−	−	−	−	−	
CD31	−	−	+	+	Not done	Not done	−	+	
CD8	Not done	−	−	−	−	−	−	−	−
CD1a	−	−	−	−	−	−	−	−	
CD68	−	−	−	−	−	−	−	−	
CD163	Not done	−	−	−	−	−	−	−	−
CD14	+	+	+	+	−	+	−	+	
SMA	−	−	+	−	−	−	−	−	
EBER	−	−	−	−	−	−	−	−	

In addition, fibroblastic reticular cell sarcoma has been described as a new subtype of reticulum cell neoplasms, based on the expression of vimentin, smooth muscle actin, and desmin [1]. The diagnosis among reticulum cell sarcomas can only be made by a combination of morphology and immunohistochemistry. The most reliable immunohistochemical markers that delineate tumors of the dendritic cell lineage are CD21, CD23, CD35, CD1a, and S100. Further, newly identified markers like CNA42, K-FDC1p, Ki-M4p, Ki-M9, CD163, and desmoplakin have not enhanced the diagnostic specificity for FDCs compared to the above-mentioned markers [5, 10, 13–15, 18]. Fascin and CD68 do not help in the differential diagnosis of dendritic cell tumors. However, recently, Grogg et al. [7, 8] described clusterin as an FDC marker with a specificity of 93% and a sensitivity of 100%.

In fact, the more immunohistochemical markers have been discovered the more confusion they caused, especially due to possible overlaps with other mesenchymal neoplasms. Most notably, in cases of extranodal tumors, inflammatory pseudotumors have to be considered in the differential diagnosis.

Here, we present a case of reticulum cell tumor which expresses typical antigens of FDCs (CD35, CD23, CNA42, Kim4p, clusterin), as well as histiocytic markers (CD14) and mesenchymal antigens (CD31, vimentin). Surprisingly, it additionally stained positive for LYVE-1 which is predominantly described to be specific for endothelial cells and which to the best of our knowledge does not stain FDCs.

LYVE-1 is a lymphatic endothelium hyaluronan receptor and has been established as a marker for lymphatic sinus endothelium. It is a type I integral membrane polypeptide with structural similarities to the CD44–hyaluronan (HA) receptor. The exact physiological function of the LYVE-1–HA receptor has not yet been fully understood. One known ligand is matrix glycosaminoglycan HA, which is a component of the skin and mesenchymal tissues and plays a major role during cell migration in inflammation, wound healing, and embryonic morphogenesis [2].

Apart from the lymphatic endothelium, LYVE-1 is also expressed on fibroblastic reticular cells of the lymphatic sinus, normal liver blood sinusoids, splenic endothelium, and activated tissue macrophages [26]. Some data indicate that LYVE-1 is expressed in angiosarcomas and Kaposi's sarcoma [27].

With evidence of various immunohistochemical markers on the presented tumor and after reviewing the literature,

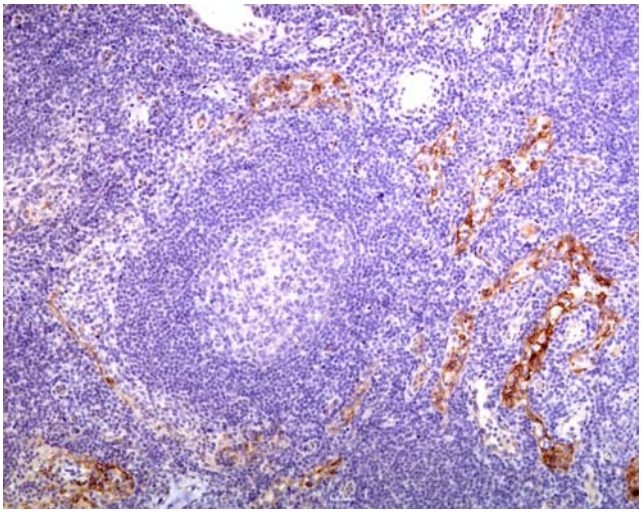


Fig. 2 LYVE-1 in reactive lymph node with follicular hyperplasia with positive membrane staining of the lymphatic endothelium (LYVE-1, ×10)

we put the given fact into question that the defined entities of reticulum cells are really separate entities rather than tumors of one common bone-marrow-derived "stem" cell in different development stages in the lymph node and extranodal lymphatic tissues, respectively.

The difficulties encountered in the reliable classification of dendritic cell neoplasms induced much effort in order to understand the development and histogenesis of these neoplasms. Previous studies investigating CD14- and CD34-positive peripheral blood mononuclear cells have demonstrated the plasticity of these circulating blood precursors showing that dendritic cells can easily differentiate in vitro either from CD34-positive stem cells upon culture with granulocyte–monocyte colony-stimulating factor (GM-CSF) and tumor necrosis factor [4, 21] or from monocytes with GM-CSF and interleukin (IL)-4 or IL-13 [17, 20, 22]. Furthermore, three independent studies proved that highly purified CD14 blood monocytes supplemented in vitro with GM-CSF and IL-4 developed into dendritic cells with the typical features [9, 16, 28].

Interestingly, D'Amigo et al. [6] could show in their experiments with in vitro cultured dendritic cells that differentiated from monocytes by exposure to granulocyte-macrophage colony-stimulating factor and IL-13 expressed CD31 and were able to migrate across endothelial cell monolayers as well as performing reverse transmigration. Furthermore, Pujol BF et al. showed that CD14-positive mononuclear cells can differentiate into endothelial like cells in the presence of angiogenic growth factors indicating a close relationship between the monocyte–macrophage system and some endothelial cells, especially microvascular endothelial cells. It is therefore conceivable that monocytes or monocyte precursors, depending on the local environment, may differentiate into either macrophages or dendritic cells or endothelial cells [19]. Simultaneous positivity for endothelial and dendritic cell markers within the same capillary endothelial cells could be demonstrated in double immunostaining analysis in palatine tonsils of newborn infants [12]. These data affirm the idea that follicular dendritic cells may derive from a group of transformed endothelial cells. The presumption that there is a close relationship between FDCs and endothelial cells could also be supported in high-resolution light microscopy—and 3D reconstruction—analysis by Sixt et al. They described that the conduit system of lymph nodes consists of basement membrane-like structures ensheathed by fibroblastic reticular cells which show molecular characteristics of lymphatic endothelial cells and a high capacity to take up soluble molecules and process tracer with greater efficiency than the sinusoidal macrophages [23].

Similar observations were made by Bofill et al. [3] who described a local differentiation pathway of fibroblastic reticular cells to mature FDCs in lymph follicles by immunohistochemical analysis.

Wacker et al. described sinus lining cells as an intermediate cell type linking monocytes–macrophages to follicular dendritic cells with the property to bind and present soluble antigens. In this context, they presented a case of a sinus lining cell reticulosarcoma [24, 25].

However, cases of LYVE-1-positive reticulum cell neoplasms—neither follicular dendritic cell sarcoma nor sinus lining cell sarcoma—have not yet been described in the literature. Concerning lymphatic tissue, our investigation could again demonstrate the high specificity of LYVE-1. This antibody was only found to bind to sinus lining cells–fibroblastic reticular cells, the histiocytes–macrophages in the sinuses, and on high endothelial venules of lymph nodes but was consistently negative in FDCs. This was also true in our control cases of angioimmunoblastic T-cell lymphoma, which is known to be associated with marked proliferation of FDCs. Furthermore, all analyzed cases of Langerhans cell histiocytosis and cases of malignant histiocytosis were negative for LYVE-1.

It might therefore be justified to describe Lyve-1-positive reticulum cell sarcomas as a new subtype or new differentiation step of reticulum cell sarcomas.

To summarize the above-mentioned studies together with our presented case, we suppose that there is an ongoing differentiation from bone-marrow-derived CD34- or CD14-positive progenitor cells to the various subtypes of reticulum cells as well as their neoplastic counterparts in the lymph node depending on microenvironmental factors. Because we could demonstrate the simultaneous expression of LYVE-1 as sinus lining cell marker and histiocytic and mesenchymal markers as well as typical dendritic cell

markers, the presented case relates to none of the established WHO entities and therefore might justify the designation as lymphatic sinus lining cell sarcoma.

Acknowledgement

Conflict of interest statement We declare that we have no conflict of interest.

References

1. Andriko JA, Kaldjian EP, Tsokos M, Abbondanzo SL, Jaffe ES (1998) Reticulum cell neoplasms of lymph nodes: a clinicopathologic study of 11 cases with recognition of a new subtype derived from fibroblastic reticular cells. Am J Surg Pathol 22 (9):1048–1058
2. Banerji S, Ni J, Wang SX, Clasper S, Su J, Tammi R, Jones M, Jackson DG (1999) Lyve-1, a new homologue of the CD44 Glycoprotein, is a lymph-specific receptor for Hyaluronan. J Cell Biol 144(4):789–801
3. Bofill M, Akbar AN, Amlot PL (2000) Follicular dendritic cells share a membrane-bound protein with fibroblasts. J Pathol 191:217–226
4. Caux C, Dezutter-Dambuyant C, Schmitt D, Banchereau J (1992) GM-CSF and TNF-alpha cooperate in the generation of dendritic Langerhans cells. Nature 360(6401):258–261
5. Chan JK, Fletcher CD, Nayler SJ (1997) Follicular dendritic cell sarcoma: clinicopathologic analysis of 17 cases suggesting a malignant potential higher than currently recognized. Cancer 79:294–313
6. D'Amico G, Bianchi G, Bernasconi S, Bersani L, Piemonti L, Sozzani S, Mantovani A, Allavena P (1998) Adhesion, transendothelial migration, and reverse transmigration of in vitro cultured dendritic cells. Blood 92(1):207–214
7. Grogg K, Lae ME, Kurtin PJ, Macon WR (2004) Clusterin expression distinguishes follicular dendritic cell tumors from other dendritic cell neoplasms: report of a novel follicular dendritic cell marker and clinicopathologic data on 12 additional follicular dendritic cell tumors and 6 additional interdigitating dendritic cell tumors. Am J Surg Pathol 28(8):988–998
8. Grogg KL, Macon WR, Kurtin PJ, Kurtin PJ, Nascimento AG (2005) A survey of clusterin and fascin expression in sarcomas and spindle cell neoplasms: strong clusterin immunostaining is highly specific for follicular dendritic cell tumor. Mod Pathol 18 (2):260–266
9. Kiertscher S, Human RM (1996) CD14+ leukocytes acquire the phenotype and function of antigen-presenting dendritic cells when cultured in GM-CSF and IL-4. J Leukocyte Biol 59:208–218
10. Middel P, Patterson BW, Ophemert I, Wacker HH, Parwaresch MR, Radzun HJ, Zschunke F (2002) Cloning of a complementary DNA encoding the unique dendritic cell antigen Ki-M9. Cell Tissue Res 307:347–355
11. Monda L, Warnke R, Rosai J (1986) A primary lymph node malignancy with features suggestive of dendritic reticulum cell differentiation. A report of four cases. Am J Pathol 149:839–843
12. Muretto P (1998) Immunohistochemical study of tonsils from newborn infants with emphasis on follicular dendritic reticulum cells. Eur J Histochem 42(3):189–195
13. Nguyen TT, Schwart EJ, West R, Warnke RA, Arber DA, Natkunam Y (2005) Expression of CD163 (hemoglobin scavenger receptor) in normal tissues, lymphomas, carcinomas, and sarcomas is largely restricted to the monocyte/macrophage lineage. Am J Surg Pathol 29(5):617–624
14. Parwaresch MR, Radzun HJ, Hansmann ML, Peters KP (1983) Monoclonal antibody Ki-M4 specifically recognizes human dendritic reticulum cells (follicular dendritic cells) and their possible precursors in blood. Blood 62:585–590
15. Perez-Ordonez B, Erlandson R, Rosai J (1996) Follicular dendritic cell tumor: report of 13 additional cases of a distinctive entity. Am J Surg Pathol 20(8):944–955
16. Pickl WF, Majdic O, Kohl, Stockl J, Riedl E, Scheinecker C, Bello-Fernandez C, Knapp W (1996) Molecular and functional characteristics of dendritic cells generated from highly purified CD14+ peripheral blood monocytes. J Immunol 157:3850–3859
17. Piemonti L, Bernasconi S Luini W, Trobonjaca Z, Minty A, Allavena P, Mantovani A (1995) IL-13 supports differentiation of dendritic cells from circulating precursors in concert with GM-CSF. Eur Cytokine Netw 6:245–252
18. Pileri SA, Grogan TM, Harris NL, Banks P, Campo E, Chan JKC, Favera RD, Delsol G, De Wolf-Peters C, Falini B, Gascoyne RD, Gaulard P, Gatter KC, Isaacson PG, Jaffe ES, Kluin P, Knowles DM, Mason DY, Mori S, Müller-Hermelink HK, Piris MA, Ralfkiaer E, Stein H, Su IJ, Warnke RA, Weiss LM (2002) Tumours of histiocytes and accessory dendritic cells: an immunohistochemical approach to classification from the International Lymphoma Study Group based on 61 cases. Histopathology 41:1–29
19. Pujol BF, Lucibello FC, Gehling UM, Lindemann K, Weidner N, Zuzarte ML, Adamkiewicz J, Elsässer HP, Müller R, Havemann K (2000) Endothelial-like cells derived from human CD14 positive monocytes. Differentiation 65:287–300
20. Romani N, Gruner S, Brang D, Kampgen E, Lenz A, Trockenbacher B, Konwalinka G, Fritsch PO, Steinmann RM, Schuler G (1994) Proliferating dendritic cell progenitors in human blood. J Exp Med 180:83–93
21. Rosenzwajg M, Canque B, Gluckman JC (1996) Human dendritic cell differentiation pathway from CD34+ hematopoietic precursor cells. Blood 87(2):535–544
22. Sallusto F, Lanzavecchia A (1994) Efficient presentation of soluble antigen by cultured human dendritic cells maintained by granulocyte/macrophage colony-stimulating factor plus interleukin-4 downregulated by tumor necrosis factor-alpha. J Exp Med 179:1109–1118
23. Sixt M, Kanazawa N, Selg M, Samson T, Roos G, Reinhardt DP, Pabst R, Lutz MB, Sorokin L (2005) The conduit system transports soluble antigens from the afferent lymph to resident dendritic cells in the T cell area of the lymph node. Immunity 22:19–29
24. Wacker HH, Heidebrecht HJ, Radzun HJ, Parwaresch MR (1992) Sinus lining cells: morphology, function and neoplasia. Verh Dtsch Ges Pathol 76:219–225
25. Wacker HH, Frahm SO, Heidebrecht HJ, Parwaresch R (1997) Sinus lining cells of the lymph nodes recognized as a dendritic cell type by the new monoclonal antibody Ki-M9. Am J Pathol 151:423–434
26. Wrobel T, Dziegiel P, Mazur G, Zabel M, Kuliczkowski K, Szuba A (2005) Lyve-1 expression on high endothelial venules (HEVs) of lymph nodes. Lymphology 38(3):107–110
27. Xu H, Edwards JR, Espinosa O, Banerji S Jackson DG, Athanasou NA (2004) Expression of a lymphatic endothelial cell marker in benign and malignant vascular tumors. Hum Pathol 35 (7):857–861
28. Zhou LJ, Tedder T (1996) CD14+ blood monocytes can differentiate into functionally mature CD83+ dendritic cells. Proc Natl Acad Sci USA 93:2588–2592

Virchows Arch (2008) 452:571–574
DOI 10.1007/s00428-007-0573-6

CASE REPORT

Wegener's granulomatosis in the thyroid mimicking a tumour

K. J. Schmitz · M. W. Baumgaertel · C. Schmidt · S. Y. Sheu · M. Betzler · K. W. Schmid

Received: 11 December 2007 / Accepted: 28 December 2007 / Published online: 28 February 2008
© Springer-Verlag 2008

Abstract Wegener's granulomatosis (WG) is a systemic vasculitis characterised by the presence of necrotizing granulomas and classically manifests as a triad of upper and lower respiratory tract involvement along with glomerulonephritis. Other rather unusual presentations of WG include ocular, salivary gland, cutaneous, gastrointestinal and cardiac involvement. We report a case in a 51-year-old woman suffering from WG with positive antineutrophil cytoplasmic autoantibodies and antibodies directed against proteinase 3. Under maintenance therapy, the patient developed two thyroid nodules suspicious for malignancy which led to thyroidectomy. Postoperative histological examination revealed a tumour-forming WG mimicking a malignant thyroid tumour. We conclude that, although extremely rare, Wegener's granulomatosis should be added to the list of differential diagnoses of tumours of the thyroid gland.

Keywords Thyroid · Wegener's granulomatosis · Histology

K. J. Schmitz · S. Y. Sheu · K. W. Schmid (✉)
Institute of Pathology and Neuropathology,
University Hospital of Essen, University of Duisburg-Essen,
Hufelandstrasse 55,
45122 Essen, Germany
e-mail: Kw.schmid@uk-essen.de

M. W. Baumgaertel
Department of Medicine II, Alfried Krupp Hospital,
Essen, Germany

C. Schmidt · M. Betzler
Department of General, Trauma and Vascular Surgery,
Alfried Krupp Hospital,
Essen, Germany

Introduction

Wegener's granulomatosis (WG) is an idiopathic systemic vasculitis characterised by the formation of necrotizing granulomas. WG classically manifests as a triad of upper and lower respiratory tract involvement along with glomerulonephritis [4]. The most common complaints include fever, malaise, cough, weight loss, chest pain and haemoptysis. The prevalence of WG is estimated at three cases per 100,000 within the USA [2]. The precise aetiology of WG remains obscure but is supposed to be autoimmune in nature. Antineutrophil cytoplasmic autoantibodies (ANCA) are the serologic hallmark of WG. In Wegener's granulomatosis, ANCA are mostly directed against proteinase 3 (PR3).

The upper airway is the most common localisation of WG with sinusitis being the most frequent initial presentation in about one half to two thirds of patients with WG [4]. Besides the upper airway, pulmonary involvement and renal disease are classical manifestations of WG. Furthermore, ocular manifestations have been reported to occur in 28% to 58% of patients with WG. Other rather unusual presentations of WG include salivary gland, cutaneous, gastrointestinal and cardiac involvement.

The disease can occur at any time from adolescence to old age but peak incidence is in early middle life (approximately 40 years). It occurs slightly more often in males. Untreated, the disease is associated with a very poor prognosis; >80% of patients die within the first year, >90% within the second. Although ANCAs are found in most patients with WG, histological examination still provides the most secure basis for diagnosis.

Clinical history

A 51-year-old woman suffering from WG was initially referred to the Department of Internal Medicine, Alfried-Krupp-Krankenhaus, Essen, Germany in order to receive cyclophosphamide chemotherapy. The patient was known to suffer from WG for 7 years. The patient initially presented with a nephritic syndrome with proteinuria, dysmorphic red blood cell casts in the urine sediment and a moderate reduction of the glomerular filtration rate. Moreover, the patient showed ophthalmologic, dermatologic, pulmonal and nasal involvement as well as arthalgias and initially positive ANCA titre (1:640) with antibodies directed against proteinase 3 (PR3-ANCA; 299 U/l). The patient's therapy was started with a corticoid bolus followed by monthly intravenous cyclophosphamide pulse therapy. After this initial therapy for 6 months, clinical remission was achieved with normalised ANCA and PR3-ANCA antibody titre. Under maintenance therapy with mycophenolate mofetil and prednisone, the WG relapsed presenting with cough, raised blood pressure, a nephritic syndrome and increasing ANCA (1:80) and PR3-ANCA serum levels (78 U/l). Physical examination showed a multinodular goitre. Subsequent thyroid scintigraphy revealed two cold nodules in the left thyroid lobe and in the isthmus region. Ultrasonography showed an inhomogeneous nodule in the left lobe with suspicion for malignancy (Fig. 1a); thyroidectomy was performed without a preoperative fine needle biopsy.

The left thyroid lobe including the isthmus measured 8.5×7.5×4 cm and the right lobe 8×6.5×3.5 cm. Two 3.4- and 2.8-cm ill-defined, grey-white solid "tumours" were demonstrated in the left lobe and the isthmus, respectively (Fig. 1b). The remaining thyroid gland showed several irregular colloid nodules partly with cystic changes.

Materials and methods

Formalin-fixed, paraffin-embedded tissue sections were stained with haematoxylin and eosin for routine examination. Ziehl–Neelsen stain, Grocott stain and periodic acid Schiff (PAS) were used to identify microorganisms. Elastic van Gieson stain was performed in order to optimise evaluation of blood vessels.

Results

Histological examination of the two "tumours" showed a necrotizing granulomatous inflammation and necrotizing vasculitis. The necrotizing granulomatous inflammation was characterised by large areas of parenchymal necrosis (Fig. 2a) bounded by epitheloid histiocytes and scattered giant cells (Fig. 2b). The necrotic zones typically were irregularly and "geographically" shaped and appeared deeply basophilic or "dirty" due to the abundant nuclear debris (Fig. 2a). Multinucleated giant cells were found frequently adjacent to a suppurative focus (Fig. 2c). There was a prominent background fibrosis. Necrotizing vasculitis of small- and medium-sized arteries with a mixed inflammatory infiltrate containing neutrophils, chronic inflammatory cells, eosinophils and epitheloid histiocytes was present in the viable parenchyma (Fig. 2d). Careful study of special stains (Ziehl–Neelsen, PAS, Grocott and Gram) did not reveal any microorganisms. Cultures were not taken.

Discussion

Thyroid gland involvement by WG seems to be an extremely rare event. A large study on 158 patients by Hoffman et al. [4] revealed no evidence of thyroid involvement. Cordier et al. [1] studied 77 patients and reported one case of hypothyroidism but the thyroid was not histologically examined. To the best of our knowledge, to date there is only one well-documented case of WG in the thyroid gland which was very recently reported by Schuerwegh and co-workers [5]. Their report deals extensively with the clinical presentation of the disease, summarising that WG should be

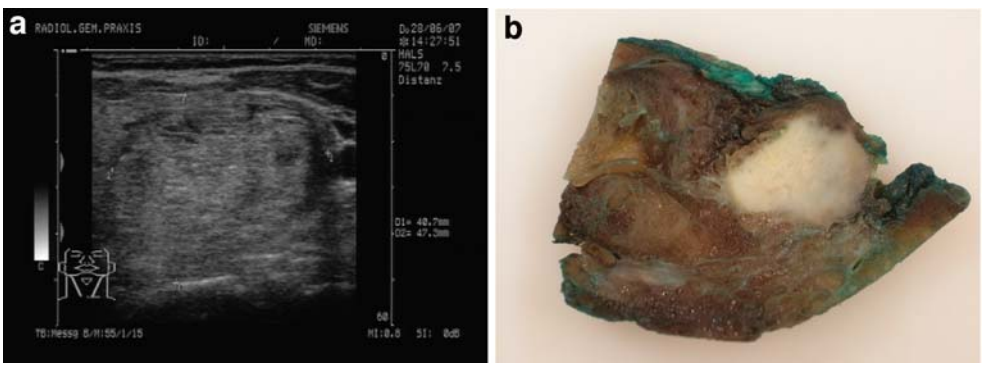


Fig. 1 **a** Ultrasonography of the left thyroid lobe suspicious for malignancy. **b** Macroscopy of a grey-white, ill-defined tumour in the thyroid

added to the differential diagnosis of inflammatory lesions of the thyroid gland; however, they only briefly report about the morphologic appearance of the thyroid lesion associated with WG.

We present the second case of a well-documented WG in the thyroid with a classical histological presentation. Although the patient suffered for years from WG with known pulmonary and renal manifestations, the presence of two distinctly nodular "tumours" in the thyroid was, particularly in ultrasound examination, suggestive of thyroid carcinoma. Surprisingly, histological examination revealed a combination of necrotizing granulomatous inflammation and necrotizing vasculitis. Although such a typical presentation is strongly suggestive of WG, it is important to rule out infectious granulomatous thyroiditis with special stains for organisms as the most important differential diagnosis especially if the patient receives immunosuppressive therapy. Moreover, it is important that vasculitis is found in viable thyroid parenchyma since vessels within any necrotic centre, regardless of aetiology, will contain necrotic cellular debris in their walls that can be mistaken for vasculitis.

WG, with the occurrence of well-formed granulomas, needs to be differentiated from other forms of granulomatous thyroiditis. Granulomatous lesions, including well-formed granulomas, can be seen in the thyroid in several conditions affecting the gland; this includes subacute granulomatous thyroiditis, so-called palpation thyroiditis, infection (e.g. tuberculosis), sarcoidosis, histiocytic reaction near haemorrhage in hyperplastic nodules or tumours, foreign body reaction and vasculitides. In contrast to subacute granulomatous thyroiditis and palpation thyroiditis, which are both relatively regular findings in thyroid specimen, infectious granulomas and granulomatous vasculitides are very rarely seen. Principally, the thyroid may be involved in any systemic vasculitis which may be confused with other granulomatous lesions affecting the thyroid. Fatal cases caused by systemic hypersensitivity vasculitis against various drugs (e.g. phenytoin and phenylhydantoin) have been described [3, 6].

The presence of granulomas with central necrosis, as found in this case, argues against sarcoidosis, De Quervain's thyroiditis as well as Riedel's disease. An early phase of De Quervain's thyroiditis may go along with microabscesses that may be part of WG as well. However, the finding of vasculitis in cases with WG is the key feature to rule out other granulomatous thyroid inflammatory diseases. Thus, careful workup of the pathological specimen especially in the periphery of the necrotizing granulomatous inflammation is critical.

In conclusion, the report describes for the first time a histologically well-documented case of Wegener's granulomatosis in the thyroid presenting as a mass. Thus, Wegener's granulomatosis should be added to the list of differential diagnoses of tumours of the thyroid gland and granulomatous thyroiditis.

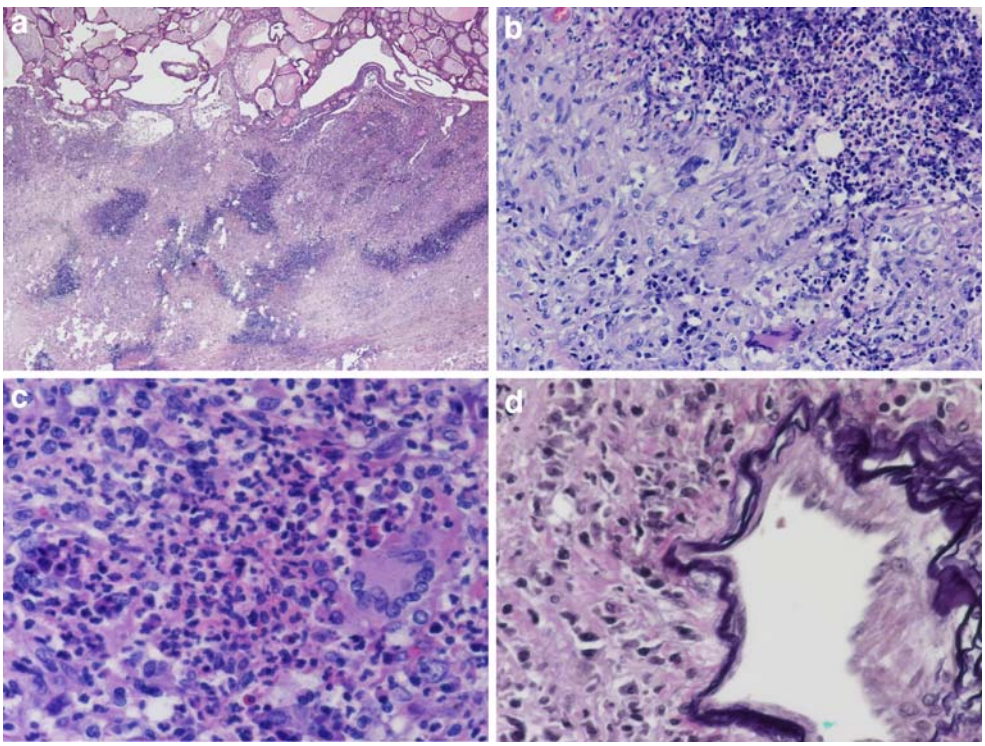


Fig. 2 Wegener's granulomatosis. **a** Low magnification of thyroid tissue showing irregular "dirty", "geographic" necrosis typically for Wegener's granulomatosis (haematoxylin–eosin, ×20). **b** Higher magnification showing necrosis (*right*) with granulomatous inflammation containing epitheloid and giant cells (haematoxylin–eosin, ×20). **c** Higher magnification showing multinucleated giant cells adjacent to a suppurative focus (haematoxylin–eosin, ×400). **d** High magnification showing necrotizing vasculitis of a small-sized artery (Elastica van Gieson, ×400)

Conflict of interest statement We declare that we have no conflict of interest.

References

1. Cordier JF, Valeyre D, Guillevin L, Loire R, Brechot JM (1990) Pulmonary Wegener's granulomatosis. A clinical and imaging study of 77 cases. Chest 97:906–912
2. Cotch MF, Hoffman GS, Yerg DE, Kaufman GI, Targonski P, Kaslow RA (1996) The epidemiology of Wegener's granulomatosis. Estimates of the five-year period prevalence, annual mortality, and geographic disease distribution from population-based data sources. Arthritis Rheum 39:87–92
3. Gaffey CM, Chun B, Harvey JC, Manz HJ (1986) Phenytoin-induced systemic granulomatous vasculitis. Arch Pathol Lab Med 110:131–135
4. Hoffman GS, Kerr GS, Leavitt RY, Hallahan CW, Lebovics RS, Travis WD, Rottem M, Fauci AS (1992) Wegener granulomatosis: an analysis of 158 patients. Ann Intern Med 116:488–498
5. Schuerwegh AJ, Verhelst J, Slabbynck H, Kockx MM, Coolen D (2007) Wegener's granulomatosis presenting as a thyroid mass. Clin Rheumatol 26:454–456
6. Yermakov VM, Hitti IF, Sutton AL (1983) Necrotizing vasculitis associated with diphenylhydantoin: two fatal cases. Hum Pathol 14:182–184

Virchows Arch (2008) 452:575–579
DOI 10.1007/s00428-008-0588-7

CASE REPORT

Report of a metaplastic carcinoma of the breast with multi-directional differentiation: an adenoid cystic carcinoma, a spindle cell carcinoma and melanoma

Aurelia Noske · Michael Schwabe · Stefan Pahl · Eva Fallenberg · Christiane Richter-Ehrenstein · Manfred Dietel · Glen Kristiansen

Received: 24 September 2007 / Revised: 21 January 2008 / Accepted: 22 January 2008 / Published online: 19 February 2008
© Springer-Verlag 2008

Abstract Metaplastic carcinoma of the breast is a heterogeneous neoplasia, generally composed of both epithelial and mesenchymal components. We report an unusual case of mammary metaplastic carcinoma in a 51-year-old female patient. Needle core biopsy from the tumour mass showed malignant epithelial and sarcomatous features. The resection specimen revealed a multi-directional tumour differentiation consisting predominantly of: firstly, a poorly differentiated basaloid epithelial cell type, consistent with an adenoid cystic carcinoma; secondly, areas of a spindle cell carcinoma; and, thirdly, areas with a melanocytic differentiation. This is the first report on a metaplastic carcinoma of the breast presenting as an admixture of an adenoid cystic carcinoma and melanoma.

Keywords Breast · Metaplastic cancer · Adenoid cystic cancer · Melanocytic differentiation

A. Noske (✉) · M. Schwabe · S. Pahl · M. Dietel · G. Kristiansen
Institute of Pathology, Charité University Hospital Berlin,
Campus Mitte, Charitéplatz 1,
Berlin 10117, Germany
e-mail: aurelia.noske@charite.de

E. Fallenberg
Department of Radiology, Charité University Hospital Berlin,
Berlin, Germany

C. Richter-Ehrenstein
Department of Gynecology and Obstetrics,
Charité University Hospital Berlin,
Berlin, Germany

Introduction

Metaplastic carcinomas of the breast are rare and comprise less then 1% of all invasive breast tumours [2]. The range of age at diagnosis as well as clinical symptoms do not differ from that of conventional invasive ductal breast cancer. Metaplastic carcinomas can be classified into purely epithelial or mixed epithelial and mesenchymal carcinomas. Generally, this tumour type can show diverse features of an adenocarcinoma or squamous cell carcinoma as well as mesenchymal components ranging from chondroid or osseus metaplasia to chondro- or osteosarcoma. In contrast, melanocytic differentiation of mammary breast cancer is extremely rare. Only very few reports presented mammary metaplastic carcinomas with melanocytic components [5, 6, 8, 10, 11]. The heterogeneous entity may be mistaken in fine needle aspiration smears or core biopsies when melanocytic cells are interpreted as a primary or secondary malignant melanoma of the breast.

So far, metaplastic carcinomas of the breast with elements of an adenoid cystic carcinoma (ACC) are not described. ACC accounts for 0.1% of breast carcinomas and the histological appearance is similar to its counterpart in the salivary glands but its prognosis is quite different [1].

Case report

Clinical history

A 51-year-old woman was admitted to the Charité Universitätsmedizin Berlin for diagnostic evaluation of a nodular mass in the breast found at self-examination. Until this time the woman was in good health. Physical examination revealed a

well-circumscribed lesion in the upper outer quadrant of the right breast. There was no tumour relation to the overlying skin. The ipsilateral axilla was inconspicuous. Ultrasound and mammography revealed a solid hypoechoic, well-delineated lesion, 30 mm in diametre, which was suspicious of malignancy (Fig. 1a, b). Simultaneously, needle core biopsies were obtained. Furthermore, a complete clinical and radiological staging including computed tomography of the chest, abdomen and pelvis was done and did not reveal any other tumour manifestation.

Materials and methods

Representative tissue specimens were fixed in 4% buffered formalin and embedded in paraffin. Histological sections were stained with hematoxylin and eosin (H & E), periodic acid-Schiff and Fontana–Masson. Immunohistochemistry using the alkaline phosphatase technique was carried out for each antibody. Primary antibodies included estrogen and progesterone receptors, c-erbB2, gross cystic disease fluid protein 15 kDa (GCDFP-15), mammaglobin, pan-cytokeratin, cytokeratin (CK) 5, 7, 14 and 18, protein S100, vimentin, cluster of differentiation 117 (CD117), human melanoma black 45 (HMB-45) and melanocyte antigen (Melan-A).

Results

Microscopic evaluation of the core biopsy showed predominantly infiltrative solid epithelial tumour cell complexes and partly atypical pleomorphic spindle-shaped cells. The preliminary diagnosis of an invasive carcinoma with a polymorphic spindle component consistent with a metaplastic breast carcinoma was reported. Subsequently, the patient underwent a lumpectomy of the right breast and an axillary sentinel lymph node excision.

The surgical specimen measured 95×85×30 mm and contained a solitary, solid, well-circumscribed tumour mass of 25×21×17 mm. The cut surface was tan-white and firm. The surrounding breast tissue was unremarkable. The lesion was excised with free resection margins of at least 6 mm to all directions.

Microscopically, the tumour showed different features, predominantly of an infiltrating epithelial component with irregular solid sheets and nests of poorly differentiated basaloid cells (Fig. 2a). These cells showed enlarged nuclei, scanty basophilic cytoplasm as well as a high mitotic rate (50 mitoses per ten high power fields). No pure tubular growth pattern was notable. Occasionally, cribriform architecture and deposits of basement membrane components outlining the tumour complexes were identified (Fig. 2b). As found in the biopsy, areas with pleomorphic spindle cells, nuclear atypia as well as bizarre nuclei were present (Fig. 2c). Chondrous or osseous metaplasia as well as squamous differentiation were not observed. At the periphery of the lesion, a strikingly different third component was detected consisting of solid aggregates of highly polymorphic bizarre cells obtaining abundant cytoplasmic granular brown to black pigment (Fig. 2d). In close vicinity, little nests of more mature naevus-cell-like cells were intermingled with the melanocytic and the epithelial elements. Intraductal carcinoma was absent. Special stains and immunohistochemistry were performed to characterise the different neoplastic cells. All tumour cells were negative for hormone receptors, c-erbB2, GCDFP-15 and mammaglobin. The epithelial tumour complexes were immunostained for pan-cytokeratin, partly cytokeratin 5, 7 and 18 (Fig. 3a), as well as protein S100 and CD117 (Fig. 3b). The

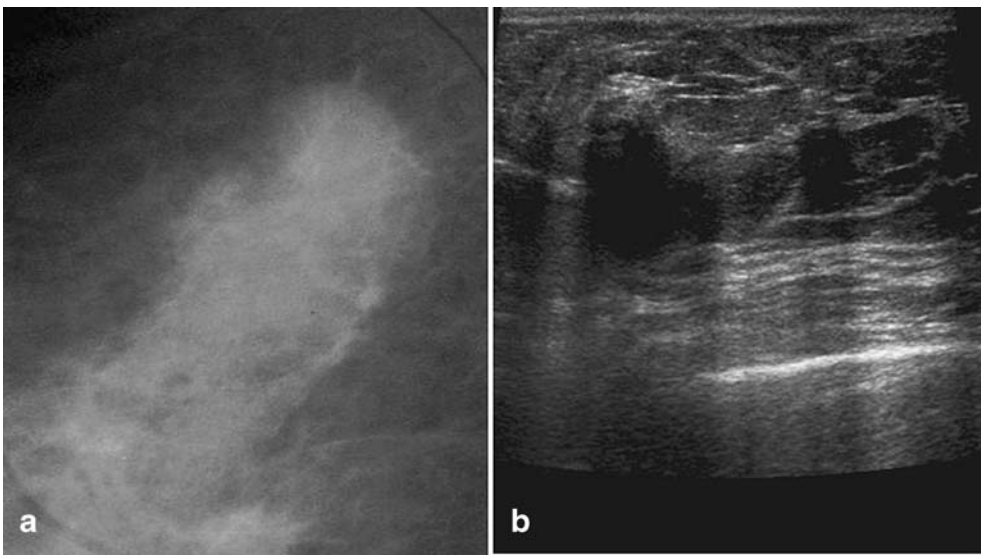


Fig. 1 Radiological findings. **a** On mammography, a well-delineated mass without any microcalcifications or ossifications is apparent. **b** Solid tumour mass with hypoechoic signals in ultrasound examination

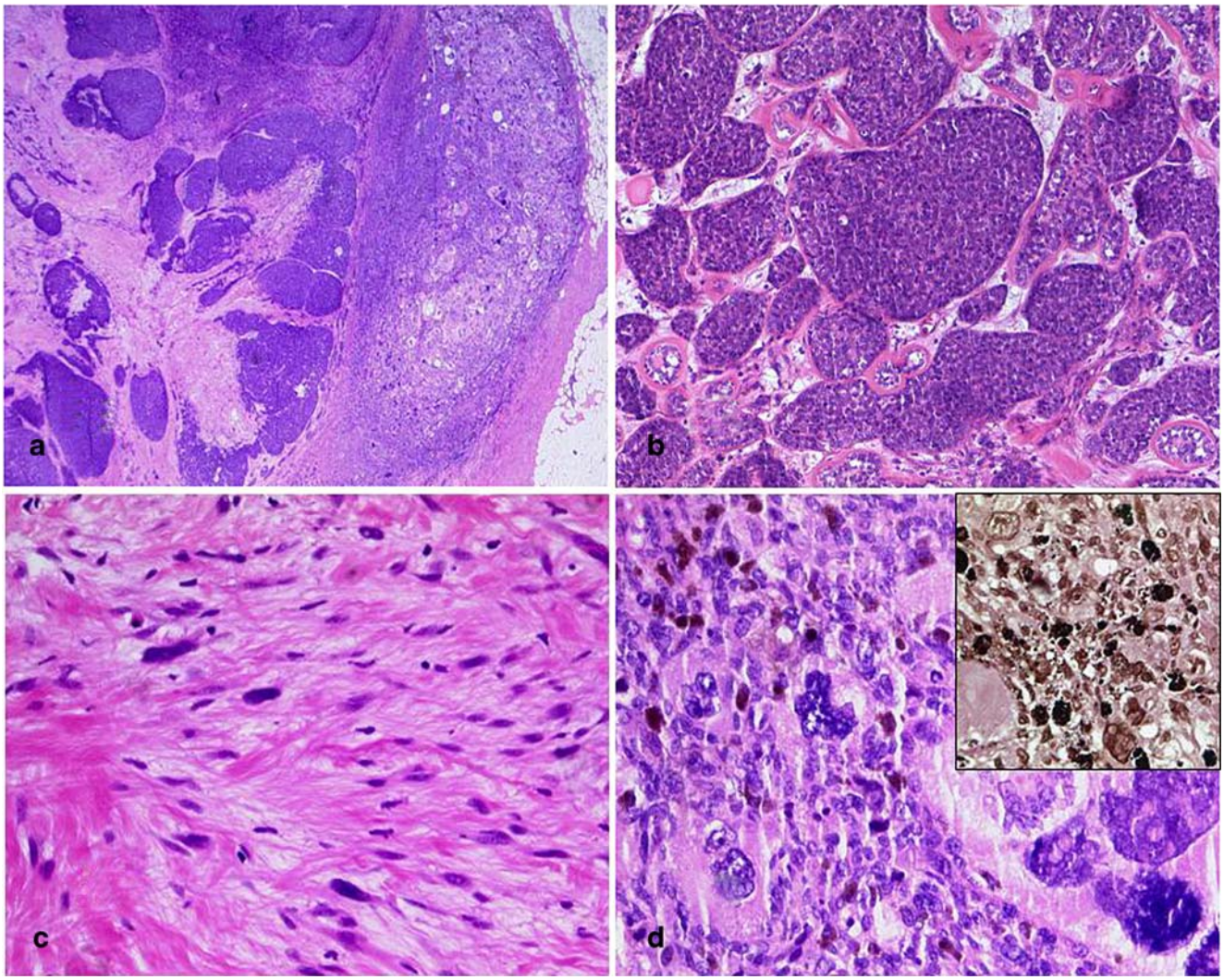


Fig. 2 Histological sections from the metaplastic carcinoma showing the triphasic differentiation. **a** Epithelial component with solid growth pattern (*left side*) as well as the melanocytic component on the *right side* (H & E, ×100). **b** Solid tumour complexes with basaloid cells, increased mitotic figures and deposits of basal lamina elements (H & E, ×100). **c** Melanocytic component with cytoplasmic pigmentation (H & E, ×400). Pigment granules give a black reaction with the Fontana–Masson stain (*inset*). **d** Pleomorphic spindle-shaped cells with atypical nuclei (H & E, ×200)

spindle cells were positive against cytokeratin 14 and vimentin. The pigmented cells displayed an expression of protein S100 and a strong expression of HMB-45 and Melan-A (Fig. 3c, d). On the basis of these findings, the tumour was classified as a metaplastic carcinoma consisting of an adenoid cystic carcinoma, spindle cell carcinoma as well as a melanocytic differentiation. Axillary sentinel lymph node did not show any metastatic spread.

Discussion

This is the first report on a metaplastic breast carcinoma with uncommon features of an adenoid cystic carcinoma as well as areas of melanocytic differentiation. Generally, mammary metaplastic carcinomas consist of an adenocarcinoma and squamous or spindle cell areas as well as mesenchymal elements to varying degrees. The squamous cell and spindle cell carcinomas may present in a pure form.

We observed a multi-directional differentiated invasive carcinoma with melanocytic component but without intraductal cancer. These findings are in line with Yen et al. [11], while other case reports described bi-directional differentiated metaplastic carcinomas with adjacent intraductal cancer [6, 8]. To date, there are only few reports on metaplastic carcinomas with a melanocytic component in the literature [5, 6, 8, 10, 11]. Since a collision tumour of a primary breast carcinoma and a manifestation of a primary or metastatic malignant melanoma appear unlikely, we assume a genuine multi-directional tumour differentiation with at least three components comparable to the report of Yen and colleagues [11]. Although little is known about the genesis of

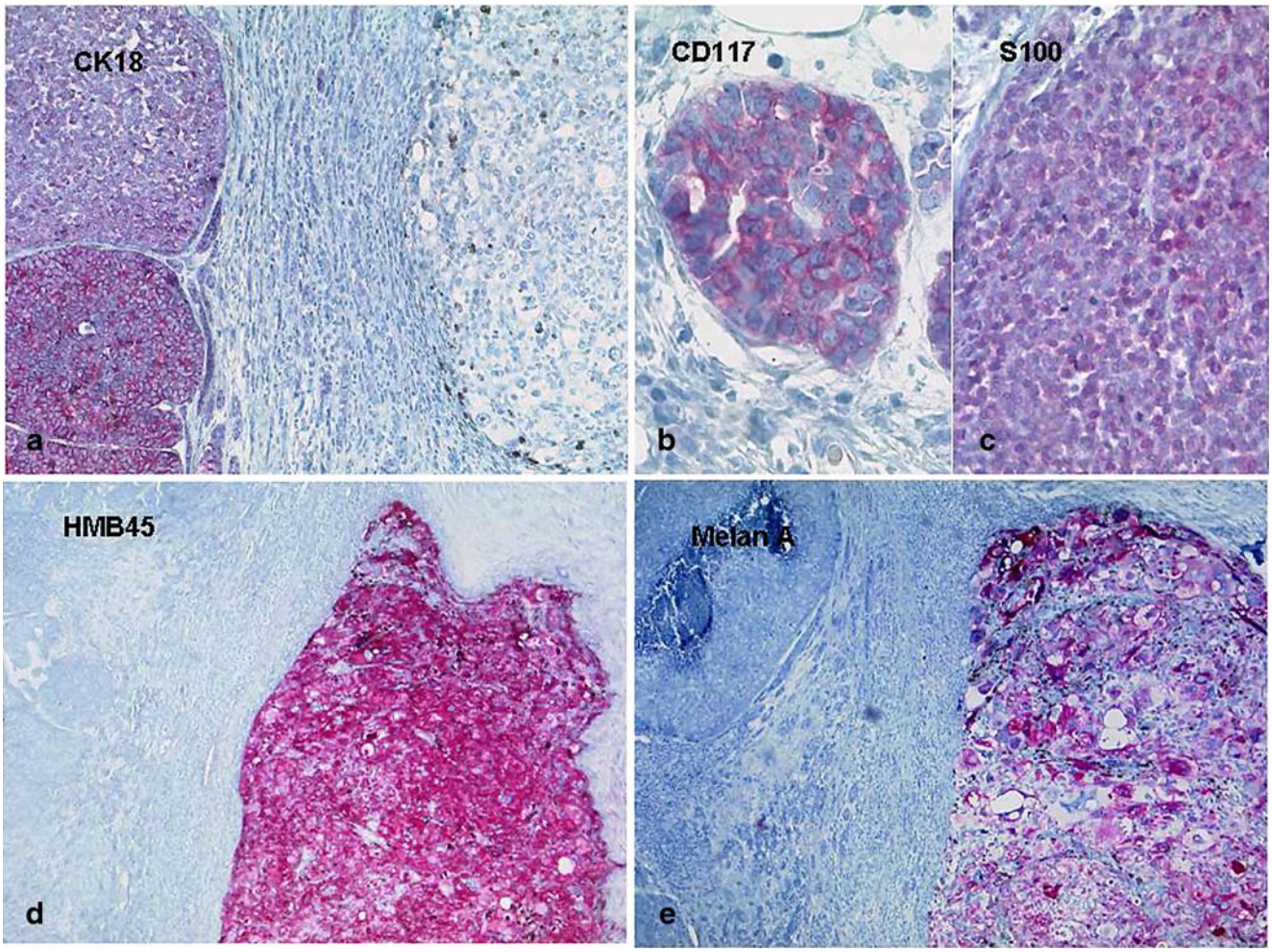


Fig. 3 Immunoprofile of the different tumour elements. **a** Epithelial tumour cells with expression of cytokeratin 18 (*left side*) and negativity in the melanocytic area (*right side*). **b**, **c** Expression of CD117 as well as protein S100 in the carcinoma cells. **d**, **e** Melanocytic cell express strong HMB-45 and Melan-A

melanocytic differentiation in breast carcinomas, it appears likely that both components arise from the same progenitor cell, since molecular studies from invasive ductal carcinomas with melanocytic differentiation revealed no different genetic alterations [5]. It is of interest to note that primary carcinomas of the breast can acquire melanin pigmentation due to the phagocytosis of melanin by tumour cells but still retain an epithelial immunophenotype [9]. In general, the histogenesis of metaplastic carcinoma remains uncertain until now. Previous studies suggest that the sarcomatoid component derives from myoepithelial cells [3, 4].

So far, features of an adenoid cystic carcinoma in metaplastic carcinomas were not described. This tumour type is morphologically very similar to its salivary gland counterpart but is associated with a favourable prognosis [1, 7]. In our case, we observed a solid variant of an ACC with a predominant basaloid cell population. The second cell type with luminal differentiation was identified immunohistochemically by cytokeratin 18 expression. Additionally, a focal expression of CD117 which was reported previously in ACC of the breast was noted [1]. However, it is difficult to distinguish between an invasive ductal carcinoma with basal phenotype and an adenoid cystic carcinoma with solid growth pattern. Since the epithelial component did not convincingly express "basal-like" markers like CK5, CK14 or vimentin but showed positive immunoreaction against CK7, protein S100 and CD117, we conclude that these tumour complexes belong to a solid adenoid cystic carcinoma.

In summary, data from previous reports and our findings show that metaplastic carcinomas are a heterogeneous group of breast cancer, usually recognised in an advanced tumour stage (>30 mm in diametre) and frequently negative for hormone receptors and c-erbB2 [2]. Patient prognosis depends on the complete and wide tumour excision as well as on the different histological sub-types. Although metaplastic carcinomas are rare, there appears to be an increasing incidence [2] which warrants further study of this uncommon tumour type.

Acknowledgments We gratefully thank Professor V. Eusebi for the evaluation of the tumour tissue. We also thank Mrs. M. Eickmann for the editorial assistance.

Conflict of interest statement The authors declare that no conflicts of interest exist.

References

1. Azoulay S, Laé M, Fréneaux P, Merle S, Ghuzlan A, Chnecker C, Rosty C, Klijanienko J, Sigal-Zafrani B, Salmon R, Fourquet A, Sastre-Garau X, Vincent-Salomon A (2005) KIT is highly expressed in adenoid cystic carcinoma of the breast, a basal-like carcinoma associated with a favourable outcome. Mod Path 18:1623–1631
2. Barnes PJ, Boutilier R, Chiasson D, Rayson D (2005) Metaplastic breast carcinoma: clinical–pathologic characteristics and HER2/neu expression. Breast Cancer Res Treat 91:173–178
3. Eusebi V, Cattan MG, Ceccarelli C, Lamovec J (1989) Sarcomatoid carcinoma of the breast: an immunocytochemical study of 14 cases. Prog Surg Pathol 10:83–99
4. Kaufman MW, Marti JR, Gallager HS, Hoehn JL (1984) Carcinoma of the breast with pseudosarcomatous metaplasia. Cancer 53:1908–1917
5. Nobukawa B, Fujii H, Hirai S, Kumasaka T, Shimizu H, Matsumoto T, Suda K, Futagawa S (1999) Breast carcinoma diverging to aberrant melanocytic differentiation: a case report with histopathologic and loss of heretozygosity analyses. Am J Surg Pathol 23:1280–1287
6. Padmore RF, Lara JF, Ackerman DJ, Gates T, Sigurdson ER, Ehya H, Cooper HS, Patchefsky AS (1996) Primary combined malignant melanoma and ductal carcinoma of the breast: a case report of two cases. Cancer 78:2515–2125
7. Pia-Foschini M, Reis-Filho JS, Eusebi V, Lakhani SR (2003) Salivary gland-like tumours of the breast: surgical and molecular pathology. J Clin Pathol 56:497–506
8. Ruffolo EF, Koerner FC, Maluf HM (1997) Metaplastic carcinoma of the breast with melanocytic differentiation. Mod Path 10:592–596
9. Shin SJ, Kanomata N, Rosen PP (2000) Mammary carcinoma with prominent cytoplasmic lipofuscin granules mimicking melanocytic differentiation. Histopathology 37:456–459
10. Tavassoli FA (1999) Pathology of the breast, 2nd ed. p 550
11. Yen H, Florentine B, Koss Kelly L, Bu X, Crawford J, Martin SE (2000) Fine-needle aspiration of a metaplastic breast carcinoma with extensive melanocytic differentiation: a case report. Diagn Cytopathol 23:46–50

Virchows Arch (2008) 452:581–583
DOI 10.1007/s00428-008-0582-0

LETTER TO THE EDITOR

A case of multiple diffuse gastric carcinoma with regional expression of mutant E-cadherin

Masamichi Bamba · Hiroyuki Sugihara · Karl-Friedrich Becker · Ingrid Becker · Heinz Höfler · Takanori Hattori

Received: 24 September 2007 / Revised: 23 November 2007 / Accepted: 11 January 2008 / Published online: 5 February 2008
© Springer-Verlag 2008

Dear Editors,

E-cadherin is a cell adhesion molecule that is normally localized to the cell–cell interface and it has been reported that downregulation of E-cadherin expression is associated with invasion and metastasis of human cancers. About 50% of diffuse gastric carcinomas have revealed mutations of the E-cadherin gene and frequently have in-frame skipping of exon 9 at the early stage of progression. Becker et al. developed a specific antibody E-cad delta 9-1 (clone 7E6; D9) against an epitope that spans the fusion junction region between exons 8 and 10 of E-cadherin and immunohistochemically demonstrated tumor cells that lacked E-cadherin exon 9 [3]. Using this antibody, we examined a case of multiple diffuse gastric carcinoma and demonstrated the presence and absence of exon 9 skipping of E-cadherin in several tumor lesions.

A 28-year-old woman, whose familial history was not examined, underwent total gastrectomy due to an advanced cancer. The operation specimen revealed two flat-depressed (IIc type of Japanese Classification of Gastric Carcinoma) lesions, 18 mm and 9 mm in greatest diameter, at the posterior wall and the anterior wall of the antrum, respectively, as well as a small ulcerated lesion, 23 mm in greatest diameter, with converging folds at the posterior wall of the lower corpus. This tumor reached the subserosa. The larger IIc-type tumor focally invaded the submucosa and the smaller one was confined to the mucosa. Additionally, microscopic examination of the background mucosa disclosed more than one hundred minute, intramucosal lesions within 5 mm in diameter (Fig. 1a and b). No lymph node metastasis was detected. All the lesions were diffuse carcinomas including signet ring cells, but in situ carcinoma as reported by Carneiro et al. in familial diffuse gastric cancer [4] was not detected. Macroscopically discernible, the three lesions were subjected to immunohistochemistry with D9 and E-cadherin monoclonal antibody (mAb) clone 36 (Transduction Laboratories, Lexington, MA, USA; 1:1500), recognizing the intracytoplasmic domain common to both mutant and normal E-cadherin. The three lesions and their surrounding non-neoplastic epithelia were positive for mAb clone 36, whereas only the larger IIc-type tumor, which invaded the submucosa, was positive for D9 (Fig. 1c and d). The small ulcerated lesion, which invaded the subserosa, and minute cancers were negative for D9 (Fig. 1e and f). These findings suggest that D9-positive cancer is not always aggressive although patients with D9-positive gastric carcinomas often showed poor survival.

Gastric carcinomas are characterized by various growth patterns. In particular, superficially spreading intramucosal carcinomas are peculiar to the stomach. Regarding the histogenesis of superficially spreading tumors, two concepts have confronted each other: monoclonal versus field (multiclonal) cancerization. The latter explains a wide mucosal lesion to be formed by the fusion of multiple tumors that arise independently. Histological studies on this problem have given us only circumstantial evidence. Among the diffuse gastric carcinomas, signet ring cell carcinoma has been reported to arise from the glandular

M. Bamba (✉)
Department of Pathology, Saiseikai Shiga Hospital,
Imperial Gift Foundation Inc.,
Oh-hashi 2-4-1,
520-3046 Ritto, Shiga, Japan
e-mail: mbamba@belle.shiga-med.ac.jp

H. Sugihara · T. Hattori
Department of Pathology, Shiga University of Medical Science,
Ohtsu, Shiga, Japan

K.-F. Becker · I. Becker · H. Höfler
Institut für Allgemeine Pathologie und Pathologische Anatomie,
Technische Universität München,
Munich, Germany

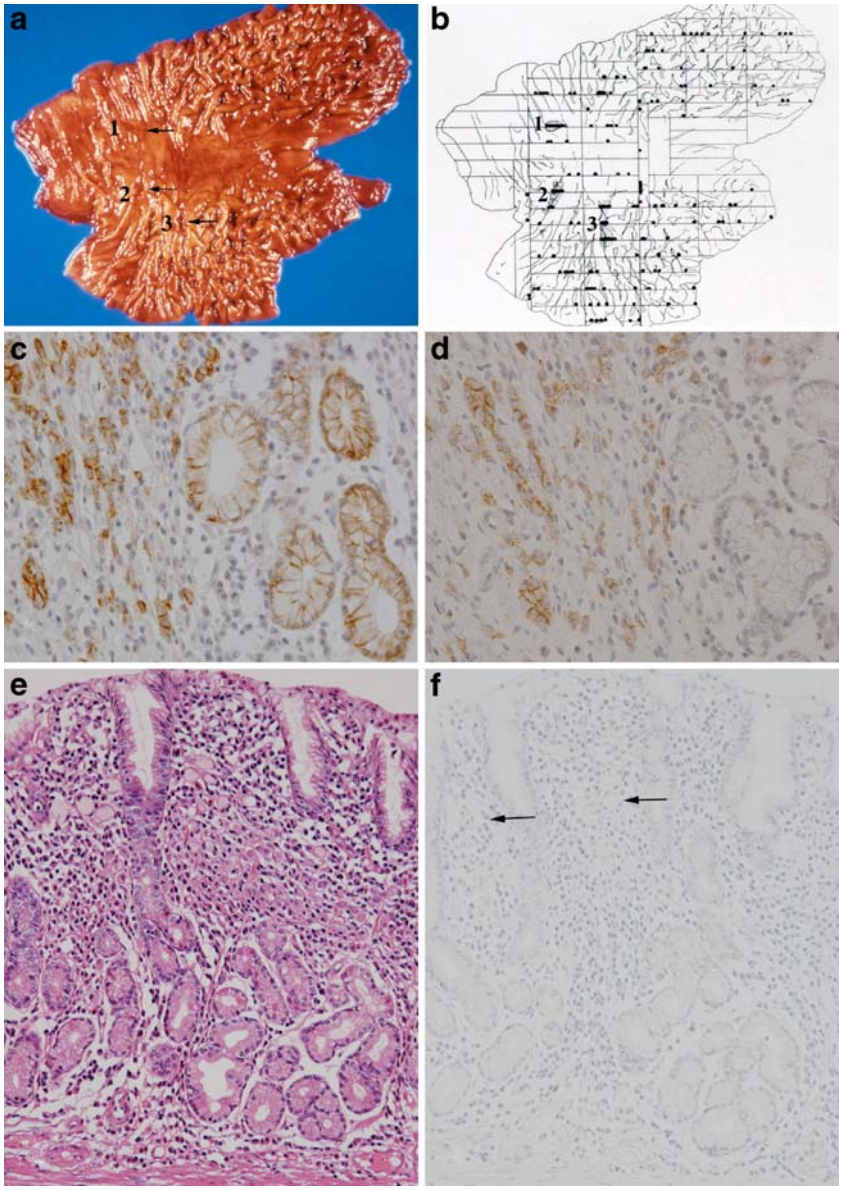


Fig. 1 A case of multiple diffuse gastric carcinoma. **a** *Arrows* show two IIc-type lesions (*nos. 1–2*) and one ulcerated lesion (*no. 3*). **b** The areas hatched with oblique lines are macroscopically discernible carcinomas: *no. 1*, an intramucosal carcinoma; *no. 2*, a submucosal carcinoma; *no. 3*, an advanced carcinoma with invasion to the subserosa. Numerous *dots* in the corpus show minute intramucosal lesions up to 5 mm in diameter, which was detected microscopically. **c**, **d** E-cadherin expression in the mucosal part of a submucosal cancer (*no. 2* in **a** and **b**). Both cancer cells and non-neoplastic epithelia are positive for intracytoplasmic domain of E-cadherin (**c**; E-cadherin clone 36, ×40), whereas cancer cells but not non-neoplastic glands are positive for exon 9 skipping (**d**; D9, ×40). (**e** and **f**) An intramucosal minute tumor shows smaller cancer cells with a small amount of mucin in the middle layer and signet ring cells with abundant mucin in the upper layer (**e**; H & E, ×20). The cancer cells, including signet ring cells (*arrows*), are negative for D9 (**f**; D9, ×20)

neck zone of the proper gastric epithelium and often shows a superficially depressed growth pattern. It is also known that this type of carcinoma shows intramucosal organized differentiation; immature and smaller cancer cells with a small amount of mucin proliferate in the middle layer at the glandular neck level, whereas terminally differentiated signet ring cells with abundant mucin are distributed in the superficial and deep parts of the mucosa [6]. The cancer cells growing to form this characteristic layered structure appear to retain the polarity of the mucosa, and do not elicit desmoplastic stromal reaction. They seem to retain normal stromal microenvironment, on which the tumor growth is dependent. These characteristics of signet ring cell carcinomas at an early stage explain how a tumor can spread superficially in the mucosa; proliferative cancer cells do nothing but spread at the gland neck zone in the mucosa until the tumor growth acquires independence from the mucosal environment. It is thus expected that such a superficially spreading tumor can be monoclonal. This notion was supported by our previous clonal analyses using Human Androgen Receptor Gene Assay (HUMARA), which demonstrated that most of the superficial gastric cancers of diffuse-type were likely to be of monoclonal origin [1]. There was also a report that intratumor heterogeneity of *TP53* mutation was demonstrated in two of the superficially spreading gastric cancers of differentiated type, suggesting a polyclonal origin [5]. However, this heterogeneity can be explained alternatively by clonal divergence within a single clone because *TP53* mutation is not the earliest event in gastric carcinomas.

The present case has demonstrated that in the D9-positive tumor, virtually all the cancer cells were positive

for D9, indicating that the mutation causing the exon 9 skipping is one of the earliest genetic events in this cancer and can be a good marker of clonality. If the lesions in the present case continue to grow superficially and are fused to each other, the combined tumor should be heterogenous in D9 positivity. However, we have not encountered such a case yet in our previous immunohistochemical analyses with D9 of 44 early signet ring cell carcinomas, of which seven were D9-positive [2]. In these seven cases as well, virtually all the tumor cells were positive for D9. These findings support the monoclonal origin of individual tumors and indicate that fusion of separate tumors in a multiple cancer case may be actually infrequent. This may be because at least one of the tumors, as in the present case, may progress to a symptomatic tumor before the fusion occurs, since the tumor spreading in the mucosa is a very slow process [1].

Acknowledgement M.B. was supported by a grant from the Alexander-von-Humboldt Foundation during a stay to research in Germany.

Conflict of interest statement We declare that we have no conflict of interest.

References

1. Bamba M, Sugihara H, Okada K, Bamba T, Hattori T (1998) Clonal analysis of superficial depressed-type gastric carcinoma in humans. Cancer 83:867–875
2. Bamba M, Sugihara H, Becker KF, Becker I, Hattori T, Stolte M, Hoefler H (2003) Clonality analysis of mutant E-cadherin-positive, diffuse-type early gastric cancers. Virchows Arch 443:387–388
3. Becker KF, Kremmer E, Eulitz M, Becker I, Handschuh G, Schuhmacher C, Mueller W, Gabbert HE, Ochiai A, Hirohashi S, Hoefler H (1999) Analysis of E-cadherin in diffuse-type gastric cancer using a mutation-specific monoclonal antibody. Am J Pathol 155:1803–1809
4. Carneiro F, Huntsman DG, Smyrk TC, Owen DA, Seruca R, Pharoah P, Caldas C, Sobrinho-Simoes M (2004) Model of the early development of diffuse gastric cancer in E-cadherin mutation carriers and its implications for patient screening. J Pathol 203:681–687
5. Iwamatsu H, Nishikura K, Watanabe H, Ajioka Y, Hashidate H, Kashimura H, Asakura H (2001) Heterogeneity of p53 mutational status in the superficial spreading type of early gastric carcinoma. Gastric Cancer 4:20–26
6. Sugihara H, Hattori T, Fukuda M, Fujita S (1987) Cell proliferation and differentiation in intramucosal and advanced signet ring cell carcinomas of the human stomach. Virchows Arch A 411:117–127

Virchows Arch (2008) 452:585–587
DOI 10.1007/s00428-008-0595-8

OpenAccess

LETTER TO THE EDITOR

Autopsy pathology should become a recognised subspecialty

Jan G. van den Tweel

Received: 25 September 2007 / Revised: 28 December 2007 / Accepted: 7 February 2008 / Published online: 6 March 2008
© The Author(s) 2008

Dear Editor,

To say that autopsy rates are declining is like kicking an open door. For more than three decades, hundreds of articles have been written to discuss this phenomenon [6]. No matter the background of the authors, clinicians and pathologists alike regret this decline and are of the opinion that this situation should be reversed in order to assure high quality medical practice [3–5, 7, 9]. However, all these papers have not had the desired effect of reversing this process. It appears that these papers served mainly to benefit the curriculum vitae of the respective authors and their list of citations. In strong contrast with this supposed lack of interest is the fact that a PubMed search for the term "autopsy" over the years 2000–2006 shows more than 10,000 links, indicating that the autopsy is still an important technique to study (mechanisms of) disease.

The reasons for this decline are well known and extensively described [3]. Relatives now are more hesitant than in the past and refuse approval for an autopsy more frequently; or, perhaps, we should say that relatives in the past were as hesitant as relatives are at present but were less likely to contradict the then-well-known (and almighty) doctor. This independence has to be accepted as a fact, there is no reason to believe that this tide will change.

Clinicians share some of the blame. Today, they are, perhaps, less persistent and even less interested in pursuing an autopsy because contacts with recently bereaved families are difficult, and many clinicians believe that modern imaging techniques supply them with enough critical information. Moreover, in today's specialty and clinic orientated practice, the clinicians have less personal contacts with the patient and the relatives, and the chance that a patient dies in the presence of his own doctor is not what it was in the past. This situation will not change in the near future. Therefore, this looser relationship has to be accepted as a fait accompli, and no drastic changes can be foreseen that will influence the autopsy numbers in this respect.

Finally, the various 'medical authorities' are also not very helpful. Requirements for specified numbers of autopsies for certification of hospitals and for residency training programmes were abolished long ago, often followed by the withdrawal of funding to perform autopsies.

So what are we left with? Do we have to accept the situation as it is, or is there something that we, as pathologists, can do? It is strange that pathologists, although we must share responsibility for the waning of the autopsy, often are left in the shadow. Sometimes, long delays in the reporting of autopsy findings is mentioned as a cause of clinical dissatisfaction, but the professional competence of pathologists is almost never an issue. Yet a lot can be gained here. What are the facts?

- Many pathologists are not interested in autopsies and/or see them as a burden.
- Many pathologists lack sufficient clinicopathological background to adequately answer the questions of their clinical colleagues.
- Reports are often so delayed that the critical features of the case have been lost from memory, and interest therefore, is low.
- Reports often do not contain the relevant answers.
- In some occasions, the reported results are evidently wrong.

J. G. van den Tweel (✉)
Department of Pathology H4 312,
University Medical Center Utrecht,
Heidelberglaan 100,
3584 CX Utrecht, The Netherlands
e-mail: j.vandentweel@umcutrecht.nl

Let us examine these facts one by one.

Many pathologists are not interested in autopsies There is nothing wrong with the fact that some, or even many, pathologists have little direct interest. We accept that we have among our colleagues dermatopathologists, GI pathologists, etc. But for some reason, there is a widely held perception that every pathologist should be able to perform, or at least supervise, autopsies "to equally share the burden", as is often said. This is a very strange and illogical perception. Nobody expects a general pathologist to diagnose a difficult myeloproliferative disorder or an unusual neurodegenerative disease or recognize a Sanderson's polster, when they see one. But we nevertheless expect him/her to perform with aplomb an autopsy on a complicated intensive care unit (ICU) patient with multiorgan disease. The same problem is also seen at resident level. The UK already offers pathology training programmes without autopsy training. At a recent course for first year pathology residents in the Netherlands, I asked the 25 residents how many of them would choose such a training if offered. Five answered positively and six indicated that they would prefer never to do autopsies as a pathologist. Worse is the situation when pathologists openly put the value of autopsies up for debate. Unfortunately, this happens with increasing frequency.

Many pathologists lack sufficient pathophysiological knowledge Performing autopsies not only requires a solid basis in the field of general pathology but also in the common problems of clinical medicine and in basic anatomy and physiology. The pathophysiology of the circulatory, respiratory and renal system, in addition to that of the clotting system, should be well known. Familiarity with ICU complications and their treatment is mandatory for adequate interpretation of what may be encountered in many autopsy cases. Also, the interpretation of the pathology of shock versus post mortem changes requires special training. We cannot expect that every pathologist has the time and interest to keep his competencies updated in such a broad and complex field, certainly if he/she, with the declining autopsy rates, will only occasionally be responsible for an autopsy.

Reports are often delayed The fact that autopsies are often reported after many weeks or even months (and sometimes not at all) is well known and constitutes a complaint in various articles discussing autopsy decline. The responsible clinician has, in the meantime, often moved to another rotation or has forgotten the details of the disease history and has also sent the final report about the patient to the GP of the patient; thus, the case is 'closed' in his/her mind. This type of disconnect certainly is a source for irritation and will contribute to reluctance in asking another autopsy approval.

Many autopsy reports do not contain relevant answers to the questions raised during life. It must be said that the autopsy request forms often contain marginal and/or incomplete information [2]. However, the questions raised should be answered and in an epilogue the morphological findings should be interpreted in the clinical context and vice versa. Only then the patient's file can be closed with confidence.

In some instances, the reports provide wrong information These types of errors can be due to misinterpretation of findings, often because of lack of detailed knowledge of the clinical course leading up to death, coupled with lack of insight in pathophysiological phenomena or due to hurry or even neglect [2]. The circumstances surrounding Dr. Shipman's cases are a good example of this situation, where deaths were reported as cardiac events without sufficient evidence for such a diagnosis [8]. Similar situations might happen everywhere. This type of publicity, certainly when combined with tissue retrieval problems, will most certainly influence the attitude towards autopsies of the general public and medical professionals.

These facts taken together raise real concern as to the contribution of 'Pathology' and pathologists in the decline in autopsy rates and, in effect, cry out for another approach by our profession to the performance of autopsies. Moreover, we cannot close our eyes to such new approaches as limited autopsies, CT and MRI procedures followed by needle biopsies and so on [1, 3]. Certainly, in the light of the declining autopsy rates, where it is difficult to acquire sufficient experience in performing, interpreting and reporting autopsies, it is necessary that the pathologists who perform autopsies are enthusiastic, interested, competent and respected for their knowledge in this field. Only then are they good sparring partners for the clinicians and good teachers for our residents.

The only way to achieve this goal is to accept Clinical Autopsy Pathology as a recognised subspecialty within our profession, in the same way as other subspecialties. A period of additional training in intensive care medicine would be desirable—to learn the language of the intensive care unit which, because of the critical condition of many ICU patients, is the source of a significant number of autopsies and certainly the most complicated ones. Or possibly, there is even a case for incorporating a year of clinical experience in Medicine and Surgery into the training of a Clinical Autopsy Pathologist, an experience

that surely contributed to the high level of competence that many of our illustrious predecessors displayed in autopsy pathology. Of course, there should be room for subspecialists who will usually perform their own autopsies, e.g. paediatric pathologists and neuropathologists.

In conclusion, the decline in autopsy rates is a progressive one. It is time for us, the pathologists, to finally do something constructive other than to weep and wail. We have to bring our best men and women in the frontline and respect their work as highly as any other recognised subspecialty. It is that or the end of the autopsy. What if our attempts do not work, and the decline continues? In that case, we have already anticipated some of the measures that must be adopted anyway. There is no way to escape the future; it is coming. But we can reshape it by acting now. I, therefore, sincerely hope that this letter will not prove to be just an addition to my list of publications.

Open Access This article is distributed under the terms of the Creative Commons Attribution Noncommercial License which permits any noncommercial use, distribution, and reproduction in any medium, provided the original author(s) and source are credited.

References

1. Benbow EW, Roberts ISD (2003) The autopsy: complete or not complete. Histopathology 42:417–23
2. Bove KE, Iery C, Autopsy Committee of the College of American Pathologists (2002) The role of autopsy in medical malpractice cases. II. Controversy to autopsy performance and reporting. Arch Pathol Lab Med 126:1032–1035
3. Burton JL, Underwood J (2007) Clinical, educational, and epidemiological value of autopsy. Lancet 369:1471–1480
4. Eresi M, Ansorge O (2007) Autopsy: not dead. Lancet 367:568
5. Hull MJ, Nazarian RM, Wheeler AE, Black-Schaffer WS, Mark EJ (2007) Resident physician opinions on autopsy importance and procurement. Hum Pathol 38:342–350
6. Roberts WC (1978) The autopsy: its decline and a suggestion for its revival. N Engl J Med 17:332–338
7. Roulson J, Benbow EW, Hasleton PS (2005) Discrepancies between clinical and autopsy diagnosis and the value of post mortem histology. Histopathology 47:551–559
8. HSMO (2003) The Shipman Inquiry, third report: death certification and investigation of death by coroners.Cm 5854. HSMO, London
9. Zarbo RJ, Baker PB, Howanitz PJ (1999) The autopsy as a performance measurement tool–diagnostic discrepancies and unresolved clinical questions: a College of American Pathologists Q-Probes study of 2479 autopsies from 248 institutions. Arch Pathol Lab Med 123:191–198

Virchows Arch (2008) 452:589–598
DOI 10.1007/s00428-008-0609-6

REVIEW AND PERSPECTIVE

Are columnar cell lesions the earliest histologically detectable non-obligate precursor of breast cancer?

Gulisa Turashvili · Malcolm Hayes · Blake Gilks · Peter Watson · Samuel Aparicio

Received: 14 February 2008 / Revised: 11 March 2008 / Accepted: 13 March 2008 / Published online: 24 April 2008
© Springer-Verlag 2008

Abstract Columnar cell lesions (CCLs) are one of the most common abnormalities in the adult female human breast, characterized by the presence of columnar-shaped epithelial cells lining enlarged terminal-duct lobular units. CCLs are being seen increasingly in core biopsies taken for the non-palpable calcifications. The increased incidence may reflect improved delineation and recognition of CCLs by pathologists or a true increase in incidence related to biological and/or environmental factors. Columnar cell-like lesions have been described under a variety of names such as blunt duct adenosis, flat epithelial atypia, and ductal intraepithelial neoplasia type DIN1a. The current histologic classification used by some pathologists divides them into simple columnar cell change and columnar cell hyperplasia, both of which can occur with or without atypia. Columnar cells lack mature luminal or basal/myoepithelial phenotype markers, but they are usually positive for estrogen receptor-α. The cellular origin of CCLs and their possible relationship to either expansion or metaplasia of a preexisting normal cell phenotype remains unclear. CCLs are frequently associated with lobular and ductal in situ tumors and invasive lobular and tubular carcinomas. The relationship and natural history of CCLs to invasive ductal carcinoma is enigmatic, but they may prove of clinical relevance when detected by screening mammography.

Keywords Columnar cell lesion · Breast cancer · Ductal intraepithelial neoplasia · Mammography

G. Turashvili (✉) · P. Watson · S. Aparicio
Molecular Oncology and Breast Cancer Program,
BC Cancer Research Centre,
675 W 10th Avenue,
V5Z 1L3 Vancouver, British Columbia, Canada
e-mail: gturashv@bccrc.ca

M. Hayes · P. Watson
Department of Pathology, British Columbia Cancer Agency,
Vancouver, British Columbia V5Z 4E6, Canada

B. Gilks
Genetic Pathology Evaluation Centre,
Vancouver General Hospital and University of British Columbia,
Vancouver, British Columbia V6H 3Z6, Canada

Introduction

Columnar cell lesions (CCLs) are one of the most common abnormalities in the adult female human breast and comprise a spectrum of histologic changes characterized by the presence of one to several layers of tightly packed, columnar-shaped epithelial cells in enlarged terminal-duct lobular units (TDLUs). CCLs may have been first recognized in by Warren in 1905 [77], who interpreted them as an abnormal pattern of involution. Subsequently, CCLs have been described by a number of authors and included in lesions termed senile parenchymatous hypertrophy [6], blunt duct adenosis [24, 40], atypical lobules, type A [78], atypical cystic lobules [38], clinging carcinoma [2, 21], hypersecretory hyperplasia with atypia [57], columnar alteration with prominent apical snouts and secretions (CAPSS) [26], enlarged lobular units with columnar alteration, columnar metaplasia [47], focal pregnancy-like changes [48], hyperplastic enlarged lobular units (HELUs) [42], monomorphic epithelial proliferation [28], columnar cell change (CCC) [60], columnar cell hyperplasia (CCH) with or without atypia [12, 60, 64], and flat epithelial atypia (FEA), originally designated as ductal intraepithelial neoplasia 1b (DIN1b) [69], and later as DIN1a [79].

The etiology of CCLs is unknown. However, for reasons that are not yet understood, they are increasingly encountered

in core biopsies taken from abnormalities identified by screening mammography [34, 52] and therefore raise important management questions [32, 36]. In particular, CCLs are found in biopsies taken for the histological assessment of non-palpable, mammographically detected calcified lesions [14, 27, 58]. Little is known about the underlying biology of microcalcifications in pre-neoplastic and pre-invasive lesions. However, since the microcalcifications that occur in CCLs are indistinguishable radiologically from those seen in atypical ductal hyperplasia (ADH; DIN1b) and ductal carcinoma in situ (DCIS), needle biopsy or excision is required for diagnosis [3, 4, 7, 37]. The increased incidence of CCLs may reflect improved recognition by pathologists or reflect the increasing representation of biopsies generated by mammographic screening. However, a true increase in incidence related to biological and/or environmental factors cannot be excluded. The increased occurrence of CCLs in biopsies has proved a challenge with regards to accurate diagnosis and distinction from other breast lesions. Furthermore, there is a need to delineate the risk of CCLs, either with regards to the likely presence of co-existent cancer in the adjacent breast or in terms of risk for subsequent development of invasive malignancy.

Morphology, terminology, and histologic classification of CCLs

CCLs of the breast represent a spectrum of lesions that have in common the presence of variably dilated TDLUs lined by columnar epithelial cells. For practical purposes, CCLs can be placed into two broad groups: CCC or CCH, both of which can occur with or without atypia [60].

CCC represents the simplest form of CCL, in which TDLUs display variably dilated acini lined by one to two layers of columnar epithelial cells with uniform, ovoid to elongated nuclei oriented perpendicular to the basement membrane. The nuclei have evenly dispersed chromatin and inconspicuous nucleoli (Fig. 1a). Apical cytoplasmic blebs or snouts are often present at the luminal surface of these columnar cells, suggesting an active apocrine secretory machinery, but this is not always as prominent or exaggerated as that associated with apocrine cells. Flocculent secretions and calcifications may be present in the lumina of the involved acini. Mitotic figures are rare [64]. We have also noted angulation in dilated acini showing CCC (Fig. 1c). This feature could be related to an altered hormonal stimulus or stromal response that may influence the evolution of CCLs.

CCH manifests with similar cytologic features to those seen in CCC but differs in that acini are lined by more than two layers of columnar cells that may also show crowding, overlapping, form small mounds, tufts, or short micropapillae (Fig. 1b). Exaggerated apical cytoplasmic snouts and intraluminal secretions are more often present than in CCC, and some of the cells may have a hobnail appearance with nuclei displaced to the luminal end of the cell. Intraluminal calcifications, sometimes with the configuration of psammoma bodies, may be present [64]. Intralobular lymphocytic infiltration is not uncommon.

Some CCLs with the architectural features of CCC or CCH show cytologic atypia characterized by cells containing round or ovoid (rather than elongated) nuclei lacking the normal perpendicular orientation to the basement membrane and showing a slight increase in nuclear/cytoplasmic ratio. The nuclear chromatin may be evenly dispersed or slightly marginated, and nucleoli are variably prominent. In some cases of CCLs with atypia, the cells may show a striking resemblance to those seen in tubular carcinoma, and these lesions may be composed of cells with cuboidal rather than columnar morphology. While atypia can be easy to distinguish in the context of some lesions, it is sometimes subtle and may be difficult to distinguish from the nuclear changes seen in apocrine cells. Furthermore, the apical decapitation secretions and cytoplasmic eosinophilia are cytoplasmic changes that are common to many CCLs and apocrine cells. Depending on the number of cell layers, atypical CCLs are designated as CCC with atypia (Fig. 1d) or CCH with atypia (Fig. 1e).

According to the current WHO classification, the traditional classification system for the intraductal proliferative lesions includes usual ductal hyperplasia (UDH), FEA, ADH, and DCIS (low, intermediate, and high grade) [79]. To overcome disadvantages of this system such as interobserver variability and to emphasize the neoplastic rather than hyperplastic nature of the process, an alternative terminology of ductal intraepithelial neoplasia (DIN) has been proposed. In this scheme, DIN is defined as a proliferation that serves no physiologic function, and the term "carcinoma" is restricted to lesions that have invaded the stroma. FEA has been previously designated as DIN1b [69]. In the latest revision of the DIN system, UDH is not included, FEA is designated as DIN1a, ADH (minute well-differentiated DCIS) as DIN1b, low-grade DCIS as DIN1c, intermediate-grade DCIS as DIN2, and high-grade DCIS as DIN 3 (Table 1) [79]. A possible criticism of the DIN classification is that it includes entities whose actual neoplastic nature has not been fully demonstrated (FEA or DIN1a). This three-tier grading system of DIN also suggests a possible progression from lower to higher grade lesions, similar to in situ lesions in other organs (e.g., cervix), but this has not been documented for the breast [75]. The WHO recommends that for purposes of clinical management and tumor registry coding, when the DIN terminology is used, the traditional terminology should be

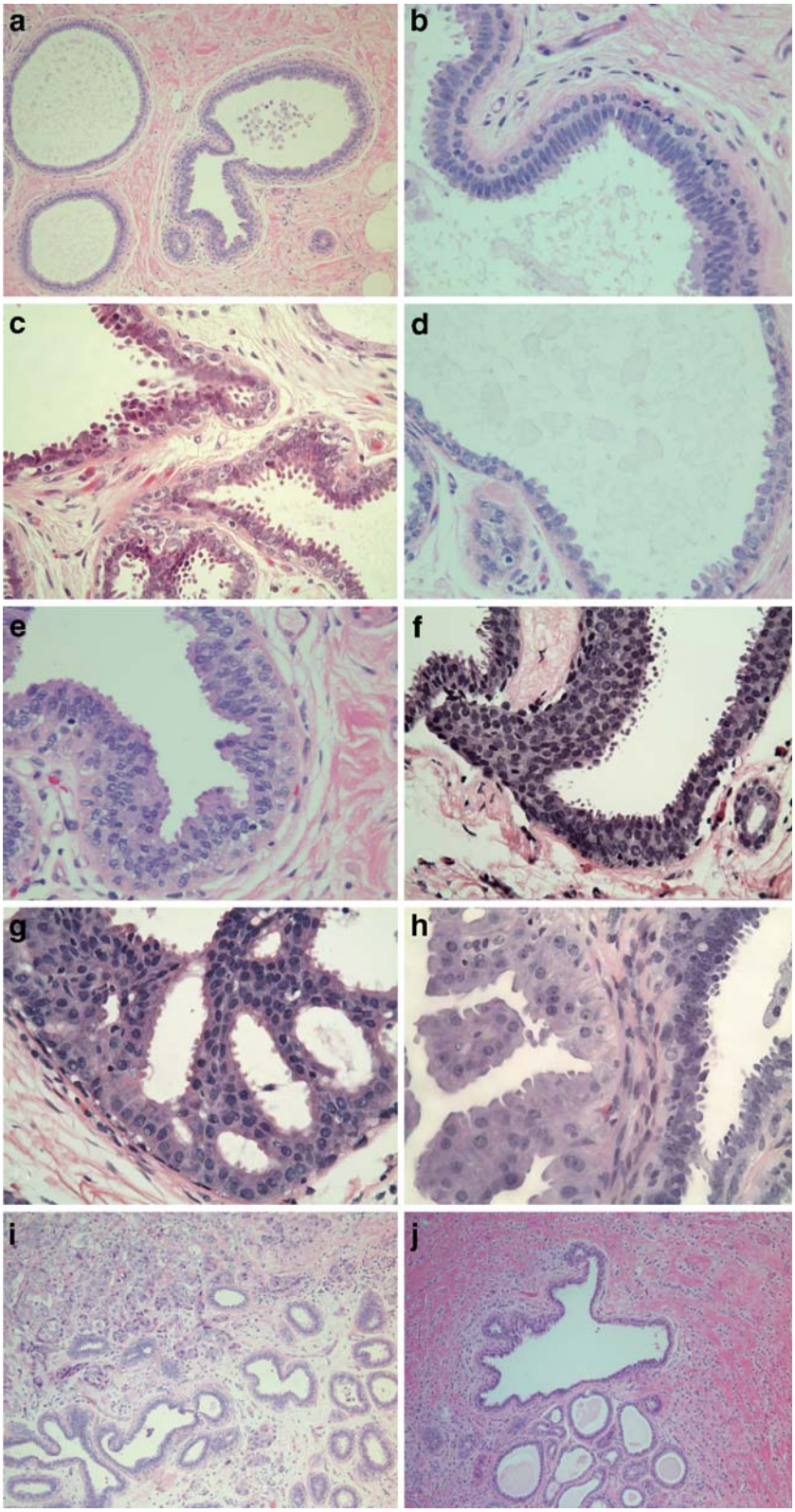


Fig. 1 **a** Columnar cell change without atypia. **b** Columnar cell hyperplasia without atypia. **c** Angulation in acini showing columnar cell change. **d** CCC with atypia (DIN1a). **e** CCH with atypia (DIN1a). **f** Flat epithelial atypia (DIN1a). **g** Atypical ductal hyperplasia with columnar cell change. **h** Columnar cell lesion and superimposed apocrine metaplasia. **i** Invasive ductal carcinoma with columnar cell lesion. **j** Invasive lobular carcinoma with columnar cell lesion. H&E, ×100 (**a**, **i**, **j**) and ×400 (**b**–**h**)

mentioned as well [79]. In our opinion, one advantage of the DIN classification is that it best describes the variation in patterns of the intraductal proliferative lesions while maintaining the concept of a morphological continuum from 'flat atypia' (DIN1a) through 'ADH' (DIN1b) to low-grade DCIS (DIN1c) and low-grade invasive cancer. It is likely that higher grades of DCIS (DIN2, DIN3) represent an unrelated process to the DIN1 spectrum. DCIS grade 1

Table 1 Classification systems of intraductal proliferative lesions

Traditional classification system [79]	Ductal intraepithelial neoplasia classification system [70, 79]	Alternative terms
Usual ductal hyperplasia	Usual ductal hyperplasia	Intraductal hyperplasia; ductal hyperplasia of usual type; ordinary intraductal hyperplasia; epitheliosis [50]
Flat epithelial atypia	Ductal intraepithelial neoplasia, grade 1a (DIN1a)	Low grade flat lesion [50]; Clinging carcinoma, monomorphic type [2]; Columnar cell hyperplasia with atypia [64]; Columnar cell change with atypia [64]; Atypical cystic lobules [10, 38]; Atypical lobules type A [78]
Atypical ductal hyperplasia	Ductal intraepithelial neoplasia, grade 1b (DIN1b)	Small (<2 mm) low grade DCIS [69]
Ductal carcinoma in situ, low grade (DCIS grade 1)	Ductal intraepithelial neoplasia, grade 1c (DIN1c)	Intraductal carcinoma, low grade
Ductal carcinoma in situ, intermediate grade (DCIS grade 2)	Ductal intraepithelial neoplasia, grade 2 (DIN2)	Intraductal carcinoma, intermediate grade
Ductal carcinoma in situ, high grade (DCIS grade 3)	Ductal intraepithelial neoplasia, grade 3 (DIN3)	Intraductal carcinoma, high grade; Clinging carcinoma, pleomorphic type [2]; High grade flat lesion [50]

has been suggested to be a multilobar/multicentric lesion involving more than one quadrant and resembling to lobular carcinoma in situ (LCIS), whereas DCIS grades 2 and 3 seem to be confined to one lobe in most cases [25]. Some variants of FEA have also been described under the term "clinging carcinoma" of the monomorphic type [2, 20, 21]. FEA shows "variably dilated acini lined by one to several layers of columnar epithelial cells with low-grade cytologic atypia"—changes that are identical to CCC with atypia and CCH with atypia described above, and we consider these lesions to be synonymous (Fig. 1f). CCL without atypia is not included in the DIN classification and should be reported separately.

Notably, flat lesions can harbor low- or high-grade cytological changes, and these should be distinguished. Flat lesions with high nuclear atypia are classified as DIN 3 (DCIS, high-grade or polymorphous variant of clinging carcinoma in situ). High- and low-grade types of clinging carcinoma were originally recognized by Azzopardi et al., who suggested that the high-grade variant tends to progress to comedocarcinoma, whereas the low-grade variant represents the precursor for low-grade micropapillary/cribriform DCIS [2]. This hypothesis has been supported by immunohistochemical [17], genetic [51], and clinical [20] studies. Furthermore, FEA should not be confused with blunt duct adenosis (BDA). In contrast to FEA, BDA shows dilated tubules with blunt lateral outlines, simultaneous proliferation of non-atypical epithelial and myoepithelial cells, and increased intralobular connective tissue. While the proliferating cells in FEA are negative for CK5/6, luminal cells in BDA often show a heterogeneous positive reaction for CK5/6 [50]. Thus, BDA is a synonymous term for some examples of CCL without atypia, whereas FEA designates CCL with atypia.

Some CCLs contain ducts that show more complex architectural patterns such as micropapillary formations, rigid cellular bridges, bars and arcades, or sieve-like fenestrations. Some degree of cellular polarization may be present within the micropapillary formations and bars or around the fenestrations. Rosen [60] suggested categorizing these lesions as CCH with moderate or severe atypia, but Schnitt [63] believed that such lesions should be categorized under the terms ADH or DCIS, depending on the severity and extent of the cytologic and architectural features. He suggested that the term "columnar cell hyperplasia with atypia" should be reserved for those lesions with cytologic and architectural features insufficient to establish a diagnosis of ADH (DIN1b) or low-grade DCIS (DIN1c; Fig. 1g). The frequent co-existence and continuity between these lesions illustrates the diverse morphology of the DIN1 process.

The simple classification of CCLs has been modified by Simpson et al. [67] to include six categories: type 1, CCC showing one to two layers of columnar cells with uniform ovoid/elongated nuclei and no/inconspicuous nucleoli; type 2, CCH showing more than two cell layers with nuclear crowding and micropapillary formations but no complex architecture (the cytology is similar to type 1 but may have hobnail cells and intraluminal calcifications); type 3, CCH with more than two cell layers with complex atypical architecture (micropapillary, tufts, fronds, arcades, rigid bridges, punched out spaces) and type 2 cytology; type 4, CCH with type 2 architecture and mild to moderate cytologic atypia, resembling that of tubular carcinoma; type 5, atypical CCH with type 3 architecture and type 4 cytology; type 6, atypical CCC with one to two cell layers and type 4 cytology.

Goldstein et al. [28] defined monomorphic epithelial proliferations (MEPs) as a slightly overcrowded, predominantly single layer of monomorphic, luminal epithelial

cells that involve TDLUs in an overgrowth extension pattern and tend to retain the architecture of the TDLU or expand the acini in an unfolded lobule-like pattern. Cytologic features in MEPs were segregated into three major subtypes: type 1, columnar cells with uniform ovoid to elongated nuclei, absent or inconspicuous nucleoli, and apical cytoplasmic snouts; type 2, cuboidal cells with mildly enlarged, round to oval nuclei with irregularly thickened nuclear membrane, punctate to prominent nucleoli, modest amounts of cytoplasm, inconspicuous cytoplasmic membranes; type 3, cuboidal to columnar cells with scant cytoplasm and round to slightly ellipsoid nuclei with irregularly thickened nuclear membrane, open or finely speckled chromatin and inconspicuous nucleoli. MEP lesions were significantly more frequent near the initial excision margin in patients with clonally related local recurrences than in patients with clonally distinct recurrences or no recurrences. Some MEPs in clonal and distinct local recurrence cases shared allelic imbalance microsatellite markers with their respective initial carcinoma. The authors concluded that MEPs seem to be the pool of partially transformed precursor lesions for most invasive carcinomas in which they could potentially be eradicated by radiotherapy, preventing new carcinomas from emerging rather than eradicating microscopic residual disease.

Complex classifications have merits for facilitating research to define different biology but are unlikely to gain acceptance or be deployed for clinical use. Perhaps more important than complexity is the issue of reproducibility. Reproducibility of histological diagnosis of CCLs using the simpler classification has been studied by several groups. O'Malley et al. [54] showed that the differential diagnosis of FEA and CCLs without atypia was highly reproducible among eight pathologists. Following review of a tutorial, the pathologists examined images from 30 CCLs and categorized lesions as either FEA or not atypical. Overall agreement was 91.8% (95% CI, 84.0–96.9%), and the multi-rater kappa value was 0.83 (95% CI, 0.67–0.94), which is within the "excellent agreement" range. In another study, Tan et al. assessed the inter/intraobserver variability in the interpretation of CCLs using 39 images presented to seven pathologists. Lesions were categorized as follows: 0, no CCC or DCIS; 1, CCC; 2, CCH; 3, CCC with architectural atypia; 4, CCC with cytological atypia; and 5, DCIS. Diagnostic reproducibility with the tutor ranged from "moderate to substantial" (kappa values, 0.439–0.697) in the first exercise. At repeat evaluation 1 week later, intraobserver agreement was "fair to perfect," whereas concordance with the tutor varied from "fair to substantial". There was unanimous agreement on more images during the second exercise, mainly because of agreement on the diagnosis of DCIS. The lowest agreement was seen for CCC with cytological atypia [68]. Notably, all pathologists were experts in breast disease and had a similar training background. Furthermore, these studies used digital images showing selected microscopic fields and used selected cases. In everyday practice, interpreting breast biopsies containing multiple heterogeneous CCLs by anatomical pathologists leads to less reproducible results.

The lack of standardized terminology has been a serious obstacle to wide recognition of CCLs by practicing pathologists and clinicians. The authors of this review currently use the "columnar cell" classification in conjunction with the DIN classification in everyday practice. The former is more widely known at present amongst clinical colleagues, but the latter terminology is gaining acceptance and avoids the inappropriate labelling of a neoplastic condition as "hyperplasia," encompasses the diversity in morphology of the lesions, many of which are composed of flat or low cuboidal rather than "columnar cells," and maintains the concept of a continuum between the various grades of the DIN1 process. We believe that the DIN terminology is the best compromise based on the current status of knowledge about these abnormalities.

Immunohistochemical markers of CCLs

To explore the question of etiology and to improve the distinction of CCLs from other breast lesions, immunohistochemical techniques have been employed. CCLs have been shown to be estrogen receptor alpha (ER-α) and progesterone receptor (PR) positive and negative for basal keratins CK5/6 and cytokeratin 14 (CK14) [67, 74]. CCH has been found to be composed of Bcl-2(+), ER(+), and PR(+) cells [44], and this specific phenotype can be used to distinguish CCLs from apocrine lesions [76]. Immunohistochemical studies of benign and malignant apocrine cells have shown that they are frequently androgen receptor (AR) positive but lack ER and PR, contrasting with the normal breast epithelium [19, 71]. This suggests that apocrine cells differ from non-apocrine luminal cells and columnar cells, not only cytologically but also biologically, and that these three types of epithelial cells in the TDLU may represent different lineages of mammary stem-cell differentiation.

In another study, expression of ER-α, PR, and AR in CCLs (described as CAPSS lesions) paralleled that of the synchronous in situ or invasive breast tumors that occurred. In some cases where the CCLs were negative for steroid hormone receptors, the coexisting in situ or invasive carcinoma was also negative for the steroid receptors. Interestingly, E-cadherin immunostaining was reduced in 81% of CCLs hinting at an immunophenotypic link between CCLs and lobular neoplasia [18].

McLaren et al. studied CCLs, termed by these authors "enlarged lobular units with columnar alteration" in 82

women who subsequently developed invasive breast cancer and compared them with a control group of 166 women who did not develop invasive breast cancer. ER-α was positive in 39% of study cases and 56% of controls. The relative risk of invasive breast cancer in women with ER-α-negative CCLs was 1.85 times that of women with ER-α-positive lesions. The presence of ER-α staining in women with CCLs was associated with a lower risk of developing subsequent invasive carcinoma [47]. However, the relatively high number of ER-negative cases in this study raises questions about its applicability to CCLs in general practice, since the majority are ER-positive lesions.

Proliferation, as measured by Ki67 index assessed by Mib-1 immunostain, is very low in simple CCC and intermediate between normal and DCIS in the CCLs with hyperplasia or atypia. Noel et al. assessed Ki67 index in CCLs without atypia, CCLs with atypia (described as FEA lesions), low-grade DCIS, and high-grade DCIS. They found the Ki67 index was extremely low in CCLs without atypia (CCC mean 0.1% and CCH mean 0.76%)—paradoxically lower than in normal TDLUs (mean 2.4%; $p<0.001$). In the presence of atypia, the Ki67 index was higher (mean 8.2%; $p<0.001$) but still lower than that seen in low-grade DCIS (mean 25.4%; $p<0.001$) [53].

Immunohistochemical analysis of some other proteins relevant to breast cancer progression has also been undertaken. CCH with atypia showed positive immunostaining for the tumor suppressor 14-3-3σ in 93% of cases. Strong immunoreactivity for 14-3-3σ was always seen in the myoepithelial cells located in the outer circumference of a dilated cystic lesion. In contrast, the inner luminal cells usually lacked immunoreactivity for 14-3-3σ. Only three (21%) of 14 lesions showed focal to diffusely positive immunoreactivity for 14-3-3σ in both luminal and myoepithelial cells. Of these three cases, only one was CK14 positive, and this case was also smooth muscle actin negative. All CCH lesions were positive for ER-α, and none were positive for p53. About half of the CCH with atypia exhibited decreased staining intensity for estrogen-responsive finger protein Efp [66]. The majority of the luminal cells exhibited expression of CK19 but not high molecular weight cytokeratins using 34 beta E-12 and CK5/6 antibodies [55]. In CCLs, 5% to 50% of the cells stained for cyclin D1 [56].

In summary, these studies showed that CCLs are commonly ER-α positive and usually lack markers associated with basal/myoepithelial or apocrine phenotypes. Nevertheless, they share many features with mature luminal cell differentiation. Since the differentiation and function of the epithelium of the normal mammary gland depends strongly on steroid and other hormones mediated by the cellular expression of receptors, it is likely that the development of CCLs is influenced by stimulation of the mammary epithelium by steroid hormones and/or growth factors.

Secretions of CCLs

The breast is considered a modified and highly specialized type of apocrine sweat gland. The latter gland produces odor, does not function prior to puberty, and probably serves a vestigial sexual function. Although apocrine sweat glands were thought to secrete their products by an apocrine mechanism, in which the apical portion of the cell is released with the secretory products, they are now believed to secrete in a merocrine fashion. During lactation and stimulation by prolactin, milk proteins are secreted by merocrine secretion (exocytosis), while lipids are secreted by an apocrine mechanism. Since both apocrine and columnar epithelial cells exhibit apical snouts, they may share the apocrine mechanism of secretion, and the secretory products are likely to be lipids and fat-binding proteins. However, this remains to be clarified. The secretory products of CCLs are abnormal in that they calcify. We have observed that some secretions in the lumina of CCLs are basophilic mucin, while others are eosinophilic and flocullent or granular. This contrasts with the pale eosinophilic non-granular secretions typically seen in normal breast ducts and lobules.

Genetic alterations in CCLs

The genetic alterations in CCLs are not well characterized. DNA microarray technology has been applied to microdissected pure epithelial cells from CCLs (described as HELUs). Changes in ERBB genes were particularly prominent, including a uniform switch in ligands for the ERBB1 receptor (14-fold decrease in epidermal growth factor and 10-fold increase in amphiregulin, respectively) in CCLs compared with normal TDLUs. These results suggest that CCLs may differ from TDLUs primarily in the activation of pathways involved in embryonic development and suppression of terminal differentiation [41].

Three cases displaying the entire spectrum of CCLs through to DCIS and including foci of invasive carcinoma were microdissected at multiple sites to evaluate any progressive relationships between these lesions. Allelic imbalance for a broad panel of microsatellite markers in proximity to known tumor suppressor genes was quantitated using polymerase chain reaction. Mutations were present in one case of CCH but not in CCC. Progressive accumulation of allelic damage was seen in CCC with atypia, DCIS, and invasive carcinoma. Low levels of allelic imbalance were demonstrated in simple CCLs, while the fractional mutation percentage increased progressively from CCH through invasive carcinoma. Allelic loss damage appeared to preferentially target loci at 9q, 10q, 17p, and 17q. The findings support the hypothesis that atypical

CCLs are morphologic precursors to invasive carcinoma [13]. This hypothesis is also supported by a comparative genomic hybridization study showing that CCLs exhibit low numbers of genetic alterations and recurrent 16q loss, features that are similar to those of low-grade in situ and invasive carcinoma. These molecular genetic profiles closely reflect the degree of proliferation and atypia in CCLs, suggesting that the lesions represent both a morphologic and molecular continuum. Overlapping chromosomal alterations between CCLs and architecturally complex lesions (DIN1b-1c) also suggests a commonality in molecular evolution [67]. Critics of these studies emphasize that the CCLs analysed were taken from cases that showed adjacent ADH or DCIS, and the results may not be applicable to CCLs occurring in the absence of such higher-grade lesions. Therefore, further studies encompassing larger cohorts are needed to explore the link between CCLs and in situ or invasive tumors and further define their premalignant potential and to elucidate factors that determine rate of progression to invasive malignancy.

Possible relationship of CCLs to mammographic density

Breast cancer is a multifactorial disease which is believed to be related to a number of risk factors such as age, nulliparity or first pregnancy at older age, genetic predisposition (BRCA1, BRCA2), personal and family history of breast cancer, previous abnormal biopsy results, mammographic density, obesity, radiation, early onset of menarche, alcohol, smoking, and hormone therapy [22, 35, 39, 46, 72]. After age and BRCA1/2 genetic predisposition, high mammographic density is the third largest population risk factor for subsequent development of in situ or invasive carcinoma ([8, 9, 49]. The basis of the risk carried by mammographic density is unknown; however, density is thought to associate with increased epithelial and stromal elements (as opposed to adipose tissue or water). It can be hypothesized that the presence of CCLs could explain the increased risk of invasive carcinoma inherent in high mammographic density. It is currently unknown whether the presence and type of CCLs correlate with mammographic density; this will be the focus of future studies.

Biological and clinical significance of CCLs

The available evidence shows that CCLs are frequently associated with many types of breast carcinoma (Fig. 1i, j). Whether the risk for subsequent development of breast cancer is due to the presence of CCLs alone or whether CCLs predict the development of higher-risk lesions such as ADH and DCIS is currently unknown. CCLs are frequently associated with both lobular and low-grade ductal in situ tumors and especially with lobular and tubular subtypes of invasive carcinoma [29, 30, 33, 61, 62]. Leibl et al. [43] studied excisional breast biopsy specimens containing lobular neoplasia (LN) but not DCIS or invasive carcinoma. They showed coexistence of LN and CCLs with atypia in 86.5% of cases ($p<0.001$). The distribution of LN was focal in 37%, multifocal in 45%, and extensive in 18% cases. CCLs were identified as focal, multifocal, and extensive in 26%, 38%, and 23% cases, respectively. Co-localization of CCLs, ADH, DCIS, and tubular carcinoma was seen in 85% patients. In most cases, these lesions displayed common cytological features. Brogi et al. [10] reported that the overall incidence of FEA (reported as atypical cystic lesions) in breast biopsies was 56%, including 60% of cases with LCIS and 46% of cases with atypical lobular hyperplasia (ALH). In another study, CCLs were seen in association with ADH in 60% of cases and low-grade DCIS in 42% of cases [1]. In a review of cases with 543 DCIS, Collins et al. showed that the presence of FEA was significantly related to low nuclear grade of the DCIS, micropapillary and cribriform architectural patterns, and absence of comedo necrosis. There was also a strong association with the presence of ADH (DIN1b) and lobular neoplasia [11].

DIN1a has been suggested to be a marker of slightly increased risk for subsequent development of invasive breast carcinoma. In a retrospective review of 1,751 core biopsies, there were found 63 cases of DIN1a, nine of which (14.3%) had diagnosed an infiltrating carcinoma on subsequent biopsies. Although an excisional biopsy is not mandatory after DIN1a is found on core biopsies, close follow-up is advised with repeat mammograms for early detection of any clinically occult carcinoma in the vicinity of DIN1a that may have been missed by the biopsy [45]. De Mascarel et al. [16] studied the occurrence of epithelial atypias that included flat epithelial atypia (DIN1a), atypical ductal hyperplasia (DIN1b), and LN in 2,833 surgical excisional biopsies from 2,375 patients performed for microcalcifications with a median follow-up of 160 months. Some patients had multiple and/or bilateral breast biopsies. FEA was seen alone in 11%, with ADH (DIN1b) in 35%, with LN in 23%, and with both ADH and LN in 31%. Epithelial atypias were found in 971 cases (34%). A concomitant cancer was present in 301 cases (31%). The associated cancer did not contain calcifications in 10% of cases, and some of the cancers were located away from the index calcifications seen in benign lesions. Concomitant cancers corresponded to DCIS with or without microinvasion (77%), invasive ductal carcinomas not otherwise specified (15%), invasive lobular carcinomas (4%), and tubular carcinomas (4%). In a group of 443 patients, the probability of developing a carcinoma within 10 years of a

diagnosis of a biopsy showing epithelial atypia alone was only 5.5%. However, 15 of the 18 cancers that developed in this group were invasive, and 14 of the cancers occurred in the homolateral breast. The authors concluded that epithelial atypia is more a risk marker of concomitant than subsequent cancer.

A few small follow-up studies of clinging carcinoma (FEA) reported to date suggest a very low risk for subsequent development of invasive cancer [5, 16, 20], but data are limited. Two features of CCLs have been related to the risk of subsequent development of invasive cancer: the presence and the extent of hyperplasia and the presence of atypia. In the retrospective study of Guerra-Wallace et al. [31], the incidence of cancer was evaluated in excision biopsy specimens after an initial core biopsy identifying CCLs (classified as CAPSS with and without atypia). During a follow-up period of 5 years, ten invasive cancers occurred in 135 patients (7.4%) previously shown to have CCLs without atypia, while 11 cases occurred in 60 patients (18.3%) previously shown to have CCLs with atypia ($p=0.023$). Furthermore, CCLs with atypia had a trend towards a higher rate of coexisting cancer on initial biopsy than CCLs without atypia (7% vs 12%, $p=0.320$). Specimens showing atypical ductal hyperplasia (DIN1b) on initial biopsy had a greater rate of coexisting cancer than CCLs with or without atypical features ($p<0.0001$). In another follow-up study by David et al., all carcinomas were found within the group of patients who had a prior diagnosis of CCH with atypia. No cancer was identified when the atypical CCLs measured less than 10 mm or when the lesion was totally removed. Therefore, these authors recommended surgical excision when vacuum-assisted core biopsies of breast show CCH with atypia larger than 10 mm or when the lesions are incompletely removed. They opine that core biopsy specimens containing CCC with atypia or CCH with atypia less than 10 mm in size or removed totally do not require further surgery [15]. However, determining the extent of CCLs in core biopsies or determining their completeness of excision is difficult in practice. Furthermore, it is unknown whether the carcinomas that subsequently developed in these patients came from the incompletely excised CCLs or from other atypical or malignant changes that were not included in the core biopsies. In practice, the size of CCLs is not routinely determined by pathologists, and we believe the management of patients based on these recommendations is not practical.

Conclusion

Both histological and molecular genetic studies suggest that CCLs represent the earliest histologically identifiable, non-obligate precursor of low-grade breast carcinomas [23, 28, 54, 58, 59, 65]. As such, it is possible and interesting to speculate that CCLs represent the first morphological evidence of the multifocal neoplastic transformation of the "sick" breast lobe conceptualized by Tot [73]. Nevertheless, the follow-up data show that the risk of local recurrence and progression of most CCLs to invasive cancer is low. This implies that categorizing and managing all CCLs as one entity may result in over-treatment [62], and the optimal clinical management of CCLs, particularly when found on core biopsy, remains unresolved [58]. In view of the pathologic diversity of DIN1 process, in which the whole spectrum of CCLs may be found, linking clinical management to subtypes of CCLs in core biopsies may be impractical and unreasonable. Furthermore, based on our own experience and the study of Goldstein and O'Malley [29], we believe that ductal in situ neoplasia is not necessarily required to progress through the different levels of architectural complexity of the DIN1 spectrum before acquiring the capacity to become an invasive carcinoma. This is especially true for tubular carcinoma, which is not uncommonly seen in association with DIN1a or DIN1b (ADH) alone in the absence of 'fully-evolved' DIN1c (low-grade DCIS). Although the risk of progression across this class of lesions appears to be low, we believe that there is sufficient evidence to recommend regular follow-up when CCLs are encountered in women participating in mammographic screening programs. Whether further excision should be recommended for CCLs detected in core biopsies remains controversial. As the natural history of CCLs is currently uncertain in any given patient, further detailed phenotype and genotype studies across the spectrum of CCLs and in the context of normal and other pre-neoplastic breast lesions will be required to delineate the biology and better define the clinical implications of CCLs.

Conflict of interest statement We declare that we have no conflict of interest.

References

1. Abdel-Fatah TM, Powe DG, Hodi Z, Lee AH, Reis-Filho JS, Ellis IO (2007) High frequency of coexistence of columnar cell lesions, lobular neoplasia, and low grade ductal carcinoma in situ with invasive tubular carcinoma and invasive lobular carcinoma. Am J Surg Pathol 31:417–426
2. Azzopardi JG, Ahmed A, Millis RR (1979) Problems in breast pathology. Major Probl Pathol 11:i–xvi, 1–466
3. Berg WA (2004) Image-guided breast biopsy and management of high-risk lesions. Radiol Clin North Am 42:935–946, vii
4. Bibeau F, Chateau MC, Masson B (2003) Management of non-palpable breast lesions with vacuum-assisted large core needle biopsies (Mammotome). Experience with 560 procedures at the Val d'Aurelle Center. Ann Pathol 23:582–592

5. Bijker N, Peterse JL, Duchateau L, Julien JP, Fentiman IS, Duval C, Di Palma S, Simony-Lafontaine J, de Mascarel I, van de Vijver MJ (2001) Risk factors for recurrence and metastasis after breast-conserving therapy for ductal carcinoma-in-situ: analysis of European Organization for Research and Treatment of Cancer Trial 10853. J Clin Oncol 19:2263–2271
6. Bloodgood J (1906) Senile parenchymatous hypertrophy of female breast. Its relation to cyst formation and carcinoma. Surg Gynecol Obstet 3:721–730
7. Bonnett M, Wallis T, Rossmann M, Pernick NL, Bouwman D, Carolin KA, Visscher D (2003) Histopathologic analysis of atypical lesions in image-guided core breast biopsies. Mod Pathol 16:154–160
8. Boyd NF, Guo H, Martin LJ, Sun L, Stone J, Fishell E, Jong RA, Hislop G, Chiarelli A, Minkin S, Yaffe MJ (2007) Mammographic density and the risk and detection of breast cancer. N Engl J Med 356:227–236
9. Boyd NF, Martin LJ, Yaffe MJ, Minkin S (2006) Mammographic density: a hormonally responsive risk factor for breast cancer. J Br Menopause Soc 12:186–193
10. Brogi E, Oyama T, Koerner FC (2001) Atypical cystic lobules in patients with lobular neoplasia. Int J Surg Pathol 9:201–206
11. Collins LC, Achacoso NA, Nekhlyudov L, Fletcher SW, Haque R, Quesenberry CP Jr., Alshak NS, Puligandla B, Brodsky GL, Schnitt SJ, Habel LA (2007) Clinical and pathologic features of ductal carcinoma in situ associated with the presence of flat epithelial atypia: an analysis of 543 patients. Mod Pathol 20:1149–1155
12. Coyne JD (2004) Columnar cell hyperplasia with intraluminal crystalloids and features of a mucocoele-like lesion. Histopathology 44:401–403
13. Dabbs DJ, Carter G, Fudge M, Peng Y, Swalsky P, Finkelstein S (2006) Molecular alterations in columnar cell lesions of the breast. Mod Pathol 19:344–349
14. Dauplat MM, Penault-Llorca F (2004) Classification of preinvasive breast and carcinoma in situ: doubts, controversies, and proposal for new categorizations. Bull Cancer 91(Suppl 4):S205–S210
15. David N, Labbe-Devilliers C, Moreau D, Loussouarn D, Campion L (2006) Diagnosis of flat epithelial atypia (FEA) after stereotactic vacuum-assisted biopsy (VAB) of the breast: what is the best management: systematic surgery for all or follow-up? J Radiol 87:1671–1677
16. de Mascarel I, MacGrogan G, Mathoulin-Pelissier S, Vincent-Salomon A, Soubeyran I, Picot V, Coindre JM, Mauriac L (2007) Epithelial atypia in biopsies performed for microcalcifications practical considerations about 2,833 serially sectioned surgical biopsies with a long follow-up. Virchows Arch 451:1–10
17. De Potter CR, Foschini MP, Schelfhout AM, Schroeter CA, Eusebi V (1993) Immunohistochemical study of neu protein overexpression in clinging in situ duct carcinoma of the breast. Virchows Arch A Pathol Anat Histopathol 422:375–380
18. Dessauvagie BF, Zhao W, Heel-Miller KA, Harvey J, Bentel JM (2007) Characterization of columnar cell lesions of the breast: immunophenotypic analysis of columnar alteration of lobules with prominent apical snouts and secretions. Hum Pathol 38:284–292
19. Eusebi V, Damiani S, Losi L, Millis RR (1997) Apocrine differentiation in breast epithelium. Adv Anat Pathol 4:139–155
20. Eusebi V, Feudale E, Foschini MP, Micheli A, Conti A, Riva C, Di Palma S, Rilke F (1994) Long-term follow-up of in situ carcinoma of the breast. Semin Diagn Pathol 11:223–235
21. Eusebi V, Foschini MP, Cook MG, Berrino F, Azzopardi JG (1989) Long-term follow-up of in situ carcinoma of the breast with special emphasis on clinging carcinoma. Semin Diagn Pathol 6:165–173
22. Falkenberry SS, Legare RD (2002) Risk factors for breast cancer. Obstet Gynecol Clin North Am 29:159–172
23. Feeley L, Quinn CM (2008) Columnar cell lesions of the breast. Histopathology 52:11–19
24. Foote FW, Stewart FW (1945) Comparative studies of cancerous versus noncancerous breasts. Ann Surg 121:197–222
25. Foschini MP, Flamminio F, Miglio R, Calo DG, Cucchi MC, Masetti R, Eusebi V (2007) The impact of large sections on the study of in situ and invasive duct carcinoma of the breast. Hum Pathol 38:1736–1743
26. Fraser JL, Raza S, Chorny K, Connolly JL, Schnitt SJ (1998) Columnar alteration with prominent apical snouts and secretions: a spectrum of changes frequently present in breast biopsies performed for microcalcifications. Am J Surg Pathol 22:1521–1527
27. Fritzsche FR, Dietel M, Kristiansen G (2006) Flat epithelial neoplasia and other columnar cell lesions of the breast. Pathologe 27:381–386
28. Goldstein NS, Kestin LJ, Vicini FA (2007) Monomorphic epithelial proliferations: characterization and evidence suggesting they are the pool of partially transformed lesions from which some invasive carcinomas arise. Am J Clin Pathol 128:1023–1034
29. Goldstein NS, O'Malley BA (1997) Cancerization of small ectatic ducts of the breast by ductal carcinoma in situ cells with apocrine snouts: a lesion associated with tubular carcinoma. Am J Clin Pathol 107:561–566
30. Gopalan A, Hoda SA (2005) Columnar cell hyperplasia and lobular carcinoma in situ coexisting in the same duct. Breast J 11:210
31. Guerra-Wallace MM, Christensen WN, White RL Jr (2004) A retrospective study of columnar alteration with prominent apical snouts and secretions and the association with cancer. Am J Surg 188:395–398
32. Harris GC (2007) Bs14 update on in situ proliferations of the breast. ANZ J Surg 77(Suppl 1):A3
33. Ho BC, Tan PH (2005) Flat epithelial atypia: concepts and controversies of an intraductal lesion of the breast. Pathology 37:105–111
34. Hoda SA, Chung SM, Gopalan A (2003) Evolving entities and changing concepts in breast pathology. Breast Cancer 10:294–300
35. Hulka BS, Moorman PG (2001) Breast cancer: hormones and other risk factors. Maturitas 38:103–113, discussion 113–106
36. Jacobs TW, Connolly JL, Schnitt SJ (2002) Nonmalignant lesions in breast core needle biopsies: to excise or not to excise? Am J Surg Pathol 26:1095–1110
37. Kim MJ, Kim EK, Oh KK, Park BW, Kim H (2006) Columnar cell lesions of the breast: mammographic and US features. Eur J Radiol 60:264–269
38. Koerner FC, Oyama T, Maluf H (2001) Morphological observations regarding the origins of atypical cystic lobules (low-grade clinging carcinoma of flat type). Virchows Arch 439:523–530
39. Laden F, Hunter DJ (1998) Environmental risk factors and female breast cancer. Annu Rev Public Health 19:101–123
40. Lanyi M, Citoler P (1981) The differential diagnosis of micro-calcification. Micro-cyst (blunt duct) adenosis (author's transl). Rofo 134:225–231
41. Lee S, Medina D, Tsimelzon A, Mohsin SK, Mao S, Wu Y, Allred DC (2007) Alterations of gene expression in the development of early hyperplastic precursors of breast cancer. Am J Pathol 171:252–262
42. Lee S, Mohsin SK, Mao S, Hilsenbeck SG, Medina D, Allred DC (2006) Hormones, receptors, and growth in hyperplastic enlarged lobular units: early potential precursors of breast cancer. Breast Cancer Res 8:R6
43. Leibl S, Regitnig P, Moinfar F (2007) Flat epithelial atypia (DIN 1a, atypical columnar change): an underdiagnosed entity very frequently coexisting with lobular neoplasia. Histopathology 50:859–865

44. Luna-More S, Weil B, Bautista D, Garrido E, Florez P, Martinez C (2004) Bcl-2 protein in normal, hyperplastic and neoplastic breast tissues. A metabolite of the putative stem-cell subpopulation of the mammary gland. Histol Histopathol 19:457–463
45. Martel M, Barron-Rodriguez P, Tolgay Ocal I, Dotto J, Tavassoli FA (2007) Flat DIN 1 (flat epithelial atypia) on core needle biopsy: 63 cases identified retrospectively among 1,751 core biopsies performed over an 8-year period (1992–1999). Virchows Arch 451:883–891
46. Martin AM, Weber BL (2000) Genetic and hormonal risk factors in breast cancer. J Natl Cancer Inst 92:1126–1135
47. McLaren BK, Gobbi H, Schuyler PA, Olson SJ, Parl FF, Dupont WD, Page DL (2005) Immunohistochemical expression of estrogen receptor in enlarged lobular units with columnar alteration in benign breast biopsies: a nested case-control study. Am J Surg Pathol 29:105–108
48. Mills SE, Fechner RE (1980) Focal pregnancy-like change of the breast. Diagn Gynecol Obstet 2:67–70
49. Mitchell G, Antoniou AC, Warren R, Peock S, Brown J, Davies R, Mattison J, Cook M, Warsi I, Evans DG, Eccles D, Douglas F, Paterson J, Hodgson S, Izatt L, Cole T, Burgess L, Eeles R, Easton DF (2006) Mammographic density and breast cancer risk in BRCA1 and BRCA2 mutation carriers. Cancer Res 66:1866–1872
50. Moinfar F (2007) Essentials of diagnostic breast pathology: a practical approach. Springer, Heidelberg
51. Moinfar F, Man YG, Bratthauer GL, Ratschek M, Tavassoli FA (2000) Genetic abnormalities in mammary ductal intraepithelial neoplasia-flat type ("clinging ductal carcinoma in situ"): a simulator of normal mammary epithelium. Cancer 88:2072–2081
52. Nasser SM (2004) Columnar cell lesions: current classification and controversies. Semin Diagn Pathol 21:18–24
53. Noel JC, Fayt I, Fernandez-Aguilar S, Buxant F, Boutemy R (2006) Proliferating activity in columnar cell lesions of the breast. Virchows Arch 449:617–621
54. O'Malley FP, Mohsin SK, Badve S, Bose S, Collins LC, Ennis M, Kleer CG, Pinder SE, Schnitt SJ (2006) Interobserver reproducibility in the diagnosis of flat epithelial atypia of the breast. Mod Pathol 19:172–179
55. Otterbach F, Bankfalvi A, Bergner S, Decker T, Krech R, Boecker W (2000) Cytokeratin 5/6 immunohistochemistry assists the differential diagnosis of atypical proliferations of the breast. Histopathology 37:232–240
56. Oyama T, Iijima K, Takei H, Horiguchi J, Iino Y, Nakajima T, Koerner F (2000) Atypical cystic lobule of the breast: an early stage of low-grade ductal carcinoma in-situ. Breast Cancer 7:326–331
57. Page DL, Kasami M, Jensen RA (1996) Hypersecretory hyperplasia with atypia in breast biopsies. Pathol Case Rev 1:36–40
58. Pinder SE, Provenzano E, Reis-Filho JS (2007) Lobular in situ neoplasia and columnar cell lesions: diagnosis in breast core biopsies and implications for management. Pathology 39:208–216
59. Pinder SE, Reis-Filho JS (2007) Non-operative breast pathology: columnar cell lesions. J Clin Pathol 60:1307–1312
60. Rosen P (2001) Rosen's breast pathology. Lippincott Williams & Wilkins, Philadelphia
61. Rosen PP (1999) Columnar cell hyperplasia is associated with lobular carcinoma in situ and tubular carcinoma. Am J Surg Pathol 23:1561
62. Sahoo S, Recant WM (2005) Triad of columnar cell alteration, lobular carcinoma in situ, and tubular carcinoma of the breast. Breast J 11:140–142
63. Schnitt SJ (2003) The diagnosis and management of pre-invasive breast disease: flat epithelial atypia–classification, pathologic features and clinical significance. Breast Cancer Res 5:263–268
64. Schnitt SJ, Vincent-Salomon A (2003) Columnar cell lesions of the breast. Adv Anat Pathol 10:113–124
65. Sewell CW (2004) Pathology of high-risk breast lesions and ductal carcinoma in situ. Radiol Clin North Am 42:821–830
66. Simooka H, Oyama T, Sano T, Horiguchi J, Nakajima T (2004) Immunohistochemical analysis of 14–3–3 sigma and related proteins in hyperplastic and neoplastic breast lesions, with particular reference to early carcinogenesis. Pathol Int 54:595–602
67. Simpson PT, Gale T, Reis-Filho JS, Jones C, Parry S, Sloane JP, Hanby A, Pinder SE, Lee AH, Humphreys S, Ellis IO, Lakhani SR (2005) Columnar cell lesions of the breast: the missing link in breast cancer progression? A morphological and molecular analysis. Am J Surg Pathol 29:734–746
68. Tan PH, Ho BC, Selvarajan S, Yap WM, Hanby A (2005) Pathological diagnosis of columnar cell lesions of the breast: are there issues of reproducibility? J Clin Pathol 58:705–709
69. Tavassoli FA (2001) Ductal intraepithelial neoplasia of the breast. Virchows Arch 438:221–227
70. Tavassoli FA (1999) Pathology of the breast. McGraw-Hill Professional, New York
71. Tavassoli FA, Purcell AP, Bratthauer GL, Man Y (1996) Androgen receptor expression along with loss of bcl-2, ER, and PR expression in benign and malignant apocrine lesions of the breast: implication for therapy. Breast J 2:261–269
72. Topal NB, Ayhan S, Topal U, Bilgin T (2006) Effects of hormone replacement therapy regimens on mammographic breast density: the role of progestins. J Obstet Gynaecol Res 32:305–308
73. Tot T (2007) The theory of the sick breast lobe and the possible consequences. Int J Surg Pathol 15:369–375
74. Tremblay G, Deschenes J, Alpert L, Quenneville LA (2005) Overexpression of estrogen receptors in columnar cell change and in unfolding breast lobules. Breast J 11:326–332
75. Viale G (2005) Histopathology of primary breast cancer 2005. Breast 14:487–492
76. Vincent-Salomon A (2003) Columnar lesions: a frequent diagnosis in breast pathology!. Ann Pathol 23:593–596
77. Warren J (1905) The surgeon and the pathologist: A plea for reciprocity as illustrated by the consideration of the classification and treatment of benign tumors of the breast. JAMA 45:149–165
78. Wellings SR, Jensen HM, Marcum RG (1975) An atlas of subgross pathology of the human breast with special reference to possible precancerous lesions. J Natl Cancer Inst 55:231–273
79. WHO (2003) World Health Organization classification of tumours. Pathology and genetics of tumours of the breast and female genital organs. IARC, Lyon, France

Virchows Arch (2008) 452:599–605
DOI 10.1007/s00428-008-0616-7

ORIGINAL ARTICLE

Morphological variability of lymphohistiocytic variant of anaplastic large cell lymphoma (former lymphohistiocytic lymphoma according to the Kiel classification)

Wolfram Klapper · Matthias Böhm · Reiner Siebert · Karl Lennert

Received: 29 January 2008 / Accepted: 8 April 2008 / Published online: 14 May 2008
© Springer-Verlag 2008

Abstract According to the WHO classification, anaplastic large cell lymphoma (ALCL) is a distinct T-cell lymphoma entity with a number of morphological variants. The characteristic feature of lymphohistiocytic variant of ALCL according to the WHO classification is the abundance of histiocytes that exceed and mask the tumour cell population. In the current, study we reanalysed a historical series of 17 lymphomas, diagnosed as lymphohistiocytic lymphoma according to the criteria of the Kiel classification, with the presence of large purple macrophages (LPM) as the decisive finding for diagnosing this lymphoma subtype. We assessed the cellular composition of the tumour and correlated the results with the definition of lymphohistiocytic variant of ALCL given in the WHO classification. Although all cases in our cohort matched the criteria of ALCL according to the WHO, in 30% of the cases, the total amount of macrophages did not exceed the number of CD30-positive tumour cells. Our results indicate that the presence of LPM might be helpful to identify this subgroup of ALCL. Because the distinction of morphological subtypes of ALCL is of clinical relevance, improved criteria for subtyping ALCL are urgently needed that might include the presence LPM as one criteria.

W. Klapper (✉) · M. Böhm · K. Lennert
Department of Pathology Haematopathology Section and Lymph Node Registry, University Hospital Schleswig-Holstein, Campus Kiel, Michaelisstrasse 11, 24105 Kiel, Germany
e-mail: wklapper@path.uni-kiel.de

R. Siebert
Institute of Human Genetics, University Hospital Schleswig-Holstein, Campus Kiel, Kiel, Germany

Keywords Anaplastic large cell lymphoma · Lymphohistiocytic variant · ALCL · Lymphohistiocytic lymphoma

Introduction

Anaplastic large cell lymphoma (ALCL) was first described in 1985 as a lymphoma consisting of large pleomorphic cells with expression of CD30. It was originally referred to as Ki-1 lymphoma in the Kiel classification [7, 16], named after the antibody Ki-1 which detects the CD30 antigen. The general acceptance of this lymphoma entity was greatly enhanced by the discovery of the translocation t(2;5)(p23; q35) that fuses the anaplastic lymphoma kinase (ALK) and the nucleolar protein nucleophosmin (NPM) gene [8]. The resulting NPM–ALK fusion gene is a constitutively active kinase that is closely associated with lymphomagenesis [13]. Molecular and immunohistochemical studies revealed that virtually all NPM–ALK-positive lymphomas are derived from T cells although an absence of T-cell marker expression was recognised [1]. Thus, in the WHO classification, ALCL are classified as a distinct entity of T-cell lymphomas [5]. With the availability of specific antibodies for detecting ALK and ALK fusion proteins in paraffin-embedded tissue, the genetic and morphological heterogeneity of the lymphoma became evident [14]. The genetic heterogeneity is reflected primarily in the variety of translocation partners of the ALK gene other than NPM, which occur in about 10% of ALCL cases [13]. A further 10% of ALCL cases do not harbour ALK translocations but resemble ALCL morphologically and to some extent immunohistochemically and are thus considered as ALK-negative ALCL according to the WHO classification [5, 14]. However, ALK-negative ALCL differ from ALK-

positive ALCL clinically and molecularly and might thus be considered as an independent entity [15, 17]. Using ALK and CD30 as markers for the malignant cells, various morphological variants of ALCL have been recognised, among which the most frequent are the small cell variant (scALCL) [6] and the lymphohistiocytic variant (lhALCL) [10].

The characteristic feature of lhALCL is the abundance of histiocytes that might mask the tumour cell population which makes up only a minor component of the infiltrate [10]. Therefore, lhALCL was not classified as a Ki-1 lymphoma in the Kiel classification but defined as a separate lymphoma entity called lymphohistiocytic lymphoma [7]. Using immunohistochemistry to detect CD30 or ALK, it became more evident that lymphohistiocytic lymphoma according to the Kiel classification resembles lhALCL. However, the morphological definition of lhALCL according to the WHO classification differs from the definition of lymphohistiocytic lymphoma according to the Kiel classification. The most important difference between the two definitions lies in the role of large purple macrophages (LPM) in establishing the diagnosis. LPM have formerly been called "LB cells" (an adaptation from a patient's name and the term that was originally used by I. Hamlin and A. Stansfeld when they presented the first cases of lymphohistiocytic lymphoma at the European Lymphoma Club in 1974). LPM resembles CD68-positive macrophages with purple cytoplasm in Giemsa staining, a bright perinuclear Golgi field and eccentric nuclei with condensed chromatin (Fig. 1). The typical morphology of LPM, thus, differs from the majority of other CD68-positive macrophages in the tumour which have a brighter grey cytoplasm and less chromatin dense nuclei (Fig. 1). Of prime importance is the fact that the macrophages in lhALCL do not resemble epithelioid cells, which are characteristic for other types of lymphomas, especially lymphoepithelioid lymphoma (so-called Lennert's lymphoma [4]), which is grouped together with other lymphomas as peripheral T-cell lymphomas, unspecified, according to the WHO classification [5]. Whereas LPM are mandatory for the diagnosis of lymphohistiocytic lymphoma according to the Kiel classification [7], this characteristic cell type is not part of the definition of lhALCL according to the WHO classification [5].

The aim of the current study was to reanalyse a historical series of lymphomas, diagnosed between 1980 and 1992 as lymphohistiocytic lymphoma according to the Kiel classification and to correlate the diagnosis of lymphohistiocytic lymphoma with the diagnosis of lhALCL according to the WHO classification. Because a subclassification of ALCL might be of clinical relevance [3], our aim was to describe the morphologic variability of this disease to improve the diagnostic criteria. For this purpose, in 17 cases of lhALCL, the expression of ALK and the cellular composition of this rare lymphoma were evaluated.

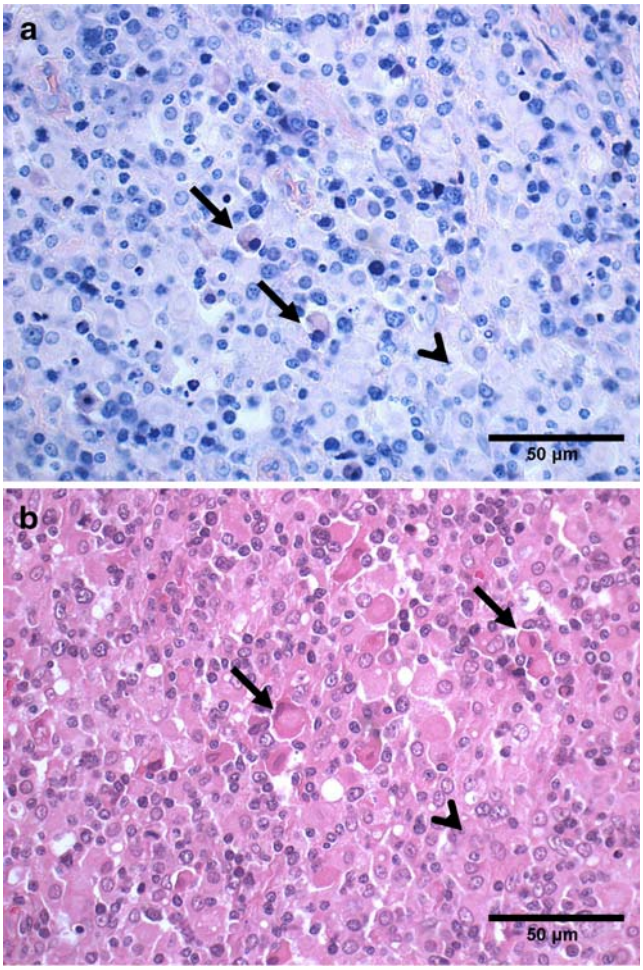


Fig. 1 Morphological examples of lymphohistiocytic lymphoma–lhALCL from the series of lymphomas examined in this study. The *arrow* indicates LPM with strongly stained cytoplasm, a bright perinuclear Golgi field and eccentric nuclei with condensed chromatin. LPM differ, strikingly in their morphology from the majority of macrophages found in lhALCL (*arrowhead*). **a** Giemsa stain, **b** H & E stain

Materials and methods

Patient samples

Samples from 17 patients were obtained from the files of the Lymph Node Registry Kiel and examined according to the local ethical guidelines. All cases in a period between 1981 and 1992 were selected for analysis. This historical cohort was defined by the following morphological criteria for lymphohistiocytic lymphoma according to the Kiel classification. The lymph node architecture was replaced by an infiltrate composed of histiocytes and T cells. A variable number of blast-like cells was detectable. To establish the diagnosis, it was mandatory that there be among the histiocytes a variable but small number of LPM (Fig. 1).

Morphology and immunohistochemistry

All cases were evaluated on slides stained according to Giemsa, haematoxylin & eosin, periodic acid–Schiff and Gomori. Immunohistochemical staining was performed for CD3, CD20, CD30, CD68, ALK (all antibodies from Dako, Glostrup, Denmark) using the alkaline phosphatase and monoclonal anti-alkaline phosphatase technique [2]. ALK staining was done using EnVision (Dako). The percentage of CD20-, CD3-, CD68- and CD30-positive cells were evaluated at a ×1,000 magnification using an ocular with a grid by counting at least ten areas of the grid. All values were calculated as percentage of positive cells in relation to all cells within the evaluated region. Cell proliferation was assessed in immunohistochemical stainings by counting 100 mitotic figures in the tumour area and indicating the percentage of mitosis occurring in the positive cell fraction.

Fluorescent double staining using antibodies against mouse anti-CD30 and rabbit anti-CD3 was performed using fluorescein-isothiocyanate-labelled anti-mouse and rhodamine-labelled anti-rabbit secondary antibodies. The fluorescent stainings were evaluated with a Zeiss Axioscop 40 equipped with a fluorescent camera and MetaVue Software.

Results

Patient characteristics

Our historical cohort included all lymphomas diagnosed as lymphohistiocytic lymphoma according to the Kiel classification between 1981 and 1992 in the Lymph Node Registry Kiel before the description of the involvement of the ALK gene. Table 1 summarises the patient characteristics. The mean age was 22 years, with only two patients being older than 40 years. The ratio of female to male patients was 8:9. The therapy was very heterogeneous and included polychemotherapy, irradiation and bone marrow transplantation. The median follow-up (time to last patient contact or death) was 23.5 months and the survival probability after 40 months only 47% (Table 1). Remarkably, two spontaneous remissions without therapy (except the excision for diagnostic purposes) were reported. Extra-nodal involvement was detected in 12 of 17 (71%) patients. The skin, bone marrow and central nervous system were the most frequently involved extra-nodal organs (Table 1).

ALK expression

For approximately half of the cases, sufficient material was available for ALK immunohistochemical staining. We found no staining in one (6%) patient, nuclear and cytoplasmic staining in six (35%) and homogeneous cytoplasmic staining in one (6%). In 53% of the patients, the ALK staining was not feasible because material was lacking or it was unrepresentative. Interestingly, one of the two spontaneous remissions without therapy except the excision for diagnostic purposes was a nuclear and cytoplasmic ALK-positive lymphoma in a 20-year-old woman during pregnancy (patient 6, Table 1 and Fig. 2a). The other spontaneous remission occurred in a lymphoma in which the ALK staining was not assessable but this patient also presented in a very limited stage (patient 10, Table 1).

Quantification of cell composition and fluorescent double staining

We quantified the tumour cell composition by assessing the percentage of CD30-positive tumour cells, CD68-positive macrophages, CD3-positive T cells and CD20-positive B cells within representative tumour areas. Furthermore, we quantified the percentage of LPM based on their morphological characteristics. As shown in Table 2, the mean percentage of CD30-positive cells was 15.0% (standard deviation [SD] 11.9%, Table 2). The mean content of macrophages (CD68+) was 23.2% (SD 9.0, Table 2). Notably, in five of 16 evaluable cases (31.3%) the number of macrophages did not exceed the number of CD30-positive tumour cells. The dominant cell population was CD3-positive T cells (29.9%, SD 13.9, Table 2). B cells (CD20) made up only a minor percentage within the tumour (7.8%, SD 6.1 Table 2).

Two cases (cases 1 and 2) with nuclear and cytoplasmic ALK expression and sufficient material were evaluated by immunofluorescent double staining for the expression of CD30 and CD3. Co-expression of CD3 on the CD30-positive tumour cells was not detectable in either case. Figure 2 shows a representative example.

Proliferation

The cell proliferation of each tumour component was evaluated by counting 100 mitotic figures using immunohistochemical stainings. The percentage of mitosis occurring in the positive cell fraction for each case is shown in Table 3. The majority of mitosis were detectable in the CD30-positive cell fraction (mean 60.9±28.1%) indicating their neoplastic nature. However, cell proliferation in the CD3-positive cells, although lower than in the CD30-positive fraction on average, exceeded the mitotic count in CD30-positive cells in some cases (cases 4, 8, 11, 16). The mitotic count in the LPM was lowest compared to all other cell components analysed (4.4±6.7%).

Table 1 Summary of patient characteristics

No.	Age at diagnosis (years)	Sex	Symptoms	Hepatomegaly–splenomegaly	Extra-nodal involvement	Affected organs	Stage	Therapy	Outcome after initial therapy	Time to first relapse in month	Survival in month, status at time of study	
1	5	M	n.a.	n.a.	+	L, S, BM	IVB	n.a.	CR	25	42	A
2	12	F	Skin involvement	n.a.	+	L, S, BM	IIIB	B-NHL, BMT	CR	12	24	D
3	30	M	Lymphadenopathy	–	−	L	IA	Irradiation with 36 u, 41 Gy	CR	84	96	A
4	12	F	Lymphadenopathy, fever, skin involvement	H	+	L, S, CNS	IIIB	COPADAM, MOPP, VBC	PR		14	D
5	28	F	Lymphadenopathy, fever, night sweat	–	+	L, S, BM	IVB	CHOP-V, DEXABEAM, KMT	CR	6	18	A
6	20	F	Fever	S	−	L	IA	No therapy	SR	–	23	A
7	26	F	Fever	n.a.	+	L, MB, S, Li, K, thymus	IVB	COPP, CVB	Progression		3	D
8	22	M	Lymphadenopathy Splenomegaly	S	+	L, BM, Li	IVB	COPLAM, IMV	CR	–	61	A
9	45	M	Lymphadenopathy, fever	n.a.	+	L, BM	IVB	MOPP	Progression		13	D
10	29	F	Lymphadenopathy	–	−	L	IIA	No therapy	SR	–	78	A
11	41	M	Lymphadenopathy, fever	S	+	L, BM	IVB	Corticoids	Progression		3	D
12	7	M	Lymphadenopathy, fever	S	−	L	IIB	B-NHL (BFM 82), Hodgkin HB82, irradiation with 35 Gy	CR	–	97	A
13	35	F	Lymphadenopathy, fever	S, H	+	L, BM, Li, Lu, K, thyroid gland	IVB	CYVADIC, McElwain, irradiation	CR	5	12	D
14	15	M	Lymphadenopathy, fever, skin involvement	S, H	+	L, S, BM	IVB	Vibramycin, corticoids, Endoxan, Urbason, Gerbebacin	Progression		4	D
15	17	M	Lymphadenopathy, skin involvement	–	+	L, S	IVB	CHOP, irradiation with 50 Gy	n.a.	>6	n.a.	n.a.
16	18	M	Lymphadenopathy	S, H	−	L	IIIB	CHOP	CR	6	144	A
17	13	F	Lymphadenopathy, skin involvement	n.a.	+	L, S, CNS	IIIB	BACOP, CVPP	CR	7	31	D

H Hepatomegaly, *S* splenomegaly, *Sk* skin, *BM* bone marrow, *L* lymphadenopathy, *CNS* central nervous system, *Li* liver, *Lu* lung, *S* spleen, *K* kidney, *CR* complete remission, *PR* partial remission, *SR* spontaneous remission, *n.a.* not available, *A* alive, *D* dead

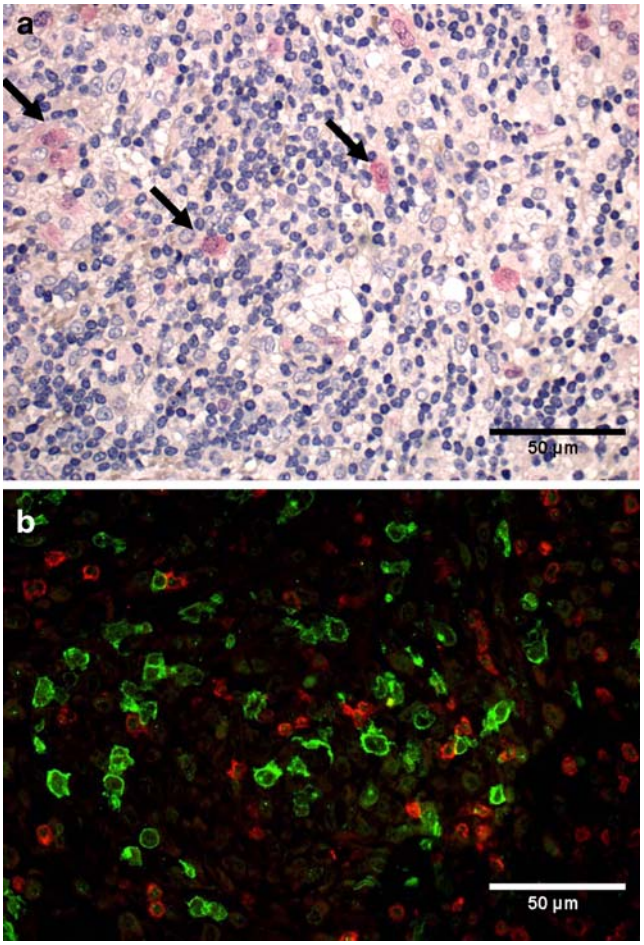


Fig. 2 **a** ALK staining by immunohistochemistry of a case of lhALCL in a pregnant woman which was reported to show a spontaneous remission without therapy. The *arrow* indicates nuclear and cytoplasmic ALK staining (original magnification ×400). **b** Fluorescent double staining for CD30 (*green*) and CD3 (*red*) in lhALCL shows no co-expression of the two markers (original magnification ×400)

Discussion

The originally described common (classical) type of ALCL (cALCL) consists of large pleomorphic blasts with abundant cytoplasm [16]. The nuclei are large with multiple nucleoli. Horseshoe-shaped nuclei characterise the "hallmark cells" of this lymphoma. The most frequent morphological variants are scALCL and lhALCL The CD30-positive tumour cells in lhALCL are often small to medium-sized and resemble those found in scALCL, making the distinction between the subtypes rather difficult [16].

To clarify the relationship of lymphohistiocytic lymphoma to lhALCL according to the criteria of the WHO classification all available cases of our historical series were stained for ALK. The majority of our cases expressed ALK. Only one assessable case was ALK-negative. The nuclear and cytoplasmic expression pattern of ALK suggests the presence of the NPM–ALK translocation in these lymphomas [13]. However, one case in our series showed only cytoplasmic staining, indicating that involvement of ALK translocation partners other than NPM occur in lhALCL [16]. In summary, the widespread expression of ALK indicates that virtually all lymphohistiocytic lymphomas defined according to the Kiel classification in our historical

Table 2 Content of positive cell fractions for each case

No.	% CD30+	% CD68+	% CD3+	% CD20+
1	7	19	39	3
2	21	23	17	12
3	25	35	39	<1
4	6	22	35	22
5	27	22	36	2
6	20	17	32	9
7	n.a.	8	36	<1
8	10	15	n.a.	n.a.
9	0	25	54	7
10	6	30	19	0
11	5	46	52	10
12	23	18	12	3
13	4	27	20	7
14	35	29	25	6
15	n.a.	n.a.	n.a.	n.a.
16	2	18	27	16
17	34	17	5	4
Average ± standard deviation	15.0±11.9	23.2±9.0	29.9±13.9	7.8±6.1

n.a. Not available

Table 3 Percentage of mitosis in the positive cell fraction for each case

No.	Mitosis in CD30+	Mitosis in CD68+	Mitosis in CD3+	Mitosis in CD20+	Mitosis in LPM
1	70	5	40	17	0
2	79	<5	30	8	0
3	85	6	77	18	0
4	32	10	42	10	8
5	52	<5	43	<5	14
6	72	25	15	0	10
7	n.a.	<5	92	62	0
8	80	n.a.	n.a.	6	n.a.
9	0	6	88	66	14
10	70	6	16	10	0
11	20	<5	78	21	0
12	79	8	24	<5	0
13	70	<5	16	<5	0
14	84	26	43	7	0
15	n.a.	n.a.	n.a.	n.a.	n.a.
16	12	<5	50	30	20
17	74	8	n.a.	21	0
Average ± standard deviation	60.9±28.1	6.3±5.6	46.7±26.0	17.7±19.3	4.4±6.7

All values as percentage of mitosis in the tumour area that occurred in the cell population staining positive for the marker indicated on top of the columns.
n.a. Not available

series fit the criteria of lhALCL according to the WHO classification.

In light of the recently described immunological response to the *ALK* gene [9, 12] and the abundance of reactive immune bystander cells in lhALCL, one might speculate that the number and characteristics of inflammatory cells in lhALCL reflect a specific immune response that characterises this subtype. However, a lymphohistiocytic morphology also occurred in one case in our series that did not show ALK staining. Our findings are in concordance with reports by other authors of ALK-negative lhALCL [11, 16]. We suggest that the specific macrophage and T-cell-rich background in lhALCL might be caused by the tumour cells themselves, e.g. by secretion of specific cytokines. Because the morphological subtype of ALCL might become of clinical relevance [3], future studies need to shed light on the mechanisms that attract so many macrophages in lhALCL. Double staining with CD30 and CD3 revealed that the CD30-positive tumour cells did not express CD3 and that the majority of CD3-positive cells were CD30-negative. The absence of T-cell markers is a common finding in ALCL in general and has been described elsewhere for cALCL [1]. Compared to bystander cells, the tumour cells are outnumbered in scALCL and lhALCL, and distinguishing tumour cells and bystander cells in stainings with only one antibody-like CD3 is difficult. To gain further insights into the immunophenotype and expression of cytokines in the tumour cells in lhALCL, double staining using ALK and CD30 in combination with other antigens needs to be performed. These future experiments might reveal similarities and differences between the tumour cells in morphological variants of ALCL in comparison to the cALCL.

The quantification of mitotic figures indicated that the cell proliferation is highest in the CD30-positive cell fraction. These data are in line with the results published previously that suggested the CD30-positive cells to be the neoplastic component of lhALCL [10]. Nevertheless, our data indicate that cell proliferation in the CD3-positive fraction might be very high, sometimes even higher than in the CD30-positive cells. However, we and others [1] have shown that the CD30-positive tumour cells in ALCL to lack CD3 in most cases. The high cell proliferation in non-neoplastic T cells might thus indicate a highly activated immune reaction. Again, the data indicate that assessing the immunophenotype of the neoplastic cells in lhALCL will be virtually impossible without double stainings since proliferating T cell might be confused with tumour cells in conventional immunohistochemistry.

Since the presence of LPM was the decisive finding for the diagnosis of lymphohistiocytic lymphoma [7], the total amount of CD30-positive tumour cells and macrophages was very variable in our cohort. In 30% of the cases that were lymphohistiocytic lymphomas according to the Kiel classification, the number of macrophages did not exceed the number of CD30-positive tumour cells. LPM are macrophages with a typical morphology that differs from other macrophages and that is rarely found in other reactive lymphadenopathies. Hemophagocytosis has been discussed as a typical feature of LPM [10]; however, the mechanism of development of these peculiar macrophages is not understood. Nevertheless, in ALK-negative cases, the detection of LPM might be useful to differentiate lhALCL from peripheral T-cell lymphoma.

A morphological subclassification of ALCL is of relevance since recent data show that the morphologic subtypes of ALCL have a prognostic impact [3]. Data from children treated within a prospective randomised trial showed that the morphological variants scALCL and lhALCL are associated with a poorer outcome than cases with classical morphology [3]. The reason for the poorer therapeutic response of scALCL and lhALCL is not yet known. Since in our series two lymphomas in a localised stage showed spontaneous regression, one might hypothesise that there might be an aggressive generalised and an indolently more localised subtype of lhALCL. However, larger cohorts of homogeneously treated lhALCL have to be studied to gain insight into the clinical course of this disease.

Our data based on the definition according to the Kiel classification indicate that the cellular composition, especially the content of macrophages, in lhALCL is variable, indicating that the cellular composition alone might be insufficient to define this subtype. Moreover, the percentage of macrophages might be even smaller than the percentage of CD30-positive tumour cells. In light of the clinical relevance, the definition of morphological variants of ALCL needs to be improved. We suggest that the presence of LPM should be part of the criteria for this subtype since these cells with their typical morphology can be easily detected in a Giemsa stain. However, to define criteria for lhALCL that are reliable, reproducible and clinically relevant, large cohorts of patients from controlled trials have to be analysed in detail for their cellular composition, the immunophenotype of the tumour cells and the presence of LPM.

Acknowledgements The authors would like to thank Olivera Batic, Monika Hauberg, Michael Weiss, Charlotte von Drathen and Christiane Stange for their excellent technical assistance and Kay Dege for editing the manuscript. This work was supported by the Kinder-Krebs-Initiative Buchholz, Holm-Seppensen.

Conflict of interest statement We declare that we have no conflict of interest.

References

1. Bonzheim I, Geissinger E, Roth S, Zettl A, Marx A, Rosenwald A, Muller-Hermelink HK, Rudiger T (2004) Anaplastic large cell lymphomas lack the expression of T-cell receptor molecules or molecules of proximal T-cell receptor signaling. Blood 104:3358–3360
2. Cordell JL, Falini B, Erber WN, Ghosh AK, Abdulaziz Z, MacDonald S, Pulford KA, Stein H, Mason DY (1984) Immunoenzymatic labeling of monoclonal antibodies using immune complexes of alkaline phosphatase and monoclonal anti-alkaline phosphatase (APAAP complexes). J Histochem Cytochem 32:219–229
3. Damm-Welk C, Busch K, Burkhardt B, Schieferstein J, Viehmann S, Oschlies I, Klapper W, Zimmermann M, Harbott J, Reiter A, Woessmann W (2007) Prognostic significance of circulating tumor cells in bone marrow or peripheral blood as detected by qualitative and quantitative PCR in pediatric NPM–ALK positive anaplastic large cell lymphoma. Blood 110:670–677
4. Geissinger E, Odenwald T, Lee SS, Bonzheim I, Roth S, Reimer P, Wilhelm M, Muller-Hermelink HK, Rudiger T (2004) Nodal peripheral T-cell lymphomas and, in particular, their lymphoepithelioid (Lennert's) variant are often derived from CD8(+) cytotoxic T-cells. Virchows Arch 445:334–343
5. Jaffe E, Harris N, Stein H, Vardiman JW (2001) Pathology and genetics of tumours of haematopoietic and lymphoid tissues. IARC, Lyon
6. Kinney MC, Collins RD, Greer JP, Whitlock JA, Sioutos N, Kadin ME (1993) A small-cell-predominant variant of primary Ki-1 (CD30)+ T-cell lymphoma. Am J Surg Pathol 17:859–868
7. Lennert K, Feller A (1981) Histopathologie der Non-Hodgkin-Lymphome. Springer, Berlin
8. Morris SW, Kirstein MN, Valentine MB, Dittmer KG, Shapiro DN, Saltman DL, Look AT (1994) Fusion of a kinase gene, ALK, to a nucleolar protein gene, NPM, in non-Hodgkin's lymphoma. Science 263:1281–1284
9. Passoni L, Gallo B, Biganzoli E, Stefanoni R, Massimino M, Di Nicola M, Gianni AM, Gambacorti-Passerini C (2006) In vivo T-cell immune response against anaplastic lymphoma kinase in patients with anaplastic large cell lymphomas. Haematologica 91:48–55
10. Pileri S, Falini B, Delsol G, Stein H, Baglioni P, Poggi S, Martelli MF, Rivano MT, Mason DY, Stansfeld AG (1990) Lymphohistiocytic T-cell lymphoma (anaplastic large cell lymphoma CD30+/Ki-1+ with a high content of reactive histiocytes). Histopathology 16:383–391
11. Pileri SA, Pulford K, Mori S, Mason DY, Sabattini E, Roncador G, Piccioli M, Ceccarelli C, Piccaluga PP, Santini D, Leone O, Stein H, Falini B (1997) Frequent expression of the NPM–ALK chimeric fusion protein in anaplastic large-cell lymphoma, lymphohistiocytic type. Am J Pathol 150:1207–1211
12. Pulford K, Falini B, Banham AH, Codrington D, Roberton H, Hatton C, Mason DY (2000) Immune response to the ALK oncogenic tyrosine kinase in patients with anaplastic large-cell lymphoma. Blood 96:1605–1607
13. Pulford K, Lamant L, Espinos E, Jiang Q, Xue L, Turturro F, Delsol G, Morris SW (2004) The emerging normal and disease-related roles of anaplastic lymphoma kinase. Cell Mol Life Sci 61:2939–2953
14. Pulford K, Lamant L, Morris SW, Butler LH, Wood KM, Stroud D, Delsol G, Mason DY (1997) Detection of anaplastic lymphoma kinase (ALK) and nucleolar protein nucleophosmin (NPM)–ALK proteins in normal and neoplastic cells with the monoclonal antibody ALK1. Blood 89:1394–1404
15. Salaverria I, Bea S, Lopez-Guillermo A, Lespinet V, Pinyol M, Burkhardt B, Lamant L, Zettl A, Horsman D, Gascoyne R, Ott G, Siebert R, Delsol G, Campo E (2008) Genomic profiling reveals different genetic aberrations in systemic ALK-positive and ALK-negative anaplastic large cell lymphomas. Br J Haematol 140:516–526
16. Stein H, Foss HD, Durkop H, Marafioti T, Delsol G, Pulford K, Pileri S, Falini B (2000) CD30(+) anaplastic large cell lymphoma: a review of its histopathologic, genetic, and clinical features. Blood 96:3681–3695
17. Zettl A, Rudiger T, Konrad MA, Chott A, Simonitsch-Klupp I, Sonnen R, Muller-Hermelink HK, Ott G (2004) Genomic profiling of peripheral T-cell lymphoma, unspecified, and anaplastic large T-cell lymphoma delineates novel recurrent chromosomal alterations. Am J Pathol 164:1837–1848

Virchows Arch (2008) 452:607–620
DOI 10.1007/s00428-008-0593-x

ORIGINAL ARTICLE

Inactivation of *p16^{INK4a}/CDKN2A* gene may be a diagnostic feature of large B cell lymphoma leg type among cutaneous B cell lymphomas

Marc-Antoine Belaud-Rotureau · Virginie Marietta · Beatrice Vergier · Guillaume Mainhaguiet · Michelle Turmo · Yamina Idrissi · Jacky Ferrer · Marie Beylot-Barry · Pierre Dubus · Jean-Philippe Merlio

Received: 7 November 2007 / Revised: 4 January 2008 / Accepted: 31 January 2008 / Published online: 1 March 2008
© Springer-Verlag 2008

Abstract The World Health Organization–European Organization for Research and Treatment of Cancer has individualized three main categories among the primary cutaneous B cell lymphoma (PCBCL): leg-type primary cutaneous large B cell lymphoma (PCLBCL leg type), primary cutaneous follicle center lymphoma (PCFCL), and primary cutaneous marginal zone lymphoma (PCMZL). The genetic features of 21 PCBCL cases (six PCLBCL leg type four PCFCL large cells, seven PCFCL small cells, and four PCMZL) were investigated by comparative genomic hybridization (CGH array). Fluorescent in situ hybridization (FISH) analysis was performed to confirm CGH array data and to detect lymphoma-associated gene rearrangements. *p14^{ARF}/p16^{INK4a}CDKN2A* gene quantification, methylation analysis, and immunohistochemical detection were also performed. CGH array showed a higher number of recurrent genetic imbalances in PCLBCL leg type (mean 62) than in PCFCL large cells (mean 34). PCFCL small cells and PCMZL exhibited fewer chromosomal alterations (mean 24 and 9). FISH analysis provided concordant results with CGH array data in 97% (98 of 101) assays and demonstrated a t(8;14)(q24;q32) in two of six PCLBCL leg type. Recurrent deletions in 9p21 (*p14^{ARF}/p16^{INK4a}CDKN2A*) were a constant finding in PCLBCL leg type (six of six). Conversely, PCFCL large cells exhibited recurrent 1p36 deletions (four of four) without deletion in 9p21 (zero of four). The diagnostic and prognostic impact of the *p16^{INK4a}CDKN2A* gene status in PCBCL should therefore be confirmed on a larger series.

Keywords B cell · Lymphoma · Skin · Cutaneous B cell lymphoma · p16

M.-A. Belaud-Rotureau (✉) · V. Marietta · B. Vergier · G. Mainhaguiet · M. Turmo · Y. Idrissi · J. Ferrer · M. Beylot-Barry · P. Dubus · J.-P. Merlio
EA 2406 Histologie et Pathologie Moléculaire des Tumeurs, Université Victor Segalen, Batiment 3B, 2ème étage, 146 rue Leo saignat, 33076 Bordeaux Cedex, France
e-mail: MA.Belaud-Rotureau@histo.u-bordeaux2.fr

M.-A. Belaud-Rotureau · B. Vergier · J. Ferrer · P. Dubus · J.-P. Merlio
Service d'Anatomie et Cytologie Pathologiques, Hôpital du Haut-Lévêque, Avenue de Magellan, 33604 Pessac Cedex, France

M. Beylot-Barry
Service de Dermatologie, Hôpital du Haut-Lévêque, Avenue de Magellan, 33604 Pessac Cedex, France

Introduction

Primary cutaneous B cell lymphomas (PCBCL) are classified by the European Organization for Research and Treatment of Cancer (EORTC) into three main histopathological groups with distinct clinical and evolutive features [34]. While primary cutaneous follicle center cell lymphoma (PCFCL) and marginal zone B cell lymphoma (PCMZL) exhibit 97% and 100% 5-year survival, respectively, primary cutaneous large B cell lymphoma leg type (PCLBCL leg type) is considered an intermediately aggressive disease with 58% 5-year survival. Their relative frequency among cutaneous lymphomas is estimated at

13%, 2%, and 3%, respectively. However, the histological features of PCBCL largely differ from those of their nodal counterparts [15]. For example, BCL2 expression is generally absent from tumor cells of PCFCL that do not carry the t(14;18)(q32;q21) translocation, a cytogenetic hallmark of nodal follicular lymphomas [13, 30]. A great step toward uniform patient diagnosis and management was taken by the World Health Organization (WHO)–EORTC classification confirming that the overall majority of PCBCL fall into three diagnostic categories: PCMZL, PCFCL, and PCLBCL leg type [32, 33]. This classification takes into account recent advances on debated entities such as PCLBCL leg type that may occur outside the leg but typically exhibit a round cell morphology and a BCL2+ phenotype, unlike PCFCL [8, 11, 28].

However, clinicopathological variants include BCL2-negative PCLBCL leg type according to the site of involvement (7% at leg site vs 23% at nonleg site) [28], BCL2-positive large PCFCL (23%) [12] more frequently observed at the leg site (38%) that may represent a subgroup of PCFCL with worse prognosis [8, 28]. The lack of gold standard phenotypic criteria when using BCL-2, MUM-1, and FOXP1 markers may account for interobserver variation in large cell PCBCL diagnosis [11, 28]. Such cases may also be included in the other categories of PCBCL by some authors [20, 31]. However, other PCLBCL might correspond more to very rare diseases such as intravascular large B cell lymphoma, T cell/histiocyte-rich B cell lymphoma, or skin presentation of plasmablastic lymphoma rather than to a wait basket category [28, 32].

Therefore, additional analyses have been used for the subclassification of PCBCL, with a relative reproducibility between series that, in turn, may be due to differences in inclusion criteria. For example, the mutational pattern of the immunoglobulin gene of both PCFCL and PCLBCL leg type was primarily considered as germinal center derived [9]. In contrast, oligonucleotide microarray analysis identified a germinal center B cell-like signature in PCFCL and an activated B cell-like signature in PCLBCL leg type that was confirmed by immunohistochemistry [16, 17]. No *IGH*,*myc*, or *bcl6* loci breakpoints were detected by interphase fluorescence in situ hybridization (FISH) in PCMZL or in PCFCL, whereas 11 out of 14 PCLBCL leg type harbored at least one of them [14]. In another report, PCLBCL leg type and nonleg type displayed the same genetic aberrations irrespective of classification, anatomic site, cell morphology, or BCL2 expression [31]. Using comparative genomic hybridization (CGH) or CGH array, the number of chromosomal alterations was generally found to be higher in PCLBCL leg type than in PCFCL, but the same recurrent chromosome abnormalities are rarely identified between series [10, 14, 24]. The use of a more sensitive and automatized CGH array procedure, restricted to academic institutions, showed high-level deoxyribonucleic acid (DNA) amplifications at 2p16.1 (63%) and deletion of chromosome 14q32.33 (68%) as the most recurrent alterations in PCFCL [6]. In the 12 PCLBCL leg-type cases, amplifications at 18q21.31-q21.33 were observed in 67% of cases. A small region at 9p21.3 involving the *CDKN2A* and *CDKN2B* loci was also observed, and the loss of *CDKN2A* by either deletion and/or promoter hypermethylation was associated with a poor outcome [6].

To extend these findings using commercially and worldwide available tools, we decided to select material from 21 PCBCL cases representative of the three main diagnostic categories of the WHO–EORTC classification. After a careful review of clinical and histopathological data, we performed CGH array. Recurrent imbalances were further investigated by FISH, and specific chromosomal losses such as 9p21 in PCLBCL leg type were confirmed. We also set up quantitative real-time polymerase chain reaction (PCR) assays to quantify the allelic loss of the $p16^{INK4a}$/*CDKN2A* and $p14^{ARF}$ genes and to determine their methylation status.

Material and methods

Patient selection

We retrieved 21 patients with PCBCL displaying both clinical and immunohistochemical characteristic features (Table 1). Inclusion was based on the review of each case by a consensus panel according to the WHO–EORTC criteria and on the presence of at least 40% of tumor cells on frozen sections. This percentage was arbitrarily fixed to ensure a minimal amount of DNA from tumor cells for the CGH array analysis. Some cases were excluded when they did not exhibit such features or when the section of the frozen tissue revealed little tumoral infiltration. In accordance with morphological criteria used in a recent review of 300 PCBCL [28], six cases with confluent sheets of cells with a centroblast or immunoblast-like morphology corresponded to PCLBCL leg type. Four cases with confluent sheets of large cleaved cells (large centrocytes) corresponded to PCFCL large cells. Seven cases had a small cleaved cell morphology and were considered as PCFCL small cell. Four cases presented with PCMZL.

Immunohistochemistry

Immunohistochemistry was performed after a heat-induced antigen retrieval technique on paraffin-embedded sections using the biotin–streptavidin peroxidase LSAB kit (Dako,

Table 1 Clinical and immunohistochemical characteristics of the 21 patients

Case number	Sex	Age	Site	Number of lesions	BCL2/BCL6/MUM1	Therapy	Relapse	Follow-up	
								Status	Months
PCLBCL leg type									
1	F	88	Leg	1	+/−/+	RT	Skin	D+	33
2	F	89	Leg	7	+/−/+	CT	Skin+EC	D+	24
3	M	60	Leg	5	+/−/−	CT	Skin+EC	D+	12
4	F	66	Leg	1	+/−/+	CT+RT	Skin+EC	D+	78
5	F	51	Leg	1	+/−/+	RT	Skin	D+	21
6	F	88	Arm	5	+/−/+	CT	Skin	D+	6
PCFCL large cells									
7	M	69	Trunk	5	−/−/−	CT+RT	No	A−	48
8	M	39	Face	3	−/+/−	RT	No	A−	68
9	F	74	Scalp	1	−/+/−	CT+RT	No	A−	72
10	M	57	Trunk	5	−/−/−	CT+RT	No	A−	120
PCFCL small cells									
11	F	70	Trunk+arm	15	−/+/−	CT	Skin	A+	74
12	M	68	Face	5	+/+/−	CT	Skin	A+	64
13	M	31	Trunk+arm	2	−/+/−	RT	No	A−	72
14	F	39	Trunk	5	−/+/−	RT	Skin	A−	78
15	F	63	Scalp	1	+/+/ND	CT	Skin	A−	132
16	F	85	Scalp	1	−/ND/ND	RT	No	A−	96
17	F	53	Trunk	5	+/ND/−	RT	No	A−	77
PCMZL									
18	M	69	Arm	3	−/−/−	RT	No	D−	48
19	M	34	Leg	1	−/−/−	RT	Skin	A−	72
20	F	35	Face	3	−/−/−	RT	Skin	A−	64
21	F	37	Arm+leg	2	−/−/−	RT	No	A−	31

F Female, *M* male, *ND* not done, *CT* chemotherapy, *RT* radiotherapy, *EC* extracutaneous relapse, *A*− alive without disease, *A*+ alive with disease, *D*+ dead as result of lymphoma, *D*− dead of other cause

Trappes, France) on an automated Chemate (Dako). The primary antibodies were directed against CD20 (Dako), CD3 (Dako), BCL-2 (Dako), BCL-6 (Dako), and CD10 (Novocastra, Leica, Rueil-Malmaison, France), follicular dendritic cell antigens CNA42 (Dako), and CD21 (Novocastra), and MUM1 (Dako). For $p16^{INK4a}$/CDKN2A immunohistochemical detection, two different antibodies and procedures were used on paraffin-embedded sections. The CINtec™ $p16^{INK4a}$histology kit including the primary antibody (clone E6H4), used at a 1:20 dilution for 1 h, was obtained from Dako together with the negative control antibody and visualization reagents. On parallel sections the monoclonal Pharmingen G175-405 monoclonal antibody (BD Biosciences, Le Pont-de-Claix, France) was used at a 1:10 dilution after a retrieval procedure at pH 8 in ethylenediamine tetraacetic acid (EDTA) buffer. Detection was further performed using the LSAB kit. On cervical intraepithelial lesions, both protocols provided a predominant nuclear staining of chromosome instability cells and a negative staining on adjacent normal epithelium. Occasional positive endothelial or fibroblast-like cells were found positive in the lamina propria. Positive controls also included tonsils with positive nuclear staining of basal epithelial cells and nodal large B cell lymphomas (n=2) with more than 50% positive cells.

CGH array

For each sample, genomic DNA was isolated from ten fresh frozen tissue sections (20 μm) according to the manufacturer's procedure after Proteinase K lysis, RNAse treatment, and isopropanol precipitation (Abbott-Vysis, Rungis, France). A qualitative control of DNA integrity was performed after electrophoresis on a 0.8% agarose gel. The DNA copy number changes in tumoral specimens were assessed by CGH array analysis using the Array 300 (Abbott-Vysis). The slides contained 287 clones spotted in triplicate including a set of subtelomeric sequences for each chromosome arm and 98 clones representing regions that have been reported to be amplified in human tumors. Genomic areas involved in homozygous or hemizygous deletion were also covered by 40 probes. DNA labeling and CGH array analysis were performed according to the manufacturer's recommendations. Briefly, the DNAs were

labeled by random priming using the Vysis kit. Then, cyanin 5 (Cy5)-isosex control and cyanin 3 (Cy3) test DNA were checked by gel analysis. After denaturation at 80°C, the DNAs were dropped on the chips, and hybridization was performed at 37°C for 60–72 h. Following hybridization and removal of the unhybridized probe, target spots were counterstained with diamidinophenylindole (DAPI). The analysis was performed using the GenoSensor Reader (Abbott-Vysis) which is a large-field multicolor fluorescence imaging system capturing an image of the hybridized chip in three color planes: Cy 3, Cy5, and DAPI blue. The included software automatically identifies each spot and, by analysis of the set of Cy3/Cy5 ratios on all targets, calculates the ratio most representative of the modal DNA copy number of the sample DNA. For each target, the normalized ratio of a target relative to the sample's modal DNA copy number is provided, indicating the degree of gain or loss of copy number. The results were displayed as target reports, image, and coded image panes. The detection of copy ratio changes is highly dependent on the relative abundance of tumor cell DNA in the tissue specimen. As immunohistochemistry showed a high content of reactive inflammatory cells in some samples, we decided to set fluorescence ratios values at less than 0.9 for a genomic loss and at greater than 1.1 for a copy number gain to increase the sensitivity threshold.

FISH analysis

Interphase FISH assay was performed on touch imprints of frozen tissues of all cases, as previously described [1]. After fixation (methanol, formaldehyde) and enzymatic digestion (pepsin), specimens and probes were codenaturated and hybridized overnight according to the manufacturer's instruction. After nuclei counterstaining by DAPI (Vector, Burlingame, USA), the cells were viewed using a fluorescent Axioplan II microscope (Zeiss, Le Pecq, France). Both dual-color dual-fusion (DCDF) and split probes (SP) were assayed. First, we sought systemic B cell lymphoma translocations t(11;14)(q13;q32), t(14;18)(q32;q21) and t(8;14)(q24;q32) by using DCDF probes LSI IGH-CCND1, IGH-BCL-2, and IGH-MYC (Abbott-Vysis). Breakpoints of *IGH* and *MALT1* gene loci were also investigated with the corresponding Split Signal DNA Probes (SP, Dako). The FISH pattern of normal nuclei was two red (R) two green (G) spots (DCDF) or two fusion (F) signals using the SP probes, whereas positive nuclei typically exhibited a 1R1G2F pattern (DCDF) or a 1R1G1F pattern (SP). All variant patterns (1R2G1F, 2R1G1F, etc.) were taken into account for the exact determination of the percentage of normal and positive nuclei.

A second set of probes was employed on cases showing imbalances by CGH array for specific chromosomal regions. The following locus-specific probes were used: LSI AML1/ETO (21q22.3/8q22), MYC and MALT1, TOP2A/HER-2/CEP17 (17q21-q22/17q21.1/Centomere 17), $p14^{ARF}$/$p16^{INK4a}$/*CDKN2A* (9p21), 1p36/1q25, 7p tel, 19q tel. FISH patterns were determined by analyzing 200 nonoverlapped nuclei. The positive threshold to assess translocation or a gene breakpoint was calculated for each probe set as the mean+3 SD of the percentage of nuclei with a positive FISH pattern in control samples. The calculated values for the IgH-BCL-2, IgH-CCND1, IgH-MYC MALT1, and IgH probe sets were 5%, 5%, 5%, 3%, and 10%, respectively. For the other probes, the cutoff values were 5% or less. This value (5%) was finally selected for all locus-specific probes with the exception of 10% for the IGH probes.

$p14^{ARF}$ and $p16^{INK4a}$/*CDKN2A* allelic assay by quantitative real-time PCR

The abovementioned genes were assayed by quantitative PCR (Q-PCR) using a primer pair for the E2 exon shared by the $p14^{ARF}$ and the $p16^{INK4a}$/*CDKN2A* genes and their corresponding probes [21]. Primers specific for the $p16^{INK4a}$/*CDKN2A* E1 exon and their specific probes did not provide reproducible Q-PCR results in our hands. The final primer and fluorescent probe concentration was 200 and 50 nM, respectively. Fifty nanograms genomic DNA was used as a template. The albumin gene served as control according to Hostein et al. [18]. Specificity was checked by melting curve analysis in preliminary experiments with SYBR green and efficiency by dilution curves. Healthy control DNA was used for normalization and showed a constant ratio between the target genes and the albumin control gene. The LN401 glioblastoma cell line (gift of Dr A. Merlo, University Hospital, Basel, Switzerland) exhibits a homozygous deletion at the INK4A locus but a normal Ct value for the control gene [21]. The Ct value for the albumin control gene was used to normalize DNA input around 10 ng (7.5±5 ng). All samples exhibited the same Ct value for albumin (less than 1 Ct variation between samples and triplicates). The relative copy number of $p16^{INK4a}$/*CDKN2A*/*p14ARF* was expressed as the ratio of target gene Ct above the Ct values [18].

$p14^{ARF}$ and $p16^{INK4a}$/*CDKN2A* methylation status

DNA methylation patterns in the CpG islands were determined by methylation-specific PCR (MSP) after bisulfite treatment of DNA to convert all unmethylated cytosines to uracils, according to Lehmann et al. with some modifications [22]. Two hundred nanograms of DNA were incubated in 200 mM NAOH at 42°C for 30 min in a total volume of 50 μL. After the addition of 275 μL of 3.6 M

bisulfite containing 1 mM freshly prepared hydroquinone, samples were incubated for 5 h at 55°C in the dark. Then, 375 μL of 6 M sodium iodine (Sigma) containing 1 mM β-mercaptoethanol and 5 μL glass milk suspension (QIAEX II suspension, Qiagen, Hilden, Germany) were added and mixed thoroughly. After 10 min at room temperature and centrifugation (8,000 rpm, 3 min), the pellet was washed three times with 70% ethanol, once with 20 mM NAOH/90% ethanol 5 min at room temperature and twice with 90% ethanol. DNA was eluted from the dried pellet with 25 μL Tris–EDTA buffer for 15 min at 55°C. From this solution, 1 μL (8 ng) was used for MSP. After an initial denaturation step at 95°C for 10 min, MSP consisted in 40 cycles with 30 s at 95°C, 60 s at 60°C, and 30 s at 72°C.

For the *p16*^{INK4a}*/CDKN2A* promoter region, MSP was performed with E5/E6 primers amplifying methylated or unmethylated DNA together with specific probes for methylated or unmethylated DNA [22]. The primers and probe concentration were 200 and 100 nM, respectively. Per reaction, the Brilliant QPCR Core reagent kit was used with 2.5 mM $MgCl_2$, 1.25 U SureStart *Taq* DNA polymerase, 0.8 mM deoxynucleotide triphosphates, and 30 nM reference dye in a total volume of 25 μL (Stratagene, Amsterdam, The Netherlands).

For *p14*^{ARF} MSP, the primer pairs amplified a region spanning six CpGs within the 5′ region of the gene [7]. Per reaction, the primer concentration was 200 nM in Brilliant QPCR Master Mix 30 nM reference dye in a total volume of 25 μL (Stratagene).

For all primers, melting curve analysis was performed, and the absence of amplification of native DNA samples prior to bisulfite treatment was checked. The American Type Culture Collection (ATCC) human genomic DNA (RPMI 8226; ATCC, Manassas, VA, USA) was used as the control for *p16*^{INK4a}*/CDKN2A* biallelic methylation. The HDLM2 cell line (gift from Dr J.F. Garcia, CNIO Madrid, Spain) was used as the methylated positive control for *p14*^{ARF} and *p16*^{INK4a}*/CDKN2A* [26]. A healthy control DNA showing no methylation for all loci was also included. The efficiency of Q-PCR for the amplification of methylated sequences was determined by serial dilutions of the methylated cell lines in the control unmethylated DNA. This allowed the detection of a 5% dilution of fully methylated DNA within the linear range.

Results

Clinical and histopathological data

Twenty-one PCBCL were included, and their characteristic features are summarized in Table 1.

Ten cases were characterized by a majority of large cells:

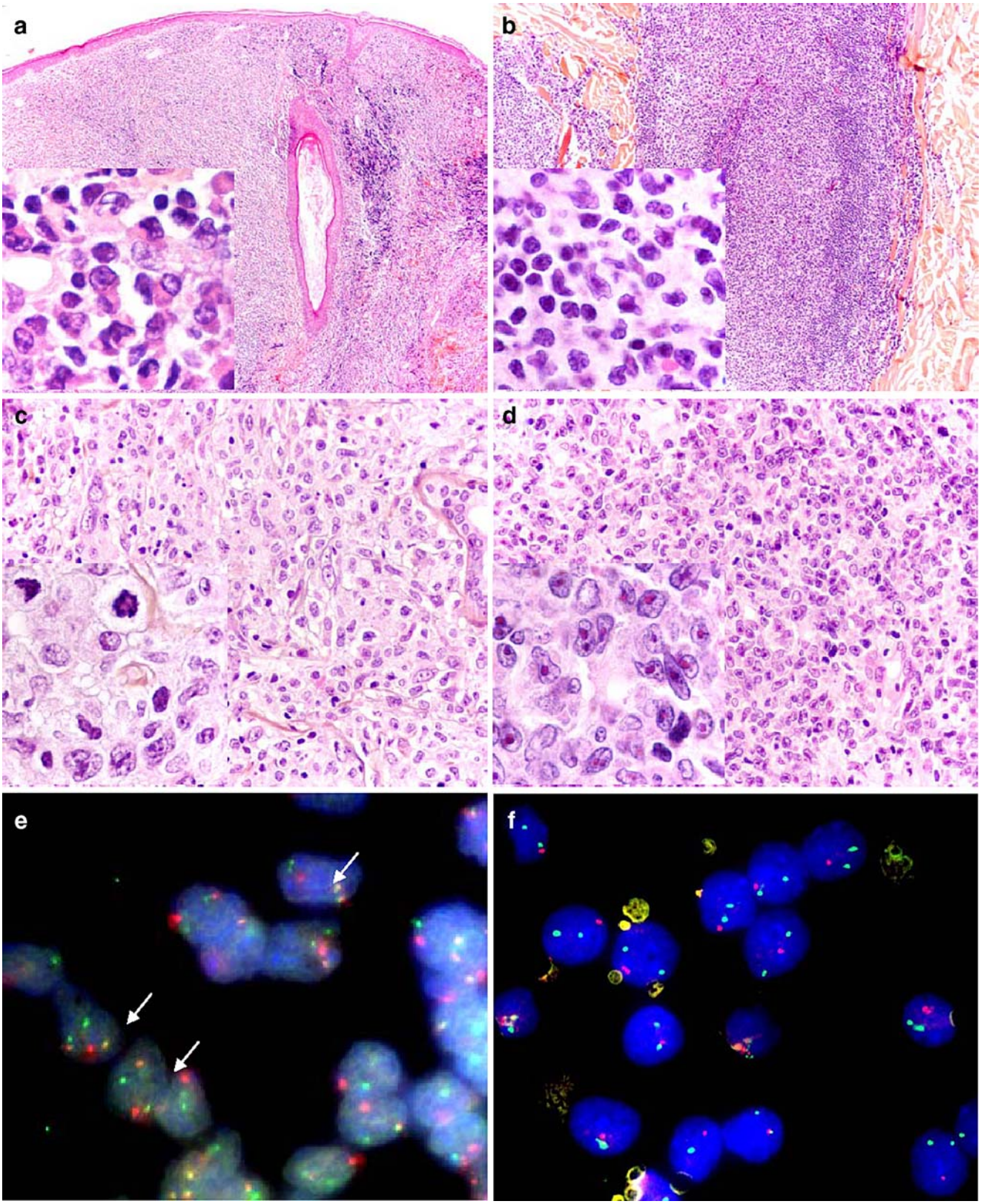
- Six cases (Fig. 1d) were characterized by a round cell morphology and were classified as PCLBCL leg type. Five out of six were located on the leg, and one was located on the arm. BCL2 was highly expressed in all cases, BCL6 and CD10 were negative, and MUM1 was expressed in five out of six cases. Three of six patients presented with extracutaneous spread, and all had cutaneous relapse. The mean overall survival was 29± 26 months.
- Four cases were classified as PCFCL large cells (Fig. 1c). They displayed a large cleaved cell morphology (large centrocytes) and were BCL2 negative. Two were BCL6 positive. The lesions were located on the face/scalp (two of four) or on the trunk (two of four). All patients are alive without disease. The mean follow-up was 7731 months.

Eleven cases were found to contain a majority of small tumoral cells:

- Seven cases (Fig. 1b) were classified as PCFCL small cells because of a follicular architecture and a predominance of small cleaved cells (centrocytes) with a few large centroblastic cells. Their usual phenotype was BCL2+/−, BCL6+, and MUM1− (Table 1). The lesions were located predominantly on the trunk (four out of seven). All patients are alive. The mean follow-up was 8523 months.
- Four cases (Fig. 1a) were classified as PCMZL and were composed of a majority of plasma cells in one case or in three cases by a mixture of plasma cell, centrocytic-like cells with some residual reactive germinal centers, and a hyperplastic follicular dendritic network. Tumor cells had a BCL2-, BCL6-, and MUM1-negative phenotype. Three patients are alive without disease, and the last one has died of another cause. The mean follow-up was 5418 months.

CGH array analysis

Both genomic losses (ratio less than 0.9) and copy number gains (ratio greater than 1.1) were detected by CGH array analysis. In the total group of PCBCL, the mean number of chromosomal aberrations was 34 (range 3 to 131 aberrations per case). Mean genomic gains (n=22) were significantly more frequent than losses (n=12, p<0.05). The mean number of chromosomal imbalances (CI) was higher in large cell lymphomas (PCLBCL leg type and PCFCL large cells, n=50) than in small cell lymphomas (PCFCL small cells and PCMZL, n=18, p<0.05). Some gains (Table 2) and losses (Table 3) were recurrently found in the total group of


a
b
c
d
e
f

◀ **Fig. 1** Histological and FISH features of PCBCL. **a** PCMZL: neoplastic proliferation with marginal zone features (×200). *Insert*: centrocytic-like cells and plasmacytoid differentiation (×1,000). **b** PCFCL small cells characterized by a follicular pattern (×400). *Insert*: predominance of small cleaved B-cells (×1,000). **c** PCFCL large cells with more than 80% of large cleaved B cells (×400). *Insert* (×1,000). **d** PCLBCL leg type characterized by a predominance of round large cells with prominent nucleoli (×400). *Insert* (×1,000). **e** FISH analysis using the LSI IGH-MYC DCDF probes (IGH: *green spots*; MYC: *red spots*). Nuclei with a 1R1G2F hybridization pattern (*arrows*) demonstrated a t(8;14)(q24;q32) in two of six PCLBCL leg-type cases (×630). **f** FISH analysis using the LSI p16 (*red spots*)/CEP 9 (*green spots*) probes. Nuclei with a 1R2G hybridization pattern indicated a hemizygous 9p21.3 deletion ($p14^{ARF}/p16^{INK4a}$ gene) in five of six PCLBCL leg-type cases (×630)

PCBCL. The most frequently observed anomalies were genomic gains in 7ptel (67%), 17q11.2 (48%), 3p21.3 (43%), 2p22.1-2p22.3 (38%), 11q13 (38%), 7q21.1 (29%), 12q12-q13 (29%), and losses in 9p11.2 (33%), 1p36 (29%), 1p36.31 (29%), 6q22-q23 (29%), 10q tel (29%), 1p36.32 (24%), 9p21 (24%), 9p21.3 (24%), 14q tel (24%) and Xp22.3 (24%).

The number of genomic alterations (mean±SD) and the recurrence of these changes were also assessed for each PCBCL subtype. These different groups showed distinct patterns of hybridization (Fig. 2a–c). PCLBCL leg type exhibited more imbalances (62±39) than PCFCL large cells (34±5), PCFCL small cells (24±19), and PCMZL (9±2). PCLBCL leg type exhibited more genomic gains (37±18) and losses (25±21) than PCFCL large cells (24±6, 10±2), PCFCL small cells (17±14, 7±5), and PCMZL (7±1, 2±2). Within the PCFCL small cell group, patients with a unique skin lesion of the head or trunk showed more genomic changes (33±21) than those with multiple lesions (13±6).

In PCLBCL leg type, the most frequent findings (>50% of cases) were genomic gains in 7ptel (five of six), 17q11.2 (five of six), 1p36.33 (four of six), 3p21.3 (four of six), 7p21 (four of six), 7q11.23 (four of six), 7q21.1 (four of six), 11q13 (four of six), 12q12-q13 (four of six), 17q21-q22 (four of six), 19q tel (four of six), and losses in 9p21 (five of six), 9p21.3 (five of six), 6q22-q23 (four of six), and 17p11.2-p12 (four of six).

In the group of PCFCL large cells, only gains in 17q11.2 were found in more than 50% of the cases (three of four). Conversely, several recurrent losses were observed in 1p36 (four of four), 1p36.31 (four of four), 1p36.32 (three of four), 1p36.33 (three of four), and 1p tel (three of four). PCFCL small cells and PCMZL showed fewer genomic alterations than the other PCBCL groups. Gains in more than 50% of cases were observed only for PCFCL small cells: 7ptel (five of seven) and 2p22.1–2p22.3 (four of seven). No genomic loss was found in PCMZL or in the majority of PCFCL small cells.

FISH analysis

Analysis of all the PCBCL showed a t(8;14)(q24;q32) in 33% (two of six) PCLBCL leg type (Fig. 1e). Neither t(11;14)(q13;q32), t(14;18)(q32;q21), *IGH*, or *MALT1* gene rearrangement was detected in the other PCBCL. FISH analysis was also performed to confirm the results of the CGH array analysis.

Both PCLBCL leg type (N=6) and PCFCL large cells (N=4) were assayed using commercially available locus-specific probes allowing the exploration of 11 loci for each of these ten cases: 1p36 (*TP73*), 7p tel, 8q22 (*ETO*), 8q24 (*MYC*), 9p21 ($p14^{ARF}/p16^{INK4a}/CDKN2A$), 11q13 (*CCND1*), 17q21 (*TOP2A*), 17q21 (*HER-2*), 18q21 (*BCL2*), 19q tel, and 21q22 (*AML1*). CGH array analysis found that these loci exhibited either a DNA loss (N=7), DNA amplification (N=35), or a normal (N=68) pattern.

Hybridization of 101 of 110 loci was successfully performed by FISH assay. Concordant results between the two techniques were obtained in 97% (98 of 101) of the cases. In each case, abnormal FISH hybridization patterns were observed in a fraction of the nuclei (9–75%, mean 29%). These patterns always associated DNA losses with hemizygous deletions and DNA amplification with a low number gain (three copies) of the locus. The three discordant results corresponded to DNA amplification (1p36.33 in two PCLBCL leg type and 21q22 in one case of PCFCL large cells) found by CGH array but not by FISH analysis (normal hybridization pattern for all three cases).

Analysis of the chromosomal aberrations led to the identification of several oncogenes and/or tumor suppressor genes present in the regions of interest.

Deletion of chromosome 1p36

CGH array analysis showed a loss of the 1p36.22–1p tel chromosomal region (seven clones) in 50% (two of four) of the PCFCL large-cell cases. Such DNA loss was not found in the other PCBCL groups. The tumor suppressor genes *PRKCZ*, *TP73*, and *CDC2L1* (*p58*) were covered by the deleted clones. According to CGH array analysis, a hemizygous deletion of *TP73* was found by FISH (LSI 1p36/1q25 probe set) in 50% (two of four) of PCFCL large-cell cases but not in the PCLBCL leg-type group. The *CDC2L1* (*p58*) gene was found deleted by CGH array in all the PCFCL large-cell cases (four of four).

Gain in chromosome 7

A DNA amplification of 5 of 12 clones hybridizing on the two arms of chromosome 7 was found by CGH array analysis in 50% (three of six) PCLBCL leg type. The oncogenes *EGFR* and *MDR1* are located in the hybridized areas. A low copy

Table 2 Recurrent gains for all PCBCL

Cytogenetic band	Candidate genes	PCBCL		PCLBCL leg type		PCFCL large cells		PCFCL small cells		PCMZL	
		Total (*N*=21)	Percent	Total (*N*=6)	Percent	Total (*N*=4)	Percent	Total (*N*=7)	Percent	Total (*N*=4)	Percent
1p36.33	–	4	19	4	67	0		0		0	
1q25-q31	*LAMC2*	4	19	2	33	0		0		2	50
1q41	*TGFB2*	2	10	2	33	0		0		0	
1q44	*AKT3*	2	10	0		0		0		2	50
1q tel	–	4	19	2	33	2	50	0		0	
2p22.3–2p22.1	–	8	38	2	33	2	50	4	57	0	
2p13-p12	*REL*	2	10	0		2	50	0		0	
2p12-q11	–	4	19	2	33	2	50	0		0	
3p25-p26	–	2	10	2	33	0		0		0	
3p25	*RAF1*	3	14	3	50	0		0		0	
3p24.3	–	2	10	2	33	0		0		0	
3p21,3-p23	–	2	10	2	33	0		0		0	
3p21.3	*RASSF1*	9	43	4	67	2	50	3	43	0	
3q21-q22	–	2	10	2	33	0		0		0	
3q26	*TERC*	2	10	2	33	0		0		0	
3q27-q29	–	6	29	2	33	0		2	29	2	50
3q tel	–	4	19	2	33	2	50	0		0	
7p tel	–	14	67	5	83	2	50	5	71	2	50
7p21	–	4	19	4	67	0		0		0	
7p12.3-p12.1	*EGFR*	3	14	3	50	0		0		0	
7q11.23	–	4	19	4	67	0		0		0	
7q21.1	*MDR1*	6	29	4	67	2	50	0		0	
7q21-q22	*CDK6*	2	10	2	33	0		0		0	
7q tel	–	7	33	2	33	2	50	3	43	0	
8q24.12–q24.13	*MYC*	2	10	2	33	0		0		0	
8q24-qter	*PTK2*	2	10	0		0		2	29	0	
9p12-q21	–	6	29	2	33	0		2	29	2	50
11q13	*MEN1*	2	10	2	33	0		0		0	
11q13	*CCND1*	8	38	4	67	2	50	2	29	0	
11q tel	–	4	19	2	33	0		0		2	50
12p tel	–	3	14	3	50	0		0		0	
12p13.1-p12	–	3	14	3	50	0		0		0	
12p11.2	*KRAS2*	2	10	2	33	0		0		0	
12q12-q13	*WNT1*	6	29	4	67	2	50	0		0	
12q13	*CDK2*	4	19	2	33	0		2	29	0	
12q13.2-q13.3	*GLI*	5	24	2	33	0		3	43	0	
12q13-q14	*SAS*, *CDK4*	2	10	0		0		2	29	0	
12q14.3-q15	*MDM2*	2	10	2	33	0		0		0	
12q tel	–	3	14	3	50	0		0		0	
14q32.32	*AKT1*	2	10	2	33	0		0		0	
16q23.2	–	2	10	2	33	0		0		0	
16q24.2	–	4	19	3	50	1	25	0		0	
17q11.2	*THRA*	10	48	5	83	3	75	2	29	0	
17q11.2–17q12	*HER-2*	2	10	2	33	0		0		0	
17q12	*PPARBP*	2	10			0		2	29	0	
17q21-q22	*TOP2A*	6	29	4	67	2	50	0		0	
17q21.3	–	2	10	2	33	0		0		0	
18q11.2	–	5	24	3	50	0		2	29	0	
18q12.3	–	3	14	0		0		3	43	0	
18q21.1	–	3	14	3	50	0		0		0	
18q21.3	*BCL2*	2	10	2	33	0		0		0	
18q tel	–	2	10	2	33	0		0		0	
19q13.1-q13.2	*AKT2*	2	10	2	33	0		0		0	
19q tel	–	4	19	4	67	0		0		0	

Table 2 (continued)

Cytogenetic band	Candidate genes	PCBCL		PCLBCL leg type		PCFCL large cells		PCFCL small cells		PCMZL	
		Total (N=21)	Percent	Total (N=6)	Percent	Total (N=4)	Percent	Total (N=7)	Percent	Total (N=4)	Percent
20q13	*TNFRSF6B*	2	10	2	33	0		0		0	
21q22	*DYRK1A*	2	10	0		2	50	0		0	
21q22.3	*AML1*	4	19	0		2	50	2	29	0	
21q tel	*PCNT2*	2	10	0		2	50	0		0	
22q11.21	–	4	19	2	33	0		2	29	0	
22q11.23	*BCR*	2	10	2	33	0		0		0	
22q13.1	*PDGFB*	2	10	2	33	0		0		0	
Xp21.1	–	2	10	0		2	50	0		0	
Xq11-q12	*AR 3′*	2	10	0		2	50	0		0	

number gain restricted to the chromosome 7p tel was also observed in 83% (five of six) of PCLBCL leg type, 50% (two of four) of PCFCL large cells, 71% (five of seven) of PCFCL small cells, and in 50% (two of four) of PCMZL. Five of these cases were assayed by FISH (LSI 7p tel probe), which demonstrated a trisomy of this locus in each case.

Gain in chromosome 11q13

CGH array analysis showed a gain in the chromosomal region 11q13 in 67% (four of six) of PCLBCL leg type, 50% (two of four) of PCFCL large cells, and in 29% (two of seven) of PCFCL small cells. FISH confirmed this finding and showed a trisomy of this locus covering the *CCND1* gene.

Gain in chromosome 12q12-q13

A gain of 11 of 13 clones covering chromosome 12 was detected by CGH array analysis in 33% (two of six) of PCLBCL leg type. A common minimal region of gain (one clone) of the chromosomal region 12q12-q13 was found in 67% (four of six) PCLBCL leg type and in 50% (two of four) PCFCL large cells. This area covered the gene *WNT1*, which triggers oncogenic conversion. Another gain in 12q13-q14 encompassing the *CDK2*, *CDK4, MDM2*, and *GLI* oncogenes was found in 29–43% (two to three of seven) PCFCL small cells.

Gain in chromosome 17q11.2-q22

A DNA amplification of the chromosomal region 17q11.2-q22 (five clones) was found by CGH array analysis in 33% (two of six) of PCLBCL leg type. Two clones in this region more frequently showed a chromosomal alteration. One encompassing the *THRA* gene was associated with DNA amplification in 83% (five of six) of PCLBCL leg type, 75% (three of four) of PCFCL large cells, and in 29% (two of seven) of PCFCL small cells. The other clone covered the *TOP2A* gene and showed a gain in 67% (four of six) of PCLBCL leg type and in 50% (two of four) of PCFCL large cells. FISH experiments (LSI TOP2A/HER-2/CEP17) demonstrated a trisomy of the loci 17q11-q12 (*TOP2A*) and 17q11.2-17q12 (*HER-2*). FISH and CGH array results were strictly correlated.

Gain in chromosome 19q tel

A gain in the 19q tel chromosomal region was found by CGH array exclusively in 67% (four of six) of the PCLBCL leg type. FISH analysis (LSI 19q tel) confirmed this observation and showed a trisomy of this locus.

Deletion of chromosome 9p21.3 involving $p14^{ARF}$ and $p16^{INK4a}$/*CDKN2A*

A loss of the 9p21.3 chromosomal region was observed in 83% (five of six) of PCLBCL leg type, in accordance with their CGH array analysis. FISH experiments using the LSI p14/p16 probe set identified a common altered region with a hemizygous 9p21.3 deletion encompassing the *CDKN2A* ($p14^{ARF}$/$p16^{INK4A}$), *CDKN2B* ($p15^{INK4B}$), and *MTAP* genes (Fig. 1f). The nondeleted PCLBCL leg-type case (no. 6) showed clinical lesions involving the arm and not the leg, as in the five other PCLBCL leg-type cases. None of the PCFCL large-cell cases (n=4) exhibited 9p21.3 deletion, in accordance CGH array data (Table 4).

$p14^{ARF}$/$p16^{INK4a}$*CDKN2A* gene quantification

The genetic analysis of a common E2 exon of $p14^{ARF}$ and $p16^{INK4a}$/*CDKN2A* genes was performed on PCLBCL leg type and PCFCL large cells. The relative copy number of $p14^{ARF}$/$p16^{INK4a}$/*CDKN2A* was expressed as the ratio of target exon Ct over the control gene Ct values [18]. Healthy control DNA as well as nondeleted samples were characterized by a Ct ratio=1.1±0.1. Cases with an exon E2-deleted ratio displayed a Ct ratio less than 0.5, and all corresponded to PCLBCL leg type, whereas PCFCL large cells displayed a normal range ratio. Due to a variable proportion between

Table 3 Recurrent losses for all PCBCL

Cytogenetic band	Candidate genes	PCBCL		PCLBCL leg type		PCFCL large cells		PCFCL small cells		PCMZL	
		Total (*N*=21)	Percent	Total (*N*=6)	Percent	Total (*N*=4)	Percent	Total (*N*=7)	Percent	Total (*N*=4)	Percent
1p tel	–	3	13	0		3	75	0		0	
1p36.33	*PRKCZ*	3	14	0		3	75	0		0	
1p36.33	*TP73*	2	10	0		2	50	0		0	
1p36.32	–	5	24	0		3	75	2	29	0	
1p36.31	–	6	29	2	33	4	100	0		0	
1p36.22	–	2	10	0		2	50	0		0	
1p36.13	–	2	10	2	33	0		0		0	
1p36	*CDC2L1(p58)*	6	29	0		4	100	2	29	0	
1p32.3	–	2	10	2	33	0		0		0	
1p31.1	–	4	19	2	33	0		2	29	0	
1p13.2	–	2	10	2	33	0		0		0	
4q24	–	2	10	0		0		2	29	0	
4q tel	–	2	10	2	33	0		0		0	
5p15.2	–	2	10	0		0		2	29	0	
6q16.3	–	3	14	3	50	0		0		0	
6q16.3-q21	–	2	10	2	33	0		0		0	
6q22-q23	–	6	29	4	67	2	50	0		0	
6q25,1	–	2	10	2	33	0		0		0	
6q tel	–	2	10	2	33	0		0		0	
8p tel	–	2	10	2	33	0		0		0	
8p22	*CTSB*	2	10	2	33	0		0		0	
8p22-p21.3	*PDGRL*	3	14	2\3	50	0		0		0	
8p22	–	2	10	2	33	0		0		0	
8p11.2-p11.1	–	2	10	2	33	0		0		0	
8q11	–	2	10	2	33	0		0		0	
8p22-q21.3	–	4	19	0		2	50	2	29	0	
9p11.2	–	7	33	2	33	2	50	3	43	0	
9p21.3	*MTAP*	5	24	5	83	0		0		0	
9p21	*P16MTAP*	5	24	5	83	0		0		0	
10q tel	–	6	29	3	50	0		3	43	0	
14q tel	–	5	24	2	33	0		3	43	0	
15q11-q13	–	3	14	3		0		0		0	
16q24.3	*FANCA*	2	10	0		0		2	29	0	
17p12–11.2	–	4	19	4	67	0		0		0	
17q23	–	3	14	3	50	0		0		0	
Xp22.3	–	5	24	3	50	0		2	29	0	
Xq11-q12	*AR 3′*	3	14	3	50	0		0		0	
Xq13.2	*XIST*	2	10	2	33	0		0		0	
Xq25	–	2	10	2	33	0		0			

tumor and reactive cells, such global technique could not determine whether the *p16* deletions were mono- or biallelic.

Finally, real-time Q-PCR correlated with both FISH and CGH array data in nine out of ten large PCBCL cases (Table 4). Case 6 displayed a deleted ratio for $p14^{ARF}$/$p16^{INK4a}$/*CDKN2A* exon2, which may correspond to cryptic deletion not detected by FISH or CGH array techniques using probes covering a much larger region.

$p14^{ARF}$ and $p16^{INK4a}$/*CDKN2A* methylation analysis

After bisulfite modification of DNA, analysis was performed in parallel with different primer pairs specific for either the unmethylated DNA or methylated DNA. Despite the use of a very sensitive real-time PCR assay with specific probe detection for $p16^{INK4a}$/*CDKN2A* methylated DNA as shown by dilution experiments, no amplification

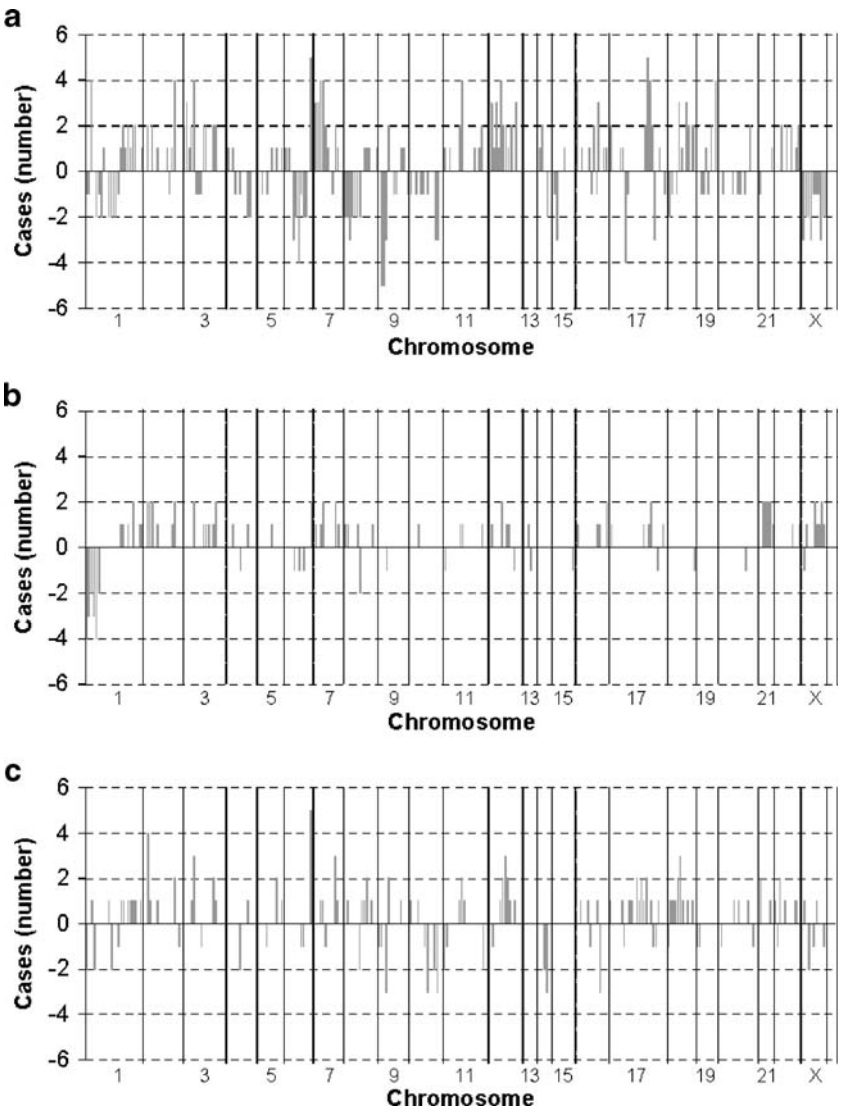


Fig. 2 CGH array analysis of PCBCL DNA was extracted from 21 tumoral skin biopsies and CGH analysis was performed using the Array 300 (Abbott-Vysis). The genomic alterations are indicated in **a** the group of PCLBCL leg type (*N*=6), **b** the group of PCFCL large cells (*N*=4), and **c** the group of PCFCL small cells (*N*=7). Positive values represent gains, and negative values represent losses

Table 4 *p16* gene status in large cells PCBCL

Case number	Diagnosis	Q-PCR	FISH	Methylation		IHC	
		p14/p16	LSI p16	p14	p16	EGH4	G175–405
1	PCLBCL leg type	Del	Del (24%)	U	NI	NI	NI
2		Del	Del (30%)	U	U	−	−
3		Del	Del (12%)	U	U	−	−
4		Del	Del (65%)	U	U	NI	NI
5		Del	Del (50%)	U	U	−	NI
6		Del	N	U	U	−	−
7	PCFCL, large cells	N	N	U	U	NI	NI
8		N	N	U	U	+ (5%)	+ (10%)
9		N	N	U	U	−	−
10		N	N	U	U	NI	NI

Del Deleted, *N* normal, *U* unmethylated, *NI* noninformative, + positive, − negative

for methylated sequences was achieved from PCLBCL leg type or PCFCL large cell samples.

p16^{INK4a}/CDKN2A immunohistochemical detection

Using two monoclonal antibodies with a different visualization system in parallel with several positive controls as described above, no labeling of tumor cell nuclei was observed in PCLBCL leg type or PCFCL large cell samples, except in case 8 with a minority of positive tumor cells (10%, data not shown). When no reactive or endothelial positive cell could be detected on consecutive sections, samples were interpreted as noninformative that could result from a sample over fixation or degradation.

Discussion

PCBCL is a heterogeneous group of B cell lymphomas falling into three main diagnostic categories: PCMZL, PCFCL, and PCLBCL leg type [32]. Our goal was therefore to analyze their genetic profiles on typical cases using commercially available tools that in turn could be used as ancillary diagnostic markers for borderline cases, especially between PCFCL and PCLBCL leg type. Therefore, we also separated large-cell PCFCL from small-cell PCFCL. The simple CGH array with a restricted set of genetic loci used in this study showed a higher number of CI (for gains or losses) in PCLBCL leg type (62±39) than in PCFCL large cells (34±5) or PCFCL small cells (24±19). PCMZL exhibited few or no CI (9±2). Moreover, FISH confirmed the CGH array data with a very high concordance (97%) when exploring the genetic status of 11 loci in ten cases of PCLBCL leg type (n=6) and PCFCL large cells (n=4). Our data are in broad accordance with previous studies using classical CGH showing a higher number of CI in PCLBCL leg type than in PCFCL [13, 14]. A combined CGH and CGH array study also found CI in 50% of diffuse large cell lymphoma, 33% of PCMZL, and in only one out of six PCFCL (8%) [23].

In our study, PCLBCL leg type was characterized in the majority of cases by a predominance of genomic gains at 1p36.33, 3p21.3, 7p21, 7ptel 7q11.23, 7q21.1, 11q13, 12q12-q13, 17q11.2, 17q21-q22, and 19q tel. Conversely, the most frequent losses were observed at 1p36, 1p36.31, 1p36.32, 1p36.33, 1p tel, 6q22-q23, 9p21, 9p21.3, and 17p11.2-p12. Our findings share some similarities with other series. Gains at 3p, 7p, 7q, and 12q and losses at 6q and 9p21 have also been reported in PCLBCL leg-type cases by other studies [6, 10, 14, 23].

In our study, PCFCL large cells displayed fewer genetic imbalances than PCLBCL leg type with rare recurrent gains at 2p, 12q12-q13, and 17q11.2 in accordance with other reports [14]. Specific gains at 2p13-p12 may indeed involve specific *REL* or *BCL11A* gene amplification as shown by FISH experiments [6, 14]. Strikingly, no other study has reported hemizygous losses at 1p36 observed by both CGH array and FISH as in our PCFCL large-cell cases.

PCFCL small cells and PCMZL showed even less frequent genomic alterations. Gains in the majority of cases were only observed for PCFCL small cells at 7ptel and 2p22.1-2p22.3: Differential diagnosis between PCMZL and PCFCL small cells may be further supported by their different genetic profiles. Some alterations such as 2p, 3q, and 11q13 gains were shared, although at different rates by PCLBCL leg type, PCFCL large cells, and PCFCL small cells, but were not seen in PCMZL cases. Despite selection of cases with marked dermal infiltration, the relative abundance of reactive cells may account for the negative CGH array results in PCMZL.

In contrast with the abovementioned reports, we did not detect any 18q21 gain in PCLBCL leg-type cases, and our CGH array data were confirmed by FISH experiments with both MALT1 and BCL2 probes. Indeed, 6q loss and 18q gain or amplification were primarily found in the majority of PCLBCL leg-type but not in PCFCL cases [10, 14, 24]. These imbalances were further detected in, respectively, 32% and 11% of PCFCL cases [6]. Differences in methodology (classical CGH vs. CGH array) and inclusion criteria prior to the WHO/EORTC classification make it difficult to correlate data obtained on different patients at heterogeneous clinical stages. BCL2 overexpression was detected by immunohistochemistry in six cases of PCLBCL leg type but was not correlated with a gain in 18q21. This observation is in accordance with a previous CGH report, which did not find any 18q gain in 9 of 16 diffuse large B cell lymphomas overexpressing BCL2 [2]. Conversely, chromosomal 18q amplifications were associated with the BCL2 overexpression in these lymphomas [25].

Interphase FISH experiments have suggested that t(14;18)(q32;q21) involving *IGH–MALT1* could be observed in a subset of PCMZL with monocytoid morphology [27]. No *MALT1* rearrangement was observed in our limited series of four MALT cases (three with monocytoid morphology), in accordance with larger reports showing the lack of *MALT1* or *IGH* rearrangement in PCMZL [5, 13, 35]. Strikingly, Streubel et al. found by FISH the t(14;18)(q32;q21) involving *IGH–BCL2* in a significant proportion (41%) of PCFCL, although consensus PCR with BIOMED-2 primers failed to amplify BCL2-JH rearrangement [29]. Such cases, which could represent borderline cases with systemic follicle center lymphoma and with unique skin presentation, were not observed in either our present or previous reports, in accordance with many other observers [3, 14, 19, 23, 30]. We also detected *IGH* breakpoints in two out of our six PCLBCL leg-type cases

that were associated with *MYC* breakpoints without amplification in a reciprocal t(8;14)(q24;q32), as reported by others [13]. Conversely, no *IGH* breakpoint was detected in other PCBCL subtypes, as in our cases [13].

Interphase FISH was found to correlate with the CGH array technique for the detection of $p16^{INK4a}$/*CDKN2A* hemizygous deletion in five of six PCLBCL leg-type cases, whereas the remaining case was found to display a cryptic $p16^{INK4a}$/*CDKN2A* deletion by semiquantitative real-time PCR. Therefore, 9p21 loss not detected in other histological subtypes appears as the most recurrent genetic imbalance of PCLBCL leg type. Such loss was not found in conventional CGH studies, which may only detect larger deletions [10, 14]. Indeed, loss of heterozygosity at 9p21 was previously described in 2 out of 36 PCBCL cases [4]. In a recent array-based study, homozygous deletion of 9p21.3 was found in only 5 of 12 patients with PCLBCL leg type and was not observed in 19 patients with PCFCL [6]. In addition, complete methylation of the promoter region of $p16^{INK4a}$/*CDKN2A* but not of $p15^{INK4b}$/*CDKN2B* was also detected in two other PCLBCL leg-type cases, including one with hemizygous deletion. Such hypermethylation was not detected in our case despite the use of a sensitive real-time PCR technique. Our data and those of Dijkman et al. for $p15^{INK4b}$/*CDKN2B* [6] also contrast with the report of both $p16^{INK4a}$/*CDKN2A* and $p15^{INK4b}$/*CDKN2B* promoter hypermethylation in 43% and 23% of PCBCL cases of different subtypes [4]. In contrast with the latter report, we were unable to analyze $p16^{INK4a}$/*CDKN2A* immunohistochemical loss confidently according to the criteria used to calibrate our immunohistochemical procedure. More interestingly, all seven patients with PCLBCL leg type and $p16^{INK4a}$/*CDKN2A* inactivation of Dijkman et al. died like our patients, which would suggest that such genetic alterations are only seen in cases with adverse prognosis.

Finally, the genetic study of a restricted set of typical PCBCL strengthens their clinicopathological subclassification into three main categories. As the most aggressive disease, PCLBCL leg type requires therapeutic intensification, and its diagnosis may require further genetic studies, especially for borderline cases with PCFCL. Therefore, interphase FISH for the detection of *IGH*, *MYC*, or *BCL6* breakpoints and especially $p16^{INK4a}$/*CDKN2A* deletion may be a valuable diagnostic tool. It would also be relevant to determine in a larger series whether $p16^{INK4a}$/*CDKN2A* deletion among PCBCL is truly specific of PCLBCL leg type.

Acknowledgments This work was supported by a grant from the Programme Hospitalier de Recherche Clinique (CHU Bordeaux) and from the Ligue Nationale contre le Cancer (comité Aquitaine Charentes). We thank Dr. Ray Cooke for his linguistic advice.

Conflict of interest statement We declare that we have no conflict of interest.

References

1. Belaud-Rotureau MA, Parrens M, Dubus P, Garroste JC, de Mascarel A, Merlio JP (2002) A comparative analysis of FISH, RT-PCR, PCR, and immunohistochemistry for the diagnosis of mantle cell lymphomas. Mod Pathol 15:517–525
2. Berglund M, Enblad G, Flordal E, Lui WO, Backlin C, Thunberg U, Sundstrom C, Roos G, Allander SV, Erlanson M, Rosenquist R, Larsson C, Lagercrantz S (2002) Chromosomal imbalances in diffuse large B-cell lymphoma detected by comparative genomic hybridization. Mod Pathol 15:807–816
3. Child FJ, Russell-Jones R, Woolford AJ, Calonje E, Photiou A, Orchard G, Whittaker SJ (2001) Absence of the t(14;18) chromosomal translocation in primary cutaneous B-cell lymphoma. Br J Dermatol 144:735–744
4. Child FJ, Scarisbrick JJ, Calonje E, Orchard G, Russell-Jones R, Whittaker SJ (2002) Inactivation of tumor suppressor genes p15 (INK4b) and p16(INK4a) in primary cutaneous B cell lymphoma. J Invest Dermatol 118:941–948
5. de la Fouchardiere A, Gazzo S, Balme B, Chouvet B, Felman P, Coiffier B, Salles G, Callet-Bauchu E, Berger F (2006) Cytogenetic and molecular analysis of 12 cases of primary cutaneous marginal zone lymphomas. Am J Dermatopathol 28:287–292
6. Dijkman R, Tensen CP, Jordanova ES, Knijnenburg J, Hoefnagel JJ, Mulder AA, Rosenberg C, Raap AK, Willemze R, Szuhai K, Vermeer MH (2006) Array-based comparative genomic hybridization analysis reveals recurrent chromosomal alterations and prognostic parameters in primary cutaneous large B-cell lymphoma. J Clin Oncol 24:296–305
7. Esteller M, Tortola S, Toyota M, Capella G, Peinado MA, Baylin SB, Herman JG (2000) Hypermethylation-associated inactivation of p14(ARF) is independent of p16(INK4a) methylation and p53 mutational status. Cancer Res 60:129–133
8. Geelen FA, Vermeer MH, Meijer CJ, Van der Putte SC, Kerkhof E, Kluin PM, Willemze R (1998) bcl-2 protein expression in primary cutaneous large B-cell lymphoma is site-related. J Clin Oncol 16:2080–2085
9. Gellrich S, Rutz S, Golembowski S, Jacobs C, von Zimmermann M, Lorenz P, Audring H, Muche M, Sterry W, Jahn S (2001) Primary cutaneous follicle center cell lymphomas and large B cell lymphomas of the leg descend from germinal center cells. A single cell polymerase chain reaction analysis. J Invest Dermatol 117:1512–1520
10. Gimenez S, Costa C, Espinet B, Sole F, Pujol RM, Puigdecanet E, Garcia-Moreno P, Sanchez J, Gallardo F, Estrach T, Garcia-Muret P, Romagosa V, Serrano S, Servitje O (2005) Comparative genomic hybridization analysis of cutaneous large B-cell lymphomas. Exp Dermatol 14:883–890
11. Grange F, Bekkenk MW, Wechsler J, Meijer CJ, Cerroni L, Bernengo M, Bosq J, Hedelin G, Fink Puches R, van Vloten WA, Joly P, Bagot M, Willemze R (2001) Prognostic factors in primary cutaneous large B-cell lymphomas: a European multicenter study. J Clin Oncol 19:3602–3610
12. Grange F, Petrella T, Beylot-Barry M, Joly P, D'Incan M, Delaunay M, Machet L, Avril MF, Dalac S, Bernard P, Carlotti A, Esteve E, Vergier B, Dechelotte P, Cassagnau E, Courville P, Saiag P, Laroche L, Bagot M, Wechsler J (2004) Bcl-2 protein expression is the strongest independent prognostic factor of survival in primary cutaneous large B-cell lymphomas. Blood 103:3662–3668
13. Hallermann C, Kaune KM, Gesk S, Martin-Subero JI, Gunawan B, Griesinger F, Vermeer MH, Santucci M, Pimpinelli N, Willemze R, Siebert R, Neumann C (2004) Molecular cytogenetic analysis of chromosomal breakpoints in the IGH, MYC, BCL6, and MALT1 gene loci in primary cutaneous B-cell lymphomas. J Invest Dermatol 123:213–219

14. Hallermann C, Kaune KM, Siebert R, Vermeer MH, Tensen CP, Willemze R, Gunawan B, Bertsch HP, Neumann C (2004) Chromosomal aberration patterns differ in subtypes of primary cutaneous B cell lymphomas. J Invest Dermatol 122:1495–1502
15. Harris NL, Jaffe ES, Diebold J, Flandrin G, Muller-Hermelink HK, Vardiman J, Lister TA, Bloomfield CD (1999) World Health Organization classification of neoplastic diseases of the hematopoietic and lymphoid tissues: report of the Clinical Advisory Committee meeting—Airlie House, Virginia, November 1997. J Clin Oncol 17:3835–3849
16. Hoefnagel JJ, Dijkman R, Basso K, Jansen PM, Hallermann C, Willemze R, Tensen CP, Vermeer MH (2005) Distinct types of primary cutaneous large B-cell lymphoma identified by gene expression profiling. Blood 105:3671–3678
17. Hoefnagel JJ, Mulder MM, Dreef E, Jansen PM, Pals ST, Meijer CJ, Willemze R, Vermeer MH (2006) Expression of B-cell transcription factors in primary cutaneous B-cell lymphoma. Mod Pathol 19:1270–1276
18. Hostein I, Pelmus M, Aurias A, Pedeutour F, Mathoulin-Pelissier S, Coindre JM (2004) Evaluation of MDM2 and CDK4 amplification by real-time PCR on paraffin wax-embedded material: a potential tool for the diagnosis of atypical lipomatous tumours/well-differentiated liposarcomas. J Pathol 202:95–102
19. Hsi ED, Mirza I, Gascoyne RD (2002) Absence of t(14,18) chromosomal translocation in primary cutaneous B- cell lymphoma. Br J Dermatol 146:1110–1111 discussion 1111–1112
20. Kodama K, Massone C, Chott A, Metze D, Kerl H, Cerroni L (2005) Primary cutaneous large B-cell lymphomas: clinicopathologic features, classification, and prognostic factors in a large series of patients. Blood 106:2491–2497
21. Labuhn M, Jones G, Speel EJ, Maier D, Zweifel C, Gratzl O, Van Meir EG, Hegi ME, Merlo A (2001) Quantitative real-time PCR does not show selective targeting of p14(ARF) but concomitant inactivation of both p16(INK4A) and p14(ARF) in 105 human primary gliomas. Oncogene 20:1103–1109
22. Lehmann U, Hasemeier B, Lilischkis R, Kreipe H (2001) Quantitative analysis of promoter hypermethylation in laser-microdissected archival specimens. Lab Invest 81:635–638
23. Mao X, Lillington D, Child F, Russell-Jones R, Young B, Whittaker S (2002) Comparative genomic hybridization analysis of primary cutaneous B-cell lymphomas: identification of common genomic alterations in disease pathogenesis. Genes Chromosomes Cancer 35:144–155
24. Mao X, Orchard G, Lillington DM, Child FJ, Vonderheid EC, Nowell PC, Bagot M, Bensussan A, Russell-Jones R, Young BD, Whittaker SJ (2004) BCL2 and JUNB abnormalities in primary cutaneous lymphomas. Br J Dermatol 151:546–556
25. Monni O, Joensuu H, Franssila K, Klefstrom J, Alitalo K, Knuutila S (1997) BCL2 overexpression associated with chromosomal amplification in diffuse large B-cell lymphoma. Blood 90:1168–1174
26. Sanchez-Aguilera A, Delgado J, Camacho FI, Sanchez-Beato M, Sanchez L, Montalban C, Fresno MF, Martin C, Piris MA, Garcia JF (2004) Silencing of the p18INK4c gene by promoter hypermethylation in Reed-Sternberg cells in Hodgkin lymphomas. Blood 103:2351–2357
27. Schreuder MI, Hoefnagel JJ, Jansen PM, van Krieken JH, Willemze R, Hebeda KM (2005) FISH analysis of MALT lymphoma-specific translocations and aneuploidy in primary cutaneous marginal zone lymphoma. J Pathol 205:302–310
28. Senff NJ, Hoefnagel JJ, Jansen PM, Vermeer MH, van Baarlen J, Blokx WA, Canninga-van Dijk MR, Geerts ML, Hebeda KM, Kluin PM, Lam KH, Meijer CJ, Willemze R (2007) Reclassification of 300 primary cutaneous B-cell lymphomas according to the new WHO–EORTC classification for cutaneous lymphomas: comparison with previous classifications and identification of prognostic markers. J Clin Oncol 25:1581–1587
29. Streubel B, Scheucher B, Valencak J, Huber D, Petzelbauer P, Trautinger F, Weihsengruber F, Mannhalter C, Cerroni L, Chott A (2006) Molecular cytogenetic evidence of t(14;18)(IGH;BCL2) in a substantial proportion of primary cutaneous follicle center lymphomas. Am J Surg Pathol 30:529–536
30. Vergier B, Belaud-Rotureau MA, Benassy MN, Beylot-Barry M, Dubus P, Delaunay M, Garroste JC, Taine L, Merlio JP (2004) Neoplastic cells do not carry bcl2-JH rearrangements detected in a subset of primary cutaneous follicle center B-cell lymphomas. Am J Surg Pathol 28:748–755
31. Wiesner T, Streubel B, Huber D, Kerl H, Chott A, Cerroni L (2005) Genetic aberrations in primary cutaneous large B-cell lymphoma: a fluorescence in situ hybridization study of 25 cases. Am J Surg Pathol 29:666–673
32. Willemze R (2006) Primary cutaneous B-cell lymphoma: classification and treatment. Curr Opin Oncol 18:425–431
33. Willemze R, Jaffe ES, Burg G, Cerroni L, Berti E, Swerdlow SH, Ralfkiaer E, Chimenti S, Diaz-Perez JL, Duncan LM, Grange F, Harris NL, Kempf W, Kerl H, Kurrer M, Knobler R, Pimpinelli N, Sander C, Santucci M, Sterry W, Vermeer MH, Wechsler J, Whittaker S, Meijer CJ (2005) WHO–EORTC classification for cutaneous lymphomas. Blood 105:3768–3785
34. Willemze R, Kerl H, Sterry W, Berti E, Cerroni L, Chimenti S, Diaz-Perez JL, Geerts ML, Goos M, Knobler R, Ralfkiaer E, Santucci M, Smith N, Wechsler J, van Vloten WA, Meijer CJ (1997) EORTC classification for primary cutaneous lymphomas: a proposal from the Cutaneous Lymphoma Study Group of the European Organization for Research and Treatment of Cancer. Blood 90:354–371
35. Wongchaowart NT, Kim B, Hsi ED, Swerdlow SH, Tubbs RR, Cook JR (2006) t(14;18)(q32;q21) involving IGH and MALT1 is uncommon in cutaneous MALT lymphomas and primary cutaneous diffuse large B-cell lymphomas. J Cutan Pathol 33:286–292

Virchows Arch (2008) 452:621–627
DOI 10.1007/s00428-008-0594-9

ORIGINAL ARTICLE

Cyclin D1 expression is induced by viral BARF1 and is overexpressed in EBV-associated gastric cancer

Thorsten Wiech · Elisabeth Nikolopoulos · Silke Lassman · Timo Heidt · Anja Schöpflin · Mario Sarbia · Martin Werner · Yuko Shimizu · Emna Sakka · Tadamasa Ooka · Axel zur Hausen

Received: 3 October 2007 / Revised: 7 January 2008 / Accepted: 6 February 2008 / Published online: 25 April 2008
© Springer-Verlag 2008

Abstract Approximately 10% of gastric carcinomas (GC) worldwide are associated with Epstein–Barr virus (EBV). GC is one of the most frequent human malignancies associated with EBV. The latent expression of the EBV-oncogene BARF1 is restricted to epithelial malignancies. To investigate the underlying BARF1-related mechanisms of oncogenic epithelial transformation, we analyzed gene expression profiles of a BARF1-transfected epithelial (HaCaT+) and the corresponding BARF1-negative (HaCaT−) cell line by cDNA microarray analysis. Real-time PCR was performed to confirm the cDNA microarray results. In addition, immunohistochemistry and fluorescence in situ hybridization were performed on a tissue microarray of 181 GC including 11 EBV-associated GC. Among other genes cyclin D1 expression was significantly upregulated in HaCaT+ on the transcriptional and protein level. Cyclin D1 protein expression in GC revealed a significant overexpression of cyclin D1 in EBV-associated GC ($p<0.012$) but not in EBV-negative GC. Cyclin D1 FISH showed that cyclin D1 overexpression was not due to gene amplification in EBV-associated GC. Cyclin D1 is induced in HaCaT+ by BARF1 and is overexpressed in EBV-associated GC indicating an interaction of viral BARF1 and cyclin D1.

Keywords Epstein–Barr virus · Gastric carcinogenesis · BARF1 · Viral oncogene · Cyclin D1

T. Wiech · E. Nikolopoulos · S. Lassman · T. Heidt · A. Schöpflin · M. Werner · Y. Shimizu · A. zur Hausen (✉)
Institute of Pathology, University Hospital Freiburg,
Breisacherstr, 115A,
79106 Freiburg, Germany
e-mail: axel.zurhausen@uniklinik-freiburg.de

M. Sarbia
Institute of Pathology, Technical University,
Munich, Germany

Y. Shimizu · E. Sakka · T. Ooka
Laboratoire de Virologie Moléculaire, UMR5537, CNRS,
Faculté de Médecine R.T.H. Laennec,
Université Claude Bernard Lyon-1,
Lyon, France

Present address:
M. Sarbia
Institute of Pathology,
Nymphenburg,
Munich, Germany

Introduction

Although the incidence of gastric cancer is declining, it still remains the fourth most common type of cancer and the second leading cause of cancer-related death worldwide [6]. The association of EBV with approximately 10% of gastric carcinomas (GC) and endemic nasopharyngeal carcinoma (NPC) is well established [18, 28]. With an incidence of approximately 88,000 new cases each year worldwide, GC is one of the most frequent EBV-associated human malignancies. However, the exact role of EBV in the carcinogenesis of GC and NPC remains to be elucidated, though very recent findings indicate an important and independent role of EBV in gastric carcinogenesis [1]. Recently, the expression of the EBV-encoded oncogene BARF1 (i.e., *Bam*HI A rightward open reading frame 1) has been reported in EBV-associated GC [15, 27, 36]. Latent BARF1 expression is restricted to epithelial EBV-associated malignancies [8, 11, 15, 24, 27, 36]. BARF1 induces malignant transformation of rodent fibroblasts and transfection of the BARF1 gene enhances the tumorigenic-

ity of BL-derived Louckes and Akata cells [26, 31, 32]. In addition, BARF1 is able to immortalize primary monkey epithelial cells [33]. Transfection of the BARF1 gene has been reported to result in growth activation of monkey epithelial cells, in which the viral sequence was specifically localized in double minute chromosomes [9]. Thus it appeared that BARF1 was implicated not only in cell immortalization but also in malignant transformation. It has been demonstrated recently that the first 54 amino acids of BARF1 are sufficient to both, induce malignant cell transformation, and activate Bcl2 expression [25]. Bcl2 activation was also observed in EBV-negative human Akata B cell transfected by BARF1 [26]. However, the oncogenic mechanism induced by BARF1 is not yet known.

Cyclin D1 is a positive regulator of the cell cycle and a proto-oncogene. Binding of cyclin D1 to cyclin-dependent kinase Cdk4 initiates phosphorylation of Rb which results in the release of E2F and transcriptional activation of S-phase genes [5]. Aberrant overexpression of cyclin D1 leads to a disturbed cell cycle regulation. Cyclin D1 gene amplification or high expression of its protein has been shown to be frequent events in diverse human malignant tumors [14, 16, 22]. Besides gene amplification, the transcription of cyclin D1 mRNA and the expression of its protein may be modulated by genetic polymorphisms [2, 12, 23].

In this study, we used gene expression profiling and identified cyclin D1 expression induced by BARF1 in a BARF1-transfected epithelial HaCaT cell line and analyzed cyclin D1 expression and gene amplifications in EBV-associated and EBV-negative gastric carcinomas. Our data underline recent findings that EBV-associated gastric carcinomas comprise a distinct clinico-pathological entity of gastric carcinoma [29, 35].

Materials and methods

Cell lines HaCaT cells were transfected by pBABE vector containing BARF1 sequence and selected by 500 μg/ml of neomycine. BARF1 sequence was at first amplified by PCR using two primers, then inserted in the *Bam*H1- and *Eco*R1-linearized pBABE vector. After amplification of BARF1 recombinant pBABE vector, HaCAT cells were transfected. At 24-h post-transfection, 500 μg/ml of neomycine was added into the culture medium, then neo-resistant cells were isolated after 3 weeks culture (E. Sakka et al., submitted).

RNA isolation, sample processing, and array hybridization Total RNA was extracted with Tri-reagent (Sigma, France) and treated twice with DNase 1 (Stratagene). The quality of total RNA and biotin-labeled cRNA of all samples was checked by calculating the ratio of absorbance at 260 and 280 nm (between 1.9 to 2.1) and agarose gel electrophoresis. Further sample processing, including labeling, hybridization, and image scanning was performed using standard Affymetrix protocol. In brief, 5 μg of total RNA from each cell line, T7-oligo(dT) primers, and Superscript II RT (GibcoBRL®) were used for first strand cDNA synthesis. After second strand synthesis, in vitro transcription was performed using IVT Transcript Labeling Kit (Ambion, Inc.) to generate biotinylated cRNA targets. cRNA targets were fragmented at 94°C for 35 min and 15 μg of biotinylated cRNA fragments was hybridized to HG-U133A chips (Affymetrix, Santa Clara, CA, USA) at 45°C for 16 h. The arrays were washed and stained with 10 μg/ml streptavidin–phycoerythrin. After signal amplification with biotinylated anti-streptavidin antibodies, the HG-U133A chips, containing 22.283 probe sets representing 14.564 human genes, were scanned using the GeneChip® Scanner 3000.

Quality control and data analysis CEL files, containing the signal intensity value and the standard deviation for each probe, were generated using the GeneChip operating software (Affymetrix, Santa Clara, CA, USA). As a quality control criterion, the ratios of 3′ signal to 5′ signal of the housekeeping gene GAPDH were between 0.9 and 3.8. The signals of the hybridization controls BioB, BioC, BioD, and Cre were in a linear relationship of intensity. Furthermore, the scale factors between the arrays did not vary by fourfold and the background intensities did not exceed 60. For every probe, the difference expression between each pair of samples was weighted by the absolute of the mean difference. We denoted this measure by the vector $m=m_$(probe_1,..., probe_22.283). Note that $m_$(probe_i) takes positive values for genes that were overexpressed in the modified sample or otherwise negative values. The probes were sorted with respect to m separately in both trials. Furthermore, we determined the pool of probes where $m>0$ in both trials and sorted the resulting lists with respect to m. cDNA synthesis and TaqMan analysis Reverse transcription of mRNA was performed using oligo(dT) primers and Superscript™ II RT 200 U/μl (GibcoBRL®).

For validation of the expression array results, a semi-quantitative real-time PCR (TaqMan, Applied Biosystems, Foster City, USA) for selected genes (cyclin D1, defensin beta 1, protease inhibitor 3 SKALP, DiGeorge syndrome critical region gene 8, DEAD box polypeptide 58) was performed. For cyclin D1 the primers, forward primer CCC TGA CGG CCG AGA AG, the reverse primer AGG TTC CAC TTG AGC TTG TTC AC, and the probe 6-FAM-AGG AGC TGC TGC AAA TGG AGC TG-TAMRA were used. For relative quantification the housekeeping gene TATA box binding protein (TBP) was amplified. For the other genes, the TaqMan® Gene Expression Assays (Applied Biosystems) were used according to the manufacturer's instructions. The ratio of the amount of the gene

to the amount of the TBP at the beginning of the reaction was determined with assumption of maximum efficiency using the formula: Sgene/STBP=2 Ct (TBP)/2 Ct (gene) with S being the starting amount and Ct the cycle number of the amount exceeding the detection threshold.

Immunohistochemistry Immunohistochemistry (IHC) for cyclin D1 was carried out as described previously [21]. A tissue microarray (TMA), which contained among others 92 carcinomas of the gastric cardia and 89 distal GC [20], was evaluated for cyclin D1 expression. The expression of cyclin D1 as tested by IHC was evaluated by light microscopy. The percentage of cyclin D1-positive tumor cells was determined according to the following category: 0 (0%), 1 (1–4%), 2 (5–24%), 3 (25–49%), 4 (50–74%), and 5 (75–100%) [21]. The cyclin D1 expression was correlated to the EBV status which has previously been described [20]. Statistical analyses were performed using Fisher's exact test. p values <0.05 were considered as significant.

Western immunoblotting To analyze cyclin D1 protein expression in BARF1-transfected and mock control HaCaT cells we performed Western immunoblotting as previously described using a 10% polyacrylamide gel [13]. The monoclonal cyclin D1 antibody (clone SP4, DCS, Germany; 1:5,000 dilution) detected the 36-kDa cyclin D1 protein. Equal amounts of protein were loaded on the gel as tested by Bradford assay, Ponceau staining, and β-actin Western immunoblotting (clone AC-15, Sigma, Germany; 1:1,000; Fig. 2b).

Fluorescence in situ hybridization For fluorescence in situ hybridization (FISH) analysis, a PathVysion cyclin D1 DNA probe kit (Vysis; Downers Grove, UK) was used according to the manufacturer's recommendations. The kit consists of directly labeled fluorescent DNA probes specific for the PRAD1/cyclin D1 gene locus (11q13.3) and a DNA probe specific for the alpha satellite DNA sequence at the centromeric region of chromosome 17 (17p11.1–q11.1). Tissue pretreatment was performed as previously described [34]. Counterstaining of nuclei was performed using diaminobenzidine. Nuclei from normal squamous epithelium or lymphocytes deposited separately on the same slide were used as controls of hybridization efficiency and specificity.

Results

Stable BARF1 transfection of epithelial HaCaT cells

Transcriptional expression of BARF1 was analyzed by RT-PCR prior to cDNA microarray analyses. RNA of the EBV-positive BARF1-expressing P3HR1 and Louckes cell line served as positive controls. Specific full-length transcripts of BARF1 were restricted to P3HR1 cells and BARF1-transfected HaCaT cells (Fig. 1) while no BARF1 transcripts were detected in vector control cells. In addition, BARF1 protein expression was tested in both transfectants and as expected the largest part of BARF1 protein was secreted into the culture medium [7, 19].

cDNA array analysis of BARF1-transfected epithelial HaCaT cells

The gene expression profile of BARF1-transfected epithelial HaCaT cells was compared to its pBABE vector control HaCaT cells. Detailed analysis revealed 1,010 genes to be differentially expressed. Most of them showed a decreased expression (94.3%) whereas only a small percentage was upregulated (5.7%). A summary of the 20 most significantly downregulated genes in BARF1-transfected HaCaT cells is given in Table 1.

Functional gene groups up- or downregulated in BARF1-transfected HaCaT cells

Analyzing the results with respect to functional groups, it is interesting that 22.9% of genes induced by BARF1 expression in the epithelial background of the HaCaT cells could be grouped to transcription (Table 2). In addition, rather unexpected no significant number of genes was found to be induced in the group of cell proliferation in HaCaT cells. The results are summarized in Table 2.

Validation of microarray results by quantitative RT-PCR and Western blotting

In order to evaluate the data obtained by microarray analysis, Taqman analysis was performed for the following genes, i.e., mad2, bcl-xl, protease inhibitor-3, DiGeorge syndrome 8, human defensin beta 1, DEAD, and cyclin D1. The results are shown in Fig. 2a with the given fold change as tested by Taqman analysis. Cyclin D1 expression was

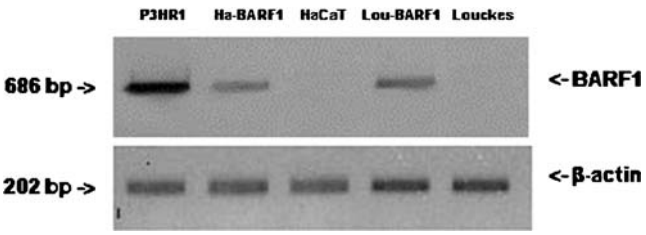


Fig. 1 *Upper panel*: specific transcription of full-length BARF1 (686 bp) in the EBV-positive epithelial cell line P3HR1 cells, BARF1-transfected HaCaT cells (*Ha-BARF1*) and BARF1-transfected Louckes cells (*Lou-BARF1*) tested by RT-PCR. No BARF1 transcripts are detected in the pBABE HaCaT and pZip Louckes cells. *Lower panel*: RT-PCR reveals β-actin transcripts in all tested cell lines

Table 1 Summary of the 20 most significantly down regulated genes in BARF1-transfected HaCaT cells

Symbol	Gene name	Accession	fc change
SKALP	*Homo sapiens* protease inhibitor 3, skin-derived (SKALP)	NM_002638.1	−19.91
ENO1L1	Human alpha enolase like 1	U88968.1	−10.48
	Human elafin gene	L10343	−9.32
	Translocase of inner mitochondrial membrane 17	BC004439.1	−6.45
	14-3-3 protein mRNA	U28964.1	−6.08
SKP1A	S-phase kinase-associated protein 1A (p19A)	NM_006930.1	−5.83
	Capping protein (actin filament)	BC005338.1	−5.7
	HSPC274 protein	NM_014145.1	−5.64
	Similar to heat shock protein, 110 kDa	BC002526.1	−5.52
SPRR1B	Small proline-rich protein 1B (cornifin)	NM_003125.1	−5.48
MTAP44	Interferon-induced, hepatitis C-associated microtubular aggregate protein (44 kDa)	NM_006417.1	−5.09
RAB1	RAB1, member RAS oncogene family	NM_004161.1	−5.07
JNK2B1	JNK2 beta1 protein kinase	U35002.1	−5.02
IL1A	Human interleukin 1-alpha	M15329.1	−5.01
SPTLC1	Serine palmitoyltransferase, long chain base subunit 1	NM_006415.1	−4.57
ANX14	Annexin 14	AF196478.1	−4.54
SCCA2b	*Homo sapiens* mRNA for SCCA2b	AB046400.1	−4.33
	Human mitochondrial NAD(P)+-dependent malic enzyme	M55905.1	4.19
RHAMM	Hyaluronan receptor	U29343.1	−4.14
IL8	Interleukin 8 C-terminal variant	AF043337.1	−4.11

found 1.53-fold upregulated in BARF1-transfected HaCaT cells by microarray analysis. A triplicate testing revealed a 2.5-fold overexpression of cyclin D1 in BARF1-transfected HaCaT cells as tested by Taqman analysis.

In addition, protein expression of cyclin D1 was assessed by Western blotting analysis. Cyclin D1 protein expression was upregulated in BARF1-transfected HaCaT cells whereas this upregulation was not found in the BARF1-negative mock control HaCaT cells (Fig. 2b).

Cyclin D1 expression in EBV-positive and EBV-negative GC

Since cyclin D1 protein expression has been implicated in gastric carcinogenesis recently [3, 4, 10, 17, 30], we

Table 2 Comparison of functional gene groups up- or downregulated in BARF1-transfected HaCaT cells

	HaCaT BARF1+	
	Gene expression induced by BARF1	Gene expression downregulated by BARF1
Genes	58	952
Apoptosis	5.7%	4.9%
Cell cycle	5.7%	6.4%
Cell proliferation	–	5.4%
Cell adhesion	2.9%	1.4%
Transcription	22.9%	10.2%
Metabolism	5.7%	9.4%
Mitosis	2.9%	1.8%

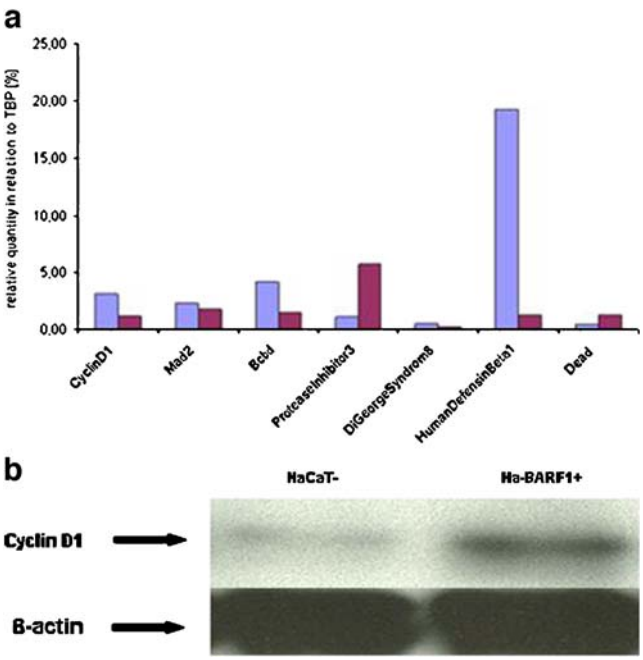


Fig. 2 **a** Results of Taqman RT-PCR analyses of selected genes up- or downregulated by BARF1 in HaCaT cells: *bars in blue* represent HaCaT BARF1-transfected cells and *bars in red* BARF1-negative vector control HaCaT cells. Y-axis indicates the relative quantity in relation to TBP. *Bars* represent the average of 3 (cyclin D1, DiGeorge syndrome 8, human defensin beta 1 and bcl-xl) and 2 (Mad2, DEAD, protease inhibitor 3) independent analyses. **b** *Upper panel*: equal amounts of protein (25 μg/lane) were loaded on a 10% SDS page gel. Western immunoblotting reveals strong protein expression of the 36 kDa cyclin D1 protein in BARF1-transfected HaCaT cells in contrast to the BARF1-negative mock control-transfected HaCaT cells. *Lower panel*: Equal loading was confirmed by β-actin protein expression

decided to test its expression in a large cohort of GC in order to assess the biological importance of cyclin D1 expression in EBV-associated epithelial malignancies. One hundred eighty-one formalin-fixed and paraffin-embedded GC specimens spotted on a tissue microarray were tested for cyclin D1 expression by immunohistochemistry. Of 181 GC, 157 were available for cyclin D1 IHC. Of 11 previously described EBV-positive GC, nine revealed a strong overexpression of cyclin D1 (Fig. 3a–b). In contrast, only 50 EBV-negative GC revealed a strong expression of cyclin D1 within the tumor cells. This difference was statistically significant with a p value <0.0012.

Cyclin D1 overexpression in EBV-associated GC is not due to gene amplification

To test whether cyclin D1 overexpression in EBV-associated GC was due to amplification, we performed cyclin D1 FISH. Five of nine EBV-associated and 25 of 50 EBV-negative GC which were shown to overexpress cyclin D1 were left to cyclin D1 FISH analysis because of multiple usage of the TMA and due to the FISH pretreatment protocol. None of the five EBV-associated GC revealed an amplification of the cyclin D1 gene (Fig. 3c). In contrast, 23 of the EBV-negative GC overexpressing cyclin D1 revealed gene amplification of the cyclin D1 gene (Fig. 3d).

Discussion

Latent expression of the viral oncogene BARF1 is restricted to epithelial EBV-associated malignancies [8, 11, 15, 24, 27, 36]. The BARF1 gene is the only viral oncogene of EBV that is expressed in EBV-associated GC. In order to investigate BARF1-mediated effects on gene transcription in epithelial cells, we analyzed the gene expression profile of BARF1-transfected HaCaT cells using Affymetrix HG-U133A expression microarray chips. The number of differentially expressed genes in HaCaT+ was 1,010 genes, and it is of interest that the majority of differentially expressed genes in HaCaT+ (94.3%) were downregulated and only a small proportion of genes were upregulated (5.7%). This might reflect that BARF1 mainly contributes to carcinogenesis by possibly downregulating genes which are involved in the maintenance of the cellular integrity and indeed the analysis of the genes downregulated (Table 2) mainly

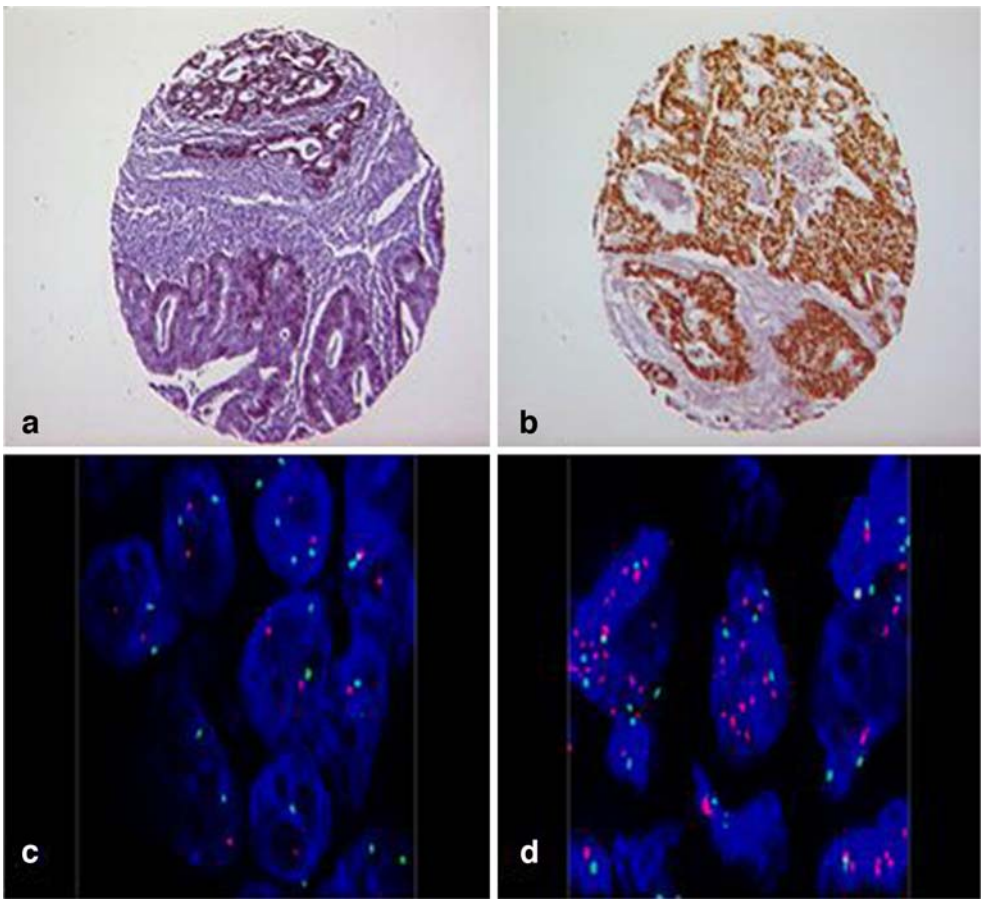


Fig. 3 **a** Specific nuclear EBER transcripts (*dark brown*) in the tumor cells of a gastric carcinoma as tested by RNA in situ hybridization. **b** Immunohistochemistry reveals strong nuclear (*brown*) cyclin D1 expression in an EBV-associated gastric carcinoma. **c** No cyclin D1 gene amplification was detected in an EBV-associated gastric carcinoma by cyclin D1 FISH (*red*: cyclin D1; *green*: centromer). **d** Cyclin D1 FISH in an EBV-negative gastric carcinoma overexpressing cyclin D1 reveals cyclin D1 gene amplification (*red*: cyclin D1; *green*: centromer)

revealed major differences in differentially expressed genes involved in transcription, cell proliferation, and metabolism.

The analysis of up- and downregulated genes in BARF1-transformed HaCaT cells reveals that BARF1 expression induces a number of significant changes in gene expression in an epithelial cell line. Some of these changes have been described previously and others have not been associated with gastric carcinogenesis before [4, 25]. Especially genes such as the human defensin beta, skin-derived protease inhibitor-3 and others with significant fold changes of the expression level are of interest for further studies. In the present study, we selected cyclin D1 to further test its importance in EBV-related gastric carcinogenesis. The finding that cyclin D1 expression is induced upon BARF1 transfection in epithelial cells on the transcriptional and protein level is of particular interest. Cyclin D1 expression has previously been associated with gastric carcinogenesis [3, 4, 10, 17, 30]. In our study, 37.6% of GC revealed overexpression of cyclin D1 as tested by IHC. Other studies show a range between 23.7% and 47% of cyclin D1 expressing GC [3, 10, 17]. In a recent study, Chang et al. report a more frequent expression of cyclin D1 in EBV-associated GC [4]. However, data on cyclin D1 gene amplification in GC are very sparse and only few reports range between 10% and 16% coinciding with a fair agreement of overexpression and amplification of the CCND1 gene [3, 10]. Prior to this study, no data about cyclin D1 gene amplification in EBV-associated GC were available. The fact that in our study none of the EBV-associated GC which overexpressed cyclin D1 revealed amplification of the cyclin D1 gene and most of the EBV-negative GC showed amplification indicates that BARF1 of EBV is able to induce cyclin D1 overexpression in these GC. As to what extent if there is a direct or indirect interaction between BARF1 and cyclin D1 is currently under investigation. Among others, BARF1 siRNA experiments will be helpful to determine the modality of BARF1 and cyclin D1 interactions.

In summary, the present study identifies new molecular targets of EBV-related carcinogenesis transcriptionally regulated by the viral oncogene BARF1. Our data strongly indicate a cyclin-D1-mediated role of BARF1 in gastric carcinogenesis. The results of the present gene expression profiling will further help to define the molecular background of BARF1-related carcinogenesis and its influence of its expression in GC.

Acknowledgments We like to acknowledge the excellent technical assistance of Mrs. Bokla and Deepa Pantulu, both from the Institute of Pathology, University Hospital Freiburg, Germany. We thank Axel Walch for helpful discussions with cyclin D1 FISH analyses.

Conflict of interest statement None declared.

References

1. Au WY, Pang A, Chan EC, Chu KM, Shek TWH, Kwong YL (2005) Epstein–Barr virus-related gastric adenocarcinoma: an early secondary cancer post hemopoietic stem cell transplantation. Gastroenterology 129:2058–2063
2. Betticher DC, Thatcher N, Altermatt HJ, Hoban P, Ryder WD, Heighway J (1995) Alternate splicing produces a novel cyclin D1 transcript. Oncogene 11:1005–1011
3. Bizari L, Borim AA, Leite KR, Gonsalves Fde T, Cury PM, Tajara EH, Silva AE (2006) Alterations of the CCND1 and HER-2/neu (ERBB2) proteins in esophageal and gastric cancers. Cancer Genet Cytogenet 165:41–50
4. Chang MS, Lee HS, Jung EJ, Kim CW, Lee BL, Kim WH (2005) Cell-cycle regulators, bcl-2 and NF-kappaB in Epstein–Barr virus-positive gastric carcinomas. Int J Oncol 27:1265–1272
5. Coqueret O (2002) Linking cyclins to transcriptional control. Gene 299:35–55
6. Correa P, Piazuelo MB, Camargo MC (2004) The future of gastric cancer prevention. Gastric Cancer 7:9–16
7. De Turenne-Tessier M, Jolicoeur P, Middeldorp JM, Ooka T (2005) Expression and analysis of the Epstein–Barr virus BARF1-coded protein from a tetracycline-regulatable adenovirus system. Virus Res 109:9–18
8. Decaussin G, Sbih-Lammali F, De Turenne-Tessier M, Bouguermouh A, Ooka T (2000) Expression of BARF1 gene encoded by Epstein–Barr virus in nasopharyngeal carcinoma biopsies. Cancer Res 60:5584–5588
9. Gao Y, Lu YJ, Xue SA, Chen H, Wedderburn N, Griffin BE (2002) Hypothesis: a novel route for immortalization of epithelial cells by Epstein–Barr virus. Oncogene 21:825–835
10. Gao P, Zhou GY, Liu Y, Li JS, Zhen JH, Yuan YP (2004) Alterations of cyclin D1 in gastric carcinoma and its clinicopathological significance. World J Gastroenterol 10:2936–2939
11. Hayes DP, Brink AA, Vervoort MB, Middeldorp JM, Meijer CJ, van den Brule AJ (1999) Expression of Epstein–Barr virus (EBV) transcripts encoding homologues to important human proteins in diverse EBV associated diseases. Mol Pathol 52:97–103
12. Hosokawa Y, Gadd M, Smith AP, Koerner FC, Schmidt EV, Arnold A (1997) Cyclin D1 (PRAD1) alternative transcript b: full-length cDNA cloning and expression in breast cancers. Cancer Lett 113:123–130
13. Kurz AK, Graf D, Schmitt M, Vom Dahl S, Haussinger D (2001) Tauroursodesoxycholate-induced choleresis involves p38 (MAPK) activation and translocation of the bile salt export pump in rats. Gastroenterology 121:407–419
14. Lung JC, Chu JS, Yu JC, Yue CT, Lo YL, Shen CY, Wu CW (2002) Aberrant expression of cell-cycle regulator cyclin D1 in breast cancer is related to chromosomal genomic instability. Genes Chromosomes Cancer 34:276–284
15. Luo B, Wang Y, Wang XF, Liang H, Yan LP, Huang BH, Zhao P (2005) Expression of Epstein–Barr virus genes in EBV-associated gastric carcinomas. World J Gastroenterol 11:629–633
16. Moonen L, Ong F, Gallee M, Verheij M, Horenblas S, Hart AA, Bartelink H (2001) Apoptosis, proliferation and p53, cyclin D1, and retinoblastoma gene expression in relation to radiation response in transitional cell carcinoma of the bladder. Int J Radiat Oncol Biol Phys 49:1305–1310
17. Muller W, Noguchi T, Wirtz HC, Hommel G, gabbert HE (1999) Expression of cell-cycle regulatory proteins cyclin D1, cyclin E, and their inhibitor p21 WAF1/CIP1 in gastric cancer. J Pathol 189:186–193
18. Rickinson AB, Kieff E (2002) Epstein–Barr virus. In: Fields BN, Knipe DM, Howley PM (eds) Fields virology. Lippincott-Raven, Philadelphia, pp 2575–2627

19. Sall A, Caserta S, Jolicoeur P, Franqueville L, de Turenne-Tessier M, Ooka T (2004) Mitogenic activity of Epstein–Barr virus-encoded BARF1 protein. Oncogene 23:4938–4944
20. Sarbia M, Hausen AZ, Feith M, Geddert H, von Rahden BH, Langer R, von Weyhern C, Siewert JR, Höfler H, Stein HJ (2005) Esophageal (Barrett's) adenocarcinoma is not associated with Epstein–Barr virus infection: an analysis of 162 cases. Int J Cancer 117:698–700
21. Sarbia M, Stahl M, Fink U, Heep H, Dutkowski P, Willers R, Seeber S, Gabbert HE (1999) Prognostic significance of cyclin D1 in esophageal squamous cell carcinoma patients treated with surgery alone or combined therapy modalities. Int J Cancer 84:86–91
22. Sauter ER, Yeo UC, von Stemm A, Zhu W, Litwin S, Tichansky DS, Pistritto G, Nesbit M, Pinkel D, Herlin M, Bastian BC (2002) Cyclin D1 is a candidate oncogene in cutaneous melanoma. Cancer Res 1:3200–3206
23. Sawa H, Ohshima TA, Ukita H, Murakami H, Chiba Y, Kamada H, Hara M, Saito I (1998) Alternatively spliced forms of cyclin D1 modulate entry into the cell cycle in an inverse manner. Oncogene 16:1701–1712
24. Sbih-Lammali F, Djennaoui D, Belaoui H, Bouguermouh A, Decaussin G, Ooka T (1996) Transcriptional expression of Epstein–Barr virus genes and proto-oncogenes in north African nasopharyngeal carcinoma. J Med Virol 49:7–14
25. Sheng W, Decaussin G, Sumner S, Ooka T (2001) N-terminal domain of BARF1 gene encoded by Epstein–Barr virus is essential for malignant transformation of rodent fibroblasts and activation of BCL-2. Oncogene 20:1176–1185
26. Sheng W, Decaussin G, Ligout A, Takada K, Ooka T (2003) Malignant transformation of Epstein–Barr virus-negative Akata cells by introduction of the BARF1 gene carried by Epstein–Barr virus. J Virol 77:3859–3865
27. Seto E, Yang L, Middeldorp JM, Sheen TS, Chen JY, Fukayama M, Eizuru Y, Ooka T, Takada K (2005) Epstein–Barr virus (EBV)-encoded BARF1 gene is expressed in nasopharyngeal carcinoma and EBV-associated gastric carcinoma tissues in the absence of lytic gene expression. J Med Virol 76:82–88
28. Takada K (2000) Epstein–Barr virus and gastric carcinoma. J Clin Pathol: Mol Pathol 53:255–261
29. van Beek J, zur Hausen A, Klein Kranenbarg E, van de Velde CJH, Middeldorp JM, van den Brule AJC, Meijer CJLM, Bloemena E (2004) EBV-positive gastric adenocarcinomas: a distinct clinicopathologic entity with a low frequency of lymph node involvement. J Clin Oncol 15:664–670
30. Wang Q, Tsao SW, Ooka T, Nicholls JM, Cheung HW, Fu S, Wong YC, Wang X (2006) Anti-apoptotic role of BARF1 in gastric cancer cells. Cancer Lett 238:90–103
31. Wei MX, Ooka T (1989) A transforming function of the BARF1 gene encoded by Epstein–Barr virus. EMBO J 8:2897–2903
32. Wei MX, Moulin JC, Decaussin G, Berger F, Ooka T (1994) Expression and tumorigenicity of the Epstein–Barr virus BARF1 gene in human Louckes B-lymphocyte cell line. Cancer Res 54:1843–1848
33. Wei MX, de Turenne-Tessier M, Decaussin G, Benet G, Ooka T (1997) Establishment of a monkey kidney epithelial cell line with the BARF1 open reading frame from Epstein–Barr virus. Oncogene 14:3073–3082
34. Werner M, Mattis A, Aubele M, Cummings M, Zitzelsberger H, Hutzler P, Höfler H (1999) 20q13.2 amplification in intraductal hyperplasia adjacent to in situ and invasive ductal carcinoma of the breast. Virchows Arch 435:469–472
35. Young LS, Rickinson A (2004) Epstein–Barr virus: 40 years on. Nat Rev Cancer 4(10):757–768
36. zur Hausen A, Brink AA, Craanen ME, Middeldorp JM, Meijer CJ, van den Brule AJ (2000) Unique transcription pattern of Epstein–Barr Virus (EBV) in EBV-carrying gastric adenocarcinomas: expression of the transforming *BARF1* Gene. Cancer Res 60:2745–2748

Virchows Arch (2008) 452:629–635
DOI 10.1007/s00428-007-0574-5

ORIGINAL ARTICLE

Mucoepidermoid carcinoma of upper aerodigestive tract: clinicopathologic study of 78 cases with immunohistochemical analysis of dicer expression

S. I. Chiosea · E. L. Barnes · S. Y. Lai · A. M. Egloff · R. L. Sargent · J. L. Hunt · R. R. Seethala

Received: 25 November 2007 / Accepted: 28 December 2007 / Published online: 1 February 2008
© Springer-Verlag 2008

Abstract MicroRNAs (miR) are small noncoding RNAs that are predicted to regulate up to 30% of protein-encoding genes. miR maturation requires functional microRNA machinery, including the Dicer protein. We review our experience with mucoepidermoid carcinoma (MEC) and characterize the prognostic value of Dicer expression. Expression of Dicer was assessed in 78 MEC by immunohistochemistry. Dicer expression was scored semiquantitatively and relative to the internal controls: large excretory/striated ducts or basal/parabasal layers of normal squamous epithelium (mucosa). Dicer scores were then correlated with clinical and pathologic parameters. Dicer over- and/or under-expression were more commonly seen in high-grade MEC (83%) than in low/intermediate grade MEC (35%; $p=0.002$) and in stage III/IV MEC (80%) than in stage I/II MEC (41%; $p=0.04$). Abnormal Dicer expression correlates with high-grade and advanced stage, acting as a univariate predictor of poor disease-specific survival (DSS) in MEC. Age and stage were independent predictors of poor DSS on multivariate analysis. Abnormal immunoexpression of Dicer in aggressive MEC suggests a role for miR and miR machinery in tumor progression.

Keywords Salivary gland tumors · Mucoepidermoid carcinoma · Dicer

S. I. Chiosea · E. L. Barnes · R. L. Sargent · R. R. Seethala
Pathology and Laboratory Medicine,
University of Pittsburgh Medical Center,
Pittsburgh, PA, USA

E. L. Barnes · S. Y. Lai · A. M. Egloff · R. R. Seethala
Otolaryngology, University of Pittsburgh Medical Center,
Pittsburgh, PA, USA

S. Y. Lai
Pharmacology, University of Pittsburgh Medical Center,
Pittsburgh, PA, USA

J. L. Hunt
Pathology and Laboratory Medicine,
Cleveland Clinic Foundation,
Cleveland, OH, USA

S. I. Chiosea (✉)
Department of Pathology and Laboratory Medicine,
University of Pittsburgh,
A711 Scaife Hall Presbyterian University Hospital,
3550 Terrace Street,
Pittsburgh, PA 15261, USA
e-mail: chioseasi@upmc.edu

Introduction

Salivary gland malignancies are rare, accounting for about 6% of all head and neck cancers. They show great morphologic diversity even within a specific tumor type. Ancillary studies such as DNA content analysis, proliferation index and p53 expression have been applied to salivary gland neoplasms in an attempt to refine diagnosis and predict biologic behavior [15, 27, 31]. More recently, several gene array studies have expanded the list of biomarkers in salivary gland tumors [9, 10, 18, 21]. It is interesting to note that, of the salivary carcinoma types evaluated to date by gene array, only two types, mucoepidermoid carcinoma (MEC) and adenoid cystic carcinoma, consistently showed distinct gene-expression profiles [18, 21]. MEC is the most common primary salivary gland malignancy in both adults and children [11, 32]. As with most salivary tumors, conventional pathologic parameters

of MEC are not completely reliable, as even MEC assigned low to intermediate grade may behave poorly [3, 4, 25]. Furthermore, current treatment modalities for high-grade aggressive MEC are poor, making biomarkers for targeted therapy desirable.

Recently, the family of classic tumor suppressors and oncogenes was expanded to include microRNAs (miR), small 18- to 21-nt noncoding RNAs that regulate diverse cellular and molecular processes including cell death and proliferation [14]. Hundreds of human miR are predicted to regulate 10% to 30% of protein-encoding genes by interactions with their 3′-untranslated regions [19]. Little is known about the mechanisms underlying miR dysregulation in neoplastic processes. The final steps of miR maturation require Dicer, an RNase III-related enzyme [13, 20]. To date, this pathway has not been investigated in salivary gland neoplasms. We present our three-decade experience with 78 well-characterized MEC and correlate Dicer immunoreactivity with traditional clinicopathologic parameters.

Materials and methods

Case selection

This study was approved by the University of Pittsburgh Institutional Review Board (IRB#0601084). One hundred cases of MEC were retrieved from the Department of Pathology archives (1973–2004). Each case was reviewed by two of the authors (R.R.S. and S.C.) and graded using the point-based grading system proposed by Brandwein et al. [5] with one exception: bone invasion was excluded as a grading feature because of its function as a staging parameter. Clinical and demographic data were obtained from the electronic medical record and the institutional Head and Neck Tumor Registry. The tumor–node–metastases (TNM) stage and American Joint Committee on Cancer/International Union Against Cancer (AJCC/UICC) stage grouping was assigned based on sixth-edition guidelines. The demographic and clinicopathologic features of the patients in this study are listed in Table 1.

Table 1 Demographic and clinicopathologic features

Features	Values
N	78
Median age (range), years	51.5 (7–81)
Gender (%)	
Female	42 (53.8)
Male	36 (46.2)
Site (%)	
Parotid	33 (42.3)
Minor salivary	
Oral/oropharynx	29 (37.2)
Sinonasal/nasopharyx	6 (7.7)
Larynx/hypopharyx	2 (2.6)
Submandibular gland	6 (7.7)
Primary intraosseous (mandible)	2 (2.6)
Grade (%)	
Low	19 (24.4)
Intermediate	25 (32.1)
High	34 (43.6)
Margin status[a] (%)	
Positive	20 (26.7)
Negative	55 (73.3)
Nodal status[b] (%)	
Positive	18 (27.7)
Negative	47 (72.3)
Stage[c] (%)	
I	3 (49.2)
II	12 (19.0)
III	6 (9.5)
IV	14 (22.2)
Recurrence[d] (%)	20 (28.7)

[a] Margins could not be assessed in three cases.
[b] Node status was unavailable in 13 cases
[c] Staging data were unavailable for 15 cases.
[d] Recurrence data were unavailable in eight cases

Immunohistochemistry

Immunoperoxidase staining was performed as previously described [6]. Briefly, the slides were incubated at 4°C overnight with anti-Dicer antibodies (Clonegene, Hartford, CT, USA) at a 1:500 dilution. Several internal controls were used: the basal/parabasal layers of non-neoplastic squamous epithelium or skin, as well as both basal and luminal layers of excretory or intercalated ducts of salivary tissue. The intensity was graded on a three-tiered scale from 1 to 3. The following criteria were used to semi-quantitatively score the Dicer staining: score of "1" was defined by a staining intensity lower than that of the internal controls, a score of "2" was defined by a staining intensity equal to that of the internal controls, and a score of "3" was defined by a staining intensity greater than that of the controls (Fig. 1). Two pathologists (R.R.S. and S.C.) independently scored the stained slides.

Statistical analysis

All statistical analyses were performed with SPSS 14.0 software (SPSS, Chicago, IL, USA) and STATA V.9.0 (StataCorp LP, College Station, TX, USA). The relative frequencies of Dicer abnormalities by immunostaining with the subgroups of various parameters (grade, stage, and margin status) were compared using Fisher's exact test (two-tail distribution). For these analyses, parameters were

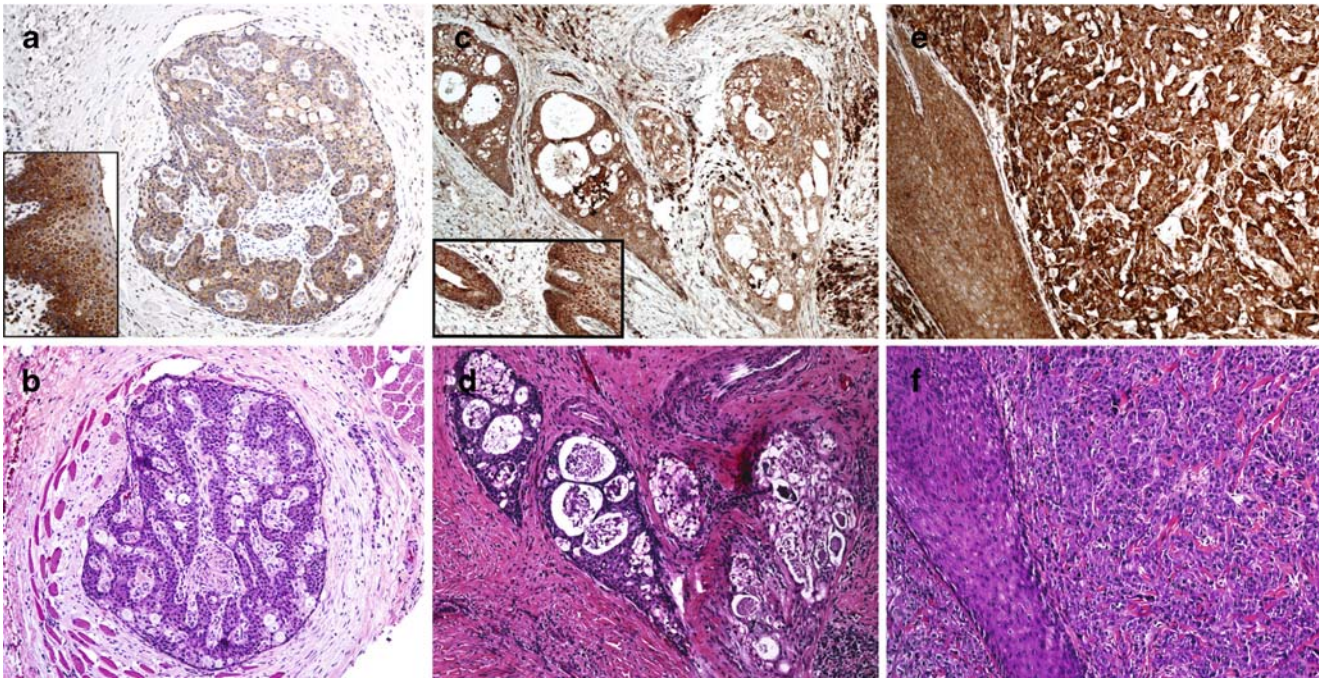


Fig. 1 Scoring of Dicer expression in MEC. **a**, **b** Intermediate-grade MEC of the palate. Dicer immunoreactivity in MEC is lower than in basal squamous cells of adjacent normal mucosa (see *inset*), Dicer 1+. **c**, **d** Intermediate-grade MEC of the oral cavity. Dicer immunoreactivity in MEC is similar to that of basal squamous cells of adjacent normal mucosa, Dicer 2+. **e**, **f** High-grade MEC arising in parotid gland. Dicer immunoreactivity in MEC is higher than that of basal squamous cells of overlying normal epidermis (*left one third of the image*), Dicer 3+. Immunohistochemistry, original magnification ×100

resolved into two-tiered groups as follows: grade—low/intermediate grade vs. high grade; stage—stage I/II vs. stage III/IV; and age—less than 55 years vs. greater than 55 years. Univariate disease-specific survival (DSS) was calculated using the Kaplan–Meier method with group-wise comparisons using the log-rank test. Multivariate analysis of DSS was performed using a Cox proportional hazards model, including all confounder variables that were significantly associated with DSS by univariate analysis and significantly associated with Dicer expression. The assumption of proportional hazards was evaluated for appropriateness by the assessment of scaled Schoenfeld residuals. A p value of less than 0.05 was considered statistically significant for all tests.

Results

Clinicopathologic features

Twenty-two of 100 cases diagnosed as MEC from 1973–2004 were reclassified as adenosquamous carcinoma (AsqCA) based on the presence of surface involvement by dysplasia, carcinoma in situ, a discrete adenocarcinoma component, significant nuclear pleomorphism, and/or presence of abundant keratinization [2].

Of the remaining 78 cases, the median age was 51.5 years (range 7–81) with a slight female predilection (F/M=1.2:1). The parotid and minor salivary glands of the oral cavity/oropharynx were the two most common sites involved. In this series, the most common MEC grade was high, followed by intermediate and low. Stage I was the most common stage for tumors, followed by stage IV. Margins were positive in 26.7% of cases, while lymph nodes were positive in 27.7% of cases. The recurrence rate was 28.7%.

Low/intermediate-grade MEC were more frequently low stage (stage I/II, 35/38, 92.1%) as compared to high grade MEC (stage I/II, 8/25, 32%; $p<0.001$). Of the three stage-III/IV tumors in the low/intermediate-grade category, all were intermediate grade. Only 4 of 45 (8.9%) low/intermediate-grade MEC had positive lymph nodes as compared to 14 of 33 (42.4%) in high-grade MEC ($p<0.001$). All cases with positive lymph nodes in the low/intermediate category were intermediate grade. Similarly, only 5 of 45 (12.2%) low/intermediate-grade MEC had recurrences, while 15 of 29 (51.7%) high-grade MEC recurred ($p<0.001$). In the low/intermediate grade-MEC with recurrences, four were intermediate grade, and only one was low-grade MEC.

Overall, the 5- and 10-year DSS were 73.6% and 69.9%, respectively. Median follow-up for surviving patients was 4.42 years (range, <1 week–20.93 years). Univariate

Table 2 Univariate predictors of DSS

Parameter	5 year DSS (%)	10 year DSS (%)	Log-rank *p* value	Degrees of freedom
Grade			<0.001	2
Low	100	100		
Intermediate	100	87.5		
High	42.7	42.7		
Stage			<0.001	3
I	100	100		
II	83.3	83.3		
III	75.0	[a]		
IV	12.9	12.9		
Margin status			0.013	1
Negative	81.9	76.7		
Positive	46.0	46.0		
Age			<0.001	1
Under 55	92.0	92.0		
Over 55	54.6	47.8		

DSS Disease-specific survival
[a] Follow-up within stage III tumors did not extend to 10 years

predictors of DSS are summarized in Table 2 and Fig. 2. Age >55 years, grade, stage, and positive margin status were all univariate predictors of poor outcome, while gender and site were not.

Dicer IHC in normal salivary glands, normal squamous mucosa

In normal salivary tissue, Dicer intensity was highest in the basal/myoepithelial and luminal epithelium of intercalated, striated, and excretory ducts (Fig. 3). Serous acini showed weaker reactivity, while mucous acini were negative. The distal myoepithelial cells surrounding the acini showed variable reactivity. In squamous mucosa, Dicer intensity was highest in the basal/parabasal layers. Generally, the stromal elements of salivary glands (fibrous tissue, adipose tissue, and nerves) were non-reactive for Dicer. The vascular endothelium was occasionally positive for Dicer.

Dicer IHC in mucoepidermoid carcinoma

Dicer was expressed predominantly in the epidermoid and intermediate cell types, both within the solid and cystic areas of MEC. Overall, 47 of 78 (60.3%) cases showed abnormalities of Dicer expression, with 22 of 78 (28.2%) showing increased expression and 25 of 78 (32.1%) showing decreased expression. Dicer over-expression was significantly more common in high-grade, stage-III/IV, margin-positive MEC. Decreased expression was significantly more common in the tumors of patients over 55 years

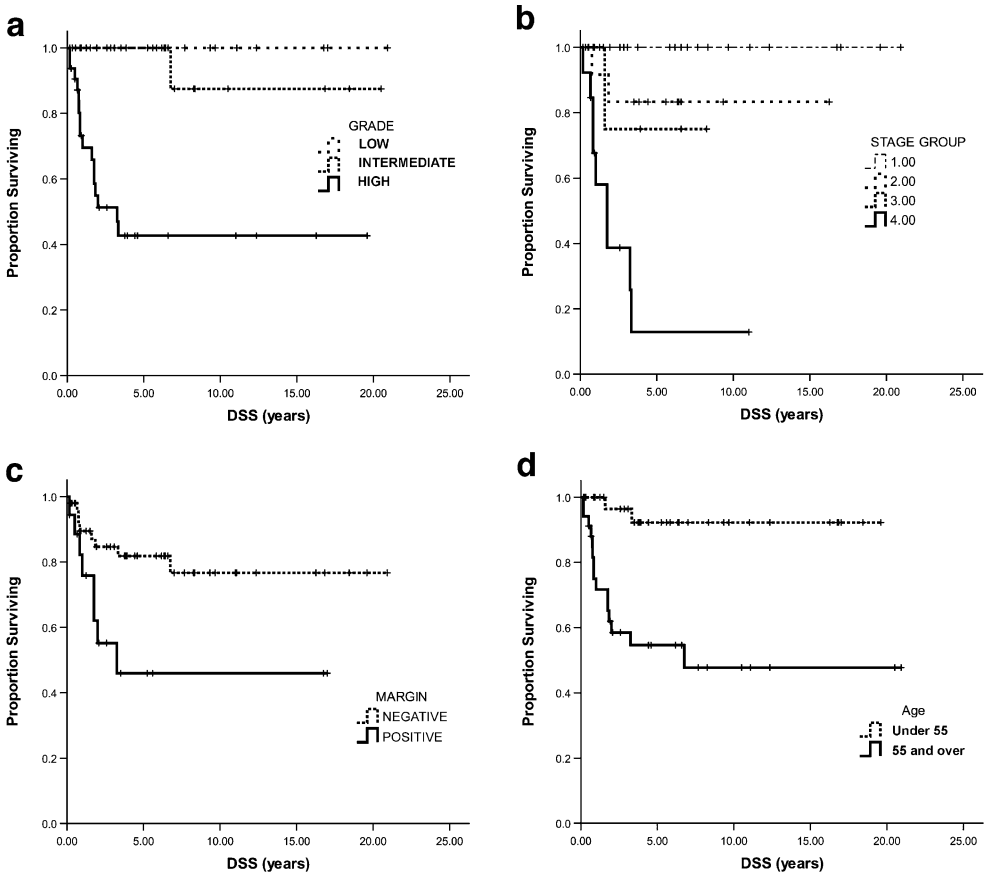


Fig. 2 Clinicopathologic analysis of 78 MEC cases. Univariate predictors of DSS. **a** Modified histologic grade. **b** Pathologic stage. **c** Margin status. **d** Patient's age, older or younger than 55 years of age

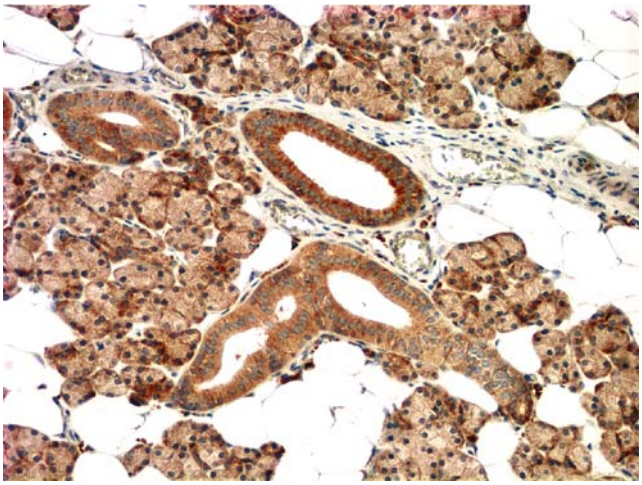


Fig. 3 Dicer immunoreactivity in normal salivary tissue**.** Expression level is highest in the striated and intercalated ducts. Immunohistochemistry, ×200 original magnification

of age. Table 3 summarizes Dicer expression levels with respect to grade, stage, and margin status. Overall, abnormal Dicer expression (both over- and under-expression combined) was significantly more frequent in high grade, stage III/IV, and tumors of patients over 55 years. By univariate analysis, both over- and under-expression of Dicer correlated with poorer survival (Fig. 4). Age and stage were independent predictors of poor DSS on multivariate analysis.

Dicer was also frequently abnormally expressed in adenosquamous carcinoma in 17 of 22 (77.3%) cases, with 8 of 22 (36.4%) showing increased immunoreactivity and 9 of 22 (40.9%) with decreased immunoreactivity.

Discussion

The current MEC cohort is among the largest single-institution experiences in the past decade and validates stage, Brandwein grade, margin status, and age as prognostic factors. Prior large series are characterized by limited application of modern grading and staging systems [25], large referral population (hence not truly a single-institution experience) [11] or a lack of adequate assessment of stage altogether [8]. The Brandwein grade is the most modern grading system and shows improved correlation with outcome as compared to the Armed Forces Institute of Pathology grading system [5]. We did not compare these grading systems directly, but we were able to provide supportive evidence for the utility of the Brandwein system. Ultimately, in our cohort, only age and stage are independent predictors of poor DSS. Grade and stage may have been too closely linked to show an independent predictive value for grade alone.

An ancillary but significant finding in our study was the high prevalence of AsqCA (22%) that were inappropriately classified as MEC. AsqCA is essentially a variant of squamous cell carcinoma with divergent glandular differentiation. Morphologic criteria for its separation from high-grade MEC include surface dysplasia/carcinoma in situ,

Table 3 Dicer expression stratified by various clinicopathologic parameters

	Dicer over-expression	Dicer under-expression	Dicer abnormal (over- or underexpression)	Dicer Score		
				2	3	1
Grade						
Low/intermediate (%)	13.3	26.7	40.0			
High (%)	48.5	39.4	87.9			
p value	0.001	0.326	<0.001			
Stage						
I/II (%)	16.7	31.0	47.6			
III/IV (%)	42.9	38.1	81.0			
p value	0.034	0.584	0.015			
Margin						
Negative (%)	28.4	34.0	56.4			
Positive (%)	50	25	75			
p value	0.024	0.574	0.184			
Age						
Under 55 (%)	24.4	22.0	46.4			
55 and over (%)	32.4	43.2	75.6			
p value	0.011	0.461	0.054			
DSS						
5 year survival (%)				96.2	67.0	52.4
10 year survival (%)				96.2	67.0	26.2
p value				0.003		

DSS Disease-specific survival

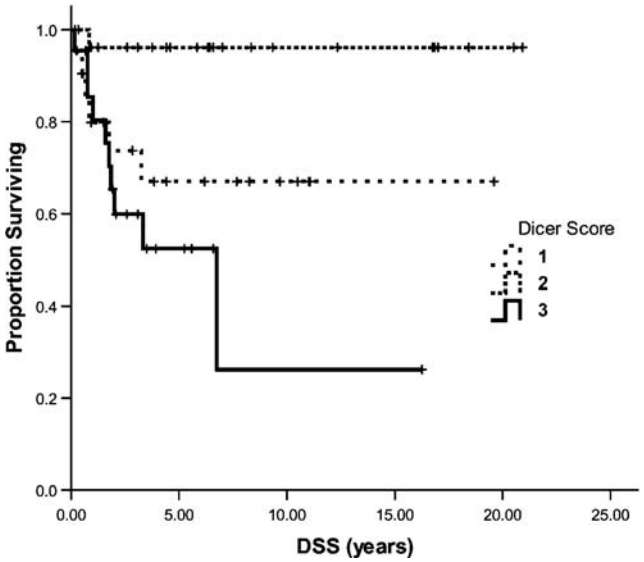


Fig. 4 Abnormal Dicer expression correlates with worse survival of MEC patients

prominent keratinization, and discrete gland formation, often present in the deeper portions of the tumor [2]. Unfortunately, separation of these entities may still be challenging, particularly on small biopsies or when surface mucosa is ulcerated. Historically, at our institution, until the mid 1980s, the distinction between high-grade MEC and AsqCA was not made, which was another contributing factor to the discrepancy rate. Both MEC and AsqCA have poor outcome, with a 5-year survival of 13–20% for AsqCA and 0–43% for high-grade MEC, and mandate aggressive management [17].

The molecular pathogenesis of MEC is not fully elucidated. Perhaps the best characterized MEC-specific genetic alteration is the *t*(11;19)(q21;p13) initially identified by traditional karyotyping [24]. This translocation was shown to generate a mucoepidermoid carcinoma translocated 1 (MECT1)–mastermind-like 2 (MAML2) gene fusion consisting of exon 1 of MECT1 fused to exons 2–5 of MAML2 [29]. Fusion-positive patients are generally younger, have smaller, well-differentiated tumors, and a significantly lower risk of local recurrence, metastasis or tumor-related death. However, a few translocation-positive aggressive high-grade MEC have been recently described [28]. The participation of the miR pathway in these molecular alterations, if any, has yet to be characterized.

To the best of our knowledge, this is the first report demonstrating correlation between Dicer protein immunoreactivity and survival in human carcinomas. Previously, another group showed correlation between the level of Dicer mRNA and post-operative survival of patients with non-small cell lung carcinoma [16]. We have recently presented additional details on Dicer expression in non-small cell lung carcinoma and showed the role of Dicer in prostate adenocarcinoma [6, 7]. Dicer expression varies in squamous cell carcinoma of the esophagus and does not show significant association with patient survival [26]. Combined with Dicer changes in MEC described here, alteration of Dicer levels may represent a previously unrecognized common theme in carcinogenesis. Differential miR expression is the most likely explanation for worse prognosis in patients with both up- or down-regulation of Dicer. miR expression in MEC has yet to be characterized. However, in cell lines of head and neck squamous cell carcinoma, 55 miR were differentially expressed [30].

We also describe the immunoexpression profile of Dicer in normal salivary/mucoserous glands. Dicer appears to be distributed at higher levels in intercalated and striated ducts, both in basal and luminal layers. The functional importance of this expression pattern might be explained by the anti-apoptotic function of Dicer [23]. It is possible that Dicer expression in normal salivary gland mirrors the cellular constituents of salivary gland with proliferative or regenerative capacity.

The implications of Dicer expression abnormalities may extend beyond prognosis. Since the disease-specific survival for high-grade/high-stage MEC is poor, additional therapeutic modalities are desirable. In recent years, understanding of RNA interference (RNAi)-based gene silencing has offered yet another therapeutic approach to cancer. Importantly, Dicer level correlates with the efficiency of RNAi. For instance, over-expression in HeLa cells leads to a 30% enhancement of a shRNA-mediated gene silencing [22].

There is increasing evidence that potential RNAi-based therapeutics will induce significant side effects, including off-target silencing and activation of the interferon system [1]. Furthermore, some adverse effects appear to be caused by competition of exogenous siRNAs with the endogenous miR for proteins of miR machinery (e.g., Exportin-5) [12]. While this remains largely speculative, the widespread changes of Dicer expression in MEC, particularly in high-grade MEC, may ultimately help to predict the efficacy of potential RNAi-based drugs.

In summary, this study represents the first comprehensive analysis of Dicer expression in a clinicopathologically well-characterized cohort of MEC patients. In addition, we herein characterize Dicer expression in normal salivary tissue. We show a higher frequency of abnormal Dicer expression in high-grade, high-stage MEC when compared to low/intermediate-grade, low stage-MEC. Almost two thirds of MEC show abnormal Dicer expression. Abnormal Dicer immunoreactivity (over- and under-expression combined or separately) correlated with poorer survival.

Acknowledgments This study was supported by a grant from the Postdoctoral Pathology Research Training Program (PPRTP, RT =

00147, CC = 99FUND) from the Department of Pathology, University of Pittsburgh Medical Center to SC. The study was also supported by the Stout Family Fund for Head and Neck Cancer Research at the Eye & Ear Foundation of Pittsburgh and the Head and Neck Oncology Registry. S.Y. Lai was supported by an NIH Mentored Career Development Award (K08 DE018061-01). Authors would like to thank Kim Marie Adams and Jennifer Ridge Hetrick for their administrative support. All experiments comply with the current laws of the USA. Authors would like to thank Marie Acquafondata for excellent technical support.

Conflict of interest statement We declare that we have no conflict of interest.

References

1. Aagaard L, Rossi JJ (2007) RNAi therapeutics: principles, prospects and challenges. Adv Drug Deliv Rev 59:75–86
2. Alos L, Castillo M, Nadal A, Caballero M, Mallofre C, Palacin A, Cardesa A (2004) Adenosquamous carcinoma of the head and neck: criteria for diagnosis in a study of 12 cases. Histopathology 44:570–579
3. Auclair PL, Goode RK, Ellis GL (1992) Mucoepidermoid carcinoma of intraoral salivary glands. Evaluation and application of grading criteria in 143 cases. Cancer 69:2021–2030
4. Batsakis JG, Luna MA (1990) Histopathologic grading of salivary gland neoplasms: I. Mucoepidermoid carcinomas. Ann Otol Rhinol Laryngol 99:835–838
5. Brandwein MS, Ivanov K, Wallace DI, Hille JJ, Wang B, Fahmy A, Bodian C, Urken ML, Gnepp DR, Huvos A, Lumerman H, Mills SE (2001) Mucoepidermoid carcinoma: a clinicopathologic study of 80 patients with special reference to histological grading. Am J Surg Pathol 25:835–845
6. Chiosea S, Jelezcova E, Chandran U, Acquafondata M, McHale T, Sobol RW, Dhir R (2006) Up-regulation of dicer, a component of the MicroRNA machinery, in prostate adenocarcinoma. Am J Pathol 169:1812–1820
7. Chiosea S, Jelezcova E, Chandran U, Luo J, Mantha G, Sobol RW, Dacic S (2007) Overexpression of Dicer in precursor lesions of lung adenocarcinoma. Cancer Res 67:2345–2350
8. Evans HL (1984) Mucoepidermoid carcinoma of salivary glands: a study of 69 cases with special attention to histologic grading. Am J Clin Pathol 81:696–701
9. Francioso F, Carinci F, Tosi L, Scapoli L, Pezzetti F, Passerella E, Evangelisti R, Pastore A, Pelucchi S, Piattelli A, Rubini C, Fioroni M, Carinci P, Volinia S (2002) Identification of differentially expressed genes in human salivary gland tumors by DNA microarrays. Mol Cancer Ther 1:533–538
10. Frierson HF Jr., El-Naggar AK, Welsh JB, Sapinoso LM, Su AI, Cheng J, Saku T, Moskaluk CA, Hampton GM (2002) Large scale molecular analysis identifies genes with altered expression in salivary adenoid cystic carcinoma. Am J Pathol 161:1315–1323
11. Goode RK, Auclair PL, Ellis GL (1998) Mucoepidermoid carcinoma of the major salivary glands: clinical and histopathologic analysis of 234 cases with evaluation of grading criteria. Cancer 82:1217–1224
12. Grimm D, Streetz KL, Jopling CL, Storm TA, Pandey K, Davis CR, Marion P, Salazar F, Kay MA (2006) Fatality in mice due to oversaturation of cellular microRNA/short hairpin RNA pathways. Nature 441:537–541
13. Hutvagner G, Zamore PD (2002) A microRNA in a multiple-turnover RNAi enzyme complex. Science 297:2056–2060
14. Hwang HW, Mendell JT (2006) MicroRNAs in cell proliferation, cell death, and tumorigenesis. Br J Cancer 94:776–780
15. Karja VJ, Syrjanen KJ, Kurvinen AK, Syrjanen SM (1997) Expression and mutations of p53 in salivary gland tumours. J Oral Pathol Med 26:217–223
16. Karube Y, Tanaka H, Osada H, Tomida S, Tatematsu Y, Yanagisawa K, Yatabe Y, Takamizawa J, Miyoshi S, Mitsudomi T, Takahashi T (2005) Reduced expression of Dicer associated with poor prognosis in lung cancer patients. Cancer Sci 96:111–115
17. Keelawat S, Liu CZ, Roehm PC, Barnes L (2002) Adenosquamous carcinoma of the upper aerodigestive tract: a clinicopathologic study of 12 cases and review of the literature. Am J Otolaryngol 23:160–168
18. Leivo I, Jee KJ, Heikinheimo K, Laine M, Ollila J, Nagy B, Knuutila S (2005) Characterization of gene expression in major types of salivary gland carcinomas with epithelial differentiation. Cancer Genet Cytogenet 156:104–113
19. Lewis BP, Burge CB, Bartel DP (2005) Conserved seed pairing, often flanked by adenosines, indicates that thousands of human genes are microRNA targets. Cell 120:15–20
20. Maniataki E, Mourelatos Z (2005) A human, ATP-independent, RISC assembly machine fueled by pre-miRNA. Genes Dev 19:2979–2990
21. Maruya S, Kim HW, Weber RS, Lee JJ, Kies M, Luna MA, Batsakis JG, El-Naggar AK (2004) Gene expression screening of salivary gland neoplasms: molecular markers of potential histogenetic and clinical significance. J Mol Diagn 6:180–190
22. Mikuma T, Kawasaki H, Yamamoto Y, Taira K (2004) Overexpression of Dicer enhances RNAi-mediated gene silencing by short-hairpin RNAs (shRNAs) in human cells. Nucleic Acids Symp Ser (Oxf) 0:191–192
23. Muljo SA, Ansel KM, Kanellopoulou C, Livingston DM, Rao A, Rajewsky K (2005) Aberrant T cell differentiation in the absence of Dicer. J Exp Med 202:261–269
24. Nordkvist A, Gustafsson H, Juberg-Ode M, Stenman G (1994) Recurrent rearrangements of 11q14–22 in mucoepidermoid carcinoma. Cancer Genet Cytogenet 74:77–83
25. Spiro RH (1986) Salivary neoplasms: overview of a 35-year experience with 2,807 patients. Head Neck Surg 8:177–184
26. Sugito N, Ishiguro H, Kuwabara Y, Kimura M, Mitsui A, Kurehara H, Ando T, Mori R, Takashima N, Ogawa R, Fujii Y (2006) RNASEN regulates cell proliferation and affects survival in esophageal cancer patients. Clin Cancer Res 12(24):7322–7328
27. Suzzi MV, Alessi A, Bertarelli C, Cancellieri A, Procaccio L, Dall'olio D, Laudadio P (2005) Prognostic relevance of cell proliferation in major salivary gland carcinomas. Acta Otorhinolaryngol Ital 25:161–168
28. Tirado Y, Williams MD, Hanna EY, Kaye FJ, Batsakis JG, El-Naggar AK (2007) CRTC1/MAML2 fusion transcript in high grade mucoepidermoid carcinomas of salivary and thyroid glands and Warthin's tumors: implications for histogenesis and biologic behavior. Genes Chromosomes Cancer 46:708–715
29. Tonon G, Modi S, Wu L, Kubo A, Coxon AB, Komiya T, O'Neil K, Stover K, El-Naggar A, Griffin JD, Kirsch IR, Kaye FJ (2003) t(11;19)(q21;p13) translocation in mucoepidermoid carcinoma creates a novel fusion product that disrupts a Notch signaling pathway. Nat Genet 33:208–213
30. Tran N, McLean T, Zhang X, Zhao CJ, Thomson JM, O'Brien C, Rose B (2007) MicroRNA expression profiles in head and neck cancer cell lines. Biochem Biophys Res Commun 358:12–17
31. Van Heerden WF, Raubenheimer EJ, Dreyer L (2005) The role of DNA ploidy and Ki-67 in the grading of mucoepidermoid carcinomas. Anticancer Res 25:2589–2592
32. Waldron CA, el-Mofty SK, Gnepp DR (1988) Tumors of the intraoral minor salivary glands: a demographic and histologic study of 426 cases. Oral Surg Oral Med Oral Pathol 66:323–333

Virchows Arch (2008) 452:637–650
DOI 10.1007/s00428-008-0605-x

ORIGINAL ARTICLE

KIT, *PDGFRα* and *EGFR* analysis in nephroblastoma

Sylvia C. Wetli · Ivo Leuschner · Dieter Harms · Alex Rufle · Anja Foerster · Michel Bihl · Norbert Graf · Roikos Furtwaengler · Michael Paulussen · Jakob Briner · Charalampos Aslanidis · Gerd Schmitz · Luigi Tornillo · Michael J. Mihatsch · Inti Zlobec · Elisabeth Bruder

Received: 3 October 2007 / Revised: 4 March 2008 / Accepted: 6 March 2008 / Published online: 14 May 2008
© Springer-Verlag 2008

Abstract Nephroblastoma prognosis has dramatically improved, but an unfavourable prognostic subgroup warrants development of novel therapeutic strategies. Selective KIT, PDGFRα and epidermal growth factor receptor (EGFR) tyrosine kinase inhibition evolved as powerful targeted therapy for gastrointestinal stromal tumours and non-small-cell lung cancer. To investigate a potential role for tyrosine kinase inhibition, we analyzed 209 nephroblastomas for immunohistochemical KIT and EGFR expression, 63 nephroblastomas for mutations in *KIT* exons 9, 11, 13, *EGFR* exons 18, 19, 20 and 21, and all 209 nephroblastomas for *PDGFRα* exons 12, 14 and 18. Twenty-two tumours (10.5%) expressed KIT, 31 (14.8%) EGFR, and 10 (4.8%) both KIT and EGFR, respectively. KIT expression was relatively more common among high-risk tumours (6/27; 22.3%) compared to low-/intermediate-risk tumours (26/181; 14.4%). Nine patients deceased, four of which had high-risk tumours with KIT expression in two of four and EGFR expression in one of four. There were no *KIT*, *PDGFRα* or *EGFR* mutations. Our results suggest no significant contribution of *KIT*, *EGFR* or *PDGFRα* mutations to nephroblastoma pathogenesis. Despite a trend towards association of immunohistochemical KIT and EGFR expression with poor outcome in high-risk nephroblastomas, statistical analysis did not yield significant correlations in this subgroup. Therefore, it remains open if KIT, PDGFRα or EGFR tyrosine kinase inhibition constitute a therapeutic target in nephroblastoma in the absence of *KIT, PDGFRα* or *EGFR* mutations.

Electronic supplementary material The online version of this article (doi:10.1007/s00428-008-0605-x) contains supplementary material, which is available to authorised users.

S. C. Wetli · A. Rufle · A. Foerster · M. Bihl · L. Tornillo · M. J. Mihatsch · I. Zlobec · E. Bruder (✉)
Institute for Pathology, Basel University Hospital,
Schoenbeinstrasse 40,
CH-4031 Basel, Switzerland
e-mail: elisabeth.bruder@unibas.ch

I. Leuschner · D. Harms
Institute for Pathology,
University Hospital Schleswig-Holstein Campus Kiel,
Michaelisstrasse 11,
24105 Kiel, Germany

N. Graf · R. Furtwaengler
Department of Paediatric Oncology,
University Children's Hospital,
Building 9,
66421 Homburg, Germany

M. Paulussen
Department of Paediatric Oncology/Haematology,
University Children's Hospital,
Römergasse 8,
CH-4005 Basel, Switzerland

J. Briner
Institute for Histologic and Cytologic Diagnostics,
Dammweg 1,
CH-5001 Aarau, Switzerland

C. Aslanidis · G. Schmitz
Institute for Clinical Chemistry and Laboratory Medicine,
University of Regensburg,
Franz-Josef Strauß Allee 11,
93053 Regensburg, Germany

Keywords Nephroblastoma · KIT-PDGFRα-EGFR mutation analysis · Tyrosine kinase inhibition · KIT-EGFR immunohistochemistry

Introduction

Nephroblastoma is the most common malignant renal tumour in childhood and affects 1 in 8,000 children [11]. Over the past three decades, multimodal nephroblastoma therapy has been a story of success. Nephroblastoma prognosis has improved dramatically, and overall 10-year survival now approaches 85% [15]. Nevertheless, a poor prognostic subgroup of nephroblastomas remains. Diffuse anaplasia, persistent blastema after chemotherapy, allelic loss at 1p or 16q, *TP53* mutations and advanced tumour stage have been identified as adverse prognostic factors [3, 10, 11, 31, 32]. Therefore, development of novel therapeutic strategies is mandatory.

Over recent years, receptor tyrosine kinases have evolved as focus of research for potential targeted tumour therapy [26]. Transmembrane receptor tyrosine kinases play an important role in the modulation of growth factor signalling [33]. Receptor tyrosine kinases KIT (v-kit Hardy-Zuckermann 4 feline sarcoma viral oncogene homologue), PDGFRα (platelet-derived growth factor receptor α) and EGFR (epidermal growth factor receptor) participate in cell growth and are implicated in malignant transformation and tumour progression. KIT is claimed to play an important role in kidney organogenesis. It is expressed during metanephrogenesis in blastema and immature epithelium and in the mature kidney in proximal and distal tubules [27]. KIT expression has been demonstrated in a subset of renal cell carcinomas, oncocytomas, mesoblastic nephromas, angiomyolipomas and a small series of nephroblastomas [22, 30]. The KIT internal tyrosine kinase component is structurally related to the platelet-derived growth factor receptor α [40]. PDGFRα overexpression has been described in carcinomas of colon, breast, lung, ovary and pancreas. Expression of activated PDGFRα in stromal cells of colon carcinomas has been associated with metastatic potential [23]. EGFR is expressed in most human tissues and plays an important role in normal cell biology. In the kidney, the human epidermal growth factor family members play a significant role in the mesenchymal to epithelial transition during renal tubulogenesis [41]. EGFR expression is found in a number of tumours, particularly squamous cell carcinomas, sarcomas, gliomas, breast, bladder and lung tumours. In nephroblastoma, EGFR expression has been described in a subset of tumours in one small series [14].

Selective inhibition of receptor tyrosine kinases has evolved as a powerful, targeted therapeutic tool in a number of tumours, and the spectrum of small molecule receptor tyrosine kinase inhibitors is rapidly expanding [26]. Imatinib/Gleevec® and Gefitinib/Iressa® are now well established as therapeutic inhibitors of KIT and EGFR, respectively. In particular, gastrointestinal stromal tumours and leukemias have been shown to be amenable to receptor tyrosine kinase inhibitor therapy [16, 17, 21, 34]. *KIT* iuxtamembranous exon 9, 11 and 13 mutations correspond with susceptibility to tyrosine kinase inhibition and improved survival in gastrointestinal stromal tumours and myeloic leukemia [8, 9, 13, 36, 38]. Up to 90% of gastrointestinal stromal tumours are *KIT*-mutated, and exon 11 mutations are most common [20, 25]. Approximately 7–12% of gastrointestinal stromal tumours without *KIT* mutations show *PDGFRα* mutations instead and are susceptible, though to a lesser degree, to imatinib treatment [7, 20, 38]. Interestingly, *KIT* and *PDGFRα* are located in the same chromosomal region 4q12 [35]. *PDGFRα* mutations are most often located in exon 18, and rarely in exons 12 and 14. In clinical phase 3 studies, a new generation of KIT/PDGFR receptor tyrosine kinase inhibitors for resistant tumours, e.g. sunitinib/Sutent®, are currently being tested [6]. Furthermore, activating *EGFR* gene mutations of exons 18, 19, 20 or 21 in non-small-cell lung carcinoma result in inhibition of apoptosis, in tumour proliferation, angiogenesis, invasion and metastasis [29, 33]. *EGFR* gene mutations confer susceptibility to gefitinib/Iressa® EGFR receptor tyrosine kinase inhibition [19].

In nephroblastomas, immunohistochemical KIT and EGFR expression has only been investigated in a small number of tumours [14], and neither *KIT*, *PDGFRα* nor *EGFR* mutations have been reported in these tumours so far. In a separate small set of 12 KIT-positive nephroblastomas, we detected mutations of *KIT* exon 11 in two tumours (Bruder et al., manuscript submitted). Moreover, no information is available so far with regard to tyrosine kinase expression and outcome. To provide a rationale for potential targeted small molecule receptor tyrosine kinase inhibition in nephroblastomas, we screened 209 nephroblastomas for immunohistochemical KIT and EGFR expression. Tumours with KIT expression were analysed for mutations of *KIT* exons 9, 11, 13. Similarly, tumours with EGFR expression were submitted to sequence analysis of *EGFR* exons 18, 19, 20 and 21. All 209 tumours were analysed for *PDGFRα* exons 12, 14 and 18 mutations.

Materials and methods

Nephroblastomas

From the archives of the Kiel Paediatric Tumour Registry, 209 nephroblastomas were compiled (1993–2002). Patient data were available on gender, age and stage at diagnosis,

tumour subtype, therapy mode and patient outcome. Male to female ratio was 1:1.27. Median patient age was 4.3 years. Preoperative chemotherapy had been administered to 181 patients according to the current International Paediatric Oncology Society (SIOP) protocol, and 28 patients underwent primary tumour resection. All nephroblastomas were classified according to the current SIOP classification [39] (Fig. 1). This current nephroblastoma classification accounts for the differential prognostic impact of blastema before and after chemotherapy and newly categorises residual blastema after chemotherapy in tumours with more than one third viable tumour tissue and more than two thirds of the viable tumour tissue of blastemal type (i.e. blastema predominant) as high-risk histology [39]. Tumours were reviewed by IL, DH, EB and SCW as well as by the SIOP nephroblastoma panel.

For tumour diagnosis, at least one block per centimeter tumour diameter was embedded. A mean of five blocks were available for tumour classification at the Kiel Paediatric Tumour Registry.

A paraffin tumour tissue microarray was constructed for efficient expression screening as previously described [24] (Fig. 2). For adult tumours, like urothelial carcinoma, one single punch cylinder per tumour was previously shown to be representative of each tumour [28]. For the present study of nephroblastoma, the paraffin tissue microarray construction technique was modified and specifically adapted to account for nephroblastoma as a heterogeneous embryonal tumour. Therefore, each histological tumour component of all 209 nephroblastomas was sampled, the respective tumour area circled on an H&E slide, and the corresponding paraffin block area marked before punching, resulting in five to six punch cylinders (mean 5.4, median 5) for each tumour on a total of three recipient blocks with a total of 1,178 punch cylinders. Normal renal parenchyma was included whenever present.

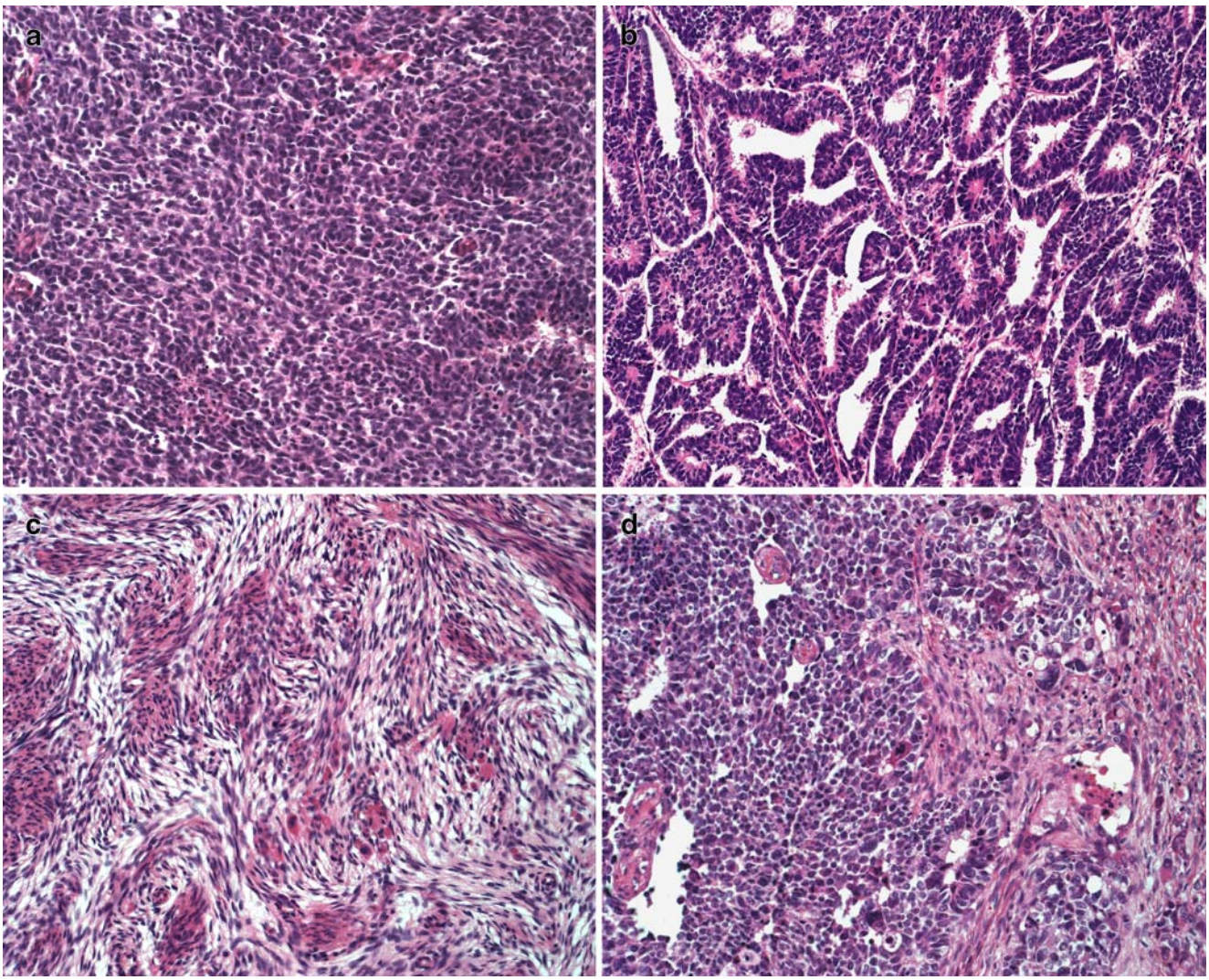


Fig. 1 Conventional histology: **a** Blastemal nephroblastoma (H&E×200). **b** Epithelial nephroblastoma (H&E×200). **c** Stromal nephroblastoma (H&E×200). **d** Diffuse anaplastic nephroblastoma (H&E×200)

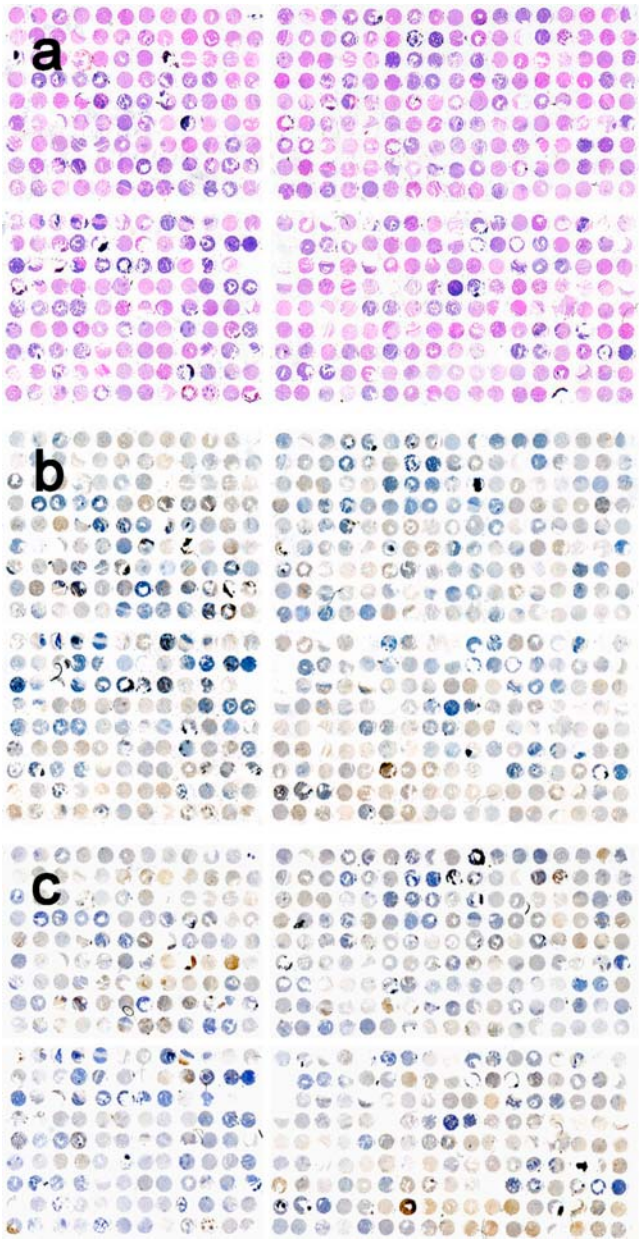


Fig. 2 Nephroblastoma array: **a**–**c** Overview of one paraffin block of the constructed nephroblastoma array (**a** H&E, **b** CD117/ KIT immunohistochemistry, **c** EGFR immunohistochemistry slide scans)

Criteria for tumour components for inclusion in the paraffin tissue microarray comprised all known histological nephroblastoma components, i.e. blastemal, epithelial, stromal and anaplastic tumour areas [11]. To carefully account for tumour heterogeneity and regional tumour variability, each histological tumour component was diligently selected for punching and was represented on the paraffin tissue microarray. Tumour punch samples originated from one or multiple blocks (median 3 blocks, mean 2.7 blocks). Punch core needle diameter was 0.6 mm as described previously [24, 28].

Immunohistochemistry

Paraffin tissue microarray sections were cut at 4 μm according to a protocol standardised in our laboratory. Immunohistochemistry for KIT receptor CD117 protein was performed on a Bond™ Immunostainer (Bond Max, Vision BioSystems; Figs. 3 and 4). For KIT/ CD117 immunohistochemistry, sections were pretreated in the manufacturer's ' Epitope Retrieval buffer 2' (Tris–EDTA buffer at pH 8.8) for 20 min at 100°C, incubated with polyclonal antibody Anti CD117 primary antibody (DAKO, 1:1000), followed by Bond polymer refine detection kit according to the manufacturer's protocol. A gastrointestinal tumour served as positive control. As it is known that KIT immunohistochemistry is prone to false positive staining results [20], the immunohistochemical reaction for KIT was carefully tested and set up in our laboratory with particular attention to negative controls so as to avoid false positive immunohistochemical staining results. For EGFR, immunohistochemistry was performed according to the EGFR pharmDx™, Code K1492 (Dako Cytomation) kit protocol. A cytospin of an EGFR-positive cell line contained in the kit served as positive control. A test array slide, containing a combination of normal and neoplastic human tissue cores, was included as negative control for each KIT and EGFR immunohistochemical reaction. Immunohistochemistry for PDGFRα was not performed because in our experience, PDGFRα immunohistochemistry is currently not reliable. Instead, all tumours were submitted to PDGFRα sequence analysis (see below).

Immunohistochemical staining for KIT/CD117 and EGFR was evaluated for each individual array punch tissue sample and recorded according to tumour tissue component and intensity of staining. Staining intensity was graded from + to +++, with + denoting faint cytoplasmatic staining, ++ intermediate cytoplasmatic staining and +++ exclusively only awarded to those tumours with distinct membranous in addition to cytoplasmic staining (Table 1). Immunohistochemical scoring was performed by SCW and EB independent of further tumour and patient information. Tumours were classified as KIT- or EGFR-positive, respectively, only in the presence of membranous KIT or EGFR expression and selected for subsequent DNA sequence analysis. Immunohistochemical scoring was amended to include the percentage of KIT- or EGFR-positive cells. In Table 1, the percentage of immunohistochemically positive tumour cells is provided.

KIT, PDGFRα and EGFR sequence analysis

For *KIT*, *PDGFRα* and *EGFR* sequence analysis, those tumours with strong immunohistochemical KIT and/or EGFR expression were selected. As in gastrointestinal

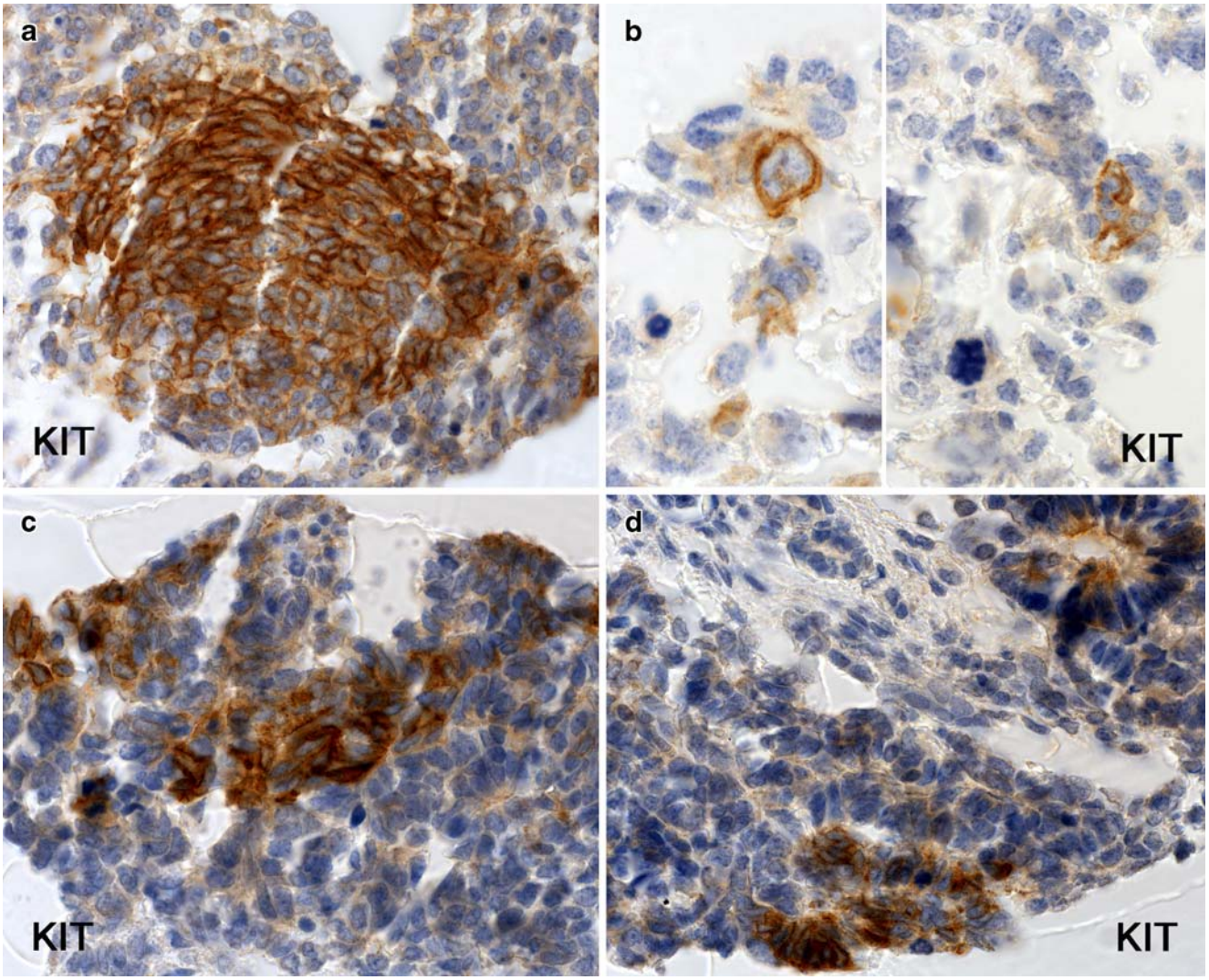


Fig. 3 KIT immunohistochemistry: **a** Membranous KIT expression in a blastemal nephroblastoma (KIT immunohistochemistry×630). **b** Focal membranous KIT expression in a nephroblastoma with diffuse anaplasia (KIT immunohistochemistry×630). **c**, **d** Focal membranous KIT expression in a nephroblastoma of mixed subtype (KIT immunohistochemistry×630). **c** Represents a blastemal component of this tumour, whereas **d** depicts a focus of KIT expression in immature epithelium in addition to a group of blastemal cells (KIT immunohistochemistry×630)

stromal tumours the presence of either *KIT* or *PDGFRα* mutations is regarded as predictive of tumour response to receptor tyrosine kinase inhibition [2], we proceeded to submit all KIT expressing nephroblastomas not only to *KIT* but also to *PDGFRα* sequence analysis. *KIT* and *PDGFRα* sequence analysis was performed on 22 of 209 tumours with strong +++ membranous and cytoplasmic CD117 expression. *EGFR* sequencing was performed on 31 of 209 tumours with strong +++ membranous and cytoplasmic EGFR expression. Ten nephroblastomas revealed both EGFR and KIT expression and were submitted to *KIT*, *PDGFRα* as well as *EGFR* sequencing analysis. Consequently, *KIT* and *EGFR* DNA sequence analysis was performed on a total of 63 nephroblastomas. In addition, in the absence of an immunohistochemical PDGFRα screening test, all 177 CD117 negative nephroblastomas were submitted to *PDGFRα* sequence analysis, resulting in *PDGFRα* sequence analysis of all 209 nephroblastomas included in this study.

For DNA extraction, one to three punch cylinders 0.6 mm in diameter were removed from identical matched tumour regions of the original paraffin tissue blocks of each selected nephroblastoma. DNA was extracted according to the SIOP 1 and the QIAamp® DNA mini kit DNA extraction protocols (Qiagen AG, Basel, Switzerland) [37]. The extracted DNA was submitted to a semi-nested or nested multiplex polymerase chain reaction (PCR) for *KIT* exons 9, 11, 13, *PDGFRα* exons 12, 14 and 18 and *EGFR* exons

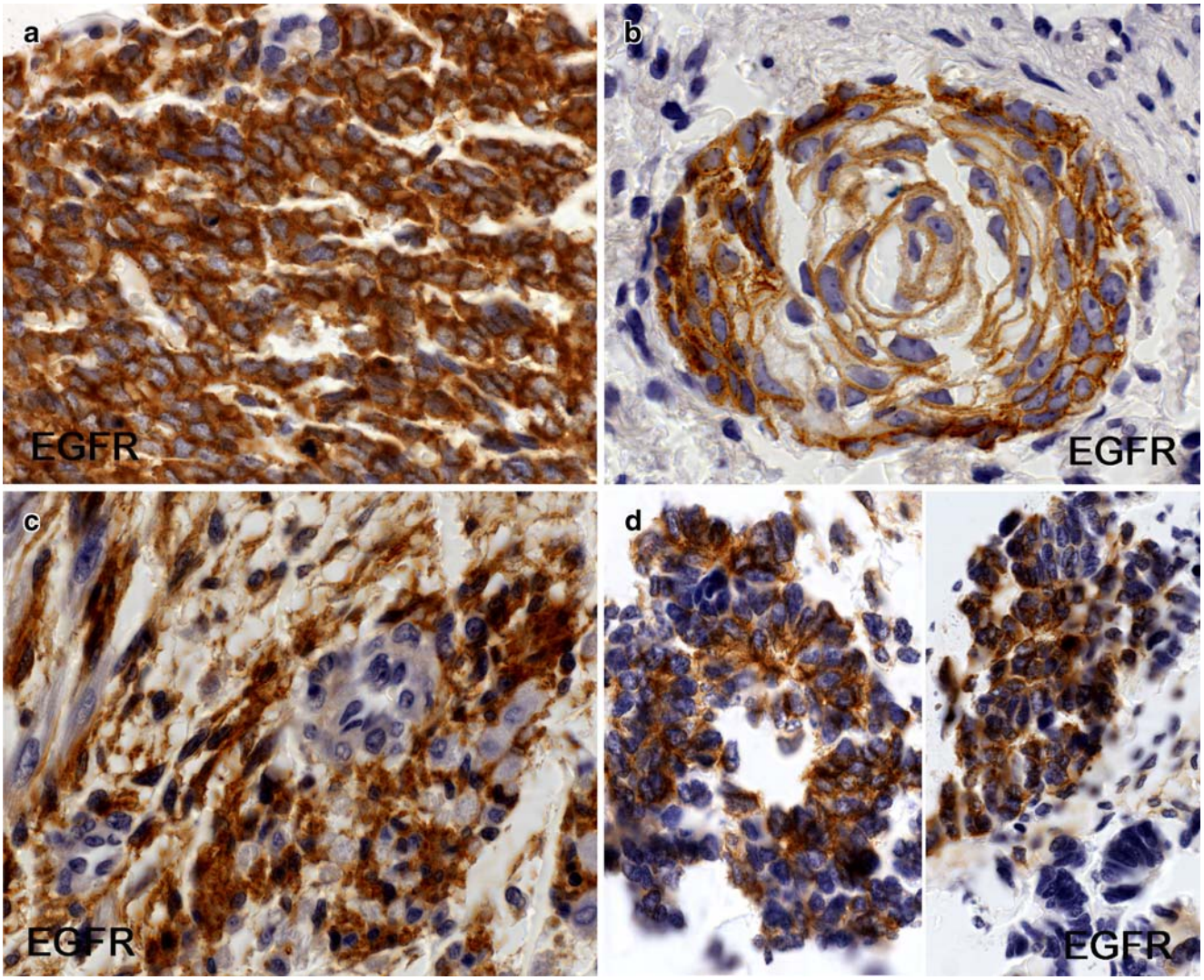


Fig. 4 EGFR immunohistochemistry: **a** Membranous EGFR expression in a blastemal predominant nephroblastoma. At the *top border* of the figure is an EGFR-negative tubule (EGFR immunohistochemistry×630). **b** Membranous EGFR expression in a focus of squamous epithelium. Surrounding stroma is negative for EGFR (EGFR immunohistochemistry×630). **c** EGFR expression in a stromal predominant nephroblastoma. Foci of rhabdomyoblastic differentiation are negative for EGFR (EGFR immunohistochemistry×630). **d** EGFR expression in blastemal foci and immature epithelium in a mixed type nephroblastoma (EGFR immunohistochemistry×630)

18, 19, 20 and 21. DNA sequencing was performed on the PCR products on an ABI PRISM 310xl Genetic Analyzer (Applied BioSystems). Sequencing primers were identical to initial PCR primers. Primer sequences are given in Table 2.

Statistical analysis

For statistical analysis, associations between follow-up data, histological nephroblastoma subtype and immunohistochemical expression of KIT and EGFR were analysed, respectively. The association between survival, recurrence and metastasis with KIT and EGFR expression was evaluated using the chi-square test or Fisher's exact test. P values<0.05 were considered statistically significant. All analyses were carried out using SAS (version 9.0, The SAS Institute, NC, USA).

Results

In this study, we analyzed 209 nephroblastomas for immunohistochemical KIT and EGFR expression, a total of 63 tumours for mutations in *KIT* exons 9, 11, 13, *EGFR* exons 18, 19, 20 and 21, as well as *PDGFRα* exons 12, 14 and 18 in the total series of 209 nephroblastomas. Tumour localisation was equally distributed between both kidneys, with 108 tumours localised in the right and 101 in the left kidney.

Table 1 Clinicopathologic characteristics and immunohistochemistry (*N*=209): risk group, nephroblastoma subtype, membranous KIT and EGFR expression, preoperative chemotherapy, adverse events, follow-up interval

Risk group	Histology	KIT expression	EGFR expression	KIT and EGFR expression	Local recurrence	Metastasis	Death of disease
Low 2 (1%)	CPDN 2 (100%)	0	0	0	0	0	0
Intermediate 179 (86%)	Blastemal (pretreatment) 9 (5%)	2	0	1	0	1	0
	Epithelial 6 (3.4%)	0	0	0	1	1	0
	Stromal 29 (16.2%)	7	7	2	1	2	0
	Mixed 91 (50.8%)	12	23	4	6	10	2
	Regressive 42 (23.5%)	4	7	2	3	10	3
	Focal anaplasia 2 (1.1%)	0	0	0	0	0	0
High 27 (12.5%)							
	Blastemal (post-treatment) 21 (77.8%)	4	2	1	4	2	3
	Diffuse anaplasia 6 (22.2%)	1	1	0	1	1	1
Unclassified (0.5%)	Unclassified 1 (0.5%)	1	0	0	0	0	0
Total 209 (100%)		22 (10.6%)	31 (14.8%)	10 (4.8%)	16 (7.6%)	27 (12.9%)	9 (4.3%)

CPDN cystic partially differentiated nephroblastoma

The 209 tumours were classified according to the SIOP classification (Table 1, Fig. 1): two low-risk tumours (1%; CPDN: cystic partially differentiated nephroblastoma), 179 intermediate-risk tumours (86%), 27 high-risk tumours (12.5%) and one non-classifiable tumour (0.5%). Tumour group details are provided in Table 1. The 179 nephroblastomas of intermediate risk were: 91 mixed (52%), 42 regressive (23%), 29 stromal (16%), nine pre-chemotherapy blastemal (5%), six epithelial (3%) and two with focal anaplasia (1%). The 27 nephroblastomas of high-risk histology were: 21 of 27 (78%) post-chemotherapy blastemal and 6 of 27 diffuse anaplastic nephroblastomas (22.3%). The nephroblastomas classified as post-chemotherapy blastemal showed more than one third viable tissue of which more than two thirds of the viable tumour tissue was of blastemal type (i.e. blastema predominant).

Follow-up between 7 and 132 months (mean 66 months) was available for all 209 patients. Of 209 patients, nine (4%) died of tumour: five intermediate-risk tumours (56%; three regressive and two mixed), four high-risk tumours (44%; three post-chemotherapy blastemal, one diffuse anaplastic nephroblastoma; Fig. 1). Of the 27 patients with a high-risk histology tumour, four died (14.8%). Thus, our study confirms the association of high-risk nephroblastomas with poor outcome. Of the nine patients deceased, four had metastases, predominantly pulmonary: two patients with intermediate-risk tumours (regressive) and two high-risk tumours (one post-chemotherapy blastemal, one diffuse anaplastic nephroblastoma). A total of 27 (13%) tumours metastasised: 24 intermediate-risk tumours [89%; ten mixed (37%), two stromal (7%), ten regressive (37%; two patients died], one epithelial (4%), one pre-chemotherapy blastemal nephroblastoma (4%) and three high-risk tumours (11%; two post-chemotherapy blastemal (7%; one patient died), one with diffuse anaplasia (4%; this patient died).

Immunohistochemistry for KIT and EGFR

Tumours with membranous immunohistochemical KIT or EGFR expression were graded +++ and classified as positive. Immunohistochemical results are provided in Table 1. In most tumours, KIT and EGFR expression was focal and observed in blastemal and immature epithelial tumour components (Figs. 3 and 4). For more precise analysis, the percentage of KIT- and EGFR-expressing tumour cells per punch was estimated and is indicated in Table 1. Assuming that each KIT- or EGFR-expressing tumour area might be of potential biological relevance, all tumours with membranous immunohistochemical KIT or EGFR expression were classified as positive irrespective of the percentage of positive tumour cells. Sixty-three (30.1%) nephroblastomas demonstrated expression of KIT, EGFR or both: 22 (10.6%) nephroblastomas were KIT-positive, 31 (14.8%) nephroblastomas were EGFR-positive, and 10 (4.8%) tumours expressed both KIT and EGFR. Consequently, a total of 32 of 209 nephroblastomas (15.3%) showed immunohistochemical KIT expression. Of these, 26 were intermediate-risk tumours (81.3%) and one was not classifiable (3.1%). KIT expression was observed in 12 (37.5%) mixed nephroblastomas, seven (21.9%) stromal, four (12.5%) regressive and three (9.4%) pre-chemotherapy blastemal nephroblastomas. Of the 27 high-risk histology

Table 2 Polymerase chain reaction primer sequences

Primer name	Primer direction	Primer sequence 5′→3′
KIT exon 9	Forward_1	TCC TAG AGT AAG CCA GGG CTT
	Forward_2 (nested)	AGC CAG GGC TTT TGT TTT CT
	Reverse	TGG TAG ACA GAG CCT AAA CAT CC
KIT exon 11	Forward	CCA GAG TGC TCT AAT GAC TG
	Reverse_1	AGC CCC TGT TTC ATA CTG AC
	Reverse_2 (nested)	ACT CAG CCT GTT TCT GGG AAA CTC
KIT exon 13	Forward_1	GCT TGA CAT CAG TTT GCC AG
	Forward_2 (nested)	TGA CAT CAG TTT GCC AGT TG
	Reverse	AAA GGC AGC TTG GAC ACG GCT TTA
PDGFRα exon 12	Forward_1	GCT CTG GTG CAC TGG GAC TTT GGT A
	Forward_2nested	TGG TGC ACT GGG ACT TTG GTA ATT CA
	Reverse_1	TTG TGT GCA AGG GAA AAG GGA GTC TT
	Reverse_2nested	GGG AAA AGG GAG TCT TGG GAG GTT AC
PDGFRα exon 14	Forward_1	CTTTCAACAGCCACGGCCAGATC
	Forward_2nested	GGGGATGGAGAGTGGAGGATTTAAGC
	Reverse_1	CAACAGCCACGGCCAGATCCAG
	Reverse_2nested	CAACCACATGTGTCCAGTGAAAATCCTC
PDGFRα exon 18	Forward_1	CAG CCA GTC TTG CAG GGG TGA TG
	Forward_2nested	GAT GGC TTG ATC CTG AGT CAT TTC TTC C
	Reverse_1	GGG AGG ATG AGC CTG TCC AGT GTG
	Reverse_2nested	GAG CCT GTC CAG TGT GGG AAG TGT G
EGFR exon 18	Forward	GCA TGG TGA GGG CTG AGG TGA
	Forward_nested	ACC CTT GTC TCT GTG TTC TTG TCC C
	Reverse	CCC CAC CAG ACC ATG AGA GGC
	Reverse_nested	GCC CAG CCC AGA GGC CTG TG
EGFR exon 19	Forward	TGC CAG TTA ACG TCT TCC TTC
	Forward_seminested	AAC GTC TTC CTT CTC TCT CTG
	Reverse	CCA CAC AGC AAA GCA GAA AC
EGFR exon 20	Forward	CCA CCA TGC GAA GCC ACA CTG A
	Forward_nested	CCA TGC GAA GCC ACA CTG ACG T
	Reverse	TCC TTA TCT CCC CTC CCC GTA TCT C
	Reverse_nested	CCC CTC CCC GTA TCT CCC TTC C
EGFR exon 21	Forward	AGC TTC TTC CCA TGA TGA TCT GTC C
	Forward_nested	TCC CAT GAT GAT CTG TCC CTC ACA
	Reverse	GGC AGC CTG GTC CCT GGT GTC
	Reverse_nested	CAG GAA AAT GCT GGC TGA CCT AAA G

nephroblastomas, six showed KIT expression (22.3%). Five of 21 post-chemotherapy blastemal nephroblastomas and one of six with diffuse anaplasia were KIT-positive. None of the six epithelial, focal anaplastic or cystic partially differentiated nephroblastomas showed KIT expression. EGFR expression was observed in 41 of 209 nephroblastomas (19.6%). Thirty-eight of them were intermediate-risk tumours (92.7%) and three high-risk tumours (7.3%). Similar to KIT, EGFR expression was observed predominantly in mixed nephroblastomas: 23 of 41 tumours (56.1%) were mixed, seven (17.1%) were stromal, seven (17.1%) regressive and one (2.4%) non-pretreated blastemal nephroblastomas. Only 3 of 27 high-risk nephroblastomas expressed EGFR, two (of 21) post-chemotherapy blastemal and one (of 6) nephroblastoma with diffuse anaplasia. None of the six epithelial, focal anaplastic or cystic partially differentiated nephroblastomas showed EGFR expression.

Immunohistochemical scoring was amended to include the percentage of KIT- or EGFR-positive cells in immunohistochemically positive tumour punches. In ESM Table 1, the percentage of immunohistochemically positive tumour cells per positive tumour punch is provided.

KIT exon 9, 11, 13, EGFR exon 18, 19, 20, 21, PDGFRα exon 12, 14 and 18 sequence analysis

Sequence analysis for *KIT* and *EGFR* was performed on a total of 63 tumours and for *PDGFRα* on all 209 tumours from 209 patients. A total of 957 exons were sequenced. Twenty-two nephroblastomas with KIT expression were

selected for *KIT* exon 9, 11, 13 and *PDGFRα* exon 12, 14 and 18 sequence analysis. All 22 tumours contained *KIT* exon 9, 11, 13 and *PDGFRα* exon 12, 14 and 18 wild-type sequences (Fig. 5). The 31 nephroblastomas with immunohistochemical staining for EGFR were selected for *EGFR* exon 18, 19, 20 and 21 sequence analysis. All 31 tumours contained *EGFR* exon 18, 19, 20 and 21 wild-type sequences (Fig. 5). The ten tumours with both KIT and EGFR expression were selected for *KIT* exon 9, 11, 13, *PDGFRα* exon 12, 14, 18 and for *EGFR* exon 18, 19, 20 and 21 sequence analysis. All ten tumours contained wild-type sequences of *KIT* exons 9, 11, 13, *PDGFRα* exons 12, 14, and 18 and for *EGFR* exons 18, 19, 20 and 21. In addition, all 177 immunohistochemically KIT-negative nephroblastomas were submitted to *PDGFRα* sequence analysis. Similar to the KIT immunohistochemically positive tumours, the immunohistochemically KIT-negative nephroblastomas contained *PDGFRα* exon 12, 14 and 18 wild-type sequences.

PDGFRα sequence analysis was performed in double independently in two separate laboratories at the Institute of Pathology at the University Hospital in Basel, Switzerland

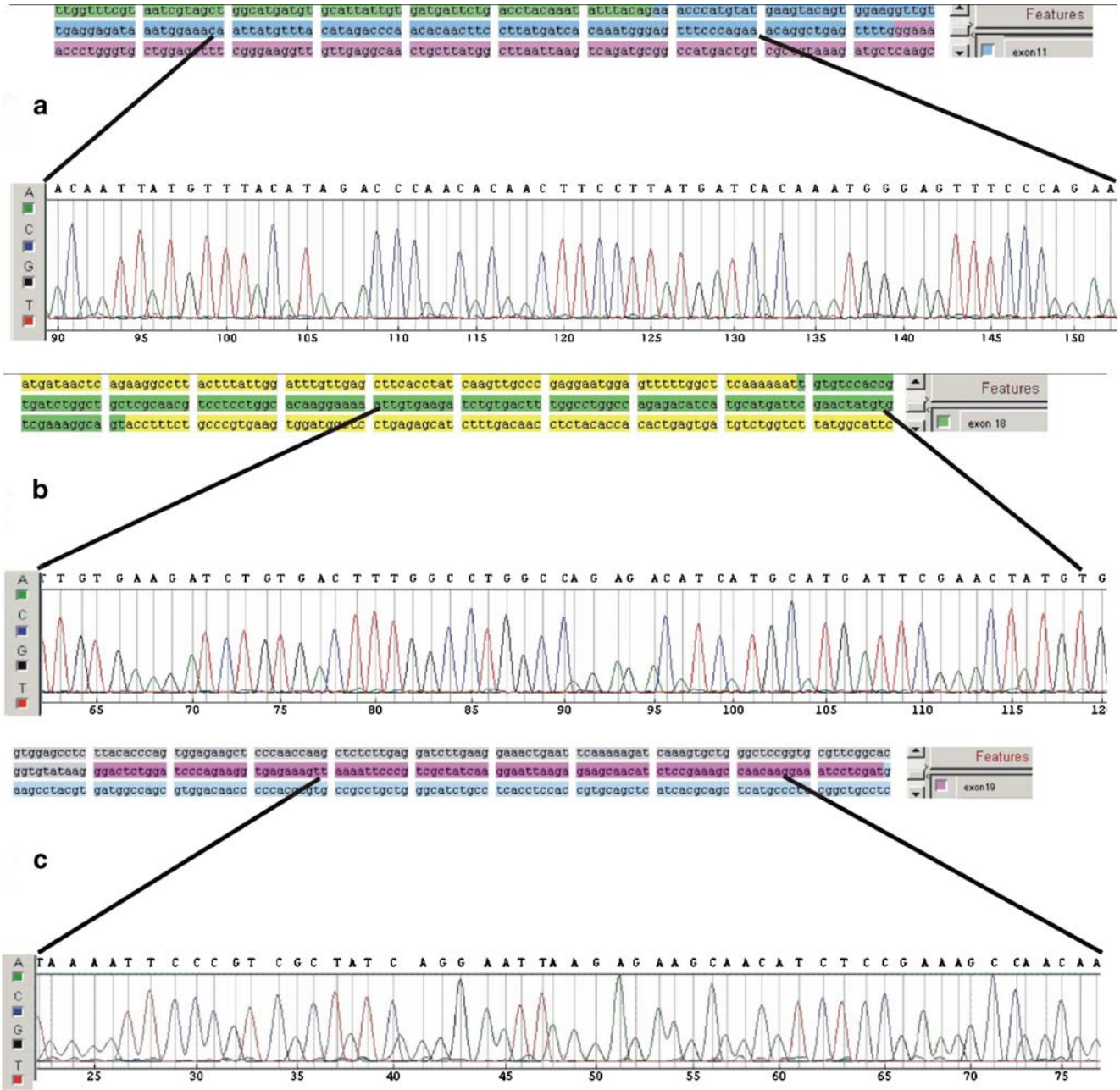


Fig. 5 KIT, PDGFRα and EGFR sequencing results: **a** KIT wild-type sequence (32 nephroblastomas). **b** PDGFRα wild-type sequence (209 nephroblastomas). **c** EGFR wild-type sequence (41 nephroblastomas)

and at the Institute for Clinical Chemistry and Laboratory Medicine at the University of Regensburg, Regensburg, Germany.

All sequencing reactions were repeated twice. Repeat mutation analyses yielded identical results.

Statistical analysis

Correlation of tyrosine kinase receptor expression and outcome

Metastases occurred in 30 patients (14.1%), tumour recurrences were observed in 17 patients (8%), and nine patients died (4.2%). Although we observed a trend for KIT expression in high-risk histology tumours with adverse events, statistically, KIT expression was not significantly associated with outcome, neither in the whole group of nephroblastomas (p=0.18) nor in the group of low- or intermediate-risk histology tumours nor in high-risk histology tumours (p=0.062). KIT expression was independent of immunohistochemical EGFR expression. Similar to KIT, EGFR expression did not correlate with adverse events for the total group of nephroblastomas analysed (p=0.224).

Comparison of treated and untreated nephroblastomas

Preoperative chemotherapy had been administered to 181 patients according to the current SIOP protocol, and 28 patients underwent primary tumour resection without preoperative chemotherapy (see Table 3). In the tumour group with preoperative chemotherapy, there were 27 high-risk histology nephroblastomas, 153 intermediate risk histology nephroblastomas and one unclassified nephroblastoma. In the tumour group without preoperative chemotherapy, there were two low-risk histology tumours and 26 intermediate-risk histology tumours, but no high-risk tumour. None of the high-risk histology tumours were treated with primary resection; all of these had received preoperative chemotherapy.

Comparing the immunohistochemical results of the total group of 209 tumours with those tumours treated preoperatively, there is no statistical difference between the total group and the group treated with preoperative chemotherapy.

Comparison of immunohistochemical expression among the preoperatively treated versus the preoperatively untreated group yields a tendency towards a higher percentage of KIT-expressing tumours in the preoperatively untreated group (p=0.069). Seven of 26 preoperatively untreated nephroblastomas of intermediate-risk histology showed KIT expression, corresponding to 27%, as opposed to 19 of 153 (12%) of intermediate-risk histology nephroblastomas with preoperative chemotherapy. As for EGFR expression, the trend is similar but to a lesser degree (p=0.443): Seven of 26 (27%) preoperatively untreated nephroblastomas of intermediate-risk histology showed EGFR expression versus 31 of 153 (21%) preoperatively treated intermediate-risk histology nephroblastomas.

However, the numbers of individual intermediate-risk histology subgroups without preoperative chemotherapy are small, and analysis of larger numbers is required to confirm such a trend. Similarly, the tumour spectrum within the preoperatively treated versus preoperatively untreated tumour group is different and is therefore likely to introduce a bias into the comparison of these two nephroblastoma groups.

As for outcome analysis among the preoperatively untreated tumours and comparison with the preoperatively treated tumours, a similar bias is likely.

None of the adverse events occurred in these 28 preoperatively untreated tumours except one surviving patient with metastases of a KIT- and EGFR-negative tumour of the intermediate-risk histology group. No patient in the preoperatively untreated group died. All other

Table 3 Comparison of immunohistochemical results in treated and untreated tumours

Chemotherapy	*N*	Histology risk group	*N*	KIT expression	EGFR expression
Yes	181				
		High	27	5 of 27 (19%)	3 of 27 (12%)
		Intermediate	153	19 of 153 (12%)	31 of 153 (21%)
		Unclassified	1	1	0
No	28				
		High	0	0	0
		Intermediate	26	7 of 26 (27%)	7 of 26 (27%)
		Low	2	0	0
Total yes and no	209				
		High	27	5 of 27 (19%)	3 of 27% (12%)
		Intermediate	179	26 of 179 (15%)	38 of 179 (21%)
		Low	2	0	0
		Unclassified	1	1	0

N=209

adverse events occurred in those patients with preoperative chemotherapy. All patients who died were in the group with preoperative chemotherapy.

Discussion

Enhanced understanding of genetic alterations in nephroblastoma and identification of key molecular markers is expected to provide the foundation for novel targeted therapies to address currently poor prognostic nephroblastoma subgroups. Transmembrane receptor tyrosine kinases play a crucial role in growth factor signalling cascades. The role of tyrosine kinases for tumour growth and angiogenesis in nephroblastomas has been described in previous studies [1, 12, 14, 41]. Constitutional protein kinase activation by somatic mutation is a frequent mechanism of tumourigenesis [33]. Targeted small molecule drugs have emerged as elegant and efficient anti-cancer strategies, and selective receptor tyrosine kinase inhibition evolves as focus of research for novel therapies. As receptor tyrosine kinases, KIT and EGFR play a significant role in renal organogenesis and expression has previously been described in a small series of nephroblastomas, we set out to determine the prevalence of KIT and EGFR expression in a large series of 209 nephroblastomas. So far, as known from the experience in gastrointestinal stromal tumours, leukemias and non-small-cell lung cancer, susceptibility to kinase inhibition appears to be linked to constitutionally activating gene mutations, which has held true for KIT as well as for EGFR. Neither KIT nor EGFR mutations have been described in nephroblastomas so far. In a separate small set of 12 KIT-positive nephroblastomas, we detected mutations of KIT exon 11 in two tumours (Bruder et al., manuscript submitted). Therefore, we also determined KIT and EGFR gene sequences of most commonly involved exons in 63 nephroblastomas and PDGFRα of all 209 nephroblastomas to investigate a rationale for potential targeted tyrosine kinase inhibitor therapy in nephroblastoma.

Among the 209 nephroblastomas investigated in this study, we found KIT and/or EGFR expression in 63 tumours. Interestingly, KIT expression was more frequent among tumours of high-risk histology (6/27; 22.3%) compared with those of low- and intermediate-risk (26/181; 14.4%). In contrast, EGFR expression was less frequent in high-risk nephroblastomas (3/27; 11%) than in intermediate- and low-risk tumours (38/181; 20%). Did KIT or EGFR expression confer a different prognosis in our set of nephroblastomas? If nephroblastomas with adverse events defined as local recurrence, metastasis or death from disease were regarded separately, adverse events occurred in 37 (17.7%) of the total series of 209 tumours and in five (12.2%) of 41 tumours with EGFR expression. Conversely, adverse events occurred in 32 (19%) of 168 tumours without EGFR expression. Furthermore, adverse events were recorded in three (9.4%) of 32 KIT-expressing tumours, as opposed to adverse events in 34 (19.2%) of 177 KIT-negative tumours. In contrast, in 200 surviving patients, KIT and EGFR were positive in 15% and 19.5%, respectively. It therefore appears that KIT or EGFR expression alone may be associated with slightly better tumour outcome if regarded independently from tumour histology. However, in nine patients who died of their tumour, two (22.3%) tumours showed strong KIT expression and another 2 (22.3%) showed strong EGFR expression, while KIT and EGFR were positive in slightly lower proportions in the 200 surviving patients, 15% and 19.5%, respectively. Moreover, if evaluated in the context of tumour histology, four of the nine patients who died of disease had tumours of high-risk histology, and among these four tumours, two strongly expressed KIT, and one was EGFR-positive ($p=0.371$). Although these findings suggest a tendency that KIT expression, and to a minor degree also EGFR expression, may potentially be associated with poor outcome in the context of unfavourable histology, we were unable to statistically prove such a correlation. This is also true for tumours of low- and intermediate-risk histology associated with adverse events in relation to KIT and EGFR expression: Of 182 tumours with low- and intermediate-risk histology, only one (3.8%) of 26 KIT-expressing tumours and four (10.5%) of 38 EGFR expressing tumours ($p=0.206$) were associated with adverse events, whereas, conversely, 31 of 156 (19.9%) KIT-negative and 28 of 144 (19.4%) EGFR-negative tumours were associated with adverse events. Even if these results might suggest a tendency that low- and intermediate-risk histology nephroblastomas with KIT and EGFR expression appear to be associated with a better prognosis, this correlation is statistically not significant. As numbers of subgroups are small, this issue requires to be addressed in a still larger study. Nevertheless, these results suggest that KIT and EGFR expression should be evaluated in the context of tumour histology and outcome. The potential correlation of KIT and EGFR expression with better prognosis in low-/intermediate-risk histology nephroblastomas in this series is an interesting and important observation.

Could a subset of nephroblastomas merit a trial of selective tyrosine receptor kinase inhibition and be susceptible to this therapeutic approach? As the presence of either KIT or PDGFRα mutations is predictive of tumour response to selective receptor tyrosine kinase inhibition with imatinib in gastrointestinal stromal tumours [2, 18, 20], though to a lesser degree for PDGFRα mutations and no KIT mutations were detected in the subset of nephroblastomas investigated in this study, we therefore proceeded to determine also *PDGFRα* sequences in those nephro-

blastomas with KIT expression, and in the absence of an immunohistochemical screening test for PDGFRα, also in those tumours without KIT expression. Moreover, we investigated EGFR-expressing nephroblastomas for EGFR sequence alterations. None of the 63 nephroblastomas investigated showed any sequence alteration in any receptor tyrosine kinase analysed. Our present study of mutation analysis of 63 and 209 nephroblastomas, respectively, suggests that neither KIT, EGFR nor PDGFRα mutations appear to play a significant role in tumour pathogenesis. KIT and EGFR expression therefore do not appear to result from constitutionally activating mutations in the investigated exons in these nephroblastomas. Why do these tumours express KIT and/or EGFR in the absence of respective gene mutations? Importantly, KIT and PDGFRα receptor tyrosine kinases may be activated by mechanisms other than gene mutation, such as gene fusion and amplification, autocrine and paracrine stimulation of the receptor by its ligand, loss of phosphatase activity, cross-activation by other kinases and epigenetic promoter activation via methylation status alteration. Therefore, absence of KIT or PDGFRα mutations does not exclude selective tyrosine kinase inhibition with imatinib as targeted therapeutic strategy in the KIT-expressing nephroblastomas [35]. Importantly, imatinib has been shown to also effectively inhibit wild-type KIT and PDGFR receptors [2]. Similarly, in a previous study correlating KIT immuno-phenotype with response to tyrosine kinase inhibitor, imatinib even showed a response in gastrointestinal stromal tumours with only weak immunohistochemical staining [4]. Of note, in non-small-cell lung cancer, EGFR receptor tyrosine kinase inhibition with erlotinib/Tarceva® has recently been found to be effective in non-small-cell lung cancer with wild-type EGFR [5]. Therefore, as numbers in this current study are small, further investigations are required to evaluate a potential benefit, and future clinical therapeutic studies might be considered for the limited poor prognostic subgroup of nephroblastomas with high-risk histology also in the absence of *KIT*, *PDGFRα* or *EGFR* mutations. Nevertheless, at present, the question remains open whether the small group of poor prognostic nephroblastomas will benefit from additional receptor tyrosine kinase inhibition.

Addressing the question of preoperative chemotherapy and evaluation of the patient outcome in relation to expression of KIT and EGFR, comparing with patients without preoperative chemotherapy, such a comparison is likely to be biased for the following reasons. According to the current SIOP protocol, most nephroblastoma patients are treated by preoperative chemotherapy [15]. Only a minority of very young patients are judged not to require chemotherapy because of a high likelihood of congenital mesoblastic nephroma. Therefore, the criteria of patient inclusion will render the preoperatively treated versus the preoperatively untreated nephroblastoma groups incongruent.

It has been argued that preoperative chemotherapy may unpredictably alter tumour protein expression and genetics; therefore, only analysis of untreated tumour tissue should be regarded as reliable. However, it is now being recognised that surviving blastemal tumour tissue after chemotherapy constitutes an indicator towards poor chemotherapy response and prognosis, and therefore, nephroblastomas of post-chemotherapy blastemal predominant histology are currently classified among the high-risk histology group accordingly, in contrast to those blastemal predominant nephroblastomas without preoperative chemotherapy. Analysis of a study population of nephroblastomas with available pre-chemotherapy pre-surgical biopsy as well as post-chemotherapy specimens of identical tumours should be undertaken in the future to further contribute to resolve this issue.

In summary, a minor proportion of nephroblastomas express KIT and EGFR. However, KIT, PDGFRα and EGFR mutations do not appear to significantly contribute to nephroblastoma pathogenesis. Hence, unlike in gastrointestinal stromal tumours, leukemia and non-small-cell lung cancer, there appears to be no comparable molecular basis for potential selective tyrosine kinase inhibition in nephroblastoma. In nephroblastomas, immunohistochemical KIT and EGFR expression does not appear to bear a direct association with outcome. Nevertheless, as numbers of high-risk histology nephroblastomas are small, further clinical evaluation studies might be considered to elucidate a potential therapeutic benefit for this poor prognostic subgroup of patients.

Acknowledgments We are grateful to Barbara Stalder, Molecular Pathology Section, Institute for Pathology, University Hospital Basel, Switzerland for excellent performance of immunohistochemistry and to Melanie Schlangstedt, Institute for Clinical Chemistry and Laboratory Medicine at the University of Regensburg, Regensburg, Germany for PDGFRα sequence analysis. The study experiments comply with the current laws in the country in which they were performed.

This study was funded by a grant of the Basel Cancer League to EB.

Conflict of interest statement We declare that we have no conflict of interest.

References

1. Alpers CE, Hudkins KL, Ferguson M, Johnson RJ, Rutledge JC (1995) Platelet-derived growth factor A—chain expression in developing and mature human kidneys and in Wilms' tumor. Kidney Int 48(1):146–154
2. Buchdunger E, Cioffi CL, Law N, Stover D, Ohno-Jones S, Druker BJ, Lydon NB (2000) Abl protein-tyrosine kinase inhibitor STI571 inhibits in vitro signal transduction mediated by c-kit and

platelet-derived growth factor receptors. J Pharmacol Exp Ther 295:139–145
3. Charles AK, Brown KW, Berry PJ (1998) Microdissecting the genetics events in nephrogenic rests and Wilms tumor development. Am J Pathol 153:991–1000
4. Chirieac RL, Trent JC, Steinert DM, Choi H, Yang Y, Zhang J, Patel SR, Benjamin RS, Raymond AK (2006) Correlation of immunophenotype with progression-free survival in patients with gastrointestinal stromal tumors treated with imatinib mesylate. Cancer 107:2237–2244
5. Cho BC, Im CK, Park MS, Kim SK, Chang J, Park JP, Choi HJ, Kim YJ, Shin SJ, Sohn JH, Kim H, Kim JH (2007) Phase II study of erlotinib in advanced non-small-cell lung cancer after failure of geftinib. J Clin Oncol 25:2528–2533
6. Chow LQM, Eckhardt SG (2007) Sunitinib: from rational design to clinical efficacy. J Clin Oncol 25:884–896
7. Corless CL, Schroeder A, Griffith D, Town A, Mc Greevey L, Harrell P, Shiraga S, Bainbridge T, Morich J, Heinrich MC (2005) PDGFRA mutations in gastrointestinal stromal tumors: frequency, spectrum and in vitro sensitivity to imatinib. J Clin Pathol 23:5357–5365
8. Dei Tos AP (2003) The reappraisal of gastrointestinal stromal tumors: from Stout to the KIT revolution. Virchows Arch 442:421–428
9. Demetri GD (2001) Targeting c-kit mutations in solid tumors: scientific rationale and novel therapeutic options. Semin Oncol 28 (5 Suppl 17):19–26
10. Dome JS, Coppes MJ (2002) Recent advances in Wilms tumor genetics. Curr Opin Pediatr 14:5–11
11. Eble JN, Sauter G, Epstein JI, Sesterhenn IA (2004) Pathology and genetics, tumours of the urinary system and male genital organs. World health organization classification of tumours. IATC, Lyon
12. Fraizer GE, Bowen-Pope DF, Vogel AM (1987) Production of platelet-derived growth factor by cultured Wilm's tumor cells and fetal kidney cells. J Cell Physiol 133:169–174
13. Frost MJ, Ferrao PT, Hughes TP, Asman LK (2002) Juxtamembrane mutant V560Gkit is more sensitive to Imatinib (STI571) compared with wild-type c-kit whereas the kinase domain mutant D816Vkit is resistant. Mol Cancer Ther 1:1115–1124
14. Ghanem MA, Van Der Kwast TH, Den Hollander JC, Sudaryo MK, Mathoera RB, Van den Heuvel MM, Noordzji MA, Nijman RJM, van Steenbrugge GJ (2001) Expression and prognostic value of epidermal growth factor receptor, transforming growth factor-a, and c-erb B-2 in nephroblastoma. Cancer 92:3120–3129
15. Graf N, Semler O, Reinhard H (2004) Prognosis of Wilm's tumor in the course of the SIOP trials and studies. Urologe A 43:421–428
16. Heinrich MC, Corless CL, Demetri GD, Blanke CD, von Mehren M, Joensuu H, McGreevey LS, Chen CJ, Van den Abbeele AD, Druker BJ, Kiese B, Eisenberg B, Roberts PJ, Singer S, Fletcher CD, Silbermen S, Dimitrijevic S, Fletcher JA (2003) Kinase mutations and imatinib response in patients with metastatic gastrointestinal stromal tumor. J Clin Oncol 21:4342–4349
17. Hirota S, Isozaki K, Moriyama Y, Hashimoto K, Nishida T, Ishiguro S, Kawano K, Hanada M, Kurata A, Takeda M, Muhammad Tunio G, Matsuzawa Y, Kanakura Y, Shinomura Y, Kitamura Y (1998) Gain-of-function mutations of c-kit in human gastrointestinal stromal tumors. Science 279:577–580
18. Hirota S, Ohashi A, Nishida T, Isozaki K, Kinoshity K, Shinomura Y, Kitamura Y (2003) Gain-of-function mutations of platelet-derived growth factor receptor alpha gene in gastrointestinal stromal tumors. Gastroenterology 125:660–667
19. Hirsch FR, Varella-Garcia M, Bunn PA Jr, Franklin WA, Dziadziuszko R, Thather N, Chang A, Parikh P, Pereira JR, Ciuleanu T, von Pawel J, Watkins C, Flannery A, Ellison G, Donald E, Knight L, Parums D, Botwood N, Holloway B (2006) Molecular predictors of outcome with gefitinib in a phase III placebo-controlled study in advanced non-small-cell lung cancer. J Clin Oncol 24:5034–5042
20. Hornick JL, Fletcher CDM (2007) The role of KIT in the management of patients with gastrointestinal stromal tumors. Human Pathology 38:679–687
21. Joensuu H, Roberts PJ, Sarlomo-Rikala M, Andersson LC, Teervahartiala P, Tuveson D, Silberman S, Capdeville R, Dimitrijevic S, Druker B, Demetri GD (2001) Effect of the tyrosine kinase inhibitor STI571 in a patient with a metastatic gastrointestinal stromal tumor. N Engl J Med 344:1052–1056
22. Kato N, Honma K, Hojo H, Sasou S, Matsuzaki O, Motoyama T (2005) KIT expression in normal and neoplastic renal tissues: immunohistochemical and molecular genetic analysis. Pathol Int 55:479–483
23. Kitadai Y, Sasaki T, Kuwai T, Nakamura T, Bucana CD, Hamilton SR, Fidler IJ (2006) Expression of activated platelet-derived growth factor receptor in stromal cells of human colon carcinomas is associated with metastatic potential. Int J Cancer 119:2567–2574
24. Kononen J, Bubendorf L, Kallioniemi A, Barlund M, Schraml P, Leighton S, Torhorst J, Mihatsch MJ, Sauter G, Kallioniemi OP (1998) Tissue microarrays for high-throughput molecular profiling of tumor specimens. Nat Med 4:844–847
25. Lasota J, Wozniak A, Sarlomo-Rikala M, Rys J, Kordek R, Nassar A, Sobin LH, Miettinen M (2000) Mutations in exons 9 and 13 of KIT gene are rare events in gastrointestinal stromal tumors. A study of 200 cases. Am J Pathol 157:1091–1095
26. Medinger M, Drevs J (2005) Receptor tyrosine kinases and anticancer therapy. Curr Pharm Des 11:1139–1149
27. Miliaras D, Karasavvidou F, Papanikolaou A, Sioutopoulou D (2004) KIT expression in fetal, normal adult, and neoplastic renal tissues. J Clin Pathol 57:463–466
28. Nocito A, Bubendorf L, Tinner EM, Süess K, Wagner U, Forster T, Kononen J, Fijan A, Bruderer J, Schmid U, Ackermann D, Maurer R, Alund G, Knönagel H, Rist M, Anabitarte M, Hering F, Hardmeier T, Schoenenberger AJ, Flury R, Jäger P, Fehr JL, Schraml P, Moch H, Mihatsch MJ, Gasser T, Sauter G (2001) Microarrays of bladder cancer tissue are highly representative of proliferation index and histological grade. J Pathol 194:349–357
29. Paez JG, Janne PA, Lee JC, Tracy S, Greulich H, Gabriel S, Herman P, Kaye FJ, Lindeman N, Boggon TJ, Naoki K, Sasaki H, Fuji Y, Eck MJ, Sellers WR, Johnson BE, Meyerson M (2004) EGFR mutations in lung cancer: correlation with clinical response to gefitinib therapy. Science 304:1497–1500
30. Pan CC, Chih-Hsueh C, Chiang H (2004) Overexpression of KIT (CD117) in chromophobe renal cell carcinoma and renal oncocytoma. Am J Clin Pathol 121:878–883
31. Peres EM, Savasan S, Cushing B, Abella S, Mohamed A (2004) Chromosome analyses of 16 cases of Wilms tumor: different pattern in unfavorable histology. Cancer Genet Cytogenet 148:66–70
32. Pritchard-Jones K (2002) Controversies and advances in the management of Wilms' tumour. Arch Dis Child 26:486–493
33. Ranson M (2004) Epidermal growth factor receptor tyrosine kinase inhibitors. Br J Cancer 90:2250–2255
34. Schnadig ID, Blanke CD (2006) Gastrointestinal stroma tumors: imatinib and beyond. Curr Treat Options Oncol 7:427–437
35. Sihto H, Sarlomo-Rikala M, Tynninen O, Tanner M, Andersson LC, Franssila K, Nupponem NN, Joensuu H (2005) KIT and platelet-derived growth factor receptor alpha tyrosine kinase gene mutations and KIT amplifications in human solid tumors. J Clin Oncol 23:49–58

36. Smithey BE, Pappo AS, Hill DA (2002) C-kit expression in pediatric solid tumors: a comparative immunohistochemical study. Am J Surg Pathol 26:486–492
37. Tornillo L, Duchini G, Carafa V, Lugli A, Dirnhofer S, Di Vizio D, Boscaiano A, Russo R, Tapia C, Schneider-Stock R, Sauter G, Insabato L, Terracciano LM (2005) Patterns of gene amplification in gastrointestinal stromal tumors (GIST). Lab Invest 85:921–931
38. Tornillo L, Terracciano LM (2006) An update on molecular genetics of gastrointestinal stromal tumours. J Clin Pathol 59:557–563
39. Vujanic GM, Sandstedt B, Harms D, Kelsey A, Leuschner I, De Kraker J (2002) Revised International Society of Paediatric Oncology (SIOP) working classification of renal tumors of childhood. Med Pediatr Oncol 38:79–82
40. Yarden Y, Kuang WJ, Yang-Feng T, Coussens L, Munemitsu S, Dull TJ, Chen E, Schlessinger J, Francke U, Ullrich A (1987) Human proto-oncogene c-kit: a new cell surface receptor tyrosine kinase for an unidentified ligand. EMBO J 6:3341–3351
41. Yokoi A, Mc Cruddden KW, Huang J, Kim ES, Soffer SZ, Frischer JS, Serur A, New T, Yuan J, Mansukhani M, O'toole K, Yamashiro DJ, Kandel JJ (2003) Human epidermal growth factor receptor signaling contributes to tumor growth via angiogenensis in her2/neu-expressing experimental Wilms' tumor. J Pediatr Surg 38:1569–1573

Virchows Arch (2008) 452:651–665
DOI 10.1007/s00428-008-0586-9

ORIGINAL ARTICLE

Replacement of α-galactosidase A in Fabry disease: effect on fibroblast cultures compared with biopsied tissues of treated patients

Jana Keslová-Veselíková · Helena Hůlková · Robert Dobrovolný · Befekadu Asfaw · Helena Poupětová · Linda Berná · Jakub Sikora · Lubor Goláň · Jana Ledvinová · Milan Elleder

Received: 18 June 2007 / Revised: 21 December 2007 / Accepted: 20 January 2008 / Published online: 20 March 2008
© Springer-Verlag 2008

Abstract The function and intracellular delivery of enzyme therapeutics for Fabry disease were studied in cultured fibroblasts and in the biopsied tissues of two male patients to show diversity of affected cells in response to treatment. In the mutant fibroblasts cultures, the final cellular level of endocytosed recombinant α-galactosidases A (agalsidases, Fabrazyme™, and Replagal™) exceeded, by several fold, the amount in control fibroblasts and led to efficient direct intra-lysosomal hydrolysis of (^{3}H)Gb3Cer. In contrast, in the samples from the heart and some other tissues biopsied after several months of enzyme replacement therapy (ERT) with Fabrazyme™, only the endothelial cells were free of storage. Persistent Gb3Cer storage was found in cardiocytes (accompanied by increase of lipopigment), smooth muscle cells, fibroblasts, sweat glands, and skeletal muscle. Immunohistochemistry of cardiocytes demonstrated, for the first time, the presence of a considerable amount of the active enzyme in intimate contact with the storage compartment. Factors responsible for the limited ERT effectiveness are discussed, namely post-mitotic status of storage cells preventing their replacement by enzyme supplied precursors, modification of the lysosomal system by longstanding storage, and possible relative lack of Sap B. These observations support the strategy of early treatment for prevention of lysosomal storage.

Keywords α-Galactosidase A deficiency · Enzyme replacement therapy · Persistent storage · Enzyme targeting · Clearance of storage lysosomes

J. Keslová-Veselíková, H.Hůlková and R. Dobrovolný contributed equally to this work.

J. Keslová-Veselíková · H. Hůlková · R. Dobrovolný · B. Asfaw · H. Poupětová · L. Berná · J. Sikora · J. Ledvinová (✉) · M. Elleder (✉)
Institute of Inherited Metabolic Disorders,
Bldg. D, Division B; Ke Karlovu 2, 128 08,
Prague 2, Czech Republic
e-mail: jledvin@cesnet.cz
e-mail: melleder@cesnet.cz

J. Keslová-Veselíková
e-mail: jana.keslova@seznam.cz

H. Hůlková
e-mail: helena.hulkova@lf1.cuni.cz

R. Dobrovolný
e-mail: robert.dobrovolny@lf1.cuni.cz

B. Asfaw
e-mail: basfaw@cesnet.cz

H. Poupětová
e-mail: helena.poupetova@lf1.cuni.cz

L. Berná
e-mail: lindaberna@yahoo.com

J. Sikora
e-mail: jakub.sikora@lf1.cuni.cz

L. Goláň
Clinical Department of Cardiology and Angiology,
First Faculty of Medicine and University Hospital,
U nemocnice 2, 128 08, Prague 2, Czech Republic
e-mail: lubor.golan@seznam.cz

Introduction

Fabry disease (MIM 301500) is an X-linked deficiency of α-galactosidase A (α-GALA, EC 3.2.1.22) leading to widespread lysosomal accumulation of glycosphingolipids with terminal α-galactosyl moieties (mainly globotriaosyl-

ceramide, Gb_3Cer). The ensuing phenotype at the clinical level is well known, including its organ-limited milder variants in hemizygous males and in females who are mosaic hemizygotes [9, 10]. The dominating therapeutic approach, enzyme replacement therapy (ERT), is based on substitution of the missing enzyme with recombinant α-galactosidases, Fabrazyme™ (agalsidase beta, Genzyme) or Replagal™ (agalsidase alfa, SHGT) [6, 13]. Despite differences in the glycosylation pattern due to different expression systems [14, 41], both enzymes appear to be functionally indistinguishable from each other [3, 23]. The essential requirement for successful ERT of Fabry disease is the delivery of a sufficient dose of the enzyme into the storage lysosomal compartment. The effect on storage has been evaluated either by monitoring the level of storage or the induction of enzyme activity [12, 21, 3, 23, 33]. However, there is not any report demonstrating complete clearance of the storage lysosomal system generally. The effect is mostly restricted to endothelia, but the partial clearance effect has been seen by some authors also in another cells, e.g., in the kidney [15].

The goal of this study was to compare effectiveness of ERT in two cell systems: by cultured mutant fibroblasts on one side, representing dynamic cell population minimally modified by low degree spontaneous storage, and transiently exposed to trace amount of tritiated substrate to follow its catabolic pathway. This in vitro experimental system was compared to the situation in vivo, represented by a series of cell types of various regeneration capacities exposed to prolonged ERT after longstanding disease course. Extreme counterpart to cultured fibroblasts was represented by cardiocytes, postmitotic cells, modified by longstanding spontaneous storage.

This is also the first study focused on delivery of the applied α-GALA into the storage cardiocytes which may contribute to better understanding of the factors responsible for the limited effectiveness of ERT in vivo.

Patients

For details of examined patients, their ERT regime, and the biopsy samples, see Table 1.

Materials and methods

The study was approved by the Ethics Committee of the General Teaching Hospital and the First Faculty of Medicine, Charles University (60/2003F), Prague. Cardiac biopsy samples were taken during coronary surgeries. Written informed consent was obtained from patients included in the study.

Cell lines Four fibroblast cell lines of patients with classic type of Fabry disease (mutations in the *GLA* gene:p. Q280K, p.R342Q, c.801ins36, c.delEx2 (c.195−?−369+? del)) came from the cell culture depository of the Institute of Inherited Metabolic Diseases. Fibroblasts with mutations c.801ins36 and p.Q280K were from patient 1 and patient 2, respectively, who underwent heart biopsy later on. All cell lines (including p.R342Q and c.delEx2) were derived from skin biopsies taken several years before ERT from patients with classical form of the disease.

Recombinant α-galactosidases A REPLAGAL (agalsidase alpha, a gift from Shire Human Genetic Therapies, Cambridge, MA, USA) sample no. 001-0229 was used without any further modification (dilution 1mg/ml solution). FABRAZYME (agalsidase beta, a gift from Genzyme, Cambridge, MA, USA) batch no. H0214AM, diluted according to manufacturer's recommendation to 5mg/ml and then further diluted to 1mg/ml with redistilled water.

Experiments in cell cultures Cultured skin fibroblasts were grown in accordance with standard protocols in Dulbecco's modified Eagle's medium (DMEM) and 10% bovine fetal serum (BFS).

Preparation of substrate The globoside, Gb_4Cer, was isolated from human erythrocyte membranes, characterized, and tritium-labeled at the ceramide moiety (330MBq/mg). The (^{3}H)Gb_4Cer was incorporated into liposome particles (a mixture of phosphatidylcholine, α-tocopherol, and phosphatidic acid, Sigma, Czech Republic) and coated with apoprotein E [2].

Feeding assays DMEM, 3 ml per 25-cm^2 flask, with 1% BFS and radiolabeled glycolipid (3.3×10^6dpm/1ml) was applied to nearly confluent Fabry fibroblasts and incubated in a 5% CO_2 incubator for 3days [2].

Uptake of enzyme Three milliliters of the enzyme solution (1.32μg of enzyme per milliliter, final activity 3.8μmol MU mg^{-1}.h^{-1}, the same for both enzymes) were placed in fresh DMEM containing 10% heat-inactivated BFS and applied to cells in 25-cm^2 flasks. The flasks were then incubated for different periods of time. At least two 25-cm^2 flasks were analyzed for each time period/enzyme combination (0, 12, 24, 48, 96, and 192 h).

Analysis of (^{3}H)Gb3Cer degradation Three milliliters of the enzyme solution (0.66μg of enzyme per milliliter, final activity 1.9μmol MU mg^{-1} h^{-1}, the same for both enzymes) were placed in fresh DMEM containing 10% heat-inactivated BFS and conduritol B epoxide (final concentration 100mM, Calbiochem-Novabiochem GmbH,

Table 1 Patients' data

Patient	Age	Phenotype	Mutation in the *GLA* gene	α-GALA activity[c] in nmol MU mg^{-1} protein h^{-1} WBC skin fibroblasts	Biopsy before ERT (year)	Biopsy in the course of ERT: Fabrazyme™ (duration in months)	LV mass (g) before ERT	LV mass (g) in the course of ERT (year of examination)
1	59[a]	Classical	c.801ins36	0.19(0.4%) 0.63(1.3%)	Skin (1998)	LV (6) saphenous v.(21) heart auricle(21) biopsy taken 3 days after last infusion	440 (2002Jul)	472 (2003Mar) 817 (2004Jun) 910 (2006Feb) 840 (2007May)
2	50[a]	Classical	p.Q280K	0.13(0.3%) 0.95(1.9%)	Skin (1980)	Heart auricle (65) skin (65) skeletal muscle (65) biopsy taken 2 days after last infusion	338 (2001Jan)	404 (2002Jun) 340 (2004Sept) 423 (2006Jan) 583 (2006Jun) 521 (2006Dec)
3	60[b]	Classical	p.H46Y	0.14(0.3%)	–	–	ND	–

LV (left ventricle) mass was measured by echocardiography according to Sahn DJ et al., Circulation 58 (1978), pp 1072–1083.
Clinical details and ERT regime: Patient 1 underwent two coronary bypass graft surgeries (April 2003, June 2004). Patient 2 underwent coronary bypass surgery in November 2006. Both patients were treated by Fabrazyme (dosage, 1 mg/kg every 2 weeks); patient 1 since October 2002 and patient 2 since July 2002. Biopsy was taken on the third day after the protocolar infusion of Fabrazyme in patient 1 and on the second day after the infusion in patient 2. Patient 3 underwent renal transplantation in 1993 and was treated by ERT (Replagal 0.2 mg/kg every 2 weeks) for 3 years since September 2001. ERT was withdrawn 1 year before death because of advanced dementia.
ND not determined
[a] Age when heart auricle biopsy was performed
[b] Age at death. Only frozen autopsy samples of the heart were available for analysis which substituted approximate status without ERT.
[c] Determined before ERT, control range for WBC 24.8–75.7 nmol MU mg^{-1} protein h^{-1} (n=65); for skin fibroblasts 33.8–70.8 nmol MU mg^{-1} protein h^{-1} (n=13)

Germany) and applied to cells in 25-cm^2 flasks preloaded with (^{3}H)Gb_4Cer and incubated for different periods of time. Analyses were performed at least in two 25-cm^2 flasks for each time period/enzyme combination (0, 9, 14, 19, and 24 h).

Cell harvesting and homogenization The fibroblasts were harvested by trypsinization. The cell pellets were homogenized in distilled water in a cuphorn sonifier filled with ice for 3 × 10s (Ultrasonic homogenizer 4710, Cole-Parmer, Chicago, IL, USA, 40% output). Protein concentration [16], enzyme activities, and uptake of the (^{3}H)Gb_4Cer tracer were determined in homogenate aliquots.

Enzyme assay The activity of α-GALA was assayed in culture medium and in cell and tissue homogenates according to the modified method of Mayes et al. [27]. Briefly, the reaction mixture contained 5mM of substrate, 4-methylumbelliferyl(MU)-α-D-galactopyranoside (Sigma, Germany), in citrate buffer (pH 4.5). For cell and tissue homogenates, the reaction also contained 100mM α-*N*-acetyl-D-galactosamine to inhibit α-*N*-acetylgalactosaminidase activity. The complete reaction mixture was incubated for 30min at 37°C, and the fluorescence of the released 4-MU was measured at excitation 365nm and at emission 448nm on a luminescence spectrometer (Perkin Elmer LS50B, Wellesley, USA).

Extraction and thin-layer chromatography analysis of (^{3}H) glycosphingolipids

The remaining cell homogenate was extracted with chloroform–methanol (2:1, *v*/*v*), and the lipids were separated on thin-layer chromatography (TLC) plates (Silica gel, Merck, Germany) using chloroform–methanol–water (70:30:05, *v*/*v*/*v*) as the solvent system. Chromatograms were evaluated using a TLC linear radioactivity analyzer (Raytest, Germany) [2].

Immunofluorescence labeling Fibroblasts were grown on glass coverslips to near-confluence using standard methods. The cells were then grown for an additional 24h in DMEM containing 10% of heat-inactivated BFS and 0.66μg/ml of the recombinant enzyme.

For the experiments using mannose-6-phosphate (M-6-P) receptor blocking, the M-6-P (Sigma, Germany) was added to the medium together with the enzymes to yield a final concentration 10mM. Cells were fixed for 10min in ice-cold methanol before immunodetection and non-specific binding was blocked with 5% BFS. Recombinant agalsidases were detected using rabbit polyclonal antibody against human α-GALA TK88 (anti α-GAL, TKT, Cambridge MA, USA) diluted to 9μg/ml, while cathepsin D was detected simultaneously using monoclonal mouse antibodies (Serotec, Oxford, UK) diluted to

20 μg/ml. Gb3Cer was located using mouse monoclonal anti-Gb3 (CD77) antibody (BGR23, code 370680, Seikagaku, Japan) diluted to 6.7μg/ml after 10min fixation with 4% phosphate-buffered paraformaldehyde and blocking with 5% BFS. The primary antibodies were visualized using Alexa Fluor 488-conjugated goat anti-rabbit IgG, Alexa Fluor 488-conjugated goat anti-mouse IgG and Alexa Fluor 568-conjugated goat anti-rabbit IgG (Molecular Probes, Invitrogen, Carlsbad, CA, USA). The samples were examined using two Nikon confocal microscope setups (1) Nikon C1, Eclipse E800 microscope equipped with a laser scanning confocal head (Nikon, Japan) and a Nikon 60X, NA 1.4 oil immersion objective or (2 Nikon C1*si* LSM head mounted on TE-2000 inverted microscope and with Nikon TIRF NA 1.49 60× oil immersion objective. All channels were recorded separately to avoid cross-talk between channels. The co-localization analysis was performed with representative images using ImageJ software [31] with JaCoP plugin [4] and Huygens image analysis software (SVI, Hilversum, The Netherlands). The degree of co-localization was assessed by coefficients described by Manders et al. [26]. Two independent experiments were done to support the results.

The image acquisition conditions were kept constant in all parameters for samples presented in Fig. 3e–h.

Histochemical and ultrastructural analyses of tissue samples Patient 1. The sample of superficial part of the left cardiac ventricle biopsied after 6months of ERT was processed for electron microscopy. Specimens of the heart auricle and part of the saphenous vein graft taken after 21months of ERT were transferred to the liquid nitrogen and stored on dry ice.

Patient 2. Samples of the heart auricle, skin, and skeletal muscle taken after 65months of ERT were frozen in liquid nitrogen or fixed with phosphate-buffered paraformaldehyde (Fluka, Buchs, Switzerland). Samples for standard ultrastructural analysis were fixed with 10% paraformaldehyde overnight, post-fixed in phosphate-buffered 1%$Os0_4$, dehydrated and embedded into Epon-Araldit mixture. Samples for electron microscopic immunostaining were fixed with 4% paraformaldehyde for 2 h, dehydrated, and embedded into LR White resin (London Resin Company, Reading, England). Skin biopsies taken before ERT start from both patients were processed for standard electron microscopy. Patient 3 (death one year after ERT termination). Postmortem frozen and resin embedded samples from the left cardiac ventricle were included into the study to substitute approximate status before ERT.

Cryostat sections were prepared from the frozen samples and used for immunohistochemical evaluation of the lysosomal storage status (Gb3Cer storage, lipopigment accumulation) for detection of the applied agalsidase protein and for histochemical evaluation of its activity.

Lysosomal storage status Gb3Cer storage was detected in cryostat sections after pretreatment with cold anhydrous acetone (at 4°C) for removal of possible apolar lipid admixture and for glycolipid fixation. They were briefly post-fixed with 4% buffered paraformaldehyde (for 5min at 4°C). After standard blockade of endogenous peroxidase (with sodium azide and H_2O_2) and non-specific protein–protein interactions (with 5% BFS), the sections were incubated with monoclonal mouse anti-Gb3Cer antibody diluted 1:100 in 5% BFS (at 37°C for 1h or at 4°C overnight). Detection of bound primary antibody was achieved using EnVision + System-HRP Anti-Mouse (DakoCytomation, Glostrup, Denmark) and the DAB + Chromogen kit (K 3460, DAKO Cytomation, Carpinteria, USA). The staining specificity was checked using total lipid extraction by chloroform (C)–methanol (M)–water (W) 4:8:3, followed by C–M 2:1 (each step for 30min at room temperature). The sections were rinsed in methanol, briefly fixed in paraformaldehyde, and used for the lipid immunodetection. Lysosomal storage status was also studied by birefringence of liquid crystals of the stored polar lipid and by detection of lipopigment autofluorescence. The latter was evaluated by epifluorescence microscopy using the Nikon BV-2A filters blocks (EX 400-440, DM 455, BA 470). The best results were obtained after brief (5min) pre-extraction of the lipids with C–M mixture (1:1, *v*/*v*) to prevent moderate non-specific autofluorescence of the stored lipid. The liquid crystalline state of the stored lipid deposits exhibited considerable instability and was best evaluated using Baker's fixative solution. The results were compared with samples from age-matched controls. Neutral term lipopigment was used throughout the manuscript because of ambiguous terminology [34].

Immunohistochemical detection of the applied enzyme protein Cryostat sections were fixed with 4% phosphate-buffered paraformaldehyde exposed to standard blocking procedures (see above) and incubated for 1h at 37°C with the primary polyclonal antibody TK 88 diluted to 4.5μg/ml in 5% FCS then washed in PBS and exposed to the detection kit (EnVision + System-HRP Anti-Rabbit, Dako-Cytomation). An alternative fixation of sections using a mixture of chloroform–acetone (1:1, *v*/*v*) for 30min at room temperature followed by paraformaldehyde was used for some of the experiments. Semi-thin 0.5-μm sections embedded into LR White medium were treated with citrate buffer pH6.0 for 40min at 90°C and incubated after the aforementioned blocking procedures with TK88 antibody for 1h at 37°C and thereafter treated with the detection kit as described above.

The sections immunostained either for Gb3Cer or for α-GALA were counterstained with Harris hematoxylin and mounted into the Immu-Mount medium (Shandon, Pittsburgh, PA, USA) which allowed simultaneous evaluation of the presence of the applied enzyme (eventually Gb3Cer), birefringent lipid and autofluorescent lipopigment.

Histochemical detection of in situ enzyme activities Activity of α-GALA was evaluated using both the post-coupling technique with 6-bromo-2-naphthyl-α-D-galactopyranoside (LaChema, Brno, Czech Republic) and Fast Blue B and the simultaneous azo-coupling technique with 1-naphthyl-α-D-galactopyranoside (Koch Light, Colnbrook Bucks, UK) and hexazonium pararosaniline; both were done on semi-permeable membranes allowing to detect activities of both bound and soluble enzymes according to the published prescriptions [24]. Semi-permeable membrane technique was used for demonstration of activities of β-galactosidase (indigogenic method), β-glucuronidase, and acid phosphatase (simultaneous azo-coupling method using in both cases naphthol ASBI-type substrates and hexazonium pararosaniline). Acid phosphatase activity was also demonstrated using the aqueous medium [24].

Mannoso-6-phosphate receptor (MPR, cation-independent) was detected using monoclonal antibody (2G11 clone, Abcam, Cambridge, UK), diluted 1:400. Polyclonal antibody against cathepsin D was purchased from DAKO and used in dilution 1:200. In both cases, the incubation was overnight at 4°C.

Results

Studies in cultured mutant cells

Uptake of recombinant enzymes into cultured Fabry cells and efficiency of Gb3Cer hydrolysis

To monitor the function of agalsidases in situ, the uptake into Fabry fibroblasts was measured over the course of 192 h (8days). Both enzymes were similarly internalized into the cultured cells, with maximum activity at 24h incubation. The uptake of agalsidase beta measured with MU-substrate was 2.5-fold greater than that of agalsidase alpha, although the enzymes were applied at the same concentration (1.32mg/ml medium). This result was confirmed by repeated experiments on three different Fabry fibroblast cell lines. After 24h, the cellular activities of both enzymes started to decline. However, even after 8days, the values exceeded several times the normal activity of healthy cells (Fig. 1). Activity in the culture medium decreased equally in both agalsidases, falling to 4–6% of its original value (Fig. 1, inner graph).

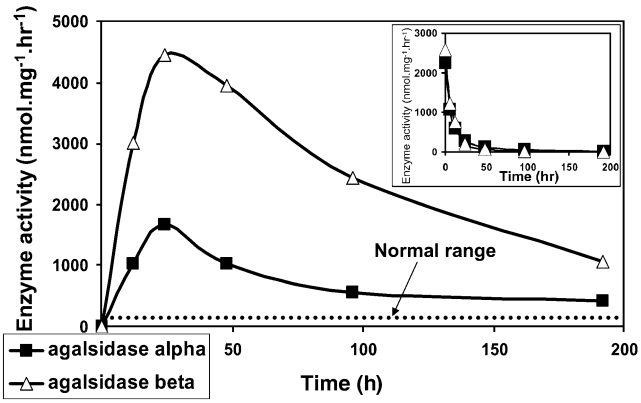


Fig. 1 Internalization of recombinant α-galactosidases A (agalsidases alpha and beta) into Fabry skin fibroblasts as a function of time. Recombinant enzymes (1.32 μg of enzyme protein per milliliter of medium) were applied into cultures of Fabry cells incubated under standard conditions. After 0, 12, 24, 48, 96, and 192 h, medium was removed, cells harvested, and analyzed in vitro with MU-substrate as described in "Materials and methods". Each value is average of duplicate flasks. Intracellular agalsidase beta activity exceeded 20 times normal levels at the maximum (24 h), while agalsidase alpha activity was eight times the normal value in healthy cells (50.3± 13.6 nmol MU mg^{-1} protein h^{-1} in controls, see *broken line*). *Insert* is a time course of agalsidases stability in the culture medium

The correction of the defect in Fabry cells was monitored with natural substrate in mutant cell cultures pre-loaded with tritium-labeled globoside (^{3}H)Gb_4Cer, the (^{3}H)Gb_3Cer precursor. The quantity of degradation products calculated from TLC-radioactivity scans reflected approximately the uptake tendencies of the respective enzymes (Fig. 2). Despite the differences in uptake (Fig. 1), both loaded agalsidases proved efficient in intra-lysosomal degradation of Gb_3Cer.

Confocal microscopic examination of internalized agalsidases with endosomal/lysosomal markers in cultured Fabry cells

Fabry fibroblasts were incubated with recombinant agalsidases for 24h. The intracellular distribution of agalsidase alpha and agalsidase beta in the cells was detected by anti α-GALA antibody (red channel, Fig. 3a,b). The lysosomes were visualized in the perinuclear region by immunodetection of cathepsin D (green channel, Fig. 3a,b). In a similar manner, the localization of intracellular Gb3Cer deposits was correlated with recombinant enzymes internalized into α-GALA deficient fibroblasts (Fig. 3g,h). The merger of the agalsidase and cathepsin D signals suggested lysosomal localization of loaded recombinant enzymes and was further documented by co-localization maps (Fig. 3c,d). Correlation of agalsidase signal with lysosomal transmembrane protein LAMP 2 was also demonstrated (data not shown).

Endogenous enzyme protein was not detected in the cells of Fabry patients (data not shown). The addition of M-6-P to the culture medium, together with agalsidases, strongly

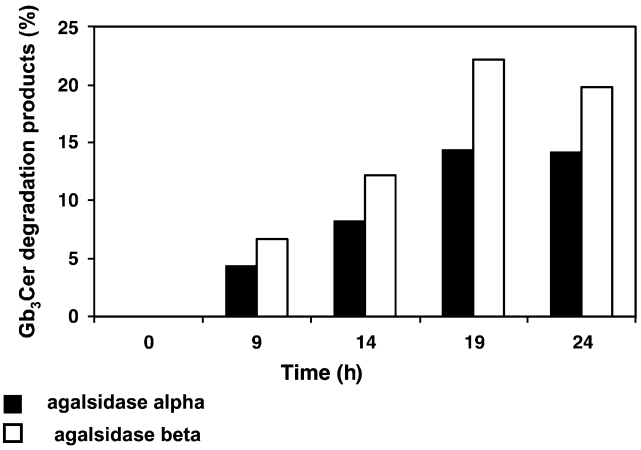


Fig. 2 Degradation of (^{3}H)Gb_3Cer by Fabry fibroblasts loaded with (^{3}H)-globoside after application of agalsidases alpha and beta. Illustration of 24-h experiments (example of one experimental set from three is shown). (^{3}H)-globoside (5×10^6 dpm), precursor of (^{3}H) Gb_3Cer, was incorporated into the liposomes coated with Apo E and added to the culture medium as described in "Materials and methods". After 3 days of incubation, the agalsidases were applied at final activity of 1.9 μmol ml^{-1} h^{-1}. After 0, 9, 14, 19, and 24 h, cells were harvested, the lipids extracted, separated by high performance thin layer liquid chromatography, and the products were quantified by TLC linear radioactivity analyzer ("Materials and methods"). Percentage of degradation products was calculated from TLC scans in relation to total cell radioactivity comprising substrate (^{3}H)Gb_3Cer and the sum of its degradation products partially transformed into products of re-synthesis (phospholipids)

inhibited the uptake of both enzymes (Fig. 3e,f), confirming that M-6-P receptor endocytosis is a major pathway of agalsidase transport into fibroblasts. The double labeling of Gb3Cer (Fig. 3g,h, green channel) and recombinant enzymes (Fig. 3g,h, red channel) did show only a few granular structures containing non-degraded Gb3Cer which were still present. The co-localization map of Gb3Cer and recombinant enzymes (Fig. 3i,j) showed only limited overlap (compare logarithmically color coded overlap coefficient in co-localization maps of Gb3Cer/α-GALA and CatD/α-GALA).

Studies in tissues

In vitro α-GALA activity in the heart samples

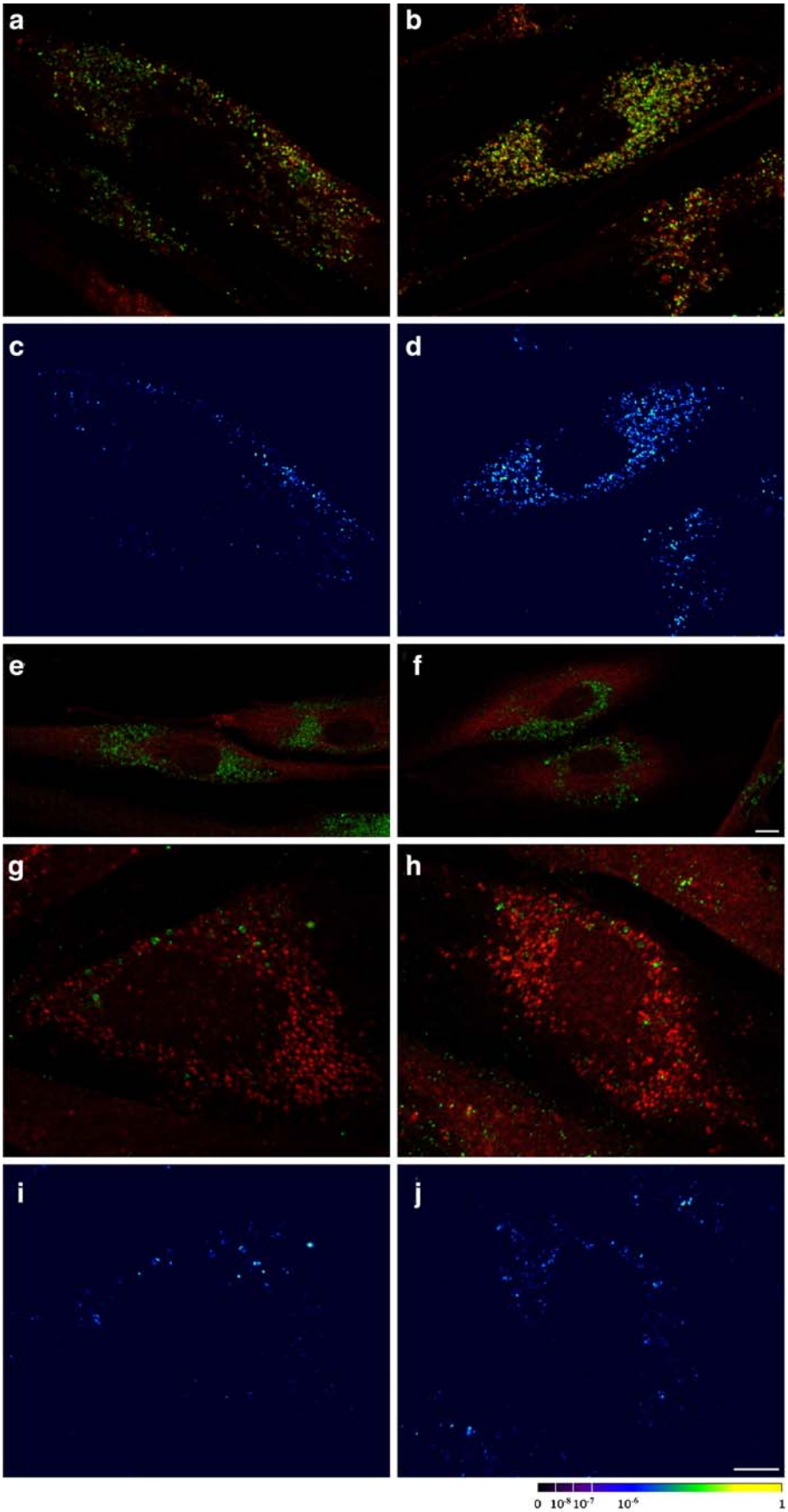
α-GALA activity determined in the auricular sample of the patient 1 was 1.53 vs. 10.18±2.32 nmol MU mg^{-1} protein h^{-1} in controls (n=5). This value represented 15% of the normal activity of the enzyme in the auricular part of the heart which implies slight increase from deficient values. There was no representative sample of the heart auricle in patient 2 for biochemical analysis. Residual enzyme activity in the autopsy sample (patient 3) was barely detectable (0.12 nmol MU mg^{-1} protein h^{-1}, i.e., about 1% of the control mean).

Immunohistochemical and ultrastructural studies

Evaluation of the lysosomal storage status Before ERT, dermal capillaries (skin biopsy available in patients 1 and 2) displayed lysosomal storage (Fig. 4a). ERT led to complete clearance of the capillary endothelium lysosomes already after 6 months (patient 1) from the stored lipid and to retraction of the originally expanded system to normal dimensions (Fig. 4b,c). Capillary basement membranes were thin and single. Capillary endothelial storage in various degrees was detectable in the postmortem heart specimen of the patient who died 1 year after ERT withdrawal (Fig. 4d).

The auricular cardiocytes in both patients on ERT displayed variable, but on average high degree, Gb3Cer storage concentrated in the large perinuclear region (Fig. 5a). Lipid storage was paralleled by increase in lipopigment (Fig. 5c). Cardiocytes free of lysosomal lipid storage and containing only lipopigment were rare, and those free of both lipid and lipopigment were exceptional. The postmortem heart specimen displayed massive and uniform lipid storage occupying the bulk of the cardiocyte cytoplasm (Fig. 5b). Lipopigment was present in the form of dispersed tiny granules (Fig. 5d). Ultrastructure of cardiocytes, studied in all three cases, showed numerous lysosomes with varying degrees of aggregation and fusion with deposits of loosely or densely packed lipid mem-

Fig. 3 Co-localization of internalized agalsidase alpha (**a**–**i**) and ▶ agalsidase beta (**b**–**j**) with cathepsin D and Gb3Cer in the Fabry fibroblasts after 24-h incubation (**a**, **b**) Confocal analysis of cells labeled for α-galactosidase A (α-GALA, *red*) and intra-lysosomal marker cathepsin D (CatD, *green*) displayed granular distribution of both signals and their parallel considerable overlap. Mander's coefficients M_{GAL} and M_{CatD} ranged from 0.209 to 0.441 and 0.53 to 0.849 in the images, respectively. M_{GAL} and M_{CatD} coefficients represent the fraction of co-localizing pixels from the overall number of pixels with intensity values above the given threshold calculated for the particular image channel. Threshold levels to filter background were set to 10% of the pixel intensity range in both channels. The co-localization of both signals is also illustrated by co-localization maps (**c**, **d**) employing overlap coefficient values (0–1), color coded by lookup table placed under this panel. Addition of 5 mM of M6P to the culture medium completely blocked the α-GALA transport to the lysosomes (**e**, **f**) and changed the signal of α-GALA from granular (intra-lysosomal) pattern to diffuse low-intensity signal virtually inseparable from nonspecific background. The co-labeling of α-GALA and Gb3Cer in the cultured fibroblasts of Fabry patients incubated 24 h with recombinant agalsidases showed very limited overlap (**g**, **h**). The distribution of co-localization of both signals is also demonstrated by co-localization map of overlap coefficient (**i**, **j**). Comparing images (**g**, **h**) and (**i**, **j**) demonstrates minimal correlation of α-GALA and Gb3Cer signals in the cells. This observation suggests that the population of lysosomes with strong α-GALA detection has already been cleared off Gb3Cer. Scale bars in **f** (valid for **e**, **f**) and **j** (valid for **a**–**d** and **g**–**j**) correspond to 10 μm


a
b
c
d
e
f
g
h
i
j
0 10-8 10-7 10-6 1

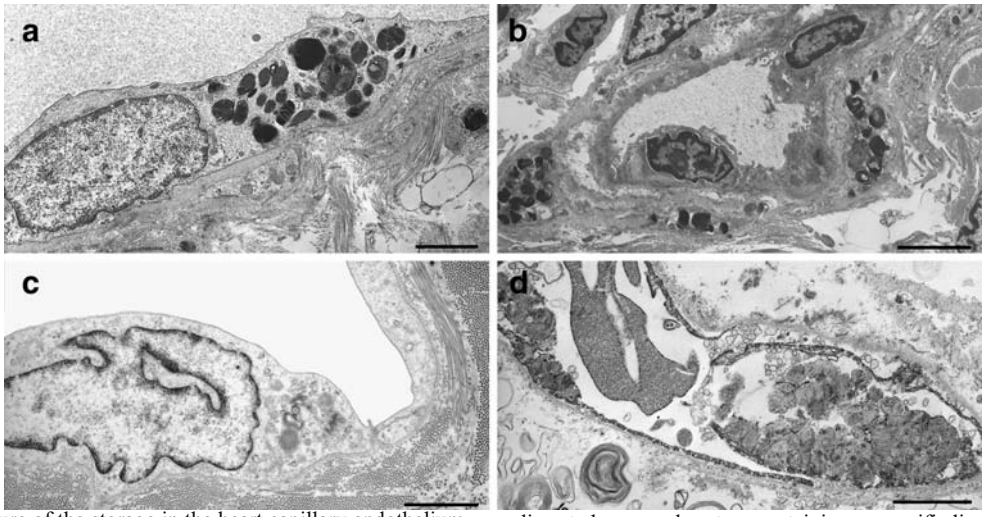


Fig. 4 Ultrastructure of the storage in the heart capillary endothelium. **a** Capillary endothelium with prominent storage before ERT. Patient 2 (*bar* 2 μm). **b** Capillary endothelium free of storage after 65 months of ERT. Persisting storage in pericapillary cells. Patient 2 (*bar* 4 μm). **c** Detail of the capillary endothelium after 6 months of ERT with discrete lysosomal system containing unspecific lipopigment. Patient 1 (*bar* 2 μm). **d** Lysosomal storage in the capillary endothelium of the heart after 1 year of ERT termination. This picture represents extreme in the wide range of capillary storage levels. Patient 3 (*bar* 2 μm)

branes often mixed with pleiomorphic lipopigment deposits (Fig. 6a). In patient 2, there were exceptional cardiocytes with discrete lysosomal lipid storage but with numerous small lucent vesicles, suggesting relatively effective lysosomal clearance (Fig. 6b).

In all cases, irrespective of the ERT, the vascular smooth muscle cells displayed marked lipid storage. Persistent storage was seen in the skin eccrine glands (Fig. 7a) in pericytes and stromal fibroblasts, especially those in the hair bulb matrix (Fig. 7b). Discrete storage was found in the skeletal muscle fibers (not shown here). In the sample of the saphenous vein graft, there was prominent lipid storage in intimal cells and in the smooth muscle cells of the tunica media (Fig. 7c), which also displayed hypertrophy and hyperplasia. Endothelial cells of the tunica intima were free of storage, as were the endothelial cells of the adventitial vessels.

Storage in some cell types was accompanied by increase in lipopigment (mostly in the cardiocytes, skeletal muscle, but almost absent in the smooth muscle cells). Electron microscopy showed densely packed lipid membranes and pleiomorphic structure of the lipopigment in lysosomes.

Evaluation of the intracellular delivery of the applied enzyme In situ immunodetection of the applied enzyme performed in heart samples of the ERT-treated patients showed relatively strong signal of variable intensity in a majority of cardiocytes (Fig. 8a). Simultaneous detection of both the immunostained agalsidase protein and the stored birefringent lipid/lipopigment in a single section showed the coexistence of both the targeted enzyme and lipid storage in a very close contact in the majority of cardiocytes (Fig. 8c). More intimate contact between the targeted enzyme and the storage compartment was seen after brief extraction of the stored lipid with chloroform–acetone mixture (see "Materials and methods"; Fig. 8d). Unfortunately, the applied enzyme proved to be fixation sensitive, so that our attempts to define its relation to the storage compartment at the ultrastructural level failed. However, in semi-thin sections exposed to intensive antigen retrieval, there were numerous positive granules of the applied enzyme interspersed between autofluorescent lipopigment granules (Figs. 8e,f). Both enzyme histochemical techniques (see "Materials and methods") showed the presence of active enzyme in the storing cardiocytes (Fig. 9a). There was also a close relation of the enzyme product to the storage lysosomal compartment better seen in simultaneous azo-coupling technique. Strong immunohistochemical signal for the enzyme protein was seen in the vascular and endocardial endothelium and in the epicardial mesothelium in both patients on ERT. Neither the enzyme protein nor its activity was detectable in cardiocytes in the Fabry postmortem heart sample without ERT (patient 3; Figs. 8b, 9b).

Other lysosomal enzymes in the cardiocytes The storage atrial cardiocytes displayed strong and uniform induction of acid phosphatase activity (Fig. 10a). In contrast, induction of β-galactosidase activity was highly irregular (Fig. 10b). Activity of β-glucuronidase was barely detectable. Activities of the above enzymes in autopsy samples were uniformly low.

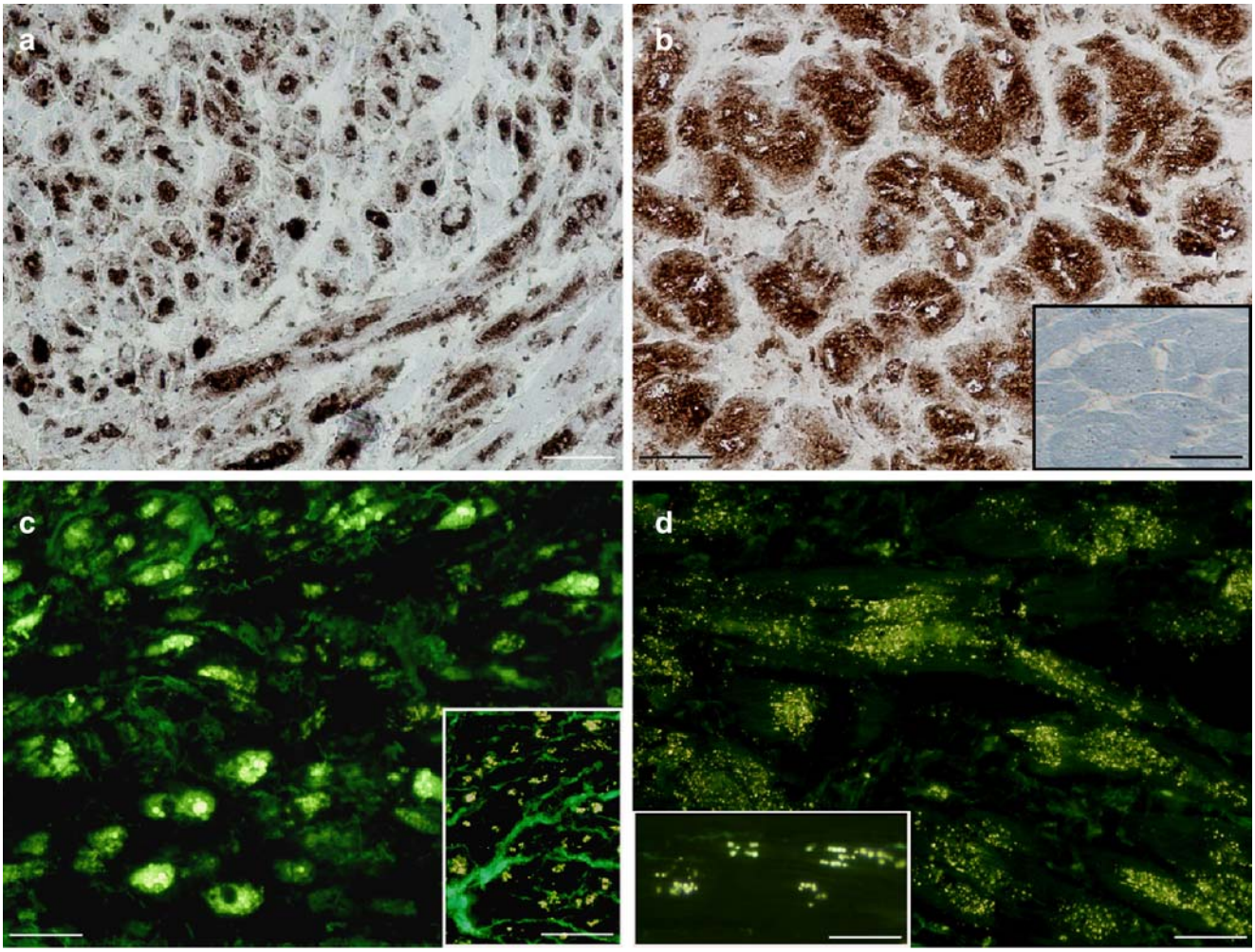


Fig. 5 Persisting lipid storage in cardiocytes. **a**, **b** Immunohistochemical demonstration of Gb3Cer. **a** Cardiocytes of the heart auricle (patient 2) after 65 months of ERT (bar 100 μm). **b** Cardiocytes of the left ventricle. Autopsy (patient 3) 1 year after ERT cessation. *Insert* shows absence of Gb3Cer staining in control cardiocytes (*bars* 100 μm). Note certain degree of variability of storage, reflecting parallel excessive lipopigment deposition. **c**, **d** Increase of the autofluorescent lipopigment demonstrated after brief lipid extraction with C–A. **c** Large lipopigment clusters in heart auricle cardiocytes (patient 2). *Insert*: age-matched control (*bars* 100 μm). **d** Cardiocytes in the left ventricle (patient 3) with dispersed numerous discrete lipopigment granules (*bar* 100 μm). *Insert*: age-matched control showing coarser lipopigment granules restricted to the perinuclear region (*bar* 50 μm)

Signals of both MPR (Fig. 10c) and cathepsin D (not shown) in the biopsy samples were remarkably heterogeneous in storage cardiocytes ranging from barely detectable to very strong intensities.

Discussion

Studies in cell culture Higher uptake of beta- than alpha-agalsidase reflected greater number of phosphorylated

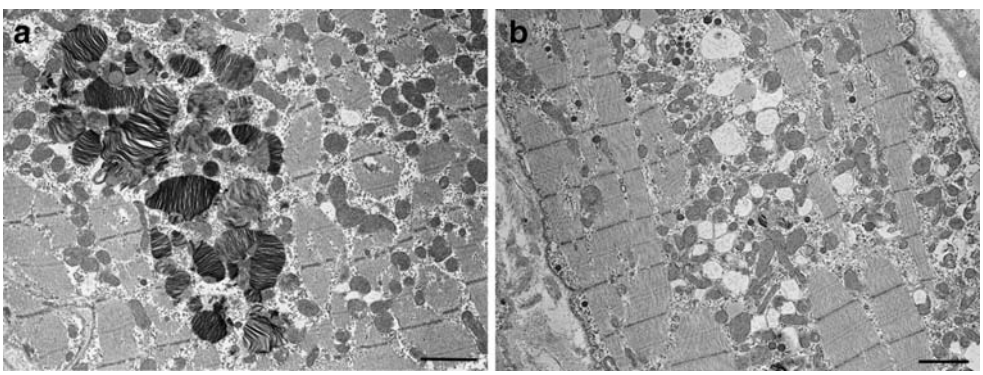


Fig. 6 Ultrastructure of the cardiocyte storage. **a** Patient 2. Atrial cardiocytes after 65 months of ERT with numerous individual lysosomes accumulating lipid dominating over lipopigment (*bar* 2 μm). **b** Exceptional finding in the same patient showing only discrete lipid storage lysosomes. There are numerous small vesicles with lucent content, which most probably represent cleared lysosomes (*bar* 2 μm)

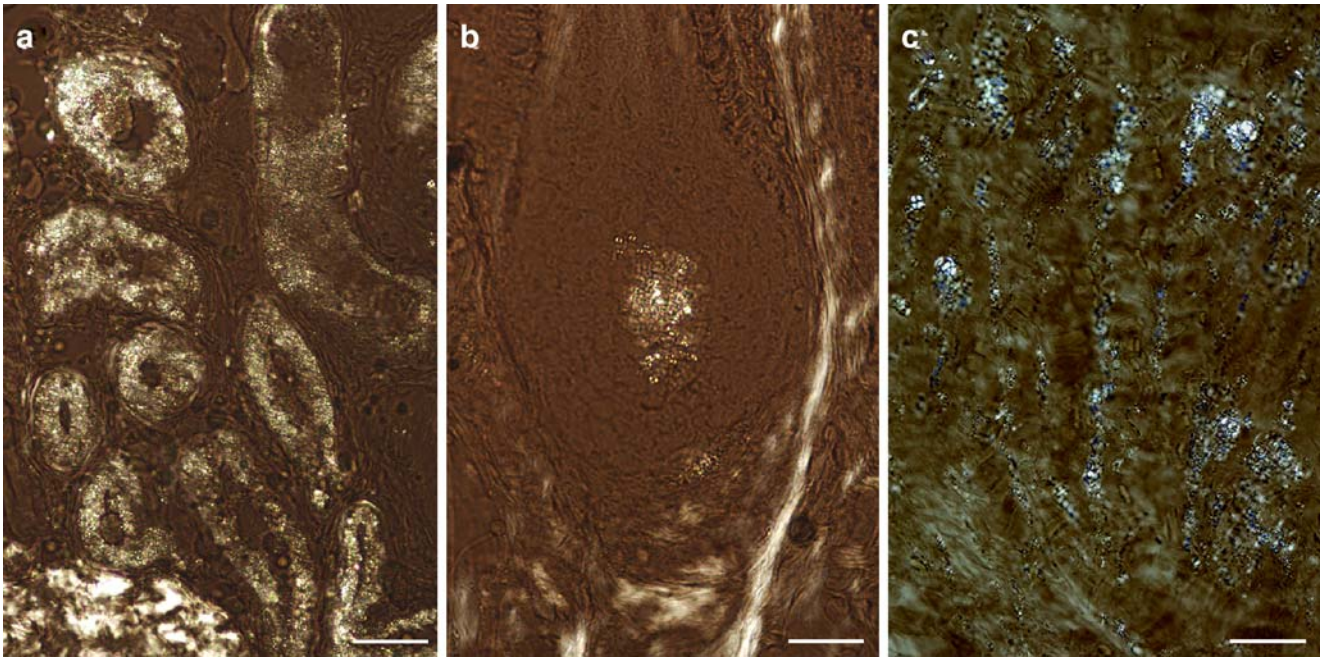


Fig. 7 Persisting storage in other cell types. **a**, **b** Patient 2 (ERT 65 months). Birefringent stored lipid in eccrine skin glands (**a**) (*bar* 100 μm) and in hair follicle matrix fibroblasts (**b**) (*bar* 50 μm). **c** Patient 1 (21 months on ERT). Graft of saphenous vein used for coronary artery reconstruction with massive birefringent deposits of the stored lipid (*bar* 100 μm)

mannose moieties per beta enzyme molecule [23, 33] and presumed principal role of MPR-mediated endocytosis [18] in skin fibroblasts which are receptor-rich. The complete inhibition of cellular uptake of both agalsidases by M-6-P is in accord with this conception.

Lysosomal targeting of the applied active enzyme was double-checked. Firstly, successful targeting of enzyme therapeutics to lysosomes has been proven through co-localization with lysosomal marker cathepsin D. Evaluation of images based on calculation of correlation and co-localization coefficients pointed to slightly lower co-localization parameters for the alpha compared to the beta enzyme.

It must be pointed out that enzyme endocytosis and trafficking via early to late endosomes is a dynamic process. Therefore, only partial co-localization with lysosomal markers can be achieved under the condition of continuous enzyme supply. Final evaluation of Gb3Cer and α-GALA signals in Fig. 3i,j strongly suggested that lysosomes in fibroblast population were almost cleared of substrate after 24-h incubation with any of the enzymes.

Secondly, the delivered enzyme was shown to degrade efficiently the natural substrate (^{3}H)Gb_3Cer produced directly in lysosomes from its radiolabeled precursor (^{3}H)Gb_4Cer. The exact quantification of lysosomal (^{3}H)Gb_3Cer degradation in situ confirmed indirect observation that recombinant agalsidases degrade accumulated Gb3Cer in a dose-dependent manner [33].

In situ (^{3}H)Gb3Cer degradation revealed lower differences between the two enzymes than in vitro assay with soluble MU-analog using the whole homogenate of agalsidase-loaded fibroblasts. This may be related to the intracellular transport and unspecified location of agalsidase in in vitro assay and to the availability of Sap B in lysosomes when supply of enzyme is high.

However, despite the different degree of agalsidase endocytosis, the cell-associated activity of both enzymes exceeded by several times the α-GALA activity of normal healthy cells (see Fig. 1), and both were found effective in cleavage of (^{3}H)Gb_3Cer. Their stability in the medium was found identical in accordance with findings in blood plasma [33].

Our experiments demonstrated effective targeting of the applied enzyme to fibroblast lysosomes using both co-localization and cleavage of its substrate locally produced from its exogenously added precursor. (^{3}H)Gb_4Cer was used for the first time as an intra-lysosomal tracer of function of recombinant agalsidases that does not increase the substrate load and can serve as a model system for evaluation of catabolic lysosomal functions and their defects.

To sum up, the ERT is effective in the cultured fibroblast system. In our view, it is because Fabry fibroblasts represent a short-lived dynamic cell population unmodified by low degree of spontaneous storage. Such cells exposed transiently to a trace amount of labeled substrate can effectively endocytose the recombinant enzyme. The

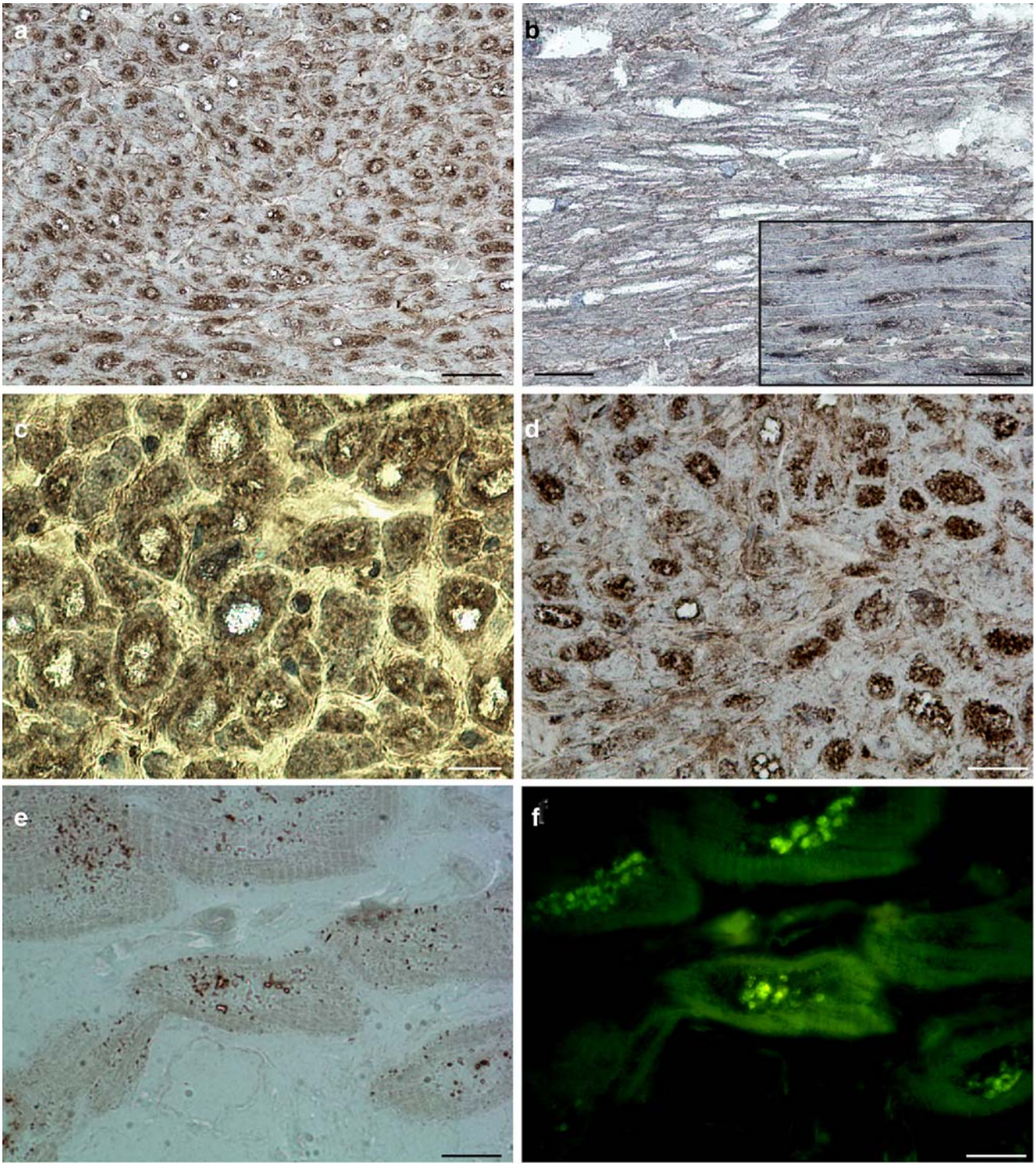


Fig. 8 Immunohistochemical detection (TK 88 antibody) of α-GALA protein in cardiocytes. **a** Strong signal for the enzyme protein in atrial cardiocytes in patient 1 (21 months on ERT; *bar* 100 μm). **b** Absence of signal in ventricular cardiocytes in patient 3 (1 year after ERT withdrawal). *Insert*: signal for endogenous α-GALA in control ventricular cardiocytes (*bars* 100 μm). **c** Simultaneous immunohistochemical detection of the enzyme and of the birefringent stored lipid showing coexistence of both in same cells. Semi-crossed Nicols (*bar* 30 μm). **d** Immunohistochemical detection of the enzyme after brief lipid pre-extraction shows close relation of the enzyme to the storage compartment (*bar* 50 μm). **e** Immunohistochemical detection of the enzyme in a semi-thin section of LR-White-embedded specimen (*bar* 20 μm). **f** The stained section was simultaneously examined under UV to show lipopigment (unstained) which represents marker of the storage compartment (*bar* 20 μm). **c**, **d** Patient 1; **e**, **f** patient 2

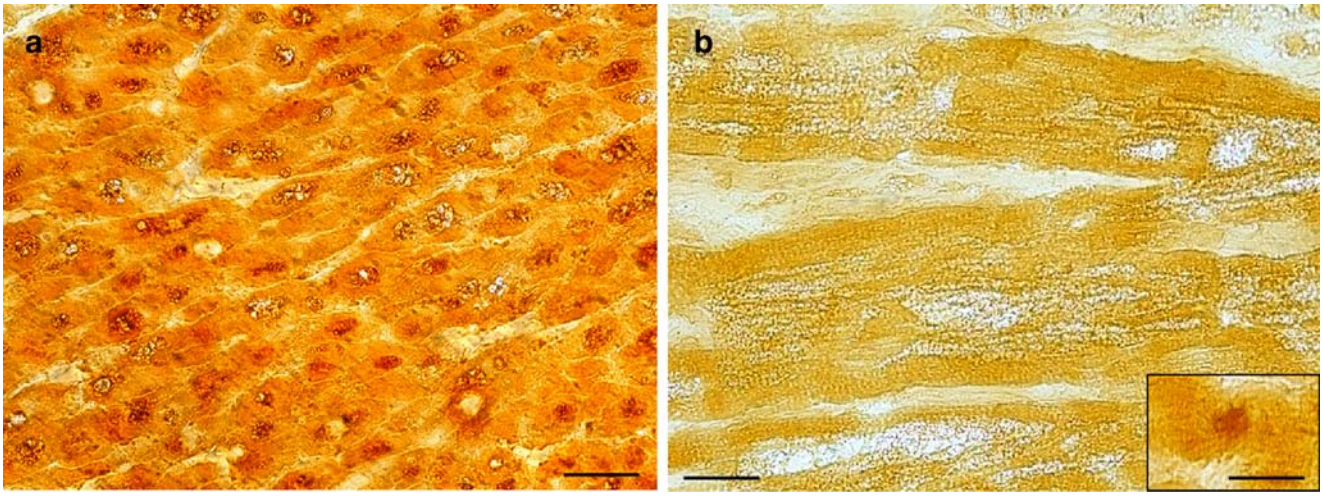


Fig. 9 Histochemical evaluation of α-GALA activity with simultaneous azo-coupling method. **a** Presence of enzyme activity in storing atrial cardiocytes of patient 1 (21 months on ERT; *bar* 100 μm). Compare with Fig. 8. **b** Absence of enzyme activity in ventricular cardiocytes 1 year after cessation of ERT (patient 3). *Insert* shows enzyme activity in control ventricular cardiocyte (*bars* 50 μm)

enzyme is delivered to the storage compartment where it exerts its degradative function. The whole process is facilitated by easy access to the applied enzyme via MPR and by the possibility to endocytose it along the entire cell perimeter of unpolarized cell.

Studies in tissues Our study showed effective clearing of endothelial cells by ERT corresponding to the published results [21, 7, 36]. The design of our study allows us to conclude that endothelial storage is resumed within 1 year after cessation of ERT. In the Fabry disease mouse model, the storage was resumed after several weeks of withdrawal of the enzyme [21].

In contrast to endothelia, the storage persisted in a set of cells despite the continuous ERT, e.g., in cardiocytes, vascular smooth muscle cells, pericytes, some fibroblasts, and perineurial cells, all repeatedly described to resist substantial storage reduction by ERT [12, 40, 7, 39, 43, 32, 33, 36]. We may add skin eccrine glands, hair bulb fibroblasts, and skeletal muscle. The design of the study did not allow detecting possible diminution of the persisting storage mentioned in some of the above-quoted reports. For instance, the cardiocyte storage pattern in both our cases admits partial clearance (Fig. 6b). Persistent storage in cardiocytes was accompanied by a notable increase in lipopigment which should be taken as irreversible. These findings may explain the absence of cardiac improvement in either patient on ERT (see Table 1).

It is not easy to explain the limited ERT effectiveness. There is the undisputed role of the physical barriers, represented by fibrous stroma and basal membranes, especially when multiplied around capillaries [11]. Free access of the applied enzyme to endocytotically active cell perimeter in non-polarized cultured fibroblasts and through fenestration in the liver sinusoidal endothelium to the hepatocyte basolateral pole may contribute significantly to the effective ERT [35] (also M.E. personal observation), similarly as the number of MPR known to be of high density in fibroblasts [42, 18]. However, the density of the latter was not shown to correlate with the level of the applied enzyme uptake [29]. In polarized storage cells (epithelia, e.g., in the sweat glands, respiratory epithelium, etc.), the applied enzyme uptake is restricted to the basolateral pole. In case of renal tubules, both poles may participate to different degree in various parts of the nephron [38]. In the case of endothelial cells, the reproducible effectiveness of ERT may be explained by the barrierless access of the enzyme to the apical pole active in endocytosis [37].

Our findings point to further potentially important facts. Before all, it is the presence of the applied active enzyme inside the storage cardiocytes in patients under ERT (not in samples from patient 3 with ERT terminated). We base this crucial finding on the following data. No enzyme protein was immunohistochemically detectable in cultured mutant fibroblasts of both patients. As the value of enzyme activity in wild-type fibroblasts is much higher (approximately fivefold) than in the heart, it excludes presence of detectable amount of endogenous mutant enzyme in atrial cardiocytes of the Fabry patients studied. This is in accord with negative results in the heart from patient 3 with ERT terminated (see Fig. 8b). The histochemically demonstrable α-GALA activity in cardiocytes of ERT-treated patients (and not in patient 3) fits perfectly with the conclusion (Fig. 9). Similarly, increase in activity was shown by biochemical assay in one auricular sample available. We would also like to stress that in our studies, we used cryostat sections because the enzyme was found to be

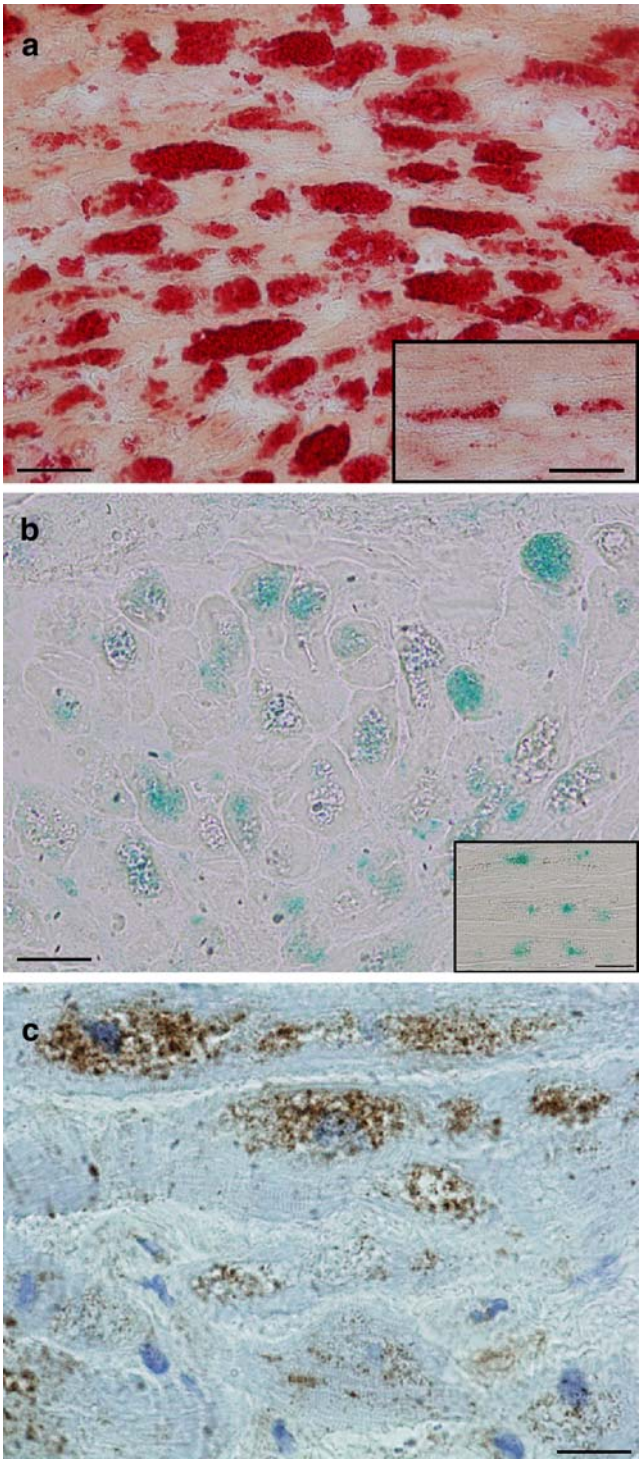


Fig. 10 Lysosomal enzyme activities and MPR immunostaining in storage atrial cardiocytes. **a** High and uniform activity of acid phosphatase (aqueous medium). *Insert* shows activity in controls (*bars* 50 mm). **b** Heterogenous activity of β-galactosidase with remarkably low values in some cardiocytes. *Insert* shows activity in control cardiocytes (*bars* 50 mm). **c** Similarly heterogeneous signal for MPR (*bar* 30 mm)

remarkably fixation-sensitive (see below). Therefore, sensitivity of our detection of the applied enzyme was higher than that in previous reports [20, 29].

The sensitivity of the applied enzyme to aldehyde fixation prevented its localization inside storage lysosomes at the electron microscope level. However, results in both cryostat and LR-White-embedded sections (Fig. 8a,d–f) indicate at least partial successive delivery of the enzyme. Its quantity may play a role, as the heart in Fabry disease may express storage even in cases with relatively high residual activity [30]. We would like to hypothesize that there may be modification of membranes of the endosomal/lysosomal compartment, induced by longstanding storage, especially in cells with low regeneration potential, cardiocytes being an ideal example. Such modification could lead to decreased effectiveness of the contact of the storage compartment with the endocytotic delivery of the applied recombinant enzyme. Decrease in MPR in many of the storage cardiocytes suggests a changed proportion of lysosomes to late endosomes, and this may result in altered fusion, inevitable for delivery of the applied enzyme cargo to the latter [8, 25]. It might also indicate disturbed contact even with the Golgi apparatus, which might explain low activities of β-glucuronidase, β-galactosidase, and cathepsin D in the cardiocyte storage compartment. Further, parallel deposition of lipopigment (see above) points to irreversible modification of storage lysosomes. Any relevant comparison with the mouse model of Fabry disease is difficult, as the mouse cardiocytes do not seem to display storage regularly [21]. Nothing is known about the effective interaction of the applied agalsidase with Sap B in Fabry disease. The disorder, featured by densely packed lysosomal lipid membranes, differs substantially from the well-defined physiologic conditions [22]. Decreased amount of Sap B in Fabry disease [28] may aggravate the situation. In sum, one of the critical factors in ERT of Fabry disease may, thus, be the degree of storage and physical status of the stored Gb3Cer and availability of Sap B. All this raises an important question whether the effective targeting of the enzyme to the storage cell is the only prerequisite for effective ERT.

The last factor awaiting evaluation is the role of storage cell turnover in Fabry disease (and in other lysosomal storage disease). In the case of endothelial cells in Fabry disease, preliminary results (J. Bultas, personal communication) showed its increase. Therefore, the positive effect of ERT might be also explained as a replacement effect of storage cells by the endothelial cell progenitors [1, 5, 17] that may easily endocytose the applied enzyme and thus prevent storage. This mechanism does not come into consideration in the case of post-mitotic storage cells, typically cardiocytes. Taken together, our observations speak in favor of the strategy of early treatment to prevent

development of storage and of irreversible modulation of post-mitotic cells or of cells with low regeneration potential (cardiocytes, smooth muscle cells) and of their lysosomes. This would be the most effective prevention of irreversible tissue changes. Studies on mouse model which would compare effectiveness of early ERT (starting immediately after birth) with its delayed application in adulthood are desirable.

Conclusions

We suggest that future studies should focus on defining the differences between the storage cell, the storage compartment and their wild-type counterparts, and on possible replacement of cell populations with higher turnover by their enzyme supplied precursors. Then, enzyme replacement treatment should probably be better conceptualized as an enzyme preventive therapy (see also [19]).

Acknowledgment We wish to thank Transkaryotic Therapies Inc., Cambridge, MA, USA for providing us with agalsidase alpha and rabbit polyclonal antibody TK88. We also wish to thank the Genzyme Corporation, Cambridge, MA, USA for providing us with agalsidase beta and the corresponding monoclonal antibodies against α-galactosidase A. We also acknowledge providing samples from patient 3 (Dr. G.A. Lammie, Univ. Hospital Wales, Cardiff) and his clinical data (Dr. P. Deegan, Department of Medicine, University of Cambridge).

This work was supported by grants from the Grant Agency of Charles University, Prague, no. 42/2005/c (to JL), from the Grant Agency of the Czech Republic, no. 303/03H065 (to JK and JL), and by the research project MSM 0021620806 from the Ministry of Education and Youth of the Czech Republic (to ME).

Conflict of interest statement We declare that we have no conflict of interest.

References

1. Asahara T, Murohara T, Sullivan A, Silver M, van der Zee R, Li T, Witzenbichler B, Schatteman G, Isner JM (1997) Isolation of putative progenitor endothelial cells for angiogenesis. Science 275:964–967
2. Asfaw B, Ledvinova J, Dobrovolny R, Bakker HD, Desnick RJ, Van Diggelen OP, De Jong JG, Kanzaki T, Chabas A, Maire I, Conzelmann E, Schindler D (2002) Defects in degradation of blood group A and B glycosphingolipids in Schindler and Fabry diseases. J Lipid Res 43:1096–1104
3. Blom D, Speijer D, Linthorst GE, Donker-Koopman WG, Strijland A, Aerts JM (2003) Recombinant enzyme therapy for Fabry disease: absence of editing of human alpha-galactosidase A mRNA. Am J Hum Genet 72:23–31
4. Bolte S, Cordelieres FP (2006) A guided tour into subcellular colocalization analysis in light microscopy. J Microsc 224:213–232
5. Boyer M, Townsend LE, Vogel LM, Falk J, Reitz-Vick D, Trevor KT, Villalba M, Bendick PJ, Glover JL (2000) Isolation of endothelial cells and their progenitor cells from human peripheral blood. J Vasc Surg 31:181–189
6. Brady RO, Schiffmann R (2000) Clinical features of and recent advances in therapy for Fabry disease. JAMA 284:2771–2775
7. Brenner BM, Grunfeld JP (2004) Renoprotection by enzyme replacement therapy. Curr Opin Nephrol Hypertens 13:231–241
8. Bright NA, Gratian MJ, Luzio JP (2005) Endocytic delivery to lysosomes mediated by concurrent fusion and kissing events in living cells. Curr Biol 15:360–365
9. Desnick R, Ioannou YA, Eng CM (2001) Alpha-galactosidase A deficiency: Fabry disease. In: Scriver CR, Beaudet AL, Sly WS, VAlle D (eds) The metabolic and molecular bases of inherited disease. McGraw-Hill, New York, pp 3733–3774
10. Dobrovolny R, Dvorakova L, Ledvinova J, Magage S, Bultas J, Lubanda JC, Elleder M, Karetova D, Pavlikova M, Hrebicek M (2005) Relationship between X-inactivation and clinical involvement in Fabry heterozygotes. Eleven novel mutations in the alpha-galactosidase A gene in the Czech and Slovak population. J Mol Med 83:647–654
11. Elleder M (2003) Sequelae of storage in Fabry disease—pathology and comparison with other lysosomal storage diseases. Acta Paediatr Suppl 92:46–53 discussion 45
12. Eng CM, Banikazemi M, Gordon RE, Goldman M, Phelps R, Kim L, Gass A, Winston J, Dikman S, Fallon JT, Brodie S, Stacy CB, Mehta D, Parsons R, Norton K, O, Callaghan M, Desnick RJ (2001a) A phase 1/2 clinical trial of enzyme replacement in Fabry disease: pharmacokinetic, substrate clearance, and safety studies. Am J Hum Genet 68:711–722
13. Eng CM, Guffon N, Wilcox WR, Germain DP, Lee P, Waldek S, Caplan L, Linthorst GE, Desnick RJ (2001b) Safety and efficacy of recombinant human alpha-galactosidase A-replacement therapy in Fabry's disease. N Engl J Med 345:9–16
14. Genzyme, Corporation (2001) Product Monograph, Enzyme replacement therapy for Fabry disease
15. Germain DP, Waldek S, Banikazemi M, Bushinsky DA, Charrow J, Desnick RJ, Lee P, Loew T, Vedder AC, Abichandani R, Wilcox WR, Guffon N (2007) Sustained, long-term renal stabilization after 54 months of agalsidase beta therapy in patients with Fabry disease. J Am Soc Nephrol 18:1547–1557
16. Hartree EF (1972) Determination of protein: a modification of the Lowry method that gives a linear photometric response. Anal Biochem 48:422–427
17. Hernandez DA, Townsend LE, Uzieblo MR, Haan ME, Callahan RE, Bendick PJ, Glover JL (2000) Human endothelial cell cultures from progenitor cells obtained by leukapheresis. Am Surg 66:355–358 discussion 359
18. Hille-Rehfeld A (1995) Mannose 6-phosphate receptors in sorting and transport of lysosomal enzymes. Biochim Biophys Acta 1241:177–194
19. Hollak CE, Vedder AC, Linthorst GE, Aerts JM (2007) Novel therapeutic targets for the treatment of Fabry disease. Expert Opin Ther Targets 11:821–833
20. Christensen EI, Zhou Q, Sorensen SS, Rasmussen AK, Jacobsen C, Feldt-Rasmussen U, Nielsen R (2007) Distribution of alpha-galactosidase A in normal human kidney and renal accumulation and distribution of recombinant alpha-galactosidase A in Fabry mice. J Am Soc Nephrol 18:698–706
21. Ioannou YA, Zeidner KM, Gordon RE, Desnick RJ (2001) Fabry disease: preclinical studies demonstrate the effectiveness of alpha-galactosidase A replacement in enzyme-deficient mice. Am J Hum Genet 68:14–25
22. Kolter T, Sandhoff K (2006) Sphingolipid metabolism diseases. Biochim Biophys Acta 1758:2057–2079

23. Lee K, Jin X, Zhang K, Copertino L, Andrews L, Baker-Malcolm J, Geagan L, Qiu H, Seiger K, Barngrover D, McPherson JM, Edmunds T (2003) A biochemical and pharmacological comparison of enzyme replacement therapies for the glycolipid storage disorder Fabry disease. Glycobiology 13:305–313
24. Lojda Z, Gossrau R, Schiebler TH (1979) Enzyme histochemistry. A laboratory manual. Springer, Berlin
25. Luzio JP, Pryor PR, Gray SR, Gratian MJ, Piper RC, Bright NA (2005) Membrane traffic to and from lysosomes. Biochemical Society Symposium, pp 77–86
26. Manders EMM, Verbeek FJ, Aten JA (1993) Measurement of colocalization of objects in dual-color confocal images. J Microsc–Oxford 169:375–382
27. Mayes JS, Scheerer JB, Sifers RN, Donaldson ML (1981) Differential assay for lysosomal alpha-galactosidases in human tissues and its application to Fabry's disease. Clin Chim Acta 112:247–251
28. Morimoto S, Yamamoto Y, O, Brien JS, Kishimoto Y (1990) Distribution of saposin proteins (sphingolipid activator proteins) in lysosomal storage and other diseases. Proc Natl Acad Sci U S A 87:3493–3497
29. Murray GJ, Anver MR, Kennedy MA, Quirk JM, Schiffmann R (2007) Cellular and tissue distribution of intravenously administered agalsidase alfa. Mol Genet Metab 90:307–312
30. Nakao S, Takenaka T, Maeda M, Kodama C, Tanaka A, Tahara M, Yoshida A, Kuriyama M, Hayashibe H, Sakuraba H et al (1995) An atypical variant of Fabry's disease in men with left ventricular hypertrophy. N Engl J Med 333:288–293
31. Rasband WS (1997–2006). "ImageJ", from http://rsb.info.nih.gov/ij/
32. Rozenfeld PA, Croxatto O, Ebner R, Fossati CA (2006) Immunofluorescence detection of globotriaosylceramide deposits in conjunctival biopsies of Fabry disease patients. Clin Exp Ophthalmol 34:689–694
33. Sakuraba H, Murata-Ohsawa M, Kawashima I, Tajima Y, Kotani M, Ohshima T, Chiba Y, Takashiba M, Jigami Y, Fukushige T, Kanzaki T, Itoh K (2006) Comparison of the effects of agalsidase alfa and agalsidase beta on cultured human Fabry fibroblasts and Fabry mice. J Hum Genet 51:180–188
34. Seehafer SS, Pearce DA (2006) You say lipofuscin, we say ceroid: defining autofluorescent storage material. Neurobiol Aging 27:576–588
35. Schiffmann R, Murray GJ, Treco D, Daniel P, Sellos-Moura M, Myers M, Quirk JM, Zirzow GC, Borowski M, Loveday K, Anderson T, Gillespie F, Oliver KL, Jeffries NO, Doo E, Liang TJ, Kreps C, Gunter K, Frei K, Crutchfield K, Selden RF, Brady RO (2000) Infusion of alpha-galactosidase A reduces tissue globotriaosylceramide storage in patients with Fabry disease. Proc Natl Acad Sci U S A 97:365–370
36. Schiffmann R, Rapkiewicz A, Abu-Asab M, Ries M, Askari H, Tsokos M, Quezado M (2006) Pathological findings in a patient with Fabry disease who died after 2.5 years of enzyme replacement. Virchows Arch 448:337–343
37. Simionescu M, Gafencu A, Antohe F (2002) Transcytosis of plasma macromolecules in endothelial cells: a cell biological survey. Microsc Res Tech 57:269–288
38. Stern AS, Klotman ME, Ioannou YA, Burrow CR, Wilson PD, Klotman PE, Lipkowitz MS (2002) Polarity of alpha-galactosidase A uptake by renal tubule cells. Kidney Int 61:52–55
39. Thurberg BL, Randolph Byers H, Granter SR, Phelps RG, Gordon RE, O, Callaghan M (2004) Monitoring the 3-year efficacy of enzyme replacement therapy in Fabry disease by repeated skin biopsies. J Invest Dermatol 122:900–908
40. Thurberg BL, Rennke H, Colvin RB, Dikman S, Gordon RE, Collins AB, Desnick RJ, O, Callaghan M (2002) Globotriaosylceramide accumulation in the Fabry kidney is cleared from multiple cell types after enzyme replacement therapy. Kidney Int 62:1933–1946
41. TKT, Europe (2001) Information Brochure, Enzyme replacement therapies for Fabry disease.
42. Wenk J, Hille A, von Figura K (1991) Quantitation of Mr 46000 and Mr 300000 mannose 6-phosphate receptors in human cells and tissues. Biochem Int 23:723–731
43. Wilcox WR, Banikazemi M, Guffon N, Waldek S, Lee P, Linthorst GE, Desnick RJ, Germain DP (2004) Long-term safety and efficacy of enzyme replacement therapy for Fabry disease. Am J Hum Genet 75:65–74

Virchows Arch (2008) 452:667–673
DOI 10.1007/s00428-008-0587-8

ORIGINAL ARTICLE

Computer-assisted validation of the synovitis score

Lars Morawietz · Frank Schaeper · Joerg H. Schroeder · Tserenchunt Gansukh · Nachin Baasanjav · Manfred G. Krukemeyer · Thorsten Gehrke · Veit Krenn

Received: 8 December 2007 / Revised: 15 January 2008 / Accepted: 22 January 2008 / Published online: 19 February 2008
© Springer-Verlag 2008

Abstract Histopathological examination of synovial specimens can contribute to the diagnosis of chronic joint diseases. A so-called synovitis score has been introduced as a standardised grading system, based on the semi-quantitative evaluation of the three determining features of chronic synovitis: enlargement of synovial lining, density of synovial stroma and inflammatory infiltrate, giving a score between 0 and 9. The present study examines the reliability of this procedure by comparison with exact measurements using computer-assisted image analysis (CAIA). Seventy-one synovial specimens from patients with osteoarthritis (OA, n=22), psoriatic arthritis (PsA, n=7), rheumatoid arthritis (RA, n=35) and from a control group (Co, n=7) were evaluated using both the synovitis score and CAIA. The measurements were transformed to semi-quantitative values analogous to the synovitis score. The differences between the transformed CAIA scores and the pathologist's scores were 0 or +/−1 in 40 cases, whereas in 31 cases the difference was greater than 1 (correlation coefficient r=0.725). The CAIA scores differed significantly between Co and RA cases (p=0.000) as well as between OA and RA (p=0.000). We conclude that the synovitis score was validated by CAIA and can be regarded a reliable grading system that contributes to the diagnostic procedure of chronic joint inflammation.

Keywords Synovitis · Arthritis · Computer assisted · Morphometry · Scoring

Lars Morawietz and Frank Schaeper contributed equally to this work.

This work has been supported by the Gemeinnuetziger Verein ENDO-Klinik e.V., the German Research Association (SFB421, project Z3) and the Federal Ministry of Education and Research, grant 01GS0413 in the framework of the national genome research network (NGFN).

L. Morawietz (✉)
Institute of Pathology, Charité University Hospital,
Charitéplatz 1,
10117 Berlin, Germany
e-mail: lars.morawietz@charite.de

F. Schaeper
Bioptic Institute and Clinic for Pathology,
Berlin, Germany

J. H. Schroeder
Center for Musculosceletal Surgery, Charité University Hospital,
Berlin, Germany

T. Gansukh · N. Baasanjav
Medical Research Institute of Mongolia,
Ulan Bator, Mongolia

M. G. Krukemeyer
Paracelsus-Kliniken Deutschland GmbH,
Osnabrueck, Germany

T. Gehrke
Department of Joint Surgery, ENDO-Klinik,
Hamburg, Germany

V. Krenn
Institute of Pathology,
Trier, Germany

Introduction

In general, the diagnosis of both degenerative and inflammatory arthropathies is based on clinical findings, and the histopathological assessment of synovial membrane specimens is often considered to be of minor importance. Although the American Rheumatism Association included histopathological diagnostics in their first version of criteria for rheumatoid arthritis (RA) in 1958, these were abandoned in the revision that took place in 1987 [3]. The

reason was not that the committee regarded the histology as irrelevant, but rather the fact that rheumatologists only rarely took a biopsy from an inflamed joint [3]. Among rheumatologists and radiologists, it has even become common practice to perform magnetic resonance imaging (MRI) for the evaluation of joint diseases [8], although this is a cost-intensive procedure. While radiologists achieve a satisfying agreement concerning cartilage and bone damage, the inter-observer variability of the evaluation of synovitis is too high when using MRI [15]. This should be a good reason to obtain tissue samples from unclear joint lesions and to perform histopathological examination more often, as it is already the case for resected material from therapeutic synovectomies and endoprosthesis implantations, which are routinely sent to pathologists.

One general problem in orthopaedic pathology is, that joint diseases often present with uncharacteristic histopathologic findings [9, 16]. Therefore, in recent years some histopathological scoring systems have been proposed in order to contribute to a standardised histopathological diagnosis of synovitis, to gain an objective standard for the effects of drug treatment in RA and to correlate the clinical severity of arthritis with synovitis by the quantification of the inflammatory infiltrate [4, 5]. One of these grading systems, the so-called synovitis score, was developed for application to all forms of chronic synovitis [11]. In a previous study, the synovitis score proved to be a feasible histopathological tool, easily applied to H&E sections of synovial biopsies and synovectomy specimens with good inter-observer reliability and good correlation to clinical diagnoses [12]. It is a numerical score, based on a semi-quantitative assessment of the three determining features of chronic synovitis, which are (1) the synovial lining, (2) the density of the synovial stroma and (3) the inflammatory infiltrate [10, 14, 21]. These are independently graded from normal (0 points) to highly pathologic (3 points). The sum of these three aspects becomes the synovitis score, ranging from 0 to 9 and leading to the following interpretation: 0–1 points = no synovitis, 2–4 points = low-grade synovitis and 5–9 points = high-grade synovitis. It was shown that low-grade synovitis is typically found in degenerative processes like osteoarthritis (OA) and posttraumatic joint injury, whereas high-grade synovitis is the histopathological equivalent of inflammatory diseases like RA and psoriatic arthritis (PsA) [12]. In a recent study by Pessler et al., the synovitis score was compared with the immunohistochemical expression of the proliferation marker Ki-67 and the macrophage marker CD68 in biopsies from various joint diseases, revealing a strong correlation between the synovitis score, immunohistochemistry and the clinical severity, which supported the presumption that the synovitis score is a valid and reliable method for the evaluation of synovial specimens [18]. Lately, it has also been applied to synovial samples from patients with Gulf War veterans' illness in order to quantify and objectify possible signs of synovitis [7].

Computer-assisted image analysis (CAIA) is a method that allows the automatic examination of digital images—such as video images from histopathological slides—by a computer. Depending on the programming of the machine, both an objective measurement of histological structures and a precise quantification of defined cell forms are enabled. Different CAIA algorithms have successfully been applied to the evaluation of chronic arthritis [6, 19], as well as for cell quantification in different fields of histopathology [22, 23]. However, most of these studies used immunohistochemically stained slides. Since the synovitis score is based on the size of the synovial lining and the number of stroma and inflammatory cells, which can be identified on H&E-stained sections, it was regarded as a good subject for computer-assisted morphometry. This study consequently has two aims: first, to ascertain whether or not the real cellularity of the lesion is reflected by the pathologist's semi-quantitative evaluation, and second, to examine the reliability of the synovitis score method for the evaluation of synovial tissue samples.

Materials and methods

Patients and tissue preparation

From our collection of synovectomy specimens we chose $n=71$ cases to encompass a broad spectrum of diagnoses and histological findings. The clinical diagnoses were based on the criteria of Altman et al. for OA ($n=22$), of the ACR for RA ($n=35$) and of Moll and Wright for PsA ($n=7$) [2, 3, 16, 17]. All specimens had been obtained at therapeutic synovectomy surgery or at the implantation of a total joint endoprosthesis. Control synovial tissue was obtained from autopsies in which there were no joint alterations (Co, $n=7$). All patients had given informed consent. Samples were fixed in formalin, embedded in paraffin, cut in microsections of 1–3 μm and stained with H&E according to routine procedures. The samples were re-evaluated according to the synovitis score by three pathologists (L.M., F.S. and V.K.). The pathologists evaluated each sample independently, and in cases of disagreement upon the score between the observers, they discussed the cases until they had formed a consensus. Then the same slides were subjected to computer-assisted morphometry.

Computer-assisted image analysis

The slides were viewed with a DMRB microscope (Leica Microsystems, Wetzlar, Germany) containing a prism in the

course of the beam, which diverts half of the light to the eyepiece and the other half to a DXC-930P videocamera (Sony Professional Solutions Europe, Berlin, Germany) with 584×720 pixel resolution. The video signal was processed to the image analysis system Quantimet Q600 (Leica) on a personal computer. The software contains the operating system QWin, which can be programmed in the language Quips, a version of Basic (Microsoft Corporation, Redmond, WA, USA). Two kinds of measurements were performed by CAIA: The synovial lining was assessed by the pathologist marking the upper and lower margins of the lining, and the computer then measuring the distance between them, whereas the assessment of the synovial stroma and inflammatory cells was fully automated.

Interactive measurement was made necessary by the inability of the software to detect the margins of the synovial lining. The pathologist evaluated the video picture on the computer monitor and marked the bottom and top of the synovial lining at ten different sites by clicking the mouse. The software then measured the distance between the bottom and top points in micrometers at all ten sites and calculated the arithmetic mean (Fig. 1). Additionally, one pathologist (F.S.) evaluated the thickness of the synovial lining by counting the number of cells at ten different locations and calculating the arithmetic mean.

The assessment of the density of the synovial stroma cells and the inflammatory cells was made fully automated by colour intensity recognition in the RGB (red, green, blue) mode. Each pixel was assigned a colour value between 0 and 255, e.g. a plain blue pixel had the value R=0, G=0, B=255. In order to "teach" the software the typical colour of the nucleus of a lymphocyte, these were marked on the screen by the pathologist (Fig. 2b), and the computer then calculated a range of colour values, e.g. 85<R<123 AND 90<G<163 AND 50<B<255, that were similar to the selected nucleus. In a new part of the slide, the software then marked all pixels which fulfilled the stated criteria and counted the nuclei, which were defined as clusters of at least 50 marked pixels. The nuclei, once recognised, were indicated on screen in yellow (Fig. 2c) and were controlled by the pathologist, who then marked nuclei that were either overlooked (false negative) or mistakenly recognised (false positive) by the software. If these corrections affected less than 5% of all nuclei, the teaching was regarded as having been successful, otherwise the margins for the colour values were adjusted and another area of the slide was used for testing the system. Once teaching was successful, the pathologist had to move the slide from one area to another and let the software count the nuclei at ×100 magnification. In order to evaluate the whole slide, four to ten visual fields were assessed in each case, and the mean number of nuclei per visual field was calculated.

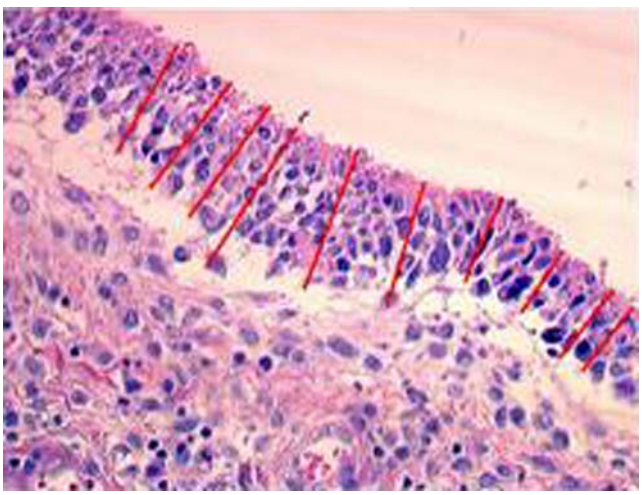


Fig. 1 Example of the interactive measurement of the synovial lining. The pathologists mark on screen the top and the bottom of the synovial lining with a mouseclick, and the CAIA draws a line between the two points and measures the distance, which is reproduced in micrometers

This method held two different sources of error. Sometimes, nuclei were situated closely together, so the software regarded them as a single and not two separate nuclei. In these cases, the pathologist was able to separate the virtual nuclei on the screen with a line drawn with the mouse (Fig. 2d). Furthermore, some cell forms had the same kind of blue stain as the desired cells. For example endothelia or stroma cells might be mistaken for lymphocytes, or lymphocytes might be regarded as stroma cells. On the other hand, some cells might be only lightly stained and therefore overlooked. In general, the software tended to record more false positive than false negative cells, delivering slightly inflated numbers (see "Results", Table 1). The most practical way to overcome this problem was to preselect the areas that were suited for CAIA, meaning that lymphocyte-rich areas were only used for the assessment of the inflammatory infiltrate and not for the stroma cells, and vice versa.

As a preliminary test, in five sample areas the cell numbers were counted exactly by F.S. and then assessed by CAIA and by three pathologists, who were given the task of estimating the cell numbers using their normal clinical practice.

Statistical evaluation

The measurements of the synovial lining and the CAIA cell count of lymphocytes and stroma cells are ratio measurements. For each case, ten measurements were made, and the arithmetic mean and standard deviation of these measurements were calculated.

In order to compare the pathologist's score for each of the three aspects and the CAIA measurement, Spearman's rho was employed as correlation coefficient, and the one-tailed significance for that correlation was computed.

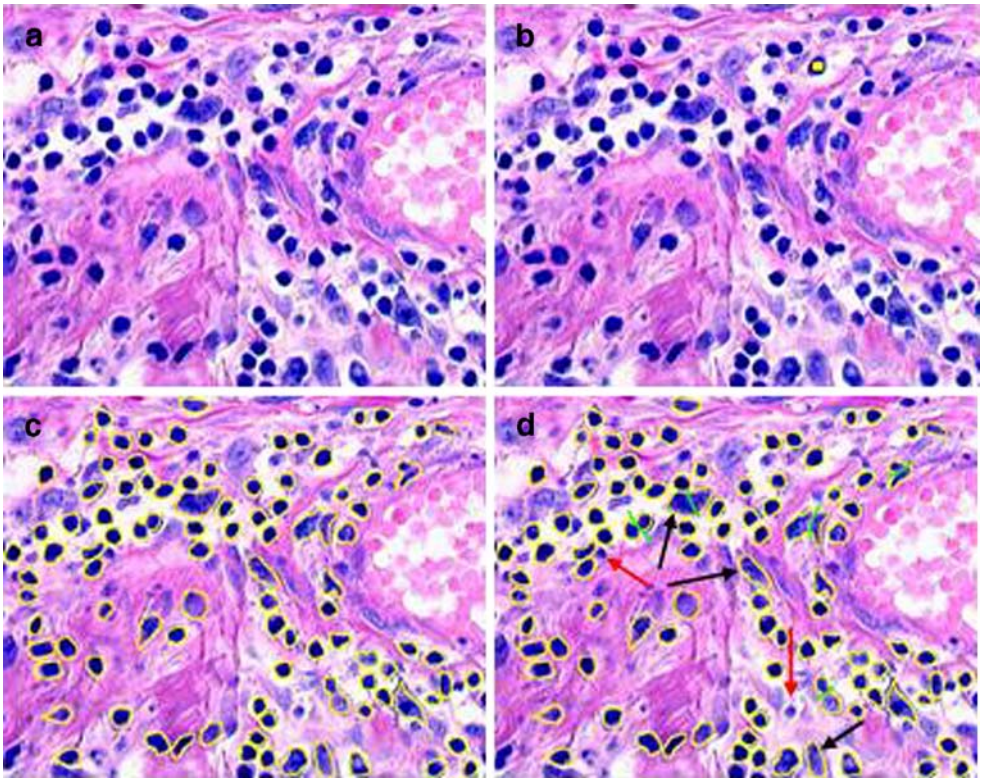


Fig. 2 Example of the CAIA count of the lymphocyte number. An adequate area of the slide is selected and viewed on the screen (**a**), then a typical lymphocyte is selected by the pathologist (*yellow dot* in **b**). CAIA marks and counts all nuclei with similar colour (*yellow circles* in **c**), and finally the pathologist can separate nuclei that are too close to each other (*green lines* in **d**). Some nuclei (*black arrows* in **d**) rather belong to fibroblasts and are therefore false positive, whereas some weakly stained lymphocytes are overlooked (*red arrows*)

In order to make the CAIA results comparable to the synovitis score, the measurements had to be transformed to semi-quantitative values. Therefore, the range of the CAIA results was divided into four equal segments. For example, the lowest mean value for stroma cells was 9.9 and the highest was 125.4, so the values between 9.9 and 38.7 were set at "0", values between 38.8 and 67.6 were set at "1", values between 67.7 and 96.5 at "2" and values between 96.6 and 125.4 at "3". From these values, a synovitis score was calculated and compared to the pathologist's score, using the Wilcoxon signed ranks test for two related samples.

The Kolmogorov–Smirnov test was used to determine any significant differences in the CAIA-based synovitis scores between the four patient groups.

All calculations were executed with SPSS 12.0 (SPSS Inc., Chicago, IL, USA).

Results

In the preliminary test, the CAIA cell count differed from the real cell numbers by two to 24, which corresponded to 0.7–8.3%. The CAIA cell counts were always higher than the exact cell numbers. The deviations of the three pathologists were higher and ranged between nine and 209 cells (12.7–72.3%, Table 1). Each pathologist had the tendency to either over- or underestimate the cell numbers in all five cases. Based on these results, the CAIA measurement was regarded sufficiently exact, so the study could be continued as planned.

All of the 71 cases were successfully evaluated by CAIA. The description of the CAIA measurements of the three aspects of synovitis is given in Table 2.

For each aspect of synovitis, a correlation between the pathologist's score and the CAIA measurement was calculated. Spearman's rho was $r=0.458$ for the synovial lining, $r=0.525$ for the stroma cell number and $r=0.733$ for the lymphocyte count. The number of lining cells assessed later by a pathologist as a check had a correlation coefficient of $r=0.921$ to the CAIA measurement. All correlations were highly significant ($p=0.000$, one tailed).

The CAIA values were transformed to semi-quantitative values and summarised to obtain synovitis scores. These were compared to the pathologist's synovitis scores. There

Table 1 Results of the preliminary test on five slides by CAIA and three pathologists (path 1–3)

Test slide	Exact cell number	CAIA count	Path 1	Path 2	Path 3
1	293	295 (+2)	200 (−93)	400 (+107)	100 (−193)
2	289	313 (+24)	260 (−29)	400 (+111)	80 (−209)
3	193	195 (+2)	120 (−73)	250 (+57)	50 (−143)
4	71	74 (+3)	90 (+19)	80 (+9)	30 (−41)
5	198	210 (+12)	160 (−38)	350 (+152)	60 (−138)

Table 2 Descriptive statistics of the CAIA measurements

	Synovial lining thickness (μm)	Stroma cell count	Lymphocyte count
Minimum	6.2	9.9	0.0
Maximum	73.3	125.4	392.2
Arithmetic mean	29.7	50.8	169.1
Standard deviation	16.9	32.2	151.9

Minimum and maximum are the arithmetic means of ten visual fields per case

were no significant differences (p=0.543, Wilcoxon test) between CAIA scores and pathologist's scores. The correlation coefficient was r=0.725 (Spearman's rho).

The differences between the coded CAIA scores and the pathologist's scores were calculated. In 20 cases, both were exactly the same, in another 20 cases, the difference was +/−1, and in 31 cases the difference was more than 1. The maximum differences were −5 and +5, the arithmetic mean of the differences was 1.42 and the standard deviation was 1.89. A histogram of the differences is given in Fig. 3.

The CAIA results were also compared between the patient groups. The descriptive statistics are given in Table 3. The synovitis scores based on CAIA values were also evaluated to ascertain any significant difference between the four patient groups. Significant differences were found between Co and RA and between OA and RA

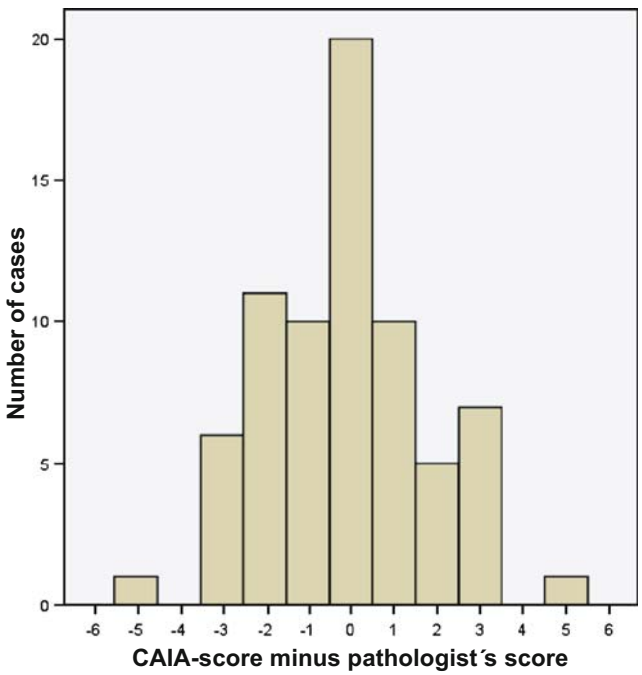


Fig. 3 Histogram of the difference between the synovitis score based on the CAIA values minus the pathologist's synovitis score (x-axis, difference, y-axis, number of cases, total n=71). In two RA cases, the difference was −5 and +5, respectively. In more than half of the cases, the differences was between −1 and +1

Table 3 Descriptive statistics of the CAIA scores grouped by clinical diagnoses

	Co (n=7)	OA (n=22)	PsA (n=7)	RA (n=35)
Minimum	0	0	0	0
Maximum	1	5	6	8
Arithmetic mean	0.6	1.3	2.9	5.4
Standard deviation	0.5	1.4	2.5	1.7

(p=0.000). All p values are given in Table 4 (Kolmogorov–Smirnov test).

Discussion

The present study was motivated by two questions. The first and more general query was, is the pathologist able to make a good semi-quantitative evaluation of tissue changes? This is a frequent task in histopathological diagnostics, not only with regard to synovial tissue specimens, but even more frequently on, e.g. gastric mucosa biopsies [20]. Secondly, the study questioned the ability of the synovitis score, which was introduced for the assessment of synovial tissue in 2002, to reflect the real numbers of inflammatory cells and deliver reliable results that can be substantiated by exact measurements and cell counts [11].

The first preliminary test, which was executed on five slides, already showed that CAIA is a system that can count cell numbers with an error rate of around 5% (0.7–8.3%), which is superior to three pathologists who had error rates between 12.7% and 72.3%. But even though the exact number is hardly ever met by pathologists, they are very often able to estimate the cell number within the correct dimension. Deciding if a pathological change is absent, slightly, moderately or strongly developed must also be determined when making a semi-quantitative evaluation.

The three aspects of the synovitis score were graded independently in this semi-quantitative way, and the results were correlated to the CAIA measurements. The correlation coefficients for the thickness of the synovial lining (r=0.458) and for the stroma cell number (r=0.525) were sufficient, and the correlation for the lymphocyte number (r=0.733) was adequate. This is best explained by the fact that lymphocytes are a very distinct, easily detectable cell

Table 4 Probability values as calculated by Kolmogorov–Smirnov test for the differentiation of the patient groups by CAIA scores, significant differences marked with asterisk

	OA	PsA	RA
Co	0.484	0.203	0.000*
OA		0.172	0.000*
PsA			0.128

form. They have small, dark, round and monomorphic nuclei, whereas the stroma cells have lighter and more irregularly shaped nuclei that are more easily confused with other cells. The lower correlation coefficient for the synovial lining indicates that this is the most difficult part of the synovitis score. Two reasons might account for this. First, the enlargement of the synovial lining is quite variable within one specimen, and on the edges an enlargement can be simulated by tangential cutting of the slide. Second, the range of the pathologic changes is rather narrow, so small differences in the lining layer can lead to much larger differences in the score. In order to further examine the synovial lining, one pathologist counted the cell layers in all 71 cases at ten different sites and calculated the arithmetic mean. These values then correlated very well (r=0.921) with the thickness measured by CAIA. The conclusion drawn from this result is that the reliability of the scoring of the synovial lining should be enhanced by not only estimating but rather counting the cell layers at ten different sites, calculating the arithmetic mean and scoring according to the following scheme: 0.0–1.7=score 0, 1.8–3.5=score 1, 3.6–5.3=score 2 and more than 5.3=score 3. Similar results were found by Cunnane et al., who compared automated with conventional microscopy on synovial biopsies from patients with chronic arthritis of the knee joints [6]. However, as a marker for the synovial stroma, they evaluated the area occupied by blood vessels, which resulted in an insignificant correlation between conventional and automated microscopy.

In our study, the overall correlation between CAIA and the pathologist's scoring was adequate (r=0.725), and in more than half of the cases (40 out of 71), the CAIA score was equal or differed only by +/−1 from the pathologist's score. In only two cases was there significant disagreement of +5 and −5, respectively. This disagreement is most likely caused by the selection of the scoring sites. As the distribution of the inflammatory changes is known to be very heterogeneous within one sample, selection of areas that are most representative for the lesion is recommended. Interestingly, this heterogeneity, which is obvious in histopathological examination, is also reflected on the molecular level, as has been demonstrated by evaluating gene expression profiles from different biopsies of the very same joint [13].

The correlation of the CAIA scores with the clinical diagnoses showed that the score is able to discriminate between RA and OA (p=0.000) and RA and Co (p=0.000). No significant differences were found between Co and OA (p=0.484), which is consistent with our previous findings [6, 7] and well in line with the recent immunohistochemical findings by Pessler and coworkers [18]. In disagreement with our previous study, the differences between Co and PsA (p=0.203), OA and PsA (p=0.172) and RA and PsA (p=0.128) were not significant using CAIA. However, this may be due to the smaller number of only n=7 PsA cases in the present study.

Summarising the present study, CAIA is a reliable method to evaluate different kinds of histopathologic changes, however it is a time-consuming technique that—at least to date—is unsuitable for routine histopathological diagnostics. CAIA results correlate well with synovitis scores determined by pathologists, but the assessment of synovial specimens should be sharpened by counting rather than estimating the synovial lining cells. The score can be recommended as a standard procedure for the routine histopathological assessment of synovial specimens and it might be a valuable contribution to rheumatological diagnostics.

Acknowledgements This work is part of the promotion thesis of F.S. We wish to thank Mrs. Gabriele Fernahl for excellent technical assistance and Mrs. Kelley Wilder for proofreading.

Conflict of interest statement We declare that we have no conflict of interest.

References

1. Adamopoulos IE, Danks L, Itonaga I, Locklin RM, Sabokbar A, Ferguson DJ, Athanasou NA (2006) Stimulation of osteoclast formation by inflammatory synovial fluid. Virchows Arch 449:69–77
2. Altman R, Asch E, Bloch D, Bole G, Borenstein D, Brandt K et al (1986) Development of criteria for the classification and reporting of osteoarthritis. Classification of osteoarthritis of the knee. Diagnostic and Therapeutic Criteria Committee of the American Rheumatism Association. Arthritis Rheum 29:1039–1049
3. Arnett F, Edworthy S, Bloch D, McShane DJ, Fries JF, Cooper NS et al (1988) The American Rheumatism Association 1987 revised criteria for the classification of rheumatoid arthritis. Arthritis Rheum 31:315–324
4. Bresnihan B, Tak PP, Emery P, Klareskog L, Breedveld F (2000) Synovial biopsy in arthritis research: five years of concerted European collaboration. Ann Rheum Dis 59:506–511
5. Bresnihan B, Gerlag DM, Rooney T, Smeets TJ, Wijbrandts CA, Boyle D et al (2007) Synovial macrophages as a biomarker of response to therapeutic intervention in rheumatoid arthritis: standardization and consistency across centers. J Rheumatol 34:620–622
6. Cunnane G, Bjork L, Ulfgren AK, Lindblad S, FitzGerald O, Bresnihan B et al (1999) Quantitative analysis of synovial membrane inflammation: a comparison between automated and conventional microscopic measurements. Ann Rheum Dis 58:493–499
7. Diaz-Torne C, Schumacher HR, Yu X, Gomez-Vaquero C, Dai L, Chen LX, Clayburne G, Einhorn E, Sachdeva RM, Singh JA, Pessler F (2007) Absence of histologic evidence of synovitis in patients with Gulf War veterans' illness with joint pain. Arthritis Rheum 57:1316–1323

8. Frick MA, Wenger DE, Adkins M (2007) MR imaging of synovial disorders of the knee: an update. Magn Reson Imaging Clin N Am 15:87–101
9. Fritz P, Laschner W, Saal JG, Deichsel G, Tuczek H V, Wegner G (1989) Histological classification of synovitis. Zentralbl Allg Pathol 135:729–741
10. Kim HJ, Krenn V, Steinhauser G, Berek C (1999) Plasma cell development in synovial germinal centers in patients with rheumatoid and reactive arthritis. J Immunol 162:3053–3062
11. Krenn V, Morawietz L, Haupl T, Neidel J, Petersen I, Konig A (2002) Grading of chronic synovitis—a histopathological grading system for molecular and diagnostic pathology. Pathol Res Pract 198:317–325
12. Krenn V, Morawietz L, Burmester GR, Kinne RW, Mueller-Ladner U, Muller B et al (2006) Synovitis score: discrimination between chronic low-grade and high-grade synovitis. Histopathology 49:358–364
13. Lindberg J, af Klint E, Ulfgren AK, Stark A, Andersson T, Nilsson P, Klareskog L, Lundeberg J (2006) Variability in synovial inflammation in rheumatoid arthritis investigated by microarray technology. Arthritis Res Ther 8:R47
14. Magalhães R, Stiehl P, Morawietz L, Berek C, Krenn V (2002) Morphological and molecular pathology of the B cell response in synovitis of rheumatoid arthritis. Virchows Arch 441:415–427
15. McQueen F, Lassere M, Bird P, Haavardsholm EA, Peterfy C, Conaghan PG, Ejbjerg B, Genant H, O'Connor P, Emery P, Østergaard M (2007) Developing a magnetic resonance imaging scoring system for peripheral psoriatic arthritis. J Rheumatol 34:859–861
16. Mohr W (2000) Chronische Gelenkentzündungen. In: Mohr W (ed) Gelenkpathologie. Springer, Berlin, pp 307–392
17. Moll JM, Wright V (1973) Psoriatic arthritis. Semin Arthritis Rheum 3:55–78
18. Pessler F, Ogdie A, Diaz-Torne C, Dai L, Yu X, Einhorn E et al (2008) Subintimal Ki-67 as a synovial tissue biomarker for inflammatory arthropathies. Ann Rheum Dis 67:162–167
19. Rooney T, Bresnihan B, Andersson U, Gogarty M, Kraan M, Schumacher HR et al (2007) Microscopic measurement of inflammation in synovial tissue: inter-observer agreement for manual quantitative, semi-quantitative and computerized digital image analysis. Ann Rheum Dis 66:1656–1660
20. Stolte M, Meining A (2001) The updated Sydney system: classification and grading of gastritis as the basis of diagnosis and treatment. Can J Gastroenterol 15:591–598
21. Walsh DA, Bonnet CS, Turner EL, Wilson D, Situ M, McWilliams DF (2007) Angiogenesis in the synovium and at the osteochondral junction in osteoarthritis. Osteoarthr Cartil 15:743–751
22. Weaver DL, Krag DN, Manna EA, Ashikaga T, Harlow SP, Bauer KD (2003) Comparison of pathologist-detected and automated computer-assisted image analysis detected sentinel lymph node micrometastases in breast cancer. Mod Pathol 16:1159–1163
23. Went P, Mayer S, Oberholzer M, Dirnhofer S (2006) Plasma cell quantification in bone marrow by computer-assisted image analysis. Histol Histopathol 21:951–956

Virchows Arch (2008) 452:675–688
DOI 10.1007/s00428-008-0591-z

ORIGINAL ARTICLE

Elastase-induced lung emphysema in rats is not reduced by hematopoietic growth factors when applied preventionally

Andreas Schmiedl · Tobias Lempa · Heinz G. Hoymann · Susanne Rittinghausen · Daniela Popa · Thomas Tschernig · Heinz Fehrenbach · Reinhard Pabst · Marius M. Hoeper · Jens M. Hohlfeld

Received: 2 August 2007 / Revised: 7 January 2008 / Accepted: 27 January 2008 / Published online: 25 April 2008
© Springer-Verlag 2008

Abstract We hypothesized that formation of pulmonary emphysema could be diminished after previous activation of stem cells. Animals received either a daily dose of the hematopoietic growth factors (GF; recombinant rat stem cell factor plus recombinant granulocyte colony stimulating factor; n=6, Elastase/GF group) or vehicle (n=9, Elastase/Sham group) starting 3 days before intratracheal instillation of elastase or vehicle and continued for another 25 days. Control animals were treated with NaCl (n=9, Sham/Sham group). On day 25, in all animals, a 2-mL pump was implanted subcutaneously that delivered 200 μg/h 5-bromo-2-desoxyuridine (BrdU) until study termination. Compared to controls, the Elastase/Sham group exhibited elevated total lung capacity (TLC) and functional residual capacity (FRC), significantly increased mean free alveolar pathway, alveolar volume, and decreased septal density. The Elastase/GF group showed (1) a significant increase of TLC and FRC, (2) a significant increase in alveolar size and volume, (3) a significant reduction of septal density, volume, and thickness. Proliferation in lung parenchyma and in terminal bronchioles remained significantly decreased in the Elastase/Sham group and the Elastase/GF group. Blood cell number has significantly increased in the Elastase/GF group.

The application of GF-enhanced pulmonary emphysema, presumable because of increased inflammatory activity, was a result of a preventive treatment.

Keywords Rat · Lung emphysema · Stem cell factors · Stereology · Lung function

Supported by the DFG, SFB 587

A. Schmiedl (✉) · T. Lempa · D. Popa · T. Tschernig · R. Pabst
Department of Functional and Applied Anatomy,
Hannover Medical School,
Carl-Neuberg-Straße 1,
30625 Hannover, Germany
e-mail: Schmiedl.Andreas@mh-hannover.de

H. G. Hoymann · S. Rittinghausen · J. M. Hohlfeld
Fraunhofer Institute of Toxicology and Experimental Medicine,
Hannover, Germany

H. Fehrenbach
Clinical Research Group "Chronic Airway Diseases",
Faculty of Medicine, Philipps-University Marburg,
Marburg, Germany

M. M. Hoeper · J. M. Hohlfeld
Department of Respiratory Medicine, Hannover Medical School,
Hannover, Germany

Background

Lung emphysema is a lung disease involving damage to the alveoli. It is defined as permanent destructive enlargement of the airspaces distal to the terminal bronchioli without obvious fibrosis combined with progressive destruction of alveolar septa resulting in the development of large air cysts. Lung emphysema as part of chronic obstructive lung disease (COPD) is one of the leading causes of morbidity and mortality throughout the world and is the only common cause of death in the industrialized world whose prevalence has been steadily increasing [1]. The pathogenesis of pulmonary emphysema is still incompletely understood. However, several lines of evidence suggest that an imbalance of noxious and protective factors leads to destruction of lung parenchyma and alveolar walls resulting in a loss of alveolar surface area and elastic recoil [6, 35, 42]. Pulmonary emphysema is notoriously unresponsive to

medical treatment and no currently available drug has been shown to slow or halt progression of the disease (except for selected patients with alpha-1-antitrypsin deficiency who may have some gradual benefit from alpha-1-antitrypsin augmentation therapy). Therefore, lung transplantation remains the only "cure" for patients with advanced emphysema [7]. Recent cardiovascular research suggests that the concept of irreversible tissue destruction may no longer be valid. There are possible therapeutic approaches and therapeutic relevance of stem cell factors for treatment of infarcted myocardium [23, 30]. In myocardial infarction, which was considered to be an irreversible destruction of cardiac tissue, several groups have recently shown that pluripotent stem cells are able to infiltrate infarcted myocardium and to differentiate into cardiomyocytes and endothelial cells. These cells may obtain histological and functional features indistinguishable from "normal" myocardium [28, 29, 39]. Orlic et al. have shown that bone marrow cells mobilized by SCF and G-CSF move into the infarct area forming new cardiomyocytes and capillaries in a mouse infarct model. Furthermore, the infarcted area was reduced and heart function was improved [29]. Based on these observations, we speculate that pulmonary emphysema may also be prevented in the presence of a high number of activated stem cells. This concept is principally supported by earlier studies of Massaro et al., who have shown that induced emphysema or emphysema caused by a genetic failure of septation was reversible after administration of retinoic acid [25, 26]. To test our hypothesis, we designed experiments in a well-established rat emphysema model [5, 20, 31].

According to Orlic [29], we treated rats with SCF (stem cell factor) and G-CSF (granulocytes colony stimulating factor) because the combination of both factors has resulted in a strong mobilization of peripheral blood stem cells in other models [9, 10, 2].

We assessed the hypothesis that activation of stem cells before and after elastase instillation may result in a reduction in elastase-induced emphysema.

Materials and methods

Animals

Male Lewis rats (Charles River Wiga GmbH, Sulzfeld, Germany) weighing 195 to 230 g were used in the experiments. Animals were housed, watered, and fed as described before [14]. Care and use of experimental animals was strictly performed according to the "Guide for the Care and Use of Laboratory animals" published by the National Institute of Health (NIH publication 85-23, revised 1985) and the study was approved by the Institutional Review Board as well as by the state government of Hannover, Germany (AZ:TS-539).

Study design

All rats underwent splenectomy 2 weeks prior to the treatment phase of the study (day −17) to minimize immune response. On day −3, animals were randomized into three groups: rats in the "Elastase/GF" (n=6) received elastase intratracheally on day 0 and were treated once daily with hematopoietic growth factors subcutaneously throughout the study period (day −3 until day 28, see below). The "Elastase/Sham" (n=9) received elastase intratracheally on day 0, but was given saline subcutaneously from day −3 to day 28. The "Sham/Sham" (n=9) served as control group and received saline both intratracheally on day 0 and subcutaneously from day −3 to day 28.

Treatment

Starting on day −3, once daily subcutaneous treatment with either hematopoietic growth factors (GF; 150 μg/kg recombinant rat stem cell factor (rratSCF) plus 50 μg/kg recombinant human granulocyte colony stimulating factor (rHuG-CSF); n=6; Elastase/GF group), both kindly provided by Amgen, Thousand Oaks, CA, USA or saline at a volume of 1 ml/kg (n=9; Elastase/NaCl group) was performed for 31 days. On day 0, animals were anesthetized with 2% halothane/30% oxygen and intubated orally with a tracheal cannula. They received a single intratracheal bolus of either 250 U/kg elastase (EC 3.4.21.36, Roche, Mannheim, Germany) at a volume of 1 ml/kg or (n=9; Sham/Sham group) saline as indicated above.

Pulmonary function measurements

Pulmonary function was assessed in all animals on day −3 prior to start of treatment and at day 28. Respiratory function variables, including forced expiratory maneuvers, were measured in anesthetized, orotracheally intubated, spontaneously breathing rats by body plethysmography as described before [15, 17]. At first, spontaneous pulmonary function variables such as tidal volume, breathing frequency, minute ventilation, dynamic lung compliance, lung resistance, and tidal midexpiratory flow were determined [12]. Second, forced lung function maneuvers were performed during temporary apnea and included forced vital capacity (FVC), forced expiratory volume in 0.1 s, peak expiratory flow, maximum mid-expiratory flow, and forced expiratory flow at 75%, 50%, and 25% of FVC. Functional residual capacity (FRC) and quasistatic pressure–volume curves were derived during two subsequent apnea periods and allowed for calculation of quasistatic

compliance, total lung capacity (TLC), and residual volume (RV). Animals in all treatment groups were studied on each study day in randomized order (Fig. 1).

Histological studies

After pulmonary function testing on day 28, animals were killed by an overdose of intraperitoneal pentobarbital. A cannula was inserted into the trachea via tracheotomy. The chest was opened and the heart–lung blocks were removed. The lungs were fixed by tracheal instillation at a constant pressure of 20 cm H_2O in a special instillation device. The fixation solution consisted of 4% paraformaldehyde plus 1% glutaraldehyde in 0.2 M HEPES buffer. After instillation fixation, the lungs were immersed in the same fixation solution overnight at 4°C. After fixation, lungs were separated in the right and left lung and each lung was embedded into 2% aqueous agarose and cut into equidistant slices of 3 mm thickness from apical to basal by means of a tissue slicer. The slices were taken for light and electron microscopy in an alternating manner [32]. From each single lung, four to five slices were obtained for paraffin embedding.

Qualitative and quantitative investigations of were carried out by a light microscope (Orthoplan, Leitz, Wetzlar, Germany). Stereological analysis was carried out on-line using a digital camera (Olympus DP 50, Olympus DP-soft; SIS GmbH, Muenster, Germany). The final magnification was ×325. At this magnification, alveoli and alveolar ducts could be clearly differentiated and were evaluated separately.

Stereological analysis

Both lung lobes of all animals per group were evaluated. From each animal, up to six tissue blocks per lung were studied.

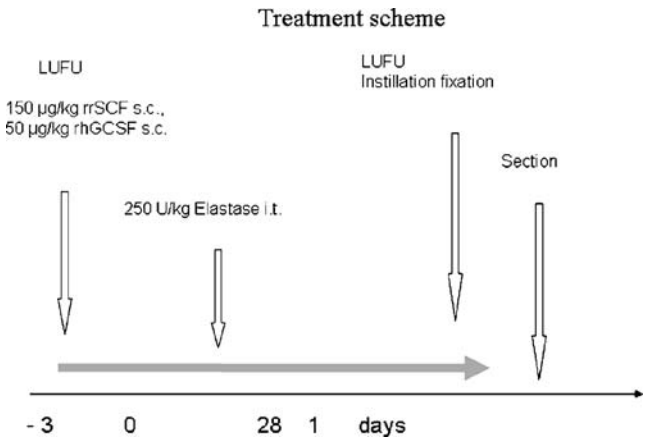


Fig. 1 Treatment protocol

Systematic uniform random test fields of view were obtained using the *x*- and *y*-axis of the microscope stage micrometers by applying the systematic random sampling method [37]. Starting at a random position outside the section, e.g., the upper left side, the microscope stage was moved at fixed intervals along both axes until the whole section was examined. This method guarantees that each area of the section had the same chance of being evaluated.

Stereological parameters

Volume densities (V_V), surface densities (S_V) and volume to surface ratios (V_S ratio) of alveolar septa and parenchymal alveolar air spaces were determined according to the point and intersection counting [16, 37]. Therefore, a coherent multipurpose test system with 15 test lines and 30 test points was used.

Alveolar volume

The volume-weighted mean volume was evaluated by using point sampled intercepts method [11, 13]. This technique gives information about the mean volume and variability of size of alveoli [11]. The following procedure was applied as described elsewhere [11, 33]. Briefly, a transparent test system composed of test lines with intercepts was superimposed on an orientation frame with a systematic random choice. Alveoli chosen by the intercepts were measured in the direction dictated by the test-line using a logarithmic ruler (L_{15}=100 mm) composed of a series of 15 classes. ∇_V was obtained using the formula: $\nabla_V=\pi/3\times l_0^3$. The factor 3 in the denominator represents the reference standard ruler of L=3 mm from which all other rulers were constructed [11]. ∇_V were then calculated according to the formula [3]: $\nabla_V=\pi/3\times((L_{15}\times 1{,}000)/3\times\text{magnification})^3\times l_0^3(\mu m^3)$. ∇_V (μm^3) is a parameter for alveolar volume.

Alveolar septa

We characterized the density of alveolar septa by determining the septal volume density (V_V) (%) and the septal thickness by the barrier thickness (V_S ratio) of alveolar septa (µm). Both estimators give information about the reduction or new formation of alveolar septa provided that there is no overexpansion.

Alveoli

The V_V of alveolar air space (%) was regarded as a measure for enlargement or reduction of the air space. The surface density (S_V) of septa ($\mu m^2/\mu m^3$) was used to evaluate the gas exchange surface. The V_S ratio ($\mu m^3/\mu m^2$) of alveoli is a parameter for alveolar size.

Absolute volumina

Absolute volumina of alveolar septa and air spaces were determined according to the following formula: V-septa (cm^3) = V_V-septa/parenchyma × V_V-parenchyma/lung × V-lung.

Total alveolar surface area

Total surface area of alveolar septa was determined according to the following formula: S_V-septa (cm^2/m^3) = S_V-septa/parenchyma × V_V-parenchyma/lung × V-lung.

Cytological analyses

All animals were subcutaneously implanted with a 2-mL pump (Alzet, Charles River Wiga GmbH, Sulzfeld, Germany) that delivered 200 μg/h 5-bromo-2-desoxyuridine (BrdU) until study termination on day 25.

Detection of proliferating cells in lungs by immunohistochemistry

Three-micrometer-thick paraffin sections were used. Enzyme pre-treatment for removal of protein cross links was done with protease (Sigma P/6911), 1% in PBS buffer (pH 7.2) for 2 min. After washing, hydrolysis was performed with 4 N HCl for 30 min. After washing again, the slides were incubated with normal goat serum (Vector, 1:20 diluted in PBS) for 20 min. The slides were then incubated with the primary antibody (mouse anti-bromodesoxyuridine, BioGenex, San Ramon, CA, USA, clone IIB5, 1:100) for 1 h. Again, after washing, the slides were incubated with the secondary antibody (goat-anti-mouse-biotin-SP, IgG, rat adsorbed, Jackson ImmunoResearch, Cambridgeshire, UK, 1:1,600) for 30 min, and further, after washing in Tris–NaCl buffer (pH 7.6), with streptavidin–biotin–alkaline phosphatase complex (Vector Laboratories, Burlingame, CA, U.S.A., 1:800) for 30 min. After washing in Tris–NaCl buffer (pH 7.6), visualization followed by fast red (BioGenex, San Ramon, CA, U.S.A.) for 15 min. All steps were performed at room temperature. The slides were counterstained with Mayer's hemalaun (Merck, Darmstadt, Germany).

Quantification of cell proliferation index in the lungs by light microscopy

From each lung, immunostained slices from two or three lung blocks per animal were taken. Cell proliferation was determined by counting the BrdU-positive nuclei in representative areas, using an image analysis system (Analysis Pro, SIS; Muenster, Germany).

a) Cell proliferation in terminal bronchioli

For quantification of cell proliferation in the epithelium of terminal bronchioles, the ULLI (Unit Length Labeling Index) was estimated [27]. For the ULLI of longitudinally sectioned terminal bronchioli, starting at the transition to alveoli, for each bronchiole, 500 μm of the airway surface of the respiratory epithelium was measured. The number of BrdU-positive bronchiolar epithelium cells per micrometer of airway surface for these regions was counted using a 20× magnification.

b) Cell proliferation in alveolar parenchyma

For quantification of cell proliferation in the alveolar parenchyma, the LI (labeling index) was estimated using a 40× magnification and a measurement grid within the optical path. For each evaluated bronchiole, the LI of four adjacent parenchyma areas was determined. A minimum of 2,000 alveolar cells was counted per lung slide and classified as positive or negative cells, respectively. The number of positive nuclear profiles/number of total nuclear profiles was estimated and given as labeling index.

Evaluation of the number of blood cells

Cytospins of the peripheral blood leukocytes were fixed in ethanol and washed in Tris-buffered saline containing 0.05% Tween 20. Incubation (30 min, room temperature) with primary antibodies recognizing epitopes was followed by incubation with rabbit anti-mouse IgG and then with the APAAP complex (Dako, Hamburg, FRG; both 15 min). The last two steps were repeated and the color reaction was developed using fast red (Sigma, St. Louis, USA) as the substrate for alkaline phosphatase. Leucocyte subsets were analyzed with monoclonal antibodies characterizing monocytes (ED1+ cells) and lymphocytes (mix of B cell and T cell marker, His14/R73+ cells) [38]. After surface staining, the DNA was denaturated with 0.025 N NaOH (30 s at 70°C) and the slides were incubated with anti-BrdU (Becton Dickinson, Heidelberg, Germany). The following steps were performed as described above, with the exception that fast blue (Sigma) was used as a chromogene. Slides were counterstained with hematoxylin and mounted in glycerol (Dako). Stainings were performed for neutrophils and monocytes as described previously [38]. Counting at least 300 monocytes or lymphocytes, the proliferation index has been determined. For evaluation of the percentage of subsets of the proliferated cell fraction, all BrdU-labeled cells have been evaluated.

Screening for parenchymal infiltration with inflammatory cells

Three H & E-stained sections of five rat lungs per group were evaluated using a light microscope (Eclipse 80i fluorescence microscope; Nikon, Düsseldorf, Germany). Parenchymal infiltration with inflammatory cells (macrophages, granulocytes) was counted by systematic uniform random sampling using a stereo investigator system (MicroBrightField, Williston, VT).

Briefly, in each section, 50 test fields (size of the test frame: 150×150 μm) were evaluated with a variable grid distance between the test fields in the *x*- and *y*-axes. The counted cells in lung parenchyma (alveoli, septa) were given as cell number per square millimeter (cell density) using the following formula: Q=number×grid size (μm)/150×150 (μm).

Statistics

Results are expressed as mean values±SEM. Statistical differences between mean values of treatment groups were determined by unpaired *t* test. Differences of changes after treatment in comparison to baseline within a group were tested for their statistical significance by paired *t* test. Correlations were assessed by Spearman Rank test. *p* values of less than 0.05 were considered significant.

Results

Body weight and lung weight

In animals treated with elastase, the weight gain was reduced; however, the lung weights were comparable The development of body weight is shown in Fig. 2. After emphysema induction, weight gain was delayed. While animals in the Elastase/Sham group had a slowed weight gain over four days, animals in the Elastase/GF group transiently even lost weight. Thereafter, lines of weight gain run in parallel, but the overall weight gain was lower in elastase-treated rats.

The weight of instilled lungs measured by fluid displacement was comparable in all groups (Sham/Sham: 10.26±0.35, Elastase/Sham: 10.31±0.23, Elastase/GF: 10.33±0.19)

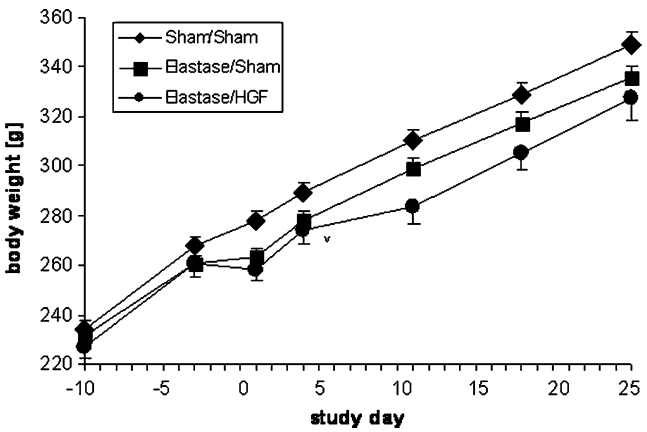


Fig. 2 Body weight development of the experimental groups (means± SEM)

Effect of hematopoietic growth factors (GF) on respiratory function

Compared to controls, the TLC and FRC were significantly increased in the Elastase/GF group At baseline, total lung capacity and residual volume were identical in all treatment groups (data not shown). During the study period, TLC increased at 22% in the Sham/Sham group; at 31%, in the Elastase/Sham group; and at 39%, significantly, in the Elastase/GF group (Fig. 3a).

Functional residual capacity at baseline was comparable in all groups. After treatment, the increase of FRC from baseline was significantly higher in the Elastase/GF group compared to the other groups (Fig. 3b).

Further differences in the residual volume and lung resistance are listed in Table 1.

Effect of hematopoietic growth factors (GF) on lung parenchyma

Both the Elastase/Sham group and the Elastase/GF group exhibited an emphysema with inhomogeneously expanded alveoli Compared to controls (Fig. 4a,b), alveoli appeared more expanded and alveolar size showed an inhomogeneous distribution in the Elastase/Sham group. Furthermore, areas with alveoli appearing only slightly more expanded altered with such of remarkably large alveoli (Fig. 5a,b). Also, a very inhomogeneous alveolar size distribution was seen in the Elastase/GF group (Fig. 6a–d). To get information about possible reduction in emphysematous alterations after GF treatment, stereological analysis was carried out.

Elastase instillation with/without application of GF resulted in less and smaller alveolar septa Compared to controls, septal volume fraction (Fig. 7a) decreased significantly in the Elastase/Sham group at 22%, and in the Elastase/GF group at 29%. Also, the total volume of alveolar septa was significantly reduced in the Elastase/Sham group compared to the Sham/Sham group. After application of GF, the septal volume remained decreased (Table 2).

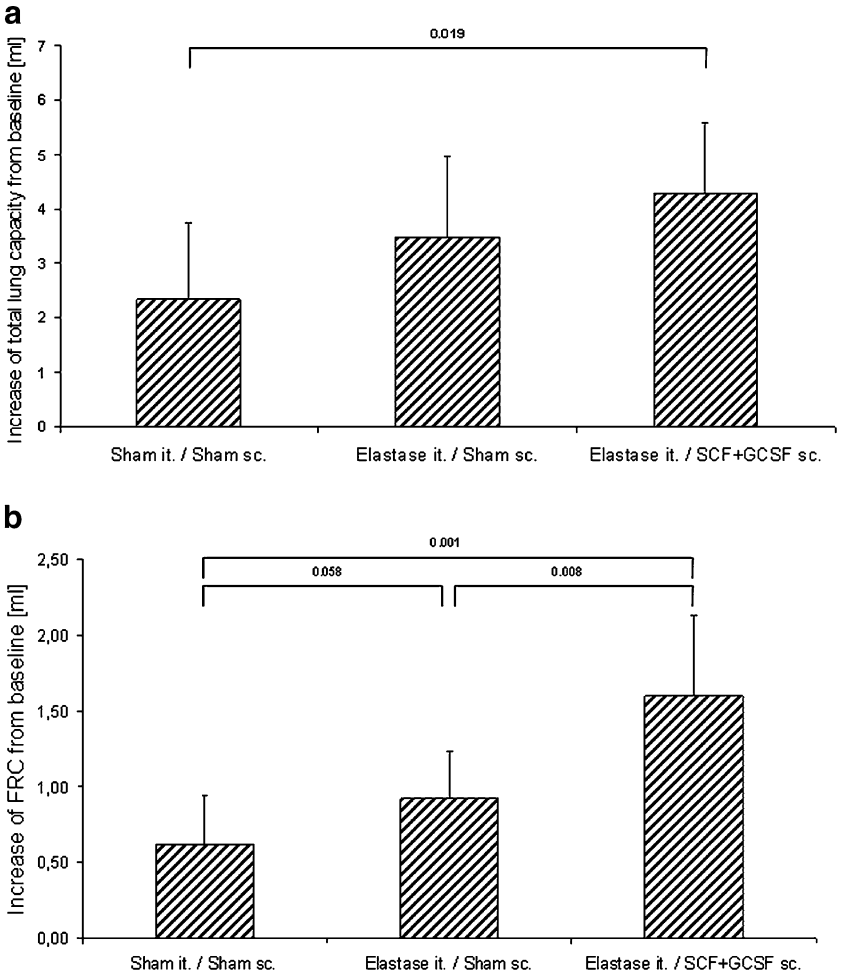


Fig. 3 Increase of total lung capacity (**a**) and functional residual capacity (**b**) from baseline in the study groups. Values are given as means±SEM and exact *p* values are indicated

The thickness of alveolar septa (Fig. 7b) had a tendency to lower values (5.74 μm) compared to controls (7.19 μm). There was a significant decrease to 5.35 μm in the Elastase/GF group.

The S_V-septa showed in the Sham/Sham group with 0.038±0.004 μm^{-1}, the highest levels. There was a reduction to 0.033±0.004 μm^{-1} in the Elastase/Sham group and to 0.035±0.002 μm^{-1} in the Elastase/GF group.

Table 1 Lung ventilatory parameters

	Sham/Sham (n=9)	Elastase/Sham (n=9)	Elastase/HGF(n=6)
V_T [ml]	0.21±0.05	0.19±0.04	0.19±0.05
f [min^{-1}]	−10.90±2.80	−10.50±4.80	−15.80±8.10
C_{dyn} [ml/cmH_2O]	0.06±0.02	0.03±0.02	0.06±0.01
R_L [cm H_2O/ml/s]	0.009±0.01	0.006±0.012	−0.030±0.011*·***
$FEV_{0.1}$ [ml]	0.70±0.20	0.50±0.20	0.30±0.20
FEF_{75} [ml/s]	8.70±3.70	4.10±4.50	3.10±2.60
FEF_{50} [ml/s]	6.60±3.80	0.60±3.30	−2.10±2.20
FEF_{25} [ml/s]	1.20±2.20	−5.30±1.90	−2.10±3.00
C_{qs} [ml/cmH_2O]	0.32±0.15	0.46±0.10	0.54±0.19
RV [ml]	0.29±0.19	0.39±0.26	1.37±0.31**·***

Difference of pulmonary function variables tidal volume (V_T), breathing frequency (f), minute ventilation (MV), dynamic lung compliance (C_{dyn}), lung resistance (R_L), expiratory flow at 50% vital capacity (EF_{50}), forced vital capacity (FVC), and forced expiratory volume after 0.1 s ($FEV_{0.1}$), peak expiratory flow (PEF), maximum mid-expiratory flow ($MMEF$), forced expiratory flow at 75% of forced vital capacity (FEF_{75}), 50% FVC (FEF_{50}), and 25% FVC (FEF_{25}), quasistatic compliance (C_{qs}), and residual volume (RV) at day 28 compared to baseline on day −3 in the treatment groups. Values are given as means±SEM. *p<0.05 and **p<0.01 compared to sham/sham group. ***p<0.05 compared to Elastase/Sham group.

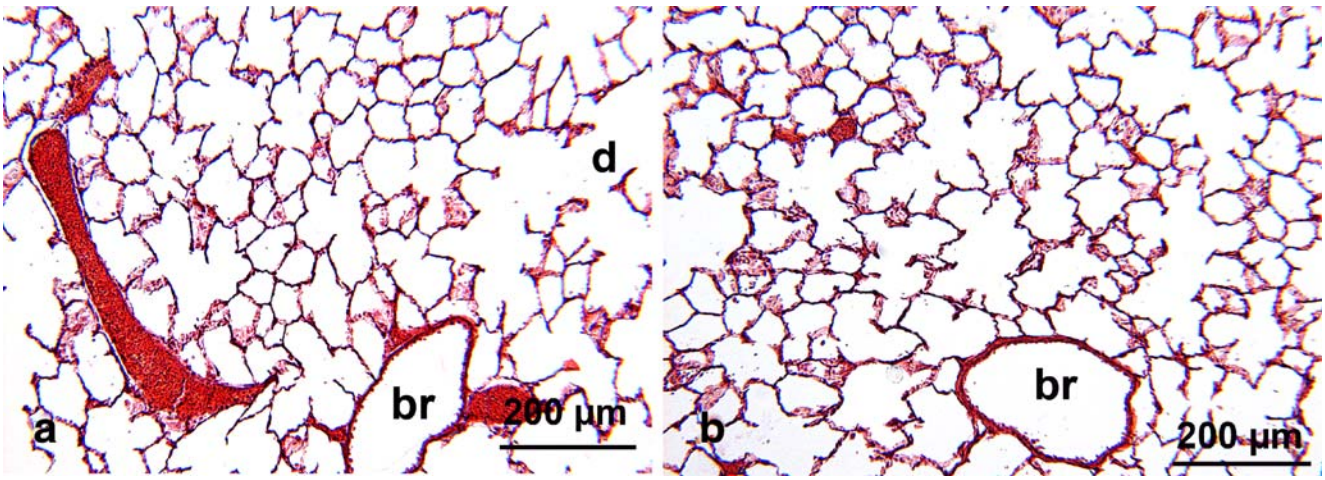


Fig. 4 Lung parenchyma of control lungs fixed by instillation. Lung parenchyma with more or less homogeneously opened alveoli. **a** Vessels filled with erythrocytes, a branching ductus alveolares (*d*) and a bronchiolus (*br*) are seen in lung parenchyma. **b** Sacculi alveolares and a bronchiolus (*br*) are visible

However, the differences were not significant. Also, the total alveolar surface area exhibited no significant differences in all groups (Table 2).

Elastase instillation and application of GF increased significantly the air space as well as mean free path and volume of alveoli The volume density of alveolar air space was significantly increased in the Sham/Sham group and in the Elastase/Sham group at 11% (Fig. 7c). Air space values remained significantly reduced in the GF group (Fig. 7c). The total volume of air spaces within lung parenchyma increased significantly after application of elastase compared to controls (Sham/Sham group; $p<0.04$). In the Elastase/GF group, total volume of air spaces was also significantly reduced compared to the Sham/Sham group (Table 2; $p<0.04$).

According to these findings, the V_S ratio of alveoli as a measure of the mean alveolar free path increased significantly from 16.8 $\mu m^3/\mu m^2$ to 20.8 $\mu m^3/\mu m^2$ in the Elastase/Sham group and to 19.4 $\mu m^3/\mu m^2$ in the Elastase/GF group (Fig. 7d). The volume-weighted mean volume of alveoli increased significantly from 3.76×10^6 μm^3 at 22% after Elastase application and at 41% in the Elastase/GF group (Fig. 8a).

There was a significant correlation between alveolar volume and FRC or alveolar volume and TLC independent from the experimental group Correlation analysis of alveolar volume with lung function parameters (see below) showed that there was a significant correlation between mean alveolar volume and the functional residual capacity as well as with the total lung capacity (Fig. 8b,c).

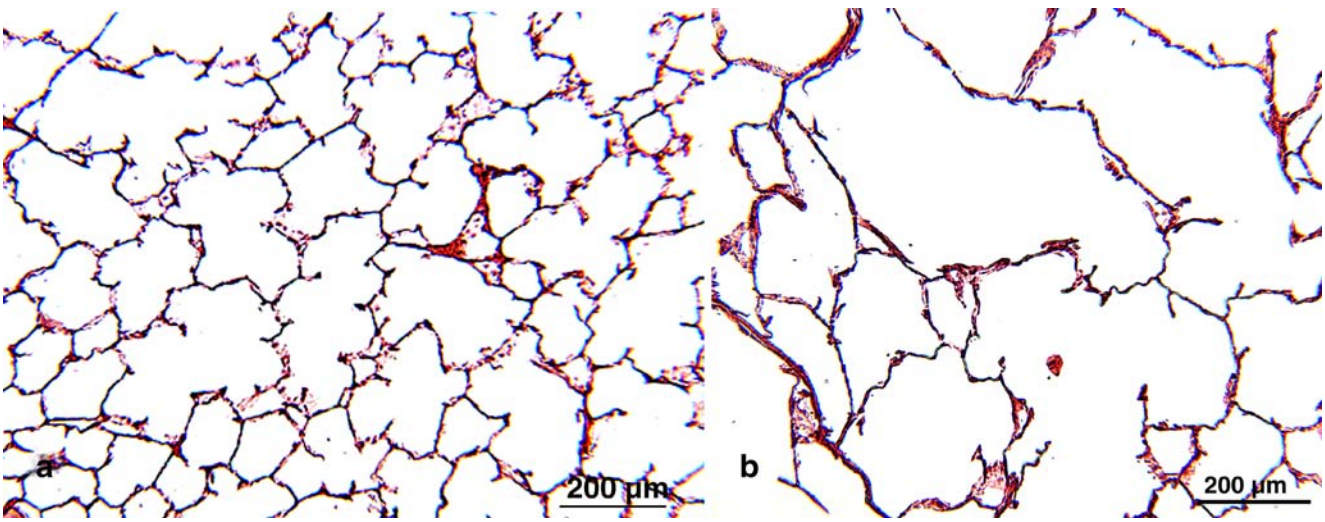


Fig. 5 Lung parenchyma of Elastase-instilled lungs. **a** Lung parenchyma with remarkably enlarged alveoli, **b** Lung parenchyma with sparse partly pronounced enlarged alveoli

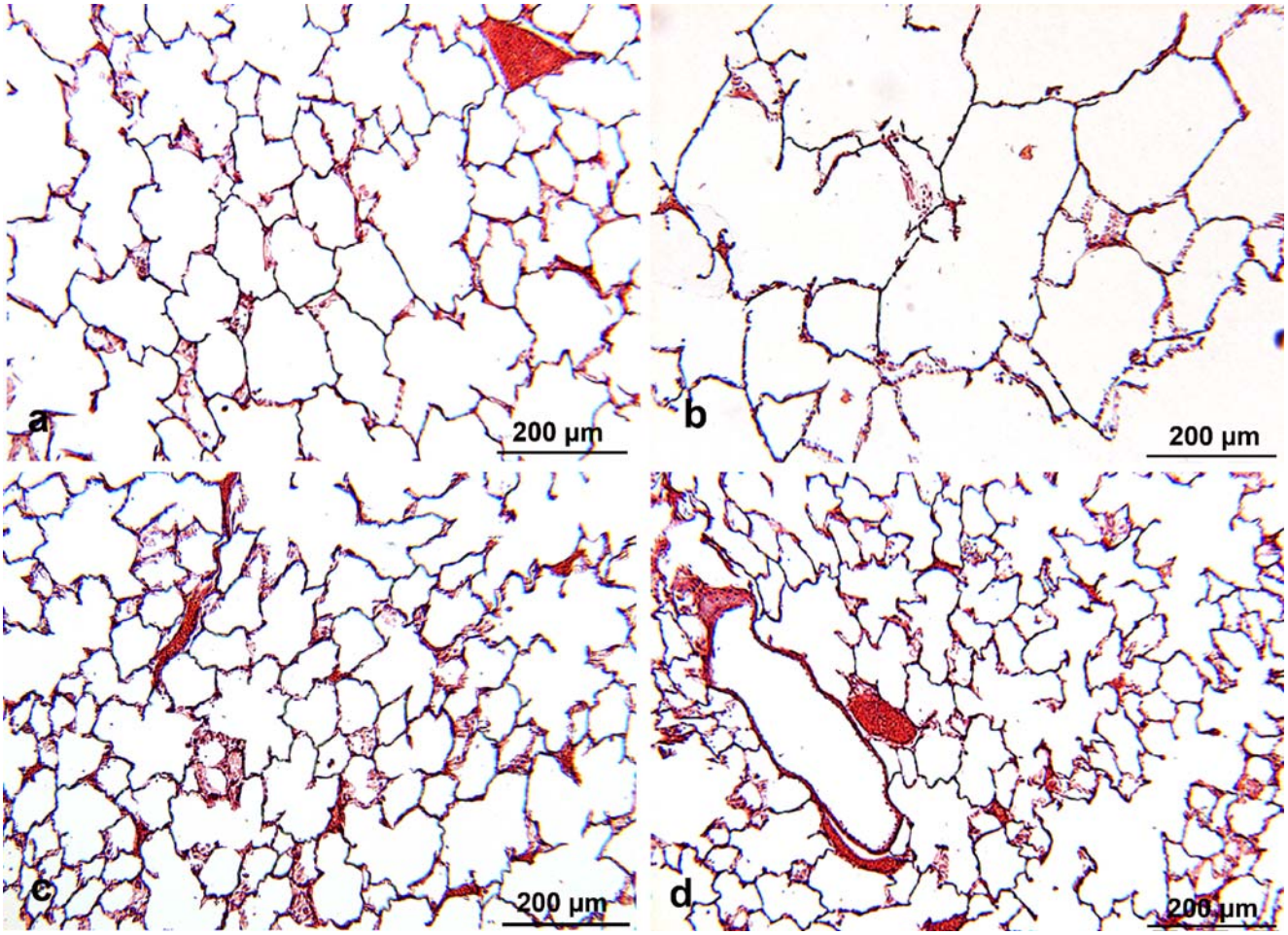


Fig. 6 Lung parenchyma after application of GF and emphysema induction Alveoli exhibit a very inhomogeneous size distribution. **a** Remarkably widened alveoli **b** extremely enlarged alveoli **c** moderately opened alveoli **d** alveoli and ductus alveolares comparable with controls

Cell proliferation

Compared to controls, proliferation decreased significantly in the Elastase/Sham group without increase in the Elastase /HGF group The labeling index as a measure of cell proliferation in the lung parenchyma (Fig. 9a,b) decreased significantly after elastase treatment. Elastase plus GF have led to values which are comparable to the Elastase/Sham group (Fig. 10a). The unit length labeling index of terminal bronchioles (Fig. 9c,d) showed the significant highest values in controls. The proliferation rate was significantly lower in the Elastase/Sham group and remained significantly reduced in the Elastase/GF group (Fig. 10b). Within the bronchioalveolar duct junction, only sporadical BrdU-labeled cells were detected. No tissue section contained more than two positive cells.

Parenchymal infiltration

Lung parenchyma exhibited no local clusters of inflammatory cells Septa and alveoli were only moderately infiltrated with macrophages and neutrophils in the emphysematic groups (Elastase/NaCl group: nearly 20/mm^2; Elastase/GF group: about 26/mm^2 compared to controls: nearly 13/mm^2). However, the highest numbers were found in the Elastase/GF group.

Number of blood cells

The total number of blood cells has significantly increased in the Elastase/GF group The total number of leukocytes was $2.9\pm0.4\times10^6$/ml in controls, $3.0\pm0.4\times10^{6/}$ml in the Elastase/Sham group, and $5.6\pm0.8\times10^6$ in the Elastase/GF group. Thus, the number of leucocytes was significantly elevated in the GF treated group. However, there were no differences in the percentages of subsets.

Discussion

This study was designed to induce emphysema by elastase instillation and to reduce or prevent the development of

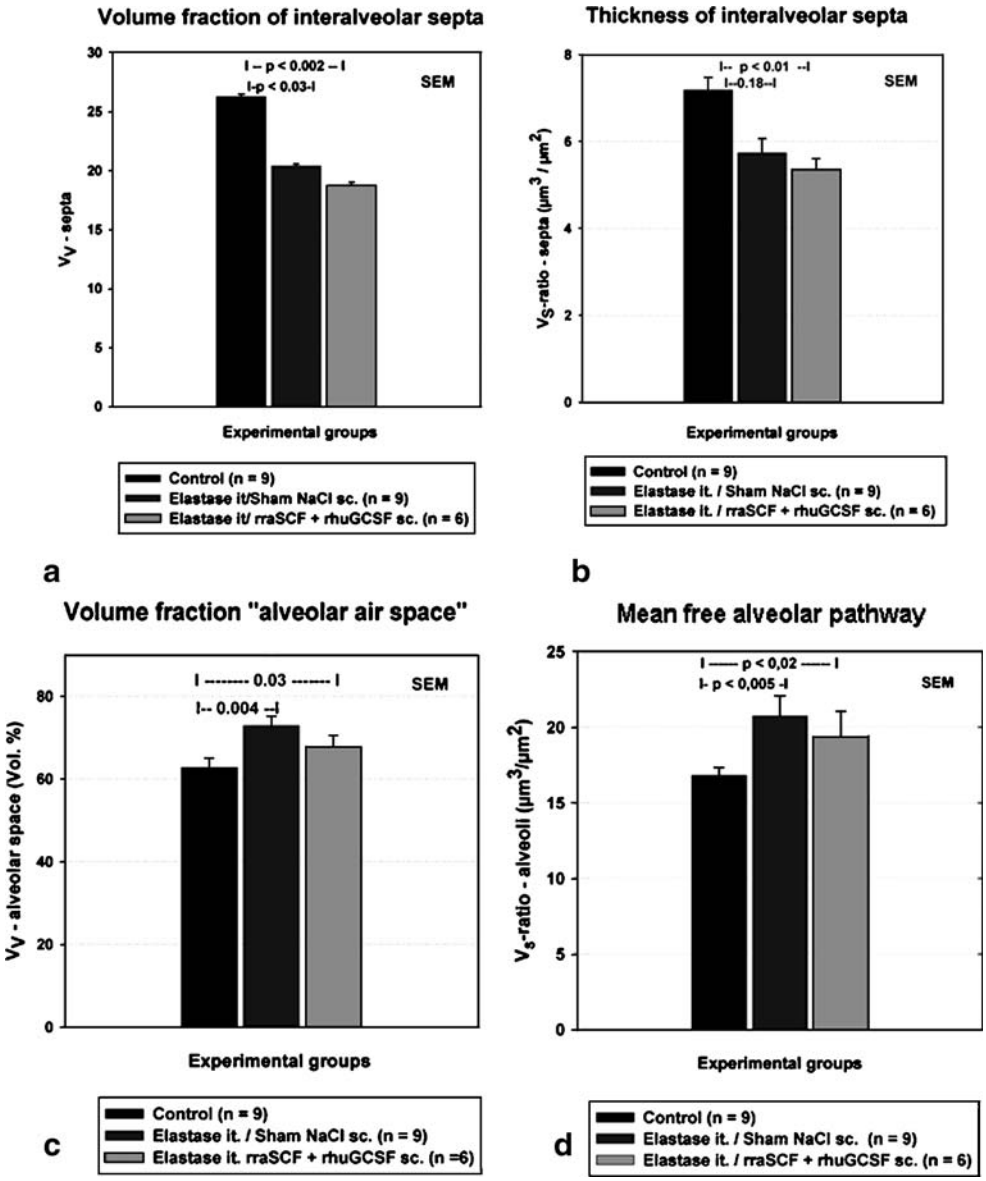


Fig. 7 **a** The volume fraction of alveolar septa is significantly higher in controls than in the Elastase/Sham as well as than in the Elastase/HGF group. **b** The volume to surface ratio of alveolar septa as a measure for septal thickness shows after Elastase instillation a tendency to lower values. Application of HGF reduced the arithmetric thickness significantly. **c** The volume fraction of alveolar air space is significantly lower in controls than in both experimental groups. **d** The volume to surface ratio as measure of the mean free alveolar path has significantly increased in the Elastase group as well as in group which received growth factors and Elastase

experimental emphysema by utilizing the presumptive regenerative potential of hematopoietic growth factors (GF). We determined the degree of emphysema with more or less pronounced and inhomogeneously distributed lesions (see Fig. 4) using stereological methods. The significant change of emphysema specific stereological parameters clearly indicates an emphysema induction by elastase instillation. The increase of total lung capacity and

Table 2 Total volumes and surfaces of alveolar septa and air spaces

Groups	Total volumes (cm^3)		Total surface (cm^2)
	V-septa	*V*-air spaces	
Sham/Sham	2.36±0.11	6.65±0.32	3,596±180
Elastase/Sham	1.91±0.14*	7.36±0.15*	3,194±180
Elastase/GF	1.77±0.03*	7.44±0.19*	3,305±100

Total volumes of septa and airspaces differ significantly compared to controls. Total septal volume is significantly reduced after elastase instillation with and without HGF application. The total air volume is significantly increased independent of HGF treatment. Total surface area was not significantly reduced in the treated groups. Values are given as means±SEM. *$p<0.05$ compared to the sham/sham group.

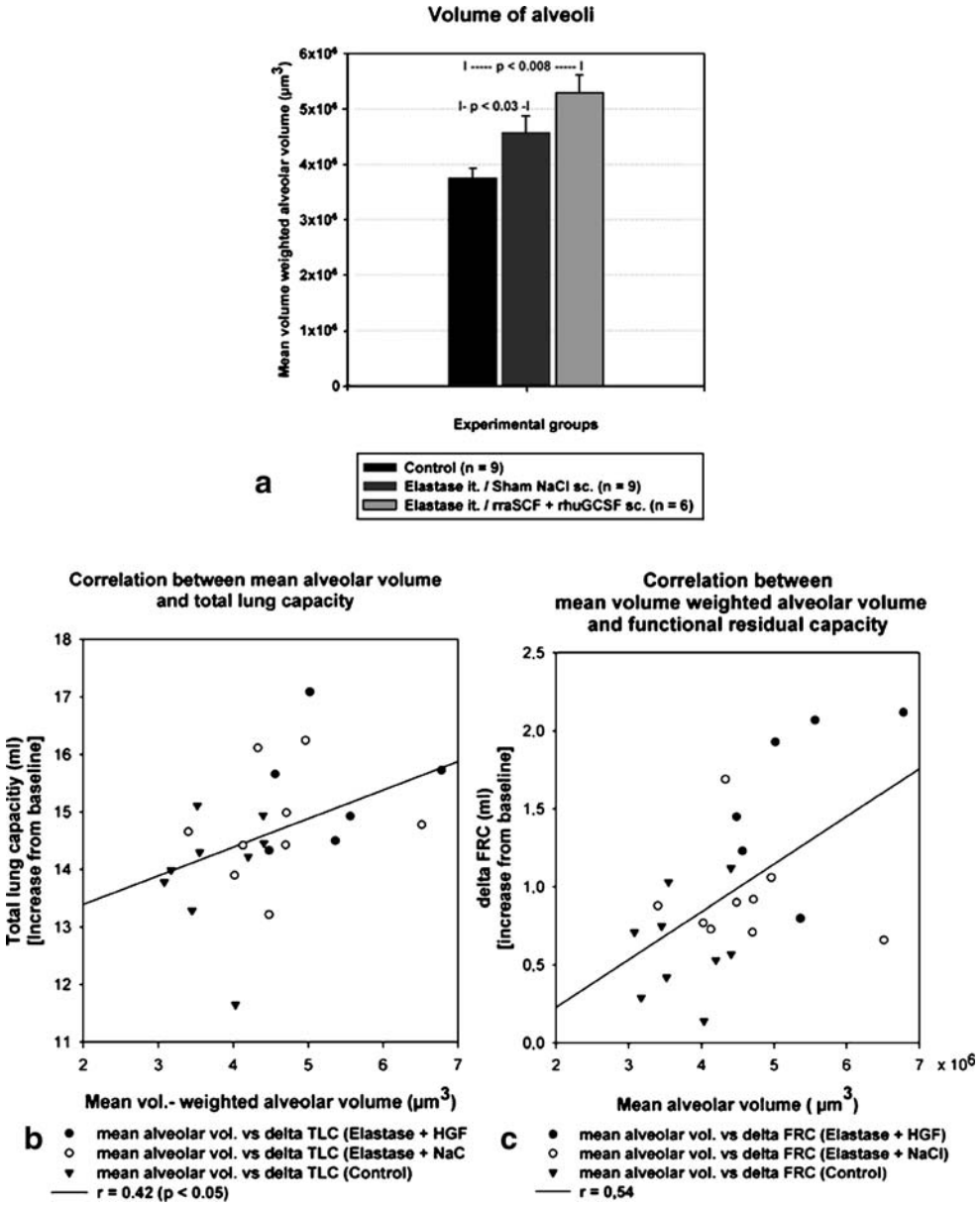


Fig. 8 **a** The volume-weighted mean volume of alveoli. Elastase instillation with and without HGF application increased the mean volume significantly compared to controls. **b** Correlation analysis of alveolar volume with functional residual lung capacity. Mean alveolar volume and functional residual capacity exhibited a close significant correlation independent of the experimental group. **c** Correlation analysis of alveolar volume with functional residual lung capacity. Mean alveolar volume and functional residual capacity exhibited a close significant correlation independent of the experimental group

functional residual capacity support the stereologic results. Furthermore, correlation analysis between stereological and functional parameters indicates a close structure–function relationship independent of the treatment.

To check our hypothesis that hematopoietic GF will reduce elastase-induced emphysema, we started the treatment with GF 3 days before induction of emphysema and continued the administration to day 25. The timing of the treatment as well as the choice of the hematopoietic GF was adapted to Orlic et al. [28]. In their protocol, both hematopoietic GFs were given 5 days before and 3 days after induction of an infarction by ligature of the left coronary artery. At day 27, they found a significant reduction of the infarct size as well as a functional and structural recovery of the heart. They postulated that mobilization and activation of bone marrow cells (BMC) by hematopoietic GF could be a non invasive therapeutic strategy for regeneration of ischemic myocardium [29].

Application of SCF and G-CSF was undertaken because both induce a synergistic activation of different genes involved in propagation of mitogenic signals in hematopoietic cells [9]. Both factors lead to an increase of circulating stem cells in the blood [2, 18] with the potential to differentiate into different mature cells of many organs [22]. These progenitor cells should have the potency to adopt to the phenotype of alveolar epithelial cells and endothelial cells by spontaneous cell fusion or by differentiation and, therefore, reduce the induced emphysema as shown by Ishizawa et al. [18]. However, in their study, alveoli remained significantly enlarged compared to con-

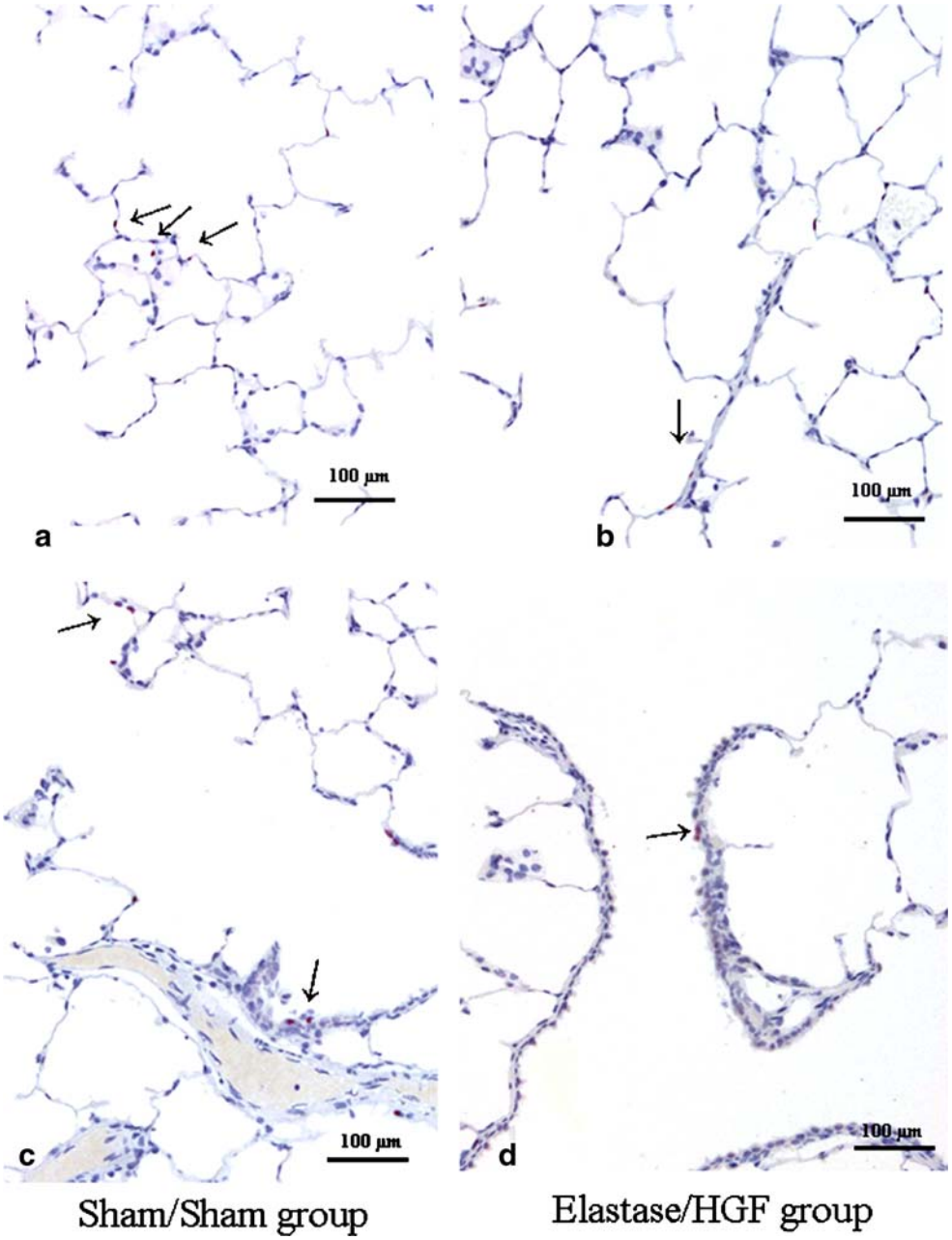


Fig. 9 BrdU-positive cells are seen in alveolar septa in both groups (*arrows*). **a** Controls **b** Elastase/HGF BrdU-positive cells are also seen in bronchioli terminales (*arrows*) in both groups. **a** Controls **b** Elastase/HGF

trols [18]. They have shown that green fluorescent protein (GFP)-positive BMCs increased in lung parenchyma after HCG treatment in C57BL/6 mice that have been irradiated and completely reconstituted with BMCs of GFP mouse origin, but they could not prove whether the occurrence of GFP-positive endothelial and epithelial cells was generated by BMC differentiation or fusion with existing cells [18].

Yet, in our study, treatment with hematopoietic GF did not reduce, but rather promoted emphysematous changes. Not only did the lung capacity and functional residual capacity increase significantly compared to control conditions, but also the alveolar volume accompanied by a significant reduction of alveolar septa. These results indicate clearly an enhancement of emphysema. We found no increase of proliferating cells in lung parenchyma or terminal airways. Therefore, we assume that there was no migration of activated pluripotent bone marrow cells into the lung parenchyma and/or no transdifferentiation and therefore no participation in tissue regeneration. Furthermore, BrdU-labeled cells are only rarely found at bronchioalveolar duct junctions in all three groups. Therefore, we assume that there is no evidence for proliferation of peripheral stem cells expressing CC10 and SP-C. Instead, our application protocol may have mobilized bone marrow cells, which promote lung inflammation and tissue damage by supplying pro-inflammatory effector cells such as

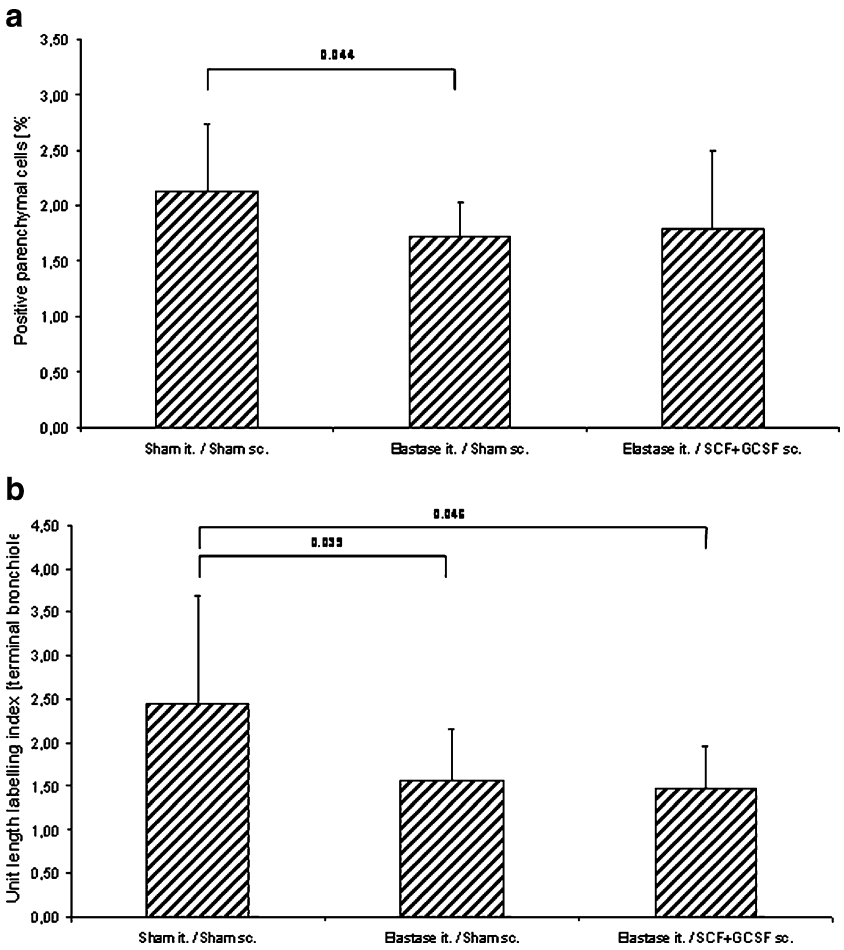


Fig. 10 There is no increase of BrdU-positive cells in the Elastase/HGF group. BrdU labeling index in lung parenchyma (*upper panel* **a**) and unit length labeling index of terminal bronchioles (*lower panel* **b**) in control rats (sham it) or rats after emphysema induction (elastase it) following 28 days of sc-treatment with either vehicle (sham sc) or stem cell factor plus granulocyte colony stimulating factor (SCF+G-CSF sc). Values are given as means± standard deviation. Exact *p* values are indicated

granulocytes and monocytes changing to alveolar macrophages at the onset of emphysema induction [8]. This may be supported by the determined significant increase of the number of leucocytes in the blood and more inflammatory cells predominantly macrophages in the lung parenchyma. It seems reasonable to assume that this higher abundance of inflammatory cells would contribute to a more pronounced tissue destruction, especially since injection of hematopoietic growth factors was started 3 days prior to elastase instillation. The possibility that polymorphonuclear leukocytes (PMN) recruiting into the lung have the capability to damage alveolar septa was confirmed by investigations of Cavarra et al. on several mice strains [4]. They found a similar PMN influx in alveolar spaces and an increase in bronchoalveolar lavage total cell count as well as a decrease in lung elastin content combined with a development of significant emphysema after an intratracheal instillation of the neutrophil activator FMLP (Formyl-Methionyl-Leucyl-Phenylalanine) [4]. Some heart studies also showed lack of regeneration when CSF was applied after or during heart infarction [34, 36].

The apparent choice of timing for administration of GF may be supported by new findings showing that stem cells should be applied not earlier than 5 days after the heart infarction because there are beneficial colonization conditions when onset of repair occurs [24]. G-CSF/SCF therapy 5 days after myocardial infarction leading to improved cardiac function and increased number of blood vessels and cells of cardiomyogenic lineage [19] confirmed these assumptions. Furthermore, Yuhgetsu et al. found significantly better pulmonary function and smaller alveolar airspaces as well as increased numbers of proliferative Ki-67-positive cells in rabbits 4 weeks after application of both elastase and bone marrow cells, compared to animals that received porcine pancreatic elastase (200 U/kg) alone [41].

Progenitor cells have the potential to reduce lung injury as shown in an LPS lung injury mice model. Suppression of bone marrow progenitor cells by irradiation in LPS-induced emphysema and reconstitution of bone marrow with fetal liver cells from GFP mice led to an emigration of progenitor cells from bone marrow to the injured lung combined with a differentiation in endothelial and epithelial cells and reduction of lung emphysema [40]. However, detection of GFP-labeled stem cells in lung parenchyma by immunofluorescence may be overestimated by autofluorescence, dead cells, and contaminating blood cells [21].

Kotton et al. demonstrated that if those cells were excluded from analysis, no detectable reconstitution of lung alveolar epithelial cells by unfractionated bone marrow cells or purified hematopoietic stem cells was detectable in bleomycin-induced lung injury [21].

Thus, our results support the broad spectrum of publications showing very different results concerning the possibility to repair structural damage with stem cell factors or stem cells.

However, the hematopoietic GF might have a therapeutic potential in emphysema. It is possible that an increased number of inflammatory cells and possibly, hematopoietic stem cells may have detrimental effects only in the initial phase of elastase-induced emphysema formation. Theoretically, administration of hematopoietic growth factors at a later time point may be capable of supporting regenerative processes. Further studies have to address this question.

Finally, our results support the concept that inflammatory cells contribute to emphysema formation because hematopoietic stem cell activation prior to emphysema induction caused harm. Furthermore, the present findings highlight the adverse potential of a therapeutic strategy and warn us to be cautious when further exploring regenerative strategies using hematopoietic stem cells as potential new tools for the treatment of emphysema.

Acknowledgements The authors wish to thank Amgen, (Thousand Oaks, CA, USA) for providing the hematopoietic growth factors for this study, M. Hanke, B. Philippens, R. Korolewitz and V. Rehse for technical assistance.

Conflict of interest statement We declare that we have no conflict of interest.

References

1. Barnes PJ, Kleinert S (2004) COPD—a neglected disease. Lancet 364:564–565
2. Bodine DM, Seidel NE, Gale MS, Nienhuis AW, Orlic D (1994) Efficient retrovirus transduction of mouse pluripotent hematopoietic stem cells mobilized into the peripheral blood by treatment with granulocyte colony-stimulating factor and stem cell factor. Blood 84:1482–1491
3. Braendgaard H, Gundersen HJ (1986) The impact of recent stereological advances on quantitative studies of the nervous system. J Neurosci Methods 18:39–78
4. Cavarra E, Martorana PA, Gambelli F, de Santi M, van Even P, Lungarella G (1996) Neutrophil recruitment into the lungs is associated with increased lung elastase burden, decreased lung elastin, and emphysema in alpha 1 proteinase inhibitor-deficient mice. Lab Invest 75:273–280
5. Chen XJ, Hedlund LW, Moller HE, Chawla MS, Maronpot RR, Johnson GA (2000) Detection of emphysema in rat lungs by using magnetic resonance measurements of 3He diffusion. Proc Natl Acad Sci U S A 97:11478–11481
6. Churg A, Wright JL (2005) Proteases and emphysema. Curr Opin Pulm Med 11(2):153–159
7. Cote CG, Celli BR (2005) New treatment strategies for COPD. Pairing the new with the tried and true.. Postgrad Med 117:27–34
8. Denburg JA, van Eeden SF (2006) Bone marrow progenitors in inflammation and repair: new vistas in respiratory biology and pathophysiology. Eur Respir J 27:441–445
9. Duarte RF, Frank DA (2000) SCF and G-CSF lead to the synergistic induction of proliferation and gene expression through complementary signaling pathways. Blood 96:3422–3430
10. Duarte RF, Frank DA (2002) The synergy between stem cell factor (SCF) and granulocyte colony-stimulating factor (G-CSF): molecular basis and clinical relevance. Leuk Lymphoma 43:1179–1187
11. Fehrenbach A, Ochs M, Wittwer T, Cornelius J, Fehrenbach H, Wahlers T, Richter J (1999) Stereological estimation of the volume weighted mean volumes of alveoli and acinar pathways in the rat lung to characterise alterations after ischaemia/reperfusion. J Anat 194(Pt 1):127–135
12. Glaab T, Hoymann HG, Hohlfeld JM, Korolewitz R, Hecht M, Alarie Y, Tschernig T, Braun A, Krug N, Fabel H (2002) Noninvasive measurement of midexpiratory flow indicates bronchoconstriction in allergic rats. J Appl Physiol 93:1208–1214
13. Gundersen HJ, Jensen EB (1985) Stereological estimation of the volume-weighted mean volume of arbitrary particles observed on random sections. J Microsc 138(Pt 2):127–142
14. Hohlfeld J, Hoymann HG, Molthan J, Fabel H, Heinrich U (1997) Aerosolized surfactant inhibits acetylcholine-induced airway obstruction in rats. Eur Respir J 10:2198–2203
15. Hohlfeld JM, Hoymann HG, Tschernig T, Fehrenbach A, Krug N, Fehrenbach H (2004) Keratinocyte growth factor transiently alters pulmonary function in rats. J Appl Physiol 96:704–710
16. Howard CVRM (1998) Unbiased stereology. BIOS Scientific, Oxford
17. Hoymann HG (2007) Invasive and noninvasive lung function measurements in rodents. J Pharmacol Toxicol Methods 55:16–26
18. Ishizawa K, Kubo H, Yamada M, Kobayashi S, Numasaki M, Ueda S, Suzuki T, Sasaki H (2004) Bone marrow-derived cells contribute to lung regeneration after elastase-induced pulmonary emphysema. FEBS Lett 556:249–252
18. Kanellakis P, Slater NJ, Du XJ, Bobik A, Curtis DJ (2006) Granulocyte colony-stimulating factor and stem cell factor improve endogenous repair after myocardial infarction. Cardiovasc Res 70(1):117–125
20. Karlinsky J, Fredette J, Davidovits G, Catanese A, Snider R, Faris B, Snider GL, Franzblau C (1983) The balance of lung connective tissue elements in elastase-induced emphysema. J Lab Clin Med 102:151–162
21. Kotton DN, Fabian AJ, Mulligan RC (2005) Failure of bone marrow to reconstitute lung epithelium. Am J Respir Cell Mol Biol 33:328–334
22. Krause DS (2002) Plasticity of marrow-derived stem cells. Gene Ther 9:754–758
23. Lee MS, Lill M, Makkar RR (2004) Stem cell transplantation in myocardial infarction. Rev Cardiovasc Med 5:82–98
24. Lenzen-Schulte M (2006) Cells for ailing hearts. Medical solutions 6:1–10
25. Massaro GD, Massaro D (1997) Retinoic acid treatment abrogates elastase-induced pulmonary emphysema in rats. Nat Med 3:675–677
26. Massaro GD, Massaro D (2000) Retinoic acid treatment partially rescues failed septation in rats and in mice. Am J Physiol Lung Cell Mol Physiol 278:L955–960
27. Nolte T, Kaufmann W, Schorsch F, Soames T, Weber E (2005) Standardized assessment of cell proliferation: the approach of the RITA-CEPA working group. Exp Toxicol Pathol 57:91–103

28. Orlic D, Kajstura J, Chimenti S, Jakoniuk I, Anderson SM, Li B, Pickel J, McKay R, Nadal-Ginard B, Bodine DM, Leri A, Anversa P (2001) Bone marrow cells regenerate infarcted myocardium. Nature 410:701–705
29. Orlic D, Kajstura J, Chimenti S, Limana F, Jakoniuk I, Quaini F, Nadal-Ginard B, Bodine DM, Leri A, Anversa P (2001) Mobilized bone marrow cells repair the infarcted heart, improving function and survival. Proc Natl Acad Sci U S A 98:10344–10349
30. Orlic D (2003) Adult bone marrow stem cells regenerate myocardium in ischemic heart disease. Ann N Y Acad Sci 996:152–157
31. Rubio ML, Sanchez-Cifuentes MV, Peces-Barba G, Verbanck S, Paiva M, Gonzalez Mangado N (1998) Intrapulmonary gas mixing in panacinar- and centriacinar-induced emphysema in rats. Am J Respir Crit Care Med 157:237–245
32. Schmiedl A, Hoymann HG, Ochs M, Menke A, Fehrenbach A, Krug N, Tschernig T, Hohlfeld JM (2003) Increase of inactive intra-alveolar surfactant subtypes in lungs of asthmatic Brown Norway rats. Virchows Arch 442:56–65
33. Schmiedl A, Krug N, Hohlfeld JM (2004) Influence of plasma and inflammatory proteins on the ultrastructure of exogenous surfactant. J Electron Microsc (Tokyo) 53:407–416
34. Terrovitis J, Charitos C, Dolou P, Papalois A, Eleftheriou A, Tsolakis E, Charitos E, Mponios M, Karanastasis G, Koudoumas D, Agapitos E, Nanas JN (2004) No effect of stem cell mobilization with GM-CSF on infarct size and left ventricular function in experimental acute myocardial infarction. Basic Res Cardiol 99:241–246
35. Valenca SS, da Hora K, Castro P, Moraes VG, Carvalho L, Porto L (2004) Emphysema and metalloelastase expression in mouse lung induced by cigarette smoke. Toxicol Pathol 32 (3):351–356
36. Valgimigli M, Rigolin GM, Cittanti C, Malagutti P, Curello S, Percoco G, Bugli AM, Della Porta M, Bragotti LZ, Ansani L, Mauro E, Lanfranchi A, Giganti M, Feggi L, Castoldi G, Ferrari R (2005) Use of granulocyte-colony stimulating factor during acute myocardial infarction to enhance bone marrow stem cell mobilization in humans: clinical and angiographic safety profile. Eur Heart J 26:1838–1845
37. Weibel ER (1979) Stereological methods. Practical methods for biologiical morphometry, vol. 1. Academic, New York
38. Westermann J, Persin S, Matyas J, van der Meide P, Pabst R (1993) IFN-gamma influences the migration of thoracic duct B and T lymphocyte subsets in vivo. Random increase in disappearance from the blood and differential decrease in reappearance in the lymph. J Immunol 150:3843–3852
39. Wollert KC, Meyer GP, Lotz J, Ringes-Lichtenberg S, Lippolt P, Breidenbach C, Fichtner S, Korte T, Hornig B, Messinger D, Arseniev L, Hertenstein B, Ganser A, Drexler H (2004) Intracoronary autologous bone-marrow cell transfer after myocardial infarction: the BOOST randomised controlled clinical trial. Lancet 364:141–148
40. Yamada M, Kubo H, Kobayashi S, Ishizawa K, Numasaki M, Ueda S, Suzuki T, Sasaki H (2004) Bone marrow-derived progenitor cells are important for lung repair after lipopolysaccharide-induced lung injury. J Immunol 172:1266–1272
41. Yuhgetsu H, Ohno Y, Funaguchi N, Asai T, Sawada M, Takemura G, Minatoguchi S, Fujiwara H, Fujiwara T (2006) Beneficial effects of autologous bone marrow mononuclear cell transplantation against elastase-induced emphysema in rabbits. Exp Lung Res 32:413–426
42. Zheng T, Zhou Z, Zhongde W, Homer RJ, Ma B, Riese RJ, Chapman HA, Shapiro SD, Elias JA (2000) Inducible targeting of IL-13 to the adult lung causes matrix metalloproteinase-and cathepsin-dependent emphysema.. J Clin Invest 106:1081–1093

Virchows Arch (2008) 452:689–696
DOI 10.1007/s00428-008-0580-2

CASE REPORT

Complex t(5;8) involving the *CSPG2* and *PTK2B* genes in a case of dermatofibrosarcoma protuberans without the *COL1A1-PDGFB* fusion

Laurence Bianchini · Georges Maire · Bernard Guillot · Jean-Marie Joujoux · Philippe Follana · Marie-Pierre Simon · Jean-Michel Coindre · Florence Pedeutour

Received: 13 November 2007 / Accepted: 11 January 2008 / Published online: 6 February 2008
© Springer-Verlag 2008

Abstract Dermatofibrosarcoma protuberans (DFSP) is a rare, dermal neoplasm of intermediate malignancy. It is made of spindle-shaped tumor cells in a storiform pattern positive for CD34. Cytogenetically, DFSP cells are characterized by either supernumerary ring chromosomes composed of sequences derived from chromosomes 17 and 22 or more rarely of translocations t(17;22). These chromosomal rearrangements lead to the formation of a specific chimeric gene fusing *COL1A1* to *PDGFB*. So far, the *COL1A1-PDGFB* fusion gene remains the sole fusion gene identified in DFSP. However, some observations suggest that genes, other than *COL1A1* and *PDGFB*, might be involved in some DFSP cases. We report in this paper a DFSP case presenting as a unique chromosomal abnormality a complex translocation between chromosomes 5 and 8. This is the first report of a DFSP case where the lack of chromosomes 17 and 22 rearrangement and the absence of *COL1A1-PDGFB* fusion gene have been demonstrated. Using fluorescence in situ hybridization analysis, we showed that the *CSPG2* gene at 5q14.3 and the *PTK2B* gene at 8p21.2 were disrupted by this rearrangement. Although rare, the existence of cases of DFSP negative for the *COL1A1-PDGFB* fusion has to be taken in consideration when performing molecular diagnosis for a tumor suspected to be a DFSP.

Keywords Dermatofibrosarcoma protuberans · Translocation t(5;8) · *CSPG2* · *PTK2B* · Cytogenetics) · FISH

L. Bianchini · G. Maire · P. Follana · F. Pedeutour
Laboratoire de Génétique des Tumeurs Solides,
Faculté de Médecine, Centre Hospitalier Universitaire de Nice,
Université de Nice-Sophia Antipolis,
Nice, France

L. Bianchini · G. Maire · P. Follana · M.-P. Simon · F. Pedeutour (✉)
CNRS UMR 6543, Centre-Antoine-Lacassagne,
Nice, France
e-mail: florence.pedeutour@unice.fr

B. Guillot
Département de Dermatologie, Hôpital Saint-Eloi,
Centre Hospitalier Universitaire de Montpellier,
Montpellier, France

J.-M. Joujoux
Département de Pathologie,
Centre Hospitalier Universitaire de Nîmes,
Nîmes, France

J.-M. Coindre
Département de Pathologie, Institut Bergonié,
Bordeaux, France

Present address:
G. Maire
Princess Margaret Hospital, Ontario Cancer Institute,
Toronto, ON, Canada

Introduction

Dermatofibrosarcoma protuberans (DFSP) is a rare, slow-growing dermal neoplasm of intermediate malignancy. The classic histologic form shows a storiform or cartwheel cellular pattern with a strong immunopositivity for CD34 [1, 12]. DFSP cells most often contain supernumerary ring chromosomes composed of sequences derived from chromosomes 17 and 22. Balanced or unbalanced t(17;22) translocations are also observed, especially in pediatric

cases [34]. These chromosomal rearrangements lead to the formation of a chimeric gene resulting from the fusion of *COL1A1* (17q21) with *PDGFB* (22q13) [32].

So far, the *COL1A1-PDFGB* fusion gene remains the only fusion gene identified in DFSP and variant tumors such as giant cell fibroblastomas and Bednar tumors, and its detection is a useful tool for diagnosis. To date, among more than 50 DFSP karyotypes that have been published, only 4 cases showed chromosomal anomalies other than ring chromosomes or t(17;22) [20, 34]. These four variant karyotypes included a t(X;7)(q21.2;q11.2) in a pediatric case [7], a t(9;22)(q32;q12.2) [35], a t(2;17)(q33;q25) [33], and a complex unbalanced translocation involving chromosomes 3, 5, 7, and 22 [27]. These observations suggest that genes other than *COL1A1* or *PDGFB* might indeed be involved in a small subset of DFSP cases.

We report in this paper a case presenting a translocation between chromosomes 5 and 8 with no rearrangement of either chromosome 17 or chromosome 22 as a unique karyotypic abnormality. This is the first report of a DFSP case with an abnormal karyotype where the absence of *COL1A1-PDGFB* rearrangement has been demonstrated.

Clinical history

A 66-year-old man presented with a brownish plaque and nodule of 2 cm diameter located on the right thigh developing for the past 5 years. His medical history was unremarkable except for a prostate adenoma resected 1 year before. A biopsy was performed. Histologically, the tumor was composed of spindle fibroblast-like cells arranged in fascicles and a few histiocytic cells without any mitosis. On the basis of the histologic examination, the tumor was diagnosed as a benign histiocytofibroma. The CD34-immunoreactivity was not tested on this first biopsy because CD34 antibody was not commercially available at that time. The tumor was surgically removed and recurred as a nodule of 2.5×3 cm in size 10 years later. The biopsy examination of the recurrent tumor showed that it was made of spindle-shaped cells organized in a storiform pattern characteristic of DFSP (Fig. 1a). The cells were positive for CD34 (Fig. 1b) and negative for S100 protein and alpha smooth muscle actin. Based on the histologic findings and the CD34-immunoreactivity, the tumor was diagnosed as a DFSP. The diagnosis of DFSP was confirmed by a pathologist expert in soft tissue tumors (JMC). The initial biopsy of the primary tumor was also re-examined and diagnosed as a DFSP as well. The patient underwent a complete surgical resection of the tumor with surgical margins of 4.5×3.5 cm followed by reparative skin graft. After a 10-year follow-up, the patient remained free of disease.

Materials and methods

Cytogenetic and fluorescence in situ hybridization analysis

After surgical resection of the recurrent tumor, a fresh fragment was prepared for cytogenetic analysis according to established procedures [17]. All probes used for the study are described in Table 1. Commercially available probes were used according to the manufacturer's recommendations. Yeast artificial chromosomes (YAC) were from the Centre d'Etudes du Polymorphisme Humain (CEPH, Fondation Jean Dausset, Paris, France) and selected using the GDB Human Genome Database (http://www.gdb.org). Bacterial artificial chromosomes clones (BAC) from the Roswell Park Cancer Institute library were selected according to their location in the University of California Santa Cruz genome browser (http://genome.ucsc.edu/) and obtained from the Children's Hospital Oakland Research Institute (CHORI; http://bacpac.chori.org/). YAC and BAC probes were prepared for fluorescence in situ hybridization (FISH) analysis according to standard procedures [19]. Microscopic analysis was performed using an Axioplan II imaging microscope (Carl Zeiss, Jena, Germany). FISH images were processed using the ISIS software (Metasystems, Altlussheim, Germany).

RNA isolation and RT-PCR analysis

Total RNAs were extracted from paraffin-embedded tumor tissue samples [37] and from short-term cultured cells using the Trizol method according to the manufacturer's recommendations (Invitrogen, Carlsbad, CA). Detection of the *COL1A1-PDGFB* fusion gene was performed on RNA by multiplex reverse transcriptase polymerase chain reaction (RT-PCR) as described in Maire et al. [20] and Terrier-Lacombe et al. [37].

Results

Rearrangement of chromosomes 5 and 8

Eight RHG-banded metaphases were analyzed. The karyotype showed a rearrangement involving the chromosome 5 long arm at 5q13–14 and the chromosome 8 short arm at 8p21 (Fig. 1c). The der(5) was identified by RHG-banding and FISH analysis using whole chromosome painting (WCP) probes for chromosomes 5 and 8 as resulting from a t(5;8)(q13–14;p21). An additional deletion or inversion of the translocated 5q fragment was suspected on the der(8). Trisomy 8 was observed in approximately 10% of tumor cell metaphases.

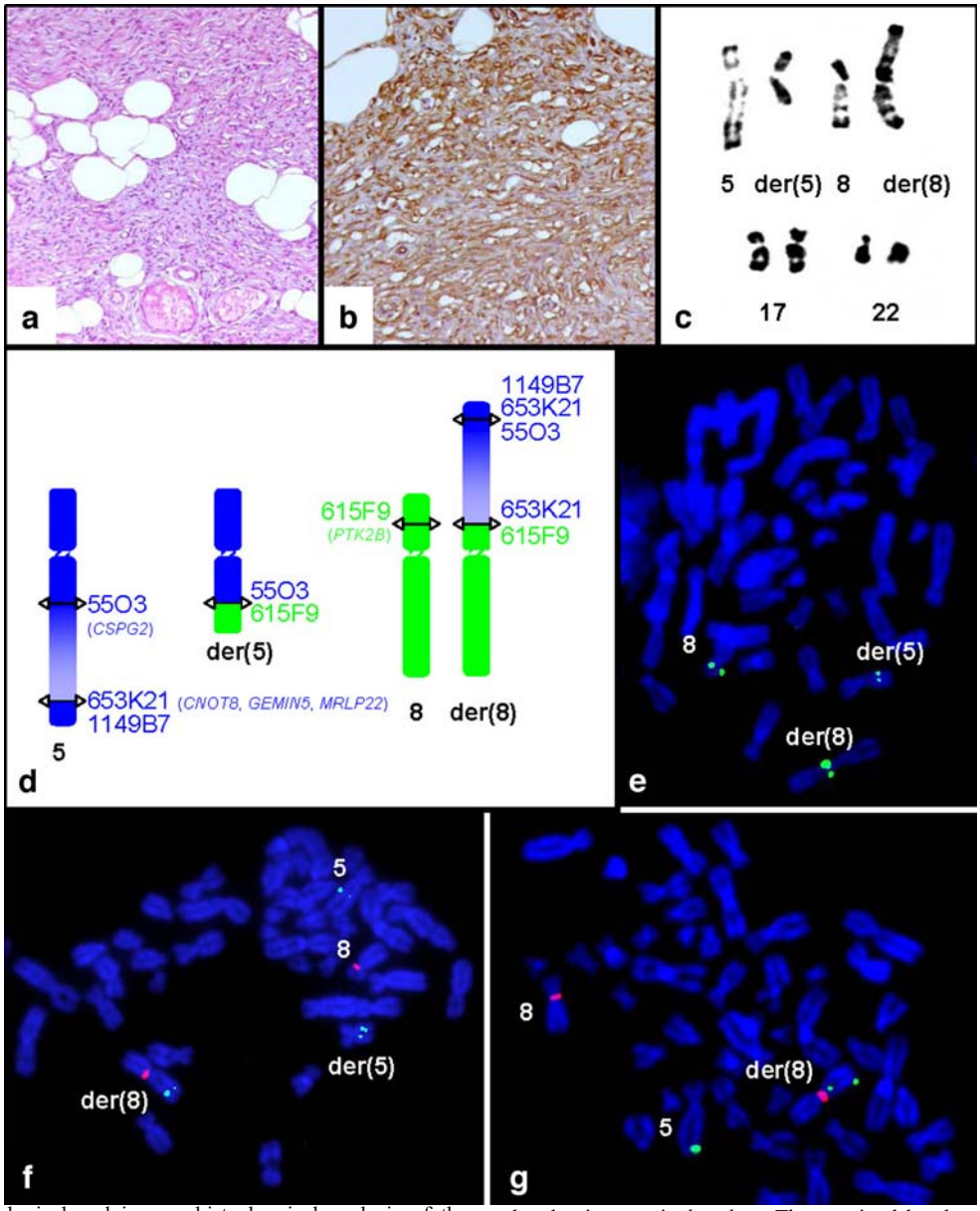


Fig. 1 **a**, **b** Histological and immunohistochemical analysis of the tumor (×100 magnification). **a** Hematoxylin–eosin staining is showing spindle-shaped cells organized in a storiform pattern characteristic of dermatofibrosarcoma protuberans. **b** Tumor cells strongly express the CD34, as shown by the immunohistochemical staining. **c**–**g** Molecular cytogenetic analysis. **c** Partial RGH-banded karyotype showing abnormal chromosomes 5 and 8—der(5) and der(8)—resulting from a translocation t(5;8) and a paracentric inversion of 5q on the der(8). The chromosomes 17 and 22 are apparently normal. According to the International System for Human Cytogenetic Nomenclature [30], the karyotype was 46,XY,der(5)t(5;8)(q14;p21),der(8)t(5;8)inv(5)(q14q33)/47,idem, +8/47,XY,+8. **d**–**g** Fluorescence in situ hybridization (*FISH*) on tumor cell metaphases. **d** Schematic representation of the breakpoints (*double arrows*) within chromosomes 5 (*blue*) and 8 (*green*). The der(5) resulted from a translocation with chromosome 8, while the der(8) resulted from the t(5;8) and from a paracentric inversion of a 71-Mb fragment comprised between 5q14.2 and 5q33.2. The orientation of the 5q14.2–q33.2 is identified by a gradient of *blue*: *dark* on the 5q14.2 extremity and *light* on the 5q33.2 extremity. All BAC probes presented are from the RP11 library. Genes present in breakpoints are in *brackets*. The proximal breakpoint of the 5q14.2–q33.2 inverted fragment was identified by a split of the RP11-5503 probe containing CSPG2. The distal breakpoint was identified by a split of the BAC clone RP11-653K21 containing *CNOT8*, *GEMIN5*, and *MRPL22*. **e** Signals of the BAC probe RP11-615F9 (*green*), containing the *PTK2B* gene (8p21.2) are observed on both der(5) and der(8) indicating that the 8p21 breakpoint is located in *PTK2B*. **f** Co-hybridization of centromeric probe for chromosome 8 (*red*) and BAC clone RP11-55O3 (*green*) containing the *CSPG2* gene (5q14.2) showed green signals on both der(5) and der(8) indicating that the 5q14.2 breakpoint was located in *CSPG2*. In addition, the presence of the green signal on the der(8) on the distal position close to the telomere confirmed the inversion of the 5q14.2–q33.2 fragment on the der(8). **g** Co-hybridization of the centromeric probe for chromosome 8 (*red*) and the BAC clone RP11-653K21 (containing *CNOT8*, *GEMIN5*, and *MRPL22*) showed two green signals on the short arm of the der(8), indicating that the distal breakpoint of the inverted 5q14.2–q33.2 fragment was located on the der(8) close to the centromere

Table 1 Description and origin of the FISH probes used for the characterization of the complex t(5;8) in a case of dermatofibrosarcoma protuberans without *COL1A1-PDGFB* fusion

Result: chromosomal localization	Probe name	Type	Chromosomal location/accession number/ gene of interest		Origin/reference(s)
Whole chromosome painting probes					
Normal	WCP17		Chromosome 17		Euro-Diagnostica
Normal	WCP22		Chromosome 22		Euro-Diagnostica
der(5)/der(8)	WCP5		Chromosome 5		Euro-Diagnostica
der(5)/der(8)	WCP8		Chromosome 8		Q-Biogene
Gene- and locus-specific probes					
Chromosome 22					
Normal	RP11-1149b8	BAC	22q13.1	58 kb centromeric to *PDGFB*	RPCI
Normal	RP11-434E5	BAC	22q13.1	79 kb telomeric to *PDGFB*	RPCI
Normal	RP11-101B10	BAC	22q13.1		RPCI
Chromosome 8					
der(5)	965_d_3	YAC	8p22	*PDGFRL*	CEPH
der(5)	RP11-203E8	BAC	8p21.2		RMC
der(5)	767_g_4	YAC	8p21.2	*NEFL*	CEPH
der(5)	RP11-199N14	BAC	8p21.2		RPCI
der(5)	CTD-3000I12	BAC	8p21.2		Invitrogen
der(5)/der(8)*	RP11-615F9	BAC	8p21.2	*PTK2B*	RPCI
der(8)*	RP11-138J2	BAC	8p21.2	*PTK2B*	RPCI
der(8)*	SCB-212E3	BAC	8p21.1	AF311103/*PTK2B*	LIAR-FLI
der(8)*	RP11-360M9	BAC	8p21.1	AC011132	RMC
der(8)*	778_b_12	YAC	8p21.1		CEPH
der(8)*	901_e_10	YAC	8p12		CEPH
der(8)*	815_e_8	YAC	8p12		CEPH
der(8)*	978_b_9	YAC	8p12	*HGL*	CEPH
der(8)*	953_h_12	YAC	8p12	*FGFR1*, *WRN*	CEPH
der(8)*	959_a_4	YAC	8p11.23	*FGFR1*	CEPH
Chromosome 5					
der(5)	RP11-195E2	BAC	5q13.2		RPCI
der(5)	RP11-172K14	BAC	5q13.3		RPCI
der(5)	RP11-1H14	BAC	5q14.1		RPCI
der(5)	RP11-1E10	BAC	5q14.1		RPCI
der(5)	RP11-47N20	BAC	5q14.2		RPCI
der(5)/der(8)**	CTD-3143O9	BAC	5q14.2–14.3	*CSPG2* (exons 1 to 12)	Invitrogen
der(5)/der(8)**	RP11-275E14	BAC	5q14.2	*CSPG2* (all exons)	RPCI
der(5)/der(8)**	RP11-55O3	BAC	5q14.2	*CSPG2* (exons 6 to 15)	RPCI
der(8)**	RP11-95A21	BAC	5q14.3		RPCI
der(8)*	RP11-136E22	BAC	5q33.1	*PERC, PDEGA*	RPCI
der(8)*	RP11-21I20	BAC	5q33.1	*PDGFRB*	RPCI
der(8)*	RP11-754J8	BAC	5q33.1	*PDGFRB*	RPCI
der(8)*	RP11-368O19	BAC	5q33.1	*PDGFRB*	RMC
der(8)*	RP11-759G10	BAC	5q33.1		RPCI
der(8)*	RP11-802B10	BAC	5q33.1–q32		RPCI
der(8)*	RP11-802B10	BAC	5p33.1		RPCI
der(8)*	RP11-59F21	BAC	5q33.1		RPCI
der(8)*	RP11-963P19	BAC	5q33.1		RPCI
der(8)*	RP11-109B15	BAC	5q33.1		RPCI
der(8)*	RP11-91G17	BAC	5q33.2		RPCI
der(8)*	RP11-282L23	BAC	5q33.2		RPCI
der(8)*	CTD-2332P4	BAC	5q33.2	*CNOT8*	Invitrogen
der(8)*/der(8)**	CTD-2527O23	BAC	5q33.2	*CNOT8*, *GEMIN5*, *MRPL22*	Invitrogen
der(8)*/der(8)**	RP11-452J22	BAC	5q33.2	*CNOT8*, *GEMIN5*, *MRPL22*	RPCI
der(8)*/der(8)**	RP11-653K21	BAC	5q33.2	*CNOT8*, *GEMIN5*, *MRPL22*	RPCI
der(8)**	RP11-1149B7	BAC	5q33.2		RPCI

Table 1 (continued)

Result: chromosomal localization	Probe name	Type	Chromosomal location/accession number/ gene of interest	Origin/reference(s)
der(8)**	RP11-1082K13	BAC	5q33.2	RPCI
der(8)**	RP11-31B18	BAC	5q33.2–q33.3	RPCI
der(8)**	RP11-117L6	BAC	5q35.1	RPCI

All BACs probes were chosen according to their localization on the University of California Santa Cruz genome browser version March 2006 (http://www.genome.ucsc.edu); YAC probes were chosen according to their localization on the GDB Human Genome Database (http://www.gdb.org).

BAC Bacterial artificial chromosome; *YAC* yeast artificial chromosome; *WCP* whole chromosome painting probe; *RPCI* Roswell Park Cancer Institute; *CEPH* Centre d'étude du polymorphisme Humain (http://www.cephb.fr); *RMC* Resources for Molecular Biology (University of Bari, Bari, Italy; http://www.biologia.uniba.it/rmc); *LIAR-FLI* Leibniz Institute for Age Research-Fritz Lipmann Institute (Jena, Germany: http://genome.imb-jena.de/); *der(8)** the signal is observed on the p arm of the der(8), close to the centromere; *der(8)*** the signal is observed on the p arm of the der(8), close to the telomere; Invitrogen, Carlbad, CA; Euro-Diagnostica, Arnhem, The Netherlands

Absence of chromosomes 17 and 22 rearrangement and *COL1A1-PDGFB* fusion

The karyotype analysis (Fig. 1c) and FISH experiments with WCP probes for chromosomes 17 and 22 showed no evidence for rearrangements of chromosomes 17 and 22 (Table 1). In addition, FISH with *PDGFB* "break-apart" probes RP11-1149B8 (3′), RP11-434E5 (5′), and RP11-101B10 (5′) showed no rearrangement and no extra signal in addition of the signals on the two normal chromosomes 22 (Table 1). The RT-PCR analysis was negative for the *COL1A1-PDGFB* fusion gene detection.

Mapping of the 8p breakpoint

A collection of 15 probes located between 8p11.23 and 8p22 were hybridized on tumor cell metaphases (Table 1). The breakpoint was identified at 8p21.2, between the probes CTD-3000I12 (distal side), and RP11-138J2 (proximal side) within a 870-kb interval. The hybridization of the probe RP11-615F9 spanning this interval exhibited signals on both der(5) and der(8) (Fig. 1d,e). According to the detailed map of this region (USCS Genome Browser; chr8:27,364,183–27,365,993; Mar. 2006), the breakpoint was located within the intron 2 of the *PTK2B* (*protein tyrosine kinase B*) gene.

Detailed characterization of the chromosome 5 rearrangements

The characterization of the 5q rearrangement was performed using a collection of 30 BAC probes located within the 5q13.2–q35.1 region (Table 1). Probes comprised between RP11-195E2 (5q13.2) and RP11-47N20 (5q14.2) were observed on the der(5), while the probes located between RP11-95A21 (5q14.3) and CTD-2332P4 (5q33.2) were detected on the der(8). As suggested by the conventional cytogenetic analysis, the position of the 5q probes on the der(8) showed the presence of a paracentric inversion of the 5q14.2–q33.2 fragment in addition to the t(5;8). Indeed, probes from the 5q14.3 region and probes of the 5q33-qter region located distally to RP11-1149B7 were positioned close to the telomere of the der(8) short arm, while the probes from the 5q33.2 region located proximally to CTD-2332P4 were positioned on the short arm of the der (8) close to the centromere. These results indicated that the 5q paracentric inversion was generated by the occurrence of two breakpoints, one at 5q14.2 and one at 5q33.2, respectively. Probes RP11-275E14 and RP11-55O3 located at 5q14.2 (Table 1) exhibited two fluorescent signals, one on the der(5) and one on the der(8), respectively (Fig. 1f). Probe CTD-3143O9 exhibited a bright signal on the der(5) and a very faint signal on the der(8). The signals on the der (8) were observed close to the telomere of the der(8) short arm. Analysis of the detailed map of this region (UCSC genome browser version Mar. 2006; chr5:82,736,091–82,981,443) identified the breakpoint within the *CSPG2* gene (*Chondroitin Sulphate Proteoglycan 2* or *Versican*) between exons 9 and 12 (Table 1 and Fig. 1f). The distal breakpoint on chromosome 5 was located within the 5q33.2 cytoband. Each of the probes CTD-2527O23, RP11-452J22 and RP11-653K21 showed two signals on the short arm of the der(8): one close to the telomere, the other close to the centromere (Table 1 and Fig. 1g). The analysis of the genomic interval delineated by these three probes on the USCC map (chr5:154,193,027–154,416,284; version Mar. 2006) indicated that the area of the breakpoint contained three genes: *GEMIN5* (*GEM-Associated Protein 5*), *MRPL22* (*Mitochondrial Ribosomal Protein L22*), and *CNOT8* (*CCR4-NOT transcription complex, subunit 8*).

Discussion

Abnormal fusion genes resulting from simple chromosomal translocations are frequent in leukemias and sarcomas and have recently been identified also in carcinomas [23]. Over

the last decades, the progressive discoveries of fusion genes have been crucial for establishing novel tumor classifications. Moreover, the detection of specific fusion genes by FISH or RT-PCR is now used routinely for diagnosing tumors or after residual diseases. When fusion genes are identified in a type or subtype of sarcoma, it is usual that most cases exhibit a "major" type of fusion gene, while a small subset of cases presents "variant" fusion genes. These "variant" fusion genes are usually made of the fusion of one of the gene involved in the "major" type with another partner gene. For instance, the predominant fusion gene in peripheral neuroectodermic tumors (PNET) is *EWS-FLI1*, present in 90–95% of cases. Genes of the ETS family other than *FLI1*, such as *ERG*, *FEV*, *ETV1*, or *ETV4* are also found to be fused with *EWS* in PNET [28]. In some other types of tumors, two major types of fusion are observed: for instance, in pleomorphic adenoma of the salivary gland, fusion genes involving either *PLAG1* at 8q12 (*CTNNB1-PLAG1*, *LIFR-PLAG1*, and *TCEA1-PLAG1*) [3, 14, 39] or *HMGA2* at 12q15 (*HMGA2-NFIB*, *HMGA2-FHIT*, and *HMGA2-WIF1*) [10, 11, 25] are detected.

Only one type of fusion gene — the *COL1A1-PDGFB* fusion — had been identified in DFSP so far [4, 34]. We have described in this paper the first DFSP case with a "variant" molecular rearrangement. This DFSP case had no clinical or histological particularity and was characterized by a complex rearrangement of chromosomes 5 and 8 involving three breakpoints located at 8p21, 5q14, and 5q33, respectively. Strikingly, the *PDGFRB* gene that encodes the receptor of PDGFB is located at 5q33. It has been shown that the chimeric COL1A1-PDGFB protein is able to undergo cleavage and acts as a ligand for PDGFR, therefore, leading to activation of the PDGFR signaling pathway [31]. This abnormal stimulation of PDGFR is inactivated by the tyrosine kinase inhibitor imatinib mesylate and allows an efficient pharmacological treatment for metastatic or non-operable DFSP [22]. Moreover, *PDGFRB* is a gene that is prone to the formation of fusion genes resulting from chromosomal translocations. Indeed, chimeric genes generated by the fusion of *PDGFRB* with *PDE4DIP*, *HIP1*, *H4*, or *ETV6* have been reported in myeloproliferative disorders and leukemias [16]. The *PDGFRB* gene was therefore a likely candidate for being involved in the 5q33 breakpoint of the present DFSP case. However, we showed that the breakpoint at 5q33.2 was located in the region of the *CNOT8*, *MRPL22*, and *GEMIN 5* genes. *PDGFRB* was located on the short arm of the der (8) at distances of 63 Mb from the proximal breakpoint and 153 Mb from the distal breakpoint, respectively (Table 1). These large distances excluded *PDGFRB* from being directly or indirectly involved in this rearrangement. We identified that the breakages in 5q14 and 8p21.2 were located in the *CSPG2* and *PTK2B* genes, respectively. We mapped the 8p breakpoint within the intron 2 of *PTK2B* (also called *PYK2*) and the 5q14 breakpoint between the exons 9 and 12 of *CSPG2*. The genomic rearrangement generated by the t(5;8) and the paracentric 5q inversion may potentially lead to the formation of three fusion genes: *CSPG2-PTK2B* on the der(5), *PTK2B-CNOT8* (or *PTK2B-MRPL22* or *PTK2B-GEMIN5*) on the proximal side of the der(8) short arm, and *CNOT8-CSPG2* or (*MRPL22-CSPG2* or *GEMIN5-CSPG2*) on the distal side of the der(8) short arm. However, because of their 5′–3′ orientation, some of these putative fusion genes might not be functional. The sole genomic configurations compatible with the production of in frame fusion transcripts are *MRPL22-PTK2B*, *CNOT8-PTK2B*, or *GEMIN5-CSPG2*. PTK2B is a cytoplasmic tyrosine kinase structurally related to the focal adhesion kinase [29]. The activation of PTK2B leads to the activation of the MAP kinase pathway via interaction with a Src kinase protein [15]. The breakage of *PTK2B* in intron 2 is able to preserve the tyrosine kinase domain integrity. Therefore, the functional consequences of the PTK2B activation could be similar to the PDGFRB activation observed in "classical" DFSP by stimulating the MAP kinase pathway. The overexpression of *PTK2B* has been reported in hepatocellular carcinomas as a marker of poor prognosis; in glioma, *PTK2B* promotes cellular migration and invasion [18, 36]. We described in this paper the first case of genomic involvement of *PTK2B* in a chromosomal rearrangement. In the hypothesis of a *MRPL22-PTK2B* fusion, *MRPL22*, which encodes a ribosomal protein part of the 39S subunit, could be able to drive an abnormal expression of *PTK2B* by its "housekeeping" promoter [9]. *CNOT8* encodes the 8 subunit of the *CCR4-NOT* complex, which acts as an ubiquitous transcription regulator [2]. *CNOT8* is a relevant candidate to form a fusion gene with *PTK2B*, as one or both of the genes involved in chromosomal translocations often encode transcription factors. *CSPG2* codes for a large chondroitin sulfate proteoglycan found in the extracellular matrix; it modulates cell adhesion, migration, proliferation, and differentiation [40]. High levels of CSPG2 have been detected in a variety of malignant solid tumors, such as pancreatic carcinomas, breast carcinomas, prostate carcinomas, brain tumors, melanomas, and malignant fibrous histiocytomas [5, 13, 21, 24, 26, 38]. *GEMIN5* encodes a WD-repeat scaffolding protein involved in ribonucleoprotein assembly [8]. The domains downstream exon 9 of *CSPG2* have been reported to enhance cell proliferation via the EGF-like motifs in a model of NIH3T3 fibroblasts and in a sarcoma cell line [6, 41]. As these motifs are potentially preserved in the 3′ end of the *GEMIN5-CSPG2* fusion gene, *GEMIN5* promoter could act as an activator for the transcription of *CSPG2*.

In conclusion, we have described in this paper the first case of DFSP without a molecular rearrangement of

COL1A1 and *PDGFB*. We have identified a novel rearrangement of chromosomes 5 and 8 involving the *CSPG2* and *PTK2B* genes. Three other genes located at 5q33, *CNOT8*, *MRPL22*, and *GEMIN5*, might also be involved in this rearrangement. The identification of variant fusion genes in DFSP is of importance for improving the molecular diagnoses of this tumor. Indeed, while the positive detection of the *COL1A1-PDGFB* fusion gene in a tumor sample ascertains the diagnosis of DFSP, a negative result has to be carefully interpreted. This negative result indicates in most cases that the tumor is not a DFSP. However, in a small number of cases, it could reflect the presence of a molecular variant, as in the case described in this paper. The characterization of these variant cases is mandatory to provide not only a more accurate diagnosis but also a better understanding of the molecular and biological mechanisms that are involved in the DFSP tumorigenesis.

Acknowledgments We thank M. Rocchi (University of Bari, Italy), M-J Pébusque, M. Chaffanet, and D. Birnbaum (Institut Paoli Calmettes, Marseille, France) for kindly providing some of the BAC and YAC clones used in this study. This work was supported by the Comité des Alpes-Maritimes de la Ligue Nationale contre le Cancer, the Association pour la Recherche sur le Cancer, the Institut National du Cancer, and the Fondation pour la Recherche Médicale (master grant to P. Follana). The experiments described in this study comply with the current laws of France.

Conflict of interest statement We declare that we have no conflict of interest.

References

1. Aiba S, Tabata N, Ishii H, Ootani H, Tagami H (1992) Dermatofibrosarcoma protuberans is a unique fibrohistiocytic tumour expressing CD34. Br J Dermatol 127:79–84
2. Albert TK, Lemaire M, van Berkum NL, Gentz R, Collart MA, Timmers HT (2000) Isolation and characterization of human orthologs of yeast CCR4-NOT complex subunits. Nucleic Acids Res 28:809–817
3. Asp J, Persson F, Kost-Alimova M, Stenman G (2006) CHCHD7-PLAG1 and TCEA1-PLAG1 gene fusions resulting from cryptic, intrachromosomal 8q rearrangements in pleomorphic salivary gland adenomas. Genes Chromosomes Cancer 45:820–828
4. Bianchini L, Maire G, Pedeutour F (2007) [From cytogenetics to cytogenomics of dermatofibrosarcoma protuberans family of tumors]. Bull Cancer 94:179–189
5. Brown LF, Guidi AJ, Schnitt SJ, Van De Water L, Iruela-Arispe ML, Yeo TK, Tognazzi K, Dvorak HF (1999) Vascular stroma formation in carcinoma in situ, invasive carcinoma, and metastatic carcinoma of the breast. Clin Cancer Res 5:1041–1056
6. Cattaruzza S, Schiappacassi M, Kimata K, Colombatti A, Perris R (2004) The globular domains of PG-M/versican modulate the proliferation-apoptosis equilibrium and invasive capabilities of tumor cells. FASEB J 18:779–781
7. Craver RD, Correa H, Kao Y, Van Brunt T (1995) Dermatofibrosarcoma protuberans with 46,XY,t(X;7) abnormality in a child. Cancer Genet Cytogenet 80:75–77
8. Fierro-Monti I, Mohammed S, Matthiesen R, Santoro R, Burns JS, Williams DJ, Proud CG, Kassem M, Jensen ON, Roepstorff P (2006) Quantitative proteomics identifies Gemin5, a scaffolding protein involved in ribonucleoprotein assembly, as a novel partner for eukaryotic initiation factor 4E. J Proteome Res 5:1367–1378
9. Gan X, Kitakawa M, Yoshino K, Oshiro N, Yonezawa K, Isono K (2002) Tag-mediated isolation of yeast mitochondrial ribosome and mass spectrometric identification of its new components. Eur J Biochem 269:5203–5214
10. Geurts JM, Schoenmakers EF, Roijer E, Astrom AK, Stenman G, van de Ven WJ (1998) Identification of NFIB as recurrent translocation partner gene of HMGIC in pleomorphic adenomas. Oncogene 16:865–872
11. Geurts JM, Schoenmakers EF, Roijer E, Stenman G, Van de Ven WJ (1997) Expression of reciprocal hybrid transcripts of HMGIC and FHIT in a pleomorphic adenoma of the parotid gland. Cancer Res 57:13–17
12. Gloster HM Jr (1996) Dermatofibrosarcoma protuberans. J Am Acad Dermatol 35:355–374 (quiz 375–356)
13. Isogai Z, Shinomura T, Yamakawa N, Takeuchi J, Tsuji T, Heinegard D, Kimata K (1996) 2B1 antigen characteristically expressed on extracellular matrices of human malignant tumors is a large chondroitin sulfate proteoglycan, PG-M/versican. Cancer Res 56:3902–3908
14. Kas K, Voz ML, Roijer E, Astrom AK, Meyen E, Stenman G, Van de Ven WJ (1997) Promoter swapping between the genes for a novel zinc finger protein and beta-catenin in pleiomorphic adenomas with t(3;8)(p21;q12) translocations. Nat Genet 15:170–174
15. Lev S, Moreno H, Martinez R, Canoll P, Peles E, Musacchio JM, Plowman GD, Rudy B, Schlessinger J (1995) Protein tyrosine kinase PYK2 involved in Ca(2+)-induced regulation of ion channel and MAP kinase functions. Nature 376:737–745
16. Lierman E, Cools J (2007) TV6 and PDGFRB: a license to fuse. Haematologica 92:145–147
17. Limon J, Dal Cin P, Sandberg AA (1986) Application of long-term collagenase disaggregation for the cytogenetic analysis of human solid tumors. Cancer Genet Cytogenet 23:305–313
18. Lipinski CA, Tran NL, Menashi E, Rohl C, Kloss J, Bay RC, Berens ME, Loftus JC (2005) The tyrosine kinase pyk2 promotes migration and invasion of glioma cells. Neoplasia 7:435–445
19. Maire G, Forus A, Foa C, Bjerkehagen B, Mainguene C, Kresse SH, Myklebost O, Pedeutour F (2003) 11q13 alterations in two cases of hibernoma: large heterozygous deletions and rearrangement breakpoints near GARP in 11q13.5. Genes Chromosomes Cancer 37:389–395
20. Maire G, Fraitag S, Galmiche L, Keslair F, Ebran N, Terrier-Lacombe MJ, de Prost Y, Pedeutour F (2007) A clinical, histologic, and molecular study of 9 cases of congenital dermatofibrosarcoma protuberans. Arch Dermatol 143:203–210
21. Mauri P, Scarpa A, Nascimbeni AC, Benazzi L, Parmagnani E, Mafficini A, Della Peruta M, Bassi C, Miyazaki K, Sorio C (2005) Identification of proteins released by pancreatic cancer cells by multidimensional protein identification technology: a strategy for identification of novel cancer markers. FASEB J 19:1125–1127
22. McArthur G (2004) Molecularly targeted treatment for dermatofibrosarcoma protuberans. Semin Oncol 31:30–36
23. Mitelman F, Johansson B, Mertens F (2007) The impact of translocations and gene fusions on cancer causation. Nat Rev Cancer 7:233–245
24. Paulus W, Baur I, Dours-Zimmermann MT, Zimmermann DR (1996) Differential expression of versican isoforms in brain tumors. J Neuropathol Exp Neurol 55:528–533
25. Queimado L, Lopes CS, Reis AM (2007) WIF1, an inhibitor of the Wnt pathway, is rearranged in salivary gland tumors. Genes Chromosomes Cancer 46:215–225

26. Ricciardelli C, Mayne K, Sykes PJ, Raymond WA, McCaul K, Marshall VR, Horsfall DJ (1998) Elevated levels of versican but not decorin predict disease progression in early-stage prostate cancer. Clin Cancer Res 4:963–971
27. Rubin BP, Schuetze SM, Eary JF, Norwood TH, Mirza S, Conrad EU, Bruckner JD (2002) Molecular targeting of platelet-derived growth factor B by imatinib mesylate in a patient with metastatic dermatofibrosarcoma protuberans. J Clin Oncol 20:3586–3591
28. Sandberg AA, Bridge JA (2000) Updates on cytogenetics and molecular genetics of bone and soft tissue tumors: Ewing sarcoma and peripheral primitive neuroectodermal tumors. Cancer Genet Cytogenet 123:1–26
29. Sasaki H, Nagura K, Ishino M, Tobioka H, Kotani K, Sasaki T (1995) Cloning and characterization of cell adhesion kinase beta, a novel protein-tyrosine kinase of the focal adhesion kinase subfamily. J Biol Chem 270:21206–21219
30. Shaffer J, Tommerup N (2005) ISCN 2005: an international system for human cytogenetic nomenclature. Krager, Basel
31. Simon MP, Navarro M, Roux D, Pouyssegur J (2001) Structural and functional analysis of a chimeric protein COL1A1-PDGFB generated by the translocation t(17;22)(q22;q13.1) in Dermatofibrosarcoma protuberans (DP). Oncogene 20:2965–2975
32. Simon MP, Pedeutour F, Sirvent N, Grosgeorge J, Minoletti F, Coindre JM, Terrier-Lacombe MJ, Mandahl N, Craver RD, Blin N, Sozzi G, Turc-Carel C, O'Brien KP, Kedra D, Fransson I, Guilbaud C, Dumanski JP (1997) Deregulation of the platelet-derived growth factor B-chain gene via fusion with collagen gene COL1A1 in dermatofibrosarcoma protuberans and giant-cell fibroblastoma. Nat Genet 15:95–98
33. Sinovic J, Bridge JA (1994) Translocation (2;17) in recurrent dermatofibrosarcoma protuberans. Cancer Genet Cytogenet 75:156–157
34. Sirvent N, Maire G, Pedeutour F (2003) Genetics of dermatofibrosarcoma protuberans family of tumors: from ring chromosomes to tyrosine kinase inhibitor treatment. Genes Chromosomes Cancer 37:1–19
35. Sonobe H, Furihata M, Iwata J, Ohtsuki Y, Chikazawa M, Taguchi T, Shimizu K (1999) Dermatofibrosarcoma protuberans harboring t(9;22)(q32;q12.2). Cancer Genet Cytogenet 110:14–18
36. Sun CK, Ng KT, Sun BS, Ho JW, Lee TK, Ng I, Poon RT, Lo CM, Liu CL, Man K, Fan ST (2007) The significance of proline-rich tyrosine kinase2 (Pyk2) on hepatocellular carcinoma progression and recurrence. Br J Cancer 97:50–57
37. Terrier-Lacombe MJ, Guillou L, Maire G, Terrier P, Vince DR, de Saint Aubain Somerhausen N, Collin F, Pedeutour F, Coindre JM (2003) Dermatofibrosarcoma protuberans, giant cell fibroblastoma, and hybrid lesions in children: clinicopathologic comparative analysis of 28 cases with molecular data—a study from the French Federation of Cancer Centers Sarcoma Group. Am J Surg Pathol 27:27–39
38. Touab M, Villena J, Barranco C, Arumi-Uria M, Bassols A (2002) Versican is differentially expressed in human melanoma and may play a role in tumor development. Am J Pathol 160:549–557
39. Voz ML, Astrom AK, Kas K, Mark J, Stenman G, Van de Ven WJ (1998) The recurrent translocation t(5;8)(p13;q12) in pleomorphic adenomas results in upregulation of PLAG1 gene expression under control of the LIFR promoter. Oncogene 16:1409–1416
40. Wight TN (2002) Versican: a versatile extracellular matrix proteoglycan in cell biology. Curr Opin Cell Biol 14:617–623
41. Zhang Y, Cao L, Yang BL, Yang BB (1998) The G3 domain of versican enhances cell proliferation via epidermial growth factor-like motifs. J Biol Chem 273:21342–21351

Virchows Arch (2008) 452:697–702
DOI 10.1007/s00428-008-0612-y

CASE REPORT

Perivascular epithelioid cell tumor of the rib

Ikuko Torii · Nobuyuki Kondo · Teruhisa Takuwa · Seiji Matsumoto · Yoshitomo Okumura · Ayuko Sato · Fumihiro Tanaka · Takashi Nishigami · Seiki Hasegawa · Tohru Tsujimura

Received: 15 December 2007 / Revised: 18 March 2008 / Accepted: 27 March 2008 / Published online: 24 April 2008
© Springer-Verlag 2008

Abstract We present a rare case of perivascular epithelioid cell tumor (PEComa) in the right 6th rib of a 28-year-old man. A plain computed tomography scan showed a round osteolytic lesion in the right 6th rib. The resected tissue contained a globular-shaped, soft tumor. Histologically, the tumor was rich in vasculature and exclusively composed of perivascular epithelioid cells with clear cytoplasm. Immunohistochemically, the tumor expressed diffusely a melanocyte marker, human melanoma black-45, and focally a myogenic marker, α-smooth muscle actin, but not an epithelial marker, AE1/AE3. Fontana–Masson-positive melanin pigments were present and c-*kit* receptor tyrosine kinase (CD117), involved in the development of melanocytes but not myogenic cells, was expressed in tumor cells. These findings indicate that the tumor is PEComa with some differentiation into melanocytes. Notably, owing to the unique location of the occurrence, the tumor occupied bone marrow tissues of the rib, resulting that the tumor has the potential for hematogenous metastasis. In spite of the lack of cells with severe atypia, necrosis, and numerous mitoses, tumor cells invaded into surrounding tissues and overexpressed cyclin D1. To the best of our knowledge, this is the first case report of PEComa arising from the rib with the signs of malignant potential.

I. Torii · A. Sato · T. Nishigami · T. Tsujimura (✉)
Department of Pathology, Hyogo College of Medicine,
1-1 Mukogawa,
Nishinomiya, Hyogo 663-8501, Japan
e-mail: tohru@hyo-med.ac.jp

N. Kondo · T. Takuwa · S. Matsumoto · Y. Okumura · F. Tanaka · S. Hasegawa
General Thoracic Surgery, Hyogo College of Medicine,
Nishinomiya, Hyogo 663-8501, Japan

Keywords Perivascular epithelioid cell tumor (PEComa) · Rib · Melanin · c-*kit* receptor tyrosine kinase · HMB-45 · Cyclin D1

Introduction

Perivascular epithelioid cell tumor (PEComa) is a rare mesenchymal tumor composed of perivascular epithelioid cells (PECs) [9]. Histologically, PECs are characterized by an epithelioid appearance with a clear to granular cytoplasm, a round to oval, centrally located nucleus, and an inconspicuous nucleolus, but they may have also spindle-shaped and pleomorphic features [2, 3, 8, 9, 12]. Immunohistochemically, PECs are positive for melanocytic and myogenic markers, such as human melanoma black (HMB)-45, Melan-A, microphthalmia transcription factor, NKIC3, smooth muscle actin (SMA), calponin, muscle myosin, and, less commonly, desmin [2, 3, 8, 18]. However, as for epithelial markers, PECs are exclusively negative [2, 8, 18]. PECs characterized by epithelioid features are strongly positive for HMB-45 and slightly for actin. On the other hand, PECs characterized by muscular features with a spindle shape show a stronger positivity for actin than for HMB-45 [10]. The PEComa family of tumors includes angiomyolipoma (AML), clear cell "sugar" tumor (CCST) of the lung, lymphoangioleiomyomatosis (LAM), clear cell myomelanocytic tumor of the falciform ligament/ligamentum teres, and unusual clear cell tumors of the pancreas, rectum, abdominal serosa, uterus, vulva, thigh, heart, and skin [2, 3, 8, 11, 18, 22, 24]. Most of the patients with the PEComa family are female, and some of them suffer from tuberous sclerosis complex (TSC) simultaneously [10]. PEComas other than AML, CCST, or LAM are exceedingly rare.

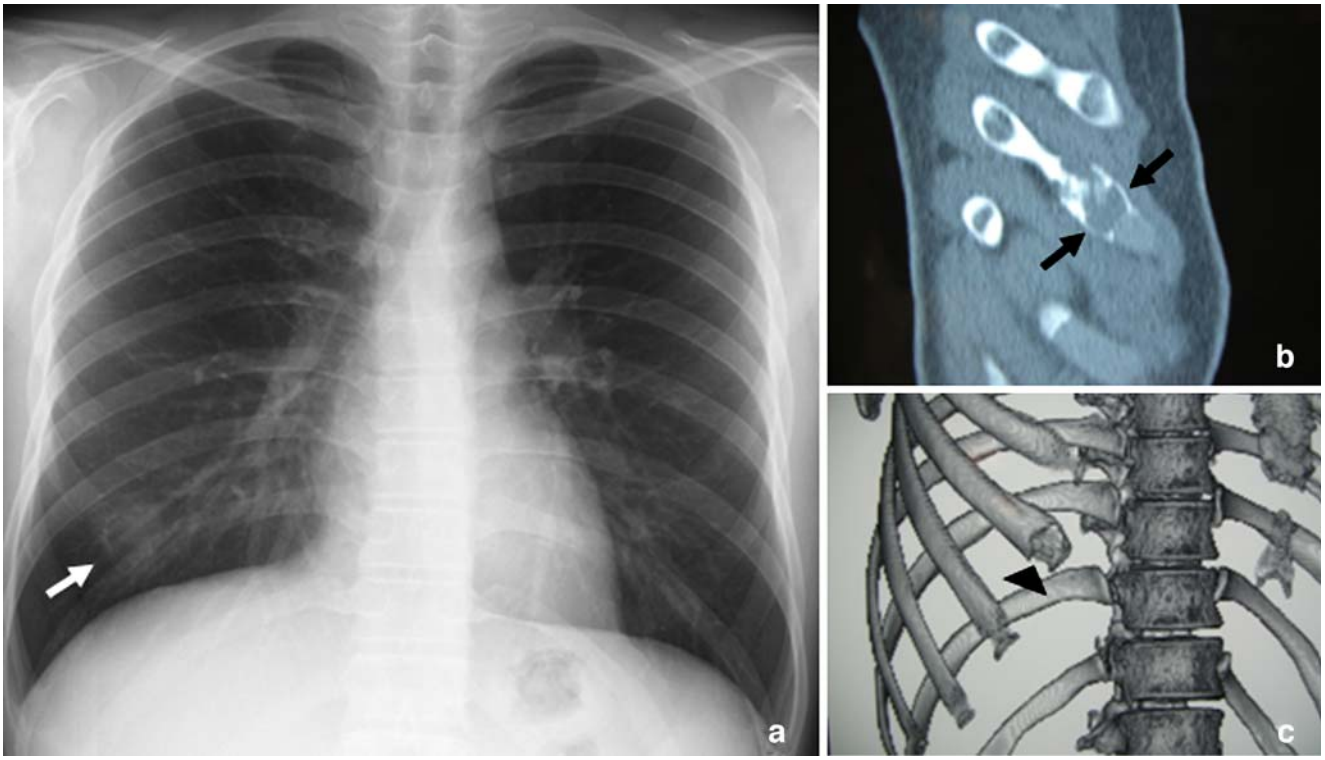


Fig. 1 Radiographic features. **a** Chest radiograph shows a round radiopaque nodule in the right lower lobe (*arrow*). **b** Reconstructed computed tomography scan of the chest shows a round osteolytic lesion in the right 6th rib (*arrows*). **c** Three-dimensional view reconstructed from the chest CT scan clearly demonstrates an osteolytic lesion in the right 6th rib adjacent to the costicartilage (*arrow head*)

While most reported PEComas have behaved in a benign fashion, malignant PEComas have occasionally been documented [5–8, 11, 15, 19]. Based on the reviews of previously reported PEComa, the stratification of "benign", "uncertain malignant potential", and "malignant" has recently been introduced into the prognosis of PEComa [8]. However, it is still hard to accurately predict the biological behavior of PEComas. Here, we report a case of PEComa arising from an exceedingly rare site, the rib, with signs of malignant potential.

Clinical history

A 28-year-old man with no history of TSC noticed the increase of pain in the right anterior rib that has been continued for the last few years. No pigmented lesions were observed in the skin. The laboratory data were all within normal limits. A plain computed tomography (CT) scan showed a round osteolytic lesion in the right 6th rib, but positron emission tomography/CT did not detect the extensive uptake of ^{18}F-2-deoxy-D-glucose in the lesion. One month later, a partial resection of the right 6th rib including the lesion was performed. Most part of the lesion could be resected easily, but a part of the posterior surface hardly due to the extensive adhesion to the visceral pleura. Histological and immunohistological examinations showed that the osteolytic lesion of the right 6th rib was PEComa. Because some tumor cells were histologically found on the lateral margin of the resected tissue, an additional operation was performed immediately. Complete resection of the tumor was confirmed by the final histological examination and the patient was stable postoperatively (Fig. 1).

Materials and methods

The resected tissue of the right 6th rib was fixed with 10% formalin solution, and a part of the tissue was decalcified with a decalcification solution (Hayashi Pure Chemical Ind., Ltd., Osaka, Japan). Then, the tissue was embedded in paraffin, cut into 5-μm thick sections, stained with hematoxylin and eosin, and histologically examined. The Fontana–Masson stain with or without bleaching by a potassium permanganate was performed to examine the melanin pigments. Immunohistochemical analysis was performed with the Dako autostainer (Dako Cytomation, Glostrup, Denmark). Immunoreacted cells were visualized with diaminobenzidine tetrahydrochloride (Dako Cytomation), and nuclei were lightly counterstained with hematoxylin. Primary antibodies were listed in Table 1.

Table 1 Antibodies used in this study and immunohistochemical findings

Antigen (antibody clone)	Source	Result
S-100 (n/a)	Biomeda	–
Calponin (CALP)	Dako Cytomation	–
CD68 (PG-M1)	Dako Cytomation	–
Melan-A (A103)	Dako Cytomation	–
Factor VIII (polyclonal)	Dako Cytomation	–
c-*kit* (polyclonal)	Dako Cytomation	+++
Cytokeratin (AE1/AE3)	Dako Cytomation	–
Ki-67 (MIB-1)	Immunotech	3%
CD34 (QBEND10)	Immunotech	–
Cyclin D1 (SP4)	Nichirei Biosciences Inc.	>50%
α-SMA (1A4)	Shandon Immunon	+
HMB-45 (HMB-45)	Shandon Immunon	+++
Desmin (D33)	Shandon Immunon	+
Vimentin (V9)	Shandon Immunon	+

– Negative, + focal positive, +++ diffuse positive

Results

The resected tissue from the right 6th rib contained a tumor, which was globular-shaped, 2×2×2 cm in size, soft, and tan to partially black in color. Tumor was covered by the periostium except for the minor area to which the visceral pleura was adhered. No obvious necrotic lesion was observed on the cut surface.

Microscopically, epithelioid tumor cells were arranged in nests or cords traversed by a delicate vasculature consisting of a rich network of sinusoid-type blood vessels (Fig. 2a). The tumor was comprised a rather uniform population of polygonal cells with abundant, clear, or granular cytoplasm and occasionally contained brown pigments (Fig. 2b). These brown pigments in the tumor cells were intensely decorated with the Fontana–Masson staining (inset of Fig. 2b), but clearly disappeared when the bleaching was performed on the specimen before staining with the Fontana–Masson (data not shown). Tumor cells had a round to oval nucleus, sometimes with a prominent nucleolus, and exhibited a mild nuclear pleomorphism. Occasionally, intranuclear inclusion bodies were observed in the tumor cells (Fig. 2c). The number of mitoses was only three per high-power fields. Some tumor cells were growing in the intraperiostium and invading into the neighboring connective tissues (Fig. 2d). The bone marrow in the lesion of the right 6th rib was completely replaced by tumor cells.

Immunohistochemical findings of the tumor are summarized in Table 1. Tumor cells exhibited strong and diffuse positivity for the melanogenesis-related marker, HMB-45, and were partially positive for α-SMA and vimentin (Fig. 3a and b). The striking expression of c-*kit* receptor tyrosine kinase (CD117) was also observed on the membrane of tumor cells (Fig. 3c). On the other hand, tumor cells failed to react with antibodies against Melan-A,

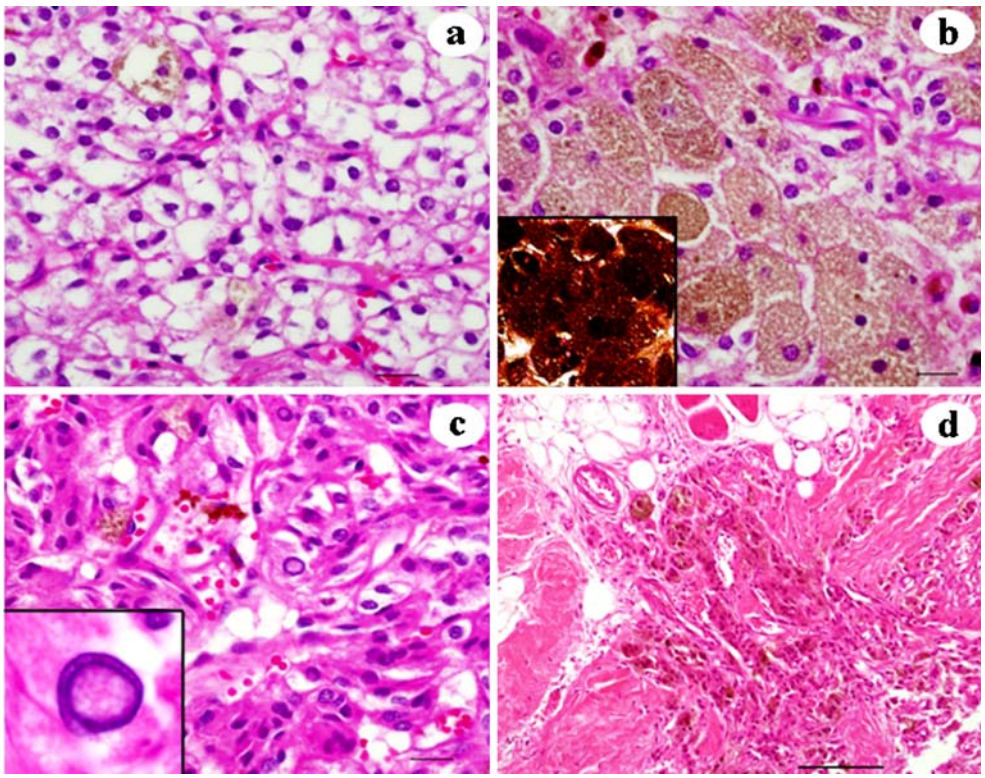


Fig. 2 Microscopic features. **a** Polygonal tumor cells with abundant clear cytoplasm are arranged in the nests or cords traversed by a delicate vasculature consisting of a rich network of sinusoid-type blood vessels. Some tumor cells demonstrate clear small nucleoli. **b** A large number of tumor cells contain abundant brown pigments and are intensely decorated with the Fontana–Masson staining (*inset*). **c** Spindle-shaped tumor cells with granular cytoplasm contain prominent intranuclear cytoplasmic inclusion bodies (*inset*). **d** Invasive growth across the periostium. *Bars* represent 20 μm in **a**, **b**, and **c** and 100 μm in **d**

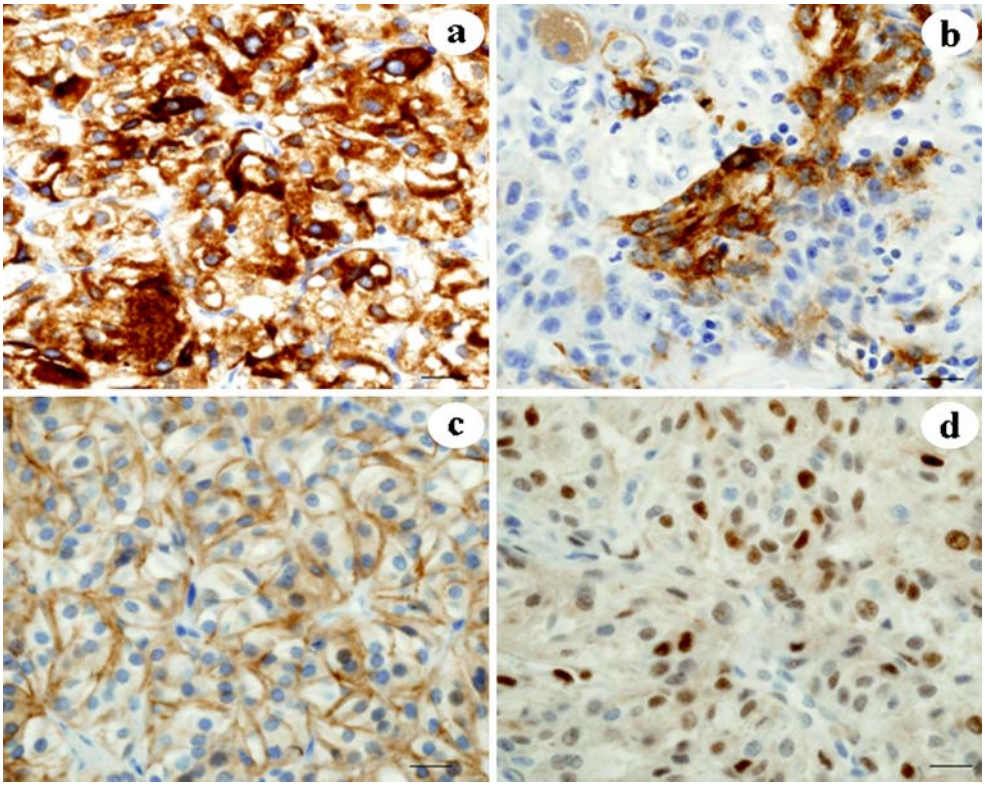


Fig. 3 Immunohistochemical findings. **a** Tumor cells are diffusely stained for a melanocytic marker, HMB-45. **b** Tumor cells are stained for α-SMA in small areas. **c** Uniformly strong membranous staining for c-*kit* receptor tyrosine kinase (CD117) is observed in the tumor cells. **d** Numerous nuclei of the tumor cells are positively stained for cyclin D1. *Bars* represent 20 μm

S-100, calponin, desmin, AE1/AE3, CD34, CD68, and factor VIII. Mib-1 (Ki-67) was expressed in only 3% of the tumor cells, but more than 50% of tumor cells were positive for cyclin D1, indicating that cyclin D1 is overexpressed in the tumor cells (Fig. 3d).

Discussion

PEComa has been characterized by the dual–melanomyocytic differentiation. The present tumor was positive for both melanogenic (HMB-45) and myogenic (α-SMA) markers, showing that the tumor was a PEComa. Occasionally, it is necessary to distinguish PEComa from the clear cell carcinoma, gastrointestinal stromal tumor (GIST), and melanoma/clear cell sarcoma. Clear cell carcinoma expresses an epithelial marker, AE1/AE3, but PEComa does not [8, 9]. GIST generally expresses CD34 as well as the *c-kit* receptor tyrosine kinase (CD117), but PEComa shows no expression of CD34 [6]. Melanoma/clear cell sarcoma strongly expresses S-100, but no expression of S-100 is a feature of PEComa [21]. Because the present tumor showed no expression of AE1/AE3, CD34, and S-100, it can be clearly discriminated from the clear cell carcinoma, GIST, and melanoma/clear cell sarcoma.

It is interesting that the markers of melanocytes, HMB-45 and Melan-A, show the contradictory expression in the present case: positive for HMB-45 and negative for Melan-A. HMB-45 was reported to react with the fetal retina and melanocytes but not adult retina and mature/resting melanocytes [4, 14]. Melan-A was shown to react with the adult mature melanocytes [4]. These findings suggest that the expression of HMB-45 and Melan-A is dependent on the differentiation stage of melanocytes and that no expression of Melan-A in the present tumor reflects the immature property of tumor cells. The expression of S-100 is also usually seen in melanocytes, but PEComa does not express S-100. S-100 is strikingly expressed in neuroglia and Schwann cells in the nervous system, suggesting that S-100 expression reflects the differentiation into neuroglia and Schwann cells rather than melanocytes. Thus, it is unlikely that S-100 might be expressed in PEComa characterized by the dual–melanomyocytic differentiation.

Folpe et al. reported that 55 of 61 PEComa cases occurred in women and six in men, with a median age of 38 years [8]. PEComas were found in various tissues, such as gynecologic, soft, cutaneous, and visceral tissues [1, 6, 13, 15, 16, 18, 20, 21, 23]. In addition, the following rare two cases have been reported. One reported case was the tibia-derived monotypic epithelioid angiomyolipoma with no recurrence during the 12 months of follow-up [13]. Another case was the skull base-derived malignant PEComa with the aggressive invasion into the spinal canal [15]. In the latter case, the tumor might arise from the meninges or the metastatic tumor from elsewhere, so it is doubtful whether the tumors directly developed from the

bone. Therefore, this case seems to be the second PEComa arising in the bone and the first as for the rib.

While most reported PEComas have behaved in a benign fashion, malignant PEComa with the overexpression of cyclin D1 have been reported [25, 26], suggesting that the cyclin D1 plays an important role in the genesis of malignant PEComa and serves as a marker of biological behaviors of PEComa. Recently, Folpe et al. have proposed the provisional classification of PEComa to "benign", "uncertain malignant potential", and "malignant" [8]. The PEComa displaying nuclear pleomorphism and/or more than 5 cm in size without any other malignant features can be classified as "uncertain malignant potential". Although the present tumor did not fill the criteria of "uncertain malignant potential", it requires close follow-up as a PEComa with malignant potential because of the having some critical factors such as the growth in bone marrow tissue with the potential for hematogenous metastasis, overexpression of cyclin D1, and invasion into the surrounding tissues.

PEComas with abundant Fontana–Masson-positive melanin pigments and definite melanosome have been reported [1, 21, 22]. Moreover, the expression of *c-kit* receptor tyrosine kinase (CD117), which is involved in the development of melanocytes but not myogenic cells, is reported in AML [13, 17]. These results indicate that some PEComas may differentiate into melanocytes. In the present case, both Fontana–Masson-positive melanin pigments and c-*kit* expression were observed in tumor cells, showing that the tumor is a PEComa with some differentiated into melanocytes.

Acknowledgments We thank Mr. T. Yamamoto and Ms. R. Nishikawa of Hyogo College of Medicine for their technical assistance.

Conflict of interest statement We declare that we have no conflict of interest.

Reference

1. Adachi S, Hanada M, Kobayashi Y, Tsutahara K, Fukuhara S, Mori N, Hara T, Mukai H, Shimasaku E, Kawai M, Kishikawa N, Yamaguchi S (2004) Heavily melanotic perivascular epithelioid clear cell tumor of the kidney. Pathol Int 54:261–265
2. Bonetti F, Martignoni G, Colato C, Manfrin E, Gambacorta M, Faleri M, Bacchi C, Sin V-C, Wong N-L, Coady M, Kwok-cheung JC (2007) Abdominopelvic sarcoma of perivascular epithelioid cells. Report of four cases in young woman, one with tuberous sclerosis. Mod Pathol 14:563–568
3. Bonetti F, Pea M, Martignoni G, Doglioni C, Zamboni G, Capelli P, Rimondi P, Andrion A (1994) Clear cell ('sugar') tumor of the lung is a lesion strictly related to angiomyolipoma: the concept of a family of lesions characterized by the presence of the perivascular epithelioid cells (PEC). Pathology 26:230–236
4. Busam KJ, Chen YT, Old LJ, Stockert E, Iversen K, Coplan KA, Rosai J, Barnhill RL, Jungbluth AA (1992) Expression of melan-A (MART1) in benign melanocytic nevi and primary cutaneous malignant melanoma. Am J Surg Pathol 22:976–982
5. Dimmler A, Seitz G, Hohenberger W, Kirchner T, Faller G (2003) Late pulmonary metastasis in uterine PEComa. J Clin Pathol 56:627–628
6. Evert M, Wardelmann E, Nestler G, Schultz H-U, Roessner A, Röcken C (2005) Abdominopelvic perivascular epithelioid cell sarcoma (malignant PEComa) mimicking gastrointestinal stromal tumor of the rectum. Histopathology 46:115–117
7. Fink D, Marsden DE, Edwards L, Camaris C, Hacker NF (2004) Malignant perivascular epithelioid cell tumor (PEComa) arising in the broad ligament. Int J Gynecol Cancer 14:1036–1039
8. Folpe AL, Mentzel T, Lehr H-A, Fisher C, Balzer BL, Weiss SW (2005) Perivascular epithelioid cell neoplasms of soft tissue and gynecologic origin. Am J Surg Pathol 29:1558–1575
9. Folpe AL (2002) Neoplasms with perivascular epithelioid cell differentiation (PEComa). In: Fletcher CDM, Unni KK, Mertens F (eds) World Health Organization classification of tumors: pathology and genesis of tumors of soft tissue and bone. Lyon, IARC, pp 221–222
10. Martignoni G, Pea M, Reghellin D, Zamboni G, Bonetti F (2008) PEComas: the past, the present and the future. Virchows Arch 452:119–132
11. Harris GC, McCulloch TA, Perks G, Fisher C (2003) Malignant perivascular epithelioid cell tumor ('PEComa') of soft tissue: a unique case. Am J Surg Pathol 28:1655–1658
12. Hornick JL, Fletcher CDM (2006) PEComa: what do we know so far? Histopathology 48:75–82
13. Insabato L, De Rosa G, Terracciano LM, Fazioli F, Santo FD, Rosai J (2002) Primary monotypic epithelioid angiomyolipoma of bone. Histopathology 40:286–290
14. Kapur RP, Bigler SA, Skelly M, Gown AM (1992) Anti-melanoma monoclonal antibody HMB-45 identifies an oncofetal glycoconjugate associated with immature melanosomes. J Histochem Cyrochem 40:207–212
15. Lehman NL (2004) Malignant PEComa of the skull base. Am J Surg Pathol 28:1230–1232
16. Mai KT, Belanger EC (2006) Perivascular epithelioid cell tumor (PEComa) of the soft tissue. Pathology 38:415–420
17. Makhlouf HR, Remotti HE, Ishak KG (2002) Expression of KIT (CD117) in angiomyolipoma. Am J Surg Pathol 26:493–497
18. Mentzel T, Reißhauer S, Rütten A, Hantschke M, Soares de Almeida LM, Kutzner H (2005) Cutaneous clear cell myomelanocytic tumor: a new member of the growing family of perivascular epithelioid cell tumors (PEComas). Clinicopathological and immunohistochemical analysis of seven cases. Histopathology 46:498–504
19. Pan C-C, Yang A-H, Chiang H (2003) Malignant perivascular epithelioid cell tumor involving the prostate. Arch Pathol Lab Med 127:e96–e98
20. Parfitt JR, Bella AJ, Izawa JI, Wehrli BM (2006) Malignant neoplasm of perivascular epithelioid cells of the liver. Arch Pathol Lab Med 130:1219–1222
21. Park SH, Ro JY, Kim H-S, Lee ES (2003) Perivascular epithelioid cell tumor of the uterus: Immunohistochemical, ultrastructural and molecular study. Pathol Int 53:800–805
22. Ribalta T, Lloreta J, Munné A, Serrano S, Cardesa A (2000) Malignant pigmented clear cell epithelioid tumor of the kidney: clear cell ("sugar") tumor versus malignant melanoma. Human Pathol 31:516–519
23. Tan J, Peach AH, Merchant W (2007) PEComa of the skin: more common in the lower limb? Two case reports. Histopathology 51:135–136

24. Tazelaar HD, Batts KP, Srigley JR (2001) Primary extrapulmonary sugar tumor (PEST): a report of four cases. Mod Pathol 14: 615–622
25. Weinreb I, Howarth D, Latta E, Ghazarian D, Chetty R (2007) Perivascular epithelioid cell neoplasms (PEComas): four malignant cases expanding the histopathological spectrum and a description of a unique finding. Virchows Arch 450: 463–470
26. Yamamoto H, Oda Y, Yao T, Oiwa T, Kobayashi C, Tamiya S, Kawaguchi K, Hino O, Tsuneyoshi M (2006) Malignant perivascular epithelioid cell tumor of the colon: report of a case with molecular analysis. Pathol Int 56:46–50

Virchows Arch (2008) 452:703
DOI 10.1007/s00428-008-0598-5

LETTER TO THE EDITOR

The case of the purple colon

Gábor Cserni · Lajos Kocsis

Received: 15 February 2008 / Accepted: 15 February 2008 / Published online: 19 April 2008
© Springer-Verlag 2008

Abstract Purple discoloration of the large bowel at autopsy was related to beetroot ingestion and post-mortem changes.

Keywords Autopsy · Colon · Purple

Sir,

The autopsy of a 56-year-old female diagnosed with pulmonary and pleural metastases of breast cancer yielded the uncommon finding of complementary colours in the abdominal cavity consisting of the common yellow fat of the great omentum, mesenterium and mesocolon and the unexpected purple of the colon (Fig. 1). Several ad hoc theories were formed to explain the discoloration, including putrefaction and colonisation by a chromogenic bacterium, intoxication, drug-related colouration or the consumption of colourant substances. No clinical history of gastrointestinal symptoms, coloured therapeutics or intoxication could be gained, but the patient was reported to consume large quantities of beetroot (*Beta vulgaris*) as adjunct to her anti-cancer drugs. This is the first case which was observed in our department performing over 1,000 autopsies per year, but we are aware of another case of "purple colon" which was also related to beetroot ingestion and was seen by one of us at autopsy in another hospital. The purple colour vanished during fixation in buffered formalin, and on histology, the bowel mucosa showed only some degrees of autolysis and melanosis. Therefore, it is probable that post-mortem changes help the diffusion of the colourant from the bowel lumen to the serosal surface and that such discolouration cannot be found in vivo, e.g. during laparoscopy or open abdominal surgery. As many patients ingest herbs and other substances (including beetroot amongst other vegetables) believed or proven to support and/or complement their medical treatment, pathologist should be ready to explain this uncommon finding.

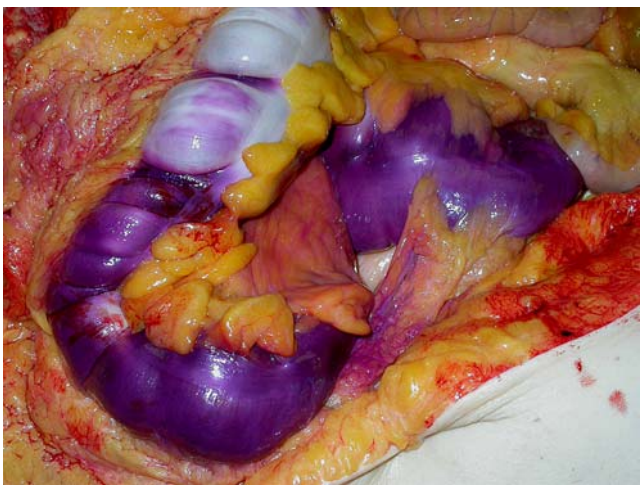


Fig. 1 A large proportion of the colon was purple

G. Cserni (✉) · L. Kocsis
Bács-Kiskun County Teaching Hospital,
Nyiri ut 38.,
6000 Kecskemét, Hungary
e-mail: csernig@freemail.hu

Virchows Arch (2008) 452:705
DOI 10.1007/s00428-008-0614-9

LETTER TO THE EDITOR

Letter to the editor

Milan Elleder

Received: 7 February 2008 / Accepted: 29 March 2008 / Published online: 7 May 2008
© Springer-Verlag 2008

Askari H, Kaneski CR, Semino-Mora C, Desai P, Ang A, Kleiner DE, Perlee LT, Quezado M, Spollen LE, Wustman BA, Schiffmann R. Cellular and tissue localization of globotriaosylceramide in Fabry disease. *Virchows Arch* 2007 Oct;451(4):823–34.

Dear Editor,

I read with great interest the paper by *Askari et al*. dealing with alpha galactosidase A deficiency (Fabry disease) describing a new aspect of lysosomal lipid storage—extralysosomal accumulation of the critical lipid globotriaosylceramide (Gb_3Cer). A substantial part of the study was carried out using organic solvent dehydrated paraffin-embedded samples from a set of tissues which are typically affected by this lysosomal storage disorder. Lipid localization was followed, at the histological level, with immunohistochemical detection combined with markers of several subcellular compartments. All the results were correlated with control samples which had been processed in the same way.

I highly appreciate the attempt to demonstrate the extralysosomal presence of Gb_3Cer in a condition which is characterized primarily by its deficient intralysosomal degradation. Such an approach would certainly help to extend our knowledge of the biology of lysosomal storage beyond the limit of the storage lysosome itself. However, the bulk of the results are based on techniques that include a sequence of dehydrating steps in organic solvents that are known to be able to dissolve Gb3 and so can hardly be considered conclusive. The results presented defined only that part of the stored Gb_3Cer which resisted the embedding procedure and simultaneously underwent certain degree of diffusion. This can explain the authors' finding that in some locations the staining of Gb_3Cer was diffuse, colocalized with various cell compartments, and absent from sites that are well known for having lysosomal lipid inclusions, e.g., in cardiocytes. It is also questionable as to whether or not the normal (nonstoring) tissues represented an optimal control. However, the pre-embedding techniques, although not completely eliminating the possible diffusion of GB3 in the processed material, can shed new light on this biologically very interesting topic. The paper by *Askari et al*. would be greatly enhanced if the pre-embedding techniques, both at the light and ultrastructure levels, was included to a greater extent and presented with all the necessary controls, measurements, and statistics. All future studies, designed to address the important topic of extralysosomal lipid accumulation in lysosomal storage disorders, must utilize samples that guarantee that the actual position of the extralysosomal lipids are unchanged. Whenever possible, the use of organic solvents and heat-mediated procedures (e.g., dewaxing, antigen retrieval) should be kept to a minimum or eliminated.

M. Elleder (✉)
First Medical Faculty, Charles University in Prague,
Institute of Inherited Metabolic Disorders,
Ke Karlovu 2, Bldg. D, First Floor,
120 00 Prague, Czech Republic
e-mail: melleder@cesnet.cz

Virchows Arch (2008) 452:707–708
DOI 10.1007/s00428-008-0615-8

LETTER TO THE EDITOR

The sub-cellular localization globotriaosylceramide in Fabry disease

Raphael Schiffmann

Received: 2 March 2008 / Accepted: 29 March 2008 / Published online: 7 May 2008
© Springer-Verlag 2008

Dear Editor,

We thank Professor Milan Elleder for his comments on our paper (Askari et al. Cellular and tissue localization of globotriaosylceramide in Fabry disease. Virchows Arch 451 (4):823–34). We do agree that one cannot completely exclude the possibilities of loss and some diffusion in immunohistochemistry and even immunogold electron microscopy. However, we used three independent in situ immuno-detection methods including a pre-embedding immunogold EM technique. We studied autopsy, biopsy, and cell culture samples from different patients and organs as well as primary-unlabeled and normal controls. All three methods showed similar cellular and sub-cellular localization of globotriaosylceramide (Gb_3), the main glycolipid that accumulates in Fabry disease. We hope that others using the advice of Professor Elleder will confirm our work.

The extra-lysosomal localization of Gb_3 in Fabry disease, the main finding of our paper, is not surprising. Gb_3 is normally a cell membrane receptor (CD77) that is internalized when it is attached to its ligands [4, 5, 10, 13]. In both health and in Fabry disease, Gb_3 is also located in the extra-cellular space by virtue of its presence in the circulation. This fact implies that Gb_3 is secreted by cells and therefore is transported throughout the cellular endosomal network. Recently, it has been shown in the Fabry mouse model that Gb_3, as well as other related glycosphingolipids, markedly accumulate in cellular rafts [11]. These structures are located in the cellular membrane and include endothelial nitric oxide synthase (eNOS). A dysfunction of eNOS pathways in Fabry disease as a mechanism of increased production of reactive oxygen species, possible through eNOS decoupling, has been previously suspected [1, 2, 6, 7]. The finding of a wide intracellular distribution of Gb_3 in Fabry disease joins similar finding in Gaucher disease [9], GM1-gangliosidosis [3, 12] and GM2-gangliosidosis [3, 8] where both localization and molecular interaction and disruption of extra-lysosomal functions have been found.

R. Schiffmann (✉)
Institute of Metabolic Disease, Baylor Research Institute,
3812 Elm Street,
Dallas, TX 75226, USA
e-mail: Raphael.Schiffmann@Baylorhealth.edu

References

1. Altarescu G, Moore DF, Pursley R, Campia U, Goldstein S, Bryant M, Panza JA, Schiffmann R (2001) Enhanced endothelium-dependent vasodilation in Fabry disease. Stroke 32:1559–1562
2. Bodary PF, Shen Y, Vargas FB, Bi X, Ostenso KA, Gu S, Shayman JA, Eitzman DT (2005) Alpha-galactosidase A deficiency accelerates atherosclerosis in mice with apolipoprotein E deficiency. Circulation 111:629–632
3. Ginzburg L, Li SC, Li YT, Futerman AH (2008) An exposed carboxyl group on sialic acid is essential for gangliosides to inhibit calcium uptake via the sarco/endoplasmic reticulum Ca2+ -ATPase: relevance to gangliosidoses. J Neurochem 104:140–146
4. Jarvis RM, Chamba A, Holder MJ, Challa A, Smith DC, Hodgkin MN, Lord JM, Gordon J (2007) Dynamic interplay between the neutral glycosphingolipid CD77/Gb3 and the therapeutic antibody target CD20 within the lipid bilayer of model B lymphoma cells. Biochem Biophys Res Commun 355:944–949
5. Khine AA, Firtel M, Lingwood CA (1998) CD77-dependent retrograde transport of CD19 to the nuclear membrane: functional relationship between CD77 and CD19 during germinal center B-cell apoptosis. J Cell Physiol 176:281–292
6. Moore D, Scott LJC, Gladwin MT, Altarescu G, Kaneski C, Suzuki K, Pease-Fye M, Ferri R, Brady RO, Herscovitch P, Schiffmann R (2001) Regional Cerebral Hyper-Perfusion and Nitric Oxide Pathway Dysregulation in Fabry Disease: reversal by Enzyme Replacement Therapy. Circulation 104:1506–1512

7. Moore D, Ye F, Brennan ML, Gupta S, Barshop BA, Steiner RD, Rhead WJ, Brady RO, Hazen SL, Schiffmann R (2004) Ascorbate decreases Fabry cerebral hyperperfusion suggesting a reactive oxygen species abnormality: an arterial spin tagging study. J Magn Reson Imaging 20:674–683
8. Pelled D, Lloyd-Evans E, Riebeling C, Jeyakumar M, Platt FM, Futerman AH (2003) Inhibition of calcium uptake via the sarco/endoplasmic reticulum Ca2+ -ATPase in a mouse model of Sandhoff disease and prevention by treatment with N-butyldeoxynojirimycin. J Biol Chem 278:29496–29501
9. Pelled D, Trajkovic-Bodennec S, Lloyd-Evans E, Sidransky E, Schiffmann R, Futerman AH (2005) Enhanced calcium release in the acute neuronopathic form of Gaucher disease. Neurobiol Dis 18:83–88
10. Schweppe CH, Bielaszewska M, Pohlentz G, Friedrich AW, Buntemeyer H, Alexander Schmidt M, Kim KS, Peter-Katalinic J, Karch H, Muthing J (2008) Glycosphingolipids in vascular endothelial cells: relationship of heterogeneity in Gb3Cer/CD77 receptor expression with differential Shiga toxin 1 cytotoxicity. Glycoconj J 25:291–234
11. Shu L, Shayman JA (2007) Caveolin-associated accumulation of globotriaosylceramide in the vascular endothelium of alpha-galactosidase A null mice. J Biol Chem 282:20960–20967
12. Tessitore A, del PMM, Sano R, Ma Y, Mann L, Ingrassia A, Laywell ED, Steindler DA, Hendershot LM, d'Azzo A (2004) GM1-ganglioside-mediated activation of the unfolded protein response causes neuronal death in a neurodegenerative gangliosidosis. Mol Cell 15:753–766
13. Tetaud C, Falguieres T, Carlier K, Lecluse Y, Garibal J, Coulaud D, Busson P, Steffensen R, Clausen H, Johannes L, Wiels J (2003) Two distinct Gb3/CD77 signaling pathways leading to apoptosis are triggered by anti-Gb3/CD77 mAb and verotoxin-1. J Biol Chem 278:45200–45208

Virchows Arch (2008) 452 (Suppl 1):S1–S286
DOI 10.1007/s00428-008-0613-x

O-1

The epithelial-to-mesenchymal transition protein periostin is associated with higher tumour stage and grade in non-small cell lung cancer

Alex Soltermann; Laura Morra; Stefanie Arbogast; Peter Wild; Holger Moch, Glen Kristiansen
Institute for Surgical Pathology Zürich, Switzerland

Background: The epithelial-to-mesenchymal transition (EMT) is vital for morphogenesis and has been implicated in cancer invasion. EMT of carcinoma cells can be defined by morphological trans-differentiation, accompanied by permanent cytosolic overexpression of mesenchymal proteins, which are normally expressed in the peritumoural stroma. We aimed for correlating the expression levels of the EMT indicator proteins periostin and vimentin with clinico-pathological parameters of non-small cell lung cancer (NSCLC). Method: 538 consecutive patients with surgically resected NSCLC were enrolled in the study and a high density tumour tissue micro-array, containing 2 cores per tumour, was constructed. Immunohistochemistry with antibodies against periostin and vimentin was performed and the protein expression levels in either stroma or cytoplasma were measured by semi-quantitative scores 0 to 3+. EMT was defined as cytoplasmic overexpression with score 2+ to 3+. Results: Of the 538 patients, 384 (71%) were men and 154 (29%) women; the median age being 64 years. Adenocarcinoma was diagnosed in 245 (46%), squamous cell carcinoma in 275 (51%) and adenosquamous carcinoma in 18 (3%) cases. EMT was observed in 30% (periostin) and 12.5% (vimentin) of all tumours, respectively. Overexpression of periostin in both stroma and cytoplasm was significantly associated with the squamous cell carcinoma subtype, a higher pT-stage, a higher histological tumour grade and an increased tumour size of >4 cm (p-values<0.05). Overexpression of stromal periostin only was associated with a higher pN-stage and a higher clinical stage (p-values<0.05). For vimentin, overexpression of cytoplasmic protein only was associated with a higher histological grade (p-value<0.05). Conclusion: To define EMT in NSCLC, the expression levels of the mesenchymal proteins periostin and vimentin have to be measured in both peritumoural stroma and carcinoma cell cytoplasm. Overexpression of periostin is closely associated with increasing TNM stage and grade.

O-2

Squamous cell carcinoma of the lung: polysomy of chromosome 7 and wild type of exon 19 and 21 were defined for the EGFR gene

Vitor Sousa; Maria Silva; Ana Alarcão; Patrícia Couceiro; Ana Gomes; Lina Carvalho
Instituto de Anatomia Patológica - Faculdade de Medicina da Universidade de Coimbra, Portugal

BACKGROUND: The use of tyrosine kinase inhibitors after first line chemotherapy, induced several studies to determine molecular characteristics in non-small-cell lung cancer to predict the response to those drugs.
The present study was delineated to clarify the status of *EGFR* gene by Fluorescence *in situ* Hibridization(FISH), Polimerase Chain Reaction (PCR) and Immunohistochemical protein expression in 60 cases of squamous cell carcinoma of the lung after surgical resection of tumours in stages IIb/IIIa.
METHOD: Representative sections were selected and submitted to tissue microarray construction for determination of EGFR protein expression by applying the antibody Mouse anti-EGFr, Clone 31G7 (Zimed Laboratories) and *EGFR* gene copy number was searched with LSI EGFR/CEP 7 probe (Vysis, Abbot Molecular). Also LP34, CK7, Chromogranin A and CD56 antibodies were applied to correctly define the squamous differentiation of each tumour. Genomic DNA was extracted from selected malignant cells by microdisection in 40 cases. PCR was performed to verify deletions in exon 19 and the pontual mutation in exon 21 of *EGFR* gene, assessed by capillary electrophoresis and restriction fragment length polymorphism (RFLP), respectively.
RESULTS: Immunohistochemical EGFR protein overexpression was identified in 35 cases, by the application of Hirsh scoring system. Increased gene copy number was observed in 32 cases by FISH, according to Cappuzzo method. Through capillary electrophoresis, the deletion in exon 19 of EGFR gene was detected in 3 cases; the exon 21 of *EGFR* was expressed in its wild type by RFLP, in all cases.
CONCLUSIONS: Our study concerning only cases of squamous cell carcinoma of the lung in surgical stages is the first to be done, to the best of our knowledge, after reviewing the published medical literature. In published studies performed in non-small-cell lung cancer in advanced stages, the cases of squamous cell carcinoma referred, expressed

higher levels of the parameters included in the present study. The results obtained showed that squamous cell carcinoma in surgical stages, independently of the presence of lymph nodes metastases, express EGFR protein and have high chromosome 7 polysomy in 50% of the cases and the gene remains without molecular alterations. These conclusions have to be correlated with follow-up of these patients to define potential recurrence related with the results obtained.

O-3

Inflammatory pseudotumour and myofibroblastic tumour of the respiratory tract: just one entity?

A.Ambrosini-Spaltro; C.Ligorio; M.Boaron; S.Asioli; A.Cancellieri; A.Cavazza; M.G. Di Rocco; A.Dubini; D.Galletta; L.Laurino; B.Murer; G.Pelosi; T.Ricchetti; G.Rossi; G.Sartori; S.Damiani

Anatomic Pathology University of Bologna; Division of Thoracic Surgery and Anatomic Pathology of Maggiore Hospital of Bologna, University of Turin, University of Modena, European Institute of Oncology Milan, Humanitas Hospital Milan; General Hospitals of Reggio Emilia, Forlì, Mestre and Treviso, Italy

Background. The nature and the cell of origin of lesions variously described as inflammatory pseudotumour (IP), pseudosarcomatous proliferation or inflammatory myofibroblastic tumour (IMT) are still debated. Most cases behave as benign, reactive lesions, but rarely may have an aggressive course. We analysed the clinicopathological and molecular features of a series of IMTs of the respiratory tract, with the aim to verify if they represent a single entity or a heterogeneous group of lesions.

Methods. Histological features of thirty-eight cases diagnosed as IMT or IP in various Institutions were reviewed. Immunohistochemistry was performed for the following antibodies: CAM 5.2, MNF116, CD34, CD21, CD35, beta-catenin, CD68, HHV8 and 6, smooth muscle actin, desmin, ALK, ki67, IgG4. Molecular investigations included in situ hybridization for EBV and DNA sequencing for c-kit, c-met, EGFR, PDGFR alpha and beta.

Results. Histologically, tumours were subdivided in two groups: type A (8 cases) included lesions with a predominance of inflammatory cells and no prominent spindle cell proliferation; type B (27 cases) included lesions composed of uniform proliferation of spindled cells, sometimes with myxoid features. Three cases had borderline features between type A and B and were classified as "type AB". All cases were negative for cytokeratins, HHV8, HHV6 and CD21 and beta-catenin. Cases from all subtypes were variously positive with muscular markers, CD34, CD68 and IgG4. ALK antibody stained only 4 cases of B type. No cases showed mutations in the genes studied.

Conclusions. Under the designation of IMT or IP are actually included different lesions. In the present series, we identify histologically two main groups: one which represents more likely true myofibroblastic tumoral proliferations, and a group which is represented by non-tumoural, reactive lesions. At moment, however, it appears that there are no immunohistochemical or molecular markers to distinguish the two types of lesions.

O-4

Expression of vascular endothelial growth factor (VEGF) and its receptors in lung carcinoids. A focus on neoangiogenesis.

Cinzia Giacometti1; Giovanna Rizzardi2; Federico Rea2; Chiara Martini3; Francesca Lunardi1; Massimo Rugge1; Marialuisa Valente1; Fiorella Calabrese1.

1 Department of Medical-Diagnostic Sciences and Special Therapies; 2 Department of Cardiothoracic Sciences; 3 Department of Medical and Surgical Sciences, University of Padua, Padua, Italy

BACKGROUND: Angiogenesis is an essential process in the progression of different tumour types. Vascular endothelial growth factor (VEGF) is considered one of the most important angiogenic factor in *vivo*. Its expression and role in human lung carcinoid remains unclear. The aim of the present study was to investigate the expression of VEGF and its receptors VEGF-R1, 2 and 3. The expression was then correlated with tissue neoangiogenesis measured by endoglin (CD105). immunohistochemistry.

METHODS: Between 2003 and 2007, 45 patients (mean age±SD 46.45±15.66 yrs, range 16–75 yrs, M:F=1:1.7) underwent thoracic surgery for pulmonary carcinoid. In each case, immunohistochemical analysis of VEGF and its receptors (VEGF-R1, 2, and 3) and CD105 was performed on serial paraffin sections. VEGF was also evaluated by western blot analysis. Nonneoplastic lung tissues at distance from the primary tumor were also analyzed as controls.

VEGF was quantified in a semi quantitative manner (% of positive cells X intensity staining score, from 0 to 3, range 0 to 300). The micro vessel density (MVD) was assessed as the number of CD105 microvessel positive/mm^2.

RESULTS: All the cases were classified according to WHO as atypical (AC), 12 cases, and typical (TC), 33 cases. VEGF and its receptors VEGF-R1, 2 and 3 expression was mainly detected in the cytoplasm of tumor cells. AC had a higher expression of VEGF (mean±SD 112.28±87.1 vs 44.35± 84.52, p=.03) and a higher MVD (mean±SD 38±26.69 vs 14.1±21.87, p=.03) than TC. VEGF values were directly correlated with MVD (p=.02). No significant differences were found in the expression of VEGF-R 1, 2 and 3 between AC and TC.

CONCLUSIONS: Our data suggest that lung tumor cells are the most important source of VEGF in human lung carcinoids. Neoangiogenesis, which is more pronounced in AC than TC, seems to be highly influenced by VEGF.

O-5

Epidermal growth factor receptor expression in 334 non small cell lung carcinoma patients; prognosis and correlation between gene copy number and protein expression

Jens Enoksson; Monica Haglund; Maria Planck; Per Jönsson; Karin Jirström; Leif Johansson
Department of Pathology, University Hospital UMAS, S-205 02 Malmö, Sweden

Background: Lung cancer is one of the most frequently occurring neoplastic disorders and overall survival is less than 15%. Some patients with advanced non-small cell lung cancer (NSCLC) may benefit from treatment with tyrosine kinase inhibitors directed against the epidermal growth factor receptor (EGFR). Patients can be identified by EGFR gene copy number determined by fluorescence in situ hybridising (FISH) and EGFR protein expression determined by immunohistochemistry (IHC). However, it is difficult to get enough tumour tissue from patients with advanced non small cell lung cancer (NSCLC) to construct high throughput tissue micro arrays (TMA). We studied 369 patients surgically treated for NSCLC during the time periods 1981–83 and 1995–97.
Materials and methods: A TMA with three cores from each case was constructed and evaluated for EGFR protein expression by IHC and FISH for gene copy number. It was scored with IHC as 0–3+ and with FISH as negative (non amplified) or positive (polysomy or amplified). Both tests were evaluable for 334 cases.
Results: *IHC*; 0+=132, 1+=63, 2+=67, 3+=2. *FISH*; non amplified=196, polysomy=115, amplified=23. All cores containing viable tumour tissue could be evaluated for both tests. The correlation between IHC and FISH was highly significant (p=0.0007). *Survival*; Kaplan-Meyer plots showed that EGFR IHC 1–3 was and adverse factor for survival (p=0.02) but not EGFR FISH (p=0.35).
Conclusion; This is one of the first studies to show a highly significant correlation between EGFR FISH and IHC. Also, EGFR IHC 1–3 was a negative prognostic factor for survival. The results suggest that testing for EGFR FISH and IHC should be performed before treating patient with EGFR tyrosine kinase inhibitors.

O-6

STAT1 expression is associated with EBV status in T/NK-cell lymphomas

Patricia Escrivá; Marylène Lejeune; Ramon Bosch; Carlos López; Miriam González; M.Teresa Salvadó; Joaquín Jaén; Lluis E. Pons; Tomás Alvaro
Department of Pathology and Department of Otorhinolaryngology, Hospital de Tortosa Verge de la Cinta. Spain

Background: T-cell and NK-cell lymphoma subtypes exhibit a high association with the Epstein-Barr virus (EBV). The role of cytotoxic T cells (CTL) and macrophages in the control of EBV infection is well established. Moreover, the signal transducer and activator of transcription 1 (STAT1) plays a pivotal role in the initiation and maintenance of certain cancers. The relevance of STAT1 expressing tumor associated macrophages (TAM) has been previously demonstrated in the outcome of follicular lymphoma. We examined the possible relationship between EBV status and the presence of these immune cells in these tumors.
Method: Thirty pathologic specimens with the diagnostic of anaplastic large cell lymphoma (ALCL, n=9), peripheral T-cell lymphoma, unspecified type (PTCLU, n=13), extranodal T-cell lymphoma, other type (ETCLO, n=6) and extranodal NK/T-cell lymphoma, nasal-type (NKTCL, n=2) were incorporated in tissue microarrays. EBV expression was detected by in situ hybridization (ISH) and infiltrated immune cells were detected by immunohistochemistry (IHC). The presence of CTL cells (TIA-1, Granzyme B), macrophages (CD68) and STAT1 into representative areas of the tumor was automatically quantified with the image analysis software Image-Pro Plus 5.0 implemented with appropriated algorithms.
Results: In total, 7 cases (22.6%) were detected EBV-positive: 5 PTCLU (38.46%) and 2 NKTCL (100%). All of ALCL and ETCLO were negative for EBV. The expression of STAT1 correlated with EBV expression (rho=0.489; p=0.011) and with the presence of CD68-positive macrophages (rho=0.616; p=0.001). The tumor tissue of EBV-positive cases presents a significant overexpression of STAT1 (mean 189.86±133.59 vs. 51.24±84.57; p=0.013) as compared to EBV-negative cases. No significant differences in the level of CTL and macrophages were observed in relation to the EBV status.
Conclusion: The association of STAT1 expression with the EBV status and the level of infiltrated macrophages suggest a possible role of STAT1-positive TAM in the immune response against T cell lymphoma.

O-7

Adult T-cell leukemia/lymphoma (ATL) presenting in the skin: clinicopathological and immunohistochemical features of 46 cases

Achiléa L Bittencourt; Helenemarie S. Barbosa; Maria das Graças Vieira; Lourdes Farré

Hospital Prof. Edgar Santos - Universidade Federal da Bahia. Brazil

Background - Adult T-cell leukemia/lymphoma (ATL) is a severe and fatal form of HTLV-I-associated leukemia/lymphoma with frequent skin involvement. We describe the clinicopathologiasl and immunohistochemical findings of 46 cases with histologically-proven skin involvement and investigate whether there is any relationship between the deepness of dermo-hypodermal infiltration and CD8 positivity and median survival time (MST).

Methods - All cases were HTLV-I+ and HIV-, and had known follow-up. Search for HTLV-I proviral integration was performed in 19 cases.

Results - The skin lesions were always multiple and generally disseminated. Twenty-five cases were primary to the skin (smoldering and primary cutaneous tumoral), and 21 were secondary. In all 19 cases imonoclonal integration of the virus was demonstrated, including 9 cases that survived more than 5 years. Twenty-nine cases were histologically diagnosed as peripheral T-cell lymhoma, 16 as mycosis fungoides, and one as anaplastic large-cell lymphoma. Immunophenotype: CD3+, CD4+, CD5+, CD8-, CD45RO+, CD25+, CD7-, and CD20-, but 14 cases were CD8+. 17.4% of the patients are still alive with diesase (6 smoldering and 2 chronic). The overall MST was 21 months. The MST of the cases with superficial versus deep skin infiltration was 20 months and 22 months, respectively. The CD8+ and the CD8- cases had MSTs of 48 and 21 months, respectively.

Conclusions - There are no characteristic histological and immunohistochemical features that enable the pathologist to diagnosis ATL without knowing the results of serologic or molecular studies. No correlation was observed between the degree of skin infiltration and the MST. The MST was longer in CD8+ cases, but the difference between these and the CD8 negative cases was not statistically significant. The smoldering cases had a much longer MST (60 months) in relation to the primary cutaneous tumoral cases (20 months), confirming the importance of clearly defining these two types of primary ATL.

O-8

FOXP3 positive regulatory T-cells in cutaneous T-cell lymphomas

Lise Mette Gjerdrum, Andreas Woetmann, Niels Odum, Elisabeth Ralfkiaer

Department of Pathology, Rigshospitalet, Copenhagen University Hospital. Denmark

Background: FOXP3 is a unique marker for CD4+ CD25+ regulatory T-cells (Tregs). In solid tumours, high numbers of Tregs are associated with a poor prognosis. Knowledge about the implications of Tregs for the behaviour of haematological malignancies is more limited.

Methods: Skin biopsies from 86 patients with either Mycosis Fungoides (MF) or cutaneous T-cell lymphoma (CTCL) unspecified and 27 patients with CD30 positive cutaneous lymphoproliferations (lymphomatoid papulosis (LyP) or primary cutaneous anaplastic large cell lymphoma (C-ALCL)) were analyzed for the expression of FOXP3 on tumour cells and tumour-infiltrating Tregs using immunohistology.

Results: Labelling of the neoplastic cells was seen in a case classified as an aggressive epidermotropic CD8+ cytotoxic CTCL and a case of C-ALCL. In the remaining cases, the neoplastic infiltrate was FOXP3-negative. By contrast, all biopsies showed varying numbers of strongly FOXP3+ tumour-infiltrating Tregs. MF with early or infiltrated plaques had significantly higher numbers of FOXP3+ Tregs than CTCL unspecified or advanced MF with tumours or transformation to large cell lymphoma. Similar results were obtained in 27 cases of primary cutaneous CD30-positive lymphoproliferations. In these conditions, the proportion of Tregs was significantly higher in LyP than in C-ALCL.

Conclusion: Our data indicate that the presence of FOXP3+ Tregs in CTCL is associated with disease stage and patient survival.

O-9

Primary MALT lymphoma of the thymus in a black patient

Carlos Santonja; Guadalupe Renedo; Alicia Cazorla; Raquel Mata; Hans-Konrad Mueller-Hermelink

Departamento de Anatomía Patológica, Fundación Jiménez Díaz, Madrid, Spain

Background. Thymic extranodal marginal zone B-cell lymphoma of mucosa associated lyhmphoid tissue has been included in the recently published WHO classification of tumors of the thymus. 42 cases have so far been reported in the world medical literature. A large percentage of patients are Asians (i.e. Japanese, Korean or Chinese), and many suffer either Sjögren's disease or Rheumatoid Arthritis. We

report a case occurring in a black patient with no history of autoimmune disease.

Method. A 47-year-old man from Angola with pneumococcal sepsis and meningitis underwent aortic valve replacement in January of 2005 because of severe regurgitation due to endocarditis. At the time of surgery, a biopsy was taken of a large, partly cystic anterior mediastinal mass that by imaging techniques had been interpreted as tuberculosis, lymphoma or cystic thymoma.

Results. The submitted 3.5 cm grayish mass consisted of lobules of lymphoid tissue with a vaguely nodular pattern, with interspersed sheets of plasma cells and rare epithelial cysts and Hassall's corpuscles. An extensive network of epithelial cells infiltrated by CD20-positive centrocytoid lymphocytes was disclosed by immunohistochemistry. The plasma cells were monoclonal (kappa) and expressed IgG and IgM. By PCR a clonal IgH rearrangement was demonstrated, in an oligoclonal T background. A RT-PCR for detection of the t(11;18) translocation was negative. The patient was treated with chemotherapy (CVP-Rituximab), with partial decrease in size of his residual mediastinal mass.

Conclusion. This is to our knowledge the first black patient with a MALT lymphoma of the thymus to be reported. The three proposed pathogenic pathways for this entity are: sistemic autoimmunity, spread from a primary gastric or parotideal MALT lymphoma, and aberrant paraneoplastic chemokine secretion from a coexisting micronodular thymoma. No associated autoimmune diseases or MALT lymphoma involving other organs have so far been detected in our patient.

O-10

A diagnostic challenge: Cystic carcinoma of the thyroid with papillary and squamous differentiation.

Thierry Rausch; Michel Sutter; Snezana Andrejevic-Blant.

Institute of Pathology, CHUV-Hospital, Faculty of Medicine and Biology, University of Lausanne. Switzerland

BACKGROUND: It is well known that squamous metaplasia and dysplasia can occur in association with thyroid papillary carcinoma. However, the well-differentiated papillary thyroid carcinoma associated with squamous cell carcinoma denotes rare tumors of the thyroid and present highly difficult task for both, surgeon and pathologist. METHOD: We present a case of a 82 years old female with a painless left latero-cervical swelling, increased in size over the last 6-months. The ultrasonography revealed a large cystic mass, measuring 6 cm. Fine needle aspiration suggests a differential diagnosis of a squamous cell carcinoma, cystic variant, or a branchial cyst with atypia. RESULTS. The neck dissection involving the left lobe of the thyroid and cervical lymphnode was performed. The histopathological examination yielded two intermingled morphologically different patterns including conventional papillary thyroid carcinoma and poorly differentiated squamous cell carcinoma, cystic variant. Four lymphnodes out of 18, presented admixed metastases of both components.

CONCLUSION: Three differential diagnosis were considered: 1) primary papillary carcinoma of the thyroid, with squamous differentiation; 2) a collision tumor involving the papillary thyroid carcinoma and metastatic squamous cell carcinoma with unknown primary and 3) branchial cleft cyst cancerisation associated with papillary carcinoma on ectopic thyroid tissue. The metastatic origin was excluded by the absence of primary head and neck carcinoma. The branchial cleft cyst cancerisation was not retained because of the anatomical localization, absence of preexistent bronchial cyst or precancerous lesions in the cystic part of the tumor. Despite the advanced stage of the disease, the immunophenotype especially of the squamous component, with partial expression of TTF-1, thyroglobulin and p53 overexpression, was consistent with the diagnosis of a papillary thyroid carcinoma with squamous differentiation. This particular presentation of the thyroid carcinoma seems to have a poor prognosis with high recurrence rate and metastases over distant sites in about 20% of the cases.

O-11

Study of vascular invasion in thyroid carcinoma and its relation with histopathology of tumor

Saeed Kareghar;Shokouh Taghipour;Vahid Vahabzadeh

Pathology and surgery wards of shahid sadoughi medical university main hospital, yazd. Iran

Background: Papillary and follicular carcinoma are the two most common thyroidal malignancies. Recent data showed that histopathologic vascular invasion should be considered as a sign of higher tendency to hematogenic and lymphatic invasion. The aim of this study is determine the relation between microvascular invasion with type, stage, and grade of the papillary and follicular carcinoma and patients sex and age.

Method: This cross sectional study was performed on 100 patients (f=77, m=23)referred to shahid sadoughi university hospitals during 1991–2006. Pathologic vascular invasion was assessd with a new scoring system based on number of blood vessels invasion in microscopic fields. Score0=no blood vessel invasion,score 1=in one field seen, score 2=in 2–3 fields seen,scpre3=in 3–4 fields seen, score4=>4 fields invasion seen

Results:The increase of vascular invasion (score3,4)was seen in tumors with poor differentiation (pv=0.001)and

higher stage (tumor size and lymphnode involvement) (pv=0.03). Patients older than 45 years had higher scores (pv=0.036)The number of females was approximately three times more than males but males had a highest score(3,4)Largest tumors had the highest score.patients with lymph node involvement(15%) had highest scores (73.3%had score 3,4)(pv=0.02). There was no significant difference between vascular invasion and metastasis.(pv=0.169)and vascular invasion and type of tumor (pv=0.131) Conclusion: Higher scores of vascular invasion were seen in patients with higher stage and grade,in males and age over45 years. So this study suggest that vascular invasion should be considered as a prognostic factor in thyroid neoplasms. Additional studies need to approve it

O-12

In situ steroidogenesis in Differentiated Papillary Thyroid Carcinoma

Armando Gamboa; Fernando Candanedo; Aura Jiménez; Daniela Domville; Sharon Ortiz

Instituto Nacional de Ciencias Médicas y Nutrición Salvador Zubirán. Mexico

The influence of steroid hormones on the thyroid has been suggested in epidemiologic, case series and in vitro studies. Aim: Identify if aromatase and 17-betaHSD1 expression are associated with morphologic variables and prognosis in DPTC. Design: Analytical comparative study Material and Methods: In a cohort of similarly treated PTC (n=378), we select those patients with differentiated tumor >1 cm submitted to total thyroidectomy. Clinical charts and slides were reviewed. Tumor sections and paraffin blocks were selected to perform tissue arrays and immunohistochemistry for aromatase (Abcam ab18995, Cambridge MA), and 17-beta HSD1(Epitomics EP1682Y, Burlingame CA) was performed. A masked review of cytoplasmic expression was performed and a 10% cutoff was considered for positive cases with both antibodies. Recurrence development was the outcome. Descriptive statistics, Chi square and Fisher exact test were used when necessary. Results: 304 cases were studied, 93% were women, mainly premenopausic (68%) with a mean age of 40 and a 7 year follow up. Classic histotype was observed in 88% and stages I and II were identified in 70% of the cases. Six percent and 29% were positive for aromatase and 17-beta HSD1, respectively. In situ steroidogenesis did not correlate with recurrence, nevertheless positivity for one protein or both was associated with single tumor (p=0.022) and extrathyroid invasion (p=0.042). The percentage of positive cases for aromatase was significantly higher in men than in women (p<0.0001) and this difference was also observed in 17-beta HSD1 when more than 50% of the cells were stained. Conclusion: Single tumors with local invasion produce steroidogenic enzymes, without influence in prognosis at a mean follow up of 7 years. Additional studies including larger groups of recurrent cases or the aggressive variants of PTC should be conducted.

O-13

MERITS OF THE PMiT (PAPILLARY MICROTUMOR) TERMINOLOGY IN THE DEFINITION OF INDICENDAL PAPILLARY CARCINOMAS OF THE THYROID: EXPERIENCE OF FIFTY CASES

Sofia Asioli; Marco Volante; Chiara Odasso; Luigia Macrì; Nicola Palestini; Gianni Bussolati

Department of Biomedical Sciences and Oncology, University of Turin, Italy.

Background: The term “papillary thyroid microcarcinoma (PTMC)” is generally employed to designate an incidental papillary carcinoma measuring 1 cm or less witch manifests extremely indolent behaviour. PTCMs are often detected by chance in thyroids removed for benign clinical nodules or widespread processes. There has been an exponential increase in the detection of PTCMs thanks to the recent improvement and application of ultrasonography in the management of thyroid lesions. However, no definitive treatment guideline has been developed to indicate how best to treat and manage these small tumours. For this reason the surgeon and patients may become alarmed when the pathologist reports the presence of PTMC and this may lead to re-operation, radical dissection of the neck or extensive irradiation, all of which are deemed unnecessary. On the other hand, the pathologist is concerned in defining as a “carcinoma” a lesions which he considers benign. For these reasons, Rosai et al proposed the term Papillary Microtumour of the thyroid (PMiT) during the 12th Annual Cancer Meeting in Porto (2003) and reported strict definition criteria for such entities.
Methods: Since 2003, we have adopted, the Porto proposal criteria for PMiT in agreement with clinicians and surgeons. Here we report a series of 50 consecutive cases designed as PMiT (during the interval from March 2003 to August 2007) collected and treated at Molinette Hospital, University of Turin.
Results: Patients (39F 11 M, median age 55.3 years) underwent to total thyrodectomy (47/50) or to lobectomy (3/50). No further treatment was performed. At histology, PMiT are often associated with benign nodules (19/50) or diffuse hyperplasic goitre (29/50), more rarely to parathyroid adenoma (1/50) and Thymoma B1 (1/50). All patients are alive and well after a median of 31.6 months follow-up (range from 5 to 57 months).
Conclusions: In our experience this terminology, is well accepted by both clinicians and patients, since it decreases the

danger of over-treatment, minimizes the psychological anxiety engendered by a diagnosis of carcinoma, and maintains the patient's eligibility for life insurance unalterated.

O-14

New isoforms of human periostin expressed in the thyroid gland

Yanhua Bai; Gengyin Zhou; Misa Nakamura; Ichiro Mori; Tomoko Wakasa; Akira Miyauchi; Yaqiong Li; Zhiyan liu; Kennichi Kakudo
THE SECOND DEPARTMENT OF PATHOLOGY, WAKAYAMA MEDICAL UNIVERSITY, JAPAN

Periostin is an extracellular matrix protein. Eight isoforms of human periostin (h-periostin) have been identified, which are generated by alternative splicing of the C-terminus. Recently, expression of h-periostin has been linked to carcinoma invasiveness and metastasis, but the role of each h-periostin isoform in the carcinoma invasiveness and metastasis are still little known. The expression and biological roles of h-periostin isoforms in the thyroid tissue and thyroid carcinogenesis have not been established. In the present study, we identified eight isoforms of h-periostin in thyroid tissue by RT-PCR and confirmed their identity by direct DNA sequence analysis. Four of these isoforms were unique to this study and have not been previously identified in any tissue. Especially three of them haven't been previously reported in any species. This is the first report that identified the other four isoforms in the thyroid gland, which have been reported in other human organs. Each of the isoforms was coexpressed in both thyroid carcinoma and matched non-neoplastic tissues. The results suggest that although the expression of these periostin isoforms is a common phenomenon in thyroid physiology, yet their roles in thyroid function and carcinogenesis still remain unknown.

O-15

TIME FOR CHANGE IN FIGO CLASSIFICATION OF MACROINVASIVE CERVICAL CARCINOMA (CX) – BASED ON HISTOPATHOLOGY

Karl Bilek, Bettina Hentschel, Uta Fischer, Dana Galle, Lars-Christian Horn
Institute of Pathology, Division of Gynecologic Pathology, University Leipzig. Germany

Background: Limited knowledge exists about extranodal extension of the tumor outside the lymph node capsule, i.e. extracapsular spread (ECS) the prognostic impact of micrometastatic disease (i.e. metastatic deposits ≤0.2 cm = pN1mic) and for tumor size in FIGO-stage II tumors. *Methods:* 245 cases of FIGO stage II CX who received upfront surgery, were evaluated regarding tumor size. Pelvic nodes of 894 surgically treated CX FIGO IB to IIB were re-examined. In cases with lymph node involvement, the metastatic deposits were measured and extranodal spread of the metastatic deposits outside the lymph node capsule (ECS) was recognised.
Results: FIGO-stage II patients with bulky tumors (113/245) showed reduced 5-year overall survival (67.7% [95% CI: 58.2–74.8] vs. 49.5% [95% CI: 36.8–59.1]; p=0.0015). Patients with metastatic disease represented reduced recurrence free survival (RFS) time (pN1mic: 112.6+6.8 and pN1: 122.5+9.6 months), when compared to pN0 (190.9+3.0 months; p<0.0001). 5-year-overall survival (OS) was also decreased in metastatic disease (pN0: 86.6%, pN1mic: 63.8%, pN1: 48.2%; p<0.0001). The 5-year overall survival rate was significant lower in patients with ECS (33.5% [95% CI: 20.6% - 46.3%] vs. 60.5% [95% CI: 52.3% - 68.6%]; p<0.001). In multivariate analysis, tumor stage, pelvic lymph node involvement and maximal tumor size and ECS, were independent prognostic factors.
Conclusions: The results indicate that micrometastases and extracapsular spread (ECS) of pelvic lymph node metastases is of prognostic impact. A revised FIGO/TNM classification system for pelvic lymph node disease is recommended: pN1mic = micrometastatic disease (≤0.2 cm), pN1 = macrometastases; ECS 0 = lymph node involvement without extranodal spread of the metastatic deposits and ECS 1 = lymph node involvement with extranodal spread of the metastatic deposits as it is for FIGO stage II CX: stage IIA1 and stage IIB1 for tumors with <4 cm and IIA2 and IIB2 for tumors >4 cm (i.e. bulky disease).

O-16

Evaluation of cervical (pre) neoplastic lesions by in situ hybridization and immunohistochemistry: a tissue microarray study

Mohammad Arafa; Jacques Boniver; Philippe Delvenne
Department of Anatomic Pathology and Cytology, GIGA-Cancer, University of Liege, Belgium

Background: Management of (pre) invasive human papillomavirus (HPV) induced cervical diseases depends on the histologic confirmation of the lesions. Misinterpretation of their morphologic criteria leads to a significant diagnostic disagreement. In addition, many benign changes mimic cervical preneoplastic lesions such as immature squamous metaplasia and atrophy. For these reasons, a continuous effort is still going on in order to discover surrogate markers which could help to reach an accurate definitive diagnosis. The aim of this study was to evaluate the usefulness of a panel of biomarkers in the characterization

of cervical intraepithelial neoplasia (CIN), invasive squamous cell carcinoma (SCC) and glandular lesions.
Methods: Archival biopsies of normal ecto- and endocervical tissues, squamous metaplasia, cervical intraepithelial neoplasia (CIN), squamous cell carcinoma (SCC), adenocarcinoma in situ (AIS) and adenocarcinoma (ADC) were retrieved to construct a tissue microarray (TMA). A panel of markers was tested on the TMA obtained slides by in situ hybridization (ISH) (HPV DNA) and immunohistochemistry (IHC) (p16, involucrin, Ki-67 and HPV L1 proteins).
Results: The sensitivity to detect high risk HPV DNA increased with lesion's severity. ISH signals suggesting integrated viral physical status predominated in CIN II/III, SCC and glandular (pre) neoplastic lesions. The p16 and Ki-67 protein expression increased from CIN I to CIN III and to infiltrative lesions. Involucrin positivity was better appreciated in well differentated diagnostic entities (ectocervix, mature metaplasia and CIN I). HPV L1 antibody detected the viral capsid protein in a low proportion of CIN I and II.
Conclusions: Using a panel of cervical biomarkers improves the final reporting of the various HPV induced epithelial lesions. Carefully constructed TMA with single spots of 1 mm diameter is a powerful search tool having a high reliability in representing the archival biopsies.

O-17

Androgen receptor expression in cervical carcinogenesis

Isabelle Fayt, Jean-Christophe Noel.
Department of Pathology, Erasme University Hospital, ULB, Brussels. Belgium

Background: If in vitro studies have demonstrated a potential interaction between HPV and androgen receptor (AR), their expression i vivo during cervical carcinogenesis remains unknown.
Methods: To clarify the issue, we have tested by immunohistochemistery the expression of AR in LSILs (CIN1) (n=30); HSILs (CIN2–3) (n=30) and invasive squamous cell carcinoma (ISCC) (n=13) linked to high risk HPVs (HR-HPVs). 30 cases of normal epithelium served as controls. A H-score system was used for quantification nd a H-score >50 was considered as positive.
Results: AR expression was observed in 100% of normal epithelium (30/30) and LSILs (30/30) but only in 63% of HSIL (19/30) and 23% of ISCC (3/13). A statistically difference ($p<0,05$) concerning this expression was found between normal epithelium and HSILs or ISCC, between LSILs and HSILs or ISCC and between HSILs and ISCC.
Conclusions: This is the first study study describing that the loss of AR expression is a frequent and common event in HSIL and ISCC resulting probably from complex interactions between HR-HPVs and these receptors. These data provide new insights concerning to potential role of androgen and AR in cervical carcinogenesis which should be confirmed in furthers studies.

O-18

PTEN AND KI-67 EXPRESSION IN NORMAL ENDOMETRIUM, ENDOMETRIAL HYPERPLASIA AND ENDOMETRIOID ADENOCARCINOMA

Funda Eren; Leyla Citak; Husnu Gokaslan
Marmara University School of Medicine Department of Pathology. Turkey

PTEN is a tumor suppressor gene that inhibits cell proliferation by regulating intracellular signaling pathways. The aim of this study was to evaluate the expression of PTEN and Ki-67 in normal endometrium, endometrial hyperplasia and adenocarcinoma.
We studied PTEN and Ki-67 expression in 70 endometrial adenocarcinoma, 37 endometrial hyperplasia and 21 normal endometrium immunohistochemically. We evaluated the correlation between PTEN and Ki-67 expression and the most important prognostic parameters (tumor grade, myometrial invasion, lymphovascular invasion and stage) in carcinomas as well as the correlation between carcinomas, precancerous lesions and normal endometrium.
The expression of PTEN and Ki-67 index was the highest in the proliferative phase and PTEN –null glands were also seen in normal endometrium.
We found that the expression of PTEN in hyperplastic endometrium was significantly lower than normal endometrium and carcinoma ($x^2=11.90$, $p=0,003$). In accordance with this PTEN-null glands were significantly higher in hyperplastic endometrium ($x^2=16.55$, $p=0.00$). The difference in Ki-67 staining was not significant. When the subgroups of endometrial hyperplasia was evaluated PTEN-null gland ratio was significantly higher and PTEN staining ratio was significantly lower in hyperplasia without atypia ($x^2=7$, 48, $p=0,02$). No significant correlation in expression was found between subgroups of carcinoma, and the evaluated prognostic parameters. There was no correlation between PTEN and Ki-67 expression.
In conclusion our findings suggest that PTEN is not a distinctive factor in endometrial carcinogenesis but PTEN loss may be an important underlying mechanism for endometrial hyperplasia by causing susceptibility of cellular proliferation under the influence of estrogen.

O-58

Small Size Virtual Slides in Pathology

O. Ferrer-Roca, F. Marcano, J.J. Quintana

UNESCO Chair of Telemedicine. Department of Pathology. Faculty of Medicine. University of La Laguna. Spain

BACKGROUND: Small Size Virtual Slide (SSVS) is a novel technique used by TEXCAN-II® software to make diagnosis on pathology slide images through an intranet or internet environment as these slides were seen under the microscope, with diagnostic quality, in a fast and reliable way, minimizing storage requirements.
MATERIAL & METHODS: SSVS technique was implemented in the TEXCAN-II® software. The system provide a online test where pathology samples were tested using a 5-degree scale of difficulty. Images corresponded to fluid, gynaecology smears and histological samples, captured and digitised using the TEXCAN-II®. JPEG2000 file format and JPIP server technology were chosen to optimise retrieving and transmission of virtual slides through any network.
RESULTS: The results showed coincidences of diagnosis at distance and under the microscope. Retrieving and transmission of images through intranet/internet were significantly faster than similar non-based JPEG2000/JPIP image sharing tools, keeping a optimum diagnostic quality of images.
CONCLUSION: The SSVS technique has been proved as a technique useful for delivering fast and accurate quality pathology images, offering a framework to digitise slides in relatively short time with a high compression rate, keeping the diagnostic quality of acquired images.
INDEX TERMS – Pathology, Telepathology, Telemedicine, Small Size Virtual Slide, TEXCAN -II®, JPEG 2000, JPIP server

O-59

Pathorama – atlas of virtual slides for various target groups

Katharina Glatz; Dieter Glatz

Institute of pathology, university hospital of Basel. Switzerland

ProjectDescription:
Histologic andcytologic preparations form an integral part of pathology education from basictraining to continuing education. At all levels of education the provision of adequatereference material poses a problem. In particular, from small biopsies andcytologic material only very few representative slides can be produced. Thisproblem can be circumvented by virtual slides i.e. fully digitized histologicand cytologic preparations that can be investigated microscopically over theinternet by an unlimited number of students.

Main objectivesof Pathorama at http://pathorama.ch/:

– Development of an open access online atlas with premiumquality histologic and cytologic reference slides for a visually orienteddiscipline.
– Provision of learning material for active and self-guidedlearning for a modern medical educationby allocating slides that can be interactively microscopied instead of static images.
– Pathorama has an integrative function for the institutionand for the society of pathologists and dermatologists by providing referencematerial for the application in different contexts (teaching, research, dailydiagnostics) in one location and readily accessible for all target groups.
– Modular technical concept allowing for the reuse of thecontents in different contexts and for a cost-saving support independent oftechnical experts.
– Integration of Pathorama slides in already existing awardwinning course modules at all levels of education.

Pathorama is used in three ways:

As a self-contained atlas:extensive metadata allow all users to find adequate slides.
As a supplement for existingmodules: our preexisting online pathology courses have been completed by virtualslides which allow the student to «microscope» each diagnosis.
As a foundation for new applications: for students, residents, and experts

O-60

Application programme for tumour bank authorisation in the Andalusian Network: The quality challenge

Ana Isabel Sáez Castillo; Irene Fernández, Mercedes Gómez

Red de Bancos de Tumores de Andalucía. Spain

Usually the creation of tumour banks (TBs) is an initiative of research-active centres seeking access to tumoral samples that have been conserved in excellent conditions. The situation differs in Andalusia because the Public Health System promotes the organisation of TBs as whatever other hospital service. The objectives are to improve treatment of oncological patients (especially their diagnosis) and promote research.
How may we set up a new service in a hospital that fulfils the requirements of treatment and academic interest, and that involves a range of professional disciplines and resources?
RESULTS
A programme has been designed for setting up and authorising TBs based on:

- Familiarisation of the centre's management team. Advantages of establishing the TB:
  - Improvement of diagnosis of oncological patients.
  - Promotion of research. Prospective availability of samples provided with the patients' permission.
  - Review of procedures for sending samples from sites of extraction to places of diagnosis.
  - Review of traceability of samples (identification, processing, storage, policy for obtaining samples, etc.).
- Election of person responsible for the TBs (Pathology)
- Analysis of each centre, specific adaptation of accredited guides for good practice. Policy for control of deviations.
- Familiarisation of all professionals involved.
- Trial period. Adjustment of procedures.
- External authorisation through auditing

In three years, of the 30 Andalusian hospitals, twelve are putting the process in place and four have already been authorised.

IMPROVEMENTS

- To increase institutional investment, allowing TBs to be organised more rapidly.
- To ensure information about the TB is available to professionals and patients. To improve the strategy of informed consent for obtaining permission to use samples: training of professionals, divulging policies for patients.
- Expansion of expectations for treatment (updating of molecular diagnostic hospital service).
- Development of scientific policy ensuring direct benefits to professionals.

O-61

Major discrepancy in clinical and autopsy cause of death: clinical doubt in only a minority of cases.

Miriam Marichal; Tamara Verslijpe; Jacques Sennesael
Universitair Ziekenhuis Brussel, Belgium

Background: With progress in in vivo diagnostic methods, the role of autopsies in clinical medicine is sometimes questioned. We used autopsy request forms and reports to compare the postmortem findings with the clinicians' confidence in their cause of death (COD) diagnosis and with their judgment on the clinical relevance of the requested autopsies. Method: A consecutive series of 2414 clinical non-pediatric autopsies, performed between 2001 and 2006, was analyzed and compared with the autopsy request forms stating the clinicians' COD diagnosis and their rating of the clinical importance of the autopsy as minor, major or essential. Staff pathologists and a senior internist identified the cases with major discrepancies in COD diagnosis. Discrepancies were listed as class I or II, depending on whether or not pre-mortem knowledge of the correct diagnosis would have changed management with benefit in terms of life prolongation or cure.

Results: In 16% of autopsies, a major discrepancy was found between postmortem and clinical COD diagnosis. 61% of autopsies were judged of minor clinical importance, 30% of major importance and 9% essential. Major discrepancies were 14, 17 and 20% respectively. When doubt was expressed (12% of requests), major discrepancy was found in 26% (4% class I and 22% class II). In the large "no doubt" group, 14% showed major discrepancy (4% class I and 10% class II). Clinicians expressed doubt in 20% of discrepant cases.

Conclusion: Clinicians considered most autopsies of minor clinical importance. In 16% of autopsies major discrepancy was found between postmortem and clinical COD. Knowledge of correct diagnosis would have led to different treatment with clinical benefit for 4% of the patients. Clinicians had expressed no doubt on their diagnosis in 80% of discrepant cases. These data underscore the necessity for autopsies as a quality control tool in evidence-based medicine.

O-62

TMA-Match: automatic spot correspondence in TMA serial sections

Musodiq Bello; Ali Can; Xiaodong Tao; Maximillan Seel; Michael Gerdes
GE Global Research, Niskayuna, NY 12309. USA

Background: Tissue Microarray (TMA) technology enables various high throughput RNA, gene and protein expression studies. For multiple studies on the same set of patients, TMAs are typically prepared from adjacent serial-sections of the 'recipient' paraffin block. During preparation, some tissue cores may fall off, making it a challenge to match spots across serial sections or relate them directly to clinical information, especially when a whole slide image is not available.

Method: We have developed automated tools that determine the spotcorrespondence between serial TMA slides and match the image numbers toabsolute coordinates (rows and columns), which in turn are matched toclinical information provided by pathologists. The tool relies entirely on the coordinates of the tissue spots obtained from the microscope and does not require the availability of a whole slide image. The whole slide image can be used when the spot coordinates are not available. We provide tools for visual validation as well.

Results: We used TMA-Match on ten TMA slides from a recipient tissue block originally consisting of 217 breast tissue cores from 55 patients. Six of the slides were conjugated with immuno-fluorescent (IF) dyes and examined under fluorescent microscopy. The remaining four slides were examined with bright field microscopy after Diaminobenzidine tetrahydrochloride (DAB) staining. The whole slide scan was not available for the DAB slides and one of the IF slides. Pathologists provided a TMA map for the block. All the spots were matched across all the serial sections with 100% accuracy. The TMAs were similarly matched with the TMA-map and hence clinical information without any error. The process of matching one TMA to another takes about 45 seconds on a Pentium M Windows PC. Visual images of the overlaid TMAs were generated for verification along with the spreadsheet file that lists the correspondences.

Conclusion: The ability to relate tissue spots in adjacent TMAs is very important for correlating multiple biomarker expressions in immuno histochemistry studies. TMA-Match is simple to use, and the required input is either the whole slide image or the relative x-y coordinates of the tissue spots on the slide. The coordinates can be easily obtained from the microscope. Spreadsheet files with the correspondences are automatically generated along with visual display of the correspondences for validation.

O-63

TMA-Q: A tissue quality assurance tool for sequentially multiplexed TMAs

Ali Can; Musodiq Bello; Xiaodong Tao; Maximillan Seel; Michael Gerdes

GE Global Research, Niskayuna, NY 12309. USA

Background: Tissue Microarray (TMA) technology enables various high throughput RNA, gene and protein expression studies. Technologies to automatically quantify the expression of multiple proteins, genes or RNA on the same tissue by sequentially staining the tissues with dyes attached to biomarkers are the current focus of research in this area. One major challenge with the chemical-based sequential multiplexing approach is tissue folding and progressive tissue loss as the number of staining/bleaching steps increases. Also, the registration of corresponding images from sequential steps has to be verified before performing further analysis.

Methods: We have developed a workflow and quality assurance productivity tool that compares tissue images at any given step with the corresponding baseline images and computes metrics for registration failure, tissue folding or loss as well as tissue viability. This is automatically done for every step of a multiplexed study. The results are presented as a spreadsheet that can be further verified by a user. The quality assurance results are also illustrated graphically with annotated thumbnail images. The tool also allows the user to visualize all the tissue cores on a TMA from multiple sequential steps all at once and compare the results with the automatic evaluation.

Results: We conducted a number of experiments to quantify the performance of TMA-Q in speeding up the QA process. As shown with receiver-operating characteristic (ROC) curves, most of the image-to-image metrics evaluated perform well in identifying good quality tissues. For example, correlation coefficient (CC) gives up to 98.0% true positive rate at 4.9% false positive rate. Also, the tissues were automatically classified into Good Tissues, Partial Fold, and Tissue Loss and compared to manual labeling by an individual. About 94.4% of the images fall on the diagonal of the 3×3 matrix comparing the automated with manual annotation, indicating correct classification. This implies that the user will modify the spreadsheet output of TMA-Q in less that 6% of the images. It is interesting to note that no good tissue was classified as tissue loss (or vice versa) by the algorithm. The errors are in neighboring classes, some of the images of which are borderline cases.

Conclusion: A single TMA can have up to a few-hundred tissue spots and a multiplexed study may involve performing tens of sequential steps on the TMA. It is very crucial for the quality of each tissue spot at each step to be ascertained in order to avoid errors in consequent image analysis and tissue scoring. TMA-Q saves time in the quality assurance process by evaluating each tissue spot image based on registration accuracy, tissue quality, and tissue viability. Compared with examining the tissues one-at-a-time, the tool gives more than 15-fold productivity for validating a typical TMA.

O-64

RECURRENT LUPUS NEPHRITIS IN RENAL TRANSPLANT RECIPIENTS. A REVIEW OF 8 PATIENTS

Esther Roselló-Sastre; Natalia Camarasa; Ana Ávila; Luis Pallardó

Departments of Pathology and Nephrology. Hospital U. Dr Peset. Valencia. Spain

Kidney transplantation in Lupus Nephritis (LN) patients has become a successful treatment for this population. Recurrent LN (RLN) was previously considered rare, but its exact incidence is difficult to establish. We present a review of 8 renal transplant recipients secondary to LN followed for a long period, to establish our RLN rate.

PATIENTS AND METHODS. 8 women, mean age 40 years (y), graft from cadaveric donor (mean age 41 y).

First graft in 7 cases; second graft in 1 case. Mean Time on dialysis before transplantation, 48 months. Mean time to biopsy after transplantation, 28 m (7 d-90 m). Number of biopsied patients: 6, number of biopsies 12 (light microscopy LM and Immunofluorescence IF study). Mean follow-up: 71 m (15–126 m). Maintenance immunosupression: Ciclosporine A, Tacrolimus, or Mycophenolate mofetil and Prednisone. Outcome: graft survival is 100% at one year and 70% at 5 years.

RESULTS. LM study showed: Acute tubular necrosis (4/12), acute rejection (3/12), chronic rejection (2/12), CS-toxicity (4/12) and RLN (5/12). The 5 RLN biopsies belonged to 2 patients, with time to biopsy 11 m-60 m, and were graded as WHO stage 3 (4 cases) and stage 4 (1case). They showed extensive double contours and increased mesangial matrix, with semilunes in 4/5 cases. Compared to the non-RLN group, the only specific parameter was the presence of semilunes (0/7). IF showed glomerular mesangial and subendothelial deposits of IgG-IgA-C3 in 5/5 cases of RLN and in none case of the non-RLN group. Clinical outcome: C3-C4 in normal range in 8/8 patients, graft lost in 2 cases (1 chronic rejection, 1 RLN), proteinuria-increased Creatinine in 1 RLN.

CONCLUSIONS. RLN rate is 25% in our series, all of them as late RLN. Differential diagnosis with chronic transplant glomerulopathy is difficult and requires IF studies. RLN hastens in our series a bad prognosis, increasing the risk of graft lost.

O-65

Gastroesophageal reflux disease (GERD) is highly frequent in lung transplanted patients: the Padua experience

Giovanna Rizzardi2; Cinzia Giacometti1; Laura Zanatta3; Monica Loy2; Giuseppe Marulli2; Francesca Lunardi1; Mario Costantini3; Federico Rea2; Fiorella Calabrese1

1 Department of Medical and Diagnostic Sciences and Special Therapies;2 Department of Cardiothoracic Sciences; 3 Department of Surgical Sciences, University of Padua, Padua, Italy

Background: In lung transplanted recipients, gastroesophageal reflux disease (GERD) is associated with increased incidence of acute rejection, earlier onset of chronic rejection and higher mortality. We report the prevalence of GERD in all patients undergoing single (SLTx) or double (DLTx) lung transplantation from December 2006 to June 2007.

Methods: Sixteen patients (14 females, 2 males, mean age 49.5 yrs) were evaluated. Our protocol included: programmed spirometry, transbronchial biopsy and broncholaveolar lavage (BAL) for routine follow-up testing and lipid-laden macrophage index (LLMI) in the BAL for detection of GER-related lung aspiration, upper endoscopy, gastric emptying study, esophageal manometry and 24-hour pH-monitoring for detection of GER episodes. The median time to enter the scheduled protocol was 5 months from transplantation (range 2–84 mos).

Results: Gastric emptying was prolonged in almost all patients (12/16, 75%). GERD had a prevalence of 56% (9/16), documented at pH-monitoring. Oesophageal manometry revealed abnormal esophageal motility in 37% (6/16); endoscopy revealed the presence of esophagitis in 31% (5/16). LLMI suggestive for lung aspiration (cut-off value >85) was positive in 62% (5/8) patients with GERD and in 43% (3/7) patients without GERD. However, 2/3 patients with normal pH-assay showed moderate gastro-esophagitis at histology. In one case BAL collection was not available.

Conclusions: Our experience confirms the high frequency of GERD in lung transplanted patients. High values of LLMI are correlated with GERD, thus LLMI seems to be a sensitive diagnostic tool for lung aspiration.

PFP-1

Hybrid tumors in renal oncocytosis: the missing link between oncocytoma and chromophobe renal cell carcinoma?

Liang Cheng 1; Stefano Gobbo 1,2; Albino Eccher 2; John Eble 1; Brett Delahunt 3; David Grignon 1; Hemamali Samaratunga 4; Guido Martignoni 2; Shaobo Zhang 1; Mingsheng Wang 1; Paolo Cossu-Rocca 5; Matteo Brunelli 2

Departments of Pathology and Laboratory Medicine 1, Indiana University School of Medicine, Indianapolis, Indiana, USA; Dipartimento di Patologia 2, Universitá di Verona, Verona, Italy; Department of Pathology and Molecular Medicine 3, Wellington Medical School, Wellington, New Zealand; Sullivan Nicolaides Pathology 4, Brisbane, Queensland, Australia; Dipartimento di Patologia 5, Universitá di Sassari, Sassari, Italy.

Background: The term "hybrid" tumor was proposed to describe tumors with morphologic features of both oncocytoma and chromophobe renal cell carcinoma. These tumors are composed of mixed histologic components in the same nodule, often showing transition features characterized by nuclear irregularity and perinuclear halos. The pathogenesis and genetic relationship between oncocytoma, hybrid tumor, and chromophobe renal cell carcinoma are uncertain.

Method: We analyzed the genetic pattern of hybrid tumors, oncocytomas and chromophobe renal cell carcinomas from three cases of renal oncocytosis comparing them with those found in 6 cases of multiple renal oncocytoma. Fluores-

cence in situ hybridization was performed to analyze chromosomes 1, 2, 6, 10, and 17 that are typically lost in chromophobe renal cell carcinoma and numerically normal in oncocytoma. X-chromosome inactivation analyses were also performed in women.
Results: The tumors studied from renal oncocytosis included 7 hybrid tumors, 3 oncocytomas and 1 chromophobe renal cell carcinoma. All three hybrid tumors from one oncocyotosis case showed gains of all five chromosomes tested, one hybrid tumor had gains of chromosomes 2 and 10; no numerical chromosomal alterations were detected in the other three hybrid tumors. In a third oncocytosis, three oncocytomas showed no loss or gain and the chromophobe renal cell carcinoma showed loss of chromosome 1, 6, 10 and 17. Twelve tumors from the patients with multiple oncocytomas showed no loss of any of the chromosomes; two other oncocytomas had loss of chromosome 1 only. A concordant pattern of nonrandom X-chromosome inactivation in the coexisting multiple lesions was seen in both cases of renal oncocytosis and multiple oncocytomas. **Conclusion**: Our data suggest that renal oncocytoma does not progress to chromophobe renal cell carcinoma or to hybrid tumor. These three renal neoplasms seem to be distinct and not related to each other.

PFP-2
PROGNOSTIC VALUE MICROMETASTASIS AND EXTRACAPSULAR SPREAD OF PELVIC LYMPH NODES IN CERVICAL CANCER PATIENTS
Bettina Hentschel; Lars-Christian Horn; Dana Galle; Karl Bilek
Institute of Pathology, Division of Gynecologic Pathology, University Leipzig. Germany

Background: Limited knowledge exists about extranodal extension of the tumor outside the lymph node capsule, i.e. extracapsular spread (ECS) the prognostic impact of micrometastatic disease (i.e. metastatic deposits ≤0.2 cm = pN1mic) in cervical carcinoma (CX).
Methods: Pelvic nodes of 894 surgically treated CX FIGO IB to IIB were re-examined regarding metastatic disease. In cases with lymph node involvement, the metastatic deposits were measured using ocular micrometer and extranodal spread of the metastatic deposits outside the lymph node capsule (ECS) was recognised.
Results: 29.7% (266/894) patients represented with pelvic lymph node involvement. 22.1% of these patients showed micrometastases (pN1mic). Patients with metastatic disease represented reduced recurrence free survival (RFS) time (pN1mic: 112.6+6.8 and pN1: 122.5+9.6 months), when compared to patients without metastatic disease (pN0: 190.9+3.0 months; $p<0.0001$). 5-year-overall survival (OS) was also decreased in metastatic disease (pN0: 86.6%, pN1mic: 63.8%, pN1: 48.2%; $p<0.0001$).
ECS was seen in 30.9% of cases with metastatic disease. Occurrence of ECS showed a correlation to advanced stage disease ($p=0.02$), number of involved nodes ($p<0.001$) and the size of metastatic deposits ($p<0.01$). The 5-year recurrence free survival rate in patients with ECS was significant lower, compared to patients without ECS (59.75% [95% CI: 46.3% - 73.2%] versus 67.2% [95% CI: 58.9% - 75.5%]; ($p=0.04$). The 5-year overall survival rate was significant lower in patients with ECS (33.5% [95% CI: 20.6% - 46.3%] vs. 60.5% [95% CI: 52.3% - 68.6%]; $p<0.001$).
Conclusions: The results indicate that micrometastases and extracapsular spread (ECS) of pelvic lymph node metastases is of prognostic impact. A revised FIGO/TNM classification system for pelvic lymph node disease is recommended: pN1mic = micrometastatic disease (≤0.2 cm), pN1 = macrometastases; ECS 0 = lymph node involvement without extranodal spread of the metastatic deposits and ECS 1 = lymph node involvement with extranodal spread of the metastatic deposits.

PFP-3
VEGF and TSP-1 expression in basal/luminal subtype of breast carcinoma.
Luis Vicioso; Elena Gallego; Martina Álvarez; Isabel Hierro; Lidia Pérez-Villa; Rafael Trujillo*; Emilio Alba*; Alfredo Matilla
Department of Pathology and Oncology. Hospital Universitario Virgen de la Victoria. Málaga. Spain*

Tumour progression depends, at least in part, on recruitment of new vessels or angiogenesis. This process depends on a balance between angiogenic and antiangiogenic factors. Vascular Endothelial Growth Factor (VEGF) is the main proangiogenic factor in breast cancer. Its secretion by tumour cells has shown prognostic relevance in most of the studies. Trombospondin-1 (TSP-1) is a well-known antiangiogenic factor that inhibits tumour growth and metastases in animals. However, its clinical relevance in breast cancer is equivocal. Some data suggest that TSP-1 can promote the increased expression of angiogenic factors by cancer cells reaching a greater propensity to metastasize successfully to distant organs. The aim of this study is to determine any association between TSP-1 and VEGF expression and to investigate their relation with the basal/luminal phenotype of breast cancer.
Method.- Paraffin-embedded tumour sections from 130 breast cancer patients were stained immunohistochemically for ER, PR, HER2, EGFR. Ck18, Ck19, Ck5,6, Ck14, TSP-1 and VEGF expression. Basal subtype was defined by

Ck5,6 and/or Ck14 positivity. Luminal subtype was defined by positivity of Ck18 and/or CK19.

Results.- A basal phenotype was found in 14% of the cases. ER and PR positivity were directly correlated with luminal subtype and inversely correlated with the basal one ($p<0.0001$). VEGF expression was considered as positive in 69 cases (53,5%). TSP-1 showed stromal stain in 78 cases (60%). An association between VEGF and luminal phenotype (Ck18) was found ($p=0,03$) while only 33% of the basal carcinomas showed VEGF positivity. TSP-1 stain was seen in most of the basal carcinomas (78,9%) although statistical signification was not reached ($p=0,06$). In addition, association between VEGF and TSP-1 was found.

Conclusions.- Our results suggest that luminal and basal subtype of breast carcinoma has different way of angiogenesis, with VEGF playing a relevant role mainly in luminal subtype. On the other hand, TSP-1 stromal expression is frequently found in basal carcinomas and its role in the angiogenic process must be investigated.

PFP-4

Clusterin expression in urothelial bladder tumors

Majid Akbari; Elaheh Akbari; Kiril Trpkov

Anatomical Pathology, Rockyview General Hospital, Calgary, Alberta, Canada

Background: Clusterin is a stress-associated cytoprotective protein, which is upregulated in many cancers and confers treatment resistance when overexpressed. To our knowledge, clusterin expression in urothelial tumors has been evaluated only in one study, but the relationship between the tumor grade and the clusterin expression has not been previously studied.

Method: We constructed tissue microarray (TMA) that included 153 urothelial tumors: 13 papillomas, 14 papillary urothelial neoplasms of low malignant potential (PUNLMP), 20 papillary non-invasive low-grade carcinomas and 106 high grade urothelial carcinomas (21 non-invasive, 21 with lamina propria invasion, 21 with muscularis propria invasion, 43 recurrent cases with muscularis propria invasion). The cases were selected from our institutional database. Immunostaining was performed using anti-goat clusterin antibody (Santa Cruz Biotechnology, Inc.). Clusterin expression was scored 0–3+ in the tumor cell cytoplasm, with a cut-off of >10% of positive cells.

Results: Clusterin was not expressed in benign or borderline urothelial tumors. Only one case (5%) of non-invasive low grade tumors showed clusterin expression. In contrast, 19% of non-invasive high grade tumors and 29% of all invasive high grade tumors, were positive, regardless of the depth of invasion. When the positive cases were grouped as low grade tumors vs. high grade tumors, there was a significant difference in the clusterin expression in high grade tumors ($p=0.0004$). No significant differences were found in the clusterin expression in relation to the depth of invasion (lamina propria vs. muscularis propria invasion) and when invasive recurrent and non-recurrent tumors were compared.

Conclusions: Clusterin expression correlated strongly with the urothelial tumor grade, which suggests that clusterin may play a role in the progression of the urothelial tumors. These findings may introduce a new target for nucleotide-based therapy and may lead toward better selection of patients who would benefit from additional aggressive chemotherapy.

PFP-5

Gene expression profiling in gliomas and immunohistochemical evaluation of IGFBP-2

Gianluca Marucci; Moira Ragazzi; Luca Morandi; Enrico Franceschi*; Rossella Miglio#; Daniela Calò#; Annalisa Pession; Maria Pia Foschini; Vincenzo Eusebi.

*Section of Anatomic Pathology "M. Malpighi", Bellaria Hospital, University of Bologna, Bologna, Italy; *Section of Oncology, Bellaria Hospital, Bologna, Italy; #Department of Statistic Science, University of Bologna, Bologna, Italy.*

Background. The differential behaviour of low and high grade gliomas and the possibility to develop novel selective agents that specifically target tumour-associated proteins in gliomas stimulate the research of molecules playing a role in glioma progression.

Method. In the present paper gene expression microarray using about 20,000 genes allowed the study of the gene expression profile in 39 glial neoplasias (28 glioblastomas (GBM) and 11 low grade gliomas, namely 4 oligodendrogliomas, 5 pilocytic astrocytomas (PA), 2 fibrillary astrocytomas (FA)).

Results. Unsupervised classification through hierarchical cluster analysis identified 4 groups of tumours: 2 groups mainly composed of low grade malignant tumours (all the 11 low grade gliomas and 4 GBM), the other 2 were constituted by GBM. 276 genes resulted informative in all the tests. Among them 15 genes were underexpressed in low grade gliomas, but overexpressed in GBM; on the contrary 27 genes were underexpressed in GBM, but overexpressed in low grade tumours. In all GBM there was overexpression of IGFBP-2, that on the contrary was underexpressed in all low grade tumours. This protein, that acts as carrier of IGFs, is synthesized in many tissues to inhibit or enhance IGF actions but it may also have ligand-indipendent activity. Furthermore it is also frequently

overexpressed in various malignant tumours outside the central nervous system. IGFBP-2 immunohistochemical staining was found to be positive in only one low-grade glioma (1/10=10%; 95%CI 0,3–44,5%), while it was found positive in 24 out of 27 GBMs (88,8%; 95%CI 69,7–95,1%).

Conclusion. Gene expression profiling and immunohistochemistry suggest that IGFBP-2 may play a role in glioma progression. IGFBP-2 appears to be a novel immunohistochemical marker of malignancy in glial tumours and probably is the basis for targeted chemotherapy.

PFP-6

Mammalian target of rapamycin (MTOR) signaling activation patterns in neuroendocrine tumors of the lung

Luisella Righi, Marco Volante, Veronica Tavaglione, Rosj Rosas, Pierluigi Filosso*, Silvia Novello, Francesco Ardissone, Mauro Papotti

*Department of Clinical and Biological Sciences at San Luigi Hospital, Orbassano, and *Thoracic Surgery Unit at Molinette Hospital, Turin, University of Turin, Turin, Italy*

Background. Adjuvant therapeutic strategies in metastatic lung neuroendocrine tumors (NETs) are still incompletely settled and are mostly planned on the degree of differentiation of the tumor. Clinical trials testing the efficacy of mTOR inhibitors in lung NETs are ongoing, despite little is known about mTOR activation patterns in this spectrum of neoplasms.

Method. We analyzed the expression of phosphorylated-mTOR and of its major targets p70-S6K and 4EBP-1 by means of immunohistochemistry in a large series of 162 surgically resected lung NETs with complete clinical and follow up information available; the series included 53 typical carcinoids (TC, of which 16 with metastases), 50 atypical carcinoids (AC), 33 large cell neuroendocrine carcinomas (LCNEC) and 26 small cell carcinomas (SCC).

Results. Higher levels of mTOR were detected in well differentiated lung NETs (TC and AC), as compared to poorly differentiated LCNEC and SCC (Mann Whitney test $p=0.01$), whereas 4EBP-1 was more expressed in poorly differentiated tumors ($p=0.02$). A strong correlation between mTOR and p70-S6K expression was observed (Spearman test $p<0.0001$) whereas 4EBP-1 was unrelated to mTOR expression ($p=0.89$), possibly due to the fact that 4EBP-1 antibody does not recognized specifically the phosphorylated form. Low mTOR expression was correlated to the presence of lymph node metastases in AC tumor group (Chi-square test $p=0.018$) and to residual/recurrent disease and disease-related deaths in the poorly differentiated tumor group ($p=0.03$) However, mTOR did not correlate with adverse outcome both in well differentiated and poorly differentiated tumor groups at univariate survival analysis. 4EBP-1 and p70-S6K were both unrelated to specific clinical features.

Conclusion. Peculiar mTOR activation patterns are present within the spectrum of lung NETs, with possible clinico-prognostic implications. The definition of mTOR pathway activation profile in lung NETs is of potential interest to test its predictive value in patients treated with mTOR-targeted therapies.

PFP-7

Squamous cell carcinoma of the vulva: HPV detection and its correlation with p16INK4a and p53 overexpression.

Belen Lloveras; Maria Alejo; Jaume Ordi; August Vida;, Omar Clavero; Joellen Klaustermeier; Nuria Guimerà; Marleny Vergara; Xavier Vallès; Suzanne Garland; Hai-Rim Shin; Jorge Salmerón; Elena Kasamatsu; Antonio Cubilla; Eugénia Cruz; Cheng-Yang Chou; Enrique López; Gustavo Hernández; Efren J. Domingo; Ashrafun Nessa; Edgar Kestler; Asha Jain; Václav Mandys; Sara Tous; Rebeca Font; Wim Quint; Nubia Muñoz; Silvia de Sanjose; F.Xavier Bosch

INSTITUT CATALÀ D'ONCOLOGIA. SPAIN

Objective To assess the correlation of HPV DNA detection with p16INK4a and p53 over expression in relation to histology classification of vulvar carcinomas.

Methods Paraffin blocks corresponding to vulvar cancers are being collected from pathology departments archives. HE slides are cut and reviewed by 2 pathologists. Histological classification includes conventional keratinizing, warty and basaloid squamous cell carcinoma, as well as other less common variants. HPV detection is done by SPF-10 PCR subsequently followed by DEIA and genotyping by $LiPA_{25}$ (version 1). Samples are tested at HPV laboratory at ICO (Barcelona, Spain). Immunohistochemical detection of p16INK4a (clone E6H4, provided by mtm laboratories) and p53 (clone BP53–12–1, Biogenex) staining is carried out using standard procedures and read blinded to HPV results.

Results Data are presented on 196 cases. HPV DNA was detected in 43 samples. All 23 HPV positive cases with warty/basaloid pattern showed p16 overexpression (sensitivity 100%). Among 155 non warty/basaloid carcinomas HPV was detected in 20 samples, of which 16 were p16 positive (sensitivity 80%). p53 was positive (>25%) in 93 (49,2%) cases, of which only 5 were HPV positive. In HPV negative cases, p53 was detected in 88 (59,4%).

Conclusion P16INK4a over expression strongly correlates with HPV detection in cancer of the vulva. In contrast, p53 positivity has a high negative predictive value (94.6%) for HPV detection, both in warty/basaloid carcinomas (90%) and in non warty/basaloid (95,2%). The combination of

p16INK4a and p53 staining appears useful to identify carcinomas related to HPV.

PFP-8

Different microRNA profile in hyalinizing trabecular tumours of the thyroid and papillary thyroid carcinomas

Sien-Yi Sheu; Esther Vogel; Karl Worm; Suzan Schwertheim; Florian Grabellus; Kurt Werner Schmid
Institute of Pathology and Neuropathology, University Hospital of Essen, University of Duisburg-Essen, Essen, Germany

Aims: There is much controversy about hyalinizing trabecular tumours of the thyroid (HTT) regarding their biological behaviour. Because of morphologic (nuclear features) and pathogenetic (Ret/PTC rearrangements) similarities with papillary thyroid carcinomas (PTC) they are considered to be a variant of PTC. Using a set of microRNA typically upregulated in PTC we compared the microRNA expression profile of PTC with those of HTT.
Methods: Paraffin-embedded tissue specimen of 20 patients with HTT were investigated for the expression of a set of microRNAs (miR-146b, -181b, -21, 222 and -221) using real-time quantitative stem-loop RT-PCR. Tissues of 10 multinodular goiter and 10 PTC served as control.
Results: miRNA expression profiles of PTC and HTT are completely different. PTC show an upregulation of all investigated types of microRNAs whereas HTT and nodular benign tissue disclose a similar regulation profile.
Conclusions: Although there are similarities between HTT and PTC in histopathology and some molecular pathologic features the different regulation of the investigated microRNAs is against the assumption of HTT being a variant of PTC probably faouring its classification as a benign tumour.

PFP-9

MUM1 translocations in primary cutaneous anaplastic large cell lymphoma

Andrew Feldman; Mark Law; Ellen Remstein; Ahmet Dogan
Mayo Clinic, Rochester, Minnesota, USA

BACKGROUND: Anaplastic large cell lymphoma (ALCL) is a heterogeneous entity composed of ALK+ and ALK- systemic types and a primary cutaneous (CUT) type. ALCL previously was reported to express the transcription factor MUM1. We recently observed a case of peripheral T-cell lymphoma, unspecified, with a translocation involving the MUM1 and T-cell receptor-alpha (TCRA) genes. We therefore studied a series of ALCLs for MUM1 translocations using fluorescent in situ hybridization (FISH).
METHODS: We evaluated 27 cases of ALCL, including 10 ALK+, 12 ALK-, and 5 CUT. Mean ages in the 3 groups were 31 y, 61 y, and 58 y, respectively. MUM1 staining was performed using immunohistochemistry; staining in tumor cells was scored as diffuse (>30% of tumor cells), partial (10–30%), or negative (<10%). FISH for MUM1 was performed using a home-brew, two-color breakapart probe. Data from G-banded karyotypes were reviewed when available.
RESULTS: MUM1 staining was positive in 8/10 ALK+ (80%, diffuse staining), 10/12 ALK- (83%; 8 diffuse, 2 partial), and 2/3 CUT (67%; diffuse). Overall, 20/25 cases were positive (80%). Two cases could not be scored. FISH showed a MUM1 translocation in 2/27 (7%); both were CUT cases and were diffusely MUM1 positive by staining. Additional FISH showed no evidence of TCRA or IgH as a translocation partner. Neither case had G-banded karyotyping available. Of 11 cases with available karyotypes, 3 were abnormal. Each showed multiple aberrations, but no anomalies involving the 6p25.2 MUM1 locus were seen.
CONCLUSIONS: Occasional cases of ALCL contain translocations involving the MUM1 gene locus. In this study, such cases were restricted to CUT ALCL. Further study is necessary to evaluate (1) the biologic significance of MUM1 expression in ALCL, and (2) the possibility that the presence of MUM1 translocations might be helpful in distinguishing primary cutaneous ALCL from systemic cases.

PFP-10

Caspase 8, survivin and XIAP expression in Ewing Sarcoma Family Tumors (ESFT)

Maria Tsokos; Susana Galli
Laboratory of Pathology, National Cancer Institute, National Institutes of Health, Bethesda, MD, USA

Background: ESFT are common pediatric bone and soft tissue tumors with only 60% cure rate, because of drug-resistant tumor cells with impaired apoptosis. TRAIL, a novel agent, which induces apoptosis by activating caspase 8 and circumventing the mitochondrial pathway, may offer alternative therapeutic possibilities. However, because the balance of the pro-apoptotic caspase 8 and the anti-apoptotic proteins survivin and XIAP may affect the response of ESFT cells to TRAIL, we studied the expression of these proteins in ESFT tissues and cell lines.
Method: Archival, paraffin-embedded ESFT tissues from the Laboratory of Pathology, NCI were studied by immunohistochemistry for the expression of XIAP (48 samples), caspase 8 (38 samples) and survivin (37 samples). An immunohistochemical score was generated by multiplying the intensity of staining (scored as 0, 1+, 2+, 3+) with the percentage of positive cells (0, 1=<10%, 2= 10–50%, 3=51–80%, 4=>80%). Low expression was

defined as score 1–3, medium as 4–6 and high as 7–12. We also examined the expression of these proteins by Western blotting in 15 ESFT cell lines (TC-32, TC-71, TC-248, TC-268, 5838, SK-N-MC, TC-300, TC-324, TC-389, TC-390, TC-392, TC-393, TC-394, TC-399, TC-400). Commercially available antibodies were used.

Results: Moderate to high expression of caspase 8 was seen in 92% and of XIAP in 70% of the specimens. Survivin was expressed in 54% of the specimens. In 24 cases, in which staining for all 3 proteins was available, over-expression of both survivin and XIAP co-existed in 58%. ESFT cell lines showed generally high expression of caspase 8 and XIAP. Survivin expression was variable, similarly to the immunohistochemical data in the tissues.

Conclusion: Our data demonstrate that ESFT express high caspase 8 and therefore, may be amenable to treatment with TRAIL. High XIAP and survivin expression suggests that they may serve as therapeutic targets in selected cases.

O-19

Paediatric Barrett's oesophagus: clinico- pathological features of a rare condition in this age group.

Marta C Cohen; Dhandapani Ashok; John Bishop; Jenny Walker; Mike Thomson; Mudher Al-Adnani

Sheffield Children's Hospital NHS Foundation trust. UK

Background: Barrett's oesophagus (BE) is a common condition in adults but is quite rare in children. We describe the clinical, endoscopic and histological features of all cases of BE diagnosed at our institution between 2000 and 2007.

Method: Information was collected with respect to age, symptoms, treatment, endoscopic and histological features (colonic-like, small bowel-like, cardia-like and a mixture) from patient case notes and pathology computer data base.

Results: Nine children (8 males and 1 female) with a median age of 11 (5 to 15) years were diagnosed with BE. In 8/9 the presenting features were typical of gastro-oesophageal reflux (GOR), 4/9 cases had symptoms of dysphagia (one had a signet ring cell adenocarcinoma of the stomach infiltrating the BE). Two cases had a co-existing Helicobacter Pylori gastritis. The 9 patients underwent 23 endoscopies. These showed features of GOR with various degrees of erythema and superficial ulceration. A stricture was noted in 3/9. Histology confirmed BE in 21/23 endoscopies with: a) colonic-like mucosa in 3/21, b) small bowel-like in 3/21, c) cardia –like in 11/21 and d) mixed in 4/21. None of the cases had fundic-type gastric mucosa. Intestinal metaplasia (IM) was present in all our cases of BE. Sialomucins were present in 21/21 and sulphomucins in 17/21 samples. Both mucins expressed more in columnar than in goblet cells.

The estimated prevalence of BE in the paediatric population of South Yorkshire (North of England) is 0.0018%, 0.6% in children referred for upper GI endoscopy and 9% in the children with reflux oesophagitis. All patients in whom subsequent biopsies were done had intestinal metaplasia. BE is an endoscopic diagnosis that requires histologic confirmation.

Conclusion: BE is rare in childhood, although it has become a less rare diagnosis in our institution in the last few years. Standardised documentation of endoscopic landmarks by the paediatric gastroenterologist and conveying that information to the pathologist is essential for an accurate diagnosis of BE.

O-20

THE USE OF MLPA FOR CYTOGENETIC DIAGNOSIS IN NEUROBLASTOMA TUMOURS

Eva Villamón; Marta Piqueras; Samuel Navarro; Rosa Noguera

Department of Pathology, Medical School, University of Valencia, Valencia, Spain

Background: Neuroblastoma tumour cells show complex combinations of acquired genetic aberrations, including amplification of the *MYCN* oncogene, deletions of chromosome arms 1p and 11q, and gain of chromosome arm 17q. Up to date, many different methods have been used for the detection of deletions and gains including chromosome analysis, Southern blot, fluorescence in situ hybridization (FISH) and methaphasic-comparative genomic hybridization (mCGH). However, these methods have some limitations. Studies using array-CGH (aCGH) are necessary to map the breakpoints precisely. A new methodology called multiplex ligation–dependent probe amplification (MLPA) has been developed. This new approach is based on polymerase chain reaction (PCR) amplification of ligated probes hybridized to target sequences. Furthermore, the MLPA reaction is fast, relatively inexpensive, and easy to perform, and the equipment needed for MLPA analysis is present in most molecular laboratories. In this study we used MLPA technique to detect the genetic alterations in 100 patients with neuroblastoma.

Method: Specifically designed set of probes for testing for chromosomal abnormalities in neuroblastoma, SALSA MLPA Kit P251/P252/P253 (MRC-Holland) was performed in all patients. P251 probemix contains 38 probes for chromosomes 1, 3 and 11; P252 probemix contains 36 probes for chromosomes 2 and 17; P253 probemix contains 32 probes for chromosomes 4, 7, 9, 12 and 14.

Results: The results obtained by MLPA were validated with FISH (*MYCN* amplification; 1p loss), mCGH and aCGH, showing a high concordance. The genetic alterations were used to group neuroblastic tumour in: (a) *MYCN* amplification; (b) segmental chromosome imbalance; (c) entire chromosome imbalance.

Conclusion: The use of MLPA as routine technique will be very interesting procedure to detect the implication of the

common genetics alterations in neuroblastoma that will permit obtain important information for estimation of prognosis and therapy available for patients.
This work is supported by grants RTICC RD/06/0020/0102 (Instituto de Salud Carlos III, Ministerio de Sanidad y Consumo; PI8/07–62 (Conselleria de Sanitat, Generalitat Valenciana); PI4/07–36 (Fundación Sociedad Española de Oncología Pediatrica)

O-21
Implications of high feto-placental weight ratio in appropriate for gestational age (AGA) infants

Olimpia Curran; Liina Kiho; Fiona Warburton; Irene Scheimberg
Royal London Hospital, Barts and The London NHS Trust. UK

Background: Feto-placental weight ratio (FPR) is a reliable indicator of fetal growth and uteroplacental function in small-for-gestational age (SGA) fetuses. However, a diagnosis of high risk appropriate-for-gestational age (AGA) infants is clinically difficult. We propose that an abnormally high FPR can reliably identify high risk AGA infants at any gestational age (GA).
Methods: Placental and fetal measurements were available from a group of 208 singleton intrauterine deaths (IUD), identified through an audit of perinatal post mortems, who died at 24–43/40. A second group of live births (LB) included 277 neonates born at 33–42/40 at two London hospitals and 50 neonates delivered at 30–36^{+6}/40, whose placentas were sent for histological examination. All placentas were fixed and trimmed prior to weighing. All cases were categorized into four groups according to the FPR percentiles by GA (<10th, 10–89th, 90–97th and >97th). The relationship between FPRs and survival was analysed using Chi-square test. Logistic regression was conducted to adjust for GA and birth weight (BW).
Results: The Chi-squared test showed that survival was significantly related to FPRs ($p<0.001$). Logistic regression demonstrated that after adjusting for GA and BW, FPR remained significant ($p<0.001$) with infants with >97th FPR 9.80 times more likely to die than infants with 10^{th}-89^{th} FPR ($p<0.001$, 95% CI 4.57–21.28). In infants with >97th FPR, 75.6% (n=34) were IUD and 24.40% (n=11) were LB. Of the IUD, 17.6% were less than 34^{+6}/40, 8.8% were between 35–36^{+6}/40, and 73.5% were older than 37/40. For each gestational age, 67%, 67%, and 76%, respectively, were AGA.
Conclusions: A substantial proportion of AGA fetuses can be reliably identified as at risk by measuring FPRs at any GA. This emphasises that placental and fetal weights are both important to identify AGA babies at risk, who may subsequently be rescued by an appropriate clinical intervention.

O-22
Congenital granular cell tumor in a newborn, a case report and literature review

Fatemeh Eghbalian
Bessat Hospital. Hamadan University Of Medical Siencies. Hamedan - Iran

Congenital Epulis is a rare tumor of the newborn, also known as granular cell tumor of the newborn or congenital gingival granular cell tumour because of its histological features(this tumor arises from the mucosa of the gingival). Neumann first described CE in 1871. CE is usually benign tumor. Epulis is seen only in the newborn and is a different entity from other granular cell tumors. CE has a female predilection with 8:1 ratio. Epulis is most frequently located on the anterior maxillary alveolar ridge and usually occurs as a single mass although 10% cases occur as multiple. CE clinically appears as a pedunculated protuberant mass which may interfere with respiration or feeding. In cases with large lesions mechanical oral and nasal obstruction can impair fetal deglutition and neonatal respiratory efforts resulting in polyhydramnios prenatally or respiratory impairment postnatally. The exact histiogenesis is still uncertain, various theories of origin are epithelial, undifferentiated mesenchymal cells, pericytes, fibroblast, smooth muscle cells and nerve related cells. The recommended treatment is prompt surgical resection. Recurrences of the tumor and damage to future dentition have not been reported. Spontaneous regression of congenital epulis has been reported in a few cases. However, surgical excision is generally indicated due to interference with feeding or respiration. We report a female neonate with Congenital Epulis (multiple tumors in the anterior maxillary alveolar ridge) and review the relevant literature. The tumors was rejected by surgical excision. The intra- and postoperative course was uneventful. Follow-up for three months didn't show recurrence.
Key words: Congenital epulis, Congenital granular cell tumor, new born.

O-23
Umbilical Cord Stricture Is Not a Genetic Anomaly

Adrián Mariño Enríquez; Pablo Lapunzina*; Alejandra Caminoa Lizarralde; Judith Suárez Aguado; José I. Rodríguez
*Departamento de Anatomía Patológica. *Departamento de Genética Médica. Hospital Universitario La Paz. Universidad Autónoma de Madrid. Spain*

Background: Umbilical cord stricture (UCS) at the fetal insertion is a poorly understood cause of fetal demise. Little is known about its epidemiology and pathophysiology. It has been traditionally considered a sporadic entity with a

very low risk of recurrence in subsequent pregnancies. However, a genetic cause for UCS has been proposed, based on two recent reports on recurrent cases.
Methods: We reviewed 130 cases of UCS located at the fetal insertion, diagnosed among 2,067 fetal and infantile autopsies we performed during the last 10 years, focusing on 2 recurrent episodes and 16 cases occurring in multiple pregnancies. Zygosity was analyzed by placental histology and/or a panel of 12 microsatellite markers to classify twins as monozygotic (8) or dizygotic (8).
Results: UCS was found in 6.2% of the autopsies. All cases were macerated stillborn fetuses and 54.6% were ≤20 weeks of gestational age. There is not a higher incidence of UCS in multiple gestations. Among twins, males were affected more than females (2.2:1), although no statistical significance was found. Associated umbilical cord anomalies were present in 8/16 cases, consisting in hypocoiling (3 cases), hypercoiling (2), excessive length (1), vascular tortuosity (1) and single umbilical artery (1). The most frequent placental finding was obliterative endovasculopathy (6). All eight genetically identical twins were discordant for the anomaly and two dizygotic twins with UCS had co-twins that were also affected.
Conclusion: UCS is not a genetic condition and parents with a fetal demise due to UCS should be counseled as having a low-recurrence risk for subsequent pregnancies. Twinning should not be considered a risk factor for UCS.

O-24

Cardiac Stem Cells in human right ventricular remodelling after surgical palliation for Hypoplastic Left Heart Syndrome

Chiara Castellani, Massimo Padalino, Silvia Toffoli, Mila della Barbera, Ornella Milanesi, Giovanni Stellin, Marialuisa Valente, Gaetano Thiene, Annalisa Angelini
University of Padua, Medical School. Italy

Introduction: The recognition that myocytes and vascular structures could be formed from primitive cells homed to myocardium from circulation or from resident cardiac stem cells was accompanied by the idea that increased cardiac mass in cardiac hypertrophy could result from a combination of myocytes hypertrophy and hyperplasia. Hypoplastic Left Heart Syndrome is a complex congenital heart disease, characterized by severe hypoplasia of the left-sided heart and right ventricular hypertrophy. Aim of the study was to identify the role of cardiac stem cells in the right hypertrophy remodelling in a group of patients affected by Hypoplastic Left Heart Syndrome.
Aim of the study was to identify the role of cardiac stem cells in right ventricular remodeling of patients affected by Hypoplastic Left Heart Syndrome after Norwood surgical procedures.
Methods: Eleven hearts of the affected patients (ages 9 to 365 days) were compared with age-matched controls. Samples taken from the inflow and outflow tracts of the right ventricle were evaluated at histology and immunohistochemistry for stem cells markers.
Results: we observed a recruitment of cardiac precursor stem cells (CPSCs) CD117 and CD105 positive, both in the inflow and the outflow tract in operated hearts compared to the controls (*CD117* inflow: controls 7.8±3.3, operated hearts 18.09± 15.85 cells/field, with p=0.06; outflow: controls 9±4.73, operated patients 17.81±13.61cells/field with p=0.01; *CD105* inflow: controls 1.3±0.9, operated patients 9.18±3.8 cells/field, p=0.07; outflow: controls 1.8±1.6, operated patients 6.2±3.1 cells/field, p=0.1). CPSCs seem to be mainly mobilized by acute injury (early death patients) rather than by chronic processes (late death patients) since a higher presence of putative cardiac stem cells (CD105) was detected in operated patients. The major fraction of CPSCs were found to be localized near collagen III. Rare cycling cardiac precursor cells, positive both for myosin and Ki67 markers were found.
Conclusions: During right ventricle hypertrophy we observed a recruitment of CPSCs, suggesting an active role of endothelial precursor progenitor cells in cardiac remodelling mainly involving the interstitial and endothelial tissues.

O-25

Synovial sarcoma: Presentation of seven cases reports with unnusual localization

Telma Meizoso; M[a] Jesús Fernández-Aceńero; Maria Garrido-Ruiz* M[a] José Mestre; Teresa Rivera; Teresa Aramendi; Concepción Villanueva; Raquel Sánchez-Simón: Luis Cortés.
Department of Surgical Pathology of Hospital de Móstoles and Hospital 12 de Octubre, Madrid, Spain*

BACKGROUND: Synovial sarcoma is a rare soft tissue tumor that most often occurs in the extremities of young adults. On exceptional occasions it is also encountered in areas without any apparent relationship to synovial structures, as in the retroperitoneum, pleura, mediastinum, parapharyngeal region, or abdominal wall.
MATERIAL AND RESULTS: Our report included 7 patients who ranged in age from 12 to 57 years with neoplasm. Primary site were mandible articulation, larynx, wrist, arm, forearm, abdominal wall, and chin. Histological and immunohistochemically these tumors were classified into monophasic and biphasic variants of synovial sarcoma. Complete surgical excision was the treatment of choice. Chemotherapy was administer in 6 cases in the postoperative period and in one case preoperatively. Local recur-

rence was developed in two patient and distant metastasis in three. Four of the patients were alive and three free of the disease.
Synovial sarcoma is a rare soft tiisue neoplasm. Only 3% of these mesenchymal malignant tumors occur in the head and neck region and only 13 cases with endolaryngeal loalization have been reported so far. We report 6 new cases, three of them in the mandible articulation, larynx and chin. The clinical and pathologic feattures of these cases, as well as a practical approach to the diagnosis, is presented.
CONCLUSIONS: Synovial sarcoma needs a differential diagnosis with other neoplasms. More than 50% of the cases shows recurrence and have a high rate of distant metastases. Accurate diagnosis of these tumors requires adequate tissue sampling, immunohistochemical staining and characteristic chromosomal traslocations findings. The poor prognosis of this sarcoma justified a radical surgery wth postoperative neoadyuvant treatment.

O-26

Is beta-catenin Useful in Evaluating Surgical Resection Margins in Desmoid Tumors?

Qihui
The Methodist Hospital Well College of Medicine Cornell University. USA.

Background: Immunostain of beta-cateninis reported useful in confirming a diagnosis of desmoid tumor, which isa locally aggressive spindle-cell neoplasm that requires negativesurgical margins to prevent recurrence. However, H&E sections aredifficult to be sure of a negative margin due to the infiltrativegrowth pattern and bland cytology. The use of beta-catenin staining to evaluate the adequacy of surgical margins in desmoid tumor has not been documented. We investigated beta-catenin staining in a series of desmoid tumors to determine if tumor cells with nuclear expression of -catenin were present at surgical resection margins previously diagnosed as free of tumor by H&E alone.
Design: Paraffin embedded sections from 48 cases of desmoid tumor were immunohistochemically stained with -catenin(1:100, clone CAT-5H, Novocastra). Sections were evaluated for nuclearand cytoplasmic staining. Eight cases of desmoid tumor previouslydiagnosed as having free resection margins by H&E were reviewed,and all sections (n=42) of these margins were immunostained with beta-catenin. These sections were evaluated for the presence of tumor cells (identified by nuclear beta-catenin staining) at the margins.
Result: Nuclear and cytoplasmic staining for beta-cateninwas seen in 46 of 48 cases (96%) of desmoid tumor. One case had onlycytoplasmic staining, and one case had no staining. Tumor cells withnuclear staining were seen infiltrating the inked margins in 5 of the 8cases (63%), represented by 12 out of the 42 margin sections, in whichwe reevaluated margins using beta-catenin immunostain.
Conclusion: Nuclear expression of beta-catenin is a frequent finding in desmoid tumors in our series. Beta-cateninimmunostaining enabled us to identify desmoid tumors with positivemargins that were previously diagnosed as negative by H&E. Therefore, the use of beta-cateninimmunostain may be helpful in detecting foci of tumor cells involvingthe margins, subsequently enabling optimal treatment of the patient.

O-27

Peculiarities of cryptococcosis combined with HIV infection

V.A. Zinserling; N.V. Vassilieva; A.G. Rakhmanova; A. A. Stepanova; V.E. Karev; A.M. Velichko.
Institute of Medical Mycology and Chair of Infectious Diseases Medical Academy of Postgraduate Medical Training, SP Botkin Hospital of Infectious Diseases, St. Petersburg, Russia

Cryptococcosis (C) remains one of the most important complication of HIV-infection on the stage of AIDS. We observed C up to 14,9% as the immediate course of lethal outcomes. On the clinical material prevailed the lesions of the central nervous system; their diagnostics was based upon mycological culture and cytological investigation of CSF with revealing of typical capsulated fungi. In cases the early diagnostics of C allowed the effective treatment.
In the lethal cases C always combined with other infections, recently in most cases tuberculosis. We succeeded to evaluate C. lesions in meninges, brain, lungs, lymph nodes, kidneys, spleen, adrenals and heart. Practically always there was no exudative reactions in the tissues. C varied in seize and thickness of the capsule. Of particular interest was one our case with long term clinical course of HIV, C, and tuberculosis. The patient of 24 years received VAART therapy, fluconazol, amfotericin B etc, died after 6 years history of illness. At the autopsy there were found the hallmarks of HIV infection at stage C: candida pharyngitis, esophagitis; widespread C.: meningoencephalitis, nephritis, splenitis, hepatitis, tuberculosis of lungs with dissemination in kidneys, liver spleen. Some C. were revealed just in the focuses of caseous necrosis. We considered the leading role in the lethal outcome of C lesions of the CNS with numerous polymorph fungi in the histological slices. In order to study the peculiarities of the ultrastructure of the tissue forms of C we refixed for electronic microscopy according our modification specimens of brain and

meninges. The relative good storage of the tissue allowed evaluating the state of C We succeeded to reveal 4 different variants of their degradation, totally intact fungi were absent. Some of the C were phagocyted by macrophages and had undergone degradation. In the macrophages were observed also the signs of catabolic and anabolic processes at once. The time and mechanisms of C degradation in the patients with HIV-infection has to be investigated specially.

O-28

Clinico-pathological discrepancies in the diagnosis of causes of maternal mortality in sub-Saharan Africa

M.R. Ismail, C. Carrilho, C. Romagosa, F. Saute, N. Osman, F. Machungo, A. Bardaji, J.A. Bombí, J. Balasch, P.L. Alonso, C. Menéndez, J. Ordi

Departments of Pathology, Maputo Central Hospital, Maputo, Universidad Eduardo Mondlane, Maputo, Mozambique and Hospital Clinic, University of Barcelona, Spain

Background: Maternal mortality in sub-Saharan Africa continues to be a major public-health problem insufficiently recognized. Extreme differences in maternal mortality rates between developed and developing countries indicate that most of these deaths are preventable. Diagnostic errors may play an important role in this burden.

Methods: We carried out a retrospective analysis of clinico-pathologic correlation, using necropsy as the gold standard for diagnosis. All maternal autopsies during the period from October 2002 to December 2004 at the "Maputo Central Hospital, Mozambique were included and major diagnostic discrepancies, those involving the cause of death, were analyzed.

Results: Major diagnostic errors were present in 56 (40.3%) cases. A high rate of false negative diagnoses was observed for infectious diseases which showed sensitivities under 50%: HIV/AIDS related conditions (33.3%), pyogenous bronchopneumonia (35.3%), pyogenous meningitis (40.0%) and puerperal septicemia (50.0%). Eclampsia, was the main source of false positive diagnoses, showing a low predictive positive value (42.9%).

Conclusion: Clinico-pathological discrepancies were very frequent. They may have a significant impact on maternal mortality in sub-Saharan Africa. Increasing clinical awareness of the impact of obstetric and non-obstetric infections with their inclusion in the differential diagnosis, together with a thorough evaluation of cases clinically thought to be eclampsia could have a significant impact on the reduction of maternal mortality.

O-29

Comparative study of HER2/neu, CD34 AND SMA expression in benign, In situ and invasive ductal breast carcinoma.

David Parada D1; Karla B. Peña G2.

1Servicio de Anatomía Patológica, Hospital Vargas, Caracas. Venezuela. 2Servico de Anatomía Patológica Instituto Oncológico "Luis Razetti", Caracas, Venezuela.

Background: Tumor-stromal interaction plays an important role in tumor invasion and metastasis of breast cancer. The purpose of this study was to evaluate HER2/neu expression in relation with CD34 and smooth muscle actin (SMA) expression in breast fibroblasts.

Methods: Immunohistochemistry for HER2/neu (HERCEPTEST), CD34 and SMA was performed on 159 cases including 10 normal, 20 cases of ductal carcinoma in situ (DCIS) and 129 infiltrating ductal carcinomas. The relation between staining pattern and histopathological features was recorded as positive, negative, or reduced.

Results: Mean age was 52±11 years. 50% were clinical stage II and III. Fibroblasts around normal duct–lobule units were CD34 positive and mainly SMA negative. In contrast, fibroblasts around invasive carcinoma were CD34 negative and SMA positive. In DCIS, loss of CD34 was significantly more frequent in high grade tumours than in low or intermediate grade ones. Her2/neu was seen in 25% of infiltrating ductal carcinomas and 60% of DCIS. There was no correlation between Her2/neu and SMA expression (Rho>0.05).

Conclusions: These results show that loss of CD34 is strongly related to the malignant phenotype, in both pre-invasive and invasive disease. SMA positive myofibroblasts were strongly associated with invasive ductal carcinoma. HER2/neu expression in DCIS and invasive ductal carcinoma showed similar findings compared with otherx studies. Loss of CD34 probably is not related with HER2/neu expression. The functional relevance of altered CD34 and SMA expression is unclear but focal changes implicate local signaling mechanisms probably of epithelial origin, independent of HER2/neu expression.

O-30

Prognostic significance of Aquaporin 1 (AQP1) in human breast cancer

Agnes Bankfalvi; Friedrich Otterbach; Rainer Callies; Rainer Kimmig; Kurt W. Schmid

Institute for Pathology and Neuropathology, University Clinic, Essen, Germany

Background Aquaporin1 (AQP1) is a water channel protein widely expressed in endothelial and epithelial cells

in different organs, where it facilitates water flux across cell membranes. In the human female breast, AQP1 is expressed in endothelial and myoepithelial cells, but its function in resting, lactating and malignant breast tissues is largely unknown. There is increasing evidence that AQP1 is also expressed in high-grade tumour cells of different origin and it may play a role in tumour angiogenesis, cell migration and metastasis.

Methods The aim of this study was to assess for the first time the immunohistochemical expression of AQP1 in a well-characterised cohort of 203 invasive breast carcinomas with long-term follow up to unravel possible associations with patient and tumour characteristics and outcome data.

Results AQP1 expression was found in 5.4% of cases, all belonging to the group of basal-like carcinomas. Accordingly, significant correlations of AQP1 expression were found with high tumour grade (P=0.049), medullary-like histology, absence of oestrogen receptors (ER), "triple-negativity" for ER, progesterone receptor (PR) and HER-2, cytokeratin 14 (Ck 14) and smooth muscle actin expression (SMA) (P<0.000 for each). In univariate analysis, AQP1 was highly significantly associated with poor prognosis (P<0.000). Multivariate analysis showed that AQP1 expression has an independent value in predicting outcome if stratified by age, tumour size, lymph node status, histological grade and ER status (P=0.002).

Conclusions Our results suggest that AQP1 expression is a novel characteristic feature of a particularly aggressive subgroup of basal-like breast carcinomas, which are poor responders to standard chemotherapy. Such patients need new treatment options.

O-31
Quantitative Digital Image Analysis of Estrogen Receptor Immunostaining As a Model for Morphological Screening of Nuclear Immunomarkers

N.Makretsov, W.Howart, P.Pharoah, S-J.Dawson, E.Provenzano, F.Bows, K.Driver, C.Caldas.
Cancer Research UK, Cambridge Institute, Department of Onclogy, University of Cambridge and Addenbrooke's Hospital Department of Histopathology, Cambridge, UK

Background: The application of tissue microarrays (TMAs) to histopathology has dramatically increased the productivity and reproducibility of the immunohistochemical analysis of biomarkers, and required the development of analytical tools for the rapid and accurate assessment of new biomarkers. The aim of this study was to evaluate the clinical utility of automatic analysis of immunomarkers with nuclear staining pattern.

Methods: We used TMAs containing 288 breast carcinomas and estrogen receptor (ER) immunostaining. The TMA slides were digitalized by ARIOL imaging system and scored manually by a pathologist using clinically validated guidelines, considering staining intensity (scores 0–3) and proportion (scores 0–5), resulting in a combined score 0–8. The images were digitally edited by the pathologist and tumor cells selected, where possible. Any images without tumor cells were excluded from the further analysis. The original and edited images were then scored automatically by both ARIOL (Applied Imaging Inc.) and ImageJ (NIH) software. The prognostic significance of all scores was measured by Kaplan-Meier analysis. Receiver-Operator Curve (ROC) analysis was used to measure the sensitivity and specificity of automatic analysis. Kappa-statistics were used to measure agreement between automatic and manual scoring systems.

Results: The automatic scoring of ER (produced by either method) was of prognostic significance in Kaplan-Meier analysis ($p<0.001$). Using original images and manual scores as gold standard in ROC analysis (optimal cut-off of 4–5% positive nuclei) the ARIOL showed 85% sensitivity and 95% specificity compared to 80% sensitivity and 85% specificity for ImageJ scoring (areas under ROC curve 0.94 and 0.88 accordingly). The ARIOL performance improved for edited images (ROC area 0.96) showing 97% specificity, and had no effect on sensitivity. Kappa statistics showed substantial agreement between manual and automatic scoring (Kappa 0.6–0.7, $p<0.001$).

Conclusion: Automated digital image analysis of nuclear immunomarkers is a robust high-throughput screening tool with potential clinical application.

O-32
Evaluation of the axillary clearance rest material, Telemark Hospital-preliminary observation

Bernard Majak; Ivar Guldvog; Torunn Soland
Department of Pathology, Telemark Hospital, Skien, Norway

Sentinel lymph node (sln) examination in the breast cancer patients is well established and performed in all cases of invasive, microinvasive carcinoma and DCIS grade 3 diagnosed patients. A positive result of sln by frozen section, imprint cytology or routine histology causes the axillary node sampling, and the histologic diagnosis has prognostic and therapeutic consequences.

In our study we have spared the rests of axillary clearance material and performed a "second look" cut up,especially searching for not previously found lymph nodes. New sections have been taken and also sections from all negatively reported lymph node remnants-were stained by AE1/AE3 cytokeratin. Our preliminary observation consists of 150 cases In the group of 31 "new lymph nodes" we found 8 micrometastases, while in negatively reported rest material 11 micrometastase have been detected.

Our short study shows, that there are differences in detected lymph nodes in axillary sampling between cut up performing pathologists. The reexamination and a use of simple cytokeratin stain increase the number of detected positive lymph nodes, what may contribute to the better assesment of prognosis and therapy.

O-33

Frequent exon 20 PIK3CA mutations in Her-2 positive breast carcinomas

Enrique Lerma; Lluis Catasus; Alberto Gallardo; Gloria Peiro; Ignacio Aranda; Agustí Barnadas; Jaime Prat
Hospital de la Santa Creu i Sant Pau, Barcelona. Spain

PIK3 mutations are mainly located in exons 9 and 20 and may be important events in breast cancer (BC) progression.. We studied the these mutations in aggressive tumours with Her-2 over-expression or triple-negative BC (negative for ER, PR and Her-2). Forty-nine cases of breast carcinomas with negativity for oestrogen receptors (ER) and progesterone receptors (PR) were collected: 20 with Her-2 over-expression and 29 with triple negative (TN) BC. Clinicopathological data were reviewed and DNA was extracted from frozen tumour or paraffin embedded tissues using standard procedures. PIK3 mutations were assessed by PCR amplification and subsequent sequencing analysis for exons 9 and 20. Five exon 20 PIK3CA mutations were identified among the 20 Her-2 positive BC, whereas one exon 9 PI3K mutation appeared in TN BC (p=0.03). No correlation was found with prognosis. Over-expression of p110α was related with exon 20 PI3KCA mutations (p=0.001), whereas no correlation was found with PTEN loss, Akt over-expression, or other pathological features. Although exon 9 and 20 PI3K mutations are rare in TN, PI3KCA mutations in exon 20 may be relevant in Her2 BC.

TN BC (p=0.03). No correlation was found with prognosis. Over-expression of p110α was related with exon 20 PI3KCA mutations (p=0.001), whereas no correlation was found with PTEN loss, Akt over-expression, or other pathological features. Although exon 9 and 20 PI3K mutations are rare in TN, PI3KCA mutations in exon 20 may be relevant in Her2 BC.

O-34

Nature and prognostic signification of ckit gene expression changes in breast cancer

Dolores Bautista; Isabel Arranz; Ana Jimenez; Maria Luisa Bernal; Bernardo Weil; Sebastian Luna
Hospital Regional Universitario Carlos Haya, Spain

Background: The c-kit gene encodes a transmembrane tyrosine kinase growth factor receptor involved in the development of certain neoplasms. Conflicting results concerning its expression have been reported in malignant breast lesions. Using immunohistochemistry approaches, c-kit expression seems to be lost in most breast neoplasms. However, an increase of c-kit expression has been associated with aggressiveness and poor outcome. The objective of this study was to better characterize the c-kit gene expression within the spectrum of breast ductal carcinoma.
Method: One hundred and twenty eight randomly selected cases of invasive ductal carcinoma containing normal and neoplastic areas were obtained from the local Tumor Bank. The expression of c-kit was analyzed by immunohistochemistry and mRNA expression was evaluated by real time polymerase chain reaction (QPCR). C-kit mRNA was selectively quantified in normal and neoplastic breast epithelial cells using cytokeratin 18 expression as internal reference. We also correlated the findings with tumor size, WHO grade, proliferative activity by Ki67 expression, lymph node metastasis, and expression of HER-2, estrogen receptor (ER)-α, and progesterone receptor (PR).
Results: Using immunohistochemistry and QPCR, protein and mRNA expression of c-kit was high in normal mammary gland. Analyzing tumor regions the different methodologies gave somewhat different results. Protein expression was lost in most invasive breast cancer (89,84%) and was only maintained in few tumors with high tumor size (≥2 cm), high proliferative activity, and estrogen receptor expression. However, mRNA expression maintained a normal index in many neoplasms (51,72%) and the decrease of expression on neoplastic cells was statistically associated to high tumor size and high WHO grade.
Conclusion: These results suggest that the c-kit pathway plays an important role in the maintenance of normal mammary epithelium and that malignant transformation and progression is accompanied by its loss.

O-35

Impact of American Society of Clinical Oncology/ College of American Pathologists guideline recommendations on HER2 testing in breast cancer

Sejal S. Shah; Rhett P. Ketterling; Edith A. Perez; Beiyun Chen
Mayo Clinic Rochester and Jacksonville, USA

Background: Testing for HER2 gene amplification by fluorescent in-situ hybridization (FISH) and protein expression by immunohistochemistry (IHC) plays a critical role in management of patients with invasive breast cancer. The new 2007 guidelines by ASCO/CAP define a HER2 IHC staining of 3+ as uniform intense membrane staining in >30% of invasive tumor cells as compared to previously defined >10% strong staining. We set out to study the

impact of this change on the results of HER2 IHC testing and its correlation with FISH results.
Method: One hundred forty cases of invasive breast carcinoma with IHC of 3+, scored according to the HercepTest interpretation guidelines of strong membrane staining of >10% cells, were retrieved from the archive of Mayo Clinic Rochester. The HER2 IHC slides were re-reviewed and results recorded as percentage of 3+, 2+, 1+, and 0 staining. HER2 FISH analyses were performed in tumors with 11%-30% of IHC 3+ staining.
Results: Of the 140 cases, 14 cases (10%) showed intense membrane staining in 11–30% of the invasive tumor cells and would have been scored as 2+ according to the new ASCO/CAP guidelines. Of the 14 cases, 5 cases were negative for HER2 gene amplification by FISH (HER2/CEP17 ratio of <1.8), 2 cases were equivocal (ratio of 1.8–2.2), 6 cases were positive (ratio >2.2), and 1 case showed dramatic intratumoral heterogeneity with high level amplification (ratio of 12.2) in the IHC 3+ area and no amplification (ratio of 1.0) in the IHC 1+/2+ areas.
Conclusion: The new ASCO/CAP guidelines down-scored 10% of tumors from 3+ positive to 2+ equivocal in this study, and half of these tumors are positive for HER2 gene amplification. Clinical study is needed to determine whether the new guidelines would be better at predicting response to anti-HER2 therapy.

O-36

Basal- and non-Basal Phenotypes in Triple-Negative Breast Cancers

Zeinab Elsawaf; Hans-Peter Sinn
Dept. of Pathology, Univ. of Heidelberg, Germany

Background: Triple negative breast cancers are characterized by lack of expression of oestrogen, and progesterone hormone receptors, and lack of HER2 overexpression. Frequently they are associated with a basal phenotype, but there is a distinct subgroup of "quadruple-negative" cancers which not basal-like, and are yet ill defined yet. Therefore, in the present study, we have analyzed the expression of basal and other markers the triple negative breast cancers.
Methods: 158 triple-negative invasive breast carcinoma were selected from the archives and used for construction of tissue microarrays. A panel of immunohistochemical markers, which included ER, PgR, HER2, CK5/6, CK14, CK18, EGFR, p53, c-KIT, MKI-67, bcl-2, and p16 was used to further characterize these tumours.
Results: 102 tumours (66%) showed a basal phenotype by being positive for either CK5/6 or CK14 using a cutoff value of 10%. The non-basal triple-negative cancers differed from the carcinomas with a basal phenotype by having a lower proliferative rate ($p=0.04$), and were less frequently CD117 positive (14% vs. 32%, $p=0.01$) and less frequently overexpressed p16 (31% vs. 52%, $p=0.01$). No differences were seen for bcl-2 (9% vs. 10%) and p53 overexpression (37% vs. 36%).
Conclusions: Non basal-like triple-negative breast cancers differ from basal-like triple-negative breast cancers in several aspects, and have a lower malignant phenotype. Therefore, this subgroup of triple-negative breast cancers is important to distinguish from the basal-like triple-negative breast cancers.

O-37

Role of intraoperative imprint cytology for evaluation of surgical margins in breast cancer: a prospective controlled study about 400 lumpectomy

François D'Halluin; Patrick Tas; Olivier Coué; Cécile Bendavid; Jérôme Blanchot; Fabrice Foucher; Jean Vialard; Habiba Meshba; Jean Levêque
Centre Eugène Marquis, Comprehensive Breast Cancer Center, Rennes, France

Objective: The aim of this study is to assess the efficacy of intraoperative imprint cytology (IIC) in conservative surgery for early stage of breast cancer.
Materials and methods: This is a prospective controlled study led at the Comprehensive Cancer Center of Rennes, France. We reviewed a total of 736 patients who underwent lumpectomy for unifocal breast cancer from January 2004 to 31st December 2005. 400 procedures were finally included. After a standardised surgical procedure, the lumpectomy specimens were intraoperatively oriented by he surgeon and were submitted fresh to pathology for cytologic assessment. The IIC consisted of touching the four faces of interest (superior, inferior, and laterals) onto the glass slide.
Results: We evaluated 1665 separate margins. The correlation between IIC and permanent sections was 91.5%. Sensitivity was 88.6%, and specificity was 92.2%. Positive predictive value was 73.6%, and negative predictive value was and 97%. The analysis of the false positives, show significantly ($p<0.001$), that the lesions of fibrocystic mastopathy were more frequently identified in the lumpectomy. The rate of false positives was significantly increased when the technique used more than four apposition slides ($p=0.0019$). The ductal carcinoma in situ was statistically greater represented among the false negatives ($p<0.005$), above all when its size was ≥30 mm ($p<0.005$). The intraoperative reexcisions not requested by the pathologist were tumour free in 93.9% of cases; conversely there was 71.2% residual tumour when the pathologist requested these reexcisions. The global rate of postoperative reexcisions was 13.25% and IIC avoided a second intervention for 47 patients.
Conclusion: Intraoperative imprint cytology is a rapid, simple, reliable and cost-effective method to analyse the margin status

of lumpectomy in patient undergoing breast conservative surgery. This technique allows a survey of the entire surface area of the lumpectomy specimen. This method is enables to reduce the number of second operative procedures.

Keywords: Imprint cytology, Margins, Breast cancer, Lumpectomy

O-38

Luminal and basal phenotypes in salivary duct carcinomas

Mats G Karlsson

Dept of pathology, Örebro univrsity hospital and School of Health and Medical Sciences, Örebro university, Sweden

Background Salivary duct carcinoma (SDC) is a morphological look-alike to ductal breast carcinoma. Molecular studies have identified four subgroups of breast carcinomas, oestrogen receptor (ER) positive, luminal cell, basal cell and non-specific types. Luminal carcinomas are characterized by HER-2 amplification, basal cell type by cytokeratin 5 positivity and epidermal growth factor receptor (EGF-R) overexpression. SDC are not associated with ER expression whilst HER-2 receptor overexpression is frequent. A group of non-HER-2 amplified SDC exists. Thus, the question emerged whether there is a basal type of SDC.

Method 28 SDC were available for analysis. The cases where either *de novo* or carcinomas ex plemorphic adenoma with SDC morphology.

CK5, p63 and EGF-R were immunohistochemically stained. Cases with >10% cytoplasmatic (CK5), nuclear (p63) and membranous staining (EGF-R) were considered positive.

Fluorescence in situ hybridization for HER-2 was performed. A ratio (HER-2:centromere) of ≥2.2 was considered amplified, high (not countable) HER-2 signal were considered as clusters. HER-2 data has previosly been reported.

Results HER-2 clusters were found in 14 tumours, two tumours were heterogeneous with non-amplified areas. One case showed low-level amplification.

18 SDC showed basal phenotype, 17 of these with EGF-R overexpression. Nine were HER-2 negative, 5 showed HER-2 gene clusters while the three remaining cases were heterogenous or low level concerning HER-2.

CK5 and/or p63 positivity occurred in 9 of the tumours with basal phenotype, two of the cases showed HER-2 gene amplification.

Discussion Luminal and basal phenotypes occurs in SDC. There is a group of tumours with both HER-2/luminal as well as EGF-R/basal associated molecular events in SDC. Emerging interests in molecular targeted therapies highlights the need to characterize tumours concerning several oncogenetic pathways. In the case of SDC, these results indicate that targeted therapies for both EGF-R and HER-2 need to be evaluated.

O-39

ESR1 hypermethylation in prostatic adenocarcinoma correlates with high Gleason score

Dilek Ertoy-Baydar; Sevilay Karahan; Haluk Ozen

Hacettepe University Medical School, Turkey

Background: Abnormal DNA methylation of the gene promoter regions is linked to numerous cancers through silencing the expression of tumor suppressor and other regulatory genes. It refers to covalent bonding of a methyl group to the 5′-cytosine of the dinucleotide, CpG. Aberrant promoter methylations have been reported for several genes in prostate carcinoma. We have evaluated the methylation status of estrogen receptor alpha gene (ESR1) and investigated its value in the disease prognosis.

Method: Sixty eight radical prostatectomies from clinically localized prostate cancer patients were included in the study. Preoperative and post-operative data were obtained from the hospital charts. Slides were reviewed to note prognostically important pathological parameters. Paraffin blocks were used to isolate tumor DNA from each case. The presence of ESR1 CpG island hypermethylation was determined by real-time methylation specific polymerase chain reaction.

Results: Gleason score of the tumors ranged from 6 to 9 while pathological stage ranged from T2N0Mx to T3BN1. ESR1 gene was found methylated in 11 cases. Unfavorable prognostic features were more frequent in radical prostatectomies with ESR1 hypermethylation. The rates of extraprostatic extension, seminal vesicle invasion, lympovascular permeation, PSA relapse, Gleason score ≥7 and pT ≥3a were 68.4%, 22.8%, 14%, 31.4%, 73.6% and 68.4% respectively in hypermethylated group in comparison to 72.7%, 45.5%, 27.3%, 40%, 90.9% and 72.8% in non-methylated group. The correlation between presence of hypermethylated gene and high Gleason score was statistically significant ($p=0.028$).

Conclusion: ESR1 hypermethylation is rare in prostate carcinoma, seen in 16% of cases. Our findings suggest that the patients with methylated ESR1 are more likely to present with adverse prognostic features. ESR1 silencing may play a role in the progression of the disease.

O-40

Invasion front: Cadherin-shift and tumorproteases in prostatic cancer

Peter E. Stoemmer; Ingrid K. Bayer

Forschungslabor Prof.Dr.Dr.Stoemmer; Gemenschaftspraxis für Pathologie. Germany

Background: *I*ntratumoral heterogenity in prostatic cancer (PC) leads to different architectural classifications. Studies of the expression of cellmembrane-adhesion-molecules and

proteases considered only the Gleason-Score of the tumor but not the localisation of different cadherin- expressing cells in respect of centrally located tumorcells versus cells of the invasionfront and epithelial-mesenchymal transition zone (EMT), being probably more important for its biological behaviour.

Method 60 EMT-zones of PC were analysed in respect to their expression of E-cadherin(Biologo,Dr.Schultheiss, Kronshagen,Klon 5H9), N-cadherin (Biozol,Eching, GeneTex; IgG,polyclonal), β-catenin (Dianova,Hamburg; rabbit polyclonal) and hepsin (Cayman Chemical; IgG) in comparison to adjacent nontumor epithelia and carcinomacells in the central parts.

Results *E-Cadherin:* Membranous expression in non-neoplastic glands. Low expression in tumor-cell-membranes Gleason-Pattern 3 and 4; good expression in peripheral parts of cribriform areas and in small tubular and trabecular parts of the tumor. Loss of E-cadherin in the inasionfront and EMTs.

N-Cadherin: No N-cadherin in non-neoplastic glands; high cyoplasmic and membranos expression in tumorcells of EMTs corresponding to the loss of E-Cadherin (E-cadherin: N-cadherin-shift).

β-Catenin: Membranous localisation in non-neoplastic glands; membranous and granular intracytopamic deposits in tumor-center; intranuclear β-catenin in cells of the invasionfront.

Hepsin: low expression in non-tumor glands; mediocre expression in centrally localised carcinomacells; very high expression in epithelia of invasionfront and EMTs.

Conclusion: Tumorcells in EMTs show extensive remodelling of shape and function: shift of intercellular connections (cadherins), nuclear translocation of β-catenin, inducing wnt-pathway, abundance of serin-protease (hepsin), fostering invasion by dissolvin collagens and dissolution of tight cell-adhesions in the invasion front influencing the tumor's biology and architecture.

O-41
CORRELATION BETWEEN BIOPSY and PROSTATECTOMY - PREDICTIVE FACTORS

Isabel Español; Noemi Vidal; Isabel Trias
HOSPITAL PLATÓ. SPAIN

Background: The increase in detection of the PSA has taken to a rising number of prostate biopsies (bx) that plays an important role at the time of making therapeutics decisions. We have tried to correlate biopsy and prostatectomy (p) that allows us to predict the neoplasia stage.

Materials and Methods Radical prostatectomy was performed in 77 patients between 2005–2006. We have 48 biopsies, 17 of them with information of Gleason(G). The age average is 66.5. We have reviewed in bx as well as in p: PSA measurement before and after the treatment, Gleason (G), extraprostatic extension, perineural invasion, volum in %, pT and surgical margins status (irregular/regular, focal/extensive).

Results The score correlation between bx and p is of 58% rising to 85% for G=7. In 1,5% there is an overgrading and infragrading in the 30%. PSA before p was between 12.5 and 4.4 ng/ml. We have found bilaterally in 15 bx, and 100% is confirmed in p. All of the p had bx with intraprostatic cancer. The majority of the cases (46/77) are T2C, 3/77 of them had previous treatment and one case was not valuable by fragmentation. The rest is distributed in T3A, B, T2A, B. The resection margins were not valuables in 2, affected in 21, and free in the 53. 13/21 cases have been submitted to RDT treatment. Only one of the cases that have PSA measurement post-treatment, has detectable PSA.

In the biopsies, 8 cases had perineural invasion. 4/8 turned out to be T2C, and 4/8T3A-B had affected margins. Of those without perineural invasion, 71% were T2C and only 5% T3A, and 20% had affected margins. There are not significant differences with theGleason.

Conclusions It is significantly important to evaluate a series of parameters in the biopsy, because they will be decisive by the time of making a suitable treatment, and to establish a reliable prediction. The perineural invasion biopsy is a factor that predicts an advanced local stage. In our series, the resection of margins status has no influence in the short time prognostic (two years). It is necessary longer pursuit to take out conclusions. Pathologist accurate valuation of the biopsy is vital, so that a strict professional discipline is very important at the time of biopsy grading.

O-42
PIK3CA MUTATIONS IN PROSTATE CANCER

Laia Agell, Silvia Hernández, Silvia de Muga, José Antonio Lorente, Núria Juanpere, Raquel Esgueva, Antoni Gelabert, Sergi Serrano, Josep Lloreta
Hospital del Mar, Departament d'Anatomia Patològica. Spain

Background: An important goal in cancer research is the identification of genes involved in tumor initiation and progression. One of thecrucial genes is PI3K, specifically its catalytic subunit p110α, also known as PIK3Ca, has been found to be mutated in different tumor types such as colon, breast and bladder cancer. There have been no reports of studies on this gene in prostate cancer. The aim of our project is to analyze the frequency of mutation of this oncogene in a well-defined group of prostate tumors.

Methods: A total of 35 cases with prostate cancer were selected from the files of the Department of Pathology (Hospital del Mar, Barcelona). DNA was extracted from formalin-fixed, paraffin-embedded tissue in which representative tumor areas were selected and manually microdissected. 5 consecutive 10 μm sections were deparafinized and DNA was extracted using Dneasy Tissue Kit (Qiagen GmbH, Hilden, Germany). We studied the exons 9 and 20, in which most of the reported mutations have been discovered. Mutational analysis was performed by direct sequencing from the purified PCR product.
Results: Only one change was found in a total of 35 radical prostatectomy cases containing clinically significant tumors, 15 with a Gleason grade ≤6; 14 with a Gleason Score of 7 and 6 with a Gleason Score ≥8). The only change occurred in intron 9 (IVS9+91) producing a transition C-T in different tumor areas of the same patient.
Conclusion: Our findings indicate that PIK3Ca mutations could be an uncommon abnormality in prostate cancer, but further analysis in larger series of patients must be carried out.
Supported by FIS 06/1411, FIS 965190005 and Spanish Association Against Cancer.

O-43
DISTINCT CELLULAR EXPRESSION PATTERNS OF NEUTRAL ENDOPEPTIDASE (CD10) IN PROSTATE CANCER PREDICT DIVERGING CLINICAL COURSES

A. Fleischmann; T. Schlomm; H. Huland; M. Graeten; Ph. Simon; M. Mirlacher; R. Simon; G. Sauter; A. Erbersdobler
Institute of Pathology, University of Bern, Switzerland; Dept. of Pathology, University Medical Center Hamburg-Eppendorf, Germany

Background: Prostate cancer is a heterogeneous disease with variable clinical courses. Individual prediction of outcome is relevant to select the appropriate therapies and avoid overtreatment. CD10, a cell surface bound endopeptidase, has been suggested as a potential molecular marker for prostate cancer.
Methods: 3261 prostate cancer patients treated homogeneously by radical prostatectomy were evaluated using tissue microarray (TMA) technology. Immunohistochemically, the cellular domain (membranous, membranous-cytoplasmatic, cytoplasmatic only) of CD10 expression was analyzed and correlated with various clinical and histopathological and immunohistochemical tumor features.
Results: CD10 expression was present in 62.2% of the cancer samples and occurred preferentially in higher Gleason pattern. CD10 expression positively correlated with adverse tumor features like elevated preoperative PSA, higher Gleason score and advanced stage ($p>0.0001$ each). Survival analyses showed that PSA recurrence was significantly associated with CD10 expression intensity and also staining pattern. Outcome significantly declined with increasing staining intensity ($p<0.0001$) and from negative over apical, apical-cytoplasmatic to exclusively cytoplasmatic CD10 expression ($p<0.0001$). In multivariate analysis CD10 expression was an independent predictor for PSA failure.

O-44
The role of allelic imbalance at 8p in cases of atypical adenomatous hyperplasia of the prostate and its implications on prostatic carcinogenesis

Rafael J Luque; Ana Quintero Cabello(*); Mª Dolores Martín Salvago; José María Martínez de Victoria; Isabel Ruiz Ávila; Antonio López-Beltrán(*).
Pathology Department, Complejo Hospitalario de Jaén and (*)University of Córdoba, Spain

Background: The putative precursor for prostate cancer is Prostatic Intraepithelial Neoplasia (PIN), that shares morphological, functional and genetical features with intermediate-grade Prostate Cancer (PCA). However, little is known about the origin of low-grade PCA. Atypical adenomatous hyperplasia (AAH-adenosis) has been proposed as such preneoplastic lesion. The goal of this study is to investigate the role of Allelic Imbalance (AI) at 8p -a common feature of PCA- in AAH, trying to define different populations of AAH indicating a possible transition to PCA.
Method: We studied 40 formalin-fixed, paraffin-embedded samples from simple prostatectomies which contained 42 foci of AAH, coexisting with NH and transition zone well-differentiated PCA. Stereological studies were performed determining mean nuclear volume, volume fractions of stroma and basal cells and relative number of nucleoli in acinar cells. Immunohistochemical demonstration of p21, p27 and MIB-1 was made and corresponding labelling indices were determined. Also they were tested for AI at four different loci of 8p (D8S133, D8S261, D8S254 and DS258) using standard methods. Statistical analysis was done using Student t test to compare cases with or without AI.
Results: 33 cases were informative. Of them, 13 cases showed AI at different loci of 8p. When stereological and immunophenotypical features of these cases were compared with Normal (N) cases, an increase in the relative number of nucleoli (N: 0.85%, AI: 1.85%, $p>0.001$) and p21LI (N: 9.13%, AI:13.66%, $p=0.006$) and a decrease in p27LI

(N:45.72%, AI:31.55%, N.S.) was noted, The rest of parameters showed similar values for N and AI groups.
Conclusion: AI at 8p seems to be related with morphological and functional changes in a subset of AAH, more similar to those noted in previous studies for well differentiated PCA. This group should be more likely to be the immediate precursor of PCA of the transition zone of the prostate.

O-45

Clear-cell papillary renal cell carcinoma: a distinct histopathological and molecular genetic entity

Stefano Gobbo 1,2; Albino Eccher 2; John Eble 1; David Grignon 1; Guido Martignoni 2; Gregory MacLennan 3; Rajal Shah 4; Shaobo Zhang 1; Matteo Brunelli 2; Liang Cheng 1

Departments of Pathology and Laboratory Medicine 1, Indiana University School of Medicine, Indianapolis, Indiana, USA; Dipartimento di Patologia 2, Universitá di Verona, Verona, Italy; Departments of Pathology and Laboratory Medicine 3, Case Western Reserve University, Cleveland, Ohio; Departments of Pathology and Laboratory Medicine 4, University of Michigan, Ann Arbor, MI USA

Background: Tumors composed of cells with clear cytoplasm arranged in papillary patterns have been recently described in kidneys with end-stage renal disease.
Method: We investigate the cytogenetic and immunohistochemical phenotypes of papillary tumors entirely composed of clear cells showing the same peculiar features previously described in tumors arising from kidney with end-stage renal disease but arising also in kidneys unaffected by end-stage renal disease. Interphase fluorescence in situ hybridization was performed with centromeric probes for chromosomes 7, 17 and Y, to analyze the typical chromosomal alterations seen in papillary renal cell carcinoma. We also tested deletion of 3p usually seen in clear cell renal cell carcinoma using centromeric probe for chromosome 3 and subtelomeric probe for 3p25.
Results: Seven tumors from 5 patients (age range: 53 to 64 years, mean: 60 years; 3 male and 2 female) were identified. Only one patient had end stage renal disease. All 7 tumors (ranging from 4 to 50 mm in diameter) were stage pT1. None showed recurrence or metastasis after a mean follow-up of 24 months. Six tumors showed no chromosomal losses or gains of chromosomes 7, 17 or Y; one case had gains of chromosome 17. Chromosome 3p deletion was not detected in any case. Cytokeratin 7 and CA-IX were strongly positive in all cases. CD10 immunoreactivity was negative in six tumors and focal in one case, Alpha-methylacyl-CoA-racemase and TFE3 were negative.
Conclusion: Clear-cell papillary renal cell carcinoma may arise in otherwise normal kidneys as well as kidneys with end-stage renal disease. This tumor has immunophenotypic and genetic profiles distinct from those of either classic papillary or clear cell renal cell carcinomas.

O-46

FLUORESCENCE IN SITU HYBRIDIZATION, FLOW CYTOMETRIC AND KARYOTYPING ANALYSES IN THE DIFFERENTIAL DIAGNOSIS BETWEEN RENAL ONCOCYTOMA AND CHROMOPHOBE RENAL CELL CARCINOMA.

Matteo Brunelli; Brett Delahunt; Stefano Gobbo; Albino Eccher; Liang Cheng; Regina Tardanico; Piera Balzarini; Claudia Parolini; Samantha Bersani; Fabio Menestrina; John Nelson Eble; Guido Martignoni.

Department of Pathology, University of Verona, Italy.

Background: Cytogenetic analysis usually reveals low number of chromosomes 1, 2, 6, 10 and 17 in chromophobe renal cell carcinoma and a normal numerical complement of chromosomes in renal oncocytoma. However, different chromosomal patterns have been rarely reported in both renal cell neoplasms.
Method: We investigated 23 renal cell neoplasms (11 chromophobe renal cell carcinomas, 12 renal oncocytomas)by metaphase karyotyping and interphase FISH for chromosomes 1, 2, 6, 10 and 17 and flow cytometric analyses on tissue sections.
Results: FISH showed losses of two or more chromosomes in 10 chromophobe renal cell carcinomas (91%) and gains of multiple chromosomes in one (9%). Six (50%) renal oncocytomas were totally disomic, five (42%)showed one chromosomal loss (chromosome 1 in 3 cases), one case (8%) two losses. Among 9 chromophobe renal cell carcinomas with available istograms 6 (67%)showed aneuploid stemlines whereas the three remaining and 8/9 (89%) renal oncocytomas were diploid.
Karyotypically, 3 hromophobe renal cell carcinomas (33%) were hypodiploid, 3 (33%) were polydiploid, one (11%) was diploid. Nine out of 12 (75%) renal oncocytomas were diploid, one showed -Y (8%), one 47XX (8%), one multiple different clones (9%). All chromophobe renal carcinomas which failed to grow and 2/3 (75%) showing gains by metaphase analyses displayed multiple chromosomal losses by FISH. Eight renal oncocytomas with normal DNA content and those three with additional chromosomal abnormalities (91%) by karyotyping showed normal complement of chromosomes by FISH.
Conclusion: 1) chromophobe renal carcinomas usually display multiple chromosomal losses by FISH analysis in spite of a different spectrum found by karyotyping and flow

cytometric analyses; 2) chromophobe renal carcinomas that fail to grow in culture are characterized by chromosomal losses in FISH; 3) renal oncocytomas usually show a normal DNA content by both interphase and metaphase analyses.

O-47
ROLE OF POLYSOMY 17 IN TRANSITIONAL CELL CARCINOMA OF BLADDER (TCC). IMMUNOHISTOCHEMICAL STUDY OF HER2/neu EXPRESSION AND FISH ANALYSIS OF c-erbB-2 GENE AND CHROMOSOME 17.

Sara Simonetti1, Rosa Russo2, Giuseppe Ciancia1, Chiara Mignogna1, Gaetano De Rosa1, and Luigi Insabato1.

1) Department of Biomorphological and Functional Science, Anatomic Pathology Section, Faculty of Medicine, University "Federico II", Naples, Italy. 2) Department of Pathology, S. Giovanni di Dio e Ruggi D'Aragona Hospital, Salerno, Italy.

Background: We investigate HER2-neu gene and chromosome 17 alterations by FISH analysis and HER2/neu overexpression in transitional cell carcinoma of urinary bladder correlating with tumor grade and stage.
Methods: Sixty-three cases of TCC retrieved from the files of two departments of Pathology were studied for chromosome 17 aberrations and HER2-neu amplification by FISH and for HER2/neu overexpression by immunohistochemical analysis. Five tumors were low grade (G1), 29 tumors were intermediate grade (G2) and 29 tumors were high grade (G3); 32 tumors had stage T1, 18 had stage T1 and 13 were T2.
Results: We found polysomy of chromosome 17 in 37/63 (58.7%) TCC with average chromosome copy number > 2.26; increased number of HER2/neu gene copy (cut-off > 2.00) was observed in 42/63 (66.7%) of tumors. HER2-neu amplification occurred in 4/63 (6.3%) of tumors. Immunohistochemically 38/63 (60.3%) TCC overexpressed HER2/neu. All tumors with polysomy showed simultaneously increase of HER2/neu gene copy number whose 34/37 (92%) with protein overexpression. A significant correlation between polysomy of chromosome 17 and tumor stage ($p=0.0003$) and tumor grade ($p<0,0001$) was found: none of low grade tumors(G1), 8/29 (27.6%) of intermediate grade tumors (G2), and 29/29 (100%) of high grade tumors (G3) showed polysomy of chromosome 17; in 22/50 (44%) of non-invasive tumors (8/32 Ta and 14/18 T1) and 13/13 (100%) of deep invasive tumors (T2) polysomy 17 was observed. Moreover we found that 7 superficial tumors (1 Ta and 6 T1) showed high polysomy with average of chromosome 17 copy number ≥ 3.76 as observed in all invasive tumors (T2).
Conclusions: Our study suggests that HER2/neu gene amplification in invasive and high grade TCC is a rare event. However polysomy of chromosome 17 is fairly frequent, and it is correlated with tumor stage and grade, providing important information on tumor progression. Further work is needed to directly study these issues.

O-48
EXTRATESTICULAR EXTENSION IN GERM CELL TUMORS

Asli Yilmaz; Kiril Trpkov; Tina Cheng

Calgary Laboratory Services and University of Calgary; Tom Baker Cancer Centre

Background;Extratesticular extension (ETE) in germ cell tumors (GCT) is defined as tumor penetration through tunica albuginea. Depending on the site of invasion tumor may involve various extratesticular structures including tunica vaginalis (TV), hilar soft tissue, epididymis or spermatic cord. We investigated the frequency and morphological patterns of ETE in GCT with special focus to involvement of hilar structures including the rete testis. Method:We reviewed all 289 primary testicular GCT (209 seminoma and 80 nonseminoma) at our center between October 1999, and December 2006. Pathology slides and reports were reviewed. When ETE was identified, extension of tumor into the following structures; TV, epididymis, hilar soft tissue and spermatic cord were assessed. Results:ETE was identified in 58 (20%) patients which represented 16% (34/209) of seminomas and 30% (24/80) of nonseminomatous GCT. 97% of all ETE was through the hilum. Direct invasion of the rete testis was identified in 83% (48/58) of the cases. Hilar soft tissue was involved 62% (36/58) and epididymis was involved in 27% (16/58) of cases. Spermatic cord involvement was identified in 17% (10/58) of ETE cases, one of which showed tumor in lymphovascular spaces only. In four cases where hilar involvement were extensive, reliable distinction of paratesticular soft tissue involvement from a true spermatic cord invasion was difficult. TV was involved only in 2 cases (0.6% of total GCT and 3% of ETE cases). Conclusion: ETE is more frequent in nonseminomatous GCT. TV invasion is rare in GCT and the least common type of ETE. Most common form of ETE is through the hilum into the hilar soft tissue via direct invasion of the rete testis. Since there is no established anatomical landmark present between paratesticular soft tissues and spermatic cord pathological staging in a subset of patients can be problematic.

O-49

EVALUATION OF MSPATH SCORE COMPARED TO REVISED BETHESDA GUIDELINES FOR DETECTING LYNCH SYNDROME IN A CONSECUTIVE SERIES OF 225 COLORECTAL CARCINOMAS

Catherine Julié; Alain Beauchet; Tresallet Christophe; Christine Muti; Florence Coulet; Antoine Brouquet; Catherine Boileau; Florent Soubrier; Bernard Nordlinger; Philippe Rougier; Brigitte Franc; Hélène Radvanyi.
Ambroise Paré Hospital (AP-HP). France

Introduction: The Bethesda guidelines (BG) for Lynch syndrome were developed to preselect patients for microsatellite instability (MSI) testing before germline mutation screening. Among the 5 revised criteria, 1 focuses on particular pathology features. MsPath score (MsPS), based on site of the tumor, age at diagnosis and pathology features was recently shown to predict high-MSI (MSI-H) tumors in patients diagnosed before age 60 years. Our aim was to compare this score with the BG for detecting Lynch syndrome in unselected patients.

Methods: A consecutive series of 225 resected colorectal invasive adenocarcinomas from 214 patients was collected in our institution. All tumors were reviewed by a senior pathologist. Familial history, pathology features, site and age at diagnosis were obtained. MSI analysis was performed for all tumors. Germline mutations in the mismatch repair genes pointed out by immunohistochemistry were searched for MSI-H tumor patients.

Results: Ninety (42%) patients met the BG. MsPS was ≥1 in 105 patients (49%). Twenty-one patients (9.8%) had MSI-H tumors. Germline testing identified 8 mutations (3.7%) (MSH2, n=5; MLH1, n=2; MSH6, n=1). The BG failed to identify 2 of the 8 probands. All patients with Lynch syndrome had MsPS ≥2.3. The sensitivity and the specificity of the BG in combination with MSI were 75% and 98.5%, versus 100% and 54% for MsPS ≥1.

Conclusion: In our study, the MsPS identified all the patients with germline mutation, while a quarter of them were missed by the BG. Furthermore, MsPS increased only slightly the number of patients who should be tested for MSI (49% versus 42% for the BG). These data suggest the MsPS could replace the BG for preselecting patients for MSI testing. Further studies in larger series are needed to confirm these data and to determine a MsPS value which would increase specificity with no decreasing sensitivity.

O-50

Prognostic Value of Vessel Location in Angioinvasive Colorectal Cancer

Verena S. Pollheimer; Marion J. Pollheimer; Richard A. Lindtner; Peter Kornprat; Andrea Schlemmer; Peter Rehak; Cord Langner
Institute of Pathology, Medical University, Graz, Austria

Background: Lymphatic and venous invasion represent established prognostic parameters in colorectal cancer. Whether the prognostic significance of these parameters is related to intra- and/or extramural vessel location remains to be elucidated.

Method: 381 patients (215 men, 166 women; ratio 1.3:1) with colorectal cancer operated upon between 1992 and 2000 were randomly selected for analysis. Mean and median age of patients was 69.9 and 68.5 years, respectively. Patient records and histopathological slides were re-evaluated with respect to tumour stage, tumour grade and presence of intra- and/or extramural lymphatic and/or venous invasion. Follow-up data were available from 92% of patients (median time of follow-up 61 months).

Results: Lymphatic invasion was observed in 126/381 (33%) patients and was significantly associated with tumour stage ($p<0.001$) and grade ($p<0.001$). Intramural (L1a), extramural (L1b) as well as both intra- and extramural lymphatic invasion (L1ab) was seen in 44%, 6% and 50% of cases. Venous invasion was observed in 87/381 (23%) patients and was significantly associated with tumour stage ($p<0.001$) and grade ($p<0.001$). Intramural (V1a), extramural (V1b) as well as both intra- and extramural venous invasion (V1ab) was seen in 16%, 62% and 22% of cases. Presence of extramural lymphatic (L1b, L1ab) and venous (V1b, V1ab) invasion was significantly associated with high tumour stage ($p<0.001$) and grade ($p<0.001$). In addition, extramural lymphatic invasion (compared with intramural invasion) proved to be a significant prognostic variable in both univariate ($p<0.001$) and multivariate ($p=0.01$) analysis, whereas presence of extramural venous invasion (compared with intramural invasion) demonstrated prognostic significance only in univariate analysis ($p=0.02$).

Conclusion: Patient outcome was significantly associated with presence of lymphatic and/or venous invasion. With respect to lymphatic invasion, extramural lymphatic permeation proved to be a new independent prognosticator (compared with intramural lymphatic permeation). Its presence should thus be recorded during routine pathological work-up of colorectal cancer specimens.

O-51

Prognostic Value of pT Subclassification in Colorectal Cancer

Marion J. Pollheimer; Verena S. Pollheimer; Richard A. Lindtner; Peter Kornprat; Andrea Schlemmer; Peter Rehak; Cord Langner

Institute of Pathology, Medical University, Graz, Austria

Background: Tumour stage is the most important prognostic parameter in colorectal cancer. Our study aimed to assess the prognostic significance of a pT2 and pT3 subclassification.

Method: 381 patients with colorectal cancer operated between 1992 and 2000 were randomly selected for analysis. PT2 classification was subdivided as follows: pT2a with infiltration of the inner circumferential and pT2b with infiltration of the outer longitudinal layer of the muscularis propria. pT3 classification was subdivided by measuring the maximal tumour invasion beyond the muscularis propria: pT3a ≤1 mm, pT3b >1–5 mm, pT3c >5–15 mm and pT3d >15 mm. Follow-up data were available from 92% of patients, mean and median time of follow-up being 64 and 61 months, respectively.

Results: pT1 classification was noted in 28 (7%), pT2a in 37 (10%), pT2b in 22 (9%), pT3a in 49 (13%), pT3b in 83 (22%), pT3c in 53 (14%), pT3d in 33 (9%) and pT4 in 65 (17%) patients. 168 (44%) patients presented with nodal metastasis at time of diagnosis. 4/37 pT2a (11%) and 10/33 (30%) pT2b ($p=0.07$) as well as 12/49 (24%) pT3a, 32/83 (39%) pT3b, 36/53 (68%) pT3c and 23/33 (70%) pT3 tumours ($p<0.001$) showed nodal disease. Regarding patient outcome, no significant difference was detected between patients with pT2a or pT2b tumours. The pT3 subclassification, however, proved useful in predicting disease progression: 11/47 (23%) pT3a, 23/75 (31%) pT3b, 29/49 (59%) pT3c and 14/24 (58%) pT3d cases developed progressive disease ($p<0.001$; log-rank test). These data were confirmed in a Cox's multivariate analysis using the 5 mm cut-off level (pT3a/3b vs. pT3c/3d; $p<0.01$).

Conclusion: pT3 subclassification proved feasible in our patients, a cut-off level of 5 mm maximal tumour invasion beyond the outer border of the muscularis propria is recommended. Although the proposed pT2 subclassification tended to correlate with nodal status, no prognostic significance was observed.

O-52

Serrated adenomas and their relationship to colorectal carcinoma: Histopathological reevaluation of colorectal epithelial lesions diagnosed before the WHO (2000) classification

Mirosław Kiedrowski, Michał Kamionek, Janina Orłowska

Histopathology Laboratory of Department of Gastroenterology and Hepatology, Medical Center for Postgraduate Education; Department of Pathology, Maria Sklodowska-Curie Memorial Cancer Center and Institute of Oncology, Warsaw, Poland

Objectives:

1. To revise previously established diagnoses of colorectal epithelial lesions according to the WHO 2000 classification with special emphasis on serrated adenomas.
2. To characterize the frequency of focal CA arising from or CA coexisting with benign epithelial lesions depending on sex, age, localization and size.

Materials and methods: During the period of 1981–1994 in the Department of Gastroenterology of Medical Center for Postgraduate Education 24 000 consecutive endoscopic examinations of GIT were performed. Sigmoido- or colonoscopy revealed 2285 colorectal epithelial polyps and tumors in 1753 patients (mean age 59,9). There were 1544 adenomas: 1146 tubular (TA), 359 tubulo-villous (TVA), 39 villous (VA); furthermore there were 5 transitional polyps (TP), 128 hyperplastic polyps (HP) and 487 carcinomas (CA) (50,15%; 15,71%; 1,71%; 0,22%; 5,60%; 18,69%, respectively). The patients with familial adenomatous polyposis (FAP) were excluded from the study.

In 2007 the previously established diagnoses of all colorectal epithelial lesions were verified microscopically to disclose serrated adenomas (SA) according to the WHO 2000 classification. Multivariate logistical regression statistical analysis was applied.

Results: 128 of 2285 epithelial lesions were reclassified (5,6%). Most of them were SA (121 cases), which constituted 7,27% of all adenomas. 81 of 204 formerly diagnosed HP (39,7%) were reclassified as SA but 2 HP (0,98%) as TP. Focal CA arising from benign epithelial lesions was found in 60 cases. There were 7/46 focal CA in VA (15,22%), 28/387 in TVA (7,24%), 23/1169 in TA (1,97%) and 2/128 HP after revision (1,67%), however none CA was found in SA. CA coexisting with benign polyps of any kind in other localizations was found in 44 of 1753 patients (2.51%). Surprisingly, it was most common in patients with SA (5/57=8.8%) in contrast to lower frequency in groups with TVA (14/358=3,91%), TA (28/759=3,69%), VA (1/39=2,56%), and quite similar to the

latter one in HP (2/100=2,00%). HP and SA were generally small (≤5 mm), in contrast to large (>10 mm) TVA, VA and CA. Adenomas were significantly more frequent in older people, in the sigmoid colon and rectum. Most differences were statistically significant.
Conclusions: Introduction of WHO 2000 classification caused reevaluation of essential part of previous HP into SA. HP, formerly thought to be harmless, may have malignant potential, which was similar to TA in our material. All adenomas and HP may coexist with CA, however SA most frequently.

O-53

Nuclear expression of the splice factor Tra2β in ductal epithelium adjacent to ductal pancreatic carcinomas predicts poor patient outcome

Anna Kordelia Kurz; Kai Wagner; Frank Makowiec; Claudia Bauer, Elmar Stickeler, Axel zur Hausen
Institute of Pathology, University Hospital Freiburg, Germany

Background: Alternative splicing represents an important regulatory mechanism of gene expression. Tra2β, a member of the extended family of serine-arginine rich (SR) splicing factors regulates alternative splicing of exons with C/A-rich enhancer sequences. Biological important genes (e.g. CD44, vegf, insulin receptor, BRCA2, SYK) are alternatively spliced and contain these C/A rich sequences. **Methods:** We investigaetd expression levels of Tra2β in a matched pair analysis of microdissected tumor samples and normal tissues in tissues of invasive ductal pancreatic cancer by qRT-PCR (n=6) and immunohistochemistry (IHC, n=58). **Results:** Tra2β transcript expression was twofold upregulated in ductal pancreatic cancer. IHC revealed high Tra2β expression in 36, and low Tra2β expression in 22 pancreatic carcinomas. Tra2β expression within the tumor tissue did not have impact on patient survival. Of the corresponding histological normal duct epithelia 24 revealed weak and 18 revealed strong nuclear expression of Tra2β. Of interest, high nuclear Tra2β expression in the corresponding normal ductal epithelia correlated significantly with poor patient survival. **Conclusion:** Our data support a biological relevance of Tra2β in ductal pancreatic cancer. Tra2β expreesion might have a potential as a marker of patient outcome in ductal pancreatic cancer. In addition, high Tra2β expression level possibly reflects changes in alternative splicing patterns in ductal pancreatic carcinogenesis.

O-54

Correlation of EGFR expression with clinicopathological features in Pancreatic Ductal Carcinomas

Ovgu Aydin; Sibel Erdamar, Berke Ozucer; Nihan Karatas; Konstantinos Kouladouros; Desire Campoy Castano; Umar Gursu; Gokhan Demir; Gulen Dogusoy; Suha Goksel
Cerrahpasa Medical Faculty Pathology Department. Turkey

Background: The Epidermal growth factor reseptor (EGFR) is a receptor tyrosine kinase of the ErbB family that is abnormally activated in many epithelial tumors. The effect of overexpression EGFR in pancreatic carcinoma is not clear. We examined the EGFR expression and its relation with clinicopathological in invasive ductal adenocarcinomas of pancreas.
Method: Using tissue microarray technology, 70 histologically confirmed pancreatic ductal adenocarcinomas were cored twice and re-embedded in paraffin blocks. TMA slides were immunostained with antibody for EGFR obtained commercially and evaluated by two pathologists on light microscopy.
Results: Five of cases had to be eliminated from the study group. The mean age was 61,8 and F/M was 24/41 (n=65). EGFR expression was seen in 30/65 cases (46,2%). There was significant negative correlation between EGFR expression and lymphatic vessel invasion (r:-,265; p: 0,03). The frequency of lymph node metastases was lower in EGFR positive group. Thirteen of cases were death of disease with mean time of 17 months. Survival time was shorter in cases who had blood vessel invasion and longer in cases who had EGFR expression but these did not reach statistical significance.
Conclusion: Immunohistochemical analysis of EGFR expression has useful information for biological behaviour, although this analyse does not demonstrate prognostic value in pancreatic ductal adenocarcinomas.

O-56

Correlation of Hepatitis B surface antigen (HBsAg) and Hepatitis B Core Antigen (HBcAg) immunohistochemistry on liver biopsy specimens and serum HBV DNA levels

Funda Yılmaz; Deniz Nart; Rukiye Vardar; Fulya Günşar; Galip Ersöz; Zeki Karasu; Rüçhan Sertöz; Selda Erensoy; Tankut İlter; Ulus Salih Akarca
Ege University Faculty of Medicine Departments of Pathology Gastroenterology and Microbiology Izmir Turkey

Hepatitis B core antigen (HBcAg) and hepatitis B surface antigen (HBsAg) expressions in the liver may reflect the status of the balance between viral replication and the host immune reaction.

Aim: We aimed to search the correlation between serum HBV DNA levels and the percentage of positive cells and the staining patterns of HBsAg and HBcAg on liver biopsy specimens (LBS).
Patients and Methods: 162 patients with chronic hepatitis B were included in the study (mean age: 43±10, M/F: 107/55). The activity of hepatitis on LBS was assessed by using Ishak's score. HBsAg and HBcAg immunohistochemistry was performed using an automated immunohistochemical stainer according to the manufacturer's guidelines (streptavidin-peroxidase protocol; BenchMark,Ventana, USA). The staining pattern (membranous, cytoplasmic, nuclear, mixed) and the percentage of positive cells were assessed semi quantitatively.
Results: Mean HBV DNA level was 5.49±1.64 log copies/ml. On LBS, 32 out of 162 cases (19%) were HBcAg(+) and 145 (89%) were HBsAg(+). There was a positive correlation between the serum HBV DNA levels and percentage of HBcAg ($r=0.593$; $p<0.0001$) and HBsAg ($r=0.568$; $p<0.0001$) positivity. In all cases with HBV DNA > 8 log copy/ml HBcAg was found to be positive. There was no HBcAg positivity in cases with HBV DNA < 4.2 log copy/ml. The immunostaining of HBcAg on LBS indicated that serum HBV DNA level is over 6.25 log copy/ml with 91% specificity and 81% sensitivity. When HBcAg is taken ≥0.01, specificity and sensitivity rose to 96.4% and %81 respectively. The correlation of HBcAg and HBsAg staining was statistically significant ($r=0.470$; $p<0.0001$). There was no relationship between the staining pattern of HBcAg (nuclear, nuclear dominant mixed, cytoplasmic dominant mixed) and serum HBV DNA level. Whereas, HBsAg staining pattern tended to shift from the membrane to the cytoplasm with higher HBV DNA levels ($r=0.356$; $p<0.0001$). HBeAg positivity was not related to HBsAg staining, but HBeAg ($p<0.0001$).
Conclusions: The HBcAg expression in the liver is highly related with HBV DNA level in the serum (100% in HBV DNA>8 log copies/ml; 0% in HBV DNA<4.2 log copies/ml). HBcAg immunostaining is a reliable method for the demonstration of viral replication.

O-57

Mesothelin and p53 expression in pancreatic adenocarcinoma

Ali Abed Al-Mhsin;Jasim Radhi
McMaster University Hamilton Ontario Canada

Background: Mesothelin is an emerging marker for cancer diagnosis and target based therapy. In addition to mesothelial malignancies, mesothelin expression in malignancies from the ovary, and more recently from the pancreas has been demonstrated. The purpose of this study is to evaluate the expression of this monoclonal antibody in pancreatic carcinoma, chronic pancreatitis and compare it to the expression of p53 protein.
Methods: The authors reviewed 100 cases of pancreatic ductal carcinomas from the files of McMaster University Medical Centre. Representative blocks of tumour and adjacent non-neoplastic pancreas were selected for immunohistochemistry. Immunohistochemistry was performed using mesothelin monoclonal antibody (5B2, Nova Castra) and p53 protein (DO-7 Dako). Mesothelin staining of greater than 25% of tumour cells was considered to be strongly positive, less than 1% was considered negative, and the remaining cases were called focally positive. Intensity of staining was semi quantitatively graded on a scale of 1–3 (weak, moderate and strong) Up to 5% of p53 staining was considered negative.
Result: Mesothelin staining was seen in 90% of pancreatic ductal carcinomas, of which 78% of cases showed staining in 25% or more of the tumour cells. The staining intensity was graded as 2 in the majority of the positive cases. Cases of chronic pancreatitis showed only occasional focal positive staining in 5% of cases. The normal pancreatic tissue was negative in all cases. 75% of carcinomas expressed p53 in the range of 10–60%. Less than 2% of chronic pancreatitis cases were positive.
Conclusion: We conclude that mesothelin is a useful marker for the diagnosis of pancreatic ductal carcinoma and may be helpful in discriminating cases from chronic pancreatitis. However, p53 showed higher specificity but less sensitivity and the expression can be complementary

O-66

Myocardial Chromogranin A (GCA) protein expression in chronic heart failure is negatively regulated by left ventricular assist devices, but its plasma levels fail to reflect hypertrophy regression

Jeremias Wohlschlaeger, MD; Moritz von Winterfeld; Hendrik Milting, PhD; Aly El Banayosy, MD; Klaus Jürgen Schmitz, MD; Atsushi Takeda, MD; Nobuakira Takeda, MD; Petra Azhari, MD; Christof Schmid, MD; Christian August, MD; Kurt Werner Schmid, MD; Hideo Andreas Baba, MD
Institute of Pathology, University Hospital of Essen, University of Duisburg-Essen, Germany

Aims: In chronic heart failure (CHF), among increased expression of natriuretic peptides (NPs), recently Chromogranin A (GGA) was found to be up-regulated and associated with disease severity. Significant decrease of both NPs and hypertrophy after mechanical ventricular suppoprt (LVAD) was demonstrated.

Methods and results: Prior to and after support, ANP-, BNP, CGA and NCAM/CD56 expression was investigated by immunohistochemistry and morphometrically quantified in 33 paired myocardial samples. In 40 patients, ANP-, BNP- and CGA plasma levels were evaluated. In CHF, ANP-, BNP- and CGA levels were increased compared to controls and decreased significantly after LVAD. However, CGA levels did not show significant intergroup differences after multiple comparisons (post-hoc testing) and no significant differences of CGA plasma levels were outlined after support. Colocalization of BNP and CGA was found before, but not after ventricular unloading. CGA and NCAM/CD56 were not correlated with cardiomyocyte diameters.
Conclusions: Similar to NPs, CGA is significantly decreased by LVAD. BNP and CGA are colocalized in CHF, but not after unloading. Neither CGA nor NCAM/CD56 are associated with cardiac hypertrophy. In contrast to NPs, changes in myocardial CGA expression are not reflected by plasma levels, thus CGA does not appear to be an approriate biomarker of hypertrophy regression after unloading.

O-67

Cell culture as a testing system for lipid-lowering substances

Sergei V. Jargin
Peoples' Friendship University of Russia, Moscow, Russia

In the large series of publications started by Chazov EI, Orekhov AN et al. in 1986 (The Lancet, 2:595) and continuing until today (e.g., several presentations at the ISA Symposium in Rome, 2006) it has repeatedly been reported that incubation of cultured macrophages, smooth muscle and other cells with the serum from patients suffering from coronary heart disease caused significant lipid accumulation in cytoplasm, whereas serum from healthy individuals had no effect on lipid content in cultured cells. The ability of serum to cause lipid infiltration in vitro was named atherogenicity; and the method has been used by the same group of researchers for testing anti-atherogenic drugs and food components. Extract from garlic added to the "atherogenic" serum significantly reduced lipid infiltration and proliferation of cultured smooth muscle cells in vitro. Interestingly, the same effect was observed ex vivo: blood serum taken two hours after oral administration of garlic "caused substantially less cholesterol accumulation in cultured cells". Numerous substances have been reported to be efficient against serum atherogenicity: dibutyryl cyclic AMP, calcium antagonists, lipoxygenase inhibitors, carbacyclin and many others. The method was applied for assessment of hormonal influences: glucagon, estrogens and testosterone reduced serum atherogenicity and suppressed proliferation of cultured cells. The authors claim to have developed a novel principle of direct anti-atherosclerotic therapy based on inhibition of cholesterol deposition in the arterial wall without giving any plausible explanation of mechanisms of its action directly upon the serum. According to the current knowledge, anti-atherogenic substances can act on lipid metabolism in the liver, on intestinal absorption of lipids or on the endothelial receptor- or gene-mediated mechanisms. All these targets are absent in the cell cultures used. Therefore, reliability of reported results and recommendations for praxis appears questionable.

O-68

Pathological study of primary cardiac and pericardial tumours in a specialist UK centre: surgical and autopsy series

Junaid Patel; Mary Sheppard
Royal Brompton Hospital, London. UK

Background: Primary cardiac and pericardial tumours are rare with a prevalence of between 0.001 and 0.3%. Thus pathologists do not see them. Although uncommon, cardiac tumours represent an important cause of morbidity and mortality. Modern advances in cardiac imaging have increased the number of patients identified with a primary cardiac tumour in its early stage and also improved prognosis. At the Royal Brompton Hospital, London, which is a tertiary cardiac referral centre, we conducted a study to investigate the pathological features of primary cardiac and pericardial tumours and compared our findings to other centres.
Methods: All pathologic records at the Royal Brompton Hospital, between 1990 and 2007 were reviewed to identify patients with a confirmed diagnosis of primary cardiac tumours. A total of 94 patients with a histological diagnosis of primary cardiac and pericardial tumours were identified and formed the study population. Both surgical and autopsy specimens were included.
Results: The majority (n=67, 71.3%) of cases were benign cardiac tumours. Myxoma was the most common histologic type accounting for 28.7% of total tumours. Among cases with malignant tumours (n=27, 28.7%), unclassified sarcoma (n=11), leiomyosarcoma (n=5) and lymphoma (n=4) were the most common histologic types of primary malignant tumour. Primary cardiac tumours occurred more commonly on the left side of the heart (n=56, 59.6%), with the majority being benign tumours (n=43/56, 76.8%). When the tumours were present only in the right side of the heart, nearly half of them (8/20, 40.0%) were primary cardiac malignancies.
Conclusion: This study demonstrates a large spectrum of cardiac tumours (surgical and autopsy cases) seen in recent cardiologic practice and confirms that myxoma is

the most common primary cardiac tumour, but more fibroelastomas are being diagnosed. Moreover, the study shows that right sided tumours are more likely to be malignant.

Key words: heart, myxoma, sarcoma, leiomyosarcoma.

O-69

Carotid fibromuscular dysplasia: the main pathohistologic features

Yuliya Kuzyk

Institute of clinical pathology of Danylo Halytsky Lviv National Medical University. Ukraine

Background Fibromuscular dysplasia (FMD) is a non-atherosclerotic, noninflamatory vascular disease that most commonly affects the renal and internal carotid arteries. The major task of this study is to determine the main pathohistologic features of carotid FMD.

Materials and Methods The biopsy material of carotid arteries of 211 patients being operated on account of carotid stenosis (CS) for six years (2001–2006) was investigated. The operating material was analysing macroscopically; pathohistological examination including H&E staining, resorcine-fuxin, picrofuxin, trichrome Masson.

Results The analyse shows, that FMD ranks as the second cause (15%) of CS after atherosclerosis (71%). Men and women are in nearly equal ratio. The age of patients varied from 18 to 69 years. In 12.5% carotid FMD was asymptomatyc, in others clinical presentations were variable. Most often carotid FMD was observed in the middle and in the upper parts of the internal carotid artery (95%), bilateral involvement – in 60% of cases. Amongst pathological deviation discovered in one third of cases, the most frequent were kinking (62%) and atherosclerotic plaques (21,8%). Pathohistologically the most frequent type of FMD was medial fibroplasia (65,6%), rarely – intimal fibroplasia (34,4%). Medial fibroplasia was characterized by fibrosis of the media, segmental hyperplasia of the intima, and adventitia was invariable. Under intimal fibroplasia the subendothelial collagen deposits were revealed with ruptures of internal elastic membranes, while media and adventitia were invariable.

Conclusions Finally, the investigation showed that FMD is not characterized by sexual and age-specific features; clinically it may be symptomless; pathohistologically it is displayed by medial and intimal fibroplasias. We are not yet in a position to explane ethiology and morphogenesis of FMD and further research is needed with larger groups of patients.

O-70

Cardiac Histiocytosis. A Clue To The Erdheim-Chester Disease.

Ana Botelho(1); Alexandre Antunes(1); José Carlos Almeida(2); Miguel Abecassis(3); Rosa Henriques de Gouveia(4); Ana Paula Martins(4); A.M.Leitão Marques(1)

Cardiology(1) and Hematology(2) Departments, Centro Hospitalar de Coimbra, Coimbra; Cardiothoracic(3) and Pathology(4) Departments, CHLO - Hospital de Santa Cruz; Portugal

Background: Erdheim-Chester Disease (ECD) is an uncommon entity, whose etiology and pathophysiology still remain unclear. It may present multisystemic involvement and the diagnosis requires high level of suspicion. The authors report a case where apparently unspecific histiocytic infiltration of the heart pointed out the diagnosis.

Material and Methods: A 58 year-old male with complex cardiological clinical history, underlying multiple hospital admissions and therapeutic procedures since 1998, was refered to surgical treatment of severe mitral insufficiency. The marked thickning of both atrial walls - obstacle to the valvular correction - and a previous diagnosis of Langerhans Cell Histiocytosis in a tooth alveolus lesion, led to the hypothesis of a cardiac manifestation of the disease. Yet, during a second attempt of valvular approach, samples procured from right atrial wall and peri-aortic fat de novo "infiltration" were submitted to macroscopic and microscopic examination (including immunohistochemical characterization with a panel of markers).

Results: Macroscopically, the fragments were white-pinkish and elastic, measuring from 9 mm to 2.3 cm. Microscopy revealed "moderate to severe multifocal aggregates of histiocytic cells, lymphocytes, plasmocytes and other inflammatory cells in a background of fibrous tissue and residual cardiac muscle". The immunohistochemical profile of the histiocytic cells was CD68 +, lisozime +, alfa1-antiquimiotripsine + and S100 protein negative, among other negative markers.

Conclusion: Although apparently reactive, the density of the macrophagic/histiocytic infiltration suggested the possibility that it might represent Erdheim-Chester Disease, which was confirmed by examination of the skeleton (namely bone scintigraphy). This case not only highlights the possible histiocyte intra-mutation fenomena, allowing the coexistence of the two entities - Langherhans Cell Histiocytosis and Non-Langherhans Cell Histiocytosis (ECD) - in the same patient (1); but also emphasizes the Histopathology contribution for the diagnosis of such a specific entity, despite the cardiac microscopic unspecific features (2).

O-71
EFFECT OF SWIMMING ON MYOCARDIAL VASCULARIZATION IN SPONTANEOUS HYPERTENSIVE RATS

Flávia A. Oliveira; Rodrigo L. Moura; Octávio Barbosa Neto; Rosana R. Miranda; Renata C. Rossi; Marlene A. Reis; Vicente P. A. Teixeira; Valdo J. Dias da Silva
Pathology Department, Tropical Pathology and Public Health Institute of the Federal University of the Goiás (UFG), Goiânia, GO, Brazil; General Pathology Department of the Federal University of the Triângulo Mineiro (UFTM) and Physiology Department of the UFTM, Uberaba-MG, Brazil

Background: hypertensive cardiopathy caused by pressure overload is characterized by myocardiocyte hypertrophy, followed by microvascular rarefaction in the myocardium due to exacerbation of the vasoconstrictors responses. Moderate physical exercise, in the long run, can cause anatomical alterations that attenuate hypertension and its harmful effects. The aim was to describe the quantitative effects of physical training by swimming on the myocardial vascularization of spontaneous hypertensive rats (SHR). Methods: the male rats were divided into four groups: sedentary Wistar-Kioto (WKY C), trained WKY (WKY T), sedentary SHR (SHR C) and trained SHR (SHR T). The quantification of the vessels was done in myocardium of the left ventricle using HE, and the interative software "AxionVision 3.1". Fifity fields of each case were analyzed with ×40 magnification. Results: After the swimming protocol it was observed that there was no have significant difference in the number of vessels between the hypertensive groups and the WKY groups. Groups SHR presented a significantly bigger number of vessels than the WKY. The correlation between the weight of the heart and the number of vessels presented was negative, being significant only in SHR C. The correlation of arterial pressure and the number of vessels was not significant. Conclusion: According to the results, the swimming was not capable of stimulating increase of vessels, however it proved to not be harmful because it did not cause a reduction in the already existing number of vessels in the myocardium. Moreover, it can be inferred that the SHR has a bigger vascular proliferation capacity than the WKY perhaps as a mechanism of protection against hypertension.

O-72
Medianecrosis of aorta – Gsell-Erdheim syndrome: the main pathohistologic features

Dmitry Zerbino; Julia Kuzyk
Institute of clinical pathology of Danylo Halytsky Lviv National Medical University. Ukraine

Background Today a great part of progressively increasing amount of aortic dissection is associated with medianecrosis of aorta – Gsell-Erdheim syndrome. It may be explained by insufficient studying of morphologic features of aortic dissection and especially of nonatherosclerotic aneurysms of aorta.

Materials and methods 24 cases of Gsell-Erdheim syndrome during 2004–2006 were analyzed: 20 men (83,4%) and 4 women (16,6%) from 22 to 69 years. Aortic wall was studied at all parts. The pathohistologic examination included: H&E staining, resorcine-fuxin (Hart), picrofucxin (Veigert) trichrome Masson, alcian blue.

Results Irregular focal thickening of the intima; focal accumulations of alcian+ mucoid substances, single cystic cavities, focal irregular anucleated zones with disoriented fibers of the media were seen in the areas, distant to the rupture of the aortic wall. Medial lamina elastica interna was partially straightened, fragmented, with the zones of hyperelastosis and multiplication. Adventitial edema, rarely focal sclerosis and perivascular sclerosis of vasa vasorum were typical.

Signs of total medial disorganization were seen near the area of rupture: focal accumulations of mucoid substances, ribbon-like anucleated zones, chaotic orientation of smooth muscle cells with severe degeneration; irregular sclerosis. Elastic fibers showed focal hyperelastosis, fragmentation. Areas of severe elastrolyses and zones filled by amorphous masses with altered tinctorial properties and fragmented elastic fibers were revealed near the rupture of the aortic wall. Adventitia showed severe hemorrhagic infiltration, dilated vasa vasorum.

Conclusions In aortic medianecrosis pathologic process was revealed in the whole vessel, not only in the area of aneurysm and dissection. Manifestations of variable severity of the same process were seen in different parts of aortic wall.

Aortic medianecrosis – Gsell-Erdheim syndrome – is a disease of aorta, associated with the lesions of elastic fibers of the media and with some other typical morphologic changes. Clinically dissecting aortic aneurysms manifests it.

O-73

Clinical morphology of acute coronary syndrome

Lev Kakturskiy; Alexey Philippov
Research Institute of Human Morphology of the Russian Academy of Medical Sciences. Russia

Background. Acute coronary syndrome (ACS) is "a useful operational term to refer to any constellation of clinical symptoms that are compatible with acute myocardial ischemia" (Braunwald E. et al., 2002). ACS's symtoms include unstable stenocardia without or with increased troponins and also early acute myocardial infarction without or with Q wave.

Methods. Autopsy material from 43 cases of ACS has been examined (33 males, 10 females, 39–60 years). Macro- and microscopic tests on myocardial ischemia were used including NBT-macrotest, polarizing microscopy, PAS-, Rego-, Lie, Sudan III-, Heidenhein-stain. In 7 cases morphofunctional comparisons with vital ECG data have been carried out.

Results. Vulnerable atherosclerotic plaques with focal hemorrhages into coronary intima have been found in all cases. The fibrous caps of plaques are loosened, infiltrated by mononuclear and foamy cells, and also impregnated by plasma proteins. As a sign of myocardial ischemia sarcomere hyperrelaxation has been found by polarizing microscopy associated with multiple contracture. Wavy deformation of muscular fibers was permanently seen. Microcirculatory disorders as an additional sign of ischemia were visible. NBT-test revealed focuses of myocardial ischemia in the left vantricle wall and in interventricular septum. On preliminary data by comparing the ECG with NBT-test, it was apparent that in early ischemia without Q wave (but with microscopic signs of ischemia) NBT-test was positive only with addition of lactate as substrate. In later stages of ischemia (myocardial infarction with Q wave) NBT-test was constantly positive.

Conclusion. Morphological basis of ACS is a myocardial ischemia provoced by rupture of vulnerable atherosclerotic plaques. Ischemia is detected on the lots of morphological signs on macro- and microscopic levels. Macroscopic test with NBT allow to define and to distinguish both early ischemia (unstable stenocardia) without Q wave and early necrosis (acute myocardial infarction) with occurence of Q wave.

O-74

Perivascular deposits - The role of EM in diagnosis of CADASIL and Nephrogenic Fibrosing Dermopathy (NFD) associated to gadolinium containing contrast agents.

Josef Schroeder; Ferdinand Hofstaedter
Pathology Department, University Hospital Regensburg. Germany

Peculiar small-sized perivascular deposits, preferable studied by electron microscopy (EM), play an important role in two different diseases. The first disease, known since 1993 as CADASIL (**Cerebral Autosomal-Dominant Arteriopathy with Subcortical Infarcts and Leukoencephalopathy**), is an adult-onset neurologic disorder with recurrent strokes and progressive dementia caused by mutations in Notch-3 gene. Degeneration of arterial vascular smooth muscle cells and concurrent accumulation of granular osmiophilic material (**GOM**), which major component is the ectodomain of Notch-3, typify CADASIL. The pathognomonic GOM deposits were originally described in small blood vessels of the central nervous system. Later on involvement of many systemic tissues - including skin - was reported. Today it is common practice to utilize deep skin biopsies for CADASIL diagnosis confirmation. We report GOM deposits of two genetically confirmed CADASIL patients, whose skin biopsies were processed with and without routine postosmication. The EM evaluation revealed a similar deposit appearance in both tissue samples. This finding substantiates suspicions, that GOM is not truly osmiophilic and the term "GOM" seems to be a misnomer. In consequence, we propose to rename it: **VSMD = Vessel Smooth Muscle Deposit.**

Nephrogenic Fibrosing Dermopathy (NFD), now termed **Nephrogenic Systemic Fibrosis (NSF)**, is a recently emerged acquired disorder of the skin and systemic tissues. It is observed exclusively in patients with renal insufficiency exposed to gadolinium (Gd) used in contrast agents for MRI. Our EM study of skin samples of an NSF patient, utilizing electron spectroscopic imaging (ESI) and electron energy loss spectroscopic (EELS) microanalysis, revealed **Gd deposits** in a wide perivascular zone of the skin vessels. **Simultaneously iron was detected** in some Gd-deposits as well as in the adjacent tissue. This finding supports the Gd transmetallation hypothesis and its trigger function for the circulating fibroblasts. We provide ultrastructural evidence for the ability of lesional fibroblasts to differentiate into myofibroblastic cells.

O-75

Comparative ultrastructure of interstitial Cajal-like cells from different normal tissues

Mihail Eugen Hinescu; Mihaela Gherghiceanu; Laurentiu Mircea Popescu
Victor Babes Institute of Pathology; Bucharest; Romania

Background Interstitial Cajal-like cells (ICLC) were identified in the last few years in a series of digestive and non-digestive organs. However, there is no available data describing similarities and differences between such cells, in terms of ultrastructure.

Method In this study we comparatively examined the ultrastructural features of ICLC identified in pancreas, gallbladder, mesentery, mammary gland, myometrium, and atrial or ventricular myocardium. Tissue samples were processed for ultrastructural investigation according with the usual protocol. Electron microscopy examination was performed with a Philips CM 12 transmission electron microscope at 60 kV. The images were recorded with Morada 11 megapixel CCD camera and analyzed with iTEM SIS software (Olympus).

Results Cells were identified using accepted transmission electron microscopy (TEM) criteria for ICLC: location in interstitium, vicinity to capillaries, nerve bundles, or other interstitial cells, very characteristic long cell processes, as well as quantitative data about organelles, plasmalemmal or cytoskeletal structural components. The processes of different ICLC were particularly long (e.g. from tens of μm in myocardium or pancreas to a mean length of 24.91 μm, in mesentery). A convolution index was calculated in order to measure the potential length of the very typical cell processes (e.g. 2.32 for mesentery, 2.47 for gallbladder). Appearance and spatial orientation in different tissues were revealed by measuring mean distances vs. main target cells of ICLC - nerve bundles, vessels, other connective cells and macrophages (e.g. 110.69, 115.80, 205.07 and 34.65 nm respectively in mesentery) or measuring distances at the level of close contacts with other cell types (e.g. 26.17 nm in a ICLC-smooth muscle contact in or 74 nm in an ICLC-eosinophil cell contact in myometrium).

Conclusion ICLC recognized in different tissues share significant ultrastructural features allowing ICLC to be viewed as a distinct interstitial cell type.

O-76

Exogenous surfactant causes direct lung injury and acivates lymphocyte-macrophage axis - electron microscope and flow cytometry studies

Andrzej Marszalek; Monika Seget; Lidia Gackowska; Ewa Florek; Elzbieta Kaczmarek; Wieslawa Biczysko
Department of Clinical Pathomorphology Collegium Medicum Nicolaus Copernicus University Bydgoszcz, POland and Dept. of Clinical Pathomorphology Poznan Univesity of Medical Sciences, Poland

Background: the cause of unsatisfactory results of surfactant treatment of acute respiratory insuficiency in adults remain unclear.

Methods: pathogen-free rats were given a single dose (150 mg of lipids/kg of b.w.) of semi-natural surfactant (curosurf). After 1, 6, 24 hours, 5, 10, 21, 42 days lungs from at least 5 animals were taken. Tissue secimens were prepared and examined by by light and transimission elecron microscope as well as morphometric studies were performed. We used cell cultures (macrophages and lymphocytes separated or mixed) for the studies of increasing surfactant concentration effect on cell proliferation. All results were statistically evaluated.

Results: in experimantal lungs average air-less areas (AALA) were fluctuating during observations, but in all time-groups they were greater than in controls ($p<0.0001$). In lungstaken short after treatment we found a raise of AALA from 28.15% (at 1 h) to 35.31% (at 24 h; $p<0.001$) and then a decrease. At this time experimental lungs were collapsed with parenchymal/intraalveolar edema. At 1 h observations in some samples only about 10% of area was aerated (vs. controls 82%; $p<0.0001$). Since 24 h enomous inflow of pulmonary macrophages into areas with abundance of exogenous surfactant was found and followed by proliferation of type II pneumocytes. In experimental lungs at 42nd day of observation AALA was 30.57% vs. 21.73% in controls ($p<0.001$). Alveolar septa were widened by the proliferation of fibroblasts as well as deposits of estracellular components (mainly collagen). Cell cultures revealed activation of macrophages with increasing doses of surfactant. The macrophage proliferation was augmented by the presence of pre-stimulated lymphocytes.

Conclusions: our results suggest that surfactant treatment possibly destroys normal lung tissue. Rapidly developing changes are partially reversible. Unfortunately they might lead to lung fibrosis. The lymphocyte-macrophage axis is activated depending on surfactant concentration.

O-77

Pathological evaluation of lentigo maligna

Leonard N, Brown S, Lawrence CM

Royal Liverpool University Hospital and Royal Victoria Infirmary, Newcastle-upon-Tyne.UK

Background: The pathological features of lentigo maligna (LM) can be subtle and difficult to evaluate in sun-damaged skin.

The aim of this project was to compare cases of LM with controls. We assessed 28 cases of LM. Eleven cases were formalin-fixed Mohs resections from difficult-to-treat recurrent or ill-defined LM with a control biopsy taken from the opposite side to the tumour. One case had another lesion removed at the time of surgery which was used as a control. The remaining 16 cases were matched with biopsies of basal cell carcinomas matched for sun damage and age.

Methods: Numbers of melanocytes per high power field were assessed by H&E and using a Melan A immunostain. HMB45 immunostaining was also used. Cases were graded as high grade if they possessed two or more of the following: cells above the dermo-epidermal junction; nests of melanocytes; confluence of melanocytes at the dermo-epidermal junction; a more uniform population of cells.

Results: Twenty cases were judged to be high grade and eight low grade LM. Four high grade lesions recurred in contrast to no low grade lesions.

Melanocyte counts in each case were compared with its control and a ratio was calculated. Cases where this ratio was greater than 2:1 were judged as highly informative. 21/27 (78%) cases were highly informative using H&E staining only and 17/24 (71%) cases were highly informative using a Melan A stain.

HMB45 staining was less well defined but was positive in all LMs and negative in 24/28 controls.

Conclusions:

1. Grading in LM is useful as all recurrences in this study occurred in high grade cases.
2. The use of a control biopsy alongside LM is helpful as the control: case ratio is usually greater than 2.
3. Positive HMB45 staining distinguished between cases and controls.

O-78

Consistent expression of the stem cell renewal factor BMI-1 in primary and metastatic melanoma

Daniela Mihic-Probst; Ariana Kuster; Sandra Kilgus; Beata Bode-Lesniewska; Barbara Ingold-Heppner; Carly Leung; Martina Storz; Burkhardt Seifert; Silvia Marino; Peter Schraml; Reinhard Dummer; Holger Moch

Institute of Surgical Pathology, Department Pathology, University Hospital Zurich. Switzerland

Background: Stem cell-like cells have recently been identified in melanoma cell lines, but their relevance for melanoma pathogenesis is controversial. To characterize the stem cell signature of melanoma, expression of stem cell markers BMI-1 and nestin was studied in primary and metastatic melanomas. Because BMI-1 functions as a transcriptional repressor of the Ink4a/Arf locus, $p16^{ink4a}$ and $p14^{Arf}$ expression was also analyzed.

Method: 64 cutaneous melanomas, 165 melanoma metastases as well as 53 melanoma cell lines were investigated for BMI-1, Nestin, $p16^{ink4a}$ and $p14^{Arf}$ expression using immunohistochemistry.

Results: Increased nuclear BMI-1 expression was detectable in 41 of 64 (64%) primary melanomas, 117 of 165 melanoma metastases (71%) and 15 of 53 (28%) melanoma cell lines. High nestin expression was observed in 14 of 56 primary melanomas (25%), 84 of 165 melanoma metastases (50%) and 21 of 53 melanoma cell lines (40%). There was a significant correlation between BMI-1 and nestin expression in cell lines ($p=0.001$) and metastases ($p=0.02$). Cell lines obtained from melanoma metastases showed a significant higher BMI-1 expression compared to cell lines from primary melanoma ($p=0{,}001$). Further, primary melanoma lacking lymphatic metastases at presentation (pN0, $n=40$) were less frequently BMI-1 positive than melanomas presenting with lymphatic metastases (pN1; $n=24$) (52% versus 83%; $p=0.01$). In addition a high BMI-1/low $p16^{ink4a}$ expression pattern in primary melanoma was a significant predictor of metastasis by means of logistic regression analysis ($p=0.005$).

Conclusions: These data indicate that cells in primary melanomas and their metastases have stem cell properties. BMI-1 expression in primary melanoma appears to induce a metastatic tendency.

Furthermore BMI-1 mediated repression of $p16^{ink4a}$ seems contributing to an increased aggressive behavior of stem cell-like melanoma cells. Besides being of prognostic relevance, these data may provide new insights in melanoma tumor genesis.

O-79

TYROSINASE AND TRP2 EXPRESSION IN HIPOMELANOTIC MALIGNANT MELANOMA

Alexandra Bastian*; Gabriela Negroiu; Florica Staniceanu* ***; Sabina Zurac* ***; Luciana Nichita***; Razvan Andrei*; Stefana Petrescu**;**
NOTE: Bastian and Negroiu should be regarded as first authors in equal contribution
* *Colentina University Hospital;* ** *Institute of Biochemistry of the Romanian Academy;* *** *Carol Davila University of Medicine and Pharmacy, Bucharest, Romania*

Background: Amelanotic malignant melanoma (MM) can be sometimes difficult to diagnose on hematoxilin-eozin (H&E) slides. Since the expression of consecrated melanoma markers may widely variated from case to case, new immunohistochemical markers should be used in order to establish the melanomatous characteristics of the tumor.
Method: We studied 24 cases of nodular MM, 4 of them with minimal focal production of melanin and 2 cases of malignant peripheral nerve sheath tumor (MPNST). We analyzed the expression of several immunohistochemical markers as S100 protein, HMB45, Melan A, tyrosinase and TRP2.
Results: All the MM cases presented S100 protein, HMB45 and melan A positivity, very variable in intensity or distribution. For S100 protein, 3 of the hipomelanotic cases had intense diffuse positivity, the other having faint diffuse positivity. HMB45 and melan A were unevenly distributed within the tumoral mass both in pigmented and hipomelanotic tumors with one case of hipomelanotic MM with very few positive cells. Tyrosinase and TRP2 were positive in some of the tumoral cells in pigmented nodular MM while the hipomelanotic MMs had intense diffuse pattern of positivity. Tyrosinase has fine granular cytoplasmic positivity while TRP2 has dot-like paranuclear and faint cytoplasmic pattern of positivity.
Both of the MPNST cases showed diffuse positivity for S100 protein while HMB45 and melan A stained small groups of tumoral cells. None of the MPNSTs had positivity for either tyrosinase or TRP2.
Conclusion: Tyrosinase and TRP2 are useful markers to be added to the immunohistochemistry panel of antibody when a diagnosis of hipo/amelanotic MM is suspected. Also, they may be used to exclude a MPNST.
Supported by National Authority for Scientifical Research, Excellence Research Program, 2006–2008

O-80

Difficulties in the diagnosis of vulval inflammatory disease

Sharma N; Hashim N; Hickey S; Bell H; Leonard N
Dept of Pathology and Dermatology, Royal Liverpool and Broadgreen University Hospitals.UK

Background: Diagnosis of vulval inflammatory disease can be difficult both clinically and histologically. The major problem is the distinction of lichen sclerosus (LS) from lichen planus (LP), when the features are not well established, is particularly challenging as both present with lichenoid inflammation. Some authors have suggested specific histopathological features to aid differentiation of these diseases and this study evaluated them.
Methods: 38 biopsies from 26 patients seen in Dermatology clinics were reviewed along with their clinical histories. Nine patients required more than one biopsy: 6 patients had 2 biopsies and 3 patients had 3 biopsies. An initial H&E diagnosis was made. Two different sets of diagnostic criteria as described by Fung et and al and by Regauer et al were used and the diagnoses reached by using these criteria were compared with the original biopsy diagnosis and the final clinical impression.
Results: Nine biopsies showed features of other inflammatory diseases: bullous pemphigoid; eczema; psoriasis; Hailey Hailey disease. Two biopsies showed unequivocal features of LP and 9 biopsies showed unequivocal features of LS. Sixteen biopsies were initially judged as non-specific. Ten of these scored for LS using one or both of Regauer's and Fung's criteria. Some so-called specific features such as loss of elastin from the papillary dermis and basement membrane thickening were found in LS and LP.
Conclusions:

1. 16 of 38 biopsies were initially called non-specific. 10 of these had features of LS according to criteria described by Fung et al and Regauer et al. This could mean either that LS is being significantly under-reported by pathologists using established criteria or that the reported criteria for early disease are too broad and include a range of non-specific entities.
2. Some so-called specific features were seen in both LS and LP making them unhelpful in making such a distinction.

O-81
Evaluation of Bcl-2 Expression in Aggressive and Non-aggressive Basal Cell Carcinomas

Elham Amini; Pirooz Salehian
Pirooz Pathobiology Laboratory. Iran

Bcl-2, a well-known anti-apoptotic gene, promotes cell viability without cell proliferation. Expression of the bcl-2 oncogene is reported in certain low grade neoplasms including Basal Cell Carcinomas(BCCs). Bcl-2 expression in BCCs is contradictory, with 67–100% immunopositivity being reported. The purpose of this study was to evaluate bcl-2 expression in the indolent variants of BCC, namely superficial and circumscribed subtypes and their aggressive counterparts; infiltrative and morphea-like subtypes. Anti-human bcl-2 monoclonal antibody was used to identify its protein product in formalin-fixed tissue from 33 BCCs. 22 histopathologically non-aggressive and 11 aggressive subtypes were investigated. Quantity of decoration of tumor cells for bcl-2was graded in the following fashion: 0 to 25%, 26% to 50%, 51% to 75%, 76% to 100%. Intensity of decoration was evaluated as slight, moderate and intense. Bcl-2 expression was observed in all of the BCCs, but high bcl-2 expression was statistically a significant feature of non-aggressive BCCs($P=0.001$). Different bcl-2 expression in various non-aggressive and aggressive histopathological subtypes of BCCs suggests that despite the common derivation of these tumors from a primitive basaloid stem cell and a limited potential for metastasis, they form a heterogenous group of tumors. While the superficial and circumscribed BCCs are indolent slow-growing tumors with high bcl-2 labeling, the aggressive BCCs are infiltrative and morphea-like tumors with low bcl-2 labeling. High expression of bcl-2 may indicate a more favorable prognosis in BCCs.

O-82
PILAR LEIOMYOMA: A REVIEW OF 12 CASES WITH PARTICULAR EMPHASIS ON THE SYMPLASTIC VARIANT

Empar Mayordomo; Jose María Martín; Ana María Calatayud; Francisco Giner; Carlos Monteagudo
Hospital Clinico Universitario, University of Valencia, Spain

Background: Benign smooth muscle neoplasms of the skin have been classified into three categories: pilar leiomyomas, angioleiomyomas and genital leiomyomas. Previous studies have defined their clinico-pathological features. However, only few cases on the symplastic variant have been reported. Further studies on the clinico-pathological and immunohistochemical features of this variant, and its differential diagnosis with cutaneous leiomyosarcoma, are needed.

Method: We have studied the clinical and histological features of 12 consecutive cases of pilar leiomyoma with special emphasis on the symplastic variant, the potential diagnostic value of the immunohistochemical expression of smooth muscle and proliferative markers such as desmin, caldesmon and Ki67, and a correlation with clinical outcome.
Results: Piloleiomyomas are presented as dermal spindle cell proliferations usually organized in interlacing and short fascicles, with eosinophilic cytoplasm, elongated blunt-ended nuclei and loose chromatin. Three out of the twelve cases showed multifocal significant nuclear pleomorphism and prominent nucleoli resembling the symplastic leiomyomas of the uterus. 0 to 2 typical mitotic figures were found in these three cases, with a Ki67 proliferative index lower than 2%. Interestingly, one of the symplastic piloleiomyomas showed a prominent epithelioid component and 5% of Ki67 expression. All of them showed a smooth muscle immunophenotype.
Conclusion: Symplastic piloleiomyomas are not exceptional. In our series they represent the 25% of the cases, showing multifocal hyperchromatic and pleomorphic nuclei and a low proliferative rate, from less than 2%, in most cases, both conventional and symplastic type, and 5% in the epithelioid symplasic case. To the best of our knowledge, epithelioid symplastic pilar leiomyomas have not been previously described. Recognition of the spindle and epithelioid symplastic variants of piloleiomyoma, complemented with the proliferative index, may allow its distinction from cutaneous leiomyosarcoma.

O-83
Cutaneous Leishmaniasis

Sujatha Fernando
Central West Pathology Services. Australia

Leishmaniasis is a parasitic disease caused by a haemoflagellate protozoan organism of the genus Leishmania. Cutaneous Leishmaniasis (Oriental Sore and Espundia) and the other main type Visceral Leishmaniasis (Kala-azar); are broadly classified as old world and new world depending on the endemic geographical area.
This disease is not endemic in Australia and all reported cases are imported, with the incubation period spanning from 2 to 30 years.
The case presented is a 32-year-old male migrant of Indian origin who was referred to a dermatologist for a painless, erythematous and scaly papule on his right cheek. A punch biopsy of the lesion was received which demonstrated plentiful Leishmania organisms in the histiocytes.

The life cycle, clinical features, Dermatopathologic Differential Diagnosis, of similar organisms in lesions will be discussed.

O-93
CHARACTERIZATION OF DIABETIC MASTOPATHY BY FINE NEEDLE ASPIRATION

Rosario Granados; Carmen Gimenez; Teresa Corrales
Hospital Universitario de Getafe. Spain

Background: Diabetic mastopathy occurs in patients with a long-standing insulin-dependent disease, and it courses with nodules that clinically and radiographically mimic breast cancer. The lesions may be multiple and bilateral. There are few cytological reports of this entity, most of them with non-conclusive findings or with insufficient samples.
Methods: We report the cytological findings of two different breast nodules arising in the right breast of a 35 year-old diabetic woman. Ultrasound-guided FNAB was performed with a 22-gauge needle, and the material smeared onto glass slides. After air-drying, the samples were stained with Diff-Quick, and immediately interpreted by a pathologist and a cytotechnologist.
Results: Both nodules yielded numerous blood vessels of the capillary type surrounded by a large number of lymphocytes. These cells had different sizes, predominating the small lymphocytes, and lacked atypical features. There were no epithelial cells in our samples. The diagnosis of diabetic (lymphocytic) mastopathy was rendered, avoiding unnecessary biopsy or excision of the tumors.
Conclusions: The presence of a capillary mesh admixed with a polymorphus lymphocytic cell population in an FNAB of a clinically malignant breast mass from a diabetic patient, provides sufficient information as to avoid unnecessary surgical procedures. Therefore, FNAB is a very useful tool in the management and follow-up of breast lesions in young diabetic women.

O-94
EVALUATING THE HEALTH OF THE VAGINAL FLORA USING CULTIVATION-INDEPENDENT METHODS

Mathilde E. Boon; Johanna M. Klomp; Banut-Sabine M. Verbruggen; Hans Korporaal; Pauline de Jong; Gerco C. Kramer; Maarten van Haaften; A. Peter M. Heintz
Leiden Cytology and Pathology Laboratory, Leiden, the Netherlands; Department of Obstetrics and Gynecology, Diakonessenhuis, Utrecht, the Netherlands; Department of Surgical Gynecology and Oncology, University Medical Center Utrecht, Utrecht, the Netherlands

Background: A healthy vaginal flora is of paramount importance. Our objective was to determine the morphotype of the adherent bacteria in liquid-based cytology (LBC) in smears with healthy and disturbed vaginal flora and to use PCR technology on the same fixed cell sample to establish DNA patterns of the 16S RNA genes of the bacteria in the sample.
Method: Thirty samples were randomly selected from a large group of cervical cell samples suspended in a commercial coagulant fixative "(BoonFix)". PCR was used to amplify DNA of five bacterial species: *Lactobacillus acidophilus*, *Lactobacillus crispatus, Lactobacillus jensenii, Gardnerella vaginalis* and *Mycoplasma hominis*. The LBC slides were then analyzed by light microscopy to estimate bacterial adhesion.
Result: DNA of lactobacilli was detected in all cell samples. Seventeen smears showed colonization with *Gardnerella vaginalis* (range 2.6×102 - 3.0×105 bacteria/μl BoonFix sample). Two cases were identified as dysbacteriotic with high DNA values for *Gardnerella vaginalis* and low values for *Lactobacillus crispatus*. The sample with the highest concentration for the (unhealthy) bacteria *Gardnerella vaginalis* showed an unequivocal *Gardnerella* infection. This cultivation independent method reveals a strong inverse relationship between *Gardnerella vaginalis* (unhealthy flora) and *Lactobacillus crispatus* (healthy flora).
Conclusion: This study indicates that the vaginal flora in liquid-based cervical samples can be evaluated because these samples are suitable for quantitative PCR analysis allowing evaluation of the health of the vaginal flora.

O-95
Regional differences in proliferation, DNA repair enzymes and p53 mutations in gliomas. Where to biopsy?

A.H. Gene1; M. Brell2; F. Santandreu3; I. Barceló4; A. Guerrero5; J. Fiol1; P. Roca3; J. Oliver3; M.E. Couce1.
1Servicio de Anatomía Patológica, 2Servicio de Neurocirugía, 4Servicio de Neurología, 5Servicio de Radioterapia, Hospital Universitario Son Dureta (HUSD); 3 Grup de Metabolisme Energètic i Nutrició, Universitat de les Illes Balears (UIB). Spain

Background: Gliomas comprise a spectrum of different tumor subtypes that share a diffuse infiltration of brain tissue and intratumor heterogeneity, which can be an issue when assessing tumor grade in small tissue samples. Invasion is regarded as one of the main reasons for poor therapeutic success. Mutations in the p53 gene are common in gliomas and are thought to arise early in the development of a malignant tumor. Methylguanine-methyltransferase (MGMT) is a DNA repair enzyme with an important role in cancer cell resistance to O6-alkylating drugs.
Design: The aim of this project was to study intra-tumor heterogeneity in gliomas, by investigating the differences between central and peripheral regions of 21 brain tumors (16 gliomas and 5 metastatic tumors) from gross total resection specimens, when these were readily available for

analysis. We studied the status of p53, Ki-67 and MGMT. We compared these results with the clinical outcome and response to therapy in these patients. Statistical analysis were done using SPSS computer program. Data were tested for significance by T-student test.

Results: Of the 16 gliomas, 15 were positive in at least one region for p53 and 11 showed MGMT immunoreactivity with significant differences between central and peripheral regions. Ki-67 expression was variable, with values ranging from 5 to 90% and a significantly higher central proliferation.

Patients with the diagnosis of gliomas received the established therapeutic protocol according to STUP which included quimio- (Temozolomide) and radiotherapy in high grade gliomas.

Of the 16 patients, 6 were alive and free of disease, 7 were alive with residual/recurrence tumor and 3 were dead of disease.

Conclusions: The results obtained in this study, reveal that clear differences exist between central and peripheral regions in brain tumors, particularly in regards to proliferation, and reinforce the importance of the selection of the sampled tumoral region in these cases. Although a larger study is ongoing, we believe that this work will contribute to advance the knowledge of the physiopathology of gliomas and may have an impact in treatment protocol designs.

O-84

Role of chromatin remodeling mediated by the HIV-1 Tat protein in the genesis of the HIV-1-associated malignancies

Giulia De Falco; Giovanna Cerino; Eleonora Leucci; Joshua Nyagol; Mario Cocco; Anna Onnis; Piero Tosi; Antonio Giordano; Lorenzo Leoncini

Dpt. Human Pathology and Oncology, University of Siena, Italy and Sbarro Institute For Cancer Research & Molecular Medicine, Temple University Philadelphia PA 19122, USA

BACKGROUND:The incidence of non-Hodkin's lymphoma (NHL) is greatly increased in HIV-infected individuals. Malignant lymphoma occurs in association with acquired immunodeficiency syndrome (AIDS). The vast majority of neoplasms are clinically aggressive, monoclonal B-cell neoplasms that exhibit Burkitt's, immunoblastic, or large cell lymphoma histopathology. The Tat protein of HIV is a likely candidate to contribute to tumour pathogenesis in HIV-infected patients. Extensive evidence indicates that Tat is a cofactor in the development of AIDS-related neoplasms and the protein has also been found to have an oncogenic role in vitro and in vivo. Deregulation of cellular genes and functions by Tat can also cause abnormalities that may contribute to the development of AIDS-associated disorders. The molecular mechanism underlying Tat's pleotropic activity may include the generation of heterodimers of Tat with cell cycle proteins.

RESULTS AND CONCLUSIONS: We have previously shown that Tat interacts with the RB2/p130 tumour suppressor gene product, resulting in uncontrolled cell proliferation. The interaction of Tat with cell cycle regulatory proteins alone may not be sufficient for neoplastic transformation in vivo and other cofactors may be required. Another mechanism, through which Tat may influence HIV-mediated transformation, is by hyper-activation of transcription by interacting with chromatin remodelling complexes. Recent findings indicate a complex interplay between viral proteins and host transcription regulatory machineries, including histone deacetylases (HLACs), histone acetyltransferases (HATs), cyclin-dependent kinases (CDKs), and histone metyltransferases (HMTs). The chromatin structure presents a significant barrier to transcription. These modifications and alterations of chromatin structure increase DNA accessibility to transcription factors and activators, thus promoting transcription initiation and efficient elongation. Many reports in the last several years have linked Tat transactivation to chromatin remodelling in vitro and in vivo. The aim of our study is to investigate whether Tat-mediated chromatin remodelling may have a role in HIV-associated transformation.

O-85

Proteomics characterization of formalin fixed breast cancer tissues

Elena Bonanno, Andrea Urbani, Alfredo Colantoni, Maurizio Ronci, Giorgio Federici, Luigi Giusto Spagnoli

Università di Roma Tor Vergata, Dipartimento di Biopatologia, Istituto di Anatomia Patologia. Italy

Background: Breast cancer is a complex disease only incompletely characterized by clinicopathological parameters. Even though tumoral proteins are good markers and allow the identification of targets for specific treatment their limited number hampers the selection of the most appropriate diagnostic or therapeutic strategy. Proteomic techniques complement and further enlarge the wealth of information generated by genomics. In particular MSE data acquisition is a novel parallel peptide fragmentation protocol that allows high peptide detection efficiency, ideal for protein identification from very complex samples. Archival formalin-fixed paraffin-embedded (FFPE) tissues could represent an incredible source for examining the clinical course of diseases.

Methods:In the present study we compared the efficiency of protein identification from FFPE human breast cancers

samples with the unfixed counterpart. In order to explore different protein unlocking procedures which might enable a suitable recovery of polypeptides we have developed an in vitro approach using "tissue surrogate" samples for MSE analysis.
Results: Our results outline the possibility to obtain comparable peptide mass spectra both from unfixed and FFPE samples. The number of the identified proteins from unfixed cancer tissue was 160 (sequence coverage 48%); from Trypsin/EDTA treated FFPE tissues was 150 (sequence coverage 39%); whereas from FFPE untreated tissues the number of identified proteins was 35 (sequence coverage of 32%). Among the identified proteins the most relevant were annexin, ubiquitin, calmodulin, histonic proteins, MIF, tenascin.
Conclusions: Appropriate pretreatment to unlock the fixed proteins allowed us to obtain suitable protein expression profiles from FFPE tissues. Improvements of sequences analysis software could further increase the number of protein detected. The study of large numbers of archival FFPE tumors may represent an useful approach to assess breast cancer heterogeneity defining more reliable diagnostic/prognostic factors to selectively targeting the tumor cells.

O-86

Linear Discriminant Analysis of transcriptomic data reveals a 7-gene signature diagnostic of prostate cancer

Raquel Bermudo; David Abia; Berta Ferrer; Iracema Nayach; Alberto Benguria; Ángel Zaballos; Elías Campo; Ángel R. Ortiz; Timothy M. Thomson; Pedro L. Fernández
IBMB-CSIC, Barcelona; IDIBAPS, Barcelona; CBM-CSIC-UAM, Madrid; Hospital Clínic, Barcelona; CNB-CSIC-UAM. Spain

Background: Transcriptional profiling studies have unveiled new molecular markers of cancer, that are being applied to diagnosis in actual clinical environments. Quantitative PCR determinations for selected transcripts should be useful adjuncts for diagnosis, prognosis and monitoring of neoplasia. We have identified a small gene set that is diagnostic of prostate cancer, and have explored its applicability as a diagnostic aid.
Methods: We have used prostate carcinoma samples with homogeneous epithelial representations, normal prostate and pure stromal tissue and analysed them with Affymetrix Human Focus microarrays. Results were validated by low-throughput QPCR in whole tissue samples and micro-dissected specimens as well as by immunohistochemistry for selected genes.
Results: By microarray analysis, we have identified gene signatures that are highly discriminant of prostate cancer. Subsequent Linear Discriminant analysis (LDA) of micro-array and QPCR data supported a 7-gene signature which allowed robust discrimination between normal and tumoral prostate samples in 100% of cases, including samples distinct from those used in the original microarray analysis. In support of their tumor vs normal discriminant capacity, individual genes in this signature showed similar expression profiles when external datasets were interrogated.
Conclusions: Our transcriptomic studies of highly selected prostate cancer samples coupled to extensive validations and linear discriminant analyses have yielded a highly discriminant 7-gene transcriptional signature with diagnostic potential in clinical practice.
Supported by grants from the Ministerio de Educación (GEN2001–4856-C13, GEN2001–4865-C13–10 and SAF2005–05109), Ministerio de Sanidad (PI020231), Fundació Marató TV3, RTC of the Instituto Carlos III (ISCIII-RETIC RD06/0020) and the Fundación Ramón Areces.

O-87

Genomic alterations associated with the progression to invasive breast cancer revealed by array comparatlive genomic hybridization

Vladimir Iakovlev 1, 2, 3, 8; Nona Arneson 1; Vietty Wong 1; Chunjie Wang 1; Stephanie Leung 1, 2; Gaiane Iakovleva 7; Keisha Warren 1; Melania Pintilie 5; Susan Done 1,3,4,6
1 Division of Applied Medical Oncology, Ontario Cancer Institute/Princess Margaret Hospital; 2 Department of Laboratory Medicine and Pathobiology, University of Toronto; 3 Division of Pathology St. Michael's Hospital; 4 Department of Pathology, University Health Network; 5 Department of Biostatistics, Ontario Cancer Institute/Princess Margaret Hospital, 6 Department of Medical Biophysics, University of Toronto; Toronto, Ontario, Canada. 7 Department of Pathology, University of Manitoba, Winnipeg, Manitoba, Canada. 8 Canadian Institute for Health Research training program in Oncologic Molecular Pathology, Canada.

Background: Our knowledge of molecular events during breast cancer progression is limited. Preinvasive breast cancer (also known as duct carcinoma in situ, DCIS) is a heterogeneous group of lesions of difficult to predict prognosis. Genomes of DCIS and infiltrating duct carcinoma (IDC) have been compared previously and show a similarity of genomic alterations. We hypothesized that significant events can be detected by comparing lesions with a broader range of behavior: from pure DCIS (without IDC) to IDC associated with lymph node metastasis.
Method: Array comparative genomic hybridization was calibrated by self-self hybridization of normal DNA and used to analyze 6 cases of pure DCIS, 17 cases of paired

DCIS and IDC where 8 tumors had metastases in the axillary lymph nodes.

Results: We found a higher number of genomic alterations in pure DCIS than DCIS and IDC components of invasive tumors. In-situ and invasive components of the same tumor had similar genomic profiles. Pure DCIS differed from DCIS associated with IDC while the latter showed similarity within the group. IDCs positive for metastatic spread also showed similarity between tumors. Several alterations were detected preferentially in IDC and associated DCIS compared to pure DCIS. Gain on 17q22–24.2 was associated with higher histological grade, large IDC size, lymphatic/vascular invasion and lymph node metastasis ($p<0.05$).

Conclusion: These findings suggest that specific genomic events occur at different stages of breast cancer progression. DCIS associated with IDC may represent a clone with high invasive potential or an established invasive clone spreading inside the ducts. Gain on 17q22–24.2 is a candidate region for testing as a marker for high risk of invasion and nodal metastasis, which may prove useful for limited biopsy material.

O-88

Detection and genotyping of human papillomavirus DNA in 914 samples from a specialized Cervical Pathology Service

Paloma Martín[1]; Linah Kilany[1]; Dolores Suarez[1]; Clara Salas[1]; Rosario Sanchez-Yuste[1]; Denise Soutar[1]; Ana M Lopez[1]; Fernando Salazar[*]; Enrique Iglesias[*]; Carmen Bellas[1]

*[1]Department of Pathology and *Department of Obstetrics and Gynaecology. Hospital Universitario Puerta de Hierro, Madrid, Spain*

Background: Cervical cancer represents the second most common malignancy in women worldwide. Almost all cases are caused by persistent infection with about 15 genotypes of human papilloma virus (HPV). A clear understanding of the molecular epidemiology of HPVs and the availability of powerful molecular diagnostic techniques has provided the background for prevention strategies of HPV-related carcinomas. The aim of this study was to investigate the frequency and genotype distribution of HPV infection in cervical brushings from women followed in a Cervical Pathology Service.

Methods: Cervical samples of 914 patients were collected for cytopathological and molecular test in the Pathology Cervical Service from May 2006 through October 2007. HPV infection was searched by PCR and viral typing was performed by dot blot hybridization.

Results: Out of the total number of tested women, 436 (47.7%) of them were positive to HPV Polymerase chain reaction (PCR). This high rate of HPV DNA positivity (adjusted prevalence of 6.8% in Southern Europe) is ascribed to our study population (women who attended to a specialized Gynaecological Service of cervical Pathology). The most frequent genotype detected in our series was HPV16, found in 18.1% of all positive samples, followed by HPV31 in 10.5%, HPV53 in 8.9%, HPV52 in 6.8%, HPV58 in 6.5%, HPV44 in 6.5%, HPV18 in 5.6%, HPV66 in 5.5% and HPV39 in 5%. Genotypes 56, 6, 33, 42, 59, 68, 35, 45 and 51 follow this group, with frequencies lower than 5%. A coinfection with two or more virus was found in 132 samples (30.3% of positive cases), 41 of these had HPV16 with other genotype. Correlation with cytological data will be done.

Conclusions: HPV16 alone or in coinfection is the most frequent type detected. According with other Spanish studies HPV18 is not a frequent type in our series. HPV31 and HPV53 are the second and third commonest types.

HPV types differ geographically and with the social phenomena of immigration HPV type-specific prevalence are varying; hence additional work should be done in providing information on frequency of different genotypes in Spain and to understand the mechanisms of HPV carcinogenesis.

O-89

FATTY ACID SYNTHASE AND KU80 AS NEW MARKERS FOR HER2 TRASTUZUMAB RESPONDER POPULATION SELECTION. MOLECULAR FOCUS ON A COMPLEX CROSS TALK

Pucci S.; Bonanno E.; Mazzarelli P.; Luigi Giusto Spagnoli

Dept.of Biopathology, University of Rome Tor Vergata. Italy

Background Over expression of the EGFR family member Her2 is found in approximately 30% of breast cancers. Her2 currently represents one of the most appropriate targets for specific therapy. The determination of Her2 overexpression has become necessary for the selection of breast cancer patients responder to Herceptin therapy. Immunohistochemistry in combination with FISH is currently the most used method for this detection that still provide controversial results in term of selection of responder patients. In fact, a consistent number of Her2-positive tumors is not firstly responsive to HER2-driven therapy, indicating the need of a multiparametric approach on receptor functionality to improve the selection of real responder patients. We analysed the complex cross talk among the functional activated Her2 receptor and the

activation of the molecular target cascade closely linked to its functionality. Recent studies in breast cancer cells have revealed a bi-directional connection between Her-2/neu and fatty acid synthase (FASN), a major lipogenic enzyme catalyzing the synthesis of long-chain saturated fatty acid-sHer-2/neu overexpression stimulates the FASN promoter and concomitantly the presence of nuclear Ku80DNArepair protein, usually loss in advanced tumors, suggesting an indirect evidence of Her-2 transduction activity.

Methods In the present study we observed the pattern shift expression of Ku80 and FASN in 20 ductal infiltrating breast cancer biopsies matching their localization and expression to Her2 status determined by FISH and immunohistochemistry.

Results We observed that the overexpression of Her-2 due to polysomy, aneuploidy was correlated to the absence of Ku80 in the nuclei. Conversely, patients with Her2 ratio >>2 correlated to Ku80 and FASN overexpression only in 64%of cases.

Conclusions Data obtained could explain at least in part the existence of a cohort that lacks Her2 functionality and therefore do not respond to the therapy. These screening may further enhance the efficacy of trastuzumab therapy by selecting those patients most likely to respond.

O-90

Clusterin and IL-6: a new twin set of non-invasive molecular markers for colorectal cancer detection

Fabiola Sesti; Sabina Pucci; Paola Mazzarelli; Elena Bonanno; Luigi Giusto Spagnoli

Institute of Anatomic Pathology, Dept. of Biopathology, University of Rome Tor Vergata, Italy

Background. Clusterin is an ubiquitous glycoprotein implicated in a large number of physiological processes and IL-6 is a pleiotropic cytokine with a broad range of functions on immune and non-immune cells. The expression of both Clusterin and IL-6 is regulated by TGF-β which plays an important role in the development of colorectal cancer and both proteins are involved in proliferation and apoptosis. These opposite effects are carried out by two different isoforms of Clusterin (cytoplasmic/secreted and nuclear, respectively) and by different signalling pathways that IL-6 is able to activate in cells.

We have already shown that in the adenoma-carcinoma sequence of colorectal cancer the pro-apoptotic nuclear Clusterin is lost, while there is an increase in the production of secreted Clusterin.

Method. Secreted Clusterin and IL-6 levels were assessed by ELISA in serum of healthy individuals and of patients with colorectal cancer. Clusterin was also assessed in stool specimens and immunohistochemistry was performed on surgical specimens.

Results. We evidence a significant increase of secreted Clusterin in serum and stool of patients with colorectal cancer compared to healthy individuals. The level of secreted Clusterin correlates with the grade and the metastatic potential of the tumour. The increase of secreted Clusterin was also observed by immunohistochemistry performed on surgical specimens of patients when tumour and normal mucosa were compared. Moreover an increase of IL-6 in serum and *in situ* was also shown to correlate with colon carcinoma stage.

Conclusion. The correlation among IL-6 and Clusterin levels and tumour progression suggests a role for these proteins as *in situ* and circulating prognostic markers for non-invasive colorectal cancer screening. Besides, the evaluation of Clusterin level in stool and in serum after surgical resection could be a good parameter to evaluate the relapse of the disease and for early detection of an ongoing metastatic process.

O-91

FGFR3 pathway identification by oligonucleotide microarrays

Jose Javier Gomez Roman; Edurne Entrena; Dietmar Fernandez; Gorka Ochoa; Lourdes Osaba; Jose Luis Gutierrez; Jose Fernando Val-Bernal

Hospital Universitario Marques de Valdecilla. Facultad de Medicina. Universidad de Cantabria. Spain

There are two capital pathways in transitional cell carcinomas of the urinary bladder development, FGFR3 pathway for pTa and pT1 carcinomas and the p53 pathways for pT2 muscle infiltrating cases. The cellular human line RT-112 (from urinary bladder transitional cell carcinoma) has been showed to have FGFR3 overexpressed. Otherwise, PD173074 is a FGFR3 tyrosin-kinase activity inhibitor molecule developed by Pfizer. Our aims are to explore the different molecules implied in FGFR3 transduction pathway by oligonucleotide microarrays after inhibiting tyrosin-kinase activity in RT112 cells with PD173074

Methods: Four experiments were performed. RT112 cells were subjected to PD173074, FGFalpha plus heparin, FGFalpha plus heparin plus PD173074 and lastly RT112 control cells without treatment. Every experiment was performed by triplicate with and without DMSO (solvent of PD173074), in order to avoid the possible spurious effect of it. The analysis of gene expression has been realized using the technology GeneChip of Affymetrix (Human Genome U133 Plus 2.0). For the identification of changes in expression statistically significant between the groups of samples parametric tests were applied taking like significant those changes in $p<0.05$

Results: Hierarchical Clustering of the samples analyzed showed 30 sequences that were capable to differentiate gene expression between the four experiments. When we used the criteria of a fold change >2 to identificate significative sequences, we obtained a list of 50. 10 of them were included in MAPK signalling pathway, 6 in cytokine-cytokine receptor interaction and 4 in hemapoietic cell lineage signal transduction.
Conclusions: We have identified several molecules implied in FGFR3 signal transduction that are affected by tyrosin-kinase activity inhibition that could be used as diagnostic or therapeutical targets in urinary bladder carcinoma development.

O-92

WT1 EXPRESSION AS A MARKER OF ADVANCED STAGES OF PRIMARY MALIGNANT MELANOMA

Garrido-Ruiz MC, Rodriguez-Pinilla M*, Rodriguez-Peralto JL

Hospital Universitario 12 de Octubre, Madrid and Centro Nacional de Investigaciones Oncológicas CNIO, Madrid. Spain*

Background Cutaneous malignant melanoma remains the leading cause of skin cancer death. Clinical and histological variables predicting survival including Breslow's index or ulceration have been identified. Although the potential relevance of biological variables still awaits an in-depth study, recently, a group of biological markers ($p16^{INK4a}$, Ki-67 and Bcl-6) have been related to prognosis.
WT1 was first identified as tumor suppressor gene, involved in the development of Wilms' tumor of the kidney. Contradictory functions have been described to the protein WT1; it can develop a role as a tumor suppressor in some cancers, but as a potential oncogene in others. Since WT1 has been identified as a molecular target for cancer immunotherapy, immunodetection of WT1 in tumor cells has become an essential step in cancer studies. Two isolated studies report the expression of WT1 gene in human melanoma cells.
Methods In the present study we compare the expression of WT1 among different types of nevi and different stages in primary malignant melanoma progression. Tissue microarrays containing normal tissues and 271 primary melanocytic lesions samples (163 primary malignant melanomas and 108 benign nevi) were studied by immunohistochemistry.
Results The present study shows staining for WT1 in 39, 6% of MM. WT1 expression is increased in advanced stages of MM progression: a significant ($p<0.05$) increased of expression WT1 was detected in vertical cases 46.5% vs. radial cases 16.0%, in high levels of Clark (IV, V) 57.6% vs. low levels (I, II, III) 29,4% and in thick melanomas (>1 mm) 52,4% vs. thin ones (≤1 mm) 23,8%. No significant change in WT1 expression was detected when focusing on ulceration, vascular invasion, tumor size, "satellites" or clinical variables.
Conclusions Our study demonstrates: 1. WT1 is predominantly expressed in the cytoplasm of the tumor cells as in other adult cancers; 2. WT1 expression is increased in advanced stages of MM progression; 3. We establish an association of WT1 protein expression with shorter overall survival.

Posters

Displayed on Sunday, May 18
Pulmonary Pathology

P-1

DEMOGRAPHIC, ETIOLOGIC AND HISTOLOGIC PULMONARY ANALISYS IN PATIENTS WITH HIV/AIDS AND ACUTE RESPIRATORY FAILURE – AN AUTOPSY STUDY

Alexandre de Matos Soeiro; André Luiz Dresler Hovnanian; Mauro Canzian; Edwin Roger Parra; Cecília Farhat; Vera Luiza Capelozzi

Department of Pathology, University of São Paulo Medical School, São Paulo, Brazil.

BACKGROUND: The different aspects of pulmonary pathology in HIV/AIDS are unknown in autopsies. In this study were described the demographic data, etiologic and histologic pulmonary findings in different associated pathologies of 353 autopsies of patients with HIV/AIDS and acute respiratory failure (ARF) as cause of death between 1990 and 2000.
METHOD: Were obtained following data: age, sex, and major associated diseases (found at autopsy and/or previously the death). Pulmonary histopathology was categorized as: diffuse alveolar damage (DAD); pulmonary edema (PE); alveolar hemorrhage (AH); and acute interstitial pneumonia (AIP). Odds ratio (OR) of the AIDS-associated diseases develop specific histopathologic pattern was determined by logistic regression.
RESULTS: Were observed 263 HIV/AIDS-infected men and 90 women. The mean age was 35 years. Bacterial bronchopneumonia was present in 29% (154 cases), *Pneumocystis jiroveci* pneumonia (PJP) in 15% (78 cases), tuberculosis in 11% (55), severe sepsis and/or shock septic in 8% (41), cytomegalovirus in 7% (37). Pulmonary histopathology showed AIP in 28% (99 patients), DAD in 25% (89), PE in 9% (33) and AH in 8% (29). Multivariate analysis demonstrated significantly positive association

between PJP and AIP (OR, 4.51; 95% CI, 2.46 – 8.24; $p<0.001$), severe sepsis and/or shock septic and DAD (OR, 3.60; 95% CI, 1.78 -7.27; $p<0.001$), cytomegalovirus and AIP (OR, 2.22; 95% CI, 1.01 – 4.93; $p=0.05$).

CONCLUSION: For the first time we showed in autopsies the demographic data, etiologic diagnosis and respective histopathologic findings in patients with HIV/AIDS and ARF as cause of death. More studies are necessary to elucidate the complete pulmonary fisiopathologic mechanism involved with each AIDS-associated disease.

P-2

ENDOTHELIAL APOPTOSIS AND VASCULAR COLLAGEN V INTERACTION IN SYSTEMIC SCLEROSIS: A PRELIMINARY STUDY

Edwin Roger Parra; Armando Costa Aguiar Júnior; Walcy Teodoro; Vera Luiza Capelozzi

University of São Paulo Medical School, Department of Pathology. Brazil

Background: Systemic sclerosis (SSc) is a multisystem disorder characterized by inflammation, fibrosis and vascular damage. One of the pathogenetic mechanism proposed is related to direct binding of collagen V epitopes on endothelial cells, enhancing synthesis of collagen by fibroblasts or myofibroblasts. Prolonged attack can provoke basement membrane injury and exposition of hidden collagen V epitopes, originating neoantigens, which will trigger an auto-immune disease. The aim of this study was to examine in vascular and lung septal interstitium the relationship among collagen types I, III and V, endothelial and alveolar epithelial apoptosis and pulmonary function tests in patients with SSc.

Method: We examined the amount of collagen types I, III and V in vascular and septal interstitium using immunofluorescence and morphometric analysis. Endothelium and epithelium apoptosis expression was determined by TUNEL and quantified by point counting technique in 10 open lung biopsies of patients with SSc without pulmonary hypertension. The pulmonary function tests were analyzed in theses cases and correlated with collagen and apoptosis results.

Results: We observed, in decreased order, amount of collagen type III, I and V in septal interstitium. In vascular interstitium, the collagen type I was increased, followed by types V and III. The apoptosis index was higher in endothelial cells than alveolar cells. An inverse correlation was found between CVF, endothelial and alveolar cells apoptosis (p=0.01 and p=0.02, respectively).

Conclusions: We concluded that endothelial apoptosis and vascular collagen V interaction reinforce the vascular pathway in the SSc pathogenesis. Further studies are needed to determine whether this relationship is causal or consequential.

Financial Support: FAPESP, CNPq

P-3

DIFFERENCES IN AIRWAY REMODELING AMONG THE MAJOR HISTOLOGICAL PATTERNS OF IDIOPATHIC INTERSTITIAL PNEUMONIAS?

Gustavo Sousa Noleto; Edwin Roger Parra, Vera Luiza Capelozzi

University of São Paulo Medical School. Department of Pathology. Brazil

Background: Structural alteration of the airways and lung parenchyma "remodeling" is a recognized feature of pulmonary fibrosis. In this study, we sought to validate the importance of relationships between bronchiolar collagen/elastic system, pulmonary functions tests and survival in the major histological patterns of idiopathic interstitial pneumonias (IIPs).

Method: We examined bronchiolar collagen/elastic system fibers in non-specific interstitial pneumonia (NSIP/NSIP=13), idiopathic pulmonary fibrosis (IPF/UIP=13), acute interstitial pneumonia (AIP/DAD=17) and bronchiolitis obliterans with organizing pneumonia (BOOP/OP=6) cases. We used the Picrosirius-polarization method, Weigert's resorcin-fuchsin histochemistry and morphometric analysis to evaluate the amount of bronchiolar collagen/elastic fibers, and their association with pulmonary function tests and survival.

Results: The bronchiolar measurement of collagen fibers was significantly higher in OP when compared with UIP; in the other groups (NSIP, DAD) there weren't significant differences. Analysing the amount of elastic fibers in the four groups we didn't observed statistically significant differences. The increase of collagen fibers in UIP was directly associated with dyspnea grade ($p=0.03$). Elastic fibers was directly associated with PaO_2 ($p=0.01$). In DAD we observed a direct significant correlation between amount of collagen fibers and PCO_2 ($p<0.001$) and an inverse correlation with VEF1 ($p=0,005$) and VEF1/ CVF (p=0,002). The most important predictor of survival in DAD was the amount of bronchiolar collagen deposited ($p=0.005$).

Conclusion: We concluded that a progressive bronchiolar fibroelastosis occurs in IIP histological patterns, probably indicating evolutionary adapted responses to airway injury. The more important spectrum of bronchiolar remodeling in OP and DAD suggests a more direct participation of the airways in their pathogenesis than UIP and NSIP. Further studies are needed to determine whether this relationship is causal or consequential.

Financial Support: FAPESP, CNPq

P-4

ARTERIAL AND INTERSTITIAL REMODELING PROCESSES IN NONSPECIFIC INTERSTITIAL PNEUMONIA: SYSTEMIC SCLEROSIS VERSUS IDIOPATHIC

Erika Franco de Carvalho; Edwin Roger Parra; Alexandre Muxfeldt A'b Saber; Vera Luiza Capelozzi.
Departments of Pathology, University of Sao Paulo Medical School. Brazil

Background: Recently, the nonspecific interstitial pneumonia (NSIP) pattern was described as more prevalent in the collagen vascular disease (CVD) group, including systemic sclerosis (SSc). In this regard, some authors have studied pathogenetic mechanisms in idiopathic and CVD associated lung fibrosis to discover factors that might relate to better treatment and prognosis. As the pathogenesis of these two diseases seems to be different, we hypothesize that the repair mechanisms involving the collagen/elastic system also differ, leading to a diverse remodeling process.
Methods: Pulmonary biopsy specimens were examined from 40 patients, 22 with idiopathic-NSIP and 18 with nonspecific interstitial pneumonia associated with SSc. We compared the septal and vascular matrix remodeling (collagen/elastic fibers) by an image analysis system, vascular occlusion by semiquantitative analysis, pulmonary function tests and survival between the two groups.
Results: The content of septal collagen and elastic fibers, as well as the elastic fibers in the vascular interstitium, were higher in the SSc group ($p=0.01$, $p=0.001$ and $p<0.0001$, respectively). Among pulmonary function tests the DLCO/VA was affected to a greater extent in the SSc group (59% of the predicted value in SSc and 97% in the idiopathic group). There were no differences in the collagen content of the vascular interstitium, arterial occlusion, or survival between the two groups.
Conclusions: Although the fibrotic process is more intense in the SSc group, it does not affect the prognosis of these patients. Because the elastotic process is higher in the SSc group, this might suggest that autoimmune inflammatory mechanisms affecting the elastic fiber system could play a greater role in the pathogenesis and pulmonary remodeling process of SSc-NSIP than in idiopathic-NSIP.
Financial Support: FAPESP, CNPq.

P-5

Comparison of the dysadherin and E-cadherin expression in primary lung cancer and metastatic sites.

Antigony Mitselou, Anna Batistatou, Konstantinos Charalabopoulos, Yukihiro Nakanishi, Setsuo Hirohashi, Niki J. Agnantis, Theodoros Vougiouklakis.
Department of Forensic Pathology - Medical School - University of Ioannina. Greece

Dysadherin, a cancer associated cell membrane glycoprotein, has been reported to downregulate E-cadherin. Aberrant expression of E-cadherin has been associated with the development of metastases in patients with cancer. Even though the expression of dysadherin and E-cadherin has been studied in primary non-small cell lung carcinoma, little is known about its expression at the distant metastases sites. We investigate by immunohistochemistry the ralationship between E-cadherin and dysadherin in 123 cases of primary lung carcinomas (53 squamous cell carcinomas, 21 adenocarcinomas, 13 large cell carcinomas, 24 small cell carcinoma and 12 epithelioid mesotheliomas), and their distant metastases. The intensity, the expression pattern and the percentage of neoplastic cell staining were recorded and the results were correlated with clinicopathological findings of the subjects. Dysadherin expression was expressed in 61 (49.59%) of the cases and increased dysadherin expression was significantly correlated with tumour size ($p=0.003$), distant metastases ($p=0.0034$), and metastasis size ($p=0.0008$). Reduced E-cadherin expression was noted in 58 (47.2%) of the cases, and was correlated with high grade tumour ($p=0.02$), infiltrative growth pattern ($p=0.042$), and advanced stage ($P=0.032$). Although the correlation between the expression of dysadherin and E-cadherin was not significant, a group of patients showed reduced E-cadherin expression with dysadherin overexpression. In lung carcinomas dysadherin expression seems to reflect tumour aggressiveness and may be considered a positive marker of poor prognosis when considered alone or/and in combination with downregulation of E-cadherin.

P-6

STRUCTURAL AND FUNCTIONAL CHANGES ASSOCIATED WITH PULMONARY OVERLOAD IN PIGS: PRELIMINARY STUDY

Flávio Brito Filho*; Edwin Roger Parra; Humberto Álvares de Oliveira*; Eduardo de Gálio; Cesar Augusto Melo e Silva*; Josué Fernandes*; Kleber Nogueira de Campos*; Paulo Manuel Pêgo Fernandes*.**

Department of Thoracic Surgery of Hospital de Base de Brasília and Department of Pathology** of Faculdade de Medicina da Universidade de São Paulo. Brazil*

Background: The precise mechanism of the lung microvascular barrier injury in patients with hemodynamic pulmonary overload is unclear. The aim of this study was to examine the structural and functional pulmonary changes after different levels of pulmonary overload.

Methods: This study was approved by the Institutional Ethical and Scientific Committees. Twenty Large White pigs were anesthetized and then placed on mechanical ventilation. After bilateral thoracotomy, the pulmonary arteries were exposed and the animals were divided into four groups: sham (n=5); clamp level I (n=5) with right lung overload by clamping of the left pulmonary artery; clamp level II (n=5) with right lung overload by clamping of the left pulmonary artery and right pulmonary artery branches to the inferior lobe and clamp level III (n=5) with right lung overload by clamping of the left pulmonary artery and right pulmonary artery branches to the inferior and mediastinal lobes. The arteries were clamped by 60 minutes using microvascular clamps and the pulmonary function was evaluated for dynamic gas changes (PaO_2/FiO_2). The pigs were sacrificed; the lungs were removed *in bloc*, weighed and processed using standard histological techniques to morphometric analysis.

Results: We observed that acute pulmonary overload in all levels of clamping produced a rapid and significant perivascular and interlobar edema when compared to the sham group and edema increased according to incremental levels of occlusion ($p<0.05$). Minimal alveolar hemorrhage and alveolar edema were occasionally present in the clamping groups. Mechanical pulmonary function changes were observed in the clamping groups characterized by decrease of PaO_2/FiO_2 correlated with different occlusion grade ($p>0.01$). Proportional increases of the overloaded lobes weigh in relation to the occlusion level were also observed in ($p>0.01$).

Conclusion: The acute pulmonary overload caused by increase of overload is an important factor for the damage of the alveolar/capillary barrier in lung mechanical stress injury.

Financial Support: FAPESP

P-7

Solitary fibrous tumours of pleura as a cuase of non-islet cell tumour hypoglycemia

Jelena Stojsic, Branislava Milenkovic, Dragana Jovanovic, Motohiko Aiba

Institue for lung diseases and tuberculosis, Clinical Centre of Serbia

Background The solitary fibrous tumours of the pleura (SFTP) originate from submesothelial fibroblasts mostly arising from visceral pleura as localized, pedunculated and well circumscribed tumour protruded into pleural cavity. Majority of non-islet cell tumour hypoglycemia (NICTH) are SFTPs. The association of SFTP with hypoglycemia is referred as Doege-Potter syndrome. This syndrome is described in 2–4% of SFTPs.

Patients: Fourty-eight SFTPs were diagnosed during the last 15 years in our institution and two of them with Doege–Potter syndrome. We performed EnVision System immunostaining (DAKO) with 3,3′-diaminobenzidine as a chromogen without antigen retrieval. We proved positivity of IGF-II and pro-IGF-II in the tumour cells confirmed that SFTP was the cause of hypoglycemia. *Clinical data:* The both patients were women, age of 55- and 68-years. They both suffered of headache and consciousness. Endocrine tests in the both patients showed an extremely reduced glucose level, blood concentration of insulin and C-peptide and large pleural mass, occuping almost the whole hemithorax was diagnosed in chest x-ray and CT examination. *Pathology:* Small, uniform sized spindle- and round- shaped tumour cells with scanty cytoplasm and without nuclear pleomorphism and mitoses were alternated in hypercellular and hypocellular areas. Tumour cells exhibited diffuse cytoplasmatic positivity of vimentin, strong and uniform reactivity of CD34 and positivity for bcl-2 also. The tumours were diagnosed as benign SFTPs. Dot-like reaction for insulin-like growth factor II (IGF-II) and pro-insulin-like growth factor II (pro-IGF-II) products were deposited in Golgi area of spindle tumour cells, proving that SFTPs were the cause of hypoglycemia.

Conclusion: Pathologists can confirm the suspicion that SFTP is a source of hypoglycemia appling IGF-II and pro-IGF-II on paraffin embeeded tissue spacemans, obtained on percutaneous needle biopsy as well as on surgical resection.

P-8

Studies of prevalence of ventilator-associated pneumonia in intensive care unit of the University Braz Cubas – Mogi das Cruzes Hospital (Brazil) and factors and characterize patient evolution

Silvia Froes Bassini; Edson Costa; Leila Moussa Costa; Sonia Maria Almeida; Marcelo Fabiano Rodrigues
Universidade Braz Cubas. Brazil

Introduction: Pneumonia is the second leading nosocomial infection and presents high mortality rates. Ventilator-associated pneumonia (VAP) is the leading infection in intensive care units (ICUs). The incidence ranges from 9% to 68%, depending on the diagnostic method used and on the population studied. Its lethality is high, ranging from 33% to 71%, and the case fatality rate can reach up to 55%. Of all cases of hospital-acquired pneumonia, 86% are associated with mechanical ventilation(MV). However, only 9% to 27% of mechanically ventilated patients develop pneumonia. The prevalence reported is 21.7 to 35.6 cases/1000 MV days, compared with 3.2 cases/1000 days for patients not on ventilation. The proportion of intubated patients who develop pneumonia varies from 10% to 50%, with an approximaterisk of 1% to 3% per day of endo tracheal intubation.
Objective: To determine the prevalence of ventilator-associated pneumonia in an intensive care unit, as well as to identify related factors and characterize patient evolution. Methods: This study evaluated 98 patients on mechanical ventilation for more than 24 hours in a university hospital. Results: Ventilator-associated pneumonia developed in 43.2% of the patients, translating to 39.6 cases/1000 ventilator-days: 55.8% were caused by gram-negative agents (Pseudomonas aeruginosa accounting for 27%); and multidrug resistant organisms were identified in 43.4%. In the ventilator-associated pneumonia group, time on mechanical ventilation, time to mechanical ventilation weaning, hospital stays and intensive care unit stays were all longer ($p<0.001$). In addition, atelectasis, acute respiratory distress syndrome, pneumothorax, sinusitis, tracheobronchitis and infection with multidrug resistant organisms were more common in the ventilator-associated pneumonia group ($p<0.05$). Mortality rates in the intensive care unit were comparable to those observed in the hospital infirmary. Associations between ventilator-associated pneumonia and various factors are expressed as odds ratios and 95% confidence intervals: acute sinusitis (41.1; 3.4–441); > 10 days on mechanical ventilation (7.9; 4.1–14.2); immunosuppression (4.3; 1.3–14.3); acute respiratory distress syndrome (3.5; 1.4–9.0); atelectasis (3.8; 1.2–7.3); cardiac arrest (0.19; 0.05–0.66); and upper gastrointestinal tract bleeding (0.05; 0.009–0.62). The variables found to be associated with in-hospital death were as follows: chronic renal failure (26.1; 1.9–350.7); previous intensive care unit admission (15.6; 1.6–152.0); simplified acute physiologic score II > 50 (11.9; 3.4–42.0); and age > 55 years (4.4; 1.6–12.3). Conclusion: Ventilator-associated pneumonia increased the time on mechanical ventilation and the number of complications, as well as the length of intensive care unit and hospital stays, but did not affect mortality rates.

P-9

Mucinous bronchioloalveolar carcinoma with rhabdoid features

Stefania Damiani; Gianluca Marucci; Kenji Kawamukai; Claudia Ligorio; Guido Collina; Maurizio Boaron
Section of Anatomic Pathology and Thoracic Surgery, Bellaria Hospital, University of Bologna. Italy

Background: A unique case of lung carcinoma with combined features of bronchioloalveolar carcinoma, invasive adenocarcinoma and rhabdoid poorly differentiated carcinoma is described.
Clinical history and Methods: The patient, a 63-year-old man, presented with cough and chest pain. CT scan revealed a giant mass located in the right lower lobe. The lobectomy specimen showed a mass of 10 cm in diameter that invaded the visceral pleura. Tissue were fixed in 10% buffered formalin, paraffin embedded and stained with haematoxylin-eosin. Immunohistochemistry was done with Ventana automated stainer. Results: Histologically, the lesion showed three patterns of growth: most of the lesion (40%) was composed of columnar mucus-secreting cells with a typical lepidic growth, consistent with mucinous bronchioloalveolar carcinoma (BAC). In addition, areas of invasive adenocarcinoma were present (30%- second pattern). Finally, the third pattern was constituted by a solid proliferation (30% of the lesion) composed of rhabdoid cells showing abundant deeply eosinophilic cytoplasm and large vesicular nuclei with prominent nucleoli. In these areas, the neoplastic cells were arranged in a diffuse pattern, without glandular formation and nuclei were two /three times bigger than in the other two components. Binucleated cells were also frequently seen. Immunohistochemically, the neoplastic cells had a similar phenotype in all the three components: they were positive with cytokeratin 7 and vimentin. Vimentin was strong and diffuse in the rhabdoid elements, while it was weak and focal in the other two components. Muscular markers (desmin, myogenin and striated actin) were consistently negative. The patient survived for 37 months after surgery.
Conclusions: The occurrence of a rhabdoid phenotype is most frequently seen in association with poorly differentiated carcinomas. An association with well differentiated carcinomas with BAC pattern is very rare. The present case

is the second case in which rhabdoid features are seen in association with a mucinous BAC

P-10

PULMONARY MALACOPLAKIA ASSOCIATED WITH RHODOCOCCUS EQUI INFECTION IN A PATIENT WITH AIDS

Ángela Hens; Antonio Calvo; Gloria Muñoz; Mª Isabel Moreno; José Rivas (in memoriam).
Hospital Universitario Puerto Real (Cádiz). Spain

We describe a 35-year-old man infected with the human immunodeficiency virus, who on initial examination was found to have cavitary tumoral lung lesion in right lower lobe. Histologic examination revealed sheets of foamy intraalveolar macrophages with the typical histologic features of Michaelis-Gutmann bodies that contained coccobacillary organisms and some "targetlike" cytoplasmic inclusions, so pulmonary malacoplakia probably associated to Rhodococcus equi was diagnosed. Cultures of blood yielded growth of Gram-positive coccobacilli subsequently identified as Rhodococcus equi.

Rhodococcus equi is a pathogen for some animal species, an Gram-positive coccobacillus that cause pulmonary infections in immunocompromised people. Pulmonary malacoplakia associated with this opportunistic coccobacillus is unusual, and pseudotumoral lesions are exceptional, and the recognition of this unique entity is important because of its responsiveness to therapy.

P-11

Epithelial to mesenchymal transition phenotype correlates with clinicopathological features and brain metastases in non-small cell lung cancer

Ludmila Prudkin; Diane D. Liu; Menghong Sun; Natalie C. Ozburn; Kathlynn C. Brown; B. Nebiyou Bekele; Cesar Moran; Ignacio I. Wistuba
The University of Texas MD Anderson Cancer Center. USA

Background: In epithelial to mesenchymal transition (EMT) has been implicated in the progression and metastasis of epithelial tumors. In lung cancer, individual EMT markers' expression has been studied and correlated with prognosis.

Methods: To better define the EMT phenotype of lung cancer we studied the immunohistochemical (IHC) expression of 6 proteins, E-Cadherin (ECad), N-Cadherin (NCad), β-Catenin (β-Cat), MMP-9, Integrin-β6 (Int-β6) and Vimentin in 209 adenocarcinomas (ADC) and 116 squamous cell carcinomas (SCC). EMT expression was correlated with EGFR and p-EGFR IHC and *EGFR* mutational status. We also analyzed EMT markers expressions' in 55 paired lung cancers with brain metastases.

Results: Tumors showed high expression of ECad in 37.5%, NCad 68.2%, β-Cat 95.9%, MMP-9 93.1%, Int-β6 56.2% and Vimentin 45.8% of cases. Female gender associated with higher ECad intensity and lower NCad cytoplasmic score. ADC correlated with higher ECad class and intensity, and NCad membrane and cytoplasmic intensities. Smoking correlated with lower ECad intensity and higher NCad membrane class and cytoplasmic score. Never smokers showed higher ECad and Int-β6 intensities, and former smokers had significant higher NCad membrane class and cytoplasmic score. EGFR class correlated positively with β-Cat membrane class, but negatively with Ncad membrane and cytoplasmic intensities. PEGFR class correlated with NCad membrane and cytoplasmic intensities, but associated negatively with higher Vimentin staining. Higher Int-β6 showed worse overall survival (HR=4.4). No correlations were seen between markers' expression and *EGFR* mutations. ADC brain metastases associated with higher Vimentin score and intensity, and MMP9 cytoplasmic intensity but with lower NCad cytoplasmic intensity.

Conclusions: Our findings indicate that in lung cancer EMT is a frequent phenomenon and correlates with tumor histology, smoking history and survival. The process may have a role in brain metastases occurrence in ADC. Further EMT characterization in lung cancer will provide better understanding of tumor progression and metastasis. (UT Lung Cancer SPORE P50CA70907)

P-12

Basaloid Carcinoma of the lung: a histologic and immunohistochemical study of 8 cases.

F Pérez; G Barraza; M Turell; M Casas; E Díaz; R Ortiz; L Bernadó.
Hospital Universitari de Girona Doctor Josep Trueta. Spain.

Background: Basaloid carcinoma (BC) and large-cell neuroendocrine carcinoma (LCNEC) are 2 recently recognized variants of large-cell lung carcinomas that may overlap in their morphology, and are discriminated by expression of neuroendocrine markers and TTF-1 in LCNEC, and CK34βE12 in BC.

Method: BC was classified according to the 2004 WHO classification as variant of non-small cell lung carcinoma. Immunohistochemistry was performed using antibodies against the following markers: TTF-1, CK34βE12, CK 5/6, synaptophysin, chromogranin, CD10, p63 and C-Kit (CD117).

Results: 8 men had a mean age of 70 (range 59–77 years). The histopathological features were similar in all cases with

a lobular growth pattern of small cells with moderately hyperchromatic nuclei, with no prominent nucleoli, and with scant cytoplasm, a high mitotic rate, and peripheral palisading. All cases were negative for TTF-1, chromogranin and synaptophysin. CK34βE12 was diffusely expressed in 3 cases and focal in 5. CK 5/6 was stained focally in 5 cases and negative in 3. CD10 was strongly expressed in 6 cases, focal in 1 and negative in 1. p63 nuclear staining was positive in 3 cases and negative in 5. C-Kit was stained in variable intensity and distribution in 7 cases and negative in 1. **Conclusions:** These data show that TTF-1 and CK34βE12, in association with specific neuroendocrine markers and CD10, represent a useful panel of antibodies in differentiating carcinomas presenting with a solid pattern, palisading, or pseudorosettes. The morphologic and immunohistochemical phenotype suggest that BC is derived from a basal bronchial epithelial stem cell.

P-13

HER-2/neu in Squamous Cell Lung Cancer

Lina Carvalho; Maria Silva; Ana Alarcão; Patrícia Couceiro; Ana Gomes;Vitor Sousa

Instituto de Anatomia Patológica- Faculdade de Medicina da Universidade de Coimbra, Portugal

BACKGROUND: The present study was delineated to know the status of *HER-2/neu* gene in 60 cases of squamous cell carcinoma of the lung. Either immunohistochemical protein expression and *HER-2/neu* gene and chromosome 17 copy number by fluorescent *in situ* hybridization were characterized. The cases were collected from surgical specimens in stages IIB/IIIA of squamous cell carcinoma.

METHOD: Tissue microarrays were constructed from paraffin-embedded tissue tumors after selection of representative areas from each specimen. Immunohistochemistry for HER-2/*neu* protein expression was verified with polyclonal rabbit anti-human c-erbB-2 oncoprotein. Fluorescence *in situ* hybridization was also performed in tissue microarrays to measure HER-2/neu gene copy number and its the amplification status by applying the probe LSI Her-2/neu/CEP17 (Kreatech, Biotechnology).

RESULTS: It was not verified positivity for protein expression of HER-2 in all cases. None of the 60 squamous cell carcinoma of the lung assessable by FISH exhibited HER-2/neu gene amplification as defined by HER-2/neu/chromosome 17 ratio = or >2. High polysomy for chromosome 17 with increase in HER-2/neu gene copy number was determined in 27 cases. No statistically significant association was observed between absolute chromosome 17 or HER-2/neu and protein expression levels.

CONCLUSION: Gene amplification and protein expression of HER-2 in squamous cell carcinoma in this series suggest to be an infrequent event. High HER-2 gene copy number present in this study reforces the value of HER-2 as a member of EGFR/HER family of receptors and an important partner of EGFR heterodimeration, influencing the response to tirosine kinase inhibitors. Our results are a complement to the published studies to understand the status of either HER-2 protein expression and its gene amplification in a series of squamous cell carcinoma in surgical stages, independently of the presence of lymph node metastasis. It may be understood as a basic study, to correlate with those where patients have been submitted to tyrosine kinase inhibitors in advanced stages after determination of squamous differentiation, as in general, the published data is enlarged to non-small-cell carcinoma, without clear specification of histological patterns.

P-14

Intrathoracic splenosis mimicking intrathoracic neoplasm: a case report.

Wided Stita; Soumaya Rammeh; Lilia Ben Yakoub; Amel Trabelsi; Atef Ben Abdelkader; Sarra Mestiri, Badreddine Sriha; Sadok Korbi

Departement of Pathology, Farhat Hached Hospital, Sousse, Tunisia

Background: Splenosis is a rare condition described as ectopic splenic tissue implantation generally after a splenic rupture. Most of the reported cases are intraabdominal; thoracic splenosis is even much rarer and is typically a result of thoraco-abdominal trauma. It is usually an incidental finding. Hematopoiesis associated with splenosis was rarely reported in the literature. To our knowledge, recurrence of the disease was not yet reported.

Method: We report a case of a thoracic splenosis in a 32 year-old woman and we discuss the clinicapathologic features of this entity.

Results: Our patient had a history of a mini-thoracotomy secondary to a basi-thoracic pain and a right pleural effusion. A multinodular tumor inside the visceral pleura was excised and the resected tumor was diagnosed histologically as an inflammatory pseudotumor. Nine years later, the patient presented with a recurrence of her pleural effusion. Thoracic computed tomography showed a solid and necrotic tumor at the level of the right lobe. During the intra operative observation, a dark colored, soft, multinodular lesion inside the visceral pleura over an area of 6× 3 cm in dimension was observed. The lesion was excised. The histopathological examination of the specimen showed

splenic tissu in the pleura with hematpoiesis, so the lesion was accepted as splenosis and the diagnosis was redressed. Conclusion: Our report is particular by the intrathoracic localization of the splenosis, its association with hematopoiesis and its recurrence after surgical resection.

P-15

Congenital cystic adenomatoid malformation presenting in adulthood in association with adenocarcinoma

Maja Jerse; Miha Sok

Institute of Pathology, Medical Faculty, University of Ljubljana; Clinical Department of Thoracic Surgery, University Clinical Centre Ljubljana. Slovenia

Background: Congenital cystic adenomatoid malformation (CCAM) is a rare pulmonary malformation and refers to a disorganized lung tissue with different degrees of cystic changes. Stocker described five distinct types according to the size of the cysts and the microscopic appearance. It mostly affects newborn infants, but some lesions may be delayed until school age. The adulthood presentation is reported in fewer than 40 cases. Malignoma arising in CCAM is a very rare event.
Methods: A 33-year-old male, non-smoker, presented with chronic productive cough, dyspnoea, left thoracic pain and haemoptysis. He was complaining about recurrent episodes of purulent sputum and fever, diagnosed three times as having bronchopneumonia in the last year. X-ray examination revealed opacity in the left lower lobe, while additional CT scan confirms a large area of consolidation with cystic lesions. The patient underwent left lower lobectomy after suspicion of CCAM.
Results: Macroscopically, solid and mucoid surface areas were demonstrated with multiple cysts, measuring from 0.5–3 cm. Histologically, cystic bronchiolar-like structures were lined by pseudostratified columnar epithelium intermixed with mucogenic cells that exhibited a lepidic growth pattern in adjacent alveoli, characterizing a bronchioloalveolar carcinoma (BAC). Focally, some areas showed greater cellular atypias with invasion of the underlying stroma. However, there was no invasion into pleura or lymph nodes. Based on light microscopy morphology, the diagnosis of CCAM type I in association with BAC and foci of adenocarcinoma was established. After 2-year-follow-up there is no progression of malignancy.
Conclusions: The occurence of CCAM with rhabdomyosarcoma or BAC is rarely documented. We presented the twenty-first case of late-onset CCAM associated with BAC. Because BAC is seen in type I CCAM, mucinous cells could play a neoplastic precursor role. Since CCAMs poses risk of malignant transformation, many advocate early surgical resection, even in asymptomatic patients.

P-16

Immunohistochemical detection of Simian Virus 40 (SV40) in 30 mesothelioma and 97 sarcoma

Isabela Werneck da Cunha; José Vassallo; André Almeida Schenka; Fernando Augusto Soares

Hospital do Cancer SP and State University of Campinas, SP, Brazil

Introduction: SV40 has been associated to human neoplasia, as mesothelioma, brain tumors and lymphoma. The viral protein *Tag* is thought to inactivate host p53. These data have been subject of controversies, as some authors did not find evidences to support relationship between this virus and human neoplasia. In our country, there have been no studies addressing this issue.
Objective: To contribute in the study of the oncogenic potential of SV40 by immunodetection of *Tag* in cases of mesotelioma and sarcoma, diagnosed at our laboratory.
Material and Methods: Thirty mesothelioma and 97 sarcoma had their formalin fixed, paraffin embedded tissue arranged in two tissue microarrays and submitted to immunohistochemical detection of SV40 (monoclonal antibody Ab-2, clone Pab416, Oncogene Research Products, San Diego, CA, USA). Positive cases were graded as 1 = up to 30% positive nuclei; 2=30–70%+; 3 = more than 70% +.
Results: Ten mesothelioma were non reactive for SV40 (33.3%), 4 were grade 1 (13.3%), 6 grade 2 (20%) and 6 grade 3 (20%). In 4 cases evaluation was not possible (13.3%). None of the 97 sarcoma showed any reactivity.
Discussion/Conclusion: Although some authors criticize immunohistochemistry as a method not sufficiently sensitive and specific for some purposes, it is noticeable that 53.4% of our mesothelioma showed immunoreactivity for SV40, or 61.5% of the valid cases (data from the literature using PCR=40–85%). Sarcomas were all negative. Our data furnish further support to a pathogenetic role of SV40 in mesothelioma. Divergence among studies might be due to geographic variation. (FAS and JV are supported by the National Council for Scientific Research, CNPq).

P-17

Mesothelial hyperplasias of the pleura

Roger Llatjós; Isabel Català; Ignacio M Ballarín; Claudia Guevara; Ruth Tascón; Enric Condom

Hospital Universitari de Bellvitge. Spain

Background. Specimens from patients presenting with pleural effusion are usually obtained to rule out malignancy. The separation of benign from malignant mesothelial proliferations remains one of the most difficult

problems in the pathology of the serosal membranes. Inconclusive cases may be termed either Reactive Mesothelial Hyperplasia (RMH) or Atypical Mesothelial Hyperplasia (AMH), since it is far better than overdiagnosing Malignant Mesothelioma (MM). True stromal invasion seems to be the most accurate indicator of malignancy. Clinical, radiological and macroscopic data are relevant. Cytologic atypia and immunohistochemistry are often not helpful.

Method. We looked for patints with noninfectious pleural effusion and a diagnosis of mesothelial hyperplasia, during a nine year period, and studied their characteristics and clinical outcome. Those who finally had pleural metastasis were excluded.

Results. 36 cases were included. Mean age was 62 years. 20 were men. 31 had unilateral pleural effusion. In 30 patients the initial daignostic procedure was a thoracocenthesis. The first cytology report was: benign 11, acute inflammation 7, chronic inflammation 6, RMH 6, AMH 1, MM 2 and other malignancy 3. Final diagnosis was done with open pleural biopsy in 17 cases, thoracoscopy in 10, thoracocenthesis in 3 and tru-cut biopsy in 3. It was: RMH in 13 cases, MM in 11, AMH in 7, nonspecific chronic pleuritis in 2 and inconclusive in 3. The mortality rate was of 61%; 82% in patients with MM.

Conclusion. In patients with recurrent pleural exudates and a pathologic diagnosis of RMH, invasive diagnostic procedures are recommended, along with clinical and radiological follow up, to rule out MM.

P-18
EPITHELIAL-MYOEPITHELIAL TUMOUR: AN INFREQUENT FORM OF SALIVARY GLAND-TYPE PULMONARY NEOPLASIA

Felipo F, Muñoz G, Marquina I, Fuertes A, Pascual M, Sota P, del Agua C

Department of Pathology; HU Miguel Servet, Zaragoza. Spain

BACKGROUND Tracheobronchial submucosal glands can be considered as pulmonary counterpart of minor salivary glands and, therefore, they can develop most of the tumours originated by them. However, in spite of the fact that these glands are widely distributed along tracheobronchial tree, salivary gland-type pulmonary tumours are rare.

METHODS We present the case of a 76 year-old female, with no significant personal history, to whom a pulmonary nodule is detected while studying unknown origin neutropenia. Upper right lobectomy is performed.

RESULTS After gross and microscopic examination and immunohistochemical profile, a diagnose of epithelial-myoepithelial tumour is made.

COMMENTS Salivary gland-type pulmonary tumours are rare. Among them, mucoepidermoid carcinoma and adenoid cystic carcinoma are the most frequent, whereas mixed neoplasias with epithelial and myoepithelial components are extraordinarily infrequent. In the lung, they are considered as low malignant potential tumours with capacity for local recurrence and less frequently for metastasize. No case with vascular, lymphatic or perineural invasion, neither with distant mestastases.

It has been suggested that myoepithelial cells play an important role in this type of tumours, based on a different immunostain pattern for p27/kip-1 between both neoplastic components. An aberrant subcelular location of this protein into myoepithelial cells would provoke loose of its growth inhibition function and would contribute to tumorigenesis because of a lack of restriction of myoepithelial component proliferation.

P-19
THE VEGF-SIGNALLING PATHWAY IN VASCULAR AND PERIVASCULAR TUMORS OF THE LUNG

Elvira Stacher1; Ulrike Gruber-Moesenbacher2; Mauro Papotti3; Angelo P. Dei Tos4; Lina Carvalho5; Monika Huber6; Iris Halbwedl1; Margit Gogg-Kamerer1; Elisabeth Grygar1; Alberto Cavazza7; Helmut H Popper1

1Institute of Pathology, Medical University of Graz, Graz, Austria; 2Institute of Pathology, Teaching Hospital Feldkirch, Feldkirch, Austria; 3Pathology, Dip. Scienze Biomediche E Oncologia Umana, Torino, Italy; 4Pathology, University of Treviso, Treviso, Italy; 5Pathology, University of Coimbra, Coimbra, Portugal; 6Institute of Pathology, Otto Wagner Hospital, Vienna, Austria;7Unita Operativa di Anatomia Patologica, Ospedale S. Maria Nuova, Reggio Emilia, Italy.

Background: Vascular Tumors (such as Haemangiopericytomas, Epitheloid Haemangioendotheliomas and Angiosarcomas) of the lung are very rare lesions. Due to their rare incidence no standardized therapy regimen is established. So far surgery is the only option of treatment. Especially in Haemangioendotheliomas, which can present as a diffuse or multifocal lesion, surgical resection is sometimes incomplete. A blockade of vascular endothelial growth factor receptors (VEGFR2 and VEGFR3) either by antibodies for their ligands or by kinase inhibitors have been increasingly used for the therapy of solid tumors.

Method: We investigated several factors of the VEGF-signalling pathway in two Haemangiopericytomas, seven

Epitheloid Haemangioendotheliomas and eleven Angiosarcomas by means of immunohistochemistry using commercially available antibodies for VEGFA, VEGFB, VEGFC, VEGFD, VEGFR2, VEGFR3 and endothelium specific kinase Tie2.
Results: The tumor cells of the haemangiopericytomas, epitheloid haemangioendotheliomas, and angiosarcomas reacted positively for Tie2, either VEGFR2 and/or VEGFR3. They showed a diverse reaction pattern for their ligands, revealing VEGFA and VEGFB the most predominant. In general, the tumor cells of the angiosarcomas showed a stronger positivity for the ligands.
Conclusion: The observed positivity for the factors of the VEGF-signalling pathway points towards a possible new therapeutic option by inhibiting VEGFR2 and VEGFR3.

P-20

EGFR EXPRESSION AND GENE AMPLIFICATION IN NON-SMALL CELL LUNG CARCINOMAS: CORRELATION BETWEEN GENE COPY NUMBER AND PROTEIN EXPRESSION

Ji Eun Kim;Hyun Ju Lee;Gheeyoung Choe;Sanghoon Jheon;Sook Whan Sung;Choon-Taek Lee;Jin-Haeng Chung
Seoul National University Bundang Hospital. South Korea

Progress in lung cancer biology led to the identification of the epidermal growth factor receptor (EGFR) signaling pathway as a therapeutic target leading to the development of tyrosine kinase inhibitors (TKIs). We determined EGFR protein overexpression by immunohistochemical analysis and EGFR gene amplification by fluorescence in situ hybridization (FISH) in 132 formalin-fixed, paraffin-embedded lung tumors including squamous cell carcinoma (SCC; 68 patients), adenocarcinoma (ADC; 50 patients) and other non-small cell carcinoma (14 patients). Protein expression was assessed by immunohistochemistry and gene copy number was evaluated by fluorescent in situ hybridization (FISH). EGFR protein overexpression was observed in 67% of the NSCLC, more frequently in SCC than ADC (75% vs 44% $p<.001$). There were no statistical diffrences in EGFR expression with respect to sex, smoking history, BAC feature, nodal status or stage. EGFR FISH-positivity as represented by high polysomy and gene amplification was observed in 33.2% of the NSCLC patients. The FISH patterns were disomy (29.6%) and low polysomy (37.2%), high polysomy (21.9%) and gene amplification (11.4%). Protein expression levels significantly correlated with the gene copy number per tumor cell ($p=0.000$). The proportions of EGFR-expressing tumors according to the gene copy status were: 90% of gene amplified cases, 75% of high polysomy, 40% of low polysomy, and 25% of disomy cases. EGFR overexpression or high gene copy numbers had no significant influence on tumor recurrence. EGFR overexpression is frequent in NSCLC, is most prominent in SCC, and correlates with increased gene copy number per cell. Additional studies are needed to determine whether EGFR gene amplification or protein expression bears any informative value in predicting response to EGFR inhibitor therapy.

P-21

FOLLICULAR BRONCHIOLITIS. A REVIEW OF 11 CASES.

Eduardo Alcaraz Mateos; Francisco Ignacio Aranda López; Encarnación Barroso Medel; Juan Arenas Jiménez; Maria Planelles Asensio; Ana Teruel Del Valle; Santiago Romero Candeira
Hospital General Universitario de Alicante. Spain

BACKGROUND: Follicular bronchiolitis (FB) is a histopathologic finding that occurs in diverse clinical contexts such as hypersensitivity reactions, immunodeficiency, toxic exposure and collagen diseases. Is characterized by bronchiolar lymphoid tissue with germinal follicles. The current study was conducted to characterize histopathological features, and clinical-radiologic correlation.
METHODS: From 352 lung biopsies between 1999 and 2007, 11 cases (3.1%) of FB were diagnosed. Medical synthoms, radiologic and morphological findings were recorded.
RESULTS: The patients included 5 men and 6 women; the median age at diagnosis was 47 years (range, 15–73). Main symptoms were repeated respiratory infections and variable degree of dyspnea. Some patients had underlying systemic deseases that included: In one patient FB was associated with advanced AIDS, other 3 patients had Sjögren's Syndrome (one of them also with Systemic Lupus Eritematous, SLE), other an undifferentiated connective tissue disease and another with prolonged exposure to polyethylene-flock. CT findings included reticular and ground-glass opacities and small nodules. FB was the major histopathology pattern in 8 patients, associated secondary with nonspecific interstitial pneumonia, organizing pneumonia, and isolated cases of bronchiolitis obliterans, non epitelioid granulomas and interstitial fibrosis with anthracosis and silice (using polarized light), all of them associated to the FB. The immunochemical stain for lyfocites B and T was positive in all cases using CD20 and CD3. Clinical course was characterized by relative stability with partial response to steroid or anti CD4 monoclonal antibody therapy, but in one case the progressive worsening caused the death.
CONCLUSIONS: FB is a non very unusual pathology found associated with other diseases. The major lesion of FB is the lymphoid follicles around distal airways. The clinical course and prognosis for most patients is relatively good, but progressive lung disease is possible.

P-22

Pseudoangiosarcomatous carcinoma of the lung: a clinicopathologic study of four cases.

Nuria Santonja; Liria Terradez; Jaime Ferrer.

Department of Pathology.Hospital Clínico Universitario de Valencia. Spain

Background: Pulmonary pseudoangiosarcomatous carcinoma (PPAC) is a rare type of lung cancer, defined by the presence of infiltrating, anastomosing channels that resemble vascular spaces. The 1999 WHO classification places it into the pleomorphic carcinoma (PC) category. A putative different prognosis of PPAC within the PC group has not been studied yet.

Methods: Four cases of resected PPAC and four cases of PC were studied. Immunohistochemical stains against cytokeratin 7(CK7), cytokeratin 5/6 (CK5/6), and TTF-1 were performed. Stains against CD31, CD34 and factor VIII-related antigen (FVIII) were made in PPAC cases, in order to rule out a true pulmonary angiosarcoma. Clinicopathologic comparison was undertaken between both groups. Survival curves were evaluated by the Kaplan-Meier method, and satistical signification estimated with the log-rank test.

Results: Patients with PPAC (mean age=70 years)had a mean tumor diameter of 11.3 cm. All cases were positive for CK7, at least focally; TTF-1 was positive in one case; CD31, CD34 and FVIII were negative. Three patients were in pathologic stage IIIa (two of them died at 0.7 and 5.8 months, one is alive with disease progression at 3 months) and one in stage IIb (alive and well at 4 months). Patients with PC (mean age=58.7 years) had a mean tumor diameter of 4.05 cm. All cases showed a weak positivity for CK7; TTF-1 was positive in one case. Two patients were in stage IIb, one in stage IIIa, and one in stage IV (all alive with disease progression, with a mean follow up of 16.5 months). No significant differences were observed between both groups in terms of survival.

Conclusions: Clinical data suggest an aggressive behavior of PPAC. However, the limited number of cases analyzed does not permit to establish this histologic subtype as a predictor of survival within the PC group.

P-23

RECURRENT PRIMARY LUNG LIPOSARCOMA (A CASE REPORT)

***Dilek Yavuzer; *Sevinc Hallac Keser; **Recep Demirhan; *Aylin Ege Gul; *Dilek Şakirahmet; *Nimet Karadayi**

**Dr. Lutfi Kirdar Kartal Educational and Research Hospital, Pathology Department, ISTANBUL/TURKEY **Dr. Lutfi Kirdar Kartal Educational and Research Hospital, Department of Thoracic Surgery, ISTANBUL/TURKEY*

Background: Liposarcoma is one of the most common malignant soft tissue tumors in adults and the most frequent primary sites are the extremities and retroperitoneum. Intrathoracic origin is unusual, and most of those develop in the mediastinum. Primary pulmonary liposarcoma has been reported in only a limited number of cases worldwide. The clinical behavior and prognosis seem to correlate with the histologic classification of the tumor. The extend of surgical resection is one of the most important prognostic factor. Local recurrence may occur if the tumor is not completely excised. Metastasis to various structures including lung, pleura, liver, mediastinal lymph nodes and bone are described, specially in the poorly differentiated varieties.

Case Report: There was 10 cm in diamater mass, in the patient's chest x-ray whose applied to our hospital with the complaints of chest pain and dispnea. A mass which was thought to be recurrent, surgically resected and submitted to our pathology department. Surgical materials were couple of tissue pieces which 5×4×3 cm in diameters is the largest and have yellow, shiny and diffuse appearance in their cut surfaces. Microscopically, the tumour consisted of proliferating lipoblasts with considerable nuclear pleomorfism in a stroma containing a rich capillary network. The case was diagnosed as liposarcoma after histopathological and immunohistochemical analysis. Patients previous history revealed that she had been operated and diagnosed as liposarcoma of the right lung in another institution and put in to postoperative chemoteraphy programme. In order to exclude the possibility metastasis from primary tumor, whole body scan performed but there was no one, and this tumor is accepted as the primary.

Conclusion: Primary pulmonary liposarcoma has been reported in only limited number of cases worldwide. Although it is extremely rare, primary pulmonary liposarcoma should be included in the differential diagnosis of lung tumors.

P-24

Amiodarone induces pulmonary toxicity and fibrosis via phospholipidosis mediated apoptosis

Eftihia Kapatou; Angelos Skyrlas; Christianna Zachariou; Theofilos Kolettis; Agathocles Tsatsoulis; Dimitrios Stefanou; Maria Bai; Vassiliki Malamou-Mitsi

Departments of Pathology, Cardiology and Internal Medicine-Endocrinology, Medical School, University of Ioannina. Greece

Background Amiodarone (AMD) is a potent anti-arrhythmic drug frequently used for treating ventricular and supraventricular arrhythmias. The use of AMD is limited by its toxic side effects, the most severe of which is the Amiodarone-Induced Pulmonary Toxicity (AIPT). The pathology of AIPT, which includes alveolitis, phospholipidosis, and irreversible fibrosis, is well described. However, the mechanism underlying the involvement of AMD to the pathogenic molecular machinery of the disease remains unclear.

Apoptosis of alveolar epithelial cells appear to play an important role in AIPT. It is known that an individual stimulus may initiate apoptosis; however, the pathways transducing these signals are often regulated by other cellular events such as phospholipidosis. In the present study we investigate the involvement of AMD induced phospholipidosis to the triggering and regulation of apoptosis.

Method The immunohistochemical expression of phospholipase C gamma-1 (PLC-γ1), activated-caspase-3, activated-caspase-8, Bcl-2, Survivin, and c-Flip, was studied in 33 samples of pulmonary tissue from Wistar rats after oral administration of AMD for 14 days at the minimum therapeutic dose (30 mg/kg/day). Apoptosis was detected by the TUNEL method and the apoptotic index (AI) was calculated.

Results Our results indicated that administration of AMD was correlated with increased apoptosis, increased expression of activated caspases-3 and -8, and decreased expression of PLC-γ1, Bcl-2, Survivin and c-Flip. The expression of pro-apoptotic proteins activated caspase-3 and -8 showed significant positive correlation with the AI, while the anti-apoptotic molecule Bcl-2 was positively correlated with the inhibitors of apoptosis Survivin and c-Flip. Activated caspase-8 exhibit significant negative correlation with c-Flip and Bcl-2. Finally, the expression of PLC-γ1 was positively correlated with Bcl-2 and Survivin.

Conclusion Our data indicate that administration of AMD enhances apoptosis of alveolar epithelial cells mediated by inhibition of PLC-γ1. Activated caspases-3 and -8 seem to act as the effector molecules of apoptosis in AIPT.

P-25

Diagnostic of mesothelioma in routine practice

Izidor Kern

University Clinic of Respiratory and Allergic Diseases, Golnik, Slovenia

Pathological confirmation, either cytological and or histological diagnosis, is recommended in any patient in whom mesothelioma is suspected. The aim of study was to analyse our routine diagnostic practice in mesothelioma patients.

We retrospectively reviewed all patients with pathological diagnosis of mesothelioma in the last ten years. Pathological diagnosis was obtained from pleural effusion fluid cytology and or histhology of various pleural specimens (blind or guided needle biopsy, medical or surgical thoracoscopic biopsy, pleurectomy). Cytospins were done out of pleural effusion samples, further on stained by MGG and Papanicolaou. Immunocytochemistry was done on cytospins and on cell blocks. Tissue specimens were formalin fixed and paraffin embedded. Slides were HE stained and sometimes additional stainings were done, AB and PAS with diastase pretreatment. Immunohistochemistry was performed using different antibodies. Histopathological classification into three main groups was done according to WHO.

In ten years period 183 cases of mesothelioma were diagonosed in our lab. There were 145 cases diagnosed from pleural effusion fluid cytology and 123 cases had histological diagnosis from tissue specimens (91 needle biopsies, 64 medical thoracoscopic biopsies, 25 surgical biopsies and 4 pleural resected specimens). There were 99 cases with both cytological and histological diagnosis of mesothelioma. Epithelioid type was the most predominant one, biphasic was diagnosed in larger histological specimens and there was no case of cytologicaly diagnosed sarcomatoid type. Ten years ago we used pankeratin, vimentin, CEA along with histochemistry (AB and PAS with diastase). Then came period of testing various mesothelioma markers (thrombomodulin, WT-1, CD15, HBME-1, mesothelin). In the last years a panel of four antibodies was applied strictly (BerEP4, MOC31, CK5/6 and caretinin).

Our routine diagnostic practice for mesothelioma disclosed high percentage of cases being diagnosed from cytology, while almost one half of cases were confirmed cytologicaly and histologicaly. Immuncyto- and immunohistochemistry revealed three different panels of antibodies used through ten years period.

P-26

Bronchocentric granulomatosis associated with pulmonary hidatidosis

Adnène Moussa; Leïla Njim; Rym Hadhri; Abdelmajid Dhouibi; Nada Touil; Houda Mahmoudi; Abdelfatteh Zakhama

Department of Pathology, Fattouma Bourguiba University Hospital, 5019 Monastir, TUNISIA

Background Bronchocentric granulomatosis (BG) is a non-specific necrotizing granulomatousreaction surrounding the peripheral conducting airways. In asthmatic patients, BG is considered a hypersensitivity reaction to intrabronchial fungi. However, non-asthmatic patients may develop BG without signs for endobronchial fungal infections, but probably as a consequence of other pulmonary conditions.

Method & Results We report the case of a 31-year-old woman, previously healthy, referred to our hospital because of an intermittent cough and hemoptysis. Radiographs and CT scan of the chest disclosed 2 cystic masses in the right lobe with typical appearance of hydatic cysts. A surgical resection of the two cysts was done. Pathological examination of the resected specimens confirmed the diagnosis. Histology revealed anassociated bronchocentric granulomatosis with foreign-body giant cells containing fragments of hydatic membrane and scolex.

Conclusion BG associated with hydatidosis is exceptionally rare. To our knowledge, this is the fourth case reported. Although the aetiology of BG has not been fully elucidated, the current pathogenetic mechanism is considered to be an immunologic reaction against endobronchial antigens.

P-27

Steroid hormone receptors in non small cell lung carcinomas

Christina Karlsson; Oswaldo Frenandes; Mats G Karlsson

School of health and medical sciences, Örebro university and Örebro university hospital, Sweden

Background Steroid hormone receptors have been studied in non-small cell lung carcinomas (NSCLC) in the perspective of gender-associated differences in tumour types and prognosis. During recent years receptor subtypes for both oestrogen (ERα/ERβ) and progesterone (PRA/PRB) have been identified and conflicting results concerning their expression have been reported.

Methods A consecutive material of 270 NSCLC surgically treated at Örebro University hospital between 1990 and 1995 has been studied. The tumours consisted of 126 squamous cell carcinomas (SCC), 140 adenocarcinomas (ADCA), 3 adenosquamous carcinomas and one large cell carcinoma. 172 of the patients were males and 98 females. Immunohistochemistry was performed, including heat epitope antigen retrieval, with monoclonal antibodies to ERα, ERβ, PRA and PRB using Envision® visualization procedure. Nuclear positivity was scored positive when >10% of tumours cells were stained.

Results ERα expression was focally present in 4 adenocarcinomas.

ERβ was present in 63 tumours. ERβ expression was more frequent in SCC, 29%, then in adenocarcinomas, 19%, p= 0.04 (Pearson chi^2-test).

The differences between histological types could be seen in the male group (p 0.03) while it failed to reach statistical significance amongst women. Overall, female tumours were ERβ positive in 28% whilst male tumours in 21%, (ns, chi^2-test). There was no difference concerning mean age between ERβ groups in either gender.

None of the tumours expressed PRA or PRB.

Discussion Taking our and previously published data into consideration, discrepancies in ERα expressions seems to be antibody dependent. Our data supports that only a very small fraction of NSCLC expresses ERα. The absence of PR expression is in concordance with the absence of functional ERα signalling.

ERβ expression occurs frequently with a slight predominance in SCC compared to ADCA, without influence of gender. Whether ERβ mediated effects occurs in NSCLC remains to be studied.

P-28 WITHDRAWN

P-29

VEGF ROLE IN THE SPECIFIC PATTERN OF PULMONARY DAMAGE INDUCED BY MTOR INHIBITION WITH HIGH BLOOD LEVELS IN A RAT MODEL.

Joaquim Carreras4, MD,Jordi Rovira, PhD1, E. Marcelo Arellano, MD1, 2, Fritz Diekmann, MD1,3, Daniel Moya-Rull1, Josep Ramirez, MD4, Maria José Ramírez-Bajo, PhD1, Elisenda Bañón-Maneus, PhD1 and Josep M. Campistol, MD1.

1LENIT, Hospital Clínic, Barcelona, Spain; 2Nephrology, H.U.-José E.González-, Monterrey, México;3Nephrology, Charite Campus Mitte, Berlin, Germany; 4Pathology, Hospital Clínic, Barcelona, Spain

Background: Pulmonary toxicity is an infrequent, but possibly severe side effect of mTOR inhibitor treatment. Its pathophysiology remains unknown so far.

Methods: 8 Wistar rats were treated with sirolimus with three weekly intraperitoneal injections of 1 mg/kg BW each

for three months (SRL group), and 8 rats were treated with vehicle (VEH group). After three months the animals were sacrificed for analysis. Pulmonary tissue was put in 3.5% formalin and frozen in OTC for further analysis. HE, PAS and oil red stains were performed. The histological features were quantified by a blinded lung pathologist according to severity on a scale of 0 to 3 (0=none, 1=low, 2=moderate, 3=severe). Immunohistochemical VEGF staining was quantified according to the same intensity scale.
Results: Whole blood trough concentrations after three months were 39 ng/mL. The lungs of SRL-treated rats showed a marked perivascular infiltrate of small-sized vessels (1.4±0.7 vs. 0.25±0.5; $p<0.01$). Furthermore, lungs of SRL-treated animals showed segments with marked accumulation of intra-alveolar macrophages and material (macrophages SRL vs. VEH 2.1±0.6 vs. 0±0, $p<0.01$; intra-alveolar material SRL vs. VEH 2.0±0.8 vs. 0±0, $p<0.01$). This material was intracellular, parts of it being PAS-positive and other parts oil red positive. The lungs of SRL-treated rats showed less intense staining for VEGF in vessels and interstitial.
Conclusion: In an experimental model exposure to high-dose SRL treatment leads to a histological pulmonary characterized by perivascular infiltrate and intra-alveolar macrophages and proteinaceous and lipidic material, which is associated with less intense VEGF staining.

Haematopathology

P-30
Primary Cutaneous Small-Medium CD4+ T-Cell Lymphomas. A Heterogeneous Group of Tumors with Different Clinicopathologic Features and Outcome

A. Garcia-Herrera, L. Colomo, M. Camós, J. Carreras, O. Balague, A. Martinez, A. Lopez-Guillermo, T. Estrach, E. Campo
Departments of Pathology, Hematology and Dermatology, Hospital Clinic, IDIBAPS, University of Barcelona, Spain.

Purpose: To define the clinical and pathologic characteristics of primary cutaneous small/medium CD4+ T-cell lymphoma (PCSM-TCL) and identify parameters of prognostic significance.
Patients and Methods: We have investigated 24 patients with primary cutaneous lymphomas composed of small/medium mature T-cells with a βF1, CD3, CD4+ and/or non cytotoxic, CD8- and CD30- phenotype. The proliferation index and CD8+ infiltrating cells were quantified with an automated image analysis system.
Results: Sixteen patients presenting with solitary or localized plaques or small nodules (<3 cm) had an indolent course. Only three patients experienced repeated cutaneous relapses and none of them died of the disease after 1–168 months (median 17 months) of follow-up. The tumors had a low proliferation (median Ki-67, 9% ±5) and an intense infiltrate of reactive CD8+ (median, 20% ± 11.7). Five patients presenting with rapidly evolving large tumors or nodules (≥5 cm) had an aggressive disease and died with extracutaneous dissemination 18–36 months after diagnosis (median 23 months). These tumors had a significantly higher proliferation (median Ki-67, 22% ±11.3) ($p<0.05$), and lower number of infiltrating CD8+ (median, 1% ±3) ($p<0.05$) than the previous group. A third group of three patients had a peculiar clinical presentation with multifocal relapsing lesions without extracutaneous dissemination after a long period of follow-up ranging from 41 to 92 months. Histologically these cases had an intense infiltrate of eosinophils.
Conclusion: PCSM-TCL is a heterogeneous group of tumors with differentiated clinical and pathological characteristics with impact in the outcome of the patients.

P-31 WITHDRAWN

P-32
Peripheral cutaneous T-cell lymphoma, unspecified, rich in giant cells: a case report

Thamy Yamashita; Rafael Gaiolla; Lílian Valéria Guerra da Silva Pinto Bezerra; Hamilton Ometto Stolf; Lígia Niero; Mariangela Esther Alencar Marques; Maria Aparecida Custódio Domingues
Faculdade de Medicina de Botucatu - Universidade Estadual Paulista "Júlio de Mesquita Filho". Brazil

Background: Peripheral unspecified T lymphoma are T lymphocyte neoplasias with innumerous morphological subtypes corresponding to distinct clinical aspects, renown for their difficulty for inclusion in specific entities. The report highlights a rare association of this entity with granulomatous reaction in multinucleated giant cells, which could obscure the main diagnosis. Case report: A 28 year-old Caucasian male presented infiltrated erythematous violaceous lesions, 20 cm in diameter on the right thigh and gluteus for 3 years. Examination revealed a right groin lymphadenomegaly measuring 2 cm in diameter, negative for B symptoms. The initial clinical hypothesis was non-Hodgkin lymphoma. Results: Microscopy revealed an infiltrated lymphoid neoplasia occupying surface and deep dermis with destruction of adjoining tissues, constituted by small lymphocytes. Immunohistochemical studies were

positive for CD3, CD4 in the lymphoid cells and CD68 and lisozime in the giant cells. T cell clonality proved positive by the genotyping method; BAAR and fungi tests were negative. The final diagnosis was peripheral T-cell lymphoma unspecified rich in giant cells. The CHOMP scheme was indicated. Conclusion: Peripheral T lymphoma is an entity that includes innumerous morphological aspects, though its association with granulomatous reaction rich in foreign-body type giant cells is rare. Presence of such cells can occur in other non-Hodgkin lymphomas like B lymphomas, angioimmunoblastic T lymphomas and classic Hodgkin lymphoma. The presence of giant cells could lead to an inconsistent diagnosis of infectious disease, requiring the exclusion of specific agents using special stains and confirmation of lymphoproliferative disease thorough auxiliary studies.

P-33

An unusual presacral mass in a thalssemic patient

Nouira Aminaa; Faten Limaiem; Kais Nouira; Ines Chelly; Haifa Azzouz; Khedija Bellil; Selma Bellil; Slim Haouet; Nidhameddine Kchir; Moncef Zitouna

Hospital La Rabta. Tunisia

Background: Extramedullary hematopoiesis occurs as a compensatory mechanism for bone marrow dysfunction in chronic hemolytic anemias including thalassemia. It most often involves the liver, spleen and lymph nodes. The presacral area is an unusual site of extramedullary hematopoiesis as only 21 cases have been reported in literature.

Case report: in this paper, the authors describe a new case of a symptomatic presacral extramedullary hematopoiesis in a 53-year-old man with thalassemia intermedia. Diagnosis was suggested by the association of imaging findings and knowledge of the clinical context. Histopathological examination of a CT-guided core biopsy and fine needle aspiration of the mass established the diagnosis of extramedullary hematopoiesis.

Conclusion: We conclude that CT-guided biopsy and fine needle aspiration are efficient means to obtain final diagnosis of atypical extramedullary hematopoiesis localizations.

P-34

Immunohistochemical expression and methylation status of MGMT in diffuse large B-cells lymphomas

Silvia Uccella; Claudia Placidi; Silvia Marchet; Ileana Carnevali; Roberta Cerutti; Daniela Furlan; Cristina Riva; Carlo Capella

Anatomia Patologica, Dipartimento di Morfologia Umana, Università dell'Insubria, Varese, Italy

BACKGROUND: Loss of O6-methylguanine-DNA-methyltransferase (MGMT) expression and presence of MGMT promoter methylation have been both proposed as favourable prognostic markers in diffuse large B-cell lymphomas (DLBCLs). However, there are very few studies which evaluate the relationship between the lack of immunoreactivity (IR) for MGMT and the methylation status of its promoter.

MATERIALS AND METHODS: We studied 74 patients with primary nodal DLBCL, all treated with cyclophosphamide-containing regimens and with available follow-up information. MGMT-IR was detected using a specific monoclonal antibody (Chemicon International Inc, Temecula, CA) and Ultravision Amplification System. The immunohistochemical results were evaluated in a semiquantitative way, using a four-titered score: 0 (no expression), L (Low, IR in 5–25% of neoplastic cells), I (Intermediate, IR in 20–50%), H (High, IR in more than 50%). In addition, the metilation status of MGMT promoter was analyzed in a subset of cases using a quantitative method based on Real Time methylation-specific PCR (Lo et al., 1999). For each sample we determined a methylation index (MI) and we considered cases with MI $\geq$20 as methylated.

RESULTS: At immunohistochemical analysis18 cases scored 0, 10 scored L, 16 scored I and 29 scored H. We considered all cases with score 0 or L as lacking MGMT expression (28 out of 74 cases, 38%), and all of them were studied for MGMT promoter metilation. We also analyzed the metilation status of 20 cases with score I (10 cases) or H (10 cases). The results of metilation analysis showed that all but 1 cases with immunohistochemical (IHC) score of I or H were unmetilated, while, only 52% of cases with IHC score of 0 or L (15 out of 28 cases), with no difference between the two groups, showed MGMT promoter metilation. In addition, the survival analysis showed significantly longer overall survival and lymphoma-free survival in DLBCLs with MGMT promoter metilation compared with unmetilated cases, while the difference was not statistically significant when the cases with IHC score of 0/L and I/H were compared.

CONCLUSIONS: These data suggest that the MGMT promoter metilation status, and not the loss of protein expression, is a favourable prognostic factor in primary

nodal DLBCLs treated with cyclophosphamide-containing regimens. On the other hand, immunohistochemistry seems to be an useful tool to identify unmethylated cases, while a methylation analysis should be performed when there is no or low expression of MGMT.

P-35

The evaluation of relation between staging of Hodgkin disease

Monsef Esfahani ar; Abbasi m; Eghbalian fa
Pathology Dept.Hamadan University. Iran

Hodgkin lymphoma is an uncommon cancer of the lymphatic system, mostly of the young. The staging system of the disease has been effectively used for treatment decision making. lt has recently been proposed that some serologic factors such as Lactate Dehydrogenase(LDH), Erythrocyte sedimentation rate (ESR)and C-reactive protein (CRP)are useful markers. In this study we aimed at making out the the evaluation of relation between staging of Hodgkin disease and serum levels of ESR, CRP and LDH of the known cases of Hodgkin.
Methods and Materials: Known cases were assessed for age, sex, LDH, ESR, CRP, tumor histologic type and stage, in hematological ward of Farshchian hospital, Hamedan provience, during a three year period. The data were analyzed by SPSS version.10
Results: The mean age was 32.84 years. 52% were male and 48% were female. Regarding the types we found 42% of Mixed cellularity, 40% of Nodular Sclerosis, 18% of Lymphocyte Prodominace. Stage of Them was 32%,34%, 7%, 16% respectively.
The erythrocyte sedimentation rate (ESR) was over 30 in 34% of patients. CRP was identified in 30% of all samples. LDH was over 32 .in 24% of patients
There was a significantly relationship between ESR over 30 and stage of diseases ($p=0.001$) and age over 45 years of patients ($p=O.OOO$). we also found a significant relationship between LDH over 220 and stage of diseases ($p< 0.05$). The relationship between ESR over 30 and sex and tumor type were not significant ($p>0.05$). The relationship between CRP and age, sex, tumor type and stage were not significant ($p>0.05$). Also we could not find any significant relationship between. LDH and age, sex and tumor type ($p>0.05$)
Conclusion: This study found a significant relationship between serum levels of ESR and stage of diseases and age over 45 years of patients. Also a significant relation between LDH over 220 and stage of Hodgkin disease.

P-36

Correlation between human herpesvirus-8 with multiple myeloma

Mohammad Hadi Sadeghian; Mehrdad Katebi; Hossein Ayatollahi; Mohammad reza keramati
MASHHAD UNIVERSITY OF MEDICAL SCIENCE.Iran

Introduction: Multiple myeloma is a plasma cell neoplasm characterized by involvement of the skeleton at multiple sites.some viruses such as HHV-8 implicated in pathogenesis of disease but this role is not clear.
The goal of our study was to show direct evidence of HHV-8 in multiple myeloma patients with use of immunohistochemical technique.
Materials and Methods: 30 cases of Multiple myeloma and equal number of normal bone marrow tissue were selected and Immunohistochemstry was performed with HHV-8 marker. slides were examined for immunoreactivity in cells nuclei and positive or negative results were reported.The data studied and analysed with pearson chi-square test,also 2×2 contingency tables and Fischer's exact test by specialist of statistics and Differences with p-value under 0.05 ($P\leq0.05$) assumed valuable.
Results: 73.3% of patients was male and 26.7% was females. The age ranged was 58.70 ± 13.52 for mean ± standard deviation. Fisher exact test showed no difference between two group of case and control ($P=0.11$) for HHV-8 Immunoreactivity and positive staining in MM was seen in 4 cases (13.3%) and zero (0%) in control group.
Conclusions: Our finding showed that HHV8 infection did not seem influence on pathogenesis of multiple myeloma.
Key words: herpesvirus - multiple myeloma-Immunohistochemistry.

P-37

Association between ABO and Rhesus blood group systems among confirmed Human T Lymphotropic Virus-1-infected patients in Northeast Iran

Hossein Ayatollahi; Houshang Rafatpanah; Mohammad Esmaeil Khayyami; Delaram Sayadpour;Mehrangiz Ravarian, Mohammad Hadi Sadeghian;Nafiseh Izadi; Mahdi Khabbaz Khoob
Mashhad University of Medical Sciences. Iran

Background:The distribution of ABO and Rhesus blood group types was investigated in 984 randomely selected Human T Lymphotropic Virus-1(HTLV-1) infected blood donor from April 2004 to March 2007.One thousand and eighty one healthy controls who admitted for blood donation in this period,were enrolled in this study.
Study design: Infected and control individuals were from the same region and their ABO/Rhesus blood group

systems were determined by the standard tube test technique.
All blood samples were screened for HTLV-1 using enzyme-linked immunosorbant assay (ELISA) and positive samples were confirmed by Western blot (WB).
Results: The unmached analyses showed significant differences in frequency of A+ blood group between healthy controls and HTLV-1 infected individuals(OR=0.8,95%CI=0.66–0.97) and also significant association was observed between these two groups(OR=1.42,95%CI=1.1–1.99,P=0.021).
No significant difference of blood group (A-, B+, B-, O+, O- and AB-) was observed between cases and controls.
Conclusion: Our results might suggest that A+ blood group decrease the risk of HTLV-1 infection in healthy controls, while the AB+ blood group is more frequent in HTLV-1 carriers and increase the risk of HTLV-1 infection.
Keyword: ABO Blood group, Rhesus blood group, Human T Lymphotropic virus-1.

P-38

Clonality study in malignant lymphomas - immunoglobulin gene rearrangement

Tibor Mezei; Simona Gurzu; Pap Zsuzsanna; Zoltán Pávai; Zoltán Szentirmay; János Jung
Pathology Department, University of Medicine and Pharmacy of Targu Mures. Romania

Introduction: Immunoglobuline gene (IgH) rearrangementstudy permits the analysis of the lymphoid cell line. This is possible due tothe fact that in a normal tissue (after somatic mutation of the immunoglobulingenes took place) there are numerous different cellular clones arising from thesame progenitor cell. Tumoural cells have the same IgH genes. This permits us,by the amplification of certain segments of the immunoglobulin gene, toevaluate the clonality of lymphoid tissue.
Materials and methods: We performed our study on 25 cases of malignant lymphoma,using paraffin embedded tissue samples. IgH gene rearrangement study was used toassess clonality, using PCR method (primers used: forward VH, reverse JH;framework region 3). For the analysis of the PCR products we used twodifferents methods: capillary electrophoresis and conventionalgel-electrophoresis. In the meantime we reviewed the available literature inorder to summarize the latest developments in the field.
Results: From the total of 25 cases 14 proved to be monoclonal, 2oligoclonal, 7 policlonal and 2 not interpretable. There are important differencesbetween the two methods and the costs are also different. The literature offersa great source of information highlighting the importance and utility ofclonality assessment in lymphomas.
Conclusions,discussions: The assessment of clonality by the analysis of IgH generearrangements with PCR offers additional information in the study of malignantlymphomas offering valuable information about the clonality of the cells. Therelatively high costs of the method does not permitted us the application of iton a large scale, however does not hinder its use in research and even in thediagnosis of difficult cases.

P-39

Atypical Hodgkin-like lymphadenopathy associated with CMV infection in a patient with hyper-IgM syndrome

André Almeida Schenka; Maria Marluce dos Santos Vilela; Patrícia Nishizawa; Paulo Latuf Filho; Natália Schenka, José Vassallo
State University of Campinas, São Paulo, Brazil

Introduction: CMV is a common DNA virus which causes up to 7% of cases of the mononucleosis syndrome. In contrast to EBV, CMV infection has never been formally reported in association with an “atypical” lymphadenopathy with Hodgkin-like features, although, in CMV lymphadenitides, infected cells may sometimes vaguely resemble variants of Reed-Sternberg (RS) cells.
Aims: We describe the histopathological and immunohistochemical features of an atypical lymphadenopathy with classical RS cells, associated with CMV infection, in a patient with hyper IgM syndrome.
Case report: A 16-year-old boy with a long history of recurrent infections and a previous diagnosis of hyper-IgM syndrome, presented with a persistent massive lymphadenopathy for the past six years. Lymph node biopsies showed follicular and paracortical nodular hyperplasia, rare foci of “dirty necrosis” and worrisome features, such as thickening of capsule and frequent atypical cells in interfollicular areas. Some of these were activated immunoblasts, but others were indistinguishable from classical RS cells. The diagnosis of CMV infection was established by serology, PCR and immunohistochemistry, with both types of atypical cells, a few neutrophils and sparse lymphocytes being consistently positive for the virus. Hodgkin’s lymphoma was ruled out by the lack of CD15 positivity and of characteristic clinical and evolutive features.
Conclusion: From the data presented, one cannot assume that the atypical changes found in the lymph node were due to a direct action of CMV or to the hyper-IgM syndrome itself. Most important, however, is to recognize that classical RS cells may occur in the context of CMV infection and that they should not prompt a misdiagnosis of

Hodgkin's lymphoma. (JV is supported by the National Council for Scientific Research, CNPq).

P-40

Aberrant CpG island methylation profiles of multiple genes in non-Hodgkin's lymphomas

Ji-Eun Kim; Sun Och Yoon; Young A Kim; Jin Haeng Chung[1], Chul Woo Kim

Department of Pathology, Seoul National University Boramae Hospital, Seoul, South Korea, Seoul National University Bundang Hospital[1]. South Korea

Background: Aberrant methylation of CpG islands in promoter regions is one of the major mechanisms for silencing of tumor suppressor genes in various types of human cancers including non-Hodgkin's lymphomas (NHL). In this study, we investigated the aberrant promoter methylation status of known or suspected tumor suppressor genes in NHLs and compared the methylation profiles between B-cell and T/NK-cell NHLs. Methods: 54 cases of B-cell NHLs and 16 cases of T/NK-cell NHLs were examined for the methylation status of eight tumor-related genes using methylation specific PCR.

Results: CpG islands methylation was variously found in eight genes as follows; *DAPK* (71%), *MT1G* (70%), *p16* (53%), *CDH1* (53%), *THBS1* (56%), *MGMT* (27.1%), *COX2* (13%), and *RUNX3* (11.4%), in order of frequency. In six cases (8%), methylation was not observed in any of theses genes. Overall methylation index of B-cell NHLs (0.48) was significantly higher than that of T/NK-cell NHLs (0.32). And *THBS1* gene methylation was much more prominent in B-cell NHLs (67%) than in T/NK-cell NHLs (20%).

Conclusion: This study suggests that aberrant CpG island methylation is a frequent event in NHLs, and T/NK-cell and B-cell NHLs show overlapping but distinct methylation profiles between each other.

P-41

Primary diffuse large b-cell lymphoma of bone: unusual presentation

Francisco Dario Rocha Filho; Gabrielle Gurgel Lima; Francisco Valdeci Almeida Ferreira; Ronald Feitosa Pinheiro; Ana Carolina Leite Vieira Costa.

Institute of Cancer of Ceara. Brazil

Introduction: Primary lymphoma of bone (PLB) is an extremely rare condition, habitually confused with others bone primary injuries. Any localization of skeleton can be involved, but a trend exists to reach bones with persistent bone marrow. Pelvic bones and vertebral column are usually reached. The aim of this report is to present a case of PLB. The patient had a rare lesion im vertebral column. This led us to review the literature for a survey of incidence of PLB.

Method and results: A 41-year-old woman was admitted with a six-month history of low back pain that moves to the inferior limb. In radiography, there is bone destruction with pathological fractures in L1 vertebral body. A lumbosacral spine CT showed increase on the soft paravertebrates between T12 to L3 and fractures at T12 to L1. Immunohistochemistry revealed positives CD20 and CD45. She was diagnosed with primary diffuse large B-cell lymphoma of vertebral column. She was treated with combination chemotherapy consisting of cyclophosphamide, adryamicin, vincristine, predonisolone and etoposide, followed by radiotherapy in the thoracolumbar region. There was no evidence of recurrence at the 12-month follow-up.

Conclusion: Primary non-hodgkin's lymphoma of bone constitutes 3% to 7% of all bone malignant tumors and approximately 3% of all extra nodal lymphomas. Although the radiographic appearance of disease is variable and non-specific, one typical pattern is a solitary lytic lesion near the end of the long bone. On the basis of present case and a comprehensive review of similar cases in the literature involving patients with PLB, it appears that younger age, advanced-stage disease, multiple-bone involvement, and non-large-cell histology are associated with decrease survival compared with older age, localized disease, single-bone involvement, and large-cell histology, respectively. The scarcity of cases in the literature with this localization and morphology confirm the rarity of case.

P-42

Primary non-hodgkin's lymphoma involving the proximal phalanx of the right thumb and the femur: case report

Gabrielle Gurgel Lima; Francisco Dario Rocha Filho; Francisco Valdeci Almeida Ferreira; Ronald Feitosa Pinheiro; Ana Carolina Leite Vieira Costa.

Institute of Cancer of Ceara. Brazil

Introduction: Primary lymphoma of bone (PLB) represents an uncommon bone tumour with relatively homogeneous morphology and clinical behaviour. Distinguishing PLB from other bone tumors is important because the former has a better response to therapy and a better prognosis, specially when compared with patients with systemic disease. Long bones are usually compromised. Femur is the most common isolated site (25%). The authors

discussed a case of PLB involving the proximal phalanx of right thumb and right distal femur. Method and results: A 63-year-old man was admitted with a four-month history of difficulty in walking and pain in right knee joint. Physical examination revealed a mass in the right knee joint. He also complained for pain of the right thumb. Two months before, a plain radiograph showed pathologic fractures of right distal femur and proximal phalanx of right thumb with periosteal reaction. Biopsy of the tumour demonstrated proliferation of abnormal lymphoid cells. Immunohistochemistry revealed positive CD20. She was diagnosed with primary diffuse large B-cell lymphoma of femur. He was treated with combination chemotherapy consisting of cyclophosphamide, adriamycin, vincristine, predonisolone and etoposide, followed by radiotherapy on the right distal femur and proximal phalanx of right thumb. There was no evidence of recurrence at 14-month follow-up. Conclusion: PLB constitutes 3% to 7% of all bone malignant tumours and approximately 3% of all extranodal lymphomas. Although radiographic appearance of disease is variable and non-specific, one typical pattern of primary bone malignant lymphoma is a solitary lytic lesion near the end of long bone that has a permeative pattern. Appropriate treatment depends on histologic type and stage. Review of the literature has shown that combined modality therapy does confer a better prognosis for patients having PLB. The scarcity of cases in the literature with this localization and morphology confirm the rarity of the case.

P-43

SYSTEMIC ANAPLASTIC LARGE CELL LYMPHOMA - A MULTICENTRIC CLINICO-PATHOLOGICAL STUDY

Camelia Dobrea 1,2,3; Dan Colita 2; Anca Lupu 3,4, Ana-Maria Vladareanu 3,5; Constantin Arion 3,6, Carmen Ardeleanu 1,3; Alina Nicolae 1; Cristina Iosif 1; Florina Vasilescu 1; Dana Terzea 1; Mihaela Mihai 1; Florin Andrei 1; Adriana Colita 2,3; Leny Caban 2; Andreea-Delia Moicean 2,3; Dan Coriu 2,3; Razvan Stoia 2; Emilia Niculescu-Mizil 2; Otilia Georgescu 2

1.- "V Babes" National Institute, Bucharest, Romania; 2.- "St Berceanu" Centre of Hematology& Marrow Transplantation, Fundeni Clinical Institute, Bucharest, Romania; 3.- "Carol Davila" University of Medicine, Bucharest, Romania; 4.- Dept of Hematology, "Coltea" Clinical Hospital, Bucharest, Romania; 5.- Dept of Hematology, University & Urgency Hospital, Bucharest, Romania; 6.- Dept of Pediatry, Fundeni Clinical Institute, Bucharest, Romania

First described by H Stein in 1985, Anaplastic Large Cell Lymphoma (ALCL) comprises only about 5% of Non-Hodgkin's Lymphoma (NHL), but represent the 4th NHL for children. The WHO Classification recognizes a primary systemic and a primary coutaneous ALCL. 50–80% of the systemic ALCL present the translocation t(2;5)(p23;q35) with a better prognosis. We present the results of a multicentric clinico-pathological study. We included in this study 71 cases of primitive systemic ALCL (with available clinical data) diagnosed in our institutes between July 1st, 1997 and May 31st, 2007. The diagnosis was made by histopathology and immunohisthochemistry methods; clinical data were from the patient clinical card; data were statistically processed using SPSS program, version 13 and the new version of program STATA. Histological, the common variant of ALCL was the most frequently (76.4%), followed by small-cell variant (8.8%) and lympho-histiocytic variant (5.8%). All the cases expressed CD30; 72.1% were T-cell type, and 27.9% null cell type. Most of the T-cell ALCL were CD4+CD8- (40%) or CD4-CD8- (40%). 81.8% of cases were EMA positive (all ALK+, frequently associated with T-cell type,). Half of the cases expressed ALK (83.6% nuclear and cytoplasmic, associated with translocation t(2;5), and 16.6% only cytoplasmic, indicating a X-ALK translocation). CD15 was positive in 28.5% of cases, and all the cases expressed NF-kB; the protein of RANK oncogene was positive in 82.4% cases, uncorrelated with bone determination; only 44% cases expressed RET, 82% of these ALK+. The patients were predominantly male (M/F=2.08) with a median age 41.0 years, with a bimodal age distribution. For 67.6% of the patients (74% for ALK+ cases) the diagnosis was made in a disseminated clinical stage (III/IV Ann Arbor); B symptoms were present in 81.7% cases. 50.7% of the cases presented extranode disease (skin 28.9%, pleuro-pulmonary 26.3%; bone 21%, bone marrow 18.4%; liver 18.4%), frequently associated with EMA+. Because of the younger age, lower LDH and good performance status, the International Prognosis Index (IPI) was low/intermediate-low for 66.7% of the patients. The treatment was very varied, uncorrelated with ALK expression (63.6% CHOP or CHOP-derived cures). The complete remission (CR) rate was 60%; the evolution was difficult, with multiple relapses (57% in the first year); at 3 years, the overall survival (OS) was 69%, and disease free survival (DFS) only 23%; 20.3% of the patients died, 3/4 on the first 3 months after diagnosis. The pediatric lot included 11 cases (3–18 years old); 77.7% of cases were ALK+, and all expressed EMA. Extranode disease was more frequently (82.0%). For our lot, the favorable prognosis factors included ALK+, EMA+, the absence of extranode disease, IPI 0–2, RET-; the unfavorable factors were ALK-, skin infiltration, mediastinal mass, IPI 3–5, EMA-, RET+.

The ALCL diagnosis remains a difficult one. The expression of ALK identify a better prognosis group; for ALK-cases, the group EMA+ (more disseminated clinical stage,

lower IPI, extranode disease) appear more related with ALK+ group comparing with EMA- group

P-44

Immunohistochemical expression of DNA topoisomerase IIalpha in diffuse large B-cell lymphomas

Alexandra Papoudou-Bai; Evaggelia Ioannidou; Anna Goussia; Evangelia Lambri; George Pentheroudakis; Nikolaos Pavlidis; Vasiliki Malamou-Mitsi; Panagiotis Kanavaros; Maria Bai

Departments of Pathology, Oncology and Anatomy-Histology-Embryology, Medical School, University of Ioannina. Greece

Background Topoisomerase IIalpha (Topo IIα) protein is involved in DNA replication and transcription and is the target for a number of chemotherapeutic drugs. Topo IIα immunohistochemical expression is a marker of cell proliferation in many human malignancies. Therefore, diffuse large B-cell lymphomas (DLBCL) were studied for the expression of Topo IIα protein in relation to 1) proliferation associated proteins and 2) the bcl6/CD10/MUM1 differentiation immunophenotypes.

Method Sixty four cases of de novo DLBCL were studied by immunohistochemistry for the expression of Topo IIα protein. The expression of the protein was analyzed in relation to the previously reported expression of major cell cycle proteins (p53, HDM2, p21, p14, Rb, p16, p27, Ki67/MIB1 and cyclins A, B1, D2, D3 and E) and the bcl6/CD10/MUM1 differentiation immunophenotypes. Spearman's correlation coefficient and Mann-Whitney tests were used for the statistical analysis.

Results Expression of the Topo IIα protein was observed in all DLBC cases (Mean: 74.53%, Std Deviation: 19.26). Significant positive correlations were found between Topo IIα and the expression of Ki67, Rb, and cyclin D2 proteins ($p=0.002$, $p=0.018$ and $p=0.028$, respectively). In addition, Topo IIα protein was positively correlated with CD10 ($p<0.001$) and bcl6 ($p=0.010$) proteins and was expressed more frequently in germinal center (GC: bcl6+/CD10±/MUM1- and bcl6-/CD10+/MUM1-) B-cell-like DLBCL than in non-germinal center (non-GC: bcl6±/CD10-/MUM1+) B-cell-like DLBCL ($p=0.048$).

Conclusion The above findings indicate that Topo IIα is highly expressed in DLBCL and is associated with increased proliferation status. Moreover, DLBCL with GC B-cell-like immunophenotypic profile are associated with higher expression of Topo IIα protein in comparison to DLBCL with non GC B-cell like profile. This finding might be related with the better prognosis of GC-DLBCL since Topo IIα isoenzyme is target for anthracycline-based chemotherapy.

P-45

Primary bone lymphoma: a descriptive study of 11 patients

Maria Pané (1); Fina Climent (1); Isabel Alarcón (1); Eva Domingo (3); José Antonio Narváez (2); Isabel Català (1); Vicens Romagosa (1); Enric Condom (1)

(1) Servei d'Anatomia Patològica. IDIBELL. Hospital Universitari de Bellvitge. (2) Servei de Radiologia.IDIBELL. Hospital Universitari de Bellvitge. (3) Servei d'Hematologia Clínica. IDIBELL. Institut Català d'Oncologia. L'Hospitalet de LLobregat. Barcelona. Spain

Background: Primary bone lymphoma is a rare entity that constitutes less than 5% of all extranodal lymphomas. A retrospective analysis was performed to describe clinical features, radiology, histological type and immunophenotype of primary bone lymphomas (PBL) in our institution.

Methods: We identified 11 patients with PBL between 1998–2007. Diagnosis was made based on x-ray, CT scans, MRI, bone biopsy, and in some cases, gallium scan, bone marrow biopsy and fine needle aspiration. We reviewed the clinical features, radiology findings and morphology. The cases were reclassified according to the WHO 2001 classification after examination of H&E slides and available immunohistochemical stains.

Results: Our series comprises 9 men and 2 women with a median age of 57 years (range 29–75). One third of them had disease in long bones, 18% in the spine and 27% had politopic disease. Radiological findings were lytic, sclerotic or mixed lesions often misdiagnosed as sarcoma. The clinical stage was IV in 8 cases and I in 3 cases. Ten patients had diffuse large B-cell lymphoma (DLBCL) and 1 patient had anaplastic large cell lymphoma. Six (60%) cases of DLBCL had an activated phenotype and four (40%) cases had a germinal center phenotype. All patients were treated with chemotherapy and 36% reached complete remission.

Conclusions: In our study, PBL was located in long bones or spine in 45% of cases. The main histological type was DLBCL with an activated phenotype in 60% of cases.

P-46

INTRAVASCULAR LARGE B-CELL LYMPHOMA MIMICKING PULMONARY INTERSTITIAL DISEASE

Alexandra Pignatelli; Cristina Ferreira; Ana Cristina Mendes; Afonso Fernandes

Departments of Pathology and Pneumology, Hospital de Santa Maria, Lisbon, Portugal

Introduction: We present a case of an intravascular lymphoma which manifested by fever, fatigue and weakness. The initial diagnosis was pulmonary interstitial disease.

Clinical Case: Fifty-four-year-old female patient with thalassemia minor ankylosing spondylitis taking methotrexate and corticosteroids until one month before the appearence of fever, night sweats, anorexia, weight loss, fatigue and weakness. Laboratory tests revealed persistently elevated inflammatory parameters, elevated LDH and partial respiratory insufficiency. The thoracic C.T. scan demonstrated a reticular pattern with interlobular septal thickening and bilateral ground glass appearence. A diagnosis of pulmonary fibrosis was made and the patient was medicated with azathioprine and corticosteroids. The surgical pulmonary biopsy performed demonstrated a diffuse intravascular proliferation of large lymphoid cells with starry sky pattern not only within the bronchiolar vessels but also within the alveolar capilares; these cells were immunoreactive for B-cell markers and were negative for cyclin D1 and TdT. The final diagnosis was intravascular large B-cell lymphoma and the patient started treatment with CHOP and Rituximab with remarkable clinical improvement, being discharged and maintainig treatment in an ambulatory regimen.
Comments: Intravascular large B-cell lymphoma is a rare entity and its presentation as pulmonary interstitial disease is exceptional. The starry sky pattern that we observed has never been previously described. This type of lymphoma usually has a bad prognosis; however, like in the few cases in which an early diagnosis was made, it had a good response to chemotherapy.

P-47
Differential expression of VEGF and its receptors in plasmacytoma and multiple myeloma

Azza HM Zidan; Wael Swelam
King Faisal University, Saudi Arabia

Background & Objective: Vascular Endothelial Growth Factor (VEGF) has an established role as multifunctional cytokine that potently stimulate tumorigenesis and angiogenesis in many solid tumors. However, the significance of VEGF expression in hemopoietic, especially plasma cell, neoplasms need further analysis to clarify their tumorigenic role. Materials & Methods: Fifteen cases diagnosed as Solitary Plasmacytoma (SP) of bone in addition to another fifteen cases diagnosed as Multiple Myeloma (MM) were selected. All cases will be investigated for the expression of vascular markers namely vascular endothelial growth factor (VEGF), and type IV collagen, in addition to VEGF receptors Flt-1 and Flk-1, and Bcl-2 was also used as an anti-apoptotic marker. Numbers of blood vessels were counted by using a micrometer in 500 unit squares (1 mm2) in SP and MM tumor tissues. Results & Conclusions: Most of the immunohistochemically revealed vessels within the tumor tissues were non-muscular venules. Statistically micro vessel density was higher in MM compared to SP according to site dependant analysis. Meanwhile, VEGF and Flt-1 show significant increase in their cytoplasmic expression in MM tumor cells compared to SP, indicating tumorigenic role for VEGF when its signal is perceived either paracrinally or autocrinally by Flt-1 receptor on neoplastic clonal plasma cells.

P-48
Plasmablastic lymphoma: a review of 15 cases

Rafael Navas; María C. Garrido; Ana Belen Enguita; M.Angel Martínez
Hospital 12 de Octubre. Spain

Plasmablastic lymphoma is considered a variant of Diffuse Large B Cell Lymphoma in the WHO classification. Initially these lymphomas were recognized as proliferations of large B cells with immunoblastic morphology and plasma cell immunophenotype resembling the terminally differentiated B cell, characterized by negative or weak expression of mature B-cell markers (CD20) and positivity for plasma-cell associated antigens (CD38, CD138). They are more frecuent in patients infected with HIV and they have presented commonly in the mucosa of the oral cavity, other locations include stomach, rectum and lungs. The clinical behaviour is aggressive with poor reponse to therapy and short survival. On the other hand several studies have now recognized other lymphomas with similar morphological and phenotypic plasmablastic features but with diverse clinical and molecular characteristics suggesting that they may correspond to different disease entities. We submit 15 cases from our hospital to provide their clinical and pathological characteristics and to illustrate the diversity of these tumors.

P-49
Intranodal kaposi sarcoma

Akyıldız Igdem A. Celik E. Sahan E. Mavis O. Karatas S. Erdogan N.
Taksim's Education and Training Hospital,Pathology Department,İstanbul/TURKEY
Taksim's Education and Training Hospital, Department, Internal Medicine, İstanbul/TURKEY

75 years old patient presenteal with dispne, and caughing to the Internal Medicine Department of Taksim's Education and Research Hospital. Multiple mediastinal, bilaterally axillary, inguinal, celiak, vertebral and paraaortic lymphadenomegaly had seen by MRI, CT and USG. Hemathologically there was trombocytopenia and normokrom normocyter anemia. Be-

cause his PSA was high, prostatic biopsy was planned. And the result of the biopsy was prostatic adenocarsinoma. Besides axillary lymph node was excized and the histopathological result was intranodal kaposi sarcoma. HIV markers were negative. Before he had the diagnosis of chronic renal failure. Because of prostatic adenocarcinoma and chronic renal failure was immunologically insufficient, this prepared the situation for intranodal kaposi sarcoma. We present the case because it is quiet rare in literature.

P-50

Angiocentric T/NK cell lymphoma-sinonasal type

Ljiljana Tomic; Sanja Milenkovic; Vesna Sretenovic; Milosav Kiurski; Tanja Terzic; Andrej Grubor

Department of Clinical Pathology, Vukova 9, KBC"Zemun", 11000 Belgrade, Serbia

BACKGROUND: MGS-"midline granuloma syndrome" is a clinical description of a broad spectrum of diseases, which are characterized by aggressive and progressive destruction of mucosa and adjacent structures of midface and upper aerodigestive tract. The differential diagnosis includes: Wegener's granulomatosis-WG and malignant lymphoma. After exclusion of WG and by immunophenotyping, nearly all remaining cases presenting as MGS are peripheral sinonasal angiocentric T-and/or NK-cell lymphoma. The natural history of these lymphomas is characterized through a rapidly progressive course with a poor prognosis.

METHOD: A 63 year old Serbian woman, presented with the complaint of persistent chronic, recurrent sinusitis-ozena. After development of "midline" destructive disease which involved the maxillar and ethmoid sinus also the soft and hard palates, operation revealed a diffuse infiltration of partly necrotic tissue. Histologic features were identified and immunophenotyping performed.

RESULTS: The histological features showed coagulative "geographic"necrosis, heavy inflammatory infiltrates including plasma cells, histiocytes end eosinophils. The polymorphous cell population obscured the neoplastic cells that were pleomorphic, small and medium sized cells to large hyperchromatic cells with irregular and elongated nuclei, prominent nucleoli and clear cytoplasm. Angiocentric growth was common with infiltration and destruction of the vessel wall. Tumor cells showed immunopositivity towards: CD3, CD45, CD30, Ki67(80%) while negative towards: CK, EMA, NSE, Chromogranin, Synaptophysin, CD20, CD79a, CD8, bcl 2.

CONCLUSION: ATNKCL in european population is rare and clinically of aggressive behavior because of mutilant and destructive process and consequently multiorgan failure. Because of its poor prognosis it should be included early into the differential diagnosis.

P-51

PROGRESSION OF LYMPHOMATOID GRANULOMATOSIS TO DIFFUSE LARGE B CELL LYMPHOMA

Petrusevska Gordana, Kodjmanovska Svetlana, Cvetkovski P.

Institute of pathology, Medical faculty, University of Skopje. Macedonia

Background: Lymphomatoid granulomatosis (LYG) is comprised of Epstein Barr virus (EBV) - positive B cells admixed with various proportion of reactive T cells. We present two cases of cutaneous LYG progressed to diffuse large B cell lymphoma over a period of 5 years.

Methods: We used clinical histories of 56 years old female and 61 years old male, and paraffin sections from surgically excised skin lesions. Paraffin sections were stained for H. H., Giemsa, Reticulin-Gomori, Zeil-Nilsen, and immunohistochemically for T cell, NK cell associated and B cell antigens, as well as for LMP1.

Results: The lesions started as multiple erythematous dermal papules on the back of both patients. Histological analysis in the first case revealed perivascular polymorphic infiltrate of lymphocytes without cellular atypia and absent necroses, that was defined as chronic vasculitis. In the second case there were found lymphocytic infiltrates in papillary dermis, and diagnosis of mycosis fungoides followed. The patients were treated intermittently with corticosteroids and PUVA, respectively. After a period of 5 years the lesions progressed to large subcutaneous tumor nodules overlayed with an atrophic livid skin mostly disposed at the back. These lesion demonstrated marked slightly nodular to diffuse lymphohistiocytic infiltrate, involving the upper and deep dermis, and subcutaneous fat tissue. On special stains one could see angiocentric invasive lesions and granulomas with few giant cells. The infiltrate consisted from large lymphoid cells that were positive for CD20, CD79a, bcl6+, with proliferative rate more than 80%, as was determined with Ki67. They were diffusely admixed with CD68+ histiocytes and CD3+, CD5+ T cells, mostly at the periphery of the nodules and lesion. Some of the cells were positive for LMP1.

Conclusion: These cases confirm that LYG is a rare angioinvasive and destructive lymphoproliferative disease with B cell origin and probably pathogenetically connected with EBV infection

Endocrine Pathology

P-52

A case of Somatostatin producing Endocrine (D-cell) tumour of Duodenum with literature review.

Carmalita Senaratah, Sujatha Fernando
Central West Pathology Services. Australia

Somatostatinomas are rare tumours accounting for 1–2% of endocrine tumours of the gastroenteropancreatico-hepatic axis. Somatostatin is produced from the D-type cells of pancreatic islets, gastrointestinal tract and central nervous system. Ganda et.al (1977) reported the first case originating in the pancreas. The primary extrapancreatic stomatostatinomas originating in the descending part of the duodenum, ampulla of vater and peri-ampullary areas was first documented by Alumets et.al in 1978.

In contrast to its pancreatic counterpart, the duodenal somatostatinomas are asymptomatic rarely accompanied by the somatostatinoma syndrome.

We report a case of a non-functional Somatostatin producing duodenal endocrine tumour in a seventy four year old female, who presented with melaena and anaemia, with a literature review of duodenal endocrine tumours.

P-53

MUCINOUS VARIANT OF PAPILLARY THYROID CARCINOMA

José M Arrinda-Yeregui, José Cameselle-Teijeiro, Iñaqui Zabalza-Estévez, Clara Ruíz-Ponte, Manuel Sobrinho-Simões
Department of Anatomic Pathology, Hospital Comarcal del Bidasoa, Hondarribia, Guipúzcoa, Spain. Department of Anatomic Pathology, Clinical University Hospital, University of Santiago de Compostela, Santiago de Compostela, Spain. Department of Anatomic Pathology, Hospital de Galdakao, Galdakao, Vizcaya Spain; Fundación Pública Galega de Medicina, Xenómica, Clinical University Hospital, Santiago de Compostela, Spain; IPATIMUP Instituto of Molecular Pathology and Inmunology, University of Porto,Porto, Portugal

Background: Mucin production in the human thyroid gland is an unusual event that can occur in follicular adenoma, and papillary (PTC), follicular, medullary, and mucoepidermoid carcinomas. Mucinous carcinoma of the thyroid is an extremely rare tumor characterized by clusters of neoplastic cells surrounded by extensive extracellular mucin deposition. Follicular and papillary carcinomas displaying focal mucin production should not be regarded as mucinous carcinoma. Metastatic carcinoma, on the other hand, must always be considered as a differential diagnosis when dealing with a thyroid tumor with a mucinous component.

Method: We describe the histopathological, immunohistochemical (Dako EnVision Peroxidase/DAB), and molecular features of a tumor presented in the thyroid gland in a 69-year-old-woman with multinodular goiter.

Results: The 1.5-cm tumor located in the isthmus was encapsulated and microscopically composed of cells with ribbon-like, solid, or follicular growth patterns with extensive extracellular mucin positive for mucicarmine and Alcian blue (pH 2.5). Some cytoplasmic vacuoles were found and nuclei were oval, enlarged, with irregular contours, nuclear grooves and occasional intranuclear inclusions. The nuclei exhibited dusty chromatin but no mitotic figures were found. Tumor cells were positive for TTF-1, CK7, CK19, galectin-3, HBME-1, p63, and vimentin. Focal positivity for thyroglobulin and thyroperoxidase was also found, but no reaction was detected for calcitonin, CK20 or p53. The proliferative index (MIB-1) was<2%. No mutations were found in exon 11 nor 15 of the *BRAF* gene.

Conclusion: The mucinous variant represents an extremely uncommon metaplastic variant of PTC that we should be aware of to avoid potential pitfalls of misdiagnosis.

Supported by grant PI060209 from Instituto de Salud Carlos III, Spain.

P-54

Cell Monotony, Mitotic Activity and Necrosis are Associated with Malignant Pheochromocytoma/ Paraganglioma

J Malik, B Klingenberg, J Adler, H Chen and W Huang
Department of Pathology and Laboratory Medicine, University of Wisconsin-Madison. USA

Background: Adrenal pheochromocytoma and extra-adrenal paraganglioma are uncommon neoplasms. So far no definite histologic features are able to predict aggressive behavior of pheochromocytoma or paraganglioma. This study is an attempt to identify morphologic features associated with malignant pheochromocytoma or paraganglioma.

Design: We reviewed 55 cases of pheochromocytoma and 43 cases of extra-adrenal paraganglioma from pathology archive at University of Wisconsin. After excluding cases without at least two year follow-up information or cases with tumor embolization prior to surgery, only 30 of the 98 cases are included in this study. 8 of the 30 cases are malignant (tumor metastasized to other organ or tissue). 22 cases of the 30 are clinical benign pheochromocytoma or paraganglioma, and are further classified as sporadic (n= 10) and hereditary (associated with MEN2A or von Hipple

Lindau syndrome) (n=6) pheochromocytoma, paraganglioma of head and neck region (n=6). Morphologic features of the tumors such as tumor architecture, sclerosing/hyalinizing changes, necrosis, capsular and vascular invasion, pleomorphism, nuclear hyperchromasia, cell size, nuclear and cytoplasmic (N/C) ratio and mitotic activity were examined by two pathologists.
Result: We found that relatively uniform tumor cells, small cell size, necrosis and mitotic activity are associated with malignant pheochromocytoma or paraganglioma (Table 1, below). Vascular invasion is an infrequent feature found in pheochromocytoma or paraganglioma. N/C ratio, nuclear hyperchromasia, sclerosing/hyalinizing changes and tumor architecture are indiscriminative features.
Conclusion: Tumor cell monotony, small cell size, necrosis and mitotic activity may be indicators of aggressive pheochromocytoma or paraganglioma of non-head/neck region.

P-55

A mixed medullary- follicular thyroid carcinoma discovered by fine needle aspiration.

Haefa Kamoun,Amina Mekni,Inès Chelly,Khadija Bellil,Selma Bellil,Nidhameddine Kchir,Slim Haouet, Samia Sahtout, Ghazi Besbes, Moncef Zitouna.
Department of pathology, LA RABTA Hospital. Baba Saadoun. TUNISIA.

Mixed medullary and follicular cell carcinoma (MMFCC) of the thyroid is a rare neoplasm, constituting less than 5% of thyroid medullary carcinoma. A 57 year old female patient with tyroid enlargement was admitted in our institution. Thyroid ultrasonography revealed a 2 cm solid nodule within the right thyroid lobe. The fine needle aspiration was highly cellular and showed two seperate tumoral populations. the first one was made of several three dimensional cohesive clusters of follicular cells with round oval nuclei, and scant cytoplasm in a backgrounddevoid of significant colloid. The second one was made of rare non cohesive polygonal and pleomorphic shaped cells with eccentric nuclei, and an abundant granular cytoplasm.The aspiration biopsy was reported as malignant, the diagnosis of MMFCC was suspected. The patient underwent bilateral total thyroidectomy with bilateral mediastinorecurentiel lymphadenectomy.The diagnosis of MMFC of the thyroid was established by histological investigation using immunohistochemical staining.

P-56

Diagnostic usefulness of HMBE1 and CK19 AND EVALUATION OF THEIR EXPRESSION IN FOLLICULAR-PATTERNED LESIONS WITH QUESTIONABLE FEATURES OF PAPILLARY THYROID CARCINOMA.

Amina Mekni, Heifa Azouz, Inès Chelly, khadija Bellil, Selma Bellil, Nidhameddine Kchir,Slim Haouet,Samia Sahtout,Ghazi Besbes,Moncef Zitouna.
Hospital La Rabta-Bab Saadoun. TUNISIA

Objective: To evaluate the expression of HBME1 and cytokeratin 19 and their usefulness in diagnosis of follicular variant of papillary carcinoma.
Materiels and methods: We evaluated 30 follicular patterned thyroid carcinomas including 15 papillary carcinomas (PC) and follicular carcinomas (FC). All casers were examined by immunohistochemistry.
RESULTS:87% of papillary carcinomas expressed HBME1 as well as 13% of foliicular carcinomas. CK19 marked 73% of papillary carcinomas (the one negative case for CK19 was of oncocytic variant), and 13% of follicular carcinomas.
CONCLUSION: These results suggest that CK19 is a specific and sensitive marker for papillary carcinoma which is very helpful in the diagnosis of its follicular variant; the combination of HMBE1 increases its specificity.

P-57

CD10 expression in follicular patterend thyroid nodules

Nabeel Al-Brahim; Mahmoud Ahmad
Department of Pathology, Farwaniya Hospital, Kuwait

Background: Follicular patterned thyroid nodules are a common problem in thyroid pathology and sometimes distinguishing benign from malignant nodules can be challenge. CD10 was studied and founded to be expressed in 79% of follicular patterned malignant thyroid nodules (i.e. follicular carcinoma and follicular variant of papillary carcinoma) and negative in benign counterparts. However, no further evaluation has been done in literature on this stain. Therefore, we conducted this study to evaluate CD10 expression in follicular patterned thyroid nodules.
Material & Methods: Fifty four cases of follicular patterned thyroid nodule were selected from Farwaniya hospital files as follow: Nodular hyperplasia 18 cases, follicular adenoma 16, follicular variant of papillary carcinoma 17 and follicular carcinoma 3 cases. CD10 was tested on one representative block from each case. The stain was reviewed by the two authors to reach an agreement and 10% was considered a cutoff point for positive result.
Results: The CD10 was expressed in different follicular patterned thyroid nodules as follow: 6/18 nodular hyper-

plasia, 2/16 follicular adenoma, 4/17 follicular variant of papillary carcinoma and 0/3 of follicular carcinoma. CD10 was expressed in 23.5% of benign nodules and 20% of malignant nodules.
Conclusion: CD10 is neither sensitive nor specific in distinguishing follicular patterned thyroid nodules.

P-58

Relationship between thrombospondin-1 and syndecan-1 in thyroid pathologies

Antigony Mitselou; Anna Batistatou; Dimitrios Peschos; Irene Zinovieva; Konstantinos Charalabopoulos; Niki Agnantis; Theodoros Vougiouklakis.
Deparment of Pathology, Medical School, University of Ioannina - Ioannina - Greece

Thrombospondin-1 (TSP-1) is a multifunctional matrix protein implicated in cancer cell adhesion, migration, invasion, inhibition of angiogenesis, and activation of latent transforming growth factor-β. Syndecan-1 (SYN-1), is a transmembrane heparin sulphate proteoglycan that is evolved in cell-cell adhesion, organization of cell matrix adhesion and regulation of growth factor signalling. The purpose of this study was to examine the relationship between TSP-1 and SYN-1 in pathological human thyroid glands, using immunohistochemical methods in paraffin-embedded tissue. We studied 42 carcinomas, 14 adenomas, 30 cases of hyperplastic disorders, and 16 normal thyroid glands. Statistical analysis was performing using the SPSS for windows (versio 6.0) statistical package. Normal thyroid tissues showed immunostaining for TSP-1 confined to the interfollicular stroma, and to the vasculature endothelium. A similar degree of reactivity was found in hyperplastic lesions and adenomas. TSP-1 was strongly expressed in papillary carcinomas with desmoplastic stroma, but weak to moderate in cancer epithelium. SYN-1 was expressed in normal, hyperplastic and neoplasic thyroid cells. Reduction of SYN-1 was found in carcinomas compared with normal thyroid tissue ($p=0.04$). No relationship was found between TSP-1 and SYN-1. TSP-1 expression was restricted to stroma and might be act as protective effect against tumor progression; on the other hand, SYN-1 expression in epithelial tumor cells seems to show a close association with preserved epithelial morphology and differentiation.

P-59

Neoplastic transformation of thyroid gland is accompanied with changes of sialyltransferases expression in the affected tissue

Pavol Janega; Andrea Cerna; Eva Brabencova*; Pavel Babal
*Department of Pathology, Faculty of Medicine, Comenius University, Bratislava, Slovak republic; Institute of normal and pathological physiology, Slovak Academy of Science, Bratislava, Slovak Republic and *Department of Pathology, Service d'anatomie pathologique, Reims, France*

Background: Thyroid cancer belongs to the most frequent endocrine diseases. The factor often complicating its histopathological evaluation is the difficult differential diagnosis between benign and malignant lesions. Abnormal sialylation of cell structures is an important factor of the neoplastic transformation. This work evaluated the association between the neoplastic process and the changes of sialyltransferases expression in the thyroid gland.
Methods: The cases of thyroid gland tumors (papillary, follicular, oncocytic, medullary and anaplastic carcinomas, follicular adenomas) and parenchymatous goiter were analyzed. The total RNA was isolated from formalin-fixed in paraffin embedded material and analyzed by real-time RT-PCR using the specific primers for sialyltransferase-1 (alpha-2,6 linkage of sialic acid) and 4A, 4B and 4C (alpha-2,3 linkage). The results were correlated with the quantitative evaluation of protein sialylation by lectin histochemistry.
Results: The significant increase of sialyltransferase-4C level and sialyltransferase-4B to 4A index was reported in well differentiated follicular and papillary carcinoma when compared to the parenchymatous goiter and benign adenomas. The sialyltransferase-1 has not shown any changes in expression. These results correlate with the finding of strong luminal positivity found in well differentiated carcinomas especially in the alpha-2,3 linkage. Follicular cells in normal thyroid gland, adenomas and benign goiter showed weak expression of sialic acid.
Conclusion: The data showed only weak membrane-bound sialic acid positivity in benign adenomas and goiters in comparison with malignant papillary and follicular carcinomas, with alpha 2,3-linked sialic acid predomination. Increased membrane sialic acid expression may be the result of the increase of sialyltransferase-4C expression in transformed tissue. The presented molecular changes in thyroid gland may be an important diagnostic finding in the future, especially in respect to aspiration cytology evaluation and the differential diagnostics of thyroid gland follicular lesions.
This work was supported by APVT grant N° 20–025204

P-60

Changes of inducible nitric oxide synthase expression in thyroid gland diseases

Pavel Babal; Andrea Cerna; Pavol Janega

Department of Pathology, Faculty of Medicine, Comenius University and Institute of normal and pathological physiology, Slovak Academy of Science, Bratislava, Slovak Republic

Background: Nitric oxide is a pleiotropic molecule with a variety of effects participating in the regulation of cellular functions under physiological and pathological conditions. Lately, it became an important topic in molecular biology research. The presented study evaluated the changes of NO synthase expression in thyroid gland diseases.
Methods: Inducible NO synthase expression was analyzed immunohistochemically in cases of papillary and follicular carcinomas, follicular adenomas, autoimmune Graves-Basedow and Hashimoto diseases and parenchymatous goiters of the thyroid gland. Slides were evaluated in optical microscope semiquantitatively and by morphometry.
Results: Weak and inconsistent membrane expression of i-NOS was found in parenchymatous goiter or benign follicular adenoma at the luminal site of follicular cells. Cytoplasmatic membrane, cytoplasm and colloid were negative. The increase of cytoplasmatic i-NOS expression was found in Hashimoto disease. Hyperplastic epithelium in Graves-Basedow disease showed strong nuclear expression of i-NOS with just inconsistent luminal membranes and apical cytoplasmatic positivity. The infiltrating lymphocytes were strongly positive in Hashimoto, but showed no i-NOS expression in Graves-Basedow disease. The moderate increase of strictly cytoplasmatic i-NOS expression was found in the cases of well differenciated follicular and papillary carcinoma.
Conclusion: Inducible nitric oxide synthase has been described to play a role in carcinogenesis as a mediator of DNA damage, neovascularization, vasodilatation, and metalloproteinase activation. Presented study indicate the increase of i-NOS expression in autoimmune diseases and in well differentiated thyroid tumors, but show only weak expression in benign follicular adenoma and normal thyroid gland tissue. It can be concluded that changes in NO synthase activity can be an important factor in the development of autoimmune thyroiditis, can play a role in neoplastic transformation and be a potential target for anticancer therapy in the future.
This work was supported parcially by grant APVT N° 20–025204 and grant MZSR N° 2006/23-UK-02

P-61

SOLID CELL NEST HYPERPLASIA AND PAPILLARY THYROID CARCINOMA

José Cameselle-Teijeiro; Ihab Abdulkader; Raquel Pérez-Becerra; Angel Vázquez-Boquete; Nuria Caramés; Clara Ruíz-Ponte; Manuel Sobrinho-Simões

Department of Anatomic Pathology, Clinical University Hospital, University of Santiago de Compostela, Santiago de Compostela, Spain. Fundación Pública Galega de Medicina Xenómica, Clinical University Hospital. Santiago de Compostela. Spain. IPATIMUP-Institute of Molecular Pathology and Immunology, University of Porto, Porto, Portugal

Background: Solid cell nests (SCNs) of the thyroid gland, usually considered as the remnants of the ultimobranchial body, are single or multiple foci of clusters of 2 types of cells referred to as “main cells” and “C cells”. The main cells of SCNs harbor the minimal properties of a stem cell phenotype, and may thus represent a pool of stem cells of the adult thyroid. We report a peculiar case of hyperplasia of SCNs associated with papillary carcinoma. Method: We describe the histopathological, immunohistochemical (Dako EnVision Peroxidase/DAB), and molecular features observed in the study of the right lobe of the thyroid in a 48-year-old man. The entire lobe was included in 25 formalin-fixed, paraffin-embedded tissue blocks. Results: The surgical specimen weighed 209 g, measured 12×7×6.5 cm, and showed a well-circumscribed nodule of 9 cm in diameter. Microscopically, the nodule was a follicular adenoma (FA) with focal calcification and cystic changes. Extranodular thyroid tissue showed an average of 18 (range 1–88) clusters (nests) of main cells of SCNs per section in the 25 tissue blocks. In one block, a solid nest of main cells merged with a follicular variant of papillary microcarcinoma (1.5 mm). The SCNs were positive for p63 and galectin-3, and negative for thyroglobulin. The papillary microcarcinoma was positive for thyroglobulin and galectin-3, and negative for p63. Tissue samples were obtained by laser captured microdissection and the same BRAFV600E mutation was found both in a pool of 5 solid nests we examined, as well as in the papillary microcarcinoma. Nodular hyperplasia and lymphoid aggregates occasionally associated with SCNs were also found in the histological study. No BRAF mutations were detected outside the SCNs and the papillary microcarcinoma. Conclusion: Our findings support the assumption that the solid cell nest hyperplasia may serve as a precursor lesion of papillary carcinoma of the thyroid. Supported by grant PI060209 from Instituto de Salud Carlos III, Ministerio de Sanidad y Consumo, Spain.

P-62

Immunohistochemical Expression of Galectin-3, Cytokeratin 19 and HBME-1 in Papillary Microcarcinoma of the Thyroid Gland

Sang Sook Lee, Jin Hwan Kim

Keimyung University School of Medicine. South Korea

With wide use of US and FNA of the thyroid gland, the incidence of papillary microcarcinoma of the thyroid (PMCT) is rapidly increasing. We analysed the immunohistochemical expression of galectin-3, CK 19 and HBME-1 in 37 cases of PMCT to evaluate the diagnostic value of these molecular markers. Immunohistochemically, galectin-3 and HBME-1 expression was found in all cases. CK 19 expresseion was found in 36 cases. The adjacent normal thyroid parenchyma and accompanying benign lesions are negative for these markers. There are scattered foci of incomplete positive staining in cases of Hashimoto's thyroiditis, however.

Our findings suggest that the immunohistochemical staining using antibodies for galectin-3, CK 19 and HBME-1 is an useful adjunctive method for the histopathological diagnosis of PMCT.

P-63

BRAF MUTATION IN A THYROID GLAND WITH CONCURRENT ONCOCYTIC FOLLICULAR CARCINOMA, ONCOCYTIC PAPILLARY CARCINOMA, CLASSIC PAPILLARY MICROCARCINOMA AND HASHIMOTO THYROIDITIS.

MLuisa Gómez Dorronsoro; Alicia Córdoba; Miren Arrechea; Ihab Abdulkader; Clara Ruiz-Ponte; José Cameselle-Tejeiro

Hospital de Navarra. Pamplona; Clinical University Hospital, University of Santiago de Compostela, Spain

Background: Oncocytic (oxyphilic, Hürthle cell) lesions are composed predominantly of cells with abundant eosinophilic granular cytoplasm due to accumulation of mitochondria. For many years considered a special category of follicular cell tumors, in the most recent WHO classification of thyroid tumors, oncocytic carcinomas have been considered as variants of papillary, follicular, medullary or poorly differentiated carcinomas.

Method: We describe the histopathological, and molecular features (*BRAF* gene) of a peculiar thyroid mass presented in a 65-year-old man.

Results: Histological examination revealed, within a background of Hashimoto thyroiditis, an oncocytic follicular carcinoma, 6 cm in diameter and angioinvasive in the right lobe, concurring with two papillary carcinomas, one a Warthin tumor-like variant, 3 cm in diameter, and the other, a classical-type papillary microcarcinoma in the left lobe. The mutational study of exons 11 and 15 of the *BRAF* gene showed V600E mutation of exon 15 only in the Warthin tumor-like variant of papillary carcinoma, but not in the other two neoplasms nor in the Hashimoto thyroiditis sample.

Conclusion: Our findings support the view considering the oncocytic tumors as variants of different tumor types rather than a special follicular tumor category.

Supported by grant PI060209 from Instituto de Salud Carlos III, Ministerio de Sanidad y Consumo, Spain.

P-64

HMGA2 as single marker for thyroid carcinomas

Gazanfer Belge1*; Anke Meyer1*; Markus Klemke1*; Käte Burchardt2; Corinna Stern3; Werner Wosniok4; Siegfried Loeschke1, 5; Jörn Bullerdiek1

*1 Centre for Human Genetics, University of Bremen, Bremen, Germany; 2 Department of Pathology, General Hospital Bremen-Mitte, Bremen, Germany; 3 Department of Pathology, General Hospital Altona, Hamburg, Germany; 4 Institute of Statistics, University of Bremen, Bremen, Germany; 5 Department of Pathology, Aalborg Hospital, Aalborg, Århus University hospital, Denmark; * G. Belge, A. Meyer and M. Klemke contributed equally to this paper and thus should be considered first authors.*

Background: HMGA2 expression was reported of many tumours but not of tumour-free tissue. In some tumours, for example pancreas-carcinomas HMGA2 expression can be used for discrimination of carcinomas from chronic inflammatory changes.

In diagnostics of thyroid tumours, it can be very difficult to distinguish adenomas from micro invasive carcinomas by histology and quite impossible by cytology.

The aim of this study was to investigate whether the *HMGA2* expression can be used to detect malignant thyroid tumours.

Methods: 64 formalin-fixed paraffin-embedded thyroid tissues including normal tissue (n=3), thyroiditis (n=2) and follicular adenomas (n=19) as well as follicular (n=9), papillary (n=28), and anaplastic (n=3) carcinomas were tested for *HMGA2* expression using qRT-PCR. Immunohistochemistry was performed in a subgroup of five adenomas, two samples from healthy thyroid tissue, six FTCs, one poorly-differentiated FTC and five PTCs with an antibody raised against the HMGA2 protein.

Results: qRT-PCR showed expression differences of up to 400-fold between benign and malignant thyroid tumours. Based on *HMGA2* expression alone, it was possible to distinguish between benign and malignant thyroid tissues with a sensitivity of 95.0% and a specificity of 95.0%.

There was a highly significant ($p<0.001$) concordance with histology of the tumours which is the current gold standard of thyroid tumour diagnostics. Immunohistochemistry was clearly positive in all proven malignant tumours and negative in normal thyroid tissues and all the adenomas.
Conclusion: HMGA2 expression is a promising marker of malignancy in thyroid tumours. Further investigations will be undertaken for conformation of the retrospective results in advance and practice.

P-65

CONCURRENT THYROID CARCINOMAS IN AN ADOLESCENT GIRL: AN UNUSUAL PRESENTATION WITH AGGRESSIVE CLINICAL COURSE.

Magali Gremaud; Patrick Meyer; Frédéric Triponez; Jean-Claude Pache; Neeta Kumar; Christian Seemayer; Massimo Bongiovanni

Department of Pathology, University Hospital, Geneva, Switzerland

Background Follicular carcinoma is usually seen in the fifth decade and commonly presents as an asymptomatic intra-thyroidal mass. In contrast, papillary carcinomas commonly occur at a younger age, although they are rare before the age of 20. We describe a case of a young girl with concurrent follicular and papillary carcinomas. To the best of our knowledge, this is the first report of such a case.
Method A 17 years-old girl presented with a history of multiple enlarging thyroid nodules slowly increasing in size. She had no history of radiation exposure. No family history of thyroid carcinoma was recorded. Three core biopsies, followed by two fine needle aspirations (FNAs) at three months interval were taken in 2004 from different nodules. Three years later, total thyroidectomy was performed as rapid increase in size of some of the nodules.
Results In biopsies and FNAs, macrofollicular lesions with papillary hyperplasia were detected. Total thyroidectomy specimen showed a multinodular thyroid weighting 111 gms, with multiple distinct nodules in both lobes and an unremarkable isthmus.
Microscopically, the left lobe demonstrated two angioinvasive follicular carcinomas (3.2 cm and 1.8 cm) with >50% poorly differentiated insular component, focal necrosis and a high mitotic count (14 mitosis/10 hpf). In the right lobe, one angioinvasive follicular carcinoma and one papillary carcinoma, follicular variant, were discovered. Both were 3 cms in greatest dimension. Postoperatively, the patient received radiotherapy (160 mCi) in a single dose two months after the surgery and she is well at 4 months follow up.
Conclusion Follicular thyroid carcinoma is a rare entity in children, but it is important to include them in the differential diagnosis of thyroid nodules in this age-group. In presence of rapidly increasing nodules (even with negative FNA), surgical excision may be warranted.

P-66

Genetics of radiation-induced thyroid tumors: an array-CGH (comparative genomic hybridization) study in a mouse model

Gabriele Hölzlwimmer; Alberto Jimenez-Schumacher; Michael Rosemann; Mike Atkinson; Leticia Quintanilla-Martinez

GSF - National Research Center for Environment and Health, Neuherberg, Germany

Background: Thyroid cancer is the most common endocrine malignancy in man. Although rearrangements of the ret/PTC-oncogenes are strongly correlated with the human irradiation-associated PTC, further genes are supposed to be essentially involved in tumorigenesis. The genetic mechanisms of human FTC indeed remain widely unknown up to now. Therefore, we performed a high resolution genome-wide array-CGH study in a mouse model of radiation-induced thyroid tumors to gain insights into carcinogenetic mechanisms.
Method: Iodine-deficient fed mother mice were injected with radioiodine to induce thyroid tumors in their litters. The DNA was isolated from the formalin-fixed paraffin-embedded thyroid tissue of 21 different (non-irradiated and radioiodine-treated) mice: two normal thyroids, 13 goiters, two FTA, and eight FTC. The analysis was done using a 1-Megabase BAC array-CGH.
Results: In 46% of the hyperplasias, a variety of small chromosomal gains and losses (0.5 to 119 Mb) was observed. Regional polyploidies on the chromosomes 4 and 5 (about 20 Mb) were demonstrated in an FTA. The FTCs exhibited frequent partial or complete chromosomal losses, predominantly of the chromosomes 4 (88%; p16), 9 (50%), and 14 (38%; Rb1).
Conclusion: The random gains and losses of hyperplasias represent genetic instability predisposing to malignant transformation. In similarity to the human counterpart, aneuploidies were demonstrated to be characteristics of the murine FTC, and seem to critically influence tumor development. In that respect, certain chromosomes have an increased risk for genomic damage. The commonly altered regions in FTCs and the polyploid amplification of the FTA give us a hint for the location of candidate tumor suppressor genes resp. oncogenes with effects on thyroid tumorigenesis. Losses of the tumor suppressor genes p16 and Rb1 are putative candidates playing a key role. Furthermore, in mice, histology and genomic alterations due to irradiation are similar to them in spontaneous tumors.

P-67

PHEOCHROMOCYTOMA WITH DIVERGENTE DIFFERENTIATION (COMPOSITE PHEOCHROMOCYTOMA) IN VON HIPPEL-LANDAU (VHL) DISEASE

Martha Quezado; Ruben Ronchetti; Karel Pacak; W. Marston Linehan; Maria Merino

National Cancer Institute, National Institutes of Health. USA

Background: Composite pheochromocytomas are rare tumors histologically characterized by features of pheochromocytoma/paraganglioma with those of ganglioneuroma, ganglioneuroblastoma, neuroblastoma or peripheral nerve sheath tumor. They have been described in association with NF1, MEN2A, and possibly neurocutaneous phakomatosis. The ocurrence of such tumors in the setting of VHL is unclear.
Methods: Thirty two cases of pheochromocytomas, 13 sporadic and 19 VHL associated, were retrieved from the NCI surgical pathology files. H&E sections and available IHC stains (chromogranin, synaptophysin, S100, and NFTP) were reviewed. Tumors with divergent differentiation were defined as neoplasms of a mixed phenotype exhibiting pheochromocytoma histology plus areas of an additional tumor type, supported by IHC stains.
Results: Among the VHL associated neoplasms, seven (7/19) pheochromocytomas with divergent differentiation were encountered. In all cases, the phenotype was that of focal to nearly equal admixtures of pheochromocytoma and ganglioneuroblastoma-like tumors. In one of the VHL associated cases, the ganglioneuroblastoma tumor showed increased mitotic activity and necrosis. Remainder VHL associated cases (12/19) and all sporadic tumors (13/13) were of classical histology.
Conclusions: Pheochromocytoma with divergent differentiation (composite pheochromocytoma) appears to frequently affect patients with VHL syndrome, at an younger age. Long term follow up may be necessary since metastasis from composite tumors are derived from the ganglioneuroblastoma component.

P-68

ENDOGENOUS AVIDIN BIOTIN ACTIVITY (EABA) IN THYROID PATHOLOGY – ARTIFACT OR MARKER

Barbara Nikiel; Mykola Chekan; Michal Jarzab; Dariusz Lange; Barbara Jarzab

Maria Skłodowska-Curie Memorial Center and Institute of Oncology, Gliwice Branch. Poland

BACKGROUND Immunohistochemicalmethods that use a high affinity of avidin and biotin (e.g. ABC, LSAB) arecharacterized by high sensitivity and wide known. However, non-specificreaction can be observed in frozen tissues and in paraffin embed material,increasing after heat induced epitope retrieval (HIER). The reaction caused byendogenous biotin or any another chemical compound that is an extremely highaffinity for avidin may cause diagnostic mistakes. The aim of ourinvestigation, is to study presence of endogenous avidin biotin activity (EABA)in thyreocytes originating from various thyroid pathological lesions(neoplastic and non-neoplastic).
Material and methods Theimmunohistochemical study was performed on paraffin-embedded specimenssurgically resected thyroid tissue from 75 patients with thyroid diseases: 11patients with nodular goiter, 9 with lymphocytic thyroiditis (LT), 8 withfollicular adenoma, 65 patients with papillary carcinoma (PTC) (typical,follicular, oxiphilic and cribriform-morular variants), 4 patients withfollicular carcinoma. In papillary carcinoma immunohistochemical study wasperformed both in primary tumors and metastases. After HIER incubation withstreptavidin from LSAB+ kit 25 min was done.
RESULTS Strong cytoplasmic EABA wasobserved in 56 of 65 (87.5%) PTC and in 8 of 9 cases of LT. Correlation betweenEABA in primary tumor and EABA in metastases was noted. Normal surroundingthyroid tissues show absence or weak EABA. Aberrant intranuclear localizationof biotin was noted in morules of cribriform-morular variant of PTC. Nostatistically significant correlation between patient's age, sex, metastasespresence and EABA was observed.
CONCLUSIONS Using of visualization systemsthat do not contain avidin or biotin (e.g. EnVision+ System-HRP) is preferablyfor immunohistochemistry of thyroid diseases. The nature of this reaction inPTC and LT needs further investigations.
Mykola Chekan was a fellow of our Fellowship Programtotally supported by the National Cancer Institute – Office of InternationalAffairs, NIH, Bethesda, MD, USA.

P-69

Expression of RegIV and Hath1 in neuroendocrine tumors

Kukka Heiskala; Johanna Arola; Leif Andersson

Department of Pathology, Haartman Institute University of Helsinki, Helsinki, Finland and HUSLAB, Division of Pathology, Helsinki, Finland

Background: RegIV (RELP) is a c-type lectin with an unknown physiological function. It is expressed in selected neuroendocrine cells of the intestinal epithelium and it has also been found in certain gut-derived adenomas and carcinomas and in some neuroendocrine tumors. The basic helix-loop-helix (bHLH) transcription factor Hath1 is associated with neural development and with neuroendo-

crine differentiation of the gut epithelium. We investigated a panel of neuroendocrine tumors by immunohistochemistry and in situ hybridization for the expression and co-expression of these two proteins.
Methods: A total of 56 paraffin embedded endocrine tumor samples from different organs were immunohistochemically stained by monoclonal and polyclonal antibodies to RegIV and by a polyclonal antibody to Hath1. The specificity of the anti-Hath-1 antibody was validated by in situ hybridization.
Results: A robust expression of RegIV was seen in carcinoids of the gut and the stomach, in parathyroid adenomas, in Merkel cells carcinomas of the skin, and in pulmonary small-cell carcinoma. Mucocellular (signet ring cell) cancer of the stomach stained strongly for RegIV. In the gut carcinoids, only the marginal cells layers of the tumor in direct contact with the stroma expressed RegIV. Virtually no staining was seen in the pheochromocytomas, in pancreatic islets or in tumors of endocrine pancreas (insulomas). The staining pattern of Hath1 was similar that of RegIV in the intestinal carcinoids. Pancreatic islets, insulomas, and pheochromocytomas expressed Hath1, while the tumors of the stomach remained negative. The expression of Hath1 was consistently found in the cytoplasm of the neoplastic cells despite the function of the protein as a bHLH transcription factor.
Conclusions: The expression pattern of RegIV and Hath1 is partly overlapping but not identical, implying different regulatory mechanisms. The different staining patterns might add to the diagnostic and follow up tools for neuroendocrine tumors.

P-70
Immunohistochemical profile in metastatic neuroendocrine carcinomas (MNCs)

Alina Georgescu1; Florina Vasilescu1; Cristina Iosif1; Dorel Arsene1; Mihaela Mihai1; Dana Terzea1,2; Florin Andrei1; Camelia Dobrea1,2; Enache Simona1; Mihai Ceausu1,2; Ariana Visan1; Diana Ene1; Maria Neagu1; Valentina Muntean1; Alina Anghel1; Tatiana Petre1; Elena Ion1; Florin Eremia1; Georgeta Butur1; Carmen Ardeleanu1,2
1 "Victor Babes" National Institute of Pathology, Bucharest, Romania; 2 "Carol Davila" University of Medicine and Pharmacy, Bucharest, Romania

Background: Neuroendocrine tumors (NETs) are heterogeneous, developing from a large variety of tissues. Histopathological aspects and neuroendocrine (NE) immunohistochemical (IHC) markers do not differentiate them, being frequently difficult to establish their primary origin. MNCs are relatively common encountered, representing 10–15% of unknown primary tumors (UPTs). UPTs have a particular biology with rapid progression and atypical metastases. The primary location of MNCs has impact on therapy and survival. We studied the expression of NE markers and cytokeratins (CK) in MNCs of UPTs, and looked for correlations with their histogenesis.
Method: 21 MNCs (M:F, 13:8; age range: 25–73 years, median: 52.7 years) from 53 consecutively archived in one year, formalin fixed paraffin embedded samples of NETs were reviewed. Three microns sections have been assessed using H&E stain and indirect tristadial ABC IHC method for a panel of 21 antibodies for NE differentiation, digestive - including pancreas, pulmonary, thyroid, and other origins.
Results: The sites of metastases in our study were: lymphnodes (8/21), liver (3/21), bone (2/21), brain (1/21), spleen (1/21), peritoneum (3/21), subcutis (1/21), and multiple site metastases (2/21). Beside the positivity for NE markers, in 9 tumors (42.85%) (moderate or well differentiated MNCs) the origin could be suggested by these results: digestive (2 cases): ChromograninA+/Synaptophisin+/-, NSE+/-, Gastrin+/-, Somatostatin+/-, CK7-/CEA-/CK20+/-; pancreatic (2 cases): NSE+/Synaptophisin+/CD56+/ChromograninA+/-, Gastrin+/Glucagone+/Insulin-/Somatostatin-/KL1+/MNF116+/CK7-/CK20-/VIM+/S100+/PGR+/-; pulmonary (2 cases): ChromograninA+/S100+/CD56+/-, NSE+/-, Synaptophisin+/-, TTF1+/Calcitonin-/KL1+/CEA+/CK7+/CK19+/CK20-; thyroid (3 cases): NSE+/ChromograninA+/Synaptophisin+/-, Calcitonin+/Thyreoglolbulin+/-, TTF1-/VIM+/S100+/KL1+/-, CK19+/-, CK7+/-. Some unusual particularities of immunophenotype were observed: digestive metastases were negative for CEA, and thyroidian metastases had no expression of TTF1. In our cases of poorly differentiated/undifferentiated metastatic carcinomas with NE differentiation, the primary origin could not be detected by IHC.
Conclusion: Histological diagnosis, associated with IHC algorithms, could suggest the primary origin in well or moderate differentiated MNCs. The origin of majoriry of poorly differentiated/undifferentiated NETs remains unclear after an IHC study.

P-71 WITHDRAWN

P-72
Anaplastic thyroid carcinoma with the remnants of a preexisting papillary thyroid carcinoma - case report

Aleksandra Salapura and Ljiljana Tadic Latinovic
Clinical Centre Banja Luka. Bosnia and Herzegovina

Anaplastic thyroid carcinoma is an uncommon malignant tumor, more common in women than in men and it typically occurs in elder patients (7th decade or elder).

Clinically it is presented as a neck or thyroid mass that rapidly enlarges over a short period. In a high percentage of cases anaplastic carcinoma develops in patients with a preexisting thyroid lesion such as papillary carcinoma, but the probability of anaplastic transformation is considered low. CASE REPORT: A 70-year-old woman was admitted to hospital with a large bulky mass that distort the appearance of the neck and was firm to hard, and fixed to the adjacent structures, causing dysphagia and dyspnea. Ultrasonography showed hypofunctioning (cold) lesion. Bilateral total thyroidectomy was performed. Grossly, the tumor measured 11×9, 5×5 cm and occupied the whole thyroid gland, with extrathyroidal invasion. The cut surface was tan-white and firm to hard focally mottled and soft owing to necrosis and hemorrhage. Microscopically, the tumor had a solid nested growth pattern and was composed of epithelioid tumor cells, devoided of giant cells. The neoplastic cellular infiltrate was poorly differentiated, without colloid formation, markedly pleomorphic, with associated foci of confluent necrosis and individual cell necrosis. Tumor cells infiltrated extensively intrathyroidal and extrathyroidal tissue (muscle, nerves, and vessels) and vascular spaces. Remnants of preexisting papillary carcinoma of conventional and follicular type were present. Immunohistochemically tumor cells were positive for mixed high- and low-molecular weight keratins, EMA, vimentin and negative for thyroglobulin, chromogranin and calcitonin. As anaplastic thyroid carcinoma with the remnants of a preexisting papillary thyroid carcinoma is uncommon thyroid malignant tumor, it should be reported in order to increase the data in literature.

Gynaecological Pathology

P-73 WITHDRAWN

P-74
Morphologic and functional characteristic of smooth muscles' new growth of uterus un-der amplification of nucleolar organizers.

A.F.Lazarev, A.M.Avdalyan, I.P.Bobrov, V.V. Klimatchev
Altay's office of ROSC by N.N.Blochin, Russia

It was recently discovered participation of argyrophilic proteins of nucleolar organizer areas in regulation of mitotic cycle and correlates with that of transcript activity of ribosome genes and also with indexes of proliferate cells activity.

Objective of the work is investigation of the activity of nucleolar organizers in leiomyomas and leiomyosarcoma corpus uteri myocytes.

Materials of investigation are 41 uterus, removed on account of myoma. 12 cases were cellular leiomyomas; 10- fibromyoma; 8 – bizzare leiomyomas; 6 - high-grade differentiated leiomyosarcomas and 5 are low-grade differentiated leiomyosarcomas. Histological sections of tumours were $AgNO_3$ imbued by two-stage method and calculated the average number of silver granules per 1 myocyte nucleus.

Results of the investigation made demonstrated that despite phase of the menstrual cycle in cellular leiomyoma, high-differentiated and low-differentiated leiomyosarcoma number of silver granules per 1 myocyte nucleus totaled 6,01±0,22, 12,11±0,46 and 18,8±1,06 respectively (ð<0,05). In bizzare leiomyoma number of silver granules totaled 6,6±0,33. The minimal number of silver granules was recorded in fibroma with marked sclerosis and hyalinosis i.e. 2,1±0,19.

Conclusion. Thus, calculation of the number of silver granules per 1 myocyte nucleus can be assume as a basis to differential diagnostics between cellular leiomyoma and high-differentiated leiomyosarcoma. Step growth of amplification of ribosome genes in chain from simple leiomyoma toward proliferating (mitotic activity) and further to leiomyosarcoma coupled with other molecular and biological criterion can be indexes of processes of growth of cellular anaplasia comparable with processes of dysplasia in epithelial structure. Presence of high level of silver granules in nucleus of atypical myocytes can be a sign of retrogression of their differentiation.

P-75
Intraoperative assessment of myometrial invasion in endometrioid adenocarcinoma

Francisco Tresserra; Maria Angeles Martinez; Nadwa Kanjou; Maria Teresa Cusido; Rafael Fábregas; Ramón Labastida.
Instituto Universitario Dexeus. Spain

Background: Intraoperative assessment of myometrial invasion in endometriod adenocarcinoma of the uterus can determine the surgical approach.

Methods: This is a retrospective study of 93 endometrioid adenocarcinomas surgically treated with hysterectomy, salpingooforectomy and pelvic lymphadenectomy with or without aortic lymphadenectomy during 11 years. The myiometrial invasion assessed by frozen sections during the surgical procedure is correlated with the one assessed in paraffin embedded tissue. Myometrial invasion is also correlated with other features such as age, histological grade according FIGO and lymph node involvement.

Results: Intraoperative study revealed absence of myometrial invasion in 19 cases, invasion of the inner half (IH) in 61 and of the outer half (OH) in 13. Definitive study showed absence of myometrial invasion in 9 cases, invasion of the IH in 68 and invasion of the OH in 16. The positive predictive value was 47% (95% CI: 25–70%) for absence of invasion, 93% (83–98%) for IH invasion, and 92% (82–100%) for OH invasion. In 10 cases intraoperative study was of absence of invasion and the definitive study revealed myometrial invasion (nine of them smaller than 2 mm). In four cases intraoperative study diagnosed invasion of the IH of the myometrium whereas the definitive diagnosis was of invasion of the outer myometrial half. In all of theses cases the uterus showed myomas and the tumor extensive necrosis. In one case the intraoperative diagnosis was of invasion of the OH and in definitive study only IH invasion could be demonstrated. In this case an endometrial ablation was done three weeks before. Myometrial invasion showed statistically significant relationship with age, histological grade and lymph node involvement.
Conclusions: Intraoperative assessment of myometrial invasion is a useful tool to establish the involvement of the inner or outer half. The absence of myometrial invasion by frozen section is less accurate.

P-76

Coexistence of a mature cystic teratoma and a serous cystadenoma in the same ovary

Irini Zinovieva; Evfimia Balassi; Nafsica Simou; Antigony Mitselou; Niki Agnantis
Department of Pathology, Ioannina Universtity Hospital. Greece

AIM: To describe a rare coexistence of two different benign cystic tumors in the same ovary, i.e. a mature cystic teratoma and a serous cystadenoma.
MATERIALS AND METHODS: A 32 year old female presented with a cystic tumor in the right adnexa. The tumor excision followed. We received a cystic specimen which measured 7.6×6×3 cm with two separated cystic lesions. Its surface was smooth. Ovarian tissue measuring 2.5×1×0.3 cm was also recognized. The first cyst was filled by serous fluid and had micropapillary architecture in limited regions of the inner surface. The mural thickness measured 0.2 cm. The second cyst was filled by sebum and hairs and its mual thickness measured between 0.2 to 0.4 cm. Multiple sections were taken, embedded in paraffin and stained with hematoxylin-eosin.
RESULTS: The microscopical examination showed the presence of two cystic tumors. The first was a serous cystadenoma and teh second was a mature teratoma. In the latter, skin, sebaseous and eccrine glands, hair follicles, intestinal and respiratory epithelium, cartilage, smooth muscle and adipose tissue were detected. No spsecific changes were identified in the excised ovarian tissue.
CONCLUSION: We believe that due to the rarity of this coexistence, after an exhaustive search of the literature, the pathologist should have it in mind.

P-77

The implementation of prognostic index and risk grouping in surgically treated cervical carcinoma patients: A prospective validation study

Neli Basheska; Irina Prodanova; Katerina Kubelka-Sabit; Slavica Veljanovska; Oliver Arsovski; George Zografski
Department of Histopathology and Clinical Cytology, Institute of Radiotherapy and Oncology, Medical Faculty, Skopje, Republic of Macedonia

BACKGROUND: The objective of this prospective study was to validate the prognostic criteria defined by the results of our previous study in an independent population of surgically treated cervical carcinoma patients. METHOD: The study group consisted of 340 patients who underwent abdominal hysterectomy with pelvic lymphadenectomy as primary therapy between 2000 and 2005. Based on the scores of the variables (blood vessel invasion, lymph node metastases, tumor diameter, degree of inflammatory reaction at the invasive front, and minimum thickness of uninvolved cervical stroma/parametrial extension) and calculated prognostic index (PI) values, the patients were divided into three prognostic groups. RESULTS: During the follow-up period (range, 1.6–89.7, mean, 39.7± 22.2 months) recurrences were observed in 1% (1/97), 12.2% (16/131) and 23.2% (26/112) of the low-, intermediate-, or high-risk group patients, respectively. The 5-year disease-free survival (DFS) rates of the low, intermediate, and high-risk groups were 98.82%, 84.57%, and 74.01%, respectively. The differences in DFS rates were statistically significant ($P<0.0001$). In order to validate the model from our previous study, we have compared DFS rates between the groups. There was no difference in DFS rate between low-risk groups, in spite of the fact that majority of the patients in this study were not irradiated, while radiotherapy was administrated invariably to all the patients included in the original study. Similarly, DFS did not differ significantly between the intermediate-risk groups from both studies, which could be expected since radiotherapy was administrated to majority of the patients (125/131) in this study. In contrast, the high-risk group patients in this study had significantly higher DFS rate (74.01% vs. 44.24, $P=0.0010$), probably as the result of

the adjuvant chemotherapy administrated to 69% of them. CONCLUSION: PI could be a sound and reliable basis for an appropriate planning of the following therapeutical strategy of the surgically treated cervical cancer patients.

P-78

Extraovarian granulosa cell tumor: first case report from Colombia

Ernesto Garcia Ayala, Julio Alexander Diaz P, Jorge Andres Garcia V
Universidad Industrial de Santander, Colombia

Objective: To describe the case of an extra ovarian GCT in a Colombian woman and to discuss about these malignancies.
Case Report: 69 years old female Patient, who came to the doctor with an abdominal pain, vomiting and no depositions, with 8 days of evolution.The woman presented pre existing conditions of hysterectomy with bilateral salpingoophorectomyfor placental acretism. At physical examination a mass was identified, locatedin the hypochondrium and left flank of 10×15 cm. This was confirmed inthe echogram and tomogram studies. Therefore the patient was taken to surgery,and a encapsulated retroperitoneal tumour was found.
PathologicalStudy: The pathology service received a 12×11.5×10 cm.and 950 gr. solid-cystic mass. The heterogenic surface court was well encapsulated, with a solid area (70%)and a cystic area with hemorrhagic contain (30%). The courts stained with hematoxylin andeosin were identified neoplastic lesion formed by round-nucleus cells withlongitudinal cleft and few eosinophil cytoplasms, arranged in nests, trabeculaeand solid sheets with plenty Call-Exner corps formation. Immunohistochemistry was positive forinhibin and negative for Melan A Calretinina. Making an extraovaric adult type GCTdiagnose.
Conclusions: The GCT can be originated from extraovarictissues in extremely rare cases, only 8 cases reported globally. These caseshave been informed in the broad ligament, adrenal glands, uterus and retro peritoneum. This case was originated in the retro peritoneum. Itis believed that the origin from ectopic gonadal tissue, or directly from themesonephron.

P-79

PBNIP-3-EXPRESSION AND ITS ASSOCIATION TO PATTERN OF INVASION AND PERITUMORAL STROMAL RESPONSE IN CARCINOMA OF THE CERVIX UTERI

Cornelia Leo; Lars-Christian Horn; Bettina Hentschel; Michael Höckel, Jens Einenkel, Ulf-Dietrich Braumann
Institute of Pathology, Division of Gynecologic Pathology, University Leipzig. Germany

Background: Finger-like and spray-like pattern of invasion represent the most common types of tumoral growth patterns in carcinoma of the cervix uteri (CX) invading host tissue (Horn et al. 2006). Infiltrative growth usually induce new matrix formation by activating the peritumoral stromal cells; that is, desmoplastic stromal reaction (DSR) at the front of invasion (juxtatumoral stroma). Infiltrative growth and peritumoral stromal remodelling might be involved by apoptosis of tumor cells. BNIP3 is a mitochondrial protein and a proapoptotic member of the Bcl-2 family and expressed in different types of human cancer. Nothing is known regarding the association of BNIP-3 expression in CX and parameters of infiltrative growth.
Method: Biopsies of 50 cervical cancers (FIGO stage IB to IV) were stained with an anti-BNIP3 antibody. In accordance to own previous studies (Leo et al. 2006), cytoplasmic as well as nuclear staining results were counted as positive. Staining was counted performing an immunoreactive score (IRS = staining intensity (0–3) x calculated percentage of positive stained tumor cells (1–4). The IRS was correlated to pattern of invasion (finger-like and spray-like) and the grade of DSR. DSR was scored as none/weak and moderate/strong.
Results: Spray-like pattern of invasion was associated with high expression of BNIP-3 (mean-IRS 5.8 vs. 3.2; $p=0.17$). High juxtatumoral stromal remodelling, characterised by strong desmoplastic change was also associated with BNIP-3 overxpression (mean IRS 3.6 vs. 5.7; $p=0.082$).
Conclusions: The results suggest that alteration of the mitochondrial pro-apoptotic BNIP-3 is involved in the mode of pattern of invasion (representing the grade of tumor cell dissociation) and juxtatumoral stromal remodelling in carcinoma of the cervix uteri.

P-80

PATTERN OF INVASION IS OF PROGNOSTIC IMPACT IN CARCINOMA OF THE CERVIX UTERI

Jens Einenkel, Lars-Christian Horn; Bettina Hentschel; Uta Fischer, Ulf-Dieter Braumann, Karl Bilek

Institute of Pathology, Division of Gynecologic Pathology, University Leipzig. Germany

Background: Different patterns of invasion (representing different grades of tumor cell dissociation) are associated with prognostic outcome in cancer. We evaluated the prognostic value of different patterns of invasion (PI) in cervical carcinomas (CX).

Methods: 611 surgically treated CX (FIGO IB to IIB) were re-evaluated histologically regarding the PI, using a three-level scoring system. Closed PI was defined as cohesive growth with well-delineated (pushing) borders. In finger-like PI the tumor grows in solid cords/trabecles. Highly dissociative growth in small groups or single cells was defined as spray-like PI. Types of PI were correlated to tumor stage, histomorphologic factors and prognostic outcome.

Results: 60% of the tumors showed a spray-like PI, 30% a finger-like PI, and only 7.4% were of the closed type. Spray-like PI showed a significant correlation with advanced stage disease, lymphovascular space involvement, poorly differentiated tumors and pelvic lymph node metastases. Spray-like PI was accompanied by a reduced 5-year overall survival when compared to the finger-like and closed PI (68.7% vs. 80.9% vs. 88.5%; p=0.0004). The prognostic impact of the PI disappeared in node-positive patients (p=0.06), but persisted in patients without pelvic lymph node disease (p=0.03). In multivariate analysis, using COX-regression model, the PI represented as independent prognostic factor.

Conclusions: Spray-like PI, (i.e. highest degree of tumor cell dissociation) is associated with advanced tumor stages, increased rate of recurrency and a reduced overall survival. In separate analysis of patients with and without lymph node metastases, the impact of PI persisted only in node-negative cases as an prognostic factor.

P-81

TUMOR SIZE IS AN INDEPENDENT PROGNOSTIC FACTOR IN FIGO STAGE II CERVICAL CARCINOMA

Lars-Christian Horn; Uta Fischer; Georgios Raptis, Bettina Hentschel, Karl Bilek

Institute of Pathology, Division of Gynecologic Pathology, University Leipzig. Germany

Background: Tumor size is a well recognised prognostic factor in early stage cervical carcinoma (CX). But, limited knowledge exists about the value of timor size in surgically treated CX with extrauterine extension.

Methods: 245 cases of local advanced CX (FIGO stage IIA and IIB) who received upfront surgery, were evaluated regarding tumor size, regarding the prediction of pelvic lymph node involvement, recurrence free and overall survival during a median follow-up time of 54 months (95%-CI 45.4 – 62.6 months). Tumors larger than 4 cm were defined as bulky stage disease.

Results: Bulky disease was seen in 46.1% (113/245). 60.2% of these patients showed pelvic lymph node involvement, compared to 42.4% (56/132) in non-bulky tumors (p= 0.006; odds ratio: 2.2 [95% CI: 1.3 – 3.6]). Patients with bulky tumors showed an increase of recurrent disease (40.2% vs. 28.0%; p=0.045). The relative risk for recurrent disease was 1.97 (95%-CI: 1.3–3.0). The 5-year overall survival rate was significant lower (67.7% [95% CI: 58.2–74.8] vs. 49.5% [95% CI: 36.8–59.1]; p=0.0015).

In multivariate analysis, tumor stage, pelvic lymph node involvement and maximal tumor size, were independent prognostic factors.

Conclusions: The results suggest that tumor size, defining bulky disease as tumors larger than 4 cm, is of prognostic impact also in FIGO stage II cervical carcinomas. A revised FIGO/TNM classification system similar to the subgrouping of stage IB CX is recommended for stage II using a cut-off value of 4 cm as discriminator: stage IIA1 and stage IIB1 for tumors with ≤ 4 cm and IIA2 and IIB2 for tumors > 4 cm (i.e. bulky disease).

P-82

HEPATOID CARCINOMA OF THE OVARY

Adamandia Zizi-Sermpetzoglou; Xanthippi Grammatoglou; Chryssoula Glava; Evangelia Skafida; Nerantzoula Petrakopoulou

Department of Pathology, Tzaneion General Hospital of Piraeus, Athens, Greece

Backround: Hepatoid carcinoma (HC) of the ovary is an ovarian carcinoma showing areas morphologically comparable to those of hepatocellular carcinoma. These areas are composed of cords of polygonal cells separated by sinusoids, occasionally featuring bile production and/or bile canaliculi formation. Hepatoid carcinoma is thought to be a different subtype from hepatoid-type yolk sac tumor based upon its pathologic features. In contrast to the much younger age of patients with ovarian hepatoid yolk sac tumor, the ages of the patients with hepatoid carcinoma ranged from 42 to 78 and none of them had gonadal dysgenesis or recognizable germ cell components within their tumors. The histiogenesis of HC is unknown but it has been described an association with tubular adenocarcinoma and serous carcinoma. This sug-

gests that it is a metaplastic tumor and represents a variant of the surface epithelial-stromal tumor.
Method and results: We describe a case of a 42 year-old woman who presented with abdominal pain. Physical examination and CT-scan revealed a large tumor in the left adnexal. She underwent a total hysterectomy and bilateral salpingo-oophorectomy with omentectomy. A left ovarian mass measuring 11×7×7 cm was found. The tumor was diagnosed as hepatoid carcinoma of the left ovary.
Conclusion: Based on the review of the literature we discuss the histological and immunohistochemical findings of these tumor and their differential diagnosis from other ovarian neoplasms, especially from hepatoid yolk sac tumors.

P-83

Immunolocalization of neurotrophin receptors tyrosine kinase receptors in Endometriosis Associated Ovarian Cancer (EAOC).

Elias R.1 Faghih M.1 Boutross-Tadross O. 2 Elit L.1 Foster W.G.1,3,

1Department of Obstetrics & Gynecology, McMaster University, Hamilton, Ontario. 2Department of Molecular and Cellular Pathology, McMaster University, Hamilton, Notario. Canada

Neurotrophins and their receptors have been localized in reproductive tract tissues including the ovary and endometrium. Of the neurotrophin receptors, tyrosine kinase receptor B (TrkB) is thought to be important in regulating malignant epithelial cancer cell resistance to attachment free mediated programmed cell death (Anoikis). Therefore, our objective was to immunolocalize TRK B in patients with a diagnosis of ovarian cancer and endometriosis. Endometriosis-associated ovarian cancer (EAOC) is a rare disease of unknown etiology that appears as either a low-grade tumor of endometrioid cell type or as a clear cell tumor in young women. Archived samples of formalin-fixed, paraffin embedded blocks from 15 women were obtained from the Department of Pathology at McMaster University Medical Center. Tissue sections of ovarian tumor, ovarian endometriosis, eutopic endometrium, and normal ovarian stroma were incubated with a polyclonal rabbit anti-human TrkB (1:250), Vectastain ABC Reagent, diaminobenzidine tetrahydrochloride as the chromagen, and counterstained with hematoxylin. TrkB positive epithelial cells were present in sections from 2/2 subjects with grade II ovarian endometriod tumors, 3/3 ovarian papillary serous tumors, and 2/2 with ovarian clear cell tumors. By comparison, ovarian endometrioid grade I tumors were negative (7/7), and immunostaining was generally absent in ovarian endometriosis (11 negative, 3 weak staining and 1 positive) and the eutopic endometrium (12 negative, 1 positive, and 1 weakly positive). TrkB is expressed in epithelial cells of more aggressive EAOC compared with less aggressive tumors or benign tissues.

P-84

Undifferentiated endometrial sarcoma with sex cord and smooth muscle immunophenotypical differentiation: a case report

Manuela Pelmus*;Yves-André Bureau*;Anca Lazaroiu; Alex Ferenczy*****

Sherbrooke University Hospital, Canada;Bucharest University Hospital, Romania;***Jewish General Hospital Montreal, Canada*

Backgound: Endometrial stromal sarcomas are rare tumours with two morphologically distinct entities; one is classified as low grade endometrial stromal sarcoma and the other as undifferentiated (high grade) sarcoma. Sometimes the classification of these tumours is a challenge because different histological cell types may be encounted in the same lesion. We present a case where immunohistochemistry was influential in the final histiotypic classification of uterine sarcoma.
Method: A retrospective review of a uterine tumour difficult to classify by histology alone. The lesion occurred in a 58 year-old lady and mesured 12×11×8 cm.
Result: The lesion involved the entire myometrium and replaced the endometrial lining. It was made of an admixture of two different sarcomatous growths. The main component consisted of a monotonous, small round cell proliferation with occasional sex cord like pattern and the alterations were compatible with a low-grade endometrial sarcoma. The second component contained a pleomorphic mesenchymal proliferation resembling a poorly differentiated epithelioid leiomyosarcoma. The low-grade cellular component reacted strongly and diffusely for actin, desmin, cladesmon, CD56 and ER but not for CD10. On the other hand, the high-grade carcinomatous areas stained strongly but focally for CD10 but not for smooth muscle immunomarkers. Neither component stained for PR, inhibin, calretinin, chromogranin, synaptophysin, CD99, epithelial markers and S-100 protein.
Based on these findings, the diagnosis of undifferentiated endometrial sarcoma with sex cord and smooth muscle differentiation was favoured.
Conclusion: In the field of gynaecological sarcomas, histological classification is sometimes difficult. Correlating morphological features with immunohistochemistry may help to better histiotype uterine sarcomas.

P-85

Ki-67 and P16ink4a immunoexpression strongly correlates with increasing grade of CIN and HPV infection

M VERDU 1,2;R ROMAN 1; C PUBILL 2; M CALVO 3; A VIDAL 1,2; and X PUIG 1,2.

1 BIOPAT. Biopatologia Molecular, SL, Grup Assistencia, Barcelona, Spain; 2 Histopat Laboratoris, Barcelona, Spain and 3 Statistics Department, Universitat de Barcelona, Barcelona, Spain.

Background: MIB-1 immunoquantitative features have been correlated with the grade of dysplasia in cervical epithelium, while P16 accumulation has been related to the presence of high grade intraepithelial lesions (HSIL) and detection of human papillomavirus (HPV). The aim of this study was to assess the value of these markers in assisting CIN grading.

Method: Our series included 7 normal cases, 8 HPV-suspicious, 42 CIN I, 31 CIN II, 35 CIN III and 2 invasive cervical squamous-cell carcinomas collected from 109 women. Immunohistochemical analysis of formalin-fixed, paraffin-embedded samples was performed by ABC immunoperoxidase staining, using mouse monoclonal antibodies Ki-67 and $P16^{INK4A}$. Results were reviewed by two pathologists. MIB-1 was classified in four categories according to the extension of nuclear staining within the epithelial thickness. Nuclear or nuclear and cytoplasmic diffuse strong staining was considered positive for P16. The presence of HPV was assessed by a commercial PCR-based assay and typified by hybridization to a low density microarray.

Results: A highly significant association ($p<0.0001$) was observed using Kendall's tau-c between increasing grade of CIN and MIB-1 expression. Further Chi-squared analysis of the 2 by 2 contingency table proved MIB-1 especially useful in discriminating the presence of CIN ($p=1.004e-^{09}$). Equally, a significant relation ($p=2.2\ e^{-16}$) was found between P16 immunoexpression and the presence of HSIL lesions, with 98% specificity, 98% positive predictive value and 78% negative predictive value. P16 accumulation was also indicative of the presence of HPV which was detected in 51 out of 53 P16 positive samples. Furthermore, 50 (98%) of these HPV positive cases contained High Risk HPV.

Conclusion: The combined use of these two markers provides a valuable tool in assessing the grade of CIN, the presence of HR-HPV infection and verifying the diagnosis of equivocal cases.

P-86

SYNCHRONOUS PRIMARY GYNOCOLOGICAL

Thouraya Achach, Soumaya Rammeh, Wided Stita, Mounir Trimech, Sonia Ziadi, Mohamed Taher Yacoubi, Moncef Mokni, Sadok Korbi.

Department of Pathology. Farhat Hached Hospital, Sousse. Tunisia

Background Synchronous tumor of endometrium and ovary may indicate either independently developing neoplasms or metastatic disease. Synchronous primary cancer occurring in both organs is relatively rare. Ovarian carcinosarcoma is very rare and aggressive tumor representing less than 2% of ovarian cancers. Papillary serous endometrial adenocarcinoma is a frequent endometrial tumor that is thought to occur under the influence of the estrogen receptor pathway. The etiology of synchronous malignancies is not clear, but the response of embryologically similar tissues to simultaneous carcinogens has been postulated

Method We report a rare case of simultaneous ovarian carcinosarcoma and papillary serous endometrial adenocarcinoma occurring in a 56-year-old-woman and we discuss clinicopathologic features and histogenesis of this association

Results The patient was admitted for post menopausal uterine bleeding, leucorrhoea and pelvic pain. Radiological explorations showed endometrial thichning with a left latero-uterine mass infiltrating the rectum. Histological examination of total abdominal hysterectomy with bilateral salpingo-oophorectomy specimen concluded to ovarian carcinosarcoma associated with papillary serous endometrial adenocarcinoma.

Conclusion To our knowledge, this is the first case in aspect of accompanying ovarian carcinosarcoma to papillary serous endometrial adenocarcinoma.

P-87

Gestational Choriocarcinoma. Study of an autosy case

Carrillo P; Ramos R; Forteza AV; López K; Gene AH; Canet R; Couce ME

Department of Pathology. Hospital Universitario Son Dureta. Palma de Mallorca. Spain

BACKGROUND: Gestational Choriocarcinoma may occur subsequent to a molar pregnancy, abortion, ectopic pregnancy or an uneventful gestation. Abnormal vaginal bleeding is one of the most frequents signs of presentation. However, occasionally, the discovery of the disease is associated with the presence of metastasis, being the lung the most frequent site, and haemoptisis the presenting symptom.

CASE REPORT: A thirty weeks pregnant, thirty-nine year old caucasian woman, presented at a local hospital with fever, dyspnoea, haemoptisis and toxic syndrome. Intersti-

tial alveolar infiltrates were seen in the thorax plain x-ray. Abdominal ecography demostrated a retropubic solid tumor suggestive of lymph node. She was admitted to the intensive care unit and underwent emergency caesarean surgery. During the intervention, a biopsy of the retro pubic lymph node was taken.
RESULTS: Pathology examination of the retro pubic lymph node was diagnosed as metastatatic choriocarcinoma. Thoracic CAT scan, obtained after the caesarean intervention, was rendered compatible with metastatic disease affecting both lungs. In spite of appropriate chemotherapy treatment, the patient took an unfavourable course and died. At autopsy, a necrotic vaginal nodule of 4 cm in diameter was identified. Aditionally multiple necrotic nodules were found in both lungs, affecting the pleura. Microscopic examination revealed diffuse alveolar damaged.
CONCLUSIONS: Although gestational choriocarcinoma may occur subsequent to a molar pregnancy, is not infrequent to see it in an otherwise normal gestation, and is a diagnosis to be considered when confronted with haemoptysis in a pregnant woman.
Patients at high risk have a survival rate of 85–95%. Death caused by choriocarcinoma is usually associated, as in our case, with distant haemorrhagic events and respiratory insufficiency.

P-88
P16INK4A IN CIN1. IS IT THE BIOMARKER OF PROGRESSION TO HIGH GRADE CIN ? A FOLLOW-UP STUDY of 154 PATIENTS CORRELATED TO HPV STATUS.

Gerlinde Lang-Avérous1; Gabrielle Fritz2; Paul Walter1; Sabrina Croce1; Alina Onea1; Jean-Pierre Bellocq1; Jean-Jacques Baldauf2.
1Department of Pathology and 2Department of Gynecology University Hospital Strasbourg, France.

Background: The management of CIN1 is difficult due to the lack of predictive criteria of progression. The objective of our retrospective study was to determine whether there is a correlation between the immunohistochemical staining pattern of $p16^{INK4A}$, a surrogate marker of HR-HPV activity in cervical epithelia, the HPV status and the outcome of CIN1.
Method: Biopsies of 154 patients with initial diagnosis of CIN1 and a mean follow-up of 76.8 months (12 – 240 months) without treatment were reviewed by two pathologists in a double-blind manner. Immunohistochemistry of $p16^{INK4A}$ (clone 16P07) and HPV detection by in situ hybridisation (Inform HPV III, Ventana) were performed on serial sections of paraffin embedded tissue from initial and control biopsies of the cervix. According to the evolution, three groups were defined: regression, persistence and progression.
Results: Reviewers confirmed 80 CIN1 (51.9%), whereas 18 biopsies were considered as normal, 21 as CIN2 and 35 as "squamous atypia NOS" (κ=0.64). Among 80 CIN1, 51 regressed (63.8%), 18 persisted (22.5%) and 11 progressed (13.8%).
$P16^{INK4A}$ staining was diffuse (>25% of cells), sporadic/focal (< 25%) or negative (< 1%) in 56 (70%), 18 (22.5%) and 6 (7.5%) cases respectively. All 56 HR-HPV positive CIN1 showed positive $p16^{INK4A}$ staining (45 diffuse, 11 focal). The 11 CIN1 with progression were all $p16^{INK4A}$ positive: 10 diffusely, 1 focally. Among the CIN1 without progression, 63 were $p16^{INK4A}$ positive (91.3%) and 6 negative (8.7%). Considering progression, $p16^{INK4A}$ positive staining has a sensibility, specificity, PPV and NPV of 100%, 8%, 14.9% and 100% respectively.
Conclusion: $P16^{INK4A}$ is an excellent diagnostic marker for HR-HPV induced CIN. Its low PPV for progression does not support the hypothesis of a prognostic marker. On the other hand, with a NPV of 100%, the absence of $p16^{INK4A}$ staining is highly correlated to the regression of CIN1.

P-89
IMMUNOHISTOCHEMICAL ASPECTS OF DIFFERENTIAL DIAGNOSIS IN MATURE AND IMMATURE TERATOMAS

Mariana Aschie; Ionut Poinareanu; Antonela-Anca Craciun; Andreea Iliesiu; Anca Florentina Papuc; Anca Dobre; Diana Badiu; Sezghin Osman; Ion Aschie; Constantin Tica
UNIVERSITY OVIDIUS CONSTANTA. ROMANIA

Background: Teratomas usually manifest as masses in descended or undescended testes, in extratesticular tissues where germ cells tumors occur and in ovary in females. Teratomas are germ cell tumors composed of an array of tissues derived from two or three embryonic layers in any combination. Immature teratomas occur predominantly in children and young people and represents 3% of ovarian teratomas and 5% of testicular teratomas.
Method: Our report presents two cases of immature teratomas. The first patient is a 34 year old man admitted in Surgical Department of County Hospital of Constanta for left testicular increased size in last six months and the second case is a 15 years old girl hospitalized in the same department for retroperitoneal tumoral mass. CT scan shows in both cases o testicular and ovarian mass with nonhomogeneous structure, surrounded by liquidian areas.
Results: Histological exam revealed in both situations immature teratoma with mesenchimal, epithelial adenocarcinoma and neuroepithelial features and mature zones with

condroid tissues. There are no specific immunohistochemical markers for teratoma, but individual antibodies can be used to identify particular tissues. In both cases, chromogranin, synaptophysin and AFP were positive. There was no correlation found for the rest of IHC markers used for these cases, markers that were positive or negative (PLAP, beta-HCG, CD 117, S 100 and other). Prognosis was favorable after surgery on young man, but the young woman was given chemotherapeutical support.
Conclusions: Immature teratomas are rare germ cell tumors. The incidence in children is 2% to 3% of ovarian and testicular tumors. Microscopic exam shows the certain diagnosis. In both cases the IHC confirms immature teratoma diagnosis. Imature intestinal-type of glands were positive for AFP, and neuroepithelial structures were positive for chromogranin and synaptophysin, that sustain immature teratoma.

P-90

Galectin-3 Expression in Human Endometrium and Decidua During The Menstrual Cycle and in Gestation

Nevra Dursun*, Melin Ozgun Gecer, Pelin Yildiz*, Nimet Karadayi**, Erol Rustu Bozkurt***

**The Ministry of Health Istanbul Training and Research Hospital Pathology Department Istanbul/Turkey, ***The Ministry of Health Dr.Lutfi Kirdar Kartal Training and Research Hospital Pathology Department Istanbul/Turkey*

Galectin-3, one of the member of beta-galactozide binding lectin family, binds to basal membrane glycoprotein and has a role in many biological events. Galectin-3 is important mediators of inflammation. Endometrial function and implantation involve many inflammatory mediators, galectin-3 might contribute to the modulation of the endometrial immune system. Galectin-3 have been shown to play an important role in cell adhesion, migration and chemotaxis. Galectin-3 may be involved in the establishment of endometrial receptivity by regulating the proliferation and adhesion of endometrial cells. In our study, the secrotory *endometrium* (n=30), proliferative endometrium (n=34) and *decidua* (n=41) were collected from patients undergoing *currettage* for benign reasons and from *induced abortions*. Expression of galectin-3 during the proliferative phase was considerably low ($p<0.001$). Expression of galectin -3 increased significantly in the late secretory phase *endometrium* and in the decidual tissue ($p<0.001$). This shows that galectin-3 plays an important role in implantation and beta-galactozide binding lectin family agents, like galectin-3, which take role in adhesion and inflammation can be used for the treatment of abortus in future.

P-91

Endometrial intraepithelial neoplasia and carcinoma- correlations between immunohistochemical markers expression

Cornelia Amalinei; Raluca Balan; Irina Caruntu; Corina Cianga; Petre Cianga; Stefan Butureanu

University of Medicine and Pharmacy "Gr. T. Popa" Iasi, Romania

Background: Identification of endometrial precancers has implemented EIN (endometrial intraepithelial neoplasia), defined on a combined molecular, histomorphometric, and clinical outcome diagnostic schema. Our research was designed to identify immunohistochemical markers, focused on several directions: hormonal receptors (ER, PR), proliferation (PCNA), apoptosis system (Fas, FasL), and matrix enzymes (MMP-2, MMP-9). Method: Immunohistochemistry was applied on 12 cases of non-neoplastic endometrium, 15 cases of EIN, and 6 cases of endometrial carcinomas. Results: ER and PR showed a concordant expression, with an increased expression in EIN compared to anovulatory endometrium, both in glandular and stromal components, and occasionally endothelial staining. ER and PR presented a focal overexpression in G1 and G2 endometrial endometrioid carcinomas and a weak expression or absence in undifferentiated (G3) endometrial carcinomas. PCNA index was variable but high in EIN and carcinomas, in glandular, stromal, and endothelial cells, correlated with ER and PR expression, with the maximum staining in the carcinomatous front of invasion. Fas/FasL system showed a deregulated expression in EIN and carcinomas, with a reduced Fas expression and a low FasL expression, in epithelial and immune cells. MMPs expression was increased in EIN, both in glandular and stromal components. Furthermore, MMP-9 expression was higher than that of MMP-2 and supplementary noticed in migrated cells and in myometrium. Conclusions: Overexpression of steroid receptors in EIN demonstrates the role of hormonal stimulation in carcinoma pathogenesis. PCNA, ER and PR coordinated increased expression suggests a correlation between hormonal status and cellular proliferation. Deregulated expression of Fas/FasL system probably enhances endometrial proliferation, immunohistochemical aspects suggesting that FasL positive epithelial endometrial cells, together with immune cells, may induce apoptosis in Fas positive cells. As markers of extracellular matrix degradation, MMP-2 and MMP-9 demonstrate the role of epitheliostromal interactions in the development and progression of endometrial neoplasia.

P-92

Prevalence of high risk types of human papillomavirus in previously unscreened, bosnian women in last eight years

Ermina Iljazovic; Elmir Cickusic; Silvija Avdic; Zinaida Karasalihovic; Jasminka Mustedanagic – Mujanovic; Jugoslav Stahov

University Clinical Center Tuzla, Polyclinic for Laboratory Diagnostic, Pathology Department. Bosnia Herzegovina

Background: Cervicalcancer is an important public health problem for adult women in developingcountries where it is the most or second most common cancer among women. Thevast majority of cervical cancer cases are caused by infection with certainsubtypes of human papilloma virus (HPV). Worldwide, cervical cancer claims thelives of 231 000 women annually, over 80% of whom live in developing countries.In developed countries, initiation and sustenance of cervical cytologyprogrammes involving the screening of sexually active women annually, or oncein every 2–5 years, have resulted in a large decline in cervical cancerincidence and mortality. Testing women ≥age 30 for high risk HPV is more sensitive as a primari screen than currently practiced cervical cytology.

Method: Identification of the presence of human papilomavirus was carried out by the Digene Hybride Capture II test for all patients.

Results: 4696 previously unscreenedwomen were tested for the presence of the HPV. 33.36% were positive for theHRHPV. We also analized the age of the women at the moment of the testing andassociation with some other type of infection (bacterial or fungal).

Conclusion: Data of the genitalHPV DVA prevalence in representative samples of populations in difierentcountries are lirnited, in spite of the largc number of rcports alreadypublished. When available the HPV DNA prevalence would be useful in makingprediction of expecting incidence and likely time trends of cervical cancer.Typical y the proportion of the HPV female carriers have been placed in the15–40% in the young, sexually active age group and between 3–10% in the 35 andabove age group.

P-93

LYMPHOEPITHELIOMA-LIKE CARCINOMA OF THE FEMALE GENITAL TRACT. AN IMMUNOHISTOCHEMICAL AND MOLECULAR STUDY OF 5 CASES.

Daniel Badia;Carmen Blazquez;Felicia Marginean, Josep Castellvi;Angel Garcia;Carmen Ruiz Marcellan; Javier Hernandez;Mercedes Martinez;Santiago Ramon y Cajal

ANATOMIA PATOLOGICA HOSPITAL VALL D'HEBRON. SPAIN

Introduction: Lymphoepitheliomas were originally described as a nasopharingeal neoplasm related to Epstein-Barr virus. Lymphoepithelioma like carcinoma (LELC) can also be found in the female genital tract (uterine cervix, endometrium and one case, not reported previously, in the fallopian tube). Importantly, LELC has better prognosis than squamous cell carcinoma variants, therefore its differential diagnosis has great importance. It's association with Epstein-Barr virus is still controversial in the uterine cervix. In addition, HPV is also a well known risk factor related to development of cervical cancer although the role that HPV plays in LELC development is not well studied. The aim of this study is to evaluate possible relationships between HPV, EBV and LELC in the female genital tract.

Material and methods: 4 cases of LELC of the uterine cervix and 1 case of the fallopian tube have been collected. Immunohistochemistry for p16, p53, Ki67, PCR based methods to detect EBV (EBNA2 and LMP1) and HPV serotyping by the HPV Clinical Arrays Kit, have been performed.

Results: The five cases were negative for EBV sequences. In two cases HPV was detected (serotypes 16 and 31) and, in three cases was negative. Immunohistochemistry showed overexpression of p16 in all cases and interestingly, p53 was positive in one of the cervical carcinomas (with HPV16 serotype) and in the tubaric carcinoma. In all cases, the Ki67 index was higher than 35%.

Conclusions: HPV was not found in every LELC and no EBV infection could be demonstrated in our series. On the contrary, p16 was overexpressed in all cases, including those without HPV infection. Our results together with some other reported series, suggest that other factors may be related with the development of gynecological LELC. Finally, our findings indicate that p16, p53 and HPV serotyping does not seem to help in the differential diagnosis with other squamous cell carcinoma variants.

P-94

Heterologous Mixed Mallignant Mullerian Tumor of the uterus. A case report and review of the literature.

1 Biteli Maria; 1 Koniaris Efthymios; 1 Sevastiadou Maria; 2 Derdelis Grigoris; 1 Apostolaki Aikaterini.

1 Pathology dpt. of Anticancer Oncological Hospital of Athens 'St. Savvas', Athens, Greece; 2 Gynecology dpt. of Anticancer, Oncological Hospital of Athens, 'St. Savvas', Athens, Greece.

Background: Heterologous Mallignant Mixed Mullerian Tumor (HMMMT) of the female genital tract is a rare and highly malignant neoplasm with poor prognosis occurring mainly in postmenopausal women. Endometrium is the most frequent location of HMMMTs accounting for 1.5% of all uterine malignancies. Here we present such a case.

Method: A 70-year old patient admitted to our hospital with a stagonoid uterine bleeding and pain in the hypogastrium. Ultrasonographically the endometrium was thickened measuring 7 mm. The patient underwent a total hysterectomy measuring 11.5×11.5×6 cm and bilateral oophorectomy. We also received a specimen measuring 46×11×2 cm from the omentum and a tissue specimen from the urinary bladder wall measuring 2.5×2×1.5 cm.
Results: Grossly the tumor was soft and friable, tan to grey in color and accompanied by focal and extensive hemorrhage and necrosis. After thorough histological examination it was about a HMMMT involving most of the myometrial wall, the endometrium, the left salpinx and the mesosalpigium. Histologically the tumor consisted of high cellular spindle cells, compact small round cells and bizarre giant cells resembling leiomyosarcoma or fibrosarcoma. The stroma of the tumor was myxoid and highly vascular. Heterologous elements in the form of cartilage and bone were also present and the mitotic activity was marked. Immunoreactivity with keratin and EMA was found and excluded any carcinomatous component. SMA and myoglobulin was also performed to exclude rhabdomyosarcomatous component.
Conclusion: HMMMT is regarded by many authors as a subtype of uterine sarcoma with a significantly worse prognosis than FIGO grade 3 endometrial carcinomas. Breast Cancer survivors who were treated with aromatase inhibitors for many years are reported to have higher incidence of uterine sarcomas. Stage appears to be important prognostic factoring HMMMTs, although heterologous components are not certain whether are important in the prognosis. Only those HMMMTs with rhabdomyosarcoma differentiation were linked with worse prognosis.

P-95

How to differentiate Uterine Smooth Muscle Tumors with standard smooth muscle differentiation.

1 Koniaris Efthymios; 1 Biteli Maria; 1 Sevastidou Maria; 2 Derdelis Grigoris; 1 Apostolaki Aikaterini.
1 Pathology dpt. Of Anticancer, Oncological Hospital of Athens, 'St. Savvas', Athens, Greece. 2 Gynecology dpt. of Anticancer Oncological Hospital of Athens 'St. Savvas', Athens, Greece.

Background: Many variants of leiomyoma mimicking malignancy exist. Here we present three rare cases of a Symplastic Leiomyoma (SL), Smooth Muscle Tumor of Low Mallignant Potential (SMTLMP) and High Cellular leiomyoma (HCL).
Method: The 1st case was about a 52-year old patient presented with hemorrhage, urgency and constipation. She underwent a total hysterectomy and a whitish-grey, circumscribed tumor measuring 25×22 cm was found in the uterus. The 2nd case was an incidental finding of leiomyoma-like lesion discovered ultrasonographically and involved a 32-year old patient treated for infertility. Myomectomy was performed and two tumors measuring 5×4.5 cm were obtained. The 3rd case was a 38 year old woman presented with menorrhagia. Total hysterectomy was performed and on dissection a voluminous cystic mass was observed measuring 9 cm.
Results: We examined in all three cases the degree of cellularity, atypia, mitosis and coagulative necrosis. Microscopically the 1st and the 2nd tumor were composed mainly of multinucleated, giant cells with hyperchromatic, prominent chromatin with moderate cellularity and pseudonuclear cytoplasmic inclusions. In the 3rd case the tumor was composed of monotonous appearing cells with round nuclei with evenly dispersed chromatin, small nucleoli and scant cytoplasm and high degree of cellularity. Atypia was observed only in the first case. The mitotic rate in all cases was low (<10/10HPF), and coagulative necrosis was found only in the 2nd case. According to our findings the first case was about a SL, the second was a SMTLMP and the third was HCL.
Conclusion: The diagnosis is based mainly on exclusion and the trivariate rule introduced by Kempson et al., that uses mitotic index, the degree of atypia and the coagulative tumor cell necrosis is helpful. Some authors use the term SMTLMP and some others instead use the term Smooth Muscle Tumor of Uncertain Unknown or Undetermined Malignant Potential.

P-96

Evaluation of angiogenesis in ovarian mucinous epithelial tumors: comparative analysis of new methods of semiautomated quantification

Ivan Rebouças; Jacqueline Araújo; Adriana Yoshida; Luís Sarian; Sophie Derchain; Natália Schenka; José Vassallo; Liliana Andrade; André Almeida Schenka
State University of Campinas, São Paulo, Brazil

Background: In some neoplasms, angiogenesis seems to favor not only growth, but also tumor spreading, therefore, bearing diagnostic/prognostic value. In ovarian mucinous tumors, due to shortage of studies and their methodological variability, the role of angiogenesis is not yet established.
Aims: to evaluate the diagnostic role of angiogenesis in ovarian epithelial mucinous neoplasms, comparing and validating different methods of microvessel quantification.
Methods: Twenty-one mucinous epithelial tumors (twelve benign, four borderline and five malignant), diagnosed at the Department of Pathology of our institution, from 01/1997 to 12/2003, were assessed through immunohisto-

chemical technique, using CD34 marker. Microvessel density (MVD) and parameters based upon endothelial area (total endothelial area [tENDA], mean endothelial area [mENDA] and percentual endothelial area [%ENDA]) were quantified using manual and semiautomated protocols with Imagelab (version 2.4). These different quantification methods were tested and compared for their relative ability to discriminate between the three diagnostic entities.

Results: In general, angiogenesis estimates were higher in the borderline (MVD=111.0±52; tENDA=15140.35±3000; mENDA=7.95±2) and malignant groups (MVD=95.6±60; tENDA=17712.13±17771; mENDA=31.83±68), in comparison to the benign group (MVD=94.5±46; tENDA=15292±9475; mENDA=7.94±3), except for % ENDA, whose mean estimates were higher within the benign and borderline groups. However, in none of these parameters the difference between groups reached statistical significance.

Conclusion: The present data, while preliminary, showed no significant association between parameters of vascular quantification and biological behavior of ovarian mucinous tumors, regardless of quantification method. The small number of cases and wide dispersion of values may have contributed for this finding. (JV and LA are supported by the National Council for Scientific Research, CNPq).

P-97

Selection of image format (TIFF vs. JPEG) in semi-automatic quantitative analysis of ovarian tumor angiogenesis

Jacqueline Araújo, Ivan Rebouças, Adriana Yoshida, Luís Sarian, Sophie Derchain, Natália Schenka, José Vassallo, Liliana Andrade, André Almeida Schenka
State University of Campinas, São Paulo, Brazil

Background: Although well-established in many neoplasms, the role of angiogenesis in ovarian tumors is still controversial. Computer Image Analysis Systems (CIAS) potentially improves accuracy and reproducibility of current vascular quantification. In CIAS, the use of high quality images (e.g., TIFF) is preferred over compressed images (JPEG) because, theoretically, loss of information observed in the latter could jeopardize quantitative analysis. However, this has not yet been formally demonstrated.

Aim: to compare distinct image formats with respect to different protocols of angiogenesis quantification.

Methods: Forty epithelial ovarian tumors (14 serous and 26 mucinous, including benign, borderline and malignant specimens) were included. Using a Nikon E200 microscope, adapted to a Nikon 995 Coolpix CCD camera, one TIFF and two distinct JPEG images ("basic and fine") were obtained from a single low-power field of a vascular 'hotspot', per case. Later, two more types of JPEG ("high and low") were obtained from the conversion of the TIFF images, using Adobe Photoshop. All five image types were assessed for microvessel density (MVD) and mean endothelial area (mENDA), using Imagelab 2.4 software.

Results: mean differences between TIFF and JPEGs were significantly different from zero ($p<0.001$) and varied from 89,5 to 1234,8, for MVD, e between -0,2 e -9,1, for mENDA. In both variables, the agreement between image formats (mean difference ±2X the standard deviation) was higher between TIFF and high quality JPEGs ("fine/high"). Furthermore, Spearman's correlation coefficient was high between TIFF and all (0.82–0.99) but JPEG "low" (0.61–69).

Conclusion: the significant differences found between TIFF and JPEGs precludes direct comparison between angiogenesis values obtained from different format images. Nevertheless, given their high degree of agreement/correlation with TIFF, high quality JPEGs can be used instead of TIFF images, whenever memory and computer processing speed are limiting factors. (JV and LA are supported by the National Council for Scientific Research, CNPq).

P-98

Malignant struma ovarii

Sun Young Kwon; Yu Na Kang; Hae Ra Jung; Mi Sun Chei; Sang Pyo Kim; Kun Young Kwon; Sang Sook Lee
Department of Pathology, Keimyung University School of Medicine. South Korea

Malignant struma ovarii is a very rare form of germ cell tumor. Malignancy is represented by follicular carcinoma, papillary carcinoma or a mixed pattern, similar to the types of thyroid carcinoma. It is difficult to find out the real incidence of malignant struma ovarii, due to the different criteria for its diagnosis. Some authors described an incidence as high as 37% of struma ovarii cases and others estimated an incidence lower than 5%. Anyway, the malignant transformation is an uncommon event. Here we report one case of malignant struma ovarii. The 69-year-old woman complained of a three-month history of abdominal distension. A pelvic computed tomogram imaging study indicated a large irregularly-marginated complex mass in the right pelvic cavity and large amount of ascites. Total abdominal hysterectomy with bilateral salpingo-oophorectomy was performed. On operation, the right ovary was enlarged and partially ruptured. The right pelvic cavity showed large amount of a little bloody ascites about 2000 cc. On gross examination, the right ovary measured 10.5×2.5×5.7 cm and weighed 134.0 gm. The right ovary was multinodular and multicystic mass. It contained gelatinous material and sebum-like material with hairs.

Partial solid portion is pale tan to white and firm. No endophytic papillary growth is present in any of the loculi. The right ovary was predominantly composed of follicular structure of thyroid gland. Within the struma ovarii, a small focus of papillary thyroid carcinoma was found. Immunohistochemically, the tumor was positive for thyroid transcription factor-1.

P-99

Atypical localization of lymphoblastic lymphoma-case report

Mariana Aschie; Andreea Iliesiu; Antonela-Anca Craciun; Ion Aschie; Ionut Poinareanu; Anca Dobre; Anca Papuc; Lazar Irimiea; Diana Badiu

Ovidius University Constanta. Romania

Background. Lymphoblastic lymphoma with uterine localization is a rare malignant neoplasm, present in 1% of women with extranodal lymphoma. 25% of malignant lymphomas have extranodal sites and only 1% of them have uterine localization. Uterine malignant lymphoma spreads frequently in cervix and vagina. Beside ovarian lymphoma, uterine lymhoma affects females of all ages, especially the ones in the 4-th decade. The cytological diagnosis of uterine lymphoma becomes more difficult because of the infiltrative evolution in the muscular layer.
Method. This paper reports a case of uterine lymphoma diagnosed in a 36 years old patient hospitalized in Gynecology Clinic of Clinical Emergency County Hospital, Constanta. The clinical diagnosis was massive pelvi-abdominal tumor, myelodisplastic syndrome and secondary anemia.
Results. The specimen of uterine corpus (9/6/6 cm) presents on cut surface a region with firm consistency, infiltrative character and whitish-gray with hemorraghic zones apparance. The microscopic examination reveled: malignant difuse lymphoma with small and large cells associated with lymphoblastic Burkitt-like lymphoma. Immunohistochemical exam reveal CD20 positive which confirm the diagnosis. CD20 is a specific marker for differentiation and proliferation of B lymphocytes. CD10 is a specific antibody for Burkitt lymphoma, diffuse large cell lymphoma, relevant for our diagnosis. Also we examined CD3 and CD68, that gives negative reaction because of their specificity for T lymphocytes. We made the differential diagnosis between T cell lymphoblastic lymphoma, undifferentiated carcinoma, histiocitary and anaplastic lymphoma.
Conclusions. Uterine lymphoma is a rare pathological entity. Because of high malignity lymphoblastic components, the evolution of the patient was unfavorable. The immunohistochemical tests confirms the morphological diagnosis. As a consequence of high malignity lymphoblastic lymphoma the patient's evolution was worse and she died because of leucemic convertion. Necroptic exam reveled macroscopic metastasis on skin, liver, stomach, cardiac papillary muscles.

P-100

Expression of TWIST is frequently observed in epithelial ovarian cancer.

Marta Mendiola; Adrian Mariño-Enriquez; Jorge Barriuso; Gines Hernandez-Cortes; Belen San Jose; Andres Redondo; Juan Angel Fresno Vara; Asuncion Suarez; Manuel Gonzalez-Baron; David Hardisson

Hospital Universitario La Paz, Universidad Autonoma de Madrid. Spain

BACKGROUND: Ovarian carcinoma is the most important cause of gynaecological cancer-related mortality in the western world with a poor 5-year survival. TWIST, a basic helix–loop-helix transcription factor, has been reported to be associated with the development and progression of human cancer. The aim of this study was to analize the distribution and expression of TWIST in ovarian carcinomas and to examine its clinical significance.
MATERIALS AND METHODS: The study was conducted on 65 ovarian carcinomas treated by surgery followed by paclitaxel plus carboplatin-based chemotherapy. The clinicopathologi factors evaluated were histological type (serous vs non-serous), tumor grade, FIGO stage, response to treatment (surgery and chemotherapy), progression-free survival and overall survival. Tissue samples were formalin fixed and paraffin embedded and were immunostained against TWIST antibody (Abcam, 1:100) using the Envision (Dako) method. Staining for the TWIST protein was nuclear. The intensity and percentage of cells that exhibited immunostaining was evaluated.
RESULTS: Overall, 46.15% (n=30) of ovarian carcinomas showed expression of TWIST. When categorized into negative vs positive expression (>5% of tumor cells), TWIST was not associated with any of the clinicopathological parameters examined.
CONCLUSION: Expression of TWIST is frequently observed in ovarian carcinomas and has been recently described as a useful marker in these patients as it appears to increase the risk for recurrence and for poor survival. However, these results could not be confirmed in our series of epithelial ovarian carcinomas. Thus, additional studies including larger patient samples seem necessary to validate the prognostic significance of TWIST expression in ovarian carcinomas.

P-101

Lymph node involvement in deep infiltrating endometriosis

Jean-Christophe Noel, Isabelle Fayt

Department of Pathology, Erasme University Hospital, ULB, Brussels. Belgium

Background: Lymph node involvement by endometriosis is considered to be uncommon and the status of lymph nodes in endometriosis remains obscure because at evidently lymph node dissection is usually not performed for a so-called benign disease.

Methods: In the present study, we have analyzed the lymph node involvement by endometriotic foci in surgical specimen from rectosigmoid endometriosis (n=26) where the lymph nodes are easily accessible.The lymph node involvement was correlated with the size and the wall layers affected by endometriotic lesions, the number of lymph nodes retrieved, and the presence of lymphovascular invasions as demonstrated by CD 31 and D2–40 antibodies.

Results: Lymph node involvement by endometriosis was observed in 11 of the 26 patients (46,3%) and correlated with the size of the lesions, the number of lymph nodes retrieved and the presence of lymphovascular invasions.

Conclusions: Our data confirm that lymph node involvement by endometriotic foci is a frequent event in rectosigmoid endometriosis and may result at least partially from a lymphatic spread of the disease.

P-102

IS THERE A RELATIONSHIP BETWEEN THE VIRAL LOAD IN CYTOLOGY SAMPLES AND P16 IMMUNOREACTIVITY IN BIOPSY SAMPLES?

Raquel.Murillo (1), Teresa.Gomez (2), Laura.Lopez (1), Javier Gimeno (1), Jordina Santos (1), Sandra Planella (1), Marta Pallarols (1),), Emilia Romero (1), Imma Soler (1), Eulalia Gimferrer (1), Sara Albert (1), Lara Pijuan (1) Gemma Mancebo (2), Fernando Larrazabal (2), Ramon Carreras (2) Sergi Serrano (1). Francesc.Alameda (1),

HOSPITAL DEL MAR. (1)DEPT. OF PATHOLOGY. (2)DEPT. OF OBSTETRICS AND GYNECOLOGY. AUTONOMOUS UNIVERSITY OF BARCELONA. SPAIN

OBJECTIVE: To assess the possible relationship between viral load and p16 immunoreactivity in cytology and biopsy samples, in cervical dysplasia cases.

MATERIALS AND METHODS: 82 cervical biopsies diagnosed as a cervical dysplasia obtained between 2 and 6 months posterior to cytologic diagnosis. An immunohistochemical study of p16 in each case. Review of previous diagnostic cytology in order to know the viral load determined by Hybrid Capture II

RESULTS: 54 cases were mild dysplasias and 28 cases were moderate/severe dysplasias.

11 of 54 mild dysplasia cases showed p16 immunoreactivity (20.4%). Of these, 10 showed RLU greater than 1 (Considered as positive) in previous cytology, with a mean of 1472. These 10 cases were the 23.8% of all RLU positive cases, thus 76.2% of RLU positive cases, didn't show p16 immunoreactivity in biopsy samples. The mean RLU of these cases was 820.

18 of 28 moderate/severe dysplasia cases showed p16 immunoreactivity (64.3%),. Of these, 17 had positive RLU with a mean of 1595. These 17 cases were the 62.9% of all RLU positive cases, thus the 37.1% of RLU positive cases didn't show p16 immunoreactivity in the corresponding biopsy samples. The mean RLU of these cases was 972.

CONCLUSIONS: Apparently doesn't exist correlation between viral load and p16 immunoreactivity but if we consider the biopsy diagnosis there is an increase of correlation in moderate/severe dysplasia cases related to mild dysplasia cases. Also a RLU increase is observed in p16 positive cases, in both groups.

P-103

Concurrent pregnancy and endometrial carcinoma

Marina Kos

Clinical Department of Pathology "Ljudevit Jurak", Clinical Hospital "Sisters of Mercy", Zagreb, Croatia

Introduction: Endometrial carcinoma in women of reproductive age is rare. We describe a case of accidental diagnosis of endometrial adenocarcinoma in a curretage done because of a missed abortion.

Case report: A 35-year patient with established pregnancy of 9 weeks gestation was admitted to the hospital because of bleeding. A missed abortion was diagnosed, D&C was done and the tissue was sent for histopathological examination. Abundant material was received and was examined completely. On paraffin embedded, H-E stained tissue sections the remains of gestational sac surrounded with immature, partially hidropic chorionic villi were found. In the decidua, there were scarce, confluent and cribriform endometrial glands showing atypical endometrial cells with mitotic activity. The same cells covered the surface of decidual fragments. The diagnosis of endometrioid adenocarcinoma of endometrium was made. After that, the patient underwent a series of imaging diagnostic procedures (US, 4D-US, Doppler, MRI), none of which showed suspicious findings. The patient had menarche at the age 14, she claimed that her periods were always extremely regular, that she has never taken any hormonal preparations, and was not treated because of infertility. However, she had a spontaneous abortion 1,5 year ago, but it has happened at

home, and no histopathological analysis could be done. Since she wants to become pregnant again, she was adviced to control regularly.

Discussion: Women of reproductive age who develop endometrial adenocarcinoma are rare, and usually have a history of infertility and hormonal treatment. It was not the case in this patient, and according to histopathological and imaging studies we can assume that the carcinoma was probably limited to endometrium and caused the failure of pregnancy development.

P-104

THE RELATIONSHIP OF C-ERB B-2 EXPRESSION WITH ESTROGEN RECEPTOR, PROGESTERONE RECEPTOR AND PROGNOSTIC PARAMETERS IN ENDOMETRIAL ADENOCARCINOMAS

Aylin Ege Gul; Sevinc Hallac Keser; Nilufer Onak Kandemir; Nimet Karadayi; Nagehan Ozdemir Barişik; Çaglar Çakir; Sibel Şensu

Dr. Lutfi Kirdar Kartal Educational and Research Hospital, Pathology Department, ISTANBUL/TURKEY

BACKGROUND: The transmembrane receptor encoded by the HER-2 cellular oncogene is amplified in several types of human carcinomas. There are prognostic and therapeutic implications associated with the overexpression of this transmembrane protein. HER-2/neu, the transmembrane receptor encoded by the c-erbB2 gene, is overexpressed by immunohistochemistry in <10% of endometrial cancer. The aim of this study was to investigate the expression of cerbB2 in endometrial cancer with attention both to membranous and cytoplasmic staining, to study its correlation to established prognostic parameters and to elucidate the significance of cytoplasmic signaling.

METHODS: This study is performed on 73 cases between 2004–2007 at Dr Lutfi Kirdar Training and Educational Hospital Pathology Clinic. Parafine embedded tumoral tissue with endometrial adenocarcinoma are examined immunohistochemically (IHC). Immunoreactivity of c-erbB-2 is localized in the cell membrane and is scored semiquantitatively using the following Food and Drug Administration (FDA) approved scoring system: 0, no immunostaining; 1+, incomplete membranous immunostaining of <10% of tumor cells; 2+, weak complete membranous immunostaining of >10% of tumor cells; 3+, strong complete membranous staining of >10% of tumor cells. Scores of 0 or 1+ indicate a negative result, while scores of 2+ and 3+ are regarded as positive c-erbB-2 expression. The relation between CERB-2, estrogen – progetsreone receptor status, histological grade, myometrial invasion depth and vascular invasion is investigated. Estrogen receptor (ER) and progesterone receptor (PR) status are analysed based on the percentage of stained cells and the intensity of nuclear stain. The percentage of positive cells is graded as follows: 1=0 to 25% of the nuclei stained; 2=26 to 75%of nuclei stained, 3= more than 76% of the nuclei stained. The staining intensity is scored as follows: 1= absent or weak, 2= strong, 3= very strong. The sum of both parameters give the IHC score. Tumors are divided into three categories depending on the IHC score. Category I corresponds to a score of 2, category II to a score of 3 or 4, and category III to a score of 5 or 6. Category I tumors are considered as immunonegative, whereas category 2 and 3 tumors are considered as immunopositive. SPSS (Statistical Package for Social Sciences) for Windows 10.0 software is used for the statistical analysis. For the comparison of quantitative data, Qui-square and Fisher's Exact test are used. Results are analysed at $p<0.05$ significance and 95%confidence interval.

RESULTS: In this study, we found a statistically significant relation between C-erb B2 and progesterone receptor ($p<0.05$). In progesterone receptor negative cases, expression of C-erb B2 was statistically significantly high. Membranous C-erb B2 statining and estrogen receptor did not show a statistically significant relation ($p>0.05$). However, it is noteworthy that, in estrogen receptor negative cases, C-erb B2 expression was high. There was no significant difference between C-erb B2 and histological grade ($p>0.05$). The highest levels of C-erb B2 was found in Grade 2 cases. There was not observed any statistically significant relation between C-erb B2 and myometrial invasion depth or vascular invasion ($p>0.05$).

CONCLUSION: In our study, there is found a significant relation between C-erb B2 and progesterone receptor. We conclude that, to observe a negative correlation between progesteron receptor positivity which is considered as a favorable feature in endometrial adenocarcinomas and c-erb B 2 expression will lead us in studies with larger series and will play an important role in therapeutic approach to patients.

P-105

THE RELATIONSHIP OF COX-2 EXPRESSION WITH ESTROGEN RECEPTOR, PROGESTERONE RECEPTOR AND PROGNOSTIC PARAMETERS IN ENDOMETRIAL ADENOCARCINOMAS

Sevinc Hallac Keser; Aylin Ege Gul; Nagehan Ozdemir Barişik; Nimet Karadayi; Nilufer Onak Kandemir; Sibel Şensu

Dr. Lutfi Kirdar Kartal Educational and Research Hospital, Pathology Department, ISTANBUL/TURKEY

BACKGROUND: In recent years, the design of new antineoplastic agents that can halt the progression of human

malignancies with minimal systemic damage has been at the forefront of cancer research, with cyclooxygenase-2 (COX-2) as a major target molecule. Cox-2 and its role in the pathophysiologic processes is well known. In this study immunohistochemical expression of COX-2 in the endometrial adenocarcinomas (EC) and its relationship with estrogen receptor, progesterone receptor and other prognostic parameteres are investigated.

METHODS: The study is performed on 73 endometrial adenocarcinoma cases diagnosed between 2004–2007 at Dr Lutfi Kirdar Training and Educational Hospital Pathology Clinic. Parafine embedded tumoral tissues are examined immunohistochemically (IHC). Staining intensity is evaluated as negative (0), weak (1), moderate (2), strong (3), and the percentage of positive tumor cells is categorised as follows: 0=0% to 5%, 1=6% to 25%, 2=26% to 50%, 3= 51% to 75%, and 4=76% to 100%. The sum of the intensity and extend score is used as the final staining score (0–7) for COX-2. Tumors having a final staining score of ≥4 are considered as showing strong expression. Estrogen receptor (ER), and progesterone receptor (PR) examinations are done based on the percentage of stained cells and the intensity of nuclear stain. The percentage of positive cells is graded as follows: 1=0 to 25% of the nuclei stained; 2=26 to 75%of nuclei stained, 3= more than 76% of the nuclei stained. The staining intensity is scored as follows: 1= absent or weak, 2= strong, 3= very strong. The sum of both parameters gives the IHC score. Tumors are divided into three categories depending on the IHC score. Category I corresponds to a score of 2, category II to a score of 3 or 4, and category III to a score of 5 or 6. Category I tumors are considered as immunonegative whereas category 2 and 3 tumors are considered as immunopositive. The cases are grouped according to FIGO histological grade as Grade I, Grade II and Grade III and besides they are investigated in three groups according to myometrial invasion as limited to endometrium, invasive in less than 1/2 of myometrium and invasive in more than 1/2 of myometrium. These prognostic parameteres as well as estrogen and progesterone receptor existance are compared with COX-2. SPSS (Statistical Package for Social Sciences) for Windows 10.0 software is used for the statistical analysis. For the comparison of quantitative data, Qui-square and Fisher's Exact test are used. Results are analysed at $p<0.05$ significance and 95% confidence interval.

RESULTS: When compared with Cox 2 scores, histological grade, myometrial invasion level and estrogen-progesterone receptor status of the cases did not show any statistically significant difference ($p>0,05$).

CONCLUSION: Since we could not find any statistically significant relation between COX-2 and estrogen–progesterone receptor status and other parameteres, we conclude that COX-2 can be used as an independent prognostic factor.

P-106

Uterine müllerian adenosarcoma with massive ovarian stromal sex cord-like component in two tamoxifen treated patients

Simona Stolnicu1, Krishna Balachandran2, M A Aleykuty2, Olga F.Garcia-Galvis3, Ovidiu Preda1, Monica Boros1, Andrada Loghin1, Angela Borda1, Doinita Radulescu4, Francisco F. Nogales3

From the Departments of Pathology, University of Medicine Targu Mures,Romania1. Histopathology Centre Trivandrum, Kerala, India2. University of Medicine Granada, Spain3. University of Medicine Iasi, Romania4

Introduction: To date, 68 cases of uterinetamoxifen-related uterine sarcomas have been reported. Of these, 13 corresponded to adenosarcomas. We present two further cases of adenosarcoma of the uterus in patients with breast cancer treated with tamoxifen, both of them presenting the particular feature of having a massive stromal component composed by an ovarian sex cord-like proliferation. To our knowledge, this is the first time that this association is reported in tamoxifen treated patients.

Material and methods: Two 71 and 64 year old postmenopausal patients previously diagnosed with infiltrating ductal carcinoma were treated with mastectomy, chemotherapy and tamoxifen (20 mg/day for a period of 5 and 3 years respectively). Presently, both were admitted for vaginal bleeding and subsequently treated by total abdominal hysterectomy with bilateral salpingo-oophorectomy. Follow up is uneventful.

Pathology Results: Macroscopy revealed large intracavitary polypoid tumours of 2.5 and 5 cm in diameter respectively, conformed by a foliaceous, translucent tissue with soft consistence where multiple yellow streaks were present. Myometrial limits were lineal. Microscopically, benign endometrioid, mucinous and ciliated epithelia lined dilated tubulo-cystic glandular spaces often with intraluminal phyllodes-like projections. The mesenchymal component had CD10 positive endometrial stromal periglandular cuffs present as a subepithelial cambium layer. The remaining stroma, comprising more than 80% of the mass, was of ovarian sex-cord type with luteinized cells, luteinized sertoliform tubules andepithelioid trabecular cords that were positive in different proportions and intensity for CAM5.2, Actin, Desmin, Calponin, CD 10, Inhibin,Calretinin.

Conclusions: This is the first report of adenosarcomas containing a predominant sex cord-like elements in patients under tamoxifen treatment. Adenosarcomas with stromal sex-cord elements have been reported in only three previous papers in Endometrium1 (8 cases), cervix2 (1 case) and ovary3 (6 cases) none of them associated with long term tamoxifen treatment. Both our cases had a massively luteinized sex-cord componentand only a minor

periglandular endometrial stromal component. Immunohistochemistry was characteristic of uterine tumours resembling ovarian sex cord tumours. Clinically, both behaved in a benign fashion.

References:
1. Clement P.B., Scully R.E.: Mullerian adenosarcoma of the uterus with sexcord-like elemenys. Am J Clin Pathol. 1989;91:664–672.
2. Hirschfield L., Kahn L.B., Chen S., Winkler B., Rosenberg S.: MullerianAdenosarcoma with ovarian sex cord-like differentiation. Cancer. 1986;57:1197–1200.
3. Eichhorn J.H., Young R.H., Clement P.B., Scully R.E.: Mesodermal (Mullerian)adenosarcoma of the ovary. A clinicopathologic analysis of 40 cases and areview of the literature. Am J Surg Pathol. 2002;26:1243–1258.

P-107
ATYPICAL POLYPOID ADENOMYOMA OF THE UTERUS. A REPORT OF ELEVEN CASES.

Katerina Kubelka-Sabit; Irina Prodanova; George Zografski; Neli Basheska
Department of Histopathology and Clinical Cytology, Institute of Radiotherapy and Oncology, Medical Faculty, Skopje, Republic of Macedonia

Background: Atypical polypoid adenomyoma (APA) is a rare uterine polypoid tumor occurring in women in their reproductive age.
Method: Eleven cases of atypical polypoid adenomyoma have been diagnosed at our department in the last five years (2003–2007). The mean age of the patients was 37 (range 26–46 years). The most common clinical diagnosis was abnormal uterine bleeding, leiomyoma or endometrial polyp. In one patient the clinical diagnosis was endometrial hyperplasia, while two were examined for primary sterility. In one case the diagnosis was established in a curettage material from a spontaneous abortion. Apart from the conventional hematoxylin and eosin, additional histochemical and immunohistochemical stainings were also performed.
Results: Macroscopically, white-gray polypoid fragments measuring 0.5–2 cm were found in the curettage materials. Histologically, the APAs were composed of atypical endometrial glands surrounded by smooth muscle stroma. Squamous morules were a common finding. In three cases, the APA was accompanied by foci of invasive endometrial adenocarcinoma. The immunohistochemical stains confirmed the smooth muscle nature of the stroma (alpha-smooth muscle actin, desmin and caldesmon positive). The morules were positive for CD10 marker, whereas Ki-67 proliferative index was low (5–15%), except in the foci of invasive adenocarcinoma. All tumors were hormone responsive. One of the patients was surgically treated for advanced endometrial adenocarcinoma in FIGO IIIC stage. Complete regression of the disease after tumor extirpation and consecutive high dosage progesterone therapy was achieved in four of the patients, in one the disease persisted after two years due to suboptimal therapy, whereas five were lost to follow up (four of which diagnosed in the last 10 months).
Conclusion: APA is considered to be a benign form of mixed epithelial and mesenchymal uterine tumors. This tumor can be associated with sterility and rarely with endometrial carcinoma, therefore recognition and correct diagnosis of this entity is important.

P-108
EVALUATING THE THE MALIGNANCY POTENTIAL IN ENDOMETRIAL HYPERPLASIA THROUGH PROLIFERATION MARKERS KI-67 AND PCNA AND TUMOR SUPPRESSOR GENE DESIGNATED PTEN

Maria Sajin; Alina Elena Chefani; Anca Mihaela Lazaroiu; George Simion; Mariana Costache; Mariana Georgescu; Irina Draga Caruntu; Diana Secara; Monica Carstoiu
Department of Pathology of Universitary Emergency Hospital Bucharest, Romania

Introduction: Endometrial Hyperplasia (increase in gland/stroma ratio, disorder number and shape of the glands like modifications of the glandular epithelium: exhibits loss of nuclear polarity, stratification, etc) is a lesion frequently associated with the uterine leiomyomas
Purpose: The Study was realized at the Universitary Emergency Hospital Bucharest, Romania on 294 endometrium biopsies taken in the period 2004–2006 from women with ages between 45 and 55.
Material and methods: Hematoxylin –eosin stained slides of endometrial formalin fixed, paraffin embedded tissue has emphasized in 143 cases the simple hyperplasia (SH), in 101 cases the complex hyperplasia (CH), in 19 cases the simple atypical hyperplasia (SAH) and in 35 cases the complex atypical hyperplasia (CAH). We performed the indirect tristadial ABC method of IHC for 3 antibodies: PTEN, Ki-67 and PCNA on formalin fixed embedded tissue taken by biopsies from 80 cases (14 SH, 12 CH, 54 SAH and CAH).
Results: PTEN was focal positive for SAH, diffuse for CAH and for 1–2 cases of SH and CH. Ki-67 and PCNA were also very frequent in group SAH and CAH.
Conclusion: PTEN, Ki-67 and PCNA take part in the process of endometrial carcinogenesis following probably molecular pathways and determine the malignity potential of atypical hyperplasia of endometrium.

P-109

Struma ovarii with peritoneal implants.

Nada Touil; Néjib Ben Yahia; Leila Njim; Rym Hadhri; Houda Mahmoudi; Abdelfettah Zakhama; Adnène Moussa

Department of Pathology, Fattouma Bourguiba University Hospital, 5019 Monastir, TUNISIA

Background: Struma ovarii is an ovarian monodermal teratoma composed entirely or predominantely of thyroid tissue. It is a rare form of ovarian neoplasm which represents less than 3% of ovarian teratomas. We have experienced a rare case of struma ovarii complicated by peritoneal implants and report it with a review of the main histological findings and differential diagnosis of this entity.
Methods & Results: A 26-year-old female, with no significant medical history, complained for abdominal pain and fever. The pelvic ultrasound showed a left ovarian cystic mass. Surgical removal of this mass and of multiple peritoneal nodules was achieved.
The pathological examination of the cystic mass was consistent with a mature teratoma in which the thyroid tissue had overgrown all other tissues. No atypia or malignant features was identified. The peritoneal deposits were composed of benign thyroid tissue. This condition is termed "benign strumosis".
Conclusion: Struma ovarii is a rare ovarian tumour that is characterized by the presence of at least 50% of thyroid tissue on histologic examination. This tumour is generally benign and has an excellent prognosis. Its association with peritoneal implants is very uncommon and has no side effects.

P-110

Massive chronic intervillositis. A clinicopathological study of 21 cases

Abdelmajid Dhouibi; Leila Njim; Rym Hadhri; Néjib Ben Yahia; Houda Mahmoudi; Abdelfettah Zakhama; Adnène Moussa

Department of Pathology, Fattouma Bourguiba University Hospital, 5019 Monastir, TUNISIA

Background: Massive chronic intervillositis (MCI) is an infrequently recognized placental lesion thought to be of immunologic origin that has been associated with poor fetal outcome. It is characterized by a proeminent histiocytic infiltrate in the intervillous space. Here in, we describe clinical and pathologic aspects of 21 cases of MCI.
Methods: In this retrospective study we evaluated 21 cases of MCI diagnosed between 2004 and 2006. Perinatal outcome, other associated clinical features, histopathology and immunohistochemical aspects were assessed.
Results: Overall incidence of MCI among placental specimens submitted during the 3-year period of this study was 1%. Overall perinatal mortality rate was 28%. Six of 21 patients had spontaneous abortions (28%). Intrauterine growth restriction complicated 5 pregnancies (23%). Most case (71%) occurred in the third trimester. Characteristic placental histology included infiltration of intervillous space and occasional villi by mononuclear inflammatory cells withfibrin. Immunohistochemical staining showed an infiltrate composed predominantly of histiocytic, CD68 positive cells.
Conclusion: The mononuclear nature of the inflammatory cell infiltrate and its association with increased fibrinoid material suggests an immunological origin. Although uncommon, MCI is an important cause of recurrent spontaneous abortion and in some cases, loss at later gestational ages.

P-111

Bilateral ovarian serous borderline tumour in a four-year-old girl

Leila Njim; Nada Touil; Rym Hadhri; Néjib Ben Yahia; Houda Mahmoudi; Mohsen Belghith; Abdelfettah Zakhama; Adnène Moussa

Department of Pathology, Fattouma Bourguiba University Hospital, 5019 Monastir, TUNISIA

Background: Epithelial tumours of the ovary account forabout 15% of paediatric ovarian masses. Such tumours are extremely rare before menarche. The purpose of this report is to describe clinical and pathological aspects of bilateral ovarian serous borderline tumour (SBT) in a premenarchal girl and to discuss the approach to both treatment and outcome of this type of tumours.
Methods: We describe bilateral ovarian SBT in a girl aged 4 years. Data regarding clinical presentation, treatment, pathology, and outcome were collected from the medical record.
Results: The child presented with abdominal distension and discomfort. Ultrasound and CT scan revealed multiloculated cystic masses in both ovaries. Cysts were surgically removed, with preservation of normal ovarian tissue, and histopathological findings showed a SBT of both ovaries. The girl is well with no evidence of recurrence at a follow up period of 19 months.
Conclusion: Epithelial ovarian neoplasms are rarely seen in the paediatric population, especially in the first decade of life. These tumours, nearly always, are of low grade and stage despite their large size. To preserve fertility, conservative treatment,whenever feasible, is recommended.

P-112

Appendiceal metastasis from ovarian cancer

Doinita Radulescu; Simona Stolnicu; Sorin Dumitriu; Loredana Ungureanu

University of Medicine and Pharmacy"Gr.T.Popa" Iasi; University of Medicine and Pharmacy Tg. Mures. Romania

Ovarian cancer has a well-established widespread peritoneal dissemination. Although the surface of the appendix constitues less than 1% of the peritoneal cavity, it is suggested as a frequent metastatic site. The aim of this study was to detect microscopically appendiceal metastasis from ovarian cancer as a part of surgical staging and to evaluate the prognostic of these tumors. A total of 13 patients with ovarian carcinoma and appendiceal metastatis who had undergone appendectomy were retrospectively evaluated. We detected microscopic metastasis in only 8 cases. In conclusion, according to our findigs, the identification of the gross and microscopic appendiceal involvement, offers new clinicopathologic data used for surgical staging and routine appendectomy may be justified in all ovarian cancer patients.

P-113

A NEW CASE OF SPONTANEOUS COMPLETE HYDATIFORM MOLE COEXISTENT WITH TWIN NORMAL FETUS

Nejib BEN YAHIA(1); Leila NJIM(1); Rim HADHRI (1); Houda MAHMOUDI(1); Adnène MOUSSA(1); Zahra SAIDANI(2), Abdelfatteh ZAKHAMA(1)

(1)Department of Pathology, Fattouma Bourguiba University Hospital, 5019 Monastir, TUNISIA

BACKGROUND The association of Complete Hydatiform Mole (CHM) and normal twin fetus is a rare phenomenon. Its incidence is between 1/10 000 and 1/100 000 pregnancies. The aim of this report is to discuss the difficulty of clinical management, pathological diagnosis and the main differential diagnosis.

METHODS AND RESULTS A 21-year-old woman, gravida 2, para 1 (G2P1) with a history of spontaneous abortion, consulted at 21 weeks of spontaneous pregnancy. The ultrasound scan performed identified a normal viable fetus and normal placenta in association with a molar placenta. A medical interruption of pregnancy was indicated. Pathological findings of the placenta addressed to our department of pathology showed two separate placentas. The first was a normal placenta. The second was molar with obvious grap-like pattern. The main differential diagnosis was partial hydatiform mole; this hypothesis was rejected for two criteria: first the sharp separation between molar mass and normal placenta, second the absence of fetal malformation.

CONCLUSION The association CHM and normal twin fetus necessitate a precise prenatal diagnosis. The management of such pregnancy must be the result of possibility of further pregnancies, risks of medical complications of the molar pregnancy and the hope of the mother.

P-114 WITHDRAWN

P-115

PROLIFERATING TRICHILEMMAL TUMOUR AND EPIDERMOID CARCINOMA OF THE VULVA

Sonia García Hernández; Hugo Álvarez-Argüelles-Cabrera; José-Luis Carrasco Juan: Javier de la Torre*; Eduardo Salido Ruiz; Nieves Hernández León; Candelaria García Castro; Alejandro Brito García; Leticia Melgar Vilaplana; Lucio Díaz-Flores**

From Services of Pathology and Gynecology(*) and Unit of Investigation(**). Canary University Hospital. La Laguna. Tenerife. Canary Islands. Spain.

BACKGROUND The case of a patient with a proliferating tumour of the vulva (PT) with an exceptional location of the lesion is presented here. Its association with a metachronic epidermoid carcinoma (EC) in the same place suggests a possible etiopathogenic connection between the two processes.

METHOD The tissue samples from the biopsy, fixed in 4% formalin, were subjected to processing, inclusion in paraffin and usual sectioning, and stained with hematoxiline-eosine. The presence of DNA in the HPV 6, 11, 16 and 18 was evaluated by the PCR technique.

RESULTS A 78 year old patient presented a vulvar PT which developed into an EC in the same location four years later. The initial lesion histochemically consisted of a cutaneous structure with a multicystic formation without connection to epidermis, which showed a parietal epithelial proliferation with an abrupt intracystic keratinization, similar to that present in the external radicular sheath at the level of the isthmus of the hair follicle. Some koilocytic vacuolization cells of a viral appearance were observed, as well as similar changes to those focally observed in the posterior EC.

CONCLUSION The fourth case of PT of the vulva is reported here, which later developed into an EC, a connection which we do not have any previous experience, therefore suggesting a possible etiopathogenic relationship with the HPV.

P-116

Immunohistochemical profile of high-grade endometrial adenocarcinomas. Expression of p53, Ki67 and hormonal receptor status in hysterectomy specimens.

Irmgard Costa; Maria Rosa Escoda; Neus Combalia; Jesus Montesinos; Jordi Antoni; Manuel Corona; Mercè Rey

CENTRE DIAGNÒSTIC UDIAT. CORPORACIÓ PARC TAULÍ. SABADELL. SPAIN

Background: High-grade endometrial adenocarcinomas include different histological subtypes. We analyzed their immunohistochemical profile in order to better characterize them and to detect additional prognostic factors.

Method: Immunohistochemical determination of Progesterone (PR) and Estrogen (ER) receptors, p53 and Ki67 in 25 high-grade endometrial adenocarcinomas, with clinicopathological data. The immunoreactive index (IRI) = intensity of staining (0 to 3) x proportion of positive tumor cells (0, 1:1–10%, 2:11–50%, 3:51–80%, 4:>80%): IRI= 3:7–12, IRI=2:4–6, IRI=1:<4.

Results: We collected 9 grade (G) 3 and 2 G2 FIGO endometrioid (EC), 9 serous (SC), 3 clear cell (CCC) and 2 mixed adenocarcinomas (MC) (1 EC/CCC and 1 EC/SC). 1 (G2 EC) and 5 adenocarcinomas (one G2 and one G3 EC, one SC, and the EC component of the MCs) presented an IRI RE and RP=3, respectively. Ki-67 was highly expressed in 11 adenocarcinomas (5 SC, 2 CCC, 3 G3 and 1 G2 EC) and in the serous component of one MC. p53 was highly expressed in 8/9 SC, in 2/3 CCC and in 2/9 G3 EC. 4/11 patients with EC died with disease (DWD) (one G2, pT3aN0, IRI ER 0 and PR=2; and 3 G3: one with with vascular invasion (VI), one IRI Ki67 and p53=3, and one with all IRI=1, pT3aN1 and VI), all with recurrences. One G3 EC alive with disease (AWD) presented recurrence, VI and an IRI Ki67=3. 6/9 patients with SC DWD (all IRI p53= 3 and 4 with recurrences). Two patients were alive without disease (one IRI p53=1 and one pT1aN0) and one AWD (IRI PR=3). 2 of 3 patients with CCC DWD (with recurrence, VI and IRI Ki67=3). The patients with MA showed no recurrences, one alive and one death, both without disease.

Conclusions: Additional immunohistochemical detection on high-grade endometrial adenocarcinomas can better subtipify them and could have prognostic significance.

P-117

THE HISTOPATHOLOGIC PROFILE OF MIXED TYPES OF ENDOMETRIAL CARCINOMA

Raluca Balan; Cornelia Amalinei; Irina Draga Caruntu

Department of Normal and Pathologic Morphology, University of Medicine and Pharmacy, Iasi, Romania

Background. Endometrial carcinoma may present combinations of two or more such neoplasms of the endometrium. A mixed carcinoma has at least one other component comprising at least 10% of the tumor. Method. Our study presents 7 cases of mixed endometrial carcinomas in women with age between 47 and 64 years old. All patients presented clinically abnormal vaginal bleeding and all were treated with total abdominal histerectomy and bilateral salpingo-oophorectomy. The specimens were fixed, paraffin-embedded and routinely stained with H&E. Immunohistochemical techniques were performed for p53 and BCL-2. Results. The histopathological diagnostic was: mixed endometrioid and serous carcinoma of the endometrium (4 cases), mixed endometrioid and serous carcinoma with areas of clear cell carcinoma (2 cases), and mixed endometrioid and clear cell carcinoma (1 case). All these tumors presented more than 25% of the serous component. The clear cell carcinoma was more than 10% in 2 cases and more than 25% in 1 case. The endometrioid component presented in typical form or as villoglandular carcinoma, was well-differentiated, FIGO grade 1. Because of the clear cell and serous components, the endometrial carcinomas were overall high grade, deeply invasive, and in an advanced stage. Immunohistochemically, the tumors presented less frequent expression of p53 in clear cell component than in serous carcinoma. The BCL-2 protein expression was higher in endometrioid than in serous and clear cell components. Conclusions. All mixed types of endometrial carcinomas presented in this study behave as aggressive carcinomas because of the significant percent of serous and clear cell components. The loss of BCL-2 expression was associated with other features of poor prognosis as depth of invasion, FIGO stage, and aggressive cell types.

P-118

MALIGNANT VAGINAL NEOPLASMS

Benedicta Caserta, Daniel Mazal, Mabel Cedeira, Valentina Porro

Autors:Laboratory of Pathology and Cytology. Woman's Hospital Pereira Rossell. MSP. Uruguay

INTRODUCTION AND OBJECTIVE: Malignant vaginal neoplasms (MVN) are uncommon lesions, that has been reported as representing a range between 2 and 3% of all genital malignancies. We analysed histological type, origin, and the overall result of our revision were compared with those reported previously.

MATERIALS AND METHODS: We reviewed cases of patients with complete clinical data and slides for revision wich includes pathological evaluation, correlation with clinical data, personal history, and vaginal citology when available.

RESULTS: We studied 47 cases of MVN. As already described, bleeding was the most frequent clinical finding. Macroscopically, neoplasms appeared either as vegetant polypoids or pigmented lesions, blind fistulas or ulcers. Frequently neoplasms emerged as tumors at the vaginal cul-de-sac.

In 43 cases lesions were secondary (91.5%) and 4 primary (8.58%). Fifteen cases were squamous carcinomas, 1 clear cell carcinoma, 19 adenocarcinomas, 1 choriocarcinoma, 7 poorly differentiated carcinomas, 1 primary melanoma, 1 mixed sarcoma and two primary pure sarcomas. The most frequent primitive squamous origin was the cervix whereas the vulva was identified as the second most common origin. Adenocarcinomas were identified as secondary tumors being the uterus, the cervix, the ovary and the rectum the location of the primary lesion.

The primary MVN were rare (malignant melanoma, poorly differentiated carcinoma lymphoepithelioma like, and two sarcomas). Dissemination can be due to a spread by direct extension (upper third), vascular embolism (lower third), or by directly implantation (often in anterior wall).

CONCLUSIONS: Among primary genital tumors, MVN are very infrequent lesions. Therefore, the possibility of a secondary origin must be first ruled out. The vaginal topography of tumors is related with to the its origin as well as with its way of dissemination.

P-119

PIK3CA, p53 and E-cadherin alterations in high grade endometrial carcinomas

L. Catasús, A. Gallardo, M. Cuatrecasas, Pons C, and J. Prat

Department of Pathology. Hospital de la Santa Creu i Sant Pau, Autonomous University of Barcelona, Spain

Background: Mutations in the *PIK3CA* oncogene are frequently identified in endometrioid endometrial carcinomas (EEC). We have recently confirmed coexistence of *PIK3CA* mutations with MI and mutations in *PTEN, CTNNB1, K-RAS*, and *B-RAF* in EEC, providing evidence that tumors carrying *PIK3CA* mutations are often high-grade carcinomas associated with myometrial invasion. We wanted to determine the impact of *PIK3CA* mutations in high-grade carcinomas (EECs, mixed, and NEECs).

Design: Genomic DNA was obtained from 59 high-grade endometrial carcinomas (29 grade 3 EEC, 6 serous (SC), 4 clear cell (CC), and 20 mixed (9 EC-CC, 7 EC-SC, and 4 CC-SC). Mutational screening for *PIK3CA* (exons 9 and 20), p53 (exons 5–8), *PTEN*, and *K-RAS* were performed. Microsatellite instability (MI) for five different loci (BAT25, BAT26, D2S123, D5S346, and D17S250) was also done. Tissue-arrays were performed for immunohistochemical analysis of p53 and E-cadherin. Clinicopathologic data was obtained.

Results: *PIK3CA* mutations were detected in 34% (20/59) of cases distributed in all histologic groups. Exon 20 mutation occurred in 90% (18/20) of cases. p53 overexpression was detected in 35% (18/51) being more frequent in NEEC, and mixed tumors ($p=0.037$). *PIK3CA* mutations coexisted with p53 overexpression in 11% (6/51) of either pure EEC or mixed carcinomas with endometrioid component. We found that *PIK3CA* mutations coexisted with *PTEN, K-Ras* mutations, and MI in pure EEC but not in mixed carcinomas with endometrioid component. Lack of immunoexpression of E-cadherin was detected in 14% (7/48) of cases and coexisted with p53 alterations more frequently in NEEC and mixed tumors.

Conclusions: Our results show that exon 20 PIK3CA mutations are frequent in high grade endometrial carcinomas of any histological type, whereas p53 overexpression and loss of E-cadherin immunoexpression are more frequent in NEEC, and mixed tumors. Our results confirm the role of PIK3CA as an alternative pathway in high-grade endometrial carcinomas.

P-120

Deregulation of Stathmin/OP18 in ovarian carcinomas is not due to its direct upstream regulator PAK1.

M.Romero-Sánchez, R.Nadal, C. Pons, M.Cuatrecasas, A.Barnadas, J.Prat.

Department of Pathology. Hospital de la Santa Creu i Sant Pau, Autonomous University of Barcelona, Spain

Background: Rho GTPases play an important role in cancer by regulating cell motility and invasion. PAK1 and Stathmin control the microtubule polymerization and filopodia emission. The role of these two proteins in ovarian metastasis deserves further research.

Design: Tissue-microarrays (TMA) from 70 FIGO stage II-IV ovarian carcinomas (51% serous, 12% endometrioid, 13% poorly differentiated, and 24% clear cell carcinomas) treated with CBCDA-Paclitaxel. TMAs included normal tissue, primary and metastatic tumor. Tumors were stratified into 2 groups according to onset of recurrence after chemotherapy: sensitive > 6 months; and resistant < 6 months. Immunohistochemistry (IHC) for PAK1 and OP18/Stathmin were performed.

Results: We found a statistically increase of Stathmin protein levels in tumor ($p<0.001$) and metastasis ($p<0.001$) in comparison with normal tissue. Stathmin and PAK showed low correlation only in metastatic tumors ($p=0.05$, $r=0.26$). We found a statistical increase in Stathmin levels in resistant metastasis ($p=0.05$), however no signif-

icant differences between resistant and sensitive tumors (p= 0.18) nor metastasis (p=0.45) were found in PAK1.
Conclusion: Deregulation of Stahmin in ovarian tumors and metastasis is not due to its direct regulator PAK1, other collateral proteins may be affecting Stathmin/OP18 protein levels in ovarian carcinogenesis/metastatization.

P-121

Epithelial-mesenchymal transition (EMT) in early stages of endometrioid endometrial carcinomas

N. Montserrat, L. Catasús, J. Pena, A. Gallardo, M. Cuatrecasas, X. Matias-Guiu*, and J. Prat
Departments of Pathology. Hospital de la Santa Creu i Sant Pau, Autonomous University of Barcelona, and Hospital U Arnau de Vilanova, University of Lleida. Spain*

Background: Epithelial-mesenchymal transition (EMT) is involved in the development of invasion and metastasis. Twist is a transcription factor that regulates the EMT program. We investigated some of the EMT genes and other molecular alterations in early stages of endometrioid endometrial carcinomas (EEC).
Design: Genomic DNA was obtained from 26 early stage EEC (8 Ia, 4 Ib and 14 Ic). Ic samples both from surface and myoinvasive fronts were taken. Mutational analysis for *PIK3CA* (exons 9 and 20), *PTEN*, *K-RAS* and *CTNNB1* were performed. Loss of heterozygosity (LOH) at the PTEN locus was measured by analyzing 3 different microsatellite markers (D10S579, D10S532, D10S2491). Microsatellite inestability (MI) for 5 different loci (BAT25, BAT26, D2S123, D5S346 and D17S250) was also done. Tissue-arrays for immunohistochemical analysis of Twist, E-cadherin and vimentin was done. Expression of Twist, E-cadherin, Snail, and HMGA2 was evaluated by RT-PCR. Clinicopathologic data was obtained.
Results: LOH of *PTEN* (5%), MI (38%) and mutations of *PTEN* (62,5%), *KRAS* (12,5%) and *PIK3CA* (exon 20) (12,5%) were found in Ia carcinomas. LOH of PTEN (14,5%) and mutations of *PTEN* (58%), *KRAS* (14,3%), *CTNNB1* (7,15%) and PI3KCA (exon 9 and 20) (14,5%) were detected in Ic cases both in surface and myoinvasive fronts of the tumor. Exons 9 and 20 *PIK3CA* mutations (50% each) were found in Ib tumors. *KRAS* mutations coexisted with exon 8 *PTEN* mutations in all cases (p= 0.00). Twist, vimentin, HMGA2, and SNAIL expressions were found to be increased in the myoinvasive front compared with normal tissue (p<0,05).
Conclusion: Although molecular alterations were similar in Ia, Ib, and Ic carcinomas. The expression of EMT markers was higher in the myoinvasive front.

Infectious diseases

P-122

Intralesional IgA in mice infected with Leishmania mexicana

Marina Calcagno; Zulay Maizo de Segnini; Silverio Díaz
Laboratorio de Inmunología de Parasitosis, Departamento de Biología, Facultad de Ciencias, Universidad de Los Andes. Mexico

Background The presence of immunoglobulin deposits in leishmaniasis lesion is a striking histological feature in man and experimental animals infected with *Leishmania* parasites. Previously, we described the immunocytochemical pattern of intralesional antibody isotype profiles (IgG1–4 and IgA) and plasma cells in human patients with localized American cutaneous leishmaniasis from Mérida state in Venezuela. To further characterize the presence of IgA in the lesion, we have evaluated this isotype in lesions of mice experimentaly infected with *Leishmania mexicana* (MHOM/VE/72/AZV).
Methods The presence and distribution of IgA immunostained deposits, in skin biopsies from inoculated footpads of infected resistant C57BL/6 and susceptible BALB/c mice were compared to the corresponding contralateral non-inoculated footpad's skin from the same animal, after 8 weeks of infection, using two different antibodies directed against mouse IgA by immunocytochemical procedures.
Results IgA deposits were detected in all inoculated mice footpads active lesions, from both mice strains, but they were absent in the skin of the control contralateral non-inoculated footpads. The pattern of IgA distribution in the lesion, of both mouse strains, with the two distinct IgA antibodies was the same. IgA was found in different components of the infiltrated dermis (connective tissue, macrophages, plasma cells, giant cells, granuloma, blood vessels and parasites) and in the ulcerated epidermis of BALB/c mice.
Conclusion The domonstration of IgA immunostaining in plasma cells of mice with active lesions together with the absence of IgA deposits in non-infected skin gives further support to the concept of local production of IgA. The nature of the antigen recognized by IgA in the leshmaniasis lesion appears to be non-specific, since the immunoreactivity observed with rat or goat anti mouse IgA, albeit amastigotes localization in other components of the skin lesion.

P-123

Hpv prevalence in hyperplastic tonsillary and adenoid tissues in children and young adults in Turkey

Huseyin Baloglu; Atila Gungor; Aptullah Haholu; Zafer Kucukodaci; Gozde Yasayan; Simge G Orscelik
Gulhane Medical Academy, Haydarpasa teaching Hospital, Istanbul, Turkey

Background: The aim of the study was to determine the frequency of HPV and genotypes in children and young adults which suffered for upper airway obstruction and treated with tonsillectomy and/or adenoidectomy.
Method: Archival resection materials of 258 patients threated between 2003–2007 were retrived for HPV detection and typing. Six patients were excluded because of inadequate quality of DNA extraction. Age range of remaining 252 patients was 5 to 21 (11.94±4.20). MY/GP consensus primers were used for screeing PCR. Four different set of primers covering 18 HPV types were used for M-PCR HPV typing.
Results: Sixteen of 252 samples namely, 9 of 114 tonsillectomy, 4 of 87 adenoidectomy and 3 of 51 tonsiloadenectomy tissues were found to be containing HPV virus genome by screeing PCR (6.34%). HPV-16 was dominant genotype and found in 8 tonsillectomy, 2 tonsiloadenectomy and, and 1 adenoidectomy. HPV-6 was detected in 3 tonsiloadenectomy and 1 tonsillectomy materials. HPV-31 genome was found only in 1 samples. None of the samples in the series were found to be containing multiple HPV genotypes.
Conclusion: HPV prevalence in children and young adults which suffering upper airway obstruction because of non-tumoral tonsillary and/or adenoid over growth were found 6.34% in Turkish population. HPV-16 was encountered as the most frequent genotype.

P-124

HISTOLOGIC AND ELECTRONMICROSCOPIC STUDIES IN HIV-1 ENCEPHALOPATHY

Tchavdar Georgiev[1], Adrian Paloff[2] , Dimka Hinova-Palova[2], Todor Todorov[1], Alexandar Alexandrov[1], Stanislav Hristov[1], Georgi Gergov[1]
[1] Center of Pathology and Forensic medicine; [2] Chair of Anatomy, Medical Faculty - Sofia, Bulgaria

The HIV-1 retrovirus attacks directly CNS in HIV-1 patients. The light- microscopic studies of the brains among 52 mortal cases with AIDS exhibit brain cortex atrophy, perivascular mononuclear cell infiltrates and single foci of neuronophagia. Parallel ultrastructural findings in 10 cases proved to be macrophages containing viral particles in their surface and extracellular spase. The virions measuring 100–120 nm in diameter reveal circular envelopes transected by inner lucid cores. Subplasmalemmal linear densities are prominent featuring the virus-associated cells. The visualized myelin-like bodies in the cytoplasm of the activated macrophages is a sign of brain degeneration. Giant mononuclear cells are identified in adition.

P-125 WITHDRAWN

P-126

Seroprevalence of Blood-Borne Infections Among Blood Donors in Venezuela, 2001–2002

Jesús A. Benitez,1; and Alfonso J. Rodríguez-Morales,2
1Ministry of Health, Maracay, Venezuela; 2Universidad de Los Andes, Trujillo, Venezuela

Objectives: From the data collected at the Ministry of Health from whole nation public and private blood banks (BB) find out the proportion of blood units discarded for being seropositive HBV, HCV, HIV, syphilis and *Trypanosoma cruzi*, and the seroprevalence of these infections among their donors. *Methods*: ELISA serological testing was done with 715,393 donors seen at 535 blood banks between 2001 and 2002. Samples that were repeat reactive (RR) with the ELISA underwent supplementary Western blot (WB) testing. *Results*: Of the 715,393 blood banks donors, 9,294 of them (1.3%) were positive for syphilis (VDRL), 6,107 (0.85%) for HBV (anti-HBc), 4,825 (0,67%) for *T. cruzi*, 3,859 (0.54%) for HCV and 1,870 (0.26%) for HIV. *Conclusions*: Although syphilis or *Treponema pallidum* infection was the most important blood-borne disease found in this study, the seroprevalence found is lower than others reported in other countries in the region (e.g. Goiânia, Brazil, 1989, 4.1%). For HBV and HCV, the seroprevalence estimates were also similar than those found in other countries in the region (such as Río de Janeiro, Brazil, where in 2005 the anti-HBc was 2.05% and 0.79% in 2004 for HCV), indicating high rates of infection by HBV and HCV and a persistent risk of HBV and HCV transmission by transfusion. For Chagas disease is also lower than others reported in other countries in the region (e.g. Goiânia, Brazil, 1989, 3.3%). Finally for HIV the found seroprevalence is similar to that reported in Mexico (Irapuato, Mexico, 2003, 0.24%). But as seen herein, those seroprevalences are regional, and our report is nationwide. Further epidemiological research is expected.

P-127

Prevalence of Chlamydia penumoniae in paediatric populations of Alto Tiete region (Brazil) and the clinical implications of these infections.

Leila Moussa Costa; Edson Costa; Marcelo Fabiano Rodrigues; Sonia Maria Almeida
Universidade Braz Cubas. Brazil

Introduction: Chlamydia pneumoniae is a human respiratory tract pathogen. Seroepidemiological studies indicate that C. pneumoniae infection is most common in school-aged children and infrequently detected in younger children.
Objective: The aims of this study were to further elucidate the prevalence of C. pneumoniae in paediatric populations and to describe the clinical implications of these infections.
Patients and Methods: The study population consisted of 154 children of Alto Tiete region (Brazil) with respiratory tract diseases, 231 presumed healthy children at day-care, 44 children undergoing adenoidectomy and 886 children from a population based cohort. Family members to infected day-care children were investigated. The laboratory methods used were polymerase chain reaction (PCR) on specimen from upper respiratory tract, serology by micro-immunofluorescence (MIF), and immunohistochemistry (IHC) on adenoid tissue specimen. Personal data and medical history were obtained by the means of questionnaires and by the study of patient records.
Results: In children younger than five years, the prevalence of C. pneumoniae was 11% as detected by PCR. This prevalence started to increase with increasing age from two years of age. The corresponding increase in serology as detected by MIF started at the age of four years. The prevalence at day-care centres varied from 8 to 33%. Both PCR and MIF underestimated the prevalence of C. pneumoniae detected by IHC. Families to infected children were investigated: mothers were more often infected than fathers were.Most C. pneumoniae infections in small children were confined to the upper respiratory tract. These infections were usually mild or asymptomatic. Symptomatic disease may be of prolonged nature. No subsequent illness after C. pneumoniae infection was detected at follow-up after four years. In general, no association between C. pneumoniae and asthma was found, but C. pneumoniae may be of importance for asthma in some susceptible individuals. Previous C. pneumoniae infection reduced the risk for later atopy.
Conclusion:The C. pneumoniae is a common finding in small children and most often causes relatively mild disease. If the acquisition of this infection early in life will have any implications for future health remains to be investigated.

P-128

Sinonasal mucormycosis: A report of 3 cases

Bellil Selma; Faten Limaiem; Ines Chelly; Amina Mekni; Haifa Azzouz; Khedija Bellil; Slim Haouet; Nidhameddine Kchir; Moncef Zitouna
Hospital La Rabta Bab saadoun Tunis-Tunisia

Background: Mucormycosis, also known as "zygomycosis" or "phycomycosis" is a rare opportunistic infection caused by fungi that are commonly found in soil and among decaying vegetation. It is an aggressive and often fatal disease which occurs mainly in patients with immune disorders. It involves the rhinofacial-cranial area, lungs, gastrointestinal tract, skin and less commonly other organs.
Aim of study: To highlight clinicopathologic features of this opportunistic infection with special emphasis on prognosis and differential diagnosis.
Case Reports: we report 3 new cases of sinonasal mucormycosis that occurred in 3 female patients aged between 40 and 68 year old with a medical history significant for diabetes mellitus, who presented with complaints of nasal obstruction, purulent rhinorrhea and postnasal drip. The biopsy from the nasal mucosa revealed the presence of aseptate, broad and pleomorphic hyphae with right-angled branching which are typical of mucormycosis evidenced by special stains for fungi. In all patients, CT scan showed involvement of ethmoid and maxillary sinuses along with retro-orbital extension. The three patients were managed with lipid complex amphotericin B coupled with repeated surgical debridement. During the 3-month follow-up period, one patient died whereas, the other patients are still alive.
Conclusion: Greater awareness of this opportunistic infection and rapid clinical intervention have resulted in improved prognosis. Aggressive treatment with antifungals, antibiotics and wide debridement are the key to successful management of sinonasal mucormycosis.

P-129

Bone marrow in acquired immunodeficiency syndrome: a histologic, hematologic and microbiologic study

Seema Sharma; Sharad Goel
Sanjay Gandhi Postgraduate Institute of Medical Sciences, Lucknow, India

Background: Bone marrow (BM) examination in HIV infected patients is performed for a variety of indications including pyrexia of unknown origin, diagnosis of cytopenia and for diagnosis or staging of lymphoma. BM studies offer the possibility of providing relatively rapid information about the presence of opportunistic infections in

addition to information about co-existent hematologic abnormalities.

Materials and Methods: We retrospectively evaluated 52 bone marrow trephine biopsies from HIV-infected persons in last five years. Fever of unknown origin, unexplained anemia or cytopenia were main indications for bone marrow studies.

Results: Seventy six percent marrow biopsies were normocellular or hypercellular; 24% were hypocellular. Marrow plasma cells were increased in 67% of patients. Histopathological examination of BM alone led to the diagnosis of specific condition in 17 (32%) patients (granuloma 11 cases, 2 cases of Histoplasma capsulatum and megaloblastic anemia and 1 case each of high grade B cell lymphoma and Idiopathic thrombocytopenic purpura). Ziehl -Neelsen stain for acid-fast mycobacteria was positive in 5 trephine biopsies. In 20 (38%) cases with pyrexia of unknown origin infectious pathology could be identified on histopathologic and microbiologic studies. The commonest being Mycobacterium tuberculosis in thirteen cases and Mycobacterium avium intracelluare in three cases, two cases of Histoplasma capsulatum and one case each of Cryptococcus neoformans and Candida species. Ninety four percent patients were anemic with iron studies showing a pattern consistent with anemia of chronic disease in majority of these. Forty four percent patients showed leucopenia, 51% had thrombocytopenia and 94% showed markedly reduced CD4+ T lymphocytes

Conclusion: Bone marrow biopsy may be a useful method for early diagnosis of opportunistic mycobacterial and fungal infection in patients with HIV infection presenting with persistent pyrexia. This may allow the treatment to be initiated before microbiological confirmation especially in Indian scenario.

P-130

Resolution of refractory TTP after successful treatment of a fulminant colitis due to Entamoeba histolytica.

Forteza AV*; Ballester Ruiz C **; Visvesvara GS*; Muncunill Ribas J**; Besalduch Vidal J**; Couce Matovelle ME***

* *Department of Pathology. Hospital Universitario Son Dureta. Palma de Mallorca. Spain*

Background We report the case of a 33-years old female patient with history of long standing refractory TTP who recently presented with an acute abdomen.

Case description The patient was most recently hospitalized to evaluate new purpuric marks on her legs, with no additional symptoms. Initial examination revealed serum platelets lower than 5000. She was started on plasmaferesis and steroid therapy.

A week later, the patient suffered a sudden thoracic pain and dyspnea with haemoptysis. Thoracic plain X-ray showed bilateral infiltration that was interpreted as TRALI (Transfusion related acute lung injury) and treated with oxygen therapy. During her treatment the patient presents with acute abdominal symptoms indicative of severe peritonitis, potentially due to cecal perforation, and required emergency surgery. The presumptive diagnosis was that of steroid induced colitis with cecal perforation. Pathology examination of the right hemicolectomy specimen, revealed the presence of numerous amoebic forms, compatible with *E. histolytica, associated* with multifocal ulceration and perforation of the bowel wall. She received treatment with metronizadol and paromomicina with complete recovery. Furthermore, at ten months of follow up, there is no evidence of TTP.

Conclusion This is a very interesting and challenging case, since is the first described of a refractory TTP which resolves after treatment for E. histolytica infection. Amoebic infection needs to be considered as a potential cause for TTP. The pathobiology of this association requires additional studies.

P-131

Primary ovarian carcinosarcoma: a case report and review of the literature

Amel Trabelsi; Wided Stita; Soumaya Rammeh; Atef Ben Abdelkader; Sarra Mestiri; Moncef Mokni; Sadok Korbi

Departement of Pathology, Farhat Hached Hospital, Sousse, Tunisia

Background: Ovarian carcinosarcoma is a rare malignant neoplasm characterized by an admixture of malignant epithelial and stromal elements. This tumor grow very rapidly and is usually in advanced stages when diagnosed. Most patients are postmenopausal. About 77 per cent of the patients are dead of their disease within 1 year.

Method: We report a case of a primary ovarian carcinosarcoma in a 74 years old woman and we review the clinicopathological features and prognostic factors in ovarian malignant mixed Mullerian tumors.

Results: The patient presented with acute abdominal pain. Clinical examinaion and computed tomoraphy revealed a left-side pelvic mass. The patient underwent an exploratory laparotomy and a right ovariectomy. Histological examination of operative specimen revealed malignant epithelial and mesenchymal components. The patient had than total hysterectomy with left annexectomy. Despite postoperative chemotherapy, she died from the disease 8 months after surgery.

Conclusion: Ovarian carcinosarcoma is a distinct entity with a poor overall prognosis. The management of this tumour is difficult and randomised trials are needed to

accrue sufficient patient numbers and demonstrate optimal therapy.

P-132

SIMULTANEOUS EVALUATION OF T LYMPHOCYTE SUBPOPULATIONS IN THE LIVER AND IN PERIPHERAL BLOOD CELLS OF HCV, HBV-CHRONIC INFECTED PATIENTS

Georgeta Butur1;M. Ceauşu1,2;Florina Vasilescu1; Cristina Iosif1; Camelia Dobrea1,2; Dana Terzea1,2; Maria Neagu1;Alina Georgescu1;Florin Andrei1; Carmen Ardeleanu1,2

"VICTOR BABES" NATIONAL INSTITUTE. ROMANIA

T lymphocytes population are believed to be involved in the immunopathogenesis and evolution of chronic viral hepatitis.

In this study, we evaluated both intrahepatic (by immuno-histochemistry) and peripheral blood (by flow cytometry) T lymphocytes CD3+, CD4+ and CD8+, in 15 HBV and 38 HCV chronic infected patients, serologically proven. Simultaneously, histological lesions were assessed.

In peripheral blood, CD4+ T lymphocytes had increased values in HBV infection, while in HCV infection the values were normal/slightly increased. Compared to the average of normal values (41.5%) of CD4+ lymphocytes from healthy donors (HD) we have observed an increased tendency (~10%) of this subpopulations in case of HBV infection, while for the HCV infection, the values were almost normal. CD8+ lymphocytes presented a significant decrease in both types of chronic viral infections. Compared to the normal average values of 35.5% of CD8+ T cells from HD we have noticed a decreased value (~10%) for this subset in HBV and HCV infection.

At hepatic level,comparative statistic analysis between CD4+ and CD8+ T cells, in case of HBV chronic infection demonstrated a reverse proportion statistically significant ($r=-0.7$, $p=0.05$), the increasing number of CD4+ T cells being associated with the decreasing number of CD8+ T cells. In HCV chronic infection approximate 80% of cases have shown a low positive percentage of CD8+ T cells (no more than 5–15% cells from inflammatory infiltrate); no correlation between T cells subsets was noticed at hepatic level. It was found a correlation between intrahepatic CD8+ T lymphocytes and the severity of histological lesions. The imbalance of T lymphocytes subpopulations, especially CD8+ cells, may be associated with failure to clear the virus and a chronic course of disease, facilitated the liver damage.

P-133

Fine needle aspiration biopsy in the Hospital Central de Maputo, Mozambique

C. Carrilho, M.R. Ismail, C. Lorenzoni, F. Fernandes, M. Amigo, E. Galano, I. Rodriguez, J. Ordi

Departments of Pathology, Maputo Central Hospital, Universidad Eduardo Mondlane, Maputo, Mozambique and Hospital Clinic, University of Barcelona, Spain

Background: Fine needle aspiration (FNA) biopsy is an important adjuvant to the diagnosis of a palpable lesion which often permits the complete assessment of patients. There is limited information on the use of this technique in sub-Saharan Africa. The main objective of this study was to determine the clinical benefit of a FNA service at a tertiary referral hospital in Maputo, Mozambique.

Methods: All FNA biopsies performed at the Hospital central de Maputo during a whole year (January-December 2006) were retrospectively reviewed and analyzed.

Results: A total of 2479 FNA biopsies were performed during this period. 1599 (65%) were females and 874 (35%) males. Most biopsies were performed in children (14.5%) or young to middle aged adults (56.8%). Lymph nodes (43%), breast (23%), soft tissues (15%), thyroid (4%), salivary gland (3%) and liver (3%) were the most frequently biopsied organs. In the lymph nodes, granulomatous inflammation/tuberculosis (38%) and reactive hyperplasia accounted for 65% of the diagnoses, whereas only 2% of metastatic carcinomas were identified. Breast lesions were predominantly benign (88%). Overall, only 10% of FNA-biopsy specimens were malignant.

Conclusions: Benign conditions and particularly granulomatous diseases/ tuberculosis, probably related to HIV infection/AIDS, account for a significant number of biopsies, whereas malignant diseases represent only 10% of the aspirations. Our study shows the clinical benefit and cost-effectiveness of FNA services in a tertiary hospital in sub-Saharan Africa.

Molecular Pathology

P-134

Gene networks common to cancer stem cell status and malignant progression

Timothy M. Thomson; Toni Celià; Óscar Meca; Juan José Lozano; Nuria Rubio; Julia Calvo; Jerónimo Blanco; and Pedro L. Fernández

Institut de Biologia Molecular de Barcelona, CSIC, Barcelona, Spain

Malignant progression in cancer is closely linked to the emergence of populations of cancer stem cells (CSCs) endowed with capabilities for unlimited self-renewal, survival under stress, and establishment of distant metastases. By high-throughput transcriptome analysis, we have observed that cancer progression and CSC-like populations are associated with a limited number of tightly clustered gene/protein networks. The most significant progression-associated networks control (a) mitotic transitions and checkpoints, (b) DNA replication, and (c) DNA damage recognition and repair. The activation of these networks is associated with malignant progression and poor prognosis in most, if not all, solid tumors, independent of their tissue of origin. Inappropriate activation of these networks may provide unifying molecular and mechanistic explanations for the emergence and maintenance of metastatic cancer stem cells, and thus the aggressive phenotype of the majority of tumors.

P-135

Comparison of Formalin and Finefix in Preserving DNA Material in Small Biopsies.

Fatemeh Mahjoub; Abdolmajid Zarei; Issa Jahanzad; Soudabeh Derakhshandeh.
Tehran University of Medical Sciences. Iran.

Aim: Formalin is a routine fixative in surgical pathology wards. Although morphologic assessment is very desirable in formalin fixed tissues but DNA and RNA are not preserved well and molecular studies can not be performed with reliable results. In this study we wanted to compare DNA preservation of a newly introduced alcohol based fixative with formalin in small biopsies.
Materials and Methods: Seventy small gastric biopsies taken in endoscopic ward was put in formalin and finefix in equal number. Standard processing was performed for two groups. DNA extraction and conventional PCR for Beta globulin gene (amplicon length: 256 bps) was performed for each case. Statistical analysis with Chi – square test for comparison of two groups was performed.
Results: In formalin fixed group, 20 of 35 specimens show Beta globulin band, but 30 out of 35 finefix group revealed this band. The difference between these two groups in preserving DNA for this gene is statistically significant (p value: 0.008).
Discussion: Although formalin is a good preservative for morphological purposes but molecular studies especially in small biopsies is not desirable and other fixatives such as finefix may be substituted.
Keyword: formalin, finefix, fixative, molecular studies, small biopsies.

P-136

The role of NKG2d and MICA genes in susceptibility to cervical cancer

Armando Méndez.Javier Guerrero, Salvador Huerta, Guadalupe Alcantar
Laboratorio de Patologia Experimental Facultad de Medicina,Universidad Veracruzana. Mexico

Cervical intraepithelial carcinoma represents the precursor of invasive neoplasias.This concept is of great importance because it represents morphological abnormalities and molecular characteristics. These are typical changes in malignant neoplasias when they have been associated with mutational viral lesions, even though these high grade types are not clinically apparent.The MICA gene expression has a restricted tissue distribution, and it is transcribed in epithelial cells when the protein is constitutively expressed in surface cervical cells.
MATERIAL AND METHODS: We have studied 167 patients in the hospital`s displasia clinical department.These patients were subjected to colposcopy, citology and biopsy. Of the total number of patients, fifteen were diagnosed using PCR and by immunocytochemically P16 as having papova viral lesions.
In these fifteen patients, MICA gene polimorphism was studied with PCR.SSCP technique which encoded allelic variants of MICA by polimorphisms in exons 2,3,and 4. This encoded the extracellular protein domains. This has led to the concept that MICA is a product of a marker of epithelial cells stress. This is consistent with induced virus where MICA proteins are incremented in the cell's surface. A total of 20 combinations of sense and antisense primers were selected for the analysis of MICA alleles 001–016. The putative MICA alleles was recognized, and the predicted size of PCR products studied in the 15 patients with VPH lesion.
The polymorphism of NKG2D gene was studied in these fifteen patients to determine the function of CD8 and NK cells and the capacity to destroy the host cells that express MICA.

P-137

Obtention and typification of prostate carcinoma explants and primary cultures

Julia Calvo; Daniel Benítez; Ramón Vilella; Eva Fernández; Timothy Thomson; Pedro Luis Fernández
Hospital Clínic de Barcelona - Institut d'Investigacions Biomèdiques August Pi i Sunyer. Spain

Background In vitro studies on prostate cancer are mainly based on commercially available cell lines obtained from metastatic implants or artificially transformed normal

prostate epithelium such as PC3, LNCap, RWPE1 and RWPE2. Therefore, extrapolation of results obtained from such material to hormone-dependent primary tumours can be questionable. Thus, obtention and use of tumour explants and derived cell lines could be and important tool in molecular studies on prostate carcinoma.

Method Thin fresh tissue sections from radical prostatectomies with identifiable tumours were washed and cultured in serum-free medium supplemented with androgens. Of them, 10 primary cultures of epithelial cells survived more than one month and were subjected to several culture passes. RNA and DNA were extracted and CGH and 8 K Affymetrix Human Focus microarray analyses were performed. Further typification was carried out with immunocytochemistry for several markers including CD133.

Results Unsupervised cluster analyses of our primary cultures showed a relatively common profile with overexpression of basal/stem cell markers, which was very different from that of commercial cell lines and primary source tumours. Immunohistochemical expression of stem cell markers such as CD133 was also observed.

CGH analysis did not show significant structural abnormalities in 4 cases analysed.

Conclusion Contrarily to initial expectations, the primary cultured obtained from prostate cancer did not show evidence of malignant transformation, with scarce or no structural abnormalities, but and overall resemblance to basal/stem cells, whose RNA profile is very different to that of commercially available malignant prostate cell lines. We believe that the cell lines here presented have a great potential for future uses in *in vitro* models in the study of prostate cancer.

P-138

CDKN2A and TP53 mutational analysis in metastatic squamous cell carcinoma of the skin

Heidi V.N. Küsters-Vandevelde; Arjanne Van Leeuwen; Marian A.J. Verdijk; Maurits N.C. de Koning; Wim G.V. Quint; Willem J.G. Melchers; Marjolijn J.L. Ligtenberg; Willeke A.M. Blokx

Departments of Pathology, Radboud University Nijmegen Medical Center and Canisius Wilhelmina Hospital, Nijmegen, the Netherlands

Background: At present, prognosis of cutaneous squamous cell carcinoma (CSCC) is mainly determined by TNM stage and certain histological features as poor differentiation grade. So far, molecular features of metastatic CSCCs are relatively unexplored. In non-metastasized sporadic CSCCs, the *TP53* gene is mutated in up to 50% of cases. More recently, also mutations in the *CDKN2A* (*INK4A-ARF*) locus were reported in up to 24% of CSCCs, while combined *TP53/CDKN2A* mutations are rare (5%). In addition, in skin carcinogenesis, several studies have suggested an oncogenic role for cutaneous and mucosal HPV types.

Material and methods: The aims of this study were to assess a possible role for *CDKN2A* and *TP53* in metastatic CSCCs, by performing mutational and immunohistochemical analyses on 35 metastases and their corresponding primary tumors, and to detect persistent beta-PV and mucosal HPV infections, by using PCR based assays.

Results: We detected a *CDKN2A* mutation frequency of 37% (13/35) and a combined *CDKN2A/TP53* mutation frequency of 14% (5/35). *TP53* was mutated in 18/35 cases (51%). P53 protein expression proved to be significantly associated with missense type of *TP53* mutation (P=0.001), while effects of *CDKN2A* mutations on p16 and p14 expression were less clear. Finally, no persistent HPV types were detected in the metastases.

Conclusion: Our data demonstrate a higher frequency of *CDKN2A* mutations and combined *CDKN2A/TP53* mutations in metastatic CSCCs, compared to frequencies reported in literature for non-metastatic sporadic CSCC, possibly indicating a higher metastatic potential in CSCCs. Our data do not support a role for beta-PV and mucosal HPV in metastatic CSCCs.

P-139

EXPRESSION OF VEGF-A IN WOUND HEALING BY SECOND INTENTIONAND ITS RELATION TO CELLULAR PARAMETERS

Lovorka Batelja, Bruno Vuletić, Sanja Kapitanović, Luka Brčić, Stanko Jukić, Predrag Sikirić, Sven Seiwerth

Department of pathology, Medical faculty of Zagreb. Croatia

Introduction: VEGF is the most important mediator of angiogenesis, while both neutrophils and macrophages have a role in VEGF-A transcription.

Pentadecapeptide BPC 157 has beneficial influence on healing process.

AIM: to analyze wound healing by second intention through expression of mRNA VEGF A, number of neutrophils and macrophages and attempt of compare them in control group and treated group.

Methods: Full-thickness excisional wounds were made on the back of adults rats. The animals were treated as follows: BPC 157 10 μg/ kg i.p., control group; equivolumen of saline. Wounds were left uncovered, animals were harvested 4, 6, 12, 24, 48, 72, 120, 168 hrs after wounding. For histology analysis was taken half of the full thickness skin wound area and subcutis of the wound for molecular analysis (RT-PCR).

Results: In control group expression of mRNA VEGFA followed the published data (VEGF levels peaked at 6 and 48 hrs post-injury) and in treated group mRNA VEGF showed a sinusoidal curve with three positive and two negative peaks tending toward basal level. Difference in number of neutrophils and macrophages in different part of skin, at the same post-injury time is evident in control and treated animals. Number of neutrophils was significantly elevated in control group of animals; subcutis: 4, 12, 24, 72 hrs post-injury, low third of dermis: 12, 24, 120 hrs post-injury, middle third of dermis: 24, 120 hrs post-injury, high third of dermis: 24, 48 hrs post-injury. Number of macrophages was significantly elevated in control group of animals; subcutis: 6, 12, 24, 48 hrs post-injury, low third of dermis: 48, 72 hrs post-injury, middle third of dermis: 72, 120, 168 hrs post-injury, high third of dermis: 72 hrs post-injury.
Conclusion: Control group shows that in vivo wound healing by second intention confirms results of in vitro studies. Treatment with BPC 157 results with better controlled healing process through influence on mRNA VEGF-A expression and downregulation of number of neutrophils and macrophages. Correlation between neutrophils, macrophages and VEGF-A expression is evident, in both groups of animals.

Transplantation pathology

P-140
HISTOLOGICAL, IMMUNOMORPHOLOGICAL AND ULTRASTRUCTURAL CHANGES IN A TRANSPLANTED KIDNEY

T. Todorov; Tch. Georgiev; D. Popov; A. Alexandrov; S. Hristov;A. Paloff; D. Hinova-Palova; E. Paskalev; P. Simeonov
Center of Pathology and Forensic medicine – Sofia. Bulgaria

The present investigation was carried out on 148 punctural renal biopsies of transplanted kidneys during the period between 1999 an 2006. All materials were investigated with the standard methods of nephromorphology:

1. Histological and histochemical – hemalaun – eozine, PAS-reaction, trichrome – Mason, silver impregnation of Wilder, Congo – rot;
2. Immunomorphological – direct immunofluorescence with antiserums for IgA, IgG, IgM, C1q, C3c, C4c and fibrin;
3. Eighty-six of the biopsies underwent electronmicroscopic investigation.

Using the classification of Banff 1997, we divided the results we obtained into the following groups:

1. Acute transplant rejection – 43 cases;
2. Chronic transplant nephropathy – 88 cases;
3. Cyclosporine lesions of the allograft – 7 cases;
4. Postoperative necrosis in renal allograft – 4 cases;
5. Glomerulopathy recidive – 6 cases.

The results of the electronmicroscopic investigation gave us valuable data for particularization of the morphological diagnosis in some cases of chronic transplant nephropathy, cyclosporine lesion of the transplanted kidney as well as in recidives of the main kidney disorder.
Although the present study is concerned with morphological diagnosis, we have to point out the undoubted role of the clinical data about the state of the patients.

P-141
Cholesterol embolization in cadaveric donor kidneys

Sergio Herrero; Montse Gomà; Jordi Casalots; Itziar Navarro; Carlota González; August Vidal; Enric Condom
Department of Pathology. Hospital Universitari de Bellvitge. L'Hospitalet de Llobregat, Barcelona. Spain

INTRODUCTION Cholesterol embolization (CE) is rarely seen in renal allograft specimens. In contrast to CE in native kidneys, its natural history and prognostic significance are not as well characterized.
MATERIAL AND METHODS Archival samples from 42 preimplant biopsies of cadaveric donor kidneys (November 2006 to November 2007) were reviewed, as well as the clinical charts and additional pathology samples of the patients found to have CE.
RESULTS Three cases with CE were found. In the first two cases, the donors had atherosclerotic risk factors and kidneys were refused. CE were present in the nephrectomy specimen (but not in the preimplant cortical biopsy) together with associated ischaemic changes. The third case was from a 66 year-old male without known cardiovascular risk factors who died of a stroke. A preimplant frozen biopsy from the left kidney showed a unique intravascular CE. The two kidneys were grafted in two different patients. The left one failed on the fourth day after transplant. The nephrectomy specimen showed diffuse ischaemic necrosis with several CE and marked arterial occlusion. The right kidney performed well and a five months protocol posttransplant biopsy revealed borderline acute rejection, without CE.
CONCLUSIONS We have found a 7% incidence of CE in preimplant biopsies of donor kidneys which is higher than previously reported for implanted kidneys. It is probably due to the policy in our center of accepting a more

extensive donor age. Intraoperative preimplant frozen sections appear not to be a suitable method to rule out CE in donor kidneys. The prognostic significance of finding CE in preimplant biopsies of donor kidneys remains unclear.

P-142

Positivi capillary staining for C4d associated with viruses molecular detection in monitoring endomycardial biopsiesof cardiac transplanted patients

Chiara Castellani, Annalisa angelini, Elisa Carturan, Francesco Tona, Fiorella Calabrese, Alida Caforio, Antonio Gambino, Francesca Poli, Elena Benazzi, Gino Gerosa, Mrialuisa Valente, Gaetano Thiene
University of Padua, Medical School. Italy

Objectives: The finding of complement deposition in linear pattern by monoclonal antibodies for the activated complement split product C4d by immunofluorescence or immunohistochemistry is recognized to be insufficient for the diagnosis of antibody-mediated rejection.
It has been recognized that early ischemic injury and viral infection can produce a positive capillary staining for C4d. In heart transplant no data are available which correlate C4d capillary positivity with virus infection. Aim of our study was to assess the frequency of C4d positivity with the molecular detection of virus.
Material and methods: 183 endomyocardial biopsies were studied. C4d was performed on paraffin embedded specimens and C4d staining was graded according to a score from 0 to 4. PCR/RT-PCR analysis for detection of viral genome of more common cardiotrophic viruses (CMV, EBV,EV, HSV,PV,B19) in EMB was carried out.
Results: Among the 183 EMB analyzed, 29 EMB of different patients were positive for viral detection (15,8%). Of these, thirteen EMB showed a C4d staining of grade 1 and 2 (44%), according to the score from 0–4 and 3 EMB showed a C4d staining of grade 3 and 4(10%), the other 13 EMB were negative for C4d staining. The viruses detected were CMV in 8 EMB with grade 1–2 of C4d staining, EBV in 5 EMB with grade 1–2 and, EV in 3 EMB with grade 3–4 of C4d staining.
Conclusions: C4d positivity on EMB can be detected during viral infection. In our population EV was the most frequent virus associated with severe C4d staining suggesting that a capillary positivity for C4d should be further assessed for cardiotrophic viruses myocarditis

Posters
Displayed on Monday, May 19

Paediatric Pathology

P-143

Detection of fusion gene trasncripts in formalin-fixed paraffin-embedded tissue sections of rhabdomyosarcoma after reverse transciptase-polymerase chain reaction and fluorescence in situ hybridization

Eguia-Aguilar P; Perezpeña-Diazconti M; Ponce-Castañeda V; Nieto-Matínez K; Ruiz-Sanchez E; Kofman-Alfaro S
Hosptial Infantil de Mexico Federico Gomez; Hospital General de Mexico; Hospital de Pediatria Centor Medico Nacional Siglo XXI. Mexico

Introduction: Rhabdomyosacoma is the most common soft tissue sarcoma in childhood. The histology of rhabdomyosarcoma correlates with prognosis; alveolar rhabdomyosarcoma (ARMS) has a survival of 55%. ARMS have one of two chromosome translocation detected in 85% of the cases, t(2;13)(q35;q14) more common and t(1;13)(p36, q14). RT-PCR and FISH are powerful tools for the retrospective analysis or formalin-fixed paraffin-embedded tissue.
Methods: We designed a descriptive, cross sectional, comparative studies. The study population consisted of 30 cases of ARMS from archival paraffin-embedded biopsy samples. The negative controls were consistently in all cases. For RNA extraction from paraffin-embedded tissue was made using the acid guanidinium-phenol-chloroform method. Each RNAsample was studied using RT-PCR for three differente primer pairs: PGK fwd/rev (quality of theRNA), PAX3-FKHR, PAX7-FKHR. Amplified products were separated on 2% agarosa gel electrophoresis. For FISHassay we used bacterail artificial chromosome (BAC) probe sets. Two color FISH studies were performed. Probeswere directly labeled for nick translation with either spectrum green (FKHR) or spectrum orange PAX7 and PAX3).Images were adquired by use of CytoVision Applied Image.
Results: ten cases of PAX3-FKHR were found, one case of PAX7-FKHR and ten cases with no translocation. In nine cases we did not get RNA. We also compared the results between the two techniques. The oldest paraffin-embedded tissue had 14 years old.
Conclusions: There are a number of methodologies that can be used for the detection of tumor specific fusion trsncripts from archival paraffin-embedded tissue. In our hospital is posible to do it in retrospective studies, prospective studies and for the analysis of low incidence diseases. The fusion status is an essential molecular marker

in the prognosis or ARMS and makes the molecular biology methods an invaluable tool in the treatment assignment.

P-144

Cryptosporidium Infection in Pediatric Patients with Lymphohematopoietic Malignancies

Nona Zabolinejad; Fariba Berenji; Hamidreza Kianifar; Zahra Badeii; Abdollah Banihashem; Simin Hiradfar
Department of Pathology, Dr. Sheikh Children Hospital, Mashhad University of Medical Sciences, IR Iran

Objective: Cryptosporidium parvum is a common protozoan pathogen with worldwide distribution. It localizes on the intestinal cells and prolonged diarrhea in immunocompromised patients. The aim of this study was to estimate the prevalence and the clinical features of enteric cryptosporidiosis in pediatric patients with lymphohematopoietic malignancies.
Material & Methods: In this cross-sectional study stool samples were collected from 100 children (67 boys, 33girls) with lymphohematopoietic malignancies who underwent chemotherapy between the ages of 6 months and 17 years (mean age 7.5 years). All of the specimens were examined for the oocysts of C. parvum by modified Ziehl Neelsen (MZN) staining technique and coproantigens of C. parvum by ELISA.
Findings: Cryptosporidium infection was detected in 22 patients. 16 (72.7%) of the infected patients were male and 6 (27.3) female. 7 (31.8%) patients were <5 years, 8 (36.4%) 5–10 years and 7(31.8) >10 years old. Parasites were detected in 19/85 (86.4%) patients with ALL, 2 of 5 (9.1%) with AML, and 1 of 10 (4.5%) with NHL. Clinical symptoms were found in 11 (50%) of the patients. We found longer duration of chemotherapy in patients who were positive for cryptosporidium infection (Mean= 2067 days) in comparison to negative group (Mean= 258.5 days) (ANOVA, f=2.82, P=0.04).
Conclusion: The incidence of cryptosporidium infection was 22% among pediatric patients with lymphohematopoietic malignancies. We recommend evaluation of these patients with at least two different diagnostic methods in order to prevent possible life threatening outcomes.

P-145

Immunohistochemical expression of P53 protein in histologically favorable Wilms tumor and its relationship to tumor stage at presentation

S. Mirsadraee, N. Zabolinejad N. Sharifi, A. Tabatabaee, A. Merikhi Ardabili
Department of Pathology, Dr. Sheikh Children Hospital, Mashhad University of Medical Sciences, IR Iran

Objective: Wilms tumor, as the most common renal tumor of children, has been associated with chromosomal abnormalities. Although a correlation between anaplasia and mutations of P53 tumor suppresser gene has been found in Wilms tumor, significance of these mutations in different clinical stages of favorable-Wilms tumor, remains largely unresolved. The goal of this study was to determine the frequency of P53 expression in histologically favorable Wilms tumors and its correlation to tumor-stage at presentation.
Materials and Methods In this retrospective study, 48 cases of confirmed Wilms tumor with favorable-histology were retrieved from the files of departments of pathology in three hospitals in Mashhad University of Medical Sciences between 1990 and 2004. Histological characteristics and clinicopathological staging were in accordance with National Wilms Tumor Study guidelines. P53 expression was determined by the immunohistochemical method. For each section, the proportion of neoplastic cells exhibiting nuclear positivity was broadly quantified and their intensity of staining was charted, based on visual impression, elever by two pathologists.
Results A total of 48 cases of histologically favorable Wilms tumor were assessed. Eleven cases (23%) showed positivity for P53 which were 3 (27.3%) with stage II, 3 (27.3%) with stage IV, 2 (18.2%) with stage I, 2 (18.2%) with stage III and 1 case (9.1%) with stage V. The P53 immunopositivity was seen in 1–25% of tumor cells in 9 cases (18.8%), in 26 to 50% of tumor cells in 1 case (2.1%) and in >75% of tumor cells in the other one case (2.1%). The intensity of staining was moderate in 6 cases (12.5%), weak in 4 (6.3%) and strong only in one case (4.2%). The most common component with P53 immunoreactivity was blastemal in 11 cases (100%). In 4 cases (36.4%) there was also positivity in epithelial and in 2 cases (18.2%) in mesenchymal components.
Conclusion We found no correlation of P53 immunoreactivity and its intensity to tumor stage at presentation in individuals with histologically favorable Wilms tumors (p= 0.66, p=0.52 respectively).

P-146

Ameloblastic fibrosarcoma of the maxillary sinus in an infant: a case report with long-term follow up

Nona Zabolinejad; Mehran Hiradfar; Kazem Anvari; Alale Shoja Razavi
Department of Pathology, Dr. Sheikh Children Hospital, Mashhad University of Medical Sciences, IR Iran

Ameloblastic fibrosarcoma (AFS) or ameloblastic sarcoma is an extremely rare odontogenic neoplasm. The authors report ameloblastic fibrosarcoma (AFS) in the maxillary sinus of a

4-monthold boy. The tumor composed of odontogenic epithelium, resembling that of ameloblastoma and a mesenchymal part exhibiting features of fibrosarcoma. We also found some areas with deposition of dentinoid material closely adjacent to ameloblastic epithelium. Although AFS has been occurred in a wide age range, this is the first report of this tumor in infancy with long term follow up.

P-147

Sialolipoma of the parotid gland with diffuse sebaceous differentiation in a female child

Maryam Kadivar;Shahriar Zohourian Shahzadi; Morteza Javadi

Rasoule-Akram Hospital;Tehran;Iran

Sialolipoma of the salivary gland is a tumor with ambiguous histogenesis.Histologically,this lesion is composed of mature adipose tissue and salivary glandular components.To the best of our knowledge,only twelve documented cases of sialolipoma have been reported in the literature.Except for one congenital case,all of the cases were found in adult patients.In this report,we present a unique case of sialolipoma with diffuse sebaceous differentiation in a 3-year-old female child.The differential diagnoses are discussed.

P-148

SIRENOMELIA IN SIAMESE TWINS. FIRST CASE REPORT OF THE LITERATURE

Julio Cesar Mantilla Hernández, Mario Alexander Melo Uribe, Julio Alexander Diaz Pérez and Ernesto Garcia

Universidad Industrial de Santander. Colombia

Background. The sirenomelia as the presentation of Siamese twins are extremely rare birth defects, and its presentation as a whole is even more unusual.

Objective. To describe and make a discussion of the morphological features of a case of Siamese twins in which one of them had sirenomelia.

Case report. Thoracopagus Siamese Twins, with a gestational age of 15 weeks, product of the fifth pregnancy of a 26 years old woman, who arrives to the obstetrics service with clinical symptoms of uterine activity and genital bleeding. Obstetrical ultrasound showed Siamese twins pregnancy. Subsequently presents delivery of thoracopagus Siamese fetus.

Autopsy. We received two male fetuses bodies, weighing both 320 grams, each with a length crown to ankle 13 centimeters, cranial circumference of 11.5 centimeters and a length of the sole of 20 millimeters, with multiple external malformations common to both fetuses as broad defect in the abdominal and thoracic anterior wall with exposure of the heart and abdominal viscera, agenesia of the lumbar spine and anal atresy; also one of the fetuses showed fusion of the lower limbs by the middle line to the ankles. With the above findings, diagnosis of Thoracopagus Siamese Twins and Sirenomelia type 1 was made.

Conclusions. We present a case of an unusual combination between two rare congenital anomalies; in a search in MedLine literature from January 1964 to November 2007 there where no citations. This mixture is characterized by submitted in conjunction with other alterations of the thoracic wall, vascular, renal, gastrointestinal and spinal system that make it incompatible with life.

P-149

Ezrin immunohistochemical expression in pediatric tumors by tissue array

Pérez Noelia; Rodríguez Eva; de Torres Carmen; Medina Marilyn; Suñol Mariona; Mora Jaume; Cusí Victoria

Hospital de Sant Joan de Deu.Spain

Background Ezrin is a cytoplasmic cytoskeleton-linker protein. In normal cells, ezrin is involved in polarity and cell-to-cell signal transduction, whereas in some tumor cell types it is believed to play a role in regulating growth and metastatic capacity. Its prognostic significance has been described in some adult neoplasms and osteosarcoma. The aim of this study was to analyze ezrin expression in several pediatric tumors and to determine if ezrin expression in the primary tumor correlates with a higher metastatic rate.

Methods Tissue microarray blocks were constructed, including 56 neuroblastomas (NB), 23 Ewing's sarcomas (ES), 12 synovial sarcomas (SS) and 19 fibroblastic proliferations (FP). Whole-tissue sections were studied whenever needed. A commercially available antibody (Ab1; 3C12 clone; Neomarker, Lab Vision Corp, CA) at 1/100 dilution was used. The intensity and localization of the immunohistochemical expression were recorded.

Results and conclusion Out of the 56 NB, 42 were evaluable and all showed positive staining (100%) with no definite pattern. Ten out of the 12 SS could be evaluated and they were all positive (100%). The fusiform and epithelial portions showed cytoplasm labeling, being the epithelial component the more intensely stained. The FP tissue array included 19 cases, of which 13 could be evaluated and displayed positive cytoplasm immunoreactivity. Twenty two of the 23 ES evaluated were positive (95.6%). Fourteen exhibited membrane reinforcement and eight showed cytoplasm diffuse positive staining alone.

There were no differences in the metastatic rate and outcome in these two subsets of ES patients.
In conclusion, intense and widespread ezrin immunoreactivity was observed in several pediatric tumors, including NB, SS, FP and ES. Further investigation is warranted to determine its clinical relevance.

P-150
INTRARRENAL TERATOMA OCCURRING IN INFANCY. REPORT OF A CASE WITH DISCUSSION OF EVALUATION AND DIAGNOSIS

Carmen Fuenmayor Meza1; Maryori García Ruiz1; Carlos Marín2; Maria de Gamboa3
Unidad de Anatomía Patológica1, Unidad de Cirugía Pediatrica2, Unidad de Pediatria3. Venezuela

BACKGROUND: Germ cell tumors are neoplasms that occur relatively infrequently and are most commonly encountered in the gonads. Nonetheless, such tumors have also been described in other locations, such as the pineal gland, retroperitoneum, mediastinum and sacral area. Very rarely teratomas and tumors derived from germ cell can arise within the kidney.
METHODS: The clinical and radiological features a three month old female infant with abdominal mass and review of the literature.
RESULTS: This cases presented during the year 2000 represent the casuistry of the University Hospital of The Andes (IAHULA), Mérida, Venezuela. The infant was asymptomatic with progressive abdominal distention. Serum α-fetoprotein, routine hematological and serum chemical results were normal. The X-ray and ultrasound study showed a retroperitoneal tumor of left kidney heterogeneous and amorphous calcifications. During the surgery, the tumor was excised completely and the specimen weighed 420 g. Macroscopically, the tumor was described within the kidney parenchyma. The tumor multicystic with of fat, sebaceous and mucinous materials, hair, and blood. The histological examination revealed the presence of neoplastic cells derived from more that one germined status.
CONCLUSIONS: The teratoma renal is an uncommon neoplasm with a benign clinical course and good prognosis. The suspicion clinical is based in the anamnesis, examination physical and imaging technology. Surgery should thus be the first choice for treatment with excised completely of tumor. Histopathologic differential diagnosis with Wilms' tumor with teratomatous areas is mandatory. Twelve years later, there was no evidence of tumor recurrence.

P-151
Pathology of the thymus and immunodeficiency in pediatric mortality and experiments

Larisa Volkova
Kursk State Medical University. Russia

Severe or generalized infections are one of the main causes of death in pediatric mortality and associate with congenital or acquired immunodeficiency (ID). The actual problem is post-mortem diagnostics of ID with comparison to clinical and laboratory data. *The aim of investigations* is evaluation of thymus pathology and ID in pediatric mortality from infectious diseases and experiments.
Methods. Diagnostics of ID was based on retrospective analysis of pediatric autopsy in comparison to manifestations of infections, in some groups - with symptoms of SIRS. Experimental model of poststress accidental involution (AI) was worked out to study the thymus pathology and mechanisms of acquired ID (Volkova L.V., 1996). H&E/Van Geison methods, morphometry, correlation and systemic analysis were used.
Results. The main variants of post-mortem histological diagnosis were following: *accidental involution of thymus* of different degree (1–2-"starry sky", 3- inversion of cortex and medulla, 4–5 - atrophy of thymus), *thymomegaly, dysplasia* and *hypoplasia* of the thymus. It was revealed the high rate of AI and thymomegaly. AI of 3–5 degree was the variant of acquired ID and in some cases associated with pathology of pregnancy, artifical nutrition of newborns, repeated or severe infections in postnatal period. Morphology and mechanisms of AI were examined in experiments with morphometry, systemic and correlation analysis. High synchronism of quantitative alterations of cytological profiles in structural zones of the thymus, spleen, peripheral blood and expressed changes of lymphoid cell population in AI 2–3 were revealed. The facts can be used in post-mortem diagnostics and clinical laboratory examinations of patients with ID and infections. High rate of AI in cases of lethal infectious diseases in pediatric pathology associates with acquired ID and possibilities of prophylaxis.

P-152
Study of respiratory infection caused by Chlamydia pneumoniae in children in the departament of pediatrics - the Ipiranga Hospital, Mogi das Cruzes (Brazil)

Marcelo Fabiano Rodrigues; Edson Costa; Leila Moussa Costa; Sonia Maria Almeida
Universidade Braz Cubas. Brazil

Introduction: *Chlamydia pneumoniae* is a pathogen usually associated with respiratory pathology. It has been estimated

that this agent causes 5 to 15% of all pneumonias but its incidence among hospitalized children with respiratory infections is unknown.
Objective: Characterization of the *Chlamydia pneumoniae* respiratory infections in hospitalized children.
Patients and Methods: Retrospective longitudinal study of the *Chlamydia pneumoniae* respiratory infections in children admitted between January 2005 and June 2007 in the Department of Pediatrics in the Ipiranga Hospital - Brazil. Sex, age, race,socio-economic status, number of scholar siblings, frequency of nursery/school, parents smoking habits, familiar atopy, personal history, clinical presentation, diagnosis,treatment and follow-up were analyzed for each child.
Results: 55 cases were documented, 67% males and 52% whites. The age on admission varied between 14 days and 16 years-old, with a higher incidence below 6 years-old (57%). Twenty-three (40%) of the children were in nursery or in school and 12 (43%) had siblings at school-ages. Parent smoking habits were documented in 21 (56%) and familiar atopy in 21 (48%) children. Respiratory atopy (9 children), gastroesophageal reflux (5), cerebral palsy(1), cleft palate (3) and prematurity (3). Pneumonia was the most frequent clinical presentation (67%), followed by bronquiolitis (29%). The clinical presentation was not specific, with cough (86%), respiratory distress (69%) and fever (66%) beingthe most frequent signs. The most prevalent radiological pattern was the interstitial(49%). Coinfection by other agents occurred in five cases: *S. pneumoniae* (2), *H.influenzae* tipo b (1), *P. aeroginosa* (1) and tuberculosis (1). Complications weredocumented in 32 (58%) children: hypoxemia (24), pleural effusion (11), atelectasis (5) and atelectasis and hypoxemia (5). Macrolids were prescribed in 49% cases.
Discussion: This study calls the attention to the fact that *Chlamydia pneumoniae* infection is an etiology to be considered in children with respiratory infection and hospitalizationcriteria. This infection can occur in all ages. Because the clinical presentation is not specific and complications can occur, a high leveI of suspicion is necessary for its diagnosis.

P-153

THE EXPRESSION OF HISTONE ACETYLTRANSFERASE PCAF IN PEDIATRIC ASTROCYTOMAS, IT'S ROLE TO RESPONSE TO THERAPY AND MORE HIGHLY ACETYLATED HISTONE H4.

Francisco Arenas-Huertero; Mario Perezpeña-Diazconti; Pilar Eguía-Aguilar; Fernando Chico-Ponce de León; Félix Recillas-Targa.
Hospital Infantil de México Federico Gómez. Mexico

Background. Central Nervous System tumors (CNST) are the third neoplastic disease in childhood and astrocytomas represent 20%. Currently, there is not a tumoral marker that correlates with astrocytoma. Characterisitcs as expression of chromatin modifiers and acetylated histones could be considered as tumoral markers not-described in astrocytomas.
Method. We analyzed the expression of PCAF and p300 by semi-quantitative RT-PCR in CNST surgically obtained. Also we isolated total histones from nuclei and they were electrophoresed. The median of expression of PCAF and p300 was calculated and compared against benign tumors (BT). The correlations were performed with clinical data.
Results. PCAF was not expressed in BT but it was in 100% of CNST. PCAF was expresssed with a median of 134 DU in CNST against 82.4 DU in BT; the differences were significant ($p<0.05$). CNST treated with chemoterapy revealed 110 DU and chemo plus radioterapy 124 DU; comparison to CNST not treated were also significant. 92% CNST presented di- and triacetylated H4 against 0% of triacetylated H4 in BT.
Conclusions. PCAF gene expression could be a molecular marker in CNST. The increased pattern of histone H4 acetylated also can represents a malignant marker correlated to high PCAF expression. Actually we are going to evaluate PCAF as prognostic marker.

P-154

Clinico-morphological criteria for differential diagnosis of septicenia in labor and puerpperal sepsis.

Andrey Milovanov; Alexander Matsionis; Nina Mikhanoshina; Galina Reznikova
State Research Institute of Human Morphology of the Russian Academy of Sciences (Moscow); Rostov Region Insitut of Pathology (Rostov-on-Don). Russia

Background -Pyoseptic desease still rank the third among the causes of maternal death after hemorrhages and gestoses. The purpose of our research was to develop clinico-morphological criteria for differential diagnosis of such special forms of obstetric sepsis as septicemia in labor and puerperal sepsis.
Methods -We studied 24 autopsies of puerperas who died over a 10 year period (1996 - 2006) of pyoseptic diseases in the Rostov Region, and analyzed their placentas and partum histories. Microscopic examination of uteri, spleens and lymph nodes and placentas was performed by standard methods of light microscopy, with hemotoxillin and eosin staining and PAS reaction. We used antibodies of DAKO, Denmark for immunohistological verification of cells from the inflammatory infiltration.
Results - Microscopic and immunohistochemical examination of the uterus in cases of septicemia in labor showed

low-grade infiltration with granulocytes, macrophages, T-lymphocytes in endometry. With puerperal sepsis there was diffuse infiltration with plasmacytes and macrophages in endometry and myometry. Some cells in the infiltrate were positive with TNF.
In cases of septicemia in labor the inflammatory infiltrate in the placental fetal membranes was represented by a great number of granulocytes, plasmacytes, macrophages, and rare T-lymphocytes. Some cells in the infiltrate were positive with TNF. There were no inflammatory infiltrate in fetal membranes in puerperal sepsis.
Conclusion - With septicemia in labor the onset of clinical symptoms was observed within the first 24 haurs after the delivery and in cases of puerperal sepsis the symptoms developed 3–5 days later. With septicemia in labor the focus of infection was in placenta, and in cases of puerperal sepsis the infection developed from the uterus. Our conclusion is confirmed by the presence of the key antiinflammatory mediator TNF (i.e. development of cytokins as a response to the focal damaging effect of microorganisms and their toxins) in placenta or in uterus respectively.

P-155

Medulloblastomas: Review of 51 cases. Study of INI1 to disclose atypical teratoid/rhabdoid tumours

Mariona Suñol; Ofelia Cruz; Eva Rodríguez; Marylin Medina; Noelia Perez; Victoria Cusí.
Departments of Pathology and Oncology. Hospital Sant Joan de Déu. Esplugues de Llobregat. Barcelona. Spain

Background: The aim of this study is to verify histological and immunohistochemical (IHC) markers of medulloblastoma, which can help us in the differential diagnosis and survival correlation.
Method: The study included 51 patients with a diagnosis of medulloblastoma recorded from 1982 to 2004. Histological variants, mitotic activity, microvascular proliferation, pseudopalisading necrosis and neuroblastic rosettes were analyzed. Additionally, a tissue microarray was performed including synaptophysin, NSE, GFAP, NF68, EMA, vimentin, WT1, c-erbB2, p53, INI 1 and ki67 expression.
Results: The average age at diagnosis was 5.6 years old. The overall survival (OS) was 37.5%, although survival improved in recent cohorts. According to the histological parameters studied we found that desmoplastic type and extensive nodularity were histological variants with better prognosis and high OS, whereas tumours with more than 20 mitosis/10HPF were associated with a worse prognosis and low OS. IHC analysis showed expression of synaptophysin in 76.6% of cases, NSE 100%, GFAP 31.9%, NF68 36.2%, EMA 8%, vimentin 34%, WT1 (cytoplasmic) 25.6%, c-erbB2 4.4%, p53 6.7%, INI 1 93.5%. Ki67 expression was >50% in 23.5% of cases, 20–50% in 41.2% and <20% in 35.3% of cases. Lack of INI 1 expression in 3 tumours previously diagnosed as medulloblastoma suggested the diagnosis of atypical teratoid/rhabdoid tumour (AT/RT). This was confirmed by hSNF5/INI 1 gene mutation analysis.
Conclusion: Long survival correlates with desmoplastic and extensive nodularity; likewise with less than 20 mitosis/10HPF. AT/RT can show similar histology and IHC markers as medulloblastoma. Lack of INI 1 expression is only detected in AT/RT tumours. INI 1 study in embryonal tumours in children is essential in order to disclose a possible AT/RT.

P-156

Morphological patterns of the intrauterine

Olga Reshetnikova; Sergiy Morozov; Pavlo Fedorenko
Lugansk State Medical University. Ukraine.

Background: Epidemiological studies demonstrated a relationship between impaired fetal growth and risk of adult diseases. Animal models support the hypothesis that some pathologies may originate early in gestation.
The aim of present investigation was to find out the relationship between impaired placental growth and restriction in growth of fetal organs and body at late gestation.
Fetal autopsy and placenta study were performed in 23 cases of termination of pregnancy for socio-economic reasons at 23–25 weeks of gestation. Fetal weight (FW), length, body mass index, circumferences of the chest (Cch), head (Ch), abdomen (Ca), and placental weight (PW) were recorded. Besides these, fetal organs weights were found, including liver (LW), kidneys (KW), heart (HW), pancreas (Pn W). Some indices were then calculated: PW/FW; PnW/PW; KW/PW; HW/PW; LW/PW, etc. Results: The high PW/FW index (0.31±0.02) has made it possible to identify group which shows disproportionate growth patterns between the fetus and placenta. (IUGR group). This group had smaller parameters of LW/PW (0.18±0.01), KW/PW (0.03±0.00) and HW/PW (0.02±0.00) than in controls (0.21±0.01, $p<0.04$; 0.05±0.01, $p<0.05$; 0.03±0.01, $p<0.00$ respectively).Conclusion. The results showed that a stressful intrauterine environment at 23 weeks of gestation results in series of placenta-fetal responses including disproportional growth patterns between placenta, fetal kidneys, heart and liver.

P-157

Neuronal maturation in an experimental model of brain tissue heterotopia in the lung

Paulo Roberto Veiga Quemelo; Deise Lúcia Chesca Simões; Luiz Cesar Peres

Department of Pathology - Ribeirão Preto School of Medicine - University of São Paulo. Brazil

Neural maturation involves diverse interaction and signaling mechanisms which are essential to the development of the nervous system. However, little is known about the development of neurons in heterotopic brain tissue in the lung, a rare abnormality occasionally observed in malformed babies and fetuses. The aim of this study was to identify the neurons and to investigate its maturation in experimental brain tissue heterotopia both during fetal and neonatal periods. Twenty four pregnant female Swiss mice were used to induce brain tissue heterotopia on the 15th gestational day. Briefly, the brain of one fetus of each dam was extracted, disaggregated and injected into the right hemithorax of siblings. Six of these fetuses with pulmonary brain tissue implantation (PBI) were collected on the 18th gestational day (group E18) and six other on the 8th postnatal day (group P8). The brain of fetuses from dams not submitted to any experimental procedure was collected on the 18th gestacional day (group CE18) and on the 8th postnatal day (group CP8) to serve as a control. Immunohistochemical staining for NeuN was used to assess neuron quantification and maturation. NeuN Labelling Index (LI) was greater in postnatal than fetal period both for the experimental and control groups (P8 > E18 and CP8 > CE18), although there were fewer neurons in experimental than in control groups (P8 < CP8 and E18 < CE18) ($P < 0.005$). These results indicate that fetal neuroblasts/neurons not only survive a dramatic event such as the one secondary to mechanical disaggregation, similar to what happens in human cases, but they keep its development in heterotopia irrespective of local tissue influences.

P-158

Retroperitoneal extralobar pulmonary sequestration

Isabel Marquina*; Francesc Felipo; Mar Pascual**; Ana Fuertes**; Guillermo Muñoz**; Celia Del Agua**; Patricia Sota****

**Hospital de Alcañiz; ***Hospital Universitario Miguel Servet. Spain*

Background: Pulmonary sequestration is a pulmonary mass anatomically separated from bronchial tree with sistemic blood supply. Intralobar variety shares visceral pleura with normal lung. Extralobar variety (EPS) is covered by its own pleura; it can be thoracic, intradiaphragmatic or infradiaphragmatic, which happens because of the entrapment of developing pulmonary tissue into the infradiaphragmatic space before pleuroperitoneal membranes close (5th-8th gestational week).

Case report: One month-old female newborn. An intra-abdominal mass is detected by ecography at 26th gestational week. Delivery occurs at 40th week. Abdominal ultrasound and sanner reveal an image in left hypochondrio the suggests differential diagnosis between cystic neuroblastoma and pulmonary sequestration. Left adrenalectomy and excision of cystic tumour are performed. The specimen is 7 g and includes adrenal gland of 5 cm and a rounded 2 cm mass, covered by a smooth tissue; cut surface is fleshy and microcystic.

Results: Histologically the nodule is composed by tubular structures that remain pulmary airways, some cystic, with papillary projections into the lumens, covered by a single layer of ciliated cylindrical cells. Arterial vessels with thickended walls, dilated lymphatic vessels, lymphoid aggregates, nerves, striated and smooth mucle fibers and cartilaginous tissue are seen in interstitium.

Comments: EPS may be composed by almost normal pulmonary tissue, may have reactive changes if secondary infection, or may have an image similar to congenital airway malformation. Finding striated muscular tissue in interstitium is usual, although its clinical importance is not already known. EPS can associate with cardiac and gastric anomalies or diaphragmatic hernia. Usually it is diagnosed in prenatal ultrasound controls, until first six months. Diagnosis is adults is rare. Differential diagnosis of a prenatal diagnosed abdominal mass must include neuroblastoma, pulmonary sequestration, adrenal hemorrage, renal tumours and malformations, gastric duplication, teratoma, lymphangioma and hemangioma. Microscopically, pulmonary sequestration, teratoma and rabdomyosarcoma must be considered.

P-159

Congenital paranchymatous diseases of the lungs, incidence, distribution and relation with extrapulmonary malformations in pediatric autopsies and biopsies

Orhan Diclehan; Altan Ilhan; Kale Gulsev

Hacettepe University Faculty of Medicine Division of Pediatric Pathology. Turkey

Among the autopsies and biopsies performed between 1977–2005 at Hacettepe University Children's Hospital, Division of Pediatric Pathology, cases diagnosed as congenital paranchymatous diseases of the lung were investigated. In congenital paranchmatous diseases of the lung, incidence, distribution and relation with extrapulmonary malformations were retrospectively evaluated. In this

period totally 44 553 biopsies ve 3483 autopsies were performed. Of the cases, 61 (0.13%) and 85 (2.4%) were diagnosed with congenital paranchymatous disease of the lung in biopsies and autopsies respectively. The most commonly encountered congenital paranchymatous diseases of the lungs were pulmonary agenesis, aplasia and hypoplasia. Less commonly congenital pulmonary airway malformation, congenital pulmonary emphysema, bronchogenic cysts, enteric cysts, pulmonary sequestrations and congenital pulmonary lymphangiectasis were seen respectively. In 83.5% of autopsy cases, one or more extrapulmonary malformations were detected. The most frequent encountered extrapulmonary malfomations were craniofascial and genitourinary system malformations. Except congenital pulmonary lymphangiectasis, other congenital paranchymatous diseases of the lung are commonly associated with extrapulmonary malformations. When a congenital paranchymatous diseases of the lung are detected in a patient, detailed investigations on extrapulmonary malformations should be done. In conclusion, the exact true incidence and mortality of all congenital paranchymatous diseases of the lung are displayed by this study including not only operated on congenital bronchopulmonary malformations but also with autopsy findings of neonates and stillbirths.

P-160

Alobar Holoprosencephaly in Monosomy 45,X0 with a Male Phenotype

L. Kiho, I. Salas Villar, J. Waters, W. Squier, I. Scheimberg

The Royal London Hospital, Barts and The London NHS Trust. UK

An individual with a karyotype 45,X0 is typically a short female with webbed neck and ovarian digenesis that are the most consistent features of X0 monosomy or Turner syndrome. Maleness in association with karyotype 45,X0 is an infrequent finding. The male-specific region of the Y chromosome, the MSY, differentiates the sexes and comprises 95% of the chromosome's length.The presence of the testicular determinant gene SRY on the short arm of Y chromosome is crucial for the development of male-type genitalia. Apart from the XY/X0 mosaics, in X0 males the maleness is due to a *de novo* Y/autosome translocation derived from the father. Depending on the type of deletion and the autosome involved, the phenotype could show a broad spectrum of congenital malformations.

We report on a case of Y/autosome translocation with loss of 18p and distal Yq material in a holoprosencephalic fetus. The fetus presented with a normal male phenotype and 45, X0 karyotype without evidence of mosaicism or apparent translocation on the routine cytogenetic analysis. The further cytogenetic and molecular studies indicated 45,X, der(18)t(Y;18)(p11.3;p11.3) arisen *de novo*. Parental blood karyotypes were normal showing no evidence of rearrangement involving the short arm of chromosome 18. To our knowledge, only 4 cases of Yp/18 translocation in a 45,X0 holoprosencephalic male have been previously reported.

P-161

Unclassified sex cord/ stromal tumors with spindle cells tumour occurring in a 3 months old boy

I Salas-Villar; D Berney; I Scheimberg

The Royal London hospital, Barts and The London NHS Trust. UK

The incidence of prepubertal testis tumours is approximately 0.5 to 2/100,000, accounting for 1% of all paediatric solid tumours. Sex cord-stromal tumours (SCST) account for ~4% of all testicular tumours and ~8–30% of all paediatric testicular tumours. These tumours may be composed of Leydig, Sertoli, or granulosa cell types, existing as either pure or mixed populations. A minority of SCST shows no definitive differentiation. Among the unclassified SCST there is a small, extremely rare group of tumours composed predominantly of spindle cells.

We report a case of a sex cord-stromal tumour with spindle cells occurring in a 3 months old boy. A firm solid nodular mass was noticed by the parents. The serum level of α-fetoprotein was mildly elevated, and other tumoral serum markers were negative. USS was not suggestive of cyst or infection. With the clinical diagnosis of testicular teratoma, the patient underwent radical left orchiectomy.

Microscopic examination revealed a non encapsulated circumscribed tumour composed of interlacing bundles of spindle cells with some compressed trapped tubules and frequent mitoses. There were no germ cells present. Immunohistochemically, neoplastic cells were diffusely and strongly positive for vimentin, inhibin and α-SMA, with focal positive staining for S-100 and calretinin.

To the best of our knowledge only nine cases of Unclassified SCST of the testis composed predominantly of spindle cells are reported. The majority of the cases reported are immunochemically SMA+, S100+, Vim+, CK-. The youngest case reported was 5 months old baby in which limited IHC was performed. A recent case with brain metastasis has been described. The histological features of unclassified SCST with predominance of spindle cells do not predict the biological behaviour of this tumour. As only one case with metastasis has been reported and there are few cases in the literature, long term follow up is recommended.

P-162

Pulmonary neuroendocrine cell hyperplasia of infancy: study of 3 cases

Joan Carles Ferreres; Cristina Jou; Antonio Moreno*; Silvia Gartner*; Irene Sansano; Dolores Sáez-Lagos; Santiago Ramón y Cajal; Núria Torán

Servei d'Anatomia Patològica and Unitat de Pneumologia Pediàtrica*. Hospital Universitari Vall d'Hebron. Barcelona. Spain

Introduction: Pulmonary neuroendocrine cell hyperplasia of infancy (NEHI), also known as persistent tachypnea of infancy, is a rare entity presenting as interstitial lung disease (ILD). NEHI affects young children like ILD, with persistent tachypnea, hypoxia, retractions or respiratory crackles, and with nonspecific and nondiagnostic lung biopsy findings.

Material and method: Three infants, aged three weeks, six months and two years, presented as non-filiated ILD. Chest radiographs demonstrated hyperinflation and high-resolution computed tomography, exhibited hyperinflation and ground-glass densities.

Results: The lung biopsies from all patients, showed no significant interstitial involvement or inflammation, but mild and nonspecific changes as increased alveolar macrophages and mild airway smooth muscle hyperplasia. Immunohistochemistry was performed using antibodies to synaptophisin, chromogranin A and bombesin. Immunopositive cells and neuroepithelial bodies in lobular parenchyma and in the bronchioli were observed, in larger numbers than in control samples. The patients were treated with oxygen-therapy and symptomatic bronchodilatador drugs for a long time, with gradual improvement in time.

Discussion: Neuroendocrine cells are specialized epithelial cells, distributed as solitary cells along the conducting airways, and as innervated clusters, the neuroepithelial bodies (NEB), in the lobular parenquima. These cells synthesize and release amines and a variety of neuropeptides. During the early stages of lung development, they act as modulators of fetal lung growth and differentiation, and after birth, as airway oxygen sensors involved in neonatal adaptation. These cells and NEB are related to different pediatric lung diseases as congenital lung disorders, bronchopulmonary dysplasia, disorders of respiratory control, cystic fibrosis, bronchial asthma and NEHI. The precise etiology and pathogenesis of NEHI remains unknown. It is not clear if a relation exists with the idiopathic diffuse hyperplasia of pulmonary neuroendocrine cells described in adult patients.

P-163

Pathological features in 3 cases of venous ductus agenesis associated to hydrops fetalis.

Núria Torán; Joan Carles Ferreres; Elena Carreras; Juan Carlos Blanco; Manuela Segarra; Sílvia Planas; Santiago Ramón y Cajal

Servei d'Anatomia Patològica. Hospital Universitari Vall D'Hebron. Barcelona. Spain.

Introduction. The venous ductus (VD) is a fetal vessel that takes oxygenated blood from the placenta through the umbilical vein (UV) to the fetal heart. Three main patterns of abnormal VD circulation were documented:

– 1) UV bypassing the liver and connecting directly into the right atrium (46% in the reported cases)
– 2) UV bypassing the liver and connecting into the inferior vena cava maintly through one of the iliac veins (25%).
–3) UV connecting to the portal circulation, without developing a true VD (21%)

Material and method. We show three cases which each represent an example of these mentioned patterns of UV drainage in patients with VD agenesis. The three pregnancies ended in postnatal death at 45 minutes, 4 days and 11 days respectively, with severe hydrops fetalis.

Discussion. In two cases, the cause of the fetal hydrops, could have been that most of the umbilical blood was bypassing the liver and drained directly into the heart or into the inferior caval vein, causing a cardiac overflow and under perfusion of the liver. In the patient whose umbilical blood drained directly into the hepatic sinusoids, hepatic hyper perfusion and portal hypertension could have caused damage to the liver cells, and an impaired fetal plasma protein synthesis and secretion. This could be a contribution to fetal hypoproteinemia causing hydrops.

The VD agenesis is a rare malformation and should be investigated in cases of prenatal diagnosis of hydrops fetalis or in hydropic newborns.

P-164

Non-immune hydrops fetalis: autopsic series of 53 cases

Carmen Blázquez; Joan-Carles Ferreres; María-Eugenia Semidey; Montserrat Sierra; Santiago Ramón y Cajal; Núria Torán

Servei d'Anatomia Patològica. Hospital Universitari Vall d'Hebron. Barcelona. Spain

Introduction: 'Hydrops fetalis' is used to describe the presence of generalized edema, together with liquid

accumulation in serous cavities. Despite the fact that it is a well-known pathology, it can be difficult to ascertain the cause, even in detailed autopsy studies. Its incidence has decreased notably since the exhaustive control of Rh isommunization. Although systematic complementary studies are not necessary in all cases, cytogenetic, metabolic and microbiologic studies should be carried out to obtain the etiological diagnosis. The aims of this study were to establish the prevalence of hydrops diagnosis in a recent autopsic series and analyse its causes.

Material and method: The diagnosis of hydrops has been reviewed from the records in autopsies of fetuses and infants up to 1 year of age, carried out at the Vall d'Hebron Universitary Hospital, from January, 2000 to November, 2007.

Results: In 1919 fetal and 179 newborn autopsies, the diagnosis of hydrops was confirmed in 53 cases (43 fetus and 10 newborns), representing 2.5% of the total. Grouped into categories, a metabolic disease was proved in 7 (13.2%) cases, an infection in 7 (13.2%) cases (2 of these - parvovirus B19), a placental pathology in 6 (11.3%) cases (4 of them - feto-fetal transfusion). A variety of congenital anomalies were found in 25 (47.1%) cases, (among these, 8 chromosomal abnormalities, 3 lymphatic dysplasia, 3 ductus venous agenesis, 2 achondrogenesis and 4 polimalformative anomalies). It was impossible to establish the cause in 8 (15.1%) of the cases.

Conclusions: The diagnosis of 'hydrops fetalis' represents 2,5% of cases in a recent autopsic series and its aetiology can be established in 84.9% of them.

P-165
POST-MORTEM EXAMINATIONS IN A SPECIALIZED PAEDIATRIC PATHOLOGY SERVICE 2005–2007

Scheimberg I; Salas Villar I; Dilly S; Kiho L
The Royal London Hospital, Barts and The London NHS Trust. UK.

Between January 2005 and November 2007 a total of 998 prenatal, perinatal and infant autopsies were performed by the Paediatric and Perinatal Unit at The Royal London Hospital's Department of Cellular Pathology. In the vast majority of cases (91.3%) the cause of death or important information was obtained at autopsy.

The post-mortems were divided in groups according to gestational age and neonates.

In the gestational age group less than 17 weeks gestation, 119/150 (79.33%) of the post-mortems performed revealed significant information, in 14/150 (9.33%) not enough clinical information was available to make a diagnosis, and in only 17/150 (11.33%) no relevant condition was identified.

Between 17 and 24 weeks gestation relevant information was obtained in 92% of the cases, only 28/351 of the post-mortems (8%) were unclassified.

The ReDeCo (Relevant Condition at Death) classification was used for babies over 24 weeks gestation. In stillborns (24 to 42 weeks gestation) relevant information was obtained in 327/349 (93.7%). Only 6.30% (22/349) were considered as "unclassified"; of these there was not enough clinical information and/or placenta in 6 of the cases (1.7%), the remaining 16 (4.6%) cases were considered as "No relevant condition identified".

In the group of neonatal post-mortems (less than 1 month old babies) the cause of death was identified in 71/73 (97.3%) of the cases, but relevant information was obtained in all of them.

In post-mortems performed in older babies and children (1 month to 13 years old) the cause of death o relevant information were obtained in 69/75 (92%) of the cases.

Before the use of the ReDeCo classification the percentage of unclassified cases was 16% in 2001–2003 and is now 8.7% in 2005–2007. Post-mortem performed by specialist Paediatric Pathologists offers more information to clinicians to improve prenatal care and is important for parental counselling.

P-166
Immunohistochemical analysis of tissue factor expression and microvessel density in Wilms tumor

Vinicius Duval da Silva, Elines O. Maciel; Gustavo F. Carvalhal; Eduardo F Carvalhal; Bernardo Garicochea; Henrique S. Barata.
Pontificia Universidade Católica do Rio Grande do Sul (PUCRS), Porto Alegre, Brazil.

Background: Wilms tumor is the most commonsolid renal malignancy in childhood. Even among patients with favorablehistology and staging, the most significant prognostic factors demonstrated sofar, some recur and eventually die from the disease. Novel prognostic factorscould be especially useful in the management of these children. Tissue factor(TF), a protein linked to the extrinsic coagulation pathway, is highlyexpressed in various tumors, and has been associated to the development ofmetastases and to a poor prognosis. Our study describes, for the first time,the expression of TF in paraffin-fixed specimens of Wills tumors from 41patients treated at Hospital Sao Lucas da PUCRS and Hospital da Crianca Conceicao,Porto Alegre, Brasil.

Method: The immunohistochemical expression of TF and microvasculardensity (MVD) assessed by CD34 underwent morphometric analysis with the digitalimage analysis system Image Pro Plus 4.5 (Mediacybernetics, USA).

Theseresults were compared to other established prognostic criteria, such as age,staging, histology and tumor recurrence, overall and cancer-specific mortality.
Results: Increased TF expression was correlated to a higher chance oftumor recurrence (p=0,01) and death (p=0,02). However, there was no significantcorrelation between TF expression and other established prognostic factors.Likewise, TF expression was not correlated to an increased MVD.
Conclusion: the results strongly suggest that further studies are neededto asses the potential of TF as a prognostic marker. Eventually TF may be testedas a predictive factor, considering the emergence of monoclonal antibody drugstargeting TF.

P-167
Recurrent left atrial myxoma
Milena Djukic; Slavisa Djuricic; Mila Stajevic; Vladimir Milovanovic; Sanja Rakic; Vladislav Vukomanovic; Vladimir Kuburovic
Department of Clinical Pathology,Mother and Child Health Care Institute of Serbia "dr Vukan Cupic",Radoja Dakica 6–8, 11070 Novi Beograd,Serbia

BACKGROUND: Cardiac myxoma is the most frequent primary benign cardiac tumor, occuring sporadically in adults. Pediatric cases are rare and familial cases occure in younger adults.
METHOD: We analyzed clinicopathological aspects of cardiac tumors in13 year-old female patient.
RESULTS: A 13 yr-old girl, was admitted at our institution, in May 2006 after cerebrovascular insult. Echocardiography revealed left atrial tumor. Dark red-grey, friable, gelatinous tumor mass, measuring 4.5×4×1 cm, attached by fibrous stalk to the tip of interatrial septum was resected. Microscopically, tumor tissue consisted of capillary-rich myxoid stroma, with foci of hemorrhage and chronic inflammatory infiltration, and superficial necrotic tissue. Tumor cells were spindle and stellatous, dispersed discohesivly, with no mitotic activity. Postoperative neurologic sequela was left hemiparesis. In November 2006, the follow-up ehocardiography revealed the new left atrial tumor and NMR showed that tumor mass attached on the upper frontal wall of the left atrium. In January 2007, reoperation was performed and dark red, friable tumor mass measuring 1.1×0.8×0.7 cm, attached by fibrous stalk to the middle of the interatrial septum was resected. The location of the second tumor, near the fossa ovalis, was clearly separated from the previously resected tumor. Microscopically tumor had the same texture as the previously diagnosed one. In the medical family history, parents have nevi and "spotty" efflorescence. On the grounds of clinical aspect and family history of recurrent atrial myxoma, facial and backbone nevi, oral cavity pigmentation, vulvar and perianal nevi and hirsutism, the diagnosis of Carney complex was established. Patient is on regular follow-up.
CONCLUSION: Cardiac myxoma in young adults is rare and clinically behave aggressively because it recurres frequently and is associated with embolism. The surgery is treatment of choice and regular follow-up of the patient is recomended.

Soft Tissue, Joint and Bone

P-168
Clinicopathological features of a series of 10 cases of malignant triton tumors diagnosed over 10 years at a teriary cancer hospital, Mumbai, India
Bharat Rekhi; Nirmala A Jambhekar; Ajay Puri; Manish Agrawal; R F Chinoy
Department of Pathology, Tata Memorial Hospital, Dr E.B. Road, Parel, Mumbai, India

Background: A rhabdomyoblastic differentiation in a malignant peripheral nerve sheath tumor (MPNST) is designated as a malignant triton tumor (MTT). Clinicopathological features and outcomes of 10 such cases, diagnosed over a 10 year period, are presented.
Method: H & E stained microsections were available in all the cases. Immunohistochemical (IHC) markers included vimentin, S100, desmin, myoglobin, CD34, MIC2 and glial fibrillary acidic protein (GFAP). p53 and MIB-1 staining were carried out in all cases.
Results: The average age of occurrence was 30 years, with maximum cases (60%) in the second decade, including males outnumbering the females. 62.5% cases were identified in the setting of neurofibromatosis. Average tumor size was 12.6 cms. On histology, 80% cases were of high grade. Distinct rhabdomyoblastic cells in form of 'strap' cells and pleomorphic forms were noted in 3 cases, each, respectively. The distribution of rhabdomyoblastic cells was focal, especially in close proximity to vessels and nerves in most of the cases that displayed features a MPNST. IHC showed varying S-100 expression, along with desmin and myoglobin positivity in all cases. Two cases showed GFAP positivity, including 1 case that also showed neuroectodermal differentiation. Surgery was performed in form of wide excision in 4 cases; marginal excision in 2, amputation in 2 and intracapsular excision in 2 cases. Adjuvant chemotherapy (CT) and/ or radiotherapy (RT) were offered in 9 cases. On follow-up, out of 7 cases, 3 showed local recurrences, including 1, which, in addition to other 2 cases, showed lung metastasis. One patient succumbed to the disease. This case along with another high grade case displayed diffuse MIB-1 and p53 positivity.

Conclusion: MTT is an uncommon tumor, invariably of high grade and stage and displays an aggressive behavior. High MIB-1 counts and p53 positivity indicate a dismal prognosis. Surgery with clear margins is the treatment mainstay. Adjuvant RT is effective.

P-169

Ossifying Fibromyxoid Tumor of Soft Tissue

Liliana G.Olvi; Antonio Arra; Horacio Solars; Osvaldo Peralta; Marcela Ortiz Mayor; Eduardo Santini Araujo.
Laboratory of Orthopaedic Pathology. Argentina.

Ossifying Fibromyxoid Tumor (OFMT) is a distinctive and rare soft tissue neoplasm of uncertain lineage, first described by Enzinger in 1989. The purpose of this study is to report four cases and review the literature.
We report four cases of our consultation files, all adult males aged between 32 and 53 years old. The involvement sites were abdominal wall, the supraclavicular area, lower extremity and shoulder.
All lesions were superficial soft tissue tumors with a diameter ranged from 3 to 10 centimeters. Patients complained of a painless sucutaneous mass which had been present from 2 to 15 years. Available X-ray and mamographic studies of the surgical specimen in 3 of the 4 cases revealed a circumscribed mass with irregular calcification inside it, surrounded by an incomplete ring of bone. On cut sections these masses were white, firm and rubbery-textured. Histologically showed encapsulated and lobulated tumors composed of small, uniformly-round cells with eosinophilic cytoplasm, arranged in cords and rows in a myxoid, fibromyxoid or hialinized stroma. Immunohistochemistry showed S100 protein positive in 3 of 4 cases.
Differential diagnosis was made with heterotopic ossification, extraskeletal myxoid chondrosarcoma and extraskeletal osteosarcoma. None of the cases showed atypical features neither increased mitotic activity nor cellularity. The treatment in all the 4 cases was the surgical resection of the tumoral mass without recurrence in six years, three years, 18 months and 6 months, respectivelly.

P-170

Abberant Cdx2 expression in pyloric gland adenoma of the gallbladder

Yoji Wani; Kaori Uchino; Kenji Notohara; Choutatsu Tsukayama
Department of Pathology, Kurashiki Central Hospital

Introduction: The aim of the study is to survey cdx2 expression in pyloric gland adenoma (PGA) of the gallbladder and whether the cdx2 expression is related to intestinal differentiation, to beta-catenin expression, or to spindle cell metaplasia (SM).
Materials and methods: We reviewed 25 cases of PGAs. With immunostaining, the antibodies (Cdx2, beta-catenin, MUC2, MUC6, HIK1083) were reacted and detected with Envision plus. The immunostaining was scored as follows: 0: negative, 1+: <10% positive cells, 2+: 10-<30%, 3+: 30-<50%, 4+:50-<70%, 5+: 70–100%. The number of positive nuclei for cdx2 and beta-catenin was counted in the well-labeled high power fields (HPFs). The mean labeling indices (LIs; %) were calculated by counting 1000 cells in the three HPFs. Separately, positive cells(%) were calculated in the SM foci.
Results: PGA was ranged in size from 3 to 16 mm. Four cases (16%) showed SM. In the background mucosa, cdx2 was not expressed. Although low score(1 or 2), cdx2 was expressed in 23 cases (92%). However, Muc2 was only positive in the small number of goblet cells in three cases (12%). The cdx2 score was not correlated with that of Muc6, HIK1083 and not strongly with beta-catenin. The LIs of Beta-catenin was correlated with those of cdx2 ($r = 0.705$). In all PGA cases with SM, positive cells(%) in the SM foci were higher than the mean LIs.
Conclusion: Cdx2 expression is specific to PGA with high frequency (92%) despite lacking any expression in the background mucosa, and is not related to goblet cells-type intestinal differentiation. The correlation of mean LIs between cdx2 and beta-catenin was identified, whereas the cdx2 score was generally low and was not strongly correlated with that of beta-catenin. Especially, high expression of cdx2 and beta-catenin in the SM foci raises a possibility that the mutation of beta-catenin genes promotes cdx2 expression.

P-171

Metachronous adenocarcinoma of the large intestine in a male patient with aggressive angiomyxoma

John Venizelos; Zoi Tatsiou; Anastasios Chatzitolios; Alexandra Moulla; Lampros Kampas
Department of Pathology, Hippokration Hospital, Thessaloniki, Greece

Aggressive angiomyxoma (AA) is a rear, locally infiltrative, but nonmetastasizing soft-tissue tumor that usually arises in the pelvis or perineum of premenopausal women. Only 44 cases of AA occurring in male patients have been reported in the English literature. Sites frequently involved include

the scrotum, spermatic cord, inguinal region and perineum. Correlation with carcinomas has not been reported.

We report the case of a 56-year-old man who presented with an inguinal hernia. During the operation, a nodular mass was identified attached to the spermatic cord. The hernia was subsequently repaired and the mass was excised. Histological examination showed features compatible with AA. The patient received no further treatment and had no evidence of systemic disease. Three months after the diagnosis of AA was made he presented with anemia and rectal bleeding. Colonoscopy demonstrated a large infiltrative tumor of the rectum, partially obstructing the lumen. Histological examination of the biopsies taken, revealed a moderate differentiated adenocarcinoma of the rectum. Because the tumor was unresectable the patient received systemic chemotherapy and radiotherapy and 10 months later is in good condition without evidence of metastatic disease.

In the present study we present an extremely rare case of AA in a male patient. To our knowledge, this is the first reported case of an AA with a metachronous adenocarcinoma. Correlation or common pathogenetic mechanisms are presently unknown.

P-172

A case of sarcoidosis established by gastrocnemius muscle biopsy.

Ioannis Veniselos; Zoi Tatsiou; Eleutherios Anagnostou; Anastasios Chatzitolios; Christina Nikolaidou; Despoina Alataki

Department of Pathology, Hippokration Hospital, Thessaloniki, Greece

Sarcoidosis is a multisystem disorder of unknown cause, characterised by granuloma formation in affected organs. Its diagnosis is established by the combination of clinical, laboratory, radiological and histological findings. Symptomatic muscle involvement is reported to be between 0.5 and 1.4% of known cases of sarcoidosis.

We report the case of a 42-year-old man who was admitted to our hospital due to bilateral painful enlargement of the ankle joints of 20 days duration with coexisting arthralgies especially in the hands, feet and knees as well as myopathic symptoms. On physical examination there was swelling of the ankle joints with rubor and pain during the palpation. There was no peripheral lymphadenopathy or hepatosplenomegaly. His autoantibody profile was negative. Inflammatory markers like C reactive protein and erythrocyte sedimentation rate were raised. His lactate dehydrogenase, creatine kinase as well as transaminases and fibrinogen levels were also elevated. Complete blood count was normal. Vidal-Wright reactions and Mantoux test were negative. A chest x-ray showed bilateral hilar lymphadenopathy. Thereafter, he underwent a 67Ga-Citrate scintiscan which showed 67Ga collection in hilar lymph nodes and in lesser amount in the joints. A gastrocnemius muscle biopsy was performed and histological examination showed the presence of epithelioid non-necrotic granulomas. In accordance with the clinical and histological findings, the diagnosis of sarcoidosis affecting the skeletal muscle was made. The patient received treatment with high dose methylprednisolone followed by oral prednisolone and 7 months later is in good condition.

We report the case of sarcoidosis presenting with polyarthritis and myopathic syndrome confirmed with gastrocnemius muscle biopsy. The impressive sensitivity of muscle biopsy, its safety and ease of performance, along with the extreme rarity of muscle involvement by other granulomatous diseases, may render it as the procedure of choice for the histologic confirmation of sarcoidosis.

P-173

Diagnostic usefulness of synovial biopsy in monoarthritis and oligoarthritis: A retrospective analysis of 146 synovial biopsies over 11 years (1990–2000)

Khedija Cherif;Faten Limaiem; Amina Mekni; Ines Chelly; Selma Bellil; Khedija Bellil; Haifa Azzouz; Nidhameddine Kchir; Moncef Zitouna; Slim Haouet

Hospital La Rabta; Bab Saadoun Tunis. Tunisia

Background: Synovial biopsies are seldom used for diagnostic purposes. In general, patient interview, clinical examination, routine laboratory testing, radiographic examination and synovial fluid analysis usually suffice to establish a correct diagnosis. Synovial biopsy analysis is only justified in cases with a high degree of suspicion of atypical infectious agents, evaluation for intra-articular tumours and diseases with characteristic histological features.

Aim of study: Our goal is to assess the utility of synovial biopsy in establishing correct diagnosis of oligoarthritis and monoarthritis through a confrontation of histological findings with clinical diagnoses. We will also discuss its limitations and compare our results with those reported in literature.

Materials and Methods: Between January 1990 and December 2000, 146 patients have undergone arthroscopic or surgical synovial biopsies as a diagnostic procedure for monoarthritis and oligoarthritis of unknown etiology. For each case, we proceeded with a confrontation of histological diagnoses with clinical findings after a mean follow-up period of 5 years.

Results: Our study group included 69 men and 77 women aged between 7 and 85 years (mean=41.2 years). One hundred and twenty nine patients (88.4%) had monoarthri-

tis and 17 patients (11.6%) had oligoarthritis. Diagnosis yielded by synovial biopsy was concordant with clinical findings in 84.2% of the cases. Discordant diagnoses were mainly related to rheumatoid arthritis (n=5), osteochondrmatosis (n=1), chondrosarcoma (n=1) and tuberculous arthritis (n=1).

Conclusion: Our results are similar to those reported in literature and show that synovial biopsy is reliable in establishing correct diagnosis of oligoarthritis and monoarthritis.

P-174

Accuracy of fine needle aspiration biopsy in soft tissue tumors diagnosis - Diagnostic meta-analysis

Luciana Schmidt Kirschnick; Omar Moreira Bacha; Maria Isabel Edelweiss

Universidade Federal do Rio Grande do Sul - Hospital de Clinicas de Porto Alegre - Brazil

Context - Accurate diagnosis is relevant for the treatment and prognosis of soft tissue tumors (STT). Open incisional and/or excisional biopsy are still gold-standard in the diagnosis of these neoplasias. The real accuracy of fine needle aspiration biopsy (FNAB) in the diagnosis of soft tissue tumors is still controversial in literature.

Objective - To assess the accuracy of FNAB compared to gold-standard in STT diagnosis.

Methods - Systematic research on MEDLINE, EMBASE and COCHRANE databases (1996–2007) for STT accuracy diagnostic studies was done. Six studies were included, showing 310 cases in the assessment of malignant and benign diagnosis and 190 cases for specific diagnosis. Articles were assessed through STARD checklist criteria and Oxford levels of evidence and grades of recommendation. Only the ones compared to gold-standard were included. Non-mesenchymal tumors and articles that did not allow for the exclusion of these cases despite having good methodological quality were excluded. There was no language restriction. MetaDisc software for statistical analysis was used.

Results - In the malignant and benign diagnosis, scores of 89.8% (95% CI; 84.3–93.8) for sensitivity; 88.8% (95% CI; 82.2–93.6) for specificity; 6.807 (95% CI; 4.262–10.874) for positive likelihood ratio (LR); 0.136 (95% CI; 0.083–0.224) for negative LR and 63.499 (95% CI; 28.818–139.91; p=0.425 and I2=0.0%) for diagnostic odds ratio (DOR) were found. For specific diagnosis, scores of 55.5% (95% CI; 45.7–64.1) for sensitivity; 51.1% (95% CI; 40.3–61.8) for specificity; 1.245(95% CI; 0.963–1.609) for positive LR; 0.803 (95% CI; 0.587–1.099) for negative LR and 1.644 (95% CI; 0.896–3.018; p=0.560 and I2= 0.0%) for DOR were found.

Conclusions - FNAB, based on current literature data, presented high accuracy in malignant and benign diagnosis and low accuracy in the specific diagnosis of STT.

P-175

Prostheses-related sarcomas of the hip and knee

Beatriz Fernández-Rodríguez;Patricia Domínguez-Dorado;Carlos Aliste;Pablo Lorenzo-González;Ihab Abdulkader;Juan Varela-Durán;Jerónimo Forteza;José Manuel Suárez-Peñaranda

Hospital Clínico Universitario de Santiago de Compostela. Spain

Background: Prostheses-related sarcomas are unusual butserious complications of orthopaedic surgery. Patients have an average age of 66 years and the mean time between surgery and the diagnosis is 6 years. They are usuallylocated in the hip area and the most common type is malignant fibroushistiocytoma. Prognosis is poor and most patients died in the first year.

The reason of this association is not known.Although some of the prostheses components, like chromium, nickel or cobalt,have been implicated, a casual association cannot be ruled-out.

Case Reports:

Case 1: A 78-year old woman with total hipreplacement twenty years ago. She complaint of pain in the right femur for oneyear, that increased the last week. Radiological examination revealed apathological bone fracture with associated lesion in the surrounding softtissues, which was considered of infectious origin. Examination of thecurettage specimen showed a neoplasm with histopathological immunohistochemicalfeatures of malignant fibrous histiocytoma. The patient alive with livermetastases, four months after surgery.

Case 2: A 65-year old woman with bilateral kneereplacement fifteen and one year ago. She complaint of pain from the moment ofthe last surgery. Radiological studies showed non-specific findings. The prosthesiswas removed and pathological examination revealed a soft tissue neoplasm. Histopathology and immunohistochemistry showed to be a leiomyosarcoma. Supracondylealamputation was performed and the patient is free of disease four months aftersurgery.

Conclusions: We report two unusual cases of sarcomas. Theassociation with prosthetic implants is well documented, but far from clear.Moreover, our case 2 is a leiomyosarcoma, which has been only rarely reportedin this context. The lapse of time from surgery is short, but some reportedcases have demonstrated even shorter intervals.

In patients with prosthetic devices and softtissue lesions is mandatory to exclude a neoplasm.

P-176
CEMENTIFYING FIBROMA- CLINICAL CHARACTERISTICS, HISTOLOGICAL FEATURES AND CORRELATION

Jelena Sopta; Goran Tulic; Vesna Mijucic; Vera Vojinovic
Institute of pathology, School of medicine, Belgrade. Serbia

Cementifying fibroma (CF) is a fibro-osseous lesion which produces cementum. The aim of the current study was to further refine its clinical and hystological features and to make clinico-pathological correlations. The authors report 10 cases of cementifying fibroma diagnosed on the Institute of pathology School of Medicine, Belgrade during the 15-years (1995–2005.). CF showed no sex predilection (5 males and 5 fimales). The youngest patient was male 14 years old, and the oldest was female 54 years old (the average years were 27,1). The maxila was the most frequent site (80%), just 1 patient had lesion in the baseos cranii with invasion of sella turcica. All the patients reported history of pain and edema lasting from 3 to 20 months (midle 10,4 months). The other clinical simptoms were: face assimetry, tooth dislocation and bulbus protrusion. The evolution of the tumor was longer and clinical cours indolent in the patients with mandibular localisation (mandibula-12,3 months, maxilla -9,5 months).
Clinical cours and longitude of anamnessis are in the correlation with histological feature of CF. The main histomorphological diagnostic criterium for CF are «psammoma like structures». There number and mineralisation of bone spheruls varyed during the tumor maturation. In old lesions with long anamnessis increase the number of "psammomatoid" bodys. In the opposit, dramatic clinical simptoms were discrabed in the CF with stromal haemorrhage and inflammation. We had one patient with secondary superposition of aneurysmal bone cyst on the prime CF.
Differential diagnosis of cementifying fibroma and other fibro-osseous lesion of cranial bones just by histological evaluation is often difficult and asked for permanent cooperation between clinical doctors and pathologists.
Kee words: cementifying fibroma, psammoma like body

P-177
Three-dimensional collagen-chondroitin sulfate-hydroxyapatite composite scaffolds for bone regeneration

Oana Craciunescu1; Lucia Moldovan1; Elena Iulia Oprita1; Mirela Balan1; Alexandra Gaspar1; Otilia Zarnescu2
1Department of Cellular and Molecular Biology, National Institute R&D for Biological Sciences, Bucharest, Romania; 2Faculty of Biology, University of Bucharest, Romania

Background. Osteogenesis is a natural repair mechanism that occurs in the human body but in critical sized bone defects, a transplantation of bone tissue or bone substitute is needed to regain bone integrity. In recent years, scaffolds built from synthetic or natural materials for guiding the proliferation and spread of different cell types were developed. The aim of our study was to characterize new biomaterials composed of collagen type I (COL), chondroitin sulfate (CS) and hydroxyapatite (HA), and to investigate their in vitro effect on a human osteoblast culture.
Methods. Two variants of COL-CS-HA composite scaffolds were prepared by mixing natural polymers with HA in different weight ratios (COL:CS:HA 1:0.5:1 (I); 1:0.5:2 (II)). Their structure and morphology was analyzed by scanning electron microscopy (SEM). Scaffold biodegradability in the presence of collagenase was measured. Osteoblast viability, adhesion and morphology were assessed by MTT test and DAPI-staining of cell nuclei.
Results. SEM micrographs showed a highly porous structure with small white aggregates of HA, non-homogenously scattered in the COL framework. The porosity decreased proportional with the increase of the HA quantity. In vitro biodegradability test demonstrated that the exposure to ultraviolet light increased the resistance of porous composites to collagenase digestion. The MTT test indicated the highest cell viability for variant I. Nuclear staining with DAPI showed that cells retained their normal morphology and adhered, spread and proliferated inside the porous scaffolds.
In **conclusion**, porous COL-CS-HA composites with good physico-chemical and biological properties were developed by HA powder integration in a mixture of COL-CS. Both composite variants were biocompatible with human osteoblasts in vitro. These biomaterials could be used as scaffolds for bone regeneration.
This work was supported by Romanian Programme 4 "Partnership in Strategic Domanis", Project No. 61012.

P-178
Clinicopathologic features of retroperitoneal tumors.

Oleko Dmitrievich Mishnev, Elena Alexeevna Dubova, Konstantin Anatol'evich Pavlov, Alexandr Ivanovich Shchegolev
FGU Vishnevsky Institute of Surgery Rosmedtechnologiy. Russia

Introduction: Actuality of investigation of retroperitoneal tumors is connect with considerable difficulties, such as their clinicolaboratorial and morphological diagnosis.
Method: Complex clinicomorphological (histological, immunohistochemical, cytological, electron microscopic) investigation of biopsy and surgical materials of 74 patients

(19 men and 55 woman, aged 22–75), treated in 2001–2007 for retroperitoneal tumors, was performed.

Results: In 6 cases neoplasms affected viscera (kidney, adrenal glands, uterus), in 3 cases cancer metastases (2 – adenocarcinomas, 1 – epidermal cancer) without detection of primary focus were diagnosed, in 3 cases – hematomas with sing of formation, in 1 cases – benign hyperplasia of lymphatic nods. In 61 cases (21%) of non-organic retroperitoneal tumors affections cystic tumors were detected: 6 cases – celomitic cysts, 7 cases – cystic lymphangiomas; in 21% of the cases lypolitic tumors were revealed: 3 – lipoma, 10 – lyposarcoma, in 18% - muscular tumors: 1 – leiomyoma, 10 – leiomyosarcoma (Ki67 - 23%). In 9 patients peripheral nerves tumors were detected: 5 – neurofibroma, 2 – neurinoma, 2 – malignant neurinoma (Ki67 - %). In 13% of the cases fibrous tumors were diagnosed: 7 malignant fibrous histiocytoma (Ki67 - 12%), 1 – fibrosarcoma (Ki67 - 22%). In 3 cases nonchromaffin paraganglioma (Ki67 - %), in 2 – hemangioma, in 1 – venous-cavernous angiodisplasia, in 1 – gastrointestinal stromal tumor (CD117+, CD34+, Ki67 - 12%) were detected.

Conclusion: Final decision regarding the origin of retroperitoneal tumors can be drawn after complex morphological study with obligatory application of immunohistochemical methods.

P-179

A multilocular large gastrointestinal stromal tumors of the small intestine

Sahin O;Dilek H;Aktepe F;Polat C;Çalış O

Afyon Kocatepe Univ. School of Medicine, Dept. of Pathology, Turkey, Afyon Kocatepe Univ. School of Medicine, Dept. of General Surgery, Turkey

BACKGROUND Gastrointestinal stromal tumors (GIST) are the most common mesenchymal neoplasms arising from the gastrointestinal tract and typically occur in adults older than 40 years with a peak incidence in the sixth and seventh decades. Gastro-intestinal stromal tumours are a heterogenous group of mesenchymal tumours mostly arising from the stomach and small intestine which may be benign or malignant. In the present case we reported a patient with multilocular large GIST and discussed the relevant literature on this topic.

METHODS: A 48-year man presented with abdominal pain and progressive distension of abdomen. Preoperative CT evaluation revealed two masses; one superior to bladder with septas and the second 7×5 cm solid mass. Both masses were interrelated and included some calcified areas. Microscopically, the tumour consisted of anaplastic spindle cells with high mitotic activity (90 mitoses per 50 high-power fields). Immunohistochemically, the spindle cells were positive for c KIT and CD34. The final diagnosis was high-grade malignant gastrointestinal stromal tumour of the jejunum.

CONCLUSION Considering the recent advances in the diagnosis and treatment of GIST, this neoplasm should be taken into account in the differential diagnosis of the tumours appearing in the jejunal region.

P-180

A case of synovial sarcoma; a solid mass in the inguinal region

Sahin O, Dilek H, Aktepe F, Yilmaz S, Çalış O

**Afyon Kocatepe Univ. School of Medicine, Dept. of Pathology, Turkey; Afyon Kocatepe Univ. School of Medicine, Dept. of General Surgery, Turkey*

BACKGROUND Synovial sarcomas in this location have been characterized by slow growth, intense pain in some which is not explained by the microscopic image, intense vascularity and, macroscopically, by precise peripheral limits.The great majority of the tumors known as synovial sarcomas are found in the extremities, near to, but not directly continuous with joint spaces.In the present case we reported a patient with synovial sarcoma presented as right inguinal fine defined mass that was presented as lymphadenopathy.

METHODS: A 21 years old female was presented with restlesness, weight loss and mass in the groin. History revealed inguinal mass that was present for 3–4 monthes and pain. The postoperative diagnosis revealed that the tumor was positive for vimentin and CK 7. The mass was diagnosed as biphasic synovial sarcoma.

CONCLUSION We suggest that the clinical and pathologic data concerning the origin, location and microscopic appearance of these tumors infer that they might better be named synovial sarcoma.

P-181

THE PROGNOSTIC AND PREDICTIVE VALUE OF ANGIOGENESIS IN RHEUMATOID ARTHRITIS

Ioan Jung; Simona Gurzu; Tibor Mezei

University of Medicine and Pharmacy Tg. Mures, Romania

Background: Angiogenesis is an important process in a number of physiological and pathological processes, such as inflammation, tissue repair and neoplasia. In rheumatoid arthritis (RA) the angiogenesis is a fundamental component of pannus development, which covers and erodes the articular cartilage.

Material and methods: In synovial biopsies, we determined the immunohistochemical expression of the following antibodies, provided by Lab-Vision: CD31, CD34, CD105 (Endoglin) and VEGF. We used the immunoperoxidase method. We measured the positive vessels' area versus total tissues' area.
Results: In RA, high levels of VEGF, FGF1,2, TGF-beta and other angiogenic growth factors are present in the synovial fluid. We observed a high expression of VEGF in the hyperplasic synovial cells, respectively CD105 in neoformed vessels and in the activated endothelial cells.
Conclusions: The angiogenesis may have important diagnostic, prognostic and predictive value in RA. It correlated with the progression of joint destruction and with the activity of the disease. The antiangiogenic therapy could stop the progression of RA. We belive that the synovial biopsy could be an important method in the estimation of the RA evolution.

P-182

Pleomorphic Hyalinizing Angiectatic Tumor of Soft Parts: A case report

Mi Sun Chei; Yu Na Kang; Hae Ra Jung; Sun Young Kwon; Sang Pyo Kim; Kun Young Kwon; Sang Sook Lee
Department of Pathology, Keimyung University School of Medicine. South Korea

Pleomorphic hyalinizing angiectatic tumor (PHAT) is a rare, recently recognized neoplasm occurring predominantly in the subcutaneous tissue of the lower limbs of adults. We report a case of PHAT in an 71-year-old man who presented with a 4.5×4.0×3.5 cm mass in the deep subcutaneous layer of his left inguinal area. The left inguinal mass was growing slowly in two years. No symptom was detected. Ultrasonographic findings showed a well-defined, slightly lobulated, heterogeneous, echogenic mass in the deep subcutaneous layer. The possibility of malignancy could not be excluded. Excisional biopsy was done. Histologically, the tumor was well circumscribed by a thin fibrous capsule and predominantly composed of fusiform cells with eosinophilic cytoplasm and round-to-oval or pleomorphic nuclei. The tumor had irregular-shaped mono- or multinuclear cells and marked bizarre cells with prominent intranuclear cytoplasmic inclusion. Also prominent angiectatic vesssels showing the endothelial lining with a thick eosinophilic and hyalinotic amorphous material. The positivity of CD68 and CD34 immunohistochemical stains was detected.

P-183

Atypical organizing seroma following treatment for soft tissue sarcomas of the extremities

Annarita Palomba; Giovanni Beltrami; Rodolfo Capanna; Alessandro Franchi
Dipartimento di Patologia Umana ed Oncologia. Italy

Background Postoperative seromas are a well recognized complication in patients who have undergone excision of extremity soft tissue sarcomas. Due to atypical MRI findings, these lesions may be surgically explored to exclude the possibility of sarcoma recurrence or of development of a radiation induced sarcoma.
Method We retrospectively reviewed 6 cases of postoperative seroma occurring in patients treated at our center for soft tissue sarcoma of the extremities, who were biopsied or surgically treated with the clinical suspicion of recurrence or radiation induced sarcoma. The initial diagnosis were leiomyosarcoma in 4 patients, synovial sarcoma in one and myxoid liposarcoma in one. All patients had been surgically treated and 4 had received radiation therapy. Hematoxylin and eosin stained slides were retrieved for each case and immunohistochemical staining were performed on paraffin embedded sections according to standard protocols.
Results All lesions contained fibrin clots partially covered by a single layer of flattened cells, with inconspicuous cytoplasm and oval, sometimes bulging, nucleus, either forming interconnected pseudovascular spaces containing erythrocytes or solid sheets. In two cases, there were focal areas showing a papillary architecture, with fibrin cores lined by flattened cells. Scattered cells, both lining pseudovascular spaces and within the fibrin clots, showed enlarged nucleus with prominent nucleolus, but no real pleomorphism as well as mitotic figures were observed. CD 34 immunostaining was observed in 5 cases, while CD31 and D2–40 were detected in 4 cases. At least one marker was expressed in all cases. MIB-1 nuclear staining was present in all cases (18–35% of cells).
Conclusions We present the histological features of a small series of soft tissue lesions following treatment for sarcoma clinically simulating a recurrence or a radiation induced neoplasm. The primary importance of recognizing these lesions lies in their possible misdiagnosis as angiosarcoma under histologic examination.

P-184

TETRASPANINS EXPRESSION ANALYSIS IN SOFT - TISSUE TUMORS

Kátia C Carvalho; Marcilei E C Buim; Luis F L Reis; Fernando A Soares; Isabela W Cunha
Fundação Antonio Prudente - Hospital A C Camargo. Brazil

Background: Tetraspanins are transmembrane proteins with at least 33 members in humans. These proteins can be associated each other and with a large number of different transmembrane proteins. They are involved in cellular processes like cell adhesion, motility, differentiation and proliferation, and the profile of expression or the role of these proteins in soft tissue tumors (STT) are unknown. The aim of this study was to evaluate expression of tetraspanins CD9, CD37, CD81, CD63 and CD82 by immunohistochemistry in several histological types of STT.
Methods: We analized the protein expression in 352 samples of STT (including fibromatosis, leiomyosarcoma, liposarcoma, synovial sarcoma, fibrosarcoma, pleomorphic sarcoma, schwannomas and others) spotted in duplicated in 3 tissue microarray paraffin blocks. Correspondent normal mesenchymal tissues were also analyzed. We classified the profile of the expression in 4 groups based on intensity of reaction (negative, weak, moderate and strong positive). For statistical analysis, we evaluated some clinical-pathological parameters such as hystological grade and metastasis.
Results: There was no expression of CD37 in normal or tumor tissue. Expression of CD63 was detected mainly in pleomorphic sarcomas (51%) and leiomyosarcomas (40%). CD81 and CD82 were found in almost every tumors tissue types, but in weak intensity. Expression of CD9, mainly moderated, was detected in leiomyosarcomas (28%) and pleomorphic sarcomas (22%). We found significant difference of expression of CD63, CD9 (both with $p<0{,}001$) and CD81 ($p<0{,}036$) between malignant and benign tumors.
Conclusion: all tetraspanins, except CD37, were present in soft tissue tumors. CD63 and CD9 were the most expressed, mainly in pleomorphic sarcomas and leiomyosarcomas. Our results showed that tetraspanins role in soft tissue tumors must be better investigated.

P-185
HHV-8 (LNA-1) POSITIVE MULTIFOCAL INFLAMMATORY MYOFIBROBLASTIC TUMOR

Nilufer Onak Kandemir; Banu Dogan Gun; Burak Bahadir; Gamze Numanoglu; Nimet Karadayi; Sukru Oguz Ozdamar
Zonguldak Karaelmas University, School of Medicine, Department of Pathology,Zonguldak, TURKEY

Background: Inflammatory myofibroblastic tumor (IMT) is a rare soft tissue tumor with intermediate biological potential. It is mostly found in lungs, generally in children and young adults. Proliferation of myofibroblastic spindle cells accompanied by inflammatory infiltrate characterizes its histology. Anaplastic lymphoma kinase (ALK) gene translocations are observed in almost 50% of the cases. Recent detection of EBV and human herpes virus (HHV)-8 in some cases may indicate the possible role of infectious agents in pathogenesis.
Case: An 80-year-old male presented with abdominal pain, fever, and loss of weight. Subsequent to detection of tumoral lesions in his right scrotum and mesentery of ileum, partial ileum resection and right orchiectomy were performed. Grossly, scrotal tumor neighboring epididimis was well-circumscribed and 2 cm in its greatest diameter. The larger $11\times10\times9$ cm mesenteric tumor infiltrating the ileal wall without obvious mucosal destruction exhibited focal cystic areas, necrosis, and hemorrhage. Microscopically, both tumors consisted of spindle-shaped myofibroblastic cells, ganglion-like giant cells, and inflammatory cells of mixed type settled in a myxoid stroma. Tumor cells demonstrated evident pleomorphism, but no mitosis was noted. Spindle cells immunohistochemically expressed vimentin, smooth muscle actin and HHV-8 (LNA-1). No reaction with epithelial membrane antigen, pan-cytokeratin, ALK, HMB45, CD34, factor VIII, desmin, S-100, CD68, CD 117(C-kit) and glial fibrillary acidic protein was observed in tumor cells. Considering the histopathological and immunohistochemical findings, the case was diagnosed as multifocal inflammatory myofibroblastic tumor.
Conclusion: IMT is an uncommon tumor with varying clinic and histopathologic characteristics. The current case is presented with literature review considering its concurrent existence in two separate extra-pulmonary locations and immunohistochemical HHV-8 (LNA-1) reaction of tumor cells.
Key words: Inflammatory myofibroblastic tumor, human herpes virus-8, immunohistochemistry.

P-186
Angiomatoid Malignant Fibrous Histiocytomas

Loredana Ungureanu; Doinita Radulescu; Simona Stolnicu; Sorin Dumitriu
University of Medicine and Pharmacy "Gr. T. Popa" Iasi, University of Medicine and Pharmacy Tg. Mures. Rumania

We studied four cases of angiomatoid malignant histiocytoma. The patient's ages ranged from 20 to 39 years. There

was a marked female predominance with a female-to-male ratio of 3:1. There was a predilection for the extremities (2 out of 4 cases). Three patients had tumors within subcutaneous tissue. The tumors ranged in size from 2 to 8 cm in greatest diameter. They consisted of partially cystic, circumscribed masses surrounded by a thick layer of connective tissue where a cuff of chronic inflammatory cells with formation of lymphoid follicles was present in variable amount. The cystic cavity was filled with blood and had no endothelial lining. The cytology of the tumor was bland with presence of uniform, spindle-shaped or ovoid cells forming clusters or lobules. Hemosiderin pigment was invariably present. Three of these patients had clear surgical margins at the time of the original excision and remained free of disease. Only one patient was clinically diagnosed with hematoma which was incised and drained. The tumor had been growing for 14 months and was excised, and the patient was free of tumor after 80 months. Our study shows that Angiomatoid Malignant Fibrous Histiocytomas is better treated by surgical excision, and appears to follow a low grade malignant course, characterized by local aggressiveness.

P-187

EXTRASKELETAL OSTEOCHONDROMA OF THE CHEST WALL: A CASE REPORT

Houda Mahmoudi-Brahim; Leila Njim; Abdelmajid Dhouibi; Nada Touil; Nejib Ben Yahia; Adnene Moussa; Abdelfattah Zakhama.

Department of Pathology, Universitary Hospital Center, Monastir, TUNISIA.

Background: Extra skeletal osteochondroma are benign soft tissue tumors occurring in extra-osseous and extra-synovial locations, predominantly composed of adult mature hyaline cartilage, with prominent ossification. The majority of tumours occurs in the region of the fingers and is rare in atypical sites such as chest wall.

Method- Results: We present an unusual case of an extra skeletal osteochondroma of the chest wall in a 31-year-old woman and illustrate the clinical, radiographic and histological features of this entity.

We review the literature and discuss the differential diagnoses.

Conclusion: An integrated clinical-pathologic diagnosis helps to clarify the nature of extra skeletal cartilaginous tumors that can arise at unusual site. Complete local surgical excision is the management of choice.

Presenting author: Adnene Moussa, Department of pathology, Universitary Hospital Center,Monastir-Tunisia. adnmoussa@yahoo.com

P-188

Isolated intraosseous gouty tophus in hallux sesamoid. A case report

Antoni Urban Ramón; Anna Domingo Amela**; Ramón Rochera Vilaseca***

**Centro Médico Teknon (Barcelona), **Hospital Sant Jaume, Calella (Barcelona). Spain*

INTRODUCTION Gout is a systemic disorder associated with the deposition of sodium urate crystals in the joints and soft tissue. Often, but not invariably, the serum urate levels are elevated as a result of overproduction or underexcretion of urid acid. Intraosseous gotty invasion is a relatively rare condition. We are reporting an unusual case of intraoosseous tophus of a great toe sesamoid, presenting as a persistent pain without prior history of gouty attack or underlying systemic disorders.

CASE REPORT An otherwise healhty 38-year-old man had had left great toe pain intermittently for about one year, after a car accident. On physical examination there was no inflammatory signs and analysis was normal. Radiograph, CT scan and Radionuclide scintigraphy showed a sesamoid fracture and a probable bone necrosis. Sesamoid bone was removed and the tissue obtained showed numerous tophaceousdeposits composed of crystalline material with surrounding histiocytes, giant cells, chronic inflammatory cells, and fibrosis in the destroyed bone. The pathologic diagnosis was intraosseous gout in sesamoid. Serum urate levels were never abnormal in posterior analyses. Three months later the patient had a characteristic attack of acute arthritis and began treatment. He had had no other clinical symptoms until now, six months after the diagnosis.

CONCLUSION Gout is a common disease in adults and tophaceous deposits usually appear after a long time of hyperuricemia; in fact, most of the previous cases of intraosseous gout have been described in long standing hyperuricemic patients. Thus, in our case the final diagnosis was completely unexpected. It is important to be aware of this entity as a source of sesamoid pain that can be cured by medical therapy

P-189

Malignant Psammomatous Melanotic Schwannoma Of The Axilla. A Case Report

Kalliopi Diamantopoulou; Stavroula Chranioti; Penelopi Korkolopoulou; Efimia Thoma-Tsagkli

Department of Pathology General Hospital Asklepieio Voulas and Medical School University of Athens. Greece

Background: A 46-year-old woman with neurofibromatosis 1, but not Carney's complex, presented with a mass of the right axilla, without history from her breast. A

malignant psammomatous melanotic schwannoma was diagnosed, a rather unusual case, as malignant schwannomas have been reported in only 3,1% of patients with Von Recklinghausen's neurofibromatosis.
Method: A solid, partly cystic mass of ~9,5 cm of the right axilla with orange brown pigmentation was excised. Paraffin-embedded tissue was stained with H-E, PAS, Gomori and Fontana. Immunohistochemistry was performed with the antibodies: S-100, Vimentin, HMB-45, NSE, Collagen IV, Desmin, SMA, HHF-35, EMA and CK8,18,19.
Results: Spindle-shaped and epithelioid neoplastic cells, with large vesicular nuclei and eosinophilic nucleoli, were observed. Multinucleated cells and cells with cytoplasmic vacuoles like mature adipose tissue, were also present. Mitotic activity was increased, with abnormal figures. Numerous laminated calcispherites (psammoma bodies-PAS+) and melanin pigment as brown/black granules (Fontana +) were also observed. Zones of necrosis were present, especially near cystic parts of the tumor. An inter- and pericellular reticulin staining pattern was revealed. Immunohistochemistry: S-100(+), HMB-45(+), Vimentin (+), NSE(+), laminin(+), focally Collagen IV(+). The main and most difficult differential diagnosis is with neurotropic malignant melanoma, depending on clinical course and presence of giant melanosomes ultrastructurally.
Conclusion: Our case, a malignant psammomatous melanotic schwannoma of the axilla (involvement of cervical spinal nerve) is extremely rare, as psammomatous type of melanotic schwannomas usually involves alimentary tract tumors. Most melanotic schwannomas are benign, slowly growing tumors, psammomatous form of which usually presents with Carney's complex, (a dominantly transmitted autosomal disorder), not our case. Tumors may follow a malignant course, usually after local reccurence.

P-190

Utrophin assay in Becker Muscular Dystrophy

Elahe Keyhani;Kimia Kahrizi;Yousef Shafeghati;Mehdi banan;Elham Darabi;Jalal Gharesouran;Hossein Najmabadi
Genatics Research Center. Iran

Background: Utrophin(Dystrophin Related Protein) is a protein which show marked homology with Dystrophin.It is normally found in neuromuscular junction and peripheral nerves but is absent in sarcolemma.In Dystrophinopathies, Utrophin is increased in normal position of Dystrophin and could be detected by Immunohistochemistry & Immunoblotting.Methods:10 clinically suspected BMD (Becker Muscular Dystrophy) were selected.Muscle biopsy was performed from Deltoid muscle for allof the cases.Immunostains (Spectrin,D1,D2,D3& Utrophin) were done on frozen muscle sections followed by Western blot analysis of protein extract for each muscle sample.Result: All of the patients showed an on & off pattern of all subtypes of Dystrophins & were confirmed as BMD using Immunoblotting technique.Abnormal expression of Utrophin is also evident in BMD patients (confirmed by both immunostaining & immunoblotting).This pattern is not evident in other subtypes of Muscular Dystrophies.Conclusion:Utrophin assay is an important & complementary tool for the diagnosis & differentiation of muscular Dystrophies.

P-191

SUBSCAPULAR ELASTOFIBROLIPOMA

José-Luis Carrasco Juan; Hugo Álvarez-Argüelles Cabrera; José-Antonio Perera Molinero*
Department of Pathology. Faculty of Medicine. La Laguna University. La Laguna. Tenerife. Canary Islands. Spain.
(*) Service of Pathology. La Candelaria University Hospital. Tenerife. Canary Islands. Spain.

BACKGROUND Elastofibrolipoma is a rare entity that was first described by De Nictolis et al. in 1995, and that, at the present, only two cases of which have been reported.
METHOD Tissue samples were fixed in 10% buffered formalin, embedded in paraffin blocks; 0,4-mm-thick histologic sections were taken and stained with hematoxylin and eosin, Verhoeff elastin and Masson trichrome stains.
RESULTS A 72-year-old male patient presented with a recidivant subscapular lipoma (previously studied and diagnosed in other institution). On gross examination, it was a 5× 4×2-cm mass with a capsulated and yellow-brown appearance. The cut surface was solid and lipomatous, showing streaks of white tissue irregularly alternating with areas of yellow tissue. Microscopic examination revealed that the lesion has a thin fibrous capsule. The mass consisted of bands of hypocellular, fibrous connective tissue, which separated numerous lobules of mature adipose tissue. In addition, numerous elongated or globe-like, eosinophlilic deposits, sometimes arranged linearly, were haphazardly distributed throughout the fibrous connective tissue. These deposits were strongly colored with an elastic stain. A diagnosis of benign mesenchymal tumor, i.e. elastofibroma, was made.
CONCLUSION Our findings supports that the elastofibrolipoma is a true benign neoplasm. This rare and recently recognized entity, must be bear in mind in the differential diagnosis of subscapularly located, deep-seated, well-circumscribed masses.

P-192

Intranodal kaposi sarcoma

Akyıldız Igdem A;Celik E, Sahan E; Erdogan N
Taksim's Education and Training Hospital,Pathology Department,İstanbul/ TURKEY

75 years old patient presented with dispne, and coughing to the Internal Medicine Department of Taksim's Education and Research Hospital. Multiple mediastinal, bilaterally axillary, inguinal, celiak, vertebral and paraaortic lymphadenomegaly had seen by MRI, CT and USG. Hematologically there was trombocytopenia and normochromic normocyter anemia. Because his PSA was high, prostatic biopsy was planned. And the result of the biopsy was prostatic adenocarsinoma. Besides axillary lymph node was excized and the histopathological result was intranodal Kaposi sarcoma. HIV markers were negative. Before he had the diagnosis of chronic renal failure. Because of prostatic adenocarcinoma and chronic renal failure he was immunologically insufficient, this prepared the situation for intranodal Kaposi sarcoma. We present the case because it is quite rare in literature.

Liver and Pancreas Pathology

P-193

Cellular senescence in pancreatic ductal adenocarcinoma protection

Marta Cañamero, Manuel Collado, Carmen Guerra, Mariano Barbacid and Manuel Serrano
Centro Nacional de Investigaciones Oncológicas (CNIO). Spain

K-Ras oncogenic activation is a very frequent genetic alteration in human Pancreatic Ductal Adenocarcinoma (PDA). The generation of a mouse model with controlled temporal expression of K-RasG12V under its endogenous promoter in acinar and centroacinar cells has allowed us to study the generation of preneoplastic lesions, PanINs, and their evolution to PDA1. It has been recently described that preneoplastic lesions of the lung developed by mice with widespread expression of K-RasG12V were enriched of cells positive for markers of cellular senescence2. For this reason, we decided to characterize the senescence response during pancreatic neoplasia, since senescence has proved to be a relevant tumor suppressive mechanism *in vivo*3.
Moreover, the characterization of pancreatic neoplastic lesions by oncogenic K-Ras in mice revealed that K-RasG12V expression in adult animals does not result in neoplastic development unless accompanied by chronic pancreatitis. Thus, we decided to explore how continuos low doses of caerulein, a treatment causing mild pancreatitis, can affect the senescence response.
Finally, since a high percentage of human PDA has been firmly linked with chronic pancreatitis, we wondered whether halting the pancreatitis treatment would allow the control of the neoplastic development, if senescence has a role in this control and how effective would the senescence response be in controlling tumor development.

P-194

Inflamatory Myofibroblastic Tumor presenting as a pancreatic mass

Antonio Calvo; Ángela Hens; Luis Miguel Marín; Alonso Camacho; Gloria Muñoz; María Isabel Moreno.
Hospital Universitario Puerto Real (Cádiz). Spain

Inflammatory myofibroblastic tumor of the pancreas is extremely rare, an entity previously known as an inflammatory pseudotumor. It has generally been considered a benign pseudosarcomatous inflammatory lesion which may have an infectious aetiology, very rare in the pancreatico-biliary region. We report a case of a 63-year-old man with a 3,5 cm pancreatic mass originally diagnosed as malignancy, which required surgical exploration and complete resection. Histologically the tumor consisted of a smooth muscle actin and CD68-positive spindle cell population and a more abundant mononuclear inflammatory cell population, primarily composed of T-lymphocytes and few macrophages. Genomic hybridization analysis of the tumor showed no chromosomal imbalances, with polyclonal rearrangement of IGH gene (CDRII, CDRIII).
It can be extremely difficult to differentiate inflammatory myofibroblastic tumour from pancreatic malignancies, and most cases require surgical exploration and complete resection to obtain an accurate diagnosis. The relation of the pancreatic IPT to autoimmune pancreatitis is reported.

P-195

Assessment of liver biopsy specimens in chronic viral hepatitis (B,C)and autoimmune hepatitis referred to shahid sadoughi hospital yazd, Iran

Shokouh Taghipour;Jamshid Ayatollahi
shahid sadoughi university of Medical Sciences and Health services,general hospital Yazd, Iran

Background:we decided to evaluate liver biopsies in chronic viral hepatitis (B,C) and autoimmune hepatitis based on sex,age,clinical signs and symptoms with staging and grading of the disease. Methods:This descriptive study was conducted through case series method all the patients are positive for Hbs Ag,HCV Ab or autoimmune hepatitis, so liver biopsies were assessted for staging and grading by using scheuer system. Other data accumulated from

hospital folders, data analyzed statistically using SPSS 13 and chi-squqre test.Results:120 patients were included in this study, forty-eight were HbsAg+,fifty- eight HCV +, sixteen had autoimmune hepatitis, and twoof them had both (B,C).there is significant relation between HCVAb with sex (pv:0.000),cirrhosis and age(pv:0.00),cirrhosis and sex (pv:0.00),staging of hepatitis with duration of clinical signs and grading of disease (pv:0.00),frequency of cirrhosis and beginning of clinical signs (pv:0.00)and significant relation between incidence of autoimmune hepatitis and sex. Conclusion:we advised all patients with chronic hepatitis diagnosed based on clinical signs and serological markers undergone liver biopsy and assisted by sceuher or other staging and grading system to prevent and decreased progression into the end stage phase

Keywords:viral hepatitis,autoimmune hepatitis,cirrhosis

P-196

Spectrum of Alpha-Methylacyl-CoA Racemase expression in the hepato-billiary system and pancreas: a wide tissue microarray analysis of normal and neoplastic epithelia

Ana Mozos, Ana Petit, Manel Solé, Rosa Miquel, Eva Fernández, Laura Gelabert, Pedro Luís Fernández.
Hospital Clínic, Barcelona. Spain

Background: AMACR is a mytocondrial and peroxisomal enzyme involved in the β-oxidation of dietary fatty acids. It was initially described as a diagnostic marker of prostatic carcinoma, although recent reports indicate its expression in other neoplasms, especially colorectal carcinoma. In order to precisely establish the frequency, significance and possible clinical utility of AMACR expression in the hepatobilliary system, we have performed a wide screening of AMACR expression including normal, preneoplastic and neoplastic tissues using tissue microarray (TMA) technology and immunohistochemistry.

Design: A total of 204 samples of normal (76) and tumoral (128) human tissues from the hepatobilliary and pancreatic system were selected from the surgical pathology archives. Immunohistochemical studies were carried out using anti-AMACR (Policlonal, 1:100, Dako) and the Envision System (Dako). The staining was classified as negative, weak or strong, according to intensity and percentage of positive cells.

Results: Hepatocellular carcinomas (HCC) showed a stronger expression of AMACR when compared to normal, cirrhotic liver ($p=0.015$) and to high grade dysplastic nodules ($p=0.023$), but we found no differences in AMACR expression between single and advanced HCC, and between normal and cirrhotic liver. Well differentiated neoplasms showed increased expression of AMACR when compared to poorly differentiated tumors ($p=0.007$). Normal biliary ducts were frequently negative. Three out of 14 colangiocarcinomas showed strong AMACR expression and 6 stained weakly. Interestingly, HCC showed a statistically significant stronger staining for AMACR compared with cholangiocarcinomas ($p<0.001$). Neoplastic and pre-neoplastic lesions arising in the pancreas only showed a mild AMACR expression, mainly in PANIN lesions.

Conclusions: AMACR is strongly positive in some neoplastic and preneoplastic lesions of the hepatobilliary system and may be a marker of malignant transformation. In that context, it may be a useful marker in daily practise to help the pathologist to find the origin of metastatic lesions to or from the liver.

P-197

HEPATOCELLULAR CARCINOMA WITH AN UNUSUAL NEUROENDOCRINE COMPONENT

Boujelbene Nadia, Rammeh Soumaya, Trabelsi Amel, Trimech Mounir, Sriha Badreddine, Mokni Moncef, Korbi Sadok
Department of pathology. Farhat Hached Hospital, Sousse, Tunisia.

Background: Primary hepatocellular carcinoma is a well known liver condition. It exhibits histologic polymorphism even within a single nodule. The neuroendocrine character has been observed immunohistochemically and ultrastructually in some tumor cells within some hepatocellular carcinoma nodules. Only few cases of coexisting neuroendocrine carcinoma within hepatocellular carcinoma with clear boundaries have been reported.

Method: We describe a case of a tumor of the liver with features both of primary hepatocellular carcinoma and neuroendocrine carcinoma. The clinicopathological features and pathogenesis of this rare association are studied.

Results: A 56-year-old man was referred to the department of surgery for nodular lesions of the liver detected at abdominal ultrasonography at the time of exploration of a persistent fever with lost of weight and anorexia. Serum α-fetoprotein (AFP) was 15 ng/mL. The carcinoembryonic antigen (CEA) was within normal limits. Viral hepatitis serological testing was negative.

Intraoperatively, the liver, the spleen and the peritoneum showed numerous nodules associated with ascite. A liver surgical biopsy was performed. Histologically, the majority of the tumor was a hepatocellular carcinoma that was positive for hepatocellular antigen and alpha-fetoprotein. This component was focally intermingled with large nests of small round cells that were positive for chromogranin and synaptophysin corresponding to a moderately differen-

tiated neuroendocrine carcinoma. The patient died one month later.

Conclusion: The admixture of hepatocellular carcinoma and neuroendocrine tumor with clear boundaries is rare. The origin of neuroendocrine tumors in the liver is controversial. They may represent a differentiation of the malignant liver cells into a neuroendocrine tumor or the two tumors grow independently of each other. More cases need to be documented to obtain a better insight on the pathogenesis of this association.

P-198

AUTOIMMUNE PANCREATITIS, AN UNDERDIAGNOSED ENTITY. DIAGNOSIS IMPORTANCE OF IgG4.

MT.Salcedo;H.Córdoba;MA.Montero;S.Ramon y Cajal;J.Olsina;H.Allende

Hospital Vall d'Hebron, Barcelona. Spain

BACKGROUND: Autoimmune pancreatitis (AIP) seems to be a disease with an heterogeneous appearance, that produces pancreatic nodular areas with duct estenosis, wich can mimic carcinoma. Patients often show elevated serum IgG4 and they usually respond to corticosteroid treatment, so it is important to differentiate AIP from pancreatic ductal adenocarcinoma. Our intention is to establish some key histopathological criteria and evaluate the diagnostic relevance of biopsy specimens.

MATERIAL AND METHODS: Histopathological, clinical and radiological features were recorded from 12 patients from 2000 up to 2006: 10 pancreaticoduodenectomy specimens (Whipple resections) and two biopsy specimens. The specimens displayed chronic pancreatitis and there was no evidence of pseudocysts, calculi, irregular duct dilatations, pancreas divisum and/or duodenal wall inflammation. The severity and the situation of the chronic inflammation as well as the intensity of IgG4- positive plasma cell infiltration were graded. The storiform pattern of the fibrosis and obliterative phlebitis were also determined.

RESULTS: Using previously published criteria the cases were subdivided into AIP "*concluent*" (n=1) showing periductal lymphoplasmacytic infiltrate, obliterative phlebitis, storiform fibrosis and abundant (>10 cells/HPF) IgG4 positive cells; "*suggestive*" (n=3) showing periductal lymphoplasmacytic infiltrate, storiform fibrosis and moderate (5–10 cells/HPF) IgG4 positive cells and "*doubtfu*l" (n=2) showing periductal lymphoplasmacytic infiltrate without IgG4 positive cells or lymphoplasmacytic parenchymatous infiltrate with IgG4 (<5 cells/HPF) positive cells. Ordinary chronic pancreatitis (alcohol or gallstones associated) showed lymphoplasmacytic infiltration and fibrosis without or minimal expression of IgG4.

CONCLUSIONS: 1. Benign biopsies proved to be a very helpful tool to establish the diagnosis prior to Whipple resection. 2. Autoimmune pancreatitis is characterized histologically by a dense periductal lymphoplasmacytic infiltration, with variable number of IgG4-positive plasma cells, fibrosis and venulitis. 3. IgG4-positive plasma cells are a useful immunohistochemical marker for the morphological diagnosis of AIP.

P-199

Solitary fibrous tumor of the liver. A case report.

Sevastiadou Maria; Koniaris Efthymios; Biteli Maria; Apostolaki Aikaterini

Pathology dpt. Of Anticancer, Oncological Hospital of Athens, 'St. Savvas', Athens, Greece.

Background: Solitary fibrous tumor (SFT) is a rare neoplasm of the adulthood. For many years it has been referred to the serous surfaces of the body, namely pleura, peritoneum and pericardium; recently cases arising in mesenchymal organs such as lung, mediastinum, liver and paranasal sinuses were also reported. Our aim is to present a new case of (SFTs) of liver.

Methods: A 81 year old female presented to our hospital with jaundice. Grossly the lesion was a well-circumscribed, encapsulated, firm, lobulated, gray-white to yellow-white mass. On dissection the tumor had frequent whirling and fasciculation and measured 18×13×8 cm.

Results: Microscopically the tumor showed alternating cellular with relatively acelular areas. The cellular areas were composed of uniform collagen forming spindle cells which were arranged in interlacing fascicles, while the acelular areas were edematous with stretched out tumor cells. The neoplastic cells were usually oval-shaped and contain bland nuclei with scattered chromatin and inconspicuous nucleoli surrounded by an indistinct rim of amphophilic cytoplasm. In some areas the cells are arranged around ectatic vessels in a haemangiopericytoma-like pattern. The tumor characteristically expressed Vimentin, CD-34, bcl-2 and reacted negatively to epithelial markers (CK), desmin, neurofilaments, NSE, S-100, SMA, CD117, CD31 and Factor VIII.

Conclusions: Our differential diagnosis included Peripheral Nerve Sheath Tumors which express NSE and S-100. The number of SFTs of the liver reported to date is too limited and overall experience is limited to confirm the definite prognosis of the tumor. Although most SFTs are benign, some may have malignant histological features and recur locally or metastasize. Malignancy should be considered when there is greater cellularity, cellular pleomorphism and increased mitotic activity. Treatment of choice for solitary fibrous tumors is extensive surgical resection.

P-200

Mutation and overexpression of β-catenin in hepatocellular carcinomas and hepatoblastomas

Hae Ra Jung; Yu Na Kang; Sun Young Kwon; Mi Sun Chei; Sang Pyo Kim; Kun Young Kwon; Sang Sook Lee
Department of Pathology, Keimyung University School of Medicine. South korea

Hepatocellular carcinoma is the major primary malignant tumor in the human liver, but the molecular changes for β-catenin has not yet been investigated in hepatocellular carcinoma and hepatoblastoma. We have examined the status of the β-catenin gene in 19 hepatocellular carcinomas and 3 hepatoblastomas by methods of RT-PCR, SSCP, western blot and immunohistochemical stain. In addition, mutation in the β-catenin gene is evaluated for 10 hepatoma cell lines such as SNU 182, 354, 368, 387, 398, 423, 449, 475, HepG2, Hep3B. Three cases out of nineteen hepatocellular carcinomas (16%) and Hep3B cell line had activating somatic mutations in exon 3 of the β-catenin gene. One case with β-catenin gene mutation showed β-catenin gene expression of stronger density by RT-PCR, and β-catenin overexpression by immunohistochemical stain in tumor than non-tumorous tissue, but no evidence of truncated β-catenin protein in western blot. And this case was also poorly differentiated tumor and had numerous mitoses. β-catenin overexpression had been detected mainly in the cell membrane of seventeen hepatocellular carcinomas (89%) and in the nuclei of three hepatoblastomas (100%). Thus β-catenin gene alterations are involved during liver tumorigenesis and suggest that disregulation of wnt-β-catenin pathway is a major event in the development of hepatocellular carcinoma and hepatoblastoma in humans.

P-201

The role of life-long feeding with different dietary lipid sources on the development of non-alcoholic steatohepatitis (nash) in aged rats

Cesar L. Ramirez-Tortosa; Jose L. Quiles; Julio J Ochoa; M Carmen Ramirez-Tortosa; Pedro Camacho; Sergio Granados; Jose Mataix.
COMPLEJO HOSPITALARIO DE JAÉN. Spain.

Background. Morphofunctional studies suggest that the liver, compared with other organs, ages fairly well. Nevertheless, age does not spare the liver. Dietary fat has been related with changes in the susceptibility to suffer several liver diseases and with the aging process itself. We investigated the role of feeding rats life-long on different dietary fat sources (virgin-olive, sunflower or fish oils) differing in their fatty acids (mainly n-9 monounsaturated, n-6 polyunsaturated or n-3 polyunsaturated) on the susceptibility to develop NASH with aging.

Method. One-hundred and forty seven male wistar rats were fed life-long on three semysinthetic, normolipemic (4% w/w) and isoenergetic diets differing in the lipid source (virgin-olive, sunflower or fish oils). At the age of 24 months, twelve rats per group were slaughtered and the liver, blood plasma and urine were collected. A portion of the liver was processed for histopathological studies and another portion was used for mitochondrial isolation.

Results. Animals fed on fish oil showed a significantly higher NASH grade than those fed on virgin-olive oil (animals fed on sunflower oil were not different from the rest of groups). These results positively correlated very well with finding on centrolobulillar inflammatory infiltrate. Also a good positive correlation was found between NASH grade and the liver:body weight ratio and pro-inflammatory soluble factors (MCP1, ICAM and IL-6). Concerning oxidative stress findings, animals with the lowest NASH grade reached the highest levels of the mitochondrial antioxidant coenzyme Q, the lowest activity for mitochondrial catalase as well as the lowest concentration of urinary F_2-isoprostanes

Conclusion. Our results indicate that fish but not virgin-olive oil, when fed life-long leads to the development of NASH. That might be related with inflammatory and oxidative-stress processes intrinsic to each dietary fat source.

P-202

Comparative immunohistochemical profile and identification of programmed cell death (apoptosis) in hepatocellular carcinoma and cholangiocarcinoma.

V.Herlea1, C.Pechianu1, C. Stroescu2, Liliana Paslaru[3], Monica Hortopan1, Elena Stoica-Mustafa1, Mihaela Mihai1, Andreea Vacarasteanu1, Iuliana Sobaru1, Luiza Driu1,C. Vasilescu2, M. Ionescu2, V.Tomulescu2, Simona Dima2. Dragnea2 and I. Popescu2
Department of Pathology - Fundeni Clinical Institute, Bucharest, Romania

BACKGROUND: The histological diagnosis of poorly differentiated hepatocellular carcinoma (HCC) can be complicated by difficulty in differentiation from intrahepatic peripheral cholangiocarcinoma (PCC) and metastatic carcinoma, often requiring the use of immunohistochemistry for diagnosis. The reproducible identification of apoptotic cells in malignant tumours of the liver is important in so far as apoptosis occurs in later stages of carcinoma development.

METHOD: Our aim was to analyse the immunohistochemical profile of the 73 primary liver tumors, diagnosed, between 2002–2007. Primary antibodies used are: CEA,

CK 7, CK 8/18, CK 19, CK 20, CD34, Bcl-2, VEGF, Ki 67, PCNA, p53. For detection of apoptosis we used the terminal deoxynucleotidyl transferaze (TdT)-mediated deoxyuridine triphosphate (dUTP) - nick end-labeling TUNEL method, in 24 from our 73 cases.

RESULTS: From the 73 primary liver tumors, 47 were HCC and 26 were PCC. CK 7 was positive in 42,36% from cases with PCC and in 11,11% from cases with HCC. CK 19 stained positively in 82,34% from PCCs and in 30,34% from HCC. On the other hand CK 20 was positive in 17,15% from cases with PCC, and in 10,89% from cases with HCC. 58,23% of PCC stain positively with CEA and 9,78% of HCCs show patchy staining with CEA. In CD 34 reactions we noticed the strongest reaction in sinusoidal endothelial cells around HCCs. The PCNA–labeling index was higher in PCC than in HCC.

CONCLUSIONS: -The percentage of apoptotic cells is significantly higher in PCC than in HCC, suggesting that the degree of apoptotic cell death is severe in PCC, but is relatively mild in HCC.

– The apoptotic cells are consistently negative for PCNA and vice versa, suggesting that apoptotic cells do not show proliferative activity.
– IHC results should be interpreted in the larger context of the case.

P-203

Clinicopathological Characteristics of Turkish Patients with Invasive Pancreatic Ductal Cancers

Sibel Erdamar; Nihan Karataş, Berke Ozucer; Ovgu Aydin; Gulen Dogusoy; Suha Goksel, Gokhan Demir, Ilknur Erenler

Cerrahpasa Medical Faculty Pathology Department. Turkey

Background: Pancreatic ductal adenocarcinoma (PDAC) is the major pancreatic tumor and carries an extremely poor prognosis. The aim of this study was to identify these prognostic factors in patients undergoing primary curative resection.

Method: The study retrospectively analyzed 90 patients with PDAC who were operated with whipple resection. Their clinicopathological parameters revised, documented and statistically analysed for correlations.

Results: Average age of study group was 61,5 year and F/M was 1/1,5. Most prominent location was head of pancreas (44,4%), and the second was periampullary region (40%). Lymph node metastases were found in 54%. The rates of lymph vessel (LVI) and perineural invasion (PNI) were 90% and 82%, respectively. 25% of patients had blood vessel invasion (BVI). Mean of tumor size was 3,4 cm (1–11 cm). Pancreatic intraductal neoplasia (PANIN) was seen 33% of patients. 20% of cases was associated with IPMN. There was significant correlation between tumor location and mean tumor size (2,8 cm for periampullary; 3,8 cm for head; 6,7 cm for corpus; and 6,8 cm for tail of pancreas; PNI was also associated with distal location and lymph node metastasis.

Conclusion: Our preliminary study support that PDAC which is located in tail of pancreas seem to have larger size, lymph node positivity and blood vessel invasion. Tumor location may be considered as poor prognostic factors in pancreatic adenocarcinomas.

P-204

Intraductal papillary neoplasm of the bile duct associated with Clonorchis sinensis infection

Kee-Taek Jang; Seung-Mo Hong; Ji Eun Kim; Jin Haeng Chung; Jae Hoon Lim

Samsung Medical Center; Johns Hopkins Medical Institution; Seoul National University Boramae and Bundnag Hospital. South Korea

Intraductal papillary neoplasm of bile duct (IPNB) is one of the precursor lesions of cholangiocarcinoma. Only one preexisting condition, hepatolithiasis has been extensively studied in association with IPNB. However, to the best of our knowledge, there was no comprehensive study regarding IPNB association with Clonorchiasis. We performed immunohistochemical studies of mucin proteins (MUC1, MUC2, MUC5AC, CDX2) and cytokeratin (CK7, CK20) pancels of 12 IPNB cases with Clonorchis sinensis infection. Four cases were non-ivasive IPNB (1 borderline and 3 carcinoma in-situ) and 8 contained an invasive carcinoma component (7 tubular carcinoma and 1 colloid carcinoma). Tumors were located in extrahepatic bile duct (EBD) in 7 cases, intrahepatic bile duct (IHD) in 4 cases, and both EBD and IHD in 1 case. Seven cases were positive for MUC1 and 11 for MUC5AC, while only 2 cases were positive for MUC2. The predominant immunolabeling pattern was pancreatobiliary type (MUC1 / MUC5AC /CK7) and it was associated with tubular carcinoma and has higher stage than colloid carcinoma case. Our data revealed different immuno-phenotype with that of IPNB from hepatolithiasis, which was known to be related with an intestinal type. These results suggest that IPNB with Clonorchiasis may have a different tumorigenesis pathway than IPNB with hepatolithiasis.

P-205

ANGIOGENESIS IN HEPATOCELLULAR CARCINOMA AND CIRRHOSIS: IMMUNOHISTOCHEMICAL STUDY WITH ENDOTHELIAL MARKERS

Juliana Paschoal; Adriana Caroli-Bottino; Nathalie Henriques Silva; Leila Chimelli; Vera Lucia Pannain

Department of Pathology; Federal University of Rio de Janeiro. Brazil

Background: Hepatocellular carcinoma (HCC) is a highly vascularized tumor and angiogenesis has been studied in this neoplasia. During the hepatic carcinogenesis, structural and functional changes characterized by sinusoid-like vessels, take place in the vascular architecture. Studies have demonstrated that in the HCC the capillary vessels express CD34. The CD105 is a glycoprotein associated with endothelium cell proliferation and is identified as a marker of neoangiogenesis, but its expression is controversial in HCC.

Aims: To evaluate the expression and the distribution of CD105 and CD34 proteins in HCC and surrounding cirrhotic regenerative nodules (RN).

Methods: Tissue samples of tumors and cirrhotic regenerative nodules were obtained from 16 explanted livers. Thirty-four RN and 25 HCC were studied by immunohistochemistry with human CD34 and CD105 monoclonal antibodies. Immunoexpression was semiquantitatively evaluated in sinusoidal area as follows: group 1 (negative); group II (positive to 30%); group III (positive >30%).

Results: The HCC showed CD34 and CD105 expression in 24/25 (96%) and 22/25 (88%), respectively. However in cirrhotic parenchyma the CD34 value changes 24/34 (70%) of the RN while the CD105 was similar 30/34 (88%). An important observation was the semiquantitative evaluation of the immunoexpression. CD 105 was higher in RN than in HCC. It was observed in more than 30% of the sinusoidal area in 21/34 (61.7%) of the RN, and only in 5/25 (20%) in the HCC. Conversely, the HCC showed high CD34 expression in 21/25 (84%), a difference statistically significant when compared with RN 2/34 (5.8%). CD105 showed diffuse positive immunostaining in all HCC and RN. CD34 expression was also diffuse in all the HCC, whereas only 2/34 (5.8%) of the RN were positive.

Conclusion: The higher expression of CD105 in cirrhosis when compared to the HCC suggests that may not be a good endothelial marker of the hepatic carcinogenesis as opposed to CD34.

P-206

Pancreatic tuberculosis in non immunocompromised patients: report of three cases.

Ahmed Jahid; Fouad Zouaidia;Hafsa El ouazzani; Laila Laraki; Raouf Mohssine; Abdelkader Belkouchi; Zakia Bernoussi; Fatima Mansouri; Najat Mahassini.

Department of pathology, Ibn Sina Hospital, Rabat; Morocco

Introduction Isolated pancreatic tuberculosis is rare and can mimic pancreatic carcinoma.

Cases We report three cases of pancreatic tuberculosis.

34 years old and 50 years old women presented with obstructive jaundice. For the first patient, abdominal CT scan showed suggested tuberculosis and resection was avoided. The second underwent whipple procedure.

Third case was 48 years old alcoholic man who presented with recent history of painful mass of left hypochondre. Cystic tumor of pancreas tail was suggested in CT scan. A bloc resection of tumor pancreas tail and spleen was performed.

The three patients had antitubercular therapy after histological confirmation of pancreatic tuberculosis. Follow-up was respectively 3 years, 5 months and 2 years free recurrence.

Conclusion Tuberculosis origin of an isolated pancreatic mass may be suspected in young, especially in endemic areas.

Electron Microscopy

P-207

Ultrastructural alterations of large intestine before and after endovascular hemostasis in treatment of acute intestinal hemorrhages in experiment

Ganna Mylovydova; Yuriy Avdosyev; Olena Pasternak; Igor Nalcha

Laboratory of Pathomorphology, Institute of General and Urgent Surgery of Academy of Medical Sciences of Ukraine

Background: The aim of this study was to prove at ultrastructural level the possibility of carrying out the roentgen-endovascular hemostasis at acute intestinal hemorrhages without risk of occurrence of irreversible changes in wall of mucosa of large intestine.

Method: The material for morphological research were the sites of large intestine on which different methods of roentgen-endovascular hemostasis were spent. Extracture of tissue pieces of large intestine for electron microscopic research spent at animals from three groups in different terms after endovascular interventions.

Results: The analysis of ultrastructural alterations after roentgen-endovascular hemostasis by means of microspirals has shown, that ultrastructural architectonics of column

epitheliocytes, goblet exocrinocytes vascular capillaries and smooth myocytes of the muscular layer of the large intestine of rats endured basically compensative-adaptable reorganisation. Alterations of organellas were in limits of physiological indemnification. Nevertheless, there were observed moderately expressed dystrophic disturbances, leading of which were mitochondrial dysfunction, structurally expressed in swelling of mitochondrions, loss of electron density of the matrix, disorganization of cristas and partial focal lysis of external membranes. These alterations testify to disturbance of oxidation-reduction reactions, that in their turn involves also disturbance of synthetic and reparative intracellular processes. It is necessary to notice, that the described alterations, according to depth and expression degree, are reversible.
Conclusion: Having been carried out electron microscopic researches of large intestine after roentgen-endovascular hemostasis by mechanical damage of an intima artery by guide wire or spiral, and also simultaneous introduction of chemodrugs with vasospastic and haemostatic drugs have shown convertibility of the ultrastructures alterations of mucosa of large intestine. The convertibility of ultrastructural alterations that was revealed during the experiment allowed to recommend the use of given methods of roentgen-endovascular hemostasis in clinic for treatment of patients with intestine hemorrhages.
Conclusion: Having been carried out electron microscopic researches of large intestine after roentgen-endovascular hemostasis by mechanical damage of an intima artery by guide wire or spiral, and also simultaneous introduction of chemodrugs with vasospastic and haemostatic drugs have shown convertibility of the ultrastructures alterations of mucosa of large intestine. The convertibility of ultrastructural alterations that was revealed during the experiment allowed to recommend the use of given methods of roentgen-endovascular hemostasis in clinic for treatment of patients with intestine hemorrhages.

P-208

Solitary fibrous tumour. An ultraestructural and immunohistochemical study of 11 cases

Yolanda Rodríguez-Gil; Javier Salamanca; Claudio Ballestín; Miguel A. Martínez
Hospital Universitario 12 de Octubre

BACKGROUND Solitary fibrous tumour (SFT) is a rare ubiquitous mesenchymal neoplasm of probable fibroblastic type with a prominent haemangiopericytoma-like vascular pattern. Since their initial description as arising from the pleura, SFTs have been reported in a variety of extraserosal sites. It is now commonly accepted that this neoplasm is derived from mesenchymal cells but histogenesis is not well known. In addition, because of the variability of morphological patterns, SFT may be easily misdiagnosed, specially when appears in an unusual location. We have performed the analysis of 11 cases correlating clinicopathological, immunohistochemical and ultrastructural features in order to understand the biology and help in diagnosis of this entity.
METHODS We gathered data on eleven patients diagnosed between 1986 and 2006. Histopathological evaluation was performed on hematoxylin and eosin previously stained slides. Tissue-arrays were constructed assembling two cylinders from representative areas, to perform inmunohistochemical tests. For electron-microscopic examination tissue was processed with Karnovsky reactive and embedded in epoxy resin.
RESULTS Eigth of the lesions arose in thoracic cavity and three cases were extrathoracic. One case died within the next 5 months following surgery and other was diagnosed during autopsy. Three cases recurred but there were not metastatic disease. Histopathological study showed varying degrees of cell density and mitotic activity which correlated with clinical behaviour. Inmunohistochemically all tumours stained positively for Vimentin, CD99 and CD34 and only 7 cases for bcl-2. Ultraestructural appearance of the eleven tumors showed myofibroblastic differentiation in all cases with focal smooth muscle features in three of them. In addition nine cases showed perivascular undifferentiated cells.
CONCLUSION SFT is an uncommon neoplasm with different histological patterns and clinical behaviour. We have hypothetised that the perivascular undifferentiated cells found might correspond to a quiescent stage of adult stem mesenchymal cell and may be implied in pathogenesis of SFTs.

Breast Pathology

P-209

Quickscore assessment in Bcl- 2 and Bax protein expression in invasive ductal carcinoma of breast and relation with other molecular Markers.

Noorieh Sharifi; Hossein Ayatollahi;Kamran Ghaffarzadegan;Mohammad Taghi Ghiasi; Mohammad Javad Farahmand;Amir Hossein Jafarian
Department of Pathology,Faculty of Medicine,Mashhad University of Medical Sciences.

Objective: Different score such as H- score, multiplicative and additive quickscore were used for ER status by Immunohistochemistry (IHC) methods.
This study investigates the incidence of Bcl- 2 and Bax expression with IHC method and quick score assessment, in invasive ductal carcinoma(IDC) of breast relative to their

prognostic factor and other biological markers including ER and PR status.

Materials and Methods 92 cases of formalin fixed paraffin embedded tissue of IDC of breast were selected and immunostained using primary antibody to Bcl- 2, Bax, Ki- 67, ER and PR quantified with H- score, multiplicative and additive quickscore.

Results: There were high significant positive correlation between ER, PR with Bcl- 2 and significant negative correlation between Ki- 67 with Bcl- 2.

There were high significant correlation between H- score ER and PR and multi and additive quick score ER and PR with multi and additive quick score Bcl- 2.

Conclusion: Bcl- 2 is associated with good prognostic factor in IDC of breast. Bax expression with both quickscores does not necessarily correlate with quickscore and H- score of ER and PR. We can use quickscore in evaluation of ER and PR status instead of H- score.

Keyword: Bax, Bcl- 2, Invasive ductal carcinoma, Ki- 67, Oestrogen receptor, Progestron receptor.

P-210

PRIMARY BREAST AMYLOIDOSIS PRESENTING AS MICROCALCIFICATIONS

Placide Ngendahayo; Danie Faverly; M-Anne Blaude
Institut de Pathologie et de Génétique; Centre Hospitalier Grand HORNU?; Laboratoire CMP BELGIUM

Primary breast amyloidosis presenting solely as microcalcifications is extremely rare. We report a case of a 73 year old woman with persistent radiologically suspicious microcalcifications without palpable mass. The diagnosis of amyloidosis was established histologically by the presence of an amorphous eosinophilic material which was positive for Congo red and was dichroic under polarized light. Paraffin immunohistochemistry showed the presence of kappa light chains (AL-type amyloidosis. The amyloid deposits were associated with microcalcifications. A complete workup was performed to exclude other localisations and was negative. The primary beast amyloidosis presenting solely as microcalcifications is discussed and a brief review of the litterature is presented.

P-211

Interpretation of estrogen and progesterone receptor immunohistochemistry may be biased by laboratory technique and observer expertise

Michael Linden
Henry Ford Hospital, Detroit, MI, USA

Background: Estrogen (ER) and progesterone receptor (PR) status plays an importantrole in treatment of breast carcinoma patients. ER and PR immunohistochemistry (IHC) is the current standard forassessment. However, the subjectivenature of IHC interpretation may lead to inaccurate receptor status andpossibly inappropriate therapy.

Method: 100 consecutive breast carcinoma cases were studied. Interpretation was compared between a single-pathologist with expertise in IHC (EP) and ten general pathologists (GP) withvarying IHC experience. Percentage of nuclear immunoreactivity wassemi-quantitated: positive, negative, and focal positive. Focal positive tumors showed < 5%immunoreactivity and/ or weak staining.

Results: There was 91% agreement for both ER and PR.21 and 27 cases were negative for ER and PR, respectively for both observers.There were 18 discrepancies, ER: 4 cases were negative by GP but positive byEP. Three focal positive cases by GP were positive by EP. There were 6 caseswith discordance between positive and negative for the GP and EP. For PR, 96% concordance between positive andnegative. Three cases were negative by GP but positive by the EP and 1 case wasnegative by GP and positive by the EP. Five focal positive cases by GP werepositive by EP.

Conclusions: Concordance between GP and EP was 94% and 96%, respectivelyfor ER and PR. For ER and PR similar rates of discordance between negative byGP and positive by EP were observed (4 and 3%) as well as focal positive by GPand positive by EP (3 and 5%). Subjective interpretation and technicalvariations may limit accurate quantitation in an inherently qualitative test.Discrepant rates of 4–6% may have a clinically significant impact on patienttreatment and therefore survival.

P-212

Infiltrating micropapillary carcinoma of the breast and sentinel lymph node biopsy.

M[a] Angeles. Martinez; Francisco Tresserra; Jaume Feu; Luciano Lopez-Marin; Rafael Fabregas; Máximo Izquierdo.
Institut Universitari Dexeus.

BACKGROUND: To evaluate the indications of sentinel lymph node (SLN) biopsy in patients with infiltrating micropapillary carcinoma (IMPC) of the breast and the results of this procedure when it has been performed.

METHODS: During the last ten years in our Center SLN biopsy has been performed in 494 patients. During the

same period 52 IMPC have been diagnosed. This is a retrospective and descriptive study of the technique used for nodal staging in these patients, and the reason why SLN biopsy was not performed. The results of SLN biopsy in those patients with IMPC were compared with the results of this technique in patients with other histologial types of breast cancer.
RESULTS: SLN biopsy could be done in only 15 (29%) patients with IMPC and in 10 (67%) cases in was involved. Five had metastases, three micrometastasis and two isolated tumor cells. Only one patient showed more lymph nodes involved in the axilla. In those patients in whom the SLN biopsy could not be done, positive fine needle aspiration under ulltrasonographic guidance and multifocal breast involvement were the main contraindications. In 1036 breast cancer of non IMPC diagnosed in the same period, SLN biopsy could be done in 479 (46%), being involved in 146 (31%) cases.
CONCLUSION: SLN biopsy is infrequently indicated in those patients with IMC and, when performed, the percentage of lymph node metastasis is high but mostly limited to SLN.

P-213

Sarcoma of the female breast in Zaria

Modupeola Samaila
ahmadu bello university teaching hospital,shika-zaria, Nigeria

Background:Breast cacinoma,an epithelial tumour is the second commonest tumour among women in zaria,and is a leading cause of cancer-related death in women in developing countries.However,tumours of the mesenchymal origin also occur in the breast.
Materials and Method: A seven year analysis of consecutive women with breast sarcoma from January 2000 to December 2006.tissue biopsies were processed in paraffin waxand histology sections were stained with haematoxylin and Eosin,reticulinand periodic acid Schiff.
Results:9 females were studied.Their ages ranged fron20 years to 60 years with a median age of 32 years. Clinically, these women presented with progressively increasing breast lumpsof varying sizesassociated with pain. One patient presented with a recurrent lump associated with skin ulcer which ruptured spontaneously.the duration of symptoms was from 1 year to 3 years.Examination revealed well circumscribed breast lumps and axillary lymph nodes enlargement. Clinical diagonosis included fibroadenoma and advanced carcinoma.Three women had exicisional biopsy,while swix had mastectomywith axillary clearance.Histologic diagonosis of the sarcoma subtypes included stromal sarcom-7, osteogenic sarcom-1 and Angiosarcoma-1.Microscopically, they were cellular lesions composed of spindle cells having hyperchromatic to vesicular nuclei and moderate amount of cytoplasmarranged in whorls,fascicles and herringbone pattern.They showedvarying degree of myxoid degenerationand necrosis.Variable number of mitotic figures were seen. All sampled nodes showed reactive hyperplasia only.
Conclusion:Breast carcinoma,though uncommon,affects younger women compared to carcinoma in our setting. Tumour spread is haematogenous hence the sparing of lymph nodes.Additional diagonostic methods are helpful in differentiating the various subtypes.This is important in patient care and management.

P-214

A STANDARD, HIGH SENSITIVITY, IHC PROTOCOL AND SCORING METHOD WITH THE AID OF IMAGE ANALYSIS FOR THE DETECTION OF HUMAN ESTROGEN RECEPTOR ALPHA

Therese Phillips; Joachim Schmid; Vaishali Tanna; Lee Ryan; Kurt Pii; Miu Chau
Dako North America, Carpinteria, CA, USA

Background: Immunohistochemical (IHC) assays of differing sensitivity and scoring systems with varying positive/negative cut-off values for estrogen receptor (ER) are major causes of inconsistent results between laboratories. The ER/PR pharmDx™ kit has been developed and 510(k) cleared, and provides a standard protocol for staining and scoring ER and PR with a defined cut-off. Here we describe the development of the ER cocktail antibody, automated IHC protocol, and a prototype image analysis algorithm aimed at improving staining and scoring consistency. **Method:** The epitopes for mouse anti-ER clones 1D5, ER-2–123, and 6F11 were characterized by SPOT analysis and a synthetic array. Clones 1D5 and ER-2–123 were tested separately or in combination in a highly sensitive IHC assay. Staining with the optimized ER cocktail antibody was evaluated on two automated platforms, Autostainer Plus and Autostainer Plus Link. Image analysis was performed using a prototype ER pharmDx™ algorithm on ACIS III. **Results:** Anti-ER antibody clones 1D5 and ER-2–123 demonstrated reactivity with discrete epitopes on ER; ER-2–123 and 6F11 reacted with the same epitope. IHC results using a cocktail of anti-ER clones, 1D5 and ER-2–123, revealed a synergistically increased sensitivity compared to results with individual clones. ER staining on two automated platforms showed equivalent and reproducible results. Image analysis using a prototype ER pharmDx™ algorithm showed promising results as an aid to consistent scoring. **Conclusion:** The sensitivity and quality of immunohistochemical staining of ER is dependent on selection of ER antibody and IHC protocol. Two complementary ER antibody clones were

combined to increase assay sensitivity and are provided as part of a standard protocol in the ER/PR pharmDx™ kit. The kit protocol includes a validated scoring system with defined cut-off, which combines staining intensity and proportion scores. Automated staining improved workflow and staining reproducibility. A prototype ER pharmDx™ image analysis algorithm facilitated consistent scoring.

P-215

Phyllodes tumour of the breast with features of malignant triton tumour

Francesco Vasuri; Alberto Righi; Stefania Damiani
Section of Anatomic Pathology, University of Bologna, Italy

Background: Malignant phyllodes tumour of the breast represents a rare biphasic neoplasm with epithelial and stromal components. Approximately 10–20% of all breast phyllodes tumours are malignant, most commonly with an homogeneous sarcomatous differentiation. Anyway, multiple heterologous lineages of differentiation are occasionally found in these neoplasms. Here we report a case of malignant phyllodes tumour showing features of rhabdoid and schwannian differentiation. Clinical history and Methods: The patient, a 80-year-old lady, presented with a 9 cm mass in outer superior quandrant of the right breast. At quadrantectomy, the lesion was greyish in colour, had poorly defined borders and a microcystic appearance. Tissue were fixed in 10% buffered formalin, paraffin embedded and stained with haematoxylin-eosin. Immunohistochemistry was performed with Ventana automated stainer. Results: Histologically, the tumour was constituted by a hypercellular stromal proliferation. Stromal cells had a marked nuclear atypia and numerous mitoses (up to 10 /10 HPF). Only scattered residual mammary glands were present. In most part of the lesion, neoplastic cells were round shaped and had abundant eosinophilic cytoplasm and round vesicular nuclei with prominent nucleoli. These elements merged with areas of spindle cells with elongated nuclei and wavy cytoplasm. By immunohistochemistry, the rounded cells were strongly and diffusely positive with rhabdomyoblastic markers (myogenin, desmin, striated actin) and focally positive with nervous markers (Neu-N and S100 protein). An opposite phenotype was found in the spindle cell population, as they were diffusely positive with Neu-N and S100 protein and only focally expressed rhabdomyoblastic markers. Conclusions: These histological and immunohistochemical findings are consistent with malignant triton tumour, a rare soft tissue neoplasm characterized by divergent differentiation towards skeletal muscle and Schwann cells. To the best of our knowledge, this is the first documented case of phyllodes tumour with features of malignant triton tumour.

P-216

PROGNOSTIC SIGNIFICANCE OF IMMUNOHISTOCHEMICAL EXPRESSION OF CATHEPSIN D, CYCLIN D1, AND THYMIDINE KINASE 1 IN INVASIVE DUCTAL BREAST CARCINOMAS WITH PREDOMINANT INTRADUCTAL COMPONENT

Guldal Yilmaz(1), Pinar Geyik(2), Omer Uluoglu(1)
(1)Gazi University, School of Medicine, Department of Pathology, Ankara, Turkey; (2)Hacettepe University, School of Medicine, Department of Biostatistics, Ankara, Turkey

Background: Breast cancer is the most common malignant neoplasm in women and, in the light of recent studies, new therapeutic strategies keep on developing. We present an immunohistochemical study that was performed in order to evaluate the expression of cathepsin D (CD), thymidine kinase 1 (TK1), and cyclin D1 (CycD1) in invasive ductal breast carcinomas with predominant intraductal component and to determine their prognostic value.
Method: The examination of slides stained with Haematoxylin-Eosin of 70 patients were performed retrospectively, and clinical and prognostic data were reached. The histopathological grading of invasive tumour component was done by using the Nottingham modification of Bloom-Richardson grading system, and staging by using the system proposed by American Joint Committee on Cancer. Pearson's chi-square, Likelihood ratio, Fisher's exact tests, Kaplan-Meier survival analysis were used as statistical tests and the significance of observed differences was set at $p<0.05$.
Results: Intraductal component showed higher degree of staining for CD than invasive tumour component. A correlation was found between the CD expression and the reactive stromal cells and also the increasing degrees of invasive tumour. The negativity or weak expression for CD, TK1, and CycD1 in non-tumoural areas was found to be significant. CycD1 expression is found to be lower in advanced and/or high grade carcinomas and is found to be related to better survival rates in patients with invasive ductal carcinoma.
Conclusion: The finding of significantly higher expressions of CD, TK1, and CycD1 in the tumour component compared to the non-tumoural areas, raised the possibility of usage of all three antibodies in determining the malignant character of breast lesions. CD expression in intraductal component or in the reactive stromal cells may be used as an indicator of invasive potential of the tumoural lesion. CycD1 expression may be related to a better prognosis.

P-217

A study of twenty-eight 9-gauge vacuum assisted breast biopsies for microcalcifications: Columnar Cell Lesions, a frequently detected entity in patients with microcalcifications.

Alberto Pérez Rodríguez, Joaquín González-Carreró Fojón, Pablo Fernández Vázquez, Juan Luis Ríos González

Complexo Hospitalario Xeral-Cíes de Vigo, Spain

BACKGROUND: Columnar cell Lesions are a group of proliferative lesions of the terminal duct lobular units (TDLUs) characterized by dilatation of TDLUs lined by columnar epithelial cells with prominent apical snouts and intraluminal secretions. There is currently no internationally accepted classification or terminology for this group of lesions. CCL are considered as a candidate precursor in the progression to low grade ductal carcinoma in situ (low grade DCIS) and low grade invasive carcinoma. METHOD: We have revised twenty-eight 9-gauge vacuum assisted breast biopsies for microcalcifications performed between July and November 2007, and looked for CCL. We performed immunostaining for CK5 and ER in cases where CCL were suspected histologically. RESULTS: CCL were detected in 22 (78,6%) of 28 cases, showing strong overexpression of ER and CK5 negativity. None of these lesions expressed CK5. 6 (85,7%) of 7 cases of any grade DCIS and 5 (83,3%) of 6 cases of any grade infiltrating ductal carcinoma were associated to CCL. 7 (63,6%) of 11 cases diagnosed as non-malignant presented CCL. 2 (50%) of 4 cases diagnosed as Columnar Cell Hyperplasia displayed Flat Epithelial Atypia (FEA). FEA was present in 15 (61,2%) of 22 CCL. CONCLUSIONS: CCL are frequently detected in patients with microcalcifications, and they are often associated with DCIS and invasive ductal carcinomas of any grade. FEA was the most common form of CCL detected. CCL can be frequently underdiagnosed. Immunostaining for CK5 and ER is a useful diagnostic aid and it can discriminate between CCL and its mimics, like apocrine metaplasia. All the CCL detected in this revision showed a pure epithelial (luminal, glandular) immunohistochemical phenotype.

P-218

Risk of additional axillary-node metastases in women with breast cancer and positive sentinel lymph nodes.

V Marco; F Tresserra; F García; MA Carrasco; G Florensa; MA Martinez; I Rubio; C Muñoz

Hospital Quirón, Institut Universitari Dexeus, and Hospital General de Catalunya, Spain

Background: The involvement of sentinel lymph nodes (SLN) is classified as macrometastases (M) (>2 mm), micrometastases (mic) (2 to >0.2 mm), and isolated tumor cells (ITC) (<0.2 mm). Although the risk of additional axillary metastases is significant in patients with **M**, the risk in patients with **mic** and **ITC** is less known, and the indication for completion of axillary dissection is controversial.

Design: 640 patients with breast and SLN biopsy were studied. Patients and primary tumor characteristics included: age, tumor size, histologic type, grade, lymphatic invasion, number of positive SLN, number of patients with additional axillary lymph nodes (AALN), number with positive AALN and size of metastases in AALN.

Results: 28% (n=181) of the patients had positive SLN. According to the size of the metastases, the cases were classified as **M**, 42.5%(n=77); **mic,**36.4% (n=66); and **ITC,** 20.9% (n=38). The number of SLN studied per patient was 1 to 5, and the number of positive SLN 1 to 3. **AALN** were obtained in 159 patients, 98.7% (n=76) with **M,** 93.9% (n=62) with mic, and in 55.2% (n=21) with **ITC.** Of the patients with **M** in the SLN, 34.2% (=26), had positive AALN, 25 were **M** and 1 was **mic**.Of the patients with mic in the SLN, 16.2% (=10), had positive AALN, all were **M.** Of the patients with **ITC** in the SLN, 9.5% (=2) had positive AALN, one **M** and one **mic**.

Conclusions: The risk of AALN metastases is related to the size of the metastases in the SLN, and most AALN metastases are **M**. Completion of axillary dissection is indicated in patients with **M** in the SLN. In patients with **mic** and **ITC** in the SLN, assessment of predictive factors of metastases in AALN is recommended, because there is a risk of macrometastases.

P-219

Methods of differential diagnostics of the locally extended thymomas at myasthenia

Elena Klimova; Valeriy Boyko; Sergey Sushkov; Larissa Drosdova; Anatoliy Bozhkov; Alexander Kudrevich; Ganna Mylovydova

Diagnostic Laboratory with Immunoenzyme and Radioisotopic Analysis, Institute of General and Urgent Surgery of Academy of Medical Sciences of Ukraine, Ukraine

Background: There were studied the diagnostic importance of specific immunophysiological markers associated with various types of local extended thymomas at myasthenia.

Methods: There were defined the phenotype and the density of leukocytic antigens HLA-DR of II class, the expression of differenciative markers CD3, CD4, CD8,

$\tilde{N}$D16, $\tilde{N}$D19, contents of serumal cytotoxic factors, concentration of cytokines and presence organ-specific antibodies to the tissue of liver, lungs, heart.

Results: The immunocytochemical methods of research have found the following types of thymomas: lymphoepithelial thymoma (LEÒ) – 59%, epithelial (EÒ) – 24%, lymphoid (LÒ) – 9% and granulomatous thymoma (GÒ) – 8%. The locally extended thymomas more often associated with the phenotype of antigens HLA-DR1, HLA-DR3 and HLA-DR7. Patients with LÒ have phenotype HLA-DR1 and HLA-DR5, and patients with LET have HLA-DR3 and HLA-DR7, patients with EÒ have phenotype HLA-DR1 and HLA-DR3. Phenotype HLA-DR5 and HLA-DR52 is associated with GÒ. In patients with LT $CD4^+$ T-helpers, $CD16^+$ are significantly increased and level $CD8^+$ is decreased. The increase of $CD19^+$ and $CD16^+$ in 2 times in comparison with referential values has been found at patients with LET. There was found the significant increase of $CD2^+$ at LÒ and GÒ in 1,5 times. Subpopulation of $CD3^+$ at EÒ and LEÒ is significantly decreased. Subpopulation of $CD4^+$ at LET and EÒ is considerably decreased. Cytotoxic $CD8^+$ cells in these groups of patients were also below the control parameters in 2 times. At GÒ the level of $CD3^+$, $CD4^+$ and $CD8^+$ does not differ from control value.

Conclusion: The alterations of immunophysiological reactions at various types of thymomdependent myasthenias allows to carry out differential diagnostics of thymomas, to make a choice of treatment tactics, including excisions of the thymus and to prognosticate the current of disease.

P-220

Immunoexpresion of HER family in Invasive Ductal Carcinomas of the Breast

Ipek Erbarut; Handan Kaya
Marmara University School of Medicine, Turkey

Aim: To investigate the frequency of expression of erbB/Her family of growth factor receptors in invasive ductal carcinomas of the breast.

Material Method: 59 invasive carcinomas ductal carcinomas of the breast has been studied for EGFR, c-erbB-2, c-erbB-3 and c-erbB-4 by streptavidin- biotin horseradish method and only for c-erbB-2 by FISH technique. The frequency of expression of the antibodies, their coexpressions, correlation of immunohistochemistry results and FISH for c-erbB-2 and correlations with the histopathological prognostic parameters as tumor stage, grade, lymph node status, hormonal status, age, and patients' 3 years clinical follow-up, have been investigated.

Results: Of the 59 tumours 44 (75%) were ER+, 37 (63%) PR+, 4 (7%) EGFR+, 6 (10%) c-erbB-2, 6 (12%) c-erbB-3, 14 (24%) c-erbB-4 by immunohistochemistry. Seven of eleven c-erbB-2 ++ (equivocal) cases were positive by FISH. Thus, c-erbB-2 amplification increased to 22%. Statistically significant correlations between tumor stage and lymph node status and between ER and PR status were found ($p<0.05$). There has been a statistically significant correlation with ER negativity and EGFR overexpression ($p<0.05$); a borderline positive correlation with EGFR and c-erbB-2 has also been noted ($p=0.064$). C-erbB-2 overexpression demonstrated significant correlation with the tumour high grade, PR negativity, and c-erbB-3 immunoexpression. C-erbB-3 expression and c-erbB-4 expression were found to be statistically correlated ($p<0.05$). Also significant association with c-erbB-4 expression and the patients good clinical out come ($p<0.05$) were found.

Conclusion: The results of our study suggests a subgroup of invasive ductal carcinomas of the breast which are ER-negative, EGFR positive or PR negative, c-erbB-2 positive. These groups correlate with high tumor grade, high stage, and lymph node metastasis.

P-221

CYCLİN D1 AND P21 ASSESMENT AT TAOXİFEN RESİSTANT BREAST CANCER

MİNE CAYİRCİ, NİMET KARADAYI, AYLİN GÜL, DİLEK YAVUZER
Dr.lutfi kirdar kartal egitim ve arastirma hastanesi, Turkey

Introduction: Cyclin D1 is an important nuclear protein which is necessary for progression of cells through the G1 to S phases of the cell cycle. p21 activated kinase plays inhibitor role at cell cycle. Quantifying of their proliferative potential may help in prediction of biological behavior of tumors with comparable histology.

The aim of this study was to explore the usefullness of Cyclin D1 and p21 expression as proliferative and predictive markers at tamoxifen resistant invasive ductal breast carcinomas and compare these two markers with classical prognostic parameters (tumor size, histological and nuclear grade, perineural and vascular invasion, estrogen and progesteron reseptor status, cerb-B2 positivity, axillar lymph node status).

Materials and methods: We investigated 66 cases of invasive ductal breast carcinomas of which diagnosed between 2002–2007 in our hospital. Paraffine-embedded archival tissue was used with monoclonal antibodies against Cyclin D1 and p21.

Conclusions: In this study, there was no statistically significant relationship with tamoxifen resistance and Cyclin D1 and p21 expression but we found association between estrogen and progesteron receptor positivity with Cyclin D1 expression.

P-222
HIGH AGREEMENT BETWEEN FISH AND CISH BASED TESTING FOR HER2 AND TOP2A GENE AMPLIFICATION

K. D. Hoff, J. T. Jørgensen, S. Müller, O. F. Rasmussen and A. Schønau
Dako Denmark A/S, Denmark

Background. We have developed a prototype CISH visualization kit, which used on top of FISH gene probes converts the fluorescence signals into stainings that can be evaluated by bright field microscopy. The Dako CISH kit is a dual color assay that detects both the *HER2* or *TOP2A* gene and CEN-17 on the same slide. The dual color technique makes it easier to distinguish true gene amplifications or deletions from chromosomal aneuploidy compared to single color CISH assays. The aim of the present study was to investigate the concordance between CISH and FISH technologies for detection of *HER2* or *TOP2A* gene amplifications/deletions
Method. The study was divided into two parts, one comparison for *HER2* gene detection and one for *TOP2A* FISH gene detection, including 24 and 20 FFPE breast cancer specimens, respectively. The CISH and FISH analyses were performed on serial sections. Evaluation was done blinded.
Results. For both the *HER2* and *TOP2A* status, the concordance was 100% and the corresponding Kappa values were 1,0. The correlation of the gene copy number to CEN-17 ratios were similarly high, with a correlation coefficient (r) for both *HER2* and *TOP2A* above 0,95.
Conclusion. The results from the study showed a complete agreement between CISH and FISH technologies, and a larger study is in planning to confirm the findings in the present study.
The data indicates that the technology used for the Dako prototype CISH assay holds significant promise as a future method.

P-223
Cell membrane and cytoplasmic immunoreactivity of MIB-1 in invasive breast carcinoma

José Antonio Ortiz-Rey; Carolina Gómez de María; Pastora Durán-Barbeito; Andrea Fernández-Almeida; Belén Rodríguez-Fernández; Alfonso Fernández-Costas; Iosu Antón
Servicio de Anatomía Patológica. Hospital POVISA, Spain

Background The monoclonal antibody MIB-1 recognizes the nuclear Ki67 antigen and is used to assess proliferative activity of tumors. In the last years a peculiar cell membrane or cytoplasmic MIB-1 staining has been occasionally reported in a few tumors, including breast carcinoma. We investigated clinicopathologic features of invasive breast carcinomas with non-nuclear MIB-1 immunoreactivity.
Method 295 invasive breast carcinomas stained with MIB-1 from May 2002 to September 2007 were reviewed. They were 236 usual ductal carcinomas, 35 lobular carcinomas and 24 special types. Staining method was LSAB2 (185 cases) or Envision (110) (Dako). MIB-1 antibody was diluted 1:25 and 1:75 respectively. Non-nuclear immunostaining was evaluated as + (isolated cells), ++ (focal, minority of cells) or +++ (diffuse and strong staining). In positive cases GCDFP-15, CD10, alcian blue and PAS-diastase techniques were done.
Results Fourteen cases (4.7%) showed non-nuclear reactivity (3 +, 4 ++, 7 +++): in lateral cell membrane (6 cases), luminal membrane (6) and cytoplasm (4), both with LSAB2 (9 cases, 4.8%) as with Envision (5 cases, 4.5%). Staining did not correlate with GCDFP-15 or CD10 reactivity. Positive cases were 8 usual ductal carcinomas, one pleomorphic lobular carcinoma and 5 other types, staged pN0 (6 cases), pN1(4), pN2 (1), pN3 (1) or pNx (2). Bloom-Richardson grade was low (5 cases), intermediate (5) or high (4). Estrogen receptors were positive in 8 cases and progesterone receptors in 7 tumors. PAS-diastase and alcian blue were positive.
Conclusion Cell membrane or cytoplasmic MIB-1 immunoreactivity is a rare feature of invasive breast carcinomas (4.7%). It does not depend on the visualization technique and is related to a cross-reactivity of this antibody with other epitope, probably a glycoprotein. It occurs in different types of breast carcinoma and no special clinicopathologic features have been identified, although larger series need to be investigated.

P-224
Myxoid Liposarcoma of the Breast in Female-case raport

1 Ljiljana Tadic Latinovic 2 Aleksandra Salapura
Department of Pathology Clinical Centar Banja Luka, Bosnia and Herzegovina

Breast liposarcoma is very rare malignant breast tumor and it have an incidence of 0,3% of all breast sarcomas.
A 66- year old woman presented with a tumorous mass of the left breast. The excided part of breast measured 6×5×3,5 cm. The serial sections revealed well-circumscribed nodular mass yellowish, glistened and lobular. Tumor mass measured 3,2×3×3 cm. Histological examination showed proliferation of spindle shaped cells and signet-ring lipoblasts in myxoid matrix as well as delicate branching capillaries were noted.Cytoplasm of tumor cells were positive staining for Sudan III dye. Ultrastructuraly numer-

ous fatty vacuoles of variable size were found. Phylodes tumor was excluded becauseof abscense of epithelial component.
Aditional mastectomy was done and adjuvant therapy has not been given.

P-225
Nuclear comparative morphometric study between DCIS and normal resting mammary gland tissue

Mariana Deacu; Mariana Aschie; Madalina Bosoteanu
Constanta "Ovidius" University, Medicine Faculty, Romania

Background. DCIS is the malignant epithelial cells proliferation that affect only ducts, including lobular, without basement membrane interruption. Benign or malignant cells phenotype is concerned by nuclear appearance. Morphometric analysis could provide quantitative information about nuclear profile in several lesions. In this study we proposed to assess nuclear morphometric features of mammary epithelial cells in DCIS compared to normal resting mammary tissue.
Methode. The study comprise breast tissue from 20 women histopathologically confirmed with DCIS. Normal resting breast tissue were obtained from another 20 women surgically treated for fibroadenoma, tumor condition that associate low risk of cancer development. Nuclear morphometry was performed on H&E slides, using a light microscope Nikon E600 with a Nikon camera linked to a computer and Lucia Net Software. For each case 300 ductal epithelial nuclei were randomly selected at a magnification 400×. We assess: Nuclear Area (μm^2), Nuclear Perimeter (μm), Maxim Diameter (μm), Minim Diameter (μm), Elongation and theirs standard deviations (dst). t-Test and ANOVA were used to compared morphometric parameters between selected groups ($p<0,05$).
Results. Following microscopical exam of normal resting breast tissue, 10 cases were included in follicular phase of menstrual cycle and another 10 in luteal phase. Morphometric assessment showed insignificant size diferences between ductal epithelial nuclei in follicular and luteal phases. The means values were: Nuclear Area 23,63± 3,63 μm^2; Perimeter 17,12±1,34 μm; Maxim Diameter 6,45±0,61 μm; Minim Diameter 4,66±0,56 μm; Elongation 1,41±0,24. Microscopical features of DCIS selected for morphometric assessment were: comedo, cribriforme, solide and papillary. The means values for ductal epithelial nuclei in DCIS were: Nuclear Area 83,29±15,25 μm^2; Perimeter 32,46±2,97 μm; Maxim Diameter 12,2± 1,33 μm; Minim Diameter 8,57±1,17 μm; Elongation 1,45±0,25. Applying t-Test for all evaluated morphometric parameters we obtained $p<0,05$.
Conclusions. Morphometric assessment showed that in DCIS ductal epithelial nuclei presents pronounced polimorphism and high size levels that in normal resting mammary tissue.

P-226
Expressıon of PTEN and Survıvın Correlates wıth Apoptosıs ın In Sıtu and Invasıve Breast Cancer

Fatma Aktepe*; Caner Kır *; Dursun Ali Sahin; Hüsniye Dilek ***
**Department of Pathology, ***Department of Surgery, Afyon Kocatepe University, Faculty of Medicine, Turkey*

Background: During epithelial homeostasis proliferation, migration, differantiation, and apoptosis (programmed cell death) occur. Disturbance of these processes leads to tumorigenesis. Survivin is a recently identified inhibitor of apoptosis and PTEN plays an important role in arrangement of signals required for cell growing and apoptosis. In case of absence or mutations of PTEN, tumor cells can protect themselves against apoptosis by the way of lipid signal transduction.
Methods: In this study, the relationship of PTEN and survivin expression with apoptosis was investigated by the means of immunohistochemical method in 39 patients with invasive breast cancer (IBC) and ductal carcinoma in situ (DCIS) within the same breast tissue.
Results: A decrease or loss in PTEN expression was observed in an important portion in DCIS(46.7%) and IBC (71.8%). In cases with invasive ductal carcinomas, strong staining with survivin was observed in 33.3% of cases, while there was weak staining in 61.6% and no staining in 5.1% of cases. All of the DCIS, tumor cells were positive with survivin but staining was weak. Apoptotic index was higher in IBC than in DCIS, but there was no significant differences. No relationship was found between apoptosis and PTEN or survivin expression.
Conclusion: Our results suggested that a decrease in PTEN expression and increase in apoptosis be important in progression of IBC. Further studies with large case series are needed to clarify importance of PTEN and survivin in progress of IBC and their relationship with apoptosis.

P-227
Presence of basement membrane material around the tubules of tubulolobular carcinoma

Gabor Cserni
Bacs-Kiskun County Teaching Hospital, Hungary

Published guidelines recommend both myoepithelial and basement membrane stains (the latter including collagen IV

and laminin) in the differential diagnosis of tubular or well differentiated ductal carcinomas versus microglandular adenosis or complex sclerosing lesions. Differentiating these lesions in core needle biopsy specimens may be difficult.

Two core needle biopsy samples are presented, both of them containing small acinar (tubular) proliferations arranged in an infiltrating pattern. A basement membrane like staining with collagen IV was seen in both cases, whereas the laminin immunostain was obviously negative. (A positive EMA and a negative S100 stain were also features against the diagnosis of microglandular adenosis.) The tumours were classified as tubulolbular carcinomas after excision.

The collagen IV staining around invasive glands of tubulolobular carcinomas (and probably other well differentiated tubule forming carcinomas of the breast) partially challenges the recommendation of using this immunostain in the differential diagnosis of benign versus malignant lesions of the breast. Knowledge of this phenomenon (the possible presence of a basement membrane like staining with collagen IV around the glands of a malignant lesion) may help in classifying some lesions as B5 (diagnostic of malignancy) instead of B4 (suspicious for malignancy) on core needle biopsy specimens.

P-228

E-cadherin expression in invasive breast cancer correlates with grade of the tumor

Cristian Suciu; Anca Maria Cimpean; Dragos Izvernariu; Marius Raica

"Victor Babes" University of Medicine and Pharmacy, Department of Histology&Cytology, Timisoara

Background E-cadherin is a calcium-dependent transmembrane adhesion protein, with molecular weight of 120 kDa, belonging to the type I classical cadherins family, and is localized in adherens junctions. Data from the literature support the tumor supressor activity of this protein, based on the lost of expression and function during tumorigenesis and tumour progression in different types of cancer. The aim of this study is to evaluate the expression of E-cadherin in invasive breast cancer and its correlation with tumor grade and the number of tumor metastases.

Material and methods There were investigated 22 cases of primary invasive breast carcinoma. E-cadherin expression was assessed immunohistochemically, with the monoclonal antibody (incubation with the primary anti-E–cadherin antibody clone NCH-38 was done for 30 minutes, dilution 1:75) and LSAB+ working system.. The expression of the immunostaining was considered *normal* if over 70% of the tumour cells were positive, and *aberrant* if less than 70% were positive.

Results Normal glandular structures showed an intense positive immunostaining, with membrane pattern, both in luminal and basal cells. From the invasive breast carcinomas, 45.5% (n=10) have presented normal reaction, whereas 54.5% (n=12) have presented aberrant reaction. The percent of cases with aberrant expression of E-cadherin decreases along with growth of the tumour grade. Thus, 100% of the tumors with G1 grade showed aberrant expression, which decreases to approximately 44.5% for G2 and to 37.5% in G3 tumors. The tumors with less than 2 cm in diameter had aberrant expression in 83.3% of the cases, and the percent decreased to 56.25% in the case of the tumors with over 2 cm in dimensions.

Conclusions E-cadherin immunohistochemical expression decreases in ductal invasive breast cancers as compared with normal mammary tissue. The percent of the cases with aberrant expression of E-cadherin decreases with the increase of the tumor grade.

P-229

A survey in EBV genome frequency in breast cancer of iranian population

Mahmud Khaniki; Isa Jahanzad; Fatemeh Sehati

Cancer Institute of Iran, Iran

Background: Breast cancer is the frequently diagnosed malignancy of women & is the second cause of death from cancer in women. As the etiology & progression of breast cancer remain incompletely understood, novel mechanism of disease pathogenesis is needed to be considered. Recent interest has focused on Epstein-Barr virus (EBV) an oncogenic herpes virus. Investigation of this association could not only broaden understanding of breast cancer etiology but also have implications regarding early detection, treatment and prevention. Studies of an association of this virus with breast cancer have had notably inconsistent results, marked by varying EBV presence from nil to 50% of tumors.

Objective: To assess EBV presence in breast cancer of Iranian series & investigation of this frequency with some tumoral indexes or some factors relevant to the patients.

Method: To evaluation of the presence of LMP genome of EBV by PCR on paraffin embedded blocks of 100 Iranian females with breast cancer.

To differentiate EBV in tumor cells from EBV in background immunocytes, on positive cases, we did microdissection & PCR, and then we investigated this finding with different factors.

Results: Expression of LMP genome was observed primarily in 8 of 100 cases & it was positive in 6 cases after microdissection.
No significant association was observed EBV expression & some tumoral index such as morphology, histological grade, lymph node involvement, skin & perineural & vascular invasion, tumoral necrosis, & some index included ER,PR,P53,Her-2 markers($p<0.005$).
It seems this is due to low frequency of this genome in the cases of breast cancer in Iran.

P-230

Vimentin, p-cadherin and basal type cytokeratins expression in invasive breast carcinoma.

Renata Kusinska, Piotr Potemski, Dorota Kupnicka, Grażyna Pasz-Walczak, Radzislaw Kordek
Department of Pathology, Medical University of Lodz, Copernicus Memorial hospital, 4 Paderewski St., 93–509 Lodz, Poland.

Background: Basal-type breast carcinomas defined by the CK5/6, CK14 and CK17 expression and ER and HER2 negativity are related with poorer outcome. There were suggestions that these tumours more often present vimentin and p-cadherin expression and these antigens characterise high grade and ER-negative tumours.
Method: We investigated the expression of vimentin, p-cadherin, cytokeratins: 5/6, 14, 17 and ER, PGR, HER2, Cyclin E and Ki67 in 193 invasive ductal breast cancer by immunohistochemistry, to find out the relationship among vimentin and p-cadherin expression and basal cell phenotype. We check also association of analysed antigens with clinical and morphological factors.
Results: Forty one (21,2%) cases expressed vimentin, whereas 111 (57,5%) tumours were p-cadherin-positive. Expression of CK5/6 showed 66 (34,2%) tumours, 48 (24,9%) were CK17-positive and 48 (24,9%) CK-14 positive. Expression of vimentin showed 32 (45,7%) cases from the group of "CK5/6 or CK14 or CK17" - positive tumours and 9 (7,4%) remaining tumours ($p<0,001$). P-cadherin was positive in 73,2% and 48,4% ($p<0,001$) cases accordingly.
Conclusions: P-cadherin and vimentin expression are more often present in the group of basal cytokeratin positive tumours, but can not be regarded as sensitive markers of basal-type tumours.

P-231

Metaplastic breast carcinoma. a clinico-pathologic review of 24 cases

Angels Lerín*; Teresa Soler*; Fina Climent*; Ruth Tascón*; Anna Gumà; Laura Esteller***; Mar Varela****;Maria Jesús Pla*****; Enric Benito*****; Jaume Mora******; Enric Condom***
Servei d'Anatomia Patològica, Servei de Radiologia**, Servei de Ginecologia***** i Servei de Cirurgia Plàstica******, IDIBELL, Hospital Universitari de Bellvitge; Servei d' Oncologia Mèdica*** i Banc de Tumors****, IDIBELL, Institut Català d'Oncologia, L'Hospitalet de Llobregat, Spain*

INTRODUCTION Metaplastic breast carcinoma (MBC) is characterized by an admixture of adenocarcinoma and metaplastic elements, wich can be homologous or heterologous. MBCs account for 1–3.7% of breast carcinomas. Our aim was to analyse the clinico-pathological features of a series of MBCs.
MATERIAL AND METHODS MBCs diagnosed between 1996 and 2007 were reviewed. Patient's age, size, tumor type, border appearance, presence of necrosis, osteoclast-like cells and lymph node status were assessed. Immunostains for oestrogen (ER) and progesterone receptors (PR), HER2, p53, p63, CK5–6, EGFR, vimentin, smooth muscle actin (SMA), bcl-2 and CD10 were performed.
RESULTS Twenty-four cases were found. The age ranged from 31 to 94 years (mean 47.8). By ultrasonography, the most part of tumours were lobulated. MBC was diagnosed or suggested by cytology and/or biopsy in 10 cases. 41.6% were grossly expansive. The mean size was 50.1 mm. Lymph node metastasis were seen in 41.6% of cases. 33% of patients presented recurrence between 2 and 37 months after surgery.
13 of 24 cases (54.1%) were ductal adenocarcinoma with squamous metaplasia, 12,5% pure squamous carcinoma, 12.5% with spindle differentiation, and 20.8% had condroid elements. Osteoclast-like giant cells were seen in 33.3% of cases.
62.5% of cases were positive for p53, 79.2% for p63, 50% for bcl-2, 95.8% for CK5–6, 41.7% for EGFR, 87.5% for vimentin, 16.7% for SMA and 54.2% for CD10.
21 of 24 tumours (87.5%) were negative for ER, PR, and HER2. Of these, 33% expressed EGFR, 95.8% CK5–6, 76.1% p63 and 61.9% expressed CD10.
CONCLUSIONS Most of MBC have lobulated, expansive margins.
The most frequent component is squamous metaplasia.
A high percentage are triple negative tumors. Most of them express basal and myoepithelial markers.
Recurrence is observed in 33% of cases in a shorter interval than conventional ductal adenocarcinoma.

P-232

Radiation impact on breast carcinoma after chernobyl accident

Anca Craciun; Anca Dobre; Mariana Aschie; Ionut Poinareanu; Anca Papuc; Andreea Iliesiu
Ovidius University, Constanta, Romania

Background: The accident at the Chernobyl nuclear power plant in 1996 caused radionuclides release over large areas. Radioactive Caesium-137 has a half-life of 30 years and Strontium-90 has a half-life of 50 years. In the atmosphere were also spread vapors of Iodine-131 and Plutonium-239. These radionuclides are incriminated in increase numbers of breast, thyroid, urinary cancer and leukemia.
Method: Statistical study of breast carcinoma cases new diagnosed between 1986- 2006, in Morphopathology Department of County Hospital, Constanta, following a few parameters: sex, age, tumor stage, microscopic features.
Results: From our study resulted an increasing number of new diagnosed breast cancer between 1986 - 2006 (144 cases in 1986 to 204 cases in 2006), this increase being due to life conditions change, new diagnose methods and to latency period needed for genetic mutations provoked by post-Chernobyl emission of radiations to accumulate. The study showed anticipation phenomena with a lot of new cases diagnosed between 30–50 years (20 cases in 1986 to 56 cases in 2006). Anticipation phenomena observed may be due to radiation level but further studies are needed. For this period the number of breast cancer diagnosed in first stages increased (64 cases in 1986 to 160 cases in 2006). Number of breast cancer with mixed histological features increased between 1986 -2006 (16 cases in 1986 to 100 cases in 2006). Predominance of breast cancer in female patients maintains in this period but from 1986 to 2006 had been diagnosticated cases of breast cancer in man patients.
Conclusions:

- Breast cancer is continuously increasing because radionuclides half-life.
- In breast cancer cases evolution it is observed an anticipating phenomena.
- Radiations determined an increasing in number of mixed histological features of breast cancer specimens.
- Cases of breast cancer in man are more frequent.

P-233

BREAST CANCER STEM CELLS RESIST APOPTOSIS THROUGH THE REGULATION OF BCL2

Madjd Z; Zare Mehrjerdi A; Sharifi A; Molanaei S; Zohoorian S; Asadi Lari M
Iran University of Medical Sciences, Iran

Background: cancer stem cells arise from their normal stem cell counterparts that undergo accumulation of genetic changes until the cells acquire a malignant phenotype. Breast epithelial stem cells are the primary targets in the etiology of breast cancer. The capacity of breast tumour development has been shown to be restricted to CD44+/CD24$^{-/low}$ epithelial tumour cells. Identification of breast cancer stem cell is important because of its implication on development of new therapeutic strategies. Stem cells can resist apoptosis through some mechanism such as the regulation of Bcl2.
Methods: The present study included 150 primary operable breast cancer patients with a median age of 46 years, in order to investigate the prevalence of cancer stem cells. Iimmunohistochemistry was applied to identify the population of CD44+/CD24$^{-/low}$ cells in the paraffin embedded tissues. The prevalence of cancer stem cells are then correlated with level of expression of anti-apoptotic protein Bcl2, Estrogen Receptor (ER), Progesterone Receptor (PR), also with prognostic factors including tumour size, lymph node stage, differentiation and metastasis.
Results and conclusion: Univariate analysis showed a significant correlation between higher level of expression of Bcl-2 and smaller tumour size (P=0.001), and lower grade of breast tumours (p=0.007). There was a strong correlation between the presence of Bcl-2 and the presence of ER and PR (p=0.042). Moreover, a positive correlation was found between CD44 and Bcl2 expression; i.e. CD44+ cells express higher levels of Bcl2, therefore can resist apoptosis. Anticancer therapy including chemotherapy normally target non-tumorigenic cells in tumour, while cancer stem cells are still survive and leading to tumour recurrence. Therefore, targeting this population of cells which are more resistance to apoptosis in combination with current treatments will be more effective in breast cancer patients.

P-234

Comparison of diagnostic accuracy of Triple Test Score with pathologic findings of breast masses

Fakhrjoo A., Montazeri V., Naeimi E., Nami F.
Tabriz university medical siences,- Department of Pathology, Imam Khomeini,Teaching and Research Hospital

Introduction:palpable masses of breast are common and usually benign.Combination of physical examination, imaging and Fine Needle Aspiration (FNA) for diagnosis of malignant or benign breast masses are useful.
The Aim: comparison of accurate diagnosis in combination of physical examination, imaging, FNA(Triple Test Score) with pathologic findings that obtained from biopsy or mastectomy of breast masses
Material and Method: 100 women with different ages with breast mass that physical examinations were performed, devided in to 3groups:

Scor = 1 for benign cases, Score=2 for doubtful cases,and Score =3 for malignant.Then these patients were sent to imaging and were given scores on basis of benign, doubtful and malignant. Finally FNA were done and prepared smears,and were stained by Papa and Geimsa.Then pathologic results of biopsy and mastectomy are compared with findings of TTS.

Result: 100 patients were studied by physical examination, imaging and FNA. In this survey,63cases were 3–4 points in TTSscoring, and all of them were benign,and 32 cases which were TTS> or =6, in the final diagnosis were malignant.Therefor, TTS had 100% speciality and 100% sensitivity in diagnosis of breast masses.

Coclusion: the TTS was 100% accurate in the diagnosis of palpable breast masses when all three elements were concomitant.

Key words: Fine Needle Aspiration, Imaging, Palpable masses.

P-235
HER-2/NEU IN BREAST CANCER. IMMUNOHISTOCHEMICAL COMPARISON USING MONO AND POLYCLONAL ANTIBODIES. HYBRIDIZATION IN SITU CHROMOGENICA (CISH) AMPLIFICATION.

Ma.Isabel Pérez R; Jorge Ugalde P; Gabriela Picon M.
Instituto del Cáncer SOLCA. Cuenca-Ecuador

Breast cancer is placed as the fourth most common cancer pathology in our region, with a standard rate of 20.4 per 1000 000 women. There are prognostic and predictive indicators in breast cancer. An available molecular marker is Proto oncogen Her-2/neu. The aim of the present work was to determine by means of immune histochemistry (IHC) with monoclonal and polyclonal antibodies the over expression of the protein. Genes of patients 2+ and 3+ were amplified using in situ chromogenic hybridization CISH).

Methodology: 246 patients diagnosed with breast cancer were evaluated with IHC and CISH panels. Data obtained were related to age, histological type, histological grade and lymph node metastasis.

Results: 96.3% of the results were infiltrated ductal carcinoma; from this group 80.9% were NTH II. Age prevalence was 40 – 49 years old, Of the cases studied. 67 patients (27.2%) expressed the protein by means of polyclonal antibodies (AO485), 70 cases (28.5%) used monoclonal antibodies (CB11). Amplification by CISH was 24% and 23.58%, respectively. Polyclonal antibodies sensitivity was 98.33%, with a specificity of 50% and monoclonal antibodies sensitivity was 96.97%, with a specificity of 25%. The group of patients submitted to MRM (38) with node metastasis, 28 amplified the gene (73.68%). Sensitivity and specificity of CISH 3+ were 100%.

Conclusions: Expression of Her-2 protein by IHQ for both monoclonal and polyclonal antibodies is a high sensitive technique, being less specific to monoclonal antibodies. Based in our results, we recommend CISH as a genetic expression validation test in 2+ cases.

P-236
DEDIFFERENTIATED ADENOID CYSTIC CARCINOMA OF THE BREAST WITH AGGRESSIVE BEHAVIOUR.

Alberto Righi, Luca Morandi, Federica Flamminio, Dario De Biase, Maria P. Foschini
Section of Anatomic Pathology "M. Malpighi," University of Bologna, Bellaria Hospital, Bologna, Italy.

The present paper describes a case of adenoid cystic carcinoma (AdCC) of the breast with dedifferentiated features and aggressive behaviour. A 63-year-old woman presented a 4 cm mass of the right breast. On histology, the tumour showed an in situ and an invasive component, both with typical features of AdCC intermingled with areas of solid, poorly differentiated carcinoma. The poorly differentiated areas loose markers of myoepithelial differentiation, while were diffusely positive for low weight cytokeratin. At the genetic point of view, the Neighbor Joining tree derived from mtDNA D-loop sequence analysis showed that areas of typical AdCC and dedifferentiated were similar. Furthermore both components revealed some genetic alterations in common identified by aCGH (amplifications in 5q, 6p22, 8q24, 19p13.2, 21q22.3). Additionally dedifferentiated areas showed three peculiar deletions in 2q21.1, 6q25, Xp11.22 and six peculiar amplifications in 6p21.33, 9q34.3, 11p15.5, 11q13.1, 14q32.3, 16q13.

One axillary node metastasis was evident at presentation. Presently, six years after surgery the patient is alive with bone and lung metastasis.

AdCC of the breast even if presenting solid areas is usually associated to good prognosis. The present case differs from those previously reported as showed an overgrowth of a dedifferentiated epithelial component similarly to dedifferentiated AdCC of salivary glands. These features should be better known also in breast as associated to more aggressive behaviour.

P-237

Malignant transformation of breast adenomyoepithelioma

Mar Pascual*; MJosé Ríos*; Esther Gimeno*; MIgnacia Valero*; Isabel Marquina **; Ana Fuertes*, Guillermo Muñoz*; Patricia Sota*

**Hospital Universitario Miguel Servet; **Hospital de Alcañiz, Spain*

Background: Breast adenomyoepitheliomas are rare tumours composed by a double cell population. They are usually considered benign, although they can recur locally.
Case report: We present the case of a 54 year-old female whose radiological study reveals two polilobated cystic nodules in upper outer quadrant and central region of right breast. These two nodules are resected.
Results: Histological study of the two lumpectomy specimens shows a double component, epithelial and myoepithelial. Thus, they are diagnosed of adenomyoepitheliomas with stromal overgrowth. Besides, resection margins are affected, so the patient is reoperated. In the specimen of re-excision of margins malignancy is found, in the way of myoepithelial carcinoma growing from adenomyoepithelioma. Then, mastectomy is performed and multiple adenomyoepitheliomas are seen all over breast parenchyma. Seven months after surgery the patient presents two subcutaneous nodules in the surgical area, which consist in two foci of myoepithelial carcinoma infiltrating major pectoralis muscle. Six months after treatment, there is no recurrence.
Comments: Myoepithelial carcinoma growing from adenomyoepithelioma is rareness. Histological features that indicate malignancy (atipia, necrosis, high mitotic index and infiltration) are more frequent in recurrences. Although myoepitheliomas are considered benign, there is a rank of behaviour that includes local recurrence, malignization and rarely distant metastases.

P-238

Correlation between pathological features of breast tumors and stem cell content as measured by sphere formation ability

Arrate Eguiara; Kepa Elorriaga*; Maria Diaz-Nuñez**; Angel Garcia Martin**; Ricardo Rezola***

* S^0 *Patología. Instituto Oncológico. San Sebastian.*
** *Fundación Inbiomed. San Sebastian. Spain*

Background Breast cancer stem cells have been defined as $CD44^+CD24^-Lin^-$ cells, however only about 20% of this population has the ability to recontitute the original tumor. Therefore, a further definition of breast cancer stem cells is required for its use in the clinic as prognostic criteria. By using the unique ability of stem cells to grow as floating spheres in culture we aim to identify and quantify the presence of stem cells in tumor sprecimens and correlate with clinical, phenotypic and immunohistochemical features of the tumor.
Methods We analyzed 60 breast carcinomas diagnosed at Instituto Oncologico in 2007, for which clinico-pathological data was collected. These data includes age, treatment (when applicable), size, grade, histological type, estrogen and progesterone receptors, Her2 and Ki67 expression. A fragment homogeneus for tumor tissue content was used to isolate tumor cells by enzimatic digestion and single cells cultured on non-adherent conditions to allow for sphere formation. Spheres were counted after 10–14 days in culture, time when they were disaggregated to demonstrate presence of cancer stem cells.
Results & Conclusion We have used the number of spheres formed as representative of the content of stem cells in the original tumor (SFU, sphere forming units). While only 30% of the tumors were capable of forming spheres in vitro, irrespective of the number of cells isolated, we found association between the ability to form spheres and several clinico-pathological features of the tumor, such as Her2. This association suggests that the content of stem cells may be of prognostic value. Furthemore, the identification of tumors with highest stem cell content will make possible the identification of specific stem cells markers for use in breast cancer prognosis by directing the search to those tumors.

P-239

Microvessel density in breast cancer patients with polymorphism in the endostatin gene

Gustavo Lourenço; André Almeida Schenka; Natália Schenka; C Cardoso Filho; Glauce Aparecida Pinto; José Vassallo; M S C Gurgel; Carmen Silvia Passos Lima

State University of Campinas, São Paulo, Brazil

Introduction: Angiogenesis is an important step in breast cancer (BC) development and progression. In addition to producing proangiogenesis cytokines, neoplastic cells also play a role in the generation of endogenous antiangiogenic proteins, including endostatin (ES). ES is a terminal fragment of collagen XVIII, the product of the *COL18A1* gene. The *COL18A1* gene polymorphism (D104N) in homozygosis is associated with an increased risk for sporadic breast cancer (SBC). Microvessel density (MVD) is the most commonly used technique to quantify intratumoral angiogenesis in BC. **Aims:** To test whether D104N polymorphism altered MVD in BC patients. **Patients and Methods:** Genomic DNA was obtained from peripheral blood samples from 84 untreated female patients with SBC and was analyzed using the polymerase chain reaction followed by restriction endonuclease digestion with *Mse*I, to evaluate the presence of D104N polymorphism. The

MVD of formalin-fixed paraffin-embedded tissues of all patients was determined in CD34-immunostained sections using the Imagelab software for morphoanalysis. Statistical significance of the median intratumoral MVD differences between groups was calculated by Kruskal-Wallis and Wilcoxon tests. **Results:** The median intratumoral MVD was different when we compared the patients with wild-type (DD), heterozygous (DN) and homozygous (NN) genotypes (19.00, 12.83 and 28.66, respectively; $P=0.02$). Surprisingly, there were no significant differences between the median intratumoral MVD in DD plus DN, in comparison with NN patients (18.50 *vs* 28.66; $P=0.08$). **Conclusion:** It was not possible to conclusively determine any association between D104N polymorphism in *COL18A1* gene with the degree of angiogenesis in BC. (Supported by FAPESP and CNPq).

P-240

Thymoma mimicking a primary breast cancer

Sabrina Croce; Martine Prévot-Maupoix; Selenia Casnedi; Annick Wittersheim; Alina Onea; Jean-Pierre Bellocq; Marie Pierre Chenard

Department of Pathology University Hospital Strasbourg France

Background. Most tumours of the breast originate in mammary tissue. Metastases to the breast mimicking a primary breast cancer are uncommon and direct invasion from a tumour located to the thorax is rare. We report a case of a thymoma which was diagnosed on a core biopsy of a breast mass.

Case report. A 83-year old woman presented with a palpable polycyclic 3 cm large mass in the UEQ of the left breast. Her medical history was significant for an asymptomatic mass of the anterior mediastinum, incidentally detected on radiographic imaging 12 years ago, but never histologically documented. Histological analysis of breast core biopsy showed a mixture of small ovoid or spindle-shaped cells with clear cytoplasm, bland cytologic features and trabecular or hemangiopericytoma-like growth pattern and small round basophilic cells. The clear cells were immunoreactive for pan cytokeratin, CK7, CK5/6, and p63, with a very low Ki-67 index. The basophilic cells expressed CD3, CD1a, TdT and had a Ki-67 index of 100%. The breast tumour was diagnosed as an extension of a mediastinal type AB thymoma (WHO classification). TDM confirmed the presence of a large intrathoracic mass occupying most of the left pleural space.

Discussion. Without knowledge of the past history of the patient, a solid variant of lobular carcinoma, a myofibroblastoma or a myoepithelial tumor would have been considered. Stage III thymomas may invade surrounding organs such as lung, pleura or pericardium. Rare cases of thymoma with endobronchial growth or transdiaphragmatic extension to the liver have also been described, but to our knolwledge direct invasion of the breast mimicking primary breast cancer has never been reported.

Conclusion. In case of histologic features unusual for a primary breast tumor, the possibility of metastasis to the breast, but also of direct extension of an advanced thymoma should be considered.

P-241

P53 and c-myc in advanced breast cancer. a tma immunohistochemical evaluation.

Marcello Fabiano de FRANCO; Fiorita GL MUNDIM; Angela Flavia LOGULLO; Luciana LOGULLO; Fernando SOARES; Joaquim Soares ALMEIDA; Miriam FB ENGELMAN; Clayton Aparecido de PAULA; Joao PR de LIMA

EPM-UNIFESP Pathology Department (São Paulo, BRAZIL)

Background - *c-myc* and p53 genes were frequently deregulated in invasive ductal carcinomas of the breast (IDC), but *c-myc* role in mammary carcinogenesis remains controversial.

Method - To determine if the concomitant expression of the two oncogenes might have prognostic value, stage, a retrospective series of 40 samples of lymph nodes with metastasis; hormone receptor status and survival of 80 consecutive IDC patients and clinical data were analyzed in the light of p53 and *c-myc* expression assessed by immunohistochemistry in a TMA block.

Results - Positive *c-myc* and p53 staining was detected in neoplastic epithelial cells respectively in 89% and 40% of the cases. Respective lymph nodes expressed *c-myc* in 38/40 cases and p53 in 12/40. Concomitant p53 and *c-myc* positive immunolabelling in lymph nodes emerged in 12 out of the 80 cases. Clinicopathological parameters and overall-survival of patients were not associated with the immunoreactivity of p53 or *c-myc* considered separately or grouped in subsets.

Conclusion - p53 and *c-myc* expression in tumor or compromised lymph nodes were not capable to predict outcome ou correlate to prognostic variables in advanced breast cancer.

P-242

Cytokeratin 5 as a prognostic marker in invasive ductal carcinoma

Luciana LOGULLO; Fiorita GL MUNDIM; Angela Flavia LOGULLO; Fernando SOARES; Joaquim Soares ALMEIDA.

EPM-UNIFESP Pathology Department (São Paulo, BRAZIL)

Background - Cytokeratin (CK) 5 is a marker of basaloid carcinoma in breast cancer. CK expression is considered a primordial cell feature and related to worse prognosis. To evaluate this hypothesis we assessed CK5 immunohistochemical expression in 80 advanced invasive ductal carcinoma (IDC) and correlated to classical clinicopathological prognostic variables.
Method - In a retrospective series of 80 T2-T4 NxMx IDC samples of invasive tumor and 40 compromised lymph nodes were selected to construct a Tissue Micro Array. Immunohistochemical essay with CK5, Estrogen receptor (ER), Progesterone receptor (PR), c-erbB2, MIB-1 and p53 were performed in an ABC streptoavidin method. More that 10% of stained cells were considered positive. Chi-square correlations with T-Test were performed with SPSS statistical software.
Results - CK5 staining were positive in 14 cases, negative in 63 and missing in 3. Positive cases correlated to CK expression at the lymph node (p=0,003); histological grade (p=0,03); lymph node status (p=0,01) and p53 status (p= 0,02). Proliferation, hormone receptors and c-erbB2 status did not correlate to CK5 expression.
Conclusion - We found that CK5 reflects important prognostic variables and has a potential value as a predictive marker in advanced IDC.

P-243

Immunohistochemical assessment of axilar positive lymph nodes in breast cancer patients.

Fiorita GL MUNDIM; Angela Flavia LOGULLO; Luciana LOGULLO; Fernando SOARES; Joaquim Soares ALMEIDA.

EPM-UNIFESP Pathology Department (São Paulo, BRAZIL)

Background - Lymph node (LN) metastasis is considered a worse prognosis feature in invasive breast cancer (IBC). However, little is know about the biological behavior of metastatic neoplastic cells compared to primaty tumor source. Objetive to evaluate the immunohistochemical profile of LN metastasis of advanced invasive ductal carcinoma (IDC) compared to primary tumor by Immunohistochemical method.
Method - In a retrospective series of 80 T2-T4 NxMx IDC samples of invasive tumor and 40 compromised lymph nodes were selected to construct a Tissue Micro Array. Immunohistochemical essay with CK5, Estrogen receptor (ER), Progesterone receptor (PR), c-erbB2, MIB-1, *c-myc*, EGFR, c-KIT and p53 were performed in an ABC streptoavidin method. More that 10% of stained cells were considered positive. Chi-square correlations with T-test were performed in SPSS statistical software.
Results - c-KIT was negative in IDC and LN samples. *c-myc* was positive in 89% of IDC and 80% of LN samples. CK5 positive cases correlated to CK5 expressionl at the lymph node (p=0,003); p53, c-erbB2 and EGFR IDC expression did reach a positive correlation to LN.
Conclusion - We conclude LN metastatic cancer does not necessarily develop the same primary IDC profile, with may reflect the polyclonal feature of neplastic cells. Luminal and basaloid cells managed to maintain the same similar markers as ER and CK5 in IDC and LN.

P-244

C-erbB-2 amplification in Turkish patients with invasive ductal carcinomas of the breast

Burcu Tuzuner; Handan Kaya; Ipek Erbarut; Fulya Cakalagaoglu

Marmara University Hospital, Department of pathology, Istanbul, Turkey

Aim: The aims were two-fold: 1) To determine the frequency of the immunoexpression and amplification of c-erbB-2 inTurkish patients with invasive ductal carcinoma of the breast, and 2) to search the correlation of the estrogen receptor (ER), progesterone receptor (PR), tumor histologic grade, stage andamplification of the c-erbB-2 in these cases.
Material - Method: Onehundred thirty three invasive ductal carcinomas of the breast have been studied for c-erbB-2, by streptavidin - biotin horseradish peroxidase method and FISH technique. The correlations with the histopathological prognostic parameters as tumor stage, grade, lymph node status, hormonal status, and c-erbB-2 amplification have been studied.
Results: Of the 133 tumours 14% (19/133) were 3+, 9% (12/133) 2+ for c-erbB-2 by immunohistochemistry. Eight of12 c-erbB-2 equivocal (2+) cases demonstrated amplification by FISH. Overall, c-erbB-2amplification found to be 20,3% of the cases. 33% (9/27) of the c-erb-B2amplified cases were grade 3, 67% (18/27) were grade 2. While 67% (18/27) ofthe cases were stage II, 26% (7/27) of the cases were stage I. 7,4% (2/27) ofthe cases were stage III. ER /PR negativity was found to be 63% (17/27) of the c-erbB-2 amplified cases.
Conclusion: In the recent study the frequency of the amplificationhas found to be 20,3% for c-erbB-2 in Turkish patients with invasive ductal carcinomas ofthe breast. c-erbB-2 amplification apppears to be correlated with ER / PR negativity.

P-245
CORRELATION OF CD24, CD44 AND GALECTIN-1 EXPRESSIONS WITH TUMOR DIFFERENTIATION AND POTENTIAL LYMPH NODE METASTASIS IN INFILTRATING DUCTAL CARCINOMA OF BREAST

Sacide Colak; Burak Bahadir; Sibel Bektas; Figen Barut; Nilufer Onak Kandemir; Nimet Karadayi; Sukru Oguz Ozdamar
Zonguldak Karaelmas University, School of Medicine, Department of Pathology, Zonguldak, TURKEY

Background: Breast cancer is one of the most common cancers in women and infiltrating ductal carcinoma constitutes the most common type. Axillary lymph node metastasis is found in 40–50% of the cases. Many immunohistochemical markers that may reflect the nature of the tumors have been used to establish early diagnostic methods, new targets for therapeutic strategies, and predictive parameters. In this study, the correlation of CD24, CD44 and Gal-1 expressions in infiltrating ductal carcinoma with tumor differentiation and potential lymph node metastasis as well as clinicopathologic parameters such as age, localization, tumor size, lymphovascular invasion was investigated.
Method: The study group consisted of 40 cases of infiltrating ductal carcinoma diagnosed in the Pathology Department of Zonguldak Karaelmas University School of Medicine between 2001 and 2007. Slides from each case were reevaluated in terms of grade, lymhovascular invasion and lymph node metastases and immunohistochemistry for CD24, CD44 and Gal-1 were performed.
Results: CD44 had no statistically significant correlations. There were significant correlations between tumor grade and size ($p=0.030$) as well as between lymphovascular invasion and lymph node metastasis ($p=0.011$). CD24 immunoreactivity correlated with lymph node metastases ($p=0.012$) and grade ($p=0.05$). Statistically significant associations were also observed between Gal-1 immunoreactivity and the number of metastatic lymph nodes ($p=0.05$); between Gal-1 expression in primary tumor cells and in metastatic tumor cells ($p=0.004$); and between Gal-1 expression in stromal cells in the primary tumor and in stromal cells in the metastatic foci ($p=0.003$).
Conclusion: The current study suggests that CD44 has no predictive value in infiltrating ductal carcinoma of breast. On the other hand, CD24 expression seems closely related with tumor differentiation and metastatic potential of tumors. Importantly, increased Gal-1 expression in human breast carcinoma tissues underlies the potential key role of Gal-1 particularly in tumor-stroma interaction.
Key words: CD24, CD44, Galectin-1, Breast carcinoma, Immunohistochemistry

P-246
SENTINAL LYMPH NODE BIOPSY IN BREAST CARCINOMA

Handan Kaya; Emine Bas; Ahmet Midi; Fulya Cakalagaoglu; Bahadir Gulluoglu
Marmara University Medical School Hospital Pathology Department Istanbul, Turkey

Aim: Sentinal lymph node (SLN) procedure enables selective targeting of the first draining lymph node where the initial metastases will form. A negative SLN predicts the absence tumour metastases of the other regional lymph node with high accuracy. The aim of the study was to search the reliability of intraoperative frozen section investigation of the SLN to detect metastases.
Material and Method: Ninety three SLNs were detected by gamma probe detection of nanocolloid and visual accumulation of patent blue in breast carcinomas. The identified SLNs were immediately investigated by frozen section and imprint cytological investigation. Diagnosis were confirmed on paraffin material, and in case of negative frozen sections and hematoxylin and eosin and immunochemistry were performed.
Results: While 66 SLNs (70,96%) were negative for metastasis, 17 (18,27%) of the cases contained metastesis by the frozen section procedure. Ten cases (10,75%) were false negative as they were found to be metastatic LNs on the paraffin sections. While the sensitivity of the frozen section procedure was found to be 62,9%, spesivity of the procedure was 100%. Mong the SLN positive cases 37% (10–27) were T1N1 and 51,8% (14–27) were T2N1. 77,7% (21–27) of the positive SLNs were estrogen and progesterone positive.
Conclusions: Intraoperative frozen section analysis is a reliable procedure by which a high percentage of SLN metastases can be detected in breast cancer patients without false negative results. In up to 10% of the cases the final paraffin sections will reveal micrometastases that were not detected by the frozen section and in these patients axillary lymph node dissection will have to be performed in a second session.

P-247
The relation of COX-2 expression with other prognostic parameters in invasive ductal carcinomas

Nagehan Özdemir Barışık; Sevinç Keser;Aylin Gül,; Mine Çayırcı; Nimet Karadayı; Mahmut Gümüş;Mehmet Eser
Dr.Lütfi Kırda Kartal Education and Reserach Hospital Department of Pathology, Dr.Lütfi Kırda Kartal Education and Reserach Hospital Department of Oncology, Dr.Lütfi Kırdar Kartal Education and Reserach Hospital Department of General surgery, Turkey

BACKGROUND: Cyclooxygenase (COX) is an enzyme catalysing the conversion of arachidonic acid to prostaglandins. The inducible form cox-2 is known to be essential in promotion of carcinogenesis, invasion and angiogenesis. In studies, cox 2 overexpression is observed in about 40% of human breast cancers. This overexpression is reported to be related with especially c erb B2 overexpression. The aim of this study is to investigate the relation between clinicopathological parameters such as histological grade, metastasis, ER, PR, c erb B2 and cox 2 expression in invasive ductal carcinomas.
MATERIAL&METHODS: Cox 2 expression is examined immunohistochemically by using peroxidase antiperoxidase method in slides prepared from paraffine blocks of 62 invasive ductal carcinomas patients. Data on other clinicopathological parameters, c erb B2 expression and hormonal status (ER, PR) are obtained from patient files.
RESULTS: Cox 2 expression was present in 47 of 62 cases (75.81%). There was a negative correlation between Cox 2 expression and estrogen receptor positivity and a statistically significant result was obtained ($p<0.008$). However, a statistically significance was not found between histological grade, progesteron receptor positivity and c erb B2 expression ($p>0.005$).
CONCLUSION: Regarding the statistically significant relation between cox 2 expression and estrogen receptor, cox 2 expression in breast carcinomas should be considered as a poor prognostic parameter.

P-248

Analysis of the Pathologic Response to Neoadjuvant Chemotherapy (NC) in Patients with Locally Advanced Breast Cancer (LABC), according to Hormonal Receptors (ER/PR) and ERBB2 Status.

Sara Fernandez; Francisco Javier Andreu; Amparo Saez; Maria Rosa Escoda; Esther Sanfeliu; Luis Fernandez; Merce Rey.
UDIAT-Centre Diagnostic. Corporacio Parc Tauli. Sabadell (SPAIN)

PURPOSE: Gene expression analysis identifies several breast cancer subtypes. We examined the relationship of NC response to outcome among these breast cancer subtypes, defined by immunohistochemical profile (IP) as surrogate of molecular classification. EXPERIMENTAL DESIGN: We used IP (ERBB2+ and ER/PR- for HER2+ type; ERBB2-and ER and/or PR+ for luminal type; ERBB2- and ER/PR- for basal-like type; and ERBB2+ and ER and/or PR+ for HER2+ plus hormone receptor (HR)+type) to subclassify a prospectively maintained series of patients treated with neoadjuvant anthracycline-based (doxorubicin plus cyclophosphamide) chemotherapy. We analyzed each subtype for pahtologic response to NC (evaluated by Miller&Payne system, G1-G5 from no response to complete pathologic response) and examined the relationship of pathologic response to overall (OS) and disease-free survival (DFS). RESULTS: Of the 117 patients tested, 23 (20%) were basal-like; 55 (47%) were luminal; 20 (17%) were HER2+; and 19 (16%) were HER2+/HR+. Pathologic complete response (G5) occurred in 50% of HER2+, 39.1% of basal-like, 31.6% of HER2+/HR+ group and in 7.3% of luminal type (p

P-249

Tumors initiated by constitutive Cdk2 activation contain an invasive basal component

Peter Nørgaard; Pat Corsino; Bradley Davis; Nicole Teoh Parker; Mary Law; Brian Law
Department of Pathology, Copenhagen University Hospital Herlev, Denmark and Department of Pharmacology and Therapeutics and the Shands Cancer Center, University of Florida, Gainesville, USA

Background: The basal-like subtype of breast cancer is associated with invasiveness, high recurrence rates, and poor prognosis. Aside from inactivation of the *BRCA1* tumor suppressor gene, little is known concerning the mechanisms that cause basal breast cancer or the mechanisms responsible for its invasiveness.
Method: Cell lines were isolated from MMTV-CyclinD1-Cdk2 transgenic tumors. These cell lines were examined for the expression of luminal and myoepithelial differentiation markers by immunoblot. The cell lines were injected into the mammary fat pads of wild type syngeneic FvB mice to form tumors. The mechanisms responsible for the invasiveness of the tumors and lack of cell-cell cohesion were investigated by immunohistochemical analysis (IHC) of the tumors and immunoflourescence (IF) analysis of cells grown *in vitro*.
Results: Heterogeneous MMTV-Cyclin D1-Cdk2 (MMTV-D1K2) transgenic mouse mammary tumors contain regions of spindle-shaped cells expressing both luminal and myoepithelial markers. Cell lines cultured from these tumors exhibit the same luminal/myoepithelial "mixed-lineage" phenotype that is associated with human basal

breast cancer, and express a number of myoepithelial markers including Cytokeratin 14 (CK14), P-Cadherin, -Smooth Muscle Actin, and Nestin. The cell lines form highly invasive tumors when injected into mouse mammary glands. Invasion is associated with E-Cadherin localization to the cytoplasm, or loss of E-Cadherin expression. E-Cadherin localization to the cytoplasm correlates with lack of colony formation and β-Catenin and $p120^{ctn}$ localization to the cytoplasm. The MMTV-D1K2 cancer cell lines also express the proinvasive proteins Nestin and Zyxin.

Conclusion: Together the results suggest that constitutive Cdk2 activation may contribute to the formation of basal breast cancers, provide explanations for the invasive behavior of basal breast cancers, and indicate that it may be possible to suppress tumor invasiveness by restoring cell-cell adhesive functions pharmacologically.

P-250

TOP2A - EGFR correlations in triple-negative (TN) breast cancer

Carmen Ardeleanu1,2; Mihaela Mihai1; Florina Vasilescu1; Cristina Iosif1; Dana Terzea1,2; Florin Andrei1; Alina Georgescu1; Camelia Dobrea1,2; Dorel Arsene1; Enache Simona1; Mihai Ceausu1,2; Ariana Visan1; Maria Comanescu1; Diana Ene1; Maria Neagu1; Georgeta Butur1; Florica Staniceanu2

1 "Victor Babes" National Institute of Pathology, Bucharest, Romania; 2 "Carol Davila" University of Medicine and Pharmacy, Bucharest, Romania

Background. The basal type breast cancer as identified by gene profiling expresses immunophenotypically, basal cytokeratins and EGFR. It is negative for ER, PGR, and Her2/neu proteins, and has an agressive biologic behavior. Topoisomerase II alpha (TOP2A) is involved in the anthracyclins responsivity. EGFR is a basal type marker and a molecular therapeutic target. We studied the EGFR expression in TOP2A positive TN and nonTN invasive ductal carcinomas (IDC), as a possible associated therapeutic target.

Method. We analyzed retrospectively 102 consecutive IDC positive for TOP2A (files of "Victor Babes" Institute), tested also for ER, PGR (Novocastra), cerbB2, Ki67, p53 (Dako), and for EGFR (Dako). The TN tumors were selected. The IHC bistadial indirect technique was performed using producer's development kit.

Results. From 102 breast IDC (G2 and G3) (age range: 28–83 years), 18 TN cases were founded (only 4 cases aged under 45 years). Top2A was positive in: 1 to 50% of tumoral cells in TN and 1 to 30% in nonTN tumors. The EGFR positivity was localized in tumoral cells (4/14 TN and 16/81 nonTN tumors tested), but also in vascular endothelium (3/14 TN and 18/81 nonTN tumors tested). The EGFR positivity in tumoral cells was associated with absence of cerbB2 in all 4 cases of TN tumors and with a high percentage (>20%) of Ki67 and p53. The EGFR positivity in nonTN tumors was associated in 13 cases with cerbB2 negativity, but only in 2 cases, with a high percentage of Ki67 and p53.

Conclusion. In TOP2A positive selected cases, the patients' age is higher than ussually for TN tumors. The associated TOP2A/EGFR positive tumoral cells appear in cerbB2 negative cases, but with a high percentage of positivity for Ki67 and p53, known as poor prognosis markers. The association between TOP2A and EGFR could represent a combined therapeutic target.

P-251

Insulin-like Growth Factor 1-Receptor (IGF1R) activity and mRNA expression levels in early breast carcinoma with local recurrence

Gloria Peiró; Susana Benlloch; Laura Sánchez-Tejada; Encarna Adrover; Francisca M Peiró; Enrique Lerma; José Sánchez-Payá and F. Ignacio Aranda

Hospital General Universitario de Alicante, Spain

Background. The IGF1R regulates cell survival signals and apoptosis mainly through the PI3K/Akt signaling cascade. Whether the receptor activity or mRNA levels have an impact on clinical outcome in patients with early invasive breast carcinoma (IBC) undergoing breast-conserving surgery (BCS) and radiation therapy (RT) is not well known.

Method. Our series of 197 eligible BC patients in stage I-II treated with BCS and RT, included 33 (16.8%) who developed a local recurrence (LR) and 16 (8.1%) with distant metastasis. Median follow-up was 100 months. Clinical and pathological features were assessed. Immunohistochemistry (IHC) for the phosphorylation of IGF1R beta-subunit (active form), Estrogen and Progesterone receptors (ER/PR) were performed. In addition, in tissue samples from 85 primary BC (42 without recurrence, 31 with LR and 12 with distant metastasis) and 31 LR, we evaluated the IGF1R mRNA expression by quantitative real-time PCR (qRT-PCR). The relationship between pathologic, IHC and qRT-PCR results were studied and correlated with the outcome.

Results. LR was significantly associated with high grade, PR-negative, lower expression of p-IGF1R (all $p>0.05$) and as a trend with extensive *in situ* component (EIC) ($p=0.06$). However, there were no differences regarding the mRNA levels ($p>0.05$; Kruskall-Wallis test). For local disease free survival, histologic grade, EIC, PR and p-IGF1R emerged by multivariate analyses as significant breast relapse predictors (all $p\leq0.05$; Cox regression analysis).

Conclusion. Patients with early BC treated with BCS and RT, those with tumors showing lower p-IGF1R and PR-negative expression, high histologic grade and EIC developed more frequently LR. Therefore, the IGF1R active form content is a favourable prognostic indicator.

P-252

CGH Analysis of Basal-Like Type of Breast Cancer. Comparison with Chromosomal Imbalance Pattern in HER2+ Type.

Francisco Javier Andreu; Ruben Carrera; Amparo Saez; Maria Angeles Rigola*; Sara Fernandez; Maria Rosa Escoda; Esther Sanfeliu; Jose Antonio Vazquez; Merce Rey.

*UDIAT- Centre Diagnostic, Corporacio Parc Tauli, Sabadell (SPAIN), and * Cellular Biology, Universitat Autonoma de Barcelona, Barcelona (SPAIN).*

PURPOSE: The most consistent immunophenotype seen in the basal-like tumours of the breast, identified by gene-expression profile, is negativity for hormone receptors and HER2 (triple-negative type), and positivity for vimentin, EGFR, cytokeratin 8/18, and cytokeratin 5/6, with variable expression of myoepithelial markers (SMA, p63, CD10). We have investigated whether this group of breast cancers has a distinguishing pattern of genetic alterations, defined by CGH. EXPERIMENTAL DESIGN: CGH performed on frozen material from 12 cases of breast cancer triple-negative type. Immunophenotypic profile evaluation with cytokeratin 5/6, cytokeratin 17, EGFR and p63. Comparison of the results with the chromosomal imbalance pattern observed in a series of 10 cases of HER2+ breast cancer (previously reported). RESULTS: Of the 12 cases, 10 (80%) showed positivity for EGFR and for cytokeratin 5/6 and/or cytokeratin 17. CGH found gains at 1q (91.6%), 8q (75%), 3q, 7q (66.6%) and 1p, 6q, 11q, 12p, 2q (50%); and losses in 17p (75%), 19p (66.6%), 1p (58.3%) and 8p, 16p, 17q (41.6%). CGH in HER2+ group showed gains in 17q (90%), 1q, 8q (80%), 16p, 19q, 20q (60%) and 7q (50%); and losses in 3p, 5q, 11q, 14q (50%), 4q, 9p, 13q (40%) and 6q, 8p, Xq (30%). CONCLUSIONS: 1) Chromosomal imbalance pattern of basal-like group showed an increased prevalence for losses at 16p, 17q (alterations associated with pure myoepithelial carcinomas) and 19p, opposite to those of HER2+ group, with gains in these regions and at 20q and 7q; 2) Gains at 6q and 11q are present in up to 50% of basal-like group, while HER2+ group showed losses at these regions; 3) Gains at 1q and 8q indicate shorter disease-free and overall survival times, and are common to both groups; 4) The different CGH profiles demonstrate the inherent differences in the molecular evolution of these tumour groups.

P-253

Pigmented mammary Paget's disease simulating malignant melanoma

M Teresa Soler; Teresa Serrano; M. Àngels Lerin; Emili Masferrer*; Anna Gumà; Amparo García***; J Miguel Gil****; Enric Condom.**

Departments of Pathology, Dermatology, Radiology** and Gynaecology***. Hospital Universitari de Bellvitge. Department of Medical Oncology****. IDIBELL. Institut Català d'Oncologia. L' Hospitalet de Llobregat. Barcelona, Spain*

Paget's disease of the nipple represents a cutaneous manifestation of an underlying breast malignancy. Pigmented mammary Paget's disease represents a rare variant of this entity that clinically and histopathologically simulates a melanoma. We describe a case of pigmented lesion involving the nipple with an underlying intraductal and infiltrating breast carcinoma.

A 57-year-old woman presented with a pigmented lesion in the right-breast nipple. On physical examination, nipple demonstrated a heterogeneous, dark, pigmented lesion with irregular borders. There was no evidence of erythema or excoriation, neither palpable breast mass. A skin-punch-biopsy showed an intraepidermal neoplasm characterized by cells with enlarged and pleomorphic nuclei with pale cytoplasm, some of which contained melanin pigment. The cells were arranged in a pagetoid pattern and involved all levels of the epidermis. There was infiltration of the dermis by cells forming nests and cords. Immunohistochemical studies demonstrated that the tumor cells were positive for keratins(Cam 5.2) and negative for HMB-45 and S-100 protein. Both oestrogen and progesterone receptors and HER-2 were positive, supporting the diagnosis of mammary Paget's disease. Mammographic and ultrasound studies revealed no abnormalities. A lumpectomy with excision of nipple-areola complex with sentinel lymph node evaluation was performed. Grossly the only pathological change was the nipple pigmentation. Histologically there was a 2 mm. grade 2 infiltrating ductal carcinoma and two lactiferous ducts with intraductal carcinoma. The epidermal lesion simulated a malignant melanoma. The lymph node was negative.

Comment: Pigmented mammary Paget's disease should be differentiated from melanoma clinical and histopathologically. The differentiation is based on histopathologic and immunohistochemical criteria.

Local production of melanocytic chemotactic factor by neoplastic cells when they reach the dermoepidermal junction has been postulated as the cause of the hyperpigmentation. Another possibility is the phagocytosis of melanin from melanocytes to the intraepidermal neoplastic cells of the breast carcinoma.

P-254

Value of phenotype in invasive breast carcinoma evaluated by needle core biopsy

F. Ignacio Aranda López; Adel Abuomar; Gloria Peiró; María Planelles; Eduardo Alcaraz; María Niveiro; Javier Seguí.

S. de Patología. Hospital General Universitario de Alicante, Spain

Background: Phenotype of invasive breast carcinoma (IBC) based on immunohistochemical findings, shows prognostic and therapeutic implications. The aim of this study is to evaluate the value of the phenotype from NCB in relation with the surgical specimen (SS).

Methods: 183 cases of IBC with NCB and SS, without neoadjuvant chemotherapy, were evaluated. Immunohistochemical expression of estradiol and progesterone receptors, Her-2 and Ki-67 were obtained in FNB and compared with the same variables in SS. The classification is based on immunophenotype: a)luminal A (ER/PR+/Her-2 -/Ki-67<20%) b) luminal B (ER/PR+/Her-2 -/Ki-67≥20%) c) Her-2+ (Herceptest 3+/2+ confirmed by FISH) d) triple-negative (ER/PR -/Her-2 -). Concordance and kappa value of NCB and SS were assessed.

Results: ER: sensibility 89%, specificity 87%, kappa= 0.712 (p=0.000). PR: sensibility 85%, specificity 76%, kappa=0.601 (p=0.000). Ki-67: sensibility 63%, specificity 79%, kappa=0.423 (p=0.000). Phenotypes in NCB and in SS: luminal A 59% and 56%, luminal B 25% and 12%, Her-2 12% and 17%, triple-negative 15% and 15%, respectively. Luminal A: sensibility 82%, specificity 80%, kappa=0.615 (p=0.000). Luminal B: sensibility 39%, specificity 91%, kappa=0.283 (p=0.000). Her-2: sensibility 96%, specificity 95%, kappa=0.784 (p=0.000). Triple-negative: sensibility 89%, specificity 99%, kappa=0.893 (p=0.000). Kappa global: 0.615 (p=0.000)

Conclusions: Estradiol and progesterone receptors, Her-2, Ki-67 and phenotype obtained in FNB showed a good level of concordance with SS and can be used for diagnostic purposes.

P-255

C-kit and egfr are mostly negative in advanced breast cancer. a tma study

Angela Flavia LOGULLO; Fiorita GL MUNDIM; Luciana LOGULLO; Fernando SOARES; Joaquim Soares ALMEIDA.

EPM-UNIFESP Department Pathology (São Paulo, BRAZIL)

Background - Receptor tyrosine kinases (RTKs) constitute attractive targets, as quite often their abnormal signaling has been associated with tumor development and growth. Abnormally elevated EGFR activity is associated with the most common human solid tumors and has been detected at all stages of tumor progression. The proto-oncogene C-KIT encodes a transmembrane tyrosine growth factor receptor, plays an important role in the development of certain neoplasms. Several investigators report conflicting results concerning its expression especially in malignant breast lesions.

Method - In retrospective series of 80 T2-T4 NxMx Invasive Ductal Carcinomas (IDC) samples were selected to construct a Tissue Micro Array (epithelium and stroma). Immunohistochemical essay with C-KIT, EGFR and CK5, performed in an ABC streptoavidin method. More that 10% of stained cells were considered positive.

Results - Immunohistochemically stained TMA samples for EGFR (epithelium) were positive in 16 cases, negative in 62 cases and missing in 2 cases. EGFR (stroma) were negative in 80 cases. C-KIT (epithelium) was positive in 9 cases, negative in 63 cases and missing in 8 cases. C-KIT (stroma) were positive in 10 cases, negative in 69 cases and missing in 1 case. CK5 positive/C-KIT negative were expression in 13/80 cases.

Conclusion - We conclude that C-KIT and EGFR mostly negative in advanced breast cancer. These results suggests that tumors expressing EGFR result from multiple genetic changes leading to the expression of additional receptor and nonreceptor TKs that play roles in tumor growth. C-KIT is consistently expressed in normal epithelium cells of the terminal duct lobular unit (TDLU) and poorly expressed in IDC. Correlation with CK5 positive suggests that C-KIT negative invasive breast carcinomas are of basal type.

P-256

HISTOMORPHOLOGICAL CHANGES IN BREAST CANCER WIHT NEOADJUVANT PROTOCOLS. Preliminary observations of pathological responses.

Soledad de la Peña; Benedicta Caserta

Laboratory of Pathology and Cytology.Woman's Hospital Pereira Rossell. MSP

INTRODUCTION AND OBJECTIVE: Preoperative chemotherapy (QT) is used in cases of locally avanced breast cancer. Tumor size remains as the best parameter for evaluating residual tumor. This study was conceived as an initial step aimed at evaluating the pathological response of breast cancer with neoadjuvant protocols.

MATERIALS AND METHODS: We analyzed retrospectively 20 patients with breast cancer treated with neoadjuvant protocols.In each case the presence of residual tumor was evaluated macroscopically. Sections stained with hematoxylin and eosin were used to confirm the presence of tumor, to determine it histologic type as well as the presence of lymph node metastasis. We also used inmunohistochemical analysis to evaluate hormone receptor and Her 2/neu protein expression.
RESULTS: A minimal pathological response was observed in 50% of cases with macroscopically evident nodes (size between 20×15 mm and 7×7 mm). In the remaining cases the pathological study showed only an area of fibrosis. Seven cases had lymph node metastases. Most of the residual tumors were negative for hormone receptors and did not show Her 2/neu protein overexpression.
CONCLUSIONS: This preliminary study indicate that neoadjuvant protocols were apparently most effective in a 50% of cases whereas the remaining 50% showed only a minimal response.Poorly differentiated carcinomas were most sensitive to QT when compared with moderately differentiated infiltrating ductal carcinomas NOS (this histological type usually associated minimal response). We found no significant differences between the minimal and maximal response related with the presence or absence of axilary lymph node metastases.
According to the literature, most of the cases studied had low antigenicity for hormone receptors and the over-expression of Her 2/neu.

Neuropathology

P-257
FEATURES OF CENTRAL NERVOUS SYSTEM TUMORS FROM UNIVERSITY HOSPITAL OF SANTANDER, BUCARAMANGA COLOMBIA

Carlos Alberto García Ramírez, Julio Alexander Díaz Pérez, Jorge Andrés García Vera, Ernesto García Ayala, Luís Alejandro Rivero Rendón and Javier Mauricio Olarte Villamizar
Universidad Industrial de Santander, Bucaramanga, Colombia

Objective. It identified the pathologic features of patients served by tumor lesions of the central nervous system in the Hospital Universitario de Santander, between 1998 to 2006. **Materials and Methods.** A retrospective observational study was made, with a population that corresponds to the patients of the Hospital Universitario de Santander. There were interrogated different sociodemographic, clinical and pathological findings. **Results.** We studied 213 patients with neoplastic lesions of the Central Nervous system (CNS), with age between 1 to 89 years old, with average of 38.385±20.947 years old. The male:female ratio was 1:1. There were identificated 4 CNS cysts, all of them were epidermoid cysts (1.87%). The glial tumors contribute with 51.7% of the lesions, with 93 astrocytics tumors (43.66%), 7 oligodendroglial tumors (3.3%), 8 ependymal tumors (3.75%), 7 gliomas of the mixed type (3.28%), 1 neuro-epithelial tumor of uncertain origin (0.47%) and 1 neuronal-glial tumor. Nonglial tumors contribute with 39.9% of the tumors, 12 were embryonal tumors (5.63%), 3 choroid plexos tumors (1.4%), 2 pineal tumors (0.94%), 31 meníngeals tumors (14.55%), 1 germinal (0.47%), 20 tumors of cellar region (9.39% and 16 mesenquimals tumors (7.51%). At least, 8 metastátics tumors were find (3.75%), three of them with indentificated primary lesion, 1 of ovaric tumor, 1 parotid tumor and 1 breast tumor. **Conclusions.** The central nervous system neoplasms are rare, but their behavior in many regions of the world is known,however is not available studies in Colombia, in this study it was demonstrated that these neoplams have a particular behavior in our population.

P-258
The Correlation between MDM2 Protein and Histologic Grading of Cerebral Astrocytomas

Mahzouni P MD*, Yazdi zadeh M MD, Sanei MH MD*****
Isfahan University of Medical Sciences, Isfahan, Iran

Background: $MDM_2$is a protein factor that plays an important role in inhibition of $P_{53}$and P_{73} related apoptosis. The aim of this study was to investigatethe correlation between MDM_2 expression and histologic grading ofcerebral astrocytomas in order to reduce misdiagnosis of this tumor incontroversial cases.
Methods: In this study,104 cases of astrocytic tumors including 4 different grades were selectedrandomly. We prepared 4 μm sections of paraffin blocks of tumors. Then theslides were stained by anti MDM_2 antibody.
Findings: The intensityof nuclear staining for MDM_2 marker had a statistically significantcorrelation with histologic grading. There was no significant correlationbetween percentage of nuclear staining for MDM_2 and histologic-grading. The positivity of MDM_2 marker, as well as the multiplicationof intensity and percentage of nuclear staining in S.Score had a significantcorrelation with histologic grading. The S.Score correlation with grading ofastrocytic tumors was analyzed by ROC Cure analysis method and showed that atthe cut off point of 6, this score can be indicative for differentiation of Glioblastom multiform from other grades with specificity of 95.3%.

Conclusion: Our resultsconfirm the role of the MDM_2 protein as a oncogenic factor inprogression of astrosytic tumors. Evaluation the MDM_2 expression inastrocytic cerebral tumors can be specifically indicative for distinction ofglioblastom multiform from other grades of astrocytic tumors.

Key Words: Cerebralastrocytic tumors, MDM_2 protein factor, histologic grading.

P-259

CRIPTOCOCOMA OF THE CENTRAL NERVUOS SYSTEM IN A PATIENT IMMUNOCOMPETENT

Gustavo Pradilla;Julio Alexander Díaz Pérez; Julio Cesar Mantilla Hernández; Jorge Andrés García Vera; Ernesto Garcia

Universidad Industrial de Santander, Bucaramanga, Colombia

Background. The criptococosis of the Central Nervous System is an important cause of morbidity and mortality in inmunocomprometidos patients; nevertheless, its presentation in inmunocompetentes patients extremely rare, is caused different a clinical phantom, since it is pronounced in this group of people like granulomatosas masses denominated criptococomas. **Objective.** A intracerebral case of criptococoma in a taken care of inmunocompetente woman in the University Hospital de Santander will be described and a discussion of the most excellent aspects of this pathology will be made. **Clinical case.** Patient of feminine sex of 24 years of age, that enters to present/display generalized clónica tonic convulsion, with deviation of the glance upwards, lost sialorrea and of knowledge, without data that suggest inmunosupresión. The Computerized Axial Tomografía of skull demonstrates mass of possible inflammatory origin versus. Neoplásico. Craneotomía with excisional biopsy is taken to surgery practicing. By means of pathological analysis the diagnosis becomes of cerebral Criptococoma and antimicótico handling begins, with favorable evolution, at the moment the patient is in good state of health without evidence of active disease. **Conclusions.** the presence of masses of criptococico origin of the central nervous system, had to a chronic granulomatosa reaction, rarely is reported, these appear in almost all the cases in competent patients inmuno, in these patients is important to discard all the causes of cellular immune commitment. Also I diagnose of these injuries must be considered before the presence of intracraneales masses that show inflammatory characteristics.

P-260

Cell counting in brain tumors using semi-automatic system

Tomasz Markiewicz(1,2); Bartlomiej Grala(1); Stanislaw Osowski(2,3); Wojciech Kozlowski(1); Robert Koktysz(1); Michal Kruk(2)

(1)Department of Pathology Military Institute of the Health Services,Poland, (2)Warsaw University of Technology, Poland, (3)Military University of Technology, Poland

Background Recognition of the cells with Ki-67 staining isimportant for medical diagnosis of brain tumor. Usually it is done manually byvisual inspection of the viewing field of the histological slide. This paperpresents the automatic system for cell counting. Only the viewing field of themicroscope and camera is selected manually, the rest is processed automaticallyby the system.

Method The tissue of the brain tumor is processed using Ki-67staining. The viewing field of the image, selected by the expert, is processedautomatically in order to count and recognize the immunopositive andimmunonegative cells. This is done by the developed automatic system. Thesystem uses thresholding operation, filtering, watershed algorithm and otherstandard morphological operations for extracting and counting tumor cells. Nextthe artificial neural network (Support Vector Machine) is used for recognitionof immunopositive and immunonegative cells.

Results The developed system was applied for cell counting inmeningiomas and oligodendroglioma at assessment of the cell density. 24patients with the meningothelial meningioma and 26 patients with theoligodendroglioma of grade II according to WHO classification were evaluated. We have found that the density of cells within the viewing microscope field ischanging significantly. For meningioma the mean number of cells was 652 with std=141. Most images (95%) contained 390–879 cells. For oligodendroglioma themean value of cells was 448 with std=107. Mostimages (95%) contained 285–669 cells. Even for the same patient standarddeviation was significant: in meningioma 12.3% of mean, in oligodendroglioma12.8% of mean. The results of counting have been compared to the human expertscore. The average discrepancy between these results at Ki-67 index for 50patients (over 500 images) was 0.18% at the investigated levels from 0.6% to7.8%.

Conclusions The semi-automatic system checked on over 50 patientsdelivered the sufficiently accurate results and we hope it may be useful forsupporting the medical diagnosis of brain tumors.

P-261

Subependymomas: A clinicopathological study of 7 Tunisian cases

Ben Haha Salma; Faten Limaiem; Khedija Bellil; Haifa Azzouz; Ines Chelly; Amina Mekni; Slim Haouet; Moncef Zitouna; Nidhameddine Kchir.
Hospital La Rabta, Tunisia

Background: Subependymomas are rare slow-growing, benign tumours which commonly involve the fourth or lateral ventricle. They are designated as grade I neoplasms in the latest WHO classification and are histologically characterized by clusters of ependymal cells arranged against a gliofibrillary matrix with frequent microcystic change. Most subependymomas are incidental findings discovered at autopsy; however, they may grow large enough to be symptomatic.
Aim of study: This study retrospectively reviews the clinical, radiological and pathologic features of a series of 7 subependymomas.
Patients and Methods: Between 1997 and 2007, 7 cases of subependymomas were diagnosed at the pathology department of La Rabta hospital. Medical records and microscopic slides were available in all cases and were retrospectively reviewed.
Results: Our study group included 6 men and one woman aged between 24 and 47 years (mean=38.5 years). The most common clinical presentations included headache (n=7), nausea/vomiting (n=6) and seizures (n=1). CT scan was performed in all cases. Six tumours were intraventricular and one was intraparenchymal. Six patients underwent gross total resection whereas one patient had subtotal resection. Histologically, the tumours were characterized by clusters of ependymal cells arranged against a fibrillary background. Focal cystic degeneration was seen in 6 tumours. Mitotic figures, vascular endothelial proliferation and necrosis were not seen in any of these tumours.
Conclusion: Compared with other ependymal tumours, subependymomas have the lowest rate of cell proliferation as evidenced by MIB-1 immunostaining. Following surgical resection, long-term prognosis is excellent.

P-262

Hydatid disease of the central nervous system: a clinicopathological study of 20 Tunisian cases

Limeiem Feten; Salma Bellil; Ines Chelly; Amina Mekni; Haifa Azzouz; Khedija Bellil; Slim Haouet; Nidhameddine Kchir; Moncef Zitouna
Hospital La Rabta Bab Saadoun Tunis-Tunisia

Background: Hydatid disease of the nervous system (echinococcosis) is rare and represents the development of vesicles or cysts by the larval stage of the tapeworm *Echinococcus granulosus* in the cerebrum. Cerebral hydatidosis accounts for 0.2% of all intracranial tumours. Primary hydatid cyst of the brain represents approximately 1–5% of all echinococcosis cases, showing evidence of infestation during childhood. Such cysts are much rarer in adults and constitute only 0.7% of all echinococcosis cases.
Patients and Methods: Between January 2000 and October 2007, 20 patients were operated for cerebral or spinal hydatid cysts at the neurosurgery department of La Rabta hospital. Medical records and microscopic slides were available for review in all cases and were retrospectively analyzed.
Results: Our study group comprised 8 male and 12 female patients aged between 2 and 65 years. CT scan was performed in all cases and demonstrated a round or oval well-defined cystic mass located in cerebral parenchyma (n=15), posterior fossa (n=1) and spinal cord (n=4). All patients were operated and total removal of the cyst without rupture was achieved in all cases. The size of the cysts varied between 2.5 and 8 cm in diameter. pathological examination was consistent with hydatid cyst in all cases. All patients were followed up for at least 5 years after surgery. There were no recurrences and their postoperative recovery was uneventful.

P-263

The status of MGMT methylation and TP53 mutations in patients with glioblastoma.

Dorota Jesionek-Kupnicka 1; Izabela Zawlik 2; Emilia Jesien-Lewandowicz 3; Malgorzata Szybka 1; Dominika Kulczycka 1; Renata Kusinska 1; Radzislaw Kordek
1 Department of Tumor Pathology, Chair of Oncology, Medical University of Lodz, Poland 2 Department of Molecular Pathology and Neuropathology, Chair of Oncology, Medical University of Lodz, 3 Department of Radiation Oncology, Copernicus Memorial Hospital, Lodz, Poland

Background MGMT (O-6-methylguanine-DNA-methyltransferase) is a DNA-repair enzyme that specifically removes promutagenic alkyl groups from the O-6 position of guanine and protects cells from cytotoxic and mutagenic effects. Epigenetic silencing of O(6)-methylguanine-DNA methyltransferase(MGMT) by promoter methylation can leads to lack of DNA-repair, increased sensitivity to alkylating chemotherapeutic agents and a higher susceptibility to TP53 transition mutations, especially G:C @@@ A:T transitions. The aim of our study was to assess the correlation of promoter methylation of the MGMT gene with TP53 mutations and the clinical characteristics of glioblastomas.
Methods: Tumor samples were obtained from 32 patients with primary glioblastoma (15 males and 17 females, aged

from 40 to 75 years). The methylation-specific PCR (MSP) was performed in a two-step approach.The PCR products were separated on 3% agarose gel containing ethidium bromide and documented using the Gel Doc1000 Bio Rad Image System. For each PCR reaction, methylated and unmethylated DNA were included as positive and negative control.

For statistical analysis Fisher exact test and Cox regression analysis were use.

Results: Methylation of the MGMT promoter was detectedin 72% (23 of 32) of tumors. 31% (10 of 32) of all tumors presented TP53 mutations. 90% of TP53 mutations were detected in tumors that also presented MGMT methylation. We further correlated the results with survival.

Conclusions:

1) Methylation of the MGMTpromoter gene is a frequent molecular event in glioblastoma but there was no statistical correlation between TP53 mutations MGMT methylation (Fisher exact test p=0.223)
2) No corralation between met MGMT and patients survival (HR 0,74, 95%CI, from 0,32 to 1,69, p=0,45
3) Coexistence of MGMTmethylation and TP53 mutations in patients with glioblastoma was not associated with the better prognosis.

P-264

Primary meningeal malignant melanoma

Pablo Lorenzo-Gonzalez; Carlos Aliste-Santos; Beatriz Fernandez-Rodriguez; Julian Castro-Castro; Ana Maria Torea-Filgueira; Xiana Rodriguez-Osorio; Susana Arias-Arias; Jeronimo Forteza-Vila; Jose Manuel Suarez-Peñaranda.

Complejo Hospitalario Universitario de Santiago de Compostela, Spain

BACKGROUND: Primarydiffuse meningeal melanomatosis arising in the leptomeninges is a highlyunusual lesion with only few cases reported. The correct and precociousdiagnosis of the disease is a medical challenge and most commonly this is madeonly after autopsy. It is an aggressive neoplasm with poor prognosis.

CASE REPORT: We report a case of a 41-year-old woman withheadache and vision impairment, most severe in the right eye, starting inOctober 2006. Physical examination shows meningism and bilateral paralysis ofthe VIth cranial nerve. A ventriculoperitoneal CSF shunt is created. The MRimages demonstrate subarachnoid infiltration with abnormal contrast enhancementin T1-weighted images. The CSF is negative for malignant cells thoughhypoglucorrarquia is present. A biopsy is performed in October 2007. Onmacroscopic examination, leptomeninges are black-tanned and diffuselythickened. Microscopic examination of brain specimen reveals diffuse neoplasticmeningeal infiltration spreading along the Virchow-Robin spaces. Thetumour cells were fusocellular with vesicular nuclei, coarse cromatin,prominent nucleoli and dusty cytoplasmic melanin pigment. Mitotic activity islow. Parenchymal infiltrating tumour nodules can be seen. Theinmunohistochemical staining reveals diffuse and strong positivity of tumourcells for S-100, HMB45, Melan-A, BCl-2 and p53 but lack EMA reactivity.Ultrastructural images show abundant well-developed melanosomes.

CONCLUSION: Primarydiffuse meningeal melanomatosis is a very rare neoplasia originated fromleptomeningeal melanocytes. The base of the brain is the most common locationand the tumour spreads along the Virchow-Robin spaces reaching the parenchyma.In our case, radiological findings and clinical history of the patient werehighly suspicious and a biopsy was performed. Meningioma and PigmentedSchwannoma were ruled out based on the histopathological findings and theabsence of staining with EMA. Histological, inmunohistochemical,ultrastructural and clinical data (no other primary malignant melanoma wasfound elsewhere) allowed the diagnosis of primary malignant melanoma of theCNS.

P-265

Meningioangiomatosis non Associated with Neurofibromatosis Type 2: Report of Two Cases

Aliste C; Fernández-Rodríguez B; Lorenzo-González P; Abdulkader I; Vieites B; Forteza J; Suárez-Peñaranda JM.

Department of Pathology. University Hospital of Santiago de Compostela. Spain

Background: Meningioangiomatosis (MA) is an uncommon condition of disputed nature, which commonly affects children and young adults. Although most cases are sporadic, the association with familial type 2 neurofibromatosis (NF) is well known. The sporadic type usually presents with seizures, whereas that associated with NF is often asymptomatic. Occasionally, it is associated with a neoplasm, most commonly a meningioma. Surgical treatment is recommended and, in most cases, it is gratifying.

Case Report:

Case 1: A 44-year-old woman presented with a history of generalized seizures refractory to different therapeutic

regimens. T2-weighed MRI images demonstrated a heterogeneous lesion on the left temporal lobe. The lesion was removed and histopathological examination revealed a plaque-like proliferation of meningothelial and fibroblasts-like cells, in a richly vascularised stroma, involving the meninges and Virchow-Robin spaces.
Case 2: A 2-year-old child presented with headache and seizures. Neuroradiological studies showed a lesion on the left temporal lobe, with isointense and hypointense areas in MRI. Histopathologic examination showed a lesion characterized by proliferation of small blood vessels accompanied by spindle cells that arrayed in fascicular or storiform patterns and trapping islands of gliotic cortical tissue. Immunohistochemistry showed strong and diffuse staining for vimentin and EMA, while GFAP was negative.
None of the cases was associated to type 2 NF.
Discussion: MA is a benign lesion of unclear pathogenesis but without malignant potential. Two different etiological theories have been proposed. The first holds that the lesion arises from an initial angiomatous component, while the other suggests that MA represents a variant of meningioma. It is important to distinguish MA from other possible cortical lesions since it is a surgically curable cause of seizures. The main pathological differential diagnosis is with meningeal or glial neoplasms.

P-266

Nonsmall cell bronchial carcinoma with paraneoplastic meningoencephalitis

Elka Ivanova, Georgi Gergov, Marin Daskalov, Gueorgui Maximov, Sevdalin Nachev
Medical Faculty, Medical University - Sofia, Bulgaria

Background: Paraneoplastic encephalitis is a multifocal inflammation of central nervous system, associated with malignant tumors (small cell bronchial carcinoma in 80% of cases). Immunologicaly anti-Hu, anti-Yo and P/Q antibodies are found.
Patient and Methods: D.G.S., 49 year aged man suddenly develop a loss of memory, desorientation and neuropsychic disorders (dysarthria, aphasia, general weakness, dizziness and diplopia). It was found to be afebril, with normal vesicular respiration, normal heard rhythm and variantional blood presure. Neurological examination was normal except the presence of partial aphasia. Computed tomography of the brain showed no focal changes. Cerebrospinal fluid: Protein-140,4 mg%, Ly-48%, Mo-48%, CMV-320 Ulml (+), VZV-400 Ulml (+), HIV (-), Wass. (-), HSV (-). In MRI on T1 - weighted images and T2 - small lesions (ovoid and linear) in corona radiata (bilaterally), corpus callosum, left putamen and left cerebral peduncule were found. After two months the patient dead with quadripiramidal syndrome, bronchopneumonia (with pleural and pericardial effusion) and trombosis of v.saph.magna.
Results: At autopsy a bronchial adenocarcinoma (0,5 sm. in diameter) was found. Systemic examination of the brain showed the presence of multiple punctiform, linear (oval) inflamatory necrosis with neuronal decomposition, neuronophagy and reactive astroglyosis, associated with scanty perivascular lymphoid infiltrations and lymphocytar meningistis. The changes were localized in the striatum, occipital region (paraventricular), hippocampus, mesencephalon (cerebral peduncle), near to substancia nigra, pons and cerebellum, associated with considerable loss of Purkinje cells.
Conclusion: The course of the disease with leading neurological syndroms and characteristic changes in central nervous system associated with nonsmall cell bronchial carcinoma turn to the diagnosis paraneoplastic meningoencephalitis.

P-267

Apoptosis in Glioblastoma Xenograft: Immunohistochemical expression of caspase 3, 8, 9 and Bax

Zarnescu Otilia; Brehar Felix Mircea; Chivu Mihaela; Teodorescu Daniela
Faculty of Biology, University of Bucharest, Romania; Neuroscience Basic Research Department, Clinical Hospital Bagdasar-Arseni, Bucharest, Romania; Stefan S Nicolau Institute of Virology, Bucharest, Romania

Background: Development of new therapies for glioblastoma requires animal models that mimic the biological characteristics of human brain tumors. On the other hand, potential antitumoral effects of a new therapeutic strategy are often established by evaluation of tumor cells apoptosis. Caspases are key mediators in the regulation and execution of apoptosis. Caspase-8 mediates the extrinsic pathway of apoptosis triggered by signaling through receptors while caspase-9 is activated during the intrinsic pathway downstream of mitochondria. Caspase-3 is an effector caspase that initiates degradation of the cell in the final stages of apoptosis. Bax is a pro-apoptotic member of the Bcl-2 family that play key roles in the regulation of intrinsic apoptotic signalling. In the present study we investigated the immunohistochemical distribution of caspase 3, 8, 9 and Bax in intracranial glioblastoma xenograft. **Method:** Orthotopic xenografts were establish by injecting 5×10^5 tumor cells from glioblastoma multiforme cell line U87 into the right striatum of Balb/c nude mice. Tumor growth was monitored *in vivo* by serially sectioning the xenograft

brains at 1, 7, 21, and 28 days postinjection. Immunohistochemistry were performed for detection of the expressions of caspase 3, 8, 9 and Bax. Nuclear morphology of tumor cells was assessed in fluorescence microscopy after 4′-6-Diamidino-2-phenylindole (DAPI) staining. **Results:** Immunohistochemistry showed that some glioblastoma cells with apoptotic morphology were positive for caspase 3, caspase 9 and Bax and negative for caspase 8. The percentage of caspase 3, caspase 9 and Bax positive cells varied in individual mice. However, the expression of caspase 9 was significantly higher than that of caspase 3 and Bax. **Conclusion:** Taken together, these results suggest that glioblastoma cells in vivo have the molecular components associated with intrinsic apoptotic pathway.

This work was supported by Romanian CEEX Programme, Project No. 176/2006.

P-268

Intraventricular dysembryoplastic neuroepithelial tumor

Onder Onguru; Halil İbrahim Secer; Engin Gonul; Omer Gunhan

GATA Pathology Department, Turkey

Background: Dysembryoplastic neuroepithelial tumor (DNT) is a glial-neuronal tumor characterized by usually supratentorial cortical location. Cases of DNTs in and around lateral ventricles have been reported very rarely. Here we report another extracortical case of DNT with typical morphology in lateral ventricle.

Case Presentation: A 21-year-old male patient was presented with recent onset of seizure in January 2007. As a result of single episode of seizure, he sustained a head injury with occipital linear fracture. Magnetic resonance imaging (MRI) of the brain demonstrated 2×1.5 cm hypointense mass lesion in the frontal horn of right ventricle on T1-weighted images without contrast enhancement after gadolinium injection. Right ventricle was asymmetric and enlarged compared to left ventricle due to obstructed foramen of Monro.

Materials and Methods: After routine histopathological processing and staining, immunohistochemistry was performed using primary antibodies against glial fibrillary acidic protein (GFAP; MAb, 1:100, Neomarkers), S-100 protein (MAb, 1:100, Neomarkers), synapthophysin (PAb, 1:100, Neomarkers), Ki-67 (MAb, 1:80, Neomarkers).

Results Histopathology: Histologically, the lesion was hypocellular and composed of oligodendrocyte-like cells (OLC) with small uniform round nuclei in an abundant basophilic pale mucinous matrix. Some of these cells were situated around delicate ramifying capillaries. Mature neuronal cells ("floating neurons") were observed in mucinous matrix of cystic areas. Immunohistochemically, those cells were positive for synaptophysin. However, OLCs were not immunoreactive for synaptophysin. Scattered glial fibrillary acid protein-positive reactive astrocytes were also seen. Ki-67 proliferation index was less than 1%. We considered that the lesion was consistent with simple form of DNT.

Conclusion: The present case shows the importance of correct histopathologic diagnosis in this unusual presentation of DNT to avoid overtreatment (chemotherapy or radiotherapy), because of favorable outcome after surgical resection of these benign lesions. Derivation from a secondary germinal layer was considered for the unusual presentation of ectopic DNTs.

P-269

PROGESTRONE RECEPTOR STATUS AND PROLIFERATIVE MARKER KI67, AS A GUIDE IN GRADIND OF MENINGIOMA

Nasrin Shayanfar;Masoud Mashayekh;Alireza Sadeghipour

Department of Pathology,Rasoul Akram Hospitasl,Iran University of Medical Science,Tehran,Iran

Background: Meningiomas are slow-growing neoplasms which recur locally.Their morphologic grading is simple but do not always correlate with patient outcome.The aim of present study is to evaluate the status of progestrone receptor(PR) and Ki67 in various grades of meningioma in a group of iranian patients.

Methods:78 cases of meningioma were selected from the file of a university hospital.All archival H&E stained sections were reviewed and regraded according to WHO 2000 criteria.Immunohistochemical analysis for PR and Ki67 was performed on formalin-fixed,paraffin-embedded material.The PR status considered positive if >10% tumor cell's nuclei were strongly immunoreactive,or if > than 50% of nuclei were stained with medium intensity..The Ki67 labeling index (LI) is defined as the percentage of positively immuno-reactive tumor cell nuclei in the area with the strongest immunostaining.

Results:PR were positive in 61/63(96.8%)of grade I tumors,2/10(20%) of grade II,and 0/5(0%) of grade III tumors.Ki67 LI was %2.98±2.27 in grade I tumors,%9.30± 5.79 in grade II tumors and %34.00±5.47 in grade III tumors.For both markers,differences between grade I,II and III tumors were significant($P<0.001$).There was a reverse relationship between mean of Ki67 LI and PR status,with increasing grade of tumor.

Conclusion: Evaluation of PR status and Ki67 LI together with conventional histologic evaluation can help in providing more information about the biologic behaviour of meningiomas,especially for those that histological grading is not straightforward.

P-270

Establishment and characterization of a new human cell line derived from a recurrent glioblastoma

Laura Mihaela Stefan, Elena Utoiu, Viorica Coroiu, Felix Brehar*, Wanda Buzgariu

*National Institute of Research-Development for Biological Sciences, * Bagdasar-Arseni Clinical Hospital, Romania*

Background. Glioblastomas are the most frequent and aggressive malignant brain tumors in adults which may occur de novo, especially in the frontal and temporal lobes of the brain or may result from progression of low-grade astrocytomas. Despite advances in surgical techniques, radiotherapy and chemotherapy the median survival rate for pacients with glioblastoma is only 1 year. Consequently, gliomas cell lines are useful as models for drug screening and cellular and molecular studies of these brain tumors. The aim of our study was the establishment and characterization of a human glioblastoma cell line derived from a recurrent tumor.

Method. Cell culture was carried out by enzymatic digestion from a tumor specimen removed from a 58-year old woman diagnosed with glioblastoma of the left temporal lobe. Cells were subcultured from more than 100 passages in DMEM with 10% FBS and antibiotics. Morphology, growth kinetics, specific markers expression and chromosome characteristics of this cell line were studied.

Results. Morphologic examination using light microscopy showed a polymorphic culture with spindle cells, star-shaped cells with large round nucleus and giant cells with one or more nuclei. Cell line retained immunopositivity for vimentin but was negative for GFAP. Other specific markers such as S-100 protein, PDGF, p53 protein, NSE, nestin and CD 133 have been also examined. Metaphases analysis of tumor cells revealed hyperdiploid cells with a very complex karyotype. The chromosome number varied between 55 and 72.

Conclusion. Our results have revealed that the new cell line have presented a polymorphic aspect, hyperdiploid cells and was stained negative for GFAP although the cell culture was immunopositive for this marker at first passages. This cell line may be a useful tool for understanding the biology of gliomas and for testing new drugs in the treatment of this malignant primary brain tumor.

P-271

GLIOBLASTOMA MULTIFORME WITH EXTENSIVE NEURONAL DIFFERENTIATION: CASE REPORT

Burak Bahadir; Nilufer Onak Kandemir; Nimet Karadayi; Sukru Oguz Ozdamar

Zonguldak Karaelmas University, School of Medicine, Department of Pathology,Zonguldak, TURKEY

Background: Glioblastoma multiforme (GBM) is the most aggressive, and the most frequent primary tumor of the brain in adults. The presence of poorly differentiated areas displaying small cell architecture and often immunoreaction for neuronal markers lacking glial fibrillary acidic protein (GFAP) expression is an uncommon phenomenon in GBM. The bases of this type of differentiation and its prognostic significance have remained vague.

Case: A 61-year-old woman with a 1-month history of headache and drowsiness presented with a sudden onset of left facial paresis. Magnetic resonance imaging revealed an enhanced mass lesion located in the right fronto-temporal lobe, exhibiting solid and cystic components and extending into corpus callosum and contralateral hemisphere, suggesting a diagnosis of GBM. Microscopically, the neoplasm was composed of two evidently perceptible areas. The predominant component was characterized by neoplastic cells with pleomorphic, atypical nuclei, and abundant eosinophilic cytoplasm lying on a fibrillary network. Numerous mitoses, blood vessels with endothelial cell proliferation and large areas of necrosis were also noted. Immunohistochemically these neoplastic cells as well as the fibrillary network were positive for GFAP. The second component dispersed throughout the tumor was composed of numerous small and densely packed cells with slightly elongated, hyperchromatic nuclei and scant cytoplasm. These primitive-looking neoplastic cells were immunohistochemically negative for GFAP and chromogranin but expressed synaptophysin, neurofilament protein and NeuN. Considering the age of the patient and high proportion of glial component, it was concluded that the current case represents a GBM with poorly differentiated small cell component expressing neuronal markers.

Conclusion: The significance of neuronal cells in an otherwise ordinary astrocytoma requires further investigations. Therefore, each case must be reported in detail to constitute a sufficient data.

Key words: Glioblastoma multiforme, immunohistochemistry

P-272

99mTc-tetrofosmin brain spect in the assessment of meningiomas. Correlation with histological grade and proliferation index

Anna Goussia; Michael Doukas; George Alexiou; Spyridon Tsiouris; John Nesseris; Andreas Fotopoulos; Maria Bai; Vasiliki Malamou-Mitsi; Athanasios Kyritsis

Departments of Pathology, Neurosurgery, Nuclear Medicine and Neurology, Medical School, University of Ioannina, Greece

Background Meningiomas are common brain tumors. Although benign meningiomas (WHO grade I) have a

favorable clinical course, atypical and anaplastic tumors (WHO grade II and III, respectively) are associated with high recurrence rate and aggressive biological behavior. The expression of the cell proliferation marker Ki67/MIB1 has been used as a useful adjunct for predicting recurrence and tumor behavior. SPECT (single photon emission computed tomography) by various radiotracers can metabolically characterize intracranial tumors. Therefore, in the present study we investigated whether ^{99m}Tc-Tetrofosmin (TF) uptake in meningiomas correlates with histological grade and tumor cell proliferation.

Method Fifteen patients (4 males, 11 females; mean age 62.3 years) with suspected meningioma on structural brain imaging (CT/MRI) were prospectively enrolled.

Brain SPECT by TF had been performed within a week prior to surgical tumor excision. TF uptake was assessed visually and semiquantitatively, by calculating the lesion-to-normal (L/N) uptake ratio. In the excised tumor specimens, the immunohistochemical expression of the Ki67/MIB1 protein was evaluated. Pearson's correlation analysis was performed between the level of tracer uptake (as expressed by the L/N ratio) and Ki-67/MIB1 expression and tumor grade. Statistical significance was set at $p<0.05$.

Results Intensity of TF uptake in the region corresponding to the CT/MRI findings ranged from faint to profound. On histological examination, twelve cases were diagnosed as benign meningiomas and three cases as anaplastic meningiomas. The expression of the Ki67/MIB1 protein ranged from 0.5% to 20%. A significant positive correlation between TF uptake and tumor grade ($r=0.834$, $p<0.001$) as well as between TF uptake and Ki67/MIB1 expression ($r=0.702$, $p=0.004$) was observed.

Conclusion The findings of this pilot study suggest that TF brain SPECT may be useful in differentiating benign from malignant meningiomas and may be a potential indicator of tumor proliferation activity.

P-273

Elevated expression of Cav-1 in brain tumors and its correlation with angiogenic markers – VEGF, bFGF

Tanase Cristiana; Arsene Dorel; Codorean Eleonora; Raducan Elena; Ogrezeanu Irina, Cruceru Maria Linda; Nicolescu Mihnea Ioan; Leabu Mircea; Hinescu Mihail Eugen

"Victor Babes" National Institute of Pathology; "Bagdasar-Arsenie" Hospital; "Carol Davila" University of Medicine, Bucharest

Background Caveolins, structural proteins of caveolae, are involvedin many cell functions, including endocytosis, signal transduction and cellproliferation. Their role is explored in tumor growth regulation.

We analysed the potential role of Cav-1 expression inbrain tumor progression and the association between its level of expression andthe one of VEGF and bFGF.

Methods Specimens from 20 glial tumors of various histologictypes and grades were immunohistochemical assayed for caveolin-1, VEGF and bFGFreactivity. Level of Cav-1 in selected samples was determined by Western Blot.

Results In tumoral tissue, both tumor cells and blood vesselsexpressed Cav-1 with a higher percentage compared to peritumoral areas, whereCav-1 expression was confined only to endothelial cells.Western Blot analysisconfirmed overexpression of Cav-1 in tumoral tissue lysates.

Immunoreactivity for VEGF and bFGF was expressed in both endothelial and tumor cells,with increased levels following tumor invasiveness.

Cav-1 expression in tumoral areas had a good correlation-with angiogenic markers. Significantly higher Cav-1 expression was encounteredin cases with increased VEGF and bFGF.

Conclusion Cav-1 was overexpressed in studied brain tumors, alongwith VEGF and bFGF, with a higher score in highly aggressive ones.

Future studies about interrelation between caveolins andangiogenic markers will be of majorinterest as possible therapy targets.

P-274

Correlations between clinical and morphological aspects in hypertensive patiens dead with severe primary intracerebral haemorrhage

Stelian Danut Enache; Iancu Emil Plesea; Oltin Tiberiu Pop; Simona Bondari; Corneliu Cristian Georgescu; Dan Cioroianu; Alexandru Camenita

Craiova University of Medicine and Pharmacy, Department of Pathology, Romania

Aims. The study is a retrospective integrated assesment of clinical, imagistic and morphological parameters in severe intracerebral hemorrhages (ICH) complicated with intra-

ventricular extension (IVE) and/or subarachnoid effusion (SE).

Method. The material consisted of patient's medical records (clinical charts, CT scans, autopsy protocols and histopathology records) from 106 cases with ICH associated with IVE and/or SE hospitalised in the Emergency County Hospital of Craiova. The evaluated parameters were clinical (season relation, age, sex, arterial blood presure - HT, motor deficit - MD, Glasgow score at admission - GS) and morphological (ICH sites, size, perilesional edema - pE, microhemorrhages - mH and mass effect - ME).

Results. 65% of the cases showed only IVE and 22% had both complications. Both IVE and SE were more frequent in cold seasons, but IVE in autumn whereas SE in winter. Sex distribution was almost equal, with slight male predominence in VE and slight female predominence in SE. IVE and SE were more frequent in ICH before 60 years, with no predilection for a certain age group. Around 70% of the patients had IIIrd and IVth stage HT at admission, 85% had MD and almost 50% Glasgow scores lower than 6. In half of all cases IVE involved at least one of the lateral ventricles. VE was more frequent in lobar ICH while SE was more frequent in non-lobar ones. In lobar sites involving more than one lobe, arround 85% of hematomas had huge dimensions, half of the CT investigated cases showing ME. CT and HP examinations often revealed multiple mH both near and distant to ICH, and pE.

Conclusion. ICH associated with IVE and/or SE and one or more clinical and morphological poor outcome predictors (HT, MD, low GS, pE, mH and ME) result in patient's death, despite any sustained therapeutical intervention.

P-275

Central neurocytoma: a clinical-pathological study of eight cases

Concha Fiaño Valverde; Juan Luis Rios González; Pablo Fernández Vázquez; Alberto Pérez Rodríguez; Rebeca Fernández Victoria; Joaquin González- Carreró
Complejo Hospitalario Universitario de Vigo. Hospital Xeral-Cíes, Spain

Background: Central Neurocytomas (CN) are uncommon tumours of the central nervous system, with neuronal differentation, generally found in young adults, in the lateral or third ventricles. Typically, they have a favourable prognosis after surgical total resection, but in some cases the clinical course is more agressive.

Material and methods: Our series are about eight patients (M:F=3:5: men age, 28.6 years) diagnosed between 1995–2007. All are intraventricular tumours showed typical radiological, histological and inmunohistochemical features. Most patients received craniotomy with complete removal of the tumour, except one patient who underwent partial resection.The clinical, pathological and surgical data of these patients were reviewed and analyzed.

Results: Seven tumours showed typical features of CN. Anaplastic features (mitosis, vascular proliferation and necrosis) were observed in one case. Inmunochemistry showed in all reactivity for neuronal markers and negativity for GFAP. Two tumours called atypical neurocytoma presented high proliferative activity (MIB-1 labelling index >5%), one with anaplastic features. Except one case that succumbed two month afteer surgery for another tumour, the remaining seven were alive and apparently asymptomatic during follow-up period wihch ranged from 5 to 80 months (mean 38,7).

Conclusions: CN is an infrequent neoplasm with low incidence, (0.3% in t. series). The most frequent presentation is like intraventricular masses in young adults. Definitive diagnostic require neuronal markers and/or molecular studies (LOH 1p/19q), especially in extraventricular forms. Typically, CN are associated with favourable outcome, althought cases called atypical have more agressive clinical course with local recurrences.

P-276

Metastatic hemangiopericytoma after long free disease interval; presentation of two cases

Iren Amat Villegas; M[a]Assunsión Arrechea Irigoyen; Raquuel Beloqui Perez; M[a] Rosario Mercado y M[a] Luisa Gómez-Dorronsoro
Hospital de Navarra, Spain

Background Hemangiopericytomas (HPC) are rare spindle cell tumors constituting 2,5% of soft tissues neoplasms but only a 0,4% of central nervous system (CNS) tumors. The majority of the tumors are superficially located and attached to the dura with no evidence of infiltration of the CNS parenchyma. HPC are frequently higly aggressive and they have a tendency to recur and metastasize outside de CNS.

Method We describe the cytological and histologycal finfings in a 57-year-old man and a 56-year-old woman who previously presented meningeal HPC and at this moment develop metastatic disease. After a free disease interval of fourteen and nine years respectively they present metastases in liver and pancreas.

Results Metastatic specimens showed a monotonous tumour composed of randomly oriented plump cells with ill-defiened cytoplasm and prominent highly-branched "stag-horn-like" vascular channels. The neoplastic cells were positive for CD·34 and CD99 and negative for CD·31 and keratin, supporting a diagnosis of metastases from the patint's cerebral tumor.

Conclusions Meningeal HPC is a diagnostic challenge due to its propensity to metastasize peripherically despite treatment. Surgical excision is the most common therapy recommende and the use of postoperative radiotherapy is debatable. Recurrences are frequent and metastases may be multiple, the liver is the most common location followed by bone, skin and soft tissues.

P-277

MGMT protein expression and MGMT promoter methylation status in a series of 63 glioblastomas

Cristina Carrato; Carmen Balañá; Eva Musulén; Carolina Sanz; Mireia Berdiel; José Luis Ramírez; José Javier Sánchez; Pilar Teixidor; Rafael Rosell; Aurelio Ariza.

Hospital Germans Trias i Pujol, Spain

Background: DNA repair protein O^6-methylguanine-DNA methyltransferase (MGMT) removes alkyl groups from DNA and thus prevents cell death induced by alkylating agents. Almost 30% of glial neoplasms show *MGMT* inactivation, mostly caused by promoter methylation. This phenomenon has been correlated with sensitivity to methylating agents. Additionally, some studies suggest a direct relationship between chemotherapy response and MGMT protein immunohistochemical (IHC) detection. Nonetheless, few data are available concerning the relation between IHC MGMT protein expression and *MGMT* promoter methylation status.
Method: We have studied both MGMT protein expression by IHC and MGMT promoter methylation status by methylation-specific PCR (MSP) in a series of 63 glioblastomas. Two tissue microarrays were constructed for IHC assessment. A total of 100–600 cells were counted in every case and results were expressed as percentage of MGMT-positive cells.
Results: In our series, the percentage of IHC MGMT-positive cells ranged from 5% to 93.5%. On the other hand, *MGMT* promoter methylation was detected in 39 cases. A relation between protein expression and gene promoter methylation status was observed (ROC 0.70 [0.56–0.84]; p=0.007). Placing the cut-off value of MGMT-positive cells at 12%, IHC was a sensitive tool (92.3%) in predicting non-methylation status, although with a low specificity (25%). Using the 12% cut-off value, 53 cases (84.1%) were IHC-positive and 10 were IHC-negative.
Conclusion: In our hands, although MGMT IHC detection could predict non-methylation status with a high sensitivity, its specificity was so low as to need confirmation by *MGMT* promoter methylation status determination. For this reason, we think that implementation of MGMT IHC is not justified for routine clinical management of patients.

P-278

Identification of novel candidate genes associated with recurrent meningiomas by analysis of microarrays

Rocio Juárez, Elisa Pérez-Magán; Yolanda Ruano; Angel Rodríguez de Lope; Concepción Fiaño; Juan Fernando García; Yolanda Campos-Martín;Jesús Andrade, Manuela Mollejo, Teresa Ribalta; Barbara Melendez

Hospital Virgen de la Salud, Toledo; Centro Nacional de Investigaciones Científicas, Madrid; Hospital Xeral Cíes, Vigo; Hospital Clínic-IDIBAPS-Universitat de Barcelona, Barcelona, Spain

Background and Aim: Meningiomas (MNGs) account for about 24–30% of primary intracranial tumours, with an annual incidence rate of up to 13 per 100000 individuals. Most of these tumours are benign (WHO grade I) and can be cured by surgical resection. Although generally considered benign, recurrences occur between 10% and 25% of the cases undergoing gross total resection of the tumor and represent the major factor influencing patient's outcome. Molecular mechanisms associated to recurrence are still unclear. The aim of this study was to carry out gene expression profiling in primary and recurrent MNGs in order to identify potential predictive target genes and/or molecular markers of recurrence.
Experimental design: Forty-six tumours (17 WHO grade I, 17 grade II, 7 recurrent MNGs grades I and II) and 5 non-neoplastic meninges were analysed by using oligonucleotide microarrays. Expression profiling results from primary tumors were compared to those of recurrent tumours. Statistical analyses were performed by using GEPAS (CIPF, Valencia, Spain) and GSEA (Broad Institute, Cambridge, Massachussetts).
Results: Unsupervised hierarchical clustering of the samples showed two clusters of tumours, one of them containing all of the recurrences. In addition, using a discriminant approach analysis we identified 899 genes with differential expression between primary and recurrent tumours (FDR<0.15). These genes were related to the Wnt, MAPK, regulation of actin cytoskeleton, insulin, and VEGF signaling pathways.
Conclusions: We have identified gene expression profiles and candidate markers associated to recurrent meningioma.

Additional studies on these candidate genes are warranted to assess its utility as diagnostic and/or prognostic markers.

P-279

Gene expression profiling in diffuse gliomas

Yolanda Ruano; Elisa Pérez-Magán; Concepción Fiaño; José Luis Hernández-Moneo; Yolanda Campos-Martín; Juan Luis Orradre; David Blesa; Juan Cruz-Cigudosa; Juan Fernando García; Manuela Mollejo; Teresa Ribalta; Barbara Melendez

Hospital Virgen de la Salud, Toledo; Centro Nacional de Investigaciones Científicas, Madrid; Hospital Xeral Cíes, Vigo; Hospital Clínic-IDIBAPS-Universitat de Barcelona, Barcelona, Spain

Diffuse gliomas are the most common primarybrain tumours in adults. They are currently classified histologically inastrocytoma (AST), oligodendroglioma (OLIG), and mixed oligoastrocytoma (MOA). However,some gliomas show ambiguous morphology and can be difficult to classify. High-throughput analyses of gene expression has shown to be helpful inidentifying new key genes, networks and pathways which may be clinicallyrelevant. We investigated thepattern of gene expression in 37 gliomas of different types (9 AST, 19 OLIG and9 MOA) and grades (WHO grades II and III) by using oligonucleotidemicroarrays.

Functional analyses by using GEPAS (CIPF, Valencia, Spain)and GSEA (Broad Institute, Cambridge, MA, USA) comparing tumours of WHO grade IIand III revealed a set of genes significantly up-regulated in grade III thatwere involved in cell cycle, cell proliferation and metabolism processes. Moreover, comparing the gene expression profiles between AST, OLIG and MOA, thelatter group showed a gene expression profile more similar to AST than to OLIG.We also found significant up-regulation of ANXA1 in ASTs and MOAs while thisgene was downregulated in OLIGs. Immunohistochemical validation studies in anindependent series of 66 diffuse gliomas confirmed ANXA1 overexpression in 41% of ASTs, but only in 18% of MOA and 5% of MOAs.

Our findings support the molecular relevance of the astrocytic component inthe gliomas with a mixed morphology, and disclose a set of candidate genes ofpotential diagnostic interest.

P-280

Immunohistochemical study for O6-methylguanin-DNA methyltransferase (MGMT) in gliomas: A tissue microarray study of 244 cases.

Eva Bailón; Anna Ventolà; Manuela Mollejo; Yolanda Ruano; Bárbara Meléndez; Concha Fiaño; Virginia Cardós; Avelina Tortosa; Francesc Graus and Teresa Ribalta (in the name of the Neuro-oncology group of the Hospital Clinic)

Hospital Clinic, IDIBAPS, Universitat de Barcelona, Barcelona; Hospital Vírgen del Rocio, Toledo; Hospital Xeral Cíes, Vigo, Spain

Background and aim Hypermethylation of the MGMT promoter has been recently found associated to longer survival and improved response to chemotherapy in patients with glioblastoma (GBM) who receive alkylating agents. The benefit derived from alkylating drugs has been linked to reduced expression and activity of the DNA repair gene MGMT. When the DNA lesions produced by the drug are not repaired by MGMT, cell death is induced. Epigenetic silencing of MGMT occurs between 41% and 47,7% of GBMs and in 39% of anaplastic astrocytomas (AIII). Low expression of MGMT by immunohistochemistry (IHC) has been reported in 32% of GBM, 42% of AA, and 55% of anaplastic gliomas (all types). However, most studies have shown a lack of correlation between MGMT status and MGMT protein expression. Knowing the DNA repair enzyme status of the tumour is becoming a crucial parameter for prognosis and optimizing treatment decisions in glioma patients, however, molecular analyses are not a routine clinical practice in most institutions and a standardized immunohistochemical method for this analysis is not available yet. The present study examines expression of MGMT in a large series of gliomas of adult patients.

Material and methods Tissue microarrays including 128 astrocytomas (A; 98 GBM, 11 grade III, 19 grade II, 13 grade 1), 16 oligodendrogliomas (O; 8 grade III, 8 grade II), 15 oligoastrocytomas (OA; 9 grade III, 6 grade II), 8 ependymomas (E; grade II), 2 subependymomas (SE), and 4 normal brain tissues (NB) were used for the immunohistochemical study. Based on immunostain results tumours in each category were stratified into low expressors and high expressors (strong positivity in >5% of tumour cells).

Results Most positive cases showed a heterogeneous pattern of immunostaining. Low expression was observed in 47% GBM, 54% A III, 53% A II, 38% A I, 62% O III; 37% O II: 53% OA, 37% E, and 0% SE. Low-grade tumours as a group were more expressors than high grade

gliomas. Only 4/98 GBM were strongly positive. All 8 anaplastic Oligodendrogliomas were negative.
Conclusion We conclude that MGMT is differentially expressed in gliomas and that there is an inverse correlation to tumor grade, especially in oligodendrogliomas. Further studies are necessary to determine the precise clinical utility of MGMT expression studies in the different glioma types and grades.

Poster displayed on Tuesday, May 20
Head and Neck Pathology

P-281
EVALUATION OF FINE NEEDLE ASPIRATION BIOPSY WITH HISTOPATHOLOGIC REFERENCE TESTING IN THE DIAGNOSIS OF CANCER OF THE PAROTID GLAND IN A COLOMBIAN POPULATION
Álvaro Antonio Herrera Hernández, Julio Alexander Díaz Pérez, Carlos Andrés García, Luís Carlos Orozco Vargas, Paola Aranda, Loren Paola Herrera, Ernesto Garcia
Universidad industrial de santander, Bucaramanga, Colombia

Background. Fine Needle Aspiration Biopsy (FNAB) is used commonly in the study of neoplastic lesions of the parotid gland, however, there exists controversy in its accuracy. **Objective.** To evaluate the performance of the FNAB in the diagnosis of the parotid gland carcinoma. **Materials.** 46 patients with masses in the parotid area from 7 health centers of Bucaramanga, Colombia were selected. **Results.** The mean age of the patients was of 51.78± 16.32 years old, the 58,7% were female. The FNA had a Sensitivity of 53,8%, a Specificity of 90,9%, a PPV of 70%, a NPV of 83,3%, a LR+ of 5,92 a LR- of 0,5 and kappa of 0.48 in the identification of parotid gland carcinoma, in a population with a prevalence of the disease of 28.26%. **Conclusions.** The FNAB had a moderate performance in the diagnosis of the parotid gland carcinoma, which agrees with other previous studies. Its low sensitivity and LR- indicates its limitations as a screening test; in addition its low Kappa shows little correlation in its diagnosis. Therefore, it's advisable to improve the criteria used in its interpretation, as well as to make emphasis on the development of new technologies that allow a better, valid and precise diagnosis of this pathology, and that like the FNAB, offers its service at low cost and with ease of implementation.

P-282
VEGF Biosynthesized in Adenoid Cystic Carcinoma; its role in tumor architectural histogenesis and its impact on tumor behavior
Wael Mohamed Swelam
Tanta University, Faculty of Dentistry, Oral Pathology Department, Saudi Arabia

Background Adenoid Cystic Carcinoma (ACC), the most common malignant tumor of salivary glands, is characterized by its variable histogenitic architecture. Duct-like structures together with few ductal elements constitute the prototypical patterns that typifies the tumor. Vascular endothelial growth factor (VEGF) is a potent tumorigenic growth factor, which is upregulated by hypoxic conditions for tumor cells. It is a must for tumor cells to feasibly gain their nutrients and get rid of their metabolites. How ACC tumor cells can achieve this objective though their poor vascularity, still an open question.
Aim of the work To characterize epigenetic and protein expression related to different ACC histopathology patterns.
Methods To achieve this purpose we will demonstrate the immunohistochemical distribution of VEGF and VEGF receptors (VEGFR) mainly VEGFR-1 (Flt-1) and VEGFR-2 (Flk-1) in different ACC components. Also, show how VEGF and VEGFR architecture-related expression can work to induce the characteristic tumor histogenesis, and how this can influence tumor survival and proliferation. RNA expression of different VEGF spliced variants will be demonstrated in ACC cells in culture,by competitive RT-PCR.
Results Our results immunoprofiled ACC components show strong VEGF/ Flk-1 co-localization in tumor duct-like structures indicates that VEGF functions in formation and maintenance of ductal structures when it is recognized by Flk-1. Enhanced tumor cell proliferative and anti-apoptotic signals surrounding duct-like structures demonstrated by Ki-67, Bcl-2, and Survivin compared to other tumor components.
Conclusion Our evidences suggest an active role for duct-like structures to enhance proliferation and survival.

P-283
OCULAR JUVENILE PILOCYTIC ASTROCYTOMA IN A 7 YEAR OLD NIGERIAN GIRL A RARE FINDING.
M.A. NZEGWU, E.N ONWASIGWE, A.E AGHAJI, U. AGWU-UMAHI, E.F.NNAKENYI.
UNIVERSITY OF NIGERIA TEACHING HOSPITAL ENUGU. NIGERIA.

INTRODUCTION: Most optic nerve gliomas are juvenile pilocytic astrocytomas (JPA). Most occur in individuals

between the ages of 2–6 years,and are frequently associated with von Recklinghausen neurofibromatosis type1 (NF1). JPAare uncommon clinical entities rarely seen in our environment.
DESIGN /CASE REPORT. We present a case of JPA seen recently in a 7 year old girl who presented at the eye clinic of the University of Nigeria Teaching hospital with an 18 month history of painless protrusion of the right eye ball, associated marked diminution of vision. Externally an 8 mm non-pulsatile, non-axial proptosis, resistant to retropulsion was noticed on the clinical presentation. Skull x-ray and orbital ultrasound done were indeterminate, while computerized axial tomography of the head yielded a diagnosis of optic nerve glioma. Exision biopsy following exanteration showed a histological diagnosis of optic nerve JPA.
Macroscopically, the tumor is a well circumscribed and envelops the right optic nerve. Cut surface showed a predominantly solid lesion. Microscopically, the lesion demonstrates well-differentiated pilocytes with hairlike glial processes associated with microcysts that contain mucopolysaccharide material. Capillary formationa was present.
DISCUSSION; This case represent the first time juvenile optic nerve astrocytoma is being reported internationally from our environment. Aetiologic factors are unknown. Our patient had no feature of NF1. Transformation to a malignant high-grade tumor is rare. Patients with optic pilocytic astrocytomas associated with NF1 usually have better outcomes than those of other patients with juvenile pilocytic astrocytomas because the tumor is more likely to be confined to the optic nerve. Bilateral optic gliomas are more common in patients with NF1.Patient is currently being reevaluated as to the next line of management.

P-284
PRIMARY CARCINOMAS OF THE UVULA. CLINICO-PATHOLOGICAL STUDY OF 17 CASES

Maddi Garmendia; Ayman Gaafar; Lorena Mosteiro; Verónica Velasco; Francisco José Bilbao; Rebeca Ruiz; Francisco Javier Ortega; Mari Carmen Etxezarraga; José Ignacio López; Cosme Ereño
Hospital de Basurto and Hospital de Cruces, Osakidetza, Universidad del País Vasco-Euskal Herriko Unibertsitatea, Spain

Background: We analyse clinicopathological features of a series of carcinomas of the uvula (CU) collected in two hospitals.
Design: All the CUs resected in both hospitals during 13 years period were included. Clinical and pathological data have been collected in all cases [age and sex, adjuvant therapy, follow-up, local recurrences, loco-regional extension, second primary tumours (SPT), tumour diameter (TD), growth pattern (GP), histological type (HT) and grade (G), predominant pattern of invasion (PPOI), worst pattern of invasion (WPOI), tumour-associated tissue eosinophilia (TATE), Ki-67 index, pT and pN status].
Results: All patients except one were males. Average age was 61.3 years. In 7 cases surgical resection was followed by radiotherapy and/or chemotherapy. Average follow-up was 27.8 months. In one case local recurrence was detected. Nine cases had SPTs, all of them located in UADT. Three- and 4-year overall survival was 62.7% and 50.2% respectively. Survival associated to SPT did not show significant differences in comparison with the rest. Ten cases showed exophytic GP, 4 were ulcerated-infiltrating and 3 were flat. Average TD was 15.2 mm. HT was as follows: squamous cell carcinoma in 16 cases (mostly G2), and one lymphoepithelioma-like undifferentiated carcinoma. PPOI was pushing in 8 cases, infiltrating in 7, and nested in 2. WPOI was infiltrating in 9 cases. TATE was intense in 3 cases, mild to moderate in 11 and it was absent in 3. Ki-67 index oscillated between 40% and 80%. Staging was: pT1 88.2%; pT2 11.8%; pN0 94.8%; and pN1 5.7%.
Conclusions: Most CUs are diagnosed in males, over the sixth decade, correspond to squamous cell carcinomas diagnosed in early pathological Stages. The prognosis of these patients is worsened by the high incidence of SPTs.

P-285
CARCINOMAS OF THE PYRIFORM SINUS. CLINICOPATHOLOGICAL STUDY OF 40 CASES

Cosme Ereño, Maddi Garmendia, Rebeca Ruiz, Ayman Gaafar; Aitziber Ugalde; Mari Carmen Etxezarraga; José Ignacio López; Francisco José Bilbao
Hospital de Basurto and Hospital de Cruces, Osakidetza, Universidad del País Vasco-Euskal Herriko Unibertsitatea, Spain

Background: Carcinomas of the pyriform sinus (PS) are rare and aggressive laryngeal tumours. This study reviews the clinicopathological features and clinical outcome of 40 cases.
Design: We diagnosed 40 carcinomas of the PS during the last 9 years. Age, sex, smoking and alcohol abuse, location (L), size, histological type, node status (N), extraganglionar extension (EE), distant metastases (M), local recurrence (LR), second primary tumors (SPT), stage and survival-rates (SR) were evaluated.
Results: Average age was 60.9 years with males predominance (39M/1F). Smoking and alcohol abuse was confirmed in 62.5% of cases. L was as follows: left PS 50%; right PS 45%; bilateral 5%. Surgery+radiotherapy was the

mostly applicated treatment (35%). Squamous cell carcinoma was the most frecuent type (87.5%), followed by basaloid-squamous cell carcinomas (10%), and 2.5% corresponded to carcinoma not otherwise specified. Average TS was 30.8 mm. Node metastases were positive in 67.5% cases, 44.4% of them showed EE. Distant metastases were found in 17.5% cases. LR occurred in 20% of cases and 7 cases had a SPT diagnosis. Most tumors were in advanced stage at diagnosis (I: 2.5%; II: 5%; III: 27.5%; IV: 47.5%) and 17.5% cases were not staged. Follow-up study showed high mortality (16) but most patients are still alive (23). One case was lost on the follow-up. Three- and 5-year overall survival was 41.7% and 34.7% respectively. Three-year survival comparing N and M categories did not show significant differences [(N+ 41.6% vs. N− 59%) (M+, 38% vs. M− 49.3%)].

Conclusions: Most carcinomas arising in PS are conventional squamous cell carcinomas and behave aggressively. Advanced pathological Stage at diagnosis, strong tendency to metastasize, and high incidence of SPT are findings frequently observed in these tumours.

P-286
THYROGLOSSAL DUCT CARCINOMA: CONTRIBUTION OF FOUR NEW CASES FROM COLOMBIA

Edgar Julián Ferreira B., Julio Alexander Díaz Pérez, Álvaro Antonio Herrera and Ernesto García Ayala
Universidad Industrial de Santander, Colombia

Justification. The thyroglossal duct carcinoma is an uncommon disease, which has only an aproximate of 200 reported cases worldwide, 5 of this reported in Colombia. Objective. To describe the features of the thyroglossal duct carcinoma cases diagnosed at the *Hospital Universitario de Santander* (HUS), between 2002 - 2006. **Design.** Descriptive study. **Results.** During the four years of this study, were atended four cases of thyroglossal duct carcinoma at the *HUS*, all of them in women, with ages between 35 and 45 years. All the patients consulted for neck mass, 2 of them previous and the other 2 low to the hyoid bone, with a size between 1.5 and 6 centimeters, from 6 months to 6 years of evolution, and all of them with a rubbery consistence. In this patients the malignancy was discovered ante-surgically in 3 cases, by cytology of a sample obtained with fine needle aspiration. The Sistrunk's procedure was practiced to all the patients, finding thyroid papillary carcinoma in the pahologic study, 2 of them of classic variety and the other 2 of follicular variety. At present, the patients are asymptomatic without relapse signs. **Conclusions.** The thyroglossal duct carcinoma is an uncommon disease in our Hospital, despite that the thyroglossal duct cyst was the most frequent congenital anomaly in the neck, which matches with other series reports. In our experience the antesurgical diagnosis was made on the 75% of the cases, different from the commonly informed. We found thyroid papillary carcinoma in all the cases, data that matches with all the other consulted series and the treatment used was Sistrunk's procedure, which eradicated the disease.

P-287
Morpho-functional peculiarities of the gum tissues at the jaw fractures area due to plasma enriched with platelets application

Volodimyr Gavrilov; Sergiy Morozov; Pavlo Fedorenko
Lugansk State Medical University, Kiev National Medical University, Ukraine

Background: Posttraumatic inflammation is a common complication of the fractures of the lower jaw. The aim of present investigation was to study clinical and morphological effect of plasma enriched with platelets on the course of the gum tissues inflammation in the lower jaw fractures area.Methods: 53 volunteers enrolled while receiving dental care in cases of uncomplicated lower jaw fractures. Thirty gums biopsies were taken from patients who got the reposition and fixing of jaws fragments by the teeth fixating devices without plasma application (group of comparison) and 23- from the patients who additionally routine methods had the applications of plasma, enriched with platelets at the area of the jaw fracture. Histological slides stained with H&E and Van Gison, and then studied microscopically and stereologically. The results showed the positive effect of the application of thrombocytes membrane developed from thrombocytes gel at the area of the lawyer jaw fracture under the mucosal and periosteum layers. Plasma rich with platelets filled the alveolus of the tooth (or teeth) extracted from the line of the fracture. Clinical, macroscopical and radiological control under the patient's treatment confirmed the acceleration of the bone repair. The formation and maturation of a bone callous at the zone of the lower bone fracture stimulated by platelets growth factors. The histological evaluation clearly demonstrated a reduction of the inflammation. The number of the vessels and the intensity hyperemia was smaller. Cell infiltrates and areas of connecting tissue dystrophy revealed occasionally. Conclusion: The results showed the positive effect of the plasma application at the area of posttraumatic inflammation due to the stimulation of repair processes within bones and jaw

soft tissues by the plasma growth factors. These processes accompanied with the reduction of morphological and clinical signs of inflammation at the area of jaw fracture.

P-288

Orbital metastasis as primary clinical manifestation of thyroid carcinoma: case report and literature review

Gabrielle Gurgel Lima; Francisco Dario Rocha Filho; Francisco Valdeci Almeida Ferreira; Adriana Alencar Araújo Costa; Ricardo Pinto Gondim

Institute of Cancer of Ceara, Brazil

Introduction: Papillary thyroid carcinoma (PTC) is regarded as curable malignance with favorable prognosis. However, a minority of patients may present, or subsequently develop, locoregional and distant metastases that may adversely affect survival. Metastatic thyroid carcinoma (TC) rarely involves the orbit. They constitute 5% to 6.5% of total orbital neoplasms. We report the clinical and pathological features of metastases in orbit from a primary TC. Method and Results: Patient female, 66 years, was admitted with history of unilateral ptosis on right eye for one year. She was submitted a surgery in right orbit with biopsy, which diagnosis of metastases with PTC. Thyroid was palpable during the swallow with a nodule on right lobe. The orbit computed tomographic scan confirmed expansive solid injury projected to upperside of right associated to frontal bone injury with superficial intracranial invasion. Percutaneous US-guided biopsy of right thyroid reveled two solid and hypoecogenic nodes with follicular cells proliferation. The patient was submitted total thyroidectomy. The microscopy showed epithelium heterotype formed by cells in ground-glass and nuclear crank distribution mostly solid and slicly papillary area. The patient involved with spinal toracolombar pain. Began radiotherapy in right orbit. The bone scintillography showed radio contrast hipercaptation in right orbit and T8 to T10. The orbit immunohistochemistry reveld HBME 1, CK-19 and GAL-3 positives. Currently, patient is taking chemistry with Clodronate with palliative care finality. Conclusion: The orbit and globe are not in the list of common sites to which systemic carcinoma metastases. Rarely, the presence of distant metastasis may be the only initial manifestation of TC without clinically apparent disease in thyroid region. The related case shows the importance of immunohistochemistry to strengthen the malignant character of metastatic tumor. This was demonstrated through homogeneous expression of immune markers HBME 1, CK-19 and GAL-3, that are associates to TC.

P-289

Prevalence of the papillomavirus infection in squamous-cell carcinomas (SCC) of the oral cavity and oropharynx in a spanish population.

Dolores Suarez Massa; Paloma Martin Acosta; Maria Teresa Pinilla; Carolina Frias; Maria Rosario Sanchez Yuste; Carmen Bellas

Hospital universitario Puerta de hierro, Spain

The association between oncogenic HPVs and cancer has been well established for uterine cervical carcinomas and other anogenital cancers. Substantial molecular evidence suggests a role for human HPV in the pathogenesis of a subgroup of SCC of the head and neck. The prevalence of this association varies broadly, depending on the population studied, geographical area and type of histological samples tested. The aim of this study was to investigate the association between SCC of the head and neck and HPV infection and its prevalence.

A retrospective study of 83 paraffin blocks diagnosed of SCC was included. Data regarding sex, age, anatomical localization, and toxic habits were analyzed. Samples were tested for HPV DNA by PCR and genotype identification was performed by RFLP.

HPV DNA was detected in 12 out of 83 (14.5%) samples. Of the 12 positive cases 8 were genotyped as HPV16 and the remaining 4 could not be classified. In our series, most carcinomas were classic SCC (78 cases) and also included some variants; 2 basaloid, 2 verrucous and a papillar one. HPV DNA was detected in the two basaloid and in the papillar one. Regarding anatomical location, 10 out of 47 cases from oropharynx and 2 out of 36 from oral cavity were positive for HPV. Mean age at the time of diagnosis in positive cases was 49.6 years. No significant association was found between the presence of HPV and other risk factors, including tobacco use and alcohol use.

Our prevalence is in agreement with the IARC multicontinent studies. HPV-16 is the most frequent type detected in our series and 14.5% of oral SCC was positive for the virus. In the Spanish studied population HPV associated SCC was higher in oropharynx than in the oral cavity and patients with HPV positive tumours were younger than negative ones.

P-290

LOW GRADE ADENOCARCINOMA OF EAR LOBE WITH APOCRINE DIFFERANTIATION (CERUMINOUS ADENOCARCINOMA?): A CASE REPORT

Cem Leblebici*, Nevra Dursun*, Zeynep Alkan, Ozgur Yigit**, Erol Rustu Bozkurt***

**The Ministry of Health Istanbul Training and Research Hospital Pathology Department Istanbul/Turkey, ***The Ministry of Health Istanbul Training and Research Hospital Head and Neck Surgery Department Istanbul/Turkey*

CONTEXT: Ceruminous glands are tubuloalveolar apocrine glands in the external auditory meatus. Ceruminous gland tumors are rare neoplasms. Histologically auricle essentially a cutaneous structure composed of keratinizing, squamous epithelium with associated cutaneous adnexial structures that include hair follicles, sebaceous glands and ecrine sweat glands. Apocrine glands in ear are located external ear canal. Apocrine adenocarcinoma of ear lobe is uncommon.

CASE REPORT.: 42 year old man was presented with 3-month history of painless mass at the right ear lobe. No history of trauma was noted. On physical examination nonulcerated mass was seen on external ear lobe. A wide local resection was performed. Histological examination showed low grade apocrine adenocarcinoma with occasinal mitotic activity. Immunohistochemically tumor showed cytokeratin 7, S100, GCDFP-15 expression.

CONCLUSION: There was no apocrine carcinoma on ear lobe at literature. Ceruminous adenocarcinomas located external auditory meatus. Apocrine and ceruminous adenocarcinomas posses glandular structure with evidence of apocrine differantiation. Only ceruminous carcinomas show dense fibrosis that seperates neoplastic proliferation. In our case localization is uncommon. Histological apperarence resembled ceruminous carcinomas. But in literature there was no apocrine glands at ear lobe; so it was difficult to name this tumor.

P-291

CLINICOPATHOLOGICAL FEATURES OF ORAL CARCINOMA: ANALYSIS OF 240 CASES

D.Micello; A.Ciatti; G.Tosti; G.Tagliabue; C.Riva

Department of Human Morphology, University of Insubria, Varese, Italy

BACKGROUND Oral carcinoma (OC) is a neoplasia of old men. Tumors may arise in any part of the oral cavity and the most common sites vary geographically. The aim was to analyze clinicopathological features of a series of OCs and to evaluate outcome according to the location and tumor stage.

METHOD A series of 240 consecutive primary OCs collected from 1985 to 2005 was investigated for following parameters: age, sex, anatomic site, size, macroscopic appearance, histotype, grade, type of surgery, surgical margins, stage and follow up. RESULTS: OCs were more frequent in males (76%), with an average age at diagnosis of 63.1 years (vs women age 70.1 ys). Most frequently tumors were ulcerated (73%), the size ranged from 0.4 to 7 cm (average: 2.3 cm) and surgical margins were free in 87.1% of the cases. SCC was the most common histotype (93%) and the majority of cases were G2 (62.9%) or G1 (23.8%) tumors. Early stages (T1 and T2) were most commonly observed (83%) and cervical node involvement was present in 36/88 (42%) patients.The locations of OCs were tongue (38.3%), mouth floor (16.6%), lip (15%), palate (10.4%), retromolar pad (7.5%), gingiva (4.5%), cheek (2.5%) and oral cavity NOS (4.5%); subsites mostly involved were lateral tongue and lower lip. Retromolar tumors showed a male predilection, while gingival ones were more frequent in females. The survival rate was 51% (mean follow up:62.2, range: 3–96 months), while 19% of patients died of disease and 30% of other cause. OCs of lip, cheek and gingiva showed a favourable outcome while retromolar, oral cavity NOS, tongue and floor tumors had a worst prognosis.

CONCLUSION OC is more frequently observed in early stages, in males over age of 60 years, the more common site is the tongue. The site of presentation may play a role in survival outcome.

P-292

Activated MAP-kinases show coordinated expression in salivary gland adenoid cystic carcinoma

A. Handra-Luca, P. Menard, P. Fouret

APHP, GHU Paris Nord et Ouest, Institut Gustave Roussy, France

Background: Little is known regarding the mitogen-activated protein kinase(MAPK) activation state in salivary gland adenoid cystic carcinoma(ACC).

Methods: We evaluated expression of the phosphorylated forms of ERK(pERK), JNK(pJNK), P38(pP38), and Ki67 by immunohistochemistry in 61 paraffin-embedded tumour specimen. The median value of the H-score (the proportion of stained tumour nuclei multiplied by the staining intensity of nuclei) and of the percentage of the Ki67 tumour nuclei were used as cutoff for classifying tumours as with high or low expression.

Results: The sex ratio was 15 men to 46 women. The median age was 50 years. Forty-two out of 61 tumors

(69%) developed in the minor salivary glands. The median tumour size was 20 mm. The 23 cases with stage IV presented with bone infiltration (17), skin or facial nerve extension (3), or metastases to the lungs (3). pERK, pJNK, and pP38 were expressed at high levels in 57%, 79% and 63% ACC, respectively. The rankings of scores for pairs of activated MAPK across tumours were correlated (pERK, pP38 tau 0.38 p=0.0004;pERK,pJNK tau 0.33 p=0.002; pP38, pJNK tau 0.45 p<0.0001). The Ki67index was high in 33/60 ACC.Among clinicopathologic characteristics, perineural invasion was correlated with high pJNK and high Ki67 index (p=0.005 and p=0.03, respectively). In the 42 patients with follow-up complete data for more than 5 years, pP38 (adjusted risk ratio 0.91, 95% CI 0.86 - 0.97) and Ki67 (adjusted risk ratio 1.05, 95% CI 1.00–1.10) could be used to fit a Cox regression model to overall survival (p=0.009). In univariate analysis, patients with pP38 positive tumours survived longer than those with pP38 negative tumours.

Conclusion: This study provided evidence that the activated MAPK pERK, pJNK and pP38, were coordinately expressed in salivary gland ACC. Perineural invasion was correlated to high Ki67 index and high pJNK expression.

P-293

Release of the soluble alpha chain of IL-15 receptor: a new tumor evasion mechanism associated with poor clinical outcome in head and neck cancer patients.

Cécile Badoual, Gregory Bouchaud, Nour El Houda Agueznay, Erwan Mortier, Stéphane Hans, Alain Gey, Fahima Fernani, Severine Peyrard, Pierre Laurent Puig, Patrick Bruneval, Xavier Sastre, Ariane Plet, Laure Garrigue-Antar, Françoise Quintin-Colonna, Wolf H Fridman, Daniel Brasnu, Yannick Jacques, Eric Tartour

EA 4054 Université Paris-Descartes. Faculté de Medecine. Ecole Nationale Vétérinaire d'Alfort. 94704 Maisons Alfort. Service d'Anatomie Pathologique. Hopital Européen Georges Pompidou. 75015 Paris. INSERM, U601, Groupe de Recherche Cytokines et Récepteurs, Institut de Biologie, 44035 Nantes. France. Department of Otorhinolaryngology-Head and Neck Surgery, Hôpital Européen Georges-Pompidou. 75015 Paris. Service d'Immunologie Biologique. Hopital Européen Georges Pompidou. Paris France. Centre d'Investigations Cliniques, Assistance Publique des Hopitaux de Paris, Paris. France. Université Paris-Descartes, Inserm, UMR-S775. 75006 Paris. France Service d'Anatomie Pathologique. Institut Curie. 75005 Paris. France.

IL-15 is a proinflammatory cytokine, as it induces the production of cytokines (IL-6, TNFα, IL-17...) which play a role in various inflammatory processes. A correlation between high intratumoral IL-15 concentrations and poor clinical outcome in lung and head and neck cancer patients has been recently reported. The purpose of this study was to investigate the role of the soluble chain of IL-15 receptor (sIL-15R), a natural regulator of IL-15, in head and neck cancer. Increased serum sIL-15R concentrations were found in head and neck cancer patients, as mean concentrations of sIL-15R were 5.8 pM for head and neck cancer patients and 0.35 pM for healthy donors (p<0.0001). Serum sIL-15R levels were significantly correlated with both locoregional control and survival. The locoregional control rate at 12 months was 78% for head and neck patients with no detectable serum sIL-15R versus only 48% for cancer patients with detectable sIL-15R (p=0.04). In addition, the 12-month survival rate in patients with no serum sIL-15R levels was 89%, versus 69% for patients with detectable sIL-15R levels (p=0.04). Multivariate analysis, including tumor stage, TNM grading, serum sIL-2R levels - considered as a powerful prognosis marker –, showed that the only significant prognostic factor independently related to locoregional control was the serum sIL-15R level (P=0.0065; relative risk, 1.078). On Cox multivariate analysis, only serum sIL-15R levels influenced overall survival probability (p=0.0059; relative risk 1.086). From these clinical results we tried to characterize this sIL-15R , determine its origin and propose some mechanisms to explain its association with poor prognosis. sIL-15R was mainly produced by tumor cells which express IL-15R *in situ* and *in vitro* both at protein and mRNA levels. This expression of IL-15R was found in 17 out of 48 tumors tested. In contrast, normal epithelium did not significantly express IL-15R Various arguments strongly suggest that sIL-15R is produced via proteolytic cleavage of IL-15R mediated by ADAM-17. A correlation was observed between ADAM-17 expression in tumor cells and serum sIL-15R concentrations. Tumor cells coexpress IL-15R and ADAM-17 *in vivo*. Surprisingly, sIL-15R did not act *in vitro* as an IL-15 antagonist but rather as an enhancer of IL-15-induced proinflammatory cytokines (IL-6, TNF , IL-17) that may promote tumor progression. This new tumor evasion mechanism based on amplification of the intratumoral inflammatory reaction is probably not restricted to head and neck cancer, as other tumors have been shown to release sIL-15R . Overall, these results support for the first time an original role of sIL-15R in inflammation and cancer.

P-294

Immunoexpression of hgfa in different degrees of invasion of carcinoma ex-pleomorphic adenoma

Cristiane Furuse; Albina Altemani; Ney Soares de Araújo; Vera Cavalcanti de Araújo

São Leopoldo Mandic Dental Research Center, Brazil

Carcinoma ex pleomorphic adenoma (CXPA) is a salivary gland tumour derived from the malignization of a benign tumour, the pleomorphic adenoma, usually from a long-standing or a recurrent pleomorphic adenoma. Hepatocyte Growth Factor (HGF) is a cytokine that induces many biological functions in not only hepatocytes but also in many epithelial cells. It plays roles in promoting cell migration and proliferation, angiogenesis, and apoptosis inhibition. Immunoexpression of HGFA has been investigated in CXPA using sixteen cases in different degrees of invasion– intracapsular, minimally and frankly invasive carcinoma. To this aim, we have analyzed positive cells in different areas. In residual pleomorphic adenoma, only the cells in the condroid and myxoid areas were positive. *In situ* areas of CXPA presented strong expression in all luminal cells. In intracapsular type, immunoexpression was detected in 2 of 4 cases, with positive cells only in focal areas next to the capsule. Minimally invasive ones presented increased area of positive cells, with variable pattern among the tumours, including areas of in situ carcinoma and small nests in invasive areas. In frankly invasive CXPA with only epithelial component, 2 cases were negative and 3 positive. An increased number of positive cells was observed when compared with the previously described subtypes. In well-circumscribed large cellular blocks, most of the cells were strongly positive for HGFA. In the small nests, strong immunostaing was observed even in individually detached cells. Some small nests with basaloid cell profile were negative. In all the four cases of frankly invasive CXPA with epithelial and/or myoepithelial component studied, the cells were negative. HGFA was present in CXPA with epithelial component, with increased number of positive cells following tumour progression. This fact may indicate a possible role of the HGFA in the invasion progress.

P-295
Angiogenic switch in salivary carcinomas with and without myoepithelial differentiation

Ana Flavia Costa; Vera Lúcia Leite Bonfitto; João Felipe Leite Bonfitto; Cristiane Furuse; Vera Cavalcanti de Araújo; Konradin Metze; Altemani A
Department of Pathology, Medical Science Faculty, University of Campinas (UNICAMP); CPO São Leopoldo Mandic, Brazil

BACKGROUND: Tumor angiogenesis has been considered a putative target for cancer therapy. In a previous study we have shown salivary carcinoma with myoepithelial component arising in pleomorphic adenoma presented lower angiogenesis than those without such differentiation. The process of angiogenesis is influenced by the net balance between angiogenic factors that stimulate and those that inhibit vessel growth, and in vitro syudies have suggested that myoepithelial cells may inhibit angiogenesis. In order to investigate the hypothesis whether other salivary carcinomas (non ex-pleomorphic adenoma) with and without myoepithelial differentiation could also present difference regarding degree of angiogenesis, we compared tumor vascularization between mucoepidermoid carcinomas (neoplasias without myoepithelial component) and adenoid cystic carcinomas (neoplasias with myoepithelial component). These tumors are considered the two more frequent salivary carcinomas. METHOD: In 37 mucoepidermoid carcinomas (MEC) and 31 adenoid cystic carcinomas (ACC) tumor vascularization was assessed by measuring microvessel density (MVD) in sections stained for CD34 (a pan-endothelial marker) and CD105 (a neoangiogenesis marker). For both markers MVD was calculated in three hot spot areas in intratumoral as well as in peritumoral regions. RESULTS: Whereas the CD34 values did not differ among the tumors, MVD for CD105 was significantly higher in MEC than in ACC (p=0,0004). In both carcinomas, the intratumoral region was the site with more marked angiogenesis (MEC - mean 12.91; ACC - mean 5.10). Regarding histological tumor grade MVD for CD105 did not differ significantly between: a) high grade and intermediate/lowgrade MECs and b) solid and tubular/cribriform ACCs. CONCLUSIONS: The antibody CD105 reflects better the salivary carcinoma's angiogenic switch than CD34. The degree of neoangiogenesis differs significantly between MEC and ACC suggesting that tumors with myoepithelial component, such as ACC, possibly have an angiogenic phenotype that leads to a low tumor-induced angiogenesis.

P-296
Chondromyxoid fibroma of the zygoma

Esther Diaz; Maria Rosa Ortiz; Graciela Barraza; Mariana Turell; Josep Puig; Lluis Bernado
Hospital Universitari de Girona Doctor Josep Trueta, Spain

Background: Chondromyxoid fibroma (CMF) is a rare benign neoplasm of bone with an extremely unusual involvement of facial skeleton, most often the mandible and maxilla. Zygoma involvement is even more uncommon and to date only two cases have been reported in this location. We report a case of CMF arising on the zygomatic arch in a young woman.
Method: Diagnosis was established following the WHO definition. Immunohistochemistry (IHC) was performed using antibodies against smooth muscle actin (SMA), CD 34 and S-100 protein.

Results: A 34 year-old woman presented with light expansion over her right zygomatic region of 6 month duration. She revealed a radiolucent well-circumscribed lesion of about 3 cm in diameter in the right zygoma with scalloped borders, expansion and apparent disruption of the cortical bone. A surgical curettage was performed. Light microscopy showed a tumor with a lobular-like arrangement. It was composed of hypocellular myxochondroid areas with randomly arranged stellate or spindle shaped cells. The tumor cells were devoid of pleomorphism, atypia or mitoses. The lesion also revealed densely cellular regions containing sparse osteoclast-like multinucleated giant cells. No areas of necrosis were identified. Focal coarse calcification was observed. By IHC the tumoral cells expressed SMA and showed negativity for S-100 protein and CD 34. The patient has no symptoms or signs of recurrence 3 years after the curettage.
Conclusion: CMF is an important consieration when diagnosing facial chondroid tumors, particularly in young patients. It should be distinguished from myxoid chondrosarcoma, especially in small biopsies.

P-297

Fetal rhabdomyoma of the head and neck: clinicopathologic features of one case with comparative genomic hybridization (CGH) analysis

Amparo Sáez; M.Rosa Escoda; Mireia Yébenes; Rubén Carrera; Ruth Orellana; Francisco Javier Andreu; Oscar Escuder; Jesús Luelmo; Merçè Rey.
UDIAT Centre Diagnòstic. Corporació Sanitària Parc Taulí, Spain

Background: Extracardiac rhabdomyomas are exceptionally rare benign tumors that have a proclivity to occur on the head and neck region. Cytogenetic study of an adult rhabdomyoma has demonstrated clonal chromosome (Chr) abnormalities (reciprocal translocation between Chr15 and 17 and abnormalities of the long arm of Chr 10). CGH analysis of rhabdomyosarcoma has identified chromosomal gains and several regions of loss, such in Chr 16. We report a fetal intermediate rhabdomyoma analysed by CGH. **Method:** Freshly frozen tumor samples were obtained. CGH was performed as described by Kallioniemi, reagents and protocol modifications from Vysis® and preparations were analyzed using Isis™ software, (Metasystems®). Gains and losses were determined when the 95% confidence interval of the immunofluorescence ratio did not contain the value 1.0. Positive and negative controls were included. **Results:** A 30-year-old man with a 17-year history of an asymptomatic, solitary mass on the filtrum crest of the nose. Physical examination disclosed a whitish, firm nodule, 2×2 cm in diameter. Magnetic Resonance Imaging revealed a soft tissue mass, ruling out the presence of cartilage or bone involvement. A surgical excision was carried out. Histopathologycal examination disclosed a tumor with broad fascicles of spindled cells simulating a smooth muscle tumour and strap-like striated muscle cells without cytological atypia. Immunohistochemical studies revealed immunoreactivity for vimentin, muscle specific actin (HHF35), desmin, smooth muscle actin and bcl2. Moreover, the cells showed focal expression of myoglobin, CD117, and were negative for CD34, CD31, EMA, S100 Protein, HMB45 and CAM 5.2. No chromosomal imbalances in the entire tumor genome were detected by CGH. **Conclusions:** The histopathologycal features of this case correspond to a fetal intermediate rhabdomyoma. No gains and losses of chromosomal regions were detected by CGH analysis of the case. However, balanced translocations cannot be excluded utilizing CGH technique.

P-298

The characteristics of inflammatory restoration period in different skin wounds of facial area during experiment

Tatiana Fedorina; Tatiana Brailovskaya
Samara State Medical University,Russia

Optimizing factors in treating wounds of mandibular-facial area is rather urgent, that's why our *aim* was to give morphofunctional estimation of skin wound edges and surrounding tissues depending on the mechanism of injury, changes in adjacent and remote tissues, location, depth and direction of wound defect, it's form and degree of wound edge tension, time of putting stitches. *Materials and methods.* Experiment was carried out on adult white lab rats of both genders, weight about 300 grams. Under aether anaesthesia (with the help of anaesthesia mask developed for rats) animals were inflicted different kinds of wounds. Operative treatment, including mobilization of tissues with the following putting stitches with different materials, was carried out under aether anaesthesia in early stages after trauma (15 minutes – 4 hours) and late stages (1–7 days). Animals were not excluded from the experiment; taking tissues for morphological investigation was performed under local anaesthesia with novocain during surgical intervention; it was also performed on decapitated animals on the same stages after putting stitches. *Results of investigation.* With the help common histological, histochemical, immunohistochemical, enzyme-chemical, cytological, morphometrical methods of investigations we revealed a certain dependence of wound process on the original stages of wound defect edges, surrounding and remote tissues, degrees of wound edges tension, type of stitch material, time of putting stitches. *Conclusion.* Morphofunctional investigation of inflammatory restoration

process in skin and soft tissues characteristics in experimental animals will help to increase efficacy of surgical treatment for patients with different wounds and their locations, in particular in mandibular facial area.

P-299

Evaluation of EGFR, Her-2/neu and Cyclin D1 Protein and Gene Copy Number in Head and Neck Squamous Cell Carcinomas

Tim Helliwell; Nisreen Gaber; Andrew Jones
University of Liverpool, UK

Background The EGFR signalling pathway is considered to be important in controlling the growth of squamous carcinomas of the head and neck (HNSCC) and is a potential therapeutic target.
Methods Tissue microarrays of 200 cases of HNSCC (45 oral cavity, 72 pharynx and 83 larynx) and their nodal metastases (83 cases) have been constructed. This study has evaluated the immunocytochemical expression of epidermal growth factor receptor (EGFR), phosphorylated EGFR, Her-2 and cyclin D1 proteins, and of EGFR and HER-2 gene expression by FISH. Protein expression was defined as high or low according to the median value of % positive cells. Gene amplification was present when the ratio of signals for the gene and centromeric probes was >2. Minimum clinical follow-up is five years and the main clinical end points were nodal metastasis and survival.
Results Median survival was 14 months, and overall survival was longer in cases without nodal metastasis (log-rank, $p=0.011$). Expression of EGFR was observed in 86%, Her-2/neu in 37% and cyclin-D1 in 94% of cases by immunocytochemistry. High EGFR and cyclin-D1 expression were associated with poorly-differentiated carcinomas ($p<0.037$; <0.001 respectively); high cyclin-D1 expression was associated with pharyngeal site ($p<0.001$) and nodal metastasis ($p<0.013$).
EGFR and HER-2 gene amplification were seen in 13 and 11 cases respectively. Polysomy for centromeric probes was seen in 84% cases for chromosome 7 and 53% for chromosome 17. Protein and gene expression for EGFR and HER-2/neu were significantly correlated in primary carcinomas ($p<0.018$, 0.033 respectively) and in nodal metastases. Gene expression was not associated with prognosis.
Conclusions Immunocytochemical labelling for cyclin-D1 is of prognostic value in HNSCC. FISH analysis of EGFR and HER-2 does not provide additional prognostic value.

P-300

Unusual Localisation of a Bronchogenic Cyst

Zeynep Türkşen; Ayla Tezer; Gulcin Guler Simsek; Heyecan Ökten; Ömer Faruk Taner
Kecioren Eğitim Araştırma Hospital, Turkey

Bronchogenic cysts are rare, most commonly seen in the skin and subcutaneous tissues of just above the sternal notch: usually on the anterior of the neck or on the chin.
In our case, the cyst lined with pseudostratified columnar epithelium with cilia and goblet cells, was located on the eyelid. The patient is 19 years old and nothing know about the lesion until this time.

P-301

BUCCOMAXILLOFACIAL LESIONS IN THE ELDERLY: A STUDY OF 545 CASES

Ana Lídia T. Costa; Wanessa M. Silva; Denise Tavares; Flávia A. Oliveira; Eneida F. Vêncio
Department of Oral Pathology, School of Dentistry, Federal University of Goiás (UFG) and Department of Pathology, Tropical Pathology and Public Health Institute of the UFG, Goiânia, GO, Brazil

Background: studies of the lesions in the buccomaxillofacial area in elderly patients were not frequently related. The aim of this study was to describe the epidemiological aspects of buccomaxillofacial lesions in elderly patients. Method: the archives from the Oral Pathology Laboratory of the Federal University of Goiás were reviewed and the data obtained were from 1956 to 2006. Results: of a total of 4885 cases, 11.1% (545) were elderly patients ≥60 years old. The median age was 65 (60 to 95) years, and seventh decade of life (60 to 69 years) being the most frequent (42.4%, 231). There was a predominance of females in 63.1% (344) of the cases. The maxilla was the most affected (30.7%, 151), followed by the mandible (26.6%, 131) and jugal mucosa (19.1%, 94). Inflammatory lesions were the most frequent (62.9%, 343), being 76.7% (263) fibroepiteliais hyperplasias (traumatic lesions). Tumors were the second most frequent category, 9.2% (50) of the cases affected by malignant tumors and 6.4% (35) by benign tumors. Conclusion: among the elderly studied the lesions in the buccomaxillar area predominated in women and in the maxilla. The inflammatory lesions were the most frequent.

P-302

INTRAORAL MINOR SALIVARY GLAND TUMOR: AN EPIDEMIOLOGICAL STUDY OF 85 CASES

Claúdia T. Taveira; Aline A. Máximo; Flávia A. Oliveira A; Rita C. Alencar; Eneida F. Vêncio

Oral Pathology Department, School of Dentistry, Federal University of Goiás; Pathology Department, Cancer Hospital Araújo Jorge and Pathology Department, Tropical Pathology and Public Health Institute (IPTSP/UFG), Goiânia-GO, Brazil

Background: salivary gland tumors are uncommon, and they represent 2 to 6.5% of all head and neck neoplasms. Among them, intraoral minor salivary gland tumors corresponding to 9 to 23%. Few studies have shown epidemiological data of intraoral minor salivary gland tumors. The aim of this study is to present an epidemiological study of intraoral minor salivary gland tumors in a Brazilian population. Methods: the demographic data and diagnosis was reviewed in the anatomo-pathologic archives and corresponded to period of 10 years (1996 to 2005). Results: of 599 salivary glands tumors retrieved, 87 cases (14.5%) affected minor salivary glands. Women were the most affected with 61% (53 cases) in a male:female ratio of 1:1.6. The age ranged from 15 to 87 years old (with median age of 48 years). The palate was the most affected site with 70% of cases (61), followed by jugal mucosa with 6.9% (6) and tongue with 5.7% (5). Malignant tumors were the most frequent with 57.5% (50) of the cases, being the mucoepidermoid tumor and the adenoid cystic carcinoma the most frequent histopathologic types with 32% (16) of cases. Among benign tumors, pleomorphic adenoma was verified in 86.5% (32) of cases. Malignant tumors were more frequent in women with 62% (31) of the cases, $p>0.05$. Both adenoid cystic carcinomas and mucoepidermoid tumors predominated in women with 68.7% and 62.5% of cases, respectively, $p>0.05$. Conclusion: an epidemiological study of intraoral minor salivary gland tumors in a Brazilian population is presented. The palate was the most frequent location; malignant tumors predominated and women were more affected.

P-303

Tracheal chondrosarcoma

Ana Fuertes; Francesc Felipo; Isabel marquina*;Mar Pascual; Guillermo Muñoz; Patricia Sota; Celia Del Agua

*Hospital Universitario Miguel Servet. *Hospital de Alcañiz, Spain*

BACKGROUND The most frequent tracheal malignant tumour is squamous cell carcinoma (80–90%). Respiratory tract chondrosarcomas represent just 0,2% of all malignant neoplasias; despite this, it is the most common mesenchimal tumour. Cricoid cartilage is its most usual location.
METHODS We present the case of a 73 year-old male whose scanner showed a 32 mm solid mass with numerous inner calcifications, infiltrating anterior wall of the trachea, destroying cartilage and growing into the lumen. Resection of the lesion is performed.
RESULTS Pathological examination reveals a rounded lesion of 45 mm in its greatest dimension, hard and well delimitated. Surface cut is shiny, gray-white with calcified areas. Histologically it corresponds to grade 1 chondrosarcoma that affects resection margins.
COMMENTS Tracheal chondrosarcoma is an extremely rare tumour. In our literature review we have found just 15 published cases. In most of them the patients are males, the tumour is low grade and clinical presentation is airway obstruction. Main differential diagnosis is with chondroma, which is a less celular benign tumour, with no atipia or infiltration, never larger than 20 mm, as recommended by WHO.

P-304

HUGE RETROPHARYNGEAL LIPOMA CAUSING OBSTRUCTIVE SLEEP APNEA: A CASE REPORT

Grzegorz Namysłowski; Dariusz Lange; Wojciech Ścierski; Maciej Misiołek; Natalia Urbaniec; Agata Stanek-Widera

Department of Otolaryngology, Silesian Medical University, Zabrze and Institute of Oncology Gliwice, Poland

Lipoma of the retropharyngeal space is a very rare benign tumor often causing unspecific clinical symptoms. The most common symptoms are dysphagia and/or respiratory disturbances. The clinical diagnosis may be difficult. The radiological imaging techniques (CT and MRI) can provide adequate information with regard to the composition and extension of the tumor, although final histological confirmation is essential. Surgery is the treatment of choice. We present a case of 40-year-old male patient complaining of obstructive sleep apnea symptoms (respiratory disturbances, excessive daytime somnolence, morning headache). The radiological examination (CT) showed a huge (11.7× 7.2 cm) lipoma of the retropharyngeal space extending from the nasopharynx to the superior mediastinum. The tumor was removed via transcervical approach with complete amelioration of symptoms.

P-305

Tight junction claudin-7 downregulation is implicated in advanced stages of oral squamous cell carcinoma

Silvia Vanessa Lourenço; Cláudia Malheiros Coutinho-Camillo; Marcilei E. C. Buim; Ana Carolina de Carvalho; Roberta Cardim Lessa; Cláudia Pereira; André Luiz Vettore; André Lopes Carvalho; Luiz Paulo Kowalski; Fernando Augusto Soares

Department of General Pathology, Dental School, University of São Paulo; Hospital A.C. Camargo; Department of Biological Sciences, Federal University of São Paulo - Brazil

Background: Claudins, a large family of essential tight junction (TJ) proteins are abnormally regulated in human carcinomas, suggesting that they might represent potential targets for cancer detection, diagnosis and therapy. In a previous study, we have showed that several claudins are altered in the oral squamous cell carcinoma (OSCC) cases analyzed and that there is an association between these alterations and clinico-pathological characteristics of these tumors. **Method:** In this study, using a Tissue Microarray (TMA) comprising 133 cases of OSCC, we have analyzed the expression of claudin-7 by immunohistochemistry. We have also studied the expression of claudin-7 mRNA transcripts and methylation status of the claudin-7 promoter region. **Results:** Claudin-7 was almost absent in the majority of the cases - 9.1% of the cases showed strong expression of claudin-7 and 90.9% of the cases showed mild or no expression of claudin-7. Loss of claudin-7 was associated with advanced stages of OSCC ($p=0.044$) and tended to be more frequent in moderately/poorly differentiated tumors ($p=0.055$). Loss of claudin-7 was also associated with depth of invasion higher than 3 mm ($p=0.020$). Disease-free survival is significantly shorter in claudin-7 negative patients ($p=0.015$). Expression of the mRNA transcript of claudin-7 gene was assessed and down-regulation of claudin-7 transcripts was detected in 77.78% of the cases analyzed. As methylation is one of the mechanisms involved in downregulation of claudins, the methylation status of the promoter region of claudin-7 was investigated. We found that treatment of O28 cells (that did not express claudin-7 mRNA transcripts) with 5-Aza-2′-Deoxycytidine (5-Aza-dC) leaded to the re-expression of claudin-7 mRNA transcript. **Conclusion:** Our data suggests that loss of claudin-7 expression might be associated with the tumorigenic process of OSCC and it is associated with a poor prognosis. Furthermore, claudin-7 downregulation is problaby due to its promoter hypermethylation.

P-306

Primary oral mucosal melanoma: analysis of tetraspanin CD63 in a tissue microarray of 35 cases

Marcilei Eliza Cavicchioli Buim; Sheyla Batista Bologna; Cláudia Malheiros Coutinho-Camillo; João Gonçalves Filho; Gilles Landman; Fernando Augusto Soares; Silvia Vanessa Lourenço

Department of Pathology, Hospital A.C. Camargo; Department of General Pathology, Dental School, University of São Paulo; Department of Head and Neck, Hospital A.C. Camargo, São Paulo - Brazil

Background: Tetraspanins comprise a family of proteins with functional roles in a wide array of cellular processes and have been reported to be associated with the biological behaviour of solid tumors, especially with their metastatic potential. CD63, a tetraspanin membrane protein, has been suggested to play important role in the regulation of skin melanoma progression, being strongly expressed in early stages of the disease and downregulated in advanced stages. Little is know on the adhesion and molecular mechanisms of oral mucosal melanomas due to the rarity of the lesions. These melanomas are in general very aggressive and have poor prognosis. Modulation of CD63 may be involved with the aggressive behaviour of oral mucosal melanomas, but no studies investigated this possibility. **Method:** The present study analyzed the expression of the tetraspanins CD63 is oral melanoma using immunohistochemistry. Tissue Microarray (TMA) of 35 cases of oral melanoma and 09 normal tissue of oral cavity were evaluated immunomorphologically and semi-quantitatively, and results were compared to the clinical-pathological features and qui-square test were used for statistical analysis. **Results:** Expression of CD63 was observed in the cytoplasm of all melanocytes in the controls of normal oral mucosa. Downregulated/negative expression was observed in 23/35 (66.0%) of oral melanomas included in the array. Loss/downregulation of CD63 in oral melanoma was statistically significant when compared with the normal controls ($p<0.001$). There was no correlation between expression of CD63 and clinical-pathological parameters analysed, such race, age, sex, metastasis, recurrence, histological grade and size of tumor. **Conclusion:** Our results suggest that reduction or loss of CD63 expression is involved with the complex mechanisms of oral melanomas, and possibly contribute with other mechanisms that culminate with disease progression.

P-307

Transforming Growth Factor beta 1, beta 2 and beta 3 in human developing teeth: immunolocalization according to the odontogenesis phases

Fernando Augusto Soares; Cláudia Malheiros Coutinho-Camillo; Marcilei Eliza Cavicchioli Buim; Ana Paula Sassá Benedette; Ana Paula Veras Sobral; Silvia Vanessa Lourenço

Hospital A.C. Camargo; Department of General Pathology, Dental School, University of São Paulo; Universidade Estadual de Pernambuco - Brazil

Background: Transforming Growth Factor beta (TGF beta) is a multifunctional growth factor that has several biological effects in vivo, including control of cell growth and differentiation, cell migration, lineage determination, motility, adhesion, apoptosis, synthesis and degradation of extracellular matrix, and plays an important role in regulating tissue repair and regeneration. **Method:** Our study analyzed the participation of TGF beta 1, beta 2 and beta 3 in the different stages of morphogenesis and differentiation of human developing dental organ using immunohistochemistry. For this purpose maxilla and mandible of 10 human embryos ranging from 8 to 23 weeks of gestation were employed, according to the approval of the Ethical Committee. **Results:** TGF beta subunits – beta 1, beta 2, beta 3 were present in the various stages of tooth development, but the expression varied according to the differentiation stage, tissue and TGF beta subunit. TGF beta-1 was strongly expressed in the enamel epithelium from dental lamina up to late bell stage where it was detected in the external epithelium, stellate reticulum, stratum intermediate, preameloblasts and ameloblasts. TGF beta-2 presented mild positivity from bud stage, mainly in the enamel organ epithelium and this positivity was maintained up to bell stage. TGF beta-3 was mainly negative, with sparce positivity detected only in the dental papilla and odontoblasts. **Conclusion:** Our results indicated that TGF beta-1 is closely related to differentiation of enamel organ and initiation of matrix secretion, TGF beta-2 to cellular differentiation and TGF beta-3 to mineral maturation matrix.

P-308

Human salivary gland morphogenesis: expression of galectins-1 and -3 during the different developmental phases

Cláudia Malheiros Coutinho-Camillo; Jee Hee Park; Marcilei Eliza Cavicchioli Buim; Fernando Augusto Soares; Silvia Vanessa Lourenço

Hospital A.C. Camargo; Department of General Pathology, Dental School, University of São Paulo - Brazil

Background: Galectins are members of animal lectins that bind b-galactosides through the sequence elements of carbohydrates recognition-binding domain (CRD). Fourteen members of galectin family have been identified and galectins 1 and 3 (Gal-1 and Gal-3) are the best-studied members. They participate in biological processes such as development, differentiation, cell adhesion, cell/matrix interactions, growth, apoptosis, tumorigenesis and metastasis. Expression of these proteins has been described in salivary gland neoplasms, but their participation in salivary gland morphogenesis, which involves co-ordinated events and molecules have not yet been determined, and may be an important key for the understanding of tumorigenesis. **Method:** The present work analysed the expression of Gal-1 and Gal-3 during developmental stages of human salivary glands using immunohistochemistry. The specimens were obtained from foetuses ranging from 8 to 24 weeks of gestation, according to the approval of the Local Ethical Committee. **Results:** In adult fully developed salivary glands (controls) Gal-1 was detected in the cytoplasm of acinar cells and Gal-3 was expressed in ductal cells along the entire extension of the ductal system (from intercalated duct up to excretory portion). In human developing glands, Gal-1 was detected in the glandular stroma in all phases of morphogenesis and in the cytoplasm of rudimentary acinar cells. Gal-3 was not detected in the bud stage of gland development but its expression was increasingly observed in epithelial cells during canalization and branching phases and its greatest expression occurred in the ductal system of the advanced stages of salivary gland development (advanced cytodifferentiation). **Conclusion:** Expression of gal-1 and gal-3 in developing human salivary glands is gradual and complementary during the different phases of glandular morphogenesis. This pattern is probably related to the fully developed salivary gland functions.

P-309

Alveolar rhabdomyosarcoma of the maxillary sinus in an adult

Abdelfettah Zakhama; Leila Njim; Abdelmajid Dhouibi; Rym Hadhri; Néjib Ben Yahia; Houda Mahmoudi; Adnène Moussa

Department of Pathology, Fattouma Bourguiba University Hospital, 5019 Monastir, TUNISIA

Background: Sites in the head and neck region are among themost frequent locations of rhabdomyosarcoma (RMS) in patients younger than 15 years. However, comparable neoplasms in adults are very uncommon and often of embryonal type. We report a case of alveolar RMS of the maxillary sinus in an adult with a review of the main

findings concerning pathology, molecular biology and differential diagnosis.
Methods A 31-year-old female, with no significant medical history, complained for paranasal sinus tumefaction associated with ophtalmic manifestations. CT scan documented a maxillary sinus mass involving the orbital floor. There was no evidence of direct extension into the orbit. Surgical biopsy of this mass was achieved.
Results: The pathological examination of the mass biopsy was consistent with an alveolar RMS which demonstrated the presence of round to oval cells arranged predominantly in sheets. Immunohistochemically the cells were positive for desmin and myogenin. The molecular biology showed the characteristic PAX3-FKHR fusion gene. Despite combination chemotherapy and radiation, the patient died of her illness within one year with disseminated metastases.
Conclusion: RMS, notably of the alveolar type, rarely present in the head and neck of adults, but should be considered in the differential diagnosis of a small cell neoplasm in patients during the third and fourth decade of life. Genetic testing may be successfully used for diagnosis and may guide therapy in future clinical trials. Despite the poor prognosis, prompt diagnosis and palliative radiotherapy may improve the qualityof life for patients with terminal disease.

P-310
TELOMERASE CATALYTIC SUBUNIT HTERT EXPRESSION IN PATIENTS WITH PRECANCEROUS LESIONS OF THE LARYNX

Józef Kobos (1); Wioletta Pietruszewska (2), Marcin Durko (2),
(1)Department of Pathology of the Age of Development, Medical University of Lodz (2) Department of Otolaryngology, Chair of Otolaryngology, Medical University of Lodz, Poland

Telomerase is a specific enzyme which functions as a reverse transcriptase. It synthesizes telomeric repeats at the chromosomes' endings, protecting them from excessive shortening and damaging important genes. The correlation between telomerase activity during cellular immortalization and reactivation in tumours has led to the view that telomerase reactivation is required for tumour growth. Nevertheless the telomerase reactivation in precancerous lesions is still unclear. The diagnosis and treatment of premalignant lesions of larynx has been frustrated because of failure to adequately define the histologic changes that may predict the potential for progression to invasive squamous cell carcinoma.
The aim of our study is the evaluation of catalytic subunit of telomerase (hTERT) expression in precancerous lesions of the larynx as well as its impact on possibility of neoplasm progression.
Patients and methods: The research was conducted on the group of 104 patients with precancerous lesions of the larynx, which were operated in direct microlarygoscopy. Immunohistochemical staining of paraffin sections was performed using monoclonal antibody NCL-hTERT (Novocastra) against telomerase protein and avidine – biotin – peroxydase detection system ABC.
Results: Telomerase expression was detected in 100% patients with precancerous lesions with the intensification between 5% and 75% as nuclear reaction in the form of brown granulations. The mean hTERT expression equalled 18,4% in simple hyperplasia, 24,8% in abnormal hyperplasia, 46% in atypical hyperplasia and 55,7% in carcinomas in situ.
Statistically significant dependence in hTERT expression was stated between simple hyperplasia in relation to abnormal and atypical hyperplasia as well as to carcinoma in situ ($p=0{,}001$; $p=0{,}002$; $p<0{,}01$). Similar observation was made between abnormal and atypical hyperplasia ($p=0{,}003$), whereas no statistically relevant dependence was found in telomerase expression between atypical hyperplasia and carcinoma in situ ($p=0{,}07$).
Conclusion: Telomerase expression increases in conjunction with the progression of the precancerous lesion and is potential factor which will facilitate diagnostication and making a prognosis in patients with precancerous lesions and cancer of the larynx.

P-311
POTENTIAL PROGNOSTIC IMPORTANCE OF MMP-1, 2 AND 9, AS WELL AS TIMP-1, 2 AND 3 IN PATIENTS WITH LARYNGEAL SQUAMOUS CELL CARCINOMA

Pietruszewska W.(1), Durko T.(1), Bojanowska-Pozniak K.(1), Kobos J.(2)
(1) Department of Otolaryngology, Chair of Otolaryngology, Medical University of Lodz, (2) Department of Pathology of the Age of Development, Medical University of Lodz, Poland

Matrix metalloproteinases (MMPs) are a family of proteolytic enzymes implicated in the invasion and metastasis of many cancers, because of their ability to degrade components of extracellular matrix. Their activity is regulated by specific tissue inhibitors of matrix metalloproteinases (TIMPs). MMPs and TIMPs was identified in many carcinomas, including cancers of head and neck region, lung, breast and colon. In most of the researches a strong

dependence between MMPs and TIMPs expression and clinical course of the disease was observed.
The aim of the research was to evaluate the expression of MMP-1, -2 -9 and TIMP-1, -2 -3 in laryngeal cancer cells and to investigate the prognostic impact of these factors in patients with laryngeal cancer.
Material and method: 104 patients with laryngeal cancer, that underwent surgical treatment were included in the study. Only cases with at least a 5-year follow-up were included. Immunohistochemical studies were performed on formalin fixed, paraffin embedded sections by using monoclonal antibodies against MMP-1, -2, -9 and TIMP-1, -2, -3 antigen and ABC detection system.
Results: For all of the markers diffuse, cytoplasmatic staining of tumorcells and some surrounding stromal cells was observed. There was a correlation between TIMP-2 and TIMP-3 overexpression and advanced carcinomas (p= 0,037 and p=0,022, respectively). Regarding the otherenzymes investigated we could not find any correlation between their expression and tumor's stage. We observed a strong association between MMP-2 expression and the presence of nodal metastses (p=0,013). It was found that the TIMP-2 overexpression was significantly more frequent in the tumors of patients facing lymph node metastases during the follow-up period compared with those having no nodal relapses (p=0,05). No correlation was observed between other enzymes expression and nodal status and nodal or local recurrences. We found that positive immunostaining of MMP-1, -2, -9 and TIMP-1, -2 was significantly related with higher tumor grade. Specially strong correlation was seen between TIMP-2 and differentiation (p<0,001). There was no association between TIMP-3 expression and grading. We found that tumors expressing TIMP-2 were significantly associated with a poorer prognosis. Patients with TIMP-2 positive expression had diminished both overall and disease-free survival (p= 0,049). Besides the overall survival was shorter in cases with positive MMP-9 expression. This correlation was statistically borderline (p=0,07). The survival analysis revealed no difference between overall and disease-free survival time of patients in groups with positive and negative expression of MMP-1, -2 and TIMP-1, -3.
Conclusions: Our data suggest the existence of correlation between expression of MMPs and TIMPs and clinicopathological features of laryngeal carcinoma. Moreover TIMP-2 is a significant prognostic parameter for patients with laryngeal cancer.
We observed a strong association between MMP-2 expression and the presence of nodal metastses (p=0,013). It was found that the TIMP-2 overexpression was significantly more frequent in the tumors of patients facing lymph node metastases during the follow-up period compared with those having no nodal relapses (p=0,05). No correlation was observed between other enzymes expression and nodal status and nodal or local recurrences. We found that positive immunostaining of MMP-1, -2, -9 and TIMP-1, -2 was significantly related with higher tumor grade. Specially strong correlation was seen between TIMP-2 and differentiation (p<0,001). There was no association between TIMP-3 expression and grading. We found that tumors expressing TIMP-2 were significantly associated with a poorer prognosis. Patients with TIMP-2 positive expression had diminished both overall and disease-free survival (p=0,049). Besides the overall survival was shorter in cases with positive MMP-9 expression. This correlation was statistically borderline (p=0,07). The survival analysis revealed no difference between overall and disease-free survival time of patients in groups with positive and negative expression of MMP-1, -2 and TIMP-1, -3.

P-312
Fhit and Wwox Expression in Mucoepidermoid and Adenoid Cystic Carcinomas

Nazmiye Dincer 1; Gaye Guler Tezel 1; Cigdem Himmetoglu 1; Kay Huebner 2; Gulnur Guler 1; Arzu Sungur 1

1 Hacettepe University Faculty of Medicine Department of Pathology; 2 Ohio State University, Department of Molecular Virology, Immunology and Medical Genetics, USA

Background: Mucoepidermoid carcinoma (MEC) and adenoid cystic carcinoma (ACC) are salivary gland neoplasms with divergent morphological features and clinical behaviour. ACC is a basaloid tumor whereas MEC is a glandular-epithelial neoplasm. FHIT and WWOX are tumor suppressor genes that encompass the FRA3B and FRA16D fragile sites at chromosomes 3p14.2 and 16q23.3–24.1, respectively. In our previous studies, we have shown concordant loss of Fhit and Wwox expression in breast cancer, significantly more in basal like phenotype. To test if there is a similar association in salivary gland neoplasms, we designed this study on tissue microarrays (TMA).
Methods:TMAs were constructed from 25 MEC and 19 ACC of salivary gland. Fhit, Wwox, CK14, CK5/6, CK19, SMA and p63 immunostainings were performed on TMAs. Expression in more than 10% of tumor cells was accepted as positive for CK14, CK5/6, CK19, SMA and p63. Expression of Fhit and Wwox in more than 50% of neoplastic cells were assessed as positive while any other expression level was accepted as reduced. Correlations between immunohistochemical markers and their relation with histological type were determined.

Results: Reduced Fhit and Wwox expression was significantly more common in ACC (p=0.012, p=0.003, respectively). There was a negative association between Fhit and Wwox with SMA (p=0.004, p=0.01, respectively). The relation between Fhit and Wwox expression and CK5/6, CK19 and p63 were not significant. Wwox and CK14 expression related negatively (p=0.02) while there was no relation between Fhit and CK14.
Conclusion: Our results suggest that reduced Fhit and Wwox expression might have a role in the pathogenesis of basaloid differentiation in salivary gland neoplasms similar to breast cancer. Studies designed on basaloid tumors of other organ systems may show similar findings and these results may have implications on treatment modalities designed for basal like tumors.

P-313
INTERGRIN LINKED KINASE (ILK) AND p-Akt EXPRESSION IN LARYNGEAL CANCER.

Anastasios K. Goulioumis, Helen Papadaki, Vasiliki Bravou, Panos Goumas and Ioannis Varakis.
Anatomy- Histology- Embryology department, medical Faculty, University of Patras, Patras, Greece

Background Laryngeal carcinoma has an ominous progression because of local invasiveness and nodal metastasis. It is evidenced in cases of many epithelial cancers that the ILK is a central molecule in many pathways that are being activated during the cancer formation which endow the cancerous cells with molecular and phenotypic traits that potentiates the cell to metastasize. Moreover p-Akt seems to be a downstream intervener of the ILK-activated molecular pathway which regulates many crucial events for the cancerous cell, like altered adhesion, inhibition of apoptosis and induction of angiogenesis.
Methods In order to examine the role of ILK and p-Akt in the pathogenesis of laryngeal cancer we evaluated the expression of these molecules using immunohistochemical methods in paraffin embedded tissue samples from 97 (n= 97) squamous laryngeal cancers. Statistical analysis was performed by SPSS for windows. The correlation between the expressions of the two proteins was evaluated by Spearman statistical test.
Results It was detected an increase expression of ILK and p-Akt in 81% and 76% of tumor specimens respectively, comparing to the normal controls. The correlation of expression pattern between ILK and p-Akt was statistical significant (p=0,003).
Conclusion The nodal role of ILK for the transition of a cancerous epithelial cell to a cell with all the proper molecular mechanisms that potentiates it to invade has been already described in cancer. This was the first time, to the best of our knowledge, the enhanced expression of ILK in laryngeal cancer to be described. Besides we have evidence that its action is applied probably through the already described pathway of PI3K-pAkt to which are attributed many of the aggressive characteristics of a metastatic cell. By making progress to the comprehension of the molecular mechanisms of the metastatic process, the nodal role of molecules, like ILK and p-Akt, are highlighted.

Uropathology

P-314
Extracellular matrix alterations in conventional renal cell carcinomas by tissue microarray profiling influenced by chronic low-dose ionizing radiation exposure in humans

Luisa Morell Quadreny1, Alina Romanenko2, David Ramos1, Valentin Nepomnyaschy2, Anna Iemelianova2, Alexander Vozianov3, Antonio Llombart-Bosch1
1Department of Pathology, Medical School of Valencia University, Valencia, Spain. Departments of 2Pathology and 3Urology, Academy of Medical Sciences of Ukraine, Kiev, Ukraine

Background. The accident at the Chernobyl power plant in Ukraine on April 1986, introduced for the first time the problem of chronic persistent low-dose exposure to ionizing radiation (IR). Redox homeostatic processes in the microenvironment, involving interaction between cell-cell and cell-extracellular matrix (ECM), asociated with cell-cell comunication in conventional (clear cell) renal carcinomas (cRCCs) in patients living more than 20 years after the Chernobyl accident in Cesium (137Cs) - contaminated areas of Ukraine.
Material an method. The ECM major components such as fibronectin, laminin, E-cadherin/β-catenin complexes as well as p53 tumor suppressor gene protein and transforming growth factor beta 1 (TGF-β1) were immunohistochemically (IHC) evaluated in cRCCs from 59 Ukrainian patients, wich represented 18 living in non-contaminated areas and 41 from 137Cs - contaminated areas. A control group of 19 Spanish patients with analogue tumors were also investigated. For IHC evaluation a tissue microarray technique was used.
Results. Decrease or loss and abnormal distribution of fibronectin, laminin, E-cadherin/β-catenin complexes accompanied by elevated levels of p53 and TGF-β1 were detected in the Ukrainian cRCCs from 137Cs- contaminated areas with statistically significant differences.
Conclusion. Our study suggests that chronic long-term, low-dose IR exposure migth result in global remodelling of

ECM components of the cRCCs with disruption in peri-epithelial stroma as well as epithelial basement membranes that leads to loss of cellular differentiation. These factors may also become relevant targets for novel therapeutic strategies.
Supported with a grant of the "Conselleria de Sanitat de la Comunitat Valenciana". Ref N° 909/2007
Supported with a grant from the University of Valencia

P-315

ALTERATION OF APOPTOTIC REGULATORY MOLECULES IN CONVENTIONAL RENAL CELL CARCINOMA INFLUENCED BY CHRONIC LONG-TERM LOW-DOSE IONIZING RADIATION EXPOSURE IN HUMANS REVEALED BY TISSUE MICROARRAY*

Alina Romanenko1, David Ramos2, Luisa Morell-Quadreny 2, Anna Iemelianova1, Alexander Vozianov3, Antonio Llombart-Bosch2**
DEPARTMENT OF PATHOLOGY. UNIVERSITY OF VALENCIA. MEDICAL SCHOOL. SPAIN

Background. During the 20-year period subsequent to the Chernobyl accident the morbidity of malignant renal tumours in Ukraine has increased from 4.7 to 9.0 per 100,000 of total population. Cesium 137 (^{137}Cs), which accounts for 90% of the internal radioactivity in the Ukrainian population exposed to long-term low-dose radiation and 90% of the more labile pool of ^{137}Cs, is excreted via the kidneys. The goal of our present study was to evaluate the status of pro- and anti-apoptotic regulatory molecules in conventional renal cell carcinomas (cRCCs) in Ukrainian patients.
Materials and Methods. Bcl-2, Bcl-x, BAX, death receptor (DR5), and transcriptional nuclear factor kappa B (NF-kB, with p50 and p65 subunits) were immunohistochemically (IHC) investigated using a tissue microarray technique in cRCCs from 56 Ukrainian patients, consisting of 18 patients living in non-contaminated areas and 41 patients from ^{137}Cs-contaminated areas. As a comparison, 19 Spanish patients with analogue tumours were also investigated.
Results. Our findings showed that BAX and DR5-positive cRCCs tend to increase among the Ukrainian patients living in the radio-contaminated areas along with the suppression of anti-apoptotic molecules (Bcl-2 and Bcl-x) and with p65 and p50 over-expression in these same tumours, with statistically significant differences.
Conclusions. Our study suggests that chronic long-term, low-dose radiation exposure might result in the alteration of apoptotic regulatory mechanisms, which in turn, could lead to enhanced tumour progression and resistance to apoptosis. These factors may also become relevant targets for novel therapeutic strategies.
*Supported with a grant of the "Conselleria de Sanitat de la Comunitat Valenciana". Ref. N 909/2007
**Supported with a grant from the University of Valencia

P-316

Gene amplification and protein expression of epidermal growth factor receptor (EGFR) in prostatic adenocarcinoma after hormonal therapy

Rebecca Marks 1; Stefano Gobbo 1,2; Rodolfo Montironi 3; Antonio Lopez-Beltran 4; Shaobo Zhang 1; Gregory MacLennan 5; Zhong Jiang 6; Suqin Zheng 1,7; Darrell Davidson 1; Liang Cheng 1
Departments of Pathology and Laboratory Medicine 1, Indiana University School of Medicine, Indianapolis, IN; Department of Pathology 2, Universitá di Verona, Verona, Italy; Institute of Pathological Anatomy and Histopathology 3, School of Medicine, Polytechnic University of the Marche Region (Ancona), United Hospitals, Ancona, Italy; Department of Pathology 4, Cordoba University, Cordoba, Spain; Department of Pathology 5, Case Western Reserve University, Cleveland, OH; Department of Pathology 6, University of Massachusetts Medical School, Worcester, MA; and Department of Pathology 7, North China Coal Medical College, Tangshan, China

Background: Previous investigations have provided support for the contention that EGFR may be responsible for prostate cell growth. Evidence that over-expression of EGFR in hormone refractory prostate cancer may provide a rationale for new therapeutic strategies.
Methods: The current study was conducted to investigate whether there is significant EGFR over-expression and gene amplification in a population of patients treated with hormonal therapy using fluorescence in situ hybridization and immunohistochemical staining method.
Results: Immunohistochemically, EGFR expression was demonstrable in 57 of 71 tumors. Membranous immunostaining for EGFR was observed in >75% of tumor cells in 11% of cases, in 51–75% of tumor cells in 20% of cases, in 26–50% of tumor cells in 21% of cases, in 11–25% of tumor cells in 21% of cases, and in 1–10% of tumor cells in 7% of cases. No immunostaining for EGFR was seen in 20% of cases. FISH for EGFR gene amplification was performed in all 71 cases. EGFR gene amplification was present in 1 of 71 tumors. Polysomy (more than two copies of CEP7 and EGFR/CEP7 ratio < 2) of chromosome 7 was present in 24 of 71 tumors. Disomy was present in the remaining 46 specimens. There was no statistically significant association between the EGFR expression and other clinicopathologic characteristics including patients' ages,

different hormonal therapy regimens, and metastatic status. There was no correlation between EGFR protein expression and gene amplification.

Conclusion: Our findings provide additional evidence that EGFR plays a significant role in the progression of prostate cancer to an androgen-independent state. Future studies are needed to evaluate the overall significance of the amplification of EGFR and its potential use in anti-EGFR therapies.

P-317

Standard Gleason grading system vs 2005 WHO/ISUP modified grading: A comparative study based on 172 needle prostatic biopsies.

Athanase Billis; Marbele S. Guimarães; Leandro L.L. Freitas; Luciana Meirelles; Luís A. Magna. Ubirajara Ferreira

Department of Pathology, School of Medicine, State University of Campinas (Unicamp, Brazil

Background: In 2005, the Gleason grading underwent its first major revision. The aim of our study was to compare the concordance of pattern and change of prognostic group between these two readings. Additionally, to check any disciminative power of the modified grading we compared the time of biochemical (PSA) progression-free outcome according to prognostic groups.

Method: The study was based on 172 biopsies of patients that were subsequently submitted to radical prostatectomy (RP). Four prognostic Gleason grading groups were considered: scores 2–4, 5–6, 7, and 8–10. Several clinicopathologic variables were studied. The second reading based on the modified grading was done by the same reviewer (AB). Time to biochemical progression was studied using the Kaplan-Meier product-limit analysis.

Results: Comparing the two readings, there was concordance in 83.14%, 63.3%, and 68.02% for Gleason primary pattern, Gleason secondary pattern, and Gleason score, respectively. The second reading reflected in a change towards a higher Gleason grading group in 46/172 (26.74%) patients. The distribution of the prognostic groups for the standard reading was 1 (0.58%), 117 (68.03%), 44 (25.58%), and 10 (5.81%) biopsies, respectively, for the groups 2–4, 5–6, 7, and 8–10; for the modified reading was 0 (0%), 85 (49.42%), 68 (39.53%), and 19 (11.05%), respectively. The Kaplan-Meier curve showed no significant difference among patients stratified according to prognostic groups with the standard Gleason reading (log-rank, $p=0.524$) but a significant difference in outcome for patients stratified according to the revised reading (log-rank, $p=0.010$).

Conclusion: The highest impact of the modified grading is on the secondary pattern resulting in a change towards higher prognostic groups resulting in a significant biochemical progression outcome following RP in our study. The findings favor that the WHO/ISUP modified grading is a valuable refinement for the standard Gleason grading system.

P-318

Clinicopathologic findings and biochemical (PSA) progression following radical prostatectomy of patients with microscopic bladder neck involvement: A study in Brazil.

Marcelo Noronha; Luciana Meirelles; Leandro L.L. Freitas; Luís A. Magna; Ubirajara Ferreira; Athanase Billis

Dep. of Pathology, School of Medicine, State University of Campinas (Unicamp)

Background: It is controversial whether microscopic invasion of the bladder neck has a high risk for biochemical progression following radical prostatectomy. The TNM classification for prostate cancer considers bladder neck involvement to be pT4 disease, however, it does not specifies whether the invasion is macroscopic or microscopic.

Method: The study was based on 290 whole-mount consecutive radical prostatectomies. Biochemical progression was defined as PSA $\geq$0.2 ng/mL. Time to biochemical progression-free outcome was compared using the Kaplan-Meier product-limit analysis. To assess individual variables for risk of biochemical progression we created a univariate Cox proportional hazards model, and to assess the influence of several variables simultaneously, we developed a final multivariate Cox proportional hazards model of the statistically significant covariates.

Results: Bladder neck invasion was present in 55/290 (18.96%) surgical specimens and absent in 235/290 (81.03%). Patients with bladder neck invasion had significantly higher preoperative PSA ($p<0.001$), higher Gleason score ($p<0.001$), higher positive surgical margins ($p=0.049$), and a more advanced pathological stage ($p=0.002$). At 5 years, the progression-free outcome was 42%, 44%, and 28% for patients with microscopic bladder neck invasion, extraprostatic extension, and seminal vesicle invasion, respectively. The relative risks for PSA progression by univariate Cox analysis were 1.60, 1.85, and 2.35 for the same variables, respectively. The multivariate Cox proportional hazards models determined that the PSA progression relative risk in patients with bladder neck involvement was not significant when combined either with extraprostatic extension or seminal vesicle invasion.

Conclusion: Patients with bladder neck invasion have significantly higher preoperative PSA, higher Gleason score, higher positive surgical margins, and more advanced pathological stage compared to patients without bladder neck invasion. However, the outcome following radical prostatectomy compared either to patients with extraprostatic extension or seminal vesicle invasion do not favor considering microscopic bladder neck invasion as stage pT4.

P-319

Histological, histochemical, and immunohistochemical study of normal Skene's glands: An aid for establishing the origin from these glands of a case of adenocarcinoma of the female urethra negative for prostate-specific antigen.

Daniel Teixeira; Rafael F. Stelini, Leandro L.L. Freitas; Luciana Meirelles; Athanase Billis

Dep. of Pathology, School of Medicine, State University of Campinas (Unicamp)

Background: Female primary urethral tumors are rare. Detailed microscopic descriptions of normal Skene's glands are not found in histology textbooks as well as in descriptions of tumors originating from these glands. A detailed histological, histochemical, and immunohistochemical study of normal Skene's glands was the clue for establishing the origin from these glands of an adenocarcinoma negative for prostate-specific antigen (PSA) in a 43-year-old female.

Method: We studied the histology of normal Skene's glands from autopsies and noninvolved glands in periurethral tumors. The histochemistry and immunohistochemistry study included: PAS, mucicarmin, alcian blue (pH 2.5), alcian blue (pH 0.4), alcian blue (pH 1), alcian blue/PAS (pH 2.5), colloidal iron, colloidal iron/PAS, bcl2, S-100, Ki-67, estrogen and progesterone receptors, 1A4, AE1/AE3, CK7, CK20, p53, p63, CD10, 34betaE12, CEA, and PSA.

Results: The female urethral mucosa is lined in most of its extension by a squamous nonkeratinizing epithelium that is continuous to the invaginated Skene's ducts. After a short distance, this epithelium is abruptly substituted by a transitional type epithelium lined in its luminal border by columnar eosinophilic cells. At the every end of the ducts, the columnar cells form alveolar outpouchings of clear cells. The strongest reactions showed positivity for CEA and AE1/AE3 (squamous nonkeratinizing epithelium); p63 and 34betaE12 (transitional type epithelium); CK7 (columnar eosinophilic epithelium); and PAS, alcian blue/PAS (pH 2.5) and colloidal iron (clear secretory cells). Only scattered secretory clear cells in some glands showed PSA positivity in the luminal part of the cytoplasm.

Conclusion: The microscopy of the periurethral adenocarcinoma reproduced all tissues of normal Skene's glands as well as the correspondent histochemical and immunohistochemical findings. Mucinous stromal pools stained similarly to the secretory cells of normal glands. In spite of negative PSA, the findings of the tumor were consistent for an origin from Skene's glands.

P-320

Malignant Solitary Fibrous Tumor of the Urinary Bladder. An Immunohistochemical and Electron Microscopic Study of 1 case.

M Casas; G Barraza; M Turell; F Pérez; E López-Bonet; L Bernadó.

Hospital Universitari de Girona Doctor Josep Trueta, Spain

Background: Solitary Fibrous Tumor (SFT) may occur at any site, but it has been most frequently described in the pleura. In a search of the literature, we could only identify 11 cases of SFT arising in the urinary bladder.

Method: SFT was determined to have malignant component if there was focal areas of marked increased cellularity (≥ 5% of the tumor), with greater than 4 mitoses/10 HPF, with or without foci of necrosis. Immunohistochemical studies were performed using the Dako Envision + Kit and the following primary antibodies: pan-keratin (CK22), CK AE1/AE3, EMA, vimentin, smooth muscle actin (SMA), muscle specific actin (MSA), calponin, desmin, S-100 protein, ALK, CD34 and bcl-2. Tissue for electron microscopy was also taken and fixed in 2.5% glutaraldehyde and processed according to standard methods.

Results: a 74-year- old man presented with a recent history of gross hematuria. The patient underwent cystoprostatectomy without complications. Grossly, the tumor was a polypoid white mass that measured 10 cm and was attached by a short pedicle to the bladder wall. Microscopically, the tumor was comprised of densely packed spindled cells with a high mitotic rate (>30/10 HPF), wich form interlacing bundles resembling fibrosarcoma. The tumor cells stained diffusely for vimentin, CD34 and bcl-2, and focally for SMA by immunohistochemistry but were negative for CK22, CK AE1/AE3, EMA, MSA, calponin, desmin, S-100 and ALK. Ultrastructurally, the tumor cells had spindle or ovoid nuclei with irregular nuclear contorns and small nucleoli. The cytoplasm contained ribosomes, mitochondria, and dilated rough endoplasmic reticulum. These features were suggestive of primitive mesenchymal or fibroblast-like cells.

Conclusion: SFT is a rare mesenchymal tumor of the urinary bladder, but should always be considered in the

differential diagnosis of spindle cell neoplasms encountered in the lower urinary tract.

P-321

Nuclear fractal dimension in the study of prostate cancer.

Petroula Kakouri 1; Petros M. Pavlopoulos 1,2; Efthymios Koniaris 3; Aikaterini Apostolaki 3; Sofoklis Bouzoukas 1

1 1st Social Security Hospital, Urological Clinic, Athens, Greece, 2 Department of Pathology, National University of Athens Medical School, Athens, Greece; 3 Department of Pathology, Anticancer Oncological Hospital of Athens "St. Savvas", athens, Greece

Background: Fractal dimension provides a measurable, precise and reproducible approximation of nuclear structure properties and especially nuclear shape complexity. Considering the applications of fractal analysis in the field of histopathology many studies have been published evaluating fractal dimension as an indicator of complexity and irregularity of tumor tissues. However, extended fractal analysis studies of prostate cancer are lacking.
Methods: Archival pathologic material from 42 radical prostatectomy specimens was examined and the pertinent medical files were reviewed. Histological sections from the 42 carcinomas as well as from non-malignant adjacent areas from 12 cases were stained with Feulgen for nuclear complexity evaluation. Two randomly selected high power fields from each case were digitally archived. These files were automatically transformed to binary images suitable for fractal analysis, through a non-supervised histogram-based clustering procedure. The nuclear fractal dimension (FD) on each image was estimated by using an implementation of the widely used box-counting algorithm in a specially designed application.
Results: Prostate carcinomas presented higher mean values of nuclear FD compared to areas of normal prostate. The difference was statistically significant ($p<0.01$). Well-differentiated neoplasms had significantly lower FD values than poorly differentiated ones. FD was significantly and positively correlated with nuclear size morphometric parameters ($r=0.67–0.75$, all $p<0.05$), as well as with Gleason score ($R=0.61$, $p<0.05$).
Conclusions: Prostate cancer nuclear FD seems to be an important morphometric parameter possibly valuable for the diagnosis as well as for the future development of an unbiased and reproducible image analysis system for the study of prostate cancer pathology.

P-322

Collecting duct renal cell carcinoma with divergent sarcomatoid components: a case report with potential implications in the pathogenesis of renal cancer dedifferentiation.

M[a] Carmen Faus; Rebeca Alcalá; Stephan Ghünthner; Pilar Soriano; David Ramos

Department of Pathology.Medical School.University of Valencia, Spain

BACKGROUND: Sarcomatoid components in renal cell carcinomas (RCC) has been described in up to 10% of cases and considered a high grade lesion in terms of tumor differentiation related to poor patient outcome. Collecting duct carcinoma represents only 1% of all histologic types in RCC. We present a case of a 75-year-old man with a collecting duct RCC presented in our hospital with abdominal pain and hematuria. Magnetic resonance imaging (MRI) and sonography revealed both a heterogenous tumor of the left renal parenchyma 11 cm in diameter with tumor areas resembling osteo- and chondrosarcoma in addition to the more frequent fusiform and storiform areas resembling a fibrosarcoma. METHODS: After radical left nephroureterectomy all tumor fragments were formalin-fixed and paraffin-embedded, and representative sections were stained with hematoxilyn & eosin and, immunohistochemically, with vimentin, CD10, 34betaE12 antigen, S-100, SOX9, osteonectin, osteocalcin, actin, desmin, COX2, CD117 (c-KIT) and Her2-Neu. RESULTS: The tumor demonstrated areas displaying irregular ducts characteristic of collecting duct RCC. Tumor areas with collecting duct appearance show specific immunoreactivity against 34betaE12 antigen along with reactivity against mesenchymal antigens (osteonectin, osteocalcin and SOX9) and vimentin. Otherwise, dedifferentiated fusocellular zones presented specific immunostaining with mesenchymal antigens such as osteonectin, osteocalcin, SOX9 and vimentin), whereas areas of typical osteosarcoma and chondrosarcoma demonstrated the presence of osteoid material and intense immunoreactivity with osteogenic antigens in the former, and intense reactivity against S-100 and SOX9 in the latter. Otherwise, dedifferentiated fusocellular zones presented specific immunostaining with mesenchymal antigens such as osteonectin, osteocalcin, SOX9 and vimentin), whereas areas of typical osteosarcoma and chondrosarcoma demonstrated the presence of osteoid material and intense immunoreactivity with osteogenic antigens in the former, and intense reactivity with S-100 and SOX9 in the latter. Interestingly, this neoplasm showed an intense Her2-Neu immunostaining in all histologic subtypes in contrast to the diffuse lack of immunostaining with c-Kit and COX-2.

CONCLUSION: Our study appears to demonstrate, at least in the current case, that in dedifferentiated types of RCC the epithelial component demonstrated a specific cytokeratin immunophenotype, whereas the both epithelial and sarcomatoid components expressed indistinctly mesenchymal markers at the immunohistochemical level.

P-323

Atheromatous embolization (AE) diagnosed on bladder transurethral resection (B-TUR) specimens: a report on nine cases

Isabel Alarcón; Maria Pané; August Vidal; Ainhoa Laborda; Josep Muñoz-Seguí; Enric Condom

Hospital Universitari de Bellvitge (Departments of Pathology and Urology); Hospital de Viladecans (Department of Urology, Spain

Background: Atheromatous embolization (AE) is an underrecognized medical disorder due to vascular migration of cholesterol crystals from atherosclerotic plaques. It is though to be associated with a high mortality rate. Since it has been very rarely reported on B-TUR specimens its true clinical relevance for this group of patients is largely unknown.

Objectives: To assess the clinical profile of patients and the prognostic relevance of finding AE on B-TURs performed for bladder cancer.

Methods: Review of clinical charts and pathology slides from patients codified as having AE on B-TUR specimens between 1988 and 2007 at the Department of Pathology, Hospital Universitari de Bellvitge.

Results: Nine patients were identified. All of them were male, aged 51 to 87 years, and all had some risk factor known to be associated with AE. Eight were or had been smokers. Four patients were under treatment for hypertension. Three had received anticoagulant or antiagregant therapy. One patient had a past history of cardiovascular surgery. In five patients AE appeared to be a spontaneous phenomenon with no precipitating factors. No patient had evidence of AE involving other anatomical sites. AE was seen as needle-shaped cholesterol clefts occupying the lumen of small arterial vessels mainly in the deep subepithelial tissue or submucosal layer of the bladder. There were two deaths, due to tumor progression, one and three years after the diagnosis of AE in bladder carcinoma. No deaths attributable to cardiovascular causes were recorded till date.

Conclusion: AE is an unusual, though not exceptional, incidental finding on B-TUR performed for bladder cancer. It is often a spontaneous phenomenon, with more than half of the patients lacking an obvious precipitating factor. In contrast with AE involving other organ systems, AE as an isolated finding on B-TUR specimens does not seem to have prognostic impact on survival.

P-324

Unusual Presentation of an abdominal seminoma

Hakan buluş; Ayla Tezer; Gulcin Guler Simsek; Heyecan Ökten; Ali Coşkun

Kecioren Eğitim Araştırma Hospital, Turkey

45 years old man presented with 3–4 months history of progressive abdominal pain and lower quadrant mass. CT scans showed 9×8×7 cm.s diameter well-defined bulky mass with smooth border and compressed bladder base. It was supposed to be a mesenteric cyst in abdomen. Macroscopically a gray-cream homogenous lobulated mass, composed of multiple distinct nodules, the biggest of which was 7 cm in diameter. Microscopically, tumor showed a histopathology of a seminoma. Mitoses were numerous in tumor cells. It was emerged on undescended testis and limited in the testis, and there wasn't any lymph node and other metastases until this time. Although he has got no testis and seminal vesiculum at right side, he wasn't infertile.

P-325

Squamous cell carcinoma of the urinary bladder. A clinical immunohistochemical study.

Papathanasaki Antigoni; Papaevangelou Maria; Sevastiadou Maria; Biteli Maria; Koniaris Efthymios; Apostolikas Nikiforos.

Pathology Dpt. Of Anticancer, Oncological Hospital of Athens, 'St. Savvas', Athens, Greece.

Background: Squamous Cell Carcinoma (SCC) arising in the urinary bladder consists 2–7% of all urothelial infiltrating cancers and is thought to arise through a process of squamous metaplasia. In areas were Schistosomiasis is edemic this percentage rises up to 70%.

Methods: We re-evaluated 102 cases of urinary bladder carcinomas in a two year period (2006–2007) and we reported 3 cases of SCC of the urinary bladder. The majority of the cases concerned Papillary Urothelial Carcinomas (PUC) (97 cases- 96.08%), one case was metastatic from the prostate (0.98%) and 3 cases were pure SCC (2.94%). The mean age of patients with SCC in this series was 66 years and the male to female ratio was 3:0. Hematuria was the presenting symptom in all the cases.

Results: Grossly the first two cases were biopsy tissue samples from the urinary bladder measuring 1.7 cm and 3 cm respectively, while the third case was a total cystectomy. In the latter case the tumor located in the

bladder neck adjacent to the paraurethral side of the prostate and measured 4.8×4.5×2 cm. All cases infiltrated the smooth muscle wall of the urinary bladder and were staged pT3b(i) the first 2 cases and pT3b(ii) the 3rd. According to Bergkvist grading system the two first cases were grade IV, while the third was grade III with extensive keratin formation. No squamous metaplasia was found adjacent to the tumors. The immunocytochemical analysis showed strong positivity for Cytokeratin (CK) 7, 8 and Pankeratin, while CK20 was not immunoreactive. In situ hybridization for HPV was performed.

Conclusion: Because none of the patients had a history of Schistosomiasis or irradiation, we suspect that SCC of the urinary bladder maybe associated with chronic irritation and inflammation. One of our patients had multiple surgical procedures which maybe set the stage for subsequent development of SCC.

P-326

A case of nephrogenic adenoma in the female urethral diverticulum.

Anna Domingo Amela; Antoni Urban Ramón**; José Emilio Batista***

**Centro Médico Teknon (Barcelona), **Hospital Sant Jaume de Calella, Spain*

INTRODUCTION. Nephrogenic adenoma is a rare benign lesion that can occur at several sites along the urogenital tract that is typically preceded by some form of genitourinary injury. It is composed of small glandular structures that develop along the urothelium. Their pathogenesis is controversial. Generally presumed to be a metaplastic process of the urothelium, recent evidence suggest that it may be derived from detached renal tubular cells implanting along the urothelial tract in previously injured areas. It is important to recognize this entity and to be aware of its histologic characterisitcs to avoid misdiagnosis of malignant neoplasms occurring at the same sites.

CASE REPORT 44 year old female with a history of periurethral pain for the last 3–4 years. A urethral diverticulum was observed by magnetic resonance and cistoscopy and partially resected. Histologic examination revealed a diverticulum with an urothelial epithelium, squamous metaplasia and chronic inflammation. In some sites we saw clusters of glandular or tubular proliferation, along the urothelium lining, in an edematous and inflammatory stroma, without significant cytologic atypia and few mitoses. The CAM 5.2 expression on basal cells confirmed that it was a benign process.

CONCLUSION The most frequent localisation of Nephrogenic adenoma is in bladder trigon (79%), ureter (19%) and urethra. It is more frequent in males than in females (3:1). It can be confused with malignant neoplasms occurring at the same sites as clear cell carcinoma, nested or microcystic variants of urothelial carcinoma and prostatic adenocarcinoma. There is no specific immunohistochemical profile to distinguish this lesion from its malignant mimickers. Clinicopathologic correlation with careful attention to morphology is the most important way to achieve a correct diagnosis.

P-327

Development of a testicular germ cell tumor model in nude mice for the study of tumor biology and resistance to cisplatin treatment

August Vidal; Alberto Villanueva; Josep Maria Piulats; Fina Climent; Marga Nadal; Wilmar Castillo; Marc Gallegos; Sara Puertas; Francesc Vinyals; Javier García del Muro; Ferran Algaba; Gabriel Capellà; J Ramón Germà and Enric Condom

Servei d'Anatomia Patològica. Hospital Universitari de Bellvitge, Spain

Introduction: Testicular germ cell tumor (TGCT) is the most frequent cancer in young males. Chemotherapy based on cisplatin together with surgery, leads to a very high curation rate. Nevertheless, 15–20% of patients, mainly in the non-seminomatous germ cell tumors (NSEGCT) group, will no achieve a complete remission after treatment. Most of these patients are refractory to cisplatin and die of disease. Little is known about the mechanisms of resistance to cisplatin. ***Aim:*** To identify genes involved in the development of TGCT and in the resistance to cisplatin-based treatment. ***Results:*** We have developed a model for the study of NSEGCT, based on orthotopic implantation of primary human NSEGCT in nude mice. Eleven of 28 NSEGCT (39.3%) grew as orhotopic implants in nude mice, maintaining the pathological features of primary tumors. Five tumors developed metastasis 6–8 months after orchiectomy performed when tumors raised a palpable size. Whole genome analysis (Nimblegen microarrays, 60.000 bp resolution) and expression profiles analysis (Affymetrix microarrays) were performed in perpetuated tumors as well as in paired cases of tumors/metastases obtained after orchiectomy in mice. Our genetic analysis confirms previous results, identifying recurrent regions of gain and loss in TGCT. Presence of gene mutations and epigenetic methylation changes were studied for a subset of

genes. *In vivo* response pattern to cisplatin was established in 9 tumors. Five of these tumors became resistant to cisplatin after exposure to increasing doses of the drug. Comparative whole genome and expression profiles analysis are being performed in paired cisplatin-sensible/resistant tumors in order to identify genes involved in the acquisition of resistance. ***Conclusions:*** We have developed a new model for the study of NSEGCT biology and the mechanisms of resistance to cisplatin treatments. This is a suitable preclinical model to assay new therapeutic approaches for improving prognosis of patients refractory to cisplatin.

P-328

Testicular tumour with an unusual histological pattern

Muñoz G, Felipo F, Pascual M, Fuertes A, Sota P, Marquina I, del Agua C.

Department of Pathology; HU Miguel Servet, Spain

BACKGROUND Polyembryoma is a distinctive form of mixed germ cell tumour of the gonads composed of embryonal carcinoma and yolk sac tumour, sometimes with teratomatous components that are arranged in a pattern resembling the presomitic embryo. This tumour was first described by Peyron at 1939.

METHODS We present the case of a 19 year-old male with a testicular painless mass of 7 cm in its greatest dimension, predominantly solid.

RESULTS Diagnose was mixed germ cell tumour constituted by 20% seminoma and 80% polyembryoma (yolk sac tumour + embryonal carcinoma + teratoma, with abundant embryoid bodies). The embryo-like formations consist of a central "germ disc" composed of embryonal carcinoma epithelium and two cavities, a dorsal one recapitulating the amniotic cavity and a ventral one recapitulating the yolk sac cavity. The later is separated from the germ disc by a thin layer of yolk sac epithelium. Surrounding the embryoid bodies there is a loose, primitive, extraembryonic mesenchyme, giving rise to a very distinctive low-power appearance.

COMMENTS These unique histological features lead some authors to categorize it as a separate tumour. However, in the WHO histological classification of testis tumours it is classified as a tumour of more than one histological type. We agree with the opinion that is preferable to consider polyembryoma as a unique and distinctive form of highly organized mixed germ cell tumour, given that it behaves and is treated like other mixed germ cell tumours with similar components. Moreover, as in our case, polyembryomatous foci always comprise a part of a mixed germ cell tumour, and to our knowledge, polyembryoma has not been reported in pure form in the testis.

P-329

Lymphoepithelioma – like Carcinoma of the Urinary Bladder

1 Papaevangelou Maria; 1 Papathanasaki Antigoni; 1 Sevastiadou Maria; 1 Thodoropoulou Georgia; 1 Koniaris Efthymios; 2 Arvanitakis T; 1 Apostolikas Nikiforos

1 Pathology Dpt. of 'St. Savvas' Hospital, Athens, Greece; 2 Urology Dpt. of 'St. Savvas' Hospital, Athens, Greece

Background: Lymphoepithelioma-like carcinoma (LLC) of the urinary bladder is a rare type of infiltrating urothelial carcinoma with only 53 cases reported to date. We report an additional case of a pure LLC which was recently diagnosed in our hospital.

Method: A 50-year old man with a history of heavy smoking was admitted with heamaturia and with the diagnosis of an urothelial carcinoma (T2, Grade III). The patient underwent a partial cystectomy and excision of the outer right and outer left iliac lymph nodes.

Results: Grossly we received 6 tissue specimens measuring in total 2.3×4.5×5.3 cm, of soft consistency and brownish color. Microscopically a tumor developed in the subepithelial connective tissue of the bladder invading the superficial muscle and focally the deep muscle of the bladder. No conventional solid invasive transitional cell carcinoma and no urothelial dysplasia or carcinoma in situ were identified. The tumor composed of nests and sheets of undifferentiated large cells with pleomorphic nuclei and prominent nucleoli. A prominent lymphoid stroma was present throughout the tumor and consisted mainly of small lymphocytes and eosinophils. All the excised lymph nodes were free of metastases.

Immunostaining with antibodies against pankeratin, cytokeratin 7, 8 and P53 showed positivity within carcinoma tumor cells and negativity for cytokeratin 20. The lymphocytes between the tumor cells stained with antibodies against CD3 and CD 20.

Conclusion: The undifferentiated character of the tumor, the heterogeneous nature of the inflammatory infiltrate and the epithelial nature of the tumor cells establish the diagnosis of LLC. Our case was grade IV according to Bergkvist classification or undifferentiated carcinoma according to WHO. It has been suggested that LLC of the bladder has a relatively favorable prognosis and should be treated by stage like other bladder carcinomas.

P-330

Pathologic analysis of 1000 cases of transrectal ultrasound-guided systematic prostate biopsy: establishment of new sample processing method and diagnostic utility of immunohistochemistry

Chang Lim Hyun; Hee Eun Lee; Haeryung Kim; Hye Seung Lee; So Yeon Park; Jin Haeng Chung; Gheeyoung Choe

Department of Pathology, Seoul National University Bundang Hospital, Seoul National University College of Medicine, Korea

Background: We developed a new processing method for extended prostate needle biopsy, and evaluated diagnostic utility of routine immunohistochemistry in 1000 consecutive unselected cases of transrectal ultrasound-guided systematic prostate biopsy. **Materials and Methods:** Four to five biopsy cores were embedded in one paraffin block. All the biopsy cores were immunohistochemically stained with basal cell markers. **Results:** The new sample processing method was technically perfect for making a diagnosis from extended prostate needle biopsy. Among 1000 cases, there were 323 cases (32.3%) of adenocarcinoma, 5 cases of other malignant tumors, 9 cases of high-grade prostatic intraepithelial neoplasia without a carcinoma, and only 8 cases of atypical small acinar proliferation. Among the 323 cases of adenocarcinoma, there were 38 cases (11.8%) of microcarcinomas <0.1 cm and 101 cases (31.3%) of small adenocarcinomas <0.3 cm in length. In the needle biopsy specimens, 59 cases (18.3%) were classified as clinically insignificant carcinomas. Among them, 37 cases underwent radical prostatectomy, which turned out to be clinically significant carcinomas in 24 cases (64.9%). **Conclusions:** Routinely performed immunohistochemistry combined with the new sample processing method is very effective for detecting microscopic carcinoma foci as well as differentiating carcinoma from benign conditions mimicking cancer.

P-331

Morphology of testis at atherosclerosis

Nikolay M. Krupnov, Alexander F. Astrakhantsev, Yriy I. Uchov

Ryazan Clinical Hospital, Russia

Background.Up to now in the field of morphology of reproductive system of men the problems of testis involution and morphogenesis at atherosclerosis haven't been thoroughly investigated.

Methods.We have investigated histologically and ultrastructurally testicles of 63 died patients aged 36–89 with general atherosclerosis and testicles of 38 men aged 36–89 with minimal manifestations of atherosclerosis died in an accident.

Results.The absolute volume of rete of testicle of patients being ill with atherosclerosis decreases by 65–80% in comparison with the age control. Absolute volume of convoluted seminiferous tubules and interstitial tissue decrease by 24–27%. The lumen of arterioles also progressively decreases. Together with it at atherosclerosis there is Leidig cells volume expansion to 80%. At general atherosclerosis in testis there are zones of focal sclerosis of seminiferous tubules, whose area goes as far as 12.7% of shear section area. It was revealed that on the periphery of sclerosis zones there is a reduction of transaction area of seminiferous tubules by 20–33% with Sertolli cells quantity reduction by 17–24%. Ultrastructural investigation of Sertolli cells has revealed zones of dissociations of endoplasmatic reticulum and activization of lysosomes with a great number of lipid inclusions of various electron density. It has been stated the downward changes in index of spermatogenesis in convoluted seminiferous tubules by 63–65.6%, accounted for the quantity reduction of all kinds of cells. In some visual fields we revealed the destruction of spermatogenous cells up to the syndrome "only Sertolli cells" and intensifying processes of spermatogenous cell endoreproduction in seminiferous tubules.

Conclusion.Morphological changes of testis at general atherosclerosis consist in focal sclerosis of convoluted seminiferous tubules, reduction of transaction area of remaining seminiferous tubules, Sertolli cells quantity reduction and downward changes in index of spermatogenesis. These changes characterize «atherosclerotic testiculopatie», caused by chronic ischemia of testis.

P-332

Primary diffuse large B-cell lymphoma of the urinary bladder

Luis Alfaro; Mª Jośe Roca; José M. Castillo

Hospital Rey Don Jaime. Castellón. Spain

Primary urinary bladder lymphomas are very uncommon. Among them low grade lymphomas mainly MALT type occur most frequently, and they don't create important diagnostic problems because cell morphology is easily distinguished from urothelial neoplasms. High grade lymphomas from the urinary bladder are extremely rare, and can simulate undifferentiated carcinomas. Distinction is important as chemotherapy will replace usual surgical treatment.

We report a case of a large B-cell lymphoma developed in a 42-years-old woman. She initially presented hematuria, and cystoscopy showed an ill defined non-papillary mass. Small biopsies were taken, with broad necrotic areas and isolated

large atypical cells. No epithelial nest were found, although small pseudocordonal patterns suggested a poorly differentiated carcinoma. A new transuretral resection was performed, and histological study revealed a neoplasm composed of large occasionally epithelioid cells, with pale or clear cytoplasm, and atypical irregular nuclei. High mitotic rate was found and normal or slightly hyperplastic superficial urothelium was present in some areas. There was wide parietal infiltration with muscular invasion and again necrotic and hemorrhagic regions.
Immunohistochemically neoplastic cell expressed intensely B-cell markers (CD20 and CD79a). All low and high molecular weight cytokeratins were negative. Blc2, bl6, CD30 and ALK were also negative. Ki-67 (mib-1) expression was around 30%
Imaging revealed no pelvic lymphadenopathy and extension study of the patient couldn't find dissemination of the disease at the time of diagnosis. Low number of cases and studies makes optimal management still controversial. Our patient was treated with chemotherapy, and although follow up is still short no complications non recurrence have been detected.

P-333

Pathological features of latent prostate cancer: an autopsy study with complete prostate embedding and alpha-methyl-coacetate-racemase staining

Núria Juanpere; José Antonio Lorente; Raquel Esgueva; Silvia Hernández; Laia Agell; Silvia de Muga; Antoni Gelabert; Sergi Serrano; Josep Lloreta
Department of Pathology and Department of Urology, Hospital del Mar; Departament de Ciències Experimentals i de la Salut, University Pompeu Fabra and Autonomous University of Barcelona, Barcelona, Spain.

BACKGROUND Prostate cancer (Pr Ca) is the second cause of cancer-related death in males of Western countries. Previous autopsy studies suggested that Pr Ca might be more prevalent than it seems by its clinical detection rate. Thus, the concept of latent Pr Ca was coined mostly to refer to cases detected at autopsy, in patients dying from unrelated causes. The purpose of this ongoing project is to investigate the real incidence and the features of latent Pr Ca in a detailed clinico-pathological study.
DESIGN A total of 21 autopsy prostate specimens (age range: 56–87 years; mean age: 73.9 years) are the subject of this report. All the prostates were completely embedded. The tumor foci were measured and mapped. Doubtful cases were confirmed with α-methyl-CoA-racemase and p63 staining.
RESULTS The prevalence of Pr Ca in this preliminary series is 61.9%. PSA level is < 4 ng/ml in 71.5% of these cases. The most common Gleason pattern is 3+3 (53.8%) followed by 3+4 and 3+5 patterns (23.1% each). From these cases, 53.85% meet the criteria of insignificant Pr Ca, while the remaining 46.15% would have been considered clinically significant if previously detected. The age distribution was similar in the insignificant and significant subgroups. Overall prevalence of high grade PIN (hg PIN) is 76.2%. Pr Ca was found in 62.5% of patients with hg PIN and in 60% of patients without hg PIN.
CONCLUSION The prevalence of latent Pr Ca in our series is similar to those reported in the literature. Most of the tumors appeared in men older than 65 years and were most frequently insignificant, with Gleason pattern 3+3, but there was a remarkable proportion of potentially significant and higher grade tumors. The proportion of cancer was similar in patients with and without hg PIN. Besides, PSA levels were clinically low in the majority of patients with tumor. Therefore, hg PIN and PSA levels do not seem good predictors of latent Pr Ca. Nevertheless, a high number of cases must be included in order to draw more definitive conclusions on latent Pr Ca.
This study has been funded by grants FIS/ISCIII 06/1411, FIS 965190005, and Asociación Española Contra el Cáncer-Barcelona-2006.

P-334

Basal cell hyperplasia of the prostate with unusual morphologic pattern

Angela Borda; Andrada Loghin; Mihai Turcu; Nicole Berger
University of Medecine and Pharmacy Tirgu Mures, Romania, Hopital Lyon Sud, Lyon, France

Background. Basal cell hyperplasia (BCH) is a microglandular proliferation of the prostatic transition zone, usually easy to diagnose. However, in rare cases this well-described lesion displays unusual morphologic patterns, causing confusion and difficulties in differentiating it from malignant lesions.
Method. We report the case of a 58 years old man who underwent adenomectomy for urinary tract obstruction symptoms. The histologic evaluation was made on haematoxyline-eosine stained sections. The presence of a focus with unusual morphologic pattern imposed an immunohistochemical study with monoclonal antibodies against Prostatic Specific Antigen (PSA), high molecular weight cytokeratin 34βE12 (HMWCK), S-100 protein, P504S and p63.

Results. On a backgroud of a benign prostatic hyperplasia (BPH) we noticed a circumscribed nodule of BCH which had the usual aspect at the periphery and a cribriform pattern in the centre. The cribriform structures were medium sized, centred by small luminal spaces and separated by an unremarkable stroma. At higher magnification cells were small, with scant cytoplasm and regular hyperchromatic oval nuclei. No mitotic figures, no necrosis and no infiltration were noticed. In immunohistochemistry prostatic basal cells markers (HMWCK, p63) were positive, but only as a single layer at the periphery of the glands. In the cribriform structures all the other cells were negative for these markers. Some adluminal cells expressed PSA marker. S-100 protein and P504S were negative in all cells.
Conclusion. The proposed terminology for this lesion is adenoid cystic-like BCH. This diagnosis is sustained by the identical bland morphology of the cells of both cribriform and classical BCH, even if not all these cells expressed basal cell markers. Cells labeling PSA markers represented residual secretory cells.Adenoid cystic-like BCH is a florid benign histologic variant of the BPH, important to recognise and to distinguish from cribriform PIN and the rarest adenoid-cystic and basaloid carcinoma.

P-335

Outcome prediction for renal cell carcinoma in adults: a ten-year review with 150 tumours

Ana González Piñeiro; Antonio Ojea Calvo; Concepción Fiaño Valverde, Rebeca Fernández Victoria; Juan L. Ríos González; Pablo Fernández Vázquez
Compexo Hospitalario Universitario de Vigo. Xeral-Cíes, Spain

Background: A wide of histopathological parameters have been investigated for their prognostic significance in renal cell carcinoma. Recent investigations have focused upon tumor diameter, invasion within the renal sinus, and the presence of tumour necrosis.
Methods: To study the significance of these parameters in the cases from our hospital, 150 nephrectomy specimens (from 1995 to 2005) were evaluated, assesing the pT classification, histologic subtype, tumor size and grade, presence of histologic tumor necrosis, perirenal, sinus, adrenal and vascular invasion (microvascular peritumoral and renal vein).
Objectives: Statistical analysis were performed to asses the morphologic features associated with metastasis-free survival and cancer-specific survival in our series and compared with literature.

P-336

IMMUNOHISTOCHEMICAL QUANTITATIVE ASSESMENT OF THE EXPRESSION OF GSTP1, iNOS AND COX-2 IN PIA, PIN AND CARCINOMA IN THE PROSTATE GLAND

Milen Karaivanov; Krasimira Todorova; Soren Hayrabedyan
Department of general and clinical pathology, Medical University of Pleven, Bulgaria;Institute of Biology and Immunology of Reproduction, Bulgarian Academy of Sciences

Background: The term “proliferative inflammatory atrophy” has been proposed for the first time by De Marzo and Marchi in 1999 to unite the common atrophy and postatrophic hyperplasia, combined with chronic or acute inflammation.It has been hypothesized that the proliferative inflammatory atrophy (PIA) is a neopastic precursor of the prostatic intraepithelial neoplasia (PIN) and of the prostatic carcinoma(PCa).The present study was intended to quantitatively asses and compare the levels of expression of the GSTP1, iNOS and COX-2 in PIA, PIN and PCa.
Materials ant methods: Archived tissue sections obtained after radical prostatectomy from cases (n=30) comprising of PIA, PIN and PCa were testet using immunohistochemistry with monoclonal antibodies against GSTP1, iNOS, and COX-2 (Labvision) and visualised by biotin-streptavidin-alkaline kit (DAKO LSAB 2 kit).The chromogen abundance was qantified using modified quantitative immunohistochemistry approach and measured as eu/pix ± standard error of mean.
Results: The mean values for the intensity of the expression GSTP1 were 122,1±8,64 for PIA, 69,4±11,2 for PIN and 53,8±12,5 for PCa.The mean values for the intensity of the expression iNOS were 78,1±10,16 for PIA, 17±13,12 for PIN and 45,7±11,36 for PCa.The mean values for the intensity of the expression COX-2 were 154,7±4,14 for PIA,113,2±3,95 for PIN and 80,5±4,63 for PCa.
Conclusion: The statistically different levels of expression provide opportunity these markers to be utilized as differential diagnostic and prognostic tools.

P-337

Multiple synchronous renal cell tumors

Dmitry Pasechnik
Rostov Medical University, Rostov Regional Hospital №2, Department of Pathology, Russia

The use of the nephron-sparing surgery demand research of multiple renal cell tumors.

We conducted a retrospective analysis of nephrectomies and autopsies performed in our clinic.
Of 240 renal cell tumors 52 (21, 7%) were multifocal. Most of the patients were men. 24 cases were present where the histological subtype of the largest tumor was clear cell. Satellite tumors were clear cell carcinoma (14), papillary adenoma (10), angiomyolipoma (7), renomedullary fibroma (4), Bellini duct carcinoma (1). 12 multiple renal cell tumors were found with T1, 3 with T2, 9 with T3A primary tumors. 8 patients had bilateral neoplasms. 28 cases were present only multiple papillary adenomas and carcinoma. Usually there were small tumors no more than 3 cm in diameter. In 15 cases multiple tumors originated on a background of nephrosclerosis of various genesis (chronic pyelonephritis, gouty nephropathy, amyloidosis).
When conservative surgery is performed, it should be remembered that 20% patients with renal cell tumor have multiple neoplasms which may cause local recurrence. The origin of multiple renal cell tumors can be bound up with hereditary predisposition or nephrosclerosis creating multifocal tumor field.

P-338
PROSTATE NEEDLE BIOPSY FINDINGS IN PATIENTS WITH BIOCHEMICAL FAILURE AFTER BRACHYTHERAPY

Casalots J; Herrero S; Suarez-Novo JF; Pera J; Alvarez T; Condom E

Departments of Pathology and Urology, Hospital Universitari de Bellvitge, and Department of Radiation Oncology (Institut Català d'Oncologia), IDIBELL, L'Hospitalet de Llobregat, Barcelona, Spain

Introduction. Brachytherapy (BT) is gaining favor as a treatment option for organ-confined prostate carcinoma (PC) with excellent survival results. As a consequence of that, growing numbers of PC patients treated with BT are eventually going to be biopsied because of Prostate Specific Antigen (PSA) levels rises during follow-up.
Objective. To summarize the histological findings in needle biopsies of the prostate in patients with biochemical failure after BT for PC.
Material and methods. Retrospective analysis of the pathology material of patients with a previous history of prostate BT performed at the author's institution.
Results Fourteen BT patients with biochemical failure (according to ASTRO 1997 criteria) were found to have been biopsied. One patient was biopsied twice. So, fifteen biopsies were available for review. All the biopsies showed radiation-related changes in non-tumour tissue, mainly consisting of acinar atrophy, pseudo-infiltrative duct distortion, marked duct cell atypia and stromal fibrosis. Six biopsies from 5 patients were negative for tumour while carcinoma was seen in the other 9 biopsies from 9 patients. Carcinoma was bilateral in 4 out of 9 cases. A Gleason pattern was not reported in 6 cases. The other 3 were classified as Gleason 3+3; 3+4 and 4+3. Immunohistochemical stains for Cam 5.2 and CK903 were performed for diagnostic purposes in six cases (3 of which were finally reported as positive and 3 as negative).
Conclusions. Biopsies are found to be positive for cancer in two thirds of patients with PSA relapse after BT. In nearly half of these cases the tumour is bilateral and in two thirds the Gleason pattern cannot be estimated. Radiation induced changes are found in non-tumour prostate tissue in all cases. Difficulties in the interpretation of these post-BT biopsies are illustrated by the frequent (40%) use of immunohistochemical stains.

P-339
APPROACH TO ETIOPATHOGENIC STUDY OF BLADDER'S TRANSITIONAL TUMORS. CLINICAL-HISTOPATHOLOGICAL AND IMMUNOLOGICAL CORRELATION

M.C.Sánchez Fernández de Sevilla*, Y. Pallás Costa, J. E. Blasco Alfonso.

Department of Pathology. Valencia's University. Pathology and Urology Units from Hospital General de Requena, Spain

FOREWORD
Bladder cancer is the second urological neoplasm more frequently found in men worldwide.Several factors are involved in the epidemiology of this neoplasm as follows:
Eventhough their relation is thoroughly established in some of them (such as in schistosomiasis and bladder's epidermoid carcinoma), in others such as transitional carcinoma, which is the most often histological type, there's no evidence whatsoeverregarding their activating factors which are stated above.
There seem to be unanimity regarding their function as cocarcinogenics, though.
METHOD We are carrying out a study comprising all patients affected by bladder's TCC (transitional cell carcinoma) for the last fifteen years at Eighth HealthCare Area from Comunidad Valenciana (Spain). This widens through a 3,979.82 km2 area and gets a population of 58,414 dwellers.
We compare the implication of serial exogenous factors as: chemicals (tobacco,agriculture plaguecides, industrial and grape-growing toxics), physicals(Lithiasis, BPH, nuclear radiations), biologicals (parasites, bacteria, viruses.);and endogenous factors as: immunized state both tumoral Igs

(IgA) as cellular(T4/T8) and hormonal state in order to check if there is any relation among them.

RESULTS We will proceed to show and discuss the preliminary results out of the study related to geographical localization since we deal with a settled population inland Comunidad Valenciana (Spain) where a nuclear power station (Cofrentes) was founded 30 years ago.

We will set its relationship to a range of both clinical parameters (size, localization,multiplicity, recurrence, response to immunotherapy) and morphologic ones(grade, stage, 'CIS" association and immunohistochemical (ki67, p53, p16)

CONCLUSION TCC aetiology study reveals a multifactor behaviour, however, the fact of having checked a moderate increase of its incidence besides "CIS", makes us believe the presence of possible cocarcinogens in the studied area.

P-340

Hybrid renal cell carcinoma with papillary and clear cell features. Case report

Nadia KOURDA, Jihene KOURDA, Amine DEROUICHE, Faten FARAH, Mohamed CHEBIL, Sarah BALTAGI BEN JILANI, Rachida ZERMANI.
Pathology department Charles Nicolle Hospital, Tunisia

Introduction: Clear cell (CRCC) and papillary (PRCC) renal cell carcinomas (RCC) are the two most frequent subtypes of RCC. RCC displaying an hybrid morphology with areas of PRCC and CRCC or which contained papillary structures with clear cell changes (CCC) are rarely reported.

Case report: We report a new case of hybrid renal cell carcinoma with papillary and clear cell features. 73-years old man a heavy smoker, who presented with a history of presenting with left back pain associated with episodes of total macroscopic haematuria. Imaging showed a mass in the upper pole of the left kidney. Grossly, there were tow distinct tumor the first we found a well-circumscribed, greyish-white tumor the second lesion was nodular lesion; which protrudes beyond the normal contour of the kidney. Its cut surface was variegated, composed of soft, bright yellow parenchyma with areas of hemorrhage and necrosis. Histologically, the first tumor was composed of a typical PRCC the second one was consisting with CRCC. In the papillary areas, the tumor cells were arranged around delicate fibro-vascular tissue fronds containing foamy histiocytes or lymphoplasmocytic infiltration. The cells covering the papillae commonly showed an eosinophilic cytoplasm. Both tumors were of nuclear grade 2. The CRCC, was typically formed by a network of a small blood vessels witch invests alveolar clusters of carcinoma clear cells. Immunohistochemistry showed very intense labeling of tumour cells of both component with cytokeratins: KL1 and vimentin while p504 showed an intense labeling of PRCC component only. The diagnosis of hybrid renal cell carcinoma with papillary and clear cell features was made.

Conclusion: Few authors studied and identied RCC with papillary structures and a possible admixture between CRCC and PRCC. It seems to be important to recognize this type of tumor with hybrid morphologic features of typical PRCC and CRCC due to its more aggressive biologic behavior compared to classical PRCC. Its recognition may also facilitate the classification of RCC with ambiguous morphologies.

P-341

AN USUAL VARIANT OF PRIMITIVE NEUROECTODERMAL TUMOR

Elouni Ahlem, Selma Bellil, Ihsen Zemmel, Khadija Bellil, Ines Chelly, Amina Mekni, Slim Haouet, Nidhameddiine Kchir, Mohamed Moncef Zitouna
Departement of pathology, La Rabta Hospital, Tunisia

Primitive neuroectodermal tumors (PNET) are rare and aggressive tumors seen predominantly in young adults. PNETs may include small round cell tumors showing different degrees of neuroectodermal differentiation and some histological variants. Between 10 and 20% of neuroepithelioma will display spindled areas that ressemble a primitive fibrosarcoma or malignant schwannoma.

We repoet a case of PNET arising in the third cervical nerve root of a 28-year-old woman who's presented with neck mass evolving for two months. Clinical examination found a neurological disturbances with right hemiplegia, left hemiparesia and parasthesia. Neuroimaging schowed a voluminous mass measuring 56×30 mm intersting the left posterior cervical space extending to the cerviccal canal with cord compression evoking in first a tumor of nervous origin. Histological examination of the surgical specimen revealed a malignant prolifferation of spindle cells dissociated by necrotic areas. Immunohistochemical analysis showed positivity for CD99, NSE, Vimentin and PS100 and negativitycytokeratin, EMA, CD34 and desmin.

Through this case and a review of the litterature, we discuss the microscopic features of PNET with spindle cells as well as differential diagnoses.

P-342

STUDY OF KIT EXONS 9,11 AND PDGFRA EXONS 12,18 IN SARCOMATOID RENAL CELL CARCINOMA

Anna Petit; Mireia Castillo; Albert Gaspa; Dolors Colomer*; Xabier García-Albéniz^, Carolina Moreno*, Mireia Camós*, Begoña Mellado^, Carme Mallofré.

Departament d'Anatomia Patològica, Secció d'Hematopatologia (*) i Departament d'Oncologia (^). Hospital Clínic de Barcelona. Universitat de Barcelona, Spain

Background: Sarcomatoid renal cell carcinoma (SRCC) represents high-grade transformation in different Renal cell Carcinoma subtypes. It is associated with poor prognosis because of local aggressiveness, high metastatic rate and absence of effective therapy. Imatinib a selective tyrosine kinase inhibitor of ABL-BCR, KIT and PDGFRA has recently been incorporated for the treatment of neoplasms such as Chronic Myeloid Leukemia (CML) and Gastrointestinal Stroma Tumour (GIST). Immunohistochemical expression of KIT and PDGFRA in the sarcomatoid part of SRCC has been found suggesting the promising use of Imatinib for this neoplasm. Different studies support the concept that mutation-mediated activation of these two tyrosine kinase receptors is a condition for successful therapy with Imatinib as it has been described in GIST. The aim of our study was to sequence exons 9,11 of KIT and 12 and 18 of PDGFRA, where gain of function mutations have been most commonly found in GIST.

Method: Six SRCC cases that showed immunohistochemical expression of KIT (DAKO dil:1/100) and PDGFRA (Santa Cruz dil:1/100) in the sarcomatoid part were selected. Genomic DNA was extracted of formalin-fixed, paraffin-embedded blocks containing sarcomatoid differentiation. DNA was amplified by polymerase chain reaction using the primers corresponding to KIT exon 9,11 and PDGFRA exon 12 and 18 being the product directly sequenced and analysed.

Results: Neither KIT nor PDGFRA mutations were identified in any of the cases tested.

Conclusion: Lack of mutations in KIT exons 9, 11 and PDGFRA exons 12, 18 in sarcomatoid differentiation of RCC does not support the effective use of Imatinib for this neoplasm.

P-343

Molecular alterations of PTEN in prostate cancer

Silvia de Muga; Silvia Hernández; Laia Agell; José Antonio Lorente; Núria Juanpere; Raquel Esgueva; Antoni Gelabert; Sergi Serrano; Josep Lloreta

Department of Pathology and Department of Urology, Hospital del Mar; Departament de Ciències Experimentals i de la Salut, Universitat Pompeu Fabra, and Autonomous University of Barcelona, Barcelona, Spain.

Background: Prostate cancer is the most prevalent non-cutaneous tumour and the second cause of cancer-related death in males of Western countries, as well as one of the most frequent cancers worldwide. Although many different tumour suppressor genes, including *RB1*, *PTEN* and *TP53*, are thought to be involved in prostate cancer, to date no specific gene has been found to be the key in prostate cancer progression. PTEN is a tumor suppressor gene that is able to dephosphorylate the product of PI3K. It has been studied in many cancers and it is known to be deleted or inactivated in many tumor types including endometrial, breast, prostate, lung and bladder among others. Our objective is to analyze the frequency of PTEN mutations in a well-defined group of prostate tumors.

Material and methods: 56 prostate adenocarcinomas have been studied. The series consisted of 44 clinically significant (biopsy or prostatectomy) cases, 9 autopsy tumours, and 3 bone metastases. Gleason grade was ≤7 in 43 and >7 in 11 cases. DNA was extracted (Dneasy Tissue Kit, Qiagen GmbH, Hilden, Germany) by manual microdissection from selected tumor areas of formalin-fixed, paraffin-embedded tissue. Exons 5 to 8 were amplified by PCR from intronic primers and mutational analysis was performed by direct sequencing from purified PCR products.

Results: 3/56 (5,3%) tumours showed PTEN mutations. One case, with Gleason 7, had the mutation K222K in exon 7. In two cases, the mutations have been identified in exon 5. One of them, with Gleason >7, had a deletion leading to a stop codon and the other one, with Gleason <7, had the mutation P95S.

Conclusions: The frequency of PTEN mutations in this series of prostate tumors is around 5%. We have not detected differences in the prevalence of mutations among the different tumor groups. Further analysis including a lager number of cases is being carried out.

This study has been funded by grants FIS/ISCIII 06/1411, FIS965190005, and Asociación Española Contra el Cáncer-Barcelona-2006.

P-344

FGFR3 alterations in prostate cancer

Silvia Hernández; Silvia de Muga; Laia Agell; Nuria Juanpere; Raquel Esgueva; José Antonio Lorente; Sergi Serrano; Josep Lloreta

Departament de Ciències Experimentals i de la Salut, Universitat Pompeu Fabra; Departments of Pathology and Urology, Hospital del Mar; Autonomous University of Barcelona; Barcelona, Spain

Background: Prostate cancer is the second most common cause of cancer-related death in men in the western world, and its incidence is increasing. Fibroblast growth factor receptors (FGFR1–4) regulate diverse cellular processes including cell growth, differentiation, and angiogenesis. In prostate tumors, there is a differential and changing expression of the FGFRs. FGFR3 gain-of-function mutations have been reported in multiple myeloma, cervix, and bladder cancer. However, the functional role of FGFR3 and its alterations in prostate cancer are not known.Our objective is to study the prevalence of *FGFR3* genetic mutations in a large group of prostate tumors classified by stage and Gleason grade.
Method: 98 prostate tumors were recruited prospectively from the files of the Departament of Pathology, Hospital del Mar, BCN. 73 were biopsy or prostatectomy tumors, 16 were latent tumors (from autopsy), and 9 were metastases. The cases were classified as Gleason ≤7 (n=75) and Gleason >7 (n=23). DNA was extracted from formalin-fixed, paraffin-embedded tissue in which representative tumor areas were selected and manually microdissected. Exons 7 and 10 of *FGFR3* were amplified by PCR and the mutational analysis was performed by direct sequencing.
Results: 9 tumors presented *FGFR3* mutations (9%). The most common mutation was the S249C substitution (89%), followed by A393E, found in only 1 tumor (11%). 8 of 75 (11%) tumors classified as Gleason ≤7 vs 1 of 23 (4%) tumors with Gleason grade >7 carried a mutation ($p<0.05$). The F386L germline single nucleotide polymorphism was detected in two samples (2%), both of them with a Gleason grade=7.
Conclusion: In conclusion, *FGFR3* mutations are present in about 9% of the prostate cancers, with a higher prevalence in low grade tumors.
This study has been funded by grants FIS/ISCIII 06/1411, FIS 965190005, and Asociación Española Contra el Cáncer-Barcelona-2006.

Gastrointestinal Pathology

P-345
Clinicopathologic study of 106 gastrointestinal stromal tumors. Experience at two medical institutions in Venezuela.

Karla B. Peña G2; David Parada D1
2Servicio de Anatomía Patológica, Instituto Oncológico Luis Razett, Caracas. Venezuela. 1Servicio de Anatomía Patológica Hospital Vargas, Caracas, Venezuela

Background: Gastrointestinal Stromal Tumors (GIST) are the most frequent sarcomas of gastrointestinal tract, with variable biologic behavior. Due to the availability of molecular-targeted therapy for GIST it is important to distinguish GIST from other mesenchymal tumors of gastrointestinal tract. The aim of this study was to evaluate the clinical, morphological and immunohistochemical features in a GIST group.
Methods: Cases of gastrointestinal mesenchymal tumors between 1997 and 2007 were reclassified according to modern criteria. Haematoxylin-eosin stained sections and clinical information were reviewed. Immunohistochemistry for vimentin, CD117, CD34, smooth muscle actin, desmin, S-100 protein and epithelial membrane antigen was performed. Clinical data were obtained from clinical histories or biopsy reports.
Results: A total of 106 cases were studied. There was a slightly female predominance, with an age range between 17 to 75 years (Mean: 45.83). Gastrointestinal bleeding was the most common symptom. The tumors were located in the stomach (48%), small intestine (31%), large bowel (12%), abdominal tumor (7%) and liver metastasis (2%). Macroscopically, tumors ranged in size from 1.5 to 44 cm (mean, 11.53 cm). Cystic degeneration was present in 15% of the tumors. The cell types observed included pure spindle cell type in 71% cases, followed by pure epithelioid cell type (15%), and mixed epithelioid/spindle (14%). Intermediated and high risk tumors were the most frequent finding. CD117 positivity was detected in 96% tumors, and CD34 was found in 62% cases. 25% were positive for smooth muscle actin, 6.12% cases were positive for S-100 and desmin was present in 4.17% tumors.
Conclusions: In Venezuela, gastrointestinal stromal tumors have similar clinicopathologic and immunohistochemical features compared with other countries. Histologically, it is not always easy to distinguish GIST from other soft tissue lesions. An adequate immuhistochemical study should be used to confirm the pathologic diagnostic.

P-346
CLINICS AND PATHOLOGIC FEATURES OF PATIENTS SCREENED FOR GASTRIC CANCER IN A COLOMBIAN POPULATION DURING 2004–2005

Luís Alejandro Rivero Rendón, Carlos Alberto García Ramírez, Julio Alexander Díaz Pérez, Javier Mauricio Olarte Villamizar, Edgar Julián Ferreira Bohorquez and Ernesto García Ayala
Universidad Industrial de Santander, Bucaramanga, Colombia

Justification: The gastric cancer is one of the most frequent neoplasms. In Colombia this disease is the principal cause of death by cancer. Its early diagnosis is

difficult, for that reason, the mass screening, using endoscopy and histopathological evaluation of biopsy specimens has been imposed as detection method of the early gastric cancer. **Objective:** To describe the clinical and pathological characteristics of the patients who went under screening of gastric cancer at the *Liga Santandereana de Lucha Contra el Cancer* during 2004 and 2005. **Materials and Methods:** A retrospective observational study was made, with a population that corresponds to the people who went under screening of gastric cancer at the *Liga Santandereana de Lucha Contra el Cáncer*. There were interrogated different sociodemographic, clinical and physical examination variables, besides of endoscopic and pathological findings. **Results:** 155 patients were studied, 103 men (66,5%) with a rank of ages between 15 to 93 years old, with an average of 45.43±14.15 years old. The principal referred symptoms were epigastric pain 63.4%, pyrosis 55.5%, regurgitation 26.5%, weight loss 26.5%, metheorism 18%, nausea 16%, vomit 14.8% and abdominal distention 14.8%. The most frequent antecedents were toxicological 25.5%, followed by the massive corn intake 11.6%, having A+ blood type 58% and having history of cancer in the first degree family 21.3%. The only sign found was abdominal mass in the 0.6%. Finally, the most frequent pathological findings were chronic gastritis 31.61%, chronic follicular gastritis 16.77%, peptic ulcer 1.29%, follicular peptic ulcer 1.29% and adenocarcinoma 1.29%. **Conclusions:** Sifting for gastric cancer allows detecting multiple alterations of the upper gastroenteric tract, including diverse neoplastic and preneoplastic lesions. In the studied population the most of the patients, had symptoms and/or antecedents that suggested gastrointestinal lesions. Finally, it must be encouraged the continuity in the programs of early detection of preneoplastic lesions.

P-347

EVALUATION OF ENDOSCOPY VISUALIZATION IN THE IDENTIFICATION OF PREMALIGNES GASTRIC LESSIONS IN A COLOMBIAN PEOPLE WITH HISTOPATHOLOGIC REFERENCE TEST

Julio Alexander Díaz Pérez, Edgar Julián Ferreira Bohorquez, Paola Aranda Valderrama, Luís Alejandro Rivero Rendón, Javier Mauricio Olarte Villamizar and Ernesto García Ayala.
Universidad Industrial de Santander, Bucaramanga, Colombia.

Justification. The gastric cancer is one of the main causes of mortality and morbidity in the world, its high mortality is due to its difficult early diagnosis, and so it's identified in advanced stages. Therefore diverse methods of early detection for gastric cancer and preneoplastic lesions have been studied. However, these methods have had a low cost-effectiveness. **Objective.** To evaluate the yield of endoscopic visualization, to the identification of gastric premalignant lesions, with examination of histopathological biopsy samples as a reference test, in Bucaramanga, Colombia. **Materials and Methods.** There were selected the patients of the *Liga de Lucha Contra el Cáncer*, from Bucaramanga Colombia. A statistical analysis was made by a cross-sectional sampling, to evaluate the gastrointestinal endoscopy in the diagnosis of preneoplastic gastric lesions, using the histopathological examination as a reference test. **Results.** 155 patients were studied, with a mean age of 45.43± 14.15 years and an approximated male:female relation of 2:1. The endoscopic visualization had a sensitivity of 87.84%, a specificity of 55.56%, a Positive Predictive Value of 64.36%, a Negative Predictive Value of 83.33%, a Likelihood Ratio+ of 1.98, a Likelihood Ratio - de 0.22 and a kappa of 0.4272, in the identification of preneoplastic lesions of the stomach in a population with a disease prevalence of 47.74%. **Conclusions.** The endoscopic visualization of the gastrointestinal mucosa, allows a mild identification of early preneoplastic lesions. Therefore its use as the sole test for the detection of lesions preneoplasic is not recommended, making it necessary to evaluate the gastric mucosa through biopsy.

P-348

ASSOCIATED FACTORS WITH THE IDENTIFICATION OF GASTRIC PRENEOPLASIC LESSIONS IN LA LIGA SANTANDEREANA DE LUCHA CONTRA EL CANCER DURING 2004 TO 2005.

Javier Mauricio Olarte Villamizar, Julio Alexander Díaz Pérez, Carlos Alberto García Ramírez, Luís Alejandro Rivero Rendón, Edgar Julián Ferreira Bohorquez, Mario Alexander Melo Uribe and Ernesto García Ayala.
Universidad industrial de Santander, Colombia

Justification. Gastric cancer is one of the malignancies that cause an increased mortality and morbidity with a major impact in Colombia, however the factors associated with the identification of preneoplasic lessions have not been studied. **Objective.** To determine the factors associated with the identification of preneoplasic gastric lesions in Bucaramanga, Santander Colombia. **Materials and Methods.** A study was conducted cross-sectional in Liga Santandereana de lucha contra el cancer with a population of 155 patients who were screened for gastric cancer, who were conducts a survey on different clinical characteristics. **Measurements and Main Results.**155 patients were studied, 103 men (66,5%) with a rank of ages between 15 to 93 years, with an average of 45.43±14.15 years. We was

determined that the infection by H. Pylori (PR 1.69; IC 95% 1.15–2.5), the daily consumption of red meat (RP 1.76; IC 95% 1.265- 2.445) and daily consumption of corn (RP 1.9; IC 95% 1.459- 2.566) were significantly associated with the identification of lesions in patients preneoplasic screenings. **Conclusión.** We identified different characteristics associated with preneoplasic injuries, which are similar to those associated with gastric cancer identified by other studies, this supports the chain of events for the development of this malignancy, and indicates that its eradication would control in the development of this disease.

P-349

PRIMARY MONOPHASIC SYNOVIAL SARCOMA OF THE DUODENUM: CASE REPORT AND REVIEW OF THE LITERATURE

María M Company Campins, Magdalena Garcia Bonafé, Rafael Morales, Carlos Dolz, Angels Vilella, Pere Huguet*
SON LLATZER HOSPITAL, PALMA DE MALLORCA AND VALL D'HEBRON UNIVERSITY HOSPITAL, BARCELONA, SPAIN*

Synovial sarcoma is an uncommon malignant neoplasm of the soft tissues. It mainly affects the soft tissues of the extremities in close proximity to the joints, and less often other sites lacking synovial and periarticular structures, including the head and neck, abdominal wall, intra-abdominal cavity, intracranial cavity, mediastinum, bones, vessels, nerves and visceral organs, such as the lung, heart, kidney and prostate. The gastrointestinal tract is an unusual location with 12 cases described in the literature to date. We report a case of primary synovial sarcoma of the duodenum in a 69-year-old woman. First histologic examination was made in the endoscopic biopsy of the duodenal mucosa and showed infiltration of the tissue by a proliferation of mesenchymal spindle cells whose morphology and immunophenotype suggested monophasic SS. The patient underwent cephalic duodenopancreatectomy. Inmunohistochemical analysis revealed diffuse positivity for antibodies against vimentin, CD56 and bcl-2 expression, partial positivity for EMA and focal AE1/3 positivity. Cytogenetic analysis confirmed the diagnosis, with detection of the X;18 translocation. The patient presented postoperative complications and died at one month following the intervention. The 12 cases described in the literature occurred in the esophagus (8) and the remaining in the gastroesophageal junction, gastric antrum, distal duodenum, jejunum, and colon. Macroscopically as polypoid masses; two intramural cases have been described, one of them ours. Histologically, the biphasic type predominates over other histological types. SS of the gastrointestinal tract is unusual, and may be an underdiagnosed or erroneously diagnosed condition. The differential diagnosis for monophasic SS of the small intestine are gastrointestinal stromal tumor (GIST) and other malignant spindle cell tumors. Cytogenetic study plays a key role in the diagnosis of monophasic types arising in exceptional locations such as the small intestine.

P-350

A CASE OF INCOMPLETE MECHANICAL BOWEL OBSTRUCTION CAUSED BY CYSTIC ENLARGED APPENDIX

Manol Kalniev[1]; Liudmil Velchev[2]; Lidia Karadjova[a]; Todor Todorov[3]; Alexandar Alexandrov*; Georgi Gergov*; Stanislav Hristov*
*[1]Chair of Anathomy, Histology and Embriology; [3]Institute of hepato-biliary surgery–Paris, France; [a]Chair of Emergency Center–Sofia; [3]Chair of Pathology; * Chair of Forensic Medicine, Bulgary*

The author's team presents a case of incomplete mechanical bowel obstruction caused by cystic enlarged appendix, filled with mucus and designated mucocele, that presses the sigmoid colon. As an etiological factor for the occurrence of the appendiceal lumen is accepted the chronical obstruction of the appendiceal lumen, and the pathologoanatomically it is observed a different stage of mucosal hyperplasia, leading to accumulation of the mucus and cystic dilatation. The histological features can be benign or malign. In the complicated forms one can observe infection, perforation with peritonitis and intra abdominal dissemination of the malign form. The treatment is operative.

Reference:

1. Aho AJ, Heinonen RQ, Lauren P. Benign and malignant mucocele of the appendix. Histological types and prognosis.Acta Chir Scand 1973; 139:392–400.
2. Arancha GV, Reys CV. Primary epithelial tumors of the appendix and a reappraisal of the appendiceal "mucocelle". Dis Colon Rectum 1979; 22:472–6
3. Carr NJ, McCarty WF, Sobin LH.Epithelial noncarcinoid tumors and tumor like lesions of the appendix.A clinicopathologic study of 184 patients with a multivariate analysis of prognostic factors. Cancer 1995; 75:757–68.
4. Gibbs NM. Mucinous cystadenoma and cystadenocarcinoma of the vermiform appendix with particular reference to mucocele and pseudomyxoma peritonei. J Clin Pathol 1973;26:413–21.
5. Gonsales JE, Hann SE, Trujillo YP. Mixoglobulosis of the appendix. Am J Surg Pathol 1988;12:962–6.
6. Mac Gillivray JB. Mucosal metaplasia in the appendix. J Clin Patho. 1972; 25: 809–11.

P-351

INTRAEPITHELIAL LYMPHOCYTOSIS AND CD10 EXPRESSION OF DUODENAL MUCOSA IN IRON DEFICIENCY ANEMIA

Sare Kabukcuoglu1; Tuncay Temel2; Aysegul Harmanci2; Ertugrul Colak3

Departments of Pathology1, Gastroenterology2 and Biostatistics3 Eskisehir Osmangazi University School of Medicine, Turkey

Background: Diet iron is absorbed by the proximal small intestine. In coeliac disease the greatest damage is found in this site. Iron deficiency anemia is a common finding in newly diagnosed coeliac disease. The first aim of the study was to determine the frequency of increased intraepithelial lymphocytosis (IELs) in patients with iron deficiency anemia. The second aim of the study was to evaluate CD10 expression pattern of duodenal mucosa in iron deficiency anemia and coeliac disease.

Method: Duodenal biopsies of patients with iron deficiency anemia (n=17), coeliac disease (n=15), and patients with other disease (n=8) were included in the study. Duodenal bopsies were stained for expression of CD3 and CD10 in mucosa using immunohistochemistry. CD10 expression in mucosa and IELs were scored on a five point scale. Villous architecture was scored as a three point scale.

Results: When these study groups were compared according to IELs, it was found that there were more IELs in coeliac patients ($P<0.001$). There was no significant difference in terms of CD10 staining pattern between the coeliac and iron deficiency anemia groups ($P>0.05$). A significant correlation between the IELs and flattening of the mucosa was found in these study groups ($r=0.523$, $P=0.00053$). There was no significant difference in terms of H. pylori infection between the coeliac and iron deficiency anemia groups ($P>0.05$).

Conclusion: CD10 (CALLA), is defined also as an intestinal mucinous marker and stains normal intestinal brush border continously. Various degree of CD10 staining was observed in the duodenal biopsies of iron deficiency anemia and coeliac disease. This study suggested that partial loss of CD10 staining is an early finding of small intestinal mucosal damage.

P-352

Fibroblastic polyps of the colon and colonic perineuriomas: two names for a single entity

Gabriel Groisman; Sylvie Polak-Charcon

Hyllel Yaffe Medical Center, Israel

Background: Fibroblastic polyps and perineuriomas of the colon are unusual mucosal lesions with identical clinical and histologic features and apparent different immunohistochemical and ultrastructural characteristics. Immunohistochemical distinction however, was solely based on results obtained with epithelial membrane antigen (EMA), an antibody whose reactivity on perineuriomas is difficult to demonstrate. Likewise, accurate ultrastructural diagnosis may be flawed by sampling error, preservation artifacts or paucity of specific diagnostic features. In a recent short communication it was suggested that both lesions may represent a single entity. To further evaluate this hypothesis we studied by immunohistochemistry and electron microscopy a series of 28 polyps with clinical and histologic characteristics of fibroblastic polyps/perineuriomas.

Methods: Twenty eight colorectal polyps with clinical and histological features of fibroblastic polyps/perineuriomas were stained immunohistochemically for 4 markers of perineurial differentiation: claudin-1, GLUT-1, collagen type IV and EMA (the latter performed using an extended protocol for antigen retrieval and a kit for signal amplification). Electron microscopy was carried out in 4 cases.

Results: EMA and claudin-1 stained 26 of 28 cases (93%) polyps whereas GLUT-1 and collagen IV were expressed by all the lesions. EMA staining was mostly focal and weak while the other markers exhibited a diffuse and strong signal. Ultrastructurally, tumor cells showed long, very thin cytoplasmic processes, discontinuous external lamina, pinocytotic vesicles and rare thight junctions.

Conclusion: Our findings support the hypothesis that fibroblastic polyps and perineuriomas of the colon represent the same entity. We suggest reclassifying fibroblastic polyps reactive to perineurial markers as perineuriomas. To reach and accurate diagnosis, we recommend employing at least 2 markers of perineurial differentiation, and performing EMA immunostaining with high antibody concentration, prolonged incubation time, and/or extended protocol for antigen retrieval.

P-353

HIGH FEASIBILITY OF HMLH1, HMSH2 AND HMSH6 PROTEIN EXPRESSION AND MICROSATELLITE INSTABILITY ANALYSIS (PENTAPLEX SYSTEM) TO SCREEN PATIENTS WITH CLINICAL CRITERIA OF LYNCH SYNDROME.

Felicia Marginean; Stefania Landolfi; Javier Hernández; Ines de Torres; Marta Garrido; Daniel Badia; Carmen Blazquez; Miriam Cuatrecasas; Santiago Ramón y Cajal

Department of Pathology, Vall d'Hebron University Hospital, Barcelona (Spain)

Background: The Lynch Syndrome (LS), the most prevalent genetic disease in hereditary non-poliposys

cancers (HNPCC), is characterized by germinal mutations in the Mismatch Repair (MMR) genes and by microsatellite instability (MSI). MSI consists of DNA insertions and deletions in microsatellite sequences. In order to select patients for further genetic studies, nowadays the techniques used are immunohistochemestry (IHC) of MMR proteins and MSI analysis by PCR, using a panel of three-dinucleotide and two-mononucleotide repeats (Bethesda Panel). A recent NCI workshop suggested a more sensitive panel of five-mononucleotide repeats.

Method: We evaluated the concordance between IHC and the presence of MSI with the new pentaplex system (five-mononucleotide and two-pentanucleotide repeats). We collected 107 patients with colorectal cancer (CCR) selected by Bethesda clinical criteria of LS. We evaluated by IHC the nuclear expression of MLH1, MSH2 and MSH6 proteins in the neoplastic areas. We extracted DNA from a paired normal-tumor samples for each patient and evalueted MSI using a pentaplex method with BAT25, BAT26, MONO27, NR21 and NR24 microsatellites enclosed in the "MSI Analysis System" kit (Promega Corp.).

Results: We detected loss of nuclear expression of MMR proteins in 18% of the samples (19/107) (MLH1: 14/19, MSH6: 3/19 and MSH2-MSH6: 2/19). About MSI analysis by PCR, we detected MSI-positivity in 13% (14/107) of the patients: 13/14 with High-MSI (in 2 or more MS) and 1/14 with Low-MSI (in BAT26). We found complete concordance between MSI-positivity by PCR and loss of expression of any MMR protein by IHC (14 cases). 5 cases was MLH1-negative by IHC without MSI.

Conclusion: The combination of MSI analysis (pentaplex-system) and IHC allows us the selection of patients who will benefit from further germinal mutation studies. Both techniques are complementary, but other factors must be considered to improve the knowledge of the difference between hereditary and sporadic CCR.

P-354

Is acetylcholine an autocrine growth factor in human colon cancer cells?

Ann Pettersson; Linn Nilsson; Karin Edsparr; Gunnar Nylund; Amir Khorram-Manesh; Per Albertsson; Svante Nordgren; and Dick Delbro.

School of Pure and Applied Natural Sciences, University of Kalmar, Kalmar, Sweden

Background: Acetylcholine (ACh) is an ubiquitos signalling molecule in the organism, in neuronal, as well as non-neuronal tissue, binding at muscarinic and nicotinic receptors (mAChRs; nAChRs). Moreover, ACh has been suggested to serve as an autocrine/paracrine growth factor in several types of tumor or tumor cell lines, but, so far, studies of nAChRs in human colon cancer or colon cancer cell lines are sparse. The 7 homopentamer (7nAChR) convey anti-inflammatory, as well as pro-proliferative effects by ACh-stimulation, as noted in the human colon cancer cell line, HT-29.

The aim of the current study was to investigate whether ACh is an autocrine mediator in the HT-29 cells. This was undertaken by studying the expression of 7nAChRs, and the enzymes being responsible for ACh formation and degradation, choline acetyltransferase (ChAT) and acetylcholine esterase (AChE), respectively. We also investigated the effect of nicotine on the invasive-metastatic properties of the cells. This was achieved by analysis of the secretion of urokinase type plasminogen activator (uPa).

Methods: HT-29 cells were studied with RT-PCR (ChAT, AChE), Western blotting- immunocytochemistry (α7nAChRs, ChAT, AChE), and ELISA (uPa). The cells were challenged with nicotine tartrate (1–1000 nM) for 24 h.

Results:α7nAChRs and ChAT showed strong expression while that of AChE was weak. Nicotine administration to the cells resulted in increased uPa-secretion with a peak at a concentration of 10 nM.

Conclusion:ACh may serve as an autocrine mediator in the HT-29 cells, since the enzymes for its synthesis and degradation, are expressed as well as a receptor for the ligand. Previous reports showed that nicotine increases tumor cell proliferation and here, we demonstrate that this ligand causes increased invasive-metastatic properties. The current findings may point at the development of receptor blocking agents in the prevention of metastasizing colon cancer.

P-355

HER2 over-expression and classic histological features correlation in gastric cancer

Gabriela Acosta; Isabel Frahm; Graciela Lozano;Silvia Vornetti;Ana Cabane; Valeria Cáceres

Instituto María Curie, Hospital De San Isidro, Sanatorio Mater Dei, Productos Roche, Argentina

Background *HER2* is over-expressed in a variety of solid human cancers and related to poor prognosis.

By testing for HER2 over-expression, physicians can accurately select patients likely to benefit from therapy.

There is growing interest in its role in prognosis, pathogenesis and treatment implications for gastric cancer (GC) patients, with the future introduction of trastuzumab therapy.

The aim of this study was to examine HER2 over-expression in GC and to correlate in our population with

age and classic histological features, such as: histological type and grade.
Material and methods 100.H&E-stained, formalin fixed paraffin embedded invasive gastric carcinomas tissue samples with required criteria were collected.
Routine histological parameters were assessed according to *WHO Tumor classification.*
HER-2 analysis was performed using policlonal antibody anti Her 2 (DAKO), microwave antigenic recovery, detection system EnVision (Dako) and developed with diaminobenzidine. Results were interpreted as hercepTest® guideline's.
Results Median age was 64.2 years, histological grades were: G1: 23, G2: 39, G3: 37. HER2+ was over-expressed in 13 patients (13.0%)
With multivariate analysis, age (p=0.1059) and histological grade (p=0.168) were non statistically linked with HER2+ tumors.
Conclusions HER2+ prevalence in our sample (13%) is in line with previously published ones.
Identifying HER2+ patients enables specific therapy leading to a significant change in treatment and prognosis.
Technique standardization is a key to success in identifying HER 2 over-expression in an accurate, precise and truthful way.
Due to the small sample set we couldn't correlate HER2 over-expression with age and classic histological features.

P-356
EFFECT OF MELATONIN ON PROLIFERATION OF LARGE INTESTINE CARCINOMA CELLS SENSITIVE (LOVO) OR RESISTANT (LOVO DX) TO DOXORUBICIN IN VITRO TESTS

Piotr Dziegiel1, Magdalena Fic1, Marzena Podhorska-Okolow1, Malgorzata Drag-Zalesinska1, Teresa Wysocka1, Maciej Zabel1,2
1Department of Histology and Embryology, Medical University of Wroclaw, Wroclaw, Poland 2Department of Histology and Embryology, University of Medical Sciences, Poznan, Poland

Melatonin (MLT) is a pineal hormone affecting proliferation of cultured neoplastic cells. Mechanism of its action has not been fully recognized. It is known to inactivate free radicals, which are generated in the body, i.e. during turnover of anthracyclines (e.g., doxo- and daunorubicin). Also, it has been found that MLT does not alleviates the toxic action of cytotoxic drugs exerted to neoplastic cells. It seems that there exists a potential for overcoming by MLT the multidrug resistance (MDR) of neoplastic cells to doxorubicin (DOX).
This study aimed at evaluation of *in vitro* effects of MLT on proliferation of colonic-originating carcinomas sensitive (LoVo) and resistant ($LoVo_{DX}$) to DOX cells.
The experiments were conducted in *in vitro* conditions on LoVo and $LoVo_{DX.}$ cells. Cells were exposed to MLT in concentrations of 0.1 mM and 1.0 mM and to DOX in concentrations of 0.005 μg/ml (K3), 0.05 μg/ml (K2) or 0.5 μg/ml (K1). The extent of proliferation inhibition in cell cultures was evaluated using staining with SRB technique and readout of optical density in an automatic microplate densitometer (Elx 800). The type of lesions developing in cell nuclei was estimated by comet test. Statistical analysis was performed by using Mann-Whitney's test.
In both cell lines inhibition of tumor cell proliferation (%) clearly increased in parallel to growing DOX concentration but the resistant cell line proved to be definitely less sensitive. MLT significantly inhibited proliferation of LoVo and $LoVo_{DX}$ cells but increase in MLT concentration did not intensify the cytotoxic effect. However, in the case of LoVo cells MLT intensified cytotoxicity of DOX at the concentration of K3. In parallel, MLT significantly overcome resistance to DOX of $LoVo_{DX}$ line cells.
The obtained data confirmed the anti-proliferative effects of MLT on some neoplastic cell lines and its role in overcoming resistance to DOX in resistant cell lines.

P-357
Automatic recognition of colon cells in inflammatory bowel disease

Michal Kruk; Robert Koktysz; Stanislaw Osowski; Wojciech Kozlowski; Tomasz Markiewicz
Department of Pathology Military Institute of the Health Services, Poland; Warsaw University of Technology, Poland; Military University of Technology, Poland

Background: The histological diagnosis of inflammatory boweldisease and other forms of colitis may be subjective. One of the most importantcriterion is inflammatory infiltration of the lamina propria by eosinophils,plasma cells, lymphocytes and other cells. This paper presents the automaticsystem for these cells recognition and counting.
Methods: Analysis has been performed on images taken from 60 randomlyselected cases of colitis patients primarily divided by human experts into 3groups depending on subjective assessment of inflammatory infiltrationintensity: low, moderate and high. There were 6 to 12 tissue samples taken fromeach individual IBD patient The recognition of four main type of inflammatorycells has been done on photographs randomly taken from biopsy specimens. Usingthe basic morphological operations like thresholding, filtering, watershedtransformation, the individual cells are extracted and then used to diagnosticfeatures generation,

based on the texture, geometry and histograms of cellimages. Next the set of five artificial neural networks (MLP, RBF, SVM, KNN,FLD) was used for recognition of four main types of inflammatory cells. Theprocess is fully automatic.

Results: The difficulties of automatic extraction of cells-differ significantly and the probability of error increases for each casedepending on severity of inflammatory changes. Measurements has been performedon images taken from 60 randomly selected cases primarily divided by humanexperts into 3 groups depending on subjective assessment of inflammatoryinfiltration intensity. All cases were divided into: low, moderate and highintensity of inflammatory changes. The results of automatic cell typerecognition and counting were compared with the appropriate results of humanexperts. The average relative discrepancies between scores including all celltypes were as follows: for first group 11.55% (std=3.89%), for second group14.11% (std= 5.44%) and for third group 18.48% (std=5.14%).

Conclusions: The developed computer aided system hasconfirmed its usefulness at automatic processing of medical image of the colonbiopsy specimens leading to recognition and counting subsets and distributionof inflammatory cells.

P-358

Colon Collision Tumor: Adenocarcinoma and Carcinoid Tumor. Case Report and Literature Review

Andrea Prada Serrano; Ana María Uribe
Hospital Universitario San Ignacio, Colombia

BACKGROUND A 63 year old female patient came to the hospital with a chief complain of abdominal distention and constipation. Colonoscopy revealed a 4 cm elevated mass in the ascending colon. The biopsy reported a tubulovillous adenoma. The patient underwent a right hemicolectomy and a ileotransverstomy.

METHOD The tissue obtained at surgery was fixed in 10% buffered formalin and embedded in paraffin. Routine histological sections were stained with hematoxylin and eosin. Immunohistochemical staining was performed.

RESULTS The anatomopathologic study revealed a 5× 3 cm tumoral lesion coming from the colonic mucosa, with an exophytic aspect that infiltrated the wall macroscopically up to the submucosa. Histologically, the lesion was composed by two zones. The first one contained multiple glandular structures, the second had multiple lobules composed of cells with ovoid nuclei, chromatin in a "salt and pepper" conformation, and scarce cytoplasm. Immunohistochemical staining for CK AE1/AE3 revealed strong and diffuse positivity in the cytoplasm of adenocarcinoma cells and carcinoid cells. The carcinoid component revealed positive staining for chromogranin A and synaptophysin. The twelve dissected lymph nodes were found to be negative for tumoral involvement.

CONCLUSION The histologic and immunophenotypic studies of this tumoral lesion confirmed the diagnosis of a colon collision tumor composed by a carcinoid and a moderately differentiated adenocarcinoma infiltrating up to the submucosa. This is a rare diagnosis; with few reported cases in the literature. Prognosis of these types of tumors remains unclear, with some authors suggesting it depends on the two types of isolated components, and other studies suggesting that collision tumors and composite tumors have a worse prognosis.

P-359

Epstein-Barr virus in gastric carcinoma in situ hybridization study of 25 Tunisian cases

Faten Limaiem; Amina Mekni; Ines Chelly; Haifa Azzouz; Khedija Bellil, Salma Bellil; Jalel Boubaker; Nidhameddine Kchir; Moncef Zitouna; Slim Haouet
Hospital La Rabta, Tunisia

Background: The Epstein-Barr virus (EBV) is a ubiquitous human herpes virus implicated in the etiology of many human lymphoid and epithelial malignancies including gastric carcinoma. The presence of EBV DNA in gastric carcinomas was first documented in 1990 using the polymerase chain reaction. EBV-associated gastric carcinoma occurs worldwide, with varying degrees of incidence in different countries. Our study is the first to describe the frequency of EBV in gastric carcinoma in Tunisia.

Aim of study: To evaluate the prevalence of EBV in gastric carcinomas through a series of 25 Tunisian cases.

Methods: Twenty-five gastric adenocarcinomas were retrospectively investigated for the presence of EBV using in situ hybridization. Control cases included samples obtained from 8 antrectomy specimens for duodenal ulcer.

Results: Our study group comprised 15 intestinal type and 10 diffuse type gastric carcinomas. In situ hybridization detected EBV in 68% of gastric adenocarcinomas and 12.5% of control cases with a statistically significant difference between the two studied groups. The proportion of EBV+ gastric carcinomas was 80% in cardial carcinomas, 75% in carcinomas of the fundus and 62.5% in antral carcinomas. Epstein-Barr virus involvement was found more in the diffuse (80%) than the intestinal type (60%) with a statistically significant difference.

Conclusion: Our findings show a higher prevalence for EBV infection in gastric carcinoma than literature. Such results need to be confirmed by other larger series and by Polymerase Chain Reaction.

P-360

HOW DISTANT FROM THE PRIMARY TUMOR SHOULD LYMPH NODES BE RECOVERED IN COLORECTAL CARCINOMA SURGICAL SPECIMENS ?

Marc Pusztaszeri 1, Anne Kuonen 3, Maurice Matter 2 and Hanifa Bouzourene 1.

1 Department of Pathology and 2 Department of Surgery. 3 Medical student. Centre Hospitalier Universitaire Vaudois (CHUV). Lausanne. Switzerland.

Background: the nodal stage of colorectal cancer (CRC) is a major prognostic factor. The total number of nodes examined from CRC surgical specimens has been associated with improved survival possibly because of increased accuracy in staging. However, systematic sampling of lymph nodes located far from the CRC is time and money consuming and few studies have addressed it's value.

Material and Methods: this is a retrospective study of lymph node status from 349 CRC where the mesocolic and perirectal fat was divided into two parts: 1/ close to the tumor (5 cm of both sides of the tumor); 2/ distant from the tumor (above 5 cm of both sides of the tumor).

Results: Tumors were located as follows: caecum (61), ascending (31), transverse (33), descending (31), sigmoid (103) and rectum (90). The median number of nodes recovered from the fat close to and distant from the tumor was respectively 13 (range 0–66) and 4 (range 0–33). There were 175 pN0, 104 pN1 and 70 pN2 cases. In all pN1 cases, metastatic lymph nodes were located close to CRC, except for 5 cases in the rectum and 1 case in the colon where metastatic lymph nodes were only present in the distant fat. In pN2 cases, the median number of positive nodes close to and distant from the CRC was respectively 5 (range 3–29) and 0 (range 0–9).

Conclusion: In the colon, lymph nodes should be recovered only from the pericolic fat close to the tumor. In the rectum, systematic sampling of nearby and distant lymph nodes is mandatory since rare cases of metastasis arise in distant lymph nodes only. This quantitative restriction of lymph node sampling for CRC surgical specimens might induce a cost effect without having deleterious effects on patient treatment and outcome.

P-361

solitary rectal ulcer syndrom: a clinico-pathological study of 10 cases

Naser Al-awadhi; Nabeel Al-Brahim; Saleh Al-Enezi; Mahmoud Ahmad

Department of Pathology and Medicien; Farwaniya Hospital; Kuwait

Background: Solitary rectal ulcer syndrome (SRUS) is a rare disorder and has a wide spectrum of clinical presentation and variable endocscopic findings. To further characterize the clinical and pathological features, a retrospective, hospital based clinico-pathological study was conducted.

Materials & Methods: All cases of SRUS diagnosed at Farwania Hospital, Kuwait between 2002 and 2007 were retrieved. The histological slides were reviewed by two authors to confirm the diagnosis. Immunohistochemical stain for smooth muscle actin (SMA) was performed. The clinical files were reviewed for clinical features and endoscopic findings.

Results: Ten cases were identified 6 males and 4 females with an age range of 22–67. Rectal bleeding, constipation and abdominal pain were the most common clinical presentation and were seen in 80% of cases. Rectal ulceration was the most common endoscopic finding seen in 70% of the cases. Thirty percent of cases had multiple ulcerations. Two patients (20%) had polyps one of them was multiple. The histological examination of 11 biopsies (1 patient had 2 sets) reveled that all cases had surface serration, fibromuscular obliteration and crypts distortion. Forty five percent of the cases had diamond crypts. Ectatic mucosal vessels were a common finding. SMA expression was seen in all examined cases.

Conclusion: SRUS is a rare disorder and only ten cases were diagnosed in Farwania hospital over 6 years period. The clinical presentation of our patients is typical for SRUS. The presence of polyps and multiple ulcerations in the endoscopic findings further support that SRU is a misnomer. Surface serration, fibromuscular obliteration and crypts distortion are the most diagnostic features. Presence of Diamond crypts is additional diagnostic feature.

P-362

How is the importance of inflammatory cells in the pathogenesis of colitis?

Sanei MH1*, Hadizadeh F2, Alavi SA2

Department of Pathology, Alzahra hospital, Iran

Introduction: Free radical effects are one of the known mechanisms responsible for inducing inflammatory bowel disease (IBD). In addition to inflammatory cells, tissues are another origin for free radicals. The first origin can be controlled by steroids but tissue oxidizing agenoidsts are not affected by these drugs. Identifying the role of each mechanism can lead to a better treatment for IBD. This study is conducted to identify inflammatory cells role as the basic pathogenesis for colitis and also to evaluate the efficacy and importance of steroids in IBD treatment.

Methods & Materials: In an analytical-experimental study, 30 healthy male mice were divided into 6 groups, each consists of 5 members. Group 1 had induced colitis with acetic acid enema. Groups 2 was exposed to acetic acid like group 1, after immune suppression, and in group 3 the distal of colon which was extracted, was exposed to acetic acid. All of these groups had one control group that was exposed to water injection instead of acetic acid. Following sacrificing and laparotomy, their tissues were studied and compared on the basis of histologic and biochemical factors.
Results: Considering neutrophilic infiltration there were significant differences between group 1 and its control group and also between groups 2 & 3 ($p<0.05$).
There were significant differences among groups 2, 3 and their control ones and also between groups 1 and the control of group 3 in terms of Goblert depletion.
Based on tissue originated H2O2 we found significant differences between group 1 and its control one and group 3 and also between groups 2 and the control of group 3. All the three groups were significantly different with their controls based on FRAP and such differences were seen between groups 1 & 2 and also between their control groups ($p<0.05$).
Discussion: This study not only presents that neutrophiles aren't the only cause of oxidation process and production of tissue free radicals, but also make suspicions about steroids effect in IBD treatment because of the increasing amount of H2O2 in the presence of steroids and steady state of FRAP in such condition.
Keywords: colitis, acetic acid, steroid

P-363
COLUMNAR-LINED ESOPHAGUS AND FETAL ESOPHAGUS: IMMUNOHISTOCHEMICAL PHENOTYPE COMPARISON

Timur Akhmetov, Semyon Petrov, Michael Burmistrov
Kazan Cacer Centre (Kazan, Russia); Kazan State Medical University (Kazan, Russia)

Background. Although columnar lined esophagus (CLE) attracts much attention of investigators due to its role in development of esophageal adenocarcinoma nowadays, its nature is still being discussed.
Purpose. To compare immunohistochemical (IHC) phenotype of CLE and fetal esophagus.
Methods. 6 autopsy cases of 12–24 weeks gestation fetuses and 67 biopsy cases of CLE were studied prospectively using IHC (antibodies to CK7, CK20, CK5, CK14, villin, CEA and Ki-67).
Results. At 12–16 weeks of gestation (3 cases) fetal esophagus was lined by stratified cuboidal epithelium positive for CK7 (moderately), CK20 (from weak to moderate- reaction only in distal esophagus), CK5&14 (weakly) and CEA (weakly). At 16–18 weeks of gestation (1 case) esophagus was lined by stratified squamous epithelium positive for CK7 (weakly), CK5&14 (brightly) and CEA (moderately). At 18–24 weeks of gestation (2 cases) esophagus was lined by stratified squamous epithelium positive only for CK5&14 (brightly) and CEA (moderately). Proliferation level in basal layer of esophageal epithelium in studied fetuses was low (3,6±0,3%).
CLE was divided into gastric type (28 cases), intestinal type-Barrett's esophagus (23 cases) and predominant gastric epithelium with small islets of intestinal epithelium (13 cases). CLE with gastric type was CK7 positive and CK20 negative, weakly positive for villin and CEA. CLE with intestinal type was CK7 and CK 20 positive, strongly positive for villin and CEA. We revealed positive reaction in columnar epithelium for CK5&14 in 20 cases of CLE.
Conclusions. Similarities of IHC phenotype in CLE and fetal esophagus may support hypothesis of return to fetal state of epithelium in pathogenesis of CLE. Expression of CK7&14 (markers of squamous differentiation) in CLE supports its metaplastic nature.

P-364
CAPILLARY HEMANGIOMA OF THE ILEUM PRESENTING AS AN INTUSSUSCEPTION

Ahlem Blel; Amina Mekni; haikel Bdioui; Inés Chelly; Selma Bellil; Khadija Bellil; Slim Haouet; Nidhameddine Kchir; Moncef Zitouna.
Department of Pathology, La Rabta Hospital Tunis, Tunisia.

Hemangiomas of the small intestine are rare benign tumors; accounting for only 0,05% of all intestinal neoplasms and 7–10%of all benign tumors of small bowel. These tumors may be solitary or multiple and usually present with overt bleeding or chronic anemia. The majority of gastrointestinal hemangioma are cavernous type and situated in the middle jejunum. We report a new case of polypoid capillary hemangioma of the ileum. A man of 20 years admitted in emergency for abdominal pain and vomiting. Abdominal ultrasound and computed tomography scan showed a large lobulated mass of terminal ileum suggestive of an intussusception. A resection of terminal ileum and coecum was made. Gross pathological examination revealed a polypoid ileal tuminal tumor mesuring 10×3×2 cm that was myxoid at section. Microscopy revealed a capillary hemangioma of terminal ileum. We discuss the differential diagnoses of vasoformative intestinal lesions and review the litterature on enteric hemangiomas.

P-365

UNUSUAL FOLLICULAR ADENOMA OF THYROID GLAND: MUCINOUS VARIANT

Ahlem Ouni; Amina Mekni; Inés Chelly; Sélima Kharrat; Selma Bellil; Khadija Bellil; Slim Haouet; Nidhameddine Kchir;Samia Sahtout; Moncef Zitouna.
Department of Pathology, La Rabta Hospital Tunis, Tunisia.

Follicular cells of the thyroid may undergo squamous, oncocytic or mucinous metaplastic changes. Of these, the mucinous change is the most unusual, and mucinous follicular adenoma of the thyroid is extrrmrly rare. It's a variant of adenoma characterised by accumulation of abundant extracell mucin, often accompanied by a microcystic growth pattern. We describe a case of mucinous follicular adenomaof thyroid gland in a 36-year-old euthyroid woman. She's presented with a 1-year history of a right anterior neck mass. The patient underwent a hemithyroidectomy; the cut surface of the 7×3,5 cm lesion was solid and tanned orange. Microscopy of the tumor showed a mucinous follicular adenomawhich follicular cells were positive for alcian blue.

P-366

Ileoceacal actinomycosis: Diagnosis difficulties and management, a case report.

Inès Chelly, Heifa Azouz, Amina Mekni, Selma Bellil, Khadija Bellil, Nidhameddine Kchir, Slim Haouet, Moncef Zitouna
Hospital LA RABTA, BAB SAADOUN. TUNIS-TUNISIA.

INTRODUCTION: Actinomycosis is an unusual chronic granulomatous disease. Actinomyces israelli has been found to be related to infectious process in those patients with affected skin integrity leading to abcess formation, fistulae or mass lesions. Actinomycosis mainly presnts in three forms cervicofacial (20%), gastrointestinal (20%) and thoracic (15%). Primary bowel involvement is rare, although it has been increased in frequency over the last years. The most common sites of the disease are the transverse colon and the caecum with the appendix.
CASE REPORT: The patient was a 55 year old man who presented with abdominal discomfort and a palpable right lower quadrant mass defined on CT scan. He underwent en bloc resction of the mass for a presumed diagnosis of tumour of uncertain type with intestinal involvement. The diagnosis was reversed, when histology revealed filamentous organisms consistent with actinomyces. He was treated with high dose penicillin for several weeks and was discharged from the hospital taking penicillin.
COMMENTS: Preoperative diagnosis of abdominal actinomycosis is difficult. An accurate diagnosis is always obtained in a histological or microbiological examination, often requiring surgical resection. Recognition is important because successful treatment requires combined surgery and prolonged penicillin treatment. The diagnosis and management of abdominal actinomycosis will be discussed through a review of the literature and a case report from our own institution.

P-367

Carcinogenetic pathways in synchronous or metachronous colorectal carcinomas

Eva Musulen; María Teresa Fernandez-Figueras; Laura Layos(1); Ariadna Quer; Aurelio Ariza
Departments of Pathology and Oncology(1), Hospital Universitari Germans Trias i Pujol, Badalona, Barcelona, Spain

Background: Synchronous or metachronous (S/M) neoplasms arising in the same organ system of an individual provide an interesting model to unravel the mechanisms of carcinogenesis. The aim of our study was to elucidate whether those pathways are differentially involved in S/MCRC according to inheritance pattern, microsatellite instability (MI) status, location, or stage.
Method: Expression of p53, β-catenin, PTEN, p21, p16, cyclinD1, hMLH1, hMSH2, and hMSH6 was immunohistochemically studied in a series of 43 S/MCRC from 20 patients (P) (14M/6F; age range, 41–88 years). Nineteen tumors (T) were located in the right side and 24 in the left. Thirteen T were confined to the intestinal wall (T1+T2), whereas 30 were advanced T (T3+T4). Twenty-one T showed negative lymph nodes (N0), while 22 has metastasized to lymph nodes (N1+N2). Formalin-fixed, paraffin-embedded tissue from these 43 T was used to build a TMA block. Different expression patterns were evaluated for β-catenin, p21, and p16. Expression intensity was semiquantitatively evaluated as 0=negative; 1=low; 2=moderate; 3=high. Medical records were searched for a history of familial cancer.
Results: Four P fullfied Amsterdam criteria for familial CRC. All their 10T were unstable. The remaining 16P showed sporadic CRC. Of their 33T, 4 were unstable and 29 were stable. An identical expression patterns of all markers investigated was only observed in 15 sporadic T from 7P. Nevertheless, a correlation was found between evidence of β-catenin mutation and expression of both p53 and cyclinD1 ($p=0.028$ and 0.055, repectively) when analyzing all T as a single group.
Conclusions: S/MCRC do not show a specific pattern of cell cycle abnormalities even when they are segregated according to type of inheritance, MI status, location, or stage. Random factors, therefore, must be operative in the

development of these T, which fail to reveal a differential involvement of the known carcinogenetic pathways of CRC.

P-368

Expression of cell adhesion molecule CD44 in gastric adencocarcinoma and its correlation with cliniclopathological characteristics and survival time

Kamran Ghafarzadegan; Hamidreza Raziee; Hamidreza Sima; Mostafa Jafarzadeh; Ehsan Esmaeili Shandiz; Hanieh Hosseinnezhad; Maryam Bahrani; Ali Taghizadeh kermani; Omeed Moaven; Mohammadreza Ghavam Nasiri

Gastric Cancer Research Group, Mashhad University of Medical Science, Mashhad, Iran.

BACKGROUND: Gastric carcinoma is one of the leading causes of cancer death worldwide. The invasion depth and lymph node metastasis result from the polygenes and their protein expression in gastric carcinoma. Two types of gastric adenocarcinoma can be distinguished histopathologically: diffuse and intestinal type. We have examined the cell surface molecule CD44, which is attracting interest because of reports that isoforms are associated with metastasis. This transmembrane glycoprotein is involved in cell-cell and cell-matrix interactions and in cell trafficking and, thus, may play a role in tumor metastasis and/or local invasion. In the present study we measured the expression of CD44 in diffuse and the intestinal type adenocarcinoma and its effect on survival time in the patients.

METHOD: Paraffin wax embedded gastric adenocarcinoma cases were selected from the Omid University Hospital (Mashhad, Iran) pathology archive and were assessed by immunohistochemistry method. The patients comprised 74 males and 26 females, who had undergone curative surgery without any prior treatment between 2000 and 2006. Their mean age was 63.31 years (from 26 to 82). Adjacent normal mucosa was used as control.

RESULTS: A total of 100 gastric adenocarcinoma cases were included in the study. The tumors were categorized into intestinal (74%), diffuse (21%) and mixed type (5%). CD44 staining showed that, 64% of patients were positive (51 patients had CD44 only on surface membrane of the tumoral cells and in 13 patients CD44 was detected both in membrane and cytoplasm) and 36% were negative for CD44. 100 normal gastric mucosa showed no CD44 staining. There was a relationship between histological type of tumor and CD44 staining. 70% of intestinal types, 42% of diffuse types and 80% of mixed type gastric cancers showed positive CD44 staining. CD44 was more expressed in intestinal types (P=0.02) and there was a significant difference between well differentiated types in compare with others. The survival analaysis has shown that CD44 cause a poor prognosis for the patients (P=0.05).

CONCLUSION: The CD44 expression rates in three types of gastric cancer were different significantly (P<0.05). Expression of CD44 was related to the genesis and prognosis of gastric cancer, and is one of the biological markers indicating metastasis and poor prognosis.

P-369

Gastrointestinal stromal tumors recognized as ovarian neoplasms before surgical operation.

WandaMichej;.Zbigniew.Nowecki;Piotr Rutkowski; Włodzimierz Olszewki;Włodzimierz Ruka

Cancer Centre Instytute Warsaw Roentgena 5 Str.. Poland

Gastrointestinal stromal tumors (GISTs) are the most commonneoplasms of mesenchymal origin ofstomach and small bowel. They derive from precursors of Cajal's cells andexpress positive reaction with CD117 antibody. This immunohistochemicalexamination is currently a base of recognition them and allows to treat with imatinib – they are resistant to classic chemotherapy and radiotherapy. Theymetastatic mainly to the liver and peritoneal cavity. Surgical resection is the most important treatment of them, butit is very often is impossible toremoved them completely. In such cases treatment with imatinib reduces size oftumors, and makes possibility to resect them completely. Aim of the study was histopathologic analysis of tumors diagnosedpreoperatively as ovarian neoplams in women, whereas postoperative pathologicrecognition revealed, that they were gastrointestinal stromal tumors (GISTs).

Materials and methods Between 2002 and 2007 in Department of Pathology of Cancer Center inWarsaw there were diagnosed 130 gastrointestinal stromal tumors of small bowelin women confirmed by positive reaction of CD 117. The postoperative materialoriginated from gynaecological department of our Institute, but most of them became from anotherhospitals from surgical and gynaecological wards for consultation.

All GISTs in women	GISTs of small intestine in women	GISTs recognized as ovarian neoplams preopratively
130cases	44cases	16 cases
100%	34%	12%

Results Grossly the tumor's diameter ranged from 10 to 15 cm, cream - coloured,sometimes with many haemorrhages. Most of them were attached to small bowel. Afew of them were connected to large intestine. In two cases they looked likebig leiomyomas of uterus. Microscopically: the spindle cells were seen mostlymixed with epitheliod and

signet –ring ones. There were no big atypia..There were skenoid fibers in a few tumors. Mitotic figures were counted in 50high power fields. They ranged from 5 to 20. Neoplams expressed a positivereaction with CD 117 antibody. The most of them were no resected completely, sothey demanded postoperative treatment.
Conclusions In case of uncharacteristic tumor of ovarian with similarmorphology to GIST, it is necessary to make immunohistochemical examination with antibody CD117, to make wellrecognition and in a consequence to introduce therapy with imatinib or othersinhibitors of kinase tyrosinase..

P-370
DECIDUOSIS IN A CASE OF AN ACUTE APPENDICITIS MIMICKING HISTIOCYTIC NODULES OF MALAKOPLAKIA

Sibel Gelecek Geyik; Gulcin Guler Simsek; Ayla Tezer; Heyecan Ökten; Servet Güreşçi; Ali Coşkun
Kecioren Egitim & Arastırma Hospital, Turkley

Deciduosis is a rare event, usually located in the ovaries, cervix and uterus, but may also be located on peritoneal surfaces of pelvic organs. Usually it is an incidental finding that has not been associated with clinical symptoms. Our patient had chronic abdominal pain that was increased in pregnancy. She was taken into an operation with a clinical diagnosis of an acute appendicitis. Pathological examination of the appendix showed nodules of decidual cells containing intrcytoplasmic blue vacuoles, in a dense acute inflammatuar stroma. These mucin vacuoles may mimic calculospherules that are characteristic of malakoplakia. Calculospherules appear refractile and stain with iron and calcium but decidual cells do not. They may also suggest adenocarcinoma however the vacuoles within the decidual cells contain acidic rather than neutral mucin.

P-371
TUMOR ANGIOGENESIS IN GASTRIC CARCINOMA: CORRELATION WITH CLINICO-PATHOLOGICAL FACTORS AND SURVIVAL OF THE PATIENTS

Sorina Tăban; Daniela Lazăr; Elena Lazăr; Alis Dema; Marioara Cornianu; Ioan Sporea; Adrian Goldiş
University of Medicine and Pharmacy "V. Babes" Timisoara, Romania, Department of Pathology

Aim: To evaluate the relationship between microvessel density (MVD), VEGF expression, clinico-pathological factors and survival in patients with gastric cancer.
Methods: We performed a prospective study regarding the outcome and aggressiveness of gastric carcinoma on a five year period, including 61 patients (43 men, 18 women), mean age 59,34 years. For the immunohistochemical assessment of tumor angiogenesis, we used the monoclonal antibodies anti-CD34 and anti-human VEGF by LSAB technique. Angiogenesis was quantified by measuring MVD. Immunohistochemical expression of VEGF was assessed by using a score representing the sum between the percentage of positive cells and the intensity of the staining.
Results: Gastric carcinomas were characterized by an intense neoangiogenesis, especially in the front of invasion, with numerous microvessels and CD34 positive "hot spots" among the malignant structures. MVD in gastric carcinomas ranged between 12 and 65, with a mean value of 38,7± 24,3, significantly increased in comparison with normal mucosa (12,5±9,8, $p<0.001$ ES). Increased MVD correlated with diffuse type of gastric cancer, poor differentiation, presence of vascular invasion and advanced TNM stage. For patients with MVD>38 (34 cases – 55,7%), the 5-year survival rate was significantly decreased in comparison with patients with MVD<38 (7,4% vs. 23,5%). We obtained positive immunostaining for VEGF in 40 cases of gastric carcinomas (65,6%), significantly more frequent than gastric normal mucosa (6,5%, $p<0.0001$ ES). For gastric carcinomas with VEGF +~++, the overall 5-year survival rate was 12,5%, significantly decreased than for patients with VEGF negative carcinomas (23,8%).
Conclusions: Our study demonstrates a strong correlation between VEGF expression and MVD, these two markers of neoangiogenesis playing an important role for the biological behavior, progression and prognosis of gastric carcinoma.

P-372
RELATIONSHIP BETWEEN THE EXPRESSION OF CYCLOOXIGENASE-2, VEGF, TUMOR ANGIOGENESIS AND PROGNOSIS OF THE PATIENTS WITH GASTRIC CANCER

Daniela Lazăr; Sorina Tăban; Ioan Sporea; Mărioara Cornianu; Adrian Goldiş; Elena Lazăr
University of Medicine and Pharmacy "V. Babes" Timisoara, Romania; Clinic of Gastroenterology

Aim: To assess the immunohistochemical expression of cyclooxigenase-2 (COX-2) in gastric carcinomas and peritumoral mucosa with different lesions, by analyzing the correlation with clinico-pathological factors, angiogenesis and survival of the patients.
Methods: Our prospective study included 61 patients operated for gastric cancer (43 men and 18 women, mean age 59,34 years). COX-2 and VEGF immunohistochemical expressions were evaluated by semi-quantitative analysis. We assessed microvessel density (MVD) and VEGF

expression in COX-2 negative group and COX-2 positive group of gastric carcinomas.

Results: COX-2 immunostainings were observed significantly more frequent in gastric carcinomas, in comparison with peritumoral normal mucosa (57,4% vs. 4,9%). Areas of dysplasia surrounding carcinomas of intestinal type expressed COX-2 in 35,5% cases, significantly more frequent than normal mucosa (p=0.000384 ES). COX-2 immunostainings were significantly more frequent in the intestinal type of gastric carcinomas than diffuse type (68,4% vs. 29,4%, p<0.001 ES). COX-2 expression correlated with the dept of tumor invasion, presence of nodal metastasis and advanced TNM stage, but didn't influence the 5 year survival rate of the patients. Mean MVD values (39,4) was significantly higher in COX-2 positive carcinomas (35 cases). We observed a strong direct correlation between COX-2 and VEGF in gastric carcinomas (r=0.562, p<0.001 ES). VEGF negative carcinomas expressed COX-2 in only 19% of cases, in comparison with those VEGF positive, associated with COX-2 immunoreactions in 77,5% cases.

Conclusions: COX-2 immunoreaction appears to be in our study an early event of the sequence involved in the development of the intestinal type of gastric carcinoma. Our results showed a strong correlation between the immunohistochemical expression of COX-2, VEGF and MVD in gastric carcinomas, demonstrating an intense angiogenesis in COX-2 positive tumors.

P-373
IMMUNOHISTOCHEMICAL EXPRESSION OF E-CADHERIN IN GASTRIC CANCER: CORRELATION WITH CLINICO-PATHOLOGICAL FACTORS AND SURVIVAL

Elena Lazar; Daniela Lazar; Sorina Taban; Alis Dema; Marioara Cornianu; Ioan Sporea; Iulia Ratiu

University of Medicine and Pharmacy "V. Babes" Timisoara, Romania, Department of Pathology

Background: To investigate the immunohistochemical expression of E-cadherin in gastric carcinomas and in adjacent mucosa (normal or with lesions of chronic atrophic gastritis, intestinal metaplasia or dysplasia).

Methods: We included 61 patients with gastric cancers operated in Clinical Emergency County Hospital Timisoara. We analysed the E-cadherin immunohistochimical expression, the correlation with clinical and pathological factors and the outcome of the patients. The positive homogeneous pattern of staining for the cellular membranes is considered normal. Aberrant E-cadherin expression was represented by the negative or the heterogeneous pattern (both in the cytoplasm and on the membrane).

Results: Areas of chronic atrophic gastritis and intestinal metaplasia presented a normal pattern of immunostaining for the membranes. Aberrant E-cadherin expression was noticed in 30 cases of gastric carcinomas (49,2%) and in 11 cases (35,5%) of epithelial dysplasia, significantly more frequent in comparison with the surrounding normal mucosa (p<0.001 ES). Our results showed no correlation between E-cadherin expression and gender, age, tumor location, pT, pN, pTNM and lympho-vascular invasion. Aberrant E-cadherin immuostainings were significantly more frequent in diffuse-type carcinomas in comparison with the intestinal-type carcinomas (82,4% vs.31,6%)(p= 0.000491 ES). Signet-ring carcinomas and anaplastic carcinomas presented a high proportion of aberrant immunostainings (82,4% and 100%), as well as poor differentiated carcinomas (61,5%). Carcinomas with distant metastasis presented significantly more aberrant immunostainings than those without metastasis (71,4% vs.42,6%). The 5 year survival rate was significantly lower in patients with aberrant E-cadherin expression in comparison with the patients presenting normal staining (10% vs. 22,6%).

Conclusions: Our data suggest a strong correlation between Lauren classification of gastric carcinomas and E-cadherin immunohistochemical expression. Assessment of the survival curve of the patients highlighted the role of prognostic factor for the aberrant immunohistochemical E-cadherin expression.

P-374
Monocarboxylate transporter expression correlates with CD147 and HIF-1α in gastric cancermonocarboxylate transporter expression correlates with CD147 and HIF-1α in gastric cancer

Céline Pinheiro, Adhemar Longatto-Filho, Kleber Simões, Luísa Ferreira, Venâncio A.F.Alves, Fernando Schmitt, Fátima Baltazar

Life and Health Sciences Research Institute, School of Health Sciences, University of Minho, Braga, Portugal

Background: Acid efflux through *M*ono*C*arboxylate *T*ransporters (MCTs) constitute one of the most important mechanisms involved in the maintenance of tumor intracellular pH and, as a result, MCTs constitute an attractive target in cancer therapy, which has not been explored yet. Recently, it was demonstrated that CD147 is required for proper expression of MCT1 and MCT4 at the cell surface as well as for catalytic activity of the transporters. On the other hand, silencing studies showed that maturation and cell surface expression of CD147 depends on MCT1 and MCT4 expressions. Also, it was described that MCT1 is induced by hypoxia and that MCT4, but not MCT1, is up-regulated by the hypoxia-inducible factor-1-α (HIF-1α).

Method: Gastric samples, including normal, metaplastic, tumoral and metastasis tissues, were obtained from the Faculty of Medicine, São Paulo University (Brazil). Analysis of the expression of MCT1, MCT4, CD147 and HIF-1α was performed by immunohistochemistry with specific antibodies, using the avidin-biotin-peroxidase complex assay. Immunoreactions were evaluated both qualitative and semi-quantitatively.
Results: We found significant correlations between CD147 expression and both MCT1 and MCT4 expressions. Also, and as supported by the literature, HIF-1α expression correlated with MCT4 expression but not with MCT1. CD147 expression was also associated with HIF-1α expression and nodal metastasis. In addition, CD147, MCT1, MCT4, HIF-1α expressions were associated with intestinal-type gastric carcinoma (Lauren classification).
Conclusion: Our data support the evidence that MCT1 expression is regulated by CD147 and that MCT4 expression is regulated by both CD147 and HIF-1α, for the first time in human tumour samples. These observations contribute to the understanding of the metabolic alterations in cancer and might be of value in the development of new therapeutic strategies.

P-375
IMMUNOHISTOCHEMICAL EXPRESSION IN GASTROINTESTINAL STROMAL TUMORS (GISTs) AND EXTRAGASTROINTESTINAL STROMAL TUMORS(EGISTs).

Simona Enache 1; Mihaela Mihai 1; Florina Vasilescu 1; Cristina Iosif 1; Florin Andrei 1; Dana Terzea1,2; Mihai Ceausu1,2; Alina Georgescu1;Camelia Dobrea1,2; Dorel Arsene1; Valentin Enache3; Georgeta Butur1; Neagu Maria1; Diana Teletin1;Carmen Ardeleanu1,2
1.National Institute of Pathology"Victor Babes", Bucuresti, Romania 2.University of Medicine and Pharmacy"Carol Davila" Bucuresti 3.Clinical Hospital "Sf. Ioan" Bucuresti, Romania

GISTs are the most common primary mesenchymal tumors of the gastrointestinal tract.
They are CD117 (stem cell factor receptor) - positive mesenchymal spindle or epithelioid cells neoplasms, believed to originate from interstitial cells of Cajal (intestinal pacemaker cells) or related stem cells. Most GISTs arise in the stomach and small bowel, while rare cases occured elsewhere in the gastrointestinal tract are known as EGISTs. An improvement of histopathological diagnosis is required by their malignant potential and also by recent advances in their management with Glivec.
They typically express CD117, as well as CD34, SMA and S100. Recently it was reported Nestin (intermediate filament of neuroectodermal stem cells and progenitor skeletal muscle cells) positivity.
Aim: We analized the immunohistochemical expression of CD117,CD34, SMA, S100 and Nestin in GISTs, compared with EGISTs, for establishing morfo-immunohistochemical correlations with possible therapeutic implications.
Method: 63 GISTs and 8 EGISTs were morphologically and immunohistochemically evaluated using hematoxiline-eosine standard method and immunohistochemical ABC method for CD117, CD34, ACT, S100 and Nestin.
Results: 74,6% of GISTs and 50% of EGISTs were positive for CD117. CD34 and S100 expression was 84,2% and 87, 9% while ACT was positive in 49, 2% of GISTs and 25% of EGISTs. Nestin was highly expressed in GISTs: 80,9% and correlated with CD117 expression in 70% and with CD34 expression in 69%. In EGISTs, Nestin was positive in 50% and correlates with CD117 and CD34 expression in 50%. Spindle-cells GISTs were positive for CD117 in 43% while spindle-cells EGISTs were CD117 positive in 100%, suggesting a possible better response in Glivec therapy.
Conclusions: The Nestin expression in GISTs and EGISTs could be considered a good marker together with CD117 and CD34 in establishing the tumoral variants; its positivity could support the stem cell-Cajal cell origin and also to represent new possible therapeutic targets.

P-376
CDX2 and Villin are useful markers for metastatic colorectal cancer.

Jeanette Musser; Sussie Steen Jensen; Betsy Spaulding
Dako North America, Inc., USA

CDX2 and Villin are immunohistochemical markers that have been demonstrated to be of diagnostic value in identifying tumors derived from intestinal epithelium. CDX2 is a transcription factor expressed in cells of intestinal epithelium and is thought to play an important role in their proliferation and differentiation. Villin is a 95 kDa calcium-regulated actin-binding protein that regulates actin filament assembly. It is a major constituent of the brush border of epithelial cells, forming absorptive surfaces in the microvilli of intestinal and renal proximal tubular epithelia. Using monoclonal mouse anti-Villin (clone 1D2 C3) and a newly developed monoclonal mouse antibody to CDX2 (clone clone DAK-CDX2), we evaluated CDX2 and Villin expression in a series of primary and metastatic tumors to assess the utility of the antibodies in distinguishing metastatic colorectal cancer from tumors arising from other organs.
Method: Formalin-fixed, paraffin-embedded tissue specimens were procured from primary and metastatic colorectal, lung and breast carcinomas and from metastatic

prostate, renal and pancreatic carcinoma. Immunostaining was performed using monoclonal mouse antibodies to CDX2 (clone DAK-CDX2) and Villin (clone 1D2 C3) on tissue pretreated with Tris/EDTA target retrieval solution. Bound antibody was visualized with the Dako FLEX detection system.
Results: Anti-CDX2 and Villin demonstrated similar immunoreactivity on colorectal carcinomas, staining the majority of both primary (17/17 CDX2+: 16/17 Villin+) and metastatic (6/7 CDX2+: 7/7 Villin+) specimens tested. None of the primary breast or lung carcinomas (excluding neuroendocrine tumors) were postive with anti-CDX2, wheras Villin expression was observed in 3/17 lung carcinomas. Among the 14 metastatic tumors tested from sites other than colon, 13/14 were unreactive with anti-CDX2 and 11/14 with anti-Villin.
Conclusions: In this study we have demonstrated that CDX2 and Villin are highly expressed in both primary and metastatic colorectal carcinoma. Antibodies to CDX2 and Villin can be used to better differentiate metastatic colorectal cancers from other cancers when evaluating tumors of unknown origin.

P-377

Idiopathic Myointimal hyperplasia of mesenteric veins: A rare cause of intestinal ischemia in young patients.

Breier D; Lppez R; Ojanguren I; Bargallo A; Ariza A
Department of Pathology, Hospital Germans Trias i Pujol, Autonomous University of Barcelona, Badalona, Spain.

Nonthrombotic occlusion of mesenteric veins is a rare cause of intestinal ischemia that has been previously described in association with systemic lupus erythematosus, Behcet`s disease and mesenteric inflammatory veno-occlusive disease. Idiopathic myointimal hyperplasia of mesenteric veins (IMHMV) is a rare, recently described entity that must be added to these associations. Its etiology remains unclear but previous trauma has been hypothesized in some cases
We describe the case of a 32-year-old female who consulted for abdominal discomfort and tenesmus and was diagnosed with intestinal pneumatosis by CT scan. The patient progressively worsened and was finally admitted due to severe abdominal pain with bloody stools requiring sigmoidectomy. The surgical specimen showed a severely thickened, well-demarcated segment of colon with pneumatosis as well as steatonecrosis of pericolonic fat. Additionally, there were severe ischemic mucosal necrosis and striking intimal circumferential thickening of small mesenteric veins in the muscularis propia and submucosa. These changes resulted in complete or near complete luminal occlusion and gave rise to tortuous hyalinized capillaries in the lamina propria, with frequent thrombus formation. Neither vasculitis nor arterial involvement was present.As already described in similar cases, the patient recovered rapidly after surgery.
IMHMV, an uncommon condition that mostly affects previously healthy young male patients, must be differentiated from other causes of ischemia such as vasculitis or connective tissue diseases requiring a very different therapeutic approach.

P-378

Digestive neoplasms malt tipe - pathological study

Anca Dobre; Mariana Aschie; Ionut Poinareanu; Anca Craciun; Anca Papuc; Andreea Iliesiu
Ovidius University, Constanta, Romania

Background: Digestive neoplasms are a vast and freqent pathology. In this pathology are included MALT lymphomas wich represents 3% of digestive neoplasms and 7–8% of B cell lymphomas. Slight female predisposition has been reported for MALT. Its simptoms vary and they mimic other digestive deseases.
Method: Statistical study of MALT lymphoma cases new diagnosed between 2000 – 2007, in Morphopathology Department of County Hospital, Constanta, following a few parameters: sex, age, tumor localization, signs and symptoms, immunohistochemistry pattern, disease extension.
Results: From our study resulted an increasing in number of new diagnosed MALT lymphoma between 2000 - 2007 (5 cases in 2000 to16 cases in 2006), MALT lymphoma representing less than 1% of intestinal pathology diagnosed in this period. From all MALT cases the most frequent localization was stomach with 57% off all MALT cases, followed by intestinal localization (23%) and colo-rectal localization (10%). There were a few cases of gastro-intestinal localization associated with non-gastro-intestinal localization (5%). Sex ratio didn't show any preference for a sex determinism excepting gastric localization with slighted predisposition for mans patients. Medullar invasion was present in 35% of cases. Non-specific symptoms were present in 5% cases for increased LDH, 35% for weight loss, 3% for fever and 40% for anemia. Immunohistocemical analysis showed that MALT lymphomas are negative for CD43 (98%), CD5 and CD10 (100%), Ki67 (99%) and positive for CD11c (60%), CD20 (95%).
Conclusions:
- MALT lymphomas are a rare pathology.
- MALT lymphomas are more frequent at gastric level and they show a slighted predisposition for mans patients at this level.
- There are no cases of esophageal MALT lymphomas.
- Paraclinical most frequent syndrome is anemia.

– Symptoms mimic other digestive diseases implying morphological and immunohistochemical exam.
– IHC showed that MALT lymphomas are most frequent negative for CD5 and CD10 and positive for CD20.

P-379

Enterogenous cyst of the hepatoduodenal ligament: case report.

Alexandr Ivanovich Shchegolev, Elena Alexeevna Dubova, Oleko Dmitrievich Mishnev

FGU Vishnevsky Institute of Surgery Rosmedtechnologiy, Russia

Introduction: Enterogenous cysts (enteric duplication cysts) are hollow, epithelium-lined, spherical or tubular structures that are tightly attached to some portion of the gastrointestinal tract. They are located in or adjacent to the wall of part of the gastrointestinal tract and found most commonly in the distal ileum, the posterior mediastinum, and the third part of the duodenum. Rarely, enteric cysts can occur distant from the gut.

Case report: A 47-year-old woman presented with an incidentally found abdominal mass. The preoperative diagnosis was a cystic neoplasm the head of pancreas. Laparotomy showed a cystic mass in the hepatoduodenal ligament. It had no connection to the pancreas, stomach, small bowel, or large bowel. The gross specimen showed a cystic lesion with smooth and red-gray external surface 3,3×3×2,5 cm. On cut section, the mass expelled turbid fluid. The inner surface was relatively smooth and the wall of the cyst was thick (1 cm). Histopathologic findings showed that the cystic wall composed of irregulary oriented smooth muscle, and the cyst is lined with mucin-secreting columnar epithelium gastric and intestinal types with mucous glands.

On immunohistochemistry, the majority of cells were positive for CK7, CK8, CK18, CK19, CK20, MUC1, MUC2, MUC4. A few cells also immunoreactivity with MUC5AC. The final diagnosis of a completely isolated enterogenous cyst was made.

Conclusion: No communication or connection with the adjacent alimentary tract but the presence of a typical histopathologic and immunohistochemical features of a enterogenous cyst has been described as an isolated enterogenous cyst.

P-380

PROGNOSTIC IMPORTANCE OF ANGIOGENESIS IN GASTRIC CANCER

Filip Vukmirovic

Department of Pathology, Clinical Center of Montenegro, Montenegro

BACKGROUND: The new blod vessels which generation tumor inducer is a important in process of growth, prognosis and metastasis of tumors. We investigate the relationship between the angiogenesis and clinicopathologic features to related with prognosis in gastric cancer patients.

METHODS: To asses tumor angiogenesis, microvascular density (MVD) were analyzed immunohistochemically in 83 primary gastric cancers. Any single brown-stained cell with Factor VIII, that indicates an endothelial cell, was counted as a single vessel. Branching structures were counted as a single vessel unless there was a discontinuity in the structure. Vessels were counted in 4 regions, with the highest vascular density, at 200-magnification, and the average number of microvessels was recorded.

RESULTS: The microvascular density for 83 tumor specimen ranged from 17,5–51,5 with a mean MVD of 33,17± 7,95. Mean microvascular density was chosen as the cut-off point, 38 patients were categorized as a low MVD and 45 patients as a high MVD. There was no significant relationship between angiogenesis and age, sex, and histological type of gastric cancer. A significant correlation was found between the angiogenesis in early and advanced gastric cancer, and between gastric cancer with and without regional lymph node metastasis. Angiogenesis was significantly associated with poor survival. Multivariate survival analysis showed that stage of dissease and angiogenesis were independent prognostic factors.

CONCLUSION: Angiogenesis is one of the most important prognostic factors for gastric cancer patients, and therapeutic inhibition of angiogenesis may advance poor prognosis of gastric cancer patients.

P-381

ANGIOGENESIS AND VESSELS' MATURATION GRADE IN COLORECTAL CARCINOMAS

Gurzu Simona, Anca Maria Cimpean, Marius Raica, Ioan Jung, Tibor Mezei, Leonard Azamfirei

University of Medicine and Pharmacy of Tg. Mures, Romania

Background: It is very difficult to identify, based on the immunohistochemically (IHC) aspects, the cases with colorectal carcinomas (CRC) in which the angiogenesis inhibition could prolonge life. In CRC the double immu-

nostain (DIHS) with CD105 (endoglin) and SMA (Smooth Muscle Actin) was studied in a few papers.
Methods: 20 CRC surgical specimens were IHC studied utilizing the antibodies CD31 and CD105. The DIHS realized with CD105 and SMA.
Results: With DIHS we identified more type of vessels. The endothelial isolated cells were represented by non-irrigated endothelial cells, did not have lumen and marked only with CD105 in DIHS. The immature vessels presented lumen, were marked only with CD105 and were not have pericytes. The intermediary vessels were marked with both CD105 and SMA. The wall was very thin, the lumen was small, they did not have pericytes neither smooth muscle cells. The mature vessels were marked only with SMA, they had pericytes and a smooth muscle layer. CD105 in DIHS was correlated with CD105 in simple immunostain (SIHS) at 400× but not at 200× magnification. CD105 in both SIHS and DIHS was correlated with CD31 immunostain at 400× magnification. The microvascular density of intermediary vessels was correlated with the histological grade of non-mucinous CRC. The positive area of intermediary vessels was higher in well differentiated CRC (2±0,03) than in moderate (0,14±0,02) or poorly differentiated ones (0,07±0,01). Their high density was also observed in displasia and polypoid CRC. This type of vessels could not be identified with SIHS and we believe that this is the argument for using DIHS in study of CRC angiogenesis.
Conclusions: The density of intermediary vessels, evidentiated only with DIHS, could be one of the reasons for success or failure of antiangiogenic treatment. The DIHS could be utilised for the study of vessels' maturation grade.

P-382

Cyclooxygenase (COX-2) and Matrix Metalloproteinase 9 (MMP-9) expression in human colonic angiodysplasia

Ines de Torres; Esteve Saperas*; Stefania Landolfi; Marta Garrido; M[a] Eugenia Semidey; Irene Sansano; JR Malagelada * and Santiago Ramon y Cajal.
Pathology Department and Digestive Research Unit. Hospital General Vall d'Hebron, Autonomous University of Barcelona, Spain.

BACKGROUND: Gastrointestinal angiodysplasia (AGD) is an acquired vascular pathology of the elderly and a major cause of chronic or recurrent bleeding. We previously showed that angiodysplasia strongly express vascular endothelial growth factor, a key effector molecule of angiogenesis. Angiogenesis is tightly controlled by multiple effector molecules and pathways. Among them, COX-2 and MMP-9 appear to play a role in the signaling pathway that mediate angiogenesis in colorectal cancer.
AIMS: To investigate whether these molecules participate in the process of vascular remodeling of human colonic angiodysplasia we examined the immunohistochemical expression of COX-2 and MMP-9.
METHODS: Immunohistochemistry was performed in sections of formalin-fixed, paraffin-embedded specimens obtained from 20 patients with colonic angiodysplasia and from seven patients with colon cancer and its adjacent, histologically normal margins of resection, as controls. We used affinity-purified rabbit polyclonal antibodies for COX-2 (4H12, Novocastra) and MMP9 (2C3, Oncogen Research) at 1:100 and 1:200 dilutions with the Envision method.
RESULTS: Strong vascular immunoreactivity for COX-2 was seen in 9 (45%) specimens of angiodysplasia and in 5 (71%) of colon cancer. In contrast, no immunoreactivity was found in normal colon. In angiodysplasia, staining for COX-2 was homogeneously distributed in the endothelial lining of blood vessels. Positive specimens were mostly graded as 2+ or 3+ intensity. Semiquantitative analysis revealed that the intensity of vascular staining in angiodysplasia (2.0+0.2) was similar to that of colon adenocarcinoma (1.6+0.2) (p=NS). Vascular immunoreactivity for MMP-9 was seen in 10 (50%) specimens of angiodysplasia and 4 (57%) of colon cancer, but not in normal colon. Vascular staining for MMP- 9 in angiodysplasia was focally distributed in endothelium as well as in pericytes, and was similar to that of colon cancer
CONCLUSION: Induction of COX-2 and MMP 9 expression support their role in the development and/or progression of human colonic angiodysplasia and provides potential therapeutic targets for the prevention of bleeding from these vascular lesions.

P-383

Podoplanin expression and lymphatic microvessel density in colorectal carcinomas. Correlation with histopathologic types

Anca Maria Cimpean*; Marius Raica*; Simona Gurzu; Ioan Jung****
Department of Histology, University of Medicine and Pharmacy Victor Babes Timisoara, Romania;*Department of Pathology, University of Medicine and Pharmacy Tirgu Mures, Romania*

Background. Podoplanin expression in human colon cancer is less studied. Some data suggest that level of podoplanin is greater in colon tumors with lymph node metastasis compared with those without it. There are controversies concerning the presence of intratumoral lymphatic vessels. The involvement of podoplanin in the metastatic process is supported by expression in tumor cells

at primary and metastatic sites from many tumors but is not certified in colon neoplasms. The aim of the present study was to describe the podoplanin expression in tumor cells, lymphatics and stroma components of colon tumors. **Methods.** Specimens from 30 cases with colorectal carcinomas were evaluated for microscopic diagnosis on routine stained slides. Immunohistochemistry for podoplanin was performed using anti-podoplanin antibodies, clone 18H5 followed by application of catalyzed signal amplification working system. **Results.** In colon dysplasia podoplanin was expressed weakly in glandular cells with cytoplasmic granular pattern. An intense staining for podoplanin was observed in tumor cells of adenocarcinomas. Mucinous adenocarcinomas showed strong reaction in tumor cells, stroma, and high number of positive lymphatic vessels closely linked with mucus quantity. A more intense expression was found in undifferentiated tumor cells. Clusters of tumor cells invading stroma at distance from the core of the tumor also expressed podoplanin more intensely than primary tumor cells. Positivity in tumor cells was associated with low intratumor lymphatic vessels density. Lymphatic vessels were more numerous at distance from the tumor. Positive stromal cells were grouped between tumor areas with and without necrosis or scattered between stromal components. **Conclusions.** Podoplanin expression in tumor cells was mainly found in mucinous adenocarcinoma and undifferentiated tumors. Our results suggest that podoplanin could be used as prognostic marker of invasion and metastasis in colorectal carcinomas.

P-384

Mutation and Expression of APC/β-Catenin/E-cadherin in Colorectal Adenocarcinoma

Sang Sook Lee; Kun Young Kwon, Yu Na Kang; Hae Ra Jung; Sun Young Kwon; Mi Sun Chei; Sang Pyo Kim; Sang Sook Lee

Department of Pathology, Keimyung University School of Medicine, South Korea

Purpose: The pathogenesis of colorectal adenocarcinoma is described as a sequential multistep accumulation of genetic alterations. Adenomatous polyposis coli (APC) somatic mutations are the earliest known abnormalities in the development of sporadic colorectal tumors. Recently, accumulation of β-catenin by β-catenin mutation in colorectal carcinoma cell lines without APC mutation was demonstrated, which also occurred in some sporadic primary colorectal tumors. Most research into the development of colorectal cancer has focused on the detection of mutation of particular gene, but the elucidation for the interaction of these mutated genes with cell adhesion molecules is also important to understand the colorectal tumorigenesis. Methods: To elucidate the role of APC/β-catenin/E-cadherin in the colorectal adenocarcinoma, we identified APC/β-catenin/E-cadherin mutation and expression in forty two colorectal adenocarcinomas. Results: Mutations of APC exon 15 and β-catenin exon 3 were detected in eleven cases (26.2%) and one case (2.4%) out of forty two colorectal adenocarcinomas. But there was no evidence of aberrant shift in E-cadherin exon 6–9. APC and E-cadherin promoter methylations were found in five cases (11.9%) and twenty five cases (59.5%) out of forty two colorectal adenocarcinomas. The membranous staining of APC and E-cadherin was decreased in thirty cases (71.4%) and thirty seven cases (88.1%) out of forty two colorectal adenocarcinomas. The β-catenin expression was increased in the membranes in thirty four cases (81.0%), cytoplasms in seventeen cases (40.0%) and nuclei in twenty one cases (50.0%) out of forty two colorectal adenocarcinomas. At the invasive areas of tumor growth, nuclear expression of β-catenin was common. The degree of reduced E-cadherin expression and the grade of tumor differentiation were statistically significant. Conclusion: Down-regulation of APC and E-cadherin by genetic mutation or epigenetic change such as methylation as well as β-catenin mutation was closely related with increased expression of β-catenin protein in colorectal adenocarcinoma. Decreased expression of APC and E-cadherin and increased β-catenin expression were commonly found in colorectal adenocarcinoma, which may be helpful to understand the pathogenesis of colorectal adenocarcinoma. But increased β-catenin expression is caused by secondary change arising from APC inactivation or competitive binding of β-catenin to APC and E-cadherin than by carcinogenic effect directly involved in tumorigenesis of colorectal adenocarcinoma.

P-385

hMLH1 Abnormality in 180 Sporadic Colorectal Carcinomas

Yu Na Kang; Hae Ra Jung; Sun Young Kwon; Mi Sun Chei; Sang Pyo Kim; Kun Young Kwon; Sang Sook Lee

Department of Pathology, Keimyung University School of Medicine, South Korea

Colorectal carcinomas in South Korea is increasing due to the increase of lipid-rich diet and meat intake. Pathogenesis of colorectal carcinomas has known to be involved with numerous chromosomes and genetic abnormalities. One of them is microsatellite instability (MSI) due to defective DNA mismatch repair (MMR) genes (hMLH1, hMSH2, hMSH6, PMS1, PMS2). The MMR gene abnormality is associated with promoter methylation as well as genetic mutation. Recently immunohistochemical detection of DNA MMR protein is able to suggest of the presence of MMR gene abnormality. The aim of this study was to

evaluate the role of immunohistochemical stain of hMLH1 as a screening tool for carcinomas with defective DNA mismatch repair (MMR) genes. In this study, 180 colorectal carcinoma tissue were obtained in the fresh status for MSI phenotype, hMLH1 promoter methylation, hMLH1 mutation analysis. The tissue microarray slides made of 180 formalin-fixed, paraffin-embedded colorectal carcinomas were examined for hMLH1 immunohistochemistry. High frequency of MSI (MSI-H) indicates at least two of five standard MSI markers (D2S123, D5S346, D17S250, Bat-25, and Bat-26). Of the 180 colorectal carcinomas, nine cases (5.0%) were MSI-H, nine cases (5.0%) had hMLH1 mutation on exon 1, 7, 12, and 16. Twenty one cases (11.7%) showed loss of hMLH1 protein expression on immunohistochemistry, and sixty one cases (33.9%) were methylated at the hMLH1 promoter. Status of MSI-H was correlated with younger age below 50 years old ($p=0.004$), tumor location of right colon ($p<0.0001$), and mucinous carcinoma ($p=0.025$). Presence of hMLH1 mutation was correlated with tumor location of right colon ($p=0.022$), and mucinous carcinoma ($p=0.015$). Immunohistochemical stain of hMLH1 was correlated with only younger age below 50 years old ($p=0.029$), but hMLH1 promoter methylation was not significant correlation with any clinicopathologic feature. Average of tumor size was larger in the groups of MLH1-H and hMLH1 gene mutation than MSS/MLH1-L and none mutation. Patients' age was younger in the group of MLH-H than MSS/MLH1-L. And immunohistochemical stain of hMLH1 was correlated with the results of MSI-H (<0.0001), hMLH1 promoter methylation ($p<0.0001$), and MLH1 mutation ($p=0.039$). In conclusion, most hereditary non-polyposis colorectal carcinomas was known to be associated with DNA MMR genetic mutation, but in sporadic colorectal carcinomas hMLH1 promoter methylation (34%) than hMLH1 gene mutaion (5%) is more frequently detected. And immunohistochemical stain of hMLH1, as single simple test, is able to apply for effective detection method of MLH1 abnormality.

P-386

The Value of Magnifying Colonoscopy In Determining Serrated Polyps In Asymptomatic Individuals

Berna Savas; Mehmet Bektas; Ali Emre Tuzun; Hulya Cetinkaya; Murat Toruner; Arzu Ensari

Ankara Universitiy, Medical Faculty, Department of Pathology & Gastroenterology, Turkey

BACKGROUND: The genetic pathway model for the pathogenesis of colorectal cancer (CRC) is mainly based upon the concept of an adenoma-carcinoma sequence. In recent years, however, a "serrated pathway" involving hyperplastic polyp-serrated adenoma-carcinoma sequence has been proposed. This prospective study was designed to evaluate the value of magnifying colonoscopy in determining serrated polyps in asymptomatic individuals.
METHODS: One hundred and seventy four asymptomatic individuals over the age of 50 years were included in the study. After identifying the lesions at colonoscopy, 0.2% indigocarmine solution was sprayed and a magnified view of the stained crypt orifice at a maximum of 100 times magnification was obtained. The observed pit patterns were classified into 6 categories (I, II, IIIL, IIIS, IV, and V) according to Kudo's classification. Types I and II were designated as non-neoplastic patterns whereas types III-V were considered as neoplastic. All polypoid lesions were histopathologically examined on a routine basis. Chi-square test was used for statistical analysis.
RESULTS: There were 93 females and 81 males, with a mean age of 58,78±9,13 years. During magnifying colonoscopy, a total of 182 polyps, including 103 serrated polyps (SP) (78 hyperplastic polyps, 23 sessile serrated adenomas, 2 traditional serrated adenomas), and 79 conventional adenomas were identified. The majority of the polyps were located in the left colon (76,2%) while 23,8% were observed in the right colon. According to the pit pattern analysis 80,4% of the polyps revealed types I-II while 19,6% showed types III-V. Types I-II were significantly more frequently observed in SP ($p<0,001$) while types III-V were significantly higher in adenomas ($p<0,001$).
CONCLUSIONS: Magnifying colonoscopy proves to be useful in differentiating serrated polypoid lesions of the colon even in asymptomatic individuals according to pit pattern analysis which seems to correlate with histopathologic subtyping.

P-387

FOXP3+ REGULATORY T CELLS IN MICROSCOPIC COLITIS.

Jaume Casalots; Fernando Fernández-Bañares*; Antonio Salas; Esther Ferré; Karina Caci; Clarisa González; Xavier Tarroch; Pilar Forcada; Guadalupe González.

Departments of Pathology and Gastroenterology.Hospital Mútua Terrassa. Barcelona. Spain.*

Background: Regulatory T cells (Treg) contribute to the control of immunologic tolerance, autoimmunity and immune response phenomena of human diseases. Treg cells express IL-2Ralpha (CD25) and they are specifically identified by FOXP3 expression, which is the main regulating gen involved in these immunological processes. The pathogenesis of microscopic colitis is unknown, but it has been suggested an autoimmune basis as well as alterations in the immune response against several antigens.

Objective: The aim of this study is to assess the presence of Treg cells in patients with collagenous (CC) and lymphocytic colitis (LC) in comparison with patients with chronic diarrhea and nonspecific colonic inflammation.
Materials and Methods: We studied colonic biopsies from 41 patients with microscopic colitis (21 CC and 20 LC), 17 patients with chronic diarrhea and nonspecific inflammation of the colonic mucosa (NC), and 10 control patients without diarrhea (CO). Immunohistochemical stains in formalin fixed, paraffin-embedded tissue for CD3 (intraepitelial lymphocytes; %), CD25 (0–3 score), and FOXP3 (0–3) were performed. The results were expressed as mean±SEM or median and compared by the Kruskal-Wallis one-way analysis of variance, and the Freeman-Halton extension of the Fisher test for a 2×3 table.
Results: We found CD25 expression in 1/17 NC, 19/20 LC y 14/21 CC ($p<0.0001$), with a subepithelial predominance. There was no expression of CD25 in the control group (CO). Immunoreactivity for FOXP3 with predominant subepithelial distribution was observed in the cases of CC and LC with CD25 expression.
Conclusions: Treg cells CD4+/CD25+/FOXP3+ are increased in lamina propria in patients with CC y LC, suggesting that they may play a role in the pathogenesis of these diseases

P-388
THE EXPRESSION OF SNAIL AND E-CADHERINE IN COLORECTAL ADENOMATOUS POLYPS

Aso Manso,S; Romero Gúzmán G.; Campos Martín Y; Cruz Pérez G; Navarro Sanchez; Mollejo Villanueva M; Orradre Romeo JL; Rodríguez Merlo R.
Hospital Virgen de La Salud, Toledo, Spain

Background: The Snail gene family is composed of Snail (sna 1) and Slug (Sna2). Snail gene downregulate E-Cadherine expression, which is essential for epithelial to mesenchymal transition (ETM). This process takes place in the embryonic phase, during nervous central system development and in tumorigenesis.
Snail is overexpressed in some carcinomas in both epithelial and mesenchymal component, but its expression is unknown in colorectal adenomatous lesions. To investigate expression of Snail in the colorectal adenoma-carcinoma sequence, we examined expression of different types of adenoma.
Methods: A series of 50 colorectal adenomatous polyps have been selected. Five normal colonic mucosa and 5 colorectal carcinoma has been included for comparative purposes. Immunohistochemical studies for Snail, E-Cadherine, Mib 1 and p53 were perfomed in paraffin blocks.
Results: Transcriptional factor Snail is expresssed in 10% tubular adenoma and in 56% villous adenoma. In normal mucosa, the bottom crypt cells are slightly positive for epithelium, whereas colorectal carcinoma showed strong nuclear snail expression in epithelial and mesenchymal cells. E-cadherina is overexpressed in tubular and villous adenoma with light- moderate dysplasia. However its expression is decreased in adenoma with severe dysplasia.
Conclusions: Expression of Snail protein varies according to histological subtype of adenoma, dysplasia grade and cellular phenotype (epithelial or mesenchymal), however positivity for E-Cadherine depends on dysplasia grade. The role of nuclear expression of Snail as a biomarker for progression of adenoma needs further study.

P-389
Slow Transit Constipation and decreased Interstitial Cells of Cajal

Karina Caci; Clarisa González; Esther Ferré; Jaume Casalots; Pilar Forcada; Xavier Tarroch; Guadalupe González; Antonio Salas
Hospital Mutua de Terrassa, Spain

Background: Chronic constipation is a common pathology affecting mainly younger women. Slow Transit Constipation (STC) is the most severe form, frequently refractory to therapeutic measures, needing a surgical approach. The causes of STC are still poorly understood, but are thought to be related to abnormal colonic motility. Decrease in colonic Interstitial Cells of Cajal (ICC) has been reported in patients with STC.
Case: A 33 years old woman diagnosed with nervous anorexia from age 12 to 24. At 25 she presented severe chronic constipation, showing slow colon transit at the right colon and a neuropathic pattern in the gastrointestinal manometry. Due to non-response to medical treatments, she underwent subtotal colectomy.The ascending and transverse colon were slightly dilated without other alterations. Histological sections were normal; submucous and intermuscular plexus showed ganglionar cells normally distributed at all levels. Immunohistochemical *c-kit* stains were done at different levels to demonstrate the presence of ICC. The sections from ascending and transverse colon showed decrease of ICC, with total loss in some areas. The distribution of ICC at descending colon and terminal ileum was normal, compared with normal surgical specimens used as controls.
Discussion: ICC are thought to play an important role in the control of gut motility, acting as pacemakers. They are localized mainly at the mienteric plexus and muscular

layers along the entire colon, and express consistently *c-kit*, so immunodetection of *c-kit* in tissue is a simple and reproducible method to evaluate alterations in number or distribution of ICC in the bowel. Our case is similar to others previously reported, supporting the role of ICC anomalies in the pathogenesis of at least some cases of STC.

Conclusion: In surgical specimens, from patients with intestinal motility disturbances, immunohistochemistry for *c-kit* is very useful to disclose ICC alterations in an otherwise histologically normal colon.

P-390

Prognostic role of HER-2/neu over expression in colorectal cancer

Mohamad Hasan Emami [2], Sanei Mohammed Hossein[1], Sedghi Azadeh[3]

Isfahan University of Medical Sciences Lzahra hospital, Iran

BACKGROUND: The Her-2/neu (c-erbB2) oncogene is one of the members of thyrosine kinas family.this oncogene encodes a 185 KD transmembrane protein which is involved in pathways of cell proliferation and differentiation because of its extensive homology and relation to epidermoid growth factor receptor.Her-2/neu is over-expressed in 30–40% of breast and ovarian cancers. This over-expression has been shown to correlate with poor prognosis of such malignancies. Monoclonal antibody-directed therapy has been used as an effective treatment for the patients with over-expressed tumors. We investigated over-expression of Her-2/neu in colorectal cancer, and its correlation with survival of the patients.

METHODS: Over-expression of Her-2/neu was examined by immunohistochemistry in 50 patients with colorectal cancer. The patients had undergone curative sugery at Alzahra Hospital since 2002 till 2005.

RESULTS: Over-expression of Her-2/neu was detected in 52%(26) of patients. There was no relationship between over-expression of Her-2/neu and prognosis.

(Respectively the mean survival in over-expressed and non over-expressed patients, were 44.46 +/- 2.68 vs 40.47 +/- 3.95 months).

CONCLUSION: Immunohistochemistry did not reveal any correlation between Her-2/neu over-expression and survival in colorectal cancer.

Key words: colon cancer,her2-neu, prognosis.

P-391

Mucins expression in gastric neoplasms

Cristina Colarossi 1; Eleonora Aiello 1; Salvatore Scarpulla 1; Tiziana Perin 2; Lorenzo Memeo 1; Vincenzo Canzonieri 2

1 Pathology Unit, Mediterranean Institute of Oncology, Catania, Italy; 2 Division of Pathology, CRO, Aviano, Italy

Gastric cancers constitute a highly heterogeneous group of tumors with respect to epidemiology, genetics, histopathology and biological behaviour.

Epithelial mucins MUC2, MUC5 and MUC6 whose genes are clustered on chromosome 11p15.5 are involved in the mucus gel formation. MUC5 and MUC6 are the major mucin components in normal gastric mucosa. MUC5 is highly expressed in mucous cells of the superficial and foveolar epithelium, whereas MUC6 is present in mucous neck cells and in mucous glands of cardia and antrum. Moreover, MUC2 and MUC5 which are absent or barely detectable in normal gastric tissues have been reported in gastric carcinoma. MUC2 expression has been related more specifically to the mucinous carcinomas of WHO classification whereas MUC5 has been associated with poor tubular differentiation and high mucin content. However, coexpression of multiple mucins is frequently observed in gastric carcinomas. In an effort to bring additional information in understanding the diversity of gastric neoplasms,we investigated the expression of MUC2, MUC5 and MUC6 in a series of gastric neoplasms.

We studied the immunohistochemical expression of MUC2, MUC5, MUC6, gastrin, villin and chromogranin in a cohort of 28 gastric neoplasms (7 adenocarcinomas, 11 undifferentiated carcinomas, 4 neuroendocrine tumors and 6 tubular adenomas).

We found MUC2 expression in 3 (43%) adenocarcinomas, 6 undifferentiaded carcinomas (55%) and 2 tubular adenomas (33%); MUC5 was expressed in 1 adenocarcinoma (15%), 1 undifferentiaded carcinoma (9%) and in all 6 tubular adenomas (100%); MUC6 was expressed in 1 adenocarcinoma (15%), 1 undifferentated carcinoma (9%) and in 4 tubular adenomas (66%). No expression of the the 3 studied mucins was found in neuroendocrine carcinomas. These data, even if in a small cohort, suggest that mucins could be useful, together with the classical neuroendocrine markers to identify an epithelial rather then a neuroendocrine origin of the neoplasia.

P-392

Mixed exocrine-endocrine carcinoma of the stomach associated with sarcoid-like granulomas

Zorica Stojsic; Miodrag Stojiljkovic; Darko Babic; Tomislav Randjelovic; Dragan Gacic

University Hospital Bezanijska kosa Belgrade, Institute of Pathology School of Medicine University of Belgrade, Serbia

Mixed exocrine-endocrine carcinomas are defined as epithelial malignant tumors characterised by a combination of a predominant exocrine component (conventional adenocarcinoma) and a neuroendocrine tumor component represented by at least one-third of the tumor area. These tumors are rare in the stomach, and only 28 cases have been reported so far. We describe a further case in a 36-year-old man who underwent subtotal gastrectomy with regional lymph node dissection for an intestinal-type adenocarcinoma on initial biopsy. However, the resected tumor consisted of two components: a poorly differentiated intestinal-type adenocarcinoma with focal glandular areas and a poorly differentiated neuroendocrine carcinoma occupying approximately 30% of the tumor mass. The latter component was composed of diffuse sheets of small cells with high nuclear/cytoplasmic ratio. The adenocarcinomatous areas were immunopositive for cytokeratin 7, cytokeratin 20 and CEA, but the neuroendocrine component was negative. Neuroendocrine markers, including chromogranin A, synaptophysin and neuron-specific enolase, were diffusely positive in the neuroendocrine portions of the tumor, and only in scattered neuroendocrine cells within glandular structures of the adenocarcinomatous component. Perigastric lymph node metastases corresponded either to neuroendocrine or adenocarcinomatous component. Our case is unique in its association with sarcoid-like granulomas existing in the entire gastric mucosa and all perigastric lymph nodes. Numerous giant cells within granulomas exhibited laminated Schaumann bodies, and some of them contained asteroid bodies, too. The abscence of any clinical manifestations and the negative results of chest radiograph and laboratory test for the serum angiotensin converting enzyme excluded the possibility of systemic sarcoidosis. The association of mixed exocrine-endocrine carcinoma of the stomach and sarcoid reaction has never been reported previously.

P-393

Cell cycle proteins alterations in gastric cancer

Maria D Begnami; José H Fregnani; Sueli Nonogaki; Carlos Nascimento; Fernando A Soares

Hospital A C Camargo, Brazil

Background: Progression of the cell cycle is governed by cyclin-dependent kinases (cdks), whose activity is inhibited by the cdk inhibitors. Dysregulated expression of cyclins, cdks, and cdks inhibitors is closed linked to uncontrolled proliferation and malignant transformation of the cell. In gastric cancer (GC) increasing evidence suggests that alterations in cell cycle proteins are associated with poor prognosis but the results still contradictory. The aim of this study was determinate the expression of cell cycle proteins in gastric cancer by immunohistochemistry (IHC) and their prognostic significance. **Material and methods:** Using IHC, expression of p27, p21, p16, pRb, p53, cyclin D1, cyclin A, and cyclin B1 was evaluated in a high throughput tissue microarray containing 482 GC in duplicate. According with literature criteria, positive cases were determinate when nuclear or cytoplasmatic staining was observed in >10% of the tumor cells. **Results:** Expression for p53, p27, p16, p21, and pRb was observed in 137 out 458 (30%), 231 out 457 (50%), 50 out 463 (10.8%), 64 out 458 (14%), and in 313 out 458 (68%) GC. 220 out 449 (49%), 316 out 458 (69%), and 229 out 460 (49%) GC was positive for cyclin D1, cyclin A, and for cyclin B1. Intestinal type of GC frequently showed expression of p21 and p53 and loss cyclin B1 and pRb staining compared with diffuse type of GC. Diffuse type of GC with p53 expression showed poorer prognosis than the p53 negative cases ($p<0.001$). **Conclusion:** Alterations in cell cycle proteins expression are common events in gastric cancer. Loss of p21 and p16 staining with overexpression of cyclin D1, cyclin A, and cyclin B1 are the major findings. Poor prognosis is associated with p53 expression in diffuse type of GC. This marker could be used to identify individuals that are at high risk.

P-394

THE WAY IMUNO-MARKERS APOPTOTIC GENES, PROLIFERATION FACTORS AND ENDOTHELIAL ANTIGENS TURN UP IN BARRETT ESOPHAGUS AND ITS COMPLICATIONS

Anca Mihaela Lazaroiu; Maria Sajin; Alina Elena Chefani; George Simion; Mariana Costache; Mariana Georgescu; Carmen Fierbinteanu Braticevici; Costica Balan; Alina Stanescu; Victoria Hurduc

Department of Pathology of Universitary Emergency Hospital Bucharest, Romania

Introduction. The most serious complication of the chronic reflux esophagitis, or Barrett esophagus (BE), with glandular metaplasia is secondary esophagial adenocarcinoma. **Purpose:** Checking the link between the progress of Barrett's metaplasia to adenocarcinoma and the application of tumor markers involved in increased proliferation

aspects with presence of apoptotic genes (p-53, bcl-2) proliferation factors (PCNA, Ki-67) and endothelial antigenes (CD 34)

Material and methods. The study included 102 cases, mainly males, aged between 23 and 65, who were subjected to endoscopic and histopathologic investigation. Biopsies were fixed in 10% formol and parafin included.. Than ue used HE and histochemical staining for neutral and acid mucopolysaccharides and IHC staining: (indirect tristadial Avidine-Biotine-Peroxidase method).

Results: The 102 cases, diagnosed by endoscopic and histologic methods, classified as follows: 35 cases of Barrett esophagus with specialised epithelium, 11 cases of non-determined metaplasia, 9 cases of initial intraepithelium neoplasic lesions, 10 cases of advanced intraepithelium neoplasic lesions and 17 cases of moderate and undifferentiated carcinoma (one of them abounding in Russell bodies).

Immunohistochemical, Mutated tumor marker p-53 evidentiation was expressed in 61% cases (high grade of displasya of Barrett's esophagus and adenocarcionoma). The second antiapoptotic marker bcl-2 was inconstantly positive, especially in the lymphocytes of lamina propria. Monoclonal PCNA and 85% of Ki-67 antibodies were positive especially in the undifferentiated carcinoma. Endothelial antigenes (CD 34) were positive especially in the areas with the highest vascularization of well differentiated carcinoma. Follow-up studies are necessary to evaluate the prognostic value of BE complications.

Conclusion: To diagnose the distal esophagus precancerous and cancerous conditions, assess the prognosis and risk of progression and to determine effective treatment, a wider panel of tissue tumour markers could help.

P-395

Macro and microscopic assessment of activitiy in ulcerative colitis

Maria Rosa Ortiz; Manuel Adrados; Ferran Gonzalez-Huix; Esther Diaz; Graciela Barraza; Montse Figa; Lluis Bernado

Hospital Universitari de Girona Doctor Josep Trueta, Girona, Spain

Background: Medical treatments have changed morphological features ol ulcerative colitis (UC) giving unusual patterns of colonic involvement. In this setting we try to assess the ability of macro and microscopic parameters to determine the activity of UC in treated and untreated patients.

Method: 113 consecutive patients with active and inactive UC (64 men, 49 women; mean age 45 years, range 18–81 years) in their first attack (16 cases) or with established colitis (97 cases) were prospectively assessed. They underwent a complete ileocolonoscopy with sequential biopsies of terminal ileum and all colonic segments (total= 625 samples). Endoscopic and histopathological parameters were evaluated using two different scores in which acute and chronic signs of inflammation were considered separately. Five diagnostic categories (normality, remission, mild, moderate and severe disease) and the continuous/patchy extension were established. The degree of agreement between scores was characterized by kappa statistics.

Results: kappa values between scores were 0,469 (concordance=59.2%) for the different categories and 0.748 (concordance=87.6%) when only inflammatory activity was considered. Endoscopy didn't detect normality in 5.4% of samples and overdiagnosed remission in 8.8% of them. Histology revealed more inflammatory activity respect endoscopy in 3.3%. In patients in their first attack there was an excellent correlation on the inflammatory activity (k=1.000) in contrast with that seen in established colitis (k=0.529–0.758). Patchiness was determined in 38/113 (33.6%) of patients by both endoscopic and histological parameters. Histological rectal sparing was detected in 7 of 113 (6.2%) patients.

Conclusion: Correlation between macro and microscopic scores is frequently bad in longstanding UC. Endoscopy underestimates normality and inflammatory activity and overestimates remission. Endoscopic parameters are insufficent to detect normality. Rectal sparing and patchiness are frequentlly seen in treated longstanding UC.

P-396

Clinicopathological and immunohistochemical prognostic factors in stage II (T3/4N0M0) colorectal carcinoma

Matej Bračko; Zdravko Štor; Snježana Frković Grazio

Institute of Oncology Ljubljana, Slovenia

Background: Several proteins have been suggested to represent prognostic factors in colorectal cancer; however, the prognostic role of their expression in the group of stage II (T3/4N0M0) carcinomas has only rarely been studied and compared to the prognostic value of classical clinicopathological factors. We studied these relations with the use of tissue microarray (TMA) technology in a large tumor series.

Methods: Data on stage II colorectal carcinomas from 251 patients who underwent R0 resection, received no adjuvant treatment and were followed for a minimum of 5 years were retrieved from pathology reports. In addition, 2 mm cores were obtained from paraffin blocks of these tumors and used for the construction of TMAs, which were stained immunohistochemically for p53, cyclin-D1, E-cadherin,

HER2, and EGFR. Associations with overall survival were assessed by univariate (Kaplan-Meier and log rank test) and multivariate (Cox regression) analysis.
Results: The overall 5-year survival was 72.5%. Older age, presence of lymphovascular invasion, higher pT category (pT4), rectal location, lower number of examined lymph nodes (<12) and presence of perineural invasion were significantly associated with decreased survival in univariate analysis; tumor grade and patients' sex were not related to survival. In multivariate analysis, older age, male sex, and presence of lymphovascular and/or perineural invasion were the only independent adverse prognostic factors. None of the features studied by immunohistochemistry were significantly associated with survival in univariate or multivariate analysis.
Conclusion: Our findings suggest that classical clinicopathologic parameters are superior to some immmunohistochemical features in predicting survival in stage II colorectal carcinoma and should be included in future studies of potential prognostic value of new molecular markers.

P-397

Correlation Of Clinical And Histopathologic Features Of Celiac Disease

Gulen Bulbul Dogusoy; Tugce Esen; Sibel Erdamar Cetin; Suha Goksel; Fugen Cullu; Tufan Kutlu; Tulay Erkan; Aykut Ferhat Celik; Ibrahim Hatemi
Istanbul University Cerrahpasa Medical Faculty Pathology Department

Aim: Endoscopic, clinical and histopathologic findings of Celiac disease is well described. In this study we aimed to investigate the relationship between these findings.
Methods: First, 420 cases were collected who had duodenal biopsies because of suspicion of malabsorption from the archives of Pathology Department. We reexamined the biopsies for histopathologic features in them. Then clinical features and serologic findings of the cases were reviewed. The relationship between the histopathologic features and endoscopic, clinical and serologic results were investigated statistically, using chi square and Multiple Comparison Tests.
Results: After the microscopic examination, 99 cases were diagnosed as Celiac disease. 20 of them had previous biopsies, among whom, 16 had complete response and 4 had no response to diet. No definite diagnosis could be given in 19 cases. Among all patients, male to female ratio was 0,52 and 102 of them were under the age of 19, while 35 were adults. The most common clinical finding is diarrhea (42 cases), followed by failure to thrive in 24, abdominal meteorism in 17 and weight loss in 13 cases. 2 cases were diagnosed as Hashimoto thyroiditis and 3 cases were diagnosed as cystic fibrosis. Endoscopic examination was diagnostic in 2 cases with the loss of folds mostly. 138 cases were gathered and 69 of them had clinical findings. Antigliadin G, A, and antiendomysium antibodies were positive in 59%, 58%, and 58% of the patients respectively. After the histopathologic review all cases were found to be have villous atrophy, and increase in number of intraepithelial lymphocytes. The results of correlations between age, gender, histopathologic, endoscopic and serologic findings were discussed.
Conclusion: In clinically symptomatic cases of celiac disease, endoscopic and serologic findings are usually suggestive, however, as the sensitivity and specifity of histopathologic features are the highest, duodenal biopsies should be always performed for correct diagnosis.

P-398

Venous invasion in lymph node negative colorectal carcinomas

Daniel Baumhoer; Thore Thiesler; Christoph A. Maurer; Andreas Huber; Gieri Cathomas
Kantonales Institut für Pathologie, Liestal; Department of Surgery, Kantonsspital, Liestal, Department of Surgery, Kantonsspital Bruderholz, Switzerland

Introduction: Patients diagnosed with lymph node negative colorectal carcinomas (UICC Stage I and II) undergo surgical tumor resection with curative intent, yet up to 30% of these patients suffer recurrent or metastatic disease within 5 years of surgery. Vascular invasion has been associated with inverse outcome but major differences in the detection rate and the impact in respect to the localization of venous invasion has been reported.
Material and Methods: We retrospectively evaluated Stage I and II colorectal carcinomas for the presence of intra- and/or extramural venous invasion ($V1_{IM}/V1_{EM}$). All available tumor sections were stained with H&E and Elastica van Gieson (EvG) and the findings were correlated with the clinical outcome.
Results: A total of 185 colorectal cancers, including 39 stage I and 146 stage II, were reanalyzed. On an average, 3.7 tumor sections were evaluated per case and median clinical follow-up was 32 months (range 0 to 153 months). Venous invasion was present in 43 (23.2%) patients (26 intramural, 17 extramural), including 37 (86.1%) cases in which venous invasion was previously not detected by H&E. Venous invasion was more common in stage II compared to stage I cancers (28.8% versus 2.6%; $p<0.001$). Survival analyses of patients with and without venous invasion showed 5-year survival rates of 65% and 69%, respectively, which did not reach statistical significance (p=

0.382). Comparison between $V1_{IM}$ and $V1_{EM}$ did not show significant differences either (5-year survival rates 62% vs. 65%, p=0.663).

Conclusion: Venous invasion is common in stage II colorectal cancers, but elastic stains to highlight vascular structures are mandatory for reliable detection. In our serie, however, the presence of venous invasion, irrespective of localization does not have a prognostic impact.

P-399

Analyis of FGFR4 Gly388Arg polymorphism as a prognostic factor in resected hepatic metastases of colorectal cancer.

Nuria Baixeras; Laura Padullés; David G. Molleví; Teresa Serrano; Enric Condom; Emilio Ramos; Jaume Torras; Ramón Salazard;Gabriel Capella; Alberto Villanueva

Institut Català d'Oncologia (ICO), Hospital Duran i Reynals and Hospital Universitari de Bellvitge. L'Hospitalet de Llobregat, Barcelona, SPAIN

Background: Colorectal carcinoma (CRC) is the second cause of cancer-related mortality in the Western world. In the majority of patients, CRC is detected with lymph node metastases and a significant number of cases have distant spread, mainly in the liver. To improve patient treatment it becomes important dispose of genetic markers that select better the patients. Presence of fibroblast growth factor receptor-4 (FGFR4) Gly388Arg polymorphism has been associated with a poor prognosis in several neoplasms including colorectal and breast tumors. The aim of this study is to analyze the prognosis value of the presence of Gly388Arg polymorphism in a series of resected colorectal hepatic metastases. ***Methods:*** From 2001 until 2006 a series of 156 patients harboring CRC liver metastases underwent radical surgery. Histological confirmation was made for all cases, and fresh-frozen hepatic metastases and paired non-adjacent normal liver parenchyma was simultaneously collected for all patients. Prospective clinical follow-up is avalaible for all patients. DNA and RNA was obtained for all cases by standard methods. Presence of Gly388Arg polymorphism was analized by a BstNI-RFLP (Restriction Fragment Length Polymorphism) method. ***Results:*** Presence of FGFR4 (Arg 388) allele was identified in the 42.15% of the patients, in 65 patients heterozygous and in 7 patients homozygous. In a preliminary analysis we did not identified any association between the presence of FGFR4 (Arg 388) allele and the clinicopathological variables analyzed. Similary, in our preliminary prognostic data presence of FGFR4 (Arg 388) allele seems not correlates with survival parameters. ***Conclusion:*** To improve our study we are analyzing: (i) the correlation between this polymorphism and the degree of fibrosis present in liver metastases; and (ii) establish the association between the presence of FGFR4 (Arg 388) allele and the FGFR4 expression levels determined by quantitative real-time PCR (qPCR). Our study will permit to establish the prognostic significance of FGFR4 (Arg 388) allele in colorectal liver metastases.

P-400

Intestinal graft versus host reaction in patients with Good's syndrome – case report

Andrzej Mroz; Maria Cwikla

Department of Gastroenterlogy and Hepatology, Medical Centre for Postgraduate Education, Poland

60 year old patient was admitted to our Gastroenterology Unit due to bloody diarrhea of about month duration. The patient had been operated on mediastinal thymoma (AB type) two months earlier. In laboratory studies he presented hypogammaglobulinemia but no overt infection was appreciated. Stool was collected for microbiological studies but they were constantly negative for bacteria or fungi presence.

Biopsy specimen were taken from stomach, right colon, sigmoideum and rectum. According to endoscopic depiction large bowel mucosa were oedematous and hyperaemic with many ulcers and changes in vascular pattern what gave the suggestion of nonspecific inflammatory bowel disease.

In histological picture many extensive ulcers and mucosal sloughing were seen. No architectural crypt changes occurred and many apoptotic bodies were present in crypts' epithelium. These changes were so pronounced and numerous in rectal mucosa that it would correspond with what is called in literature "exploding crypt cells". Interestingly, inflammatory infiltrate, in the areas remote from necrosis, was quite sparse.

Additional the immunohistochemical studies for CMV were performed and turned out negative as the serology for cytomegalovirus was.

No histological changes were seen in gastric mucosa.

Conclusion: Graft versus host like reaction is rare complication in non-transplanted patients but should be taken into differential diagnosis of diarrhea in patients with Good's syndrome. Intestinal histological features could include, next to characteristic apoptotic bodies, quite extensive and deep ulcers. Slight distortion of crypts can be appreciated but no pronounced mucosal remodeling occurs.

Acute infectious colitis should always be the matter of differential diagnosis debate as the CMV infection is. CMV colitis could have very similar histological picture and the adjunctive immunohistochemistry or in situ hybridization use seems mandatory.

P-401

TUMORATION IN THE JEJUNUM WITH HISTOPATHOLOGIC FEATURES OF SARCOMA OF CLEAR CELLS

Hugo Álvarez-Argüelles-Cabrera; José-Luis Carrasco Juan; Sonia García Hernández; Vicente Medina Arana*; Rafael Ramos Asensio; Juan-Cruz Cigudosa García***; Nieves Hernández León; Candelaria García Castro; Alejandro Brito García; Leticia Melgar Vilaplana; Lucio Díaz-Flores**

*Service of Pathology. Canary University Hospital. Tenerife. Spain. *Service of Surgery. Canary University Hospital. Tenerife. Spain. **Service of Pathology. Son Dureta University Hospital. Mallorca. Spain. ***CNIO. Madrid.*

BACKGROUND Clear cell sarcoma (CCS), also known as malignant melanoma of soft parts, is a soft tissue sarcoma of the lower limb in adolescents and young adults. Other anatomical sites of this tumour such as gastrointestinal tract are extremely rare. In particular, the location in the jejunum of this neoplasm is exceptional, so we performed a review of the literature with an emphasis on its histopathological differential diagnosis.

METHOD The biopsy material, for the pathologic study was fixed in 4% formalin according to the usual methods for processing and inclusion in paraffin, and the posterior sections were stained by hematoxiline-eosine, PAS and Wilder's reticuline. Some sections were choosed for immunohistochemical study and for an evaluation of chromosome 22 translocation using FISH.

RESULTS A 41 year old male patient presented a neoplasia, measuring 7.7 cm along the major axis, in the jejunum which affected all the parietal strata with local adenopathic conglomerate metastasis. Microscopically this was a tumour with a pattern of solid growth in the form of masses, nests and ribbons which were composed of atypical epithelioid cells with eosinophile or clear cytoplasm (positive PAS) and a vesiculose nucleus with macronucleoli and frequent mitosis. There was also the presence, in some cases, of osteoclastic type cells. The tumoural cells were immunohistochemically positive for S-100 protein, vimentine and bcl-2, and negative for other markers, including CD-117, HMB-45 and Melan A.

CONCLUSIONS After a review of the literature, a fourth case of CCS in the jejunum, with a genetic study, is presented here. A differential diagnosis with GIST, malignant schwannoma melanomas and carcinomas, was made given the extremely uncommon location of the tumour.

P-402

Impact of small lymph nodes (<2 mm) on N-stage in colorectal cancers

Thore Thiesler; Niels Willi; Christoph A. Maurer; Andreas Huber; Gieri Cathomas

Kantonales Institut für Pathologie, Liestal; Department of Surgery, Kantonsspital Liestal; Department of Surgery, Kantonsspital Bruderholz, Switzerland

Introduction: Lymph node metastasis is an important prognostic factor of colorectal cancers. A minimal requirement of 12 lymph nodes has been proposed by the UICC/TNM. However, several authors feel that this number is too low and therefore a cumbersome search for small lymph nodes is initiated. In the present study, we evaluated the impact of small lymph nodes in tumour staging.

Material and methods: Retrospectively, lymph nodes of surgical specimen of colorectal cancers were analyzed.

Results: A total of 464 colorectal carcinomas were evaluated. Lymph node metastasis was detected in 216 (46.6%) of specimens (130 patients N1, 86 patients N2). Of 7659 lymph nodes, 899 (11.7%) show tumour involvement. The size of lymph nodes with metastasis was significantly larger than lymph nodes free of tumour (median diameter 5.76 mm versus 3.52 mm; $p<0.0001$). The size of lymph nodes in 65 patients with a single lymph node metastasis was also significantly larger (5.76 mm versus 3.44 mm; $p<0.0001$). Metastatic involvement of lymph nodes <2 mm was significantly less common than of larger lymph nodes (2.2% versus 13.2%; $p<0.0001$). Only in 2 patients, metastasis of a solitary lymph node <2 mm led to an upstaging from N0 to N1. Using a cut off of <3 mm, 10 (2.2%) patients would have been upgraded from N0 to N1 whereas a cut off <5 mm would understage 45 (9.6%) patients inadequately as N0.

Conclusion: A careful evaluation of lymph nodes in colorectal surgical specimen is crucial in the management of patients with colorectal carcinomas. This includes also lymph nodes smaller than 5 mm; however, lymph nodes <2 mm are seldom involved by carcinoma and rarely (0.4%) lead to an inadequate N0 staging.

P-403

Colo-rectal micropapillary carcinoma: A clinicopathological and molecular study of 27 cases.

Ruth Roman1; August Vidal1,2; Montse Verdú1,2; Miquel Calvo3; and Xavier Puig 1,2

1 BIOPAT. Biopatologia Molecular, SL, Grup Assistencia, Barcelona, Spain; 2 Histopat Laboratoris, Barcelona, Spain and 3 Statistics Department, Universitat de Barcelona, Barcelona, Spain.

INTRODUCTION. Invasive micropapillary carcinoma (MC) is associated with frequent lymph node metastasis and adverse clinical outcome. It has been reported in ovary, breast, urinary bladder, ureter, lung, parotid gland and, recently, in colon. Little is known about the morphological and molecular profile of this type of colonic carcinoma.
AIM. To analyze the clinico-pathologic features and molecular findings of colorectal MC and to compare with non-MC carcinoma.
MATERIAL AND METHODS. Clinicopathological features of a cohort of 333 patients with primary colo-rectal cancer were retrospectively reviewed. All slides avalaible from each tumor were reviewed by two pathologists, looking for the presence of micropapillary pattern (small papillary cell clusters surrounded by lacunar spaces). An estimation of the proportion of this component was recorded. The parameters evaluated in each case included: age, sex, location of primary tumor, tumor size, growing pattern (infiltrative or expansive), grade, depth of invasion (pT), lymphovascular and perineural invasion, nodal status (pN) and number of positive lymph nodes Genetic assesment of microsatellite instability (MIN), chromosome 18q status, p53 and Kras mutation were performed on DNA extracted from sections of formalin-fixed, paraffin-embedded specimens.
RESULTS. Twenty seven cases (8.1%) had micropapillary component, ranging from 10 to 95% of the tumor. They showed higher frequency of infiltrative pattern, lymphovascular and perineural invasion, a higher depth of invasion, and more positive lymph nodes when compared with conventional adenocarcionoma. These differences were statistically significative ($p</=0.0001$). There were not statistical significative differences in molecular findings between the two groups, but MC had a tendency to carry p53 mutations ($p=0.03945$).
CONCLUSIONS. Colorectal MC appears to be more aggressive than conventional colorectal adenocarcinoma. They present at a higher tumor stage with frequent lymphovascular and perineural invasion and nodal metastasis compared with conventional adenocarcinoma and have more tendency to carry p53 mutations.

P-404

IMMUNOHISTOCHEMICAL AND MORPHOMETRICAL EVALUATION OF THE NEUROENDOCRINE CELLS AND PROLIFERATIVE ACIVITY OF GASTRIC EPITHELIUM IN SUPERFICIAL (gchs) AND DEEP (gch) CHRONIC GASTRITIS

1.Kozłowski Wojciech.; 2.Jochymski Cezary; 1,2.Markiewicz Tomasz; 2.Osowski Stanisław; 1.Koktysz Robert; 1.Dąbek Andrzej; 1.Patera Janusz
1. Department of Pathology Military Institute of the Health Services, Poland;2. Warsaw University of Technology, Poland

Background Neuroendocrinecells exist almost in the whole alimentary canal. These cells have an influence on secretory functions and normal gastric mucosa histostructure. Up to nowinvestigations confirmed participation of these cells in e.g. HCl and gastrinsecretion regulation and in some of the proliferative states of gastric mucosa.The aim of the study was to estimate participation of neuroendocrine cells andstatus of the proliferative activity gastric epithelim in gchs and gch.
Method Paraffin blocks from gastricoligobiopsies were the material which was collected from 35 women (of average-age-52) and 34 men (of average age-54). Chronic inflammations were gradedaccording to modified Whitehead's classification. Helicobacter pylori wasevaluated according to the system from Sydney.Neuroendocrine cells and proliferative antigen expression of gastric mucosawere counted after proper immunohistochemical stains (Chromogranin A, Serotonin,Somatostatin and PCNA) in circular, oblique short, oblique long and oblong mucosalgastric glands sections. All measurements were conducted separately for gastricmucosa prepyloric part and gastric corpus. Next we use the thresholdingoperation sequentially and apply the artificial neural network of SVM type formeasurement of the same objects. The results of quantitative evaluations wereanalysed with the use of statistic methods. Results In gastricmucosa antrum there were twice more Chromogranin A,Serotonin and Somatostatincells in comparison with corpus. Gastric mucosa inflammatory type did not havea significant influence on cells localization in gastric mucosa. The number of ChromograninA cells diminished in gchs gastric antrum among patients who were over 50 yearsold,whereas the same number increased in corpus inflammations of this type.The increase of Chromogranin A cells number was found in gchs gastric antrumwith Helicobacter pylori colonization.and higher proliferative activity of thegastric epithelium. In these cases Serotonin and Somatostatin cells numberdiminished. Any differences were found in proliferative activity gastricepithelium depending on histotopography of samples, age and Helicobacter pyloricolonization.
Conclusion

1. Chronic superficial gastritis coexists with higher proliferative activity in the prepyloric part and Chromogranin A cells number increase. In these cases Somatostatin and Serotonin cells number decreases.
2. Changes of the proliferative activity in chronic gastritis do not depend on its age and Helicobacter pylori colonization in the gastric mucosa
3. In chronic gastritis quantitative changes of Chromogranin A, Somatostatin and Serotonin cells run differently in gchs and gch both in prepyloric part and in gastric corpus.

P-405

Expression of survivin in colorectal carcinomas

Ioannis KAlliakmanis; Chariklia Kouvidou; George V Papatheodoridis; Dimitrios Anagnostakis; Ioannis Koskinas; Athanasios J Archimandritis

Departments of Pathology, Gastroenterology and Medical Oncology, Elpis Hospital, Athens,Greece; 2nd Department of Internal Medicine, Athens University School of Medicine; Hippokration General Hospital of Athens, Greece

Background: Survivin is a new member of the IAP family that has a dual function as mitotic regulator and apoptosis inhibitor. Survivin is prominently expressed in transformed cell lines and in many human cancers including colorectal carcinoma. The aim of the study was to investigate the expression of survivin in colorectal carcinomas and to correlate it with clinicopathological parameters and patient survival. **Materials and Methods:** Formalin-fixed paraffin embedded tissue from 60 cases of colorectal carcinomas was stained by immunohistochemistry for survivin. **Results:** Survivin was mainly detected in the bottom of the glands of the normal mucosa and the localization was mainly cytoplasmic. No reactivity of the survivin antibody was found in the infiltrating lymphocytes, fibroblasts, smooth-muscle cells or neural tissue. Survivin predominantly cytoplasmic and minimal nuclear staining was found in 36/60 (60%) carcinomas. A slight tendency for a relationship between survivin expression and tumor differentiation (p-value=0.32) was observed. Survivin expression was not statistically significantly correlated with the others clinicopathological variables. The survival curves did not differ according to survivin expression. **Conclusion:** Overexpression of survivin suppress the apoptotic checkpoint during mitosis, promote aberrant progression through mitosis and seems to provide a survival advantage for tumor progression.

P-406

Detection of MLH1 and MSH2 expression in colorectal carcinomas of patients less than 50 years old in Costa Rica

Fernando Brenes; Mónika Núñez

Servicio de Patología, Hospital México, San José, Costa Rica

Background: Microsatelite instability (MSI) is detected in more than 90% of cases with hereditary non-polyposis colorectal cancer (HNPCC). Immunohistochemistry analysis of MLH1 and MSH2 expression can be used in colorectal carcinomas to identify patients with a possible DNA mismatch repair defect related with HNPCC. Besides, it has been demostrated that MLH1 or MSH2-deficient colorectal carcinomas have better prognosis. **Method:** Fourty three colorectal adenocarcinomas ocurring before 50 years of age were retrieved from the Laboratory of Pathology of Hospital México, Costa Rica. They were studied by immunohistochemistry in paraffin-embedded surgical samples for MLH1 (Biocare, clone G168–15) and MSH2 (Zymed, clone FE11) protein expression. Absence of tumor cell nuclear staining with positive internal control was considered negative. **Results:** 10 (23.3%) tumors showed loss of MLH1 or MSH2. We found significant differences regarding to patients' age (negative expression 35.6±2.8; positive expression 40±1.4). There was a higher percentage of colorectal cancer familiar history in patients negative for MSH1 or MLH2 (negative expression 30.0%; postive expression 12.0%). A trend regarding tumor size was found (negative expression 10.9 cm; positive expression 15.3 cm). The two groups were not different for tumor site, differentiation, pTNM stage, vascular and perineural invasion and 5-year survival rates. **Conclusions:** MLH1 or MSH2-deficient colorectal adenocarcinomas of less than 50 years old patients exhibit some features similar or sugestive of HNPCC. This study confirms that immunohistochemistry is a useful tool for the routine study of patients with suspicion of HNPCC in Costa Rica.

P-407

The role of the gastric biopsy for the diagnosis of the Biermer's disease, about 64 moroccan cases.

Fouad Zouaidia; Ahmed Jahid; Nadia Tazi; Leila Laraki; Zakia Bernoussi; Fatima Mansouri; Najat Mahassini.

Department of pathology, Ibn Sina Hospital, Rabat; Morocco.

Introduction: Pernicious anemia, also called Biermer'sdisease, is an autoimmunne gastritis limited to the fundus of the stomach. In addition to fundic atrophy, the patient presents reduced secretion of gastric acid and intrinsic factor as well as vitamin B12 malabsorption. Prevalence was estimated to 9–17 new cases/100000 H/year in the occidental countries.

Methods: We report 64 cases of the pernicious anemia colliged in 2006–2007. This study is based on the gastric biopsy specimens made for patients with pernicious anemia or for the other symptomatology.the pathological criteria for diagnosis of the pernicious anemia were intestinal metaplasia, fundic atrophy and hyperplasic of the fundic endocrine cells.

Results: There were 34 females and 30 males with a median age of 53 year. We have 18 patients recorded with pernicious anemia. 17 patients had macrocytosis. 19 patients had hyperplasia of the fundic endocrine cells. In follow up, 6 patients developed neuroendocrine tumors. Helicobacter pylori was diagnosed in 23 patients.
Conclusion: There is evidence that the gastric biopsy is an essential tool for diagnosis, prognosis and confirmation of clinically suspected cases.

P-408
Specific features of small bowell gastrointestinal stromal tumors

Vuka Katic, Goran Stanojevic, Dejan Janjic, Katarina Katic, Ivan Ilic, Suncica Janjic
Institute for Pathology, Medical faculty Nis, Serbia

Background:Small bowell Gastrointestinal Stromal Tumors (GIST) are rare mesenchymal tumors originating in the wall of the gastrointestinal (GI) tract.The cell origin of these tumors is thought to be a stem cell that differentiates toward the interstitial cell of Cajal. Aim: Different clinical and morphological characteristics of the small bowell GISTs from the stomach GISTs, are the reason for this study. **Material and methods:** We have discovered 14 small bowell GISTs on surgical material, during last five years. Paraffine sections were stained with HE, PAS, HID-AB pH =2,5 and immunohistochemical LSAB2 methods, by using the antibodies: CD117, CD34, Ki-67, Melan A, S-100 protein, Desmin, Vimentin, NSE and panCytokeratin (Galen Fokus- Kopenhagen). **Results:** 14 patients (9 female and 5 male) were identified. The mean age of patients were 52 years, range 8, 17 (two children) to 72 years. Based on microscopical features of malignant potential of GISTs, disease was localized in 5 patients, locally advanced in 7 patients and with multiple primary lesions in 2 patients, associated with recurrent disease (after 7 months from surgical therapy in one) and spreading within the abdominal cavity (in the other), but never to lymph nodes. The most impressive finding was the discover of intracellular lipofuscin-like and melanin pigments in the spindled cells that showed strong expression the specific kit tyrosine-kinase receptor (CD117). Important histological diagnostic feature of the small bowell GISTs was globoid extracellular collagen accumulations (so-called skenoid fibers). **Conclusion:** It has been concluded that small bowell GISTs behave more agressivelly than gastric tumors, produce lipofuscin-like and melanine pigments and occur in the children as well as in adults.

P-409
Both histological and immunohistochemical study of rare duodenal neuroendocrine tumor - gangliocytic paraganglioma

Ivan Ilic; Vuka Katic; Vera Todorovic; Miroslav Stojanovic; Miljan Krstic; Marija Matic; Dusan Mihajlovic
Institute for Pathology, School of Medicine Nis, Serbia

Background. Duodenal gangliocytic paraganglioma is very rare, accounting for about 9% of all gut endocrine tumors. Though considered benign the disease can spread to regional lymphatics. **Case presentation.** We report a case of a 25 - year - old woman presenting with a 2-week history of melena and was found to have periampullary mass. The tumor was resected with pyloris-preserving pancreatico-duodenectomy and was found to represent an infiltrative lesion of large size (9 cm in diameter). The resection margins were free of tumor. Histologically, the tumor had triphasic cellular appearance: 1. Spindle cells resembling Schwann cells or sustenticular cells, positive for neurofilament and S- 100 protein. 2. Ganglion-like cells, in nests, resembling the “zellballen” of classical paragangliomas, positive for synaptophysin and glial fibrillary acidic protein. 3. Endocrine cells arranged in nests, trabeculae, papillae and gland-like structures, positive for pancreatic polypeptide and neurone specific enolase, but staining for chromogranine was negative. There were areas of stromal hyalinization resembling amyloid, with focal calcification. She is alive and well one year following resection. **Discussion.** The authors have reviewed the current literature pertaining to this entity and have discussed the biological behavior of the tumor.

P-410
ADENOMYOMA OF THE GASTROINTESTINAL TRACT. REPORTS OF FOUR CASES AND REVIEW OF THE LITERATURE

Krstic Miljan, Basic Marin, Ilic Ivan, Stoiljkovic Simonida, Katic Vuka
Institute of Pathology, School of Medicine, Nis, Serbia

Background. Adenomyoma of the gastrointestinal tract is a rare benign tumor-like condition characterized histologically by a mixture of glandular structures lined by tall columnar epithelium with intervening bundles of smooth muscle. The pathogenesis of adenomyoma is considered to be either a form of myoepithelial hamartoma or a pancreatic heterotopia. **Reported cases.** We describe four cases of adenomyoma. One was the jejunal adenomyoma that presented with intussusception occuring in a 48-year-old man. The other was gastric antral adenomyoma found incidentally in a 62-year-old man, during cholecistectomy. It had intra-abdominal localisation, origining from the

antral subserous region. The third had just below the cardia intramuscular localisation, inducing both the cardiac stenosis and cardiac ulcer, found after gastrectomy. The fourth was the Vater's papilla adenoma, discovered during the autopsy in a 54-year-old woman. Clinical diagnosis was dysfunction of the papilla Vateri, associated with severe obstructive jaundice induced by its cancer. Formaldehyde fixed, paraffin sections were stained with H&E, Van Gieson, PAS and HID-AB methods. Immunohistochemical LSAB2 method was used for verification of epithelial, mesemchymal, smooth muscles and myoepithelial tissues as well as nuclear proliferative activity (DacoCytomation). On histological examination, the lesions consisted of hyperplastic glandular lobules of the pylorus, exocrine pancreas and jejunum, covered by single-layer epithelium of cuboidal and columnar cell type. The cells showed no atypia; some ducts showed cystic changes. The hyperplastic glandular lobules were surrounded by hyperplastic mesenchymal tissue, composed of bundles of smooth muscle. Immunohistochemically, intense expression of panCytokeratin (epithelial marker), vimentin (mesenchymal marker), desmin (smooth muscle marker) as well as actin (myoepithelial cell marker) has been found. Ki-67 activity (proliferative activity marker) was negative. **Conclusion.** Adenomyoma of the gastrointestinal tube is a rare benign lesion. The differential diagnosis from adenocarcinoma, especially in a frosen section, might be difficult. The main features are the absence of cytological abnormalities, the absence of desmoplastic stroma and the presence of smooth muscle bundles encircling the cysts.

Posters Displayed on Wednesday, March 21

Cytopathology

P-411

chordoma – preoperatve diagnosis using fine needle aspiration cytology: a cytologic, histologic, radiological & immunohistochemical correlation.

Dr. lopa Modi, Dr. Rohit Jain, Dr. Trupti patel, Dr. Manoj J Shah

The Gujarat Cancer & Research Institute, Ahmedabad, India

BACKGROUND- Chordoma is a rare tumor arising fromprimitive notochord located along the axial skeleton. The fine needleaspiration biopsy findings are described, correlated with histology, radiologyand immunohistochemistry and compared with previously reported descriptions of Chordoma.

STUDY DESIGN –During years 2006 & 2007 clinically unsuspected four cases of Chordoma werediagnosed preoperatively in the department of cytology, The Gujarat Cancer& Research Institute, Ahmedabad, India. Cytological material includedsmears and cell blocks. Immunostains were performed in all four cases onhistological material. Multiple cytological parameters were studied andcompared with previously reported description of Chordoma.

RESULTS- All four cases were male patients (mean age 58.7 years, range 45–65 years)had tumor involving sacrum (2 cases) and coccyx (2 cases). Pain was thepresenting symptom in all four cases. All smears were cellular with myxoidbackground; chondroid background was noted in one case. Cells with clear,vacuolated cytoplasm constituted the predominant cellular component. Small epithelial like cells were seen inthree cases. However, true physaliphorous cells were rare. Binucleated andmultinucleated cells were present in all.

CONCLUSION- Cytomorphologic findings are characteristic and when taken in context withradiological study allow differentiation of Chordoma from other primary ormetastatic lesion in axial skeleton. Chordoma is often an unsuspected diagnosisand fine needle aspiration biopsy can lead to a correct preoperativediagnosis.FNA may be utilized to document recurrence and thus facilitate theevaluation and management of the patients with these lesions.

P-412

Low Grade Squamous Intraepithelial Lesion/Human Papilloma Virus: Retrospective Cytologyc Study of the South East of Mexico

Fiandesio Ada Cecilia; Trinidad Hernández Sagrario; Ángeles Arturo

Instituto Nacional de Ciencias Médicas y de la Nutrición Salvador Zubirán, Mexico

Background: Uterine cervix carcinoma (CCU) is the second cause of women oncologic death in the world. Human papilloma virus (HPV) is associated with low grade squamous lesions (LSIL) and these ones are associated withthe development of cervix carcinoma. The objective is to evaluate the relationship between HPV and LSIL of Mexican and foreign women from Cozumel Island and its associated risk factors.

Methods and Materials: 305 pap smears were evaluated from The Cozumel Medical Center from November/2004 to May/2005. Papanicolaou technique was selected for evaluation, and interpretation was made by Bethesda System/ 2001. We excluded gyn-citologies with other sexually transmission deseases.

Results: Respective and correspondent percentage of total cases was: ASC, 11.07%; LSIL, 4.56% and HSIL, 0.65%. 30 years old was the average for LSIL, 8 (15.7%) were foreigners and 8 (0.3%) were native patients; 2 corresponded to HSIL (1 foreign case, 35 years old and the other a local one, was 74 years old, with later diagnosis of differentiated squamous uterine cervix carcinoma).
Conclusions: Cozumel's total population is a risk one. Average of foreign patients with LSIL is higher than native patients average. Tourism would be a risk variablefor transmission and infection with HPV.

P-413

Metaplastic endometrial cells as a possible pitfall in cervical/vaginal smears

Naver A. Sarkissian, MD, PhD; Marietta Kintiroglou, MD; Michael Dardik, MD
Department of Pathology, Saint Barnabas Medical Center, Livingston, New Jersey, U.S.A.

40-year old patient with a history of uterine spotting had a cervicovaginal smear with endometrial cell clusters demonstrating cytologic features of eosinophilic metaplasia. A concurrent endometrial biopsy showed shedding endometrium with eosinophilic metaplasia including clusters of cells identical to those seen in the Pap smear. According to the 2001 Bethesda system the presence of endometrial cells should be reported in all women of 40 years of age or older. Since benign metaplastic changes can alter the morphology of endometrial cells, it is possible that the presence of endometrial cells in Pap smears can be substantially underdiagnosed. Endometrial metaplastic changes can cause endometrial cells to resemble columnar endocervical, squamous metaplastic, eosinophilic, clear or tubal cells. This report raises awareness of an unusual metaplastic change that may prevent recognition of the cells as endometrial. Reports of metaplastic endometrial cells as a possible pitfall in the diagnosis of endometrial cells and/or malignancies is severely lacking in the cytology literature. While it is admittedly difficult to diagnose endometrial metaplasia in Pap smears alone, the fact remains that endometrial cells may not appear as the "typical" three dimensional clusters of small cells with high nuclear/cytoplasmic ratio and inconspicious nucleoli in Pap smears, especially in women 40 years of age or older when endometrial metaplasia is quite common.

P-414

ENDOSCOPIC ULTRASOUND-GUIDED FINE NEEDLE ASPIRATION OF PANCREATIC CYSTIC AND SOLID MASS LESIONS.

M Magdalena Garcia-Bonafe, Maria M Company, Angels Vilella, Arantxa Quiñoa
Son Llatzer Hospital, PALMA DE MALLORCA, SPAIN

EUS-FNA of pancreatic masses has shown to be a very effective diagnostic technique. We evaluated our series.
Material and Method A total of 66 EUS-FNAs in 62 patients with either cystic (21) or solid (45) pancreatic masses (40 head, 23 body, 3 tail) were performed. The mean age was 66 years (range 34–90).The final diagnosis was based on histology, clinical and/or imaging follow-up or biochemical and tumor markers.
Results: A median of 2 needle passes were performed (range, one to five). Histological correlation was available on 13 patients.The cytological diagnoses included: 30 (28 solids, 2 cystics) malignant (25 ductal adenocarcinoma, 1 mucinous cystadenocarcinoma, 1 intraductal papillary mucinous neoplasm with invasive carcinoma, 2 neuroendocrine tumors and 1 lymphoma), 28 benign (17 cyst: 11 serous and 4 mucinous cysts and 2 pseudocysts), 2 suspicious, and 6 nondiagnostic. All malignant diagnoses were confirmed.One suspicious case was a false-positive identified as chronic pancreatitis. All false-negatives (n=3) corresponding to a solid mass (1 head, 1 body, 1 tail).Six unsatisfactory cases (3 head, 3 body) corresponded to 4 ADC, 1 serous cyst and 1 mucinous cystadenoma.
Sensitivity, specificity, and positive and negative predictive values were 91,18%, 96,15%, 96,88%, and 89,29%, respectively. The diagnostic accuracy was 91%.
Conclusions EUS-FNA is an effective method for diagnosis in patients with suspected pancreatic malignancy, as well as in evaluation of cyst. The appearance and biochemical analysis of the fluid aid in precise diagnostic of cystic aspirates.The location was not in determining the suitability of the samples.False-negative diagnoses were attributed to sampling error and the false-positive were due to the presence of scant atypical cellularity. To avoid false-negative and nondiagnostic results in highly suspicious malignant lesions, we should increase the number of needles passes until we achieve the malignant cytological diagnosis on-site.

P-415

A quality control study on concordance in Pap Test among cytotechnologist (CT) and cytopathologist (CP)

Massimo Bongiovanni; Barbara De Saussure; Neeta Kumar; Magali Gremaud; Jean-Claude Pache.
University Hospital, Geneva, Switzerland

Background Quality-control is an important issue in Pap Test screening. The accuracy of Pap Test is largely dependent on CT's expertise. We performed a CT-CP concordance study to analyse areas of discordance. This could be used to target remedial actions for continuous quality improvement.
Methods An experienced staff pathologist (MB) out of three CPs, recorded in an excel datasheet the diagnoses of all cases referred to him for review by nine CTs over one year period. He compared their provisional diagnosis with his final diagnosis according to the Bethesda System 2001 and analyzed the discordant categories.
Result A total of 10,453 Pap Tests were screened by CTs during one year out of which 933 were referred to MB for final diagnosis. The most problematic diagnoses were "negative, inflammation" and "ASC-H" with concordance rates of 29% and 37.5% respectively. The range of agreement in the other diagnostic categories was 67% to 80%.
In the "negative, inflammation" category, the overall CTs-CP discordance was 71% (112/158). Among 112 misclassified cases, 84 (75%) were overcalled ASC-US and 17 (15%) cases were marked negative by CTs. For "ASC-H" the overall CTs-CP discordance was 62.5% (20/32). Among 20 misclassified cases, 13 (65%) were under interpreted as ASC-US and 4 (20%) as HSIL by CTs.
In 4 cases few malignant cells and necrotic debris were present and a definitive diagnosis of "suspicious for neoplasia" was rendered by CP. CTs diagnosed only one case correctly and called the rest as AGC (2) and negative (1).
Conclusion. We used an objective procedure to evaluate CTs's performance and observe dispersion of discordance. These data allow us to direct financial resources for education to specific diagnostic categories. The inflammatory category was the most problematic; therefore a specific education session describing inflammatory changes in squamous epithelium could be useful to improve concordance.

P-416

Liqui prep a new liquid based cervical cytology method in comparison with conventional pap smear

Mahmood Khaniki; Nadereh Behtash; Zeinab Nazari
Department of Pathology, Medical faculty of Tehran university, Iran

Background: The aim of the study was to compare, the screening performance of a new liquid-based cytology method, LiquiPREP™,with conventional Pap in a low risk population, using colposcopy followed histology as "gold standard".
Materials and Method: This prospective study was performed in a general gynecology clinic in ValiAsr University Hospital, Tehran, Iran from February 2005 to March 2007. The split-sample method was used for preparing conventional and liquid-based cytology.A new technique of liquid-based cytology; Liqui-PREP™ was used in this study. All positive result of smears and 10% of negative results in each group were submitted to colposcopy and a biopsy taken when any atypical transformation zone was seen. Sensitivity, specificity, positive and negative predictive values, and overall accuracy of both conventional and LiquiPREP™ methods were computed in relation to histology.
Results: A total of 506 patients were analyzed by two cytology methods and in 65 (12.84%) of cases histologic diagnosis was performed. There were more adequate samples with LiquiPREP™ (94.7%) than with conventional (92.1%) smears. There was not any LSIL and HSIL report in two groups. ASCUS was diagnosed significantly more with conventional than with LiquiPREP™ smear (1.56% vs. 0.79%). Pathologically 50% of ASCUS in Liqui-PREP™ and 12.5% in CP had squamous abnormality. LiquiPREP™ had a significantly higher sensitivity (66% vs. 83%) and specificity (86% vs. 98%) than the conventional Pap smear to detect ASCUS+ at histology.
Conclusion: This study confirms the superiority of the LiquiPREP™ method to detect cervical lesions.
Key Words: Cervical carcinoma; Screening; Conventional smear, Liquid based smear

P-417

Evaluation of morphometric diagnosis accuracy in thyroid cytology

Mazir Ghafouri MD, Zahra Forouhesh MD
Shariati hospital, Tehran university of medical sciences, Iran

Introduction: Decision making in pathology is changing toward quantitative criteria. Quantitative measurements obviously can demonstrate minimal differences, not readily identifiable to human vision. Morphometry is quantitative description of geometric characteristics of objects. This study tends to test feasibility of this new technique using available instruments and softwares and to select useful parameters and their thresholds for discrimination of benign versus malignant lesions of thyroid.
Materials & Methods: Cases have been selected among received fine needle aspiration specimens of thyroid in pathology department of Dr. Shariati hospital from October 2003 to March 2004. Patients whose surgical pathologic reports were not available have been excluded due to impossibility of comparing diagnoses. At least 100 cells have been measured for each patient. The cells were selected by a zone guided manner. Totally 67 patients were entered to the study, 36 with benign pathology diagnosis

and 31 with malignant lesions. In a pilot study to test reproducibility of measurements, a single cell was selected and measured for 20 times.
Result: Coefficient of variation remained below %2 for all measurements but nuclear diameter which has been excluded from analysis. Benign cells were different from malignant ones in mean nuclear perimeter (Peri), mean nuclear area (Area), nuclear area to perimeter ratio (A/P), cluster diameter, mean gray level (in 256 gray levels) and standard deviations of Peri, Area and A/P (P-values<0.05); but not in CV of nuclear area, intercellular standard deviation of gray levels, intracellular CV of gray levels and its standard deviation. a Receiver Operator Characteristic curve analysis was performed for parameters with significant difference and sensitivities and specificities calculated for different cut-off values.
Conclusion: The highest sensitivity has been reached for nuclear perimeter, nuclear area, cluster diameter and nuclear area to perimeter ratio equal to %93.55 and for cluster diameter equal to %89.55. The results are comparable to classic cytology practice thus this technique is recommended to screen thyroid FNA specimens.
Keywords: Morphometry, Cytology, Pathology, Thyroid, Needle Aspriration

P-418

Fine needle aspiration of axillary lymph node in breast carcinoma. Cytohistological correlation with sentinel lymph node.

Neus Combalia; M[a] Rosa Escoda; Ruth Orellana; Sara Fernandez; Xavier Andreu; Ampar Saez; Merce Rey.
Servei de Patologia UDIAT-CD Corporació Sanitaria Parc Tauli, Spain

Introduction: Axillary lymph node metastases is one of the most important prognostic parameters in patients with breast cancer. Axillary limphadenectomy is substituted by the technique of sentinel lymph node (SLN) biopsy in patients without palpable lymph nodes. Currently the ultrasound guided fine needle aspiration of axillary lymph node (FNALN) has been proposed, to determine the best treatment for each patient, but FNALN not always is done in SLN.
Objective: To evaluate the FNALN we correlated cytological findings with SLN study, and axillary lymphadenectomy.
Material and methods: 179 FNALN were studied between 2005 and 2006, and correlated to 45 cases with SLN study and with surgical lymphadenectomy specimen.
Results: The FNALN was positive in 64 cases (35,7%), negative in 95 (53%) and inadequated in 20 (11,11%).
There were histological correlation in 46 of 64 positive cases; in 38 the diagnosis was confirmed, and in 8 cases the lymph nodes were negative, all of them treated with neoadjuvant chemotherapy.
The 95 negative cases had histological correlation in 71. In 45 of them SLN technique was made; at the cytologic intraoperative study 8 were positive and 37 negative, 5 of them showed micrometastases in the exhaustive histological and immunohistochemistry study. Of 26 cases without SLN study, 5 presented metastases in the axillary lymphadenectomy.
Excluding the 8 negative cases after neoadjuvant chemotherapy, the Efficiency of the FNALN in our experience was: Sensitivity: 66,6%; Specificity: 100%; VPP: 100%; VPN: 73,2%; and Accuracy: 77%.
Conclusions: The FNALN has moderate sensitivity, high specificity and high accuracy to detect metastases and to stage breast cancer. It is very useful to establish the best treatment for each patient, and to avoid the study of SLN in a high rate of cases.

P-419

Unusual Findings of Papillary Carcinoma in Aspiration Cytology

Ayla Tezer; Gulcin Guler Simsek; Heyecan Ökten
Kecioren Eğitim Araştırma Hospital, Turkey

FNA biopsy is highly accurate in diagnosis of Papillary thyroid carcinoma (PTC).The smear of PTC is usually cellular and it has papillary structures of various types. The cytoplasm of follicular cells are squamoid,and have septate vacuoles in PTC. In nucleus, grooved membrane,INCIs, fine pale chromatin,marginated nucleoli, are other findings in PTC. Psammoma bodies, epitheloid giant cells, gummy colloid are seen in some PTC cases.Sometimes you can't see any characteristic finding in PTC such as in our case.
In cytology, we saw irregular membranes, grooved nuclei in follicular cells arranged in flat sheets. Furhermore nuclei were much bigger than normal. Flame cells were found in some areas they were thought to be a finding of hyperthyroidi, less commonly seen ın neoplasm.Accordıng to all of these fındıng we thought benign cytology and cellular nodule which presented hyperactivite finding.
After operation, histopathological findings showed that diagnosis as papillary carcinoma with follicular varyant and tumour cells extended to surgical margins.
On conclusıon, if you see bigger nuclei with grooves ın most cells and you don't see any colloid or a little colloid, you must be careful when you writing diagnosis. Perhaps it is better to write suspicious cytology as a diagnosis

P-420

LANGERHANS CELL HISTIOCYTOSIS IN ORBIT- DIAGNOSED BY FINE NEEDLE ASPIRATION CYTOLOGY (FNA):TWO CASES REPORT

Fahimeh Asadi Amoli; Hedieh Moradi Tabriz; Ali Sadeghi Tari; Naser Kamalian
Farabi hospital (eye research center) Iran

Background: langerhans cell histiocytosis is a benign lesion that rarely occurred in orbital bone. Most cases present before the age of 20 and the majority of lesions are monostotic. FNA cytologic findings of this disorder have been well described, but using of this method in the diagnosis of orbital lesions is a recent experience. We were aimed to report two cases of langerhans cell histiocytosis in the orbital bone that diagnosed by FNA and later confirmed by routine H&E histopathology and Immunohistochemistry methods.
Material and method: Case report. We performed our study in Farbi eye hospital, a referral ophthalmologic center in Tehran University of Medical Science during two years, 2005 and 2006.
Results: The first case was a one year old boy with a left upper lid mass. CT scan showed a solid tumor with orbital bone invasion and erosion, suspicious for malignancy. The other case was a three years old boy with right lower lid edema. Radiographic study revealed a mass with peripheral condensation and orbital bone defect. FNA of both lesions showed a mixed cell population of eosinophils, neutrophils and lymphocytes admixed with neoplastic histiocytes with folded nuclei; so called "coffee- bean" nuclei. Some of these cells were binuclear or multinucleated. So the cytologic diagnosis was langerhans cell histiocytosis. After open surgery and mass excision, that diagnosis was confirmed by the routine histopathologic examination. In both cases IHC for CD1a were also performed.
Conclusion: In the hands of experienced ophthalmologists and pathologists, FNA can provides a rapid and reliable diagnostic method in orbital lesions suspicious for langerhan's cell histiocytosis.

P-421

CYTOKERATIN 20 IN URINE LIQUID-BASED CYTOLOGY SMEARS: A POTENCIAL MARKER FOR THE DETECTION OF UROTHELIAL CARCINOMA

Sara Fernández; Neus Combalia; Ruth Orellana; M Angeles Cabezuelo; M Rosa Escoda; Esther Sanfeliu; Anna Ferran; Lluís García; Mercè Rey
Corporació Parc Taulí, Sabadell, Spain

Background: The expression of CK 20 is useful to differenciate bening processes (such reactive urothelial atypia and degenerative changes secondary to calculi, trauma, instrumentation, infection or even intravesical terapy) of urothelial carcinoma, to avoid false positives, when the basis of morphology alone, may be difficult in some cases.
Method: 70 voided urine samples were evaluated by liquid-based cytology and CK 20 immunoexpression was detected. We reviewed using cytologic-histologic correlation, the histologic diagnosis was considered the "gold standard".
Results: Diagnosis of urine cytology were: 9 cases bening urothelial cells, 13 cases reactive urothelial atypia, 6 cases papillary lesion, 17 cases atypical urothelial cells, 7 cases atypical urothelial cells suspicious of malignancy and 18 cases of malignant cells.
CK 20 was positive in twenty-three cases, seventeen of them showed urothelial carcinoma in the biopsy, and six cases the biopsy was normal.
The fifty-seven cases with negativity to CK 20 immunostaining, twenty-three cases corresponded to cytologic diagnosis of atypical cell, atypical cell suspicious of malignancy and malignant cells, of these sixteen biopsies did not show alterations, in four cases had urothelial carcinoma, in two urothelial displasia and one case atypia of unknown significance.
Conclusions: Urothelial carcinoma shows strong immunoexpression of CK 20 in urine liquid-based cytology, except in a few cases, could be explained, because the expression is not found in 10% of cellularity. The CK 20 therefore aid to differenciate bening processes from the urothelial carcinoma, disminishing the false positives cases and increased diagnosis accurancy.

P-422

INTRA-OPERATIVE CYTOPATHOLOGY: A LITERATURE REVIEW

Marilene F Nascimento; Eliane P Dias; Ana Lucia Eisenberg; Giuliana Silva
Instituto Nacional de Cancer

Background: Intra-operative cytopathology (IOC) is a diagnostic technique used in many pathology departments around the world, alone or in association with tissue frozen section (FS). Although it was developed over 80 years before the FS, it never replaced it. Likely, the main reason for this is the inexperience of pathologists in interpreting the findings. The purpose of this study is to determine the current profile of IOC.
Methods: A literature review was performed in MEDLINE for articles published between 1927 and November 2007.

The inclusion criterion was that every specimen examined by IOC had a corresponding histologic section. A database was created cataloging the following variables: country of origin, total number of cases, organs/tissues examined, method of material collection, staining and accuracy.
Results: Two hundred ninety seven articles addressing IOC were selected. Most studies originated in the United States, Japan and Germany. In conjunction, 61,846 cases were examined, and, overall, the most commonly studied organs/tissues were central nervous system lesions (25.2%), lymph nodes (22.7%) and breast (8.7%). Within the last 15 years sentinel lymph nodes, central nervous system tumors, pancreatic lesions and mediastinal tumors became the most common evaluated tissues. In most cases, material for IOC was obtained using imprint and smear techniques, and stained by Papanicolaou and May-Grunwald-Giemsa methods. After correlation with histologic samples, the accuracy of IOC ranged between 80 and 100%.
Conclusion: The vast majority of articles recognized that IOC is a safe, simple, inexpensive and rapid technique option for intra-operative diagnosis. In addition, it is an effective way to prevent production of FS artifact in tissues. The practice acquired during IOC in examining cytomorphologic details can aid in improving fine needle aspiration diagnosis skills.

P-423

Clinical significance of diagnosis of ASC-US and ASC-H in cervicovaginal cytology: comparison between premenopausal and postmenopausal women

Ferré Esther; Caci Karina; Casalots Jaume; Tarroch Xavier; García Federico; Surrallés María Lluïsa; González Clarisa; Morlius Xavier; Forcada Pilar; González Guadalupe; Salas Antonio.
HOSPITAL MÚTUA DE TERRASSA

BACKGROUND: Some studies in order to evaluate the clinical significance of the cytological diagnosis of ASC-H (Atypical Squamous Cells cannot exclude H-SIL) in cervicovaginal cytology of postmenopausal women, comparing with other age groups, have shown opposed conclusions regarding their posterior management.
MATERIALS AND METHODS: We have reviewed the cytohistologic follow-up during the first year after diagnosis of ASC-US (Atypical Squamous Cells Undetermined Significance) or ASC-H in our department between 1997 and 2006 in premenopausal (< 45 years), perimenopausal (45–54 years), and postmenopausal women (> 54 years). In this period, in a total of 141669 smears examined, 611 (0.4%) cases of ASC-US (568) or ASC-H (43) were identified, and 490 of them (455 ASC-US and 35 ASC-H) had cytohistologic follow-up.
RESULTS: In the follow-up, 139 of the 455 cases initially diagnosed of ASC-US evolved into Low grade Squamous Intraepithelial Lesion (L-SIL), High grade Squamous Intraepithelial Lesion (H-SIL) or Positive For Malignant Cells (PFMC), and 17 of the 35 cases initially diagnosed of ASC-H changed into H-SIL or PFMC. The positive predictive value (PPV) of ASC-US for L-SIL/H-SIL/PFCM was: 32.5% in premenopausal, 24.7% in perimenopausal, and 28.3% in postmenopausal women. The PPV of ASC-H for H-SIL/PFCM was: 38% premenopausal, 60% perimenopausal, and 66.6% postmenopausal women. We have found statistically significant differences between age and diagnosis of H-SIL/PFCM in the follow-up of ASC-H ($p=0.02$), but not in ASC-US ($p=0.35$)
CONCLUSIONS: Our experience suggests that diagnosis of ASC-H in postmenopausal women would justify a close surveillance, because these patients have risk to develop a more aggressive lesion. In the case of ASC-US it would not be justified to make differences in the management of patients with regard to age group.

P-424

Cloacogenic (basaloid) carcinoma of the anus metastatic to the uterine cervix diagnosed by Liquid Based Cytology

Zoi Tatsiou; Natalia Vladika; Rosalia Valeri; Despoina Sioutopoulou; Charalampos Charalampidis; Chariklia Destouni
Department of cytopathology, Theagenion Cancer Hospital, Thessaloniki, Greece

Carcinomas of the anal canal and anus comprise fewer than 10% of the carcinomas in the distal colon. Most of these are epidermoid carcinomas and only 3% constitute the cloacogenic (basaloid) subtype. Extrauterine tumors metastatic to the cervix are very rare. The most frequent primary sites are the ovaries, gastrointestinal tract and breast. Among them only 2 cases of primary cloacogenic (basaloid) carcinoma of the anus metastatic to the uterine cervix and detected by Papanikolaou test have been reported in the English literature.
We present an extremely rare case of a cloacogenic (basaloid) carcinoma of the anus metastatic to the uterine cervix incidentally detected by a routine Papanikolaou smear. A 57-year-old woman was treated for squamous cell carcinoma, cloacogenic (basaloid) subtype of the anus, stage IIIA, with partial resection of the tumor, followed by 5 courses of systemic chemotherapy and radiotherapy. One year later, a routine Papanikolaou test was performed. The material was processed by Liquid Based Cytology (ThinPrep) technique. Evaluation of the cervicovaginal smear revealed a few well circumscribed aggregates of small,

uniform squamoid cells with hyperchromatic nuclei and peripheral palisading. Immunocytochemistry showed strong positivity for Cytokeratines 8/18, CEA and p53. Infection with 'high risk' human papillomavirus (HPV) was not detected by polymerase chain reaction (PCR). Diagnosis was based on the cytomorphologic and immunocytochemical characteristics as well as the patient's history and concerned a metastatic involvement of the uterine cervix by a squamous cell carcinoma, cloacogenic (basaloid) subtype. The patient received 3 courses of systemic chemotherapy and radiotherapy and is in partial remission.

Cervicovaginal smear screening in extrauterine malignancies is of high clinical significance to monitor these patients for possible metastasis and evaluate the stage of the disease or even to detect a second primary neoplasm.

P-425
EXPRESSION OF VASCULAR ENDOTHELIAL GROWTH FACTOR (VEGF) AND PLATELET-DERIVED GROWTH FACTOR RECEPTOR (PDGFR) IN MALIGNANT ASCITIC FLUIDS OF PATIENTS WITH OVARIAN CARCINOMAS

Natalia Vladika; Rosalia Maria Valeri; Anastasios Chatzitolios; Zoi Tatsiou; Kiriaki Boglou; Chariklia Destouni

Department of Cytopathology, Theagenion Cancer Hospital, Thessaloniki, Greece

Background: Angiogenesis plays a crucial role for growth, invasion and metastasis of solid tumours. Various molecules and their receptors have been studied to evaluate the mechanism of angiogenesis. Among them, vascular endothelial growth factor (VEGF) and platelet-derived growth factor receptor (PDGFR) induce proliferation of endothelial cells and promote the activation of tumour cells.

We investigated the immunoexpression of VEGF and PDGFR in ascitic fluids from various types of ovarian cancer.

Method: The study consisted of 38 ascitic fluids, including 14 cases with a cytomorphological and immunocytochemical diagnosis of type I(10 low-grade serous, 3 endometrioid, 1 clear cell carcinomas) and 24 cases of type II (19 high-grade serous, 2 undifferentiated carcinomas and 3 carcinosarcomas) ovarian malignancies. The material was processed using Liquid Based Cytology (ThinPrep) technique. Then, we applied antibodies against VEGF and PDGFR.

Results: VEGF showed granular/homogeneous cytoplasmic or membrane staining. The VEGF expression was much stronger in type II (15/24) ovarian carcinomas in comparison with those of type I (5/14). PDGFR was expressed in 23/38 of ovarian malignancies showing cytoplasmic and nuclear staining also with prevalence in type II carcinomas. Moreover, in five cases of type II ovarian carcinomas, weak PDGFR staining was observed even though VEGF was negative.

Conclusion: Co-expression of VEGF and PDGFR in tumours of the ovary suggests that the two pathways interconnect and may play an important role in angiogenesis of ovarian cancer, subsequent proliferation of tumour cells, and further tumour progression. This study supports the hypothesis that inhibition of VEGF signaling in ovarian cancer might induce suppressive effects in tumour cell proliferation. Anti-angiogenesis therapy targeting VEGF and PDGFR may be a promising therapeutic approach for patients with ovarian carcinoma, especially for those with overexpression of VEGF and PDGFR.

P-426
The role of L1 protein and of p16 INK4a gene in the prognosis of changes of the cervical endothelium.

L. Kampas, Ch. Charalampidis, Ch. Papaloukas, A. Fiska, R.M. Valeri, Ch. Destouni, Th. Dimitriou.

Department of Anatomy, Democritus University of Thrace, Alex/polis – Greece, and Department of Cytology, Theagenion Anticancer Hospital, Thessaloniki – Greece.

Introduction Immunocytochemical detection methods using HPV L1 capsid protein and the tumour suppressing gene p16 ^{INK4a} seem to help in the prognosis and follow up of precancerous changes related to the HPV (Human Papilloma Virus).

The aim of this study was to investigate the expression of the two biochemical markers in vaginal-cervical smear in the prognosis of progress of precancerous changes as well as the comparative assessment of their values in relation to the cell morphology and the follow-up.

Material and Methods: Two hundred vaginocervical samples from women (with or without changes in cell morphology) were studied. Thirty of them were followed up. The samples were processed by ThinPrep Thehnique followed by immunocytochemical detection of the L1 protein and of the gene p16 ^{INK4a}.

The results from the two techniques were compared as well as their correlation to the cell morphology and follow up, where possible.

Results: L1 was mainly expressed in low grade endothelial changes and was correlated to a good prognosis while p16 ^{INK4a} was detected in all the high grade endothelial changes indicating an unfavourable prognosis. Most of the followed

up cases showed a change of expression of the indices in accord with the cell morphology and colposcopy image.
Conclusions: This study showed that the immunocytochemical indices L1 and $p16^{INK4a}$ are two reliable aids in assessing the prognosis of precancerous changes of the cervix. Their routine application combined with the cytological examination and colposcopy can improve the treatment of women with HPV infection.
Key words: Pap-test, HPV, L1 capsid protein, $p16^{INK4a}$ gene, follow up, ThinPrep technique

P-427

IS VIRAL LOAD A PROGNOSTIC FACTOR IN LSIL CASES?

Laura Lopez (1), Teresa Gomez (2), Raquel Murillo (1), Javier Gimeno (1), Jordina Santos (1), Sandra Planella (1), Marta Pallarols (1), Emilia Romero (1), Imma Soler (1), Eulalia Gimferrer (1), Sara Albert (1), Lara Pijuan (1) Gemma Mancebo (2), Fernando Larrazabal (2), Ramon Carreras (2) Sergi Serrano (1). Francesc Alameda (1),
HOSPITAL DEL MAR. DEPT. OF PATHOLOGY. DEPT. OF OBSTETRICS AND GYNECOLOGY

Objective. To asses if viral load is a prognostic factor related to persistence/progression in LSIL cases.
Materials and Methods 134 patients diagnosed as LSIL using liquid based cytology ThinPrep (Cytyc), in a one-year period. The same sample was used to determine HPV and viral load using Hybrid Capture II (Digene). The patients were followed by cytology and/or biopsy.
Results: 55 (41%) cases regressed and 79 (59%) cases persisted or progressed. The mean of viral load in cases that regressed was 366.13 URL and the mean in cases that persisted was 861.5 RLU. The difference is statistically significant. If we consider the HPV positive cases when the value of RLU is 1, we obtain a sensitivity of 89% and a specificity of 22%, related to the persistence/progression of the disease. On the other hand. the specificity higher than 95% is obtained when we consider a RLU equal or greater than 1250. In these circumstances the sensitivity decreases around 30% but the predictive positive value is greater than 90%.
Conclusions: We think reasonable to suggest that patients diagnosed as LSIL with a viral load equal or greater than 1250 RLU should be submitted to surgical procedures. Using these data and based in our cases, 17% of the patients diagnosed as LSIL would be classified in this category.

P-428

3Q (HTERC) AMPLIFICATION AS A PERSISTENCE/PROGRESSION PREDICTIVE FACTOR IN LSIL CASES. A STUDY IN FROZED MATERIAL

Javier Gimeno (1), Blanca Espinet,(1), Jordina Santos (1), Raquel Murillo (1), Laura Lopez (1), Emilia Romero (1), Imma Soler (1), Eulalia Gimferrer (1), Sara Albert (1), Lara Pijuan (1) Gemma Mancebo (2), Fernando Larrazabal (2), Ramon Carreras (2) Sergi Serrano (1) and Francesc Alameda (1),
HOSPITAL DEL MAR. DEPT. OF PATHOLOGY. DEPT. OF OBSTETRICS AND GYNECOLOGY.

Objective: To assess the relationship between 3q26 (HTERC) amplification and persistence/progression in LSIL cases.
Material and Methods: 48 cased studied using liquid based cytology (ThinPrep, Cytyc), 24 normal cases used as controls and 24 LSIL cases used as a problem cases. All of the problem cases were followed on a control 6 months after diagnosis. 12 of them showed persistence/progression of LSIL and 12 showed regression of the lesion. Using the frozed material corresponding to first diagnosis, a study of copy number of HTERC was performed applying FISH techniques.
Results: The normal cases showed a mean of 5.3% of cells with only one copy of HTERC and a mean of 3.9% of cell with more than 2 copies of HTERC. There was no differences between trofic and atroffic cases.
None of LSIL cases showed cells with only one copy of HTERC.
The mean of cells with more than 2 HTERC copies in LSIL with regression was 4.9% and the mean of cells in LSIL cases with persistence/progression, was 11.75% ($p<0.05$)
Conclussion: HTERC amplification may be used as a predictive factor for the persistence/progression of LSIL

P-429

FINE NEEDLE ASPIRATION CYTOLOGY (FNAC) AS A VERY RELIABLE DIAGNOSTIC METHOD IN BONE LESIONS: A REVIEW OF 1040 CASES, FOCUSING ON 347 METASTATIC CARCINOMA.

C. Dinarès; C. Iglesias; A. Rivas*; M. Alberola; P. Huguet; V. Peg; MT. Salcedo; S. Planas; E. Martinez; S. Ramon y Cajal; N. Tallada.
*Departament of Pathology, *Departament of Radiology, Hospital Universitari Vall d'Hebron. BARCELONA (Spain)*

BACKGROUND: FNAC is a non-invasive and very useful method and a proved cost-effective technique in the diagnosis of neoplastic lesions. This study was designed to evaluate our experience with the use of FNAC, its utility and reliability, focusing on the diagnosis of bone metastatic carcinoma (MC).
DESIGN: We reviewed 1040 CT-guided FNAC of bone lesions performed between 1990 and 2007. We selected 347 MC positive cases. Aspirated material was air-dryed for Diff-Quik stain and fixed in ethanol for Papanicolaou staining. Tissue cell block was available in 330 cases. Immunohistochemical (IHC) techniques were performed in 177 samples.
RESULT: Of the 1040 reviewed FNAC, 808 aspirates were adequate for evaluation, 209 were insufficient, 347 positive for MC, and 494 from miscellaneous entities (lymphoma, multiple mieloma, primary lesions, inflammatory and negatives results).
Foccusing on the 347 MC FNAC, the patients ranged in age from 29 to 88 years, with 216 male and 136 female. In 74/347 cases with known primary tumour 61/74 were malignant aspirates confirming the patient's primary malignancies, 13/74 reveled a second metastatic tumour. The most frequent radiological and clinical presentation were as lytic lesion, pain and nodules/masses. The spine was the most frequent aspirated site (lumbar, dorsal and cervical), followed by ilium bone, ribs and femur. Of MC cases, carcinoma with different subtypes and origin were 162 (61.1%), 139(43.84%) corresponded to adenocarcinomes, 9 (2.83%) were small cell carcinoma (neuroendocrine) and 7 (2.2%) undifferentiated tumours. The primary tumour site was breast, lung, pancreatic and gall bladder area, kidney and prostate in order of frequency.
CONCLUSION: FNA is a non-invasive and very reliable method in the diagnosis of bone lesions. The use of the thicker-gauged needles in the last few years, has improved significantly the technique in order to obtain satisfactory samples, avoid inssufficient specimens and get high diagnostic accuracy. When previous history of malignancy is unknown, performing IHC markers on tissue cell block has proved determinant to establish site origin of the primary tumour. In our experience CK7, CK20, CK19, PSA, Hormonal Receptors and TTF-1 are the most used/useful markers. To summerize, on satisfactory FNAC specimens, the cytomorphology combined with IHC techniques, viewed in a clinical-radiological context, asses high diagnostic accuracy rate over 95%.

P-430

The new protocol for cervical cancer screening in catalonia: results in women with inadequate screening history.

María Alejo; Belen Lloveras; Silvia de Sanjose; Raquel Ibañez; Monica Olivera; Josep María Borras; Pilar Castro; Judith Moreno; F.Xavier Bosch; Mercé Peris.
Hospital General de Vic (Barcelona), Spain

Introduction Cervical cancer screening in Spain is opportunistic. Cytology covers 50–70% of the population and about 80% do so every year. However, 80% of invasive cervical cancers appear in women without a previous Pap smear. Since June 2006 in Catalonia, a new protocol of screening activities has been implemented to increase coverage and to reach a 3 years interval between screening Pap smears.
The new protocol includes HPV detection in 3 circumstances: inadequate screening history (IS), triage of ASC-US, and follow up of patients treated for cervical lesions (PT). We report the results of the first year of the new protocol on the IS group.
Material and methods Women attending primary health care centers are questioned by sentinels (nurses, midwives, medical doctors) about screening history. IS is considered when a > 40 y.o. woman doesn't have a Pap smear in the previous 5 years. HPV and cytology are offered to the women. Hybrid Capture 2 (HC2, Digene) is being performed in 12 different laboratories. Cytology is reported following Bethesda classification.
Results The new protocol has generated 7649 HPV detections, distributed as follows: 56.5% from IS, 27.8% from ASC-US, 5.3% from PT and 10.4% from other cause. From the samples corresponding to IS 72.4% (n=3127) followed the criteria and HPV was detected in 5.7% of these samples. Cytology and biopsy results from 3 areas are being recruited.
Conclusion
- The protocol has been able to identify 179 women at risk of developing cervical cancer (40 y.o. and HPV+).
- HC2 has been easily implemented in the reference laboratories.
- Follow up of these patients as well as the results of cytology and histology will determine the real impact of the new protocol in cervical cancer screening.

P-431

Fine needle aspiration cytology of large cell neuroendocrine carcinoma of the lung. A cyto-histologic correlation study of 11 cases

Jose Jimenez Heffernan, Pilar Lopez Ferrer, Blanca Vicandi, Adrian Mariño, Eva Tejerina, Jose M Viguer
University Hospitals Puerta de Hierro, La Paz and Monteprincipe, Madrid, Spain

Background: The classification of pulmonary neuroendocrine neoplasms is particularly controversial. Among them, large cell neuroendocrine carcinoma (LCNEC) has emerged as a separate entity. Regardless terminological considerations there is a problem that pathologists face periodically: aspirates from pulmonary tumors showing neuroendocrine features but composed of large cells. Their specific recognition is important since prognosis is worse than for other large cell carcinomas. Few cytologic studies concerning this entity are available. The objective of the present study is to describe cytologic features of LCNEC, in an attempt to separate them from other pulmonary carcinomas.
Method: A cyto-histologic study of 11 surgical lobectomy specimens classified as LCNEC. In all of them preoperative fine needle aspiration cytology material was available for review.
Results: Cytologic features were rather similar resulting in a repetitive pattern. Most smears were hypercellular with numerous single, medium to large cells. Naked nuclei were abundant but a variable subset of cells showed evident cytoplasm. Groups were three-dimensional, of variable size, some of them large. Nuclear pleomorphism, molding and mitosis were common findings. A necrotic background was evident in 6 cases. In at least 6 cases, neoplastic groups showed peripheral nuclear palisading. Rosette-like structures were present in samples from five patients. In four cases immunocytochemistry for the detection of synaptophysin was performed with positive results.
Conclusions: Our experience, with 11 FNA cases of LCNEC, has led us to believe that their cytologic image is peculiar and recognizable in many cases. Nevertheless, it is a difficult diagnosis and immunocytochemistry plays a critical diagnostic role.

P-432

Positive urine cytology in patients with lung cancer without obvious urine tract metastases.
A single center study.

Evangelos Voulgaris; Vassiliki Malamou-Mitsi; Lina Pappa; Maria Bafa; Evdoxia Sintou; Urania Skoufi; Evangelos Papadiotis; George Pentheroudakis; Nikolaos Pavlidis.
Departments of Medical Oncology and Pathology, Ioannina University Hospital, Ioannina Greece

Background: Urine cytology is widely used for the diagnosis of primary tumors of the urinary tract as well as the detection of metastases in the urinary tract. The presence of positive urine cytology in patients without obvious urine tract metastases is not expected and only few cases had been reported in the literature.
Method: Our department recently reported this phenomenon in 5 such patients. They all had metastatic lung cancer and positive urine cytology without urinary tract metastases. This is an ongoing study and up to now we have studied the cases of 35 patients with metastatic lung cancer (small and non small cell lung cancer).
Results: The urine sediment cytology of those patients revealed 9 cases with positive for malignancy results. None of these patients had radiological verification of metastasis to urinary tract. The morphological appearance of the cells from the primary lung biopsy and the urine cytology were identical.
Conclusion: Urine cytology is a reliable method for the detection of malignancy. In combination with immunocytochemical and molecular techniques it can identify the exact origin of the malignant cells.

P-433

A STUDY OF ATYPICAL GLANDULAR CELLS (AGC) ON CONVENTIONAL CERVICAL SMEARS AND ITS HISTOPATHOLOGICAL CORRELATION.

Güzin Deveci; M. Salih Deveci
Department of Pathology, Gulhane Military Medical Academy (GATA), School of Medicine, Ankara, Turkey.

OBJECTIVE: The aim of this study is to correlate the atypical glandular cells (AGC) diagnosed on conventional Pap smears with subsequent biopsy diagnosis retrospectively.
MATERIALS AND METHODS: We retrieved 28 cases of atypical glandular cells diagnosed cytologically in conventional Pap smears from the archieves of Gulhane Military Medical Academy, Pathology Department and correlated their cervical biopsies, endocervical and endometrial curettages during the follow-up period of two years.
RESULTS: Biopsy findings of cervical smears were as follows: of 28 smears, 14 cases showed bening lesions (cervicitis, endometritis, endocervical and endometrial polyp, tubal metaplasia and squamous metaplasia, keratosis, fetal and placental tissues, ectopic pregnancy and microglandular adenosis, irregular proliferative endometrium coexisting adenomyosis, endometrial hyperplasia and cervical endometriosis), 4 cases had sguamous intraepithelial lesion (2 LGSIL and 2 high grade SIL), 4 cases showed malignancy (2 cases adenocarcinoma in situ, in which one of them was associated with low grade squamous intraepithelial lesion (LGSIL), and 2 case adenocarcinoma).

Correlation of 6 cases with histopathology and follow up was not achieved.
CONCLUSION: Biopsy follow-up of conventional cervical smears diagnosed as atypical glandular cells (AGC) revealed mainly benign reactive epithelial changes, some of them squamous cervical intraepithelial lesions and as well as glandular lesions (adenocarcinoma in situ and adenocarcinoma). The diagnosis of glandular lesions in conventional smears are often not recognized due to lack of experience. However, in our small series, one third of the cases were malignant and premalignant lesions. Therefore, a careful examination can be helpful in diagnosing the glandular lesions.

P-434

FINE NEEDLE ASPIRATION CYTOLOGY OF A PAPILLARY-CYSTIC TYPE ACINIC CELL CARCINOMA OF THE SALIVARY GLAND.

M. Salih Deveci; Güzin Deveci
Department of Pathology, Gülhane Military Medical Academy, School of Medicine, Ankara, Turkey

OBJECTIVE: To impress the importance of brown hemosiderin-like pigment in fine needle aspiration cytology (FNAC) of salivary gland lesions.
MATERİAL AND METHOD: A case of acinic cell carcinoma of salivary gland diagnosed by FNAC in 20 year old male patient. Patient complained of a mass (2 cm) localized in right parotid gland. Fine needle aspiration biyopsy was performed. Microscopical examination of Papanicolaou-stained slides showed cellular aggregates arranged in sheets or papillary clusters. The cells had round to oval nuclei, some with enlarged nucleoli. The cytoplasmic vacuoles were small and some contained brown pigment. Differential diagnosis included papillary thyroid carcinoma, malignant melanoma and primary salivary gland carcinoma. In cytology slides, the pigment in cytoplasms were stained with Prussian blue and they did not express HMB45 and thyroglobulin, immunocytochemically. Final diagnosis was malignant epitelial cells present and cytological findings are consistent with malignant epithelial tumor favored acinic cell carcinoma. The excision specimen was diagnosed as acinic cell carcinoma, papillary cystic type.
CONCLUSION: Acinic cell carcinoma accounts for 12–17% of primary salivary gland carcinomas. In tissue section its morphological features are clear cut and well defined but diagnosis on FNAC is more difficult. Herein we discuss the cytological findings and hemosiderin pigment which is only seen in papillary-cystic type acinic cell carcinoma and are clue to the diagnosis.

P-435

MOLECULAR HPV TYPIFICATION IN ATYPICAL GYNECOLOGICAL CYTOLOGIES: DESCRIPTION OF OUR SERIES

R.Conejo; C.Iglesias; J.Hernandez; C.Dinarès; M.Alberola; C.Centeno; M.Ochoa; C.Cachot; M.Serra; R.Campos; S.Ramon y Cajal and N.Tallada
Department of Pathology. Vall d'Hebron, University Hospital, Barcelona (SPAIN)

BACKGROUND: HPV is the main cause of cervical cancer. The detection and genotyping in women with atypical cytology improves their clinical management
METHODS: We have analyzed 1715 samples from 1223 patients with previous cytological abnormalities, by liquid cytology and molecular typing of HPV (Clinical Arrays, Genomica). The DNA was obtained following the manufacturer protocols.
RESULTS: 782 cases (600 patients) were positive (POS) for HPV. In decreasing order of frequency the prevalence of HPV types was: 16(19.3.%), 53 (10.2%), 6 (8.69.%), 66, 51,31, 61, 18, 11, 33, 52, 84, 59, 70, 81, 56, 83, 62, 39, 45, 54, 73, 68, 82, 72, 44, 71, 35, 89, 42, 89, 43 and 40, with 182 co-infections.The more frequent high-risk(HR) types were 16, 53, 58, 51, 66, 31, 18; low-risk(LR) 6 and 61, indetermined-risk(IR) 84 and 83. The HPV types associated to LSIL were 16 (18.4%),53,6,31 and 51. HPV 16 was predominant in HSIL(47.5%). 275 cases were POS for HPV with normal (N) cytology. The predominant types in this group were: LR: 6 (12%) and 61 (10%); HR 16 (12%) and 53 (11%); IR: 84 (4%) and 83 (1.5%). Thirteen of these 275 cases showed atypical cytology in the next control (6 LSIL, 6 ASC-US and 1 HSIL). HPV 53 and 66 have been classified as low risk in some series, in our series both are associated to atypical cytology as a single agent: HPV 53, 71% and HPV 66, 77%.
CONCLUSION: HPV typing combined with cytology is an effective method to control patients with SIL, due to its ability to detect new infections, viral clearance and co-infections. From the biological point of view, the molecular test allows to best define the oncogenic role of each type and clinical follow-up. According to our dates HPV 53 and 66 should be reconsidered of high risk group.The high sensitivity of the HPV test allows to detect infections without cytological changes

P-436

Correlation between estrogen and progesterone receptor status in fine-needle aspiration biopsies and surgically resected specimens in 74 breast cancer patients

Ulrika Klopčič*; Nataša Nolde*; Janez Lamovec; Boštjan Luzar*****

Department of Cytology and Pathology**, Institute of Oncology, Zaloška 2 and Institute of Pathology***, Korytkova 2, Ljubljana, Slovenia*

Background: Estrogen (ER) and progesterone (PgR) receptors in breast cancer are predictive factors for response to adjuvant hormone therapy. Hormone receptor analysis has been traditionally performed on surgically resected specimens. Therefore, the aim of the study was to correlate estrogen and progesterone receptor status in fine needle aspiration biopsies (FNAB) and surgically resected specimens from the same breast cancer patients.

Methods: FNABs from 74 breast cancer patients were immunostained for ER (Novocastra, NCL-ER-6F11, dilution 1:10) and PgR (Novocastra, NCL-PGR-AB, dilution 1:10) by automated immunostainer (Ventana, NexEs™M), without pretreatment. Immunohistochemical analysis for ER (Neomarkers, RM-9101-S, dilution 1:100, pretreatment in Tris EDTA, PT module) and PgR (Dako, M 3569, dilution 1:50, pretreatment in Dako Pascal) was performed on surgically resected specimens from the same patients by automated immunostainer (Lab Vision). ER and PgR stain was considered positive if unequivocal strong staining was detected in more than 10% of cells.

Results: ER and PgR detection in FNAB had a sensitivity of 93.4% and 91.4%, a specificity of 100% and 85.1%, a positive predictive value of 100% and 91.4%, and a negative predictive value of 76% and 85.1%.

Conclusions: Automated immunostaining for ER and PgR in FNAB samples is a safe and reliable method for assessment of hormone receptor status in breast cancer patients. This method is especially suitable for patients with inoperable breast cancer, tumours inaccessible to surgical biopsy and general contraindications for surgery. Furthermore, sensitivity of hormone receptor analysis in FNABs can even be increased by repeating FNAB and the test in ER or PgR negative patients, thus increasing the negative predictive value of the test.

P-437

CYTOLOGICAL FEATURES OF THE SEBACEOUS LYMPHADENOMA OF THE PAROTID GLAND

Mª Carmen Martín Corríente; Rosa-Nieves Rodriguez; Cipriano Manzano Sanz; José-Luis Carrasco Juan; Rafael Méndez Medina; Hugo Alvarez-Argüelles Cabrera; Nieves Hernández León; Sonia Garcia Hernández; Mª Candelaria García Castro

Canary University Hospital, Spain

INTRODUCTION Primary sebaceous tumours of the salivary glands are uncommon (0.2%). Although sebaceous metaplasia has an 11% presence in the parotid gland and a 6% presence in the submaxilar gland, sebaceous lymphadenoma accounts for only 0.1% of all adenomas in the salivary gland.

A case of sebaceous lymphadenoma, whose cytological picture suggests a differential diagnosis between a tumour of the salivary gland or adenopathy, is reported here.

RESULTS A 74 year old female patient presented a left parotid tumoration of an evolution of months. A FNA of the lesion was performed and slides were obtained which were stained with Diff-Quick and Papanicolaou.

Its removal was recommended because a suspected probable Warthin's tumour. A parotidectomy was performed and a histological study was carried out with a diagnosis of a sebaceous lymphadenoma of the parotid gland.

DISCUSSION FNA is an efficient method for the diagnosis of salivary gland lesions. The most common tumours have well established cytological features, but it is also necessary to bear in mind the less common forms, which may lead us into diagnostic mistakes.

In the FNA study, in this case, a prominent lymphoid background was identified suggesting a series of possible diagnoses such as Warthin's tumour, sebaceous lymphadenoma, lymphoepithelial carcinoma, as well as other benign possibilities like sialoadenitis, or malignant possibilities such as lymphoma or metastatic illness.

P-438

Value of the cytodiagnosis as a screening method for the periodontal disease

Atena Galuscan;Liliana Vasile; Elena Lazar; Razvan Simulescu; Pusa Gaje; Adina Valeanu

University Of Medicine Timisoara, Romania

Write the text... *Background:* Periodontal disease describes a large number of clinical entities that affect gingiva, gingival attachment, periodontal ligament, cementum and supporting alveolar bone. Unique ecologic ninches are

observed in most areas of the mounth such as gingiva margins and tooth surface. The aim of the study is to qualified the significance of the cytodiagnosis for the identification and evolution in the periodontal disease. *Method:* Between 2004–2005 we have selected 345 pacients with lesional and non-lesional periodontum. Periodontal disease was classified in seven major categories including periodontitis as a manifestation of systemic disease. The cytological samples were obtained by aspiration, brushing or imprints of the periodontal areas. The samples were air-dried or alcohol fixed before staining with cytological methods (Papanicolau, Blue-Polichrom-Tanin-Dragan, MGG)
The cytodiagnostic was corelated with clinical data and the histodiagnosis by histochemical methods (Alcian Blue, PAS, Silver impregnation) or immunohistochemical stainings (Cks, S100protein, Vim, Desm, Lymphoid markers and Ki-67).
Results: According to clinical examination we have found 3 groups of lesions: C1-C2-C3 (a,b) depending of the inflammation, tissue destruction, bone resorbtion and impaired tissue regenerationIn C1-C2 samples most of the examined cells were epithelial scuamous with different nucleo-cytoplasmic alterations. In C3a-C3b samples, according with the cytological features we have found numerous conjunctive-inflammatories cells. The periodontal disease has a grading of severity from level I to III, coresponding with the deepness of the tissue loss (1 mm to 3 mm). Bacterial flora is qite similar to all the 3 categories of lesions depending on the host individual defence. *Conclusion:* We agreed that the cytodiagnosis is an important method for the screening and the management in periodontal lesions with a sensitivity of 82%, specificity of 76% and false-negative fraction of 12–15%.

P-439

Cytological aspects in the hyperglucidic stress - study of the mesenchymal stem cells, dental pulp cells and on oral samples from diabetic patients

Liliana Vasile; Roxana Oancea; Pusa Gaje; Razvan Simulescu; Viorica Bocan, Raluca Ceausu
University Of Medicine Timisoara, Romania

Background. Extracellular matrix with volume and inappropriate composition for the cellular metabolism influences the K+, Na+ and Ca+ ionic pumps, the intercellular junctions, the membrane pumps and the proteic synthesis. The behavior of the cells in the host organism and of the pathogenic microflora in the hyperglucidic medium is dictated by the intervention of various factors of oxidative and mechanic stress which lead to modifications of the cellular cycle partially explaining the cavities in diabetic patients and the periodontal disease.
Method In 2007 there have been taken in study 150 specimens from diabetic patients from both sexes with the age between 23 and 57 years with cavities and periodontal problems, a lot of patients without oro-dental evolutional lesions as witness lot, and samples from stem cells cultures from the pulp, collected in conformity with the ethic and asepsis regulations, from 3 subjects 7–8 years of age. The samples were harvested from the global saliva and from the gingival gap, and for the cellular cultures reactives from Sigma Aldrich, Redox Treding-Romania and Promo Cell Heidelberg Germany. The coloration of the samples was made with May-Grunwald-Giemsa and the original Blue-Polichrom-Tanin-Dragan methods.
Results We have reached the following results: at the diabetic patients without drugs control the samples were highly supurative and litical and the dominant flora is fusospirilaris and fungical on an acidic Ph background. At the stem cellsin hiperglucidic enviroment, the density, the nuclear and cellular volume are increased, we can observe citoplasmatic vacuolation and variations in shape and borders of the cells.
Conclusions: These findings suggest possible consequences of the tissue substitution in diabetic patients.

Miscellaneuos

P-440

Importance and Repercussions of Renal and Cardiovascular Pathology on Stroke in Young Adults: An Anatomopathologic Study of 52 Clinical Necropsies

Gabriel Arismendi-Morillo; Mary Fernández-Abreu; José Cardozo-Duran; Gustavo Vilchez-Barrios
Instituto de Investigaciones Biológicas, Facultad de Medicina, Universidad del Zulia. Venezuela

BACKGROUND: Stroke in young adults has seldom been studied in a necropsy series. The objective of the present clinical necropsy-based investigation was to analyze stroke and its relationship with cardiovascular and renal pathology in young adults.
METHODS: The protocols of 52 clinical necropsies with diagnoses of stroke in patients aged 18 - 49 years, performed between the years 1990–2006, were reviewed.
RESULTS: Hemorrhagic stroke was diagnosed in 36 patients (69.3%), whereas the remaining 16 (30.7%) had ischemic stroke. Hypertensive cardiopathy was evident in 88.4% of the cases. Chronic renal pathology, directly or indirectly related to hypertension, was observed in 55.7%

of the patients. Ischemic stroke as a result of occlusive atherosclerotic disease was seen in 50% of cases. Cardiogenic emboli were found in 25% of the cadavers. Hemorrhagic stroke was associated with hypertension in 43% of the cases, with ruptured vascular malformations in 29%, and coagulopathies in 17% of the cases. Hypertensive cardiopathy was present in patients with either ischemic or hemorrhagic stroke (81.2% and 91.6%, respectively). The most frequently observed renal ailments were chronic pyelonephritis (23%) and nephrosclerosis (21.1%). These were associated with ischemic stroke in 43.7%, and 12.5% of the cases, respectively, and with 13.8% and 25% of the hemorrhagic stroke cases.

CONCLUSION: Hypertensive cardiopathy, occlusive atherosclerotic disease, chronic pyelonephritis and nephrosclerosis are among the pathophysiologycal mechanisms that apparently and eventually interact to induce a significant number of cases of stroke in young adults. A chronic systemic inflammatory state appears to be an important related condition because it possibly constitutes an accelerant of the pathophysiologycal process.

P-441
AN EVALUATION OF INTRAOPERATIVE FROZEN-SECTION BIOPSY IN PHILIPPINE HEART CENTER: A 10-YEAR RETROSPECTIVE STUDY

Katherine D. Sia; Marissa A. Orillaza; Carmela D. Tan
Philippine Heart Center,Philippines

Background: Frozen section is a very helpful ancillary procedure for the surgeon in guiding him in his decision intraoperatively. Indications include: to establish the presence and nature of lesion, determine adequacy of surgical margins and to establish whether the tissue obtained contained diagnosable material. The accuracy of frozen section varied depending on the author and type of tissue.

Objective: To review and evaluate the accuracy of frozen section in the Philippine Heart Center from 1994–2005.

Methodology and Result: This is a retrospective study where we reviewed 114 lesions that underwent frozen section from 1994–2005. The most common site sent for frozen section diagnosis was the mediastinum, followed by the lung and breast. There were 47% true positive, 54% true negative and 2.7% false negative. There were no cases of false positive frozen section diagnosis. Cases with false negative diagnosis includes 3 cases of mediastinal tumors which were diagnosed as thymoma on frozen section but was later signed out as lymphoma on permanent sections. There was also a single case of breast tissue with a deferred diagnosis. Our study revealed that our frozen section diagnosis has a very good sensitivity (94.5%) and specificity (100%) in diagnosing tumors.

Conclusion: We conclude that frozen section is very accurate in diagnosing mediastinal, pulmonary and breast lesions. Since frozen section has some limitations, we recommende good communication between the surgeon and pathologist to avoid misdiagnosis.

P-442
PATOMORFOLOGY OF THE UTERO-PLACENTARY COMPLEX AT BREACH OF PATRIMONIAL ACTIVITY

F.G.Zabozlaev, A.P.Milovanov, T.G.Barkhina
Institute of Human Morphology of the Russian Academy of Medical Sciences, Russia

MATERIAL AND METODS: Complex research of patomorfology utero-plasentary complex was lead at 145 women: In 47 cases at weakness of patrimonial activity, in 45 supervision at premature fall off normally located placenta and in 53 - at discoordination the patrimonial activity, accompanied breaks of corpse and cervical part of a uterus. Histologic, macro-histostereometric and ultramicroscopic methods of research were used.

RESULTS: At weakness of patrimonial activity absence of adequate expansion of a gleam miometral segments of utero-placentary arteries placentary laying down and pathological immaturity fleecy of horion with development of chronic placentary insufficiency was precisely combined with weak lacunary transformation of a dividing venous sine of a body of a uterus and a formed bottom segment. These changes, being the structural precondition of decrease morfofunctional capacities of venous depot of a uterus at development of the patrimonial activity, accompanied unproductive hypotonic fights, in turn, lead to infringement of processes of maturing cervical part a uterus.

At hypertonic dysfunction of a uterus the formed uteroplacentary form of chronic placentary insufficiency, incomplete hestation reorganization both endo-, and myometrial segments of utero-placental arteries, reduction morfometrics parameters of a vascular vessel myometrium. Ultramicroscopical research has revealed law of damages of communication communications between myocytous.

At premature fall off normally located placenta authentic dependence between defective gestational transformation of utero-placental arteries placentary laying down, expressed hemoreological infringements fleecy horion, preliminary venous lacunary transformation of a vascular layer of a body of a uterus with a thrombosis of a dividing venous sine and critical increase of pressure in intervillous space with progressing hipoxia a condition at a fetus is certain.

At dyscoordination the patrimonial activity, accompanied breaks of cervical part and bodies of a uterus processes expressed lacunary transformations of a dividing venous sine of a body of a uterus and dystalis parts of the generated bottom segment with progressing reduction in a direction to it proximalis parts and cervical part a uterus not ready to deformation reconstruction develop on a background inadequate, stimulating patrimonial activity, therapies in a combination to an accompanying initial pathology cervical part of a uterus.
CONCLUSION:Research patomorfology corpse, lower segment and cervical part of a uterus, placentary laying down and placentae at infringement of patrimonial activity has allowed to reveal a morphological basis of a system pathology of a utero-placental complex.

P-443

Pathomorphology of endocrine glands during chronic drug intoxication

Vugar K. Huseynov; Edalet B. Hasanov
Forensic medical expertise and pathological anatomy Unification of Azerbaijan Republic

Introduction. The peculiarities of morphological changes and opportunities for differential forensic-pathologic diagnostics were studied during chronic drug intoxication on the basis of analysis of pathomorphologic changes in hypophysis and adrenal.
Materials and methods. 110 autopsies, including 83 forensic and 27 postmortem examinations of bodies (from various acute or chronic recurrent infectious diseases) of individuals suffering from chronic intravenous abuse of narcotics, were carried out. Among the dead individuals were 95 men (86.4%) and 15 women (13.6%) aged between 17 and 36.
Result. During the microscopic examination of drug addicts, who abused narcotics for less than two years, morphological changes in hypophysis and adrenal were of a mainly hypertrophic, hyperplastic and dystrophic nature, with acute microcirculatory disorders as a reaction of strain. In the cases of drug abuse for up to ten years by older drug addicts, necrotic, atrophic and sclerotic changes of parenchyma and intersticium of glands associate with the aforesaid pathologies in the hypophysis-adrenal group. The atrophic changes in endocrine glands testify to lingering high functional load on these organs, which leads to exhaustion of their functions (polyendocrinopathy syndrome).
Conclusion. Thus, changes taking place in the neuroendocrine organs during chronic drug intoxication develop within realization of general adaptation syndrome [theory of H. Selye], like in all strong stresses. In this case, high-toxic drug addiction (chronic "chemical stress") plays the role of a stressor. From this viewpoint, phase change of hormonal homeostasis happens during chronic drug intoxication. The morphological differences in the examined endocrine glands are likely related in different cases to "longevity" of rug abuse, i.e., the duration of drug addiction, different effects of various doses and individually constitutional peculiarities of drug addicts.
Similar changes in hypophysis and adrenal require determination of hormonal balance and its correction in patients with chronic drug addiction.

P-444

Morphology of immunodeficiency state during chronic drug addiction

Edalet B.Hasanov
Forensic medical expertise and pathological anatomy Unification of Azerbaijan Republic.

Introduction. The peculiarities of morphologic changes taking place during chronic drug addiction were studied at its different development stages on the basis of analysis of pathomorphologic changes in the organs of immune system (thymus, spleen, glands and lymphoid follicles of intestines).
Materials and method. 135 autopsy observations of individuals, who have become victims of various kinds of violent death or died of acute or chronic recurrent infectious diseases, were investigated. All of these individuals also suffered from chronic drug addiction through intravenous abuse of narcotics (mainly opium). The dead persons were 118 men and 17 women aged between 17 and 40. Depending on the duration of drug abuse, all observations were divided into two groups: the first group – chronic drug addiction with misuse of narcotics for up to a year or two; the second group – chronic drug addiction with misuse of narcotics from two to ten years.
Result. In the first group, the observations of morphologic changes in the immune system were of a mainly reactive-hyperplastic and dystrophic nature, with acute microcirculatory disorders. The morphologic changes in the immune system at the early stage of chronic drug addiction are formed from "acute atrophy" defined lymphoid devastation of thymus and spleen caused by amplification of emigration of lymphocytes, their redistribution and, to a considerably lesser extent, apoptosis.
In the second group, morphologic changes of an atrophic and sclerotic nature were revealed during the observations of drug addicts, who committed intravenous abuse of narcotics for over two years (up to ten years). The depletion of compensatory capabilities of the immune system occurred and secondary B- and T-cell immunodeficiency states developed in these patients.
Conclusion. The reduced data confirm that during intravenous chronic drug intoxication the "reserve" forces of

organs of the immune system get activated first in order to overcome the increasing immunosuppression (compensation stage). The stages of temporary activation and resistance are followed by the late stage of immunodeficiency states (decompensation stage), i.e., lymphoid tissue of the immune organ feels real exhaustion. Morphologically, this process occurs due to decrease in the number of lymphoid cells and T- and B-zone atrophies, appearance of great number of changed cells, activation of apoptosis of lymphocytes and development of atrophic and sclerotic changes in lymphoid organs.

P-445
Withdrawn

P-446
A rare case of combined thymic epithelial tumor (thymic carcinoma and type B2 thymoma) in a 51-year-old female

Maricel Ribo; Minnie Jane Pineda; Arlene de Luna; Bernadette Asuncion
Philippine Heart Center, Biological and Clinical Laboratory Division, Rhilippines

Background: Combined thymic epithelial tumors are extremely rare neoplasm having at least two distinct areas each corresponding to one of the histological thymoma and thymic carcinoma. Prognosis is dependent upon the most aggressive histologic subtype. Therefore careful diagnosis should be made especially with the presence of two distinct histologic types.
Case Methodology: This is a case of a 51-year old female with a chief complaint of right eye ptosis, right sided weakness of the face and upper extremities for three months. Chest CT scan revealed an anterior mediastinal mass measuring 3.3×5.0×6.0 cm. FNAB of the anterior mediastinum was done. Open thoracotomy with wedge resection of the lung was performed and specimen was submitted for histopathology. Patient was discharge with good condition.
Result: CT guided FNAB of the anterior mediastinal mass revealed cytomorphologic features consistent with thymoma, favor A or AB subtype. The specimen submitted for histopathology is tan-brown, irregular firm mass with nodulations and measures 7.5×6.0×4.5 cm. Histologically, the tumor was composed of a mixture of lymphocyte-poor and lymphocyte-rich component. The lymphocyte-poor component contains spindle-shaped cells with bland irregular nuclei, dispersed chromatin and inconspicuous nuclei in solid sheet and hemangiopericytoma-like appearance. The lymphocyte-rich component consists predominantly of small polygonal epithelial cells with small, round, oval or spindle nuclei showing dispersed chromatin and inconspicuous nucleoli admixed with mature lymphocytes. With these finding, a diagnosis of combined thymic epithelial tumor (thymic carcinoma and type B2 thymoma) is made.
Conclusion: A combination of thymic carcinoma and type B2 thymoma is an exceptionally rare thymic epithelial tumor accounting for <1%. In our institution it is the 1.5%. Fine needle aspiration may reveal one of the two components if not both components. Depending on the sampling, the malignant area maybe missed. Tissue confirmation is thus imperative.

P-447
PATTERN OF PLEURAL DISEASES SEEN IN EASTERN NIGERIA.A review of 75 histopathological biopsies seen over a five year period from January1, 2000-December31, 2004.

***M.A.Nzegwu1 *D.B Olusina, *E.F NNAKENYI*C.I AKUSOBA.**
University of nigeria teaching hospital ENUGU NIGERIA.

BACKGROUND. There is a dearth of authentic information regarding pleural and respiratory lesions in our environment. I then sought to determine the pattern of pleural lesions diagnosed in our environment by biopsies sent to us at UNTH.Enugu, Nigeria over a 5-year period as a base line data.
DESIGN. A retrospective study, involving analysis and review of slides of trucut needle biopsies received and processed at UNTH, in Enugu.Nigeria, over a five-year period.
RESULTS. From a total of 75 biopsies received, males (n=49) were 68.1%, while females were 31.2%(n=26). The mean age was 42.6 years ranging from 1.5 years to 86 years.The causes of the lesions as found by biopsy were as follows. Tuberculosis (n=8) constituting 10.7%, metastatic breast carcinoma (n=7) was responsible for 9.3%, chronic non-specific bacterial pleuritis was the most common indication for pleural biopsy (n=22) constituting 29.3%. Three biopsies were false 4%, empyaema thoracis was responsible for 18.7%(n=14),with three cases of bronchogenic carcinoma; squamous cell variety was two (2.8%), while bronchial adenocarcinoma variant had one case(1.3%). Non-Hodgkin's Lymphomas was responsible for 2.7%(n=2). Metastatic prostate cancers (n=3) constituted 4%. There were two cases of haemathorax (2.7%). Two cases each of metastatic sarcomas and a metastaic

unclassified carcinoma in the females,each constituting 2.7%. Lymphogranulomatosis n=1 was 1.3%.
CONCLUSION The commonest indication for pleural biopsy here remains infective causes n=22,or its complication of empyaema n=14.Then tuberculosis n=8 and

P-448

Clinical and laboratorial findings of spontaneous bacterial peritonitis in patients of Universidade Braz Cubas- School Hospital, Mogi das Cruzes, Brazil.

Sonia Maria Almeida; Edson Costa;Leila Moussa Costa;Silvia Froes Bassini;Marcelo Fabiano Rodrigues
Universidade Braz Cubas, Brazil

Introduction: spontaneous bacterial peritonitis (SBP) is a severe complication in patients with liver cirrhosis and ascitis, with mortality rate around 20–37%. Objectives: to review the literature and establish the clinical manifestation and laboratorial characteristics of the patients diagnosed as SBP. Patients and methods: a retrospective study of 19 medical documents in period from January, 2005 to July, 2007 was performed in Universidade Braz Cubas- School Hospital Results: the mean age of the patients was 75, predominantly men. The average hospitalize period was 9 days. The most common symptoms were: abdominal pain, ascitis and jaundice. The most common cause of chronic hepatophaty was viral Hepatitis C, present in 33% of cases. The majority of SBP was communal with leucometry over 250 polymorphonuclear leukocyte/mm^3 in 78% of cases, only one presenting positive culture of the ascitic fluid, isolating Staphylococcus aureus, whereas 50% of the hemocultures were positive, with Escherichia coli isolated. Only one case presented bacterioscopic exam positive, with Gram positive coccus. The laboratory blood exams present the following average results: leukocyte count 9216,67/mm^3 with 75,33% neutrophil, prothrombin time was 54,3%, creatinine 1,58 mg/dl and albumin 2,44 g/dl. The treatment used was third and fourth generation cephalosporins per 10 days. The outcome of the patients was: upturn and released from hospital in 17 cases, 1 death and 1 case hospital transference. Conclusions: findings correspond to the literature, less the fact of the ascitic fluid collection were done by routine method. Nowadays, the best method used to collect ascitic fluid is direct inoculation of ascites into hemoculture bottle method with a higher positivity of 49,8%. Therefore, the knowledge about SBP is essential, as diagnosed methods and clinical manifestations looking for early treatment to reduce the mortality.

P-449

Identification of the predominance bacterial pathogen of community acquired orofaringitis (OF) at Hospital Geral in Guarulhos, Brazil.

Claudio Costa; Edson Costa; Marcelo Fabiano Rodrigues; Leila Moussa Costa; Sonia Maria Almeida
Universidade Braz Cubas, Brazil

OFs remain the common infections diagnosed in out-patients as well as hospitalized patients, current knowledge on antimicrobial susceptibility pattern is essential for appropriate therapy and the aim of this study was to determine the distribution and antibiotic susceptibility patterns of bacterial strains isolated from patients with community acquired infections (OFs) at Guarulhos as well as identification of ESBL producers in the population of different oral pathogens throught exsudate isolates from symptomatic OFs cases attending to the Hospital Geral at Guarulhos were identified by conventional methods (2006-april 2007) and antimicrobial susceptibility testing was performed by Kirby Bauer's disc diffusion method. Isolates resistant to third generation cephalosporin were tested for ESBL production by double disk synergy test method and the results points that of the 157 tested sample 71 samples showed growth of pathogens among which the most prevalent were *Streptococcus pyogenes* (78%)followed by *S.aureus* (35%) and the majority (70.25%) resistance was observed against ampicillin and co-trimoxazole. Most of the isolates were resistant to 3 or more number of antibiotics, the forty nine percent of isolates were detected to produce ESBL among which 41,21% were *Streptococcus* isolates.
This study revealed that *Streptococcus pyogenes* was the predominant bacterial pathogen of community acquired OFs in Guarulhos,it also demonstrated an increasing resistance to Co-trimoxazole and production of ESBL in OF pathogens in the community.

P-450

Immunohistochemical study of prognostic markers in Retinoblastoma

Seema Kashyap; Neelam Pushker; Seema Sen; Supriyo Ghose;Bidhu Mohanty
Ocular Pathology department;Dr. Rajendra Prasad Centre for Ophthalmic Sciences;All India Institute of Medical Sciences;New Delhi

Background-Prognosis of Retinoblastoma has tremendously improved due to improved modalities of treatment and early diagnosis. This study was designed to correlate expression of p53, apoptosis and ki-67 with histological differentiation.

Methods- Retinoblastoma cases were retrieved from our departmental records from 1996–2002. Immunohistochemistry was performed on 90 wax blocks of retinoblastoma for p53,apoptosis and ki-67.
Results - Total no. of unilateral and bilateral Retinoblastoma(RB) cases were 69 & 21 repectively with a M:F ratio of 61:29. Age ranged from 3 mths-132 mths. Total no. of cases which showed positive staining for p53, ki- 67 and apoptosis were 37(41%), 74(82%) and 37(41%) respectively. More no. of ki-67 positive cases were obtained in poorly differentiated retinoblastoma(PDRB) i.e 52 as compared to p53 in PDRB i.e 26. Similarly larger no. ki-67 positivity was found in Well differentiated Rb (22) than p53(11).
Conclusion - We thus conclude that ki-67 is an important risk factor/prognostic marker as compared to p53 and apoptosis.There was no statistically significant correlation between histological differentiation and immunohistochemical markers studied.

P-451
Morphological characteristics of tissue reaction to implantation of polypropylene meshes

Elena Alexeevna Dubova; Alexandr Ivanovich Shchegolev; Natalia Vladimirovna Filatkina; Dmitry Vsevolodovich Chizhov; Valery Nikolaevich Yegiev
Department of Pathology Federal State Institution "A.V. Vishnevsky Institution of Surgery Rosmedtechnologiy", Moscow; Department of Surgery and Oncology People Friendship University of Russia, Russian Federation, Moscow

Introduction: Mesh polypropylene endoprostheses are most often used in herniology. We studied the morphology of tissue reaction to implantation of PROLEN (Ethicon), ESFIL (Linteks), Biomesh P1 Mesh (Cousin Biotech) mesh and unwoven polypropylene endoprostheses - Biomesh NK 2 Mesh (Cousin Biotech).
Methods: Experimental study was carried out on mice, implanted polypropylene prostheses. On days 3, 7, 14, and 28 after the intervention the animals were sacrificed and material was resected for morphological study.
Results: We found that after 3 implantation of Esfil and the unwoven endoprosthesis caused a more pronounced inflammatory reaction of tissues. Solitary fibroblasts and new vessels were detected around all implants. By day 7 formation of granulation tissue was observed. After 14 days numerous collagen fibers were seen in the presence of a moderate count of fibroblasts. The total count of fibroblasts in the zone of implantation of the unwoven prosthesis was lower than with the meshes. Implantation of the meshes was associated with an increase in the number and thickness of collagen fibers, some these fibers grown between the implant fibers. After implantation of unwoven endoprosthesis a fine capsule was seen at the implant periphery against the background of pronounced tissue edema and there were many loose collagen fibers and fibroblasts between the endoprosthesis elements, virtually each polypropylene fiber was surrounded by collagen fibrils. By day 28 cellular reaction was presented mainly by fibroblasts. The connective tissue capsule enveloping the unwoven prosthesis was much thinner and the connective tissue components totally grew into the implant.
Conclusion: Implantation of the unwoven endoprosthesis caused a more pronounced inflammatory reaction. The growth of connective tissue components between the implant fibers with the formation of a fine connective tissue capsule enveloping the prosthesis was observed during earlier period of experiment.

P-452
Severe infantile carnitine palmitoyltransferase II (CPT II) deficiency in 19-week fetal sibs

Karen Meir; Stanley Korman; Vardiella Meiner; Ilana Ariel
Hadassah - Hebrew University Medical Center. Israel

Background: Long chain fatty acid oxidation in mitochondria is regulated by two carnitine palmitoyltransferases (CPT) and by carnitine:acylcarnitine translocase. In the inner mitochondrial membrane, CPT type II (CPT II) converts palmitoylcarnitine to carnitine and palmitoyl-CoA. CPT II deficiency typically manifests in adolescence with muscle pain and rhabdomyolysis following vigorous exercise. Presentation in infancy is less common. Antenatal presentation has been rarely reported.
Methods: Fetal autopsies and CPT gene sequencing were performed.
Results: Prenatal ultrasound at 19-weeks gestation showed a fetus with enlarged polycystic kidneys. A previous pregnancy five years earlier ended in termination for polycystic kidneys. The suspected clinical diagnosis was Meckel-Gruber syndrome. At autopsy, the renal parenchyma was largely replaced by cysts which appeared to increase in diameter toward the medulla. The liver showed diffuse microvesicular steatosis. A subsequent pregnancy was terminated for polycystic kidneys and Dandy Walker malformation. Fetopsy was not performed.
Fetopsy of the present case showed micrognathia, hypospadias, cystic renal dysplasia with cyst diameter increasing toward the medulla, and microvesicular hepatosteatosis. Fatty accumulation in the liver, renal tubular epithelium, myocardium, and skeletal muscle was demonstrated by Oil red O staining. Diffuse microvascular proliferative changes associated with small old and recent hemorrhages were

seen in the cerebral cortex. A diagnosis of glutaric aciduria or related beta-oxidative enzyme deficiency was suspected. Analysis of the CPT II gene showed a homozygous del1237AG truncating mutation in exon 4. This mutation has been previously reported in Ashkenazi Jewish patients. *Conclusions*: Since abnormal cerebral findings different from our case have only been reported once previously in a fetus with CPT II deficiency, CPT II deficiency should be included in the differential diagnosis in fetuses with cystic dysplastic kidneys, particularly with unusual cerebral findings, in Ashkenazi Jewish families.

P-453

FLEX Ready-to-Use antibodies – a high quality and standardized IHC solution

Majken Nielsen, Lotte Pfeifer, Ole Feldballe Rasmussen, Tony Knoll, Uffe Lovborg
Dako Denmark A/S, Denmark

Background Pathology laboratories face major challenges to deliver high quality results in a timely and cost efficient manner. An increasing number of cases are evaluated by means of immunohistochemistry (IHC), and the need for high quality and standardized IHC solutions is growing in order to ensure correct patient diagnosis and efficient work flow in the laboratories. A key prerequisite is high performance antibodies. In an international study supported by eight independent international experts, new ready-to-use (RTU) antibodies have been demonstrated to match world wide IHC performance acceptance criteria. When used with associated instrumentation, these will support standardization in laboratories across the world.
Method The study was designed with eight independent experts who evaluated the results in terms of diagnostic relevance. The antibodies were developed to match instruments with dedicated protocols so that the end result was easy to standardize. The final formulation of each antibody was defined to assure optimal sensitivity and specificity by using antibody specific "quality indicators". These were divided into high expression (HE) and low expression (LE) structures that typically were identified in normal tissues (control tissues). The HE structures were used to assure staining capacity, whereas the LE structures were considered as sensitivity markers of the IHC performance.
Results and conclusion A range of 60 clinical important RTU antibodies with high sensitivity and specificity has been studied. The series include key antibodies such as Ki67, CD79α, CK5/6 and Calretinin. Review of the resulting performance with the eight independent experts, demonstrated that it is possible to conduct testing in a standardized way using RTU antibodies and associated instruments and protocols that satisfy performance acceptance criteria world wide. The RTU antibodies are developed to provide the same IHC result world wide, thus contributing not only to obtaining standardized results, but also a diagnostically correct result.

P-454

Acute lung injury and histopathological findings in illicit drugs users with toxicologic corelation

1Mitrovic S; 2 Todorovic M; 2 Azanjac G; 2 Matejic S
1 Department of Pathology,Faculty of Medicine University of Kragujevac,Serbia 2 Department of Forensic Medicine, Faculty of Medicine University of Kragujevac,Serbia

BACKGROUND:Illicit drugs and psychoactive substances affect all anatomical lung compartments to produce diverse morphological changes. Major classes of drugs wich cause respiratory manifestations are opiates,stimulants and cannabinoids.The intrapulmonary site of injury and the histological pattern of response depend not only on the pharmacological agents, but also on the dose,chronicity of use,route of delivery and presence of additives and adulterants. The pulmonary pathohistological findigs most common include oedema, pulmonary haemorrhage and haemosiderosis,panacinar emphysema,bronchiolitis obliterans, ineterstitial pneumonia or fibrosis.
MATERIALS AND METHODS:The investigation was included 48 judicial autopsies of heroin or other drug consumers who suddenly died from 1995–2007 year. Autopsies, postmortem toxicologic studies and serological research of anti-HIV/HBV/HCV antibodies were performed. Histological sections of all cases were reviewed and dominant pathomorphological changes are finded in the pulmonary tissue and liver.
RESULTS:Cases were mostly male 35/48(72,9%) and all white.The deceased patients ranged in age from 19 to 49 (mean,31 years). 22 patients had serological evidence of hepatitis C virus infection,9 had hepatitis B virus surface antigen and one was HIV positive.A postmortem toxicologic examination was performed on all of the deceased patients,and drugs in the fatal range were identified in only four of them(8,33%),in the toxic range in six(12,5%) and in minimal concetrations in nine of the deceased patients (18,7%).Drugs are identified in the fatal, toxic or minimal range included heroin, morphine,methadone,diazepam,cocaine and amphetamine.
Pulmonary oedema was the cause of death in 42 patients (87,5%)of the 48 drug users.Of the remaining patients as cause of death,four had acute myocardial infarction and two had massive intracranial bleeding.Under light microscopy, the histopathological analysis of lung tissue from the deceased patients indicated oedema,diffuse alveolar damage, emphysema, alveolar haemorrhage and haemosidero-

sis,interstitial fibrosis,bronchiolitis obliterans, arterial medial hypertrophy and inhaled particulates.The most common histological features observed in drug users were acute alveolar haemorrhage 37/48 (77,1%), haemosiderosis40/48 (83,3%) and emphysematous changes 39/48(81,3%).
CONCLUSION:The pulmonary disease is a most common cause of death in drug users.

P-455
MULTILOCULAR CYSTIC THYMOMA:A CASE REPORT
Vesna Stankovic 1;Mitrovic Slobodanka 1; Milisavljevic Slobodan 2;Stanko Mrvic 2; Azanjac Goran 2;
1 Department of Pathology,Clinical Center Kragujevac, Serbia;2 Surgical Clinic,Clinical Center Kragujevac,Serbia

BACKGROUND:Primary anterior mediastinal neoplasms comprise a diverse group of tumors and account for 50% of all.Thymic cysts are rare and represent approximately 1 to 3% of all anterior mediastinal masses.Their etiology is contraversal:may be congenital or acquired,either due to inflammation or in association with an inflammatory neoplasm such as Hodgkin`s lymphoma,seminoma or thymoma.
CASE PRESENTATION:A rare case of multilocular cystic thymoma is presented.The patient is a 49 year-old woman who came to consult with a persistent dyspnea and cough. The chest computed tomographic scan revealed a solitary, lobulated and nonenhancing mass,11 cm in maximum diametar,near the right atrium and aorta ascending.Physical examination and laboratory work-up were within normal limits.Total tumorectomy was performed via medial sternotomy.Histopathological examination on the resected specimen revealed a thymoma stage I,with cystic appearance,according to the classification of Masaoka.The postoperative course was uncomplicated.
CONCLUSION:Encapsulation and resectability of thymoma is associated with good prognosis. Complete surgical resection is the cornestone of curative therapy.

P-456
Utility of Atomic Force Microscope (AFM) in identification of membranne characteristics of different neoplasms
Manuel Vaquero; Jose Iñaki Alava*; Roberto Muñoz*
Donostia Hospital and INASMET Fundation, Spain*

The atomic force microscope (AFM) is a very high-resolution type of scanning probe microscope, with demonstrated resolution of fractions of nanometre. Samples viewed by AFM do not require any special treatment. It can work perfectly well in liquid environment without any vacuum system. The AFM works in the same way as ours fingers which touch and probe the environment when we cannot see it. Initial applications in Biology are coming but structural analysis and manipulation of cellular membranes and applications of antibodies on probing tip to localise determinates antigens or receptors of signal vies are interesting challenges.
Method – AFM at mode contact in aqueous media was used to study cultivated cells from malignant mesotelioma and mammary carcinoma. As a first stage, differences between both types of cells and correlation with optical microscope dates of same cells were made to analyse utility of AFM in classify morphological dates for differentiate characteristic types of cells.
Results -AFM provides a true three-dimensional surface profile. Typical patrons of malignant mesotelio and carcinoma cells can be obtained to differentiate between both types of cancer. A more irregular surface and larger protrusion of nucleus were typical of malignant mesotelioma cells, and correlation with optical microscope image was apparent.
Conclusion-AFM is a unique imaging technique that allows high resolution studies of cells in a native state with a topographic map of the membrane surface. This surface can be characteristic of cellular type and to change dynamically in response to external and internal stimuli.

P-457
In vitro and in vivo testing of biocompatibilized polyurethane materials for medical use
Lucia Moldovan1; Oana Craciunescu1; Elena Utoiu1; Traian Leau2; Cornelia Vasile3; Otilia Zarnescu4
1Department of Cellular and Molecular Biology, National Institute R&D for Biological Sciences, Bucharest, Romania; 2Faculty of Veterinary Medicine, USAMV, Bucharest, Romania; 3"Petru Poni" Institute of Macromolecular Chemistry, Iassy, Romania; 4Faculty of Biology, University of Bucharest, Romania

Background. Polymeric biomaterials fulfill several medical uses as artificial organs, prostheses, in dentistry, bone repair, drug delivery systems and regenerative tissue engineering. In order to be safely used in patients, their biocompatibility has to be tested on *in vitro* and *in vivo* models. The aim of our study was to investigate the *in vitro* biocompatibility and *in vivo* tissue response for two new polymeric biomaterials, prepared by compounding polyurethane (PU) with collagen (COL) and with a collagen-elastin (COL-EL) mixture, respectively, compared to PU material.
Methods. *In vitro* biological evaluation of the biomaterials in direct contact with human dermal fibroblasts (HDF) was

performed. Cell viability and proliferation were assessed by MTT test and cell adhesion and morphology were observed by light microscopy. Material biodegradation was measured by the collagenase degrading test. *In vivo* biocompatibility of polymeric biomaterials was evaluated following subcutaneously implantation in rats, for periods of up to 6 weeks. The biomaterials together with surrounding tissue were fixed, processed and paraffin-embedded for histopathological evaluation.

Results. MTT test results indicated the highest HDF viability for PU-COL composite. Light micrographs showed that cells adhered, spread and proliferated onto the surface of all polymeric biomaterial variants. It was also observed that HDF retained their normal phenotype. The degradation of PU-COL-EL composite was slower than that of PU-COL material. Histological and immunohistochemical analysis of polymeric implants showed that they induced a focal but chronic inflammatory reaction, which was limited to a small area around the materials. A moderate foreign body reaction was seen around the implant surface.

Conclusion. Both cell culture studies and *in vivo* experiments showed that the two composites PU-COL and PU-COL-EL exhibit a better biocompatibility than PU alone. They could be used as bioactive scaffolds for tissue engineering and medical device fabrication.

This work was supported by Romanian Project CEEX-CALIST No. 6114.

P-458
Withdrawn

P-459
AGE-ASSOCIATED LOSS OF NEURONS IN BRAIN STEM STRUCTURES.

Alexey Kolomiytsev
Taganrog Pathoanatomical Bureau, Russia

Background. Age-associated loss of neurons in central nervous system was an axiom in biology for a long time. Stereological techniques have failed to confirm these earlier findings, there is evidence of focal neural death and synaptic or receptor loss. Focal damages in vital nervous centres may play a significant role in aging and age-related pathology.

Methods. The research was undertaken on autopsy material. We studied the state of nucleus dorsalis n. vagi,nucleus sensorius superior n. trigemini.

Autopsy material has undergone standard histological processing. Serial cross-sections of medulla oblongata were prepared. The calculation of neurons in the right and left nucleus dorsalis n. vagi and nucleus sensorius superior n. trigemini was undertaken with mean number identification.

Results. 70 autopsies were studied. The age varied from 22 to 80 years. The study revealed a 22% decrease of mean number of neurons in n. dorsalis n. vagi in age group of 71–80 years comparing with age group of 21–30 years. A strict correlation between the alterations in n. vagus dorsal nuclei and persistence of chronic atrophic pyloroantral gastritis and chronic atrophic duodenitis was also revealed. This correlation plays also an important role in cases of gastric and duodenal ulcer persistence when the decrease of neurons takes place in age groups of 31–40, 41–50 and 51–60 years. The revealed decrease of neurons in nucleus sensorius superior n. trigemini in the same age groups was 34,4%.

Discussion. Age-related focal neuronal loss is constant feature as neuronal regeneration is resrticted by low amount of neural stem cells in adult organism. It may result in persistence of a number of pathologic processes and a decrease of life duration.

P-460
Efficiency of fetoplacental unit study in fetal death: Review of a series of 339 cases.

M.R.Bella Cueto; R.Orellana Fernandez; M.R.Escoda Giralt; J.C.Ferreres Piñas; E.Sanfeliu Torres; S.Fernandez Ferrer; A.Casalots Casado; N.Combalia Soriano; N.Baena Diez; J.Costa Colomer; M.Rey Ruhi.
Corporacio Parc Taulí, Sabadell; Hospital Vall d'Hebron, Barcelona. Spain.

Background: Fetoplacental unit study in fetal death is important, to try to determine its cause and to improve the follow-up of next gestations.

Objective: To determine how often can be determined the cause of fetal death based on the fetoplacental study, clinical data and cytogenetic study of fetal tissue, and the prevalence of the different causes.

Material: 339 consecutive cases of fetal death between 12 and 41 weeks of gestation, in wich fetal autopsy and histopathologic study of the placenta have been done, happened between 1997 and 2006.

Method: Review of clinical, cytogenetic, autopsy and histopathologic reports, and review of autopsy and histopathologic material in selected cases.

Results: Alterations highly suspicious to be the cause of death could be determined in 265 cases (78%), being placental pathology (96), amniotic fluid infection (87), funicular pathology (40) and malformations (18) the more prevalent. Other less common causes were oligohydramnios (7), immaturity (10), cervical incompetence (5), maternal death (1) and abortive drug (1).

There were more cases between 12 and 24 gestation weeks (227/339). The proportion of unknown cause was slightly higher in this period also, so there were more cases between 12 and 24 gestation weeks (55/74) in with no cause was found.
Amniotic fluid infection, malformations and other less common causes had higher incidence before week 24, while placental and funicular causes had higher incidence after weeks 24 and 31 respectively.
Conclusion: In our series of 339 cases of fetoplacental study in fetal death, cause could be determined in 78% of cases, with varying percentages of the different causes depending on the weeks of gestation.

P-461

Calcitonin targets extracellular signal-regulated kinase signaling pathway in cancers

Misa Nakamura; Bo Han1;Yanhua Bai;Ichiro Mori; Kennichi Kakudo
Deapartment of Pathology, Wakayama Medical University, Japan

[Backgrounds] The mitogen-activated protein kinase (MAPKs) signaling pathway is a potential target in cancer therapy. Constitutive phosphorylated extracellular signal-regulated kinase (ERK1/2), which is one of the MAPKs has been detected in a variety of tumors. Calcitonin (CT) is a polypeptide hormone secreted by the thyroid gland and has been used to treat the osteoporosis and humoral hypercalcemia of malignancy. The purpose of this study was to determine the mechanism of the effects of CT on ERK1/2 phosphorylation in breast cancer cell line and to further investigate the therapeutic usefulness of CT targeting ERK1/2. [Methods] Fourteen human cell lines were used to detect ERK status using Western blotting. To investigate the effect of CT for tumor growth, Female athymic BALB/c nu/nu mice were used. All protocols for in vivo studies were approved by the Institutional Animal Care and Use Committee of Wakayama Medical University. [Results] CT decreased ERK1/2 phosphorylation in cancer cells, MDA-MB-231, MDA-MB-435, T24, DU145, CaR-1 and VMC-RCW, showing constitutive phosphorylated ERK1/2. However CT had no effect on cancer cells, MCF-7, T47D, MRK-nu-1, TT, FTC-133, KP-1NL, KP-3, and CCK81, showing non-constitutive phosphorylated ERK1/2. In MDA-MB-231 cells, a breast cancer cell line, CT phosphorylated c-Raf at Ser^{259} via the PKA pathway, resulting in suppression of ERK1/2 phosphorylation. CT significantly reduced the tumor volume of MDA-MB-231 cells compared with saline buffer *in vivo*. However, CT did not exert any significant effects on the proliferation of MCF-7 cells, a breast cancer cell line. [Conclusion] CT decreased constitutive ERK phosphorylation in cancer cell lines. In addition, CT suppresses the *in vivo* proliferation of cancer cells with constitutive ERK phosphorylation. CT would be a candidate for the treatment of cancer patients with accompanying osteoporosis, and could also be used in combination with a complex hormone therapy.

P-462

Low-passage tumour cell lines: A challenge for biorepositories

Ana M[a] Sánchez López; Héctor Navarro Linares; Raquel Gómez Ramírez, Paloma de la Cueva,; Manuel Medina; Manuel Beltrán, Ana Isabel Sáez Castillo
Red de Bancos de Tumores de Andalucía, Spain

Low-passage tumour cell lines are those generated from tumoral tissue with the least possible number of passes, by which means it is aimed to preserve the characteristics of the original tumour as best as possible. These lines represent an excellent in vitro model for the study of human tumours and they are the tool of choice for transcriptional modification experiments using RNAi, and for drug-sensitivity studies, etc. Despite their usefulness, there exist no standard or guides for its characterisation.
The most critical problems are related to:

- Exhaustive morphological and phenotypical characterisation, and their study in the context of the molecular profile of the original tumour.
- Identification of the degree of transformation of the cells in culture, their replicative capacity and their ability to avoid the process of senescence.

Two of the objectives of the Andalusian Tumour Repository Network are to generate cell lines of this type and to distribute them to researchers. Characterisation and distribution must be carried out employing some minimun quality standards. We are working towards obtaining good markers that will improve the characterisation of these lines.

- The characterisation panel must be developed for each type of cell line. The most common features is the loss of markers typical of the lineage. For example, carcinomas may have a defect in their cytokeratin expression.
- The most widely accepted sign of cellular transformation is the presence of “foci transformation”. These are structures of cells distributed in layers. Our analysis shows that they have a cell cycle arrest profile that is different from all other cells in culture. The cells in these foci have a low proliferation ratio, and exhibit expression of p16 and p27 and a loss of expression of cyclin D1.

P-463

Age related morphological changes in the seminiferous tubule wall

Iancu Emil Plesea; Stelian Danut Enache; Oltin Tiberiu Pop; Petrica Badea; Liviu Riza

Craiova University of Medicine and Pharmacy, Department of Pathology, Romania

Background. Possible correlations between ageing and morphologic changes in lamina propria (LP) of the seminiferous tubules (ST) were assessed.

Method. The studied material consisted of testicular tissue samples from 28 cases with orchiectomy for prostate adenocarcinoma. Tissue samples were processed by the classical histological technique and stained, on serial slides, with Hematoxilin-Eosin, Goldner trichrome and immunomarked for smooth muscle Actin (SMA) and collagen IV (CIV).

Images were acquired and measurements were performed with an image analysis software, after previous calibration. The assessed parameters were: LP thickness (LP-Th) and Hyalin "Collar" thickness (HyC-Th). 30 tubules were randomly selected, with X40 objective, for each case and 5 random determinations for each tubule and for each parameter were performed. Mean thickness (M) for each ST (M-x-Th/ST), case (M-x-Th/C) and age group (M-x-Th/A) were calculated (x = assessed parameter). Regression line (RL), Slope (m) and Significance test for Slope ("p") were calculated to assess the correlation of each parameter with ageing.

Results. M-LP-Th showed a discrete decreasing trend with ageing, but without an obvious statistical correlation (SC). The internal LP layer, apposed to BM (usually formed of a loose, reticular, fibrillary network), revealed, not rarely, areas of collagen focal denseness which often showed foci of hyaline degeneration. Sometimes, these foci had circumferential, "collar"-like disposal around the tubule. M-HyC-Th had a discrete decreasing trend with ageing but without an obvious SC. The percentage occupied by HyC in LP had also a mild decreasing trend but without SC with ageing.

Conclusion. LP of the seminiferous tubule undergoes, with ageing, a wide variety of degenerative changes, with "mosaic", focal distribution and no tendency to advance with ageing as demonstrated by the great variety of morphologic measurements (ranging from total absence to surrounding the entire circumference of the tubule) and statistical determinations.

P-464

Tuberous sclerosis complex in a fetus of 25 weeks gestation:autopsy findings

A.Konstantinidou; H.Zorzos; P.Kaminopetros; E.Patsouris

Department of Pathology-Medical School-National University of Athens, Greece

Background: Tuberous Sclerosis Complex (TSC) is an autosomal dominant multisystem disorder in which CNS, eyes, kidneys,skin and heart are most commonly affected by malformative,hamartomatous or neoplastic lesions.We present a case of TSC in a 25 wk-gestation fetus.

Method & Results: Prenatal ultrasound at 24 weeks had shown rhabdomyoma of the left atrium and cystic dysplasia of the left kidney.Fetal autopsy revealed multiple neocortical tubers and subependymal nodules (SENs) of the fixed brain, atrial rhabdomyoma and generalized myocadial rhabdomyomatosis, a multicystic left kidney with histological features pathognomonic of TSC and hamartomatous lesions of the lungs.

Conclusion: Typical pathological features of TSC are already present at 25 weeks of gestation.Ultrasonographical detection of cardiac rhabdomyoma should rise suspicion of TSC, especially when combined with renal lesions.Typical brain lesions evade prenatal ultrasound detection at this age.

P-465

Thresholding challenges in quantification of immunohistochemical cytoplasmic stain

Dorina Gui; Garrett Gerney; Ngan Doan; Galen Cortina; Steven Ohsie; Sarah Dry; Jonathan Said

UCLA Department of Pathology and Laboratory Medicine, Los Angeles, California, USA

Immunohistochemical stain is widely used in clinical and research laboratories to obtain measurements of neoplastic biomarkers. The protein level was shown to be correlated to immunohistochemical stainings and this fact has led to the development of computer-assisted analysis of immunostains. But image segmentation/thresholding that works well in other fields is not as good when it comes to quantify the cytoplasmic expression of various proteins.

We propose the use of no-counterstained images to allow automated and accurate identification of diaminobenzidene (DAB)-labelled antigens. For this study, we have used a set of sixteen images. Initially, the slides were DAB stained only, images were captured, then the slides were counterstained with hematoxylin and images were captured again.

DAB chromogen develops a brown coloration; the brown color is a mixture of red, blue, and yellow color. The hematoxylin which is normally used for counterstaining, has a blue color. So, when a hematoxylin counterstained image is thresholded for DAB, the resulting mask will always include nonspecific areas due to the blue component that is part of the DAB brown coloration. A statistical analysis has shown differences between thresholding the no-counterstained and the counterstained images.
Many computerized applications are inconsistent in quantifying DAB staining due to the nonspecific background, but our method was consistent for all staining levels.

P-466

Survivin expression in posterior uveal melanoma: an immunohistochemical study.

Mihaela Mera(1); Carmen Georgiu(1); Simona Mera(2); Dan Gheban(1); Dan Călugăru(3); Aurelian Georgiu(4)
(1)University of Medicine and Pharmacy "Iuliu Haţieganu"- Department of Pathology, (2)County Hospital – Department of Infectious Disease, (3)University of Medicine and Pharmacy "Iuliu Haţieganu"- Department of Ofthalmology,(4) Individual Medical Center 81, Cluj Napoca, Romania

PURPOSE: Survivin, an inhibitor of apoptosis (IAP) protein, acting in the G2/M phase of the cell cycle, is expressed in several human cancers. The aim of this work was to study the survivin expression in primary posterior uveal melanomas treated with enucleation without prior radiotherapy. **METHODS:** It was performed immunohistochemical staining for survivin (DAKO clone 12C4, with specificity for an epitope present in the first 34 N-terminal amino acids of the survivin protein), with melanin bleaching, in formalin-fixed, paraffin-embedded blocks from thirty two uveal posterior melanomas. Specimens were divided according to size, cell type and extracellular matrix deposition. The intensity of survivin immunostaining was scored for both, cytoplasmic and nuclear staining independently, as follows: 0, absent; 1+, weak; 2+, moderate; and 3+, intense. **RESULTS:** There was a high expression of survivin in uveal posterior melanoma. Twenty three cases (69,6%) of 32 uveal melanomas expressed survivin protein, among them, 13 cases positively expressed in the cytoplasm (7 intense, 4 moderate, 2 weak), 3 cases expressed predominantly and intensely in the nuclei, and 7 cases expressed moderately in both nuclei and cytoplasm. The intranuclear staining had a particular dotted pattern. The survivin was also weakly positive in the extra cellular compartment that is in the aqueous humor of the eye of 15 cases. The Pearson chi-square analysis demonstrated a significant correlation (p=0,0034) of survivin expression to epithelioid or mixed cell type being absent mostly in the spindle cell tumors. Similarly, the nuclear expression of survivin correlated to epithelioid cell types (p=0,0008), the isolated nuclear expression being associated exclusively to epithelioid tumors with extensive necrosis. It also strongly correlated with the largest basal dimension and the loops or network pattern of extracellular matrix deposition. **CONCLUSION:** This study suggests the possible role of nuclear survivin in the progression of uveal melanoma, the survivin being associated to the known risk factors of uveal melanomas which are the epithelioid cell type, extracellular matrix deposition in looping patterns and monosomy 3. The extracellular presence of the survivin in the aqueous humor of the eyes may reflect also the possible role of survivin in the secondary processes unleashed by the tumor that is neoangiogenesis and immunomodulation, which both need antiapoptotic mediators.

PURPOSE: Survivin, an inhibitor of apoptosis (IAP) protein, acting in the G2/M phase of the cell cycle, is expressed in several human cancers. The aim of this work was to study the survivin expression in primary posterior uveal melanomas treated with enucleation without prior radiotherapy. **METHODS:** It was performed immunohistochemical staining for survivin (DAKO clone 12C4, with specificity for an epitope present in the first 34 N-terminal amino acids of the survivin protein), with melanin bleaching, in formalin-fixed, paraffin-embedded blocks from thirty two uveal posterior melanomas. Specimens were divided according to size, cell type and extracellular matrix deposition. The intensity of survivin immunostaining was scored for both, cytoplasmic and nuclear staining independently, as follows: 0, absent; 1+, weak; 2+, moderate; and 3+, intense. **RESULTS:** There was a high expression of survivin in uveal posterior melanoma. Twenty three cases (69,6%) of 32 uveal melanomas expressed survivin protein, among them, 13 cases positively expressed in the cytoplasm (7 intense, 4 moderate, 2 weak), 3 cases expressed predominantly and intensely in the nuclei, and 7 cases expressed moderately in both nuclei and cytoplasm. The intranuclear staining had a particular dotted pattern. The survivin was also weakly positive in the extra cellular compartment that is in the aqueous humor of the eye of 15 cases. The Pearson chi-square analysis demonstrated a significant correlation (p=0,0034) of survivin expression to epithelioid or mixed cell type being absent mostly in the spindle cell tumors. Similarly, the nuclear expression of survivin correlated to epithelioid cell types (p=0,0008), the isolated nuclear expression being associated exclusively to epithelioid tumors with extensive necrosis. It also strongly correlated with the largest basal dimension and the loops or

network pattern of extracellular matrix deposition. **CONCLUSION:** This study suggests the possible role of nuclear survivin in the progression of uveal melanoma, the survivin being associated to the known risk factors of uveal melanomas which are the epithelioid cell type, extracellular matrix deposition in looping patterns and monosomy 3. The extracellular presence of the survivin in the aqueous humor of the eyes may reflect also the possible role of survivin in the secondary processes unleashed by the tumor that is neoangiogenesis and immunomodulation, which both need antiapoptotic mediators.

P-467

UNUSUAL SITES OF METASTASIS: PRESENTATION OF THREE CASES

MA Arrechea Irigoyen, ML Gómez Dorronsoro, I Amat Villegas, R Beloqui Pérez, A Córdoba Iturriagagoitia, JM Martínez-Peñuela Vírseda

Servicio de Anatomía Patológica. Hospital de Navarra, Spain

Introduction: The improved survival of patients with carcinoma together with aging of population has led to a higher incidence of metastasis in unusual sites. We report herein the cases of three patients with cancer in the past who presented metastatic disease in non-common sites. **Material and methods:** The first case corresponds to a 73-year-old man presenting a solitary duodenal mass seven years after a nephrectomy for a Renal Cell Carcinoma. The second one relates to a 55–year-old woman with a history of meningeal hemangiopericytoma nine years earlier, who presented with ictericia and abdominal pain. The third case corresponds to a 57-year-old man with lung cancer and multiple disseminated metastases. **Results:** The histopathology of the resected specimen on the first case confirmed a metastatic renal cell carcinoma in duodenum. A pancreatic mass was found on the second case which microscopically was diagnosed as being a hemangiopericytoma. Ten years after the initial diagnosis, distant metastasis to liver were also found. An autopsy was requested on the third case when he passed away and a lung adenocarcinoma metastasizing into a non-previously diagnosed 7-cm-renal cell carcinoma was described. **Discussion:** In patients with a previous history of cancer and newly diagnosed symptoms, the possibility of local recurrences or metastasis should be kept in mind. We would like to highlight the importance of long-term follow up in order to provide accurate diagnosis and exclude the presence of possible metastasis.

P-468

Vascular endothelial growth factor A expression in uveal melanoma.

Carmen Georgiu(1), Mihaela Mera(1), Simona Mera(2), Dan Gheban(1), Dan Călugăru(3), Aurelian Georgiu(4)

(1)University of Medicine and Pharmacy "Iuliu Haţieganu"- Department of Pathology, (2)County Hospital – Department of Infectious Diseases, (3)University of Medicine and Pharmacy "Iuliu Haţieganu"- Department of Ophthalmology,(4)Individual Medical Center 81, Cluj Napoca, Romania

AIMS. Immunohistochemical investigations of the VEGF A expression in uveal melanomas revealed variable results. The aim of this study was to evaluate the expression of vascular endothelial growth factor A (VEGF A) in the anterior and posterior uveal melanomas and his relationship with the extracellular matrix deposition pattern and other parameters of high risk significance. **METHODS.** Thirty two posterior uveal melanomas and 3 cilliary body melanomas were investigated, using melanin bleaching and immunohistochemistry for VEGF A (Dako). The extracellular matrix deposition was assessed using PAS without haematoxylin counterstaining. No eyes had received prior treatment. The intensity of VEGF A was scored as the following: (0) <5%; (1) 5–25%; (2) 25–50%; (3) 50–75%; and (4) >75%. The mitotic index was assessed on each tumor on 10 field delimited by a Weibel reticle of 0,658 mm square, eliminating the necrotic areas. **RESULTS.** Tumor cell type, location, necrosis, mitotic index and extracellular matrix were analyzed by using light microscopy. Histopathologically, the tumor cell types were spindle cells in 12 (34,3%) of the cases, mixed cells in 16 (45,7%), and epithelioid cells in 7 (20%) tumors. Positive reaction for VEGF-A was present in 80% of the tumors. The intensity of VEGF A was weak (1) in 15/35 (43%), moderate (2) in 12/35 (34%) and high in 8/35 (23%) cases. The VEGF A was also present in all positive cases in the extra cellular compartment of the eye, in the aqueous humor. The mitotic index varied between 3 and 35 mitosis on 10 field occupied by tumor cells. Microvascular loops/networks were seen in 15 (42,8%) of the tumors, in 9 (25,7%) the arc pattern sometimes with branches, in 6 (17,2%) parallel pattern with or without crosslinking, the rest of 5 (14,3%) displaying the straight pattern. The intensity of the VEGF A was correlated with the other prognostic factors. On multivariate analysis, the correlation between VEGF-A expression and the epithelioid cell type especially with necrosis, associated with high mitotic rate and the loop/network patterns, was found to be statistically significant (p=0,0037). It displayed any relationship with

the tumor location, tumor size and age. **CONCLUSIONS.** Our data suggest that increasing VEGF-A expression can be used as a dependent prognostic factor for high risk posterior uveal melanoma beside the other well known parameters as the epithelioid cell type, extracellular matrix deposition in looping/network patterns and monosomy 3.

P-469

Balloon cell nevus of the conjunctiva (case report)

Cermik Hakan, Yumuşak Erhan, Güllü Levent, Sahin Ömer
Etimesgut Military Hospital, Turkey

Background Balloon cell nevus (BCN) is an uncommon variation of melanocytic nevi characterized histologically by a preponderance of peculiarly large nevomelanocytes with clear foamy or finely vacuolated cytoplasm(1) Balloon cells are altered melanocytes with clear vacuolated cytoplasm caused by a defect in the process of melanogenesis. Although rare, balloon cell change has been observed in a variety of melanocytic proliferations, particularly intradermal melanocytic nevi and melanoma. When present, such features may lead to difficulties in diagnosis, particularly with other clear cell neoplasms. The diagnosis should be made when more than 50% of the tumour shows balloon cell change.

The balloon cell nevus is a rare variant of the conjunctival nevi.

Case report A 22-year old asymptomatic man was admitted to our hospital with a pigmented lesion of the right eye. He reported that the lesion had become noticeable 6 weeks earlier. His ophthalmologic history wasn't any remarkable symptom. On examination, a slightly elevated, movable, tan-yellow nodule with a deep brown area was observed on the bulbar conjunctiva of the right eye. No other bulbar pigmentation was noted. An excisional biopsy was performed. A $0.7 \times 0.4 \times 0.2$ cm. conjunctival specimen was white-yellow and contained a slightly central dark brown pigmented lesion.

Histologic examination: The tumor mass involved the papillary and superfisial dermis and consisted of large cells with deeply basophilic, small, centrally-placed nuclei and abundant, slightly eosinophilic vacuolated or granular cytoplasms with microvesicles. Some cytoplasms has moderate amounts of intracelluler melanin. Some multinucleate cells were also noted. Some areas showed small aggregates of small lymphocytes between balloon cells. There was no mitotic figure. Diagnosis was made as a balloon cell nevus of the conjuctiva.

Cardiovascular Pathology

P-470

HYPERTROPHIC CARDIOMYOPATHIES OF ISCHEMIC ETHIOLOGY

Liliana Parascan*, Gabriela Mutiu, Vasile Candea*, Nikki J. Agnantis*****
Greece

Aim: The multidisciplinary analysis of particularly necropsic aspects related to arterial hypertension of myocardial ischemia. **Material and methods:** 200 autopsies were made sampling fragments from myocardial aries injuried as well as from neighbouring territories. Fragments from miscellaneous organs were gathered too. Histological techniques used were: H.E., V.G., Weigert, Lee, PAS, PAS-Alcian, Gomori, achieving photo images from zones with ischemic lesions. **Results:** The correlations among pathological versus clinical and paraclinical data are tested according to the chronological recording of their appearance, starting with the risk factors, going to the collection of symptoms presented in admised moment, then to the actual clinical signs and paraclinical investigations registered during the hospitalization stage and submitted as graphical representations (ECG, PHONO) or iconic drawings (ECHO, CT). The first table shows the risk factors as: arterial hypertension (HTA), hypercholesterolemia (colesterol), smoking (fumat), diabetes mellitus (diabet zaharat or DZ), overweight (obezitate) and dislipidemia described in terms of standard deviations on age groups for male patients. **Conclusions:** 1. Compensated systemic HHD may be asymptomatic an suspected only in the appropriate clinical setting by ECG or echocardiographic indications of left ventricular enlargement. 2. Other causes for such hypertrophy must be excluded. 3. In many patients, systemic HHD comes to attention by onset of atrial fibrillation (owing to left atrial enlargement) or CHF with cardiac dilation, or both. 4. Depending on the severity, duration and the underlying basis of the hypertension and on the adequacy of therapeutic control, the patient may: (1) enjoy normal longevity and die of unrelated causes, (2) develop progresive IHD owing to the effects of hypertension in potentiating coronary atherosclerosis, (3) suffer progressive renal damage or cerebrovascular stroke, (4) experience progressive heart failure. 5. The risk of sudden cardiac death is also icreased. 6. The electronmicroscopy can thoroughly describe the bio-morphology of extracellular matrix, the modification of it being important in the

evolution of the ischemic cardiopaty. 7. The abundance of data given by the necropsy examinations, followed by hystopathology studies supplies the area of paraclinic investigations being needed the sampling of myocardial biopsies in view of microscopy diagnosis of patitents during life, as well as the necropsy of all cases of ischemic cardiopaties, including all known and multi-disciplinary investigated cases.

P-471

Cardiac 'MICE' What is it really?

Rosa Henriques de Gouveia; Ana Paula Martins
Pathology Department, CHLO - Hospital de Santa Cruz, Portugal

Background: Mesothelial/Monocytic Incidental Cardiac Excrescence (Cardiac MICE) is an entity first described by Rosai et al in 1979. The authors present two cases and put forward their view concerning its still controversial histogenesis. **Material and Methods:** One of the cases refers to a 66-year-old woman with floppy mitral valve and coronary atherosclerosis that was submitted to diagnostic coronary angiography and afterwards to mitral valve surgery and aortocoronary bypass; and whose lesion was detected inside the left atrium during surgery, and macroscopically accepted as a thrombus. The other case concerns a 76-year-old man with a pacemaker due to complete atrioventricular block, that after having undergone surgical revision as a consequence of electrode exteriorization one year after its insertion, had the electrode removed the next year, in the context of infection resistent to antibiotherapy. The surgical specimen, obtained from the right side of the heart, was attached to the electrode and considered as a vegetation. **Results:** Histological evaluation of both samples disclosed a lesion made up of fragments of mesothelium and macrophages/histiocytes supported by a fibrin meshwork. On the second case, it was associated to real organizing thrombus and "pannus" enveloping the electrode. **Conclusion:** Cardiac MICE is a rare begnin tumoral lesion (1). It may be located in any of the four heart chambers depending upon each clinical setting (2). Finally, the common element shared by both cases - cardiac manoeuvres - emphasizes the intracardiac shifting of pericardial mesothelium fragments during surgical/interventional cardiac procedures as the mechanism of origin (3) and consolidates its classification as an Iatrogenic Disease.

P-472

TGF-BETA PATHWAY IS ACTIVATED IN LEAFLETS OF NON SYNDROMIC MITRAL VALVE PROLAPSE

Stefania Rizzo; Gino Gerosa; Adolfo Paolin; Gaetano Thiene; Cristina Basso
Departments of Medico-diagnostic Sciences and Special Therapies and of Cardiac, Thoracic and Vascular Sciences, University of Padua Medical School, Padua-Italy

BACKGROUND Mitral valve prolapse (MVP) is the leading cause of mitral valve incompetence in western countries. Although its etiopathogenesis remains uncertain, a genetic defect has been recently identified in some syndromic (ie, Marfan syndrome) and non syndromic cases. The finding that TGF-beta dysregulation may play an important role in the development of MVP prompted us to evaluate whether the Smad receptor-mediated intracellular TGF-beta pathway is activated in isolated MVP as well.
METHODS Myxomatous mitral valve specimens were obtained at surgery from patients (13 cases, 11 males and 2 females, mean age 55.5±12.7 years) who underwent valve repair or replacement due to MVP. Other connective tissue disorders or familial valve disease were excluded. Age and sex-matched control samples of mitral valve were obtained from homograft Tissue Bank (5 cases, mean age 49± 9 years). Valve morphology, mucoid substance, elastic fibers and mitral valve thickness were assessed on routinely stained histology sections. Specific primary antibodies recognizing active phosphorylated form of Smad2 (P-Smad2, Dako) in valvular myofibroblasts (vimentin and smooth muscle myosin positive) were used. Picro-Sirius staining was applied to examine the amount of collagen I and III.
RESULTS MVP leaflets exhibited alterations in architecture with fourfold increase in thickness (2,5±0,8 vs 0,6± 0,3 mm, $p<0.0001$) and increased cell density in the spongiosa (110,9±64,6 vs 51,8±27,5 cells per high power field, $p=0.04$) compared to the normal valves. A higher density of nuclear staining for P-Smad2 (38% vs 12%, $p< 0.0001$) was also observed, indicating an increased activation of TGF-beta pathway. Collagen I and III have higher expression in MVP leaflets than in controls.
CONCLUSION Our data support the hypothesis that an increased activation of the intracellular TGF-beta response pathway may contribute to the pathogenesis of non syndromic MVP.

P-473

The evaluation of angiologic distortions (involutive-structural) in the appearing of cerebral stroke

Lilian Birzoi

National Centre for Emergency Medicine, Chisinau, Republic of Moldova

Background and aims: We have studied the involutive-structural element and the stroke. The cerebral stroke in the practice of emergency medicine frequently causes the death of patients. Actually, its appearing is noted in subjects of "professionally active" age of the modern society (30 - 40 - 45 years). **Method:** We have analyzed the macro- and microscopic morphologic panorama of the altered region in 300 deceased patients. **Results:** We have noted frequently in the complex of distortions of the cerebrovascular circulation the acceleration of involutive structural modifications in the angio-phlebolic system. Among the components of the constituents which predispose to cerebral stroke, well known and described in detail up to date, attention is attracted towards the phenomenon of "elastolysis": the behaviour of elastic structures, the biomolecular, physico-chemical state of the elastic tissue. **Conclusion:** This state might influence substantially the advancement of pathomorphologic processes, which result in serious consequences (stroke). The premature appearing of involutive factors results in precocious senescence of the subject. The phenomenon of "elastolysis" becomes an associated factor in the appearing of cerebral stroke.

P-474

Myocardium fluorescence in human myocardial infarction

Ilie Tsiple; Vasile Anestiadi

Centre for Pathobiology and Pathology, Academy of Sciences, Chisinau, Moldova

Background and aims: The study aimed towards finding new criteria forthe determination of the duration in time of myocardial infarction (MI).

Method: Fifty-two hearts from persons (PRS) deceased from MI, in which MI beginning was documented clinically and by ECG, were selected. Thirty hearts of PRS deceased almost instantaneously from traumas served as controls. In each case we did 1000 measurements of myocardial primary fluorescence (MPF) at the wavelength of 360 nm, both in the necrotic (ischaemic) zone (NZ) and in extrainfarctic zones (EZ).

Results: During 8–12 h from MI beginning, the MPF decreased concordantly in both zones, being 89.6±2.3% of controls. At 24 h after MI onset MPF in NZ was 78.8±4.3%, in EZ 84.4±3.1% of controls. Minimal NZ MPF was on Days 4–5 and 9–10 (66.3±2.5% and 62.6±2.1% of controls, $p<0.001$). EZ MPF on Days 4–5 was 77.4±3.5%, on Days 9–10 82.3±2.2% and on Days 14–15, 85.7±2.8%, remaining even up to Days 30–35 of MI 7.3±0.8% below controls. MPF variations in time were approximated by splines.

Conclusion: By solving a system of equations, which included formulae for EZ and NZ MPFs, it was possible to determine the time elapsed from the MI onset, with an accuracy of 9.6 hours.

P-475

Mediastinal nonleukemic granulocytic sarcoma with cardiac infiltration: case report and literature review

Adriana Alencar Araújo Costa; Gabrielle Gurgel Lima; Francisco Dario Rocha Filho; Francisco Valdeci Almeida Ferreira

Institute of Cancer of Ceara, Brazil

Introduction: Granulocytic Sarcoma (GS) is a rare extramedullary tumor composed of immature myeloid cells. It is usually associated with leukemia or other myeloproliferative disorders but can also occur without overt hematologic diseases. The involvement of heart is very rare and usually diagnosed at autopsy. We reported the clinical and pathological features of an isolated mediastinal GS with cardiac infiltration with no evidence of leukemia involving bone marrow or peripheral blood, and reviewed the literature. Method and results: Patient male, 31 years old, was admitted with history of dry cough and progressive dyspnea for five months. He had done previously transthoracic-eco, which revealed mass occupying approximately 65% of the left atrium. The mass invates da cavity of the left ventricle in diastole through the mitral valve, which caused great restriction on the filling. The previous morphological and immunohistochemistry studies were angiossarcoma, paraganglioma and small cell carcinoma. The chemotherapy was started with etoposide and cisplatin, no good clinical response. Three months later, the thorax computed tomographic scan showed the mediastinal expansive mass, with right pleural effusion and pericardial spill. The case was reviewed showing positive for myeloperoxidase and CD99, favoring the diagnosis of GS. Treatment was directed to GS with daunorrubicina and cytarabine, with clinical remission. Meanwhile patient presented febrile neutropenia, envolving to death ten months after start of symptons. Conclusion: Previous literature showed that almost half of the patients with heart primary GS was misdiagnosed initially. GS most often represent relapse or initial presentation of AML. We reported a case of isolated heart GS without a history or subsequent development of AML

at last follow-up. Immunohistochemistry is extremely helpful for recognizing isolated myeloid sarcoma. The research in literature disclosed the presence of only five of GS unrelated to the leukemia to exclusively mediastinal presentation and only one with cardiac infiltration.

P-476
ANATOMOCLINICAL CORRELATIONS IN COMPLICATED CONGENITAL LEFT ATRIAL CARDIOVASCULAR DISEASE

Vasile Candea*, Liliana Parascan*, Gabriela Mutiu**
**Cardiovascular Diseases Institute "Prof.Dr.C.C.Iliescu"-Bucharest ROMANIA*

Aim: The presentation of a rare case of a left cardiac malformation hart with non surgical resolving.
Material and methods: During year 2000 there have been done necropsies on 19 years old women known with coarctation of aorta and endoluminal isthmoplastia with balloon and mitral supravalvular diaphragm through incomplete identified mechanism and pulmonary hypertension releaved by the presence of media hypertrophy and vasoconstriction between focal siderophagia on histological cups of both lang certified by ordinary and specific stains: HE, VG, Weigert, PAS.
Results: On the secondary irreversible pulmonary hypertension background through necrotized arteritis and plexiform lesions have appeared bronchopneumonic centers with hyaline intraalveolar membranes and interruptions of basal kidney glomerular membrane.
Discussion: The complicated histopathological aspect of pulmonary lesions leads to etiology of final episode about presence of immune complexes of circulatory anti basal membrane auto-antibodies against of non-collagen domain of α-3 chain of collagen what is on the basis of pathogenesis of Goodpasture syndrome to explain the final pulmonary and renal inflammatory lesions.
Conclusions: The correctly and in time diagnosis of patients with congenital left cardiac lesions that may be classified in Shone syndrome characterized by four obstructive cardiac lesions situated in left heart: supravalvular mitral ring, deformation on mitral valve in parachute, supraaortic stenosis and aortic coarctation is the first step to the heavy surgical treatment of these cases.

P-477
LEFT ATRIAL MYXOCHONDROSARCOMA RELAPSE

Gabriela Mutiu*, Liliana Parascan*, Carmen Ardeleanu**, Vasile Candea***
**Cardiovascular Diseases Institute "Prof.Dr.C.C.Iliescu"-Bucharest ROMANIA*

CASE PRESENTATION
Ten months before the examination, the 76-year old female patient had suffered from periodical dyspnea and from congestive cardiac insufficiency symptoms. The echocardiographic test detected the presence of a tumoral mass in the left atrium, on the interatrial septum. The tumoral mass was extirpated by surgery (dr Vasile R.'s team) and white-grey fragments displaying firm areas, of medium consistency, and measuring between 3 cm and 0.5 cm, were submitted to histological exams, alongside other, hard fragments. The histological aspects detected through HE, VG, PAS-Alcian, Gomori colorations varied in the different examined territories, as follows: subendocardially there appeared myxoid images showing round, fusiform and faintly starred cells, images of chondroid and osteoid metaplasia, alcianophile matrixes alongside fascicled areas with numerous larger, hyperchromatic, bi-nucleate atypical cells. The reappearance, ten months later, of the initial clinical symptoms called for reexamining the patient, especially echocardiographically, which made it possible to detect the relapse of the left atrial tumor. Surgery was performed and a cauliflower-like tumor measuring 5/4/3 cm, of firm consistency and hard at the implantation basis was removed. Numerous histological sections as well as the same colorations, including immunohistochemical ones, were performed at the Victor Babes Institute, which showed images similar to those detected in the primary tumor. However, there prevailed the chondrosarcomatose aspects with osteoid differences and cells having atypical aspects.

P-478
The Clinical Role of Recurrently Elevated Macro Creatine Kinase Type 1

Ju-Feng Hsiao; Hsiao-Chen; Po-Wen Gu;Pao-Hsien Chu
Department of Cardioloyg, Chang Gung Memorial Hospital, China

The typical creatine kinase (CK) isoenzymes include CK-BB, CK-MB and CK-MM. Macro CK type 1, one of the atypical CK enzymes, has been identified in human serum, but the clinical significance still remains uncertain. In our laboratory, 105 patients who expressed serum macro CK isoenzyme type 1 were identified from March 2004 to May 2007. We found macro CK type 1 recurred after a least one month in 16 patients.
Clinical diagnoses were myopathy in 15 patients, and one had acute coronary syndrome. The averages of serum total CK, macro CK type 1 were 10,784 and 2,249 (U/L), respectively. The linear regression analysis between macro CK and total CK revealed a good correlation ($y=3.5054x+2381.3$, $R^2=0.7822$, $P<0.001$). Three patients had critical

illness, including one respiratory failure and two mortalities. Good linear correlation is documented between total CK and macro CK type 1. In conclusion, the macro CK type I isoenzyme recurred in patients with myopathy mostly.

P-479

Arrhytmogenic right ventricular dysplasia cases in forensic autopsies year 2004 in Barcelona

MT Marrón; JC Canós; JC Borondo; MJ Leal; JM Tortosa; J Castellà; JL Valverde; S Crespo.
INSTITUT MEDICINA LEGAL CATALUNYA. INSTITUT NACIONAL TOXICOLOGIA-CF, BARCELONA. SPAIN

SUB-HEADING. Arrhytmogenic right ventricular dysplasia in forensic autopsies.
BACKGROUND. Arrhytmogenic right ventricular dysplasia (ARVD) is a progressive heart muscle disease often familial characterized by structural and functional abnormalities of the right ventricle due to replacement of the muyocardium by fatty and fibrous tissue extending in some cases to the left one (a factor considered of bad prognosis). Clinical presentation consists of arrythmias of RV origen that include, premature ventricular beast, ventricular tachycardia, ventricular fibrilation and sudden death. Most cases are related to young people performing exercise.
METHOD. Retrospective review of cases about (ARVD) after performing complete forensic autopsies an histologic examinations at the INT-CF Barcelona in 2004.
RESULTS. Out of a total 875 studies performed at the National Institute of Toxicology in Barcelona (2004), 47.3% (n=414) were due to sudden death and only one case diagnosed as (ARDV).
CLINICAL CASE: A 46 y. old caucassian man were studied at the cardiology department because of syncope episodes. Electrophysiologic studies were normal and he was allowed to performed exercise. While he was playing his first tennis match he underwent a loss of consciousness and sudden death. A complete judicial autospy was performed with toxicologic screening.
Macroscopic Findings (Gross): A 405 g heart, showed epicardial fat thickened with focally dilated right ventricle. Minimal atherosclerotic changes of about 30% stenosis at main and left coronary artery. Neither aneurysmal changes nor wall thinning were related.
Histopathology: Transmural fibrofatty infiltration of the right ventricle with foamy/bubbly myocardiocystes wth left ventricle involvement (biventricular). No inflammatory changes were related.
Vitreous humor test were negative. Toxicologic analysis showed paracetamol and metamizol in blood and bile.
DISCUSSION. About 0.24% of all sudden death cases studied at the histopathology service of the INTCF (Barcelona) in 2004 were classified as ARVD.
ARDV is a well-known disease related to sudden death as result of ventricular fibrilation during exercise and the diangosis is of paramount importance in terms of genetic counseling to other family members.

P-480

Role of myocardial endothelial permeability in the development of heart failure following open-heart surgery

E. Stefanovic, P Otasevic, L.Lausevic-Vuk, P.Milojevic, D.Nezic, B Djukanovic
"Dedinje" Cardiovascular institute, Belgrade, Serbia

Introduction During open heart surgery some damages of cardiomyocytes and myocardial capillary endothelium occure, with the consequences to the structure and function of cardiomyocytes as well.
This lesions are the result of the usage of the cold multicomponent cardioplegic (CPL) solution, long term hypoxia and reperfusion.
Aim The aim of the study is to assess the influence of intraoperative changes of myocardial capillaries on the severity of heart failure (HF) in the postoperative course.
Methods Two groups were analysed. Group A, consisting of 13 patients who underwent open-heart surgery and with signs and symptoms of mild HF in the postoperative course. Group B – 7 patients who died from second to tenth postoperative day due to HF. The ischemic period was 77,6±4,2 min in gr.A, and 94,2±5,2 min in gr. B. Myocardial intraoperative biopsies from the right ventricle, taken during different time during the ischemic period and reperfusion, were analysed by electron microscope using quantitative stereological analyses.
Results Myocardial ultrastructural analysis showed increase in permeability of the capillary wall, edema and degenerative changes of cardiomyocytes that were similar in both groups. Stereological analysis of endothelial cells organelles revealed decrease of 48% in volume fraction of basic pinocyte vesicles in gr.B after release of the cross-clamp as compared to immediate preoperative level, suggesting that the elimination of metabolic products from interstitium to microcirculation is altered.
Conclusion Ischemic changes of myocardial capillary endothelium during the open-heart surgery, as assessed by stereological analysis, are more profound in patients who died due to HF, suggesting that the disturbance of trans-endothelial transport may play certain role in the development of HF.

P-481

Detection of apoptosis in myocardial infraction with the use of a single-stranded DNA (ss-DNA) monoclonal antibody.

Angelos Tsipis; Anna-Maria Athanassiadou; Pauline Athanassiadou; Nicolaos Kavantzas; George Agrogiannis; Efstratios Patsouris.

1st Department of Pathology, Medical School, University of Athens, Greece.

Background: Cardiac myocyte death during ischemic injury has been thought to occur exclusively by necrosis, but recently several studies have demonstrated that large numbers of myocytes undergo apoptosis in response to ischemic disorders. Apoptotic cells are usually identified by terminal deoxynucleotide transferase-mediated dUTP nick end-labeling (TUNEL), but recently, a single-stranded DNA (ss-DNA) monoclonal antibody has been reported to be sufficiently sensitive to detect apoptosis. The aim of this study was to investigate and quantify the presence of apoptosis in acute and chronic ischemic cardiac disorders.
Method: We studied myocardial samples of hearts with histologic findings of acute myocardial infraction (group A, n=20), old myocardial infraction (group B, n=20), and chronic ischemic heart disease (group C, n=20). Myocardial samples of normal heart were also included in this study (control group, n=10). An immunohistochemical method was performed with the use of anti-ss-DNA monoclonal antibody (mAb), in order to investigate the presence of apoptosis in ischemic cardiac disorders.
Results: In all cases of acute myocardial infraction (group A), the infracted area included extensive presence of both apoptosis and necrosis. In the tissue bordering on and away from the obviously infarcted areas, positive nuclei were intermingled with non stained normal myocytes. The number of positive nuclei decreased with the distance from the infraction foci. Stained nuclei were dispersed with intermingled normal cardiomyocytes, in salvaged areas at the old stage of infraction and in chronic ischemic disease. Absence of ss-DNA-positive cells was confirmed in normal control myocardium.
Conclusions: The results suggest that cardiomyocyte apoptosis in the border zone is responsible for cellular loss in the acute stage of myocardial infraction and may play a role in the evolution of the chronic heart failure in patients with old myocardial infraction and chronic ischemic disease.

P-482

Cardiac myxoma: new biomolecular insights for a classificatory re-consideration

Augusto Orlandi, Amedeo Ferlosio, Luigi Giusto Spagnoli

Anatomic Pathology, Dept. Biopathology, Tor Vergata University of Rome, Italy

Background and methods. Cardiac myxoma is the most common primary cardiac tumour but its classification remains difficult, being retained of unknown origin. We used biomolecular investigation in conjunction with ancillary methods to a large series (n=30) of these tumours.
Results. Mixoma tissue was constituted from abundant hypocellular myxoid and oedematous matrix, resembling primordial cardiac jelly. Immunohistochemical investigation revealed that mixoma cells express -smooth muscle actin, whereas alpha-cardiac and alpha-skeletal actin isoforms were almost absent. Co-expression of CD34 and α-smooth muscle actin by double immunohistochemisty and confocal microscopy suggested loss of stem endothelial markers and the acquirement of myocytic antigens Early cardiac differentiation markers were also investigated by RT-PCR. We documented the presence of transcripts for Sox9 (100%), Notch1 (87.5%), NFATc1 (37.5%), Smad6, metalloproteinases 1 and 2 alone or in variable combinations and the absence of ErbB3 and WT1. Myxoma cells maintained phenotypic heterogeneity in vitro, including the expression of alpha-SMA and the presence of stress fibres.
Conclusions. These results strongly suggest the cardia myxoma cell exhibit a phenotype resembling embryonic endothelial-to-mesenchymal transformation preceding terminal differentiation of endocardial cushions.

Skin Pathology

P-483

Basal Cell Carcinoma of Vulva

Carlos Mario Rangel, Sergio Andrés Torres, Julio Alexander Díaz, Ernesto García Ayala

Universidad Industrial de Santander, Bucaramanga, Colombia

Background. The basal cell carcinoma is the malignant neoplasm more prevalent in the world; nevertheless, its location in vulva is infrequent. **Objective.** To describe a case of basal cell carcinoma of the vulva from the Hospital Universitario de Santander. **Clinical case.** Female patient of 62 years old, that consults to display a lesion in mayor labia of 3 years of evolution. In the physical examination an ulcerated lesion of 2.5×1.2 cm, poorly delimited, with bleeding and necrosis was observed. A made skin ellipse excision, in the pathological study was recognized a basal cell carcinoma of vulva. The patient at the moment is asintomatic without displaying signs of recurrence of the disease. **Conclusions.** The basal cell carcinoma of vulva is a cancer little frequent, rare time is metastasizing but sometimes it's locally aggressive. One has been associated to numerous factors; nevertheless its etiologic is not

completely known. Its clinical presentation is varied and it does not specify, which makes difficult diagnose of precocious way. The election treatment is the surgical split with clean margins. The basal cell carcinoma presents foretell good but due to his rate of recurrence it is necessary to carry out periodic monitoring after the treatment

P-484

ANNULAR ACQUIRED ELASTOTIC HEMANGIOMA TREATED WITH IMIQUIMOD.

F. Terrasa; J. Ibarra; A. Llambrich; J*. I. Torné*; C. Nadal*.

Pathology and Dermatology Departments of Hospital Son Llàtzer, Spain*

BACKGROUND Acquired Elastotic Hemangioma is a distinctive clinicopathological variant of hemangioma described by Requena et al in 2002. It seems to be an underrecognised entity. Because of the shortage of published cases, some dermatoscopic, clinical features or therapies of AEH are to be described. We describe an annular clinical presentation of AEH in a man treated with imiquimod. The dermatoscopic pattern of another case of AEH is presented.

METHOD Three cases of acquired elastotic hemangioma are described. The histological, clinical, and inmunohistochemical features are studied. Topical use of imiquimod 5% cream was used for the treatment of one case of AEH.

RESULTS Acquired elastotic hemangioma is a vascular proliferation that appears on sun-damaged skin of middle aged or elderly people. For the first time, to our knowledge, we describe a case in a man, and an annular clinical presentation of AEH. Dermatoscopy pattern of the other case located on the forehead of a woman shows generalised erythema, linear irregular vessels and white patches maybe due to fibrotic or elastolytic changes. We don't see typical vascular lagoons that we commonly see in vascular lesions as angiomas. One of the cases was treated with topical Imiquimod and the other two cases were followed up with no other treatment.

CONCLUSIONS Acquired elastotic hemangioma is a distinctive clinicopathological variant of acquired hemangioma. AEH is presented in the sun exposed skin of patients in the adulthood, not exclusively in women. The typical clinical presentation is an erythematous plaque. The first case of annular clinical presentation of AEH is described. The clinical differential diagnosis of annular lesions must include AEH. The dermatoscopic pattern of one case of AEH is described as generalised erythema, linear irregular vessels and white patches. Topical imiquimod could avoid surgical excisions after a punch biopsy of AEH.

P-485

Cutaneous Gamma-Delta T-cell Lymphoma arising in the setting of Behcet's disease

Ennaifer Ines; Faten Limaiem; Selma Bellil; Amina Mekni; Haifa Azzouz; Khedija Bellil; Haouet Slim; Moncef Zitouna; Nidhameddine Kchir.

Hospital La Rabta, Tunisia

Cutaneous Gamma-Delta T-cell lymphoma is an uncommon lymphoma composed of a clonal proliferation of mature activated gamma-delta T-cells expressing a cytotoxic phenotype. Malignant lymphoma is rarely associated with Behcet's disease as only 12 cases have been reported in literature including a case of cutaneous t-cell lymphoma. We report a new case of cutaneous gamma-delta T-cell lymphoma emerging in the course of Behcet's disease in a 40-year-old man. Diagnosis of cutaneous gamma-delta T-cell lymphoma was established based on the combination of clinical, histological, immunophenotypical and molecular findings. Through a review of the current literature, we analyze the unique clinicopathological, molecular and immunohistochemical features of this rare cutaneous lymphoma.

P-486

An inaugural association in skin tumours:melanoma and trichoblastoma: A new entity.

Heifa Azouz, Amina Mekni,Inès Chelly,Khadija Bellil, Selma Bellil, Nidhaleddine Kchir, Moncef Zitouna, Slim Haouet.

Department of pathology, Hospital LA RABTA,BAB-SAADOUN. TUNISIA.

INTRODUCTION: The coexistence of two neoplasms within a single cutaneous lesion is rather uncommon. The combination of malignant melanoma and basal cell carcinoma within a single tumour is an unusal finding. We report herein, the association of malignant melanoma and trichoblastoma that had never been reported yet at our knowledge.

CASE REPORT: we report a case of a melanoma colliding with a trichoblastoma on the head of a 69 year old north african man, the patient had a prior history of multiple trichoblastomas on the scalp. He presented with 3/2/1 cm purple, black firm exophytic and eroded mass on the scalp. He had surgical excision. Histologically, the tumour presented a dual pattern of trichoblastoma intermingled with typical features of malignant melanoma..Immunohistochemical studies for cytokeratin highlited the epithelial componement and studies for S100 protein and HMB45 confirmed the melanocytic componement.

To our knowledge, this is the first description of melanoma with non pigmented trichoblastoma. The diffrential diagnosis, pathogenesis and prognosis of this collision tumour are discussed.

P-487

Nodular form of Kaposi sarcoma.

Cegan M., Dvorackova J.,Ceganova L., Uvirova M., Tichy M.Ticha V., Cejka P., Machackova A., Sterba J., Ziak D.

CGB laboratory Corp. Ostrava, FNO Ostrava, LFUP FN Olomouc, Pathology Department Sumperk, Czech Republic

Hereby we report a case of a 67 years old female. Examined skin biopsy from upper thigh of patient with negative anamnesis. The lesion had ovoid-nodular borders growth patern, without encapsulation (4×3 mm) formed with spindle elements, with high mitotic and proliferation aktivity.

Kaposi's sarcoma (KS) is an aggressive localized tumor of endothelial cells (including blood and lymph vessels) that is characterised by the multifocal skin lesions. Mucous membrane, lymphatic glands and internal organs might be affected as well. While KS is classified as tumorigenic, it is not very well understood whether it occurs as a monoclonal proliferation of a single malignant cell or whether it is of a polyclonal, hyperplastic-reactive origin. The results of several studies indicate that at the onset of the disease is an altered hyperplastic-recative cell that further proliferate. The disease is typically described in association with HHV-8 (human herpes virus-8) infection and several genetic abnormalities including gain of 8q and 1q, loss of 3p and 7q22, 8p11, 13q11 and 19q13 rearrangements. However, the data obtained from either earlier or later stages utilizing comparative genomic hybridization remain controversial. Here, we show in our case monosomy of chromosome 17 utilizing FISH method on paraffin sections. Interestingly, we did not observe the previously reported abberations of gain of 1q and 3q associated with diagnosed KS.

P-488

A SERIES OF 10 CASES OF PRIMARY CUTANEOUS DIFFUSE LARGE B-CELL LYMPHOMA, LEG TYPE, & THEIR RELATION TO EBV

A.Padron, M. Arumi-Uria, F. Gallardo1, C.Barranco, R.Pujol1, A.Munne, S.Serrano.

Pathology and Dermatology Deparment1, Hospital del Mar-IMIM, Barcelona, Spain.

Background: In general, primary cutaneous B-cell lymphomas present an indolent course, but a subtype having a worse prognosis and specific immunophenotypical characteristics has been recognized by the EORTC. This subtype is known as diffuse large b-cell lymphoma, leg type, and it predominantly affects the inferior extremities of the elderly. It is made up of sheets of large lymphoid cells with rounded nuclei and prominent nucleoli, similar to centroblasts or immunoblasts. In an intense manner, cells express Bcl-2, Bcl-6 and Mum-1. They do not express CD30. We present here a peculiar case of this type of lymphoma in which the expression of CD30 was observed to coincide with infection by EBV. We carried out a study on a series of 10 cases. In the literature, very few similar cases have been cited, and it is unknown if a relationship between EBV and the physiopathology of this entity exists or if this is only a chance discovery.

Material and methods: We selected 10 cases with a diagnosis of primary cutaneous diffuse large B-cell lymphoma, leg type, which were reviewed from morphological, immunohistochemical, molecular and cytogenetic perspectives by two independent pathologists. After conducting a study using *in-situ* hybridization, we found the expression of CD30, along with the presence of RNA for EBV, in this series.

Results and Conclusions: We observed the coincidence of the expression of CD30 and the presence of RNA for EBV in the tumoral cells of only one of the 10 cases studied. The similarity of this case, in particular, with the case described in the Literature leads us to suspect that a relationship, not yet studied, exists between both variables. In order to prove this, perhaps it would be necessary to increase the number of cases in the series for study.

We observed the coincidence of the expression of CD30 and the presence of RNA for EBV in the tumoral cells of only one of the 10 cases studied. The similarity of this case, in particular, with the case described in the Literature leads us to suspect that a relationship, not yet studied, exists between both variables. In order to prove this, perhaps it would be necessary to increase the number of cases in the series for study.

We observed the coincidence of the expression of CD30 and the presence of RNA for EBV in the tumoral cells of only one of the 10 cases studied. The similarity of this case, in particular, with the case described in the Literature leads us to suspect that a relationship, not yet studied, exists between both variables. In order to prove this, perhaps it would be necessary to increase the number of cases in the series for study.

P-489

ROLE OF STEROID RECEPTORS IN BIOLOGICAL BEHAVIOUR OF CUTANEOUS MELANOMA

Stefania Staibano1, Massimo Mascolo1, Guido Molea2, Massimiliano Scalvenzi3, Gennaro Ilardi1, Loredana Nugnes1, Maria Luisa Vecchione1, Anna Somma1, Gaetano De Rosa1

1Department of Biomorphological and Functional Sciences, Pathology Section; 2 Dpt Plastic Surgery; 3 Dpt Dermatology, "Federico II" University, Naples, Italy

Background: In the last two decades, the incidence of skin cancers and, in particular of cutaneous malignant melanoma (CMM), has shown a progressive increase. Recent improvement of diagnostic techniques have lead us to diagnose most CMM at an early stage: nevertheless, the death rates from CMM have not yet significantly decrease. The traditional clinical and pathological parameters are unable to provide a precise outcome prevision. For this reason, attempts continue to be made to find new molecular prognostic markers for this tumour. Experimental and clinical evidence indicate that sex hormones have a pivotal role in the growth of several type of human cancers.

The data existing about the relationship between the biological behaviour of CMM and sex hormones are conflicting. Epidemiological data indicate that melanomas metastasize with higher frequency in male than in female, and that the survival after metastasis is longer in female than in male patients.

The aim of this study was to analyze whether sex hormones (oestrogen, progesterone and androgens) could be have a significant role in determining CMM growth.

Methods: The study was performed by immunohistochemistry: oestrogen receptor (ER)-alpha, ER-beta, progesterone receptor and androgen receptor (AR) expression was evaluated on a selected series of CMM (formalin-fixed, paraffin-embedded tissue).

Results: The results were correlated with the clinical and pathological data and with patient's outcome. In addition, the findings were correlated with the age-group category of patients (young patients: 0–44 years versus older patients) and, for female, with pre-menopausal, post-menopausal, or pregnancy state.

Conclusion: The significance of the different expression of steroid receptors in our series of CMM was discussed. Moreover, consideration about the use of steroids as therapeutic targets in the treatment of CMM was also made.

P-490

GLYCERALDEHYDE 3-PHOSPHATE DEHYDROGENASE (GAPDH) AND GROWTH ARREST PROTEIN 7 (GAS7): TWO NOVEL CANDIDATE GENES INVOLVED IN THE PROGRESSION OF CUTANEOUS MALIGNANT MELANOMAS

David Ramos, Ana Pellín, Jaime Agustí, Martín Abba, Liria Terrádez, Esperanza Jordá, Antonio Pellín, Carlos Monteagudo

Department of Pathology. Medical School. University of Valencia. Spain

Background: The glycolitic function of glyceraldehyde-3-phosphate dehydrogenase (GAPDH) has been widely reported in nearly all cell types. However, the non-glycolitic role of this molecule has been recently described with prognostic importance in diverse tumor models such as breast and renal cancer, and, interestingly, also in melanoma patients. Otherwise, the biological role of growth arrest protein 7 (GAS7) as a tumor suppressor gene or as an immunomodulator has been only elucidated in central nervous system neoplasms and in malignant cutaneous melanomas.

Methods: A molecular and immunohistochemical study was carried out in a series of 74 melanoma patients including primary (< 1 mm, 15 patients; and ≥ 1 mm lesions, 16 patients) and metastatic conditions (in-transit, lymph node and organ metastases; 17, 13 and 13 patients, respectively). GAPDH and GAS7 gene expression was evaluated by means of immunohistochemistry (protein) and quantified by Real Time PCR (mRNA). For the immunohistochemical study, a tissue microarray was constructed and each case was analyzed by triplicate. Additionally, the presence of point mutations in specific exons within these two genes (codon 175 in GAPDH and codon 225 in GAS7) was analyzed by using a c-DNA sequenciation methodology. To determine the statistical correlation between variables and the distinct melanoma groups, univariate statistical tests were utilized (chi-square, ANOVA and Fisher's tests).

Results: In univariate statistical studies, a remarkable loss of GAPDH and GAS7 m-RNA expression levels demonstrated the strongest statistical differences between primary and metastatic melanomas ($p<0.05$). This finding was also corroborated at the immunohistochemical level. Unfortunately, point mutations in specific exons were not encountered.

Conclusion: Differences in GAPDH and GAS7 gene expression levels in human malignant cutaneous melanomas may act as the trigger changes leading tumor cells through the final phases of the disease.

Supported by a specific grant: "AP060/07 de la Conselleria de Salut. Generalitat Valenciana. Valencia. Spain".

P-491

Podoplanin expression in tumor cells of canine mastocytoma. A case report

Marius Raica (1); Pusa Gaje (1); Narcisa Mederle (2); Anca Maria Cimpean (1)

(1) "Victor babes" University of Medicine and Pharmacy, Department of Histology and Cytology, Timisoara, Romania; (2) University of Agricultural Sciences, Faculty of Veterinary Medicine, Timisoara, Romania

Background. Mastocytoma is a frequent tumor in dogs and rare in human. In the dog, mastocytoma represents between 9 and 15% from all tumors of the skin. The histochemical and immunohistochemical features are highly specific for the diagnosis, but the molecular profile is not completely characterized. Podoplanin is a well known marker of the lymphatic endothelium, but is not entirely specific. Its expression was found in some malignant human tumors and it was not reported in animal tumors. The present case report shows a multiple mastocytoma with tumor cells with expression of podoplanin. Case report. A 9 years old dog was admitted with four tumors, located in the skin of the nose and abdomen. One ulcerated tumor from the nose and one non-ukcerated from the abdomen were removed and specimens were fixed and embedded in paraffin. Sections were stained with haematoxylin-eosin, toluidine blue, alcian blue-safranin pH1.42, mast cell tryptase, CD117, and podoplanin (clone 18H5).Results. A diffuse proliferation with medium sze polygonal shaped cells was found in the dermis, extended to the subcutaneous tissue. Nuclear atypia were moderate and rare mitotic figures were found. All tumor cells were positive for toluidine blue and alcian blue-safranin. The diagnosis was confirmed by immunohistochemistry with mast cell tryptase and CD117. All tumor cells were positive with strong of moderate intensity for podoplanin, with diffuse cytoplasmic.pattern. There were not found differences in the expression of the markers used in the study between the two specimens.Conclusion. It is reported a case of a multiple canine mastocytoma with tumor cells expressing podoplanin. To the best of our knowledge, it is the first report on podoplanin expression in mastocytoma tumor cells.

P-492

Syringocystadenoma papilliferum with features of proliferating trichilemmal tumor

Gulcin Guler Simsek; Ayla Tezer; Heyecan Ökten; Servet Güreşçi; Hakan Buluş; Ali Coşkun

Kecioren Eğitim Araştırma Hospital, Turkey

Syringocystadenoma papilliferum is an uncommon benign tumor of an apocrine type appendages. It usually arises upon nevus sebaseus. This case is an unusual one with dense keratinization of trichilemmal type and inwards of squamous epithelium looking as nests of squamous cells simulating squamous cell carcinoma.

P-493

Masson's Hemangioma: A Lesion Often Mistaken for Angiosarcoma

Heyecan Ökten; Gulcin Guler Simsek; Ayla Tezer; Sibel Gelecek Geyik; Ali Coşkun

Kecioren Egitim & Arastırma Hospital, Turkey

Intravascular papillary endothelial hyperplasia (Masson's hemangioma) is an unusual benign, non-neoplastic, vascular lesion characterized histologically by papillary fronds lined by proliferating endothelium. The main significance of intravascular papillary endothelial hyperplasia is its clinical and histological resemblance to soft-tissue sarcoma and possible misinterpretation as such. An otherwise healthy 52-year-old white man had nodular lesion of the foot. Pathologic analysis demonstrated the mass to be a Masson's hemangioma, a papillary proliferation of thin-walled capillaries intimately associated with thrombus. Considered a benign intravascular lesion, the treatment of choice is complete excision. The lesion has a propensity to occur in the head, neck, fingers, and trunk. There is only one case in the literature, described this lesion on the foot. In 1923, Masson regarded this disease as a neoplasm inducing endothelial proliferation, however, now it is considered to be a reactive vascular proliferation following traumatic vascular stasis. The recognition of the morphologic features of this lesion and its inclusion in the differential diagnosis of vascular mammary tumors will reduce the likelihood of its misdiagnosis as an angiosarcoma and avoid unnecessary and aggressive therapy.

P-494

Histopathological spectrum of Grover's disease: a review of 52 cases

Pablo Cannata; M Teresa Fernandez-Figueras; Miriam Cuatrecasas*; Rosa M Penin; Luis Puig*; Carlos Ferrandiz; Aurelio Ariza**

Hospital Universitari Germans Trias i Pujol. Hospital de la Santa Creu i Sant Pau. Area de Diagnòstic Anatomopatològic**, Spain*

Background: Grover's disease ("transient acantholytic dermatosis") is a dermatosis of unknown cause, characterized microscopically by acantholisis that frequently is associated with dyskeratosis of individual keratinocytes. Histopathologically, the lesions tend to adopt features

similar to pemphigus (P), Darier's disease (D), Hailey-Hailey's disease (H-H) and spongiotic (E). A superficial lymphohistiocytic infiltrate is usually present and eosinophils are a common finding.
Method: Microscopical evaluation of 52 cases of Grover's disease.
Results: In 28 cases, the lesions involved ≥2 mm of the epidermal suface. The patterns observed where D: 25, P:24, E:12 and H-H:7. In 14 cases there was coexistence of more than one pattern. In two cases the infiltrate extended deeply into the dermis and in most biopsy specimens (43) eosinophils where found in significant amounts. Neutrophils where also common at the base of the lesions or forming subcorneal pustules (42) and in 35 cases vasculopathic changes such as endothelial tumefaction, erythrocyte extravasation or iron deposition where identified.
Conclusions: In our study the lesions tended to involve wider areas of the epidermal surface than is stated in the literature and we frequently found hints of vascular damage and neutrophilic infiltrate. These findings that have been overlooked in previous studies.

P-495

Superficial acral fibromyxoma. A review of five cases

Esther Sanfeliu; Ruth Orellana; Amparo Saez; Maria Rosa Escoda; Sara Fernandez; Merce Rey
Corporació Sanitària Parc Taulí de Sabadell, Spain

BACKROUND: Superficial acral fibromyxoma (SAFM)is a rare soft tissue tumour which has recently been described by Fetsch, as aproliferation of spindle/stellate cells embedded in a predominantly myxoidmatrix with accentuated microvasculature. METHOD: Five resected cases of SAFMwere reviewed from our files (2003 to 2007). Collected clinicopathologic datawere: sex, age, location, visit's reason, cellular type, atypia, mitosis count,stroma, other histological findings, immunoreactivitiy (CD34, vimentin, CD99,EMA, S-100 protein and muscle specific actin) and surgical borders. RESULTS: There were four men and one woman (age range:28 to 73 years). Toe was common affected site. Reasons for visit were nodulararappearance in three patients, cystic lesion and posttraumatic onychogryphosisin others. All cases had proliferation of spindle cells, increase number ofblood vessels and mast cells. Three showed myxoid stroma and two myxoid andcollagenous matrix. Tumour cells had slight nuclear atypia in two cases andfocally moderate in one case. Mitotic figures were infrequent or inexistent.All cases showed immunoreactivity for CD34 and vimentin, and negativity forS-100 protein and muscle specific actin (HHF35); three stained for CD99 and twostained weak focal for EMA. Surgical borders were invaluable in two, affectedin other two and free in last one. No tumour recurrence appeared (follow-up 53to 2 months). CONCLUSION: SAFM represents a new entity in spectrum of softtissue tumours, including myxoid and mesenchymal neoplasms. Moreover, the widerange of appearances required making a differential diagnosis with fibroushistiocytoma, dermatofibrosarcoma protuberans, superficial angiomyxoma,acquired fibrokeratoma, sclerosing perineurioma, acral myxoinflammatoryfibroblastic sarcoma, digital myxoma, ossifying fibromyxoid tumour, low-grade myxofibrosarcoma,myxoid neurotheketoma, myxoid neurofibroma and solitary fibrous tumour.

P-496

TYROSINASE A USEFUL MARKER FOR IDENTIFYING PAGETOID INVASION IN MALIGNANT MELANOMA

Sabina Zurac* **; Gabriela Negroiu*;
Florica Staniceanu* **; Alexandra Bastian**; Razvan Andrei**; Luciana Nichita*; Stefana Petrescu***;
NOTE: Zurac and Negroiu should be regarded as first authors in equal contribution**
Carol Davila University of Medicine and Pharmacy; **Colentina University Hospital; * Institute of Biochemistry of the Romanian Academy, Bucharest, Romania*

Background: In most of the cases, malignant melanoma (MM) is diagnosed based on hematoxilin-eozin (H&E) appearance, supplemental investigations being performed in a minority of cases. We address our study to differentiation between particular types of nevocellular naevi (predominantly junctional, lentiginous or displastic) and MM. In these cases, one of the clues of differentiation is the presence of melanoma cells within the superficial layers of the epidermis (pagetoid growth). This feature is not always easy to interpret on H&E, immunohistochemical stains being necessary.
Method: We studied 23 cases of thin MM (nontumorigenic MM with Breslow score less than 1 mm). We analyzed the presence of pagetoid growth in consecutive slides stained with H&E, S100 protein, HMB45, tyrosinase and TRP2. The number of the invading melanoma cells was counted in each high power field, the highest figure being attributed as the score for each slide. The scores recorded in immunohistochemical stains were compared with those recorded in H&E for the same case. Statistical analysis was performed using EXCEL and EPIINFO programs (statistical significance $P<0.05$).

Results: The presence of epidermal invasive melanoma cells was noticed in all but 3 cases in H&E stains. The extent of pagetoid invasion revealed by S100 protein and H&E was similar. HMB45 was intense positive in all the cases with slightly more numerous intraepidermal invasive cells comparing with H&E (statistically unsignificant). TRP2 showed slightly more numerous cells in pagetoid growth than HMB45 but not significant comparing with H&E. Tyrosinase highlighted most numerous pagetoid spreading cells, the differences being statistically significant comparing both with HMB45 and H&E.
Conclusion: Tyrosinase is a useful marker for pagetoid invasion comparing with other immunohistochemical markers or H&E, helping in differentiating MM form naevi with prominent intraepidermal compartment.
Supported by National Authority for Scientifical Research, Excellence Research Program, 2006–2008

P-497

Multicentric reticulohistiocytosis. Report of a case presenting with clinical features of dermatomyositis.

Flavia Guzmán; Anna Mozos; Antonio Guilabert; Esteve Darwich; Marc Juliá; Josep Palou; José Manuel Mascaró; Llúcia Alós
Pathology and Dermatology Departments. Hospital Clinic, Universitat de Barcelona. Spain.

Background: Multicentric reticulohistiocytosis (MRH) is rare disease of unknown etiology and probable immunologic basis, characterized by a skin papulonodular eruption. This disorder often courses with destructive polyarthritis, and can be associated with other diseases and malignancy. The clinical presentation of MRH mimicking dermatomyositis has been reported previously.
Case Report: A 72 year man presented with muscular weakness and skin lesions for six month. The skin lesions were confluent papules and nodules in the extension areas of both hands, fingers, elbows and knees. Moreover, small periungual nodules (coral beads) and in both ears were seen. Muscular biopsy was normal. The biopsies of two of these skin lesions showed a superficial and deep dermal infiltration of histiocytes, some of them multinucleated, with large eosinophilic, granular cytoplasm with ground-glass appearance. These histologic characteristics were diagnostic of MRH. The patient had also arthritis in both knees. Screening for neoplasms was negative.
Conclusion: MRH can present with clinical features of dermatomyositis. Our case emphasizes the usefulness of histologic study of the skin lesions to differentiate both conditions and perform a correct diagnosis and treatment.

P-498

Clinico-pathological findings in a series of cutaneous sea-urchin granuloma

Begoña Vieites; Iosu Antón; José Antonio Ortíz-Rey; Emilio del Río; Hugo Váquez-Veiga; José Manuel Suárez-Peñaranda
Complejo Hospitalario Universitario de Santiago de Compostela, Spain

Background:Injuries cause by sea-urchin spines are only rarely reported in the medical literature. They occur usually in the hands and feet and tend to heal after forced or spontaneous extrusion of most of the foreign material. Rarely, papules or small nodules appear after some weeks in the sites of injury, and tend to persist unless treatment, usually surgery, is applied. Histologically, they show granulomatous inflammation, classically described as sarcoid-type.Results:We have retrospectively evaluated 23 skin biopsies from 20 patients (16 males, 4 females, ages ranging from 23 to 68 years) with the diagnosis of sea-urchin granuloma and definite antecedent of sea urchin injury. Most lesions were solitary and located in the dorsum of the hands (8 cases), fingers (7 cases) and forearm (4 cases). Intervals from puncture ranged from 2 weeks to three years, and it was usually comprised between 1 and 6 months (9 cases). The lesions were most commonly described as nodules (13 cases).Histopathological examination revealed the presence of granulomas in all but one case. In 14 out of the 23 biopsies, the inflammation was predominantly granulomatous. Sarcoid granulomas were the predominant inflammation pattern (11 cases) but suppurative and necrobiotic granulomas were also common. In many cases, more than one type of granuloma could be seen. In 4 cases, acute or chronic, non-granulomatous, inflammation was the predominant finding. Surgery was the elective treatment in all cases and antibiotics were added in four.Conclusion:Sea-urchin granuloma encompasses a wide morphological spectrum of granulomatous reaction involving the dermis and the subcutaneous fat tissue. Histopathological findings are not specific and mixed patterns of inflammation are common. Documentation of previous sea-urchin injury and clinico-pathological correlation are necessary for the diagnosis.

P-499

Malignant proliferating trichilemmal tumour of the scalp: Report of a case and review of the literature.

Nesrine Knani, Amel Trabelsi, Wided Stita, Badreddine Sriha, Soumaya Rammeh, Sadok Korbi
Departement of Pathology, Farhat Hached Hospital, Sousse, Tunisia

Bakckground: Malignant proliferating trichilemmal tumour is a rare skin tumour that originates from the root sheath of the hair. It mimicks poorly differential squamous cell carcinoma ant its biological behaviour is unpredictable, because rarely can produce distant metastases.
Methods
Results: we report on a case of a malignant proliferating trichilemmal tumour of the scalp in a 76-year-old man and we discuss the clinicopathologic features of this entity.
Results: Our patient proceeded with a cystic lesion in the scalp measuring 8 cm. The lesion was removed with wide excision. The histological examination of the lesion revealed a malignant proliferating trichilemmal tumour. Eleven months after the excison, the patients is free of disease.
Conclusion: Malignant proliferating trichilemmal tumours are rare malignant lesions that affect mainly older women. The appropriate treatment includes wide resection and dose postoperative follow-up of the patient to facilitate the early diagnosis of distant metastases.

P-500

intravascular lobular capillary hemangioma: a rare intravascular tumor (report of two cases)

Raquel Beloqui; Maria Luisa Gomez-Dorronsoro; Palmira Malo; Carla Valentí; Irene Amat; Maria Asunción Arrechea; María del Rosario Mercado
Hospital de Navarra, Spain

BACKGROUND Lobular capillary hemangioma (LCH), also known as pyogenic granuloma is a frecuent benign vascular tumor. Intravascular lobular capillary hemangioma (ILCH) is a rare form of LCH in which the angiomatous proliferation is confined within a lumen of a vein.
METHOD We report 2 cases of ILCH involving the periophthalmic region in two male patiets (25 and 65 years old).
RESULTS The two lesions are similar and consist of an intraluminal polyp attached to the vein wall and composed of lobules of capillaries lined by flattened or rounded endothelial cells and separated by a fibromyxoid stroma. Angiomatous lobules usually can be demostrable in the adjacent venous media.
CONCLUSION ILCH was described by Cooper et al. in 1979. They described 18 cases, all of which arose in veins of the superficial soft tissues in the neck or upper limbs of young or middle aged adults. Since then only 4 cases have been described in the periocular adnexa region. Distinction from other primary intravascular neoplasm like intravascular papillary endothelial hyperplasia (Masson's tumor), malignant endovascular papillary angioendothelioma (Dabska tumor) and epithelioid hemangioendothelioma is straightforward.
ILCH is a benign lesion that is usually cured by local excision.

P-501

CXCR2 Expression and Progression of Cutaneous Melanoma

Liria terrádez; Núria Santonja; Carlos Monteagudo
Hospital Clínico Universitario, University of Valencia, Spain

BACKGROUND: Incidence of cutaneous malignant melanoma (MM) has been increasing worldwide in the last decades. There are evidences supporting a role for chemokines and their receptors in MM progression and metastasis. In this regard, expression of CXCR1 and CXCR2 receptors in MM has been suggested to be involved in vessel density, aggressiveness and metastatic potential.
METHODS: We examined the expression of CXCR2 in human MM by inmunohistochemical analysis of 71 tumors on tissue arrays from formalin-fixed, parafin-embebed specimens including 30 primary cutaneous MM: 14 thin, and 16 thick; and 41 metastatic MM: 16 in transit metastases, 12 metastases in regional lymph nodes, ans 13 distant metastases. A histoscore was established to evaluate the intensity of the immunostaining and the percentage of positive tumor cells.
RESULTS: Comparative analysis of the expression between the different groups of tumors yielded the following results:

- CXCR2 expression was lower in thin than in thick MM.
- The expression of this receptor was higher in "in transit" metastases than in thin primary tumors.
- A lower expression of CXCR2 was found in lymph node and distant metastases compared to primary MM and "in transit" metastases.

CONCLUSIONS: Differences on CXCR2 expression between thin and thick primary MM may reflect differences in metastatic potential between both groups. Our results support the implication of CXCR2 overexpression in cutaneous "in transit" metastases of MM, but not in lymph node and distant metastases.

P-502

Nevoid basal cell carcinoma syndrome- the importance of early diagnosis and proper treatment

Boris Vodopivec (1); Ciril Trcek(2); Boris Jancar(3); Maja Jerse(1)

(1) Insitute of Pathology, Medical Faculty, University of Ljubljana; (2)Department of Otorinolaringology and Cervicofacial Surgery, University Medical Centre Ljubljana; (3) Institute of Oncology Ljubljana, Zaloška 2, Slovenia

Background: Nevoid basal cell carcinoma syndrome (NBCCS) is a rare autosomal dominant disorder, caused by mutation of a tumour supressor gene (PTCH) on chromosome 9q22.3-q31. It is characterized by multiple basal cell carcinoma (BCC) of the skin, odontogenic keratocysts, skeletal anomalies, ectopic calcification and a predisposition of additional neoplastic processes.

Methods: We are presenting 30-year-old male, mentally retarted, with NBCCS, who had undergone resection of multiple BCC of his forehead 6 years earlier. Also facial dismorphisms, as flat occipital area, broad forehead, deep set eyeballs, hypertelorism, epicanthus, broad nasal root and tip, thin upper lip and tooth anomalies, had been observed. Three years later BCC of the forehead and a new tumour mass at the left mandibular angle had occured. CT scan had revealed destruction of the frontal bone with tumour invasion into the frontal lobe of the brain. Irradiation therapy had achieved significant improvement. After two years he had presented with metastases of BCC, confirmed by fine-needle biopsy, in the right submandibular and preauricular area, that had been successfully treated by irradiation therapy. At current examination, he was hospitalized due to massive haemoptysis and died the same day after admission.

Results: Autopsy macroscopically revealed extensive destruction of frontal and ethmonasal bones by tumorous mass, that was observed also in the right submandibular region. As well, lamellar calcification of the falx cerebri and palmo-plantar pits were detected. On the trunk and extremities numerous exophytic masses were presented. Histology showed numerous BCC metastases in the lungs, mediastinal lymph nodes, liver and spleen. The observed lesions of the skin were confirmed as BCC or epidermoid cysts.

Conclusions: BCC occurence in young person other than in NBCCS is exceptional. The diagnosis, carefull monitoring and proper treatment, such as surgical wide excision is mandatory. As well, avoiding sun exposure and radiation is essential.

P-503

Mesenchymal tumour in dermis

Carlos Hörndler*; Mar Pascual*; Isabel Marquina; Ana Fuertes*; Guillermo Muñoz*; Patricia Sota***

**Hospital Universitario Miguel Servet; **Hospital de Alcañiz, Spain*

Background: Dermatomyofibroma is a distinct clinicpathological entity into the group of mesenchymal cutaneous neoplasias with myofibroblastic differentiation. It is frequently found in young women, in the region of the shoulder and also in the upper trunk.

Case report: We present the case of a 13 year-old female with an acquired lesion in presternal skin, with no traumatic antecedents. A sample of skin is received,which has a superficial, lightly raised, greyish lesion of 5×4 mm in its great dimension.

Results: Histologically, a proliferation in upper dermis is observed, formed by cells with ill-defined citoplasm and oval nucleus with no atipia; these cells are characteristically arranged in bundles and fascicles parallel to the skin surface. Immunohistochemically, cells express vimentin and smooth muscle actin and are negative for desmin, CD 34, S100 and epithelial markers. Diagnosis is dermatomyofibroma.

Comments: Dermatomyofibromas are benign mesenchymal cutaneous tumours with myofibroblastic differentiation, with a typical arrangement of fascicles parallel to skin surface. This entity was first described by Kamino et al. in 1992 with this name and previously in 1991 by Hügel as "dermic fibromatosis plaque-like". Less than 60 cases of dermatomyofibroma have been reported, mostly in adult women. Differential diagnosis includes hypertrophic scar, dermatofibroma, pilar leiomioma, neurofibroma, adult myofibromatosis, extraabdominal fibromatosis and dermatofibrosarcoma protuberans plaque-stage. For the latter, the immunohistochemical pattern helps; our case is positive for smooth muscle actin and vimentin and negative for factor XIIIa, CD 34 and S100. As for behaviour, they are benign tumours that usually do not recur.

P-504

Metastatic renal cell carcinoma: an able mimicker of a wide range of skin lesions

John Lara; M Teresa Fernández-Figueras; Oria Rosiñol; Purificación Parrales; Gustavo Tapia; Aurelio Ariza

Hospital Universitari Germans Trias i Pujol, Spain

Background: Cutaneous and mucosal metastases from renal cell carcinoma are uncommon, although in some cases they

can be the first manifestation of the disease, causing serious problems of differential diagnosis due to their similitude to certain dermatological neoplasms.
Method: The clinicopathological characteristics of four patients with skin metastasis at the time of presentation are reviewed.
Results: All patients were males and their ages ranged from 43 to 74 years. One case presented with multiple papules on the trunk with microscopical appearance similar to a sweat gland carcinoma. The other three lesions were solitary and located in the tongue, thorax and foot. The lingual lesion was composed of nests of spidle and epithelioid cells that showed focal epitheliotropism simulating a melanoma. The other two ones simulated clear cell sweat gland tumors.
Conclusion: Cutanous metastatic renal cell carcinoma is an able mimicker of a wide range of primary skin neoplasms. It is important to keep in mind this option in the differential diagnosis of clear cell, spindle cell and ductal tumors. In suspicious cases, a panel of immunohistochemical markers and ultrastructural studies can be helpful to rule out or confirm this possibility.

P-505

MERKEL CELL CARCINOMA OF THE SKIN STAINING PATTERN

Natalia Camarasa Lillo; Esther Roselló Sastre; Jorge Escandón Álvarez; Maria Luisa Pérez Ebri
Hospital Universitario Doctor Peset, Spain

Background Merkel cell carcinoma (MCC) is an unusual and aggressive primary neuroendocrine carcinoma of the skin, that mainly affects sun-exposed areas of elderly people. They recurre locally in 22–46% of patients, have regional metastases in up to 75% of patients, and have a five year survival between 30 and 64%. The aim is to determine an immunohistochemical pannel to allow distinguishing MMCs from other small round blue cell tumours and to study plausible of the prognostic markers.
Method Six cases and 2 recurrences of MCCs were identified over the last 8 years in a retrospective analysis of the cutaneous tumour registry from our hospital. Paraffin sections were stained for chromogranine, CK20, BCL-2, TTF-1, C-KIT, P53, P16, Ki67, EGFR and CD99.
Results Reactivity with chromogranine, BCL-2 and P16 was demostrated in all cases, as well as CK20. The staining patterns for CK20 ranged from punctate (perinuclear) to localized or diffuse. No one expressed nor TTF-1 neither CD99. C-KIT and EGFR were focally positive in 2 cases. P53 was positive in 3 cases in more than 80% of neoplastic cells. Ki67 was expressed in more than 35% of cells in 4 cases and in less than 10% in 2 cases.
Conclusion We note that the classically described perinuclear dotlike keratin staining pattern is the predominant but not the only one. We differ from the literature that nor the majority neither one third of MMCs express C-KIT and CD99 respectively. Universal staining for P16 can be used for diagnostic purpose and it raises the possibility of an HPV relation. Positive staining for EGFR could predict sensitivity for specific treatment. Both the positive and negative elements of the staining profile of MCCs provide additional useful diagnostic information for the differential diagnosis between MCC and other carcinomas that may simulate it.

P-506

Combined malignant melanoma and basal cell carcinoma tumor of the intermingled type: case report and rewiew of the literature

Carmen Admella Salvador; Gemma Sais Puigdemont; Maria Jose Fantova Cosculluela; Carmen Ferrer Cassado; Olga Garcia Vidal
Mataró Hospital. Consorci Sanitari del Maresme, Spain

Background: The coexistence of two different malignant skin tumors in the same histologic specimen is an unusual finding.
Case Report: A 76-year-old man with a nodular tumor on the front showing a combination of malignant melanoma (MM) and basal cell carcinoma (BCC).
Results: A 1,2 cm. nodular non-pigmented lesion on the front was considered clinically as BCC or epidermal appendages tumor. Histologic examination showed a nodular tumor consisting of a BCC nodulocystic variant and a nodular MM located adjacent as well as admixed within the epitelium of the BCC. The MM showed no junctional component and measured 6 mm in thickness.The diagnosis of the two neoplasms were confirmed by immunohistochemical studies: BCC cells showed a keratinocytic phenotype (cytokeratins, p63) and tumor cells of the MM a melanocytic phenotype (HMB-45, Melan-A, S100 protein).
Conclusion: The combination of MM and BCC in a single tumor is extremely rare and a chance occurrence. These tumors were described as combined, colliding, basomelanocytic, biphasic, contiguous or even parasitic or metastasic. The few cases reported were located on the upper part of the body, mainly in the trunk/back and are more frequent in male being the mean age of 61 years. The clinical picture is rather variable and does not point to the diagnosis. There are two variants: a collision type in which components of each cell type are clearly demarcated and an intermingled type in which both cell types grow intimately together almost on a single-cell level.

P-507

Cutaneous reactive intravascular histiocytosis

Susana Moyano; Lluis Colomo; Jose Manuel Mascaró; Antonio Martínez; Elías Campo; Llúcia Alós

Departments of Pathology and Dermatology, Hospital Clínic, IDIBAPS, University of Barcelona, Spain

BACKGROUND Reactive intravascular histiocytosis is a rare entity, of unclear pathogenesis. It has a broad clinicopathologic spectrum, and some cases have been associated with rheumatoid arthritis and other systemic diseases. It has been related to early stages of reactive angioendotheliomatosis.

CASE REPORT A 60 year-old man presented with asymptomatic thoracic cutaneous lesions. They were erythematous and reticulated papules, some of them with purpuric appearance, clinically suggestive of a vascular lesion. A complete clinical study ruled out any associated disease. Two biopsies of these lesions were performed and both showed similar histological characteristics. In the papillary and reticular dermis irregular dilated vascular structures were seen. In the lumina of these vessels there were mononuclear cells with abundant cytoplasm, of histiocytic appearance, without atypical cytologic features. These cells were positive for CD68 and CD31. Other tested markers (CD1a, S-100, CD45, CD20, CD79a, CD3 and CD34) were negative.

CONCLUSION The cutaneous reactive intravascular histiocytosis is a benign process that can present without any other condition, and probably represents an initial phase of reactive angioendotheliomatosis. The differential diagnoses include benign and malignant vascular lesions, and intravascular large B-cell lymphoma, which has an aggresive clinical course.

P-508

Prognostic relevance of mitotic rate in patients with melanoma

Sorin Dumitriu; Doinita Radulescu; Simona Stolnicu; Loredana Ungureanu

University of Medicine and Pharmacy "Gr.T.Popa" Iasi, University of Medicine and Pharmacy Tg. Mures, Romania

Background Interest in the prognostic clinical relevance of biological variables has focused on a small number of factors, and among the different markers, cell proliferation can reasonably be supposed to be related to tumor aggressiveness. Recently, a renewed interest was witnessed in one of the proliferation markers first used, the mitotic rate, which is the fraction of cells in mitosis at any given time. The aim of this study was to evaluate the prognostic value of mitotic activity and the relationship with overall survival.

Method The prognostic relevance of mitotic rate was analyzed in a series of 49 patients with histologically confirmed cutaneous melanoma. Mitotic figures were counted in areas selected on the basis of the following criteria: presence of good cellularity and high density of mitotic figures.

Results The mitotic rate was categorized in 3 groups: $1/mm^2$, $1–4/mm^2$, and $>4/mm^2$ and was significantly related to 5-year overall survival (95%, 91% and 74%). In conclusion, a high number of mitotic figures is associated with a higher probability of developing distant metastases and a shorter survival. Our study shows that mitotic activity is an independent prognostic factor, possibly even more important than other biomarkers known.

P-509

Hypertrophic scars arising at the biopsy site of melanocytic lesions

Aikaterini Zioga*;Anna Batistatou*;Sevasti Kamina*; Anna Goussia*;Michael Doukas*;Evangeli Lampri*; Christina Fotika; Vassiliki Malamou-Mitsi***

Departments of Pathology and Dermatology**, Medical School, University of Ioannina, Greece*

Background: Hypertrophic scar (HS) results from an abnormal response to wounding and has been noted after a variety of local injuries. Hypertrophic scars have not been reported after biopsy of melanocytic lesions, one possible explanation being that such lesions are not biopsied in routine clinical practice. Herein, we report two cases of HS arising after biopsy of melanocytic lesions, located at the epidermis. The aim of this study was to investigate their histopathological features and pathogenesis.

Method: The patients, one male, 25-years-old, and one female, 61-years-old, underwent a 4 mm punch biopsy. The diagnoses were dysplastic junctional naevus, and lentigo maligna, respectively. After approximately two months the lesions were excised. The specimens were fixed in buffered formalin and processed for routine histopathological study. Immunostaining for vimentin, α-SMA, desmin, CD68, CD3, CD1-α, tryptase, S-100 and Ki-67 (MIB-1 clone) was also performed.

Results: In both lesions, at the area of previous biopsy, histopathological features consistent with HS were noted. These included flattening and slight acanthosis of the overlying epidermis, scarring of the papillary dermis, prominent vertically oriented blood vessels and nodular aggregates of collagen with fibroblasts. The scar remained within the boundaries of the previous biopsy. The lesional cells expressed vimentin and focally α-SMA, consistent

with their fibroblastic/myofibroblastic nature. There was no increase in the number of macrophages and T-lymphocytes, while an increase in Langerhans and mast cells was noted. Interestingly, the number of basal keratinocytes within the cell cycle (as indicated by MIB-1 immunostaining) was increased.

Conclusion: Hypertrophic scars can develop after biopsy of melanocytic lesions that do not involve the dermis, indicating that the pathogenetic mechanism is more complex than isolated dermal phenomena. The persistence of activated keratinocytes in HS epidermis indicates that epidermal processes may stimulate dermal changes. Langerhans and mast cells might be mediators in this process.

P-510

THE CORRELATION OF P53 AND P63 EXPRESSIONS WITH HISTOPATHOLOGIC SUBTYPE AND NUCLEAR MORPHOMETRIC FEATURES IN BASAL CELL CARCINOMAS

Gurkan Kertis; Burak Bahadir; Banu Dogan Gun; Sibel Bektas; Figen Barut; Nimet Karadayi; Sukru Oguz Ozdamar

Zonguldak Karaelmas University, School of Medicine, Department of Pathology,Zonguldak, TURKEY

Background: Basal cell carcinomas usually have low recurrence rate and very low metastatic potential. However, tumors with aggressive course may cause tissue destruction as well as high recurrence and metastatic rate, eventually leading to death. Since histopathological subtyping can be inadequate in determining tumor aggressiveness, immunohistochemical and morphometric parameters have also been considered. The aim of this study is to establish histopathological subtypes of basal cell carcinoma, immunohistochemical expressions of p53 and p63, and morphometric features of tumor cell nuclei by computer-assisted analysis system and eventually investigate the correlations between these parameters.

Method: 100 tumors from 92 cases, which had been diagnosed as primary basal cell carcinoma from 2001–2007 in the Pathology Department of Zonguldak Karaelmas University School of Medicine were included. The study group consisted of 92 patients, 47 male and 45 female, with an age range between 38 and 88 (average 64.34). The aggressiveness and histopathological subtypes of tumors were ascertained and p53 and p63 immunohistochemical stains were performed. About 100 nuclei with sharply demarcated contours were also included for morphometric analysis in all cases. Statistical analysis was performed; however since most tumors were nodular type and numbers of the cases with other subtypes were inadequate, correlation between histopathological subtypes and the other parameters could not be investigated by statistical analysis.

Results: Correlation between p53 and p63 staining intensity and the nuclear morphometric parameters as well as tumor aggressiveness were not statistically significant. There was a significant correlation between age and p53 staining intensity ($F=3.54$, $p=0.017$).

Conclusion: Larger series are to be studied to establish the precise correlations, if any, between the stated parameters. Nevertheless, the correlation between age and p53 staining intensity probably denoting the pathogenesis of basal cell carcinoma is noteworthy.

Key words: Basal cell carcinoma, immunohistochemistry, p53, p63, nuclear morphometry

P-511

Cutaneous manifestations of cowden syndrome

A. Palacín, Eva Bailón; Susana Puig; Antonio Mas; Josep Palou; José Manuel Mascaró; Llúcia Alós.

Departments of Pathology and Dermatology of Hospital Clínic, University of Barcelona, Spain.

Background: Cowden disease, also known as multiple hamartoma syndrome, is a rare autosomal dominant genodermatosis, with variable expression, that results from a mutation in the PTEN tumour suppressor gene. It is associated with multiple cutaneous lesions and neoplasias or hamartomas in internal organs, which especially develop in gastro-intestinal tract, thyroid and breast.

Case report: A 40 year-old male presented with small cutaneous papules in the face and upper trunk. These lesions had a smooth surface or were verrucoid, as well. In palms and soles showed traslucent punctate keratoses. The patient had a past history of testicular seminoma at the age of 20 and thyroid goiter. Few months ago also presented several polyps in esophagus, stomach and colon.

The histological study of four skin lesions were perfomed. They were trichilemmoma, an inverted follicular keratosis, a seborreic keratosis and a sclerotic fibroma.

Conclusion: In Cowden syndrome the cutaneous signs may be diverse but allow early recognition of the disease. It is important to suspect the syndrome in order to rule-out internal malignancies and perform a familial screening.

P-512

Howitt and pelisse syndrome with stenosis of vagin: A case report

Mahnaz Banihashemi. M. D.

Department of dermatolog of medical science -Mashhad-Iran

Hewitt and pelisse syndrome with stenosis of vagin: A case report
Vulvovaginal-gingival lichen planus is a distinctive erosive form of lichen planus, it is clinically very similar to mucous membran pemphigoid.
Vulvovginal ginginal lichen plans principally affect the inner aspect of labia minore, vestibula and gingival,servix may also be involved and oral lichen plan can occur. The condition is chronic and painful. Vaginal synechia and adhesion develops and leading in some cases to vaginal stenosis The manifestation of this syndrome do not necessarily all occur synchronously.
We report tow cases that had this syndrome with stenosis of vagin and oral lichen plan and gingivitis.

P-513

Langerhans cell histiocytosis of the adult presenting as a localized cutaneous lesion. A report of six cases

Eva Tejerina, Jose Jimenez Heffernan, Luis Ortega, Jesus Cuevas, Antonio Gonzalez, Felix Contreras
Hospitals Puerta de Hierro, Monteprincipe, and La Luz, Madrid, and Pathology Laboratory, Leon, Spain.

Background: Most frequently Langerhans cell histiocytosis (LCH) presents as a multisystemic disorder of young patients. Since the introduction of immunohistochemistry atypical clinicopathologic forms of LCH have been described. Among them, we would like to highlight its presentation as a single cutaneous lesion in adults. In these cases there is no clinical suspicion and the diagnosis is based on the pathologic study.
Methods: We reviewed pathologic and clinical data of six patients with LCH that presented as a single cutaneous lesion with no evidence of extracutaneous involvement.
Results: Patients age varied from 24 to 67 years. Lesions were located in the arm (3), trunk (2) and genitalia (1). Clinically they were regarded as epitheliomas (2) or non-specific tumoral lesions. Histology was similar in five cases and consisted of a polymorphous dermal infiltrate of eosinophils, lymphoid and histiocytic cells. The latter showed eosinophilic cytoplasm and a characteristic irregular nuclei with grooves. Multinucleation was seen in four cases. Eosinophils were abundant and intimately mixed with the histiocytic population. No emperipolesis or granulomas were seen. The sixth case showed a neoplastic proliferation of poligonal to spindle cells with few lymphocytes. Nuclear atypia and mitotic figures were common. In all cases histiocytes strongly expressed S-100 protein and CD1a. Isolated cells were positive for CD68. There was no expression of HMB45 or Melan A. In the follow up of these patients, no other cutaneous or extracutaneous lesions related to LCH were detected.
Conclusions: LCH may present as a localized cutaneous disease affecting adults. The most common form resembles eosinophilic granuloma located elsewhere. Immunohistochemistry is needed to confirm the diagnosis and to exclude arthropod bites. More rarely, it may present as a monomorphous neoplastic proliferation of atypical cells. These cases should be considered when faced with an atypical cutaneous tumor that strongly expresses S-100 protein.

P-514

APOCRINE HIDRADENOCARCINOMA: AN INFRECUENT SWEAT GLAND NEOPLASIA.

Alvarez R; Sota P; Alfaro J; Pascual M; Fuertes A; Muñoz G; Marquina I*; Felipo F; Del Agua C.
*Hospital Universitario MIguel Servet. * Hopital de Alcañiz, Spain*

BACKGROUND The diagnosis of hidradenocarcinoma is very difficult because nomenglature has been inconsistent, it's a rare neoplasia and variable morphology of cells composing the neoplasm.Face, hands and feet are the most usual localitations. Inmunochemistry of this tumor has been reported in only one case report.
METHODS We present the case of a 81 year-old female, with no significant personal history, to whom an asyntomatic eye nodule is detected. The diagnose before surgery was epidermoid carcinoma.
RESULTS After gross (a white, rounded nodule of 10 mm in its greatest dimension) and microscopic examination, a diagnose of apocrine hidradenocarcinoma is made.
COMMENTS Sweat glands tumours are rare. In our literature review we have found 71 published cases, and only 47 of these cases, there are clinical information. The patients are 50 year-old and these tumours are more frequents in males. These neoplasias are considered as malignant potencial tumours with capacity for lymphatic invasion and for metastasize. No case de vascular o perineural invasion. All cases have scattered atypical cells and mitosis.
Inmunohistochemical profile, ki-67 and p53, may be helpful in the diagnosis of difficult lesions.Others inmunohistochemical markers such as CEA, S-100, EMA, have not clarified the question of apocrine differentiation.

P-515

Significance of immunohistochemical expression of cyclooxygenase-2 in actinic keratosis of the skin.

Anna Maria Athanassiadou; Andreas C. Lazaris; Efstratios S. Patsouris; Kyriaki Aroni.
Dermatopathology Unit, 1st Depart. of Pathology, Medical School, National and Kapodistrian University of Athens, Athens, Greece.

BACKGROUND Cyclooxygenase-2 (COX-2) is a catalyzing enzyme in the conversion of arachidonic acid to prostaglandins; COX-2 is not usually detectable in normal tissues but is induced in inflammation and carcinogenesis. Aktinic keratosis is a common intraepidermal neoplasm of sun damaged skin characterized by various atypia of keratinocytes.
MATERIAL AND METHODS Our aim was to investigate the expression of COX-2 by means of immunohistochemistry in a series of 30 cutaneous actinic keratoses of the atrophic (n=20) and hypertrophic type (n=10). The cut-off point of COX-2 immunopositivity was set at 10 , only strong staining intensity of the keratinocytes was regarded as positive.
RESULTS COX-2 was positively expressed in 12 samples (40) and the percentage of immunoreactive keratinocytes rarely exceeded 20 . Positive immunostaining demonstrated a cytoplasmic pattern. COX-2 immunopositive cells were mainly located close to the dermoepidermal junction, away from areas of hyperkeratosis or parakeratosis. In half of the COX-2 immunopositive specimens, a heavy inflammatory infiltrate of the papillary dermis was noticeable.
CONCLUSION COX-2 appears to be expressed in a considerable number of actinic keratoses, though at rather low percentages of keratinocytes. The observation of COX-2 positive keratinocytes away from areas of keratinization may be related to COX-2 role as an anti-apoptotic growth promoter since keratinization is known to be strongly correlated with the apoptotic potential of keratinocytes.

Kidney Pathology

P-516
Costimulatory molecule b7-h3 is overexpressed in renal angiomyolipoma

Yuri Sheinin; Stephen A. Boorjian, Paul L. Crispen; Christine M. Lohse; Bradley C. Leibovich; Eugene D. Kwon
Departments of Urology and Immunology, Mayo Clinic Rochester, USA

BACKGROUND. Renal angiomyolipoma (AML) is a highly vascular renal tumor, the pathogenesis of which has not been well established. We recently demonstrated high expression of the T cell coregulatory molecule, B7-H3, in the tumor vasculature of renal cell carcinoma. Here, we investigated expression of the coregulatory molecule B7-H3 in surgically resected renal AML.
METHOD. We evaluated tumor specimens from 110 patients who underwent partial or radical nephrectomy for renal AML at our institution between 1970 and 2004. Immunohistochemistry was performed using anti-B7-H3 antibodies to stain paraffin-embedded surgical tumor sections.
RESULTS. B7-H3 expression was found in the AMLs from all 110 patients. Diffuse expression was noted on the membrane and within the cytoplasm of the smooth muscle, vascular and lipoid components of the tumors. Seven patients demonstrated 20%-30% of tumor cells staining for B7-H3, 14 patients had 30%-60% of cells positive, and 91 patients had greater than 60% of cells expressing B7-H3, including 61 patients with greater than 90% expression. Also, 52 patient specimens contained normal renal tissue adjacent to the AML in which no B7-H3 expression was observed. Levels of B7-H3 expression, as determined by percentage of cells within the AMLs that demonstrated immunoreactivity, did not correlate with patient age ($p=0.43$), gender ($p=0.27$), tumor size ($p=0.21$), or symptomatic presentation ($p=0.35$).
CONCLUSION. B7-H3 is uniformly expressed by renal AMLs. These results support potential use of B7-H3 as a marker of renal AML. Further evaluation is necessary to ascertain the role of B7-H3 in AML pathogenesis or treatment of these tumors.

P-517
AMYLOIDOSIS – MORPHOLOGICAL FINDINGS IN THE KIDNEY

A. Alexandrov; T. Todorov; Tch. Georgiev; D. Popov; S. Hristov; A. Paloff; D. Hinova-Palova; E. Paskalev; P. Simeonov
Center of Pathology and Forensic medicine – Sofia, Bulgaria

Although amyloidosis is a well-known disease with typical histochemical and electronmicroscopic characteristics, which give enough reasons for diagnosing the illness, it could sometimes cause differentialdiagnostic difficulties. We had the chance to observe 3 cases; during the lightmicroscopic investigation in two of them, we found some interesting changes in the podocytes; in the third case we applied an ultrastructural investigation and observed different osmiophilic depositions in the glomerules. We could diagnose amyloidosis in the cases with podocyte changes in the second punctural renal biopsy, which was carried out after a year, mainly with Congo-rot stain in polarized light; in the third case we used the same method and diagnosed amyloidosis in the first biopsy.
We conducted an amyloidosis typification which proved the presence of type AL deposition. We observed depositions in the cytoplasm of the podocytes and in the glomerul endothelial cells, which probably represent some of the precursors of the amyloid fibrils. In the three cases we could not prove a disease, which could cause amyloidosis.

P-518

High grade transitional cell carcinoma of the renal pelvis with divergent differentiation mimicking a renal abscess

Jonathan F. Lara MD; Naver A. Sarkissian MD PhD
Department of Pathology, Saint Barnabas Medical Center, Livingston, New Jersey, USA

We describe an unusual case of high-grade transitional cell carcinoma of the renal pelvis with sarcomatoid and squamous differentiation that presented as a left renal abscess. The patient had originally been treated for minimally invasive transitional cell carcinoma of the urinary bladder and ureteral orifices five years prior. Computerized tomography scan findings were consistent with an abscess of the left kidney. Percutaneous nephrostomy with drainage afforded no clinical improvement. Nephrectomy was performed and tissue was removed piecemeal because of the diagnosis of an abscess. Macroscopically the tissue was fragmented and necrotic with patches of gray-tan abscess. Microscopic sections revealed a biphasic neoplasm with squamous and sarcomatous elements that were co-existent with evident morphologic transition. There was also evidence of residual papillary transitional cell carcinoma in the renal pelvis. The sarcomatoid component was immunoreactive for cytokeratin and vimentin. A malignant process must always be considered as an underlying cause when patients present with an abscess especially when there is a prior history of malignancy.

P-519

BRIDGING PODOCYTES IN HUMAN CRESCENTIC GLOMERULONEPHRITIS

Mandache Eugen; Gherghiceanu Mihaela; Penescu Mircea
"V. Babes" National Institute of Pathology, Bucharest, Romania

The concepts concerning the cellular composition of extracapillary proliferation in crescentic nephropathies have evolved during the last decade. Epithelial cells, both parietal and visceral, and macrophages have been found to participate in crescents formation. Several years ago Le Hir M. & coll. (2001) found, in an experimental crescentic glomerulonephritis (GN), podocytes adhering to both glomerular basement membrane and parietal basement membrane, and thus, forming bridges between the glomerular capillary tuft and the Bowman's capsule. Consequently, he proposed that the spreading of podocytes on the capsular membrane initiates the crescentic proliferation.
Twenty-eight renal biopsies from patients with extracapillary proliferative GN have been examined both in light and electron microscopy. From these cases we have selected five patients (two anti-GBM GN, one post-infectious GN and two ANCA associated vasculitis) showing only, or mostly cellular crescents. The EM investigation was targeted to identify some ultrastructural markers of the cells making up the crescents.
The two cases of ANCA associated vasculitis showed very large cellular crescents. Among their cellular components we found elongated cells having one end applied in close contact, on the glomerular basement membrane, and the opposite end stretched toward the Bowman capsule in between the neighboring cells. These elongated cells, identified as podocytes with modified phenotype, showed a much developed rER and some electron-dense vesicles. The majority of the large neighboring cells had an euchromatic nucleus and cytoplasmic glycogen granules. Since the glycogen rosettes are a cytoplasmic particularity of parietal epithelial cells, we considered them as such.
These facts endorse the le Hir & coll. theory, and also suggest the validity of the podocyte bridges formation in the human crescentic nephropathies.

P-520

ROLE OF NF-KB IN CELL APOPTOSIS AND PROLIFERATION IN RAT RENAL TUBULES AFTER ACUTE EXERCISE

Aleksandra Piotrowska1, Marzena Podhorska-Okolow1, Ilona Izykowska1, Maciej Zabel1,2, Piotr Dziegiel1
1Department of Histology and Embryology, Medical University of Wroclaw, Wroclaw, Poland 2Department of Histology and Embryology, University of Medical Sciences, Poznan, Poland

It is widely accepted that an acute physical exercise can induce pathological changes in untrained organism. Our previous studies have demonstrated that exercise-induced apoptosis was confined to the renal distal tubular cells. Under the normal condition, in response to the tubular cell's injury occurs the process of regeneration via neighboring cells proliferation. NF-κB is a transcription factor that plays a pivotal role in the expression of various target genes regulating both, cell proliferation and apoptosis.
The aim of this study was to examine if NF-κB could control exercise-induced apoptosis and cell proliferation in renal proximal and distal tubules.
Material and methods: Twenty male Wistar rats formed groups of running (n=10) and control animals (n=10). The animals from the exercise group were subjected to running on a treadmill at 1.0 km/h until exhaustion. The control animals remained in their cages throughout the experiment. Apoptosis was detected in paraffin sections by the TUNEL technique. Expression of Ki-67 and NF-κB was examined on paraffin sections by immunohistochemistry, using

mouse monoclonal antibody and rabbit polyclonal antibody, respectively.

Results: Apoptosis was detected only in cells of distal tubules. Expression of nuclear proliferation marker Ki-67 was more prominent in distal renal tubular cells. Expression of NF-κB was different in both renal tubules; in proximal tubular cells was confined to the nucleus while in distal tubular cells to the cytoplasm.

Conclusion: The obtained results could suggest that apoptosis of distal tubular cells is followed by cell proliferation what could allow the regeneration of damaged cells. The nuclear translocation of NF-κB could be involved with the protection of proximal tubular cells against apoptosis while the cytoplasmic location could suggest that apoptosis inhibition in distal tubular cells does not exist.

P-521

Kidney carcinoma associated with TFE3 gene fusion coexistent with ureteral transitional cell carcinoma-case report-

Madalina Bosoteanu; Mariana Aschie; Catalin Bosoteanu; Mariana Deacu

Department of Pathology, Faculty of Medicine, "Ovidius" University of Constantza, Romania

Background. Renal carcinomas associated with TFE3 gene fusions, included in the new WHO classification of kidney tumors (2004), have interesting morphological and biological features. In addition, the coexistence with ureteral carcinoma represents a challenge for the pathologist.

Material and method. The aim of this study is to analyse the morphological and immunohistochemical profile of a case: 55 y.o. male patient, Turkish ethnic, with both renal and ureteral carcinoma (Constantza has a Turkish minority representing 6,4% of population).

Results. Macroscopically: nephroureterectomy specimen of 10/8/6 cm with polycyclic outline; at the upper pole, a 3/3/2,5 cm intraparenchimatous nodular lesion, well circumscribed, yellowish, soft, with hemorrhage and necrosis; upper third of the ureter with a soft, grayish 1,5/0,5 cm mass with papillary surface. Histopathologically, renal tumor exhibits papillary growth patterns of polygonal cells, eosinophilic granular cytoplasm, hyaline inclusions, pseudostratified nuclei of Fuhrmann grade 3; foamy macrophages in papillary cores, necrosis; immunolabeling: CK7+, RCC-Ma+, EMA+, Ulex europaeus-, WT1-. This morphological features determined us to establish, initially, the diagnosis of papillary renal carcinoma, excluding other renal tumors that share similarities with it (classic renal cell carcinoma with papillary architecture, collecting duct carcinoma, metanephric adenoma). Surprisingly, our diagnosis was invalidated by the evidence of TFE3 protein overexpression, assessed by immunohistochemistry (strong nuclear reaction). This finding allows us to certify that the renal tumor belongs to the new class of kidney carcinoma associated with TFE3 gene fusion. Ureteral tumor was a high grade transitional cell carcinoma (G3), with positive immunolabeling for p63, that excludes the ureteral invasion by the renal malignant lesion.

Conclusions. This report emphasizes the utility of immunomarkers in cases with overlapping features. Also, it reveals distinct morphogenetic characteristics of the tumoral association in the Turkish patient: TFE3 gene fusion and p63 overexpression, creating a distinct molecular profile - target for further research.

P-522

Experimental substantiation of nephropathies because of the food dye consumption (E 102)

Galina Gubina-Vakulik; Antonina Yakovtsova; Ganna Mylovydova; Kuame Magest

Department of Pathologic Anatomy, National medical university, Kharkov, Ukraine

Background: Last decades the quantity of various nephropaties at children increasing. Probably, to this process concern not only negative ecological factors, but also some food factors. For an experimental research yellow food dye tartrasine (Å 102) has been selected. It is used in fruit-drops, cakes, wafers, fruit water manufacturing.

Methods: Female rats Wistar received a tartrasine solution daily in an adequate doze (at extrapolation on the person 0.5 liters of fruit water) during 1 month before pregnancy, then during the period of time of pregnancy and feedings of posterity. Kidneys of rats before pregnancy, after pregnancy and feeding, and kidneys of one-month rat posterity were investigated morphologically with the using of immunomorphological and morphometric techniques.

Results: At adult female rats the glomerulas are reduced in sizes. In mesangium the number of macrophages (CD16+) is increased, in basal membrane of capillaries IgG is found in places. Epithelium of proximal canalicules is injured: PAS-positive apical parts of epitheliocytes are frequently absent, accelerated apoptosis is observed.

The consuming of tartrasine during 4 months adult rats have kidneys with microscopic signs of proceeding mainly mesangeal-proliferative glomerulonephritis with sclerosis of separate glomerulas and interstitial-tubularis nephritis. A plenty of apoptosed changed nucleus of canalicularis epithelium is combined with reduction of their average size. At one-month rats which intrauterinally had influence with tartrasine and consumed it with parent milk, dysplastic glomerulas presence, large cortex areas without glomerulas

are observed. Mesangium of glomerulas contains the increased number of macrophages, IgG presences, accumulation of collagen I type is marked.
Conclusion: The food dye tartrasine (Å 102) is dangerous for kidneys because of toxic and xenobiotic actions.

P-523

An atypical case of huge type 1 papillary renal cell `carcinoma with like-type 2 aggressive behaivor

Gabriel Arismendi; gustavo Torres; Nathalia Medina; Mary Fernández; Mirida González; Madeline Fernández; Zoila Romero
Hospital General del Sur "Dr. Pedro Iturbe", Venezuela

Background: Type 1 papillary renal cell carcinoma is associated with favorable outcome, while the type 2 tumor is associated with higher metastatic progression and larger tumor size. However prognosis of the papillary renal cell carcinoma remains debatable in the literature. In Venezuela, papillary renal cell carcinoma is particularly unusual. **Case Presentation:** Authors report clinicopathological features of an unusual case of papillary renal cell carcinoma (type 1) with vascular invasion in a 70 years old male with hematuria of two month of evolution. The tumor was located on the upper lobe of the right kidney, and his size was 10×9 cm. Total nephrectomy was done. Grossly, well-circumscribed tumor with considerable hemorrhage and necrosis areas were seen. Microscopically, the tumor displayed a papillary architecture, papillae covered with a single layer of small cuboids cells with scanty cytoplasm and nucleoli, foam cells in stroma, tumoral necrosis and hemorrhage, renal vein was involved. Immunohistochemically was intensely reactive for CK7 and CD10. **Conclusions:** Contradictorily, to the generally reported in type 1 papillary renal cell carcinoma, this case presented threatening characteristics, such as; vascular invasion, tumor size (>7 cm), and extensive necrosis, these elements are more linked to type 2 papillary renal cell carcinoma. The fact that papillary tumors represent a heterogeneous group of different entities whose identification at cytogenetic and molecular level is currently being studied, possibly explain the more aggressive behavior in this patient.

P-524

The correlation of pathological findings in kidney biopsy and first clinical and laboratory manifestations of Primary focal and segmental glomerulosclerosis

Diana Taheri, Ali Chehrei, Pargol Samanianpour, Amar Hassanzadeh, Shohreh Sadrarhami,Shiva Seyrafianpour
Isfahan University of medical sciences, Isfahan, Iran

Background: The first clinical presentations and morphologic features of FSGS are various among patients and they are important predictor of prognosis in them. The aim of this study was to analyze the correlation of clinical, laboratory and pathological features at presentation of FSGS.
Methods: In this cross-sectional study, pathological findings of 64 cases of primary FSGS were reviewed by single renal pathologist without knowledge of patient identity or outcome. Clinical and laboratory data will be obtained on each patient at the time of biopsy. The data include systolic and diastolic blood pressure, the level of plasma creatinine, BUN, glomerular filtration rate (GFR), serum albumin, and the level of proteinuria. Then compare histopathological findings with clinical and laboratory data at the time of biopsy.
Results: The mean of Serum creatinin level was significantly higher in the patients with the presence of synechiae with the Bowman's capsule, and the presence of interstitial fibrosis and the presence of the global scars in their biopsies(p value<0.05), and also there were significant different in the mean level of GFR in the patients with the presence of interstitial fibrosis in their biopsies in the comparison with the patients without the interstitial fibrosis (p value<0.05).Also we discovered positive correlation between the level of plasma creatinin and global sclerosis (r=2,21,p-value=0.04),and between the level of GFR and global sclerosis(r=2.01,p-value=0.02). All the patients with renal insufficiency had intrestial fibrosis in their biopsies in comparison of only the 24 patients (48%) of the group without renal insufficiency (p value<0.05). There were no significant difference between patients with and without hypertension and nephrotic- ranged proteinuria.
Conclusion: in our studies we found that in addition to the interstitial fibrosis, global scars and the synechiae of Bowman's capsule are correlated with serum creatinin level and the level of plasma albumin and GFR.Although the prognostic role of these laboratories and the pathological features have not been proved until now, but because the prognostic role of the laboratory findings such as Pcr which is correlated with these pathological features, has been proved,there is a hypothesis that these two pathological features could have prognostic roles in FSGS patients.
Key words: Focal and Segmental Glomerulosclerosis (FSGS), creatinin, Albumin, BUN, interstitial fibrosis, global scar, synechiae with the Bowman's capsule.

P-525

Useful Markers for Differential Diagnosis of Oncocytoma, Chromophobe Renal Cell Carcinoma and Conventional Renal Cell Carcinoma

Bita Geramizadeh, Mahmoud Ravanshad, Marjan Rahsaz

Pathology Department, Shiraz University of Medical Sciences, Iran

ABSTRACT: Renal oncocytoma, conventional RCC (with granular cell type), and chromophobe RCC have different prognosis. Some times differentiation between them is difficult in H & E slides. In study of 128 renal tumors during 5 years, we selected 76 cases (30 conventional RCC (CRCC),16 papillary RCC, 21 chromophobe RCC (ChRCC), 8 oncocytoma, 1 collecting duct carcinoma and staining with Hale's colloidal iron, CK7, CK8, CK18, CK19, CK20, Vimentin, EMA, CD10 and RCC marker were done. No significant difference was seen between renal tumor subtypes with CK8, CK19, CK18, CK20 and EMA. The most useful markers were vimentin, CK7, CD10, RCC marker and Hale's colloidal iron. Hale's colloid iron staining with diffuse reticular fine cytoplasmic pattern was present in ChRCCs, but was absent in other subtypes and oncocytomas.Vimentin, CK7, CD10, RCC marker and Hale's colloidal iron can be used for the differential diagnosis of the problematic epithelial tumors of kidney (CRCC, ChRCC and oncocytoma), i.e. ChRCC: Vimentin, CD10 and RCC marker negative, CK7 positive and diffuse fine reticular cytoplasmic pattern of Hale's colloidal iron. Oncocytoma: Vimentin, CK7, RCC marker and CD10 negative, Hale's colloidal iron negative. CRCC: CK7 negative, Vimentin, CD 10 and RCC marker positive, and Hale's colloidal iron negative.

P-526

Pathological changes in kidney biopsies from patient with drug-induced nephropathy

Galina Reznikova; Alexander Matsionis; Mihail Batuchin; Olga Dmitrieva; Patrisia Povilaitite

Rostov Regional Institute of Pathology; Rostov-on-Don, Russia

Background: The influence of variety drugs on the kidney first of all associate with an allergic acute tubulointerstitial nephritis. But durable excessive usage nonsteroidal anti-inflammatory drugs (NSAID) or analgesics often results in chronic renal failure with decrease of function. We aimed to examine clinical and pathomorphological correlations in such chronic secondary drug-induced nephropathy.

Methods: Our study included 21 kidney biopsies from patients with tubulo-interstitial nephritis without any other renal diseases (after careful clinical and morphological examination), with long history of chronic usage of NSAID (1–22 years). The mean age of the group 39,5 years, 12 men, 9 women.

Results: Diffuse interstitial fibrosis and diffuse weak nonspecific inflammatory infiltration of interstitium by various cellular elements with admixing of eosinophilic granulocytes were observed in 90,5% of patients. Marked tubular changes (atrophy, subatrohy) were showed in 47,6% cases, not numerous casts in 67,7%. The focal changes of glomerular capillaries (total or segmental gialinosis, sclerosis of basement membrane, weak mesangial hypercellularity) had 57% of patients. Electron microscopy examination of glomeruli showed marked changes of podocytes - focal fusion and even desquamation of foot processes, microvillous transformation of the cell membrane in 76% of cases. Analysis of clinical features and its correlations to morphological changes showed interrelation between the level of proteinuria and the level of interstitial and glomerular fibrosis/gialinosis.

Conclusion: Analyses of clinical and pathological features let us to develop the score system for the calculation the risk of the probable morphological changes progressing in the kidney under the influence of NSAID.

P-527

FIBRILLARY GLOMERULONEPHRITIS: A REPORT OF TWO CASES

Fulya Çakalağaoğlu, Serap Şirvancı, Zeynep Tosuner Sever, Hakkı Arıkan, Handan Kaya

Marmara School of Medicine, Turkey

Background: Fibrillary glomerulonephritis (FGN), is identified in about 1% of patients who undergo native kidney biopsy. FGN is defined by electron microscopic finding of randomly arranged, straight nonbranching fibrils ranging in diameter from 10 to 30 nm. The deposits do not stain with Congo Red. We have reported two cases of FGN.

Method-Results

Case 1: The kidney biopsy performed from a-15 year-old boy presented with hematuria with a serum creatinine level above 7.0 mg/dL. Microscopically while 8 of the 18 glomeruli were globally sclerosed 4–5 glomeruli showed cellular crescents. The other glomeruli demonstrated mesangial hypercellularity. Congo Red Stain was negative for amyloid. Minimal interstitial inflammation and focal atrophy of the tubules were observed. The histomorphology of the extraglomerular vessels were normal. Ultrastructurally extensive 15–20 nm fibrils deposition within the

glomeruli were noted. The final diagnosis of the case was FGN.
Case 2: A 36 year old man presented with nephrotic syndrome. The kidney biopsy consisted of the renal cortex with 16 glomeruli; 4 of these were globally sclerosed and mesangial hypercellularity were seen in the other glomeruli. The basement membranes of the peripheral capillary walls were markedly and regularly thickened. While the tubules showed focal atrophy, the vessel walls showed mild sclerosis. Congo Red stain was negative for amyloid in the glomeruli, interstitium and vessels. The immunofluorescence microscopy showed fine granular deposition for polyclonal IgG, IgM, IgA, and C3 along the glomerular capillary walls. One of the glomerulus was examined ultrastructurally and numerous fibrillary deposits (30 nm diameter) in the expanded mesangium was seen. All of these findings suggested the diagnosis of FGN.
Conclusion: The finding of Congo red negative organized deposits on renal biopsy should prompt a careful search for FGN by ultrastructural analysis.

P-528
COLLAGENOFIBROTIC GLOMERULOPATHY: A DESCRIPTION OF TWO CASES

Marlene Antonia dos Reis; Fabiano Bichuette Custodio; Renata Diniz Rabelo Ferreira; Maria Laura Pinto Rodrigues; Eumenia Costa Cunha Castro; Vicente de Paula Antunes Teixeira.
Federal school of Triângulo Mineiro - UFTM, Uberaba, MG, Brazil

Collagenofibrotic glomerulopathy (CG) is a recently discovered entity characterized by massive accumulation of spiraled and frayed collagen fibrils in mesangial and subendothelial areas: clinically it presents with nephritic syndrome. The reported cases are still rare, principally in the West counties, as it is the knowledge in the diagnosis of this disease. Case 1: female patient, 21 years old, white; patient was previously healthy. No familiar history of renal diseases. She showed for routine exams and in the urine analyses she had proteinuria (1,6 g/24 h) and microscopic haematuria with one year of evolution. Case 2: female patient, 15 years old, white, began the disease with edema and hypertension for two months; urine analyses showed proteinuria of 2,49 g/24 h and dyslipidemia (total colesterol: 426 mg/dl and triglycerides: 264 mg/dl), without other alterations; she presented partial answer to the use of corticosteroids. Renal biopsy: in both cases, at light microscopy, the only alteration was discrete mesangial hipercelularity; the immunofluorescence was negative. The electronic microscopy found massive accumulation of spiraled and frayed collagen fibrils in mesangial and subendothelial areas compatible with collagen type III. At picrosírius method under polarized light, the fibers displayed birefringence and greenish staining, highly suggestive of type III collagen. These two cases of CG are probably the first ones to be reported in Brazil and in South America. Even being rare the CG deserves distinction as a differential diagnosis in the cases of nephritic syndrome, mainly in adolescents/young adults. The CG illustrates the importance of electronic microscopy for diagnosis and best understanding of glomerulopathies.
Grant: CNPq, Fapemig, Funepu, UFTM

P-529
HEREDITARY PROTEINURIA: DIFFUSE MESANGIAL SCLEROSIS AND FINNISH TYPE NEPHROPATHY

Fabiano Bichuette Custodio; Maria Laura Pinto Rodrigues; Eumenia Costa Cunha Castro; Vicente de Paula Antunes Teixeira; Marlene Antonia dos Reis
Federal University of Triângulo Mineiro - UFTM, Uberaba, MG, Brazil

The nephrotic syndrome in the childhood (NSC), congenital or within the first years, is a rare condition which has an elevated rate of mortality and an evolution to an end-stage renal disease (ESRD). With the genetic studies and recent discoveries on the molecular structure of the glomerular filtration barrier (diaphragm slit proteins, like nephrin and podocin), there was an increase in the knowledge of these pathologies, but there is still a small amount of cases reported. Between the main pathologies that have features of NSC are the diffuse mesangial sclerosis (isolated or associated with Denys-Drash syndrome) and the Finnish type nephropathy (FN). Case 1: six-month-old African-American female, born at term; at five months old, began with diarrhea which fast evolution to oliguria, anasarca and hipertension. Exams showed high proteinuria and loss of renal function. Renal biopsy diagnostic was of DMS. Case 2: 13 years-old white boy; routine exams showed creatinine (Cr)=2,1 mg/dl and proteinuria 5,2 g/24 h. In the past history (two years old) he went to a nephrectomy (Wilms' tumor). He has bilateral cataracts and cryptorchidism. Renal biopsy showed the diagnosis of DMS, probably as a part of the Denys-Drash syndrome. Case 3: white female patient, 24-days-old, born at 36 weeks due to a placenta abruption (weights 2080 g). She presented intense edema and severe proteinuria. Renal biopsy showed severe tubular dilatations (cysts) and the electronic microscopy showed absence of the slit diaphragm between the foot processes, which was

highly suggestive of FN. Although new studies had been published in the past few years in this area, the discussion about the diagnosis between clinicians and pathologists was still the best way to deal with the NSC.
Grant: CNPq, Fapemig, Funepu, UFTM

P-530

Renal Carcinoma of Collecting Duct of Bellini.

Sevastiadou Maria; Papaevangelou Maria; Koniaris Efthymios; Biteli Maria; Papathanasaki Antigoni; Apostolikas Nikiforos
Pathology dpt. Of Anticancer, Oncological Hospital of Athens, 'St. Savvas', Athens, Greece.

Background: Collecting Duct Carcinoma of Bellini (CoDCB) is a very rare renal malignancy (less than 1%) with poor prognosis since most of the cases are metastatic at presentation. Although the diagnosis should be considered in patients presenting with marked deterioration of the general status and/or the presence of a very large invasive renal tumour on abdominal CT scan.
Methods: From January 2003 up to the end of December 2007 two cases of CoDCB (2.9%) were diagnosed among 68 renal malignancies in our department. The first case was about a 50-y.o. male patient with gross hematuria. The patient underwent a radical right nephrectomy. On dissection a whitish tumor, measuring 11.5×9×8 cm, was found on the posterior surface of the kidney, infiltrating the perinephric fat. The second case was about a 52 year old female with a renal tumor (m.d. 8 cm) that invaded the renal fat but also the renal vein.
Results: The tumors fulfilled the major and minor criteria of Sringly et al. More specifically our cases showed the typical irregularity of tubular architecture with high nuclear grade (hobnail cells, Fuhrman 3&4). Small papillary architecture and desmoplastic stroma with numerous inflammatory granulocytes were noted. In the second case although the tumor was smaller than the first, invasion of the renal vein was found because of its central. The immunohistochemical staining supported the diagnosis (soy bean agglutinin, CK8, 18, high molecular weight Keratin, EMA, vimentin).
Conclusion: Our cases, besides the other typical morphological characteristics, showed the characteristic positive immunohistochemical profile and the positive staining for soy bean agglutinin, a marker of the distal nephron. CoDCB presents with a very poor prognosis and our cases were staged pT3a and pT3b respectively.

P-531

Immunohistochemical profile of Chromophobe renal cell carcinoma. A four year review.

Papaevangelou Maria; Biteli Maria; Koniaris Efthymios; Papathanasaki Antigoni; Theodorakopoulou Georgia; Apostolikas Nikiforos
Pathology dpt. of Anticancer, Oncological Hospital of Athens, 'St. Savvas', Athens, Greece.

Background: We re-evaluated 62 cases of Renal Cell Carcinoma (RCC) which were diagnosed in our department from January 2003 to December 2007. According to the strict morphologic criteria of WHO classification, we estimated the immunohistochemical diagnostic utility of various antigens, for the assessment of Chromophobe (Chr) subtype renal cell carcinoma.
Methods: Seven carcinomas from the total 62 cases were classified as Chr (11.3%). According to the Furrhmann grading system 1 case was grade II, 5 cases were grade III and 1 case grade IV. No case was grade I. The following antibodies were applied to all the cases: CK7, EMA, CD10, CD117 and Vimentin (Vim).
Results: The immunohistochemical phenotype of Chr showed strong positivity for CK7, CD 117 and EMA while all the Chr RCCs were negative for Vim and CD10.
Conclusion: We conclude that whenever the differential diagnosis included eosinophilic variant of RCC the most sensitive markers were CD117and CK7 in combination with the negativity of CD 10, and Vim.

P-532

Malignant Fibrous Histiocytoma of the kidney. A rare case.

Biteli Maria; Papaevangelou Maria; Koniaris Efthymios; Sevastiadou Maria; Apostolikas Nikiforos.
Pathology dpt. Of Anticancer, Oncological Hospital of Athens, 'St. Savvas', Athens, Greece.

Background: Various types of sarcomas have been reported so far in the adult kidney and among them Malignant Fibrous Histiocytoma (MFH) is a very rare neoplasm in that special location. It was first described by O'Brian in 1964. Usually MFH of the kidney arise from the renal parenchyma or from the renal capsule. Also retroperitoneal soft tissues often develop MFH.
Methods: A 59-year old patient presented with hematouria and general malaise and underwent a left nephrectomy. Part of the descending colon was also excised. We received the left kidney measuring 19×12×10 cm along with the perinephric fat. The left colon was attached to the kidney

and its length was 19 cm. Grossly the tumor had whitish-yellow color, hard-elastic consistency, while on sectioning it had solid, partly lobular and fasciculating appearance and was measuring 12×12×8 cm. The tumor was found to occupy the lower pole approaching to the middle of the kidney, infiltrating part of the renal pelvis and part of the ureter which was also removed. It was also infiltrating the perinephric fat up to the serosal layer of the excised left colon. Renal artery and vein appeared to be free of tumor infiltration.

Results: Histological examination the tumor demonstrated spindle shaped fibroblast-like cells arranged in a storiform pattern with fibrous stroma and clusters or sheets of rounded histiocyte-like cells. Pleomorphic giant cells with bizarre nuclei (Tuton cells) were also observed. Our diagnosis was also supported immunohistochemically with and the tumor was immunoreactive for Cytokeratin, CD10 and CD117.

Conclusion: MFH is unusual urological malignancy and differential diagnosis includes leimyosarcoma, sarcoma and sarcomatoid carcinoma. Their distinction is based mainly on immunohistochemistry. Histogenesis of MFH is linked to mesenchymal cells from renal capsule. On conclusion MFH has strong predilection for local recurrence and its prognosis is poor, therefore close and life-long follow-up is advised.

P-533
WITHDRAWN

P-534
SARCOMATOID CARCINOMA OF THE RENAL PELVIS AND URETER: A CASE REPORT WITH IMMUNOHISTOCHEMICAL FINDINGS

Sibel Bektas; Figen Barut; Burak Bahadir; Aydin Mungan; Nimet Karadayi;Sukru Oguz Ozdamar
Zonguldak Karaelmas University, School of Medicine, Department of Pathology,Zonguldak, TURKEY

Background: Sarcomatoid carcinoma is a rare tumor of the urothelium. In this case report we present a sarcomatoid carcinoma of the renal pelvis and ureter and discussed its morphological and immunohistochemical aspects.

Case: A 69-year-old male presented with gross hematuria and abdominal pain. Clinical imaging work up revealed severe hydronephrosis with dilated right renal pelvis and extensively large right kidney. Suspicious of renal cell carcinoma, right nephrectomy and periton biopsy were performed. Histopathologically, the tumor was composed of epithelial and sarcomatous areas. The epithelial component was a high-grade papillary urothelial carcinoma in renal pelvis and ureter. The sarcomatous component had spindle, chondroid and rhabdomyoid appearance. Immunohistochemically, the epithelial component was reactive for epithelial membrane antigen, pankeratin, cytokeratin 7 and 20. The sarcomatous elements were positive for vimentin, smooth muscle actin and focally desmin and epithelial membrane antigen but negative for S-100, myoglobin, pankeratin, cytokeratin 7 and 20. Only the sarcomatous component of the tumor infiltrated through the renal parenchyma and extended to perirenal fat tissue. Similarly, periton biopsy revealed only sarcomatous elements. The patient died a day after the nephrectomy.

Conclusion: Sarcomatoid carcinoma of the renal pelvis and ureter is a high-grade malignant neoplasm with poor prognosis. Demonstration of epithelial characteristics in sarcomatous component by means of immunohistochemistry confirms the diagnosis.

Key words: Renal Pelvis, Ureter, Sarcomatoid carcinoma, Immunohistochemistry

P-535
Multilocular cystic renal cell carcinoma.

Koniaris Efthymios 1; Kakouri Petroula 2; Sofoklis Bouzoukas 2; Pavlopoulos Petros 2,3
1 Pathology dpt of Anticancer Oncological hospital of Athens 'St. Savvas', Athens, Greece; 2 1st Social Security Hospital, Urological clinic, Athens, Greece; 3 Department of Pathology, National University of Athens Medical School, Athens, Greece.

Background: Multilocular Cystic Renal Cell Carcinoma (MCRCC) is a rare variant of the Clear Cell Renal Carcinoma (CCRC) with a favorable outcome and still not well-known clinical significance and biological behavior.

Method: A 47-year old patient presented to our hospital with dysuric problems. On ultrasound and MRI scan a space occupying cystic mass was found. Similar findings were also observed on CT scan. The patient underwent a radical kidney excision and on dissection a cystic, whitish tumor measuring 5 cm in its greater diameter was found.

Results: Microscopically the tumor appeared partly solid with neoplastic cells organized in islands or tubular structures being separated by each other by thin, slender fibrovascular septa. The neoplastic cells were cuboidal and in some places polygonal with a central nucleus, without nucleoli and clear cytoplasm (grade 1 according to Furhman grading system). In other areas the tumor appeared cystic composed mainly of thin-walled cysts of varying size and shape. The neoplastic cells that were investing the wall of these cystic spaces were epithelial clear cells. These cysts were filled with eosinophilic amorphous material. The tumor was examined immunohistochemically and reacted

for Pankeratin (AE1/AE3), Vimentin, EMA, CD10 and NSE. Negativity was observed for the following antigens: Cytokeratin 7, Cytokeratin 20, p53 and MIB-1.

Conclusion: MCRCC has a benign clinical course and many authors suggest nephron-sparing surgical treatment. Preoperative diagnosis is difficult and has to be differentiated from other space-occupying cystic renal lesions. Our case appeared to be limited to the kidney with no invasion of the perinephric fat or the Gerota's fascia. The renal vessels and the ureter were also free of direct invasion by the neoplasm. According to the 1997 criteria of tumor-node-metastasis (TNM) classification our case was stage pT1b.

P-536

Hepatocyte growth factor (HGF) and transforming growth factor (TGF-β1) expression in 42 renal biopsy from lupus nephritis patients. Role of the HGF/TGFB1 ratio as a prognostic factor.

Gianfranco Zannoni1, Vincenzo Arena1, Elisa Gremese2, Stefano Costanzi3, Arnaldo Capelli1, Gianfranco Ferraccioli2.
Department of Pathology (1), Rheumatology (2) and Nephrology (3), Catholic University of the Sacred Heart, School of Medicine, Catholic University of Rome, Italy

Background. The identification and validation of molecular markers of prognosis are the future for several pathologies. Until now in lupus nephritis (LN) the prognostic value of different clinical and histological factors remains debated. Several animal models demonstrate that HGF and TGF-β_1 are implicated in renal damage.

Objective. To evaluate HGF and TGF-β_1 expression in renal specimens of LN patients and their role to predict the renal outcome after six months of immunosuppressant therapy.

Methods. 42 consecutive patients with newly diagnosed LN were included in the study. Renal biopsy specimens were classified according to the WHO criteria. Immunohistochemical expression of HGF and TGF-β_1 was evaluated. We divided patients in two groups on the basis of the response to therapy at 6th month in responders (R) and non responders (NR).

Results. Immunohistochemistry confirmed that HGF and TGF-β_1 are expressed in the tubuli but not in the glomeruli. The TGFβ_1 extension score directly correlated with the chronicity index ($r=0.40$, $p=0.03$). We did not find any correlations with clinical parameters of renal involvement (proteinuria, creatinine clearance) as well as serum complement levels and antiDNA antibodies. The 29 R differs from the 13 NR only for the HGF extension score ($p<0.001$) and intensity score ($p<0.001$) and HGF/TGF ratio either for extension ($p<0.001$) and intensity score ($p=0.001$). A cut-off value >1 for the ratio HGF/TGFb1 is predictive of remission with a PPV of 95% and with an OR of 15.2 (95% IC 2.5–92, $p<0.0001$).

Conclusions. Consistent with these findings, our studies provide strong evidence supporting the biological significance and clinical relevance of HGF/TGFb1 ratio at baseline for the identification of patients with a good response to standard SLE therapy. Immunohistochemical assessment of HGF/TGFb1 ratio as a prognostic factor could be an efficient approach in the routine study of LN patients.

P-537

WITHDRAWN

P-538

Nephrotoxicity by cyclosporine-a: the role of TGF-β1, apoptosis and intersticial fibrosis

María Virgilia Soto Abraham; José Ramón Paniagua Sierra; Armando Medina Cruz; María del Carmen Ávila Casado
Department of Pathology, Instituto Nacional de Cardiología "Ignacio Chávez"; Research Unit for Nephrological Diseases, Hospital de Especialidades del CMN siglo XXI, IMSS; Department of Pathology, Hospital General de México

Background: Acute and chronic Cyclosporine-A (CyA) nephrotoxicity prevalence varies from 15% to 30% in different series. Chronic toxicity is the more frequent of both two and is characterized by acelular interstitial fibrosis and arteriolopathy. Interstitial fibrosis could be the result of and important profibrotic growing factor and apoptosis inductor i.e., TGF-β1.

Objective: To demonstrate that there is an increase expression of TFG-β1 and apoptosis in renal allograft biopsies in patients with histological data of CyA-toxicity.

Methods: Renal biopsies from 40 transplanted patients of living related donor were retrospectively reviewed. All patients have had a renal biopsy performed at the time of the transplant (immediate). Second biopsies were taken by protocol of early CyA withdrawal, at least after 6 months of treatment. Biopsies were reviewed looking for vascular or interstitial fibrosis as well as the expression of TGF-β1, immunomarkers of apoptosis and TUNEL. Vascular damage was scored as mild, moderate and severe. Expression of immunomarkers was measured by morphometry using image analyzer software. Pearson correlation was performed between the percentage of interstitial fibrosis and

TGF-β1 expression, immunomarkers of apoptosis and TUNEL.
Results: There was a clear correlation between expression of TGF-β1 and interstitial fibrosis in the first biopsy; however this correlation was highly significant in the second biopsy under the treatment with CyA. There was also a direct correlation between interstitial fibrosis and apoptosis (i.e., Bcl-6). TUNEL results showed an increase in apoptosis in the interstitium in the second biopsies compared to those biopsies taken immediately. However, this showed an affected cortex surface maximal increase in all those second biopsies with fibrosis scored grade 1 and 2, while there was a diminution in those biopsies scored as grade 3.
Conclusions: Data supports that CyA chronic toxicity in the renal allograft is mediated by TGF-β1 and the apoptosis induction.

P-539

MIXED EPITHELIAL AND STROMAL TUMOR OF THE KİDNEY: A CASE REPORT

***Caglar Cakir;*Aylin Ege Gul;*Mine Cayirci;**Cihangir Cetinel; *Nimet Karadayi; **Selami Albayrak**
**Dr. Lutfi Kirdar Kartal Educational and Research Hospital, Department of Pathology Istanbul/ TURKEY.* ***Dr. Lutfi Kirdar Kartal Educational and Research Hospital, Department of Urology Istanbul/ TURKEY*

Background: Mixed epithelial and stromal tumors of kidney are characterized by a mixture of epithelial and stromal elements that form solid and cystic growth patterns. Cystic areas composed of large cysts, microcyst and tubules. Solid areas consist of proliferations of spindle cells admixed focally gland-like structures. The stromal component ranges from hypocellular and fibrotic to more cellular with fibroblastic and myofibroblastic foci to cellular ovarian-like stroma. Smooth muscle cells may be prominent.These tumors were reported previously in the literature under various names, including adult mesoblastic nephroma. All have been adults and the mean age is perimenopausal.
Case: The case is a 44 years old woman with chronic hepatitis B. Abdominal ultrasonography showed a multi-lobulated mass with solid and cystic areas at the middle-lower pole of the left kidney and a hemangioma of the liver. Radical nephrectomy was performed. Macroscopic examination revealed a well- circumscribed 6×5×5 cm mass with solid and cystic components of the mid-lower poles of the left kidney.Microscopically the tumor was composed of a mixture of a spindle cell proliferation of variable cellularity and microcysts, tubules and large cysts are lined by columnar and cuboidal epithelium. Immunhistochemically spindle cells reacted with antibody to smooth muscle actin, desmin, vimentin, and estrogen, progesterone receptors. Epithelial elements of the tumor were positive for cytokeratin and vimentin.
Conclusion: We present a case of mixed epithelial and stromal tumor of the kidney by reviewing the literature.

P-540

Primary renal leiomyosarcoma, case report

M. Fawaz Dawamneh,M.D.
Pathology Services Division, Dhahran Health Center, Saudi Aramco Medical Services Organization, Saudi Arabia

Background: Primary renal leiomyosarcoma is a very rare adult malignant neoplasm constituting about 1% of all primary malignant kidney tumors and 60% of all renal sarcomas. It carries a poor prognosis and fails most treatment modalities.
Method: The patient was 43 years old male who presented with two-month history of right flank pain without hematuria. Radiologic studies revealed a large right kidney mass compressing the inferior vena cava. Radical nephrectomy was performed. Subsequently, the patient developed multiple lung and liver metastases and local tumor recurrence. He did not response to multiple chemo and radiation treatment regimens and died one year after surgery.
Results: The right kidney was largely involved by a large tumor measuring 23 cm with nodular, lobulated, solid and fleshy cut surface and focal hemorrhage and necrosis. Microscopically, the tumor consisted of cellular growth of spindly cell with elongated plump moderately pleomorphic and hyperchromatic nuclei. Increased mitotic activity is noted (11/10 hpf). Some highly atypical cells are present. Areas of necrosis, hemorrhage, hyalinization and myxoid changes are present. The tumor cell arranged in short intersecting fascicles. The tumor cells were strongly positive for vimentin, actin and desmin, weakly positive for CD117 and negative for CD34, F-VIII, EMA and cytokeratin.
Conclusion: Although primary renal leiomyosarcoma is very rare, it should be considered in the differential diagnosis of spindle cell proliferation because of the poor prognosis and bad outcome despite aggressive therapy. It should be differentiated from other sarcomas and from sarcomatoid renal cell and urothelial carcinomas which have different treatment strategies and outcome. The distinction is based on the morphologic and immunohistochemical findings. The tumor may arise from renal capsule, wall of renal pelvis, hilar blood vessels or intrarenal small blood vessels. No specific cytogenetic abnormalities have been found.

Author Index by Abstract

Abba, Martín P-490
Abbasi, M P-35
Abdelkader, Atef Ben P-131, P-14
Abdulkader, I P-265
Abdulkader, Ihab P-175, P-61, P-63
Abecassis, Miguel O-70
Abia, David O-86
Abraham, María Virgilia Soto P-538
Abuomar, Adel P-254
Achach, Thouraya P-86
Acosta, Gabriela P-355
Acosta, Paloma Martin P-289
Adler, J P-54
Adrados, Manuel P-395
Adrover, Encarna P-251
Agell, Laia O-42, P-333, P-343, P-344
Aghaji, A E P-283
Agnantis, Niki J P-5, P-58, P-76, P-470
Agrawal, Manish P-168
Agrogiannis, George P-481
Agua, Celia Del P-158, P-303
Aguado, Judith Suárez O-23
Agueznay, Nour El Houda P-293
Aguiar Júnior, Armando Costa P-2
Agustí, Jaime P-490
Agwu-Umahi, U P-283
Ahlem, Elouni P-341
Ahmad, Mahmoud P-361, P-57
Aiba, Motohiko P-7
Aiello, Eleonora P-391
Aikaterini, Apostolaki P-199, P-94, P-95
Akarca, Ulus Salih O-56
Akbari, Elaheh PFP-4
Akbari, Majid PFP-4
Akhmetov, Timur P-363
Aktepe, F P-179, P-180, P-226
AKUSOBA, C I P-447
Akyildiz, Igdem A P-49, P-192
Al-Adnani, Mudher O-19
Al-awadhi, Naser P-361
Al-Brahim, Nabeel P-57, P-361
Al-Enezi, Saleh P-361
Al-Mhsin, Ali Abed O-57
Alameda, Francesc P-102, P-427, P-428
Alarcão, Ana O-2, P-13
Alarcón, Isabel P-45, P-323
Alataki, Despoina P-172
Alava, Jose Iñaki P-456
Alavi, SA P-362
Alba, Emilio PFP-3
Albayrak, Selami P-539
Alberola, M P-429, P-435
Albert, Sara P-102, P-427, P-428
Albertsson, Per P-354
Alcalá, Rebeca P-322
Alcantar, Guadalupe P-136
Alcaraz, Eduardo P-254
Alejo, María P-430, PFP-7
Alencar, Rita C P-302
Alexandrov, A P-140, P-517, P-350
Alexiou, George P-272
Aleykuty, M A P-106
Alfaro, J P-514
Alfaro, Luis P-332
Alfonso, J E Blasco P-339
Algaba, Ferran P-327
Aliste-Santos, Carlos P-264
Aliste, C P-265
Aliste, Carlos P-175
Alkan, Zeynep P-290
Allende, H P-198
ALMEIDA, Joaquim Soares P-241, P-242, P-243, P-255
Almeida, José Carlos O-70
Almeida, Sonia Maria P-8, P-127, P-152, P-448, P-449
Alonso, P L O-28
Alós, Llúcia P-497, P-507, P-511
Altemani, A P-295
Altemani, Albina P-294
Álvarez-Argüelles-Cabrera, Hugo P-401
Álvarez, Jorge Escandón P-505
Álvarez, Martina PFP-3
Alvarez, R P-514
Alvarez, T P-338
Alvaro, Tomás O-6
Alves, Venâncio A F P-374
Amalinei, Cornelia P-91, P-117
Amat, Irene P-500
Ambrosini-Spaltro, A O-3
Amel, Trabelsi P197
Amela, Anna Domingo P-188, P-326
Amigo, M P-133
Aminaa, Nouira P-33
Amini, Elham O-81
Amoli, Fahimeh Asadi P-420
Anagnostakis, Dimitrios P-405
Anagnostou, Eleutherios P-172
Andersson, Leif P-69
Andrade, Jesús P-278
Andrade, Liliana P-96, P-97
Andreas Baba MD, Hideo O-66
Andrei, Florin P-43, P-70, P-132, P-250, P-375
Andrei, Razvan O-79, P-496
Andrejevic-Blant, Snezana O-10
Andreu, Francisco Javier P-248, P-252, P-297
Andreu, Xavier P-418
Andrzej, Dąbek P-404
Anestiadi, Vasile P-474
Angelini, Annalisa O-24, P-142
Anghel, Alina P-70
Antigoni, Papathanasaki P-325, P-329, P-530, P-531
Antón, Iosu P-223, P-498
Antoni, Jordi P-116
Antonio, Salas P-423
Antunes, Alexandre O-70
Anvari, Kazem P-146
Apostolaki, Aikaterini P-321
Arafa, Mohammad O-16
Aramendi, Teresa O-25
Arana, Vicente Medina P-401
Aranda, F Ignacio P-251
Aranda, Ignacio O-33
Aranda, Paola P-281
Araujo, Eduardo Santini P-169
Araújo, Jacqueline, P-97
Arbogast, Stefanie O-1
Archimandritis, Athanasios J P-405
Ardabili, A Merikhi P-145
Ardeleanu, Carmen P-132, P-250, P-375, P-43, P-477, P-70
Ardissone, Francesco PFP-6
Arellano MD, E Marcelo P-29
Arena, Vincenzo P-536
Arenas-Huertero, Francisco P-153
Argüelles-Cabrera, Hugo Álvarez- P-115
Arias-Arias, Susana P-264
Ariel, Ilana P-452
Arion, Constantin P-43
Arismendi-Morillo, Gabriel P-440
Arismendi, Gabriel P-523
Ariza, A P-377
Ariza, Aurelio P-277, P-367, P-494, P-504
Arıkan, Hakkı P-527
Arneson, Nona O-87
Arola, Johanna P-69
Aroni, Kyriaki P-515
Arra, Antonio P-169
Arranz, Isabel O-34
Arrechea, Maria Asunción P-500
Arrechea, Miren P-63
Arrinda-Yeregui, José M P-53
Arsene, Dorel P-250, P-375, P-70
Arsovski, Oliver P-77
Arturo, Ángeles P-412
Arumi-Uria, M P-488
Asadi, Lari M P-233
Aschie, Ion P-89, P-99
Aschie, Mariana P-225, P-232, P-378, P-521, P-89, P-99
Asensio, Maria Planelles P-21
Asensio, Rafael Ramos P-401
Asioli, S O-3
Asioli, Sofia O-13
Astrakhantsev, Alexander F P-331
Asuncion, Bernadette P-446
Athanassiadou, Anna Maria P-515, P-481
Athanassiadou, Pauline P-481
Atkinson, Mike P-66
August MD, Christian O-66
Avdalyan, A M P-74
Avdic, Silvija P-92
Avdosyev, Yuriy P-207
Ávila, Ana O-64
Ávila, Isabel Ruiz O-44
Ayala, Ernesto García P-257, P-286, P-346, P-347, P-348, P-483, P-78
Ayatollahi, Hossein P-209, P-36, P-37
Ayatollahi, Jamshid P-195
Aydin, Ovgu O-54, P-203
AYLİNGÜL, P-221
Azadeh, Sedghi P-390
Azamfirei, Leonard P-381
Azanjac G P-454
Azhari MD, Petra O-66
Azouz, Heifa P-366, P-486, P-56
Azzouz, Haifa P-128, P-173, P-261, P-262,

P-33, P-359, P-485

Babal, Pavel P-59, P-60
Babic, Darko P-392
Bacha, Omar Moreira P-174
Badea, Petrica P-463
Badeii, Zahra P-144
Badia, Daniel P-353, P-93
Badiu, Diana P-89, P-99
Badoual, Cécile P-293
Badreddine, Sriha P197
Bafa, Maria P-432
Bahadir, Burak P-185, P-245, P-271, P-510, P-534
Bahrani, Maryam P-368
Bai, Maria P-24, P-272, P-44
Bai, Yanhua O-14, P-461
Bailón, Eva P-280, P-511
Baixeras, Nuria P-399
Balachandran, Krishna P-106
Balague, O P-30
Balan, Costica P-394
Balan, Mirela P-177
Balan, Raluca P-117, P-91
Balañá, Carmen P-277
Balasch, J O-28
Balassi, Evfimia P-76
Baldauf, Jean-Jacques P-88
Ballarín, Ignacio M P-17
Ballester, Ruiz C P-130
Ballestín, Claudio P-208
Baloglu, Huseyin P-123
Baltazar, Fátima P-374
Balzarini, Piera O-46
Banan, Mehdi P-190
Banihashem, Abdollah P-144
Banihashemi MD, Mahnaz P-512
Bankfalvi, Agnes O-30
Bañón-Maneus PhD, Elisenda P-29
Barata, Henrique S P-166
Barbacid, Mariano P-193
Barbera, Mila della O-24
Barbosa, Helenemarie S O-7
Barceló, I O-95
Bardaji, A O-28
Bargallo, A P-377
Barişik, Nagehan Ozdemir P-104, P-105, P-247
Barkhina, T G P-442
Barnadas, A P-120
Barnadas, Agustí O-33
Barranco, C P-488
Barraza, G P-12, P-320
Barraza, Graciela P-296
Barraza, Graciela P-395
Barriuso, Jorge P-100
Barut, Figen P-245, P-510, P-534
Bas, Emine P-246
Basheska, Neli P-77, P-107
Bassini, Silvia Froes P-8, P-448
Basso, Cristina P-472
Bastian, Alexandra O-79, P-496
Batelja, Lovorka P-139
Batista, José Emilio P-326
Batistatou, Anna P-5, P-58, P-509
Batuchin, Mihail P-526
Bauer, Claudia O-53
Baumhoer, Daniel P-398
Bautista, Dolores O-34
Bayer, Ingrid K O-40
Bdioui, haikel P-364
Beauchet, Alain O-49
Begnami, Maria D P-393
Behtash, Nadereh P-416
Bekele, B Nebiyou P-11
Bektas, Mehmet P-386
Bektas, Sibel P-245, P-510, P-534
Belge, Gazanfer P-64
Belghith, Mohsen P-111
Belkouchi, Abdelkader P-206
Bell, H O-80
Bellas, Carmen O-88, P-289
Bellil, Khadija P-33, P-55, P-56, P-128, P-173, P-261, P-262, P-289, P-341, P-359, P-364, P-365, P-366, P-485, P-486
Bellil, Salma P-33, P-55, P-56, P-173, P-262, P-341, P-359, P-364, P-365, P-366, P-485, P-486
Bello, Musodiq O-62, O-63
Bellocq, Jean-Pierre P-240, P-88
Beloqui, Raquel P-500
Beltrami, Giovanni P-183
Beltrán, Manuel P-462
Benazzi, Elena P-142
Bendavid, Cécile O-37
Benedette, Ana Paula Sassá P-307
Benguria, Alberto O-86
Benítez, Daniel P-137
Benitez, Jesús A P-126
Benito, Enric P-231
Benlloch, Susana P-251
Berdiel, Mireia P-277
Berenji, Fariba P-144
Berger, Nicole P-334
Bermudo, Raquel O-86
Bernadó, L P-12, P-320
Bernado, Lluis P-296, P-395
Bernal, Maria Luisa O-34
Berney, D P-161
Bernoussi, Zakia P-206, P-407
Bersani, Samantha O-46
Besbes, Ghazi P-55, P-56
Bezerra, Lilian Valéria Guerra da Silva Pinto P-32
Biase, Dario De P-236
Biczysko, Wieslawa O-76
Bilbao, Francisco José P-284
Bilbao, Francisco José P-285
Bilek, Karl P-80, P-81, PFP-2
Billis, Athanase P-317, P-318, P-319
Birzoi, Lilian P-473
Bishop, John O-19
Bittencourt, Achiléa L O-7
Blanchot, Jérôme O-37
Blanco, Jerónimo P-134
Blanco, Juan Carlos P-163
Blaude, M-Anne P-210
Blazquez, Carme n P-353, P-164, P-93
Blel, Ahlem P-364
Blesa, David P-279
Blokx, Willeke A M P-138
Boaron, M O-3
Boaron, Maurizio P-9
Bobrov, I P P-74
Bocan, Viorica P-439
Bode-Lesniewska, Beata O-78
Boglou, Kiriaki P-425
Bohorquez, Edgar Julián Ferreira P-346, P-347, P-348
Boileau, Catherine O-49
Bologna, Sheyla Batista P-306
Bombí, J A O-28
Bonafé, Magdalena Garcia P-349
Bonanno, E O-89
Bonanno, Elena O-86, O-90
Bondari, Simona P-274
Bonfitto, João Felipe Leite P-295
Bonfitto, Vera Lúcia Leite P-295
Bongiovanni, Massimo P-415, P-65
Boniver, Jacques O-16
Boon, Mathilde E O-94
Boorjian, Stephen A P-516
Borda, Angela P-106, P-334
Borondo, JC P-479
Boros, Monica P-106
Borras, Josep María P-430
Bosch, F Xavier P-430, PFP-7
Bosch, Ramon O-6
Bosoteanu, Catalin P-521
Bosoteanu, Madalina P-225, P-521
Botelho, Ana O-70
Boubaker, Jalel P-359
Bouchaud, Gregory P-293
Boutross-Tadross O P-83
Bouzoukas, Sofoklis P-321, P-535
Bouzourene, Hanifa P-360
Bows, F O-31
Boyko, Valeriy P-219
Bozhkov, Anatoliy P-219
Bozkurt, Erol Rustu P-290, P-90
Brabencova, Eva P-59
Bračko, Matej P-396
Brailovskaya, Tatiana P-298
Brasnu, Daniel P-293
Braticevici, Carmen Fierbinteanu P-394
Braumann, Ulf-Dieter P-80
Braumann, Ulf-Dietrich P-79
Bravou, Vasiliki P-313
Brčić, Luka P-139
Brehar, Felix P-270
Breier, D P-377
Brell, M O-95
Brenes, Fernando P-406
Brouquet, Antoine O-49
Brown S O-77
Brown, Kathlynn C P-11
Brunelli, Matteo O-45, O-46, PFP-1
Bruneval, Patrick P-293
Buim, Marcilei E C P-184, P-305
Buim, Marcilei Eliza Cavicchioli P-306, P-307, P-308
Bullerdiek, Jörn P-64

Buluş, Hakan P-324, P-492
Burchardt, Käte P-64
Bureau, Yves-André P-84
Burmistrov, Michael P-363
Bussolati, Gianni O-13
Butur, Georgeta P-132, P-250, P-375, P-70
Butureanu, Stefan P-91
Buzgariu, Wanda P-270

C Garrido, María P-48
Caban, Leny P-43
Cabane, Ana P-355
Cabello, Ana Quintero O-44
Cabezuelo, M Angeles P-421
Cabrera, Hugo Álvarez-Argüelles P-191, P-437
Cáceres, Valeria P-355
Cachot, C P-435
Caci, Karina P-387, P-388
Caforio, Alida P-142
Caja, Santiago Ramón y P-353
Cajal, S Ramon y P-198, P-429, P-435
Cajal, Santiago Ramón y P-162, P-163, P-164
Cajal, Santiago Ramon y P-93, P-382
Çakalagaoglu, Fulya P-244, P-246, P-527
Çakir, Çaglar P-104, P-539
Calabrese, Fiorella O-4, O-65, P-142
Calatayud, Ana María O-82
Calcagno, Marina P-122
Caldas, C O-31
Çalış O P-179, P-180
Callies, Rainer O-30
Calò, Daniela PFP-5
Călugăru, Dan P-466, P-468
Calvo, Antonio Ojea P-335
Calvo, Antonio P-10, P-194
Calvo, Julia P-134, P-137
Calvo, M P-85
Calvo, Miquel P-403
Camacho, Alonso P-194
Camacho, Pedro P-201
Camarasa, Natalia O-64
Camenita, Alexandru P-274
Cameselle-Teijeiro, José P-53, P-61, P-63
Camós, M P-30
Camós, Mireia P-342
Campins, María M Company P-349
Campistol MD, Josep M P-29
Campo, E P-30
Campo, Elías O-86, P-507
Campos, Kleber Nogueira de P-6
Campos, Martín Y P-388
Campos, R P-435
Campos-Martín, Yolanda P-278, P-279
Can, Ali O-62, O-63
Cañamero, Marta P-193
Cancellieri, A O-3
Candanedo, Fernando O-12
Candea, Vasile P-470, P-476, P-477
Candeira, Santiago Romero P-21
Canet R P-87
Cannata, Pablo P-494
Canós, JC P-479
Canzian, Mauro P-1
Canzonieri, Vincenzo P-391
Capanna, Rodolfo P-183
Capella, Carlo P-34
Capellà, Gabriel P-327, P-399
Capelli, Arnaldo P-536
Capelozzi, Vera Luiza P-1, P-2, P-3, P-4
Caramés, Nuria P-61
Cardós, Virginia P-280
Cardozo-Duran, José P-440
Carnevali, Ileana P-34
Caroli-Bottino, Adriana P-205
Carrasco, José-Luis P-115
Carrasco, MA P-218
Carrato, Cristina P-277
Carrera, Ruben P-252,
Carrera, Rubén P-297
Carreras MD, Joaquim P-29
Carreras, Elena P-163
Carreras, J P-30
Carreras, Ramon P-102, P-427, P-428
Carrilho, C O-28, P-133
Carrillo P P-87
Carstoiu, Monica P-108
Carturan, Elisa P-142
Caruntu, Irina Draga P-108, P-117
Caruntu, Irina P-91
Carvalhal, Eduardo F P-166
Carvalhal, Gustavo F P-166
Carvalho, Ana Carolina de P-305
Carvalho, André Lopes P-305
Carvalho, Erika Franco de P-4
Carvalho, Kátia C P-184
Carvalho, Lina O-2, P-13, P-19
Casado, A Casalots P-460
Casado, María del Carmen Ávila P-538
Casalots, J P-338
Casalots, Jaume P-387, P-388
Casalots, Jordi P-141
Casas, M P-12, P-320
Caserta, Benedicta P-118, P-256
Casnedi, Selenia P-240
Cassado, Carmen Ferrer P-506
Castano, Desire Campoy O-54
Castellà, J P-479
Castellani, Chiara O-24, P-142
Castellvi, Josep P-93
Castillo, Ana Isabel Sáez O-60, P-462
Castillo, José M. P-332
Castillo, Maa P-332
Castillo, Mireia P-342
Castillo, Wilmar P-327
Castro-Castro, Julian P-264
Castro, Candelaria García P-115, P-401, P-437
Castro, Eumenia Costa Cunha P-528, P-529
Castro, Maa-Candelaria García P-437
Castro, Pilar P-430
Català, Isabel P-17, P-45
Catasús, L P-119, P-121
Catasus, Lluis O-33
Cathomas, Gieri P-398, P-402
Cavazza, A O-3
Cavazza, Alberto P-19
Cayirci, Mine P-221, P-539
Çayirci, Mine P-247
Cazorla, Alicia O-9
Ceauşu, M P-132
Ceausu, Mihai P-250, P-375, P-70
Ceausu, Raluca P-439
Cecilia, Fiandesio Ada P-412
Cedeira, Mabel P-118
Cegan M P-487
Ceganova L P-487
Cejka P P-487
Celià, Toni P-134
Celik E P-192, P-49
Celik, Aykut Ferhat P-397
Centeno, C P-435
Cerino, Giovanna O-84
Cerna, Andrea P-59, P-60
Cerutti, Roberta P-34
Cetin, Sibel Erdamar P-397
Cetinel, Cihangir P-539
Cetinkaya, Hulya P-386
Cezary, Jochymski P-404
Charalabopoulos, Konstantinos P-5, P-58
Charalampidis, Ch P-426
Charalampidis, Charalampos P-424
Chatzitolios, Anastasios P-171, P-172, P-425
Chau, Miu P-214
CHEBIL, Mohamed P-340
Chefani, Alina Elena P-108, P-394
Chehrei, Ali P-524
Chei, Mi Sun P-182, P-200, P-384, P-385, P-98
Chekan, Mykola P-68
Chelly, Ines P-128, P-173, P-261, P-262, P-33, P-341, P-359, P-364, P-365, P-366, P-486, P-55, P-56
Chen, Beiyun O-35
Chen, H P-54
Chenard, Marie Pierre P-240
Cheng, Liang O-45, O-46, P-316, PFP-1
Cheng, Tina O-48
Cherif, Khedija P-173
Chimelli, Leila P-205
Chinoy, R F P-168
Chizhov, Vsevolodovich P-451
Choe, Gheeyoung P-20, P-330
Chou, Cheng-Yang PFP-7
Chranioti, Stavroula P-189
Christophe, Tresallet O-49
Chu, Pao-Hsien P-478
Chung, Jin Haeng P-204, P-330, P-40, P-20
Ciancia, Giuseppe O-47
Cianga, Corina P-91
Cianga, Petre P-91
Ciatti, A P-291
Cickusic, Elmir P-92
Cimpean, Anca Maria P-228, P-381, P-383, P-491
Cioroianu, Dan P-274
Citak, Leyla O-18
Clarisa, González P-423
Clavero, Omar PFP-7
Climent, Fina P-231, P-327, P-45
Cocco, Mario O-84

Cohen, Marta C O-19
Colak, Ertugrul P-351
Colak, Sacide P-245
Colantoni, Alfredo O-86
Colarossi, Cristina P-391
Colita, Adriana P-43
Colita, Dan P-43
Collado, Manuel P-193
Collina, Guido P-9
Colomer, Dolors P-342
Colomer, J Costa P-460
Colomo, L P-30
Colomo, Lluis P-507
Comanescu, Maria P-250
Combalia, Neus P-116, P-418, P-421
Company, Maria M P-414
Condom, E P-338
Condom, Enric P-17, P-231, P-253, P-323, P-327, P-399, P-45
Conejo, R P-435
Contreras, Felix P-513
Córdoba, Alicia P-63
Córdoba, H P-198
Coriu, Dan P-43
Cornianu, Marioara P-371, P-373
Cornianu, Mărioara P-372
Coroiu, Viorica P-270
Corona, Manuel P-116
Corrales, Teresa O-93
Corriente, M[a] Carmen Martín P-437
Corsino, Pat P-249
Cortés, Luis O-25
Cortina, Galen P-465
Cosculluela, Maria Jose Fantova P-506
Coşkun, Ali P-324, P-370, P-492, P-493
Cossu-Rocca, Paolo PFP-1
Costa, Adriana Alencar Araújo P-288, P-475
Costa, Ana Carolina Leite Vieira P-41, P-42
Costa, Ana Flavia P-295
Costa, Ana Lídia T P-301
Costa, Claudio P-449
Costa, Edson P-8, P-127, P-152, P-448, P-449
Costa, Irmgard P-116
Costa, Leila Moussa P-127, P-152, P-448, P-449, P-8
Costa, Y Pallás P-339
Costache, Mariana P-108, P-394
Costantini, Mario O-65
Costanzi, Stefano P-536
Couce ME P-87
Couce, M E O-95
Couceiro, Patrícia O-2, P-13
Coué, Olivier O-37
Coulet, Florence O-49
Coutinho-Camillo, Cláudia Malheiros P-305, P-306, P-307, P-308
Craciun, Anca P-232, P-378
Craciun, Antonela-Anca P-89, P-99
Craciunescu, Oana P-177, P-457
Crespo, S P-479
Crispen, Paul L P-516
Cristiana, Tanase P-273
Croce, Sabrina P-240, P-88
Cruz-Cigudosa, Juan P-279
Cruz, Armando Medina P-538
Cruz, Eugénia PFP-7
Cruz, Ofelia P-155
Cruz, Pérez G P-388
Cserni, Gabor P-227
Cuatrecasas, M P-119, P-120, P-121
Cuatrecasas, Miriam P-494
Cubilla, Antonio PFP-7
Cueto, M R Bella P-460
Cuevas, Jesus P-513
Cullu, Fugen P-397
Cunha, Isabela W P-184
Cunha, Isabela Werneck da P-16
Curran, Olimpia O-21
Cusí, Victoria P-149, P-155
Cusido, Maria Teresa P-75
Custodio, Fabiano Bichuette P-528, P-529
Cvetkovski, P P-51
Cwikla, Maria P-400

Da Silva, Valdo J Dias O-71
Damiani, S O-3
Damiani, Stefania P-215, P-9
Daniela, Teodorescu P-267
Darabi, Elham P-190
Dardik MD, Michael P-413
Darwich, Esteve P-497
Daskalov, Marin P-266
David, J O-28
Davidson, Darrell P-316
Davis, Bradley P-249
Dawamneh MD, M Fawaz P-540
Dawson, S-J O-31
De Araújo, Ney Soares P-294
De Araújo, Vera Cavalcanti P-294, P-295
De Gálio, Eduardo P-6
De la Cueva, Paloma P-462
De la Peña, Soledad P-256
De la Torre, Juan Javier P-115
De León, Fernando Chico-Ponce P-153
De Lope, Angel Rodríguez P-278
De María, Carolina Gómez P-223
De Sanjose, Silvia PFP-7
De Sevilla, M C Sánchez Fernández P-339
De Torres, Carmen P-149
De Victoria, José María Martínez O-44
Deacu, Mariana P-225, P-521
Dei Tos, Angelo P P-19
Del Agua C P-328, P-18, P-514
Del Muro, Javier García P-327
Del Río, Emilio P-498
Del Valle, Ana Teruel P-21
Delahunt, Brett O-46, PFP-1
Delbro, Dick P-354
Delvenne, Philippe O-16
Dema, Alis P-371, P-373
Demir, Gokhan O-54, P-203
Demirhan, Recep P-23
Derakhshandeh, Soudabeh P-135
Derchain, Sophie P-96, P-97
DEROUICHE, Amine P-340
Destouni, Ch P-426
Destouni, Chariklia P-424, P-425
Deveci, Güzin P-434
Deveci, İ Güzin P-433
Deveci, M Salih P-433, P-434
Dhandapa, ni Asho k O-19
Dhouibi, Abdelmajid P-110, P-187, P-26, P-309
Di Rocco, M G O-3
Diamantopoulou, Kalliopi P-189
Dias, Eliane P P-422
Díaz-Flores, Lucio P-115, P-401
Diaz-Nuñez, Maria P-238
Díaz, E P-12
Diaz, Esther P-296, P-395
Diaz, Julio Alexander P P-78, P-483
Díaz, Silverio P-122
Diclehan, Orhan P-159
Diekmann MD, Fritz P-29
Diez, N Baena P-460
Dilek H P-179, P-180
Dilek, Hüsniye P-226
Dilly, S P-165
Dima, Simona P-202
Dimitriou, Th P-426
Dinarès, C P-429, P-435
Dincer, Nazmiye P-312
Djukanovic, B P-480
Djukic, Milena P-167
Djuricic, Slavisa P-167
Dmitrieva, Olga P-526
Dmitry, Filatkina P-451
Doan, Ngan P-465
Dobre, Anca P-232, P-378, P-89, P-99
Dobrea, Camelia P-132, P-250, P-375, P-43, P-70
Dogan, Ahmet PFP-9
Dogusoy, Gulen Bulbul P-397
Dogusoy, Gulen O-54, P-203
Dolz, Carlos P-349
Domingo, Efren J PFP-7
Domingo, Eva P-45
Domingues, Maria Aparecida Custódio P-32
Domínguez-Dorado, Patricia P-175
Domville, Daniela O-12
Done, Susan O-87 Dorel, Arsene P-273
Dorronsoro, ML Gómez P-467
Dorronsoro, MLuisa Gómez P-63
Doukas, Michael P-272, P-509
Drag-Zalesinska, Malgorzata P-356
Driu, Luiza P-202
Driver, K O-31
Drosdova, Larissa P-219
Dry, Sarah P-465
Dubini, A O-3
Dubova, Elena Alexeevna P-178, P-379, P-451
Dumitriu, Sorin P-112, P-186, P-508
Dummer, Reinhard O-78
Durán-Barbeito, Pastora P-223
Durko, Marcin P-310
Dursun, Nevra P-290, P-90
Dvorackova J P-487
Dziegiel, Piotr P-356, P-520

Eble, John Nelson O-46
Eble, John O-45, PFP-1
Ebri, Maria Luisa Pérez P-505
Eccher, Albino O-45, O-46, PFP-1
Edelweiss, Maria Isabel P-174
Edsparr, Karin P-354
Efthymios, Koniaris P-199, P-325, P-329, P-530, P-531, P-532, P-535, P-94, P-95
Eghbalian, Fatemeh O-22
Eguia-Aguilar P P-143
Eguía-Aguilar, Pilar P-153
Eguiara, Arrate P-238
Einenkel, Jens P-79, P-80
Eisenberg, Ana Lucia P-422
El Banayosy MD, Aly O-66
Elena, Raducan P-273
Eleonora, Codorean P-273
Elias R P-83
Elit L P-83
Elorriaga, Kepa P-238
Elsawaf, Zeinab O-36
Emami, Mohamad Hasan P-390
Enache, Simona P-375
Enache, Stelian Danut P-274, P-463
Enache, Valentin P-375
Ene, Diana P-250
Ene, Diana P-70
ENGELMAN, Miriam FB P-241
Enguita, Ana Belen P-48
Enoksson, Jens O-5
Enríquez, Adrián Mariño O-23
Ensari, Arzu P-386
Entrena, Edurne O-91
Erbarut, Ipek P-220, P-244
Erbersdobler, A O-43
Erdamar, Sibel O-54, P-203
Erdogan N P-192
Eremia, Florin P-70
Eren, Funda O-18
Erenler, Ilknur P-203
Ereño, Cosme P-284, P-285
Erensoy, Selda O-56
Erhan, Yumuşak P-469
Erkan, Tulay P-397
Ersöz, Galip O-56
Ertoy-Baydar, Dilek O-39
Escoda, M Rosa P-297, P-421
Escoda, Ma Rosa P-418
Escoda, Maria Rosa P-116, P-248, P-252, P-495
Escrivá, Patricia O-6
Escuder, Oscar P-297
Esen, Tugce P-397
Eser, Mehmet P-247
Esfahaniar, Monsef P-35
Esgueva, Raquel O-42, P-333, P-343, P-344
Español, Isabel O-41
Espinet, Blanca P-428
Esteller, Laura P-231
Esther, Ferré P-423
Estrach, T P-30
Etxezarraga, Mari Carmen P-284, P-285
Eugen, Hinescu Mihail P-273
Eugen, Mandache P-519
Eusebi, Vincenzo PFP-5

Fa, Eghbalian P-35
Fabregas, Rafael P-212, P-75
Faghih M P-83
Fakhrjoo, A P-234
Falco, Giulia De O-84
FARAH, Faten P-340
Farahmand, Mohammad Javad P-209
Farhat, Cecília P-1
Farré, Lourdes O-7
Faus, Ma Carmen P-322
Faverly, Danie P-210
Fayt, Isabelle O-17, P-101
Federici, Giorgio O-85
Federico, García P-423
Fedorenko, Pavlo P-156, P-287
Fedorina, Tatiana P-298
Feldman, Andrew PFP-9
Felipo, F P-328, P-18, P-514
Felipo, Francesc P-158, P-303
Ferenczy, Alex P-84
Ferlosio, Amedeo P-482
Fernandes, Afonso P-46
Fernandes, F P-133
Fernandes, Josué P-6
Fernandes, Paulo Manuel Pêgo P-6
Fernández-Abreu, Mary P-440
Fernández-Almeida, Andrea P-223
Fernández-Bañares, Fernando P-387
Fernández-Costas, Alfonso P-223
Fernandez-Figueras, M Teresa P-494, P-504
Fernandez-Figueras, María Teresa P-367
Fernández-Rodríguez, B P-265
Fernández-Rodríguez, Beatriz P-175, P-264
Fernandez, Dietmar O-91
Fernández, Eva P-137, P-196
Fernández, fIrene O-60
Fernandez, Luis P-248
Fernández, Madeline P-523
Fernández, Mary P-523
Fernández, Pedro L O-86, P-134
Fernández, Pedro Luis P-137, P-196
Fernandez, R Orellana P-460
Fernandez, Sara P-248, P-252, P-418, P-421, P-495
Fernando, Sujatha O-83, P-52
Fernani, Fahima P-293
Ferraccioli, Gianfranco P-536
Ferran, Anna P-421
Ferrandiz, Carlos P-494
Ferré, Esther P-387, P-388
Ferreira, Cristina P-46
Ferreira, Edgar Julián P-286
Ferreira, Francisco Valdeci Almeida P-288, P-41, P-42, P-475
Ferreira, Luísa P-374
Ferreira, Renata Diniz Rabelo P-528
Ferreira, Ubirajara P-317, P-318
Ferrer-Roca, O O-58
Ferrer, Berta O-86
Ferrer, Jaime P-22
Ferrer, Pilar Lopez P-431
Ferrer, S Fernandez P-460
Ferreres, Joan Carles P-162, P-163, P-164
Feten, Limeiem P-262
Feu, Jaume P-212
Fiaño, Concepción P-278, P-279
Fiaño, Concha P-280
Fic, Magdalena P-356
Figa, Montse P-395
Filho, C Cardoso P-239
Filho, Flávio Brito P-6
Filho, Francisco Dario Rocha P-288, P-41, P-42, P-475
Filho, João Gonçalves P-306
Filho, Paulo Latuf P-39
Filosso, Pierluigi PFP-6
Fiol, J O-95
Fischer, Uta O-15, P-80, P-81
Fiska, A P-426
Flamminio, Federica P-236
Flávia, A P-302
Fleischmann, A O-43
Florek, Ewa O-76
Florensa, G P-218
Fojón, Joaquín González-Carreró P-217
Font, Rebeca PFP-7
Forcada, Pilar P-387, P-388
Forouhesh MD, Zahra P-417
Forteza AV P-87
Forteza-Vila, Jeronimo P-264
Forteza, AV P-130
Forteza, J P-265
Forteza, Jerónimo P-175
Foschini, Maria P P-236
Foschini, Maria Pia PFP-5
Foster W G P-83
Fotika, Christina P-509
Fotopoulos, Andreas P-272
Foucher, Fabrice O-37
Fouret, P P-292
Frahm, Isabel P-355
Franc, Brigitte O-49
Franceschi, Enrico PFP-5
Franchi, Alessandro P-183
FRANCO, Marcello Fabiano de P-241
François, O-37
Fregnani, José H P-393
Freitas, Leandro L L P-317, P-318, P-319
Frenandes, Oswaldo P-27
Frias, Carolina P-289
Fridman, Wolf H P-293
Fritz, Gabrielle P-88
Fuertes, A P-328, P-18, P-514
Fuertes, Ana P-158, P-237, P-303, P-503
Furlan, Daniela P-34
Furuse, Cristiane P-294, P-295

Gaafar, Ayman P-284, P-285
Gaber, Nisreen P-299
Gabriela, Picon M P-235
Gacic, Dragan P-392
Gackowska, Lidia O-76
Gaiolla, Rafael P-32
Gaje, Pusa P-438, P-439, P-491
Galano, E P-133

Gallardo, A P-119, P-121
Gallardo, Alberto O-33
Gallardo, F P-488
Galle, Dana O-15, PFP-2
Gallego, Elena PFP-3
Gallegos, Marc P-327
Galletta, D O-3
Galli, Susana PFP-10
Galuscan, Atena P-438
Gambino, Antonio P-142
Gamboa, Armando O-12
Gamboa, Maria de P-150
García, Alejandro Brito P-115, P-401
García, Amparo P-253
Garcia, Angel P-93
García, Carlos Andrés P-281
Garcia, Ernesto P-148, P-259, P-281
García, F P-218
Garcia, Jorge Andres V P-78
García, Juan Fernando P-278, P-279
García, Juan-Cruz Cigudosa P-401
García, Lluís P-421
García-Albéniz, Xabier P-342
Garcia-Bonafe, M Magdalena P-414
Garcia-Galvis, Olga F P-106
Garcia-Herrera, A P-30
Garicochea, Bernardo P-166
Garland, Suzanne PFP-7
Garmendia, Maddi P-284, P-285
Garrido-Ruiz, MC O-92
Garrido, Marta P-353, P-382
Garrigue-Antar, Laure P-293
Gartner, Silvia P-162
Gaspa, Albert P-342
Gaspar, Alexandra P-177
Gavrilov, Volodimyr P-287
Gecer, Melin Ozgun P-90
Gelabert, Antoni O-42, P-333, P-343
Gelabert, Laura P-196
Gene AH P-87
Gene, A H O-95
Georgescu, Alina P-132, P-250, P-375, P-70
Georgescu, Corneliu Cristian P-274
Georgescu, Mariana P-108, P-394
Georgescu, Otilia P-43
Georgia, Thodoropoulou P-329
Georgiev, Tch P-140, P-517
Georgiev, Tchavdar P-124
Georgiu, Aurelian P-466, P-468
Georgiu, Carmen P-466, P-468
Geramizadeh, Bita P-525
Gerdes, Michael O-62
Gergov, Georgi P-124, P-266, P-350
Germà, J Ramón P-327
Gerney, Garrett P-465
Gerosa, Gino P-142, P-472
Gey, Alain P-293
Geyik, Pinar P-216
Geyik, Sibel Gelecek P-370, P-493
Ghafarzadegan, Kamran P-368, P-209
Ghafouri MD, Mazir P-417
Gharesouran, Jalal P-190
Gheban, Dan P-466, P-468
Gherghiceanu, Mihaela O-75
Ghiasi, Mohammad Taghi P-209
Ghose, Supriyo P-450
Ghünthner, Stephan P-322
Giacometti, Cinzia O-4. O-65
Gil, J Miguel P-253
Gimenez, Carmen O-93
Gimeno, Esther P-237
Gimeno, Javier P-102, P-427, P-428
Gimferrer, Eulalia P-102, P-427, P-428
Giner, Francisco O-82
Giordano, Antonio O-84
Giralt, M R Escoda P-460
Gjerdrum, Lise Mette O-8
Glatz, Dieter O-59
Glatz, Katharina O-59
Glava, Chryssoula P-82
Gobbo, Stefano O-45, O-46, P-316, PFP-1
Goel, Sharad P-129
Gogg-Kamerer, Margit P-19
Gokaslan, Husnu O-18
Goksel, Suha O-54, P-203, P-397
Goldiş, Adrian P-371, P-372
Gomà, Montse P-141
Gomes, Ana O-2, P-13
Gómez-Dorronsoro, Maaa Luisa P-276, P-500
Gómez, Mercedes O-60
Gomez, Teresa P-102, P-427
Gondim, Ricardo Pinto P-288
Gonul, Engin P-268
Gonzalez, Antonio P-513
González, Carlota P-141
González, Clarisa P-387, P-388
González, Guadalupe P-387, P-388
González, Juan L Ríos P-335
González, Juan Luis Ríos P-217, P-275
González, Miriam O-6
González, Mirida P-523
Gonzalez-Baron, Manuel P-100
González-Carreró, Joaquin P-275
Gonzalez-Huix, Ferran P-395
Goran, Azanjac P-455
Gordana, Petrusevska P-51
Goulioumis, Anastasios K P-313
Goumas, Panos P-313
Goussia, Anna P-272, P-44, P-509
Gouveia, Rosa Henriques de O-70, P-471
Grabellus, Florian PFP-8
Graeten, M O-43
Grala, Bartlomiej P-260
Grammatoglou, Xanthippi P-82
Granados, Rosario O-93
Granados, Sergio P-201
Graus, Francesc P-280
Grazio, Snježana Frković P-396
Gremaud, Magali P-415, P-65
Gremese, Elisa P-536
Grignon, David O-45, PFP-1
Grigoris, Derdelis P-94, P-95
Groisman, Gabriel P-352
Gruber-Moesenbacher, Ulrike P-19
Grubor, Andrej P-50
Grygar, Elisabeth P-19
Gu, Po-Wen P-478
Guadalupe, González P-423
Gubina-Vakulik, Galina P-522
Guerra, Carmen P-193
Guerrero, A O-95
Guerrero, Armando Méndez Javier P-136
Guevara, Claudia P-17
Gui, Dorina P-465
Guilabert, Antonio P-497
Guimarães, Marbele S P-317
Guimerà, Nuria PFP-7
Gul, Aylin Ege P-104, P-105, P-23, P-539
Gül, Aylin P-247
Guldvog, Ivar O-32
Guler, Gulnur P-312
Gulluoglu, Bahadir P-246
Gulsev, Kale P-159
Gumà, Anna P-231, P-253
Gümüş, Mahmut P-247
Gun, Banu Dogan P-185, P-510
Gungor, Atila P-123
Gunhan, Omer P-268
Günşar, Fulya O-56
Güreşçi, Servet P-370, P-492
Gurgel, M S C P-239
Gursu, Umar O-54
Gurzu, Simona P-181, P-38, P-383
Gutierrez, Jose Luis O-91
Guzmán, Flavia P-497

Haaften, Maarten van O-94
Hadhri, Rim P-113
Hadhri, Rym P-109, P-110, P-111, P-26, P-309
Hadizadeh, F P-362
Haglund, Monica O-5
Haholu, Aptullah P-123
Hakan, Cermik P-469
Halbwedl, Iris P-19
Han, Bo P-461
Handra-Luca, A P-292
Hans-Konrad, O-9
Hans, Stéphane P-293
Haouet, Slim P-128, P-173, P-261, P-262, P-33, P-341, P-359, P-364, P-365, P-366, P-486, P-55, P-56
Hardisson, David P-100
Harmanci, Aysegul P-351
Hasanov, Edalet B P-443, P-444
Hashim, N O-80
Hassanzadeh, Amar P-524
Hatemi, Ibrahim P-397
Hausen, Axel zur O-53
Hayrabedyan, Soren P-336
Heffernan, Jose Jimenez P-431, P-513
Heintz, A Peter M O-94
Heiskala, Kukka P-69
Helliwell, Tim P-299
Hens, Ángela P-10, P-194
Hentschel, Bettina O-15, P-79, P-80, P-81, PFP-2
Herlea, V P-202
Hernandez-Cortes, Gines P-100
Hernández-Moneo, José Luis P-279
Hernández, Álvaro Antonio Herrera P-281

Hernández, Gustavo PFP-7
Hernandez, J P-435
Hernández, Javier P-353, P-93
Hernández, Julio Cesar Mantilla P-148, P-259
Hernández, Silvia O-42, P-333, P-343, P-344
Hernández, Sonia García P-115, P-401, P-437
Herrera, Álvaro Antonio P-286
Herrera, Loren Paola P-281
Herrero, S P-338
Herrero, Sergio P-141
Hickey, S O-80
Hierro, Isabel PFP-3
Himmetoglu, Cigdem P-312
Hinescu, Mihail Eugen O-75
Hinova-Palova, D P-124, P-140, P-517
Hiradfar, Mehran P-146
Hiradfar, Simin P-144
Hirohashi, Setsuo P-5
Höckel, Michael P-79
Hoff, K D P-222
Hofstaedter, Ferdinand O-74
Hölzlwimmer, Gabriele P-66
Hong, Seung-Mo P-204
Horn, Lars-Christian O-15, P-79, P-80, P-81, PFP-2
Hörndler, Carlos P-503
Hortopan, Monica P-202
Hosseinnezhad, Hanieh P-368
Hovnanian, André Luiz Dresler P-1
Howart, W O-31
Hristov, S P-140, P-517
Hristov, Stanislav P-124, P-350
Hsiao-Chen, Hsiao P-478
Huang, W P-54
Huber, Andreas P-398, P-402
Huber, Monika P-19
Huebner, Kay P-312
Huerta, Salvador P-136
Huguet, P P-429
Huguet, Pere P-349
Huland, H O-43
Hurduc, Victoria P-394
Huseynov, Vugar K P-443
Hyun, Chang Lim P-330

Iakovlev, Vladimir O-87
Iakovleva, Gaiane O-87
Ibañez, Raquel P-430
Ibarra, J P-484
Iemelianova, Anna P-314, P-315
Iglesias, C P-429, P-435
Iglesias, Enrique O-88
Ilardi, Gennaro P-489
Ilhan, Altan P-159
Ilic, Ivan P-408, P-409
Iliesiu, Andreea P-232, P-378, P-89, P-99
Iljazovic, Ermina P-92
İlter, Tankut O-56
Ines, Ennaifer P-485
Ingold-Heppner, Barbara O-78
Insabato, Luigi O-47
Ioan, Nicolescu Mihnea P-273
Ioannidou, Evaggelia P-44
Ion, Elena P-70
Ionescu, M P-202
Iosif, Cristina P-132, P-250, P-375, P-43, P-70
Irigoyen, MA Arrechea P-467
Irimiea, Lazar P-99
Irina, Ogrezeanu P-273
Ismail, M R O-28, P-133
Iturriagagoitia, A Córdoba P-467
Ivan, Ilic P-410
Ivanova, Elka P-266
Izadi, Nafiseh P-37
Izquierdo, Máximo P-212
Izvernariu, Dragos P-228
Izykowska, Ilona P-520

J, Kobos P-311
Jacques, Yannick P-293
Jaén, Joaquín O-6
Jafarian, Amir Hossein P-209
Jafarzadeh, Mostafa P-368
Jahanzad, Isa P-229
Jahanzad, Issa P-135
Jahid, Ahmed P-206, P-407
Jain, Asha PFP-7
Jain, Dr Rohit P-411
Jambhekar, Nirmala A P-168
Jancar, Boris P-502
Janega, Pavol P-59, P-60
Jang, Kee-Taek P-204
Janjic, Dejan P-408
Janjic, Suncica P-408
Janusz, Patera P-404
Jargin, Sergei V O-67
Jarzab, Barbara P-68
Jarzab, Michal P-68
Jaume, Casalots P-423
Javadi, Morteza P-147
Jensen, Sussie Steen P-376
Jerse, Maja P-15, P-502
Jesien-Lewandowicz, Emilia P-263
Jesionek-Kupnicka, Dorota P-263
Jheon, Sanghoon P-20
Jiang, Zhong P-316
JILANI, Sarah BALTAGI BEN P-340
Jimenez, Ana O-34
Jiménez, Aura O-12
Jiménez, Juan Arenas P-21
Jimenez-Schumacher, Alberto P-66
Jirström, Karin O-5
Johansson, Leif O-5
Jones, Andrew P-299
Jong, Pauline de O-94
Jönsson, Per O-5
Jordá, Esperanza P-490
Jørgensen, J T P-222
Jose, Belen San P-100
Jou, Cristina P-162
Jovanovic, Dragana P-7
Juan, José-Luis Carrasco P-191, P-401, P-437
Juanpere, Núria O-42, P-333, P-343, P-344
Juárez, Rocio P-278
Ju-Feng, P-478
Jukić, Stanko P-139
Juliá, Marc P-497
Julié, Catherine O-49
Jung, Hae Ra P-98, P-182, P-200, P-384, P-385
Jung, Ioan P-181, P-381, P-383,
Jung, János P-38

K, Bojanowska-Pozniak P-311
Kabukcuoglu, Sare P-351
Kaczmarek, Elzbieta O-76
Kadivar, Maryam P-147
Kahrizi, Kimia P-190
Kakouri, Petroula P-321
Kakturskiy, Lev O-73
Kakudo, Kennichi O-14, P-461
KAlliakmanis, Ioannis P-405
Kalniev, Manol P-350
Kamalian, Naser P-420
Kamina, Sevasti P-509
Kaminopetros, P P-464
Kamionek, Michał O-52
Kamoun, Haefa P-55
Kampas, L P-426
Kampas, Lampros P-171
Kanavaros, Panagiotis P-44
Kandemir, Nilufer Onak P-105, P-185, P-245, P-271
Kang, Yu Na P-98, P-182, P-200, P-384, P-385
Kanjou, Nadwa P-75
Kapatou, Eftihia P-24
Kapitanović, Sanja P-139
Karadayi, Nimet P-23, P-90, P-104, P-105, P-185, P-221,P-245, P-247, P-271, P-510, P-534, P-539
Karahan, Sevilay O-39
Karaivanov, Milen P-336
Karasalihovic, Zinaida P-92
Karasu, Zeki O-56
Karatas, Nihan O-54, P-203
Karatas, S P-49
Kareghar, Saeed O-11
Karev, V E O-27
Karina, Caci P-423
Karla, B O-29
Karlsson, Christina P-27
Karlsson, Mats G O-38, P-27
Kasamatsu, Elena PFP-7
Kashyap, Seema P-450
Katebi, Mehrdad P-36
Katic, Katarina P-408
Katic, Vuka P-408, P-409
Kavantzas, Nicolaos P-481
Kawamukai, Kenji P-9
Kaya, Handan P-220, P-244, P-246, P-527
Kchir, Nidhaleddine P-486
Kchir, Nidhameddine P-33, P-55, P-56, P-128, P-173, P-261, P-262, P-341, P-359, P-364, P-365, P-366, P-485
Keramati, Mohammad reza P-36
Kermani, Ali Taghizadeh P-368

Kern, Izidor P-25
Kertis, Gurkan P-510
Keser, Sevinc Hallac P-23, P-104, P-105
Keser, Sevinç P-247
Kestler, Edgar PFP-7
Ketterling, Rhett P O-35
Keyhani, Elahe P-190
Khaniki, Mahmood P-416
Khaniki, Mahmud P-229
Kharrat, Sélima P-365
Khayyami, Mohammad Esmaeil P-37
Khoob, Mahdi Khabbaz P-37
Khorram-Manesh, Amir P-354
Kianifar, Hamidreza P-144
Kiedrowski, Mirosław O-52
Kiho, L P-160, P-165
Kiho, Liina O-21
Kilany, Linah O-88
Kilgus, Sandra O-78
Kim, Chul Woo P-40
Kim, Haeryung P-330
Kim, Ji Eun P-20, P-40, P-204
Kim, Jin Hwan P-62
Kim, Sang Pyo P-98, P-182, P-200, P-384, P-385
Kim, Young A P-40
Kimmig, Rainer O-30
Kintiroglou MD, Marietta P-413
Kır, Caner P-226
Kirschnick, Luciana Schmidt P-174
Kiurski, Milosav P-50
Klaustermeier, Joellen PFP-7
Klemke, Markus P-64
Klimatchev, V V P-74
Klimova, Elena P-219
Klingenberg, B P-54
Klomp, Johanna M O-94
Klopčič, Ulrika P-436
Knani, Nesrine P-499
Knoll, Tony P-453
Kobos, Józef P-310
Kofman-Alfaro S P-143
Koktysz, Robert P-260, P-357
Kolettis, Theofilos P-24
Kolomiytsev, Alexey P-459
Koniaris, Efthymios P-321
Koning, Maurits N C de P-138
Konstantinidou, A P-464
Korbi, Sadok P-14, P-86, P-131, P-499
Kordek, Radzislaw P-230, P-263
Korkolopoulou, Penelopi P-189
Korman, Stanley P-452
Kornprat, Peter O-50, O-51
Korporaal, Hans O-94
Kos, Marina P-103
Koskinas, Ioannis P-405
Kouladouros, Konstantinos O-54
KOURDA, Jihene P-340
KOURDA, Nadia P-340
Kouvidou, Chariklia P-405
Kowalski, Luiz Paulo P-305
Kozlowski, Wojciech P-260, P-357
Kramer, Gerco C O-94
Kristiansen, Glen O-1
Krstic, Miljan P-409
Kruk, Michal P-260, P-357
Krupnov, Nikolay M P-331
Kubelka-Sabit, Katerina P77, P-107
Kuburovic, Vladimir P-167
Kucukodaci, Zafer P-123
Kudrevich, Alexander P-219
Kulczycka, Dominika P-263
Kumar, Neeta P-65, P-415
Kuonen, Anne P-360
Kupnicka, Dorota P-230
Kurz, Anna Kordelia O-53
Kusinska, Renata P-230, P-263
Kuster, Ariana O-78
Küsters-Vandevelde, Heidi V N P-138
Kutlu, Tufan P-397
Kuzyk, Julia O-72
Kuzyk, Yuliya O-69
Kwon, Eugene D P-516
Kwon, Kun Young P-98, P-182, P-200, P-384, P-385
Kwon, Sun Young P-98, P-182, P-200, P-384, P-385
Kyritsis, Athanasios P-272

Labastida, Ramón P-75
Laborda, Ainhoa P-323
Lambri, Evangelia P-44
Lamovec, Janez P-436
Lampri, Evangeli P-509
Landman, Gilles P-306
Landolfi, Stefania P-353, P-382
Lang-Avérous, Gerlinde P-88
Lange, Dariusz P-68, P-304
Langner, Cord O-50, O-51
Lapunzina, Pablo O-23
Lara, John P-504
Laraki, Laila P-206
Laraki, Leila P-407
Larrazabal, Fernando P-102, P-427, P-428
Latinovic, Ljiljana Tadic P-72, P-224
Laurino, L O-3
Lausevic-Vuk, L P-480
Law, Brian P-249
Law, Mark PFP-9
Law, Mary P-249
Lawrence CM O-77
Layos, Laura P-367
Lazăr, Daniela P-371, P-372, P-373
Lazăr, Elena P-371, P-372, P-373, P-438
Lazarev, A F P-74
Lazaris, Andreas C P-515
Lazaroiu, Anca Mihaela P-108, P-394
Lazaroiu, Anca P-84
Leal, MJ P-479
Leau, Traian P-457
Leblebici, Cem P-290
Lee, Choon-Taek P-20
Lee, Clara Sang Sook P-61
Lee, Hee Eun P-330
Lee, Hye Seung P-330
Lee, Hyun Ju P-20
Lee, Sang Sook P-62, P-98, P-182, P-200, P-384, P-385
Leeuwen, Arjanne Van P-138
Leibovich, Bradley C P-516
Lejeune, Marylène O-6
Leo, Cornelia P-79
León, Nieves Hernández P-115, P-401, P-437
Leonard N O-77, O-80
Leoncini, Lorenzo O-84
Lerín, Angels P-231
Lerin, M Àngels P-253
Lerma, Enrique O-33, P-251
Lessa, Roberta Cardim P-305
Leucci, Eleonora O-84
Leung, Carly O-78
Leung, Stephanie O-87
Levent, Güllü P-469
Levêque, Jean O-37
Li, Yaqiong O-14
Ligorio, C O-3
Ligorio, Claudia P-9
Ligtenberg, Marjolijn J L P-138
Lillo, Natalia Camarasa P-505
Lim, Jae Hoon P-204
Lima, Carmen Silvia Passos P-239
Lima, Gabrielle Gurgel P-41, P-42, P-288, P-475
LIMA, Joao PR de P-241
Limaiem, Faten P-33, P-128, P-173, P-261, P-359, P-485
Linares, Héctor Navarro P-462
Linda, Cruceru Maria P-273
Linden, Michael P-211
Lindtner, Richard A O-50, O-51
Linehan, W Marston P-67
Liu, Diane D P-11
Liu, Zhiyan O-14
Lizarralde, Alejandra Caminoa O-23
Llambrich, A P-484
Llatjós, Roger P-17
Llombart-Bosch, Antonio P-314, P-315
Lloreta, Josep O-42, P-333, P-343, P-344
Lloveras, Belen P-430, PFP-7
Lluïsa, Surrallés María P-423
Loeschke, Siegfried P-64
Loghin, Andrada P-106, P-334
LOGULLO, Angela Flavia P-241, P-242, P-243, P-255
LOGULLO, Luciana P-241, P-242, P-243, P-255
Lohse, Christine M P-516
Longatto-Filho, Adhemar P-374
López, K P-87
Lopéz, Ana M O-88
López, Ana Mª Sánchez P-462
López, Carlos O-6
López, Enrique PFP-7
López, F Ignacio Aranda P-254
López, Francisco Ignacio Aranda P-21
López, José Ignacio P-284, P-285
Lopez, Laura P-102, P-427, P-428
López-Beltrán, Antonio O-44, P-316
López-Bonet, E P-320
Lopez-Guillermo, A P-30
Lopez-Marin, Luciano P-212

Lorente, José Antonio O-42, P-333, P-343, P-344
Lorenzo-González, P P-265
Lorenzo-González, Pablo P-175, P-264
Lorenzoni, C P-133
Lourenço, Gustavo P-239
Lourenço, Silvia Vanessa P-305, P-306, P-307, P-308
Lovborg, Uffe P-453
Loy, Monica O-65
Lozano, Graciela P-355
Lozano, Juan José P-134
Lppez, R P-377
Luelmo, Jesús P-297
Luna, Arlene de P-446
Luna, Sebastian O-34
Lunardi, Francesca O-4, O-65
Lupu, Anca P-43
Luque, Rafael J O-44
Luzar, Boštjan P-436

Machackova A P-487
Machungo, F O-28
Maciel, Elines O P-166
MacLennan, Gregory O-45, P-316
Macrì, Luigia O-13
Madjd, Z P-233
Magest, Kuame P-522
Magna, Luís A P-317, P-318
Mahassini, Najat P-206, P-407
Mahjoub, Fatemeh P-135
Mahmoudi-Brahim, Houda P-187
Mahmoudi, Houda P-26, P-109, P-110, P-111, P-113, P-309
Mahzouni MD, P P-258
Majak, Bernard O-32
Makowiec, Frank O-53
Makretsov, N O-31
Malagelada, JR P-382
Malamou-Mitsi, Vasiliki P-24, P-44, P-272, P-432, P-509
Malik, J P-54
Mallofré, Carme P-342
Malo, Palmira P-500
Mancebo, Gemma P-102, P-427, P-428
Mandys, Václav PFP-7
Mansouri, Fatima P-206, P-407
Marcano, F O-58
Marcellan, Carmen Ruiz P-93
Marchet, Silvia P-34
Marco, V P-218
Marginean, Felicia P-93, P-353
Maria, Biteli P-94, P-95, P-199, P-325, P-530, P-531, P-532
Maria, Neagu P-375
Maria, Papaevangelou P-325, P-329, P-530, P-531, P-532
Maria, Sevastiadou P-94, P-95, P-199, P-325, P-329, P-530, P-532
Marichal, Miriam O-61
Marin, Basic P-410
Marino, Silvia O-78
Marín, Carlos P-150
Marín, Luis Miguel P-194
Mariño, Adrian P-431
Mariño-Enriquez, Adrian P-100
Markiewicz, Tomasz P-260, P-357
Marks, Rebecca P-316
Marques, A M Leitão O-70
Marques, Mariangela Esther Alencar P-32
Marquina, I P-18, P-328, P-514
Marquina, Isabel P-158, P-237, P-303, P-503
Marrón, MT P-479
Marszalek, Andrzej O-76
Martignoni, Guido O-45, O-46, PFP-1
Martin, Angel Garcia P-238
Martín, Jose María O-82
Martín, Paloma O-88
Martinez, A P-30
Martínez, Antonio P-507
Martinez, E P-429
Martínez, M Angel P-48
Martinez, Ma Angeles P-212
Martinez, MA P-218
Martinez, Maria Angeles P-75
Martinez, Mercedes P-93
Martínez, Miguel A P-208
Martini, Chiara O-4
Martins, Ana Paula O-70, P-471
Marucci, Gianluca P-9, PFP-5
Marulli, Giuseppe O-65
Mas, Antonio P-511
Mascaró, José Manuel P-497, P-507, P-511
Mascolo, Massimo P-489
Masferrer, Emili P-253
Mashayekh, Masoud P-269
Massa, Dolores Suarez P-289
Mata, Raquel O-9
Mataix, Jose P-201
Matejic S P-454
Mateos, Eduardo Alcaraz P-21
Matias-Guiu, X P-121
Matic, Marija P-409
Matilla, Alfredo PFP-3
Matsionis, Alexander P-154, P-526
Matter, Maurice P-360
Maurer, Christoph A P-398, P-402
Mavis, O P-49
Máximo, Aline A P-302
Maximov, Gueorgui P-266
Mayor, Marcela Ortiz P-169
Mayordomo, Empar O-82
Mazal, Daniel P-118
Mazzarelli, P O-89
Mazzarelli, Paola O-90
MD, Jonathan F Lara P-518
Meca, Óscar P-134
Medel, Encarnación Barroso P-21
Mederle, Narcisa P-491
Medina, Manuel P-149, P-155, P-462
Medina, Nathalia P-523
Medina, Rafael Méndez P-437
Meiner, Vardiella P-452
Meir, Karen P-452
Meirelles, Luciana P-317, P-318, P-319
Meizoso, Telma O-25
Mekni, Amina P-55, P-56, P-128, P-173, P-261, P-262, P-341, P-359, P-364, P-365, P-366, P-485, P-486
Melchers, Willem J G P-138
Melendez, Barbara P-278, P-279, P-280
Mellado, Begoña P-342
Memeo, Lorenzo P-391
Menard, P P-292
Mendes, Ana Cristina P-46
Mendiola, Marta P-100
Menéndez, C O-28
Menestrina, Fabio O-46
Mera, Mihaela P-466, P-468
Mera, Simona P-466, P-468
Mercado, María del Rosario P-500
Merino, Maria P-67
Meshba, Habiba O-37
Mestiri, Sarra P-14, P-131
Mestre, Maa José O-25
Metze, Konradin P-295
Meyer, Anke P-64
Meyer, Patrick P-65
Meza, Carmen Fuenmayor P-150
Mezei, Tibor P-38, P-181, P-381
Micello, D P-291
Michej, Wanda P-369
Midi, Ahmet P-246
Miglio, Rossella PFP-5
Mignogna, Chiara O-47
Mihaela, Chivu P-267
Mihaela, Gherghiceanu P-519
Mihai, Mihaela P-43, P-70, P-202, P-250, P-375
Mihajlovic, Dusan P-409
Mihic-Probst, Daniela O-78
Mijucic, Vesna P-176
Mikhanoshina, Nina P-154
Milanesi, Ornella O-24
Milenkovic, Branislava P-7
Milenkovic, Sanja P-50
Miljan, Krstic P-410
Milojevic, P P-480
Milovanov, A P P-442
Milovanov, Andrey P-154
Milovanovic, Vladimir P-167
Milting PhD, Hendrik O-66
Miquel, Rosa P-196
Miranda, Rosana R O-71
Mircea, Brehar Felix P-267
Mircea, Leabu P-273
Mircea, Penescu P-519
Mirlacher, M O-43
Mirsadraee, S P-145
Mishnev, Oleko Dmitrievich P-178, P-379
Misiołek, Maciej P-304
Mitrovic S P-454
Mitselou, Antigony P-5, P-58, P-76
Miyauchi, Akira O-14
Moaven, Omeed P-368
Moch, Holger O-1, O-78
Modi, Dr lopa P-411
Mohanty, Bidhu P-450
Mohssine, Raouf P-206
Moicean, Andreea-Delia P-43
Mokni, Moncef P-86, P-131

Molanaei, S P-233
Moldovan, Lucia P-177, P-457
Molea, Guido P-489
Molinero, José-Antonio Perera P-191
Mollejo, Manuela P-278, P-279, P-280
Mollejo, Villanueva M P-388
Molleví, David G P-399
Moncef, Mokni P197
Montazeri, V P-234
Monteagudo, Carlos O-82, P-490, P-501
Montero, MA P-198
Montesinos, Jesus P-116
Montironi, Rodolfo P-316
Montserrat, N P-121
Mora, Jaume P-149, P-231
Morales, Rafael P-349
Moran, Cesar P-11
Morandi, Luca P-236, PFP-5
Morell-Quadreny, Luisa P-315
Moreno, Antonio P-162
Moreno, Carolina P-342
Moreno, Judith P-430
Moreno, Ma Isabel P-10
Moreno, María Isabel P-194
Mori, Ichiro O-14, P-461
Morozov, Sergiy P-156, P-287
Morra, Laura O-1
Mortier, Erwan P-293
Mosteiro, Lorena P-284
Moulla, Alexandra P-171
Mounir, Trimech P197
Moura, Rodrigo L O-71
Moussa, Adnène P-26, P-109, P-110, P-111, P-113, P-187, P-309
Moyano, Susana P-507
Mozos, Ana P-196
Mozos, Anna P-497
Mroz, Andrzej P-400
Mrvic, Stanko P-455
Mueller-Hermelink, O-9
Muga, Silvia de O-42, P-333, P-343, P-344
Müller, S P-222
MUNDIM, Fiorita GL P-241, P-242, P-243, P-255
Mungan, Aydin P-534
Munne, A P-488
Muñoz, G P-328
Muñoz, C P-218
Muñoz, G P-18, P-514
Muñoz, Gloria P-10, P-194
Muñoz, Guillermo P-158, P-237, P-303, P-503
Muñoz, Nubia PFP-7
Muñoz, Roberto P-456
Muñoz-Seguí, Josep P-323
Muntean, Valentina P-70
Murer, B O-3
Murillo, Raquel P-102, P-427, P-428
Musser, Jeanette P-376
Mustedanagic-Mujanovic, Jasminka P-92
Musulén, Eva P-277, P-367
Muti, Christine O-49
Mutiu, Gabriela P-470, P-476, P-477
Mylovydova, Ganna P-207, P-219, P-522
Nachev, Sevdalin P-266
Nadal, C P-484
Nadal, Marga P-327
Nadal, R P-120
Nadia, Boujelbene P197
Naeimi, E P-234
Najmabadi, Hossein P-190
Nakamura, Misa O-14, P-461
Nakanishi, Yukihiro P-5
Nalcha, Igor P-207
Nami, F P-234
Namysłowski, Grzegorz P-304
Nart, Deniz O-56
Narváez, José Antonio P-45
Nascimento, Carlos P-393
Nascimento, Marilene F P-422
Nasiri, Mohammadreza Ghavam P-368
Navarro, Itziar P-141
Navarro, Samuel O-20
Navas, Rafael P-48
Nayach, Iracema cancer tissues O-86
Nazari, Zeinab P-416
Neagu, Maria P-70, P-132, P-250
Negroiu, Gabriela O-79, P-496
Nepomnyaschy, Valentin P-314
Nessa, Ashrafun PFP-7
Nesseris, John P-272
Neto, Octávio Barbosa O-71
Nezic, D P-480
Ngendahayo, Placide P-210
Nichita, Luciana O-79, P-496
Nicolae, Alina P-43
Niculescu-Mizil, Emilia P-43
Nielsen, Majken P-453
Niero, Lígia P-32
Nieto-Matínez K P-143
Nikiel, Barbara P-68
Nikiforos, Apostolikas P-325, P-329, P-530, P-532
Nikiforos, Georgia Apostolikas P-531
Nikolaidou, Christina P-172
Nilsson, Linn P-354
Nishizawa, Patrícia P-39
Niveiro, María P-254
Njim, Leila P-26, P-109, P-110, P-111, P-113, P-187, P-309
NNAKENYI, E F P-283, P-447
Noel, Jean-Christophe O-17, P-101
Nogales, Francisco F P-106
Noguera, Rosa O-20
Nolde, Nataša P-436
Noleto, Gustavo Sousa P-3
Nonogaki, Sueli P-393
Nordgren, Svante P-354
Nordlinger, Bernard O-49
Nørgaard, Peter P-249
Noronha, Marcelo P-318
Notohara, Kenji P-170
Nouira, Kais P-33
Novello, Silvia PFP-6
Nowecki, Zbigniew P-369
Nugnes, Loredana P-489
Numanoglu, Gamze P-185
Núñez , Mónika P-406
Nyagol, Joshua O-84
Nylund, Gunnar P-354
NZEGWU, M A P-283
Nzegwu, M A P-447

Oancea, Roxana P-439
Ochoa, Gorka O-91
Ochoa, Julio J P-201
Ochoa, M P-435
Odasso, Chiara O-13
Odum, Niels O-8
Ohsie, Steven P-465
Ojanguren, I P-377
Okolow, Marzena Podhorska P-356
Ökten, Heyecan P-300, P-324, P-370, P-419, P-492, P-493
Oliveira, A P-302
Oliveira, Flávia A O-71, P-301
Oliveira, Humberto Álvares de P-6
Oliver, J O-95
Olivera, Monica P-430
Olsina, J P-198
Olszewki, Włodzimierz P-369
Olusina, D B P-447
Olvi, Liliana G P-169
OnakKandemir, Nilufer P-104
Onea, Alina P-240, P-88
Onguru, Onder P-268
Onnis, Anna O-84
ONWASIGWE, E N P-283
Oprita, Elena Iulia P-177
Ordi, J O-28, P-133
Ordi, Jaume PFP-7
Orellana, Ruth P-297, P-418, P-421, P-495
Orillaza, Marissa A P-441
Orlandi, Augusto P-482
Orłowska, Janina O-52
Orradre, Juan Luis P-279
Orradre, Romeo JL P-388
Orscelik, Simge G P-123
Ortega, Francisco Javier P-284
Ortega, Luis P-513
Ortiz, Ángel R O-86
Ortiz, Maria Rosa P-296, P-395
Ortiz, R P-12
Ortiz, Sharon O-12
Ortiz-Rey, José Antonio P-223, P-498
Osaba, Lourdes O-91
Osman, N O-28
Osman, Sezghin P-89
Osowski, Stanislaw P-260, P-357
Otasevic, P P-480
Otilia, Zarnescu P-267
Otterbach, Friedrich O-30
Ouazzani, Hafsa El P-206
Ouni, Ahlem P-365
Ozburn, Natalie C P-11
Ozdamar, Sukru Oguz P-185, P-245, P-271, P-510, P-534
Ozen, Haluk O-39
Ozucer, Berke O-54, P-203

Pacak, Karel P-67
Pache, Jean-Claude P-65, P-415,
Padalino, Massimo O-24
Padron, A P-488
Padullés, Laura P-399
Palacín, A P-511
Palestini, Nicola O-13
Pallardó, Luis O-64
Pallarols, Marta P-102, P-427
Paloff, A P-124, P-140, P-517
Palomba, Annarita P-183
Palou, Josep P-497, P-511
Pané, Maria P-45, P-323
Pannain, Vera Lucia P-205
Paolin, Adolfo P-472
Papadaki, Helen P-313
Papadiotis, Evangelos P-432
Papaloukas, Ch P-426
Papatheodoridis, George V P-405
Papotti, Mauro P-19, PFP-6
Papoudou-Bai, Alexandra P-44
Pappa, Lina P-432
Papuc, Anca Florentina P-89
Papuc, Anca P-99, P-232, P-378
Parada, D O-29
Parada, David P-345
Parascan, Liliana P-470, P-476, P-477
Park, Jee Hee P-308
Park, So Yeon P-330
Parker, Nicole Teoh P-249
Parolini, Claudia O-46
Parra, Edwin Roger P-1, P-2, P-3, P-4, P-6
Parral, Purificación P-504
Paschoal, Juliana P-205
Pascual M P-18, P-328, P-514
Pascual, Mar P-158, P-237, P-303, P-503
Pasechnik, Dmitry P-337
Paskalev, E P-140
Paskalev, E P-517
Paslaru, Liliana P-202
Pasternak, Olena P-207
Pasz-Walczak, Grażyna P-230
Patel, Dr Trupti P-411
Patel, Junaid O-68
Patsouris, E P-464
Patsouris, Efstratios P-481, P-515
PAULA, Clayton Aparecido de P-241
Pavlidis, Nikolaos P-44, P-432
Pavlopoulos, Petros M P-321
Pavlov, Konstantin Anatol'evich P-178
Pechianu, C P-202
Peg, V P-429
Peiró, Francisca M P-251
Peiro, Gloria O-33, P-251, P-254
Pellín, Ana P-490
Pellín, Antonio P-490
Pelmus, Manuela P-84
Pelosi, G O-3
Peña, G O-29
Pena, J P-121
Peña, Karla B P-345
Penin, Rosa M P-494
Pentheroudakis, George P-44, P-432
Pera, J P-338
Peralta, Osvaldo P-169
Pereira, Cláudia P-305
Peres, Luiz Cesar P-157
Perez, Edith A O-35
Pérez, F P-12, P-320
Pérez, Julio Alexander Diaz P-148, P-257, P-259, P-281, P-286, P-346, P-347, P-348
Pérez, Ma Isabel R P-235
Pérez, Noelia P-149, P-155
Pérez, R Beloqui P-467
Pérez-Becerra, Raquel P-61
Pérez-Magán, Elisa P-278, P-279
Perezpeña-Diazconti M P-143
Perezpeña-Diazconti, Mario P-153
Pérez-Villa, Lidia PFP-3
Perin, Tiziana P-391
Peris, Mercé P-430
Peschos, Dimitrios P-58
Pession, Annalisa PFP-5
Petit, Ana P-196
Petit, Anna P-342
Petrakopoulou, Nerantzoula P-82
Petre, Tatiana P-70
Petrescu, Stefana O-79, P-496
Petros, Pavlopoulos P-535
Petroula, Kakouri P-535
Petrov, Semyon P-363
Pettersson, Ann P-354
Peyrard, Severine P-293
Pfeifer, Lotte P-453
Pharoah, P O-31
Philippov, Alexey O-73
Phillips, Therese P-214
Pietruszewska, Wioletta P-310
Pignatelli, Alexandra P-46
Pii, Kurt P-214
Pijuan, Lara P-102, P-427, P-428
Pilar, Forcada P-423
Piñas, J C Ferreres P-460
Pineda, Minnie Jane P-446
Piñeiro, Ana González P-335
Pinheiro, Céline P-374
Pinheiro, Ronald Feitosa P-41, P-42
Pinilla, Maria Teresa P-289
Pintilie, Melania O-87
Pinto, Glauce Aparecida P-239
Piotrowska, Aleksandra P-520
Piqueras, Marta O-20
Piulats, Josep Maria P-327
Pla, Maria Jesús P-231
Placidi, Claudia P-34
Planas, S P-429
Planas, Sílvia P-163
Planck, Maria O-5
Planella, Sandra P-102, P-427
Planelles, María P-254
Plesea, Iancu Emil P-274, P-463
Plet, Ariane P-293
Podhorska-Okolow, Marzena P-520
Poinareanu, Ionut P-89, P-99, P-232, P-378
Polak-Charcon, Sylvie P-352
Polat C P-179
Poli, Francesca P-142
Pollheimer, Marion J O-50, O-51
Pollheimer, Verena S O-50, O-51
Ponce-Castañeda V P-143
Pons, C P-119, P-120
Pons, Lluis E O-6
Pop, Oltin Tiberiu P-274, P-463
Popescu, Dragnea I P-202
Popescu, Laurentiu Mircea O-75
Popov, D P-140, P-517
Popper, Helmut H P-19
Porro, Valentina P-118
Potemski, Piotr P-230
Povilaitite, Patrisia P-526
Pradilla, Gustavo P-259
Prat, J P-119, P-120, P-121
Prat, Jaime O-33
Preda, Ovidiu P-106
Prévot-Maupoix, Martine P-240
Prodanova, Irina P-77, P-107
Provenzano, E O-31
Prudkin, Ludmila P-11
PUBILL, C P-85
Pucci, S O-89
Pucci, Sabina O-90
Puertas, Sara P-327
Puig, Josep P-296
Puig, Luis P-494
Puig, Pierre Laurent P-293
Puig, Susana P-511
PUIG, X P-85
Puig, Xavier P-403
Puigdemont, Gemma Sais P-506
Pujol, R P-488
Puri, Ajay P-168
Pushker, Neelam P-450
Pusztaszeri, Marc P-360

Qihui, O-26
Quadreny, Luisa Morell P-314
Quemelo, Paulo Roberto Veiga P-157
Quer, Ariadna P-367
Quezado, Martha P-67
Quiles, Jose L P-201
Quiñoa, Arantxa P-414
Quint, V P-138
Quint, Wim PFP-7
Quintana, J J O-58
Quintanilla-Martinez, Leticia P-66
Quintin-Colonna, Françoise P-293

Radhi, Jasim O-57
Radulescu, Doinita P-106, P-112, P-186, P-508
Radvanyi, Hélène O-49
Rafatpanah, Houshang P-37
Ragazzi, Moira PFP-5
Rahsaz, Marjan P-525
Raica, Marius P-228, P-381, P-383, P-491
Rakhmanova, A G O-27
Rakic, Sanja P-167
Ralfkiaer, Elisabeth O-8
Ramirez MD, Josep P-29
Ramírez, Carlos Alberto García P-257, P-346, P-348

Ramírez, José Luis P-277
Ramírez, Raquel Gómez P-462
Ramírez-Bajo PhD, Maria José P-29
Ramirez-Tortosa, Cesar L P-201
Ramirez-Tortosa, M Carmen P-201
Rammeh, Soumaya P-14, P-86, P-131, P-499
Ramón, Antoni Urban P-188, P-326
Ramos R P-87
Ramos, David P-314, P-315, P-322, P-490
Ramos, Emilio P-399
Randjelovic, Tomislav P-392
Rangel, Carlos Mario P-483
Raptis, Georgios P-81
Rasmussen, O F P-222
Rasmussen, Ole Feldballe P-453
Ratiu, Iulia P-373
Rausch, Thierry O-10
Ravanshad, Mahmoud P-525
Ravarian, Mehrangiz P-37
Razavi, Alale Shoja P-146
Raziee, Hamidreza P-368
Rea, Federico O-4, O-65
Rebouças, Ivan P-96, P-97
Recillas-Targa, Félix P-153
Redondo, Andres P-100
Rehak, Peter O-50, O-51
Reis, Luis F L P-184
Reis, Marlene A O-71
Reis, Marlene Antonia dos P-528, P-529
Rekhi, Bharat P-168
Remstein, Ellen PFP-9
Rendón, Luís Alejandro Rivero P-257, P-346, P-347, P-348
Renedo, Guadalupe O-9
Reshetnikova, Olga P-156
Rey, Mercè P-116, P-248, P-252, P-297, P-418, P-421, P-495
Reznikova, Galina P-154, P-526
Rezola, Ricardo P-238
Ribalta, Teresa P-278, P-279, P-280
Ribo, Maricel P-446
Ricchetti, T O-3
Righi, Alberto P-215, P-236
Righi, Luisella PFP-6
Rigola, Maria Angeles P-252
Ríos, MJosé P-237
Riva, C P-291
Riva, Cristina P-34
Rivas (in memoriam), José P-10
Rivas, A P-429
Rivera, Teresa O-25
Riza, Liviu P-463
Rizzardi, Giovanna O-4, O-65
Rizzo, Stefania P-472
Robert, Koktysz P-404
Roca, M[a] José, P-332
Roca, P O-95
Rodrigues, Marcelo Fabiano P-127, P-152, P-448, P-449
Rodrigues, Maria Laura Pinto P-528, P-529
Rodríguez, Alberto Pérez P-217, P-275
Rodríguez, Eva P-149, P-155
Rodriguez, I P-133
Rodríguez, José I O-23
Rodríguez, Merlo R P-388
Rodríguez, Rosa-Nieves P-437
Rodríguez-Fernández, Belén P-223
Rodríguez-Gil, Yolanda P-208
Rodríguez-Morales, Alfonso J P-126
Rodriguez-Osorio, Xiana P-264
Rodriguez-Peralto, JL O-92
Rodriguez-Pinilla, M O-92
Romagosa, C O-28
Romagosa, Vicens P-45
Roman, Jose Javier Gomez O-91
ROMAN, R P-85
Roman, Ruth P-403
Romanenko, Alina P-314, P-315
Romero, Emilia P-102, P-427, P-428
Romero, Gúzmán G P-388
Romero, Zoila P-523
Romero-Sánchez, M P-120
Ronchetti, Ruben P-67
Ronci, Maurizio O-85
Rosa, Gaetano De O-47, P-489
Rosas, Rosj PFP-6
Rosell, Rafael P-277
Roselló-Sastre, Esther O-64
Rosemann, Michael P-66
Rosiñol, Oria P-504
Rossi, G O-3
Rossi, Renata C O-71
Rougier, Philippe O-49
Rovira PhD, Jordi P-29
Ruano, Yolanda P-278, P-279, P-280
Rubio, I P-218
Rubio, Nuria P-134
Rugge, Massimo O-4
Ruhi, M Rey P-460
Ruíz-Ponte, Clara P-53, P-63
Ruíz-Ponte, Jin Hwan Kim P-61
Ruiz-Sanchez E P-143
Ruiz, Eduardo Salido P-115
Ruiz, Maryori García P-150
Ruiz, Rebeca P-284, P-285
Ruka, Włodzimierz P-369
Rull, Daniel Moya P-29
Russo, Rosa O-47
Rutkowski, Piotr P-369
Ryan, Lee P-214

S, Aso Manso P-388
Saber, Alexandre P-4
Sadeghian, Mohammad Hadi P-36, P-37
Sadeghipour, Alireza P-269
Sadok, Korbi P197
Sadrarhami, Shohreh P-524
Saez, Ampar P-418
Saez, Amparo P-248, P-252, P-297, P-495
Sáez-Lagos, Dolores P-162
Sagrario, Trinidad Hernández P-412
Sahan E P-192, P-49
Sahin O P-179, P-180
Sahin, Dursun Ali P-226
Sahtout, Samia P-365, P-55, P-56
Said, Jonathan P-465
SAIDANI, Zahra P-113
Sajin, Maria P-108, P-394
Şakirahmet, Dilek P-23
Salamanca, Javier P-208
Salapura, Aleksandra P-224, P-72
Salas Villar, I P-165, P-161
Salas, Antonio P-387, P-388
Salas, Clara O-88
Salazar, Fernando O-88
Salazard, Ramón P-399
Salcedo, MT P-198, P-429
Salehian, Pirooz O-81
Salma, Ben Haha P-261
Salmerón, Jorge PFP-7
Salvadó, M Teresa O-6
Salvador, Carmen Admella P-506
Salvago, Ma Dolores Martín O-44
Samaila, Modu peola P-213
Samanianpour, Pargol P-524
Samaratunga, Hemamali PFP-1
Sanchez, Navarro P-388
Sánchez-Payá, José P-251
Sánchez-Simón, Raquel O-25
Sánchez-Tejada, Laura P-251
Sánchez-Yuste, Rosario O-88
Sánchez, José Javier P-277
Sanei MD, MH P-258
Sanei, MH P-362
Sanfeliu, Esther P-248, P-252, P-421, P-495
Sanjose, Silvia de P-430
Sansano, Irene P-162, P-382
Santandreu, F O-95
Santonja, Carlos O-9
Santonja, Nuria P-22, P-501
Santos, Jordina P-102, P-427, P-428
Sanz, Carolina P-277
Sanz, Cipriano Manzano P-437
Saperas, Esteve P-382
Sarian, Luís P-96, P-97
Sarkissian MD PhD, Naver A P-413, P-518
Sartori, G O-3
Sastre, Esther Roselló P-505
Sastre, Xavier P-293
Saussure, Barbara De P-415
Saute, F O-28
Sauter, G O-43
Savas, Berna P-386
Sayadpour, Delaram P-37
Scalvenzi, Massimiliano P-489
Scarpulla, Salvatore P-391
Scheimberg, I P-160, P-161, P-165
Scheimberg, Irene O-21
Schenka, André Almeida P-16, P-239, P-39, P-96, P-97
Schenka, Natália P-239, P-39, P-96, P-97
Schlemmer, Andrea O-50, O-51
Schlomm, T O-43
Schmid MD, Christof O-66
Schmid, Joachim P-214
Schmid, Kurt W O-30
Schmid, Kurt Werner PFP-8
Schmitt, Fernando P-374
Schmitz MD, Klaus Jürgen O-66
Schønau, A P-222

Schraml, Peter O-78
Schroeder, Josef O-74
Schwertheim, Suzan PFP-8
Ścierski, Wojciech P-304
Secara, Diana P-108
Secer, Halil İbrahim P-268
Seel, Maximillan O-62, O-63
Seemayer, Christian P-65
Segarra, Manuela P-163
Seget, Monika O-76
Segnini, Zulay Maizo de P-122
Seguí, Javier P-254
Sehati, Fatemeh P-229
Seifert, Burkhardt O-78
Seiwerth, Sven P-139
Selma, Bellil P-128
Semidey, Ma Eugenia P-382
Semidey, María-Eugenia P-164
Sen, Seema P-450
Senaratah, Carmalita P-52
Sennesael, Jacques O-61
Şensu, Sibel P-104, P-105
Serra, M P-435
Serrano, Andrea Prada P-358
Serrano, Manuel P-193
Serrano, S P-488
Serrano, Sergi O-42, P-102, P-333, P-343, P-344, P-427, P-428
Serrano, Teresa P-253, P-399
Sertöz, Rüçhan O-56
Sesti, Fabiola O-90
Sever, Zeynep Tosuner P-527
Seyrafianpour, Shiva P-524
Shafeghati, Yousef P-190
Shah, Dr Manoj J P-411
Shah, Rajal O-45
Shah, Sejal S O-35
Shahzadi, Shahriar Zohourian P-147
Shandiz, Ehsan Esmaeili P-368
Sharifi, A P-233
Sharifi, N P-145
Sharifi, Noorieh P-209
Sharma, N O-80
Sharma, Seema P-129
Shayanfar, Nasrin P-269
Shchegolev, Alexandr Ivanovich P-178, P-379, P-451
Sheinin, Yuri P-516
Sheppard, Mary O-68
Sheu, Sien-Yi PFP-8
Shin, Hai-Rim PFP-7
Sia, Katherine D P-441
Sierra, José Ramón Paniagua P-538
Sierra, Montserrat P-164
Sikirić, Predrag P-139
Silva, Cesar Augusto Melo e P-6
Silva, Giuliana P-422
Silva, Maria O-2, P-13
Silva, Nathalie Henriques P-205
Silva, Vinicius Duval da P-166
Silva, Wanessa M P-301
Sima, Hamidreza P-368
Simeonov, P P-140, P-517
Simion, George P-108, P-394
Simões, Deise Lúcia Chesca P-157
Simões, Kleber P-374
Simon, Ph O-43
Simon, R O-43
Simona, Enache P-250, P-70
Simona, Gurzu P-381
Simonetti, Sara O-47
Simonida, Stoiljkovic P-410
Simou, Nafsica P-76
Simsek, Gulcin Guler P-300, P-324, P-370, P-419, P-492, P-493
Simulescu, Razvan P-438, P-439
Sinn, Hans-Peter O-36
Sintou, Evdoxia P-432
Sioutopoulou, Despoina P-424
Şirvancı, Serap P-527
Skafida, Evangelia P-82
Skoufi, Urania P-432
Skyrlas, Angelos P-24
Slim, Haouet P-485
Slobodan, Milisavljevic P-455
Slobodanka, Mitrovic P-455
Soares, Fernando A P-184, P-393
Soares, Fernando Augusto P-16, P-305, P-306, P-307, P-308
SOARES, Fernando P-241, P-242, P-243, P-255
Sobaru, Iuliana P-202
Sobral, Ana Paula Veras P-307
Sobrinho-Simões, Manuel P-53, P-61
Soeiro, Alexandre de Matos P-1
Sok, Miha P-15
Soland, Torunn O-32
Solars, Horacio P-169
Solé, Manel P-196
Soler, Imma P-102, P-427, P-428
Soler, M Teresa P-253
Soler, Teresa P-231
Soltermann, Alex O-1
Somma, Anna P-489
Sopta, Jelena P-176
Soriano, N Combalia P-460
Soriano, Pilar P-322
Sota P P-328, P-18, P-514
Sota, Patricia P-158, P-237, P-303, P-503
Soubrier, Florent O-49
Soumaya, Rammeh P197
Sousa, Vitor O-2, P-13
Soutar, Denise O-88
Spagnoli, Luigi Giusto O-85, O-89, O-90, P-482
Spaulding, Betsy P-376
Sporea, Ioan P-371, P-372, P-373
Squier, W P-160
Sretenovic, Vesna P-50
Sriha, Badreddine P-14, P-499
Stacher, Elvira P-19
Stahov, Jugoslav P-92
Staibano, Stefania P-489
Stajevic, Mila P-167
Stanek-Widera, Agata P-304
Stanescu, Alina P-394
Staniceanu, Florica O-79, P-250, P-496
Stanisław, Osowski P-404
Stankovic, Vesna P-455
Stanojevic, Goran P-408
Stefan, Laura Mihaela P-270
Stefanou, Dimitrios P-24
Stefanovic, E P-480
Stelini, Rafael F P-319
Stellin, Giovanni O-24
Stepanova, A A O-27
Sterba J P-487
Stern, Corinna P-64
Stickeler, Elmar O-53
Stita, Wided P-131, P-14, P-499, P-86
Stoemmer, Peter E O-40
Stoia, Razvan P-43
Stoica-Mustafa, Elena P-202
Stojanovic, Miroslav P-409
Stojiljkovic, Miodrag P-392
Stojsic, Jelena P-7
Stojsic, Zorica P-392
Stolf, Hamilton Ometto P-32
Stolnicu, Simona P-106, P-112, P-186, P-508
Štor, Zdravko P-396
Storz, Martina O-78
Stroescu, C P-202
Suarez, Dolores O-88
Suarez-Novo, JF P-338
Suárez-Peñaranda, JM P-265
Suárez-Peñaranda, José Manuel P-175, P-264, P-498
Suarez, Asuncion P-100
Suciu, Cristian P-228
Sun, Menghong P-11
Sung, Sook Whan P-20
Sungur, Arzu P-312
Suñol, Mariona P-149, P-155
Sushkov, Sergey P-219
Sutter, Michel O-10
Svetlana, Kodjmanovska P-51
Swelam, Wael Mohamed P-282
Swelam, Wael P-47
Szentirmay, Zoltán P-38
Szybka, Malgorzata P-263

T, Arvanitakis P-329
T, Durko P-311
Tăban, Sorina P-371, P-372, P-373
Tabatabaee, A P-145
Tabriz, Hedieh Moradi P-420
Taghipour, Shokouh O-11, P-195
Tagliabue, G P-291
Taheri, Diana P-524
Takeda MD, Atsushi O-66
Takeda MD, Nobuakira O-66
Tallada, N P-429, P-435
Tan, Carmela D P-441
Taner, Ömer Faruk P-300
Tanna, Vaishali P-214
Tao, Xiaodong O-62, O-63
Tapia, Gustavo P-504
Tardanico, Regina O-46
Tari, Ali Sadeghi P-420
Tarroch, Xavier P-387, P-388
Tartour, Eric P-293
Tas, Patrick O-37
Tascón, Ruth P-17, P-231
Tatsiou, Cytology Zoi P-424
Tatsiou, Zoi P-171, P-172, P-425
Tavaglione, Veronica PFP-6
Tavares, Denise P-301

Taveira, Claúdia T P-302
Tazi, Nadia P-407
Teixeira, Daniel P-319
Teixeira, Vicente de Paula Antunes P-528, P-529
Teixeira, Vicente P A O-71
Teixidor, Pilar P-277
Tejerina, Eva P-431
Tejerina, Eva P-513
Teletin, Diana P-375
Temel, Tuncay P-351
Teodoro, Walcy P-2
Terradez, Liria P-22, P-490, P-501
Terrasa, F P-484
Terzea, Dana P-250, P-375, P-43
Terzea1, Dana P-132, P-70
Terzic, Tanja P-50
Tezel, Gaye Guler P-312
Tezer, Ayla P-300, P-324, P-370, P-419, P-492, P-493
Theodorakopoulou, P-531
Thiene, Gaetano O-24, P-142, P-472
Thiesler, Thore P-398, P-402
Thoma-Tsagkli, Efimia P-189
Thomson, Mike O-19
Thomson, Timothy M O-86, P-134
Thomson, Timothy P-137
Tica, Constantin P-89
Ticha V P-487
Tichy M P-487
Todorov, T P-124, P-140, P-517
Todorova, Krasimira P-336
Todorovic M P-454
Todorovic, Vera P-409
Toffoli, Silvia O-24
Tomasz, Markiewicz P-404
Tomic, Ljiljana P-50
Tomulescu, V P-202
Tona, Francesco P-142
Torán, Núria P-162, P-163, P-164
Torea-Filgueira, Ana Maria P-264
Torné, J I P-484
Torras, Jaume P-399
Torres, E Sanfeliu P-460
Torres, gustavo P-523
Torres, Ines de P-353, P-382
Torres, Sergio Andrés P-483
Tortosa, Avelina P-280
Tortosa, JM P-479
Toruner, Murat P-386
Tosi, Piero O-84
Tosti, G P-291
Touil, Nada P-109, P-111, P-187, P-26
Tous, Sara PFP-7
Trabelsi, Amel P-131, P-14, P-499
Trcek, Ciril P-502
Trecasas, Miriam Cua P-353
Tresserra, F P-218
Tresserra, Francisco P-212, P-75
Trias, Isabel O-41
Trimech, Mounir P-86
Triponez, Frédéric P-65
Trpkov, Kiril O-48, PFP-4
Trujillo, Rafael PFP-3
Tsatsoulis, Agathocles P-24
Tsiouris, Spyridon P-272
Tsipis, Angelos P-481
Tsiple, Ilie P-474
Tsokos, Maria PFP-10
Tsukayama, Choutatsu P-170
Tulic, Goran P-176
Turcu, Mihai P-334
Turell, M P-12, P-320
Turell, Mariana P-296
Türkşen, Zeynep P-300
Tuzun, Ali Emre P-386
Tuzuner, Burcu P-244

Uccella, Silvia P-34
Uchino, Kaori P-170
Uchov, Yriy I P-331
Ugalde, Aitziber P-285
Ugalde, Jorge P P-235
Uluoglu, Omer P-216
Ungureanu, Loredana P-112, P-186, P-508
Urbani, Andrea O-86
Urbaniec, Natalia P-304
Uribe, Ana María P-358
Uribe, Mario Alexander Melo P-148, P-348
Utoiu, Elena P-270, P-457
Uvirova M P-487

Vacarasteanu, Andreea P-202
Vahabzadeh, Vahid O-11
Val-Bernal, Jose Fernando O-91
Valderrama, Paola Aranda P-347
Valeanu, Adina P-438
Valente, Marialuisa O-24, O-4, P-142
Valentí, Carla P-500
Valeri, R M P-426
Valeri, Rosalia Maria P-425
Valeri, Rosalia P-424
Valero, MIgnacia P-237
Vallès, Xavier PFP-7
Valverde, Concepción Fiaño P-335
Valverde, Concha Fiaño P-275
Valverde, JL P-479
Vaquero, Manuel P-456
Váquez-Veiga, Hugo P-498
Vara, Juan Angel Fresno P-100
Varakis, Ioannis P-313
Vardar, Rukiye O-56
Varela-Durán, Juan P-175
Varela, Mar P-231
Vargas, Luís Carlos Orozco P-281
Vasile, Cornelia P-457
Vasile, Liliana P-438, P-439
Vasilescu, C P-202
Vasilescu, Florina P-132, P-375, P-43, P-70
Vasilescu1, Florina P-250
Vassallo, José P-16, P-239, P-39, P-96, P-97
Vassilieva, N V O-27
Vasuri, Francesco P-215
Vázquez-Boquete, Angel P-61
Vazquez, Jose Antonio P-252
Vázquez, Pablo Fernández P-217, P-275, P-335
Vecchione, Maria Luisa P-489
Velasco, Verónica P-284
Velichko, A M O-27
Veljanovska, Slavica P-77
Vêncio, Eneida F P-301, P-302
Veniselos, Ioannis P-172
Venizelos, John P-171
Ventolà, Anna P-280
Vera, Jorge Andrés García P-257, P-259
Verbruggen, Banut-Sabine M O-94
Verdijk, Marian A J P-138
VERDU, M P-85
Verdú, Montse P-403
Vergara, Marleny PFP-7
Verslijpe, Tamara O-61
Vettore, André Luiz P-305
Vialard, Jean O-37
Vicandi, Blanca P-431
Vicioso, Luis PFP-3
Victoria, Rebeca Fernández P-275, P-335
Vida, August PFP-7
VIDAL, A P-85
Vidal, August P-141, P-323, P-327, P-403
Vidal, Noemi O-41
Vidal, Olga Garcia P-506
Vieira, Maria das Graças O-7
Vieites, B P-265
Vieites, Begoña P-498
Viguer, Jose M P-431
Vilaplana, Leticia Melgar P-115, P-401
Vilaseca, Ramón Rochera P-188
Vilchez-Barrios, Gustavo P-440
Vilela, Maria Marluce dos Santos P-39
Vilella, Angels P-349, P-414
Vilella, Ramón P-137
Villamizar, Javier Mauricio Olarte P-257, P-346, P-347, P-348
Villamón, Eva O-20
Villanueva, Alberto P-327, P-399
Villanueva, Concepción O-25
Villar, I Salas P-160
Villegas, I Amat P-467
Villegas, Iren Amat P-276
Vinyals, Francesc P-327
Vírseda, JM Martínez-Peñuela P-467
Visan, Ariana P-250, P-70
Visvesvara, GS P-130
Vladareanu, Ana-Maria P-43
Vladika, Natalia P-424, P-425
Vladimirovna, Natalia P-451
Vodopivec, Boris P-502
Vogel, Esther PFP-8
Vojinovic, Vera P-176
Volante, Marco O-13, PFP-6
Volkova, Larisa P-151
Vornetti, Silvia P-355
Vougiouklakis, Theodoros P-5, P-58
Voulgaris, Evangelos P-432
Vozianov, Alexander P-314, P-315
Vuka, Katic P-410
Vukmirovic, Filip P-380
Vukomanovic, Vladislav P-167
Vuletić, Bruno P-139

W, Pietruszewska P-311
Wagner, Kai O-53
Wakasa, Tomoko O-14

Walker, Jenny O-19
Walter, Paul P-88
Wang, Chunjie O-87
Wang, Mingsheng PFP-1
Wani, Yoji P-170
Warburton, Fiona O-21
Warren, Keisha O-87
Waters, J P-160
Weil, Bernardo O-34
Werner Schmid MD, Kurt O-66
Wild, Peter O-1
Willi, Niels P-402
Wim, G P-138
Winterfeld, Moritz von O-66
Wistuba, Ignacio I P-11
Wittersheim, Annick P-240
Woetmann, Andreas O-8
Wohlschlaeger MD, Jeremias O-66
Wojciech, Kozłowski P-404
Wong, Vietty O-87
Worm, Karl PFP-8
Wosniok, Werner P-64
Wysocka, Teresa P-356
Xavier, Morlius P-423
Xavier, Tarroch P-423

Yacoubi, Mohamed Taher P-86
Yahia, Néjib Ben P-109, P-110, P-111
YAHIA, Nejib BEN P-113
Yahia, Nejib Ben P-187, P-309
Yakoub, Lilia Ben P-14
Yakovtsova, Antonina P-522
Yamashita, Thamy P-32
Yasayan, Gozde P-123
Yavuzer, Dilek P-23, P-221
Yébenes, Mireia P-297
Yegiev, Valery Nikolaevich P-451
Yigit, Ozgur P-290
Yildiz, Pelin P-90
Yilmaz S P-180
Yilmaz, Asli O-48
Yilmaz, Guldal P-216
Yılmaz, Funda O-56
Yoon, Sun Och P-40
Yoshida, Adriana P-96, P-97
Yuste, Maria Rosario Sanchez P-289

Zaballos, Ángel O-86
Zabalza-Estévez, Iñaqui P-53
Zabel, Maciej P-356
Zabel1, Maciej P-520
Zabolinejad, N P-145
Zabolinejad, Nona P-144, P-146
Zabozlaev, F G P-442
Zachariou, Christianna P-24
Zadeh M MD, Yazdi P-258
Zakhama, Abdelfattah P-187, P-113, P-26, P-109, P-110, P-111, P-309
Zanatta, Laura O-65
Zannoni, Gianfranco P-536
Zare, Mehrjerdi A P-233
Zarei, Abdolmajid P-135
Zarnescu, Otilia P-177, P-457
Zawlik, Izabela P-263
Zemmel, Ihsen P-341
Zerbino, Dmitry O-72
ZERMANI, Rachida P-340
Zhang, Shaobo O-45, P-316, PFP-1
Zheng, Suqin P-316
Zhou, Gengyin O-14
Ziadi, Sonia P-86
Ziak D P-487
Zidan, Azza HM P-47
Zinovieva, Irene P-58
Zinovieva, Irini P-76
Zinserling, V A O-27
Zioga, Aikaterini P-509
Zitouna, Mohamed Moncef P-341
Zitouna, Moncef P-128, P-173, P-261, P-262, P-33, P-359, P-364, P-365, P-366, P-485, P-486, P-55, P-56
Zizi-Sermpetzoglou, Adamandia P-82
Zografski, George P-107, P-77
Zohoorian, S P-233
Zoltán, Pávai P-38
Zorzos, H P-464
Zouaidia, Fouad P-206, P-407
Zsuzsanna, Pap P-38
Zurac, Sabina O-79, P-496